

Edited by Herbert Sixta

 WILEY-VCH

# Handbook of Pulp

Volume 1



**Handbook of Pulp**

*Edited by  
Herbert Sixta*

*Further of Interest*

H. Holik (Ed.)

**Handbook of Paper and Board**

2006, ISBN 3-527-30997-7

# Handbook of Pulp

*Edited by*  
*Herbert Sixta*



WILEY-  
VCH

WILEY-VCH Verlag GmbH & Co. KGaA

**Editor**

**Dr. Herbert Sixta**

Lindenweg 7  
4860 Lenzing  
Austria

All books published by Wiley-VCH are carefully produced. Nevertheless, authors, editors, and publisher do not warrant the information contained in these books, including this book, to be free of errors. Readers are advised to keep in mind that statements, data, illustrations, procedural details or other items may inadvertently be inaccurate.

**Library of Congress Card No.:** applied for  
**British Library Cataloguing-in-Publication Data**  
A catalogue record for this book is available from the British Library.

**Bibliographic information published by  
Die Deutsche Bibliothek**  
Die Deutsche Bibliothek lists this publication in the Deutsche Nationalbibliografie; detailed bibliographic data is available in the Internet at <<http://dnb.ddb.de>>.

© 2006 WILEY-VCH Verlag GmbH & Co. KGaA, Weinheim

All rights reserved (including those of translation into other languages).  
No part of this book may be reproduced in any form – nor transmitted or translated into machine language without written permission from the publishers. Registered names, trademarks, etc. used in this book, even when not specifically marked as such, are not to be considered unprotected by law.

Printed in the Federal Republic of Germany.  
Printed on acid-free paper.

**Cover** Grafik-Design Schulz, Fußgönheim  
**Typesetting** Kühn & Weyh, Satz und Medien, Freiburg

**Printing** Strauss GmbH, Mörlenbach

**Binding** Litges & Dopf Buchbinderei GmbH, Heppenheim

**ISBN-13:** 978-3-527-30999-3

**ISBN-10:** 3-527-30999-3

*This book is dedicated to my friend and teacher,  
Professor Dr. Dr. h.c. Josef (Joe) S. Gratzl.*

## Contents

**Preface** XXIII

**List of Contributors** XXVII

**List of Abbreviations** XXIX

### Volume 1

#### **Part I Chemical Pulping** 1

##### **1 Introduction** 3

*Herbert Sixta*

##### 1.1 Introduction 3

##### 1.2 The History of Papermaking 4

##### 1.3 Technology, End-uses, and the Market Situation 8

##### 1.4 Recovered Paper and Recycled Fibers 14

##### 1.5 Outlook 15

##### **2 Raw Material for Pulp** 21

*Gerald Koch*

##### 2.1 Wood 21

##### 2.1.1 Chemical Composition of Wood 22

##### 2.1.1.1 Cellulose 23

##### 2.1.1.2 Hemicelluloses 28

##### 2.1.1.3 Lignin 30

##### 2.1.1.4 Extractives 33

##### 2.1.1.5 Inorganic Components 39

##### 2.1.2 Wood Structure and Morphology 41

##### 2.1.2.1 Ultrastructure and Distribution of Cell Wall Components 41

##### 2.1.2.2 Lignification of the Cell Walls 44

##### 2.1.2.3 Functional Elements of the Conducting System 46

*Handbook of Pulp*. Edited by Herbert Sixta (Ed.)

Copyright © 2006 WILEY-VCH Verlag GmbH & Co. KGaA, Weinheim

ISBN: 3-527-30999-3

- 2.1.3 The Microscopic Structure of Wood 48
  - 2.1.3.1 Cell Types 48
  - 2.1.3.2 Softwood and Hardwood Structure 50
  - 2.1.3.3 Reaction Wood 54
  - 2.1.3.4 Juvenile Wood 56
  - 2.1.3.5 Secondary Changes 56
- 2.2 Outlook 59
  - 2.2.1 Nano-structure of Fibers 59
  - 2.2.2 Topochemical Distribution of Lignin and Phenolic Extractives 61

**3 Wood Yard Operations 69**

*Jörg B. Ressel*

- 3.1 Raw Material Storage 69
- 3.2 Debarking 71
  - 3.2.1 Debarking Methods 72
    - 3.2.1.1 Drum Debarker 72
    - 3.2.1.2 Rotary Debarker 76
    - 3.2.1.3 Ring Debarkers 77
- 3.3 Chipping and Screening 79
  - 3.3.1 Disc Chipper 80
  - 3.3.2 Drum Chipper 84
  - 3.3.3 The Andritz HQ™-Sizer and Rechipper 86
  - 3.3.4 Chip Conditioner 87
  - 3.3.5 Chipper Canter Line: Profiling Line in Softwood Sawmills 88
- 3.4 Chip screening 89
  - 3.4.1 Mechanical Screening 89
  - 3.4.2 Wind Screening 93
  - 3.4.3 Air Density Separator (ADS) 94
- 3.5 Process Control and Automation 95
- 3.6 Transport and Handling Systems 95
  - 3.6.1 Log Handling 97
  - 3.6.2 Stationary Conveyor Systems 97
  - 3.6.3 Chip Storage 98
    - 3.6.3.1 Chip Storage Systems 101
  - 3.6.4 Wood Yard Losses and Waste Reduction 104
    - 3.6.4.1 Specific Causes of Waste Generation 105
    - 3.6.4.2 Pollution Prevention Options 105

**4 Chemical Pulping Processes 109**

*Herbert Sixta, Antje Potthast, Andreas W. Krottschek*

- 4.1 Introduction 109
- 4.2 Kraft Pulping Processes 111
  - 4.2.1 General Description 111
  - 4.2.2 Kraft Cooking Liquors 113



4.2.3	Mass Transfer in Kraft Cooking	122
4.2.3.1	Purpose of Impregnation	122
4.2.3.2	Heterogeneity of Wood Structure	123
4.2.3.3	Steaming	130
4.2.3.4	Penetration	133
4.2.3.5	Diffusion	138
4.2.3.6	Diffusion Model	151
4.2.3.7	Effect of Impregnation on the Uniformity of Delignification	159
4.2.3.8	Numerical Solution of the Diffusion Model	163
4.2.4	Chemistry of Kraft Cooking	164
	<i>Antje Potthast</i>	
4.2.4.1	Lignin Reactions	164
4.2.4.2	Reactions of Carbohydrates	174
4.2.4.3	Reactions of Extractives	181
4.2.4.4	An Overview of Reactions During Kraft Pulping	183
4.2.4.5	Inorganic Reactions	184
4.2.5	Kraft Pulping Kinetics	185
	<i>Herbert Sixta</i>	
4.2.5.1	Introduction	185
4.2.5.2	Review of Kraft Cooking Models	188
4.2.5.3	Structure of a Selected Kinetic Model for Kraft Pulping	211
4.2.6	Process Chemistry of Kraft Cooking	229
4.2.6.1	Standard Batch Cooking Process	229
4.2.6.2	Modified Kraft Cooking	235
4.2.6.3	Polysulfide and Anthraquinone Pulping	306
4.2.7	Multistage Kraft Pulping	325
4.2.7.1	Prehydrolysis	325
4.2.7.2	Prehydrolysis: Kraft Pulping	345
4.2.8	Pulping Technology and Equipment	366
	<i>Andreas W. Krottschek</i>	
4.2.8.1	Batch Cooking <i>versus</i> Continuous Cooking	366
4.2.8.2	Batch Cooking Technology and Equipment	367
4.2.8.3	Continuous Cooking Technology and Equipment	377
4.3	Sulfite Chemical Pulping	392
	<i>Herbert Sixta</i>	
4.3.1	Introduction	392
4.3.2	Cooking Chemicals and Equilibria	395
4.3.3	Impregnation	403
4.3.4	Chemistry of (Acid) Sulfite Cooking	405
	<i>Antje Potthast</i>	
4.3.4.1	Reactions of Lignin	407
4.3.4.2	Reactions of Carbohydrates: Acid Hydrolysis	416
4.3.4.3	Reactions of Extractives	425
4.3.5	Process Chemistry of Acid Sulfite Pulping	427
	<i>Herbert Sixta</i>	

- 4.3.5.1 Basic Technology 427
- 4.3.5.2 Influence of Reaction Conditions 449
- 4.3.6 Alternative Sulfite Pulping Concepts 465
  - 4.3.6.1 Magnesite Process 466
  - 4.3.6.2 Two-Stage Neutral Magnesite (Bisulfite-MgO) 467
  - 4.3.6.3 Sivola Processes 468
  - 4.3.6.4 Stora Processes (Hydrogen Sulfite or Monosulfite-Acid Sulfite) 472
  - 4.3.6.5 Alkaline Sulfite Pulping 475

## 5 Pulp Washing 511

*Andreas W. Krottscheck*

- 5.1 Introduction 511
- 5.2 Pulp Washing Theory 512
  - 5.2.1 Overview 512
  - 5.2.2 Drainage 513
  - 5.2.3 Compressive Dewatering 517
  - 5.2.4 Diffusion 517
  - 5.2.5 Sorption 519
- 5.3 Principles of Washing 523
  - 5.3.1 Dilution/Extraction Washing 524
  - 5.3.2 Displacement Washing 524
  - 5.3.3 Compressive Dewatering 525
  - 5.3.4 Multi-Stage Washing 526
  - 5.3.5 Fractional Washing 528
- 5.4 Washing Parameters 528
  - 5.4.1 Overview 528
  - 5.4.2 Dilution Factor 529
  - 5.4.3 Feed and Discharge Consistencies 532
  - 5.4.4 pH 533
  - 5.4.5 Entrainment of Air 534
  - 5.4.6 Temperature 535
  - 5.4.7 Equipment-Specific Parameters 535
- 5.5 Washing Efficiency 537
  - 5.5.1 Overview 537
  - 5.5.2 Wash Yield 537
  - 5.5.3 Displacement Ratio 538
  - 5.5.4 Norden Efficiency Factor 539
  - 5.5.5 Standardized Norden Efficiency Factor 545
- 5.6 Washing Equipment 547
  - 5.6.1 General Remarks 547
  - 5.6.2 Rotary Drum Washers 547
    - 5.6.2.1 Conventional Drum Washers 547
    - 5.6.2.2 Drum Displacer 549
  - 5.6.3 Belt Washers 551

5.6.4	Diffusion Washers	552
5.6.4.1	Atmospheric Diffuser	552
5.6.4.2	Pressure Diffuser	554
5.6.5	Roll Presses	556
5.6.6	In-Digester Washing	557
<b>6</b>	<b>Pulp Screening, Cleaning, and Fractionation</b>	<b>561</b>
	<i>Andreas W. Krottscheck</i>	
6.1	Introduction	561
6.2	Screening Theory	563
6.2.1	Introduction	563
6.2.2	Flow Regime	564
6.2.3	Fiber Passage and Reject Thickening	566
6.2.4	Selective Fiber Passage	570
6.3	Screening Parameters	572
6.3.1	Equipment Parameters	572
6.3.1.1	Screen Basket	572
6.3.1.2	Rotor	573
6.3.2	Operating Parameters	575
6.3.2.1	Reject Rate	575
6.3.2.2	Accept Flow Rate	575
6.3.2.3	Feed Consistency	577
6.3.2.4	Temperature	577
6.3.2.5	Rotor Tip Velocity	577
6.3.3	Furnish Parameters	578
6.3.3.1	Pulp Fibers	578
6.3.3.2	Contaminants	579
6.3.3.3	Entrained Air	579
6.4	Centrifugal Cleaning Theory	579
6.4.1	Introduction	579
6.4.2	Flow Regime	580
6.4.3	Sedimentation	581
6.4.4	Underflow Thickening	584
6.4.5	Selective Separation	585
6.5	Centrifugal Cleaning Parameters	586
6.5.1	Cyclone Parameters	586
6.5.2	Operating Parameters	587
6.5.2.1	Flow Rate and Pressure Drop	587
6.5.2.2	Feed Consistency	587
6.5.2.3	Temperature	587
6.5.3	Furnish Parameters	587
6.5.3.1	Pulp Fibers	587
6.5.3.2	Contaminants	588
6.6	Separation Efficiency	588

- 6.6.1 Screening and Cleaning Efficiency 588
- 6.6.2 Fractionation Efficiency 590
  - 6.6.2.1 Removal Efficiency 590
  - 6.6.2.2 Fractionation Index 591
- 6.7 Screening and Cleaning Applications 592
  - 6.7.1 Selective Contaminant Removal 592
    - 6.7.1.1 Knots 593
    - 6.7.1.2 Shives 593
    - 6.7.1.3 Bark 593
    - 6.7.1.4 Sand and Stones 593
    - 6.7.1.5 Metals and Plastics 594
  - 6.7.2 Fractionation 594
- 6.8 Systems for Contaminant Removal and Fractionation 594
  - 6.8.1 Basic System Design Principles 594
  - 6.8.2 Systems for Contaminant Removal 596
    - 6.8.2.1 Arrangement 596
    - 6.8.2.2 Fiber Loss *versus* Efficiency 598
  - 6.8.3 Systems for Fractionation 599
- 6.9 Screening and Cleaning Equipment 601
  - 6.9.1 Pressure Screens 601
  - 6.9.2 Atmospheric Screens 604
    - 6.9.2.1 Secondary Knot Screens 604
    - 6.9.2.2 Vibratory Screens 605
  - 6.9.3 Hydrocyclones 605

**Volume 2**

- 7 Pulp Bleaching 609**  
*Herbert Sixta, Hans-Ullrich Süss, Antje Potthast, Manfred Schwanninger, and Andreas W. Krottscheck*
- 7.1 General Principles 609
- 7.2 Classification of Bleaching Chemicals 610
- 7.2 Bleaching Operations and Equipment 613  
*Andreas W. Krottscheck*
- 7.2.1 Basic Rheology of Pulp-Liquor Systems 614
- 7.2.2 Generic Bleaching Stage Set-Up 616
- 7.2.3 Medium Consistency Pumps 617
- 7.2.4 Medium Consistency Mixers 619
  - 7.2.4.1 High-Shear Mixers 620
  - 7.2.4.2 Static Mixers 621
  - 7.2.4.3 Atmospheric Steam Mixers 622
- 7.2.5 Medium Consistency Reactors 623
  - 7.2.5.1 Atmospheric Upflow Reactors 623

7.2.5.2	Atmospheric Downflow Reactors	624
7.2.5.3	Pressurized Reactors	625
7.2.6	Blowtank	627
7.2.7	Agitators	627
7.2.8	Washing	628
7.3	Oxygen Delignification	628
7.3.1	Introduction	628
7.3.2	Chemistry of Oxygen Delignification	632
	<i>Manfred Schwanninger</i>	
7.3.2.1	Bleachability	634
7.3.2.2	Lignin Structures and their Reactivity	634
7.3.2.3	Oxygen (Dioxygen) and its Derivatives	641
7.3.2.4	A Principal Reaction Schema for Oxygen Delignification	649
7.3.2.5	Carbohydrate Reactions in Dioxygen-Alkali Delignification Processes	657
7.3.2.6	Residual Lignin–Carbohydrate Complexes (RLCC)	666
7.3.2.7	Inorganics (Metals) and their Role in the Protection/ Degradation of Cellulose	668
7.3.3	Mass Transfer and Kinetics	671
	<i>Herbert Sixta</i>	
7.3.3.1	Kinetics of Delignification	672
7.3.3.2	Kinetics of Cellulose Chain Scissions	685
7.3.3.3	Application of Surfactants	687
7.3.4	A Model to Predict Industrial Oxygen Delignification	688
7.3.4.1	Theoretical Base of the van Heiningen Model	690
7.3.4.2	Case Study	695
7.3.5	Process Variables	701
7.3.5.1	Temperature	701
7.3.5.2	Retention Time	702
7.3.5.3	Alkali Charge	703
7.3.5.4	pH Value	704
7.3.5.5	Final pH	705
7.3.5.6	Alkali Source	706
7.3.5.7	Oxygen Charge, Oxygen Pressure	707
7.3.5.8	Consistency	708
7.3.6	Pulp Components and Impurities	708
7.3.6.1	Effect of Metal Ion Concentration	708
7.3.6.2	Residual Lignin Structures	713
7.3.6.3	Carry-Over	716
7.3.6.4	Xylan Content	719
7.3.6.5	Selectivity of Oxygen Delignification	720
7.3.7	Process and Equipment	721
7.3.7.1	MC <i>versus</i> HC Technology	721
7.3.7.2	Process Technology	722
7.3.7.3	Process Equipment	731

- 7.3.8 Pulp Quality 733
- 7.4 Chlorine Dioxide Bleaching 734
  - 7.4.1 Introduction 734
  - 7.4.2 Physical and Chemical Properties and Definitions 735
    - 7.4.2.1 Behavior of Chlorine Dioxide in Aqueous Solution 737
    - 7.4.2.2 Inorganic Side Reactions during Chlorine Dioxide Bleaching of Wood Pulps 737
  - 7.4.3 Generation of Chlorine Dioxide 741
  - 7.4.4 Chemistry of Chlorine Dioxide Treatment 745  
*Manfred Schwanninger*
    - 7.4.4.1 Chlorination Products 752
    - 7.4.5 Performance of Chlorine Dioxide Bleaching 754
      - 7.4.5.1 Standard Chlorine Dioxide Bleaching 754
      - 7.4.5.2 Chlorine Dioxide Bleaching of Oxygen-Delignified Kraft Pulps 759
      - 7.4.5.3 Modified Chlorine Dioxide Bleaching 761
    - 7.4.6 Technology of Chlorine Dioxide Bleaching 770  
*Andreas W. Krotscheck*
    - 7.4.7 Formation of Organochlorine Compounds 771
  - 7.5 Ozone Delignification 777
    - 7.5.1 Introduction 777
    - 7.5.2 Physical Properties of Ozone 778
    - 7.5.3 Ozone Generation 782
    - 7.5.4 Chemistry of Ozone Treatment 785  
*Manfred Schwanninger*
      - 7.5.4.1 Ozone Decomposition 786
      - 7.5.4.2 Degradation of Lignin 790
      - 7.5.4.3 Degradation of Carbohydrates 794
    - 7.5.5 Process Conditions 798
      - 7.5.5.1 Mass Transfer 798
      - 7.5.5.2 Mixing and Mixing Time 802
      - 7.5.5.3 Effect of Pulp Consistency 806
      - 7.5.5.4 Effect of pH 811
      - 7.5.5.5 Effect of Temperature 813
      - 7.5.5.6 Effect of Transition Metal Ions 814
      - 7.5.5.7 Effect of Carry-Over 816
      - 7.5.5.8 Effect of Pretreatments and Additives 818
      - 7.5.5.9 Effect of Sodium Borohydride after Treatment 822
      - 7.5.5.10 Effect of Alkaline Extraction 824
    - 7.5.6 Technology of Ozone Treatment 826  
*Andreas W. Krotscheck*
      - 7.5.6.1 Medium-Consistency Ozone Treatment 826
      - 7.5.6.2 High-Consistency Ozone Treatment 827
      - 7.5.6.3 Ozone/Oxygen Gas Management 828
    - 7.5.7 Application in Chemical Pulp Bleaching 829
      - 7.5.7.1 Selectivity, Efficiency of Ozone Treatment of Different Pulp Types 829

- 7.5.7.2 Effect of Ozonation on the Formation of Carbonyl and Carboxyl Groups 840
- 7.5.7.3 Effect of Ozonation on Strength Properties 841
- 7.5.7.4 Typical Conditions, Placement of Z in a Bleaching Stage 843
- 7.6 Hydrogen Peroxide Bleaching 849
  - Hans-Ullrich Süß*
  - 7.6.1 Introduction 849
  - 7.6.2 H<sub>2</sub>O<sub>2</sub> Manufacture 850
  - 7.6.3 Physical Properties 850
  - 7.6.4 Chemistry of hydrogen peroxide bleaching 853
    - Manfred Schwanninger*
    - 7.6.4.1 Decomposition of H<sub>2</sub>O<sub>2</sub> 854
    - 7.6.4.2 Residual Lignin 856
    - 7.6.4.3 Carbohydrates 859
  - 7.6.5 Process Parameters 860
    - Hans-Ullrich Süß*
    - 7.6.5.1 Metals Management 860
    - 7.6.5.2 Alkaline Decomposition of H<sub>2</sub>O<sub>2</sub> 862
    - 7.6.5.3 Thermal Stability of H<sub>2</sub>O<sub>2</sub> and Bleaching Yield 863
    - 7.6.5.4 Pressurized Peroxide Bleaching 866
  - 7.6.6 Technology of H<sub>2</sub>O<sub>2</sub> Bleaching 866
    - Andreas W. Krottscheck*
    - 7.6.6.1 Atmospheric Peroxide Bleaching 866
    - 7.6.6.2 Pressurized Peroxide Bleaching 867
  - 7.6.7 Application in Chemical Pulp Bleaching 868
    - Hans-Ullrich Süß*
    - 7.6.7.1 Stabilization of Brightness with H<sub>2</sub>O<sub>2</sub> 873
    - 7.6.7.2 Catalyzed Peroxide Bleaching 877
    - 7.6.7.3 Application in TCF Sulfite Pulp Bleaching 877
    - 7.6.7.4 Activators for H<sub>2</sub>O<sub>2</sub> Bleaching 880
- 7.7 Peracetic Acid in Pulp Bleaching 880
- 7.8 Hot Acid Hydrolysis 883
- 7.9 Alternative Bleaching Methods 885
- 7.10 Bleach Plant Liquor Circulation 887
  - Andreas W. Krottscheck*
  - 7.10.1 Introduction 887
  - 7.10.2 Intra-Stage Circulation and Circulation between Stages 888
  - 7.10.3 Open and Closed Operation of Bleaching Stages 890
  - 7.10.4 Construction Material Compatibility 893
  - 7.10.5 Implications of Liquor Circulation 893

- 8 Pulp Purification 933**  
*Herbert Sixta*
- 8.1 Introduction 933
  - 8.2 Reactions between Pulp Constituents and Aqueous Sodium Hydroxide Solution 935
  - 8.3 Cold Caustic Extraction 942
    - 8.3.1 NaOH Concentration 942
    - 8.3.2 Time and Temperature 944
    - 8.3.3 Presence of Hemicelluloses in the Lye 945
    - 8.3.4 Placement of CCE in the Bleaching Sequence 948
    - 8.3.5 Specific Yield Loss, Influence on Kappa Number 949
    - 8.3.6 Molecular Weight Distribution 951
  - 8.4 Hot Caustic Extraction 952
    - 8.4.1 Influence of Reaction Conditions on Pulp Quality and Pulp Yield 953
      - 8.4.1.1 NaOH Charge and Temperature in E, (EO), and (E/O) Treatments 953
      - 8.4.1.2 Xylan *versus* R18 Contents 957
      - 8.4.1.3 Purification *versus* Viscosity 959
      - 8.4.1.4 Purification *versus* Kappa Number and Extractives 960
      - 8.4.1.5 Composition of Hot Caustic Extract 961
    - 8.4.2 MgO as an Alternative Alkali Source 962
- 9 Recovery 967**  
*Andreas W. Krotscheck and Herbert Sixta*
- 9.1 Characterization of Black Liquors 967
    - 9.1.1 Chemical Composition 967
    - 9.1.2 Physical Properties 970
      - 9.1.2.1 Viscosity 970
      - 9.1.2.2 Boiling Point Rise (BPR) 970
      - 9.1.2.3 Surface Tension 971
      - 9.1.2.4 Density 971
      - 9.1.2.5 Thermal Conductivity 972
      - 9.1.2.5 Heat Capacity [8,11] 972
    - 9.2 Chemical Recovery Processes 973
      - 9.2.1 Overview 973
      - 9.2.2 Black Liquor Evaporation 974
        - 9.2.2.1 Introduction 974
        - 9.2.2.2 Evaporators 975
        - 9.2.2.3 Multiple-Effect Evaporation 977
        - 9.2.2.4 Vapor Recompression 979
      - 9.2.3 Kraft Chemical Recovery 980
        - 9.2.3.1 Kraft Recovery Boiler 980
        - 9.2.3.2 Causticizing and Lime Reburning 986
        - 9.2.3.3 The Future of Kraft Chemical Recovery 992
      - 9.2.4 Sulfite Chemical Recovery 994



- 10 Environmental Aspects of Pulp Production 997**  
*Hans-Ulrich Süß*
- 10.1 Introduction 997
- 10.2 A Glimpse of the Historical Development 998
- 10.3 Emissions to the Atmosphere 1002
- 10.4 Emissions to the Aquatic Environment 1004
- 10.5 Solid Waste 1006
- 10.6 Outlook 1007
- 11 Pulp Properties and Applications 1009**  
*Herbert Sixta*
- 11.1 Introduction 1009
- 11.2 Paper-Grade Pulp 1010
- 11.3 Dissolving Grade Pulp 1022
- 11.3.1 Introduction 1022
- 11.3.2 Dissolving Pulp Characterization 1024
- 11.3.2.1 Pulp Origin, Pulp Consumers 1024
- 11.3.2.2 Chemical Properties 1026
- 11.3.2.3 Supramolecular Structure 1041
- 11.3.2.4 Cell Wall Structure 1047
- 11.3.2.5 Fiber Morphology 1051
- 11.3.2.6 Pore Structure, Accessibility 1052
- 11.3.2.7 Degradation of Dissolving Pulps 1056
- 11.3.2.8 Overview of Pulp Specification 1060
- II Mechanical Pulping 1069**  
*Jürgen Blechschmidt, Sabine Heinemann, and Hans-Ulrich Süß*
- 1 Introduction 1071**  
*Jürgen Blechschmidt and Sabine Heinemann*
- 2 A Short History of Mechanical Pulping 1073**  
*Jürgen Blechschmidt and Sabine Heinemann*
- 3 Raw Materials for Mechanical Pulp 1075**  
*Jürgen Blechschmidt and Sabine Heinemann*
- 3.1 Wood Quality 1075
- 3.2 Processing of Wood 1076

- 3.2.1 Wood Log Storage 1076
- 3.2.2 Wood Log Debarking 1076
- 3.2.3 Wood Log Chipping 1078
  
- 4 Mechanical Pulping Processes 1079**  
*Jürgen Blechschmidt and Sabine Heinemann*
- 4.1 Grinding Processes 1079
  - 4.1.1 Principle and Terminology 1079
  - 4.1.2 Mechanical and Thermal Processes in Grinding 1080
    - 4.1.2.1 Softening of the Fibers 1080
    - 4.1.2.2 Defibration (Deliberation) of Single Fibers from the Fiber Compound 1083
  - 4.1.3 Influence of Parameters on the Properties of Groundwood 1084
  - 4.1.4 Grinders and Auxiliary Equipment for Mechanical Pulping by Grinding 1087
    - 4.1.4.1 Pocket Grinders 1089
    - 4.1.4.2 Chain Grinders 1090
    - 4.1.4.3 Pulp Stones 1092
  - 4.1.5 Pressure Grinding 1095
- 4.2 Refiner Processes 1098
  - 4.2.1 Principle and Terminology 1098
  - 4.2.2 Mechanical, Thermal, and Chemical Processes in the Refiner Process 1100
  - 4.2.3 Machines and Aggregates for Mechanical Pulping by Refining 1104
  
- 5 Processing of Mechanical Pulp and Reject Handling: Screening and Cleaning 1113**  
*Jürgen Blechschmidt and Sabine Heinemann*
- 5.1 Basic Principles and Parameters 1113
- 5.2 Machines and Aggregates for Screening and Cleaning 1114
- 5.3 Reject Treatment and Heat Recovery 1121
  
- 6 Bleaching of Mechanical Pulp 1123**  
*Hans-Ulrich Süss*
- 6.1 Bleaching with Dithionite 1124
- 6.2 Bleaching with Hydrogen Peroxide 1126
- 6.3 Technology of Mechanical Pulp Bleaching 1134
  
- 7 Latency and Properties of Mechanical Pulp 1137**  
*Jürgen Blechschmidt and Sabine Heinemann*
- 7.1 Latency of Mechanical Pulp 1137
- 7.2 Properties of Mechanical Pulp 1138

<b>III</b>	<b>Recovered Paper and Recycled Fibers</b>	<b>1147</b>
	<i>Hans-Joachim Putz</i>	
<b>1</b>	<b>Introduction</b>	<b>1149</b>
<b>2</b>	<b>Relevance of Recycled Fibers as Paper Raw Material</b>	<b>1153</b>
<b>3</b>	<b>Recovered Paper Grades</b>	<b>1157</b>
<b>3.1</b>	<b>Europe</b>	<b>1157</b>
<b>3.2</b>	North America and Japan	<b>1161</b>
<b>3.2.1</b>	United States	<b>1162</b>
<b>3.2.2</b>	Japan	<b>1163</b>
<b>4</b>	<b>Basic Statistics</b>	<b>1165</b>
<b>4.1</b>	Utilization Rate	<b>1167</b>
<b>4.2</b>	Recovery Rate	<b>1170</b>
<b>4.3</b>	Recycling Rate	<b>1173</b>
<b>4.4</b>	Deinked Pulp Capacities	<b>1174</b>
<b>4.5</b>	Future Development of the Use of Recovered Paper	<b>1175</b>
<b>5</b>	<b>Collection of Recovered Paper</b>	<b>1177</b>
<b>5.1</b>	Pre-Consumer Recovered Paper	<b>1178</b>
<b>5.2</b>	Post-Consumer Recovered Paper	<b>1178</b>
<b>5.2.1</b>	Pick-Up Systems	<b>1178</b>
<b>5.2.2</b>	Drop-Off Systems	<b>1179</b>
<b>5.3</b>	Efficiency of Different Collection Systems	<b>1180</b>
<b>5.4</b>	Municipal Solid Waste	<b>1181</b>
<b>6</b>	<b>Sources of Recovered Paper</b>	<b>1183</b>
<b>7</b>	<b>Sorting, Handling, and Storage of Recovered Paper</b>	<b>1187</b>
<b>7.1</b>	<b>Sorting</b>	<b>1187</b>
<b>7.2</b>	Handling	<b>1189</b>
<b>7.3</b>	Storage	<b>1190</b>
<b>8</b>	<b>Legislation for the Use of Recycled Fibers</b>	<b>1191</b>
<b>8.1</b>	Europe	<b>1192</b>
<b>8.2</b>	United States of America	<b>1195</b>
<b>8.3</b>	Japan	<b>1198</b>
	<b>Appendix: European List of Standard Grades of Recovered Paper and Board (February, 1999)</b>	<b>1203</b>

<b>IV</b>	<b>Analytical Characterization of Pulps</b>	<b>1211</b>
	<i>Erich Gruber</i>	
<b>1</b>	<b>Fundamentals of Quality Control Procedures</b>	<b>1213</b>
1.1	The Role of QC	1214
1.2	Basics of QC-statistics	1214
1.3	Sampling	1216
1.4	Conditions for Testing and/or Conditioning	1216
1.5	Disintegration	1217
<b>2</b>	<b>Determination of Low Molecular-Weight Components</b>	<b>1219</b>
2.1	Moisture	1219
2.2	Inorganic Components	1219
2.2.1	Ashes	1220
2.2.1.1	Total Ash	1220
2.2.1.2	Sulfated Ash	1220
2.2.1.3	Acid-Insoluble Ash	1220
2.2.2	Determination of Single Elements	1221
2.2.2.1	Survey of Chemical Procedures	1221
2.2.2.2	Atomic Absorption Spectroscopy (AAS)	1222
2.2.2.3	X-ray Fluorescence Spectroscopy (XFS)	1223
2.2.2.4	Electron Spectroscopy for Chemical Application (ESCA)	1223
2.3	Extractives	1224
2.3.1	Water Extractives	1224
2.3.1.1	Test Water	1224
2.3.1.2	Cold Water Extraction	1225
2.3.1.3	Hot Water Extraction	1225
2.3.1.4	Analysis of Water Extracts	1225
2.4	Chlorine Compounds	1225
<b>3</b>	<b>Macromolecular Composition</b>	<b>1227</b>
3.1	Lignin Content	1227
3.2	Extent of Delignification	1228
3.2.1	Roe Number	1228
3.2.2	Chlorine Number	1228
3.2.3	Kappa Number (Permanganate Number)	1228
3.3	Alkali Resistance and Solubility	1229
3.3.1	Alkali-Soluble Components	1229
3.3.2	$\alpha$ -, $\beta$ -, and $\gamma$ -cellulose	1229
3.3.3	R <sub>18</sub> and S <sub>18</sub> values	1230
3.4	Composition of Polysaccharides	1231
3.4.1	Determination of Monosaccharides after Hydrolysis	1231
3.4.1.1	Gas Chromatography	1231
3.4.1.2	Thin-Layer Chromatography	1232

- 3.4.1.3 Liquid Chromatography 1232
  - 3.4.2 Determination of Pentosans after Hydrolysis 1233
  - 3.4.3 Determination of Uronic Acids after Hydrolysis 1233
  - 3.5 Functional Groups 1234
    - 3.5.1 Carbonyl Functions 1234
      - 3.5.1.1 Copper Number 1235
      - 3.5.1.2 Sodium Borohydride Method 1236
      - 3.5.1.3 Hydrazine Method 1236
      - 3.5.1.4 Oxime Method 1236
      - 3.5.1.5 Girard-P Method 1237
      - 3.5.1.6 Cyanohydrin Method 1237
      - 3.5.1.7 Fluorescent Dying 1237
    - 3.5.2 Carboxyl Functions 1238
  - 3.6 Degree of Polymerization (Molecular Mass) 1239
    - 3.6.1 Solvents for Cellulose 1240
      - 3.6.1.1 CUOXAM 1241
      - 3.6.1.2 CUEN 1241
      - 3.6.1.3 Iron Sodium Tartrate (EWNN) 1241
    - 3.6.2 Diverse Average Values of Molecular Mass and Index of Nonuniformity 1241
    - 3.6.3 Methods to Determine Molar Mass (“Molecular Weight”) 1243
      - 3.6.3.1 Osmosis 1243
      - 3.6.3.2 Scattering Methods 1245
    - 3.6.4 Viscosity Measurements 1248
      - 3.6.4.1 Solution Viscosity as a Measure of Macromolecular Chain Length 1248
      - 3.6.4.2 Viscosity Measurements on Cellulose Pulps 1251
    - 3.6.5 Molecular Weight Distribution 1251
      - 3.6.5.1 Fractional Precipitation or Solution 1251
      - 3.6.5.2 Size-Exclusion (Gel-Permeation) Chromatography 1252
- 4 Characterization of Supermolecular Structures 1257**
- 4.1 Crystallinity 1257**
    - 4.1.1 Degree of Crystallinity 1257
      - 4.1.1.1 X-Ray Diffraction 1259
      - 4.1.1.2 Solid-phase NMR-Spectroscopy 1261
      - 4.1.1.3 Reaction Kinetics 1262
      - 4.1.1.4 Density Measurements 1262
    - 4.1.2 Dimension of Crystallites 1263
    - 4.1.3 Orientation of Crystallites 1265
  - 4.2 Accessibility, Voids, and Pores 1265
    - 4.2.1 Porosity 1266
    - 4.2.2 Accessible Surface 1267
  - 4.3 Water and Solvent Retention 1268

4.3.1	Total Water Uptake	1268
4.3.2	Free and Bound Water	1268
<b>5</b>	<b>Fiber Properties</b>	<b>1269</b>
<b>5.1</b>	<b>Identification of Fibers</b>	<b>1269</b>
5.1.1	Morphological Characterization	1269
5.1.2	Visible and UV Microscopy	1271
5.1.3	Electron Microscopy	1271
5.2	Fiber Dimensions	1272
5.2.1	Fiber Length and Width	1273
5.2.1.1	Microscopic Methods and Image Analysis	1273
5.2.1.2	Fiber Fractionation by Screening	1274
5.2.2	Coarseness	1275
5.3	Mechanical Properties	1275
5.3.1	Single Fiber Properties	1275
5.3.1.1	Wet Fiber Properties	1275
5.3.1.2	Mechanical Properties of Dry Fibers	1277
5.3.2	Sheet Properties	1278
5.3.2.1	Preparation of Laboratory Sheets for Physical Testing	1278
5.3.2.2	Determination of Mechanical Pulp Sheet Properties	1279
5.4	Optical Properties of Laboratory Sheets	1279
<b>6</b>	<b>Papermaking Properties of Pulps</b>	<b>1281</b>
<b>6.1</b>	<b>Beating</b>	<b>1281</b>
6.2	Drainage Resistance	1281
6.3	Drainage (Dewatering) Time	1283
6.4	Aging	1284
6.4.1	Accelerated Aging	1284
<b>Index</b>		<b>1291</b>

## Preface

Pulp is a fibrous material resulting from complex manufacturing processes that involve the chemical and/or mechanical treatment of various types of plant material. Today, wood provides the basis for approximately 90% of global pulp production, while the remaining 10% originates from annual plants. Pulp is one of the most abundant raw materials worldwide which is used predominantly as a major component in the manufacture of paper and paperboard, and with increasing importance also in the form of a wide variety of cellulose products in the textile, food, and pharmaceutical industries.

The pulp industry is globally competitive and attractive from the standpoint of sustainability and environmental compatibility. In many ways, this industry is an ideal example of a desirable, self-sustaining industry which contributes favorably to many areas of our daily lives. Moreover, there is no doubt that it will continue to play an important role in the future.

Although the existing pulp technology has its origins in the 19th century, it has still a very high potential of further innovations covering many areas of science. Knowledge of the pulping processes has been greatly extended since *Pulping Processes* – the unsurpassed book of Sven A. Rydholm – was first published in 1965. Not only has the technology advanced and new technology emerged, but our knowledge on structure–property relationships has also deepened considerably. It is self-evident that the competitiveness of pulp and its products produced thereof can only be maintained through continuous innovations at the highest possible level.

A recent publication which comprised a series of 19 books on *Papermaking Science and Technology*, and was edited by Johan Gullichsen and Hannu Paulapuro, provided a comprehensive account of progress and current knowledge in pulping and papermaking. The aim of the present book, however, is initially to provide a short, general survey on pulping processes, followed by a comprehensive review in certain specialized areas of pulping chemistry and technology. Consequently, the book is divided into four parts: Part I, Chemical Pulp; Part II, Mechanical Pulp; Part III, Recovered Paper and Recycled Fibers; and Part IV, the Analytical Characterization of Pulps.

In Part I, Chapter 2 and 3 describe the fundamentals of wood structure and woodyard operations, whilst in Chapter 4 emphasis is placed on the chemistry

and technology of both kraft and sulfite pulping, the mass transfer of cooking liquor into wood structure and chemical kinetics in alkaline pulping operations. The current technologies of dissolving pulp manufacture are also reviewed, covering both multi-stage alkaline and acid sulfite pulping. Considerable effort was devoted in the subsequent chapters to present the fundamentals of pulp washing, screening, cleaning, and fractionation. These important mechanical pulping operations are followed by a comprehensive review of the state-of-the-art bleaching chemistry and technology. High-purity pulps are important raw materials for the production of high added-value cellulose products, and the necessary purification processes are introduced in a separate chapter. A short overview on chemical recovery processes and pulp properties concludes Part I.

Parts II and III provide a survey of the latest technologies on mechanical pulp and recovered paper and recycled fibers.

Finally, Part IV deals with the analytical characterization of pulps. Since the wood and pulp components are closely associated within the cell wall, the analytical characterization covers not only molecular but also supramolecular structures.

A project such as this could never have succeeded without input from contributors of the very highest standard. I would like to express my sincere appreciation to the contributors, for the high quality of their work and for their enthusiasm and commitment.

Individual sections of the manuscripts have been reviewed in detail by several friends and colleagues, and in this respect the suggestions and critical comments of Josef Bauch of the University of Hamburg, Germany (Part I, Chapter 2), Hans-Georg Richter of the BFH, Germany (Part I, Chapter 2), Rudolf Patt of the University of Hamburg, Germany (Part I, Chapters 3, 4 and 7), Othar Kordsachia of the BFH, Germany (Part I, Chapters 4, 7, 8 and 11), Richard Berry of Paprican, Point Claire, Canada (chlorine dioxide bleaching peracetic acid in pulp bleaching, hot acid hydrolysis and Chapter 10 in Part I, hydrogen peroxide bleaching in Part I and II), Chen-Loung Chen and Michail Yu. Balakshin of NC State University, USA (chemistry of kraft and sulfite pulping), John F. Kadla of the University of British Columbia, Vancouver, Canada (chemistry of oxygen-, ozone and hydrogen peroxide bleaching), Adriaan R.P. van Heiningen of the University of Maine, USA (oxygen delignification, ozone bleaching), James A. Olson of the University of British Columbia, Vancouver, Canada (Part I, chapter 6), Andrea Borgards, R&D Lenzing AG, Austria (Part I, Chapter 8), Hans Gr-stlinger of Lenzing Technik, Austria (bleaching technology), Wojciech Juljanski of Lenzing Technik, Austria (pulping technology) and Mikael Lucander, Ilkka Nurminen and Christoffer Westin of the Oy Keskuslaboratorio, Espoo, Finland (Part II, Mechanical Pulping) are gratefully acknowledged. Moreover, I am very indebted to Alois Ecker of Lenzing Technik for his valuable support for the mathematical computations of kraft cooking and oxygen delignification kinetics. I also owe sincere thanks to the management of Lenzing AG for the assistance granted to me by their library services.



In addition to my gratitude to all of these people, I also thank my family for their great patience, understanding, and inspiring support.

Last, but not least, I would like to thank the publishers for the attractive presentation of this book, and the personnel at Wiley-VCH for their cooperation and skilful editorial work.

Lenzing,  
December 2005

*H. Sixta*

## List of Contributors

### **Jürgen Blechschmidt**

Wachbergstrasse 31  
01326 Dresden  
Germany

### **Erich Gruber**

TU-Darmstadt  
Makromolekulare Chemie  
Nachwachsender Rohstoffe  
64283 Darmstadt  
Germany

### **Sabine Heinemann**

KCL Science and Consulting  
Pulp and Paper  
P.O. Box 70  
Espoo  
Finland

### **Gerald Koch**

Federal Research Centre for Forestry  
and Forest Products  
Institute for Wood Biology and Wood  
Protection  
Leuschnerstrasse 91  
21031 Hamburg  
Germany

### **Andreas W. Krotscheck**

Lenzing Technik GmbH  
Pulp Technology Division  
4680 Lenzing  
Austria

### **Antje Potthast**

University of Natural Resources and  
Applied Life Sciences Vienna  
Department of Chemistry and  
Christian-Doppler-Laboratory  
Muthgasse 18  
1190 Vienna  
Austria

### **Hans-Joachim Putz**

Paper Technology and Mechanical  
Process Engineering  
Darmstadt University of Technology  
Alexanderstrasse 8  
64283 Darmstadt  
Germany

### **Jörg B. Ressel**

Department of Wood Science  
University of Hamburg  
Leuschnerstrasse 91  
21031 Hamburg  
Germany

### **Manfred Schwanninger**

BOKU  
University of Natural Resources and  
Applied Life Sciences  
Vienna Department of Chemistry  
Division of Biochemistry  
Muthgasse 18  
1190 Vienna  
Austria

***Herbert Sixta***

Lenzing AG  
Business Unit Pulp  
Werkstraße 1  
4860 Lenzing  
Austria

***Hans-Ulrich Süß***

Degussa AG  
Global Competence Center  
Active Oxygen Products  
O2-AO-AT, 913-120  
Rodenbacher Chaussee 4  
63594 Hanau  
Germany

## List of Abbreviations

4OMeGlcA	4-O-methyl- $\beta$ D-glucuronic acid-(1 $\rightarrow$ 2)-xylose)
AAS	atomic absorption spectroscopy
AEC	anion-exchange chromatography
AF&PA	American Forest & Paper Association
AFM	atomic force microscopy
AHG	anhydroglucose
AMT	accepted modern technology
AOX	adsorbable organic halogen
ASAM	alkaline sulfite with anthraquinone and methanol
B.I.R.	Bureau International de la Récupération
BAT	best available technology
BLG	black liquor gasification
BLGCC	black liquor gasification with combined cycle
BLPS	black liquor dissolved polysaccharides
CCE	cold caustic extraction
CCOA	carbazole-9-carboxylic acid [2-(2-aminooxy-ethoxy)-ethoxy]-amide
CDE	cupri-ethylene-diamine-solution
CE	causticizing efficiency
CEPI	Confederation of European Paper Industries
CGW	chemigroundwood
CI	crystallinity index
CMP	chemimechanical pulp
COD	chemical oxygen demand
CRMP	chemi-refiner mechanical pulp
CTC	charge transfer complex
CTMP	chemi-thermomechanical pulp,
CTO	crude tall oil
CZE	capillary zone electrophoresis
DAE	differential algebraic equation
DD	drum displacer
DDA	dynamic drainage analyzer
DDJ	dynamic drainage jar

DIP	deinked pulp
DP	degree of polymerization
DSC	differential scanning calorimetry
DTPA	diethylene triamino penta-acetate
EAPC	enhanced alkali profile cooking
ECCSA	effective capillary cross-sectional area
ECF	elemental chlorine-free
EDR	equivalent displacement ratio
EDXA	energy dispersive X-ray analysis
EPA	Environmental Protection Agency
ERPA	European Recovered Paper Association
ERPC	European Recovered Paper Council
ESCA	electron spectroscopy for chemical analysis
ESR	electron spin resonance
EUGROPA	European Paper Merchants Association
FBSKP	fully bleached softwood kraft pulp
FEAD	European Federation of Waste Management and Environmental Services
FEFCO	European Federation of Corrugated Board Manufacturers
FE-SEM	field emission-SEM
FSP	fiber saturation point
FTIR	Fourier transmission infra-red
GPC	gel-permeation chromatography
GSA	General Services Administration
HCE	hot caustic extraction
HEDP	hydroxy ethylene 1,1-diphosphonic acid
HHV	higher heating value
HP-AEC	high-performance anion-exchange chromatography
HVLC	high-volume low-concentration
INTERGRAF	International Confederation of Printing and Allied Industries
IPPC	Integrated Pollution and Prevention Control
ISEC	inverse size-exclusion chromatography
I-TEQ	International Toxicity Equivalent
LCC	lignin-carbohydrate complex
LMS	laccase-mediator-system
LODP	level-off DP
LVHC	low-volume high-concentration
LWC	lightweight coated
MCC	modified cooking circulation
MFA	microfibril angle
MHW	Ministry of Health and Welfare
MITI	Ministry of International Trade and Industry
MOW	mixed office waste
MSW	municipal solid waste

MWD	molecular weight distribution
NCG	noncondensable gases
NHV	net heating value
NHWA	National Household Recovery Analysis
NMR	nuclear magnetic resonance
NPEs	non-process elements
NSSC	neutral sulfite semi-chemical
ODE	ordinary differential equation
OXE	oxidation equivalent
PAD	pulsed amperometric detection
PCDD	polychlorinated dibenzo- <i>p</i> -dioxins
PCDF	polychlorinated dibenzofurans
PDI	polydispersity index
PGW	pressure groundwood
PHK	prehydrolysis kraft pulp
PRMP	pressurized refiner mechanical pulp
PSA	pressure swing adsorption
RAC	Recycling Advisory Council
RDH	rapid displacement heating
RLLC	residual lignin-carbohydrate complex
RMP	refiner mechanical pulp
RTS	retention time, temperature, speed
SAXS	small-angle X-ray scattering
SC	supercalendered
SEM	scanning electron microscopy
SET	single electron transfer
SGW	stone groundwood
SRV	solvent retention value
SSL	spent sulfite liquor
TCF	totally chlorine free
TEM	transmission electron microscopy
TEQ	toxic equivalency quantity
TGW	thermo groundwood
TMP	thermomechanical pulp
TOC	total organic carbon
ToF-SIMS	time-of-flight secondary ion mass spectroscopy
TRS	total reduced sulfur
TSS	total suspended solids
TTA	total titrable alkali
UCC	upper cooking circulation
UMSP	scanning UV microspectrophotometry
VOC	volatile organic compounds
VSA	vacuum swing adsorption
WAXS	wide-angle X-ray scattering

WRV	water retention value
XFS	X-ray fluorescence spectroscopy
XPS	X-ray photoelectron spectroscopy

## **Part I**

# **Chemical Pulping**



# 1

## Introduction

*Herbert Sixta*

### 1.1

#### Introduction

Industrial pulping involves the large-scale liberation of fibers from lignocellulosic plant material, by either mechanical or chemical processes. Chemical pulping relies mainly on chemical reactants and heat energy to soften and dissolve lignin in the plant material, partially followed by mechanical refining to separate fibers. Mechanical pulping involves the pretreatment of wood with steam (and sometimes also with aqueous sulfite solution) prior to the separation into fibrous material by abrasive refining or grinding. Depending on its end-use, the material recovered from such processes – the unbleached pulp – may be further treated by screening, washing, bleaching and purification (removal of low molecular-weight hemicelluloses) operations.

For any given type of production, the properties of the unbleached pulp are determined by the structural and chemical composition of the raw material. The variation in fiber dimension and chemical composition of some selected fibers is detailed in Tab. 1.1.

By far, the predominant use of the fiber material is the manufacture of paper, where it is re-assembled as a structured network from an aqueous solution. Fiber morphology such as fiber length and fiber geometry have a decisive influence on the papermaking process. A high fiber wall thickness to fiber diameter ratio means that the fibers will be strong, but that they may not be able to bond as effectively with each other in the sheet-forming process. Another property which is important to fiber strength is the spiral angle of the longitudinal cellulose micelle chains which constitute the bulk of the fiber walls. Moreover, certain chemical properties of the fibers and the matrix material in which they are embedded must also be taken into account.

Tab. 1.1 Fiber dimensions and chemical composition of some selected agricultural and wood fibers (adopted from [1–6]).

Fiber type	Cell dimensions				Chemical Composition				
	Length [mm]		Diameter [ $\mu\text{m}$ ]		Cellulose %	Pentosan %	Lignin %	Ash %	SiO <sub>2</sub> %
	average	range	average	range					
Stalk fibers (grass fibers)									
Cereal straw (wheat, corn, rice)	1.4	0.4–3.4	15	5–30	29–35 <sup>a</sup>	26–32 <sup>a</sup>	16–21 <sup>a</sup>	4–9 <sup>a</sup>	3–7 <sup>a</sup>
Bamboo	2.7	1.5–4.4	14	7–27	26–43 <sup>a</sup>	15–26 <sup>a</sup>	21–31 <sup>a</sup>	1.7–5 <sup>a</sup>	1.5–3 <sup>a</sup>
Sugarcane bagasse	1.7	0.8–2.8	34		32–44 <sup>a</sup>	27–32 <sup>a</sup>	19–24 <sup>a</sup>	1.5–5 <sup>a</sup>	0.7–3 <sup>a</sup>
Bast fibers (single fibers)									
Flax	33.0	9–70	19	5–38	64.1 <sup>d</sup>	16.7 <sup>d</sup>	2 <sup>d</sup>	2–5 <sup>a</sup>	
Hemp	25.0	5–55	25	10–50	78.3 <sup>d</sup>	5.5 <sup>d</sup>	2.9 <sup>d</sup>	0.5 <sup>d</sup>	
Jute		2–5	20	10–25	59.4 <sup>d</sup>	18.9 <sup>d</sup>	12.9 <sup>d</sup>	0.6 <sup>d</sup>	<1 <sup>a</sup>
Kenaf	3.4 <sup>d</sup>	1.5–11 <sup>d</sup>	24 <sup>d</sup>	12–36 <sup>d</sup>	31–39 <sup>a</sup>	21–23 <sup>a</sup>	15–18 <sup>a</sup>	2–5 <sup>a</sup>	
Leaf Fibers									
Abaca (long)		3–12 <sup>d</sup>	10 <sup>d</sup>	6–46 <sup>d</sup>	61 <sup>a</sup>	17 <sup>a</sup>	9 <sup>a</sup>	<1 <sup>a</sup>	<1 <sup>a</sup>
Sisal (long)	3.3 <sup>d</sup>	0.8–8 <sup>d</sup>	21 <sup>d</sup>	7–47 <sup>d</sup>	43–56 <sup>a</sup>	21–24 <sup>a</sup>	8–9 <sup>a</sup>	0.6–1.0 <sup>a</sup>	<1 <sup>a</sup>
Seed and fruit fibers									
Cotton lint (raw)		20–50 <sup>c</sup>		8–19 <sup>c</sup>	88–96 <sup>c</sup>			0.7–1.6 <sup>e</sup>	<1 <sup>a</sup>
Cotton linters (second cut, raw)		2–3 <sup>c</sup>		17–27 <sup>c</sup>	80 <sup>c</sup>			2 <sup>c</sup>	<1 <sup>a</sup>
Wood fibers									
Softwood	3.3	1.0–9.0	33	15–60	40–44 <sup>b</sup>	(25–29) <sup>b</sup>	25–31 <sup>b</sup>		
Hardwood	1.0	0.3–2.5	20	10–45	43–47 <sup>b</sup>	25–35 <sup>b</sup>	16–24 <sup>b</sup>		

Adopted from Refs. [1<sup>a</sup>, 2<sup>b</sup>, 3, 4<sup>c</sup>, 5<sup>d</sup> and 6<sup>e</sup>].  
Values in parentheses indicate total hemicellulase.

## 1.2 The History of Papermaking

The history of papermaking can be traced back to about AD 105, when Ts'ai-Loun created a sheet of paper using old rags and plant tissues. In its slow travel westwards, the art of papermaking reached Arabia in the middle of the eighth century, from where it entered Europe via Spain in the 11th century. By the 14th century, a number of paper mills existed in Europe, particularly in Spain, France, and Germany. For centuries, paper had been made from linen, hemp and cotton rags. After cleaning, sorting and cutting, these were boiled with potash or soda ash to remove the remaining dirt and color. The operation was continued in a “breaking engine” by adding fresh water until the cloth was separated into single fibers.

Until the paper machine was constructed in 1799 by Louis-Nicholas Robert, the final sheet-formation process was carried out manually.

Throughout the 18th century the papermaking process remained essentially unchanged, with linen and cotton rags furnishing the basic fiber source. However, the increasing demand for paper during the first half of the 19th century could no longer be satisfied by the waste from the textile industry. Thus, it was evident that a process for utilizing a more abundant material was needed. Consequently, major efforts were undertaken to find alternative supplies for making pulp. As a result, both mechanical and chemical methods were developed for the efficient production of paper from wood. Mechanical wood pulping was initiated in 1840 by the German Friedrich Gottlob Keller. The wood-pulp grinding machine was first commercialized in Germany in 1852 (Heidenheim) on the basis of an improved technology developed by Voelter and Voith. However, mechanical pulping did not come into extensive use until about 1870 when the process was modified by a steam pretreatment which softens the inter-fiber lignin. Paper made from mechanical wood pulp contains all the components of wood and thus is not suitable for papers in which high brightness, strength, and permanence are required.

The clear deficiencies compared to paper made from cotton rags made it necessary to strengthen the development of chemical wood pulping processes, focusing on the removal of accessory wood components such as lignin and extractives.

The first chemical pulping process was the soda process, so-named because it uses caustic soda as the cooking agent. This process was developed in 1851 by Hugh Burgess and Charles Watt in England, who secured an American patent in 1854. A year later, the first commercial soda mill using poplar as raw material was built on the Schuylkill River near Philadelphia under the direction of Burgess, who served as manager of the mill for almost 40 years. Because this process consumed relatively large quantities of soda, papermakers devised methods for recovering soda from the spent cooking liquor through evaporation and combustion of the waste liquor and recausticizing of the sodium carbonate formed. To compensate for the losses, sodium carbonate had to be added to the causticizing unit. Since the preparation of sodium carbonate from sodium sulfate was rather expensive by using the Leblanc process, Carl Dahl in Danzig tried to introduce sodium sulfate directly in place of soda ash in a soda pulping recovery system. This substitution produced a cooking liquor that contained sodium sulfide along with caustic soda. Fortunately, the pulp so produced was stronger than soda pulp and was called "kraft" pulp, so named from the Swedish word for "strong". The process, which was patented in 1884 by Dahl, has also been termed the sulfate process because of the use of sodium sulfate (salt cake) in the chemical make-up. As a consequence, many soda mills were converted to kraft mills because of the greater strength of the pulp. Kraft pulp, however, was dark in color and difficult to bleach compared to the competing sulfite pulp. Thus, for many years the growth of the process was slow because of its limitation to papers for which color and brightness were unimportant. With the development of the Tomlinson [7,8] combustion furnace in the early 1930s, and with the discovery of new bleaching techniques, par-

ticularly using sodium chlorite (1930) and later chlorine dioxide (1946), bleached kraft became commercially important. The availability of pulp of high brightness and high strength and the expanding demand for unbleached kraft in packaging resulted in rapid growth of the process, making kraft the predominant wood-pulping method.

In 1857, shortly after the discovery of the soda pulping process, Benjamin Tilghman, a US chemist, invented acid sulfite pulping. In 1867, the US patent was granted to Tilghman on the acid sulfite cooking process, using solutions of sulfur dioxide and hydrogen sulfite ions at elevated temperature and pressure. Tilghman observed that the presence of a base such as calcium (to form hydrogen sulfite ions) was important in preventing the formation of burned or discolored pulp. His invention, however, did not result in commercial use due to severe technical difficulties (leakages, etc.), although the product he obtained was satisfactory.

In 1870, Fry and Ekman in Sweden carried these studies further and their improved process, which came into use in 1874, used rotary digesters and indirect heating to produce magnesium-based sulfite pulp. This process was applied in the first American mill, the Richmond Paper Co., built in 1882 at East Providence, Rhode Island, with a capacity of about 15 tons of book and newsprint per day.

Immediately after the German/French war of 1870/1871, Alexander Mitscherlich began to work on the development of calcium hydrogen sulfite cooking with an excess of dissolved sulfur dioxide. The process was characterized by its low temperature (ca. 110 °C), low pressure and long retention time, thus producing rather strong fibers. Heating was carried out indirectly by means of steam in copper coils within the digester. The German sulfite pulping industry was built 1880 on the basis of the Mitscherlich process. In 1887, the first commercially successful sulfite mill in America was built by G. N. Fletcher in Alpena, Michigan. This mill continued in active production until 1940.

Between 1878 and 1882, the Austrians Ritter and Kellner developed an acid calcium-based hydrogen sulfite process using upright digesters with direct steaming. The time of cooking was considerably reduced by applying high temperature and high pressure ("quick cook" process). The patent rights for the Ritter–Kellner process which covered the digester, the method of making the acid cooking liquor, and all features of the system were acquired about 1886 by the American Sulfite Pulp Co.

Following the introduction of the upright digesters, progress was rapid and sulfite pulping became the leading cooking process using spruce and fir as the preferred species. The good bleachability and low costs of the applied chemicals were the main reasons for the advantage over the soda and kraft processes. In 1925, the total production of chemical wood pulp showed a distribution of 20% soda, 20% kraft and 60% unbleached and bleached sulfite pulps. While for sulfite pulp manufacture, a single-stage treatment of pulp at low consistency, using calcium hypochlorite satisfied most requirements, this simple bleaching treatment was not practical for kraft that is difficult to bleach, nor can it retain maximum strength.

Since 1937 the sulfite cooking technology lost ground to the kraft process despite the introduction of soluble sodium and ammonium bases and the recov-

ery of cooking chemicals in case of magnesium (e.g., the Lenzing [9], the Babcock & Wilcox [10], and the Flakt [11] Mg base systems) and sodium (e.g., the Stora [12], the Rauma [13–15] and the Tampella [16] systems) bases. As previously mentioned, advances in kraft pulping technology comprising the introduction of the modern combustion furnaces by Tomlinson, the improvement of the white liquor recovery system and the development of continuous multi-stage bleaching using chlorination (C), alkali extraction (E) and hypochlorite (H) bleaching and later chlorine dioxide (D) were the key elements of achieving the predominant position in chemical wood pulping. Kraft pulping enables the use of practically all species of wood to produce pulps with high degrees of purification and brightness while maintaining high strength.

Until the end of the 19th century, the exclusive role of pulp production was to supply the paper industry with raw materials. At that time, the first patents were applied for the production of cellulosic products involving chemical conversion processes. The most important technology for the production of regenerated cellulose fibers, the viscose process, was developed by Charles F. Cross and Edward J. Bevan who, with C. Beadle, received a patent on the process in 1892 [17]. The discovery of cellulose diacetate by Miles [18] in 1904 and Eichengrün [19] in 1905 marked the breakthrough of cellulose acetate production, which subsequently developed as the second highest consumer of dissolving pulp until the present time.

Dissolving pulp refers to pulp of high cellulose content which was produced until World War II solely from purified cotton linters or, in case of lower demands on purity (as for viscose), according to the acid sulfite process using somewhat higher temperature and acidity together with prolonged cooking to remove the greater part of the hemicelluloses. The regular kraft pulping process is not capable of removing hemicelluloses completely; in particular, residual pentosans interfere with the chemical conversion of cellulose to either viscose, cellulose ethers or acetates. The hemicelluloses can only be effectively solubilized when exposing wood chips to acid hydrolysis prior to alkaline pulping. The prehydrolysis-kraft (PHK) process was finally developed during World War II in Germany, with the first mill operating in Königsberg (Kaliningrad). In the prehydrolysis step, the wood chips are treated either at temperatures between 160 and 180 °C for between 30 min and 3 h with direct steaming, or in dilute mineral acid (0.3–0.5% H<sub>2</sub>SO<sub>4</sub>) at temperatures between 120 and 140 °C. This pretreatment liberates organic acids (e.g., acetic, formic) from the wood, and these hydrolyze the hemicelluloses selectively to produce water-soluble carbohydrates. Since the 1950s, the PHK process, with its various modifications, has been installed, particularly in the United States and South America. One of the advantages of this process is its applicability to most wood species; in contrast, sulfite pulping has been restricted to spruces, hemlock, fir, and a few hardwoods. The latest development of the PHK – the Visbatch® and VisCBC processes – combine the advantages of both steam hydrolysis and displacement technology [20].

### 1.3

#### Technology, End-uses, and the Market Situation

Today's pulping processes have advanced significantly since their emergence during the second half of the 19th century, and have progressed towards more capital-intensive and increasingly large-scale automated production processes, with continuous emphasis on improvements in product quality, production efficiency and environmental conservation. Thus, the pulp and paper industry has become a very important sector of the economy.

At present, more than 90% of the pulp (virgin pulp fiber) produced worldwide is wood pulp. The first species of trees to be used in great quantities for paper-making were pine and spruce from the temperate coniferous forests located in the cool northern climates of Europe and North America. However, during the past few decades a gradual shift to hardwood species has occurred, mainly driven by lower costs, better availability and advances in pulping and papermaking processes. Today the main species comprise birch, beech, aspen and maple, in the United States and central and western Europe, pine in Chile, New Zealand and United States, eucalyptus in Brazil, Spain, Portugal, Chile and South Africa. Eucalyptus pulp was first introduced as a market pulp during the early 1960s. Brazilian eucalyptus shows a seven-year growth cycle; this is the shortest of all trees worldwide, and translates into very high forest productivity. Eucalyptus plantations yield an average of  $45 \text{ m}^3 \text{ ha}^{-1} \text{ year}^{-1}$  of wood, whereas the average for North American forests is  $2\text{--}4 \text{ m}^3 \text{ ha}^{-1} \text{ year}^{-1}$ . A shorter growth cycle means lower investments and wood production costs, and thus a more rational utilization of natural resources and more available space for other equally important land uses.

Worldwide, the largest stock of hardwood undoubtedly exists in South America, and that of softwood in Russia, Canada and in the South of the United States, respectively. It may be expected that, in the long run, South America and Russia are promoted to the dominating pulp producers. A gradual shift from today's dominating bleached softwood kraft pulp to cheaper bleached hardwood kraft pulp will take place for the years to come, due mainly to the higher growth rate and the better delignifying properties of the latter.

Wood pulps are categorized by the pulping process as either chemical or mechanical pulps, reflecting the different ways of fiberizing. Chemical pulping dissolves the lignin and other materials of the inter-fiber matrix material, and also most of the lignin which is in the fiber walls. This enables the fibers to bond together in the papermaking process by hydrogen bond formation between their cellulosic surfaces. As noted previously, kraft pulping has developed as the dominating cooking process, and today the kraft pulps account for 89% of the chemical pulps and for over 62% of all virgin fiber material (Tab. 1.2). In 2000, the annual global virgin pulp fiber production totaled 187 million tonnes, while only about 50 million tonnes or 27% accounted for market pulp [21]. The remaining 73% stems from integrated paper and cellulose converting mills (captive use).

Due to distinct disadvantages of the sulfite cooking process (including all its modifications) over the kraft pulping technology (see above), the share of sulfite

Tab. 1.2 Global pulp production by category, 2000 [21].

Pulp category	Pulp production [Mio t]
Chemical	131.2
Kraft	117.0
Sulfite	7.0
Semichemical	7.2
Mechanical	37.8
Nonwood	18.0
Total virgin fiber	187.0
Recovered fiber	147.0
Total fibers	334.0

pulps in total fiber production steadily decreased from 60% in 1925 [22] to 20% in 1967 [22], to 9.2% in 1979 [23], and finally to only 3.7% in 2000 [21] (see Tab. 1.2).

The superiority of kraft pulping has further extended since the introduction of modified cooking technology in the early 1980s [24]. In the meantime, three generations of modified kraft pulping processes (MCC, ITC and Compact Cooking as examples for continuous cooking and Cold-blow, Superbatch/RDH and Continuous Batch Cooking, CBC, for batch cooking technology) have emerged through continuous research and development [25]. The third generation includes black liquor impregnation, partial liquor exchange, increased and profiled hydroxide ion concentration and low cooking temperature (elements of Compact Cooking), as well as the controlled adjustment of all relevant cooking conditions in that all process-related liquors are prepared outside the digester in the tank farm (as realized in CBC). However, the potential of kraft cooking is not exhausted by far. New generations of kraft cooking processes will likely be introduced, focusing on improving pulp quality, lowering production costs by more efficient energy utilization, further decreasing the impacts on the receiving water, and recovering high added-value wood byproducts [25].

During the 1980s and 1990s, many of the developments in chemical pulp production of both sulfite and kraft processes were driven by severe environmental concerns, especially in Central Europe and Scandinavia [26]. Increasing pulp production resulted in increasing effluent loads. The need to reduce the amount of organic material originating mainly from bleach plant effluents was most pronounced in highly populated countries, where filtered river water was used as a source of drinking water. The biodegradability of the bleach plant effluents, particularly from the chlorination (C) and extraction stages (E), turned out to be very poor due to the toxicity of halogenated compounds. Finally, the detection of polychlorinated dioxins and furans in chlorination effluents and even in final paper

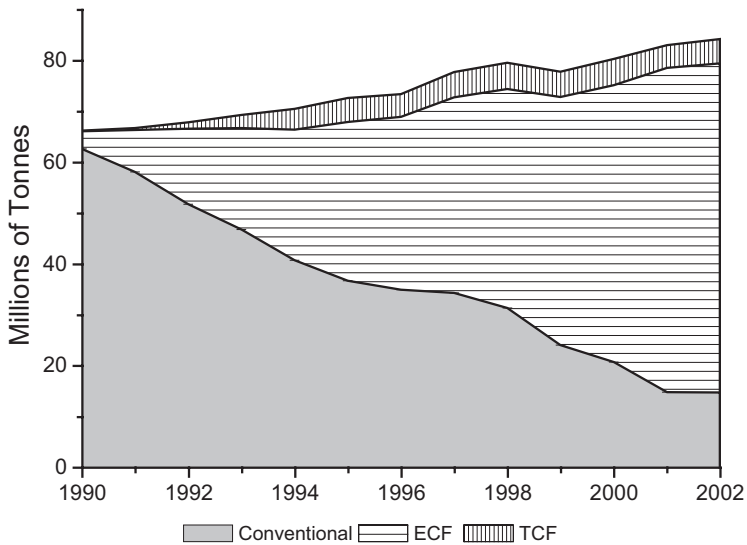


Fig. 1.1 World bleached chemical pulp production: 1990–2002 [29].

products during the 1980s caused a rapid development of alternative, environmentally benign bleaching processes [27]. The initial intention was the complete replacement of all chlorine-containing compounds, resulting in Totally Chlorine Free (TCF) bleaching sequences. This could be easily accomplished with sulfite pulps due to their good bleachability. Kraft pulp mills have been converted dominantly to Elemental Chlorine Free (ECF) bleaching rather than to TCF bleaching, because the latter, by using ozone or peracids to yield high brightness, deteriorates pulp quality. ECF bleaching, comprising chlorine dioxide (D)-containing bleaching sequences, such as DEOpDEpD, is acknowledged as a core component of the best Available Technology (BAT), since numerous field studies have shown that ECF bleaching is virtually free of dioxin and persistent bioaccumulative toxic substances [28]. ECF pulp, bleached with chlorine dioxide, continues to dominate the world bleached chemical pulp market. In 2002, ECF production reached more than 64 million tonnes (Fig. 1.1) [29]. Market data show that ECF production grew by 17% in 2001, whereas TCF pulp production remained constant, maintaining a small niche market at just over 5% of world bleached chemical pulp production. The transition to ECF is essentially complete in Europe, the United States and Canada, with ECF production now representing more than 96% of the whole bleached chemical pulp production.

Dissolving pulps represent specialty pulps within the chemical pulp segment. They are chemically refined bleached pulps composed of more than 90% pure cellulose ( $\alpha$ -cellulose). As mentioned above, two basic processes are used to produce dissolving pulp. The sulfite process produces pulp with an  $\alpha$ -cellulose content of 90–92%, whereas the PHK process typically produces pulp with an  $\alpha$ -cellulose content of 94–96%. Special alkaline purification treatments can yield even higher



cellulose levels of up to 96% for the sulfite and up to 98% for the PHK processes. The low-level  $\alpha$ -cellulose pulps are predominantly used to manufacture viscose staple fibers, whereas the high-level  $\alpha$ -cellulose pulps are converted to viscose yarn for industrial products such as tire cord, high-purity cellulose ethers, various cellulose acetates and other specialty products.

Although world production of dissolving pulp has been reduced constantly since the mid-1970s, the developments of the past two years have signaled a slight change in this trend. With an annual global production averaging 3.65 million tonnes in 2003, dissolving pulp accounted for only 2.8% of the total wood pulp production. However, the high demands for cellulose purity and reactivity, as well as its manifold routes of utilization, are the main reasons for the advanced state of technology within the pulp industry.

Viscose staple fibers and viscose filaments (both textile and technical) had the lion's share of the total production, at 2.2 million tonnes (60%), while 0.53 million tonnes (15%) stemmed from the manufacture of a variety of cellulose acetate products (cigarette filters, filaments, plastics, etc.). The remaining 25% were accounted for by the production of cellulose ethers, cellophane, microcrystalline cellulose (MCC), specialty papers and nitrocellulose (Tab. 1.3).

Tab. 1.3 World production of dissolving pulp by end-use in 2003 [30].

Cellulose product	End-use	Mio t
Regenerated fibers	Staple, filaments	2.20
Cellophane	Incl. sponges, casings	0.10
Cellulose acetate	Tow, filament, plastic	0.53
Cellulose ether	Non-ionic, ionic (CMC)	0.47
MCC	Incl. moulding powder	0.09
Others	Nitrocellulose, speciality papers	0.26
<b>Total</b>		<b>3.65</b>

Unlike paper-grade pulping the acid sulfite process is the dominant process for the production of dissolving pulps, and accounted for 60–63% of the total production, while 22–25% originated from PHK process in 2003. The remaining 12–16% was produced from cotton linters which, for purification and viscosity control, is treated by alkaline cooking and subsequent hypochlorite bleaching. Purified cotton linters represents the dissolving pulp of highest cellulose purity particularly used for manufacturing acetate plastics and high-viscosity cellulose ethers. However, in China cotton linters is used as a raw material for the manufacture of viscose fibers, both staple and filaments.

Similar to paper-grade pulps, a gradual shift from softwood to hardwood can be observed. This development is mainly driven by better availability and lower costs. The slight increase in the world's dissolving pulp production predicted for the next five years is mainly attributed to new installations of viscose fiber plants in Asia and to the continuous growth of the cellulose ether and acetate tow markets.

Semichemical pulping processes are characterized by a mild chemical treatment preceded by a mechanical refining step. Semichemical pulps, which apply to the category of chemical pulps, are obtained predominantly from hardwoods in yields of between 65 and 85% (average ca. 75%). The most important semichemical process is the neutral sulfite semichemical process (NSSC), in which chips undergo partial chemical pulping using a buffered sodium sulfite solution, and are then treated in disc refiners to complete the fiber separation. The sulfonation of mainly middle lamella lignin causes a partial dissolution so that the fibers are weakened for the subsequent mechanical defibration. NSSC pulp is used for unbleached products where good strength and stiffness are particularly important; examples include corrugating medium, as well as grease-proof papers and bond papers. NSSC pulping is often integrated into a kraft mill to facilitate chemical recovery by a so-called cross-recovery, where the sulfite spent liquor is processed together with the kraft liquor. The sulfite spent liquor then provides the necessary make-up (Na, S) for the kraft process. However, with the greatly improving recovery efficiency of modern kraft mills, the NSSC make-up is no longer needed so that high-yield kraft pulping develops as a serious alternative to NSSC cooking. Semichemical pulps is still an important product category, however, and account for 3.9% of all virgin fiber material (see Tab. 1.2).

The second category of pulping procedures – mechanical pulping processes – can be classified as stone grinding (groundwood pulping: stone groundwood, SGW, and pressure groundwood, PGW) and refiner pulping processes (refiner mechanical pulp, RMP, pressurized refiner mechanical pulp, PRMP, thermomechanical pulp, TMP, chemigroundwood, CGW, chemi-refiner mechanical pulp, CRMP, and the chemi-thermomechanical pulp, CTMP).

Groundwood pulp shows favorable properties with respect to brightness ( $\geq 85\%$  ISO after bleaching), light scattering and bulk, which allows the production of papers with low grammages. Moreover, the groundwood process also offers the possibility of using hardwood (e.g., aspen) to achieve even higher levels of brightness and smoothness [31]. Groundwood pulp has been the quality leader in magazine papers, and it is predicted that this situation will remain [31].

The most important refiner mechanical pulping process today is thermomechanical pulping (TMP). This involves high-temperature steaming before refining; this softens the inter-fiber lignin and causes partial removal of the outer layers of the fibers, thereby baring cellulosic surfaces for inter-fiber bonding. TMP pulps are generally stronger than groundwood pulps, thus enabling a lower furnish of reinforcing chemical pulp for newsprint and magazine papers. TMP is also used as a furnish in printing papers, paperboard and tissue paper. Softwoods are the main raw material used for TMP, because hardwoods give rather poor pulp strength properties. This can be explained by the fact that hardwood fibers do not

form fibrils during refining but separate into short rigid debris. Thus, hardwood TMP pulps, characterized by a high-cleanness, high-scattering coefficient, are mainly used as filler-grade pulp. The application of chemicals such as hydrogen sulfite prior to refining causes partial sulfonation of middle lamella lignin. The better swelling properties and the lower glass transition temperature of lignin results in easier liberation of the fibers in subsequent refining. The CTMP pulps show good strength properties, even when using hardwood as a fiber source, and provided that the reaction conditions are appropriate to result in high degrees of sulfonation. Mechanical pulps are weaker than chemical pulps, but cheaper to produce (about 50% of the costs of chemical pulp [31]) and are generally obtained in the yield range of 85–95%. Currently, mechanical pulps account for 20% of all virgin fiber material (see Tab. 1.2). It is foreseen that mechanical paper will consolidate its position as one major fiber supply for high-end graphic papers. The growing demand on pulp quality in the future can only be achieved by the parallel use of softwood and hardwood as a raw material.

The largest threat to the future of mechanical pulp is its high specific energy consumption. In this respect, TMP processes are most affected due to their considerably higher energy demand than groundwood processes. Moreover, the increasing use of recovered fiber will put pressure on the growth in mechanical pulp volumes.

Almost 10% of the total pulp production is made from nonwood plant fibers, including stalk, bast, leaf and seed fibers (see Tab. 1.1). In view of the enormous annual capacity of nonwood fiber material (mostly as agricultural waste) as a potential source for pulp production of 2.5 billions tons, the current nonwood pulp annual production of only 18 million tons is rather low [32,33]. Assuming an average pulp yield of 50%, the utilization of nonfiber material as a source for pulp production accounts only for 1.4%. In 1998, the major raw material sources for nonwood pulp were straw, sugar cane bagasse and bamboo, with shares of 43%, 16%, and 8% of the total nonwood pulp capacity, respectively [32]. With regard to the fiber length, the nonwood pulps can be divided into three groups: (a) those with fiber length >4 mm, represented by cotton lint, abaca, flax and hemp; (b) those with fiber lengths of 1.5–4 mm, represented by bamboo, bagasse, kenaf and reed; and (c) those with a fiber length <1.5 mm, represented by all kinds of straw pulps [34]. Technically, the nonwood pulps belong to the group of chemical pulps, and are predominantly produced according to the soda cooking process. Kraft cooking processes are applied using selected substrates such as bamboo, kenaf, sisal, or others.

The complex logistics of harvesting, transporting and storing a bulky seasonal commodity, particularly in regions of the world where wood supplies are adequate, has prevented the emergence of nonwood plant fibers as a source of cost-competitive pulp for both printing/writing and cellulose products. The use of nonwood fibers, however, is common in wood-limited countries, such as China and India, which are the two largest producers of nonwood pulp. In China, the nonwood pulping capacity amounts to approximately 80% of the country's total pulping capacity, while in India it is 55% [21]. In Western countries, nonwood pulp

has established niches in specialty paper production. Flax, hemp and abaca have confirmed good results as reinforcing pulps for thin applications such as cigarette paper, bank notes, and bibles. Cotton papers are known to be superior in both strength and durability to wood-based papers, and this favors their use as acid-free, high-end fine papers. In general, the higher costs of nonwood pulps limit their use to high-end products often marketed as “eco-friendly” papers. Even bigger players are now beginning to enter the market for eco-papers more seriously, and are positioning themselves in the as yet tiny niche of eco-friendly nonwood printing/writing grades. Small (but growing) niches have been developed for “tree-free” papers. The most popular fiber sources for these papers are kenaf, hemp, flax, bamboo, wheat straw and other grasses. The emerging use of blends from nonwood and deinked fibers increasingly blurs the border between tree-free and other eco-friendly papers. In order to expand the use of nonwood pulps in applications beyond the current niche markets, it will be necessary to develop cost-effective pulping processes, and particularly innovative recovery methods to handle the high silica content.

Mastering the technological and logistical requirements of harvesting, storing and processing large quantities of bulky fibers will continue to be a major challenge.

#### 1.4

#### **Recovered Paper and Recycled Fibers**

After wood, the second largest share of pulp produced worldwide is pulp made from recovered paper (see Tab. 1.2). Apart from good economic reasons, a major force in this drive to recycling is derived from public pressure to reduce the amount of used paper that is landfilled as waste. In the recycling process, recovered paper is reduced to pulp principally by mechanical means, followed by separation and removal of inks (de-inked paper, DIP), adhesives, and other contaminants, through both chemical and mechanical processes. Recovered fibers generally differ from virgin wood fibers in terms of their fiber morphology and physical properties. Strength, as well as swelling and optical properties, tend to deteriorate due to the recycling process. To a large extent, modern processing technology can compensate for the inherent disadvantages of recovered fibers which, however, contribute to higher costs. Modern mechanical refining is used, for example, to resurrect surface fibrils, and modern papermaking machines and coatings can enhance sheet strength and surface properties, while the efficiency of contaminant removal has been improved by modern deinking systems.

The proportion of recovered fiber has grown substantially during the past few years, and continues to expand. Its share of the global fiber flow increased from 22.5% in 1978 to 33.5% in 1992, and to 44% in 2000. The extent to which recovered paper is used varies greatly from country to country. In Central Europe, where there is a fiber deficiency, it accounts about half of the total fiber raw material (utilization rate 47%, collection rate 57.3% in 2003 [35]), whereas in countries

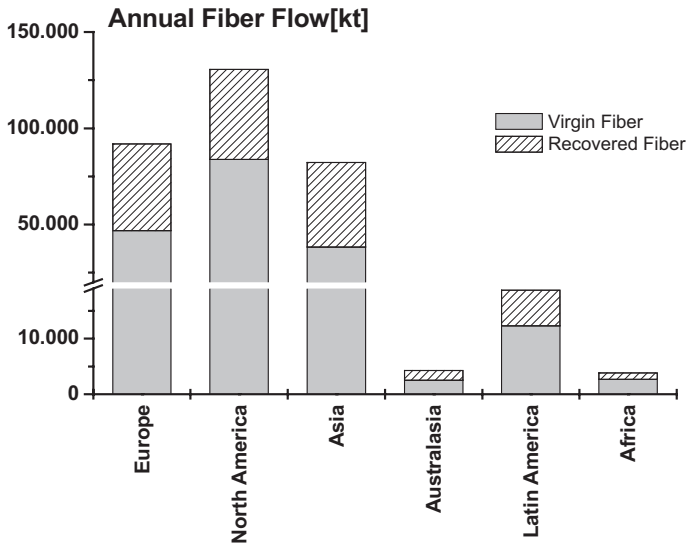


Fig. 1.2 Global annual flow of virgin and recovered fibers by region in 2000 [21].

such as Scandinavia and Canada, recycling levels are much lower. The share of virgin and recovered fiber by region is illustrated in Fig. 1.2.

On a European level, about 50% of the collected volumes are derived from trade and industrial sources, 40% from households, and the remaining 10% from offices. These proportions differ greatly between countries as well as collection systems. The future potential clearly lies in households, but as these consist of numerous small sources, the costs and quality of recovered paper are placed under pressure.

Among users of recovered paper, packaging grades are the major user at almost two-thirds of the total recovered paper. In Europe, case materials represent 23% of total paper and board production, have a utilization rate of 90%, and use 45% of the total recovered paper consumption [35]. The utilization rate of newsprint, representing about 12% of total paper and board production, has increased steadily over the years and reached 74% in 2003. The challenge for the future is certainly the use of recycled fiber for the manufacture of printing and writing papers. Currently, the utilization rate of these grades is slightly below 9% [35].

## 1.5 Outlook

Recoverable raw materials undoubtedly will play a decisive role in the future. Nature is producing an enormous amount of plant biomass, approximately 170 billion tons per year [36]. Although renewable raw materials offer many opportunities for use, they have been only rarely applied so far. In particular, the increased

use of renewable raw materials for the production of chemical products would promote future developments towards a lasting supply of resources. Renewable raw materials are advantageous because they are part of the closed cycle of the biosphere. Therefore, using renewable raw materials is an opportunity to supply all substances needed without polluting the biosphere with foreign and hazardous substances.

With an estimated average annual growth rate of 2.2%, the world's consumption of pulp fibers is expected to rise from 334 million tons in 2000 to over 400 million tons in 2010 [37]. New pulp and paper capacities are now shifting to Asia and South America, where many new mills are currently under construction. By comparison, very few mills have been built in North America and Europe over the past few years.

Within the past three decades, enormous efforts have been devoted to the development of new pulping processes in an attempt to overcome the shortcomings of alkaline cooking, which mainly comprise air and water pollution as well as high investment costs. A serious alternative to kraft pulping could be possible, if a new process were available that had the following characteristics [38]:

- Selective delignification to increase pulp yield and preserve pulp strength properties.
- Pulp quality at least equal to that of kraft pulps.
- Low energy input and even temperature profile throughout whole fiber line processes in order to minimize energy demand.
- Low chemical consumption to enable an efficient and simple chemical recovery system.
- The possibility of closing the chemical cycle of the process (closed-loop operations) without impairing processability and pulp quality.
- Selective bleaching without chlorine-containing compounds.
- Minimum restriction in the use of raw material sources.
- Minimum air and water pollution; to avoid any malodorous emissions, the process should be totally sulfur-free.
- Recovery of valuable byproducts with competitive costs.
- Profitable smaller production units requiring lower set-up costs.

Organosolv pulping – that is, the process of using organic solvents to aid in the removal of lignin from wood – has been suggested as an alternative pulping route [39]. The pioneering studies on organosolv pulping began with the discovery in 1931 by Kleinert and Tayanthal that wood can be delignified using a mixture of water and ethanol at elevated temperature and pressure [40,41]. During the following years, a rather wide variety of organic solvents have been found to be suitable for pulp production. The intrinsic advantage of organosolv over kraft pulping processes seems to be the straightforward concept of recovering the solvents by using simple distillation. Furthermore, organosolv processes are predicated on the bio-refining principle – that is, the production of high amounts of valuable byproducts. The advantage of small and efficient recovery units which could fulfill the demand

for profitable smaller production units is, however, limited to very simple solvent systems such as ethanol-water derived from the Kleinert process. For example, the use of acid-catalyzed organosolv pulping processes such as the Formacell and Milox processes clearly complicates an efficient recovery of the solvents, and this in turn diminishes the advantage over existing pulping technologies [42]. The reason for this is the nature of the solvent system. The spent pulping liquor contains water, formic acid, and acetic acid which form a ternary azeotrope. The complexity of efficient solvent recovery, together with the limitation to hardwood species as a raw material and, moreover, the clearly inferior strength properties of organosolv pulps compared to kraft pulps, indicates that organosolv pulping processes are not ready to compete with the kraft process at this stage of development. [42]. The challenge of organosolv pulping for the future is to identify solvents with better selectivity towards lignin compared to those available today which simultaneously allow simple, but efficient, recovery.

Parallel to the research on alternative pulping processes, the kraft process has undergone significant improvements since the discovery of the principles of modified cooking during the late 1970s and early 1980s at the department of Cellulose Technology of the Royal Institute of Technology and STFI, the Swedish Pulp and Paper Research [43,44]. In the meantime, the third generation of modified cooking technology has been established in industry and, together with an efficient two-stage oxygen delignification stage prior “ECF-light” bleaching, the impact on the environment has been reduced dramatically within the past two decades. The specific effluent COD and AOX emissions after the biological treatment plant of today’s state-of-the-art kraft pulping technology are at a level of about  $7 \text{ kg adt}^{-1}$  and  $<0.1 \text{ kg adt}^{-1}$ , respectively [25]. Simultaneously, continuous effort on closing the loops led to a significant decrease in the total effluent flow from values higher than  $100 \text{ m}^3 \text{ adt}^{-1}$  in the 1970s to about  $16 \text{ m}^3 \text{ adt}^{-1}$  today. The successful technological improvements in the past, as well as the current developments focusing on new generations of alkaline cooking, clearly signal that kraft pulping will remain the dominant cooking process in the future.

It is commonly agreed [25,45] that the only serious alternative to kraft pulping is ASAM pulping (alkaline sulfite with anthraquinone and methanol) developed by Patt and Kordsachia [46,47]. In order to overcome the problem with the additional recovery of methanol, a new attempt was made to improve the efficiency of alkaline sulfite pulping, AS/AQ, in the absence of methanol [48]. The AS/AQ process, by using a split addition of alkali charge to ensure a rather even alkali profile throughout the cook, produces pulp with strength properties that are equal or even slightly superior to those of kraft pulp whilst revealing a distinct yield advantage, even at low kappa number [49,50]. Even though odor abatement is quite powerful in modern kraft mills, pulping processes based on AS/AQ are clearly advantageous in this respect. The principal stumbling block to implementing AS/AQ pulping has been the inability to regenerate sodium sulfite with the Tomlinson recovery cycle. An important prerequisite for the successful introduction of AS cooking is that a new chemical recovery technique based on black liquor gasification can be implemented.

It is most likely that, similar to the situation before 1930 when kraft pulping became the dominant cooking process through the development of the Tomlinson recovery boiler, a new generation of black liquor incineration combined with efficient energy and chemical recovery – namely black liquor gasification/combined cycle (BLGCC) – will mark a further breakthrough of alkaline pulping. BLGCC is certainly the key element to entering into a new era of pulping technology. Black liquor gasification technology is classified by operating temperature into high-temperature (~1000 °C) and low-temperature gasification (below 700 °C). The temperature level of the former is sufficient to convert the inorganic components into a smelt, whereas operating below 700 °C ensures that the inorganics leave as dry solids. If the gas is combusted in a combined cycle (as is the case in a BLGCC installation), there is the potential to produce at least twice more electric power from the same amount of black liquor than with a Tomlinson furnace – and this is the most compelling reason for pursuing this new technology [45]. Moreover, gasification also provides a significant separation of sulfur from sodium in that the reduced sulfur accumulates in the product gas in the form of hydrogen sulfide. The separation of sulfur from sodium is an important prerequisite for the application of modified alkaline cooking technologies including split sulfidity pulping, polysulfide pulping and AS/AQ pulping [51]. The prospects for commercializing BLGCC appear quite promising, and although a number of open technical issues have still to be solved, commercialization is expected within the next five to ten years [25].

## References

- 1 Hurter AM, in Tappi Pulping Conference, Vol. 1, Tappi, New Orleans, 1988, p. 139.
- 2 Klemm D, Philipp B, Heinze T, Heinze U, Wagenknecht W, *Comprehensive Cellulose Chemistry*, Vol. 1. Wiley-VCH Verlag GmbH, Weinheim, Germany, 1998.
- 3 Rowell R, Young RA, Rowell J, *Paper and composites from agro-based resources*. Lewis Publishers, 1997.
- 4 Temming H, Grunert H, Huckfeldt H, *Temming Linters: technical information about cotton cellulose*. J.J. Augustin, Glückstadt, 1972.
- 5 Batra SK, *Other long vegetable fibres*, Vol. 15. Marcel Dekker, Inc., Jerusalem, Israel, 1998.
- 6 Wakelyn PJ, Bertoniere NR, French AD, Zeronian SH, Nevell TP, Thibodeaux DP, Blanchard EJ, Calamari TA, Triplett BA, Bragg CK, Welch CM, Timpa JD, Franklin WE, Reinhardt RM, Vigo TL, *Cotton Fibres*, Vol. 15, Marcel Dekker, Inc., Jerusalem, Israel, 1998.
- 7 Tomlinson GHT, Schwartz JN, *Pulp Paper Mag. Can.*, 1946; 47: 71.
- 8 Tomlinson GHT. US Patent 2406867 19460903, 1946.
- 9 Hornke R, *Wochenbl. f. Papierf.*, 1972: 98: 895.
- 10 Clement JL, *Tappi*, 1966; 49: 127A.
- 11 Herrlander B, *Pulp Paper Can.*, 1982; 83: T208.
- 12 Bernhard R, Backman K, in *TAPPI Pulping Conference*, 1981, p. 329.
- 13 Reilama I, in *CPA Sulphite Committee: Chemical Recovery Workshop*, Montreal, 1979, p. 186.
- 14 Reilama I, Hassinen I, Rasanen R, *Pulp Paper Can.*, 1981; 82: T37.
- 15 Reilama I, Hauki T, *Tappi Proceedings*, 1982, 41.



- 16 Vuojolainen TJ, Romantschuk H, in *International Sulphite Conference*, Montreal, 1978, p. 19.
- 17 Cross CF, Bevan EJ, Beadle C, British Patent 8700, 1892.
- 18 Miles GW, A.P. 838 350, 1904.
- 19 Eichengrün A, Becker, Guntrum, D.R.P. 252,706, 1905.
- 20 Wizani W, Krotscheck A, Schuster J, Lackner K, in WO9412719 PCT Pub., 1994.
- 21 Toland J, Galasso L, Lees D, Rodden G, in *Pulp Paper International*, Vol. Paperloop, 2002, p. 5.
- 22 Ingruber OV, *Sulfite Science & Technology*, Vol. 4, Tappi, CPPA, Atlanta, Montreal, 1985.
- 23 Fengel D, Wegener G, *Wood, Chemistry, Ultrastructure, Reactions*, W. Degruyter, Berlin, New York, 1989.
- 24 Teder A, Olm L, *Pap. Puu*, 1981; 63: 315.
- 25 Axegard P, Backlund B, STFI, Swedish Pulp and Paper Research Institute, Stockholm, Sweden, 2003.
- 26 European Commission, 2001.
- 27 d. Souza F, Kolar MC, Kringstad KP, Swanson EE, Rappe C, Glas B, Tappi, 1989, 147.
- 28 Bright D, Hodson P, Lehtinen K-J, McKague B, Rodgers J, Solomon K, Evaluation of ecological risks associated with the use of chlorine dioxide for the bleaching of pulp. Scientific Progress since 1993. SETAC Press, 2003.
- 29 T. A. f. E. T. AET, 2003.
- 30 Sixta H, Lenzing AG, Lenzing, 2004.
- 31 Arppe M, *Das Papier*, 2001, 45.
- 32 Atchison JE, *Tappi*, 1996; 79: 87.
- 33 Atchison JE, in *North American Non-wood Fiber Symposium*, Tappi, 1998.
- 34 Judt M, *Das Papier*, 2001, 41.
- 35 CEPI, in *Special Recycling 2003 Statistics – Confederation of European Paper Industry*, 2004.
- 36 Krässig HA, *Cellulose: Structure, Accessibility and Reactivity*, Vol. 11. Gordon and Breach Science Publishers, 1993.
- 37 World paper markets up to 2015, in know-how wire, *Jaakko Pöyry Magazine*, 2003, p. 5.
- 38 Franzreb JP, *Papier*, 1989; 43: V94.
- 39 Hergert HL, *Developments in organosolv pulping – an overview*. John Wiley & Sons, Inc., 1998.
- 40 Kleinert TN, Tayenthal K, in AT 124738 19310515, 1931.
- 41 Kleinert TN, Tayenthal KV, *Angewandte Chemie*, 1931; 44: 788.
- 42 Muurinen E, PhD thesis, University of Oulu (Oulu), 2000.
- 43 Hartler N, *Svensk. Papperstidn.*, 1978; 15: 483.
- 44 Teder A, Olm L, *Paperi ja Puu – Papper och Trä*, 1981; 4: 315.
- 45 Larson ED, McDonald GW, Yang W, Frederick WJ, Iisa K, Kreutz TG, Malcolm EW, Brown CA, *Tappi*, 2000; 83: 1.
- 46 Patt R, Kordsachia O, Deutsches Patentamt 1985, DE 3518005 A1, 1.
- 47 Patt R, Kordsachia O, *Das Papier*, 1986; 40: 1.
- 48 Patt R, Kordsachia O, Rose B, *Wochenbl. f. Papierf.*, 2002, 892.
- 49 McDonough TJ, van Drunen VJ, Paulson TW, *J. Pulp Paper Sci.*, 1985; 11: 167.
- 50 Patt R, Kordsachia O, Rose B, in *Seventh International Conference on New Available Technologies*. SPCI, Stockholm, Sweden, 2002, p. 26.
- 51 Dahlquist E, Jones A, *Tappi*, 2005; 4: 15.

## 2

### Raw Material for Pulp

Gerald Koch

#### 2.1

##### Wood

In order to understand the behavior of wood during pulping, as well as the resulting pulp quality, it is indispensable to have a basic knowledge on the chemical composition and structure of this natural raw material. The final cellulose and lignin content and its variation, as well as fiber strength properties are typical essential characteristics of the pulp which depend significantly on the chemical composition as well as the structure of the various components of wood.

In the literature, five structural levels of observation have been distinguished for the characterization of wood [1]:

- Integral level (stem structure)
- Macroscopic level (tissue structure)
- Microscopic level (cell structure)
- Ultrastructural level (cell wall structure)
- Biochemical level (biochemical composition of the cell wall)

On each level, structural variations influence the chemical and mechanical properties of wood, and these differences are extremely important for the different applications of the material.

This chapter begins by detailing the chemical composition of wood, followed by the submicroscopic structure of the cell wall, the microscopic structure of wood, and finally considers aspects of the macroscopic structure of both softwoods and hardwoods. The structure of phloem or bark is not described; neither are the primary and secondary growth due to meristem (cambium) activities (e.g., cell division in the cambial region, cell differentiation and cell growth) considered in detail in this chapter. Nevertheless, these are characteristic features which must be taken into account in order to explain certain chemical properties of wood. For such information, the reader is referred to special literature.

## 2.1.1

**Chemical Composition of Wood**

Wood is an organic material – that is, it contains carbon. With very little variation between different species, woody matter is composed of the three main elements carbon, oxygen, and hydrogen (Tab. 2.1). Nitrogen as well as some inorganic elements, such as sodium, potassium, calcium, magnesium, and silicon [2], are also essential material compounds that are mostly involved in the metabolism of the living cells during wood formation and growth [3,4].

**Tab. 2.1** Elementary composition of wood [5].

	Element(s)	Content [%]
Carbon	C	49
Hydrogen	H <sub>2</sub>	6
Oxygen	O <sub>2</sub>	44
Nitrogen	N <sub>2</sub>	<1
Inorganic elements	Na, K, Ca, Mg, Si	<<1

At a higher level, these elements form macromolecules – that is, polymers – which represent the main cell wall compounds of *cellulose*, *hemicelluloses*, and *lignin*. These are the main constituents of all wood species (Tab. 2.2). To a lesser extent, low molecular-weight substances (e.g., extractives and inorganic substances (ash)) can also be found, and these are representative of individual plant taxa.

The proportions and chemical composition of lignin and hemicelluloses differ in softwoods and hardwoods, while cellulose is a relatively uniform component of all woods (Tab. 2.3). In wood from temperate zones, the portions of the high-polymeric compounds which constitute the cell wall account for 97–99% of the woody material. For tropical woods, this value may decrease to an average of 90%, with 65–75% of the woody material consisting of polysaccharides [6].

**Tab. 2.2** Macromolecular substances of the wood cell wall [5].

	Content [%] Softwoods	Compound Hardwoods
Cellulose	40...44	40...44
Hemicelluloses	30...32	15...35
Lignin	25...32	18...25

**Tab. 2.3** Chemical comparison of various wood species (% of dry wood weight; adopted from [7]).

Species	Common name	Extrac- tives <sup>a</sup>	Lignin	Cellulose	Gluco- mannan	Glucuro- noxytan	Other polysac- charides
Softwoods							
<i>Abies balsamea</i>	Balsam fir	2.7	29.1	38.8	17.4	8.4	2.7
<i>Pseudotsuga menziesii</i>	Douglas fir	5.3	29.3	38.8	17.5	5.4	3.4
<i>Tsuga canadensis</i>	Eastern hemlock	3.4	30.5	37.7	18.5	6.5	2.9
<i>Juniperus communis</i>	Common juniper	3.2	32.1	33.0	16.4	10.7	3.2
<i>Pinus radiata</i>	Monterey pine	1.8	27.2	37.4	20.4	8.5	4.3
<i>Pinus sylvestris</i>	Scots pine	3.5	27.7	40.0	16.0	8.9	3.6
<i>Picea abies</i>	Norway spruce	1.7	27.4	41.7	16.3	8.6	3.4
<i>Picea glauca</i>	White spruce	2.1	27.5	39.5	17.2	10.4	3.0
<i>Larix sibirica</i>	Siberian larch	1.8	26.8	41.4	14.1	6.8	8.7
Hardwoods							
<i>Acer rubrum</i>	Red maple	3.2	25.4	42.0	3.1	22.1	3.7
<i>Acer saccharum</i>	Sugar maple	2.5	25.2	40.7	3.7	23.6	3.5
<i>Fagus sylvatica</i>	Common beech	1.2	24.8	39.4	1.3	27.8	4.2
<i>Betula verrucosa</i>	Silver birch	3.2	22.0	41.0	2.3	27.5	2.6
<i>Betula papyrifera</i>	Paper birch	2.6	21.4	39.4	1.4	29.7	3.4
<i>Alnus incana</i>	Gray alder	4.6	24.8	38.3	2.8	25.8	2.3
<i>Eucalyptus globulus</i>	Blue gum	1.3	21.9	51.3	1.4	19.9	3.9
<i>Acacia mollissima</i>	Black wattle	1.8	20.8	42.9	2.6	28.2	2.8

a. Extraction with CH<sub>2</sub>Cl<sub>2</sub>, followed by C<sub>2</sub>H<sub>5</sub>OH.

### 2.1.1.1 Cellulose

#### 2.1.1.1.1 Significance and Occurrence

In terms of quantity, *cellulose* is the most abundant renewable polymer resource available worldwide. It has been estimated that, by photosynthesis, 10<sup>11</sup> to 10<sup>12</sup> tons are synthesized annually in a rather pure form (e.g., in seed hairs of the cotton plant), but mostly are combined with lignin and other polysaccharides (hemicelluloses) in the cell wall of woody plants [8]. Further cellulose-containing materials include agriculture residues, water plants, grasses, and other plant substances.

Commercial cellulose production concentrates on harvested source such as wood or on naturally highly pure sources as cotton (Tab. 2.4).

A rather new approach to synthesize pure cellulose is the laboratory-scale production of the polymer by acetic acid-producing bacteria, such as *Gluconacetobacter xylinum* and *Acanthamoeba castellanii*. Algae constitute another source for cellulose (e.g., *Valonia ventricosa* and *Chaetomorpha melagonicum*). The cellulose obtained is highly crystalline and is useful for studying polymorphs of the polymer [9]. In addition, there are several celluloses of animal origin, one of which is tunicin, a cell wall component of ascidians that has been extensively studied by Klemm et al. [8].

**Tab. 2.4** Chemical composition of some typical cellulose-containing materials (adopted from [8]).

Source	Composition [%]			
	Cellulose	Hemicelluloses	Lignin	Extract
Hardwood	43–47	25–35	16–24	2–8
Softwood	40–44	25–29	25–31	1–5
Bagasse	40	30	20	10
Coir	32–43	10–20	43–49	4
Corn cobs	45	35	15	5
Corn stalks	35	25	35	5
Cotton	95	2	1	0.4
Flax (retted)	71	21	2	6
Flax (unretted)	63	12	3	13
Hemp	70	22	6	2
Jute	71	14	13	2
Sisal	73	14	11	2
Wheat straw	30	50	15	5

#### 2.1.1.1.2 Structure of Cellulose

Cellulose is a strictly linear homopolymer consisting of  $\beta$ -1,4-glycosidic linked D-glucopyranose units (anhydroglucose units, AGU) (Fig. 2.1). With cellobiose as the basic unit, cellulose can be considered as an isotactic polymer of cellobiose. Every anhydroglucose unit carries hydroxy groups at positions C2, C3 and C6, able to undergo all the typical reactions of primary and secondary alcohols. While the terminal hydroxyl group at C4 behaves also like a typical aliphatic hydroxyl, the reducing OH at C1 shows a totally different behavior. The C1 end, being pres-

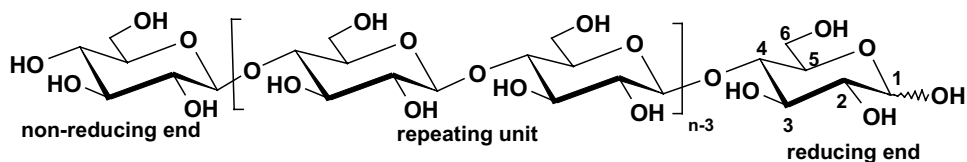


Fig. 2.1 The molecular structure of cellulose.

ent in the form of a semiacetal, has a reducing character, and the C4 hydroxy group is nonreducing. The conformation of the AGU in the cellulose chain is assumed to be a chair of the  ${}^4C_1$  type. In this conformation the free hydroxy groups are positioned equatorially, while the hydrogen atoms are placed in axial positions.

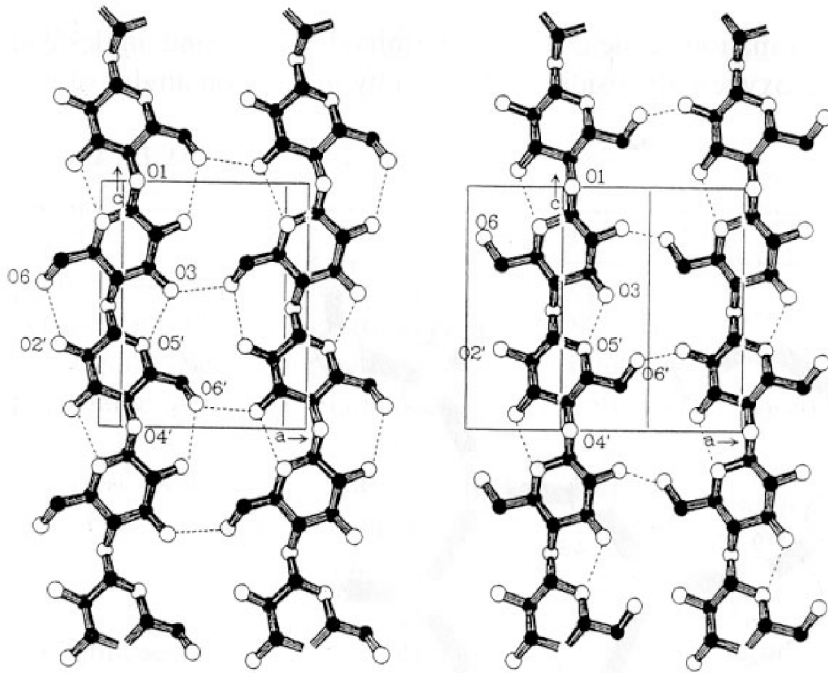
Cello-oligomers up to a degree of polymerization (DP) of 7–8 are (partly) water-soluble, and the solubility decreases strongly with increasing DP. Higher oligomers (DP >30) already behave in polymer-like fashion, especially with regard to their spectroscopic properties.

Celluloses from industrial sources show deviations from the “ideal” molecular structure. This is mainly caused by the isolation procedure (pulping and bleaching), since cellulose in higher plants is always incorporated into a matrix of hemicelluloses, lignin and low molecular-weight substances. During pulping and bleaching a number of other functionalities, such as carboxyl and carbonyl groups, or lactones, are introduced (for a more detailed description of oxidized structure anomalies in cellulose, see Section 2.4).

Although the molecular structure of cellulose appears to be rather simple, the supramolecular organization makes cellulose an extremely complex substance and complicated material, with an inherent ability to form different types of hydrogen bonds, either within the same cellulose chain (intramolecular) or between different chains (intermolecular). The presence of intramolecular hydrogen bonds is of great relevance with regard to chain stiffness and conformation [8,10]. Intermolecular bonds are responsible for the formation of supramolecular aggregates, such as crystalline domains or fibrils (Fig. 2.2).

#### 2.1.1.1.3 Supramolecular Structure

The various types of intermolecular hydrogen bonds in cellulose result in a very complex organization which in turn is responsible for a majority of its properties. The supramolecular cellulose structure can be described best on the basis of hierarchical categories, starting at the lowest level with the homoglucon chains with intermolecular hydrogen bonds, which cause their high tendency to organize into arrangements of crystallites, the basic elements of supramolecular structure in cellulose [12]. Such highly ordered domains are referred to as “crystalline”, since they exhibit a distinct X-ray pattern; less-ordered regions are described as “amorphous”, sometimes also as noncrystalline, but having a certain degree of order as in associated glucon chains (nematic ordered cellulose) [13]. Fundamental studies



**Fig. 2.2** Intra- and intermolecular hydrogen bonds in cellulose I (left) and cellulose II (right) (according to [11]).

on the cellulose crystal structure were carried out during the 1930s [14] and again later during the 1970s [15].

Native crystalline cellulose occurs in a metastable form, known as cellulose I, consisting of rod-like crystalline microfibrils containing parallel chains with a two-fold screw symmetry along the chain axes, which is due to the  $\beta$ -1,4-linkage of the  $D$ -glucose subunits. First discovered in 1984 [16] through an analysis of line splitting in  $^{13}\text{C}$ -CPMAS NMR spectra, two phases coexist within native cellulose I, known as  $I_\alpha$  and  $I_\beta$  [17]. The ratio of  $I_\alpha/I_\beta$  in the native state is unique to the species producing them. The  $I_\beta$  phase predominates in cotton and wood, and may be transformed by a hydrothermal treatment to cellulose  $I_\alpha$ , which is the prevailing allomorph in bacteria and algae. Also, during kraft pulping of spruce, distorted wood cellulose as well as small initial amounts of cellulose  $I_\alpha$  have been converted to the  $I_\beta$  form, and this has resulted in a higher degree of order in the final kraft pulp [18].

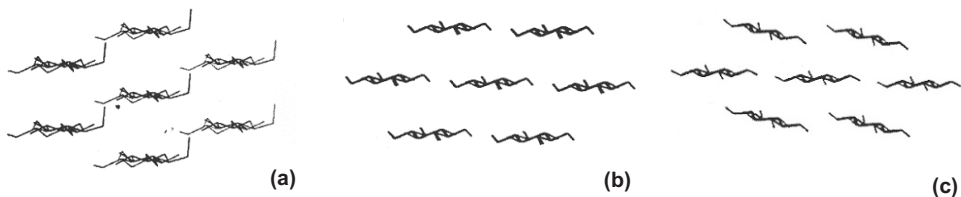
Cellulose  $I_\beta$  can be modeled by a monoclinic space group  $P2_1$  containing two parallel, but conformationally distinct chains [19]. The cellulose  $I_\alpha$  form is thought to possess a triclinic unit cell. The hydroxymethyl groups are arranged *trans-gauche* (tg), leading to intramolecular hydrogen bonds between O-2(H) and O-6' within two glucose units. Other H-bonds are situated between O-3(H) and O-5' as well as between O-6(H) and O-3. The cellulose polymorph (i.e., the crystal struc-

ture and unit cell type) is the second category in the hierarchical order of the cellulose structure. Recently, the crystal structure of cellulose I as well as the hydrogen bond patterns have been extensively investigated [20,21].

Cellulose II, as the more stable allomorph, can be obtained by two different processes: mercerization and regeneration from solution. Regeneration involves either the dissolution of cellulose in an appropriate solvent or the formation of a soluble metastable derivative, both of which afford cellulose II upon regeneration at room or slightly elevated temperature. Mercerization of cellulose I – that is, treatment with aqueous sodium hydroxide – forms sodium cellulose I as an intermediate, which is subsequently converted to cellulose II upon neutralization. Mercerization involves intracrystalline swelling in concentrated aqueous sodium hydroxide, followed by washing and recrystallization [21]. Based on high-resolution synchrotron X-ray results, Langan et al. [21] suggested for mercerized cellulose an anti-parallel chain arrangement in a monoclinic unit cell with different conformations of the chains, but with the hydroxymethyl groups of both chains predominantly near the *gt* conformation. Due to the mechanistic problems of converting the parallel chains in cellulose I into the antiparallel chain assortment in cellulose II merely by mercerization, it was also proposed that cellulose II has a parallel structure [22,23]. Even though the antiparallel model finds increasing acceptance, there is – as yet – no final answer to this issue.

The hydrogen bond network of cellulose II is more complex as compared to that of cellulose I (see also Fig. 2.2): From neutron diffraction analysis, an intramolecular three-center hydrogen bond is observed in both chains involving O3 as the donor and O5 and O6 as the acceptors. Intermolecular hydrogen bonds are observed between O2 and O6. Four-center H-bonds between the center and origin chain are also proposed [24].

The other cellulose polymorphs (III<sub>I</sub>, III<sub>II</sub>, IV<sub>I</sub>, and IV<sub>II</sub>) are obtained by special treatments of cellulose I, and are of only minor importance. The structure of cellulose and its polymorphs has been comprehensively reviewed [25]. Figure 2.3 shows a comparison of the packing in the crystalline lattice in cellulose I<sub>α</sub> and I<sub>β</sub> with a dimeric cellulose model compound.

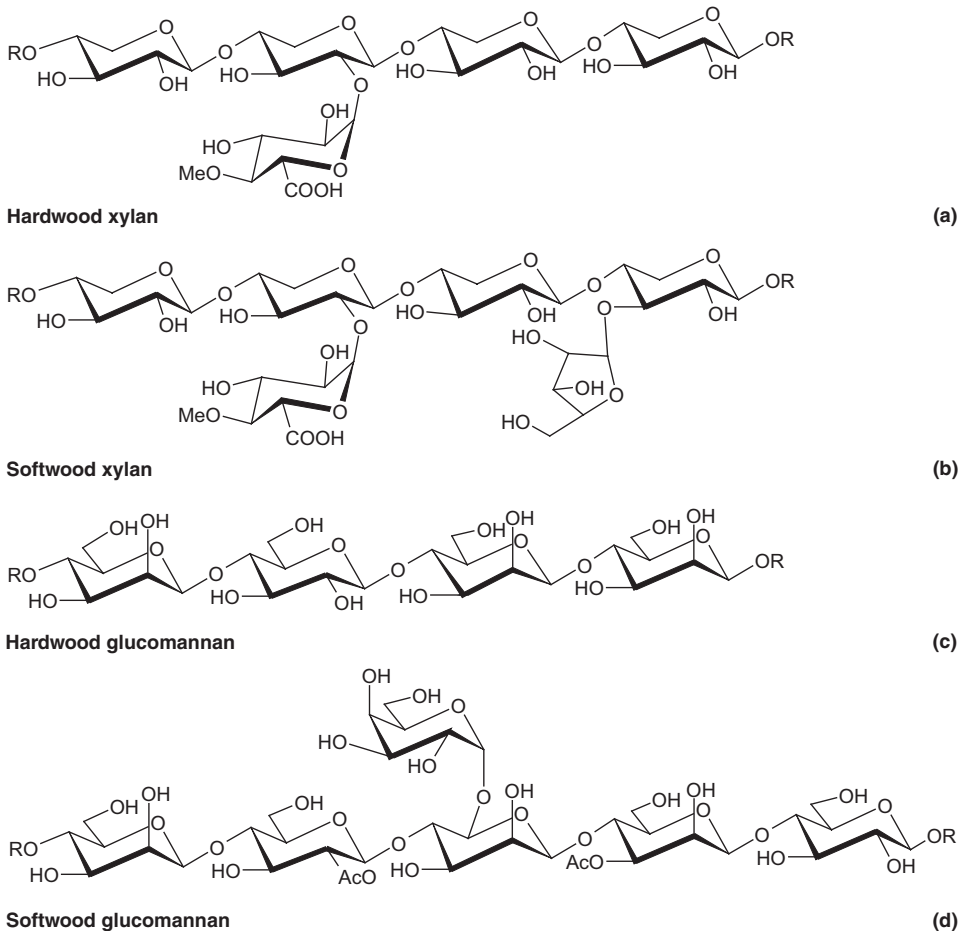


**Fig. 2.3** Packing in the crystalline lattice of (a): Model compound 4'-O-Me- $\beta$ -D-Glcp-(1 $\rightarrow$ 4)- $\beta$ -D-GlcpOMe (phase 1); (b) cellulose I <sub>$\alpha$</sub> ; and (c) cellulose I <sub>$\beta$</sub>  [26].



### 2.1.1.2 Hemicelluloses

Hemicelluloses are heteropolysaccharides, and differ from cellulose in that they consist of several sugar moieties, are mostly branched, and have lower molecular masses with a DP of 50...200. The sugar units (anhydro-sugars) making up the supramolecular structures of hemicelluloses (within the biosynthetic pathways) can be subdivided into groups such as pentoses ( $\rightarrow$  xylose and arabinose units), hexoses ( $\rightarrow$  glucose and mannose units), hexuronic acids ( $\rightarrow$  glucuronic acid) and deoxy-hexoses ( $\rightarrow$  rhamnose units). The main chain of the hemicelluloses can consist of only one unit (homopolymer; e.g., xylans), or of two or more units (heteropolymer; e.g., glucomannans) (Fig. 2.4). Some of the units are always (or sometimes) side groups of a main chain (backbone), for example 4-O-methylglucuronic acid, galactose.



**Fig. 2.4** Molecular structure of xylans and glucomannans in hard- and softwoods. (a) Hardwood xylan; (b) softwood xylan; (c) hardwood glucomannan; (d) softwood glucomannan.

There are also significant differences between softwoods and hardwoods in relation to the type and content of the various hemicelluloses in the wood cell walls. With regard to the nonglucosic sugar units present in wood, it is apparent that softwoods have a high proportion of mannose units and more galactose units than hardwoods, whilst hardwoods have a high proportion of xylose units and more acetyl groups than softwoods (Tab. 2.5).

**Tab. 2.5** Nonglucosic units of the hemicelluloses in various woods (adopted from [6]).

Species	Man [%]	Xyl [%]	Gal [%]	Ara [%]	Uronic acid [%]	Rha [%]	Acetylated [%]
Softwoods							
<i>Abies balsamea</i>	10	5.2	1.0	1.1	4.8	–	1.4
<i>Larix decidua</i>	11.5	5.1	6.1	2.0	2.2 <sup>a</sup>	–	–
<i>Picea abies</i>	13.6	5.6	2.8	1.2	1.8 <sup>a</sup>	0.3	–
<i>Picea mariana</i>	9.4	6.0	2.0	1.5	5.1	–	1.3
<i>Pinus strobus</i>	8.1	7.0	3.8	1.7	5.2	–	1.2
<i>Pinus sylvestris</i>	12.4	7.6	1.9	1.5	5.0	–	1.6
<i>Tsuga canadensis</i>	10.6	3.3	1.8	1.0	4.7	–	1.4
Hardwoods							
<i>Acer rubrum</i>	3.3	18.1	1.0	1.0	4.9	–	3.6
<i>Betula verrucosa</i>	3.2	24.9	0.7	0.4	3.6 <sup>a</sup>	0.6	–
<i>Fagus sylvatica</i>	0.9	19.0	1.4	0.7	4.8 <sup>a</sup>	0.5	–
<i>Fraxinus excelsior</i>	3.8	18.3	0.9	0.6	6.0	0.5	–
<i>Populus tremuloides</i>	3.5	21.2	1.1	0.9	3.7	–	3.9
<i>Ulmus americana</i>	3.4	15.1	0.9	0.4	4.7	–	3.0

a. 4-O-Methylglucuronic acid.

In hardwoods, the *xylan* chains are laced at irregular intervals with groups of 4-O-methylglucuronic acid with an  $\alpha$ -(1,2)-glycosidic linkage at the xylose units (Fig. 2.4a) [27]. Furthermore, many of the OH-groups at C2 and C3 of the xylose units are substituted by O-acetyl groups producing O-acetyl-4-O-methylglucuronoxylan, the main hemicellulose component in hardwoods (10–35%). Besides the main units, hardwood xylans contain small amounts of rhamnose and galacturonic acid. Further studies showed that the reducing end of xylans consists of a combination of xylose, rhamnose and galacturonic acid units which is seen to be

responsible for the alkali resistance of the xylan molecule, as the galacturonic acid makes it stable after the removal of the reducing xylose unit [28]. In general, softwood xylans differ from hardwood xylans by the lack of acetyl groups and by the presence of arabinose units linked by  $\alpha$ -(1,3)-glycosidic bonds to the xylan backbone (Fig. 2.4b). Thus, the softwood xylans are arabino-4-O-methylglucuronoxylans in an amount varying from 10 to 15%.

*Mannans* from wood are characterized by a heteropolymer backbone consisting of mannose and glucose units (so-called glucomannans). The simplest structure is shown in hardwood glucomannans, as they consist only of glucose and mannose units linked by ( $\beta$ -(1,4) glucosidic bonds forming slightly branched chains (Fig. 2.4c). Softwoods contain about 15–20% (25%) mannans that consist of a glucomannan backbone to which acetyl groups and galactose residues are attached, forming *O*-acetylgalactoglucomannans (Fig. 2.4d) [6].

In addition to cellulose and hemicelluloses, wood contains other polysaccharides, chief among them being starch and pectin.

*Starch*, the main reserve polysaccharide of a tree, consists of two components: (a) the linear amylose; and (b) the branched amylopectin, both of very high molecular weight, in the case of amylopectin considerably higher than that of cellulose. The glucose units of amylose are linked by  $\alpha$ -(1,4)-glycosidic bonds; in amylopectin  $\alpha$ -(1,6)-glycosidic linkages are also present. The  $\alpha$ -glycosidic linkages can easily be split, a fact which is important for mobilization during metabolic processes. Due to this linkage the pyranose rings are tilted at an angle of about 120° or less, and this results in a helical structure of the starch molecules with six glucose units per turn. Starch therefore exists only in form of granules and not as fibrils [6]. Nevertheless, the various amyloses are able to crystallize [29].

*Pectin* is more abundant in bark than in wood, where it is formed only during the earlier stages of cell development. On hydrolysis, pectin usually gives galacturonic acid and minor quantities of arabinose and galactose. The general structure of the pectic polymers consists of homogalacturonan linear chains interspersed with highly branched galacturonic chains, the backbone of which is composed of repeats of arabinans, galactans and arabinogalactans being attached to O-4 of rhamnosyl residues. Pectins are more of special interest as these polymers are known to modulate cell wall porosity and electrostatic potential [30]. Moreover, they are deposited very early in the apoplasm, which suggests that they may also intervene in the first steps of cell differentiation [31,32].

### 2.1.1.3 Lignin

#### 2.1.1.3.1 Significance and Occurrence

The third major cell wall polymer is *lignin*. Next to cellulose, lignin is the most abundant and important polymeric organic substance in plants. It is a characteristic chemical and morphological component of the tissue of higher plants such as pteridophytes and spermatophytes (gymnosperms and angiosperms), where it typically occurs in the vascular tissue, specialized for liquid transport and mechan-

ical strength [6]. The amounts of lignin present in different plants is quite variable. Whilst in wood species the lignin content ranges from 20 to 40%, aquatic and herbaceous angiosperms as well as many monocotyledons are less lignified [33]. Additionally, the distribution of lignin within the cell wall and the lignin contents of different parts of a tree are not uniform. For example, large amounts of lignin are characteristic for softwood branches and compression wood [34].

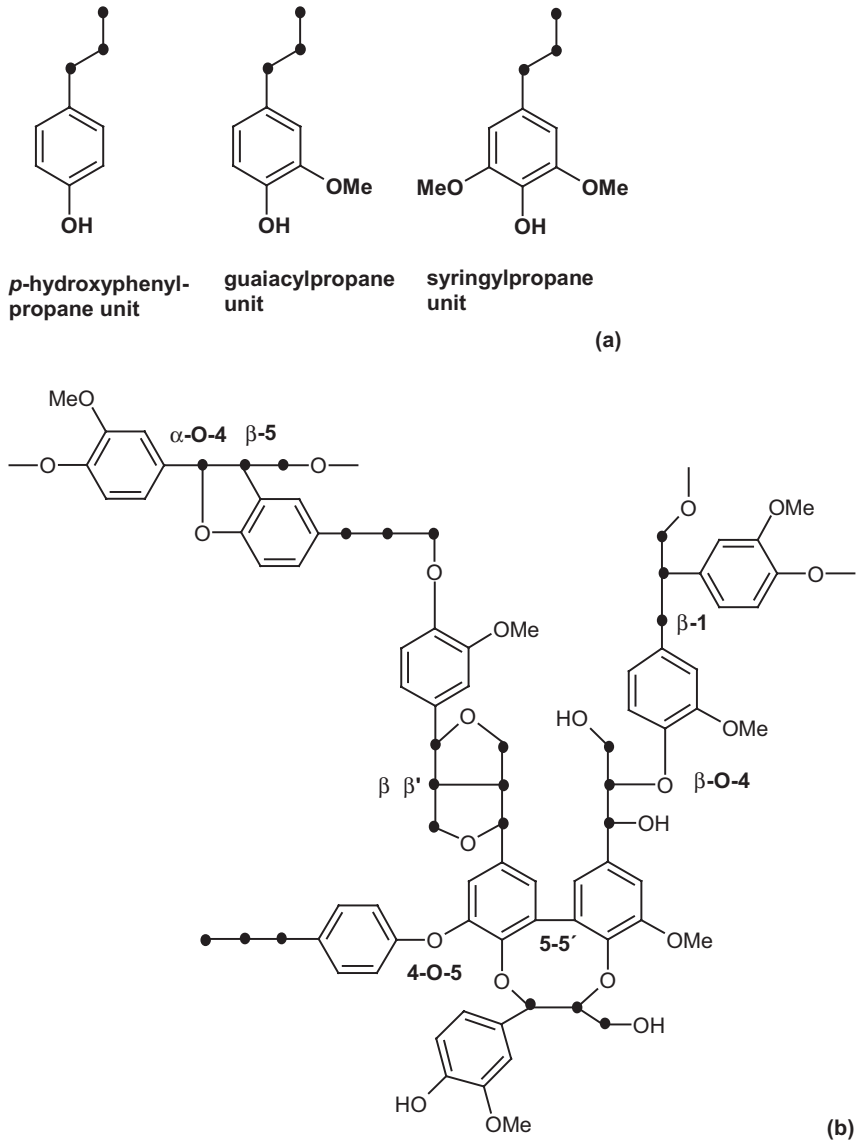
In most cases of wood utilization, lignin is used as an integrated part of wood cell walls. Only in the case of pulping and bleaching is lignin more or less released from wood in degraded and altered forms, representing a large potential carbon source for chemical and energy purposes.

#### 2.1.1.3.2 Structure of Lignin

Lignin is a complex phenolic polymer formed by radical coupling reactions of mainly three hydroxycinnamyl alcohols or monolignols (Fig. 2.5a): *p*-coumaryl (4-hydroxy-cinnamyl), coniferyl (3-methoxy-4-hydroxy-cinnamyl), and sinapyl (3,5-dimethoxy-4-hydroxy-cinnamyl) alcohol, which are synthesized via the phenylpropanoid pathway [35,36]. The complex structure of lignin arises from its biosynthesis, in which the last step is a nonenzymatic, random recombination of phenoxy radicals of coniferyl, sinapinyl, and *p*-coumaryl alcohols. The synthesis of the monolignols (precursors) and the formation of lignin macromolecules comprise complicated biochemical and chemical reactions which have been extensively studied and repeatedly reviewed [33,36–38]. According to Terashima [39], the polymerization of the monolignols is considered to proceed primarily via the following steps: (a) the formation of monolignol radicals by hydrogen peroxide and peroxidase or laccase and oxygen [40]; (b) the production of dilignols and dilignol quinone methides by coupling of the radicals; (c) addition of water, lignol or carbohydrates to the quinone methides [33,41]; and (d) formation of phenol radicals on oligo- and polyphenols and coupling with monolignol radicals to synthesize the polyphenol. The mode of polymerization can be affected by relative amounts of radical types participating in the reaction. The first products of the coupling of monolignol radicals are  $\beta$ -O-4,  $\beta$ -5, and  $\beta$ - $\beta$  dimers (Fig. 2.5b), whereas in the next stages of polymerization bulk-type oligomers and endwise polymers are formed. As a result, a globular macromolecule is formed which is composed of bulk polymers inside and endwise polymers in the outer part [42].

Variations in the chemical reactivity of lignin are based on the proportions of the three monolignol structural units [guaiacyl (G), syringyl (S) and *p*-hydroxyphenyl (H) units] (Fig. 2.5a), in different wood species as well as in different tissues and even cell wall layers. Whereas coniferous lignin consists mainly of guaiacylpropane (4-hydroxy-3-methoxyphenylpropane) units (G), hardwood lignins also contain up to 50% syringyl (3,5-dimethoxy-4-hydroxyphenyl) groups (S). Guaiacyl lignins (G-lignins) are predominantly polymerizates of coniferyl alcohol, while guaiacyl-syringyl-lignins (GS-lignins) are composed of varying parts of the aromatic nuclei guaiacyl and syringyl in addition to small amounts of *p*-hydroxyphenyl units.

Based on extensive  $^{13}\text{C}$ -NMR spectroscopic investigations, the lignins of monocotyledons and grasses contain up to 30% *p*-hydroxyphenylpropane (H) units, and are distinguished as GSH lignins from the lignins of dicotyledons (GS-lignins) [35].



**Fig. 2.5** (a) Molecular structure of the basic phenylpropane building blocks of lignin. (b) Model of important lignin linkages (modified model adopted from [43]).

Although softwood (coniferous) lignins are generally described as rather uniform, no general G:S:H ratio can be given for different softwood species. Distinct ratios were only reported for spruce (*Picea abies*) (G:S:H = 95:1:5) and for pine (*Pinus taeda*) lignin (G:S:H = 86:2:13) [44]. The reaction wood of softwoods (compression wood) has not only a higher lignin content than normal wood but also a considerably higher percentage of H units (up to 70%) than normal softwood G-lignins, and may therefore be classified as a GH-lignin [6,34].

Hardwoods are characterized by a higher variability of lignin composition than softwoods. The syringyl content of the typical hardwood GS-lignins varies between 20 and 60%, and the range is even wider if herbaceous plants are included (10–65%). A distinct ratio for beech (*Fagus sylvatica*) lignin was given by Nimz [45] (G:S:H = 56:40:4). Other examples of lignin heterogeneity are the higher syringyl content found in the heartwood of hardwoods as compared to the corresponding sapwood [46] and the higher quaiacyl content of root lignin in comparison with the corresponding stem lignin of beech. The composition of lignin is also influenced by its age, as shown in the case of poplar wood (*Populus nigra*) [47]. The ratio of syringaldehyde to vanillin obtained by nitrobenzene oxidation was high in the mature xylem and decreased in the younger xylem and in the phloem. The primary xylem yielded only vanillin.

Investigations on bark lignins from several softwoods and hardwoods showed that the softwood bark lignins are typical G-lignins with increased amounts of H-units as compared to the corresponding wood lignins. The hardwood bark lignins are GS-lignins with higher portions of G-units than the wood lignins [6].

A very important aspect of lignin heterogeneity was elaborated by Fergus and Goring [48], who were the first to show that the composition of birch lignin differs depending on its location. Ultraviolet microscopy applied to ultrathin sections revealed that the lignin in the secondary wall of the vessels and in the middle lamellae is predominantly a G-lignin. The secondary wall lignin of fibers and ray parenchyma, however, is mainly composed of syringyl units. Lignin from the middle lamellae and cell corners of the fiber and ray cell tissue is a typical mixed GS-lignin. Musha and Goring [49] extended these results by correlating the distribution of S- and G-residues in hardwood lignins from different morphological regions with the ratio of methoxyl groups per C<sub>9</sub> unit (OCH<sub>3</sub>/C<sub>9</sub>) of the overall wood lignin. The principal findings were confirmed by results obtained by isolation and characterization of lignin fractions assigned to certain cell wall regions [50], and support the idea of an intracellular biosynthesis of lignin [39].

#### 2.1.1.4 Extractives

In addition to its major structural components, cellulose, hemicelluloses and lignin, wood contains also an exceedingly large number of other low- and high-molecular weight (organic) compounds, the so-called *accessory compounds* or *extractives* (Tab. 2.6). These compounds can be extracted from wood with organic solvents (terpenes, fats, waxes, and phenols) or hot water (tannins and inorganic salts). In some cases, they are also classified as secondary metabolites – that is,

waste products of the plant metabolism, playing a nonintrinsic role in physiological processes. Depending on the quantity and the class of compound, which are specific to the tree type and genus to some extent, the extractives affect the chemical, biological, physical, and optical properties of the wood to varying degrees. As the swelling and biodegradability may be significantly reduced by lipophilic resins they improve the dimensional stability and durability of wood, while other chemical and physical properties – for example, during mechanical and chemical pulping – are negatively affected [51].

**Tab. 2.6** Major classes of wood extractives (adopted from [52]).

<b>Volatile oils</b>	<b>Wood resins</b>	<b>Fats and waxes</b>
<i>Mainly softwoods</i>	<i>Mainly softwoods</i>	Minor, less than 0.5%
Terpenines, monoterpenes, turpentine, tropolens	Acidic diterpenes; resins of softwoods, basis of tall oil	Suberin
Tannins	Lignans	Carbohydrates
<i>Hardwoods and softwoods</i>	<i>Hardwoods and softwoods</i>	<i>Typically food reserves</i>
Hydrolyzable tannins built upon glucose and gallic acid; Condensed tannins, flavonoid-based	Optically active lignin dimers (controlled free radical coupling process)	

The content of accessory compounds in the wood of trees from temperate zones amounts approximately from 2 to 5%, but the concentration can be much higher in certain parts of a tree, for example, the branch bases, heartwood, roots, and areas of sore irritation. Relatively high amounts (up to 20% of dry matter) of extractives are found in certain tropical and subtropical woods.

Although the content and composition of extractives vary among the wood species (Tab. 2.7), there are also variations depending on the geographical site and season [51]. In particular, unsaturated compounds such as fats and fatty acids are degraded during the growing season. This fact is important for the production of pulp as certain extractives in fresh wood may cause yellow discolorations (pitch troubles) or a yellowing of the pulp. Extractives may also influence the strength of refiner pulp, the gluing and finishing of wood as well as the drying behavior.

**Tab. 2.7** Percentage of the extractives in the sap- and heartwood of *Pinus sylvestris* and *Quercus robur* (based on dry wood) (adopted from [53]).

	<i>Pinus sylvestris</i>		<i>Quercus robur</i>		Extractives
	Sapwood	Heartwood	Sapwood	Heartwood	
Petroleum ether	2.20	8.60	0.15	0.15	Free fatty acids, triglycerides, neutral diterpenes, phenolic compounds, fats and waxes
Ether	0.06	0.80	0.35	0.15	Free fatty acids, sterine, resin acids, phenolic compounds
Acetone/water (9/1)	0.30	0.70	5.80	3.60	Monomer carbohydrates, phenolic compounds, hydrolyzable tannins
Ethanol/water (8/2)	0.40	0.40	1.80	0.90	Cyclite, hydrolyzable tannins, low molecular-weight lignin
Water <sup>[a]</sup>	–	–	0.65	0.40	Soluble hemicelluloses

a. Two hot-water extractions (temperature 60 °C).

#### 2.1.1.4.1 Accessory Compounds of Softwoods

Coniferous woods contain mainly terpenes, which can be obtained from pines by resinification of the living tree or as turpentine (monoterpenes) and tall oil (diterpenes, resin acids) from kraft (sulfate) pulping effluents. The common chemical characteristic of terpenes is their composition of isoprene (2-methyl butadiene) units [54]. According to the number of isoprene units linked in a terpene, the terpenes are subdivided into several classes: (a) monoterpenes (2 units); (b) sesquiterpenes (3 units); (c) diterpenes (4 units); (d) sesterterpenes (5 units); and (e) triterpenes (6 units). The monoterpenes can be subdivided into acyclic, monocyclic, and bicyclic compounds. The most important ones are  $\alpha$ - and  $\beta$ -pinene and limonene, which are apparently present in all softwoods. Further components of the volatile softwood oils are those belonging to the sesquiterpenes. Among these are the acyclic nerolidol, the monocyclic germacrene, the bicyclic cadinene and cadinol, and the more complex longifolene and longipinene. These compounds are present in pine and spruce species [6]. Sesquiterpenic tropolone derivatives called nootkatin and hydronootkatinol were isolated from extractives of *Cupressus*, *Chamaecyparis* and *Juniperus* species [55]. Furthermore, the oleoresin of softwood species contains a relatively high percentage of diterpenes and diterpenoidic acids apart from fats, fatty acids, and alcohols. The neutral diterpenes consist of hydrocarbons (thunbergene), oxides (manoyl-oxide), alcohols (abienol, pimarinol), and aldehydes (levopimaral). The resin acids are mostly tricyclic compounds [6]; their



total amount is in the range of 0.2–0.8% (based on dry wood) as determined for various pine species and spruce. The composition of the resin acid fraction of various softwoods is summarized in Table 2.8. It is clear that there are also variations in the composition of the resin acids of sapwood and heartwood.

**Tab. 2.8** Composition of the resin acid fraction of various softwoods (adopted from [6]).

Wood species	$\alpha$ -Pinene [%]	$\beta$ -Pinene [%]	$\Delta^3$ -Carene [%]	Camphene [%]	Limonene [%]	p-Cymene [%]	Terpinene [%]	Myrcene [%]	Terpinolene [%]	Sabinene [%]	$\beta$ -Phellandrene [%]
<i>Abies alba</i>	39.0	3.0	4.5	trace	53.5	–	–	–	trace	–	trace
<i>Abies grandis</i>	13.0	18.5	0.5	34.5	5.0	–	–	–	0.5	–	26.0
<i>Picea abies</i>	58.0	24.0	2.1	3.0	4.5	0.5	–	0.4	–	–	–
<i>Pinus eliottii</i>	62.6	20.6	–	1.4	1.7	–	–	0.4	1.7	–	8.1
<i>Pinus monophylla</i>											
– sapwood	46.0	2.0	3.0	1.0	7.0	–	5.0	4.0	22.0	–	8.0
– heartwood	67.0	2.0	–	1.0	3.0	–	1.0	1.0	20.0	–	3.0
<i>Pinus strobus</i>	67.0	18.0	–	2.9	0.9	–	–	0.5	0.9	–	0.5
<i>Pinus taeda</i>	64.0	28.0	–	1.3	1.5	–	–	–	2.0	–	0.5
<i>Pseudotsuga menziesii</i>	31.0	36.0	10.0	0.5	5.0	–	–	5.5	1.0	9.5	1.5

After sulfate pulping, the resin acids are recovered in tall oil which is separated from black liquor.

Long-chain fatty acids are also present in tall oil, and arise from fats and waxes in the wood. *Fats* are defined as esters of higher carbonic acids (fatty acids) with glycerol, whereas *waxes* are esters of fatty acids with higher alcohols. Fats and waxes are extractable from wood with organic solvents (diethyl ether, petroleum ether, acetone). The content of fats is about 0.3–0.4%, that of waxes about 0.08–0.09% (based on dry wood), as determined for *Picea abies* and *Pinus sylvestris* [6]. Apart from fats and waxes, free fatty acids and alcohols are also components of the wood extractives. In softwoods more than 20 different fatty acids have been identified. In general they are saturated, monomeric, dienic and trienic acids with 16–22 carbon atoms, but lower acids ( $C_{10}$ – $C_{14}$ ), higher ones ( $C_{24}$ – $C_{30}$ ) and tetraenic ones were also reported.

The extractives of softwoods also contain a large number of various *phenolic compounds* which are believed to be residues and byproducts of lignin biosynth-

esis. Among the simple phenols which can be isolated from spruce extractives are vanillin, *p*-hydroxybenzaldehyde, coniferyl aldehyde, quaiacylglycerol and *p*-ethylphenol, as well as coniferin and syringin [56]. By fractionating the extractives obtained by a supercritical gas extraction of spruce wood, guaiacol, eugenol, isoeugenol, cresols and further phenols were also identified. However, because of the high temperatures applied in this process these compounds probably derive from early stages of lignin degradation [6].

A second group are the *lignans*; these are compounds consisting of two phenylpropane units linked in a different manner. Some of these compounds represent dimeric structures which are also present in the lignin molecule (see p. 32). Many lignans, as identified in the extracts of *Picea*, *Pinus*, *Larix*, *Abies*, and *Tsuga* species, contain a tetrahydrofuran ring, such as pinoresinol, lariciresinol, and conidendrin [56]. The location and nature of the lignan deposits indicate that their biosynthesis probably takes place at the sapwood–heartwood boundary during heartwood formation.

A further group of the aromatic compounds in softwoods are the *stilbenes*, which are particularly present in the heartwood of pines. These compounds – mainly 4-hydroxystilbene, 4-methoxystilbene, pinosylvin, and pinosylvin mono- and diether – are responsible for the light-induced darkening of the wood as well as for difficulties during acidic pulping [6].

A large group of various vegetable extractives are summarized as flavonoids, which comprise subgroups such as flavones, flavanes, flavanones, and isoflavones. In softwoods, several flavonoids have been identified such as chrysin and taxifolin [51]. Catechin is also a structural unit of condensed tannins or phlobaphenes which can be extracted from the heartwood of various conifers in yields of 0.2 to 6%. These extractives, however, show a high content of methoxyl, which can be explained by the presence of a considerable amount of lignin. The presence of catechin in the wooden tissue is seen to be responsible for discolorations, as this compound is able to form chromophoric polymers with quinone structures [57].

#### 2.1.1.4.2 Accessory Compounds of Hardwoods

The hardwoods contain a lower content of terpenes in comparison to the softwoods. Mostly, triterpenes (e.g., squalene) and acetylated methyl betulinate in birch wood (*Betula* spp.) or betulin and taraxerol in oak species (*Quercus* spp.) have been identified [6]. Moreover, in tropical woods some mono-, sesqui- and dipertenes can be detected. One of the most prominent monoterpenes is camphor from the true camphorwood (*Cinnamomum camphora*). Examples of sesquiterpenes are  $\alpha$ - and  $\beta$ -santalol, which comprise more than 90% of the oil from sandalwood (*Santalum album*), and the tropolone derivate apitonene which is found in *Dipterocarpus* species [51]. Like softwoods, hardwoods also contain steroids. In species of *Betula*, *Populus*, *Quercus* and *Ulmus*, steroids – mainly  $\beta$ -sitosterol – were found. Some of the steroids present in wood are esterified with fatty acids. The triterpenes and steroids may survive the pulping process and are degraded during bleaching. The resulting products are seen to be jointly responsible for the

yellowing of pulps. Furthermore, polyterpenes (compounds containing more than six isoprene units) are present in some tropical hardwoods, for example, in the form of gutta and caoutchouc (*Tectona grandis*, *Guaiacum officinale*), both being polymers that differ in their chain conformation. While the isoprene units in gutta are arranged in the “trans” form, those in caoutchouc are arranged in “cis” form. In both compounds the isoprene units are linked mainly by 1,4-bonds; only a small percentage is linked by 3,4 bonds. Hardwoods contain fats, waxes, fatty acids and alcohols similar to those found in softwoods. Most of the fatty acids isolated from *Betula*, *Populus* and *Quercus* were bound as triglycerides, mainly consisting of linoleic and lignoceric acid [6].

The extracts of hardwoods also contain low molecular-weight phenols, some of them probably degradation products of compounds which can easily be hydrolyzed during extraction or steam distillation. Among these are *p*-hydroxybenzoic, vanillic, syringic, ferulic acid, vanillin and syringaldehyde in *Populus* and *Salix* species, or sinapinaldehyde, coniferylaldehyde syringaldehyde and *p*-hydroxybenzaldehyde in the extracts of *Quercus* species. A further group always mentioned with the softwood extractives are lignans. From hardwoods – particularly *Alnus*, *Quercus* and *Ulmus* species – lignans such as syringaresinol and lyoniresinol have been isolated [6]. Some of them are linked with rhamnose or xylose as glucosides. Earlier studies also revealed the presence of lignans in *Populus* species as well as in a number of subtropical and tropical woods [58].

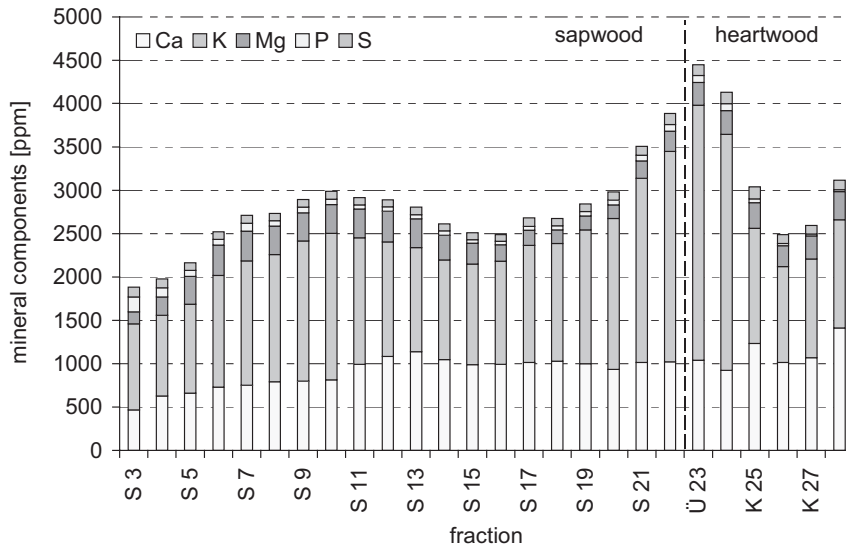
A major group of extractives (phenolic compounds) in hardwoods are the tannins and flavonoids, ranging from simple phenols to condensed flavonoids systems. The tannins are subdivided into hydrolyzable tannins and nonhydrolyzable or condensed tannins (phlobaphenes). The hydrolyzable tannins are esters of gallic acid and its dimers (digallic, ellagic acid) with monosaccharides, mainly glucose. They are often subdivided into gallotannins yielding gallic acid after hydrolysis, and ellagitannins yielding ellagic acid after hydrolysis [6]. The study of the behavior of ellagitannins with alkali showed that, under the conditions of cold soda and alkaline groundwood pulping, the tannins are notably resistant [55]. Under conditions comparable to kraft and soda pulping, the decarboxylation of gallic and ellagic acid is the major reaction. The main components of the condensed tannins are the catechins (flavan-3-ols) and the leucoanthocyanidins (flavan-3,4-diols). These compounds belong to the group of flavonoids. The flavonoids can be derived from flavone which itself is interpreted as a 2-phenyl benzopyrone. Its derivatives containing a hydrated pyrane ring are called flavanes. Other derivatives of the basic flavone structure are the flavanones and the isoflavones. Structures containing an open pyrone ring are called chalcones, and those with a furanone ring aurones [6]. Some of the flavonoids and related compounds determine the color of the respective wood (e.g., fisetin, morin, santal), while others (e.g., butein, sulfuretin, rengasin) are responsible for colored specks in pulps from tropical woods. They are often present in wood as colorless leuco-compounds, and the color must be developed by biochemical and chemical reactions [57]. The color and its gradation can be influenced by further treatments with acids, alkali, or metal salts. Various studies are concerned with the utilization of condensed tannins [6]. Experi-

ments have been performed yielding simple phenols by fusion processes, and adhesives for plywood and particleboard by autocondensation, condensation with formaldehyde, or sulfitation.

On the cellular level, the extractives are concentrated in the parenchymal cells and the resin canals; smaller quantities are also found in the middle lamellae, intercellular and cell walls of tracheids and libriform fibers [57,59].

### 2.1.1.5 Inorganic Components

The inorganic constituents of wood are entirely contained in the ash, the residue remaining after burning the organic matter. The content of the inorganic components is low, and amounts in wood of temperate zones comprise 0.1 to 1.0% of the ash [2]; by comparison, in woods of tropical and subtropical zones the inorganic components comprise up to 5% of the ash [6]. There is a certain dependence of the mineral content and composition on environmental conditions (site, climate, soil) and on the location within the tree [4,60]. With regard to the whole tree, the highest content of inorganic components is found in the leaves or needles, respectively. The sequence of decreasing ash content is, subsequently: bark, roots, branches, and stem. Analyses of the elemental distribution across a stem of beech (*Fagus sylvatica*) showed an increase of the mineral content from the outer part of the sapwood towards the heartwood (red heart) (Fig. 2.6). The mineral



**Fig. 2.6** Qualitative and quantitative distribution of mineral components (Ca, K, Mg, P, S) in sapwood and heartwood tissue of beechwood (*Fagus sylvatica*) determined by ICP-OES analyses [62].

components of wood are mainly oxalates, carbonates or glucuronates of calcium (40–70%), potassium (10–30%), magnesium (5–10%), iron (up to 10%), and sodium (Tab. 2.9). Cytological investigations indicated the importance of potassium for the cell enlargement (osmoregulation) during primary wall formation of differentiating xylem cells [4,61]. Calcium is involved in the synthesis of cellulose and hemicelluloses, and also in the lignification of the cell wall. Many other elements such as Al, Zn, Cu, and Ni are also cations present in concentrations of less than 50 ppm. These must be defined as trace elements, and are important for several biochemical syntheses. By using electron microscopy combined with energy dispersive X-ray spectroscopy (SEM/TEM-EDXA), it can be shown that the minerals are not only incorporated into the cell walls but are also deposited in the lumina of parenchymal cells, and consist mostly of calcium oxalate, calcium carbonate (in the form of prismatic or polyhedric crystals), or noncrystalline silicate.

**Tab. 2.9** Inorganic composition of several softwoods and hardwoods (modified and adopted from [6]).

Species	Ca [%]	K [%]	Mg [%]	Mn [%]	Na [%]	P [%]	Al [%]	Fe [%]	Zn [%]
Softwoods									
<i>Abies balsamea</i>	830	770	270	127	–	–	–	13	11
<i>Picea abies</i>	1800	250	160	440	100	50	–	14	20
<i>Pinus strobus</i>	210	290	70	28	–	–	–	10	11
<i>Pinus</i> spp.	764	39	110	97	28	–	6	–	–
<i>Pseudotsuga menziesii</i>	295	–	41	25	44	–	13	–	–
<i>Tsuga</i> spp.	750	400	110	145	–	–	–	6	2
Hardwoods									
<i>Acer rubrum</i>	820	690	120	72	29	30	2	11	29
<i>Betula papyrifera</i>	740	270	180	34	–	150	23	10	28
<i>Fagus sylvatica</i>	1150	880	320	250	120	–	–	–	10
<i>Populus</i> spp.	1130	1230	270	29	–	100	–	12	17
<i>Quercus alba</i>	674	780	11	2	3	8	6	–	–
<i>Tilia americana</i>	1125	543	117	11	74	–	15	–	–

## 2.1.2

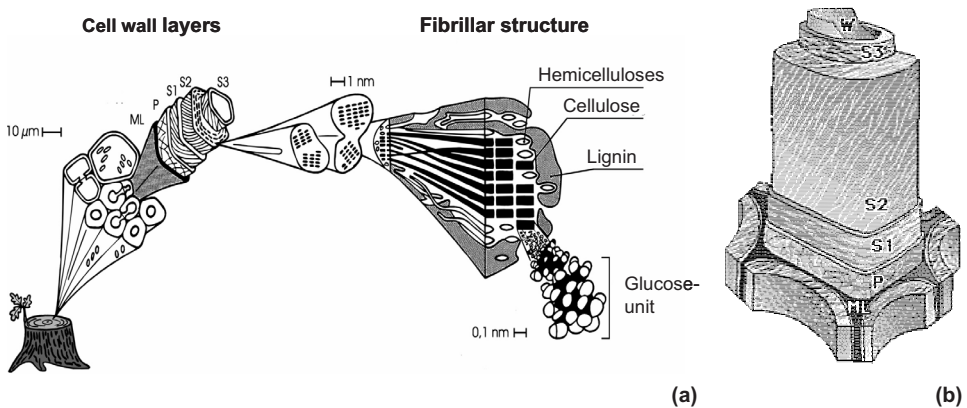
## Wood Structure and Morphology

## 2.1.2.1 Ultrastructure and Distribution of Cell Wall Components

The wood cell walls are composed of the above-described three groups of structural substances *cellulose*, *hemicelluloses*, and *lignin* which are classified respectively as framework, matrix, and encrusting materials. The framework substance is cellulose, which occurs in the form of microfibrils. Hemicelluloses and other carbohydrate materials (excluding cellulose) are incorporated into the cell wall as the matrix substances, whereas lignin is incrustated in the microcapillary regions of the cell walls.

## 2.1.2.1.1 Fibrillar Structure of Cellulose

Of the three cell wall components, cellulose has a partially ordered crystalline structure, whereas the hemicelluloses and lignin are amorphous. Because of regular hydrogen bonds, the cellulose chains are ordered to form *elementary fibrils* with a diameter of about 3.5 nm and alternating crystalline (micelles) and amorphous regions [6,63]. Recent electron microscopic and WAXS (wide-angle X-ray scattering) data indicate that the diameter of elementary fibrils may differ in the range of 3 to 35 nm depending on the source of cellulose. As the next larger morphological unit, *microfibrils* are composed of aggregates of elementary fibrils shrouded by shorter hemicelluloses chains. The diameters of microfibrils are approximately 10 to 30 nm. The microfibrils form so-called *macrofibrils* between which the lignin and the hemicelluloses are deposited. Chemical bonds are formed between the



**Fig. 2.7** (a) Schematic illustration of the individual cell wall layers and their chemical composition (illustrated by Per Hoffmann). (b) Cell wall model with the fibrillar structure of the cell wall layers. ML = Middle lamella; P = Primary wall; S = Secondary wall (S1, S2, S3); W = Warty layer. (Adopted from [64].)

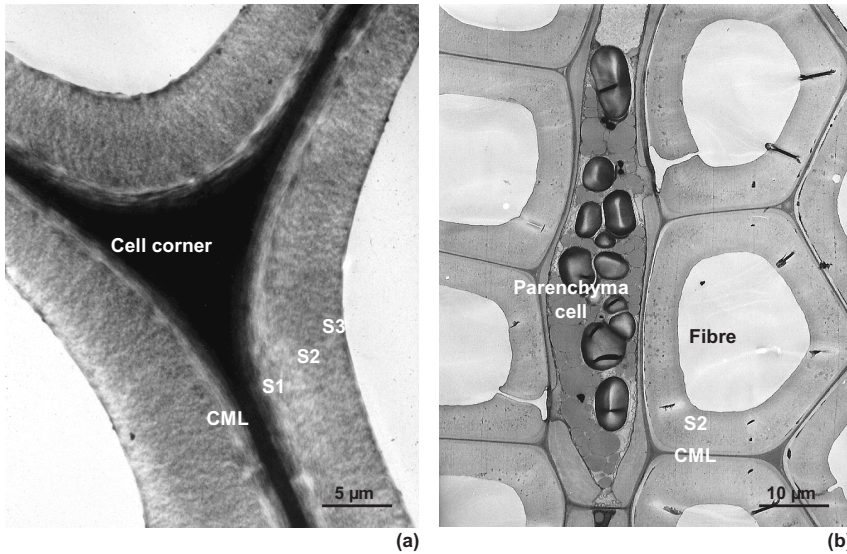
$\alpha$ -C atoms of lignin and the hydroxyl groups of the hemicelluloses (benzyl ethers), which prevent the leaching of lignin from the wood by neutral organic solvents. Irregular hydrogen bonds also exist between the hydroxyl groups of lignin, the hemicelluloses, and the cellulose through which a close, but irregular network of the three components is formed.

#### 2.1.2.1.2 Ultrastructure of the Cell Wall

The micro- and macrofibrils represent the construction units of the cellulose fiber cell wall architecture, which consists of several layers (Figs. 2.7 and 2.8). The concentric arrangement of the individual cell wall layers is caused by differences in the chemical composition and by different orientations of the structural elements, which are synthesized during cell division and cell differentiation [65]. The cell wall formation starts with the division of a cambial initial. A daughter cell becomes separated first at the equatorial plane by a thin, tangential wall which consists mainly of pectic material. This initial layer, which is common to both adjacent cells, is termed the *middle lamella* (ML) and functions as a “cementing” substance between the cells.

At this early developmental stage the wood cell begins to deposit new wall material against the ML. Contrary to the ML, this new layer contains cellulosic material embedded in a pectin and hemicelluloses containing matrix. This layer represents the first formed cell wall layer and is called the *primary wall* (P). The thin primary wall (thickness 0.1  $\mu\text{m}$ ) consists of a loose aggregation of microfibrils arranged randomly on the outer surface and oriented more or less transverse to the cell axis on the inner surface. The cellulose molecules have DPs between 2000 and 15 000 anhydroglucose units in long, nonbranched chains. These cellulose chains are twisted along the axis of the glucan chains ( $180^\circ$ ) and stabilized by hydrogen bonds between the chains [8]. At the cell corners, the primary wall is often thickened into a rib-like structure that extends along the length of the cell. Both the middle lamella and primary wall are extensible to allow cell expansion during differentiation. Cellulose fibrils and matrix material are continuously incorporated into the growing wall, accompanied by some wall protein.

As the developing wood cell wall approaches final thickness, deposition of the stiff *secondary wall* occurs (Fig. 2.8). Secondary walls in most cases show a subdivision into three layers (S1, S2, S3), with the narrow S1 (0.12–0.35  $\mu\text{m}$ ) as the first-formed layer next to the primary wall, the S2 layer generally representing the thickest portion (2–5  $\mu\text{m}$ ) (Tab. 2.10), and the sometimes barely discernible, thin S3 layer (0.1–0.14  $\mu\text{m}$ ) constituting the interface with the cytoplasm in living cells or the cell lumen in dead cells. The S2 layer of the secondary wall contributes most to the bulk of cell wall material, as well to its physical and mechanical properties. It is a compact region with a high degree of parallelism of the microfibrils. The number of lamellae composing the S2 may vary from the 30 or 40 in thin-walled or earlywood cells to 150 or more in thick-walled latewood elements. The S3, when present, is a thin layer of helically arranged microfibrils similar to the S1, probably not exceeding five or six lamellae in thickness.



**Fig. 2.8** Transmission electron micrographs of ultrathin sections of the cell wall layers of (a) softwood tracheids (*Picea abies*) and of (b) hardwood fiber and parenchymal cells (*Betula* spp.) which show the various wall layers: CML= compound middle lamella; P = primary wall; S = secondary wall (S1, S2, S3) [68].

**Tab. 2.10** Average thickness and percentage of the wall layers in spruce tracheids (*Picea abies*) (adapted from [66]).

Wall layer	Earlywood		Latewood	
	[ $\mu\text{m}$ ]	[%]	[ $\mu\text{m}$ ]	[%]
ML/P	1.00	33.1	1.00	19.1
S1	0.26	8.6	0.38	7.3
S2	1.66	55.0	3.69	70.8
S3	0.10	3.3	0.14	2.8
Total wall	3.02	–	5.21	–

These three layers of the secondary wall are organized in a plywood-type of structure. Electron- and polarized light microscopy indicate that the microfibrils of the inner and outer layers are oriented more or less perpendicular to those of the middle layer (S2). In the S1 there occurs a crossed fibrillar texture. The microfibril orientation generally ranges from 50° to 70° relative to the cell axis. In the S2, the angle of microfibril orientation varies between 10° and 30° depending on



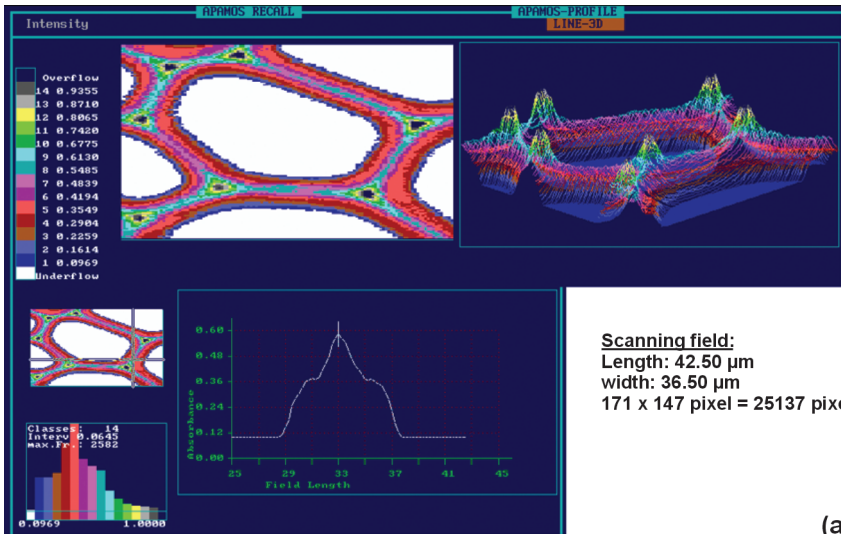
the type of cell, earlywood or latewood, and in the S3 the microfibrils are oriented at an angle of between 60° and 90° relative to the cell axis (see Fig. 2.7b). These varying fibril orientations in the particular layers produce a mechanical locking effect, leading to very high stiffness of the overall cell [67]. In some wood species, helically oriented thickenings or *spiral thickenings* (spirally arranged ridges of microfibril bundles) on the inside of the cell wall are formed with the development of the S3 layer. They are distinctly separated from the S3 layer and only rarely parallel to the microfibril orientation of this wall layer. Spiral thickenings are a characteristic feature of few softwood species, for example in Douglas fir (*Pseudotsuga menziesii*) and Himalaya spruce (*Picea smithii*), and more common in hardwood species, for example in maple, some birches, and cherry [5].

#### 2.1.2.2 Lignification of the Cell Walls

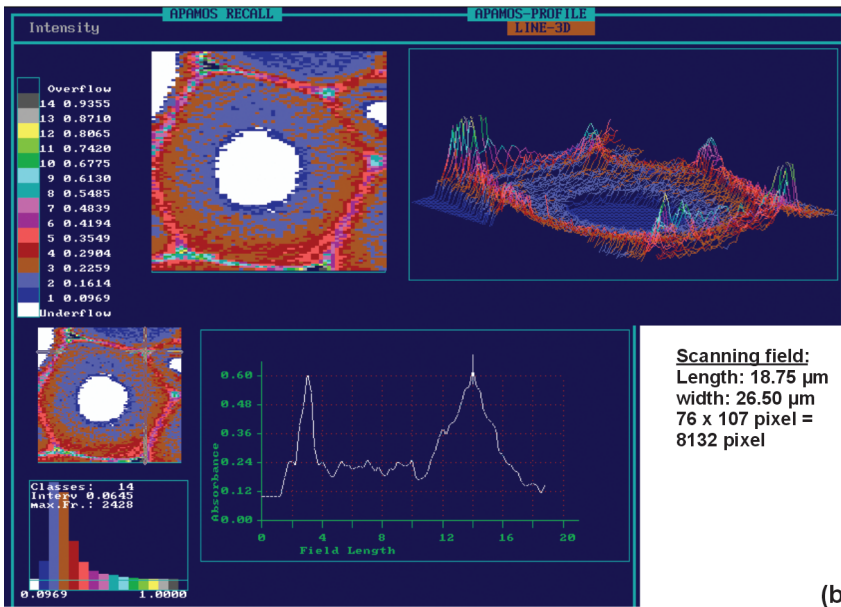
The incorporation of *lignin* within the polysaccharide cell wall framework is generally seen as the final phase of the differentiating process of the typical secondary xylem cell wall. Results from ultraviolet, fluorescence and light autoradiographic microscopic studies, as well as from electron microscopic studies, have confirmed that lignin is most probably deposited initially in the cell corners (Fig. 2.9) when the surface enlargement of the cell is finished, and just before the S1 starts to thicken. The lignification proceeds in the intercellular layer (middle lamella, ML) and the primary wall (P), starting at the tangential walls and spreading centripetally [69]. The lignification of the compound middle lamella (ML and adjacent primary wall) continues during differentiation of the S1 and S2 layers, and even until the formation of the secondary wall 3 (S3). Lignification of the secondary wall layers proceeds slowly in a first stage, but becomes more rapid after thickening of the S3 wall has been completed [69]. These findings indicate a permanent lignification process throughout the entire period of cell wall differentiation, with a considerable delay as regards the synthesis of cellulose and hemicelluloses.

According to data obtained from cellular UV spectroscopy and chemical analysis, almost 60% of the substance of the compound ML consists of lignin, while only 20% is found in the secondary wall. However, the bulk of the lignin (63–74%) is concentrated in S2, as this layer is the thickest one since it also contains 90% of the cellulose and 70–80% of the hemicelluloses.

The image profiles of spruce tracheids (Figure 9a) are characterised by a high UV absorbance at the cell corners and compound middle lamellae as compared to the adjacent S2 layers with a lower, slightly varying lignin distribution. As found by Fergus et al. (1969) [71] the average lignin content in the compound middle lamella is about twice that in the S2 of the tracheids. The scanned beech fibre (Figure 9b) shows a different absorbance level as compared to the softwood tracheids. In particular, the broad S2 layer reveals a lower absorbance. The uniform level of absorbance in this wall layer corresponds to earlier results reported by Saka and Goring (1988) [72], who predicted lignin distribution across the width of the whole S2 should be homogeneous. The compound middle lamella is distinguished by higher absorbance values as compared to those of the spruce tracheid.



(a)



(b)

Fig. 2.9 UV microscopic image profiles of an individual (a) tracheid of *Picea abies* and (b) fibre of *Fagus sylvatica* scanned with a geometrical resolution of  $0.25 \mu\text{m}^2$ . The color scales indicate the different UV-absorbance values at a wavelength of 278 nm (absorbance maximum of softwood lignin) and 278 nm (absorbance maximum of hardwood lignin) [70].[70].

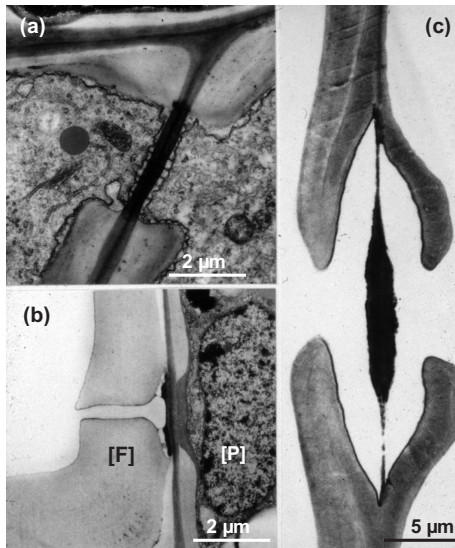
### 2.1.2.3 Functional Elements of the Conducting System

In all cell types, the secondary wall layers show specific openings or gaps, the so-called *pits* (Figs. 2.10 and 2.11). These pits serve as valve-like canals, allowing liquids to flow between adjoining cells (e.g., water flow to the top of the tree, controlled by the suction force emanating from evaporation from leaves or needles). Pit structure and shape varies with the type of the cells that they are connecting, and also with the wood species concerned. Three different types of pits must be distinguished:

- simple pits connecting two parenchymal cells;
- bordered pits connecting vascular cells (*vessels, fibers, tracheids*);  
and
- half-bordered pits connecting parenchymal cells to vascular cells

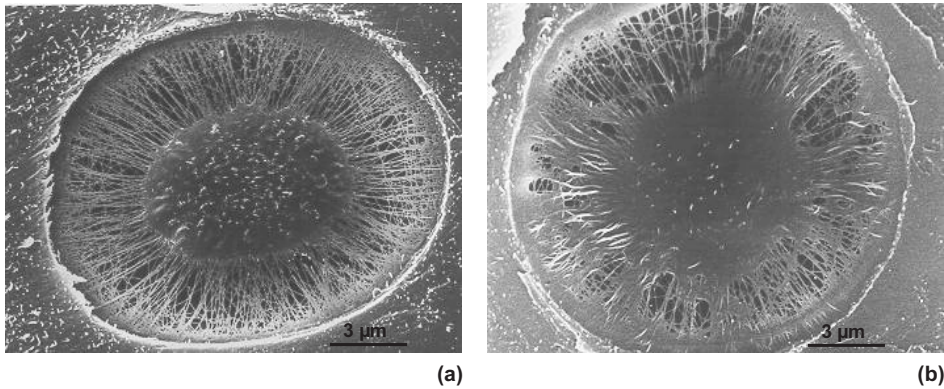
Simple pits are holes in adjacent cell walls, interrupted by a membrane in the region of the compound middle lamella. Simple pits appear only in and between parenchymal cells. For the exchange of plasmatic material, the pit membranes are interlaced with plasmatic threads, the so-called *plasmodesmata*.

The *bordered pits* belonging to the vascular cells (*vessels, fibers, tracheids*) have a somewhat different structure. The openings (apertures) in both cell walls enlarge towards the pit membrane forming a cavity. The shape of the aperture of the



**Fig. 2.10** The various types of pits in hardwoods and softwoods. Ultrathin sections, transmission electron micrographs. (a) Simple pits between parenchymal cells in oak (*Quercus robur*). The membranes are interlaced with plasmodesmata. (b) Half-bordered pit between a parenchymal cell (P) and

a fiber (F) in birch (*Betula pendula*). At the parenchymal side, the pit membrane is covered with a protective layer. (c) Bordered pit between two tracheids in spruce (*Picea abies*) in open conditions. The disk-like torus lies in the center of the porus. (Adopted from [68].)

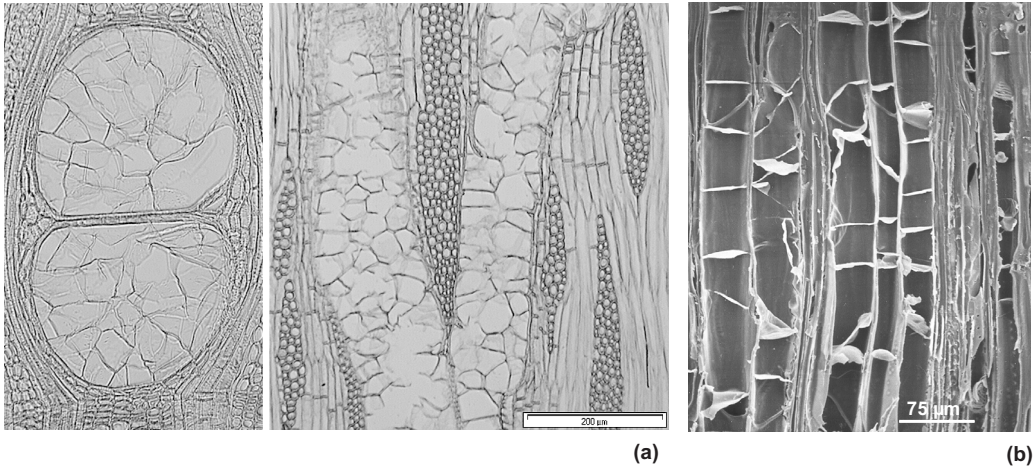


**Fig. 2.11** Cross-section of bordered pits in (a) earlywood and (b) latewood of *Picea abies*. The pit membrane in earlywood shows relatively wide interspaces in the margo. The pit membrane in the corresponding latewood shows an extremely dense margo (scanning electron micrographs) [75].

bordered pits can be very different depending on the species, the cell type, earlywood and latewood, etc. The pit membrane is formed by the primary cell walls of both adjoining cells and the sandwiched middle lamella. It is rich in pectins and reinforced by cellulose microfibrils. During cell wall growth in softwoods, the central portion of the membrane is altered through accumulation of densely packed microfibrils which form the so-called *torus*, held in place by radially arranged microfibrils (the margo) which is formed over the existing primary wall (Fig. 2.11). Subsequently, the pectine matrix of the margo is decomposed enzymatically, providing enough open voids for water flow between the adjoining cells. With further growth of the cell wall the secondary wall overarches the margo and torus, forming the pit chamber. The principal structure of hardwood bordered pits is similar, but the membrane is quite different: no torus is developed and no dissolution of primary wall components is visible.

The *half-bordered pits* connect parenchymal cells to vascular cells. On the parenchyma side, they consist of a simple pit, whereas on the vascular side one half of a bordered pit is formed. In softwoods, half-bordered pits have a central thickening (torus) at the tracheid side. Special forms of half-bordered pit are the “window-like” and “pinoid” cross-field pits between ray parenchymal cells and longitudinal tracheids with large membranes, large apertures and small borders [73,74].

Closing (aspiration) of the pits is caused by injuring the tree, or during the course of natural heartwood formation. The pits with a torus in their membranes can be very effectively closed by pressure differences between adjacent cells. By pressing the torus against the aperture, the pit is closed irreversibly. During this process the outer part of the margo is stretched by some reorganization of the fibrils which are aggregated to strands. During heartwood formation, the margo



**Fig. 2.12** Formation of tyloses in hardwoods of (a) *Robinia pseudoacacia* and (b) *Fagus sylvatica* (red heart). The tyloses grow out from an adjacent ray or axial parenchymal cell through a pit in a vessel wall, partially or completely blocking the vessel lumen.

can be encrusted with amorphous material (phenolic extractives) so that movement towards the aperture is no longer possible [76].

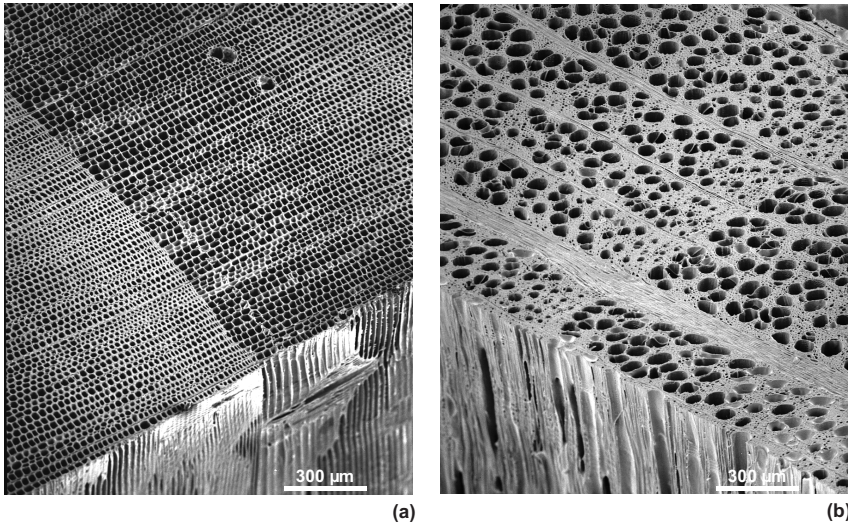
The movement of water within the vessels of several hardwoods may be blocked by the formation of *tyloses*, the formation of which is a natural physiological process linked to heartwood formation and to the death of living sapwood cells, respectively. It may also be initiated by mechanical damages or fungus and virus infection [77]. Tyloses (protective layer) are thin membranes, the growth of which starts at the pits bordering the associated parenchymal cells, and then extends like balloons into the vessels (Fig. 2.12). The tylosis wall consists of two or more layers, containing cellulose, hemicelluloses and lignin, and in areas where two tylosis walls are in contact a middle lamella-like layer as well as simple pits are developed between them.

### 2.1.3

#### The Microscopic Structure of Wood

##### 2.1.3.1 Cell Types

The wooden tissue consists of various cell types which can be readily observed at both the light and electron microscopic level (Fig. 2.13). During growth and maturation, from the fusiform initials they change in size, shape and structure to fulfill specific requirements of their genetically predetermined function in the living tree (Fig. 2.14). According to their individual morphology and function, four groups of cell types can be distinguished:



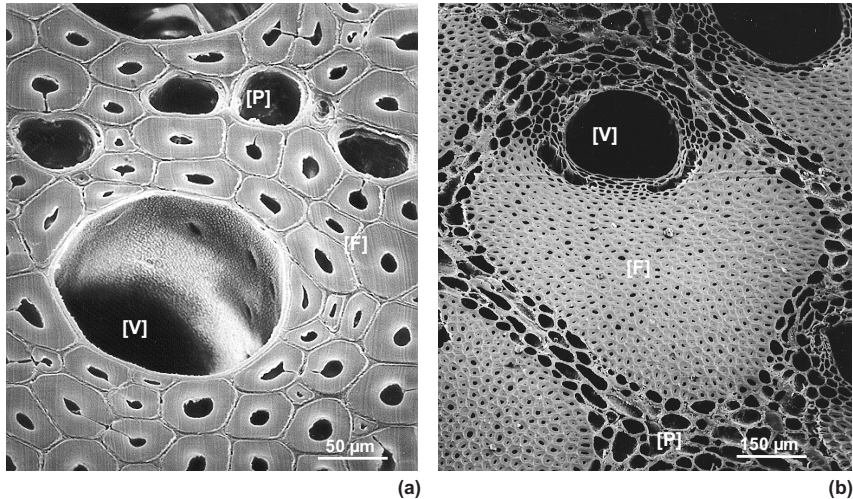
**Fig. 2.13** Transverse sections of a (a) softwood (*Picea abies*) and a (b) hardwood (*Fagus sylvatica*) showing the transition between earlywood and latewood within the annual ring. Scanning electron micrographs.

- parenchymal cells
- tracheids
- fibers
- vessels.

*Parenchymal cells* in living wood contain cytoplasm and are involved in various processes such as metabolic pathways, short-distance transport, and storage; they form horizontal bands (rays) as well as axially oriented strands. Axial parenchyma is much more frequent in hardwoods, where it tends to form distinctive patterns, particularly in tropical timber species. These cells usually have thin secondary walls.

*Tracheids* are the predominant axial cell elements in softwoods; they provide both water conduction and mechanical support. Tracheids also occur in some hardwoods. They are located adjacent to the vessels (vasicentric tracheids), or they resemble vessels (vascular tracheids) with the sole function of water transport. In softwoods, these cells serve as conduction paths (thin-walled earlywood tracheids) and provide the necessary mechanical stiffness (thick-walled latewood tracheids).

*Fibers* occur exclusively in hardwoods, and represent specialized elements for mechanical support. Slight differences in morphology have given rise to a differentiation between “libriform-fibers” and “fiber-tracheids”. However, since continuous intergrading exists between them, the general term fiber is commonly employed [78].



**Fig. 2.14** (a) Transverse section of a diffuse porous hardwood (*Fagus sylvatica*). The basic tissue contains spacious earlywood vessels (V), parenchymal cells (P) and fibers (F).

(b) Microscopic structure (transverse section) of monocotyledons (rattan) with the basic cell types: vessels (V), parenchymal cells (P) and fibers (F).

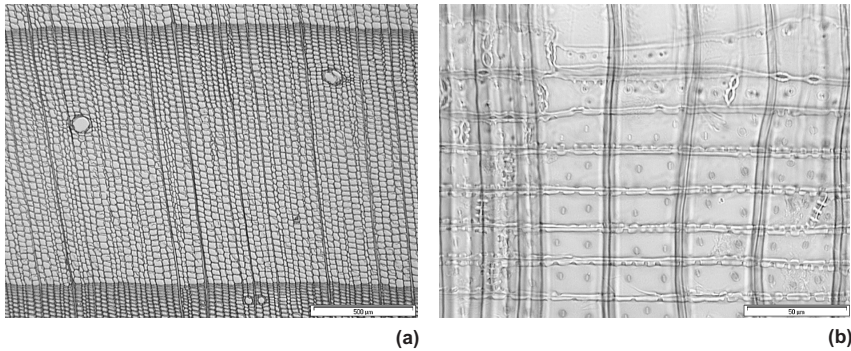
*Vessels* are specialized elements for the long-distance transport of water and mineral solutes in hardwoods; they are composed of individual vessel members that are associated to form a continuous duct with a length of 50–60 cm in some genera (*Populus*, *Fagus*) or even longer, as in oaks (*Quercus* spp.). During maturation of the vessels the end walls of the individual members abutting on other members above and below are removed partly or entirely by enzymatic action; this process results in a rather different appearance of the so-called vessel perforation plates.

Tracheids and vessels reach functionality only after the death of their cytoplasm. Fibers have also commonly been considered to be dead cells, but in some species a few cells retain their cytoplasm over a long period after completion of wall thickening; in the extreme case until heartwood formation. These fibers are termed living fibers, and may store starch.

### 2.1.3.2 Softwood and Hardwood Structure

The major anatomical distinction between softwoods and hardwoods is based on the structure of their wood and cell elements.

*Softwoods* (coniferous woods) exhibit a simpler structure than the more advanced hardwoods (deciduous woods). They are basically composed of tracheids as the principal cell type (ca. 90–95% of total volume) (Figs. 2.13a and 2.15). *Tracheids* of softwoods are mainly oriented in the longitudinal direction, with only a small amount being radially oriented within the rays. The length to width ratio of



**Fig. 2.15** Microscopic structure of softwood (*Picea abies*) in (a) transverse and (b) radial directions.

the longitudinal tracheids is about 100:1 or even greater (length ca. 3–4 mm, diameter ca. 25–45  $\mu\text{m}$ ) (Tab. 2.11). Cell size, wall thickness and lumen diameter vary greatly, with thin walls and wide lumina in earlywood tracheids and extreme wall thickening and narrow lumina in the latewood tracheids. The latter contribute mainly to mechanical strength, whereas the earlywood tracheids are conductive rather than supporting elements.

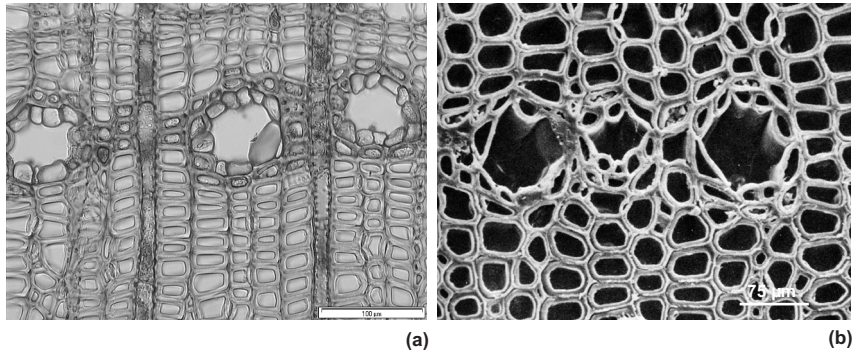
Tracheids may also be horizontally oriented, forming lower and upper margins of the rays in some genera of Pinaceae. The *rays* consist entirely either of parenchymal cells (homocellular ray), or both ray parenchyma and ray tracheids (heterocellular ray). On tangential surfaces, the shape of the rays resembles tiny spindles that are just one or two cell(s) in width (*uniserate* – *biserate rays*) and from few to many cells in height [79].

In some softwoods, *axial parenchyma* is either absent (e.g., *Picea*, *Pseudotsuga*) or sparse (e.g., *Larix*); in others, it is of regular occurrence (e.g., *Podocarpus*, *Juniperus*). Only a few softwood species have thin-walled longitudinal parenchymal cells to a smaller extent (ca. 1–2% of the overall volume), for example redwood (*Sequoia sempervirens*) and some cedars (*Thuja* spp.).

Axial and radial resin ducts are characteristic features of some genera of Pinaceae (e.g., *Picea*, *Larix*, *Pinus*, *Pseudotsuga*), and are lined by parenchymatous epithelial cells responsible for the production and posterior secretion of resin into the duct system, often in response to injury or harmful and traumatic events. These canals form a three-dimensional network in longitudinal and radial direction in the tree (Fig. 2.16). In the radial direction, these canals are embedded in (fusiform) rays.

The margin of a growing period or annual ring is marked by an abrupt change in cell wall thickness. The transition between earlywood and latewood regions within one annual ring varies from gradual (e.g., in soft pines; *Pinus* spp.) to abrupt (e.g., in Douglas fir; *Pseudotsuga menziesii* and hard pines, *Pinus* spp.) [79].





**Fig. 2.16** Transverse sections of softwood (*Picea abies*) with resin canals which are surrounded by epithelial cells (a) Light microscopy; (b) scanning electron microscopy.

**Tab. 2.11** Average cell dimensions and percentages of some wood species (adapted from [66]).

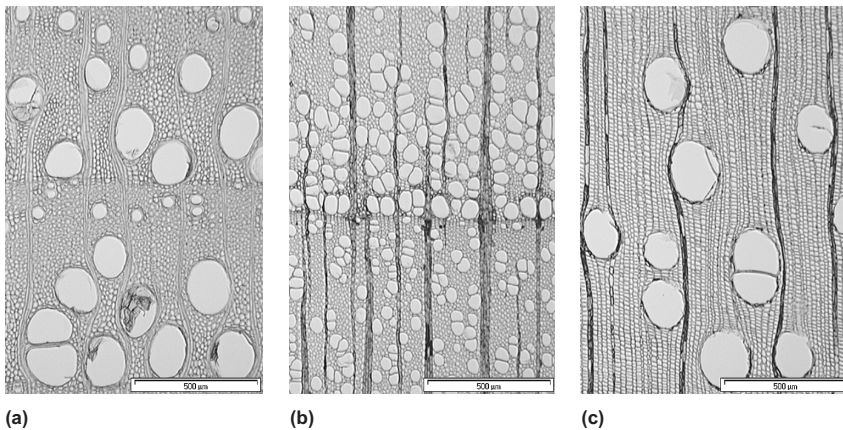
	Softwoods			Hardwoods		
	<i>Abies alba</i>	<i>Picea abies</i>	<i>Pinus sylvestris</i>	<i>Fagus sylvatica</i>	<i>Quercus robur</i>	<i>Populus</i> spp.
<i>Cell dimensions</i>						
Tracheids/fibers						
Length [mm]	3.4–4.3–4.6	1.7–2.9–3.7	1.4–3.1–4.4	0.6–1.3	0.6–1.6	0.7–1.6
Diameter [ $\mu\text{m}$ ]	25–50–65	20–30–40	10–30–50	15–20	10–30	20–40
Vessels						
Length [mm]				300–700	100–400	500
Diameter [ $\mu\text{m}$ ]				5–100	10–400	20–150
<i>Cell percentages</i>						
Tracheids/fibers [%]	90.4	95.3	93.1	37.4	51.2	61.8
Vessels [%]				31.0	39.6	26.9
Axial parenchyma [%]	scarce	1.4–5.8	1.4–5.8	4.6	4.9	
Rays [%]	9.6	4.7	5.5	27.0	22.8	11.3

The evolutionary advanced *hardwoods* possess a functionally and morphologically more diversified structure. The most distinctive feature is the occurrence of vessels, alternatively called “pores” when observed on transverse surfaces.

*Vessels* vary in size and distribution, especially within a discernible growth increment. This diversity is termed “porosity”, and its various patterns represent a very important feature for the identification of hardwoods attributed to three groups: ring-porous; semi-ring-porous; and diffuse-porous (Fig. 2.17):

- Ring-porous woods show distinct differences in the size of vessels within one growth increment; earlywood vessels being larger in diameter than latewood vessels, with an abrupt transition between both. Hence, in some cases the earlywood portion becomes clearly visible as a pore-ring, even with the unaided eye.
- Semi-ring-porous woods are characterized by a gradual change from large-diameter earlywood vessels to small latewood vessels.
- Diffuse-porous woods display vessels of nearly the same diameter throughout on growth increment.

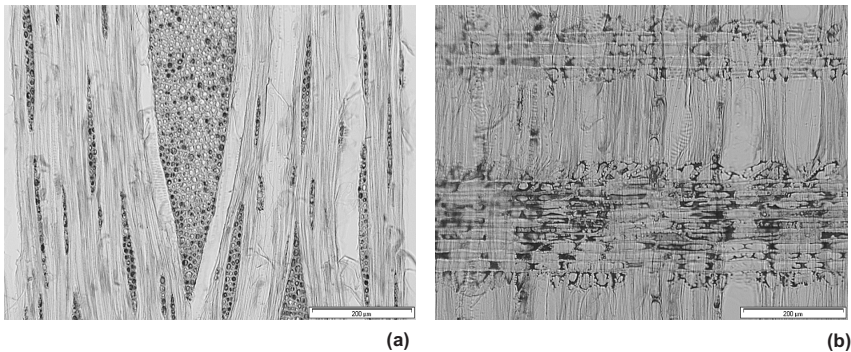
The variation within a species, however, may range sometimes from ring-porous to semi-ring-porous, or from semi-ring-porous to diffuse porous.



**Fig. 2.17** Distinction between (a) ring-porous (*Fraxinus excelsior*), (b) semi-ring-porous (*Prunus* spp.), and (c) diffuse porous hardwoods (*Aucoumea klaineana* = Okoumé) (Light microscopy).

The vessels may be arranged in tangential bands, may exhibit a diagonal or radial pattern, or may reveal a branched appearance to form a dendritic pattern. Vessel may also occur in solitary fashion, as groups in radial multiples of four or more, or as irregular clusters. As vessels are specialized in water conduction, the end walls of the single elements are typically perforated by unrestricted openings during the cell maturation process. The pattern of these perforation plates is either *simple*, *scalariform* or *foraminata*. The lateral connection between adjoining vessels is provided by numerous closely packed bordered pit pairs. The pattern type of the perforation plates, as well as the pitting arrangement, do not change within a given species; both patterns are very useful for microscopic wood identification. Connections to fibers, longitudinal and ray parenchyma and other cell types also occur through pits.

Rays in hardwoods are generally much larger in height and width (up to about 30 cells in a tangential direction) compared to softwoods; they can constitute up to 30% or more of the total xylem volume, with an average of about 17%. The rays consist only of parenchymal cells (*homocellular rays*), but are different in shape and configuration (Fig. 2.18). Most of these brick-like parenchymal cells have their long axis oriented radially, and they appear to be lying down. In some species, ray cells on the upper and lower margins of the ray stand upright on end, with their long axis vertically or parallel to the grain. These two types of ray configurations are termed *homogeneous* and *heterogeneous* rays, respectively. On tangential surfaces, rays are either arranged in a diffuse pattern or in definite, tangential tiers – that is, in a storied arrangement. In the latter case, rays show roughly the same size in height and width and they all begin at about the same level along the grain. A storied arrangement of rays constitutes a very useful tool in wood identification.



**Fig. 2.18** Microscopic structure of hardwood (*Fagus sylvatica*) in the (a) tangential and (b) radial anatomical directions, showing the rays.

*Axial parenchymal* cells are much more abundant in hardwoods than in softwoods. On a transverse section, axial parenchyma (storage elements) are recognized by their thin cell walls. These cells are either elongated and tapered or brick-shaped, or form an epithelium around resin canals. Often, crosswalls subdivide these longitudinal cells into smaller compartments. The position of axial parenchymal cells in relation to vessels is used for a general subdivision into two types of parenchyma. The term “apotracheal parenchyma” reflects the isolation of vessels against axial parenchyma by other cells, whereas “paratracheal parenchyma” describes the association of axial parenchymal strands with vessels. The amount and various distributional patterns display a marked diversity.

### 2.1.3.3 Reaction Wood

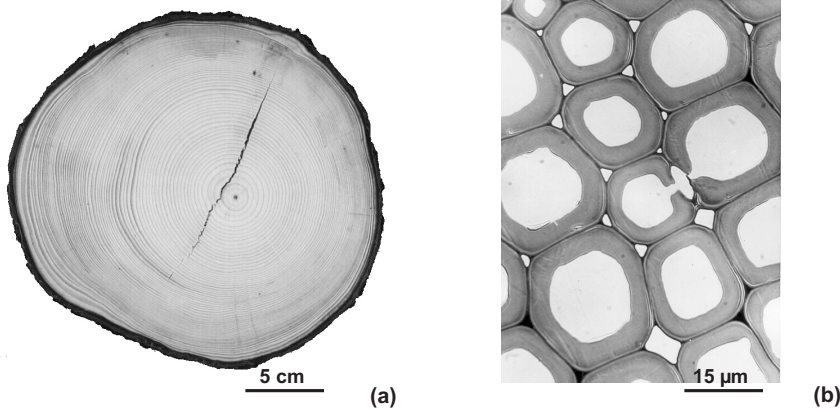
The shape of the cells, particularly of tracheids and fibers, is influenced not only by seasonal changes but also by mechanical forces [80]. Trees react to strain forces

acting on stems and branches (e.g., by high wind or geotropic erection) by forming *reaction wood* in the zones of compression or tension. Softwoods (coniferous trees) develop compression wood in the compressed ranges, and hardwoods (deciduous trees) develop tension wood in the tensile ranges. Compression and tension tissues differ in anatomical, chemical and physical properties from each other, as well as from the normal wood tissue.

#### 2.1.3.3.1 Compression Wood

The main characteristics of compression wood are its dark color, which is caused by a relatively high lignin content, rounded tracheids with intercellular spaces, an absence of the S3 wall, and a secondary wall with helical cavities [34] (Fig. 2.19).

The angle of the fibrils in the S2 of compression tracheids is about  $45^\circ$  in relation to the fiber axis. Compared to normal tracheids, compression wood tracheids are shorter (about 30%), possess a higher lignin and hemicelluloses content (ca. 8–9% higher) and a lower cellulose content (ca. 10% less) [81]. This different property profile leads to some undesired disadvantages when using wood containing compression wood zones. For example, local density is increased, some strength properties are significantly reduced (compared to normal wood of a similar density), and the longitudinal shrinkage is increased to 1–2% (compared to 0.1–0.2% for normal wood).



**Fig. 2.19** (a) Stem section of spruce (*Picea abies*) with compression wood characterized by an eccentric growth and darker color in the region of the reaction wood.

(b) The tracheids of compression wood are rounded with intercellular space, and show higher UV absorbance (UV micrograph recorded at 280 nm wavelength).

#### 2.1.3.3.2 Tension Wood

Tension wood contains fewer and smaller vessels than normal wood, and the fibers are provided with a special wall layer, the so-called *gelatinous layer* or G-layer. Depending on the species, the G-layer may be present instead of the S2, the S3 wall or deposited in addition to the normal wall layers [82]. The G-layer consists of

concentric lamellae of cellulose microfibrils aligned in the direction of the fiber axis. The microfibrils are almost parallel to the grain at an angle of only 5°. The cellulose is highly crystalline, and the content of hemicelluloses and lignin amounts only to a few percent. The thickness of the G-layer varies along the axis of a tension wood fiber, and is thicker in the central region.

Due to these particular features the strength properties of tension wood are reduced (compared to normal wood of similar density), and the longitudinal shrinkage is increased up to 1%. The reason for high tension wood shrinkage is the loose contact between the G-layer and the remaining cell wall which does not prevent the outer cell region (i.e., the P and S1 layers) from contracting during drying [5].

#### 2.1.3.4 Juvenile Wood

During the early years of their life span all trees produce juvenile wood, which occupies the inner core of xylem surrounding the pith. The time during which juvenile wood is formed is termed the juvenile period. This period varies among individuals, with species, and with environmental conditions. The transition from juvenile to mature wood is rather gradual, with a progressively decreasing proportion of cells exhibiting juvenile wood characteristics with increasing distance from the pith.

The microfibril angle in the S1 layer is almost perpendicular to the grain, so this layer tends to shrink longitudinally when water is removed. A firmly attached S2 layer to the adjoining S1 layer – as in normal wood – will provide shrinkage restraint and overall longitudinal shrinkage will be reduced significantly.

In juvenile wood the cells are smaller and structurally less developed than those of the outer, mature xylem. Particular differences exist in the length of the cells as well as in the structure of the layered cell wall. The proportion of latewood in juvenile wood is very small, leading to a relative low density and thus low strength properties. Another disadvantage of juvenile wood is the spiral grain – that is, the fiber orientation deviates significantly from the stem axis. This is the reason for extensive twisting of dried timber containing juvenile wood. At the ultrastructural level, the microfibril angle in the S2 layer is greater than in cells of the mature tissue. Analogous to compression wood, this causes a higher degree of longitudinal shrinkage as well as a reduced tensile strength. In practice, juvenile wood is very difficult to identify because there is no clear demarcation between the former and adult wood [5,83,84].

#### 2.1.3.5 Secondary Changes

With increasing age and secondary thickening of a woody plant, the more centrally located xylem of many species undergoes natural changes. Consequently, the xylem must be subdivided into two parts. In a living tree, the xylem portion close to the cambium serves as a pathway mainly for water and mineral solutes, but it also has a storage function; its parenchymal cells are physiologically active and involved in various metabolic processes.

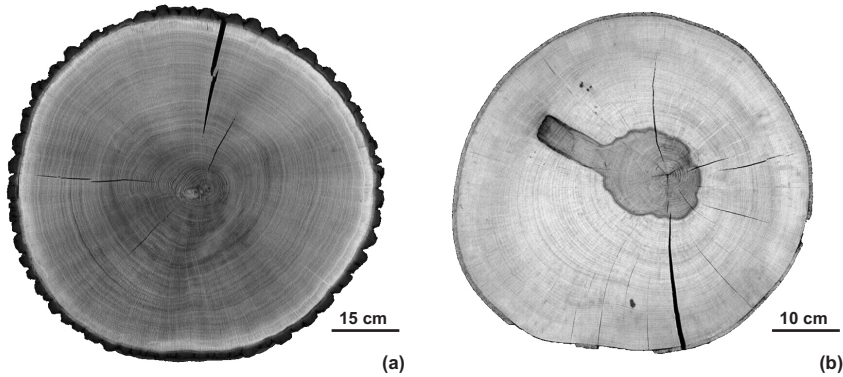
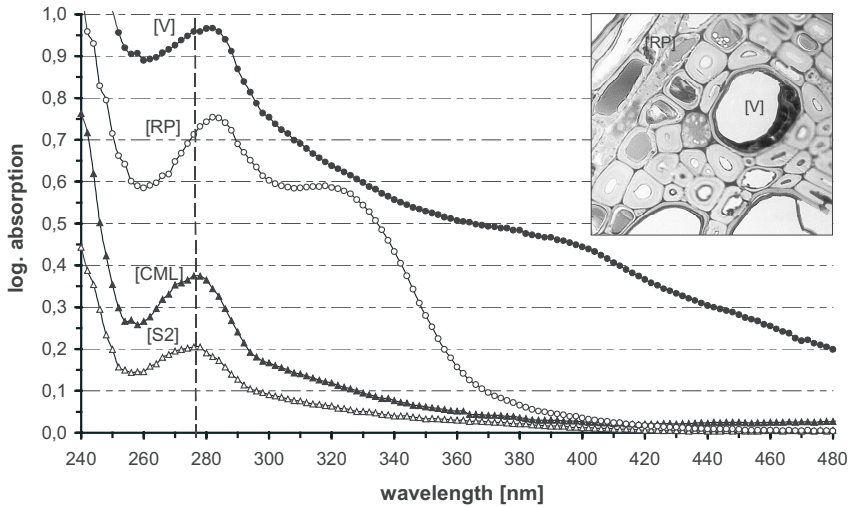


Fig. 2.20 Obligate heartwood formation in (a) *Quercus robur* and (b) facultative heartwood formation in *Fagus sylvatica*.

The more centrally located wood portion in mature trees, however, does not contain living parenchyma [85]. In general, the terms sapwood for the outer, and heartwood for the central portions are used. Transition from sapwood to heartwood usually occurs within a narrow zone of few cell rows, resulting in a slightly undulating sapwood–heartwood boundary. In many species, the heartwood has a significantly darker color than the surrounding sapwood, with certain variation of sapwood width between and within species (Fig. 2.20). Besides the obligatory formation of such a distinctly colored heartwood, some tree species develop less-colored or almost colorless heartwood; all of those species are therefore considered to form a regular heartwood [86].

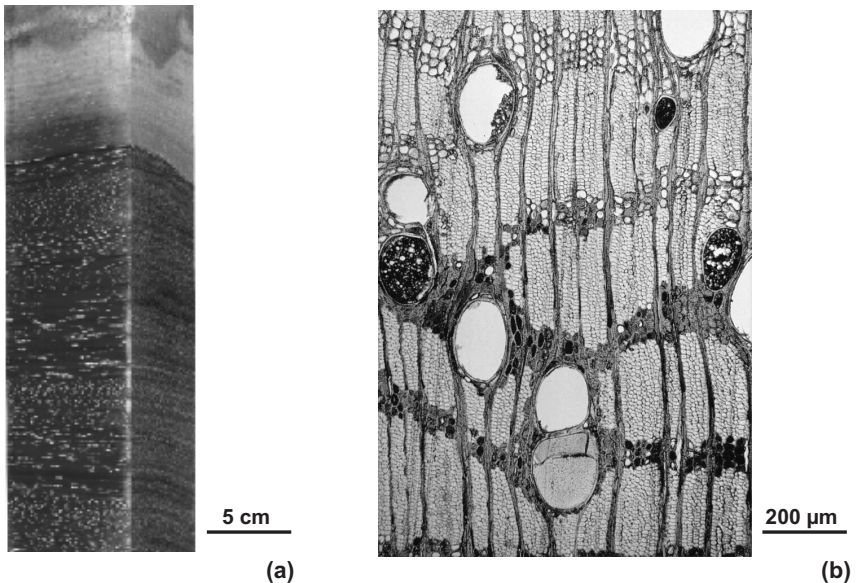
Other trees species such as *Betula* or *Fraxinus* do not form heartwood under normal growth conditions. However, all woody plants develop discolored wood as a result of environmental influences (e.g., injury, attack by microorganisms, severe frost). The boundary between unaffected and discolored wood often extends across a larger number of growth increments with an irregular periphery. Discolorations may also be induced in regular heartwood as a secondary process. The misleading terms “false heartwood”, “pathological heartwood”, and “frost heartwood” are often used for these environmentally initiated changes.

The main criteria for the differentiation between regular heartwood and discolored wood are as follows: regular heartwood is characterized by increased natural durability and lower moisture content in comparison to sapwood; in discolored wood, however, the durability does not considerably increase, and the moisture content may rise even above the sapwood level. The change from sapwood to heartwood during natural heartwood formation in hardwoods is frequently accompanied by the occlusion of vessels. The lumina of some species are more or less filled with dark-colored organic material secreted from adjacent parenchymal cells (Fig. 2.21). Other species develop tyloses – that is, balloon-like protrusions from parenchymal cells through the pits into adjacent vessels.



**Fig. 2.21** Representative UV absorbance spectra of deposited phenolic compounds in the woody tissue of beechwood with red heart (high condensed phenolic compound in the lumen of a vessel [V], low molecular-weight

phenolic compound in the lumen of a ray-parenchymal cell [RP]; compound middle lamella [CML] and secondary wall [S2] of a fibre).



**Fig. 2.22** (a) Stem section and (b) transverse light micrograph of Bongossi (*Lophira alata*), with increasing deposition of extractives from sapwood to heart/wood.

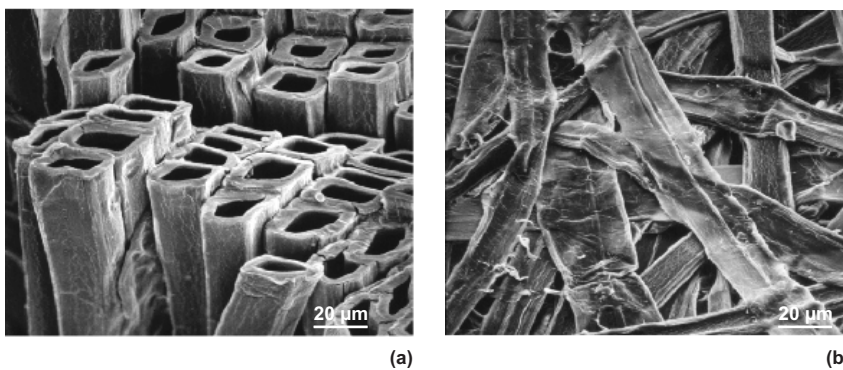
The conversion of sapwood to heartwood is commonly associated with a color change caused by the deposition of chemical compounds or extractives (Figs. 2.21 and 2.22). The extractives also impart the durability to the wood against fungal decay and insect attack. The degree of durability varies widely among different species [87].

## 2.2 Outlook

### 2.2.1 Nano-structure of Fibers

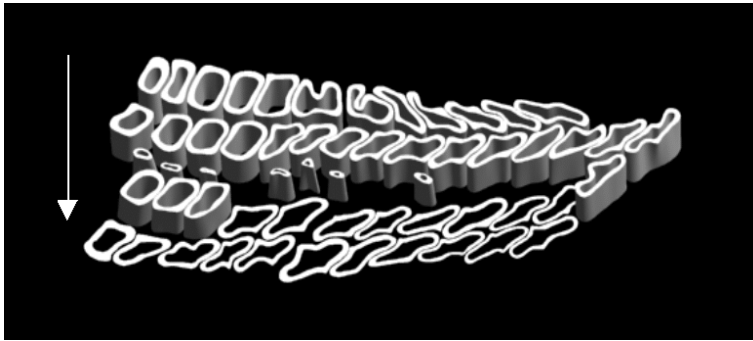
The nano-structure and physico-chemistry of pulp fibers has been of considerable interest to paper research in recent years, as it is realized that the improvement and development of new fiber products can only be achieved by a better knowledge of the fundamental structure of fibers. For example, the fiber surface – and particularly fiber fibrillation – is considered to play a major role as regards inter-fiber bonding in paper products, while the nano-structure of the fiber cell wall as a whole (including the surface layers) are considered to govern the properties related to paper strength (Fig. 2.23). Furthermore, the hierarchical architecture of wood and the tilt angle of the cellulose fibrils against the longitudinal cell axis (microfibril angle; MFA) are believed to play a decisive role in determining the mechanical properties of wood [88].

A better understanding of these aspects should provide important clues as to how improvements in paper products can be achieved. The revived interest has primarily been prompted by the availability of more refined microscopy techniques and preparation methods that allow scientists to come closer to visualizing the “true” pulp fiber structure. This, in turn, provides a means for allowing



**Fig. 2.23** (a) Scanning electron micrographs of spruce wood during the ASAM pulping process and (b) the surface of ungrounded paper [90].





**Fig. 2.24** Three-dimensional reconstruction (40  $\mu\text{m}$  thick) of transverse sections of embedded Kraft cooked fiber bundle. The horizontal rows are numbered 1 to 5 from top to bottom [91].

comparisons of the effects of different pulping processes on fiber structure (Fig. 2.24).

Techniques currently being adapted to study the nano-morphology or surface chemistry of wood and pulp fibers include:

- scanning electron microscopy (SEM);
- transmission electron microscopy (TEM);
- atomic force microscopy (AFM);
- spectroscopic techniques (e.g., X-ray photoelectron spectroscopy; XPS);
- time-of-flight secondary ion mass spectroscopy (ToF-SIMS);
- wide-angle and small-angle X-ray scattering methods (WAXS);
- and
- scanning UV microspectrophotometry (UMSP).

Scanning electron microscopy, and in particular FE-SEM (Field Emission-SEM) and environmental-SEM, have now been used widely to reveal new aspects of fiber wall structure ranging from the micro- to the nano-structural level. More recently, the use of TEM metal replicas to study pulp fiber surface and intracellular nano-structure has shown a revival of the earlier applications developed by Côté et al. [64] to study fiber cell wall structure [89].

Atomic force microscopy has also been applied very successfully to study fiber surfaces under both wet and dry conditions [92], and also sections of resin-embedded pulp fibers [93,94]. Although XPS was not considered previously as a nano-technique, and was originally applied to study paper surfaces [95,96], it has been used recently to study individual fibers and fiber bundles. Within conjunction with FE-SEM, this technique allows comparative chemical and morphological studies on the same fiber region [89].

The application of ToF-SIMS is also being used for studies of the chemistry of pulp fiber surfaces, and is recognized as having great potential. With some care,

this technique should also be useful for studying fiber surfaces/bundles, as shown with XPS-FE-SEM. Wide-angle and small-angle X-ray scattering methods were found to be powerful, nondestructive tools to characterize MFA in wood tissues without extensive sample preparation [97,98].

### 2.2.2

#### Topochemical Distribution of Lignin and Phenolic Extractives

Scanning UV microspectrophotometry (UMSP) has been established as a useful technique for the topochemical detection (analysis) of lignin and phenolic extractives on a cellular and subcellular level. This improved analytical approach enables direct imaging of the lignin distribution within individual cell wall layers (resolution of  $0.25 \mu\text{m}^2$ ), and offers a variety of graphical and statistical analyses [99].

In a comparative study, the delignification of spruce tracheids during bisulfite pulping was analyzed on a subcellular level using scanning UMSP [100]. The results of the study revealed that delignification starts in the region of the pit canals and proceeds homogeneously across the entire S2 (Fig. 2.25) [101–104]. The start of delignification becomes evident as localized areas of the S2 with significantly reduced absorbance values ( $\text{abs}_{280 \text{ nm}}$  0.1–0.2). As a specific feature, a partial delignification of the radial compound middle lamella can be detected at this cooking stage. Jayme and Torgersen [105] assumed that the cooking liquor penetrated the radial middle lamella from the pit system, whereas the tangential middle lamella was not yet penetrated at this early cooking stage. On completion of the pulping process, the tissue revealed a homogeneous delignification throughout the cell wall. Only parts of the cell corners could be distinguished by the UV scanning technique, showing low absorbance values in the range of  $\log \text{Abs}_{280 \text{ nm}}$  0.3. Due to the shape of the tracheids, the radial cell walls were characterized by higher absorbance values caused by the shorter distance between the cell corners in a radial direction.

Scanning UMSP can also be used to detect and quantify aromatic compounds associated with the woody tissue [57]. The presence of extractives can easily be visualized as spherical conglomerations of high absorbance as compared with the surrounding tissue. In Fig. 2.26, the local deposition of extractives in the lumina of ray parenchymal cells of beech heartwood is emphasized by a significantly higher absorbance ( $\text{abs}_{280 \text{ nm}}$  0.68–1.00) as compared to the cell wall-associated lignins. The phenolic compounds are generally synthesized by parenchymal cells *in situ*, and are highly condensed, making it impossible for them to penetrate into the interfibrillar spaces of the cell walls [51]. The adjacent fibers do not seem to be impregnated, as evidenced by lower absorbance levels in these cells. The scanned fibers and parenchymal cells show the typical absorbance profile originating from lignification of the different cell wall layers. In contrast to wood species with an obligatory heartwood formation, the cell walls of beech fibers are not impregnated, and the deposited phenolic extractives in the cell lumina do not contribute to decay resistance (cf. [106]).

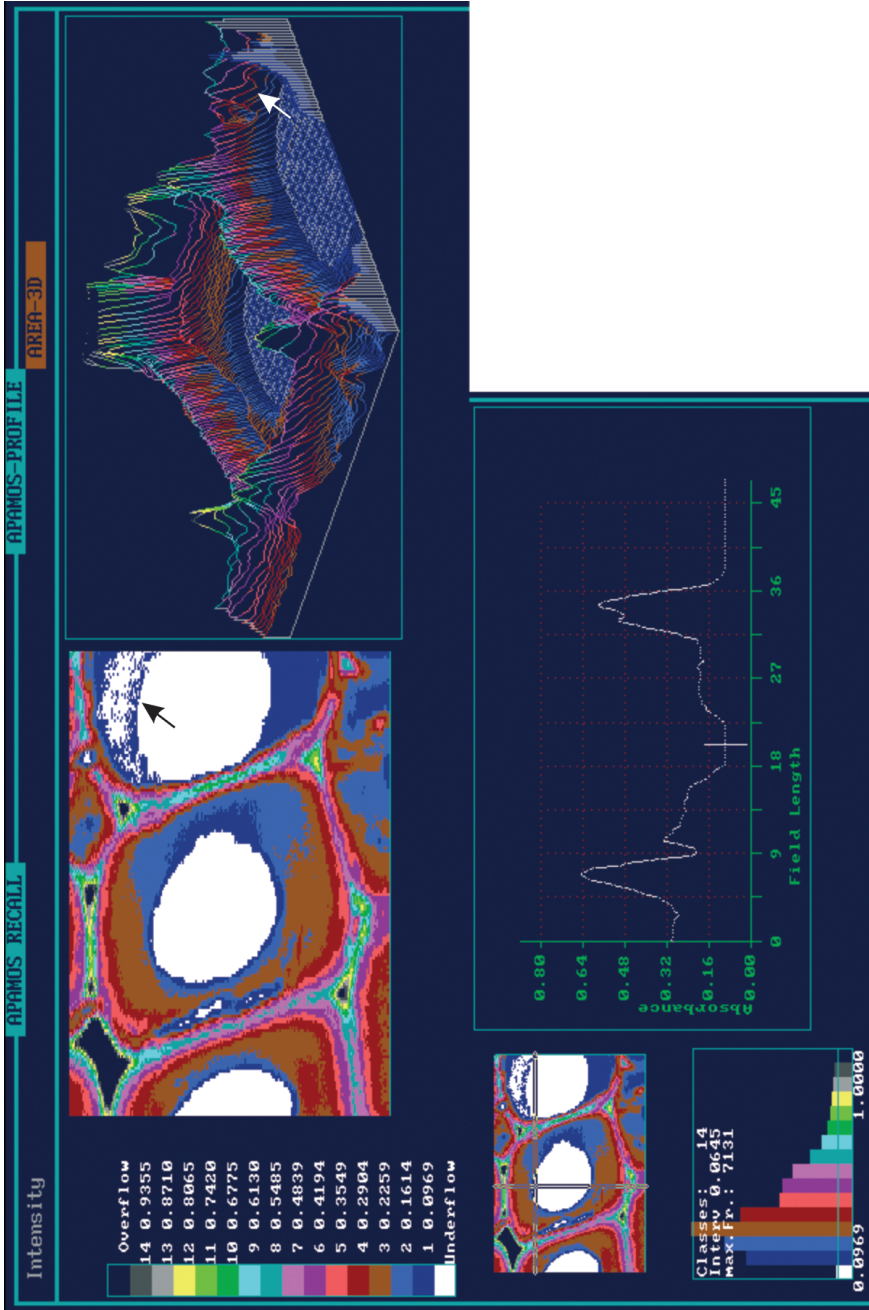


Fig. 2.25 UV-microscopic image profiles of bisulfite-pulped *Picea abies* latewood tracheids (cooking stage 60 min). The color scales indicate the different UV-absorbance values at a wavelength of 280 nm [70].

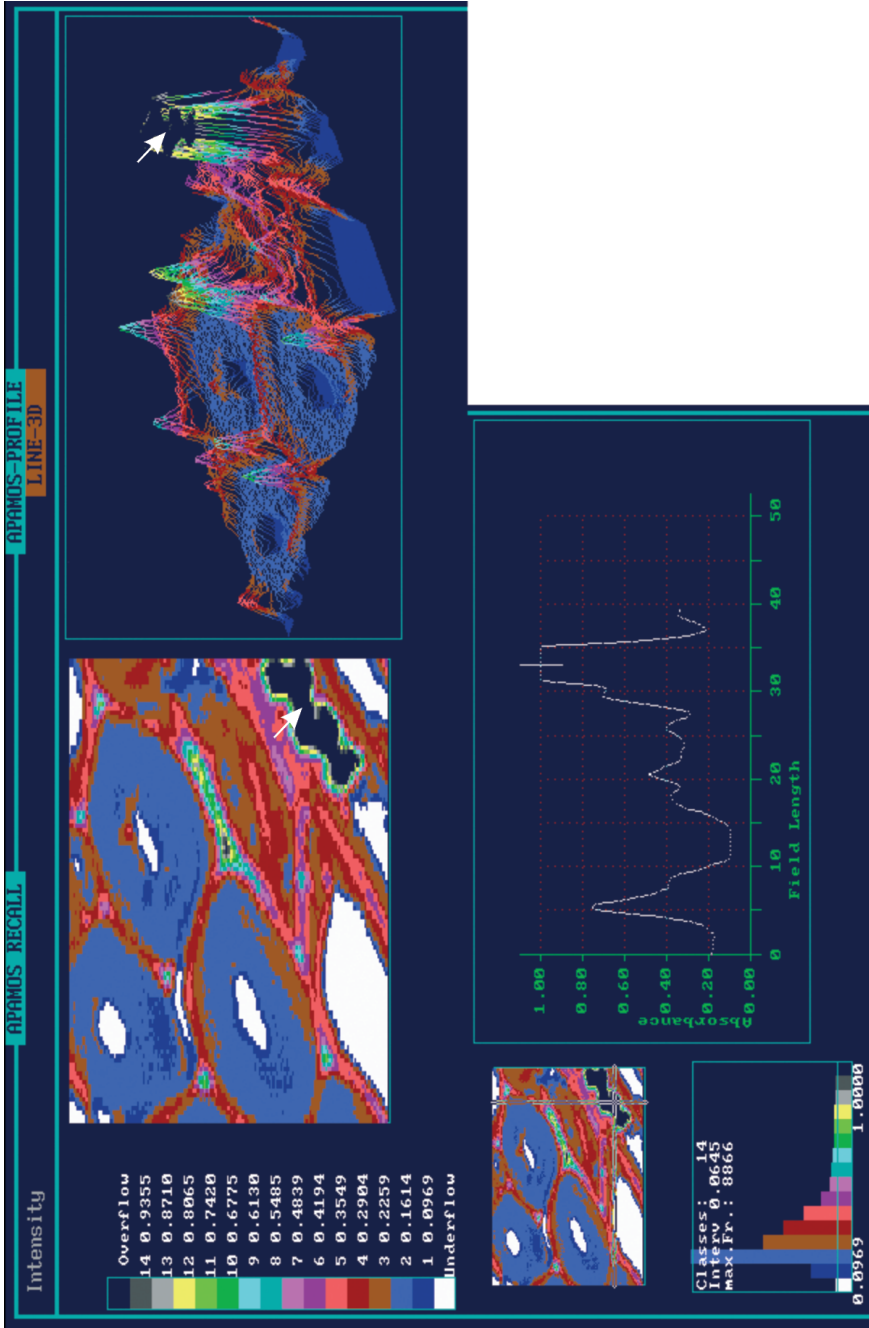


Fig. 2.26 UV microscopic image profiles of *Fagus sylvatica* tissue measured at  $\lambda_{278\text{ nm}}$  showing the deposition of phenolic extractives (arrows) in lumina of ray parenchymal cells [70].

## References

- 1 Jane F. W. 1970: *The structure of wood*. Second edition. Adam & Charles Black, London.
- 2 Rademacher P., Ulrich B., Michaelis W. 1992: *Bilanzierung der Elementvorräte und Elementflüsse innerhalb der Ökosystemkompartimente Krone, Stamm, Wurzel und Boden eines belasteten Fichtenbestandes am Standort "Postturm"*. Eds. W. Michaelis and J. Bauch. GKSS 92/E/100, pp. 149–186.
- 3 Aloni R. 1991: Wood formation in deciduous hardwood trees. In: *Physiology of trees*. Ed. Raghavendra A.A., Wiley and Sons Inc., New York, pp. 175–197.
- 4 Dünisch O., Bauch J. 1994: Influence of mineral elements on wood formation of old growth spruce (*Picea abies* [L.] Karst.). *Holzforschung*, 48, 5–14.
- 5 Haygreen J.G., Bowyer J.L. 1982: *Forest products and wood science*. Iowa State University Press.
- 6 Fengel D., Wegener G. 1989: *Wood – Chemistry, Ultrastructure, Reactions*. Walter de Gruyter, Berlin, New York.
- 7 Sjöström E. 1993: *Wood Chemistry, Fundamentals and Applications*. Second edition. Academic Press, San Diego.
- 8 Klemm D., Schmauder H.-P., Heinze T. 2002: Cellulose. In: *Biopolymers: Biology, Chemistry, Biotechnology, Applications*, Eds. E. Vandamme, S. De Baets, A. Steinbüchel, Wiley-VCH, Weinheim, Vol. 6: Polysaccharide II; pp. 277–319.
- 9 Yamamoto E., Bokelman G.H., Lewis N.G. 1989: Phenylpropanoid metabolism in cell walls. In: *Plant cell wall polymers, biogenesis and biodegradation*. Eds. Lewis N.G., Paice M.G., ACS Symp. Ser. 399, American Chemical Society, Washington DC. pp. 66–88.
- 10 Klemm D., Philipp B., Heinze T., Heinze, U., Wagenknecht, W. *Comprehensive Cellulose Chemistry*; Wiley-VCH: Weinheim, 1998; vols. 1 & 2.
- 11 Kroon-Batenburg L.M.J., Kroon J., Nordholt M.G. 1986: *Polym. Commun.*, 27, 290.
- 12 Krässig H.A. 1993: *Polymer Monographs. Bd. 11: Cellulose: Structure, accessibility and reactivity*. Yverdon: Gordon and Breach Science Publishers.
- 13 Kondo T., Togawa E., Brown R.M. 2001: *Biomacromolecules*, 2, 1324.
- 14 Meyer K.H., Misch L. 1937: *Helv. Chim. Acta*, 20, 232.
- 15 Gardner K.H., Blackwell J. 1974: *Biopolymers*, 13, 1975.
- 16 Atalla R.H., Van der Hart D.L. 1984: *Science*, 223, 283.
- 17 Baker A.A., Helbert W., Sugiyama J., Miles M.J. 2000: *Biophys. J.*, 79, 1139.
- 18 Hult E.L., Larsson P.T., Iversen T. 2000: *Cellulose*, 7(1), 35.
- 19 Nishiyama Y., Langan P., Chanzy H. 2002: *J. Am. Chem. Soc.*, 124, 9074.
- 20 Sugiyama J., Vuong R., Chanzy H. 1991: *Macromolecules*, 24, 4168.
- 21 Langan P., Nishiyama Y., Chanzy H. 2001: *Biomacromolecules*, 2, 410.
- 22 Fengel D. 1993: *Das Papier*, 12, 695.
- 23 Kroon-Batenburg L.M., Bouma J., Kroon J. 1996: *Macromolecules*, 29, 5695.
- 24 Langan P., Nishiyama Y., Chanzy H. 1999: *J. Am. Chem. Soc.*, 121, 9940.
- 25 Atalla R.H. 1999: In: *Comprehensive natural products chemistry*. Barton D., Nakanishi K., Meth-Cohn O., Eds.; Pinto B.M., Vol. Ed.; Vol. 3. Carbohydrates and their derivatives including tannins, cellulose, and related lignins. Elsevier: Oxford (UK), Chapter 16, pp. 529.
- 26 Rencurosi A., Röhrling J., Pauli J., Potthast A., Jäger C., Perez S., Kosma P., Imberty A. 2002: *Angew. Chem. Int. Ed.*, 41(22), 4277.
- 27 Timell T.E. 1964: Wood hemicelluloses: Part I. *Adv. Carbohydrate Chem.*, 19, 247–302.
- 28 Ericsson T., Petersson G., Samuelson O. 1977: Galacturonic acid groups in birch xylan. *Wood Sci. Technol.*, 11, 219–223.
- 29 Marchessault R.H., Sarko A. 1967: X-ray structure of polysaccharides. *Adv. Carbohydrate Chem. Biochem.*, 22, 421–482.
- 30 Carpita N.C., Gibeaut D.M. 1993: Structural models of primary cell walls in flowering plants: consistency of molecular structure with the physical proper-

- ties of the wall during growth. *Plant J.*, 3, 1–30.
- 31 McCann M.C., Roberts K. 1996: Plant cell wall architecture: the role of pectins. In: *Pectins and Pectinases*. Eds. Visser J., Voragen A.G.J., Elsevier, Amsterdam, pp. 91–107.
  - 32 Micheli F., Ermel F.E., Bordenave M., Richard L., Goldberg R. 2002: Cell walls of woody tissues: cytochemical, biochemical and molecular analysis of pectins and pectin methylesterases. In: *Wood formation in trees*. Ed. Chaffey N., Taylor and Francis, London, New York, pp. 179–200.
  - 33 Sarkanen K.V., Hergert H.L. 1971: Classification and distribution. In: *Lignins: Occurrence, Formation, Structure and Reactions*. Eds. Sarkanen K.V., Ludwig C.H., Wiley Interscience, New York, pp. 43–49.
  - 34 Timell T.E. 1986: *Compression wood in gymnosperms*. Springer-Verlag, Berlin, Heidelberg, New York.
  - 35 Nimz H.H. 1981: Carbon-13 NMR spectra of lignins, 8 structural differences between lignins of hardwoods, softwoods, grasses and compression wood. *Holzforschung*, 35, 16–26.
  - 36 Boerjan W., Ralph J., Baucher M. 2003: Lignin biosynthesis. *Annu. Rev. Plant Biol.*, 54, 519–546.
  - 37 Glasser W.G. 1980: Lignin. In: *Pulp and paper. Chemistry and chemical technology*. Ed. Casey J.P., Wiley-Interscience, New York, pp. 39–111.
  - 38 Terashima N., Fukushima K., He L., Takabe K. 1993: Comprehensive model of lignified plant cell wall. In: *Forage cell wall structure and digestibility*. Eds. Jung H.G., Buxton D.R., Hatfield R.D., Ralph, J. Am. Soc. Agr. Madison, WI, pp. 247–270.
  - 39 Terashima N. 2000: Formation and ultrastructure of lignified plant cell walls. In: *New Horizons in wood anatomy*. Eds. Kim Y.S., Chonnam National University Press, Korea, pp. 169–180.
  - 40 Dean J.F.D., Eriksson K.E. 1994: Laccase and the deposition of lignin in vascular plants. *Holzforschung* 48, 21–33.
  - 41 Higuchi T. 1997: *Biochemistry and molecular biology of wood*. Springer-Verlag, Berlin.
  - 42 Terashima N., Nakashima J., Takabe K. 1998: Proposed structure for protolignin in plant cell walls. *ACS Symp. Ser.* 697, American Chemical Society, Washington DC, pp. 180–193.
  - 43 Kindl H., 1991: *Biochemie der Pflanzen*, 3. Auflage, Springer Verlag Berlin, Heidelberg, New York.
  - 44 Glasser W.G., Glasser H.R. 1981: The evaluation of lignin's chemical structure by experimental and computer simulation techniques. *Pap. Puu*, 63, 71–83.
  - 45 Nimz H.H. 1974: Das Lignin der Buche – Entwurf eines Konstitutionsschemas. *Angew. Chem.*, 86, 336.
  - 46 Parameswaran N., Faix O., Schweers W. 1975: Zur Charakterisierung des Sklereiden- und Holzlignins von *Entandrophragma candollei*. *Holzforschung*, 29, 1–4.
  - 47 Hergert H.L. 1971: Infrared Spectra. In: *Lignins. Occurrence, formation, structure and reactions*. Eds. Sarkanen K.V., Ludwig C.H., Wiley-Interscience, New York, pp. 267–297.
  - 48 Fergus B.J., Goring D.A.I. 1970: The distribution of lignin in birch wood as determined by ultraviolet microscopy. *Holzforschung*, 24, 118–124.
  - 49 Musha Y., Goring D.A.I. 1975: Distribution of syringyl and guaiacyl moieties in hardwoods as indicated by ultraviolet microscopy. *Wood Sci. Technol.*, 9, 45–58.
  - 50 Takabe K., Miyauchi S., Tsunoda R., Fukazawa, K. 1992: Distribution of guaiacyl and syringyl lignins in Japanese beech (*Fagus crenata*): variation within annual ring. *IAWA Bull.*, 13, 105–112.
  - 51 Hillis W.E. 1987: *Heartwood and tree exudates*. Springer-Verlag, New York.
  - 52 Helm R.F. 2002: Wood. <http://www.chemistry.vt.edu/chem-dept/helm/home.htm>.
  - 53 Faix O. 2001: Akzessorische Bestandteile und Repetitorium. Materialien zur Lehrveranstaltung 'Grundlagen der Holzchemie' des Studienganges Holzwirtschaft an der Universität Hamburg (als Manuskript vervielfältigt).
  - 54 Newman A.A. 1972: *Chemistry of terpenes and terpenoids*. Academic Press, London, New York.

- 55 Hillis W.E. 1971: Distribution, properties and formation of some wood extractives. *Wood Sci. Technol.*, 5, 272–289.
- 56 Ekman R. 1976: Analysis of lignans in Norway spruce by combined gas chromatography-mass spectrometry. *Holzforforschung*, 30, 79–85.
- 57 Koch G., Bauch J., Puls J. 2003: Topochemical characterisation of phenolic extractives in discoloured beechwood (*Fagus sylvatica* L.). *Holzforforschung*, 57, 339–345.
- 58 Hathway D.E. 1962: The Lignans. In: *Wood extractives and their significance to the pulp and paper industries*. Ed. Hillis W.E., Academic Press, New York, London, pp. 159–190.
- 59 Grosser D., Fengel D., Schmidt H. 1974: Tamrit-Zypresse (*Cupressus dupreziana* A. CAMUS). *Beitrag zur Ökologie, Anatomie und Chemie – Forstwiss. Centralbl.*, 93, 191–207.
- 60 Dünisch O., Bauch J., Müller M., Greis O. 1998: Subcellular quantitative determination of K and Ca in phloem, cambium and xylem cells of spruce (*Picea abies* L. Karst) during earlywood and latewood formation. *Holzforforschung*, 52, 582–588.
- 61 Kuhn A.J., Schröder, W.H., Bauch J. 1997: On the distribution and transport of mineral elements in xylem, cambium and phloem of spruce (*Picea abies* [L.] Karst.). *Holzforforschung*, 51, 487–496.
- 62 Koch G. 2004: Biologische und chemische Untersuchungen über Inhaltsstoffe im Holzgewebe von Buche (*Fagus sylvatica* L.) und Kirschbaum (*Prunus serotina* Borkh.) und deren Bedeutung für Holzverfärbungen. *Mitteilungen der Bundesforschungsanstalt für Forst- und Holzwirtschaft* Nr. 216, p. 82.
- 63 Heyn A.N.J. 1977: The ultrastructure of wood pulp with special reference to elementary fibril of cellulose. *Tappi*, 60, 159–161.
- 64 Côté W.A., Koran Z., Day A.C. 1964: Replica techniques for electron microscopy of wood and paper. *Tappi*, 47, 477–484.
- 65 Chaffey N. 1999: Cambium: old challenges – new opportunities. *Trees*, 13, 138–151.
- 66 Fengel D., Grosser D. 1976: Holz, Morphologie und Eigenschaften. In: *Ullmann's Encyklopädie der technischen Chemie*, Fourth edition, Vol. 12, Verlag Chemie, Weinheim, pp. 669–679.
- 67 Booker R.E., Sell J. 1998: The nanostructure of the cell wall of softwoods and its functions in a living tree. *Holz als Roh- und Werkstoff*, 56, 1–8.
- 68 Schmitt U. 1996: Biology of Wood. In: *Ullmann's Encyclopedia of Industrial Chemistry*. Eds. Nimz H., Schmitt U., Schwab E., Wittmann O., Wolf F. VCH Verlagsgesellschaft mbH Weinheim pp. 305–356.
- 69 Takabe K., Fujita M., Harada H., Saiki H. 1981: The deposition of cell wall components in differentiating tracheids of sugi. *Mokuzai Gakkaishi*, 27, 249–255.
- 70 Koch G., Grünwald C. 2004: Application of UV microspectrophotometry for the topochemical detection of lignin and phenolic extractives in wood fibre cell walls. In: *Wood Fibre Cell Walls: Methods to Study their Formation, Structure and Properties*. Eds. U. Schmitt, P. Ander, J. Barnett, A.M. Emons, P. Saranpää and S. Tschegg, Swedish University of Agricultural Sciences, Uppsala, pp. 119–130.
- 71 Fergus B.J., Procter A.R., Scott J.A.N., Goring D.A.I. 1969: The distribution of lignin in sprucewood as determined by ultraviolet microscopy. *Wood Sci. Technol.*, 3, 117–138.
- 72 Saka S. Goring D.A.I. 1988: Localization of lignins in wood cell walls. In: *Biosynthesis and biodegradation of wood components*. Ed. Higuchi, T. Academic Press, New York, pp. 51–62.
- 73 Grosser D. 1977: *Die Hölzer Mitteleuropas*. Springer-Verlag, Berlin, Heidelberg, New York.
- 74 Wagenführ R. 1999: *Anatomie des Holzes*. Fifth edition. DRW Verlag Leinfelden-Echterdingen.
- 75 Koch G. 1999: Sekundäre Veränderungen im Holz dynamisch beanspruchter Fichten (*Picea abies* [L.] Karst.) aus immissionsbelasteten und windexponierten Hochlagenbeständen. In: *Mitteilungen der Bundesforschungsanstalt für Forst- und Holzwirtschaft*, Nr. 192, p. 196.

- 76 Bauch J., Liese W., Schultze R. 1972: The morphological variability of the bordered pit membranes in gymnosperms. *Wood. Sci. Technol.*, 6, 165–184.
- 77 Core H.A., Côté, W.A., Day, A.C. 1979: *Wood. Structure and identification*. Second edition. Syracuse University Press.
- 78 Wheeler E.A., Baas P., Gasson P.E. 1989: IAWA list of microscopic features for hardwood identification. *IAWA Bull.*, 10(3), 219–332.
- 79 Richter H.G., Grosser D., Heinz I., Gasson P. 2004: IAWA list of microscopic features for softwood identification. *IAWA*, 25, 1–70.
- 80 Wodzicki T.J. 2001: Natural factors affecting wood structure. *Wood Sci. Technol.*, 35, 5–26.
- 81 Timell T.E. 1982: Recent progress in the chemistry and topochemistry of compression wood. *Wood Sci. Technol.*, 16, 83–122.
- 82 Casperson G. 1965: Über endogene Faktoren der Reaktionsholzbildung. *Faserforschung Textiltechnik*, 16, 352–359.
- 83 Zobel B.J., Sprague J.R. 1998: *Juvenile wood in forest trees*. Springer-Verlag, Berlin, Heidelberg, New York.
- 84 Larson P.R. 2001: *Formation of juvenile wood in Southern Pines*. USDA, FPL-GTR-129.
- 85 Ziegler H. 1968: Biologische Aspekte der Kernholzbildung. *Holz als Roh- und Werkstoff*, 26, 61–68.
- 86 Bauch J. 1980: Variation of wood structure due to secondary changes. In: *Natural variations of wood properties*, Proceedings of IUFRO All Division 5 Conference in Oxford, UK (1980). Ed. Bauch J., Mitteilungen der BFH 131, pp. 69–95.
- 87 SWST 2002: Society of Wood Science and Technology – <http://www.swst.org/teach/set2/struct1.html>.
- 88 Burgert I., Keckes J., Frühmann K., Fratzl P., Tschegg S.E. 2002: A comparison of two techniques for wood fibre isolation – Evaluation by tensile tests on single fibres with different microfibril angle. *Plant Biol.*, 4, 9–12.
- 89 Duchesne I., Daniel G., van Leerdam G.C., Basta J. 2003: Surface chemical composition and morphology of ITC kraft fibres as determined by XPS and FE-SEM. *J. Pulp Paper Sci.*, 29, 1–11.
- 90 Patt R., Schmitt U., Neumann J., Kordsachia O. 1992: Vom Holz zum Papier. *Physik in unserer Zeit*, 23, 129–136.
- 91 Bardage S.I., Daniel G. 2004: Three-dimensional morphological aspects of spruce wood and pulp fibres. In: *Wood Fibre Cell Walls: Methods to Study their Formation, Structure and Properties*. Eds. Schmitt, U., Ander, P., Barnett, J., Emons, A.M., Saranpää, P., Tschegg, S., Swedish University of Agricultural Sciences, Uppsala (comp. Nr. 70), 221–233.
- 92 Hanley S.J., Gray, D.G. 1994: Atomic force microscopy images of black spruce sections and pulp fibers. *Holzforschung*, 48, 29–34.
- 93 Fahlén J., Salmén L. 2002: On the lamellar structure of the tracheid cell wall. *Plant Biol.*, 4, 339–345.
- 94 Fahlén J., Salmén L. 2003: Cross-sectional structure of the secondary wall of wood fibers as affected by processing. *J. Mater. Sci.*, 38, 119–126.
- 95 Laine J., Stenius P., Carlsson G., Ström. G. 1994: Surface characterization of unbleached kraft pulps by means of ESCA. *Cellulose*, 1, 145–160.
- 96 Laine J., Stenius P., Carlsson G., Ström. G. 1996: The effect of ECF and TCF bleaching on the surface chemical composition of kraft pulp as determined by ESCA. *Nordic Pulp Pap. Res. J.*, 11, 201–210.
- 97 Daniel G., Duchesne I. 1998: Revealing the surface ultrastructure of spruce pulp fibers using field emission-SEM. In: *7th International Conference Biotechnology in the Pulp and Paper Industry, Proceedings*, Vancouver, Canada, pp. 81–84.
- 98 Duchesne I., Daniel G. 2000: Changes in surface ultrastructure of Norway spruce fibres during kraft pulping – Visualization by Field emission-SEM. *Nordic Pulp Paper Res. J.*, 15, 54–61.
- 99 Koch G., Kleist G. 2001: Application of scanning UV microspectrophotometry to localise lignins and phenolic extractives in plant cell walls. *Holzforschung*, 55, 563–567.



- 100 Koch G., Rose B., Patt R., Kordsachia O. 2003: Topochemical investigations on delignification of *Picea abies* [L.] Karst. during alkaline sulfite (ASA) and bisulfite pulping by scanning UV microspectrophotometry. *Holzforschung*, 57, 611–618.
- 101 Procter A.R., Yean W.Q., Goring. D.A.I. 1967: The topochemistry of delignification in kraft sulphite pulping of spruce wood. *Pulp Paper Mag. Can.*, 68, 445–460.
- 102 Whiting P., Goring D.A.I. 1981: The topochemistry of delignification shown by pulping middle lamella and secondary wall tissue from black wood. *J. Chem. Technol.*, 1, 111–122.
- 103 Saka S., Whiting P., Fukazawa K., Goring D.A.I. 1982: Comparative studies on lignin distribution by UV microscopy and bromination combined with EDXA. *Wood Sci. Technol.*, 16, 269–277.
- 104 Wu S.C., Wang H., Wang. H.H. 1987: Microanalysis of lignin and cellulose in leucaena pulps at different cooking stages. *Proc. Natl. Sci. Council Rep. China, Part B-Life Sci.*, 11, 194–205.
- 105 Jayme G., Torgersen H.F. 1967: Topochemie der Delignifizierung beim Aufschluss von Fichtenholz nach dem Sulfite- und Sulfatverfahren. Teil I: Ultraviolettmikroskopische Untersuchungen an teilweise delignifizierten Fichtenholz. *Holzforschung*, 21, 110–116.
- 106 Kleist G., Bauch J. 2001: Cellular UV microspectrophotometric investigation of Sapelli heartwood (*Entandrophragma cylindricum* Sprague) from natural provenances in Africa. *Holzforschung*, 55, 117–122.

### 3

## Wood Yard Operations

*Jörg B. Ressel*

The characteristic purposes of a wood yard are to receive logs, wood residues and chips, to debark logs, to chip logs and residues, and to store bark and chips for further processing. The raw materials are delivered by truck or rail and stored in stacks or piles to ensure continuous production. Logs are handled either by rail-mounted cranes or large wheeled vehicles. The storage of logs and chips follows an inventory management procedure that reduces weathering and spoiling. An example of the material flow and processing steps at a pulp mill wood yard is illustrated in Fig. 3.1.

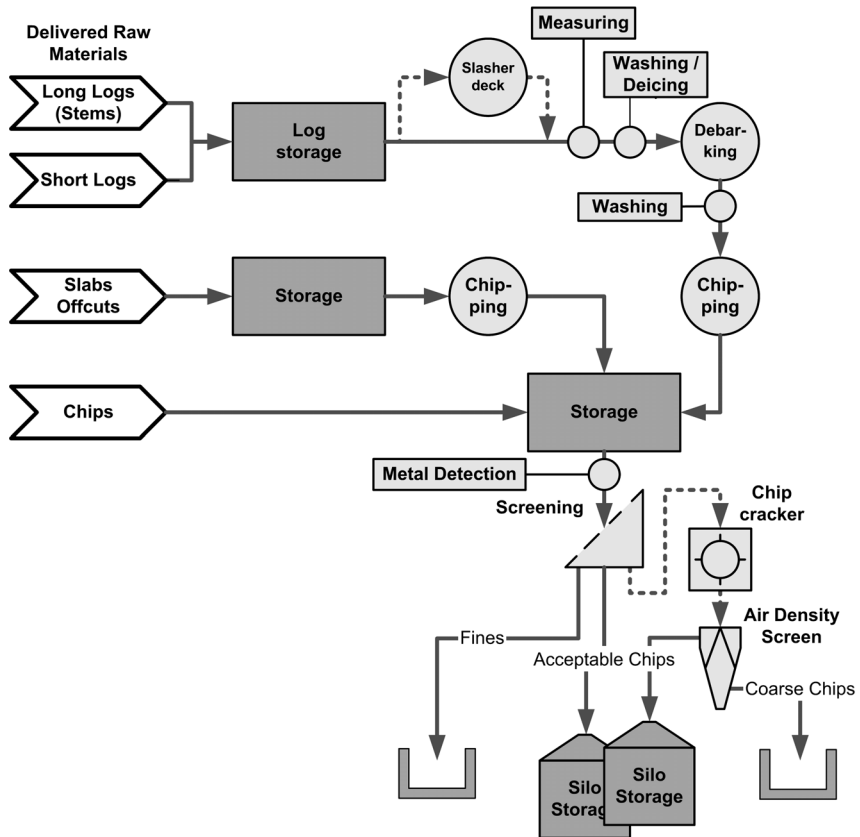
Small-diameter logs (e.g., from thinnings) and sawmill residues are the most important fresh raw material sources for fiber production. Additionally, plantation-grown species are a common, less expensive source. Traditionally used softwoods include spruce and pine, which offer an excellent fiber morphology. Hardwood species (e.g., birch, beech, poplar and, in particular eucalyptus) are also important raw material resources.

Individual wood species require particularly adapted process parameters in pulping, and thus should be separately processed in order to obtain optimal pulps. The mixing of wood species – for example, softwood and hardwood or tropical hardwood species – should be avoided.

### 3.1

#### Raw Material Storage

Accordingly, the raw materials delivered (stems, logs, sawmill chips and other sawmill residues) must be stored separately. Particular measures are required during the storage period to reduce losses caused by biodeterioration. Wood decay mainly depends on storage duration, climatic and storage conditions. Microbiological deterioration causes wood substance losses and wood quality losses – that is, decreasing strength properties of the fibers, and discoloration, leading to drawbacks in further processing and economical losses. This occurs especially when the wood moisture content is in the range of 25–55%. Regularly piled up logs undergo mass losses of approximately 2–3% during the first year of open-air



**Fig. 3.1** Raw material processing and schematic material flow in a pulp mill wood yard.

storage, but  $<0.1\%$  when stored in or under water. Nevertheless, a decrease of wood moisture and resin content is advantageous in open-air storage, apart from providing an even raw material flow to the mill. Today, after harvesting, logs are mostly piled up and stored in the forests for several weeks up to months. Transport to the mill is on call, and the average storage in a pulp mills' wood yard may vary from only a few days up to weeks.

Log storage conditions affect the processability of the wood materials in pulping and bleaching. In recent investigations with beech (*Fagus sylvatica* L.) by Sixta et al. [1], logs were stored for approximately 15 months under dry and wet conditions. Significant differences have been reported related to the demand of bleaching chemicals. For pulp made from dry-stored logs, between 60 and 300% more bleaching chemicals – expressed as OXE – were necessary to achieve a comparable target brightness to pulp made from fresh chipped or wet-stored logs. During wood drying, chromophore compounds were developed from polyphenolic compounds which negatively affect acid bisulfite pulping and thus final pulp quality.

Wet storage of beech logs effectively prevents the formation of these compounds and leads to a chip quality as made from fresh-cut logs.

Investigations published by Liukko [2] and Elowsson and Liukko [3] are related to the water management of wet-stored pine log piles (*Pinus sylvestris* L.) and wood moisture content development. To maintain the quality of fresh logs, the period between felling and starting wet-storage (e.g., water sprinkling) must be as short as possible. Additionally, climate-controlled water sprinkling – that is, sprinkling adapted to the local evaporation rate – prevents negative impact on groundwater and the environment and results in the same wood moisture content development as intensive sprinkling. The moisture content development of logs during wet storage is to a great extent dependent on the wood handling prior to sprinkling. According to the authors, the (water) buffering capacity in a log pile is low. However, sprinkling of pulp wood is not a standard treatment in wood yards; it may be a recommended treatment in emergency cases. It leads to additional costs and may cause some problems in further processing, for example, the leaching of bark components into the wood. A more general report of von Aufseß [4] provides further information on wood quality changes during log storage; these data are less related to pulping, rather, this author mostly describes differences between sound and decayed trees.

Logs should be carefully piled up on a well-prepared log yard, ensuring sufficient water drainage and air circulation. Adequate measures are also required for the drained water to prevent against ground water pollution by soluble wood and bark substances. In this respect, local regulations related to ground water protection must also be considered [5]. (Chip storage is described in detail in Section 3.6.3.1.)

## 3.2 Debarking

The debarking of wood subjected to pulping processes is a very important subject; a too-high bark content of the chips reduces the brightness, leads to yield reduction and extended cooking times, to increased bleaching chemicals consumption, and finally results in bad pulp properties.

The lowest acceptable bark content is required for groundwood logs. In particular, phenolic substances in the outer bark lead to problems in sulfite pulping due to reactions with lignin. The yield of fiber material decreases and the process requires additional chemicals to achieve a sufficiently low final lignin content. Sulfate pulping is least susceptible to bark contamination, but a too-high bark content requires more chemicals, results in a longer cooking time, poor bleaching ability and yield and fiber strength reduction. Insufficient bark removal carries sand and dust particles into the pulping process, requiring extended subsequent cleaning steps. Finally, the ash content of the bark interferes strongly with the recovery of process chemicals.

Adhesion between wood and bark as well as log shape affect the debarking success. Bark adhesion varies with wood species, harvesting time, storage duration and conditions. During the winter period, frozen bark is extremely difficult to remove, and requires a suitable de-icing pre-treatment, for example, by using hot water or steam. A washing station is recommended at the debarker infeed. Log washing and hot water pre-treatment contributes to effluent treatment costs due to an increased biochemical oxygen demand (BOD), and requires suitable extensive wastewater treatment facilities. Depending on the debarking equipment and the chipping technology applied, the logs may be cut to length by passing a so-called “slasher deck” prior to debarking.

### 3.2.1

#### Debarking Methods

The state-of-the-art debarking technology is summarized by Goldie [6]. The overall intention is to remove the bark completely at the cambium with no fiber losses or damage to wood, little log end damage due to excessive tool pressure, and high throughput. The most common debarking technologies in forest products industries include:

- Drum debarker                      Simultaneously continuous or batch-wise
- Rotary or cradle debarker      debarking of a bundle of logs
- Ring debarker
- Flail debarker
- Rosserhead debarker              Subsequent debarking of individual logs
- Mobile debarker

Debarking based on water jets or radiofrequency, or formerly used pocket debarkers, are no longer of interest in forest products industries due to their low capacity and high costs (high energy consumption, wastewater treatment, substantial fiber losses).

In pulp mills, the use of rotating drum debarkers and rotary debarkers is widespread, whilst ring debarkers are less often utilized. Other debarker types are found only occasionally, and will not be described in detail at this point.

##### 3.2.1.1 Drum Debarker

In rotating-drum debarkers, the logs are tumbled or rolled by the drums’ rotation, and this causes the bark to be removed from the logs as they are abraded against each other and against either the corrugated interior of the drum or alternatively built-in steel staves which act as “lifters”. As the logs pass the rotating drum, bark removal is started with breakage of the bark-to-wood bond, and subsequently edge bond failure between the loosened patch and the still-intact area. The logs move ahead slowly through the length of the drum because the drum slopes down towards the discharge opening. More recently, the batch drum debarking procedure has developed into continuous debarking, with less wood losses and improved log cleanliness.

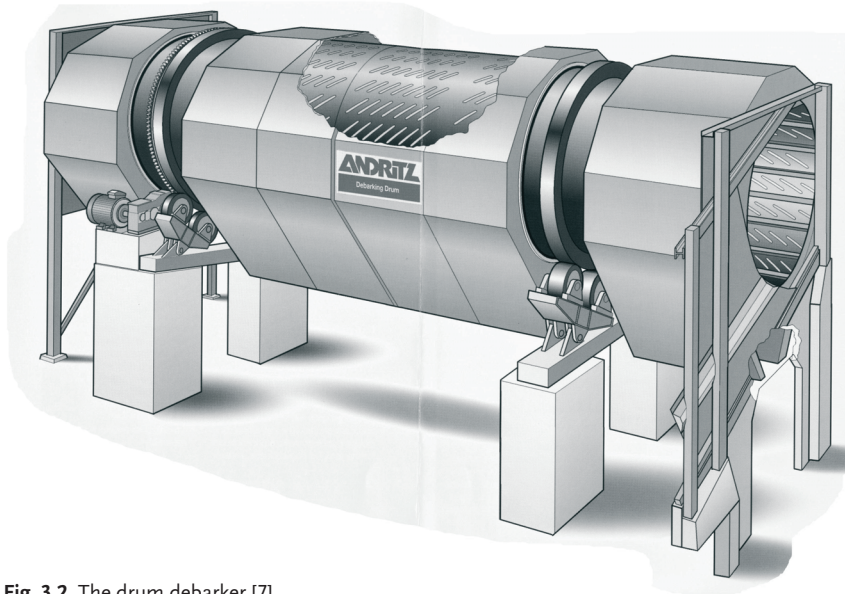
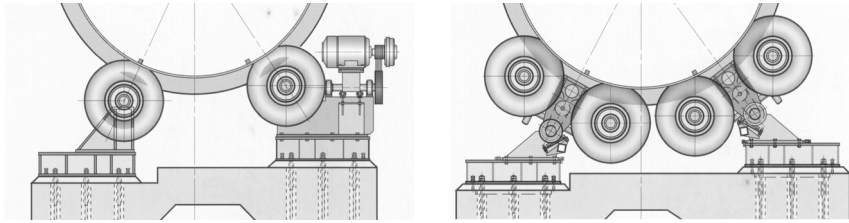


Fig. 3.2 The drum debarker [7].

The drum size ranges in length from 6 to 60 m (mainly 16–40 m), while the diameter ranges from 2 to 5.5 m (mainly 4–5.5 m), depending on the capacity and production conditions required by the respective mill (Fig. 3.2). The attainable surface speed on the interior drum shell ranges between 50 and 200  $\text{m min}^{-1}$  (equivalent to 7 to 30 r.p.m.), depending on the drum diameter. The debarking capacity ranges from 50 to 350  $\text{m}^3$  solid wood over bark per hour.

The drums' shell is constructed from thick, solid steel plates, which contain slots for bark removal. The open slot area can be up to 8% of the total shell area, depending on the drum size. Steel lifters are fitted along the total length of the drum interior, or optionally, cast steel lifters or rubber staves contribute to the debarking procedure. Rigid support rings are fixed to the outside of the shell.

The drum is carried on cast steel wheels, either as single or as bogie wheel assembly (Fig. 3.3). Alternatively, a flexible rubber tire support is available, which reduces vibration transfer to the concrete foundations. The support wheel system is assembled to the prefabricated base beam for smooth erection procedure and trouble-free operation. Girth sprockets, gearing, or friction drives ensure drum rotation to achieve the optimal surface speed on the drum surface. The power for drum rotation is transmitted from electric motors via V-belts to gear-reducers. Close tooth contact between the drive pinion and the master gear is ensured by fixing the master gear to the rigid support ring, and by compact design of the motor/reducer system. Depending on the debarking capacity and wood species, one or two electric motors are required to rotate the drum (power 250–450 kW each). A multi-motor drive ensures a high availability of the plant, because debarking can be continued even if one motor drive is out of service [8].



**Fig. 3.3** Drum support and driving unit. Left: axle supported system by each drive, drum is driven from one side only. Right: bogie supported drum, two motors by each gear reducer, all tires are driven [7].

With modern drum debarking technology, the logs are fed into the drum and discharged continuously. The latter is achieved by adjusting the discharge gate position to maintain an even discharge rate from the drum. The retention time in the drum is directly related to drum length; thus, with increasing drum diameter and rotation speed, the passage time decreases. Drum diameter, bark removal efficiency and retention time influence each other; hence, the ratio of drum diameter to length is important. Wood depth and the wood filling gradient over the drum length are controlled by the discharge gate position.

Although a greater cleanliness is achieved with wet debarking, dry debarking is more common in industry due to its lower costs per cubic meter debarked. Wet debarking requires longer drums, larger drum diameters and additional equipment as for effluent treatment, as well as hot water or steam generation. Dry debarking avoids the pollution problems that are inherent in the wet system. Even in cold northern regions, the dry debarking is applied, aided mostly by steam pre-treatment or hot-water de-icing on the infeed conveyor [9,10].

With modern drum debarkers the log length/drum diameter ratio is  $<0.7$ , ensuring effective debarking for short logs and degrees of cleanliness, with the final bark content being  $\leq 1\%$ .

For the debarking of long, straight logs (log length  $>$  drum diameter), “parallel debarking” (as drum speed increases, short logs become oriented parallel to the drum axis, and debarking occurs in parallel mode) offers certain clear advantages [9,11]:

- Increased plant capacity;
- High yield of acceptable chips (less log ends);
- Less wood losses (reduced log breakage and “brooming” of log ends);
- Higher chip quality (less log ends); and
- Less re-chipping compared to tumbling short wood debarking systems.

Recent developments from Metso Paper Oy – that is, the GentleFeed™ and the GentleBarking™ systems – offer further process improvements [10]. With the GentleFeed system the logs are fed into the drum not randomly via a conventional

chute, but in bundles on a specially designed conveyor system. This simple charging system reduces wood losses (less end breakage) and maintenance costs, and enhances uptime. The system may be extended by additional washing and de-icing equipment. The objectives of GentleBarking™ are particularly related to bark separation, not via slots in the drum shell but exclusively from the chipper feed line attached to the debarking drum and discharge gate, respectively. The significant feature of this system is a shorter debarking drum, which allows less retention time and results in fewer wood losses and less wood breakage.

The discharge gate operating mode has also been changed by Metso Paper Oy whereupon the discharge gate, instead of operating like a sluice-gate, functions as a regulating device, causing minimal interference to the uniformity of the log flow. Setting of the discharge gate depends on the prevailing debarking conditions, and is not used to control throughput of the line. The line capacity is controlled by the amount of logs fed into the drum – that is, the log receiving deck and the feeding conveyor. When interruptions occur in the line the outlet is not closed as usual; rather, the whole line is stopped and restarted after the hold-up has been cleared [8].

The bark morphology of individual wood species leads to requirements for separate debarking treatment by flexible adjustment of infeed speed (e.g., with the Andritz PowerFeed™; [12]) and drum speed. Depending on log length, the drum is either run in tumble debarking mode for short log length, or in parallel debarking mode for long log length (up to 6 m and more). Rotational speed is also adjusted according to the wood quality and species. For debarking eucalyptus in particular (Fig. 3.4), the equipment has been developed by Andritz. Between

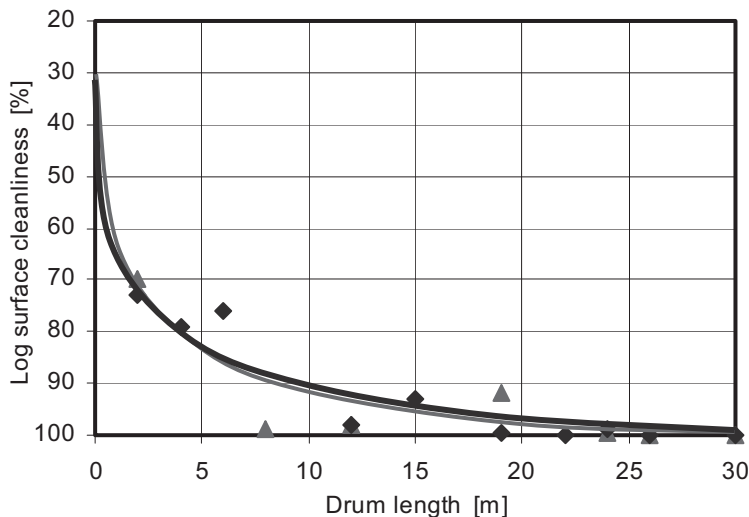


Fig. 3.4 Log cleanliness investigations. Field test results from debarking green eucalyptus in Spain, according to Tohkala [8]. The symbols refer to two different test series.



20–30% of the eucalyptus bark is removed in the debarking drum, whilst the remaining bark, which leaves the drum together with the logs, is extracted by the so-called EucaRoller™. This particularly designed outfeed conveyor removes the remaining bark via engineered gaps between the rollers. The debarked logs are moved sideways by reverse and shaking rollers, enabling the loose eucalyptus bark to fall through the gaps [12].

### 3.2.1.2 Rotary Debarker

Rotary debarkers, as designed by Fuji Kogyo Co. Ltd., Japan, and built under license by CAE Machinery Ltd., US, consist of a fixed trough assembly containing pair-wise openings in the bottom. Rotors driven by electric motors (each up to about 100 kW) via chain transmission are located in each opening, mounted at the ends on roller bearings. Debarking plates are fixed on the surface of the rotors. The debarker comprises three sections, each of approximately 9 m length. Each minute, between 15 and 30 logs (length ca. 2.5 m) are fed continuously into the debarker, whereupon spinning plates hit the logs and begin bark removal by breaking the fiber bonds at the cambium layer (Fig. 3.5). These plates also cause the logs to spin and to hit each other. The machinery is installed at a declined angle, thereby ensuring continuous log motion towards the discharge end as they are being debarked [14].



**Fig. 3.5** Rotary debarker: the rotating plates spin the logs in the casing [14].

Dingwell's North America Ltd. also manufactures rotary debarkers for forest product industries. These have interchangeable, especially designed abrasion tools which produce superior performance in loose reclaimed material (sawmill residues) and extremely stringy, fibrous bark species, for example, eucalyptus, cedar, basswood and tropical acacia. In order to suit any need and flexibility, different modules are available with rotor options that include variable body sizes to accom-

moderate various stem diameters. The debarkers are equipped with heavy-duty, operator-managed hydraulic or mechanical electrically driven systems in permanent, semi-portable or mobile portable configurations [6].

### 3.2.1.3 Ring Debarkers

Ring debarkers are used for the subsequent debarking of individual logs. Compared to drum debarkers, the use of ring debarkers leads to significantly lower investment costs in addition to a power consumption of only about one-sixth of that required by drum or rotary debarkers.

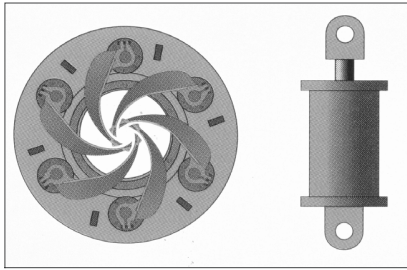
With ring debarkers, debarking is carried out by curved, scraping-tipped tools mounted on a rotating ring. Up to six of these tools are pivoted at the ring and pressed against the log by springs or rubber bands, or by hydraulic or air pressure. The applied radial and tangential forces shear the bark off at the cambium layer as the log passes the ring. The rotational speed of the tool-carrying ring varies between 90 and 450 r.p.m., depending on the log diameter. Rotational speed, the number of tools mounted on the ring and the overlap of successive tools on their helical path over the log surface (up to 50%, depending on the required debarking quality) determine the feeding speed, which ranges from approximately 20 to 65 m min<sup>-1</sup>. The shape of the tools, and also their scraping tips, must be adapted to the processed wood in order to minimize wood losses. Any feedworks should be as close as possible to the debarking ring to achieve the best centering of crooked logs (for further details, see Ref. [9], p. 1657).

Ring debarkers are equipped with either one single debarking ring or as a tandem debarker carrying two successive rings. Debarking and processing rings with different pressure systems are shown in Fig. 3.6. Tandem ring debarkers are used for extra clean debarking or better bark removal with higher feed speeds. The first ring removes the majority of the bark, while the second ring gently cleans up any remaining bark.

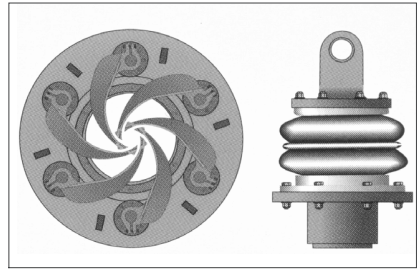
Most ring debarkers are composed of individual modules with their own feedwork, either at the infeed or the outfeed side depending on where the module is arranged in the machinery. Debarking modules are provided with pullout rings for easy and safe maintenance.

For wood species with fibrous bark (e.g., eucalyptus, cedar and redwood), a particular stringy bark splitter ring is recommended. Three to six special knives mounted on a rotating ring cut the bark in a helical pattern, so that a second standard debarking ring can remove the resulting short bark segments without jamming. The splitter ring is generally used as the first ring in a tandem ring debarker. Special add-on debarking modules, either stand-alone or post-processing modules (e.g., a four roll module), a centering infeed conveyor module or a flared butt reducer ring allow adaptation of ring debarkers to individual debarking tasks [15].

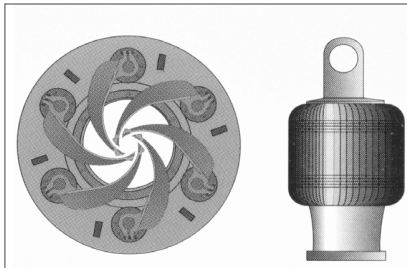
According to Goldie [6], Nicholson Manufacturing Co. (Figs. 3.7 and 3.8), ForMin Inc., USNR [delivering the Cambio debarker series made by Kockums Cancar and Forano (all US)] and Valon Kone Brunett Ltd. (CAN), are well-known suppliers of ring debarkers.



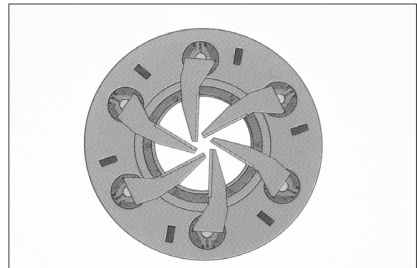
Variable pressure air seal debarking ring (Ø 31...183 cm)



Variable pressure bellow air seal ring (Ø 31...56 cm)

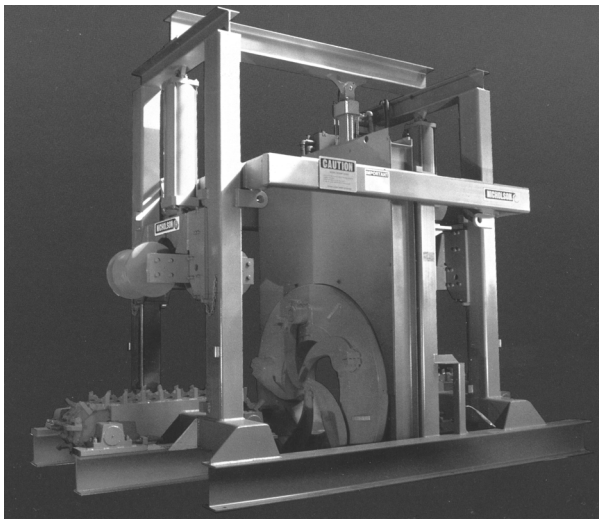


Variable pressure air cell debarking ring (Ø 31...112 cm)



Stringy bark splitter ring for difficult species (Ø 56...89 cm)

**Fig. 3.6** Debarking and processing rings [15].



**Fig 3.7** Nicholson A2 Debarker with powered chain feedworks and air cylinders on hold-down rolls to clamp the logs [15].



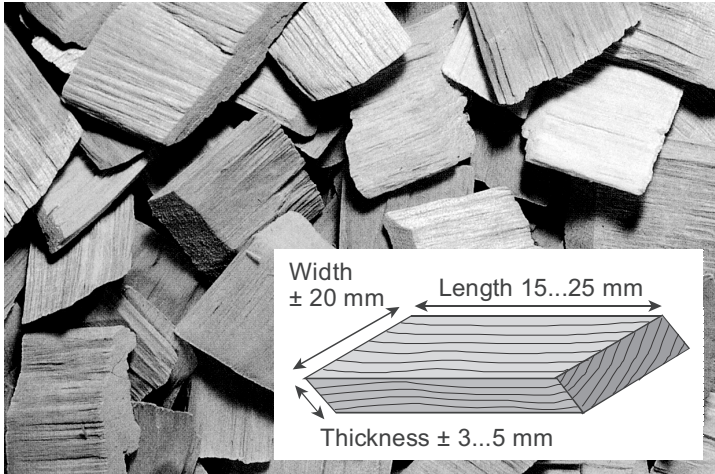
Fig. 3.8 Nicholson A8 Debarcker with tandem debarking rings [15].

### 3.3 Chipping and Screening

Wood chips used for chemical pulp must be of relatively uniform size, though optimum size may vary depending on the wood species. Penetration of the pulping chemicals and thus the cooking time is considerably determined by chip length; doubling the chip length requires a fourfold impregnation and cooking time! In batches of mixed chip sizes, excessive absorption and side reactions in smaller chips could slow the delignification of larger chips by depleting chemicals in the liquor penetrating the chips. When cutting chips, wood and fiber damage respectively should be as low as possible; chip length must also be adapted to the fiber length of individual species in order to achieve good paper strength properties. Chip size will always be a compromise between mechanical fiber damage caused by the cutting process and liquor impregnation. Standard average chip dimensions are shown in Fig. 3.9 (according to [9], p. 2195).

Chips can be generated in different modes with specially designed machinery, the power consumption of which depends mainly on the selected cutting direction, knife geometry (notably the rake angle), knife sharpness and wood properties such as specific gravity, moisture content and temperature.

Chipping inevitably leads to mechanical damage of the wood fibers. High-quality chips have a clearly cut surface without any ripped-out or sheared-off fibers. Rough surfaces and fractures are caused by shear forces, compression forces, buckling, etc., and may occur in the middle lamella between adjacent fibers as well as inside the cell wall between particular wall layers (e.g., between the S1-



**Fig. 3.9** Recommended chip dimensions and shape.

and S2-layers). These failures open additional penetration paths for chemical liquids during pulping, and this results in increased cell wall swelling, substantial hydrolysis (especially of the crystalline cellulose regions) and finally leads to reduced fiber strength. Earlywood is more susceptible to such damages than thick-walled latewood. Especially in sulfite pulping, these strength properties are unfavorably affected by such damages; according to Patt [5], the observed strength losses are up to 10–20%, and are accompanied by yield losses. These effects are less pronounced in kraft pulping.

In order to optimize results, the chipping process must be carefully controlled, any blunted chipper knives must be exchanged regularly, and all of the machinery must be kept in good repair.

Disc chippers are used most frequently in pulp mills for chipping whole logs. In modern softwood sawmills equipped with chipper canter or profiling lines side cuts, slabs and edgings are directly converted into chips by twin-disc chippers and edge cutter heads. Other sawmill residues may be converted into chips by horizontally fed drum chippers; occasionally, these chippers are also used for chipping whole logs, either end-feed or side-feed.

### 3.3.1

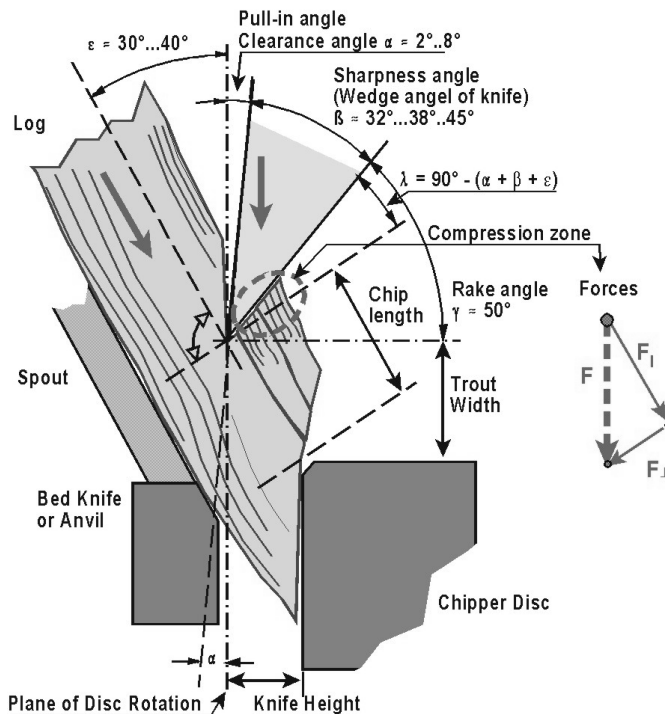
#### **Disc Chipper**

The cutting direction in conventional disc chippers is between 90–90 and 90–0 plane (corresponding to a plane which is slightly tilted to the transverse section). Several straight knives are mounted on a heavy, rigid disc in more or less radial arrangement, and the disc revolves in either a vertical or in a slanted plane. The generated chips pass through slots in the disc and may be discharged from the top, bottom or sides of the disc housing. The supply of logs or sawmill residues is

maintained via an infeed spout at an angle between the face of the disc and the spout axis which is usually 30–40°.

When the knife edge cuts the wood, the fibers are more or less compressed in a longitudinal direction; depending on the cutting geometry, either splitting and cleavage or shearing occurs. Figure 3.10 shows the cutting action of a knife in a disc chipper in detail:

- $\alpha \approx 1\text{--}7^\circ$  Clearance angle or pull-in angle; decreasing  $\alpha$  reduces the pull-in rate of logs.
- $\beta = 30\text{--}40^\circ$  Sharpness angle or wedge angle of knife; with increasing  $\beta$ , splitting of the chips turns into shearing. The knife life decreases with decreasing sharpness angle.
- $\gamma$  Rake angle
- $\varepsilon \approx 30\text{--}40^\circ$  Feed-in angle; the chip length is increased as  $\varepsilon$  is decreased
- $\lambda = 90^\circ - (\alpha + \beta + \varepsilon)$  Complementary angle, responsible for either split or sheared chips; specific power consumption decreases with decreasing  $\lambda$ .



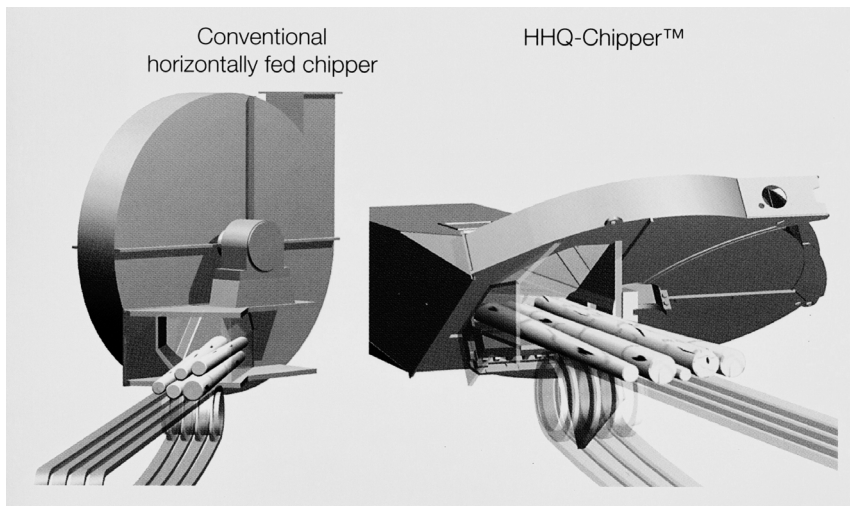
**Fig 3.10** The cutting action of a wedge-shaped knife in a disc chipper: cross-section through the disc and knife (wedge angle  $\beta = 32^\circ$  leads to splitting or cleavage;  $\beta = 45^\circ$  leads predominantly to chip shearing).

The thickness of chips depends to a great extent on the force  $F$  caused by the wedge-shaped knife. The force which is effected parallel to the grain,  $F_{\parallel}$ , increases with increasing depth of the cutting edge; only a small part  $F_{\perp}$  of the penetrating force acts perpendicularly to the grain. Chip thickness decreases with increasing  $F_{\parallel}$ . Wood strength perpendicular to the grain, moisture content, temperature, cutting speed and cutting direction each determine chip width. Chip width does not have a large effect on the pulping process in the digester. Chip length is adjusted by the cutting edge position of the knife above the disc surface (knife height) as well as the feed-in angle. Initially, the chips produced first resemble the parts of pre-broken wooden discs, still adhering to each other to some extent. The final chip width and breakage respectively are achieved by additional fingers mounted peripherally on the chipper disc.

The wood moisture content (mc) is of major importance for chip quality; at high mc, the chips are more fragile (especially perpendicular to grain) and become thinner. At low mc, the wood tends to split and the amount of fines and pins increases. Frozen wood behaves similarly to very dry wood. Fungi-attacked wood has considerably reduced strength properties, and this results in fractures rather than in clear cuts; hence, the fines content increases.

Sawmill residues (e.g., slabs, timber trims and edgings) are of low value for chip production. Pre-damage and wide dimensional variations lead to a broad range of chip size distribution. In addition, feeding these raw materials into the chipper requires particular aligning measures.

According to disc alignment and feeding system, two types of disc chippers must be distinguished: (a) primarily gravity-fed chippers with a vertical spout angle and vertically rotating disc; and (b) horizontally fed chippers, with wood



**Fig 3.11** Single log layer chipping by a horizontal chain or belt conveyor ensures a controlled feeding rate and optimum log orientation [7].

delivery by a powered conveyor and disc rotation in a plane tilted towards the feeding direction (Fig. 3.11) ([9], p. 2197).

Orientation of the infeed spout in relation to the disc surface ensures a particular feed-in angle, which primarily determines chip length. Monitored log infeed via a horizontal band conveyor guarantees high chip quality due to controlled infeed rate and correct log alignment. A stable position of the logs during chipping contributes to uniform chip size distribution and a high level of accepts. The gentle side discharge minimizes the production of pins and fines.

The modular design of modern disc chippers (e.g., the Andritz HQ™ and HHQ™) (Figs. 3.12 and 3.13) offers optimal adaptation to individual production requirements of the pulping process [16,17]:

- Chipping geometry
  - Fast chip length adjustment
- Different disc speed–chipper knife combinations for various process requirements
  - Knife system
  - Particular HQ-Plus™ knife system with service agreement (regrindable knives, clamping system, spare parts and continuous service)
  - Face-mounted knives (QuickClamp™ system)
  - Insert knives

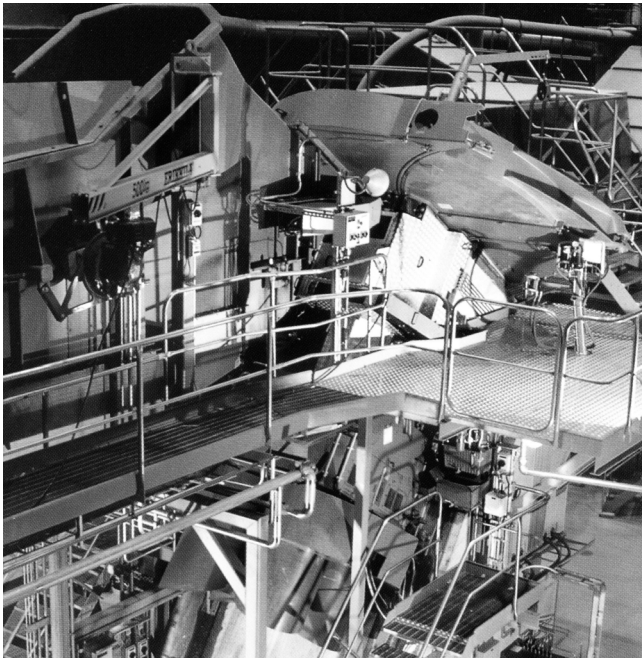
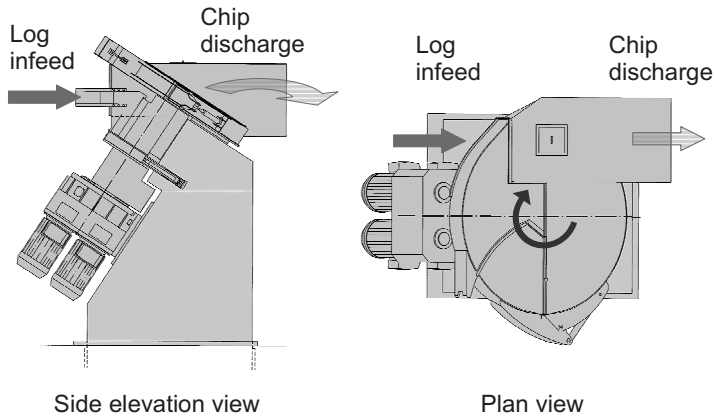


Fig 3.12 The Andritz HHQ™ chipper in a log yard setting [17].





**Fig 3.13** Schematic diagram (side and elevation views) of the Andritz HHQ™ chipper [17].

- Drive alternatives
  - Four motors with one gear reducer
  - One synchronous motor
  - One or two squirrel cage motors with gear reducer

Depending on size, the capacity of modern disc chippers varies between 50 and 350 m<sup>3</sup> per hour. The disc diameter is 1200 mm to 4500 mm (in most cases 2000–3500 mm), disc thickness is 100–250 mm, and its weight is up to 30 tons and more (high moment of inertia!). Between four and 16 knives are bolted to the disc, which rotates between 220 and 900 rpm. The rated driving power ranges from 400 kW to more than 2 MW; the disc is either belt-driven or directly driven via an inserted gear reducer.

Andritz AG has developed a so-called TwinChipper™, which corresponds to a vertical disc chipper with horizontal infeed for long logs and an additional, second infeed, designed as drop feed spout. To avoid interruptions of the chipping process by jammed short, broken logs fed into the chipper horizontally together with long logs and to ensure constant high chip qualities, the log fragments are separated from the main feed by a breakage dropout. These parts are collected by a particular conveyor and fed into the chipper via an additional breakage spout just above the main horizontal spout. The large disc diameter allows a sufficient large spout opening which is also capable of swallowing crooked wood pieces. In order to reduce pins and fines fraction to minimum, the cutting speed is decreased and chips are discharged laterally [17].

### 3.3.2

#### Drum Chipper

Drum chippers operate in a different mode to that of disc chippers. They are most suitable for processing waste wood and wood residues, and therefore they are

more common in sawmills and wood-based panel industry than in pulp mills. With this machinery, logs or wood residues are either fed by gravity or horizontally by mechanical infeed rollers. Two to four straight knives are mounted on the periphery of a rotating drum and aligned either parallel or slightly slanted to the drum axis. The wood is cut between the knife edge and an anvil which is fixed at the bottom end of the infeed spout. The cut chips are caught in pockets, while larger pieces are further broken down by specially designed bridges. Additional breakage of oversized chips occurs when the chips pass the rigid screen which partially surrounds the drum. Chips are fed out either by bottom discharge or by momentum discharge from the rear of the chipper. The drum chipper often has a wider infeed opening, and this eliminates most hang-ups in the chipper spout.

During the cutting action the knife follows an arched path through the wood; when chipping larger logs, the initial knife penetration begins at an angle of about  $40^\circ$  perpendicular to the supplied material. The cutting geometry and conditions respectively vary steadily according to the cutting circle. This leads to a wider spread of chip dimensions, with even compressed cut ends of the chips and an increasing fines content. Chip shape varies from cuboid to a more or less slim prism. Those chips that are too large to pass the screen immediately are carried around to the chipping area to be chipped a second time to their final size. Essentially, the feed speed, rotation speed and number of knives determine average chip dimensions.

Drum chippers (Fig. 3.14) are available in many different sizes, with production capacities ranging from  $20 \text{ m}^3$  to  $300 \text{ m}^3$  round wood per hour (5 to 150 metric tons dry substance per hour). The rotor diameters range from approximately 600 mm to 2800 mm, and the spout dimensions (width  $\times$  height) extend from  $400 \times 250 \text{ mm}^2$  to about  $1600 \times 1000 \text{ mm}^2$ .



Fig 3.14 Drum chipper [18].

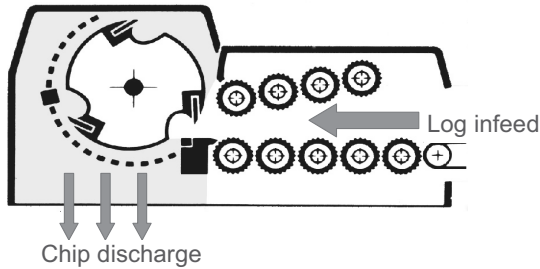


Fig 3.15 Drum chipper PHT: side elevation [19].

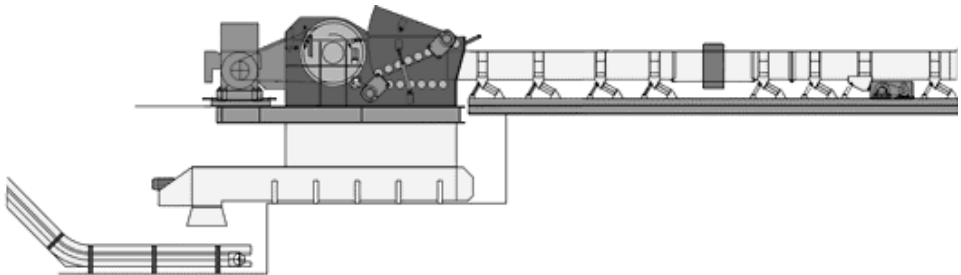


Fig 3.16 Layout of drum chipper including feeding conveyor (belt or vibration conveyor) and gravity discharge onto a belt conveyor [19].

The drum is belt driven by an electric motor (150 kW to >1500 kW) which ensures rotation speeds between approximately 400 rpm and 900 rpm. Additional features, including a swing-away safety anvil, large anvil access doors on both sides of the casing (for anvil replacement and knife-to-anvil adjustment), entire hydraulic top casing opening for full knife access, fast knife clamping and adjusting device, replaceable and adjustable screen, etc., reduce downtime and improve maintenance (Figs. 3.15 and 3.16) [19].

### 3.3.3

#### The Andritz HQ™-Sizer and Rechipper

The origin of “overs” during log chipping is caused by log ends, breakage and log faults (e.g., knots). In order to convert oversized and thicker chips after screening into “accepts”, special rechippers have been developed, the demands of which are:

- To convert as much as possible of the overs into accepts.
- To generate as little as possible fines and dust.
- To cause minimal mechanical damages to the fibers.
- To have low operational and maintenance costs.

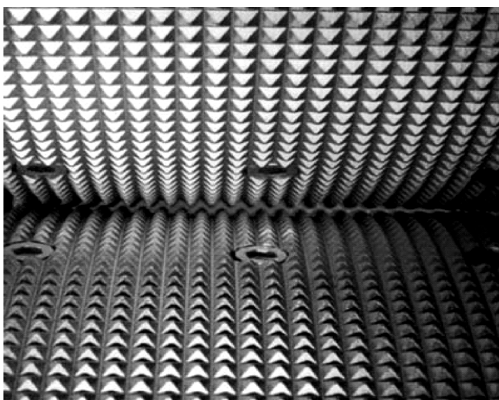
The Andritz HQ™-Sizer is a conventional disc chipper with horizontally rotating disk driven by a vertical shaft. Oversized chips are gravity-fed from above into the

chipper via a V-shaped chute and a centrally arranged vertical infeed spout. The supplied chips lay flat on top of the rotating disc, and the cut occurs according to their thickness. The multiple anvil arrangement and specially designed knives allow a 4- to 8-mm gap adjustment (between knife and bed knife) corresponding to the required final chip thickness. The sealed anvil to knife design forces the carefully aligned accepts to pass the cutting knife without any fiber damage, while overs cannot pass the thickness adjustment. Chip discharge occurs tangentially to the disc. The Andritz rechipper is used to upgrade the oversize chip fraction, mainly knots and splinters, into accepts. Compared to drum chipper-based rechipper or shredders, this machine offers significant advantages, mainly with regard to fines generation and low fiber damage [12].

#### 3.3.4

#### Chip Conditioner

Chip conditioners are used to fissure overthick chips to insure proper pulping liquor penetration for better digestion and higher yield. The conditioner consists of two parallel rollers, which move in opposite directions, and have specially designed textured stainless steel segments mounted on their surfaces. The chips are fed between the rollers and fissured as they pass through the interlaced pattern of the segments, depending on the adjusted gap between the rollers (Fig. 3.17). One roller is stationary, while the other is dynamic, being held in place by two independent hydraulic cylinders. This maintains the required pressure for desired chip fissuring and protects the unit by retracting when over-pressure is sensed in the hydraulic system. Oversized contaminants can pass the gap with minimum damage to the replaceable segments. The rollers are driven by a self-contained hydraulic power unit. Efficient operation requires an even distribution of the infeed material over the entire roller length; this is achieved by a specially designed distribution chute, equipped with adjustable and removable deflector plates [20].



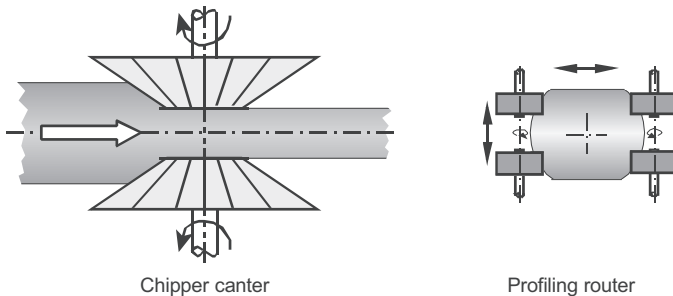
**Fig 3.17** The textured stainless steel segments of a Dyna Yield chip conditioner [20].

## 3.3.5

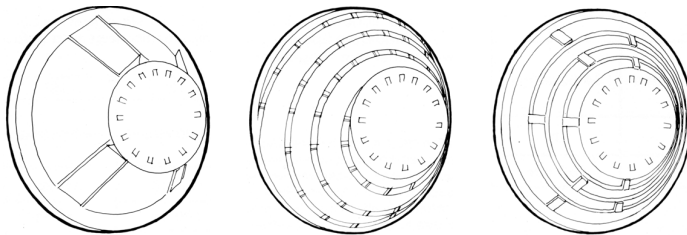
**Chipper Canter Line: Profiling Line in Softwood Sawmills**

Chipper canter lines and so-called profiling lines are notably installed in large softwood sawmills. Slabs and timber trims of wane-edge boards are directly converted into chips when the logs pass the chipper canter and profiling router, with feeding speeds of up to  $130 \text{ m min}^{-1}$ . Two pairs of two parallel chipper canter discs remove the slabs, while two groups of four or eight symmetrically arranged profiling routers convert the wane of sidings directly into chips already before cutting the sidings off from the remaining two-sided or four-sided cant. The final sawmill products are straight-edge boards, resawn cants, and wood residues as sawdust and chips. According to the steadily changing cutting conditions, chipper canter knives generate chips of various shape and size. Knife orientation and arrangement on the surface of the chipper disc (which is shaped like a truncated cone), the number of knives, rotation speed and feeding speed determine chip dimensions (Figs. 3.18 and 3.19). Considerable efforts have been made to improve chip quality and to achieve uniform chip dimensions; however, screening is absolutely necessary to obtain chips suitable for pulping.

For further details on the chipping process and additional chipper types, the reader is referred to Koch [9].



**Fig 3.18** Tool arrangement in chipper canter (plan view, left) and profiling router (front view, right) in softwood sawmills.



**Fig 3.19** Chipper canter disc types. Knife arrangement: left to right: chopper disc (four long straight knives) to produce cross-cut, large chips; spiral disc (up to 114 small knives) to produce cuts in a tangential plane; stepped disc (up to 30 knives) to produce cross-cut, small chips [13].

### 3.4 Chip screening

In order to obtain desired pulp properties, to maximize yield, to minimize chemical and liquor consumption – and thus to ensure a most economical production – almost uniform chips are required as raw material to supply the digester. However, due to log dimensions, wood imperfections and process-related variations, the generated chips will vary in size and shape; hence, chip classification by size and dimension is essentially. Accepts must be separated from rejects, oversized rejects must be re-chipped to increase the yield of the available raw material, and fines and dust must be excluded from subsequent processes. For example, chips purchased from sawmills must meet delivery specifications agreed in advance. In addition to chip dimensions, these cover wood species, moisture content, maximum storage duration, contaminations, maximum bark content, quality control procedures and random sampling, analysis methods, volume or weight determination on delivery, change of ownership, payment, etc. Comprehensive guidelines are available, for instance, from Papierholz Austria Ges. m.b.H.: Übernahmerichtlinien, Revision 5a. (o.J.) [38]; the LWF-Report 21 (2000) [39] also contains useful hints to determine quality criteria for chips.

The equipment for screening chips must comply with the following requirements:

- Reliability and high fractioning capacity.
- Effective separation of chips into up to five different fractions.
- Maximum screening yield, selective fines separation and pinch recovery.
- Low downtime for continuous supply of subsequent processes.
- Low maintenance and repair.
- Self-cleaning features.

Basically, two different screening methods can be distinguished:

- Mechanical screening
  - Vibrating screening machines
  - Gyrotory screening machines
  - Vibrating tumbler screening machines
  - Disc or roller screening machines
  - Diamond roll screening machines
- Wind screening (air screening)
  - JetScreen™ [12]
  - Air density separator [40]

#### 3.4.1

#### Mechanical Screening

Vibrating, rotating and gyrotory chip screens are of a round, six-or eight-sided or rectangular shape, either suspended by cables fixed to an outer frame or supported from below by stiff legs mounted on pivots. The casing of rectangular gyrotory

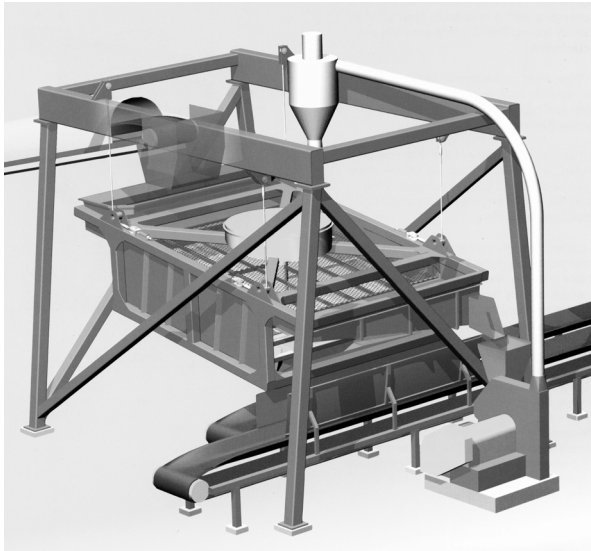


Fig 3.20 CS Chip screen [21].

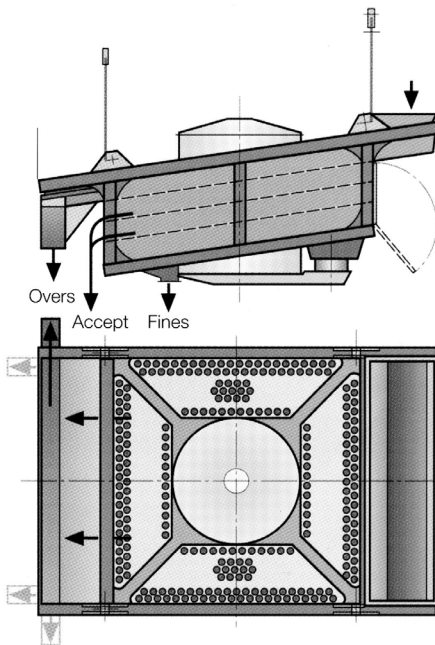
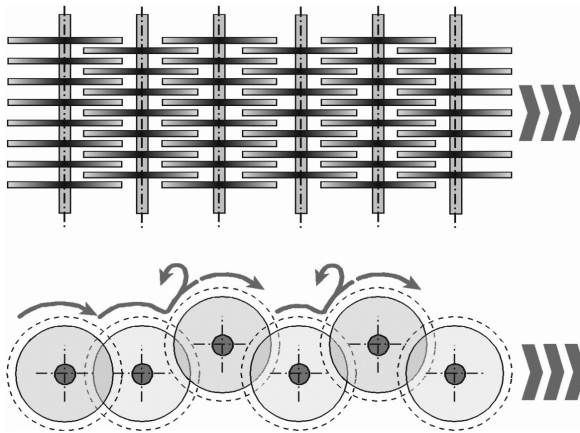


Fig 3.21 CS Chip screen: side elevation and plan view [21].

screens is slightly tilted, while the others swing in a horizontal plane. A swinging circular motion is achieved by electrically driven rotating counterweights spreading infeed chips from the top of the machine evenly over the screen plates. Fractioning is achieved by a multi-layered arrangement of screen plates, containing round holes or slits (decreasing diameter or width from top to bottom, e.g., 45 mm, 8 mm, 7 mm, 3 mm). Oversized chips and slivers slide over the top deck to the rejects chute. Passed chips collected on the following deck(s) as accepted fraction are discharged via the accept chute. Fines pass through all decks and are collected at the bottom of the screen and discharged via an appropriate opening (Figs. 3.20 and 3.21).

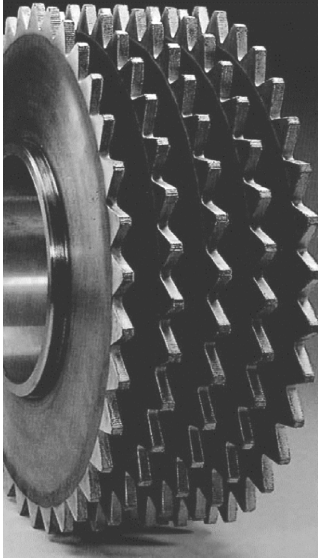
Depending on the desired fractioning capacity, these screens are provided with up to six decks; standard screens contain three to four decks. The capacity of chip screens ranges between approximately 150 to 650 to 1000 m<sup>3</sup> h<sup>-1</sup>. The chip load per deck can be reduced by additional screen plates. Standard decks are made of mild steel; for abrasive conditions (e.g., chips contaminated with sand), more resistant stainless steel decks are also available. The top of the screen is either more or less open or is totally covered by a dust protection with an infeed opening.

Another mechanical chip separation method is based on a particular arrangement of rotating dentated discs. Fixed on up to 30 parallel aligned shafts, these discs (thickness 6 mm) mesh with each other, forming a particular disc arrangement through which the traveling chips must pass. The synchronously driven shafts are either aligned on one level, (e.g., with the Winbergs™ Thickness, Scalping or Fines Screen; [12]), or alternately elevated resulting in an undulating path to break the infeed chip mat (e.g., the RaisedRollDisc Thickness Screen; [40]) (Figs. 3.22 and 3.23).



**Fig 3.22** Raised Roll Disc Thickness Screen: plan view (top) and side elevation view (bottom) [40].



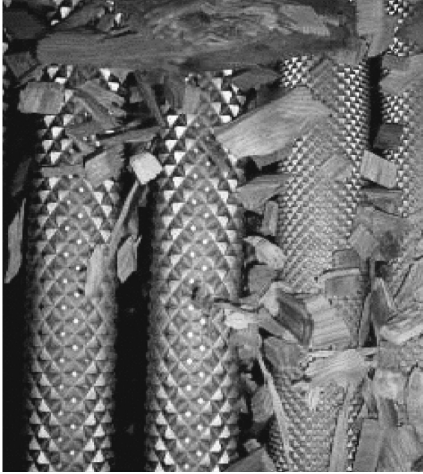


**Fig 3.23** Dentated discs in a RaisedRollDisc Thickness Screen [40].

Depending on the interfacial opening of the accurately placed discs – that is, the gap between adjoining discs (1–3 mm up to 10 to 80 mm) – the chips are selectively separated into fractions while traveling in the rotating direction of the shafts. This very gentle and efficient method maximizes chip yield, chip quality and uniformity. Screen widths are between 600 mm and 3500 mm, and screen lengths reach up to approximately 10 m. The screening capacity is up to about  $2000 \text{ m}^3 \text{ h}^{-1}$ .

A similar recent development of thickness screening is based on parallel aligned solid rolls with textured knurl pattern surfaces, so-called “diamond rolls”. These rolls rotate and agitate the chips as they are fed from the infeed of the screen, allowing the smaller chips to pass between the rolls. Gradually the larger chips accumulate above the rolls and are finally outfed at the end of the screen. The pre-adjusted space between adjoining rolls – variable inter-roll openings – and the size of the diamond roll pattern changes over the length of the screen (Fig. 3.24). Fines and acceptable chips pass these gaps at different traveling distances and are discharged from below the roll carpet by a conveyor system. The thickness screen section can be extended by an additional scalping screen section.

With a scalping screen, the surface of the rolls is cut with a deeper knurl pattern, and the gaps are set to 20–30 mm. Knots, large strings and cards still present in the oversize chip flow are rejected in this section to protect the following over-thick chip processing equipment. Diamond roll thickness screens are available in different sizes with up to 100 diamond rolls in series; the width is up to 4 m, and length up to 8 m [40].

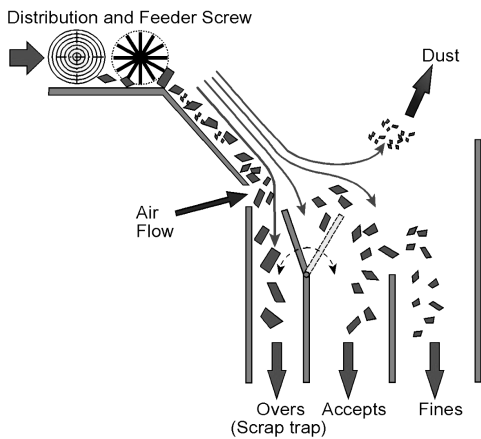


**Fig 3.24** Textured surface of Diamond Roll Thickness Screen [40].

### 3.4.2

#### Wind Screening

Wind screening is based on the impact effect of an air stream on falling particles (Fig. 3.25). Depending on chip size (shape) and weight (density), the air impact causes variable trajectories. Fed-in chips are evenly distributed on a sloped slide plane over the entire width of the screen. When sliding down, the chips pass a longitudinal air nozzle and are scattered by the air stream. Depending on the trap arrangement, the overall chip flow is separated into different fractions.



**Fig 3.25** The principle of wind screening (side elevation view).

The heavier particles are caught in a scrap trap. Guided by an adjustable gate, the oversize reject fraction is forwarded to the reject screw. Separation of fines – the particles with the furthest trajectory – is adjusted by setting the air flow. Accepts are carried across the overs gate to the accept screw and the accepts conveyor respectively for further processing. The oversize screw is equipped with a by-pass gate to the accepts conveyor. Dust particles are suctioned from the upper part of the screen into a cyclone and removed via an airlock feeder to the fines conveyor. The air stream partially circulates from the cyclone by means of a suction fan; a small amount is replaced by fresh air from the environment (see Jet-Screen™; [12]).

### 3.4.3

#### Air Density Separator (ADS)

The air density separator (ADS) (Fig. 3.26) is used to remove metal, stones and knots from the oversized chip fraction. The ADS infeed airlock distributes the overthick chips into a precisely controlled vertical air stream. Separation is achieved by the different floating velocities of contaminants versus chips; the cleaned chip fraction is separated in a specially designed cyclone, while the rejects drop out of the air stream. Material as small as 3 mm in diameter is efficiently removed. Large nuts and bolts, and broken stones as small as a match head, will fall out consistently. The system includes a centrifugal fan, silencers and a control system, which self-adjusts the air volume for various feed rates [20,40].

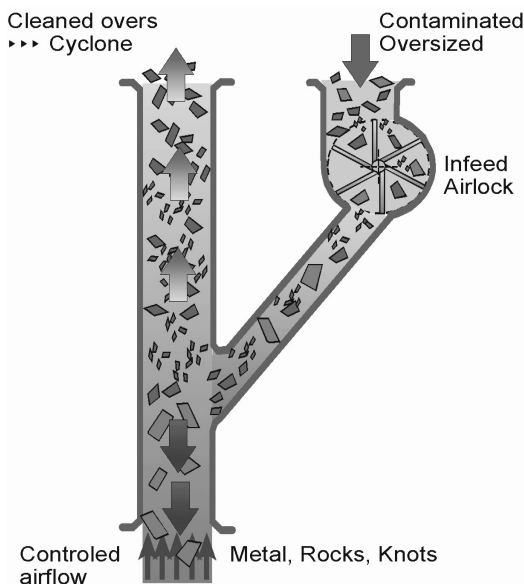


Fig 3.26 Air density separator ADS [40].

### 3.5

#### Process Control and Automation

In order to achieve target production capacity and desired chip quality (cleanliness, chip size, etc.) suppliers such as Metso Paper Oy and Andritz AG have developed advanced control and automation systems for overall wood yard operations.

The GentleMatic™ system from Metso Paper Oy [10] optimizes both debarking and chipping process; the extension by the VisiBark™ measurement system promises reduced wood losses and improved chip cleanliness. The similar DrumMatic™ system by Andritz AG (Fig. 3.27) [22] controls the debarking process to achieve both highest possible production and optimum economy.

Compared to earlier control systems, the advantages of the latest generation of process control system are summarized by the manufacturers as follows:

- Reduced wood losses by 0.5–3% (optimized filling degree and retention time in the drum debarker).
- Increased production (shorter retention time in the drum debarker, higher capacity).
- Better chip quality (uniform discharge rate, improved operation of stone and short end trap).
- Minimized down-time (uniform discharge rate, correct adjustment to irregularities).
- Minimized energy consumption (reduced de-icing and debarking energy consumption).

The DrumMatic™ system operates in a supervisory mode on a control level above the controlling systems of the individual processing units. Distinguishing features comprise an optimization program including hardware and software, a data logging program and field devices. The status of the parameters and the total process is based on the transmitted data. Based on the Fuzzy Control technology, this information is compared to calculated and stored optimum data, and the process is guided to the desired direction. The operator mainly determines target capacity and log cleanliness [22].

### 3.6

#### Transport and Handling Systems

Wood yard operations require transportation and handling systems for unloading delivered raw materials, as logs, sawmill residues and chips, for intermediate storage of these materials and for feeding (i.e., infeed and outfeed of the machinery concerned). Transportation systems must meet particular demands related to the size, volume and weight of the material being handled. Additional demands concern careful handling of the material, optimal use of available storage area, versatile applicability, high mobility, high availability and performance, but also in some specific cases alignment of the conveyed material and separation tasks. Economical demands are related, for example, to low operation costs, low energy consumption and low maintenance and repair.

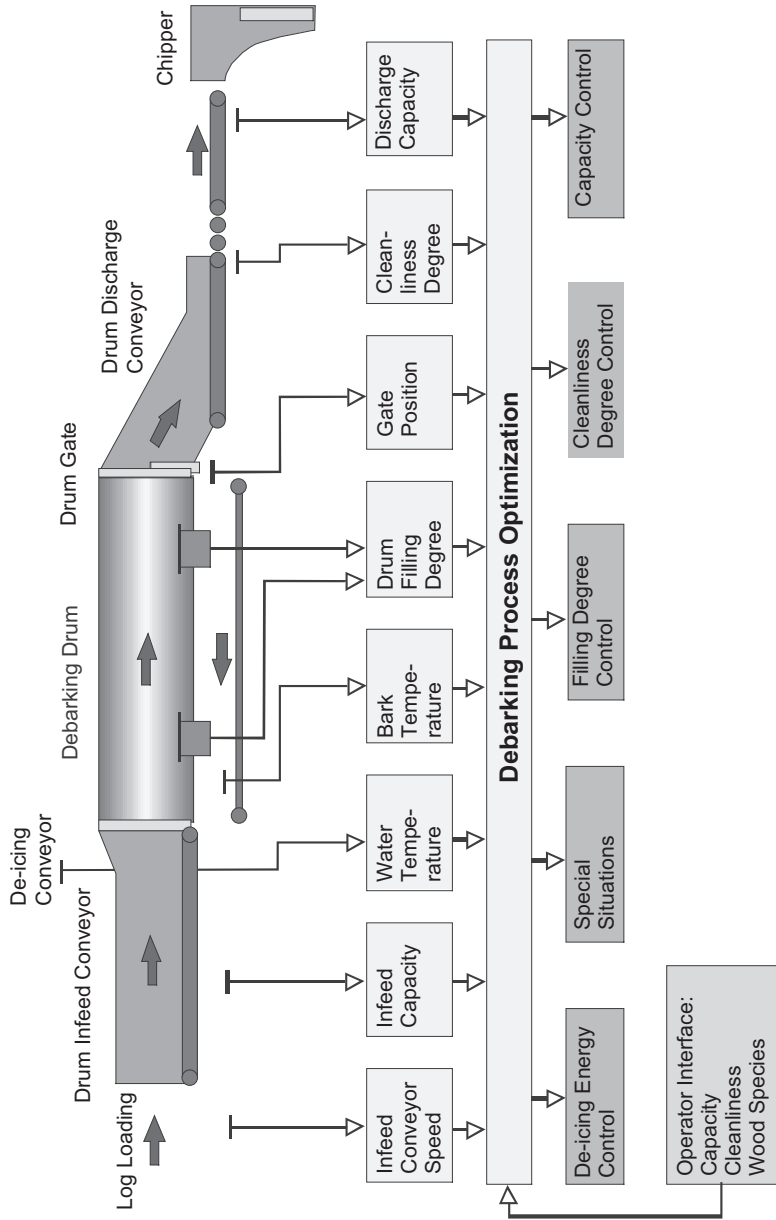


Fig 3.27 Flow chart of the DrumMatic™ process control system for pulp mills [22].

### 3.6.1

#### **Log Handling**

At log yards, the unloading of delivered logs is carried out either by rail-based crane systems (e.g., a portal crane) or by wheel-based vehicles such as wheel loaders or wheeled excavators.

Electrically powered portal cranes require less space and are environmentally friendly compared to wheel-based systems. Ground compression and soil contamination by fuel, oil and wood fibers are very low. Less wood yard preparation is required, and the network of stabilized roads by gravel, asphalt or concrete can be reduced considerably. Versatility is achieved by grasping tools (wood tongs) adaptable to individual handling tasks. More advantages accrue from the considerable stacking heights between 15 and 25 m, the selective access to stored logs, and lifting the load over the storage pile. Only one operator can manage the discharge activities as well as feeding the wood yard machinery. If the crane is the only available handling system, it might be the bottleneck of the wood yard operations. An inability to handle bulk materials such as bark, chips or other particles is another disadvantage of porter crane systems.

The versatile availability of wheel loaders or wheeled excavators is based on their flexibility and frequency of working cycles, even if the handled load per cycle is less compared to crane systems. Per vehicle, one operator is required as well as a sufficiently paved road network. Different grasping tools, tongs and buckets are available, and can be employed according to the material to be handled. Some disadvantages arise from environmental impacts, caused by fuel, oil, emissions and soil compression, respectively.

The decision to use either of these principally different systems, or for combined handling systems, depends on a careful analysis of the individual site conditions at the mill.

### 3.6.2

#### **Stationary Conveyor Systems**

Stationary, fixed conveyor systems handle the material before and after processing. Depending on the size, volume and weight of the materials being handled, various conveyor systems are in use, partially completed by special equipment (e.g., washing station, de-icing station, metal detector). The most common mechanical conveyor systems utilized are listed in Table 3.1 (Pneumatic systems are not included in this table as they are rarely used in wood yard operations due to their limited capacity; other disadvantages include damage to conveyed particles while passing a fan, high energy demand, dust emission rate, and drying effects on the material being transported.)

Transport capacity, reliability (under different environmental conditions), uptime, maintenance and repair, required space, energy consumption, break-up of material jams, investment costs, etc. are additional decisive characteristics of conveyor systems.

**Tab. 3.1** Stationary conveyor systems and materials to be handled.

System	Conveyed materials	Remarks
Chain conveyor	Long and short logs, sawmill residues	Heavy-duty conveyor systems, used as receiving decks, e.g., for drum debarkers; optionally equipped with swinging plates on dampers for infeed zones
Roller conveyor	(slabs, timber trims)	
Steel plate conveyor		Chipper infeed, additionally preceding roller conveyor (stone trap, bark separation, short end trap), metal detector and washing station
Vibrating conveyor	Logs, slabs, bulk materials	Swinging metal trough, system capable of orientating slender parts in grain direction, to separate and screen particles according to size
Belt conveyor	Bulk materials (particles, chips, bark, sawdust)	Rubber belt, sliding in a plate trough or on idler rollers
Bucket elevator		Buckets mounted on cord-reinforced rubber belt running in a vertical steel housing, less space required, high capacity
Scraper conveyor		Metal plates fixed between two parallel conveyor chains moving in a housing, either acting from above or from below the trough bottom, optional discharge openings along conveyor path
Screw conveyor		Rotating steel screw running in a round or U-shaped trough, dust-proofed conveyor, little space required

Depending upon the storage mode of particles, mostly chips (but also bark) specialised reclaiming systems have been developed, and these are described below.

### 3.6.3

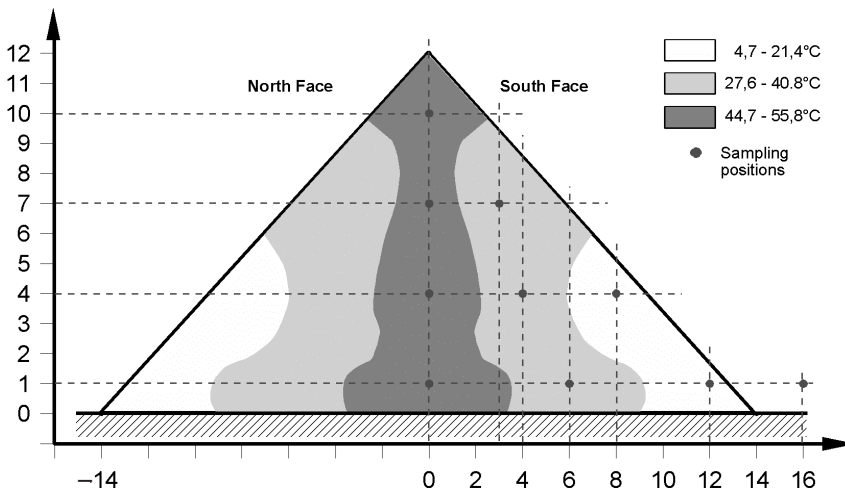
#### Chip Storage

Chip storage at the end of all log yard operations is required to ensure a continuous supply of the subsequent pulping process, and to compensate for seasonal fluctuations in raw material supply. Compared to logs, chip handling and storage is more advantageous; in relation to the required equipment, storage area and quality losses, it offers more economical benefits. However, chip storage requires well-suited storage conditions to avoid chip deterioration and resultant substance losses, reduced fiber yield and discolorations [23,24]. Sap stain and decay fungi are responsible for chip deterioration. Several investigations on factors affecting chip quality – most of which relate to the development of internal micro-climate

and micro-organism growth in the chip pile and the interaction between both – have emphasized the need for an adequate chip pile inventory [23,25–27].

According to Hulme and Hatton [28,29], the respiration of wood cells, chemical oxidation and micro-organism activity cause changes in the chip pile. With respiration of still-living parenchymal cells in fresh-cut, “green” chips, the temperature within the chip pile increases rapidly, as does the carbon dioxide concentration [30–32] during the beginning of storage. In the investigations of fresh built-up softwood chip piles by Wolfhaardt and Rabie [27], a maximum temperature of 55 °C was achieved within the initial two weeks, followed by a clearly pronounced temperature drop during the following week. Temperature zones and measurement points in the pile are presented in Fig. 3.28; significant daily temperature differences were also detected. The temperature gradient between internal and ambient temperature drives aeration of the chip pile. The temperature in the center part of the pile did not show significant fluctuations, and thus was independent of ambient temperature fluctuations.

Increasing temperature in the inner part of the pile initiates a convective air movement; fresh air is drawn into the pile through its flanges, humidified by passing fresh chips, and finally leaves the pile at the top. The air flow through the pile also causes heat redistribution by evaporation and condensation processes. At about 40 °C, autoxidation (an initially temperature-driven reaction of chemical wood components with oxygen; further reaction is catalyzed by the product of the initial reaction) and hydrolysis of carbohydrates occurs; these chemical reactions become more important with rising temperature. When heat losses to the environment are equal to heat generation by microbial activities, a stable temperature



**Fig 3.28** Softwood chip pile dimensions (*Pinus patula* (40%), *P. elliottii* (40%) and *P. taeda* (20%), approximately 3000 tons of chips, oven dry), monitoring positions within

the pile and extent of temperature zones developed in the pile after three weeks of outside storage. Dots represent sampling positions. (Based on Fig. 2 of [27].)



level is achieved finally. After only one week, the CO<sub>2</sub> level was maximal (12.7%) at the bottom center of the pile, but decreased during the following weeks. Significant differences in CO<sub>2</sub> levels were identified between day and night.

During storage, a redistribution of chip moisture content occurs; a significant reduction in mc (up to 28% on dry-mass basis) has been detected in the center bottom region of the pile. Subsequently, a mc-migration into the top region of the pile occurs parallel to the air flow. Similar findings have been reported previously by Hulme and Hatton [28], who developed a so-called “chimney-model” for large chip piles.

Investigations on the storage of maple chips (*Acer saccharum*) have been reported by Hulme [29]. The central area of a chip pile was simulated in two silos, filled either with fresh chips or chips previously dipped into a borax solution. During the first 100 days of storage, weight loss, temperature, fungal growth and screened yield of kraft pulp were observed. In the untreated chip pile, higher temperatures developed, pulp losses were stated to be negligible during 100 days’ storage, and no protective treatment was required.

The behavior of the silo-stored hardwood chips (*Acer saccharum*) treated with sodium carbonate, kraft pulp yields and pulping characteristics were simulated for 100 days’ storage in an insulated 8.1 m<sup>3</sup> cylinder [28]. For the first 50 days, the temperature equilibrated close to 60 °C but then slowly fell to 40 °C by 100 days. The sodium carbonate-treated chips generated more heat due to microbial oxidation of the NaAc formed from sodium carbonate by deacetylation of the wood. The temperature was 55 °C at 100 days. Chip losses for both treated and untreated chips were 3.6% of their oven dry weight during storage, but yields of kraft pulp were 5.6–6.2 % more than those from fresh chips. The treated chips required only half of the cooking time (at maximum temperature) needed by untreated chips, and alkali consumption was reduced by over 10%. The pulp strength appeared unaffected by the treatment.

Feist et al. [32] determined the loss of wood substance in outside chip storage, using both a tower to simulate a chip pile and an experimental chip pile. The change in green volume after 6 months’ storage was negligible up to a weight loss of 6.5%. No differences were found between determinations of loss in weight and loss in specific gravity.

Brightness losses are an additional concomitant problem of chip storage. The reasons are manifold, but include the oxidation of lignin and extractives, diffusion of phenolic substances from bark into wood fibers, increased lignin content and changed lignin structures due to the breakdown of carbohydrates by fungal attack, stained mycelium and bacterial metabolic products. According to Patt [5], brightness losses range from 10 to 18 points during 3 to 10 months’ chip storage. The condensation of lignin and changed lignin structures respectively require increasing use of pulping chemicals. More severe pulping conditions also result in higher carbohydrate breakdown and finally yield losses. Furthermore, losses of resin and fatty acids occur due to oxidation reactions during storage.

Average wood substance losses during chip storage are at least 1% per month. These losses are significantly higher with hardwood chips than with softwood

chips; chips made from sapwood are also more prone to microbiological decay than those from heartwood.

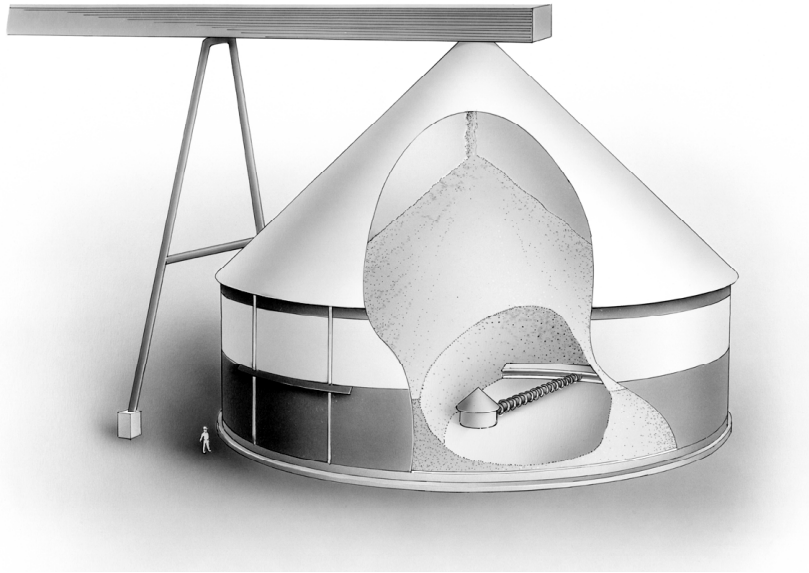
Chips should be stored on a well-prepared and drained wood yard area. To minimize storage losses, the most preferential conditions for fungal growth between 25 °C and 50 °C must be avoided. This requires small piles to be prepared during the cold winter period, and larger piles during summer time. However, the subsequent production process must also be considered with chip storage; the breakdown of resins is preferred for sulfite pulp production, whereas a high yield of resin increases the economy of sulfate pulping. To summarize, storage duration should not exceed 2–3 months, and chip accumulation to piles must match a pre-determined management schedule. Fresh-cut chips should never be accumulated on top of existing piles as rapid fungal infection will occur. Likewise, the content of fines influences the microclimate within the pile and thus wood decay by enhanced fungal growth. Thus, chip screening before storage is recommended. Preventive measures against microbial deterioration include complete pile coverage or the injection of nitrogen to reduce the aerobic activities of micro-organisms. Water storage, chemical or radiation treatment may also protect the chips from deterioration, but these procedures are less economical in application and conflict to a great extent with strict regulations for environmental protection [5].

#### 3.6.3.1 Chip Storage Systems

Guidelines to improve chip storage and inventory, related to volume, location and methods of chip storage, are provided by Maron [33]. These factors influence production costs, and must be considered in the design of a suitable storage system.

The storage of chips, either generated on the spot, or received from other mills (e.g., sawmills) is carried out in open piles or closed silos; open storing of air-worthy particles is not recommended or even inadmissible in some countries. The purchase of chips requires suitable receiving stations for trucks or railroad wagons. The chips are poured into large hoppers, equipped with sliding gates and grizzly, a particular screen and scraper system, and discharged by a screw feeder or linear stoker. Optionally, a disc screen could be interposed between hopper and silo [34].

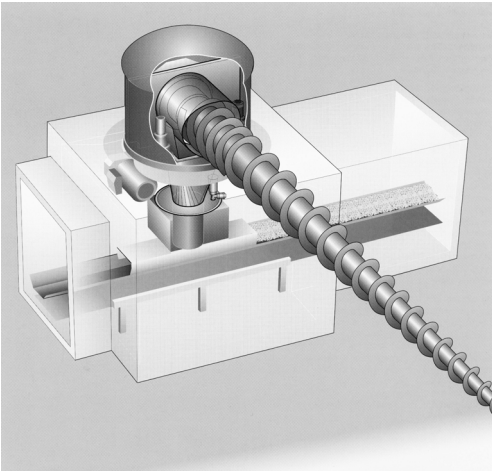
In order to overcome previously mentioned disadvantages of open-air chip storage, silo storage systems become more significant. Common chip storage bins (Fig. 3.29) or silos are either round (diameter up to more than 40 m, capacity up to 30 000 m<sup>3</sup>) or rectangular enclosing volumes up to 50 000 m<sup>3</sup>. Closed systems are either steel or concrete constructions, and may be insulated on demand. No snow problems, less or even no dust emission and environmental friendliness are important features of closed storage systems. Open-air chip storage can be done between side walls, mostly made of concrete, for pile control. The discharge system should follow the first-in/first-out mode, based on rugged and proven screw reclaimers, and ensure reliable and even outfeed.



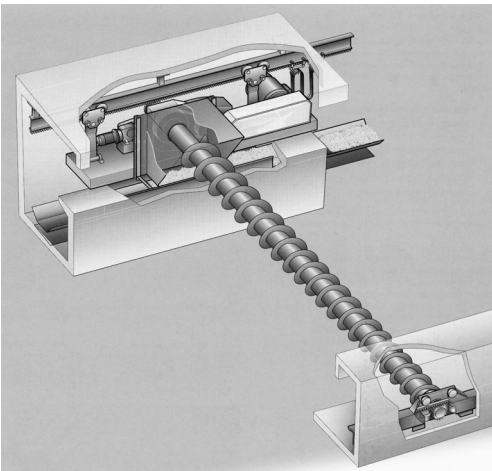
**Fig 3.29** Modern chip storage bin (surge bin) RotaRecAll™ [10].

Optimum material reclaiming conditions are ensured by special constructions of screw reclaimers, depending on stacking height, particle shape and material properties. Cantilever screw reclaimers either slew through the stored material around the central point at the bottom of a round silo, or travel forth and back at the bottom of a linear pile. The material is reclaimed through a central discharge chute onto a belt conveyor below. Tapered flights with variable pitch are welded on the thick-walled steel screw pipe, which is either of tubular or conical shape. Flight diameter and pitch increase in the direction of material flow to ensure even reclaiming across the silo area. According to the material reclaimed, stainless steel cladding and stainless steel flights with special shredder teeth are available. Screw reclaimers for larger silos, either round or rectangular, are supported at both ends – that is, at the discharge end within the central housing as well as at the opposite end via a peripheral ring or a parallel rail. Slewing drives and screw drives must be sized for a high starting torque to ensure a reliable start even under high piles and different materials (Figs. 3.30 and 3.31) [12].

The TubeFeeder™ silo reclaimer travels as a radial reclaimer under the storage pile. Both the tube equipped with reclaim slots as well as the central screw inside the tube, rotate and reclaim material to a collection conveyor below the central housing. The tube is moved by a variable speed drive controlling the rotation speed and the outfeed rate. The discharge screw inside the tube transports the chips equally off the reclaimer tube at a fixed speed. Advantages of this system are less chip damage, considerably lower power consumption (up to 75% compared to conventional screw reclaimers), even and homogenized material flow, and less wear of the conveying equipment [20,34].



**Fig 3.30** Slewing screw reclaimer; the CenterScrew™ [41].



**Fig 3.31** Traveling screw reclaimer: the ParaScrew™ [42].

The boom-type stacker reclaimer is an integrated system developed for open storing and reclaiming large volumes of bulk materials. A luffing and slewing belt-type stacker and an equally moved rake-type chain reclaimer are positioned in the center of a semicircular storage pile. The stacker and reclaimer are mounted separately on the same heavy central column with large-diameter slewing bearings. Stacking and reclaiming is carried out independently of each other, monitored and either remotely or locally controlled via PLC and PC. First-in/first-out reclaiming is gained by reclaiming the oldest storing zones first. Infeed and out-feed of the stacker reclaimer takes place via long belt conveyor systems [37].

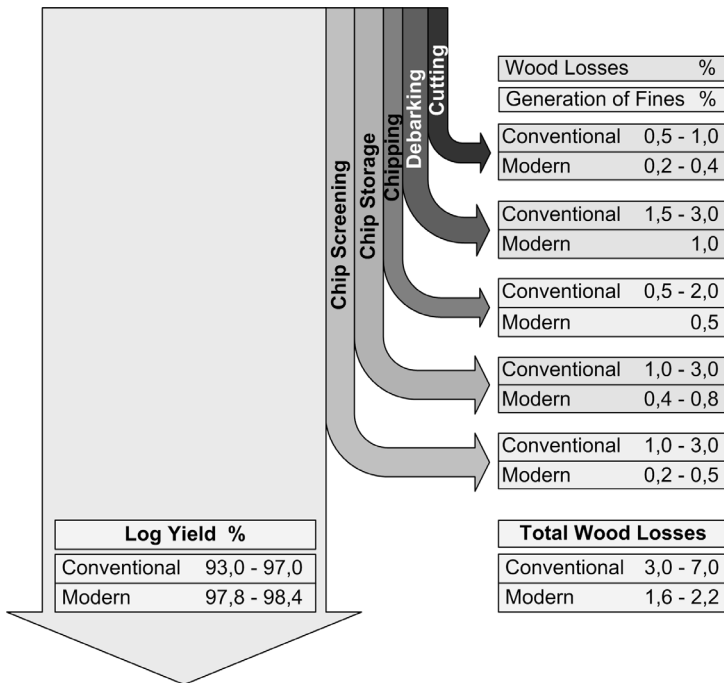
Stoker dischargers are hydraulic driven feeding modules, arranged parallel to each other at the bottom of a bunker, and alternately traveling back and forth. Supplied by wheel loaders, specially designed cross-members between the rail modules convey the bulk material into a transversely attached screw feeder at the bottom end. This “life bottom” can either be installed horizontally or inclined.

Blair [35] reported on investigations of a computer simulation to predict economic viability of adding a chip storage bin to an in-woods chipping operation. A chip storage bin such as this improves chipper and chip van utilization significantly. The simulation program developed by the Forest Engineering Research Institute of Canada (FERIC) is used to evaluate the economics of using a chip storage bin (referred to as a “surge bin”) under a variety of in-woods chipping scenarios, and to develop chip van schedules for operations with and without such a surge bin.

3.6.4

**Wood Yard Losses and Waste Reduction**

Depending upon the technology used, overall wood yard losses range from 3 to 7% of the total log volume input (conventional processing technology). However, by thorough utilization of modern equipment, these losses may be reduced significantly from 1.6–2.2% in total (data from Metso Paper Oy [10]; see also Fig. 3.32).



**Fig 3.32** Common wood yard losses and achievable reduction of losses by improvements of processing technology (according to [10]).

Not all of the material delivered to the wood yard is usable for pulping. Bark, soil-contaminated chips, small limbs, oversized logs, metal-containing logs and mold-damaged chips are waste materials and must be used for other purposes such as fuel, as raw material for horticulture, or as landfill cover. Fuel for log-handling vehicles and their exhaust gases, grease and lubrication oils used for all movable machinery generate additional wastes.

#### 3.6.4.1 Specific Causes of Waste Generation

Crumpler [36] provides a very useful summary on pollution prevention on pulp mill wood yards. His report contains many hints how to improve wood yard operations with regard to environmental pressure reduction.

Tab. 3.2 Wood yard waste: causes and countermeasures (according to [36]).

Waste	Causes and countermeasures
Soil-contaminated bark and chips	Materials not usable as fuel or for pulping; avoidable/reducible by partially/completely paved wood yard; log washing station in front of the debarking equipment.
Oversized logs	Materials too large for processing by mill equipment; inadequate delivery specifications or poor control of incoming material; improved inspection, reselling logs to sawmill.
Wooden debris	Limbs and other debris (e.g., soil, stones, sand) attached to logs or delivered with bark and chips manufactured offsite (mobile chipper); screening of incoming material (e.g., by vibratory screen systems), washing station in front of debarker infeed.
Metal-containing logs	Wire, nails, bullet and grenade fragments only detectable by metal detector, installed ahead the chipper feeding line.
Decayed wood	Microbiological decay caused by fungi and bacteria; reduced storage time, depending on weather conditions, suitable inventory management program, storage in or under water.

#### 3.6.4.2 Pollution Prevention Options

Depending on the amount of limbs, wood debris and undersized logs, additional debarking and chipping equipment can be used for these raw materials (e.g., mobile chippers). Metal-containing wood, identified by metal detectors, can either be cut off or used as fuel or landfill cover.

Specialized vibratory screens, and to some extent washing stations, are very efficient in separating soil and stones from contaminated chips and bark. The cleaned material could be further processed or used as fuel or for horticulture. Soil and fines can be used as landfill cover or other soil use.

A paved log yard (bearing in mind the weight of the load-carrying trucks) and the use of wheel-based transportation vehicles significantly reduces the contamination of logs, chips and bark. Chips and bark can be collected directly from the paved areas. Maintenance costs for handling systems, debarkers, chipping and screening equipment decline remarkably.

The log yard layout and the applied handling systems are of major importance for the energy consumption of all necessary transportation tasks. In particular, fuel consumption and maintenance costs can be significantly reduced by minimizing traveling distances by an improved wood yard layout, based on time and material flow studies as for instance conducted in manufacturing plants [36].

## References

- 1 Sixta H., Promberger A., Koch G., Gradinger C., Messner K. 2004. Influence of beech wood quality on bisulfite dissolving pulp manufacture. Part 1: Influence of log storage on pulping and bleaching. *Holzforschung*, 58(1): 14–21.
- 2 Liukko K. 1997. Climate-adapted wet-storage of sawn timber and pulpwood: An alternative method of sprinkling and its effect on freshness of groundwood and environment. *Acta Universitatis Agriculturae Sueciae – Silvestria* (No. 51): 44 pp + papers i–v.
- 3 Elowsson T., Liukko K. 1995. How to achieve wet storage of pine logs (*Pinus sylvestris*) with a minimum amount of water. *For. Prod. J.*, 45 (11/12): 36–42.
- 4 von Aufseß H. 1986. Lagerverhalten von Stammholz aus gesunden und erkrankten Kiefern, Fichten und Buchen. *Holz Roh- Werkstoff*, 44: 325–330.
- 5 Patt R. 1998. Lecture handout “Chemische Holztechnologie”. University of Hamburg, Dept. of Wood Science, Section Chemical Wood Technology.
- 6 Goldie S. 2003. Tech Updates – Debarkers. [http://www.forestnet.com/archives/Dec\\_Jan\\_03/tech\\_update.htm](http://www.forestnet.com/archives/Dec_Jan_03/tech_update.htm), 4 pages; accessed 25.06.2004.
- 7 Andritz AG 2002. Debarking drum. Company leaflet SP298en, Rev. D01/2003.
- 8 Tohkala A. 2003. GentleBarking™ – a log debarking method for higher yield. *Fiber & Paper, Metsä Paper Customer Magazine*, 3: 12–14.
- 9 Koch P. 1982. *Utilization of hardwoods growing on Southern Pine sites. Vol. 1 – The raw materials, Vol. 2 – Processing, Vol. 3 – Products and prospective.* Washington D.C., U.S. Dept. of Agriculture, Forest Service, Agriculture Handbook No. 605.
- 10 Metso Paper Oy. 2004. Company web site. <http://www.metsopaper.com/>, accessed 26.06.2004 and personal communication.
- 11 Mälzer K., Fritsch R. 2004. Contract chip facility that supplies eucalyptus chips to Japan.... [http://www.paperloop.com/db\\_area/archive/p\\_p\\_mag/2004/0004/woodyard.html](http://www.paperloop.com/db_area/archive/p_p_mag/2004/0004/woodyard.html), 10 pages; accessed 02.07.2004.
- 12 Andritz AG 2004. Company web site. <http://www.andritz.com.ANO-NIDZD804C4FC6CBD4732/ppp.htm>; accessed 01.07.2004.
- 13 Söderhamn Eriksson AB. 1987. Spannerscheiben. Söderhamns Verkstäder. Reg. Nr. 2714–740.
- 14 Cody H. 2002. Woodyard modernization lowers costs, improves fiber quality at St. Mary’s Paper. [http://www.paperloop.com/db\\_area/archive/p\\_p\\_mag/2002/0007/woodyard.htm](http://www.paperloop.com/db_area/archive/p_p_mag/2002/0007/woodyard.htm), 5 pages; accessed 02.07.2004.
- 15 Nicholson Manufacturing Co. 2004. Company brochures, and web site. See: <http://www.nicholsonmfg.com/enghm/mainframe.htm>; accessed 14.07.2004.
- 16 Andritz AG 1996. HQ-Plus™. Company leaflet SP 480 en 5/96.

- 17 Andritz AG 2002. HHQ-Chipper™. Company leaflet 6999en 11/2002.
- 18 Bruks-Kloeckner 2004. Company brochure and web site. See: <http://www.torex.ch/Kloeckner.htm>; accessed 14.7.2004.
- 19 Pallmann GmbH 2004. Pallmann drum chipper "PHT". Company brochure and web site. See: <http://www.pallmann-online.de/seiten/holz/>; accessed 14.07.2004.
- 20 Ward L.A. 2002. A unique upgrade of the chip handling and storage process at Green Bay Packaging's Morrilton, Ark., mill. *Pulp & Paper Magazine*, 5, 5. See: [http://www.paperloop.com/db\\_area/archive/p\\_p\\_mag/2002/0005/warehousing.htm](http://www.paperloop.com/db_area/archive/p_p_mag/2002/0005/warehousing.htm); accessed 06.08.2004.
- 21 Andritz AG 2000. CS chip screen. Company leaflet SP 502en Rev. A 01/2000.
- 22 Andritz AG 1998. DrumMatic™ – Debarking process optimization system. Company leaflet SP348en, Rev. B05/98.
- 23 Bergmann Ö., Nilsson T. 1979. An experiment on outdoor storage of whole-tree chips. *Swed. Univ. Agric. Sci. R.*, 109, 1–21.
- 24 Vanderhoff J.E. 1992. Handling chips. *Papermaker*, October: 22–24.
- 25 Hatton J.V., Hunt K. 1972. Effect of prolonged outside chip storage on yield and quality of kraft pulps from *Picea glauca* and *Pinus contorta* chips. *Tappi J.*, 55(1): 122–126.
- 26 Fuller W.S. 1985. Chip pile storage – A review of practices to avoid deterioration and economic losses. *Tappi J.*, 68(8): 48–52.
- 27 Wolfhaardt F., Rabie C. 2003. Evaluation of the microclimate in a stored softwood chip pile for biopulping. *Holzforschung*, 7: 295–300.
- 28 Hulme M.A., Hatton J.V. 1978. Silo-stored hardwood chips treated with sodium carbonate – kraft pulp yields and pulping characteristics. *Tappi J.*, 61(12): 47–50.
- 29 Hulme M.A. 1975. Chip storage in silos. I. Hot storage and borax preservatives. Report, East. For. Prod. Lab., Canada, No. OP-X-136 E: 13 pp.
- 30 Springer E.L., Hajny G.J., Feist W.C. 1970. Spontaneous heating in piled wood chips. I. Initial mechanisms. *Tappi J.*, 53(1): 85–86.
- 31 Springer E.L., Hajny G.J., Feist W.C. 1971. Spontaneous heating in piled wood chips. II. Effects of temperature. *Tappi J.*, 54(4): 589–591.
- 32 Feist W.C., Springer E.L., Hajny G.J. 1972. Determining loss of wood substance in outside chip storage: a comparison of two methods. USDA For. Serv. Res. Paper, For. Prod. Lab., Madison, No. FPL-189: 8 pp.
- 33 Maron G.F. 1982. Proper chip storage methods can reduce wood and byproduct losses. *Pulp Paper*, 56(6): 65–67.
- 34 Rader Companies. 2004. Company web site. <http://www.rader.com>; accessed 17.08.2004.
- 35 Blair C.W. 1998. Using a chip storage bin to improve in-woods chipper efficiency and reduce chip van cycle times. Technical note. *For. Eng. Res. Inst. Canada (FERIC)*, No. TN-274: 8 pp.
- 36 Crumpler P. 1996. An analysis of pollution prevention opportunities and impediments in the pulp and paper manufacturing sector in Georgia. <http://www.ganet.org/dnr/p2ad/pblcations/pulp.html>, 5 pages; accessed 13.07.2004.
- 37 Andritz AG 2004. Overcoming the "bark with a bite" at Valdivia. Andritz AG. *Fiber Spectrum* 2: 4–5.
- 38 Papierholz Austria Ges. m.b.H. 2002. Holzübernehmerrichtlinien, Revision 5a. See: <http://www.papierholz-austria.at/co.hdl/1/144/H%C3%9C-Richtlinien%20Rev%205A.doc>; accessed 17.08.2004.
- 39 Bayerische Landesanstalt für Wald und Forstwirtschaft. Informationen aus der Wissenschaft 2000 – LWF Report 21, Abschnitt 4.6 Qualitätskriterien und Möglichkeiten der Qualitätsbeurteilung. See: <http://www.lwf.bayern.de/lwfbericht/lwfber21/>; accessed 25.06.2004.
- 40 Acrowood Corporation. 2004. Diamond-Roll Thickness Screen; DiamondRoll Fines Screen; Raised Roll Disc Thickness Screens; DiamondRoll Separation System; Chip Slicers. See: <http://acrowood.com>; loaded 06.08.2004.
- 41 Andritz AG. 1999. CenterScrew. Company leaflet SP330en Rev. C 10/99.
- 42 Andritz AG. 1997. ParaScrew. Company leaflet SP379en Rev. A 03/97.

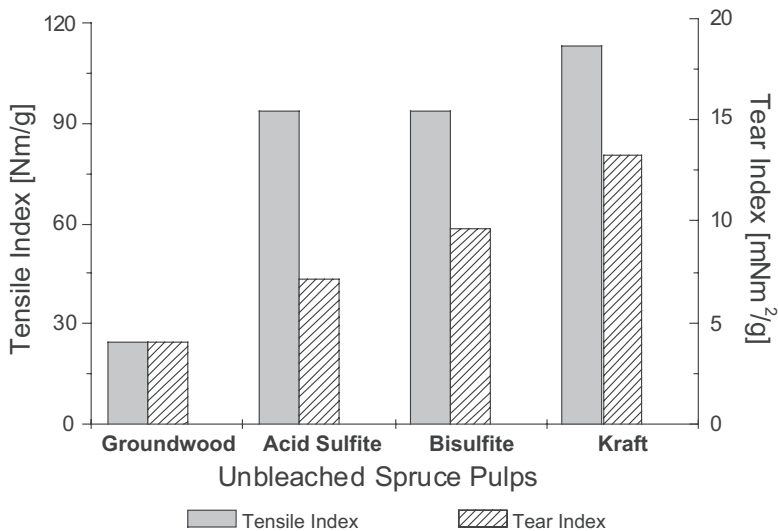


## 4 Chemical Pulping Processes

Herbert Sixta, Antje Potthast, Andreas W. Krottschek

### 4.1 Introduction

Pulping represents the process by which wood or other lignocellulosic material is reduced to a fibrous mass, denoted as pulp. The process of defibration can be accomplished mechanically, chemically, or by a combination of both treatments. The corresponding commercial processes are then classified as mechanical, chemical and semi-chemical. Pulps produced in different ways have different properties that make them suited to particular products. Figure 4.1 illustrates the effects of different pulping processes on the strength properties of unbleached spruce pulps [1].



**Fig. 4.1** Paper properties of unbleached spruce pulps at 45° SR, showing the effect of different pulp processes (according to Annergren and Rydholm [1]).

On a global scale, pulps are predominantly produced by chemical pulping processes. In 2000, the chemical pulps accounted for more than 77% of all wood-based fiber material worldwide (see Tab. 2 in Chapter 1, Introduction) [2]. In chemical pulping, lignin is degraded and dissolved through chemical reactions at elevated temperatures (130–170 °C). The fibers can be separated without further mechanical defibration only after about 90% of the lignin has been removed. Unfortunately, delignification is not a selective process. Parallel to the lignin removal, significant parts of the hemicelluloses and some cellulose are also degraded. The total fiber yield ranges from 45 to 55% (at a given extent of delignification of about 90%), depending on the wood source and the pulping process applied. Continuing cooking beyond a certain extent of delignification inevitably results in disproportionately large yield losses due to preferred carbohydrate degradation. Hence, the chemical reactions must be stopped at a point when the lignin content is low enough for fiber separation, and where acceptable yield can be still attained. In a complete fiber line, further delignification is achieved by bleaching processes downstream of the digester.

The main commercial chemical pulping techniques comprise the sulfate or kraft, the acid sulfite, and the soda processes. The dissolution of wood components during pulping is characteristic for each pulping process which, at a given residual lignin content, is reflected in the carbohydrate yield and composition. Cellulose is largely preserved in sulfite pulps, whereas xylan is most stabilized in kraft pulps. The high resistance of xylan towards alkali is the main reason for the

**Tab. 4.1** Yields of main pulp components after acid Mg sulfite [4,5] and kraft pulping [4,6] of beech and spruce wood.

Constituents	Spruce			Beech		
	Wood	Sulfite pulp Acid Mg-Sulfite	Kraft pulp CBC	Wood	Sulfite pulp Acid Mg-Sulfite	Kraft pulp Conventional
Carbohydrates (CH)	70.6	50.9	47.2	73.3	46.6	48.6
Cellulose	42.2	42.0	39.1	42.0	40.4	36.2
Galactoglucomannan (GGM)	19.0	5.3	3.2			
Glucomannan (GM)	2.0	0.4	0.1			
Arabinglucuronoxylan (AX)	9.4	3.6	4.9			
Glucuronoxylan (X)	27.8	5.8	12.3			
Other carbohydrates				1.5		
Lignin (L)	27.2	1.7	1.6	24.5	1.2	1.3
Extractives, Ash	2.2	0.4	0.2	2.2	0.2	0.1
Sum of components (Total Yield)	100.0	53.0	49.0	100.0	48.0	50.0

yield advantage of kraft over sulfite pulps in case of hardwoods (Tab. 4.1). On the other hand, galactoglucomannan (GGM) is less degraded during sulfite pulping, which in turn contributes to the higher yield of softwood sulfite pulps as compared to kraft pulps. The yield advantage even increases when the pH is shifted to neutral conditions in the first stage of a two-stage sulfite process due to an increased retention of glucomannan [3]. It has been shown that neutral conditions at elevated temperature are sufficient to account for almost complete deacetylation of glucomannan. In this state, glucomannan may bind more closely via hydrogen bonds to the cellulose microfibrils, thus being more resistant toward acid hydrolysis.

Kraft pulping has developed as the principal cooking process, accounting for 89% of the chemical pulps and for over 62% of all virgin fiber material. In comparison, only 5.3% of the world chemical pulp production is obtained by the sulfite process [2]. The soda process, using aqueous sodium hydroxide solution as cooking liquor, is used primarily for the pulping of annual plants and, in combination with small amounts of anthraquinone (ca. 0.05% on wood), also for the pulping of hardwoods.

## 4.2 Kraft Pulping Processes

### 4.2.1 General Description

The main active chemical agents in the kraft process are hydroxide and hydrosulfide anions which are present in the kraft cooking liquor, an aqueous solution of caustic sodium hydroxide and sodium sulfide, denoted as white liquor. The hydrosulfide ion plays an important role in kraft pulping by accelerating delignification and rendering nonselective soda cooking into a selective delignifying process. Delignification can be divided into three phases, namely the initial, bulk, and residual or final phases. In the initial phase, delignification is caused by the cleavage of  $\alpha$ -aryl and  $\beta$ -aryl ether bonds in the phenolic units of lignin which accounts for approximately 15–25% of native lignin. In this stage, the predominant part of the total carbohydrate losses can be observed. In the bulk delignification phase the main part of the lignin is removed while at the same time only minor carbohydrate losses occur. The cleavage of  $\beta$ -aryl bonds in nonphenolic units of lignin is assumed to be the main delignification reaction. In the residual delignification phase, only approximately 10–15% of the native lignin is removed. However, with continuous delignification, the dissolution of carbohydrates extensively increases. In order to maintain high yields and to preserve a sufficiently high quality of the pulp, delignification is limited to a certain degree of delignification, targeting kappa numbers of about 25–30 for softwood and 15–20 for hardwood kraft pulps.

After cooking, the pulp and the black liquor (which is white liquor enriched with degraded wood components with a residual hydroxide ion concentration of

ca.  $0.25 \text{ mol L}^{-1}$ ) are discharged at reduced pressure into a blow tank. After removing the knots through screening on knotter screens, the black liquor is removed after countercurrent washing of the pulp and further processed within the recovery line. The washed pulp is mechanically purified by pressurized screens prior entering the bleach plant.

The volatile fraction of the wood extractives – the crude turpentine – is removed during presteaming and condenses from the relief condensates (the average yield of crude turpentine of pine is  $5\text{--}10 \text{ kg t}^{-1}$  pulp, with monoterpene compounds as the main fraction). The tall oil soap, which originates from the nonvolatile fraction of the wood extractives, is removed during evaporation of the black liquor by skimming. Through the addition of sulfuric acid, the resin and fatty acids are liberated to yield crude tall oil (CTO) in an amount of approximately  $30\text{--}50 \text{ kg t}^{-1}$  of pulp. Further purification of the main fractions of the CTO is achieved by vacuum distillation.

During kraft pulping, malodorous and toxic compounds such as methyl mercaptan ( $\text{CH}_3\text{SH}$ ), dimethylsulfide ( $\text{CH}_3\text{SCH}_3$ ), dimethyldisulfide ( $\text{CH}_3\text{SSCH}_3$ ) and other reduced sulfur compounds, referred to as “total reduced sulfur” (TRS), are formed during the course of nucleophilic substitution reactions with predominantly lignin moieties. Great efforts must be made to collect TRS containing gases (relief gases from cooking, blowing, evaporation of black liquor, etc.) to convert them to harmless compounds by oxidation, mainly through incineration.

The regeneration of the black liquor to fresh white liquor comprises the following principal steps of the recovery line:

- Evaporation of the black liquor
- Incineration of thick liquor
- Causticizing of smelt from recovery boiler
- Calcination of the lime

The weak black liquor, including the filtrates from oxygen delignification, must be evaporated to a solid content of up to 80% by multiple-effect evaporators; this includes a concentrator prior to entering the Tomlinson-type recovery furnace. Make-up sodium sulfate is added to the concentrated black liquor to compensate for the losses of sodium and sulfur. Combustion of the dissolved organic compounds generates heat, which is transformed to process steam and electric power. A modern kraft pulp mill is designed such that it is self-sufficient with respect to both power and heat. In fact, it even has the potential to generate surplus energy. The inorganic smelt, which contains mainly sodium carbonate and sodium sulfide, is dissolved in water to yield the so-called green liquor which, after clarification, is subjected to the causticizing reaction where sodium carbonate is converted to sodium hydroxide by treatment with calcium hydroxide (slaked lime) according to the Eq. (1):



After calcium carbonate is precipitated and separated from the liquor, the resultant white liquor is ready for re-use for cooking. To close the cycle, the lime is

reburned in a rotary kiln (lime kiln) to produce calcium oxide, which in turn is slaked to form calcium hydroxide [Eq. (2)]:



Make-up calcium carbonate is added to the lime kiln to compensate for the losses of calcium hydroxide.

#### 4.2.2

#### Kraft Cooking Liquors

The active chemicals in kraft or sulfate pulping are the hydroxide and hydrogen sulfide ions,  $\text{OH}^-$  and  $\text{HS}^-$ . In commercial kraft cooking, the active agents are supplied as an aqueous solution consisting of sodium hydroxide and sodium sulfide, denoted as white liquor. The white liquor preparation includes the conversion of sodium carbonate ( $\text{Na}_2\text{CO}_3$ ) in the smelt to sodium hydroxide ( $\text{NaOH}$ ) in a recausticizing plant. Thereby, a certain amount of inert salts and nonprocess elements are accumulated in the white liquor, according to equilibrium conditions. The composition of the main components of a typical white liquor is given in Tab. 4.2.

Tab. 4.2 Composition of a typical white liquor [7].

Compounds	Concentration [g/l]	
	as NaOH	as compound
NaOH	90.0	90.0
Na <sub>2</sub> S	40.0	39.0
Na <sub>2</sub> CO <sub>3</sub>	19.8	26.2
Na <sub>2</sub> SO <sub>4</sub>	4.5	8.0
Na <sub>2</sub> S <sub>2</sub> O <sub>3</sub>	2.0	4.0
Na <sub>2</sub> SO <sub>3</sub>	0.6	0.9
Other compounds		2.5
Total alkali (TA)	156.9	170.6
Total Sulfur (TS)	47.1	19.7
Effective alkali (EA)	110.0	
Active alkali (AA)	130.0	

In kraft cooking technology, the concentration of active chemicals are expressed according to the following terminology:

- Total alkali (TA) comprises the sum of all sodium salts, the amount of total titratable alkali (TTA), the sum of sodium hydroxide, sodium sulfide and sodium carbonate. Most important for the characterization of the cooking liquor are the expressions effective alkali (EA), active alkali (AA) and sulfidity (S), which are defined according to Eqs. (3–5).
- The EA-concentration (eq. 3) is equivalent with the concentration of hydroxide ions because the sulfide ions are completely dissociated to hydrogen sulfide ions and hydroxide ions under the conditions occurring throughout kraft pulping (see Fig. 4.2).

$$EA = NaOH + 0.5 Na_2S \quad (3)$$

- The AA-concentration (eq. 4) includes the whole sodium sulfide concentration and can be used to express the sulfidity of the aqueous solution according to Eq. (5):

$$AA = NaOH + Na_2S \quad (4)$$

$$S = \frac{Na_2S}{AA} \cdot 100\% \quad (5)$$

For simplicity, all the chemicals are calculated as sodium equivalents and expressed as weight of NaOH or Na<sub>2</sub>O (see Tab. 4.2).

- The inter-relationship between EA- and AA-concentrations can be displayed by Eq. (6):

$$EA = AA(1 - 0.5 \cdot S)$$

$$AA = \frac{EA}{(1 - 0.5 \cdot S)} \quad (6)$$

where S is expressed as a fraction.

In pulping chemistry, molar units are preferred over weight units. As mentioned previously, the OH<sup>-</sup> ion concentration is equivalent to the effective alkali concentration. The HS<sup>-</sup> ion concentration, however, corresponds to only half of the sodium sulfide concentration. The OH<sup>-</sup> ion and the sulfide ion concentrations in molar units of the white liquor introduced in Tab. 4.2 are depicted in Tab. 4.3.

Based on molar units, the sulfidity of the white liquor can be calculated by using Eq. (7):

$$S = \frac{2 \cdot [HS^-]}{[HS^-] + [OH^-]} \cdot 100\% \quad (7)$$

Tab. 4.3 Molar concentrations of hydroxide ions, hydrogen sulfide ions and carbonate ions in the white liquor presented in Tab. 4.2.

Species	mol/l
$\text{OH}^-$	2.75
$\text{HS}^-$	0.50
$\text{CO}_3^{2-}$	0.25

Reversed, the molar concentration of  $\text{H}_2\text{S}$  may be derived from sulfidity (fraction) and  $[\text{OH}^-]$  according to Eq. (8):

$$[\text{HS}^-] = \frac{S \cdot [\text{OH}^-]}{(2 - S)} \quad (8)$$

Residual amounts of sodium carbonate in the white liquor are determined by the extent of the causticizing reaction, which is an equilibrium reaction. The efficiency of this reaction is characterized by the causticity (C) or causticizing efficiency, and thus the concentration of sodium carbonate according to Eq. (9):

$$C = \frac{\text{NaOH}}{\text{NaOH} + \text{Na}_2\text{CO}_2} \cdot 100\% \quad (9)$$

expressed as sodium hydroxide equivalents.

The causticity is a function of reaction time and the total salt concentration (e.g., TTA). In dilute aqueous solutions and with longer retention times, the equilibrium is shifted to the sodium hydroxide side, which in fact corresponds to a higher causticizing efficiency. Table 4.2 shows also oxidized sulfur compounds, such as sodium sulfate, sodium sulfite or sodium thiosulfate, which can be considered inert with respect to the pulping reactions. From a process point of view, the amount of oxidized sulfur compounds must be kept at the minimum achievable level. The ratio between the reduced sulfur compounds (sodium sulfide) and the total sulfur is designated as degree of reduction (DR). Actually, DR can be related to both the total sulfur or the sulfate sulfur only, respectively [Eq. (10)]:

$$DR_{\text{tot}} = \frac{\text{Na}_2\text{S}}{\text{Na}_2\text{S} + \text{Na}_2\text{SO}_4 + \text{Na}_2\text{SO}_3 + \text{Na}_2\text{S}_2\text{O}_3} \cdot 100\% \quad (10)$$

$$DR_{\text{SO}_4^{2-}} = \frac{\text{Na}_2\text{S}}{\text{Na}_2\text{S} + \text{Na}_2\text{SO}_4} \cdot 100\% \quad (10)$$

Table 4.4 lists the characteristics of the white liquor given in Tab. 4.2 by using the expressions of Eqs. (5), (9) and (10).

**Tab. 4.4** Sulfidity and efficiency of transformation to active cooking chemicals based on the white liquor composition given in Tab. 4.2.

Combined parameters	Unit	Value
Sulfidity (S)	%	30.8
Causticity (C)	%	82.0
Degree of reduction (DR)	% on total S	81.5
	% on SO <sub>4</sub>	89.9

The density of the white liquor is an important property for mass balance considerations of white liquor management, and correlates with the effective alkali concentration and sulfidity according to the following relationships [Eq. (11)]:

$$\begin{aligned}\rho_{WL} &= 0.692 \cdot EA^{0.092} \cdot S^{0.017} \\ \rho_{WL} &= 1.051 \cdot [OH^-]^{0.078} \cdot [HS^-]^{0.014}\end{aligned}\quad (11)$$

Using Eq. (11), the density of the white liquor characterized in Tabs. 4.2–4.4 corresponds to a value of 1.126 g mL<sup>-1</sup>.

The following equilibria occur in the aqueous solution of white liquor, comprising the active compounds sodium hydroxide, sodium sulfide, and sodium. Sodium hydroxide is a strong base and is therefore completely dissociated according to Eq. (12):



An aqueous sodium sulfide solution dissociates into sulfide, S<sup>2-</sup>, hydrogen sulfide, HS<sup>-</sup>, and dissolved hydrogen sulfide, H<sub>2</sub>S<sub>aq</sub> according to the equilibrium conditions. Their relative proportions are determined by the OH<sup>-</sup> ion concentration and the equilibrium constants, which are particularly dependent on temperature and ionic strength. Since the pK<sub>a</sub> of the protolysis of hydrogen sulfide has been agreed as ca. 17.1, the equilibrium in Eq. (13) strongly favors the presence of HS<sup>-</sup> ions; this concludes that, under conditions prevailing in the white liquor, sulfide ions can be considered to be absent [8,9]:



where the pK<sub>a,HS<sup>-</sup></sub> and pK<sub>b,S<sup>2-</sup></sub> equal 17.1 and -3.1, respectively.

Most older publications deal with a pK<sub>a</sub> value of HS<sup>-</sup> ions lower than the pK<sub>w</sub> value, which in turn provides a wrong picture of the electrolyte equilibria, especially at initial cooking conditions. Stephens selected a value of pK<sub>a</sub> = 13.78 based on calorimetric and thermodynamic consideration, whereas Giggenschach derived a



value of  $pK_a = 17.1$  from an ultra-violet study that involved reassigned absorption bands [8]. This value was confirmed by Meyer based on Raman spectra for *in-situ* measurement of the H–S stretch in high-pH solutions [9]. It has been agreed that  $pK_a$  values below 15, which were published previously, were due to oxygen contamination.

Aqueous  $HS^-$  ions dissociate according to Eq. (14):



where the  $pK_{a,H_2S}$  and  $pK_{b,HS^-}$  equal 7.05 and 6.95, respectively.

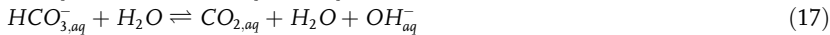
The formation of  $H_2S$  becomes significant when the pH approaches values of about 8. The dissolved  $H_2S$  is involved in an equilibrium with hydrogen sulfide in the gas phase, which only has to be considered in the sodium sulfite recovery systems where  $H_2S$  is expelled from the green liquor by carbonation processes (e.g., Stora and Sivola processes) [10,11]:



where

$$K_g = \frac{[H_2S_g]}{[H_2S_{aq}]}$$

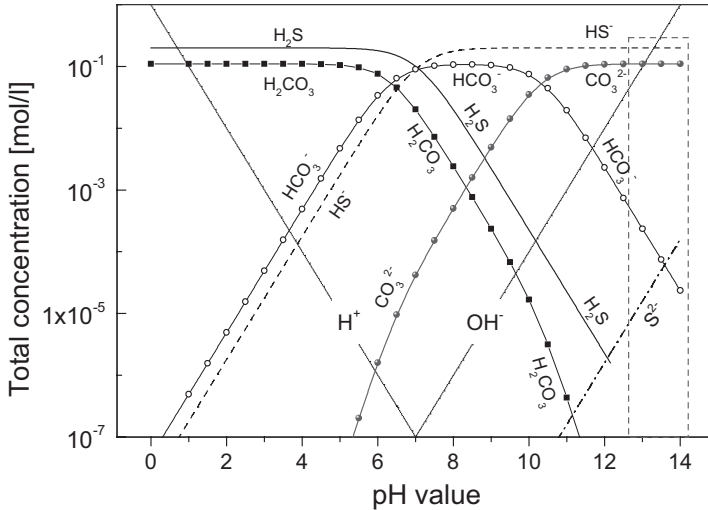
Sodium carbonate is also involved in the acid–base equilibria of white liquor according to Eqs. (16) and (17):



where the  $pK_{a,HCO_3^-}$  and  $pK_{b,CO_3^{2-}}$  are 10.33 and 3.67 and the  $pK_{a,CO_2}$  and  $pK_{b,HCO_3^-}$  are 6.35 and 7.65, respectively. The acid dissociation constants of the involved equilibria in white liquor are summarized in Tab. 4.5.

**Tab. 4.5** Acid dissociation constants of important acid–base equilibria in the white liquor.

Compound	Acid	Conjugated Base	$pK_a$
Sodium sulfide	$HS^-$	$S^{2-}$	17.10
	$H_2S$	$HS^-$	7.05
Sodium carbonate	$HCO_3^-$	$CO_3^{2-}$	10.33
	$CO_2 \cdot H_2O$	$HCO_3^-$	6.35



**Fig. 4.2** Bjerrum diagram of the electrolyte system prevailing at the beginning of a conventional kraft cook, assuming a hydroxide concentration of  $1.15 \text{ mol L}^{-1}$ , a hydrogen sulfide ion concentration of  $0.20 \text{ mol L}^{-1}$ , and a carbonate concentration of  $0.11 \text{ mol L}^{-1}$ .

The initial concentrations of the active cooking chemicals in a conventional kraft cook, assuming an EA charge of 18.4% NaOH on wood and a liquor-to-wood ratio of 4:1, are shown by the Bjerrum diagram over the whole pH range (Fig. 4.2).

The shaded area in Fig. 4.2 represents the pH range typical for a kraft cook. The results depicted in the figure confirm that, during the whole kraft cook, the equilibria strongly favor the presence of  $\text{HS}^-$  ions and carbonate ions. The sulfide ion and the hydrogen carbonate ion concentrations are below  $0.1 \text{ mmol L}^{-1}$  and thus of no importance in the electrolyte equilibria of the cooking liquor.

A titration curve of the white liquor at room temperature illustrates the presence of three equivalence points characterizing the acid–base equilibria shown in Eqs. (14), (16) and (17). The equilibrium conditions for the titration of salts of weak acids and strong bases with a strong acid can be expressed according to Eq. (18):

$$\sum [\text{AH}] + [\text{H}^+] = [\text{A}^-] + [\text{OH}^-] \quad (18)$$

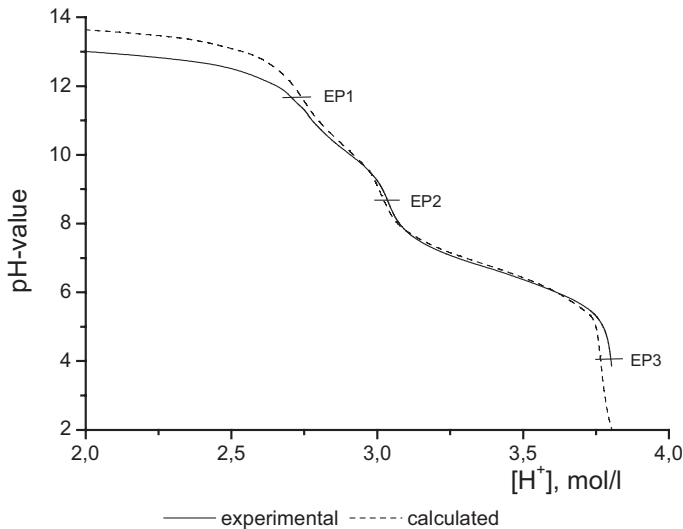
where  $[\text{AH}]$  corresponds to the concentration of the conjugated acid of the titrated weak base (e.g., the carbonate ions). Assuming the total concentration of the sum of the conjugated base  $[\text{A}^-]$  and the acid  $[\text{AH}]$  to be  $C$  (in  $\text{mol L}^{-1}$ ), and  $k_B$  the equilibrium constant of the conjugated base, the concentration of the acid  $[\text{AH}]$  is calculated according to Eq. (19):

$$[AH] = \frac{k_B \cdot C}{(k_B + [OH^-])} \quad (19)$$

The concentration of  $A^-$  can be expressed as the difference between the molar amount of the titrator acid,  $C^*$ , and the molar concentration of the strong bases available in the white liquor sample, equivalent to the EA concentration. The titration curve can be calculated on the basis of Eq. (18) and by considering the acid–base equilibria present in the white liquor [Eqs. (14), (16) and (17)]. The  $pK_b$  values are used from Tab. 4.5:

$$\frac{k_{B,CO_3^{2-}} \cdot C_{CO_3^{2-}}}{(k_{B,CO_3^{2-}} + [OH^-])} + \frac{k_{B,HCO_3^-} \cdot C_{HCO_3^-}}{(k_{B,HCO_3^-} + [OH^-])} + \frac{k_{B,HS^-} \cdot C_{HS^-}}{(k_{B,HS^-} + [OH^-])} + \frac{10^{-14}}{[OH^-]} - (C^* - [EA]) = [OH^-] \quad (20)$$

The course of pH (or the  $[OH^-]$ ) can be calculated as a function of the molar addition of titrator acid by solving an equation of the fifth order. A synthetic white liquor comprising an effective alkali concentration of  $110 \text{ g L}^{-1}$ ,  $[OH^-] = 2.75 \text{ mol L}^{-1}$ , a sulfidity of 30.4%,  $[HS^-] = 0.485 \text{ mol L}^{-1}$ , and a sodium carbonate concentration of  $20 \text{ g L}^{-1}$  (as NaOH),  $[CO_3^{2-}] = 0.25 \text{ mol L}^{-1}$ , was titrated with hydrochloric acid of  $0.5 \text{ mol L}^{-1}$ . A comparison between the experimental and theoretical neutralization curves shows quite acceptable correspondence (Fig. 4.3). In the high-pH region, some deviation occurs mainly due to the disregarded high ionic strength which affects the activity factor of the hydroxide ions.



**Fig. 4.3** Neutralization curve of white liquor at room temperature ( $[OH^-] = 2.75 \text{ mol L}^{-1}$ ,  $[HS^-] = 0.485 \text{ mol L}^{-1}$ ,  $[CO_3^{2-}] = 0.25 \text{ mol L}^{-1}$ ) using  $0.5 \text{ mol L}^{-1}$  hydrochloric acid as titrator acid at room temperature. Experimental

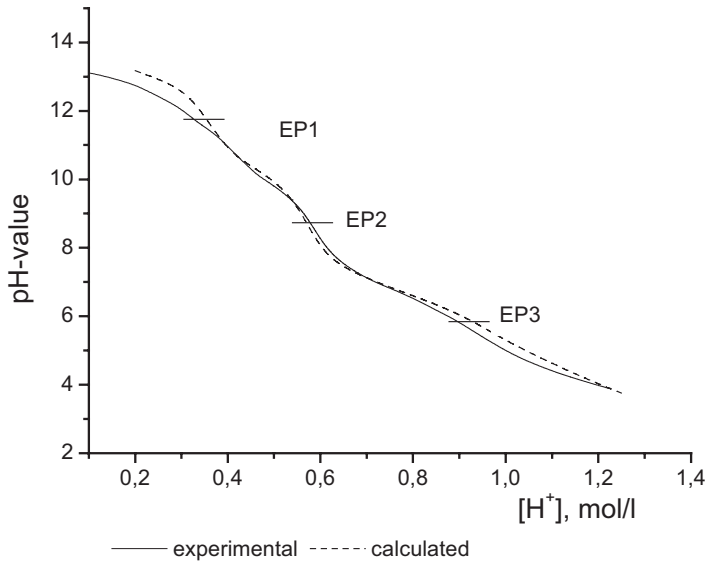
curve compared to theoretical curve using Eq. (20) (Mathematica 4.1.). Equivalence points: EP1 at pH 11.7, EP2 at pH 8.7, EP3 at pH 4.1 [7].

During the course of cooking, the white liquor gradually enriches with an extremely complex mixture of degraded lignin and carbohydrate substances, and finally converts to black liquor. The lignin part of the wood is degraded into low molecular-weight compounds which contain hydrophilic groups such as phenolate, catecholate and partly also carboxylate groups [12]. The main part of the carboxylic acids originate from carbohydrate degradation products, for example, hydroxyacids such as gluco-, xyloisosccharinic acid, lactic acid and gluconic acid [13]. In addition, rather large amounts of formic acid, glycolic acid and acetic acid are formed through fragmentation reactions. In addition to the various organic acids, which are ionized in the cooking liquor, a significant amount of inorganic substances are mostly present as dissolved species, including  $\text{Na}^+$ ,  $\text{K}^+$ ,  $\text{CO}_3^{2-}$ ,  $\text{SO}_4^{2-}$ ,  $\text{SO}_3^{2-}$ ,  $\text{S}_2\text{O}_3^{2-}$ ,  $\text{S}_n\text{S}^{2-}$ ,  $\text{HS}^-$  ions and nonprocess-elements (NPEs), comprising, for example, Mg, Al, Si, Mn, Cl, P, and transition metal ions. The alkalinity of the black liquor depends on the acid–base properties of all the dissolved and ionized compounds. The residual effective alkali concentration is a key parameter for the processability and the control of the kraft cooking process. Thus, knowledge of the hydroxide ion concentration in black liquor is of great importance, although most methods provide only approximate values [14]. Following the black liquor model from Ulmgren et al., the acid–base equilibria of four organic and three inorganic substances have been considered (Tab. 4.6).

**Tab. 4.6** Black liquor composition following the suggestion of Ulmgren et al. [14] and additional measurements [6].

Compounds	Species		Concentration mol/l	$\text{pK}_a$
	Base	Acid		
Hydroxide	$\text{OH}^-$	$\text{H}_2\text{O}$	0.347	>14
Hydrogen sulfide	$\text{HS}^-$	$\text{H}_2\text{S}$	0.217	7.05
Carbonate	$\text{CO}_3^{2-}$	$\text{HCO}_3^-$	0.180	10.33
Hydrogen carbonate	$\text{HCO}_3^-$	$(\text{H}_2\text{CO}_3)$	0.180	6.35
Formic acid	$\text{HCOO}^-$	$\text{HCOOH}$	0.300	3.45
Acetic acid	$\text{CH}_3\text{COO}^-$	$\text{CH}_3\text{COOH}$	0.200	4.75
Phenolate	$\text{PhO}^-$	$\text{PhOH}$	0.350	10.18
Catecholate	$\text{PhO}_2^{2-}$	$\text{PhO}_2\text{H}^-$	0.005	12.82
	$\text{PhO}_2\text{H}^-$	$\text{Ph(OH)}_2$	0.005	8.42

In strongly alkaline solutions only catecholic structures play a role in the acid–base reactions. Since the concentration of these compounds is very low in black liquor (Tab. 4.6), their influence on determination of the  $\text{OH}^-$  ion content is almost negligible. The (calculated) neutralization curve reveals three equivalence



**Fig. 4.4** Neutralization curve of black liquor at room temperature ( $[\text{OH}^-] = 0.347 \text{ mol L}^{-1}$ ,  $[\text{HS}^-] = 0.217 \text{ mol L}^{-1}$ ,  $[\text{CO}_3^{2-}] = 0.18 \text{ mol L}^{-1}$ ) using  $0.5 \text{ mol L}^{-1}$  hydrochloric acid as titrator acid at room temperature. Experimental curve compared to theoretical curve using Eq. (20) (Mathematica 4.1.) [6].

points at about pH 11.7, 8.8 and 5.0 which can be ascribed to the presence of  $\text{OH}^- + \text{PhO}_2^{2-}$ ,  $\text{PhO}^- + \text{CO}_3^{2-}$  and  $\text{HSO}_3^- + \text{HCO}_3^- + \text{OAc}^-$ . A fourth equivalence point at about pH 2.2 can be detected; this is probably due to carbonic acid and formic acid. Based on the shown equilibria, a neutralization curve can be calculated by using the algorithm shown in Eq. (20). The correspondence between experimental and theoretical neutralization curves is surprisingly good, although the experimental curve contains many more inflection points which are less resolved due to the many compounds present in black liquor (Fig. 4.4). Differentiation of the experimental curve reveals eight inflections points only in the pH range 13 to 4.5 (pH of 12.6, 11.9, 10.6, 9.5, 8.3, 6.4, 5.8, and 5.2).

In most cases, the hydroxide ion concentration is determined from the first inflection point or by direct titration with acid to a predetermined pH of 11.3 [15,18]. Temperature and dilution of the sample affect the acid–base properties of the inorganic and organic compounds present in the liquor [16]. For a more precise determination of the hydroxide content of black liquors, a potentiometric titration of the sample using Gran's method can be recommended [14,17].

## 4.2.3

**Mass Transfer in Kraft Cooking**4.2.3.1 **Purpose of Impregnation**

In any chemical pulping process, it is essential to achieve adequate penetration of liquids into the wood. The uniform distribution of the active cooking chemicals within the chip void system is an important prerequisite for the production of high-quality pulps, leaving no unreacted zones. Ideally, each fiber in a wood chip that is being pulped should receive the same chemical treatment which involves immersion in a pulping liquor of the same concentration, at the same temperature, and for the same time.

Alkaline pulping is carried out at temperatures in the range between 140 and 175 °C. Under these conditions, the degradation reactions of wood components are clearly diffusion-controlled. This includes the diffusion of reactants into the fiber wall and the reaction products out of the chips into the bulk liquor. With a homogeneous distribution of reagents, the kinetics of the pulping reactions will also be uniform throughout the system. At low temperatures, the process is no longer diffusion-controlled, and a reaction gradient is established inside the chip, so that reaction occurs in all parts of the chip assuring the homogeneous degradation of wood components. The key procedure to achieve an even distribution of cooking chemicals prior to pulping reactions is denoted as the “impregnation process”. The impregnation of wood corresponds to the liquid and chemical transport into the porous structure of the wood which is characterized by two main mechanisms, namely: (a) penetration into the capillaries; and (b) diffusion through cell walls, pit membranes and interfaces. Impregnation of wood is influenced by both wood properties such as wood species, chip dimensions, moisture content, air content and the capillary structure as well as the liquid properties such as pH and chemical concentration, surface tension, viscosity, temperature, and pressure [1]. The quality of impregnation relies on the homogeneity of the chemical treatment which, in turn, has an impact on the rejects content of the pulp and on the final product quality.

*Penetration* refers to the flow of liquid and associated chemicals into the air-filled voids of the wood chips under the influence of hydrostatic pressure. Penetration is the process where liquid transfers into the gas- or steam-filled cavities of the chips. Distinction can be made between forced penetration, including gas and liquid flow by an externally applied pressure differential, and natural penetration consisting of capillary rise. Mass transfer stops as the liquid approaches the wood capillaries that are at the fiber saturation point or that contain liquid–air interfaces. Hydrostatic pressurization of the system reduces the size of the air bubbles somewhat, but the effect is small, since extremely high system pressures would be required to overcome the resistance of the surface-tension forces of multiple liquid–air interfaces in the narrow capillaries. Under these conditions, entrapped air dissolves into water to some extent and also can gradually diffuse out of the pores, while the liquid diffuses into the pores countercurrently.

The second mechanism, *diffusion*, is a comparatively slow process and refers to the diffusion of ions or other soluble matter through the water layer of the cell wall and pit membrane structure under the influence of a concentration gradient. Molecular diffusion replaces the reactant chemicals as they are consumed by the chemical reactions within the chip. All transfer of new chemicals into chips and dissolved matter from the chips will occur through diffusion only after complete penetration. Thus, molecular diffusion is a very important step in chemical pulping. Industrial chips are not homogeneous in dimensions and void structure. Moreover, wood chips – even from fresh wood – contain air in the void system which must be displaced as far as possible prior to impregnation to ensure that all parts of the wood chips can be filled with liquid during penetration. Air removal can be accomplished by presteaming the chips. Part of the air inside the chips is removed due to direct expansion by heating, whereas a more complete air removal requires a successive steam condensation and evaporation in the capillary system of the chips.

In the following sections, the most decisive parameters determining the efficiency of the impregnation step, such as the heterogeneity of wood structure, presteaming, penetration and diffusion, will be introduced and discussed.

#### 4.2.3.2 Heterogeneity of Wood Structure

Wood is a very porous material. The high porosity is essential for the transport of water in the sapwood of a living tree, where water flows from the roots to the top through the cell lumina and is further distributed through the pits. Wood is, however not very permeable for gases and liquids, because flow into or through it must occur through a coarse system of capillaries. The void system of wood is different in softwoods and hardwoods, sapwood and heartwood, springwood and summerwood and additionally is also dependent on the individual wood species.

*Softwoods* consist mainly of longitudinal fibers, tracheids, with a tubular structure of an average length of approximately 3.5 mm and a diameter of 30–35  $\mu\text{m}$ . The tapered ends overlap longitudinally by about one-fourth of their length. Penetration occurs through their lumina and pits, which are covered by a membrane. There are two types of pits, namely the *simple pit* and the *bordered pit*, but all are characterized by the presence of a pit cavity and a pit membrane. In the simple pit the cavity is almost constant in width, whereas in the bordered pit the cavity narrows more or less abruptly toward the cell lumen. The pit membrane, which consists of primary wall and middle lamella, contains pores with dimensions in the range below of approximately 4 nm [2]. Within the heartwood of softwoods, mass transport is very limited because the pores in the pit membrane are often sealed by lignification or resinification.

*Hardwood fibers* are made up of several cell types, differentiated according to their special functions (see Chapter I-2). Mass transfer occurs predominantly through the lumina of the vessel elements, which are connected vertically to form long tubes. The channels thus formed contribute very efficiently to the water transport. If the vessels are plugged by tyloses, which frequently occurs during the development of heartwood, the penetration rate almost ceases (as is the case

in white oak; see Tab. 4.9). The fibers of hardwoods are interconnected by pit pairs, but they are smaller and fewer in number as compared to the softwood tracheids. They are less effective for liquid transport. Electron microscopic studies have not provided any evidence of pores through the membranes of hardwoods, thus indicating that hardwood fibers are ineffective for liquor flow [3]. Springwood is more easily penetrated than summerwood due to its wider lumina and its thinner and more fissured cell walls. Reaction wood and wood knots are very dense and thus more difficult to penetrate.

The water content of the wood determines not only the mechanical properties but also the efficiency of impregnation prior to chemical pulping. The moisture content in wood,  $MC_d$ , is defined as the water in wood expressed as a fraction of the weight of oven-dry wood [see Eq. (21)]:

$$MC_d = \frac{m_{wc} - m_{dc}}{m_{dc}} \quad (21)$$

where  $m_{dc}$  equals the mass of dry chips, and  $m_{wc}$  the mass of wet chips.

The moisture content can be related to the dry solid content,  $DS$ , expressed as a weight fraction using Eqs. (22) and (23):

$$DS = \frac{m_{dc}}{m_{wc}} = \frac{1}{1 + MC_d} \quad (22)$$

$$MC_d = \frac{1 - DS}{DS} \quad (23)$$

And thus the mass of the wet chips,  $m_{wc}$ , can be calculated according to equation (24):

$$m_{wc} = \frac{m_{dc}}{DS} \quad (24)$$

On occasion, the moisture content is based on the total weight of wet wood,  $MC_w$ , which then can be expressed as:

$$MC_w = \frac{m_{wc} - m_{dc}}{m_{wc}} = \frac{MC_d}{MC_d + 1} \quad (25)$$

The amount of moisture content,  $MC_d$ , in freshly cut green wood can vary considerably within species, and can range from about 30% to more than 200%. In softwoods, the moisture content of sapwood is usually greater than in heartwood. In hardwoods, the difference in moisture content between heartwood and sapwood depends on the species. Variability of moisture content exists even within individual pieces cut from the same tree. The average moisture contents of a selection of hardwoods and softwoods are listed in Tab. 4.7.

At the cellular level, moisture can exist as free water or water vapor in the cell lumens and cavities, and as chemically bound water within the cell walls. Earlywood tracheid lumens can hold more water because they are much larger than the latewood tracheid lumens. The cell walls are denser in the latewood tracheids and so contain more of the bound water. The bound water is held between microfibrils in the cell wall and is closely associated with the polysaccharides by means



Tab. 4.7 Average moisture content of green wood, by species according to [4].

Wood species	Moisture content [MC <sub>g</sub> ]	
	Heartwood [%]	Sapwood [%]
Ash, white	46	44
Aspen	95	113
Beech, American	55	72
Birch, paper	89	72
Birch, yellow	74	72
Cottonwood	162	146
Elm, American	95	92
Hickory, bitternut	80	54
Hickory, red	69	52
Magnolia	80	104
Maple, silver	58	97
Oak, norther red	80	69
Oak, southern red	83	75
Oak, white	64	78
Sweetgum	79	137
Yellow-poplar	83	106
Baldcypress	121	171
Cedar, western red	58	249
Douglas fir	37	115
Fir, white	98	160
Hemlock, eastern	97	119
Hemlock, western	85	170
Pine, lobolly	33	110
Pine, ponderosa	40	148
Redwood, old growth	86	210
Spruce, black	52	113
Spruce, Sitka	41	142

of hydrogen bonds. It is further assumed that the density of bound water is 1–2% higher as compared to the density of free water [5]. According to Tab. 4.7, even green wood is never completely filled with water. Consequently, wood cavities contain considerable amounts of air. Conceptually, the moisture content at which the cell wall is fully saturated with bound water and no water exists in the cell lumens is called the fiber saturation point (FSP). The FSP also is often considered as the moisture content below which the physical and mechanical properties of the wood begin to change as a function of moisture content. Although dependent on the species, for practical purposes, the FSP is generally considered to be 30%. Above the FSP, the larger capillaries contain free water which is held within the structure of wood membranes, pores and capillaries as hydrates, surface-bound water with a high apparent density, as adsorbed in multimolecular layers, and finally as capillary condensed water [6].

With an increase in pH, the wood structure swells due to an increased accumulation of water molecules as a bound layer. This enhancement of water layer adsorption also takes place on the capillary walls, with the consequence that the capillary pore diameters become much narrower, and the mass transfer is reduced. Furthermore, each capillary pore is blinded by the pit membranes which are made of primary wall and middle lamella covered with a multimolecular layer of water molecules, leaving no void micropores. Any passage of chemical through these membranes is thus controlled by diffusion [7]. The overall transportation mechanism can be considered as a diffusion mechanism which is controlled by the mass transport through the hydrated membrane pores.

To achieve pulping uniformity, the composition of the cooking liquor must be equally distributed inside the wood chips. It is apparent that the dimensions of the chips will have a considerable effect on the efficiency of chemical impregnation. Chips of different thickness are delignified very nonuniformly; wood is overdelignified at the surface, while the chip centers still show very high lignin concentrations. Only sufficiently thin chips can be uniformly delignified down to kappa numbers below 15 without a loss of yield and strength properties [8]. Extensive studies have shown clearly that chip thickness is the most critical dimension in kraft pulping [9–12]. At a given chip thickness, chip width and chip length have an insignificant influence on delignification rate and reject formation [13]. Chips produced by industrial chippers have cracks and other faults, and are thus more permeable as compared to laboratory-made chips. Kraft cooking of technical chips from *Pinus silvestris* with a thickness of 10 mm resulted in the same amount of rejects as compared to 4.8 mm hand-made chips [14]. Electron microscopy studies by using staining material confirmed that penetration of the cell wall is favored by fissures in the wood tissue produced by mechanical treatment of the samples [15].

Wood chips for chemical pulping should be uniform in size and shape. Typical wood chips are 15–25 mm long and wide and 2–5 mm thick (softwood, 25 mm × 25 mm × 4 mm; hardwood, 20 mm × 20 mm × 3 mm; denser hardwoods often tend to give thicker chips at identical chip length compared with softwoods). The three-dimensional structure of a wood chip is shown in Fig. 4.5.

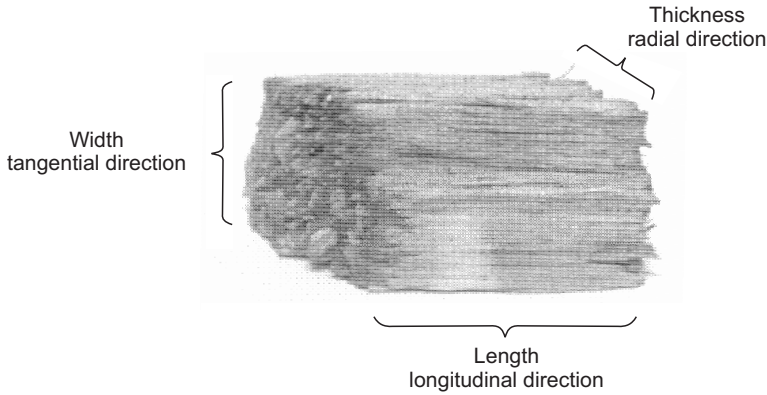


Fig. 4.5 Wood chip dimensions.

Industrial chips are formed after an initial cutting by applying a shearing force in the longitudinal direction of the wood. Longitudinal is defined as parallel to the wood capillaries, and transverse as perpendicular to them. The resulting chip geometry is characterized by chip thickness in a radial direction, chip length in a longitudinal direction, and chip width in a tangential direction. The void spaces of the wood chips consist mainly of the lumina of the cells, the vessels in the case of hardwoods, the resin ducts and other intercellular cavities which are also formed by mechanical cracks in the structure. Fresh wood contains solid material (cell walls), gas and water in cavities. The density of the solid fraction is rather constant, and can be calculated from the densities of the two main wood components, lignin and carbohydrates. Assuming an average wood composition of 28% lignin and 72% carbohydrates, the average density of the solid wood fraction can be calculated as follows:

$$\rho_{ws} = 0.28 \cdot \rho_L + 0.72 \cdot \rho_{CH} = 0.28 \cdot 1400 + 0.72 \cdot 1580 = 1530 \text{ kg m}^{-3} \quad (26)$$

where  $\rho_{ws}$  is the density of wood solids,  $\rho_L$  is the true density of lignin, and  $\rho_{CH}$  is the true density of carbohydrates. The density of the wood solids,  $\rho_{ws}$ , can be kept constant for all practical purposes.

The proportion of the void spaces or the void volume fraction,  $f_{\text{void}}$ , in a wood chip can be calculated by simply knowing the density of the dry wood chip,  $\rho_{dc}$ :

$$f_{\text{void}} = \rho_{dc} \cdot \left( \frac{1}{\rho_{dc}} - \frac{1}{\rho_{ws}} \right) = \rho_{dc} \cdot V_v = 1 - \frac{\rho_{dc}}{1.53} \quad (27)$$

where  $V_v$  is the void volume in  $\text{m}^3/\text{t}$  or  $\text{cm}^3 \cdot \text{p}^{-1}$ .

The void volume fraction of typical pulpwoods lies between 0.5 and 0.75, and depends strongly on a variety of factors such as wood species, location, climate, and season (Tab. 4.8).

Tab. 4.8 Density and void volume fraction of a selection of wood types.

Wood species	Dry density $\rho_{dc}$ [g cm <sup>-3</sup> ]	Void volume $V_v$ [cm <sup>3</sup> g <sup>-1</sup> ]	Void volume fraction $f_{void}$
Aspen, <i>Populus tremula</i>	0.37	2.05	0.76
Spruce, <i>Picea abies</i>	0.43	1.67	0.72
Pine, <i>Pinus silvestris</i>	0.47	1.47	0.69
Beech, <i>Fagus silvatica</i>	0.68	0.82	0.56
Esh, <i>Fraxinus excelsior</i>	0.65	0.88	0.58
Maple, <i>Acer pseudoplatanus</i>	0.59	1.04	0.61

The density ( $\rho_{wc}$ ) and the volume ( $V_{wc}$ ) of wet chips can be calculated according to equation (28) and (30):

$$\rho_{wc} = \frac{m_{wc}}{m_{dc}} = \frac{\rho_{dc}}{DS} \quad (28)$$

$$V_{wc} = \frac{m_{wc}}{P_{wc}} = \frac{m_{wc} \cdot DS}{P_{dc}} \quad (29)$$

The volume of the wood solids can be calculated by knowing the mass of the wet wood, the dry solids content and the density of the wood solids:

$$V_{ws} = \frac{m_{wc} \cdot DS}{\rho_{ws}} \quad (30)$$

Thus, the void volume is just the difference between the volumes of the wet wood and the wood solids:

$$V_v = V_{wc} - V_{ws} \quad (31)$$

Knowing the density of the initially present water,  $\rho_{H_2O,i}$ , the volume of this water,  $V_{H_2O,i}$  in the chip can be easily computed:

$$V_{H_2O,i} = \frac{m_{wc} \cdot (1 - DS)}{\rho_{H_2O,i}} \quad (32)$$

The change in the water volume can be estimated by considering the density of the water at the temperature  $T$ ,  $\rho_{H_2O,T}$ :

$$V_{H_2O,T} = V_{H_2O,i} \cdot \frac{\rho_{H_2O,i}}{\rho_{H_2O,T}} \quad (33)$$

During penetration, additional water or aqueous solution is introduced into the void system of the chips. The volume of the penetrated water,  $V_{H_2O,P}$  is then calculated by:

$$V_{H_2O,P} = \frac{m_{H_2O,P}}{\rho_{H_2O,T}} \quad (34)$$

where  $m_{H_2O,P}$  is the weight of the water penetrated into the chips.

The degree of penetration prior to impregnation,  $P_0$ , is estimated according to:

$$P_0 = \frac{V_{H_2O,i}}{V_v} \cdot 100 \quad (35)$$

After impregnation with *e.g.*, water, the degree of penetration,  $P$ , changes to:

$$P = \frac{(V_{H_2O,T} + V_{H_2O,P})}{V_v} \cdot 100 \quad (36)$$

**Example:** A simple example illustrates the way of calculatory the degree of penetration.

What is the degree of penetration and the density prior (300 °K) and after impregnation (373 °K) of aspen chips with 55% dry solids content (DS) and 0.37 t/m<sup>3</sup> dry density ( $\rho_{dc}$ )?

Impregnation takes place at 373 °K and increases the moisture content,  $MC_w$ , to 0.65. The densities of water at 300 °K are 0.997 t/m<sup>3</sup> and 0.959 t/m<sup>3</sup>, respectively.

(a) Prior impregnation:

$$\rho_{wc} = \frac{0.37}{0.55} = 0.67 \text{ t/m}^3$$

$$m_{wc} = \frac{1}{0.55} = 1.82 \text{ t/t dry solids}$$

One ton of dry chips contains 0.82 ton of water at 55% dry solids content.

The void volume,  $V_v$  is calculated according to equation:

$$V_v = V_{wc} - V_{ws} = \frac{1.82}{0.67} - \frac{1}{1.53} = 2.06 \text{ m}^3/\text{t dry solids}$$

The degree of penetration prior impregnation,  $P_0$ , at 300 K can be estimated using the following equations:

$$P_0 = \frac{\frac{1.82 \cdot (1 - 0.55)}{0.997}}{2.06} \cdot 100 = 39.9\%$$

This simple calculation shows that only 39.9% of the void volume of aspen chips contains liquid at a DS of 0.55.

(b) After impregnation:

During penetration the moisture content,  $MC_w$ , increases to 0.65 which equals a DS of 0.35. The mass of the wet chip,  $m_{wc}$ , calculates to:

$$m_{wc} = \frac{1}{0.35} = 2.86 \text{ t/t dry solids}$$

Assuming an even temperature rise to 373 K, the total volume of the penetrated water,  $V_{H_2O,P}$ , is calculated by:

$$V_{H_2O,P} = \frac{2.86 \cdot (1 - 0.35)}{0.959} = 1.938 \text{ m}^3/\text{t dry solids}$$

After impregnation, the degree of penetration,  $P$ , changes to:

$$P = \frac{1.938}{2.06} \cdot 100 = 94.1\%$$

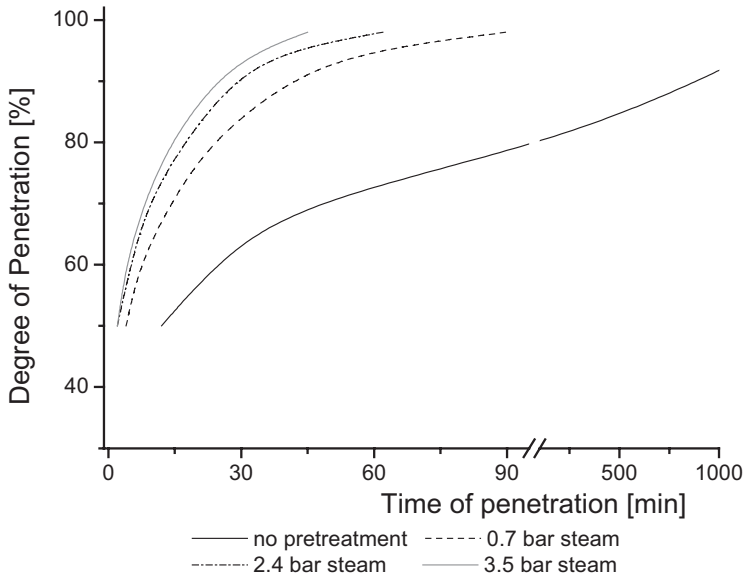
#### 4.2.3.3 Steaming

As mentioned above, rapid and uniform impregnation prior to any chemical pulping treatment is a necessary prerequisite. The importance of a thorough penetration of liquor into wood was emphasized as early as 1922 by Miller and Swanson [16]. It is generally agreed that an efficient air removal is the key for a successful penetration. In the course of the technical development of the impregnation step, three different pretreatment techniques have been investigated, though only one has gained practical acceptance.

The first pretreatment is *evacuation of the digester*, but this has proved to be not practical with commercial digesters. Numerous investigations at the laboratory scale have shown, however, that evacuation is the most efficient process for removing air from inside the chips.

An improved penetration can also be achieved by the *replacement of air* by condensable gases. The air inside the cavities of the chips can be replaced by repeated introduction of a gas which is soluble in the cooking liquor at elevated pressure, alternating with relief. A pretreatment procedure, where air is replaced by gaseous  $SO_2$  prior to introducing the cooking liquor, was developed by Montigny and Maass [17]. Although the penetration results were comparable to those of pre-evacuation, this process was not put into practice, mainly because it is more or less limited to the sulfite process and the composition of the cooking liquor cannot be determined precisely since the amount of  $SO_2$  inside the wood chips is essentially unknown.

Finally, the *steaming* process at atmospheric or superatmospheric pressure to remove interstitial air from the wood has achieved broad practical application. Steaming is intended to ensure uniformity of moisture distribution in the chips



**Fig. 4.6** Effect of steam pressure during the pre-steaming of chips from black spruce (*Picea marina*) on the rate of penetration using distilled water at 60 °C; the steaming time was kept constant at 10 min (according to Woods [18]).

and purge air from the inside of the chips. In numerous studies it has been proved that pre-steaming of chips accelerates the rate of subsequent penetration considerably. The degree of penetration is determined by both steam pressure and steaming time. The effect of pre-steaming on the rate of penetration using distilled water at 60 °C was studied by Woods for several steam pressures [18]. The results of the trials with a steaming time of 10 min are shown in Fig. 4.6.

Steaming time can be reduced without impairing the efficiency of impregnation by increasing the steam pressure. The higher degree of penetration of pre-steamed chips can be traced back by a more extensive filling of the cooking liquor (15–30% more than for non-pre-steamed chips) due to the additional space of the air removed, and also to an enhanced outward diffusion of the air. Moreover, it was shown that the cell wall becomes more accessible to water after pre-steaming. Purging according to the Va-Purge process, which includes pre-steaming with intermittent relief, has an even more pronounced effect on fiber structure [19]. When applied at equal pressures and total time, Va-purge steaming is slightly more efficient as compared to continuous steaming only if longer intermittent steaming phases are allowed.

Today, the pre-steaming of chips forms an integral part of the continuous kraft cooking process [20]. Modern batch cooking technology, however, only uses slight pre-steaming of the chips during the chip packing stage. The main objectives of pre-steaming are to preheat the wood chips from ambient temperature to 100–120 °C and to remove noncondensable gases (e.g., air) which are present in the

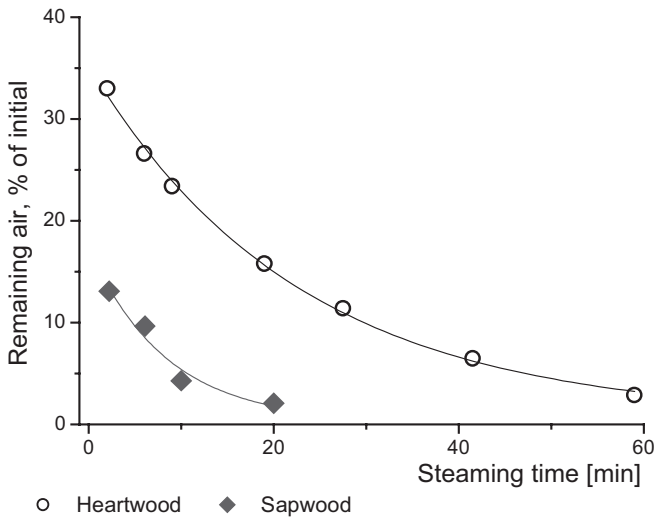
void volume of the chips. The heating of the wood chips is influenced by the wood properties, the chip dimensions, the initial chip temperature, the steam temperature and pressure, and the venting of the steam. Heating of the chip with saturated steam takes place from all three wood dimensions. Most of the heat released from the condensation of steam is consumed in the heating process. According to the simulations, the heating efficiency for sapwood and heartwood pine chips is almost the same [20]. From the results obtained, it can be concluded that the heating of wood chips of typical dimensions with saturated steam is a rapid process, and lasts for only a few minutes. Under industrial conditions, however, a longer heating period may be expected because of the limited heat transfer within the chip layer. When heating chips with saturated steam, only a small part of the water present within the wood voids will vaporize at the moment when the whole chip has been heated to the ultimate temperature. It has been shown that pre-steaming with saturated steam results only in a slight increase in the moisture content of both heartwood and sapwood. If the moisture content exceeds the fiber saturation point, then pre-steaming can even lead to a reduction of the water content [21].

The extent of air removal as a function of steaming time at atmospheric pressure can be described by a simple exponential dependency according to Eq. (37):

$$N = N_0 \cdot \text{Exp}(-k \cdot t) \quad (37)$$

where  $N$  is the amount of entrapped air.

The amount of remaining air as a function of steaming time for heartwood and sapwood from pine is illustrated graphically in Fig. 4.7.



**Fig. 4.7** Effect of steaming at 105 °C on air removal from sapwood and heartwood chips from pine (*Pinus silvestris*) (according to [20]).



In order to achieve a degree of 90% air removal from heartwood, 30 min of steaming is required, while for sapwood only 5–6 min is required.

By increasing the steaming temperature – for example, from 100 °C to 120 °C – the efficiency of penetration increases further, most likely due to a better permeability of the cell wall layers to gases. Hence, a higher temperature can accelerate the dissolution of wood substances at the pit membranes [22].

In practice, complete removal of air may be difficult to achieve, even by applying optimal steaming conditions. Some air cannot be removed because the pressure gradient at the end of pre-steaming is insufficient to overcome the surface tension forces at the liquid–air interface. Moreover, some air can be trapped within capillaries, which are sealed by extractives.

Hardwood species such as poplar, elder and beech wood are more easily penetrated after steaming as compared to spruce [21]. Spruce requires longer steaming time to achieve acceptable degrees of penetration.

Quite recently, the longitudinal permeability and diffusivity of steam in beech wood were estimated simultaneously by using a Wicke-Kallenbach-cell [23]. Both parameters increase slightly with the moisture content of wood. The average values obtained at ambient temperature (20 °C) were  $8.1 \times 10^{-6} \text{ m}^2 \text{ s}^{-1}$  for the axial diffusivity and  $2.2 \times 10^{-11} \text{ m}^2$  for the axial permeability (according to Darcy's relationship:  $V = K_p \cdot \Delta P \cdot \eta^{-1} \cdot L^{-1} v = [\text{m} \cdot \text{s}^{-1}]$   $K_p = [\text{m}^2]$   $\Delta P = [\text{Nm}^{-2}]$   $\eta = [\text{Ns} \cdot \text{m}^{-2}]$   $L = [\text{m}]$ ).

#### 4.2.3.4 Penetration

Penetration describes the flow of liquor into wood under the influence of a hydrostatic pressure gradient which is the sum of external pressure,  $p_E$ , and capillary pressure,  $p_C$ .

$$p_{\text{tot}} = p_E + p_C \quad (38)$$

The capillary pressure can be expressed by the Young–Laplace equation [Eq. (39)]:

$$p_C = \frac{2 \cdot \gamma \cdot \cos\theta}{r} \quad (39)$$

where  $\gamma$  is the surface tension of the impregnation liquor [ $\text{Nm}^{-1}$ ],  $\theta$  is the contact angle between the liquid and the solid phases, and  $r$  is the capillary radius [m].

From Eq. (39) it is clear that the penetration rate is sensitive to the diameter of the individual capillaries. The total pressure,  $p_{\text{tot}}$ , is opposed by the pressure drop due to the liquid flow in the capillaries,  $p_F$ , according to the Hagen–Poiseuille's law of laminar flow [Eq. (40)]:

$$\Delta p_F = \frac{\dot{V} \cdot 8 \cdot \eta \cdot l}{r^4 \cdot \pi} [\text{Pa}] \quad (40)$$

where  $\eta$  is the viscosity of the liquid (in Pa.s),  $V$  is the rate of volume flow (in  $\text{m}^3 \text{ s}^{-1}$ ), and  $l$  is the capillary length or penetration distance (m).

Liquid flow through the capillaries occurs as near-perfect laminar flow. When  $N$  identical capillary tubes of equal length are connected in parallel, the total flow through them equals  $N$  times that of one single tube. For the penetration of a liquid through a porous material with  $N$  parallel capillaries per unit surface area  $A$ , the flow rate of volume flow can be expressed by Eq. (41), derived from Eqs. (38–40):

$$\dot{V} = \frac{N\pi r^2 \cdot (2 \cdot r \cdot \gamma \cdot \cos\theta + P_E \cdot r^2)}{8 \cdot l \cdot \eta} \left[ \frac{m^3}{s} \right] \quad (41)$$

Thus, the penetration rate will increase with any increase in applied external pressure, increase in the capillary radius, with the surface tension of the impregnation liquor, with reduction in liquor viscosity and with the contact angle between the liquid and the solid phases. Since flow varies inversely as the fourth power of the radius of the capillaries, the size of the pit-membrane openings will control the rate of flow.

Acidic liquors penetrate faster than liquors which are sufficiently alkaline to swell the cell walls beyond their water-swollen dimensions, as in the case of soda and kraft liquors.

The ease of penetration of wood depends on the species and whether it is sapwood or heartwood [24]. In contrast to diffusion, penetration is strongly affected by the wood structure, and consequently structural differences between softwood and hardwood must be clearly distinguished. The differences are due to the presence of vessels in hardwoods, which run in the longitudinal direction and which, when unplugged by tyloses, permit rapid penetration into the interior of the wood. The number, diameter and distribution of vessels is highly dependent on the hardwood species. In ring porous woods (e.g., oak) the vessels are concentrated in the early wood, whereas in diffuse porous woods (e.g., beech) they are more uniformly distributed over the annual ring. If the vessels are plugged by tyloses (which frequently occurs), the penetration rate is exceedingly small in all directions. Softwoods are not provided with vessels. There, the tracheids and their interconnecting pit system take over the function of liquid transfer. Compared to easily penetrated hardwoods, penetration through softwoods in a longitudinal direction is less efficient, whereas transverse penetration is more rapid. This can be explained by the fact that the pits in softwood tracheids are much larger and more numerous than in hardwood fibers. The longitudinal flow of liquids is 50- to 200-fold faster than flow in the other directions. Tangential flow in softwoods is controlled by the bordered pits situated on the radial walls of tracheids, while the flow in the radial direction is controlled by ray cells [25]. The permeability of softwoods in the radial direction is considered to be more efficient than in the tangential direction [26]. Thus, it can be concluded that water penetration into softwood chips occurs through the longitudinal direction. Radial flow may contribute a small part of the total penetration, whilst flow in a tangential direction can be neglected. In hardwoods, no liquid flows in the transverse fiber direction [27]. It is assumed that the hardwood fibers are totally enclosed cells, where no liquid trans-

fer occurs. In summarizing these observations, it can be concluded that the optimum conditions for the impregnation of hardwoods is given when the fibers are water-saturated (which is the case at the fiber saturation point) and the vessels are empty, assuming that they are not plugged by tyloses. Liquor could then flow into the interior of the wood via the vessels, and the pulping chemicals could diffuse radially from the vessels into the surrounding fibers through the water present in the cell walls. In case the vessels are plugged by tyloses, which prevents penetration, the wood should be water-saturated in order to provide optimum conditions for diffusion.

A semiquantitative method to determine the penetrability of a wood has been proposed by Stone [24]. The rate of air permeability is measured using an apparatus consisting of two flowmeters in series, the restrictions in one being a glass capillary of known dimensions and the restrictions in the other being a dowel of known dimensions of the wood being tested. By applying the Poiseuille equation, the following relationship is obtained:

$$\text{Penetration Factor} = r_{\text{wood}}^4 = \frac{r_{\text{glass}}^4}{N \cdot A} \cdot \frac{p_{\text{glass}}}{p_{\text{wood}}} \cdot \frac{l_{\text{wood}}}{l_{\text{glass}}} = \text{const} \frac{p_{\text{glass}}}{p_{\text{wood}}} \quad (42)$$

where  $r$  is the radius of capillary,  $p$  the pressure drops,  $l$  the length of capillary,  $N$  the number of capillaries and  $A$  the cross-sectional area of wood.

The porosity of the wood is then defined as the fourth power of the radius of a glass capillary, which would permit the same flow of air as  $1 \text{ cm}^2$  of the wood in question. At this stage, neither  $r_{\text{wood}}$  nor  $N$  – the number of capillaries per unit cross-section – is known. To overcome this problem, all the capillaries in  $1 \text{ cm}^2$  of wood are considered to be gathered together into a single capillary which gives the same rate of flow. For any given glass capillary and length of wood dowel, the penetration factor  $= r_{\text{wood}}^4 = \text{const} \cdot p_{\text{glass}}/p_{\text{wood}}$ . Many different wood species have been characterized according to this penetration factor, and average values for a number of wood species are summarized in Tab. 4.9 [24].

Typically, the ratio of the penetration factor in sapwood to heartwood lies between 10 and greater than 1000. Aspen, beech, Douglas-fir and white oak show poor penetrability. The reason for poor penetrability is the occurrence of tyloses in the vessels which cause blockade of these passages.

Penetration of water into the chips of three selected softwood species, *Picea abies*, *Larix sibirica* and *Pinus silvestris*, was studied using a specially designed impregnator [28]. In agreement with the data listed in Tab. 4.9, penetration into heartwood chips proved to be less efficient than into sapwood chips. In the case of spruce, the degrees of penetration were 65% and 92% into heartwood and sapwood, respectively. The results were similar for the other wood species. Thickness (between 4 and 8 mm) and width do not influence the efficiency of impregnation significantly. The chip length, however, has a much more pronounced effect on the efficiency of penetration, since the longitudinal flow in softwoods is 50- to 200-fold faster than the tangential or radial flows. Impregnation of water can be controlled by adjusting the process conditions. An increase in temperature (e.g.,

Tab. 4.9 Penetrability of a selection of wood species by means of a semiquantitative method [24].

Wood type	Species	Penetration factor $\times 10^{10}$	
		Sapwood	Heartwood
Softwood	<i>Piceas engelmannii</i> , Engelmann spruce	5	3
	<i>Picea mariana</i> , black spruce	n.d.	2
	<i>Pinus contoria</i> , lodgepole pine	300	n.d.
	<i>Pinus echinata</i> , shortleaf pine	120	5
	<i>Pinus elliotii</i> , slash pine	6000	10
	<i>Pinus monticola</i> , white pine	100	10
	<i>Pinus palustris</i> , longleaf pine	4000	2
	<i>Pseudotsuga taxifolia</i> , Douglas fir	70	5
Hardwood	<i>Acer negundo</i> , box elder	1300	400
	<i>Acer rubrum</i> , maple	400	120
	<i>Betula papyrifera</i> , white birch	1300	450
	<i>Caryax</i> spp., hickory	4000	400
	<i>Fagus grandifolia</i> , American beech	1000	0.5
	<i>Fraxinus nigra</i> , American ash	80	n.d.
	<i>Liquidambar styraciflua</i> , sweet gum	1200	850
	<i>Platanus occidentalis</i> , sycamore	4000	4000
	<i>Populus deltooides</i> , cottonwood	4000	500
	<i>Populus tremula</i> , European aspen	5000	4
	<i>Populus tremuloides</i> , American aspen	2500	1
	<i>Quercus alba</i> , white oak	0.7	n.d.
	<i>Quercus coccinea</i> , scarlet oak	1000	400
	<i>Quercus falcata</i> , red oak	4000	5
	<i>Ulmus americana</i> , elm	400	70

n.d. = not determined

from 20 to 80 °C) accelerates the degree of penetration, whereas the final value for water uptake is not influenced. Increasing the pressure results in a higher compression of air within the chip voids, thus facilitating water flow into the wood capillaries (from 2 to 9 bar: the final value increased from 76% to 92%). The degree of penetration, P, can be improved from 75% to almost 94% as a result of pre-steaming the chips.

Quite recently, a mathematical model describing the process of water penetration into softwood chips was developed [29]. The model considers the important physico-chemical phenomena, including capillary rise, air dissolution and outward diffusion as well as the decrease in the permeability coefficient of wood as a function of the degree of penetration. A simulation program based on the model was able to predict the process of water penetration accurately. It was found that for simulating the process of water penetration at different temperatures, the

empirical dependence of the permeability coefficient on the temperature must be inserted into the model. The prediction of white liquor penetration into softwood chips was possible considering the dependence of chemical interactions between the constituents of white liquor and wood components on the permeability of wood chips. Black liquor penetration into softwood chips, however, cannot be simulated with sufficient precision by using the proposed model, possibly due to unknown interactions between organic molecules and wood components or to a non-Newtonian behavior of the black liquor at the beginning of the penetration process.

It was shown that pretreatment of Aspen chips (*Populus tremuloides*) with alkali increased the permeability of the individual fiber walls and thus increased the rate of diffusion of water-soluble substances [30]. The mechanism of improved penetration of pulping chemicals was attributed to the saponification of uronic acid esters of the 4-*O*-methylglucuronoxylans, which are assumed to be cross-linked with other wood components. As soon as these cross-links are broken, the wood structure is allowed to swell beyond the water-swollen state. There was also clear experimental evidence that opening of the wood structure also occurs in the middle lamella, possibly due to the cleavage of cross-link structures between galacturonic acid esters of pectic polysaccharides and lignin structures [31]. Consequently, penetration into the wood structure is improved.

Under industrial pulping conditions, the chips are impregnated with hot black liquor (HBL) [32]. Compared to water, the following physical properties from black liquor have been determined (Tab. 4.10).

Tab. 4.10 Surface properties of black liquor and water.

Liquid	Unit	Black liquor		Water	
		20	80	20	80
Temperature	°C				
Dynamic viscosity	mPas	2.60	0.81	0.99	0.36
Surface tension	mN m <sup>-1</sup>	32.6	27.7	67.3	63.0

Industrial pine (*Pinus silvestris*) was used for the impregnation tests and subsequent Superbatch<sup>®</sup> cooking. The results showed that pre-steaming of chips and increased pressure (from 2 to 9 bar) had a favorable effect on the efficiency of black liquor impregnation into heartwood and sapwood. The effect of penetration pressure was more pronounced for heartwood chips due to the high amount of air initially present within the chips. By applying 9 bar overpressure during penetration into sapwood chips, it was possible to reach a degree of penetration of 99.6%. When pre-steaming is finished and the chip temperature is reduced, condensation of water within the chip voids occurs. The vacuum thus formed facilitates the uptake of condensate from chip surface into voids. The effect of pre-steaming can

be explained primarily by the removal of air from the chip voids. In addition, de-aeration of heartwood pits during steaming could also be considered as a cause of improved penetration. The results of the Superbatch<sup>®</sup> cooking experiments confirmed that efficient liquor penetration has a favorable influence on cooking. The application of chip pre-steaming and high pressure during the initial cooking stages (warm black liquor impregnation) resulted in a lower amount of rejects and kappa number, whereas the screened yield remained unaffected. In the case of heartwood, the presence of entrapped air can be considered as the primary cause of possible heterogeneity in delignification, whereas in the case of sapwood there are diffusion limitations. With heartwood chips, the effect of liquor temperature is significant. In addition to a lower viscosity, the softening by the warm liquor of resin compounds present in the pine heartwood capillaries is likely to cause faster penetration under higher temperatures. The unbleached pulps produced with different modes of impregnation were subjected to ECF bleaching using an O-D<sub>0</sub>ED<sub>1</sub>ED<sub>2</sub> sequence [33]. To reach the full brightness of 88% ISO, 20 kg more of active chlorine (ClO<sub>2</sub>) must be used for pulp produced using no pre-steaming and low-pressure impregnation during the HBL stage, as compared to pulp which was pre-steamed and treated at higher pressure during the HBL stage. The differences in chemical consumption are caused solely by differences in the incoming kappa number of the pulps, and not by their bleachability. The equivalent chlorine multiple remains 0.35 to achieve 88% ISO in all cases.

#### 4.2.3.5 Diffusion

All transfer of cooking chemicals into chips, and dissolved matter from the chips, will occur through diffusion only after complete penetration. Consequently, molecular diffusion is a very important step in chemical pulping.

To understand the process of impregnation, much effort has been made to follow the distribution of the active cooking chemicals within the void structure of the wood by both experimental studies and theoretical considerations. McKibbins contributed the first rather complete description of the diffusion of sodium ions in kraft-cooked chips [34]. He measured the diffusivity of sodium ions by immersing the cooked chips in distilled water, and compared the measured chip sodium concentration as a function of time to those predicted by unsteady-state diffusion theory.

Data were obtained for extraction in the transverse and longitudinal directions of the wood for several temperatures and sample thicknesses.

Unsteady-state and unidirectional and isothermal diffusion in one dimension may be described by Fick's second law of diffusion according to Eq. (43):

$$\frac{\partial c}{\partial t} = D \frac{\partial^2 c}{\partial x^2} \quad (43)$$

It is assumed that diffusion occurs through a homogeneous material of constant width or thickness,  $L$ , with an initial concentration  $c_i$ , and that the solute leaves at

both faces which are maintained at a constant concentration,  $c_0$ . There is no single integral solution to this differential equation, but a variety of solutions have been derived depending on the boundary and other conditions [35].

Equation (43) may be solved by applying the following initial and boundary conditions:

- Initial conditions:  $t = 0, c = c_i$  for all  $x$
- Boundary conditions:  $x = 0, L, c = c_0$  for  $t > 0$
- $c_0$  concentration of sodium ions outside the chips
- $c_i$  concentration of sodium ions inside the cooked chips

Considering these initial and boundary conditions yields Eq. (44):

$$Y = \frac{c - c_0}{c_i - c_0} = \frac{8}{\pi^2} \sum_{n=1}^{\infty} \frac{1}{(2n-1)^2} \text{Exp} \cdot \left[ \frac{-(2n-1)^2 \pi^2 D \cdot t}{L^2} \right] \quad (44)$$

where  $Y$  equals the average fraction of unextracted sodium ions.

The solution of this infinite series reduces to a single term for values of  $(D \cdot t \cdot L^{-2}) > 0.03$ , which is accomplished when  $Y < 0.6$ . In this very likely case, Eq. (44) reduces to Eq. (45):

$$Y = \frac{c - c_0}{c_i - c_0} = \frac{8}{\pi^2} \cdot \text{Exp} \cdot \left[ -\frac{\pi^2 D \cdot t}{L^2} \right] \quad (45)$$

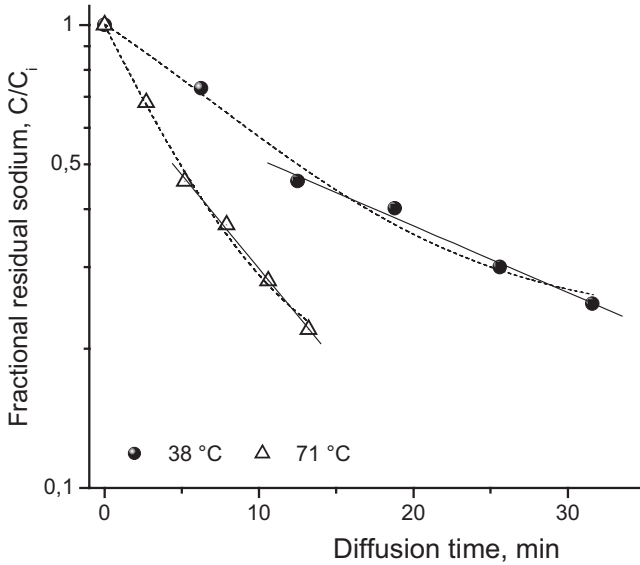
According to Eq. (45), the diffusion coefficient can be determined from the slope  $k$  of the linear correlation obtained by plotting the natural logarithm of  $Y$  against time. The diffusion coefficient  $D$  can thus be calculated using Eq. (46):

$$D = \frac{k \cdot L^2}{\pi^2} \quad (46)$$

In case diffusion occurs in more than one direction, Eq. (43) must be expanded to include the new coordinates. It has been shown that for certain geometries and sets of boundary conditions, the solution for multidirectional diffusion is the product of the solution for unidirectional diffusion for each of the coordinates involved. Considering diffusion in the  $x$ ,  $y$ , and  $z$  directions, the average concentration of a rectangular parallelepiped will be equal to the product of the concentrations obtained for each of these directions according to Eq. (47):

$$Y_{av} = Y_x \cdot Y_y \cdot Y_z \quad (47)$$

The diffusion coefficient,  $D$ , is determined by plotting the logarithm of the fractional residual sodium content against the diffusion time. The values of the diffusion coefficients are determined from the slope of the straight-line portion of these curves (Fig. 4.8).



**Fig. 4.8** Residual sodium fractions versus extraction or diffusion time for unidirectional longitudinal diffusion from 0.3175 cm-thick wood chips (according to McKibbins [34]).

The diffusion coefficients in longitudinal directions at 38 °C and 71 °C can be determined by putting the calculated slopes determined from the natural logarithm of  $Y$  against extraction or diffusion time in Fig. 4.8 into Eq. (46) according to Eq. (48):

$$D_{38^{\circ}\text{C},\text{longitudinal}} = \frac{6.95 \cdot 10^{-4} \text{ s}^{-1} \cdot (3.175 \cdot 10^{-3})^2 \cdot \text{m}^2}{\pi^2} = 7.1 \cdot 10^{-10} \text{ m}^2 \cdot \text{s}^{-1} \quad (48)$$

$$D_{71^{\circ}\text{C},\text{longitudinal}} = \frac{1.86 \cdot 10^{-3} \text{ s}^{-1} \cdot (3.175 \cdot 10^{-3})^2 \cdot \text{m}^2}{\pi^2} = 19.0 \cdot 10^{-10} \text{ m}^2 \cdot \text{s}^{-1}$$

Since the diffusion process is a rate phenomenon,  $D$  may be related to the temperature by an Arrhenius-like relation. An associated activated energy,  $E_A$ , is required according to Glasstone, Laidler and Eyring to elevate the diffusing molecules to that energy level sufficient to initiate molecular transport [36]. The diffusion coefficient may thus be related to the temperature in the following manner [Eq. (49)]:

$$D = A \cdot \sqrt{T} \cdot \text{Exp}\left(-\frac{E_A}{R \cdot T}\right) \quad (49)$$

A plot of the natural logarithm of the ratio  $D$  to the square root of the absolute temperature against the reciprocal of the absolute temperature results in a straight line with a slope dependent on the activation energy,  $E_A$ . The experimen-



tal results obtained for the diffusion coefficients and activation energies for both longitudinal and transverse direction are summarized in Tab. 4.11.

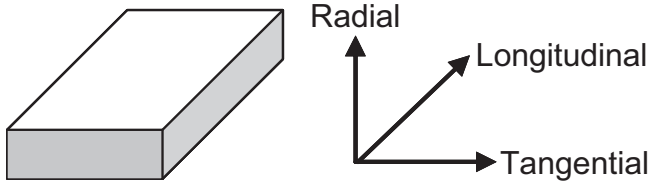
**Tab. 4.11** Diffusion coefficients as a function of temperature and activation energies according to [34] (recalculated).

Direction of diffusion	Diffusion length L [mm]	Diffusion coefficient $D \cdot 10^{10} [\text{m}^2 \text{s}^{-1}]$ at T [°C]			Frequency factor $A \cdot 10^7 [\text{m}^2 \text{s}^{-1}]$	Activation energy $E_A [\text{kJ mol}^{-1}]$
		38	52	66		
Longitudinal	3.2	7.1	12.0	18.0	8.0	25.5
	6.4	8.4	14.0	21.0	18.9	27.3
Transverse	3.2	3.6	5.8	6.8	0.5	20.2
	6.4	3.6	6.0	7.5		

The rate of diffusion in the longitudinal direction is higher as compared to the transverse direction due to the hindrance offered by the tracheid walls. The ratio is, however, rather low for cooked chips as, with the solubilization of the middle lamella, the resistance to mass movement especially in the transversal directions has been considerably reduced. A significantly higher ratio has been determined in untreated wood. Behr, Briggs and Kaufert [37] found that the ratio of coefficients for longitudinal to tangential diffusion was approximately 40 for uncooked spruce. Christensen also reported a ratio of about 40 for the diffusion of sodium chloride in uncooked pine samples [38]. Diffusion in the radial direction, however, was less restricted and the ratio between longitudinal to radial diffusion was only approximately 11 in the temperature range between 20 and 50 °C. The corresponding diffusion coefficients in longitudinal, tangential and radial directions at 20 °C were measured as  $5 \times 10^{-10} \text{ m}^2 \text{ s}^{-1}$ ,  $0.12 \times 10^{-10} \text{ m}^2 \text{ s}^{-1}$  and  $0.46 \times 10^{-10} \text{ m}^2 \text{ s}^{-1}$ , respectively (see also Tab. 4.13) [38].

McKibbins worked under neutral conditions and used cooked chips as a model substrate. Thus, the results of his investigations were primarily applicable to the washing of unbleached kraft pulps.

Talton and Cornell also studied the temperature-dependence of the diffusivity of sodium hydroxide at a pH greater than 12.9 out of uncooked chips into a water bath [39,40]. Chips from plantation-grown loblolly pine were handcut to dimensions of 25 mm (longitudinal) by 25 mm (tangential) by 3–6 mm (radial). To eliminate diffusion in the longitudinal and tangential directions, the sides of the chips were coated with an impermeable barrier, as shown in Fig. 4.9.



**Fig. 4.9** Definition of chip parameters according to Talton and Cornell [40].

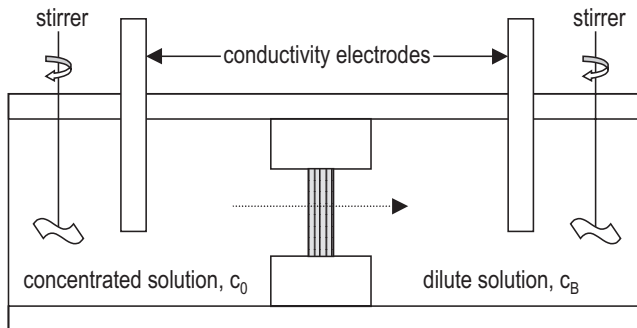
The data were correlated to temperature using Eq. (49). The results obtained for the frequency factor,  $A$ , and the activation energy,  $E_A$ , were  $1.36 \times 10^{-7} \text{ m}^2 \text{ s}^{-1}$  and  $22.3 \text{ kJ mol}^{-1}$ , respectively. Thus, a diffusion coefficient at  $38^\circ\text{C}$  in the radial direction calculates to  $4.2 \times 10^{-10} \text{ m}^2 \text{ s}^{-1}$ , which is close to the value determined by McKibbins, though for cooked chips (see Tab. 4.11). Talon and Cornell also measured the influence of the diffusion coefficient on the extent of kraft pulping in the yield range between 67% and 99% at  $30^\circ\text{C}$ . They found a linear relationship between the diffusion coefficient and the yield percentage. By combining the temperature and the yield dependency of the diffusion coefficient, the following expression can be obtained:

$$D = \sqrt{T} \cdot [1.24 \cdot 10^{-6} - 1.12 \cdot 10^{-8} \cdot Y_{perc}] \cdot \text{Exp} \cdot \left( -\frac{2688}{T} \right) \quad (50)$$

where  $Y_{perc}$  represents the pulp yield after kraft pulping.

Assuming a pulp yield of 67%, the diffusion coefficient  $D$  increases to  $15.3 \times 10^{-10} \text{ m}^2 \text{ s}^{-1}$  at  $38^\circ\text{C}$ , which is more than four-fold the value found by McKibbins.

Both McKibbins and Talton and Cornell measured the diffusion coefficients in the reverse direction, for example, from saturated uncooked or cooked wood to dilute solution, neglecting eventual hysteresis effects [41].



**Fig. 4.10** Apparatus for determining the diffusion coefficient through wood chips.

Robertsen and Lönnberg determined the diffusion of NaOH in the radial direction of spruce (*Picea abies*) using a diffusion cell consisting of two chambers which are connected by a square opening into which a wood chip fits [1,42]. The only diffusion contact between the two chambers was through the mounted wood chip. A scheme of the diffusion cell is shown in Fig. 4.10.

Both sides are provided with stirrers, the intention being to avoid concentration gradients. The chambers are equipped with conductivity measurement cells and temperature compensation probes. The concentration  $c_B$  in the dilute solution is calculated with the Debye–Hückel–Onsager equation when

$$c_B = \frac{\kappa_b}{\Lambda_B} \quad (51)$$

where  $\kappa_b$  is the conductivity and  $\Lambda_B$  is the molar conductivity of  $c_B$ .

The molar conductivity can be calculated using the Debye–Hückel–Onsager equation:

$$\Lambda_B = \Lambda_m^0 - (A + B \cdot \Lambda_m^0) \cdot \sqrt{c_B} \quad (52)$$

with  $\Lambda_m^0$  the limiting molar conductivity at infinite dilution. A and B are known functions of the Debye–Hückel–Onsager coefficients of water ( $A = 60.2$ ;  $B = 0.229$ ).

Provided that D is independent of the concentration of the impregnation liquor, the diffusion can be assumed to follow Fick's first law of diffusion:

$$J = -D \cdot \frac{dc}{dL} \quad (53)$$

where J is the alkali molar diffusive flow velocity [ $\text{mol m}^2 \text{s}^{-1}$ ], D is the diffusion coefficient in the wood [ $\text{m}^2 \text{s}^{-1}$ ], and L is the chip thickness [m].

In case steady-state conditions are attained, the diffusion rate through the plate is constant and thus J can be expressed by Eq. (54):

$$J = D \cdot A \cdot \frac{(c_0 - c_B)}{L} \quad (54)$$

where A is the effective area of the plate,  $c_0$  and  $c_B$  are the concentrations of the two liquids, and  $c_0 > c_B$ . The diffusion coefficient, D, can be computed by application of Eq. (54). The electrical conductivity of the dilute solution,  $c_B$ , is plotted against diffusion time. The slope of the resulting curve and the relationship between the solute concentration (e.g., NaOH) and conductivity, the chemical transport by diffusion can be calculated as  $\text{mol time}^{-1}$ .

The intimate contact of hydroxide ions with wood components immediately leads to deacetylation reactions [41]. Molecular diffusion can be determined alone only after completing deacetylation reactions prior diffusion experiments. Further-

more, if convective flow can be neglected, it can be assumed that for each value of time  $t$ , Fick's first law of diffusion applies according to Eq. (53).

Since  $J$  can be defined as

$$J = \frac{V}{A_i} \cdot \frac{dc_B}{dt} \quad (55)$$

where  $V$  is the diffusion cell volume which is constant over time,  $A_i$  the interface area of the wood chip in the experimental diffusion cell and combining Eqs. (53) and (55), and when assuming that the chip is very thin, then the derivative can be approximated by the incremental ratio  $\Delta c/\Delta L = (c_0 - c_B)/L$  and the relationship can be expressed in Eq. (56):

$$\frac{V}{A_i} \cdot \frac{dc_B}{dt} = -D \cdot \frac{(c_0 - c_B)}{L} \quad (56)$$

When  $c_0 \gg c_B$ , which can be assumed as the bulk concentration  $c_0$ , is kept constant, then

Eq. (56) yields to the following expression:

$$D = \frac{L \cdot V \cdot \left(\frac{dc_B}{dt}\right)}{A_i \cdot C_0} \quad (57)$$

where  $(dc_B/dt)$  is the slope of the experimental results. It must be ensured that the slope remains constant, and this can be achieved by successive experiments conducted at moderate temperatures (so that only deacetylation occurs).

The procedure to calculate  $D$  can be explained on the basis of a simple experiment described by Constanza and Constanza [43]:

As wood sample radial poplar wood chips were used:

- Temperature            298 K
- $C_0$  (NaOH)            1 mol L<sup>-1</sup>
- $L$  (chip thickness)    0.15 cm
- $V$                         1000 cm<sup>3</sup>
- $A_i$                         8.41 cm<sup>2</sup>

Three consecutive experiments were conducted to ensure that the deacetylation reactions were complete. In the third experiment, the assumption that only diffusion occurred appeared to be correct. The slope of the diffusion experiment was determined as  $5.50 \times 10^{-6}$  S cm<sup>-1</sup> · min<sup>-1</sup>. Considering a molar conductivity of NaOH of  $232 \times$  S cm<sup>2</sup> mol<sup>-1</sup>, the experimental diffusion coefficient was obtained:

$$\begin{aligned} D &= \frac{L \cdot V \cdot \left(\frac{dc_B}{dt}\right)}{A_i \cdot C_0} = \frac{0.15 \cdot 1000 \cdot \left[\frac{\text{cm}^2 \cdot \text{l}}{\text{mol}}\right]}{8.41 \cdot 1} \cdot 2.414 \cdot 10^{-5} \left[\frac{\text{mol}}{\text{l} \cdot \text{min}}\right] \\ &= 4.31 \cdot 10^{-4} \left[\frac{\text{cm}^2}{\text{min}}\right] = 7.18 \cdot 10^{-10} \left[\frac{\text{m}^2}{\text{s}}\right] \end{aligned} \quad (58)$$

This value was quite comparable to data reported previously (see Tab. 4.13).

Robertsen and Lönnberg studied the influence of NaOH concentration in the range between 0.5 and 2 mol L<sup>-1</sup> and the temperature dependence in the range of 300 to 400 K. They experienced a slight increase in diffusion with time, probably due to the progressive dissolution of wood components. Not surprisingly, due to the high level of caustic concentration, no dependency of D on the NaOH concentration was observed. The temperature dependency was evaluated according to Eq. (49). The results obtained for the frequency factor, A, and the activation energy, E<sub>A</sub>, were  $3.02 \times 10^{-7} \text{ m}^2 \text{ s}^{-1}$  and  $E_A = 23.7 \text{ kJ mol}^{-1}$ , which were close to the values found by Talton and Cornell for NaOH diffusion in uncooked loblolly pine wood.

In a recent study, Constanza et al. determined the diffusion coefficient in the radial direction of poplar wood (*Populus deltoides carolinensis*) [41,43]. A significant sigmoid dependency of D on the alkali concentration, especially in the range between 0.05 and 0.2 mol L<sup>-1</sup>, was found (Fig. 4.11).

The relationship between the pH of an aqueous solution and the diffusion was reported previously using the concept of effective capillary cross-sectional area (ECCSA) [44–46]. ECCSA describes the area of the paths available for the chemical transport which may be proportional to the diffusion coefficient. ECCSA was originally determined as the ratio of the resistance R of bulk solution to the resistance R' through the wood of the same thickness. It is a measure for the total cross-sectional area of all the capillaries available for diffusion. It is defined as the ratio of the area available for diffusion to the area which would be available if no wood at all were present. Stone [44] used aspen (*Populus tremuloides*) as a wood source for the first trials. In the longitudinal direction, ECCSA is independent of pH and time and showed a value of about 0.5, which meant that 50% of the gross external cross-sectional area would be available for diffusion. In the tangential and radial directions, however, the area available for diffusion was very limited until a pH of approximately 12.5 was reached (Fig. 4.12).

By further increasing the pH, the ECCSA in the transverse direction approaches almost 80% of the permeability in the longitudinal direction. The pH dependency may be related to the swelling effect. The increased porosity of the cell walls at pH levels higher than 12.5 can be led back to the high swelling of the hydrophilic part of the wood components, mainly the carbohydrate fraction. The interaction between the solute ions and the carbohydrate fraction reaches a maximum at a pH of 13.7, which corresponds to the pK<sub>a</sub> of the hydroxy groups. From the results obtained with uncooked chips (Stone with aspen [44], Häggglund with spruce [45]), it can be concluded that strongly alkaline aqueous solutions (>0.5 mol L<sup>-1</sup>) can be considered capable of diffusing into wood at almost the same rates in all three structural directions. Bäckström investigated the influence of ECCSA on the pulping yield using pine as a raw material. The experiments were made at a constant pH of 13.2, and the results confirmed the assumption that with progressive pulping the accessibility increases in the transverse directions (Fig. 4.13).

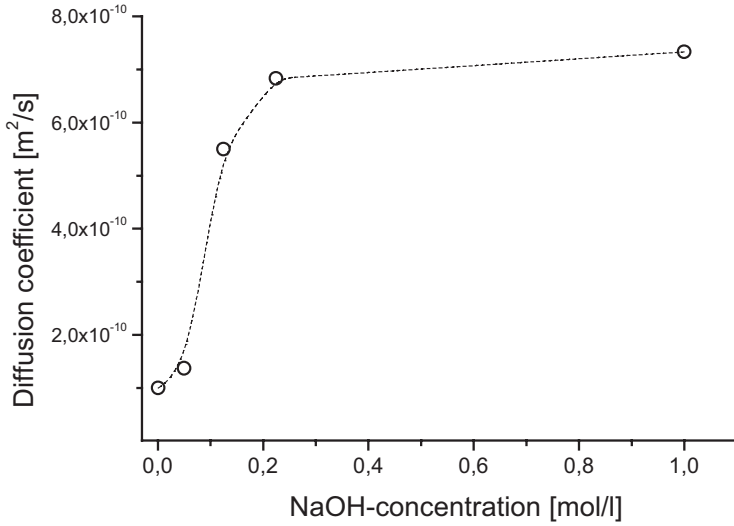


Fig. 4.11 Radial diffusion coefficient as a function of NaOH concentration (according to [41]).

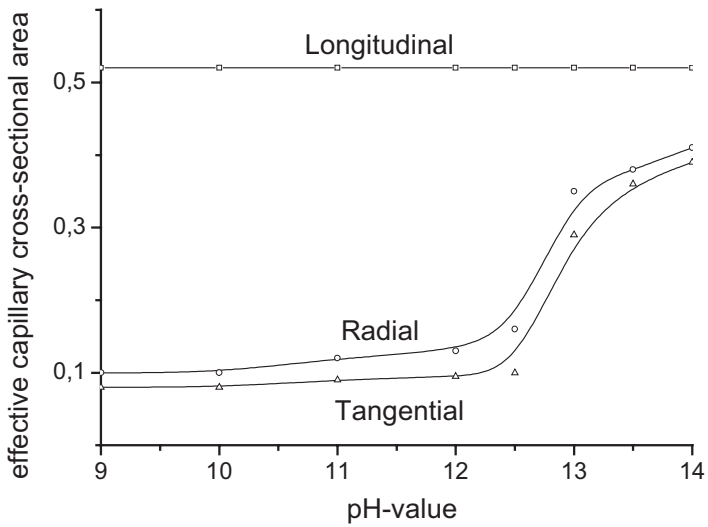


Fig. 4.12 Effective capillary cross-sectional area of aspen after 24 h of steeping in aqueous alkaline solutions as a function of pH (according to [44]).

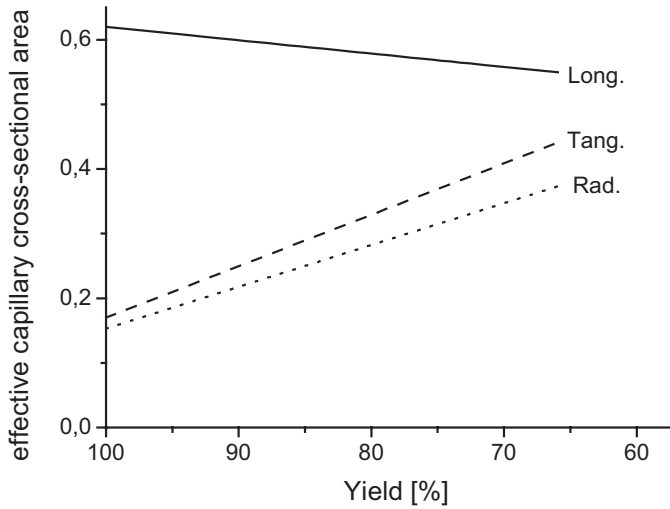


Fig. 4.13 ECCSA at a pH of 13.2 as a function of pulp yield after kraft cooking of pine (according to [46]).

ECCSA can also be related to  $D$  according to the following expression:

$$D = D_{Na^+-water}(T) \cdot ECCSA \quad (59)$$

where  $D_{Na^+-water}(T)$  is the diffusion coefficient for sodium ions in a solution of highly diluted NaOH. ECCSA compensates for the pH and the pulp yield in the diffusion of sodium ions in the uncooked or cooked wood chips [47]. Equation (59) demonstrates that the diffusion rate is controlled by the total cross-sectional area of all the capillaries, rather than their individual diameters.

Quite recently, another approach has been undertaken to determine the active cross-sectional area [48]. It is assumed that all the pores in the different directions investigated can be approximated as a bundle of linear capillaries. In the longitudinal direction, the flux of water through a wood chip is calculated by using Darcy's law:

$$J = \frac{dV}{dt} \cdot A_\phi = -\frac{k_L}{\eta} \cdot \left(\frac{dp}{dl}\right) \approx \frac{k_L \cdot \Delta p}{\eta \cdot l} \quad (60)$$

where  $dV$  is the volume of the water that passes the wood chip in time  $dt$ ,  $dp/dl$  is the pressure gradient,  $k_L$  is the longitudinal permeability, and  $\eta$  is the viscosity of water. Rearranging Eq. (60) gives the equation for the determination of the active cross-sectional area in longitudinal direction  $A_\phi$ :

$$A_\phi = \frac{\left(\frac{dV}{dt}\right) \cdot \eta \cdot l}{k_L \cdot \Delta p} \quad (61)$$

The flow of water through the wood chips is measured in the longitudinal direction by applying a small pressure ( $p$ ) according to the descriptions in ASTM 317 [49]. Several different pressures are used, and  $(k_L \eta^{-1} \cdot l^{-1})$  is measured as the slope of the assumed linear water flux.

Due to a very small flow, the active cross-sectional area in tangential direction cannot be measured accurately using the equipment described in ASTM 316 [49]. Alternatively, the active cross-sectional area in tangential direction is calculated by using the Stokes–Einstein model for diffusion:

$$D = \frac{k \cdot T}{6 \cdot \pi \cdot \eta \cdot a_{NaCl}} \quad (62)$$

where  $a$  is the mean radius of the sodium ions and  $\eta$  is the kinematic viscosity.

Assuming that NaCl does not interact with the wood, the active cross-sectional area in tangential direction can be calculated by combining Eqs. (62) and (57). Rearranging for an explicit expression of the active cross-sectional area  $A_\phi$  in tangential direction gives

$$A_\phi = 6\pi \cdot \frac{\left(\frac{\Delta c_B}{\Delta t}\right) \cdot V \cdot L \cdot \eta \cdot a_{NaCl}}{k \cdot T \cdot c_0} \quad (63)$$

The results for the active cross-sectional area for the three wood species pine, birch and spruce, as calculated with Eqs. (61) and (63) are presented in Tab. 4.12.

**Tab. 4.12** The active cross-sectional area determined for the wood species pine, birch and spruce.

Directions	Pine [m <sup>2</sup> ]	Birch [m <sup>2</sup> ]	Spruce [m <sup>2</sup> ]
Tangential	0.042	0.023	0.032
Longitudinal	0.736	0.532	0.787

The values presented in Tab. 4.12 are slightly higher in the longitudinal and lower in the tangential directions as compared to the ECCSA values published by Hartler for spruce [50] and Stone for aspen [44]. In relation to the values for spruce and pine, the calculated value for  $A_\phi$  for birch is obviously too low considering the very high diffusion coefficient (see Chapter 4.2.3.5.1).

An overall diffusion coefficient for white liquor  $D_{wL}(T)$  has been developed by using the Stokes–Einstein relationship [see Eq. (62)] to the following expression [51]:

$$D_{wL}(T) = 1.6 \cdot 10^{-9} \frac{1.083}{2.0 \cdot \eta_w(T)} \frac{T}{290} \quad (64)$$



where the coefficients are related to the value of  $D_{wl}(T)$  at 17 °C as a reference. The kinematic viscosity of the white liquor is approximated by doubling the value for water,  $\eta_w$ , which is  $1.0 \text{ m}^2 \text{ s}^{-1}$  at 20 °C and  $0.28 \text{ m}^2 \text{ s}^{-1}$  at 100 °C.

The combined dependence of the diffusivity of sodium ions on temperature, hydroxide ion concentration and the residual lignin fraction was taken into account by one single expression [52]:

$$D = 9.5 * 10^{-8} \cdot \sqrt{T} \cdot \text{Exp}\left(-\frac{2452.4}{T}\right) \cdot (-2.0 \cdot \alpha_L + 0.13 \cdot [\text{OH}^-]^{0.55} + 0.58) \quad (65)$$

where  $\alpha_L$  is the mass fraction of lignin.

This expression for the diffusion coefficient of sodium ions is integral part of the kinetic model for kraft pulping introduced in Chapter 4.2.5 (Reaction kinetics).

#### 4.2.3.5.1 Dependency of D on Wood Species

The diffusion of  $\text{Na}_2\text{S}$  and  $\text{NaOH}$  into birch (*Betula verrucosa*), pine (*Pinus sylvestris*) and spruce (*Picea abies*) was studied separately in longitudinal and tangential directions at 25 °C [48]. The apparatus used in the diffusion experiments was similar to that described by Robertsen (see Fig. 4.10) [1]. The major objective of this investigation was to measure the concentration dependence of  $D$  for the three different wood species. The results confirmed the high dependence of  $D$  on the concentration of both  $\text{HS}^-$  and  $\text{OH}^-$  ions. Tangential diffusion in birch is significantly higher for both ions as compared to the softwood species. In addition, the diffusion coefficient for  $\text{NaOH}$  in birch was more than 10-fold that in the longitudinal direction ( $D_{\text{tang},25^\circ\text{C}} = 192 \times 10^{-10} \text{ m}^2 \text{ s}^{-1}$  versus  $D_{\text{long},25^\circ\text{C}} = 14 \times 10^{-10} \text{ m}^2 \text{ s}^{-1}$  at a  $\text{NaOH}$  concentration of  $1 \text{ mol L}^{-1}$ ). The exceptionally high diffusion in the tangential direction has been attributed to the presence of transversal wood ray in birch, which offers channels with a more open structure than the pores that connect the fibers to each other. Moreover, an extremely value of  $D$  ( $\sim 300 \times 10^{-10} \text{ m}^2 \text{ s}^{-1}$ ) of  $\text{HS}^-$  in pine in the longitudinal direction with a sharp maximum at  $0.7 \text{ mol L}^{-1}$  is reported. It was speculated that both the activity of the solutions and a change in capillary effects may partly explain the large value of  $D$ . In summarizing the results, it can be concluded that the diffusion characteristics of  $\text{NaOH}$  were found to be quite similar for pine and birch. For spruce, the diffusion of  $\text{NaOH}$  proceeds very slowly, especially at low concentrations. The poor diffusion characteristics of spruce can be related to the reported difficulties in the impregnation of spruce wood under industrial conditions which results in high reject contents.

#### 4.2.3.5.2 Diffusion Rate of Lignin Macromolecules [53]

The intrinsic diffusion rate of kraft lignin within the fiber walls of a black spruce kraft pulp can be determined under alkaline conditions using a displacement cell. A very wide distribution of  $D$ -values ranging from  $10^{-13}$  to  $10^{-19} \text{ m}^2 \text{ s}^{-1}$  was

obtained by analyzing the diffusion rate with a computer model based on the mathematical solution for diffusion in a hollow cylinder. The diffusion rate increased with increasing pH (12–14). A large portion of the D-values of kraft lignin determined at pH 13 was about  $10^{-17} \text{ m}^2 \text{ s}^{-1}$ . Furthermore, it was found that the diffusion rate was affected not only by the size of lignin molecules and pores, but also by electrostatic interactions between pore walls and lignin. With increasing electrolyte concentration, the thickness of the electrostatic double layer decreases. At higher ionic strength, the repulsive forces on the diffusion of molecules with higher charge density will be reduced.

#### 4.2.3.5.3 Effect of Pressure Steaming on Ion Diffusion [48,54]

The pretreatment of pine (*Pinus sylvestris*), birch (*Betula verrucosa*) and spruce (*Picea abies*) chips with hydrothermal steaming at a temperature of 160 °C and a pressure of 6 bar affects the diffusivity of sodium salts in different ways. The water content in the voids reached approximately 100% with steaming, but only 80% after immersion in de-ionized water for 24 h. Pre-steaming affects the tangential flux less than the longitudinal, and this can be attributed to the combined effects of opening pores and swelling. In the longitudinal direction, the steaming increases both the active area of diffusion and the length of flow. The tangential diffusivity of the  $\text{OH}^-$  and  $\text{HS}^-$  ions is, however, only improved in spruce – which indicates that steaming is a very efficient pretreatment for this wood species. Nonetheless, in the transverse direction pre-steaming is an efficient way to increase the water content in the void structure of the other wood species pine and birch.

#### 4.2.3.5.4 Comparative Evaluation of Diffusion Coefficients

Table 4.13 provides a selected overview of published D-values for sodium ions from both NaOH and NaCl in radial and tangential directions of a variety of wood species. For reasons of comparison, the D-values were calculated or directly determined at 25 °C.

The measured diffusion coefficients for the important radial direction were in rather good agreement. This was very surprising, because quite different experimental set-ups (from saturated wood to dilute solution versus from high concentration in the bulk liquid to low concentration in the wood void system), analytical methods to determine the sodium ions, wood species and modes of calculation (Fick's first versus second laws of diffusion) were applied. The diffusion coefficient in the radial direction out of cooked chips, as determined by McKibbins, appeared to be comparatively low, though this may have been caused by diffusion combined with chemical reaction (deacetylation), as was noted by Constanza et al. [41]. On the other hand, their objection was quite doubtful because cooked chips no longer contain acetyl groups. Very remarkable, however, was the very low activation energy determined by Kazi and colleagues [55,56] which was almost one magnitude lower as compared to values obtained by others (see Tab. 4.13). Two

**Tab. 4.13** Comparison of published diffusion coefficients (D) of sodium ions at various conditions and wood substrates, T = 25 °C = const.

Publication	Species	Yield [% o.d.]	C <sub>NaOH</sub> [mol L <sup>-1</sup> ]	D <sub>long</sub> *10 <sup>10</sup> [m <sup>2</sup> s <sup>-1</sup> ]	D <sub>rad</sub> *10 <sup>10</sup> [m <sup>2</sup> s <sup>-1</sup> ]	A <sub>long</sub> * 10 <sup>7</sup> [m <sup>2</sup> ·s <sup>-1</sup> ·K <sup>-0.5</sup> ]	E <sub>A, long</sub> [kJ mol <sup>-1</sup> ]	A <sub>rad</sub> * 10 <sup>7</sup> [m <sup>2</sup> s <sup>-1</sup> · K <sup>-0.5</sup> ]	E <sub>A, rad</sub> [kJ mol <sup>-1</sup> ]
McKibbins, 1960	Spruce	x50	neutral	4.7	2.6	7.97	25.5	0.53	20.2
Christensen, 1951	Pine	100	neutral	5.7	0.5	0.57	18.5	0.02	16.6
Talon & Cornell, 1987	Lobolly pine	99	pH > 12.9		2.9			1.36	22.3
Talon & Cornell, 1987	Lobolly pine	67	pH > 12.9		10.5			4.90	22.3
Robertsen & Lönnberg, 1991	Spruce	°99	> 0.5		3.7			3.02	23.7
Constanza, 2001	Poplar	°99	0.05		1.4				
Constanza, 2001	Poplar	°99	1.00		7.3				
Kazi, 1997	Spruce	°99	2.27	54.0	1.5	0.01130	3.2	0.00027	2.8

x Estimation based on permanganate number.

° Assumed after NaOH treatment.

reasons have been quoted as being responsible for the low activation energy – namely, the application of Fick’s second law of diffusion, which does not consider surface area, and the special experimental set-up used (impregnator) where no NaOH-desorption step from the wood block (which also needs activation) was considered. Nevertheless, the numerical values of D in radial directions were quite comparable, such that any of these values can be used for modeling the impregnation process by diffusion.

#### 4.2.3.6 Diffusion Model

(The numerical solution of the diffusion model is described in Section 4.2.3.8.)

The presented diffusion model is essentially based on the studies of Kazi and Chornet [2,55,56]. This model has been selected because it is applicable to different impregnation temperatures and pressures, and also demonstrates the main parameters influencing the efficiency of impregnation. As mentioned previously, any impregnation process comprises both liquid impregnation into the capillaries and diffusion through cell walls, pit membranes and other structural elements of the fibers. To avoid any significant chemical reactions, impregnation should be conducted at a lower temperature, preferably below 100 °C. When the cell wall pores are filled with water – or, in other words, when the moisture content in the

chip is well above its fiber saturation point – the chemical impregnation is controlled by diffusion.

#### 4.2.3.6.1 Model Structure

The impregnation model is limited to the following assumptions:

- Chemical impregnation follows Fick's second law of diffusion.
- The model considers axial and radial diffusion. Both axial and radial diffusion coefficients are independent of radial and axial position in the cylindrical samples. However, radial and tangential diffusion are not distinguished and are treated equally.
- The solute concentration (NaOH) in the impregnation solution remains constant.
- The temperature is uniform throughout the sample.
- No chemical reactions occur between the matrix and the diffusing chemicals at the temperature of impregnation.
- The diffusion coefficient of NaOH into wood is considered to be independent of pH (valid for concentrations  $> 1 \text{ mol L}^{-1}$ ).
- Despite swelling, the sample geometry remains invariant with time.

In the present model,  $D$  is assumed to be dependent only on pressure, temperature and the pore structure of the chip sample.

The pressure influence on diffusion can be expressed by extending the Arrhenius-type equation [Eq. (49)]:

$$D = D_0 \cdot \sqrt{T} \cdot P^m \cdot \text{Exp} \cdot \left( -\frac{E_A}{RT} \right) \quad (66)$$

where:

- $D$  = diffusion coefficient,  $\text{cm}^2 \cdot \text{s}^{-1}$
- $D_0$  = diffusivity constant,  $\text{cm}^2 \text{ s}^{-1} \cdot \text{K}^{-0.5}$
- $p$  = dimensionless pressure term (i.e., the ratio of absolute pressure to atmospheric pressure)
- $m$  = pressure power constant

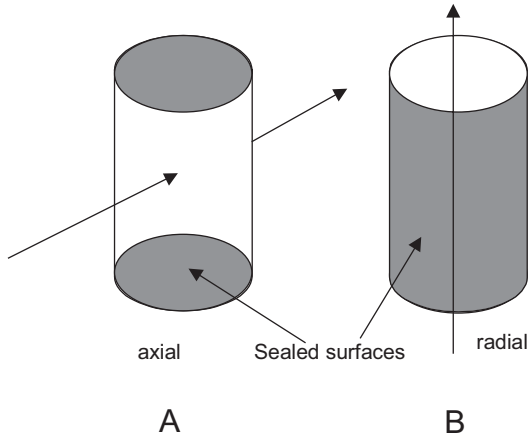
Considering all of the assumptions made above, the diffusion process can be described by Fick's second law of diffusion [35]. Its differential form in cylindrical coordinates is given by Eq. (67):

$$\frac{\partial C}{\partial t} = \left[ \frac{1}{r} \cdot \frac{\partial}{\partial r} \left( r \cdot D_r \frac{\partial C}{\partial r} \right) + \frac{\partial}{\partial z} \left( D_z \frac{\partial C}{\partial z} \right) \right] - k \cdot C^n \quad (67)$$

where  $C$  is the concentration of the diffusing species at the position  $(r, z)$ ,  $k$  is the reaction constant between chemical and matrix,  $n$  is reaction order,  $r$  is radial direction and  $z$  is axial direction.

If it is assumed that no chemical reaction (of relevance) takes place, the term  $k \cdot C^n$  can be eliminated from Eq. (67).

Radial and axial diffusion are investigated separately. Thus, the radial directional impregnation is isolated from the axial one by sealing the outer surface in the radial and axial directions. The surfaces were sealed with an appropriate sealing material, thereby creating impermeable barriers. The open faces represent then either the axial or the radial surfaces (Fig. 4.14).



**Fig. 4.14** Sketch of the wood sample prepared for unidirectional impregnation according to Kazi and Chornet [57]. (A) For radial impregnation, the axial surfaces are impermeable; (B) for axial impregnation, the radial surfaces are impermeable.

Equation (67) is divided into two separate equations: one for radial concentration and one for axial concentration only. Thus, it is assumed that there is no interaction between radial and axial diffusion processes.

#### 4.2.3.6.2 Radial Concentration Profile

A long circular cylinder in which diffusion is everywhere radial. Consequently, concentration is then a function of radius,  $r$ , and time,  $t$ , only, and the diffusion equation becomes

$$\frac{\partial C}{\partial t} = D_r \cdot \left[ \frac{1}{r} \cdot \frac{\partial}{\partial r} \left( r \frac{\partial C}{\partial r} \right) \right] \quad (68)$$

The initial and boundary conditions must be considered:

- IC:  $C = 0$  at  $0 \leq r \leq a$  at  $t = 0$
- BC:  $C = C_0$  at  $r = a$  at  $t \geq 0$   
 $C = \text{finite}$  at  $r = 0$  at  $t \geq 0$

- $C_0$  chemical concentration at the edge of the sample  
(= initial concentration)
- $a$  radius of the cylindrical sample

In contrast to the case of Kazi and Chornet, Eq. (68) is solved numerically (for an explanation, see Section 4.2.3.8).

#### 4.2.3.6.3 Axial Concentration Profile

The equation for the axial concentration profile is given as:

$$\frac{\partial C}{\partial t} = D_z \cdot \left( \frac{\partial^2 C}{\partial z^2} \right) \quad (69)$$

with the initial and boundary conditions given below:

- IC:  $C = 0$  at  $z > 0$  at  $t = 0$
- BC:  $C = C_0$  at  $z = 0$  at  $t > 0$   
 $C = C_0$  at  $z = Z$  at  $t > 0$

Again, Eq. (69) is solved numerically (see Section 4.2.3.8).

#### 4.2.3.6.4 Experimental

The heartwood section of *Populus tremuloides* was chosen as a substrate for the impregnation study. A cylindrical probe with a radius  $a = 25$  mm and a length  $Z = 150$  mm was prepared. The axis of the cylindrical sample is parallel to the fiber axis representing the longitudinal direction. The radial surface represents the radial and tangential surfaces of the wood sample.

The bare surfaces were exposed in the impregnator to a solution of  $2.3 \text{ mol L}^{-1}$  NaOH for 60 and 15 min for radial and axial impregnation, respectively, under a variety of conditions (temperature 25, 50, 75 or  $100^\circ\text{C}$ ; pressure: 200, 790, 1480 and 2179 kPa). The experimental set-up and the conditions are described in detail elsewhere [56,57]. The concentration profile of  $\text{Na}^+$  ions, the diffusing species, was determined by measuring the local X-ray intensity on the sliced sample. After completion of the impregnation, the samples were frozen and sliced at marked locations using a fine power saw. The marked samples were then subjected to scanning electron microscopy analysis. The X-ray intensity of the sodium element at the sample edge was defined as reference intensity,  $I_0$ . The X-ray intensity is directly proportional to the concentration of the  $\text{Na}^+$  ion. Thus, the X-ray intensity ratio,  $I/I_0$ , translates to the concentration ratio,  $c/c_0$ . Equations (68) and (69) can be solved using  $I/I_0$ .

#### 4.2.3.6.5 Examples and Results

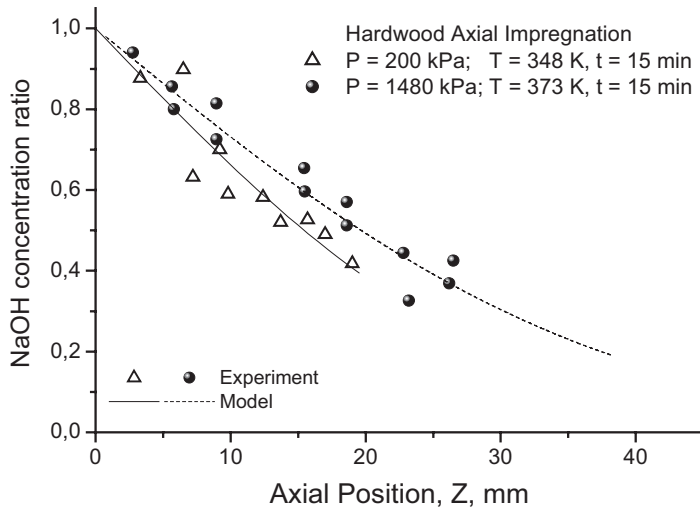
A selection of the results published by Kazi and Chornet [56] were used to evaluate the impregnation model and to calculate  $D$  at the given impregnation conditions. Axial impregnation with a  $2.3 \text{ mol L}^{-1}$  NaOH solution was calculated for two different conditions:

- Conditions A: Pressure 200 kPa, Temperature  $75^\circ\text{C}$ , time 15 min.
- Conditions B: Pressure 1480 kPa, Temperature  $100^\circ\text{C}$ , time 15 min.

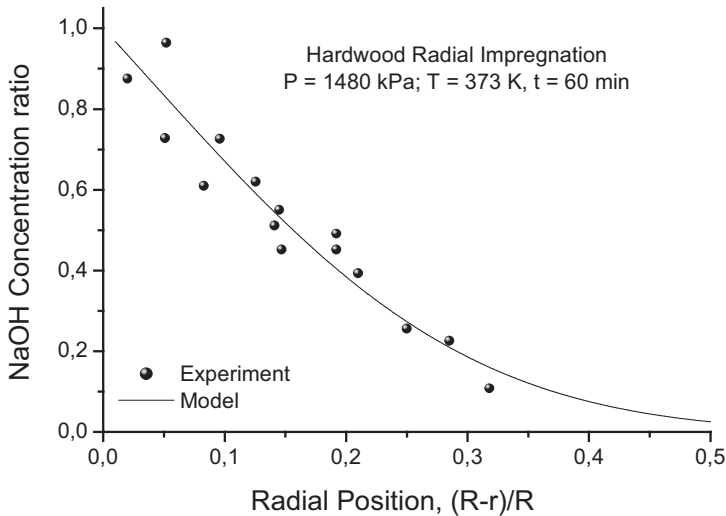
The concentration profiles obtained from model and experimental results are depicted in Fig. 4.15.

Figure 4.16 shows the radial profiles for the same impregnation conditions as in Fig. 4.15, under conditions B.

The calculated diffusion coefficients,  $D$ , at the given conditions are summarized in Tab. 4.14.



**Fig. 4.15** Profiles of concentration ratio for axial impregnation with  $2.3 \text{ mol L}^{-1}$  NaOH at specified conditions A and B (see text). Wood sample length  $Z = 150 \text{ mm}$ ; radius  $a = 25 \text{ mm}$  (data from Kazi and Chornet [56]).



**Fig. 4.16** Profile of concentration ratio for radial impregnation with  $2.3 \text{ mol L}^{-1}$  NaOH; impregnation pressure = 1480 kPa; temperature = 100 °C. Wood sample length  $Z = 150 \text{ mm}$ ; radius  $a = 25 \text{ mm}$  (data from Kazi and Chornet [56]).

**Tab. 4.14** Conditions of selected impregnation experiments [56] and calculated diffusion coefficients,  $D$ , by numerical solution (see Section 4.2.3.8).

Parameter	unit	Axial	Radial
Temperature	°C	75	100
Pressure	kPa	200	1480
Time	min	15	60
$D$ (calculated)	$10^{-5} \text{ cm}^2 \text{ s}^{-1}$	293.6	0.98

According to the results listed in Tab. 4.14, the  $D$ -value for axial diffusion is more than 500-fold higher than that for radial diffusion under the same impregnation conditions. This ratio of diffusion coefficients is thus more than 10-fold higher than that reported by Christensen [38] and Behr et al. [37].

Based on extensive impregnation experiments, Kazi and Chornet have calculated the coefficients  $D_0$ ,  $m$  and  $E_A$  from Eq. (66) for the radial and axial directions. The results are shown in Tab. 4.15.

The diffusion coefficients calculated directly by the impregnation model, and summarized in Tab. 4.14, correspond quite well with those calculated with Eq. (66) using the average diffusion coefficient parameters listed in Tab. 4.15. The activa-



**Tab. 4.15** Diffusion parameters from Eq. (66) calculated by Kazi and Chomet [56]. These values were obtained from experiments using 14 samples impregnated with a 2.3 mol L<sup>-1</sup> NaOH aqueous solution at different pressures, temperatures and times.

Parameter	unit	Axial	Radial
D <sub>0</sub>	cm <sup>2</sup> · s <sup>-1</sup> · K <sup>-0.5</sup>	1.98*10 <sup>-4</sup>	5.77*10 <sup>-7</sup>
m		0.27	0.38
E	kJ mol <sup>-1</sup>	1.235	2.700

tion energies for diffusion in the radial and axial directions are significantly lower than those obtained by others (see Tab. 4.13). Several explanations for the low activation energies have been put forward. First, when diffusion occurs from the impregnated wood to the water solution surrounding the wood sample, the effective surface area can be assumed to be significantly higher than the geometric area due to surface roughness. Second the release of the diffusing substance from the wood block comprises two process steps, namely desorption and diffusion. Accounting for both the higher effective surface area and the elimination of the desorption process step would eventually lead to lower activation energies.

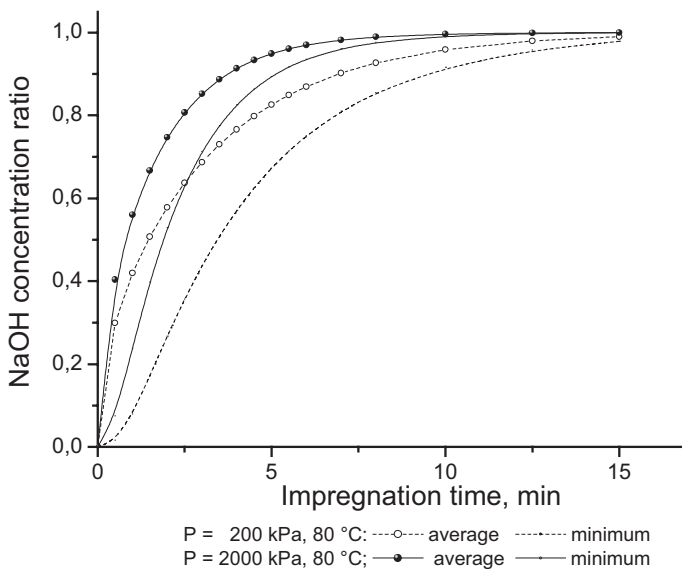
The model also considers the influence of the pressure during impregnation of wood chips. Such pressure may change the geometry of the pore system, and also affect the diffusion coefficient for chemical diffusion into the wood chip. The diffusion coefficient has been considered to be proportional to the dimensionless pressure with a power factor *m*. The pressure power factor in the axial direction is found to be smaller than that for the radial direction, which means that the influence of pressure is more significant in the radial direction (see Tab. 4.15).

The established impregnation model is able to predict the required time to reach a steady-state concentration distribution within the chips which is a prerequisite for homogeneous delignification reactions. The point concentration from the surface to the center of the chip can be simulated by considering both chip length and thickness. The course of the average and the center NaOH concentration in relation to the bulk concentration as a function of impregnation time were calculated for two different impregnation conditions (Tab. 4.16).

The simulation result is shown in Fig. 4.17. Compared to the minimum concentration at the chip center, the average concentration rises rapidly with increasing impregnation time. The increase in impregnation pressure from 200 kPa to 2000 kPa reduces the impregnation time needed to reach an average concentration of 99% (of the NaOH concentration in the bulk solution) from 15 min to only 8 min. The same concentration level at the chip center requires a prolongation of the impregnation time of up to 5 min, depending on the applied pressure.

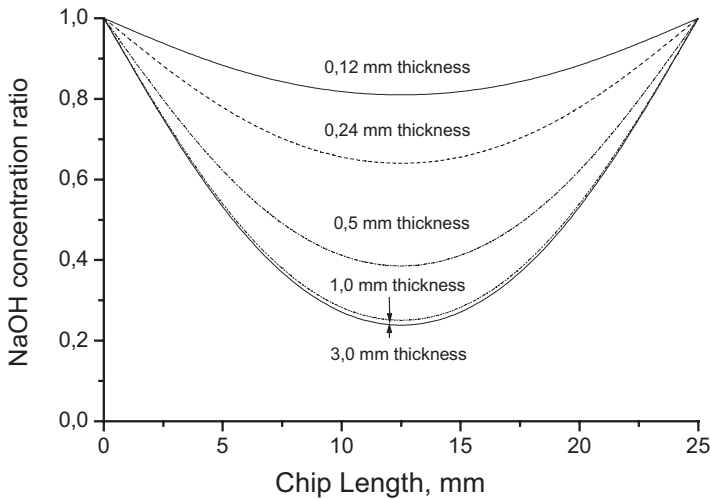
**Tab. 4.16** Conditions for the impregnation of hardwood chips: influence of pressure. Based on these conditions, the course of average and minimum concentration in a chip are simulated by the introduced impregnation model [56].

Parameter	Unit	Conditions	
		A	B
Chip length	mm	25	25
Chip thickness	mm	6	6
Pressure	kPa	200	2000
Temperature	°C	80	80



**Fig. 4.17** Course of average and minimum concentration of NaOH in a hardwood chip of thickness 6 mm and length 25 mm with impregnation time at two different pressure conditions. Impregnation model based on Kazi and Chornet [56] (numerical solution).

The simulation of point concentrations across the axial and radial directions in a chip enables determination of progression of the impregnation front for a given impregnation time. The two-dimensional concentration profile across chip length and chip thickness after an impregnation time of only 1 min (80 °C and 2000 kPa) is shown in Fig. 4.18.



**Fig. 4.18** Concentration distribution after 1 min of impregnation. Chip dimensions: thickness 6 mm, length 25 mm. Model simulation using the following impregnation conditions: pressure 2000 kPa, temperature 80 °C. Impregnation model based on Kazi and Chornet [56] (numerical solution).

As expected, the concentration gradient in both directions – axial and radial – remains very pronounced after 1 min of impregnation. In this particular case, the minimum concentration of the diffusing species, NaOH, is reached at only 1 mm beneath the chip surface (radial direction).

Chemical impregnation into wood chips having a moisture content above the fiber saturation point can be modeled by diffusion mechanisms. The introduced model considers both radial and axial diffusion processes, and is able to predict the required time to impregnate wood chips to achieve a uniform distribution of active cooking chemicals.

#### 4.2.3.7 Effect of Impregnation on the Uniformity of Delignification

The effects of chip size have been evaluated by several research groups. In a study of kraft pulping of pine chips, Backman [57] stated that above a thickness of 1 mm the reaction rate is at least partially controlled by the transport steps, while below this thickness the rate is probably controlled by the rate of the chemical reactions involved. Hartler and Östberg identified that the Roe number remained constant when the thickness was 3 mm or less [58], and Larocque and Maass found essentially the same effect of chip size [59]. Both the chip size and the uniformity of chip dimensions are very important criteria for pulp properties. In particular, chip thickness is a critical dimension which strongly controls the extent of delignification, the amount of rejects, and even strength development. Chip length and width have been shown to have a minimal influence on delignification [12], with

thick chips showing very steep delignification gradients. Wood is overdelsignified at the surface, while chip centers are almost undelsignified. Gullichsen et al. [8] reported a kappa number gradient from 14 on the surface to more than 120 in the chip center for a 8 mm-thick chip of a Scots pine cook with an average screened kappa number of 23.4 [8]. The same authors also noted that only chips with a thickness <2 mm can be uniformly delignified under conventional cooking conditions [8]. Uniform thin chips without knots and reaction wood can be produced either by efficient screening or by applying an innovative chipping technique. Another approach involves the application of chip pretreatments and optimization of impregnation conditions, aimed at improving penetration and efficient diffusion.

Recently, the effects of chip steaming and increased pressure impregnation during the hot black liquor stage on the kappa number distribution inside handmade pine chips (*Pinus silvestris*) were investigated by using reflection Fourier transmission infra-red (FTIR) spectroscopy (equipped with a microscope which enables a lateral resolution of an area of approximately  $100 \times 100 \mu\text{m}$ ) [60]. Two scenarios with different impregnation conditions have been compared with regard to the uniformity of delignification. Scenario A represents very poor impregnation conditions involving no pre-steaming and applying only 5 bar overpressure during the hot black liquor stage. Scenario D, a very efficient mode of impregnation, combines intensive pre-steaming (30 min,  $105^\circ\text{C}$ ) with a high-pressure treatment (9 bar overpressure) during the hot black liquor stage. The subsequent cooking steps and conditions were identical for the two scenarios investigated (Superbatch technology, 17% EA on wood, 40% sulfidity,  $170^\circ\text{C}$ , 890 H-factor in cooking stage). The handmade chips were cut to a length of 34 mm (longitudinal direction in wood), a width of 14 mm (tangential direction in wood) and a thickness of 8 mm (radial direction in wood). To analyze the uniformity of delignification, cooked heartwood chips were cut across the thickness dimensions at distances of 2 mm. Infrared spectra were measured along the chip length and along the chip width from the middle to the edge, with steps of 2 and 1 mm, respectively. The kappa number profiles within heartwood chips for cooking scenarios A and D are illustrated in Fig. 4.19.

In cooking scenario A, the middle part of the 8 mm-thick chip (4 mm deep) was clearly undercooked. There was a gradual transition along the chip length from the edge kappa number of 40 to the undercooked regions with kappa number over 90. In the tangential direction (along the chip width), kappa number rise was, however, very abrupt close to the chip edge, which confirmed the limited mass transfer in this direction (not seen).

In scenario D, with the application of pre-steaming and higher pressure profile, the uniformity of delignification of heartwood chips was significantly improved, though some gradient was present in the middle (4 mm deep) layer of the chip. However, the undercooked region was much narrower than in scenario A. These results confirmed the beneficial effect of reinforced impregnation conditions with regard to the uniformity of delignification.

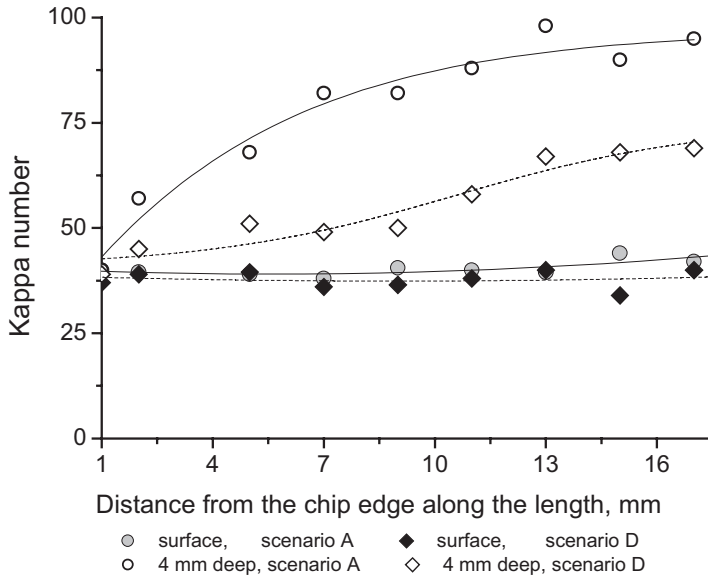
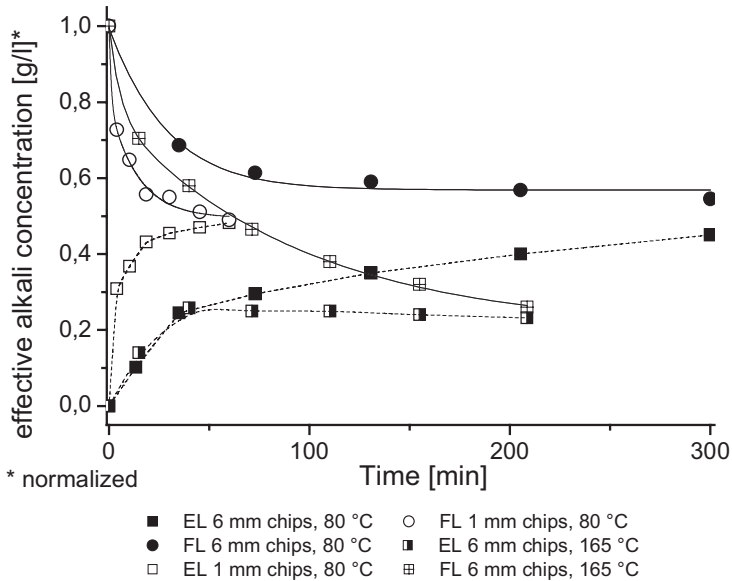


Fig. 4.19 Delignification profiles within the pine heartwood of handmade chips [60].

An alternative method has recently been introduced to determine the alkali and lignin concentration profiles in the free and entrapped liquor as a function of chip thickness [61]. *Eucalyptus globulus* chips with dimensions of about  $30 \times 30 \times 1$  mm and  $30 \times 30 \times 6$  mm were used as raw material for the impregnation and cooking studies. Impregnation trials were carried out at  $5^\circ\text{C}$  and  $80^\circ\text{C}$  using a cooking liquor with an effective alkali (EA) concentration of 19.3–22.6% on dry wood, a sulfidity of 25–30%, and an initial liquor:wood ratio of 6:8. Cooking experiments were conducted at  $165^\circ\text{C}$  using only the 6-mm chips. At the end of each trial the chips were immediately separated from the remaining free liquor and the excess liquor at the surface was carefully removed with sorption paper. The chips were then pressed to 350 bar for 2–3 min to release the entrapped liquor that had been collected in a previously inertized flask and cooled in a similar ice bath. The free and entrapped liquors were analyzed for EA and lignin concentrations according to standard methods [62,63]. The concentration profiles for EA in both free and entrapped liquors are illustrated for experiments with 1- and 6-mm chips at  $80^\circ\text{C}$ , and with 6-mm chips at  $165^\circ\text{C}$  (Fig. 4.20). The results confirmed the remarkably high difference between the entrapped and free liquor concentrations, especially at the beginning of the reaction. For the thin chips of only 1 mm thickness, the EA concentrations in both liquors were similar at about 60 min impregnation time. However, for the 6-mm chips, even after 300 min, there was no equalization of EA concentrations. Performing these experiments at a cooking temperature of  $165^\circ\text{C}$  yielded a more significant decrease in the concentration of EA in the free liquor, but this was not followed by a higher increase of EA concentration in the entrapped liquor. These findings clearly indicate that higher consumption rates of

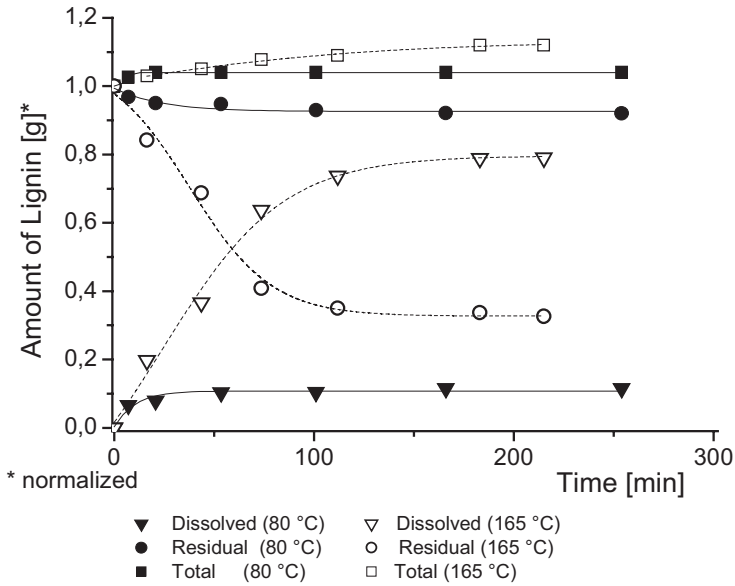


**Fig. 4.20** Effective alkali concentrations (normalized) in the free (FL) and entrapped (EL) liquid phases versus time for 1- and 6-mm chips at 80 °C and 165 °C.

alkali occur when chemical reactions are conducted at temperatures above 80 °C. Moreover, the results reveal that, in such a heterogeneous process, the alkali concentration profiles in the free and entrapped liquors do not necessarily appear as image and mirror image.

The consumption of EA does not correspond to the alkali concentration in the bulk liquor because the alkali inside the chip is not totally consumed by the wood components. It is clear that the alkali concentration in the entrapped liquor determines the dissolution of wood components, and this must be considered in the development of a heterogeneous delignification kinetic model.

The concentration profiles of dissolved kraft lignin in both entrapped and free liquors depend heavily on the reaction temperature. At 80 °C, the concentration of dissolved lignin in the bulk liquor remains very low, indicating only a small degree of delignification at this temperature. Inside the chips, the concentration rises quickly to a constant low level. When the temperature is increased to 165 °C, the dissolved lignin concentration in the entrapped liquor reaches a maximum after about 80 min. Continuing the cooking process leads to a decrease in dissolved lignin concentration in the enclosed liquor due to a slow-down of the delignification rate, and this results in an overall enhanced mass transfer of lignin to the free liquor. The whole mass balance of lignin calculated from lignin concentration profiles in the entrapped and free liquors and the lignin content in the wood chips is illustrated in Fig. 4.21.



**Fig. 4.21** Mass balance of lignin during impregnation at 80 °C and kraft cooking at 165 °C using *Eucalyptus globulus* chips with a thickness of 6 mm.

The data shown in Fig. 4.21 confirm that at a temperature of 80 °C, which is a typical temperature for impregnation, only negligible delignification occurs. At 165 °C, the expected pattern of residual lignin as a function of time can be observed. The total normalized mass of lignin increases up to 10% of its initial value being attributed to experimental errors as dissolved extractives contribute to lignin concentration using UV detection at 280 nm.

#### 4.2.3.8 Numerical Solution of the Diffusion Model

The solution of Eqs. (68) and (69) is calculated numerically by a finite difference scheme. The origin of the coordinate system is located at the cylinder center. For the radial concentration profile [Eq. (68)], the interval  $[-a, a]$  is divided into  $2n$  pieces of equal size  $\Delta h = a/n$ , for the axial concentration profile [Eq. (69)] the interval  $[-Z/2, Z/2]$  is divided into  $2n$  pieces of size  $\Delta h = Z/2n$ .  $C_i$  denotes the concentration at  $i\Delta h$ , thus  $C_i(t) = C(i\Delta h, t)$ .

The derivation of a smooth function can be approximated by a central difference quotient:

$$\frac{df}{dx}(x) \approx \frac{f(x+h) - f(x-h)}{2h} \quad (70)$$

To obtain an approximation for a second-order derivation, the second-order derivation is replaced by a central difference quotient of first-order derivations, after which the first-order derivations are replaced by central difference quotients.

The resulting difference equations for Eq. (68) are

$$\dot{C}_i(t) \approx \frac{D_r}{\Delta h^2} \left( \left(1 + \frac{1}{2i}\right) C_{i+1}(t) - 2 C_i(t) + C_{i-1}(t) \left(1 - \frac{1}{2i}\right) \right) \quad i = 1, \dots, n-1 \quad (71)$$

and

$$\dot{C}_i(t) \approx \frac{D_z}{\Delta h^2} (C_{i+1}(t) - 2 C_i(t) + C_{i-1}(t)) \quad i = 1, \dots, n-1 \quad (72)$$

for Eq. (67).

The condition that  $C$  is finite at  $r = 0$  in Eq. (68) implies  $\frac{\partial C}{\partial r}(0, t) = 0$  for  $t > 0$  and symmetry of problem Eq. (69) implies  $\frac{\partial C}{\partial z}(0, t) = 0$  for  $t > 0$ . After approximation of  $C_2, C_1, C_0$  with a quadratic polynomial this conditions transform into:

$$C_0(t) \approx \frac{4}{3} C_1(t) - \frac{1}{3} C_2(t) \quad (73)$$

After inserting Eq. (73) into Eqs. (71) and (72) respectively, a system of ordinary differential equations (ODE) is obtained which can be solved by any standard numerical ODE solver with good stability properties.

Euler's implicit method is used in the sample code. Only a set of linear equations with a tridiagonal system matrix is solved each time step.

#### 4.2.4

### Chemistry of Kraft Cooking

*Antje Potthast*

#### 4.2.4.1 Lignin Reactions

In pulping operations the lignin macromolecule must be degraded and solubilized to a major extent. Inter-lignin linkages are cleaved and the fragments dissolved in the pulping liquor. The reactivity of different lignin moieties towards pulping chemicals and pulping conditions is highly dependent on the chemical structure. An understanding of the major reactions of lignin moieties has been established by experiments applying low molecular-weight model compounds featuring lignin substructures, assisted by modern analytical techniques. The reactivity of lignin subunits differs most notably depending on whether the phenolic units are etherified, or not. In general, the reactivity of phenolic moieties is signif-

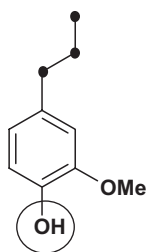


icantly enhanced over nonphenolic lignin units. In the following sections, the reactions of the more reactive phenolic units under alkaline pulping conditions will be addressed.

#### 4.2.4.1.1 Phenolic Subunits

The following reactions form the basis of the degradation/dissolution of phenolic lignin moieties during pulping under alkaline conditions:

- Ionization of phenolic groups
- Cleavage of  $\alpha$ -aryl-ether bonds and the most abundant  $\beta$ -O-4-ether links
- Liberation of free phenolic groups



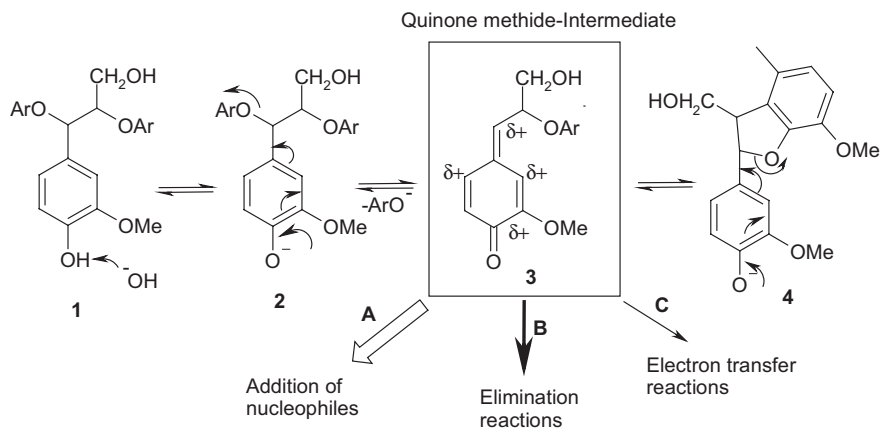
The  $\beta$ -O-4 and  $\alpha$ -O-4-ether links (cf. Scheme 4.2) taken together represent the most abundant connections between lignin units (up to 65%) [1]. Hence, the behavior of these moieties in the pulping process have been extensively analyzed in model compound and lignin studies.

The key-intermediate is the *para*-quinone methide (3), which is formed from the  $\beta$ -aryl ether structure upon ionization of the phenolic residue and elimination of the aryl substituent in  $\alpha$ -position by a vinylogous  $\beta$ -elimination [2] or by alkali-induced cleavage of the cyclic  $\alpha$ -aryl ether bonds, for example cleavage of the phenylcoumaran-type substructure via quinone methide. The reaction is reversible, but addition of a nucleophile (e.g.,  $\text{HS}^-$ ) in a subsequent reaction step leads to re-aromatization by nucleophilic addition of  $\text{HS}^-$  to the C- $\alpha$  of the quinone methide, which is the driving force. A common feature of all major pulping processes is the reaction of nucleophiles (nucleophilicity increases in the order  $\text{OH}^- < \text{HS}^- < \text{SO}_3^{2-}$ ) with electron-deficient centers at the lignin molecule, resulting in cleavage of inter-lignin linkages and a higher hydrophilicity of the resulting lignin fragments and thus a better dissolution in the pulping liquor.

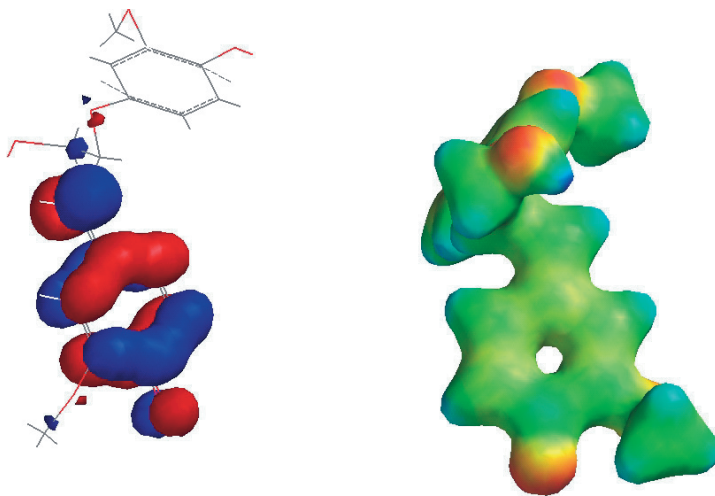
#### 4.2.4.1.2 Lignin: General Structure

Once the *para*-quinone methide has been formed, a number of reactions may proceed as outlined in Scheme 4.3, which can be divided according the type of transformation into *addition*, *elimination* and *electron transfer* reactions. The electron

density distribution at the quinone methide intermediate, as illustrated in Scheme 4.4, finally determines the pathway of subsequent processes. The size of the respective atomic orbital [Lowest Unoccupied Molecule Orbital (LUMO) distribution; Scheme 4.4, left] denotes the nucleophilicity – that is the probability of a nucleophilic attack, whilst red zones (Scheme 4.4, right) denote centers of high electron density. The electron-deficient sites are marked in Scheme 4.3 by  $\delta+$ , situated at alternating carbons starting from the keto carbon.



**Scheme 4.3** Formation of quinone-methide (3) and subsequent reaction pathways.



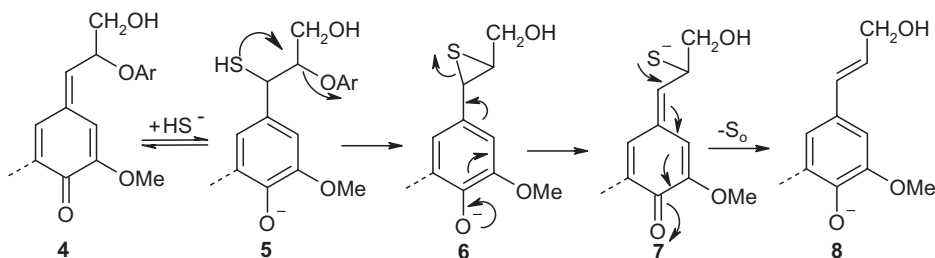
**Scheme 4.4** LUMO-distribution (left) and electron density distribution of the quinone-methide intermediate [4].

### Reaction Path A

#### Addition of Nucleophiles

In kraft cooking, the nucleophilicity of the hydrosulfide anion is higher as compared to the hydroxyl ions, which results in an improved delignification behavior in comparison to soda pulping. Other nucleophiles present in the pulping liquor, such as the carbon-centered mesomer of phenoxide anions or nucleophilic species originating from carbohydrates, may also compete for the quinone methide, finally resulting in condensation reactions rather than fragmentation.

Scheme 4.5 outlines the fragmentation of the  $\beta$ -aryl ether bond by hydrosulfide: after addition of  $\text{HS}^-$  to the quinone methide, an intramolecular attack at the neighboring  $\beta$ -carbon (neighboring group participation [5]) causes formation of a thiiran intermediate **6**. Elimination of elemental sulfur (formation of polysulfide) with concomitant re-aromatization yields coniferyl-type structures (**8**).



**Scheme 4.5** Addition of hydrogen sulfide to quinone methide structures.

Cleavage of phenolic  $\alpha$ - and  $\beta$ -aryl-ether linkages proceeds relatively easily. This reaction has thus been proposed as the major pathway occurring in the initial phase of delignification in kraft pulping [6] (see Section 4.2.5, Kinetics).

#### Condensation Reactions

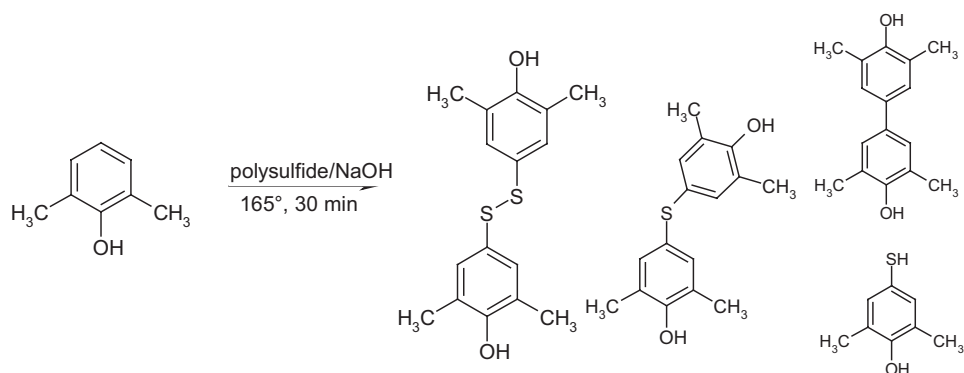
The formation of stable carbon–carbon bonds between lignin units is normally referred to as “condensation”. Such condensation processes lead to lignin structures which are more difficult to cleave. This applies mainly to the terminal phase of the kraft cook as well as to the residual lignin structures. The unoccupied 5-position in guaiacyl units is very susceptible to carbon–carbon coupling reactions, and is less frequent in kraft lignin as compared to the more genuine MWL (Milled Wood Lignin). The lignin moieties with 5–5',  $\beta$ -5, 5-O-4 and diphenylmethane structures (DPM) are considered as condensed units. Condensation reactions are thought to proceed through addition of a carbon-centered mesomer of phenoxide anions (donor) (in the carbon-centered resonance form) to a quinone methide (acceptor), and results in a novel  $\alpha$ -5-bond (primary condensation), a Michael-addition-type reaction [7]. Condensation with formaldehyde leads to stable diarylmethane units (cf. elimination reactions) (Conclusive evidence for the outlined condensation reactions during pulping and in residual lignin structures

is still missing [56].) However, it has recently been shown with 2D-NMR techniques that the amounts of DPMs are very small [below the detection limit for HSQC experiments (0.05–1%)] [8,9], while novel  $\alpha$ -5 are shown to be present only to a minor extent [10,55]. Interestingly, more  $\alpha$ -5-units are found in hardwood than in softwood lignins, and these structures are more abundant in the dissolved lignin than in the residual one. From the structures of these moieties it is concluded that condensation occurs after lignin degradation rather than before. Thus, if condensation really occurs in lignin (it can also be simply an accumulation of native lignin condensed moieties), the mechanism might be different to that hitherto comprehended.

Condensed phenolic structures can be analyzed using  $^{13}\text{C}$ -NMR, permanganate oxidation and  $^{31}\text{P}$ -NMR [11].  $^{31}\text{P}$ -NMR is a semi-quantitative technique, especially with regard to condensed moieties, and requires a good resolution of the spectra.  $^{31}\text{P}$ -NMR is limited to the analysis phenolic (condensed/non-condensed) moieties only.

Recently, Gellerstedt et al. [12] proposed a novel concept for the formation of condensed units in residual lignins based on a one-electron mechanism with elemental sulfur as the radical initiator. The products of a model study with the observed sulfur bridges are presented in Scheme 4.6. However, the model does not explain condensation reactions in soda pulping.

An increase of condensed structures in residual lignins as kraft cooking proceeds was also confirmed by solid-state NMR. However, it cannot be determined whether these structures are just enriched during pulping or are formed *de novo* [13], which is a general question dealing with condensation in lignin chemistry.



**Scheme 4.6** Model reaction to demonstrate the action of sulfur as electron-transfer reagent under kraft conditions to bring about condensation reactions in lignin (from Ref. [12]).

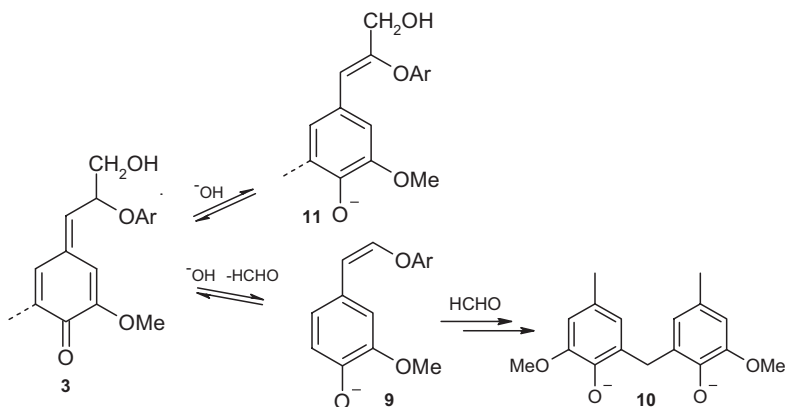
### Reaction Path B

#### Elimination Reactions

Starting from the quinone methide, the  $\gamma$ -hydroxymethyl group can be eliminated as formaldehyde, resulting in an enol ether structure. This reaction is prevalent in soda pulping, causing a lower selectivity [5], but also observed at the start of the bulk delignification phase during kraft pulping, despite a high initial charge of sodium sulfide [50]. The amount of enol-ether structures approaches a maximum at about the time when the maximum cooking temperature is reached, and is believed to have a decisive influence on the amount of residual lignin [14]. However, the total amount of enol-ether is rather small, especially in residual lignins. Interestingly, a large quantity of enol-ether units was detected in dissolved soda lignin, as expected, but not in the corresponding residual soda lignin [10].

The  $\beta$ -hydrogen can also be eliminated in another base-induced reaction. The formaldehyde, which is highly reactive, can further condense with carbon-centered mesomers of phenoxide anions leading to stable diarylmethane compounds **10** (Scheme 4.7) that have been suggested to be present in residual lignin [15,16]. The amount of these diarylmethane structures have been roughly estimated by a combination of nitrobenzene oxidation and the nucleus exchange method [15–19], though this technique has been proven to be erroneous.

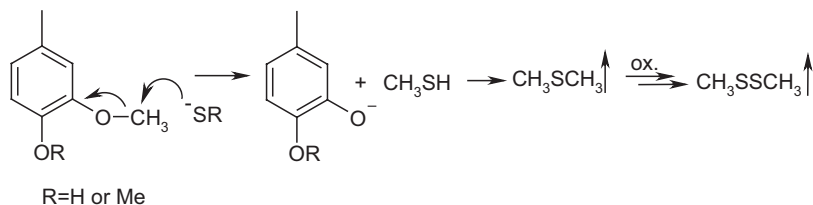
The  $\beta$ -aroxy styrene-type structures (**9,11**) show a high resistance towards alkali, and may even survive the kraft cook (cf. structure of residual lignin)[20,21].



**Scheme 4.7** Formation of enol ethers and elimination of formaldehyde with subsequent condensation to diarylmethane-type structures.

The action of the strong nucleophile  $\text{HS}^-$  also causes a partial demethylation reaction at the methoxyl groups of lignin [22]. The formed methyl mercaptane is itself a strong nucleophile, and reacts further with another methoxyl group to yield dimethyl mercaptane (Scheme 4.8), an extremely volatile (but nontoxic) compound which is responsible for the typical odor of kraft mills. Methyl sulfide can

be further oxidized to dimethyl disulfide upon exposure to air. In total, about 5% of the methoxyl groups of lignin are cleaved.

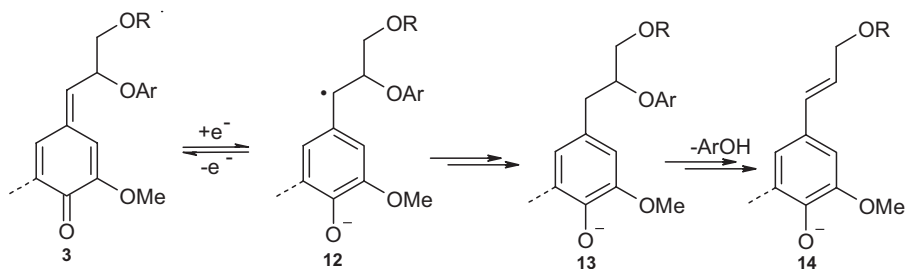


**Scheme 4.8** Demethylation reaction at lignin methoxyl groups and formation of mercaptanes.

### Reaction Path C

#### *Electron-transfer Reaction*

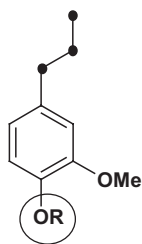
In the alkaline cooking liquor, reducing compounds such as carbohydrate moieties, or pulping aids such as AHQ (Anthrahydroquinone), are also present. Hence, the quinone methide can be reduced by different compounds, as was demonstrated by model compound studies (Scheme 4.9). The process is postulated to proceed according to a single-electron transfer mechanism involving radical intermediates (12) [23]. The structural analysis of residual lignin in pulp also supports the occurrence of such mechanisms to a minor extent [24].



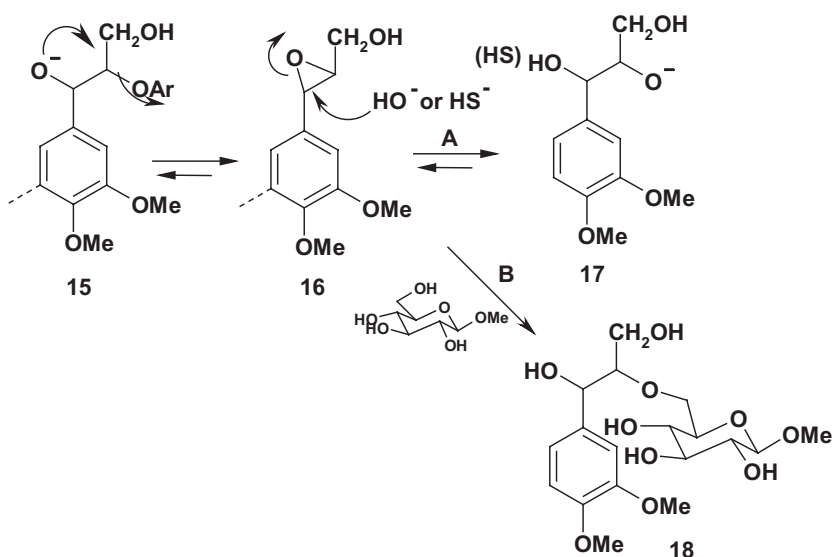
**Scheme 4.9** Reduction of the quinone methide, and formation of coniferyl-type structures.

#### 4.2.4.1.2 Nonphenolic Units

Non-phenolic units are more difficult to cleave than units with a free phenolic hydroxyl group. To a small extent, fragmentation proceeds via oxirane intermediates (13) formed by a neighboring group-assisted mechanism (Scheme 4.10).



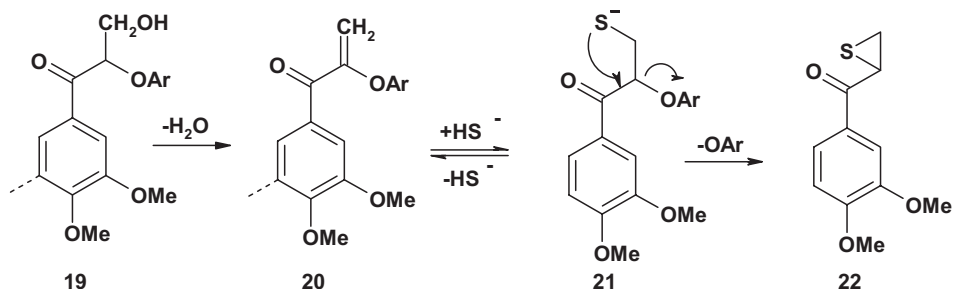
The cleavage of nonphenolic lignin units requires more drastic conditions (temperature, alkalinity), and the reaction is consequently assigned to the bulk delignification phase of a kraft cook.



**Scheme 4.10** Intramolecular formation of epoxides and nucleophilic opening of the oxirane, either by hydroxyl or hydrosulfide ions (path A) or by carbohydrate hydroxyl groups and subsequent formation of stable LCC. (path B)

Starting from epoxide 16, hydroxyl groups of carbohydrate moieties can also attack C- $\alpha$ , resulting in opening of the oxirane ring and formation of lignin-carbohydrate ether bonds. These linkages are stable to some extent under the conditions of bulk delignification, and are thus considered to be one of the reasons for alkali resistant inter-unit linkages and incomplete removal of lignin [25]. Example reactions, carried out with model compounds, also underline the necessity of high alkalinity towards the end of a kraft cook to prevent the increasing formation of stable lignin-carbohydrate-complexes (LCC) (Scheme 4.10, Path B).

For  $\alpha$ -keto lignin units (frequency of **19** in MWL of spruce approx. 0.2 per  $C_9$  unit [26,27]), a sulfidolytic cleavage as depicted in Scheme 4.11 is also possible. Nonphenolic  $\alpha$ -ether structures are stable in all phases of the kraft cook [128].

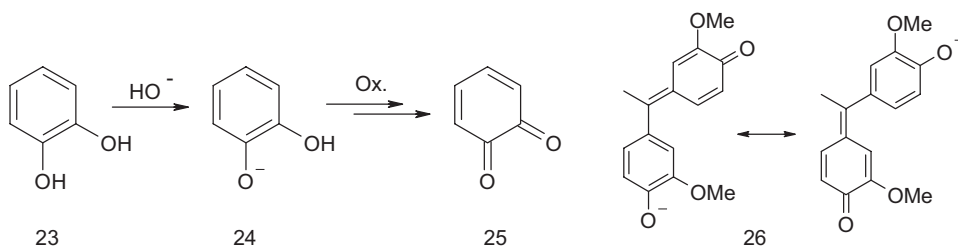


Scheme 4.11 Sulfidolytic cleavage of the b-O-4 ether at  $\alpha$ -carbonyl structures.

#### 4.2.4.1.3 Chromophore Formation

In comparison to other pulping methods (e.g., the sulfite process), residual lignin in unbleached kraft pulp has always a higher specific absorption coefficient – that is, the pulp appears darker. The reason for this can be seen in the formation of unsaturated and highly conjugated compounds. The oxidation potential of phenols is substantially lowered under alkaline conditions; hence the formation of quinoid and higher condensed structures from phenolic lignin units is favored in the presence of oxygen or air, according to Scheme 4.12.

The formation of such structures – together with the alteration within the residual lignin itself – are one reason for the decreased bleachability of kraft pulps. Chromophores can be isolated and analyzed after hydrolysis with  $BF_3$ -acetic acid complexes [28].



Scheme 4.12 Formation of chromophores from phenolic lignin substructures.



#### 4.2.4.1.4 Residual Lignin Structure (see Section 4.2.5)

The structure of the residual lignin which still remains in the pulp after cooking depends highly on the degree of delignification, as well as on the kraft process conditions. To study this lignin, an isolation procedure must be applied, with currently available approaches being enzymatic procedures and acid-catalyzed hydrolysis [29–32] or combinations thereof [33,34]. It is important to know that the procedure chosen (e.g., acidolysis) has an influence on the structure of the residual lignin [35,36], and that the yield of dioxan lignin is rather low. Enzymatic methods isolate the lignin less destructively, with a higher yield with still intact lignin carbohydrate linkages. The yields of residual lignins, for both enzymatic and acid hydrolyses, are lower for hardwood lignins [37]. Enzymatic methods introduce protein impurities which must be removed at later stages [38], but improved methods to remove the latter from lignin preparations are available [37]. An acid hydrolysis may cleave ether linkages to a certain extent, but provides lower yields and somewhat purer lignin preparations.

Residual lignin still contains intact  $\beta$ -O-4 ether structures, as well as a very small amount of enol ethers which are indicative of elimination reactions. Lignin-carbohydrate complexes are also proposed to be present in residual lignin [30,39–41], and this has been confirmed with 2D-NMR [10,55]. Residual lignins can generally be characterized by changes in the functional group distribution, or by different NMR techniques.

*Condensed structures* (5–5',  $\beta$ -5, 5-O-4 and DPM) in residual lignins are either enriched or generated during pulping, and can be roughly determined by degradation methods or NMR techniques, or combinations thereof [42–47]. However, the DFRC method showed a limited potential for quantification with lignins [48].

*Phenolic groups* determine to a large extent the reactivity of lignin, and increase its solubility. Free phenolic groups are generated by cleavage of the different ether linkages, hence the dissolved lignin contains more free phenols compared to the residual lignin, whereas in MWL the value is even less (Tab. 4.17).

**Table 4.17** Phenolic hydroxyl groups in different lignin fractions according to Gellerstedt [49,50].

Lignin type	OH-groups/100 C9
Wood	13
Residual	27
Dissolved	50–60

The same trends were subsequently confirmed later by Faix et al. [51] and Froass et al. [52,53].

*$\beta$ -Aryl ether structures:* In general, the amount of  $\beta$ -aryl ethers decreases as the kraft cook proceeds, although a substantial number of noncondensed  $\beta$ -aryl ether

structures remains in the residual lignin. The numbers of these in the dissolved lignin, and in the lignin remaining in the pulp, approach similarity towards the final phases [21,50]. However, in most dissolved lignins the amount is rather low, and it can be concluded that most of them are cleaved.

*Quinoide structures:* *o*-Quinones may result from the oxidation of *ortho*-dihydroxy benzenes (catechols), which are formed upon demethylation of the aromatic methoxyl groups (cf. Scheme 4.8 and Scheme 4.12). They exhibit a dark color, and are therefore considered to form a major part of the chromophores of kraft pulp [54]. An overview on the structure of residual and dissolved kraft lignins as visualized by NMR has been provided by Balakshin et al. [55].

#### 4.2.4.2 Reactions of Carbohydrates

The reactivity of carbohydrates in kraft pulping depends highly on structural features such as morphology, crystallinity or degree of polymerization (DP). Cellulose is more resistant towards alkaline media and suffers less degradation than hemicelluloses.

Under strongly alkaline conditions (as prevail in kraft and soda pulping), all carboxyl groups are neutralized. Swelling promotes penetration of the cooking chemicals into the wood matrix. The high pH at the beginning of the cook may also ionize part of the hydroxyl groups and lead to a deacetylation ( $T > 70^\circ\text{C}$ ) of acetyl moieties in hemicelluloses (from softwood galactoglucomannans and hardwood glucuronoxylans) with increasing temperature. The hemicelluloses, in particular, undergo base-catalyzed hydrolysis of acetoxyl groups to produce acetoxyl anions, which consume a considerable amount of base during the heating-up period of the kraft cook, and are responsible for a decrease of about 0.35 and 0.9 mol alkali per kg wood for hardwood and softwood, respectively [56]. In addition, acids formed from the carbohydrates decrease the effective alkali content.

A major portion of the deacetylated hemicelluloses dissolve in the pulping liquor. At a later stage of the cook, the hemicelluloses precipitate on the cellulose fiber, increasing the fiber strength. During the bulk phase of the cook the carbohydrates – including the deacetylated hemicelluloses – are reasonably stable. In the final residual delignification phase the decrease in the concentration of alkali tends to decline, and this leads to the aforementioned reprecipitation of hemicelluloses on the fiber matrix. The retake of xylan (addressed in detail by Meller [57]) can be analyzed spatially on the resulting fibers by using either chemical [58] or enzymatic peeling techniques [59,60]. Degradation of celluloses also occurs mostly in the final phase.

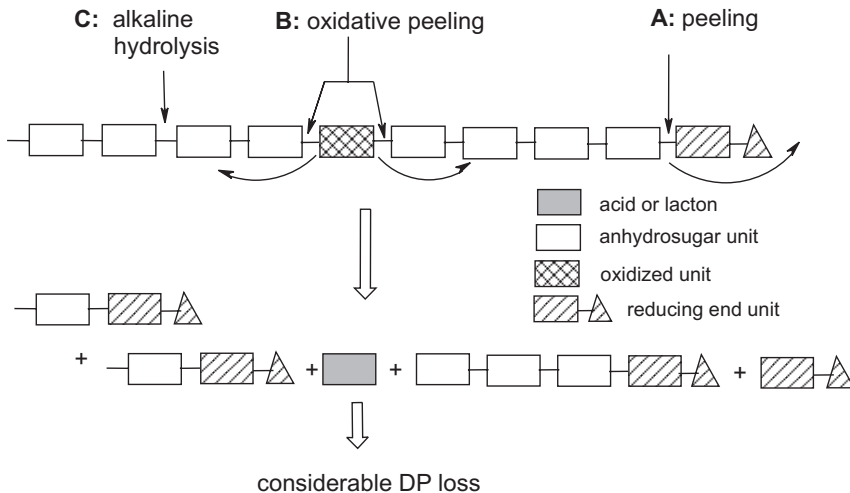
In general, the following reactions proceed with carbohydrates under kraft conditions:

- Deacetylation @  $T < 70^\circ\text{C}$
- Peeling and stopping reactions @  $T > 80^\circ\text{C}$
- Random hydrolysis (= secondary peeling) @  $T > 140^\circ\text{C}$
- Fragmentations
- Dissolution of hemicellulose

- Elimination of methanol from 4-*O*-methylglucuronic acid residues and formation of hexenuronic acid
- Re-adsorption of hemicelluloses on the fiber surface
- Stabilization of carbohydrates against peeling (oxidation)
- Formation of chromophores

#### 4.2.4.2.1 General Reactions Decreasing the DP

The degradation of wood carbohydrates can be divided into three basic reactions. End-wise peeling (**A**, Scheme 4.13) slowly lowers the DP from the reducing end, whereas oxidative peeling (**B**) cleaves the polymer chain randomly and alkaline hydrolysis (**C**), occurring at higher temperatures, is also referred to as secondary peeling. All of these processes (cf. Scheme 4.13) may occur simultaneously, their rate being highly dependent on the chemical structure and the prevailing conditions (type of monomer, branching, state of oxidation, concentration of hydroxyl ions, temperature).



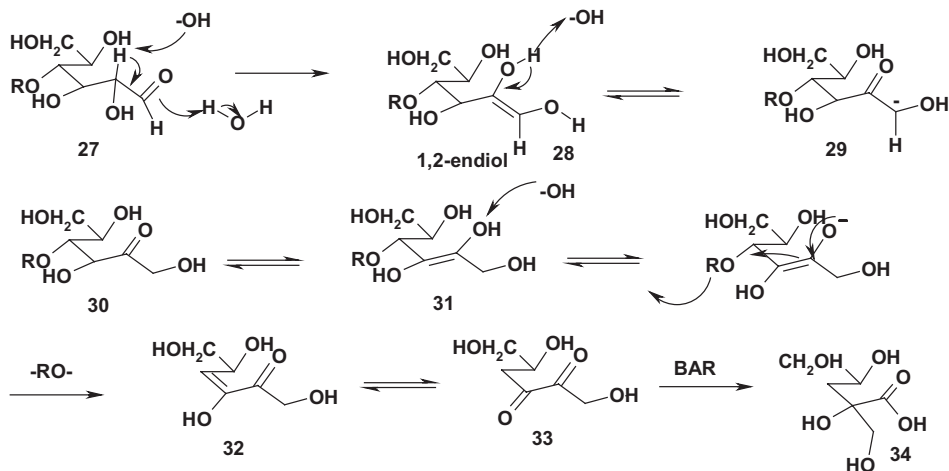
**Scheme 4.13** Schematic model of cellulose/hemicellulose degradation under alkaline conditions.

#### Peeling

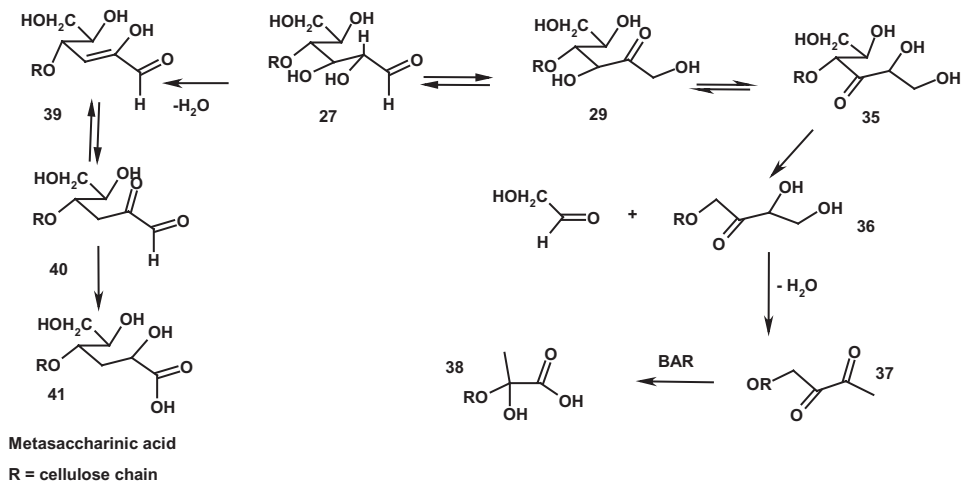
Peeling removes the terminal anhydro-sugar unit, generating a new reducing end group until a competitive stopping reaction sets in, forming a stable saccharinic acid end group. The peeling reaction starts with the well-known Lobry de Bruyn–Alberda van Ekenstein rearrangement [61], an isomerization reaction of carbohydrates under alkaline catalysis with the intermediate formation of an enediol anion species (**28**) [62,63].

The elimination of the cellulose chain in  $\beta$ -position to the anionic intermediate leads to a dicarbonyl structure (**33**) in the leaving unit, which is extremely

unstable under alkaline conditions and undergoes various degradation reactions, such as benzylic acid rearrangements or Cannizzaro reactions, eventually yielding isosaccharinic acid (34) or 2,5-dihydroxypentanoic acid, respectively, as main degradation products of cellulose (Scheme 4.14). Enolization of the starting carbohydrate as the rate-determining step is accelerated by increased  $\text{OH}^-$  concentrations. Depending on the reaction conditions, about 50–60 glucose units are peeled off before a competitive stopping reaction sets in (Scheme 4.15) [64]. Here, reducing



Scheme 4.14 Mechanism of the peeling reaction. BAR = benzylic acid rearrangement.

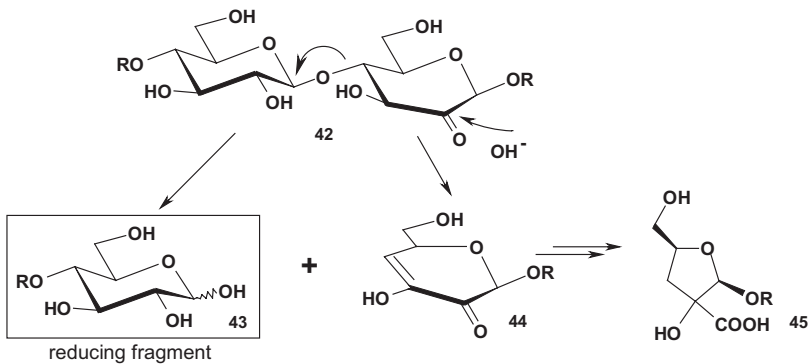


Scheme 4.15 Major stopping reaction. BAR = benzylic acid rearrangement.

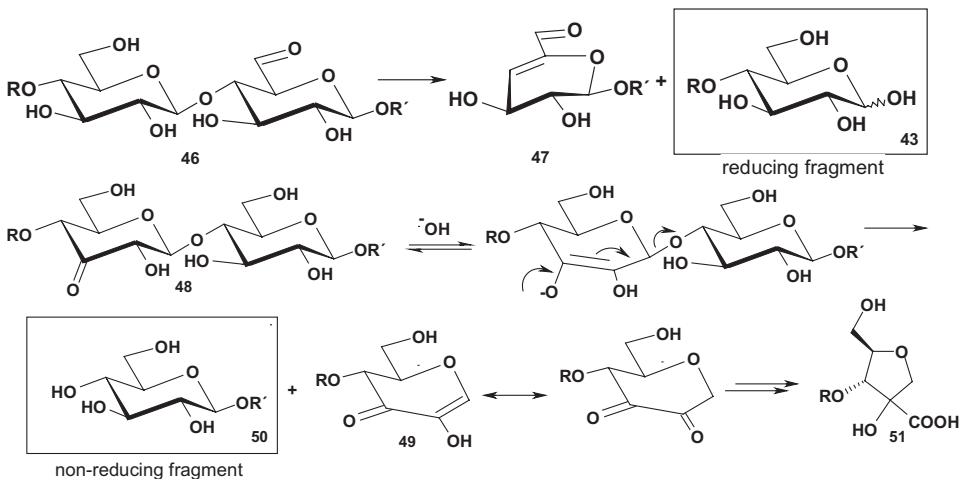
end groups are stabilized by conversion into the corresponding aldonic acid by simple oxidation, or by conversion to metasaccharinic acid (41) or 2-hydroxy-2-methyl-3-alkoxy-propanoic acid, respectively [65]. The activation energies for the peeling and stopping processes have been estimated as  $103 \text{ kJ mol}^{-1}$  and  $135 \text{ kJ mol}^{-1}$ , respectively [66]. This implies that the peeling reaction becomes less pronounced with increasing temperature.

### Oxidative Peeling

If keto or aldehyde groups are present along the cellulose chain, they generally cause cleavage of the glycosidic bond in alkaline media by  $\beta$ -alkoxy elimination (cf. Scheme 4.16). Therefore, oxidized groups in the C2, C3 or C6 position are



**Scheme 4.16**  $\beta$ -elimination reaction at C2-keto units.



**Scheme 4.17** Cleavage of the glycosidic bond by  $\beta$ -elimination at C3-keto and C6-aldehyde structures along the cellulose chain [67].

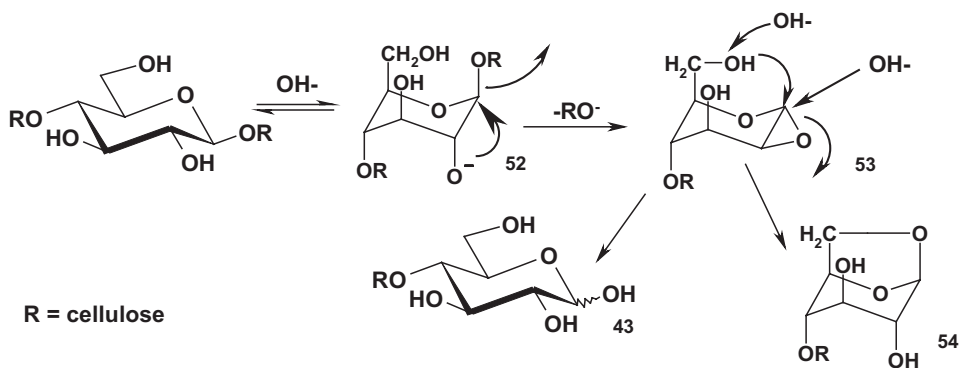
considered as “weak links” or “hot spots” along the chain. Keto groups at C2 (42) or an aldehyde at C6 (46) and the anomeric carbon are referred to as “active carbonyls”, leading to a new reducing end group (43), which might undergo further degradation reactions. A keto group at C3 (48) is considered as an “inactive carbonyl”, since  $\beta$ -elimination eventually forms a non-reducing end (50) and a stable acid (51) (cf. Scheme 4.17).

### Alkaline Hydrolysis

At elevated temperatures ( $T > 140^\circ\text{C}$ ), direct chain cleavage of cellulose commences – a process that is also referred to as alkaline hydrolysis or secondary peeling. This reaction is mainly responsible for observed yield losses during alkaline pulping. The reaction mechanism is depicted in Scheme 4.18.

Elevated temperatures facilitate a conformational change of the pyranose ring from the  ${}^4\text{C}_1$  conformer with all hydroxyl groups arranged in equatorial position to a  ${}^1\text{C}_4$  conformation, with all hydroxyl groups arranged axially (52). Starting from this molecular geometry, the ionized hydroxyl at C2 reacts by intermolecular nucleophilic attack to form an oxirane intermediate (53) under elimination of the cellulose chain in position 1. The intermediate oxirane can be opened either by reaction with hydroxyl ions (formation of a terminal glucose moiety, 43) or again by an intramolecular reaction with the ionized C6 hydroxyl, yielding an anhydrate (levoglucosan, 54). The activation energy has been determined to be  $150\text{ kJ mol}^{-1}$  for cotton [68] and  $179\text{ kJ mol}^{-1}$  in Soda-AQ-pulping for spruce cellulose [69].

The ultrastructure of cellulose also plays a crucial role in the reaction under alkaline conditions, and may also affect the reaction rate [70]. Atalla et al. [71] demonstrated by raman spectroscopy cellulose II structure is formed in kraft pulp, while Isogai et al. [72] reported the formation of cellulose IV from amorphous regions of cellulose I during kraft pulping. Amorphous regions are more readily attacked than highly ordered domains. Even though the DP is decreased, the total yield loss during alkaline hydrolysis at elevated temperatures is appreciably small.

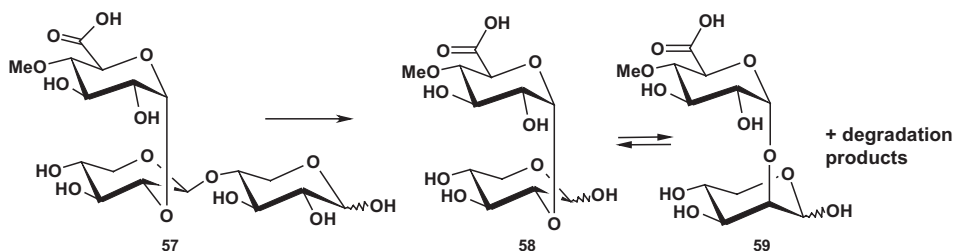


**Scheme 4.18** Alkaline hydrolysis of glycosidic linkages at elevated temperatures.

### Specific Reaction of Xylans

The side chain substituents in the xylan (either the 4-*O*-methylglucuronic acid in hardwood xylans, or the arabinopyranose in some softwood xylans; for structures, see Chapter 1) significantly hamper the alkaline degradation [73] (see above). The xylan backbone undergoes the peeling reaction until a unit with a substituent in position 2 or 3 is reached, or a stopping reaction with the formation of xylo-meta-saccharinic acid and xylo-isosaccharinic acids sets in.

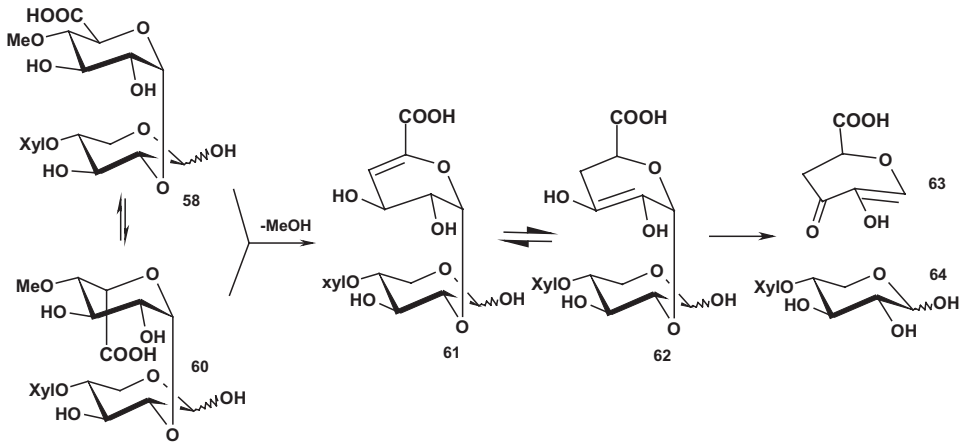
Model studies have indicated that at low temperatures the linear backbone of xylans are subjected to the peeling reaction at a higher rate compared to cellulose [74], though the peeling reaction was strongly retarded by side chain branches (4-*O*-methylglucuronic acid) in position C2 (57) [75].



**Scheme 4.19** Stopping of the peeling reaction at 4-*O*-methylglucuronic acid side chains (adopted from Ref. [75]).

Johansson and Samuelson [76,77] demonstrated that the peeling reaction is also hindered by a rhamnose substituent at C2 or an end group carrying a 4-*O*-methylglucuronic acid residue. Since these units are more stable, the peeling reaction pauses at this point until a temperature is reached at which the substituent is cleaved and the peeling process can be then resumed [78–81]. Recently, novel insights into the distribution of uronic acids within xylan showed that uronic acids are distributed rather randomly in hardwood xylan, but quite regularly in softwood xylans [82].

Also galacturonic acid end groups stabilize the xylan against peeling at lower temperature ( $T > 100\text{ }^{\circ}\text{C}$ ), but they are equally degraded at temperatures above  $130\text{ }^{\circ}\text{C}$ . 4-*O*-Methylglucuronic acid residues, partially converted into the corresponding hexenuronic acid ( $T > 120\text{ }^{\circ}\text{C}$ ) (cf. Scheme 4.20), are believed to stabilize the xylan towards depolymerization. The hexenuronic acid formed has a higher stability towards alkali, so that further peeling of the chains is prevented [83]. The arabinose units in softwood xylans also contribute to the higher alkali stability by inducing the stopping reaction. However, at elevated temperature these effects are reduced and the arabinose units are also cleaved [84].



**Scheme 4.20** Formation of HexA and cleavage of the side chain [83,90].

The hexenuronic acid side chains in xylans undergo elimination of methanol under alkaline conditions, forming hexenuronic acid residues (i.e., 4-deoxy-L-threo-hex-4-enopyranosyl-uronic acid, **61**, **62**) [85]. The reaction is promoted with both increasing alkali concentration and temperature [86,87]. After kraft pulping only about 12% of the carboxyl groups in accessible xylan are still of the 4-O-methylglucurono-type [88]. Formation of HexA is discussed as a cause for the stability of xylans during kraft cooking due to prevention of peeling reactions at the branched unit. Eventually, the hexenuronoxlyose is further decomposed to xylitol **83**. HexAs are seen as being partly responsible for the diminished brightness stabilities of bleached pulps. As under acidic conditions hexenuronic acids are unstable, an acidic treatment can be used to selectively remove HexA from the pulp [89].

Hexenuronic acids add to the total carboxyl group content in kraft pulps, and also to the kappa number. To estimate the actual amount of residual lignin in pulps, a modified kappa number has been proposed, which selectively disregards nonlignin fractions [91,92]

#### Specific Reactions of Glucomannans

Glucomannans are less stable than xylans, and undergo a rapid endwise peeling. One reason for the higher reactivity is the lack of substituents [93]. Galactose residues in galactoglucomannans are believed to have a similar stabilizing effect as the side chains in xylans [84,94]. However, Timell [95] considers the link between Gal and the backbone as a rather weak one, which will be cleaved readily under alkaline extraction conditions.

#### Xylan and Fiber Morphology

During pulping, the xylan is dissolved and also modified to a large extent. Towards the end of the cook [96,97], part of the xylan – which is still of oligomeric nature –

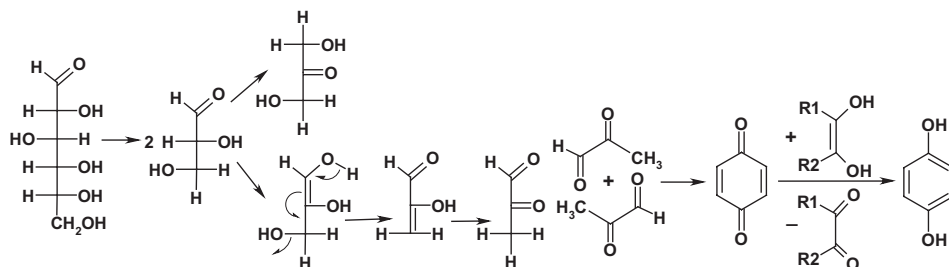


is re-precipitated at the cellulose fibers [98–102], thereby increasing pulp yield [103], changing the mechanical characteristics (increasing strength) of kraft pulps [104,105], and affecting the fiber quality. Hereby, the structure of the xylan affects the adsorption characteristics to a large extent, and increasing the removal of carboxyl groups thereby favors the retake of xylan [106].

The interaction of cellulose and hemicellulose in kraft pulps can be addressed by a number of modern analytical approaches. Differences in hemicellulose concentrations are observed between the surface and the inner layer of a kraft pulp fiber. In the pulps investigated (softwood and hardwood), the amount of hemicelluloses is generally larger at the surface as compared to the inner layer. The MWD and sugar composition of the hemicellulose deposits can be studied with MALDI and CE [107,108]. Analysis of the solid material involves CPMAS-<sup>13</sup>C-NMR studies [109–112], association and localization of hemicellulose on pulps are studied by GPC [113–116], and the use of enzymes in combination with other analytical techniques provides insights into bonding types [117–119], as well as LCC and hemicellulose structures [120,121].

### Carbohydrate-derived Chromophores

Low molecular-weight carbohydrates can undergo further reactions under the alkaline conditions of a kraft cook. Besides a series of isomerizations and further fragmentations, condensation to cyclic compounds and phenols can also occur (cf. Scheme 4.21). A number of catechols, phenols and acetophenones could be detected in model studies with glucose and xylose [122]. Some of these can also form stable radicals [123], which can also be detected in alkaline solutions from hot caustic extractions of cellulose [124]. Chromophores are also produced by oxidation reactions under alkaline conditions [125].

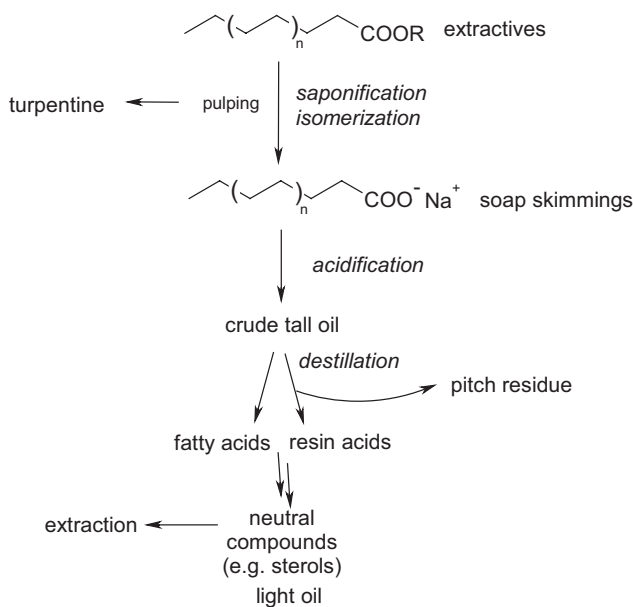


**Scheme 4.21** Formation of chromophores from carbohydrate monomers.

#### 4.2.4.3 Reactions of Extractives

Extractives are complex mixture of terpenes, fats, waxes, resin acids, fatty acids, phenols and tannins. Most extractives are soluble in alkaline solutions, and a good solubility permits the processing of wood species that are rich in extractives (including tropical woods). In kraft pulping, however, high extractive contents of wood may result in a considerable reduction in pulp yield. This in turn leads to an

increase in the consumption of chemicals, since extractives react rapidly with alkali and thus the amount of available hydroxyl ions is reduced [126]. The dissolution of extractives during pulping is of primary importance. Extractives are responsible for pitch problems in papers, they may also prevent delignification by covering parts of lignin with resinous material or simply reduce the penetrability of cooking chemicals into the wood [127], and they add to the toxicity of kraft mill effluents. The total amount of extractives which can be recovered from pulp mills varies greatly with the wood species and the storage conditions of the wood (Scheme 4.22). The highly volatile fraction is called turpentine, sulfate turpentine or tall oil (from the Swedish “tall” = pine), and is recovered from the digester relief condensate [128]. The sulfur-containing fractions (mercaptanes) need to be removed from the distillates.



**Scheme 4.22** Fractions of extractives obtained after kraft cooking [128].

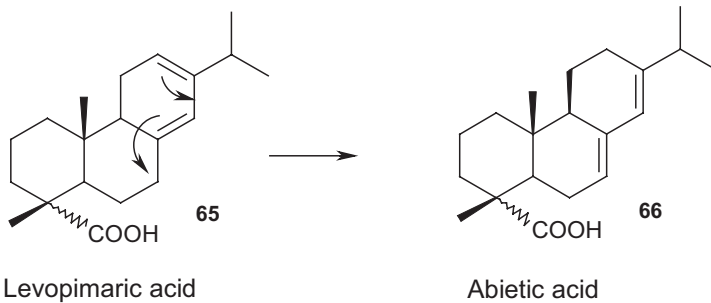
Fatty acids and resin acid esters are saponified in alkaline pulping and recovered as tall oil soap [1]. Acidification of the crude tall oil yields the corresponding free acids. This deacidification process consumes a large amount of sulfuric acid, which can be reduced by a carbon dioxide pretreatment.

Wood terpenes undergo mainly condensation reactions during pulping, and are collected as sulfate turpentine. The major reactions of extractive components are as follows:

- *Fatty acids* [129]: these undergo isomerization reactions (the shift of double bonds in the fatty acid chain from *cis* to *trans*, or *vice versa*) under alkaline pulping conditions, and are mainly dis-

solved. Nonconjugated double bonds are transformed to mainly conjugated isomers. The degree of conjugation is highly influenced by the prevailing conditions during the cook. For linoleic acid, almost no isomerization was observed at 150 °C, whereas at 180 °C almost 98% were isomerized [130]. The incorporation of fatty acids into residual lignin has recently been demonstrated [12].

- *Resin acids* [129]: these are also mainly dissolved. Part of the levopimaric acid (**65**) is converted to abietic acid (**66**), though the extent of this reaction during pulping is variable (Scheme 4.23). The acidification and heating of sulfate soap finally converts most of the levopimaric acid [131,132].



**Scheme 4.23** Conversion of levopimaric acid to abietic acid during the kraft process.

- *Waxes*: sterol esters and waxes are saponified much more slowly as compared to the glycerol esters. Waxes and triglycerides are hydrolyzed during alkaline pulping; hence, no esters are detected in sulfate soaps [129]. The sterol esters, waxes and free sterols do not form soluble soaps as do free acids, and therefore have a tendency to deposit and as such cause pitch problems.

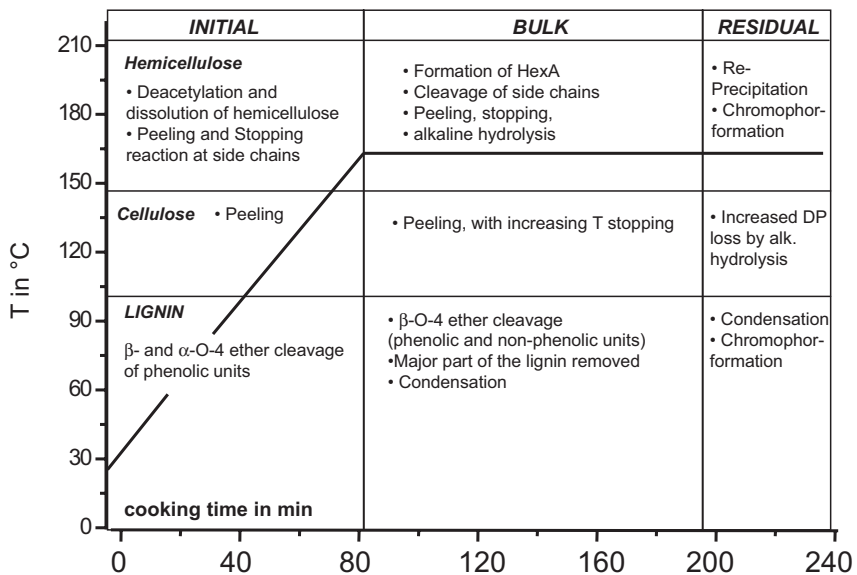
A number of extractives survive the cook more or less unchanged, and this portion is referred to as the “non-saponifiable” fraction.

#### 4.2.4.4 An Overview of Reactions During Kraft Pulping

The course of dissolution of lignin and carbohydrates reveals three distinct phases of a kraft cook: *initial*, *bulk*, and *residual* delignification which affect the single wood components as summarized in Scheme 4.24.

- *Initial phase*: the initial stage is characterized by losses in the carbohydrate fraction, which is more pronounced for hardwoods as compared to softwoods [133]. The hemicelluloses undergo deacetylation and physical dissolution, and peeling reactions also start. Cellulose degradation by peeling is negligible in terms of yield loss. Reactive phenolic lignin units, such as  $\alpha$ -O-4-ethers, are cleaved as early as the initial phase.

- *Bulk phase*: The core delignification occurs in the bulk phase and, importantly, both phenolic and nonphenolic  $\beta$ -O-4-ether bonds are cleaved. About 70% of the lignin is removed. The reactions of the carbohydrates are characterized by secondary peeling (i.e., alkaline cleavage of the glycosidic bonds), but also by stopping reactions, which are favored at elevated temperature. Methanol is liberated from 4-O-methylglucuronic acid side chains, and hexenuronic units are formed.
- *Residual phase*: the residual phase begins at a delignification rate of about 90%. Delignification has slowed down considerably due to depletion of reactive lignin units. It is believed that the chemical nature of the residual lignin hampers further degradation reactions. A slow delignification is accompanied by rapid carbohydrate degradation, causing disproportionate carbohydrate losses.

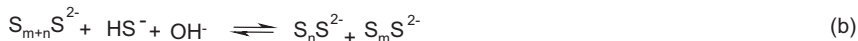


Scheme 4.24 Phases of delignification and respective reactions of wood components.

#### 4.2.4.5 Inorganic Reactions

As can be deduced from Scheme 4.5, nucleophilic attack of hydrogen sulfide results in the formation of elemental sulfur, which in turn results in a temporary loss of active hydrogen sulfide. Elemental sulfur can further react with hydrosulfide ions to polysulfide (Scheme 4.25). This polysulfide may disproportionate to thiosulfate and hydrosulfide. During a kraft cook, the amounts of polysulfide and sulfide varies [12]. Gellerstedt et al. [12] demonstrated a rather constant concentration of sulfide ions and a decrease in polysulfide towards the end of a conventional kraft cook. Teder [134] showed that the stoichiometric composition of a polysulfide

solutions depends on the alkalinity, while the average size of the polysulfide anions ( $S_nS^{2-}$ ) in equilibrium with elemental sulfur is independent on the prevailing alkalinity. However, the concentration of hydrosulfide ions decreases with increasing alkalinity.



**Scheme 4.25** Formation of polysulfide ions (a) and reaction of polysulfide ions under cooking conditions.

The analysis of inorganic compounds in cooking liquors can be performed with either ion-exchange chromatography or capillary electrophoresis [135,136]. Quinone-type compounds are thought to be responsible for the rapid oxidation of sulfide ions to sulfite and thiosulfate [134].

#### 4.2.5

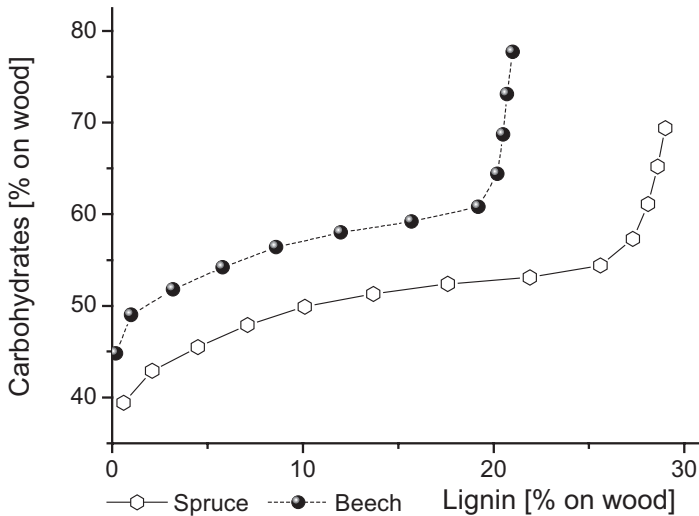
##### Kraft Pulping Kinetics

*Herbert Sixta*

##### 4.2.5.1 Introduction

The removal of lignin during kraft pulping is accompanied by the loss of carbohydrates, which mainly consist of hemicelluloses. Following a complete kraft cook, the removal of the two major wood components shows a characteristic pattern. The course of delignification in relation to the content of carbohydrates reveals three distinct phases throughout the whole cooking process. The initial stage is characterized by a substantial loss of carbohydrates, small but rapid delignification and high alkali consumption. In the second stage – generally referred to as the bulk delignification – the main dissolution of lignin takes place and the amount of carbohydrates and the alkali concentration in the cooking liquor decrease only slightly. Reaching a certain degree of delignification, the continuation of the cook results in the residual delignification phase where the degradation of carbohydrates, mainly cellulose, predominates. The low selectivity in the final phase of a conventional kraft cook is a limiting factor, as both the yield loss and the molecular weight degradation of cellulose are unacceptable. Consequently, the cook should be interrupted before the residual phase is attained. Figure 4.22 shows the course of delignification and carbohydrate degradation during alkaline pulping of beech (*Fagus sylvatica*) and spruce (*Picea abies*).

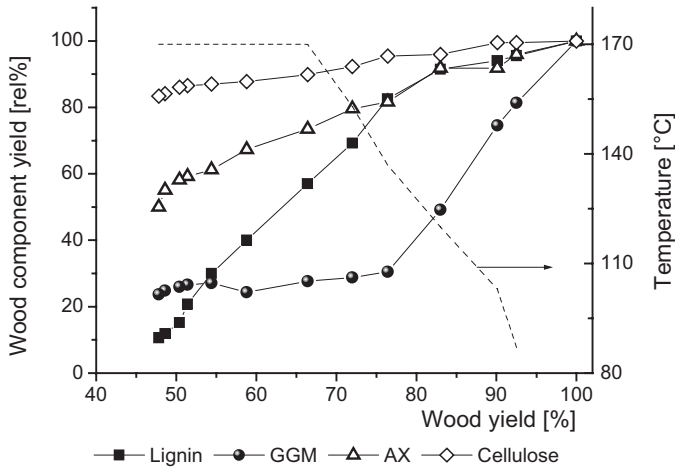
From the results in Fig. 4.22 it can be clearly seen that alkaline delignification is accomplished in three phases. In the initial phase of alkaline pulping, approximately 22% of the total polysaccharides in both spruce and beech wood are removed (which equals 15% and 16.9% of the mass of spruce and beech wood, respectively). At the same time, the removal of lignin amounts to 11.7% of the



**Fig. 4.22** Yield of total amount of carbohydrates as a function of the amount of lignin during alkaline pulping of spruce and beech at a liquor-to-wood ratio of 4:1; an EA-charge of 20.6% on wood; Results from Masura [1].

total lignin in spruce wood and 8.6% of the total lignin in beech wood (which equals 3.4% and 1.8% of the mass of spruce and beech wood, respectively). Based on the total wood yield, the removal of polysaccharides at the beginning of the cook is 4.4-fold larger for spruce wood and 9.3-fold larger for beech wood as compared to the lignin dissolution. The second cooking stage is characterized by a very selective removal of lignin. There, only 6.8% of the total polysaccharides in spruce wood and 5.9% of the total polysaccharides in beech are degraded to alkaline soluble components (equal to 4.7% and 4.5% of the mass of spruce and beech wood, respectively). Simultaneously, 52.8% of the total lignin content in spruce wood and 54.5% of the total lignin content in beech wood are dissolved (which corresponds to 15.3% and 11.4% of the masses of spruce and beech woods, respectively). This confirms that the second delignification phase is highly selective, as the amount of lignin removal is 3.2-fold that of the carbohydrates for spruce wood and 2.5-fold that of the polysaccharides for beech wood. The third phase of alkaline degradation is again characterized by a more intense degradation of the polysaccharide fraction as compared to the residual lignin. Although the carbohydrate and lignin fractions of beech wood and spruce wood differ in their molecular and structural composition, the course of delignification and carbohydrate dissolution is comparable for both species.

Removal of the single carbohydrate fractions during kraft pulping of pine (*Pinus sylvestris*), divided into cellulose (C), galactoglucomannan (GGM) and 4-O-methylglucuronarabinoxylan (AX), was studied extensively by Aurell and Hartler [2]. Figure 4.23 shows the relative content of the wood components as a function of the total yield during the whole kraft cooking process. Between 100 and 135 °C, or



**Fig. 4.23** The removal of wood components as a function of the total wood yield during kraft cooking of pine at a liquor-to-wood ratio of 4:1, an effective alkali charge of 20.3% on wood, a sulfidity of 25% with a heating-up period of 2 h, and a maximum cooking temperature of 170 °C. Data from Aurell and Hartler [2].

in the yield range between 92 and 78%, an extensive loss of GGM can be observed which contributes predominantly to the yield loss during this initial cooking phase. The loss of GGM is probably due to peeling reactions.

At 135 °C, the residual GGM remained quite stable throughout the subsequent cooking. Its stabilization cannot be explained solely by chemical stabilization (e.g., the formation of metasaccharinate end-groups), but may also be attributed to the formation of a highly ordered structure, which would significantly decrease the rate of hydrolysis of the glycosidic bonds.

The dissolution of AX and lignin follows a similar pattern up to a temperature of approximately 140 °C. The amount of AX removed is quite small even during the later phases of kraft cooking. The peeling reaction is of little importance, since the removal of xylan is not significantly influenced by the presence of sodium borohydride [2]. The comparatively high stability of the softwood xylan towards the peeling reaction is due to the arabinose substituents in the C-3 position. Arabinose is easily eliminated by means of the  $\beta$ -alkoxy elimination reaction under simultaneous formation of a metasaccharinic acid end group which stabilizes the polymer chain against further peeling [3]. The content of 4-O-methylglucuronic acid side groups of AX decrease significantly in the early phases of the cook. Simultaneously, the amount of another type of acidic group, 4-deoxyhex-4-enuronic acid (HexA), increases. The HexA is a  $\beta$ -elimination product of 4-O-methylglucuronic acid [4,5]. The highest amount of hexenuronic acid, approximately 10% of xylan, is detected at the end of the heating period. During the subsequent cooking phases, about 60% of the formed hexenuronic acids are degraded again. The removal of xylan increases during the cooking phase at maximum temperature, which in part can be attributed to dissolution and in part to alkaline hydrolysis

(secondary peeling). In addition, peeling reactions contribute to the degradation of AX. The dissolution of xylan depends strongly on the effective alkali concentration. With an increasing effective alkali concentration, the amount of AX present in the solid residue decreases. In the final cooking phase, when the effective alkali concentration drops below a certain level, the absolute yield of AX increases again due to its readsorption onto the fibers [6]. Hence, the alkalinity and the alkaline profile of the kraft cook strongly affect the amount of AX present in the pulp. During a conventional kraft cook, 10–15% of the cellulose is dissolved. The removal of cellulose starts at about 130 °C, increases to the maximum temperature, and then slows down gradually. The cellulose degradation is limited to the amorphous zones, probably involving peeling reactions, initiated at higher temperatures by alkaline hydrolysis of glycosidic bonds.

The three phases of the kraft cook are obviously governed by the different reactivity of the wood components involving different chemical and physical processes. To achieve a high-quality pulp combined with an acceptable yield, the chemical reactions must be stopped at a residual lignin content which can be selectively removed in a subsequent ECF or TCF bleaching treatment. This is the predominant aim of paper grade production. In the case of dissolving pulp production, the major target is to adjust a certain weight average molecular weight of the pulp carbohydrates, measured as intrinsic viscosity. The control of the most important process and pulp quality parameters, such as the lignin content (measured as kappa number), the molecular weight (measured as intrinsic viscosity) and the pulp yield requires a highly advanced process control system. The basis of such a cooking model is the description of the kinetics of the chemical reactions that occur in the digester. Because of the heterogeneity of the system, however, pulping reactions are complicated and can thus not be regarded in the same way as homogeneous reactions in solution.

This chapter provides first a review of both empirical and partly mechanistic models of delignification, carbohydrate degradation and cellulose depolymerization. Finally, a rather complete kinetic model for softwood kraft cooking is presented in detail. This kinetic model combines the model proposed by Andersson et al. with expressions for the kinetics of delignification and carbohydrate degradation and the modified model of Kubes et al. which describes the rate of cellulose chain scissions [7,8].

#### 4.2.5.2 Review of Kraft Cooking Models

##### 4.2.5.2.1 Model Structure

Kinetic studies are important in providing essential evidence as to the mechanisms of chemical processes. The chemical reactions occurring during the kraft pulping process in the solid-interface of wood and pulping liquor are very complex and thus not known in detail. The pulping processes therefore cannot be treated as having reaction kinetics similar to those of homogeneous reactions in solution. The present picture of the reaction mechanisms is that the swollen lignin in the



wood chip is degraded into fragments at the solid–liquid interface by the hydroxyl and hydrosulfide ions present in the pulping liquor. Assuming different lignin species, the delignification reaction of each can be approximated to a first-order reaction. The rate constant can be calculated from the simple expression:

$$-\frac{dL_j}{dt} = k_j \cdot L_j \quad (74)$$

The influence of the pulping temperature on the rate of delignification can be expressed quantitatively according to the Arrhenius equation [9]:

$$k = A \cdot \text{Exp}\left(-\frac{E_A}{R} \cdot \frac{1}{T}\right) \quad (75)$$

The validity of this simple approach has, however, been questioned on the grounds that the rate-determining reactions are unknown [10]. Nevertheless, the temperature dependence of the delignification reaction using the Arrhenius equation can be applied, provided that the reaction does not change over the temperature range studied [11].

The major objective of the development of kinetic models is to improve the control of digester operation. During the past 45 years, many studies of the kinetics and transport behavior of the kraft pulping process have been carried out. Based on the experimental results of these studies, kraft pulping models of varying complexity have been developed for control and design purposes. Basically, all models are data-driven and, according to Michelsen, can be categorized as either empirical (black box) and pseudo first-principle models (partly mechanistic) [12].

## Empirical Models

### *Delignification*

#### H-Factor concept

Process control in practical pulping is mainly based on empirical models due to their simplicity and ease of implementation. One of the earliest kinetic models was developed by Vroom and this, even today, is widely used for control purposes [13]. This model is called the H-factor, and expresses the cooking time and temperature as a single variable in batch reactors. It is defined as:

$$H = \int_{t_0}^t k_L \cdot dt \quad (76)$$

where  $k_L$  is the relative reaction rate of pulping (dimensionless). The rate at 100 °C is chosen as unity, and all other temperatures are related to this rate. An Arrhe-

nius-type equation is used to express the temperature dependence of the reaction rate. At a temperature  $T$ , it is expressed as

$$\text{Ln}(k_{L(T)}) = \text{Ln}(A) - \frac{E_{A,L}}{R} \cdot \frac{1}{T} \quad (77)$$

The reference reaction rate at 100 °C is simplified to

$$\text{Ln}(k_{L,100^\circ\text{C}}) = \text{Ln}(A) - \frac{E_{A,L}}{R} \cdot \frac{1}{373.15} \quad (78)$$

The relative reaction rates at any other temperature can be expressed by the following equation:

$$\text{Ln} \frac{k_{L(T)}}{k_{100^\circ\text{C}}} = \frac{E_{A,L}}{R \cdot 373.15} - \frac{E_{A,L}}{R \cdot T} \quad (79)$$

The activation energy values  $E_A$  for bulk delignification published in the literature range from 117 kJ mol<sup>-1</sup> [14] for birch to 150 kJ mol<sup>-1</sup> [15] for pine. Assuming an activation energy of 134 kJ mol<sup>-1</sup>, according to Vroom the H-factor can be expressed as

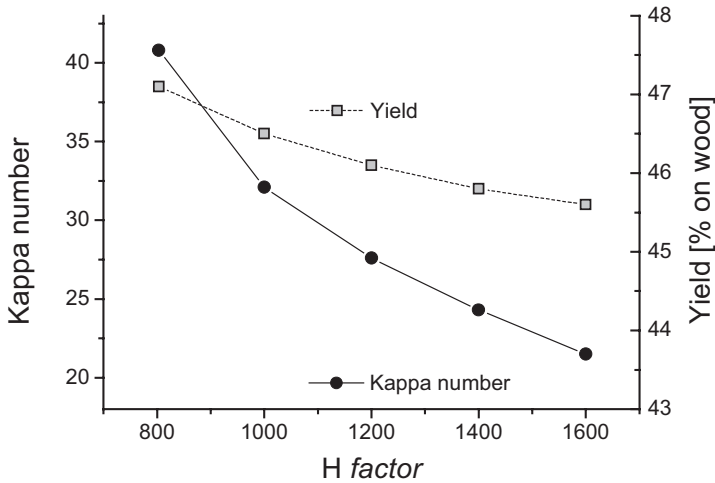
$$H = \int_{t_0}^t \frac{k_{L(T)}}{k_{100^\circ\text{C}}} \cdot dt = \int_{t_0}^t \text{Exp} \cdot \left( 43.19 - \frac{16113}{T} \right) \cdot dt \quad (80)$$

The H-factor is designated as the area under the curve of  $k$  vs. time in hours. As an example, the H-factor for 1-h isothermal cooking at 170 °C equals a value of 925. The H-factor was developed to predict the temperature or cooking time needed to achieve a given Kappa number. This means that the result is only valid when the relationship between the H-factor and the Kappa number is known, provided that the other cooking conditions such as effective alkali concentration, liquor-to-wood-ratio, etc. are kept constant. In this case, the prediction of kappa number is of sufficient precision. Figure 4.24 shows as an example the course of kappa number and yield as a function of H-factor for softwood kraft cooking.

Depending on the charge of effective alkali and the sulfidity of the cooking liquor, H-factors in the range of 1000 to 1500 are needed for a complete kraft cook [17].

A number of simple models for the relationship between two or three process variables have been developed. Hatton describes a model to predict yield and kappa number based on the H-factor and the charge of effective alkali for a variety of wood species with an equation of the form [18]:

$$Y = \kappa = \alpha - \beta \cdot [(\text{Log}H)(EA)^n] \quad (81)$$



**Fig. 4.24** Course of kappa number and yield as a function of the H-factor. Spruce/pine = 1:1; liquor-to-wood-ratio = 3.8:1; maximum temperature = 170 °C; EA-charge = 19% on wood; sulfidity 38% [16].

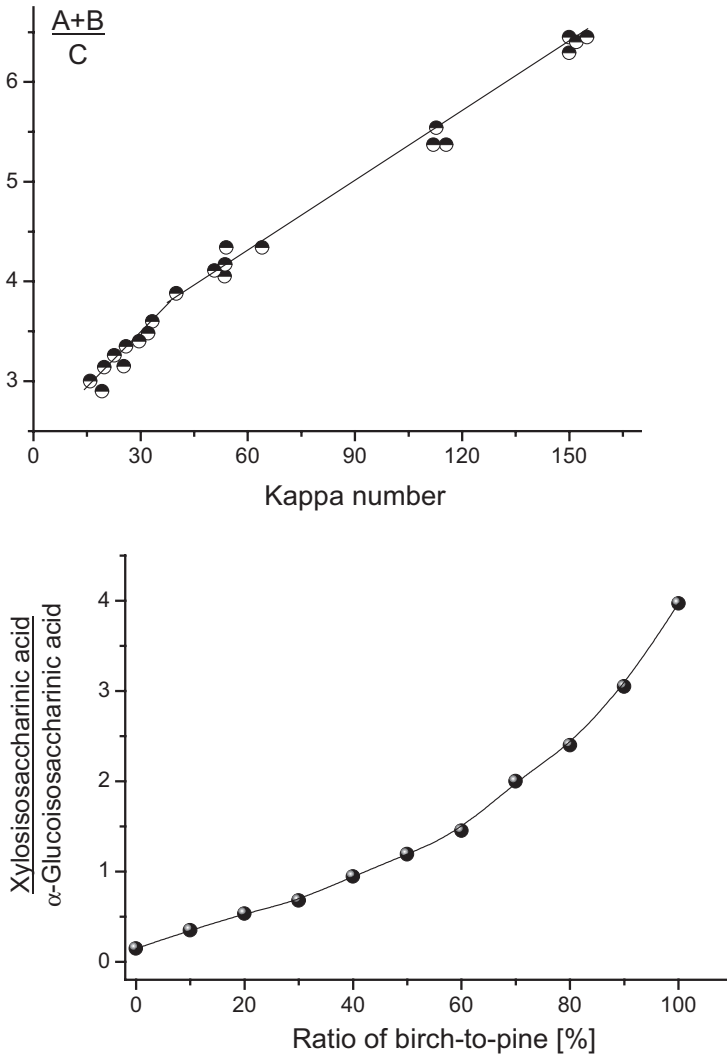
where  $Y$  is the yield,  $k$  the kappa number,  $a$  and  $b$  are adjustable parameters,  $H$  is the H-factor, and EA is the effective alkali charge based on wood.

The integration of additional process parameters into the model structure certainly improves the precision of kappa number prediction. For example, the model of Bailey et al. uses five variables in a 20-term polynomial to predict kappa number [19]. Despite the high complexity, the reliability of these models is limited to the specific cooking plant investigated.

#### Control of kraft pulping by monitoring of hydroxy carboxylic acids

A prerequisite for reliable H-factor control is that the cooking conditions are precisely known and kept strictly constant, since the prediction of the cooking time needed to reach the target kappa number is based only on temperature measurements. Typical industrial conditions, however, include uncontrollable variations in the moisture content and the quality of chips, the concentration of the active cooking chemicals, and the temperature measurements. Alternatively, it was suggested to correlate the progress of delignification with the carbohydrate degradation taken place during cooking. The majority of carbohydrates in kraft pulping are degraded to hydroxy carbonic acids according to the *peeling* reaction (see Section 4.2.4.2.1). The formation of these short-chain acids is directed by temperature and effective alkali concentration. Detailed investigations have shown that adequate information with regard to the extent of delignification can be obtained simply by analyzing the key hydroxy monocarboxylic acids as their trimethylsilyl derivatives by gas-liquid chromatography [20]. Kraft pulping of pine can be reliably controlled by following the concentration ratio comprising the sum of 3,4-dideoxypentanoic

acid (A) and anhydroglucoisosaccharinic acid (B) divided by the concentration of 2-hydroxybutanoic acid (C). This procedure is also advantageous because it avoids the difficulty of measuring the absolute concentrations.



**Fig. 4.25** (A) Acid concentration ratio versus kappa number of pine kraft pulping according to [21]. EA-charge 18–24% on wood, sulfidity 35%. A = 3,4 dideoxypentonic acid; B = anhydroglucoisosaccharinic acid;

C = 2-hydroxybutanoic acid. (B) Ratio of the concentrations of xyloisosaccharinic acid to  $\alpha$ -glucoisosaccharinic acid as a function of the wood composition consisting of birch and pine (according to [21]).

Figure 4.25A shows the concentration ratio in relation to the course of kappa numbers. Based on this relationship, it was possible to determine the end point of the cook with an accuracy corresponding to  $\pm 2$  kappa number units. However, the described method for the determination of the ratio of hydroxy monocarboxylic acids is still too time-consuming to be used for process control under industrial conditions.

The fragmentation pattern of the carbohydrates under alkaline cooking conditions is different for softwoods and hardwoods. Thus, the proportion of, for example hardwood in a wood composition consisting of a mixture of hardwood and softwood, can be detected by using this method. Among different possibilities, the ratio of xyloisosaccharinic acid to  $\alpha$ -glucoisosaccharinic acid determines the composition of the softwood and hardwood chip mixtures as seen in Fig. 4.25B, which shows clearly that the composition of the chip mixtures can be reliably determined on the basis of the analysis of the hydroxy monocarboxylic acids.

#### Carbohydrate degradation

The selectivity of kraft pulping is determined by the ratio of polysaccharide degradation and lignin removal. For the production of dissolving pulp, the most important control parameter is the average degree of polymerization, determined as intrinsic viscosity. A kinetic model for the degradation of pulp polysaccharides (cellulose and hemicelluloses) can be derived by assuming the initial number of molecules to be  $M_0$  and the initial total number of monomer units as  $N_0$ , then the initial total number of bonds is  $n_0$ , where [22]

$$n_0 = N_0 - M_0 = N_0 \cdot \left(1 - \frac{1}{DP_{n,0}}\right) \quad (82)$$

where  $DP_{n,0}$  is the initial degree of number average polymerization =  $N_0/M_0$ .

Similarly, the number of bonds in the polymer substrate remaining at time  $t$  can be described as:

$$n_t = N_t - M_t = N_0 \cdot \left(1 - \frac{1}{DP_{n,t}}\right) \quad (83)$$

where  $M_t$  is the number of polymer molecules at time  $t$ ,  $DP_{n,t}$  is the degree of number average polymerization at time  $t = N_t/M_t$ , and  $n_t$  is the number of intermonomer bonds per molecule at time  $t$ .

For first-order kinetics of bond scission, the rate is proportional to the number of unbroken bonds in the polymer and the hydroxide ion concentration:

$$-\frac{dn}{dt} = k'_c \cdot [OH^-] \cdot n \quad (84)$$

In the case of constant hydroxide ion concentration the equation simplifies to:

$$\ln\left(\frac{n_t}{n_0}\right) = -k'_c \cdot [OH^-]^a \cdot t = -k_c \cdot t \quad (85)$$

where  $k_c$  is the rate constant of the first-order reaction.

Substituting for  $n_t$  and  $n_0$

$$\ln\left(1 - \frac{1}{DP_{n,t}}\right) - \ln\left(1 - \frac{1}{DP_{n,0}}\right) = -k_C \cdot t \quad (86)$$

If  $DP_t$  and  $DP_0$  are large, which is valid in the case of pulp polysaccharides, this simplifies to a zero-order reaction:

$$\left(\frac{1}{DP_{n,t}} - \frac{1}{DP_{n,0}}\right) = CS = k_C \cdot t \quad (87)$$

where  $CS$  is the number of chain scissions per anhydroglucose unit and  $k_C$  is a reaction rate for cellulose degradation; assuming  $DP_{n,0} = 1500$  and  $DP_{n,t} = 1000$ , the number of chain scissions calculates to  $0.33 \text{ mmol AHG}^{-1}$ .

It must be taken into account that this approach is strictly applicable only if the polymer is linear, monodisperse, and there is no loss of monomer units during scission. Although the pulp carbohydrates are by no means monodisperse and there is also some loss of monomers during scission due to peeling reactions, the model is applicable to predict the degree of average polymer weight with sufficient precision. In a certain range of the degree of polymerization it can be assumed that the polydispersity remains constant during the degradation reaction.

The rate of cellulose chain scission is also strongly dependent on the hydroxide ion concentration, as expressed by Eq. (85). The value of  $a$  can be obtained as the slope of  $a$  plot of  $\ln(k_C)$  against  $\ln([\text{OH}^-])$ . Kubes et al. studied the effect of hydroxide ion concentration for both kraft and Soda-AQ pulping of black spruce [23]. Figure 4.26 illustrates the effect of  $[\text{OH}^-]$  on the rate of cellulose chain scissions at a cooking temperature of  $170^\circ\text{C}$ .

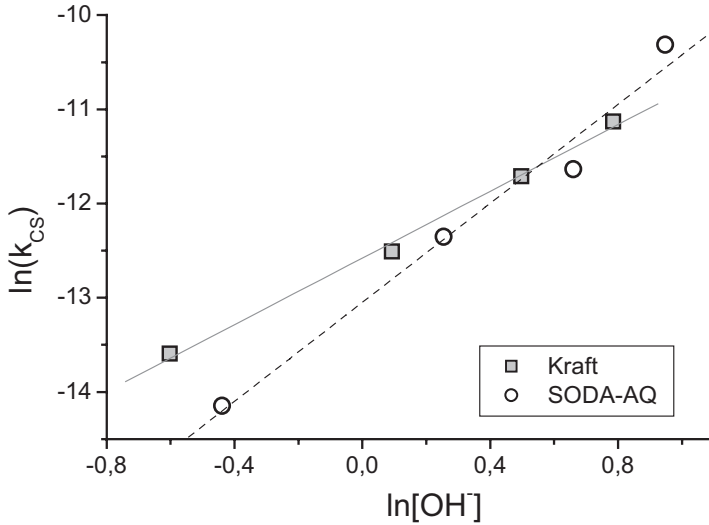
According to Fig. 4.26, Soda-AQ cooking displays a more pronounced effect on the rate of cellulose chain scissions as compared to kraft cooking. The corresponding values for the power constant in Eq. (85) have been determined to be 2.63 for Soda-AQ and 1.77 and for kraft pulping, respectively. In the case of kraft pulping, Eq. (87) can thus be modified to

$$\left(\frac{1}{DP_{n,t}} - \frac{1}{DP_{n,0}}\right) = CS = k'_C \cdot [\text{OH}^-]^{1.77} \cdot t \quad (88)$$

The temperature dependence can be described by the Arrhenius equation according to the following expression

$$k'_C = A \cdot \text{Exp}\left(-\frac{E_{A,C}}{R} \cdot \frac{1}{T}\right) \quad (89)$$

where  $E_{A,C}$  can be calculated from the slope of the graph of  $\ln k_C$  versus  $1/T$ .



**Fig. 4.26** Effect of hydroxide concentration on the rate of cellulose chain scissions in the course of kraft and Soda-AQ cooking of black spruce at 170 °C as a plot of  $\ln(k_c)$  against  $\ln([\text{OH}^-])$  with liquor-to-wood ratio amounts to 0.5–2.6 mol L<sup>-1</sup>; The Tappi Standard Viscosity Method T-230 (0.5% cuene) was converted by the equation  $\text{IV}[\text{mL g}^{-1}] = 1 \times 10^3 \times [8.76 \times \log(V) - 2.86]$  to the intrinsic viscosity (IV = SCAN-CM-15:88) which again was converted to  $\text{DP}_v$  by the appropriate equations included in the SCAN Method CM 88.

Kubes et al. obtained an activation energy of  $179 \pm 4 \text{ kJ mol}^{-1}$  for the chain scissions in both Soda-AQ and kraft pulping. This result reveals that additives such as sulfide for kraft and anthraquinone for Soda-AQ pulping do not affect pulp viscosity. This observation was confirmed quite recently, showing that the activation energies for cellulose degradation were not influenced by the addition of AQ and PS, either alone or in combination, and were in the range of 170–190 kJ mol<sup>-1</sup> [24,25].

Finally, Eq. (90) represents the complete rate equation for cellulose chain scissions of Soda-AQ and kraft pulping combining the expressions for temperature and hydroxide ion concentration dependences:

$$\begin{aligned}
 \text{SODA - AQ} : \left( \frac{1}{\text{DP}_{n,t}} - \frac{1}{\text{DP}_{n,0}} \right) &= 2.80 \cdot 10^{15} \cdot \text{Exp} \cdot \left( -\frac{21538}{T} \right) \cdot [\text{OH}^-]^{2.63} \cdot t \\
 \text{KRAFT} : \left( \frac{1}{\text{DP}_{n,t}} - \frac{1}{\text{DP}_{n,0}} \right) &= 4.35 \cdot 10^{15} \cdot \text{Exp} \cdot \left( -\frac{21538}{T} \right) \cdot [\text{OH}^-]^{1.77} \cdot t
 \end{aligned}
 \tag{90}$$

Following Vroom's approach, Kubes et al. have derived the G-factor model for viscosity loss as a means for expressing the effect of cooking time and temperature in a single variable [8,23]. Analogous to the H-factor concept, the reaction rate constant for cellulose degradation,  $k_c$ , can be related to the rate at 100 °C which is chosen as unity. Thus, the relative reaction rates at any other temperature can be expressed by the following equation:

$$\ln \frac{k_{C,(T)}}{k_{C,100^{\circ}C}} = \frac{E_{A,C}}{R \cdot 373.15} - \frac{E_{A,C}}{R \cdot T} \quad (91)$$

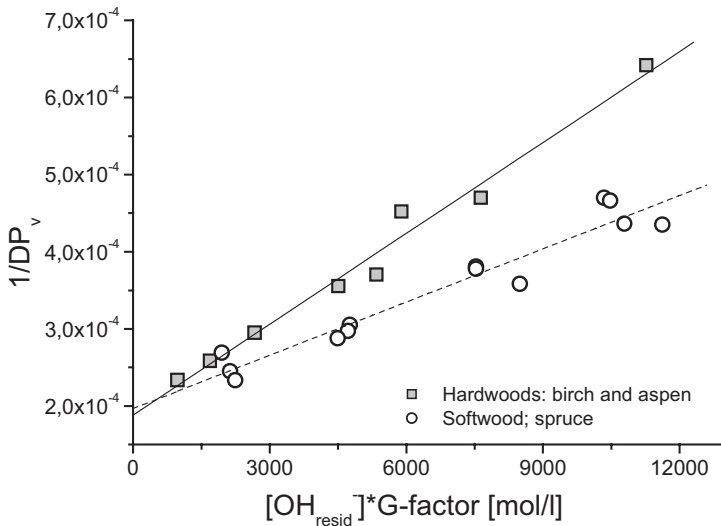
Inserting the activation energy for viscosity loss,  $179 \text{ kJ mol}^{-1}$ , leads to the following expression for the G-factor:

$$G = \int_{t_0}^t \text{Exp} \cdot \left( 57.70 - \frac{21538}{T} \right) \cdot dt \quad (92)$$

At a constant hydroxide ion concentration, the G-factor can be related to the chain scission according to Eq. (93):

$$\left( \frac{1}{DP_{n,t}} - \frac{1}{DP_{n,0}} \right) \propto G \quad (93)$$

In industrial pulping the hydroxide ion concentration varies as a function of time. Fleming and Kubes recognized a linear correlation between the cellulose chain scissions and the product from residual alkali concentration and G-factor. Figure 4.27 shows a plot of  $([\text{OH}_{\text{res}}^-] \cdot G)$  against the reciprocal viscosity average degree of polymerization,  $1/DP_v$ , for both hardwood (birch and aspen) and softwood kraft pulping.



**Fig. 4.27** Reciprocal viscosity average degree of polymerization against  $([\text{OH}_{\text{res}}^-] \cdot G\text{-factor})$  for kraft pulping of birch, aspen and spruce at 30% sulfidity and a liquor-to-wood-ratio of 5:1 (according to [26]).



The results confirmed a linear relationship between  $1/DP_v$  and the product from  $[OH_{resid}]$  and G-factor, with different slopes for hardwoods and softwood. The reason for the more intense cellulose degradation in the case of hardwood pulps might be due to the lower amount of residual lignin being a measure of protection against polysaccharide degradation. The intercept on the ordinate corresponds to a viscosity average degree of polymerizations of 5315 for hardwood and 5080 for softwood which in turn correspond to intrinsic viscosities of 1550 and 1495 mL g<sup>-1</sup>, respectively.

**Pulping selectivity:** As a consequence of its high activation energy, viscosity loss accelerates more rapidly than delignification as temperature increases. The ratio of  $k_L$  to  $k_C$  can be used to represent the pulping selectivity. The values of this ratio against the cooking temperatures have been calculated on the basis of kraft pulping of black spruce at constant alkali concentration (Tab. 4.18).

**Tab. 4.18** Pulping selectivity denoted as the ratio of  $k_L$  to  $k_C$ . Kraft cooking of black spruce wood  $[OH] = 1.1 \text{ mol L}^{-1}$ , liquor-to-wood ratio = 24:1; sulfidity = 30% according to [25] Li et al. (2002).

Temperature [°C]	$k_L^a$ [kappa min <sup>-1</sup> ]	$k_C$ [min <sup>-1</sup> ]	$k_L/k_C$
150	1.25E-04	6.70E-07	187
160	3.23E-04	2.14E-06	151
170	8.62E-04	6.79E-06	127
180	1.76E-03	1.72E-05	102

a) apparent second-order reaction kinetics.

Pulping selectivity is improved by decreasing the cooking temperature, as expected. Consequently, cooking at low temperatures makes it possible to extend kraft cooking to lower kappa numbers without impairing pulp quality.

H- or G-factor models are very useful for batch pulping as they predict the kappa number and viscosity quite satisfactorily when the relationships between these factors and pulp quality parameters for any particular pulping system are known. These models do not possess any general validity, and cannot be transferred from one system to another as they do not take into account the chemistry of the pulping operations. The H-or G-factor models must be calibrated for each single pulping system. The amounts and types of lignin, hemicelluloses and extractives in the wood vary significantly. Hardwoods contain mixtures of syringyl and guaiacyl lignins, whereas softwoods contain mainly guaiacyl lignin. Lignins also differ in the relative amounts of linkages between the phenylpropane units (see Chapter 2.1.1.3.2). The chemical composition of hemicelluloses and extractives, and the proportion of their basic constituents, are also highly dependent

upon the wood species, and even on their provenance. Thus, the reactivity of the single wood constituents towards fragmentation reactions cannot be depicted in a simple model. Therefore it seems improbable that an empirical model such as the H-factor can ever be adapted with a high degree of precision to the kraft process, in particular when using continuous-flow operation. A reasonably good model would certainly need to take into account the major chemical steps.

#### Pseudo First-principle Models

More elaborate models consider different reaction conditions such as hydroxide ion and hydrogen sulfide ion concentrations, temperature, and classification into different pulping stages or the different reactivities of wood components [7,15, 27–35]. Some models even consider chip dimensions, ion strength, dissolved solids and pulping additives such as anthraquinone or polysulfide [31,36–39]. The more comprehensive and partly mechanistic models use either the concept of parallel or consecutive reactions of the wood components [7,12]. The former is often referred to as the Purdue model, derived at Purdue University, USA [40], while the latter was developed primarily at University of Washington, USA, with Gustafson as the prominent representative [28].

Both models, however, can be traced back to the work of Wilder and Daleski [36], Kleinert [41], LeMon and Teder [27] and Olm and Tistad [35]. The Purdue model, which was developed by Smith and subsequently modified by Christensen, includes an in-depth description of the main wood components as high- and low-reactive lignin (HR-L, LR-L), cellulose (C), the hemicellulose components galactoglucomannan (GGM) and arabinoxylan (AX), dissolved solids, and extractives. The latter are assumed to react very quickly, while the digester is being filled with cooking liquor. Hydroxide ions and hydrogen sulfide ions are considered to be active species of the cooking liquor.

A plot of the non-lignin constituents removed during pulping against lignin dissolved indicates the initial, bulk and residual delignification pattern for both kraft and soda processes (see Fig. 4.22). The shape of diagram is almost independent of the operating conditions, type of wood or equipment. The kinetics of dissolution of the five wood components is expressed as a set of first-order ordinary differential equations according to the general equation:

$$\frac{dX_j}{dt} = \left[ k'(\text{OH}^-) + k''(\text{OH}^-)^a(\text{HS}^-)^b \right] \cdot (X_j - X_{j,0}) \quad (94)$$

where  $X$  is the concentration of the wood components  $j$ ,  $X_{j,0}$  is the unreactive portion of the reactant  $j$ ,  $k'$  and  $k''$  are rate constants as a function of temperature using the Arrhenius equation.

Further, mass transfer equations were provided to calculate differences in the concentration of caustic and hydrogen sulfide between the free and entrapped liquors [42]. The model also consists of mass and energy balances formulated as first-order ordinary differential equations that are solved in 50 compartments along the digester [43]. The Purdue model considers only the initial and bulk

stages. Recently, Lindgren and Lindström reported that the amount of lignin in the pulp at the transition from bulk to residual delignification is decreased by increasing the  $[OH^-]$  concentration in the final stage and the  $[HS^-]$  concentration in the bulk phase. They also concluded that the residual lignin is not created during the main part of the cook but exists already at the beginning of the bulk phase. Moreover, the amount of residual lignin is also decreased by reducing the ionic strength in the bulk phase [33]. The corresponding kinetic model can be assigned as a development of the Purdue model because it also uses the concept of parallel reactions. Lindgren and Lindström (and later also Andersson) pointed out that the existence of unreactive wood components is questionable because the amount of residual phase lignin can be lowered using reinforced conditions [44]. A comprehensive model based on the concept of three consecutive reaction steps was developed by Gustafson et al. [28]. This concept, however, suffers from the abrupt transitions between the three phases, initial, bulk and residual. The wood components are divided into two components, lignin and carbohydrates. The separation of carbohydrates into cellulose and hemicellulose was accomplished by Pu et al. [45]. The rate expression for the initial period is taken from Olm and Tistad [35], for the bulk delignification from LeMon and Teder [27] and the form of the residual delignification originates from Norden and Teder [46]. The rate expressions [Eqs. (95–97)] are:

Initial stage:

$$\frac{dL}{dt} = 36.2 \sqrt{T} \exp\left(-\frac{4810}{T}\right) * L \quad (95)$$

Bulk stage:

$$\frac{dL}{dt} = (k_1[OH^-] + k_2[OH^-]^{0.5}[S]^{0.4})L \quad (96)$$

Residual stage:

$$\frac{dL}{dt} = \exp\left(19.64 - \frac{10804}{T}\right) [OH^-]^{0.7} * L \quad (97)$$

Further, the calculation of carbohydrates is simplified by using a functional relationship between the time derivative of carbohydrates and the time derivative of lignin. Thus, the carbohydrate degradation is always a ratio of the lignin degradation, which is an inadmissible assumption following the results from Lindgren [47].

#### 4.2.5.2.2 Process Variables

In numerous studies, the influence of reaction conditions, chemical additives, wood species, chip dimensions and other factors on delignification and carbohydrate degradation have been evaluated using both consecutive and parallel reaction concepts. An overview of the reported results is provided in the following sections.

### Effect of Temperature

The process of delignification during kraft pulping can be divided into three phases depending on the rate of lignin dissolution [15]. It is commonly accepted that, in all three phases, the delignification rate is of apparent first order with respect to the remaining lignin content. The temperature dependence of the rate constants follows the Arrhenius expression according to Eq. (75). It appears reasonable to assign the degradation reactions of the different lignin structural units (e.g., alkyl-aryl ether cleavage) with different phases of the technical pulping process [48]. It has been shown by extensive studies using model compounds that the degradation of lignin during kraft pulping may be primarily ascribed to the cleavage of alkyl aryl-ether linkages [49]. The alkyl-aryl ether bond types can be classified into phenolic  $\alpha$ -aryl ether linkages,  $\beta$ -aryl ether bonds in phenolic and non-phenolic units (see Chapter 2.1.1.3.2). Thus, the facile cleavage of phenolic  $\alpha$ -aryl ether bonds has been shown to dominate the initial phase of delignification [50]. The initial period is characterized by rapid delignification, significant hemicellulose degradation, and major alkali consumption. The activation energy of the degradation reaction of a model substrate representing the *p*-hydroxy-phenylcumaran structures in the lignin ( $\alpha$ -aryl ether bond) to form *o,p'*-dihydroxystilbene in an aqueous alkaline solution of 1 M sodium hydroxide was found to be  $77.5 \text{ kJ mol}^{-1}$  [51]. Kinetic studies using wood chips or wood meal as a substrate revealed activation energies for the initial phase of delignification in the range between 40 and  $86 \text{ kJ mol}^{-1}$  (see Tab. 4.19). The low activation energy values indicate that delignification in the initial phase is mainly a diffusion-controlled process that is independent of the alkali concentration, as long as it is above a minimum level. The initial phase delignification is expressed in general as Eq. (98):

$$\frac{dL}{dt} = -A_i \cdot \sqrt{T} \cdot \text{Exp}\left(-\frac{E_a}{R \cdot T}\right) \cdot L \quad (98)$$

where  $L$  represents the percentage of lignin in the wood with respect to the initial composition,  $T$  is the reaction temperature (in K), and  $E_a$  is the activation energy (in  $\text{kJ mol}^{-1}$ ).

According to the published literature, an activation energy of  $50\text{--}55 \text{ kJ mol}^{-1}$  can be assumed for the initial phase delignification (see Tab. 4.19). The existing database does not allow any influence to be assumed of the composition of the cooking liquor (Kraft versus Soda), additives (AQ) and wood species on the activation energy of the initial phase delignification.

Kondo and Sarkanen proposed that the initial delignification in kraft pulping consists of two kinetically distinguishable periods, ID1 and ID2, resulting in the dissolution of 13% and 11% of the initial lignin, respectively. ID1 is characterized as a rapid phase of indeterminate kinetic order and an estimated activation energy of  $50 \text{ kJ mol}^{-1}$ , whereas ID2 is designated as subsequent slower phase, conforming with first-order kinetics and a determined activation energy of  $73 \text{ kJ mol}^{-1}$ .

The bulk phase delignification is associated with the cleavage of  $\beta$ -aryl ether bonds in nonphenolic arylpropane units which could be expected to constitute the rate-determining reaction [48]. Miksche investigated the alkaline degradation of

erythro-veratrylglycerin- $\beta$ -guaiacyl ether by determining the formation of guaiacol in an aqueous alkaline solution of 1 M sodium hydroxide [52]. The fragmentation reaction follows first-order kinetics with respect to the substrate and the hydroxide ion concentration. The activation energy,  $E_a$ , for this degradation reaction has been determined as 130.6 kJ mol<sup>-1</sup>. The data in Tab. 4.19 show that most published activation energies of bulk phase delignification are reasonably close to this value, and are largely independent of the wood species, the presence of hydrosulfide ions (Kraft versus soda), and additives (AQ, PS).

Tab. 4.19 Comparison of literature data an activation energies for delignification.

Phase/ period	wood source	Process	l:s ratio	EA [KJ mol <sup>-1</sup> ]	In (A <sub>i</sub> )	Model concept	Reference
<b>Initial</b>	<i>Pinus silvestris</i> L. (dry)	Kraft	20	50.0		consecutive	[35]
	<i>Pinus silvestris</i> L. (wet)	Kraft	20	61.0		consecutive	[35]
	<i>Pinus silvestris</i> L.	Kraft	10	60.0		consecutive	[15]
	<i>Tsuga heterophylla</i>	Kraft	10	50.0		one-stage	[80]
	<i>Eucalyptus regnans</i>	Soda	100	73.0		consecutive	[92]
	<i>Tsuga heterophylla</i>	Soda	75	80.1	22.1	consecutive	[93]
	Douglas fir	Kraft	50	85.8	22.5	parallel	[30]
	Indian mixed hardwood	Soda-AQ	5	20.8		consecutive	[93]
	<i>Quercus</i>	Kraft	6	38.8			[94]
	<i>Picea abies</i>	Kraft	41	50.0		parallel	[7]
<b>Bulk</b>	<i>Picea marina</i>	Soda	17	134.0		one-stage	[95]
	<i>Pinus taeda</i>	Soda	200	142.3	34.7	one-stage	[36]
	<i>Pinus taeda</i>	Kraft	200	119.7	30.2	one-stage	[36]
	<i>Picea excelsa</i>	Kraft	10	134.9		consecutive	[41]
	<i>Tsuga heterophylla</i>	Kraft	100	134.0			[76]
	<i>Tsuga heterophylla</i>	Soda	100	129.7			[76]
	<i>Pinus silvestris</i> L.	Kraft	20	134.0		consecutive	[35]
	<i>Liquidambar styraciflua</i> L.	Soda	10	130.2	32.3	bulk stage	[39]
	<i>Liquidambar styraciflua</i> L.	Soda-THAQ	10	120.1	30.5	bulk stage	[39]
	<i>Liquidambar styraciflua</i> L.	Soda-AQ	10	113.8	28.5	bulk stage	[39]
	<i>Pinus taeda</i>	Soda	100	152.0	44.7	bulk stage	[96]

Tab. 4.19 Continued.

<b>Bulk</b>	<i>Pinus taeda</i>	Soda-AQ	100	137.0	34.7	bulk stage	[96]
	<i>Pinus silvestris</i> L.	Kraft	10	150.0		consecutive	[15]
	<i>Quercus mongolica</i>	Kraft	50	119.7	27.9	consecutive	[29]
	<i>Fagus</i>	Kraft	120	147.2	37.3	consecutive	[37]
	<i>Pinus densiflora</i>	Kraft	120	162.2	39.4	consecutive	[37]
	Western hemlock	Kraft	10	113.0		consecutive	[80]
	<i>Eucalyptus regnans</i>	Soda	100	132.0		consecutive	[92]
	<i>Pseudotsuga menziesii</i>	Kraft	50	123.8	30.5	parallel	[30]
	<i>Tsuga heterophylla</i>	Soda	75	131.1	31.6	consecutive	[93]
	Hybrid poplar	Kraft	6	152.8	41.0	one-stage	[82]
	<i>Pinus elliotii</i>	Kraft	6	125.0	31.9	consecutive	[32]
	<i>Picea abies</i>	Kraft	41	127.0		parallel	[33]
	<i>Betula pubescens</i>	Kraft	47	117.0		parallel	[14]
	<i>Picea abies</i>	Kraft	32	136.0		parallel	[34]
	<i>Pinus silvestris</i> L.	Soda-AQ	85	110.0		parallel	[97]
	<i>Quercus</i>	Kraft	6	115.5			[94]
	<i>Picea mariana</i>	Kraft	24	138.5	29.8	one-stage	[25]
	<i>Picea mariana</i>	Kraft-AQ	24	126.1	27.0	one-stage	[25]
	<i>Picea mariana</i>	Kraft-PS	24	142.2	31.4	one-stage	[25]
	<i>Picea mariana</i>	Kraft-PSAQ	24	138.5	30.6	one-stage	[25]
<i>Picea abies</i>	Kraft	41	127.0		parallel	[7]	
<b>Residual</b>	<i>Picea excelsa</i>	Kraft	10	90.0		consecutive	[41]
	<i>Pinus silvestris</i> L.	Kraft	10	120.0		consecutive	[15]
	<i>Pseudotsuga menziesii</i>	Kraft	50	110.0	23.4	parallel	[30]
	<i>Tsuga heterophylla</i>	Soda	75	117.0	26.3	consecutive	[93]
	<i>Picea abies</i>	Kraft	41	146.0		parallel	[33]
	<i>Betula pubescens</i>	Kraft	47	135.0		parallel	[14]
	<i>Picea abies</i>	Kraft	32	152.0		parallel	[34]
	<i>Pinus silvestris</i> L.	Soda-AQ	85	158.0		parallel	[97]
	<i>Picea abies</i>	Kraft	41	127.0		parallel	[7]

The model concept, however, has shown to have an influence on the calculation of activation energy. Blixt and Gustavsson have shown that the assumption of parallel reactions results in a decrease of the activation energy for the bulk phase by more than 10 kJ mol<sup>-1</sup> as compared to the concept of consecutive reactions [34]. Simultaneously, the value for the residual phase delignification increases significantly so that a lower value for the bulk than for the residual phase delignification is obtained. This has also been confirmed by recalculating the data from Kleinert using a model with two parallel reactions, which in fact gives 127 kJ mol<sup>-1</sup> for the bulk phase and 138 kJ mol<sup>-1</sup> for the residual phase delignification, in contrast to the values of 135 kJ mol<sup>-1</sup> and 90 kJ mol<sup>-1</sup>, respectively, that had been obtained with a model using two consecutive reactions [41]. The higher activation energy for the bulk phase delignification using a consecutive model concept can be led back to the delignification of parts of the residual phase lignin (depending on the reaction conditions). Lindgren and Lindström assumed that the initial concentration of the residual lignin species, denoted as L3, was independent of the cooking temperature [33]. Andersson found, however, an improved fit when considering the effect of temperature, by recalculating the data from Lindgren and Lindström, particularly for the high temperature levels [7]. As a result, the activation energy of the residual phase delignification (or the delignification of L3) decreased from 144 kJ mol<sup>-1</sup> to 127 kJ mol<sup>-1</sup>, which is equal to the fitted value for the bulk delignification (or the delignification of L2). For a reliable process control of kraft pulping, it is necessary to improve the knowledge of the physical and chemical properties of the residual phase lignin. Since the first considerations were made about the kinetics of delignification, it has been assumed that the residual lignin is formed during the cook [41,53]. Models based on this assumption (consecutive concept) were found not to be very suitable for extended delignification or continuous-flow digesters, especially in those cases where [OH<sup>-</sup>] was changed [7]. On the other hand, if the residual phase lignin is assumed to be present in the wood, then the amount can be determined by extrapolation of the residual phase to the beginning of the cook. This model concept – known as the parallel concept – can be used to predict the course of extended delignification quite satisfactorily (see also Chapter 4.2.5.3).

#### Effect of [OH<sup>-</sup>] and [HS<sup>-</sup>]

The concentrations of the active cooking chemicals, the hydroxyl and hydrosulfide ions, influence the rate of delignification of the different lignin species (parallel model concept) or in the different pulping phases (consecutive model concept) in different ways. If the concentrations of hydroxyl and hydrogen sulfide ions are considered as variables for the rate equation, the constants  $k_j$  in Eq. (74) can be expressed as equation of the type:

$$k_j = k'_j \cdot [\text{OH}^-]^{a_j} \cdot [\text{HS}^-]^{b_j} \quad (99)$$

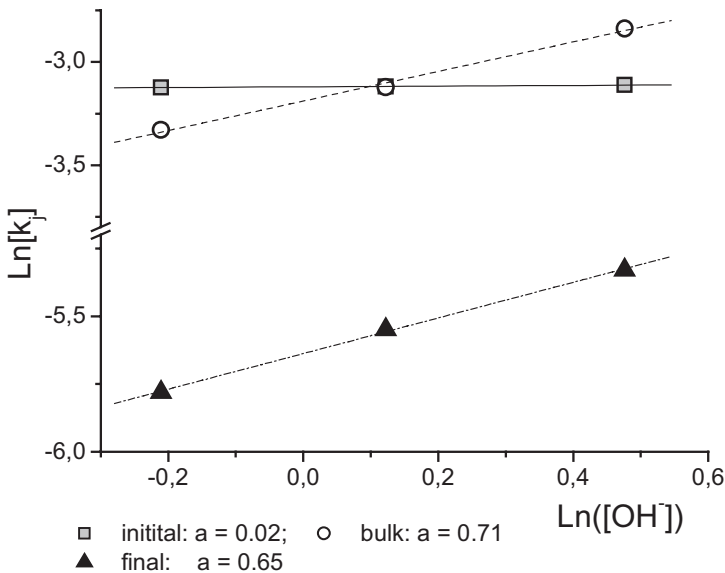
where  $k_j'$  represents the true first-order rate constant for the lignin species  $j$  or the delignification phases  $j$ ,  $a$  and  $b$  are the reaction orders with respect to  $[\text{OH}^-]$  and  $[\text{HS}^-]$ .

To investigate the effect of  $[\text{OH}^-]$  concentration on the rate of delignification, the kinetic experiments are carried out by keeping the  $[\text{HS}^-]$  concentration at a constant level, while evaluating the reaction kinetics at different levels of  $[\text{OH}^-]$  concentrations. Following this condition, Eq. (99) can be rewritten as:

$$k_j = k_j' \cdot [\text{OH}^-]^{a_j} \quad (100)$$

with  $k_j'' = k_j' [\text{HS}^-]^{b_j}$  and  $j = 1$  to 3.

The reaction order  $a$  for the lignin species  $j$  can thus be obtained as the slope of the linear relationship between the logarithm of the rate constant  $k_j$  and the logarithm of the hydroxyl ion concentrations. Similarly, the exponent  $b$  is obtained by the slope of the plot of  $\ln(k_j)$  against  $\ln([\text{HS}^-])$ . Figure 4.28 illustrates the effect of  $[\text{OH}^-]$  on the rate of the delignification for the initial, bulk and final phases using the data from Chiang and Yu [30].



**Fig. 4.28** Effect of  $[\text{OH}^-]$  on the rate of delignification; Kraft pulping with  $[\text{HS}^-] = 0.23 \text{ M} = \text{const}$ ; at three  $[\text{OH}^-]$  levels: 0.81 M, 1.13 M and 1.61 M; cooking temperature: 170 °C, liquor-to-wood ratio: 50:1. Data recalculated from Ref. [30]

The results show correspondingly (Tab. 4.20; Fig. 4.28) that the delignification reactions in the initial phase proceed with zero-order with respect to both  $[\text{OH}^-]$  and  $[\text{HS}^-]$  concentrations.



Tab. 4.20 Comparison of literature data on reaction orders with respect to reactant concentrations.

Phase/ period	Wood source	Process	l:s ratio	Reaction orders		Model concept	Reference
				[OH <sup>-</sup> ]	[HS <sup>-</sup> ] <sup>m</sup>		
Initial	<i>Picea excelsa</i>	Kraft	10	0.00	0.00	consecutive	[46]
	Douglas fir	Kraft	50	0.00	0.00	parallel	[30]
	<i>Picea abies</i>	Kraft	41	0.00	0.06	parallel	[7]
Bulk	<i>Picea marina</i>	Soda	17	0.59	n.d.	one-stage	[95]
	<i>Pinus taeda</i>	Soda	200	1.00	n.d.	one-stage	[36]
	<i>Pinus taeda</i>	Kraft	200	1.00	0.69	one-stage	[36]
	<i>Pinus silvestris</i> L.	Kraft	10	0.50	0.40	consecutive	[27]
	<i>Betula verrucosa</i>	Kraft	10	0.49	0.66	one-stage	[98]
	<i>Picea excelsa</i>	Kraft	10	0.7–0.8	0.1–0.4	consecutive	[46]
	<i>Quercus mongolica</i>	Kraft	50	0.72	0.31	consecutive	[29]
	<i>Fagus</i>	Kraft	120	1.05	0.29	consecutive	[37]
	<i>Pinus densiflora</i>	Kraft	120	0.66	0.13	consecutive	[37]
	<i>Eucalyptus regnans</i>	Soda	100	0.84	n.d.	consecutive	[92]
	<i>Pseudotsuga menziesii</i>	Kraft	50	0.62	0.39	parallel	[30]
	<i>Tsuga heterophylla</i>	Soda	75	0.70	n.d.	consecutive	[93]
	<i>Pinus elliotii</i>	Kraft	6	0.50	0.60	consecutive	[32]
	<i>Picea abies</i>	Kraft	41	1.00	0.32	parallel	[33]
	<i>Betula pubescens</i>	Kraft	32	1.00	0.41	parallel	[14]
	<i>Picea abies</i>	Kraft	41	0.48	0.39	parallel	[7]
Residual	<i>Picea excelsa</i>	Kraft	10	0.70	0.00	consecutive	[17]
	<i>Pseudotsuga menziesii</i>	Kraft	50	0.62	0.00	parallel	[30]
	<i>Picea abies</i>	Kraft	41	0.20	0.00	parallel	[7]

n.d. not determined

This seems to be understandable, as any conditions used in kraft pulping are sufficient enough to cause the cleavage of phenolic  $\alpha$ -aryl ether linkages which are the predominant structural units in the lignin of the initial phase [54]. The rate of delignification of the bulk phase lignin is, however, significantly influenced by

both  $[\text{OH}^-]$  and  $[\text{HS}^-]$  concentrations. In most published reports, the influence of  $[\text{HS}^-]$  is reported to be weaker compared to that of  $[\text{OH}^-]$ . The corresponding reaction orders with respect to  $[\text{HS}^-]$  are in the range of 0.3–0.5, and those with respect to  $[\text{OH}^-]$  are determined to be between 0.4 and 0.8 (see Tab. 4.20).

The presence of hydrogen sulfide ions (strong nucleophiles) facilitates the cleavage of  $\beta$ -ether bonds via the formation of a thiirane structure, thus increasing the delignification rate of bulk phase lignin (see Section 4.2.4.). Finally, the rate of degradation of residual lignin is influenced by the concentration of  $[\text{OH}^-]$  with an exponent of 0.6–0.7 which means that a ten-fold increase in hydroxide concentration would yield a four- to five-fold increase in the delignification rate of the residual phase lignin. It is commonly accepted that the rate of residual lignin degradation is almost unaffected by the concentration of hydrogen sulfide ion [33,53]. It has been speculated that the dominating delignification reaction in this phase is the alkali-promoted cleavage of carbon–carbon linkages originally present or generated by condensation reactions [50,54,55]. Besides an influence on the reaction rates, the concentration of the active cooking chemicals in the earlier phases affects the amount of residual lignin. An increase in hydrogen sulfide concentration in the initial phase, for example, does not affect the rate in that phase; rather, it increases the rate of delignification in the subsequent bulk phase and also decreases the amount of residual lignin. Moreover, an increase in  $[\text{OH}^-]$  concentration in the initial phase also decreases the amount of residual lignin. The amount of residual phase lignin is defined as the lignin content determined by extrapolation of the delignification rate in the residual phase to the reaction time zero [56]. Using this definition, Gustavsson et al. established a relationship between the amount of residual phase lignin,  $L_r$ , and the hydroxide and hydrogen sulfide ion concentrations according to Eq. (101):

$$L_r = 0.55 - 0.32 \cdot [\text{OH}^-]^{-1.3} \cdot \ln[\text{HS}^-] \quad (101)$$

The validity of this equation has been specified for  $[\text{OH}^-]$  concentration in the range from 0.17 to 1.4 M, and for  $[\text{HS}^-]$  from 0.07 to 0.6 M. According to Eq. (101), the influence of hydrogen sulfide ions on the amount of residual phase lignin is much stronger when the cooking is performed at low hydroxide ion concentration [57]. In the absence of a strong nucleophile (e.g., hydrogen sulfide ion) in cooks at low  $[\text{OH}^-]$  concentration, alkali-stable enol ether structures or condensation products will probably be formed from the quinone methide intermediate instead of the desirable sulfidolytic cleavage of  $\beta$ -aryl ether bonds [58]. The solubilization of lignin at a low hydroxide concentration requires the fragmentation of lignin to lower molecular-weight fractions, and this can be achieved at a high  $[\text{HS}^-]$  concentration due to sulfidolytic cleavage of the  $\beta$ -aryl ether bonds.

Knowing which concentrations of the active cooking chemicals influence the pulping performance and resultant pulp quality provides the basis for improving the selectivity of kraft cooking, and a better understanding of delignification in the final cooking phase, which is of major practical importance.

### Effect of Sodium Ion Concentration (Ionic Strength) and of Dissolved Lignin

The sodium concentration of the cooking liquor (an approximate measure of the ionic strength) exerts an influence on the amount of residual phase lignin in a similar manner as a decrease in  $[\text{OH}^-]$ . For a sodium concentration of up to  $1.9 \text{ mol L}^{-1}$  the effect is seen to be small, but in the range typical for industrial kraft pulping ( $2\text{--}3 \text{ mol L}^{-1}$ ) the amount of residual phase lignin is significantly increased. It has been reported that in kraft pulping of both birch and spruce wood, an increase in sodium ionic strength from  $1.3$  to  $2.6 \text{ mol L}^{-1}$  causes an 80% increase in the amount of residual phase lignin [38], while the rate of delignification remains unchanged. It has been speculated that this effect might be due to a decreased solubility of the lignin fragments, but this is unlikely because a reduced solubility would also result in a decreased rate of delignification – which definitely is not the case. This strengthens the hypothesis that the main influence on the amount of residual phase lignin is via the activity of the reactants. The desirable decrease in sodium ion concentration of an industrial cooking liquor below a critical level of  $1.8 \text{ mol L}^{-1}$  can only be accomplished by increasing the dilution factor, but this would require additional evaporation capacity.

The rate constant  $k_j$  in Eq. (74) is influenced by the concentration of dissolved lignin in various ways. The presence of dissolved lignin in the early stages of kraft cooking (e.g., the beginning of the bulk phase) causes an increase in the bulk delignification rate, which in turn results in a higher viscosity at a given kappa number. Moreover, the addition of dissolved lignin during the bulk delignification results in a yield increase of about 0.5% on wood (valid for the use of *Pinus silvestris* L. as a wood source) [59]. The mechanism of this increased selectivity is not known, but it has been speculated that the added lignin may increase the absorption of sulfur by the wood during the precooking stage [59]. Another reason for this positive effect might be the generation of polysulfide ions, which may accelerate the cleavage of ether linkages in the lignin via the oxidation of enone and quinone methide-type intermediates [60]. However, adding dissolved lignin at a late stage of the cook (e.g., kappa number  $<50$ ) reduces the delignification rate during the final phase. Consequently, the presence of dissolved lignin during extended delignification inevitably leads to a decrease in selectivity. The ratio of the reaction rates of bulk ( $k_b$ ) and final delignification ( $k_f$ ) is reduced by 17–50%. The reasons for this negative effect of dissolved lignin on delignification rate during the final phase are not physical effects, such as the sorption of lignin by fibers or a reduction in the rate of diffusion of released lignin fragments. Condensation reactions between the dissolved lignin and the fiber lignin or carbohydrates are thought to be responsible for the disadvantageous effect of dissolved lignin on delignification selectivity [59]. The addition of black liquor from previous cooks already in the early pulping stages (as is the case in modern displacement cooking procedures) leads to an increase in the concentration of dissolved lignin throughout the whole cooking process. The presence of dissolved lignin early in the cook almost compensates for the negative effect in the later part of the cook.

### Effect of Wood Chip Dimensions and Wood Species

As discussed earlier in this chapter, “impregnation” – the transport of chemicals into wood chips – is a combined effect of penetration and diffusion. While penetration is confined to the heating-up period, diffusion occurs during the whole cooking process. Under the conditions of alkaline cooking, the rate of diffusion of chemicals into the chip is almost the same in all three of its structural directions. Farkas studied the influence of chip length and width [61], and found both dimensions to have an insignificant influence on the rate of delignification and amount of screening rejects. The lack of influence of chip length on delignification rate was confirmed by others [62,63]. Thus, there is general agreement that chip thickness is the most critical dimension for delignification, pulp yield, and the amount of screening rejects. Chip thickness determines heterogeneity in delignification, with Backman reporting that maximum yields were generally obtained by using 3 mm-thick chips [64]. Based on a study of the kraft pulping of pine chips, Backman further concluded that above a chip thickness of 1 mm, the reaction rate is at least partially controlled by the transport steps (penetration, diffusion), whereas below this thickness the rate is probably controlled by the rates of the chemical reactions involved [65]. Hartler and Östberg reported that the Roe number (lignin content) remained constant when the chip thickness was 3 mm or less [66]. When using thicker chips, the same extent of delignification can be achieved only by a higher alkali charge and/or higher cooking intensity (H-factor), and both would result in a lower yield. Chip thickness is more critical for hardwood than for softwoods, with hardwood chip use resulting in significantly more rejects than with softwood chips of the same thickness. The reason for this higher sensitivity of hardwood chips in terms of thickness might be associated with the more heterogeneous hardwood fiber morphology (see Chapter 2.1.2; Wood Structure and Morphology), in particular in hardwoods, such as oak or ash, where the vessels are closed by tyloses that enter the vessel from the neighboring ray cells [67]. Wood density and morphology are factors which influence the rate of diffusion and thereby a critical chip thickness.

Thus, optimal chip thickness is dependent on the cooking conditions and the wood species. Delignification rates during the early kraft cooking phase were reported to increase with decreasing chip thickness when using both beech and Japanese Red Pine. This infers that the initial delignification phase is diffusion-controlled, even when using chips with thicknesses of 1.7–3.7 mm for beech and 2.6–7.2 mm for Red pine [37]. In the bulk delignification stage, the rate of delignification was not seen to depend on chip thickness for either wood species. In industrial pulping, the influence of chip thickness can also be expressed by the H-factor needed to reach a certain kappa number.

Kraft cooking of pine chips (*Pinus silvestris* L.) with an effective alkali charge of 22%, a sulfidity of 30%, a liquor-to-wood ratio of 4:1, and a maximum cooking temperature of 170 °C, requires H-factors of 2140, 2425, and 3600 to achieve a kappa level of 30 when using chips of 3, 7, and 12 mm thickness, respectively. Furthermore, pulping selectivity is impaired significantly due to the longer cook-

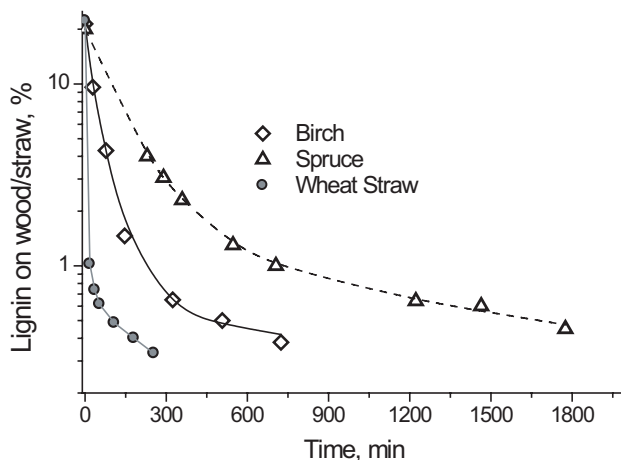
ing time. The viscosity decreased from 950 to 800 ml g<sup>-1</sup> at a kappa number of 30 when using 12-mm rather than 3-mm chips [68,69].

An increase in chip thickness also leads to a reduced cooking capacity. For example, when compared to 3 mm-thick chips, 7 and 12 mm-thick chips showed reduced cooking capacities of 5% and 21% respectively, assuming a total cooking cycle of 6 h for the 3-mm chips.

Another factor to consider in process control of kraft pulping is the difference in delignification rate among softwood and hardwood species, which can in turn be related to the specific structural building blocks of lignin. Softwood lignins are referred to as guaiacyl lignin, whereas hardwood lignins are composed of both guaiacyl and syringyl units in varying ratios (see Chapter 2.1.1.3.2, Structure of Lignin). The kinetics of the bulk and residual delignification in kraft pulping of birch (*Betula pubescens*) and spruce (*Picea abies*) were compared, with the delignification pattern being described with the same model for both wood species. The amount of residual phase lignins in cooking of both birch and spruce are affected by the reaction conditions in a similar manner. The only difference is the less pronounced influence of hydrogen sulfide ion concentration on the amount of residual phase lignin in the case of birch. This explains the well-known experience in industrial pulping that, in kraft pulping, sulfidity is less important for hardwood than for softwood. This different behavior may be traced back to the fact that native lignin in birch wood exhibits fewer cross-linked structures compared to spruce, due to the presence of syringylpropane units. The bulk delignification of birch is 2.2-fold more rapid than that of spruce (recalculated from Ref. [14]).

Hou-min Chang and Sarkanen evaluated the rates of delignification of two softwood (Western true fir and Western hemlock) and two hardwood species (Maple, Madrona) at 150 °C [70]. Their results clearly suggest that a high content of syringylpropane units in lignin promotes the rate of delignification in the kraft cooking process. This again can be explained by the fact that syringylpropane units are less susceptible to condensation reactions. The results indicate a distinct linear correlation between the rate of delignification and the syringyl content of the lignin of the initial wood species (S/G = 0, 0.52, and 1.44 for Western true fir and Western hemlock, Maple and Madrona, respectively).

The kraft pulping of wheat straw (*Triticum aestivum*) involves a third category of lignocellulosic material. It is known that wheat straw contains more *p*-hydroxyphenylpropane units and fewer  $\beta$ -aryl ether linkages than softwood or hardwood lignin. In addition, 20–30% of the lignin units are phenolic, and a large number of ester linkages exist between lignin and carbohydrates [71]. Kraft pulping experiments carried out under the same conditions with wheat straw, birch wood and spruce wood showed that the amount of residual phase lignin in wheat straw and birch wood was 33% and 53% of the amount of residual phase lignin in spruce wood, respectively [38,72]. Moreover, about 90% of the lignin in wheat straw reacts according to the rapid initial delignification kinetics, in contrast to spruce and birch wood, where only 15–25% of the lignin is removed during the early stage of the cook. In the case of wheat straw, lignin removal can therefore be explained by the hydrolysis of ester linkages and cleavage of phenolic  $\alpha$ -aryl ethers.



**Fig. 4.29** Comparative evaluation of the course of kraft delignification for spruce wood, birch wood and wheat straw using the same conditions:  $[\text{OH}^-] = 0.5 \text{ mol L}^{-1}$ ;  $[\text{HS}^-] = 0.3 \text{ mol L}^{-1}$ , temperature =  $150^\circ\text{C}$ , liquor-to-wood ratio = 100:1 (according to [38]).

A comparison of the delignification patterns in kraft pulping of spruce wood, birch wood and wheat straw, using the same reaction conditions, is shown in Fig. 4.29.

The rates of residual delignification for the three different lignocellulosic raw materials are approximately the same, but the activation energy for the residual phase was reported to be less for wheat straw as compared to spruce and birch [72].

Cho and Sarkanen found differences in the bulk delignification rates of Douglas fir, Southern yellow pine and Western hemlock on the basis of the corrected H-factor concept [73]. To obtain the same degree of delignification, Douglas fir requires a 1.28-fold higher H-factor as compared to Western hemlock. These differences in bulk delignification rate cannot be attributed to different values of the activation energy because this was identical for both species. Among a number of different factors, the lower bulk delignification rate of Douglas fir as compared to Western hemlock has been attributed to a higher degree of dehydrogenation. Interestingly, the reaction rates for sapwood and heartwood of Douglas fir were identical, indicating that wood morphology plays a minor role with regard to pulping kinetics, provided that the degree of impregnation is satisfactory.

Variations in the type of wood chips and seasonal variations in wood chip constitution can be considered by using a multiplier (the value of which is close to 1.0) to correct the frequency factors in the kinetic rate expression. Values above 1.0 indicate that the chips are more reactive with the result that, at given conditions, lower kappa numbers are obtained [74].

Wood age was also reported to have an influence on the rate of delignification [75]. Wood samples from very old eucalyptus species (e.g., *E. diversicolor*, estimated to be about 200 years old) contained appreciable amounts of lignin which was

very easily removed by a mild alkali treatment at low temperatures. It has been speculated that acids generated in the wood over a long period of time modified the wood in a manner similar to a mild prehydrolysis treatment.

#### **Effect of Chemical Additives: Soda versus Kraft; Soda-AQ, PS**

Unlike activation energies, delignification rates are significantly dependent on the presence of nucleophiles such as hydrogen sulfide ions, anthraquinone, or polysulfide. The delignification rates in soda-AQ pulping were found to be two- to three-fold higher compared to soda pulping [39]. Wilson and Procter reported a two- to three-fold higher delignification rate for kraft as compared to soda pulping [76], while Farrington et al. found that the addition of AQ to soda pulping resulted in a delignification rate equal to that of kraft pulping [77]. Labidi and Pla studied the influence of cooking additives by using poplar as a raw material [31]; their results suggested that the first delignification phase was equivalent for soda, soda-AQ and kraft cooking, indicating that during this stage the main phenomenon is not the cleavage of alkyl-aryl ether linkages but rather diffusion of the cooking chemicals. The delignification rate of the subsequent cooking phases increased, however, in the order soda < soda-AQ < kraft. Recently, Li and Kubes investigated the kinetics of delignification during kraft, kraft-AQ, kraft-PS and kraft-PSAQ pulping of black spruce using the apparent second-order kinetics in kappa number [25]. The results clearly revealed that the addition of AQ, PS and the combined addition of PSAQ accelerated delignification in the kappa number range from 10 to 60. In relation to standard kraft pulping at 170 °C, the rate constants increased to 1.7, 1.8 and 2.1, for kraft-AQ, kraft-PS and kraft-PSAQ, respectively.

The amount of residual phase lignin is lowered by 30% for spruce and 10% for birch wood, when polysulfide is added to a kraft cook [38]. One explanation for this may be that polysulfide is able to introduce carboxylic groups into the residual phase lignin, thus increasing its water solubility. The ability of polysulfides to degrade enol ether structures may however also be important.

#### **4.2.5.3 Structure of a Selected Kinetic Model for Kraft Pulping**

As mentioned previously [7], the raw material wood is characterized by four major components of lignin (L), cellulose (C), galactoglucomannan (GGM), and arabinoxylan (AX). Based on an analysis of the individual sugars, the single carbohydrate components are calculated as follows:

- AX is the simple sum of arabinose and xylose.
- GGM is the sum of galactose and mannose and a contribution from the glucose which is assumed to be one third of the mannose content [78].
- The cellulose content is estimated from the total glucose corrected for the glucose present in GGM.

The total carbohydrates, composed of C + GGM + AX, are labeled CH. According to the well-established observation of three different reaction phases, the wood

components are divided into three species of different reactivity and dissolution behavior. The model is based on the assumption that all species of the four wood components react in parallel throughout the entire cooking process; this permits a better description of transition from the bulk to the residual phase reactions when compared to the assumption of a consecutive model ([28]).

#### 4.2.5.3.1 Delignification Kinetics

The general structure of the model is derived from models introduced by Smith [40], Christensen et al. [79] and later Chiang et al. [30], by Blixt and Gustavsson [34], and later improvements of Andersson et al. [7]. The delignification is described by three parallel reactions, assuming that the single lignin species react simultaneously. A general rate equation can be expressed as:

$$\frac{dL_j}{dt} = -k_{L_j} \cdot [OH^-]^a \cdot [HS^-]^b \cdot L_j \quad (102A)$$

$$\frac{dL_j}{dt} = -k_j \cdot [OH^-]^a \cdot [HS^-]^b \cdot L_j \quad (102B)$$

for  $j =$  lignin species 1, 2, and 3.

Equation (102) is based on the assumption that the delignification is of apparent first order with respect to the lignin content in the wood [80]. Using this structure, the model is only valid for kraft cooking conditions, with  $[HS] > 0$ . If pure soda cooking must be considered (the sulfide concentration is reduced to 0), Eq. (74) must be replaced by Eq. (103), as established by LeMon and Teder [27]:

$$\frac{dL_j}{dt} = -\left(k'_j \cdot [OH^-] + k''_j \cdot [HS^-]^b\right) \cdot L_j \quad (103)$$

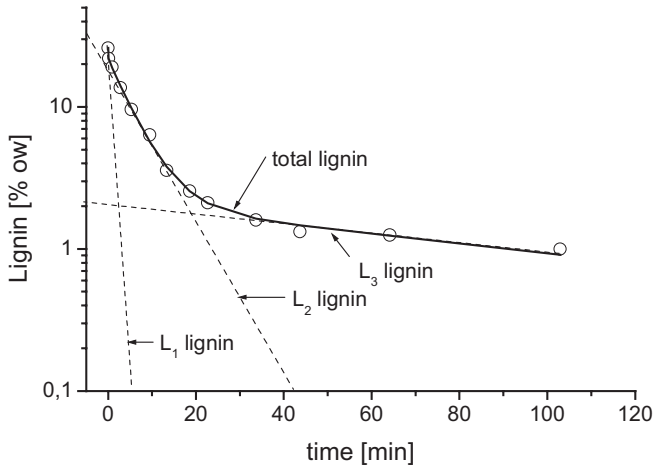
The general solution of these first-order rate equations is displayed in Eq. (104):

$$L_{tot} = \sum_{j=1}^3 L_{j,0} \cdot \text{Exp}\left(-k_{L_j} \cdot t\right) \quad (104)$$

The sum of the three lignin species corresponds to the total amount of lignin. In the special case of constant concentration cooks (high liquor-to-wood ratio), degradation of the lignin species (L1, L2, and L3) can be approximated by straight lines when plotted as a log/linear diagram (Fig. 4.30).

The sum of the three lignin species corresponds to the total amount of lignin. The proportions of the lignin species (L1, L2, and L3) can be quantified by using Eq. (104). A selection of literature data with regard to the single lignin weight fractions is provided in Tab. 4.21.





**Fig. 4.30** Degradation of the three lignin species of prehydrolyzed *Eucalyptus saligna* during the course of a subsequent kraft pulping under isothermal conditions ( $T = 160^\circ\text{C}$ ) and constant  $[\text{OH}^-]$  and  $[\text{HS}^-]$  concentrations [81].

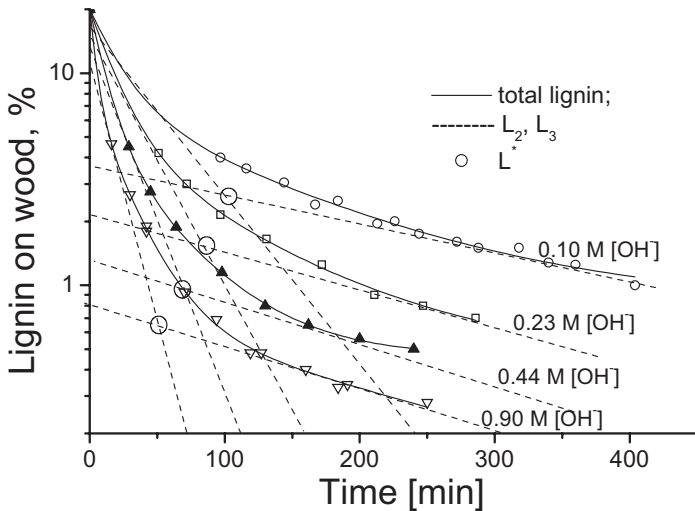
**Tab. 4.21** Lignin weight fractions, L1, L2, L3, selected from literature data.

Wood species	l : s	$L_0$ % ow	$L_1/L_0$	$L_2/L_0$	$L_3/L_0$	Reference
Lobolly pine	200 : 1	28.6	0.18			[36]
Western hemlock	10 : 1	29.4	0.24			[80]
Western hemlock	75 : 1	28.5	0.16	0.78	0.06	[93]
Douglas fir	50 : 1		0.24	0.71	0.04	[30]
Hybrid poplar	6 : 1	25.6	0.48			[82]
Poplar			0.19	0.75	0.06	[31]
Spruce	41 : 1	29.5	0.31	0.64	0.05	[7]

According to Tab. 4.21, the published lignin weight fractions corresponded quite well, except for the hybrid poplar where a very high extent of initial delignification was reported [82]. The wood from old trees was reported to contain rather high amounts of lignin that could easily be removed by alkali at low temperatures at the start of the cook. The suggestion was that the hydrolytic action of acids in the wood over a long period may have modified the wood in a manner similar to mild pulping [75].

However, most of the models do not account for any subsequent changes in alkali concentration as occurring in modern industrial batch and continuous cook-

ing processes. Lindgren and Lindström [14,33,47], Lindström [38] and Gustavsson [56] have clearly shown that the initial amount of L3 in constant composition cooks is not an homogeneous lignin, since reinforcing cooking conditions can make part of it to react as L2. The amount of L3 is strongly affected by  $[\text{OH}^-]$  and to some extent by  $[\text{HS}^-]$  and ionic strength. For spruce pulp, significant interactions between these effects have been observed. In order to reduce the amount of L3, it is important to have a low concentration of hydrogen sulfide in combination with a high hydroxide concentration. Interestingly, Lindgren and Lindström [33] could not detect a dependency of the initial concentration of L3 on cooking temperature, whereas Andersson et al., using Lindgren and Lindström's experimental data, confirmed an influence of temperature on L3, since the fit improved slightly when considering the effect of temperature [7]. Andersson et al. observed that the amount of lignin at the intersection of the log-linear extrapolations for the species L2 and L3 depends on the cooking conditions,  $[\text{OH}^-]$ ,  $[\text{HS}^-]$ , and temperature. (Ionic strength was also observed but not considered in the model.) The intersection of the log-linear extrapolations corresponds to the lignin level of equal amounts of L2 and L3, denoted as  $L^*$ , as depicted in Fig. 4.31.



**Fig. 4.31** Course of total lignin, L2, L3 and  $L^*$  during kraft pulping at 170°C and constant  $[\text{HS}^-] = 0.28 \text{ M}$  and increasing  $[\text{OH}^-]$ .  $L^*$  shows a significant influence on  $[\text{OH}^-]$ . Experimental data from Lindgren and Lindström [33]

The dependence of  $L^*$  on the three major cooking parameters, temperature,  $[\text{OH}^-]$  and  $[\text{HS}^-]$  has been evaluated by nonlinear regression analysis, assuming no cross-coupling terms. The expression for  $L^*$  is given in Eq. (105):

$$L^* = 0.49 \cdot ([\text{OH}^-] + 0.01)^{-0.65} \cdot ([\text{HS}^-] + 0.01)^{-0.19} \cdot (1.83 - 2.91 \cdot 10^{-5} (T - 273.15)^2) \quad (105)$$

The initial amounts for  $L_{1,0}$  and  $L_{\text{tot},0}$  are known and hence the sum of the initial amounts for species 2 and 3  $L_{2+3,0} = L_{\text{tot},0} - L_{1,0}$ . The initial values  $L_{2,0}$  and  $L_{3,0}$  depend on cooking conditions, and can be calculated as follows using the definition of  $L^*$ :

$$L_{2,0} = L^* \cdot \text{Exp}(k_{L_2} \cdot \Delta t) \quad (106)$$

$$L_{3,0} = L^* \cdot \text{Exp}(k_{L_3} \cdot \Delta t) \quad (107)$$

where  $k_{L_2}$  and  $k_{L_3}$  are the rate constants for the first-order reactions for species 2 and 3 in Eqs. (102) and (103), respectively and  $\Delta t$  is the time interval after which species 2 and 3 reach the same level  $L^*$ . Summing these equations yields

$$L_{2+3,0} = L^* \cdot [\text{Exp}(k_{L_2} \cdot \Delta t) + \text{Exp}(k_{L_3} \cdot \Delta t)] \quad (106)$$

which can be solved numerically for  $\Delta t$  by any standard nonlinear equation solver and obtaining  $L_{2,0}$  and  $L_{3,0}$  from Eqs. (106) and (107).

$L_2(t)$  and  $L_3(t)$  can now be calculated from Eq. (104) as long as the reaction conditions remain constant. If reaction parameters change at time  $t_c$ , the model assumes that the two lignin species,  $L_2$  and  $L_3$ , interchange reversibly and instantaneously. The situation is treated as if the cook starts at time  $t_c$  with initial values  $L_{2,c}$  and  $L_{3,c}$  exactly calculated as above from the actual total amount of species 2 and 3  $L_{2+3,c} = L_2(t_c) + L_3(t_c)$ . If reaction conditions change continuously, the calculations Eqs. (106–108) and Eq. (104) must be carried out for sufficient small time steps.

The influence of ion strength of the liquor is not considered in the model. All experimental data used for the development of the kinetic model were obtained at comparable ion strength levels of  $[\text{Na}^+] = 1.5 \text{ M}$ . Lindgren and Lindström have shown that reasonable variations of ion concentration around this value have only a slight influence on the delignification kinetics [33].

#### 4.2.5.3.2 Kinetics of Carbohydrate Degradation

Few studies have been conducted to investigate carbohydrate degradation kinetics. In order to develop a model, the experimental data as published by Matthews (slash pine) and Smith and Williams (Loblolly pine) were employed [40,83]. In the proposed model, the carbohydrates are divided into three components: C, GGM, and AX. The course of the carbohydrate components during kraft pulping also reflected the presence of three different species within each component. Thus, it appears justified to further divide the three components into three species, similar to the lignin model.

Unlike the situation in the lignin model, the  $[\text{HS}^-]$  showed no influence on carbohydrate degradation. The influence on alkali concentration was, however, more pronounced in the initial stage, where even very low concentrations led to a substantial loss of carbohydrates. An amount of 7% (based on wood) of directly dis-

solved wood components, consisting of acetyl groups and low molecular-weight hemicelluloses, was determined by Kondo and Sarkanen [80]. This value was calculated by measuring the amount of degraded hemicelluloses of wood meal stabilized against alkaline peeling by borohydride reduction and extrapolating to zero time. The insertion of a rate constant  $k_2$  into the kinetics equation reflected the observation that degradation of carbohydrates occurs easily under very mild conditions. The proposed structure for the carbohydrate kinetics is provided in Eq. (109):

$$\frac{dCH_{ij}}{dt} = -k_{CH_{ij}}([OH^-]^a + k_2) \cdot CH_{ij} \quad (109)$$

for the three components, i, C, GGM, and AX, each with three species,  $j = 1$  to 3.

Since only limited data were available for the individual carbohydrate components, only the total carbohydrates,  $CH = C + GGM + AX$ , were considered. It has been shown by Lindgren that the proportion of the carbohydrate species is also dependent on the sodium hydroxide concentration [47]. The intersection of CH2 and CH3, denoted as  $CH^*$ , was conducted from the log-linear extrapolation of the experimental data in a manner similar to that described for lignin. The relationship between  $CH^*$  and reaction conditions was derived by nonlinear regression analysis. In contrast to  $L^*$ , no dependency on temperature was found; thus, regressing  $CH^*$  against  $[OH^-]$  yields Eq. (110):

$$CH^* = 42.3 + 3.65 \cdot ([OH^-] + 0.05)^{-0.54} \quad (110)$$

The initial amounts for  $CH_{1,0}$  and  $CH_{tot,0}$  are known and hence the sum of the initial amounts for species 2 and 3  $CH_{2+3,0} = CH_{tot,0} - CH_{1,0}$ . The initial values  $CH_{2,0}$  and  $CH_{3,0}$  depend on the cooking conditions and can be calculated as follows using the definition of  $CH^*$ :

$$CH_{2,0} = CH^* \cdot \text{Exp}(k_{CH_2} \cdot \Delta t) \quad (111)$$

where  $\Delta t$  is again defined as the time interval between  $t(L^*)$  and  $t(0)$ .

The initial amount of CH3 is calculated using the expression in Eq. (112):

$$CH_{3,0} = CH_2 + CH_3 - CH_{2,0} = CH^* \cdot \text{Exp}(k_{CH_3} \cdot \Delta t) \quad (112)$$

where CH2 and CH3 are calculated by using Eq. (102), where  $k_{CH_2}$  and  $k_{CH_3}$  are the rate constants for the first-order reactions for species 2 and 3 in Eqs. (102) and (103), respectively, and  $\Delta t$  is the time interval after which species 2 and 3 reach the same level  $CH^*$ . Summing these equations yields:

$$CH_{2+3,0} = CH^* \cdot [\text{Exp}(k_{CH_2} \cdot \Delta t) + \text{Exp}(k_{CH_3} \cdot \Delta t)] \quad (113)$$

which can be solved for the time interval  $\Delta t$  using the nonlinear equation solver (see Appendix).

#### 4.2.5.3.3 Kinetics of Cellulose Chain Scissions

The kinetics of carbohydrate degradation, observed as a viscosity drop or cellulose chains scissions, have been studied to a much smaller extent than the kinetics of delignification. The rate expression describing the cellulose chain scissions, derived in Section 4.2.5.2.1, Chapter Carbohydrate degradation, can be used to calculate the average degree of polymerization parallel to model the extent of delignification and carbohydrate degradation. Equation (90) describes the cellulose chain scissions as a function of the most important reaction conditions, temperature, effective alkali concentration and time. Due to lack of experimental data, there is only one expression for the whole pulping process [see Eq. (90)].

$$\left( \frac{1}{DP_{n,t}} - \frac{1}{DP_{n,0}} \right) = 4.35 \cdot 10^{15} \cdot \text{Exp} \left( -\frac{21538}{T} \right) \cdot [\text{OH}^-]^{1.77} \cdot t \quad (90)$$

For simplicity,  $DP_v$  can be used instead of  $DP_n$ .  $DP_v$  is calculated from intrinsic viscosity according to SCAN-CM-15:88; assuming a  $DP_{n,0} \cong DP_v = 5080 = \text{Intrinsic viscosity (IV)} = (5080^{0.76}) \cdot 2.28 = 1495 \text{ ml g}^{-1}$  for softwood pulps (see Fig. 4.26), a reaction time of 120 min at 160 °C (isothermal conditions), a constant  $[\text{OH}^-]$  of 0.9 mol L<sup>-1</sup>, and a chain scission  $[\text{OH}^-]$  of, CS,  $1.10 \times 10^{-4}/\text{AHG}$  can be calculated which corresponds to a  $DP_v$  of  $1/(\text{CS} + (DP_{n,0}) DP_v = 1/(\text{CS} + DP_{n,0}^{-1}) = 3258 = \text{IV} = 1065 \text{ mL g}^{-1}$ .

#### 4.2.5.3.4 Concentration of Cooking Chemicals, $[\text{OH}^-]$ and $[\text{HS}^-]$ [28]

Experimental evidence indicates that diffusion in porous wood material may limit the pulping rates during the early stages of kraft pulping [28,35]. The transport of chemicals and dissolved solids between the wood chips and the bulk liquor includes diffusion processes [42]. The diffusivities of the wood components are zero as they are bound in the wood. The diffusion of the degradation products is not considered as the pulping reactions are assumed to be irreversible. Because of the very low consumption rate of hydrogen sulfide throughout the cook, an equal distribution between solid and liquid phases can be expected. The diffusivity of sodium hydroxide, however, must be estimated. As the diffusion process is a rate phenomenon, the diffusion coefficient may be related to temperature by an Arrhenius-type relationship [42]. McKibbins measured diffusivity by immersing cooked chips in distilled water and comparing the measured chip sodium concentration dependency on time to that predicted by non-stationary diffusion theory [42]. Diffusion was considered to be proportional to the concentration difference of the respective alkali in the entrapped and free liquor. Hence, for a set of different temperatures, the following expression was derived [Eq. (114)].

$$D = 3.4 \cdot 10^{-2} \cdot \sqrt{T} \cdot \text{Exp} \left( -\frac{2452.4}{T} \right) \quad (114)$$

where D is the diffusion coefficient (in cm<sup>2</sup> min<sup>-1</sup>) and T was temperature (in K).

Because McKibbins measured cooked chips at a given level of pH and cooking intensity,  $D$  had to be corrected with respect to these variables. This approach was made in the 1960s by Hartler [84], and earlier by Hägglund [85] and Bäckström [86]. These authors identified relationships between pH and the so-called effective capillary cross-sectional area (ECCSA), and between the pulp yield and ECCSA. ECCSA is a measure of the diffusion area in the wood chips. Thus, Eq. (114) is corrected with respect to pH and lignin content with the ECCSA data published by Hartler [84]. Benko reported that the diffusion of sodium hydroxide is approximately 12-fold faster than that of lignin fragments due to the higher molecular weight of the latter [87]. The corrected value of  $D$  is expressed in Eq. (115):

$$D = 5.7 \cdot 10^{-2} \cdot \sqrt{T} \cdot \text{Exp}\left(-\frac{2452.4}{T}\right) \cdot (-2.0 \cdot \alpha_L + 0.13 \cdot [\text{OH}^-]^{0.55} + 0.58) \quad (115)$$

where  $\alpha_L$  is the mass fraction of lignin.

The constant, 0.057, is calculated by demanding the  $D$ -values from Eqs. (114) and (115) to be equal at selected conditions:  $T = 170^\circ\text{C}$ ,  $\alpha_L = 0.03$  and  $[\text{OH}^-] = 0.38 \text{ mol L}^{-1}$ .

Neglecting transverse diffusion (across the fibers), one-dimensional wood chips with thickness,  $s$ , can be considered. At the beginning of the cook ( $t = t_0$ ), it is assumed that the average  $[\text{OH}^-]$  in the bound liquor (chip phase) depends on the wood density,  $\rho_{dc}$ , and the chip moisture according to the following equation:

$$[\text{OH}^-]_{\text{bound}} = \left(\frac{V_{bl} - MC_d}{V_{bl}}\right) \cdot [\text{OH}^-]_{\text{free}} \quad (116)$$

where  $MC_d$  [ $\text{l kg}^{-1}$  dry wood] =  $MC_w / (1 - MC_w)$ , which is the average  $[\text{OH}^-]$  resulting from diluting the penetrating liquor with chip moisture.

The volume of bound liquor,  $V_{bl}$ , can be estimated considering the following simple relationship between the dry wood density,  $\rho_{dc}$ , and the density of wood substance,  $\rho_w$  according to Eq. (117):

$$V_V = V_{wc} - V_{ws} = \frac{m_{wc}}{\rho_{dc}} - \frac{m_{wc}}{\rho_w} = \frac{1}{\rho_{dc}} - \frac{1}{1.53} \quad (117)$$

where  $V_V$  is the void volume,  $V_{wc}$  the chip volume,  $V_{ws}$  the volume of wood substance,  $m_{wc}$  the mass of wood substance, and  $\rho_w$  the density of wood substance, which is approximately 1.53 and constant for all practical purposes, wood species constant and even pure cellulosic material.

The degree of penetration,  $P$ , determines the volume of bound liquor,  $V_{bl}$ , using Eq. (116):

$$V_{bl} = P \cdot V_V \quad (118)$$

$P$  is nondimensional.

In case of full impregnation,  $V_{bl}$  equals  $V_V$ .

**Example:**

Given:  $P = 1$ ;  $\rho_{dc} = 0.45 \text{ kg L}^{-1}$ ;  $MC_w = 0.45 \text{ L kg}^{-1}$ ;  $[\text{OH}]_{\text{free}} = 1 \text{ mol L}^{-1}$ .

Result:  $V_v = V_{bl} = 1/0.45 - 1/1.52 = 1.56 \text{ L kg}^{-1}$ ;  $MC_d = 0.45/(1 - 0.45) = 0.82 \text{ L kg}^{-1}$   
 $[\text{OH}]_{\text{bound}} = \{(1.56 - 0.82)/1.56\} \times 1 \text{ mol L}^{-1} = 0.47 \text{ mol L}^{-1}$ .

During the course of the heating-up period, the pulping reactions start. The generated degradation products neutralize alkali as they diffuse out of the chips. Alkali is transported from the bulk phase to the boundary layer, and then diffuses into the chip to replace the sodium hydroxide consumed by the degradation products. Diffusion of alkali within the porous chip structure obeys Fick's second law of diffusion. The one-dimensional wood chip is divided into  $2n$  slices with the width,  $\Delta h = s/2n$ . For calculation of the gradient of the  $[\text{OH}]$  within the chip, a value of 20 was chosen for  $n$  (see Fig. 4.32).

Fick's second law of diffusion for a one-dimensional chip is expressed as:

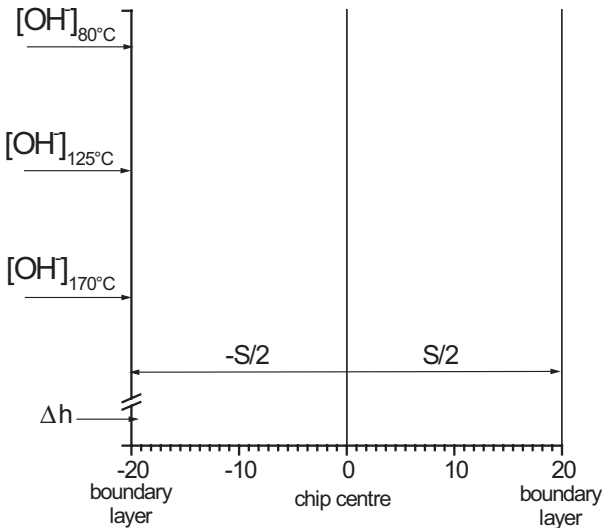
$$\frac{\partial C}{\partial t}(z, t) = \frac{\partial}{\partial z} \left( D \frac{\partial C}{\partial z}(z, t) \right) - Ra \quad \text{for } t < 0; 0 \leq z \leq s/2 \quad (119)$$

where  $C$  is the alkali concentration ( $\text{mol L}^{-1}$ ),  $D$  the coefficient of diffusion ( $\text{cm}^2 \text{ min}^{-1}$ ) and  $Ra$  the reaction rate of  $[\text{OH}]$ , ( $\text{mol L}^{-1} \times \text{min}^{-1}$ ).

The initial concentration is given as

$$C(z, 0) = C_0(z) \quad \text{for } 0 \leq z \leq s/2 \quad (120)$$

constant under assumption in Eq. (114).



**Fig. 4.32** Schematic of a one-dimensional chip stages at: the start of the cook at  $80^\circ\text{C}$  (solid model;  $s =$  chip thickness;  $2n$  slices with width curve); after reaching  $125^\circ\text{C}$  in the heat-up time  $\Delta h = s/2n$ ; the gradient of bound  $[\text{OH}^-]$  across (broken curve); and at the start of the cooking phase at  $170^\circ\text{C}$  (dotted curve).

In the chip center, the plane of symmetry, no concentration gradient occurs at  $t > 0$ , as expressed in Eq. (121):

$$\frac{\partial C}{\partial z}(0, t) = 0 \quad t > 0 \quad (121)$$

The mass flow rate at the solid–liquid interface is considered as proportional to the concentration difference of the free and entrapped liquor, and must equal the mass flow rate which is expressed by Fick’s first law of diffusion according to Eq. (122):

$$D \frac{\partial C}{\partial z}(\frac{s}{2}, t) = k(C_{bulk}(t) - C(\frac{s}{2}, t)) \quad (122)$$

where  $k$  is the mass transfer coefficient.

As it is assumed that the bulk phase is homogeneous and well-stirred, the hydroxide ion concentration in the free liquor has no concentration gradient and is described as  $C_{bulk}$ . According to the conservation of mass, the mass of free liquor decreases by the mass passing through the boundary layer. Thus, the balance on the bulk phase gives the following equation:

$$\frac{dC_{bulk} V_{bulk}}{dt}(t) = -A_C D \frac{\partial C}{\partial z}(\frac{s}{2}, t) \quad (123)$$

$V_{bulk}$  is assumed to be the constant volume of the free liquor, and  $A_C$  the surface area where the mass transfer takes place. The total area is double the circular (chip) area,  $A_C = 2r^2\pi$ . The disk (chip) volume calculates to  $V_{chip} = r^2\pi s$ , so that with  $A_C = 2V_{chip}/s$ , Eq. (123) leads to:

$$\frac{dC_{Bulk}}{dt}(t) = -\frac{2 V_{Chip}}{s V_{Bulk}} D \frac{\partial C}{\partial z}(\frac{s}{2}, t) \quad t > 0 \quad (124)$$

The system is fully described by Eqs. (119–124). A method for the numerical solution of the differential equations to determine the  $[OH^-]$  across the chip thickness is described in the Appendix.

#### 4.2.5.3.5 Alkali and Hydrogen Sulfide Consumption

One prerequisite for studying the influence of  $[HS^-]$  and  $[OH^-]$  on the rate of delignification is to use a high liquid-to-wood ratio (L/W) that ensures a constant liquor composition. During industrial kraft cooking, where L/W ranges between 3 and 5, the concentration of cooking chemicals decreases as a result of the consumption of chemicals by wood components. Consumption of the active cooking chemicals must be considered when applying rate expressions to predict the extent of delignification and carbohydrate degradation. The main alkali consump-



tion is caused by degradation reactions of carbohydrates (peeling reactions), where an average effective alkali consumption of  $1.6 \text{ mol mol}^{-1}$  degraded hexose unit has been reported [88,89]. The dissolved lignin contains approximately 0.8 phenolic groups per monomer, and finally the released carbonic acids (acetic and uronic acids) require a stoichiometric amount of caustic for neutralization. The alkali consumption can thus be expressed as a linear function of the degradation rate of the most important wood components [7,28,79,82,90]. To implement the specific alkali consumption, values reported by Christensen into the kinetic model proved to be most appropriate [79]. The specific effective alkali values are listed in Tab. 4.22.

Tab. 4.22 Specific consumption of active cooking chemicals [79].

Component	EA-consumption		NaHS-consumption	
	[kg NaOH kg <sup>-1</sup> removed]	[mol OH mol <sup>-1</sup> removed]	[as kg NaOH mol kg <sup>-1</sup> removed]	[mol HS mol <sup>-1</sup> removed]
Lignin	0.15	0.66	0.03	0.13
Cellulose	0.40	1.62	0	0
Glucomannan	0.40	1.62	0	0
Xylan	0.40	1.32	0	0

The data listed in Tab. 4.22 reflect the observation that the consumption of hydrogen sulfide ions is low during kraft pulping. A specific sulfur consumption of 5–10 g kg<sup>-1</sup> of wood due to reactions which produce thiolignin and other sulfur-containing compounds was reported by Rydholm; this exactly covers the range shown in Tab. 4.22 [91].

#### 4.2.5.3.6 Model Parameters

According to Andersson, the model parameters originate from nonlinear regression analysis of the experimental data from Lindgren and Lindström [33], the investigations of Lindgren [47], and the course of the hemicelluloses components from Matthew [83]. The initial proportions of species 2 and 3 are obtained by means of the distribution model. The influence of  $[\text{OH}^-]$  and  $[\text{HS}^-]$  was derived from the studies by Kondo and Sarkanen [80] and Olm and Tistad [35] for species 1, from Lindgren and Lindström [33] for lignin species 2 and 3, and from Lindgren [47] for carbohydrates species 2 and 3. The model parameters listed in Tab. 4.23 were obtained by re-fitting the experimental data using the distribution model [7]. Since Olm and Tistad found that the proportion of lignin and carbohydrate reactions is independent on temperature for species 1, it can be assumed that the activation energy must be similar for both reactions ( $E_a = 50 \text{ kJ mol}^{-1}$ )

[35]. This low value indicates that the degradation of this species is diffusion-controlled, and this has been considered in the model. The pre-exponential factors,  $A$ , listed in Tab. 4.23 were derived from constant composition cooks using very high  $L/W$  ratios (41:1). These values were adjusted by a correction factor,  $f_c$ , to simulate the conditions of industrial cooks with  $L/W$  ratios of between 3 and 5. In practical cooks, the increasing concentration of dissolved organic substances accelerates the reaction rates of species 2 and simultaneously retards the reaction rates of species 3; this is compared to constant composition cooks, which can be adjusted by choosing the appropriate correction factors, less than or equal to 1 (Tab. 4.23) [34,59]. The regression analysis revealed a rather large correction factor 6 to simulate the course of carbohydrate species 1, CH1, but this was most likely due to the limited experimental data points available.

The reaction rates  $k_{lj}$  and  $k_{CHij}$  can thus be calculated according to Eq. (125):

$$k_{lj}, k_{CHij} = A_c \cdot f_c \cdot \text{Exp}\left(\frac{E_A}{R} \cdot \left(\frac{1}{443.15} - \frac{1}{T}\right)\right) \quad (125)$$

The model parameters used in the distribution model are summarized in Tab. 4.23 [7].

**Tab. 4.23** Model parameters used in Eqs. (102), (109) [7].

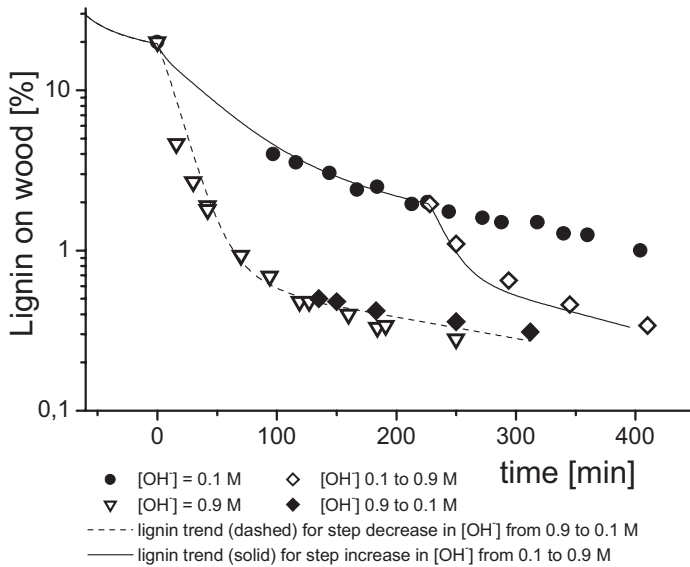
Component	Initial value [% ow] <sup>a</sup>	powers		const [k <sub>j</sub> ]	pre-exp [A <sub>j</sub> ]	corr. Factor [f <sub>j</sub> ]	E <sub>A</sub> [kJ mol <sup>-1</sup> ]
		[OH <sup>-</sup> ] <sup>a</sup>	[HS <sup>-</sup> ] <sup>b</sup>				
L1	9.0	0.00	0.06	0	0.1	1.5	50
L2	19.0	0.48	0.39	0	0.1	1.2	127
L3	1.5	0.20	0	0	4.7 · 10 <sup>-3</sup>	1	127
C1	3.0	0.10	0	0	0.06	6	50
C2	4.1	1.00	0	0.22	0.054	2	144
C3	36.4	1.00	0	0.42	6.4 · 10 <sup>-4</sup>	0.4	144
GM1	12.8	0.10	0	0	0.06	6	50
GM2	2.5	1.00	0	0.22	0.054	2	144
GM3	4.5	1.00	0	0.42	6.4 · 10 <sup>-4</sup>	0.4	144
AX1	1.1	0.10	0	0	0.06	6	50
AX2	1.6	1.00	0	0.22	0.054	2	144
AX 3	4.5	1.00	0	0.42	6.4 · 10 <sup>-4</sup>	0.4	144

a) over-dried wood

### Validation and Application of the Kinetic Model

- Prediction of delignification in the case where  $[\text{OH}^-]$  is changed.

After an initial impregnation stage, the course of delignification during a constant composition cook with a L/W ratio of 41:1 at a very low alkali concentration of  $[\text{OH}^-] = 0.1 \text{ M}$  and  $[\text{HS}^-] = 0.28 \text{ M}$  was determined [33]. After a cooking time of approximately 220 min, the cooking liquor is replaced with a high-alkalinity liquor of  $[\text{OH}^-] = 0.9 \text{ M}$  and  $[\text{HS}^-] = 0.28 \text{ M}$ . In a second run, the cook was run at a high  $[\text{OH}^-]$  concentration of 0.9 M prior to a change to a very low alkali concentration of  $[\text{OH}^-] = 0.1 \text{ M}$ . Figure 4.33 shows that the presented model developed by Andersson et al. is able to predict both scenarios very precisely [7].



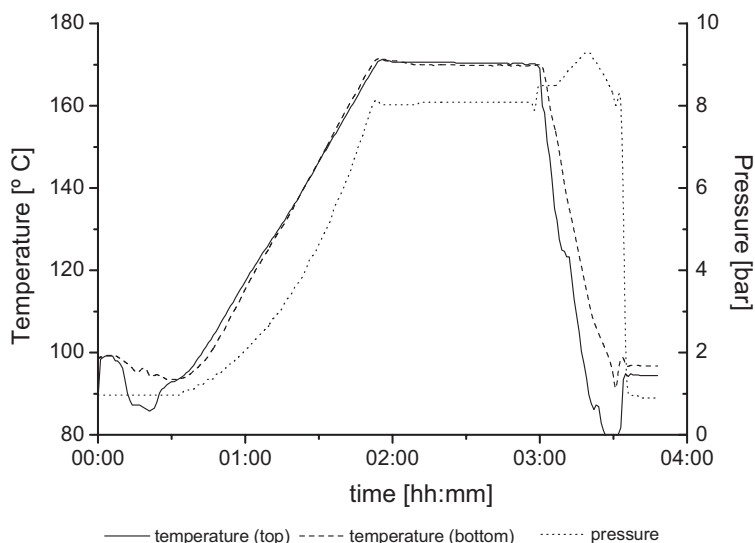
**Fig. 4.33** Model predictions of an autoclave cooking scheme. The effect of changing  $[\text{OH}^-]$  from 0.1 to 0.9 M and 0.9 to 0.1 M in the residual phase in two cooks at constant  $[\text{HS}^-] = 0.28 \text{ M}$  and maximum cooking temperature of 170 °C. Data from Lindgren and Lindström [33].

- Prediction of the unbleached pulp quality of softwood kraft pulping and the course of EA-concentration using a conventional batch process.

The wood raw material consisted of a mixture of industrial pine (*Pinus sylvestris*) and spruce (*Picea abies*) chips in a ratio of about 50:50. The chips were screened in a slot screen, and the fraction passing a plate having 7-mm round holes and retained on a plate with 3-mm holes were used. Bark and knots were removed by hand-sorting. The mean ( $\pm$  SD) thickness of the chips was  $3.5 \pm 1.5 \text{ mm}$ ; the corresponding mean length of the chips was  $25.4 \pm 6.5 \text{ mm}$ . The chips had a dry content of 49.5% and were stored frozen. The cooking trials were carried out in a 10-L

digester with forced liquor circulation. The digester was connected to three pressurized preheating tanks, which allowed precise simulation of a large-scale operation. In addition, dosage volumes, temperatures and H-factors were monitored and recorded on-line. The digester and pressurized tanks were heated by steam injection and/or a heat exchanger in circulation and/or an oil-filled jacket. Dry wood chips (1700 g) were charged, followed by a short steaming phase (7 min, 0.2 g water  $\text{g}^{-1}$  wood, final temperature 99 °C). Subsequently, the white liquor with an average temperature of 90 °C was added to a total L/W ratio of 3.7–3.8:1. The effective alkali charge (EA) of 19% was kept constant. The sulfidity varied slightly in the range between 35 and 39% (see Tab. 4.24). The conventional batch cooking procedure was characterized by a heating-up time of 90 min and a H-factor-controlled cooking phase at constant temperature. The cooking phase was terminated by cold displacement from bottom to top using a washing filtrate at 80 °C comprising an EA concentration of 0.2 mol  $\text{L}^{-1}$ , a sulfidity of 65% (equals to  $[\text{HS}^-]$  of 0.19 mol  $\text{L}^{-1}$ ) and a dry solid content (DS) of approximately 10%. The time–temperature and time–pressure profiles are shown schematically in Fig. 4.34.

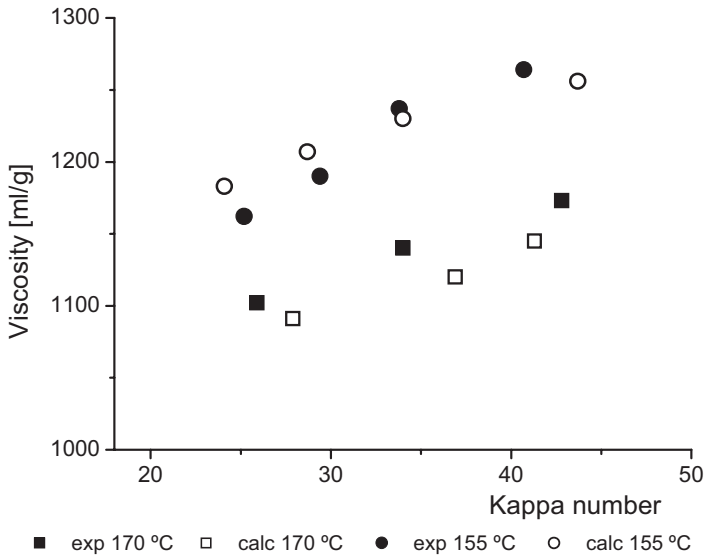
Finally, the pressure was released to fall to atmospheric by quenching with cold water. Two series of H-factors in the range between 800 and 1400 were investigated at two different cooking temperatures, 170 °C and 155 °C. Further details concerning the experimental conditions and the results are summarized in Tab. 4.24.



**Fig. 4.34** Time–temperature (top/bottom) and time–pressure profiles of a selected laboratory kraft cook using conventional batch technology (cook labeled CB 414).

**Tab. 4.24** Conditions and results of pine/spruce kraft cooking experiments. Comparative evaluation of experimental and calculated values (according to [16]).

Label	Maximum temperature [°C]	Time at max. temperature [min]	L/W ratio	Initial [OH <sup>-</sup> ] [mol L <sup>-1</sup> ]	Residual [OH <sup>-</sup> ] [mol L <sup>-1</sup> ]		Initial [HS <sup>-</sup> ] [mol L <sup>-1</sup> ]	Yield, unscr. [%]		Kappa number		Intrinsic viscosity [mL g <sup>-1</sup> ]		Carbohydrates [%]	
					Exp.	Model		Exp.	Model	Exp.	Model	Exp.	Model	Exp.	Model
CB412	170	52	3.7	1.34	0.31	0.31	0.28	50.2	50.5	42.8	41.3	1173	1145	45.6	47.7
CB413	170	60	3.8	1.32	0.26	0.30	0.26	49.2	50.0	34.0	36.9	1140	1120	45.6	47.4
CB414	170	71	3.8	1.32	0.23	0.30	0.30	49.0	49.3	25.9	27.9	1102	1091	45.3	47.3
CB430	150	185	3.7	1.35	0.30	0.32	0.31	49.9	50.7	40.7	43.7	1264	1256	45.7	47.6
CB431	150	227	3.7	1.35	0.26	0.32	0.32	49.4	50.0	33.8	34.0	1237	1230	46.0	47.5
CB432	150	266	3.7	1.35	0.26	0.31	0.32	49.1	49.5	29.4	28.7	1190	1207	45.5	47.4
CB433	150	312	3.7	1.35	0.25	0.30	0.33	49.2	49.0	25.4	24.1	1162	1183	45.2	47.2



**Fig. 4.35** Selectivity plot of pine/spruce kraft cooking: comparison of predicted and experimentally determined values (see Tab. 4.24).

The most important parameters characterizing the results of a kraft cook –for example, unscreened yield, kappa number, intrinsic viscosity and the content of carbohydrates – have been predicted by applying the kinetic model introduced in Chapter 4.2.5.3. The correspondence between the calculated and the experimentally determined values is rather satisfactory for unscreened yield, kappa number and intrinsic viscosity. The content of carbohydrates differ, however, significantly (on average, by >2%) mainly due to the fact that the measured values are based simply on the amounts of neutral sugars (calculated as polymers, e.g., xylan = xylose  $\times$  132/150). By considering the amounts of side chains (4-*O*-methylglucuronic acid in the case of AX and acetyl in the case of GGM), the difference between calculated and experimentally determined values would be greatly diminished. Moreover, the experimental determination of carbohydrates in solid substrates always shows a reduced yield due to losses in sample preparation (e.g., total hydrolysis). The predicted yield values are a little higher (average 0.5%) and show a more pronounced dependency on cooking intensity as compared to the experimentally obtained values. The selectivity, or the viscosity at a given kappa number, is predicted rather precisely which is really remarkable because modeling of the intrinsic viscosity is based on a very simple approach [see Eq. (90) and Fig. 4.35].

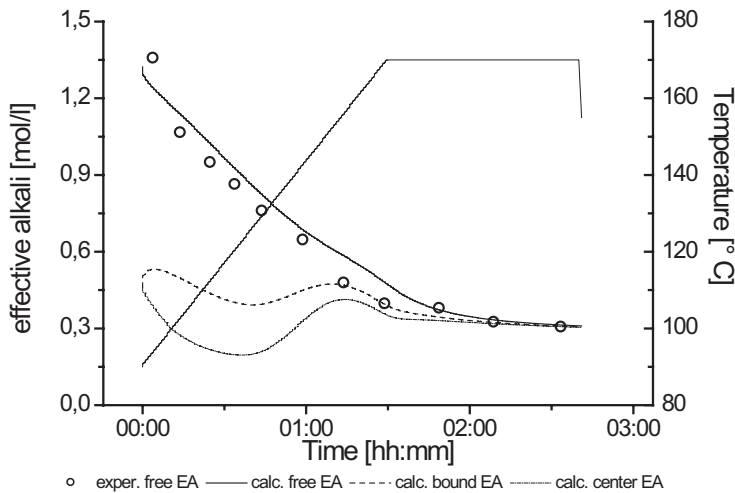
A detailed glance at the single values reveals that the calculated viscosity values show a higher temperature dependency, especially at lower kappa numbers. This might be due to several reasons, for example, a changed degradation behavior of the residual carbohydrates (degree of order increases with an increasing removal of the amorphous cellulose part and the hemicelluloses, etc.) and/or an altering

dependency on EA concentration at lower levels. The difference in predicted and experimentally determined values is however very small, considering both the model-based assumptions and the experimental errors.

Consequently, the model is appropriate for optimization studies to predict the influence of the most important cooking parameters.

The precise calculation of the time course of EA concentration in the free and entrapped liquor throughout the whole cook is an important prerequisite to reliable model kraft pulping. For a selected cook (labeled CB 414), the concentration profiles of the free effective alkali are compared for the calculated and experimentally determined values as illustrated in Fig. 4.36. The agreement between model and experiment is excellent.

The heterogeneous nature of the cooking process is clearly illustrated in Fig. 4.36, where the concentration profiles for the effective alkali in both free and entrapped cooking liquors are visualized. The difference between these profiles is remarkable up to a temperature level of approximately 140 °C. The EA concentration in the entrapped liquor has been calculated for two cases, the average value in the chip (denoted bound EA) and the minimum value in the center of the chip (denoted center EA). Interestingly, the EA concentration in the bound liquor (for both calculated cases) experiences a minimum value after a reaction time of about 40 min at 127 °C, presumably due to augmented EA consumption caused by extensive hemicellulose degradation reactions (peeling) in the initial phase. According to the selected example, the EA concentration inside the chips approaches that outside the chips only after reaching the cooking phase.



**Fig. 4.36** Course of the effective alkali concentration in the free and entrapped cooking liquor during a kraft cook (CB 414); the entrapped liquor is differentiated in “bound liquor”, which equals the average content of entrapped EA concentration, and the “center

liquor”, which corresponds to the EA concentration in the middle of the 3.5-mm chip. Model and experimental values for free EA concentration. Note that the initially ensued bound EA value has been calculated according to Eq. (116).

## 4.2.5.3.7 Appendix

**Numerical Solution of the Kinetic Model**

The numerical approximation for the solution of Eqs. (119–124) is calculated by a finite difference scheme. After replacing the spatial derivations with difference quotients, a system of ordinary differential equations for the concentration  $C$  at discrete points is obtained.

The origin of the coordinate system at the chip center is located and the one-dimensional wood chip is divided into  $2n$  slices with the width  $\Delta h = s/2n$ .  $C_i$  denotes the concentration at height  $i\Delta h$ ; thus,  $C_{i(t)} = C_{(i\Delta h, t)}$ . The derivation of a smooth function can be approximated by a central difference quotient

$$\frac{df}{dx}(x) \approx \frac{f(x+h) - f(x-h)}{2h}. \quad (126)$$

The difference quotient is applied consecutively in Eq. (119), with  $h = \Delta h/2$  obtaining the following difference equations

$$\dot{C}_i(t) \approx \frac{D}{\Delta h^2} (C_{i+1}(t) - 2C_i(t) + C_{i-1}(t)) + Ra_i \quad i = 1, \dots, n-1 \quad (127)$$

To simplify expressions, it was assumed that  $D$  does not depend on the spatial direction; the general case, however, can be solved using the same principle.

After approximating  $C_2$ ,  $C_1$ ,  $C_0$  with a quadratic polynomial and minding [Eq. (121)], we obtain

$$C_0(t) \approx \frac{4}{3}C_1(t) - \frac{1}{3}C_2(t) \quad (128)$$

The same approximation for  $C_n$ ,  $C_{n-1}$ ,  $C_{n-2}$  results in

$$\frac{\partial C(S/2, t)}{\partial z} \approx \frac{1}{2\Delta h} (3C_n(t) - 4C_{n-1}(t) + C_{n-2}(t)) \quad \text{which, after combining with Eqs. (122) and (124), yields}$$

$$C_n(t) \approx C_{Bulk}(t) - \frac{D}{k2\Delta h} (3C_n(t) - 4C_{n-1}(t) + C_{n-2}(t)) \quad (129)$$

and

$$\dot{C}_{Bulk}(t) \approx \frac{V_{Chip} D}{s V_{Bulk} \Delta h} (3C_n(t) - 4C_{n-1}(t) + C_{n-2}(t)) \quad (130)$$

Equations (127–130) define a system of differential algebraic equations (DAEs). After elimination of  $C_{0(t)}$  and  $C_{n(t)}$  by inserting Eq. (128) and Eq. (129) into Eqs.



(127) and (130), the DAEs simplify to a system of ordinary differential equations (ODE) which can be solved by any standard numerical ODE solver that has good stability properties, for example, an implicit Runge Kutta method. Euler's – which has excellent stability properties – is used in the sample code, and although a set of linear equations must be solved for every time step, the method is very fast because the system matrix is almost trigonal.

#### 4.2.6

### Process Chemistry of Kraft Cooking

#### 4.2.6.1 Standard Batch Cooking Process

In standard batch cooking, the whole amount of chemicals required is charged with the white liquor at the beginning of the cook. Certain amounts of black liquor are introduced together with white liquor to increase the dry solids content of the spent liquor prior to evaporation. The concept of conventional cooking results in both a high concentration of effective alkali at the beginning of the cook and a high concentration of dissolved solids towards the end of the cook which, according to kinetic investigations, is disadvantageous with respect to delignification efficiency and selectivity.

##### 4.2.6.1.1 Pulp Yield as a Function of Process Parameters

Pulp yield is a very decisive economical factor, as the wood cost dominates the total production cost of a kraft pulp. Consequently, the knowledge of the relationship between process conditions and pulp yield is an important prerequisite for economical process optimization. Based on the numerous published reports on conventional kraft pulping, it is known that the pulp yield generally increases by 0.14% per increase of one kappa unit for softwood in the kappa number range of 30 to 90, and by 0.16% for hardwood in the kappa number range of 10 to 90, respectively [1]. In the higher and lower kappa number range, the influence on yield is slightly more pronounced. Kappa numbers below 28 should be avoided when using conventional kraft pulping technology, because the yield and the viscosity losses increase considerably. The pulp yield is also influenced by the effective alkali charge (EA). It is reported that in pulping of softwood an increase in the EA charge of 1% NaOH on wood, will decrease the total yield by 0.15% [2]. The small overall drop in yield is explained by two oppositely directed effects, namely an increase in the retention of glucomannan and a decrease in xylan due to increased peeling reactions. The influence of EA charge is much more pronounced in case of hardwoods due to the very small amounts of glucomannans present. An increase of 1% EA charge results in a total yield loss of about 0.4% (Fig. 4.37) [3].

(127) and (130), the DAEs simplify to a system of ordinary differential equations (ODE) which can be solved by any standard numerical ODE solver that has good stability properties, for example, an implicit Runge Kutta method. Euler's – which has excellent stability properties – is used in the sample code, and although a set of linear equations must be solved for every time step, the method is very fast because the system matrix is almost triginal.

#### 4.2.6

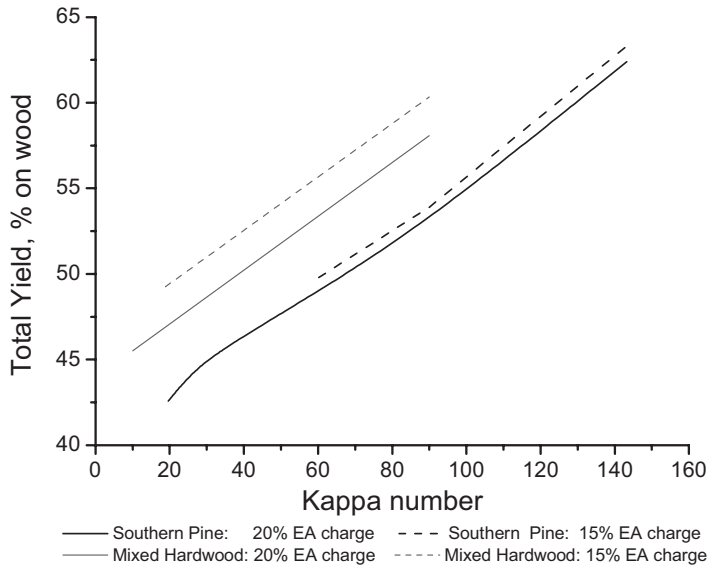
### Process Chemistry of Kraft Cooking

#### 4.2.6.1 Standard Batch Cooking Process

In standard batch cooking, the whole amount of chemicals required is charged with the white liquor at the beginning of the cook. Certain amounts of black liquor are introduced together with white liquor to increase the dry solids content of the spent liquor prior to evaporation. The concept of conventional cooking results in both a high concentration of effective alkali at the beginning of the cook and a high concentration of dissolved solids towards the end of the cook which, according to kinetic investigations, is disadvantageous with respect to delignification efficiency and selectivity.

##### 4.2.6.1.1 Pulp Yield as a Function of Process Parameters

Pulp yield is a very decisive economical factor, as the wood cost dominates the total production cost of a kraft pulp. Consequently, the knowledge of the relationship between process conditions and pulp yield is an important prerequisite for economical process optimization. Based on the numerous published reports on conventional kraft pulping, it is known that the pulp yield generally increases by 0.14% per increase of one kappa unit for softwood in the kappa number range of 30 to 90, and by 0.16% for hardwood in the kappa number range of 10 to 90, respectively [1]. In the higher and lower kappa number range, the influence on yield is slightly more pronounced. Kappa numbers below 28 should be avoided when using conventional kraft pulping technology, because the yield and the viscosity losses increase considerably. The pulp yield is also influenced by the effective alkali charge (EA). It is reported that in pulping of softwood an increase in the EA charge of 1% NaOH on wood, will decrease the total yield by 0.15% [2]. The small overall drop in yield is explained by two oppositely directed effects, namely an increase in the retention of glucomannan and a decrease in xylan due to increased peeling reactions. The influence of EA charge is much more pronounced in case of hardwoods due to the very small amounts of glucomannans present. An increase of 1% EA charge results in a total yield loss of about 0.4% (Fig. 4.37) [3].



**Fig. 4.37** Total pulp yield in kraft pulping of southern pine and southern mixed hardwoods as a function of kappa number (according to [1]).

Sulfidity exerts a significant influence on pulp yield for softwood and hardwood at sulfidity values below 15%. Compared to a pure soda cook, the addition of sodium sulfide to achieve a sulfidity of 15% enables a yield increase of approximately 2.8% for softwood and 2.4% for hardwood, respectively [4]. A further increase of the sulfidity to 40% means an additional yield increase of about 1% for softwood and only about 0.2% for hardwood. Yield is also affected by the chip dimension [5]. A reduction in chip thickness improves the uniformity of pulping, which leads indirectly to a slight increase in pulp yield. The better uniformity of pulping in case of thin chips makes it possible to reduce the EA charge which in turn results in an improved pulp yield at a given kappa number (see Chapter 4.2.3, Impregnation).

In conventional cooking, the EA concentration profile follows an exponential decrease with increasing cooking intensity measured as H-factor (see Fig. 4.36; see also Fig. 4.38). In the initial phase of hardwood (birch) kraft pulping, about 8% xylan can be dissolved in the cooking liquor, depending on the EA concentration [1]. Part of the dissolved xylan can be adsorbed onto the surface of the wood fibers in the final cooking phase as soon as the pH falls below 13.5 [6]. In the pulping of birch, a yield increase of 1–2% has been observed due to the reprecipitation of dissolved xylan [7]. The effect on yield is reported to be about half for softwood (pine) as compared to birch due to the lower amount of xylan present in both wood and cooking liquor.

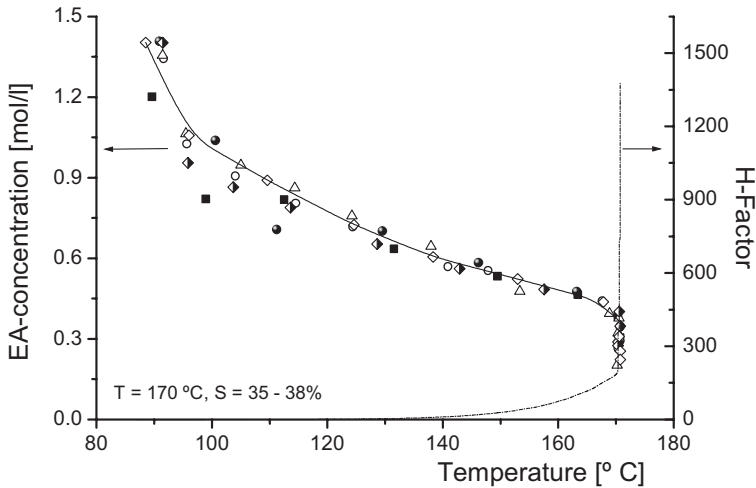
Conventional kraft pulping in batch digesters is a very simple process and comprises the following steps:

- Chip filling.
- Chip steaming.
- Introduction of an aqueous solution containing the cooking chemicals in the form of white liquor, or a mixture of white liquor and black liquor from a preceding cook.
- Heating the digester to a cooking temperature of about 170 °C by direct steam or by indirect heating in a steam/liquor heat exchanger.
- In case of indirect heating, the cooking liquor is circulated through a heat exchanger to even out temperature and chemical concentration gradients within the digester.
- Cooking is maintained until the target H-factor is reached. The pressure is controlled by continuously purging volatile substances being released during the cooking process.
- Condensable gases are partly recovered as wood by-products, such as turpentine.
- Digester content is blown by digester pressure to a blow tank.

The pulp from the blow tank is then washed and screened before it enters the bleach plant.

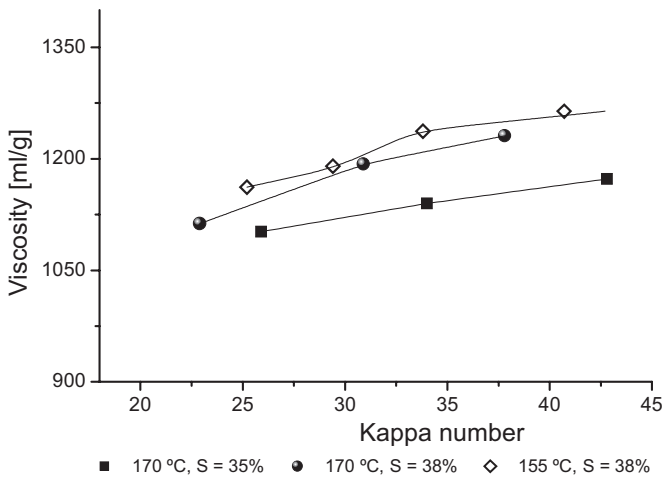
The performance of conventional kraft pulping is predominantly dependent on the wood species, the wood quality, the EA charge, the ratio of hydrogen sulfide ion to hydroxide ion concentration, the time–temperature profile, the H-factor, and the terminal displacement and pulp discharge procedure. Laboratory trials according to the description in Chapter 3 (see Section 4.2.5.3.6. Reaction kinetics: Validation and application of the kinetic model) were conducted to investigate the influence of sulfidity, cooking temperature and H-factor. A mixture of industrial pine (*Pinus sylvestris*) and spruce (*Picea abies*) in a ratio of about 50:50 was used as raw material. The time–temperature and time–pressure profiles correspond to a conventional batch cooking procedure, characterized by a long heating-up time (see Fig. 4.34). Approximately 80% of the EA is consumed already during the heating-up time, which corresponds to an H-factor of about 180 (Fig. 4.38). This leads to the conclusion that 80% of the alkali-consuming reactions occur in the course of only 15% of the total cooking intensity (180 H-factor versus 1200 H-factor to obtain a kappa number of about 25).

At the start of bulk delignification, the hydroxide concentration reaches a value of about 0.45 mol L<sup>-1</sup>. From the viewpoint of delignification kinetics, the course of hydroxide ion concentration in a conventional batch cook – with a high [OH<sup>-</sup>] during the initial and a low [OH<sup>-</sup>] during bulk and residual delignification – is very unfavorable. Moreover, delignification efficiency and selectivity are impaired due to the increasing concentration of dissolved solids in the late stages of cooking. An increase in sulfidity, even only by 3% from 35% to 38%, shows a significant improvement in delignification selectivity characterized as viscosity–kappa number relationship. The reduction in cooking temperature from 170 °C to 155 °C reveals a further slight improvement in delignification selectivity (Fig. 4.39).

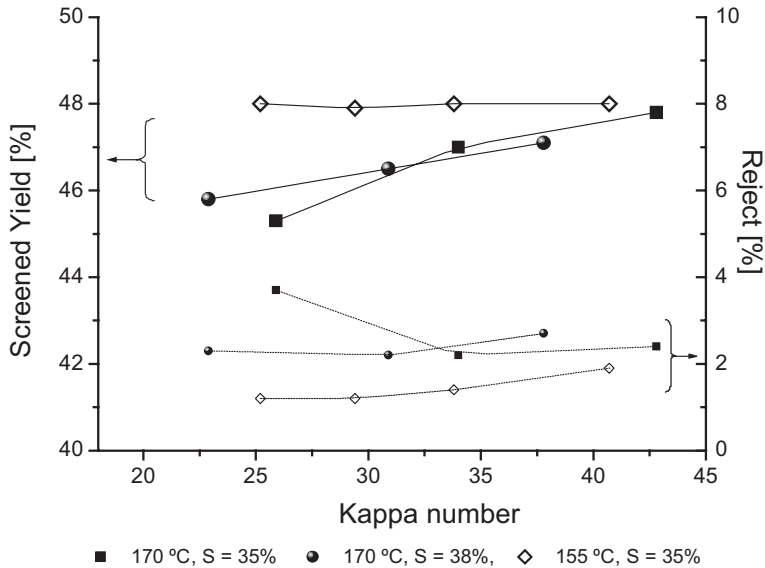


**Fig. 4.38** Course of effective alkali concentration during conventional kraft cooks as a function of cooking temperature and H-factor (according to [8]). Raw material was a mixture of industrial pine (*Pinus sylvestris*) and spruce (*Picea abies*) in a ratio of about 50:50. The EA-charge was kept constant at 19% on oven-dry wood, sulfidity varied from 35 to 38%, liquor-to-wood-ratio 3.7 L kg<sup>-1</sup>. (See also Fig. 4.36.)

Lowering the cooking temperature additionally improves the screened yield, mainly because of more homogeneous delignification reactions resulting in a lower amount of rejects (Fig. 4.40).



**Fig. 4.39** Selectivity plot (viscosity–kappa number relationship) of pine/spruce conventional kraft cooking (according to [8]). Influence of sulfidity:  $[HS^-] = 0.28$  versus  $0.31 \text{ mol L}^{-1}$  and cooking temperature: 170 °C versus 155 °C. The EA-charge was kept constant at 19% on o.d. wood, liquor-to-wood-ratio 3.7 L kg<sup>-1</sup>.



**Fig. 4.40** Pine/spruce conventional kraft cooking. Screened yield and amount of rejects as a function of kappa number (according to [8]). Influence of sulfidity:  $[\text{HS}^-] = 0.28$  versus  $0.31 \text{ mol L}^{-1}$  and cooking temperature:  $170^\circ\text{C}$  versus  $155^\circ\text{C}$ . The EA-charge was kept constant at 19% on o.d. wood, liquor-to-wood-ratio  $3.7 \text{ L kg}^{-1}$ .

The effect of sulfidity and cooking temperature on the processability and selectivity of conventional batch cooking is illustrated for a kappa number 25 softwood kraft pulp in Tab. 4.25.

Increasing sulfidity and lowering the cooking temperature to  $155^\circ\text{C}$  improves the viscosity of the unbleached kappa number 25 pulp by 60 units, and the screened yield by more than 2%. The yield increase can be attributed to a lower amount of rejects and higher contents of arabinoxylan and cellulose (Tab. 4.25). Moreover, a significant lower amount of carboxylic groups of the unbleached pulp derived from high-sulfidity and low-temperature conditions is noticeable. It can be speculated that this pulp contains a lower amount of hexenuronic acid, as it is reported that a low cooking temperature leads to a lower hexenuronic acid content at a given kappa number [9–11]

Despite the yield and viscosity advantages, the reduction of cooking temperature from  $170^\circ\text{C}$  to  $155^\circ\text{C}$  results in an extension of the cooking time by approximately 200 min (Tab. 4.25). The cover-to-cover time of a conventional batch cook would thus increase from about 265 min to 465 min, which is totally unacceptable from an economic point of view. At a given digester volume, the prolongation of the cooking cycle due to a reduction in cooking temperature would reduce the production capacity by 43% ( $1-465^{-1}/265^{-1}$ ). On the basis of conventional batch cooking, technology improvements in the pulping efficiency and selectivity are very

limited. The progressive knowledge on pulping reactions and delignification kinetics finally led to the development of modified kraft cooking concepts.

**Tab. 4.25** Production of unbleached softwood kraft pulps with kappa number 25 using a conventional batch cooking procedure. Comparison of three different cooking conditions: (a) low sulfidity (S), high cooking temperature (T); (b) high sulfidity, high cooking temperature; (c) high sulfidity and low cooking temperature, according to [8].

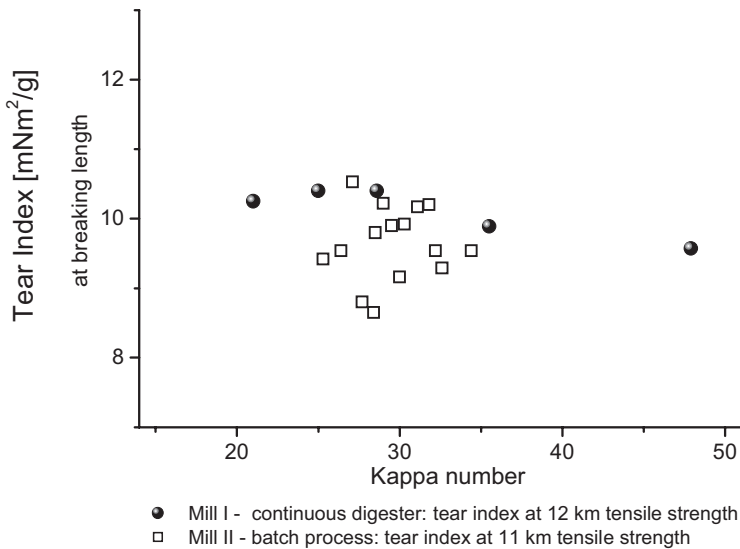
Parameter	Units	Low S, High T	High S, High T	High S, Low T
Max. temperature	°C	170	170	155
H-factor		1200	1296	1400
Total cooking time <sup>a)</sup>	min	190	200	430
[OH <sup>-</sup> ] <sub>initial</sub>	mol/L	1.25	1.26	1.27
[HS <sup>-</sup> ] <sub>initial</sub>	mol/L	0.28	0.31	0.31
[OH <sup>-</sup> ] <sub>residual</sub>	mol/L	0.25	0.26	0.26
[HS <sup>-</sup> ] <sub>residual</sub>	mol/L	0.20	0.21	0.20
[DS <sup>-</sup> ] <sub>residual</sub>	g/L	140	149	156
EA-charge	%NaOH on oven-dried wood	19.0	19.0	19.0
Yield_tot	%	49.0	48.3	49.2
Yield screened	%	45.3	46.0	48.0
Kappa number		25.9	25.0	25.2
Brightness	%ISO	31.2	32.3	32.0
Viscosity	ml/g	1102	1134	1162
Cellulose	%	75.41	75.61	75.4
AX	%	8.0	8.5	9.3
GGM	%	8.3	8.1	7.9
DCM	%	0.13	0.13	0.12
Copper	%	0.47	0.43	0.36
COOH	mmol/kg	111	128	93

a) Comprises 90 min of heating-up time, time at  $T_{\max}$  and 30 min of cold displacement and discharge.

#### 4.2.6.2 Modified Kraft Cooking

From an environmental standpoint, it would be highly desirable to lower the residual lignin content (kappa number) as much as possible before entering the bleach plant. In commercial practice, most softwood kraft pulps are, however, delignified only to a kappa number in the range from 20 to 35, depending on the technology applied. The reason for this constraint can be referred to limitations in pulp quality and pulp yield. Pulp with lower strength properties will not be accepted by customers.

The strength properties of an unbleached kraft softwood pulps reach an optimum in the kappa number range from 22 to 35. A mill study including both continuous and batch digesters revealed that conventional pulping in kraft softwood mills can be extended to kappa numbers close to 25 without deteriorating unbleached pulp strength (Fig. 4.41).

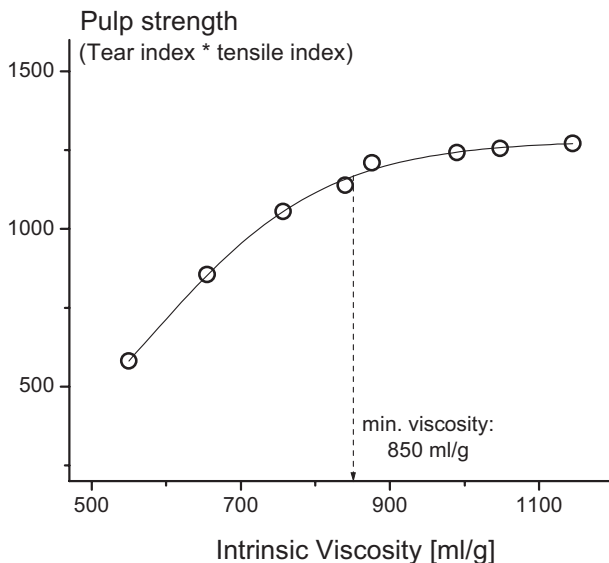


**Fig. 4.41** Tear index at given tensile strength as a function kappa number. Results from different kraft mills. Mill I operates a continuous digester using a spruce/pine mixture; Mill II operates batch digesters using softwood furnishes (according to [12]).

The optimum target kappa number, however, is determined not only by pulp strength properties but also by yield and other parameters. Reinforcing delignification from kappa number 32 to 25 reduces the yield of screened pulp from 47.2% to 45.7% in case of conventional cooking [12].

In a given process, prolonged cooking results in a gradual degradation of the carbohydrate chains, observed as a drop in viscosity and in a decrease in yield. The pulp viscosity of a softwood kraft pulp can be correlated to pulp strength, expressed by the product of specific tearing strength and tensile strength [13]. The





**Fig. 4.42** Strength, estimated by the product of tensile index and tear index, of a softwood kraft pulp related to its intrinsic viscosity (according to [13]).

relationship between viscosity and pulp strength can be approximated by the type of saturation curve shown in Fig. 4.42.

Teder and Warnquist have chosen a value of  $850 \text{ mL g}^{-1}$  as the lowest acceptable viscosity after bleaching for a softwood kraft pulp [13]. This relationship is valid for conventionally and ECF bleached pulps, including an oxygen stage. As seen from Fig. 4.42, pulp strength is seriously deteriorated when the viscosity falls below  $850 \text{ mL g}^{-1}$ . Taking a viscosity drop in the course of ECF-bleaching of approximately 150 viscosity units into account, the viscosity should be about  $1000 \text{ mL g}^{-1}$  after cooking. In the case of TCF-bleaching, the overall viscosity loss during bleaching accounts for more than 300 units, which in turn requires an unbleached viscosity of more than  $1150 \text{ mL g}^{-1}$  at a given kappa number.

The selectivity of conventional kraft cooking improves by increasing the sulfidity of the white liquor. Raising the sulfidity from 25% to 35% and further to 45% increases the viscosity by 110 and  $125 \text{ mL g}^{-1}$  at a given kappa number of 30, respectively [14]. Considering the pros and cons of high sulfidity, in general the disadvantages prevail slightly. The potential drawbacks of higher sulfidity (>35%) can be summarized as more costs for malodorous gas collection, incineration and recovery, the tendency to more corrosion in the recovery furnace, the more reduced sulfur to oxidize in the white liquor, and a higher amount of inert sulfur and sodium compounds. However, in case of high wood costs and high wastewater treatment costs, raising the sulfidity might be a favorable measure.

The need to reduce environmental pollution by simultaneously keeping the pulp quality at the desired level (see Fig. 4.42) was the basis of seeking possibili-

ties to modify the kraft cook so that selectivity would be improved. These modifications should it make possible either to enter the bleach plant with a lower kappa number, or – in order to gain also the yield advantage – to sufficiently increase the viscosity at a given kappa number (in the range of 25–30) so that a subsequent TCF- or ECF-bleaching treatment would be applicable. The principles of modified cooks, with the focus on increasing the ratio of delignification to carbohydrate degradation rates,  $r_1/r_C$ , are primarily based on the results of pulping kinetics investigations (see Section 4.2.5, Kraft Pulping Kinetics). The principles of modified cooking are summarized in the next section.

#### 4.2.6.2.1 Principles of Modified Kraft Cooking

The modified kraft cooking technique was initially developed at the Department of Cellulose Technology at the Royal Institute of Technology and STFI, the Swedish Pulp and Paper Research Institute during the late 1970s and early 1980s [15–19]. This allowed the kraft pulping industry to respond to environmental challenges without impairing pulp quality. Based on numerous investigations, it is well established that a kraft cook should fulfill the following principles in order to achieve the best cooking selectivity [20]:

- The concentration of EA should be low initially and kept relatively uniform throughout the cook.
- The concentration of  $HS^-$  should be as high as possible, especially during the initial delignification and the first part of the bulk delignification. This allows a faster and more complete lignin breakdown during bulk delignification.
- The content of dissolved lignin and sodium ions in the pulping liquor should be kept low during the course of the final bulk and residual delignification phases. This enables enhanced delignification and diffusion processes.
- The rate of polysaccharide depolymerization increases faster with rising temperature than the rate of delignification. Consequently, a lower temperature should improve the selectivity for delignification over cellulose depolymerization [21].
- Avoidance of mechanical stress to the pulp fibers, especially during the discharge operation. The digester must be cooled to a temperature below 100 °C (and the residual overpressure must be removed from the digester via the top relief valve) prior to discharge of the pulp suspension, preferably using pumped discharge [22].

#### Effect of $[OH^-]$ (Alkali Concentration Profile)

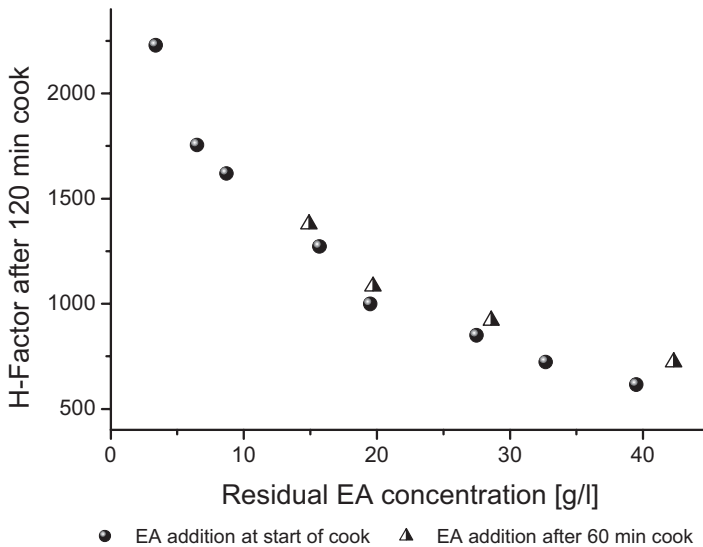
Kinetic studies have demonstrated that the rate of delignification in the initial phase of kraft pulping is independent of the alkali concentration, providing that sufficient alkali remains for the reaction to continue (see Section 4.2.5, Kraft Pulping Kinetics). A logical modification of the conventional process is therefore to

delay the addition of alkali until it is required, for example, in the bulk and residual delignification phases. The bulk delignification rate is most dependent on the EA concentration.

A low and uniform concentration of EA is favorable with respect to delignification selectivity [18]. A controlled alkali profile, where the EA concentration was maintained at levels from  $10 \text{ g L}^{-1}$  to  $30 \text{ g L}^{-1}$  throughout the cook of *Eucalyptus syberii* and *Eucalyptus globulus* resulted in higher strength properties (measured as zero span tensile and tear indices) in the kappa number range 8–18 as compared to conventionally produced kraft pulps [23].

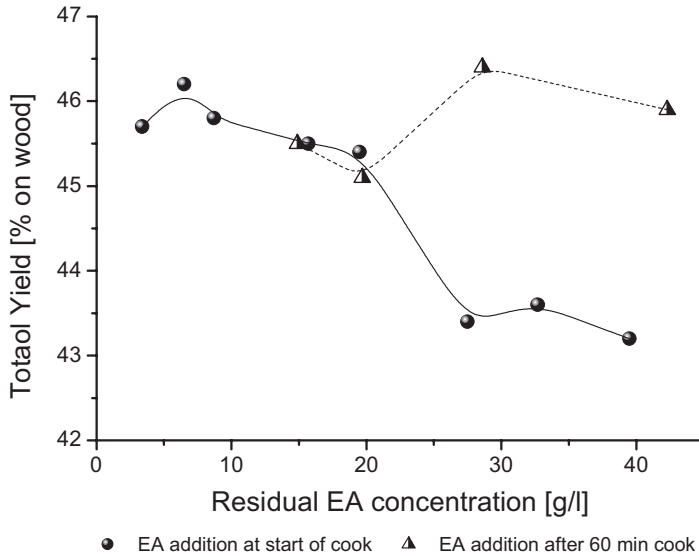
An increase in EA charge accelerates the delignification rate and the transition from bulk to final delignification phase moves towards a lower lignin content, resulting in a shorter cooking time at a given cooking temperature, or making a lower cooking temperature possible at a given cooking time to attain a given kappa number target. Thus, in industrial cooking, the level of EA concentration during bulk delignification will also determine the cooking capacity. Consequently, a compromise between productivity and pulping selectivity must be found in practice.

When the EA concentration in the final cooking stages of a softwood kraft cook is increased in a first case at the beginning of the cook (A-profile), and in a second case after a cooking time of 60 min, a clear relationship between the residual EA concentration at the end of the cooks and the H-factor required to reach a target kappa number of 25 can be established (Fig. 4.43) [24].



**Fig. 4.43** H-factor after 120 min of cooking time required to reach a kappa number 25 as a function of the residual effective alkali (EA) concentration at the end of the cook (according to [24]). Kraft pulping of Scots

pine (*Pinus sylvestris*). Sulfidity of white liquor 37%. Two different EA profiles were established due to the time of adding the final and third EA charge, simulating a modified continuous digester operation.

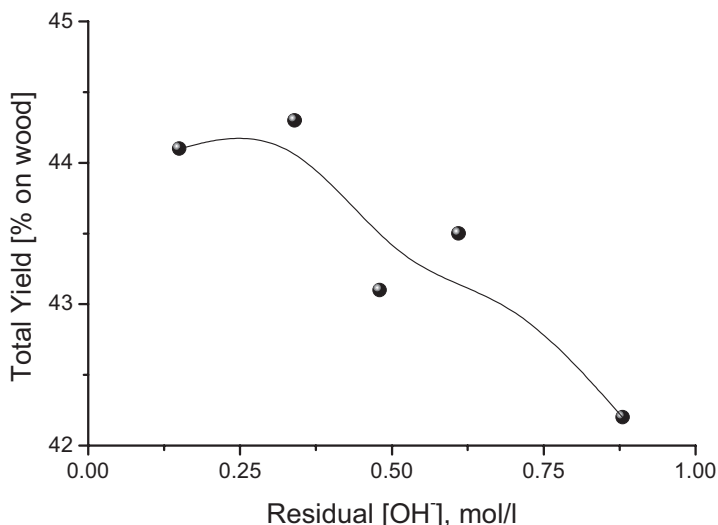


**Fig. 4.44** Total yield of Scots pine (*Pinus sylvestris*) kraft cooking to kappa number 25 as a function of the residual effective alkali concentration at the end of the cook (according to [24]). Sulfidity of white liquor

37%. Two different EA profiles were established due to the time of adding the final and third EA charge, simulating a modified continuous digester.

From these results it can be concluded that the temperature can be lowered by 15 °C when the final EA concentration is raised from 3 to 40 g L<sup>-1</sup> by simultaneously keeping the cooking time constant. The H-factor requirement of both EA profiles is quite comparable. This result agrees well with the findings of Lindgren et al., that a high EA concentration during the final cooking stage accelerates the delignification of residual lignin [25]. It is common knowledge that the pulp yield generally decreases when the EA concentration is increased [26]. The relationship between yield and EA dosage is, however, very complex and additionally depends on the temperature level and EA concentration profile throughout the whole cook. The effects of both EA profile and residual EA concentration on total yield are compared in Fig. 4.44.

The kraft cooks with the higher EA concentration at the beginning of the cooking stage experience significant yield losses when the residual EA concentration exceeds 20 g L<sup>-1</sup>. This observation is also in line with the results obtained from a two-stage kraft process comprising a pretreatment step with a constant hydrogen sulfide ion concentration ([HS<sup>-</sup>] = 0.3 mol L<sup>-1</sup>) and varying hydroxide ion concentrations [0.1–0.5 mol L<sup>-1</sup>) and a cooking stage where the initial hydroxide ion concentration is varied from 1 to 1.6 mol L<sup>-1</sup> [27]. The pulp yield decreases sharply when the residual EA concentration exceeds 0.4 mol L<sup>-1</sup> (Fig. 4.45).



**Fig. 4.45** Pulp yield of pine kraft pulps produced according to a two-stage laboratory cook at a kappa number 20 as a function of the residual alkali concentration (according to [27]).

The loss of pulp yield is mainly caused by a decrease in the xylan yield (total yield from 44.1% → 42.2% on wood parallels the change in the xylan content from 3.8% → 2.1% on wood).

The study also shows that when the comparison is made at the same total EA charge, approximately 1% higher pulp yield is achieved if the alkali charge is more shifted to the pretreatment stage ( $[\text{OH}^-]$  0.1/1.6 mol L<sup>-1</sup> versus 0.5/1.0 mol L<sup>-1</sup>).

Shifting the final EA charge to the late cooking stages, however, contributes to a preservation of the yield throughout the whole range of residual EA concentration investigated (see Fig. 4.44). Hence, high EA concentrations at the beginning of the cooking stage seem to be particularly unfavorable with respect to pulp yield. However, when the EA profile is modified in such a manner that the alkali concentration at the beginning of the cook remains relatively low and the concentration is increased only at the end of the cook, pulp yield can be preserved and viscosity can even be improved.

The higher hemicellulose content of the pulp derived from the late EA addition indicates that when the EA concentration at the beginning of bulk delignification is moderate (means below 15 g L<sup>-1</sup>), a high concentration at the end of the cook does not impair pulping selectivity with respect to pulp yield. Thus, a high EA concentration at the beginning of bulk delignification degrades hemicelluloses, predominantly xylans. The reprecipitation of xylan onto the fibers during the final cooking phase is however limited due to the high EA concentration. A further advantage of the high EA concentration at the end of the cook is partial degradation of the hexenuronic acid (HexA). However, the reduction of HexA is more pro-

nounced when the EA concentration is increased at the beginning of the cook, which is in agreement with the findings of Vuorinen et al. [28]. On the basis of these findings and appropriate process simulations, a new continuous cooking process denoted as Enhanced Alkali Profile Cooking (EAPC) has been developed [29] (see also Mill applications).

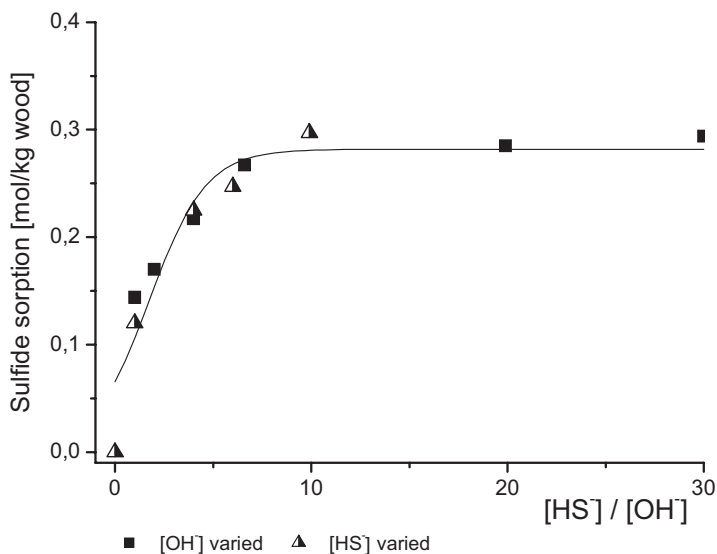
#### **Effect of $[\text{HS}^-]$ (Sulfide Concentration Profile)**

The sulfide concentration should be as high as possible to attain high delignification selectivity (yield versus kappa number and viscosity versus kappa number). This is particularly important during the transition from initial to bulk delignification, where the addition of hydrogen sulfide ions to quinone methide intermediates favors subsequent sulfidolytic cleavage of the  $\beta$ -O-arylether bond at the expense of condensation during the bulk delignification [30]. A lack of sulfide ions may also lead to a carbon-carbon bond cleavage of the  $\beta$ - $\gamma$ -linkage to yield formaldehyde and styryl aryl structures [30] (see Section 4.2.4).

The pretreatment of loblolly pine chips with sodium sulfide-containing liquors (pure  $\text{Na}_2\text{S}$  or green liquor) in a separate stage prior to kraft pulping results in a higher pulp viscosity at a given kappa number as compared to conventional kraft pulping (at a kappa number level of 25, the intrinsic viscosity – recalculated from Tappi-230 – increases from  $950 \text{ mL g}^{-1}$  to  $1080 \text{ mL g}^{-1}$ . Conditions: pretreatment: l:s = 4:1; temperature  $135^\circ\text{C}$ , EA-charge of  $\text{Na}_2\text{S}$  13.5 wt% NaOH; kraft cook: (a) after pretreatment: EA-charge 12 wt% NaOH, (b) without pretreatment: EA-charge 20.5 wt% NaOH; all residual conditions were constant). The pretreatment of wood with aqueous sodium sulfide solutions at temperatures of about  $140^\circ\text{C}$  prior to a modified kraft cook results in an additionally improved delignification selectivity [31]. The beneficial effect observed is probably related to an increased uptake of sulfur/sulfide which also leads to a faster delignification in a subsequent kraft cook.

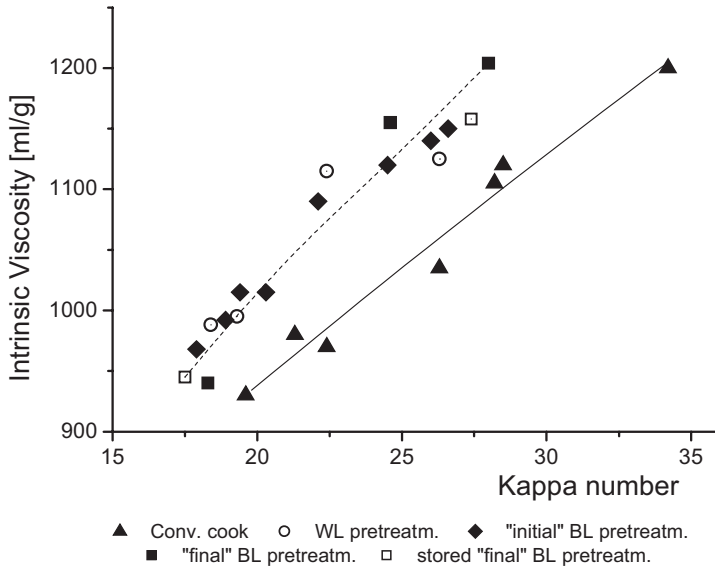
The increase in pulping selectivity can only be obtained when about 70% of the pretreatment liquor is removed ahead of the addition of white liquor in the subsequent kraft stage [32]. The high viscosity is solely due to the lower alkali requirement during the kraft cook. Thus, the increase in selectivity when pretreating the chips with hydrogen sulfide-containing liquors at temperatures around  $135^\circ\text{C}$  can be attributed to enhanced lignin degradation at any given EA dosage [32].

The treatment of wood chips with sulfide-containing liquors under conditions typical for impregnation yields sulfide absorption. The sorption of sulfide in wood chips increases with increasing hydrogen sulfide ion concentration, time, temperature, and concentration of sodium ions, but decreases with increasing hydroxide ion concentration [33,34]. At a given temperature and reaction time, there is a relationship between the sulfide sorption in wood and the ratio of the concentrations of hydrogen sulfide and hydroxide ion concentration, similar to a Langmuir-type adsorption isotherm (Fig. 4.46).



**Fig. 4.46** Sulfide sorption in wood (50% pine, 50% spruce) as a function of the ratio of hydrogen sulfide ion to hydroxide ion concentrations at a temperature of 130 °C after 30 min (according to [33]).

The saturation level of absorbed sulfide ions amounts to approximately  $0.3 \text{ mol kg}^{-1}$  wood, which corresponds to about 25 S units per 100 C9 units. The presence of polysulfide in the treatment liquor doubles the amount of sulfide sorption. Due to the high hydroxide ion concentration, the ratio of hydrogen sulfide ion to hydroxide ion concentration yields only about 0.25 at the beginning of a conventional cook ( $[\text{HS}^-] = 0.28 \text{ mol L}^{-1}$ ,  $[\text{OH}^-] = 1.12 \text{ mol L}^{-1}$  equals a sulfidity of 40%). According to Fig. 4.46, the amount of absorbed sulfide is very low. The ratio of hydrogen sulfide ion to hydroxide ion concentration governs the extent of cleavage of  $\beta$ -aryl ether linkages in phenolic structures and the formation of enol ether structures. At high ratios, the formation of enol ether structures is minimized, and the cleavage of  $\beta$ -aryl ether structures is favored. Laboratory trials demonstrated that pretreating wood chips with a solution exhibiting a ratio of hydrogen sulfide ion to hydroxide ion concentration as high as 6 prior to a kraft cook produces pulps with approximately  $100 \text{ mL g}^{-1}$  higher viscosity at a given kappa number as compared to a conventional kraft cook without pretreatment (Fig. 4.47). The results also indicate that there is no difference in selectivity after pretreatment with different types of black liquor with higher and lower molecular weights of the lignin, or with a pure inorganic solution as long as the solutions have an equal ratio of hydrogen sulfide ion to hydroxide ion concentration. This implies that the organic matter in the black liquor has no perceivable effect on the selectivity.



**Fig. 4.47** Selectivity plot – intrinsic viscosity versus kappa number – for kraft pulps made from wood chips consisting of 50% pine and 50% spruce chips, pretreated with different kinds of black liquors and for a reference kraft cook (according to [33]). Pretreatment conditions:  $[\text{HS}^-]/[\text{OH}^-] = 6$ ; 130 °C, 30 min.

In order to provide a  $[\text{HS}^-]/[\text{OH}^-]$  ratio of at least  $\geq 6:1$  to ensure sufficient sulfide sorption, it is clear that there is a need to separate the hydrogen sulfide from the hydroxide of the white liquor. The concept would be to apply the sulfide-rich liquor alone or combined with black liquor to the early phases and the sulfide lean liquors in the late stage of the cook. A novel method for the production of white liquor in separate sulfide-rich and sulfide lean streams has been proposed [35,36]. This process utilizes the lower solubility of sodium carbonate and sodium sulfide in the recovery boiler smelt to achieve a separation of these two compounds. Preliminary results have shown that the sulfide-rich white liquor fraction exhibits a sulfidity of 55%, whereas the sulfide-lean white liquor fraction shows a sulfidity of less than 5% (Tab. 4.26). Further advantages of this separation into two fractions are the significantly higher EA concentration of the combined white liquors, the 6% higher overall causticity, and the lower hydraulic load in the green liquor clarification, slaking, causticizing and white liquor separation systems. The higher causticity can be attributed to the reprecipitation of sodium carbonate from the part of the sulfide-lean liquor recycled back to smelt leaching.



Tab. 4.26 Composition of conventional and alternative white liquors (according to [36]).

Constituents	Unit	Conventional	Alternative white liquor recovery		
			Sulfide-rich	Sulfide-lean	Total
NaOH	g NaOH L <sup>-1</sup>	88.9	194.3	130.6	
Na <sub>2</sub> S	g NaOH L <sup>-1</sup>	47.9	234.3	6.2	
Na <sub>2</sub> CO <sub>3</sub>	g NaOH L <sup>-1</sup>	16.1	trace	27.9	
Active alkali (AA)	g NaOH/L <sup>-1</sup>	136.8	428.6	136.8	226.5
Effective alkali (EA)	g NaOH L <sup>-1</sup>	112.8	311.5	133.7	188.4
Sulfidity	% on AA	35.0	54.7	4.51	33.7
Causticity	%	84.7	99.9	82.41	88.6
Percentage of total EA	%	100.0	49.8	50.2	100.0

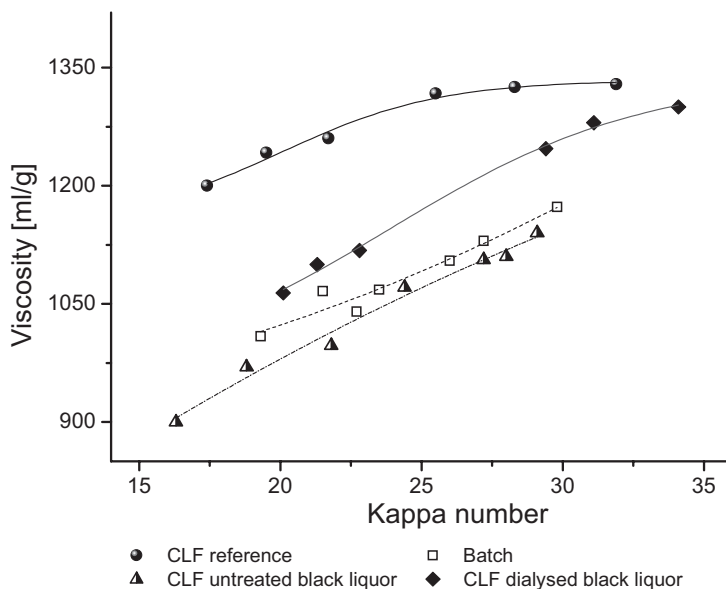
#### Effects of Dissolved Solids (Lignin) and Ionic Strength

Delignification selectivity is negatively affected by the organic substances dissolved during the cook at given liquor-to-wood ratios (3:1 to 5:1). The reason for the impaired final pulp quality can be attributed to the reduced delignification rate at a late stage of the cook due to the presence of the dissolved organic matter [18] (see Section 4.2.5.2.2, Reaction kinetics). The removal of dissolved wood components, especially xylan, during the final cooking stages is however disadvantageous to total yield as the extent of xylan adsorption on the pulp fibers diminishes. The xylan content in a pine kraft pulp would be 4–6% without adsorption compared to 8–10% after a conventional batch cooking process, and hence the total yield would be reduced by 2% from 47 to 45% [37].

The level of dissolved lignin concentration in the final cooking stage is also a major determinant of delignification selectivity in batch cooking. In order to avoid extra dilution and to preserve material balance, a lower lignin concentration in the final cooking liquor means shifting to a higher concentration in the initial stages of the cook. A linear relationship between the gain in viscosity at a given kappa number and the dissolved lignin concentration after displacement with fresh cooking liquor has been obtained [38]. A reduction in the dissolved lignin concentration from 62 g L<sup>-1</sup> to approximately 40 g L<sup>-1</sup> corresponds to an overall increase in viscosity of 100 mL g<sup>-1</sup> [38].

A detailed study on the effects of dissolved lignin has been conducted by Sjöblom et al. [39]. The results of *Pinus silvestris* kraft cooks in a continuous liquor flow digester demonstrate that the presence of dissolved lignin during the later stages of delignification (bulk and final) impairs the selectivity expressed as viscosity–kappa number relationship. The effect increases with prolonged delignification. Interestingly, the presence of lignin during the initial phase and the transi-

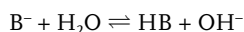
tion phase to bulk delignification results in an increase in pulp viscosity. The addition of untreated black liquor from a previous cook decreases selectivity more as compared to the addition of dialyzed black liquor or precipitated kraft lignin (Indulin AT from Westvaco) at a given lignin concentration (Fig. 4.48). Conventional batch cooking and continuous liquor flow cooking with the addition of untreated black liquor in the final part of the cook show comparable selectivity in the kappa number range 20–32. Figure 4.48 shows that, in comparison to these cooks, continuous liquor flow cooking without the addition of lignin to the cooking liquor (CLF reference) produces pulps with 200–250 mL g<sup>-1</sup> higher viscosity in the given kappa number range. The better selectivity may be explained partly by the low concentrations of dissolved lignin and sodium ions which increases the delignification rate, and partly by the continuous supply of hydrogen sulfide ions. In conventional cooking there seems to be a lack of hydrogen sulfide ions at the beginning of the bulk delignification phase, and this might increase the proportion of enolic ether structures in the lignin [40].



**Fig. 4.48** Selectivity plots of laboratory *Pinus sylvestris* kraft cooks comparing the concepts of continuous liquor flow (CLF) and conventional batch (Batch) technology, as well as the addition of untreated and dialyzed black liquor during the final cooking stage according to Sjöblom et al. [39].

CLF reference:  $[\text{OH}^-] = 0.38 \text{ mol L}^{-1}$ ;  $[\text{HS}^-] = 0.26 \text{ mol L}^{-1}$ ; Batch: 20% EA on wood, 40% sulfidity, liquor-to-wood ratio 4:1; cooking temperature 170 °C for both concepts; untreated or unchanged black liquor and dialyzed black liquor in a concentration of 50 g L<sup>-1</sup> lignin, each of which is added at the end of bulk delignification until the end of the cook.

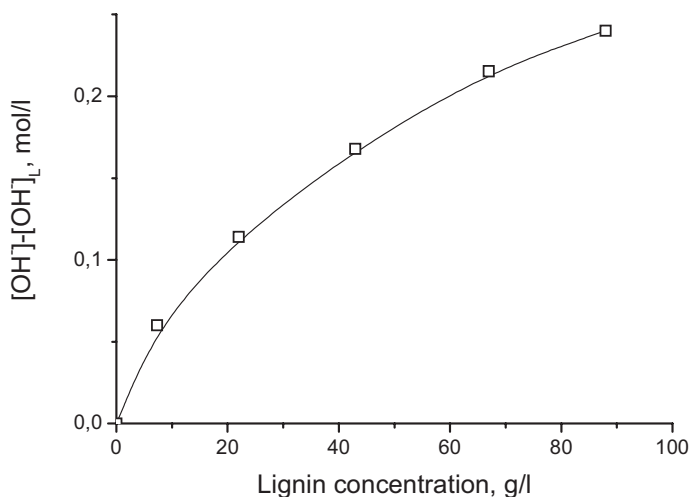
Moreover, the presence of dissolved lignin in alkaline solution leads to an increase in the alkalinity when the temperature is raised [41]. The amount of hydroxide liberated from lignin when increasing the temperature from 25 to 170 °C equals approximately the amount being consumed by dissolution of precipitated lignin at 25 °C. The effect of increased temperature on the acid/base reactions is a displacement towards the acid forms according to the following equation:



The release of hydroxide ions at high temperatures is most pronounced in the pH range 10–12, where the phenolate and carbonate ions react to form phenols and hydrogen carbonate, respectively [42].

The determination of alkali concentration at 170 °C is measured indirectly by the extent of cellulose degradation caused by alkaline hydrolysis using high-purity bleached cotton linters (stabilized with  $\text{NaBH}_4$  treatment against alkaline peeling degradation). It has been shown that in a lignin-free cooking liquor (white liquor), the alkali concentration at 25 °C must be increased by 31% in order to obtain equal alkalinities at 170 °C with that of a lignin solution of 44 g L<sup>-1</sup>. Figure 4.49 illustrates how much the EA concentration must be increased in a lignin-free solution at 25 °C to reach the alkalinity at 170 °C of a lignin solution of a given concentration. The relationship is valid at an effective alkali concentration of 0.6 mol L<sup>-1</sup> in the lignin solution at 25 °C.

The selectivity is also impaired by an increasing ionic strength (e.g., sodium ions) during the final part of the cook. The effect of dissolved lignin on selectivity is, however, greater than that of sodium ions limited to the concentration levels in



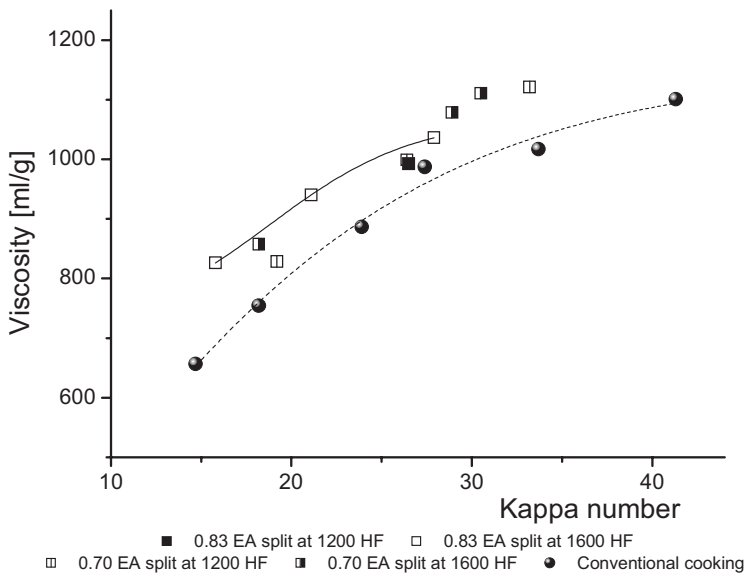
**Fig. 4.49** Difference in alkali concentration at 25 °C between lignin-free solution and lignin-containing solutions,  $[\text{OH}^-]_{170} - [\text{OH}^-]_{25}$ , as a function of lignin concentration (according to [41]).

Both solutions show the same alkalinities at 170 °C. The relationship is valid at an alkali concentration of 0.6 mol L<sup>-1</sup> at 25 °C.

normal cooks. The presence of untreated black liquor during the final part of the cook causes a lower yield of approximately 0.5% at a given kappa number. The yield loss originates from the prolonged cooking necessary to reach a given kappa number.

The sole effect of liquor displacement was studied for kraft cooking of radiata pine [43]. Liquor displacement means the replacement of black liquor by fresh white liquor in the late stage of the cook. The results from laboratory cooking experiments clearly show that if the displacement is conducted earlier in the cook (1200 H-factor), then the effective alkali split ratio has no influence on pulping selectivity. However, if displacement is delayed until 1600 H-factor, pulping selectivity increases for both effective alkali split ratios investigated (see Fig. 4.50).

In another study, a three-stage process with both high initial sulfide concentration due to a low liquor-to-wood ratio and the use of a sulfide-rich white liquor (vapor phase cook until H-factor 300) and low final lignin concentration suggests a substantial selectivity advantage compared to a modified reference cook [26,44,45]. A dissolved lignin concentration in the final cooking phase as low as  $20 \text{ g L}^{-1}$  (compared to  $40 \text{ g L}^{-1}$  for the modified reference and  $70 \text{ g L}^{-1}$  for the conventional reference cooks) is achieved through drainage of the free liquor at H-factor 1200. The bisection of the dissolved lignin concentration in the final cooking phase results in an increase of approximately 90 units in pulp viscosity at a given kappa number, which again is about 60 and 160 units higher as compared to the modified and conventional reference cooks, respectively [44].



**Fig. 4.50** Selectivity plot as viscosity–kappa number relationship for radiata pine kraft pulps (according to [43]). Influence of liquor displacement at different effective alkali split ratios at different H-factor levels in comparison

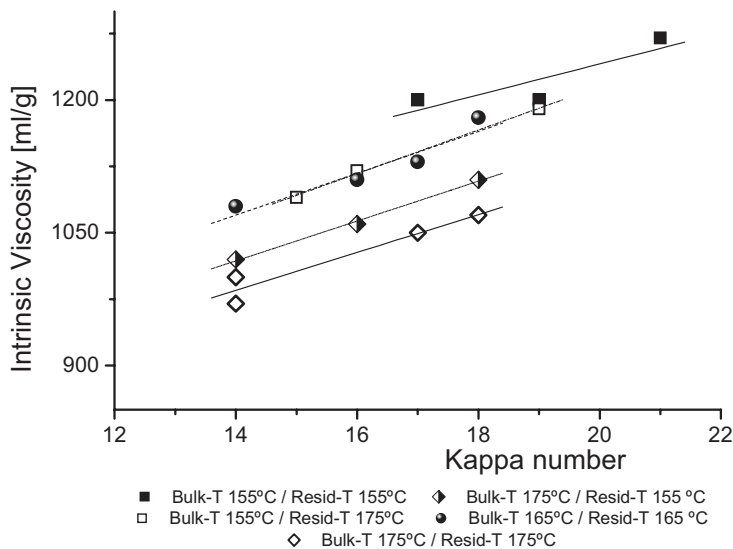
to conventional kraft batch cooking. Constant conditions: Total EA-charge 15.6% on o.d. wood; 26.5% sulfidity; max. cooking temperature 170 °C.

The application of liquor exchange at a predetermined H-factor to reduce the content of dissolved lignin and sodium ions in laboratory kraft pulping of hardwood (e.g., different *Eucalyptus* species) was also very successful in improving the relationship between pulp strength and kappa number [23]. If liquor exchange is combined with alkali profiling, the benefits gained are substantially additive.

The rate of delignification is determined by the initial fraction of EA alkali reflecting the higher alkali concentration at the start of the bulk phase. High pulping rates can be maintained at low EA split ratios if displacement is shifted to earlier cooking stage [43].

#### Effect of Cooking Temperature

The rate of carbohydrate degradation during alkaline pulping is affected by both EA concentration and cooking temperature (see Section 4.2.5.2.1, Kinetics of carbohydrate degradation). Kubes et al. determined an activation energy of  $179 \pm 4 \text{ kJ mol}^{-1}$  for the chain scissions of the carbohydrates by applying the Arrhenius equation that describes the temperature dependence in Soda-anthraquinone (AQ) and kraft pulping [21]. The corresponding activation energy for bulk delignification is known to be about  $134 \text{ kJ mol}^{-1}$  (see Tab. 4.19 in) [46]. The selectivity of kraft cook with respect to the intrinsic pulp viscosity is defined as the ratio of the rate of delignification ( $k_L$ ) to the rate of carbohydrate degradation, determined as chain scissions ( $k_C$ ). Pulping selectivity improves by decreasing the cooking temperature due to a significantly higher activation energy for the chain scissions (see Tab. 4.18). Laboratory and industrial cooking experiments according



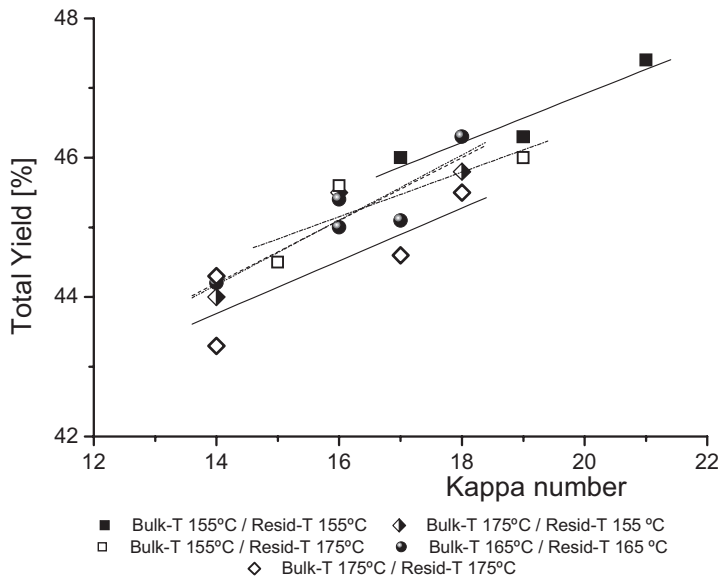
**Fig. 4.51** EMCC laboratory kraft cooks of pine/spruce mixture. Pulp viscosity versus kappa number (according to [47]). Total EA-charge 18% on wood; EA-split 80%/20%; sulfidity

40%; beginning of counter-current cooking after H-factor of 600; residual delignification is assumed to start beyond H-factor 1450.

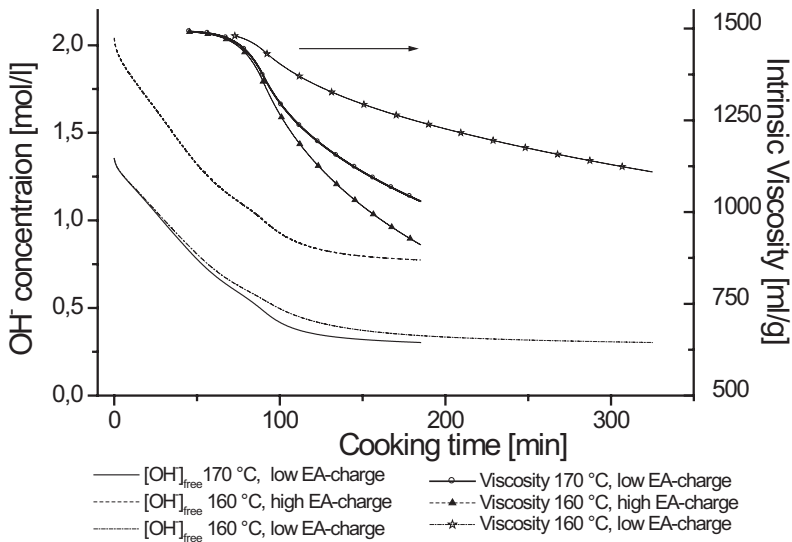
to the isothermal cooking (ITC) and extended modified cooking concept (EMCC) confirmed the predictions from kinetic investigations [47,48]. Figure 4.51 demonstrates that lowering the temperature during bulk delignification is preferable with respect to selectivity as compared to a decrease in temperature in the residual phase. When translated to the EMCC cooking procedure, this means that a low temperature during the co-current and the first counter-current cooking zones is more efficient for a selective kraft cook than a low temperature in the “HiHeat” cooking zone.

Figure 4.51 shows that a decrease in cooking temperature of 10 °C results in an increase in pulp viscosity by 80 units. Isothermal conditions at 165 °C yield pulps of equal selectivity as compared to those being produced at 155 °C during bulk and 175 °C in the course of final phase delignification. The gain in pulp yield with decreasing temperature is not clear. The results indicate that the pulp yield is increased by 0.5% on wood when the cooking temperature is decreased by 10 °C (Fig. 4.52).

In contrast to the results from industrial isothermal cooking (ITC), the strength properties of the laboratory-cooked pulps are not affected by the cooking temperatures [47,48]. A decrease in temperature was also unsuccessful in increasing the tear strength of Eucalyptus pulps, though a small improvement in pulp yield was reported [23].



**Fig. 4.52** EMCC laboratory kraft cooks of pine/spruce mixture. Total yield versus kappa number (according to [47]). Total EA-charge 18% on wood; EA-split 80%/20%; sulfidity 40%; beginning of counter-current cooking after H-factor of 600; final delignification is assumed to start beyond H-factor 1450.



**Fig. 4.53** Prediction of the course of effective alkali (EA) concentrations and intrinsic viscosities of three model cases through conventional softwood kraft pulping to kappa number 25. Case 1, high temperature, low EA charge; Case 2, low temperature, high EA charge; Case 3, low temperature, low EA charge. Kinetic model based on Ref. [50]

It is clear that to compensate for the lowering of the cooking temperature, either the cooking time or the EA charge must be increased. Prolonging the cooking time would clearly reduce the digester capacity, which would hardly be accepted in an existing digester plant. To compensate for decreasing the temperature from 170 °C to 160 °C on the kraft pulping of hardwood to a given kappa number of  $21 \pm 1$ , the EA charge (as NaOH) was increased from 16.3% to 23.1% on o.d. wood. Simultaneously, the H-factor was reduced from 1021 to 441 [49]. In this particular case, the total yield remained almost unaffected, whereas the ratio cellulose to pentosan content shifted in favor of the cellulose content. The effect of decreasing the cooking temperature on the conventional kraft pulping of softwood was investigated by using the kinetic model introduced in Section 4.2.5.3 (Fig. 4.35). The applied reaction conditions and the calculated results are summarized in Tab. 4.27 and Fig. 4.53.

According to the predicted results, cooking at low temperature and applying a high EA charge to reach the target kappa number without extending the cooking time leads to pulps with low yield and poor properties (low viscosity) compared to the high-temperature reference (case 1). If cooking time is prolonged while maintaining a low EA charge, the viscosity of the resulting pulp increases as expected, whereas the pulp yield remains unaffected. Thus, it can be concluded that the only way to improve kraft pulping selectivity with respect to viscosity is to compensate for the lowering of the cooking temperature by increasing the cooking time. For an economic optimization, a compromise between temperature, EA charge and cooking time must be found.

**Tab. 4.27** Effect of the interdependence of temperature, cooking time and effective alkali (EA) charge on process and pulp parameters of softwood kraft pulping. Values are predicted for a kappa number 25-pulp by using a kinetic model based on an extended model of Andersson (see Section 4.2.5.3, Reaction kinetics) [50]. Case 1, high temperature, low EA charge; Case 2, low temperature, high EA charge; Case 3, low temperature, low EA charge.

Parameter	unit	Case 1	Case 2	Case 3
Temperature	°C	170	160	160
Time	min	95	95	235
Liquor to wood ratio	L kg <sup>-1</sup>	3.5	3.5	3.5
[OH <sup>-</sup> ] in fresh liquor	mol L <sup>-1</sup>	1.35	2.04	1.35
[OH <sup>-</sup> ] in residual liquor	mol L <sup>-1</sup>	0.30	0.77	0.31
[HS <sup>-</sup> ] in fresh liquor	mol L <sup>-1</sup>	0.24	0.36	0.24
EA charge	% od wood	19.0	27.9	19.0
Total yield	%	48.5	47.2	48.7
Kappa number (K)		25	25	25
Intrinsic viscosity (V)	mL g <sup>-1</sup>	1030	915	1110
Selectivity (V/K)		41.2	36.6	44.4
Glucomannan	% od wood	5.3	4.8	5.3
Arabinoxylan	% od wood	5.0	4.6	5.0

### Effect on Carbohydrate Composition

It is well known that the major part of the wood hemicelluloses are degraded during the course of the initial delignification phase (see Sections 4.2.5.1 and 4.2.5.3.2, Kraft Pulping Kinetics). The carbohydrate composition of spruce (*Picea abies*) comprises 17.1% galactoglucomannan (GGM), 8.7% arabinoglucuronoxylan (AX), and 44.2% cellulose (C). It was reported that 40% of AX and 70% of GGM were removed during the heating-up time to cooking temperature [51].

In a kinetic study using constant-composition cooks (l:s = 41:1), the influence of [OH<sup>-</sup>], [HS<sup>-</sup>], [Na<sup>+</sup>] and temperature on the removal of AX, GGM, C and hexenuronic acid (4-deoxyhex-4-enuronic acid or HexA) was investigated after a pre-treatment at 135 °C, [OH<sup>-</sup>] = 0.5 mol L<sup>-1</sup>, [HS<sup>-</sup>] = 0.3 mol L<sup>-1</sup>, [Na<sup>+</sup>] = 1.3 mol L<sup>-1</sup> for 60 min [52]. HexA is formed from 4-O-methyl- $\alpha$ -D-glucuronic acid after  $\beta$ -elimination of methanol during the heating-up periods of the kraft cook [9,10]. The presence of HexA causes an increased consumption of KMnO<sub>4</sub> during kappa number determination, and thus contributes to the kappa number in a manner that 11.6  $\mu$ mol of HexA corresponds to 1 kappa unit, according to Li and Geller-



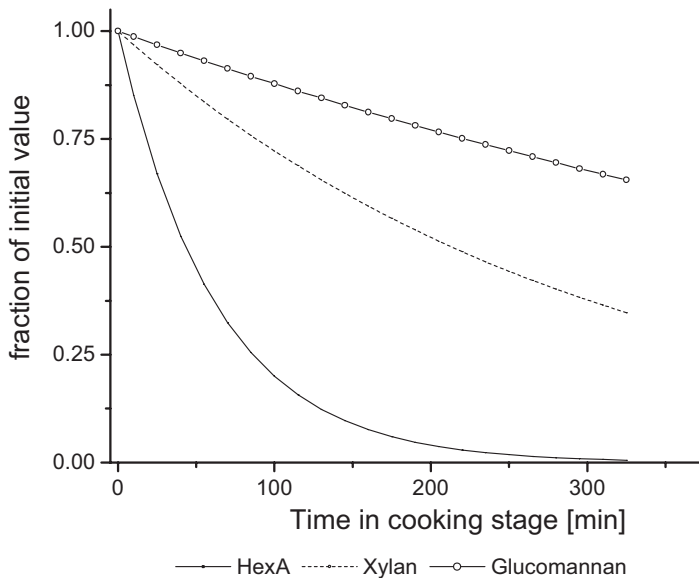
stedt [11]. The initial concentrations of AX, GGM, and HexA after the pretreatment were 4.5% on wood (-48%), 4.7% on wood (-72.5%) and 47  $\mu\text{mol g}^{-1}$  pulp (% on wood), respectively. According to the kinetic model, the rate of hexenuronic acid removal increases with increasing hydroxyl ion concentration, increasing ionic strength, increasing hydrogen sulfide concentration, and increasing cooking temperature. Taking the delignification kinetics into account, this means that at a given corrected kappa number (the kappa number of HexA is subtracted) the hexenuronic content can be reduced by applying a high hydroxyl ion concentration, a high ionic strength, a low cooking temperature, and a low hydrogen sulfide concentration. There are indications that the removed hexenuronic acid is partly dissolved together with xylan, and partly degraded. The residual xylan and glucomannan fractions are less affected by the cooking conditions as compared to hexenuronic acid, probably due to the removal of the reactive part of the compounds during the pretreatment. The rate of xylan and glucomannan degradation increases with increasing hydroxyl ion concentration, increasing hydrogen sulfide concentration and increasing cooking temperature. The rate of xylan removal decreases with increasing sodium ion concentration, whereas the rate of glucomannan removal remains unaffected by the ionic strength. This translates into a reduction of the xylan content at a given corrected kappa number with increasing hydroxyl ion concentration and decreasing hydrogen sulfide concentration.

Applying the kinetic model developed by Gustavsson and Al-Dajani, the course of degradation of the three hemicellulose-derived compounds, normalized to their initial values after the pretreatment, is compared on the basis of constant cooking conditions ( $[\text{OH}^-] = 0.44 \text{ mol L}^{-1}$ ,  $[\text{HS}^-] = 0.28 \text{ mol L}^{-1}$ ,  $[\text{Na}^+] = 1.3 \text{ mol L}^{-1}$ , and temperature 170 °C) [52]. The results, shown in Fig. 4.54, clearly demonstrate the decrease in stability at the given conditions according to the sequence: GGM > AX > HexA.

The dissolution of glucomannan takes place during the early stage of the cook, the compound being degraded to low molecular-weight fragments. Consequently, no decisive differences in the glucomannan content of differently prepared kraft pulps can be expected (see Tab. 4.28).

#### *Structural changes of softwood xylan*

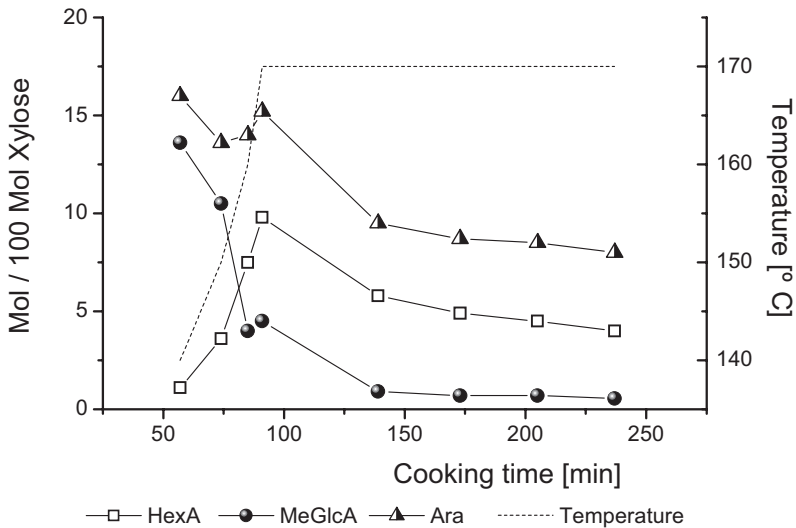
Softwood xylan is composed of a linear chain of (1→4)-linked  $\beta$ -D-xylopyranose units which are partially substituted at C-2 by 4-O-methyl- $\alpha$ -D-glucuronic acid groups, on average two residues per ten xylose units. Additionally, the  $\alpha$ -L-arabinofuranose units are substituted at C-3 by an  $\alpha$ -glycosidic linkage, on average 1.3–1.6 residues per ten xylose units [53]. In kraft pulping, the structure of the xylan undergoes extensive modifications and degradations. In one study, the xylan in pine kraft accessible to xylanase degradation was analyzed with respect to the structural modifications [54]. From the surface of the unbleached pine kraft pulp with kappa number 26, approximately 25% of the xylan was selectively solubilized. The total amount of carboxylic groups of a pine kraft pulp with kappa number 25 ranges between 110 and 120  $\text{mmol kg}^{-1}$ , depending on the cooking conditions [55]. In the accessible surface xylan, the ratio of xylose to uronic acids was reduced from 5:1,



**Fig. 4.54** Comparative evaluation of the degradation rates of the xylan, glucomannan, and hexenuronic acid fractions for the given cooking conditions ( $[\text{OH}^-] = 0.44 \text{ mol L}^{-1}$ ,  $[\text{HS}^-] = 0.28 \text{ mol L}^{-1}$ ,  $[\text{Na}^+] = 1.3 \text{ mol L}^{-1}$ , and temperature  $170^\circ\text{C}$ ) by applying the kinetics model developed by Gustavsson and Al-Dajani [52]. Values normalized to the initial values determined after a pretreatment step ( $135^\circ\text{C}$ , 60 min,  $[\text{OH}^-] = 0.5 \text{ mol L}^{-1}$ ,  $[\text{HS}^-] = 0.3 \text{ mol L}^{-1}$ ,  $[\text{Na}^+] = 1.3 \text{ mol L}^{-1}$ ,  $l:s = 31:1$ ). Spruce chips were used in these experiments.

which was present in the native wood, to 20:1 in the kraft pulp with kappa number 26. Hence, 75% of the initial uronic acids were removed during the kraft cook. Assuming a xylan content of 8% on o.d. pulp ( $606 \text{ mmol kg}^{-1}$  pulp), uronic acids accounted for approximately 28% ( $606 \times 0.05 = 30.3 \text{ mmol kg}^{-1}$ ) of the total carboxylic groups. The major part thereof (namely 88%) consisted of hexenuronic acids. The 4-*O*-methylglucuronic acid side groups were extensively degraded already in the early stages of the cook (Fig. 4.55). As mentioned earlier, the hexenuronic acid was rapidly formed during the heating-up period, attained a maximum, and then was gradually degraded parallel to the H-factor. Arabinose side groups are rather stable during a kraft cook, the degradation occurring simultaneously with degradation of the hexenuronic acids. The total degree of substitution of surface xylan comprising both the uronic acids and arabinose was reduced from 0.3 in the pine wood to 0.13 in the kraft pulp, kappa number 26.

The amount of HexA is also dependent on the wood species. It is clear that hardwoods contain more 4-*O*-methylglucuronoxylan than softwoods, and this is the main reason why about 50% more HexA is formed during hardwood pulping as compared to softwood under comparable conditions. The amount of HexA in *Eucalyptus globulus* kraft pulps passes through a maximum content of HexA, about  $55 \text{ mmol kg}^{-1}$  pulp, in the kappa number range 11–18, and then decreases rapidly



**Fig. 4.55** Course of the structural changes of the accessible part of xylan during a conventional pine kraft cook (according to [54]). The carbohydrates, solubilized by enzymatic peeling, were analyzed using  $^1\text{H}$  NMR spectroscopy.

towards a lower kappa number [56]. The minimum level remains rather high ( $30\text{--}40\ \mu\text{mol kg}^{-1}$  pulp), even when reinforced conditions are applied (high temperature, high EA dosage).

The higher selectivity in modified cooking is achieved through a more uniform concentration profile for active cooking chemicals and a minimum concentration of dissolved lignin during the final part of the cook. Dissolved xylan is therefore shifted to earlier stages of the cook, whereas the EA concentration increases towards the end of the cook. It can be expected that these two measures influence the adsorption of xylan as well as the final pulp yield [57]. Comparative kraft pulping experiments using *Pinus sylvestris* L. as a wood source concluded that the adsorption of xylan can take place at a relatively high EA concentration of about  $0.4\ \text{mol L}^{-1}$ , and also early in the cook. The xylan that is lost and not adsorbed onto the fibers through the change in cooking conditions appears to be compensated for by a reduced dissolution of carbohydrates, most likely due to the milder cooking conditions [57]. Taking these factors into account, it may be concluded that the final yield for modified continuous cooking is about the same as for conventional cooking at a given kappa number.

Pekkala reports a slight increase in the xylan yield when the cook is prolonged which is explained by the sorption of dissolved xylan back onto the fibers [58].

Results from mill trials with modified continuous cooking for extended delignification indicate that the yield at a given kappa number is even slightly higher than that in conventional continuous cooking [59].

Table 4.28 lists the carbohydrate composition of pulps from conventional batch and continuous liquor flow cooking, simulating the conditions of modified continuous cooking by introducing dissolved xylan at different phases of the cook.

**Tab. 4.28** Relative carbohydrate composition of pulps from conventional batch and continuous liquor flow cooking series. (From Ref. [57].)

Series	Cooking process	Xylan addition <sup>a)</sup> [time interval, min]	Relative composition [%]				
			Glu	Xyl	Man	Ara	Gal
CB	Conventional batch		84.6	8.5	6.4	0.5	0
CLF-early	Continuous liquor flow	70–130	86.4	7.1	5.9	0.4	0.2
CLF-late	Continuous liquor flow	90–150	85.6	7.4	6.2	0.5	0.3
CLF-ref	Continuous liquor flow	no addition	87.8	6.1	5.7	0.2	0.2

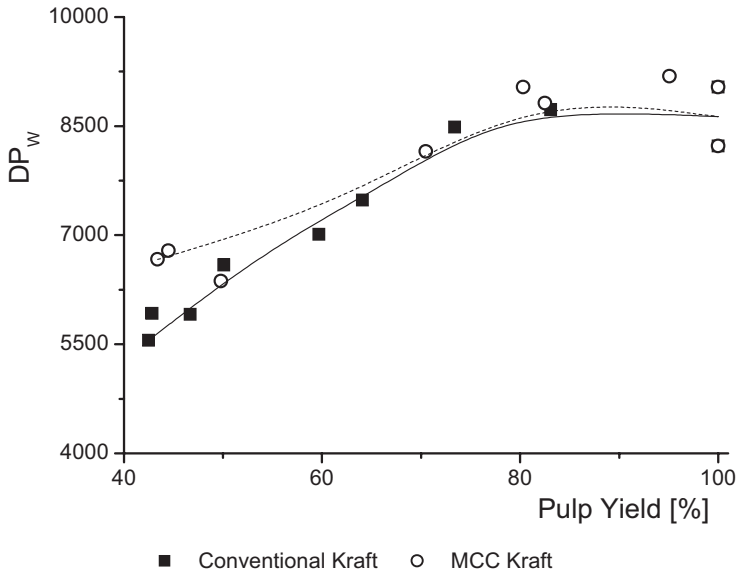
a) Xylan concentration 3.5 g L<sup>-1</sup>.

There appears to be no significant difference in the observed xylan content between the series of early (CLF-early) and late xylan addition (CLF-late), the latter simulating a conventional batch cooking system. As expected, the xylose content is highest in pulps from the conventional batch cooks, and lowest in pulps from the continuous liquor flow cooks without xylan addition (CB and CLF-ref). Pulps from pilot plant trials using a Lodgepole pine/spruce mixture as raw material indicate that the xylan content of a rapid displacement heating (RDH) pulp with a kappa number of 26.7 is slightly lower (7.9% on unbleached pulp) as compared to a pulp from a conventional batch cook with a kappa number 33.5 (8.6% on unbleached pulp) [60].

Cellulose degradation was monitored during both conventional kraft and modified continuous kraft (MCC) pulping of *Pinus radiata* using gel permeation chromatography (GPC) measurement of isolated holocellulose fractions [61]. The molecular mass of the cellulose fraction was determined by assuming that all the cellulose molecules eluted until a certain elution volume was reached. The results suggest that, in both the conventional and modified processes, cellulose degradation takes place only at pulp yields lower than 75%. From this result it can be concluded that cellulose degradation becomes apparent only after initial delignification has completed.

The extent of cellulose chain scissions during bulk and residual delignification is thus more pronounced for conventional kraft pulping as compared to MCC pulping (Fig. 4.56).

The results are in line with the experience from practice that MCC pulping is more selective with respect to cellulose degradation than conventional kraft pulping.



**Fig. 4.56** Degree of polymerization ( $DP_w$ ) of the cellulose fraction from conventional kraft and MCC pulps (according to [61]). Holocellulose was isolated according to the method of Holmes and Kurth [62] from the pulps prior to GPC measurement. The weight average mole-

cular weight was determined from the tricarbanilate, considering only the high molecular-weight peak and assuming that no cellulose is eluted with the second peak at the higher elution volume.

### Pulp Strength Delivery

Industrially produced softwood kraft pulps typically show only 60–80% of the strength performance as compared to laboratory reference pulps. The strength delivery is defined as the percentage of the tear index at a given tensile index from an industrially cooked pulp in relation to the corresponding tear index of a laboratory reference pulp from the same chip material. Extensive mill studies revealed an average strength delivery from softwood batch cooking of 72% and 73%, respectively [63,64]. The major reason for the low strength delivery of industrially cooked pulps has been attributed to the hot blow which exerts a destructive effect on the pulp fibers [22]. The development of a more gentle pump discharge improved the strength delivery to 84% as compared to only 70% using hot blow discharge [65]. Surprisingly, the deleterious effect of hot blow on strength delivery diminishes when cooking is performed according to the displacement technology, as reported for the Superbatch technology. Mill trials at the Joutseno-Pulp Oy's digester house confirmed that when using liquor displacement cooking technique the blow method made very little difference in the strength delivery. Blowing a kappa-30 displacement batch cook without terminal displacement directly at cooking temperature still resulted in about 90% strength delivery as compared to 100% in the case of a cold blow (see Tab. 4.29) [66].

**Tab. 4.29** Strength delivery (percentage of tear index at  $70 \text{ Nm} \cdot \text{g}^{-1}$  tensile index to reference laboratory pulps) of industrially cooked softwood pulps at different kappa number levels, and for both cold and hot blow (according to [66]).

Properties	Unit	Cold blow	Hot blow	Hot blow
<b>Kappa level</b>		<b>30</b>	<b>22</b>	<b>30</b>
Tear index <sup>a</sup>	$\text{mNm}^2 \text{g}^{-1}$	18	17	16
Strength delivery	%	100	94	89

a) At tensile index  $70 \text{ Nm} \cdot \text{g}^{-1}$

From the results shown in Tab. 4.29, it can be indirectly concluded that strength delivery is improved from 72% (tear index  $13 \text{ mN m}^2 \text{g}^{-1}$ ) to 89% (tear index  $16 \text{ mN m}^2 \text{g}^{-1}$ ) by applying displacement technology. An additional reduction of the severity of the discharge (e.g., by using cold pump discharge) further increases the tear index from 16 to  $18 \text{ mN m}^2 \text{g}^{-1}$ . Thus, it can be concluded that by using displacement cooking technology, pulps that are less vulnerable to the blow conditions are produced. According to Tikka et al., the improved delignification selectivity of the displacement batch cook is affected by the modified cooking chemistry, in which black liquor with a high sulfidity seems to be the key factor [66]. The pre-treatment promotes selectivity and further reduces the required cooking H-factor by 20–30%. The strength deficit is therefore due to a combination of cooking conditions and the severity of discharge methods.

### Residual Lignin Structures

The kappa number in unbleached and also bleached kraft pulps is made up of lignin and other oxidizable structures denoted as false lignin. The latter contains contributions from hexenuronic acid groups (HexA) and “non-lignin” structures [67] (one kappa number unit corresponds to  $11.6 \mu\text{mol HexA}$  [68]). The amount of true residual lignin can be measured directly using the Ox-Dem kappa number method [69]. The contribution to the kappa number of the “non-lignin” structures can then be calculated as the difference between the standard pulp kappa number and the sum of the contributions of the residual lignin and HexA. It was shown that about 24% of the kappa number in spruce kraft pulp and about 41% of the kappa number in birch kraft pulp can be attributed to false lignin structures. In absolute values, the false lignin accounts to approximately 5–6 kappa number units for both softwood and hardwood kraft pulps [67]. In the softwood kraft pulp the “non-lignin” structures dominate the false lignin fraction, whereas in the hardwood kraft pulp HexA constitutes the main part of the false lignin (Tab. 4.30).

**Tab. 4.30** Fractionation of pulp kappa number of spruce and birch kraft pulps before and after oxygen delignification (according to [67]).

Pulp	Kappa number	Ox-Dem Kappa number	Kappa from HexA	Kappa from "non-lignin"
Spruce kraft pulp				
Unbleached	22.5	17.2	1.3	4.0
O-delignified	10.7	4.6	1.2	4.9
Birch kraft pulp				
Unbleached	13.8	8.1	4.7	1.0
O-delignified	9.6	3.2	4.3	2.1

Oxygen delignification is, in fact, a highly efficient delignification agent for both softwood and hardwood pulps. Although the total kappa numbers indicate only about 52% and 30% reduction, the degree of lignin removal is about 73% and 60%, respectively. Table 4.30 also shows that the "non-lignin" structures are formed during the kraft cook, and to some extent also during the oxygen delignification stage. It has been speculated that these structures originate from carbohydrate moieties which undergo elimination of water, with the final products being aromatic structures containing catechols and chromones [70]. The elimination reactions may result in keto groups in equilibrium, with the corresponding enol structures being located along the carbohydrate chain, in for example, hemicelluloses. Successive DMSO + 5% KOH extraction experiments revealed that a decrease in the amount of xylan is accompanied by a near-equivalent decrease in the amount of "non-lignin" structures, which suggests that the accessible part of the xylan is the main source of false lignin [71]. With prolonged cooking, the content of conjugated carbonyl groups in pulp dioxane lignin increases slightly [72]. The proportion of the glucose content in pulp dioxane lignin rises during cooking, while the proportions of mannose and galactose decline and those of arabinose and xylose remain rather constant. This might indicate that the pentoses form relatively alkali-stable complexes with lignin [72].

The presence of alkali-stable chromophores based on carbohydrate structures makes it likely that lignin-carbohydrate complexes (LCC) play an important role in limiting the efficiency of oxygen delignification. The progressive removal of hemicelluloses (e.g., xylan) from a *Eucalyptus saligna* prehydrolysis kraft pulp (PHK) clearly results in a significant improvement of the oxygen delignification efficiency. The kappa number of the unbleached pulps is adjusted to a comparable level (9–12) by controlling the H-factor [73]. A selection of the most important results is displayed in Tab. 4.31.

Tab. 4.31 Influence of prehydrolysis intensity, measured as P-factor, on the efficiency of oxygen delignification (according to [73]).

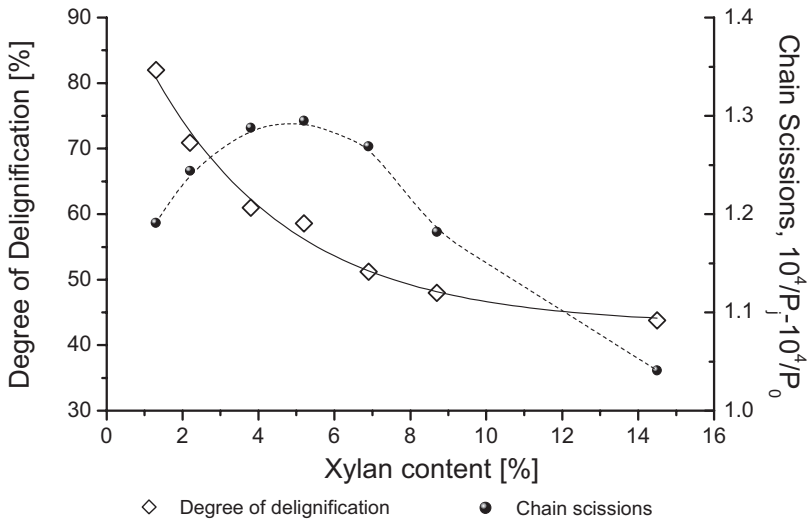
Cook #	Cooking Process		Unbleached <i>Euca</i> -PHK pulp				OO-delignified <i>Euca</i> -PHK pulp			
	P-factor	H-factor	Yield [%]	Kappa	Viscosity [mL g <sup>-1</sup> ]	Xylan [%]	Kappa	Δ kappa [%]	Viscosity [mL g <sup>-1</sup> ]	Chain scissions [0.1·mmol AHG <sup>-1</sup> ]
Ka118	0	1057	47.7	11.7	934	14.5	6.6	43.6	772	1.041
Ka121	107	708	43.7	12.3	1411	8.7	6.4	48.0	1008	1.182
Ka124	1701	708	42.91	9.0	1152	6.9	4.41	51.1	865	1.269
Ka125	210	368	41.4	9.9	1353	5.2	4.1	58.6	957	1.295
Ka127	310	368	40.6	8.8	1304	3.8	3.4	61.4	936	1.288
Ka129	710	368	36.5	9.0	1112	2.2	2.6	71.1	848	1.244
Ka131	1900	368	31.6	11.1	668	1.3	2.0	82.0	578	1.191

Oxygen delignification was performed in a two-stage reaction without interstage washing, with 15 min retention time in the first and 60 min in the second reactor, respectively. The reaction temperature was kept constant at 110 °C throughout both stages. The total alkali charge of 25 kg t<sup>-1</sup>, was added in the first stage. The data in Tab. 4.31 indicate that the efficiency of oxygen delignification improves along with the removal of the xylan content. Parallel with the reduction in the hemicellulose content, the number of chain scissions increases until a residual xylan content of approximately 5% is reached. When the residual xylan content is further reduced to below 2%, the residual cellulose fraction again becomes more resistant to degradation reactions (Fig. 4.57).

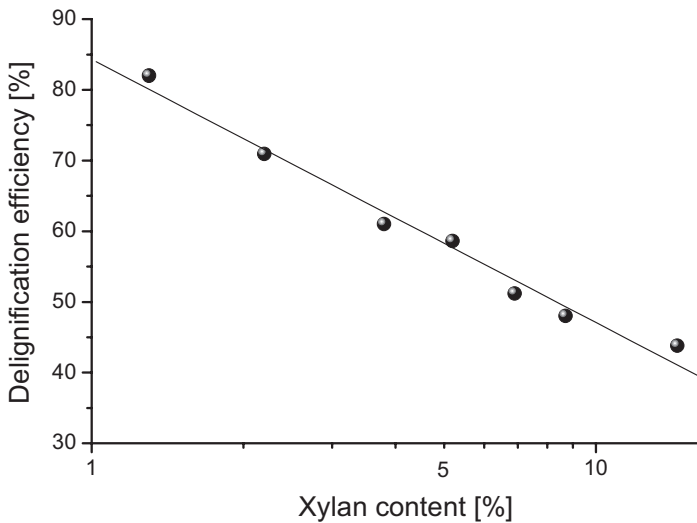
Interestingly, the degree of delignification during the oxygen delignification stage is linearly correlated with the logarithm of the xylan content of the *Eucalyptus saligna* prehydrolysis kraft pulp (Fig. 4.58).

Recently, the correlation between the residual amount of hemicelluloses and delignification efficiency during oxygen delignification was confirmed for both softwood and hardwood kraft pulps, with and without pre-hydrolysis [74]. Surprisingly, the kappa numbers of the pulps after oxygen delignification display a very similar final lignin content, expressed as Ox-Dem kappa. The kraft pulps without pre-hydrolysis (paper-grade pulps) contain a considerably higher amount of “non-lignin” and HexA structures as part of the kappa number as compared to the pre-hydrolysis kraft pulps (dissolving pulps). As shown previously, the false lignin fraction which is predominantly derived from carbohydrate structures is not susceptible to oxygen delignification. On the contrary, during oxygen delignification the proportion of “non-lignin” kappa number fractions even increases. The presence of chemical linkages between cellulose, the residual hemicellulose and the residual lignin in native wood were reported by Isogai et al. [75], and the





**Fig. 4.57** Influence of the residual xylan content of a *Eucalyptus saligna* prehydrolysis kraft pulp on the delignification efficiency and number of chain scissions in a subsequent oxygen delignification stage (OO: 15/60 min, 110 °C, 25 kg NaOH t<sup>-1</sup>) (according to [73]).



**Fig. 4.58** Influence of the residual xylan content of a *Eucalyptus saligna* prehydrolysis kraft pulp on the delignification efficiency in a subsequent oxygen delignification stage (OO: 15/60 min, 110 °C, 25 kg NaOH t<sup>-1</sup>) (according to [73]).

formation of alkali-stable ethers and carbon-carbon linkages during kraft pulping were reported by Ohara et al. [76] and Gierer and Wännström [77]. Iversen and Wännström proposed the alkali-catalyzed formation of ether bonds between carbohydrate hydroxyl groups and lignin oxiranes derived from the degradation of the lignin molecule during kraft pulping [78].

The most prominent lignin structures, which are responsible for the reactivity in subsequent bleaching treatments, are the alkyl-aryl ether linkages ( $\beta$ -O-4-structures), the methoxyl groups, the aliphatic and aromatic hydroxyl groups and the hydrophilic substituents, such as carbonyl and carboxylic groups [79]. Moreover, the macromolecular properties of the residual lignin provide additional information about the conditions during the delignification reactions. Unfortunately, there is still no method for the isolation of a representative residual lignin of unchanged physical and chemical structure. The acidolytic and enzymatic hydrolysis methods are used for the isolation of residual lignin. Additionally, a combination of enzymatic and acidic hydrolysis as a two-step procedure was proposed [80]. The latter shows some advantages with respect to the yield and the amount of impurities in comparison to the one-step procedure. The dioxane acidolysis, which is still the most common method, produces pure lignin of only about 40% yield. Unfortunately, the  $\beta$ -aryl-ether and lignin-carbohydrate linkages are cleaved during the isolation procedure, which is seen as a reduction in the molecular weight of the lignin and in an increased phenolic hydroxyl group content [81]. According to Gellerstedt et al., the formation of condensed phenolic groups during acidolysis is not probable [82]. Although residual lignin can be recovered quantitatively after enzymatic hydrolysis, the isolated lignin contains large amounts of impurities which aggravate structural lignin characterization to a significant degree.

There are some indications that modern modified cooking technologies alter the structure of residual kraft lignin beneficially for subsequent bleaching treatments. The residual lignin isolated from a hemlock EMCC kraft pulp using a dioxane acidolysis protocol shows a lower amount of condensed phenolic and higher amounts of carboxylic acids and uncondensed phenolic units as compared to the residual lignin structure from a conventional hemlock kraft pulp [83]. Comparative data from lignin characterizations are listed in Tab. 4.32.

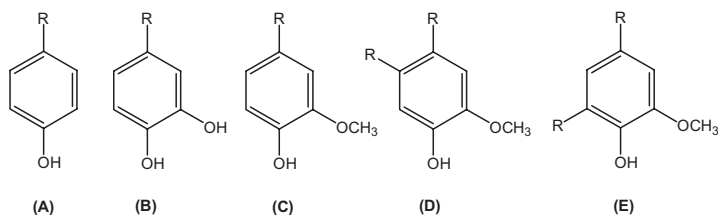
The enrichment of carboxylic groups during kraft cooking is followed by the elimination of aliphatic hydroxyl groups, which are decreased from 4.27 mmol g<sup>-1</sup> in case of the milled wood lignin to 2.14 resp. 2.15 mmol g<sup>-1</sup> for the residual lignin isolated from the hemlock unbleached kraft pulps (Tab. 4.32). This is in agreement with the growing elimination of the  $\alpha$ -hydroxyl groups present in  $\beta$ -O-4 ether units. The relatively high content of primary hydroxyl groups in the wood lignin can be expected to be diminished during pulping because of the known reactions in which the  $\gamma$ -carbon is eliminated as formaldehyde. The content of the primary hydroxyl groups is significantly higher in the residual lignin isolated from the conventional spruce kraft pulp as compared to the residual lignin from modified kraft pulp (0.24 mol per aromatic unit versus 0.33 mol per aromatic unit, respectively) [84].

**Tab. 4.32** Comparative evaluation of the residual lignin structures isolated from milled wood lignin, unbleached conventional and EMCC kraft pulps (according to [83]).

Parameters	Units	MWL <sup>b)</sup>	Hemlock kraft pulps	
			Conv. Kraft	EMCC Kraft
Kappa number			26.8	26.0
Isolation yield <sup>a)</sup>	%	14.2	49.5	46.7
Elemental composition				
C	%	61.0	65.2	62.8
H	%	5.7	5.7	5.7
O	%	32.9	27.9	29.8
S	%		1.2	1.7
OCH <sub>3</sub>	%	15.3	12.1	10.5
Carboxylic groups	mmol g <sup>-1</sup>	0.15	0.32	0.54
Hydroxyl Units				
Aliphatic hydroxyls	mmol g <sup>-1</sup>	4.27	2.14	2.15
Phenolic hydroxyls	mmol g <sup>-1</sup>	1.15	2.71	2.50
Type A	mmol g <sup>-1</sup>	0.02	0.02	0.01
Catechol (type B)	mmol g <sup>-1</sup>	0.05	0.21	0.17
Guaiacol (type C)	mmol g <sup>-1</sup>	0.62	0.23	0.56
Type D	mmol g <sup>-1</sup>	0.06	0.38	0.27
Type E	mmol g <sup>-1</sup>	0.35	1.64	1.32

a) Continuous dioxane acidolysis (dioxane-water = 85:15, 0.1 mol/l HCl).

b) Milled wood lignin from spruce.



The content of  $\beta$ -O-4-structures in residual lignin decreases with the extent of delignification. The residual lignin in the EMCC pulp with kappa number 17.9 contained less  $\beta$ -O-4 structures and a higher content of C5 condensed structures as compared to the residual lignin of conventional kraft pulp with kappa number 27.4 [85]. This is in accordance with the results obtained from the characterization of residual lignins isolated from MCC and Super-Batch pulping technologies [86]. George et al., however, made different observations comparing residual lignins isolated from spruce kraft pulps using also a dioxane acidolysis procedure [84]. The number of alkyl-O-aryl linkages, determined by  $^{13}\text{C}$ -NMR, was higher in the modified residual lignin than in the conventional residual lignins. This observation is in accordance with the higher amount of free phenolic groups present in the conventional lignin. In a recent comparative study of conventional and laboratory-simulated EMCC kraft pulps produced from *Pinus elliottii*, the residual lignin of the latter had a higher content of  $\beta$ -O-4-structures and carboxylic groups. At comparable kappa number, the amount of condensed structures was, however, similar for both residual lignins [87].

The total phenolic hydroxyl content in the residual lignin continuously increases during kraft pulping due to progressive cleavage of the  $\beta$ -O-4 bonds. The guaiacol-type of phenolic unit (type C) gradually decreases in parallel with the progress in delignification. Conditions favoring the formation of unreactive carbon-carbon bonds prevail, especially during conventional kraft cooking [88]. As shown in Tab. 4.32, the amount of phenolic units substituted at the C5 position (type E) continuously rise in both the dissolved and residual lignins. The  $\text{Ca}$ -C5 and the diphenylmethane units are described as the predominant C5 condensed structures [89]. The formation of the diphenylmethane moieties has been described as a considerably more facile reaction under soda pulping conditions as compared to kraft pulping conditions. This may be one of the reasons why the bleaching of soda pulps is more difficult compared to a kraft pulp at a given kappa number [90]. Recently, the accumulation of completely unreactive 5-5'-biphenolic hydroxyl groups was detected using quantitative  $^{31}\text{P}$ -NMR [91]. The final concentration of the 5-5' structures after softwood kraft pulping was approximately  $0.6 \text{ mmol g}^{-1}$ , and thus more than three-fold higher than the corresponding value of  $0.2 \text{ mmol g}^{-1}$  detected for the milled wood lignin.

The molecular weight of the residual lignin increases slightly towards the end of the cook, which may be an indication of progressive condensation reactions [83]. Lignin from pulps and corresponding spent liquors during kraft pulping of *Pinus sylvestris* covering the kappa number range between 116 and 17 were isolated by acidic dioxane extraction and characterized by GPC, UV and IR spectroscopy and oxidative degradation methods [72]. The average molar mass of both lignin precipitated from the spent liquor and lignins isolated from pulps increases with the progress in cooking. The lignins extracted from pulps showed a higher molar mass as compared to the spent-liquor lignins.

In accordance with the higher content of phenolic hydroxyl groups, the conventional kraft residual lignin exhibits a lower molecular mass than the modified residual lignin at a given kappa number [84]. In extending the cook from kappa

number 30 to kappa number 15, the molecular weight of the modified residual lignin continues to decrease, whereas that of the conventional residual lignin is not influenced [84]. Since the number of phenolic hydroxyl groups in the case of the residual lignins of both pulps remained constant, it may be assumed that rupture of the ether bonds immediately leads to lignin dissolution. Extending the conventional cook results in a significant decrease in the number of methoxyl groups. This trend is less pronounced with modified cooks. The loss in methoxyl groups may also be accounted for by a slight enrichment in *p*-hydroxyphenyl units toward the end of the cook. It is known that the cleavage of alkyl-aryl ether linkages is favored by the presence of methoxyl groups. Consequently, guaiacyl units can be assumed to be removed prior to *p*-hydroxyphenyl units. In contrast to the modified residual lignin, the content of quaternary carbons is significantly reduced in case of the conventional residual lignin, which may be attributed to the enrichment in *p*-hydroxyphenyl units.

#### **Influence on Bleachability**

The bleachability of kraft pulps can be defined as the consumption of chemicals required to achieve a given target brightness using a specific bleaching sequence, either ECF or TCF. To better compare the application of different bleaching chemicals, the bleaching chemical consumptions are calculated and expressed in oxidation equivalents (OXE) [92]. The unit mass of a bleaching chemical (e.g., 1 kg) corresponds to the molar equivalent of mass transferring 1 mol of electrons. The oxidation equivalents of 1 kg of the most important bleaching chemicals applied in ECF and TCF bleaching are listed in Tab. 4.33.

The bleachability of pulps can be expressed in several ways, for example, as the sum of oxidation equivalents (OXE) divided by the ingoing kappa number for each stage in a sequence or as OXE per ingoing kappa number or the kappa number removed over the whole sequence.

**Tab. 4.33** Oxidation equivalents (OXE) of the unit mass of the most important bleaching chemicals (according to [92].)

<b>Bleaching chemicals</b>	<b>OXE kg<sup>-1</sup></b>
Chlorine dioxide	74.1
Active chlorine	28.8
Hydrogen peroxide	58.8
Oxygen	125.0
Ozone	125.0
Peracetic acid	26.3

Definitions for the bleachability based on OXE:

$$\sum_{i=1}^i \frac{OXE}{Kappa_{i-1}}$$

$$\frac{\sum_{i=1}^i OXE_i}{Kappa_0}$$

$$\frac{\sum_{i=1}^i OXE_i}{\Delta Kappa}$$

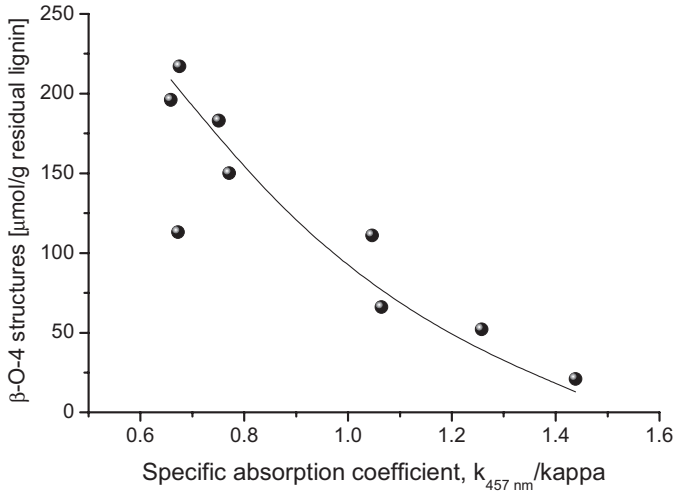
The amount of hexenuronic acid is not significantly changed during, for example, the oxygen delignification or peroxide bleaching. Thus, it can be assumed that HexA does not consume any bleaching chemical in these stages. For bleaching stages where HexA is not oxidized, the specific OXE consumption must be referred to a kappa number which is corrected for the hexenuronic acid (\*\* means that one kappa number unit corresponds to 11.6  $\mu\text{mol}$  of HexA [68]). In case of, for example ozone bleaching, the specific OXE consumption is referred to the whole kappa number as hexenuronic acid is completely oxidized by ozone. The bleachability can also be expressed by the ratio between the light absorption coefficient,  $k$ , determined at a wavelength of 457 nm, and the corresponding kappa number corrected (\*\*) or uncorrected for the content of hexenuronic acids from the pulp investigated [93]:

$$\frac{k_{457\text{ nm}}}{Kappa_{(**)}}$$

The enhanced bleachability of modified cooked pulps can be attributed to changes in by-product chemistry. In principle, the residual lignin in modified cooked pulps is less condensed and therefore likely to be more readily solubilized in subsequent bleaching stages [94]. Moreover, it has been suggested that xylan compounds which are re-deposited during the cook form a physical barrier for the extraction of residual lignin. The mass transfer limiting phenomenon is assumed to hamper delignification in both the final phase of cooking and in subsequent bleaching [95].

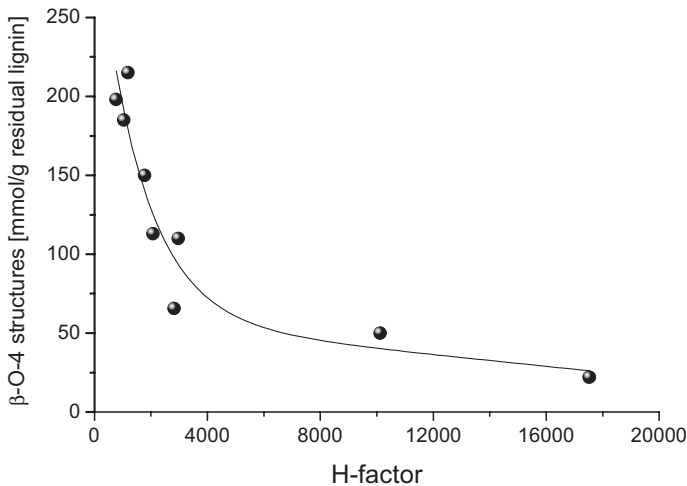
Pulp bleachability tends to correlate also with the content of  $\beta$ -aryl ether structures. Thioacidolysis can be used to estimate the amount of  $\beta$ -arylether structures in the residual lignin [96]. Pulps with a low concentration of  $\beta$ -O-4-structures exhibit a high specific absorption coefficient, as seen in Fig. 4.59.

This concludes that a large amount of  $\beta$ -O-4-linkages in the residual lignin indicates a low concentration of chromophores per kappa number unit. The  $\beta$ -O-4-structures are degraded with prolonged cooking intensity. Thus, there is a steep decrease of these structures until an H-factor of approximately 3000 is attained.



**Fig. 4.59** Relationship between the concentration of  $\beta$ -O-4-structures (determined by thioacidolysis) and the specific light absorption coefficient of the residual lignin of softwood kraft pulps (according to [97]).

Further prolongation of cooking intensity causes only an insignificant decrease in the amount of  $\beta$ -O-4-structures. A relationship between the concentration of  $\beta$ -aryl ether linkages and the H-factor of kraft cooking is shown in Fig. 4.60.



**Fig. 4.60** Course of the content of  $\beta$ -aryl ether linkages in residual lignins during kraft cooking as a function of cooking intensity expressed as H-factor (according to [97]). Softwood kraft pulps delignified to kappa number of approximately 20 with different cooking conditions, e.g., time (39 to 2602 min), hydroxide concentrations ( $[\text{OH}^-] = 0.55\text{--}1.5 \text{ mol L}^{-1}$ ), sulfidities ( $[\text{HS}^-] = 0.075\text{--}0.5 \text{ mol L}^{-1}$ ) and temperatures ( $T = 154\text{--}181 \text{ }^\circ\text{C}$ ).

The influence of pulping variables is clearly reflected in the specific amount of  $\beta$ -O-4-structures. When the  $[\text{OH}^-]$  is increased while keeping the  $[\text{HS}^-]$  and temperature constant, the content of  $\beta$ -O-4 structures is found to increase. The same observation is made when the  $[\text{HS}^-]$  is increased with the  $[\text{OH}^-]$  and the temperature constant, or when the temperature is increased with the other parameters unchanged. It is well known that an increase in  $[\text{OH}^-]$  enhances the rate of delignification. Clearly, the accelerated rate of delignification leaves a residual lignin in the pulp with a large amount of remaining  $\beta$ -O-4-structures at the given kappa number. Since hydrogen sulfide ions promote the cleavage reactions, the positive correlation with the amount of  $\beta$ -O-4 structures might be interpreted as a result of the significantly shorter reaction times at the higher  $[\text{HS}^-]$  to be the determining factor.

The color of the unbleached (kraft) pulps originates from a complex mixture of certain unsaturated structures which are denoted as chromophores. Very small amounts of conjugated structures with a very high specific absorption coefficient are sufficient to darken the pulp material. Most of the chromophores are certainly derived from lignin structures. As mentioned above, they may also originate from unsaturated structures of the polysaccharides such as hexenuronic acid (HexA) and aromatic structures containing catechols and chromones which evolve from carbohydrate moieties after the elimination of water and other molecules [70].

Moreover, metal ions bound to the unbleached pulp can originate chromophores, probably due to the formation of a complex with a catechol structure. The contribution of certain metal ions such as Mn, Cu, Fe, Mg, Al and others to the color of a pulp will be of increasing importance with the increasing closure of the water cycle in the washing and bleaching areas.

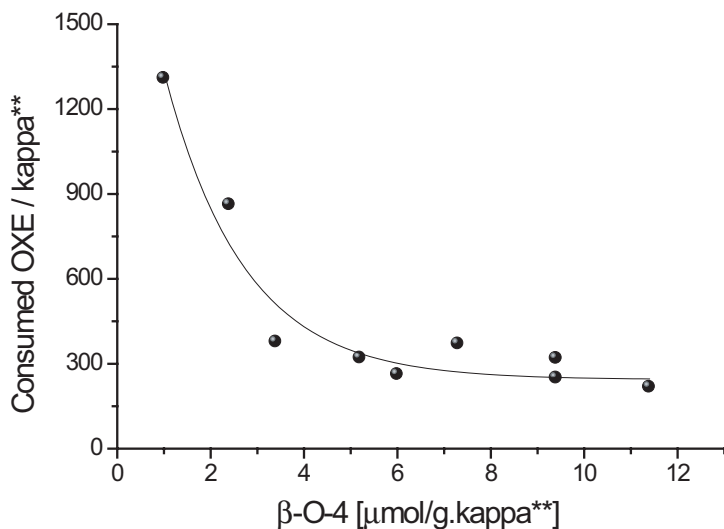
The precipitation of lignin from the black liquor might also be a source of lowering pulp brightness. The dissolved lignin shows a higher light absorption coefficient than lignin isolated from the pulp. The extent of precipitation correlates with the concentration of lignin dissolved in black liquor and with decreasing pH [97,98].

The bleachability of pulps may be related to the conditions that prevail during the kraft cook. In a detailed study, the influence of the most important parameters in kraft cooking of softwood (*Pinus sylvestris*) on TCF bleachability has been investigated [97]. It is clear that a pure peroxide-containing bleaching sequence such as a QPQP-sequence behaves more sensitively to different chromophore structures in the residual lignin as compared to an ozone-containing sequence (e.g., AZQP). The latter shows no influence on cooking temperature, whereas the former reveals an improved bleachability when the cooking temperature for pulps produced with low and medium  $[\text{OH}^-]$  is high. It is known that the bleachability of kraft pulps is improved when the EA charge is increased [99,100]. Interestingly, there is an optimum EA charge with respect to bleachability. This optimum is observed in both QPQP- and AZQP-bleaching for a hydroxide ion concentration of  $1.0 \text{ mol L}^{-1}$ . Beyond this EA concentration, the bleachability becomes impaired. The bleachability in QPQP-treatment is further improved by increasing the hydrogen sulfide ion concentration in the kraft cook. It is however almost unaffected in AZQP-bleaching. The presence of inert cations such as sodium ions in the cooking



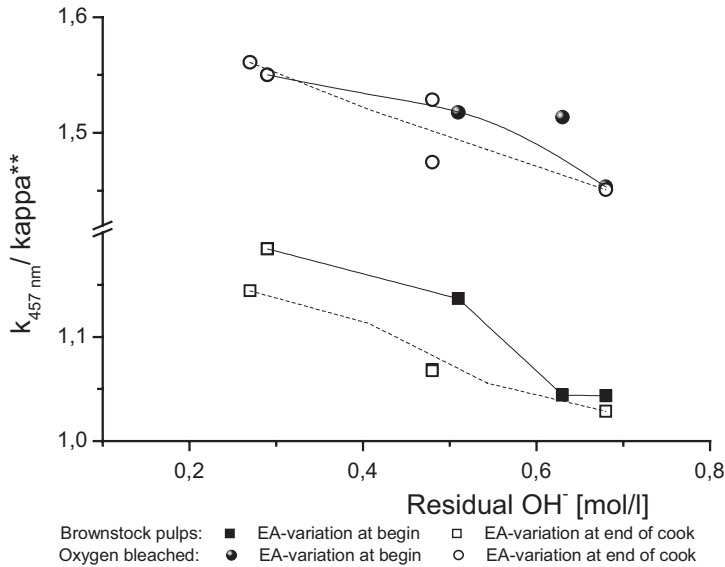
liquor contributes to the ionic strength in the liquor. It can be expected that an increased closure of the water cycles (e.g., bleach plant and recovery) leads inevitably to higher concentrations of inert cations, such as sodium ions. If the concentration of sodium ions is increased in the final part of the cook, the cooking time must be increased substantially to reach the target kappa number of about 20. In combination with low concentrations of hydroxide ion and hydrogen sulfide ion, the QPQP-bleachability is negatively influenced at an ionic strength of only  $2.9 \text{ mol L}^{-1}$ . The poor bleachability is also characterized by a lower brightness value at the given kappa number of about 20. Bleachability is not adversely affected up to a sodium ion concentration of  $2.9 \text{ mol L}^{-1}$  for pulps in which the ionic strength is adjusted after the pretreatment and then kept constant throughout the whole cook [101].

The results of the QPQP-bleaching trials reveals a clear relationship between the content of  $\beta$ -O-4 structures in the residual lignin of the unbleached pine kraft pulps and bleachability of the pulp, expressed as the consumption of oxidation equivalents per kappa number necessary to achieve a brightness level of 87% ISO (Fig. 4.61). The results clearly demonstrate that the higher the specific amount of  $\beta$ -O-4 structures, the lower the specific consumption of bleaching chemicals. Bleachability remains at an acceptably high level when the specific content of  $\beta$ -O-4 structures exceeds a value of  $5 \mu\text{mol g}^{-1} \cdot \text{kappa}^{** -1}$ . However, at a value of around  $3 \mu\text{mol g}^{-1} \cdot \text{kappa}^{** -1}$ , the bleachability changes dramatically and, below this value, becomes very poor.



**Fig. 4.61** Consumed OXE/kappa number<sup>\*\*</sup> for pine kraft pulps bleached in an OQPQP-sequence to a brightness of 87% ISO as a function of  $\beta$ -aryl-ether structures in the residual lignin after cooking according to Gellerstedt and Wafa Al-Dajani [93] and Gustavsson et al.

[97]. The peroxide charge in the first P-stage was 3.0%  $\text{H}_2\text{O}_2$ , while in the second P-stage the peroxide charge was varied between 1.5 and 6.0 %  $\text{H}_2\text{O}_2$ . In the second P-stage, 0.05% Mg-ions were added.



**Fig. 4.62** The light absorption coefficient,  $k$ , (measured at 457 nm) per kappa number corrected for the content of HexA as a function of the residual effective alkali concentration at the end of the cook (according to [102]). The unbleached pulps are produced according to an ITC-type cook with EA variation in the residual delignification phase (black liquor pretreatment and three

stages) and according to a simple two-stage process with EA variations in the beginning of bulk delignification (black liquor pretreatment and one stage). The unbleached pulps all show a kappa number around 17. Cooking temperature was 160 °C for all cooks, sulfidity 40% or at constant [HS<sup>-</sup>]. Oxygen bleaching was conducted at 100 °C, 115 min at 12% consistency, 0.7 MPa and 2.15% NaOH on pulp.

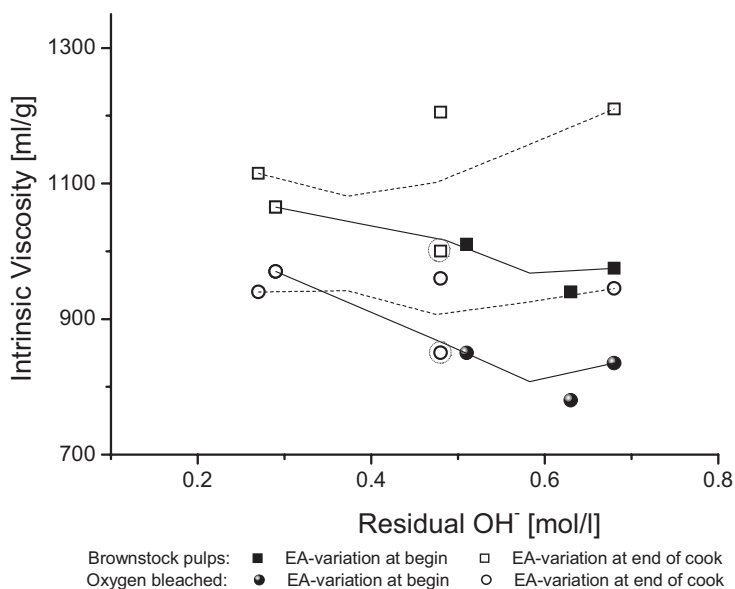
As discussed previously, unbleached softwood kraft pulps with a high remaining amount of  $\beta$ -O-4 structures can be produced by adjusting the cooking conditions such that both hydroxide ion concentration and hydrogen sulfide concentration are maintained at a high level, together with a low ionic strength. In any case, cooking conditions with high H-factors must be avoided (see Fig. 4.60) [97].

The specific light absorption of the unbleached pine (*Pinus sylvestris*) kraft pulps with kappa numbers close to 17 is lower for the ITC-type pulps as compared to the two-stage cooked pulps both with black liquor pre-impregnation. As expected, the brightness increases with raising residual alkali concentration in the black liquor after the cook (Fig. 4.62).

The lower specific light absorption coefficient after the cook at a given residual effective alkali concentration for the ITC-type pulps as compared to the two-stage pulps can be attributed to both the lower concentration of dissolved lignin in the black liquor and the lower EA concentration during the initial stage of bulk delignification [29]. The differences in the specific light absorption between the cooking procedures after a subsequent oxygen delignification stage diminishes, as shown in Fig. 4.62. Oxygen delignification clearly degrades the chromophore structures with different specific absorption coefficients equally well. The HexA

content is found to decrease with increasing alkali concentration. Due to the higher EA level in the early stage of the cook, the two-stage pulps generally reveals a lower content of HexA, which is in agreement with the results of Vuorinen et al. [28].

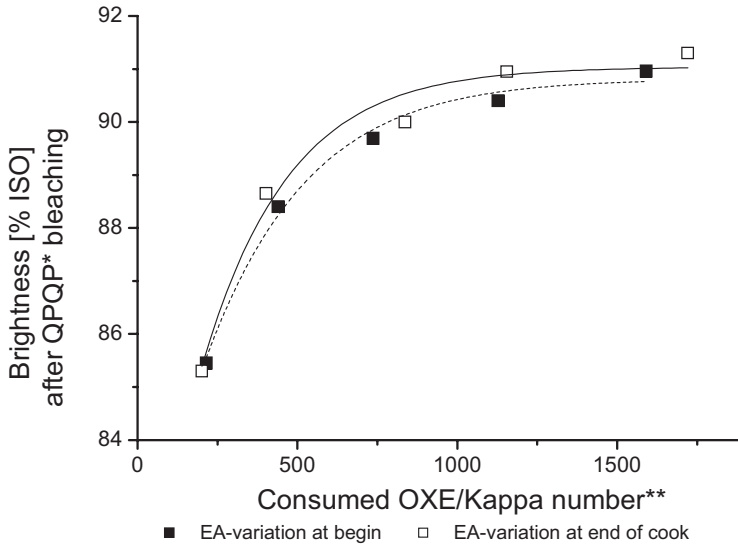
The intrinsic viscosity level is higher for the ITC-type pulps (pulps produced with an alkali concentration varied in the final part of the cook) as compared to conventional kraft pulps. In accordance with other results, the viscosity of the ITC-type pulps remains almost constant, or even shows a slight increase with increasing residual alkali concentration, whereas the pulps with the EA variation in the early stage of the cook shows a declining viscosity with increasing residual alkali concentration (Fig. 4.63) [29].



**Fig. 4.63** Intrinsic viscosity as a function of the residual effective alkali concentration at the end of the cook (according to [102] and Fig. 4.62).

The selectivity advantage for the ITC-type pulps at a given residual alkali concentration is preserved throughout oxygen delignification and QPQP final bleaching. The difference in viscosity at a given brightness in the range 85–91% ISO between the two pulping procedures even increases with increasing residual alkali concentration.

The specific OXE consumption using a QPQP bleaching sequence after oxygen delignification to reach a target brightness level is lowest for pulps with a residual alkali concentration close to  $0.5 \text{ mol L}^{-1}$ , both for the ITC-type pulps and the two-stage pulps with an EA variation in the beginning of the cook. The ITC-type pulps are slightly easier to bleach as compared to the two-stage pulps both with kappa number 17 when the comparison is made at the same residual alkali concentration (Fig. 4.64).

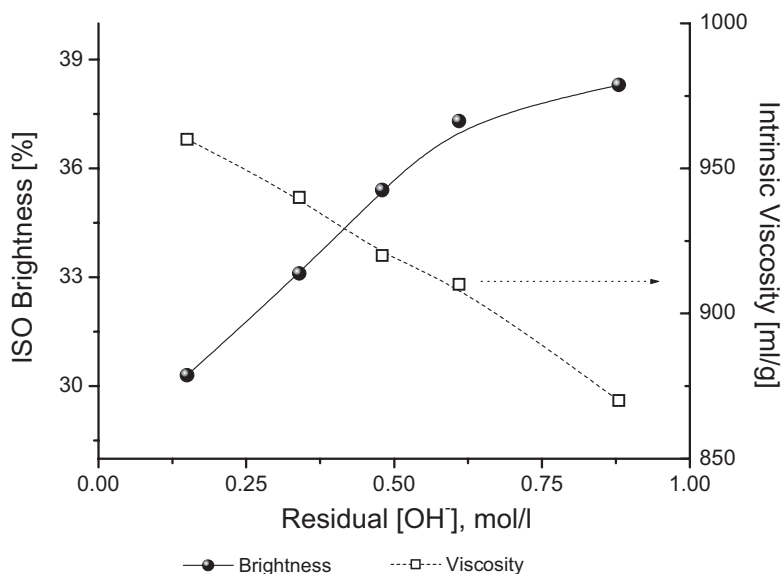


**Fig. 4.64** Brightness development after a QPQP-sequence as a function of the specific OXE consumption (OXE/kappa number\*\*) (according to [102]). The ITC-type pulps for which the alkali concentration was varied in the late stage of the cook and the two-stage pulps for which the alkali concentration was varied in the beginning of the cook both with a residual alkali concentration of about  $0.5 \text{ mol L}^{-1}$  are compared.

The differences in bleachability between the ITC-type pulps for which the alkali concentration is varied in the late stage of the cook and the two-stage cook for which the alkali concentration is modified in the beginning of the cook are, however, very small and cannot be regarded as significant.

Recently, Olm and Tormund studied the influence of different EA profiles on the bleachability of pine kraft pulps with a kappa number of about 20, using a two-stage process similar to that introduced by Sjöström, but with the difference that the former also varied the EA concentration in the pretreatment step [102]. These authors also found a clear relationship between the residual EA and the ISO brightness of the unbleached pulps (Fig. 4.65).

The poor brightness of the pulp originating from a cook with a residual alkali concentration of only  $0.15 \text{ mol L}^{-1}$  also translates into an impaired bleachability. The bleachability is evaluated as the total consumption of OXE per kappa number after the oxygen stage (and per ton of pulp) necessary to reach an ISO brightness of 89%. The specific OXE consumption amounts to  $160 \text{ OXE/kappa}_{\text{O}_2}$  for the pulp with the low residual alkali concentration ( $0.15 \text{ mol L}^{-1}$ ) as compared to only  $125 \text{ OXE/kappa}_{\text{O}_2}$  with the high alkali concentration ( $0.88 \text{ mol L}^{-1}$ ) despite the same kappa number of 20. Assuming a kappa number of 10 after the oxygen stage, the additional hydrogen peroxide charge in the last P-stage comprises approximately  $6 \text{ kg t}^{-1} [(1600 - 5_{(\text{kgO}_3/\text{t})} \times 125) - (1250 - 5_{(\text{kgO}_3/\text{t})} \times 125)] = 350 \text{ OXE t}^{-1} = 350/58.8 = 6.0 \text{ kg H}_2\text{O}_2 \text{ t}^{-1}$ . In the range of residual alkali between  $0.34$  and  $0.61 \text{ mol L}^{-1}$ , the bleachability remains almost unaffected by the hydroxide ion concentration in both

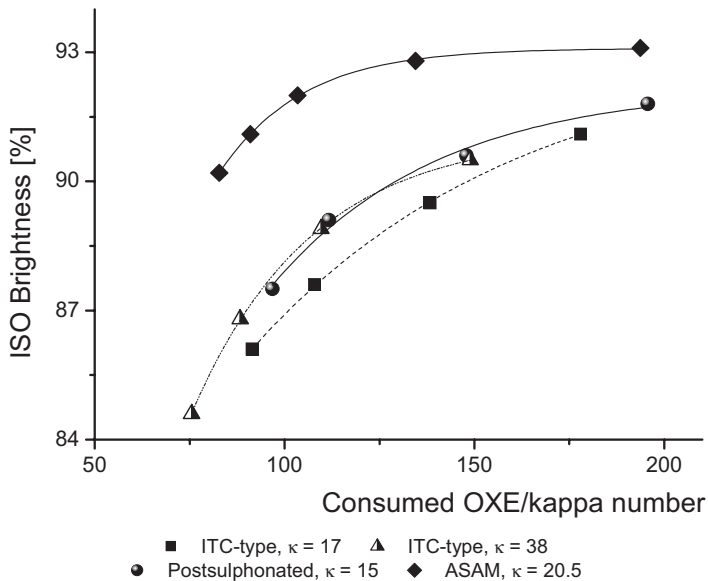


**Fig. 4.65** Brightness and viscosity of unbleached pine kraft pulps at kappa number 20 as a function of the residual effective alkali concentration (according to [27]). Laboratory cooking trials using a two-stage kraft process comprising a pretreatment step (where  $[\text{OH}^-]$  was varied from 0.1 to 0.5 mol L<sup>-1</sup>

at constant  $[\text{HS}^-] = 0.3 \text{ mol L}^{-1}$ ) and a cooking stage (where  $[\text{OH}^-]$  was varied from 1.0 to 1.6 mol L<sup>-1</sup> at constant  $[\text{HS}^-] = 0.3 \text{ mol L}^{-1}$ ). Cooking temperature was kept constant at 170 °C, and cooking time was adjusted to reach the target kappa number 20.

pretreatment and cooking stages. As expected, cooking with a high concentration of residual alkali leads to a significant loss in viscosity which, however, does not impair the strength properties measured as rewetted zero-span tensile index. On the contrary, the strength properties are about 5% lower as compared to the pulp originating from the cook with the high residual alkali concentration. The reason for this might be both the higher amount of hemicelluloses (due to enhanced xylan reprecipitation) and the significantly higher H-factor (~ 3000 versus 1000) to attain the target kappa number at this low EA charge which negatively influences fiber dimensions (average fiber length was only 2.36 mm with residual  $[\text{OH}^-] = 0.15 \text{ mol L}^{-1}$  versus 2.45 mm with residual  $[\text{OH}^-] = 0.88 \text{ mol L}^{-1}$ ).

The specific OXE consumption for modified softwood kraft pulps is significantly lower when using an A-ZQ-P-sequence following one- or two-stage oxygen delignification stages to reach a kappa number of approximately 10 prior to ozone bleaching. Bleachability in terms of specific OXE consumption is improved by interrupting the ITC-type cook at a higher kappa number and alternatively extending the delignification by applying a reinforced two-stage oxygen delignification stage (Fig. 4.66). Completing the cook at an earlier stage might prevent the formation of bonds between lignin and carbohydrates, which are difficult to remove during oxygen delignification and subsequent bleaching. Treating the



**Fig. 4.66** Brightness gain as a function of specific OXE consumption (OXE consumed/kappa number) for AZQP-bleached softwood kraft (ITC-type) and ASAM pulps (according to [107]).

ITC-pulps with  $0.3 \text{ mol Na}_2\text{SO}_3 \text{ kg}^{-1}$  o.d. wood in the final cooking stage to achieve a partial sulfonation also contributes to a slightly better bleachability as compared to the reference pulp (see Fig. 4.66).

In various pulping and bleaching experiments, it has been shown repeatedly that alkaline sulfite pulps such as alkaline sulfite with anthraquinone and methanol ASAM exhibit a better bleachability as compared to kraft pulps [103–106]. For comparative reasons, an unbleached softwood ASAM pulp with a kappa number of 20.5 is included in this TCF-bleaching study. All pulps used for TCF-bleaching are characterized before and after oxygen delignification (Tab. 4.34).

The specific OXE requirement for a given brightness level is significantly less for an alkaline sulfite pulp (e.g., ASAM pulp) as compared to the kraft pulps with or without modification, as can be seen from Fig. 4.66. The accelerated brightness development of the alkaline sulfite pulps can be led back primarily to the significantly higher brownstock brightness as compared to the kraft pulps. The brightness advantage is preserved throughout oxygen delignification. Alkaline and acid sulfite pulps show equal bleachability [107]. At a given kappa number, alkaline sulfite pulp lignin contains by far more  $\beta$ -O-4 structures as compared to a residual kraft lignin, and this agrees well with the observed superior bleachability ( $21 \mu\text{mol g}^{-1} \cdot \text{kappa}^{**}$  in the residual ASAM lignin versus  $11.4 \mu\text{mol g}^{-1} \cdot \text{kappa}^{**}$  for the residual kraft lignin, respectively) [93].

**Tab. 4.34** Characterization of softwood kraft and ASAM pulps used for TCF bleaching according to a AZP-sequence before and after oxygen delignification [107].

Pulps	Cook	Brownstock		After oxygen delignification	
		Kappa	Viscosity [ml g <sup>-1</sup> ]	Kappa	Viscosity [ml g <sup>-1</sup> ]
Reference – low kappa ITC	ITC	17.5	1165	9.0	1020
Reference – high kappa <sup>a)</sup>	ITC	38.5	1410	11.5	1055
Postsulfonated	ITC-Na <sub>2</sub> SO <sub>3</sub>	15.0	1120	8.5	1015
ASAM	ASAM	20.5	1400	10.0	1160

a) Two oxygen delignification stages with interstage acid wash.

#### 4.2.6.2.2 Comparative Kraft Cooking Results

##### Batch Cooking

###### *Cold blow*

Cold blow technology can be designated as the forerunner of the modified kraft batch cooking processes. It is characterized by one or two cooking stages and cold displacement. Another key characteristic of this technology is that there is no warm impregnation stage.

The cold blow technique comprises the process steps of chip filling, steaming, charging of cooking liquor, heating to cooking temperature, cooking, filling the digester with wash liquor to reduce the temperature below 100 °C, and finally cold blowing [108]. After chip filling and steaming, the chip temperature will rise to about 100 °C. White liquor is preheated in a heat exchanger and charged to the digester together with hot black liquor. After liquor charging, the digester content will have a temperature of ca. 130–140 °C. Raising the temperature to the target cooking temperature (160–170 °C) will be accomplished by liquor recirculation and indirect steam heating. The digester is then kept at cooking temperature until the target H-factor is reached. When cooking is completed, cold washer filtrate is introduced from the bottom of the digester to displace the cooking liquor through strainers at the top of the digester. The displaced hot black liquor is stored in the hot black liquor accumulator for use in a subsequent cook. In the next step, blowing starts by opening the blow valve. The pressure at the digester top is controlled by connecting the vapor phase of the hot black liquor accumulator with the top of the digester. The blow is more rapid and efficient than a conventional hot blow due to the reduced flashing in the blow line. The major advantages of the cold blow over the standard batch technology are the 50% shorter heating time and considerably less steam consumption. Total steam consumption during cooking could be reduced from 4.1 GJ adt<sup>-1</sup> to 2.4 GJ adt<sup>-1</sup>, corresponding a reduction of

41% [108,109]. Cold-blow cooking technology can also be run with two cooking stages. Using this technology, the cooking liquor of the first cooking stage is displaced by a mixture of weak black liquor and white liquor to reduce the dissolved lignin concentration prior to residual delignification. After displacement, the circulation is started again to evenly distribute the cooking liquor. The second cooking stage is controlled by the H-factor and the EA-concentration. Cold displacement of the cooking liquor with washer filtrate terminates the cooking stage. The two-stage cold blow cooking technology improves the pulp quality significantly. The results show that the kappa number could be reduced from 32 to about 25 while retaining the strength properties. This selectivity advantage can be expressed by an increase in viscosity of approximately 100 mL g<sup>-1</sup> at a given kappa number in the range 25–30 [110]. Today, cold blow cooking technology has been successfully replaced by further developed batch cooking technologies, and these will be introduced in the following sections.

#### *Rapid Displacement Heating (RDH) [111–113]*

The digester is steam-packed with chips using a shuttle conveyor. Next, weak black liquor from the atmospheric accumulator is used to increase chip compaction density in the digester. Air is displaced from the digesters and the discharge valves are closed. Preheated and pressurized weak black liquor with a temperature up to 130 °C is then introduced at the bottom until the digester is hydraulically full. The digester is pressurized to 7 bar just as the discharge temperature during the warm liquor fill reaches 100 °C. Liquor can enter the chips by being forced in an overpressure. It is estimated that in RDH cooking almost all the wood is impregnated by the pressure mechanism. Impregnation is carried out with warm black liquor; therefore, the ratio of hydrosulfide to hydroxide ions reaches values above 3, which ensures that cellulose is not exposed to the hydrolytic effects of high hydroxide ion concentrations as compared to a conventional cooking pattern (see Fig. 4.46).

As a result of a hydraulic cook, a rather high liquor-to-wood ratio of around 4.7 is achieved. This thorough impregnation as a separate stage assures first of all a more uniform delignification within the chips, and this results in less rejects. Secondly, it decreases alkali consumption fluctuations in the cooking phase, thereby improving cook uniformity through pre-neutralization of the degraded carbohydrate structures [114]. The high sulfide concentration achieved in the chip interior during the early stage of the cooking phase is also beneficial to delignification selectivity.

In the next step, hot black and hot white liquors are charged to the digester, displacing the warm liquor to the atmospheric accumulator. Soap is separated there and excess weak liquor is pumped to the evaporators. Digesters are thus brought to approximately 160 °C before any steam is added. Hot black liquor is continuously passed through a heat exchanger to heat the incoming white liquor, which is then stored in an accumulator for the next cook. Since liquors entering the digester are already hot, the heating-up time is very short. The amount of steam required to achieve the target cooking temperature (160–170 °C) is added directly



to the digester circulation line. After having reached the final cooking temperature, the circulation is stopped. The cooking phase is short compared to that of a conventional cook since the charging liquors are close to the cooking temperature, thus enabling an accelerated temperature elevation.

As soon as the target H-factor is reached, hot black liquor is displaced through the upper strainers with washer filtrate to immediately stop the cook. Hot black liquor with a temperature above 130 °C is displaced into the hot black liquor tank. Approximately 70% of the hot liquor displaced remains at the cooking temperature [115,116]. The displacement continues until all excess filtrate from the brownstock washing is pumped through the digester. Displaced liquors at temperatures below 130 °C pass to a second hot black liquor tank at lower temperature for reuse in a subsequent impregnation cycle. Finally, liquors with a temperature level below 93 °C are displaced into the atmospheric accumulator. The ideal displacement continues until approximately half of the free volume of digester has been pumped out. The proportion of wash liquor in the displaced liquor increases steadily.

At this point, the cook has ended and the digesters can be blown. The cooled and delignified “chips” are discharged with compressed air stored in the air receiver at significantly shorter time than conventional cooks due to the absence of flash steam. It is reported that the sulfur emissions are reduced by about 98% as compared to conventional hot blow. The TRS emissions are only constituted by methyl sulfides and very little methyl mercaptan. They are basically noncondensibles, with no affinity for water or alkali [117].

As a result of the sequence of liquor charging and displacing, the RDH-cook reveals a rather smooth alkali profile (Fig. 4.67). At the end of the cook, the residual alkali concentration remains at a higher level, in the range 0.42 to 0.5 mol L<sup>-1</sup>. The alkali concentration falls by 30% during the first 15 min, which is less when compared to conventional cooking. This can be explained by the higher liquid-to-wood ratio and the already reacted alkali during black liquor impregnation [118]. The alkali profile is also determined by the wood source applied, depending on its carbohydrate composition. Softwood galactoglucomannan (GGM) begins to react at temperatures around 100 °C according to the peeling mechanism, whereas hardwood arabinoglucuronoxylan (AX) will react only at temperatures exceeding 140 °C [118]. As a net result, the major alkali consumption in softwood pulping starts with the introduction of the hot liquor, whereas hardwood hemicelluloses are more resistant towards peeling reactions, thus keeping the alkali profile flat and at a higher level.

A reduction in total alkali consumption from 18 to 17.5% on o.d. wood has been reported at the Joutseno mill [116], and this can be assumed to be connected to the less alkali-consuming peeling reactions that take place with RDH cooking.

In the white liquor, the total amount of sulfide charged is present as free hydrogen sulfide ions, HS<sup>-</sup>. With the beginning of the cook, part of the HS<sup>-</sup> ions becomes immobilized due to both physical bonds to wood (loosely bound) and organic material in the cooking liquor and chemical bonds to lignin and lignin degradation products (chemically bound) [119,120]. The chips absorb HS<sup>-</sup> ions

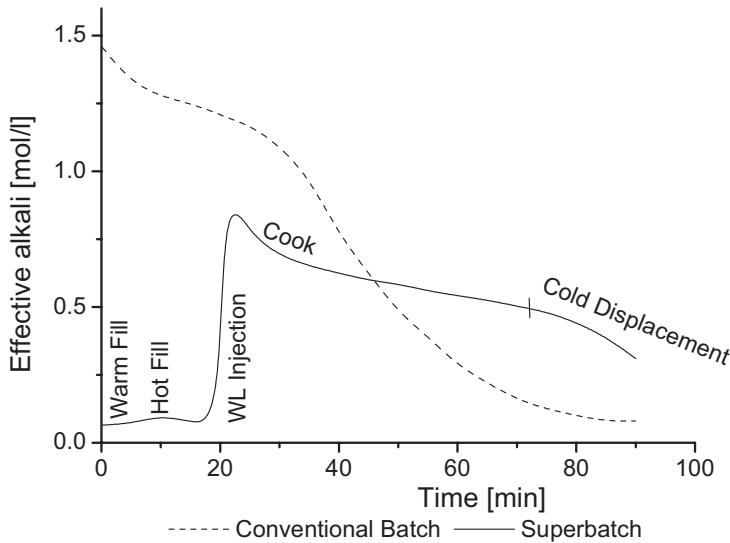
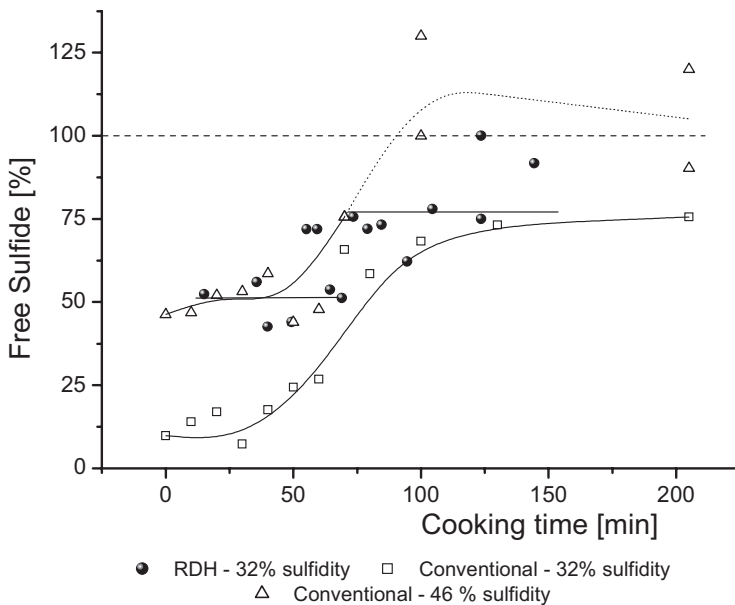


Fig. 4.67 Effective alkali profiles of RDH and conventional cooking procedures (according to [117]).

from the cooking liquor in an amount of  $0.1\text{--}0.2\text{ mol S kg}^{-1}$  wood. It is assumed that the loosely bound sulfide is not available for delignification reactions. At the end of the initial cooking phase, the loosely bound sulfide is transformed to free  $\text{HS}^-$  ions again. A deficiency of the hydrogen sulfide concentration during the initial pulping phase decreases the delignification rate in the bulk phase and promotes the formation of enol ether structures in the lignin, which results in a residual lignin that is difficult to bleach [40,121]. In the RDH cooking process, black liquor is displaced through the chips before cooking, and this counteracts the lack of available hydrogen sulfide ions. A mill study of softwood cooking according to the RDH process revealed that the content of free  $\text{HS}^-$  ions during the impregnation and charging/displacement phases was approximately four-fold higher when compared to a conventional kraft cook of the same sulfidity [119]. The graph in Fig. 4.68 shows that the initial concentration of free  $\text{HS}^-$  ions in the RDH cook is comparable to that of a conventional cook, with a sulfidity of about 46%. At the start of the bulk delignification (after 60 min cooking time), the content of free available hydrogen sulfide is approximately 10% higher in the RDH cook compared to the reference cook at the same sulfidity level (32%), although at the end of the bulk phase the levels are equal.

The measurements confirm that the displacement of black liquor through softwood chips prior to cooking promotes a sulfide accumulation in the chips, and a higher concentration of free available  $\text{HS}^-$  ions in the cooking liquor during the initial delignification phase. There is a strong indication that the better selectivity towards delignification of the RDH process can be traced back to a higher concentration of available  $\text{HS}^-$  ions in the transition from initial to bulk delignification.



**Fig. 4.68** Concentration of free sulfide ions versus cooking time in impregnation and cooking liquors in the RDH-process (Joutseno mill) and in the cooking liquor during conventional batch cooks at laboratory scale according to [119]. The method to determine the concentration of free hydrogen sulfide is described in Ref. [122]. The concentration of free sulfide ions is expressed in relative terms: 100% corresponds to the total amount of sulfide charged with white and black liquor in the reference batch cook with 32% sulfidity.

The lignin concentration in the initial phase of the RDH cook is high, and remains high throughout the whole cooking process. It increases rather rapidly following the hot liquor charges, and reaches a lignin concentration at the end of the cook which is quite comparable to that during conventional cooking [114].

RDH pulps from radiata pine contained about one-third less HexA as compared to conventional pulps of similar kappa number (Tab. 4.35). The lower content of HexA may be attributed to the greater overall alkali charge necessary to obtain the same kappa number level. Based on carbohydrate analysis, it has been determined that HexA substitution along the arabinoxylan chain was 4.0 HexA per 100 xylose for the RDH pulps, compared to 4.7 HexA per 100 xylose units for conventional pulp.

The major advantage over a conventional batch kraft process is the heat savings of more than 70%, comprising about 2.5–3.0 GJ admt<sup>-1</sup> [124–127]. A mill-scale trial of the RDH process at the Georgia Pacific mill in Port Hudson, Louisiana, resulted in a reduction in steam consumption by 61%, from 2.32 t odt<sup>-1</sup> to 0.90 t odt<sup>-1</sup> as compared to conventional batch cooking [128]. The steam reduction is verified by a comparison of starting temperatures of 63 °C for conventional cooks, and 141 °C for RDH cooks.

Further advantages comprise a reduction in cover-to-cover time by 12.5% and 15%, respectively [126].

Tab. 4.35 Hexenuronic acid (HexA) content of conventional and RDH pulps (according to [123]).

Pulp	Kappa number	HexA [mmol kg <sup>-1</sup> ]	Effective alkali [% as NaOH]
Conventional	18.4	16.3	20.6
	19.8	17.0	20.6
RDH	19.2	11.6	23.2
	19.7	11.7	23.2

Unbleached RDH pulps produced at the Joutseno Mill in Finland showed quite comparable strength properties compared to pulps from conventional cooks, and over a wide range of kappa numbers (17–29). Their corresponding tear indices at tensile index 70 Nm g<sup>-1</sup> were determined to be between 17.2 and 18.4 mN m<sup>2</sup> g<sup>-1</sup> [60]. In a pilot plant study, RDH pulps made from Lodgepole pine and spruce showed tear strengths up to 10% higher at given tensile indices as compared to conventionally produced pulps [129]. Interestingly, the trend of tear index within the RDH cooking series showed that the lower the kappa number – and thus also the viscosity – the higher the strength. The conclusion of this study was that tear index actually improves with decreasing kappa number and viscosity for RDH kraft pulps, whereas conventional kraft pulps behave in the opposite manner. The negative correlation between strength properties (tear index at given tensile index) and viscosity is, however, limited to a certain state of production (either unbleached or bleached) and kappa number range. The overall positive relationship between tear index and viscosity is of course still valid. Nevertheless, it has been shown that RDH pulps of lower kappa number with lower viscosities tend towards higher tear strengths. This phenomenon has been attributed to a lower hemicellulose content (particularly xylan), and thus a higher alpha-cellulose content [129].

Application of the RDH process to different Southern hardwoods such as white and red oak, yellow poplar, sweetgum and maple resulted – surprisingly – in a lower pulp yield at a given kappa number as compared to conventional batch cooks [130]. One possible explanation for this behavior might be the increased dissolution of xylans in hardwood pulping. The EA concentration in the final stage of an RDH cook is higher than that of a conventional cook. Thus, the amount of xylan redeposition might be less pronounced during the course of an RDH cook. Unfortunately, this hypothesis was not investigated by carbohydrate analysis.

RDH kraft pulping of *Eucalyptus urograndis* species from Brazil resulted in a 1% higher brownstock yield than when applying the conventional kraft process (total yields 54.2% and 53.2%, respectively) [131]. Despite the higher xylan retention, the viscosity of the RDH pulp of kappa number 15 was reported as being 150 units higher compared to the reference pulp of kappa 15 (intrinsic viscosity 1125 mL g<sup>-1</sup> versus 975 mL g<sup>-1</sup>, respectively; recalculated from Tappi viscosity).

The viscosity of black liquor is determined by the molecular weight distribution of the lignin fraction. In RDH pulping, the black liquor is exposed to a high tem-

perature for a longer time (during storage in the hot black liquor accumulator) and higher residual alkali concentration as compared to conventional black liquor storage. The residual active alkali in the hot black liquor accumulator might be promoting the breakdown of high molecular-weight lignin compounds. As a result, the viscosity of black liquor amounts to only 160 mPa.s at 70% dry solids content, compared to 360 mPa.s typically for black liquor originating from conventional cooking [115,116]. This provides the advantage of increasing the black liquor solids concentration by about 3–5% while maintaining the same viscosity.

#### *The Superbatch process*

The Superbatch process is characterized by a rather low impregnation temperature of 80–90 °C, which is approximately 40–50 °C less compared to the RDH process. The low temperature is chosen to avoid chemical reactions occurring on the surface of the chips during the impregnation phase in order to strictly separate the physical impregnation and chemical delignification reactions. Hot black liquor treatment follows the impregnation step by introducing hot black liquor into the bottom of the digester. The temperature reaches almost cooking temperature after completion of the liquor fill. The objective of this heating step is to utilize the residual chemicals in the black liquor for reaction with the wood components. The tankfarm of the Superbatch concept is designed to store the undiluted displaced hot liquor according to the predetermined volume in one accumulator, while the remainder of the black liquor which is diluted with wash filtrate having a lower temperature and solids content is stored in a second accumulator.

Due to the high proportion of sodium sulfide at a rather low pH, it can be assumed that sulfide reacts with the aldehyde end groups to form thioalditols, thus protecting the carbohydrates against alkaline degradation reactions [132]. The extent of delignification of this pretreatment step corresponds to a conventional cooking stage with H-factors between 400 and 1000 [133]. As a consequence, the subsequent cooking stage can be significantly shortened.

The single steps during Superbatch cooking of pine wood (*Pinus sylvestris*) comprising warm black liquor impregnation at 80 °C, hot black liquor pretreatment at 155 °C, and finally cooking at 170 °C, were monitored with respect to the dissolution of the major wood components [134]. During warm liquor impregnation a yield loss of about 7% was determined. The deacetylation of glucomannan has been identified as the main reaction during this phase. A further reduction of almost 16% of wood yield occurred during the hot liquor pretreatment. The proportion of high molecular-weight lignin increased during this stage of operation. Based on the monitoring of the concentration ratio of [2-hydroxybutanoic acid + xyloisaccharinic acid]/[3,4-dideoxypentonic acid + 3-deoxypentonic acid + glucoisaccharinic acid], representing the dissolution of xylan in relation to glucomannan, the results indicate a more rapid dissolution of glucomannan during the black liquor pretreatment stages. During the cooking stage, however, the degradation of the xylan was more pronounced. It has been speculated that the mass transfer into and out of the wood matrix is significantly improved during the course of the hot black liquor pretreatments, mainly due to the release of sub-

stantial amounts of wood components. The molecular mass distribution of the lignin fraction in the cooking stage was dependent on the alkali charge. With a lower alkali charge (AA = 18% on wood), the proportion of low molecular mass fraction decreased significantly, while the higher molecular mass increased, suggesting condensation reactions. With the higher alkali charge (AA = 22% on wood), the average molecular weight remained constant. Based on this observation, a poorer bleachability of the pulps cooked to a given kappa at a lower residual alkali concentration number can be assumed [135].

The influence of different white liquor charges after a constant two-stage pretreatment with black liquor was studied for Superbatch cooking of softwood pine chips (*Pinus sylvestris*) [135]. As expected, the rate of delignification showed a significant dependence on the alkali profile. Increasing the residual hydroxide ion concentration from 0.25 mol L<sup>-1</sup> to 0.5 mol L<sup>-1</sup> increases the delignification rate in terms of lowering the H-factor by approximately 40% to reach a given kappa number target (a kappa number of 20 requires an H-factor of 1760 with a residual [OH] of 0.25 mol L<sup>-1</sup>, and only 1060 with a residual [OH] of 0.5 mol L<sup>-1</sup>, respectively). Kinetic studies of the bulk and residual phase delignification support these findings (see Section 4.2.5.3.1, Reaction kinetics). The dependency of carbohydrate degradation on the EA charge was even more pronounced than the lignin decomposition [135]. Cooking to a residual hydroxide ion concentration of 0.5 mol L<sup>-1</sup> instead of 0.25 mol L<sup>-1</sup> resulted in a more than 50% lower H-factor demand, while keeping the carbohydrate yield constant (a carbohydrate yield of 44% requires an H-factor of 1530 with a residual [OH] of 0.25 mol L<sup>-1</sup>, and only 725 with a residual [OH] of 0.5 mol L<sup>-1</sup>, respectively). Due to the different impact of alkali concentration on lignin and carbohydrate dissolution, the yield selectivity is negatively influenced by an increased EA charge. Thus, a low alkali concentration during the cooking phase was most favorable with respect to pulp viscosity at a given kappa number of the unbleached pulp. As expected, the brightness of the unbleached pulps increases with increasing EA charge at a given kappa number. Subsequent ECF-bleaching trials confirmed the improved bleachability of pulps cooked to higher final residual alkali concentrations. Displacement batch cooking to a residual hydroxide ion concentration of 0.5 mol L<sup>-1</sup> saved approximately 10 kg of active chlorine odt<sup>-1</sup> pulp in a D(EOP)DD bleaching sequence at the same unbleached kappa number as compared to a pulp produced with a residual hydroxide ion concentration of only 0.25 mol L<sup>-1</sup>. The improved bleachability at a higher alkali charge, however, is not limited to Superbatch cooking technology, as it also occurs with conventional kraft cooking [135].

Extensive mill trials according to the Superbatch technology have been performed in two Scandinavian pulp mills, with the focus on extended delignification [136]. The cooking process was mainly adjusted by H-factor control and EA dosage. With softwood (*Pinus sylvestris*), extended delignification to a kappa number of 18 was suitable to keep the intrinsic viscosity at an acceptable level of approximately 950 mL g<sup>-1</sup>. The strength properties, measured as tear index at a tensile index of 70 Nm g<sup>-1</sup>, were close to 16 mN m<sup>2</sup> g<sup>-1</sup> and thus 10% higher than with conventionally delignified pulp with kappa 27.5 [136]. Hardwood (*Betula verrucosa*)

was cooked to kappa number levels between 12 and 20. Even though viscosity decreases when kappa level decreases, the pulp strength is preserved. Characteristic for a kappa number-12 pulp from birch is an intrinsic viscosity level of  $1030 \text{ mL g}^{-1}$  and a tear index of  $9.5 \text{ mN m}^2 \text{ g}^{-1}$  at a tensile index of  $70 \text{ Nm g}^{-1}$ .

#### *Continuous batch cooking*

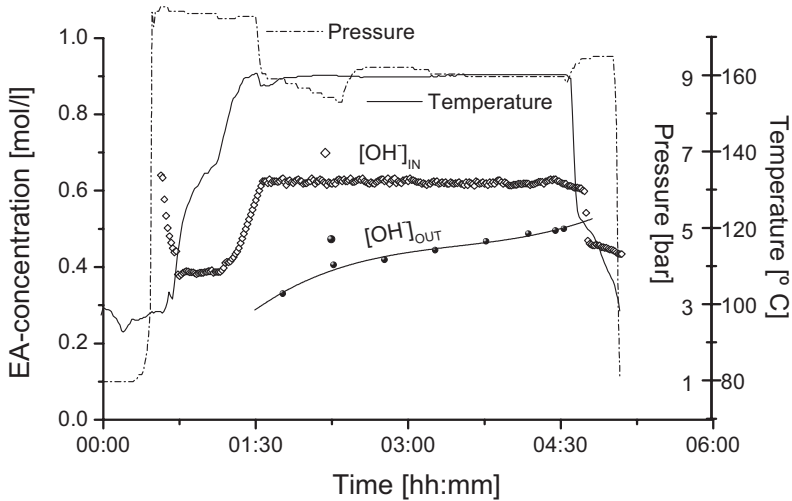
The four basic principles of modified kraft cooking can also be accomplished by combining batch displacement technology with the continuous flow of cooking liquor through the digester of constant temperature and preset cooking liquor composition. This concept of continuous batch cooking (CBC) represents the latest development of modified cooking procedures, and fully considers the rules of extended delignification and allows an even alkali profile throughout the impregnation and cooking stages [137,138]. The CBC process is characterized by the prior preparation of all process-related liquors (e.g., impregnation and cooking liquors) in the tank farm, using different tank-to-tank circulation loops. During circulation, the required reaction conditions are adjusted by the continuous addition of cooking chemicals and steam.

After chip filling, impregnation liquor is pumped through the digester from the top and bottom circulation lines, keeping the pressure at approximately 8–10 bar to ensure a uniform distribution of the cooking liquor across the chip sectional area. The ratio of  $\text{HS}^-$  ion to  $\text{OH}^-$  ion concentration of the impregnation liquor is adjusted to about 0.7 to 1.0 ( $0.25 \text{ mol HS}^- \text{ L}^{-1}$ ,  $0.25\text{--}0.37 \text{ mol OH}^- \text{ L}^{-1}$ ) to achieve a sufficient pre-sulfidation. The rapid rise in temperature further improves the sorption of sulfide in the wood chips; this is an important prerequisite of selective delignification reactions.

After about 30 min of impregnation, cooking liquor is pumped through the digester, displacing the impregnation liquor back to the impregnation tank. As soon as the whole amount of impregnation liquor is discharged, the liquor outlet is transferred to the cooking liquor system. Circulation of the cooking liquor through the digester and the cooking liquor tank continues until the preset H-factor is reached.

The cooking temperature of  $155\text{--}165 \text{ }^\circ\text{C}$  is reached within 30 min by the supply of cooking liquor only. The desired EA concentration and temperature in the cooking liquor are continuously adjusted within the cooking liquor circulation. This procedure results in a very even EA profile from the beginning of the heating-up period (transition phase from initial to bulk delignification) until the end of the cook (residual delignification) (see Fig. 4.69). The sulfidity of the cooking liquor is relatively high due to its continuous mixture with spent liquor from previous cooks. The ratio of  $\text{HS}^-$  ion to  $\text{OH}^-$  ion concentration amounts to 0.5–0.6, with a  $\text{OH}^-$  ion concentration typically between  $0.5$  and  $0.9 \text{ mol L}^{-1}$ . Towards the end of the cook, the content of dissolved solids can be reduced by continuously replacing part of the recycled cooking liquor by washing filtrate, which of course is adjusted to the desired alkali concentration and temperature. The replaced cooking liquor is fed via the impregnation liquor tank to the evaporation plant.

Similar to other batch displacement procedures, the cook is terminated by introducing washing filtrate into the digester until the whole content of the digester is



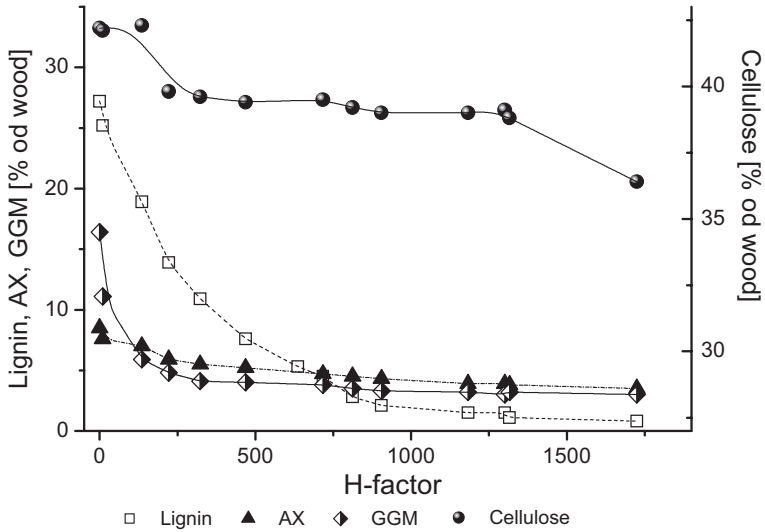
**Fig. 4.69** Course of temperature, pressure and effective alkali (EA) concentration of the cooking liquors, entering  $[\text{OH}^-]_{\text{IN}}$  and leaving the digester  $[\text{OH}^-]_{\text{OUT}}$  of a typical CBC cooking procedure using softwood as a raw material [55].

cooled to below  $100^\circ\text{C}$ . During this step, the cooking liquor is first displaced to the cooking liquor tank and, after dilution with washing filtrate, to the warm impregnation liquor tank. The cooled suspension of pulp and residual cooking liquor is then pumped to the discharge tank. The necessary consistency for pumping is controlled by a continuous dilution with washing filtrate.

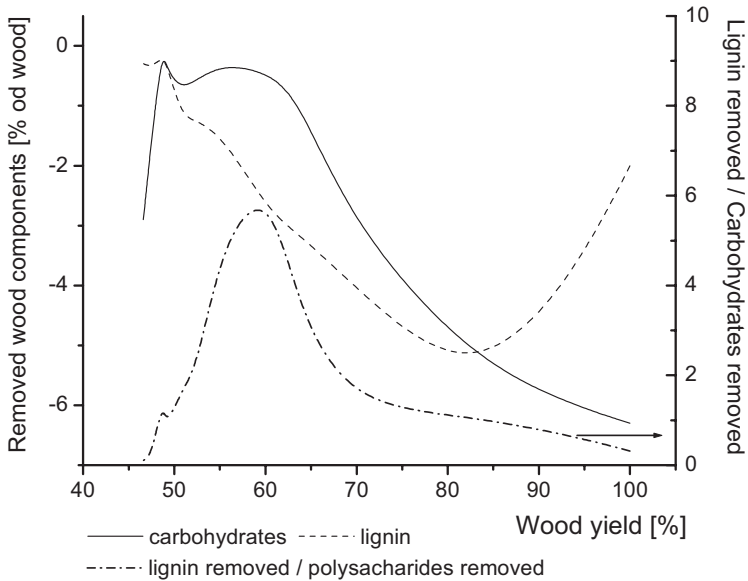
The degradation of wood components during the course of CBC cooking of spruce wood is illustrated in Fig. 4.70. Only after the short impregnation and subsequent displacement of the impregnation liquor does 7.5% of the wood components dissolve. The yield loss during this initial phase can be particularly assigned to the removal of the acetyl groups and the starting degradation of GGM. Even a small fraction of lignin is degraded during the impregnation phase. The wood yield decreases to 82% after termination of the heating-up period. As expected, the main losses can be attributed to the removal of GGM. The extent of lignin degradation is about 30%, which is unexpectedly high up to this cooking stage. The efficient lignin removal may be attributed to the favorably high ratio of  $\text{HS}^-$  ion to  $\text{OH}^-$  ion concentration of 0.79 ( $[\text{OH}^-] = 0.38 \text{ mol L}^{-1}$ ;  $[\text{HS}^-] = 0.30 \text{ mol L}^{-1}$ ) and the rapid temperature rise.

Cellulose yield is slightly reduced during the initial phase of bulk delignification, corresponding to a total wood yield of about 70%, but then remains fairly constant throughout the whole bulk delignification. The cellulose yield becomes impaired only after prolongation of the cook below a kappa number of 20. By differentiating the curve of Fig. 4.70 for the course of total wood yield, a clear minimum occurs for the carbohydrates in the residual delignification phase (Fig. 4.71).





**Fig. 4.70** Dissolution of the main wood components during CBC cooking of spruce wood (according to [55]). Impregnation liquor:  $[\text{OH}^-] = 0.38 \text{ mol L}^{-1}$ ,  $[\text{HS}^-] = 0.30 \text{ mol L}^{-1}$ . Cooking liquor:  $[\text{OH}^-] = 0.62 \text{ mol L}^{-1}$ ;  $[\text{HS}^-] = 0.34 \text{ mol L}^{-1}$ . Cooking temperature =  $160^\circ\text{C}$



**Fig. 4.71** Differential curve of the course of the carbohydrate and lignin dissolution during CBC cooking of spruce wood (according to [55]). Impregnation liquor:  $[\text{OH}^-] = 0.38 \text{ mol L}^{-1}$ ;  $[\text{HS}^-] = 0.30 \text{ mol L}^{-1}$ . Cooking liquor:  $[\text{OH}^-] = 0.62 \text{ mol L}^{-1}$ ;  $[\text{HS}^-] = 0.34 \text{ mol L}^{-1}$ . Cooking temperature =  $160^\circ\text{C}$ .

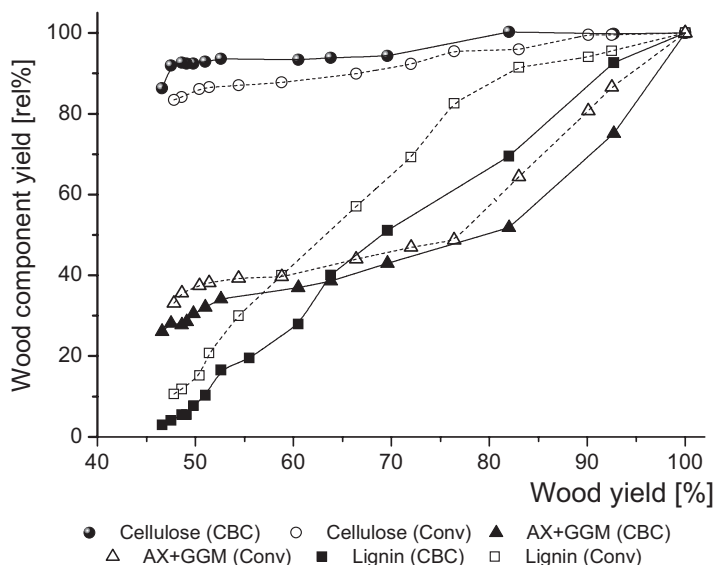
The delignification selectivity is given as the ratio of the amount of lignin removed per part of carbohydrate fraction extracted in relation to total wood yield. Figure 4.71 illustrates the highly selective bulk delignification phase ranging from about 65% to slightly below 50% wood yield. Interestingly, maximum selectivity occurs only after 70% of delignification, which corresponds to an H-factor of 470. The maximum rate of carbohydrate removal (equals the most nonselective phase of delignification) appears during both the initial and the residual delignification phases, however.

When comparing the composition of the pulp constituents of spruce CBC and conventional spruce kraft pulp, it is noted that the former always contains a higher amount of cellulose and a lower amount of hemicelluloses. These data are listed in Tab. 4.36, with a typical example of recently produced laboratory kraft pulps with a kappa number of ca. 25.

**Tab. 4.36** Characterization of unbleached spruce kraft pulps from continuous batch cooking (CBC) and conventional kraft cooking (CONV) (according to [55]).

Parameter Cooking #	Unit	CBC 65	CONV 433
Yield		47.1	48.0
Screened yield		46.8	46.8
Max. temperature	°c	155	155
Kappa number		25.6	25.2
Viscosity	mL g <sup>-1</sup>	1234	1162
Cellulose	% on pulp	77.5	75.4
GGM	% on pulp	7.8	8.3
AX	% on pulp	8.2	9.8
Residual (not analyzed)	% on pulp	6.5	6.5

The ratio of cellulose to hemicellulose concentration increases further when the EA concentration of the CBC cooking liquor is increased from 0.62 mol L<sup>-1</sup> to 0.87 mol L<sup>-1</sup>; these data are in agreement with the observations of Jiang, who investigated modified continuous cooking procedures [139]. The lower xylan content of the CBC pulps may be attributed to the lower extent of xylan reprecipitation during the late stage of the cook due to both a higher residual EA content and a lower xylan concentration in the cooking liquor (long retention time at cooking temperature favors fragmentation reactions). The more pronounced preservation of the cellulose fraction of the CBC pulp, however, cannot be identified unambiguously because the higher cellulose loss of conventionally kraft-cooked spruce



**Fig. 4.72** The removal of cellulose, lignin, and hemicelluloses (AX + GGM) as a function of total wood yield during CBC cooking of spruce [55] and conventional kraft cooking of pine [140]. CBC cooking: Impregnation liquor  $[\text{OH}^-] = 0.38 \text{ mol L}^{-1}$ ;  $[\text{HS}^-] = 0.30 \text{ mol L}^{-1}$ .

Cooking liquor  $[\text{OH}^-] = 0.62 \text{ mol L}^{-1}$ ;  $[\text{HS}^-] = 0.34 \text{ mol L}^{-1}$ . Cooking temperature =  $160^\circ\text{C}$ . Conventional kraft cooking of pine: liquor-to-wood ratio 4:1, EA-charge 20.3% on o.d. wood; 25% sulfidity;  $170^\circ\text{C}$  maximum cooking temperature (see also Fig. 4.23)

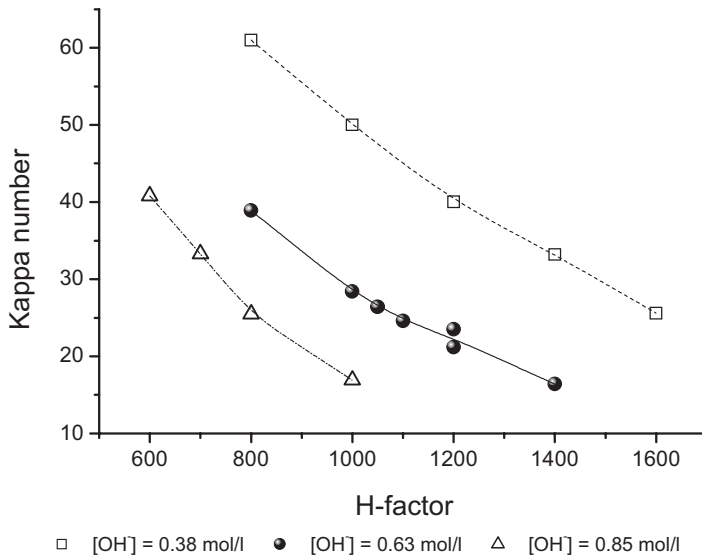
remained, even after lowering the cooking temperature to  $155^\circ\text{C}$  (see Tab. 4.36). The course of the relative content of the main wood components as a function of total wood yield (as studied by Aurell and Hartler for a conventional pine kraft cooking procedure) was compared with corresponding data obtained from spruce CBC cooking (Fig. 4.72) [140]. Although differences in the wood species (pine has higher contents of GGM and lignin, but a lower cellulose content) and the analytical methods applied may affect the results, it can be expected that the principal degradation pattern of the two kraft cooking processes should be identified. Figure 4.72 displays the removal of lignin, cellulose, and hemicelluloses (sum of GGM and AX) as a function of total wood yield.

The data illustrated in Fig. 4.72 confirm the better preservation of the cellulose fraction during CBC cooking as compared to conventional kraft cooking. The higher stability of the cellulose fraction during the initial CBC cooking phase (at about 80% yield) may be led back to the lower  $[\text{OH}^-]$  and the higher  $[\text{HS}^-]$  as compared to conventional kraft cooking. A further selectivity advantage for the CBC pulp can be observed in the final bulk and beginning residual delignification phases, where a higher  $[\text{OH}^-]$  combined with a lower content of dry solids causes a significantly higher rate of delignification, thus improving delignification selectivity. The significantly higher delignification selectivity throughout the whole cooking process, with two maxima at approximately 80% and 60% yield, com-

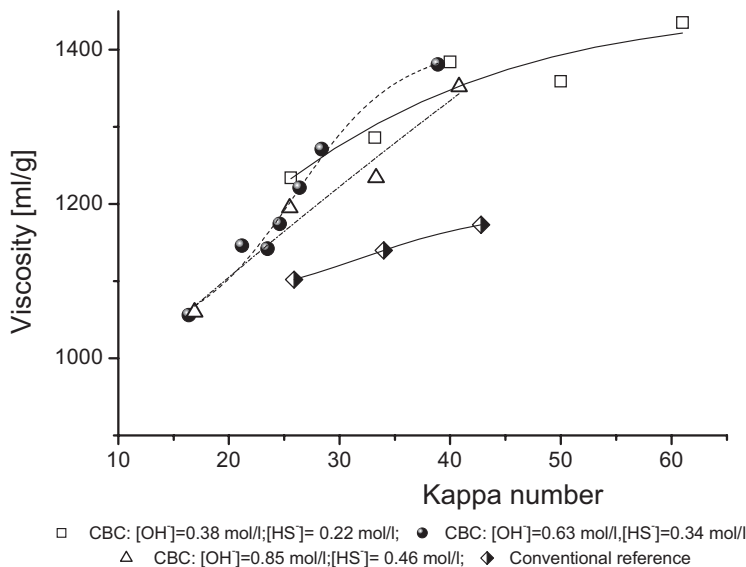
prises the main difference between CBC and conventional kraft cooking. Again, it may be speculated that the low but constant  $[\text{OH}^-]$  ion profile and the rather high ratio of  $[\text{HS}^-]$  ion to  $[\text{OH}^-]$  ion throughout the whole process may be the main reason for the higher delignification selectivity of CBC cooking. The pattern of hemicellulose dissolution proceeds in parallel up to a wood yield of about 58% (the lower values during CBC cooking in the initial delignification phase are due to the bigger gap between the determined wood yield and the sum of the identified single wood components than in the case of a conventional kraft cooking procedure). During the final cooking phases, the CBC pulp retains less hemicelluloses as compared to the conventional kraft pulp. As expected before, this behavior most probably indicates a more intense sorption of dissolved xylan back onto the fibers in the case of conventional kraft pulping.

#### *Effect of $[\text{OH}^-]$ ion in the cooking liquor*

The effect of three different levels of  $[\text{OH}^-]$  ion in the cooking liquor (0.38, 0.63, and 0.85 mol L<sup>-1</sup>) was investigated with respect to the processability of CBC cooking and the quality of the resulting unbleached pulps. As the sulfidity of the cooking liquor was kept constant at about 70%, the  $[\text{HS}^-]$  ion concentration changed correspondingly from 0.22 mol L<sup>-1</sup> to 0.34 mol L<sup>-1</sup> and to 0.46 mol L<sup>-1</sup>, respectively. Undoubtedly, the cooking intensity necessary to achieve a certain kappa number target was most influenced by the  $[\text{OH}^-]$  ion, as seen in Fig. 4.73. Using a cooking



**Fig. 4.73** Influence of  $[\text{OH}^-]$  ion concentration in cooking liquor on the course of kappa number as a function of the H-factor during CBC cooking of spruce (according to [55]). Impregnation liquor constant at  $[\text{OH}^-] = 0.39 \text{ mol L}^{-1}$  and  $[\text{HS}^-] = 0.25 \text{ mol L}^{-1}$ ; cooking temperature constant at 155 °C.

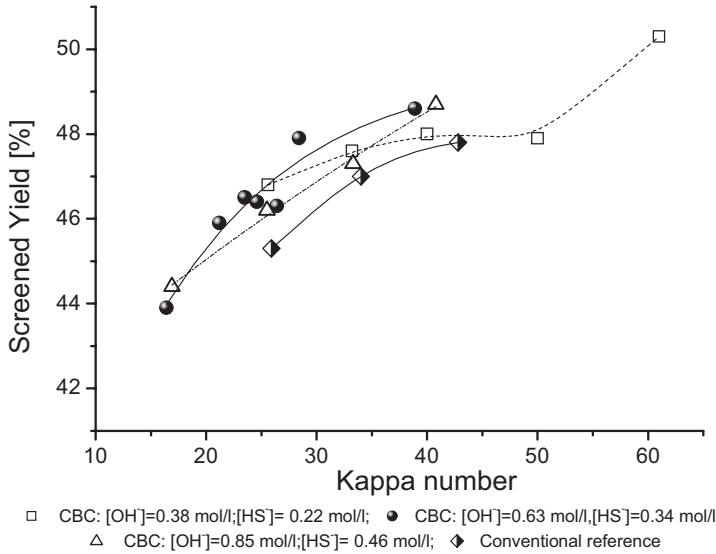


**Fig. 4.74** Selectivity plot as viscosity–kappa number relationship of CBC kraft cooking of spruce wood as a function of the  $[\text{OH}^-]$  ion concentration of the cooking liquor (according to [55]). Constant CBC cooking conditions: temperature and profile, cooking temperature  $155^\circ\text{C}$ . Conventional reference cooking conditions according to [8].

liquor with a  $[\text{OH}^-]$  ion of 0.85, 0.63, and  $0.38\text{ mol L}^{-1}$ , the corresponding H-factors to reach a kappa number of 25 comprised 820, 1080, and 1620, respectively. These H-factors translate to pure cooking times of 190 min (53), 250 min (70) and 375 min (105) at given cooking temperatures of, for example,  $155^\circ\text{C}$  ( $170^\circ\text{C}$ ), respectively (Fig. 4.73). Thus, the change from an intermediate  $[\text{OH}^-]$  ion of  $0.63\text{ mol L}^{-1}$  to  $0.38\text{ mol L}^{-1}$  results in a significant prolongation of the cooking time (to 125 min at  $155^\circ\text{C}$ ).

The delignification selectivity is only marginally influenced by the  $[\text{OH}^-]$  ion of the cooking liquor, as shown in Fig. 4.74. When cooking to kappa numbers lower than 25, the delignification selectivity tends to improve at a lower level of hydroxyl ion. The viscosity advantage at a given kappa number is at most 50 units in case of adjusting the cooking liquor to the low  $[\text{OH}^-]$  ion. Taking also the screened yield into account, the application of the medium  $[\text{OH}^-]$  ion seems to be an optimum choice (Fig. 4.74). Clearly, the amount of reject increases at higher kappa number levels and decreasing  $[\text{OH}^-]$  ion.

Independent of the  $[\text{OH}^-]$  ion of the cooking liquor, CBC cooking technology proved to be superior in delignification selectivity as compared to conventional kraft cooking (see Fig. 4.73). Again, the higher ratio of  $[\text{HS}^-]$  ion to  $[\text{OH}^-]$  ion of the impregnation liquor and the constant  $[\text{OH}^-]$  ion throughout the whole cooking process in combination with a reduced concentration of the dry solids concentration during the late stage of the cook, can be put forward as the main reasons for the selectivity advantage of the CBC cooking process. The slightly higher screened



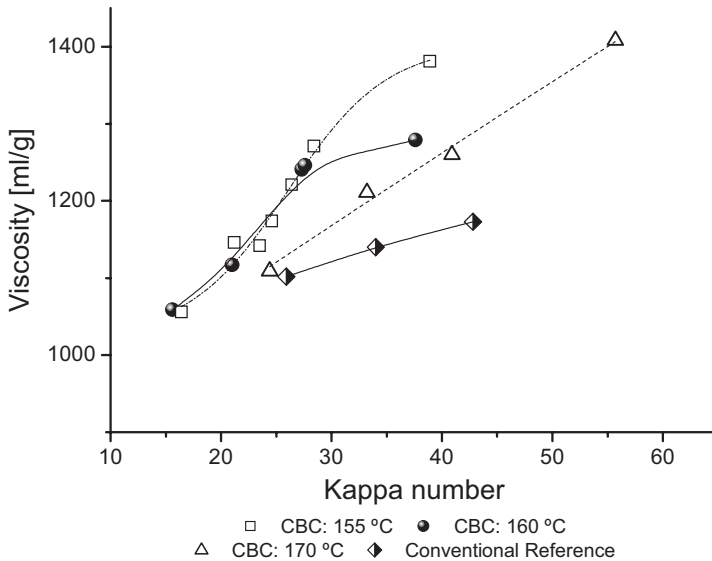
**Fig. 4.75** Selectivity plot as screened yield–kappa number relationship of CBC kraft cooking of spruce wood as a function of the  $[\text{OH}^-]$  ion concentration of the cooking liquor

(according to [55]). Constant CBC cooking conditions: temperature and profile, cooking temperature 155 °C. Conventional reference cooking conditions according to [8].

yields observed for the CBC pulps are mainly due to the lower amount of rejects as compared to the conventional kraft pulps (Fig. 4.75). The total yields are comparable for both cooking technologies, despite the significantly higher delignification selectivity of the CBC cooking technology. As mentioned above, this discrepancy can be led back to the lower extent of xylan precipitation during the final cooking phase in case of CBC cooking.

#### *Influence of the cooking temperature*

Cooking temperature is an important process parameter determining the demand of steam, the whole cooking time (cover-to-cover time) and the cooking performance (see Section 4.2.6.2.1, Principles of Modified Kraft Cooking). The effect of cooking temperature on delignification selectivity was investigated in the range between 155 and 170 °C. An increase from 155 °C to 160 °C showed no influence on delignification selectivity, provided that the kappa number stays in the range between 15 and 28 (Fig. 4.76). Beyond this kappa number range (at ca. kappa 38), the application of the higher temperature level tends to reduce the viscosity at a given kappa number. Raising the cooking temperature to 170 °C significantly impairs the delignification selectivity over the whole kappa number range. The viscosity of spruce CBC pulps at a kappa number level of 30 (40) is 50 (100) units higher as compared to conventional kraft pulps using the same cooking temperature. The selectivity advantage of the CBC pulps tends to decrease with decreasing kappa numbers. Due to the much faster heating-up time, CBC cooking technolo-



**Fig. 4.76** Selectivity plot as viscosity–kappa number relationship of CBC kraft cooking of spruce wood as a function of cooking temperature (according to [55]). Constant CBC cooking conditions (cooking liquor):  $[\text{OH}^-] = 0.63 \text{ mol L}^{-1}$ ,  $[\text{HS}^-] = 0.34 \text{ mol L}^{-1}$ . Conventional reference cooking conditions according to [8].

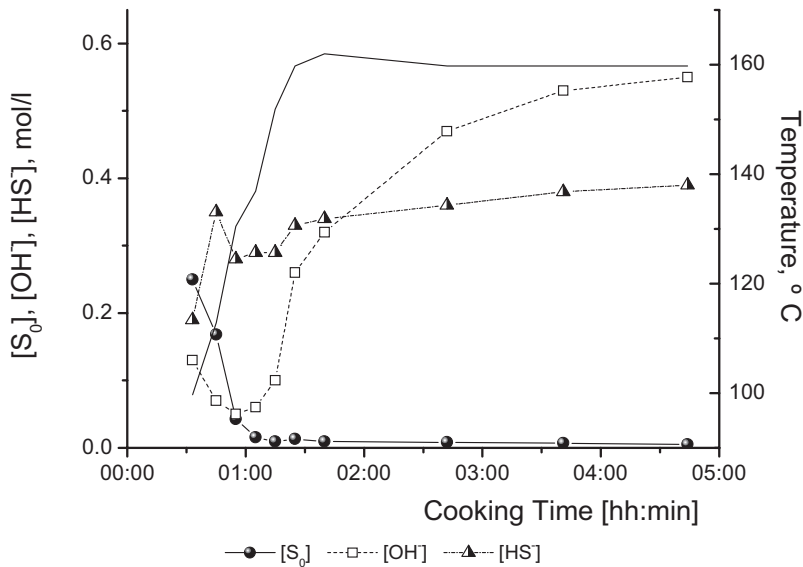
gy can be performed at a lower cooking temperature while maintaining the same cover-to-cover time as compared to a conventional kraft cook.

#### *Effect of adding polysulfide to the impregnation liquor*

The CBC cooking technology combines the advantages of both batch and continuous cooking technologies with respect to the homogeneity and selectivity of delignification (see Figs. 4.74 and 4.76). The screened yield at a given kappa number is also superior as compared to conventional kraft cooking due to the better impregnation conditions.

A secure method to further increase the pulp yield is to add polysulfide solution to stabilize the reducing end groups against alkaline peeling reactions (see Section 4.2.4.2.1, Polysulfide pulping). In some preliminary tests the effect of polysulfide on the performance of CBC cooking was investigated using spruce as a raw material [55].

Pretreatment with polysulfide solution was carried out by dissolving elementary sulfur in the impregnation liquor. The  $[\text{OH}^-]$  ion of the impregnation liquor was increased from  $0.38 \text{ mol L}^{-1}$  to  $0.50 \text{ mol L}^{-1}$  to compensate for the additional consumption of caustic during preparation of the polysulfide solution (Eq. 131). Despite this additional charge of EA, the  $[\text{OH}^-]$  ion decreases to a minimum level below  $0.1 \text{ mol L}^{-1}$  before increasing again to the target values. At the same time, the  $[\text{HS}^-]$  ion rises to values above  $0.3 \text{ mol L}^{-1}$ , thus increasing the ratio of  $[\text{HS}^-]$  ion to  $[\text{OH}^-]$  ion to a level greater than 5 to 1, which essentially leads to an improved sulfide sorption (Fig. 4.77).



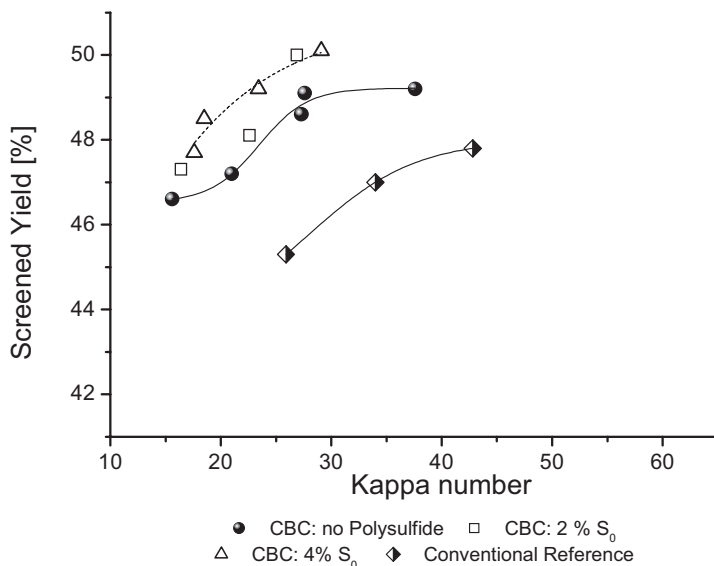
**Fig. 4.77** Polysulfide CBC cooking of spruce wood with 4% sulfur addition (according to [55]). Concentration profile of  $[OH^-]$ ,  $[HS^-]$  and  $[S_0]$  throughout the cook. Polysulfide analysis: HPLC; column Shandon Hypersil BDS C8; eluent 85% MeOH, 14.25%  $H_2O$ , 0.75% AcOH; flow rate  $0.8 \text{ mL min}^{-1}$  isocratic; detection UV 280 nm.

The polysulfide treatment must be carried out during the impregnation stage, when the temperature is still below  $120^\circ\text{C}$ , as polysulfide easily decomposes at cooking temperature. The course of the concentrations of active species throughout a typical CBC cook is illustrated graphically in Fig. 4.77. The molar polysulfide concentration (as  $S_0$ ) decreases rapidly to values below  $0.02 \text{ mol L}^{-1}$  before a temperature of  $140^\circ\text{C}$  is reached.

Two polysulfide cooking series with 2% and 4% sulfur addition on wood were conducted, respectively. As expected, the addition of polysulfide led to a substantial increase in yield at a given kappa number (Fig. 4.78).

No additional yield gain can be observed by doubling the sulfur addition from 2% to 4% on wood. The yield advantage comprises about 1.0–1.2% over the whole kappa number range investigated as compared to the CBC reference cooks. Based on carbohydrate analysis of the resulting unbleached pulps, an even higher yield gain of polysulfide CBC cooking can be assumed. The cellulose yield on wood increases by more than 2% and the GGM yield by about 0.8% at a kappa number level of about 25 (Tab. 4.37).



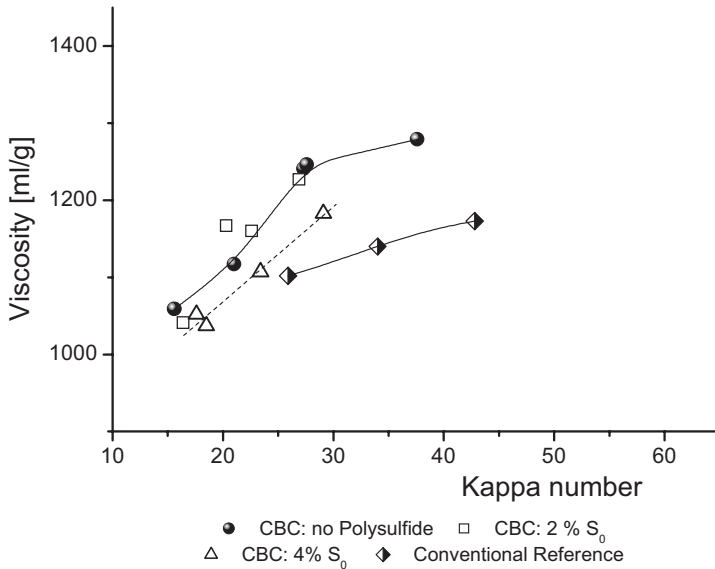


**Fig. 4.78** Effect of polysulfide addition on the screened yield kappa number relationship of CBC kraft cooking of spruce wood (according to [55]). Constant CBC cooking conditions: cooking temperature 160 °C; impregnation liquor of polysulfide cooks:  $[\text{OH}^-] = 0.50 \text{ mol L}^{-1}$ ,  $[\text{HS}^-] = 0.24 \text{ mol L}^{-1}$ ; impregnation liquor for reference CBC cooks:  $[\text{OH}^-] = 0.38 \text{ mol L}^{-1}$ ,  $[\text{HS}^-] = 0.20 \text{ mol L}^{-1}$ ; cooking liquor for all CBC cooks:  $[\text{OH}^-] = 0.63 \text{ mol L}^{-1}$ ,  $[\text{HS}^-] = 0.34 \text{ mol L}^{-1}$ . Conventional reference cooking conditions according to [8].

**Tab. 4.37** Effect of polysulfide addition on total and carbohydrate yield of spruce CBC pulps (according to [55]). Each result is an average of four or five cooking experiments, respectively.

Polysulfide [% on wood]	H-Factor	Yield [%]	Kappa	Viscosity $[\text{mL g}^{-1}]$	Cell [% on w]	AX [% on w]	GGM [% on w]	COOH $[\text{mmol kg}^{-1} \text{ w}]$
0	1200	48.1	25.8	1188	37.3	3.9	3.1	50.4
2	1100	49.2	25.1	1188	39.8	4.1	3.9	48.0
4	1250	48.9	22.2	1095	39.4	4.0	4.0	41.0

The results shown in Tab. 4.37 suggest that the polysulfide addition mainly contributes to the stabilization of the cellulose and the GGM fraction of the spruce wood, whereas the AX yield remains almost unchanged. Because of the predominant cellulose yield gain, it may be speculated that the polysulfide addition also preserves the molecular weight of the cellulose fraction. The results however demonstrate that polysulfide addition has no beneficial effect on the viscosity of the spruce CBC pulps at a given kappa number (Fig. 4.79). In fact, the polysulfide cooks with 4% polysulfide addition ultimately have a lower viscosity level.



**Fig. 4.79** Effect of polysulfide addition on the viscosity–kappa number relationship of CBC kraft cooking of spruce wood (according to [55]). Constant CBC cooking conditions: cooking temperature 160 °C; impregnation liquor of polysulfide cooks:  $[\text{OH}^-] = 0.50 \text{ mol L}^{-1}$ ,

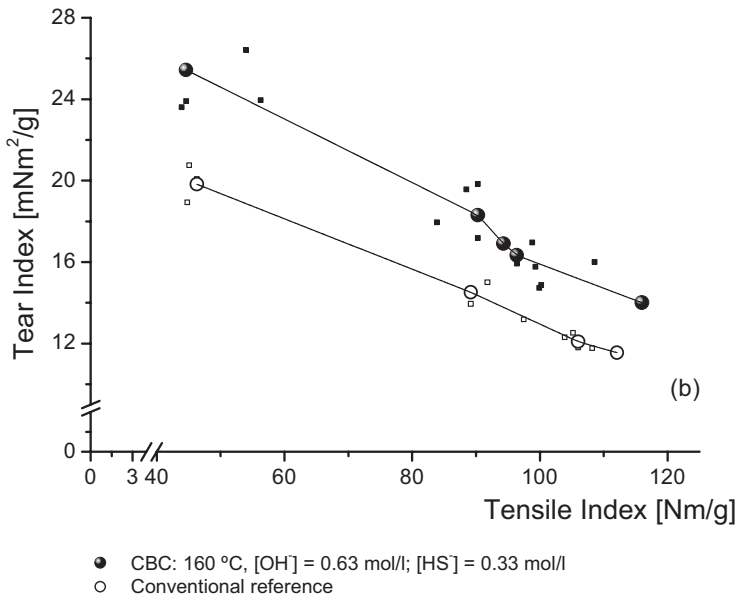
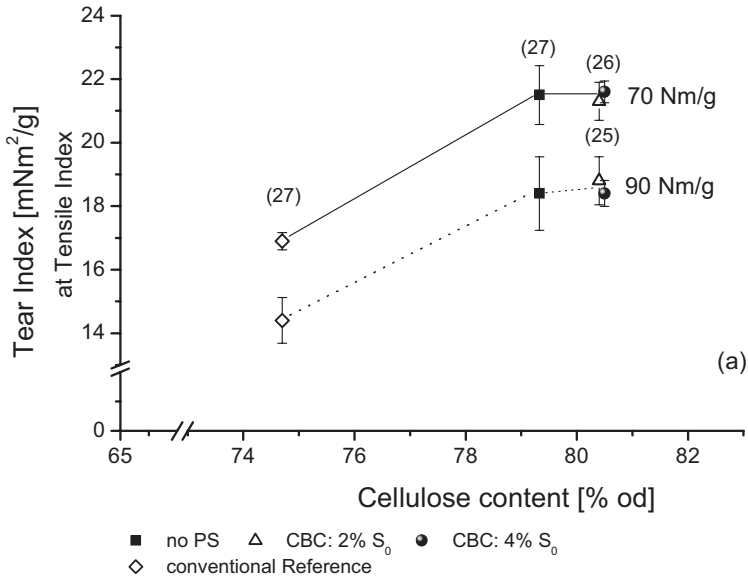
$[\text{HS}^-] = 0.24 \text{ mol L}^{-1}$ ; impregnation liquor for reference CBC cooks:  $[\text{OH}^-] = 0.38 \text{ mol L}^{-1}$ ,  $[\text{HS}^-] = 0.20 \text{ mol L}^{-1}$ ; cooking liquor for all CBC cooks:  $[\text{OH}^-] = 0.63 \text{ mol L}^{-1}$ ,  $[\text{HS}^-] = 0.34 \text{ mol L}^{-1}$ . Conventional reference cooking conditions according to [8].

Taking both the results on carbohydrate yield and viscosity measurements at a given kappa number into account, it may be speculated that besides GGM, amorphous cellulose with a low molecular weight is predominantly preserved during a polysulfide CBC cook.

#### Strength properties

The tear and tensile indices of CBC pulps and conventional kraft pulps are shown in Fig. 4.80. The results represent average values from four to five single measurements for pulps in the kappa number range 25–27. The strength properties of the CBC pulps are clearly superior as compared to those of the conventional kraft pulps. It is interesting to note that the tensile strength develops rather comparably, whereas the tear strength is significantly higher for the CBC pulps than for the conventional kraft pulps (Fig. 4.80(b)). At the same kappa number level, the CBC pulps show equal strength properties independently of the amount of additives (polysulfide), provided that comparable cooking conditions with regard to  $[\text{OH}^-]$  ion and  $[\text{HS}^-]$  ion and temperature are applied. The results clearly indicate that the superior viscosity–kappa number relationship translates into superior strength properties.

The high tear strength of the CBC pulps can be attributed to an increased fraction of high molecular weight cellulose molecules which are organized into



**Fig. 4.80** (a) Tear indexes at tensile indices of 70 and 90 Nm g<sup>-1</sup> related to the cellulose content of CBC, CBC-poly-sulfide and conventional kraft pulps made from spruce wood (according to [55]). Cooking conditions as for Fig. 4.79. (b) Tear-tensile plot of CBC and conventional kraft pulps, kappa number 27.

strands of rather undamaged cellulose microfibrils indicating rather selective cooking conditions. Fig. 80a exemplifies that the tear strength at given tensile index increases with increasing cellulose content which clearly confirms the view that an even effective alkali profile provides efficient delignification while preserving the long-chain carbohydrate fraction.

### Continuous Cooking

#### *Modified Continuous Cooking (MCC®)*

The concept of Modified Continuous Cooking (MCC) implies the process during which the main part of the cooking is performed with a low alkali concentration, while simultaneously allowing the concentration of dissolved lignin to be low. The method is not particularly new, but has been applied in Australia since the 1960s [141,142]. However, the conditions were far from optimal, and the process did not attract interest for many years. It was only after theoretical and fundamental studies at STFI and KTH in Stockholm, aimed at increasing pulping selectivity, that this type of modified cooking process regained its attraction [16,18,143–145].

Averaging the EA concentration throughout kraft pulping of *Pinus silvestris* and using a continuous two-vessel vapor/liquor-phase digester provides a more selective delignification as compared to a conventional kraft cook [146–148]. The modified kraft process is mainly characterized by lowering the initial EA concentration from  $1.45 \text{ mol L}^{-1}$  to  $0.7 \text{ mol L}^{-1}$ . This was achieved by a split addition of the white liquor between the top of the impregnator and the transfer circulation line, which takes place between the impregnator and the digester. Approximately 50% of the total white liquor charge is sent to the chip feed system prior to the impregnation stage. The remaining 50% of the white liquor is split into equal portions, with one part charging to the transfer circulation which carries chips from the impregnation vessel to the digester, and one part going to the countercurrent cooking circulation at the top of the Hi-heat washing zone [149]. The latter EA charge keeps the residual EA concentration at a level of  $0.45 \text{ mol L}^{-1}$  during the final delignification. The EA concentration profile inside the chips is considerably leveled out by the modifications compared with a conventional kraft cook in the digester as calculated by a mathematical model (max  $0.42 \text{ mol L}^{-1}$ , min  $0.18 \text{ mol L}^{-1}$  versus max  $0.95 \text{ mol L}^{-1}$ , min  $0.07 \text{ mol L}^{-1}$ , respectively) [19].

The applied temperatures in the co-current as well as countercurrent cooking stage were typically about  $165^\circ\text{C}$ .

The lignin concentration pattern is the reverse of that in conventional batch cooking. In the latter, the lignin content increases gradually to a final concentration of more than  $100 \text{ g L}^{-1}$  [150]. In MCC pulping, the highest observed lignin concentration was about  $65 \text{ g L}^{-1}$  at the extraction, and this gradually decreased to  $50 \text{ g L}^{-1}$  at the end of the countercurrent stage. It has been reported that the concentrations of dissolved lignin and sodium ions decreased by 40% at the end of the cooking zone as a result of the countercurrent flow conditions [19,147].

A single-vessel hydraulic digester was modified to operate according to the modified cooking process [151]. At a total charge of EA of approximately 24% on wood,

the optimum split was determined to be 57% to the feed, 10% to the upper circulation, and 33% to the lower circulation. Under these conditions, the same residual alkali of 8–11 g L<sup>-1</sup> in both the downflow liquor and the upflow liquor at the extraction screens could be maintained. The tear index was about 9% higher at the same tensile for the MCC pulp compared to conventional pulp. Moreover, there was less variability in pulp quality, and the pulp showed better bonding capabilities, which resulted in better runnability on the paper machines.

Based on carbohydrate analysis of mill pulps and laboratory cooks it may be assumed that, at an unbleached kappa number level of 25, the fully bleached pulp yield is approximately 0.8% higher when the modified alkali profile was applied in a continuous kraft cook [59]. The increase in yield can thus be attributed to a better cellulose retention by simultaneously keeping the hemicellulose yield [146]. Consequently, the MCC softwood pulps show a lower hemicellulose content in the kappa number range 21–42 as compared to conventional pulps (17.4–17.8% versus 18.3–18.7%) [152]. The reject level from the MCC is 1.3% lower than is experienced with conventional kraft processes (1.8% on pulp versus 3.1% on pulp at kappa number 32 [149]).

The better bleachability of MCC-cooked pulps when compared to conventional pulps, and especially at a lower kappa number, has been explained by both the higher residual alkali concentration (15 versus 10 g L<sup>-1</sup>) at the end of the counter-current cook zone, and the lower dissolved lignin concentration (50 versus 70 g L<sup>-1</sup>) at the end of the cook. Thus, the pulp produced with the MCC technique is in contact with liquor having about 50% higher alkali concentration and about half the dissolved lignin concentration of the conventional cook. It has been observed that the molecular weight of the dissolved lignin molecules increases in relation to progress of the cook [153]. Diffusion out of the fiber will be facilitated by the countercurrent cooking, and consequently less of the high molecular-weight lignin should be left in the pulp fiber. Furthermore, it has been found that the ratio of hydrogen to carbon atoms in the dissolved lignin decreases with increasing cooking time, which might correspond to a higher degree of condensation [154]. The combined effect of improving the diffusion of lignin and keeping a higher residual alkali concentration towards the end of the cook to prevent reprecipitation should result in a pulp that is easier to bleach.

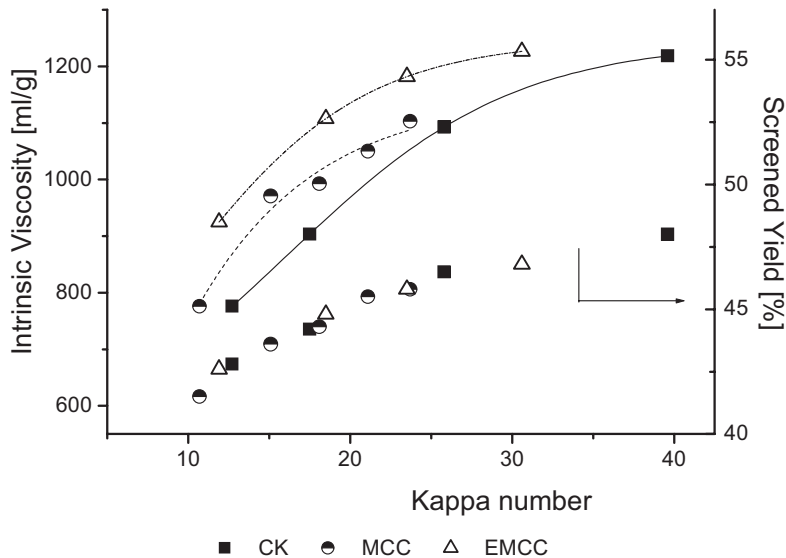
The viscosity level of the modified kraft pulp is more than 100 mL g<sup>-1</sup> higher at a given kappa number as compared to the conventional kraft pulp (1140 mL g<sup>-1</sup> versus 1000 mL g<sup>-1</sup> at kappa number 25 [147]). The unbleached kappa number could be lowered by about eight kappa numbers with maintained strength properties [154]. Hardwood pulps follow the same pattern as softwood pulps. The unbleached viscosity is about 100 mL g<sup>-1</sup> higher at the same kappa number, or about the same viscosity at 3–4 units lower kappa number. The change to modified continuous cooking of birch resulted in a better stability of the production and pulp uniformity [150]. Moreover, the kappa number was lowered from 18 to 14, and the viscosity increased from 900 to 1015 mL g<sup>-1</sup>, respectively. However, it must be stated that the performance of the batch line had previously also been on the level of approximately 1000 mL g<sup>-1</sup> [150].

The strength properties of MCC softwood pulps are reported to have a 10–30% higher tear value at a given tensile level [149]. Cooking studies using Scandinavian mixed softwood exhibit a viscosity advantage of approximately 70 SCAN units for MCC pulps over laboratory-produced conventional pulps in the kappa number range from 22 to 32. This viscosity advantage could be preserved after bleaching to a brightness of 90% ISO using a sequence (C+D)EDED.

#### Extended Modified Cooking (EMCC<sup>®</sup>)

Pulping selectivity further improves when utilizing a prolonged countercurrent cooking stage at a lower temperature [155]. The concept of extended modified cooking (EMCC) comprises the addition of white liquor at the bottom of the Hi-Heat washing zone to achieve a more even effective alkali profile and the extension of cooking to the Hi-Heat washing zone. The EMCC process is comparable to the ITC process, as the entire Hi-Heat zone is simultaneously used for both cooking and washing. The ITC and EMCC processes differ only in the equipment used for heating and circulating the white liquor in the High-Heat washing zone. The ITC uses an additional dedicated heating circulation system.

*Pinus taeda* laboratory cooks confirmed that, at the same kappa number and over the kappa number range investigated, EMCC pulps were generally found to be superior in both viscosity and strength properties as compared to MCC and conventional cook (CK) pulps (Fig. 4.81).



**Fig. 4.81** Intrinsic viscosity and screened yield versus kappa number of *Pinus taeda* kraft cooks. Results from laboratory cooks (according to [155]). Conventional cooks (CK): EA-charge 19.2–21.3% on wood, 172 °C; modified continuous cooking (MCC): EA-charge 19.6% on wood with 74:26 split addition, 171 °C; extended modified cooking (EMCC): EA-charge 19.6% on wood with 74:26 split addition and 160 °C.

The high selectivity of EMCC pulping can be explained by the low content of dissolved lignin in the final cooking stage, combined with the low temperature and thus prolonged cooking time. Diffusion of lignin into the aqueous phase is improved towards the end of the cook because of the lower dissolved lignin concentration and the longer time for diffusion. The lower pulping temperature kinetically favors delignification over cellulose chain scission, resulting in a higher pulp viscosity (see Section 4.2.5.2.1, Tab. 4.18, Kraft Pulping Kinetics).

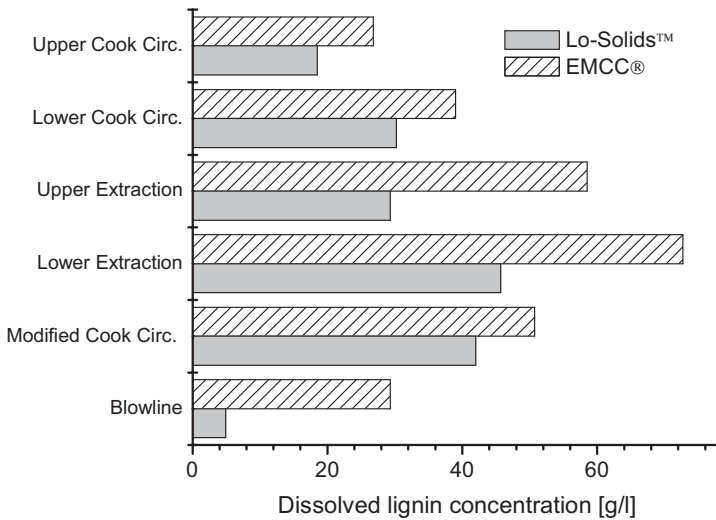
Preliminary mill trials converting from CK to the EMCC cooking concept showed an increase in intrinsic viscosity from 1160 mL g<sup>-1</sup> to 1270 mL g<sup>-1</sup> for a kappa number-12 unbleached hardwood kraft pulp. In another mill trial using northern softwoods in a single-vessel hydraulic digester, the EMCC concept was realized by adding up to 25% of the total white liquor charge to the washing zone which was operated at cooking temperature. Brownstock viscosity at kappa number 20 was significantly increased from 1030 mL g<sup>-1</sup> to more than 1200 mL g<sup>-1</sup> [155].

The knowledge from laboratory studies that the presence of dissolved solids during the bulk and final delignification stages negatively influences both the rate of delignification and pulp viscosity at a given kappa number (selectivity) led to the development of a new continuous cooking process, the Lo-Solids™ pulping [156].

#### *Lo-Solids™*

The Low-Solids™ process is based on the ITC and EMCC technologies, and is characterized by split white liquor additions, multiple extractions and split washer filtrate additions to achieve both an even EA profile, minimal cooking temperatures and minimal concentrations of dissolved lignin at the end of the cook. A typical Lo-Solids™ digester is provided with four white liquor addition points, the first before the impregnation, the second after the first extraction in the lower cook circulation (LCC) zone, the third after the second and main extraction in the modified cooking circulation (MCC) zone, and the fourth after the third and last extraction in the washing zone [157–159]. Washing filtrate is added together with white liquor at the final three addition points. Beneath the LCC there is a concurrent cooking zone, followed by the second extraction. Below the second extraction, the countercurrent cooking zones start, with the MCC screens in between. Results from mill application confirm the significant reduction in the concentration of dissolved solids within the bulk and final phases of delignification (Fig. 4.82). The low level of dissolved lignin concentration is most evident in the wash-cooking zone. Simultaneously, the final bleached viscosity of the hardwood kraft pulp increased after the transition to Lo-Solids™ pulping from 990 mL g<sup>-1</sup> (EMCC) to approximately 1100 mL g<sup>-1</sup>, which can be mainly attributed to the lower level of dissolved wood components in the final stages of pulping [157].

Softwood kraft mills which have been converted to Lo-Solids from MCC or EMCC operation have typically observed 5–10% improvements in tear strength. Laboratory trials using northwestern softwoods and simulating the time–concentration and time–composition profiles of dissolved wood solids in full-scale pulping systems even report a 28% (26%) gain in tear strength in the unbleached



**Fig. 4.82** Profile of dissolved lignin concentration at various locations on the digester. The results compare profiles for EMCC and Lo-Solids pulping (according to [157]).

(ECF bleached) pulp [160]. It has been demonstrated that pulp tear strength increases with increasing residual EA concentration. Thus, pulp yield losses can be avoided when a high EA concentration is maintained only towards the very end of the cook (see Fig. 4.44).

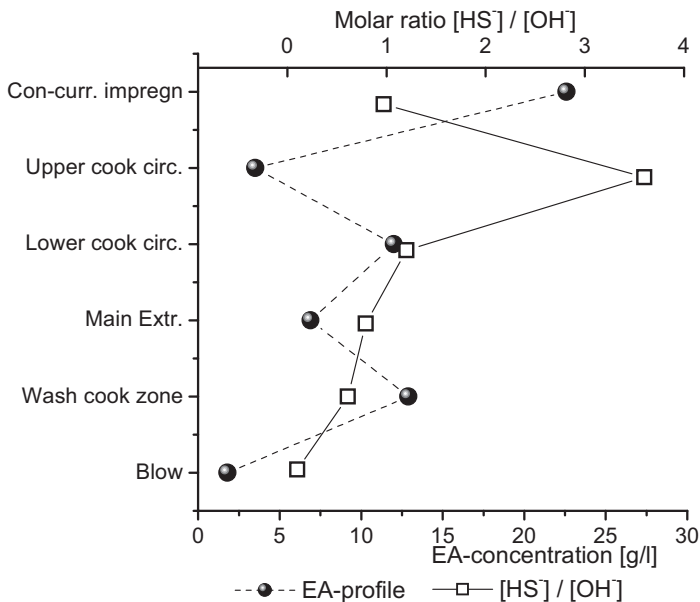
Dissolved wood solids also consume alkali in nonproductive decomposition reactions (e.g., retroaldol reactions, etc.). Based on laboratory results, it can be estimated that the dissolved wood solids present in the cooking liquors consume an equivalent of approximately 2% EA on wood due to secondary reactions [160]. The application of the Lo-Solids pulping process can reduce approximately 30% of the dissolved wood components. Based on these figures, it seems reasonable to assume a decrease of about 0.5% EA on wood. The presence of dissolved solids in the late stage of the cook also deteriorates bleachability. ECF bleaching of northern softwood pulps which were cooked according to the Lo-Solids technique without dissolved wood solids present in the cooking liquor, required 11% less amount of active chlorine to attain a brightness target of 89% ISO using a DEopDD.

Since the introduction of the Lo-Solids-pulping in 1993, there are now far more than 60 installations all over the world [161]. Fourteen rather new Lo-Solids digesters operating on different hardwoods such as mixed southern hardwoods, eucalyptus, birch and mixed Japanese hardwoods report a yield increase of 1–4% on wood compared to previous operation, mainly according to the EMCC process. The wood yield is determined either by the measurement of the wood consumption during a longer period of time, or according to a straight-line correlation of the logarithm of TAPPI viscosity ( $V$ ) divided by the square of the cellulose content fraction ( $G'$ ),  $\log(V)/G'^2$ , with the lignin-free yield [162]. The reasons for this really



significant yield advantage over conventional and even EMCC pulping processes have been mainly attributed to the even and very low EA concentration throughout the cook. This never exceeds values of ca.  $15 \text{ g L}^{-1}$ , except at the very beginning of the impregnation zone (Fig. 4.83). After impregnation, and immediately before the start of bulk delignification, the residual EA is as low as  $4 \text{ g L}^{-1}$ . At the same time, the ratio of  $[\text{HS}^-]$  ion to  $[\text{OH}^-]$  ion exceeds 3, which almost achieves the values optimized in laboratory operation [33]. The concept of Lo-Solids pulping comprises a two-stage continuous kraft process. The pre-steamed wood chips are impregnated with black liquor with a maximum ratio of  $[\text{HS}^-]/[\text{OH}^-]$ . The digester is divided into two sections, one co-current and one countercurrent. The upper half is devoted to the high sulfidity stage in a co-current flow. The sulfidity can be selectively increased by extracting the black liquor after the first treatment zone and reintroducing the withdrawn liquor with dilution liquor. In a subsequent second treatment zone a kraft cooking liquor is introduced having a higher sulfidity as compared to the first treatment zone [163].

Almost 75% of the lignin is removed in the first stage under highly selective conditions. In the lower part of the digester, the second cooking stage is performed in a countercurrent procedure. The cooking temperature can be kept at a low level, at about  $150\text{--}155^\circ\text{C}$  due to the fairly long retention time in the later stage of the cook.

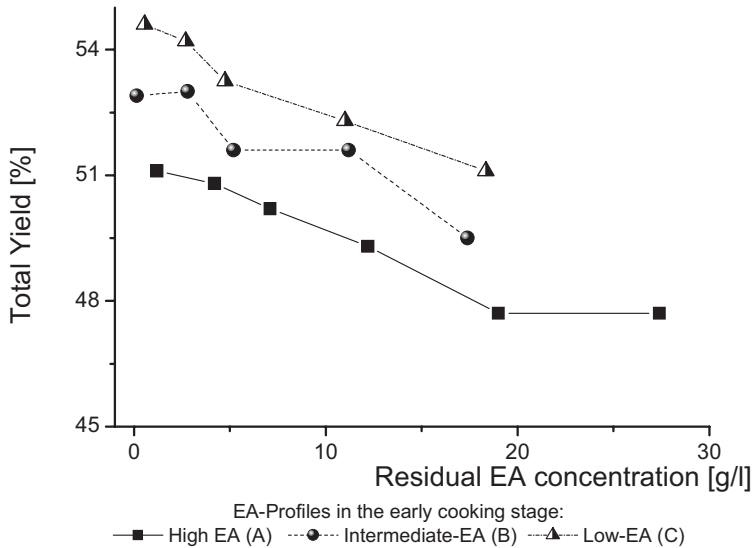


**Fig. 4.83** Profiles of effective alkali (EA) and the molar ratio  $[\text{HS}^-]/[\text{OH}^-]$  through Lo-Solids pulping (according to Refs. [161,164]) (mill data).

The low level of EA concentration, in combination with the low cooking temperature of 153 °C, decreases the extent of carbohydrate degradation reactions according to random alkaline hydrolysis and secondary peeling reactions.

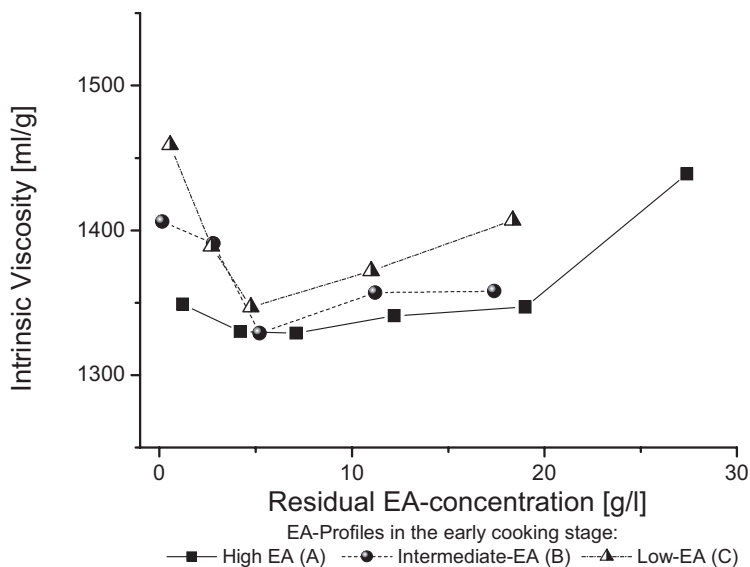
Laboratory studies on birch wood were conducted to elucidate the origin of the yield advantage of the Lo-Solids operation [165]. Three different EA-profiles (A, B, and C) were applied to the impregnation stages and during early bulk delignification. The A-profile represents a high EA-level between 8–18 g EA L<sup>-1</sup>, the B-profile an intermediate EA-concentration in the range 4–18 g L<sup>-1</sup>, and the C-profile a low EA-level in the range 2–9 g L<sup>-1</sup>. The final bulk and residual cooking phases were conducted at comparable conditions by varying the initial EA-concentration in the range 5 to 25 g L<sup>-1</sup>. The cooking temperature was kept constant at 153 °C during both cooking stages. The influence of temperature on the cooking performance was investigated in the final cooking stage, where selected trials were run at 165 °C. The cooking time or H-factor were adjusted accordingly to attain the target kappa number 18. The kappa number of the selected samples showed only minor deviations from the target kappa number (16–22), so that the kappa number can be assumed to be constant. The graph in Fig. 4.84 illustrates that the total yield is highly dependent upon the amount of EA-charge in both the early stages and the final stages of the cook.

The comparable slopes of the curves in Fig. 4.84 suggest that the yield loss is similar in magnitude for all three EA profiles investigated. A lower EA concentration at the final cooking stage is certainly favorable for xylan reprecipitation, as



**Fig. 4.84** Influence of different effective alkali (EA)-profiles in the early stages (EA-profiles A–C) and final stages of the cook (residual EA in the Figure) on the total yield of birch Lo-Solids laboratory cooks (according to [165]). All trials

were conducted at 153 °C in both cooking stages. The kappa numbers of all pulps were on average about 18 (minimum 16, maximum 22).



**Fig. 4.85** Influence of both different effective alkali (EA)-profiles in the early stages (EA-profiles A–C) and final stages of the cook (residual EA in the Figure) on the pulp viscosity of birch Lo-Solids

laboratory cooks (according to [165]). All trials were conducted at 153 °C in both cooking stages. The kappa numbers of all pulps were on average about 18 (minimum 16, maximum 22).

has been confirmed by carbohydrate analysis. The cellulose content is particularly preserved at lower EA concentration in the early stages of the cook. A high concentration of EA in the early bulk delignification phase also deteriorates pulp viscosity, as shown in Fig. 4.85. The lower cellulose content might be an explanation for the decrease in viscosity. The influence of the EA concentration in the final cooking stages, however, has an even more pronounced influence on pulp viscosity (Fig. 4.85). High viscosity levels are attained at very low residual EA concentration, despite the high extent of xylan reprecipitation. With an increasing EA charge, pulp viscosity passes through a minimum at a residual EA concentration of  $5 \text{ g L}^{-1}$  for all three EA-profiles investigated.

Higher EA charges in the residual delignification phase promote higher pulp viscosities due to unfavorable conditions for xylan retention on the fiber, while largely preserving the cellulose fraction.

By increasing the temperature from 153 °C to 165 °C in the final cooking stages, the brownstock yield is decreased by 1.2% at a given kappa number. It has been calculated that 28% of the yield loss is due to a lower cellulose yield, and 72% to a lower hemicellulose yield [165]. Hardwood kraft pulping is associated with the formation of the HexA. Kraft pulping offers only limited possibilities to reduce the HexA content prior to bleaching; however, the HexA content was shown to decrease slightly, from approximately  $73 \mu\text{mol g}^{-1}$  to about  $65 \mu\text{mol g}^{-1}$  with a higher EA concentration in both early stages and the last cooking stage.

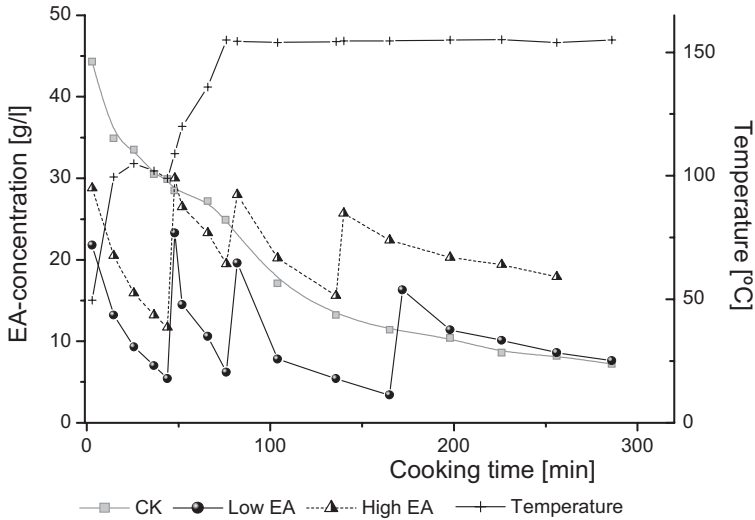


Fig. 4.86 Effective alkali and temperature profiles (according to [166]).

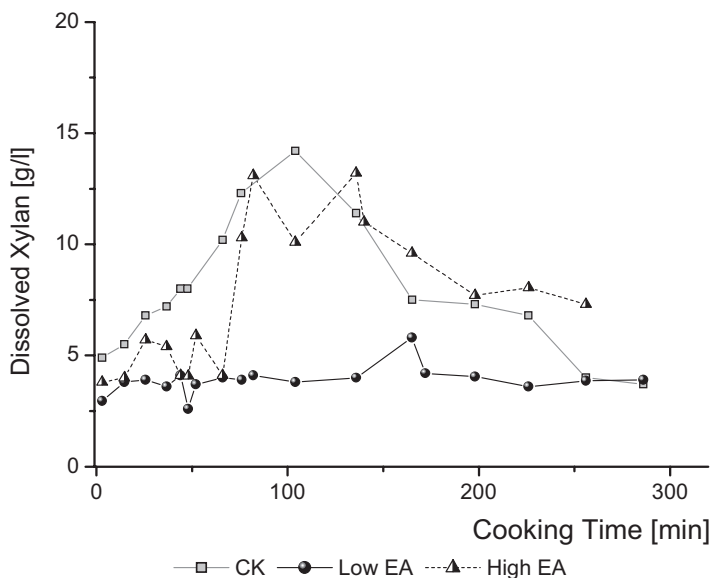
In another study, where a conventional batch cook was included for comparative purposes, it was again shown that a higher EA concentration at the start of bulk delignification tends to decrease mainly the cellulose yield, while a higher EA concentration towards the end of the cook decreases mainly the yield of xylans [139]. The corresponding alkali profiles are shown in Fig. 4.86.

For the low-EA profile, the cellulose yield is 37.5% on wood, and thus 1.5% on wood higher as compared to the conventional EA profile, whereas the xylan yield amounts to 13.7% on wood for both profiles. For the high-EA profile, the cellulose yield is 35.9% on wood and thus the same as for the conventional, but the xylan yield is 1.4% on wood lower than for the conventional and low-EA profiles.

The concentrations of dissolved xylan in the black liquor throughout the cooks reflect the amount of xylan reprecipitation onto the fiber. In the case of the conventional EA profile, the xylan concentration increases steadily to  $15 \text{ g L}^{-1}$  as it dissolves into the liquor. After having achieved maximum temperature, the xylan concentration decreases again as it reprecipitates onto the fiber. Interestingly, the dissolved xylan concentration remains constant at a very low level of about  $4 \text{ g L}^{-1}$  when cooking with a low-EA profile (see Figs. 4.86 and 4.87).

The dissolved xylan content is exactly the same after both conventional and low-EA cooks, reflecting equal xylan yields for the two cooks. As shown in Fig. 4.87, the dissolved xylan content after the high-EA cook remains at a high level when the residual EA concentration is high. This implies a direct correlation between the residual EA concentration and the xylan content of the pulp.

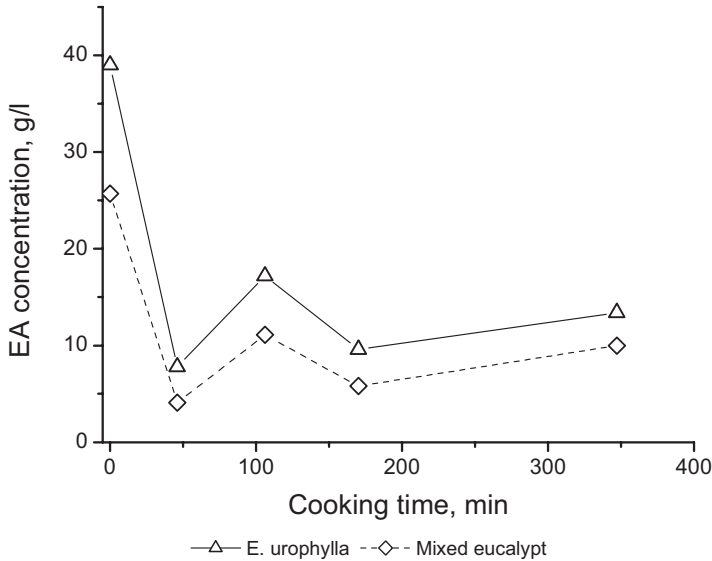
The effects of the alkali profile during Lo-Solids cooking of eucalyptus chips has been described in a recent study [167]. After the impregnation stage, a first displacement stage simulates a countercurrent heating stage by displacing part of the cooking liquor with white liquor; this is then followed by a 60-min co-current



**Fig. 4.87** Dissolved xylan concentration in the cooking liquor for cooks with different effective alkali (EA) profile (according to [139]).

cooking phase. Finally, the second displacement simulates the countercurrent cooking/washing stage at the bottom zone of a Lo-Solids digester. Again, the cooking liquor is displaced by white liquor. The maximum cooking temperature is varied in the range from 147 °C to 153 °C. Conventional batch cooks with a total EA charge of 20% NaOH on o.d. wood and a maximum temperature of 164 °C were conducted as a reference. Lo-Solids cooks were performed from both *E. urophylla* and mixed eucalypts from New Zealand, using different alkali profiles that were adjusted by adding alkali to each cooking stage. The conditions were selected such that the unbleached kappa number ranges between 14 and 17. The results indicate that pulping selectivity in terms of both yield and viscosity is clearly associated with a low and even EA profile throughout the whole cook (Fig. 4.88). Only small deviations from the optimum alkali profile would lead to a reduced pulping selectivity. The lower alkali profile (as shown in Fig. 4.88) contributes to a yield gain of 3.7% compared to the conventional batch cooks.

The Lo-Solids cooks of the mixed eucalypts showed, however, only a yield gain of 1.7% compared to the reference cook, probably due to a suboptimal EA profile. In both cases the yield gain resulted from a better retention of both cellulose (1.5–2.7% higher glucan yield) and xylan (1–1.2 % higher xylan yield) in comparison to the conventional batch cooks. Maintaining an optimum alkali profile and a low cooking temperature also improves the selectivity in terms of viscosity at a given kappa number. The viscosity/kappa number ratio for the optimized *E. urophylla* Lo-Solids cook was 82.4 (1400 mL g<sup>-1</sup> at kappa number 17)



**Fig. 4.88** Effective alkali (EA) profiles for Lo-Solids cooks of both mixed eucalypts originating from New Zealand and *E. urophylla* at the same cooking temperature of 147 °C (according to [167].)

with only 72.4 (1100 mL g<sup>-1</sup> at kappa number 15.2) for the conventional batch-cooked pulp.

A further development of the continuous cooking concept is based on the results from numerous laboratory trials in which the combination of low EA concentration at the beginning of a cook and a high EA concentration in the late stage turned out to be favorable with respect to cooking time or temperature, pulp yield, pulp viscosity, bleachability and HexA content [24]. This new continuous cooking process – denoted as Enhanced Alkali Profile Cooking (EAPC) – allows the EA profiles to be controlled in kraft cooking, without increasing white liquor consumption [29]. The first zone in the digester comprises a co-current pretreatment stage where most of the alkali introduced into the feed system is allowed to be consumed. The spent liquor with the low alkali concentration is extracted to recovery. The chips then pass the countercurrent impregnation zone where fresh alkali is added. The subsequent cooking is divided between co-current and countercurrent zones. After the first cooking zone, the cooking liquor is extracted and replaced by white liquor before entering the countercurrent cooking zone. To maintain a high EA concentration during residual delignification, white liquor is added at the end of the countercurrent cooking zone to the upflow liquor. Because of the high EA concentration, the cooking liquor from the lower extraction (of the final cooking stage) is recycled to the chip feed system to utilize the residual alkali for the subsequent cook. In this process, all black liquor to recovery is extracted from the digester between the end of the pretreatment and beginning of the

impregnation stage. The black liquor extracted from the cooking zones is to be reused in the previous stages. Thus, the continuous EAPC cooking process facilitates control of the EA profile during kraft cooking to consider the principles of modified cooking. Consequently, a wide range of alkali profiles in the cooking phase can be adjusted to partly control the unbleached pulp properties (bleachability, tear strength, etc.). Mill trials at the Enso Varkaus mill in 1996 revealed an increase in tear strength (bulk) at a given tensile strength of about 20% (10%), which confirmed the predicted improvements of unbleached pulp properties. Moreover, chlorine dioxide consumption was decreased by about 10% in a subsequent ECF bleaching sequence, suggesting an improved bleachability of the EAPC-produced softwood kraft pulps [168].

#### 4.2.6.3 Polysulfide and Anthraquinone Pulping

The peeling reactions which are responsible for a major decrease in pulp yield can be retarded if the reducing end groups are transferred into alkali stable groups. This can be achieved in three ways [1]:

- Reduction of end groups to primary alcohol groups.
- Oxidation of the end groups to aldonic acid groups.
- Blocking the end groups with agents reacting with aldehydes.

Among the wide variety of proposed methods for stabilizing the carbohydrates according to the given principles, only the oxidation of the end groups seems to be economically attractive for an industrial application. At present, there are two different technologies for the oxidative stabilization of carbohydrates against progressive alkaline peeling reactions – the polysulfide and anthraquinone methods.

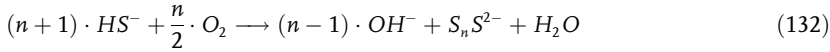
##### 4.2.6.3.1 Polysulfide Pulping

The impregnation of polysulfide liquor leads to the oxidation of the accessible reducing end groups, provided that the  $[\text{OH}^-]$  ion is sufficiently high (see Eq. (139) below) [169]. The ability of a polysulfide solution to stabilize carbohydrates increases with the concentration of elementary sulfur, and with the ratio of elementary sulfur to sulfide sulfur. The pretreatment with polysulfide solution can be carried out in different ways. One way would be to impregnate the wood chips with pure polysulfide liquor ( $\text{Na}_2\text{S}_4$ ) at temperatures between 100 and 130 °C prior to conventional cooking. After the pretreatment, the excess liquor is withdrawn and stored for reuse [170].

The polysulfide solution can be prepared by dissolving elementary sulfur in the white liquor. In the presence of  $[\text{HS}^-]$  ions, elemental sulfur is simultaneously converted to polysulfide sulfur already at rather moderate temperature:



According to Eq. (131), the dissolution of sulfur in the  $[\text{HS}^-]$  ion-containing solution consumes alkali. To maintain a target EA charge, it is necessary to add additional alkali to compensate for the alkali consumed. The polysulfide solution consists of an equilibrium mixture of different polysulfide ions, with  $n$  between 1 and 5. A second method for polysulfide production comprises a direct catalytic oxidation in which part of the hydrogen sulfide in the white liquor is oxidized to polysulfides according to the following reaction [Eq. (132)]:



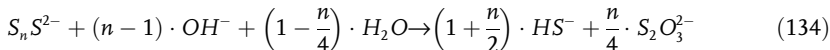
Equation (132) represents the main reaction in white liquor oxidation according to the MOXY process [171]. About 30% of the initial hydrogen sulfide will react to thiosulfate according to the following expression:



One catalyst for the MOXY system is a granular, activated carbon which has been treated with a wet-proofing agent to provide areas on the carbon surface which are not wetted by the liquid phase.

Applying the MOXY process to the whole white liquor would substantially reduce the amount of  $[\text{HS}^-]$  ions; this must be considered when choosing the appropriate conditions for modified cooking. It is thus recommended to raise sulfidity in the white liquor (i.e., in chemical recovery) from 30% to 40%, or even to 50%. It is then possible to maintain the  $[\text{HS}^-]$  ion concentration at a high level during the cook, which is important for maintaining a high intrinsic viscosity of the pulp. The MOXY process utilizes only that sulfur content normally present in the mill's liquor supply, and thereby does not alter the sulfur:sodium ratio in the black liquor, as would be the case when adding sulfur to the white liquor to produce polysulfide liquors.

Impregnation with the polysulfide-containing solution should be performed below 110 °C, as polysulfide easily decomposes to thiosulfate and sulfide under these conditions according to the Eq. (134) [172,173]:



The rate of decomposition of polysulfide solutions increases with increasing temperature, increasing  $[\text{OH}^-]$  ion and decreasing  $[\text{HS}^-]$  ion [172,174].

A recent kinetic study revealed that polysulfide disproportionation depends only on the hydrogen sulfide, polysulfide ion concentrations and on temperature according to the following rate expression [Eq. (135)] [174,175]:

$$\frac{d[S(0)]}{dt} = -7.7 \cdot 10^{13} \cdot \text{Exp}\left(-\frac{140\,000}{8.314 \cdot T}\right) \cdot [S(0)]^{1.6} \cdot [S(-II)]^{-0.8} \quad (135)$$

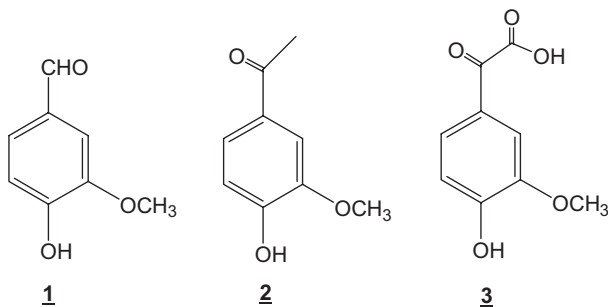


Equation (135) was derived for  $[S(0)]/[S(-II)] \leq 0.15$ , but validity can be assumed for  $[S(0)]/[S(-II)]$  as high as 0.5.

From this kinetic equation it can be concluded that a higher sulfidity in the cook will be in favor of a higher polysulfide concentration. A decrease in temperature, as employed in the latest generation of modified cooking processes (e.g., CBC, ITC), will lead to a slower decomposition of the polysulfide present. The overall result will be governed by the difference in activating energies between the production and decomposition of polysulfide sulfur.

Unbleached pulps from *Pinus sylvestris* from both conventional kraft and polysulfide cooking were compared with respect to their amounts of gluconic acid end groups. Polysulfide pulp contains significantly more glucometasaccharinic end groups than simply kraft-cooked pulps. Thus, it can be concluded that part of the reducing end groups are oxidized to aldonic acid groups during polysulfide cooking, which at least partly explains the higher yield of polysulfide cooking (50.9% at kappa number 31.5) when compared to conventional kraft cooking (45.9% at kappa number 28.1) [176].

Polysulfide also reacts with certain lignin structures, rendering them more soluble due to the introduction of, for example, carboxylic groups. Studies with model compounds revealed that polysulfide can oxidize coniferyl alcohol not only to vanillin **1** and acetovanillone **2** as shown by Nakano et al. [177] and Brunow and Miksche [178], but also to (4-hydroxy-3-methoxyphenyl)-glyoxylic acid **3** [179].



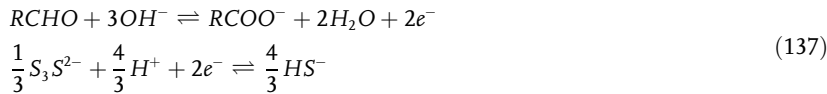
The formation of the latter requires temperatures above 135 °C, in contrast to other oxidized structures such as vanillin and acetovanillone, which already generate at lower temperatures. The formation of these compounds indicates that polysulfide can introduce not only  $\alpha$ -carbonyl groups into free phenolic structures but also carboxylic acid groups into the side chain. The oxidation products 1–3 have a strong UV-absorbance at about 350 nm. The UV spectra of black liquors from cooks with a polysulfide pretreatment show a strong absorbance at 353 nm for spruce and at 370 nm for birch [179,180]. The compound responsible for absorbance at 370 nm is identified as (4-hydroxy-3,5-dimethoxyphenyl)-glyoxylic acid. The introduction of carboxylic acid groups into lignin structures explains why more lignin is removed when part of the sulfide sulfur is added as polysulfide [175].

At a low EA concentration (e.g.,  $0.125 \text{ mol L}^{-1}$ ), the rate of bulk and residual phase delignification is increased by the addition of polysulfide, which may be led back to the better solubility of oxidized lignin structures. It has also been suggested that the amount of residual phase lignin is reduced by the polysulfide treatment, though this observation might be connected with the findings that polysulfide attacks and degrades phenolic enol ether structures at only moderate temperatures [181]. These compounds are rather stable under standard kraft cooking conditions, and consequently they are constituents of the residual phase lignin. The removal of enol ethers creates new phenolic  $\beta$ -O-4 structures which, in turn, contribute to further degradation of the lignin.

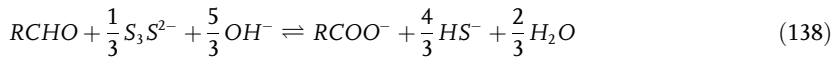
The ability of a polysulfide treatment of wood to stabilize the carbohydrates to achieve a yield increase is dependent on the ratio of elemental to sulfide sulfur,  $S(0)/S(-II)$ , the hydroxyl ion concentration,  $[OH^-]$ , and on the concentration of excess S,  $S(0)$ . The wood was pretreated with a solution containing elemental sulfur (0.1–0.5 M), effective alkali (0.3–0.01 M  $[OH^-]$ ) and hydrogen sulfide ions at  $90^\circ\text{C}$  for 1 h prior to conventional kraft cooking (l:s = 4:1, initial concentration of NaOH was 0.8 M, of NaHS 0.2 M corresponding to an EA charge of 13% and sulfidity of 40% at  $170^\circ\text{C}$  for 90 min) [169]. The redox potential of the polysulfide solution could be predicted by the following expression:

$$E_0[mV] = 606 - 49 \cdot \text{Log}[OH^-] - 37 \cdot \text{Log}[S(0)] - 56 \cdot \text{Log} \left[ \frac{[S(0)]}{[S(-II)]} - \frac{1}{4} \right] \quad (136)$$

The oxidation of reducing end groups to aldonic acids is highly dependent upon the hydroxyl ion concentration:



Total redox equation:



The ability to oxidize the reducing end groups can be predicted from the redox potential (E) by adding separate terms to consider the influence of hydroxide ion and excess sulfur concentrations to the Nernst equation according to Eq. (139):

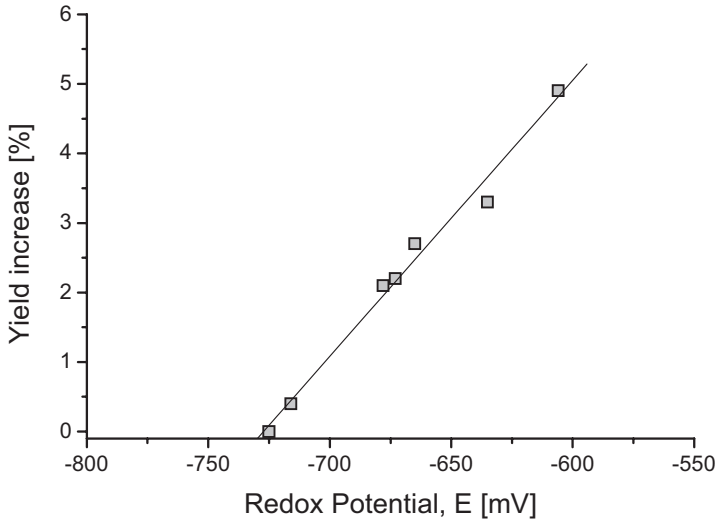
$$\Delta Y \approx E_0 + \frac{R \cdot T}{F} \cdot \left[ \frac{3}{2} \text{Ln}[OH^-] + \text{Ln}[S(0)] \right] \quad (139)$$

where  $\Delta Y$  corresponds to the yield increase compared to kraft cooking without polysulfide pretreatment.

The ability of a polysulfide pretreatment to achieve a yield increase can be described without using the redox potentials by combining expressions of the type displayed in Eqs. (136) and (139). The yield increases (in percent on wood), obtained as a result of the polysulfide pretreatment, can be calculated by Eq. (140):

$$\Delta Y = 5.0 + 1.5 \cdot \text{Log}[S(0)] + 2.4 \cdot \text{Log}[OH^-] - 2.2 \cdot \text{Log} \left[ \frac{[S(0)]}{[S(-II)]} - \frac{1}{4} \right] \quad (140)$$

The experimental results plotted against Eq. (139) are shown in Fig. 4.89.



**Fig. 4.89** The increase in yield based on wood, obtained by pretreating wood with polysulfide at 90 °C prior to kraft pulping as a function of the redox potential, E, which is composed of  $E_0$  derived from Eq. (136) and the Nernst equation derived from Eq. (139) (according to [169]).

The yield increases shown in Fig. 4.89 are dependent on the concentration of excess sulfur, the ratio of excess sulfur to sulfide sulfur ( $X_s$ ), and the alkalinity of the polysulfide solution. The conditions, as well as the calculated and measured results, are detailed in Tab. 4.38.

In Tab. 4.38,  $X_s$  is the ratio of excess sulfur to the sulfide sulfur  $[S(0)]/[S(-II)]$ ,  $E_{0,m}$  and  $E_c$  the measured redox potentials and  $E_{0,c}$  and  $E_c$  the calculated redox potentials according to Eqs. (136) and (139),  $\Delta Y_m$  the measured and  $\Delta Y_c$  the calculated yield increase according to Eq. (140).

At a given kappa number of 35, yield increases about 1.5% for every percent of elementary sulfur added in the pulping of pine and spruce. The effect can be enhanced to about 2% if the sulfur is introduced only in that part of the white liquor which is adsorbed by the wood during impregnation. According to carbohydrate analysis, polysulfide pulps have proven that the yield increases can be attrib-

**Tab. 4.38** The increase in carbohydrate yield based on wood obtained as a result of 1-h polysulfide pretreatment of wood at 90 °C prior to kraft pulping [ 169].

[S(0)] [mol L <sup>-1</sup> ]	X <sub>s</sub>	[OH <sup>-</sup> ] [mol L <sup>-1</sup> ]	E <sub>0,m</sub> [mV]	E <sub>0,c</sub> [mV]	RT/F*Ln[x] <sup>pl</sup> [mV]	E <sub>m</sub> [mV]	E <sub>c</sub> [mV]	ΔY <sub>m</sub> [%]	ΔY <sub>c</sub> [%]
0.1	2.0	0.32	-509	-511	-126.1	-635	-637	3.3	3.6
0.1	2.0	0.10	-485	-486	-180.2	-665	-666	2.7	2.4
0.1	0.5	0.32	-552	-558	-126.1	-673	-684	2.2	1.8
0.1	0.5	0.10	-538	-534	-180.2	-716	-714	0.4	0.6
0.5	2.0	0.32	-559	-537	-75.7	-606	-612	4.9	4.7
0.5	1.0	0.10	-555	-539	-129.8	-678	-669	2.1	2.4
0.5	1.0	0.01	-512	-490	-237.9	-725	-728	0	0.0

a) right part of equation (139).

uted to improved retention of glucomannan for softwood [182] and xylan for hardwood [183].

In laboratory trials a spruce-lodgepole-fir blend (80:15:5) was pulped by using a conventional batch-type schedule [184]. The polysulfide-containing cooking liquor was produced according to the MOXY process using an industrial white liquor in a pilot plant. The composition of the white liquor before and after the oxidation treatment is compared in Tab. 4.39.

**Tab. 4.39** Oxidation of white liquor according to the MOXY process [ 184].

Parameter	unit	White liquor	Orange liquor
Na <sub>2</sub> S	g NaOH L <sup>-1</sup>	54.6	19.1
NaOH	g NaOH L <sup>-1</sup>	73.0	102.2
Na <sub>2</sub> CO <sub>3</sub>	g NaOH L <sup>-1</sup>	19.4	23.1
Na <sub>2</sub> S <sub>2</sub> O <sub>3</sub>	g NaOH L <sup>-1</sup>	5.0	8.9
Polysulfide sulfur	g s L <sup>-1</sup>	0.0	9.5
Active alkali	g NaOH L <sup>-1</sup>	127.6	121.3
Effective alkali	g NaOH L <sup>-1</sup>	100.3	111.7
Sulfidity	% on AA	42.8	15.7

With a total active alkali charge of 25%, the polysulfide addition calculates to 1.9% on o.d. wood. The conventional kraft process showed a favorable response to polysulfide pulping. The yield increase was in the order of 2.6% on wood, or about 5.5% on a pulp basis. Carbohydrate analysis revealed that the yield increase found is a result of increased retention of glucans and mannans. The data suggest that 55% of the yield gain can be attributed to an increased cellulose retention, and the residual 45% to an increased galactoglucomannan retention [184].

The addition of polysulfide to EMCC kraft cooking compensates for the yield loss which occurs when pulping to kappa numbers below 20. A laboratory study using Southern pine chips confirmed that extended modified cooking and polysulfide pulping are compatible technologies [185]. The addition of 2% and 3% PS to extended modified cooking was found to increase the pulp yield by about 2% and 3% on wood, respectively, at a kappa number of 17 (Tab. 4.40).

**Tab. 4.40** Laboratory study of the effect of polysulfide (PS) addition to both conventional and extended modified kraft pulping of Southern pine chips (according to [185]).

Parameter	Unit	Conventional kraft cooks			Extended modified cooks		
		CK1	CK2	CK3	EMCC1	EMCC2	EMCC3
Polysulfide	% S od w	0	0	2	0	2	3
Sulfidity	%	30	30	30	31	30	30
Impregnation stage							
Temperature	°C	110	110	110	110	110	110
EA-charge	% NaOH od w	19.71	20.61	21.9	14.1	14.1	16.8
First cooking stage							
Temperature	°C	170	170	170	165	165	165
EA-charge	% NaOH od w				5.0	5.0	5.0
Countercurrent stage							
Temperature	°C				165	165	165
H-factor		1560	1720	1690	2960	3020	3050
Screened yield	% od w	46.2	46.1	48.7	43.4	45.3	46.7
Kappa number		29.6	27.4	27.1	16.7	17.2	17.6
Intrinsic viscosity	mL g <sup>-1</sup>	1115	1075	1150	1030	1080	1110

The addition of approximately 3% PS increases the pulp yield of an EMCC pulp with kappa 17 to a level typical for conventional pulps with kappa number 30. The results also show that charging with 2% PS increases the pulp yield by about 2.5% when cooking to kappa numbers close to 30, suggesting that the yield increase from PS addition is larger at a higher kappa number. This finding is in agreement with results from previous studies where pulp yield was found to increase by 1.2–2% for every 1% of PS added. The specific yield gain further increases when approaching higher kappa numbers [186]. In contrast to results from other studies, the addition of PS does not appear to affect pulp tear, burst or tensile properties [184]. The preservation of strength properties is also reflected in the high intrinsic viscosity levels (see Tab. 4.40). Refining energy to a given freeness can be reduced by approximately 10% and 20%, respectively, with 2% and 3% PS addition. This is in agreement with previously reported data, and can be traced back to a higher retention of hemicelluloses.

A PS kraft cook of a mixture of *Pinus sylvestris* and *Picea abies* with a 5% charge of PS on wood gave an average yield increase of about 3% on wood within a kappa number range 7 to 20 [187]. The yield increase related to PS addition is smaller than has been reported at higher kappa numbers, probably because the reinforced conditions when pulping to a lower lignin content cause a higher loss in hemicelluloses [186]. Moreover, delignification selectivity, given as kappa number–viscosity relationship, was improved as a result of the PS pretreatment. Interestingly, if the hydroxide ion concentration is too low by using, for example a  $\text{HCO}_3^-/\text{CO}_3^{2-}$  buffer system during the PS pretreatment, neither a yield increase nor a viscosity improvement can be observed.

A decrease in kappa number from 35 to 20–25 in a normal kraft cook of Scots pine reduces the pulp yield by 2–3% units. The yield loss is compensated for by the use of PS which is produced by the MOXY process [171,188]. Using a high-sulfidity white liquor (sulfidity 52%), a PS concentration of 0.32 M S(0) is produced applying the MOXY process. The conventionally bleached (CEHDED) polysulfide pulps with low kappa number (21–23) revealed similar viscosity values (ca.  $900 \text{ mL g}^{-1}$  at 88% ISO brightness) and strength properties (ca.  $14 \text{ mN m}^{-2} \text{ g}^{-1}$  tear index at  $70 \text{ Nm g}^{-1}$  tensile index) as compared to the normal kraft pulps with kappa number 35 after cooking [188]. Due to the prolonged cooking using PS-containing white liquor to compensate for the yield loss, the consumption of chlorine chemicals can be reduced by about 26% using a conventional CEHDED-sequence. In the PS process, some alkali is consumed for the reaction between the PS and the wood components according to Eqs. (137) and (138). Thus, approximately 16% more EA charge (20.4% instead of 17.6% on o.d. wood) is required in PS cooking to attain the same degree of delignification at a given H-factor.

The addition of 1.6–1.7% PS sulfur during the impregnation stages of both the MCC-type and ITC-type cooks using a mixture of *Picea abies* and *Pinus sylvestris* as wood source gave an increase in carbohydrate yields of 1.2% at kappa number 24, and of 1.5% at kappa number 19 as compared with the reference [189]. The lower yield increase for the modified cooks can probably be explained by the higher  $[\text{OH}^-]$  ion in the final cooking stages. The extraction of cooking liquor from the

digester in the Hi-Heat zone certainly counteracts the reprecipitation of dissolved hemicelluloses. The carbohydrate yield increase associated with PS pulping can be attributed predominantly to a rise in glucomannan retention. The pulps from PS pulping showed a slightly lower tearing resistance, but comparable zero-span tensile indices. Thus, it can be concluded that strength properties are not impaired by PS pulping. The bleachability in an OD(E+P)DED bleaching sequence was equal for both the PS ITC-type pulp and the reference ITC-type pulp. The latter requires 135 OXE per ton of pulp and kappa number to reach a brightness of 89% ISO, whereas the PS pulp required 133 OXE per ton of pulp and kappa number.

#### *Mill experience of PS pulping*

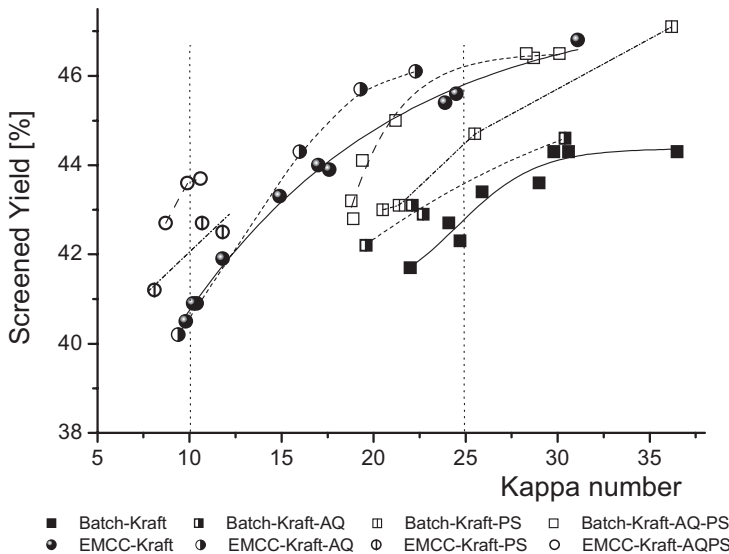
The Norwegian kraft mill, Lövenskiold-Vaekerö, Hurum Fabriker, changed to the PS process as early as 1967 [190]. Polysulfide is produced by the dissolution of elementary sulfur in the white liquor. After one year's experience, yield increases of 3.5–4.0% were obtained with a 2.2% sulfur addition on wood. The PS pulps are characterized as easy-beating pulps, with the reduction in required beating energy in the mill amounting to 25–30%. Due to the reduced fibers per unit area, a slight reduction in the tear factor of the paper product was observed. Runnability on the paper machine was, however, not significantly affected. Although economic calculations are dominated by the currently available wood, sulfur and pulp prices, a net gain of approximately 5 US\$ adt<sup>-1</sup> pulp can be expected. [190].

The additional costs in pulping due to PS addition and slightly higher EA demand must be compared with the savings in bleaching chemicals and effluent treatment costs, in order to estimate the economy of PS pulping in combination with extended modified cooking.

#### **Combined PS and Anthraquinone (AQ) Effects**

Modified pulping has made it possible to extend the cook to very low kappa numbers, without impairing strength properties. However, the significant yield losses which occur at low kappa numbers renders extended delignification economically nonfeasible. The synergetic effect on yield of the combined use of PS and AQ could compensate for the yield loss at low kappa numbers [188,191]. By applying the concept of extended modified cooking of southern pine, the sole addition of 0.1% AQ increases brownstock yield by about 1% at kappa 25 [191]. The yield increase becomes less than 0.5% by further extending delignification to kappa number 16, and is not measurable at kappa number 10. Under these conditions, only a small fraction of the AQ is available in the cooking liquor for carbohydrate stabilization. Moreover, AQ can oxidize the C-2 and C-3 hydroxyl groups in the anhydroglucose units, promoting chain cleavage and secondary peeling reactions. The addition of 2% PS, however, results in an average yield increase of about 1.5% within the kappa number range 8–12. The lower efficiency of PS in the lower kappa number range can presumably be explained by the decreasing stability of the retained hemicelluloses. The simultaneous addition of 2% PS and 0.1% AQ results in a total yield increase of 3% at kappa number 10, which is 1.6% higher

as the additive effect from applying PS and AQ individually (Fig. 4.90). As one possible mechanism which has been discussed in this regard is that PS participates in the AHQ-lignin and AQ-carbohydrate redox system, where partial regeneration of PS and/or stabilization of PS against disproportionation takes place. According to the carbohydrate analysis, the yield increase originates from an increased retention of glucomannan in the softwood pulp. The synergistic effect of the combined addition of 0.1% AQ and 1.3% PS is also reported for conventional batch cooking of southern pine in the kappa number range 20–35 [192]. At kappa number 25, the total yield advantage amounts to 3.4% at kappa number 25, which is approximately 1% more as compared to the additive yield effect from applying PS and AQ individually. If PS and AQ are used in combination, the H-factor can be reduced by 17% (from 1900 to 1580) compared to reference kraft cooking to attain kappa number 25. The sole addition of PS shows no influence on the delignification rate, whereas AQ cooking leads to a 10% reduction in H-factor to reach kappa number 25. However, the reliability with respect to delignification rate is somewhat doubtful, because in PS and PS/AQ-cooking the EA charge was 23.7% as compared to 20.8% in the case of AQ and reference kraft cooks, respectively.



**Fig. 4.90** Effect of separate and combined addition of polysulfide (PS) and AQ for both extended modified cooking [191] and conventional batch cooking [191] of southern pine. EMCC cooking conditions: 21–25% NaOH on wood, EA-split: 75% impregnation, 25% cooking, 170 °C; 0.1% AQ,

2% PS, WL sulfidity 30%; residual EA concentration 17–18 g L<sup>-1</sup> as NaOH. Batch cooking conditions: 20.8% NaOH charge on wood for reference and AQ-cooks, 23.7% for PS and PS/AQ-cooks; 30% sulfidity for reference and AQ-cooks, 16.5% for PS and PS/AQ-cooks; 166–174 °C.



On the other hand, a recent kinetic study clearly states that the PS/AQ process shows the highest delignification rate (equivalent to a H-factor reduction of approximately 20%) as compared to kraft, kraft-AQ, and PS processes [193]. In addition, compared with the kraft and kraft-AQ concepts, the PS and PS/AQ cooks have lower cellulose degradation rates.

The effect of separate and combined addition of PS and AQ for both extended modified cooking and conventional batch cooking of southern pine is illustrated in Fig. 4.90.

#### *Mill experience of combined PS/AQ pulping*

The addition of PS sulfur amounts approximately to 0.5–1.5% on o.d. wood in mill praxis. The yield increase observed is reported to be in the range of one- to two-fold the amount of PS sulfur, dependent on the impregnation and cooking techniques, kappa number and wood species [1]. However, if alkaline pulping is preceded by impregnation of the wood chips with a PS-containing liquor, the yield gain may be increased to 2.5- to 4-fold the amount of the charged PS sulfur [1]. Polysulfide pulping has been practiced at the Peterson kraft mill in Moss since 1973 [194,195]. The Moss mill is an integrated pulp and paper mill producing linerboard specialties from pine and spruce. Cooking takes place in a two-vessel steam/liquor continuous digester to a target kappa number of 65. The PS cooking is prepared by catalytic air oxidation of sulfide in the white liquor using the MOXY process [171,196]. Oxidation takes place in reactors with only a few minutes' retention time in the presence of a special carbon catalyst, where about 70% of the oxidized sulfide is converted to PS sulfur, and the remainder to thiosulfate which behaves inertly under kraft cooking conditions. At the Moss mill, the PS concentration of the cooking liquor is about 5–6 g L<sup>-1</sup> sulfur, which occurs when about 50% of the sulfide in the white liquor is oxidized. In addition, 0.35 kg AQ per o.d. pulp is added to the cooking liquor. Polysulfide-AQ pulping at the Moss mill results in an average reduction in wood consumption of about 4.3% per ton of pulp, and an increased production capacity in the digester of about 4.5% – which increases to 10% when chemical recovery evolves as bottleneck and a more easily beaten kraft pulp is produced [194].

#### **Anthraquinone (AQ) Pulping [197]**

The beneficial effects of AQ on both the pulping rate and carbohydrate yield in soda and kraft pulping were first discovered by Bach and Fiehn [198].

The stabilizing effect of AQ is explained by oxidation of the reducing end-groups to form alkali-stable aldonic acid end-groups. Convincing evidence for this type of stabilizing reaction has been provided by Sjöström [199,200] and Samuelson et al. [201]. Topochemical investigations using the method of selective bromination of the lignin in nonaqueous system and subsequent determination of the Br-L X-ray emission revealed that soda-AQ pulping was much more selective in removing lignin from the middle lamella and cell corner regions as compared to uncatalyzed alkaline processes [202]. The secondary wall, however, was delignified faster by soda, followed by kraft, and finally soda-AQ pulping. It can be speculated

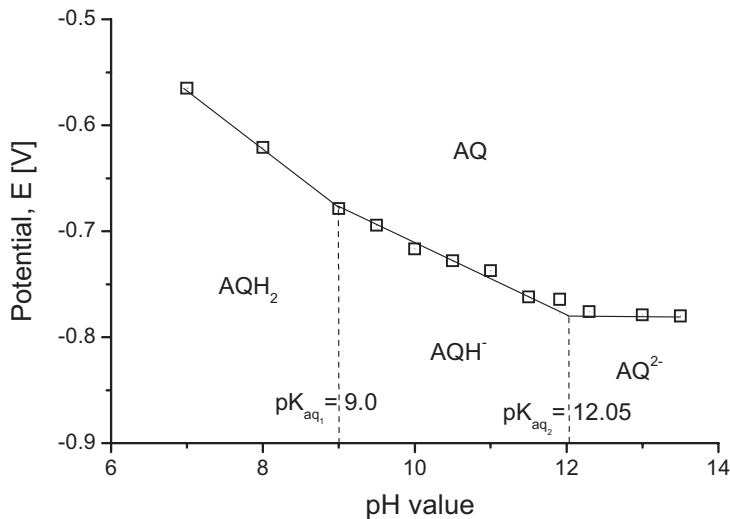
that lignin removal is retarded by the enhanced retention of carbohydrates being linked to lignin structures [203].

Anthraquinone is clearly insoluble in water, whereas its reduction product [e.g., 9,10-dihydroxyanthracene ( $AQ^{2-}$ )] is soluble in alkaline aqueous solution. In addition to the better solubility, use of the reduced form of AQ has been proposed as being advantageous because of the considerably higher rate of penetration, resulting in more homogeneous pulping [204,205]. The reduction of AQ is a reversible, two-electron process with  $AQ^{2-}$  as final product, as revealed by differential pulse polarography of AQ in aqueous solution (containing 5% DMF to solubilize AQ) [206]. The reduction of AQ in an aqueous solution can be described according to the following equilibria [Eq. (141)]:



From the intersections of linear extrapolations of the E-pH plot, the dissociation constants,  $pK_{aq1} = 9.0$  and  $pK_{aq2} = 12.05$ , can be determined. According to this result (see Fig. 4.91), the reduction product of AQ is solely present as a dianion under the conditions of kraft or soda pulping, with the standard redox potential,  $E_{AQ/AQ^{2-}}^0 = -0.778$  V (against saturated calomel electrode).

A thermodynamic study of the system  $Na_2S/AQ$  under the conditions of kraft pulping confirmed that AQ is reduced by the presence of hydrogen sulfide ions at temperatures above 100 °C. Both increasing temperature and EA are favorable for the reduction to the dianion. AQ oxidizes hydrogen sulfide ions in preference to

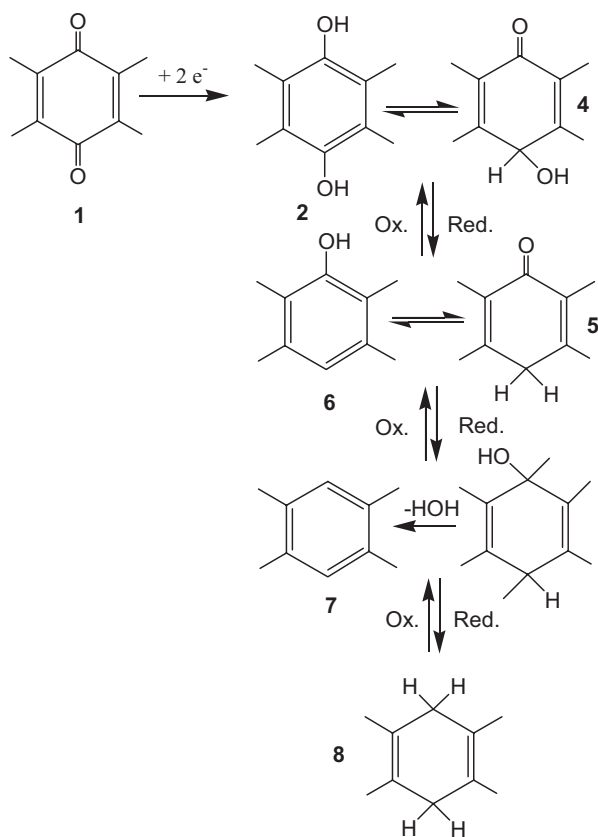


**Fig. 4.91** E-pH plot (Pourbaix diagram) for the equilibria of AQ redox reactions:  $AQ//AQH_2/AQH^-/AQ^{2-}$  measured at 25 °C in a 5% DMF aqueous solution (according to [206]).

sulfate ions and to thiosulfate ions, whereas oxidation to elemental sulfur is thermodynamically not feasible at any of the temperatures studied (298–423 K). This thermodynamic consideration suggests that AQ can be dissolved as  $AQ^{2-}$  by mixing it with white liquor at temperatures higher than 100 °C before its introduction into the digester [206].

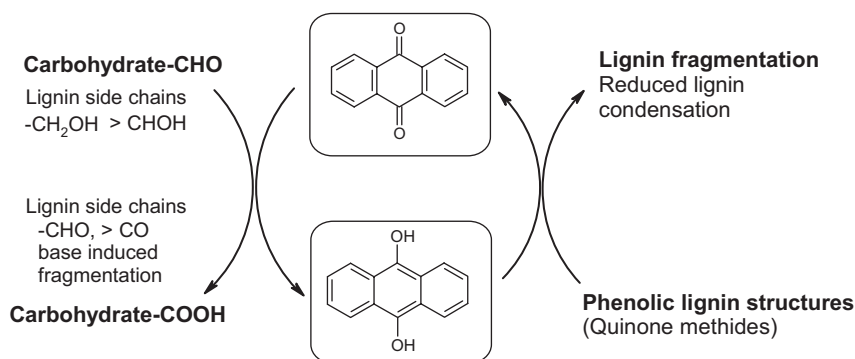
AQ is solubilized in the cooking liquor by sequential reduction, in the presence of polysaccharides. Electrons are transferred from the reducing end groups of the polysaccharide fraction in the wood. Simultaneously, the aldehyde groups are oxidized to aldonic acid groups and thus stabilized against the alkaline peeling reactions. This reaction is predominantly responsible for the increase in pulp yield, and to some extent also for some alkali savings as a result of the reduction in the formation of acids caused by suppression of stepwise depolymerization.

The AQ/AHQ redox system was extensively studied by Dence et al. [207]. During pulping, AQ **1** is reduced beyond the hydroquinone **2** to anthrone **5** and further to anthracene **7** and finally to dihydroanthracene **8**. The complete AQ/AHQ system is comprised of four individual redox systems, as shown in Scheme 4.26:



**Scheme 4.26** The AQ/AHQ system in alkaline pulping (according to [207]).

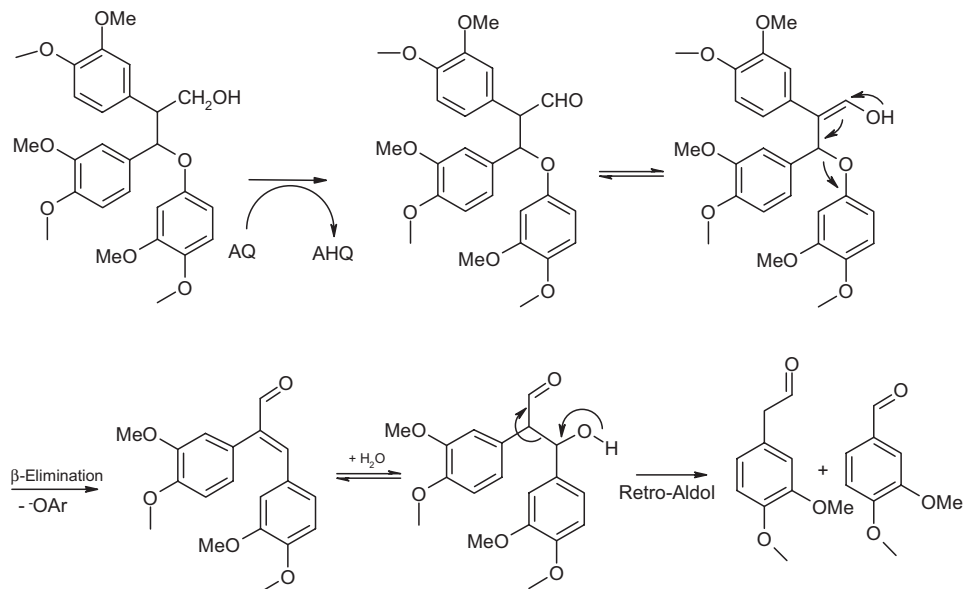
The most striking observation is the fact that the addition of extremely small amounts results in both a significant improvement of yield due to carbohydrate stabilization and in drastically enhanced delignification. An AQ charge of 0.05% on wood corresponds to a molar ratio of AQ to a phenylpropane unit (C9-unit) of about 1:500, and has a more pronounced effect on delignification as compared to a conventional kraft process with the same EA charge at 25% sulfidity. This sulfidity corresponds to a molar ratio of sulfur to C9-unit of about 1:2.5, this being two orders of magnitude less efficient in removing lignin than AQ (on a stoichiometric basis). The drastic improvements in delignification in the initial pulping stages and the substantial yield preservation achieved by extremely small quantities of AQ have been interpreted in terms of redox mechanisms. According to this highly simplified concept, the quinone is initially reduced by the carbohydrates to the hydroquinone, which in turn reduces lignin whereby the quinone is regenerated (Scheme 4.27).



**Scheme 4.27** General scheme of redox mechanisms (according to [203]).

It has been shown that in both carbohydrates and lignin, oxidative as well as reductive processes are taking place. Consequently, each could drive the redox cycle to some extent, and in particular lignin in which there appears to be a much better balance between functional groups undergoing oxidation and reduction than in the polysaccharides. The degradation of lignin is not only enhanced by reductive processes such as the cleavage of phenolic  $\beta$ -aryl ether bonds by AHQ, but also should be greatly facilitated by splitting the rather alkali-stable, nonphenolic  $\alpha$ -aryl ether substructures and the covalent carbon-carbon bonds between C- $\alpha$  and C- $\beta$  in side-chains [208]. Extensive experiments with appropriate model compounds confirmed that oxidation reactions contribute to the degradation of lignin [209]. By introducing carbonyl structures, lignin side-chains become prone to base-induced fragmentations such as reverse aldol additions and  $\beta$ -eliminations provided hydroxyl groups and ether functionalities are present in proper position in the lignin.

The degradation paths of  $\alpha$ -aryl ether structures by AQ are illustrated in Scheme 4.28.



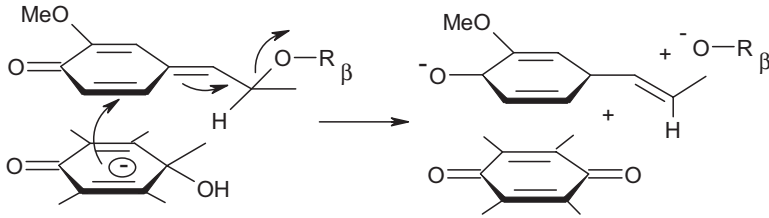
**Scheme 4.28** Degradation of  $\alpha$ -aryl ether structures by anthraquinone (AQ).

The interaction of AQ/AHQ with carbohydrates or lignin fragments can be visualized by the interaction of their  $\pi$ -electron systems, as shown in Scheme 4.29. The ionized AHQ acts as the  $\pi$ -base and forms a charge transfer complex (CTC) with the lignin quinone methide (lignin QM) intermediate ( $\pi$ -acid), allowing an electron transfer between both systems. The concomitant elimination of the  $\beta$ -aryl ether brings about a fragmentation and the regeneration of AQ. The  $\pi$ -system of AQ, now acting as  $\pi$ -acid, may accept an electron from a carbohydrate enolate ( $\pi$ -base), present in alkaline solutions, also via formation of the corresponding CTC. Here, the diketeto sugar moiety is formed and AHQ regenerated.

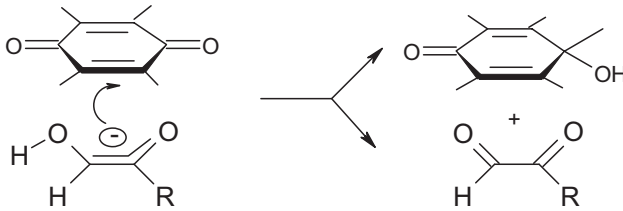
Both, the adduct and the single electron transfer (SET) mechanisms have been discussed in the literature. The adduct mechanism involves bond formation between the lignin quinone methide intermediates and AHQ, which is followed by fragmentation. The SET involves a single electron transfer between AHQ and a lignin QM, again followed by fragmentation [210]. The observation of stable radical formation within the AQ system and electron transfer to quinone methides are in favor of the electron transfer processes [211].

The effect of AQ on the pulp yield–kappa number relationship in soda pulping of water oak (*Quercus nigra*) is illustrated graphically in Fig. 4.92 [203].

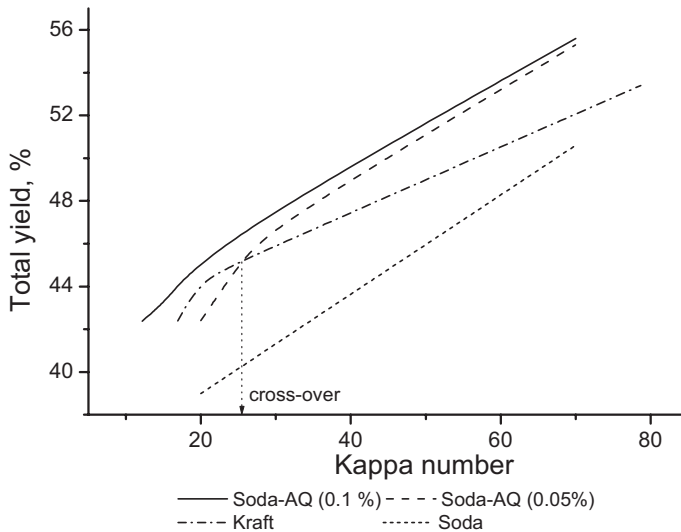
Oxidation of AHQ by lignin fragments:



Reduction of AQ by reducing end groups:



**Scheme 4.29** Proposed charge transfer complexes for the reduction of lignin fragments and oxidation of carbohydrates.

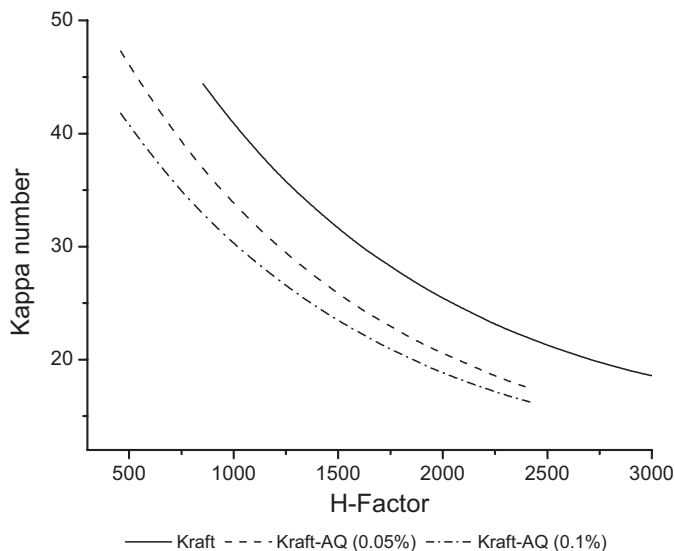


**Fig. 4.92** Soda-AQ pulping of water oak: time to = 90 min; time at = 30–80 min; active alkali 10–19%; maximum temperature 170 °C; for kraft: sulfidity 25% (according to [212]).

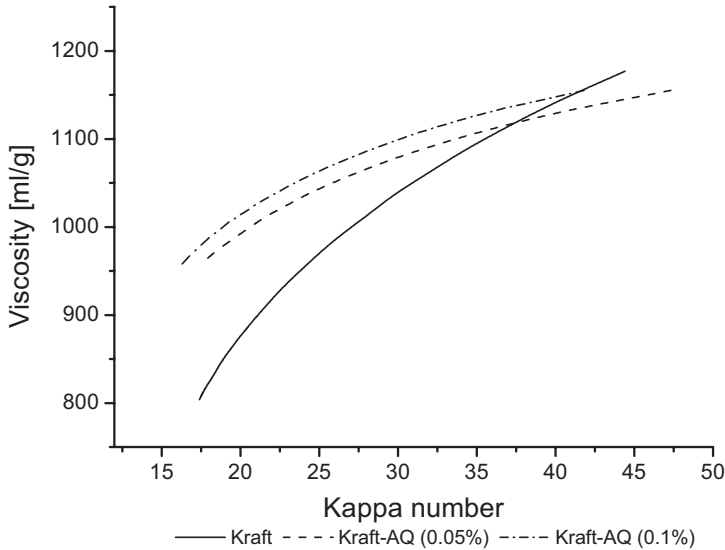
The data in Fig. 4.92 show that the additive is most effective in cooking to high kappa numbers. It is interesting to note that the regression lines for reference kraft and soda-AQ pulping with 0.05% additive charge show a cross-over at a kappa number of approximately 25. Only higher charges of AQ give a yield advantage over kraft pulping at extended delignification. Carbohydrate analysis of pulps indicated that soda-AQ pulping of water oak leads to a substantial stabilization of cellulose rather than xylans [212]. This experimental evidence is in contrast to PS pulping, where predominantly hemicelluloses are retained. The higher cellulose stability has been explained by the fact that the quinone seems to be sufficiently stable in the final cooking stage, and is thus able to stabilize the cellulose by oxidizing the reducing end groups generated by chain cleavage [203]. Further evidence for cellulose stabilization due to suppression of secondary peeling by AQ in soda pulping was provided by pulping experiments with prehydrolyzed sweetgum, where a significant increase in  $\alpha$ -cellulose yield was obtained when AQ was present [213].

The addition of AQ to conventional kraft cooking of loblolly pine revealed a significant improvement in both delignification rate and selectivity of delignification [14].

A kappa number of 30 can be achieved at 25% and 37% lower H-factors by kraft-AQ pulping by applying AQ-charges of 0.05% and 0.1% on wood, respectively (Fig. 4.93).



**Fig. 4.93** Effect of anthraquinone (AQ) charge on the kappa number–H-factor relationship (according to [14]). Constant cooking conditions: 90-min rise to a maximum temperature of 173 °C, liquor-to-wood ratio 4.0, sulfidity 35%, effective alkali charge 18% as NaOH.



**Fig. 4.94** Effect of anthraquinone (AQ) charge on the viscosity–kappa number relationship (according to [14]). Constant cooking conditions: 90-min rise to a maximum temperature of 173 °C, liquor-to-wood ratio 4.0, sulfidity 35%, effective alkali charge 18% as NaOH.

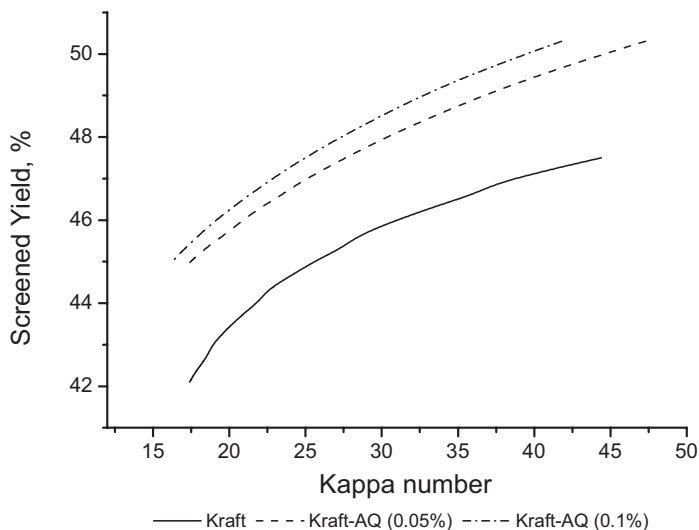
It is apparent from the data in Fig. 4.94 that the presence of AQ accelerates delignification at a given H-factor but has no effect on viscosity, and this results in an overall improvement of selectivity. The advantage in viscosity as compared to conventional kraft cooking increases with reducing kappa numbers (Fig. 4.94).

The effect of AQ addition on pulp yield being significant over the whole kappa number range investigated is not only induced by lowering the cooking intensity, but is primarily due to carbohydrate stabilization reactions. The major part of the yield advantage is already given at low AQ charges. The addition of only 0.05% AQ on wood results in a yield increase at a kappa number of 30 by 2.1%. A doubling of the AQ charge leads to a further yield increase by 0.6% at the given kappa number (Fig. 4.95).

The kraft-AQ process enables both the production of low-lignin pulps at unchanged screened yield and high-yield pulps at a given kappa number. The former are slightly more difficult to brighten in the final ECF bleaching stages of the bleaching sequence, and deliver tear strengths which are approximately 10% lower than those of conventional kraft controls. The latter, however, brings the advantage of lower wood consumption and simultaneously helps to reduce bottle-necking in the recovery area.

The addition of AQ to kraft pulping accelerates the production of southern pine chips to produce linerboard-grade pulp. Mill trials demonstrated that a charge of only 0.05% on wood allows a 25–35% reduction in H-factor combined with a 5%





**Fig. 4.95** Effect of anthraquinone (AQ) charge on the screened yield–kappa number relationship (according to [14]). Constant cooking conditions: 90-min rise to a maximum temperature of 173 °C, liquor-to-wood ratio 4.0, sulfidity 35%, effective alkali charge 18% as NaOH.

reduction in EA charge, while keeping a comparable pulp quality as produced without AQ addition [214]. At a given kappa number, yield gains of about 2–3% on wood were obtained. In another linerboard production, the effect of AQ on yield was confirmed [215], with a yield increase of 1.7% being achieved by adding 0.05% AQ to wood chips in kraft pulping of softwood to a kappa number level of 60–70. Simultaneously, the EA charge could be reduced from 14.2% to 12.6% on wood without affecting either the kappa number of the pulp or the physico-chemical properties of the linerboard.

On a chemical basis, AQ combines irreversibly with reactive parts of the lignin structure [216]. Indeed, only 10–25% of the originally added AQ can be recovered in the black liquor in an active form to be used in a subsequent cook [215]. A minor portion remains on the pulp fiber, from where it is removed quantitatively by oxidative bleaching treatment.

The effects of AQ on kraft pulping of *Pinus radiata* are less than are found for other softwoods [217]. The yield gains are in the order of only 1% when adding 0.05% AQ on wood. In fact, AQ is effective in catalytic quantities, with only 0.01% addition significantly accelerating delignification and raising the pulp yield. Comprehensive studies have shown that the most cost-effective dose of AQ for pulps in the kappa number range 25–30 is about 0.02%. At this level of addition, the yield gain is about 0.5–0.7% on o.d. wood, while the reduction in H-factor calculates to approximately 18% (which relates to a reduction in cooking time from 2.3

to 1.8 h at 170 °C). The use of AQ at this level should be economic in most applications, and particularly so for a recovery or causticizing limited mill.

The effect of AQ was slightly improved by using Scots pine in kraft pulping. At kappa number 30, the yield increase over the normal cook was about 1.7% unit with 2 kg AQ t<sup>-1</sup> wood. The reduction in H-factor was approximately 22%, while the yield gain decreased slightly to 1.3% at kappa number 25 [188]

The influence of AQ addition was studied for soda and kraft pulping using *Eucalyptus grandis* [218]. In soda pulping, a charge of 0.15% AQ on wood at given H-factor (1115) and alkali charge (EA = 20.6% NaOH) increased the extent of delignification by more than 30% (from kappa 33 to kappa 22.8), with a slight improvement in pulp yield. In kraft pulping, the addition of 0.15% AQ also led to a 30% reduction in kappa number (from 26.3 to 18.4) at 2% less alkali and 27% less H-factor. The effect on pulp yield was more pronounced (+1.4%) as compared to soda pulping (+0.4%).

#### 4.2.7

### Multistage Kraft Pulping

Alkaline pulping processes are not capable of selectively removing the short-chain hemicellulose fraction for the production of high-purity dissolving pulps, because the hemicelluloses in both hard- and softwoods are comparatively resistant under alkaline conditions. A prolonged cooking or an increased temperature will only cause excessive degradation due to alkaline hydrolysis of the glycosidic bonds, followed by peeling reactions. Thus, only a maximum of 86% alpha cellulose content is reached using softwoods. In addition, alkaline peeling reactions of the carbohydrates preferentially dissolve short-chain material of both hemicellulose and cellulose, but the adsorption of xylan on the cellulose microfibrils will cause a large amount of hemicellulose to remain on the pulp. In order to prevent precipitation of the xylans and other low molecular-weight carbohydrates, a prehydrolysis step must be applied prior to cooking to solubilize the hemicelluloses of the wood efficiently.

#### 4.2.7.1 Prehydrolysis

Prehydrolysis is generally used to remove selectively the hemicelluloses from the biomass by hydrolysis in water at 160–180 °C [1], in dilute acid (0.3–0.5% H<sub>2</sub>SO<sub>4</sub> at 120–140 °C) [2–4], or in concentrated acid (20–30% HCl at 40 °C) [3,5]. In water prehydrolysis, acetyl groups are cleaved from the β-(1–4)-linked xylan backbone and the acetic acid released acts as a catalyst for the hydrolysis of glycosidic bonds. The resulting pH in the prehydrolyzate ranges between 3 and 4. The addition of a mineral acid catalyst will, of course, greatly increase the rate of solubilization of the xylan. Hydrolysis with dilute or concentrated aqueous mineral acids is mainly applied for wood saccharification, which emphasizes the yield and quality of the released sugars. In terms of xylose production, prehydrolysis with an aqueous solution of sulfuric acid (0.4% at 170 °C) gave a higher yield of monomeric xylose as

compared to pure-water prehydrolysis [1]. The more intense degradation of xylose in the water prehydrolysis is explained by the higher hydroxyl ion concentration at a pH of 3.5 typical for water prehydrolysis. The hydroxyl ions are known to be a very effective catalyst for sugar degradation. On the other hand, glycosidic linkages, such as those in the xylan backbone, are rather stable to hydroxyl ions, but are easily cleaved in the presence of hydrogen ions [6]. The rate of hydrolysis of the glycosidic linkages decreases proportionally as solution acidity decreases, whereas the rate of xylose degradation decreases to a lesser extent due to the hydroxyl ion catalysis resulting in an overall greater xylose destruction at low acidities. The addition of mineral acids to water prehydrolysis prior to kraft pulping impairs – in the case of sulfuric acid catalysis (hydrochloric acid catalysis is not appropriate due to uncontrollable corrosion problems) – the sulfur-to-sodium ratio and renders the lignin fraction more soluble and reactive for undesirable condensation reactions, thus making the subsequent alkaline delignification more difficult.

As autohydrolysis generally is unsatisfactory for softwoods, more severe conditions must be applied in order to obtain the target purity level. Softwoods contain a higher amount of lignin which also has a greater tendency to acid condensations. In some cases, mineral acid catalysis may be appropriate for softwood prehydrolysis kraft cooking to achieve the optimum with regard to economic and pulp quality requirements.

To date, the prehydrolysis step in connection with kraft pulping is solely carried out without the addition of mineral acid. The use of water prehydrolysis with a typical liquor-to-wood ratio of 3–4:1, however, produces enormous amounts of prehydrolyzates (8–12 t adt<sup>-1</sup> pulp) containing large quantities of xylose and its oligomers. Over the years, much effort has been applied with regard to the recovery and utilization of dissolved substances. Initially, it was proposed to isolate pure xylose by crystallization from mild acid hydrolysis of beechwood hemicelluloses, using a multi-stage procedure [7–9], or to recover a pure syrup which can be used as fodder or for other purposes in the food industry [10]. The technology to recover xylose and its oligomers from the water prehydrolyzate remains a challenge for optimization. With progressive prehydrolysis, highly reactive secondary products are created as soon as the pressure is released to drain the prehydrolyzate. These hydrolysis products show a high tendency for precipitation and the formation of resinous agglutinations that are very difficult to control.

Both high yield of the released carbohydrate compounds and the production of high-value products are prerequisites for an economically feasible process. Hydrolysis products from wood are considered to be a source for chemicals, fodder, food additives, and even pharmaceutical products. To date, a wide range of research investigations are being undertaken to develop new products based on xylose and its oligomers, with the main focus on food additives [11–19]. However, at present there is no commercial utilization of the water prehydrolyzate during the course of a prehydrolysis-kraft operation for dissolving pulp manufacture. The running of a water prehydrolysis step, without utilizing the degraded wood by-products, is economically not feasible because recovery of the large amounts of prehydrolyzate requires additional equipment and evaporation capacity.

The breakthrough for cheap but low-efficiency vapor-phase prehydrolysis came with the application of displacement technology to the prehydrolysis kraft process. With the development of the Visbatch<sup>®</sup> process, the advantages of both steam hydrolysis and displacement technology were combined [20]. The efficiency of steam prehydrolysis can be significantly increased by subsequently charging a mixture of white and black liquor to the digester to further degrade and extract the acidic reaction products formed during prehydrolysis. The neutralization liquor, which contains the degraded hemicelluloses, is finally displaced by the cooking liquor to limit the effective alkali (EA) consumption and to improve the purification efficiency. This technology is presented in detail in Section 4.2.7.2, Prehydrolysis-Kraft cooking.

#### 4.2.7.1.1 Mechanisms of Acid Degradation Reactions of Wood Hemicelluloses

The treatment of polysaccharides with aqueous acidic compounds results in the occurrence of two types of reaction – glycosidic hydrolysis and dehydration. Extensive studies have been conducted on this issue, and although some aspects remain unclear, the general principles are well understood. The mechanism of glycosidic bond cleavage has been reviewed in several articles on homogeneous [21,22] and heterogeneous reactions [23]. It is agreed that hydrolytic cleavage proceeds through initial protonation of one of the hemiacetal-oxygen atoms to form a conjugated acid. In principle, two mechanisms are possible. Protonation of the glycosidic oxygen atom forms a conjugated acid, followed by fission of the exocyclic C1–O bond to give a cyclic carbenium ion, which most probably exists in the half-chair conformation having C-2, C-1, O and C-5 in a plane [24]. After reaction with water, the protonated reducing sugar and subsequently the reducing sugar is formed.

The alternative mechanism involves protonation of the ring oxygen atom to form the conjugated acid, followed by ring opening to give an acyclic carbenium ion. Again, after the addition of water the protonated hemiacetal is hydrolyzed to the free sugar [25]. The findings that methyl *D*-glucosides are anomerized in fully deuterated methanolic methanesulfonic acid with complete exchange with the solvent strengthens the mechanism with the cyclic carbenium ion intermediate [26]. It has been shown that the hydrolysis rate is highly controlled by the rigidity of the glycone ring. Thus, the hydrolysis rate of the furanosides is faster as compared to the pyranosides and substitution on the ring further decreases the hydrolysis rate. The rates in dilute acid for  $\beta$ -methylpyranosides and  $\beta$ -(1–4) disaccharides are listed in Tab. 4.41.

The major rate-controlling factors are steric diequatorial intramolecular interactions within the glycone. Based on hydrolysis experiments with cellotrioses-1-<sup>14</sup>C, it was observed that the two glycosidic bonds within the molecule behave differently. The nonreducing end of the cellotriose molecule contains an unsubstituted *D*-glucopyranose residue which enables a faster hydrolysis rate as compared to that of the bond at the reducing end of the molecule containing more bulky residues [28]. Such residues would also be expected to influence the hydrolysis of

**Tab. 4.41** Relative hydrolysis rates of methyl- $\beta$ -pyranosides and (1-4)- $\beta$ -linked disaccharides (according to Harris [27]).

Methyl pyranosides of		Disaccharides	
Substrates	Rel Rate	Substrates	Rel. Rate
$\beta$ -D-Glucose	1.0	Cellobiose	1.5
$\beta$ -D-Mannose	3.0	Glucosyl-Mannose	1.5
$\beta$ -D-Galactose	4.8	Pseudocellobiouronic acid	1.5
$\beta$ -D-Xylose	5.8	Mannobiose	2.7
		Xylobiose	11.0

the soluble cellulose molecule – that is, the glycosidic bond at the nonreducing end would hydrolyze faster than the internal bonds which would all hydrolyze at the same rate. Thus, the two kinetic constants would completely describe the homogeneous hydrolysis of cellulose.

With the exception of the arabinogalactans originating in larch that are  $\beta$ -(1-3)-linked, the backbones of the hemicelluloses present in both hard- and softwoods are joined  $\beta$ -(1-4). Their substituents are all easily cleaved under acidic conditions, leaving residual linear fragments of the  $\beta$ -(1-4) backbone. Only one substituent, 4-O-methyl- $\alpha$ -D-glucuronic acid – which occurs predominantly in hardwoods – is, however, much more resistant to acid hydrolysis than, for example  $\beta$ -(1-4) glycosidic bonds. Thus, as the uronic acid content of the hardwood xylan increases, the overall hydrolysis rate decreases. Xylan from hardwood species such as southern red oak with a low uronic acid-to-xylose ratio show a high hydrolysis rate constant. It can be concluded that the rates decrease in the order of increasing uronic acid-to-xylose ratio [4,29]. The heterogeneous backbone of the galactoglucomannan, prevalent in softwoods, hydrolyzes to expected ratios of various disaccharides and trisaccharides. The mannans of softwoods are more resistant than the hardwood xyans (due to the difference in the conformation). The heterogeneous hydrolysis rate of cellulose is one to two orders of magnitude less than that of the hemicelluloses which, fortunately, enables the selective removal of hemicelluloses during prehydrolysis. The specific morphology of the cellulose is considered to be the main reason for the high resistance towards acid hydrolysis. Apparently, the hydrolysis resistance may be ascribed to the highly ordered structure of cellulose. The hydrolytic degradation of cellulose has been comprehensively reviewed by Klemm et al. [30].

Under acidic conditions and elevated temperatures, pentoses are transformed to furfural by gradual dehydration reactions. Furfural is highly unstable under the conditions being formed, and its concentration follows a typical growth-and-decay curve. Unlike the cellulose–glucose system, the mechanism does not follow a simple pair of consecutive first-order reactions. Furfural degradation does not com-

prise a first-order reaction, and it is likely that its decomposition products are also participants. Furfural is produced during the prehydrolysis of hardwood. At the start of the reaction, the concentration is low as it depends on the furfural concentration. The mechanistic scheme and routes of furfural production from xylose have been extensively studied elsewhere [31–33].

#### 4.2.7.1.2 Kinetic Modeling of Hardwood Prehydrolysis

Water prehydrolysis is effected by the acetic acid released from labile acetyl groups present in the hemicelluloses. The extent of xylan hydrolysis is dependent upon the hardwood source, temperature, time, acidity and liquor-to-solid ratio. Control of the performance of the prehydrolysis kraft process necessitates an understanding of the kinetics of wood fractionation during the course of prehydrolysis. The aim is to establish a relationship between the intensity of prehydrolysis and the purification and delignification efficiency and selectivity under given subsequent pulping conditions.

Assuming that the xylan is completely accessible to water such that no diffusional restrictions affects the rate, and the local rate of xylan dissolution is proportional to the xylan concentration, the kinetics should follow first order in xylan. It has been shown that xylan contains fractions of different reactivity as there is a distinct slowing of the rate at about 70% conversion [29,34–36]. Transport limitations, different portions of the xylan with different reactivities and changing interfacial areas have been considered as possible explanations of the observed rate behavior [36,37]. Assuming xylan to be composed of two fractions, each of which reacts according to a homogeneous first-order kinetics law, the rate of xylan hydrolysis can be expressed as Eq. (142), according to the proposal of Veeraraghavan [38] and Conner [37]. The model is based on the presence of two types of xylan that hydrolyze via parallel first-order reactions:

$$-\frac{dX}{dt} = z_X \cdot k_{f,X} \cdot X_f + (1 - z_X) \cdot k_{s,X} \cdot X_s \quad (142)$$

in which  $X$  is the fraction of original xylan remaining in the solid residue,  $X_f$  and  $X_s$  are the fractions of the fast- and slowly-reacting xylan remaining in the residue,  $z_X$  is the fraction of the readily reacting xylan exemplified by Eq. (143):

$$z_X = \frac{(X - X_s)}{X} = \frac{X_f}{X} \quad (143)$$

and  $k_{f,X}$  and  $k_{s,X}$  are the rate constants.

A nonlinear regression (least squares) analysis is applied to determine the best values for the coefficients in the integrated form of Eq. (142), to calculate the dissolution of the wood components for each set of reaction conditions:

$$X = z_X \cdot \text{Exp}(-k_{f,X} \cdot t) + (1 - z_X) \cdot \text{Exp}(-k_{s,X} \cdot t) \quad (144)$$

The same algorithm can be used by modeling the (total) weight loss kinetics of the wood residue as the removal of xylan and its degradation products (xylo-oligomers, xylo-monomers and furfural) constitutes the bulk of the weight loss:

$$W = z_w \cdot \text{Exp}(-k_{f,w} \cdot t) + (1 - z_w) \cdot \text{Exp}(-k_{s,w} \cdot t) \quad (145)$$

in which  $W$  is the mass fraction of the remaining solid wood,  $W_f$  and  $W_s$  are the fractions of the fast- and slowly-reacting wood components remaining in the residue,  $z_w$  is the fraction of the readily reacting wood components expressed by Eq. (146):

$$z_w = \frac{(W - W_s)}{W} = \frac{W_f}{W} \quad (146)$$

and  $k_{f,w}$  and  $k_{s,w}$  are the rate constants.

The kinetics of weight loss and xylan hydrolysis is demonstrated for the water prehydrolysis of beech wood [39]. Beech wood was ground to finely divided pieces of average particle size 4 mm to minimize diffusion-controlled mass transfer. The composition of the beech wood is summarized in Tab. 4.42.

**Tab. 4.42** Composition of beech wood (*Fagus sylvatica*) [39].

Anhydride	Percentage [o.d. wood]
Glucose	42.6
Xylose	19.5
Arabinose	0.7
Galactose	0.8
Mannose	1.1
Rhamnan	0.5
Acetyl	4.5
Uronic	3.1
Klason lignin	21.0
Acid soluble lignin	3.5
Extractives <sup>a)</sup>	1.8
Ash	0.4
Sum	99.5

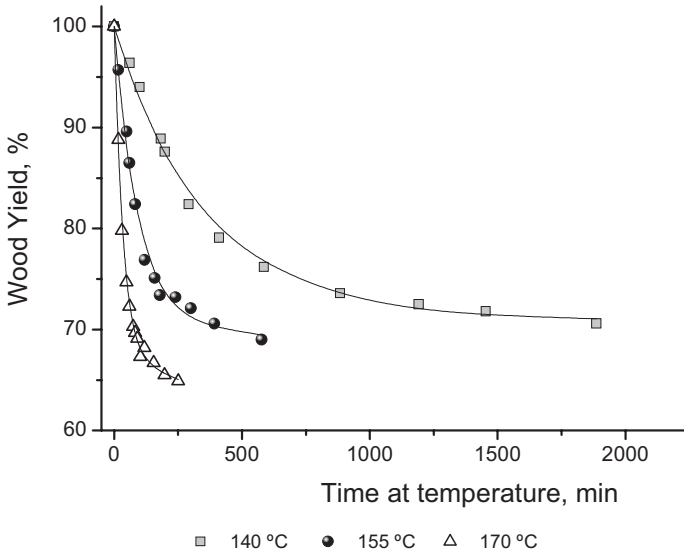
a) Ethanol and DCM extractives.

Prehydrolysis was performed at a liquor-to-solid ratio of 10:1 using a series of three 450-mL Parr autoclaves at three different temperature levels, 140 °C, 155 °C, and 170 °C. Heating-up time was kept below 20 min and corrected for isothermal conditions using the following expression [Eq. (147)]:

$$t_{T_0} = \int_{t_{T_1}}^{t_{T_0}} \text{Exp}\left(\frac{E_A}{R} \cdot \left[\frac{1}{T_{T_1}} - \frac{1}{T_0}\right]\right) \cdot dt \quad (147)$$

in which  $T_1$  is the temperature during heating-up,  $T_0$  the target temperature,  $t_{T_0}$  the reaction time at target temperature, and  $E_A$  the activation energy. The use of corrected prehydrolysis time requires an iterative procedure. First, a value is assumed, and the isothermal reaction time is calculated for each of the prehydrolysis experiments. A revised activation energy may then be calculated from an Arrhenius plot. The iterative procedure is repeated until the change in the activation energy becomes insignificant.

The results of weight-loss kinetics are shown in Fig. 4.96.



**Fig. 4.96** Mass of wood residue versus reaction time (corrected for isothermal conditions) for water prehydrolysis of beech wood. Liquor-to-solid ratio 10:1 (according to [39]).

The kinetic parameters for the fast weight-loss reaction from water prehydrolysis of beech and *Eucalyptus saligna* are compared in Tab. 4.43.



Tab. 4.43 Kinetic parameters for the weight-loss of beech wood and eucalypt according to Eq. (145).

Wood species	l:s ratio	Temperature °C	$(1 - z_w)$	$k_{f,w}$ [min <sup>-1</sup> ]	$k_{s,w}$ [min <sup>-1</sup> ]	$E_{f,w}$ [kJ mol <sup>-1</sup> ]	Reference
<i>Fagus sylvatica</i>	10.0	140	0.71	0.0028	$2.09 \cdot 10^{-6}$		[39]
		155	0.71	0.0104	$8.35 \cdot 10^{-6}$		
		170	0.68	0.0315	$9.88 \cdot 10^{-5}$	121.2	
<i>Eucalyptus saligna</i>	5.0	165	0.82	0.0300	$6.00 \cdot 10^{-5}$		[50]
		170	0.80	0.0462	$9.00 \cdot 10^{-5}$		
		170	0.83	0.0398	n.d.		
		170	0.82	0.0252	n.d.		
		180	0.79	0.0924	$1.62 \cdot 10^{-4}$	123.4	

n.d. Not determined.

The data in Tab. 4.43 show that the resistant wood fraction,  $(1 - z_w)$ , depends on wood species, and also to some extent on the reaction conditions [40]. The higher the hydrolysis temperature, the lower the amount of the resistant wood fraction. The liquor-to-solid ratio exerts an influence on the reaction rates, in a sense that with decreasing values the reaction rates decrease. This may be explained by an improved solubility of xylan degradation products with an increasing liquor-to-solid ratio.

The activation energies are very similar for both wood species investigated. The results of kinetic studies of xylan removal from beech wood are shown in Fig. 4.97 and summarized in Tab. 4.44, where they are compared to selected literature data.

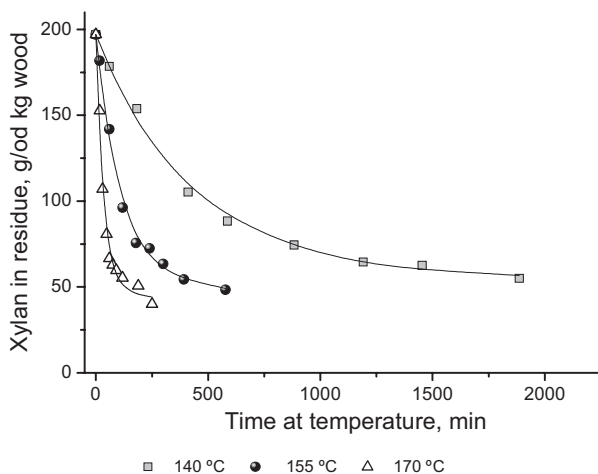


Fig. 4.97 Plot of xylan residue versus reaction time (corrected for isothermal conditions) for water prehydrolysis of beech wood. Liquor-to-solid ratio 10:1 (according to [39]).

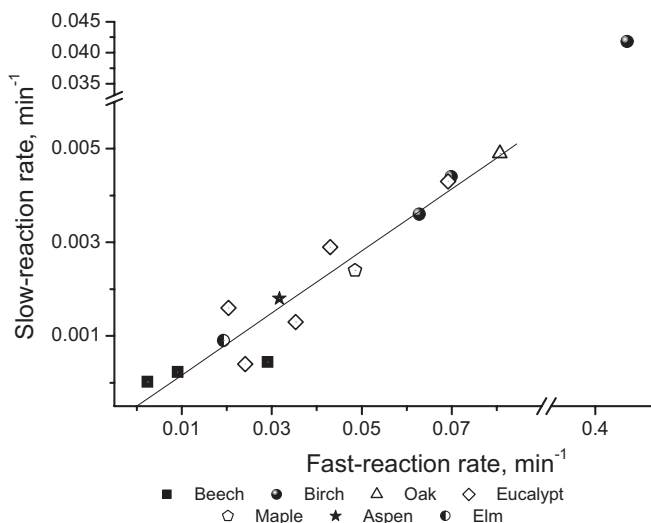
Tab. 4.44 Kinetic parameters for water prehydrolysis of xylan from various hardwoods.

Species	Reaction conditions			Model	Kinetic coefficients			Activation energy		Reference
	Medium	l : s ratio	Temperature [°C]		# of [stages]	$k_{fx}$ [min <sup>-1</sup> ]	$k_{sx}$ [min <sup>-1</sup> ]	(1-z)	$E_{fx}$ [(kJ mol <sup>-1</sup> )]	
<i>Quercus rubra</i>	water	3.0	171	2	0.0807	$4.90 \cdot 10^{-3}$	0.26			[29]
<i>Betula papyrifera</i>	water	3.0	170	2	0.0628	$3.60 \cdot 10^{-3}$	0.28			[29]
<i>Acer rubrum</i>	water	3.0	170	2	0.0485	$2.40 \cdot 10^{-3}$	0.20			[29]
<i>Populus rubrum</i>	water	3.0	170	2	0.0317	$1.80 \cdot 10^{-3}$	0.24			[29]
<i>Ulmus americana</i>	water	3.0	170	2	0.0193	$9.00 \cdot 10^{-4}$	0.16			[29]
<i>Populus tremuloides</i>	0.05–6 M HCl		60–120	1				118.0		[3]
<i>Populus tremuloides</i>	water		170	1	0.0242					[3]
<i>Betula papyrifera</i>	water		77							[3]
<i>Betula papyrifera</i>	0.082 M H <sub>2</sub> SO <sub>4</sub>	4.0	130	2	0.0699	$4.40 \cdot 10^{-3}$	0.36			[36]
	0.082 M H <sub>2</sub> SO <sub>4</sub>	4.0	150	2	0.4270	$4.18 \cdot 10^{-2}$	0.28	126.6	156.5	
<i>Liquidamber styraciflua</i>	water	10.0	155–175					126.0		
<i>Eucalyptus saligna</i>	water	5.0	160	2	0.0204	$1.60 \cdot 10^{-3}$	0.37			[50]
<i>Eucalyptus saligna</i>	water	5.0	170	2	0.0430	$2.90 \cdot 10^{-3}$	0.36			
<i>Eucalyptus saligna</i>	water	5.0	175	2	0.0692	$4.30 \cdot 10^{-3}$	0.39			
<i>Eucalyptus saligna</i>	water	5.0	180	2	0.0925	$5.60 \cdot 10^{-3}$	0.33	125.6	103.9	
<i>Eucalyptus saligna</i>	water	3.5	170	2	0.0353	$1.30 \cdot 10^{-3}$	0.35			
<i>Eucalyptus saligna</i>	water	2.0	170	2	0.0241	$4.00 \cdot 10^{-4}$	0.41			[39]
<i>Fagus sylvatica</i>	water	10.0	140	2	0.0024	$2.00 \cdot 10^{-5}$	0.29			
<i>Fagus sylvatica</i>	water	10.0	155	2	0.0091	$2.30 \cdot 10^{-4}$	0.28			
<i>Fagus sylvatica</i>	water	10.0	170	2	0.0291	$4.40 \cdot 10^{-4}$	0.28	127.2	135.7	

=>The initial xylan content in the beech wood of  $195 \text{ g kg}^{-1}$  o.d. wood comprises only the xylan backbone (xylose units), without any substituents. As shown in Tab. 4.44, the values obtained for  $(1 - z)$ , the slowly-reacting xylan fraction, are characteristic for the single wood species, and seem to be slightly dependent on the reaction temperature. The proportion of the more resistant xylan fraction is higher in *Eucalyptus* than in the other wood species (0.20–0.28). Interestingly, no correlation between the proportion of the two different xylan fractions and the reaction rates can be found. The amount of low-reacting xylan fraction may be related to both the extent of lignin-xylan or cellulose-xylan linkages and the accessibility.

The apparent rate constants at a given temperature vary from species to species. The highest rates are obtained for the xylan hydrolysis from oak, the lowest from elm (170 °C). It has been suggested that an inverse relationship between the uronic acid content and the initial rapid xylan removal exists [3,29]. As mentioned earlier, the  $\beta$ -1,4-glycosidic bonds in aldetriuronic acid are substantially less reactive as compared to the other  $\beta$ -1,4-glycosidic bonds within the xylan polymer [27]. Thus, as the uronic acid content increases, the number of easily cleaved bonds decreases. Consequently, the rate of xylan hydrolysis slows down.

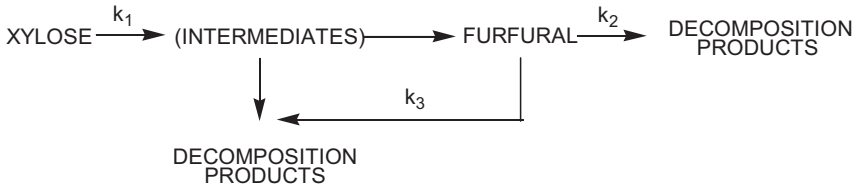
Assuming an Arrhenius temperature dependence, the activation energies determined for the fast-reacting xylan fraction are in a very narrow range, with an average value of about  $125 \text{ kJ mol}^{-1}$  (see Tab. 4.44). The corresponding values for the slowly-reacting xylan range from  $103.9$  to  $156.5 \text{ kJ mol}^{-1}$ . The higher values are more reliable, as they indicate that the hydrolysis rate may not be due to diffusional limitations. Although the apparent reaction rates for the fast- and slowly-reacting xylans vary from species to species, they are correlated for all species and even when comparing results from dilute mineral acid hydrolysis (Fig. 4.98).



**Fig. 4.98** Relationship between the rate constant for the fast and the rate constant for the slow reaction according to Conner after completion and modification [29,39].

The close relationship between the two different apparent first-order reaction rates may be attributed to the specific association with the lignin matrix rather than to variations in the polymeric structure of the xylan removed [29].

Xylan is solubilized to monomeric and oligomeric xylose that can further degrade to furfural and to unspecified condensation products. Despite the fact that the degradation of polysaccharides involves their reducing end groups, the yield of xylo-oligomers in the early stage of the prehydrolysis process is rather high (Scheme 4.30). After a certain induction period, the xylo-oligomer hydrolysis rate increases significantly.



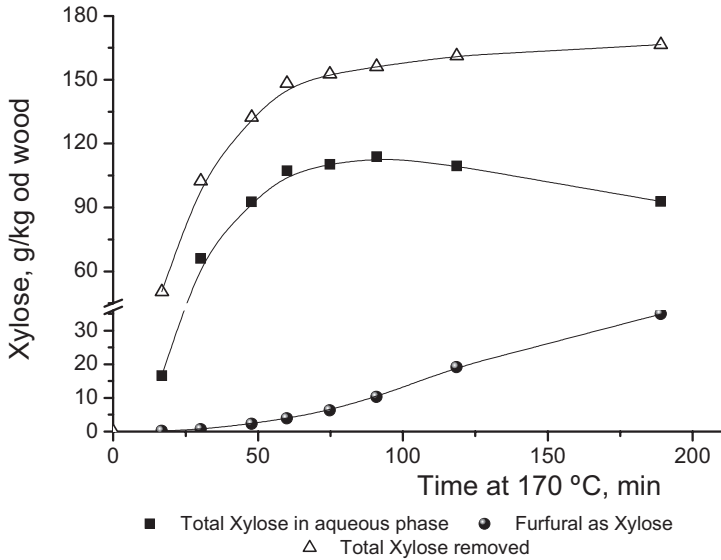
**Scheme 4.30**

Figure 4.99 shows the course of the xylose concentration in the solid residue of water prehydrolysis of beech wood at 170 °C in comparison to the concentration profiles of xylose and furfural in solution. Xylose is unstable under acidic conditions, and dehydrates to furfural. In the early stages of prehydrolysis, the concentration of furfural is low since the furfural formation rate depends on the furfural concentration. Thus, with rising reaction intensity, particularly the furfural concentration increases. Furfural production arises from a very complex group of reactions associated with the decomposition of xylose. There are at least three intermediates, all of which probably react with furfural at different rates. The mechanistic scheme of furfural production and decomposition was successfully established by Root [31].

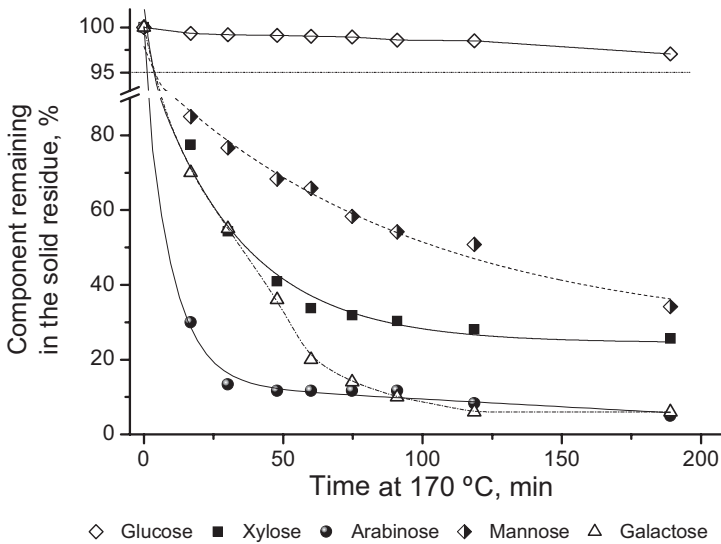
As seen from Tab. 4.42, beechwood contains also minor amounts of glucopyranoses (galactose and mannose) and arabinose. The development of the removal of these sugar compounds in relation to that of xylose and glucose originating from both glucomannan and cellulose is illustrated in Fig. 4.100.

The removal rate is largely in accordance with the conformational structure of the carbohydrates. The arabinose structure (furanoside) decomposes instantaneously, followed at some distance by galactose, xylose, and mannose. The removal rate of galactose is more rapid than would have been expected from its structural conformation. The resemblance of their degradation rates suggests the presence of polysaccharides being composed of galactose and arabinose units. The release of glucose units corresponds to the degradation of mannose in molar terms which may originate from glucomannan with a glucose-to-mannose ratio close to 1:1. With prolonged reaction time at 170 °C (>120 min), the amount of glucose removed from the wood however exceeds this stoichiometric ratio, indicating an additional loss from amorphous cellulose.

The monomeric and oligomeric sugars in aqueous solution are immediately involved in secondary reactions. Removal from the wood residue to the aqueous



**Fig. 4.99** Course of xylose in the solid residue, in solution as xylose (monomeric and oligomeric) and as furfural as a function of reaction time during water prehydrolysis of beechwood at 170 °C (according to [39]). Liquor-to-solid ratio = 10:1.



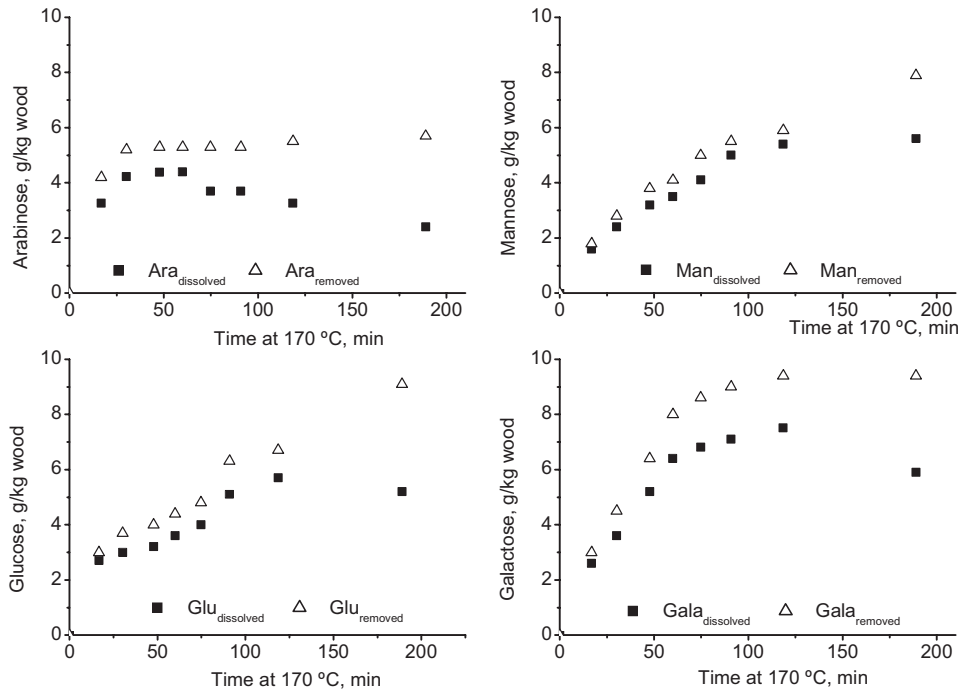
**Fig. 4.100** Course of the main carbohydrate units of beechwood in the solid residue as a function of reaction time during water prehydrolysis of beechwood at 170 °C (according to [39]). Liquor-to-solid ratio = 10:1. The initial values of the single carbohydrates are listed in Fig. 4.42.

solution and subsequent transformation to secondary products (condensation products) can be described in the simplest form as a consecutive mechanism according to Eq. (148):



The extent of the secondary reactions of arabinose, mannose, galactose and glucose in aqueous solution is demonstrated in Fig. 4.101 by comparing the difference between the amount removed from the solid residue and the amount detected in solution.

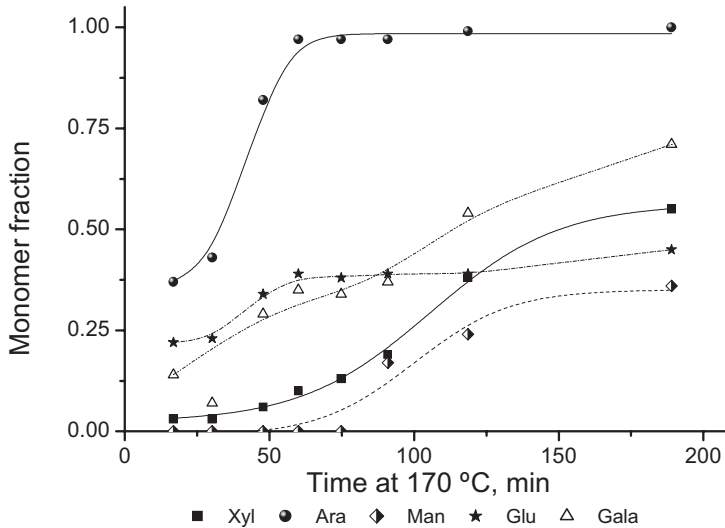
From Fig. 4.101 and Tab. 4.45 it can be seen that mannose and glucose can be recovered in high yield from solution, whereas arabinose and galactose are heavily involved in secondary reactions according to Scheme 4.30 and Eq. (148) after 1 hour retention time at 170 °C.



**Fig. 4.101** Course of arabinose, mannose, glucose, and galactose in the solid residue and in solution as a function of reaction time during water prehydrolysis of beech wood at 170 °C (according to [39]). Liquor-to-solid ratio = 10:1.

**Tab. 4.45** Course of carbohydrate removal in the solid residue of beech wood and in aqueous solution during water prehydrolysis at 170 °C at a liquor-to-solid ratio of 10:1 (according to [39]). Values include the total amount of carbohydrates denoted as monomers.

Time at 170 °C [min]	Wood Yield [%]	Glucose		Xylose		Furfural		Arabinose		Mannose		Galactose	
		dissolved [kg odt <sup>-1</sup> ]	removed [kg odt <sup>-1</sup> ]	dissolved [kg odt <sup>-1</sup> ]	removed [kg odt <sup>-1</sup> ]	dissolved [kg odt <sup>-1</sup> ]	removed [kg odt <sup>-1</sup> ]	dissolved [kg odt <sup>-1</sup> ]	removed [kg odt <sup>-1</sup> ]	dissolved [kg odt <sup>-1</sup> ]	removed [kg odt <sup>-1</sup> ]	dissolved [kg odt <sup>-1</sup> ]	removed [kg odt <sup>-1</sup> ]
0	100.0	0.0	0.0	0.0	0.0	0.0	0.0	0.0	0.0	0.0	0.0	0.0	0.0
16.8	88.8	2.7	3.0	16.6	50.4	0.2	3.3	4.2	1.6	1.8	3.0	2.6	3.0
30.2	79.9	3.0	3.7	66.0	102.4	0.7	4.2	5.2	2.4	2.8	4.5	3.6	4.5
47.8	74.7	3.2	4.0	92.6	132.3	2.3	4.4	5.3	3.2	3.8	6.4	5.2	6.4
60.0	72.4	3.6	4.4	107.2	148.3	3.9	4.4	5.3	3.5	4.1	8.0	6.4	8.0
74.8	70.3	4.0	4.8	110.2	152.6	6.3	3.7	5.3	4.1	5.0	8.6	6.8	8.6
90.9	69.1	5.1	6.3	113.8	156.2	10.3	3.7	5.3	5.0	5.5	9.0	7.1	9.0
118.6	68.2	5.7	6.7	109.5	161.2	19.1	3.3	5.5	5.4	5.9	9.4	7.5	9.4
189.0	68.4	5.2	9.1	92.8	166.5	34.9	2.4	5.7	5.6	7.9	9.4	5.9	9.4



**Fig. 4.102** Proportion of monomeric sugars as a function of reaction time during water prehydrolysis of beech wood at 170 °C (according to [39]). Liquor-to-solid ratio = 10:1.

During the early stage of water prehydrolysis, the predominant fraction of the released carbohydrates originate as oligomers. As mentioned earlier, the oligomers are easily hydrolyzed to the monomers with progressive prehydrolysis (Fig. 4.102).

Applying a prehydrolysis intensity typical for dissolving kraft pulp production (1 h at 170 °C), xylose and mannose predominantly exist as oligomers. The highest molecular weight was found to be approximately 3000 for dissolved polysaccharides isolated from the prehydrolyzates of both pine [41] and beech [42]. The degradation of polysaccharides to a size of this magnitude enables diffusion of the degraded polysaccharides from the cell wall layers into the liquor [41,43].

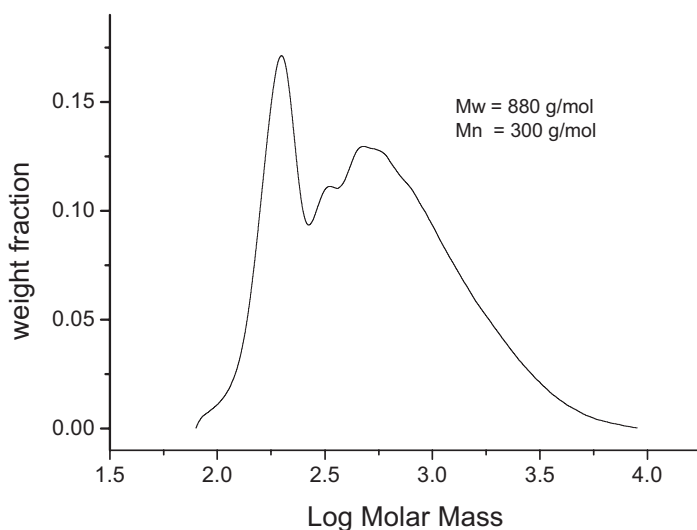
Recently, the macromolecular properties of the water prehydrolyzate from beech wood after a treatment of 1 h at 170 °C at a liquor-to-solid ratio of 10:1 was characterized by both size-exclusion chromatography and liquid chromatography, coupled with mass spectrometry [44]. Based on the carbohydrate analysis, more than 80% of the dissolved xylose is present as oligomer. With the exception of arabinose, which is quantitatively hydrolyzed to the monomer under these prehydrolysis conditions, all other neutral sugars are predominantly released as oligosaccharides (Tab. 4.46).

The molar mass distribution of the neutral sugar fraction of the prehydrolyzate revealed a trimodal distribution following the RI detection. The weight-average ( $M_w$ ) and number-average ( $M_n$ ) molecular weights were calculated from the RI-signal by universal calibration with a mix of cello-oligomer and pullulan standards (Fig. 4.103).



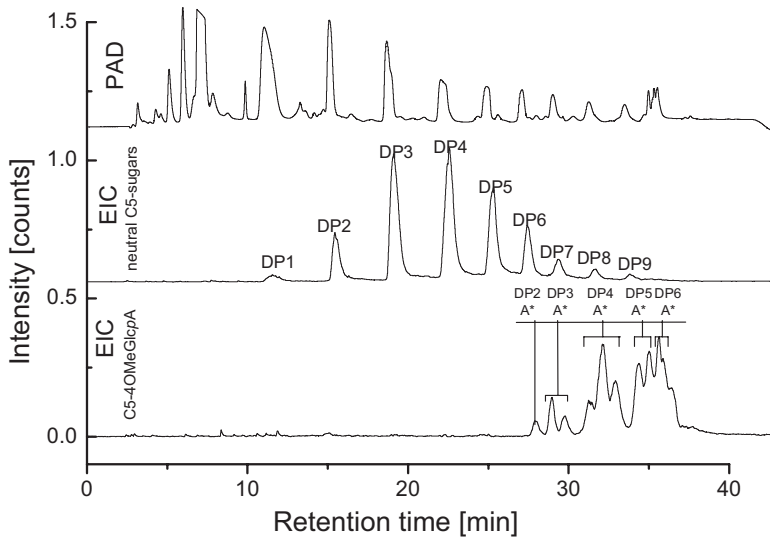
**Tab. 4.46** Mono- and oligosaccharides present in the water prehydrolyzate from beech wood after a treatment of 1 h at 170 °C at a liquor-to-solid ratio of 10:1 (according to [44]).

Constituent	Monomer	Oligomer
	[g kg <sup>-1</sup> wood]	
Xylose	18.0	100.6
Mannose	0.0	1.6
Glucose	2.5	4.9
Arabinose	3.8	0.0
Galactose	2.9	4.0
Rhamnose	2.0	1.4



**Fig. 4.103** Size-exclusion chromatography of water prehydrolyzate from beech wood after a treatment of 1 hour at 170 °C at a liquor-to-solid ratio of 10:1 (according to [44]). (PSS MCX 1000 columns; 0.5 M NaOH; flow rate 1 mL min<sup>-1</sup>).

The calculated molecular weights were significantly lower as reported from the literature [42], and comprised a weight-average degree of polymerization (DP) of about 7. These values were in agreement with those determined using high-performance anion-exchange chromatography (HP-AEC) with pulsed amperometric detection and coupled to mass spectrometry (Fig. 4.104).



**Fig. 4.104** High-performance anion-exchange chromatography HP-AEC coupled to pulsed amperometric detection (PAD) and to mass spectrometry of water prehydrolyzate from beech wood after a treatment of 1 h at 170 °C at a liquor-to-solid ratio of 10:1 (according to

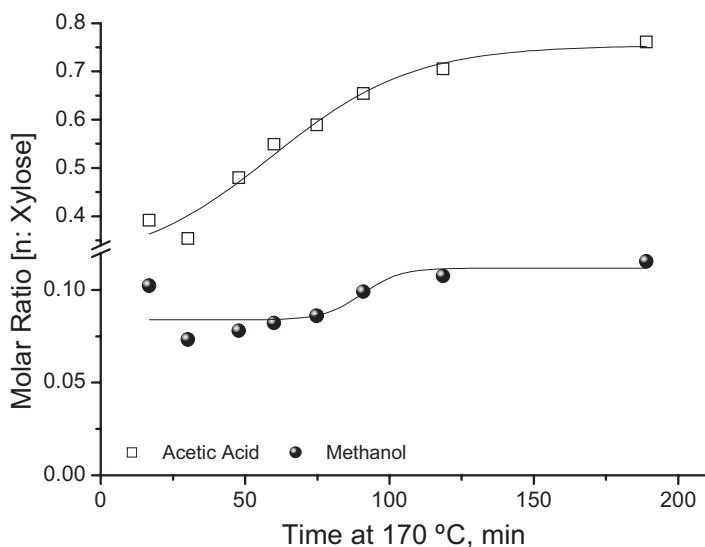
[44]). (HP-AEC-PAD: Dionex CarboPac PA100, 0.15 M NaOH/0.5 M NaAc, flow rate 0.5 mL min<sup>-1</sup>. MS-detection: Esquire 3000plus: ESI, negative mode, flow rate 0.5 mL min<sup>-1</sup>, extracted ion chromatography, EIC). A\*: 4-O-methyl-β-D-glucuronic acid.

The dissolved hemicellulose fragments undergo further acid-catalyzed hydrolysis to monosaccharides only after applying rather severe conditions. Even after 200 min at 170 °C, the proportion of xylose monomers in the prehydrolyzate amounts to only 50%. At the same time, the decomposition reactions – as shown schematically in Scheme 4.30 and Eq. (148) – begin significantly to diminish the overall xylose yield. The yield of monomer xylose can be substantially increased only by either applying prehydrolysis with dilute solutions of sulfuric acid or by raising the temperature beyond 170 °C in the case of water prehydrolysis [1].

Oligomeric arabinose structures are rapidly cleaved to monomeric sugars, however. The conversion of galactose and glucose oligomers to the monomers proceeds with intermediate reaction rates.

The deacetylation of xylan governs the efficiency of the prehydrolysis reactions. Surprisingly, the molar ratio of acetic acid in solution to xylose removed from the residue increases from 0.4:1.0 to a saturation value of slightly above 0.7:1.0 during the first 100 min of retention time at 170 °C. These results (see Fig. 4.105) indicate that deacetylation in the early stages of prehydrolysis occurs at a somewhat slower rate than xylan removal, whereas the two removal rates are almost equal during the final course of water prehydrolysis.

Figure 4.105 also displays the molar ratio of methanol released to the xylose removed. Again, in the initial phase of prehydrolysis the xylan removal rate seems to be ahead of the splitting of the methoxyl group from the xylan molecule.



**Fig. 4.105** Molar ratio of acetic acid and methanol in solution to xylose removed from the residue as a function of reaction time during water prehydrolysis of beech wood at 170 °C (according to [39]). Liquor-to-solid ratio = 10:1.

Furthermore, lignin-carbohydrate bonds and some inter-unit lignin bonds, mainly derived from the benzyl alkyl ether type, may be cleaved during water prehydrolysis. Consequently, lignin compounds are also removed from the solid wood residue. As xylan removal progresses, the amount of lignin removed passes through a maximum and then greatly decreases [1]. This apparent decrease has been attributed to a redeposition of carbohydrate degradation products on the wood residue that have been determined as lignin, as they are also insoluble in 72% sulfuric acid. Recently, lignin measurements (Klason lignin and acid-soluble lignin) on beech wood revealed that water prehydrolysis contributes to a substantial degradation of lignin compounds. At 60% xylan removal, water prehydrolysis at 170 °C and a liquor-to-solid ratio of 10:1 removes about 26% of lignin. It was reported that the so-called Hibbert ketones (e.g., vanilloyl methyl ketone and guaiacyl acetone, coniferylaldehyde and *p*-coumaraldehyde) which obviously originate from lignin, were present in the water prehydrolyzate from hemlock [45]. Coniferylaldehyde was found to be the major product of acid-catalyzed hydrolysis of guaiacylglycerol- $\beta$ -aryl ether at pH 5 and 175 °C [46]. Parallel to the decrease in the lignin content, the amount of material extractable by means of organic solvents [e.g., dichloromethane (DCM) or ethanol-benzene] increases [47]. This may be explained by the fact that, under prehydrolysis conditions, acid hydrolysis causes depolymerization of lignin and renders parts of the lignin soluble in water or organic solvents. The amount of DCM extractives in beech wood increases from 0.3% in the untreated wood to 2.0% after a 30-min vapor phase prehydrolysis treatment at 170 °C [48].

#### 4.2.7.1.3 P-factor Concept

Brasch and Free were the first to propose a prehydrolysis factor to control the prehydrolysis step [49]. These authors calculated the relative rate of prehydrolysis for any desired temperature by assuming that the prehydrolysis rate triples for each 10 °C rise in temperature, without measuring the activation energy of hydrolysis and assuming that the rate constant at 100 °C is unity. Later, Lin applied the H-factor principle to prehydrolysis using an activation energy typical for the cleavage of glycosidic bonds of the carbohydrate material in the wood [47]. According to this principle, the P-factor expresses the prehydrolysis time and temperature as a single variable and is defined as:

$$P = \int_{t_0}^t k_{rel} \cdot dt \quad (149)$$

in which  $k_{rel}$  is the relative rate of acid-catalyzed hydrolysis of glycosidic bonds. The rate at 100 °C is chosen as unity, and all other temperatures are related to this rate. An Arrhenius-type equation is used to express the temperature dependence of the reaction rate. At temperature T, it is expressed as:

$$\ln(k_{H(T)}) = \ln(A) - \frac{E_{A,H}}{R} \cdot \frac{1}{T} \quad (150)$$

in which  $k_{H(T)}$  is the rate constant of xylan hydrolysis at the temperature T, A is the pre-exponential factor, and  $E_{A,H}$  the activation energy. The reference reaction rate at 100 °C is then expressed in Eq. (151):

$$\ln(k_{H,100^\circ C}) = \ln(A) - \frac{E_{A,H}}{R} \cdot \frac{1}{373.15} \quad (151)$$

The ratio of Eqs. (150) and (151) expresses the relative reaction rates at any other temperature:

$$\ln \frac{k_{H(T)}}{k_{100^\circ C}} = \frac{E_{A,H}}{R \cdot 373.15} - \frac{E_{A,H}}{R \cdot T} \quad (152)$$

A selection of activation energies,  $E_A$ , for both bulk and residual xylan hydrolysis is provided in Tab. 4.44. A value of 125.6 kJ mol<sup>-1</sup> for the fast-reacting xylan, originating from extensive investigations of xylan hydrolysis from *Eucalyptus saligna*, has been successfully applied for P-factor calculation in a new Brazilian prehydrolysis kraft mill [50,51]. Thus, it is suggested to use this activation energy for the calculation of the P-factor. By substituting a value of 125.6 kJ mol<sup>-1</sup> into Eq. (152), the relative rate can be calculated according to Eq. (153):

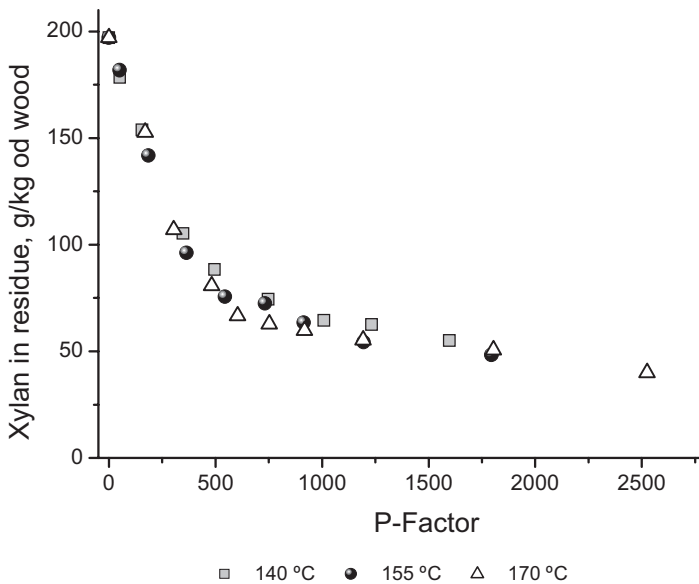
$$K_{rel} = \frac{k_{H(T)}}{k_{100^\circ C}} = \text{Exp} \cdot \left( 40.48 - \frac{15106}{T} \right) \quad (153)$$

The relative rate is plotted against time, and the area under the curve represents the “prehydrolysis factor” or “P-factor”:

$$P = \int_{t_0}^t \frac{k_{H,(T)}}{k_{100^\circ\text{C}}} \cdot dt = \int_{t_0}^t \text{Exp} \cdot \left( 40.48 - \frac{15106}{T} \right) \cdot dt \quad (154)$$

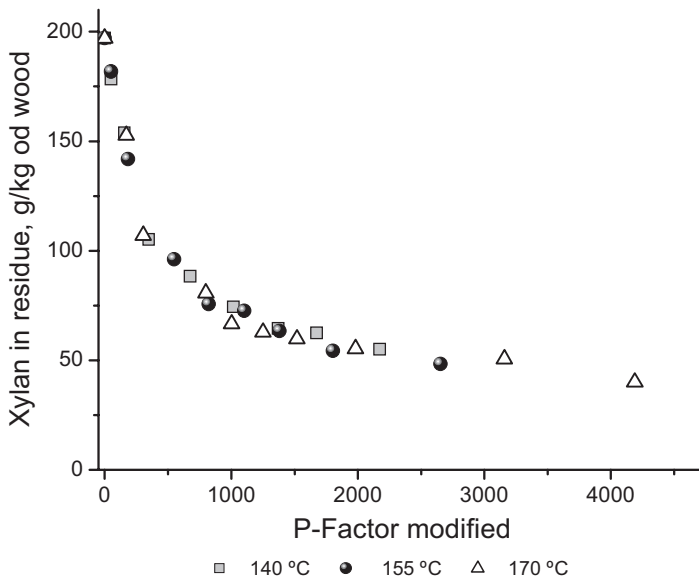
This simple concept is illustrated by calculating the P-factor for a prehydrolysis of 1 h at constant temperatures. The prehydrolysis of 1 h at 160 °C and 170 °C corresponds to P-factors of 272 and 597, respectively. The rate constants for prehydrolysis more than double for a 10 °C rise in temperature. The conclusion is that in lowering the temperature from 170 °C to 160 °C, while keeping the prehydrolysis intensity unchanged, the reaction time must be expanded from 60 min to 132 min.

The applicability of the P-factor can be examined by plotting the remaining xylan content in the beech wood obtained by water prehydrolysis three different temperatures against the P-factor, as shown in Fig. 4.106 [39] (see also Fig. 4.97).



**Fig. 4.106** Mass of xylan residue as a function of P-factor for water prehydrolysis of beech wood using a liquor-to-solid ratio of 10:1 (according to [39]).

Figure 4.106 confirms that the P-factor does indeed bear a single relationship with the amount of residual xylan in the wood at various temperatures. In the range of high P-factors, the results from low and high temperatures become slightly different. This deviation can be explained by the P-factor calculation which considers solely the activation energy of the hydrolysis of the fast-reacting xylan. The precision of the P-factor concept can be further improved by using the activation energies separately for the initial and the residual hydrolysis phases. In this



**Fig. 4.107** Mass of xylan residue as a function of the modified P-factor for water prehydrolysis of beech wood using a liquor-to-solid ratio of 10:1 (according to [39]). The modified P-factor considers two different activation energies. An activation energy of  $125.6 \text{ kJ mol}^{-1}$  is used during hydrolysis of the fast-reacting xylan, and of  $135.7 \text{ kJ mol}^{-1}$  during hydrolysis of the resistant xylan (see also Tab. 4.44).

particular case, the amount of resistant xylan has been determined by extrapolation of the hydrolysis rate of the slowly-reacting xylan to time zero. Figure 4.107 illustrates the relationship between the modified P-factor and the amount of remaining xylan in the prehydrolyzed beech wood.

The results show an improvement of the relationship between P-factor and the remaining xylan content after prehydrolysis at different temperature levels. However, the rather insignificant improvements do not justify use of the more complex modified P-factor concept.

It can be concluded that the P-factor concept is applicable to control the extent of purification during the course of a prehydrolysis-kraft process for the production of a dissolving pulp. Of course, it must be borne in mind that the removal of hemicelluloses from wood is controlled by many additional parameters, and these will be described in the next section.

#### 4.2.7.2 Prehydrolysis: Kraft Pulping

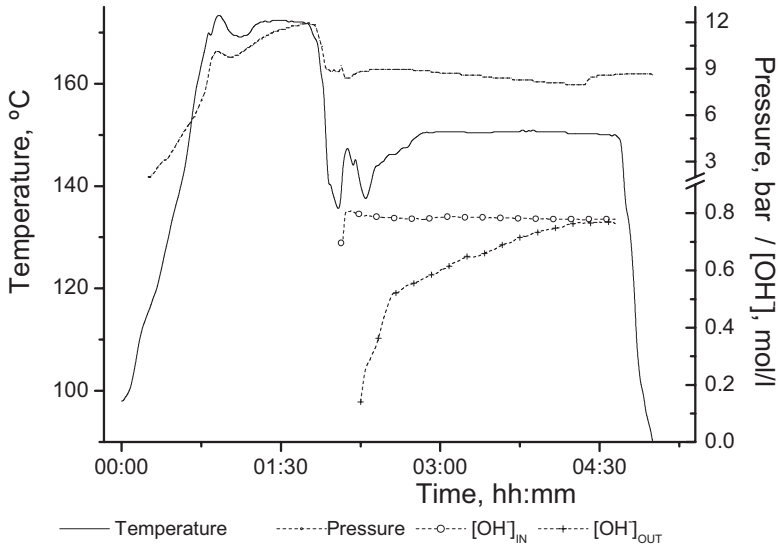
The prehydrolysis step is followed by a simple kraft or Soda-anthraquinone (AQ) process for the manufacture of a high-purity dissolving pulp. The conventional approach comprises the introduction of cold white liquor from the causticizing plant, heating-up and cooking until the desired degree of delignification is reached, after which the digester's contents are emptied to a blow tank by digester

pressure. This conventional concept has several serious disadvantages. First, water prehydrolysis may adversely affect the process behavior due to the formation of highly reactive intermediates undergoing condensation products. As a result, pitch-like compounds are formed, which separate from the aqueous phase with drainage of the prehydrolyzate, and deposit on any surface available. Moreover, the deposition of these compounds on the chip surface may affect the diffusion-controlled mass transfer. The prehydrolyzate must then be evaporated and burned together with the black liquor, which again impairs the economy of the process. Second, the two heating-up phases, prior to prehydrolysis and cooking, require large amounts of steam, and this leads to a significant prolongation of the cook.

In order to reduce the high energy costs incurred in evaporation of the prehydrolyzates, attempts have been made to replace water by steam prehydrolysis. However, this apparently simple change resulted in very poor delignification, bleachability and reactivity of the dissolving pulps. To prevent extensive condensation reactions occurring prior to the cooking stage, two measures must be undertaken. First, a pressure release must be avoided in the transition to the cooking stage. Second, the reactive hydrolysis products must be immediately neutralized, extracted and displaced prior to cooking. These requirements have been fulfilled by applying the known displacement technology to this two-stage process. The process which has been developed to overcome the described problems is known as the Visbatch<sup>®</sup> process, and it combines the advantages of displacement technology and steam prehydrolysis [20].

The prehydrolysis step is terminated by adding hot white liquor (HWL) and hot black liquor (HBL) to the digester. In this way, the organic acids are neutralized and the oligo- and monosaccharides (as well as their reactive intermediates) are subjected to extensive fragmentation reactions and solubilized in the neutralization liquor. Due to the high  $[\text{OH}^-]$  ion and the elevated temperature, delignification begins parallel to extraction of the acidic constituents of the prehydrolyzate. In the next step, neutralization liquor is displaced from bottom to top to ensure that acid-volatile substances are completely expelled from the digester. During this hot displacement step, the alkali requirement is supplied for subsequent cooking by further addition of HWL and HBL.

In a further development of the Visbatch<sup>®</sup> technology, the displacement process is continued until the predetermined H-factor is reached. This process, denoted as the VisCBC process, is based on CBC technology where the cooking liquor (CL) is prepared outside the digester (in the CL tank) by adjusting the preset alkali concentration and temperature. Cooking is terminated by displacing the cooking liquor by means of the washing filtrates. As soon as the temperature falls to less than 100 °C, the unbleached pulp suspension is pumped into the blow tank. The temperature, pressure and  $[\text{OH}^-]$  ion profiles throughout a typical prehydrolysis-kraft procedure according to the VisCBC technology is shown in Fig. 4.108. No abrupt pressure or temperature drops are detected during transition from the prehydrolysis to the cooking step; indeed, both pressure and temperature profiles develop very smoothly. The same can be observed for the  $[\text{OH}^-]$  ion profiles. The  $[\text{OH}^-]$  ion in the ingoing cooking liquor is kept constant at between 0.6 and



**Fig. 4.108** Temperature, pressure, and  $[\text{OH}^-]$  ion profiles during the course of a hardwood VisCBC cooking process (according to [52]). P-factor 700, H-factor 400; unbleached pulp: kappa number 6.6, intrinsic viscosity  $1015 \text{ mL g}^{-1}$ , R18 97.0%.

$1.0 \text{ mol L}^{-1}$ , the objective being to avoid excessive cellulose degradation and an uneven pulp quality. With continuous cooking, the difference in  $[\text{OH}^-]$  ion between the ingoing and outgoing cooking liquors gradually diminishes.

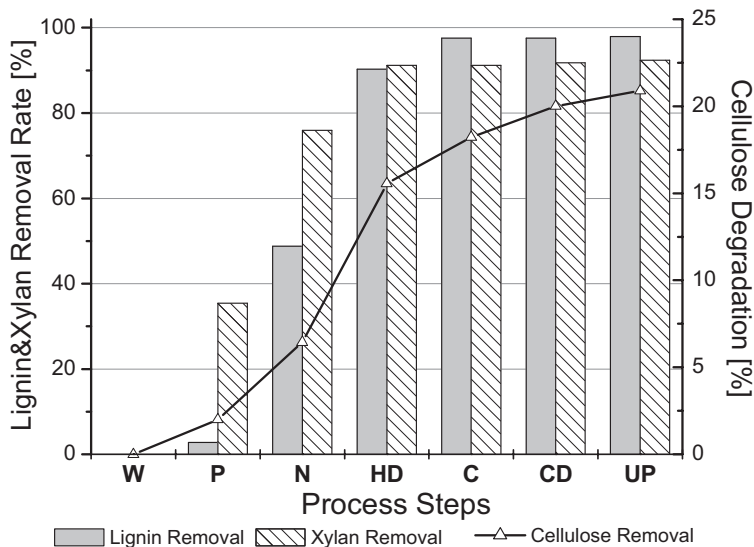
The high  $[\text{OH}^-]$  ion concentration in the later stage of the cook ensures a high delignification rate, and also prevents significant xylan reprecipitation.

#### 4.2.7.2.1 Material Balance

The prehydrolysis-kraft process according to the Visbatch<sup>®</sup> or VisCBC operations is divided into several steps. After a conventional chip filling procedure, prehydrolysis (P) is effected with saturated steam, preferably at temperatures of about  $170^\circ\text{C}$ . Depending on the wood species and the cellulose purity demanded, prehydrolysis intensity is adjusted to P-factors ranging from 300 to about 1000 (equals 30 to 100 min at  $170^\circ\text{C}$ , respectively). The absence of free water during steam prehydrolysis (the liquor-to-solid ratio ranges from 0.7 to 1.2, mainly depending on the moisture content of the wood) limits the loss of wood substance during this stage. As an example, steam prehydrolysis of *Eucalyptus urograndis* with an intensity of P-factor 300 accounts to a xylan reduction of only 38% with reference to the total xylan removed throughout the whole process (Tab. 4.47). Nevertheless, prehydrolysis degrades the major part of the hemicelluloses which then becomes solubilized in the subsequent alkaline process steps. As indicated earlier, degradation of the hydrolytically cleaved hemicelluloses is continued in the subsequent



neutralization (N) step. The major portion of the wood components degraded during the whole prehydrolysis-kraft process are removed within this step. The extensive degradation of polysaccharides requires a sufficient supply with EA to ensure their complete extraction and to prevent recondensation and reprecipitation of both carbohydrates and lignin compounds. The neutralization step is immediately succeeded by the hot displacement (HD) (Visbatch<sup>®</sup>) or cooking stage (C) (VisCBC). There, the neutralization liquor is displaced by a mixture of HWL and HBL (which in the case of VisCBC is preset to the target  $[\text{OH}^-]$  ion and temperature). The hot displacement step of the Visbatch process is most efficient with regard to both delignification and final purification, with 92% of the degradable lignin and 97% of the degradable xylan being removed at this stage (see Tab. 4.47 and Fig. 4.109). The subsequent cooking stage (C) controls the final delignification, covering a kappa number range of about 45 (at the start) to less than 10 (before cold displacement), and ensures a rather homogeneous pulp quality due to the leveled-out alkali profile (VisCBC). Although less than 4% of the wood substances are removed, the cooking phase is important for process control because the final pulp properties, viscosity and brightness, are determined. The mass balance of the most important wood components throughout a Visbatch<sup>®</sup> process typical for the use of eucalyptus wood are detailed in Table 4.47.



**Fig. 4.109** Course of lignin and xylan removal rates and cellulose yield loss throughout a Visbatch<sup>®</sup> procedure of *Eucalyptus urograndis* (according to [48]). P- and H-factors each 300, respectively. EA-charges in N and HD, 12% and 8% o.d. wood, respectively.

**Tab. 4.47** Mass balance of the most important wood components through a Visbatch® cooking process of *Eucalyptus urograndis* (according to [48]). P- and H-factors each 300, respectively. EA-charges in N and HD, 12% and 8% o.d. wood, respectively.

Process steps	Yield [%]	Cellulose [%]	Xylan [%]	GM [%]	Tot-Ch <sup>a)</sup> [%]	Tot-L <sup>b)</sup> [%]
Wood (W)	100.0	45.0	15.8	5.0	70.5	28.7
Prehydrolysis (P)	91.9	44.1	10.2	1.1	62.0	27.9
Neutralization (N)	65.8	42.1	3.8	0.7	49.6	14.7
Hot displacement (HD)	44.2	38.0	1.4	0.4	41.2	2.8
Cooking (C)	40.4	36.8	1.4	0.2	39.5	0.7
Cold displacement (CD)	38.9	36.0	1.3	0.2	38.0	0.7
Unbleached pulp (UP)	38.1	35.6	1.2	0.2	37.4	0.6

a) Carbohydrates.

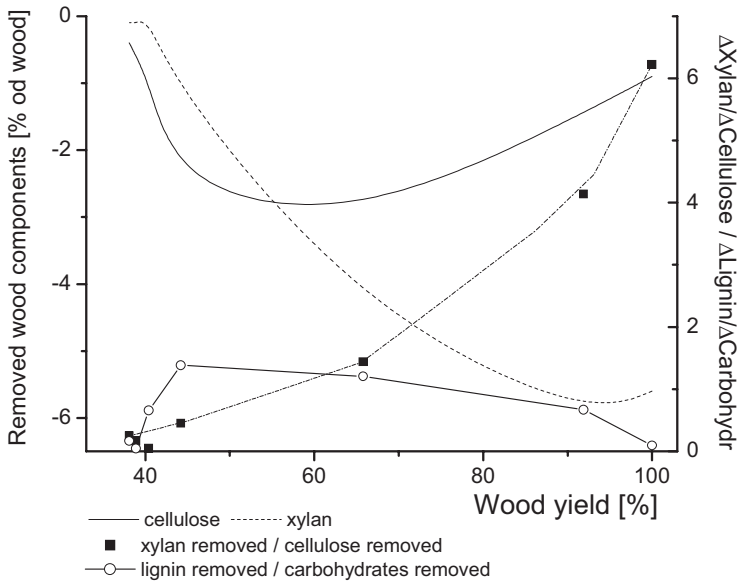
b) Lignin.

The cumulative lignin and xylan removal rates, as well as the extent of cellulose degradation, is displayed in Fig. 4.109. This shows that the cellulose yield loss is highest during neutralization and hot displacement. A limited improvement can be achieved by lowering the temperature level (especially during neutralization), but this of course impairs the heat economy.

Unlike paper-grade production, the aim of dissolving-grade cooking is to selectively remove both low-chain hemicelluloses and lignin. As mentioned earlier, delignification starts immediately after introduction of the neutralization liquor (N). Although the highest delignification rate is achieved during hot displacement, the highest delignification selectivity occurs only during the cooking stage. Purification selectivity (the ratio of xylan-to-cellulose removal) is highest during prehydrolysis and neutralization (Fig. 4.110).

The cook is terminated by cold displacement from top to bottom, using cold washing filtrate. Depending on the speed of the displacement step, the cooking is prolonged in the lower parts of the digester. Thus, some minor effects on carbohydrate yield can be observed during this final stage (see Tab. 4.47).

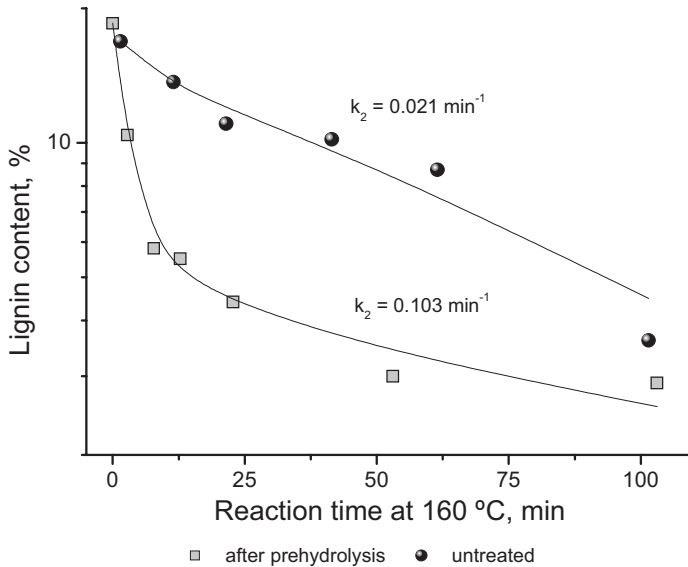
The economy of a pulping process is greatly influenced by its demand for EA. A simple balance of EA consumption can be calculated by assuming a specific alkali consumption of 1.6 mol [OH<sup>-</sup>] mol<sup>-1</sup> AHG for carbohydrate degradation, and 0.8 mol [OH<sup>-</sup>] mol<sup>-1</sup> lignin for lignin decomposition, respectively. The results of this calculation reveal an overall EA consumption of 20.3% on o.d. wood, which is in good agreement with the experimental value of 19.7% if an alkali equivalent of the exhaust gases of about 0.8% on o.d. wood is considered (Tab. 4.48).



**Fig. 4.110** Differential curves of cellulose, xylan, and lignin removals during Visbatch® cooking of *Eucalyptus urograndis* (according to [48]). P- and H-factors each 300, respectively. EA-charges in N and HD, 12% and 8% o.d. wood, respectively.

**Tab. 4.48** Calculated effective alkali (EA) consumption for the single steps through a Visbatch® cooking process of *Eucalyptus urograndis* (according to [48]). P- and H-factors each 300, respectively.

Process steps	EA-consumption [% / od wood ]		
	Carbohydrates	Lignin	Total
Wood (W)	0.0	0.0	0.0
Prehydrolysis (P)	5.6	0.1	5.7
Neutralization (N)	4.8	2.1	6.9
Hot displacement (HD)	3.8	1.9	5.7
Cooking (C)	0.7	0.4	1.1
Cold displacement (CD)	0.6	0.0	0.6
Unbleached pulp (UP)	0.3	0.0	0.3
Total	15.8	4.5	20.3



**Fig. 4.111** Effect of prehydrolysis on the delignification rates for pulping of *Eucalyptus saligna* under comparable conditions (according to [53]). Prehydrolysis-kraft: P-factor 620, l:s = 10:1,  $[\text{OH}^-] = 0.44 \text{ mol L}^{-1}$ ,  $[\text{HS}^-] = 0.076 \text{ mol L}^{-1}$ . Kraft: l:s = 10:1,  $[\text{OH}^-] = 0.44 \text{ mol L}^{-1}$ ,  $[\text{HS}^-] = 0.063 \text{ mol L}^{-1}$ .

Prehydrolysis remarkably influences delignification efficiency during the subsequent kraft cooking process. The application of a prehydrolysis step greatly facilitates lignin removal which – in practice – is expressed by both lower H-factors and lower kappa numbers. Kinetic investigations reveal that the bulk delignification rate of a non-prehydrolyzed *Eucalyptus saligna* at 160 °C comprises only one-fifth as compared to a prehydrolyzed wood (Fig. 4.111).

This impressive acceleration of the delignification rate of prehydrolyzed wood chips may be explained by both an improved permeability of the cell wall due to increased pore volumes [42] resulting in improved penetration of the cooking liquor and the (partial) hydrolytic cleavage of lignin structures and lignin–carbohydrate bonds. Moreover, it can be assumed that the formation of non-lignin chromophoric structures is impeded because of the lower content of residual carbohydrate structures. It has been shown that prehydrolyzed kraft pulps contain considerably lower amounts of non-lignin and HexA structures as part of the kappa number as compared to paper-grade kraft pulps [54].

#### 4.2.7.2.2 Influence of Process Conditions on the Performance of Prehydrolysis-Kraft Cooking

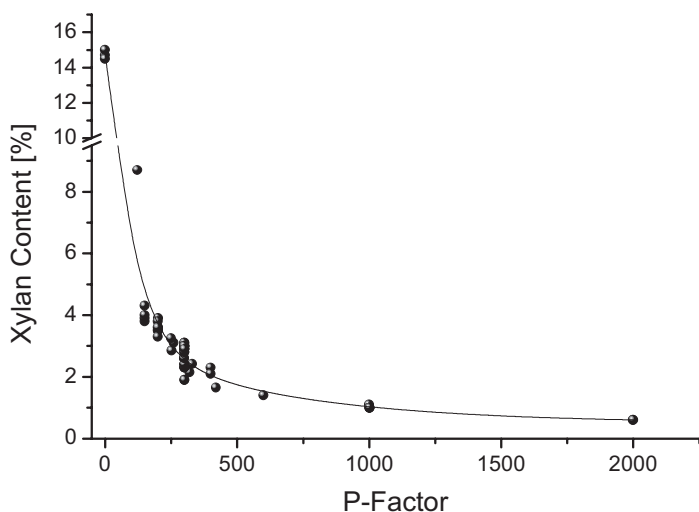
The processability of prehydrolysis-kraft cooking, as well as the properties of the resulting unbleached pulp, are significantly influenced by the conditions and the

applied technology of prehydrolysis. Furthermore, the reaction conditions of the subsequent kraft cooking process determine the final quality of the unbleached dissolving pulp. Consequently, prehydrolysis and kraft cooking conditions must be adjusted to the benefit of both process economy and desired pulp quality. The relationships between wood species, process technology and conditions with process economy and pulp quality have been reviewed in detail for various prehydrolysis-alkaline processes [50].

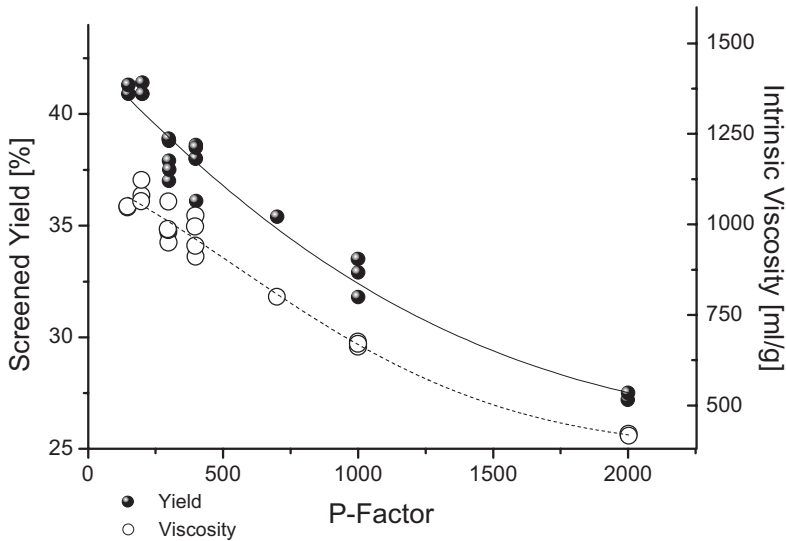
Cooking process control is determined to a considerable extent by the P-factor, the specific EA charge in neutralization, and hot displacement or cooking and cooking intensity, measured as H- or G-factors, respectively. In the following sections, the influence of the most important parameters on the unbleached dissolving pulp properties is illustrated by means of Visbatch® cooking of *Eucalyptus urograndis*.

The purity of the dissolving pulp is greatly determined by conditions during prehydrolysis. Figure 4.112 shows the change in the xylan content on varying P-factors and constant kraft cooking conditions. The course of xylan removal as a function of prehydrolysis intensity clearly reflects the presence of (at least) two types of xylans (see Section 4.2.7.1.2. Kinetic Modeling of Hardwood Prehydrolysis). Xylan removal proceeds quite substantially under mild prehydrolysis conditions. Thus, xylan contents in the range of 3–4% are easily achieved by applying P-factors less than 300.

Both yield and viscosity are highly sensitive to prehydrolysis conditions. Lowering the xylan content to values below 2%, as is demanded for the production of



**Fig. 4.112** Xylan content in the unbleached Visbatch pulp made from *Eucalyptus urograndis* as a function of prehydrolysis intensity (P-factor) at constant kraft cooking conditions: total EA-charge 22.3 % o.d. wood, 22% sulfidity, 370 H-factor at 155 °C (according to [55]).

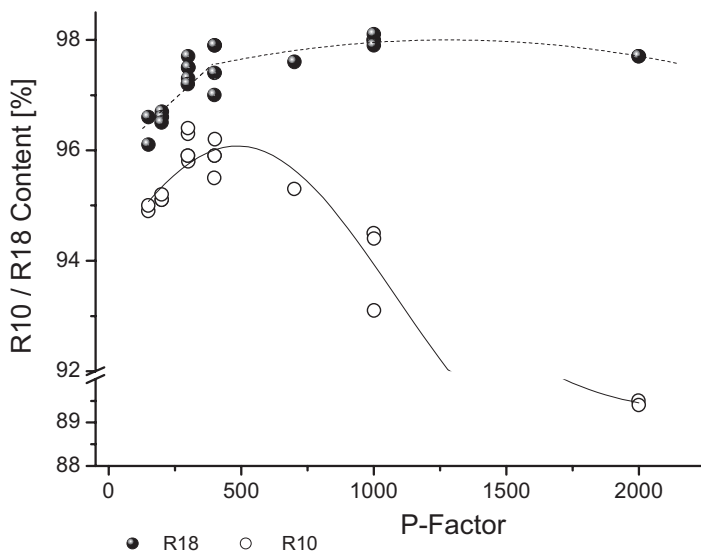


**Fig. 4.113** Yield and intrinsic viscosity of an unbleached Visbatch® pulp made from *Eucalyptus urograndis* as a function of prehydrolysis intensity (P-factor) at constant kraft cooking conditions: total EA-charge 22.5% o.d. wood, 24% sulfidity, 300 H-factor at 155 °C (according to [55]).

high-purity acetate grade pulps, is connected to high losses in yield and drastic reductions in viscosity (Fig. 4.113). The primary target value of dissolving pulp cooking is pulp viscosity at a predetermined purity level. However, the mutual dependence of viscosity and purity parameters during prehydrolysis makes it difficult to adjust one parameter independently from the other. This discrepancy becomes worse with increasing demands on purity. Thus, very high purity levels (as are demanded for special cellulose ether or cellulose acetate grades) can solely be adjusted by intensifying prehydrolysis only if, at the same time, very low viscosity levels can be accepted or even are desired.

The massive cellulose degradation induced by intensive prehydrolysis conditions (with P-factors > 600) is also reflected by the course of the alkali resistances, R18 and R10, of the resulting unbleached pulps, as shown in Fig. 4.114.

Both R-values are ascending steeply throughout the initial phase of prehydrolysis, indicating the removal of low molecular-weight hemicelluloses. With increasing prehydrolysis intensity, the R10 content decreases sharply, whereas the R18 content further increases slightly to reach a maximum at a P-factor of approximately 1500. Beyond this prehydrolysis intensity, the R18 content starts to decline. Since the difference between R18 and R10 is a measure for the low molecular-weight cellulose fraction, an increase of this difference represents an increasing polydispersity of the molecular weight distribution, indicating progressive degradation of the accessible cellulose fractions.

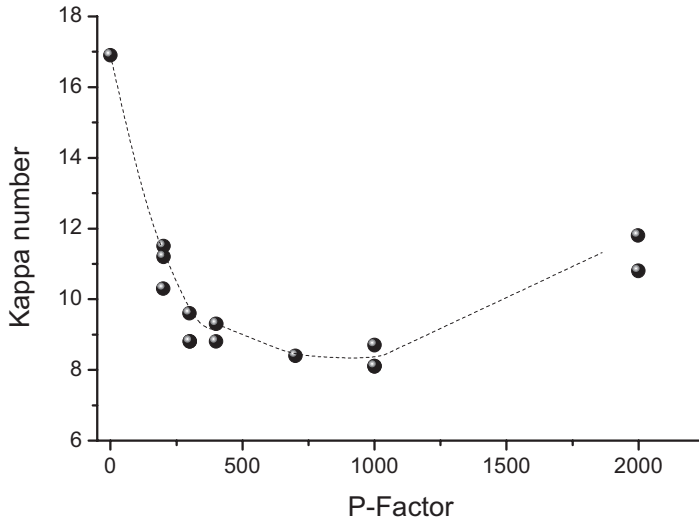


**Fig. 4.114** Course of R18 and R10 contents of unbleached Visbatch® pulps made from *Eucalyptus urograndis* as a function of prehydrolysis intensity (P-factor) at constant kraft cooking conditions: total EA-charge 22.5% o.d. wood, 24% sulfidity, 300 H-factor at 155 °C (according to [55]).

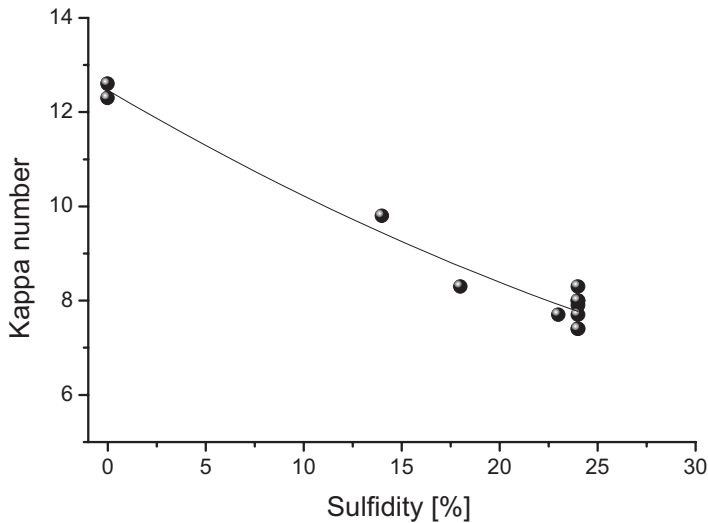
As mentioned previously, prehydrolysis facilitates subsequent alkaline delignification because of the partial hydrolytic degradation of lignin compounds, the cleavage of alkali-stable carbohydrate–lignin bonds, and improvement of the accessibility of the cooking liquor. The kappa number of the unbleached pulp therefore decreases with increasing P-factor until a value of approximately 1000 is reached. Exceeding this P-factor inevitably leads to an increase in the kappa number. This is exemplified in Fig. 4.115, where the kappa number is plotted against the P-factor for pulps made from *Eucalyptus urograndis* at constant cooking conditions.

It is known that excessive prehydrolysis will cause lignin condensation which cannot be fully compensated by adjusting the cooking conditions. These problems are less severe in the case of hardwoods, because of the lesser tendency of hardwood lignin to acid condensation and the greater ease of hardwood delignification during the kraft cook. Although the influence of sulfidity on delignification selectivity and efficiency is less pronounced as compared to paper-grade kraft cooking, the kappa number can be reduced by increasing the sulfidity of the white liquor while keeping all other parameters constant. This is illustrated in Fig. 4.116, where kappa number is plotted against sulfidity of the white liquor.

Alternatively, delignification selectivity and efficiency can be improved by adding anthraquinone to the cooking liquor in the case of low-sulfidity or pure soda cooks [50]. Both measures – the increase of sulfidity and/or the addition of anthraquinone – are known to improve delignification without simultaneously impairing viscosity or changing any other pulp quality parameter. The extent of



**Fig. 4.115** Course of the unbleached kappa number of Visbatch® pulps made from *Eucalyptus urograndis* as a function of prehydrolysis intensity (P-factor) at constant kraft cooking conditions: total EA-charge 23.5% o.d. wood, 24% sulfidity, 300 H-factor at 155 °C (according to [55]).



**Fig. 4.116** Influence of kappa number of Visbatch® pulps made from *Eucalyptus urograndis* on the sulfidity of the white liquor at constant prehydrolysis and kraft cooking conditions: P-factor 300, total EA-charge 23.0% o.d. wood, H-factor 300 at 155 °C (according to [55]).

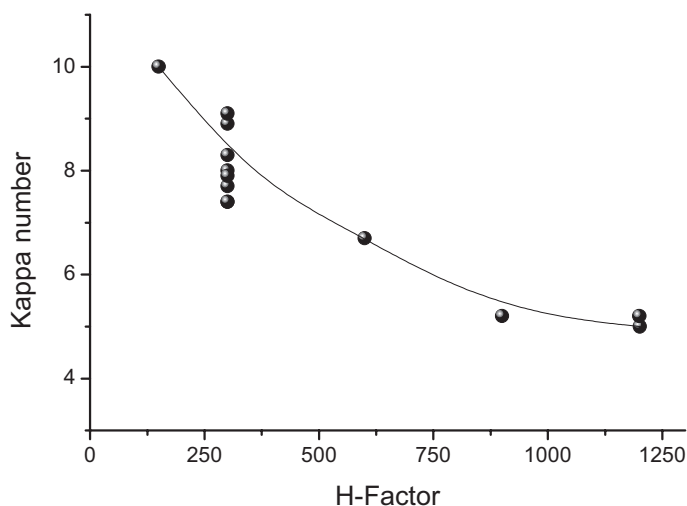


delignification and bleachability are also determined by the specific amount of EA in both neutralization and cooking, and by the cooking intensity expressed as H-factor (see Figs. 4.117 and 4.118). The kappa number decreases rapidly at H-factors ranging from 200 to 700. Following this rapid phase, delignification slows down gradually as the H-factor approaches values above 1000.

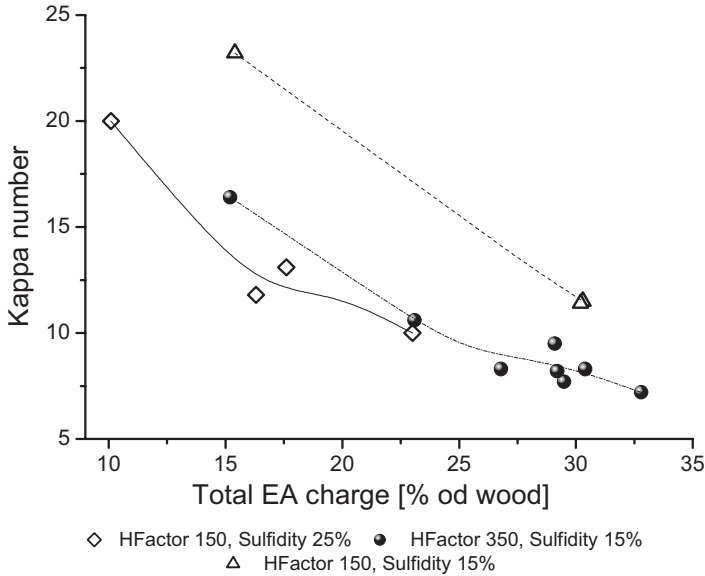
However, both the increase in EA charge and H-factor result in a degradation of the polysaccharide fraction and finally lead to yield losses. Similarly to paper-grade kraft cooking, the amount of EA determines the degree of delignification and bleachability. From kinetic considerations, it is well established that the reaction rate of the residual delignification phase depends quite significantly on the  $[\text{OH}^-]$  ion.

The H-factor – or more precisely the G-factor – relate to viscosity when the residual hydroxide ion concentration is controlled simultaneously (see Fig. 4.27). The viscosity of low-viscosity dissolving pulps, as required for Lyocell, selected cellulose ether or cellulose film production, is primarily adjusted by prolonging the cooking phase (G-factor) rather than during subsequent bleaching operations because of better viscosity control and the introduction of less-reactive functional groups (carbonyl and carboxyl groups).

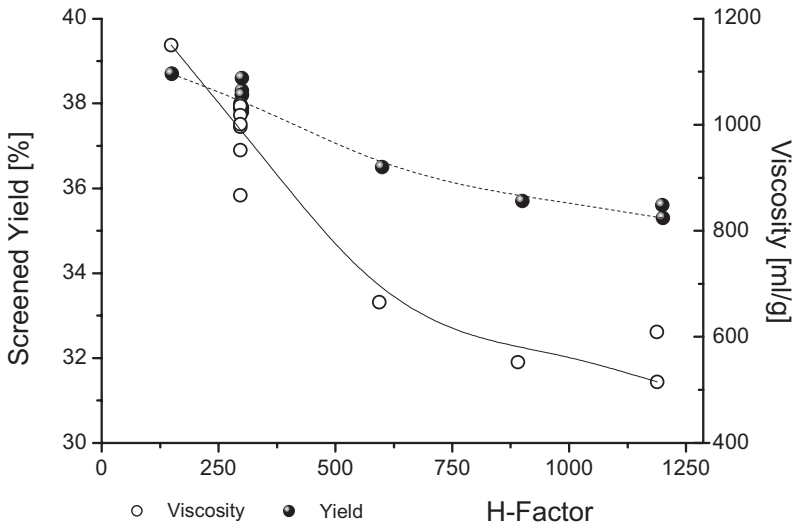
Unfortunately, extending the cooking phase is connected with additional yield losses, and thus contributes to lowering the cooking capacity (Fig. 4.119). Expanding cooking intensity from H-factor 200 to H-factor 700 is accompanied with a reduction of pulp viscosity by about 450 units (from 1080 to 630  $\text{mL g}^{-1}$ ), a yield loss of about 2.2% (from 38.4% to 36.2%), and a kappa number reduction of 3.4 units (from 9.6 to 6.2) in this particular example.



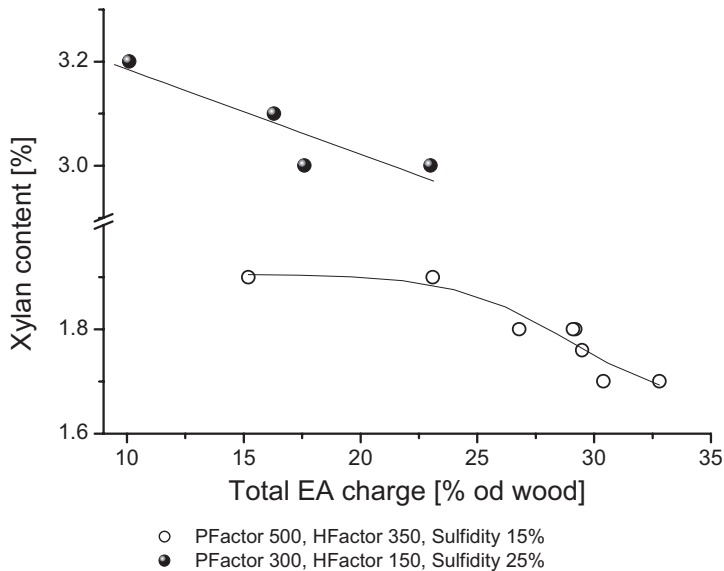
**Fig. 4.117** Course of the kappa number of unbleached Visbatch® pulps made from *Eucalyptus urograndis* with increasing H-factor at constant prehydrolysis-kraft cooking conditions. (●) P-factor 300, total EA-charge 23.0% o.d. wood and sulfidity 23% (according to [55]).



**Fig. 4.118** Development of the kappa number of unbleached Visbatch® pulps made from *Eucalyptus urograndis* as a function of the total effective alkali (EA) charge (sum of EA in N and C) under three different kraft cooking conditions: (◇) P-factor 300, sulfidity 25%, H-factor 150; (△) P-factor 500, sulfidity 15%, H-factor 150; (●) P-factor 500, sulfidity 15%, H-factor 350 (according to [55]).



**Fig. 4.119** Screened yield and viscosity of unbleached Visbatch® pulps made from *Eucalyptus urograndis* as a function of the H-factor at constant prehydrolysis-kraft cooking conditions (G-factor 6.29 times the H-factor at 155 °C, 7.28 times the H-factor at 160 °C): P-factor 300, total EA-charge 23.1% o.d. wood and sulfidity 23% (according to [55]).



**Fig. 4.120** Xylan content of unbleached Visbatch® pulps made from *Eucalyptus urograndis* as a function of the total effective alkali (EA) charge for two different prehydrolysis-kraft cooking conditions: (○) P-factor 500, sulfidity 15%, H-factor 350; (●) P-factor 300, sulfidity 25%, H-factor 150 (according to [55]).

The H-factor, however, has no influence on the degree of purification. On the contrary, extensive cooking intensity leads to a substantial degradation of the high molecular-weight cellulose fraction, thus reducing the alkali resistances of the pulp. The only way to improve slightly the pulp purity during the alkaline cooking process is to charge additional amounts of EA during both neutralization and cooking. The effect of increasing amounts of EA on the residual xylan content of the unbleached Visbatch pulp made from *Eucalyptus urograndis* is illustrated in Fig. 4.120.

The effect of increasing the alkali charge during kraft cooking preceded by a prehydrolysis step is similar to that of a hot alkali treatment applied for refining acid sulfite-dissolving pulps. The dominating reaction involved is the alkaline peeling reaction, which starts at the reducing end group of the carbohydrate chains or any other carbonyl groups introduced at other places along the chains. The effect of hot alkali purification is counteracted by a viscosity degradation which takes place simultaneously. The viscosity degradation is mainly due to alkaline hydrolysis, which is governed by both high temperature and high alkali concentration.

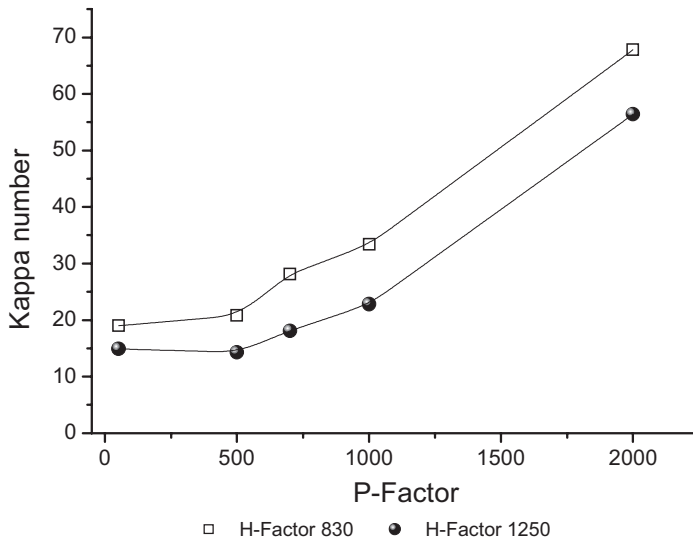
#### 4.2.7.2.3 Wood Species

Most wood species – with the exception of some very dense tropical hardwoods – can be used for the production of prehydrolysis-kraft pulps. In practical use are

pine, mixed American hardwood, Eucalyptus species and beech. In the past, aspen, birch and annual plants such as bamboo, bagasse, salai (*Boswellia serrata*) and reed have also been used for the production of dissolving-grade pulps. Some raw materials such as straw and other annual plants contain silica, which is an undesirable contaminant of dissolving pulps because it cannot be removed sufficiently during the pulping operations. More than 70% of the currently produced prehydrolysis-kraft pulps are made from hardwood species [56]. Although they are rich in pentosans, the good delignification efficiency and selectivity, the low costs, the high availability and the high density make them fairly suitable for this type of process. Softwoods are also well-suited to the prehydrolysis-kraft process but, due to their higher lignin content and the greater tendency of softwood lignin to acid condensation, intensive prehydrolysis conditions must be avoided (Fig. 4.121).

The worsening of delignification with increasing prehydrolysis intensity can partly be compensated by increasing both H-factor and EA charge, although this will cause significant yield loss and cellulose (viscosity) degradation.

Recently, the suitability of three important hardwood species (e.g., beech, birch and *Eucalyptus urograndis*) and one softwood species (e.g., spruce for prehydrolysis-kraft cooking using the Visbatch<sup>®</sup> technology) has been investigated under comparable conditions. The chemical composition of the raw material greatly determines the economy and achievable purity level of the resulting dissolving pulps. Details of the wood species used for this comparative evaluation are listed in Tab. 4.49.



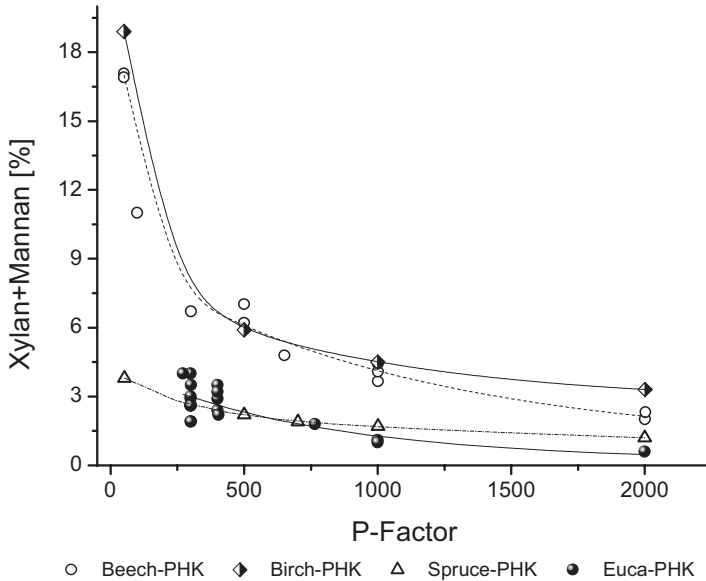
**Fig. 4.121** Influence of P-factor on the unbleached kappa number of Visbatch<sup>®</sup> pulps made from spruce at two different levels of H-factor (according to [55]). Constant reaction conditions: Total EA charge 23% o.d. wood, 30% sulfidity and 160 °C cooking temperature.

**Tab. 4.49** Chemical composition of four selected wood species used for a comparative study of prehydrolysis-kraft cooking using the Visbatch® process [57].

	<b>Beech</b> <i>Fagus sylvatica</i>	<b>Birch</b> <i>Betula pendula</i>	<b>Eucalypt</b> <i>E. urograndis</i>	<b>Spruce</b> <i>Picea abies</i>
Carbohydrates	72.8	73.6	69.5	70.0
Glucose	42.6	39.7	47.0	45.7
Xylose	19.5	22.1	13.9	6.6
Arabinose	0.7	0.5	0.4	1.0
Galactose	0.8	1.0	1.3	1.6
Mannose	1.1	1.3	1.2	12.0
Rhamnose	0.5	0.3	0.3	
Acetyl	4.5	5.1	3.2	1.4
Uronic	3.1	3.5	2.2	1.8
Lignin	24.5	23.3	28.5	27.2
Klason	21.0	19.7	25.2	27.0
Acid-Soluble	3.5	3.6	3.3	0.2
Extractives	1.8	1.9	0.4	1.0
DCM	0.2	1.9	0.4	1.0
Et-OH	1.6	n.a.	n.a.	n.a.
Ash	0.4	0.3	0.2	0.2
Total	99.5	99.0	98.5	98.5

n.a. = not applicable

The wood species with the highest glucan concentration, *Eucalyptus urograndis* and spruce, can be expected to provide dissolving pulps of the highest yield and cellulose purity. Both raw materials, however, also contain the highest lignin content of the four selected wood species (see Tab. 4.49). Thus, preservation of the high cellulose yield depends very much on the ease of selective delignification after the prehydrolysis step. Due to the high sensitivity of the spruce lignin towards reinforced prehydrolysis conditions, it can be assumed that the spruce dissolving pulp contains a significantly higher residual lignin content as compared to the hardwood pulps when preserving the high cellulose yield.



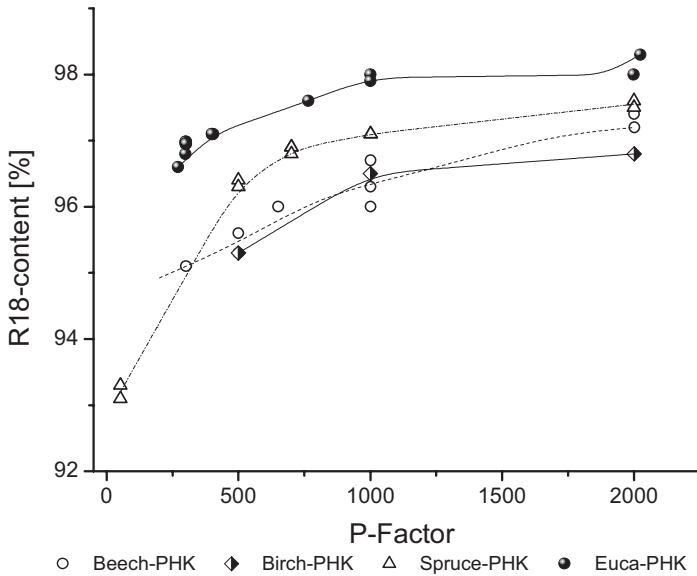
**Fig. 4.122** Course of hemicellulose content in the unbleached Visbatch® pulps as a function of the P-factor. Constant reaction conditions: Total EA charge 23% o.d. wood (all species), 24% sulfidity (beech, birch, *E. urograndis*), 30% sulfidity (spruce), 150 °C (beech, birch), 158 °C (*E. urograndis*), 160 °C (spruce), 450 H-factor (beech), 825 H-factor (birch), 300 H-factor (*E. urograndis*) and 990 H-factor (spruce) [57].

Prehydrolysis is the key process step for purification of the dissolving pulp. The efficiency of prehydrolysis is a decisive element of the economy of the whole process. The course of hemicellulose removal (xylan + mannan) thus provides a first indication about the efficiency of this process stage. The results shown in Fig. 4.122 indicate that the species with the lowest hemicellulose content – spruce and Eucalyptus – and those with the highest hemicellulose content – beech and birch – each show a similar pattern of hemicellulose removal.

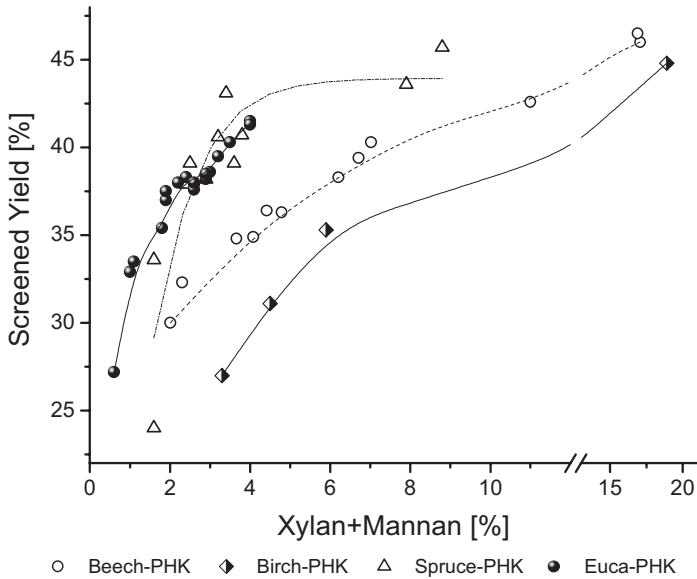
It is interesting to note, that the slow-reacting hemicelluloses fractions from spruce and birch are more resistant than those from eucalyptus and beech. This can probably be explained by both the better accessibility and the lower numbers of resistant carbohydrate–lignin bonds of the latter species.

The course of purification as a function of P-factor in terms of R18-content clearly shows an advantage for the eucalypt pulp over the spruce pulp, whereas the beech and the birch pulps develop similarly (Fig. 4.123). The lower alkali resistance of the spruce pulp can be explained by a higher amount of low molecular-weight glucan fractions deriving from both glucomannan and degraded cellulose (high H-factor!).

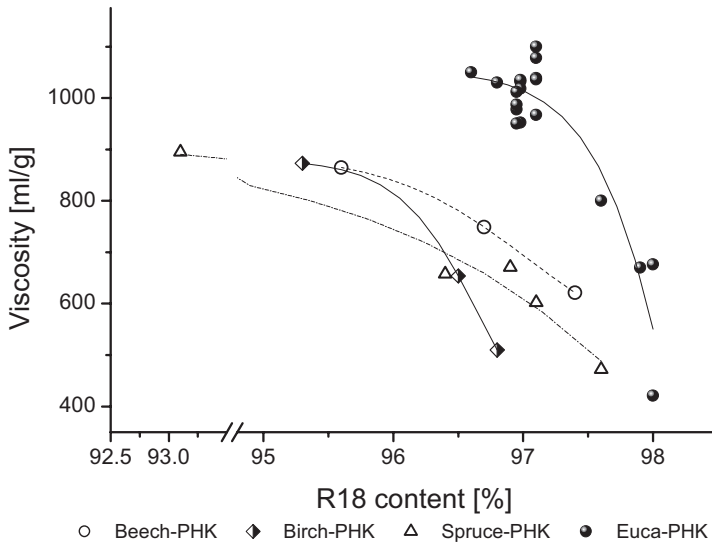
As expected from the chemical wood composition, Visbatch® cooking of eucalypt and spruce results both in a rather favorable relationship between pulp yield and residual hemicellulose content (xylan + mannan), as depicted in Fig. 4.124.



**Fig. 4.123** R18-content of unbleached Visbatch® pulps against P-factor. Constant reaction conditions: Total EA charge 23% o.d. wood (all species), 24% sulfidity (beech, birch, *E. urograndis*), 30% sulfidity (spruce), 150 °C (beech, birch), 158 °C (*E. urograndis*), 160 °C (spruce), 450 H-factor (beech), 825 H-factor (birch), 300 H-factor (*E. urograndis*) and 990 H-factor (spruce) [57].



**Fig. 4.124** Screened yield of unbleached Visbatch® pulps as a function of residual xylan and mannan content. Constant reaction conditions: Total EA charge 23% o.d. wood (all species), 24% sulfidity (beech, birch, *E. urograndis*), 30% sulfidity (spruce), 150 °C (beech, birch), 158 °C (*E. urograndis*), 160 °C (spruce), 450 H-factor (beech), 825 H-factor (birch), 300 H-factor (*E. urograndis*) and 990 H-factor (spruce) [57].



**Fig. 4.125** Relationship between viscosity and R18-content of unbleached Visbatch® pulps. Constant reaction conditions: Total EA charge 23% o.d. wood (all species), 24% sulfidity (beech, birch, *E. urograndis*), 30% sulfidity (spruce), 150 °C (beech, birch), 158 °C (*E. urograndis*), 160 °C (spruce), 450 H-factor (beech), 825 H-factor (birch), 300 H-factor (*E. urograndis*) and 990 H-factor (spruce) [57].

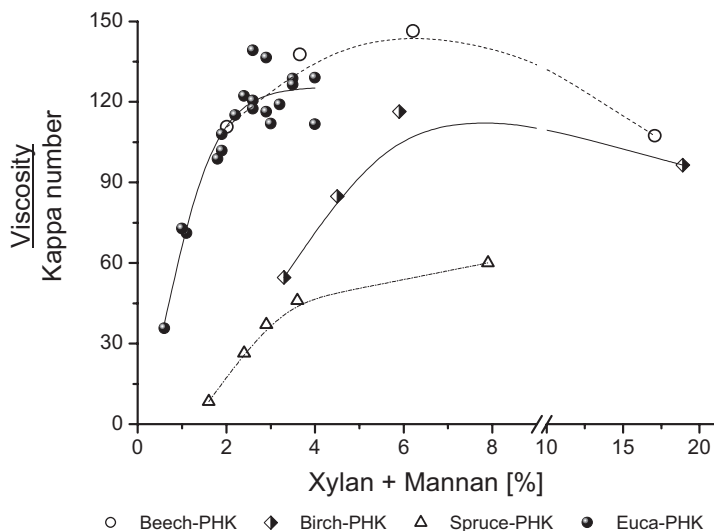
Again, efforts to reduce the hemicellulose content in spruce dissolving pulps to very low levels are offset by disproportionately high yield losses. The very low yield at a reasonably low hemicellulose content of the birch pulps can be explained by both the high hemicellulose and the low cellulose content of the raw material (see Tab. 4.49).

The purification selectivity of dissolving pulp production can be characterized as the relationship between the average molecular weight (intrinsic viscosity) and the degree of purification (R18- or cellulose content). This dependency clearly reflects the suitability of wood species for the production of high-purity dissolving pulps. High-purity and high-viscosity pulps indicate selective purification and delignification processability, whereas high-purity and low-viscosity pulps originate from wood species which contain a high cellulose content but are difficult to delignify, as seen for the spruce-Visbatch® pulps (Fig. 4.125).

The low pulp viscosity – an expression for poor delignification selectivity – arises from an increased cooking intensity that is necessary to attain reasonably low kappa numbers. The area of selective delignification and purification can easily be detected by relating the viscosity-to-kappa number ratio to the residual hemicellulose content (xylan + mannan), as illustrated in Fig. 4.126.

Figure 4.126 shows that the delignification selectivity definitely develops comparably as a function of the hemicellulose content for both beech and eucalypt Visbatch® pulps. The difference between Fig. 4.125 and Fig. 4.126 can be explained by the better delignification but worse purification selectivity of the beech pulps as compared to the eucalypt pulps (viscosities 620 mL g<sup>-1</sup> and





**Fig. 4.126** Relationship between viscosity-to-kappa number ratio and the residual hemicellulose content (xylan + mannan) of unbleached Visbatch® pulps. Constant reaction conditions: Total EA charge 23% o.d. wood (all species), 24% sulfidity (beech, birch, *E. urograndis*), 30% sulfidity (spruce), 150 °C (beech, birch), 158 °C (*E. urograndis*), 160 °C (spruce), 450 H-factor (beech), 825 H-factor (birch), 300 H-factor (*E. urograndis*) and 990 H-factor (spruce) [57].

970 mL g<sup>-1</sup> at kappa numbers of 5.6 and 8.8 for beech and eucalypt pulps with a xylan + mannan content of 2.0%, respectively).

Typical conditions for Visbatch® pulping of the four selected wood species and the properties of the resultant unbleached dissolving pulps are detailed in Tab. 4.50.

It is noted that the glucan yield is lowest for the eucalypt pulp, despite application of the lowest P- and H-factors. The order of glucan yield for different degrees of purification is as follows (see Tab. 4.50):

Beech (86.3%) > spruce (84.0%) > birch (83.0%) > eucalypt (78.5%).

This comparison is rather inadmissible, as the degree of purification is different for the pulps (see Tab. 4.49 and Tab. 4.50: degree of xylan removal: Eucalyptus (93.7%) > birch (90.3%) > beech (86.1%) > spruce (86.1%).

When comparing the purification selectivity of the different Visbatch pulps at a comparable residual hemicellulose content of about 2% (xylan + mannan), the glucan yield changes to the following order:

Eucalyptus (78.0%) > spruce (76.5%) > beech (71.7%) > birch\* (65.8%)

\* The birch Visbatch pulp is limited to a residual xylan + mannan content of 3.3%, even after applying a P-factor of 2000.

**Tab. 4.50** Process conditions of Visbatch® pulping of beech, birch, *E. urograndis* and spruce (according to [57]). Yields, properties and composition of pulp constituents of unbleached Visbatch pulps.

Parameters	Units	Unbleached PHK-Pulps			
		Beech	Birch	<i>E. urograndis</i>	Spruce
Process Conditions					
P-Factor		500	500	300	500
EA-charge	% od wood	23.2	23.1	23	23.1
Sulfidity	%	24	25	24.1	30
Temperature	°C	150	150	158	160
H-Factor		575	900	300	1050
Screened Yield	% od wood	39.3	35.3	37.8	39.9
Kappa number		7.1	7.5	8.3	17.1
Brightness	% ISO	42.9	43.6	43.4	33.6
Viscosity	mL g <sup>-1</sup>		873	970	753
R18-content	%	95.8	95.3	97.3	96.4
R10-content	%	93.4	93.2	96.4	95.2
Xylan	%	6.5	6.1	2.3	2.3
Mannan	%		0.7	0.4	1.5
Copper number	%		0.6	n.d.	0.4
Carboxylic groups	mmol kg <sup>-1</sup>	57.9	51.4	n.d.	61.1
DCM-extractives	%	0.4	0.9	0.4	0.2

n.d. = not detected.

The relatively high glucan yield of the spruce Visbatch pulp is certainly in contrast to the extremely degraded pulp of very high residual lignin content (spruce: 540 mL g<sup>-1</sup> at kappa number 39.6; beech: 705 mL g<sup>-1</sup> at kappa 9.8; birch: 510 mL g<sup>-1</sup> at kappa 9.3; eucalyptus: 950 mL g<sup>-1</sup> at kappa 9.0). The excessive prehydrolysis conditions necessary to obtain the low hemicellulose content causes lignin condensations which prevent selective delignification reactions during the kraft pulping operation.

#### 4.2.8

### **Pulping Technology and Equipment**

Andreas W. Krottschek

#### 4.2.8.1 **Batch Cooking *versus* Continuous Cooking**

Batch cooking systems process wood chips into pulp on a discontinuous basis. Today's batch digesters are usually between 300 and 400 m<sup>3</sup> in size, and a number of digesters is needed to produce the total pulp capacity of a mill. In contrast, today's continuous digesters are several thousand cubic meters in size, and the largest ones currently installed produce in excess of 3000 tons of pulp per day.

Advanced liquor management techniques have been developed over the past decades for both continuous cooking and batch cooking. These techniques allow both systems to follow the rules established from an increasing understanding of cooking chemistry for obtaining high-yield, high-strength pulp with excellent bleachability and low reject amounts. In addition, all of the above is made available at reduced consumption rates of cooking chemicals and energy.

Most – if not all – of the above benefits have resulted from the implementation of alkali and temperature profiles over the duration of the pulping process, compared to the prior art of adding all cooking chemicals to the chips at the beginning of the process.

The liquor management of modern cooking technologies generates liquor in various locations of the cooking system, which is fairly corrosive to carbon steel. That is why, today, digesters of all types are typically constructed of duplex stainless steel.

So what are the fundamental differences between batch and continuous cooking? Continuous cooking obviously offers continuous processing of wood chips and continuous production of pulp. At the same time, the consumption of cooking chemicals and utilities is continuous, reducing storage requirements and load variations imposed on other mill areas. Batch cooking excels in flexibility regarding wood furnish and pulp quality. Softwood and hardwood digesters can be operated side-by-side, and the pulp quality can be virtually switched between digesters. In addition, the modular concept using a number of identical digesters often allows an easier capacity increase.

On average, there may be certain advantages for continuous cooking with regard to the consumption of alkali and steam. For a given application, however, advanced continuous and batch cooking technologies will deliver similar pulp quality, bleachability, and rejects amount. Both will also feature in-digester washing and a similar consumption of electrical power. Any comparison in this respect must be regarded qualitative, because significant variations exist for the above factors within both batch and continuous cooking plants, depending upon the specific set-up.

Each cooking system is custom-designed under consideration of wood species, target pulp quality and other aspects. There is no general optimum system. From case to case, a specific pulping application may generate a preference for the batch or the continuous concept. Yet, in many instances the decision for a particular concept will boil down to a matter of philosophy.

#### 4.2.8.2 Batch Cooking Technology and Equipment

##### 4.2.8.2.1 Principles of Displacement Cooking

The basic idea of displacement cooking is to store process liquors from one cook and to re-use their heat and cooking chemicals in the next cook. For reasons of supply and demand, liquors need to be stored in accumulators at various levels of temperature, pressure, and chemical composition. Based on the original displacement process, technologies have developed over time which utilize the liquors in the tank farm for alkali and temperature profiling and for in-digester washing.

A typical displacement batch cooking system consists of digesters, tank farm and discharge tank, as illustrated in Fig. 4.127. At the beginning of the cooking cycle, wood chips are fed to a digester. Subsequently, liquors of various temperatures and concentrations are exchanged between the tank farm and the digester until the wood has been converted to pulp. At the end of the cooking cycle, the pulp is discharged from the digester into the discharge tank.

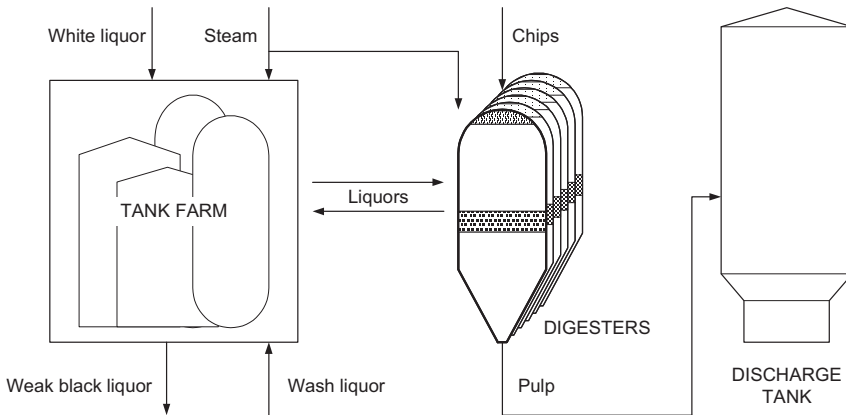


Fig. 4.127 Outline scheme of a displacement batch cooking system.

Wash filtrate from brownstock washing and cooking chemicals in the form of white liquor enter the tank farm only, and not the digester. Steam is consumed in the tank farm but may be as well directed to the digester. The weak black liquor which is not circulated back to the cooking process is subjected to fiber separation before being transferred to the evaporation plant.

##### 4.2.8.2.2 Batch Digesters

Before discussing the technology of displacement cooking in more detail, attention should be paid to the equipment at the heart of the cooking process – that is, the batch digester. Today's digesters are mostly stainless steel vessels of vertical cylindrical design (see Fig. 4.128). They have strainers constructed from perforated screen elements at different levels. The strainers hold back wood and pulp

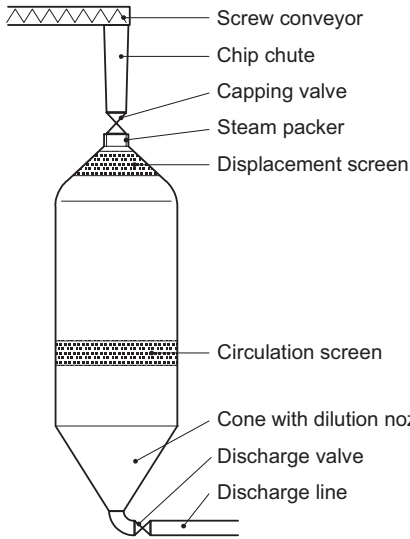


Fig. 4.128 Typical batch digester for displacement cooking.

when gas or liquor are extracted from the digester. A large ball valve (the capping valve) shuts off the digester towards the chip feed conveyor and chip chute. The bottom section of the digester is equipped with nozzles for dilution of the pulp during discharge, which occurs through the discharge elbow and discharge valve into the discharge line.

#### 4.2.8.2.3 Displacement Cooking Process Steps

While different displacement technologies follow their individual cooking cycles, the basic steps found in all these cycles are chip filling, impregnation, hot displacement, heating and cooking, cold displacement, and pulp discharge (Fig. 4.129). These steps are described in general below, and are later discussed in connection with some special displacement techniques.

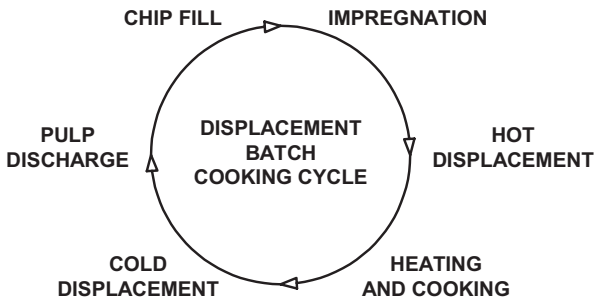


Fig. 4.129 Typical displacement batch cooking cycle.

### Chip Filling

The cooking cycle starts with chip filling, as wood chips are fed to the digester with screw or belt conveyors. Screw conveyors have the advantage that their closed design avoids the spread of wood dust which often is a nuisance with belt conveyors.

The chips drop from the conveyor into a chute and usually pass a packing device as they enter the digester. Low-pressure steam is the most-used packing medium. Introduced at an angle just as the chips enter the digester, the steam sets the chips in a spiral motion and ensures their distribution across the digester cross-section.

Packing increases the amount of wood that can be charged to a digester by 10–20%, thus leading to a higher pulp yield per digester volume. Packing also warms up the chips and improves the homogeneity of the chip column in the digester which is an important prerequisite for good liquor circulation and displacement without channeling. Decent chip filling therefore is the starting point for uniform pulp quality.

As the chips are warmed up, the air is positively displaced from inside the chips by the increasing partial pressure of wood moisture and by its own increasing volume. The residual air removal must happen by counter-diffusion of water vapor against air. During chip filling, gas is evacuated from the digester through the strainers by means of a blower.

### Impregnation

In the next step of the cooking cycle, impregnation liquor is charged to the bottom of the digester until the digester is hydraulically full. The impregnation liquor fill can in fact start before the end of the chip fill in order to shorten the cooking cycle time. At the end of the impregnation liquor fill, the digester is slightly overfilled to make sure that it is full. Overflowing liquor is returned to the atmospheric black liquor tank.

During impregnation, the wood is further preheated and residual air is removed from within the chips as liquor enters their interior. The impregnation step is supported by pressure generated by a pump to force the impregnation liquor into the chips. Good impregnation is another key to uniform pulp quality.

### Hot Displacement

After the impregnation step, the liquor in the digester is displaced by hot liquor. Ideally, the hot liquor pushes out the liquor in the digester in a plug-flow manner. As in all displacement steps, uniformity of penetration of the chip column without channeling is of critical importance for the pulp quality. There is less risk of screen pluggage by fibers when the flow rate of displacement and circulation liquors is gradually ramped up to full flow.

The liquors charged to the digester during hot displacement carry both the chemicals needed for cooking and the energy to heat the digester content. The liquors displaced from the digester are routed to their destination in the tank farm, depending on their temperature levels. At the end of the hot displacement, the digester is already close to the cooking temperature.

### Heating and Cooking

The final temperature increase required to reach the cooking temperature target can be made by injecting steam into the digester circulation line, by indirect heating in shell-and-tube heat exchangers, or by continued liquor displacement. Certain technologies allow the alkali level to be adjusted during cooking.

When the digester content has reached the cooking temperature, the circulation flow is sometimes reduced in order to protect the strainers from plugging with fibers. The cooking step continues until the desired H-factor is reached.

### Cold Displacement

The significant cooking reactions are terminated by cold displacement using filtrate from brownstock washing. Again, it is essential to have plug-flow through the digester, so that the initially displaced hot black liquor can be collected in the hot black liquor tank at the highest possible temperature for re-use in the next digester.

At some point during the cold displacement, wash filtrate begins to break through to the displaced liquor and to bring its temperature down. When the temperature drops below a set limit, the displaced liquor is switched from the hot black liquor tank in the tank farm to another tank of lower temperature. The cold displacement continues until the desired quantity of wash filtrate has been pumped through the digester. The digester contents should then be cooled down to a temperature below 100 °C.

In fact, the cold displacement step is the first brownstock washing stage. This means that, over time, there must be a balance between the wash filtrate collected from the wash plant and the liquor pumped through the digesters during the cold displacement steps.

### Digester Discharge

In the terminal step of the cooking cycle, the pulp is discharged from the digester by pumping. The pump discharge is delicate since, even at the end of the cook, the pulp in the digester still exhibits the physical structure of the wood chips. Wash filtrate is added for dilution to the lower part of the digester and to the discharge elbow. The sustainable consistency for pumping pulp from the digester is typically lower than 5%.

Besides appropriate dilution, the size of the discharge elbow and of the discharge valve are critical for a successful pump discharge. It is important for the succeeding cook that the pulp discharge is as complete as possible and that no pulp is left in the digester when the next cook starts.

### Heat Management

Hot black liquor from a previous cook is stored in the tank farm and, as it is charged to the digester, passes on its heat energy directly to the next cook. The remainder of hot black liquor not re-used in hot displacement is available for indirect heat transfer to white liquor and process water in shell-and-tube heat exchangers.

Typically excess hot black liquor, which is not needed in hot displacement, heats white liquor coming from the recausticizing plant. The temperature levels in the other black liquors are normally not high enough to be economically transferred to white liquor. Nonetheless, they are sufficiently hot for the generation of considerable amounts of hot water from warm water. The hot water temperature achievable from cooling of warm black liquor is 80–90 °C. The cooling of wash filtrate coming from brownstock washing yields somewhat lower water temperatures, because the filtrate temperature must be low enough to bring the digester contents safely beneath the boiling point.

In addition, the temperature of hot white liquor and/or hot black liquor is adjusted in the tank farm by indirect steam heating. Steam heating in the tank farm has the advantage of continuous steam consumption as compared to digester circulation liquor heating, which occurs only during the short period of heating to cooking temperature.

#### **Fiber Removal from Black Liquor**

The holes in the screens which are installed in the batch digesters need to be a few millimeters in diameter to avoid plugging during displacement and circulation. Whenever displaced liquor leaves a digester, it carries a certain amount of fibers to the tank farm. As a consequence, all liquors circulated in the tank farm contain fibers, as well as the black liquor in the atmospheric black liquor tank which is bound for chemical recovery. Since fibers are highly unwelcome in the evaporation plant, the liquor transferred to evaporation from the atmospheric black liquor tank must be subjected to fiber removal by a liquor filter or a liquor screen.

#### **Soap Skimming**

The soaps which are generated during softwood pulping can cause foaming and displacement problems if recycled back to the digester in a displacement cooking plant. Skimming of soap is a tricky undertaking because the separation of soap from the liquor occurs in narrow ranges of dry solids and pH. Usually, soap removal functions best from a liquor returning to the atmospheric black liquor tank. This liquor must then be allowed enough retention time for soap to come afloat. A dedicated, separate soap separation tank has proven most effective. The segregated soap is then pumped to the evaporation plant in a separate line or together with the black liquor.

#### **Gas Management**

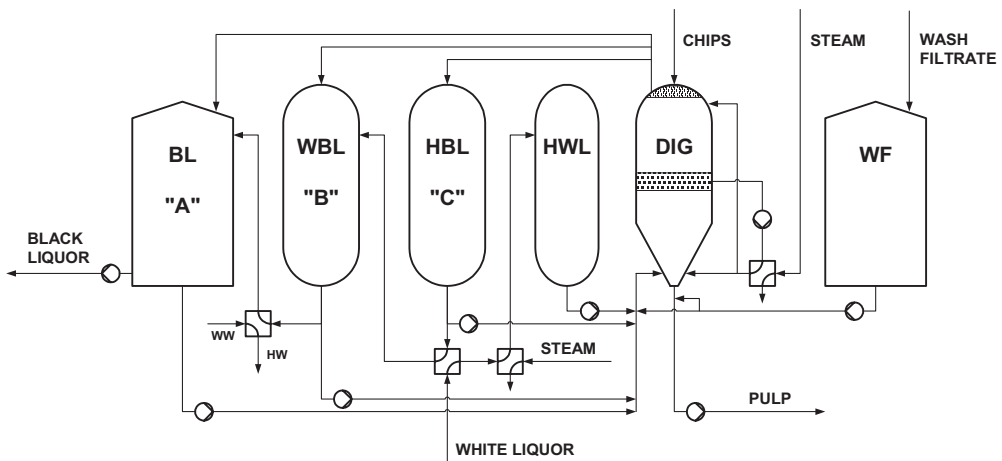
The gases vented from apparatus and equipment in the digester plant contain malodorous compounds, and must be collected for reasons of emission control and maintaining an acceptable workplace environment. Atmospheric tanks are connected to the high-volume low-concentration (HVLC) gas collection system. Such tanks include the atmospheric black liquor tank, the wash filtrate tank, and the pulp discharge tank. The air evacuated during the chip fill goes also to the HVLC gas system.



Besides non-condensable constituents, the gases vented from the pressurized tanks in the tank farm contain large amounts of moisture due to their elevated temperature. They are therefore passing condensation before proceeding to the low-volume high-concentration (LVHC) gas system. When the digester plant is being used to process softwood, the condensate contains turpentine, which is separated from the condensate by decanting.

#### 4.2.8.2.4 Rapid Displacement Heating (RDH)

A typical RDH tank farm consists of three pressurized accumulators and two atmospheric tanks (Fig. 4.130). The liquor accumulators A, B, and C are staged in temperature. Fresh alkali is provided from the hot white liquor tank. Steam is used for top-heating of white liquor in the tank farm and for bringing the digester to cooking temperature by indirect condensation.



**Fig. 4.130** Simplified Rapid Displacement Heating (RDH) process flowsheet. BL = black liquor; WBL = warm black liquor; HBL = hot black liquor; HWL = hot white liquor; DIG = digester; WF = wash filtrate; WW = warm water; HW = hot water [1].

The RDH cooking cycle is shown schematically in Fig. 4.131. After chip filling, warm black liquor (WBL) of up to 130 °C from the B accumulator is used for impregnation. Then, hot white liquor (HWL) and hot black liquor (HBL) from the C accumulator are charged to the digester during hot displacement. The displaced liquor is first returned to the A tank and then to the B accumulator. After hot displacement, the digester is brought to cooking temperature by indirect steam heating. Circulation is sometimes stopped after the target temperature has been reached. Subsequent to cooking, wash filtrate (WF) displaces the hot black liquor first into the hot black liquor accumulator C and then to the warm black liquor

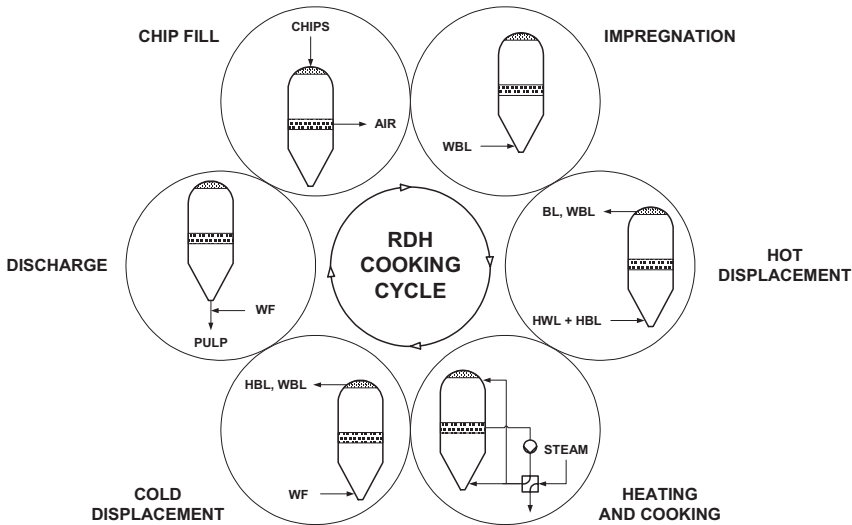


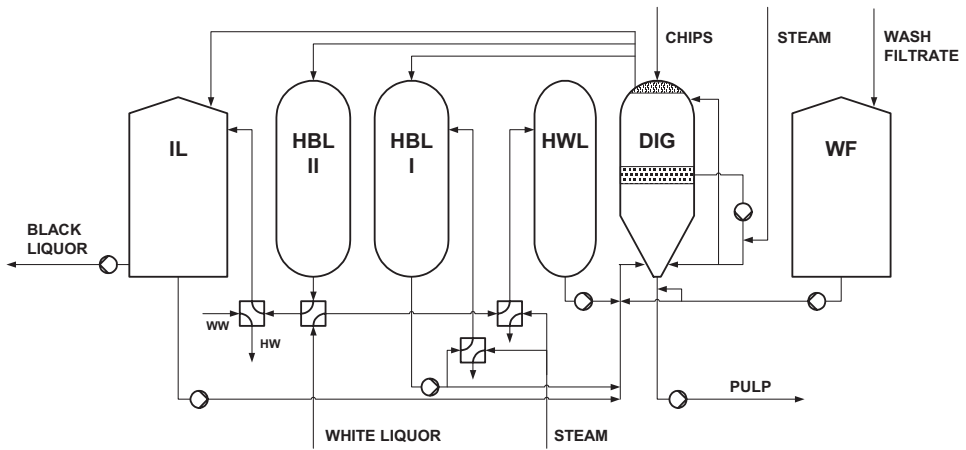
Fig. 4.131 Steps of the Rapid Displacement Heating (RDH) cooking cycle [1,2].

accumulator B. Eventually, the pulp is discharged from the digester by use of pressurized air or by pumping [1,2].

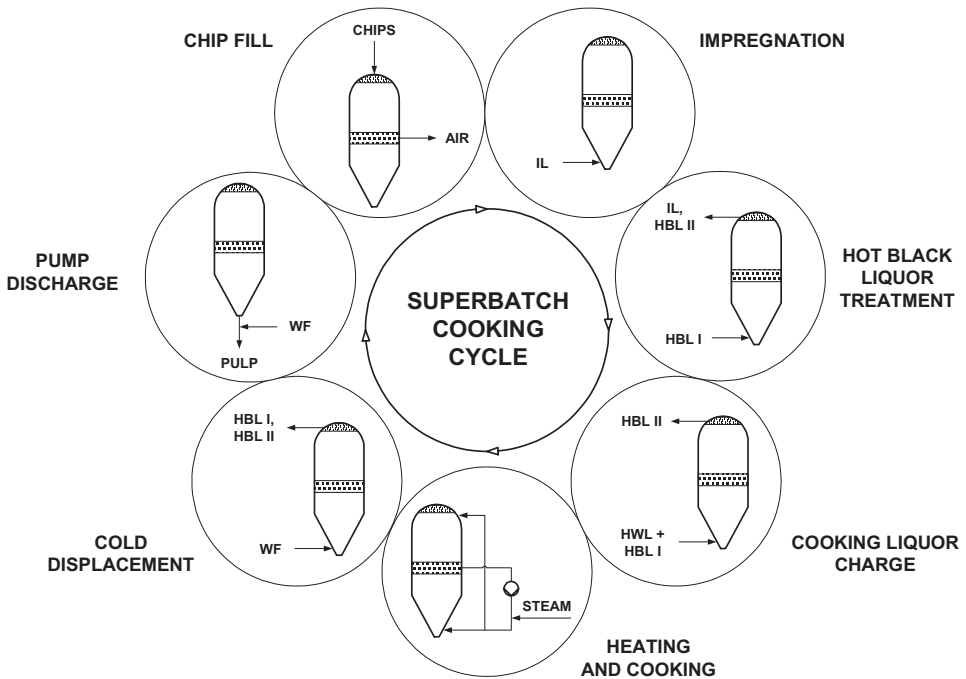
#### 4.2.8.2.5 SuperBatch

The typical SuperBatch tank farm also consists of three pressurized accumulators and two atmospheric tanks (Fig. 4.132). Again, the liquor tanks are staged in temperature and fresh alkali is supplied from the hot white liquor tank. Steam is used for controlling the temperature of both hot white liquor and hot black liquor in the tank farm, as well as for bringing the digester to cooking temperature.

The SuperBatch cooking cycle is shown schematically in Fig. 4.133. After chip filling, impregnation liquor (i.e., black liquor of below 100 °C) is used for impregnation. During the subsequent hot black liquor treatment, the impregnation liquor is displaced from the digester back to the impregnation liquor tank. The cooking liquor is then charged in the form of hot white liquor and hot black liquor, and the digester is brought to cooking temperature by steam injection into the circulation line. White liquor can be added during the cooking phase to control the alkali balance. After cooking, wash filtrate displaces the hot black liquor first into the primary hot black liquor accumulator and then into the secondary accumulator. Eventually, the pulp is discharged by pumping [3].



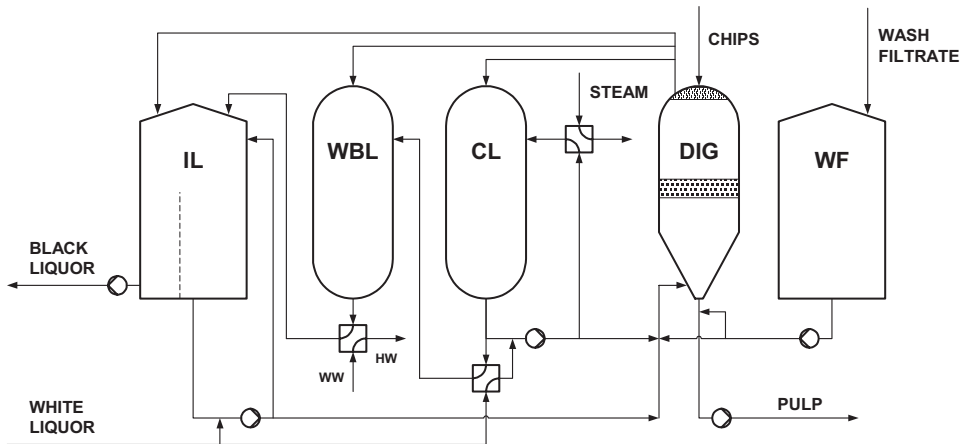
**Fig. 4.132** Simplified SuperBatch process flowsheet. IL = impregnation liquor; HBL I/II = primary/secondary hot black liquor; HWL = hot white liquor; DIG = digester; WF = wash filtrate; WW = warm water; HW = hot water [3].



**Fig. 4.133** Steps of the SuperBatch cooking cycle [3].

#### 4.2.8.2.6 Continuous Batch Cooking (CBC)

The CBC tank farm consists of two pressurized accumulators and two atmospheric tanks (Fig. 4.134). There is no hot white liquor tank, and steam is used only for heating of liquors in the tank farm. The temperatures and alkali concentrations of the impregnation liquor and the cooking liquor are adjusted in the tank farm in their respective tanks. There are also no digester circulation lines. During impregnation and cooking, the liquor circulates from the tank to the digester and back to the tank [4].



**Fig. 4.134** Simplified CBC process flowsheet.

IL = impregnation liquor; WBL = warm black liquor;  
CL = cooking liquor; DIG = digester; WF = wash filtrate;  
WW = warm water; HW = hot water [4].

After chip filling, impregnation liquor (IL) is charged to the digester. Once the digester is hydraulically full, the liquor circulates back to the impregnation liquor tank. Following the impregnation step, cooking liquor (CL) is pumped to the digester and the displaced liquor first continues to return to the impregnation liquor tank and then is switched to the warm black liquor tank (Fig. 4.135). All heating of the digester contents is carried out by the supply of hot cooking liquor. During cooking, the displaced liquor is returned to the cooking liquor tank. Subsequent to cooking, the wash filtrate displaces hot black liquor first into the hot black liquor accumulator and then to the warm black liquor accumulator. Eventually, the pulp is discharged from the digester by pumping [4].

Since the CBC cook is controlled by alkali concentrations rather than by alkali charges, the determination of chip weight in the digester is not an issue. With its straightforward design, the CBC process features the least number of sequence steps per cooking cycle, which makes its operation the easiest of all displacement cooking processes.

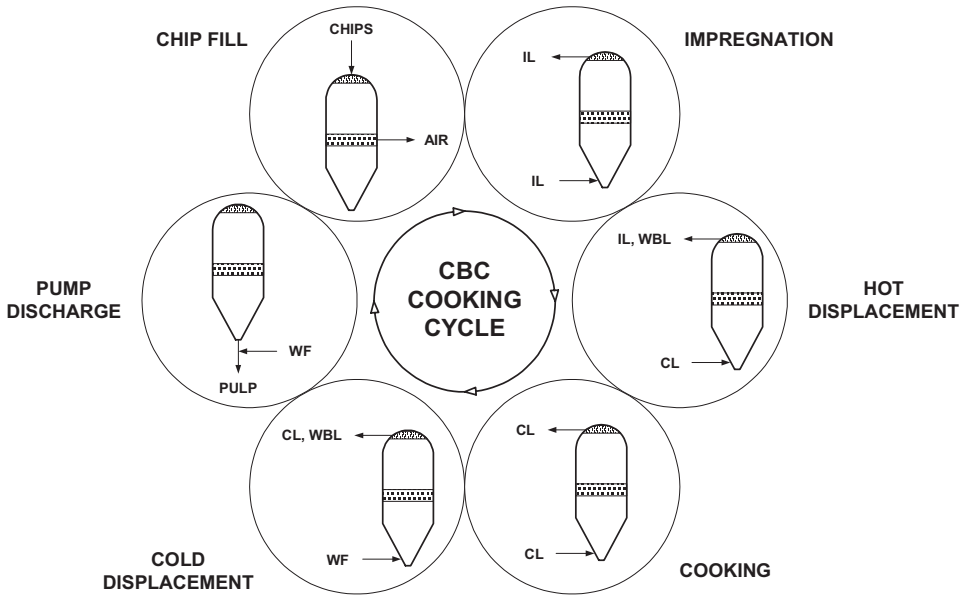


Fig. 4.135 Steps of the CBC cooking cycle [4].

4.2.8.2.7 Batch Cooking Schedule Management

In the displacement cooking plant, a number of batch digesters share a common tank farm and common supply and discharge systems. In order to make optimum use of these systems, the digester operation follows a strict program. At a given production rate, this program must account for scheduling the exclusive use of certain systems (e.g., of chip supply or pulp discharge systems), for the management of tank levels in the tank farm, and for the pulp quality.

The cooking schedule for a simple four-digester system is shown in Fig. 4.136. The chip fill in digester 2 is offset from the chip fill in digester 1, then follows digester 3, and after digester 4 it is again time for digester 1. The schedule for a particular application depends on the number of digesters, the total length of the cooking cycle as well as on the duration of the individual steps.

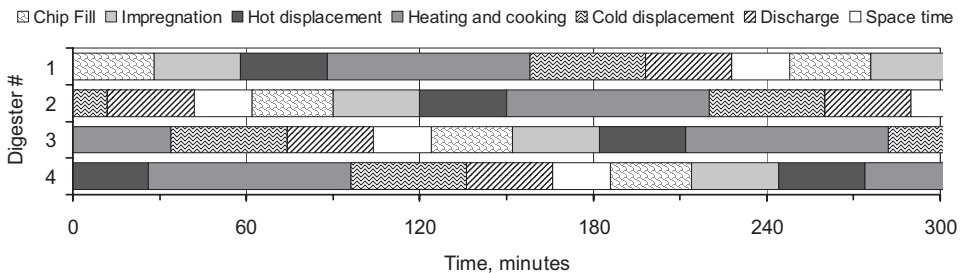


Fig. 4.136 Example for cooking schedule of four-digester displacement cooking plant.

### 4.2.8.3 Continuous Cooking Technology and Equipment

#### 4.2.8.3.1 Principles of Continuous Cooking

The basic idea of continuous cooking is to close the chain of continuous processes in the fiber line. Based on the original process, technologies have developed over time which employ in-digester washing and advanced alkali and temperature profiling.

The outline of a typical single-vessel continuous cooking system is illustrated in Fig. 4.137. Vapor recovered from the extraction liquor is used to remove air from the chips and to preheat them. The chips are then continuously transported to the digester with the help of liquor circulated between the chip feeding system and the digester top. A percentage of the cooking chemicals is charged with white liquor to the top circulation, while the remainder of the white liquor goes to the digester. A scraper and outlet device in the bottom. The digester has strainers at different levels, which hold back wood and pulp when liquor is extracted from the digester. Several liquor circulation loops are used to change the chemical regime and/or to adjust the temperature in the different zones of the digester. A central pipe discharge brings the circulation liquor back to the center of the digester near the corresponding set of circulation screens. Steam is used for liquor heating, preferably in indirect shell-and-tube heat exchangers.

The continuous digester itself is a huge vessel of vertical cylindrical design. Chips move from the top of the digester to the bottom by gravity. The vessel is equipped with a top separator, which separates the circulation liquor from the chips, and with a scraper and outlet device in the bottom. The digester has strainers at different levels, which hold back wood and pulp when liquor is extracted from the digester. Several liquor circulation loops are used to change the chemical regime and/or to adjust the temperature in the different zones of the digester. A central pipe discharge brings the circulation liquor back to the center of the digester near the corresponding set of circulation screens. Steam is used for liquor heating, preferably in indirect shell-and-tube heat exchangers.

Spent liquor which is not circulated back to the cooking process is extracted for vapor recovery. The weak black liquor is then subjected to fiber separation and cooling before being transferred to the evaporation plant.

Continuous cooking systems can be categorized into single-vessel and two-vessel systems, with hydraulic or steam/liquor phase digesters. Two-vessel systems have a separate vessel where the impregnation of chips takes place. In such a system, the chips are fed to the top of the impregnation vessel and then transferred from the bottom of the impregnation vessel to the digester top by a separate circulation loop.

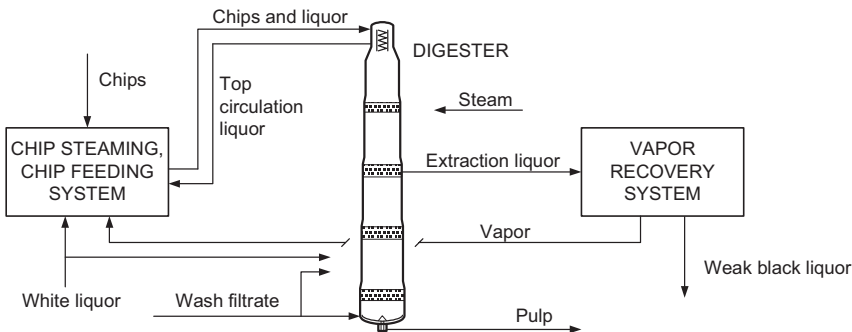


Fig. 4.137 Outline of single-vessel continuous cooking system.

*Hydraulic* digesters are completely filled with liquor, whereas *steam/liquor phase* digesters have a vapor phase at the top. In a steam/liquor phase digester, the chips reach above the liquor level. They can be heated to cooking temperature with direct steam, which in most cases requires prior impregnation and therefore makes sense mainly in a two-vessel system.

#### 4.2.8.3.2 Continuous Cooking Process Steps

While different continuous cooking technologies follow their individual concept, the basic steps found in all these systems are chip steaming, chip feeding, impregnation, cooking, washing, and pulp discharge. These steps are described in general below, and are discussed later in connection with some special continuous cooking techniques.

##### Chip Steaming

The continuous cooking process starts when the chips enter a steam environment. The target of steaming is the elimination of air from the chips to a maximum extent. As the chips are warmed up, the air is positively displaced from inside them by the increasing partial pressure of wood moisture and by its own increasing volume. The residual air removal must occur by counter-diffusion of water vapor against air.

Adequate steaming of chips must be ensured at all times, because the buoyancy of air entrapped in chips can critically influence chip column movement in the digester. Other negative effects of poor air removal include pump cavitation, feed line hammering, and inhomogeneous impregnation.

Traditionally, steaming was performed at elevated pressure in a steaming vessel and/or near atmospheric pressure in the chip bin. Lately, it has been found that pressurized steaming can be skipped when the duration of atmospheric steaming is sufficiently long.

##### Chip Feeding

Once the air is removed from the chips, they must be brought to digester pressure, which is done by a combination of rotary feeding devices and pumps. Liquor is used as the transport medium for chips from the feeding system to the digester top.

##### Impregnation

During impregnation, the cooking chemicals become distributed inside the chips. Impregnation starts as soon as the chips are subjected to digester pressure in the chip feeding system. At that time, impregnation is governed by liquor penetration into the chip voids under a pressure gradient. Once the chips are in the digester, diffusion takes control over the mass transfer as the chips and liquor move concurrently through what is commonly referred to as the impregnation zone.

Good impregnation is a key to uniform pulp quality and optimal cooking time. The aspects related to steaming and impregnation and their effects on continuous cooking have recently been extensively described [5].

### **Cooking**

The impregnation step passes into the cooking stage as the free liquor is displaced from the chip column by hot cooking liquor. Note that the liquor in the digester can be divided into a free portion moving between the chips and a bound portion trapped within the chip volume. Only the free liquor is available to displacement, whereas the bound liquor is accessible by diffusion and thermal conduction.

The cooking liquor is distributed by the central pipe discharge and flows radially towards the cooking circulation screens. It is essential that the circulation flow rate is sufficiently high to ensure uniform chemical and temperature profiles across the digester cross-section. This is of critical importance also for the other circulation operations in the digester. Otherwise, different radial temperature and/or chemical levels prevail that lead to inhomogeneously cooked fibers.

Cooking usually occurs in more than one zone. As the chip column moves down, the alkali, temperature and solid levels in the digester can be adjusted by introducing white liquor or wash filtrate into circulation loops, by indirect heating of the liquor in those loops, or by extracting spent liquor for chemical recovery.

### **Washing**

The transition between cooking and washing in a continuous digester is blurred. At the high temperature levels applied for washing, a considerable number of reactions continue in the washing zone. The in-digester washing step – termed Hi-Heat washing – was originally designed to last for up to 4 h, and this resulted in excellent washing efficiencies due to the vast time allowed for diffusion. In many mills, however, in-digester washing has been compromised for higher production rates when a part of the digester's washing zone volume was converted for cooking.

In-digester washing is the first brownstock washing stage. This means that, over time, there should be a balance between the wash filtrate collected from the wash plant and the liquor pumped into the digester. For washing to be efficient, there must be a net flow of liquor from the wash circulation located near the bottom of the digester to the liquor extraction above.

### **Pulp Discharge**

The significant cooking reactions are terminated when the cool wash filtrate from the first stage of brownstock washing brings the temperature of the digester contents down to 85–95 °C. A rotating scraper reclaims the pulp from the cross-section at the digester bottom to the outlet device. Besides cooling the pulp, the wash filtrate provides the necessary dilution before the pulp discharge. The blowline consistency is typically around 10%. Even at the end of the cook, the pulp in the digester still exhibits the physical structure of the wood chips. This structure is finally broken up as the pulp becomes defibrated during the turbulent pressure reduction at the discharge control valve.



**Heat Management**

Typically, the heat exchangers use indirect steam to raise the temperature of circulation liquors. Steam/liquor phase digesters may have direct steam addition to the digester top. The heat in the extraction liquor is usually transferred to vapor which is used for steaming of the chips, but it can also be exchanged with cooler process liquors. Additional live steam may be used for chip steaming if necessary. Some of the residual heat in the weak black liquor is spent for generation of hot water. The hot water temperature achievable from the cooling of weak black liquor is 80–90°C. The cooling of wash filtrate coming from brownstock washing yields somewhat lower water temperatures, because the filtrate temperature must be low enough to bring the digester contents safely beneath the boiling point.

**Fiber Removal from Black Liquor**

The slots in the screens installed in the digester need to be a few millimeters wide to avoid plugging. As a consequence, the extraction liquor contains fibers which are highly unwelcome in the evaporation plant. Hence, the liquor must be subjected to fiber removal before being transferred to evaporation.

**Gas Management**

The gases vented from the chip bin and steaming vessel contain malodorous compounds, and must be collected for reasons of emission control and maintaining an acceptable workplace environment. Besides noncondensable constituents, the vent gases carry certain amounts of moisture, and must therefore pass condensation before proceeding to the mill's gas collection and treatment systems. When a digester plant processes softwood, the condensate also contains turpentine, which is separated from the condensate by decanting.

**4.2.8.3.3 Chip Steaming and Chip Feeding Systems**

A conventional chip steaming and feeding system for a continuous digester is shown schematically in Fig. 4.138. The chips are fed through the airlock, a rotary star or screw feeding device, into the chip bin. Flash steam from the second extraction liquor flash tank enters the chip bin near the bottom and provides atmospheric steaming, which typically lasts for 15–25 min. The chip meter, which again is a rotary star or screw feeder, sets the pulp production rate of the digester. It discharges into the low-pressure feeder, which isolates the pressurized steaming vessel from the atmospheric chip bin. Pressurized steaming is usually continued for 1–2 min at a pressure of ca. 1.5 bar(g). A screw in the steaming vessel conveys the chips to the chip chute.

The high-pressure feeder's plug-type rotor always keeps a vertical and a horizontal flow path open for liquor circulation. When one particular pocket of the feeder is in the vertical position, the chips are sucked from the chip chute into the pocket by the chip chute circulation pump. The chips are retained in the pocket by a screen mounted in the casing of the feeder. Liquor passes the screen and returns to the chip chute via the sand separator. As the pocket turns to the horizontal

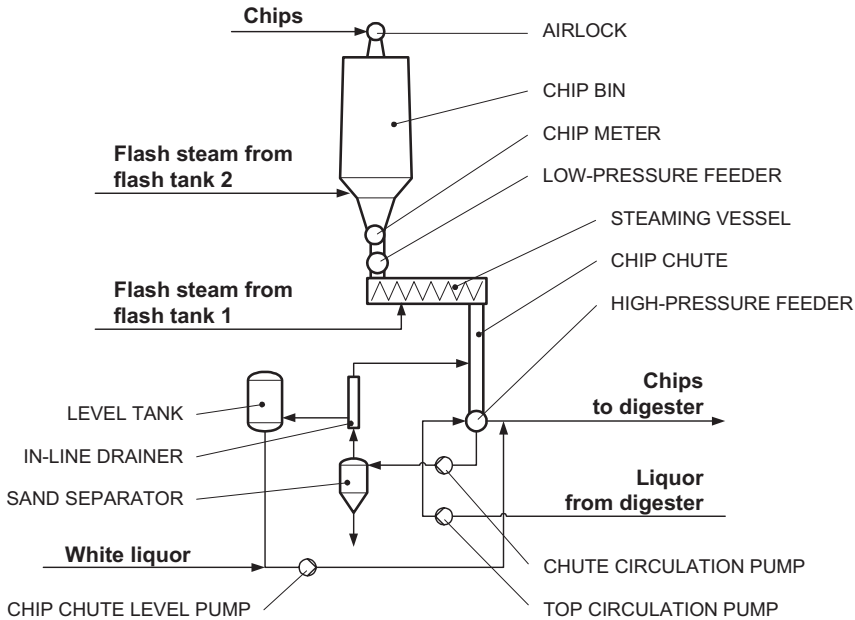


Fig. 4.138 Conventional chip feeding system for continuous digester.

position, the liquor coming from the top circulation pulp pushes the chips out of the pocket and transfers them to the digester (or impregnation vessel). There is a certain intentional leakage from the high-pressure side of the feeder (i.e. the top circulation side) to the low-pressure side (i.e. the chute side). Excess liquor in the chute liquor loop is extracted via the in-line drainer and pumped back to the top circulation by the chip chute level pump. White liquor can be added to the suction side of the chute level pump, which is therefore also referred to as make-up liquor pump.

More recently developed chip feeding systems attempt to reduce the amount of equipment installed. For example, Kvaerner Pulping's Compact Feed system (Fig. 4.139) does not require the sand separator, in-line drainer and level tank [6].

The Andritz Lo-Level Feed system skips the steaming vessel and chip chute by replacing the low-pressure feeder with a helical-screw chip pump, which directly feeds the high-pressure feeder. Recently, Andritz has developed the TurboFeed system which also eliminates the high-pressure feeder (Fig. 4.140). Chips are metered from the chip bin via twin screws into a chip tube. From there, they are forwarded to the digester by a series of specially designed pumps. The feed circulation cooler ensures that the liquor returned to the chip chute is below 100 °C. Besides easing the feed process, the system also controls the digester pressure, thereby allowing a more stable flow pattern of free liquor in the cooking zones due to a constant wash filtrate feed rate to the digester [7,8].

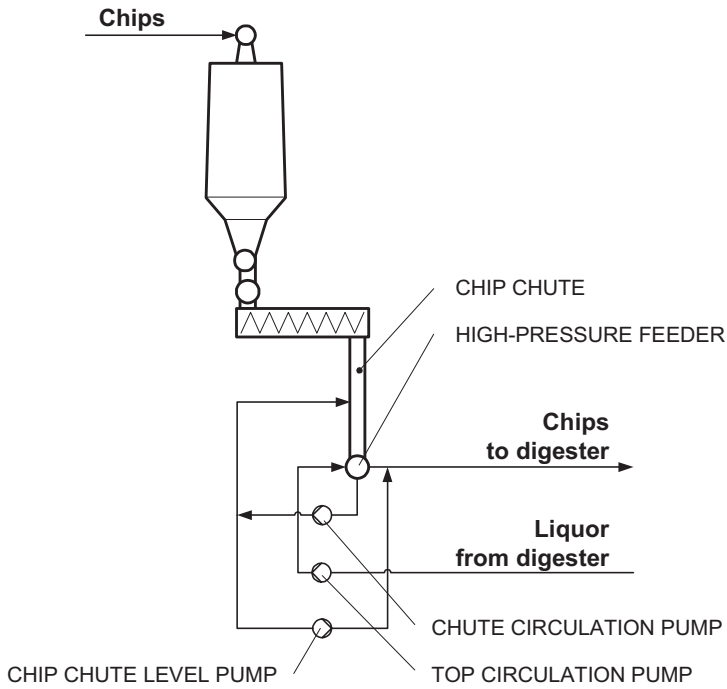


Fig. 4.139 The Kvaerner Pulping Compact Feed system [6].

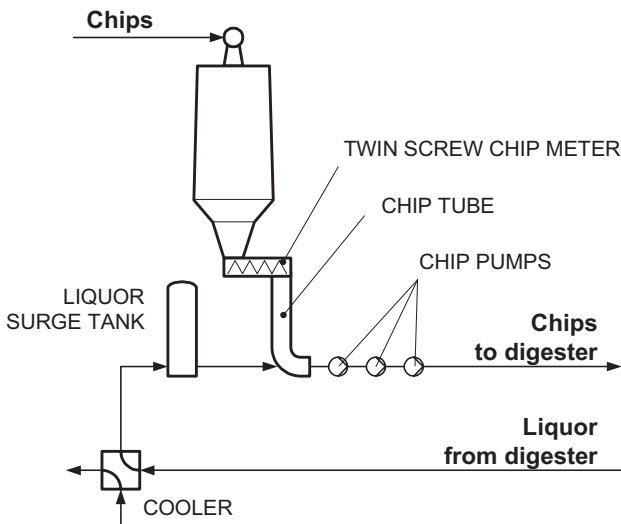


Fig. 4.140 The Andritz TurboFeed system [8].

#### 4.2.8.3.4 Modified Continuous Cooking (MCC)

Modified Continuous Cooking [9,10] was the first in a string of alterations imposed on the conventional continuous pulping process. A typical configuration of an MCC single-vessel hydraulic digester is shown in Fig. 4.141. The chips enter the top of the digester together with the top circulation liquor, and are fed to the top separator, which is a screw conveyor surrounded by a cylindrical screen. The vertical screw transports the chips downwards and also keeps the slots of the screen clean. Circulation liquor is extracted through the screen and returned to the chip feeding system, where the largest portion of the white liquor is added. The excess liquor from the top circulation travels downwards concurrently with the chips and enters the impregnation zone (see also Fig. 4.142).

Impregnation is typically performed at a temperature between 115 and 125 °C and a pressure above 10 bar(g) for 45–60 min. As the chips approach the first screen section, liquor is displaced horizontally from the central pipe discharge through the chip column to the strainers, and is then circulated back to the central pipe via the concurrent cooking heater. A small portion of white liquor is added to the cooking circulation loop. The heater is operated with indirect steam and the hot liquor introduced into the digester brings the temperature of the chip column up to the cooking temperature of 150–170 °C.

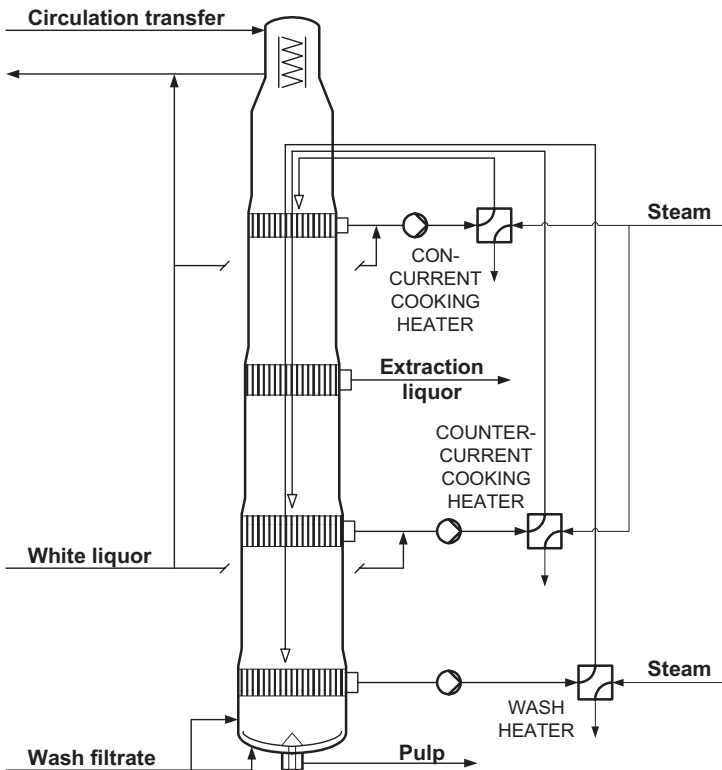


Fig. 4.141 Typical MCC single-vessel hydraulic digester [9,10].

Hot cooking liquor and chips then continue traveling downwards through the concurrent cooking zone to the extraction screens. This is where the spent cooking liquor is taken from the digester. Below the extraction screens starts the countercurrent cooking zone, where the net flow of liquor is directed upwards. The temperature in both cooking zones is roughly the same, with the countercurrent cooking heater being responsible for the temperature in the lower zone. White liquor is added to the countercurrent circulation liquor to increase the alkalinity towards the end of the cook. Typically, the total cooking time of 90–150 min is equally split between the concurrent and the countercurrent zones.

As the chips proceed into the washing zone, the countercurrent flow regime persists. The temperature in the so-called Hi-Heat washing zone decreases gradually to about 130 °C, and the dissolved wood components as well as spent cooking chemicals are removed from the pulp by diffusion washing. The final temperature in the washing zone is controlled by steam addition to the wash heater, which is installed in the lowest of the circulation loops. At the digester bottom, the pulp is cooled and diluted by wash filtrate, before it is eventually discharged from the vessel through the blow valve. The wash filtrate flow usually controls the pressure in the digester.

The major force driving behind movement of the chip column in the digester is the weight of the wood material. Forces acting against the direction of the wood's weight are the buoyancy of gas entrapped in the chips, friction between the moving chips and the digester wall, and – in zones of countercurrent flow – the drag induced by the upward liquor movement. Efficient air removal and reasonable countercurrent liquor velocities are therefore important prerequisites for smooth chip column movement.

The need to maintain high circulation flow rates brings about a considerable risk of plugging screens or screen headers because fines and other small material are carried through the chip column and accumulate at the screen surface, together with chips, or in the header. This is why techniques must be applied to keep the screens and headers clear. In a typical set of screens, profile bar screen plates are arranged at two levels above each other, with independent headers and two nozzles for each header which are positioned at opposite sides of the digester shell. This arrangement allows the automated side-to-side switching of headers and resting of screens – that is, temporary stopping of the extraction through one level of screens. When a screen rests, the movement of the chip column wipes its slots clear. When a header is switched to the other side, the flow direction is inverted, which makes the formation of deposits more difficult. In addition, back-flushing of screens may be necessary at times.

There is always a temperature and concentration gradient from the central pipe discharge along the radius of the digester to the strainers, even at high circulation rates. In particular, in large-capacity digesters it can be a major challenge to maintain gradients that are adequate for uniform cooking. Two-vessel systems provide the opportunity of heating the bottom circulation liquor returning from the digester to the impregnation vessel, thus allowing constant temperature and alkali profiles over the digester cross-section at the beginning of the bulk delignification phase. A typical impregnation vessel with top separator, outlet device and optional

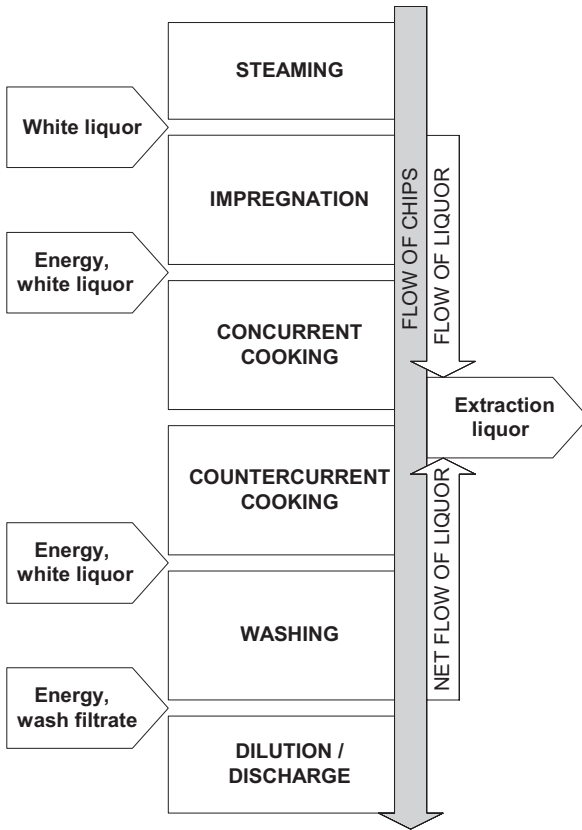


Fig. 4.142 Typical Modified Continuous Cooking (MCC) process steps and flow regime.

extraction screens, as well as its integration into the two-vessel system are shown in Fig. 4.143. If the digester in a two-vessel constellation is of hydraulic design, it is equipped with a stilling well instead of the top separator.

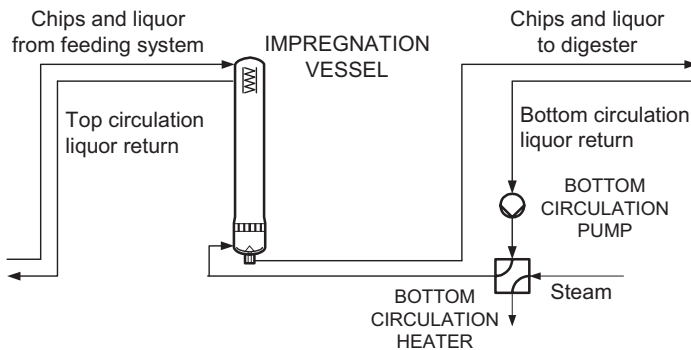


Fig. 4.143 Typical impregnation vessel in a two-vessel continuous cooking system.

In contrast to hydraulic digesters, steam/liquor phase digester have an inverted top separator, where the chips are conveyed upwards inside the screen. The liquor needed for top circulation flows back through the screen, while the chips and excess liquor overflow from the separator into the steam phase. Since in the steam/liquor phase digester the chips reach above the liquor level, direct steam can be applied for chip heating. This has some disadvantages, such as dilution of the extraction liquor, the related additional load on the evaporation plant, and a reduced amount of live steam condensate returned to the boiler house. Steam/liquor phase digesters allow compaction of the chip column to be influenced by the height of chips standing above the liquor level.

#### 4.2.8.3.5 Extended Modified Continuous Cooking (EMCC) and IsoThermal Cooking (ITC)

Extended Modified Continuous Cooking [11] and IsoThermal Cooking [12] mark the consequent prolongation of the ground broken by MCC related to the equalizing of alkali profiles and co-utilization of washing zone volume for cooking and washing.

A typical configuration of an EMCC/ITC single-vessel hydraulic digester is shown in Fig. 4.144. The initial process steps up to countercurrent cooking corre-

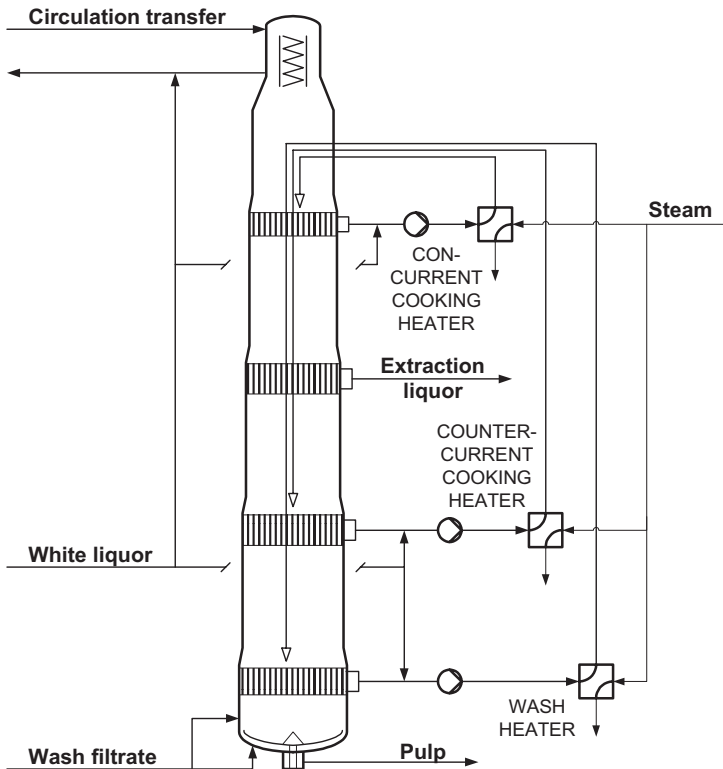


Fig. 4.144 Typical EMCC/ITC single-vessel hydraulic digester [12,13].

spond to the MCC technology described above. The additional element of EMCC/ITC lies in the extension of the cooking zone down to the lowest set of screens (see also Fig. 4.145).

There is no more dedicated high-heat washing zone between strainers. White liquor is added not only to the top circulation and countercurrent cooking circulation, but also to the wash circulation. At the same time, the temperature of the wash liquor is raised to a point where the cooking temperature is also reached in the extended zone. In Fig. 4.144, this means that the cooking temperature of typically 150–165 °C is maintained in the digester from the first set of screens down to the last.

The split of white liquor between the points of addition must ensure that a minimum residual alkali concentration is maintained in all liquors at all times, so that the detrimental re-precipitation of dissolved organic compounds is safely avoided. From a process perspective, EMCC and ITC are widely similar. Installation-wise, EMCC requires only one wash circulation, whereas ITC uses two sets of wash circulation loops with individual heaters.

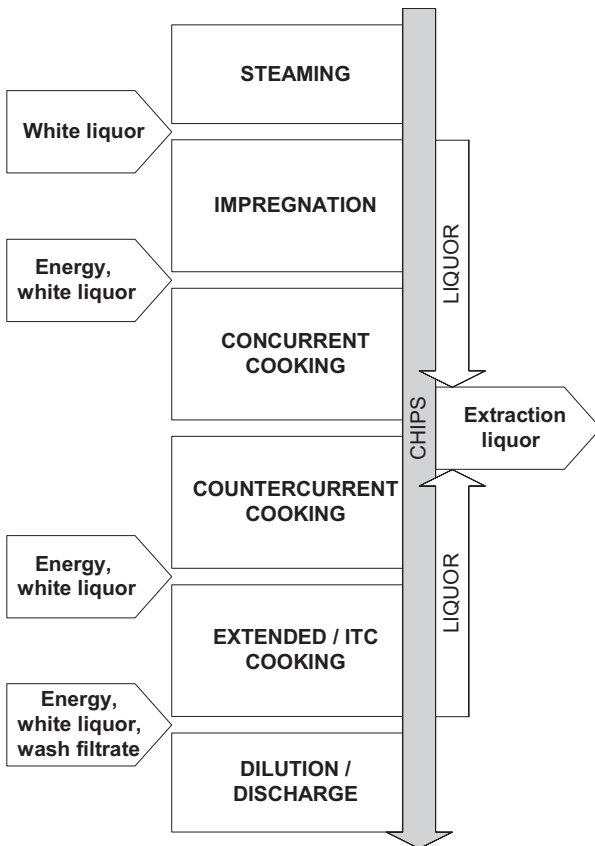


Fig. 4.145 Typical EMCC/ITC process steps and flow regime.



ITC systems have been expanded with black liquor impregnation, where a part of the extraction liquor from the cooking zone supports impregnation before being drawn from a separate extraction screen within the impregnation zone [12].

#### 4.2.8.3.6 Lo-Solids Cooking

As indicated by the name, the Lo-Solids concept [14,15] adds the feature of reduced dry solids concentration to continuous cooking. The main reduction of solids is achieved by the extraction of dissolved organic substances after impregnation and by addition of wash filtrate to the cooking zones. Compared to EMCC, Lo-Solids pulping further improves the uniform distribution of alkali and temperature over the cook.

A typical configuration of a Lo-Solids retrofit to a single-vessel hydraulic digester is shown in Fig. 4.146. The first screen section, often the former upper cooking circulation (UCC) section, is used for extraction of spent cooking chemicals and of wood material dissolved during the impregnation step. It must be remembered that 20–30% of the total wood substance is dissolved, and a considerable amount of alkali is consumed during impregnation. Below the first extraction at the UCC

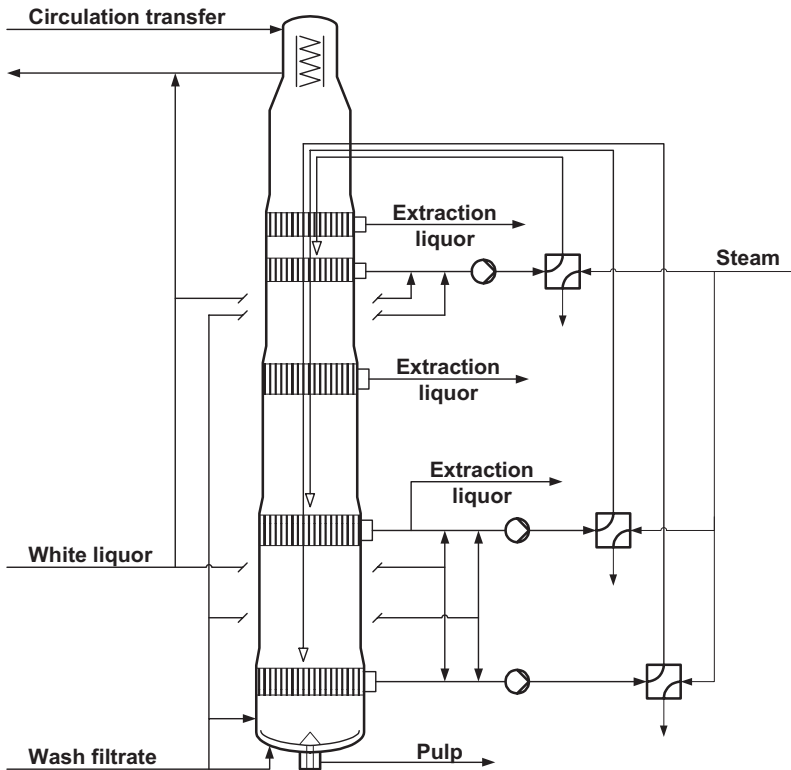


Fig. 4.146 Typical Lo-Solids single-vessel hydraulic digester [14,15].

screens follows a short countercurrent impregnation and heating zone down to the second screen section, often the former lower cooking circulation screens. White liquor and wash filtrate are added to the circulation liquor and heated to full cooking temperature.

Subsequently, the chips move into a concurrent and a countercurrent cooking zone separated by the second extraction, before proceeding into the extended cooking zone (Fig. 4.147). The third extraction occurs at the fourth set of screens. Only a part of the liquor taken from the screen is extracted, while the remainder is made up with alkali and wash filtrate and returned to the central pipe discharge. The pulp continues to travel down through the countercurrent extended cooking zone and is finally diluted and discharged. Compared to the retrofit arrangement described above, a new Lo-Solids installation would omit the fourth set of screens and respective liquor circulation.

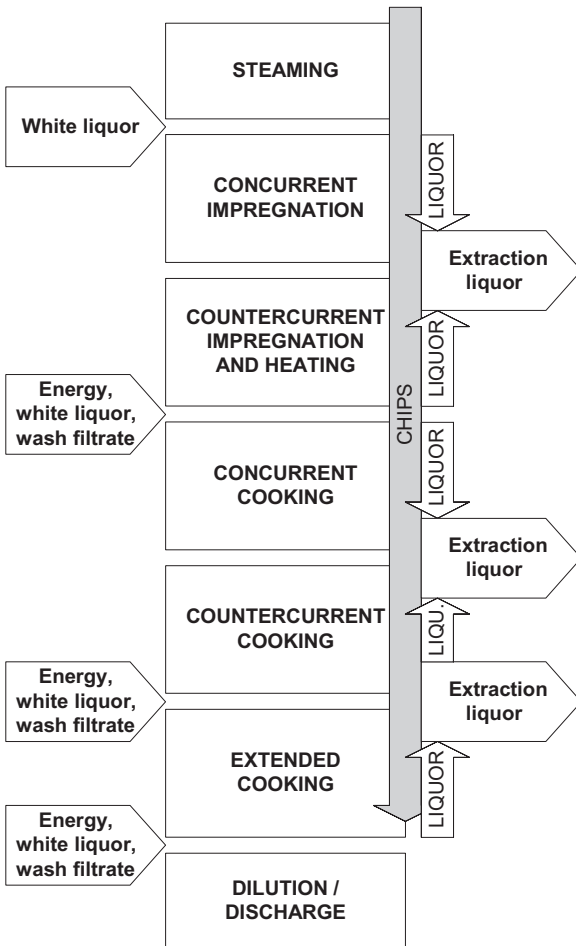


Fig. 4.147 Typical Lo-Solids process steps and flow regime [14].

The application of Lo-Solids pulping has led to reduced white liquor consumption and improved washing efficiency in the digester. The latter can be attributed mostly to higher extraction liquor flow rates. When running on a single extraction, overloaded systems often experience screen limitations and countercurrent flow restrictions. In such cases, when the digester cannot deal with the full quantity of wash filtrate, the excess filtrate must by-pass the digester to the evaporation plant. Such filtrate is lost for washing. Multiple extractions allow a larger total flow of extracted liquor without excessive load on screens, and multiple wash filtrate addition reduces the relative velocity of liquor and chip column in countercurrent zones. It has been found that the improved chip movement, when coupled with the increased extraction capacity, has boosted not only the washing efficiency but also the digester capacity.

Further information regarding the general technological aspects of continuous cooking is provided in Sections 4.2.8.3.4 and 4.2.8.3.5.

The Lo-Solids concept is undergoing continuing refinement in terms of accommodation to cooking chemistry and reduced installation efforts. Some of the related technologies are specifically addressing the requirements of a particular cooking application. Enhanced Alkali Profile Cooking (EAPC) uses black liquor from the lower extraction, together with white liquor, for impregnation [16,17]. The widely simplified process configuration of the Downflow Lo-Solids concept is shown in Fig. 4.148.

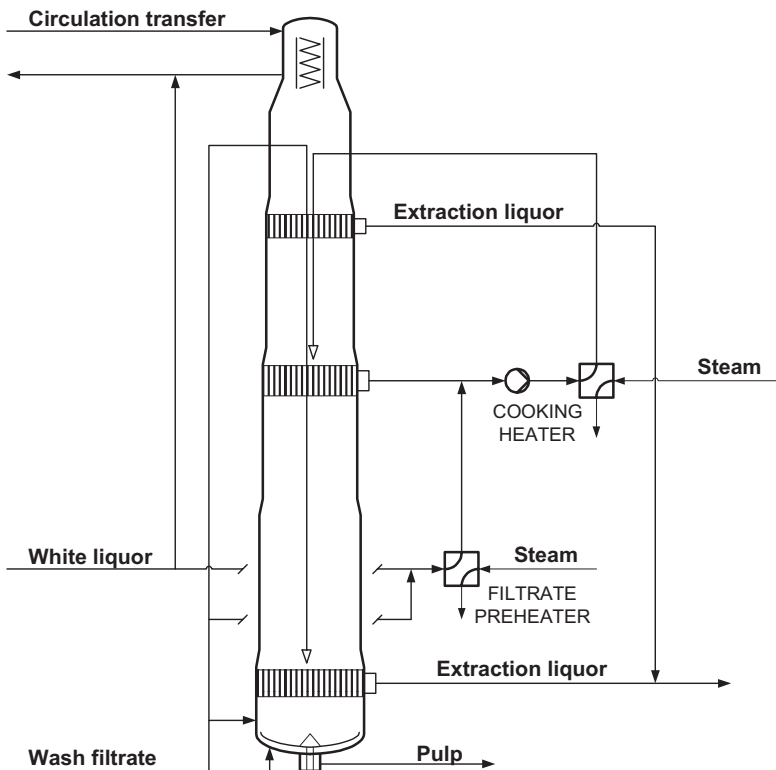


Fig. 4.148 Typical Downflow Lo-Solids single-vessel hydraulic digester [8].

#### 4.2.8.3.7 Heat Recovery Systems

Usually, heat is recovered from the extraction liquor for the generation of vapor to be used in chip steaming. The conventional heat recovery system consisting of two flash tanks installed in series is shown schematically in Fig. 4.149. Flash tank 1 is operated at a pressure of about 1.5 bar(g), and delivers flash steam to the pressurized steaming vessel. Flash tank 2 feeds the atmospheric chip bin, and is pressure-controlled at a small overpressure. The flash tanks are equipped with internals which reduce foaming by providing a special flow pattern and generous liquor surface. Any flash steam not needed for steaming is condensed, with the non-condensable gases transferred to the mill's gas collection and treatment system.

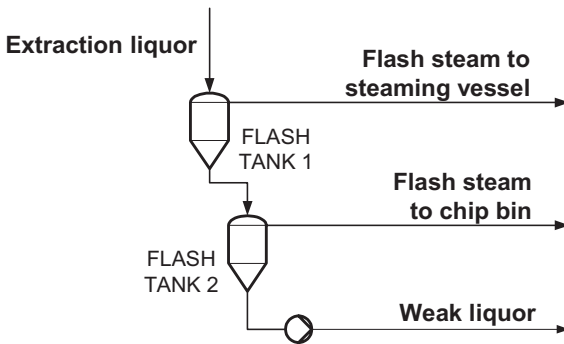


Fig. 4.149 Conventional heat recovery system.

The Lo-Level heat recovery system by Andritz (Fig. 4.150) generates clean steam from feed water by indirect heat exchange in a reboiler. The clean steam eliminates emissions of reduced sulfur compounds (TRS) from chip steaming operations. On the other hand, the water evaporation requirements and the TRS load increase in the evaporation plant.

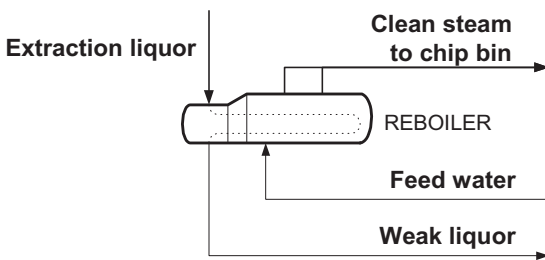


Fig. 4.150 The Andritz Lo-Level heat recovery system [8].

Modern heat recovery systems may also include indirect heat exchange between extraction liquor and cool process liquors, with the goal of improving the steam economy. Examples are the heating of white liquor before injection into a cooking circulation, or the heating of wash filtrate in a Lo-Solids cooking system.

## 4.3

**Sulfite Chemical Pulping***Herbert Sixta*

## 4.3.1

**Introduction**

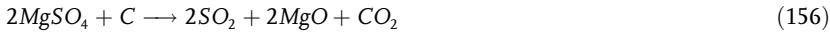
The origin of the sulfite process is attributed to the efforts of Benjamin Chew Tilghman, an American chemist, who was granted U.S. patent 70,485, dated November 1867, entitled *Treating Vegetable Substances for Making Paper Pulp*. The invention was based on the results of the experiments at the mills of W.W. Harding and Sons at Manayunk, near Philadelphia, in 1866, and covers the pulping of wood with aqueous solutions of calcium hydrogen sulfite and sulfur dioxide in pressurized reactors. However, the first sulfite mill started its production in Europe at Bergvik, Sweden, in 1874 under the direction of C.D. Ekman using magnesium hydrogen sulfite solution,  $Mg(HSO_3)_2$ , as the cooking agent. The mill was equipped with small rotating digesters heated indirectly by means of a steam jacket. In 1875, the German chemist A. Mitscherlich was developing a sulfite cooking process using a horizontal, stationary, cylindrical digester lined with brick and indirectly heated by means of coils of lead or copper pipe. Cooking was carried out under moderate temperature and pressure conditions. Consequently, the Mitscherlich process was characterized by a much higher retention time as compared to the directly heated Ritter–Kellner process, which was developed at the same time in Austria.

The sulfite process was developed around the acid calcium bisulfite process, as mentioned in the Tilghman patent. It remained the principal process for wood pulping because of the low costs and high availability until the beginning of the 1950s, when the need to recover the waste liquor and pulping chemicals slowly emerged, mainly for reasons of environmental protection. Since calcium sulfite is soluble only below pH 2.3, it can solely be used in acid bisulfite pulping in the presence of excess  $SO_2$ . At cooking temperature, the calcium hydrogen sulfite decomposes to calcium sulfite and hydrated  $SO_2$ :



Thus, high charges of free  $SO_2$  and low cooking temperatures must be maintained to prevent the precipitation of calcium sulfite. A further drawback of the use of calcium as a cation for the acid sulfite process is the formation of calcium sulfate during the course of the recovery process. The conversion to calcium sulfite is not practical, since a temperature above 1200 °C is required to achieve its complete decomposition to calcium oxide and sulfur dioxide. At this high temperature the crystal structure of calcium oxide changes, thus reducing its reactivity. Furthermore, calcium sulfite anhydride tends to disproportionate to calcium sulfate and calcium sulfide. For these reasons calcium has been replaced by more soluble bases, and is now reserved for a few pulp mills with complete by-product recovery. Today, the dominating base used in sulfite pulping is magnesium. The corre-

sponding aqueous magnesium bisulfite solutions are soluble in a pH range up to 5–6, so that acid bisulfite and bisulfite (magnefite) pulping processes in both one- and two-stage operations can be carried out. The big advantage of the magnesium bisulfite process compared to the calcium base system lies in its thermochemical behavior [1]. In contrast to the calcium system, the thermal decomposition of  $MgSO_3$  occurs at a rather low temperature, generating only a small amount of sulfide. The magnesium sulfate obtained from the combustion of magnesium sulfite spent liquor can be decomposed thermally in the presence of carbon from the dissolved organic substances to give gaseous  $SO_2$  and magnesium oxide according to Eq. (156) [2]:



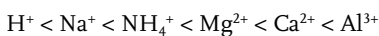
In order to avoid secondary oxidation of  $SO_2$  to  $SO_3$  in the absorption unit, the flue gas must not contain free oxygen in excess of 3%, so that the surplus of air in the combustion process must not exceed 1.5–2.0% [2].

As alternatives to calcium and magnesium, sodium and ammonium cations are also used in sulfite pulping. Since both monovalent cations are soluble over the entire pH range, they can be used in acid, bisulfite (magnefite), neutral and alkaline sulfite processes. The prevailing sulfite processes are defined according to the pH range of the resultant cooking liquor, as shown in Tab. 4.51.

**Tab. 4.51** Assignment of sulfite pulping processes according to the different pH ranges.

Nomenclature	Initial pH range at 25 °C	Base alternatives	Active reagents
Acid bisulfite	1–2	$Ca^{2+}$ , $Mg^{2+}$ , $Na^+$ , $NH_4^+$	$H^+$ , $HSO_3^-$
Bisulfite (Magnefite)	3–5	$Mg^{2+}$ , $Na^+$ , $NH_4^+$	$(H^+)$ , $HSO_3^-$
Neutral sulfite	6–9	$Na^+$ , $NH_4^+$	$HSO_3^-$ , $SO_3^{2-}$
Alkaline sulfite	10–13.5	$Na^+$	$SO_3^{2-}$ , $OH^-$

The use of monovalent cations, especially ammonium, tends to increase the rate of delignification at given process conditions [3]. Mill experience indicates that maximum temperature could be decreased by 5 °C when changing from calcium to ammonium base while keeping the cooking cycle constant [4]. The reason for the more rapid delignification in the cooks on soluble cations is not entirely known. According to the *Donnan law*, it appears that acidity in the solid phase decreases as the affinity of the cation to the solid phase increases. It is assumed that the concentration of the lignosulfonate groups in the solid phase equals about 0.3 N, corresponding to a pH level below 1.0 in the absence of cations other than protons [5]. The affinity for the solid phase is increasing in the order [6]:



The acidity of the solid phase should therefore be lower in the presence of aluminum ions, and highest in the presence of sodium ions. It is likely that the higher acidity of the solid phase in the case of monovalent bases contributes to a slightly higher extent of carbohydrate hydrolysis and somewhat greater velocity of delignification. Although the differences in rate and selectivity of delignification are not significant, mill application has revealed several advantages, such as higher pulp yield, viscosity and alphacellulose content at a given kappa number and a lower amount of rejects [7,8]. These advantages can be attributed to better penetration with cooking chemicals and a more uniform cook when changing from calcium to magnesium, ammonium, or sodium base. The brightness of the unbleached pulps is, however, clearly impaired in the case of ammonium-based pulps. There, the lower brightness is probably due to a selective reaction between the ammonium ion and carbonyl groups of lignin. This reaction is also responsible for a much darker color of the ammonium-based spent liquors. However, no differences in the bleachability of ammonium-based pulps in comparison to other sulfite pulps can be observed.

Despite some clear advantages of the monovalent over the bivalent bases with respect to flexibility (entire pH range available) and pulping operations (more homogeneous impregnation, higher rate of delignification), their use in sulfite cooking processes has been limited to a few applications, mainly due to deficiencies in recovery of the cooking chemicals. For ammonium sulfite waste liquor no economically feasible solution exists to recover the base. Ammonia recovery processes based on ion exchange have been developed to the mill level, but have not gained acceptance in praxis because of high costs. The use of ammonium base in particular has been shown to be advantageous for the production of highly reactive dissolving pulp where mill scale operations still exist. Sodium base is predominantly used in neutral and alkaline sulfite processes. The recovery of sodium-based sulfite processes combines the use of a kraft-type furnace and the conversion of the resulting sodium sulfide to sodium sulfite using carbonation processes (e.g., liberation of hydrogen sulfide from the smelt by the addition of  $\text{CO}_2$  from the flue gas, oxidizing hydrogen sulfide to  $\text{SO}_2$ , reaction of  $\text{SO}_2$  with sodium carbonate to give sodium sulfite). The technology employing carbonation of green liquor was developed in the 1950s and 1960s, but since then no decisive improvements of this recovery concept have been made. Thus, the recovery of the sodium-based sulfite cooking chemicals is significantly less efficient than the sodium-based kraft process, and this may be the main reason for the comparatively limited application of the sodium-based sulfite processes.

During the first 50 years of chemical pulp production, the sulfite process was the dominating technology, due mainly to the high initial brightness and the easy bleachability of the sulfite pulps. With the developments of both a reductive recovery boiler for the regeneration of kraft spent liquor by Tomlinson and chlorine dioxide as a bleaching agent to ensure selective bleaching to full brightness in the mid-1940s, the kraft pulping technology became the preferred method because of better energy economy, better paper strength properties, and lower sensitivity towards different wood species and wood quality. In the meantime, efficient

chemical recovery systems have been developed especially to use magnesium as a base. The high sensitivity to the wood raw material still constitutes a problem in the case of acid sulfite pulping. Most softwoods except spruce, such as pines, larches and Douglas fir, are considered less suitable for sulfite pulping. A certain part of the extractives of phenolic character such as pinosylvin, taxifolin (Douglas fir) as well as the tannins of bark-damaged spruce and oaks give rise to condensation reactions with reactive lignin moieties in the presence of acid sulfite cooking solutions.

Since the 1960s the basic and applied research has been directed almost exclusively towards alkaline pulping technologies, with kraft pulping as the key technology, due to the higher overall economic potential. Consequently, the kraft process has become increasingly important and is now the principal pulping process, accounting for far more than 90% of world pulp production. For the production of most paper-grade pulps, the strength properties are of utmost importance. Kraft pulps show clearly better strength properties, especially with regard to the tear strength as compared to sulfite pulps. Consequently, new installations for the production of paper-grade pulps are almost exclusively based on kraft pulping technology. Unlike paper-grade pulping, the acid sulfite process is the dominant technology for the production of dissolving pulps and accounts for approximately 70% of the total world production. Although a clear niche product, the dissolving pulp production is a firmly established pulp market with a predicted annual growth rate of about 5% within the next five years. The strong position of sulfite technology in dissolving pulp production of low-purity grades sufficient for regenerated fiber manufacture is based on a favorable economy, because of higher pulp yield, better bleachability and higher reactivity as compared to a corresponding prehydrolysis-kraft pulp. Therefore, the following presentation of acid sulfite pulping technology is predominantly oriented toward dissolving pulp production.

#### 4.3.2

##### Cooking Chemicals and Equilibria

In practice, the terms total, combined and free  $\text{SO}_2$  are used to characterize sulfite cooking liquors. The content of stoichiometrically base bound hydrogen sulfite and sulfite ions is referred to as combined  $\text{SO}_2$ . The difference between the total  $\text{SO}_2$  and the combined  $\text{SO}_2$  is then free  $\text{SO}_2$ . According to this definition, half of the pure hydrogen sulfite solution is free and the other is bound  $\text{SO}_2$ . The following definition is rather misleading from a chemistry point of view as no free sulfur dioxide is present in a pure hydrogen sulfite solution:



In the central European acid sulfite industry the technical sulfite solutions are characterized more closely to the chemical state of the constituents. There, the combined  $\text{SO}_2$  is equal to the pure hydrogen sulfite, whereas the (excess or true) free  $\text{SO}_2$  accounts solely for the sulfur dioxide in its hydrated form ( $\text{SO}_2 \cdot \text{H}_2\text{O}$ ) and



can be calculated as the difference between the total and the combined  $\text{SO}_2$ . The combined  $\text{SO}_2$  is calculated from the active base content, usually expressed as oxide (e.g.,  $\text{CaO}$ ,  $\text{MgO}$  or  $\text{Na}_2\text{O}$ ). The following equation demonstrates the definition of combined  $\text{SO}_2$  using magnesium hydrogen sulfite as an example:



According to Eq. (158), 1 mol  $\text{MgO}$  accounts for 2 mol combined  $\text{SO}_2$ . On a weight basis, one part of  $\text{MgO}$  corresponds to 3.179 parts of combined  $\text{SO}_2$ . A typical acid sulfite cooking liquor contains 17.5% total  $\text{SO}_2$  and 2.20%  $\text{MgO}$ , equal to 7.0% combined  $\text{SO}_2$  on o.d. wood, respectively. The amount of free  $\text{SO}_2$  calculates to 10.5% (range 7.0–17.5), representing 60% of the total  $\text{SO}_2$  as free  $\text{SO}_2$ .

For characterization of the composition of the sulfite cooking liquor, the latter definition will be used.

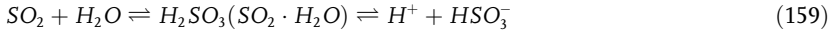
To better exemplify the differences between the two ways of cooking acid specification a comparison is provided on the basis of a typical acid sulfite cooking liquor composition, as depicted in Tab. 4.52.

**Tab. 4.52** Specification of a typical acid sulfite cooking liquor expressed in two different terms (actual definition related the more actual species concentrations as used in this book vs. the Palmrose definition according to TAPPI Standard T604 pm-79).

Parameter	units	Actual definition used in this book <sup>a)</sup>	International (Palmrose) definition
Total $\text{SO}_2$	% od wood	17.5	17.5
Free $\text{SO}_2$	% od wood	10.5	14.0
	of total $\text{SO}_2$	60	80
Combined $\text{SO}_2$	% od wood	7.0	3.5
$\text{MgO}$	% od wood	2.2	
Liquor-to-wood ratio		3.5	
Actual $\text{SO}_2$ concentration			
Total $\text{SO}_2$	$\text{mol L}^{-1}$	0.78	
Free $\text{SO}_2$	$\text{mol L}^{-1}$	0.47	
Bound $\text{SO}_2$ ( $\text{HSO}_3^-$ )	$\text{mol L}^{-1}$	0.31	

a) Denoted also as true free and true combined  $\text{SO}_2$ ; this definition may be used to convert both definitions into each other: % True free  $\text{SO}_2 = (\% \text{ Free } \text{SO}_2 - \% \text{ Comb. } \text{SO}_2)$   
 % True Comb.  $\text{SO}_2 = 2 * \% \text{ Comb. } \text{SO}_2$ .

The concentrations of the sulfur(IV) species in the aqueous cooking liquor are defined through the following equilibria:



It has been shown that the major part of the sulfur dioxide in an aqueous solution is not hydrated to sulfurous acid [6]. The hydrated and non-hydrated form of the free  $SO_2$  are combined to express the first equilibrium constant  $K_{a,1}$ :

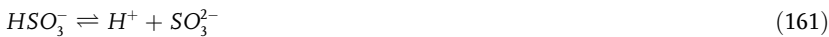
$$K_{a,1} = \frac{[H^+] \cdot [HSO_3^-]}{([SO_2] \cdot [H_2SO_3])} \quad (160)$$

The dissociation constant  $K_{a,1}$  of combined  $SO_2$  decreases clearly with increasing temperature, as seen in Tab. 4.53.

**Tab. 4.53** Temperature-dependence of the first equilibrium constant of free  $SO_2$  (according to [6]).

Temperature [°C]	pK <sub>a,1</sub>
25	1.8
70	2.3
100	2.6
110	2.8
120	3.0
130	3.1
140	3.3
150	3.5

Hydrogen sulfite ions are also in equilibrium with monosulfite ions and protons according to the following expression:



Hydrogen sulfite is a weak acid, and its equilibrium constant derived from Eq. (159), and denoted as second equilibrium constant,  $K_{a,2}$ , is expressed as:

$$K_{a,2} = \frac{[H^+] \cdot [SO_3^{2-}]}{([HSO_3^-])} \quad (162)$$

The  $pK_{a,2}$  can be approached by a value of about 7.0 at 25 °C. The change in ionization of the hydrogen sulfite ion with temperature is unknown, and is assumed to be insignificant. Consequently,  $pK_{a,2}$  is kept constant in the temperature range prevailing in acid sulfite cooking.

The concentrations of the active cooking chemicals in a pure aqueous acid sulfite cooking liquor,  $[H^+]$ ,  $[HSO_3^-]$  and  $[SO_3^{2-}]$ , can be calculated by the following simple equations:

The total  $SO_2$  concentration at any time and any pH is calculated as:

$$[SO_{2,tot}] = C_{tot} = [SO_2 \cdot H_2O] + [HSO_3^-] + [SO_3^{2-}] \quad (163)$$

The concentrations of  $[SO_2 \cdot H_2O]$ ,  $[HSO_3^-]$  and  $[SO_3^{2-}]$  can be calculated accordingly:

$$[SO_2 \cdot H_2O] = C_{tot} - ([HSO_3^-] + [SO_3^{2-}]) \quad (164)$$

$$[HSO_3^-] = C_{tot} - ([SO_2 \cdot H_2O] + [SO_3^{2-}]) \quad (165)$$

$$[SO_3^{2-}] = C_{tot} - ([SO_2 \cdot H_2O] + [HSO_3^-]) \quad (166)$$

The pH-dependent concentrations of sulfur(IV) species can be calculated by using the equilibrium equations:

$$K_{a,1} \cdot (C_{tot} - ([HSO_3^-] + [SO_3^{2-}])) = [H^+] \cdot [HSO_3^-] \quad (167)$$

The hydrogen sulfite ion concentration can be calculated by rearranging Eq. (167):

$$[HSO_3^-] = \frac{K_{a,1} \cdot (C_{tot} - [SO_3^{2-}])}{(K_{a,1} + [H^+])} \quad (168)$$

A similar procedure can be applied to calculate the monosulfite ion concentration:

$$K_{a,2} \cdot (C_{tot} - ([SO_2 \cdot H_2O] + [SO_3^{2-}])) = [H^+] \cdot [SO_3^{2-}] \quad (169)$$

$$[SO_3^{2-}] = \frac{K_{a,2} \cdot (C_{tot} - [SO_2 \cdot H_2O])}{(K_{a,2} + [H^+])} \quad (170)$$

The course of pH as a function of the concentrations of the sulfur(IV) species in a pure sulfite cooking liquor can be calculated by considering the equilibrium conditions for the titration of a weak two-basic acid with strong alkali according to the following expression:

$$\sum [A^-] + [OH^-] = [H^+] + [AH] \quad (171)$$

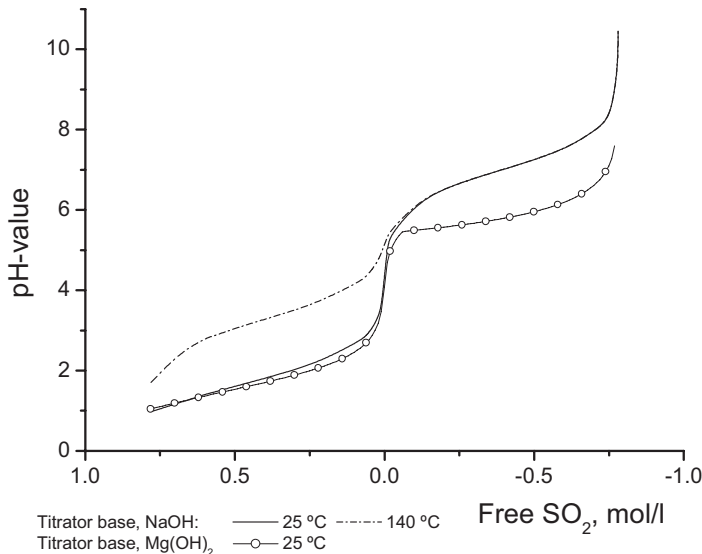
Assuming the total concentration of the sum of the conjugated bases  $[A^-]$  and the acid  $[AH]$  to be  $C_{tot}$  (in  $\text{mol L}^{-1}$ ), the acid–base equilibria can be calculated as:

$$[H^+] = \frac{K_{a,1} \cdot C_{tot}}{(K_{a,1} + [H^+])} + \frac{K_{a,2} \cdot C_{tot}}{(K_{a,2} + [H^+])} + \frac{10^{-14}}{[H^+]} - C^* \quad (172)$$

where  $C^*$  is the molar amount of the titrator base NaOH.

As an example, the course of pH of a pure aqueous sulfite solution with a total  $\text{SO}_2$  concentration of  $50 \text{ g L}^{-1}$  ( $0.78 \text{ mol L}^{-1}$ ) is calculated as a function of the free  $\text{SO}_2$  concentration (Fig. 4.151). In the first case, the titration curve is calculated according to Eq. (172), using sodium hydroxide as a titrator base. In the second approach, the titration curve is calculated by means of ASPEN-PLUS simulation software, using magnesium hydroxide as a titrator base. ASPEN-PLUS uses a high-performance electrolyte module based on the NRTL model (nonrandom, two-liquid) to calculate the thermodynamic properties of aqueous electrolyte systems [9]. The model provides an accurate description of the nonideality of concentrated aqueous solutions.

The titration curve estimated by means of Eq. (172) agrees well with that calculated by ASPEN-PLUS in the pH range 1 to 4.5, until any of the free  $\text{SO}_2$  is quantitatively converted to hydrogen sulfite ions. The course of pH beyond this point



**Fig. 4.151** Course of pH as a function of the free  $\text{SO}_2$  concentration assuming an initial total  $\text{SO}_2$  concentration of  $0.78 \text{ mol L}^{-1}$  at  $25^\circ\text{C}$  and  $140^\circ\text{C}$ . Two calculation modes: (a) titration curve calculated according to Eq. (170), using NaOH as titrator base; (b) titration curve simulated by means of ASPEN-PLUS using  $\text{Mg}(\text{OH})_2$  as titrator base.

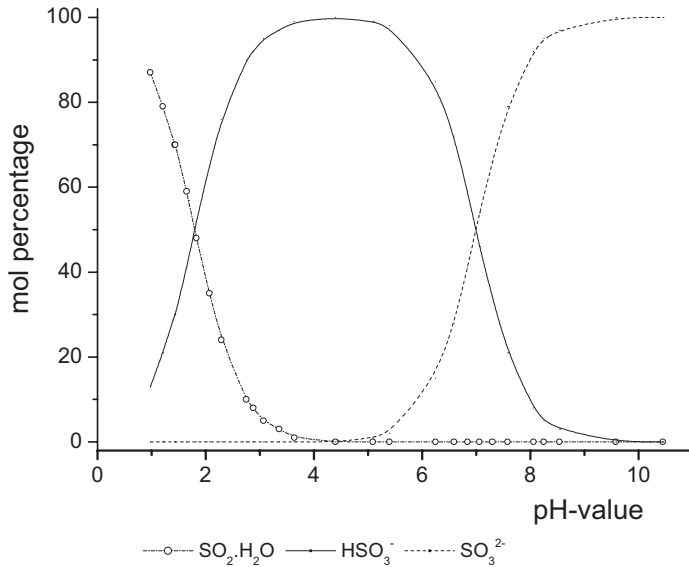
develops differently for the two bases. The addition of  $\text{Mg}(\text{OH})_2$  causes a rather even slope of pH until the equilibrium is shifted to monosulfite ions, while the addition of  $\text{NaOH}$  raises the pH more steeply.

The concentrations of ionic species of a sulfite cooking liquor are given as a function of the liquor composition (e.g., the molar content of free  $\text{SO}_2$  and active base) in Tab. 4.54.

**Tab. 4.54** Concentrations of ionic species of sulfite cooking liquor with increasing amount of active base concentration; initial free  $\text{SO}_2$  concentration  $0.78 \text{ mol L}^{-1}$ ;  $[\text{H}^+]$  calculation according to Eq. (172),  $[\text{HSO}_3^-]$  according to Eq. (168),  $[\text{SO}_3^{2-}]$  according to Eq. (170) and  $[\text{SO}_2\text{-H}_2\text{O}]$  according to Eq. (164).

Free $\text{SO}_2$ [mol L <sup>-1</sup> ]	Base [mol L <sup>-1</sup> ]	[H <sup>+</sup> ] [mol L <sup>-1</sup> ]	pH-Value	[SO <sub>2</sub> .H <sub>2</sub> O] [mol L <sup>-1</sup> ]	[HSO <sub>3</sub> <sup>-</sup> ] [mol L <sup>-1</sup> ]	[SO <sub>3</sub> <sup>2-</sup> ] [mol L <sup>-1</sup> ]	[H <sup>+</sup> ] <sup>2</sup> [HSO <sub>3</sub> <sup>-</sup> ]
0.78	0.00	$1.04 \cdot 10^{-1}$	0.98	$6.77 \cdot 10^{-1}$	$1.04 \cdot 10^{-1}$	$1.00 \cdot 10^{-7}$	$1.07 \cdot 10^{-2}$
0.58	0.20	$3.65 \cdot 10^{-2}$	1.44	$5.44 \cdot 10^{-1}$	$2.37 \cdot 10^{-1}$	$6.48 \cdot 10^{-7}$	$8.63 \cdot 10^{-3}$
0.39	0.39	$1.47 \cdot 10^{-2}$	1.83	$3.76 \cdot 10^{-1}$	$4.05 \cdot 10^{-1}$	$2.76 \cdot 10^{-6}$	$5.96 \cdot 10^{-3}$
0.28	0.50	$8.49 \cdot 10^{-3}$	2.07	$2.72 \cdot 10^{-1}$	$5.09 \cdot 10^{-1}$	$5.99 \cdot 10^{-6}$	$4.32 \cdot 10^{-3}$
0.08	0.70	$1.79 \cdot 10^{-3}$	2.75	$7.92 \cdot 10^{-2}$	$7.02 \cdot 10^{-1}$	$3.92 \cdot 10^{-5}$	$1.26 \cdot 10^{-3}$
0.00	0.78	$3.94 \cdot 10^{-5}$	4.40	$1.93 \cdot 10^{-3}$	$7.77 \cdot 10^{-1}$	$1.97 \cdot 10^{-3}$	$3.06 \cdot 10^{-5}$
-0.02	0.80	$3.97 \cdot 10^{-6}$	5.40	$1.91 \cdot 10^{-4}$	$7.62 \cdot 10^{-1}$	$1.92 \cdot 10^{-2}$	$3.02 \cdot 10^{-6}$
-0.22	1.00	$2.57 \cdot 10^{-7}$	6.59	$9.10 \cdot 10^{-6}$	$5.62 \cdot 10^{-1}$	$2.19 \cdot 10^{-1}$	$1.44 \cdot 10^{-7}$
-0.42	1.20	$8.64 \cdot 10^{-8}$	7.06	$1.97 \cdot 10^{-6}$	$3.62 \cdot 10^{-1}$	$4.19 \cdot 10^{-1}$	$3.13 \cdot 10^{-8}$
-0.62	1.40	$2.62 \cdot 10^{-8}$	7.58	$2.67 \cdot 10^{-7}$	$1.62 \cdot 10^{-1}$	$6.19 \cdot 10^{-1}$	$4.24 \cdot 10^{-9}$
-0.74	1.52	$5.68 \cdot 10^{-9}$	8.25	$1.51 \cdot 10^{-8}$	$4.20 \cdot 10^{-2}$	$7.39 \cdot 10^{-1}$	$2.39 \cdot 10^{-10}$
-0.78	1.56	$3.58 \cdot 10^{-11}$	10.45	$3.04 \cdot 10^{-13}$	$2.79 \cdot 10^{-4}$	$7.81 \cdot 10^{-1}$	$1.00 \cdot 10^{-14}$

The relative concentrations of sulfur dioxide, hydrogen sulfite, and sulfite are determined by the pH of the aqueous solution. Figure 4.152 shows that sulfur dioxide is present predominantly as  $\text{SO}_2\text{.H}_2\text{O}$  and hydrogen sulfite ions at pH 1–2, typical for acid sulfite cooking. With increasing pH, the proportion of hydrogen sulfite ion increases significantly, and in the pH range characteristic for magnesite cooking (3–5), sulfur dioxide is present almost exclusively in the form of hydrogen sulfite ions. Above this pH level, the sulfite ions start to become the dominating ionic species in the sulfite cooking liquor.



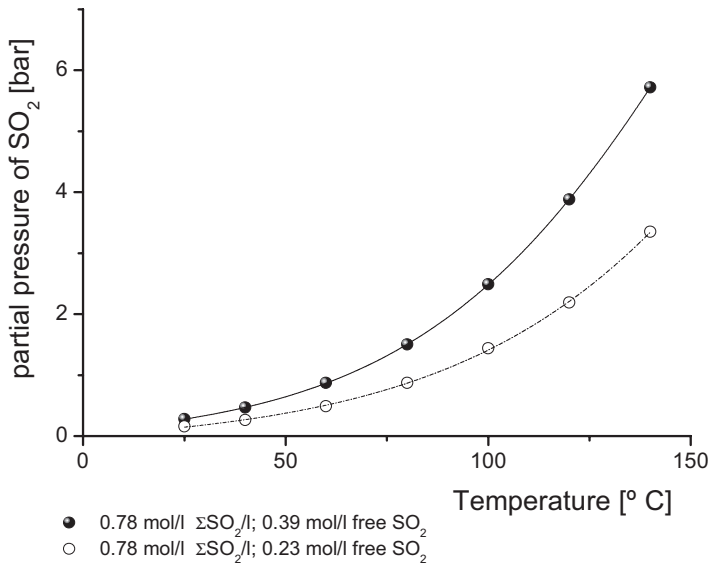
**Fig. 4.152** Relative molar percentage of  $\text{SO}_2\cdot\text{H}_2\text{O}$ , hydrogen sulfite and sulfite ions as a function of the pH at 25 °C. Data based on information in Tab. 4.54.

Due to the decrease in the acid dissociation constant of hydrated sulfur dioxide,  $K_{a,1}$ , with increasing temperature, the pH level of the acid sulfite cooking liquor is shifted to higher values at cooking temperature (Fig. 4.151, Tab. 4.51). This must be considered in acid calcium sulfite pulping by increasing the proportion of the free sulfur dioxide concentration to avoid the formation of insoluble calcium sulfite.

The ionic product,  $[\text{H}^+]\cdot[\text{HSO}_3^-]$ , is said to be proportional to the rate of delignification in the course of sulfite pulping [6]. According to Tab. 4.54, this ionic product increases exponentially with decreasing pH, which is equal to an increase in the free  $\text{SO}_2$  concentration. This result corresponds well with industrial experience. Increasing the proportion of free  $\text{SO}_2$  in the cooking acid continuously reduces the cooking time at given process conditions.

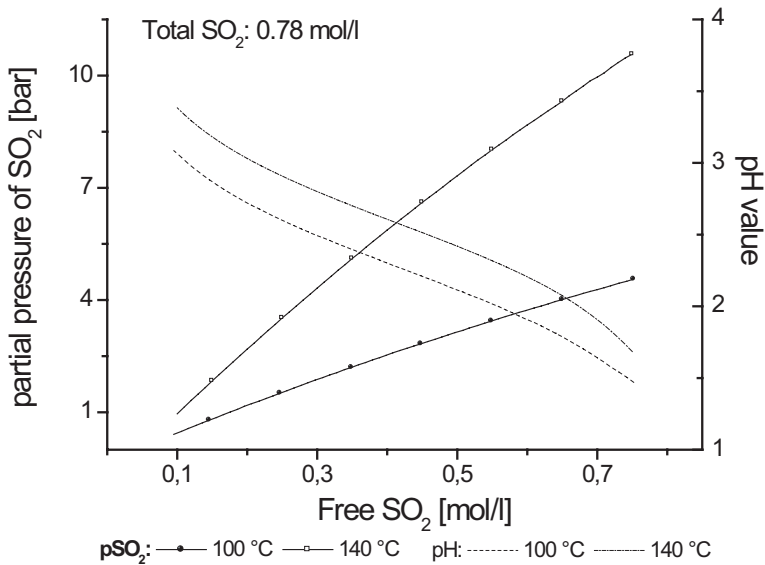
Moreover, the presence of free  $\text{SO}_2$  largely determines the vapor pressure of the cooking acid at the prevailing temperature. Figure 4.153 illustrates the development of the partial pressure of  $\text{SO}_2$  of a cooking acid with a total  $\text{SO}_2$  concentration of  $0.78 \text{ mol L}^{-1}$  containing two different amounts of free  $\text{SO}_2$ ,  $0.39 \text{ mol L}^{-1}$  (50% of total) and  $0.23 \text{ mol L}^{-1}$  (30% of total), respectively, at varying temperature levels.

The inter-relation of partial  $\text{SO}_2$  pressure, and free and total  $\text{SO}_2$  is exemplified in Fig. 4.154 for two temperatures, 100 °C and 140 °C, the latter being typical for the cooking phase.



**Fig. 4.153** Development of partial pressure of SO<sub>2</sub> of a cooking acid comprising two different proportions of free SO<sub>2</sub>, 50% and 30% of total SO<sub>2</sub> concentration (0.78 mol L<sup>-1</sup>), as a function

of temperature. The equilibrium conditions were simulated by means of ASPEN-PLUS [10] based on the pioneering studies of Hagfeldt et al. [11].



**Fig. 4.154** Development of partial pressure of SO<sub>2</sub> and pH of the three-component system magnesium oxide-sulfur dioxide-water as a function of free SO<sub>2</sub> concentration for two different temperatures, 100 °C and 140 °C,

respectively, while keeping the total SO<sub>2</sub> concentration constant at 0.78 mol L<sup>-1</sup>. The equilibrium conditions were simulated by means of ASPEN-PLUS [10] based on the pioneering studies of Hagfeldt et al. [11].

The total pressure of sulfite cooking acids containing large quantities of free  $\text{SO}_2$  is largely determined by the partial pressures of  $\text{SO}_2$ , water and, in the case of hardwood pulping, also by considerable amounts of volatile carbonic acids (e.g., acetic acid, furfural, etc.) and carbon dioxide. Digester pressures are usually limited to 8–10 bar, which means that gas must be released through the relief pressure valve during the entire cooking phase. New cooking digesters are designed to operate at higher pressures (>12 bar), which is an effective measure to further reduce cooking time.

#### 4.3.3

##### **Impregnation**

A uniform distribution of pulping chemicals within the wood chip structure is the key step of any pulping process. The impregnation step is carried out immediately after the chips have been immersed in the cooking liquor. Chemical transportation into the wood structure is accomplished by two different mechanisms. The first is the penetration of a liquid under a pressure gradient into the capillaries and the interconnected voids of the wood structure. The second is the diffusion of dissolved ions, which is governed by their concentration gradient and the total cross-sectional area of accessible pores. Since diffusion takes place in a liquid saturated environment, penetration must occur prior to diffusion.

Penetration is influenced by pore size distribution and capillary forces. Consequently, the wood structure itself affects liquid penetration. In softwoods, the impregnating liquor proceeds from one tracheid to the next through bordered pits, while the ray cells provide ways for transport in the radial direction. In hardwoods, the flow is greatly enhanced by the vessels. They are first filled with liquid, which then penetrates into ray cells and libriform fibers. Difficulties are caused by tylosis. Penetration is facilitated by a high moisture content, pre-steaming and pressure impregnation. In sulfite cooking, the introduction of the Vilamo method significantly improved the homogeneity of the cook [12–14]. Here, air is removed from the chips by sudden pressure reductions in the liquor phase. First, a hydraulic pressure of about 6 bar is applied immediately after liquor charge to full digester. The pressure increase is followed by a pressure release to approximately 2 bar by opening the top valve of the digester. Penetration is completed after several pressure pulsations. However, later investigations have been shown that pressure pulsations do not appear to give any important advantage over a constant hydrostatic pressure [15]. A suitable combination of steaming and pressure impregnation will be sufficient to complete impregnation allowing shorter cooking cycle and more uniform pulping.

Unlike alkaline pulping, the resistance to radial and transverse diffusion of cooking chemicals into the wood is much more pronounced in acid sulfite cooking. It is reported that diffusion in the longitudinal direction at room temperature is 50- to 200-fold faster than in the transverse and radial directions for softwoods [16,17]. This finding suggests that hydrogen sulfite enters the wet chip almost exclusively through the ends. Consequently, chips should be as short as possible



from the pulp quality point of view. In hot liquor, however, the wood structure is opened up and diffusion across the grain is facilitated. Steaming at atmospheric pressure may double the permeability in the tangential and radial directions. Chip thickness is therefore as important as chip length. Scanning electron microscopy (SEM) and energy dispersive X-ray analysis (EDXA) revealed that sodium sulfite diffusion at slightly alkaline conditions occurred more rapidly into aspen than into black spruce chips under comparable conditions [18]. The reason for the higher diffusivity was clearly attributed to the higher porosity of aspen, as shown by mercury porosity measurements. The reduction of interfacial energy by the addition of wetting agents seems to help in the penetration of liquids into wood. Preliminary studies confirmed that, in the presence of a surfactant in the sulfite liquor, penetration into the wood structure improved. The degree of penetration can thus be correlated with the contact angle of sulfite liquor drops on the cross-section surface of the wood [19].

The active species in sulfite cooking show different diffusion constants. The highest diffusion constant is given by hydrated sulfur dioxide, and the lowest by magnesium hydrogen sulfite (Tab. 4.55). Interestingly, ammonium hydrogen sulfite shows a rather high diffusivity, indicating a better penetration and a more uniform cook. The results indicate that in acid hydrogen sulfite cooking,  $\text{SO}_2$  tends to penetrate chips ahead of base.

**Tab. 4.55** Diffusion coefficients,  $D$ , of various sulfur(IV) species in pure aqueous solutions at 20 °C (according to [20]).

Sulfur species	$D$ at 20 °C [ $\text{m}^2 \text{ s}^{-1} \cdot 10^9$ ]
Sulfur dioxide	2.78
calcium hydrogen sulfite	1.02
magnesium hydrogen sulfite	0.96
ammonium hydrogen sulfite	1.92

Moreover, there is also some evidence that hydrogen sulfite ions migrate more rapidly into the wood structure as compared to the corresponding cations (e.g.,  $\text{Na}^+$ ) [21]. This concludes that incomplete impregnation might occur in liquid-phase cooks with a rapid temperature rise. As a consequence, the base concentration in an acid sulfite cook is not sufficient to neutralize the sulfonic acids formed. Because of the sharp drop in pH, lignin condensation reactions are favored over sulfonation reactions in the interior of the chips, and this results in uncooked regions. Correct impregnation is a prerequisite for a uniform cook. The conditions for satisfactory chip impregnation for acid sulfite cooking comprise the following steps:

- Preparation of uniform chip size with short length dimension. A short chip length ensures a better penetrability because acid liquors penetrate mainly from the cut ends. Deterioration of fiber length has been observed when chips were cut below 19 mm in length.
- Steaming at a slight overpressure (100–110 °C) until the air is displaced. Steaming at a higher temperature should be avoided due to the danger of lignin condensation reactions in subsequent acid sulfite cooking.
- Pre-steamed chips are immersed in the cooking liquor at about 80–85 °C to condense the water vapor in the chips and to fill the evacuated volume with liquor.
- Hydrostatic pressurization of the completely filled digester to 700 kPa or more by a cooking liquor pump.

The time–temperature and time–pressure profiles must be individually adjusted to the applied wood source. The permeability and anisotropy of wood is a highly variable property, not only between different species, but also within one single species. For example, heartwood is much more difficult to impregnate than sapwood. This is especially true for conifers, where heartwoods are highly resistant to penetration by sulfite liquor.

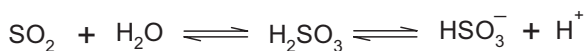
#### 4.3.4

#### Chemistry of (Acid) Sulfite Cooking

*Antje Potthast*

The composition of the spent sulfite liquor depends to a large extent on the cooking conditions chosen and the chemical composition of cooking chemicals – that is, mainly the ratio of free and combined  $\text{SO}_2$  (for details, see Section 4.3.2). The degree of delignification is directly related to the concentration of the product  $[\text{H}^+]\cdot[\text{HSO}_3^-]$ , while the concentration of  $[\text{H}^+]$  directly affects the rate of cellulose hydrolysis.

Depending on the progress of the sulfite cook, the composition of the cooking liquor changes mainly due to consumption of bound  $\text{SO}_2$  ( $\text{HSO}_3^-$ ) and changes in acidity [1].



**Scheme 4.31** Equilibrium of bound and free sulfur dioxide.

The composition of the cooking liquor in terms of free  $\text{SO}_2$  and combined  $\text{SO}_2$  (hydrogen sulfite) must be balanced in a way that assures sufficient delignification while keeping the condensation reactions to a limit. Kaufmann [2] (Fig. 4.155) illustrated the borderline ratio between total  $\text{SO}_2$  and combined  $\text{SO}_2$ , which will

either result in cooks with acceptable outcome or, if outbalanced, in so-called “black cooks”, where condensation processes preponderated. Crossing the border towards lower amounts of combined  $\text{SO}_2$  and lower total  $\text{SO}_2$  will yield pulp with highly condensed lignin fractions impracticable to bleach. Keeping the appropriate ratio is indispensable to minimize condensation effects and to allow sufficient delignification.

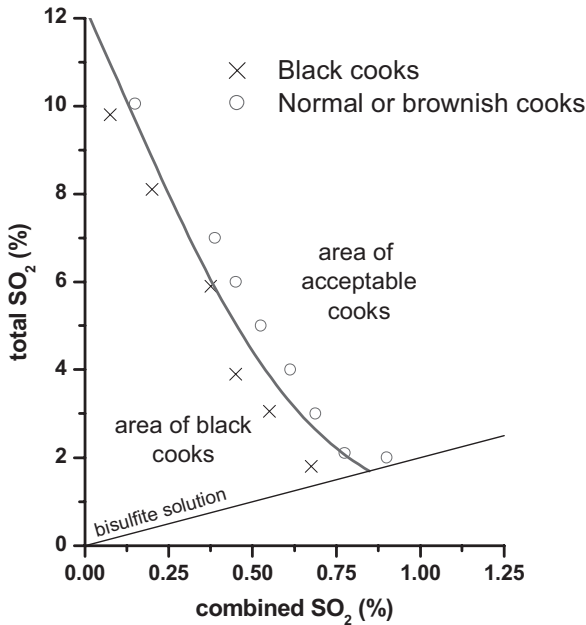


Fig. 4.155 Kaufmann diagram, indicating areas of black cooks in relation to the cooking liquor composition (adopted from [1]).

Cooking close to conditions of black cooks results in:

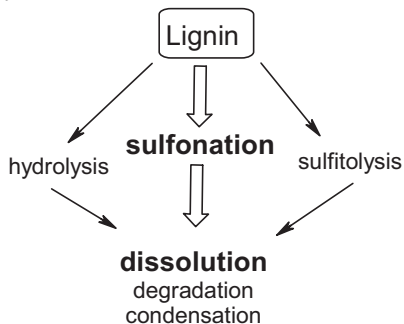
- Increasing dehydration (more free  $\text{SO}_2$ ) due to increasing temperature.
- Decreasing concentration of hydrogen sulfite due to consumption by lignin:
  - Formation of strong acid anions (lignosulfonate anions), which in turn reduce the available bound  $\text{SO}_2$
  - Less available hydrogen sulfite prevents sulfonation of lignin (delignification), but increases condensation reactions
  - Buffer capacity decreases towards the end of the cook
- Formation of new  $\text{H}^+$  ions from sulfur dioxide and water according to Scheme 4.31, hence increasing in  $[\text{H}^+]$ .

The general reactions in a sulfite cook can be divided into sulfonation, hydrolysis, condensation, and redox processes. Sulfonation reactions mainly occur with lignin and to a minor extent also with carbohydrates and low molecular-weight degradation products. Condensation is mainly observed between lignin units and lignin intermediates and extractives, and to some extent also with degradation products of carbohydrates. Carbohydrates (especially hemicelluloses) are affected by hydrolysis, but lignin moieties are also partly fragmented by this reaction type. Hydrolysis is especially important to cleave lignin–carbohydrate linkages. Redox-processes are taking place with inorganic compounds, most often with participation of the degraded carbohydrates and extractives.

#### 4.3.4.1 Reactions of Lignin

The reactions of hydrogen sulfite/sulfur dioxide with lignin are highly dependent on the pH of the reaction medium. On one hand, the pH determines the reactive species and their nucleophilicity, while on the other hand the formation of reactive intermediates within the lignin molecule is also governed by the pH. This will be further illustrated by the reactions of different lignin units occurring under acid sulfite and neutral sulfite conditions.

Lignin degrading reactions with lignin in the acidic sulfite process are characterized by three reaction principles: *sulfonation*, *hydrolysis* and, to some extent, *sulfitolysis*:



Condensation reactions are the major undesired processes counteracting delignification.

In the following section, the major reaction pathways will be illustrated. Specific reactions of different lignin units (i.e.,  $\beta$ -O-4, phenylcoumaran, and pinoreinol) are discussed exemplarily in more detail, and are used to illustrate the differences in the lignin's reaction behavior under neutral sulfite conditions.

##### 4.3.4.1.1 Sulfonation

The sulfonation is the main reaction principle under acidic conditions, which renders the lignin molecule sufficiently hydrophilic to be dissolved in the cooking liquor. The sulfonation reaction is always the fastest reaction at low pH value, and

there is a strong dependence on the pH [3]. No significant influence was observed whether the lignin units are etherified or not. However, a slightly faster rate of sulfonation was shown for phenolic units [4].

#### 4.3.4.1.2 Hydrolysis

Hydrolysis of linkages between lignin and carbohydrate, and to a smaller extent also of inter-lignin bonds, is somewhat slower than the sulfonation process [5]. Only the  $\alpha$ -benzyl ether inter-lignin linkages are cleaved to a larger extent, which decreases the molecular weight of lignin.

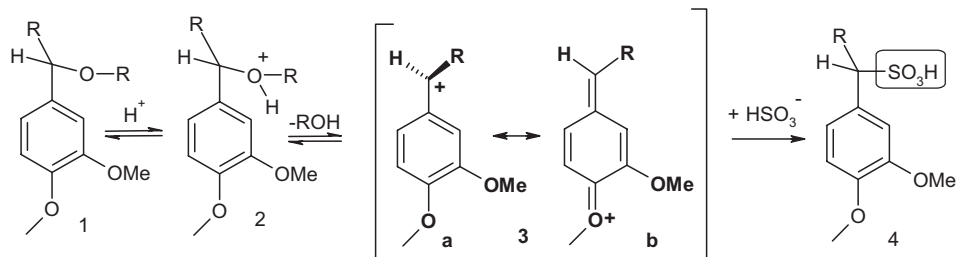
#### Major Reaction Mechanisms

Under the prevailing acidic conditions, the oxygen of the  $\alpha$ -ether or  $\alpha$ -hydroxy group is protonated. Subsequent release of the  $\alpha$ -substituent (as water or as alcohol/phenol), which is the rate-determining step, leaves behind a resonance-stabilized benzylium cation. This intermediate immediately adds hydrogen sulfite by nucleophilic addition. The electron density distribution of the benzylium cation is shown in Scheme 3 (left), where areas of high electron density are marked in red, and centers with a low electron density are marked blue. From theoretical calculations, as well as from model reactions [6], the benzylium cation (**3a**) is favored over the methylene quinone resonance form (**3b**). The latter resonance structure can only come into play if the  $\alpha$ -proton and the  $\alpha$ -substituent are fully arranged in the aromatic plane, which requires bond rotation around the benzylic carbon-carbon bond. Rotation out of this plane breaks the resonance. This bond rotation requires additional energy and time, and might be disfavored by steric factors imposed by the surrounding lignin scaffold. All of these factors favor **3a** over **3b**. A further stabilization of the intermediate is achieved by a 2-aryl substituent or by a hydroxyl in *para*-position, the latter is favoring the formation of the oxonium type resonance form (**3b**) [11].

Other nucleophiles may also add to the benzylium cation and compete with the sulfonation reaction [5]. Such nucleophiles can either be lignin moieties [6], carbohydrate compounds, or extractives. The stereochemical outcome of the sulfonation reaction was found to be consistent with a unimolecular  $S_N1$  mechanism: the pure *erythro* and *threo* forms of lignin-model compounds (e.g.,  $\beta$ -O-4 ether models) always yielded a mixture of the *threo* and *erythro* forms. The observed erosion of the stereochemistry strongly supports the intermediacy of the carbonium ion – and hence the  $S_N1$  mechanism – and dismisses an  $S_N2$  mechanism with Walden inversion.

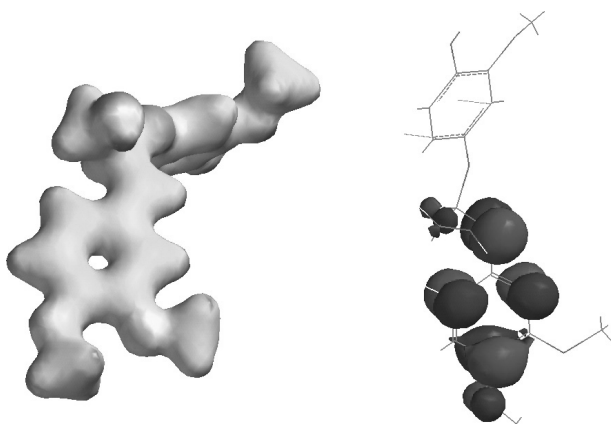
In the following, some examples on the reactions of different lignin units and their conversion under acid sulfite conditions will be given.

Phenolic and non-phenolic  $\beta$ -O-4-lignin model compounds react exclusively by sulfonation in the  $\alpha$ -position; sulfonation of the  $\gamma$ -carbon is not a relevant process [6]. No free phenolic groups are required for reactivity. In alkaline pulping systems, a major difference was seen between phenolic and nonphenolic lignin substructures: the phenolic groups were hereby always more reactive as compared to the nonphenolics. This difference is practically absent under acidic sulfite conditions.



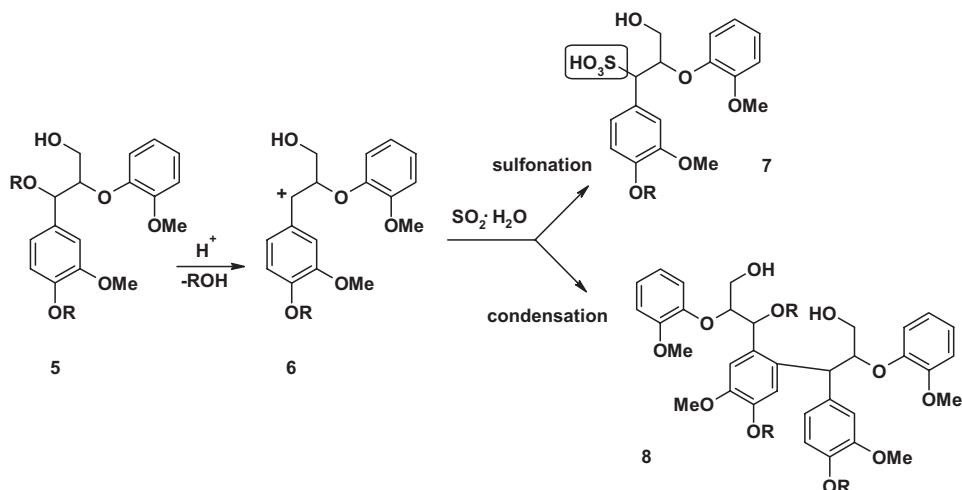
R = Alkyl; Aryl; H

**Scheme 4.32** Formation of the benzylum cation as the reactive intermediate in acid sulfite cooking.



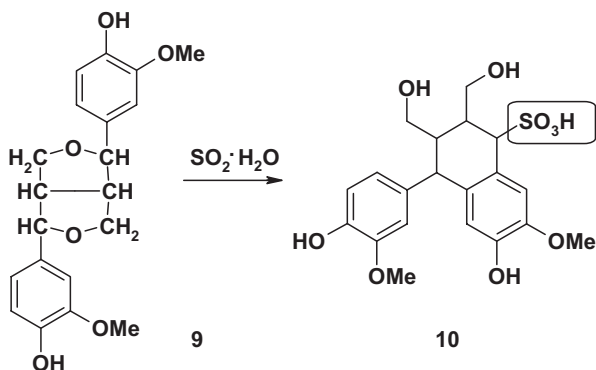
**Scheme 4.33** Electron density distribution (left) and lowest unoccupied molecule orbital (LUMO)-distribution (right) of the benzylum cation intermediate (3).

The  $\beta$ -O-4-ether bond is rather stable under acidic conditions lacking strong nucleophiles. Hence, no cleavage of the lignin macromolecule is accomplished at this point, except for  $\alpha$ -substituents (6–8% of all lignin links), although  $\alpha$ -aryl-LCC model compounds showed a high stability also in acid sulfite systems [7], as mentioned earlier. A sulfidolytic cleavage of the  $\beta$ -O-4-ether bond can only be accomplished at higher pH than acid sulfite conditions (e.g., neutral sulfite pulping [8–10]), when stronger nucleophiles are present.



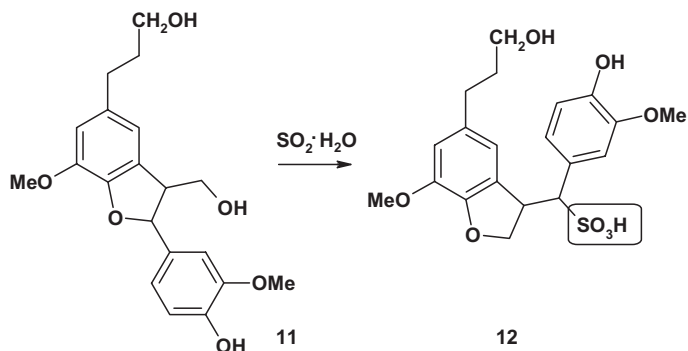
**Scheme 4.34** Reaction of  $\beta$ -O-4 aryl ether structures (according to [11]).

Phenolic *pinoresinol* structures (Scheme 4.35) are opened and the intermediate benzylium cation undergoes an intramolecular electrophilic aromatic substitution at C6 of the adjacent aromatic ring. This intramolecular condensation process is favored due to the close proximity of the adjacent ring, the  $\alpha$ -carbon of the side chain being subsequently sulfonated. Nonphenolic pinoresinols are less reactive.



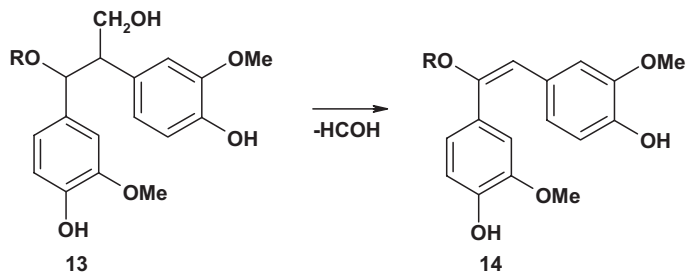
**Scheme 4.35** Reaction of pinoresinol structures (according to [11]).

Phenolic *phenylcoumaran* (Scheme 4.36) structures also show the possibility for condensation reactions if the reactive centers are close enough to the benzylium cation. Possible routes for the formation of 12 by opening the hetero-ring, recyclization and sulfonation are discussed in more detail by Gellerstedt and Gierer [6].

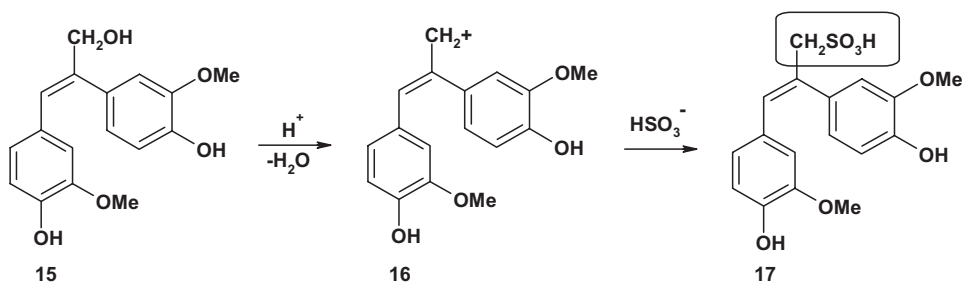


**Scheme 4.36** Reaction of phenolic phenylcoumarans under acidic sulfite conditions [5].

Sulfonation of other positions than  $C_\alpha$  has been demonstrated with  $C_\alpha^-$ -carbonyl compounds (see Scheme 4.39) and 1,2-diarylpropane structures ( $\beta$ -1, cf. Scheme 4.37). The latter is converted into stilbene structures upon elimination of formaldehyde, or to the corresponding  $\gamma$ -sulfonated product after elimination of water and addition of sulfite to the allylic carbonium ion (Scheme 4.38) [5]. The formaldehyde can be further oxidized by hydrogen sulfite to carbon dioxide and water.



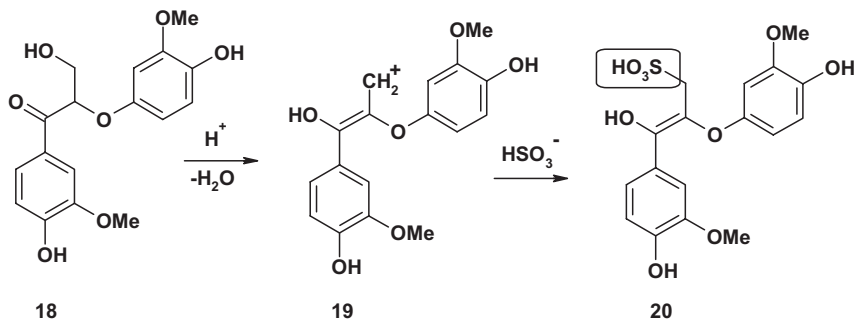
**Scheme 4.37** Reaction of  $\beta$ -1 structures to stable stilbenes [5].



**Scheme 4.38** Reaction of stilbenes [5].

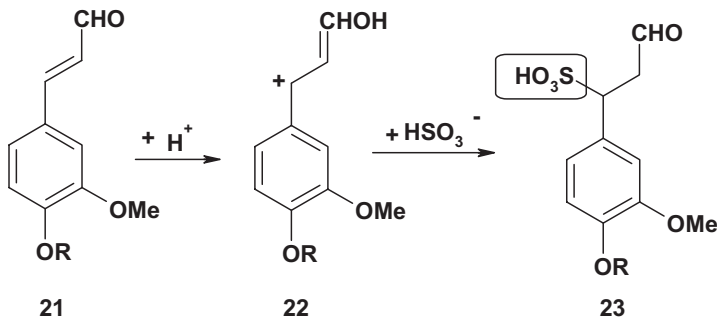


Phenylpropane  $\alpha$ -carbonyl- $\beta$ -arylether structures react also by elimination of water from the  $\gamma$ -hydroxyl group and addition of hydrogen sulfite to the generated electrophilic center (Scheme 4.39).



**Scheme 4.39** Sulfonation of phenylpropane  $\alpha$ -carbonyl- $\beta$ -arylether structures [5].

Coniferylaldehyde units are sulfonated at the  $\alpha$ -position via the allylic carboonium ion, which is formed after addition of a proton, in a Michael-type addition. Sulfonation of the  $\gamma$ -carbon is only observed under neutral sulfite cooking conditions with coniferyl alcohol and with coniferylbenzoate at a pH of 3–4 [12].



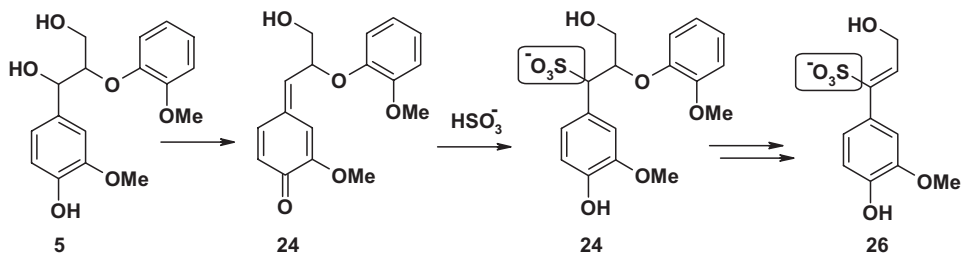
**Scheme 4.40** Sulfonation of the  $\alpha$ -position of coniferyl aldehyde-type structures.

#### Comparison to Sulfonation Reactions under Conditions of Neutral Sulfite Pulping

Sulfite and bisulfite ions are both strong nucleophiles, which are able to bring about the cleavage of ether bonds. Hence, with increasing pH values the  $\beta$ -O-4-ether groups become less stable and undergo a sulfitylytic cleavage. However, under neutral conditions only phenolic structures are reactive so that the sulfonation is more selective, proceeding moreover at a high rate. This leads to a much lower degree of sulfonation and thus a lower rate of delignification (roughly 20% of the lignin units react) [6]. Model reactions show the sulfonation to occur also at other positions than the  $\alpha$ -carbon atom (e.g., the  $\gamma$ -C) [13] as well as the existence

of two sulfonic acid groups per phenylpropane unit [5,14], which are present in different lignosulfonate fractions [13].

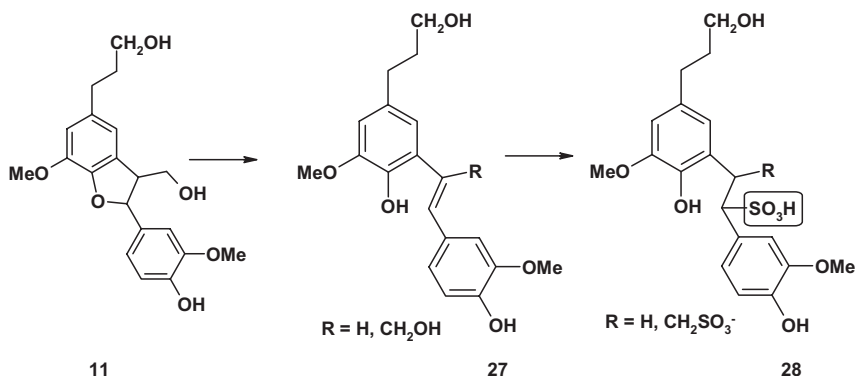
At higher pH values and long reaction times, phenolic  $\beta$ -O-4-ether groups can be converted to styrene- $\alpha$ -sulfonic acids (Scheme 4.41).



**Scheme 4.41** Reactions of  $\beta$ -O-4 ether structures during neutral sulfite pulping.

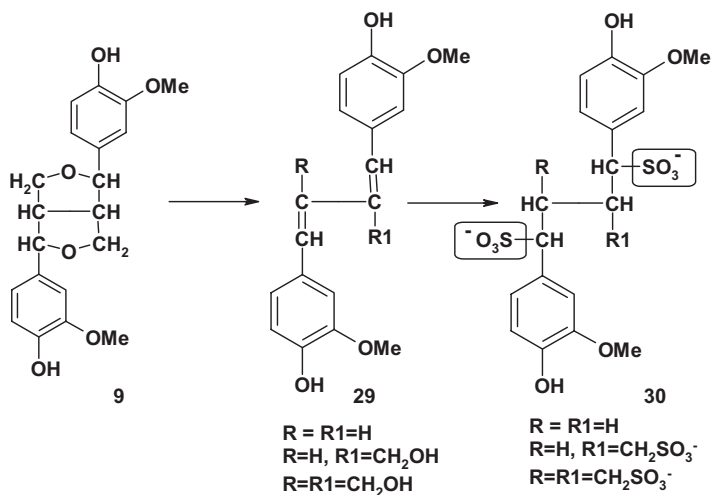
The final products obtained upon sulfonation are often similar to the sulfonated lignin fragments produced under acidic conditions (cf.  $\beta$ -O-4-units), but the mechanism of their formation is quite different. In analogy to the lignin reaction, under alkaline kraft conditions the reactive intermediate in neutral and alkaline sulfite reactions is the *quinone methide* in contrast to the *carbonium ion* (*benzylum ion*), which prevails under acidic conditions. The sulfite or bisulfite ions attacks the quinone methide at the  $C_\alpha$  as depicted in Scheme 4.41.

Phenolic  $\alpha$ -ether bonds are most completely cleaved, but the nonphenolic  $\alpha$ -aryl ether units are stable, which supports the quinone methide being the reactive intermediate. Phenolic phenylcoumarans yield the corresponding  $\alpha$ -sulfonic acids (Scheme 4.42), whereas the nonphenolic phenylcoumarans are again mostly stable. Nonphenolic pinoresinol units are cleaved at the respective  $\alpha$ -carbons and sulfonated.



**Scheme 4.42** Reaction of phenolic phenylcoumarans under neutral sulfite conditions.

Eliminated formaldehyde results in the formation of hydroxymethanesulfonic acid. At neutral pH, methoxyl groups are also removed by mechanisms ( $S_N2$ ) similar to the demethylation in kraft pulping, but with formation of the corresponding methylsulfonic acid. The rate of delignification generally decreases with increasing pH.



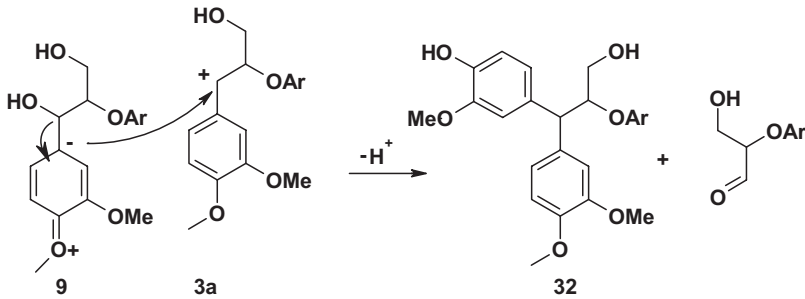
**Scheme 4.43** Reaction of phenolic pinosresinol structures under neutral sulfite conditions.

#### 4.3.4.1.3 Condensation

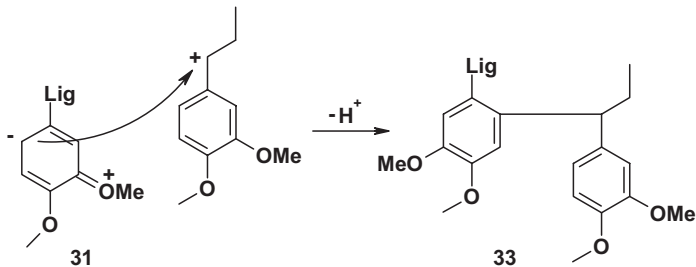
Condensations always compete with the sulfonation process, and counteract the delignification by formation of new, stable carbon–carbon bonds.

Increasing acidity, for example, towards the end of cook, favors condensation reactions between the benzylum cation (3a) and other weakly nucleophilic lignin positions, which are present due to resonance at position C1 (Scheme 4.44) and C6 (Scheme 4.45). Condensation decreases with increasing concentration of bisulfite ions (bound sulfur dioxide, cf. also the Kaufmann diagram; Fig. 4.155). The resulting stable carbon–carbon bonds cause an increased molecular weight and a lower hydrophilicity, and therefore work against the delignification process. However, the introduction of sulfonic acid groups considerably increases the solubility, which can often compensate for the increase in molecular weight by the formation of new carbon–carbon bonds [15].

Intramolecular condensations have been described for phenylcoumaran and pinosresinol structures (cf. Scheme 4.35) [6]. Due to the additional methoxyl group in the 5-position, lignins of hardwoods generally have a lower tendency for condensation reactions as compared to softwoods. Also, the sulfonation reaction is somewhat slower for hardwood than for softwood lignins. Methoxyl groups are not cleaved under acid sulfite conditions to a large extent due to the too low nucleophilicity of the cooking chemicals, whereas under neutral sulfite cooking conditions a cleavage of methoxyl groups is observed.



**Scheme 4.44** Condensation of the reactive benzylium ion with weakly nucleophilic resonance form at C1.



Lig = Lignin moieties

**Scheme 4.45** Condensation of the reactive benzylium ion with weakly nucleophilic resonance form at C6.

#### 4.3.4.1.4 Structure of Lignosulfonates

In contrast to alkaline lignin, lignosulfonates are water-soluble and often contain considerable amounts of carbohydrates – either dissolved in the liquor or still attached to the lignin polymer – which must be removed prior to analysis [20]. The removal of carbohydrates from lignosulfonates is rather tedious. The linkages between lignin and carbohydrates in bisulfite pulps have been analyzed by gel-permeation chromatography (GPC) with multiple detection [16]. A structural model for the high molecular-weight fraction of sulfite waste liquor was proposed by Hachey and Bui [17].

Monomeric lignosulfonates actually identified in sulfite waste liquor are 1-(4-hydroxy-3-methoxyphenyl)-prop-2-ene-1-sulfonate [18,19] and its isomer 1-(4-hydroxy-3-methoxyphenyl)-prop-1-ene-3-sulfonate [19].

In addition to common lignin analytics [20,21], lignosulfonates can be characterized by their degree of sulfonation ( $S/C_9$  or  $S/OMe$ ), which varies for commercial preparations from 0.4 to 0.7 sulfonate groups per phenylpropane unit [22]. Lignosulfonates carry carboxyl groups [23], and lignosulfonates have distinct polyelectrolytic characteristics, which often render chemical analysis more difficult. Recent progress has been achieved in the more accurate determination of the mo-

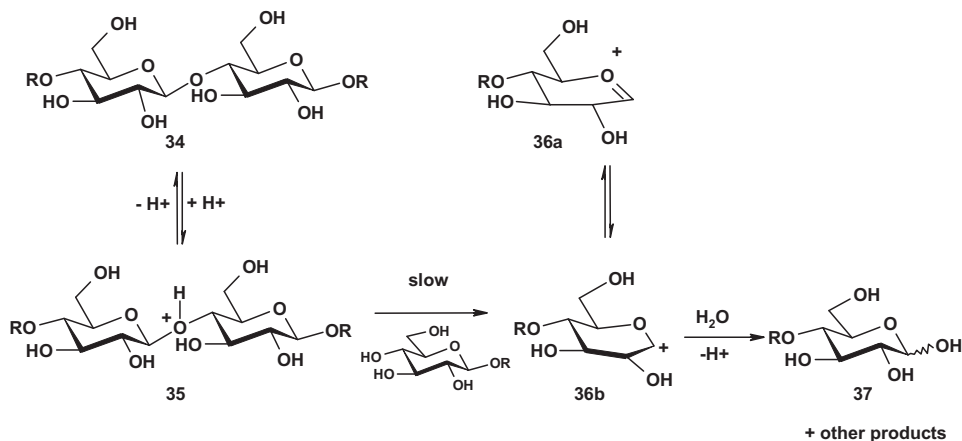
molecular weight employing size-exclusion chromatography in combination with light-scattering techniques [24].

#### 4.3.4.2 Reactions of Carbohydrates: Acid Hydrolysis

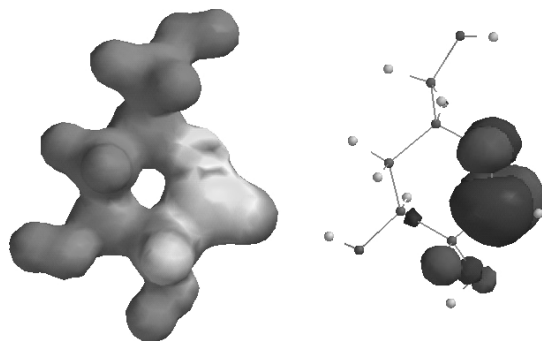
##### 4.3.4.2.1 Cellulose

Acid-catalyzed hydrolysis of glycosidic linkages constitutes a major reaction of carbohydrates under sulfite cooking conditions. The depolymerization of dissolved polysaccharides proceeds in acid sulfite processes mainly to the monosaccharide level, while oligo- and polysaccharides are more frequent in bisulfite spent liquors.

Protonation as the first step of the hydrolysis can take place either at the glycosidic oxygen (dominant pathway) or at the ring oxygen (Scheme 4.46). The protonated form releases the substituent in position C1 being converted into a *carbonium-oxonium ion* (e.g., pyranosyl cation), which is stabilized by resonance and exists in a half-chair conformation. From the electron density distribution (Scheme 4.47) a preferred localization of the positive charge at the C1 carbon can be observed, where nucleophilic attack also occurs. The addition of water leads to a new reducing end group. Hence, the formation of new reducing ends corresponds linearly with the reduction of the molecular weight (degree of polymerization, DP) [25]. As a result of the acid hydrolysis, the DP is reduced, oligomers are formed, and – depending on the severity of the conditions – the polymer can be degraded all the way to the monomers. The reaction kinetics is in agreement with a pseudo-first order rate law. The rate depends on acid concentration, temperature and the molecular environment of the glycosidic bond [26].



**Scheme 4.46** Mechanisms of acid hydrolysis of cellulose [27]

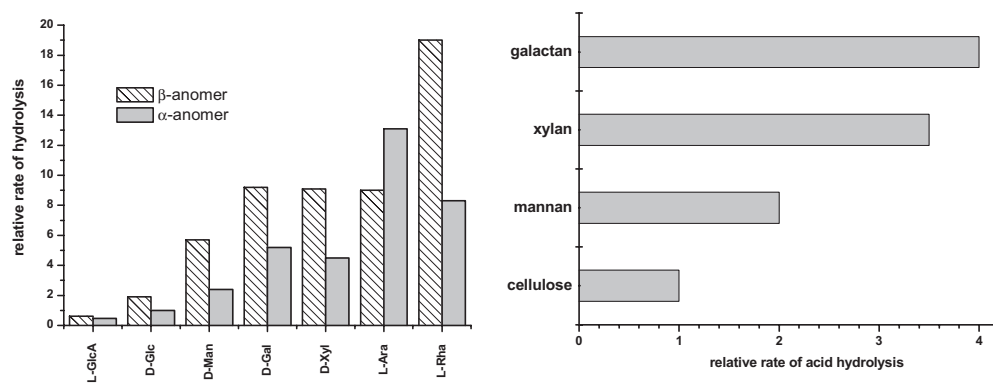


**Scheme 4.47** LUMO (right) and electron density distribution (left) of the carbonium-oxonium ion intermediate (**36**).

#### Influence of Substituents on the Rate of Hydrolysis

The glycosidic linkages between other sugar units than glucose are generally more reactive. Figure 4.156 illustrates the relative rates of the hydrolysis of the  $\alpha$ - and  $\beta$ -anomers of the corresponding methyl glycosides. Ring strain also causes a higher reactivity, in that furanoses react faster than pyranoses. A carboxyl group in position C6 decreases the reactivity, whereas an aldehyde in the same position increases the rate of hydrolysis considerably [28].

The relative rates for the monomers are not very representative for the polymeric material as the nature of the aglycone influences the hydrolysis rate. In addition, acid hydrolysis of cellulose depends not only on the chemical structure as discussed above, but also greatly on its morphology (cf. Chapter 1). The accessibility in this heterogeneous reaction is affected by the degree of crystallinity, and also by provenience or pretreatment.



**Fig. 4.156** Comparison of the relative rate of hydrolysis for monomers (left) [29] and for the polymer (right) [30].

### Hemicelluloses

As shown in Fig. 4.156, hemicelluloses are degraded much more rapidly than cellulose under acidic sulfite cooking conditions. The heterogeneous hydrolysis follows the order cellulose (1) < mannan (2–2.5) < xylan (3.5–4) < galactan (4–5) [30], which roughly agrees with the observed rates for monomers. Arabinofuranosidic bonds are hydrolyzed much more rapidly than glucopyranosidic bonds. Hence, arabinose residues appear at an early stage of the acid sulfite cook. Glucuronopyranosidic bonds are comparably stable, so that monomeric 4-*O*-methyl glucuronic acids are found at a later cooking stage, when most of the xylan backbone has been removed. Also the ratio of monomeric uronic acids to xylose in wood does not change significantly as the cook proceeds [31].

Acetyl groups of xylans and glucomannans are also removed at elevated temperature (cf. pre-hydrolysis kraft process), but in some cases are found to be rather stable.

Hardwood xylans are partly stable under acid sulfite conditions due to the presence of glucuronic acid side chains, which significantly decrease the rate of hydrolysis.

In two-stage processes for softwood, which operate at a somewhat higher pH in the first stage, an increase in the mannan content in the final pulp was observed; this was attributed to a co-crystallization of the glucomannan with the cellulose [32] after having lost most of the side chains.

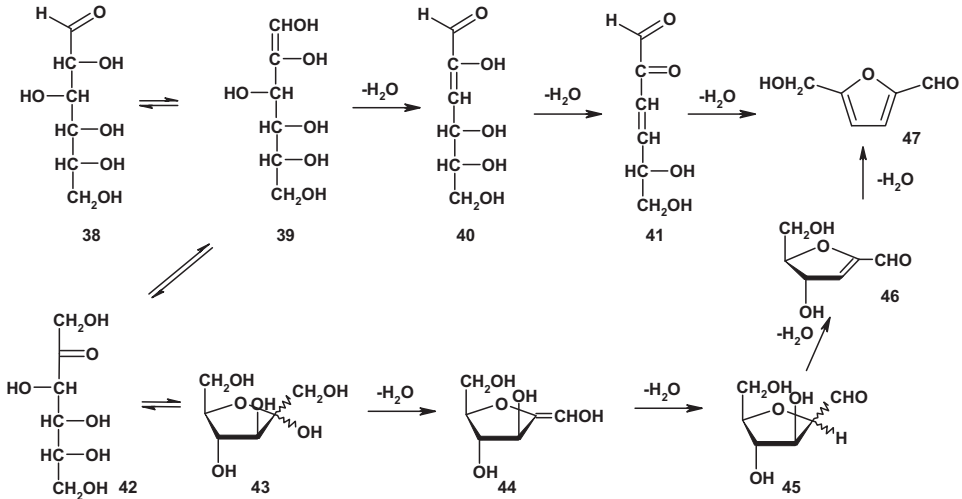
The conversion degree of aldoses to aldonic acids in acid sulfite and bisulfite cooks for birch and spruce varies in the following limits [33]: Ara and Gal: 17–51%, Xyl: 12–25%, Man and Glc: 5–12%. The concentration of uronic acids was found to be small for all liquors. Whilst for the acidic cook the total amount of carbohydrates was 25–30%, the magnesium bisulfite liquors contained only 2.5% of the carbohydrates as monosaccharides, with most of the dissolved carbohydrates remaining as polymeric or oligomeric material.

The opposite situation is true if the acidic groups in the pulp are considered. Larsson and Samuelson [34] investigated the content of uronic and aldonic acid groups in an unbleached spruce sulfite pulp, cooked according to a two-stage process. The dominating uronic acids found after total hydrolysis were 4-*O*-methylglucuronic acid and 2-*O*-(4-*O*-methylglucopyranosiduronic acid)-*D*-xylose. Only small amounts of aldonic acids, such as gluconic, xylonic and mannonic acid, besides traces of arabinonic, ribonic and galactonic acids, were found. A slight demethylation reaction of 4-*O*-methylglucuronic acid also occurred during pulping.

With increasing pH of the cooking liquor, the situation changes significantly. Nelson analyzed acidic groups in pine bisulfite and eucalypt neutral sulfite pulps [35]. The eucalypt neutral sulfite pulp yielded much larger amounts of acids than the pine bisulfite pulp, but this may be attributed to a higher xylan content of the hardwood pulp. The pine bisulfite pulp, however, contained considerably larger amounts of aldonic acids (GlcA, ManA, XylA) than the pulp cooked under neutral conditions, and also compared to pulps produced using a two-stage process [34]. This suggests that the bisulfite ion is an effective oxidant for the reducing end group, although oxidation at the reducing end did not proceed to any significant extent under acidic conditions.

#### 4.3.4.2.3 Dehydration of Carbohydrates to Aromatic Structures

Acid-catalyzed dehydration of carbohydrate monomers eventually leads to the formation of hydroxymethylfurfural (47) from hexoses as the starting material (Scheme 4.48). In a similar manner, the removal of 3 mol water from pentoses results in the formation of furfural, which can be distilled off the pulping liquor. The amount of furfural produced from degraded hemicelluloses during sulfite pulping is sufficiently large to sustain commercial usage.



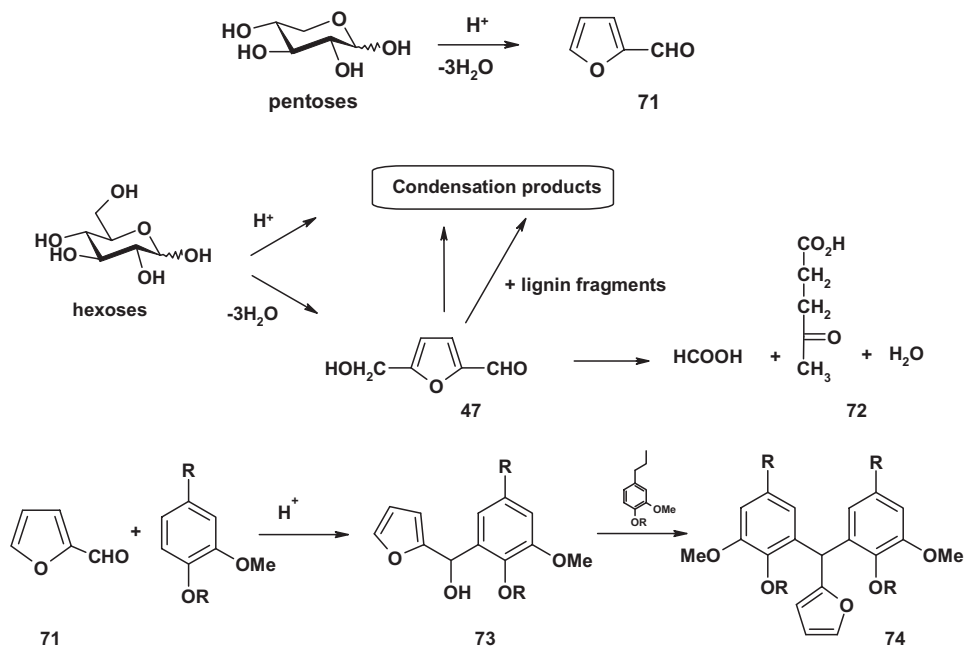
**Scheme 4.48** Formation of hydroxymethylfurfural (HMF) from glucose by acid-catalyzed dehydration.

Hydroxymethylfurfural (47) can be further converted to levulinic acid ( $\gamma$ -oxo pentanoic acid, 72) with 5-hydroxymethylfurfural as an intermediate (cf. Scheme 4.49).

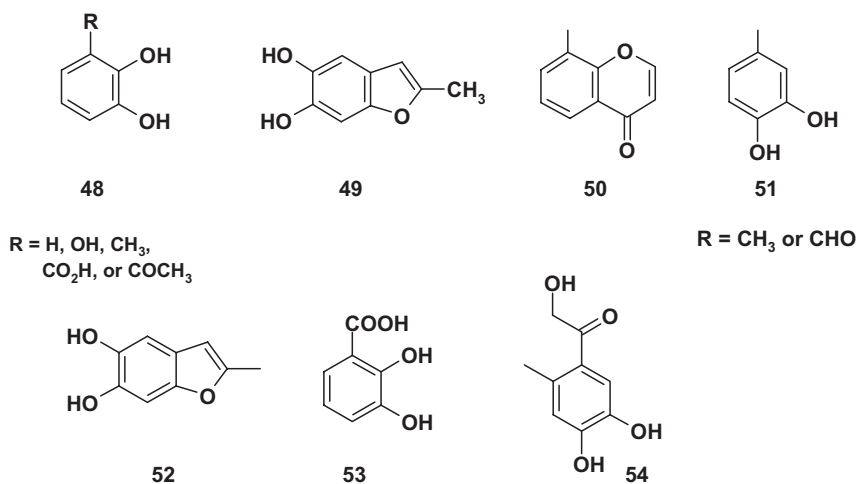
Furfural and its derivatives are highly prone to condensation reactions, either with other furfural molecules or with lignin fragments present in the liquor (Scheme 4.49). An example of such a Friedel-Craft acylation-type condensation is also shown in Scheme 4.49.

The formation of other aromatic compounds under acidic conditions has been studied extensively by Theander et al. [36–38]. Scheme 4.50 shows aromatic compounds resulting from the dehydration, degradation, and re-condensation of carbohydrates under acidic solutions. The first step comprises the formation of anhydro-sugars with intramolecular glycosidic linkages, resulting in elimination of another water molecule from two hydroxyl groups (levoglucosan). The glycosidic linkages are hydrolyzed, and further processes lead to aromatic and condensed units.





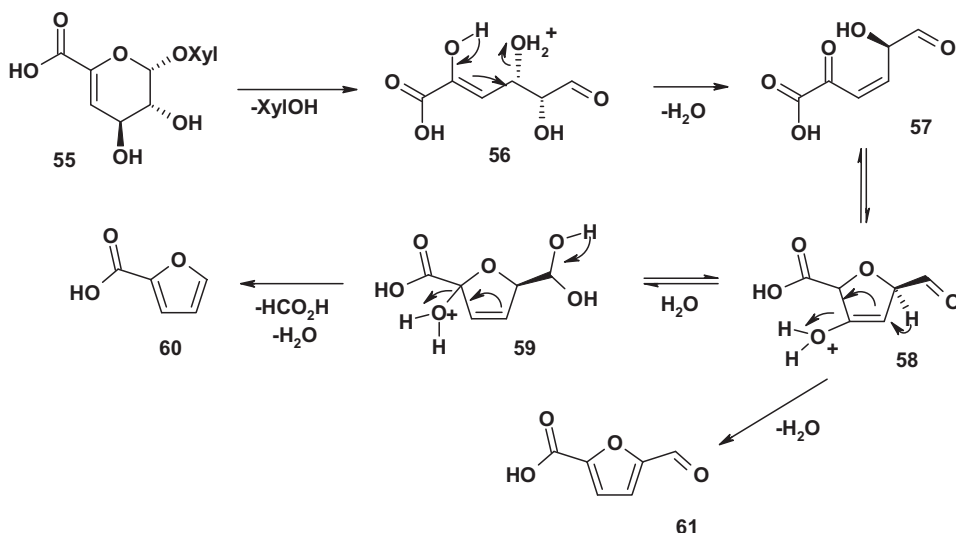
**Scheme 4.49** Degradation of pentoses and hexoses under acidic conditions and condensation of degradation products with lignin units.



**Scheme 4.50** Aromatic compounds formed from dehydration of sugars under acidic conditions [38,39].

### Reaction of Hexenuronic Acid under Acidic Conditions

Hexenuronic acids are only formed under alkaline pulping conditions (cf. reaction in kraft pulping). However, in two-stage sulfite processes with a first stage at a higher pH, their reactions in the subsequent acidic stage must be considered. According to Teleman et al. [40], hexenuronic acids are degraded under acidic conditions to 5-formyl furancarboxylic acid (**61**) according to Scheme 4.51.



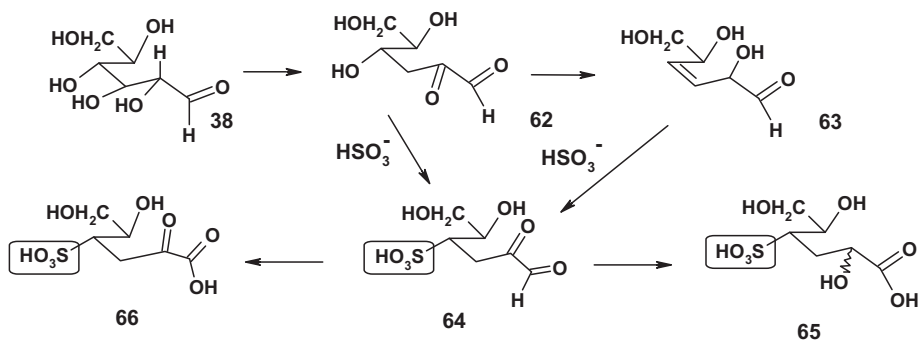
**Scheme 4.51** Formation of 5-formylfuranocarboxylic acid from hexenuronic acid [40].

#### 4.3.4.2.4 Formation of Sulfur-Containing Carbohydrates

The limited stability of sulfur-containing carbohydrate derivatives renders their isolation and identification rather difficult. (It must be borne in mind that the reaction mechanisms presented in this chapter are based on investigations carried out mainly during the period 1940–1960; no recent data are available to verify the much-esteemed work of that period with more recent analytical approaches.)

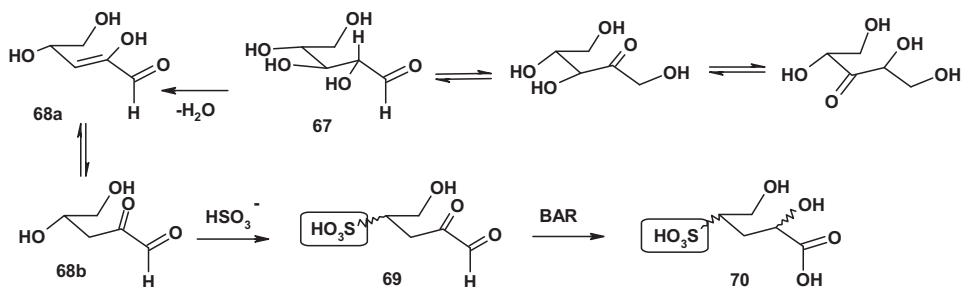
Stable products from the reaction of sulfite with both reducing and nonreducing [41] carbohydrate model compounds were obtained only with sulfite solutions of higher pH (e.g., pH 6) [42]. Adler [43] crystallized a sulfonic acid derived from glucose under the same pH.

Theander [44] showed the formation of such products to proceed in a similar manner as shown for a xylose in Scheme 4.52. Sulfonic acid **66** was formed via oxidation, and **65** by rearrangement of 4-sulfo-3-deoxy-glucosone **64**, which in turn was formed from the dicarbonyl intermediate **62** [45]. The formation of **64** from **63** was also shown to proceed [46].



**Scheme 4.52** Possible mechanism of sulfonic acid formation from glucose [45].

In a later account, Yllner [47] studied the reaction of xylose with neutral sulfite solution and isolated  $\alpha,\delta$ -dihydroxy- $\gamma$ -sulfo-valeric acid. The reaction mechanism proposed for the formation of this sulfo-sugar acid is similar to the peeling process under alkaline conditions. Neutral sulfite systems seem to be “alkaline” enough to promote the initial rearrangement and formation of the intermediate 3-deoxy-D-*glycero*-pentos-2-ulose, which reacts with the hydrogen sulfite at position C4, a benzylic acid rearrangement (BAR) finally yields the stable acid (70) (cf. Scheme 4.53).



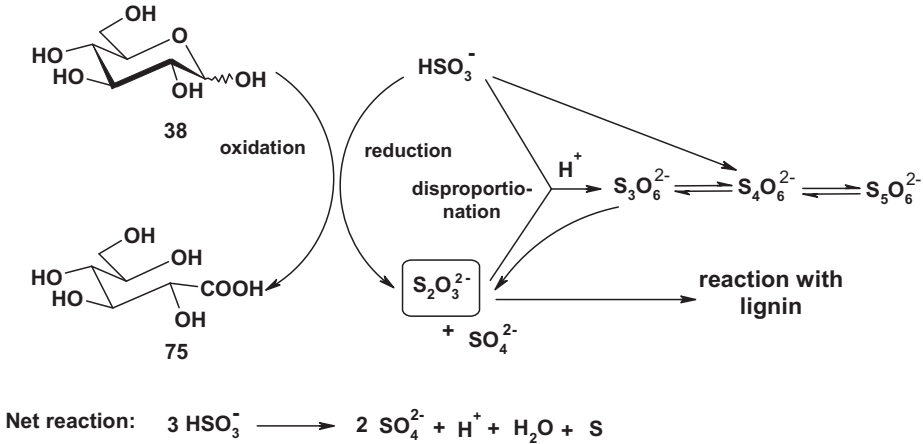
**Scheme 4.53** Possible formation of sulfonic acids from xylose intermediates under neutral sulfite conditions.

#### Side Reactions and the Role of Thiosulfate

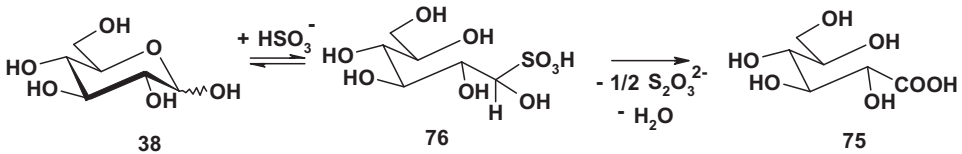
The side reactions can be divided into two categories: (a) reactions involving lignin, carbohydrate and their degradation products; and (b) reactions involving inorganic sulfur compounds only. All side reactions (Scheme 4.54) have in common the fact that they diminish the available sulfite concentration and hence destabilize the cooking liquor. Hydrogen sulfite in aqueous solutions normally acts as a reducing agent and antioxidant. However, under the conditions of the sulfite cook a major part of hydrogen sulfite is consumed by the reducing end groups of sugar monomers and other keto groups present in the liquor under formation of  $\alpha$ -hydroxysulfonates and subsequent oxidation of the reducing end to the corre-

sponding the aldonic acids, according to Scheme 4.55. The hydrogen sulfite bound as  $\alpha$ -hydroxysulfonate is classified as “loosely bound sulfur dioxide”.

The tendency to form  $\alpha$ -hydroxysulfonates and their stability depend on the type of the parent carbonyl compound. Hexoses, pentoses, and lignin carbonyls form less-stable adducts as compared to formaldehyde, furfural, or methyl glyoxal. Formic acid is converted to carbon dioxide [48] by sulfite.



Scheme 4.54 Side reactions in acidic sulfite cooking (modified from [51]).

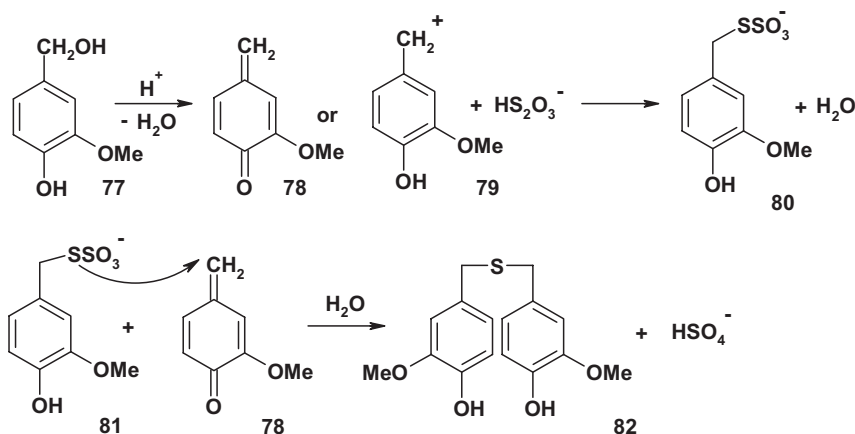


Scheme 4.55 Formation of  $\alpha$ -hydroxysulfonates (bisulfite adducts), thiosulfate and aldonic acid.

The hydrogen sulfite oxidizes aldehyde groups to the corresponding acids, which is the major process generating aldonic acids from cellulose and hemicellulose degradation products (mainly xylonic acid, gluconic acid, some mannonic and galactonic acid). Schön [63] reviewed the kinetic studies in this field, and analyzed the formation of thiosulfate under various conditions. For  $\text{pH} < 4$ , Schön showed a faster conversion of xylose as compared to mannose and glucose, the latter one reacting slightly faster than mannose. Other substances present in the cooking liquor can be oxidized in the same manner (i.e., extractives), and the oxidation of sugar alcohol has also been reported [49]. The hydrogen sulfite is in turn reduced to thiosulfate, which retards delignification [50]. The thio-sulfate plays a key role in the side reactions, as it causes detrimental decompositions of the cooking liquor that are thought to proceed autocatalytically, with thio-

sulfate being one of the catalysts [51]. High concentrations of thiosulfate may finally result in a so-called “black cook” for calcium bisulfite operations. If sodium is the base, the tolerable level of thiosulfate is considerably higher [52]. Disproportionation of hydrogen sulfite leads to thiosulfate and sulfite ion formation, which causes precipitates to occur when calcium ions are used as the base.

The reaction of thiosulfate with lignin was investigated by means of simple model compounds (Scheme 4.56). Goliath and Lindgren demonstrated that thiosulfate reacts in the same manner with the intermediate quinone methide as hydrogen sulfite does. The thiosulfate hence competes with the sulfite for reactive lignin positions. Upon prolonged reaction times or an increase in temperature, condensation to sulfides occurs. The lignin-thiosulfate condensation products are less hydrophilic, and thus have a lower solubility. Such organic excess-sulfur components are increasingly formed towards the end of the cook [54,55].



Scheme 4.56 Model reaction of thiosulfate with vanillyl alcohol (according to [53]).

#### Condensation with Phenols

Condensation with other phenolic compounds can occur in the sulfite cooking of tannin-damaged sapwood, and with the heartwood of certain species. In the first case, the phenolic compounds originate from the bark and have diffused into the wood, mainly by wet storage conditions of unbarked wood.

Phenols predominantly originate from lignin fragments, extractives and reaction products from the acid-catalyzed conversion of low molecular-weight carbohydrates. In particular, furfural and hydroxymethylfurfural – which are formed under acidic conditions from carbohydrates by intramolecular dehydration – are very prone to intra- and intermolecular condensation reactions of many types, leading also to polymeric products [56]. All intermediate compounds exhibit a pronounced tendency to condense either with lignin fragments, or with themselves. These condensation pathways may even contribute a larger share to the overall condensation reactions in the final cooking stage as compared to the reactions with sulfur compounds involved [57].

The condensation reactions of lignin-model compounds with phenols under acidic conditions have been studied extensively by Kratzl and Oburger [58,59]. Condensation reactions occur after protonation of the benzylic hydroxyl group and cleavage of water. The formed carbonium ion attacks the phenol as an electrophile, leading to formation of stable C–C-bonds. The neighboring  $\beta$ -substituent is removed by acid catalysis, and subsequent rearrangements finally also yield another stable C–C-bond at C- $\beta$ .

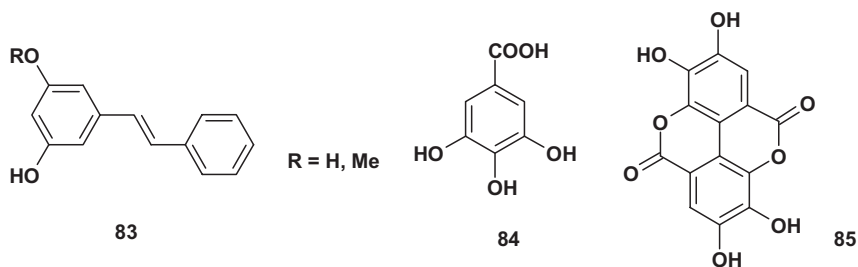
#### Methanol Formation

The formation of methanol is another side reaction that occurs during a sulfite cook. According to Häggglund [60], methanol originates from hemicellulose compounds containing methoxyl groups (e.g., 4-*O*-methylglucuronic acid side chains in xylan). However, it was demonstrated that birch wood releases more methanol than spruce, indicating that a part of the released methanol also originates from lignin methoxyl groups [61].

#### 4.3.4.3 Reactions of Extractives

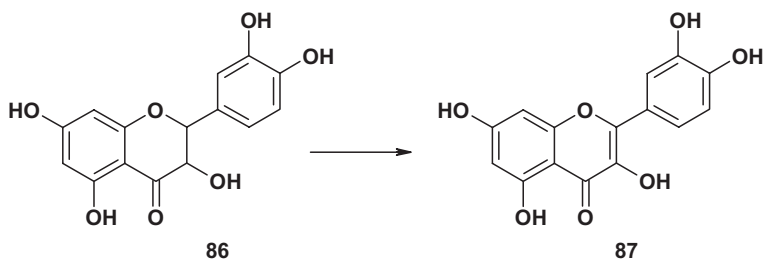
Extractives of wood can be classified according to their extraction methods. In general, extracts are differentiated in terpenes, and resins as the nonvolatile ether-solubles containing the fatty acids and alcohols, resin acids, and phytosterols. Unsaponifiable substances comprise the plant hormones, but these are of minor importance. Under acidic conditions, the various extractive classes behave differently, though they are all highly prone to condensation reactions.

Pinosylvin (pinosylvin monomethyl ether) from the heartwood of pine species efficiently inhibits the delignification during sulfite pulping, even at rather low concentrations, possibly through the formation of condensates with lignin (phenol-formaldehyde condensation) [62]. Such reactions result in larger lignin structures with a lower degree of sulfonation, and thus a lower solubility. Interestingly, gallic acid and its derivatives (ellagotannins) – which are a major extractive of Eucalyptus species – are much less prone to condensation under the same conditions, probably due to different distributions of electron densities within the aromatic ring as a result of different substitution patterns (less-activated position in C2 and C6) (cf. Scheme 4.57).



**Scheme 4.57** Pinosylvin (pinosylvin monomethylether: R = Me), gallic acid, and ellagic acid.

Extractives such as dihydroquercetin did not show a high tendency to condense, but they are oxidized to the corresponding quercetin (Scheme 4.58) with subsequent reduction of hydrogen sulfite to thiosulfate, resulting in increased liquor decomposition [65,66].

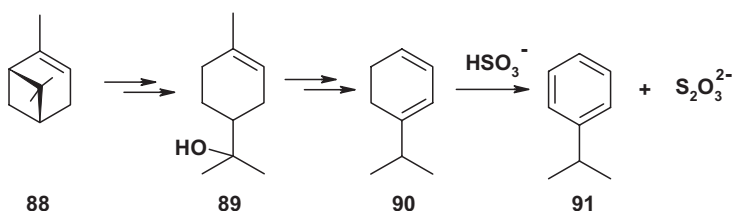


**Scheme 4.58** Formation of quercetin from taxifolin under acid sulfite conditions.

$\alpha$ -Pinene was found to be converted to cymene under sulfite conditions (Scheme 4.59).

In acidic solution, pinene is converted to terpeniol and thereafter to terpinene, which is finally oxidized to cymene by hydrogen sulfite [63]. Also in this case, the hydrogen sulfite does act as oxidizing agent as it is reduced to thiosulfate. Under acidic conditions, a number of other terpenes are unstable and undergo decomposition and rearrangement reactions [64]. Dihydroquercetin is also oxidized under the conditions of a technical sulfite cook to quercetin [65,66]. Taxifolin is converted to quercetin [67].

Acidic sulfite treatment of hydroxymatairesinol yields condendrin as the major condensation product [5].



**Scheme 4.59** Conversion of  $\alpha$ -pinene to cymene during sulfite pulping [68].

Proanthocyanidine and catechin-based tannins can polymerize up to a molecular weight of  $7000 \text{ g mol}^{-1}$ , and exhibit a brown color [69]. Proanthocyanidine is converted, under acidic conditions, to colored anthocyanidines; both are also able to co-condensate with lignin.

Components of resins (free resin globules) have the tendency to coagulate to larger droplets and to adhere to metal surfaces of machinery or fibrous material – a phenomenon referred to as “pitch”. Pitch problems appear mostly during acid pulping of coniferous wood, and this mainly limits the acid sulfite process to

hardwoods and certain softwood species. In addition to problems in the mill operation, pitch causes specks or holes on the paper surface, and in high concentration has also a negative effect on the viscose process.

Fatty acid esters are hydrolyzed to a great extent during the acid sulfite cook, the saturated resin acids remain unchanged, while the unsaturated acids decrease during cooking. Some 20–50% of the resin disappears during the cook, but no oxidation, reduction, or polymerization was observed [1].

In contrast to alkaline pulping, where most of the extractives are either dissolved or saponified, glycerol and sterol esters are not saponified in sulfite pulping.

#### 4.3.5

### Process Chemistry of Acid Sulfite Pulping

*Herbert Sixta*

#### 4.3.5.1 Basic Technology

Sulfite cooking is predominantly carried out in batch digesters with a typical volume of 200–400 m<sup>3</sup> (for technical aspects of batch cooking, see Section 4.2.8.2).

The procedure of acid sulfite cooking typically comprises the steps chip filling, steaming, cooking liquor charging, impregnation, side relief, SO<sub>2</sub> charge, heating to maximum temperature, maintaining the digester at this temperature until the desired degree of cooking is achieved, relieving the pressure (degassing), displacement of cooking liquor, and discharging the digester.

A sulfite digester cycle for dissolving pulp is illustrated by temperature, pressure and liquor diagrams according to Fig. 4.157.

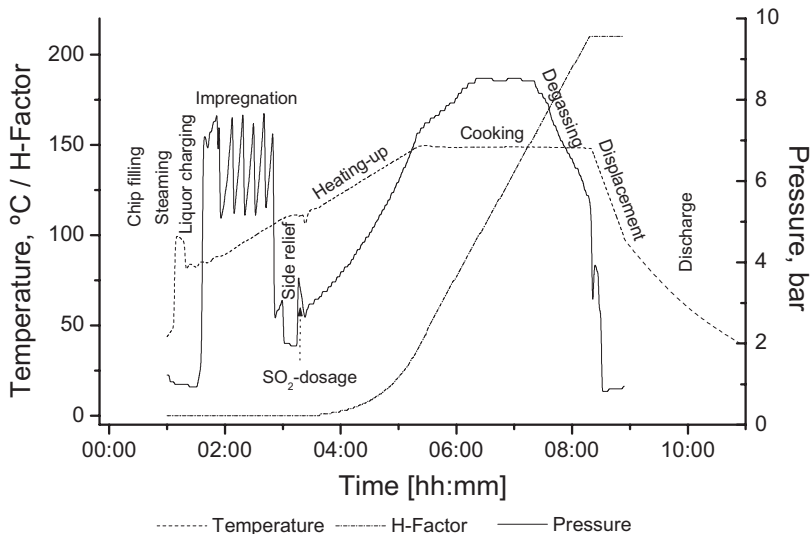


Fig. 4.157 Temperature-, pressure- and H-factor profiles of an acid sulfite cooking cycle.



#### 4.3.5.1.1 Chip Filling and Steaming

The digester is filled with chips from a chip bin above the digester, or from a conveyor transporting the chips from a chip silo at the woodyard. The weight of the wet chips is determined by a conveying weigher or, alternatively, by weighing the whole digester content by means of strain gauges. The moisture content of the chips is measured on-line on the belt conveyers using the microwave or neutron activation principle to record the moisture content of the whole chip volume.

The production of uniform pulp at maximum digester yield requires the maximum weight of chips to be distributed uniformly throughout the whole digester. Chip packers are used to obtain uniform chip distribution and greater packing density. These devices impart a tangential motion to the falling chips and produce a homogeneous horizontal surface of the chip pile inside the digester. The chip packing system of choice is chip packing with steam using the Svennson system [1]. This consists of a steam pipe with nozzles directed downward below the lower peripheral edge of the top sleeve. The amount of dry wood charged per digester volume unit is thereby increased by about 30–40%, depending on the steam pressure, the moisture content, and the density of the chips. The degree of packing is defined as the ratio of dry wood substance in a digester to the theoretical weight of dry wood substance, assuming the total digester volume to be solid wood. The following example should illustrate the term degree of packing (DP):

Digester volume (in m <sup>3</sup> )	300
Dry wood density (g cm <sup>-3</sup> )	0.68
Digester wood charge (in odt)	84

$$DP = \frac{84}{300 * 0.68} \cdot 100 = 41.2\% \quad (173)$$

#### 4.3.5.1.2 Liquor Charging and Impregnation

When the digester is full of chips, the top is sealed and hot fortified raw acid from the high-pressure accumulator is pumped in. Modern acid sulfite cooking plants add the make-up sulfur in the form of liquid sulfur dioxide directly into the digester, after adjusting the liquor-to-solid ratio. Thus, the acid charged to the digester contains a free SO<sub>2</sub> concentration as achieved by recovery of SO<sub>2</sub> from the relief flows in the pressurized accumulators. During pumping, the air vent line at the top is opened to the weak gas collecting system so that air entrained with the chips is removed from the process. Cooking liquor is added to the digester until it is hydraulically full. Even a small excess amount of cooking liquor is pumped through the digester to ensure that all void spaces are liquid-filled. The process is continued by hydraulic pressure impregnation, either using hydraulic pressure variations of the cooking liquor according to the Vilamo process, or maintaining constant hydraulic pressure [2].

#### 4.3.5.1.3 Side Relief and SO<sub>2</sub>-Dosage

Complete filling of the digester results in a rather high liquor-to-wood ratio (4–5:1 for softwoods, 3–5:1 for hardwoods) which would cause an excessive steam consumption for heating to maximum temperature, and in addition an unnecessarily high dilution of the spent liquor. Hence, cooking liquor is withdrawn through a *side relief* until a target liquor-to-wood ratio is obtained, provided that liquor circulation is ensured. Side relief of up to 30% is possible, and this decreases the liquor-to-wood ratio to about 3.5:1 for softwoods and to 2.5:1 for dense hardwoods. The following example illustrates the specific amounts of free and enclosed cooking liquor prior and after the side relief:

Wood source	<i>Fagus sylvatica</i> (beech)
Dry beech wood density	0.68 g cm <sup>-3</sup>
Dry solid density	1.53 g cm <sup>-3</sup>
Chip packing density	0.28 t m <sup>-3</sup> digester
Liquor-to-wood ratio after side relief	2.5:1
Bulk volume in digester	$V_b = 1/0.28 = 3.57 \text{ m}^3 \text{ odt w}^{-1}$
Volume of dry chip	$V_c = 1/0.68 = 1.54 \text{ m}^3 \text{ odt w}^{-1}$
Free volume between chips	$V_s = (3.57 - 1.54) = 2.03 \text{ m}^3 \text{ odt w}^{-1}$
Enclosed cooking liquor at full impregnation	$V_{el} = (1/0.68 - 1/1.53) = 0.82 \text{ m}^3 \text{ odt w}^{-1}$
Liquor-to-wood ratio prior to side relief	$V_{1,0} = 2.03 + 0.82 = 2.85 \text{ m}^3 \text{ odt w}^{-1}$
Free volume after side relief	$V_{1,1} = (2.5 - 0.82) = 1.68 \text{ m}^3 \text{ odt w}^{-1}$

As soon as the target liquor-to-wood ratio is reached, the precalculated amount of liquid SO<sub>2</sub> is added into the digester. By keeping the liquor-to-wood ratio constant, the charge of liquid SO<sub>2</sub> controls the total amount of SO<sub>2</sub> (and also the amount of free SO<sub>2</sub>), whereas the amount of combined SO<sub>2</sub> is given by the amount of active base present in the clarified raw acid.

A typical example illustrates the adjustment of final cooking liquor: The composition of the cooking liquor prior SO<sub>2</sub> charge including the dilution with water from wood and steam:

Total SO <sub>2</sub>	45	g L <sup>-1</sup>
MgO	8	g L <sup>-1</sup>
Free SO <sub>2</sub>	19.6	g L <sup>-1</sup> [(45 - 8) × 3.179]

A target of total SO<sub>2</sub> charge of 140 kg odt w<sup>-1</sup> corresponds to a concentration of 56 g L<sup>-1</sup> total SO<sub>2</sub> in case of a liquor-to-wood ratio of 2.5:1, which requires a dosage of (56 - 45) × 2.5 = 27.5 kg liquid SO<sub>2</sub> odt w<sup>-1</sup>. Thus, the final cooking liquor composition after SO<sub>2</sub> charge yields:

Total SO <sub>2</sub>	56	g L <sup>-1</sup>
MgO	8	g L <sup>-1</sup>
Free SO <sub>2</sub>	30.6	g L <sup>-1</sup>

Due to the low temperature and the low amount of free  $\text{SO}_2$  prior to liquid  $\text{SO}_2$  charge, almost no reactions occur up to this stage of the cook. At this point, the cooking process can be started by increasing the temperature.

#### 4.3.5.1.4 Cooking (Heating-up, Maintaining at Cooking Temperature)

Modern sulfite digesters practice indirect heating; this involves circulation of the cooking liquors through external heat exchangers with the aid of circulation pumps, which draw off cooking liquor through strainers in the digester walls and return the heated liquor at appropriate inlets. Circulation systems ensure a more even temperature profile as compared to direct heating systems. In acid sulfite cooking, the rate of heating should be low to allow a homogeneous distribution of active cooking chemicals within the wood structure (see Section 4.3.3, Impregnation). Thus, heating rates should be kept in the range between  $0.2^\circ\text{C}$  and  $0.4^\circ\text{C min}^{-1}$ . On increasing the temperature, the pressure increases, until top gas relief is started at a preset pressure level, approximately 2–3 bar below the design pressure of the digester. Top gas relief is typically adjusted at a pressure of about 8.5 bar abs (see Fig. 4.157), and consists of vapor containing  $\text{H}_2\text{O}$ ,  $\text{SO}_2$ ,  $\text{CO}_2$ ,  $\text{O}_2$ ,  $\text{N}_2$ , and volatile organic compounds depending on the wood source (hardwoods – acetic acid, furfural, etc.; softwoods – p-cymene from  $\alpha$ -pinene). Due to the high content of  $\text{SO}_2$ , the top gas relief is recycled to the hot accumulator acid, where it fortifies the raw cooking acid. The pressure determines the cooking liquor composition and therefore the rate of cooking. A high pressure maintains a high sulfur dioxide concentration and results in a rapid sulfite cook. An appropriate cooking control is more important for a sulfite cook as compared to a kraft cook. Although a large amount of the cooking chemicals are consumed, the acidity of the cooking liquor increases toward the end of the cook due to progressive formation of strong acid anions,  $[\text{A}^-]$ , and the simultaneous consumption of combined  $\text{SO}_2$ ,  $[\text{HSO}_3^-]$ . Hence, the concentration of hydrogen ions increases and the rate of the carbohydrate hydrolysis accelerates. The final cooking phase is very important for the production of high-purity, low-viscosity dissolving pulps. Since hypochlorite bleaching has been replaced by chlorine-free bleaching stages (e.g., ozone, hydrogen peroxide), viscosity control is predominantly carried out during the final cooking phase.

#### 4.3.5.1.5 Pressure Relief, Displacement of Cooking Liquor, and Discharge

Determination of the end-point of the cook is based on a combination of empirical cooking models and color analysis of the cooking liquor. The empirical models used for sulfite pulping are called either the S- or the H-factors [3]. The S-factor includes both the temperature and the partial pressure of  $\text{SO}_2$ . It is generally accepted that the rate of delignification is proportional to the ion product of  $[\text{H}^+]\cdot[\text{HSO}_3^-]^n$ , with n most likely being 0.75, and the rate of cellulose degradation (equals viscosity loss) to  $[\text{H}^+]$ , both being proportional to the partial pressure of  $\text{SO}_2$  [3]. Thus, the S-factor (SF) is developed from the following expression:

$$r_L = -\frac{dL}{dt} = k_L \cdot [L]^a \cdot [p_{SO_2}]^n \quad (174)$$

where  $L$  is the lignin concentration,  $k_L$  the rate constant,  $p_{SO_2}$  the partial pressure of  $SO_2$ , and  $a$  and  $n$  are constants, with  $a$  assumed to be unity. The SF calculates to the expression:

$$SF = - \int_{t_{T=100^\circ C}}^{t_{final}} \frac{dL}{L} = \int_{t_{T=100^\circ C}}^{t_{final}} \text{Exp} \left[ \frac{E_{A,L}}{R \cdot 373} - \frac{E_{A,L}}{T} \right] \cdot [p_{SO_2}]^n \cdot dt \quad (175)$$

The SF also correlates with the viscosity, provided that the activation energy is adjusted to a value determined for the carbohydrate degradation,  $E_{A,C}$ .

The energy of activation for delignification,  $E_{A,L}$ , has been found to be  $67 \text{ kJ mol}^{-1}$  in the beginning of delignification, and  $95 \text{ kJ mol}^{-1}$  at the final phase [4]. The energy of activation for the dissolution of the carbohydrates,  $E_{A,C}$ , changed only slightly in the course of cooking from about  $80 \text{ kJ mol}^{-1}$  in at the start of the cook to  $90 \text{ kJ mol}^{-1}$  at the end of the cook [4]. For cellulose degradation during acid sulfite pulping, higher values for  $E_{A,C}$  (e.g.,  $125 \text{ kJ mol}^{-1}$  and  $176 \text{ kJ mol}^{-1}$ ) have been reported, respectively [5,6]. Pressure regulation clearly has an impact on the velocity of cellulose degradation, and thus on the calculated value for the activation energy.

According to Eq. (175), the partial pressure of  $SO_2$  must be considered, though this is barely measurable. To estimate a value for the partial pressure of  $SO_2$  it has been assumed that the total digester pressure,  $p_{tot}$ , is primarily a combination of the partial pressure of  $SO_2$  and the partial pressure of water,  $p_{H_2O}$ , at the specified temperature [Eq. (176)] [7].

$$p_{SO_2} = (p_{tot} - p_{H_2O}) \quad (176)$$

It is, however, common practice that pressure and temperature are adjusted to preset values during the cooking phase (and deviate from the preset values only during the heating-up period), which therefore would maintain a rather constant partial pressure of  $SO_2$  when calculated according to Eq. (176). In view of this situation, a simple H-factor concept in combination with a color analysis of the cooking liquor would be sufficient for correct end-point determination. The activation energy for cellulose degradation,  $E_{A,C}$ , during acid sulfite pulping of beech wood with pressure control at a level of 8.5 bar, has been calculated by nonlinear regression analysis using the following approximation for H-factor determination [8]. For practical reasons, cellulose degradation is measured as loss in intrinsic viscosity.

$$H_{S,C} \propto \int_{t_0}^{t_F} \text{Exp} \left[ \left( -\frac{E_{A,C}}{R} \right) \cdot \left( \frac{1}{T} - \frac{1}{373.15} \right) \right] \cdot dt \quad (177)$$

where  $H_{S,C}$  is the H-factor for cellulose degradation during acid sulfite pulping.

Based on a total of 155 laboratory cooks, an activation energy for cellulose degradation,  $E_{A,C}$ , of  $110 \text{ kJ mol}^{-1}$  has been determined. Inserting this activation energy leads to the following expression for the  $H_{S,C}$ :

$$H = \int_{t_{T=100^{\circ}\text{C}}}^{t_{\text{final}}} \text{Exp} \left[ 35.47 - \frac{13230}{T} \right] dt \quad (178)$$

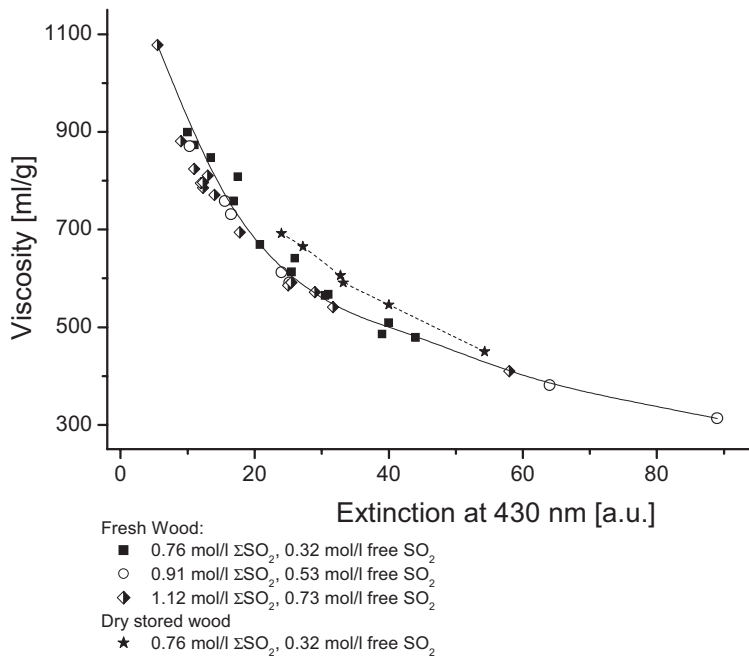
The dissolving pulp viscosity cannot be adjusted with sufficiently high precision by only using H-factor control. Cellulose degradation is additionally influenced by the composition of the cooking liquor – for example, the amounts of combined and free  $\text{SO}_2$  and the liquor-to-wood ratio. H-factor control is, however, well-suited for the precalculation of cooking times which enables the optimization of digester sequencing, steam supply and thus the prediction of production output. The real end-point determination of a sulfite cook – particularly a sulfite-dissolving cook – is very difficult for two main reasons. The first reason is that, to date, there is no capability of analyzing a representative sample from the entire cook to determine the target pulp properties. Examples include the pulp viscosity of a dissolving pulp or the residual lignin content (kappa number) for a paper grade-pulp, to be assessed either within a very short time or even on-line, such that the process operator is still in a position to adjust the process conditions accordingly. The second reason is that a sulfite cook accelerates towards the end of the process, and reactions cannot be stopped immediately at a predetermined time. Consequently, the whole process of terminating the cook including the relief of digester pressure and cold displacement – must be controlled with regard to the viscosity (or kappa number) development. Currently, only cooking liquor analysis is applied to monitor the reaction medium of the cook towards the end of the process. Although they are only indirect methods, cooking liquor tests have the advantage that the samples – which preferably are removed from the liquor circulation – represent the entire digester content, and the analysis can be carried out rapidly and even recorded on-line. Among a wide variety of possible methods listed in Table 4.56, color determination of the cooking liquor is the most important parameter for end-point determination, at least for dissolving pulp production.

Absorbance at 280 nm, which is characteristic for the lignin and furfural concentrations of the liquor, changes during the final period of dissolving pulp cook due to condensation reactions. Therefore, absorbance at this wavelength is not well-suited to measure the lignin concentration of the cooking liquor. However, absorbance in the visible region – preferably between 400 and 500 nm – correlated well with the acidity prevailing in the cooking liquor. The liquor color, which converts from light yellow to brown and finally to dark-brown, most likely originates from condensation reactions involving carbonyl groups from lignin structures induced by a lack of hydrogen sulfite ion concentration and the development of acidity [11]. In industrial practice, the color is measured at 430 nm against pure water. Development of the color is carefully monitored during the whole final

cooking phase (from the beginning of the pressure relief until the blow). Thus, absorbency at 430 nm shows a reasonably good correlation to pulp viscosity (Fig. 4.158). [13].

**Tab. 4.56** Cooking liquor analysis methods used for end-point determination of acid sulfite cooks.

Method	Reference
CE method for quantitative determination of sulfite, thiosulfate, sulfate ions	[9]
Refractive index	[10]
Color	[11]
pH-value	[12]
Conductivity	[6], [10]



**Fig. 4.158** Pulp viscosity of beech wood sulfite dissolving pulp as a function of the extinction at 430 nm at a given liquor-to-wood ratio (2.5:1), different cooking acid compositions, and differently stored beech wood (according to [13]).

Surprisingly, the absorbency–pulp viscosity relationship is not influenced by different cooking acid compositions. Clearly, the color formation is only the result of a temperature- and pH-dependent reaction. However, there are several sources of deviations in the relationship which require a current calibration of absorbance with final pulp viscosity achieved. The main factors comprise the liquor-to-wood ratio, the type of base used, the wood quality and, of course, different wood species or blends of wood furnish. As an example, the influence of different storage conditions of beech wood on the color–pulp viscosity relationship is demonstrated in Fig. 4.158. Dry storage of beech logs for 12–15 months causes some change in the relationship of liquor color and pulp viscosity as compared to the use of fresh beech wood (Fig. 4.158).

The digester pressure is first relieved to a pressure of about 3–5 bars, depending on the pressure on the hot-acid accumulator. The pressure relief is continued by simultaneously introducing cold washing liquor into the digester. To avoid SO<sub>2</sub> gas and heat losses during blowing, the temperature inside the digester must be cooled to less than 100 °C. The pulp is finally blown or pumped into the blowpit for storage.

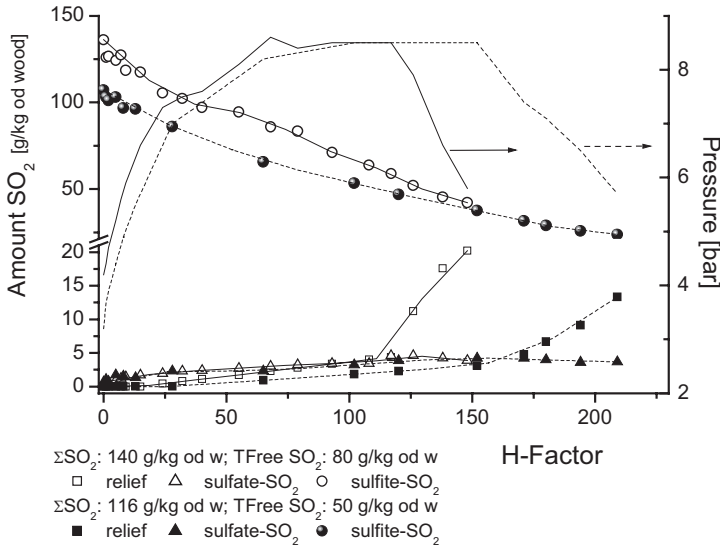
#### 4.3.5.1.6 SO<sub>2</sub> Balance

Conventional titrimetric methods, such as iodometric titration, cannot be applied to the quantitative determination of concentrations of inorganic sulfur ions present in the acid sulfite cooking liquor, mainly because the dissolved organic compounds interfere with correct measurements. A method based on capillary electrophoresis (CE) has been successfully developed for quantitative determination of thiosulfate, sulfite, and sulfate ions in acid sulfite liquors [9]. Using this CE method, it is now possible to balance the whole cook with respect to all sulfur compounds, including determination of the relieved SO<sub>2</sub> gas (top relief, pressure relief) by conventional iodometric titration. Unfortunately, the CE method cannot differentiate between free and combined SO<sub>2</sub> since the cooking liquor is immediately absorbed in an alkaline solution to prevent losses of volatile SO<sub>2</sub>.

Figure 4.159 shows the course of specific amounts of sulfite ions (hydrogen sulfite and dissolved SO<sub>2</sub> hydrate), sulfate ions, and released gaseous SO<sub>2</sub> during two magnesium sulfite cooks with different cooking liquor composition, temperature, and H-factor profiles.

As expected, the concentration of dissolved sulfur (IV) compounds continuously decreases with progress of cooking due to consumption reactions (e.g., sulfonation, redox reactions with reducing end groups, formation of ketosulfonates, etc.). Simultaneously, a slight increase in sulfate ion concentration can be observed.

As expected, the amount of gaseous SO<sub>2</sub> during the pressure release of the cook correlates with the specific amount and proportion of free SO<sub>2</sub> in the cooking acid. Assuming that the decrease in the specific amount of sulfite-sulfur compounds can be attributed solely to consuming reactions (see above), the sulfur balance can be easily completed. Although no information about the stoichiometry of reactions is available, an evaluation of the sulfur balance data reveals that the



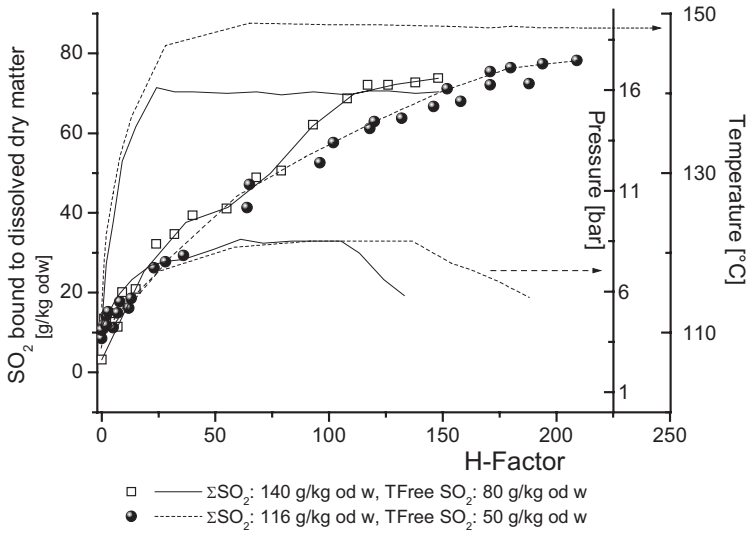
**Fig. 4.159** Specific amounts of dissolved  $\text{SO}_2$  (hydrogen sulfite and  $\text{SO}_2$  hydrate), sulfate and released gaseous  $\text{SO}_2$  during two different beech magnesium acid sulfite cooks: (a) Total  $\text{SO}_2$ : 140 g  $\text{kg}^{-1}$  o.d. wood, free  $\text{SO}_2$ : 80 g  $\text{kg}^{-1}$  o.d. wood, maximum cooking temperature: 140 °C, H-factor 148, unbleached viscosity: 590 mL  $\text{g}^{-1}$ . (b) Total  $\text{SO}_2$ : 116 g  $\text{kg}^{-1}$  o.d. wood, free  $\text{SO}_2$ : 50 g  $\text{kg}^{-1}$  o.d. wood, maximum cooking temperature: 148 °C, H-factor 210, unbleached viscosity: 590 mL  $\text{g}^{-1}$ .

sulfur consumption reactions follow a type of saturation function, which indicates that the consumption rates are highest at the beginning and level off in the later stages of the cook. The course of the consumption reactions for both cooks is shown in Fig. 4.160.

Clearly, the extent of sulfur consumption reactions is virtually independent of the cooking conditions, provided that the target viscosity is achieved. As an example, the course of one-stage acid sulfite cooking to a target viscosity of 590 mL  $\text{g}^{-1}$  comprising two different compositions of cooking acid are compared (Fig. 4.160). Despite the totally different specific amounts of total  $\text{SO}_2$  and the proportion of free and bound  $\text{SO}_2$ , the overall reaction stoichiometry during acid sulfite cooking is quite comparable for both sulfite cooks. This result is important when designing the gaseous  $\text{SO}_2$  recovery, as knowledge of the specific amount of bound  $\text{SO}_2$  compared to dissolved organic matter, allows easy calculation of the maximum amount of free  $\text{SO}_2$  recovery (Fig. 4.161).

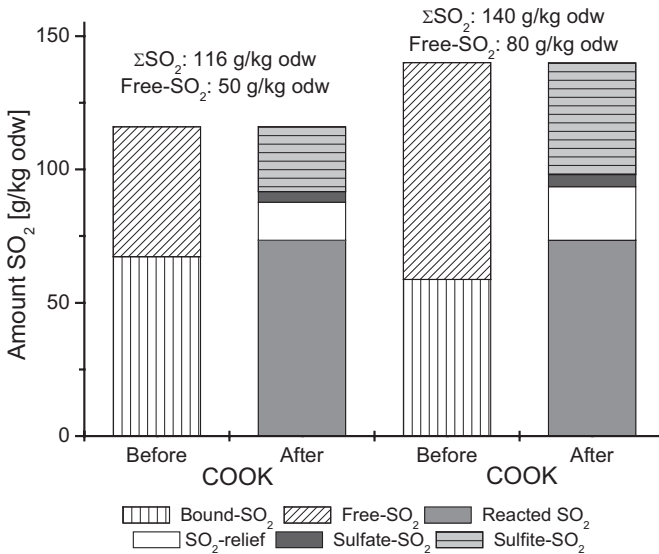
In both cooks, approximately 74 g  $\text{SO}_2$   $\text{kg}^{-1}$  o.d. wood is consumed by reactions with dissolved organic matter (e.g., to lignosulfonates, etc.). The remaining sulfur species after the cook include the released gaseous  $\text{SO}_2$  fraction (top relief and pressure relief), the dissolved sulfur(IV) compounds as hydrated  $\text{SO}_2$  or hydrogen sulfite ions, and a small fraction as oxidized sulfate ions. No thiosulfate ions have been detected on a level of  $<0.2$  g  $\text{L}^{-1}$ . The specific amounts and relative proportions of the sulfur compounds are listed in Tab. 4.57.





**Fig. 4.160** Course of the specific amount of bound  $\text{SO}_2$  to dissolved organic matter during two different beech magnesium acid sulfite cooks. (a) Total  $\text{SO}_2$ :  $140 \text{ g kg}^{-1}$  o.d. wood, free  $\text{SO}_2$ :  $80 \text{ g kg}^{-1}$  o.d. wood, maximum cooking

temperature:  $140^\circ\text{C}$ ; H-factor 148, unbleached viscosity:  $590 \text{ mL g}^{-1}$ . (b) Total  $\text{SO}_2$ :  $116 \text{ g kg}^{-1}$  o.d. wood, free  $\text{SO}_2$ :  $50 \text{ g kg}^{-1}$  o.d. wood, maximum cooking temperature:  $148^\circ\text{C}$ , H-factor 210, unbleached viscosity:  $590 \text{ mL g}^{-1}$ .



**Fig. 4.161** Gross balance of different sulfur species prior to and after two different beech magnesium acid sulfite cooks. (a) Total  $\text{SO}_2$ :  $140 \text{ g kg}^{-1}$  o.d. wood, free  $\text{SO}_2$ :  $80 \text{ g kg}^{-1}$  o.d. wood, maximum cooking temperature:  $140^\circ\text{C}$ ,

H-factor 148, unbleached viscosity:  $590 \text{ mL g}^{-1}$ . (b) Total  $\text{SO}_2$ :  $116 \text{ g kg}^{-1}$  o.d. wood, free  $\text{SO}_2$ :  $50 \text{ g kg}^{-1}$  o.d. wood, maximum cooking temperature:  $148^\circ\text{C}$ , H-factor 210, unbleached viscosity:  $590 \text{ mL g}^{-1}$ .

**Tab. 4.57** Gross balance of different sulfur species as specific SO<sub>2</sub> (g kg<sup>-1</sup> o.d. wood) after beech magnesium acid sulfite cooks of two different acid compositions: A, higher proportion of free SO<sub>2</sub>, and B, lower proportion of free SO<sub>2</sub> (57% and 43% of total SO<sub>2</sub>, respectively).

Phase	Species in g SO <sub>2</sub> kg <sup>-1</sup> odw, present as	Acid A	Acid B
		140	116 Total SO <sub>2</sub>
		80	50 Free SO <sub>2</sub>
Liquid phase	Bound to dissolved matter	73.8	73.9
	Sulfite ions (HSO <sub>3</sub> <sup>-</sup> ), hydrated SO <sub>2</sub>	42.1	24.5
	Sulfate ions (SO <sub>4</sub> <sup>2-</sup> )	4.6	4.0
	Thiosulfate (S <sub>2</sub> O <sub>3</sub> <sup>2-</sup> )	<0.2	<0.2
Gas phase	Gaseous SO <sub>2</sub> from pressure relief	20.1	14.4
Total		140.6	116.8

The released gaseous SO<sub>2</sub> amounts to 20 g kg<sup>-1</sup> o.d. wood in case of acid A, and 14 g kg<sup>-1</sup> o.d. wood in the case of the more buffered cooking acid B. This shows that most of the originally present free SO<sub>2</sub> remains dissolved as hydrated SO<sub>2</sub> or hydrogen sulfite in the cooking liquor, 42 g kg<sup>-1</sup> o.d. wood and 24 g kg<sup>-1</sup> o.d. wood, respectively. A relatively small fraction of the charged SO<sub>2</sub> is oxidized to sulfate ions, in an amount of 4–5 g kg<sup>-1</sup> o.d. wood for both cooks.

#### Degradation of wood components during acid sulfite cooking of beech wood

As mentioned earlier (see Section 4.3.2), the extent of delignification is dependent upon the ionic product, [H<sup>+</sup>]·[HSO<sub>3</sub><sup>-</sup>], whereas carbohydrate degradation is largely controlled by the acidity of the cooking liquor, [H<sup>+</sup>]. The ratio of delignification to carbohydrate removal during the sulfite cook, as given in Eq. (179):

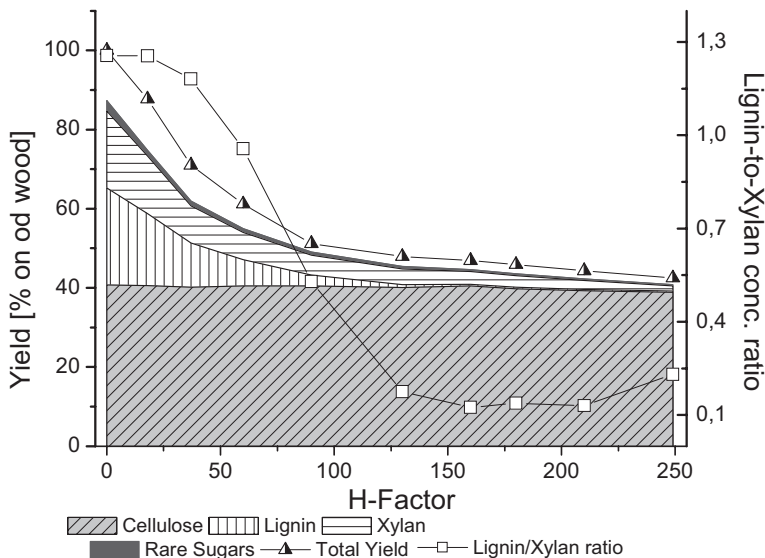
$$\frac{\text{delignification}}{\text{carbohydrate degradation}} \propto \frac{k' \cdot [H^+] \cdot [HSO_3^-]}{k \cdot [H^+]} = \frac{k'}{k} \cdot [HSO_3^-] \quad (179)$$

is therefore related to the hydrogen sulfite ion concentration. Consequently, the ratio of delignification to carbohydrate hydrolysis velocities during the sulfite cook increases with the growing buffer capacity of the cooking liquor. Moreover, both lignin and carbohydrate degradation reactions are controlled by temperature and time. Although the activation energies for delignification and carbohydrate removal are somewhat contradictory, it is agreed that the temperature-dependence of the carbohydrate degradation velocity is greater than that of the delignification rate [4,8]. This explains why the hemicellulose content in a sulfite pulp increases

with decreasing cooking temperature at a given kappa number. With progressive sulfite cooking, the ratio between the hydrogen ion and hydrogen sulfite ion concentrations increases, which consequently accelerates the hemicellulose degradation. This comparative ease of hemicellulose removal on prolonged sulfite cooking makes it possible to produce dissolving pulps of high cellulose purity.

To follow the change in the composition of the wood components during magnesium acid sulfite cooking of beech wood, extensive laboratory trials in the H-factor range from 0 to 250 have been conducted [14]. At given sulfite cooking conditions, comprising total and free  $\text{SO}_2$  concentrations of  $0.76$  and  $0.32$  mol  $\text{L}^{-1}$ , respectively, a liquor-to-wood ratio of 2.4:1 and a cooking temperature of  $148$  °C, the degradation pattern of the two main noncellulosic wood components – lignin and xylan – differs significantly, as shown by the lignin-xylan ratio in Fig. 4.162. After a short induction period, the degradation of lignin proceeds significantly faster than xylan removal, up to an H-factor of approximately 130. When prolonging the sulfite cook beyond an H-factor of 160, the xylan removal rate finally increases significantly over the delignification rate, as shown in Tab. 4.58.

The other carbohydrate components of the hemicelluloses fractions hydrolyze at different rates, depending on their chemical structure and accessibility. Furanosides are known to hydrolyze more rapidly than pyranosides, which accounts for the rapid dissolution of arabinose during sulfite cooking [15] (Tab. 4.58). In good agreement with the results from acid sulfite pulping, methyl- $\beta$ -D-mannose is cleaved about 5.7 times and both methyl- $\beta$ -D-galactose and methyl- $\beta$ -D-xylose



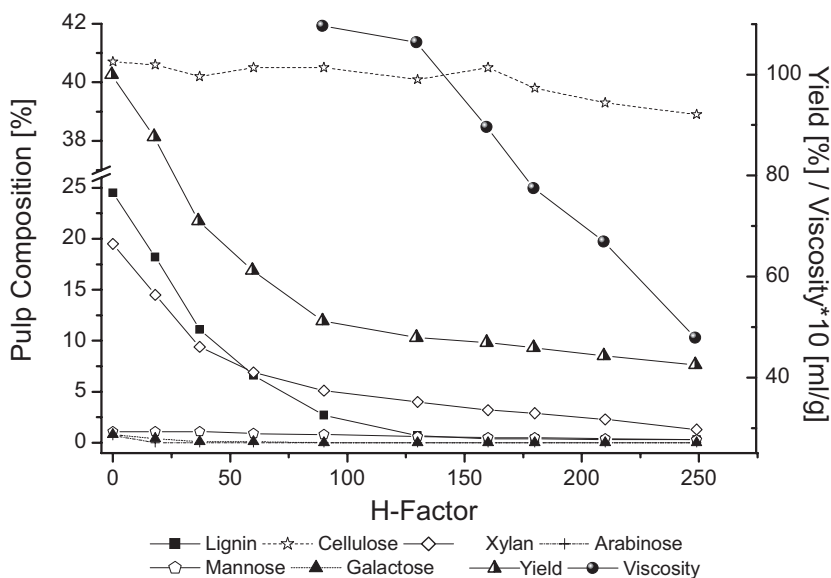
**Fig. 4.162** Course of the main wood components in the solid phase during acid magnesium sulfite cooking of beech wood [13]. Cooking conditions comprise a total  $\text{SO}_2$  concentra-

tion of  $0.76$  mol  $\text{L}^{-1}$ , a free  $\text{SO}_2$  concentration of  $0.32$  mol  $\text{L}^{-1}$  free  $\text{SO}_2$ , a liquor-to-wood ratio of 2.4:1, and a cooking temperature of  $148$  °C.

**Tab. 4.58** Characterization of the (dissolving) pulp composition through acid magnesium sulfite cooking of beech wood (according to [13]).

Label	H-Factor	Yield	Lignin	Kappa	R10	R18	Viscosity	COOH	CO	Copper#	Lignin	Glucan	Xylan	Arabinan	Mannan	Galactan	$\Delta\text{Xyl}/\Delta\text{Lign}$
		[% odw]			[% odw]	[mL g <sup>-1</sup> ]	[ $\mu\text{mol g}^{-1}$ ]	[ $\mu\text{mol g}^{-1}$ ]	[%]					[% odw]			
0	100	24.5									24.5	41.6	19.5	0.7	1.1	0.8	
Mg 433	18	87.7	20.8	100.8	65.7	69.4					18.2	40.6	14.5	0.0	1.1	0.4	1.4
Mg 434	37	71.0	15.7	79.4	70.5	73.1					11.1	40.2	9.4	0.0	1.1	0.1	1.0
Mg 435	60	61.2	10.8	62.5	74.1	76.5		78.4			6.6	40.5	6.9	0.0	0.9	0.1	0.5
Mg 436	90	51.2	5.2	25.1	84.3	86.9	1096	103.4	51.7	1.8	2.7	40.5	5.1	0.0	0.8	0.0	0.3
Mg 437	130	47.9	1.5	9.2	85.9	88.5	1064	56.3	42.9	1.7	0.7	40.1	4.0	0.0	0.6	0.0	0.3
Mg 438	160	46.9	0.9	5.6	86.2	89.6	896	41.5	41.0	1.9	0.4	40.5	3.2	0.0	0.5	0.0	1.2
Mg 439	180	45.9	0.8	5.0	86.7	90.2	775	28.0	41.0	1.8	0.4	39.8	2.9	0.0	0.5	0.0	2.7
Mg 420	210	44.3	0.6	4.0	87.3	90.6	669	27.0		1.9	0.3	39.3	2.3	0.0	0.4	0.0	4.9
Mg 408	249	42.5	0.6	3.5	86.4	92.4	479	21.9		2.2	0.3	38.9	1.3	0.0	0.3	0.0	17.0

[16,19] CO = carbonyl content

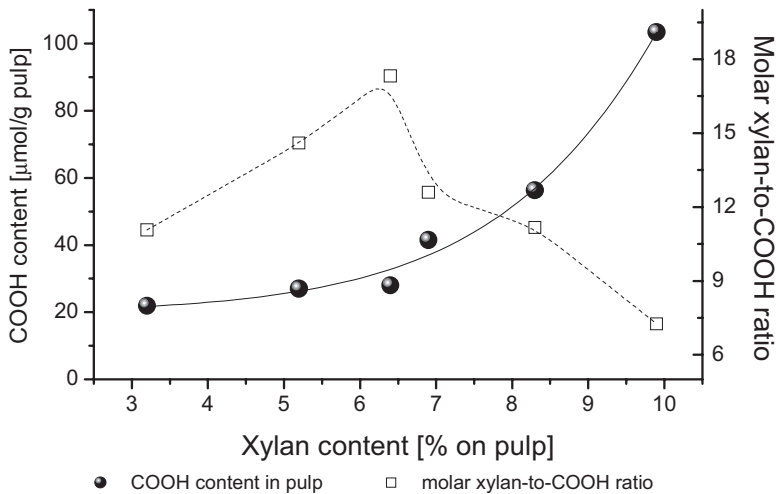


**Fig. 4.163** Course of the pulp yield and pulp viscosity, as well as the main wood components, in the solid phase during acid magnesium sulfite cooking of beech wood [13]. Cooking conditions comprise a total  $\text{SO}_2$

concentration of  $0.76 \text{ mol L}^{-1}$ , a free  $\text{SO}_2$  concentration of  $0.32 \text{ mol L}^{-1}$  free  $\text{SO}_2$ , a liquor-to-wood ratio of 2.4:1, and a cooking temperature of  $148^\circ\text{C}$ .

about 9.1 times as fast as methyl- $\beta$ -D-glucose [15]. Cellulose is, however, significantly more resistant toward acid-catalyzed hydrolysis due to its partly crystalline structure than those figures from model substrates imply. According to the material balance shown in Tab. 4.58 and Fig. 4.163, almost no cellulose is removed until very high H-factors are applied, as are necessary for the production of low-viscosity dissolving pulps.

The comparative ease of degradation of glucan-containing hemicelluloses (e.g., glucomannan) indicates that the supramolecular structure of the carbohydrates exerts a more important influence on the hydrolysis rate as compared to the conformational structure of the polysaccharides. The presence of the 4-O-methyl-D-glucuronic acid side chain of the xylan is known to stabilize the glycosidic bonds towards acid hydrolysis, and this explains the persistence of glucuronic groups during sulfite cooking. Assuming that the content of carboxylic groups in pulp is related to the glucuronic acid side chains of the xylan, it can be shown that the content of the acid side chain is reduced along with the reduction in xylan content. A closer examination of these results shows that the molar ratio xylan-to-carboxylic acid groups is increased significantly, from about 7:1 to 17:1, by reducing the xylan content of the pulp from 10% to 6%. This indicates that, at this stage of sulfite cooking, the glucuronic acid side chains are cleaved from the pulp xylan (Fig. 4.164). As the final stage of the cook is characteristic for dissolving pulp production, the molar ratio xylan-to-carboxylic acid groups decreases again to a value

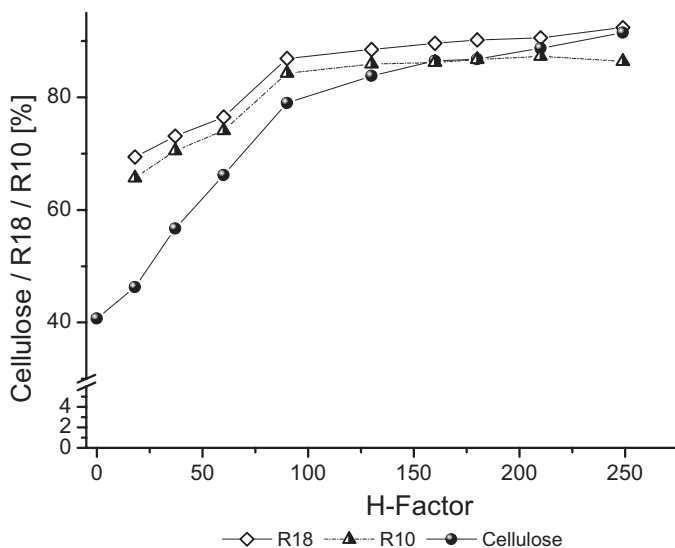


**Fig. 4.164** Carboxylic acid groups in relation to the xylan content of beech dissolving pulps produced by an acid magnesium sulfite process [13]. Cooking conditions comprise a total  $\text{SO}_2$  concentration of  $0.76 \text{ mol L}^{-1}$ , a free  $\text{SO}_2$  concentration of  $0.32 \text{ mol L}^{-1}$  free  $\text{SO}_2$ , a liquor-to-wood ratio of 2.4:1, and a cooking temperature of  $148^\circ\text{C}$ .

of about 11:1, and this can be explained by there being a preferred hydrolysis of xylan with a low degree of substitution.

Carboxylic groups may, however, also be introduced as aldonic acid groups to pulp constituents (e.g., hemicelluloses) by oxidative action of the hydrogen sulfite ions. The conclusion is that the analysis of carboxylic groups alone does not provide an unequivocally clear picture about the course of the glucuronic acid side chain concentration during acid sulfite cooking.

Along with the progress of cooking, the molecular weight of the residual carbohydrate fraction decreases. The cleavage of glycosidic bonds creates new reducing end groups, and this accounts for the increase in carbonyl groups. However, the determination of carbonyl content in the pulp by a new method using fluorescence labeling (with carbazole-9-carboxylic acid; CCOA) [16–19] reveals a reduction in the carbonyl content of pulps as sulfite cooking proceeds from H-factor 60 to about 160. This is most likely due to a disproportionately high dissolution rate of short-chain polysaccharides as compared to the degradation of the solid-phase polysaccharides (see Tab. 4.58). At the very late stage of the sulfite cook, the carbonyl content increases (as determined by the classical copper number method), despite the significant removal of short-chain hemicelluloses. Clearly, additional carbonyl groups along the chains are introduced by oxidative processes. The presence of carbonyl groups within the anhydroglucose unit (AHG) is indirectly demonstrated by an increase in the (hot) alkali solubility of these pulps, and to some extent also by a decreasing R10 content [20]. Following both the residues after a treatment in 10% and 18% NaOH concentration (R10-, R18-contents, respectively) and the cellulose content of the pulp, it can be seen that during the early stages of sulfite cooking (H-factor 20–100) much of the



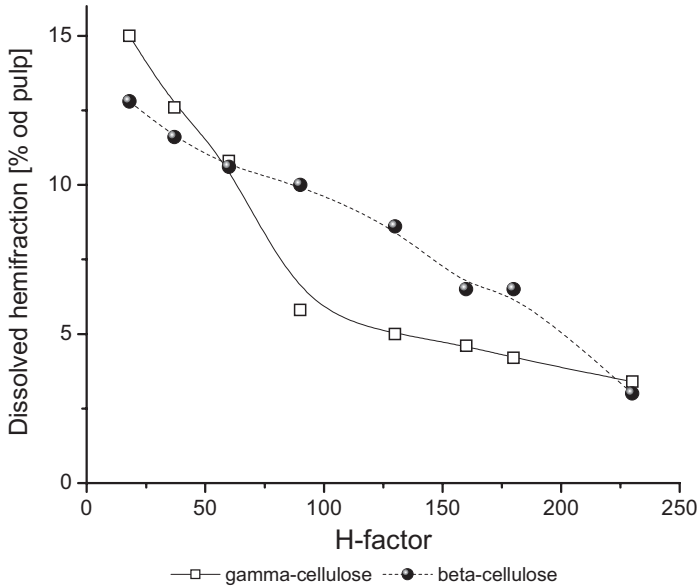
**Fig. 4.165** Course of the alkali resistances, R18 and R10, in relation to the cellulose content of beech dissolving pulps prepared by the magnesium sulfite process [13]. Cooking conditions comprise a total  $\text{SO}_2$  concentration of  $0.76 \text{ mol L}^{-1}$ , a free  $\text{SO}_2$  concentration of  $0.32 \text{ mol L}^{-1}$  free  $\text{SO}_2$ , a liquor-to-wood ratio of 2.4:1, and a cooking temperature of  $148^\circ\text{C}$ .

noncellulosic material resists alkaline treatment, indicating a high molecular weight of the hemicellulose fraction (Fig. 4.165).

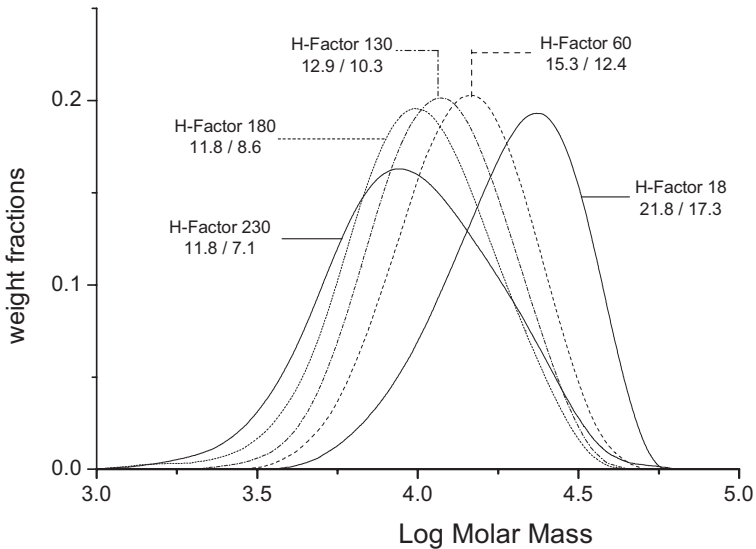
As sulfite cooking proceeds, the gap between the cellulose content and the alkali resistances diminishes. The cellulose content finally exceeds the R10 content of the pulps being produced at H-factors greater than 180. Prolonged cooking leads to a degradation of pulp cellulose, creating increasing fractions of alkali-soluble cellulose. The course of the R18-content parallels the cellulose content, and both parameters become equal after prolonged cooking (H-factor about 250). The good correspondence between the cellulose and the R18 content in sulfite pulps has yet to be confirmed in a detailed study on the quality evaluation of dissolving pulps [21].

Further information regarding the nature of the noncellulosic polysaccharide fraction in the pulp is provided by quantitative characterization of the  $\beta$ - and  $\gamma$ -cellulose fractions. According to the results shown in Fig. 4.166, the removal of  $\gamma$ -cellulose appears to occur with an initial rapid phase, followed by a second slower phase, while the  $\beta$ -cellulose content decreases almost linearly. The rapid removal of the low molecular-weight hemicellulose fraction ( $\gamma$ -cellulose) reflects the high susceptibility of the short-chain amorphous wood polysaccharides towards acid-catalyzed hydrolysis.

The molecular weight of the  $\beta$ -cellulose fraction decreases, whilst at the same time the amount of  $\beta$ -cellulose diminishes. The reduction in molecular weight decreases with increasing cooking intensity, and finally levels off at H-factors higher than 180 (Fig. 4.167). The polydispersity of the  $\beta$ -fraction appears to increase slightly when pulps are subjected to prolonged cooking.

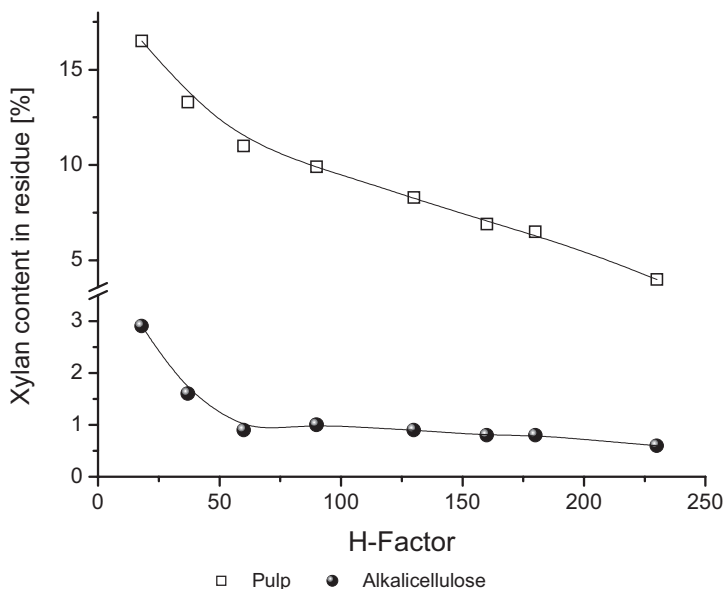


**Fig. 4.166** Course of the  $\beta$ - and  $\gamma$ -cellulose contents of beech dissolving pulps prepared by the magnesium sulfite process [13]. Cooking conditions comprise a total  $\text{SO}_2$  concentration of  $0.76 \text{ mol L}^{-1}$ , a free  $\text{SO}_2$  concentration of  $0.32 \text{ mol L}^{-1}$  free  $\text{SO}_2$ , a liquor-to-wood ratio of 2.4:1, and a cooking temperature of  $148^\circ\text{C}$ .



**Fig. 4.167** Molecular weight distribution of isolated  $\beta$ -cellulose fractions from beech dissolving pulps prepared by the magnesium sulfite process [13]. Numbers in figure represent MW (left) and MN (right), both in [kDa]. Cooking conditions comprise a total  $\text{SO}_2$  concentration of  $0.76 \text{ mol L}^{-1}$ , a free  $\text{SO}_2$  concentration of  $0.32 \text{ mol L}^{-1}$  free  $\text{SO}_2$ , a liquor-to-wood ratio of 2.4:1, and a cooking temperature of  $148^\circ\text{C}$ .



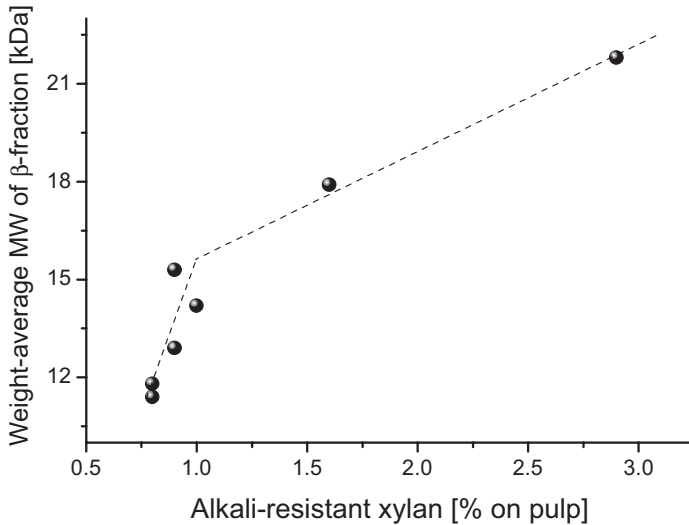


**Fig. 4.168** Course of the xylan content in pulp and regenerated alkali-cellulose derived from dissolving pulps prepared by the magnesium sulfite process [13]. Cooking conditions comprise a total  $\text{SO}_2$  concentration of  $0.76 \text{ mol L}^{-1}$ , a free  $\text{SO}_2$  concentration of  $0.32 \text{ mol L}^{-1}$  free  $\text{SO}_2$ , a liquor-to-wood ratio of 2.4:1, and a cooking temperature of  $148^\circ\text{C}$ .

The high molecular-weight xylan fraction of the wood, which is characterized by the proportion of xylan which is resistant to a treatment in 18 wt% NaOH at  $50^\circ\text{C}$  (steeping lye), is degraded within the first 60 min of sulfite cooking. As cooking proceeds beyond an H-factor of 60, the alkali-resistant xylan content in the pulp levels off and remains constant at approximately 0.8% on pulp (Fig. 4.168). As this amount of xylan is even fiber-forming (and is present in regenerated fibers), it can be assumed that this alkali-resistant xylan fraction is co-crystallized with cellulose and is thus (almost) free of side chains.

The relationship between the amount of alkali-resistant xylan and the molecular weight of the  $\beta$ -cellulose fraction reveals that a certain molecular weight must be exceeded in order for xylan to be characterized as alkali-resistant. This observation is in full agreement with the fiber-forming properties of alkali-resistant xylan (Fig. 4.169).

The amount of carbohydrates dissolved does not correspond to the yield of neutral sugars present in the sulfite spent liquor. Depending on both the composition of the cooking liquor and the cooking intensity, the dissolved carbohydrates undergo further degradation to monosaccharides (neutral sugars), aldonic acids, furfural from pentoses, acetic acid, glucuronic acid and methanol from the cleavage of the side chains and unspecified condensation products with reactive intermediates from dehydration reactions of pentoses [22,23]. In the spent liquor of a



**Fig. 4.169** Weight-average molecular weight of the  $\beta$ -cellulose fraction as a function of the amount of alkali-resistant xylan isolated from beech dissolving pulps prepared by the magnesium sulfite process [13]. Cooking conditions comprise a total  $\text{SO}_2$  concentration of  $0.76 \text{ mol L}^{-1}$ , a free  $\text{SO}_2$  concentration of  $0.32 \text{ mol L}^{-1}$  free  $\text{SO}_2$ , a liquor-to-wood ratio of 2.4:1, and a cooking temperature of  $148^\circ\text{C}$ .

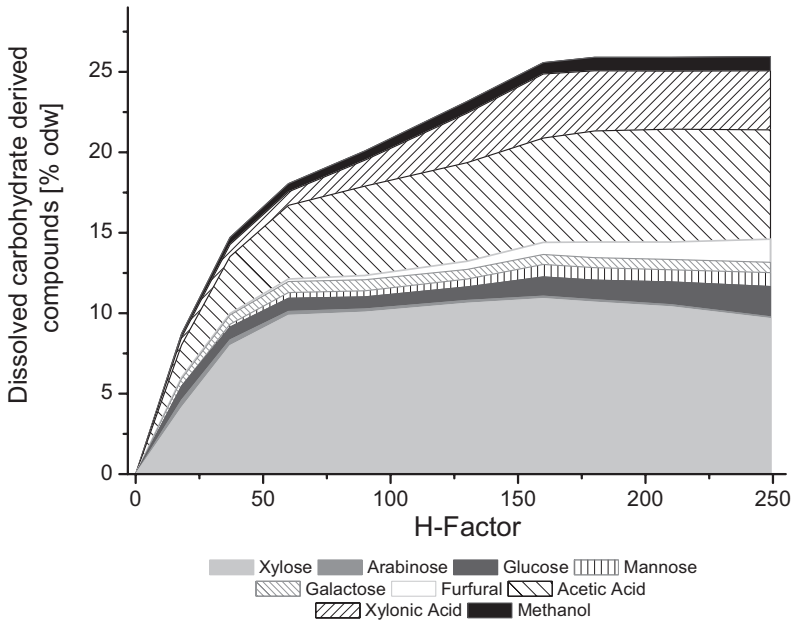
beech paper-grade pulp comprising an H-factor of 90–130, approximately 25% of the dissolved neutral sugars are still present as oligosaccharides (Tab. 4.59).

By further continuing the acid sulfite cook, the remaining oligosaccharides quickly hydrolyze to the corresponding monosaccharides. Therefore, the spent liquor of a typical dissolving cook contains only monosaccharides as neutral sugars (Tab. 4.59). The predominant monosaccharide present in the spent liquor of hardwood cooks (e.g., beech wood) is xylose, as would be expected from the carbohydrate composition of beech wood (see Tab. 4.42). The xylose yield – and also the total amount of dissolved carbohydrate-derived materials – reaches a maximum at an H-factor of 160, which corresponds to a medium- to high-viscosity dissolving pulp (Fig. 4.170).

The decrease in pentose (xylose and arabinose) concentration during the late stages of the cook indicates both the increase in furfural formation and, in addition, the occurrence of acid-catalyzed decomposition reactions to undefined condensation products. The data in Tab. 4.59 confirm the increase in furfural concentration in the spent liquor, but this does not account for the entire amount of xylan removed from the pulp. In contrast to the pentoses, the concentration of hexoses increases slightly as cooking proceeds beyond H-factors of 160. Glucose contributes the highest concentration increase, thus indicating a progressive cellulose degradation in the case of low-viscosity dissolving pulp production. During the early stages of a sulfite cook, aldoses are already oxidized to aldonic acids, with hydrogen sulfite ions serving as the oxidizing agent. In the final cooking phase,

**Tab. 4.59** Characterization of the dissolved wood components and their degradation products in the course of acid magnesium sulfite cooking of beech wood (according to [13]).

Label	H-Factor	Diss. Carboh total [% odw]	Diss. Lignin total [% odw]	Xylose		Arabinose		Glucose		Mannose		Galactose		Furfural	Acetic acid [% odw]	Xyloic acid	Methanol
				mon [% odw]	olig [% odw]	mon [% odw]	olig [% odw]	mon [% odw]	olig [% odw]	mon [% odw]	olig [% odw]						
	0																
Mg 433	18	7.3	6.3	0.2	3.9	0.4	0.0	0.3	0.5	0.0	0.0	0.1	0.4	0.1	2.0	0.4	0.2
Mg 434	37	12.2	13.4	0.9	7.1	0.3	0.0	0.2	0.6	0.0	0.2	0.1	0.5	0.1	3.5	0.8	0.4
Mg 435	60	15.0	17.9	2.7	7.2	0.2	0.0	0.3	0.5	0.0	0.4	0.2	0.4	0.2	4.6	0.8	0.5
Mg 436	90	17.1	21.8	6.0	4.6	0.2	0.0	0.4	0.3	0.1	0.2	0.4	0.3	0.3	5.6	1.6	0.6
Mg 437	130	18.6	23.8	9.0	1.0	0.2	0.0	0.7	0.2	0.4	0.1	0.6	0.0	0.5	6.1	3.1	0.7
Mg 438	160	21.2	24.1	10.8	0.2	0.2	0.0	1.0	0.2	0.5	0.3	0.6	0.0	0.8	6.5	4.0	0.7
Mg 439	180	21.5	24.1	10.7	0.0	0.2	0.0	1.1	0.1	0.6	0.2	0.6	0.0	1.0	6.9	3.7	0.9
Mg 420	210	21.6	24.2	10.4	0.0	0.2	0.0	1.4	0.0	0.8	0.0	0.6	0.0	1.1	7.0	3.6	0.9
M 408	249	21.8	24.2	9.7	0.0	0.1	0.0	1.9	0.0	0.9	0.0	0.7	0.0	1.4	6.8	3.7	0.9



**Fig. 4.170** Course of dissolved carbohydrate derived components present in the spent liquor from beech dissolving pulp production using the magnesium sulfite process [13]. Cooking conditions comprise a total  $\text{SO}_2$

concentration of  $0.76 \text{ mol L}^{-1}$ , a free  $\text{SO}_2$  concentration of  $0.32 \text{ mol L}^{-2}$  free  $\text{SO}_2$ , a liquor-to-wood ratio of 2.4:1, and a cooking temperature of  $148^\circ\text{C}$ .

when the hydrogen sulfite ion concentration is very low, only little or no aldonic acids are formed. Consequently, the amount of combined  $\text{SO}_2$  regulates the yield of the aldonic acid formation. As expected from the carbohydrate composition of the applied wood species, the spent liquor from hardwood cooks contains predominantly xyonic acid, whereas mannonic and xyonic acid are almost equally present in the spent liquor from a softwood sulfite cook. The compositions of both the pulp and spent liquor of dissolving pulp production from spruce and beech wood are listed in Tab. 4.60. This comparison is based on a viscosity of  $700 \text{ mL g}^{-1}$  for both pulps. As the free  $\text{SO}_2$  concentration is approximately 20% lower for the spruce as compared to the beech sulfite cook, the ratio of aldoses-to-aldonic acids is slightly shifted to a higher aldonic acid concentration in case of the former.

**Tab. 4.60** Pulp and spent liquor compositions of both beech and spruce sulfite cooks for the production of a dissolving pulp with an intrinsic viscosity of  $700 \text{ mL g}^{-1}$  (according to [14]).

Parameters	unit	Beech	Spruce
Cooking conditions			
Total $\text{SO}_2$	$\text{mol L}^{-1}$	0.76	0.74
Free $\text{SO}_2$	$\text{mol L}^{-1}$	0.32	0.26
Temperature	$^{\circ}\text{C}$	148	145
H-Factor		191	306
Pulp			
Yield	%	44.9	45.9
Viscosity	$\text{mL g}^{-1}$	700	700
Kappa number		5.0	3.5
R10-content	%	86.6	88.1
R18-content	%	90.8	91.1
Xylan	%	5.5	3.1
Mannan	%	0.4	2.8
Spent liquor			
Xylose	$\text{g kg od w}^{-1}$	100.9	18.4
Mannose	$\text{g kg od w}^{-1}$	7.0	58.1
Glucose	$\text{g kg od w}^{-1}$	8.4	19.8
Galactose	$\text{g kg od w}^{-1}$	4.8	n.d.
Arabinose	$\text{g kg od w}^{-1}$	1.6	0.6
Rhamnose	$\text{g kg od w}^{-1}$	2.8	<0.4
Furfural	$\text{g kg od w}^{-1}$	9.8	2.3
Acetic acid	$\text{g kg od w}^{-1}$	61.7	26.8
Xyloic acid	$\text{g kg od w}^{-1}$	29.6	15.5
Mannonic acid	$\text{g kg od w}^{-1}$	<0.5	20.2

n.d. = not determined.

The total hemicellulose content is equal for both pulps. However, the xylan-to-mannan ratio changes during spruce sulfite cooking from 0.55:1 in the wood to 1.1:1 in the pulp. This change in carbohydrate ratio is also reflected in the spent liquor composition, where the xylose-to-mannose ratio comprises a value of 0.32:1, indicating a higher resistance of the arabinoxylan as compared to the glucomannan towards acid hydrolysis. The lower furfural and acetic acid concentrations in the spent liquor of the spruce acid sulfite cook can be attributed to both the lower amount of pentoses and acetyl groups substituted at the C-2 and C-3 positions in mannose and glucose units of the glucomannan in spruce.

#### 4.3.5.2 Influence of Reaction Conditions

Knowledge of the chemistry and technology of sulfite pulping up to the year 1965 has been reviewed in detail by Rydholm [20]. In the following sections, only the most recent data relating to sulfite pulping are presented, with the main focus centered on dissolving pulp manufacture.

##### 4.3.5.2.1 Wood Species

The wood raw material has a decisive influence on the processability and final pulp quality. The heterogeneous nature of the wood structure and the chemical and physical differences between and within wood species are reflected in all pulping processes. Acid sulfite pulping technology is known to be the most sensitive process to the properties of the wood raw material, and many softwood species – and also some hardwoods – are considered to be less suited to acid sulfite pulping. The deficiencies involved with acid sulfite pulping of, for example pines or larches, are high screenings, a high residual lignin content, and thus a low screened yield. The poor pulping results are connected with either the presence of certain extractives in the wood, especially in the heartwood, or limited impregnation due to a dense wood structure. It has been found that phenolic resins – such as pinosylvin in pine heartwood or taxifolin in Douglas fir – react with lignin in acid sulfite liquors to form a condensation product that prevents delignification [24–27]. Moreover, taxifolin tends to reduce hydrogen sulfite ions to thiosulfate ions, thereby decreasing the stability of the sulfite cooking liquor [28].

Subsequently, much effort has been undertaken to modify the sulfite cooking process to overcome the problems encountered with the use of resinous wood. It was found that pretreatment of the wood with a sulfite cooking liquor of moderate acidity, as with a pure hydrogen sulfite solution, and low temperature will favor sulfonation of the reactive groups of the lignin over condensation reactions with the phenolic resins. Another prerequisite of selective sulfonation comprises an efficient pressure impregnation. This initial sulfonation stage is then followed by a conventional acid sulfite cook at temperatures and H-factors selected according to the grade desired. Hence, two-stage sulfite pulping with a preceding sulfonation stage at low acidity or even neutral pH conditions makes possible the use of pines and larches.

In the case of conventional and more simple one-stage acid sulfite pulping processes, only a limited amount of wood species can be used. Most appropriate are hardwoods with low resin contents and high density such as beech wood (*Fagus sylvatica*) and certain eucalyptus species (*E. globulus*, *E. saligna*, *E. urograndis*, etc.). Dense hardwoods with a low lignin content are favorable because of the high specific pulp yield related to the volume of the digester. Replacing spruce with, for example beech wood, results in an almost 50% higher yield at a given digester volume (280 kg o.d. beech versus 190 kg o.d. spruce per m<sup>3</sup> digester, respectively).

In the following section, four representative hardwoods – beech (*Fagus sylvatica*), aspen (*Populus tremulus*), eucalypt (*E. globulus*) and birch (*Betula pendula*) and one softwood species, spruce (*Picea abies*) – which together constitute the most important wood raw material for acid sulfite pulping, are evaluated comparatively with respect to their processability and unbleached pulp quality.

The chemical composition of the wood determines very important parameters such as pulp yield and pulp properties. The purity of dissolving pulps is governed by the content of noncellulosic carbohydrates and other impurities such as resins or inorganic components of the wood raw material used.

Chemical analysis of the hardwood samples reveals high glucan and low xylan contents for aspen and eucalypt. The low glucan and high xylan contents of birch and beech, however, indicate low cellulose yield at high residual xylan contents in the resulting dissolving pulps. Among the hardwood species, aspens shows a surprisingly high mannose content. Spruce, as the only representative of softwoods in this comparison, contains a relatively high glucan content and, together with eucalypt, the lowest amount of hemicelluloses among the species investigated. The hardwoods are characterized by a low and rather constant Klason lignin content ranging from 18.9% to 21.0%, and by a high acid-soluble lignin content, with the highest value by far determined for eucalypt. The low lignin content of the hardwoods indicates a more efficient delignification as compared to spruce at given cooking conditions.

The highest DCM-extractives contents were measured for birch and aspen, but this may relate to a pitch problem during further processing of the corresponding unbleached pulps.

Based on the chemical analysis of the main wood components, the highest cellulose yields and cellulose purities can be expected for aspen and eucalypt. The results of the chemical analysis of selected wood chips are detailed in Tab. 4.61 (see also Tab. 4.49).

The introduced five wood species were subjected to one-stage acid sulfite pulping according to the procedure described in Section 4.3.5.1 (see also Fig. 4.157). The cooking conditions applied namely the impregnation procedure, the cooking acid composition, the liquor-to-wood ratios and the maximum cooking temperatures were identical for beech, aspen, and eucalypt and comparable for spruce and birch (Tab. 4.62). The slightly different cooking acid compositions in the case of birch and spruce can be classified as rather insignificant with respect to their ion product,  $[H^+] \cdot [HSO_3^-]$ , which determines the rate of delignification.

**Tab. 4.61** Chemical composition of beech, aspen, eucalyptus, birch and spruce as used for the cooking experiments (according to [14]).

	<b>Beech</b> <i>Fagus sylvatica</i>	<b>Aspen</b> <i>Populus tremulus</i>	<b>Eucalypt</b> <i>E. globulus</i>	<b>Birch</b> <i>Betula pendula</i>	<b>Spruce</b> <i>Picea abies</i>
Carbohydrates	72.8	75.2	71.8	73.6	70.0
Glucose	42.6	49.9	48.1	39.7	45.7
Xylose	19.5	15.9	14.5	22.1	6.6
Arabinose	0.7	0.1	0.5	0.5	1.0
Galactose	0.8	0.4	1.5	1.0	1.6
Mannose	1.1	2.6	0.5	1.3	12.0
Rhamnose	0.5	0.1	0.5	0.3	
Acetyl	4.5	3.7	3.4	5.1	1.4
Uronic acid	3.1	2.5	2.7	3.5	1.8
Lignin	24.5	22.0	26.2	23.3	27.2
Klason	21.0	18.9	20.6	19.7	27.0
Acid-soluble	3.5	3.1	5.6	3.6	0.2
Extractives	1.8	1.0	0.2	1.9	1.0
DCM	0.2	1.0	0.2	1.9	1.0
Et-OH	1.6		n.a.	n.a.	n.a.
Ash	0.4	0.3	0.3	0.3	0.2
Total	99.5	98.5	98.5	99.0	98.5

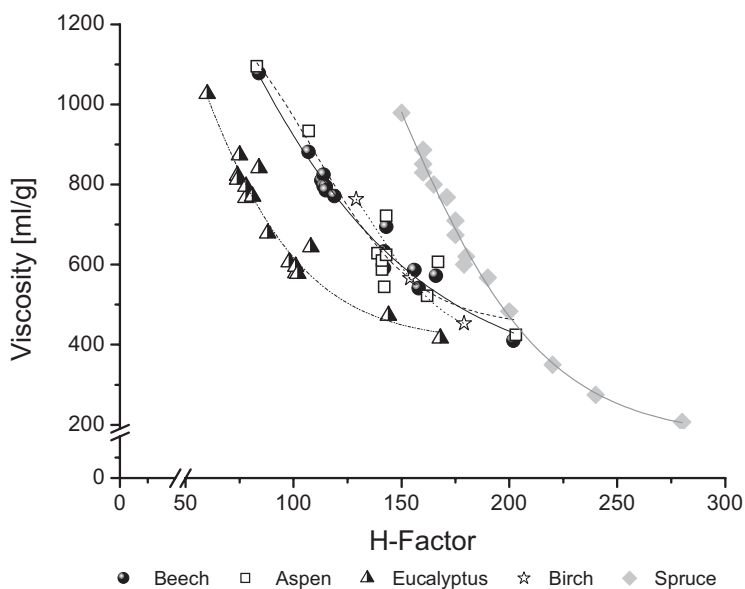
n.a. = not applicable.

The main target parameter for dissolving pulp production is the average molecular weight of the polysaccharide fraction, expressed as the CED-intrinsic viscosity; this was adjusted solely by the H-factor. All other parameters were kept constant. The relationships between viscosity and H-factor indicate the depolymerization behavior of the investigated wood species, which is an important criterion in case of blending of wood chips. The data in Fig. 4.171 show that beech, aspen and birch show virtually the same degradation characteristics, whereas (surprisingly) eucalyptus is ahead and spruce behind their course of viscosity degradation. The higher resistance towards cellulose degradation of spruce can be explained by its higher lignin content.



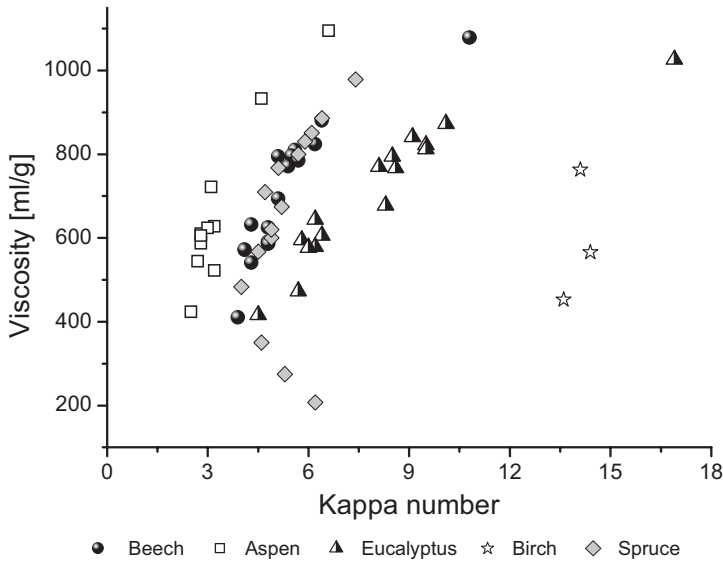
**Tab. 4.62** Important cooking parameters applied in the course of one-stage acid sulfite cooking of beech, aspen, eucalyptus, birch and spruce (according to [14]).

Wood species	$\Sigma\text{SO}_2$ [mol L <sup>-1</sup> ]	Free $\text{SO}_2$ [mol L <sup>-1</sup> ]	$[\text{H}^+]^2[\text{HSO}_3^-]$ at 25 °C, t = 0	l:s ratio	Temperature [°C]
Beech	1.04	0.68	0.0104	2.7	138
Aspen	1.05	0.69	0.0105	2.7	138
Eucalypt	1.05	0.68	0.0104	2.7	138
Birch	0.88	0.51	0.0078	2.5	145
Spruce	1.07	0.59	0.0091	3.2	145



**Fig. 4.171** Impact of H-factor during one-stage acid sulfite cooking of beech, aspen, eucalyptus, birch, and spruce on the viscosity of the unbleached pulps (according to [14]). For cooking conditions, see Tab. 4.62.

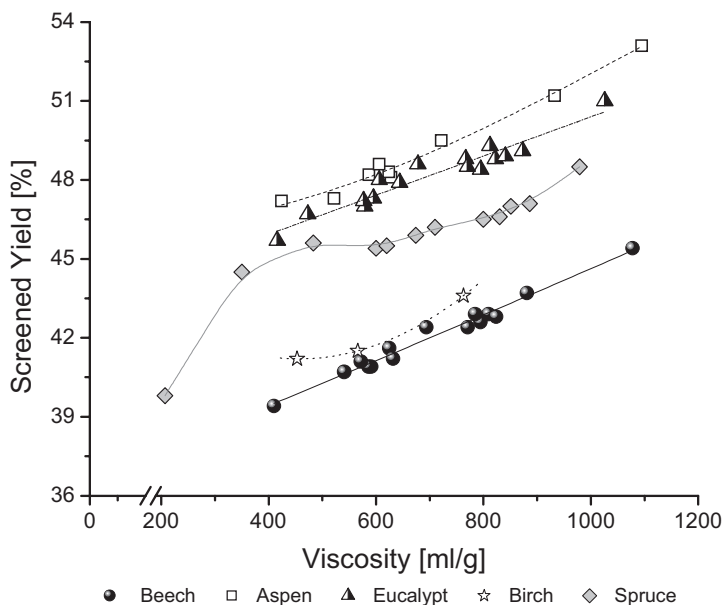
Among the wood species investigated, aspen shows by far the best delignification selectivity (expressed in terms of viscosity–kappa number relationship), followed by spruce, beech, eucalyptus and, at some distance, birch (see Fig. 4.172).



**Fig. 4.172** Delignification selectivity illustrated as viscosity–kappa number relationship of unbleached acid sulfite pulps made from beech, aspen, eucalyptus, birch, and spruce (according to [14]). For cooking conditions, see Tab. 4.62.

The limited extent of the delignification of birch wood may be attributed to a dense wood structure and the high content of extractives which can generate cross-links with lignin during acid sulfite pulping, thereby inhibiting the delignification. The fines contain a disproportionately high lignin and extractives content. Thus, removal of the fine fibers from pulp decreases the resin content of the remaining pulp [29]. The residual kappa number is unexpectedly high in the case of eucalyptus. It can be assumed that – at the given pulping conditions – the ratio of hydrolysis to sulfonation reactions is slightly shifted to the former in the case of eucalyptus. This assumption is also supported by the low degree of sulfonation, which amounts only 0.60 S/OCH<sub>3</sub> for eucalyptus in comparison to 0.73 for beech and even 0.88 for aspen, respectively. Another reason for the impaired delignification selectivity might be the accelerated cellulose degradation due to a better accessibility as compared to the other wood species.

The screened yields at given kappa numbers are highest for aspen pulp, followed by eucalyptus, spruce and with relatively clear distance beech and birch. This can be expected, as the pulp yields are in proportion to the glucan content of the respective wood species. The dependence of screened yield on kappa number is shown graphically in Fig. 4.173. Viscosity degradation during the final cooking phase is clearly connected to yield losses. The slopes of the viscosity dependent upon yield losses were comparable for all wood species investigated, and ranged from 0.7% to 0.9% per reduction of 100 intrinsic viscosity units (mL g<sup>-1</sup>).

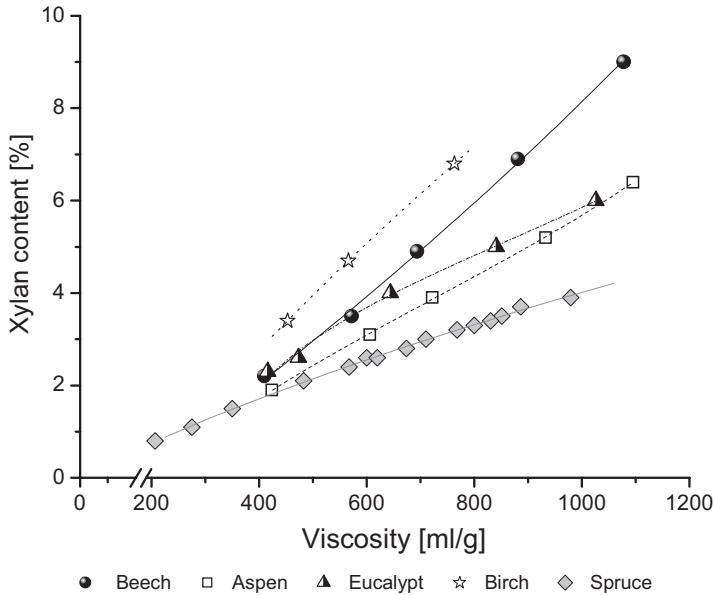


**Fig. 4.173** Screened yield as a function of viscosity of the unbleached acid sulfite pulps made from beech, aspen, eucalyptus, birch, and spruce (according to [14]). For cooking conditions, see Tab. 4.62.

As the quality of dissolving pulps is closely related to its impurities, the content of noncellulosic carbohydrates (originating from the wood hemicelluloses) in relation to pulp viscosity is an important criterion for dissolving pulp production. Xylan, the predominant hemicellulose in hardwoods, is thus related to the viscosity of the unbleached pulps (Fig. 4.174). However, at a target pulp viscosity (e.g.,  $700 \text{ mL g}^{-1}$ ), the xylan contents of the unbleached pulps are not exactly in proportion to the xylan contents of the respective wood species. The eucalypt pulp contains a higher xylan content compared to the aspen pulp, possibly due to both an accelerated cellulose degradation and a more resistant xylan of the former. Indeed, a slightly higher uronic acid content of the xylan backbone of the eucalypt xylan may be responsible for the less reactive  $\beta$ -1,4-glycosidic bonds within the xylan polymer [30,31]. Furthermore, the xylan content in the spruce pulp is higher in relation to the xylan contents of the hardwood pulps and, as would have been expected, from the xylan content in the wood.

The recovery of wood-based by-products being dissolved in the cooking liquor becomes an increasingly important criterion for the evaluation of modern pulping technologies. The results can be interpreted as a mirror-image of unbleached pulp yields – the higher the unbleached pulp yield, the lower the yield of carbohydrate-derived by-products.

The cooking liquors from hardwood acid sulfite pulping are dominated by the degradation products derived from pentosans such as xylose, arabinose, xylonic

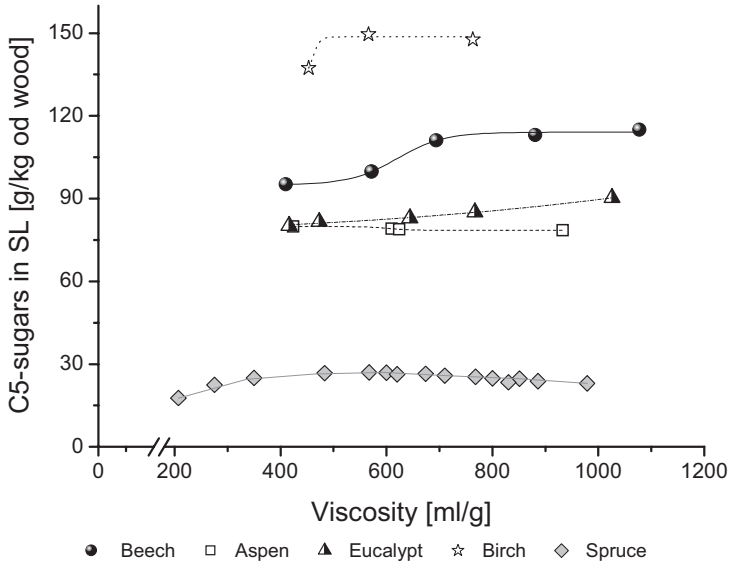


**Fig. 4.174** Xylan content as a function of viscosity of the unbleached acid sulfite pulps made from beech, aspen, eucalyptus, birch, and spruce (according to [14]). For cooking conditions, see Tab. 4.62.

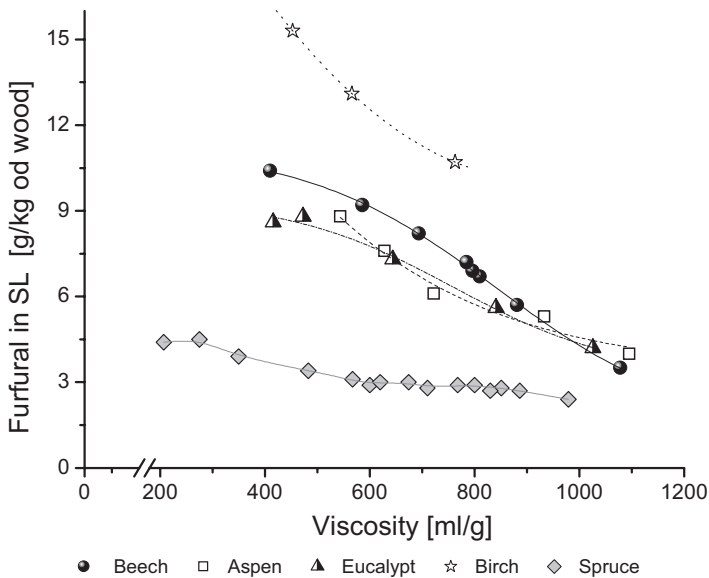
acid, and furfural. Furthermore, they also contain appreciable quantities of acetic acid. At a given acid composition, the release of pentoses (C5-sugars) is clearly dependent upon the H-factor and thus also on pulp viscosity. With prolonged cooking, a slight reduction in the pentose content of the spent liquor is observed due to further degradation reactions (Fig. 4.175), (see Scheme 4.30). The amount of pentoses present in the spent liquor is clearly proportional to the xylan content in the wood (see Tab. 4.61). Consequently, the highest yield of pentoses (xylose) is obtained with birch as a wood raw material, followed by beech, eucalypt, aspen and, at a clear distance, spruce.

The formation of furfural, derived from acid-catalyzed dehydration of pentoses, depends on both the xylan content in the wood and the cooking conditions during acid sulfite pulping (Fig. 4.176). The increase in furfural concentration with prolonged cooking is more pronounced for hardwoods than for spruce, though this may be related to the xylose concentration in the spent liquors.

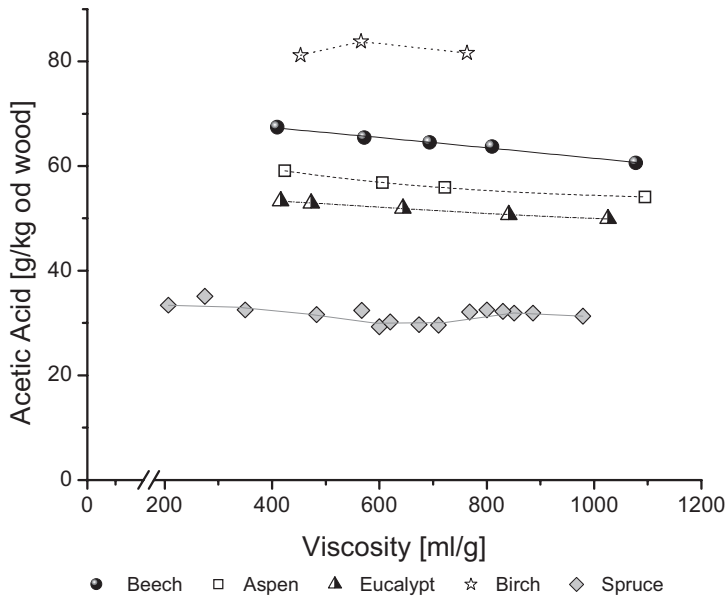
The release of acetic acid occurs during the early stages of the cook. Thus, the concentration of acetic acid in the spent liquor appears to be somewhat independent of the cooking conditions, and is directly related to the acetyl content in the respective wood species (Fig. 4.177).



**Fig. 4.175** Pentoses (C5-sugars) in spent liquor (SL) as a function of viscosity of the unbleached acid sulfite pulps made from beech, aspen, eucalyptus, birch, and spruce (according to [14]). For cooking conditions, see Tab. 4.62.



**Fig. 4.176** Furfural formation in spent liquor (SL) as a function of viscosity of the unbleached acid sulfite pulps made from beech, aspen, eucalyptus, birch, and spruce (according to [14]). For cooking conditions, see Tab. 4.62.



**Fig. 4.177** Acetic acid content in spent liquor as a function of viscosity of the unbleached acid sulfite pulps made from beech, aspen, eucalyptus, birch, and spruce (according to [14]). For cooking conditions, see Tab. 4.62.

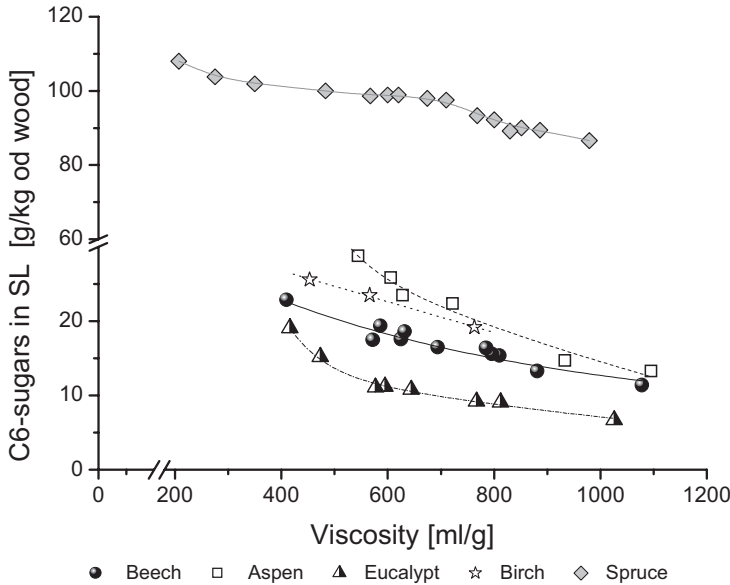
Both furfural and acetic acid are steam-volatile compounds, and thus can be recovered from the enriched evaporated condensates by liquid-liquid extraction, followed by multi-stage distillation [32].

The acid sulfite spent liquors from softwoods predominantly contain hexoses, as would be expected from the composition of their hemicelluloses. The prevailing hexose in the spent liquor is mannose in a ratio to glucose significantly higher (2.9:1) as compared to the composition in the wood (1.8:1). The higher xylan retention in softwood pulp supports this observation. Among the hardwoods, aspen releases the greatest amounts of hexoses in the spent liquor, mainly because of the high mannose content. Figure 4.178 shows an increase in the amount of hexoses with decreasing viscosity which can be substantiated by progressive cellulose degradation. The traditional use of hexoses from softwood sulfite spent liquors is that of fermentation to ethyl alcohol. Before fermentation, sulfur dioxide must be removed from the liquor to prevent inhibition of the yeast (*Saccharomyces cerevisiae*). Assuming the formation of 2 mol ethanol per mol removed hexose, up to 4–5% of ethanol (based on o.d. wood) can be produced.

A complete material balance, including both the pulp and the spent liquor composition of magnesium acid sulfite pulping of the selected five wood species, is provided in Tab. 4.63. For better comparison, the yields of pulp and spent liquor constituents are adjusted to cooking conditions appropriate for a pulp viscosity of 700 mL g<sup>-1</sup>.

Tab. 4.63 Material balance for a typical one-stage acid sulfite cook of five selected wood species (according to [14]).

Wood species	Reaction conditions				Pulp characterization						Spent liquor characterization										
	TotSO <sub>2</sub> [mol L <sup>-1</sup> ]	Free SO <sub>2</sub> [H <sup>+</sup> ][HSO <sub>3</sub> ]	H-Factor	Scr. yield [%]	Reject [%]	Kappa number	Viscosity [mL·g <sup>-1</sup> ]	Bright-ness [% ISO]	Pentosan [%]	Mannan [%]	R 10 [%]	R 18 [%]	DCM extract [%]	Xyl [%]	Man [%]	Glu [%]	Ara [%]	Furf [%]	HOAc [%]	XyLA [%]	
Beech	1.04	0.66	1.04E-02	135	42.0	0.05	5.3	700	59.0	5.0	87.0	91.6	0.3	104.2	6.2	10.9	1.6	6.0	64.4	40.3	
Aspen	1.05	0.69	1.05E-02	137	49.2	0.04	3.2	700	70.0	3.7	87.0	91.6	0.9	79.5	12.4	9.9	1.0	7.0	56.6	31.4	
Eucalypt	1.05	0.66	1.04E-02	66	46.2	0.04	7.2	700	57.6	4.3	85.8	92.2	0.3	62.5	4.1	5.7	1.5	6.7	51.5	26.1	
Birch	0.66	0.51	7.77E-03	137	43.0	0.03	14.2	700	46.0	6.1	86.6	90.2	2.6	145.6	7.0	13.6	2.1	11.5	62.0	35.1	
Spruce	1.07	0.59	9.06E-03	171	46.4		4.9	700	61.5	2.9	3.6	87.8	91.1	0.5	24.6	72.2	23.2	1.6	2.9	30.9	19.4

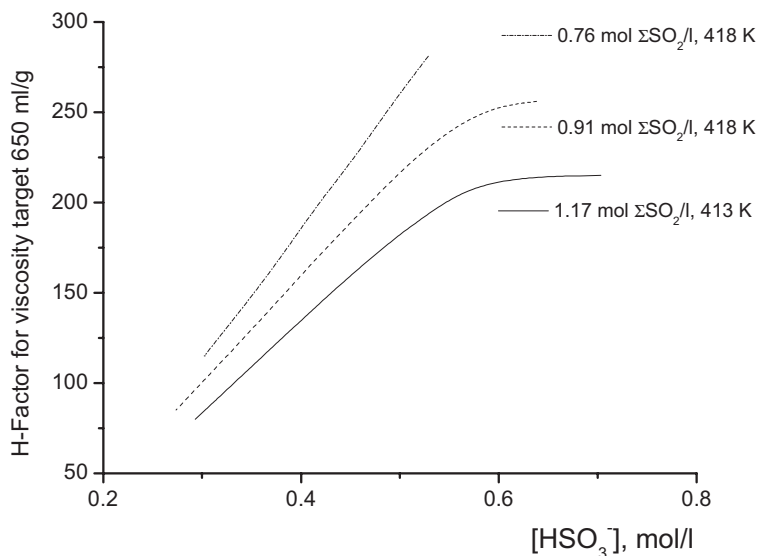


**Fig. 4.178** Content of hexoses (sum of mannose and glucose) in spent liquor as a function of viscosity of the unbleached acid sulfite pulps made from beech, aspen, eucalyptus, birch, and spruce (according to [14]). For cooking conditions, see Tab. 4.62.

#### 4.3.5.2.2 Cooking Conditions

For a given wood species, the cooking conditions determine pulp yield, pulp quality, and the composition of the spent liquor. In acid sulfite pulping the main process parameters are specified by the composition of the cooking liquor in combination with the temperature and the H-factor (cooking intensity). The acidity of the cooking liquor expressed in terms of the free  $\text{SO}_2$  concentration determines both the rate of lignin removal (proportional to the ion product,  $[\text{H}^+] \cdot [\text{HSO}_3^-]$ ) [33] and the extent of cellulose degradation (proportional to  $[\text{H}^+]$ ). At a given total  $\text{SO}_2$  concentration the acidity of the cooking liquor is controlled by the hydrogen sulfite ion concentration (combined  $\text{SO}_2$ , proportional to the base concentration). The latter must be kept above a certain limit in order to prevent uncontrolled condensation reactions due to the formation of strong acids. Lignin condensation leads to an increase in the kappa number, a significant reduction in brightness, a decrease in the homogeneity of delignification, and impaired bleachability. In serious cases, the pulp is completely blackened and destroyed (black cooks). Kaufmann has established a fairly clear picture where the transition from normal to black cooks can be drawn as a function of total and combined  $\text{SO}_2$  concentration in the cooking liquor (see also Fig. 4.155) [10]. The tolerable content of combined  $\text{SO}_2$  can be shifted to lower levels by simultaneously increasing the total  $\text{SO}_2$  concentration. Furthermore, low cooking temperatures also allow the adjustment of



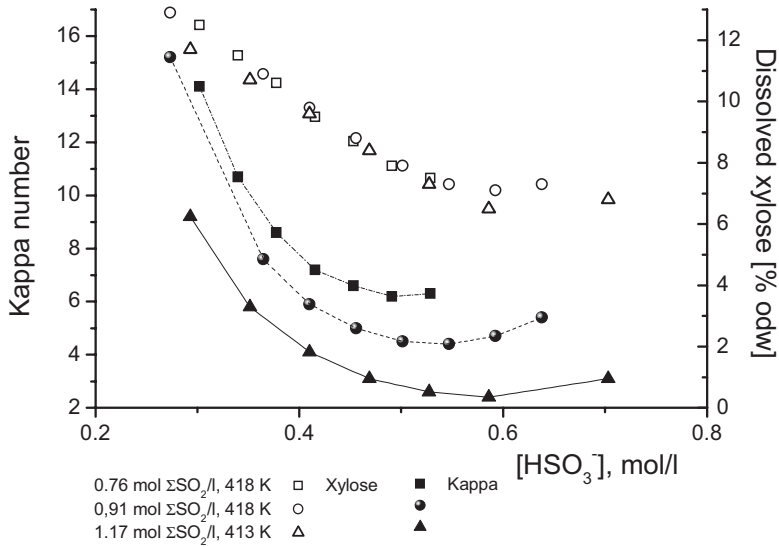


**Fig. 4.179** Hydrogen sulfite ion concentration at three different levels of total  $\text{SO}_2$  concentrations as a function of H-factor necessary to obtain a target viscosity of  $650 \text{ mL g}^{-1}$  during the course of acid magnesium bisulfite pulping of beech wood (according to [34]). The pressure relief was at 8.5 bar (abs) during cooking.

lower levels of hydrogen sulfite ion concentrations. On the other hand, the rate of delignification will decrease on increasing the combined  $\text{SO}_2$ , unless the total  $\text{SO}_2$  is increased simultaneously to keep the free  $\text{SO}_2$  concentration at a constant level. A decrease in the acidity of the cooking liquor can be compensated by an increase in temperature (and thus H-factor) to keep the cooking time within a given limit. The relationship between the hydrogen sulfite ion concentration at different total  $\text{SO}_2$  concentration levels and the required H-factor to obtain a certain target viscosity (e.g.,  $650 \text{ mL g}^{-1}$ ) is illustrated graphically in Fig. 4.179.

The data in Fig. 4.179 illustrate the significant influence of the acidity on the reaction time. Reducing the hydrogen sulfite ion concentration from  $0.6$  to  $0.4 \text{ mol L}^{-1}$  at a given total  $\text{SO}_2$  concentration of  $0.91 \text{ mol L}^{-1}$  results in a reduction of cooking time by more than half (from 330 min to 160 min), provided that the temperature is kept constant at  $145^\circ\text{C}$ . The selectivity of delignification is known to be improved with increasing hydrogen sulfite ion concentration, according to Eq. (179). This simple relationship is confirmed to a large extent by the results of acid magnesium sulfite cooks of beech wood, as illustrated in Fig. 4.180.

According to the predictions of Kaufmann, the delignification becomes more selective when increasing the total  $\text{SO}_2$  concentration at a given level of hydrogen sulfite ion concentration [10]. Interestingly, an optimum delignification selectivity exists for each cooking acid composition. The minimum kappa number is slightly shifted to higher hydrogen sulfite ion concentrations in case of increasing total  $\text{SO}_2$  concentration. Clearly, a certain amount of free  $\text{SO}_2$  seems to be necessary to



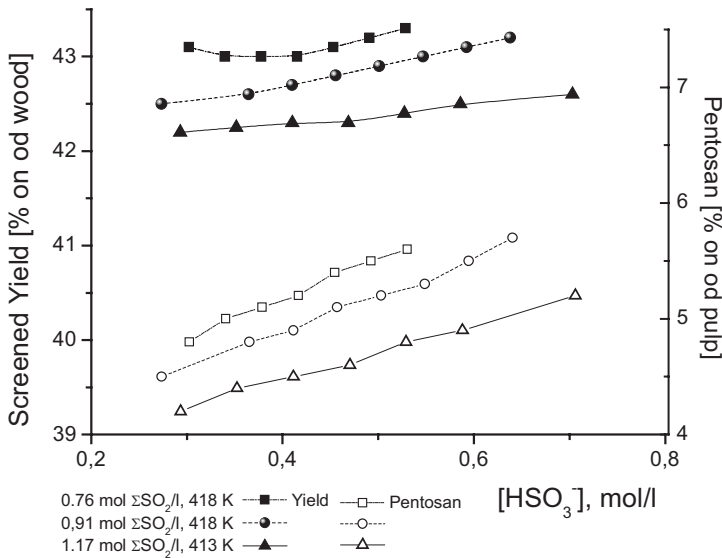
**Fig. 4.180** Kappa number of unbleached acid magnesium bisulfite dissolving pulps made from beechwood with a pulp viscosity of  $650 \text{ mL g}^{-1}$ , and the corresponding specific amount of xylose present in spent liquor as a function of hydrogen sulfite ion concentration at three different levels of total  $\text{SO}_2$  concentration (according to [34]). Pressure relief at  $8.5 \text{ bar (abs)}$  during cooking.

obtain a selective lignin separation under the prevailing conditions investigated (wood species, target viscosity, cooking temperature, liquor-to-wood ratio). In accordance with the results of Kaufmann, the use of cooking liquors with hydrogen sulfite ion concentrations below  $0.32 \text{ mol L}^{-1}$  ( $0.38 \text{ mol L}^{-1}$ ) corresponding to a total  $\text{SO}_2$  concentration of  $1.2 \text{ mol L}^{-1}$  ( $0.76 \text{ mol L}^{-1}$ ) should be strictly avoided. As previously stated, xylose (originating from beech wood) becomes oxidized to xylonic acid by hydrogen sulfite ions. This oxidation reaction is by far the most prominent side reaction responsible for the destruction of reducing sugars (see Tab. 4.63). Consequently, the xylose content in spent liquor is directly related to the hydrogen sulfite ion concentration, at least over a certain concentration range ( $0.28$  to  $0.6 \text{ mol L}^{-1}$ ).

The production of dissolving pulps with a low content of hemicelluloses (xylan in the case of hardwood pulps) at a target pulp viscosity (e.g.,  $650 \text{ mL g}^{-1}$ ) can be accomplished by both increasing the total amount of  $\text{SO}_2$  at a given amount of combined  $\text{SO}_2$ , or by reducing the combined  $\text{SO}_2$  at a given total amount of  $\text{SO}_2$ , as illustrated in Fig. 4.181.

The influence of the cooking liquor composition on cellulose lignin-free yield at a given pulp viscosity is very limited. Considering the increasing residual lignin content of pulps produced with decreasing hydrogen sulfite ion concentrations, a slight trend in cellulose yield reduction can be observed.

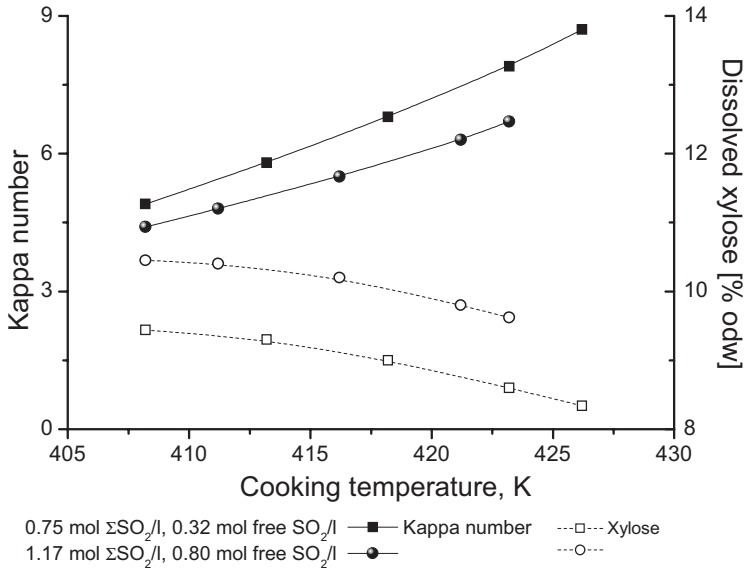
The choice of cooking temperature influences the rates of delignification and cellulose degradation, and determines the productivity of pulp production to a



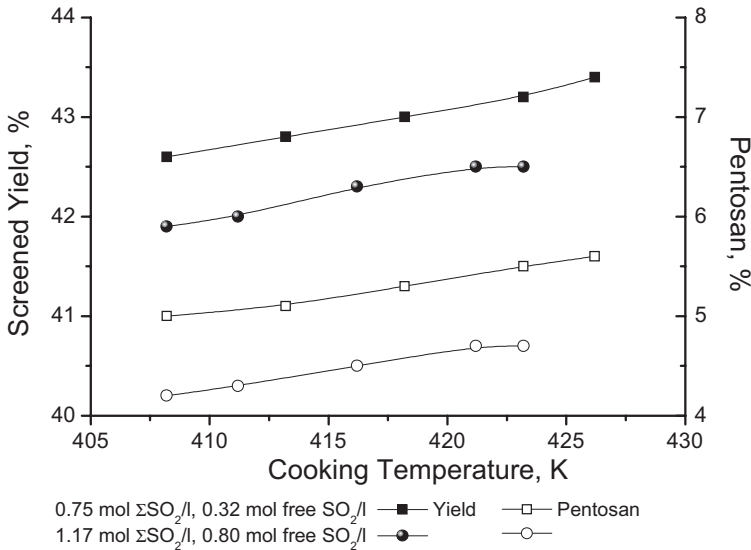
**Fig. 4.181** Screened yield and xylan content of unbleached acid magnesium bisulfite dissolving pulps made from beech wood with a pulp viscosity of  $650 \text{ mL g}^{-1}$  as a function of hydrogen sulfite ion concentration at three different levels of total  $\text{SO}_2$  concentration (according to [34]). Pressure relief at 8.5 bar (abs) during cooking.

significant degree. An increase in cooking temperature negatively affects both delignification and purification selectivity (removal of xylan in case of hardwood pulp). As shown in Fig. 4.182, the kappa number increases by approximately two units (from 4.6 to 6.6) when increasing the temperature from 410 K (137 °C) to 423 K (150 °C) at a pulp viscosity of  $650 \text{ mL g}^{-1}$ , considering the cooking acid with  $1.17 \text{ mol L}^{-1}$  total  $\text{SO}_2$ . At the same time, the xylose content in the spent liquor decreases by about 0.8% on o.d. wood, which corresponds to almost 8% of the initial value, and this is an indication of preferred side reactions. Although the temperature-dependence of the hemicellulose degradation rate is said to be stronger than that of cellulose degradation, according to the literature an increase in temperature favors cellulose degradation, as shown in Fig. 4.183 [20]. The lower purification selectivity with increasing temperature may be explained by the greater difficulty in removing the less-accessible xylan and the decreasing ratio xylan-to-cellulose towards the end of the cook. The higher residual pentosan content is, however, compensated by the higher total yield. This clearly confirms that cellulose degradation is favored over pentosan removal.

The increase in temperature of the specified range, however, accelerates the pulping reactions by a factor of 2.9, which is a significant contribution to pulping economy (H-factor ratio of  $71.1/24.5 = 2.9$  for 423 K and 410 K, respectively). In industrial practice, a compromise between cooking productivity, pulp quality and process stability must be found to optimize the production economy. A further acceleration of pulping reactions may be achieved by an increase in the digester pressure [20].



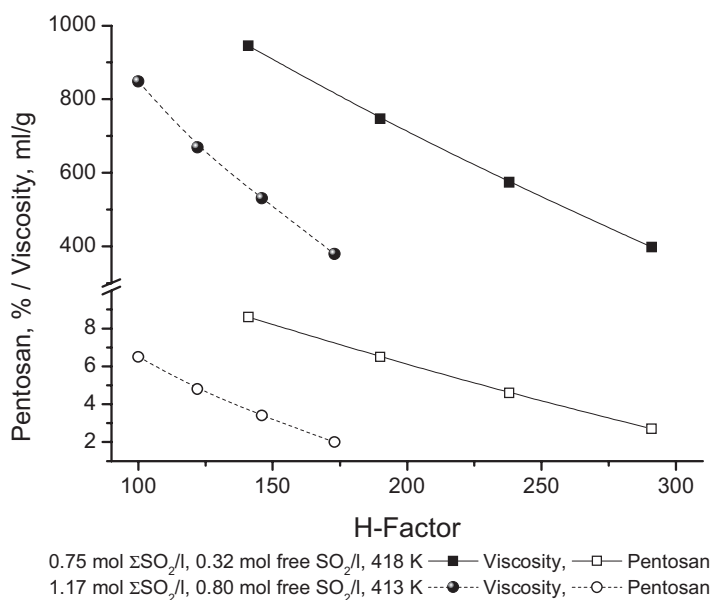
**Fig. 4.182** Kappa number of acid magnesium bisulfite dissolving pulps made from beech wood with a pulp viscosity of 650 mL g<sup>-1</sup> and the xylose content in the spent liquor as a function of cooking temperature at two different levels of total SO<sub>2</sub> concentration (according to [34]). Pressure relief at 8.5 bar (abs) during cooking



**Fig. 4.183** Screened yield and pentosan content of acid magnesium bisulfite dissolving pulps made from beech wood with a pulp viscosity of 650 mL g<sup>-1</sup> as a function of cooking temperature at two different levels of total SO<sub>2</sub> concentration (according to [34]). Pressure relief at 8.5 bar (abs) during cooking.

In industrial practice, attempts are made to keep both the composition of the cooking acid and cooking temperature at a preset level. The natural variations in wood quality (e.g., moisture content, degree of debarking, differences in storage time, different proportions in case of blending of wood species, etc.), the slight changes in cooking acid composition, and the changing steam availability – all of which influence the unbleached pulp properties (e.g., viscosity in the case of dissolving pulp and kappa number in the case of paper-grade pulp) – are compensated for by H-factor adjustment, including end-point determination by liquor analysis. H-factor control is also applied when producing dissolving pulps of different viscosity levels by utilizing the clear relationship between H-factor and pulp viscosity at a given cooking liquor composition and temperature (Fig. 4.184). Parallel to the decrease in viscosity, a reduction in pentosan content and a yield loss of about 0.9% per  $\Delta 100 \text{ mL g}^{-1}$  are observed (for comparison, see Fig. 4.173). Pentosan removal accounts for approximately 50% of the overall yield loss ( $\Delta 1\%$  of pentosan on o.d. pulp per  $\Delta 100 \text{ mL g}^{-1}$  viscosity reduction at a wood yield of about 42%, which is equal to 0.42% yield loss per  $\Delta 100 \text{ mL g}^{-1}$ ).

In the case of producing very low-viscosity pulps, the cooking temperature is appropriately adjusted to compensate for prolonged cooking.



**Fig. 4.184** Viscosity and pentosan content of acid magnesium bisulfite dissolving pulps made from beech wood as a function of H-factor for two different levels of total  $\text{SO}_2$  concentration (according to [34]). Pressure relief at 8.5 bar (abs) during cooking.

## 4.3.6

**Alternative Sulfite Pulping Concepts**

The difficulty of pulping certain resin-rich softwoods and hardwoods is certainly a serious handicap for the conventional acid sulfite process, and was one of the reasons why sulfite pulping technology lost ground to the kraft process. The development of the kraft recovery process during the 1930s, including a technically more convenient and efficient form of combustion furnace, particularly by the contributions of Tomlinson, made the pine kraft pulps highly competitive with the spruce and hemlock sulfite pulps [1–4]. Since the early days of sulfite pulping technology, much effort has been undertaken to overcome this deficiency. An initial breakthrough in the pulping of resinous wood was provided by the development of Hägglund and co-workers, who developed a two-stage concept, with the first stage more alkaline than the second [5–7]. It could be shown that condensation reactions between reactive lignin groups and some phenolic extractives (e.g., pinosylvin and its monomethylether) are greatly diminished at pH levels greater than 4. Therefore, an acceptable delignification of the extractive-rich pine heartwood in the succeeding acid sulfite stage can be obtained. This (bi)sulfite-acid sulfite two-stage concept was first realized in an industrial-scale operation by Stora Kopparberg and Svenska Cellulosa, known as the Stora and Kramfors processes for pulping pine and tannin-damaged spruce, respectively [8,9]. To change the pH from the acid to the slightly alkaline range, the so-called soluble bases (sodium, ammonia, and magnesium) are required. Sodium and ammonia both allow the possibility of changing the acidity of the liquor within the entire pH-range. Sodium is, however, to be given preference as the ammonia liquors are less stable at higher temperatures. It is also possible to use magnesium as a base up to pH levels of about 6.5 [10]. It has been shown that the solubility of magnesium monosulfite suspensions in the pH range above 5 increases significantly in the presence of recycled spent sulfite liquor or high sodium salt concentrations (e.g., NaCl or Na<sub>2</sub>SO<sub>4</sub>) [10].

The great effort into the development of alternative sulfite pulping concepts during the 1950s and 1960s, in answer to the rapid development of the kraft process, has led to the introduction of several pilot- and mill-scale applications. Among the most successful developments are the following (though this list is far from comprehensive):

- **Magnefite process (Bisulfite)**
  - Cooking base           magnesium
  - Cooking liquor       magnesium hydrogen sulfite, Mg(HSO<sub>3</sub>)<sub>2</sub>, pH 4
- **Two-stage neutral Magnefite (Bisulfite-MgO)**
  - Cooking base           magnesium
  - First stage            magnesium hydrogen sulfite, Mg(HSO<sub>3</sub>)<sub>2</sub>, pH 4
  - Second stage         magnesium monosulfite/magnesium hydroxide, pH 6–6.5
- **Sivola process(es):**
  - Bisulfite-soda
    - Cooking base       sodium
    - First stage         sodium hydrogen sulfite, pH 4–5

- Second stage sodium carbonate/sodium monosulfite, pH 8
- Acid bisulfite-soda
  - Cooking base sodium
  - First stage acid sodium sulfite, pH 1–2
  - Second stage sodium carbonate/sodium monosulfite, pH 8
- Bisulfite-acid bisulfite-soda
  - Cooking base sodium
  - First stage sodium bisulfite, pH 4
  - Second stage acid sodium sulfite, pH 1–2
  - Third stage sodium carbonate/sodium monosulfite, pH 8–10
- Stora process (hydrogen sulfite or monosulfite-acid bisulfite)

There are numerable variations to this process, but the general concept can be described as a sulfite-acid bisulfite cook.

- Cooking base sodium
- First stage sodium hydrogen sulfite, pH 4, or sodium monosulfite, pH 6–8
- Second stage acid sodium sulfite, pH 1–2.

The Billerud method, not separately introduced here, may best be described as a modification of the Stora method, the main variation occurring in the second stage of the cook (pH 3).

- ASAM (alkaline sulfite anthraquinone and methanol)

#### 4.3.6.1 Magnefite Process

The magnefite process belongs to the bisulfite processes using magnesium as base to ensure an effective and simple recovery of the cooking chemicals. The process, including a description of the magnefite chemical recovery system, was proposed by Tomlinson et al. for the pulping of conifers [11,12]. The cooking liquor consists of a more or less pure hydrogen sulfite solution comprising an initial pH value of 3.6–4.0 (25 °C) and a total SO<sub>2</sub> concentration of 4–5%, corresponding to a MgO concentration of about 1.3–1.6%. With a typical liquor-to-wood ratio of 4:1, the total SO<sub>2</sub>-charge based on wood calculates to 16–20%. Due to the low hydrogen-ion concentration, sulfonation of lignin structures is favored over the reaction with reactive phenols from extractives. Thus, pine, fir, Douglas fir, larch and other extractive-rich wood species can be satisfactorily used to produce high-grade pulp. The rate of heating is not critical, and provided that enough steam is available, digesters can be brought to cooking temperature within 1 h. The cooking temperature is about 155 °C for hardwoods and about 165 °C for softwoods. The higher reaction temperatures compared to the acid sulfite cook compensates for the lower delignification rate attributable to the significantly lower ion product,  $[H^+] \cdot [HSO_3^-]$  (see Tab. 4.66, acid sulfite pulping). Depending on the wood source and the target pulp properties, cooking is completed within only 2–3 h. In total, the cover-to-cover cycle is only 6–8 h, and allows 25–80% higher cooking capacity

as compared to conventional acid sulfite pulping. As the cook proceeds, acids that are released from the wood components tend to reduce the liquor pH. If the pH falls below 3.0 during the heating period, it is necessary to relieve some of the gas.

Since the cooking liquor contains no free  $\text{SO}_2$ , hydrolysis of the carbohydrates proceeds at a slower rate even when considering the higher temperature. Hence, pulps cooked according to the magnesite process contain a higher hemicellulose content, and yields are approximately 2–4% higher as compared to acid sulfite pulps at the same kappa number. Magnesite pulps have better strength and optical properties (brightness), and in some cases are better suited to papermaking than the corresponding acid sulfite pulps. However, the lower acidity of the cooking liquor limits the extent of delignification. Indeed, this turned out to be a serious disadvantage when the need for chlorine-free bleached grades emerged. During the course of developing ECF and TCF bleaching grades, the kappa number had to be reduced from about 30–35 to the lower 20s in order to keep the demand on bleaching chemicals and hence the effluent charges within acceptable limits. Consequently, some of the unquestionable advantages of the original magnesite process – such as the high strength properties and short cooking cycles – have been markedly diminished.

#### 4.3.6.2 Two-Stage Neutral Magnesite (Bisulfite-MgO)

The magnesite cooking process provides a number of advantages over the regular acid sulfite process, including better pulp strength properties, provided that the kappa number is kept above a certain level (e.g., 30). This, as has been outlined above, requires a high subsequent bleaching effort for obtaining pulps of full brightness (88% ISO and higher). A modification to the magnesite process – the two-stage neutral magnesite – has been introduced in which the pH is increased to about 6.0–6.5 during the latter part of the cook by the addition of magnesium hydroxide [13]. There, the first stage is carried out according to the classical magnesite process (pH 3.7) and after a period of 90 min at approximately 165 °C, (hydrated) MgO is injected into the digester until a pH of 6.5 is reached. The amount of magnesium hydroxide slurry required to reach the target pH level is equivalent to about 4.0–5.0% on o.d. wood. It is worth mentioning that the best pulp strength properties are obtained when the MgO addition is carried out when the cook is in the 60–65% yield range. The introduction of magnesium hydroxide slurry into the digester reduces the temperature of the acid by up to 15 °C. Subsequently, the temperature must be raised to 170–175 °C, which is the cooking temperature of the second stage. This temperature is maintained for about 120–150 min. The solubility of MgO can be increased by adding sodium salts, or even better by introducing it into a sulfite spent liquor from a previous cook [10]. The overall cooking time is about 1 h longer than for a one-stage magnesite cook at the same kappa number. In the case of softwoods, the yield is quite comparable to that of a regular magnesite pulp. Pulps were stronger in all categories than from single-stage magnesite, and were much stronger than from conventional acid sulfite pulping. They were said to be comparable in tensile and burst, but inferior in tear strength to kraft pulps from the same wood furnish.



Even though the unbleached brightness of the two-stage neutral pulps is lower as compared to the magnesite pulps, the bleachability of both pulps remains equally good. The combination of elevated pH levels close to neutral conditions and the high temperature causes the extraction of hemicelluloses. In the case of hardwood pulps, a very low pentosan content (6.4%) and a rather high alpha-cellulose content (90.3%) were observed [13]. This concept of two-stage magnesium-base pulping has been installed at the Weyerhaeuser mill at Cosmopolis, Washington, to produce high reactive dissolving pulps, termed "HO". In addition, the two-stage neutral sulfite pulps show slow hydrating properties and good opacity, which permits the production of pulps of a wide range of properties [14].

#### 4.3.6.3 Sivola Processes

The Sivola sulfite cooking and recovery process was developed in the early 1950s to produce either dissolving or high-grade sulfite pulp at Rauma from spruce and balsam woods [15–17]. The sodium-based, multi-stage cooking concepts of the "Sivola" type comprise the bisulfite-neutral sulfite (soda), the acid bisulfite-neutral sulfite (soda), and the bisulfite-acid sulfite-soda processes. The bisulfite-neutral sulfite process is characterized by a change of the pH level from around 3.5–4.0 in the first stage up to 7.0–8.5 (and higher) in the second stage. Differences in pulp quality are observed if the first-stage liquor is drained before alkali is added to the second stage. Pulps of superior burst and tear levels are obtained when the alkali is introduced directly into the first-stage liquor. However, when the first-stage liquor is drained before alkali is added, tearing resistances close to that of kraft pulps are obtained, but the burst was not further improved. The effect of a two-stage bisulfite-soda cooking process as compared to conventional acid sulfite and bisulfite pulping methods using aspen as a raw material is detailed in Tab. 4.64 [15].

**Tab. 4.64** Comparative evaluation of acid sulfite, bisulfite and bisulfite-soda (Sivola) cooks of aspen (according to [15]).

Acid stage			Alkaline stage				Unbleached pulps				
Liquor pH	Max. temp. [°C]	Time at max. temp. [h]	Liquor pH	Max. temp. [°C]	Time at max. temp. [h]	total time [h]	Kappa calc.	Brightness [% G.E.]	Scr. yield [%]	Tearing resistance <sup>a)</sup> [%]	Tensile strength <sup>a)</sup> [kN m <sup>-1</sup> ]
1.8	140	3.0				8.0	26.2	44.4	52.9	58	4.8
3.7	160	4.3				7.3	20.5	45.2	54.8	62	5.8
3.7	160	2.5	8.5	169	1.5	7.0	27.2	60.5	53.2	100	5.8

a) after 20 min of beating time.

The two-stage cook showed the highest unbleached brightness and superior tearing resistance compared to the one-stage cooked pulps. The yield, however, was lower than that of the bisulfite pulp when comparing at the same kappa number level.

As expected, the presence of thiosulfate exerts no undesirable effects up to very high concentration levels (up to 6–8% on o.d. wood).

A very comprehensive comparison of multi-stage sulfite pulping of both softwoods and hardwoods was presented by Sanyer et al. [18,19]. Selected results using spruce wood Jack pine as a raw material and sodium as a base are shown in Tabs. 4.65 and 4.66.

**Tab. 4.65** Unbleached pulp yield and physical properties of one-stage and multi-stage spruce pulps in comparison to a spruce kraft pulp with a permanganate number of about 20 (according to [18]).

Processes	Yield [%]	Tear factor	Breaking length
			at freeness of 500 mL [km]
BS-NS	46.3	110	13.2
BS-AS	48.1	66	12.4
NS-AS	56.7	63	11.7
BS	51.3	87	11.5
K	47.0	120	13.0

BS-NS Bisulfite-Neutral Sulfite.  
 BS-AS Bisulfite-Acid Sulfite.  
 NS-AS Neutral Sulfite-Acid Sulfite.  
 BS Bisulfite.  
 K Kraft

Pulp yield is lowest at a given residual lignin content in case of the bisulfite-neutral sulfite process (BS-NS), which can be attributed to severe hemicellulose extraction in the second, slightly alkaline stage (Tab. 4.66). However, among the sulfite pulping processes investigated, the BS-NS process has the best strength properties, as indicated in Tab. 4.65. Changing the pH regime in a way that the cook starts at neutral pH and proceeds under acidic conditions leads to a very high pulp yield due to glucomannan stabilization (Tab. 4.66). However, at the same time the tear strength is significantly impaired due to the presence of a high amount of low molecular-weight hemicelluloses, whereas the tensile properties remain at an acceptable level.

**Tab. 4.66** Carbohydrate composition of unbleached sulfite and kraft jack pine pulps with a permanganate number of about 20 (according to [18]).

Processes	Mannose	Pentose <sup>a)</sup>
	[% on total sugars]	
BS-NS	6.7	6.1
BS-AS	8.0	9.6
NS-AS	13.6	6.4
BS	7.2	7.1
K	7.6	10.7

a) includes arabinose

Further investigations showed that the combinations of bisulfite-acid sulfite (BS-AS), bisulfite-acid sulfite-neutral sulfite (BS-AS-NS; not shown in Tabs. 4.65 and 4.66), and neutral sulfite-acid sulfite-neutral sulfite (NS-AS-NS, not shown) are intermediate to the two extremes in yield and strength mentioned above.

Brightness levels are generally lowered by the second stage. The highest brightness level was obtained with the Mg system, and the lowest with the ammonium hydrogen sulfite/calcium hydroxide system [20].

The adding to a bisulfite-acid sulfite (BS-AS) process of an additional third stage at moderate alkaline conditions by adding sodium carbonate converts the Sivola process to a very flexible process for the production of dissolving pulps. The Rauma process (BS-AS-Soda), a development which parallels the Sivola process, consists of a three-stage cook for use on spruce and pine wood [21–24]. A typical cooking schedule for the Rauma three-stage sulfite cook is illustrated in Fig. 4.185.

The first stage is a bisulfite stage, pH 3–4, primarily to ensure good chip impregnation. After adding SO<sub>2</sub>, the second stage is carried out as a conventional acid sulfite stage. At the end of this stage SO<sub>2</sub> is relieved when the desired pulp viscosity is reached. In the third stage, sodium carbonate is added to extract the low molecular-weight carbohydrates. The degree of purification, denoted as alpha-cellulose content, is controlled by temperature, time and pH of cooking liquor according to Fig. 4.186. At 170 °C and a pH level of about 8, alpha-cellulose contents above 95% have been obtained [24].

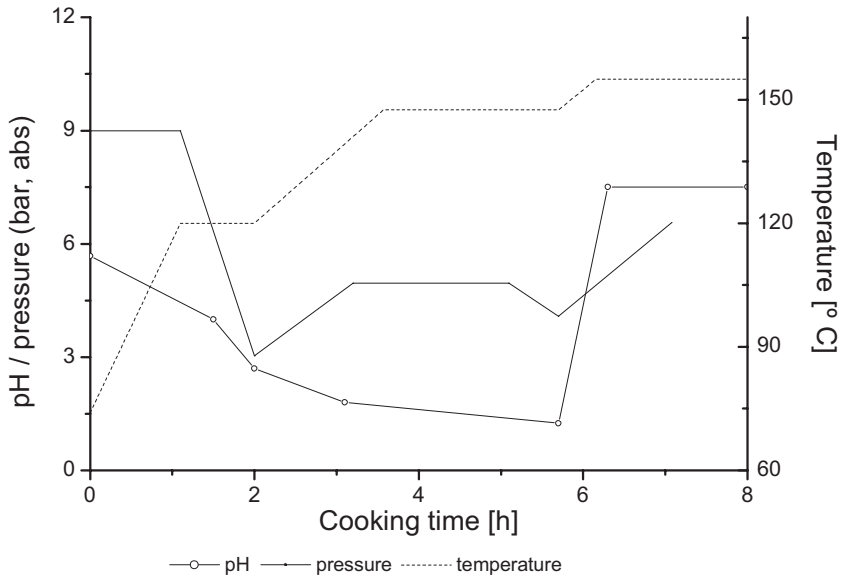


Fig. 4.185 Typical course of pH, temperature and pressure during a Rauma three-stage sulfite cook (according to [24]).

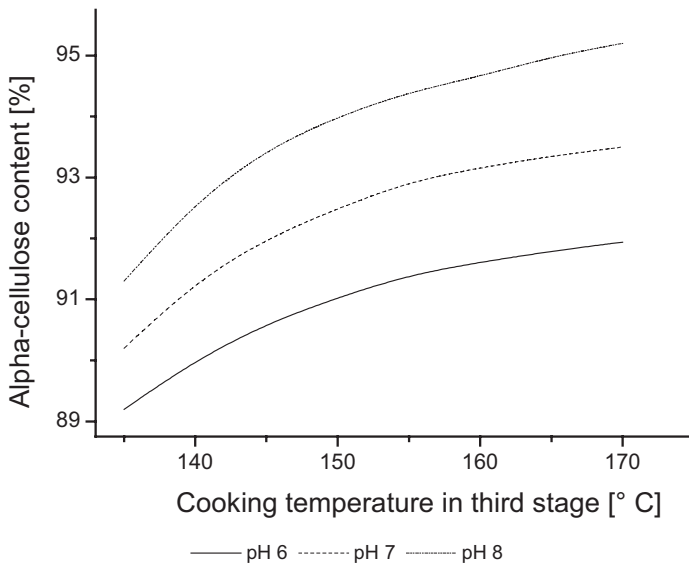


Fig. 4.186 Alpha-cellulose content as a function of third stage pH and temperature (according to [24]).

#### 4.3.6.4 Stora Processes (Hydrogen Sulfite or Monosulfite-Acid Sulfite)

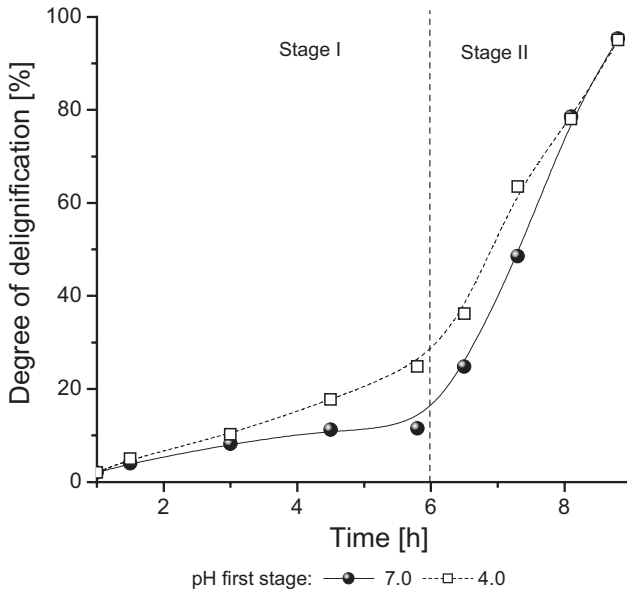
The bisulfite-acid sulfite process was primarily developed for the partial use of extractive-rich pine heartwood and tannin-damaged spruce. Yield and strength properties are reported to be slightly better compared to acid sulfite pulps, and even better than bisulfite pulps in case of breaking length (e.g., magnesite pulp) (see Tab. 4.65). The two-stage neutral sulfite-acid sulfite pulping process was developed by Stora Kopparberg for utilization of pine raw material, and was first applied in their mill at Skutskär [8,25–29]. The key principle of the Stora process involves a two-stage cooking process, comprising lignin sulfonation under slightly acidic to neutral pH conditions in the first stage, and lowering the pH by adding  $\text{SO}_2$  (liquid or hydrated) for completion of the pulping operations in a second stage. The cooking liquor for the first stage consists of about 50% of liquor drawn from a previous cook and of fresh liquor prepared in the chemical converting plant. The digester volume during the first-stage is entirely filled with cooking liquor, corresponding to a liquor-to-wood ratio for softwood of about 4.5:1, to ensure proper impregnation. Depending on the applied wood furnish, the reaction time during the first stage varies from 2–3 h (spruce) to 4–6 h (pine). After the first stage, cooking liquor is drawn to adjust a liquor-to-wood ratio of about 3.0–3.5:1. The second stage starts with the injection of  $\text{SO}_2$  and, depending on the temperature (135–145 °C), proceeds for about 2–4 h. The two cooking stages can also be characterized as sulfonation (stage 1) and delignification (stage 2) stages. A degree of sulfonation of about 0.3 S/OCH<sub>3</sub> has been identified [25].

As illustrated in Fig. 4.187, only a relatively small amount of lignin is removed during the first stage, whereas in the subsequent second stage a rapid lignin dissolution occurs.

The reaction conditions during the first cooking stage efficiently prevent condensation reactions between reactive lignin groups and the phenolic extractives originating from pine, larch, Douglas fir and other extractive-rich wood raw material. Therefore, an acceptable delignification of the extractive-rich pine heartwood in the subsequent acid sulfite cook can be obtained. Further investigations have shown that the conditions of the first stage also affects the carbohydrate yield. As shown in Fig. 4.188, the yield increase is a clear function of the pH and temperature in the first cooking stage. At higher temperature the inflexion point is shifted towards lower pH value.

Interestingly, the increase in yield proceeds parallel to a decrease in the acetyl content of the wood after the pretreatment (Fig. 4.188). After deacetylation, the molecules will be packed so closely together that acid hydrolysis and diffusion are prevented in the final acid sulfite cook.

The research group of Billerud found that the yield advantage obtained with the neutral sulfite-acid sulfite pulping concept is mainly due to a increased amount of glucomannan in the pulp [31–33]. The increased stability is thought to result from an increased degree of lateral order caused by deacetylation of the glucomannan, followed by adsorption of the linear backbone onto the cellulose surface. Surprisingly, the degree of polymerization of the retained glucomannan is about 30, independent of the cooking procedure. Both glucomannan and cellulose are located

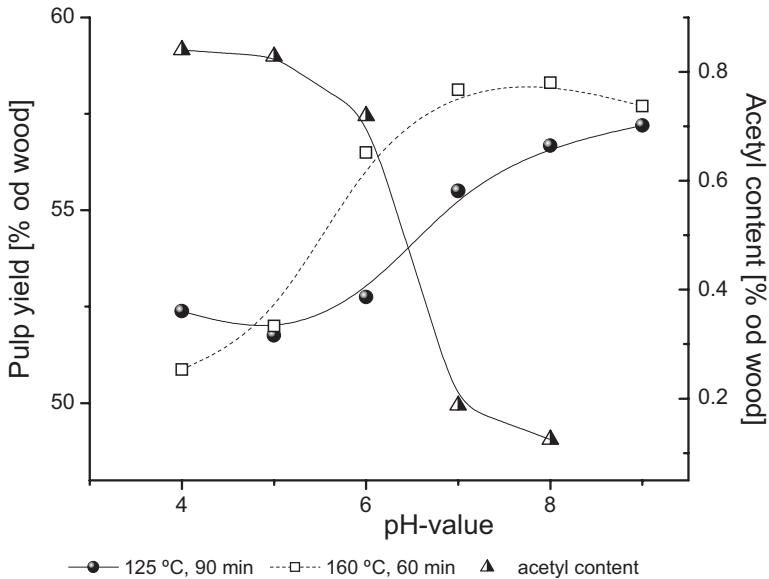


**Fig. 4.187** Delignification of pine wood in sodium-based, two-stage sulfite pulping at two different pH levels in the first stage (according to [30]).

predominantly in the S2 cell wall layer. Thus, most of the glucomannans have only a very short path of diffusion in order to be adsorbed onto the cellulose molecules.

Different results have been published regarding the stabilizing effect of hardwood pulping. Sanyer and Wenneras were unable to identify any significant yield increase for all different concepts of multi-stage sulfite cooking using oak, sweetgum, and birch [8,18,19]. The small content of glucomannan in the hardwood species was argued to be the reason for the nondetectable stabilization effect of the two-stage pulping. Janson and Sjostrom, however, reported that two-stage cooking of birch results in a 2–3% higher pulp yield as compared to conventional acid-sulfite cooking [34]. The contribution of xylan is very much dependent upon the conditions during the first stage. An increase in temperature and duration of that stage, and a decrease in temperature in the subsequent stage, appears to favor xylan retention in the final pulp [25]. In combination with a starting pH of 8–9 and a temperature of 150 °C for 1–2 h, a yield gain of up to 4–5% on o.d. wood was also reported for aspen and birch pulps when applying the two-stage Stora concept [25].

The properties of paper are influenced by the higher amounts of short-chained hemicellulose in such a way that the fibers are more easily beaten and hydrated. The fibers swell and become flexible, which promotes fiber–fiber bonding. A higher hemicellulose content means a higher beating response, a higher tensile strength and a lower tear factor and opacity at the same freeness. The two-stage



**Fig. 4.188** Pulp yield as a function of pH in the first stage of a sodium-based, two-stage sulfite pulping of spruce (according to [25]). Acetyl content of sprucewood residues after treatment at 125 °C for 90 min as a function of pH of the cooking liquor (according to [33]).

pulps attain breaking lengths which are considerably above those of acid sulfite pulps, and are also better than the bisulfite pulps. The tear strength for the two-stage pulps is however lower than for bisulfite pulps; this can be explained by the high hemicellulose content and also in part by the smaller number of fibers per gram of pulp. Surprisingly, the two-stage pulp has a higher bulk than the conventional sulfite at a certain tensile strength.

Although the use of pine heartwood creates no uncontrollable condensation reactions during two-stage sulfite pulping, the high resin content in the unbleached pulp would cause a serious pitch problem during further processing of the pulp (bleaching, papermaking). Fortunately, pitch in pine pulp can be easily extracted by using an alkaline treatment, and this is facilitated by the wide window pits in pine and the resin-rich ray parenchymal cells.

The neutral sulfite or bisulfite-acid sulfite concept has also been applied to magnesium base cooking, due to the finding that the precipitation of magnesium monosulfite/magnesium hydroxide can be avoided up to pH levels of about 6.5, as previously mentioned. The process, which was developed and realized by Weyerhaeuser, comprises a first-stage cooking at 150 °C, using a cooking liquor with a pH ranging from 5.2 to 6.0. No particular advantage was realized when cooking at pH values above 6.0, provided that the temperature was about 150 °C in the first stage [14]. At the end of the first stage, liquor is withdrawn from the digester to produce a liquor-to-wood ratio of 2:1. Liquid SO<sub>2</sub> is then injected into

the digester to adjust the acidic conditions. The second stage is carried out at 130–140 °C, adjusting the time to produce a pulp of appropriate properties. The “FB”-denoted pulp is characterized by its high hemicellulose content and resultant rapid-hydrating properties. The low opacity and low power requirement for refining makes the pulp attractive for transparent grades of paper.

The sodium-based, two-stage sulfite process is also used in the production of highly reactive spruce/pine dissolving pulp at Domsjö [24,35]. The first stage is operated at a pH of 4.5 (hydrogen sulfite), a temperature above 150 °C, and a high liquor-to-wood ratio to ensure optimum impregnation and sulfonation. At the end of the second stage, liquor is withdrawn for reuse in a subsequent cook. The acidic conditions in the second stage are adjusted by adding SO<sub>2</sub> water. Cooking is maintained until the target viscosity level between 400 mL g<sup>-1</sup> and 800 mL g<sup>-1</sup> is attained. The low content of residual lignin (kappa number 3–8) makes it possible to produce a high-brightness pulp (>92% ISO) using two-stage totally chlorine free (TCF) bleaching according to an E-P-sequence with fully closed water cycle. Before the hot caustic extraction (E), the pulp is subjected to a special depitching treatment. The alkalinized pulp is treated mechanically in screw presses, followed by Frotapulper screws. The combined chemical and physical treatments effectively disperse the resin, which then is carefully washed out [36].

#### 4.3.6.5 Alkaline Sulfite Pulping

Alkaline sulfite (AS) cooking refers to a cooking process using a cooking liquor made up of mainly NaOH and Na<sub>2</sub>SO<sub>3</sub> with a cold cooking pH of 10.0–13.5 [37]. This process was developed as an alternative to kraft pulping during the late 1960s, and the first patents on alkaline sulfite cooking were issued in 1970–1971 [38,39], at a time when many old sulfite mills had been closed in the United States, Canada, and Scandinavia. The driving force of this new pulping process was to reduce investment costs, improve bleachability and beatability and, above all, to reduce the odor problem, while maintaining strength properties at the level of a kraft pulp. Other alternatives which arose at that time were the “nonsulfur” cooking processes, the most important methods being two-stage soda-oxygen and organosolv pulping procedures, both of which have been extensively reviewed in a recent publication [40]. Soon after the first laboratory results had been obtained, the AS process was tested in pilot plant and mill trials [37,41]. The results were quite convincing, and the AS process was shown capable of producing pulp with paper properties equal to those of the kraft process, but without odor emissions. However, many disadvantages were associated with the AS process, and these eventually prevented industrial acceptance. First, the rate of delignification was very low, despite a high chemical charge. Second, the yield with softwoods was lower than that of kraft in the kappa number range typical of the production of fully bleached grades. Third, there were deep concerns about the cost and reliability of existing sodium sulfite recovery systems. In fact, the extent of delignification through AS cooking with a high Na<sub>2</sub>SO<sub>3</sub>-to-NaOH ratio is rather low because, under these conditions, lignin degradation is limited to the cleavage of β-O-4 link-



ages of phenylpropane units carrying free phenolic hydroxyl groups. Increasing the proportion of sodium hydroxide in the cooking liquor improves delignification (nonphenolic linkages are also cleaved via an oxiran intermediate; see Section 4.2.4.1, Chemistry of alkaline delignification), but at the same time the carbohydrate fraction is heavily degraded due to alkaline primary and secondary peeling reactions which reduce pulp yield and quality. The use of anthraquinone (AQ) in alkaline pulping processes initiated a renewed interest in AS cooking. In Japan, Nomura has applied for a patent for neutral sulfite and sodium carbonate cooking in the presence of AQ [42]. In many laboratory, pilot plant and even mill trials, the positive effect of AQ on the efficiency and selectivity of delignification was confirmed [43]. Compared to the kraft process, AS/AQ pulping under mildly alkaline conditions behaves very selectively, providing both a higher yield and a higher viscosity at a given lignin content or kappa number. However, the pronounced advantage of AS/AQ over kraft pulping becomes diminished as delignification is extended below a kappa number of about 40–50 [44]. Further insight into the effects of liquor composition on the rate of the dissolution of various wood components is provided by the results obtained by McDonough et al. [44]; these are summarized in Tab. 4.67.

Cooking with a pure sodium sulfite solution (in the presence of AQ) behaves very selectively towards the carbohydrates. Cellulose is completely preserved, and only 30% of the glucomannan and about 25% of arabinoxylan are removed, while about 63% of the lignin is degraded. Replacing 40% of the sodium sulfite with sodium carbonate caused a further reduction of the lignin content by 45% and a significant decrease in the glucomannan content, while the arabinoxylan fraction was only marginally affected. Replacing sodium sulfite with sodium hydroxide

**Tab. 4.67** Effect of liquor composition on yields of the major wood components using Southern pine as wood source (according to [44]).

Source	Chemical charges			Kappa no.	Total lignin [% of wood]	Total yield [%]	Cellulose [% of wood]	GGM <sup>a)</sup> [% of wood]	AX <sup>b)</sup> [% of wood]	Sulfur [% of lignin]
	[% as NaOH an od wood]	Na <sub>2</sub> SO <sub>3</sub>	Na <sub>2</sub> CO <sub>3</sub>							
Wood					31.8	100.0	37.6	17.0	8.4	
AS/AQ	31.0	0.0	0.0	95.9	12.1	68.7	37.5	10.6	6.6	3.9
AS/AQ	18.6	12.4	0.0	69.4	6.7	57.2	36.0	6.0	5.6	2.0
AS/AQ	18.6	0.0	12.4	28.9	2.4	48.0	35.6	4.8	5.4	1.5
Kraft				38.8	2.6	46.7	33.6	5.1	3.8	1.2

a) GGM: galactoglucomannan = (galactan + (4/3) mannan).

b) AX: arabinoxylan.

Cooking conditions: 0.1% AQ, I:s = 4.1, 90 min heating-up time to 175 °C, 3 h at 175 °C.

proved to be very effective in lignin removal, but also resulted in cellulose degradation and further removal of glucomannan. Thus, liquor alkalinity throughout AS/AQ cooking is the key parameter affecting delignification selectivity. It was found that pulp viscosity passes a maximum when the pulping liquor contains only a small concentration of free hydroxide ions. However, increasing the sodium hydroxide concentration beyond a certain level results in a rapid drop in viscosity. On the other hand, liquors containing no free sodium hydroxide but increasing proportions of sodium bicarbonate also produce progressively lower viscosities [44]. Another important parameter in AS/AQ cooking is the proportion of  $\text{Na}_2\text{SO}_3$  to the total alkali charged. When the proportion of nonsulfite alkali is only about 20% of the total alkali charged (calculated as  $\text{NaOH}$ ), the alkalinity prevailing during most of the cook is rather insensitive to the initial ratio of  $\text{NaOH}$  to  $\text{Na}_2\text{CO}_3$ , because the dissolved lignin and carbohydrate degradation products neutralize the charged alkali, forming an effective buffer system. In order actively to control the alkalinity of the cooking liquor, the proportion of  $\text{Na}_2\text{SO}_3$  must be reduced to about 60% of the total alkali charged. As expected, the rate of pulping increases continuously with liquor alkalinity but, unfortunately, the rate of carbohydrate degradation and dissolution is similarly affected.

The final conclusion of all investigations into alkaline sulfite pulping conducted during the 1980s was that the most promising applications of this process seem to be packaging grades and news reinforcement. Ingruber et al. showed the yield advantage of the AS/AQ over the kraft process to be about 7% on o.d. wood (62% versus 55%) at a kappa number of 80 [45]. At the same time, the tensile strength was 20% higher and the tear strength 20% lower, as compared to the corresponding kraft pulp. The advantage of AS/AQ pulps in tensile strength can be used to reduce refiner energy still further by operating at higher freeness (the beatability of the AS/AQ pulp is superior in general) while simultaneously obtaining higher tear resistance.

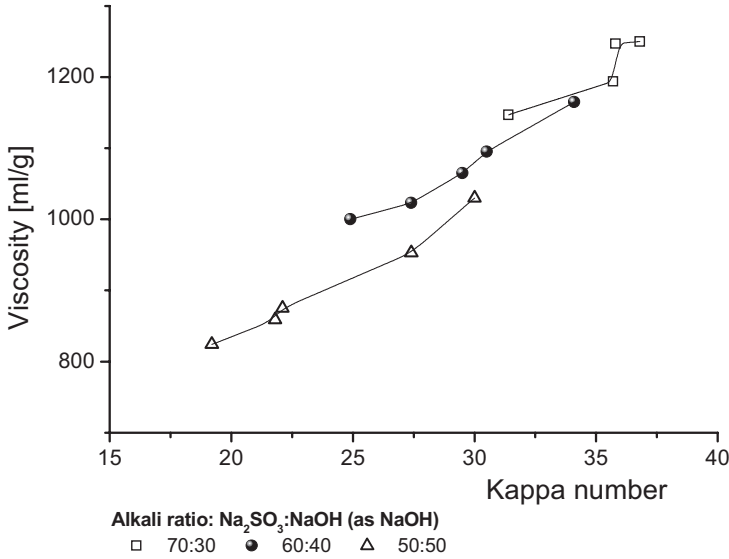
As mentioned earlier, the pronounced advantage of AS/AQ pulping diminishes as the extent of delignification is increased to obtain bleachable grades (kappa number range 20–30). Based on this conclusion, most activities on alkaline sulfite pulping were halted, with the exception of a German research group headed by Professor Patt at the University of Hamburg. This group found that the addition of methanol to the alkaline sulfite liquor improved delignification considerably, while preserving pulp viscosity. In a very systematic approach, the contribution of each single component of the pulping liquor on delignification was evaluated [46]. The experiments were carried out with a cooking liquor containing a total alkali charge of 25% on o.d. wood, calculated as sodium hydroxide, with a sodium sulfite:sodium hydroxide ratio of 80:20. The reaction conditions were kept constant, choosing a maximum temperature of 175 °C, a cooking time of 150 min, and using spruce wood as the raw material. Under these basic conditions, only 20% of the lignin could be dissolved, resulting in a kappa number of about 150. As mentioned previously, the limited extent of delignification can be attributed to the low liquor alkalinity. As soon as the charged sodium hydroxide is neutralized by the degraded wood components, delignification slows down significantly. Replacing

part of the water in the cooking liquor with methanol promoted delignification, and a final kappa number of about 100 was reached. The addition of AQ further improved alkaline sulfite delignification very efficiently, and reduced the kappa number to about 40. By combining both additives to the sulfite cooking liquor, the delignification of spruce wood was extended to kappa number 25. Based on these findings, the new pulping process – alkaline sulfite-anthraquinone-methanol (ASAM) cooking – was developed [46,47]. Throughout the next 10 years, the ASAM process was evaluated extensively on laboratory and pilot plant scale, using all sources of raw materials (softwoods, hardwoods and annual plants) [48–55]. The ASAM process has proven to yield pulps of better strength properties, higher yield and better bleachability as compared to the kraft process. The technical feasibility of this process has been proven in extensive pilot plant trials, including TCF bleaching, methanol recovery, liquor evaporation and combustion of concentrated black liquor. Despite these clear advantages over kraft pulping, the ASAM process has so far failed to become commercialized, for three main reasons:

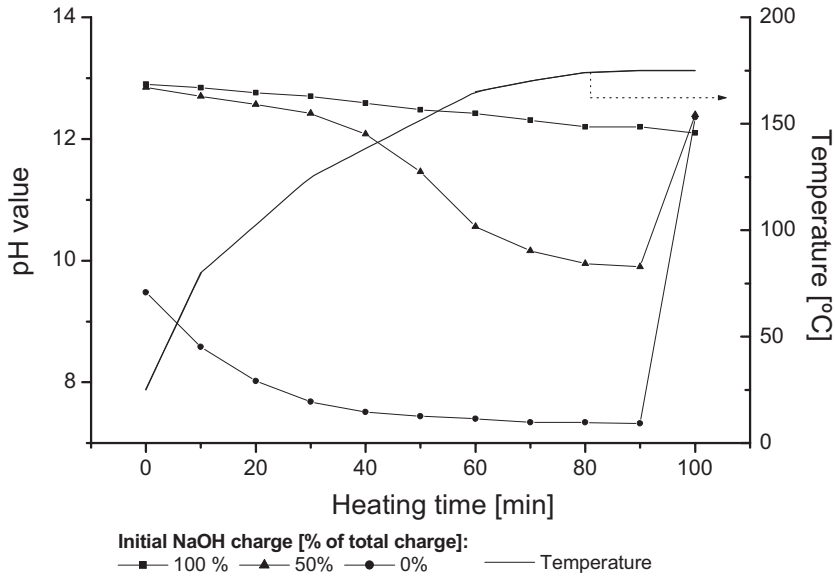
1. The presence of methanol requires explosion-proof installations and a methanol recovery system, both of which make the investment more expensive.
2. The efficiency and reliability of the available sodium sulfite recovery systems seem not to be sufficient, and measures would have to be undertaken that, again, would lead to higher costs.
3. The technology of kraft pulping has been improved extensively during the past 15 years, and this has reduced the advantages of the ASAM process (Modified kraft cooking). Furthermore, with the general acceptance of ECF bleaching procedures, the argument of a better TCF bleachability of the ASAM pulp is no longer valid.

Nevertheless, the high selectivity and bleachability of AS pulps remains an attractive basis for the development of superior pulping processes. To overcome the problem of methanol recovery, an attempt was made to improve the efficiency of AS pulping in the absence of an organic solvent. Based on the principles of modified kraft cooking, part of the sodium hydroxide is added only after having reached the maximum cooking temperature, the aim being to maintain an even alkali profile throughout the whole cooking process [56]. In an initial approach, the optimum alkali ratio with regard to delignification efficiency and selectivity was evaluated to create a sound basis for further optimization. However, as known from previous investigations [44], increasing the proportions of sodium hydroxide promotes delignification at the expense of selectivity (Fig. 4.189).

The selection of an alkali ratio of 60:40 ( $\text{Na}_2\text{SO}_3$ ; NaOH) ensures both sufficiently low kappa number and reasonably good selectivity. Splitting of the NaOH charge to different cooking stages alters the hydroxide ion concentration (pH) profile, particularly during the heating-up period, as shown in Fig. 4.190.

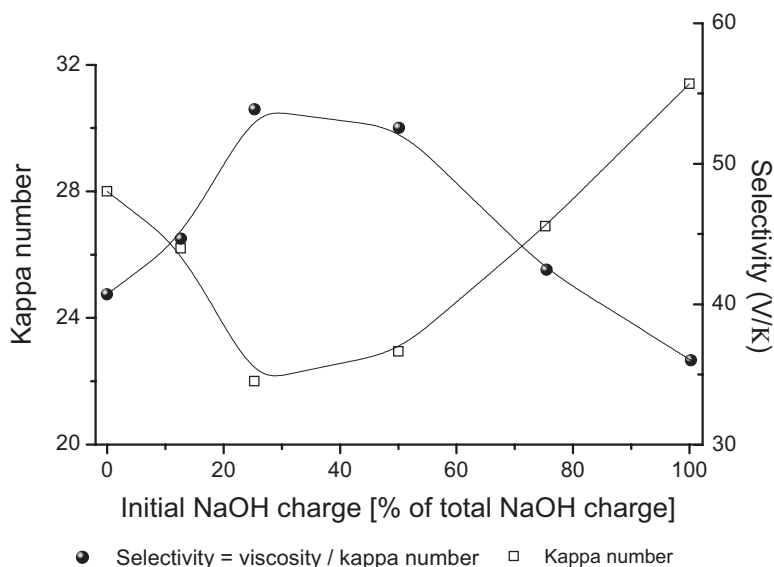


**Fig. 4.189** Effect of alkali ratio on the viscosity–kappa number relationship (according to [56]). Conditions: spruce as raw material; 27.5% total chemical charge on o.d. wood (calc. as NaOH); 0.1% AQ on o.d. wood; 90 min heating-up time; 175 °C cooking temperature; 60–270 min at cooking temperature.



**Fig. 4.190** Course of the pH of the cooking liquor (25 °C) in AS/AQ pulping with NaOH splitting (according to [56]). Conditions: pine as raw material; 27.5% total chemical charge on o.d. wood (calc. as NaOH); 0.1% AQ on o.d. wood; 90 min heating-up time; 175 °C cooking temperature.

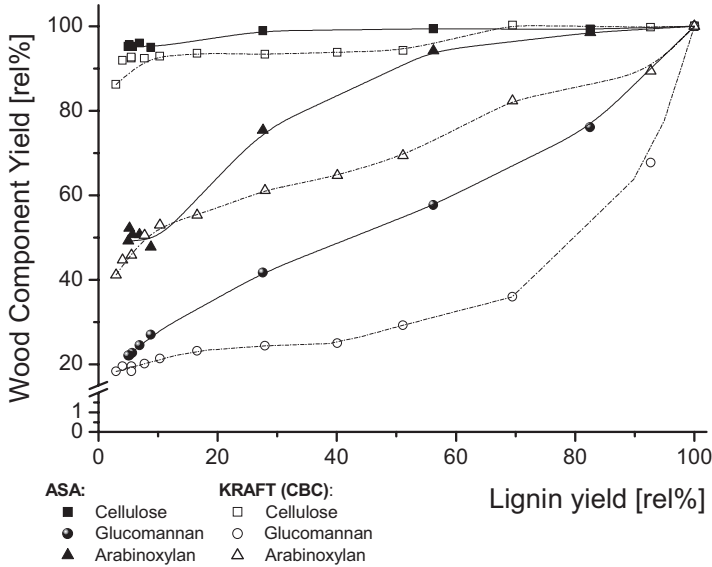
Splitting the alkali charge in a ratio 50:50 provides a rather even alkali profile throughout the cook. At the start of the cooking phase, the pH increases almost to starting level after addition of the residual amount of alkali. In the reference case – without split addition – the hydroxide ion concentration continuously decreases, leading to extensive carbohydrate degradation at the beginning of the cook and to insufficient delignification rate during residual delignification. The split addition of the NaOH charge is clearly reflected in a superior delignification efficiency and selectivity (Fig. 4.191).



**Fig. 4.191** Effect of alkali splitting in AS/AQ charge on o.d. wood (calc. as NaOH); alkali pulping on the efficiency (kappa number) and selectivity (viscosity/kappa number) of delignification (according to [56]). Conditions: pine as raw material; 27.5% total chemical charge on o.d. wood (calc. as NaOH); alkali ratio 60:40; 0.1% AQ on o.d. wood; 90 min heating-up time; 175 °C cooking temperature; 150 min cooking time.

The selectivity plot shows that optimum selectivity is obtained when the initial NaOH charge is limited to about 20–50% of the total charge. Compared to the reference case, the kappa number can be decreased from 32 to about 22, while the viscosity increases from 1130 mL g<sup>-1</sup> to about 1200 mL g<sup>-1</sup>. These convincing results clearly confirm the principles of modified cooking, where alkali profiling leads to both better selectivity and enhanced delignification. Alkaline sulfite pulping contributes to high carbohydrate yields, provided that the alkali charge remains low and cooking intensity does not exceed a certain level.

Dissolution of the main wood components during AS/AQ cooking of spruce with alkali splitting 37.5:62.5 was monitored. For comparison, the corresponding results obtained from continuous batch kraft cooking of spruce are included in Fig. 4.192 [57].

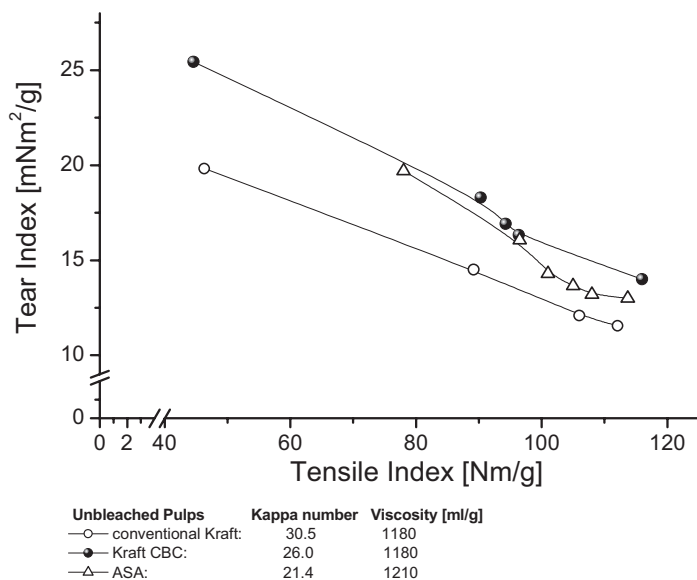


**Fig. 4.192** Dissolution of the main wood components cellulose, glucomannan, and arabinoxylan as a function of lignin content during AS/AQ and continuous batch kraft cooking of spruce. AS/AQ cooking: 27.5% total chemical charge on o.d. wood (calc. as NaOH); alkali ratio 60:40; NaOH splitting ratio 37.5:62.5; 0.1% AQ on o.d. wood; 90 min heating-up time; 175 °C cooking temperature [56,58]. For CBC kraft cooking, see Fig. 4.72, Modified Kraft Cooking [57].

The data in Fig. 4.192 confirm the better preservation of spruce carbohydrates during AS/AQ cooking as compared to CBC kraft cooking, particularly in the early and intermediate stages of the process. With progressive delignification, the yield advantage of the AS/AQ cook, including the split addition of NaOH, diminishes considerably. However, cellulose and xylan yields remain at a higher level as compared to CBC kraft pulping, even when delignification is extended to kappa numbers between 20 and 30. According to Patt et al., AS/AQ cooking of spruce with split addition of NaOH results in a kappa number 23.7 and a viscosity of 1191 mL g<sup>-1</sup> at a yield of 50.8% [56]. The corresponding results for CBC cooking of spruce are kappa number 25.8 and a viscosity of 1188 mL g<sup>-1</sup> at a total yield of 48.1% [57]. The comparison reveals a distinct yield advantage for the AS/AQ cooking procedure, even at a low kappa number. The good response of this pulp to oxygen delignification suggests that cooking should be interrupted at a higher kappa number, and continued with two-stage oxygen delignification.

The AS/AQ process produces pulp with strength properties that are equal or even slightly superior to those of kraft pulp [44]. This is illustrated in Fig. 4.193, in which tear index is shown as a function of tensile index.

Unbleached AS/AQ pulps are slightly superior in tensile strength compared to the corresponding CBC kraft pulps. As expected, the level of tear strength is below that of CBC pulps. At a given tensile strength, the tear resistance reaches a



**Fig. 4.193** Tear–tensile plots of unbleached spruce AS/AQ and CBC kraft pulps. Strength properties of spruce AS/AQ pulps are described in Ref. [58], and those of spruce CBC kraft pulps in Ref. [57].

comparable level for both pulps, especially if the better beatability of the AS/AQ pulp is considered.

Considering the manifold possibilities of modified cooking, it may be assumed that the potential of the AS/AQ cooking concept has not yet been fully exploited. For example, the rapid increase in yield loss at kappa numbers below 40 could reflect deficiencies in sulfonation of the residual lignin in relation to the hydroxide ion concentration. The introduction of displacement cooking technology may provide a better basis for adjusting the reaction conditions within all single cooking phases to further optimize the pulping performance.

One major disadvantage of AS pulping compared to kraft pulping is certainly the low delignification rate, and this will not be easy to overcome. Currently, an H-factor of about 3500 is necessary to attain a pulp of kappa number 25 in the case of AS/AQ pulping, while for CBC cooking an H-factor of about 1200 is sufficient to reach the same kappa number.

The only way finally to achieve industrial acceptance, however, is to develop a reliable, cheap, efficient and flexible chemical recovery system. Low-temperature gasification is likely to be the appropriate process that permits the highly energy-efficient pyrolysis of AS black liquor and, simultaneously, the separate recovery of sodium and sulfur components. Together, this should render possible alkali splitting in cooking (a prerequisite for modified cooking technology) and the generation of sodium hydroxide for alkaline bleaching operations.

## References

## Sections 4.1–4.2.2

- 1 Annergren G., SA Rydholm, S Vardheim, Influence of raw material and pulping process on the chemical composition and physical properties of paper pulps. *Svensk. Papperstidn.*, **1963**; 66: 196–210.
- 2 Toland J., et al., Annual review: An odyssey around the world. *Pulp & Paper International*, **2002**; 5–67.
- 3 Sjöström E., P Haglund, J Janson, Changes in cooking liquor composition during sulphite pulping. *Svensk. Papperstidn.*, **1962**; 65: 855–869.
- 4 Sixta H., et al. Comparative evaluation of sulfate-, acid sulfite-, Soda-AQ- and ASAM-processes based on beech wood. In APV-Conference, Graz, Austria, **1992**.
- 5 Sixta H., Acid magnesium sulfite cooking of beech and spruce woods. 1: Course of the degradation of wood components. R&D Lenzing AG: Lenzing, **2002**.
- 6 Sixta H., Comparative evaluation of CBC kraft pulping of pine and spruce wood chips. Internal Report, R&D Lenzing AG, **2004**.
- 7 Sixta H., *The alkalinity of white and black liquor*. Lenzing AG: Lenzing, **2004**.
- 8 Giggenbach W., Optical spectra of highly alkaline solutions and the second dissociation constant of hydrogen sulfide. *Inorg. Chem.*, **1971**; 10(7): 1333–1338.
- 9 Meyer B., et al., Second dissociation constant of hydrogen sulfide. *Inorg. Chem.*, **1983**; 22(16): 2345–2346.
- 10 Söderquist R., Natriumsulfitzellstoff. *Das Papier*, **1957**; 11(21/22): 487–491.
- 11 Pascoe, T.A. et al., The Sivola sulfite cooking and recovery process. *Tappi* **1959**; 42: 265–81.
- 12 Alén, R., Analysis of degradation products: A new approach to characterizing the combustion properties of kraft black liquor. *J. of Pulp and Paper Science*, **1997**; 23: 362–366.
- 13 Alén R., Sjöström E., Isolation of hydroxy acids from pine kraft black liquor. Part 1. Preparation of crude fraction, *Lab. Wood Chem.*, **1980**; 62(5): 328–330.
- 14 Ulmgren P., Lindström R., Printz M., The alkalinity of black liquor. *Nordic Pulp Paper Res. J.*, **1994**; 2: 76–83.
- 15 Mannbro N., Sulfite waste liquor as cooking liquor in sulfate pulping. I., *Svensk. Papperstidn.*, **1951**; 54: 19–24.
- 16 Milanova E., Dorris G.M., On the determination of residual alkali in black liquors. *Nordic Pulp Paper Res. J.*, **1994**; 9(1): 4–9.
- 17 Gran G., Determination of the equivalence point in potentiometric titrations. II., *Analyst*, **1952**; 77: 661–671.
- 18 Wilson G., Procter A.R., Baum J.W., Reactions of wood components with hydrogen sulfide. X. Formation of thiolignin during the hydrogen sulfide chip pretreatment process, *Svensk Papperstidning*, **1973**; 76(7): 253–7.

## Section 4.2.3

- 1 Robertsen, L., B. Lönnberg. Diffusion in wood. Part 1. Theory and apparatus. *Pap. Puu.*, **1991**; 73(6): 532–535.
- 2 Kazi, K.M.F., et al. A diffusion model for the impregnation of lignocellulosic materials. *Tappi J.*, **1997**; 80(11): 209–219.
- 3 Liese, W. Der Feinbau der Hoftüpfel bei den Laubhölzern. *Holz Roh- und Werkstoff*, **1957**; 15(11): 449–453.
- 4 Laboratory, F.P., *Wood Handbook – Wood as an Engineering Material*. Madison, WI: USDA, **1999**.
- 5 Weatherwax, R.C., H. Tarkow. Importance of penetration and adsorption compression of the displacement fluid. *Forest Prod. J.*, **1968**; 18(7): 44–46.
- 6 Kollman, F.F.P., Cote, W.A. Jr. Principles of Wood Science and Technology. In: *Solid Wood*. Springer-Verlag: New York, **1968**, pp. 193–194, Vol. 1: Solid Wood.
- 7 Nevell, T.P., S.H. Zeronian. *Cellulose Chemistry and Its Applications*. Ellis Horwood: Chichester, UK, **1985**, p. 31.
- 8 Gullichsen, J., H. Kolehmainen, H. Sundqvist. On the nonuniformity of



- the kraft cook. *Pap. Puu*, **1992**; 74(6): 486–490.
- 9 Worster, H.E., D.L. McCandless, M.E. Bartels. Some effects of chip size on kraft pulping of southern pine for linerboard. In: *Alkaline Pulping and Testing*. Dallas, Texas, **1976**.
  - 10 Colombo, P., et al., The influence of thickness of chips on pulp properties in kraft cooking. *Svensk. Papperstidn.*, **1964**; 67(12): 505–511.
  - 11 Hatton, J.V., J.L. Keays. Effect of chip geometry and moisture on yield and quality of kraft pulps from western hemlock and black spruce. *Pulp Pap. Mag. Can.*, **1973**; 74(1): T11–T19.
  - 12 Akhtaruzzamann, A.F.M., N.-E. Virkola. Influence of chip dimensions in kraft pulping. Part II. Present state and scope of the study. *Pap. Puu*, **1979**; 61(10): 629–634.
  - 13 Farkas, J. The dimensions of chip in kraft pulping. *Papir Celulosa*, **1965**; 20(1): 11–14.
  - 14 Hatton, J.V. Quality and kraft pulping characteristics of residual chips. *Tappi*, **1975**; 58(2): 110–114.
  - 15 Fengel, D. The distribution of aqueous solutions within wood. *J. Polymer Sci.*, **1971**; 36: 141–152.
  - 16 Miller, R.N., W.H. Swanson. *Paper Trade J.*, **1922**; 74(15): 295–305.
  - 17 Montigny, R.D., O. Maass. *Forest Service Bull.*, **1935**: 87.
  - 18 Woods, N.I. Determination of penetration rates of liquid media into wood using a quartz spiral balance. Part 2: Water and a pre-treated spruce chip. *Pulp Paper Mag. Can.*, **1956**; 57(4): 142–151.
  - 19 Hart, J.S. The Va-Purge process in chemical pulping. *Tappi*, **1954**; 37(8): 331–335.
  - 20 Malkov, S., et al. Efficiency of chip pre-steaming – result of heating and air escape processes. *Nordic Pulp Paper Res. J.*, **2002**; 17(4): 420–426.
  - 21 Flamm, E., H. Sadler. Die Durchtränkung von Laub- und Nadelhölzer. *Das Papier*, **1963**; 17(3): 94–106.
  - 22 Nicholas, D.D., R.J. Thomas. Influence of steaming on ultrastructure of bordered pit membrane in loblolly pine. *Forest Prod. J.*, **1968**; 18(1): 57.
  - 23 Mouchot, N., A. Zoulalian. longitudinal permeability and diffusivity of steam in beech wood determined with a Wick-Kallenbach-cell. *Holzforschung*, **2002**; 56(3): 318–326.
  - 24 Stone, J.E. The penetrability of wood. *Pulp Paper Mag. Can.*, **1956**; 57(7): 139–145.
  - 25 Stamm, A.J. Diffusion and penetration mechanism of liquids into wood. *Pulp Paper Mag. Can.*, **1953**; 54(2): 54–63.
  - 26 Olsson, T., et al. Study of the transverse liquid flow paths in pine and spruce using scanning electron microscopy. *J. Wood Sci.*, **2001**; 47(2): 282–288.
  - 27 Stone, J.E., H.V. Green. Penetration and diffusion into hardwoods. *Pulp Paper Mag. Can.*, **1958**; 59(10): 223–232.
  - 28 Malkov, S., P. Tikka, J. Gullichsen. Towards complete impregnation of wood chips with aqueous solutions. Part 2. Studies on water penetration into softwood chips. *Pap. Puu*, **2001**; 83(6): 468–473.
  - 29 Malkov, S., et al. Modelling the process water penetration into softwood chips. *J. Pulp Paper Sci.*, **2003**; 29(4): 137–143.
  - 30 Minor, J.L., E.L. Springer. Improved penetration of pulping reagents into wood. *Pap. Puu*, **1993**; 75(4): 241–246.
  - 31 Liyama, K., A.F.A. Wallis. An improved acetyl bromide procedure for determining lignin in woods and wood pulps. *Wood Sci. Technol.*, **1988**; 22: 271–280.
  - 32 Malkov, S., P. Tikka, J. Gullichsen. Towards complete impregnation of wood chips with aqueous solutions. Part 3. Black liquor penetration into pine chips. *Pap. Puu*, **2001**; 83(8): 605–609.
  - 33 Malkov, S., P. Tikka, J. Gullichsen. Towards complete impregnation of wood chips with aqueous solutions. Part 4. Effects of front-end modifications in displacement batch kraft pulping. *Pap. Puu*, **2002**; 84(8): 526–530.
  - 34 McKibbins, S.W. Application of diffusion theory to the washing of kraft cooked wood chips. *Tappi*, **1960**; 43(10): 801–805.
  - 35 Crank, J. *The Mathematics of Diffusion*. London: Clarendon Press, **1956**.

- 36 Glasstone, S., K.J. Laidler, H. Eyring. *The Theory of Rate Processes*. 1st edition. New York: McGraw-Hill, 1941.
- 37 Behr, E.A., D.R. Briggs, F.N. Kaufert. Diffusion of dissolved materials through wood. *J. Phys. Chem.*, 1953; 57: 476–480.
- 38 Christensen, G.N. Diffusion in wood. II. The temperature coefficient of diffusion through wood. *Australian J. Appl. Sci.*, 1951; 2(4): 430–439.
- 39 Talon, J. *The diffusion of sodium hydroxide in wood at a high pH as a function of temperature and degree of pulping*. Master Thesis, North Carolina State University: Raleigh, 1986.
- 40 Talton, J.H., R.H. Cornell. Diffusion of sodium hydroxide in wood at high pH as a function of temperature and the extent of pulping. *Tappi*, 1987; 70(3): 115–118.
- 41 Constanza, V., et al. Diffusion and reaction in isothermal pulping digesters. *Ind. Eng. Chem. Res.*, 2001; 40(18): 3965–3972.
- 42 Robertsen, L., B. Lönnberg. Diffusion in wood. Part 2. The effects of concentration and temperature. *Pap. Puu*, 1991; 73(7): 635–639.
- 43 Constanza, V., P. Constanza. Estimating pure diffusion contributions in alkaline pulping processes. *Latin American Appl. Res.*, 2002; 32: 151–159.
- 44 Stone, J.E. The effective capillary cross-sectional area of wood as a function of pH. *Tappi*, 1957; 40(7): 539–541.
- 45 Häggglund, O. *Examensarbete*. Royal Institute of Technology: Stockholm, 1959.
- 46 Bäckström, C. *Examensarbete*. Royal Institute of Technology: Stockholm, 1960.
- 47 Heinigen, A.V. Lecture notes, Department of Chemical Engineering. University of New Brunswick: Fredricton, NB, 1993.
- 48 Törnqvist, M., T. Hurme, J.B. Rosenholm. The concentration dependence of the diffusion coefficient in Pine, Birch and Spruce. *Pap. Puu*, 2001; 83(3): 204–209.
- 49 ASTM. Standard test methods for pore size characteristics of membrane filters by bubble point and mean flow pore test. p. 316–386.
- 50 Hartler, N. Penetration und Diffusionsverhalten bei Sulfatkoehung. *Pap. Puu*, 1962; 7: 365–374.
- 51 Michelsen, F.A. A dynamic mechanistic model and model-based analysis of a continuous Kamyrdigester. In: Department of Engineering Cybernetics. The Norwegian Institute of Technology. University of Trondheim: Trondheim, 1995, p. 253.
- 52 Gustafson, R.R., et al. Theoretical model of the kraft pulping process. *Ind. Eng. Chem. Process Des. Dev.*, 1983; 22: 87–96.
- 53 Li, J., A. Phoenix, J.M. MacLeod. Diffusion of lignin macromolecules within the fibre walls of kraft pulp. Part I: Determination of the diffusion coefficient under alkaline conditions. *Can. J. Chem. Eng.*, 1997; 75(2): 16–22.
- 54 Törnqvist, M., T. Hurme, J.B. Rosenholm. The effect of pressure steaming on the steady state ion diffusion and drift speed in wood. *Holz-forschung*, 2001; 55(4): 441–447.
- 55 Kazi, M.F.K. *Impregnation: A key step of biomass conversion processes*. Université de Sherbrooke: Quebec, 1996.
- 56 Kazi, K.M.F., E. Chornet. A diffusion model for the chemical impregnation of hardwoods and its significance for rapid steam treatments. *Pap. Puu*, 1998; 80(1): 41–48.
- 57 Backman, A. The influence of chip thickness on yield of cellulose and pulp quality during cooking with parallelepipedic chips. *Finnish Paper Timber J.*, 1946; 28: 200–208.
- 58 Hartler, N., K. Ostberg. Impregnation for the sulfate cook. *Svensk Papperstidn.*, 1959; 62: 524–533.
- 59 Larocque, G.L., O. Maass. The influence of penetration in the alkaline delignification of wood. *Can. J. Res.*, 1937; 15, B: 89–97.
- 60 Malkov, S., P. Tikka, R. Gustafson. Towards complete impregnation of wood chips with aqueous solutions. Part 5: Improving uniformity of kraft displacement batch pulping. *Pap. Puu*, 2003; 85(4): 215–220.

- 61 Egas, A.P.V., et al., Experimental methodology for heterogeneous studies in pulping of wood. *Ind. Eng. Chem. Res.*, **2002**; 41(10): 2529–2534.
- 62 Analysis of sode and sulfate black liquor T625 cm-85, TAPPI Standard.
- 63 Santos, A., et al. Kinetik modelling of kraft delignification of *Eucalyptus globulus*. *Ind. Eng. Chem. Res.*, **1997**; 36: 4114–4125.

#### Section 4.2.4

- 1 Fengel, D., Wegener, G. *Wood, Chemistry, Ultrastructure, Reactions*, W. Degruyter, Berlin, New York, **1989**.
- 2 Gratzl, J.S., Chen, C.L. ACS Symposium Series Vol. 742, Chapter 20. Eds. Glasser, W., Northey, R.A., Schultz T.P. ACS, **1999**: 392–421.
- 3 Modified model adopted from H. Kindl, *Biochemie der Pflanzen*, 3. Auflage, Springer-Verlag, Berlin, Heidelberg, New York, London, Paris, Tokyo, Hong Kong, Barcelona, Budapest, **1991**.
- 4 PM3 calculation using Spartan Pro 4.0.
- 5 Gierer, J. *Wood Sci. Technol.*, **1985**; 19: 289–312.
- 6 Gierer, J., Lindeberg, O. *Acta Chem. Scand.*, **1980**, 161–170.
- 7 Gierer, J., Noren, I. *Holzforchung*, **1980**; 34: 197.
- 8 Liitia, T.M., Maunu, S.L., Hortling, B., Toikka, M., Kilpelainen, I., *J. Agric. Food Chem.*, **2003**; 51 (8): 2136.
- 9 Capanema, E.A., Balakshin, M.Y., Chen, C.-L., Gratzl, J.S. In: *Proceedings of the 6th Brazilian Symposium on the Chemistry of Lignin and other Wood Components*. Guaratingueta, SP, Brazil, **1999**: 418.
- 10 Capanema, E.A., Balakshin, M. Yu., Chen, C.L., Colson, K.L., Gracz, H.S. 12th ISWPC Madison. Proceedings I, **2003**: 179.
- 11 Granata, A., Argyropoulos, D.S. *J. Agric. Food Chem.*, **1995**; 43 (6): 1538.
- 12 Gellerstedt, G., Majtnerova, A., Zhang, L. *C.R. Biologies*, **2004**; 327 (9–10): 817.
- 13 Liittä, T., Maunu, S.L., Sipilä, J., Hortling, B. *Solid State Nuclear Magn. Res.*, **2002**; 21: 171.
- 14 Gellerstedt, G.; Lindfors, E.-L. *Nordic Pulp Paper J.*, **1987**; 2: 71.
- 15 Chiang, V.L., Funaoka, M. *Holzforchung*, **1988**; 42: 385.
- 16 Chiang, V.L., Funaoka, M. *Holzforchung*, **1990**; 44: 147.
- 17 Funaoka, M., Kako, T., Abe, I. *Holzforchung*, **1990**; 44: 357.
- 18 Funaoka, M., Kako, T., Abe, I. *Wood Sci. Technol.*, **1990**; 24: 277.
- 19 Chiang, V.L., Funaoka, M. *Holzforchung*, **1990**; 44: 309.
- 20 Berthold, F., Gellerstedt, G., Lindfors, E.L. *Holzforchung*, **1998**; 52: 394.
- 21 Gellerstedt, G., Lindfors, E.-L. *Nordic Pulp Paper J.*, **1987**; 2: 71–75.
- 22 Gierer, J. *Svensk. Papperstidn.*, **1970**; 73: 571.
- 23 Dimmel, D.R., Bovee, L.F., Brogdon, B.N. *Wood Chem. Technol.*, **1994**; 14: 1–14.
- 24 Gellerstedt, G., Gustafsson, K., Lindfors, E.L., Robert, D., Proc. ISWPC, Raleigh, NC, **1989**.
- 25 Gierer, J., Wännström, S., *Holzforchung*, **1986**; 40(6): 347.
- 26 Capanema, E.A., Balakshin, M.Y., Kadla, J.K. *J. Agric. Food Chem.*, **2004**; 52: 1850.
- 27 Zhang, L., Gellerstedt, G. Sixth European Symposium on Lignocellulosics and Pulp, Bordeaux, France, Proceedings, **0000**: 7.
- 28 Rosenau, T., Potthast, A., Milacher, W., Hofinger, A., Kosma, P., *Polymer*, **2004**; 45: 6437.
- 29 Chang, H.-M. In: *Methods in Lignin Chemistry*, Eds. Lin, S.Y., Dence, C.W., Springer-Verlag, Heidelberg, **0000**: 71.
- 30 Yamasaki, T., Hosoya, S., Chen, C.L., Gratzl, J.S., Chang, H.-M. *J. Wood Chem. Technol.*, **1987**; 7(4): 485.
- 31 Gellerstedt, G., Pranda, J., Lindfors, E.-L. *J. Wood Chem. Technol.*, **1994**; 14: 467–482.
- 32 Lachenal, D., Mortha, G., Sevillano, R.M., Zaroubine, M. *C. R. Biologies*, **2004**; 327(9–10): 817.
- 33 Argyropoulos, D.S., Sun, Y., Paulus, E. *J. Pulp Paper Sci.*, **2002**; 28(2): 50.
- 34 Wu, S., Argyropoulos, D.S. *J. Pulp Paper Sci.*, **2003**; 29(7): 235.

- 35 Balakshin, M.Y., Capanema, E.A., Chen, C.L., Gracz, H.S. *J. Agric. Food Chem.*, **2003**; 51: 6116.
- 36 Jääskeläinen, J.S., Sun, Y., Argyropoulos, D.S., Tamminen, T., Hortling, B. *Wood Sci. Technol.*, **2003**; 37: 91.
- 37 Capanema, E., Balakshin, M.Y., Chen, C.-L. *Holzforschung*, **2004**; 58: 464.
- 38 Ibarra, D., del Río, J.C., Gutiérrez, A., Rodríguez, I., Romero, J., Martínez, M.J., Martínez, A.T. *Enzyme Microbial Technol.*, **2004**; 35(2–3): 173.
- 39 Lawoko, M., Henriksson, G., Gellerstedt, G. *Holzforschung*, **2003**; 57(1): 69.
- 40 Karlsson, O., Westermark, U. *J. Pulp Paper Sci.*, **1996**; 22: 397.
- 41 Iverson, T., Wännström, S. *Holz-forschung*, **1986**; 40: 19.
- 42 Tohomura, S., Argyropoulos, D.S. *J. Agric. Food Chem.*, **2001**; 49(2): 536.
- 43 Gellerstedt, G., Gustafsson, K., Lindfors, E.L. *Nordic Pulp Paper Res. J.*, **1986**; 3: 14.
- 44 Gellerstedt, G., Heuts, L. *J. Pulp Paper Sci.*, **1997**; 23: 335–340.
- 45 Jiang, Z.-H., Argyropoulos, D.S. *J. Pulp Paper Sci.*, **1999**; 25: 25–29.
- 46 Argyropoulos, D.S., Liu, Y., *J. Pulp Paper Sci.*, **2000**; 26: 107.
- 47 Lai, Y.Z., Funaoka, M., Chen, H.T., *Holzforschung*, **1994**; 48: 355.
- 48 Holtmann, K.M., Chang, H.-M., Jameel, H., Kadla, J.K. *J. Agric. Food Chem.*, **2003**; 12(4): 3535.
- 49 Robert, D.R., Bardet, M., Gellerstedt, G., Lindfors, E. *J. Wood Chem. Technol.*, **1984**; 4: 239.
- 50 Gellerstedt, G., Lindfors, E. *Svensk. Papperstidn.*, **1984**; 15: R115–R117.
- 51 Faix, O., Argyropoulos, D.S., Robert, D., Neirick, V. *Holzforschung*, **1994**; 48: 387.
- 52 Froass, P., Ragauskas, A.J. *J. Wood Chem. Technol.*, **1998**; 16(4): 347.
- 53 Froass, P., Ragauskas, A.J., Jiang, J. *Holzforschung*, **1998**; 52: 385.
- 54 Zawadzki, M., Runge, T.M., Ragauskas, A.J. *J. Pulp Paper Sci.*, **2000**; 26(3): 102.
- 55 Balakshin, M.Y., Capanema, E.A., Chen, C.L., Gracz, H.S. *J. Agric. Food Chem.*, **2003**; 51: 6116.
- 56 Gellerstedt, G. *Pulping Chemistry*. In: Hon, D.N.S., Shiraishi, N., Eds. *Wood and Cellulosic Chemistry*. 2nd edition. M. Dekker, New York, Basel, **2001**: 859.
- 57 Meller, A. *Holzforschung*, **1965**; 19(4): 118.
- 58 Fengel, D., Wegener, G., Heizmann, A., Przyklenk, M., *Cellulose Chem. Technol.*, **1978**; 12: 31.
- 59 Dahlman, O., Jacobs, A., Sjöberg, J. *Cellulose*, **2003**; 10(49): 325.
- 60 Sjöberg, J., Kleen, M., Dahlman, O., Agnemo, R., Sunvall, H. *Nordic Pulp Paper Res. J.*, **2002**; 17(3): 295.
- 61 Lobry de Bruyn, C.A., Alberta van Ekenstein, W. *Recl. Trav. Chim. Pays-Bas*, **1895**; 14: 203.
- 62 De Wit, G., Kieboom, A.P.G., van Bekkum, H. *Carbohydr. Res.*, **1979**; 74: 157.
- 63 Speck Jr., J.C. *Adv. Carbohydr. Chem.*, **1958**; 13: 63.
- 64 Franzon, O., Samuelson, O. *Svensk. Papperstidn.*, **1957**; 23: 872.
- 65 Sjöström, E., *Tappi*, **1977**; 60(9): 151.
- 66 Haas, D.W., Hrutfiord, B.F., Sarkanen, K.V. *J. Appl. Polym. Sci.*, **1967**; 11: 587.
- 67 Lewin, M., Mark, H.F. *Macromol. Symp.*, **1997**; 118: 715.
- 68 Lai, Y.-Z., Sarkanen, K.V. *Cellulose Chem. Technol.*, **1967**; 1: 517.
- 69 Kubes, G.J.; Fleming, B.I., MacLeod, J.M., Bolker, H.I., Werthemann, D.P. *J. Wood Chem. Technol.*, **1983**; 3: 313.
- 70 Gentile, V.M., Schroeder, L.R., Attalla, R.H. *J. Wood Chem. Technol.*, **1986**; 6: 1.
- 71 Attalla, R.H., Ranau, J., Malcolm, E., *Tappi*, **1984**; 67(2): 96.
- 72 Isogai, A., Akishima, Y., Onabe, F., Usuda, M. *Nordic Pulp Paper Res. J.*, **1991**; 4: 161.
- 73 Aspinall, G.O., Greenwood, C.T., Sturgeon, J.R. *J. Chem. Soc.*, **1961**, 3667.
- 74 Sartori, J., Potthast, A., Rosenau, T., Hofinger, A., Sixta, H., Kosma, P. *Carbohydr. Res.*, **2003**; 338: 1209.
- 75 Sartori, J., Potthast, A., Rosenau, T., Hofinger, A., Sixta, H., Kosma, P. *Holz-forschung*, **2004**; 58: 588.
- 76 Johansson, M.H., Samuelson, O. *Svensk. Papperstidn.*, **1977**; 80: 519.
- 77 Johansson, M.H., Samuelson, O. *Wood Sci. Technol.*, **1977**; 11: 251.
- 78 Simpsonson, R. *Svensk. Papperstidn.*, **1971**; 74(21): 691.

- 79 Johansson, M.H., Samuelson, O. *Carbohyd. Res.*, **1977**; 54: 295.
- 80 Clayton, D.W. *Svensk. Papperstidn.*, **1963**; 66(4): 115.
- 81 Hansson, J.A., Hartler, N., *Svensk. Papperstidn.*, **1968**; 71(9): 358.
- 82 Jacobs, A., Larsson, P.T., Dahlman, O. *Biomacromolecules*, **2001**; 2: 979.
- 83 Jiang, Z.-H., Lierop, B.V., Berry, R. *Tappi J.*, **2000**; 83: 167.
- 84 Hansson, J.A., Hartler, N. *Svensk. Papperstidn.*, **1963**; 66(4): 115.
- 85 Johansson, M., Samuelson, O. *Carbohyd. Res.*, **1977**; 54: 295.
- 86 Thompson, N.S., Kaustinen, O.A. Ross, R. *Tappi J.*, **1963**; 46(8): 490.
- 87 Ross, R., Thomposon, N.S. *Tappi J.*, **1963**; 46(8): 376.
- 88 Buchert, J., Telemann, A., Harjunpaa, V., Tenkanen, M., Viikari, L., Vuorinen, T. *Tappi J.*, **1995**; 78(11): 125.
- 89 Vuorinen, T., Fagerström, P., Buchert, J., Tenkanen, M., Telemann, A. *J. Pulp Paper Sci.*, **1999**; 5(25): 155.
- 90 Johansson, M.H., Samuelsson, O. *Svensk. Papperstidn.*, **1977**; 16: 519.
- 91 Li, J., Gellerstedt, G., *Nordic Pulp Paper Res. J.*, **1998**; 13(2): 153.
- 92 Li, J., Gellerstedt, G., *Nordic Pulp Paper Res. J.*, **2002**; 17(4): 410.
- 93 Lai, Y.-Z. Chemical Degradation. In: Hon, D.N.S., Shiraishi, N., Eds. *Wood and Cellulosic Chemistry*. 2nd edition. M. Dekker, New York, Basel, **2001**: 443.
- 94 Aurell, R., Hartler, N. *Svensk. Papperstidn.*, **1965**; 68(3): 59.
- 95 Timell, T.E. *Tappi*, **1961**; 44: 88.
- 96 Duchesne, I., Daniel, G. *Nordic Pulp Paper Res. J.*, **2000**; 15(1): 54.
- 97 Genco, J.M., Busayasakul, N., Medhora, H.K., Robbins, W. *Tappi J.*, **1990**; 73: 223.
- 98 Hansson, J.A., Hartler, N. *Svensk. Papperstidn.*, **1969**; 72: 521.
- 99 Yllner, S., Enström, B. *Svensk. Papperstidn.*, **1956**; 59: 229.
- 100 Yllner, S., Enström, B. *Svensk. Papperstidn.*, **1957**; 60: 549.
- 101 Clayton, D.W., Stone, J.E. *Pulp Paper Mag. Can.*, **1963**, 459.
- 102 Meller, A. *Holzforschung*, **1965**; 19: 118.
- 103 Aurell, R. *Tappi*, **1965**; 48: 80.
- 104 Sjöberg, J., PhD Thesis STFI, **2002**.
- 105 Fiserova, N., Opalena, E., Farkas, J. *Cell. Chem. Technol.*, **1986**; 21: 419.
- 106 Hansson, J.A. *Svensk. Papperstidn.*, **1970**; 73(3): 49.
- 107 Jacob, A., Dahlman, O., Sjöberg, J. *Biomacromolecules*, **2001**; 2(3): 894.
- 108 Dahlman, O., Jacob, A., Sjöberg, J. *Cel-lulose*, **2003**; 10(4): 325.
- 109 Larson, P.T. ACS Symposium Series 864 (Hemicelluloses), **2004**: 254.
- 110 Hult, E.-L., Larsson, P.T., Iversen, T. *Polymer*, **2001**; 42: 3309.
- 111 Newman, R.H., Hemmingson, J.A., Suckling, I.D. *Holzforschung*, **1993**; 47(3): 234.
- 112 Hult, E.-L., Larsson, P.T., Iversen, T. *Cel-lulose*, **2000**; 7: 35.
- 113 Sjöholm, E., Gustafsson, K., Berthold, F., Colmsjö, A. *Carbohyd. Polym.*, **2000**; 41: 1.
- 114 Sjöholm, E., Gustafsson, K., Pettersson, B., Colmsjö, A. *Carbohyd. Polym.*, **1997**; 32: 57.
- 115 Berthold, F., Gustafsson, K., Berggren, R., Sjöholm, E., Lindstroem, M. *J. Appl. Polym. Sci.*, **2004**; 94(2): 424.
- 116 Westermark, U., Gustafsson, K. *Holz-forschung*, **1994**; 48: 146.
- 117 Larsson, O., Westermark, U. *Nordic Pulp Paper Res. J.*, **1997**; 12: 203.
- 118 Karlsson, O., Westermark, U. *J. Pulp Paper Sci.*, **2001**; 27(6): 196.
- 119 Karlsson, O., Westermark, U. *J. Pulp Paper Sci.*, **1996**; 22: 397.
- 120 Buchert, J., Telemann, A., Harjunpää, V., Tenkanen, M., Viikari, L., Vuorinen, T. *Tappi J.*, **1995**; 78: 125.
- 121 Tenkanen, M., Tamminen, T., Hortling, B. *Appl. Microbiol. Biotechnol.*, **1999**; 51(2): 241.
- 122 Forsskahl, I., Popoff, T., Theander, O. *Carbohyd. Res.*, **1976**; 48: 13.
- 123 Lagercrantz, C. *Acta Chem. Scand.*, **1964**; 18(5): 1321.
- 124 Sartori, J., Potthast, A., Rosenau, Th., Sixta, H., Kosma, P. Proceedings EWLP, Turku. Book of Abstracts, **2002**: 165–168.
- 125 Luetzow, A.E., Theander, O. *Svensk. Papperstidn.*, **1974**; 77: 312.
- 126 Gardner, J.A.F., Hillis, W.E. In: *Wood extractives and their significance to the pulp and paper industries*. Hillis, W.E.,

- ed. Academic Press, New York, London, 1962.
- 127 Rydholm, S.A. *Pulping Chemistry*. R.E. Krieger Publisher Company, Malabar, Florida, 1985.
  - 128 Sjöström, E. *Wood chemistry – Fundamentals and Applications*. Academic Press, New York, London, Toronto, Sydney, San Francisco, 1981.
  - 129 Holmbom, B., Ekman, R. *Acta Academiae aboensis, Ser. B*, 1978; 38(3): 1.
  - 130 Jamieson, G.R., Reid, E.H. *J. Chromatogr.*, 1965; 20: 232.
  - 131 Holmbom, B. *J. Am. Oil Chemist's Soc.*, 1977; 54: 289.
  - 132 Takeda, H., Schuller, W.H., Lawrence, R.V., Rosebrook, D. *J. Org. Chem.*, 1969; 51: 1974.
  - 133 Lai, Y.-Z., Cerkies, A.R., Shiau, I.L. *Appl. Polym. Symp.*, 1983; 37: 943.
  - 134 Teder, A. *Acta Chem. Scand.*, 1971; 25: 1722.
  - 135 Volgger, D., Zemann, A., Bonn, G. *J. High Res. Chromatogr.*, 1998; 21(1): 3.
  - 136 Sullivan, J., Douek, M. *J. Chromatogr. A*, 2004; 1039(1–2): 215.
  - 6 Yllner, S., B. Enström, Adsorption of xylan on cellulose fibers during the sulfite cook. Part I. 1956; 59: 229–232.
  - 7 Andersson, N., D.I. Wilson, U. Germgard, An improved kinetic model structure for softwood kraft cooking. *Nordic Pulp Paper Res. J.*, 2003; 18(2): 200–209.
  - 8 Kubes, G.J., et al., Viscosities of unbleached alkaline pulps. II. The G-factor. *J. Wood Chemistry Technol.*, 1983; 3(3): 313–333.
  - 9 Arrhenius, S., N. Schmidt, *Svensk. Papperstid.*, 1924 (5).
  - 10 Yan, F.J., D.C. Johnson, *J. Appl. Polymer Sci.*, 1981; 26: 1623.
  - 11 Butt, J.B., *Reaction kinetics and reactor design*. Prentice-Hall Inc.: New Jersey, USA, 1980.
  - 12 Michelsen, F.A., A dynamic mechanistic model and model-based analysis of a continuous Kamyrdigester, in Department of Engineering Cybernetics. The Norwegian Institute of Technology, University of Trondheim, Trondheim, 1995: 253.
  - 13 Vroom, K.E., The 'H' Factor: A means of expressing cooking times and temperatures as a single variable. *Pulp Paper Mag. Can.*, 1957; 58C: 228–231.
  - 14 Lindgren, C.T., M.E. Lindström, Kinetics of the bulk and residual delignification in kraft pulping of birch and factors affecting the amount of residual phase lignin. *Nordic Pulp Paper Res. J.*, 1997; 12(2): 124–134.
  - 15 Axegaard, P., J.E. Wiken, Delignification studies – factors affecting the amount of "residual lignin". *Svensk. Papperstid.*, 1983; 86(15): R178–R184.
  - 16 Sixta, H., Conventional Kraft cooking of a mixture of 50% spruce and 50% pine. R&D Department of Lenzing AG: Lenzing, Austria, 2003.
  - 17 Rydholm, S., *Pulping Processes*. Malabar, Florida: Robert E. Krieger Publishing Company, 1965: 616.
  - 18 Hatton, J.V., Development of yield prediction equations in kraft pulping. *Tappi*, 1973; 56(7): 97–100.
  - 19 Bailey, R.N., P. Maldonado, S.W. McKibbins, M.G. Tarver, Statistical analysis and optimization procedure for the

## Section 4.2.5

- 1 Masura, V., Alkaline degradation of spruce and beech wood. *Wood Sci. Technol.*, 1982; 16: 155–164.
- 2 Aurell, R., N. Hartler, Kraft pulping of pine. Part 1. Changes in the composition of the wood residue during the cooking process. *Svensk. Papperstid.*, 1965; 68(3): 59–68.
- 3 Whistler, R.L., J.N. BeMiller, Alkaline degradation of polysaccharides. *Adv. Carbohydrate Chem.*, 1958; 13: 289–329.
- 4 Buchert, J., et al., Effect of cooking and bleaching on the structure of xylan in conventional pine kraft pulp. *Tappi J.*, 1995; 78(11): 125–130.
- 5 Teleman, A., V. Harjunpää, M. Tenkanen, J. Buchert, T. Drakenberg, T. Vuorinen, Characterisation of 4-deoxy-beta-L-threo-hex-4-enopyranosyluronic acid attached to xylan in pine kraft pulp and pulping liquor by <sup>1</sup>H and <sup>13</sup>C NMR spectroscopy. *Carbohydrate Res.*, 1995; 272(1): 55–71.

- kraft pulping process. *Tappi*, **1969**; 52(7): 1272–1275.
- 20 Alen, R., K. Niemelä, E. Sjöström, Gas-liquid chromatographic separation of hydroxy monocarboxylic acids and dicarboxylic acids on a fused-silica capillary column. *J. Chromatogr.*, **1984**; 301(1): 273–276.
  - 21 Alén, R., et al., A new approach for process control of kraft pulping. *J. Pulp Paper Sci.*, **1991**; 17(1): 6–9.
  - 22 Emsley, A.M., G.C. Stevens, Kinetics and mechanisms of the low-temperature degradation of cellulose. *Cellulose*, **1994**; 1: 26–56.
  - 23 Kubes, G.J., et al., Viscosities of unbleached alkaline pulps. II. The G-Factor. *J. Wood Chemistry Technol.*, **1983**; 3(3): 313–333.
  - 24 Håkansdotter, L., L. Olm, The influence of temperature on delignification and carbohydrate degradation in soda-AQ pulping of softwood. *Nordic Pulp Paper Res. J.*, **2001**; 16: 183–187.
  - 25 Li, Z., J. Li, G.J. Kubes, Kinetics of delignification and cellulose degradation during kraft pulping with polysulphide and anthraquinone. *J. Pulp Paper Sci.*, **2002**; 28(7): 234–239.
  - 26 Fleming, B.I., G.J. Kubes, The viscosities of unbleached alkaline pulps. IV. The effect of alkali. *J. Wood Chemistry Technol.*, **1985**; 5(2): 217–227.
  - 27 LeMon, S., A. Teder, Kinetics of the delignification in kraft pulping I. Bulk delignification of pine. *Svensk. Papperstid.*, **1973**; 11: 407–414.
  - 28 Gustafson, R.R., et al., Theoretical model of the kraft pulping process. *Ind. Eng. Chem. Process Des. Dev.*, **1983**; 22: 87–96.
  - 29 Kubo, M., et al. A kinetic model of delignification in kraft pulps. In: Second International Symposium on Wood and Pulping Chemistry, Japan, **1983**.
  - 30 Chiang, V.L., J. Yu, R.C. Eckert, Isothermal reaction kinetics of kraft delignification of douglas-fir. *J. Wood Chemistry Technol.*, **1990**; 10(3): 293–310.
  - 31 Labidi, A., F. Pla, Délignification en milieu alcalin de bois feuillus à l'aide d'un réacteur à lit fixe et à faible temps de passage. *Holzforschung*, **1992**; 46(2): 155–161.
  - 32 Vanchinathan, S., G.A. Krishnagopalan, Kraft delignification kinetics based on liquor analysis. *Tappi*, **1995**; 78(3): 127–132.
  - 33 Lindgren, C.T., M.E. Lindström, The kinetics of residual delignification and factors affecting the amount of residual lignin during kraft pulping. *J. Pulp Paper Sci.*, **1996**; 22(8): J290–J295.
  - 34 Blixt, J., C.A.-S. Gustavsson, Temperature dependence of residual phase delignification during kraft pulping of softwood. *Nordic Pulp Paper Res. J.*, **2000**; 15(1): 12–17.
  - 35 Olm, L., G. Tistad, Kinetics of the initial stage of kraft pulping. *Svensk. Papperstid.*, **1979**; 15: 458–464.
  - 36 Wilder, H.D., E.J. Daleski, Delignification rate studies. Part II of a series on kraft pulping kinetics. *Tappi*, **1965**; 48(5): 293–297.
  - 37 Kojima, M., et al. Reaction kinetics in kraft pulping: Effect of chip thickness. In: Second International Symposium on Wood and Pulping Chemistry, Japan, **1983**.
  - 38 Lindström, M.E., Some factors affecting the amount of residual phase lignin during kraft pulping. In: *Royal Institute of Technology, Pulp and Paper Chemistry and Technology*, KTH: Stockholm, **1997**.
  - 39 Vitta, S.B., Delignification kinetics and pulping characteristics of Soda-AQ and Soda-THAQ pulping of sweetgum (*Liquidambar styraciflua* L.). **1979**.
  - 40 Smith, C., *Studies of the mathematical modelling, simulation, and control of the operation of a Kamyr continuous digester for the kraft process*. Purdue University: West Lafayette, Indiana, USA, **1974**.
  - 41 Kleinert, T.N., Mechanisms of alkaline delignification. I. The overall reaction pattern. *Tappi*, **1966**; 49(2): 53–57.
  - 42 McKibbins, S.W., Application of diffusion theory to the washing of kraft cooked wood chips. *Tappi*, **1960**; 43(10): 801–805.
  - 43 Christensen, T., C.C. Smith, L.F. Abright, T.J. Williams, Modeling of batch kraft pulping and of Kamyr digesters. *Pulp and Paper Canada*, **1984**; 85(8): 55–58, 60.
  - 44 Andersson, N., D.I. Wilson, U. Germgard. Validating continuous

- kraft digester kinetic models with online NIR measurements. In: American Control Conference, Alaska, USA, 2002.
- 45 Pu, Q., W. McKean, R. Gustafson, Kinetic model of softwood kraft pulping and simulation of RDH process. *Appita*, 1991; 44(6): 399–404.
  - 46 Norden, S., A. Teder, Modified kraft processes for softwood bleached-grade pulps. *Tappi*, 1979; 62(7): 49–51.
  - 47 Lindgren, C.T., Kraft pulping kinetics and modelling, the influence of HS-, OH- and ionic strength. Royal Institute of Technology: Stockholm, Sweden, 1997.
  - 48 Gierer, J., I. Noren, On the course of delignification during kraft pulping. *Holzforschung*, 1980; 34: 197–200.
  - 49 Gierer, J., The reactions of lignin during pulping. A description and comparison of conventional pulping processes. *Svensk. Papperstidn.*, 1970; 18: 571–596.
  - 50 Ljunggren, S., The significance of aryl ether cleavage in kraft delignification of softwood. *Svensk. Papperstidn.*, 1980; 83(13): 363–369.
  - 51 Miksche, G., Über das Verhalten des Lignins bei der Alkalikochung. VI. Zum Abbau von p-Hydroxy-phenylcumaranstrukturen durch Alkali. *Acta Chim. Scand.*, 1972; 26(8): 3269–3274.
  - 52 Miksche, G.E., Zum alkalischen Abbau der p-Alkoxy-arylglycerin-b-aryletherstrukturen des Lignins. Versuche mit erythro-Veratrylglycerin-b-guajacylether. *Acta Chim. Scand.*, 1972; 26(8): 3275–3281.
  - 53 Teder, A., L. Olm, Extended delignification by combination of modified kraft pulping and oxygen delignification. *Pap. Puu*, 1981; 63(4a): 315–326.
  - 54 Gierer, J., Chemical aspects of kraft pulping. *Wood Sci. Technol.*, 1980; 14: 241–266.
  - 55 Chiang, V.L., M. Funaoka, *Holz-forschung*, 1988; 42(6): 385.
  - 56 Gustavsson, C.A.-S., C.T. Lindgren, M.E. Lindström, Residual phase lignin in kraft cooking related to the conditions in the cook. *Nordic Pulp Paper Res. J.*, 1997; 12(4): 225–229.
  - 57 Pekkala, O., Some features of residual delignification during kraft pulping of Sots Pine. *Pap. Puu*, 1983; 65(4): 251.
  - 58 Gierer, J., F. Imsgard, I. Pettersson, Possible condensation and polymerization reactions of lignin fragments during alkaline pulping processes. *Appl. Polym. Symp.*, 1976; 28: 1195.
  - 59 Sjöblom, K., Extended delignification in kraft cooking through improved selectivity. Part 5. Influence of dissolved lignin on the rate of delignification. *Nordic Pulp Paper Res. J.*, 1996; 3: 177–185.
  - 60 Brunow, G., G.E. Miksche, Some reactions of lignin in kraft and polysulfide pulping. *Appl. Polym. Symp.*, 1976; 28: 1155–1168.
  - 61 Farkas, J., The dimensions of chip in kraft pulping. *Papir Celulosa*, 1965; 20(1): 11–14.
  - 62 Hatton, J.V., Quantitative evaluation of pulpwood chip quality. *Tappi*, 1977; 60(4): 97–100.
  - 63 Hatton, J.V., Screening mill chips for sizeable savings. *Pulp Paper Canada*, 1977; 78(3): T57–T60.
  - 64 Backmann, A., Flistjocklekens inverkan på cellulosautbyte och massakvallen vid kok av parallellipedisk flis. *Pap. Puu*, 1946; 28(13): 200–208.
  - 65 Backman, A., *J. Finnish Paper Timber*, 1946; 28(13): 200.
  - 66 Hartler, N., K. Östberg, Impregneringen vid sulfatkoket. *Svensk. Papperstidn.*, 1959; 62(15): 524–533.
  - 67 Stone, J.E., The penetrability of wood. *Pulp Paper Mag. Can.*, 1956; 57(7): 139–145.
  - 68 Akhtaruzzamann, A.F.M., N.-E. Virkola, Influence of chip dimensions in kraft pulping. Part III. Effect on delignification and a mathematical model for predicting the pulping parameters. *Pap. Puu*, 1979; 61(11): 737–758.
  - 69 Akhtaruzzamann, A.F.M., N.-E. Virkola, Influence of chip dimensions in kraft pulping. Part IV. Effect on screened pulp yield and effective alkali consumption; predictive mathematical models. *Pap. Puu*, 1979; 61(12): 805–814.
  - 70 Chang, H.-M., K.V. Sarkanen, Species variation in lignin. Effect of species on the rate of Kraft delignification. *Tappi*, 1973; 56(3): 132–134.



- 71 Lee, Z.-Z., X.Q. Pau, International Symposium on Wood Pulping Chemistry, Vancouver, BC, 1985.
- 72 Epelde, I.G., C.T. Lindgren, M.E. Lindström, Kinetics of wheat straw delignification in soda and kraft pulping. *J. Wood Chem. Technol.*, 1998, 18(1): 69–82.
- 73 Cho, H.J., K.V. Sarkanen, Alternatives to H-factor measurement in the kraft process. *Pap. Puu*, 1985; 3: 121–124.
- 74 Christensen, T., et al., Dynamic modeling of the Kamyr digester: normal operation including hardwood-softwood swings. *Tappi*, 1983; 66(11): 65–68.
- 75 Olm, L., P.J. Nelson, S.-E. Campbell, The rate of delignification of *Eucalyptus disversicolor*, *E. regnans*, *E. marginata* and *E. tetradonta* woods during kraft pulping. *Appita*, 1984; 37(4): 314–318.
- 76 Wilson, G., A.R. Procter, Reactions of wood components with hydrogen sulphide: Part V. The kinetics of kraft and soda delignification of western hemlock. *Pulp Paper Mag. Can.*, 1970; 71(22): 67–71.
- 77 Farrington, A., P.F. Nelson, N. Vanderhoek, A new alkaline pulping process. *Appita*, 1977; 31(2): 119–120.
- 78 Timmel, T., *Advances in Carbohydrate Chemistry*, ed. M.L. Wolfrom. Vol. 19. New York: Academic Press, 1964.
- 79 Christensen, T., L.F. Albright, T.J. Williams. A kinetic mathematical model for the kraft pulping of wood. In: TAPPI Annual Meeting, Atlanta, Georgia, USA, 1983.
- 80 Kondo, R., K.V. Sarkanen, Kinetics of lignin and hemicellulose dissolution during the initial stage of alkaline pulping. *Holzforschung*, 1984; 38(1): 31–36.
- 81 Schild, G., W. Müller, H. Sixta, Prehydrolysis kraft and ASAM paper grade pulping of eucalypt Wood. A kinetic study. *Das Papier*, 1996; 50(1): 10–22.
- 82 Mortha, G., K. Sarkanen, R. Gustafson, Alkaline pulping kinetics of short-rotation, intensively cultured hybrid poplar. *Tappi J.*, 1992; 00: 99–104.
- 83 Matthews, C.H., Carbohydrate losses at high temperature in kraft pulping. *Svensk. Papperstidn.*, 1974; 77(17): 629–635.
- 84 Hartler, N., Penetration und Diffusionsverhalten bei Sulfatkochung. *Pap. Puu*, 1962; 7: 365–374.
- 85 Hägglund, O., *Examensarbete*. Royal Institute of Technology, Stockholm, 1959.
- 86 Bäckström, C., *Examensarbete*. Royal Institute of Technology, Stockholm, 1960.
- 87 Benko, J., The measurement of molecular weight of lignosulfonic acids and related material by diffusion. *Tappi*, 1964; 47(8): 508–514.
- 88 Rydholm, S., *Pulping Processes*. Malabar, Florida: Robert E. Krieger Publishing Company, 1965 p. 603.
- 89 Corbett, W.M., G.N. Richards, *Svensk. Papperstidn.*, 1957; 60: 791.
- 90 Giudici, R., S.W. Park, Kinetic model for kraft pulping of hardwood. *Ind. Eng. Chem. Res.*, 1996; 35(3): 856–863.
- 91 Rydholm, S., *Pulping Processes*. Malabar, Florida: Robert E. Krieger Publishing Company, 1965, p. 586.
- 92 Nelson, P.J., G.M. Gniel, Delignification of *Eucalyptus regnans* wood during soda pulping. *Appita*, 1986; 39(2): 110–114.
- 93 Dolk, M., J.F. Yan, J.L. McCarthy, Lignin 25. Kinetics of delignification of Western Hemlock in flow-through reactors und alkaline conditions. *Holzforschung*, 1989; 43(2): 91–98.
- 94 Saucedo, V.M., G.A. Krishnagopalan, Kinetics of conventional and alkali profiled hardwood cooks using on-line liquor analysis. *Appita*, 2002; 55(3): 202–207, 223.
- 95 Larocque, G.L., O. Maass, The mechanism of the alkaline delignification of wood. *Can. J. Res.*, 1941; 19(1): 1–16.
- 96 Waller, M.H., Y.N. Eyike, Soda anthraquinone pulping of loblolly pine. A kinetic study. *J. Pulp Paper Sci.*, 1983; 9(3): 83–85.
- 97 Håkansson, L., L. Olm, The influence of temperature on delignification and carbohydrate degradation in soda-AQ pulping of softwood. *Nordic pulp Paper Res. J.*, 2001; 16(3): 183–187.
- 98 Edwards, L., S.-E. Norberg, A. Teder, Kinetics of the delignification in kraft pulping. II. Bulk delignification of

birch. *Svensk Papperstidn.*, 1974; 77(3): 95–98.

#### Section 4.2.6

- 1 Kleppe, P.J., Kraft Pulping. *Tappi*, 1970; 53(1): 35–47.
- 2 Legg, G.W., J.C. Hart, Alkaline pulping of jackpine and Douglas Fir. *Pulp and Paper Mag. Canada*, 1960; 61(5): T299–T304.
- 3 Aurell, R., Kraft pulping of birch. *Svensk. Papperstidn.*, 1964; 67(3): 89–95.
- 4 Aurell, R., Nagra jämförande synpunkter. *Svensk. Papperstidn.*, 1963; 66(12): 978–898.
- 5 Nolan, W.J., Studies in continuous pulping V. The effect of chip size and preimpregnation on quality and yield. *Tappi*, 1957; 40(3): 170–190.
- 6 Yllner, S., B. Enström, Studies of the adsorption of xylan on cellulose fibres during the sulphate cook. *Svensk Papperstidn.*, 1956; 59: 229–232.
- 7 Aurell, R., *Tappi*, 1965; 48(2): 80.
- 8 Sixta, H., Conventional Kraft cooking of a mixture of 50% spruce and 50% pine. 2003, R&D Department of Lenzing AG: Lenzing, Austria.
- 9 Buchert, J., et al., Effect of cooking and bleaching on the structure of xylan in conventional pine kraft pulp. *Tappi*, 1995; 78(11): 125–130.
- 10 Buchert, J., et al. Characterization of uronic acids during kraft and superbatch pulping. In 9th International Symposium on Wood and Pulp Chemistry. Montreal, Quebec, Canada, 1997.
- 11 Li, J., G. Gellerstedt, The contribution to kappa number from hexenuronic acid groups in pulp xylan. *Carbohydrate Res.*, 1997; 302: 213–218.
- 12 MacLeod, J.M., Is unbleached softwood kraft pulp strongest at 30 kappa number? *Pap. Puu* 1991; 73: 773–777.
- 13 Teder, A., B. Warnqvist, Control of bleach plant effluents by modified cooking and oxygen bleaching, and consequences for the recovery cycle. 1980; 76(200): 10–18.
- 14 McDonough, T.J., V.J.V. Drunen, Pulping to low residual lignin contents in the kraft-anthraquinone and kraft processes. *Tappi*, 1980; 63(11): 83–87.
- 15 Teder, A., L. Olm, Extended delignification by combination of modified kraft pulping and oxygen delignification. *Pap. Puu*, 1981; 63(4a): 315–326.
- 16 Hartler, N., Extended delignification in kraft cooking – a new concept. *Svensk. Papperstidn.*, 1978; 15: 483–484.
- 17 Norden, S., A. Teder, Modified kraft processes for softwood bleached-grade pulp. *Tappi*, 1979; 62(7): 49–51.
- 18 Sjöblom, K., J. Mjöberg, N. Hartler, Extended delignification in kraft cooking through improved selectivity. Part 1. The effects of the inorganic composition of the cooking liquor. *Pap. Puu*, 1983; 4: 227–240.
- 19 Johansson, B., et al., Modified continuous kraft pulping – now a reality. *Svensk. Papperstidn.*, 1984; 87(10): 30–35.
- 20 Jameel, H. Extended Delignification Technology. In Workshop on Emerging Pulping and Chlorine Free Bleaching Technologies. Raleigh, NC, 1991.
- 21 Kubes, G.J., et al., Viscosities of unbleached alkaline pulps. II. The G-Factor. *J. Wood Chemistry Technol.*, 1983; 3(3): 313–333.
- 22 MacLeod, J.M., New, improved kraft pulp quality. *Pap. Puu*, 1990; 72(8): 780–787.
- 23 Irvine, G.M., N.B. Clark, V. Recupero, Extended delignification of mature and plantation eucalypt wood. Part I: The principles of extended delignification. *Appita J.*, 1996; 49(4): 251–257, 273.
- 24 Kettunen, A., et al., Effect of cooking stage EA concentration profiles on softwood kraft pulping. *Pap. Puu*, 1997; 79(4): 232–239.
- 25 Lindgren, C.T., M.E. Lindström, The kinetics of residual delignification and factors affecting the amount of residual lignin during kraft pulping. *J. Pulp Paper Sci.*, 1996; 22(8): J290–J295.
- 26 Mao, B., Improved modified kraft cooking. Part 5. Modified vapour-phase cooking using a conventional white liquor. *Nordic Pulp Paper Res. J.*, 1995; 10(3): 197–200.
- 27 Olm, L., D. Tormund, Kraft pulping with sulfide pretreatment. Part 2. The influence of pretreatment and cooking

- conditions on the pulp properties, bleachability in a TCF-sequence and strength properties. *Nordic Pulp Paper Res. J.*, **2000**; 15(1): 70–79.
- 28 Vuorinen, T., et al. Selective hydrolysis of hexeneuronic acid groups and its applications in ECF and TCF bleaching of kraft pulps. In 1996 International Pulp Bleaching Conference, Washington, **1996**.
- 29 Kettunen, A.K., et al., Cooking cellulose material with high alkali concentrations and/or high pH. US Patent 5,635,026. Ahlstrom Machinery, Inc.: United States, **1997**.
- 30 Gierer, J., Chemical aspects of kraft pulping. *Wood Sci. Technol.*, **1980**; 14: 241–266.
- 31 Mao, B., N. Hartler, Improved modified kraft cooking. Part 1. Pretreatment with a sodium sulfide solution. *Pap. Puu*, **1992**; 74(6): 491–494.
- 32 Andrews, E.K., H.-M. Chang, R.C. Eckert, Extended delignification kraft pulping of softwoods – Effect of treatments on chips and pulp with sulfide-containing liquors. *J. Wood Chemistry Technol.*, **1985**; 5(4): 431–450.
- 33 Olm, L., M. Bäckström, D. Tormund, Treatment of softwood with sulphide-containing liquor prior to a kraft cook. *J. Pulp Paper Sci.*, **1996**; 22(7): J241–J247.
- 34 Hultholm, T., B. Lönnberg, The effect of impregnation conditions on hydrosulfide sorption in kraft cooking. In Seventh European Workshop on Lignocellulosics and Pulp. Turku, **2002**.
- 35 Lownert, P.H. US Patent 5,507,912, **1996**.
- 36 Herschmiller, D.W., A new process for pulping with high initial hydrosulfide concentration. *Tappi J.*, **1997**; 80(3): 115–121.
- 37 Yllner, S., K. Österberg, L. Stockman, A study of the removal of the constituents of pine wood in the sulphate process using a continuous liquor flow method. *Svensk. Papperstidn.*, **1957**; 60(21): 795–802.
- 38 Hartler, N., et al. Extended delignification and its potential for environmental improvements. In EUCEPA Symposium, Helsinki, **1985**.
- 39 Sjöblom, K., et al., Extended delignification in kraft cooking through improved selectivity. Part II. The effects of dissolved lignin. *Pap. Puu*, **1988**; 70(5): 452–460.
- 40 Gellerstedt, G., et al., Structural changes in lignin during kraft cooking. Part 2. Characterization by acidolysis. *Svensk. Papperstidn.*, **1984**; 9: R61–R67.
- 41 Sjöblom, K., M.S. Lindblad, Extended delignification in kraft cooking through improved selectivity: Influence of dissolved lignin on the alkalinity. *Pap. Puu*, **1990**; 72(1): 51–54.
- 42 Gustafsson, L., A. Teder, *Svensk. Papperstidn.*, **1969**; 72(24): 795–801.
- 43 Lloyd, J.A., C.W. Horne, Extended delignification of Radiata pine by conventional and modified kraft pulping. *Appita*, **1989**; 42(1): 19–24.
- 44 Mao, B., N. Hartler, Improved modified kraft cooking. Part 4. Modified cooking with improved sulfide and lignin profiles. *Pap. Puu*, **1995**; 77(6–7): 419–422.
- 45 Mao, B., Improved modified kraft cooking. Part 6: On the chemicals and water balances for the modified vapor-phase cook. *Tappi J.*, **1996**; 79(5): 188–196.
- 46 Vroom, K.E., The 'H' Factor: A means of expressing cooking times and temperatures as a single variable. *Pulp Paper Magazine Canada*, **1957**; 58C: 228–231.
- 47 Bäckström, M., M. Häggglund, L. Olm, Effect of cooking temperature during extended delignification – selectivity, strength properties and TCF-bleachability. *Pap. Puu*, **1996**; 78(6): 392–397.
- 48 Dillner, B., Isotermisk kokning – lägre kappatal och lättblekt massa. *Svensk. Papperstidn.*, **1993**; 96(2): 22–24.
- 49 Tran, A.v., Effect of cooking temperature on kraft pulping of hardwood. *Tappi J.*, **2002**; 1(4): 13–19.
- 50 Andersson, N., D.I. Wilson, U. Germard, An improved kinetic model structure for softwood kraft cooking. *Nordic Pulp Paper Res. J.*, **2003**; 18(2): 200–209.
- 51 Sjöström, E., The behaviour of wood polysaccharides during alkaline pulping processes. *Tappi*, **1977**; 60(9): 151–154.
- 52 Gustavsson, C.A.-S., W.W. Al-Dajani, The influence of cooking conditions on the degradation of hexenuronic acid,

- xylan, glucomannan and cellulose during kraft pulping of softwood. *Nordic Pulp Paper Res. J.*, **2000**; 15(2): 160–167.
- 53 Sjöström, E., *Wood Chemistry: Fundamentals and Applications*. San Diego, California: Academic Press, Inc., **1981**
- 54 Buchert, J., et al., Effect of cooking and bleaching on the structure of xylan in conventional pine kraft pulp. *Tappi J.*, **1995**; 78(11): 125–130.
- 55 Sixta, H., Comparative evaluation of CBC kraft pulping of pine and spruce wood chips. Internal Report, R&D Lenzing AG, **2004**.
- 56 Axelsson, P., M. Ek, A. Teder, The influence of alkali charge and temperature in the kraft cook on the QPQP bleachability and the kappa number composition of birch pulp. *Swed. Nordic Pulp & Paper Res. J.*, **2002**; 17(3): 206–212.
- 57 Sjöblom, K., Extended delignification in kraft cooking through improved selectivity. Part 3. The effect of dissolved xylan on pulp yield. *Nordic Pulp Paper Res. J.*, **1988**; 1: 34–37.
- 58 Pekkala, O., Some features of residual delignification during kraft pulping of Scots Pine. *Pap. Puu*, **1983**; 65(4): 251–263.
- 59 Teder, A., P. Sandstrom, Pulp yield in continuous kraft pulping with a modified alkali profile. *Tappi J.*, **1985**; 68(1): 94–95.
- 60 Mera, F.E., J.L. Chamberlin, Extended delignification, an alternative to conventional kraft pulping. *Tappi J.*, **1988**; 71: 132–136.
- 61 Suckling, I.D., et al., Monitoring cellulose degradation during conventional and modified kraft pulping. *J. Pulp Paper Sci.*, **2001**; 27(10): 336–341.
- 62 Holmes, G.W., E.F. Kurth, Improvements in the determination of holocellulose. *Tappi*, **1959**; 42(10): 837–840.
- 63 Korhonen, H. **1987**, Helsinki University of Technology, Helsinki.
- 64 MacLeod, J.M., L.J. Pelletier, Basket cases: kraft pulps inside digesters. *Tappi*, **1987**; 70(11): 47–53.
- 65 Cyr, M.E., D.F. Embley, J.M. MacLeod. In Tappi Pulping Conference. Tappi, Seattle, USA, **1989**.
- 66 Tikka, P.O., K.K. Kovasin, Displacement vs. conventional batch kraft pulping: delignification patterns and pulp strength delivery. *Pap. Puu*, **1990**; 72(8): 773–779.
- 67 Li, J., O. Sevastyanova, G. Gellerstedt, The distribution of oxidizable structures in ECF- and TCF-bleached kraft pulps. *Nordic Pulp Paper Res. J.*, **2002**; 17(4): 415–419.
- 68 Gellerstedt, G., J. Li, The contribution to kappa number from hexenuronic acid groups in pulp xylan. *Carbohydrate Res.*, **1997**; 302: 213–218.
- 69 Rutkovsky, J., K. Perlinska-Sipa, Extended delignification with improved technological and economic pulping indices. *Cellulose Chemistry Technol.*, **2002**; 36(5–6): 483–494.
- 70 Forsskahl, I., T. Popoff, O. Theander, Reactions of D-xylose and D-glucose in alkaline, aqueous solutions. *Carbohydrate Res.*, **1976**; 48: 13–21.
- 71 Gellerstedt, G., J. Li, O. Sevastyanova. In IPBC. Halifax, Canada, **2000**.
- 72 Pekkala, O., Some effects of extended delignification on lignin in kraft cooking. *Pap. Puu*, **1985**; 67(11): 673–688.
- 73 Sixta, H. Influence of prehydrolysis on pulping and bleaching. In Book of Abstracts, 211th ACS National Meeting, New Orleans, LA, **1996**.
- 74 Antonsson, S., et al., A comparative study of the impact of the cooking process on oxygen delignification. *Nordic Pulp Paper Res. J.*, **2003**; 18(4): 388–394.
- 75 Isogai, A., A. Ishizu, J. Nakano, residual lignin and hemicellulose in wood cellulose analysis using new permethylation method. *Holzforschung*, **1989**; 43(5): 333–338.
- 76 Ohara, S., S. Hosoya, J. Nakano, Studies on the formation of lignin-carbohydrate complex during alkaline pulping processes. *J. Japan Wood Res. Soc.*, **1980**; 26(6): 408–413.
- 77 Gierer, J., S. Wannström, Formation of alkali-stable C-C-bonds between lignin and carbohydrate fragments during kraft pulping. *Holzforschung*, **1984**; 38(4): 181–184.
- 78 Iversen, T., S. Wännström, Lignin-carbohydrate bonds in a residual lignin isolated from pine kraft pulp. *Holz-forschung*, **1986**; 40(1): 19–22.

- 79 Gellerstedt, G., E.-L. Lindfors. On the structure and reactivity of residual lignin in kraft pulp fibers. In International Pulp Bleaching Conference. Stockholm, Sweden, 1991.
- 80 Argyropoulos, D.S., Y. Sun, E. Palus, A novel method for isolating residual kraft lignin. *J. Pulp Paper Soc.*, 2002; 28(2): 50–54.
- 81 Jääskeläinen, A.S., et al., The effect of isolation on the chemical structure of residual lignin. *Wood Sci. Technol.*, 2003; 37: 91–102.
- 82 Gellerstedt, G., J. Pranda, E.-L. Lindfors, Structural and molecular properties of residual birch kraft lignins. *J. Wood Chemistry Technol.*, 1994; 14(4): 467–482.
- 83 Jiang, Z.-H., D.S. Argyropoulos, isolation and characterization of residual lignins in kraft pulps. *J. Pulp Paper Sci.*, 1999; 25(1): 25–29.
- 84 George, J., D. Lachenal, D. Robert, Application of the principles of extended delignification: effects on softwood kraft residual lignin. *J. Pulp Paper Sci.*, 2000; 26(8): 271–274.
- 85 Froass, P.M., A.J. Ragauskas, J.-E. Jiang, Chemical structure of residual lignin from kraft pulp. *J. Wood Chemistry Technol.*, 1996; 16(4): 347–365.
- 86 Hortling, B., et al. in International Symposium on Wood and Pulping Chemistry. Beijing, China, 1993.
- 87 Zhan, H.-Y., et al., Structural changes of lignin during EMCC pulping of *Pinus elliottii* in Southern China. *J. South China Univ. Technol.*, 2002; 30(9): 65–70.
- 88 Gierer, J., F. Imsgard, I. Pettersson, Possible condensation and polymerization reactions of lignin fragments during alkaline pulping processes. *Appl. Polym. Symp.*, 1976; 28: 1195.
- 89 Gierer, J., Chemistry of delignification. Part 1: General concept and reactions during pulping. *Wood Sci. Technol.*, 1985; 19: 289–312.
- 90 Parthasarathy, V.R., et al., A sulfur-free, chlorine-free alternative to kraft pulping. *Tappi*, 1996; 79(6): 189–198.
- 91 Argyropoulos, D.S., L. Akim, B. Ahvazi. Salient reactions in lignin during pulping and oxygen delignification. In Pulping/process and product quality conference. Boston, MA, USA: Tappi Press, Atlanta, GA, 2000.
- 92 Grundelius, R., Oxidation equivalents, OXE – an alternative to active chlorine. *Tappi J.*, 1992; 76(1): 133–135.
- 93 Gellerstedt, G., W.A.-D. W, Bleachability of alkaline pulps. Part 1. The importance of beta-aryl ether linkages in lignin. *Holzforschung*, 2000; 54(6): 609–617.
- 94 Gellerstedt, G., E.-L. Lindfors, Structural changes in lignin during kraft pulping. *Holzforschung*, 1984; 38(3): 151–158.
- 95 Katelinen, A., et al. The role of reprecipitated xylan in the enzymatic bleaching of kraft pulp. In: 6th ISWPC, Appita, 1991.
- 96 Rolando, C., B. Monties, C. Lapierre, Thioacidolysis. In *Methods in Lignin Chemistry*, Springer-Verlag, p. 334, 1992.
- 97 Gustavsson, C., K. Sjöström, W.W. Al-Dajani, The influence of cooking conditions on the bleachability and chemical structure of kraft pulps. *Nordic Pulp Paper Res. J.*, 1999; 14(1): 71–81.
- 98 Surewicz, W., The sorption of organic components from cooking liquor by cellulose fibers; its relation to the 'Dangerous Cooking Crest'. *Tappi J.*, 1962; 45(7): 570.
- 99 Svedman, M., P. Tikka, K. Kovasin. Relations between cooking conditions, pulp quality and bleachability as studied using a New Superbatch Experimental Cooking System. In 8th ISWPC, Helsinki, Finland, 1995.
- 100 Carnö, B., M. Norrström, L.A. Ohlsson, The influence of cooking conditions on the bleachability of pine sulphate pulp. *Svensk. Papperstidn.*, 1975; 78(4): 127–129.
- 101 Sjöström, K., Influence of ionic strength on kraft pulping. *Nordic Pulp Paper Res. J.*, 1999; 14(3): 226–235.
- 102 Sjöström, K., Kraft cooking with varying alkali concentration – Influence on TCF-bleachability. *Nordic Pulp Paper Res. J.*, 1998; 13(1): 57–63.
- 103 Patt, R., et al., Chlorfreie Bleiche von Sulfit- und ASAM-Zellstoffen im Labor- und Pilotmaßstab. *Das Papier*, 1991; 45(10): 8–16.
- 104 Zimmermann, M., R. Patt, O. Kordsachia, ASAM Pulping of Douglas-Fir and

- Chlorine free Bleaching. *Tappi Proc.*, **1991**: 115–121.
- 105** Zimmermann, M., R. Patt, O. Kordsachia, ASAM Pulping of Douglas-Fir and Chlorine free Bleaching. *Tappi J.*, **1991**; 74(11): 129–134.
- 106** Teder, A., K. Sjöström, A comparison of bleachability in TCF sequences for alkaline sulphite and kraft pulps. *J. Pulp Paper Sci.*, **1996**; 22(8): 295–300.
- 107** Sjöström, K., A. Teder, Changes within the modified kraft process aiming to improve TCF bleachability. *J. Pulp Paper Sci.*, **1999**; 25(5): 176–182.
- 108** Nasman, L., B. Petterson, Commercial utilization of cold blow and extended delignification techniques in batch cooking. *Tappi Proc.*, **1985**: 77–81.
- 109** Orgill, B., commercial utilization of cold blow and extended delignification techniques in batch cooking. *IPPTA Convention Issue*, **1986**: 56–63.
- 110** Ernerfeldt, B., L.E. Nasman, D. Allen, Extended delignification in a batch cooking system – report from start-up at Karlsborgs Bruk, Sweden. *Appita*, **1986**; 39(6): 459–462.
- 111** Fagerlund, B.K.E., Process for digesting cellulosic material with heat recovery. US Patent 4,578,149, **1986**.
- 112** Fagerlund, B.K.E., Process for digesting cellulosic material with heat recovery. Canadian Patent 1 179 807, **1986**.
- 113** Bowen, I.J., J.C.L. Hsu, Overview of emerging technologies in pulping and bleaching. *Tappi J.*, **1990**; 73(9): 205–217.
- 114** Tikka, P.O., S.A. Pursiainen, I.T. Hamala, Process chemistry and control of rapid-displacement heating. *Tappi J.*, **1988**; 71(2): 51–58.
- 115** Swift, L.K., J.S. Dayton, Rapid displacement heating in batch digesters. *Pulp Paper Canada*, **1988**; 89(8): 70–76.
- 116** Swift, L.K., RDH pulping – better pulp properties through improved selectivity. *Tappi Proc.*, **1988**: 31–35.
- 117** Meredith, M.D., The chemistry of Beloit's displacement heated cooking system – RDH. *Tappi Proc.*, **1986**: 651–655.
- 118** Tikka, P., N.-E. Virkola, A new kraft pulping analyzer for monitoring organic and inorganic substances. *Tappi*, **1986**; 69: 68–71.
- 119** Vikström, B., et al. Apparent sulfidity and sulfide profiles in the RDH cooking process. In *Tappi Pulping Conference*, **1988**.
- 120** Tormund, D., A. Teder, New findings on sulfide chemistry in kraft pulping liquors. *Tappi J.*, **1989**; 72(5): 205–210.
- 121** Gellerstedt, G., E.-L. Lindfors, On the formation of enol ether structures in lignin during kraft cooking. *Nordic Pulp Paper Res. J.*, **1987**; 2(2): 71.
- 122** Tormund, D., A. Teder, B. Vikström, Ny metod bestämmer halten flyktiga föreningar. *Nordisk Cellulosa*, **1984**; 1(6): 66.
- 123** Allison, R.W., et al., Hexenuronic acid in kraft pulps from radiata pine. *Appita J.*, **1999**; 52(6): 448–453.
- 124** Sainiemi, J., S. Hiljanen, Experiences of low-energy batch cooking. *Tappi Proc.*, **1986**: 643–649.
- 125** Kaiser, M., R. Pitre. RDH at Owens-Illinois, Valdosta, Georgia – The world's first commercial scale displacement cooking plant. *Tappi Proc.*, **1986**: 627–632.
- 126** Evans, J.C.W., RDH Process boosts batch digester efficiency at U. S. and Finnish mills. *Pulp Paper*, **1987**: (5): 93–95.
- 127** Ryyänänen, H., S. Pursiainen. Management system for liquor recycling of RDH digester house. *Tappi Proc.*, **1987**.
- 128** Sherwood, R.C., Z. Chaudhri, M. Brown, Reduced steam usage in kraft batch digesters with displacement heating. *Tappi Proc.*, **1983**: 327–329.
- 129** Andrews, E.K., RDH kraft pulping to extend delignification, decrease effluent, and improve productivity and pulp properties. *Tappi J.*, **1989**: 55–61.
- 130** Matheison, B.A., R.R. Gustafson, RDH pulping of southern hardwoods. *Tappi J.*, **1996**; 79(5): 180–187.
- 131** Sezgi, U.S., J. Colodette, L. Shackford, E. Salvador, Rapid displacement heating (RDH) kraft pulping and ECF bleaching of Brazilian *Eucalyptus urograndis* – Part 1. **1997**: 137–148.
- 132** Tikka, P.O., Process for preparing kraft pulp. WO 9112368. PCT Int. Appl. 23, **1991**.

- 133 Lönnberg, B., et al. Dissolution of wood components in black liquor started displacement kraft batch cooking. In International Symposium on Wood and Pulping Chemistry. Beijing, China, 1993.
- 134 Siistonen, H., et al., Behaviour of pine wood material during displacement kraft batch cooking. *Pap. Puu*, 1999; 81(5): 379–383.
- 135 Svedman, M.A., K.K. Kovasin, and P.O. Tikka. Relations between cooking conditions, pulp quality and bleachability as studied using a new Superbatch experimental cooking system. In 8th International Symposium on Wood and Pulping Chemistry. Helsinki, Finland, 1995.
- 136 Pursiainen, S., et al., Mill-scale experiences of extended delignification with Super Batch cooking method. *Tappi J.*, 1990: 115–122.
- 137 Hepp, M.D., Process for continuously guiding liquids when digesting pulp in a digester. European Patent Specification. EP 0891 438 B1: Europe, 1997.
- 138 Wizani, W., et al. CBC – Continuous batch cooking. The revolution in kraft cooking. In Pulping process and product quality conference. Boston, MA, USA, 2000.
- 139 Jiang, J., Effect of alkali profiles on carbohydrate chemistry during kraft pulping of hardwoods. In 10th International Symposium on Wood and Pulping Chemistry. Yokohama, Japan, 1999.
- 140 Aurell, R., N. Hartler, Kraft pulping of pine. Part 1. Changes in the composition of the wood residue during the cooking process. *Svensk. Papperstidn.*, 1965; 68(3): 59–68.
- 141 Sloman, A., Continuous two stage soda pulping of eucalyptus. *Appita*, 1960; 14(2): 57–64.
- 142 Sloman, A., J. Richter, New cooking method proves successful. *Pulp Paper Int.*, 1961 (June): 18–19.
- 143 Norden, S., A. Teder, Modified kraft processes for softwood bleached-grade pulps. *Tappi*, 1979; 62(7): 49–51.
- 144 Mjoberg, P., K. Sjoblom, N. Hartler. Extensive delignification through controlled liquor concentrations. In EUCEPA, 1980.
- 145 Hartler, N., Modified kraft cooking technology. In Workshop on Emerging Pulping and Chlorine Free Bleaching Technologies. Raleigh, NC, 1991.
- 146 Backlund, E.A., Extended delignification of softwood kraft pulp in a continuous digester. *Tappi J.*, 1984; 67(11): 62–65.
- 147 Backlund, A. A progress report on continuous digester development. In XXI EUCEPA International Conference. Torremolinos, Spain, 1984.
- 148 Kortelainen, V.A., E.A. Backlund, Experiences with extended delignification of hardwood and softwood kraft pulp in a continuous digester. *Tappi J.*, 1985; 68(11): 70–74.
- 149 Greenwood, B.F., A Review of the Basis for and the Current Status of Modified Continuous Cooking. In AIChE Forest Products Division Sessions, 1988.
- 150 Dillner, B., Modified continuous cooking. *Japan Pulp Paper*, 1989; 49–55.
- 151 Whitley, D.L., J.R. Zierdt, D.J. Lebel, Mill experiences with conversion of a Kamyrdigester to modified continuous cooking. *Tappi J.*, 1990; 73(1): 103–108.
- 152 Jansson, J., A. Teder, A contribution to the determination of pulp yield by chemical analysis. Application to modified kraft cooking of pinewood. *Nordic Pulp Paper Res. J.*, 1986; 1(1): 43–45.
- 153 McNaughton, J.G., W.Q. Yean, D.A.I. Goring, *Tappi*, 1967; 40(11): 548–553.
- 154 Stromberg, B., Modified continuous cooking – an update. *Tappi Proc.*, 1987.
- 155 Jiang, J.E., et al., Extended delignification with prolonged mild counter-current cooking stage. *Appita J.*, 1992; 45(1): 19–22.
- 156 Marcoccia, B.S., J.R. Prough, R.O. Laakso, J.R. Phillips, R.C. Ryham, J.T. Richardsen, R.F. Chasse, Kraft pulp, its production with dissolved solids control and apparatus for. *PCT Int. Appl.*, 1991; 78.
- 157 Marcoccia, B.S., T.M. Poulin. A Lo-solids pulping update. In 29th Pulp and Paper Annual Meeting, ABTCP. Sao Paulo, Brazil, 1996.
- 158 Marcoccia, B.S., et al., Dissolved solids control in pulp production. US Patent 5,547,012, 1996.

- 159 Sammartino, L.S., Lo-solids cooking trials at Howe Sound Pulp & Paper Ltd. *Pulp Paper Canada*, **1996**; 97(3): 61–65.
- 160 Marcoccia, B.S., The theoretical background to Lo-Solids Pulping. In CPPA 82nd Annual meeting of the technical association. Montreal, PQ, **1996**.
- 161 Strömberg, B., Yield increases with Lo-Solids cooking. In Congresso e Exposicao Anual de Celulose e Papel. Sao Paulo, Brazil, **2002**.
- 162 Edmonds, J., W.E. Wiley. In ASKK Tech. Symposium. Tokyo, **1997**.
- 163 Prough, J.R., et al., Method for selectively increasing the sulfide ion concentration and sulfidity of kraft cooking liquor during kraft cooking of wood. US Patent 5,575,890, **1996**.
- 164 Stromberg, B., Evolution of the Andritz digester. *Internal Report, Andritz*, **1996**.
- 165 Achren, S., et al., Improved pulp yield by optimized alkaline profiles in kraft delignification of birch wood. In Tappi 'Breaking the Pulp Yield Barrier' Symposium. Atlanta, **1998**; 91–101.
- 166 Jiang, J., 10th International Symposium on Wood and Pulping Chemistry. Yokohama, Japan, **1999**.
- 167 Jiang, J.E., R.W. Allison, J.A. Lloyd, Factors responsible for yield gains from Lo-Solids pulping of *Eucalyptus* species. *Appita*, **2001**; 54(3): 304–309.
- 168 Kettunen, A., et al., Enhanced alkali profile cooking: further improvements in pulp tear strength. In **1997** Pulping Conference. San Francisco, CA, TAPPI Proceedings, **1997**; Vol. 1, p. 587–592.
- 169 Teder, A., Redox potential of polysulfide solutions and carbohydrate stabilization. *Svensk. Papperstidn.*, **1968**; 71(5): 149–160.
- 170 Taga, G., T. Nishi, S. Miyao, J. Ja, *Tappi*, **1964**; 18(1): 27–31.
- 171 Smith, G.C., S.E. Knowles, R.P. Green, All it takes is Moxy: Mead oxidation system generates polysulfide liquor. *Paper Trade J.*, **1975**; 159(13): 38–41.
- 172 Gustafsson, L., A. Teder, Alkalinity in alkaline pulping. *Svensk. Papperstidn.*, **1969**; 72(24): 795–801.
- 173 Mao, B., N. Hartler, Improved modified kraft cooking. Part 3: Modified vapor-phase polysulfide cooking. *Tappi J.*, **1994**; 77(11): 149–152.
- 174 Lindgren, C., M. Lindström, Thermal decomposition of inorganic polysulfides at kraft cooking conditions. *Nordic Pulp Paper Res. J.*, **1995**; 10(1): 41–45.
- 175 Lindström, M.E., Some factors affecting the amount of residual phase lignin during kraft pulping, PhD-Thesis, In Royal Institute of Technology, Pulp and Paper Chemistry and Technology. KTH: Stockholm, **1997**.
- 176 Alfredson, B., O. Samuelson, B. Sandstig, Carboxyl end groups in sulfate and polysulfide pulps. *Svensk. Papperstidn.*, **1963**; 66(18): 703–706.
- 177 Nakano, J., et al., Studies on polysulfide cooking. I. Behaviour of lignin during polysulfide cooking. *J. Jpn. Wood Res. Soc.*, **1964**; 10: 141–146.
- 178 Brunow, G., G.E. Miksche, Some reactions of lignin in kraft and polysulfide pulping. *Appl. Polym. Symp.*, **1976**; 28: 1155–1168.
- 179 Berthold, F., C.T. Lindgren, M.E. Lindström, Formation of (4-hydroxy-3-methoxyphenyl)-glyoxylic acid and (4-hydroxy-3,5-dimethoxyphenyl)-glyoxylic acid during polysulfide treatment of softwood and hardwood. *Holzforchung*, **1998**; 52(2): 197–199.
- 180 Berthold, F., M.E. Lindström, Polysulfide addition as a means to increase delignification in kraft pulping. *Nordic Pulp Paper Res. J.*, **1997**; 12(4): 230–236.
- 181 Berthold, F., G. Gellerstedt, Influence of polysulphide on the rate of degradation of six p-OH styrene structures at two OH- concentrations. *Holzforchung*, **1998**; 52(5): 490–498.
- 182 Kleppe, P.J., K. Kringstad, Sulphate pulping by the polysulfide process I. Investigations on spruce and pine. *Norsk. Skogind.*, **1963**; 17(11): 428–440.
- 183 Kleppe, P.J., K. Kringstad, Sulphate pulping by the polysulfide process II. Investigations on birch. *Norsk. Skogind.*, **1964**; 18(1): 13–23.
- 184 Green, R.P., Z.C. Prusas, Polysulfide pulping of two Canadian softwood blends. *Pulp Paper Canada*, **1975**; 76(9): 69–72.
- 185 Jiang, J.E., Extended modified cooking of Southern pine with polysulfide: effects on pulp yield and physical properties. *Tappi J.*, **1994**; 77(2): 120–124.



- 186 Kleppe, P.J., *Tappi*, 1975; 58(8): 172.
- 187 Lindström, M., A. Teder, The effect of polysulfide pretreatment when kraft pulping to very low kappa numbers. *Nordic Pulp Paper Res. J.*, 1995; 10(1): 8–11.
- 188 Pekkala, O., On the extended delignification using polysulphide or anthraquinone in kraft pulping. *Pap. Puu*, 1982; 11: 735–744.
- 189 Hakanen, A., A. Teder, Modified kraft cooking with polysulfide: yield, viscosity, and physical properties. *Tappi J.*, 1997; 80(7): 189–196.
- 190 Hilmo, P., K. Johnsen, Polysulfide kraft cooking proves itself in Norwegian pulp mill. *Pulp Paper Int.*, 1969(2): 39–42.
- 191 Jiang, J.E., Extended delignification of southern pine with anthraquinone and polysulfide. *Tappi*, 1995; 78(2): 126–132.
- 192 Jameel, H., et al., Extending delignification with AQ/polysulfide. *Tappi J.*, 1995; 78(9): 151–160.
- 193 Li, Z., J. Li, G.J. Kubes, Kinetics of delignification and cellulose degradation during kraft pulping with polysulphide and anthraquinone. *J. Pulp Paper Sci.*, 2002; 28(7): 234–239.
- 194 Kleppe, P.J., Emerging delignification technology. *IPPTA*, 1996; 8(1): 1–9.
- 195 Kleppe, P.J., A mill trial with the addition of a small amount of AQ to kraft and polysulfide pulping. *Pap. Puu*, 1981; 63(4): 204–210.
- 196 Smith, G.C., F.W. Sanders. US Patent 87 504, 1970.
- 197 Blain, T.J., Anthraquinone pulping: fifteen years later. *Tappi J.*, 1993; 76(3): 137–146.
- 198 Bach, B., G. Fiehn, Neue Möglichkeiten zur Kohlenhydratstabilisierung im alkalischen Holzaufschluß. *Zellstoff Papier*, 1972; 21(3): 3–7.
- 199 Heikkilä, H., E. Sjöström, Introduction of aldonic acid end-groups into cellulose by various oxidants. *Cell. Chem. Technol.*, 1975; 9(3): 3–11.
- 200 Ruoho, K., E. Sjöström, Improved stabilization of carbohydrates by the oxygen-quinone system. *Tappi*, 1978; 61(7): 87–88.
- 201 Samuelson, O., L.A. Sjöberg, Spent liquors from sodium hydroxide cooking with addition of anthraquinone. *Cell. Chem. Technol.*, 1978; 12: 463–472.
- 202 Saka, S., PhD-Thesis, North Carolina State University. Raleigh, NC 27650, USA, 1978.
- 203 Gratzl, J.S., The reaction mechanisms of anthraquinone in alkaline pulping. In Proceedings of 1980 EUCEPA Symposium. Helsinki, Finland, 1980; Vol. 2, p. 1201–1227.
- 204 Fengel, D., The distribution of aqueous solutions within wood. *J. Polymer Sci.*, 1971; 36: 141–152.
- 205 Fullerton, T.J., Soda pulping with anthrahydroquinones. *Appita*, 1978; 38: 117–118.
- 206 Revenga, J.A., F. Rodriguez, J. Tijero, Reduction Constant of anthraquinone in kraft pulping liquor. *J. Pulp Paper Sci.*, 1995; 21(3): 104–109.
- 207 Gourang, I., R. Cassidy, C.W. Dence, Reduction of anthraquinone. Soda-anthraquinone pulping of Norway spruce. *Tappi*, 1979; 62(7): 43–47.
- 208 Gratzl, J.S., Redox-processes in alkaline pulping in the presence of anthraquinone compounds – an overview. In 7th International Symposium on Wood and Pulping Chemistry. Beijing, China, 1993: Vol. 1, 1–8.
- 209 Hise, R.G., et al., Oxidative-hydrolytic processes in alkaline pulping. In 5th International Symposium on Wood and Pulping Chemistry. Paris, France, 1987; 391–398.
- 210 Dimmel, D.R., L.F. Perry, P.D. Palasz, H.L. Chum, Electron transfer reactions in pulping systems. (II): electrochemistry of anthraquinone/lignin model quinonemethides. *J. Wood Chem. Technol.*, 1985; 5(1): 15–36.
- 212 Gosh, K.L., et al., Quinone additives in soda pulping of hardwoods. *Tappi*, 1977; 60(11): 127–131.
- 213 Lin, C.K., Prehydrolysis-alkaline pulping of sweetgum wood. PhD-Thesis, North Carolina State University. Raleigh, NC 27650, USA, 1979.
- 214 Holton, H.H., F.L. Chapman, Kraft pulping with anthraquinone. *Tappi*, 1977; 60(11): 121–125.
- 215 Goel, K., A.M. Ayroud, B. Branch, Anthraquinone in kraft pulping. *Tappi*, 1980; 63(8): 83–85.

- 216 Fullerton, T.J., B.I. Fleming, *Svensk. Papperstidn.*, **1980**; 83(14): 396–397.
- 217 Fullerton, T.J., A.J. Kerr, Practical aspects of kraft-AQ pulping of *Pinus radiata*. *Appita*, **1981**; 35(2): 135–139.
- 218 Sharma, Y.K., K.S. Bhandari, Effective utilisation of cooking chemicals by use of additive. *IPPTA*, **1982**; 19(1): 12–15.

#### Section 4.2.7

- 1 Springer, E.L., J.F. Harris, Prehydrolysis of aspen wood with water and with dilute aqueous sulfuric acid. *Svensk. Papperstidn.* **1982**: 152–154.
- 2 Rydholm, S.A., *Pulping Processes*. Original Edition, 1965 ed. New York: Wiley Interscience, **1965**, p. 665.
- 3 Springer, E.L., Hydrolysis of aspenwood xylan with aqueous solutions of hydrochloric acid. *Tappi*, **1966**; 49(3): 102–106.
- 4 Springer, E.L., L.L. Zoch, Hydrolysis of xylan in different species of hardwoods. *Tappi*, **1968**; 51(5): 214–218.
- 5 Papadopoulos, J., C.-L. Chen, I.S. Goldstein, *J. Appl. Polymer Sci.*, **1983**; 37: 631.
- 6 BeMiller, J.N., Acid-catalyzed hydrolysis of glycosides. *Adv. Carbohydrate Chem.*, **1967**; 22: 25–108.
- 7 Hojnos, J., et al., Hydrolyzate from prehydrolysis of hardwood. In CS 230252 B 19861015, Czechoslovakia, **1986**.
- 8 Hojnos, J., et al., Acid prehydrolysis of wood chips. In CS 248106 B1 19880315. Czechoslovakia, **1988**.
- 9 Mozol'ová, L., E. Golis, L. Suty, Arten- und Gehaltsbestimmung der aromatischen Bestandteile der Reinigungsstufen des Buchenvorhydrolysat bei D-Xylose-Produktion. *Sammelschrift der Arbeiten der Chemisch-technologischen Fakultät der Slowakischen technischen Hochschule*, **1977**, pp. 217–221.
- 10 Hojnos, J., Useful products from beechwood hemicelluloses. *Vyskumne Prace z Odboru Papiera a Celulozy*, **1987**; 42(11): V69–V70.
- 11 Rastall, R.A., Prebiotic oligosaccharides: evaluation of biological activities and potential future developments. In *Probiotics and Prebiotics*, G.W. Tannock, Ed. Caister Academic Press: Wymondham, UK, **2002**, pp. 107–148.
- 12 Vazquez, M.J., et al., Xylooligosaccharides. Manufacture and applications. *Trends Food Sci. Technol.* **2001**; 11(11): 387–393.
- 13 Chen, H., J. Liu, Z. Li, Method for producing active oligomeric xylose. In CN 1233614 A 19991103, **1999**.
- 14 Reis, A., et al., Fragmentation pattern of underivatized xylo-oligosaccharides and their alditol derivatives by electrospray tandem mass spectrometry. *Carbohydrate Polymers*, **2004**; 55(4): 401–409.
- 15 Kabel, A.M., H.A. Schols, A.G.J. Alphons, Identification of structural features of various (O-acetylated) xylo-oligosaccharides from xylan-rich agricultural by-products: A review. ACS Symp. Ser. 864 Hemicelluloses, ACS. Series. **2004**, pp. 108–121.
- 16 Ishihara, M., Production of xylo-oligosaccharides from woody biomass. *BioIndustry*, **2001**; 18(12): 35–44.
- 17 Rycroft, C.E., et al., A comparative in vitro evaluation of the fermentation properties of prebiotic oligosaccharides. *J. Appl. Microbiol.*, **2001**; 91(5): 878–887.
- 18 Vazquez, M.J., J.L. Dominguez, J.C. Parajo, Enzymatic processing of crude xylooligomer solutions obtained by autohydrolysis of *Eucalyptus* wood. *Food Biotechnol.*, **2002**; 16(2): 91–105.
- 19 Vazquez, M.J., et al., Production of xylose-containing fermentation media by enzymatic post-hydrolysis of oligomers produced by cob autohydrolysis. *World J. Microbiol. Biotechnol.*, **2001**; 17(8): 817–822.
- 20 Wizani, W., et al., Viscose production process. In WO9412719 PCT Pub. **1994**.
- 21 BeMiller, J.N., Acid-catalyzed hydrolysis of glycosides. *Adv. Carbohydrate Chem.*, **1967**; 22: 25–108.
- 22 Vernon, C.A., *Proc. Roy. Soc. B.*, **1967**; 167(389).
- 23 BeMiller, J.N., in *Starch Chemistry and Technology*, R.L.W.a.E.F. Paschall, Ed. Academic Press: New York, **1965**.
- 24 Edward, J.T., Stability of glycosides to acid hydrolysis. *Chem. Ind. (London)*, **1955**: 1102.

- 25 Bunton, C.A., et al.,  $\alpha$ - and  $\beta$ -phenyl-D-glucopyranosides. *J. Chem. Soc.*, **1955**: 4419.
- 26 Capon, B., Mechanism of the anomerization of the methyl D-glucopyranosides. *Chem. Commun.*, **1967**; 1: 21–23.
- 27 Harris, J.F., Acid hydrolysis and dehydration reactions for utilizing plant carbohydrates. *Appl. Polymer Symp.*, **1975**; 28: 131–144.
- 28 Feather, M.S., J.F. Harris, Partial hydrolysis and acetolysis of cellotriose-1–14C. *J. Am. Chem.*, **1967**; 89(22): 5661–5664.
- 29 Conner, A.H., Kinetic modeling of hardwood prehydrolysis. Part I. Xylan removal by water prehydrolysis. *Wood Fiber Sci.*, **1984**; 16(2): 268–277.
- 30 Klemm, D., et al., *Comprehensive Cellulose Chemistry. Volume 1: Fundamentals and Analytical Methods*. Vol. 1. Weinheim, Germany: Wiley-VCH Verlag GmbH, **1998**, p. 84.
- 31 Root, D.F., et al., Kinetics of the acid-catalyzed conversion of xylose to furfural. *Forest Products J.*, **1959**: 158–165.
- 32 Dunlop, A.P., Furfural formation and behavior. *Ind. Eng. Chem.*, **1948**; 40(2): 204–209.
- 33 Harris, J.F., et al., Factors influencing dilute sulfuric acid prehydrolysis of southern red oak wood. *Prog. Biomass Conversion*, **1984**; 5: 101–141.
- 34 Nee, C.I., W.F. Yee, Hydrolysis of pentosans in bagasses pith. *J. Appl. Chem. Biotechnol.*, **1976**; 2: 283–287.
- 35 Harris, J.F., et al., Two-stage dilute acid hydrolysis of wood: an investigation of fundamentals. *J. L. for Prod. Lab.*, **1985**; p. 78.
- 36 Maloney, M.T., T.W. Chapman, A.J. Baker, Dilute acid hydrolysis of paper birch: kinetics studies of xylan and acetyl-group hydrolysis. *Biotechnol. Bioeng.*, **1985**; 27: 355–361.
- 37 Maloney, M.T., T.W. Chapman, A.J. Baker, an engineering analysis of the production of xylose by dilute acid hydrolysis of hardwood hemicellulose. *Biotechnol. Prog.*, **1986**; 2(4): 192–202.
- 38 Veerarahavan, S., et al. Kinetic modeling and reactor development for hemicellulose hydrolysis. In AIChE National Meeting. Orlando, FL, **1982**.
- 39 Sixta, H., Water prehydrolysis of beech wood. R&D Lenzing AG: Lenzing, Austria, **2003**.
- 40 Grohmann, K., R. Torget, M. Himmel, Optimization of dilute acid pretreatment of biomass. *Biotechnol. Bioeng. Symp.*, **1986**; 15: 59–80.
- 41 Casebier, R.L., J.K. Hamilton, H.L. Hergert, *Tappi*, **1969**; 52: 2369.
- 42 Smiljanski, S., S. Stankovic, Beech wood glucuronoxylan in the prehydrolysis kraft process. *Cellulose Chem. Technol.*, **1974**; 8(3): 283–294.
- 43 Stamm, A.J., *Tappi*, **1968**; 51(1): 62.
- 44 Baldinger, T., W. Milacher, Oligosaccharide characterization of water prehydrolyzate from beech wood. Lenzing AG: Lenzing, **2004**.
- 45 Goldschmid, O., *Tappi*, **1955**; 38(12): 728.
- 46 Kratzl, K., et al., *Monatsh. Chem.*, **1959**; 90: 771.
- 47 Lin, C.K., Prehydrolysis-alkaline pulping of sweetgum wood. Department of Wood and Paper Science. North Carolina State University: Raleigh, NC, USA, **1979**.
- 48 Sixta, H., Visbatch cooking of various hardwood species. R&D Lenzing: Lenzing, Austria, **1997**.
- 49 Brasch, D.J., K.W. Free, *Tappi*, **1964**; 47(4): 186–189.
- 50 Sixta, H., Zellstoffherstellung unter Berücksichtigung umweltfreundlicher Aufschluß- und Bleichverfahren am Beispiel von Chemiezellstoffen. Habilitation Thesis, Department of Pulp, Fiber and Paper Technology. Technical University of Graz: Graz, **1995**
- 51 Sixta, H., A. Borgards, New technology for the production of high-purity dissolving pulps. *Das Papier*, **1999**; 53(4): 220–234.
- 52 Sixta, H., VisCBC cooking of various hardwood species. R&D Lenzing: Lenzing, Austria, **2002**.
- 53 Schild, G., W. Müller, H. Sixta, Prehydrolysis kraft and ASAM paper grade pulping of eucalypt wood. A kinetic study. *Das Papier*, **1996**; 50(1): 10–22.
- 54 Antonsson, S., et al., A comparative study of the impact of the cooking process on oxygen delignification. *Nordic Pulp Paper Res. J.*, **2003**; 18(4): 388–394.

- 55 Sixta, H., A. Borgards, A. Lima, Influence of reactions conditions on Visbatch cooking of *Eucalyptus urograndis*. Lenzing AG: Lenzing, 1999.
- 56 Sixta, H., Dissolving-pulp market study. Lenzing AG: Lenzing, 2003.
- 57 Sixta, H., Influence of wood species on the performance of the Visbatch process. Lenzing AG: Lenzing, 2004.

## Section 4.2.8

- 1 Sezgi, U.S., et al., A combined discrete-continuous simulation model of an RDH tank farm. *Tappi J.*, 1994; 77(7): 213–220.
- 2 Scheldorf, J.J., L.L. Edwards, Challenges in modeling the RDH process: a discontinuous dynamic system. *Tappi J.*, 1993; 76(11): 97–104.
- 3 SuperBatch (product leaflet). Sunds Defibrator: Pori, Finland, 1994.
- 4 Wizani, W., et al. CBC – Continuous batch cooking, the revolution in kraft cooking. Tappi Pulping/Process & Product Quality Conference. Boston, MA, USA, 2000.
- 5 Malkov, S., Studies on liquid penetration into softwood chips – experiments, models and applications. Helsinki University of Technology: Espoo, 2002.
- 6 Compact Feed, a simplified feeding system for higher capacities. *Fiberlines, A Kvaerner Pulping Publication*, 2000(1): 26.
- 7 Poulin, T.M., W.E. Wiley, B. Stromberg. The development of an efficient continuous digester chip feeding system. Fall Technical Conference. TAPPI, 2003.
- 8 Continuous Progress in Cooking (brochure). Andritz, 2004.
- 9 Dillner, B., Modified continuous cooking. *Japan Pulp & Paper*, 1989 (3): 49–55.
- 10 Whitley, D.L., J.R. Zierdt, D.J. Lebel, Mill experiences with conversion of a Kamyr digester to modified continuous cooking. *Tappi J.*, 1990; 73(1): 103–108.
- 11 Jiang, J.E., et al., Extended delignification with a prolonged mild counter-current cooking stage. *Appita J.*, 1992; 45(1): 19–22.
- 12 Andtbacka, S., R. Tibbling, ECF and TCF bleaching of isothermally cooked (ITC) pulp. *Pap. Puu.*, 1994; 76(8): 580–585.
- 13 IsoThermal Cooking – ITC (brochure). Kvaerner Pulping: Karlstad, Sweden, 1993.
- 14 Marcoccia, B.S., R. Laakso, G. McClain, Lo-Solids pulping: principles and applications. *Tappi J.*, 1996; 79(6): 179–188.
- 15 Stanley, D., B. Marcoccia, Operating Experiences with the Lo-Solids pulping process at Willamette Industries' Johnsonburg Mill. *Tappi J.*, 2001; 84(4).
- 16 Kettunen, A., et al., Effect of cooking stage EA concentration profiles on softwood kraft pulping. *Pap. Puu.*, 1997; 79(4): 232–239.
- 17 Kettunen, A., et al. Enhanced alkali profile cooking: further improvements in pulp tear strength. Pulping Conference. TAPPI, 1997.

## Sections 4.3.1–4.3.3

- 1 Schwitzgebel, K., P.S. Lowell, *Environmental Sci. Technol.*, 1973; 7: 1147–1151.
- 2 Kann, F., R. Fuchs, Comparison of basic characteristics in burning thickened cooking liquors obtained from magnesium bisulfite and calcium bisulfite pulping. *Das Papier*, 1967; 21: 174–179.
- 3 Rydholm, S., S. Lagergren, On the delignification reactions of the technical sulfite cook. *Svensk. Papperstidn.*, 1959; 62(4): 103–122.
- 4 Barsalou, M., *Paper Trade J.*, 1957; 141(3): 34–38.
- 5 Häggroth, S. et al., *Svensk. Papperstidn.*, 1953; 56: 660–669.
- 6 Rydholm, S.A., *Pulping Processes*. Original Edn. New York: Wiley, Interscience, 1965: 439–576.
- 7 Harris, G.R., *Pulp Paper Mag. Can.*, 1957; 58(3): 284–288, 313.
- 8 Strapp, R.K., *Pulp Paper Mag. Can.*, 1957. 58(3): 277–283.
- 9 Chen, C.C., et al., Local composition model for excess Gibbs energy of electrolyte systems. Part I: Single solvent, single completely dissociated electrolyte

- systems. *AIChE Journal*, **1982**; 28(4): 588–596.
- 10 Schöggel, K., The physical properties of Mg-based sulfite cooking liquors. Internal Report, Lenzing R&D: Lenzing, **2004**.
  - 11 Hagfeldt, K., T. Simmons, U. Söderlund, Sulfur dioxide absorption in magnesium cooking acids. *Svensk. Papperstidn.*, **1973**; 76(8): 292–296.
  - 12 Vilamo, E., Old and new methods in sulfite cooks. I. Removal of air and results obtained by the new methods. *Pap. Puu*, **1954**; 36(10): 401–402.
  - 13 Vilamo, E., O. Aho, K. Aunio, Pulping according to Vilamo. *Svensk. Papperstidn.*, **1955**; 58(12): 452–457.
  - 14 Patt, R., H. Augustin, Untersuchungen über die Imprägnierbarkeit von Fichte (*Picea excelsa* L.) und Kiefer (*Pinus silvestris* L.) mit Magnesiumbisulfitaufschlußlösungen. *Wochenblatt für Papierfabrikation*, **1970** (10): 441–445.
  - 15 Aurell, R., L. Stockman, A. Teder, Chip impregnation during sulfite cooking. II. Investigation of penetration rate by means of the quartz spiral balance. *Svensk. Papperstidn.*, **1958**; 61(21): 937–944.
  - 16 Stone, J.E., H.V. Green, Penetration and diffusion into hardwoods. *Pulp Paper Mag. Can.*, **1958**; 59(10): 223–232.
  - 17 Enomoto, S., M. Okada, T. Koshizawa, Studies on penetration and diffusion of calcium-base sulfite cooking liquor into wood. *Tappi*, **1958**; 41(9): 522–526.
  - 18 Sharareh, S., P. Tessier, C. Lee, Penetration of sodium sulphite into black spruce and aspen wood chips. *Pap. Puu*, **1995**; 77(1–2): 45–50.
  - 19 Kubes, G.J., Penetration of pulping chemicals into wood structure. Web page of Pulp & Paper Research Centre, McGill, **2004**.
  - 20 Rapson, B., Queen's University: Kingston, Ontario, **1948**.
  - 21 Patt, R., Isotopentechnische Untersuchungen über das Eindringen von Bisulfitlösungen in Fichte und Kiefer und dessen bedeutung für den Zellstoffaufschluß. I. Teil: Über die Imprägnierbarkeit von Kiefer und Fichte mit Bisulfitlösungen. *Das Papier*, **1971**; 25(7): 384–390.
- ### Section 4.3.4
- 1 Rydholm, S.A., *Pulping Chemistry*. R.E. Krieger Publisher Co., Malabar, Florida, **1985**.
  - 2 Kaufmann, Z., Dissertation. ETH, Zürich, **1951**.
  - 3 Gellerstedt, G., Pulping chemistry. In D.N.S., Shirraishi, N., Eds. *Wood and Cellulosic Chemistry*. 2nd edn. M. Dekker, New York, Basel, **2001**: 859.
  - 4 Lindgren, B., *Acta Chem. Scand.*, **1949**; 3: 1011.
  - 5 Gellerstedt, G., *Svensk. Papperstidn.*, **1976**; 16: 537.
  - 6 Gellerstedt, G., Gierer, J., *Svensk. Papperstidn.*, **1971**; 5: 117.
  - 7 Tameda, H., Nakano, J., Hosoya, S., Chang, H.-M., *Wood Chem. Technol.*, **1987**; 7(4): 485.
  - 8 Gellerstedt, G., Gierer, J., *Acta Chem. Scand.*, **1968**; 22: 2510.
  - 9 Gellerstedt, G., Gierer, J., *Acta Chem. Scand.*, **1970**; 24: 1645.
  - 10 Gellerstedt, G., Gierer, J., *Acta Chem. Scand. B.*, **1975**; 29: 561.
  - 11 Gierer, J., *Svensk. Papperstidn.*, **1970**; 18: 571.
  - 12 Schubert, S.W., Andrus, M.G., Ludwig, C., Glennie, D., McCarthy, J.L., *TAPPI*, **1967**; 50(4): 186.
  - 13 Luthe, C.E., *Holzforschung*, **1990**; 44: 107.
  - 14 Parrish, J.R., *J. Chem. Soc (C)*, **1967**; 50: 1145.
  - 15 Gratzl, J.S., Chen, C.L., *Chemistry of Pulping: lignin reactions*. ACS Symposium Series Vol. 742, Chapter 20, Lignin: Historical, Biological, and Materials Perspective, Glasser, W., Northey, R.A., Schultz, T.P. Eds. ACS, Washington, DC, **1999**: 392–421.
  - 16 Karlsson, O., Pettersson, B., Westermark, U., *J. Pulp Paper Sci.*, **2001**; 27: 310.
  - 17 Hachey, J.M., Bui, V.T., *J. Appl. Polym. Sci.*, **1992**; 51: 171.
  - 18 Dahlman, O., Mansson, K., *J. Wood Chem. Technol.*, **1996**; 16(1): 47.
  - 19 Schubert, S.W., Andrus, M.G., Ludwig, C., Glennie, D., McCarthy, J.L., *TAPPI*, **1967**; 50(4): 186.

- 20 Kosikova, B., Joniak, D., Hricovini, M., Mlynar, J., Zakutna, L., *Holzforschung*, **1993**; 47: 116.
- 21 *Methods in Lignin Chemistry*, Eds. Lin, S.Y., Dence, C.W., Springer-Verlag, Heidelberg, **1992**.
- 22 Buchholz, R.F., Neal, J.A., McCarthy, J.L., *J. Wood Chem. Technol.*, **1992**; 12: 447.
- 23 James, A.N., Tice, P.A., *TAPPI*, **1965**; 48(4): 239.
- 24 Fredheim, G.E., Braaten, S.M., Christensen, B.E., *J. Chromatogr. A*, **2002**; 942: 191.
- 25 Whitmore, P.M., Bogaard, J., *Restaurator*, **1994**; 15: 26.
- 26 Klemm D., Philipp, B., Heinze, T., Heinze, U., Wagenknecht, W., *Comprehensive Cellulose Chemistry*. Vols. 1 & 2. Wiley-VCH: Weinheim, **1998**.
- 27 Lai, Y.-Z., Chemical degradation. In Hon, D.N.S., Shiraishi, N., Eds. *Wood and Cellulosic Chemistry*. 2nd edn. M. Dekker, New York, Basel, **2001**: 443.
- 28 Theander, O., *Acta Chem. Scand.*, **1964**; 18: 1297.
- 29 Feather, M.S., Harris, J.F., *J. Org. Chem.*, **1965**; 30: 153.
- 30 Gierer, J., Lenz, B., Wallin, N.-H., *Chem. Scand.*, **1964**; 18: 1469.
- 31 Hamilton, J.K., *Tappi*, **1958**; 41: 803, 811.
- 32 Annergren, G.E., Rydholm, S.A., *Svensk. Papperstidn.*, **1959**; 62: 737.
- 33 Pfister, K., Sjöström, E., *Papper ja Puu – Papper och Trä*, **1977**; 00: 711.
- 34 Larsson, K., Samuelson, O., *Svensk. Papperstidn.*, **1969**; 72: 97.
- 35 Nelson, P.F., *Svensk. Papperstidn.*, **1968**; 71: 369.
- 36 Popoff, O., Theander, O., *Carbohydr. Res.*, **1972**; 22: 135.
- 37 Popoff, O., Theander, O., *Acta Chem. Scand.*, **1976**; 30: 397.
- 38 Popoff, O., Theander, O., *Chemical Commun.*, **1970**, 1576.
- 39 Popoff, T., Theander, O., *Acta Chem. Scand. B*, **1976**; 30: 397.
- 40 Vuorinen, T., Fagerström, P., Buchert, J., Tenkanen, M., Teleman, A., *J. Pulp Paper Sci.*, **1999**; 25(5): 155.
- 41 Lindberg, B., Theander, O., *Svensk. Papperstidn.*, **1962**; 65: 509.
- 42 Häggglund, E., Johnson, T., Uerban, H., *Berichte*, **1930**; 63: 1387.
- 43 Adler, E., *Svensk. Papperstidn.*, **1946**; 49: 339.
- 44 Lindberg, B., Tanaka, J., Theander, O., *Acta Chem. Scand.*, **1964**; 18: 1164.
- 45 Theander, O., *Proceedings, First International Symposium on Delignification with Oxygen, Ozone and Peroxides*. Raleigh, NC, **1975**: 41–57.
- 46 Anet, E.F.L.J., Ingles, D.L., *Chem. And Ind.*, **1964**, 1319.
- 47 Yllner, S., *Acta Chem. Scand.*, **1956**; 10: 1251.
- 48 Stockmann, L., *Svensk. Papperstidn.*, **1951**; 54: 621.
- 49 Lindberg, B., Theander, O., *Svensk. Papperstidn.*, **1962**; 65(13): 509.
- 50 Hartler, N., Lind, L., Stockman, L., *Svensk. Papperstidn.*, **1961**; 64: 160.
- 51 Rydholm, S.A., *Pulping Chemistry*. R.E. Krieger Publisher Company, Malabar, Florida, **1985**: 525.
- 52 Pascoe, T., Buchanan, J.S., Kennedy, E.H., Sivola, G., *TAPPI*, **1959**; 42: 265.
- 53 Goliath, M., Lindgren, B.O., *Svensk. Papperstidn.*, **1961**; 64: 469.
- 54 Rosenberger, N.A., *Zellstoff- und Papier*, **1957**; 6: 361.
- 55 Regestad, S.O., Samuelson, O., *Svensk. Papperstidn.*, **1958**; 61: 735.
- 56 Gandini, A., Naceur Belgacem, M., *Prog. Polymer Sci.*, **1997**; 22(6): 1203.
- 57 Bockman, O.C., *Norsk. Skogindustri*, **1962**; 16: 320.
- 58 Kratzl, K., Oburger, M., *Holzforschung*, **1980**; 34: 11.
- 59 Kratzl, K., Oburger, M., *Holzforschung*, **1980**; 34: 191.
- 60 Häggglund, S., *Svensk. Papperstidn.*, **1944**; 47: 230.
- 61 Parck, C., Samuelson, O., *Svensk. Papperstidn.*, **1955**; 58(2): 31.
- 62 Erdtmann, H., *TAPPI*, **1949**; 32: 303.
- 63 Schöön, N.-H., *Svensk. Papperstidn.*, **1962**, 65: 729.
- 64 Mutton, D.B., in *Wood extractives and their significance to the pulp and paper industries*. Hillis, W.E., ed. Academic Press, New York, London, **1962**.
- 65 Hoge, W.H., *Tappi*, **1954**; 37: 369.
- 66 Kurth, E.F., *Ind. Eng. Chem.*, **1953**; 45: 2096.

- 67 Sjöström, E., Wood chemistry – Fundamentals and Applications. Academic Press, New York, London, Toronto, Sydney, San Francisco, 1981.
- 68 Routola, O., Pohjola, A., *Pappers- och Trävarutidskr. Finland*, 1934; 7: 289.
- 69 *Römpp-Lexikon Naturstoffe*. Eds. Falbe, J., Regitz, M. G. Thieme, Stuttgart, New York, 1997.

### Section 4.3.5

- 1 Svensson, S., Charging apparatus for cellulose digesters. SE 86978: Sweden, 1936.
- 2 Vilamo, E., O. Aho, K. Aunio, Pulping according to Vilamo. *Svensk. Papperstidn.*, 1955; 58(12): 452–457.
- 3 Yorston, F.H., N. Liebergott, Correlation of the rate of sulphite pulping with temperature and pressure. Further studies. *Pulp Paper Mag. Can.*, 1965: 272–278.
- 4 Goldfinger, G., Variation of the order and energy of activation of the delignification reaction in sulphite cooking. *Tappi Section – Paper Trade J.*, 1941: 289–291.
- 5 Rusten, D., Degradation of cellulose and solution of hemicelluloses during spruce sulfite pulping. *Norsk. Skogindustri*, 1962; 16: 328–339.
- 6 Fischer, K., I. Schmidt, Kinetics of cellulose and lignin degradation during the acid bisulfite process and the possibilities for cooking control. *Tappi J.*, 1991; 74(1): 182–185.
- 7 Haywood, S.T., An empirical cooking model for magnesium bisulphite pulp. *Pulp Paper Canada*, 1989; 90(6): 112–114.
- 8 Yaldez, R., A. Ecker, H-factor determination for viscosity degradation during acid sulfite pulping of beech wood. R&D Lenzing AG: Lenzing, 2000.
- 9 Schelosky, N., T. Baldinger, Determination of small anionic sulfur species in magnesium base bisulfite cooking liquor by capillary electrophoresis (CE). *Lenzinger Ber.*, 2000; 79: 108–112.
- 10 Kaufmann, Z., Über die chemischen Vorgänge beim Aufschluß von Holz nach dem Sulfitprozess. PhD-Thesis, ETH: Zürich, 1951.
- 11 Ivancic, A., S.A. Rydholm, Technical color reactions of lignin. *Svensk. Papperstidn.*, 1959; 16(62): 554–566.
- 12 Ingruber, O.V., *Pulp Paper Mag. Can.*, 1954; 55(10): 124–131.
- 13 Promberger, A., Influence of storage conditions of beech wood on sulfite pulping processability and final pulp properties. PhD-Thesis, In Institute of Pulp, Paper and Fiber Technology. Technical University: Graz, 2004: 191.
- 14 Sixta, H., Acid magnesium sulfite cooking of beech and spruce woods. 1: Course of the degradation of wood components. R&D Lenzing AG: Lenzing, 2002.
- 15 BeMiller, J.N., Acid-catalyzed hydrolysis of glycosides. *Adv. Carbohydrate Chem.*, 1967; 22: 25–108.
- 16 Röhrling, J., et al., A novel method for the determination of carbonyl groups in cellulose by fluorescence labelling. 1. Method development. *Biomacromolecules*, 2002; 3(5): 959–968.
- 17 Röhrling, J., et al., A novel method for the determination of carbonyl groups in cellulose by fluorescence labelling. 2. Validation and applications. *Biomacromolecules*, 2002; 3(5): 969–975.
- 18 Röhrling, J., et al., Determination of carbonyl functions in cellulosic substrates. *Lenzinger Ber.*, 2002; 81: 89–97.
- 19 Potthast, A., et al., A novel method for the determination of carbonyl groups in cellulose by fluorescence labelling. 3. Monitoring oxidative processes. *Biomacromolecules*, 2003; 4(3): 743–749.
- 20 Rydholm, S.A., *Pulping Processes*. Original edition 1965. New York: Wiley (Interscience), 1965: 439–576.
- 21 Patt, R., D.L.-K. Wang, Qualitätsbeurteilung von Chemiezellstoffen. Teil 2: Alkalilöslichkeit und Gesamtzuckeranalyse. *Das Papier*, 1987; 41(1): 7–12.
- 22 Dunlop, A.P., Furfural formation and behavior. *Ind. Eng. Chem.*, 1948; 40(2): 204–209.
- 23 Harris, J.F., et al., Factors influencing dilute sulfuric acid prehydrolysis of southern red oak wood. *Prog. Biomass Conversion*, 1984; 5: 101–141.

- 24 Erdtman, H., The phenolic constituents of pine heartwood. V. The heartwood of *Pinus strobus*. *Svensk. Kem. Tid.*, **1944**; 56: 2–14.
- 25 Erdtman, H., The phenolic constituents of pine heartwood. VIII. Ultraviolet absorption and steric configuration of pinosylvin. *Svensk. Kem. Tid.*, **1944**; 56: 134–142.
- 26 Erdtman, H., The phenolic constituents of pine heartwood. VII. The heartwoods of *Pinus nigra* Arn, *Pinus montana* Mill., *Pinus banksiana* Lamb, and *Pinus palustris* Mill. *Svensk. Kem. Tid.*, **1944**; 56: 95–101.
- 27 Erdtman, H., The phenolic constituents of pine heartwood. VI. The heartwood of *Pinus cembra* L. *Svensk. Kem. Tid.*, **1944**; 56: 26–31.
- 28 Hoge, W.H., *Tappi*, **1954**; 37: 369.
- 29 Mutton, D.B., Hardwood resins. *Tappi J.*, **1958**; 41: 632–643.
- 30 Harris, J.F., Acid hydrolysis and dehydration reactions for utilizing plant carbohydrates. *Applied Polymer Symp.*, **1975**; 28: 131–144.
- 31 Conner, A.H., Kinetic modeling of hardwood prehydrolysis. Part I. Xylan removal by water prehydrolysis. *Wood Fiber Sci.*, **1984**; 16(2): 268–277.
- 32 Sixta, H., Cellulose preparation and recycling of raw materials and auxiliaries by the Lenzinger magnesium bisulfite process. *Lenzinger Ber.*, **1986**; 61: 5–11.
- 33 Rydholm, S., S. Lagergren, On the delignification reactions of the technical sulfite cook. *Svensk. Papperstidn.*, **1959**; 62(4): 103–122.
- 34 Sixta, H., Acid magnesium sulfite cooking of beech and spruce woods. 2: Influence of cooking conditions. R&D Lenzing AG: Lenzing, **2003**.
- 2 Tomlinson, G.H., Pioneering in the chemical processing of wood. *Pulp Paper Mag. Can.*, **1948**; 49(7): 63–68.
- 3 Tomlinson, G.H., G.H.I. Tomlinson, Improved heat and chemical recovery in the alkaline pulping process. *Pulp Paper Mag. Can.*, **1946**; 47(9): 71–77.
- 4 Tomlinson, G.H., G.H.I. Tomlinson, Recovery of heat and chemicals from kraft black liquor. US 2406867 CAN 40:39740, **1946**.
- 5 Häggglund, E., J. Torsten, Contribution to the chemistry of digesting sulfite cellulose. XI. The decomposition of pine and fir wood with sulfuric acid. *Svensk. Papperstidn.*, **1928**; 31: 263–265.
- 6 Häggglund, E., The pulping of pine wood by the sulfite process. II. *Cellulose-Chemie*, **1928**; 9(4/5): 38–43.
- 7 Häggglund, E., J. Holmberg, T. Johnson, The decomposition of pine wood by means of the sulfite process. IV. *Svensk. Papperstidn.*, **1936**; 39(Special No.): 37–42.
- 8 Wennerås, S., Two-Stage Neutral Sulfite – Bisulfite Pulping of Spruce. *Norsk. Skogindustri.*, **1962**; 3: 118–126.
- 9 Evans, J.C.W., A new sulphite pulping process and a new pulp. *Paper Trade J.*, **1959**; 143(36): 42–48.
- 10 Nilsson, O., L. Stockman, Kochen von Sulfit in Magnesiumbase in zwei Schritten. *Svensk. Papperstidn.*, **1962**; 18: 711–713.
- 11 Tomlinson, G.H., et al., The magnesfite process – a new pulping method. *Pulp Paper Mag. Can.*, **1958**; 59(3): 247–252.
- 12 Tomlinson, G.H., G.H.I. Tomlinson, Recovery of heat and chemicals from an alkaline-pulping residual liquor. US Patent 2840454 19580624, **1958**.
- 13 Bryce, J.R.G., G.H. Tomlinson, Modified magnesfite pulping. The two-stage neutral process. *Pulp Paper Mag. Can.*, **1962**: 355–361.
- 14 Bailey, E.L., Recent technical advances in magnesia-base cooking. *Tappi*, **1962**; 45(9): 689–691.
- 15 Pascoe, T.A., et al., The Sivola sulphite cooking and recovery process. *Tappi*, **1959**; 42(4): 265–281.
- 16 Sivola, G., Manufacturing pulp from fibrous materials. US Patent 2701763

### Section 4.3.6



- 19550208 CAN Patent 49: 30446; AN 1955:30446, 1955.
- 17 Sivola, G., Integrated lignocellulose digestion and recovery processes. US 2730445 19560110; CAN 50:46760; AN 1956:46760, 1956.
- 18 Sanyer, N., E.L. Keller, G.H. Chidester, Multistage sulfite pulping of jack pine, balsam fir, spruce, oak, and sweetgum. *Tappi*, 1962; 45(2): 90–104.
- 19 Sanyer, N., E.L. Keller, Sulfite pulping of douglas-fir heartwood by two-stage processes using sodium, magnesium, and magnesium-ammonium bases. *Tappi*, 1965; 48(10): 545–552.
- 20 Lightfoot, R.G., O. Sepall, A study of variables in bisulphite/alkali, two-stage pulping. *Pulp Paper Mag. Can.*, 1965: 279–288.
- 21 Räsänen, R.H., L.I. Luotonen, Das Sulfit-Soda-Mehrstufen-Kochverfahren. *Zellstoff und Papier*, 1959; 10: 375–378.
- 22 Hassinen, I., Preparation of pulp by the Rauma method from various grades of wood. *Wlokna Chemiczne*, 1984; 9(4): 370–374.
- 23 Reilama, I., I. Hassinen, R. Rasanen, Rauma recovery – an environmental protection technique. *Pulp Paper Can.*, 1981; 82(1): T37–T39.
- 24 Croon, I., E. Treiber. Present situation and future trends in dissolving pulp manufacture. In TAPPI Fifth International Dissolving Pulps Conference, Vienna, Austria. Tappi, Atlanta, GA, 1980.
- 25 Croon, I., The flexibility of sodium-base two-stage neutral-acid sulphite pulping. *Pulp Paper Mag. Can.*, 1965: 71–76.
- 26 Cederquist, K.N., et al., Stora sodium-base chemical recovery process. *Tappi*, 1960; 43: 702–706.
- 27 Scholander, A., The Stora Kopparberg recovery process in the Mo & Domsjovrddoto AB Domsjovrddoto sulfite mill. *Tappi*, 1960; 43: 706–710.
- 28 Söderquist, R., Natriumsulfitzellstoff. *Das Papier*, 1957; 11(21/22): 487–491.
- 29 Lagergren, S., B. Lunden, Some recent developments in sulfite pulp making. *Pulp Paper Mag. Can.*, 1959; 60(11): T338–T341, 345.
- 30 Lagergren, S., The Stora pulping process and its implications for European paper makers. *Svensk. Papperstidn.*, 1964; 6: 238–243.
- 31 Annergren, G.E., et al., On the stabilization of spruce glucomannan in wood and holocellulose. *Svensk. Papperstidn.*, 1961; 64: 386–393.
- 32 Annergren, G.E., S.A. Rydholm, On the behavior of the hemicelluloses during sulfite pulping. *Svensk. Papperstidn.*, 1959; 62(20): 737–745.
- 33 Annergren, G.E., S.A. Rydholm, On the stabilization of glucomannan in the pulping processes. *Svensk. Papperstidn.*, 1960; 63(18): 591–600.
- 34 Janson, J., E. Sjostrom, Behaviour of xylan during sulfite cooking of birchwood. *Svensk. Papperstidn.*, 1964; 67(19): 764–771.
- 35 Lindgvist, B., K. Sondell, Experience of Domsjö sulfite pulp mill with the TCF-bleaching technology and closed water circuit. *Tsellyoloza, Bumaga, Karton*, 1997; 5–6: 1997.
- 36 Assarsson, A., et al., Controlling the resin content of pulp. *Svensk. Trävaru-och Pappersmassetidn.*, 1982; 7: 461–463.
- 37 Ingruber, O.V., G.A. Allrad, Alkaline sulphite pulping for 'Kraft' strength. *Pulp & Paper Mag. Can.*, 1973; 74(11): T354–T369.
- 38 Ingruber, O.V., C.A. Allrad, Controlled Alkaline Sulphite Pulping. US 3 630 832, 1971.
- 39 Ingruber, O.V., C.A. Allrad, Alkaline Sulfite Pulping. Can 847.218, 1970.
- 40 Young, R.A., M. Akhtar, *Environmental Friendly Technologies for the Pulp and Paper Industry*. John Wiley & Sons, Inc., 1998.
- 41 Peltonen, J.V.A. Alkaline sulphite pulp to replace kraft? Discussion of process alternatives for conversion of an existing kraft mill. In International Sulphite Pulping & Recovery Conference. Boston: TAPPI/CPPA, 1972.
- 42 Nomura, Y., M. Wakai, H.Sato, Sulphite digestion of lignocellulose materials. Japanese Patent 112 903, 1976.
- 43 Kettunen, J., N.-E. Virkola, I. Yrjälä, The effect of anthraquinone on neutral sulphite and alkaline sulphite cooking of pine. *Pap. Puu*, 1979; 11: 685–700.
- 44 McDonough, T.J., V.J.v. Drunen, T.W. Paulson, Sulphite-anthraquinone pulp-

- ing of Southern pine for bleachable grades. *J. Pulp Paper Sci.*, **1985**; 11(6): 167–176.
- 45 Ingruber, O.V., M. Stradal, J.A. Histed, Alkaline sulphite-anthraquinone pulping of eastern Canadian woods. *Pulp Paper Can.*, **1982**; 83(12): 79–88.
- 46 Patt, R., O. Kordsachia, Herstellung von Zellstoffen unter Verwendung von alkalischen Sulfidlösungen mit Zusatz von Anthraquinon und Methanol. *Das Papier*, **1986**; 40(10): 1–8.
- 47 Patt, R., O. Kordsachia, Sulfite cooking method for the production of cellulose from materials containing lignocellulose with recovery of the cooking chemicals. DE3518005, **1986**.
- 48 Kordsachia, O., R. Patt, N. Mix, Aufschluß von Pappelholz nach dem ASAM-Verfahren. *Das Papier*, **1989**; 43(7): 293–301.
- 49 Zimmermann, M., R. Patt, O. Kordsachia, ASAM pulping of Douglas fir and chlorine-free bleaching. *Tappi J.*, **1991**; 74(11): 129–134.
- 50 Schubert, H.-L., et al., The ASAM Process – a pulp technology ready for industry. *Das Papier*, **1993**; 47(10A): V6–V15.
- 51 Kordsachia, O., R. Patt, Untersuchungen zum Aufschluß von Buche nach dem ASAM-Verfahren und zur Bleiche der Zellstoffe in unterschiedlichen Sequenzen. *Das Papier*, **1987**; 41(7): 340–351.
- 52 Kordsachia, O., R. Patt, Full bleaching of ASAM pulps without chlorine compounds. *Holzforschung*, **1988**; 42(3): 203–209.
- 53 Kordsachia, O., B. Reipschläger, R. Patt, ASAM pulping of birch wood and chlorine free pulp bleaching. *Pap. Puu*, **1990**; 72(1): 44–50.
- 54 Patt, R., et al., Lignin and carbohydrate reactions in Alkaline Sulfite, Anthraquinone, Methanol (ASAM) pulping. *Das Papier*, **1991**; 45(7): 389–396.
- 55 Schubert, H.-L., O. Kordsachia, R. Patt, Pilot plant trials of ASAM pulping process. *Wochenbl. f. Papierf.*, **1990**; 118(22): 977–981.
- 56 Patt, R., O. Kordsachia, B. Rose. Progress in alkaline sulfite-AQ pulping (AS/AQ). In Seventh International Conference on New Available Technologies. Stockholm, Sweden: SPCI, **2002**.
- 57 Sixta, H., Comparative evaluation of CBC kraft pulping of pine and spruce wood chips. Internal Report, R&D Lenzing AG, **2004**.
- 58 Patt, R., O. Kordsachia, B. Rose, Modified alkaline sulfite pulping. *Wochenbl. f. Papierf.*, **2003** 131(14–15): 892–894, 896–897.

## 5 Pulp Washing

*Andreas W. Krotscheck*

### 5.1 Introduction

The purpose of pulp washing is to obtain pulp that is free of unwanted solubles. In the most basic case, this can be done by replacement of the contaminated liquor accompanying the pulp fibers by clean water. In a modern pulp mill, washing operations include also displacement of one type of liquor by another type of liquor. Aside from its washing function, washing equipment must at times also allow the effective separation of chemical regimes or temperature levels between single fiberline process steps.

Various benefits result from pulp washing, such as minimizing the chemical loss from the cooking liquor cycle; maximizing recovery of organic substances for further processing or incineration; reducing the environmental impact of fiberline operations; limiting the carry-over between process stages; maximizing the re-use of chemicals and the energy conservation within a single bleaching stage; and last – but not least – obtaining a clean final pulp product.

Ideally, pulp washing is carried out with the minimum amount of wash water in order to conserve fresh water resources and to take capacity burden from downstream areas which process the wash filtrate. Very often, pulp washing is a compromise between the cleanness of the pulp and the amount of wash water to be used.

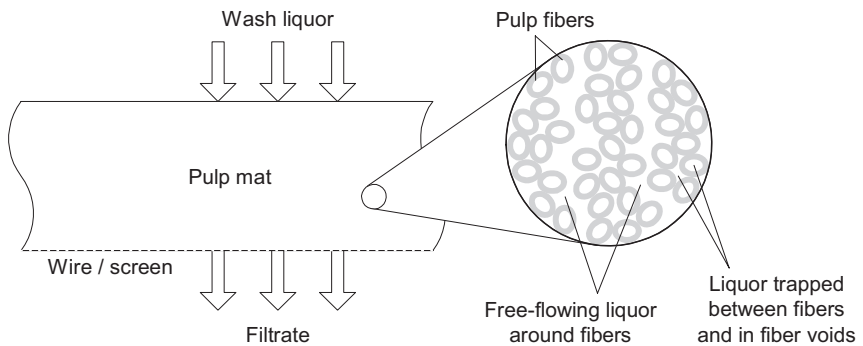
In the mill, pulp washing operations can be found in brownstock washing, in the bleach plant and, as the case may be, also in digesting and on the dewatering machine.

## 5.2 Pulp Washing Theory

### 5.2.1 Overview

First, we will examine the phenomena which influence pulp washing operations from a theoretical perspective. Due to the complexity of the involved mechanisms and a certain lack of practically applicable mathematical relationships, this theoretical discussion will be mostly qualitative in nature.

In the basic case of washing, we are dealing with a liquor-soaked network of pulp fibers – often called the “pulp mat” – which is charged with wash liquor. The pulp mat forms on the filter medium, a perforated device such as a wire or a screen, which holds back the pulp but allows the extraction of filtrate from the pulp mat (Fig. 5.1).



**Fig. 5.1** Simplified illustration of the pulp washing operation. Wash liquor is added to the pulp mat which is retained on the filter medium (wire or screen), and filtrate is extracted through the filter medium. Right side:

Simplified illustration of the pulp suspension, with free-flowing liquor around the fibers and immobile liquor trapped between the fibers and in the fiber voids.

For the purpose of facilitating the understanding of the involved processes, the phases participating in the pulp suspension can be divided into three fractions: (a) a free-flowing liquid phase around the fibers; (b) an immobile liquid phase locked in between the fibers and within the fiber voids; and (c) the fiber solid [1].

Specific considerations are applicable for each of the three fractions. On one hand, the free-flowing liquid together with the substances dissolved therein can be drained, displaced by another liquid, or pressed from the fiber network.

On the other hand, the immobilized liquid inside and in between the pulp fibers is less accessible. Removal of this liquid is limited to pressing. Otherwise, the mass transfer from the immobile liquid to the free-flowing liquid is controlled by diffusion.

As for the fiber solids, a part of the dissolved substances may be bound to the fibers by sorption and may as such be barely removable at all.

## 5.2.2

**Drainage**

Typical pulp washing operations involve the process steps of initial dewatering, actual displacement washing, and final thickening. Drainage plays a fundamental role in all of those process steps. It is driven by a pressure difference across the pulp mat which is created by applying a fluid pressure or vacuum, or by putting mechanical pressure on the pulp mat.

The liquor flow through a pulp mat is generally presumed to follow Darcy's law. This law describes how, in a laminar flow regime, the flow rate through porous media is determined by the pressure gradient and permeability:

$$\frac{\partial V}{\partial t} = -\frac{KA}{\mu} \frac{\partial p}{\partial x} \quad (1)$$

where

$\partial V/\partial t$  = volumetric flow rate of the filtrate (in  $\text{m}^3 \text{s}^{-1}$ );  $K$  = permeability (in  $\text{m}^2$ );  $A$  = filtration area (in  $\text{m}^2$ );  $\mu$  = dynamic viscosity of the filtrate (in Pa.s); and  $\partial p/\partial x$  = pressure gradient across the fiber web (in  $\text{Pa m}^{-1}$ ).

The permeability  $K$  as a qualitative property describes the ease with which a fluid passes through the porous fiber web. Under the simplifying assumption of constant parameters, the very basic equation for the drainage velocity  $v$  ( $\text{m s}^{-1}$ ) through a fiber web is [2]:

$$v = \frac{1}{A} \frac{dV}{dt} = -\frac{K \Delta p_t}{\mu d} \quad (2)$$

where  $\Delta p_t$  is the total pressure drop across the fiber web and filter medium (Pa), and  $d$  is the thickness of the fiber web (m).

We can see that the drainage velocity increases linearly with the applied differential pressure  $\Delta p_t$ . On the other hand, it decreases as the viscosity  $\eta$  goes up and as the web gets thicker. Remember that the viscosity of a liquor increases with higher dissolved solids concentration, whereas it decreases with higher temperature. Hence, drainage works better at lower dissolved solids and at higher temperature.

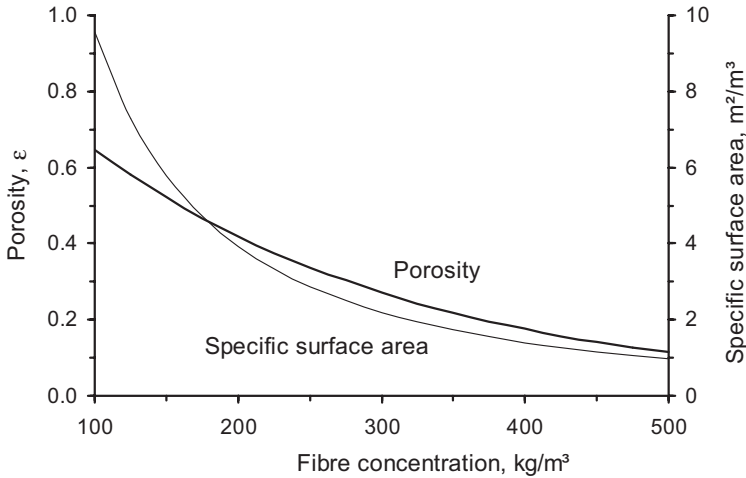
Numerous approaches have been made theoretically to derive the permeability,  $K$ . An overview over porosity–permeability functions is provided in Ref. [3]. One of the most frequently used correlations is the Carman–Kozeny relationship [4]:

$$K = \frac{\varepsilon^3}{k(1-\varepsilon)^2 S_f^2} \quad (3)$$

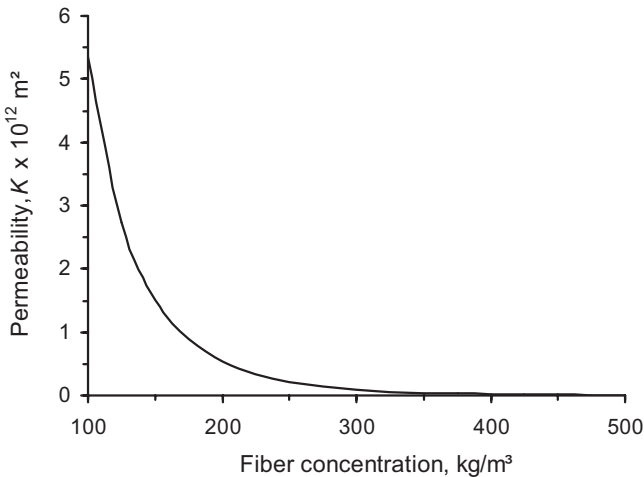
where

$\varepsilon$  = effective porosity of the fiber web (i.e., the volume fraction of the free flow channels);  $k$  = the Kozeny constant; and  $S_f$  = surface area of the free flow channels per unit volume (in  $\text{m}^2 \text{m}^{-3}$ ).

It is important to note that, for the purposes of drainage considerations, the effective porosity must not be mixed up with the total porosity – that is, the web volume not occupied by fiber solids. This is because the total volume of flow paths available for liquor to pass through the fiber web is dramatically smaller than the total filtrate volume within the web. A substantial amount of filtrate is trapped inside the fiber walls and between the fiber bundles, and is therefore not relevant to the drainage process. Both the effective porosity and the specific surface area are difficult to access. They are also fundamentally influenced by surface forces and hence by the presence of liquor components such as surfactants [5].



**Fig. 5.2** Porosity and specific surface area as a function of the fiber concentration for a bleached softwood kraft pulp [6].



**Fig. 5.3** Permeability as a function of the fiber concentration for a bleached softwood kraft pulp [6].

Figure 5.2 illustrates that the porosity and specific surface area of a pulp fiber web are dramatically reduced as the fiber concentration increases. The effect on permeability is even more pronounced (Fig. 5.3).

The specific drainage resistance  $\alpha$  ( $\text{m kg}^{-1}$ ) is defined by:

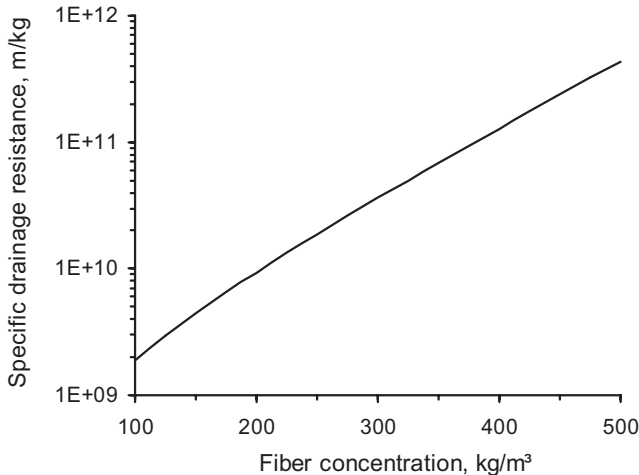
$$\alpha := \frac{d}{K} \frac{A}{W} = \frac{1}{Kc} \quad (4)$$

where  $W$  = mass of oven-dry fibers deposited on the filter medium (kg), and  $c$  = concentration of fibers in the mat ( $\text{kg m}^{-3}$ ).

By combining Eqs. (3) and (4), we can relate the drainage resistance to the structural properties of the fiber web:

$$\alpha = \frac{k(1 - \varepsilon)^2 S_F^2}{c \varepsilon^3} \quad (5)$$

The specific drainage resistance  $\alpha$  is the fundamental pulp mat parameter that characterizes the drainage behavior of a specific pulp. As expected from the permeability curve, the drainage resistance increases massively with the fiber concentration (Fig. 5.4).



**Fig. 5.4** Specific drainage resistance as a function of the fiber concentration for a bleached softwood kraft pulp (calculated from permeability data by [6]).

The specific drainage resistance also rises with the beating degree. This has been explained by the higher levels of fibrillation and fines (short fibers and fiber fragments) which result in a larger specific surface area,  $S_F$ , as well as in higher packing (i.e., reduced porosity  $\varepsilon$ ). Similarly, mechanical pulps show higher drai-

nage resistance than chemical pulps because of the mechanical pulps' larger fines fractions, and hardwood pulps have higher drainage resistance values than softwood pulps due to the presence of shorter fibers. Yet the differences between hardwood and softwood fade away when the pulps are beaten and the influences of increasing fibrillation and fines content supersede the effect of different fiber lengths [7].

The permeability of fiber webs was found to be fairly independent of the specific surface load  $W/A$  over the range applicable to pulp washing [8]. However, the specific drainage resistance may increase with the specific surface load if a pulp contains a larger amount of fines, which are washed through the outer layers of the web and accumulate near the filter medium.

With the specific drainage resistance  $\alpha$ , the drainage velocity equation [Eq. (2)] can be rewritten in the form:

$$v = \frac{-\Delta p_i}{\mu \alpha \frac{W}{A}} \quad (6)$$

Further extension to include both the drainage resistance of the fiber web and the resistance of the filter medium leads to [7]:

$$v = \frac{-\Delta p_i}{\mu \left( \alpha \frac{W}{A} + R_m \right)} \quad (7)$$

where  $R_m$  is the filtration resistance of the filter medium ( $m^{-1}$ ). The term  $\alpha W/A$  represents the filtration resistance of the fiber web.

As long as the filter medium is clean, its filtration resistance  $R_m$  depends on the design and structure of the wire. However, in industrial applications,  $R_m$  may increase to a multiple of the clean value if fines are present which tend to plug the wire.

Another important factor influencing the drainage characteristics is the amount of entrained air in the pulp fed to the washer. As the sheet forms, air bubbles are trapped in the fiber network, and these block certain liquor flow paths in the web. As a consequence, it takes longer for the liquor to pass through the remaining free flow paths. Experiments with mill pulps have shown that air entrainment can be responsible for increasing the drainage time by a factor of 3 to 4 [9].

In summary, good drainage is achievable by applying high differential pressure; limiting the mat thickness; keeping filtrate viscosity low, mainly by operating at higher temperature; controlling the fines content in the pulp and wash liquor; controlling the entrained air in the feed stock; and keeping the screen/wire clean.



## 5.2.3

**Compressive Dewatering**

Dewatering caused by high mechanical pressure follows a different mechanism than outlined above for drainage, because the fiber web's compressibility needs to be appropriately considered. Published investigations made in respect of pressing have focused on the phenomena in roll nips of paper machines, but have also a general relevance for compressive dewatering.

There are basically two models of wet pressing – the decreasing-permeability model and the limiting-consistency model. The decreasing-permeability model attributes the decrease in water removal as pressing progresses to an increasing flow resistance caused by narrower flow channels within the fiber web. The liquor remaining in the web after pressing is related to the initial consistency, the press impulse, a permeability factor and a compressibility factor [10–12]. The tenet of the limiting-consistency model is that for any dewatering system, there is a maximum, or limiting, consistency that can be reached regardless of how long a dewatering force is applied. The limiting consistency is a function of the applied pressure, initial consistency and permeability at a given compression [13].

As the fiber web is compressed, the increase in consistency goes along with a reduction in web thickness. It has been shown that, under a roll-nip-like stress pulse, the compaction of the web continues beyond the peak stress, though at a low rate [8]. When the stress is removed, the web expands again and is susceptible to rewetting. It is therefore essential for efficient compressive dewatering to leave as little pressate as possible next to the pulp network at the end of the pressing action, so that such pressate cannot be sucked back into the pulp by the expanding web.

## 5.2.4

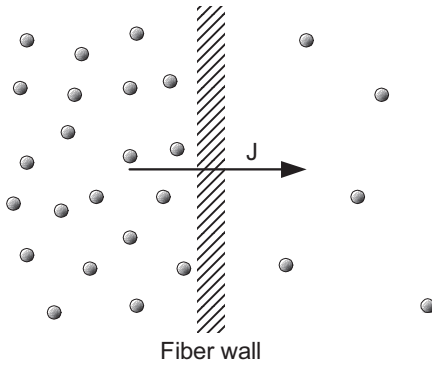
**Diffusion**

In pulp washing operations, diffusion controls the exchange of dissolved substances between the free-flowing liquor outside the fibers and the immobile liquor inside the pulp fibers or locked in between fibers. Physically, diffusion is defined as the net transport of molecules caused by their random thermal motion in an attempt to equalize concentration differences.

The basic equation describing the mass transfer related to diffusion is Fick's First Law, which states that the flux of a diffusing substance is proportional to its concentration gradient. In its one-dimensional form (see Fig. 5.5), Fick's First Law reads:

$$J = -D \frac{\partial c}{\partial x} \quad (8)$$

where  $J$  = flux of the diffusing substance ( $\text{kg m}^{-2} \text{s}^{-1}$ );  $D$  = diffusion coefficient ( $\text{m}^2 \text{s}^{-1}$ ); and  $\partial c/\partial x$  = incremental change of concentration with distance ( $\text{kg m}^{-4}$ ).



**Fig. 5.5** Simplified illustration of mass transfer by diffusion across the wall of a pulp fiber.

On a macroscopic scale,  $\partial c/\partial x$  in our simplified system expresses the concentration gradient of the diffusing substance across the fiber wall. A higher concentration difference between inside and outside the fibers gives a higher flux of the diffusing substance.

In pulp washing, the diffusion coefficient  $D$  is dependent upon the type of wood furnish, the lignin content in the fiber wall, the pH and ionic strength of the liquor, the temperature as well as the diffusing substance itself. The diffusion coefficient decreases with higher lignin content in the fiber wall, whereas it increases with rising temperature. Smaller molecules diffuse more easily, and therefore have higher diffusion coefficients than larger molecules [1,14,15].

Diffusion takes time until the concentrations equal out. According to Fick's Second Law, the time rate of concentration change is again dependent upon the diffusion coefficient:

$$\frac{\partial c}{\partial t} = D \frac{\partial^2 c}{\partial x^2} \quad (9)$$

Hence, the time-dependent equalization of concentrations is influenced by the same factors as the diffusion flux. For example, the small sodium ion diffuses very rapidly, and the equilibrium concentration inside and outside the fibers is reached within seconds, whereas it may take hours to reach the equilibrium concentration for the larger dissolved lignin molecules [15,16].

The time required for diffusion to occur must be provided by the practical design of a pulp washing system. It is essential to allow dissolved substances to pass from within the fibers to the surrounding liquor. Otherwise, the lack of time for diffusion can substantially deteriorate the washing result, especially in cases of large diffusing molecules and high initial concentration levels within the fibers, such as after digesting or oxygen delignification.

## 5.2.5

**Sorption**

Sorption is the phenomenon that makes soluble substances accumulate at the solid–liquid interface on the surface of pulp fibers. Since with pulp the phenomenon of adsorption (i.e., the retention of solutes from a solution by a solid surface) and absorption (i.e., the uptake and retention of solutes within the mass of the solid) are difficult to distinguish one from another, the term “sorption” is often used in the pulp and paper industry to cover both events. Sorption occurs when molecules accumulate on the pulp fiber because this represents their most stable situation with the lowest free energy.

Traditionally, sorption has been described by the Langmuir isotherm, which assumes a state of saturation at high solute concentrations due to space constraints on the sorbent surface [1,17]:

$$A = A_{\max} \frac{Kc}{1 + Kc} \quad (10)$$

where  $A$  = sorbed quantity of substance per unit mass of pulp ( $\text{kg odt}^{-1}$ );  $A_{\max}$  = maximum quantity of sorbed substance per unit mass of pulp ( $\text{kg odt}^{-1}$ );  $K$  = equilibrium constant ( $\text{m}^3 \text{kg}^{-1}$ ); and  $c$  = equilibrium concentration of substance remaining in solution ( $\text{kg m}^{-3}$ ).

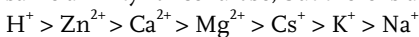
The saturation approach determines that  $A_{\max}$  is related to the sorbent’s surface area. Even if this relationship is not linear, the maximum sorption rate is substantially lower for undamaged fibers than it is for fines. In contrast, it increases massively with the accessibility of internal pore surfaces.

The equilibrium constant  $K$  depends on the charge difference between the sorbent and sorbate. It is also most fundamentally affected by changes in pH. Since the net charge of pulp surfaces is generally negative, the sorption of cations is of primary interest in pulp washing.

In kraft cooking, the predominant cation is obviously sodium. Early laboratory tests on hardwood and softwood pulps have confirmed that the pH has a significant influence on the amount of sorbed sodium [18].

The sorption behavior shown in Fig. 5.6 is characteristic of that obtained with a bifunctional ion exchanger, suggesting that sodium sorption on pulp results from the presence of two sets of functional groups [18]. While carboxylic and other acidic functional groups are made responsible for sorption already at acidic pH, phenolic hydroxyls account for the additional sorption under alkaline conditions. The amount of sodium sorbed depends on the wood species, and also on the cooking process. For a given species, sorbed sodium increases with the lignin content because higher-kappa pulps contain more carboxylic and phenolic groups.

In the multi-component system usually found in an industrial liquor, other cations compete with sodium for available sorption sites. Not all cations have the same affinity for cellulose, but there is a ranking in affinity as follows [19]:



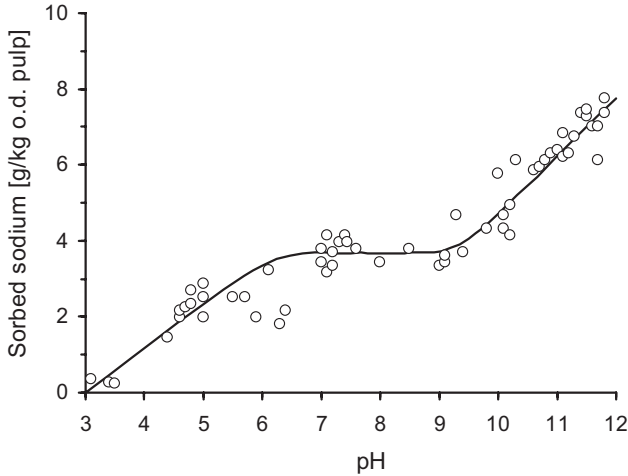


Fig. 5.6 Effect of pH on sodium sorbed by slash pine at kappa number 80 [18].

There is also a temperature-dependence of the sorption equilibrium in a way that, at higher temperatures, the ions are bound more weakly to the fiber [20].

A more recent approach to predicting the ion-exchange behavior of pulps is based on the Donnan equilibrium model, which describes the unequal distribution of ions between two parts of an aqueous system [21].

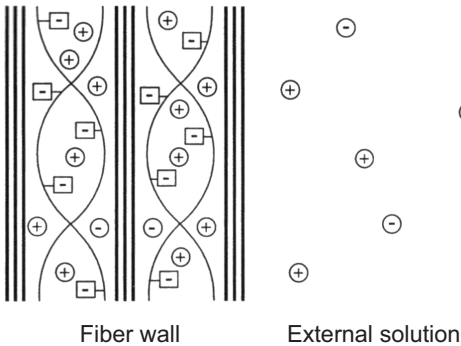


Fig. 5.7 Model of the water-swollen fiber wall in contact with an external solution [21].

Conceptually, there are two separate solutions in a pulp suspension, that is, a small volume of solution contained inside the fiber walls and a large volume of solution external to the fibers (Fig. 5.7). Within the fiber walls, the readily dissociable groups are associated with a lignin-hemicellulose gel which is located between the microfibrils. Once dissociated, the negatively charged groups cause an unequal distribution of mobile ions in a way that cations show higher concentrations within the fiber wall than in the external solution.

The Donnan theory relates the concentrations of the mobile ions in the two solutions in the form of:

$$\lambda = \frac{[H^+]_F}{[H^+]_S} = \frac{[M^+]_F}{[M^+]_S} = \sqrt{\frac{[M^{2+}]_F}{[M^{2+}]_S}} = \dots = \left( \frac{[M^{z+}]_F}{[M^{z+}]_S} \right)^{\frac{1}{z}} \quad (11)$$

where  $\lambda = \text{constant}$ ;  $[H^+] = \text{hydrogen ion concentration (kmol m}^{-3}\text{)}$ ;  $[M^+] = \text{monovalent metal ion concentration (kmol m}^{-3}\text{)}$ ;  $[M^{2+}] = \text{divalent metal ion concentration (kmol m}^{-3}\text{)}$ ; and  $[M^{z+}] = \text{concentration of multivalent metal ion (valency } z\text{) (kmol m}^{-3}\text{)}$ . The subscripts  $F$  and  $S$  denominate the concentrations in the solution inside the fibers and in the external solution, respectively.

The numerical determination of the factor  $\lambda$  is somewhat lengthy, and requires a certain knowledge about the functional groups involved [21]. Nevertheless, the charm of the theory lies in the exchangeability of metal ions in Eq. (11). When  $\lambda$  has been calculated over a range of pH values from a set of experimental distribution data available for a particular metal ion, then the pH-dependent distribution of any other metal ion can be predicted, if only the total amount of this other metal is known, by:

$$[M^{z+}]_S = \frac{1}{V + F(\lambda^z - 1)} M^{z+} \quad (12)$$

$$[M^{z+}]_F = \lambda^z [M^{z+}]_S \quad (13)$$

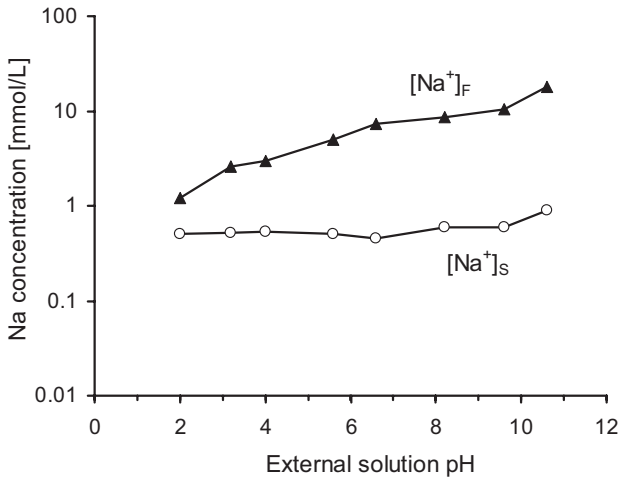
where  $V = \text{total volume of solution inside and outside fibers per unit amount of pulp (m}^3 \text{ odt}^{-1}\text{)}$ ;  $F = \text{total volume of solution inside fibers per unit amount of pulp (m}^3 \text{ odt}^{-1}\text{)}$ ; and  $M^{z+} = \text{total amount of cation with valency } z \text{ per unit amount of pulp (kmol odt}^{-1}\text{)}$ .

Equation (12) is easily obtained by combining the overall mass balance for the metal ion [Eq. (14)] with Eq. (11):

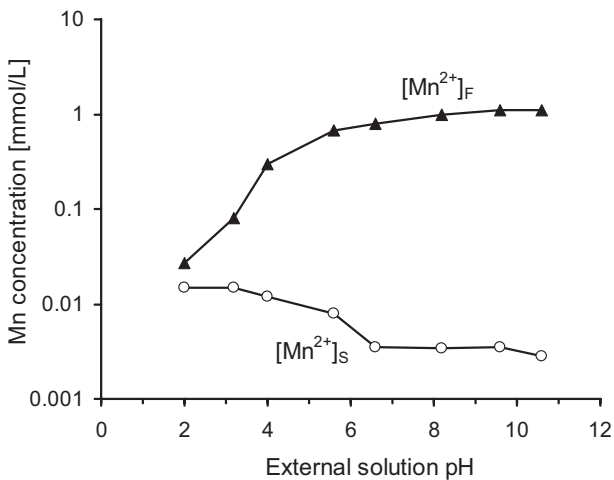
$$M^{z+} = F[M^{z+}]_F + (V - F)[M^{z+}]_S \quad (14)$$

The total volume of solution inside the fibers  $F$  (also called the fiber saturation point) has been determined to be about  $1.4 \text{ m}^3$  per oven-dried ton (odt) for northern softwood pulps [21].

It becomes apparent from Eq. (13) that the valency of the ion has a decisive influence on the distribution of a metal between the fiber wall and the external solution. For the softwood pulp investigated by Towers and Scallan [21],  $\lambda$  was about 15 in the higher pH range. A monovalent ion such as sodium can then be found at concentrations in the fiber wall which are about one order of magnitude higher than the concentrations in the surrounding liquor (Fig. 5.8). For a divalent ion such as manganese, the ratio increases to two orders of magnitude (Fig. 5.9).



**Fig. 5.8** Experimental data for the distribution of sodium between the fiber wall (F) and the external solution (S) [21].



**Fig. 5.9** Experimental data for the distribution of manganese between the fiber wall (F) and the external solution (S) [21].

Models based on the Donnan theory enjoy increasing popularity. The prediction accuracy for the metal distribution can be increased, for instance, by extending Eq. (11) with activity coefficients, and by considering the pH-dependency of the fiber saturation point [22], as well as by including models for complexation and kinetics [23].

Certain metal ions, predominantly manganese and iron, play a role in chlorine-free bleaching. They need to be removed in order to avoid catalytic decomposition

of peroxide. On the other hand, the presence of magnesium ions is desirable because they serve as an inhibitor to cellulose degradation [20]. Figure 5.10 shows the manganese concentration on pulp as a function of the pH, both with and without addition of the chelant DTPA to the dilute pulp slurry prior to dewatering.

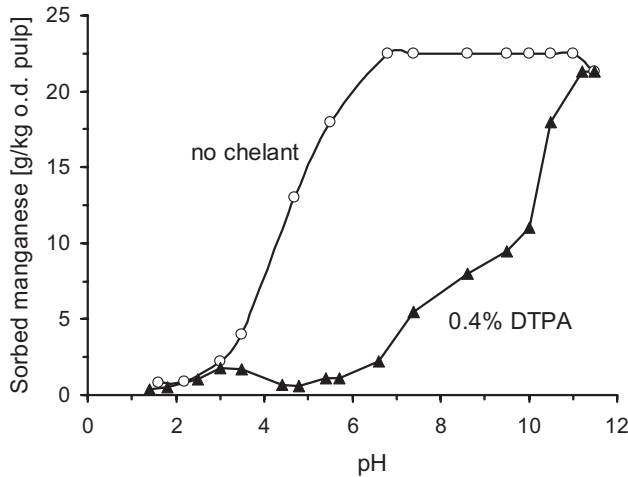


Fig. 5.10 Manganese sorbed on pulp, with and without chelant [24].

In practice, sorption can place a limit on the washing efficiency that can be reached. Since sorbed substances are not accessible to normal washing, they will remain in the washed pulp and adversely affect the washing result. Depending on the process environment, the amount of a sorbed substance may become almost insensitive to its concentration in the surrounding liquor and cannot reasonably be affected by changes in the wash liquor quantity.

However, the amount of a substance which is sorbed on pulp can be influenced by changing the pH – for example, by acidification with sulfuric acid or carbon dioxide, by changing the pulp surface charge with the aid of surfactants, or by means of additives which bind the substance otherwise in the surrounding liquor (e.g., chelating agents).

It must be well noted that sorption is a reversible process. Substances that readily desorb from pulp under changing conditions will as readily redeposit on the pulp when the environment is returned to the original conditions.

### 5.3 Principles of Washing

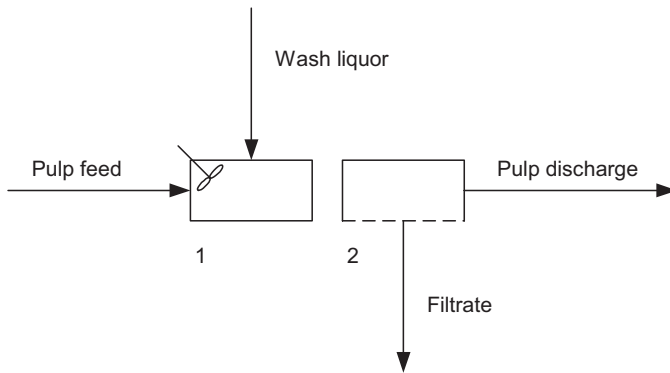
In this section, we will review the different possibilities of bringing the pulp and washing medium into contact. Pulp washing is accomplished either with clean water or, more frequently, with a washing liquid of a certain composition. Here,

the general term “wash liquor” will be used to describe both clean water and washing liquid.

### 5.3.1

#### Dilution/Extraction Washing

The simplest method of washing is by repeated dilution and extraction (Fig. 5.11). In the first step, the pulp feed is mixed with the wash liquor (1), after which the filtrate is extracted and the pulp discharged (2).



**Fig. 5.11** The principle of dilution/extraction washing.

Dilution/extraction washing will not be effective unless it is repeated many times. In theory, an infinite number of dilution/extraction washing stages is needed to bring the concentrations in the pulp discharge to their levels in the wash liquor.

The efficiency of this operation is generally low, and depends primarily on the consistencies to which the pulp is diluted and thickened. It also depends on the extent to which solute is sorbed on the fibers and the time required for solute to diffuse out of the fibers.

In a modern pulp mill, there is no room for dilution/extraction as a separate washing process. Nevertheless, dilution/extraction phenomena occur when process reasons require a dilution, whether for fiber separation during screening, for even fiber distribution in the mat formation zone of a washer, or for homogeneous mixing of chemicals.

### 5.3.2

#### Displacement Washing

Displacement washing is based on the idea of *replacing* the liquor in the pulp web with wash liquor rather than *mixing* these two liquors. Appropriate displacement washing is of primary importance in obtaining good washing efficiencies with all types of washing equipment.



The principle of displacement washing is illustrated schematically in Fig. 5.12. A volume of wash liquor is added to the pulp feed (1), in a way such that the wash liquor pushes out the liquor coming along with the pulp feed as filtrate (2). Eventually, the wash liquor occupies all the space originally held by the liquor in the pulp feed (3).

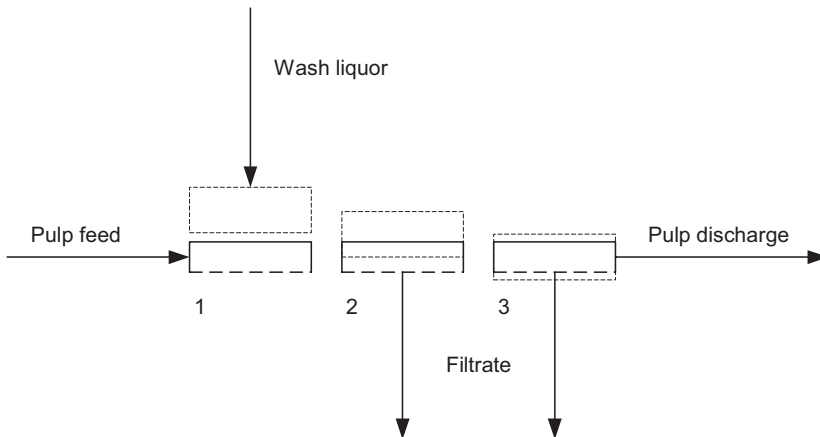


Fig. 5.12 The principle of displacement washing.

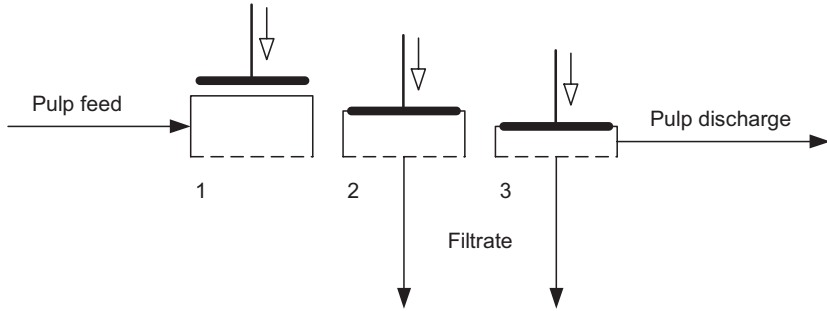
Apparently, one single stage of displacement washing is much more efficient than one single stage of dilution/extraction washing. Ideally, it would be possible to remove all the liquor in the pulp feed, together with all the soluble substances, by displacing it with the same volume of wash liquor.

The reality, however, is far from ideal: mixing occurs at the interface between the wash liquor and displaced liquor; diffusion limits the mass transfer from enclosed liquor; sorption plays its role; and inhomogeneities in the fiber web cause channeling of the wash liquor flow.

### 5.3.3

#### Compressive Dewatering

Another means of reducing the amount of unwanted substances being carried along with the pulp is liquor removal by means of mechanical pressing. The principle of compressive dewatering is illustrated schematically in Fig. 5.13. The pulp feed enters a device where it can be subjected to mechanical pressure (1). The pressure then drives the filtrate (also called the pressate) out of the pulp mat (2). Initially, the filtrate represents mainly free liquor from around the fibers. As the pressure increases, an increasing amount of the liquor is also forced out from the fiber voids (3).



**Fig. 5.13** The principle of compressive dewatering.

Unlike displacement washing, which is based on a change in liquor concentrations, compressive dewatering diminishes the amount of unwanted substances in the pulp discharge by reducing the volume of liquor. If sufficient time has been allowed before pressing for intra-fiber and extra-fiber concentrations to even out, the concentrations in the liquor entering with the pulp, in the filtrate and in the liquor leaving with the pulp are the same.

In reality, the liquor inside the fibers often has a higher concentration than the free liquor around the fibers due to sorption or due to a lack of diffusion time. The measured discharge concentration will then be higher than the measured feed concentration because highly concentrated liquor is set free from inside the fibers only in the final phase of pressing.

#### 5.3.4

#### **Multi-Stage Washing**

Frequently, one washing stage alone is insufficient to carry out the required washing. In such a case, multi-stage washing must be performed either on a number of single washers in series, or on one piece of multi-stage washing equipment. The number of stages depends mainly on the necessary washing efficiency, on the pulp furnish, applied equipment and on the liquor management.

In a multi-stage system, the maximum solute removal could be achieved if the pulp were washed in each stage with fresh water. However, this method of multi-stage washing results in a huge overall amount of very dilute filtrate, and is therefore not acceptable in practice.

Modern multi-stage wash plants utilize the countercurrent principle, where the wash medium flows countercurrent to the pulp flow. The pulp is contacted with the cleanest available wash liquor before it leaves the last washing stage. The filtrate from the last stage is sent back in the opposite direction of the pulp flow to serve as wash liquor on the next-to-last stage, and so on, until it reaches the first washing stage (Fig. 5.14). The filtrate from the first washing stage has the highest concentrations and is ready for processing elsewhere in the mill, for example, in the evaporation plant.

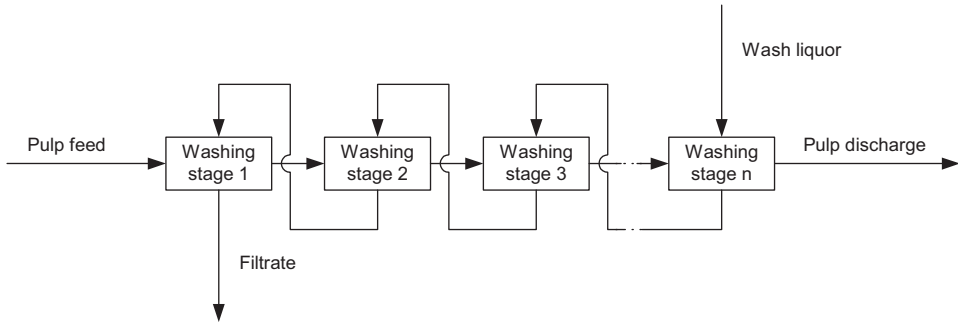


Fig. 5.14 The principle of countercurrent washing in a washing system incorporating  $n$  stages.

Besides the advantage of delivering a limited amount of filtrate at high concentrations, countercurrent washing also features a reasonable energy efficiency, as the amount of filtrate also limits the thermal energy leaving the system with this filtrate.

At a given number of washing stages, the efficiency of multi-stage washing is influenced by the method of pulp transport between stages. Intermediate mixing of the pulp slurry, for example due to pump transfer to the next stage, reduces the washing efficiency compared to the unaltered advancement of the pulp mat. In the latter case, a concentration gradient over the height of the mat is maintained between the stages, which eases washing in the second stage (Fig. 5.15).

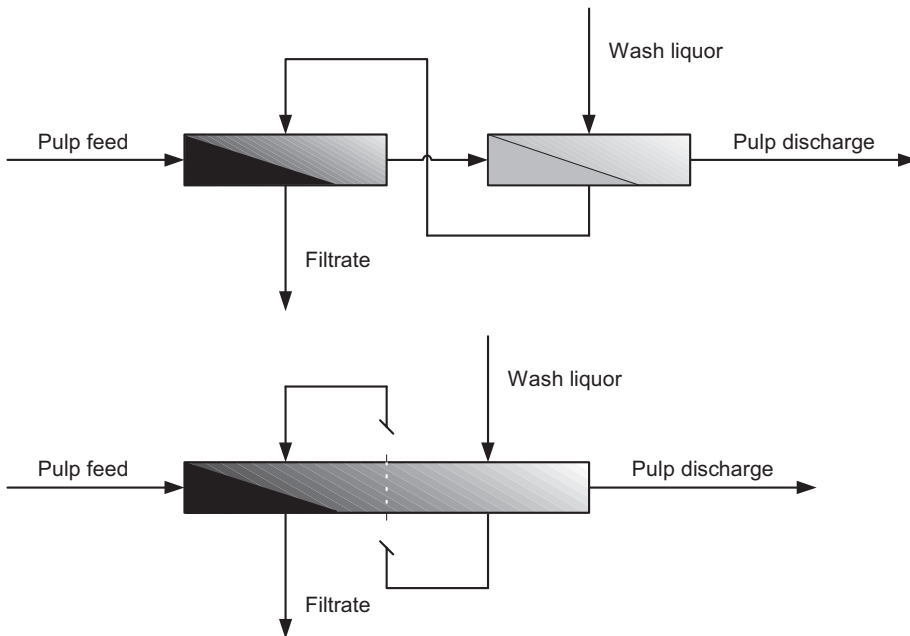


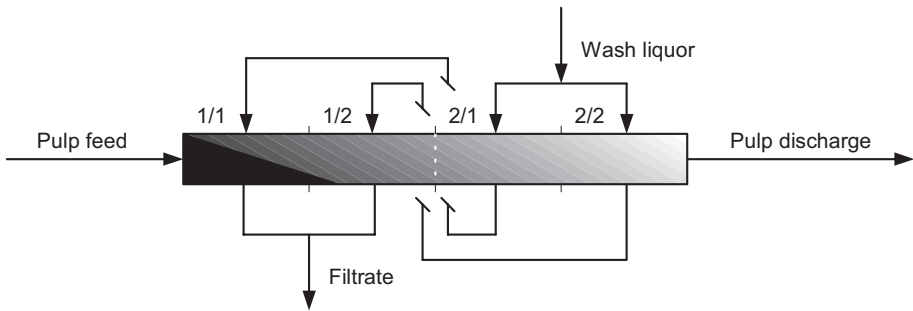
Fig. 5.15 Two-stage countercurrent washing with and without intermediate mixing.

## 5.3.5

**Fractional Washing**

Fractional washing is a specialty of countercurrent displacement washing, which improves the washing efficiency over standard multi-stage washing. The concept of fractional washing includes the split application of wash liquor and/or the split collection of wash filtrate in a single washing stage [25].

Imagine a two-stage countercurrent washing system, as illustrated in Fig. 5.16, with fresh water used as wash liquor. Following the idea of fractional washing, first the dirtier filtrate from the second stage 2/1 is used to displace the most contaminated fraction of the liquor coming with the feed into 1/1. Then, the cleaner filtrate from the second stage 2/2 is applied to stage 1/2. Filtrate from 2/2 is cleaner because it is more diluted with wash liquor.



**Fig. 5.16** The principle of fractional washing in a two-stage washing system without intermediate mixing.

## 5.4

**Washing Parameters**

## 5.4.1

**Overview**

In this section we will review the parameters that affect the operation and determine the performance of a washing system. These include process conditions such as the dilution factor, feed and discharge consistencies, pH, temperature, or entrained air. They also include equipment-specific parameters, such as a particular traveling speed, mechanical pressure, or fluid pressure or vacuum.

Some of the above parameters can be adjusted, while some are intrinsic to a special process step or piece of equipment. The chosen combination of washing parameters depends on the individual requirements of a washing application, and is usually a compromise because the optimization of single parameters often leads in opposite directions.

In addition to the equipment-specific and process-related parameters, it is essential to observe the pulp characteristics, with drainage and sorption behavior as the most important factors. The characteristic behavior of a pulp depends, *inter alia*, on the species of wood, kappa number, preceding cooking or bleaching processes and any mechanical treatment undergone. It is best determined in an appropriate laboratory test.

Here, we will discuss mainly the qualitative influences of process parameters on the washing efficiency and production capacity of pulp washing equipment. Some reference will also be made to equipment-specific parameters.

Hakamäki and Kovasin have developed an empirical model for the capacity of a rotary drum pressure washer [26]. The model was obtained from regression analysis of a very large number of laboratory test results, and was verified on an industrial scale:

$$G = 0,675 n^{0,62} N_{in}^{0,65} T^{0,26} (1 + \gamma_{air})^{-0,24} \Delta p^{0,30} \quad (15)$$

where  $G$  = specific washer surface load (i.e., pulp weight per cylindrical drum surface area and day) ( $\text{odt m}^2 \text{ day}^{-1}$ );  $n$  = washer drum rotations ( $\text{min}^{-1}$ );  $N_{in}$  = pulp feed consistency (%);  $\gamma_{air}$  = air content in pulp feed (vol. %); and  $\Delta p$  = effective filtration pressure (kPa).

The specific surface load is the ratio of the daily pulp production and the surface area of the cylindrical drum – that is, the area of the filter medium. Once the desired capacity and specific surface load for a washing application are known, the adequate washer surface can be easily calculated by dividing the first through the latter.

Although the validity of Eq. (15) is limited to pressure washers and to the tested pine kraft pulp, the basic correlations have some general significance and can, at least by tendency, also be transferred to other pieces of washing equipment. Thus, we will use the model from time to time in this section to demonstrate the principal effect of a washing parameter on washer capacity.

#### 5.4.2

##### **Dilution Factor**

Several parameters have been suggested over time to describe the ratio of liquor flows around a washer. The single most relevant parameter – which has also managed to find its way into practical application – is the dilution factor.

Imagine a pulp washer as a black box with the flows entering and leaving, as shown in Fig. 5.17. Depending on the feed consistency  $N_{in}$ , a certain amount of liquor  $L_{in}$  enters the washer with the pulp  $P$ . At the same time, a certain amount of liquor  $L_{out}$  leaves the washer with the pulp at the outlet consistency  $N_{out}$ . Wash liquor in the amount of  $WL$  is used for washing, and the filtrate quantity  $F$  is generated.

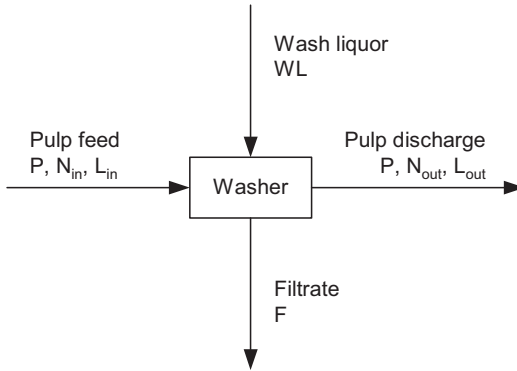


Fig. 5.17 Streams around a pulp washer.

The dilution factor is defined as the difference of wash liquor flow and liquor flow leaving with the washed pulp, related to the pulp flow:

$$DF := \frac{WL - L_{out}}{P} \quad (16)$$

where  $DF$  = dilution factor ( $\text{t odt}^{-1}$ );  $WL$  = flow rate of wash liquor ( $\text{t h}^{-1}$ );  $L_{out}$  = flow rate of liquor accompanying the discharged pulp ( $\text{t h}^{-1}$ ); and  $P$  = flow rate of pulp ( $\text{odt h}^{-1}$ ).

In practice, the dilution factor is often expressed in volumetric terms ( $\text{m}^3 \text{t}^{-1}$ ) rather than as a mass ratio ( $\text{t t}^{-1}$ ). Here, we will continue to use the mass ratio, as in this way the process engineer's calculations are simplified. (When we return to the field, it may sometimes be acceptable simply to substitute the mass ratio by the volumetric term due to the small error made compared to the variability of erratic mill data.)

The liquor flow  $L_{out}$  can be calculated from the discharge consistency  $N_{out}$  and pulp production capacity  $P$ :

$$L_{out} = P \left( \frac{1}{N_{out}} - 1 \right) \quad (17)$$

thereby providing another useful formula for the dilution factor:

$$DF = \frac{WL}{P} - \frac{1}{N_{out}} + 1 \quad (18)$$

So, why is this parameter called the dilution factor? Let us examine the overall mass balance around the washer:

$$L_{in} + WL - L_{out} - F = 0 \quad (19)$$

In another form, this equation reads:

$$WL - L_{out} = F - L_{in} \quad (20)$$

The left-hand term represents the numerator of Eq. (16). If the quantity of wash liquor  $WL$  is equal to the liquor quantity leaving with the discharged pulp  $L_{out}$ , the filtrate volume  $F$  equals the liquor volume in the pulp feed  $L_{in}$ . There is no dilution of the filtrate and the dilution factor is zero.

Any wash liquor charge which increases the amount of filtrate above the amount of liquor in the pulp feed will dilute the filtrate. In this case, the dilution factor is positive. Any wash liquor charge which reduces the amount of filtrate below the amount of liquor in the pulp feed will also reduce the amount of filtrate. Then, the dilution factor is negative.

When the dilution factor of displacement washing is negative, a portion of the contaminated liquor stays with the pulp and leaves the washer as carry-over. It is apparent that a washing stage can reach high efficiency only at positive dilution factors.

There is a clear correlation of washing efficiency and dilution factor in a way, that the washing efficiency improves with higher dilution factors. There is, however, a ceiling for the washing efficiency which is correlated to the physical limits of liquor penetration through the pulp mat.

Regardless of its undisputable beneficial effect on washing efficiency, it is important to note that a high positive dilution factor can substantially affect downstream mill areas. In the case of brownstock washing, an increased dilution factor means additional evaporation requirements; in the case of washing in the bleach plant, the increased filtrate flow places a challenge on the hydraulic capacity of the biological treatment plant or of the alternative filtrate purification system, respectively.

For a particular application, the favorable range of dilution factors is dependent upon the type and specific design of the washing equipment. As a rule of thumb, drum and belt washers are typically operated at dilution factors of 1–3 t odt<sup>-1</sup>, while wash presses usually perform best at dilution factors of 2–4 t odt<sup>-1</sup>.

In a multi-stage washing system, it is most important to note that all washers in the system must be operated at the same dilution factor in order to avoid overflows or shortage of filtrate between the stages. The dilution factor of a multi-stage system is therefore set by controlling the flow to the last washing stage.

**Example:** Calculation of wash liquor quantities in a closed, countercurrent, two-stage washing system

The pulp production capacity, the outlet consistencies of the two washers, and the desired dilution factor are known:

Pulp production capacity,  $P = 25 \text{ odt h}^{-1}$

Washer no. 1 discharge consistency,  $N_{1,out} = 11\%$

Washer no. 2 discharge consistency,  $N_{2,out} = 15\%$

Dilution factor,  $DF = 2.0 \text{ t odt}^{-1}$

In order to determine the wash liquor quantities, we first calculate the amounts of liquor leaving the washers with the pulp:

$$L_{1,out} = P \left( \frac{1}{N_{1,out}} - 1 \right) = 25 \left( \frac{1}{0,11} - 1 \right) = 202 \text{ t h}^{-1}$$

$$L_{2,out} = P \left( \frac{1}{N_{2,out}} - 1 \right) = 25 \left( \frac{1}{0,15} - 1 \right) = 142 \text{ t h}^{-1}$$

Then, the wash liquor flow rate to the first washer amounts to

$$WL_1 = L_{1,out} + DF \cdot P = 202 + 2,0 \cdot 25 = 252 \text{ t h}^{-1}$$

and the wash liquor flow rate to the second washer is

$$WL_2 = L_{2,out} + DF \cdot P = 142 + 2,0 \cdot 25 = 192 \text{ t h}^{-1}$$

Note that in a closed countercurrent washing system, the first washer must be operated with a much higher wash liquor quantity than the second washer, simply because its discharge consistency is lower.

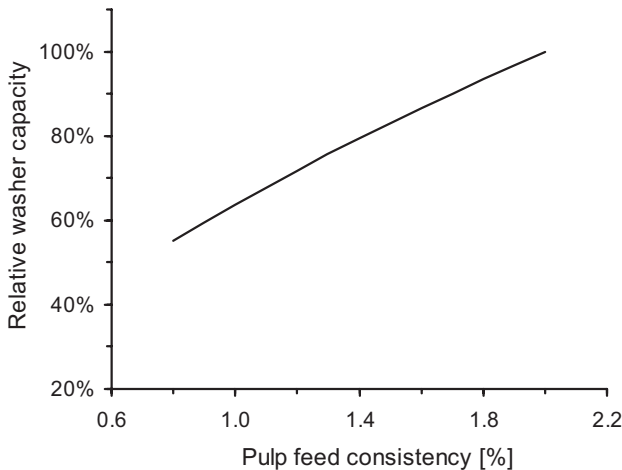
### 5.4.3

#### Feed and Discharge Consistencies

The feed consistency has a major influence on the electrical energy consumption and on the design of equipment. On the one hand, a low feed consistency means that large volumes of filtrate are pumped to dilution points before the washer, and consequently a lot of electrical energy required for pumping.

On the other hand, the feed consistency determines the amount of liquor that must be removed from the pulp suspension in the dewatering zone of the washing equipment. The lower the consistency, the larger will be the dewatering zone of the washing equipment and also the filtrate tank. For a given washer, the feed consistency has a considerable influence on the capacity (Fig. 5.18).





**Fig. 5.18** Effect of pulp feed consistency on the capacity of a pressure washer, as calculated from Eq. (15).

If the pulp discharge from the washer is at medium consistency (12–14%), the quantity of liquor leaving the equipment with the pulp exceeds the amount of pulp by a factor of 6–7. At the high discharge consistency of a press (30–35%), this factor is reduced to just two. Evidently, the liquor accompanying the pulp in the press discharge may be three times as concentrated as the liquor coming with the medium consistency discharge to still have the same per-ton washing loss.

High consistency discharge allows for a distinct separation between process stages. If a washer discharges pulp at high consistency and the next process steps occurs at medium or low consistency, the necessary dilution offers a good possibility for temperature or pH adjustment, or for chemical recycling. This usually leads to savings in chemicals, water, and energy.

#### 5.4.4 pH

The pH encountered on a pulp washer is normally a function of the preceding process step and the origin of the wash liquor. In most cases, it is not feasible to use the pH as a control parameter for washing. There are cases, however, when an adjustment of the pH is desirable and beneficial.

First, there may be a pH change on the washing equipment, for example, when alkaline feed stock is washed with acidic wash liquor. Occasionally, such a constellation provokes scaling on the surfaces of the washer due to precipitation of inorganic or organic compounds. If this is the case, process measures must be taken to move the unfavorable pH region away from the washer.

Second, pulp washing operations typically are more challenging under alkaline than under acidic conditions. On the one hand, fiber swelling under alkaline conditions is made responsible for somewhat reduced drainage rates. On the other

hand, soaps act as surfactants and induce foaming issues as well as increased entrainment of air in the filtrate. Under mill conditions, the latter effect seems to be a more critical influence on the washing performance [9].

Improved drainage can be observed as the pH of a highly alkaline pulp is lowered. It is suspected that the reason for this behavior lies in sodium phenolate soaps being converted to their protonated form, in which they no longer function as surfactants. The drainage rate begins to improve as the pH is reduced below 11, and levels out around pH 9,5. Further reduction beyond this point brings no more washing performance improvement. Instead, there is a quality risk of reprecipitation of dissolved lignin on the fibers.

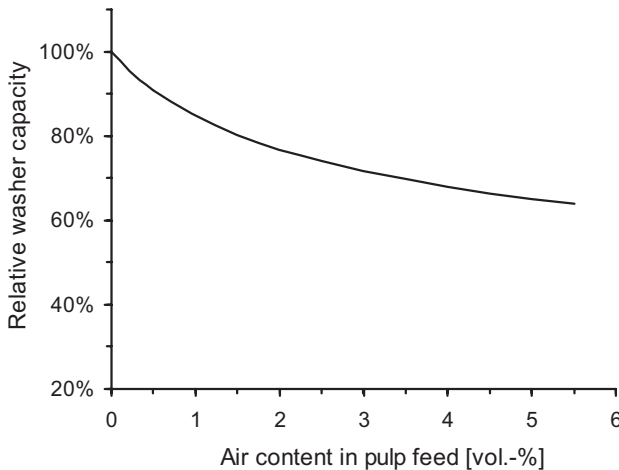
Carbon dioxide and sulfuric acid have been found to be equally effective for improving drainage and reducing foam [9], but any other inorganic acid should do as well.

For any given piece of washing equipment, improved drainage means a higher outlet consistency and consequently a higher washing efficiency. With regard to foaming, there is a trade-off between acidification and the reduced use of defoamer.

#### 5.4.5

##### Entrainment of Air

The air content or, more generally, the presence of any gas in the pulp feed to the washer negatively affects the washer capacity at only low levels (Fig. 5.19). The effect is serious, and it is of utmost importance to keep the entrained air levels low in order to maintain satisfactory washer operation and capacity [26].



**Fig. 5.19** Effect of the air content in the pulp feed on the capacity of a pressure washer, as calculated from Eq. (15).

The mechanism by which air disturbs the washing process is attributed to small bubbles which are mechanically trapped in the pulp fiber networks, thereby reducing the number of free paths through which the liquor may flow [9,27]. Thus, on the one hand the drainage rate is reduced, while on the other hand more regions are cut off from liquor displacement, which leads to reduced washing efficiency.

#### 5.4.6

##### Temperature

As the temperature rises, the increasing rate of diffusion leads by tendency to a better washing efficiency.

Compared to the other parameters, the influence of temperature on washer capacity is less pronounced. Higher temperatures bring about a moderate capacity advantage, as can be expected from improved drainage due to lower liquor viscosity (Fig. 5.20).

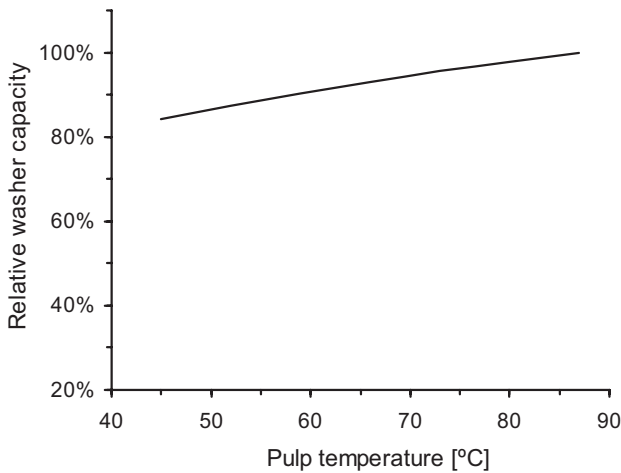


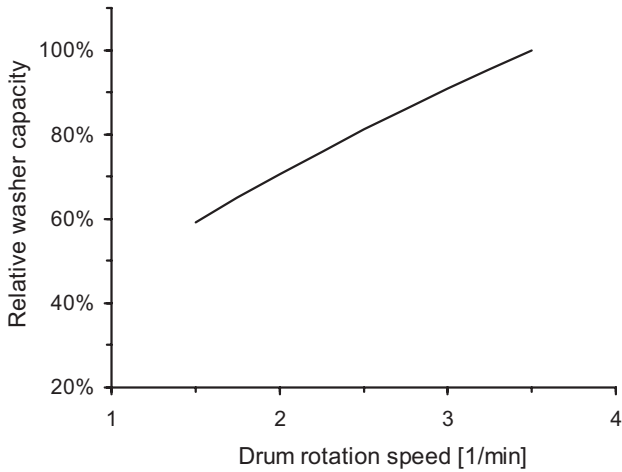
Fig. 5.20 Effect of pulp temperature on the capacity of a pressure washer, as calculated from Eq. (15).

#### 5.4.7

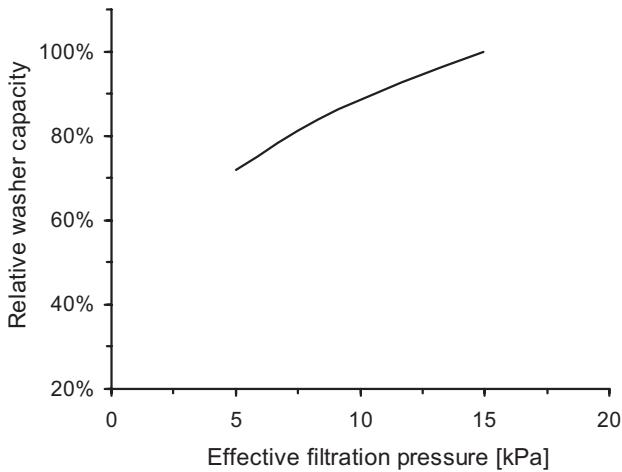
##### Equipment-Specific Parameters

In addition to the process washing parameters discussed above, different pieces of equipment allow the adjustment of individual equipment-specific parameters. These include the drum rotation speed of rotary washers and presses, the wire speed of belt washers, the pressure on baffles or press nips, and also adjustable vacuum or pressure on a particular machine.

Figures 5.21 and 5.22 illustrate graphically the influence of two equipment-specific parameters on the capacity of a rotary drum pressure washer.



**Fig. 5.21** Effect of drum rotation speed on the capacity of a pressure washer, as calculated from Eq. (15).



**Fig. 5.22** Effect of effective filtration pressure on the capacity of a pressure washer, as calculated from Eq. (15).

## 5.5 Washing Efficiency

### 5.5.1 Overview

The process engineer's focus is usually on the washing efficiency. Among the targets set for a washing application may be a recovery rate or, more frequently, a carry-over. The carry-over denotes the amount of a substance which escapes with the pulp leaving the washing system. Frequently, the carry-over is expressed as chemical oxygen demand (COD) or saltcake loss. The latter has been used traditionally because it was easy to analyze, and provided an indication of the recovery rate of inorganic chemicals. Whilst interest in the recovery of chemicals persists for economical reasons, the focus has been shifting towards organic compounds as closed cycles and environmental aspects gain increasing importance in process design.

The efficiency of a pulp washing system is judged by how much of the solute it removes and the amount of wash water required to accomplish this solute removal. While a number of schemes and nomenclatures have been developed to express the performance of washers and washing systems [19], we will focus here on the most used and most practical approaches.

Careful readers of the previous sections will suspect that the theoretical calculation of the washing efficiency without practical input is virtually hopeless. Fortunately, hands-on experience is available for all types of commercial washing equipment, which can be used for an estimation of the washing efficiency to be expected under a given set of conditions.

In this subsection, we will explore briefly the wash yield and displacement ratio, before examining more deeply today's most relevant measure for washing efficiency, the Norden E factor.

### 5.5.2 Wash Yield

Wash yield is the most basic way of expressing the washing efficiency. Consider the washer as a black box, as in Fig. 5.23. A certain amount of liquor  $L_{in}$  enters the washer with the pulp  $P$  at an inlet consistency  $N_{in}$ . At the same time, the amount of liquor  $L_{out}$  leaves the washer with the pulp at the outlet consistency  $N_{out}$ . Wash liquor in the amount of  $WL$  is used for washing, and the filtrate quantity  $F$  is generated. The single streams to and from the washer carry individual concentrations of dissolved substances  $c$ .

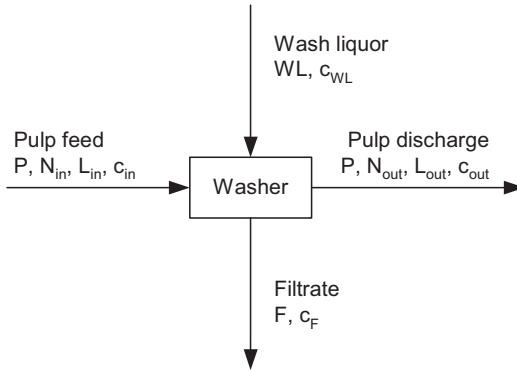


Fig. 5.23 Flows and concentrations around a pulp washer.

The wash yield  $Y$  is defined as the ratio between the amount of dissolved solids washed from the pulp and the amount of dissolved substances entering the washer with the feed pulp:

$$Y := 1 - \frac{L_{out}c_{out}}{L_{in}c_{in}} = \frac{F c_F}{L_{in}c_{in}} \quad (21)$$

Equation (21) presumes that the concentration of dissolved substances in the wash liquor  $c_{WL}$  is zero. Since in modern washing applications this often not the case, the wash yield has declining relevance.

### 5.5.3

#### Displacement Ratio

Another simple, yet more meaningful, measure for the washing efficiency is the displacement ratio. The washer is again treated as a black box (see Fig. 5.23). The displacement ratio  $DR$  is then defined as the actual washing performance related to the maximum possible washing performance at ideal displacement, expressed in concentrations:

$$DR := \frac{c_{in} - c_{out}}{c_{in} - c_{WL}} \quad (22)$$

The displacement ratio depends heavily on the amount of liquor used for washing, and is therefore only valid for the one dilution factor where the concentrations have been measured.

An equivalent displacement ratio (EDR) has been established as a mathematical tool for comparing washing equipment of different feed and discharge consistencies [28]. However, this has not won the recognition of the standardized Norden efficiency factor described below.

**Example:** Determination of the displacement ratio

The measurements around a vacuum washer in the bleach plant have given the following results:

COD concentration in pulp feed,  $c_{in} = 7900 \text{ mg L}^{-1}$

COD concentration in pulp discharge  $c_{out} = 1500 \text{ mg L}^{-1}$

COD concentration in wash liquor,  $c_{WL} = 400 \text{ mg L}^{-1}$

The displacement ratio is:

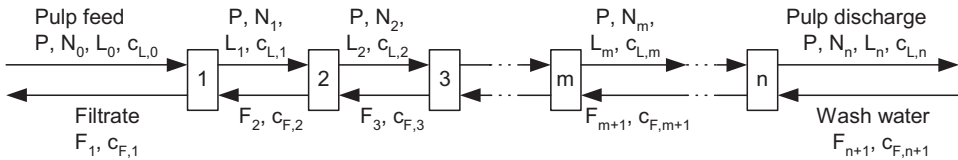
$$DR = \frac{c_{in} - c_{out}}{c_{in} - c_{WL}} = \frac{7900 - 1500}{7900 - 400} = 85\%$$

## 5.5.4

**Norden Efficiency Factor**

Currently, the Norden efficiency factor is the most practical form of specifying the washing efficiency. It is also the most widely used efficiency parameter in computer aided mass and energy balancing.

Its mathematical derivation is not well documented in the pulping literature, perhaps because it is rather lengthy. We will nevertheless derive the Norden efficiency factor here as this provides us with an opportunity to exercise some mass balancing. This section, in principle, follows Norden's original approach [29], but uses a denotation which is more practical for a pulp engineer. The model is based on a simplified form of the Kremser equation with  $n$  mixing stages in series, as shown in Fig. 5.24 [30,31].



**Fig. 5.24** Countercurrent cascade of  $n$  mixing stages in series with complete mixing in each stage.

The overall mass balance for a soluble substance over all the mixing stages can be written in the form:

$$L_0 c_{L,0} - F_1 c_{F,1} - L_n c_{L,n} + F_{n+1} c_{F,n+1} = 0 \quad (23)$$

where  $L$  = flow rate of liquor accompanying the pulp ( $\text{kg s}^{-1}$ );  $F$  = flow rate of filtrate ( $\text{kg s}^{-1}$ );  $c_L$  = concentration of soluble substance in liquor accompanying the pulp ( $\text{kg kg}^{-1}$ ); and  $c_F$  = concentration of soluble substance in filtrate ( $\text{kg kg}^{-1}$ ).

Note that this is just a liquor balance. The pulp  $P$  is assumed to pass along with  $L$ , not participating in the mass transfer, and is therefore disregarded in the equation.

A similar mass balance can be set up for only a subsection of the total system, starting from stage 1 and including  $m$  stages:

$$L_0 c_{L,0} - F_1 c_{F,1} - L_m c_{L,m} + F_{m+1} c_{F,m+1} = 0 \quad (24)$$

Complete mixing is assumed in each mixing stage  $i$ , which results in the same concentrations of accompanying liquor and filtrate leaving a stage:

$$c_{L,i} = c_{F,i} = c_i \quad (25)$$

Furthermore, a constant consistency  $N_i$  is assumed for all the pulp streams. This means that

$$L_i = L = \text{const.} \quad (26)$$

With the total liquor balance around a mixing stage

$$L_{i-1} - F_i - L_i + F_{i+1} = 0 \quad (27)$$

and consequently

$$F_i = F_{i+1} = F = \text{const.} \quad (28)$$

the mass balance [Eq. (24)] can be simplified

$$L c_0 - F c_1 - L c_i + F c_{i+1} = 0 \quad (29)$$

and solved for  $c_i$

$$c_i = \frac{F}{L} c_{i+1} + \left( c_0 - \frac{F}{L} c_1 \right) \quad (30)$$

Then, the mass balances for the single subsections are:

$$c_1 = \frac{F}{L} c_2 + \left( c_0 - \frac{F}{L} c_1 \right) \quad (31)$$

$$c_2 = \frac{F}{L} c_3 + \left( c_0 - \frac{F}{L} c_1 \right) \quad (32)$$

...



$$c_{n-1} = \frac{F}{L}c_n + \left(c_0 - \frac{F}{L}c_1\right) \quad (33)$$

$$c_n = \frac{F}{L}c_{n+1} + \left(c_0 - \frac{F}{L}c_1\right) \quad (34)$$

Nesting Eq. (34) into Eq. (33) gives

$$c_{n-1} = \frac{F}{L}\left(\frac{F}{L}c_{n+1} + \left(c_0 - \frac{F}{L}c_1\right)\right) + \left(c_0 - \frac{F}{L}c_1\right) \quad (35)$$

and further on:

$$c_{n-1} = \left(\frac{F}{L}\right)^2 c_{n+1} + \left(\frac{F}{L} + 1\right) \left(c_0 - \frac{F}{L}c_1\right) \quad (36)$$

This procedure can be repeated until

$$c_1 = \left(\frac{F}{L}\right)^n c_{n+1} + \left(\left(\frac{F}{L}\right)^{n-1} + \left(\frac{F}{L}\right)^{n-2} + \dots + \frac{F}{L} + 1\right) \left(c_0 - \frac{F}{L}c_1\right) \quad (37)$$

Solving for  $c_{n+1}$  and some rearrangement leads to

$$\begin{aligned} c_{n+1} &= c_1 \left(1 + \frac{L}{F} + \left(\frac{L}{F}\right)^2 + \dots + \left(\frac{L}{F}\right)^n\right) - c_0 \\ &\quad \times \left(\frac{L}{F}\right) \left(1 + \frac{L}{F} + \left(\frac{L}{F}\right)^2 + \dots + \left(\frac{L}{F}\right)^{n-1}\right) \end{aligned} \quad (38)$$

Remembering that the sum of a finite geometric progression is calculated by

$$s_n = \sum_{t=0}^n q^t = \frac{q^{n+1} - 1}{q - 1} \quad (39)$$

Eq. (38) can be re-written as follows:

$$c_{n+1} = c_1 \frac{\left(\frac{L}{F}\right)^{n+1} - 1}{\frac{L}{F} - 1} - c_0 \left(\frac{L}{F}\right) \frac{\left(\frac{L}{F}\right)^n - 1}{\frac{L}{F} - 1} \quad (40)$$

$$c_{n+1} \left(\frac{L}{F} - 1\right) = c_1 \left(\left(\frac{L}{F}\right)^{n+1} - 1\right) - c_0 \left(\frac{L}{F}\right) \left(\left(\frac{L}{F}\right)^n - 1\right) \quad (41)$$

$$c_1 - c_{n+1} = \left(\frac{L}{F}\right) (c_0 - c_{n+1}) - \left(\frac{L}{F}\right)^{n+1} (c_0 - c_1) \quad (42)$$

From the mass balance over the complete series of mixing stages [Eq. (23)], we obtain:

$$c_1 - c_{n+1} = \frac{L}{F} (c_0 - c_n) \quad (43)$$

Now, Eq. (42) and Eq. (43) are set equal

$$\frac{L}{F} (c_n - c_{n+1}) = \left(\frac{L}{F}\right)^{n+1} (c_0 - c_1) \quad (44)$$

and rearranged

$$\left(\frac{F}{L}\right)^n = \frac{c_0 - c_1}{c_n - c_{n+1}} \quad (45)$$

By finally taking the logarithm, the efficiency factor  $E$  is defined as the number of ideally mixed stages in a countercurrent cascade with constant liquor and filtrate flow rates:

$$E := n = \frac{\log \frac{c_0 - c_1}{c_n - c_{n+1}}}{\log \frac{F}{L}} \quad (46)$$

According to the above derivation, non-integer values for the  $E$  factor are physically meaningless. However, they are perfectly suitable to describe washing systems which perform in between the physically meaningful integer steps.

Commercial washing equipment only seldom fulfils the postulate of constant flows. In particular, the feed liquor flow  $L_0$  is mostly higher than the liquor flow leaving the washer with the discharged pulp  $L_n$ , and the wash liquor flow  $F_{n+1}$  is lower than the filtrate flow  $F_1$ . This fact is considered in the  $E$  factor model by assuming constant flow rates in all stages except in stage 1. The mass balances around stage 1

$$L_0 - F_1 - L + F = 0 \quad (47)$$

$$L_0 c_0 - F_1 c_1 - L c_1 + F c_2 = 0 \quad (48)$$

give

$$c_1 - c_2 = \frac{L_0}{F} (c_0 - c_1) \quad (49)$$

which can be inserted into the equation for the  $E$  factor for stages 2 through  $n$

$$\left(\frac{F}{L}\right)^{n-1} = \frac{c_1 - c_2}{c_n - c_{n+1}} \quad (50)$$

to give

$$\left(\frac{F}{L}\right)^{n-1} = \frac{L_0}{F} \frac{c_1 - c_2}{c_n - c_{n+1}} \quad (51)$$

and finally

$$E = \frac{\log\left(\frac{L_0}{L} \frac{c_0 - c_1}{c_n - c_{n+1}}\right)}{\log\frac{F}{L}} \quad (52)$$

This is probably the most important equation in pulp washing. Returning to the more descriptive original denotation (as per Fig. 5.23), Eq. (52) reads:

$$E = \frac{\log\left(\frac{L_{in}}{L_{out}} \frac{c_{in} - c_F}{c_{out} - c_{WL}}\right)}{\log\frac{WL}{L_{out}}} \quad (53)$$

The  $E$  factor depends on the type of washing equipment, on the mode of operation of the equipment, on the pulp furnish to be washed, on the temperature and substance loading of the involved liquors and, of course, also on diffusion and sorption phenomena. This was originally observed by Norden for rotary drum washers [29,32], but it holds true also for contemporary washing equipment.

In contrast to the displacement ratio, the  $E$  factor shows only a limited dependence on the dilution factor over the industrially relevant dilution factor range of maybe  $\pm 1$  t odt<sup>-1</sup>. This is what makes the  $E$  factor a very useful measure for washing efficiency. In most industrial washing applications, it is acceptable to regard the  $E$  factor as a constant over the range of reasonable dilution factors and also over the range of reasonable production capacities.

If two or more pieces of washing equipment with the same inlet and outlet consistencies are arranged in countercurrent mode, the  $E$  factors of the individual machines can be summed to give the  $E$  factor of the whole system.

When the performance of a washer is determined in the field, the number of measurements is limited for practical reasons. The measurements normally needed as a minimum for determination of the  $E$  factor are three of the concentrations, the feed and discharge consistencies, the wash liquor flow rate, as well as the pulp production. The fourth concentration comes from the overall mass balance, Eq. (23). In most cases this is the filtrate concentration:

$$c_F = \frac{1}{F} (L_{in} c_{in} - L_{out} c_{out} + WLc_{WL}) \quad (54)$$

**Example:** Determination of the E factor

The measurements around a multi-stage brownstock washer have given the following results:

COD concentration in pulp feed,  $c_{in} = 155\,000 \text{ mg kg}^{-1}$

COD concentration in pulp discharge  $c_{out} = 6400 \text{ mg kg}^{-1}$

COD concentration in wash liquor,  $c_{WL} = 2600 \text{ mg kg}^{-1}$

Wash liquor flow rate,  $WL = 345 \text{ t h}^{-1}$

Feed consistency,  $N_{in} = 4\%$

Discharge consistency,  $N_{out} = 13\%$

Pulp production capacity,  $P = 40 \text{ odt h}^{-1}$

First, we calculate the flow rates of liquor accompanying the pulp. These are for the pulp feed

$$L_{in} = P \left( \frac{1}{N_{in}} - 1 \right) = 40 \left( \frac{1}{0,04} - 1 \right) = 960 \text{ t h}^{-1}$$

and for the discharged pulp:

$$L_{out} = P \left( \frac{1}{N_{out}} - 1 \right) = 40 \left( \frac{1}{0,13} - 1 \right) = 268 \text{ t h}^{-1}$$

The filtrate flow rate and filtrate COD concentration are:

$$F = L_{in} - L_{out} + WL = 960 - 268 + 345 = 1\,037 \text{ t h}^{-1}$$

$$c_F = \frac{1}{F} (L_{in} c_{in} - L_{out} c_{out} + WL c_{WL})$$

$$= \frac{1}{1\,037} (960 \cdot 155\,000 - 268 \cdot 6\,400 + 345 \cdot 2\,600) = 142\,700 \text{ mg/kg}^{-1}$$

Finally, the E factor on a COD basis is:

$$E = \frac{\log \left( \frac{L_{in} c_{in} - c_F}{L_{out} c_{out} - c_{WL}} \right)}{\log \frac{WL}{L_{out}}} = \frac{\log \left( \frac{960 \cdot 155\,000 - 142\,700}{268 \cdot 6\,400 - 2\,600} \right)}{\log \frac{345}{268}} = 9,7$$

## 5.5.5

**Standardized Norden Efficiency Factor**

It is quite popular not to state the E factor for the specific operating conditions, but to use a standardized efficiency factor recalculated to a standardized outlet consistency  $L_{Std}$ :

$$E_{Std} = \frac{\log\left(\frac{L_{in} c_{in} - c_F}{L_{out} c_{out} - c_{WL}}\right)}{\log\left(1 + \frac{WL - L_{out}}{L_{Std}}\right)} \quad (55)$$

where  $L_{Std}$  is the liquor flow rate at the standardized outlet consistency  $N_{Std}$ .

The standardized E factor has a practical importance in the design of a specific piece of washing equipment for a particular purpose. Despite being often observed, it is less meaningful to use the standardized E factor for comparison of different types of washing equipment.

Remembering the definition of the dilution factor  $DF$  as per Eq. (16),

$$WL - L_{out} = P \cdot DF \quad (56)$$

and considering

$$L_{Std} = P(1/N_{Std} - 1) \quad (57)$$

the modified efficiency factor can also be expressed as

$$E_{Std} = \frac{\log\left(\frac{L_{in} c_{in} - c_F}{L_{out} c_{out} - c_{WL}}\right)}{\log\left(1 + \frac{DF}{1/N_{Std} - 1}\right)} \quad (58)$$

The most widely used standardized outlet consistency  $N_{Std}$  is 10%. Hence

$$E_{10} = \frac{\log\left(\frac{L_{in} c_{in} - c_F}{L_{out} c_{out} - c_{WL}}\right)}{\log\left(1 + \frac{DF}{9}\right)} \quad (59)$$

In analogy to Eqs. (56) and (57),

$$L_{out} = P(1/N_{out} - 1) \quad (60)$$

$$WL = P(1/N_{out} - 1) + P \cdot DF \quad (61)$$

and therefore

$$\frac{WL}{L_{out}} = 1 + \frac{DF}{1/N_{out} - 1} \quad (62)$$

The modified efficiency factor  $E_{10}$  can then be calculated from any E factor by combining Eqs. (52), (59) and (62):

$$E_{10} = E \frac{\log\left(1 + \frac{DF}{1/N_{out} - 1}\right)}{\log\left(1 + \frac{DF}{9}\right)} \quad (63)$$

**Example:** Determination of the standardized E factor

The specifications and results from the E factor example have been:

Discharge consistency,  $N_{out} = 13\%$

Pulp production capacity,  $P = 40 \text{ odt h}^{-1}$

Wash liquor flow rate,  $WL = 345 \text{ t h}^{-1}$

Liquor flow rate in pulp discharge,  $L_{out} = 268 \text{ t h}^{-1}$

E factor,  $E = 9.7$

With the dilution factor

$$DF = \frac{WL - L_{out}}{P} = \frac{345 - 268}{40} = 1,93 \text{ t odt}^{-1}$$

we get the E factor for 10% standard discharge consistency:

$$E_{10} = E \frac{\log\left(1 + \frac{DF}{1/N_{out} - 1}\right)}{\log\left(1 + \frac{DF}{9}\right)} = 9,7 \cdot \frac{\log\left(1 + \frac{1,93}{1/0,13 - 1}\right)}{\log\left(1 + \frac{1,93}{9}\right)} = 12,6$$

## 5.6 Washing Equipment

### 5.6.1

#### General Remarks

A wide variety of equipment is available for pulp washing, and many of these units exist in several design variants. In this subsection we will examine some commonly used washer types and discuss their main features. Initially, however, some general remarks are applicable.

Clearly, every washer must provide the drainage area necessary for initial dewatering, displacement and final thickening of the pulp. Apart from that, time must be provided for diffusion. In this respect, the available pieces of washing equipment show considerable differences. For example, in rotary washers and belt washers the pulp passes through one washing stage within a few seconds, whereas it takes minutes for the pulp to proceed through a diffusion washer.

In the case that the design of washing equipment involves the absence of a gas phase, the possible negative consequences of air entrainment are automatically avoided.

Washing equipment with both inlet and outlet at medium consistency does not require intermediate dilution between washing stages. Such systems are associated with relatively small flow rates of wash medium and extracted filtrate, thus reducing pumping requirements and the corresponding energy consumption. The same is true for equipment with medium-consistency feed and high-consistency discharge. The latter has the additional advantage that the pulp washing can be accomplished with a smaller quantity of wash liquor. Modern fiberline operations are increasingly based on such energy-efficient and water-saving washing solutions.

It should be noted that the aim of this chapter is to provide a certain view of industrial washing equipment. Pure dewatering equipment, such as thickeners of all types and dewatering presses, are not discussed here, despite the fact that they have many similarities. Any values mentioned below are typical and indicative. Values for a specific washing application will depend upon the many factors discussed above, and may deviate accordingly.

### 5.6.2

#### Rotary Drum Washers

##### 5.6.2.1 Conventional Drum Washers

Rotary drum washers were the first pieces of continuous washing equipment to be developed. They have undergone continuous improvement over the decades, and today exist in a wide variety of designs. Conventional drum washers can be categorized into vacuum washers and pressure washers.

Pulp of typically 0.5–1.8% consistency is fed to the washer vat. As the liquor flows through the washer wire attached to the drum, the pulp mat is formed. The pulp mat is lifted out of the vat with the rotation of the drum and enters the washing zone, where several showers layer the wash liquor onto the mat. At the end of the washing zone, the drainage may be supported by press rolls. Finally, the pulp mat is released from the wire in the discharge zone and falls from the take-off into the repulper, a shredding screw conveyor (Fig. 5.25).

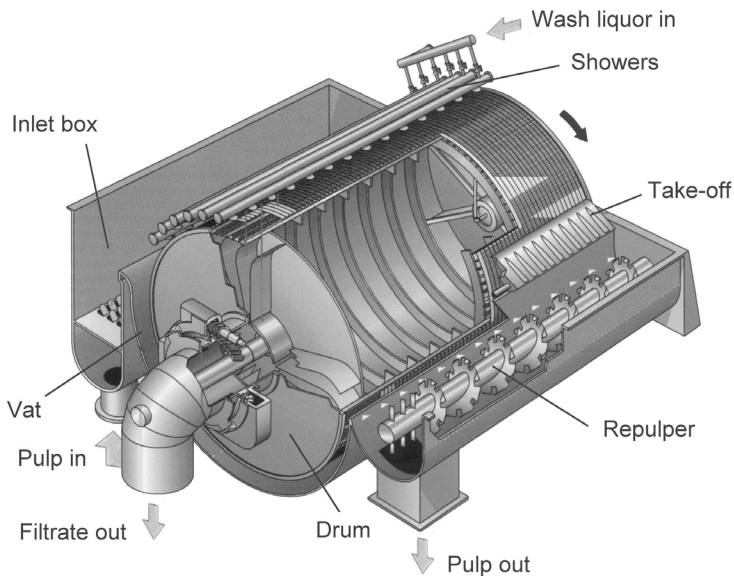


Fig. 5.25 Impco Coru-Dek vacuum washer [33].

In a vacuum washer, the vacuum which causes the liquor to flow through the pulp mat and washer wire is usually created by the downfalling filtrate in the drop leg, a vertical pipe of adequate length. This set-up requires the vacuum washer to be located at a higher level in the building. It also requires that the temperature of the filtrate does not exceed about 80–85 °C, because above this temperature the vapor pressure of water becomes a threat to the vacuum.

In pressure washers, the differential pressure across the pulp mat is created by a gas pressure maintained in the hood by a fan. No drop leg is required, and pressure washers can be operated much closer to the boiling point of the liquor than vacuum washers. The pulp enters the vat, is taken up by the drum, and is then washed in up to three countercurrent stages. After the pulp has passed the seal roll, the take-off is provoked by the pressure inside the drum which blows the pulp off the face wire. The encapsulated design minimizes emissions to the air.



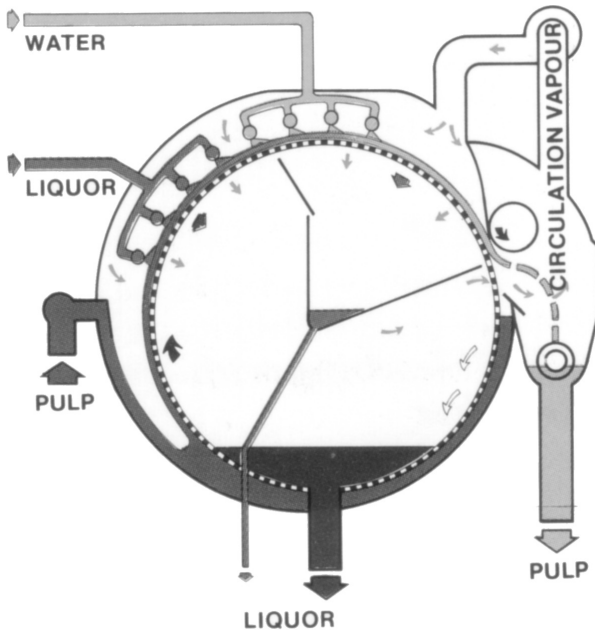


Fig. 5.26 Two-stage Sunds Rauma pressure washer [34].

The washing efficiency on a conventional drum washer depends mainly on the shower arrangement and on the washer's capability to avoid rewetting of the pulp mat with filtrate from the pockets of the drum before discharge.

As a rule of thumb, the outlet consistency is around 12%. However, it may fall well below 10% for pulp with unfavorable drainage behavior, yet may be as high as 18% for easy-draining pulp after press rolls. The E factors range from 1.5 and 3.0.

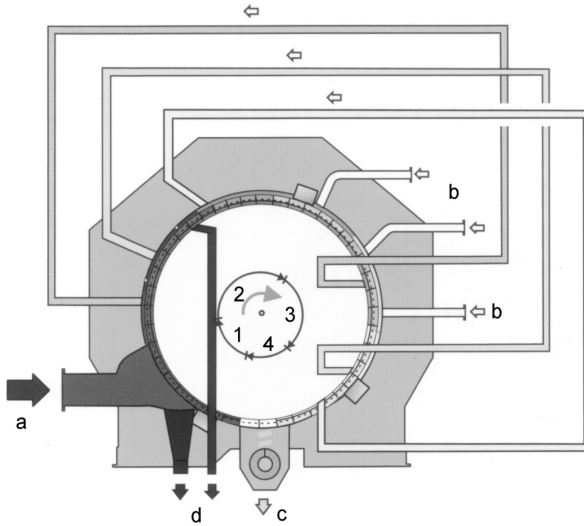
As a consequence of the design principle, conventional drum washers tend to let air through the pulp mat towards the end of the washing zone. The entrained air induces foaming in the filtrate tank, and would adversely affect drainage if recycled back with dilution filtrate before the washer. In order to avoid the latter situation, air must be given sufficient time to leave the filtrate in the filtrate tank, and this is done by providing adequate retention time and surface area.

#### 5.6.2.2 Drum Displacer

The Drum Displacer™ (DD) is a pressurized, mostly multi-stage washer which can have as many as four washing stages in one single unit. A four-stage washer may be efficient enough to serve as the only brownstock washing equipment after cooking [35].

The pulp fed to the formation section of the DD washer can be of either low consistency (3–5%) or medium consistency (8–10%). The circumference of the

rotating drum is divided into compartments, which are filled with pulp in the formation section and proceed to the washing stages. At each washing stage, the pulp is washed countercurrently with the filtrates from the succeeding washing stage. In the discharge zone, the pulp is dewatered by means of vacuum and eventually removed from the compartments by pressurized air to drop into a shredding screw conveyor (Fig. 5.27).



**Fig. 5.27** Andritz two-stage Drum Displacer™ washer. a = pulp feed; b = wash liquor inlet; c = pulp discharge; d = filtrate discharge; 1 = formation section; 2 = first washing stage; 3 = second washing stage; 4 = pulp discharge [35].

The DD washer features the specialty of fractional washing. Unlike other washers, where in one washing stage the liquor volume in the pulp is overdisplaced (dilution factor larger than zero), the DD washer has two or three liquor cycles for each stage, each operating at a negative dilution factor. As the overall washing efficiency of fractional washing is superior to the washing efficiency of other units with the same number of stages, DD washers generate rather high E factors. The E factors for two-stage, three-stage, and four-stage DD washers are 6–9, 9–12, and 11–14, respectively. The outlet consistency is usually in the range of 12–16%.

The DD washer has the smallest footprint of all multi-stage washers. The handling of wash filtrate is very compact as it is brought from stage to stage by pumps mounted on the washer itself. In the simplest arrangement, the multi-stage unit needs just one filtrate tank. More tanks are required in case the filtrate from the first stage needs to be divided into fractions of different properties (pH, temperature, chemical concentration).

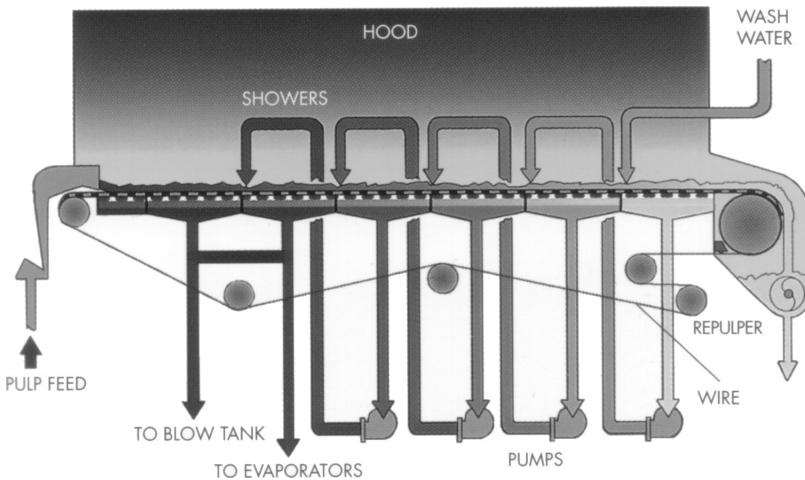
The DD washer's enclosed design and mostly submerged, gas-free operation guarantee good tolerance for high-temperature pulp feed, minimum foaming and high standards with regard to emissions to the air.

## 5.6.3

**Belt Washers**

In a belt washer, the pulp is transported on a synthetic wire through a number of countercurrent washing stages. While belt washer applications range from brown-stock washing over post-oxygen washing into the bleach plant, this type of washer is most popular where high washing efficiency is required.

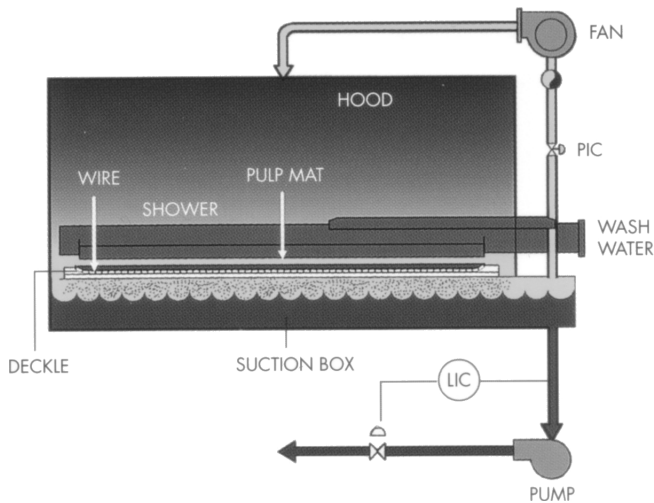
The most commonly used belt washer is the Chemi-Washer (Fig. 5.28). Pulp is fed through the headbox at a consistency of 2.0–3.5% and then distributed evenly on the moving wire. In the formation zone, the area between the headbox and the first shower, pulp is dewatered from inlet consistency to displacement consistency. Here, the pulp mat is formed on the wire while liquor flows to the suction boxes located beneath the wire. As the wire moves on, displacement washing occurs when the mat passes under the shower where filtrate from the succeeding washing stage flows onto the pulp. A pressure differential between the hood and the suction boxes pushes the liquor through the pulp mat and into the suction boxes. At each washing stage, the displaced liquor collected in the suction boxes is sent to a shower pump, which in turn pumps it to the preceding stage. When the pulp reaches the end of the washer, it is released from the wire and discharged into a shredding repulper [36].



**Fig. 5.28** Chemi-Washer (longitudinal section) [36] (used by permission of Kadant Black Clawson Inc., Mason, OH, USA).

The washing efficiency of a belt washer is optimized by controlling the vacuum profile in the suction boxes and the speed of the wire, and by adjusting the length of the dewatering and displacement zones. Typical outlet consistencies range from 10% to 14%, and normal dilution factors are  $1\text{--}2\text{ m}^3\text{ odt}^{-1}$ .

In order to maintain the differential pressure between the hood and the suction boxes, the vapor from the suction boxes is drawn into a fan and recycled back to



**Fig. 5.29** Chemi-Washer (cross-section) [36] (used by permission of Kadant Black Clawson Inc., Mason, OH, USA).

the hood (Fig. 5.29). Since the complete Chemi-Washer is efficiently sealed towards the environment, the release of odorous gases is limited to a minimum.

With up to seven washing stages in a single machine, the belt washer can provide the most efficient washing per piece of equipment of all pulp washers. The E factor per stage is usually between 2.0 and 2.5.

#### 5.6.4

#### Diffusion Washers

##### 5.6.4.1 Atmospheric Diffuser

The atmospheric diffuser is a displacement-type washer which is operated under medium consistency conditions. Its fields of application extend into the higher-temperature regions of brownstock washing and oxygen delignification, as well as into the bleach plant. The machine can be placed either directly on top of an upflow bleaching tower or on top of a storage tower for the washed pulp leaving the diffuser, which is of advantage if space is limited.

Atmospheric diffusers can be built as either one-stage or two-stage units. Double diffusers have two screen units, one above the other in mirror-image position. Each screen has its own wash liquor supply and liquor extraction arrangement. The two-stage units can therefore be used in countercurrent mode with a lower first stage and an upper second stage, or alternatively just as one stage for higher capacities [37].

Figure 5.30 shows an atmospheric diffuser with two screen units on top of a storage tower. Pulp at around 10% consistency enters the distribution cone at the bottom and approaches the first screen unit. As the pulp moves upward between

the concentric cylindrical screens, nozzles on the rotating nozzle arms distribute the wash liquor while plowing through the pulp. The wash liquor displaces the liquor from the pulp radially inward and outward into the screens where it is collected and guided through the screen arms to the liquor extraction pipes. The same displacement process is repeated in the upper section of the double diffuser. When the washed pulp reaches the top, it is shoved to the outer perimeter of the diffuser by the scraper and finally brought to the pulp outlet by the ring scraper, still at about 10% consistency.

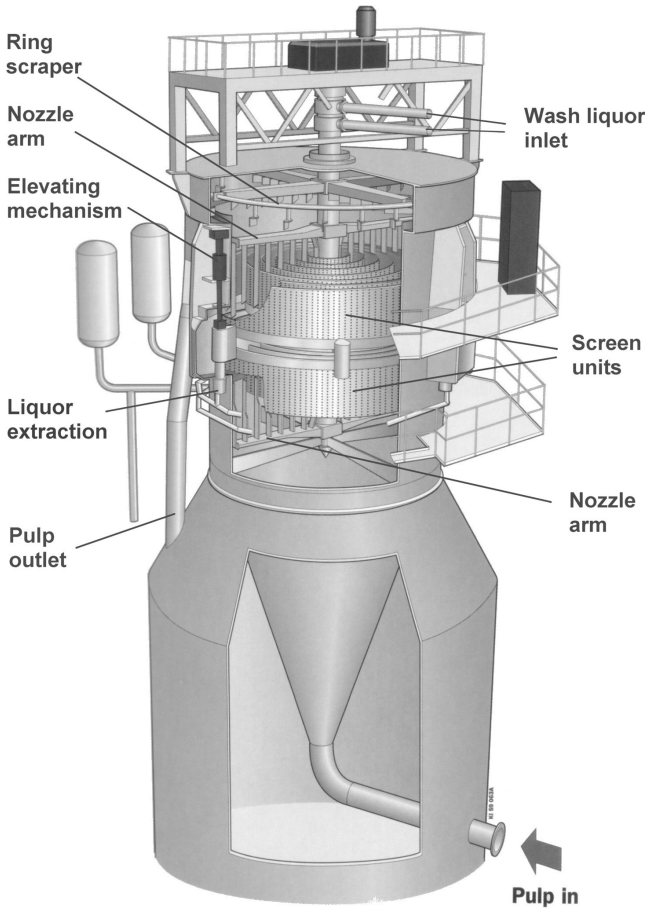


Fig. 5.30 Kvaerner Pulping double atmospheric diffuser [37].

While the pulp proceeds upwards between the screens, the complete screen units are also moving upwards at a rate slightly faster than the pulp until they reach their top position. The liquor extraction is then closed and the screens make a quick downstroke, clearing the screen holes by the combined effect of move-

ment and backflushing. From the lower position the cycle starts again and is repeated over and over. The elevating mechanism of the reciprocating screen unit is driven by a number of hydraulic cylinders.

If installed as a brownstock washer after a continuous digester, the digester pressure can be used to transfer the pulp through the diffuser without additional pumping. Generally, diffusers are amongst the washers with the lowest electrical power consumption.

Since the screen units are submerged, there is no contact of wash liquor or filtrate with the atmosphere, and this reduces the tendency to foaming. The washing efficiencies, expressed as E factors, are about 3.0–4.5 for the single diffuser and 6.0–8.0 for the double diffuser.

#### 5.6.4.2 Pressure Diffuser

A brother to the atmospheric diffuser, the pressure diffuser is a displacement-type washer which is fully enclosed and operates under pressure. It is therefore well-suited to operate under temperatures above 100 °C, and it can also serve as a heat exchanger. If installed as a brownstock washer after a continuous digester, the digester pressure can be used to transfer the pulp through the diffuser without additional pumping.

In the Kvaerner Pulping design, pulp enters the top of the pressure diffuser at about 10% consistency and is distributed into the circular space between the pressurized shell and the screen hanging in the center of the machine. The screen travels downward in a continuous, slow movement and helps the pulp on its way to the outlet at the bottom. There, a scraper ensures the uniform discharge of the pulp, still at about 10% consistency.

As the pulp passes down it is continuously washed by wash liquor introduced through a series of liquor nozzles arranged at numerous levels all around the perimeter of the shell. Baffle plates inside the shell ensure uniform circular distribution of wash liquor at each level. The wash liquor displaces the liquor in the pulp mat, and the displaced liquor is extracted through the screen holes, collected in the center of the screen unit, and finally discharged from the top of the machine.

When the screen has finished its slow downward movement, it is brought back to its upper position by a rapid upstroke. During the upstroke, the slightly conical design of the screen generates a small backflush of extracted liquor, which cleans the screen holes. The slow downward movement then starts again, and this cycle is repeated.

Featuring E factors of 4.0–5.5, the pressure diffuser has the highest per-stage washing efficiency of any washer available.

Since the pressure diffuser is hydraulically full and the washing processes occur in the absence of air, there is no risk of foaming. From an environmental perspective, the totally enclosed design eliminates any source of malodorous gas emissions.

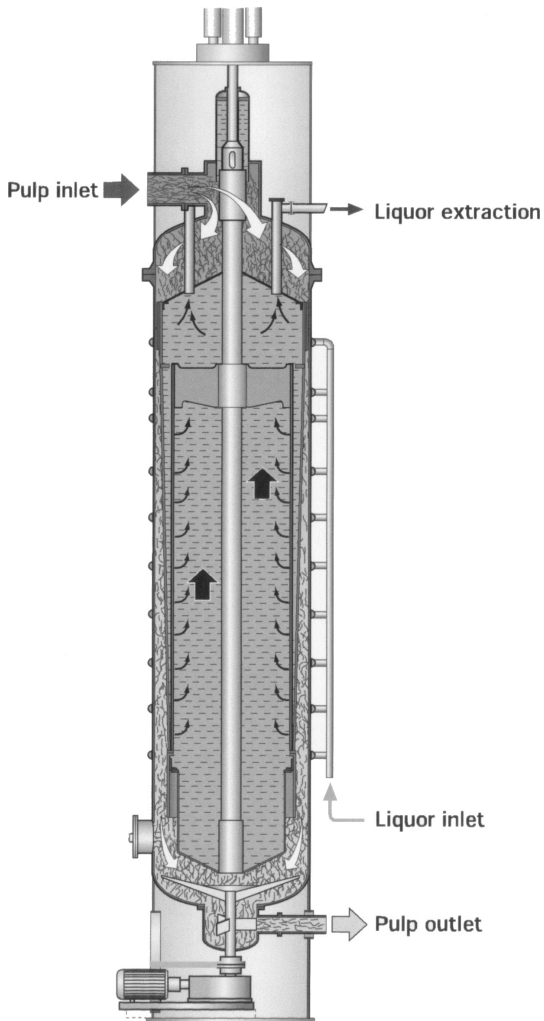


Fig. 5.31 Kvaerner Pulping pressure diffuser [38].

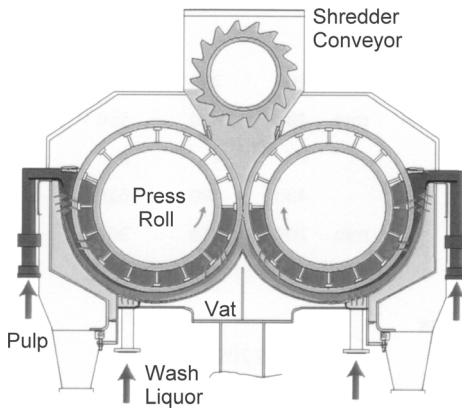
The design and operation of the Andritz pressure diffuser are similar to those of the Kvaerner Pulping unit in many respects. However, the fact that the pulp flows upwards in the Andritz pressure diffuser is advantageous if the pulp feed contains gas, as the gas leaves the diffuser with the pulp at the top without impairing the operation.

## 5.6.5

**Roll Presses**

At the prevailing design, roll presses have two counter-rotating rugged rolls installed in a machine of symmetrical layout.

Metso TwinRoll presses (Fig. 5.32) are designed for either for low (3–5%) or medium (6–10%) feed consistency. The pulp slurry enters the press and a mat is formed in the dewatering zone. There, the pulp consistency is raised to 8–12% as the stock moves on between the rotating roll and the fixed baffle and the liquor passes through holes into the inside of the roll. The clearance between the roll and baffle can be set in order to maintain an ideal flow pattern in the press. As the pulp leaves the dewatering zone and enters the displacement zone, wash liquor is added to the mat; this displaces the liquor from the pulp into the inside of the roll. In the roll nip, the pulp is pressed to a discharge consistency of 30–35%. Finally, the pulp is discharged from the nip to a shredder conveyor mounted above the rolls. The filtrate leaves the rolls through openings at the ends of the rolls [39,40].



**Fig. 5.32** The Metso TwinRoll press [40].

The Kvaerner Pulping Compact Press follows a similar operating principle. The major differences are the feed technology with inlet feeding screws for uniform distribution of pulp over the length of the press and the use of roughly three-quarters of the drum for dewatering and washing (Fig. 5.33).

Wash press E factors are around 1, and  $E_{10}$  factors range between 3 and 5. The enclosed press design generally allows high feed temperatures and minimizes foaming and emissions to air.

The biggest advantage of press washing, however, is the high outlet consistency. First, the amount of wash liquor per ton of pulp required for press washing is only about half the amount needed for a washer with medium consistency outlet. Second, the high inlet consistency to the subsequent process stage also reduces the quantity of effluent from this stage. Third, 1 ton of pulp discharged at 33%



consistency carries only 2 tons of accompanying liquor (compared to more than 7 tons if discharged at 12%), which makes temperature and pH adjustment in the subsequent dilution step an easier task.

As the pressing action places mechanical stress on the pulp up to a level where liquor is squeezed out of the fiber voids, press washing can also have some benefits in removal of extractives [42].

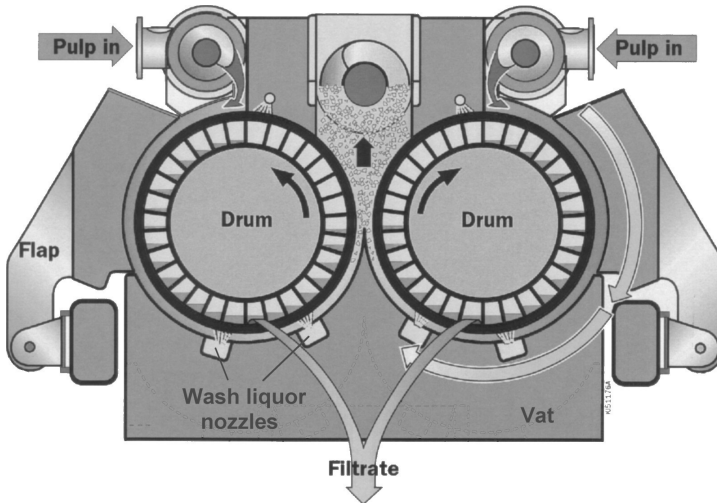


Fig. 5.33 The Kvaerner Pulping Compact Press [41].

### 5.6.6

#### In-Digester Washing

Today, most continuous cooking systems, and also modern batch displacement cooking processes, use a washing step before the digester discharge. At the end of this step the temperature of the digester content is lowered to below 100 °C, thus allowing on the one hand recovery of heat and on the other hand a gentle pulp discharge.

The regime inside the digester is characterized by the moving (continuous) or immobile (batch) pulp column and the wash liquor flowing from the point of feed to the point of extraction. Because of the large dimensions of digesters it is critical for in-digester washing to provide a homogeneous liquor distribution and to avoid channeling.

Diffusion is the other critical factor to be observed. Even at the end of the cook, the original structure of the wood chip column remains intact, with chip-sized fiber conglomerates being surrounded by cooking liquor. As the displacement front reaches a digester zone, wash liquor first displaces the free cooking liquor between the fiber bundles. Then, as the surrounding concentrations change, the

cooking liquor compounds from inside the fiber bundles begin to diffuse into the wash liquor. It is apparent that especially in such a situation, sufficient time must be provided for diffusion to occur.

Laboratory investigations on batch digesters have shown that the standardized Norden factor  $E_{10}$  for in-digester washing is about 2.5 for good displacement and about 2.0 for channeling. These figures are valid for the total of dissolved solids and for a dilution factor of 3. The  $E_{10}$  numbers for residual alkali are about 30% higher than those of the dissolved solids. Within the range of typical dilution factors for in-digester washing (1.5–3.0) the  $E_{10}$  numbers can be regarded as fairly constant. The results from the laboratory investigations correlate quite well with industrial experience. At good displacement, an  $E_{10}$  of 2.5 could be confirmed for dissolved solids. Nevertheless, really bad mill-scale channeling can bring the  $E_{10}$  down to 1.5 and below [43].

The efficiency of Hi-Heat washing in continuous digesters depends largely on the design of the cooking system. The borderline between cooking and washing is frequently indistinct, as systems have been retrofitted over time for modified and extended cooking. Due to the elevated temperature and long duration, original Hi-Heat systems have featured E factors up to 9 and a special effectiveness related to extractives removal.

## References

- Gullichsen, J., H. Östman, Sorption and diffusion phenomena in pulp washing. *Tappi J.*, **1976**; 59(6): 140–143.
- Ingmanson, W.L., An investigation of the mechanism of water removal from pulp slurries. *Tappi J.*, **1952**; 35(10): 439–448.
- Vomhoff, H., On the in-plane permeability of water-saturated fibre webs. *Nordic Pulp Paper Res. J.*, **2000**; 15(3).
- Carman, P.C., Fluid flow through a granular bed. *Trans. Inst. Chem. Eng.*, **1937**; 15: 150–167.
- Clos, R.J., L.L. Edwards, Application of the limiting-consistency web compression model to vacuum-assisted drainage cell tests. *Tappi J.*, **1995**; 78(7): 107–114.
- Wang, J., A.N. Hrymak, R.H. Pelton, Specific surface and effective volume of water-swollen pulp fibres by a permeability method. *J. Pulp Paper Sci.*, **2002**; 28(1): 13–16.
- Mantar, E., A. Co, J.M. Genco, Drainage characteristics of pulp slurries under dynamic conditions. *J. Pulp Paper Sci.*, **1995**; 21(2): J44–J50.
- Vomhoff, H., D.M. Martinez, and B. Norman, The transversal steady-stage permeability of a fibre web compressed between rough permeable surfaces. *J. Pulp Paper Sci.*, **2000**; 26(12): 428–436.
- Luthe, C., R. Berry, L. Nadeau, How does carbon dioxide improve pulp washing? Fall Technical Conference. TAPPI, **2003**.
- Kerekes, R.J., J.D. McDonald, A decreasing permeability model of wet pressing: theory. *Tappi J.*, **1991**; 74(12): 150–156.
- McDonald, J.D., R.J. Kerekes, A decreasing permeability model of wet pressing: applications. *Tappi J.*, **1991**; 74(12): 142–149.
- McDonald, J.D., R.J. Kerekes, A decreasing-permeability model of wet pressing with rewetting. *Tappi J.*, **1995**; 78(11): 107–111.
- Clos, R.J., L.L. Edwards, I. Gunawan, A limiting-consistency model for pulp dewatering and wet pressing. *Tappi J.*, **1994**; 77(6): 179–187.
- McKibbins, S., Application of diffusion theory to the washing of kraft cooked

- wood chips. *Tappi J.*, **1960**; 43(10): 801–805.
- 15 Stromberg, C.B., Washing for low bleach chemical consumption. *Tappi J.*, **1991**; 74(10): 113–122.
  - 16 Ala-Kaila, K., H.V. Nordén, Leaching of organic material in washing after oxygen delignification. *Nordic Pulp Paper Res. J.*, **1997**; 12(2): 94–102.
  - 17 Hartler, N., R. Sture, Washing of pulps, Part 1. Equilibrium studies. *Svensk Papperstidn.*, **1975**; 78(10): 367–372.
  - 18 Rosen, A., Adsorption of sodium ions on kraft pulp fibers during washing. *Tappi J.*, **1975**; 58(9): p. 156–161.
  - 19 Crotagino, R.H., N. Poirier, D.T. Trinh. The Principles of Pulp Washing. Kraft Recovery Operations. TAPPI, **1987**.
  - 20 Eriksson, G., U. Grén, Pulp washing: Sorption equilibria of metal ions on kraft pulps. *Nordic Pulp Paper Res. J.*, **1996**; 11(3): 164–170.
  - 21 Towers, M., A.M. Scallan, Predicting the ion-exchange of kraft pulps using Donnan theory. *J. Pulp Paper Sci.*, **1996**; 22(9): J332–J337.
  - 22 Bygrave, G., P. Englezos, A thermodynamic-based model and data for Ca, Mg, and Na ion partitioning in kraft pulp fibre suspensions. *Nordic Pulp Paper Res. J.*, **2000**; 15(2): 115–159.
  - 23 Räsänen, E., Modelling ion exchange and flow in pulp suspensions. Helsinki University of Technology. Helsinki, **2003**.
  - 24 Bryant, P.S., L.L. Edwards, Manganese removal in closed kraft mill bleach plants. *Tappi J.*, **1994**; 77(2): 137–148.
  - 25 Tervola, P., K. Henricson, J. Gullichsen. Mathematical model of fractional pulp washing and applications in a bleach plant. Tappi Pulping Conference. TAPPI **1993**.
  - 26 Hakamäki, H., K. Kovasin, The effect of some parameters on brownstock washing: A study made with a pulp tester. *Pulp Paper Can.*, **1985**; 86(9): T243–T249.
  - 27 Wang, J., et al., New insights into dispersed air effects in brownstock washing. *Tappi J.*, **2001**; 84(1): 101–108.
  - 28 Luthi, O., Equivalent displacement ratio – evaluating washer efficiency by comparison. *Tappi J.*, **1983**; 66(4): 82–84.
  - 29 Nordén, H.V., Analysis of a pulp washing filter. *Kemian Teollisuus*, **1966**; 4: 343–351.
  - 30 McCabe, W.L., J.C. Smith, P. Harriott. *Unit Operations of Chemical Engineering*, 6th edition. McGraw-Hill, **2001**: 632–638.
  - 31 Seader, J.D., E.J. Henley. In *Separation Process Principles*. Wiley: New York, **1998**: 242–246.
  - 32 Nordén, H.V., V.J. Pohjola, R. Seppänen, Statistical analysis of pulp washing on an industrial rotary drum. *Pulp Paper Mag. Can.*, **1973**; 56(10): 83–91.
  - 33 IMPCO Coru-Dek III Vacuum Washer (product leaflet). GL&V Pulp Group Inc.: Nashua, NH, USA, **2001**.
  - 34 PW-Pressure Washers (product leaflet). Sunds Defibrator. Rauma Oy: Pori, Finland, **1989**.
  - 35 Drum Displacer (product leaflet). Andritz: Kotka, Finland, **2000**.
  - 36 Chemi-Washer (product leaflet), Kadant Black Clawson. Mason, Ohio, USA.
  - 37 Atmospheric diffuser (product leaflet). Kvaerner Pulping: Karlstad, Sweden, **1998**.
  - 38 The Kvaerner pressure diffuser. In *Fibrelines*. Kvaerner Pulping AB: Karlstad, Sweden, **2000**: 32.
  - 39 TwinRoll-A Wash Press (product leaflet). Metso Paper: Sundsvall, Sweden, **2001**.
  - 40 TwinRoll-B Wash Press (product leaflet). Metso Paper: Sundsvall, Sweden, **2001**.
  - 41 Compact Press (product leaflet). Kvaerner Pulping AB: Karlstad, Sweden, **2002**.
  - 42 Tay, S.C.H., M.D. Ouchi, F.B. Cramer, High-intensity mechanical pretreatment and high-compression screw pressing for deresination of aspen kraft pulps. *Tappi J.*, **1996**; 79(2): 265–275.
  - 43 Timonen, O., K. Kovasin, P. Tikka. The washing efficiency of digester displacement: new aspects based on laboratory studies and improved calculation procedures. Fall Technical Conference. TAPPI, **2002**.

## 6 Pulp Screening, Cleaning, and Fractionation

Andreas W. Krotscheck

### 6.1 Introduction

After cooking, the pulp contains undesirable matter of different provenance. On the one hand, there are wood components other than separate pulp fibers, such as dense sections from branches and heartwood, bark, or uncooked chips. On the other hand, certain non-wood contaminants are carried along with the wood chips or enter the pulp mill processes by other routes. These contaminants may include stones and sand, as well as metal or plastic debris.

The objective of screening and cleaning is to remove these solid impurities from the pulp for the purposes of protecting downstream equipment, saving bleaching chemicals and last – but not least – to obtain a clean final product.

Screening and cleaning equipment can also be used for pulp fractionation. During fractionation, the totality of the pulp is divided into usable portions of different properties – for example, fiber length or fiber wall thickness – which are separately handled downstream in the process. In chemical pulping, fractionation by screens has traditionally been employed in high-kappa applications. Fractionation for low-kappa pulps has gained industrial significance only recently.

Screening operations can be located in both the unbleached and bleached sections of the fiberline. Centrifugal cleaning is usually employed for the bleached pulp, except for cleaning for sand removal which is also used in unbleached screening systems. Demands on screening operations have increased since environmentally friendly bleaching sequences have been substituted for chlorine as a bleaching agent. Shives which previously were bleachable by chlorine must now be efficiently removed.

Screening with narrow slots is emerging as a challenge to centrifugal cleaning as the process of choice for contaminant removal from bleached pulp. With regard to fractionation, pressure screens and centrifugal cleaners cover different separation tasks. While screens fractionate mainly by fiber length and fiber flexibility, cleaners fractionate mostly by wall thickness, coarseness, and fibrillation.

Traditionally, screening and cleaning have been targeted at the removal of solid impurities from pulp fibers, and for most applications this still holds true. Hence,

much of the screening and cleaning nomenclature used in the industry is related to this situation. In this chapter, however, we will at times attempt to use a more general approach to the separation phenomena encountered in screening and cleaning, which also accounts for the increasing importance of these process steps in fractionation.

Pulp *screening* can be described as solid-solid separation using a screen in a liquid environment. The larger particles are retained on the screen, while the smaller ones selectively pass through the narrow screen apertures. The mechanism of screening is separation by size. For example, large pulp fiber bundles are retained on the screen while small isolated fibers pass through.

Pulp *cleaning* is characterized by solid-solid separation using centrifugal and centripetal forces in the gravity field of a hydrocyclone. Depending on the separation task, the design of the hydrocyclone is customized so that either heavy-weight or light-weight particles are selectively separated from the main stream. The mechanism of cleaning is separation by specific weight. For example, heavy-weight sand can be separated from the light pulp fibers.

For all separation applications it is essential that the solid components can migrate freely within the pulp suspension. Unfortunately, the particle–particle interaction of pulp fibers results in flocculation even at very low consistencies. Flocs, which are stochastic clumps of fibers, constrain the free motion of both undesirable matter and good fibers. Hence, flocs must be disintegrated in order for the separation to be efficient. Only when particles do not interfere one with another does the actual size of a single particle determine whether it passes the screen aperture, or not. Likewise, the weight of a single particle determines which direction it moves in the gravity field of the hydrocyclone, but only if the particles do not interact.

The necessary deflocculation of fibers leads to a physical limitation with regard to pulp consistency in the feed to the separator. The high shear forces needed to disintegrate flocs at the consistency of pulp screening are generated mechanically, by the rotor in a pressure screen and by the vibrations of a vibratory screen. As hydrocyclones have no moving parts and require laminar flow for their correct operation, their application is restricted to lower consistencies.

Previously, screening and cleaning equipment utilized atmospheric feed and/or discharge. However, today's pressurized systems have many advantages over their atmospheric counterparts, including a higher operating consistency, an elevated operating temperature, a greater capacity, a lack of air entrainment, and a better separation efficiency.

In this chapter we will first examine, from a theoretical perspective, the phenomena and parameters that influence separation in screening and cleaning equipment. This will facilitate an understanding of the processes involved. Subsequently, screening and cleaning applications and systems design will be discussed, before focusing on separation equipment.

## 6.2 Screening Theory

### 6.2.1

#### Introduction

It is useful to start with some definitions and to develop a basic understanding of the mechanical set-up of a pressure screen before looking at the mostly mechanistic and semi-empirical models that are used to describe the process phenomena in a pressure screen.

Figure 6.1 shows the process streams around a screen. The pulp suspension containing the impurities is fed with the feed stream  $Q_F$  at the pulp concentration  $c_F$ . The clean pulp passes through the apertures in the screen plate and is discharged with the accept stream  $Q_A$  at the concentration  $c_A$ . The reject stream  $Q_R$  is rich in impurities. More in general, one fraction of a certain property is concentrated in the reject stream  $Q_R$ , while the other fraction of different property leaves the screen with the accept stream  $Q_A$ .

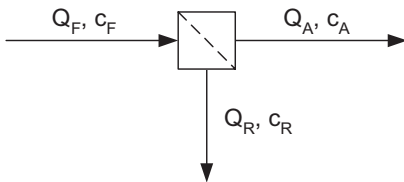


Fig. 6.1 Streams around a screen.

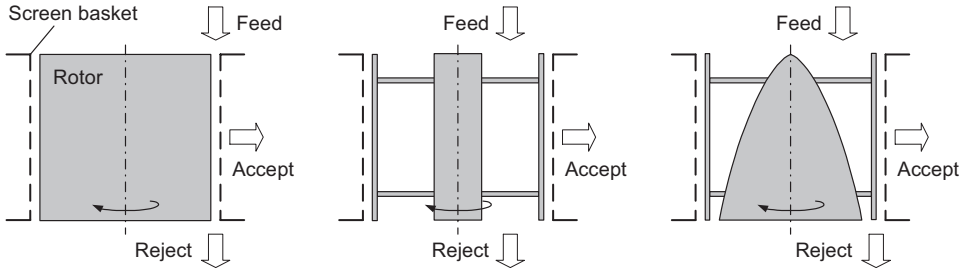
In addition to the streams shown in Fig. 6.1, most industrial pressure screens have an internal dilution by filtrate near the reject outlet. While dilution is often needed from an operational perspective to avoid plugging of the screen's reject side, we can skip internal dilution during the present theoretical considerations without losing insight.

The solid-solid separation with a pressure screen can be categorized by the type of physical separation mechanism. In *barrier separation*, particles are rejected from passage through an aperture because they are physically larger than the aperture size in any orientation. In *probability separation* the particle can pass through the aperture in at least one orientation and it depends on how the particle approaches the aperture whether it passes, or not [1,2].

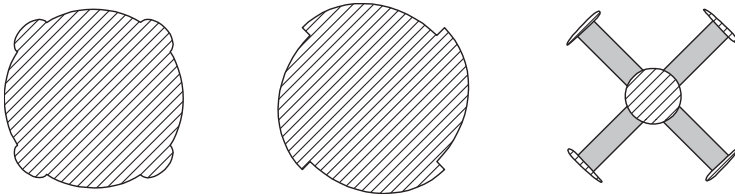
The distinction between barrier screening and probability screening is of utmost importance for all screening applications. As for screening efficiency, probability separation is apparently much more challenging than barrier separation.

The basic mechanical elements in control of separation in a simple pressure screen are the screen and the rotor. In the most common design, the screen has the shape of a cylindrical basket and is fixed in the screen housing. The apertures in the screen basket have the form of either holes or slots and the screen surface may be smooth or contoured.

Pulp is fed axially to the screening zone. The accepted material passes through the apertures in the screen basket, while the rejected material proceeds along the inside of the screen basket towards the reject outlet. The rotor revolves inside the screen basket. Over the years, a large number of different rotor designs has been developed. Most of these are based on the closed bump rotor and open foil rotor design principle (Figs. 6.2 and 6.3).



**Fig. 6.2** Rotor categories: closed rotor (left), open rotor (center), semi-open rotor (right).



**Fig. 6.3** Examples of cross-sections of simple rotors: left, bump rotor; center, step rotor; right, foil rotor.

Besides providing the tangential velocity near the screen and generating turbulence, the most important task of the rotor is to keep the screen apertures clear. This is accomplished by the regular backflush through the apertures caused by the pumping action of the rotor's pulsation elements.

### 6.2.2

#### Flow Regime

As the pulp suspension passes through the screening zone, the flow pattern near the screen can be broken down into an axial flow vector from the feed side to the reject side, a tangential flow vector induced by the rotor, and a radial flow vector through the apertures to the accept side of the screen (Fig. 6.4).

The rotor plays a most essential part in influencing the flow regime. Its motion fluidizes the pulp suspension, provides the tangential fluid velocity along the screen plate, and backflushes the screen apertures. Fluidization suppresses the particle–particle interactions and provides for quickly changing particle orienta-

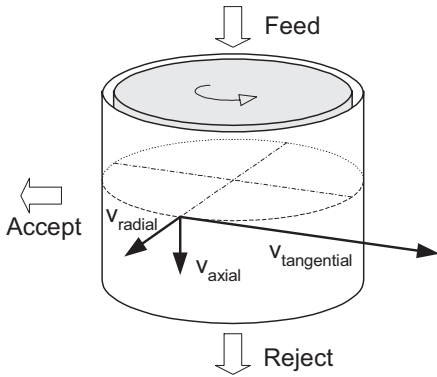


Fig. 6.4 Flow vectors near the screen basket.

tion relative to the screen aperture, thus increasing the probability for acceptable particles to pass. As the rotor element passes cyclically over the aperture, it generates a backflush through the aperture every time it passes by. The backflush removes particles trapped in the narrow screen apertures and thus keeps them clear.

While the screen performance is influenced by all the three flow vectors, the radial accept flow through the apertures is most critical for continuous operation. When the accept flow becomes limited or even completely disrupted by fibers blocking the screen apertures, the situation is referred to as “blinding” or “plugging” of the screen. Blinding leads to the formation of a fiber mat on the screen surface, and it can affect only part of the screen or the total screen. In the latter case, it may take several minutes for the screen to be blinded, but typically it takes only a few seconds. The triggering factor of blinding – that is, the build-up of fibers at the edge of a screen aperture – occurs very rapidly, within several thousands of a second [3]. Consequently, very frequent backflush is required to avoid plugging. The typical pulse frequency provoked by the rotor in a pressure screen is above 30 Hz [4].

The aperture velocity, or passing velocity,  $v$ , is often regarded as a fundamental design parameter for a pressure screen.  $v$  ( $\text{m s}^{-1}$ ) is calculated from the accept flow rate  $Q_A$  ( $\text{m}^3 \text{s}^{-1}$ ) and the open area of the screen basket,  $A_o$  ( $\text{m}^2$ ):

$$v = \frac{Q_A}{A_o} \quad (1)$$

It is important to realize that the true flow velocity through the screen apertures is considerably higher than the passing velocity calculated from Eq. (1). On the one hand, pressure pulsation as induced by the rotor action leads to a backflow from the accept side to the feed side, thus both increasing the volume to be transferred from the feed side to the accept side and reducing the time for this transfer. On the other hand, fiber accumulation at the screen apertures reduces the open area [5].



## 6.2.3

**Fiber Passage and Reject Thickening**

The essential part of the screening operation occurs in the annular gap between the rotor and the screen basket.

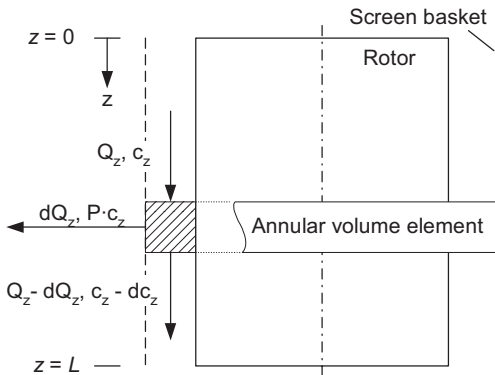
Both a mixed-flow model and a plug-flow model have been used to describe the flow pattern in a pressure screen [1,6]. Here, we will focus on the plug-flow model because it is more flexible and seems to describe the actual flow regime in a pressure screen more accurately.

The plug-flow model assumes ideal radial mixing between the rotor and the screen basket without backmixing in axial direction. Let us define a parameter called passage ratio,  $P$ :

$$P = \frac{c_s}{c_z} \quad (2)$$

where  $c_s$  is the solids concentration in the stream through a screen aperture ( $\text{kg m}^{-3}$ ) and  $c_z$  is the solids concentration of the stream just upstream of the aperture at a position  $z$  [1].

The passage ratio is a characteristic parameter of the screening system, which is influenced by many variables including screen plate and rotor design, screen operating conditions and pulp grade.  $P$  is best determined individually for a given screening application based on field measurements. A passage ratio of zero means that all the solids are retained on the screen and will be rejected. At  $P = 1$ , the concentrations in the accept and reject are equal to the feed concentration and there is no separation.



**Fig. 6.5** Flows and concentrations around an annular differential volume element.

Considering Fig. 6.5, the mass balance for pulp over the annular differential element between the screen plate and the rotor gives:

$$Q_z c_z - dQ_z P c_z - (Q_z - dQ_z)(c_z - dc_z) = 0 \quad (3)$$

where  $Q_z$  stands for the total flow rate ( $\text{m}^3 \text{h}^{-1}$ ) entering the element in axial direction and  $dQ_z$  for the flow rate leaving in radial direction, respectively.

Equation (3) can be rewritten to give:

$$\frac{dc_z}{c_z} = (P - 1) \frac{dQ_z}{Q_z} \quad (4)$$

In a first approach, it is assumed that the fiber passage ratio  $P$  is independent of the flow rate and consistency. Then, Eq. (4) can be integrated using the overall screen boundary conditions as per Fig. 6.1; that is,  $c_z = c_F$  and  $Q_z = Q_F$  for  $z = 0$ , and  $c_z = c_R$  and  $Q_z = Q_R$  for  $z = L$ .  $L$  is the length of the screening zone.

$$\frac{c_R}{c_F} = \left( \frac{Q_R}{Q_F} \right)^{(P-1)} \quad (5)$$

Note that the concentrations may relate to the totality of pulp as well as to a fraction only, for example, to shives. Then, different passage ratios will apply for total pulp and shives. When the concentrations in Eq. (5) refer to total pulp concentrations, the quotient  $c_R/c_F$  is defined as the reject thickening factor,  $T$ .  $Q_R/Q_F$  is termed the volumetric reject ratio,  $R_v$ . With these definitions we obtain a relationship between the thickening factor, total fiber passage ratio and volumetric reject ratio:

$$T = R_v^{(P-1)} \quad (6)$$

The mixed-flow model of pressure screening assumes a completely mixed volume inside the screen. In the mixed-flow model, the feed entering at the pulp concentration  $c_F$  is immediately mixed into the volume inside the screen which is at the reject concentration  $c_R$ . All accept passes through the screen apertures at the accept concentration  $c_A$ . The overall mass balance, pulp mass balance and passage ratio of this system are:

$$Q_F - Q_A - Q_R = 0 \quad (7)$$

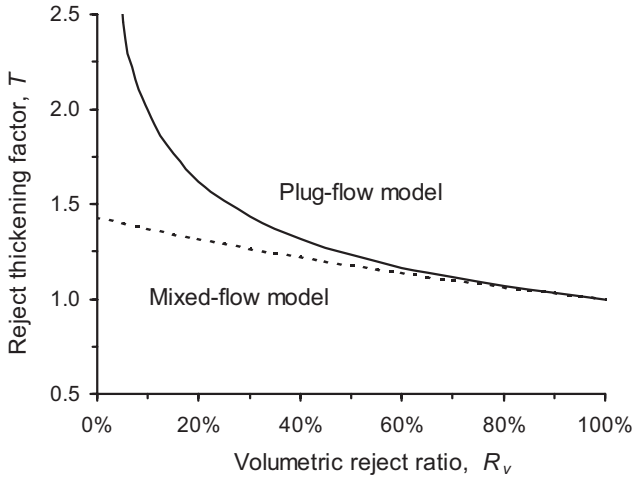
$$Q_F c_F - Q_A c_A - Q_R c_R = 0 \quad (8)$$

$$P = \frac{c_A}{c_R} \quad (9)$$

Equations (7) to (9) can be combined and rewritten using the definitions of the thickening factor and volumetric reject ratio to give the expression for the thickening factor in the mixed-flow model:

$$T = \frac{1}{P(1 - R_v) + R_v} \quad (10)$$

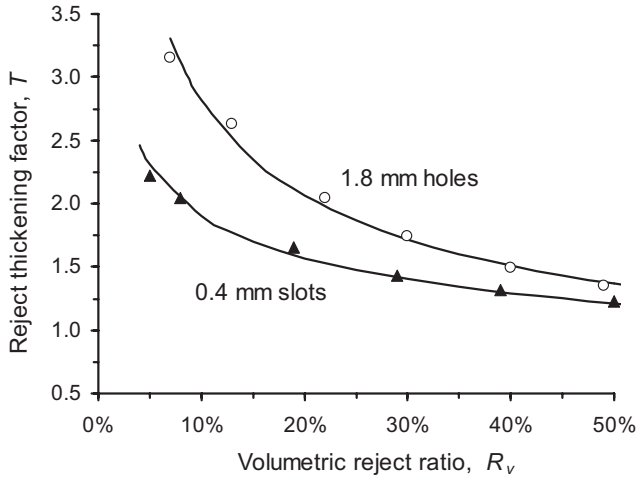
While the mixed-flow model seems worth considering for screens with open rotors, it has proven to be second to the plug-flow model at lower reject rates for virtually any screen configuration. Figure 6.6 shows, graphically, the comparison of the reject thickening behavior predicted by the mixed-flow and plug-flow models.



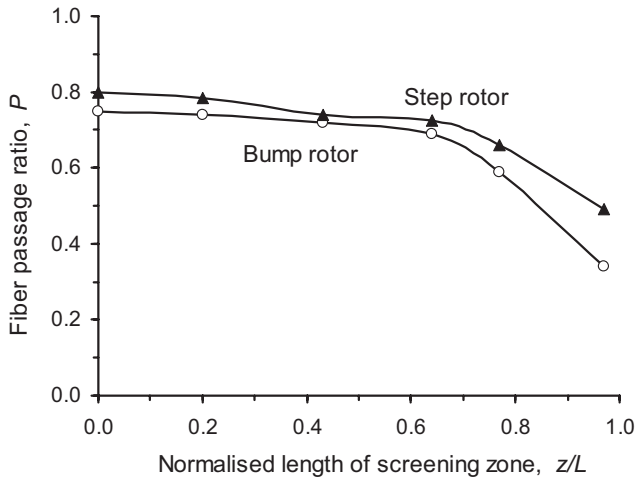
**Fig. 6.6** Reject thickening in a pressure screen predicted by the mixed-flow and plug-flow models at a constant fiber passage ratio of  $P = 0.7$ .

By examining the fit between experimental data and the curves calculated from the plug-flow model in Fig. 6.7, it can be seen that the plug-flow model describes the thickening behavior of an industrial screen quite well. Note that reject thickening increases dramatically at reject ratios smaller than 10%, and that a lower passage ratio generally leads to higher thickening.

Earlier, it was assumed that the fiber passage ratio is constant along the screening zone, which implies that the single fibers do not interact with each other. This holds true only for very low consistencies and, to a certain degree, for fiber suspensions under high shear forces in a turbulent environment. Figure 6.8 shows that the fiber passage ratio in a commercial pressure screen is fairly constant over the first two-thirds of the screen length, but then can fall significantly at the reject end of the screen [4].

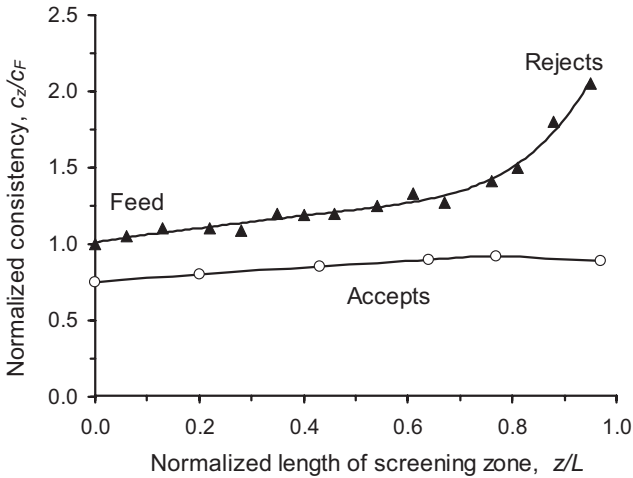


**Fig. 6.7** Example of reject thickening as a function of the volumetric reject ratio. Comparison of experimental data [6] with calculation results from the plug-flow model;  $P = 0.72$  for 0.4-mm slots,  $P = 0.55$  for 1.8-mm holes.



**Fig. 6.8** Example of fiber passage ratio as a function of the screen length and rotor geometry; smooth hole screen, eucalyptus pulp,  $R_v = 10\%$  [4].

Figure 6.9 illustrates a typical consistency profile over the length of a pressure screen. While the consistency of the accept remains fairly constant, the consistency of the pulp flow passing along the screen increases disproportionately towards the end of the screening zone. The profile explains why screens tend to blind from the reject end.



**Fig. 6.9** Example of consistencies as a function of the screen length; smooth hole screen, bump rotor, eucalyptus pulp,  $R_s = 10\%$  [4].

#### 6.2.4

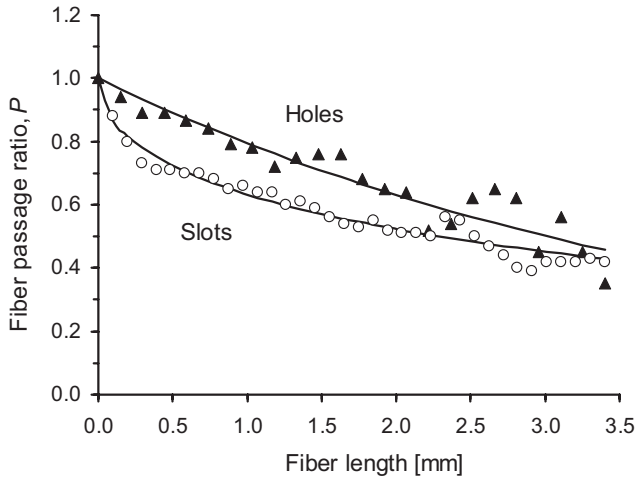
##### Selective Fiber Passage

The selective separation of the different types of solids contained in the feed stream is of major importance for all contaminant removal and fractionation applications. While the selectivity of barrier screening is essentially determined by the chosen screen, the selective separation of particles is much more challenging when screening is governed by the probability mechanism.

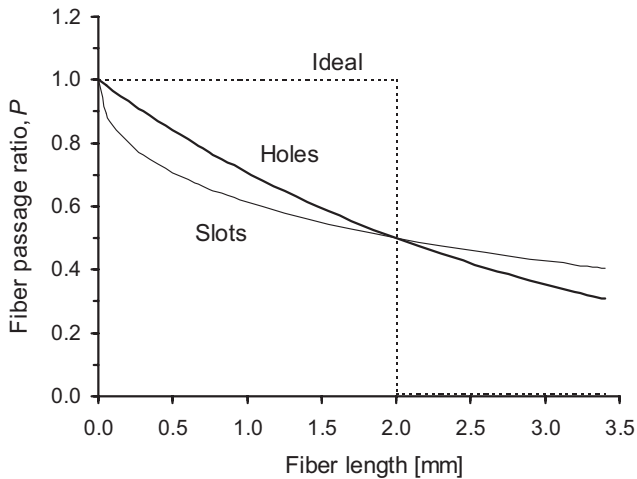
Several investigations have been made to evaluate the fiber length dependent passage of fibers through pressure screen apertures (e.g., [7–10]). It has been shown that the passage ratio can be approximated by the empirical equation

$$P = e^{-(l/\lambda)^\beta} \quad (11)$$

where  $\lambda$  is a size constant proportional to the size of the screen plate aperture and  $l$  is the fiber length.  $\lambda$  is to be determined experimentally for each screening application. The second constant was found to be  $\beta = 0.8\text{--}1.1$  for screen plates with smooth holes, and  $\beta = 0.5$  for contoured slotted screen plates. The different shapes of the fiber passage ratio versus fiber length curves in Fig. 6.10 demonstrate the divergent performance of holed and slotted screens reflected by  $\beta$ .



**Fig. 6.10** Example of fiber passage ratio as a function of the fiber length and screen type; smooth hole plate versus contoured slot plate, bump rotor, softwood thermomechanical pulp (TMP) [8].



**Fig. 6.11** Typical fiber passage ratio as a function of the fiber length; comparison of ideal profile with typical profiles of holed screen ( $\beta = 1$ ) and slotted screen ( $\beta = 0.5$ ) normalized for a fiber passage ratio of 0.5 at 2-mm fiber length [8].

It is apparent from Fig. 6.11 that currently proven screening equipment is performing far from ideally when it comes to fractionation. However, screening with holed plates leads to better length-based fractionation because the holed screen profile is closer to the ideal profile and the fiber passage ratio drops more quickly

over the fiber lengths of main interest. Remember that  $P = 1$  implies the distribution of very short fibers between accept and reject according to the respective flow rates. In contrast, very long fibers are selectively concentrated in the reject stream as  $P$  approaches zero.

For a given combination of screen plate, rotor type and pulp furnish, the length-based fiber passage ratio was shown to be independent of the reject ratio. While for slotted screen plates the fiber passage ratio increases with the aperture velocity, it is independent of the aperture velocity for holed screen plates. This behavior marks another advantage of holed screens for fractionation, because it makes the fractionation result independent of the production capacity [8]. Besides fractionation for length, pressure screens separate fibers according to their coarseness (weight per unit length) [11].

### 6.3

#### Screening Parameters

In this subsection we will review the parameters that affect the operation and determine the performance of a screening system, and their qualitative influences on screen capacity and screening efficiency.

These parameters include operating conditions, such as flow rates, feed consistency or temperature. They also include equipment-specific parameters, such as screen and rotor design or rotor tip velocity. In addition, it is necessary to observe the furnish characteristics of both the pulp fibers and the contaminants.

Some of the above parameters can be adjusted, while some are intrinsic to a special process step or piece of equipment. The chosen combination of adjustable screening parameters depends on the individual requirements of the application, and this is usually a compromise within performance limits and operating constraints, because the optimization of single parameters often leads into opposite directions.

Due to the complexity of the mechanisms involved and varying system performance depending on the specific circumstances, the discussion of parameters below will be often qualitative in nature.

#### 6.3.1

##### Equipment Parameters

##### 6.3.1.1 Screen Basket

The screen basket is fundamentally characterized by aperture size, aperture shape and aperture spacing, as well as the character of its surface. There is a basic distinction between perforated, or holed, screen plates and slotted screen plates. Both types can be furnished with contours on the side of the screen surface which faces the feed. Such contoured, or profiled, screens increase the turbulence near the screen aperture and allow the screen to be operated at a higher capacity.

Only profiled screens in combination with the wedge-wire design have made today's narrow screen slots practical and widely accepted. Slotted screens with a slot width around 0.15 mm have become state of the art for applications targeted at the removal of smaller contaminants. Wedge-wire screens consist of solid bars placed aside each other, forming long slots over the complete length of the screen basket, while machined slots are milled out of a solid screen basket. Wedge-wire slotted screens have considerable capacity advantages over machine slotted screens due to their larger open area.

Holed screens have been traditionally preferred for their high capacity and reliable operation and easy control under varying conditions. Their robustness makes them first choice for the removal of larger contaminants. The advantages of holed screens for fractionation have been discussed above. Typical hole sizes are 4–10 mm for larger contaminant removal, and about 1 mm for fractionation.

The aperture size is the most critical design variable of a screen. Holes of small diameter and slots of narrow width have advantages with regard to the screening efficiency. Their size actually determines whether a particle is rejected on the principle of barrier separation, or whether it is subject to probability separation. On the other hand, smaller apertures mean lower capacity at a given screen surface area.

Similarly, the profile depth of the screen surface causes divergent screen performance. By tendency, the additional turbulence created by a higher contour provides a greater capacity but reduces the screening efficiency. If in turn the aperture size is reduced to regain lost efficiency, the capacity of the contoured screen still remains higher [12].

It has been shown that slot spacing is important, and that longer fibers require wider slot spacing than shorter fibers. If the slots are too close, then stapling of fibers occurs as the two ends of individual fibers enter adjacent slots at the same time. Similar conclusions have been drawn for holed screens.

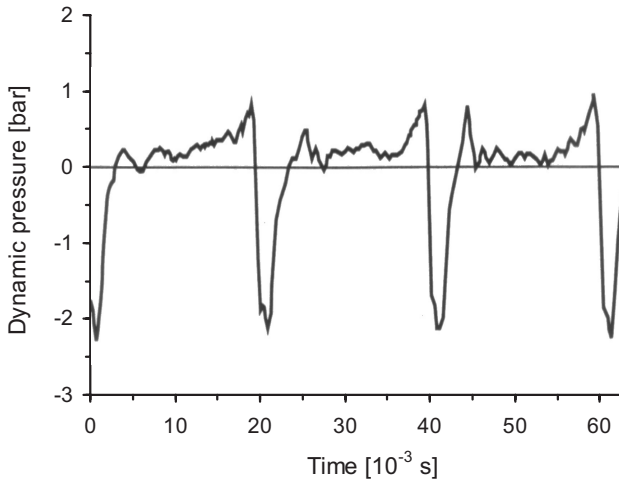
Note that the performance of a screen will deteriorate over time if the pulp furnish contains an abrasive material such as sand. Especially with heavily contoured screens, wear will significantly decrease both the capacity and the screening efficiency.

#### 6.3.1.2 Rotor

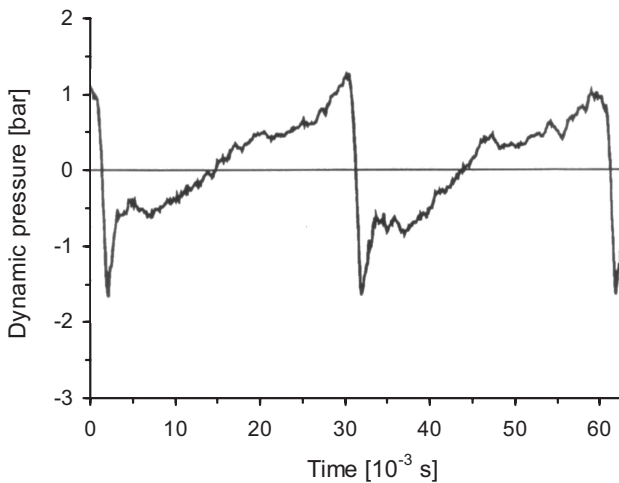
There is a variety of different rotors available, with special shapes and sophisticated local arrangements of bumps or foils. All of these are deemed to have their individual advantages regarding screen capacity, screening efficiency or power consumption.

The characteristic shape of the pressure pulse generated by a rotor depends on the design of the pulsation element, for example on the shape, length and angle of incidence of the foil, or on the shape and length of the bump. The intensity of the pulse is determined again by the rotor shape, as well as by the rotor tip velocity, the clearance between the pulsation element and the screen basket, as well as the pulp consistency and pulp furnish parameters.





**Fig. 6.12** Example of pressure pulse profile for a short foil rotor [5].



**Fig. 6.13** Example of pressure pulse profile for a contoured-drum rotor (S-rotor) [5].

Figures 6.12 and 6.13 show typical pressure pulses caused by the movement of a foil rotor and a step rotor, respectively. At a random point on the screen surface, there is in general a positive pressure pulse upstream of the rotor element, and a negative pressure pulse right after the smallest clearance between the rotor tip and the screen basket has passed by. The negative pressure is responsible for the backflush through the screen apertures.

It is evident that the profile of the pressure pulse is very different between rotors. Short negative-pressure pulses, as created by bump rotors and rotors with short foils, keep the backflush flow low. At the same time, they ensure comparatively low true

aperture velocity and low overall screen resistance. Longer negative-pressure pulses, as created by rotors with long foils and step rotors, reduce reject thickening by intensified backflushing. Higher feed consistencies require longer negative-pressure pulses to keep the consistency at the reject end of the screening zone low enough to avoid blinding. Note that the screen capacity decreases with the magnitude and duration of the negative pressure pulse.

The clearance between the pulsation element and the screen basket is quite different between rotor designs. Common clearances are between 3 and 10 mm. Reducing the clearance between the pulsation element and the screen basket leads to some increase of the pressure pulse intensity [13,14].

### 6.3.2

#### Operating Parameters

##### 6.3.2.1 Reject Rate

The reject rate is the most important operating parameter of a pressure screen. A higher reject rate improves the screening efficiency and reduces the danger of screen blinding caused by undue reject thickening (see Fig. 6.7; see also Figs. 6.23 and 6.24). The reject rate is also the only one parameter that really affects fractionation efficiency (see Fig. 6.32).

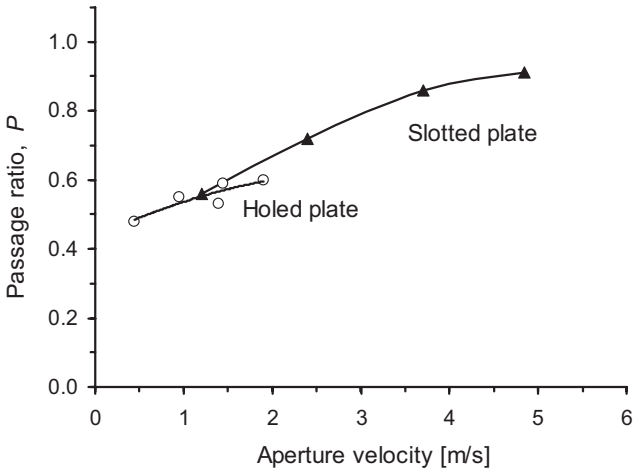
However, there is an economic boundary on the reject rate, because large reject rates inflate subsequent screening stages and thus increase both investment and operating costs. Typical volumetric reject rates for pressure screens range from 10% to 25%.

##### 6.3.2.2 Accept Flow Rate

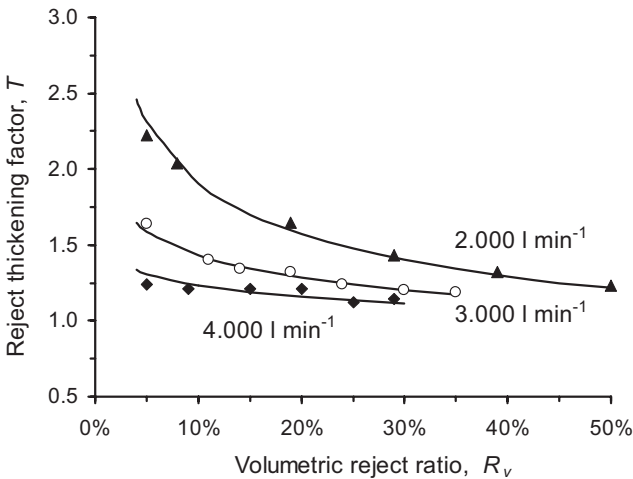
A pressure screen's capacity is given by the accept flow rate, and is often expressed in terms of the aperture velocity defined by Eq. (1). A higher aperture velocity leads to a reduction in screening efficiency [15,16]. Figure 6.14 illustrates graphically that a decreasing aperture velocity reduces the fiber passage ratio. This means that reject thickening becomes more critical at lower aperture velocities, and hence screen capacities. Note that the operation of a pressure screen below its nominal capacity may soon lead to severe operating problems caused by reject thickening (Fig. 6.15). The dependence of the fiber passage ratio on the screen capacity of holed screens is less pronounced than that of slotted screens.

As mentioned in Section 6.2.2, the gross aperture velocity calculated from Eq. (1) is a parameter of limited significance. Since the actual flow rate through the apertures depends on many factors, the meaningfulness of the aperture velocity as a parameter for evaluation of screen capacity or screening efficiency is restricted to systems of similar mechanical design, pulp furnish and operating conditions.

For a given screen geometry, pulp furnish and pulp consistency, the pressure drop across a screen is linearly related to the square of the accept flow rate, with the slope determined by the hydraulic resistance of the screen plate [17].



**Fig. 6.14** Example of fiber passage ratio as a function of the aperture velocity; experimental data, bleached softwood kraft pulp [6].



**Fig. 6.15** Example of reject thickening in a pressure screen as a function of the accept flow rate; 3000 L min<sup>-1</sup> nominal screen capacity, experimental data, bleached softwood kraft pulp [6].

Optimum levels of fractionation in slotted screens occur at low aperture velocities where the passage ratio of long fibers remains low, but that of short fibers is significant [18]. In contrast, the fractionation performance of holed screens is widely independent of the aperture velocity at the hole sizes of interest for fractionation [9].

### 6.3.2.3 Feed Consistency

The feed consistency determines the amount of liquor that has to pass the screen at a given pulp production capacity. Pressure screens can operate at feed consistencies up to 4% or 5%. The latter figure represents hardwood pulp, which generally allows higher feed consistencies than softwood pulp. The limiting factor defining the feed consistency ceiling is reject thickening. A screen's pulp capacity increases with rising feed consistency, until a point is reached when it rapidly decreases due to blinding caused by excessive reject thickening.

A screening system with a high feed consistency is more compact and requires less electrical energy than a low-consistency system due to the reduced amounts of liquor pumped around. It is, however, also more demanding to control because it operates closer to the critical point of reject thickening. At higher consistency, blinding is favored not only by the increasing population of fibers but also by a reduced backflush through the screen apertures. It has been shown that the intensity of the pressure pulse goes down considerably with increasing pulp feed consistency [13].

The passage ratio decreases as feed consistency goes up [6]. While different opinions exist about the effects of feed consistency on screening efficiency, it is likely that the latter is not significantly affected by the feed consistency [15]. However, a more dilute feed is clearly improving the fractionation efficiency [19].

Several designs of modern washing equipment require feed consistencies between 3% and 4%. If such a piece of equipment is installed downstream of the screen, only higher-end feed consistencies can provide the needed levels of accept consistency. If the accept consistency is not critical, a good compromise between screening efficiency, operability and power consumption for standard screening applications may be found in the feed consistency range of 2.5% to 3.5%, with softwood furnish at the lower end and hardwood furnish at the higher end of the range.

### 6.3.2.4 Temperature

The operating temperature affects the behavior of both liquor and solids. On the one hand, the pulp fibers become more flexible at higher temperatures (see also Section 6.3.3.1), while on the other hand the liquor viscosity decreases with higher temperatures, improving the turbulence in the screening zone. Both of these effects cause the screen capacity to rise [12].

### 6.3.2.5 Rotor Tip Velocity

As described above, the rotor is responsible for creating turbulence, providing the tangential speed of the pulp along the screen plate, and for backflushing the screen by pulsation. A higher tip velocity means a higher turbulence and a more intense pressure pulse at basically unchanged pressure pulse profile. The intensity of the pressure pulse increases with the square of the rotor tip velocity [13]. The recommended operating range of rotors is varying significantly between rotor designs and equipment manufacturers. Common tip speeds are between 10 and 40 m s<sup>-1</sup>.

Increasing the rotor tip speed improves the screen capacity and allows higher feed consistencies, while increasing the power demand of the screen. The power requirement was found to be proportional to the cylinder area and to the tip speed cubed [20]. Within the ranges of velocities recommended by rotor suppliers for their products, the screening and fractionation efficiencies are not notably affected [10,12,15].

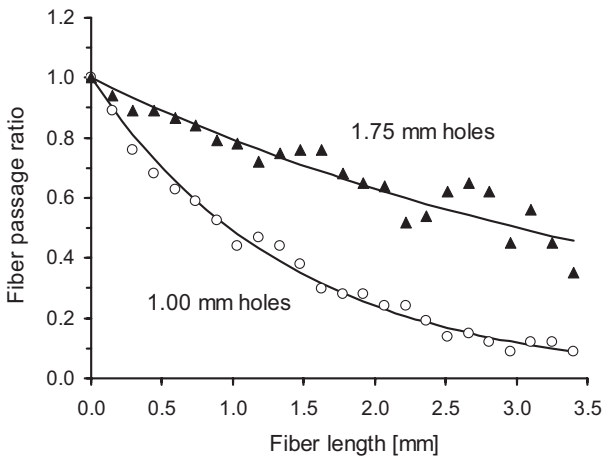
### 6.3.3

#### Furnish Parameters

##### 6.3.3.1 Pulp Fibers

With respect to screening, pulp fibers are characterized by a number of physical properties such as fiber length, fiber flexibility, freeness and disruptive shear stress of the fiber network. Together with the consistency, these properties determine the performance of the furnish in a pressure screen.

The influence of fiber flexibility on passage ratio is secondary to the influence of fiber length. Flexibility plays no role as long as the fibers are shorter than the width of the slot or the diameter of the hole. As the fibers become longer, however, the flexible fibers' passage ratios are higher than those of stiff fibers [2,18]. Note that fiber stiffness is a function of the temperature, with fibers becoming more flexible as the temperature rises. Figure 6.16 exemplifies the fiber passage ratio as a function of the fiber length and hole size.



**Fig. 6.16** Example of fiber passage ratio as a function of the fiber length and hole size; smooth hole screen, bump rotor, softwood thermomechanical pulp (TMP) [8].

Regarding the pulpwood raw material, a distinct difference can be observed between the long softwood and the short hardwood fibers. The capacity of a given slotted pressure screen with hardwood pulp is 20–30% higher than its capacity with softwood pulp.

### 6.3.3.2 Contaminants

The nature of a contaminant decides the preferred technical solution for its removal. The most important contaminant parameters for screening are the contaminant size and shape, and its deformability.

Apparently smaller contaminants require a smaller aperture size to be removed efficiently. Irregularly shaped contaminant can pose a challenge to reasonable screening, as do deformable contaminants or contaminants that break up under shear stress.

A categorization of contaminants and selective ways for their removal are highlighted in Section 6.7.

### 6.3.3.3 Entrained Air

A small or moderate air content usually has no effect on the separation of pulp in pressure screening under typical industrial conditions [16].

## 6.4 Centrifugal Cleaning Theory

### 6.4.1

#### Introduction

Hydrocyclones are gravity separators of relatively simple mechanical design, and have no moving parts. In order to function, they require an internal vortex flow as well as a difference in densities between the liquor and the particles to be separated.

Figure 6.17 shows the streams around a hydrocyclone. The pulp is fed with the feed stream  $Q_F$  at the concentration  $c_F$ . The fraction containing the heavier particles is concentrated in the underflow of the cyclone in the stream  $Q_U$  at the consistency  $c_U$ . The lighter solids are discharged with the overflow stream  $Q_O$ . The underflow is also referred to as “apex flow” and the overflow as “base flow”.

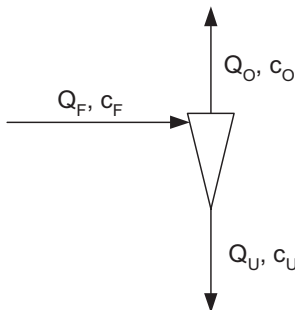
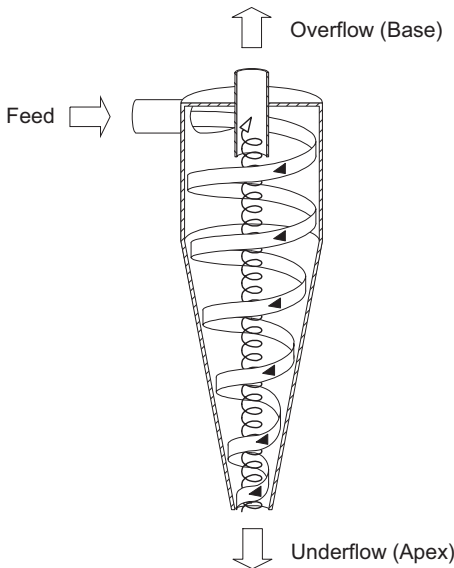


Fig. 6.17 Streams around a hydrocyclone.

## 6.4.2

**Flow Regime**

The gravitational forces which drive the separation in a hydrocyclones are generated as pressure energy is converted into rotational momentum. In the very basic design (see Fig. 6.18), the feed flow enters the cyclone tangentially at the upper end of the cylindrical section and induces a vortex around the axis of the cyclone. As the suspension swirls downward at the perimeter of the cylindrical and conical sections, heavy-weight material is concentrated near the wall and is eventually dragged to the underflow at the apex of the cone. The balance of the liquor together with the light-weight material rotates towards the axis of the cyclone and proceeds to the overflow at the opposite end of the cyclone. The overflow escapes through the vortex finder, a piece of pipe extending into the body of the cyclone which helps to limit the short-circuit flow from the feed inlet to the overflow.



**Fig. 6.18** Flow pattern in a hydrocyclone.

Hydrocyclones develop an air core when one of the outlets discharges into atmosphere. Modern cyclones used in cleaning operate at a backpressure and do not have an air core.

The geometrical form of the hydrocyclone has a major influence on the separation efficiency. While manufacturers have developed different designs mainly based on experience, all of them target at maintaining a largely laminar flow regime.

Unlike pressure screens, hydrocyclones cannot profit from turbulence and the resulting fluidization. They must be operated at low consistencies in order to minimize particle–particle interactions. Both turbulence and higher consistencies will considerably jeopardize the cleaning efficiency.

The tangential velocity profile observed in a cyclone starts with a forced vortex flow at the axis. It then passes into a free vortex flow via a transition zone before the wall effect reduces the velocity to zero again (Fig. 6.19). The axial velocity profile shows the flow towards the apex at the perimeter of the cyclone body and towards the base around the center. The pressure loss in the cyclone is a function of the friction, mainly at the cyclone walls and at the inner wall of the vortex finder.

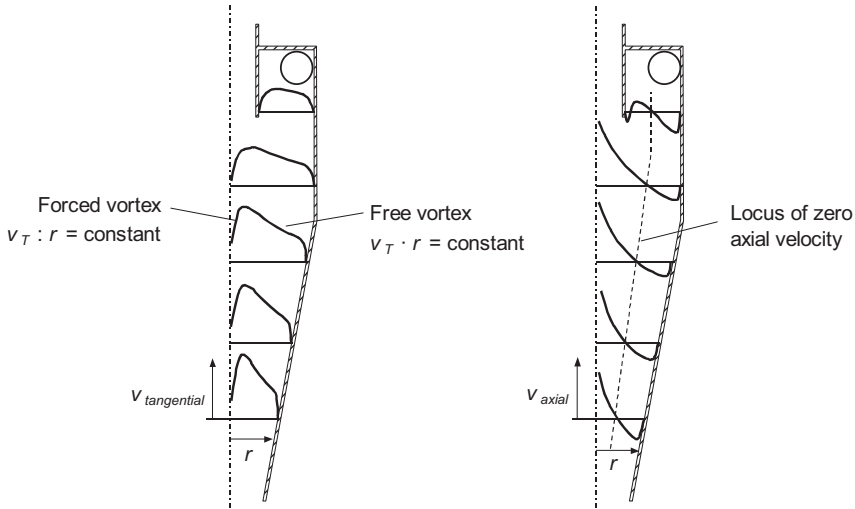


Fig. 6.19 Tangential (left) and axial (right) velocity profiles in a hydrocyclone [21].

### 6.4.3

#### Sedimentation

Let us make some basic considerations about sedimentation to better understand what is happening in a hydrocyclone. A characteristic parameter describing sedimentation is the terminal settling velocity. It describes the state where a particle moves at constant speed under the influence of frictional and gravitational forces. Figure 6.20 shows the main forces which act on a settling particle; these are the weight  $F_w$ , the buoyancy  $F_B$ , and the drag force  $F_D$ .

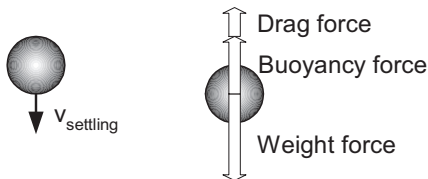


Fig. 6.20 Forces acting on a settling particle.



Weight and buoyancy depend on the specific weight of the particle and the displaced liquor, respectively. The drag force is a function of the particle movement and the particle shape. It is always directed in the opposite direction of the velocity vector. In the Earth's gravitational field, the three forces are defined as follows:

$$F_W = \rho_S V g \quad (12)$$

$$F_B = \rho_L V g \quad (13)$$

$$F_D = c_D A_P \rho_L \frac{v_s^2}{2} \quad (14)$$

where  $\rho_S$  = density of the particle ( $\text{kg m}^{-3}$ );  $\rho_L$  = density of the liquid ( $\text{kg m}^{-3}$ );  $V$  = volume of the particle ( $\text{m}^3$ );  $A_P$  = area of the particle as seen in projection along the direction of motion ( $\text{m}^2$ );  $g$  = acceleration due to gravity ( $9.81 \text{ m s}^{-2}$ );  $c_D$  = drag coefficient; and  $v_s$  = settling velocity ( $\text{m s}^{-1}$ ).

In the steady state, the forces are in equilibrium, which means that

$$F_W - F_B - F_D = 0 \quad (15)$$

Combining Eqs. (12–15) and solving for  $v_s$  yields Newton's law for the terminal settling velocity in the Earth's gravitational field:

$$v_s = \sqrt{\frac{2}{c_D} \frac{(\rho_S - \rho_L)}{\rho_L} \frac{V}{A_P} g} \quad (16)$$

In the special case of a spherical particle with the diameter  $d$  (m), where  $V = d^3\pi/6$  and  $A_P = d^2\pi/4$ , the above expression becomes:

$$v_s = \sqrt{\frac{4}{3c_D} \frac{(\rho_S - \rho_L)}{\rho_L} d g} \quad (17)$$

Note that the settling velocity increases with the density difference between the particle and the liquor and with the particle diameter. The drag coefficient depends on the size and shape of the particle, on the viscosity and density of the fluid, and on the settling velocity itself. When the sphere settles in a creeping, laminar environment, Eq. (17) converts into Stokes' law:

$$v_s = \frac{(\rho_S - \rho_L) d_s^2 g}{18\mu} \quad (18)$$

where  $\mu$  is the dynamic viscosity of the liquid ( $\text{Pa}\cdot\text{s}$ ).

The solids contained in a pulp stream are very different in shape and size. While sand particles may come close to spherical shape, pulp fibers obviously do not. Likewise, there are wide ranges of particle densities from plastics to metals. In addition, the reinforced gravitational field in the cyclone adds complexity to the matter. Consequently, meaningful theoretical models for the settling of solids in a pulp suspension during centrifugal cleaning are not available. We will therefore use the general form of Newton's law, as per Eq. (16), for the qualitative evaluation of separation in a hydrocyclone.

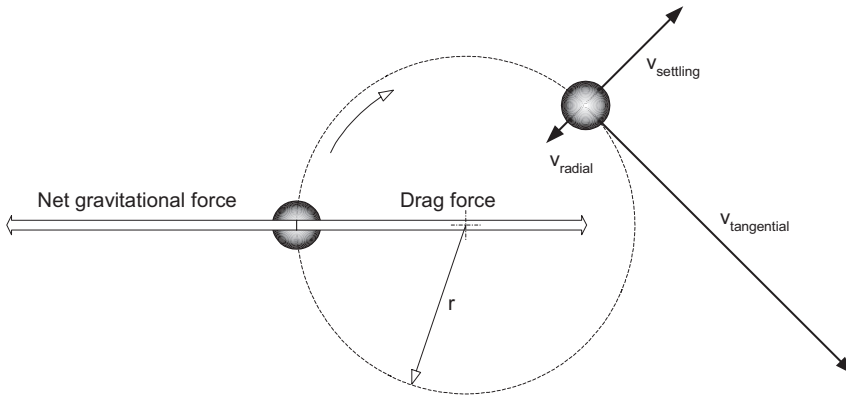


Fig. 6.21 Forces acting on a particle in a hydrocyclone.

So, what is happening to a particle in a hydrocyclone? The tangential feed provokes a tangential liquor velocity which makes the particle move along a circular path around the axis of the cyclone (Fig. 6.21). A radial flow vector describes the transport of the liquor from the feed inlet at the outer perimeter to the central vortex finder. There is also an axial flow vector which is directed towards the apex at the cyclone perimeter and towards the vortex finder around the axis. The forces acting on the particle in a plain perpendicular to the axis are a drag force pointing against the direction of the settling velocity, and gravitational forces as a function of the different solid and liquid densities.

Clearly, the settling velocity must be larger than the radial velocity in the cyclone for a particle to be separated to the underflow. Nevertheless, the tangential velocity represents the most important flow vector in the hydrocyclone because it controls the gravity forces acting on the particle.

The acceleration term is determined by the tangential velocity  $v_T$  ( $\text{m s}^{-1}$ ) and the distance between the particle and the center of rotation,  $r$  (m). When substituting the acceleration due to the Earth's gravity  $g$  by the centripetal acceleration  $v_T^2/r$ , Eq. (16) can be rewritten to give:

$$v_S = v_T \sqrt{\frac{2}{c_D} \frac{(\rho_S - \rho_L)}{\rho_L} \frac{V}{A_p} \frac{1}{r}} \quad (19)$$

Apparently, higher tangential flow velocities  $v_T$  and smaller distances  $r$  increase the settling velocity. This means that a cyclone of a smaller diameter is more efficient for the removal of small particles than a large-diameter cyclone. Likewise, higher tangential flow velocities improve the efficiency. Both the cyclone diameter and the tangential velocity are physically limited by the necessity to maintain the typical laminar flow pattern.

The density difference between the liquid and some particles (e.g., plastics or light-weight wood components) may be very low. This means that high velocities and small radii are needed for cleaning to be efficient. In a typical cleaner, the centrifugal force is so much larger than the Earth's gravity that it does not make any difference whether the cleaner is installed vertically or horizontally.

For the cleaning of pulp, the relevant solids density  $\rho_s$  is the apparent fiber density – that is, the density of the swollen fiber consisting of the liquor-saturated fiber wall and liquor-filled lumen. It has been suggested that for chemical pulp, the influence of the fiber shape on the drag force and consequently on  $c_D$  is not significant [22].

The derivations described above are valid for particles which have a larger density than the fluid. When a particle is lighter than the fluid, its weight becomes smaller than the buoyancy, and the vector for the settling velocity shown in Fig. 6.20 is directed upwards. This is when the particle begins to float to the surface rather than settle to the bottom. Consequently, the drag force points downwards. When then the terminal settling velocity is calculated in analogy to Eq. (19), the solid and liquid densities in the numerator of the density term change place:

$$v_s = v_T \sqrt{\frac{2}{c_D} \frac{(\rho_L - \rho_s)}{\rho_L} \frac{V}{A_p} \frac{1}{r}} \quad (20)$$

So, the separation of light-weight particles to the overflow is controlled by the same factors as the separation of heavy-weight particles to the underflow, the difference being that there is no need to overcome the radial velocity for separation to occur. In theory, this circumstance facilitates the separation of light-weight particles compared to heavy-weight particles. However, in practice the density difference between light-weight material and liquor is often very small, and any support for obtaining a reasonable separation efficiency is welcome.

#### 6.4.4

##### **Underflow Thickening**

In all cleaning operations, pulp fibers are heavier than liquor. Consequently, fibers become concentrated in the underflow of the hydrocyclone. In an analogy to screening, the thickening factor  $T$  is defined by:

$$T = \frac{c_U}{c_F} \quad (21)$$

The underflow thickening depends on the specific design of the cyclone applied, with typical thickening factors ranging between 1.5 and 3.0.

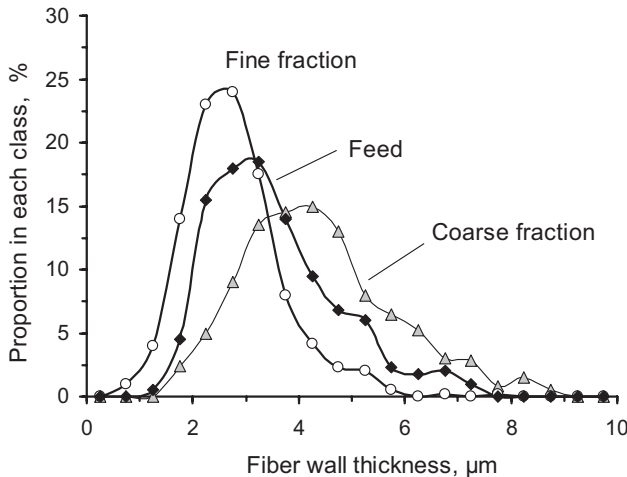
Thickening leads on the one hand to poorer separation when particle–particle interaction hinders the free movement of material to be separated. On the other hand, thickening may cause plugging of the cone which takes the cyclone out of operation. If underflow thickening is of major concern for a certain application, special cyclones with a dilution near the apex can be employed.

#### 6.4.5

#### Selective Separation

As in screening, the selective separation of different types of solids contained in the feed stream is of major importance for all contaminant removal and fractionation applications. As described earlier, separation in a hydrocyclone depends mainly on differences in the particles' densities and specific surfaces. Hence, the selectivity of separation in a contaminant removal application improves with the density difference between debris and pulp.

Likewise, the density difference between individual pulp fibers determines how selectively they can be separated in a cyclone. The apparent density of a pulp fiber results from its diameter and wall thickness. Thick-walled, smaller-diameter fibers (as found in softwood latewood) have a higher apparent density than thin-walled, larger-diameter fibers (as found in softwood earlywood). When pulp is subjected to fractionation in a cyclone, the thick-walled fibers will proceed preferably to the underflow, forming the coarse fraction. Despite their lower apparent density, thin-walled fibers are still heavier than the liquor. They report not only to the overflow (fine fraction) but also to the underflow. It is therefore easier to obtain a relatively pure fine fraction in the overflow than to obtain a pure coarse fraction in the underflow [23].



**Fig. 6.22** Example of fiber wall thickness distributions of feed and fractions after several stages of centrifugal cleaning; bleached softwood kraft pulp [23].

Separation in a hydrocyclone is influenced by a variety of factors such as the complex fiber morphology, particle–particle interactions and short-circuit flows within the cyclone. In practice, separation in a single cyclone is far from ideal, and several stages of cleaning are needed to obtain fractions of significantly different character, such as those illustrated in Fig. 6.22.

## 6.5 Centrifugal Cleaning Parameters

In this subsection, we will review those parameters that affect the operation and determine the performance of a cleaning system, and their qualitative influences on the cleaning efficiency.

These parameters include operating conditions, such as flow rate and pressure drop, feed consistency and temperature. They also include equipment-specific parameters, mainly the cyclone diameter. In addition, we need to observe the furnish characteristics of both the pulp fibers and the contaminants.

Some of the above parameters can be adjusted, but some are intrinsic to a special process step or piece of equipment. The chosen combination of adjustable cleaning parameters depends on the individual requirements of the application, and is usually a compromise within performance limits and operating constraints, because the optimization of single parameters often leads in opposite directions.

Due to the complexity of the involved mechanisms and the fact that system design is usually based on rules of thumb with supportive testing, the discussion of parameters below is of qualitative nature only.

### 6.5.1 Cyclone Parameters

Since there are no moving parts, the performance of a hydrocyclone is determined by its geometry. Design details vary between cyclone manufacturers and target, for instance, at the minimization of the short-circuit flow from the feed to the overflow, at lower or higher reject thickening, or at the prevention of cone plugging.

The major parameter affecting cleaning efficiency is the cyclone diameter. At a given pressure drop, cyclones of smaller diameter generate higher centrifugal forces, but they also process lower flow rates. Hence, the cyclone size is subject to an economical restriction given by the number of units to be installed for handling a particular production capacity. Smaller units are also more sensitive to plugging due to the small diameter of the underflow opening.

## 6.5.2

### Operating Parameters

#### 6.5.2.1 Flow Rate and Pressure Drop

A higher pressure drop, which is a synonym for an increased flow rate and a higher tangential flow velocity, improves the separation efficiency. Care must be taken not to increase the tangential velocity beyond a point where turbulence occurs. Since turbulence destroys the controlled flow pattern in the cyclone, it is highly unwelcome in cleaning and must be avoided. In addition, the pressure drop influences the operating costs of centrifugal separation, which are mainly determined by the pumping energy required to overcome the pressure drop.

#### 6.5.2.2 Feed Consistency

In order to limit flocculation, hydrocyclones are normally operated below about 0.6% feed consistency. An increase in feed consistency above this level leads to reduced cleaning efficiency.

#### 6.5.2.3 Temperature

Higher temperatures can have a positive effect on the cleaning efficiency due to the reduced liquid viscosity. The maximum operating temperature of a pressurized hydrocyclone is limited to 70–80 °C.

## 6.5.3

### Furnish Parameters

#### 6.5.3.1 Pulp Fibers

With respect to cleaning, pulp fibers are characterized mainly by their density, surface texture, size, freeness and disruptive shear stress of the fiber network. Together with the consistency, these properties determine the performance of the furnish in a hydrocyclone.

The main parameter affecting separation is the apparent density of the fiber. Depending on the nature of the furnish, this can mean that fibers are separated according to wall thickness or coarseness. At the same fiber diameter, fibers with thicker walls tend to be rejected to the underflow. At the same coarseness, fibers with smaller diameter tend to be rejected. With regard to size, larger fibers and fiber bundles go to the underflow. The influence of length alone is inferior to the influences of other fiber properties [24].

Compared to a nonfibrillated fiber, a fibrillated fiber exposes a larger specific surface area which offers more resistance to the relative flow in the gravity field of the cyclone. The larger the resulting drag force, the more likely the fibrillated fiber reports to the overflow.

### 6.5.3.2 Contaminants

The nature of a contaminant decides the preferred technical solution for its removal. The most important contaminant parameters for cleaning are the contaminant density and the contaminant shape.

Contaminants with densities that deviate far from the apparent fiber density are easier to remove. Irregularly shaped contaminants can pose a challenge to cleaning due to their inherently higher drag forces. Large contaminants may plug the underflow of the cyclone.

A categorization of contaminants and selective ways for their removal are discussed in Section 6.7.

## 6.6

### Separation Efficiency

A variety of parameters are being used to describe the separation efficiency of screening and cleaning operations. While overall parameters are usually sufficient for characterizing the separation of impurities, a more refined approach becomes appropriate especially for the purposes of fractionation.

#### 6.6.1

##### Screening and Cleaning Efficiency

The very basic definition of the separation efficiency  $E$  is

$$E = \frac{\text{amount of debris in reject}}{\text{amount of debris in feed}} \quad (22)$$

Traditionally, this equation is employed generally for screens and more or less exclusively for cleaners. There are some limitations to Eq. (22), however.  $E$  turns unity when all debris is rejected, irrespective of the reject ratio. Likewise, the operation of merely splitting a feed flow by a plain pipe tee yields a separation efficiency larger than zero. In total,  $E$  disregards the good fiber loss with debris in the reject stream.

The efficiency of a screen is usually plotted against the reject ratio due to its overwhelming influence on the efficiency. Nelson has introduced a screen performance parameter, the screening quotient  $Q$ , which can be easily determined by just two analyses [25]:

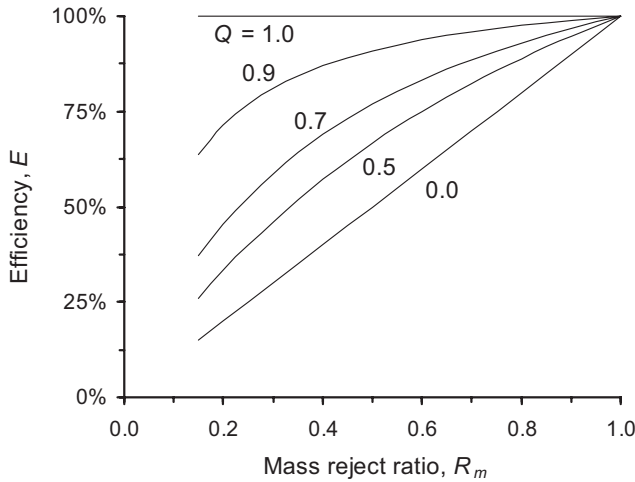
$$Q = 1 - \frac{c_{d,A}}{c_{d,R}} \quad (23)$$

where  $c_{d,R}$  = mass concentration of debris in oven-dry reject ( $\text{kg kg}^{-1}$ ); and  $c_{d,A}$  = mass concentration of debris in oven-dry accept ( $\text{kg kg}^{-1}$ ).

The screening quotient becomes zero for the pipe tee, and unity for ideal separation. When applied to measurements from a given screen,  $Q$  was found to vary only insignificantly over the range of industrially practiced reject ratios. Under consideration of the mass balance over the screen, the screening efficiency is obtained by:

$$E = \frac{R_m}{1 - Q(1 - R_m)} \quad (24)$$

where  $R_m$  is the mass reject ratio – that is, the oven-dry reject mass divided by the oven-dry feed mass. Figure 6.23 shows the screening efficiencies calculated for different values of  $Q$  over the mass reject ratio. Since the performance of a given screen is characterized by a particular  $Q$ , the screen's operating point will, in theory, move along a curve of constant  $Q$ . Typical values of  $Q$  for shives are 0.9 and larger.



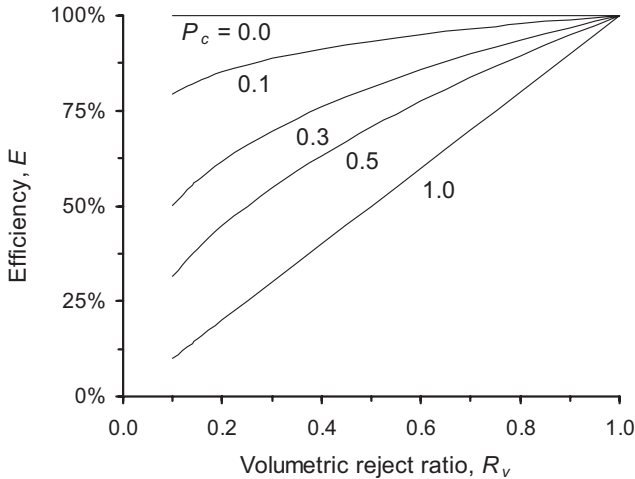
**Fig. 6.23** Screening efficiency as a function of the mass reject ratio and screening quotient  $Q$ .

Using their plug-flow model, Gooding and Kerekes [1] have derived the screening efficiency by combining Eqs. (5) and (22):

$$E = R_v^P P_c \quad (25)$$

where  $R_v$  and  $P_c$  are the volumetric reject ratio and passage ratio of the contaminants, respectively. Figure 6.24 illustrates screening efficiencies calculated for different values of  $P_c$  over the volumetric reject ratio. Again, the performance of a given screen is characterized by a particular  $P_c$ , and the screen's operating point will move, in theory, along a curve of constant  $P_c$ . Typical values of  $P_c$  for shives are 0.1 and smaller.





**Fig. 6.24** Screening efficiency as a function of the volumetric reject ratio and debris passage ratio  $P_c$ .

When comparing Fig. 6.23 with Fig. 6.24, the constant- $Q$  curves expose a steeper inclination at low reject ratios than the constant- $P_c$  curves. This holds true even after correction between mass reject ratio and volumetric reject ratio. The superiority of the plug-flow model over the mixed flow model suggests that Eq. (25) is more appropriate to describe a screen's performance than Eq. (24) [10].

It must be remembered that all efficiencies calculated from Eqs. (22), (24) and (25) above are actually contaminant-removal efficiencies. Each of these becomes 100% when the reject ratio is unity – a case which is of no industrial relevance. Clearly, the economy demands that the amount of good fibers lost with the reject from a separator is kept at a minimum. Therefore, any contaminant removal efficiency calculated as per these equations must always be evaluated in conjunction with the loss of good fibers.

## 6.6.2

### Fractionation Efficiency

#### 6.6.2.1 Removal Efficiency

In the basic case, the screening yield can be adopted for the purposes of fractionation. The fiber removal function  $e(l)$  is defined as the mass of fibers with length in the interval  $[l, l+dl]$  in the reject stream divided by the mass of fibers with the same length in the feed [26]:

$$e(l) = \frac{Q_R c_R(l)}{Q_F c_F(l)} \quad (26)$$

where  $c_R(l)$  and  $c_F(l)$  are the concentrations of the fibers with length in the interval  $[l, l+dl]$  in the reject and feed streams, respectively. Assuming a plug-flow model and constant passage ratio, this expression can be rewritten using Eq. (5):

$$e(l) = R_V^{P(l)} \quad (27)$$

While the fractionation objective above is determined by fiber length, other pulp parameters, such as wall thickness, freeness or coarseness, may be assessed similarly. In a more general form, the yield of a fiber fraction can be defined for either the accept or the reject stream, with the selection depending on which stream is of interest [11]. Then, the fractionation yield,  $Y$ , for any property of interest is defined by:

$$Y = \frac{Q_{\text{Stream of interest}} c_{\text{Stream of interest}}(\text{Property of interest})}{Q_F c_F(\text{Property of interest})} \quad (28)$$

#### 6.6.2.2 Fractionation Index

In most fractionation applications it is important to remove as high a portion of the one fraction while removing as little a portion as possible from the other fraction. Therefore, the quality of the fractionation is characterized by the removal functions of both fractions.

This can be quantified by the introduction of a fiber fractionation index,  $\Phi$ . In case of length-based fractionation,  $\Phi$  is defined as the average  $e(l)$  for long fibers,  $E_L$ , minus the average  $e(l)$  for short fibers,  $E_S$  [9]:

$$\Phi = E_L - E_S \quad (29)$$

where  $E_L$  is basically the long fiber removal and  $E_S$  is the short fiber loss. Unlike removal efficiency, the fractionation index is penalized by removal of the fraction which ought to be accepted, in the above case by the fraction of short fibers.  $\Phi = 1$  applies when the reject stream is composed only of long fibers and the accept stream is composed only of short fibers – that is, perfect separation. In addition,  $\Phi = 0$  means that the fiber length distribution remains unchanged – that is, no separation.

The fractionation index increases as the hole size is reduced below the targeted marginal fiber length, but deteriorates again as the hole size becomes smaller than about half the marginal fiber length [9]. At similar reject thickening, the fractionation index is almost twice as high for holed screen plates as for slotted ones [8].

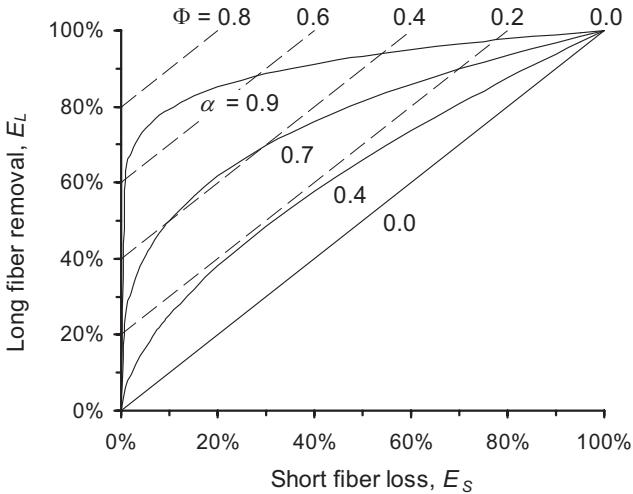
The plug-flow model delivers a fractionation parameter  $\alpha$  which is defined in terms of the passage ratios of long fibers,  $P_L$ , and short fibers,  $P_S$  [10]:

$$\alpha = 1 - \frac{P_L}{P_S} \quad (30)$$

Since the passage ratios are independent of the reject ratio,  $\alpha$  reflects the performance of a specific screen and can be used to anticipate the effect of changes in reject ratio. Applying Eq. (25) to long and short fibers and eliminating  $R_p$  yields

$$E_L = E_S^{1-\alpha} \quad (31)$$

Both the fractionation index and fractionation parameter are plotted within the field of long fiber removal versus short fiber loss in Fig. 6.25. The solid lines calculated for different values of  $\alpha$  represent the curves on which a screen's operating point will move. For a given screen, the optimum point for fractionation lies where the constant- $\alpha$  curve is tangent to a line of constant fractionation index. Typical values of  $\alpha$  are in the range of 0.4 to 0.7 [10].



**Fig. 6.25** Screen operating curves (solid lines of constant  $\alpha$ ) and fractionation index (dashed lines of constant  $\Phi$ ) plotted in a field of long fiber removal versus short fiber loss [10].

## 6.7 Screening and Cleaning Applications

### 6.7.1 Selective Contaminant Removal

The selective removal of solid pulp impurities is by far the predominant application of screening and cleaning in the production of chemical pulp. An overview over the most common contaminants and their removal is provided below.

#### 6.7.1.1 Knots

Typically, knots represent the largest fraction of impurities in the pulp coming from the digester. Knots originate from the dense sections of branches and heartwood, as well as from oversized chips which have not been cooked down to their center. Knots are rather large in size and of dark color. They can cause the failure of downstream equipment in the pulp mill if they are not efficiently removed from the pulp.

Thus, knot removal (knotting) is normally carried out before washing. Knot separation from the main stream of pulp is performed in a pressure screen. The separated knots are then subjected to removal of good fibers in a secondary, atmospheric screen. Both operations are governed by a barrier screening mechanism.

#### 6.7.1.2 Shives

Shives are smaller impurities consisting of fiber bundles from incompletely cooked wood. Their removal during screening is more difficult than that of knots. Shives cause operational problems on the paper machine. In contrast to knots, shives are mostly bleachable, but they consume higher amounts of bleaching chemicals and may still remain of darker color than the bulk of the pulp after bleaching.

Shives should be removed before bleaching. Shive separation is carried out in a system consisting of a number of pressure screens. Whether shive removal follows barrier or probability screening depends on the aperture size of the screens. As the use of very narrow slotted screens becomes common, shives tend to be removed increasingly by the barrier principle.

#### 6.7.1.3 Bark

Bark originating from incomplete debarking of the wood represents one of the most challenging impurities. Bark is of dark color, has a similar density as wood, and disintegrates easily.

There is normally no dedicated process for the removal of bark from pulp, but the primary removal of bark should take place in the woodyard before chipping. The remaining bark is removed from the pulp, together with other contaminants during the course of screening and cleaning.

#### 6.7.1.4 Sand and Stones

Sand and stones mainly come along with the wood chips, but may originate also from tiling or concrete tanks. Rocky material can cause equipment failure and is responsible for the wearing of equipment. The removal of stones and sand is therefore best carried out as soon as possible in the fiberline.

Larger stones can be separated from the pulp by screening. Cleaning takes care of any type of rocky material including sand. When narrow slotted screens are used in a screening application, sand is rejected on a barrier principle and carried through the subsequent screening stages. Special precautions must be taken in such a case to minimize wear in the system caused by sand accumulation.

#### 6.7.1.5 Metals and Plastics

Metals and plastic can enter the fiberline with the wood, they may break away from equipment, or they may enter the process accidentally. Like stones, metals can cause the breakdown of equipment and must be removed to protect sensitive machinery. Plastic contaminants adversely affect the quality of the final product by causing operational problems in paper-making.

Because of the large density difference, metals can be easily separated from pulp by centrifugal cleaning. Plastics are generally more difficult to remove, but as certain types of plastic are less dense than pulp they can sometimes be separated by reverse centrifugal cleaning.

### 6.7.2

#### Fractionation

Fiber fractionation generally follows the probability mechanism of separation. Despite the limitations placed on fractionation efficiency by currently available screening and cleaning equipment, fractionation applications are gaining increasing attention and the prospects of value-added, tailor-made fibers have stimulated the imagination of product developers.

With regard to paper-making properties, pulps containing long and thick-walled fibers generally produce a higher tear index. Pulps with thin-walled fibers, and those containing fines, have better optical properties, higher tensile strength, internal bond strength, elongation and density [23,27].

The different fractions can be separately refined or treated otherwise, and may then be recombined, or not. A market pulp producer with two dewatering machines may fractionate his pulp to increase the long fiber content of the furnish sent to one machine in order to produce a high-value reinforced pulp. A paper producer with a multi-layer headbox may direct the shorter fibers to the surface layers to improve sheet smoothness and optical properties, while placing the longer fibers in the core to provide strength [10]. Besides strength, fiber fractionation can also substantially improve the porosity of a pulp by removing the short fibers and fines that reduce porosity [28].

In total, the fractionation of pulp creates a multitude of new opportunities for the alternative utilization of the fiber raw material. Nevertheless, fractionation is practicable only in mills which can make use of all the obtained fractions.

## 6.8

### Systems for Contaminant Removal and Fractionation

#### 6.8.1

##### Basic System Design Principles

We have seen above that there are various purposes for operating a screening or cleaning system. While fractionation is of increasing interest, most applications

still target the removal of large, heavy-weight, or light-weight contaminants. There is a fundamental difference between contaminant removal and fractionation with respect to the amount of material to be separated. After fractionation, the smaller pulp fraction is seldom less than 20% of the pulp in the feed stream. In contrast, the contaminants to be removed during screening or cleaning are typically no more than 3% of the feed stream pulp.

Both contaminant removal and fractionation are subject to the condition that the rejected portion contains only a minimum of the acceptable portion. Modern screening and cleaning equipment removes unwanted matter quite efficiently from the feed stream and produces an accept stream of high purity. In order to achieve this, the reject stream must contain a relatively large amount of acceptable material in addition to the matter to be rejected.

In a contaminant-removal system, economic reasons call for the minimization of good fibers lost with the removed contaminants. Such systems usually consist of a number of separators which can be operated in different arrangements. On the one hand, contaminant removal is usually most efficient in a cascade feedback arrangement. On the other hand, generally accepted rules for designing fractionation systems are yet to be developed. In fact, it is uncertain if such rules will ever exist, as fractionation tasks are custom-designed for a particular application.

In many cases, the design of separation systems is based on experience and rules of thumb, because the interrelation of equipment, operating and pulp furnish parameters is not yet fully understood. The resulting systems are often safe to operate, but do not necessarily represent the best process solution and economy.

Screening and cleaning systems tend generally to be complex because of the large number of design and operating parameters. Their function is challenged by the circumstance that the optimum performance of the system is typically achieved with equipment working near its point of failure (i.e., plugging). As mechanistic models are further developed, the basic understanding of effects on screen capacity, reject thickening and screening efficiency will improve. Computer simulation provides valuable support in this respect [19,29].

In the following sections we will examine some common systems for contaminant removal, as well as a few potential fractionation systems. However, before doing this it may be appropriate to highlight some general aspects regarding the design of separation systems.

Slotted screen baskets are quite susceptible to damage by junk material such as metal bolts or rocks. A damaged screen basket leads to inferior screening efficiency and requires costly replacement. Therefore, it has proven advantageous to protect slotted screens from junk by the installation of an upstream perforated screen. A protective screen is also highly recommended for cleaning systems to avoid damage or blocking of hydrocyclone cones. When the amount of junk material is low, protective screens can be operated with intermittent reject discharge.

As a result of reject thickening, industrial separation techniques involve dilution at various points, both in the form of internal dilution to the equipment and in the form of dilution between stages. The objective of dilution is first, to avoid

plugging at the reject outlet and second, to adjust the feed consistency between stages. It should be noted that most of the illustrations in this chapter lack such dilution streams in order to avoid unnecessary complexity.

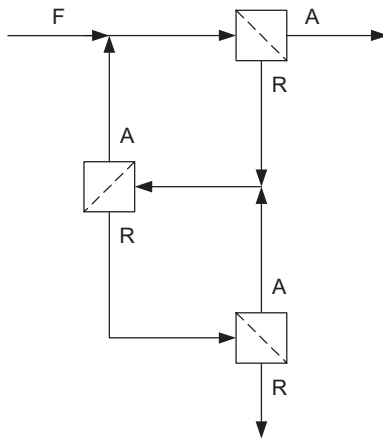
## 6.8.2

### Systems for Contaminant Removal

#### 6.8.2.1 Arrangement

As mentioned above, the contaminant level in chemical pulp is far below the mass reject ratio of industrial separation equipment. Consequently, a large portion of acceptable fibers can be found in the reject of a single separator, together with the contaminants. Economical constraints of pulping, however, require that undesirable contaminants taken from the screening system carry along as few good fibers as possible.

Hence, it is common to use a combination of separators, where, for instance, a second screen is used to reduce the amount of good fibers in the reject of the first screen, and a third screen to remove good fibers in the reject of the second one. Such a simple cascade arrangement is shown in Fig. 6.26.



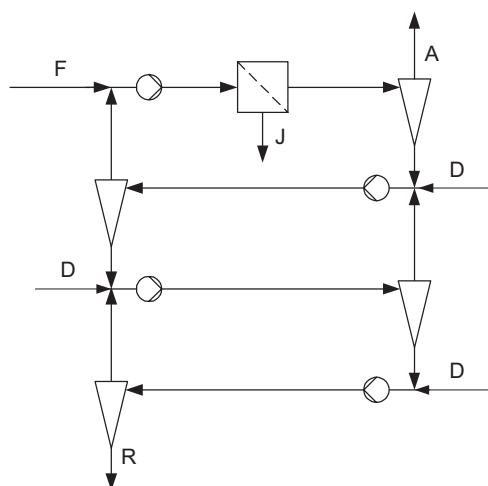
**Fig. 6.26** Three-stage screening in cascade feedback arrangement. F = Feed; A = Accept; R = Reject.

In a cascade system, the reject from one screen passes on to the feed of the screen in the next stage. In a cascade *feedback* arrangement, only the accept of the first stage proceeds to the downstream step in the pulp production process, while the accepts of the other stages are in each case brought back to the feed of the preceding stage (Fig. 6.26).

It should be noted that, in a cascade feedback screening system, sand accumulation can lead to substantial wear and to the need for frequent exchange of screen baskets. As screen slots become narrower, an increasing portion of the sand com-

ing with the feed to the first screening stage is rejected. If the following stages have screens of similar aperture size, the repeated rejection of sand effects a relative increase in the sand concentration in the reject of each stage. If one of the following stages has a screen of larger aperture size, sand may be accepted by this screen and flow back to the preceding stage, where it is rejected again. Both of these phenomena are inherent to screening systems operating with narrow slots. Depending on the sand contamination of the pulp furnish, the installation of special sand cleaners in between stages may be required to reduce the accumulation of sand in the system.

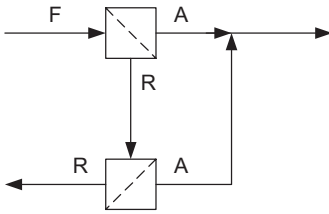
Similar to pressure screening systems, hydrocyclones are normally arranged in feedback cascades (Fig. 6.27). At four to five stages, cleaning systems often have more stages than screening systems with two to four. This is stimulated by a lower quantity of contaminants in the feed of cleaning systems and more difficult separation tasks.



**Fig. 6.27** Four-stage cleaning in cascade feedback arrangement preceded by protecting pressure screen. F = System feed; J = Junk; A = System accept; R = System reject; D = Dilution.

In a cascade *feed-forward* scenario, accepts from other stages are mixed with the primary accept. Figure 6.28 illustrates a simple two-stage feed-forward system, which is common for the barrier screening application of knot removal. The secondary screen of the knot removal system is usually a piece of equipment which combines several unit operations, including screening, washing and dewatering.



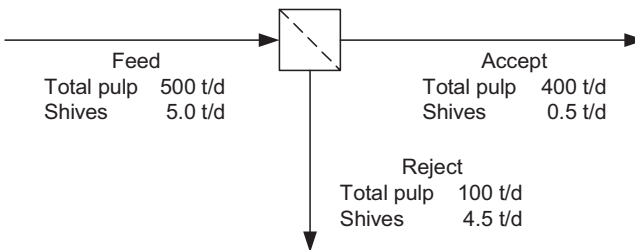


**Fig. 6.28** Two-stage screening in cascade feed forward arrangement. F = Feed; A = Accept; R = Reject.

In a cascade feed-forward system for shive removal, the reject from the secondary screen could be treated in a refiner, after which the accepts of the tertiary screen could be combined with the accepts of the primary screen, while the rejects of the tertiary screen go back to the refiner. However, the quality requirements of chemical pulps do not, in most cases, allow feed-forward operation of shive screening and, in some cases, not even reject refining.

### 6.8.2.2 Fiber Loss *versus* Efficiency

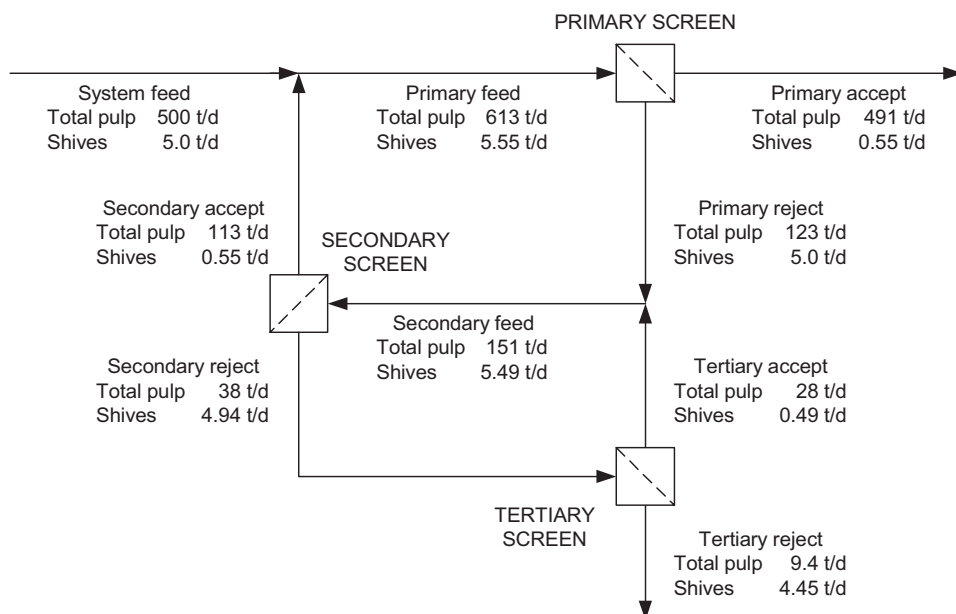
For an exemplary shive screening application where an incoming pulp contains 1% of shives, Fig. 6.29 shows the mass balance for pulp over a single screen, assuming a 20% mass reject rate and a 90% shive removal efficiency. The reject stream contains a huge amount of good fibers (in fact 95% of the rejected pulp) and almost one-fifth of the good fibers from the feed pulp are lost to the reject.



**Fig. 6.29** Mass balance for single screen; 20% mass reject rate, 90% shive removal efficiency.

Keeping the same assumptions (i.e., 20% mass reject rate and 90% shive removal efficiency in the primary screen), we can consider a three-stage screening system operated in cascade feedback mode (Fig. 6.30). Due to the repeated screening action, the amount of good fibers in the system reject is reduced to 1% of the feed pulp. In general, the good fiber loss can be reduced by adding another screening stage or by decreasing the reject ratio. However, the flow regime in the pressure screen places a physical limit on both the reject ratio and the number of stages in a multi-stage screening system. That is why there is a minimum loss of

good fibers with the system reject from the last stage of a pressure screening cascade. When the economic feasibility of equipment and operating costs versus the loss of good fibers is taken into consideration, the number of stages in a screening system for shive removal is typically three or four. As an indication, the related loss of good fibers in everyday operation seldom falls below the amount of rejected shives.



**Fig. 6.30** Mass balance for three-stage feedback cascade; 20% primary mass reject rate, 25% secondary and tertiary mass reject rates, 90% shive removal efficiency in each screen.

When comparing the single-stage and three-stage screening balances depicted in Figs. 6.29 and 6.30, another observation relates to the screening efficiency. Due to the internal circulation within the three-stage system, the accepted pulp contains 10% more shives than the accept from the single-screen case. It should be noted that multi-stage screening helps to minimize the loss of good fibers but at the same time reduces the screening efficiency.

### 6.8.3

#### Systems for Fractionation

The wide range of tasks achievable by fractionation has been repeatedly indicated above. Because of the specialty of each case, general design principles for the fractionation of chemical pulps are not yet established. Thus, the information in this subsection is restricted to some general comments.

The flow rates of the different fractions are defined by the particular application, and a low reject ratio is not necessarily part of the fractionation requirements. It may be advantageous to perform fractionation in a multi-stage system. In contrast to contaminant removal, the efficiency of fractionation can be improved by multi-stage systems. Two simple fractionation systems using screens are illustrated in Fig. 6.31.

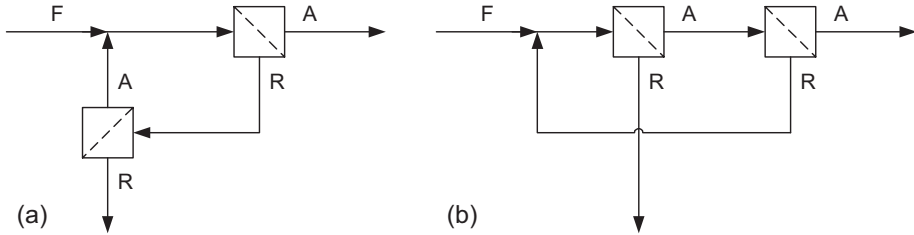


Fig. 6.31 Two-stage fractionation systems with feedback (a) cascade and (b) series.

Remember that holed screens fractionate better than slotted ones. While feedback is clearly important for obtaining a higher fractionation efficiency, it has been shown that both cascade and series arrangements may yield similar fractionation results at a given mass reject rate [19]. According to the example shown in Fig. 6.32, the best achievable fractionation occurs between about 30% and 60% mass reject ratio. Note that the location of the fractionation index peak shifts along the mass reject ratio axis dependent on of the relative amount of fractions of interest in the feed pulp.

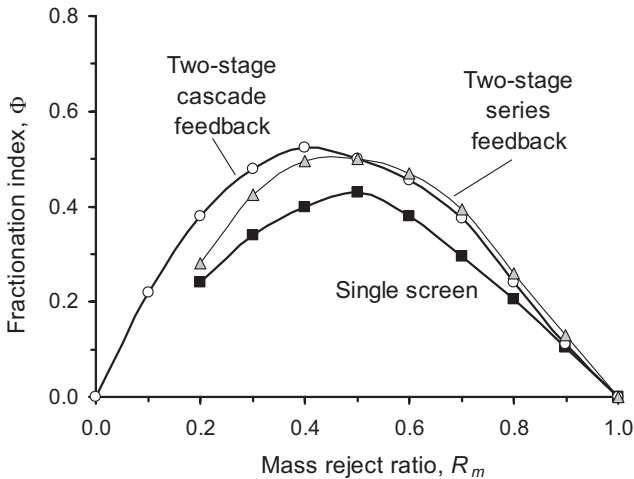


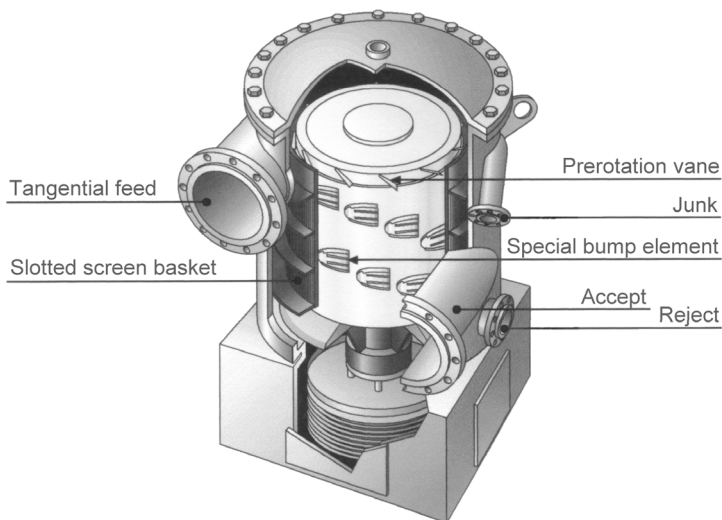
Fig. 6.32 Fractionation index as a function of the mass reject ratio for single-stage and two-stage fractionation with holed screens; length-based fractionation, simulation results [19].

## 6.9 Screening and Cleaning Equipment

There is an abundance of different types of commercial separation equipment, most of which are available as several variants. Some examples of more recent design are detailed in the following section.

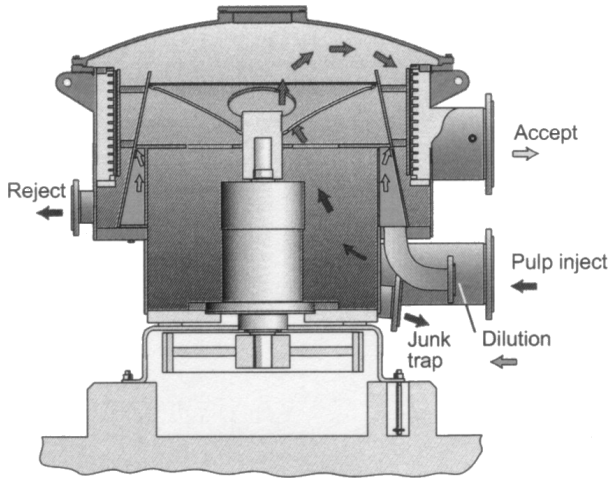
### 6.9.1 Pressure Screens

In the Impco HI-Q Fine Screen, the pulp feed enters the unit tangentially in the upper section. Heavy contaminants separate centrifugally into the junk trap. Then, as the pulp suspension enters the screening zone, prerotation vanes increase its tangential velocity to improve screening efficiency. The accept passes through the screen apertures, which are kept clean by pulsation provoked by the special bump elements attached to the closed rotor. The reject proceeds to the bottom of the screen where it is diluted and discharged through the reject nozzle [30].



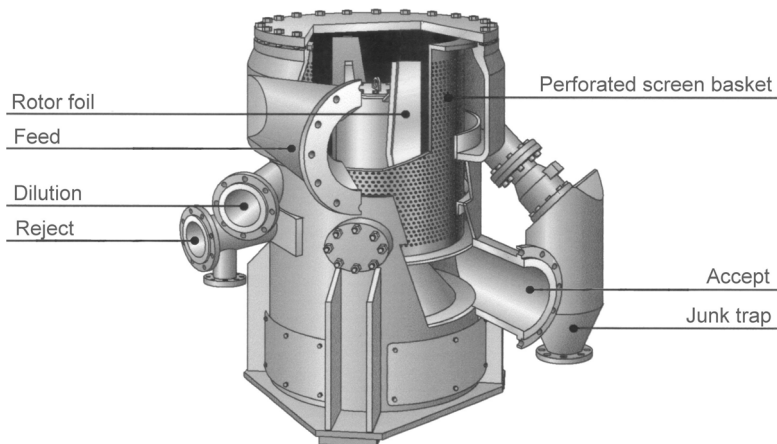
**Fig. 6.33** The GL&V Impco HI-Q Fine Screen [30].

In Metso's DeltaScreen, the pulp suspension is fed tangentially into the bottom part of the unit, where the heavy debris is trapped and can be removed through the junk nozzle. The pulp proceeds upwards through the rotor to the screening zone. The screening process takes place as the pulp moves downwards between the foil rotor and the fixed screen basket. As with some other pressure screens, the DeltaScreen can be equipped with a cyclone-type separator on top of the machine, which offers the possibility for removal of light-weight contaminants [31].



**Fig. 6.34** The Metso DeltaScreen [31].

In the Impco HI-Q Knotter, the pulp feed enters the unit tangentially in the upper section. Heavy contaminants are separated centrifugally into the junk trap. The accept passes from the outside of the screen through the screen apertures to the inside and proceeds to the accept nozzle at the bottom of the screen. Hydro-foils rotating at the accept side provide the pressure pulses which keep the screen apertures open. At the same time, the rotor action does not break up the knots. On the reject side outside the screen basket, the knots are diluted and washed as they proceed downwards to the reject nozzle [32].



**Fig. 6.35** The GL&V Impco HI-Q knotter [32].

Metso's DeltaCombi is a combined knotter and fine screen that operates in similar fashion to the DeltaScreen. In the lower section, the screen is equipped with an additional rotating screen basket with holes for knotting. The feed pulp must first pass this coarse screen basket from the outside to the inside. The pulse-generating stationary foils of the knotting section are located on the accept side of the screen basket. The coarse reject is taken out from the bottom part. The accept which has passed the coarse screen basket is led upwards through the rotor of the fine screen, and then enters the fine screening section between the foil rotor and stationary fine screen basket [33].

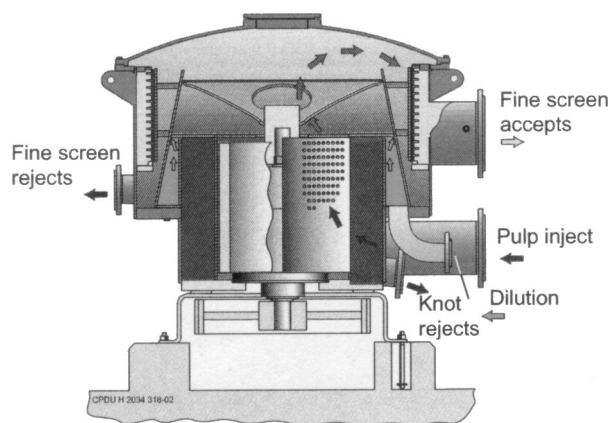
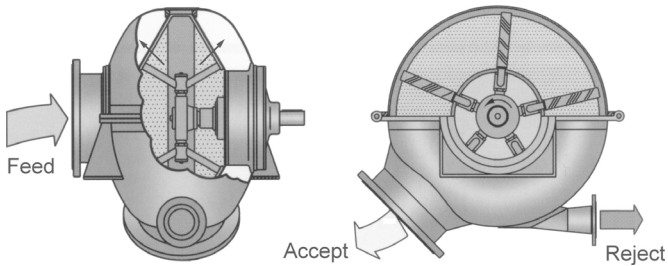


Fig. 6.36 The Metso DeltaCombi [33].

The Noss Radiscreen features a different design, with the pulp feed entering the unit in an axial direction. Accepted fibers pass through the two conical screens plates fixed in the housing, while the reject proceeds to the reject nozzle at the housing perimeter. As the rotor vanes pass along the screen plates, their peripheral velocity increases by the radius towards the reject end of the screen plates, and this leads to increased turbulence in the critical zone of higher consistency. Radiscreens are available with perforated screens for both knotting and screening applications. Their design does not require internal dilution, and features a comparatively small pressure drop and low power consumption [34].

The abundance of screen designs makes it impossible to present all variations offered by screen suppliers in this book. Tailor-made solutions are available for special applications, with recent developments including, for example, screen baskets with intermediate dilution [35] or intermediate deflocculation [36] half-way down the screen basket to reduce the effects of reject thickening, or different surface profiling along the length of the screen basket providing increased turbulence towards the reject end of the screening zone [37].



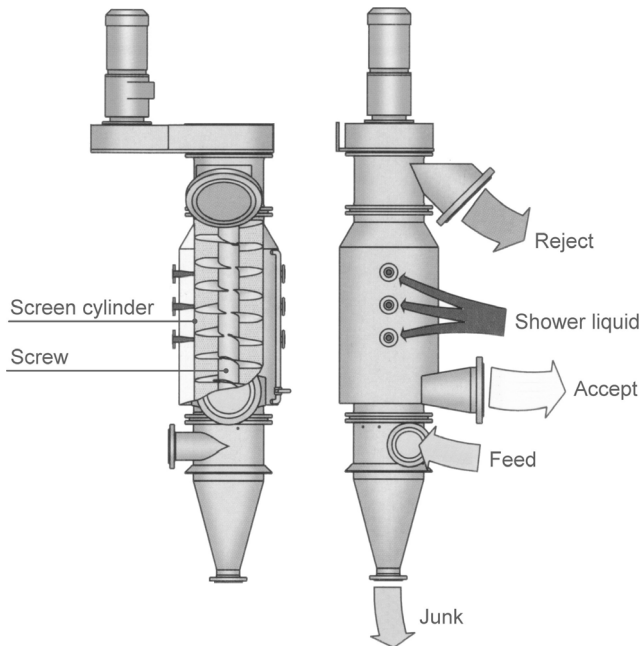
**Fig. 6.37** The Noss Radiscreen [34].

## 6.9.2

### Atmospheric Screens

#### 6.9.2.1 Secondary Knot Screens

Secondary knot screening is a barrier screening application targeted at the recovery of good fibers from the knot stream coming from the primary knotter. Modern secondary knot screens are equipped with a screw rotating inside a vertical or inclined perforated screen cylinder. The pulp feed enters the screen near the bottom. As the knots are transported upwards by the screw, accepted fibers pass



**Fig. 6.38** The Noss Raditrim [38].

through the screen apertures to the annular accept chamber. Shower liquid is added to the knots, and assists separation by washing good fibers from the knots to the accept side. A certain liquor level is maintained inside the screen, and after the knots emerge from the liquor they dewater by gravity before being discharged through the reject nozzle. The enclosed design of such secondary knot screens avoids emissions to atmosphere.

The Noss Raditrim is an example of a vertical atmospheric knot screen (Fig. 6.38). In line with other manufacturers' screen designs, shower liquid is introduced into the lower end of the screw shaft and becomes distributed through holes in the shaft.

Secondary knot screens are typically fed with an inlet consistency between 1.0% and 1.5%, and deliver knots at a consistency of 25–30%. The amount of good fibers carried along with the knots is in the range of 10% of the total reject.

#### 6.9.2.2 Vibratory Screens

The number of vibratory screens in use in the pulp industry is continuously diminishing. This may be due to the fact that vibratory screening is connected to a number of drawbacks, such as the unsuitability for fully automated control, the rather dilute accept consistency, and the mostly uncovered design impairing vent collection. However, if operated in the last stage of screening, the vibratory screen has the advantage of delivering a reject stream which contains only a minor amount of acceptable fibers.

### 6.9.3

#### Hydrocyclones

Since efficient centrifugal cleaning requires low pulp consistency and small-sized hydrocyclones, a large number of units is required to deal with the considerable flow rates. This has formerly resulted in long rows of cleaners with atmospheric reject discharge. Today, the established arrangement of large numbers of pressurized hydrocyclones is in canisters.

Figure 6.39 shows a Noss Radiclone, where the hydrocyclones are installed radially in a pressurized cylindrical canister with vertical axis. Depending on the cleaning capacity, one canister can hold several hundred cyclones. The feed enters the canister centrally from the bottom and the pulp flows to the individual hydrocyclones, where the separation takes place. The rejects and accepts from the individual cyclones are then collected in separate compartments and leave the canister through nozzles at the bottom. Typical cyclone diameters range from 80 to 125 mm. The pressure drop from the feed side to the accept side is between 1 and 2 bar [39]. In order to reduce the fiber loss from the last stage of cleaning, hydrocyclones can be equipped with apex dilution.

The above-mentioned type of hydrocyclone used for the separation of heavy-weight particles is also called a *forward* cyclone. Cleaners for the separation of light-weight contaminants are often termed *reverse* cyclones, accounting for the



inversion of accept and reject positions. Reverse cleaners can also be arranged in canisters. The flow pattern in such canisters is similar to that illustrated in Fig. 6.39, but the dimensions of the flow channels are adapted to the comparatively larger apex flow rate and smaller base flow rate. In contrast to forward cyclones, reverse cleaners do not thicken the reject, but lift the accept consistency considerably above the feed consistency. Typical thickening factors are between 1.5 and 3.0 [40].

Larger-diameter, individual cyclones are sometimes employed for the separation of heavy-weight contaminants to protect screen baskets or refiners from detrimental feed components. These cyclones are typically 200–500 mm in diameter, and may extend some meters in an axial direction. An example of a larger-diameter cyclone separator, the Metso HC cleaner, is shown in Fig. 6.40. The cleaner can be operated either on a continuous basis or with intermittent reject discharge as a junk trap. HC cleaners are designed to work with feed consistencies up to 5%, but are normally operated in the 1.5–2.5% range [41].

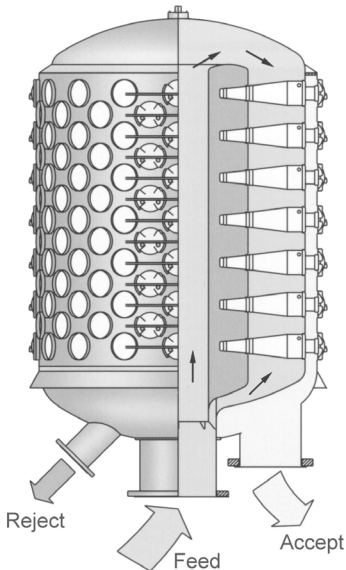


Fig. 6.39 The Noss Radiclone AM [39].

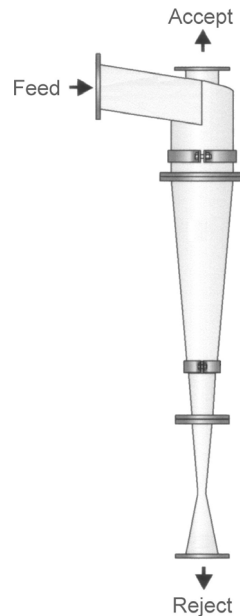


Fig. 6.40 The Metso HC cleaner [41].

## References

- 1 Gooding, R.W., R.J. Kerekes, Derivation of performance equations for solid-solid screens. *Can. J. Chem. Eng.*, **1989**; 67(10): 801–805.
- 2 Gooding, R.W., R.J. Kerekes, The motion of fibers near a screen slot. *J. Pulp Paper Sci.*, **1989**; 15(2): 59–62.
- 3 Yu, C.J., J. DeFoe, Fundamental study of screening hydraulics. Part 1: Flow patterns at the feed-side surface of screen baskets; mechanism of fiber-mat formation and remixing. *Tappi J.*, **1994**; 77(8): 219–226.
- 4 Walmsley, M., Z. Weeds. Concentration and flow variations in a wood pulp fiber separator. In APCChE Congress and CHEMECA. Melbourne, **2002**.
- 5 Yu, C.J., B.R. Crossley, L. Silveri, Fundamental study of screening hydraulics. Part 3: Model for calculating effective open area. *Tappi J.*, **1994**; 77(9): 125–131.
- 6 Gooding, R.W., R.J. Kerekes, Consistency changes caused by pulp screening. *Tappi J.*, **1992**; 75(11): 109–118.
- 7 Olson, J., G. Wherrett, A Model of Fiber Fractionation by slotted screen apertures. *J. Pulp Paper Sci.*, **1998**; 24(12): 398–403.
- 8 Olson, J.A., Fiber length fractionation caused by pulp screening, slotted screen plates. *J. Pulp Paper Sci.*, **2001**; 27(8): 255–261.
- 9 Olson, J., B. Allison, N. Roberts, Fiber length fractionation caused by pulp screening. smooth-hole screen plates. *J. Pulp Paper Sci.*, **2000**; 26(1): 12–16.
- 10 Gooding, R., J. Olson, N. Roberts. Parameters for assessing fiber fractionation and their application to screen rotor effects. International Mechanical Pulping Conference. Helsinki: TAPPI, **2001**.
- 11 Ämmälä, A., *Fractionation of thermomechanical pulp in pressure screening*. University of Oulu, **2001**.
- 12 McCarthy, C., Various factors affect pressure screen operation and capacity. *Pulp Paper*, **1988**; 62(9): 233–237.
- 13 Pinon, V., R.W. Gooding, J.A. Olson, Measurements of pressure pulses from a solid core screen rotor. *Tappi J.*, **2003**; 2(10): 9–12.
- 14 Feng, M., J. Gonzalez, J.A. Olson, C. Ollivier-Gooch, R.W. Gooding, Numerical simulation and experimental measurements of pressure pulses produced by a pulp screen foil rotor. *J. Fluids Eng.*, **2005**; 127: 347–357.
- 15 Amand, F.J.S., B. Perrin. Fundamentals of screening: effect of rotor design and fiber properties. Tappi Pulping Conference. Orlando, FL, USA, **1999**.
- 16 Rautjärvi, H., A. Ämmälä, J. Niinimäki, Effect of entrained air on the performance of a pressure screen. *Tappi J.*, **2000**; 83(9).
- 17 Gooding, R.W., D.F. Craig, The effect of slot spacing on pulp screen capacity. *Tappi J.*, **1992**; 75(2): 71–75.
- 18 Kumar, A., R.W. Gooding, R.J. Kerekes, Factors controlling the passage of fibers through slots. *Tappi J.*, **1998**; 81(5): 247–254.
- 19 Friesen, T., et al., Pressure screen system simulation for optimal fractionation. *Pulp Paper Can.*, **2003**; 104(4): T94–T99.
- 20 Olson, J.A., S. Turcotte, R.W. Gooding, determination of power requirements for solid core pulp screen rotors. *Nordic Pulp Paper Res. J.*, **2004**; 19(2): 213–217.
- 21 Slack, M. Application Challenge Cyclonic Separator. 2nd QNET-CFD Workshop. Lucerne, Switzerland, **2002**.
- 22 Li, M., et al., Characterization of hydrocyclone-separated eucalypt fiber fractions. *J. Pulp Paper Sci.*, **1999**; 25(8): 299–304.
- 23 Vomhoff, H., K.-J. Grundström, Fractionation of a bleached softwood pulp and separate refining of the earlywood- and latewood-enriched fractions. Annual General Meeting. Baden-Baden, Germany: ZELLCHEMING, **2002**.
- 24 Statie, E., et al., A computational study of particle separation in hydrocyclones. *J. Pulp Paper Sci.*, **2002**; 28(3): 84–92.
- 25 Nelson, G.L., The screening quotient: a better index for screening performance. *Tappi*, **1981**; 64(5): 133–134.
- 26 Olson, J.A., et al., Fiber length fractionation caused by pulp screening. *J. Pulp Paper Sci.*, **1998**; 24(12): 393–397.

- 27 Panula-Ontto, S., *Fractionation of unbleached softwood kraft pulp with wedge wire pressure screen and hydrocyclone*. Helsinki University of Technology, **2003**.
- 28 Olson, J., et al., Fiber fractionation for high porosity sack kraft paper. *Tappi J.*, **2001**; 84(6).
- 29 Weckroth, R., et al. Enhanced pulp screening using high-performance screen components and process simulation. APPW, Durban, South Africa: TAPPSA, **2002**.
- 30 IMPCO HI-Q Fine Screen (product leaflet). GL&V Pulp Group: Nashua, USA, **2001**.
- 31 DeltaScreen (product leaflet). Metso Paper: Sundsvall, Sweden, **2001**.
- 32 IMPCO HI-Q Knotter (product leaflet). GL&V Pulp Group: Nashua, USA, **2001**.
- 33 DeltaCombi (product leaflet). Metso Paper: Sundsvall, Sweden, **2001**.
- 34 Radiscreen-F Fine Screen (product leaflet). Noss: Norrköping, Sweden, **2002**.
- 35 Fredriksson, B., Increased screening efficiency with belt dilution. 90th PAP-TAC Annual Meeting. Montreal: PAP-TAC, **2004**.
- 36 McMinn, T., A. Serres. Intermediate deflocculation and dilution device (ID2): a new technological decisive step in the screening processes. APPW. Durban, South Africa: TAPPSA, **2002**.
- 37 AFT VariProfile (product leaflet). AFT: Montreal, Canada, **2003**.
- 38 Raditrim Secondary Knotter (product leaflet). Noss: Norrköping, Sweden, **1999**.
- 39 Radiclone AM80 (product leaflet). Noss: Norrköping, Sweden, **2002**.
- 40 Radiclone BM (product leaflet). Noss: Norrköping, Sweden, **2000**.
- 41 HC Cleaners (product leaflet). Metso: Valkeakoski, Finland, **2002**.

## 7

### Pulp Bleaching

*Herbert Sixta, Hans-Ullrich Süß, Antje Potthast, Manfred Schwanninger,  
and Andreas W. Krottscheck*

#### 7.1

##### General Principles

Unbleached chemical pulps still contain lignin in an amount of 3–6% on o.d. (oven dry) pulp in the case of softwood kraft (sulfite), and 1.5–4% on o.d. pulp in the case of hardwood kraft (sulfite) pulps. Lignin in native wood is colored only slightly, whereas residual lignin of a pulp after cooking – particularly kraft cooking – is highly colored. Moreover, unbleached pulps also contain other colored impurities such as certain extractives (resin compounds) and dirt which is defined as foreign matter having a marked contrasting color to the rest of the sheet. Dirt may originate from wood (bark, incompletely fiberized fiber bundles, sand, shives, etc.), from cooking itself (carbon specks, rust, etc.), and from external sources (grease, sand, other materials, etc.).

A continuation of cooking to further reduce the noncarbohydrate impurities would inevitably lead to a significant impairment of pulp quality due to enhanced cellulose degradation. Therefore, alternative concepts must be applied to selectively remove chromophore structures present in the pulp. Various chlorine- and oxygen-based oxidants have proven to be efficient bleaching chemicals which, being applied in sequential steps, progressively remove chromophores and impurities. As a result of the concern about chlorinated organic compounds formed during chlorine bleaching at the end of 1980s, conventional bleaching concepts were rapidly replaced by the so-called elemental chlorine-free (ECF) bleaching process, and this became the dominant bleaching technology. The complete substitution of chlorine by chlorine dioxide was the key step in reducing the levels of organochlorines (measured as adsorbable organic halogen; AOX) in pulp mill effluents. Further pressure, particularly from the environmental organization Greenpeace, and especially in the German-speaking regions of Europe, led to the development of totally chlorine-free (TCF) bleaching processes with a main emphasis on the use of oxygen (O), hydrogen peroxide (P) and ozone (Z) as bleaching agents.

Bleaching is defined as a chemical process aimed at the removal of color in pulps derived from residual lignin or other colored impurities, as outlined above.

The progress in bleaching is followed by measuring the brightness, which is in turn defined as the reflectance of visible blue light from a pad of pulp sheets, using a defined spectral band of light having an effective wavelength of 457 nm. The most common method for brightness measurement is represented by the ISO standard method (ISO 2469, ISO 2470). This method uses an absolute scale. The ISO brightness of a black, nonreflecting material is 0%, while that of a perfect diffuser is 100%. Brightness levels of pulps can range from about 20% ISO for unbleached kraft to almost 95% ISO for fully bleached sulfite (dissolving) pulps. Bleaching increases the amount of blue light reflected by the pulp sheet in that the concentration of chromophores absorbing that light is lowered. The change in brightness through a bleaching step is not proportional to the reduction in chromophore concentration. This is explained by the Kubelka–Munk remission function, which shows that the reflectance loss (brightness) is not a linear function of the chromophore concentration. At a high brightness level, the loss in brightness is governed by only a small change in chromophore concentration, while at a low brightness level the same loss in brightness is connected with a significantly higher change in chromophore concentration. The absorption coefficient,  $k$ , is proportional to the chromophore concentration and the scattering coefficient,  $s$ , is related to the surface properties of the sheet determined by the fiber dimensions and the degree of bonding.

In accordance with the Kubelka–Munk theory, the following expression defines the interrelationship between  $s$ ,  $k$  and the brightness  $B$  (reflectance factor  $R$ ):

$$B * 0.01 = \left( \frac{k}{s} + 1 \right) - \left[ \left( \frac{k}{s} \right)^2 + 2 \cdot \left( \frac{k}{s} \right) \right]^{0.5} \quad (1)$$

where  $B$  is the brightness, in percent.

Determination of the absorption coefficient at a certain wavelength or wavelength range is a usual way to monitor the chromophores contributing to pulp brightness. Figure 7.1 shows the reflectance and the absorption coefficient spectra from both unbleached and fully (TCF) bleached hardwood sulfite pulps.

The spectra in Fig. 7.1 indicate that bleaching of pulp increases reflectance predominantly at the blue end of the spectrum. The change in chromophore concentration through bleaching operations can be monitored by absorption difference spectra ( $\Delta k = k_{\text{bleached}} - k_{\text{unbleached}}$ ). This also allows estimation of the chemical structures involved in the removal of chromophores.

## 7.2 Classification of Bleaching Chemicals

Based on the knowledge of fundamental chemical reactions of bleaching chemicals with the dominant chemical structures of the chromophores in a pulp, a simplified concept has been suggested by Lachenal and Muguet to categorize the

bleaching chemicals into three groups according to their reactivity towards residual lignin structures [2–4]. This concept is summarized in Tab. 7.1.

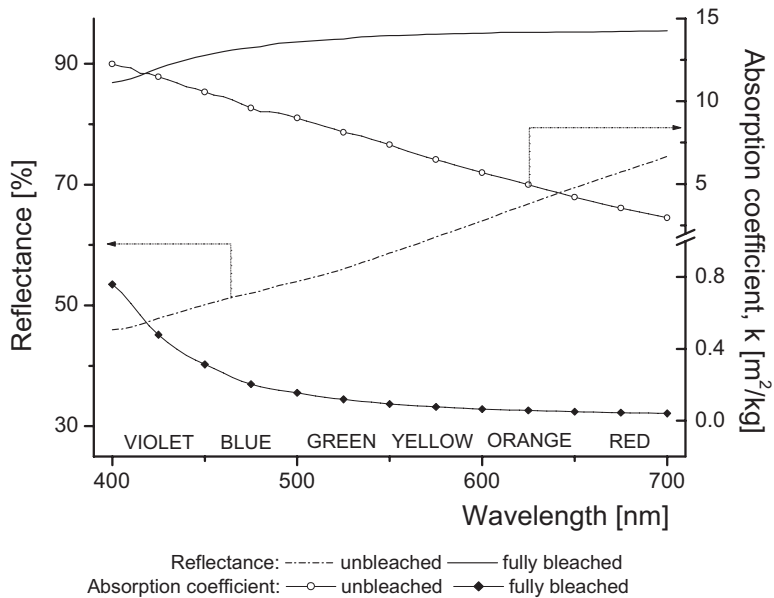


Fig. 7.1 Reflectance and absorption coefficient spectra of an unbleached and bleached hardwood sulfite pulp (according to [1]).

Tab. 7.1 Classification of bleaching chemicals with regard to their reactivity towards lignin and carbohydrate structures (according to Lachenal and Muguet [3].)

	Category		
	I	II	III
Bleaching chemicals			
Chlorine-containing	Cl <sub>2</sub>	ClO <sub>2</sub>	NaOCl
Chlorine-free	O <sub>3</sub>	O <sub>2</sub>	H <sub>2</sub> O <sub>2</sub>
Type of reaction	electrophilic	electrophilic	nucleophilic
pH level	acid	acid/alkaline	alkaline
Reaction sites in lignin structures	olefinic and aromatic	free phenolic groups, double bonds	carbonyl groups, conj. double bonds
Reaction sites in carbohydrate structures	hexenuronic acids	hexenuronic acid (only ClO <sub>2</sub> )	

The data in Tab. 7.1 show additionally that each chlorine-containing chemical has an equivalent chlorine-free counterpart. Ozone and gaseous chlorine are grouped together because they react as electrophilic agents with aromatic rings of both etherified and free phenolic structures in lignin, as well as with olefinic structures. The hexenuronic acids which contribute to the kappa number, predominantly in the case of hardwood kraft pulps, are degraded solely by electrophilic reactants in an acid environment. Chlorine dioxide and oxygen under alkaline conditions are placed in the same category because they both attack primarily free phenolic groups. Compared to chlorine dioxide, oxygen behaves rather unselectively because molecular oxygen gradually reduces to highly reactive radicals (e.g., hydroxy radicals) which also attack unchanged carbohydrate structures. Nucleophilic agents such as hypochlorite and hydrogen peroxide attack electron-poor structures (e.g., carbonyl structures) with conjugated double bonds, which are often highly colored. Nucleophilic agents thus decolorize (brighten) the pulp while being less efficient with respect to delignification as compared to electrophiles. However, peroxide bleaching changes to an efficient delignification stage when applying reinforced conditions (high temperature, high charges of sodium hydroxide and hydrogen peroxide).

Bleaching is most efficient when the bleaching sequence contains at least one oxidant from each category. From a process point of view, however, it is not advantageous to change between electrophilic and nucleophilic bleaching stages, because this is connected with a change in pH (see Section 7.10).

The classification is of course rather simplistic because it cannot take into account the fact that most of the bleaching chemicals are not stable in aqueous environment, and change to species with different reactivity towards the pulp components.

Bleaching reactions of chemical pulps are equivalent to oxidation reactions. To date, sodium borohydride is the only reductant used in chemical pulp bleaching. It is primarily applied to stabilize the carbohydrates either after hot caustic extraction or after ozone treatment, and also exerts a slight brightening effect. Oxidants accept electrons from a substrate and are thereby reduced. For example, a chlorine dioxide molecule accepts five electrons and forms one chloride ion. The equivalent weight corresponds to the weight of an oxidant transferring 1 mol of electrons. With the concept of oxidation equivalent (OXE), the oxidation capacity of any bleaching chemical can be expressed [5]. An OXE is equal to 1 mol of electrons being transferred during oxidative bleaching. A list of the most important bleaching chemicals involved in conventional, ECF and TCF bleaching is provided in Tab. 7.2 [5].

Historically, the active chlorine concept was used to quantify the oxidizing power of the different chlorine-containing chemicals such as elemental chlorine, hypochlorite and chlorine dioxide into chlorine gas equivalents. In ECF bleaching sequences this concept still prevails. The intention of the OXE concept was to compare various ECF and TCF sequences with regard to their efficiencies simply by summing all the OXEs used in the different stages. This concept is widely accepted today, although it does not allow the bleachability of a certain pulp to be

**Tab. 7.2** Oxidizing equivalents (OXE) of the most important bleaching chemicals involved in conventional, ECF and TCF bleaching of chemical pulps [5].

Oxidant	Abbreviation	Formula	Molecular weight [g mol <sup>-1</sup> ]	No. of e <sup>-</sup> transferred [e <sup>-</sup> mol <sup>-1</sup> ]	Equivalent Weight [g mol <sup>-1</sup> e <sup>-1</sup> ]	OXE kg <sup>-1</sup>
Chlorine <sup>a</sup>	C	Cl <sub>2</sub>	70.91	2	35.46	28.20
Chlorine dioxide	D	ClO <sub>2</sub>	67.46	5	13.49	74.12
Hypochlorite	H	NaClO	74.45	2	37.22	26.86
Oxygen	O	O <sub>2</sub>	32.00	4	8.00	125.00
Hydrogen peroxide	P	H <sub>2</sub> O <sub>2</sub>	34.02	2	17.01	58.79
Ozone	Z	O <sub>3</sub>	48.00	6	8.00	125.00
Peracetic acid	Paa	CH <sub>3</sub> COOOH	76.00	2	38.00	26.32

a 28.20 OXE kg<sup>-1</sup> active chlorine

expressed because the chemicals show different reactivities. Both the active chlorine and the OXE concept consider only the theoretical transfer of electrons assuming a complete redox reaction. Hence, the treatment of a pulp with different bleaching chemicals having the same amount of OXE (or active chlorine) can lead to different brightness values [6]. Alternatively, bleachability of different pulps can be evaluated by applying a specific bleaching sequence and constant bleaching conditions [7]. Nevertheless, the OXE concept is a valuable tool in comparing the efficiencies of different bleaching chemicals.

Bleaching to full brightness (> 88% ISO) requires multi-stage application of bleaching chemicals. In many cases, inter-stage washing is practiced to remove dissolved impurities, which in turn improves the bleaching efficiency of a subsequent bleaching step. Moreover, multi-stage bleaching steps take advantage of the different reactivity of each bleaching chemical and provide synergy in bleaching or delignification. The first stages of a sequence are conceived as delignification stages where the major part of the residual lignin is removed. The later stages in the sequence are the so-called “brightening stages”, in which the chromophores in the pulps are eliminated to attain a high brightness level.

## 7.2

### Bleaching Operations and Equipment

*Andreas W. Krottscheck*

In this section, we will examine the basics of the rheology of fiber-containing process streams, identify the different pieces of equipment that form the bleaching stage and discuss their function and possibilities in general. Later, the special use



of such bleach plant equipment for particular applications is considered in the subsection of the corresponding bleaching chemical.

### 7.2.1

#### Basic Rheology of Pulp-Liquor Systems

In bleach plant operations, pulp predominantly occurs in a two-phase system together with liquor. The proportion between solid fiber and liquid environment is usually characterized by the consistency – that is, the mass fraction of oven-dried pulp based on the totality of pulp and liquor. The industry uses distinctive terms to distinguish between regions of characteristic fiber concentrations.

At low consistency (LC: below 3–4%), the pulp slurry is still easy to handle, with a near-to-Newtonian flow behavior similar to that of water. A Newtonian fluid cannot store energy, and any exposure to stress will lead to a flow. As the consistency is increased towards the medium consistency range (MC: 6–14%), the pulp slurry develops non-Newtonian flow behavior [1]. When a stress is applied to a medium consistency suspension it will not flow until a certain yield stress is exceeded. At high consistency (HC: 30–40%), the pulp no longer flows but forms a firm mat. It should be noted that the numbers given for the upper and lower limits in the consistency ranges mentioned above vary among the literature.

The reason for the largely differing behavior of pulp at different consistencies lies in the fact that the fibers form networks as they contact each other. The more fibers present per volume area, the more contact points exist and the higher the network strength becomes [2,3].

When the fiber network is subjected to shear – for example during pumping or mixing – it tends to break up. At low shear stress, the break-up occurs on a macroscopic level and is controlled by friction. First, larger flocs become loose and the floc aggregates begin to flow beside each other. As the shear stress increases, larger flocs break into smaller ones until, at some point in a turbulent flow regime, all fibers are singled out from flocs and move unimpeded by network forces. This state is controlled by random flow behavior, and the fiber slurry is called “fluidized”. As soon as the pulp suspension is no longer subject to turbulent shear forces, the fibers reflocculate very quickly, within fractions of a second [4].

The fluidized state is of particular interest in the medium consistency region. The finding that a fluidized medium consistency pulp suspension develops Newtonian flow behavior [1] and thus follows Bernoulli’s law brought about a quantum leap for fiberline operations during the early 1980s. At that time, new pumping and mixing concepts began to gain widespread industry acceptance. Until today, medium consistency technology remains by far the most popular choice for bleach plant applications.

Fluidization in medium consistency pulp suspensions can be achieved only with a considerable energy input. Figure 7.2 shows the minimum power dissipation – that is, power consumption per volume unit – required to fluidize slurries of different pulp types, as determined by Wikström et al. [4]. The curve for softwood was in good agreement with data published earlier by Gullichsen and Här-

können [1]. Other authors have found substantially higher values (e.g. [5,6]). The rheology of a fiber suspension depends also on fiber length, flexibility, coarseness, freeness, as well as on liquor viscosity and chemical regime. Nonetheless, the main influencing factors are consistency and power dissipation.

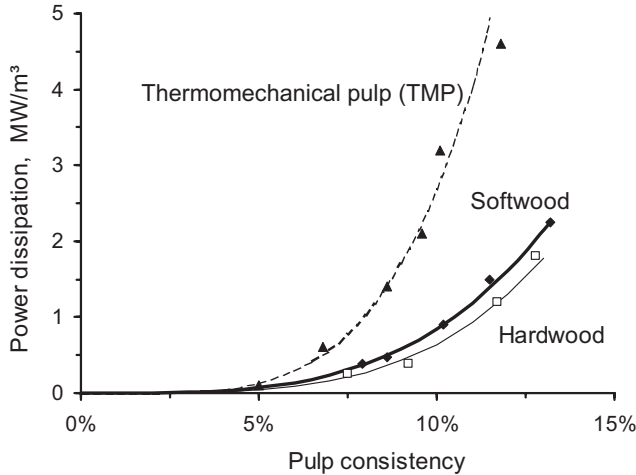


Fig. 7.2 Power dissipation as a function of pulp consistency required to fluidize different pulp types [4].

Some chemicals used for bleaching are applied in gaseous form. Then, the two-phase pulp–liquor system is converted into a three-phase system. When gas is present, the bubbles on the one hand reduce the system’s ability to transport momentum, and on the other hand they affect the turbulence as they function as turbulence dampers [7]. At a given rotor speed, the shear stress that can be applied to a three-phase system decreases with a higher gas content. In other words, fluidization in a three-phase system generally requires a higher rotor speed than in a two-phase system.

The specific behavior of pulp suspensions at different consistency levels requires customized pumping and mixing methods, and this in turn influences the design of the equipment, piping and valves. When, for example, medium consistency pulp is pumped under normal flow conditions, a plug flow is created in the pipe, which is supported by the fiber–fiber interactions in the network. If the diameter of the flow channel is reduced, there is a danger of dewatering the fiber network, and this can lead to clogging of the flow channel. This holds true not only for pipe flow but also for other contractions, for example at the outlet of a pressurized bleaching tower.

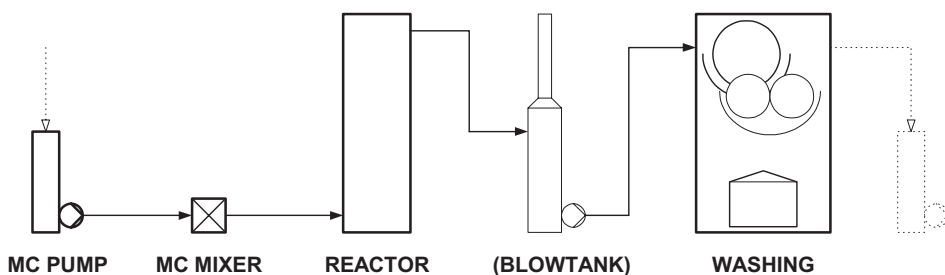
## 7.2.2

**Generic Bleaching Stage Set-Up**

Bleaching sequences consist of several stages which deal with various chemicals. Today's bleaching stages operate mostly under medium consistency conditions, between 10% and 12% consistency. Ozone bleaching is sometimes performed at high consistency (35–40%), but low-consistency bleaching is being phased out and so will not be considered in this chapter.

The basic set-up of a bleaching stage can be generalized. The generic medium consistency bleaching stage consists of a feed pump, a mixer, a reaction vessel and post-stage washing. Additional equipment and apparatus may include a blowtank or additional mixers and reaction vessels.

Figure 7.3 illustrates schematically a generic medium consistency stage. The pulp slurry is fed to the stage by a medium consistency pump, and then passes the medium consistency mixer and proceeds to the reactor. When gas is present after the reaction, it can be separated from the pulp suspension in a blowtank. Finally, the pulp is pumped to the washing equipment.



**Fig. 7.3** Generic medium consistency (MC) bleaching stage.

During the past few years, bleaching sequences have been developed which do not require washing between selected stages. In the situation when the inter-stage washing can be skipped, the pulp is forwarded to the next bleaching stage directly from the reactor or blowtank at medium consistency. The pieces of equipment used in medium consistency bleaching are described in more detail in the following subsections.

Today, high consistency bleaching is almost limited to ozonization. A modern high consistency ozone stage consists of a press, a reactor and dilution equipment, as shown in Fig. 7.4. Pulp coming from a dewatering press is fed, without dilution, to an atmospheric reactor. Once the pulp has passed through the reactor it is diluted and pumped to the subsequent stage [8].

For further information about equipment for high consistency ozone bleaching, see Section 7.5.6.2.

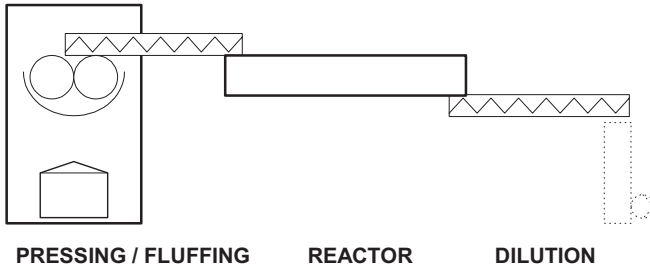


Fig. 7.4 High consistency (HC) ozone bleaching stage [8].

### 7.2.3

#### Medium Consistency Pumps

The feed pump must provide the pressure to overcome the hydrostatic head of the bleaching vessel, any backpressure controlled at the reactor top, as well as the pressure loss in piping, control valves and mixing equipment. Modern medium consistency pumps follow the centrifugal pump design with a specially designed open impeller. Compared to the previously used positive-displacement-type pumps, they operate at excellent energy economy and reduced maintenance costs.

Medium consistency pulp suspensions tend to have small gas bubbles embedded in the fiber network. As the pump feed enters the casing, gas is driven into the low-pressure zone near the center of the pump impeller. If the gas is not removed, it accumulates at the impeller up to a point where the pump fails to deliver. Therefore, medium consistency pumps are equipped with means for extracting the separated gas from the pump casing, either with an integrated or an external vacuum pump. The Kvaerner Pulping Duflo pump is an example of a medium consistency pump with an integrated vacuum system (Fig. 7.5). The air contained in the pulp feed passes through the impeller and is extracted from the back of the impeller by a liquid ring vacuum pump mounted on the same shaft as the impeller.

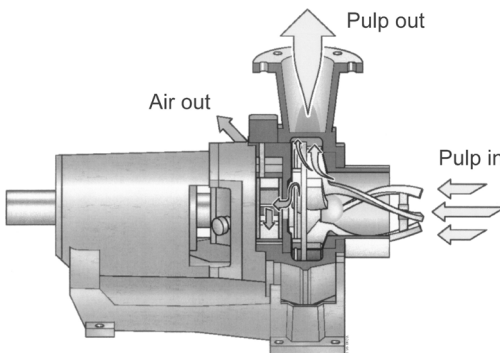
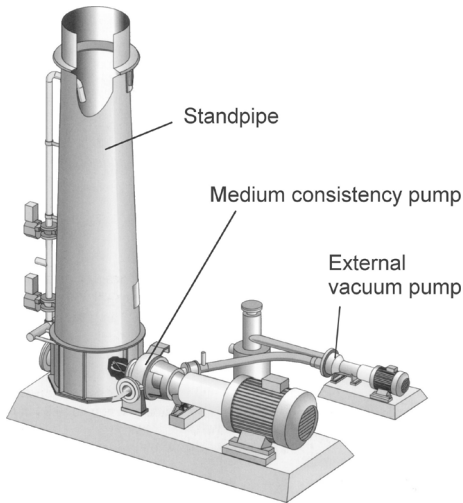


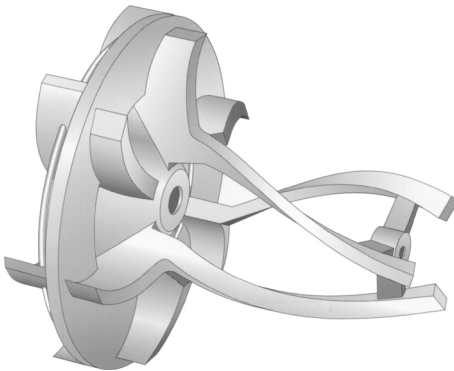
Fig. 7.5 The Kvaerner Pulping Duflo pump [9].

Centrifugal medium consistency pumps are flanged to the bottom of a standpipe which is operated at constant level, and thus provides a constant hydrostatic pressure to the suction side of the pump (Fig. 7.6).



**Fig. 7.6** Example of medium consistency (MC<sup>®</sup>) pumping system with an external vacuum pump [10] (picture from Sulzer Pumps Finland Oy).

Figure 7.7 shows a Kvaerner Pulping Duflo impeller as an example of an advanced medium consistency pump impeller. The arms which extend into the standpipe fluidize the pulp slurry at the entrance to the pump, thus helping to avoid clogging.



**Fig. 7.7** The Kvaerner Pulping Duflo impeller [11].

Following another design philosophy for medium consistency pumps, Andritz uses individual systems to provide for gas separation and pumping (see Fig. 7.13).

Suppliers of medium consistency pumps claim maximum operating consistencies to range up to 18%. In everyday plant operation, such a consistency level is seldom reached and the consistency limit for continuous, unattended operation is often in the range of 10–14%.

#### 7.2.4

#### Medium Consistency Mixers

The mixer is responsible for the distribution of bleaching chemicals in the pulp slurry and/or for increasing the slurry temperature by the addition of live steam. A uniform temperature and the homogeneous distribution of bleaching chemicals are of ultimate importance in achieving a consistent bleaching result at low chemical consumption and good selectivity.

All chemical mixers (and most steam mixers) are located downstream of the feed pump, and operate under pressure. Atmospheric steam mixers are installed upstream of the pump. The advantage of using an atmospheric steam mixer instead of a pressurized one lies in its ability to process low-pressure steam. However, the specific feed temperature limitation of subsequent pumping equipment sets a physical maximum to pulp heating with atmospheric mixers.

The required intensity of mixing depends on the chemicals applied and the temperature difference to be overcome, respectively. Gaseous chemicals such as oxygen and ozone typically require more intense mixing than liquid chemicals. In some cases, bleaching can be even done without a dedicated mixer. The bleaching chemicals are then added to the process before or into the medium consistency pump, and the mixing action of the pump is sufficient for their distribution in the pulp slurry.

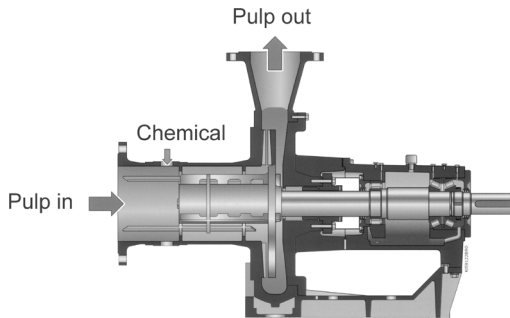
The mixing intensity can often be related to the specific energy input or power dissipation. When mixing a medium consistency pulp suspension, there is usually no point in going beyond the onset of fluidization (see Fig. 7.2).

The heating of a pulp suspension is usually carried out with direct steam. If steam is added to a pipe without using a mixing device, the very likely consequence is steam hammering – that is, the noisy implosion of large steam bubbles as they condense. Steam hammering causes wear on materials and may lead to scaling and local overheating of fibers, all of which are very undesirable. Since the steam is condensing at the gas–liquid interface, it is essential to increase and frequently to regenerate the surface of the bubbles. Turbulence and high shear stress help to avoid the formation of large steam bubbles and support rapid condensation without noticeable noise.

When it comes to heating of the pulp slurry, all mixers have certain limitations with regard to the achievable temperature difference. If the target temperature difference cannot be achieved with one mixer, then two or more units must be installed.

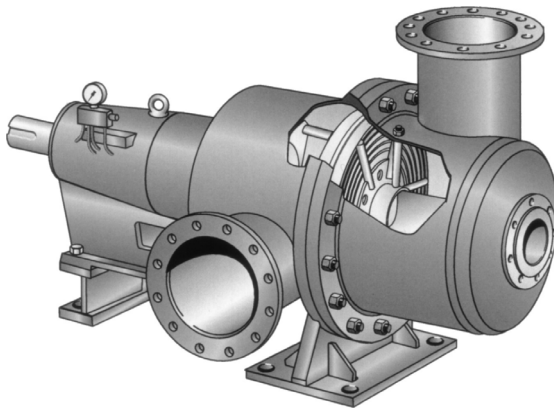
#### 7.2.4.1 High-Shear Mixers

High-shear mixers feature the highest specific energy input. They fluidize the pulp suspension and thus ensure very homogeneous distribution of both liquid and gaseous bleaching chemicals. Various designs of high-shear mixers have been developed over time. In the units with the highest specific energy input, the pulp suspension is passed through narrow gaps between the rotor and stator elements. Examples of high-shear mixers are shown in Figs. 7.8–7.10.



**Fig. 7.8** The Kvaerner Pulping Dual mixer [12].

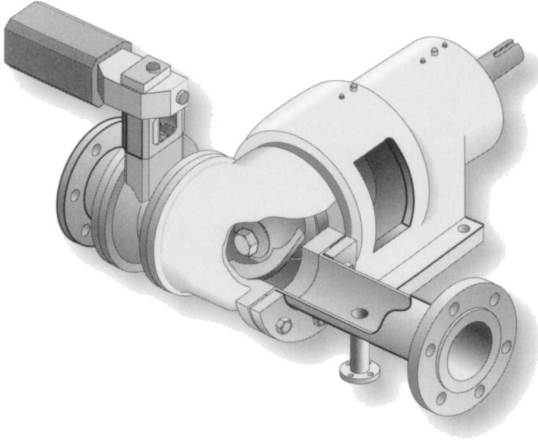
Pulp is fed axially to the Kvaerner Pulping Dual Mixer (Fig. 7.8). Chemicals are added as the pulp enters the concentric gap between the rotor and the housing. The shear stress created between the wings on the rotor and the ribs in the housing fluidizes the pulp and ensures efficient mixing. Additional turbulence is created as the pulp then passes radially through the gap between the disc rotor and the stator elements.



**Fig. 7.9** The Metso S-Mixer [13].

The feed to the Metso S-Mixer (Fig. 7.9) enters tangentially from the top and becomes mixed with chemicals added through the axial nozzle to the center of the

rotor. The mixture is then forced through fine slots between the rotating and stationary surfaces. The heavy turbulence in the slots causes efficient mixing.

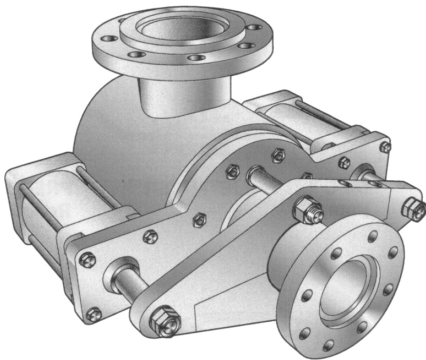


**Fig. 7.10** The Ahlmix™ Chemical Mixer [10] (picture from Sulzer Pumps Finland Oy).

The Ahlmix chemical mixer (Fig. 7.10) uses a set of rotating claws mounted perpendicularly to the pulp stream for mixing. Chemicals are added upstream of the mixer. The mixer features a comparatively low specific energy consumption, and despite the corresponding low power dissipation has proven adequate for many mixing operations.

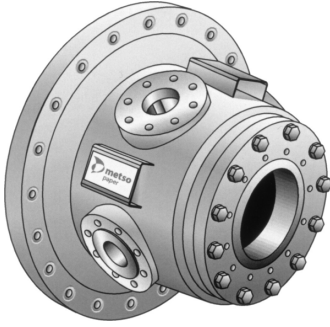
#### 7.2.4.2 Static Mixers

Static pulp mixers are mainly used for heating by injecting direct steam into the pulp suspension. In order to avoid steam hammering, the steam is fed to a turbulent zone. In the Kvaerner Pulping Jetmixer (Fig. 7.11) the turbulence is created by the



**Fig. 7.11** The Kvaerner Pulping Jetmixer [14].





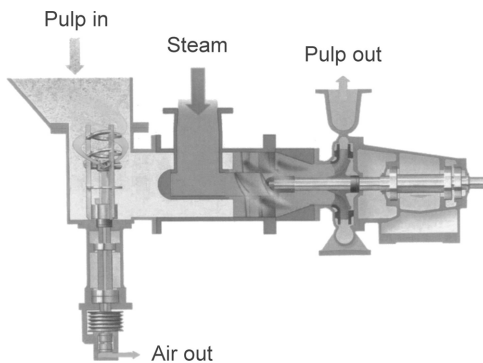
**Fig. 7.12** The Metso FlowHeater [15].

speed of the injected steam itself as pulp flows unrestrictedly through the central pipe. The steam is added to the pulp suspension through slots with adjustable length. Other mixers have elements which cause a pressure drop in the pulp stream, such as the Metso FlowHeater (Fig. 7.12), where orifice restrictions generate the necessary shear forces for homogenized mixing. The maximum achievable temperature difference in a static mixer is about 30 °C.

#### 7.2.4.3 Atmospheric Steam Mixers

Currently, the most common design of atmospheric steam mixer is the single-shaft design, which has replaced the previously popular double-shaft design. The single-shaft steam mixer has a cylindrical body which houses a central shaft equipped with paddles. Medium consistency pulp drops into the mixer at the feed end and is transported to the discharge end by means of the rotating paddles. As the pulp proceeds through the mixer, steam is added to the pulp through nozzles located at a number of points along the equipment.

The advantage of atmospheric steam mixers lies in the use of low-pressure steam instead of medium-pressure steam, as is required for pressurized mixing. A recent development is the Dynamic Steam Heater by Andritz (Fig. 7.13). This



**Fig. 7.13** The Andritz Dynamic Steam Heater [16].

mixer's rotating steam nozzles sit at the same shaft as the impeller of the medium consistency pump and plough through the pulp suspension just before it enters the impeller. With an achievable temperature level of about 100 °C, the mixer performance clearly exceeds the possibilities of shaft mixers.

### 7.2.5

#### **Medium Consistency Reactors**

The reactor provides the necessary retention time for the bleaching reactions to take place. Depending on the bleaching application, reactors may be of either the upflow or downflow type, and either atmospheric or pressurized. In addition, there may be combination reactors – for example, an upflow-downflow reactor combination for chlorine dioxide bleaching or a pressurized-atmospheric reactor sequence for peroxide bleaching.

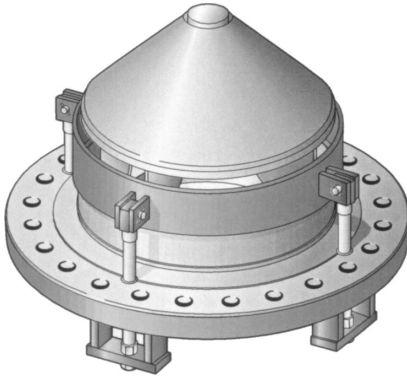
It is mandatory for any reactor design that it cares for plug flow, and that channeling is suppressed to the best possible extent. Since the bleaching towers may be up to several meters in diameter, special devices are needed for larger reactors to ensure distribution of the feed pulp across the total reactor cross-section. Similarly, discharge devices are needed for reclaiming the bleached pulp at the reactor outlet. In a pressurized reactor, the discharger also needs to minimize the risk of pulp dewatering and subsequent plugging at the reactor outlet.

Pressurized reactors normally discharge at medium consistency, whereas the discharge of atmospheric reactors is dependent upon whether further processing of the pulp requires medium consistency or low consistency.

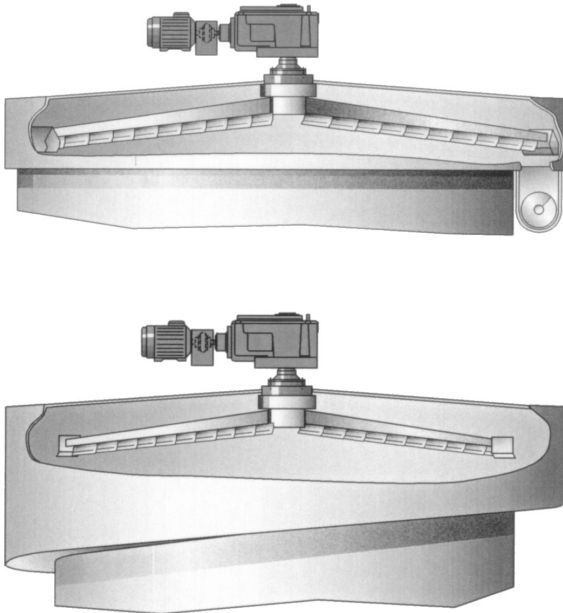
##### **7.2.5.1 Atmospheric Upflow Reactors**

Atmospheric upflow reactors with a diameter smaller than about 3 m have a conical lower part without a distributor, while larger reactors are usually fitted with a distribution device at the bottom which cares for the entering pulp to be spread out across the reactor cross-section. Some static distributors, such as Metso's FlowDistributor (Fig. 7.14), have no rotating parts, whereas others utilize rotating devices (an example being that in the base of the reactor shown in Fig. 7.18).

After the pulp has traveled to the top of the atmospheric reactor, a discharge scraper reclaims the pulp to the side of the reactor. In the case of low-consistency discharge, the reclaimed pulp drops into a circumferential spiral chute. Dilution liquor is added at the top of the chute and flushes the stock to the discharge outlet located at the bottom of the spiral chute (Fig. 7.15, lower diagram). If medium consistency discharge is desirable, the scraper is equipped with buckets at the end which carry the pulp along the perimeter of the reactor to a screw conveyor. The screw conveyor then transports the stock to the discharge chute (Fig. 7.15, upper diagram).



**Fig. 7.14** The Metso FlowDistributor [17].

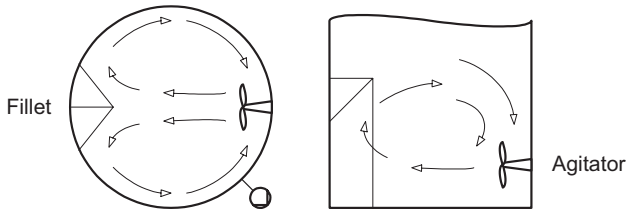


**Fig. 7.15** Metso Tower Scrapers for medium consistency discharge (upper) and low consistency discharge (lower) [17].

#### 7.2.5.2 Atmospheric Downflow Reactors

Atmospheric downflow reactors sometimes have a distribution device at the top which propels the pulp slurry across the surface and thus ensures distribution across the reactor cross-section. Once the pulp has traveled to the bottom of the reactor, it is either diluted in an agitated mixing zone and discharged at low con-

sistency (Fig. 7.16) or collected by a scraper to the standpipe of a pump for medium consistency discharge (Fig. 7.17).



**Fig. 7.16** Example of bottom of downflow reactor with low consistency discharge.



**Fig. 7.17** Metso FlowScraper for medium consistency discharge [17].

### 7.2.5.3 Pressurized Reactors

Pressurized medium consistency reactors are always of the upflow type. They have either a distributor mounted in the bottom (Fig. 7.18) or multiple inlets across the bottom, each of which receives a fraction of the total feed. In the latter case, a flow splitting device is needed outside the reactor to supply the individual inlets with the same quantities of pulp.

When the pulp slurry has reached the top of the pressurized reactor it is usually collected by the arms of a discharge scraper, which also have the task of keeping the outlet nozzle clear of pluggage (Figs. 7.18 and 7.19). In another design, a fluidizing device deals with the controlled discharge (Fig. 7.20).

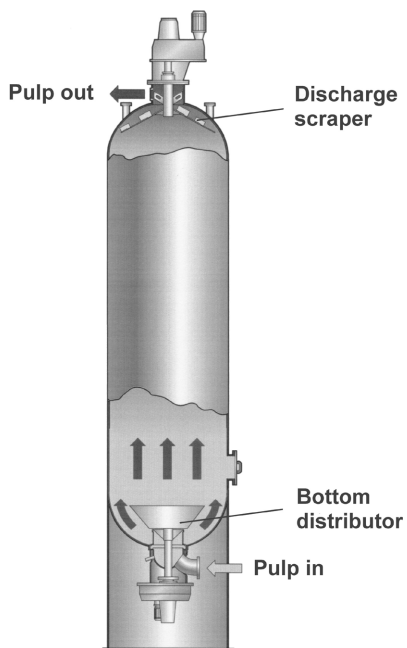


Fig. 7.18 An example of a pressurized upflow reactor [18].

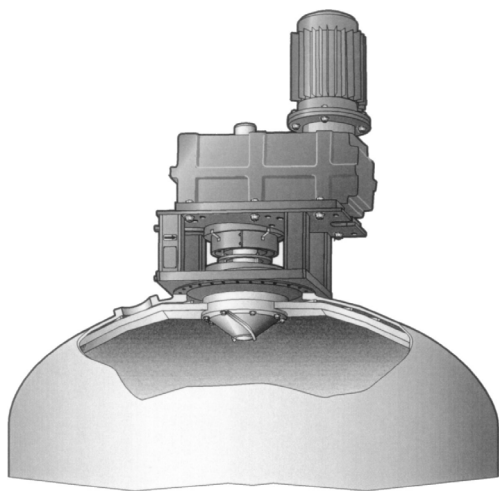
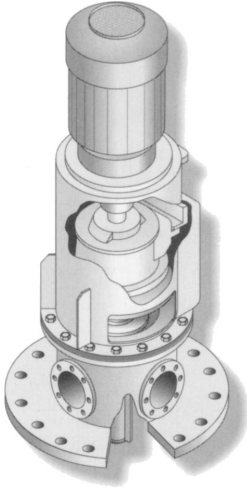


Fig. 7.19 The Metso FlowScraper [17].



**Fig. 7.20** The MC® Flow Discharger [10] (picture from Sulzer Pumps Finland Oy).

### 7.2.6

#### **Blowtank**

If the reactor outlet contains a gaseous phase, it is important to remove this gas before the pulp slurry is further processed, because a high gas content jeopardizes the operation of subsequent pumps and washers. The pulp slurry containing the gas is typically fed tangentially to the blowtank, where the slurry and the gas are separated. Gas leaves the blowtank through the vent pipe, while the pulp is pumped on to washing.

If the temperature in the reactor is higher than the boiling temperature of the liquor, steam flashes from the pulp slurry after it has passed the pressure-control valve. In such a case, the blow tank functions also as a flash tank by releasing steam to produce pulp that has cooled to the boiling point of the accompanying liquor.

The discharge from the blowtank at low or medium consistency is similar to that of an atmospheric downflow reactor (see Figs. 7.16 and 7.17).

### 7.2.7

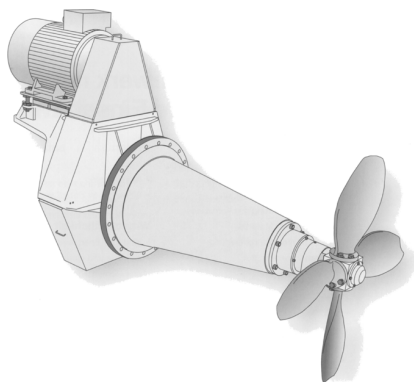
#### **Agitators**

Agitators are used in various vessels to mix and/or dilute pulp slurries. The predominant type of agitator has a horizontal shaft, and is side-mounted at the tank near the bottom in a zone of low consistency. Pulp agitators work efficiently in a consistency range up to about 5%. At higher consistencies the energy input becomes obstructive as the power requirements for agitation increase exponentially.

For practical reasons, agitation of the complete contents of a tank is limited to smaller tank volumes, as are typically used for the dilution of medium consistency

pulp coming from a washer or for blending different fiber furnishes. In contrast, bottom zone agitation is applied to large downflow tanks in order to obtain controlled dilution and discharge. If the purpose of agitation includes controlled pulp dilution, then the agitator can be equipped with a dilution system. Otherwise, separate nozzles take care of the dilution liquor addition.

The mechanical design of an agitated vessel depends on the medium to be agitated, as well as on the type and number of agitators installed. Correct agitation zone design helps to improve the homogeneity of mixing and to minimize power requirements. An example of a side-mounted agitator is shown in Fig. 7.21.



**Fig. 7.21** The Salomix® agitator [19] (picture from Sulzer Pumps Finland Oy).

### 7.2.8

#### **Washing**

The washing step targets removal of reaction products from the pulp, and also at recovering energy and/or residual chemicals. The choice of wash liquor, washing equipment and the number of washing stages depends on the bleaching stage itself, as well as on its position in the sequence. Further information about the liquor cycles in a bleach plant can be found in Section 7.10. Washing processes and washing equipment are described in more detail in Chapter 5.

## 7.3

### **Oxygen Delignification**

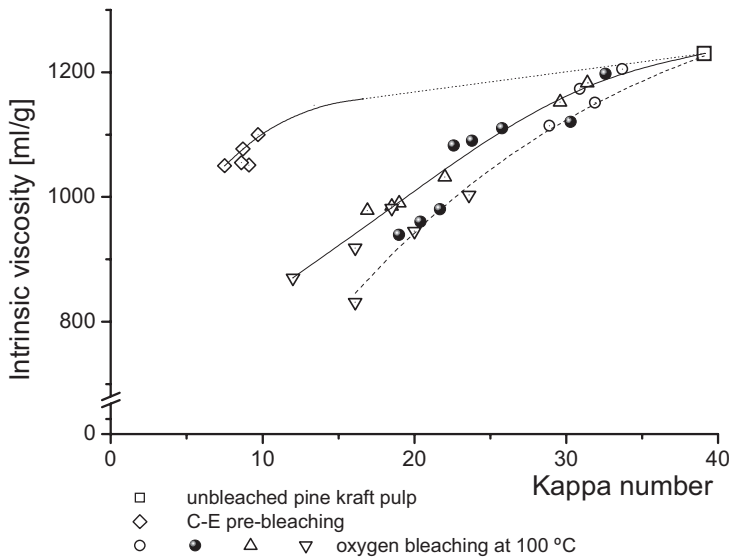
#### 7.3.1

##### **Introduction**

Environmental restrictions for bleach plant effluents and the necessity to reduce the amount of organochlorine compounds (OX) in the pulp have driven the pulp

industry to develop new environmentally benign delignification and bleaching technologies. In this context, oxygen delignification has emerged as an important delignification technology. The benefits of introducing an oxygen delignification stage are manifold, and include a lower demand for bleaching chemicals in the subsequent stages, a higher yield as compared to the final part of the cooking stage, and the possibility of recycling the liquid effluents from an oxygen delignification stage to the chemical recovery system to reduce the environmental impact with respect to color, COD, BOD and toxic compounds (e.g., organochlorine) of the bleach plant effluents. However, one of the major drawbacks of oxygen delignification is its lack of selectivity for delignification in particular beyond 50%, as this results in excessive cellulose damage which appears as a decrease in viscosity and a loss of pulp strength. The significantly lower selectivity of oxygen-alkali bleaching compared to conventional chlorine-based prebleaching sequences was one of the reasons why the introduction of oxygen delignification to industrial bleaching technology was not widely accepted by the industry. Figure 7.22 illustrates the superior selectivity performance in terms of a viscosity–kappa number relationship of a treatment with molecular chlorine followed by alkaline extraction (CE) of a softwood kraft pulp as compared to oxygen delignification with and without the addition of magnesium carbonate [1].

The potential of lignin degradation into water-soluble fragments by treatment with oxygen in alkaline solution first became apparent during the 1950s [2–6]. Oxygen delignification was successfully applied to delignify and bleach birch and spruce sulfite dissolving pulp. Several processes were patented during this early



**Fig. 7.22** Selectivity of oxygen delignification at 100 °C in comparison to chlorination followed by alkaline extraction (according to Hartler et al. [1]). The broken line denotes oxygen delignification with no MgCO<sub>3</sub> added.

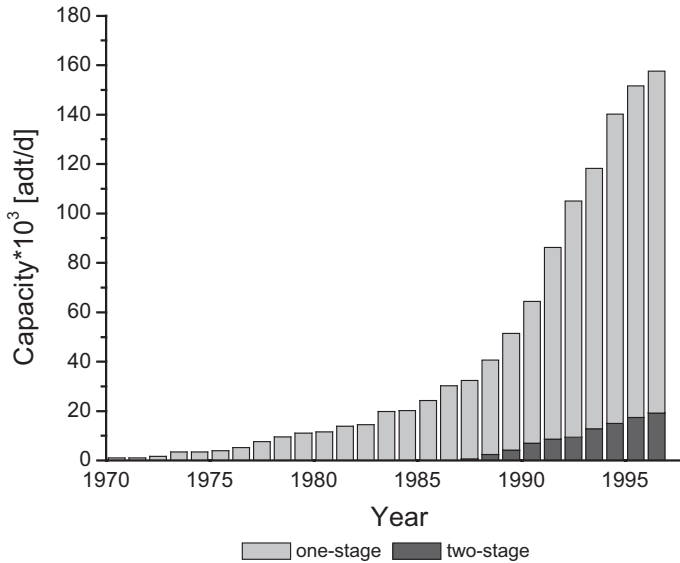


phase of research, but were not commercialized because of the observed extensive depolymerization of carbohydrates [7–9]. The poor selectivity has been explained by the formation of reactive oxygen-based radicals (e.g., hydroxy radicals) generated by oxygen attack on lignin structures [10]. A major breakthrough in oxygen delignification occurred during the 1960s, when Robert and colleagues discovered that the addition of small amounts of magnesium carbonate resulted in preservation of the strength properties of paper-grade kraft pulp [11–13]. This opened the door to the commercial development of oxygen as a delignifying agent. The first installation was a high consistency oxygen delignification plant built in South Africa at SAPPi's Enstra mill in 1970. This investment was based on a successful pilot plant operation in 1968 in Sweden, and was constructed as a cooperative effort among SAPPi, Kamyr Inc., and Air Liquide. Reported high investment costs and safety problems with the handling of combustible gases certainly retarded the acceptance and implementation of this new technology.

The development of medium consistency, high-shear mixers during the early 1980s led to a rapid increase in the installation of oxygen delignification plants due to its beneficial effects on the environment, process economy and energy savings [14,15]. This process is also more amenable to retrofit in existing mills than high consistency processes, and can be easily incorporated as intermediary stage in the sequence, for example as combined with an E-stage [16]. In 1996, there were more than 185 oxygen-delignification installations throughout the world, with a combined daily production of about 160 000 t oxygen-delignified kraft pulp [17,18]. The data in Fig. 7.23 show that 80% of these installations have come on-stream during the past 10 years, mainly driven by the stricter emission limits prescribed by regulatory authorities.

As mentioned previously, oxygen delignification also provides an economic attractive alternative to chlorine-based bleaching stages. It is reported that roughly 5 kg of oxygen can replace about 3 kg of chlorine dioxide. At a price differential of 0.61 SEK kg<sup>-1</sup> versus 8.6 SEK kg<sup>-1</sup>, respectively, the cost of using oxygen is about one-eighth that of using chlorine dioxide [19]. Moreover, the energy requirement to separate oxygen from the atmosphere is significantly less as compared to the generation of chlorine dioxide, and this is a favorable prospect for the future [20]. Presently, oxygen delignification has become a well-established technology. Because of selectivity advantages and lower investment costs, the medium consistency technology (MC, 10–18%) has dominated mill installations for the past 10 years, although high consistency installations (HC, 25–40%) are also in use. Recently, the industry has adopted the installation of two-stage oxygen delignification systems to increase both the selectivity and efficiency of the treatment. A typical 50% delignification level has thereby been increased to about 65% for a softwood kraft pulp with an unbleached kappa number between 25 and 30.

A detailed study of representative oxygen delignification installations worldwide clearly indicates the advantage of a two-stage oxygen delignification system over a one-stage system. The good performance of the high-consistency systems mainly results from better washing before the oxygen stage.



**Fig. 7.23** Daily production capacity of oxygen-delignified pulp on a worldwide basis [18].

For softwoods, evaluation of the database provides an average of 47.5% delignification, ranging from 28% to 67%. The incoming kappa number to the oxygen stage ranges from 32 to 22, and the outgoing kappa number from 22 to 8.5. For hardwoods, the performance of oxygen delignification varied from 19% to 55%, with an average of 40%. Kappa number variation is significantly reduced across the oxygen stage, from a range of 12–22 at the inlet to 7.5–13.5 at the discharge. The reason for these differences in unbleached kappa numbers of hardwood kraft pulps depends on the greater variability of hardwoods with respect to optimum yield and final pulp properties. For example, birch is often cooked to 18–20 kappa number, while many eucalypt species are only cooked to 12–14 kappa number [18]. In accordance with recent developments and the results from detailed investigations, there appears to be a lower limit of kappa number in the bleach plant for softwood kraft pulps of 8–10 and for hardwoods of 6–8 [19]. With continuing progress in oxygen delignification technology, it is expected that in future the cooking kappa will be raised to levels higher than 30, again because considerable wood yield can be preserved [21]. The yield loss during the residual cooking phase is significantly higher than during oxygen delignification. With the new highly efficient multi-stage medium consistency technology available, the overall yield can be increased by about one percentage point by increasing the cooking kappa, for example from 20 to 25.

Delignification in the oxygen stage means a smaller decrease in yield than delignification in cooking, as long as the degree of delignification in the oxygen stage remains moderate. As a rule of thumb, the yield decrease in the oxygen stage equals 0.1–0.2% on wood per 2 units of kappa number decrease, while in

cooking the yield decrease corresponds to 0.3% on wood for the same kappa number reduction [22]. Thus, oxygen delignification is more selective in terms of yield preservation than kraft cooking at kappa numbers corresponding to the final phase of a low kappa kraft cook [23].

It is generally acknowledged that an O- or OO-stage can remove 35–50% of the residual lignin in hardwood kraft pulp and 40–65% in softwood kraft pulp, without significantly impairing the selectivity of delignification and the physical pulp properties. The results of extended oxygen delignification studies indicate that distinct yield benefits can be accomplished by interrupting the cook at a high kappa number (e.g., 40–50) in the case of softwood kraft pulps include reference. The subsequent oxygen delignification of the high-kappa number pulps has been shown to provide 3–4% yield benefits over conventional cooking and bleaching technologies. These observed yield benefits are then further amplified by reducing the organic load on the recovery furnace

### 7.3.2

#### **Chemistry of Oxygen Delignification**

*Manfred Schwanninger*

Among different pulping techniques, kraft pulping is the most important process, consisting of wood treatment with a solution of sodium hydroxide and sodium sulfide at high temperature. This results in wood delignification through the degradation of lignin (and also carbohydrates) and its dissolution in pulping liquor. Although a major fraction of wood lignin (~97%) can be removed in kraft pulping, the remainder of the lignin (residual lignin) is rather resistant under the pulping conditions. In order to remove the residual lignin from pulp, oxidative lignin degradation with bleaching reagents such as dioxygen, hydrogen peroxide, ozone, and chlorine dioxide is required.

According to the general concept of the chemistry of delignification [1,2], the reactions of lignin during pulping and bleaching can be divided into two categories:

- Nucleophilic additions and displacements, which are involved in pulping processes, in later phases of lignin-degrading bleaching, and in lignin-retaining bleaching.
- Electrophilic additions and displacements, initiating the lignin-degrading bleaching processes.

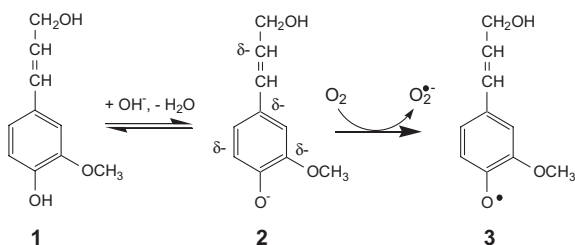
Depending on the nature of the reagent(s), the reactions can be further divided into categories of nucleophilic and electrophilic which frequently, but not always, conform to a reduction-oxidation classification.

Carbonyl carbons or the vinylogous carbon atoms in intermediates of the enone type (quinone methide intermediate; see Section 4.2.4, Chemistry of kraft pulping, Scheme 3) are the sites where the nucleophiles, which are present in pulping liquors, begin the attack [1,2]. Additionally, nucleophilic groups in the  $\alpha$ - (or  $\gamma$ -) position of the side chain attack the  $\beta$ -carbon atom in a neighboring group participation-type of reaction which, in  $\beta$ -aryl ether structures, leads to fragmentation

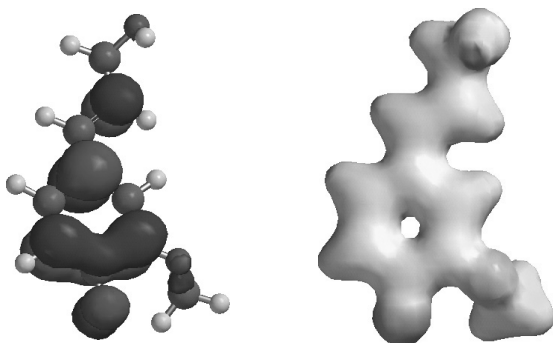
[1,2]. The initial attack by electrophiles, which are present in bleaching liquors, takes place on the aromatic rings and side chains, which are activated by free or etherified phenolic hydroxyl groups [1–4].

In order to emphasize the principal difference in delignification during pulping and bleaching, it should be stressed that delignification during pulping occurs exclusively due to nucleophilic reactions [1,2,5], whereas delignification during bleaching is primarily initiated by electrophilic reactions, which may be followed by nucleophilic processes [6–9].

This initial step of oxygen-alkali bleaching will be briefly described here. In alkaline media, the phenolic hydroxyl group (1) (Scheme 7.1) is deprotonated to produce the phenolate anion (2) that furnishes the high electron density needed to initiate a one-electron transfer. The reactive electrophilic ( $\delta^-$ ) sites marked in Scheme 7.1 (2) are situated at alternating carbons. Scheme 7.2 (left) depicts the HOMO of the phenolate ion of coniferyl alcohol. The size of the orbitals' nodes correspond to centers of high electron density, and hence to sites of preferred attack of electrophiles; thus, they determine the pathway of the subsequent reaction. The resultant electron density distribution is shown in Scheme 7.2 (right), where red zones denote centers of high electron density. Oxygen attacks at an electrophilic ( $\delta^-$ ) site and abstracts an electron, leaving a phenoxy radical (3) and/or a mesomeric cyclohexadienonyl radical, while oxygen itself is reduced to the superoxide anion radical.



**Scheme 7.1** The initial step of oxygen-alkali bleaching at electrophilic ( $\delta^-$ ) sites.



**Scheme 7.2** HOMO-distribution (left) and electron density distribution (right) of the phenylpropene unit 2 shown in Scheme 7.1 (PM3 calculation with Spartan 4.0).

### 7.3.2.1 Bleachability

Beside the differences between hardwood and softwood, it is well known that process parameters such as temperature [10–23], alkali charge and pH [10,13–15,17,19,20,22,24–34], kappa number [35], transition metal ions [34,36], surfactants [37], age of the trees [38,39], wood storage [18,40], pretreatment with chemicals or enzymes [12,19,28,31,41–45], and the formation of hexenuronic acid [10,15,46] have an impact on the bleachability of the pulp due to structural changes in lignin [47–61]. Moreover, the efficiency of delignification depends on structural features such as free phenolic hydroxyl groups, methoxyl groups, carboxyl groups, and linkages between the phenylpropane units (e.g.  $\beta$ -aryl ether linkages) in lignin contribute to a better bleachability of the pulp [29], and on the composition of the residual lignin–carbohydrate complex (RLCC) [62–67]. Notably, a new method to determine kappa number and the bleachability was recently published [68,69].

### 7.3.2.2 Lignin Structures and their Reactivity

#### 7.3.2.2.1 Composition of Lignin, Residual Lignin after Cooking and after Bleaching

The limitation of the extent to which dioxygen delignification can be used is well known in practice and research, and many investigations have focused on an elucidation of responsible lignin structures, namely those that are stable or only react slowly under dioxygen bleaching conditions. Therefore, information on the structures of the residual and dissolved lignins, isolated from pulp and the pulping solution [70,71], is of primary importance for a better understanding of the underlying mechanisms of, for example, kraft delignification and the reactivity of residual lignins in bleaching. Although extensive investigations into the isolation [72–75] and characterization of residual [76,77] and dissolved lignins using different analytical techniques have provided valuable information, their structures are not yet well established. An excellent review of the procedures used for residual lignin has recently been published [78]. Further progress in the characterization of lignins and lignin–carbohydrate complexes requires the application of advanced techniques such as nuclear magnetic resonance (NMR) [12,35,79–89] and others [77].

Based on the results of different procedures [78] applied, theoretical models for residual lignin structures have been developed, and upon these presumed structures functional groups and linkages have been selected for the study of model compounds. Although the rate of degradation in actual lignin systems is much slower and the extent of degradation is much lower [90], this might be due to the different matrices and accessibility [26,31,63,66,80,91–93]. Moreover, despite the selectivity of the chemical agents used [94], the results obtained with model compounds are valid when describing lignin degradation, as comparisons with lignin studies have revealed [90].

An excellent review of lignin model compound reactions under oxygen bleaching conditions has recently been published [90]. This presents a compilation of published data relating to functional group contents in residual kraft lignins (Tab. 7.3) and the relative reactivity of functional groups of lignin model compounds

with oxygen (Tab. 7.4). The content of free phenolic hydroxyl groups, which is important for lignin solubility and reactivity, was increased to about 25/100 C9 in residual lignin and to about 65/100 C9 in dissolved kraft lignins [90].

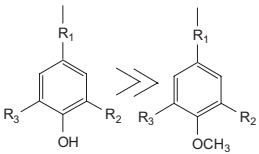
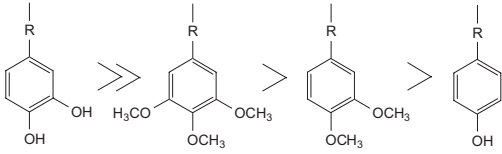
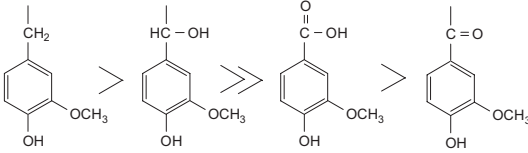
Tab. 7.3 Functional group content in residual lignin (from Ref. [90]).

Functional group	Amount relative to native lignin <sup>a</sup>	Amount	Reference
Free phenolic hydroxyl	~20% higher	25–35/100 C9	50, 95
Methoxyl group	~20% lower	Variable	60
Catechol	Formed in pulping	3/100 C9	96
Aliphatic hydroxyls	~60% lower	40/100 C9 <sup>b</sup>	81, 83
Aliphatic carbonyls	Destroyed in pulping	Negligible	82, 97
Aliphatic carboxyls	Formed in pulping	5/100 C9 <sup>b</sup>	81, 98
Aliphatic reduced units	Higher	Variable	97

a. Approximate differences for a residual kraft lignin from a 30 kappa pulp.

b. Converted literature values to groups/100 C9 using 185 g mol<sup>-1</sup> as C9 unit.

Tab. 7.4 Relative reactivity of lignin model compounds with oxygen (from Ref. [90]).

Functional group	Relative reactivity to oxygen	Reference
Phenolic hydroxyl		100
Methoxyl		100–102
Side chain		100–102

Due to lack of reactivity of nonphenolic compounds, studies on ring cleavage by oxygen have focused on compounds with free phenolic hydroxyl groups. The former can be degraded in the presence of a compound containing a free phenolic hydroxyl group that produces oxygen radical species in the reaction with oxygen [99]. Depending on the raw material (hardwood or softwood), the number of methoxyl groups varies and is also affected by alkaline demethylation reactions that form catechol groups during pulping. Although the catechol-containing compounds are by far the most reactive, their number present in residual lignin following oxygen bleaching is not significantly changed, indicating that these groups are also formed during oxidation [90].

Carboxyl groups, not present in native lignin, are formed during kraft pulping (Tab. 7.3) and oxygen bleaching through side chain and ring cleavage reactions. In contrast, muconic acid structures are the primary ring cleavage products that should be present in only minor quantities after oxygen bleaching, due to their high reactivity [90,103].

The quantity of aliphatic hydroxyl groups in softwood kraft pulp (Tab. 7.5) [80] increased after oxygen alkali treatment, while the carboxyl group content decreased after an initial increase in the residual lignin, and the quantity of all hydroxyl groups increased in the effluent lignin. Both were accompanied by a drastic increase in carbohydrates. Others have also found comparable changes in the hydroxyl group content [104,105].

**Tab. 7.5** Quantities of reactive groups (e.g., aliphatic hydroxyls, phenolic hydroxyls, carboxylic acid groups) and carbohydrate content in lignin samples (from [80]).

Group	RL [mmol g <sup>-1</sup> ]	Lig-1 <sup>st</sup> [mmol g <sup>-1</sup> ]	Lig-2 <sup>nd</sup> [mmol g <sup>-1</sup> ]	Lig-3 <sup>rd</sup> [mmol g <sup>-1</sup> ]	Lig-L1st [mmol g <sup>-1</sup> ]	Lig-L2nd [mmol g <sup>-1</sup> ]
Aliphatic OH	1.56	3.52	4.14	3.87	1.87	2.66
Condensed phenolic OH	1.02	0.77	0.52	0.55	0.91	1.10
Guaiacyl phenolic OH	0.92	0.55	0.32	0.30	0.57	0.60
<i>p</i> -hydroxyphenolic OH	–	0.09	0.06	0.07	0.13	0.22
Carboxyl OH	0.43	0.68	0.30	0.32	0.69	1.27
Carbohydrate (%)	0.9	10.4	9.8	9.5	4.8	4.2

RL: residual lignin; 1st: first stage; 2nd: second stage; 3rd: third stage of oxygen delignification, Lig-L1st: lignin from liquor after first stage of oxygen delignification.

The number of aliphatic saturated methylene and methyl groups increases significantly in residual and dissolved lignin [90], followed by a further increase during oxygen bleaching [105].

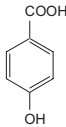
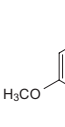
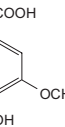
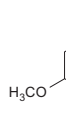
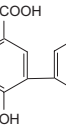
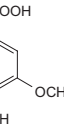
Investigations into the effect of side-chain constituents on the reactivity of model compounds to oxygen [90,100,102] revealed that structures containing methylene or methyl groups are quite reactive, followed by alcohols, carboxylic acids, aldehydes and ketones, whereas the latter three groups of compounds are only slightly reactive under oxygen bleaching conditions [90].

The frequency of linkages in kraft residual lignin (see Tab. 7.7) and the reactivity of model compounds containing these linkages under oxygen bleaching conditions (see Tab. 7.9) are presented. Though the exact nature of each linkage in kraft residual lignin has yet to be fully determined [90], and the importance of each linkage to the susceptibility of lignin to degradation by oxygen is not clear [90].

The different numbers of linkages found by researchers are mainly due to the different procedures used.

The degradation acids found in kraft pulp lignins before and after oxygen delignification presented in Tab. 7.6 show slightly higher amounts of condensed lignin structures of the 5,5' type. A similar tendency can be seen when comparing the lignin dissolving late in the kraft cook [61]. This occurrence was also reported by Fu and Lucia [80], who concluded that *p*-hydroxyphenyl and 5,5' biphenolic units are quite stable and tend to accumulate during oxygen delignification. Additionally, these authors identified oxalic acid and succinic acid [80].

**Tab. 7.6** Relative frequencies of degradation acids obtained from oxidative degradation with permanganate of various pulps and lignins (number per 100 aromatic units) (from Ref. [61]).

						
Kraft pulp	2.6	42.3	16.1	6.0	20.0	12.1
Residual lignin	1.4	40.4	16.7	6.5	22.2	12.0
O-delig. Kraft pulp	1.2	38.4	18.8	6.0	24.3	11.4
Residual lignin	1.2	33.5	19.1	5.9	26.5	13.3
Diss. lignin, 85–93%	0.7	44.8	19.5	4.2	19.9	10.4
Diss. lignin, 93–95%	0.6	40.0	20.5	4.5	22.0	11.9



The  $\beta$ -O-4 linkage, in being the most abundant in native lignin, is significantly cleaved during kraft pulping [59] and contributes to a better bleachability [29] (Tab. 7.7).

The determined numbers of diphenylmethane (DPM) -type structures formed during alkaline cooking varied over a wide range, and the validity of the method used in determining the high values has been questioned [90,106].

Tab. 7.7 Frequency of linkages in kraft residual lignin (from Ref. [90]).

Linkage	MWL [% of linkages]	Reference	Residual lignin <sup>a</sup> [relative to MWL]	Reference
$\beta$ -O-4	48	107	85% lower	52
$\beta$ -5	7–8	108, 109	Slightly greater	49, 96
	9–12	110		
$\beta$ -1	<2	107		
	3.5	111		
5–5	10–11	110		49, 96
	(16) <sup>b</sup>	109	Slightly greater	
	(24–26) <sup>b</sup>	112		
4-O-5	4–5	109, 113	Slightly greater	49, 96
$\beta$ - $\beta$				
Stilbenes	Negligible		~3% of linkages	114
Vinyl ethers	Negligible		0.5–1% of linkages	52
DPM <sup>c</sup>	Negligible		Debatable amounts <sup>d</sup>	106, 113, 115

a. Approximate differences for a residual kraft lignin from a 30 kappa pulp.

b. Values represent % of phenyl propane units containing 5,5' linkages.

c. Diphenylmethane structures of various linkages.

d. Amounts ranging from ~5% to >60% have been reported.

Gellerstedt and Zhang [61] summarized some of the residual kraft lignin features, as follows:

- A low remaining amount of  $\beta$ -O-4 structures [52].
- Linkages between lignin and polysaccharides.
- The presence of reduced structures such as methylene and methyl groups [48].
- A high degree in discoloration [116].

- A successive increase of “condensed” structures with high degree of delignification [49].
- An uneven distribution of lignin across the fiber wall.

As noted, a successive cleavage of  $\beta$ -O-4 structure takes place in the kraft cook (Tab. 7.8) ([61]). Moreover, the data in Tab. 7.8 highlight changes in the number of substructures during pulping and bleaching. An increasing number of  $\beta$ -O-4 linkages during oxygen delignification (Tab. 7.8) was also observed by Balakshin et al. [79].

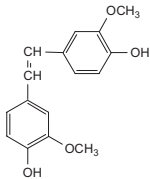
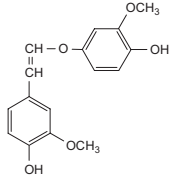
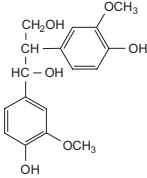
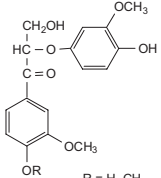
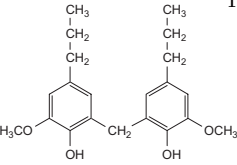
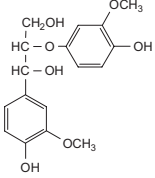
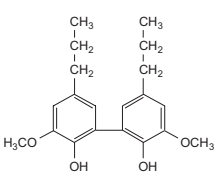
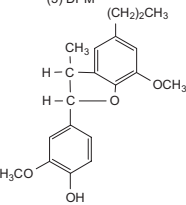
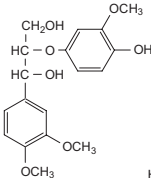
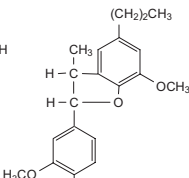
**Tab. 7.8** Number of substructures per 100 C9 in some isolated lignin samples (adapted from Ref. [61]) prepared by acid hydrolysis [117].

Lignin sample	$\beta$ -O-4	$\beta$ -5	$\beta$ - $\beta$
MWL	39 <sup>a</sup>	11	2
Residual lignin, kappa = 30	9–10	5	2
Residual lignin, kappa = 18	5–7	3	1
Dissolved kraft lignin	5	2	2
Residual lignin, from a commercial pulp, kappa = 26	11	6	2
Residual lignin, after an oxygen stage, kappa = 9.3	18	8	2

a. Includes  $\alpha$ -hydroxy- $\beta$ -O-4 and dibenzodioxocin structures.

Comparison of the relative stability and susceptibility of different structures of dimeric model compounds to degradation by oxygen is difficult due to the different conditions used, because the oxidation rate in these reactions is highly affected by system parameters such as pH, temperature, oxygen charge, and reactant charge [90,118]. Stilbene structures (Tab. 7.9) are rapidly degraded under oxygen-alkali conditions [118]. Phenolic stilbenes and vinyl ethers degrade across the double bond, whereas the stilbenes oxidize over one hundred times faster [90]. Under oxygen-alkali conditions, the model compounds in the second row of Tab. 7.9 react an order of magnitude slower than the vinyl ethers, to form phenolic aldehydes, alcohols, ketones, and carboxylic acids along with aliphatic acids as the main degradation products [90].

Tab. 7.9 Relative susceptibility of model compounds to oxygen (from Ref. [90]).

Model compounds tested (approximate order of reactivity)	Reference
<p>Very reactive</p> <div style="display: flex; justify-content: space-around; align-items: center;"> <div style="text-align: center;">  <p>(1) Stilbene</p> </div> <div style="text-align: center;">  <p>(2) Vinyl ether</p> </div> </div>	118
<p>Somewhat reactive</p> <div style="display: flex; justify-content: space-around; align-items: center;"> <div style="text-align: center;">  <p>(3) <math>\beta</math>-1</p> </div> <div style="text-align: center;">  <p>(4) <math>\beta</math>-O-4, <math>\alpha</math>-carbonyl R = H, CH<sub>3</sub></p> </div> <div style="text-align: center;">  <p>(5) DPM</p> </div> </div> <div style="display: flex; justify-content: space-around; align-items: center; margin-top: 10px;"> <div style="text-align: center;">  <p>(6) <math>\beta</math>-O-4, <math>\alpha</math>-hydroxyl</p> </div> <div style="text-align: center;">  <p>(7) 5-5</p> </div> <div style="text-align: center;">  <p>(8) <math>\beta</math>-5</p> </div> </div>	118-124
<p>Non-reactive</p> <div style="display: flex; justify-content: space-around; align-items: center;"> <div style="text-align: center;">  <p>(9) <math>\beta</math>-O-4, <math>\alpha</math>-hydroxyl</p> </div> <div style="text-align: center;">  <p>(10) <math>\beta</math>-5</p> </div> </div>	122, 124

### 7.3.2.2.2 Composition of RLCC Before and After Bleaching

The composition of the RLCC from two pulps, namely a conventional kraft pulp (CK) and a polysulfide/anthraquinone pulp (PSAQ), isolated with enzymatic hydrolysis and further purified is shown in Tab. 7.10 before and after oxygen-alkali bleaching [62]. The number of methoxyl groups decreased due to demethylation, and the number of phenolic hydroxyl groups also decreased (see Tabs. 7.3 and 7.5). Moreover, an increase in the proportion of  $\alpha$ -conjugated phenolic

**Tab. 7.10** Composition of the purified RLCC of two pulps prior and after oxygen alkali treatment (adapted from Ref. [62]).

	Kappa number	OCH <sub>3</sub> (% of C9)	PhOH (% of C9)	Proportion of $\alpha$ -conjugated PhOH (%)	Proportion of weakly acidic PhOH (%)	Molecular weight [Da]	Arabinose <sup>c</sup>	Galactose <sup>c</sup>	Glucose <sup>c</sup>	Xylose <sup>c</sup>	Mannose <sup>c</sup>
CK <sup>a,d</sup>	31.6	71	32	11	23	50 900	0.3	2.06	1.19	1.5	1.8
PSAQ <sup>a,d</sup>	33.6	72	32	12	23	45 100	0.3	2.72	1.52	1.2	3.07
Si <sup>e,f6</sup>	29.0	79	20	6	28	80 000			0.33		-0.82
CK/O <sup>a,d</sup>	17.2	62	21	18	13	33 000	0.45	1.28	1.36	1.57	1.93
PSAQ/O <sup>b,d</sup>	18.7	65	20	19	13	39 100	0.41	2.0	1.56	1.22	2.86
Si <sup>e,g</sup>	17.9	85	17	8	21	76 400			0.54		0.18

- a. Conventional kraft pulp (CK) after oxygen bleaching.
- b. Polysulfide/anthraquinone pulp (PSAQ) after oxygen bleaching.
- c. Carbohydrates in mg 100 mg<sup>-1</sup> cellulose.
- d. proRL; <sup>6f</sup> RL; <sup>7g</sup> NaCl RL; d, f and g indicate different purification procedures.
- e. Two stage neutral sulfite pulp (Si).

structures, an increase in the proportion of carboxylic acids, a decrease in the molar mass, and an increase in the hydrophilicity were observed [62]. The arabinose content increased and the galactose, as well as the mannose, content decreased during oxygen bleaching (Tab. 7.10).

Tamminen and Hortling [62] showed that the CK pulp was the most hydrophilic before oxygen delignification, with the best bleachability. The sulfite pulp lignin was structurally quite different from the alkaline pulp lignins, and seemed to dissolve during oxygen delignification without any major oxidation reactions [62].

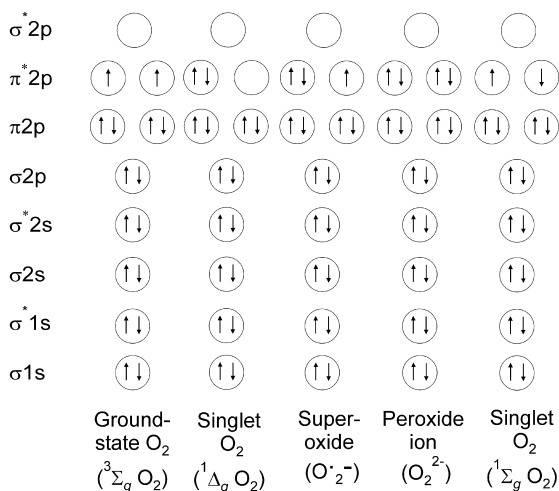
### 7.3.2.3 Oxygen (Dioxygen) and its Derivatives

The element oxygen (chemical symbol O) exists in air as a diatomic molecule, O<sub>2</sub>, which strictly should be called dioxygen. Over 99.7% of the O<sub>2</sub> in the atmosphere is the isotope oxygen-16 (<sup>16</sup>O), but there are also traces of oxygen-17 (<sup>17</sup>O, about 0.04%) and oxygen-18 (<sup>18</sup>O, about 0.2%) [125].

The solubility of dioxygen and the physical transport of dissolved dioxygen gas in an aqueous phase are important properties. The model of Broden and Simonson was used to estimate the solubility of oxygen in equilibrium conditions, as a function of oxygen pressure, temperature and hydroxide ion concentration [126].

### 7.3.2.3.1 Dioxygen: Electronic Structure

The diatomic oxygen molecule  $O_2$  has two unpaired electrons, each located in a different  $\pi^*$  antibonding orbital, having the same spin quantum number or, as is often written, having parallel spins (Fig. 7.24); this is the most stable state – or ground state – of dioxygen. If dioxygen, which can act as an oxidizing agent, attempts to oxidize another atom or molecule by accepting a pair of electrons from it, then both of these electrons must be of antiparallel spin so as to fit in to the vacant spaces in the  $\pi^*$  orbitals (Fig. 7.24). However, a pair of electrons in an atomic or molecular orbital would not meet this criterion, as they would have opposite spins in accordance with Pauli's principle. This imposes a restriction on electron transfer that tends to make  $O_2$  accept its electrons one at a time, and contributes to explaining why  $O_2$  reacts sluggishly with many nonradicals [125]. According to the law that electrons reacting with each other must have antiparallel spin, ground-state dioxygen (triplet-state) cannot react with atoms or molecules in the singlet state due to the spin restriction [127].



**Fig. 7.24** A simplified version of bonding in the diatomic oxygen molecule (16 electrons) in the ground state and of the excited state of dioxygen and his reduction products [125].

### 7.3.2.3.2 Principals of Dioxygen Activation

Due to the electron-configuration, dioxygen takes up one electron at a time – a process termed one-electron reduction [125,127]. By stepwise addition of electrons to the molecular orbital of ground state dioxygen, the reduction products of oxygen are formed (Fig. 7.25 and Scheme 7.3). On the addition of one electron, superoxide is formed. A second electron produces peroxide. Two more produces 2 separated oxides since no bonds connect the atoms (the number of electrons in antibonding and bonding orbitals are identical). Each of these species can react with protons to produce species such as  $HO_2^\bullet$ ,  $H_2O_2$  (hydrogen peroxide) and  $H_2O$ .

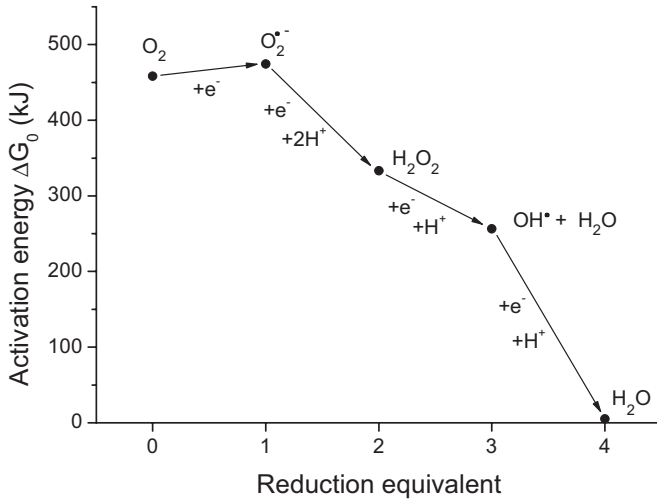
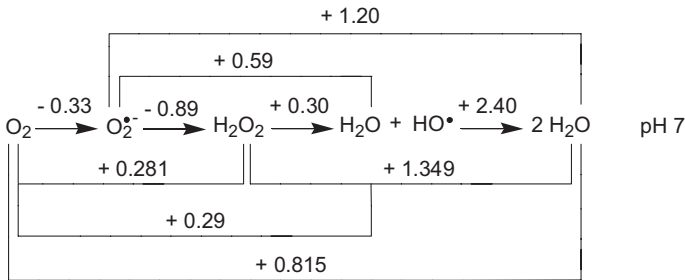
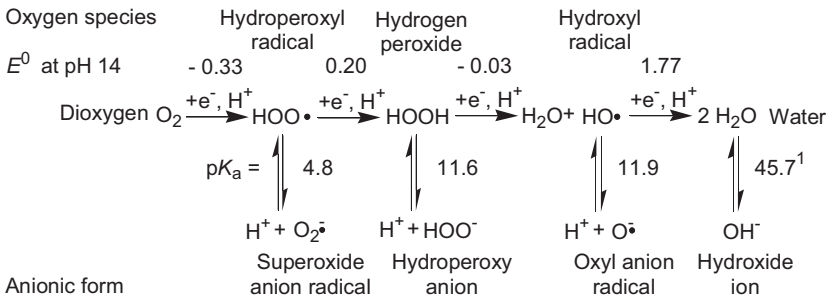


Fig. 7.25 Energetics of oxygen-reduction [127].



Scheme 7.3 Dioxygen redox potentials at pH 7 [127].

Under the conditions used in dioxygen delignification, with the pH in the range between 10 and 13, the standard redox potentials of the reactive species are substantially reduced (Scheme 7.4) due to the lower potential of the ionized form.

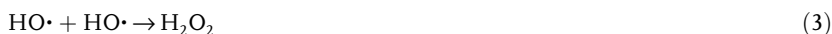


Scheme 7.4 Dioxygen reductions proceeding in four consecutive one-electron steps ( $E^0$  standard reduction potential) (according to [128]).

Therefore, in order to initiate a reaction, increases of the temperature and the ionization of functional groups (ionized phenolic hydroxyl groups on lignin) are necessary to facilitate the electron transfer to dioxygen and its related species.

### 7.3.2.3.3 The Reactions of Dioxygen and its Reduction Products

Under alkaline conditions the reaction of dioxygen with an activated lignin model compound (particularly a phenolate) generates a superoxide anion radical [3,129,130]. This is generally the rate-determining step of the oxidation requiring elevated temperatures [131] or the presence of metal ions [132], whereas the superoxide anion radical can undergo a metal-catalyzed dismutation [133–135] forming hydroperoxy anion that can further undergo a metal-catalyzed disproportionation reaction forming a hydroxyl radical. The following equations show some interconversion reactions that oxygen species can undergo. Most of these are extremely rapid, but others [Eqs. (4) and (5)] are very slow; indeed, for some reactions, metals or protons are required for catalysis [136].

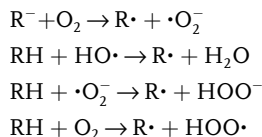


### 7.3.2.3.4 Autoxidation

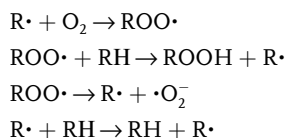
The term “autoxidation” comprises the oxidation with dioxygen [137] and a multitude of free radical reactions catalyzed by transients in the system such as hydroxyl radicals (autocatalysis) and superoxide anion radicals [1,7,138]. This chain process with various phases of autoxidation starting with the initiation of the reaction of dioxygen [131], being the least reactive, with the activated substrate (particularly a phenolate) requires an elevated temperature [137] and/or the presence of heavy metals [132], acting as redox catalysts [3], forming a superoxide anion radical and a substrate radical [Eq. (9)]. As noted, oxygen bleaching must be conducted in an alkaline environment (pH > 10) and a temperature of about 80–100 °C and beyond to ensure reasonable rates. At higher pH (alkali charge) and temperature (about 120 °C), hydroperoxides decay homolytically to hydroxyl radicals. Whilst activation

of the substrate and elevated temperatures are needed to initiate the reaction [Eq. (9)], dioxygen, on the other hand, reacts very rapidly with any substrate radical to the corresponding peroxy radical [Eq. (10), propagation]. The recombination and termination respectively is accomplished by coupling of two radicals and does not require activation by ionization, as is needed for electron transfer.

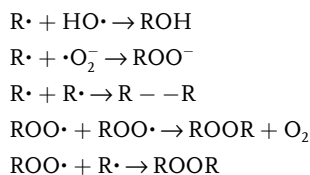
Eq. (9): Initiation [4]



Eq. (10): Propagation [4]



Eq. (11): Recombination – Termination

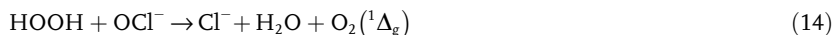


The initiation step above occurs mostly at C atoms which can produce the most stable free radicals (allylic, benzylic position, and  $3 > 2 \gg 1$  carbons). Hence, unsaturated fatty acids are extra-reactive at the methylene C that separates the double bonds.

#### 7.3.2.3.5 Singlet $O_2$ – Excited State

Singlet dioxygen, with a lifetime of about 0.06 s, can be generated from triplet dioxygen by photoexcitation [127,139]. Alternatively, it can be made from triplet oxygen through collision with an excited molecule (photosensitizer), which relaxes to the ground state after a radiationless transfer of energy to triplet oxygen to form reactive singlet oxygen [Eq. (12)] [125,140,141]. Furthermore, singlet oxygen is generated by the reaction between a hydroxyl radical and a hydroperyl radical [Eq. (13)], and between HOCl and peroxide [Eq. (14)] [142], the oxidation of the superoxide anion radicals with heavy metals [Eq. (15)] or ozone [Eq. (16)], and in consequence of the decay of polyoxides.

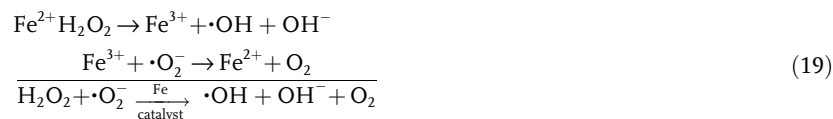
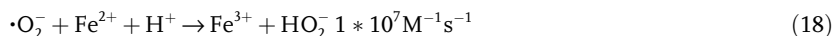




Alkenes (double-bonds) react with oxygen to form hydroperoxides, potentially through an epoxide intermediate, and dienes reacts with oxygen in a Diels–Alder-like reaction to form endoperoxides.

#### 7.3.2.3.6 Superoxide Anion Radical

This is generated during the initiation step of the autoxidation [Eq. (9)], and undergoes several interconversion reactions with other dioxygen-derived species [Eqs. (1), (4), (5), and (7)]. In the presence of metal ions, the superoxide anion radical can be oxidized to dioxygen [Eq. (17)] or reduced to the hydroperoxy anion [Eq. (18)] [125]. The reduction of  $\text{Fe}^{3+}$  by the superoxide anion can accelerate the Fenton reaction, giving a superoxide-assisted Fenton reaction [Eq. (19)] [125].

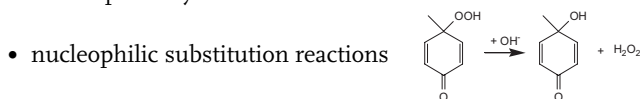


Due to its low oxidation potential, the superoxide anion radical is highly selective. It is a very strong Brønsted base capable of accepting a hydrogen from weak acidic structures, and preferentially reacting with dihydroxy structures through deprotonation followed by dehydration.

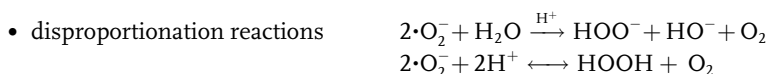
#### 7.3.2.3.7 Hydrogen Peroxide

In contrast to dioxygen, which contains multiple bonds between the O atoms, hydrogen peroxide has only one bond, which can be easily broken. Remember, bonds can be broken in a heterolytic manner (both electrons in a bond go to one of the atoms), or in a homolytic fashion, in which one electron goes to each atom.

During dioxygen delignification, hydrogen peroxide [143] and the hydroperoxide anion respectively evolve in situ from:



and



Some properties and reactions of hydrogen peroxide include the following:

- Acid/Base:  $\text{H}_2\text{O}_2 \xrightarrow[-\text{H}^+]{\text{p}K_{\text{a}1}} \text{HO}_2^- \xrightarrow[-\text{H}^+]{\text{p}K_{\text{a}2}} \text{O}_2^{2-}$  ( $\text{p}K_{\text{a}1} = 11.8$ ;  $\text{p}K_{\text{a}2} > 16\text{--}18$  [127] or 30 [128]; see Scheme 7.4)
- Reaction with  $\text{Fe}^{2+}$ : The Fenton reaction:  $\text{HOOH} + \text{Fe}^{2+} \rightarrow \text{Fe}^{3+} + \text{HO}\cdot + \text{HO}^-$ . In this reaction, a homolytic cleavage of the O–O bond occurs, generating  $\text{OH}^-$  and the hydroxyl radical ( $\text{HO}\cdot$ ), which will react with any molecule it encounters. The hydroxyl radical may be formed via an oxoiron(IV) intermediate [144]. The peroxide can also be effective as an oxidant, and in a transition metal-induced cleavage of the H–OO bond the hydroperoxyl radical ( $\text{HOO}\bullet$ ) is formed:  $\text{HOOH} + \text{Fe}^{3+} \rightarrow \text{Fe}^{2+}\text{HOO}\cdot + \text{H}^+$
- Thermal or photochemical homolytic cleavage of hydrogen peroxide:  $\text{HOO}^- + \text{HOOH} \xrightarrow{\text{Energy}} \text{H}_2\bullet + \text{HO}\bullet + \text{H}^-$

#### 7.3.2.3.8 Hydroxyl Free Radical

As mentioned earlier, this species is extremely reactive [136]. It will react with any molecule it encounters, and does so immediately. It can abstract a H atom, leaving another free radical. The anionic form, the oxyl anion radical (see Scheme 7.4), displays properties that are distinctly different from those of the hydroxyl radical. In contrast to the latter, the oxyl radical reacts predominantly by hydrogen abstraction and is therefore probably less selective than the hydroxyl radical [145].

*Note:* The terms hydroxyl free radical and hydroxyl radical are used synonymously. Care must be taken using the term hydroxyl ion, which is the synonym for the hydroxide ion ( $\text{OH}^-$ ).

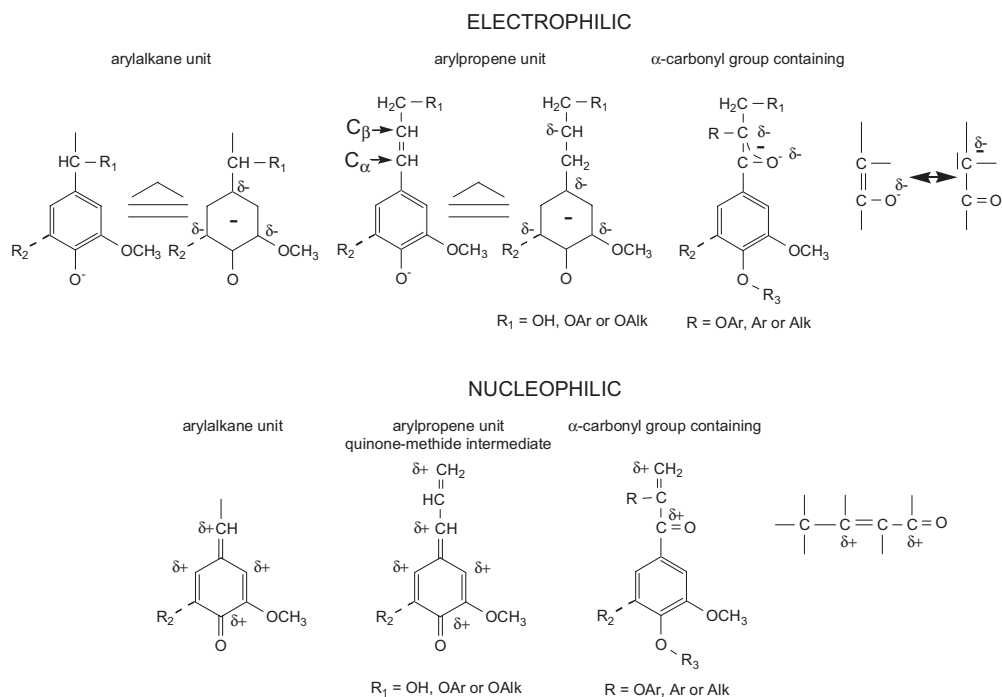
#### 7.3.2.3.9 Electrophilic–Nucleophilic Reactions

As noted, delignification during bleaching is initiated by electrophilic reactions, which may be followed by nucleophilic processes [6–9]. The reactive oxygen species (ROS) are listed in Tab. 7.11, according to their electrophilic–nucleophilic character. Under the conditions of oxygen-alkali bleaching, the hydroperoxyl radical is deprotonated to produce the superoxide anion radical. About half of the hydroxyl radical is present as its base the oxyl anion radical (Tab. 7.11; see also Scheme 7.4), and about half of the hydroperoxy anion is present as hydrogen peroxide (Scheme 7.4).

**Tab. 7.11** Reactive oxygen species (ROS) listed according to their electrophilic – nucleophilic character.

Electrophiles			
Triplet dioxygen	$^3\text{O}_2$		
Hydroperoxyl radical	$\text{HOO}\cdot \xrightarrow{pK_a=4.8} \cdot\text{O}_2^-$	Superoxide anion radical	
Hydroxyl radical	$\text{HOO}\cdot \xrightarrow{pK_a=11.9} \cdot\text{O}_2^-$	Oxyl anion radical	
Nucleophiles			
Hydroperoxy anion	$\text{HOO}^-$		
Singlet dioxygen	$^1\text{O}_2$		

The sites of electrophilic and nucleophilic attacks in lignins are shown in Fig. 7.26. The  $\pi$ -system of the aromatic ring can be overlapped by the lone electron pairs on the oxygen atom in *para*-hydroxy and the *para*-alkoxy groups, creating centers of high electron density (Fig. 7.26), that can be attacked by electrophiles. High electron density ( $\delta^-$ ) also appears at the  $\text{C}_\beta$  atom of aliphatic double bonds



**Fig. 7.26** Sites of electrophilic ( $\delta^-$ ) and nucleophilic ( $\delta^+$ ) attacks in lignin (adapted from Ref. [2]).

conjugated to the aromatic ring. By elimination of an  $\alpha$ - (see Section 4.2.4, Chemistry of kraft pulping, Scheme 3) or, in conjugated structures, a  $\gamma$ -substituent, a quinone-methide intermediate is formed from the arylalkane unit (Fig. 7.26), which involves the loss of two electrons, resulting in the generation of centers of low electron density ( $\delta^+$ ) that constitute the sites of attack by nucleophiles [2].

#### 7.3.2.4 A Principal Reaction Schema for Oxygen Delignification

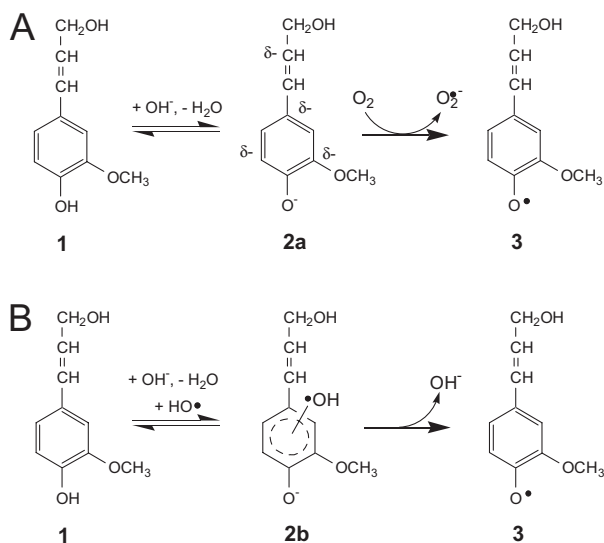
Over 30 years of research into the oxidation of lignin and lignin model compounds with dioxygen has now elapsed, and has provided insights into the reactions involved in the degradation, and their mechanisms. Based on the reaction products formed from the degradation of lignin and lignin model compounds with dioxygen and with ROS generated during bleaching, a number of mechanisms have been proposed. Several excellent reviews have been produced on the mechanisms involved in lignin degradation [1,2,4,6,7,72,101,122,138,146,147] and the reactive species present in these reactions [3,9,90,129,130], including their selectivity. The latter remains of interest [148,149], especially in connection with protective systems and additives [94,150–156]. In addition, an excellent book on oxygen delignification chemistry was published a few years ago [157]. It is impossible to cover all of these mechanisms in detail within this chapter; thus, a general summary with selected mechanisms will be provided.

Oxygen delignification is actually based on the competitive reactions of oxygen or ROS within pulp lignin and carbohydrates [94]. Lignin removal under alkali-oxygen conditions is accompanied by a kinetically less favorable oxidation of carbohydrates, whereas the oxidation of the carbohydrates becomes a more favorable process when the kappa number decreases [94]. The reaction of phenolic compounds with oxygen produces ROS, namely the hydroxyl radical ( $\bullet\text{OH}$ ), which can degrade nonphenolic (model) compounds.

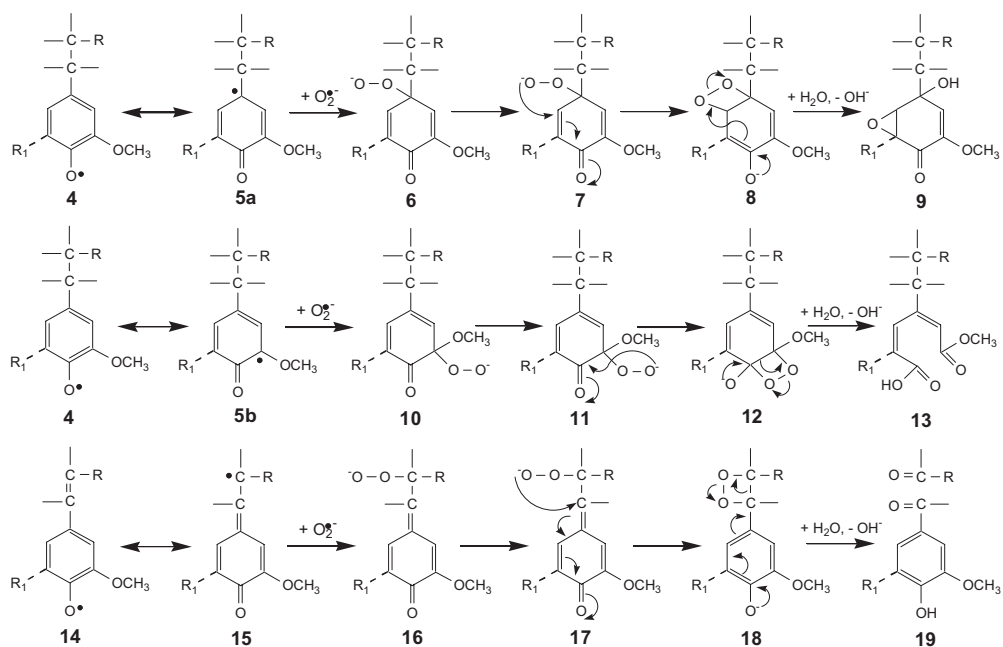
As shown previously (see Scheme 7.1), the initial step in oxygen-alkali bleaching is the formation of the phenoxyl radical as a consequence of an electrophilic attack by oxygen (Scheme 7.5A). Moreover, the hydroxyl radical formed during oxygen treatment [Eqs. (5), (6), and (19)] is also capable of generating a phenoxyl radical (Scheme 7.5B) being reduced to the hydroxide anion ( $\text{OH}^-$ ).

A principal reaction schema for oxygen delignification [3,6,7,138] starts with the generation of hydroperoxides, which are key intermediates in the oxidation of lignins and carbohydrates. They can be formed either by electrophilic or nucleophilic reactions:

- Formation of hydroperoxides [8,138]
- Fragmentation of hydroperoxides (homolytic – forming radicals; or heterolytic – forming hydrogen peroxide, singlet oxygen) [8,138]
- Involvement of the radicals in the bleaching process [3,9,129,130]

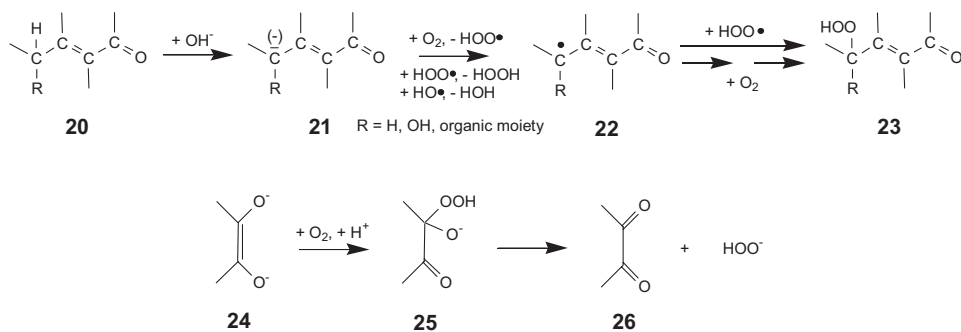


**Scheme 7.5** Formation of the phenoxyl radical by oxygen (A) and the hydroxyl radical (B).



R = H, OAr, Ar or Alk

**Scheme 7.6** Formation of hydroperoxide intermediates in alkaline media followed by an intramolecular nucleophilic attack of the hydroperoxide anions (adapted from Ref. [6]).

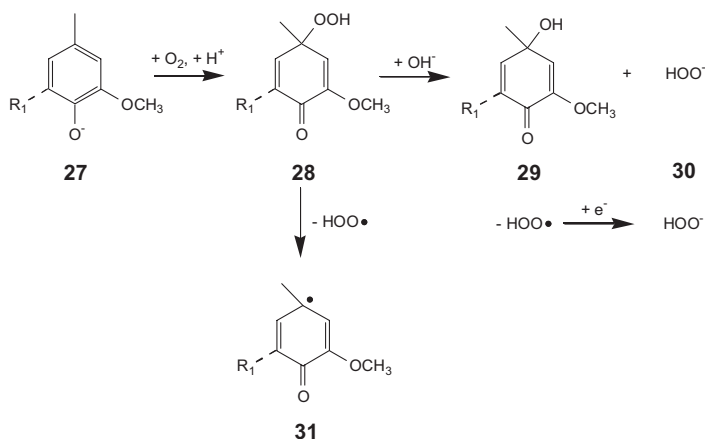


**Scheme 7.7** Formation of hydroperoxides in the autoxidation of enolisateable and enediol structures, and the formation of the hydroperoxy anion (adapted from Refs. [4,6]).

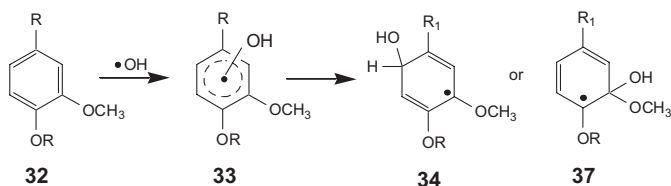
The abstraction of an electron from phenolate anions by oxygen (or the hydroxyl radical) (Scheme 7.5) yields phenoxyl radicals (Scheme 7.6, 4 and 14) and the mesomeric cyclohexadienonyl radicals (5a and 5b) or “quinone methide” radicals (15). The superoxide anion radicals then form hydroperoxide intermediates (6 and 10) with the mesomeric cyclohexadienonyl radicals or the  $\beta$ -radical (15). A nucleophilic attack by the peroxide anions on the carbonyl carbon (11) or a vinylogous carbon of the cyclohexadienone- (7) or quinone methide (17) moieties yields the corresponding dioxetane intermediates (8, 12 and 18). Intermediate 8 finally form an oxirane structure (9). The rearrangement of 12 results in an opening of the peroxide ring and heterolytic cleavage of the carbon–carbon bond, giving a “muconic acid” ester (13), and 18 is fragmented by scission of the  $\text{C}_\alpha$ – $\text{C}_\beta$  bond of the former conjugated double-bond forming the corresponding aldehydes (19) and/or a ketone, depending on the nature of R.

The hydroperoxy intermediates formed during the autoxidation of phenolic (Schemes 7.6 and 7.8) and enolic (Scheme 7.7) structures in lignin and carbohydrates can be displaced by the hydroxide ion via a  $\text{S}_{\text{N}}2$  reaction (28–29), or the bond can be cleaved heterolytically giving the hydroperoxy anion, which is described elsewhere. Homolytic decomposition of hydroperoxy intermediates produces phenoxy (31) and hydroperoxy (Scheme 7.8) radicals. The latter can be reduced to the hydroperoxy anion.

The hydroxyl radical reacts with the main components of wood, and attacks preferentially electron-rich aromatic and olefinic moieties in lignin. It also reacts with aliphatic side chains in lignin and carbohydrates, but at a lower rate. Depending on the pH, the hydroxyl radical is converted to its conjugate base, the oxyl anion radical (see Scheme 7.4). The oxyl anion radical does not react with electron-rich structures, but rather with aliphatic side chains in lignin and carbohydrates. The first step in all reactions of the hydroxyl radical with aromatic substrates (Scheme 7.9, 32) is a rapid addition to the  $\pi$ -electron system of the aromatic ring forming a short-lived charge-transfer adduct (33) that decays under alkaline conditions to give isomeric hydroxycyclohexadienyl radicals (34 and 37).



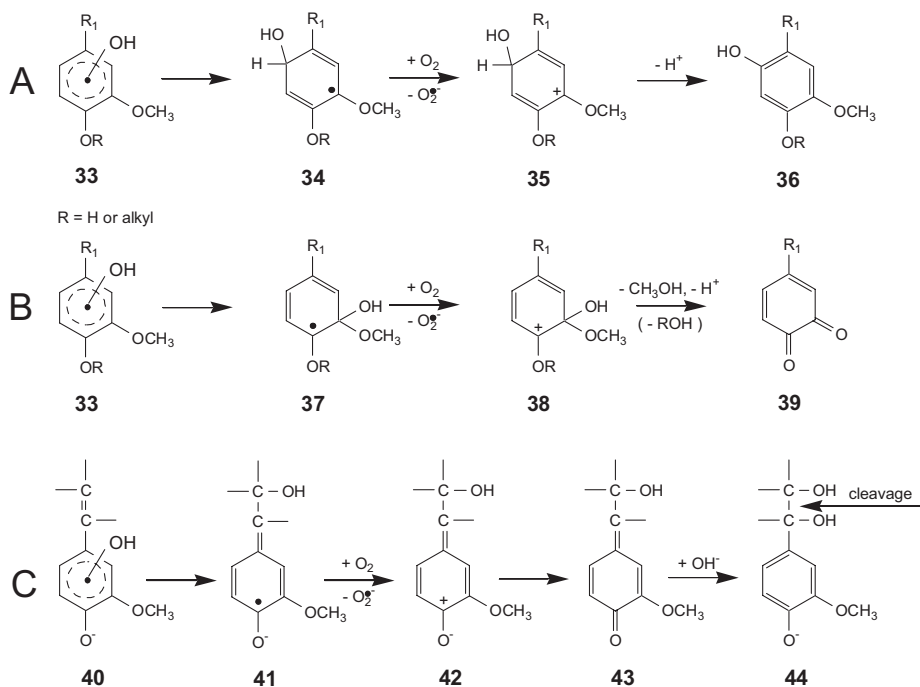
**Scheme 7.8** Formation of hydroperoxides in the autoxidation of phenolic structures, and the formation of the hydroperoxy anion (from Ref. [6]).



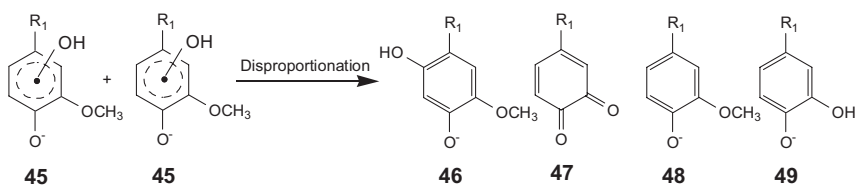
**Scheme 7.9** Formation of hydroxycyclohexadienyl radicals (adapted from Ref. [6]).

The hydroxycyclohexadienyl radical can be oxidized by addition of oxygen (Scheme 7.10) followed by alkali-promoted elimination of the superoxide anion radical forming a cation radical (**35**, **38** and **42**) and elimination of a proton (re-aromatization) leading to hydroxylation (Scheme 7.10, path A, **36**) or, in combination with elimination of methanol and cleavage of an alkyl-aryl ether bond, to dealoxylation (path B) with formation of ortho-quinonoid structures (**39**). From conjugated structures (Scheme 7.10, path C), “quinone methide” intermediates (**41**, **42** and **43**) are formed, giving glycolic structures (**44**) by adding hydroxide ions that undergo oxidative cleavage of the glycolic C–C bond (**44**) [6].

The hydroxyl radical adducts (Scheme 7.11, **45**) can undergo disproportionation reactions from which the same oxidation products (**46** and **47**) arise, together with the corresponding reduction products (**48** and **49**) [6].



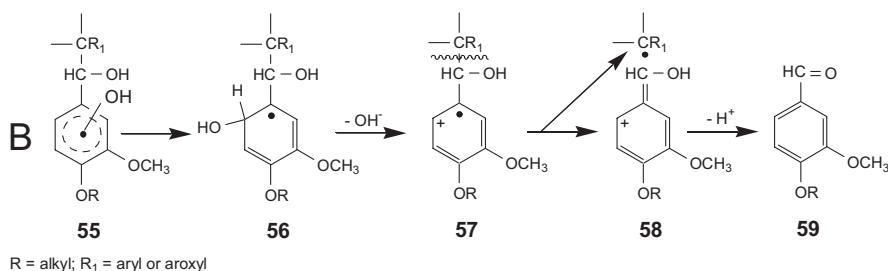
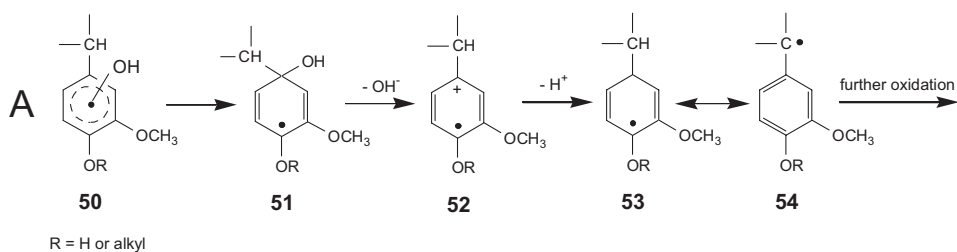
**Scheme 7.10** Reactions of the hydroxyl radical adducts of aromatic and ring-conjugated structures (adapted from Ref. [6]).



**Scheme 7.11** Disproportionation of hydroxyl radical adducts (adapted from Ref. [6]).

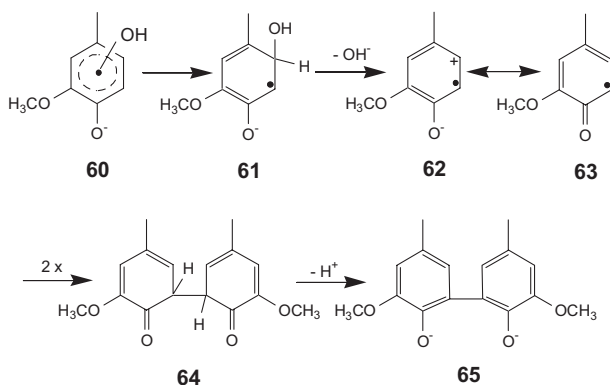
Another reaction mode of the hydroxycyclohexadienyl radical (Scheme 7.12, **51** and **56**) is the elimination of the hydroxyl radical as hydroxide anion (Scheme 7.12, paths A and B). This results in the formation of cation radicals (**52** and **57**) followed by the generation of side-chain oxidation products and products of homolytic  $C_{\alpha}-C_{\beta}$  bond cleavage (**58**). The elimination of a proton leads to a re-aromatization (**59**).





**Scheme 7.12** Reactions of the hydroxyl radical adducts of aromatic and side chain structures (adapted from Ref. [6]).

Elimination of the hydroxyl radical as hydroxide anion results in the formation of a cation radical (**62** and **63**), followed by a phenolic coupling (**64**) (Scheme 7.13) and elimination of two protons to form a diphenyl (5–5) structure (**65**). The formation of diphenyl structures is an undesirable reaction, because the 5–5 bond is very stable and can hardly be cleaved.



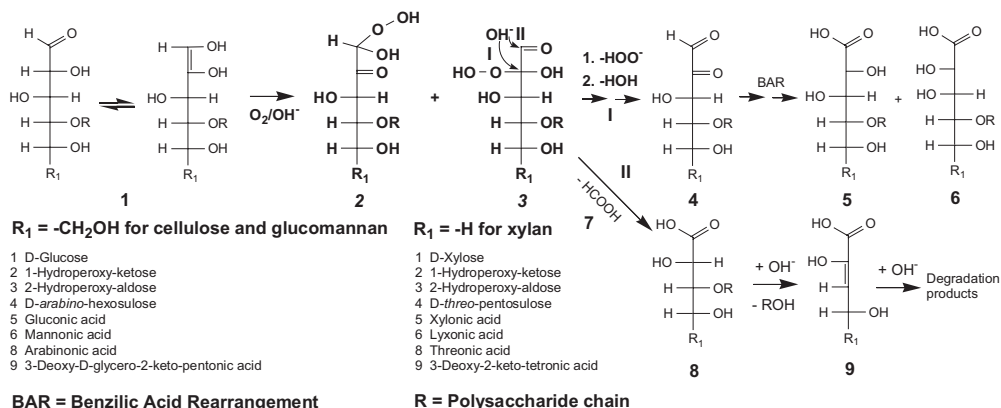
**Scheme 7.13** Phenolic coupling of the hydroxyl radical adducts of aromatic structures (adapted from Ref. [6]).

Singlet oxygen that can be generated during oxygen bleaching in different ways [Eqs. (13–16)] has been of growing research interest for the past few years [140,142,158–180]. Both, lignin model compounds and pulp have been investigated. However, in most of the studies photosensitizers, such as rose bengal

[159,162,164–167,174,179], methylene blue [140,141,160,163,169,175,177] or titanium dioxide (TiO<sub>2</sub>) [139,169,175,177] have been used to generate singlet oxygen using light from the visible range to the UV, the latter also used for direct irradiation of, for example, an  $\alpha$ -carbonyl group-containing lignin. Alternatively, singlet oxygen was produced from sodium hypochlorite (NaOCl) and hydrogen peroxide [142] according to Eq. (14). Some of these studies were performed in organic solvents [162,167,174,176] and others in aqueous alkaline solution [142,168,177,179,181], with the latter category being of main interest for this chapter. The photo- and radiation chemical-induced degradation of lignin model compounds have been summarized in a very good review [171], including other ROS, and the photochemical oxidation of lignin models in the presence of singlet oxygen has been studied by using *ab initio* calculations [178].

As mentioned, singlet oxygen has a pronounced electrophilic character, and hence reacts well with electron-rich groups such as olefinic or aromatic derivatives. These electron-rich groups tend to form an intermediate exciplex as a result of charge transfer reactions between the electron-rich substrate and the singlet oxygen. This exciplex is able to later form dioxetanes, hydroperoxides, or endoperoxides.

Photosensitized degradation studies of  $\alpha$ -carbonyl group-containing lignin model compounds (Scheme 7.14) show that a hydrogen atom transfer from the phenolic OH group (66) to <sup>1</sup>O<sub>2</sub> might occur, leading to a phenoxyl radical (67) and subsequently to quinonoid species (path A). However, formation of an endoperoxide (68) leading ultimately to *p*-quinones (70) is also possible (path B).



**Scheme 7.14** Photodegradation of  $\alpha$ -carbonyl group-containing lignin model compounds (from Ref. [171]).

Moreover,  $\alpha$ -carbonyl-containing  $\beta$ -O-4 lignin model compounds intensively used in singlet oxygen degradation studies have been degraded to products deriving from  $\beta$ -C–O bond cleavage. The main reactions were conversion of phenolic aromatic units into carboxylic acids and cleavage of the  $\beta$ -O-4 ether bonds, leading to a depolymerization of the lignin framework into smaller fragments [177]. Cleavage of the  $\beta$ -O-4 aryl ether bond has been found for phenolic as well as nonpheno-

lic derivatives [162]. Photochemical oxidation of the phenolic  $\beta$ -O-4 aryl ether gave the same type of product, which confirmed that, in this case, the presence of the carbonyl group is not indispensable for the cleavage reaction to occur [162]. When the phenoxy portion of the molecule [1-(4-hydroxy-3-methoxyphenyl)-2-(2,6-dimethoxyphenoxy)-3-hydroxy-1-propanol] shows a lower reactivity towards singlet oxygen, the oxidation of the phenol moiety to hydroquinone can occur. The photochemical behavior of this model compound can be rationalized from a reaction of singlet oxygen with the phenoxy part of the molecule [162].

Due to the unknown real contribution of singlet oxygen to lignin degradation during oxygen bleaching, and the fact that in processes interconversions between reactive species occur, this section of the text will be minimized.

One example of a rose bengal photosensitized degradation of loblolly pine (*Pinus taeda*) kraft pulp, the final product of which contained 4% by mass of residual lignin with the remainder being carbohydrates, is presented [179]. In this study, the reactivity of singlet oxygen with kraft softwood substrates with respect to the chemistry of lignin and cellulose has been investigated. The results revealed that, despite the relatively high selectivity of singlet oxygen for lignin aromatic units, degradation of the cellulose nevertheless occurred after approximately 50% removal of the lignin. A decrease was observed in the number of aliphatic hydroxyls (17%), condensed phenolics (4%), and guaiacyl phenolics (7%), and an increase in carboxylic acids (54%). This result is typical of what is observed in the reactions of ground-state oxygen with pulp or lignin, and suggests that despite the initial electrophilic reactions of singlet oxygen with lignin, it is likely that ensuing oxidations follow some of the typical reactions associated with ground-state oxygen reactions, such as ring additions by hydroperoxide and oxygen followed by ring openings to the muconic esters and acids. However, unlike ground-state oxygen reactions, the levels of condensed phenolics (e.g., conjugated lignin monomers at the C5 positions of the benzene moieties) were reduced during the singlet oxygen reactions. This may be a consequence of the high electrophilic reactivity of singlet oxygen, and was tested by subjecting substrates enriched in condensed phenolics to singlet oxygen reactions [179]. The most salient difference between this system and a typical ground-state oxygen delignification system is the absence of condensed phenolic units in the lignin. Subsequently, it was discovered that both the condensed and noncondensed (guaiacyl) units react well with singlet oxygen [179].

This finding is important since 5-condensed phenolic subunits (5-5 and diphenylmethane; DPM) in lignin are quite resistant. Their relative robustness does not, however, appear to be the main rationale for the inactivity of lignin towards oxygen delignification, but serves to suggest that the nature and reactivity of the free phenolics deserve increasing scrutiny [182].

Residual lignins isolated from unbleached and oxygen-bleached eucalyptus kraft pulps by acid hydrolysis and dissolved lignins in the kraft cooked and oxygen-bleached liquors were studied, and the results compared with the corresponding residual lignins. The data showed that etherified syringyl structures were quite resistant towards degradation in the oxygen bleaching, causing little depolymerization in residual lignin and a small increase in carboxylic acid content, but producing appreciable amounts of saturated aliphatic methylene groups [105].

### 7.3.2.5 Carbohydrate Reactions in Dioxygen-Alkali Delignification Processes

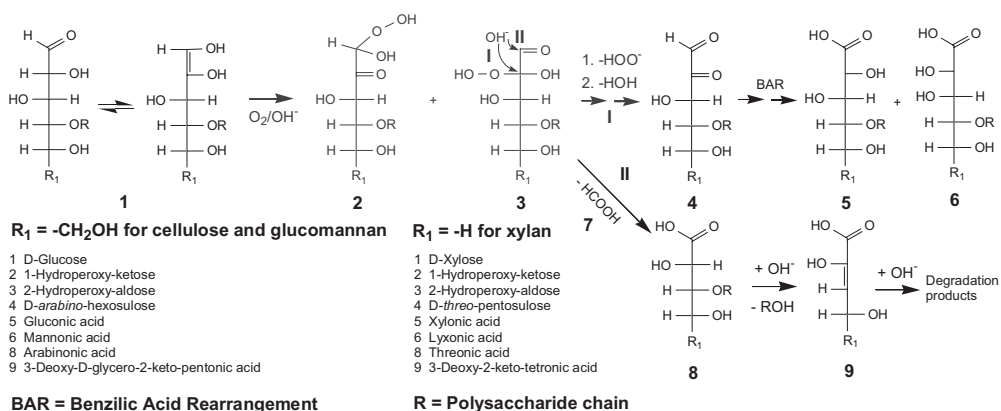
The reactions of wood polysaccharides during dioxygen-alkali treatment can be classified according to Malinen [183] into the following main categories:

- Stabilization of the reducing end-groups.
- Peeling reactions starting from the reducing end-groups.
- Peeling reactions starting from stabilized end-groups.
- Cleavage of the polysaccharide chain.

Reaction steps involving dioxygen are drawn with thicker lines (bold) and the numbers given in *italic*.

#### 7.3.2.5.1 Stabilization of the Reducing End-Groups

The rapid stabilization of the reducing end-groups of polysaccharides by transformation to aldonic acid end-residues has been considered to be one great advantage of the dioxygen-alkali delignification of wood or pulp [184–186]. Under the conditions of dioxygen-alkali treatment, oxidation of the glucose unit (**1**) may proceed via a 1-hydroperoxy-ketose (**2** [187]) and a 2-hydroperoxy-aldehyde (**3**) (Scheme 7.15). The hydroperoxy-group can easily be replaced by a hydroxide anion followed by dehydration (path **I**) resulting in a  $\alpha$ ,  $\beta$ -dicarbonyl (glucosone = *D-arabino*-hexosulose, **4**), which converts into gluconic acid (**5**) and mannonic acid (**6**) via benzilic acid rearrangement (BAR) (see Section 4.2.4.2, Carbohydrate reactions). Glucosone (*D-arabino*-hexosulose) end-groups have been suggested to be intermediates in the formation of aldonic end-residues [188,189], and Theander [185] stated that the fact that mannonic acid and gluconic acid end-residues are obtained on cellulose treatment with dioxygen in basic solution is the best support for the view that glucosone is really an intermediate. Alternatively, the hydroperoxy-intermediates are split to formic acid (**7**) and arabinonic acid (**8**) (path **II**), the latter being converted to 3-deoxy-*D-glycero*-2-keto-pentonic acid (**9**) and further degraded.



**Scheme 7.15** Stabilization of reducing end-residues through formation of aldonic acids (**5**) and mannonic acid (**6**) (adapted from Malinen [183] and Theander [185]).

In the absence of dioxygen, large amounts of 3-deoxy-pentonic acids are formed and under oxidative conditions arabinonic, erythronic and mannonic acids are the major reaction products [190]. A relative composition of aldonic acid residues from various treatments is shown in Tab. 7.12.

**Tab. 7.12** Relative composition (mol. %) of aldonic acid residues from various treatment (from Ref. [185]).

Acid	From D-glucosone			From cellulose	
	NaOH/air 0.04 M, 100 °C 4 h [189]	NaOH/O <sub>2</sub> 0.04 M, 95 °C 1 bar, 5 min [187]	NaOH/N <sub>2</sub> 0.04 M, 95 °C 1 bar, 5 min [187]	NaOH/air 18%, 25 °C 200 h [191]	NaOH/O <sub>2</sub> 0.5%, 100 °C 5 bar, 2 h [184]
Mannonic	11	18	47	15	27
Gluconic	2	5	5	2	3
Arabinonic	58	37	26	58	50
Ribonic	4	6	0	2	2
Erythronic	25	35	22	23	18

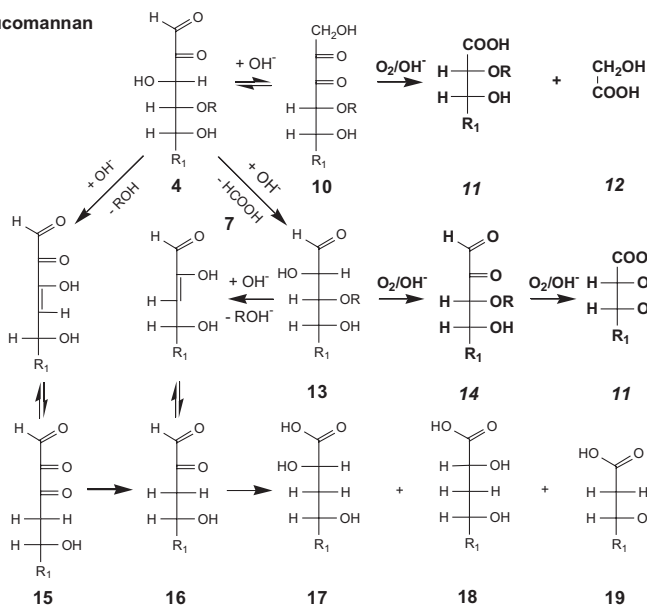
Two different pathways can form erythronic acid (**11**) (Scheme 7.16). The first entails rearrangement of the glucosone to *D*-erythro-2,3-hexodiulose (**10**), followed by an oxidative cleavage and loss of glycolic acid (**12**) [183]. In the second pathway, erythronic acid (**11**) results from alkaline and oxidative degradation of the glucosone (**4**) through arabinose (**13**) and arabinosone (**14**) as intermediates. In the absence of dioxygen arabinose (**13**, Scheme 7.16) and arabinonic acid (**8**, Scheme 7.15), it may be formed by hydroxide ion attack at C1 and C2 respectively [185]. Minor amounts of 3-deoxy-pentonic acids (**17**, **18**) are formed from an arabinose intermediate (**13**), and the main pathway starts with a direct  $\beta$ -hydroxy-elimination in the glucosone (**4**) followed by loss of the elements of carbon monoxide from the intermediate 4-deoxy-*D*-glycero-2,3-hexodiulose (**15**) [187].

The yield of 3-deoxy-pentonic acids is lower in the presence of dioxygen [185], and the formation of arabinonic and erythronic acid is particularly important. Theander [185] stated that an attack of dioxygen to the glucosone (**4**, Scheme 7.17) should give a hydroperoxide (**20**), which should further yield arabinonic acid (**8**) and carbon dioxide. A similar attack at C3 could, via formation of a hydroperoxide (**21**), result in the formation of an erythronic acid end-group (**11**) plus glyoxylic acid (**22**).

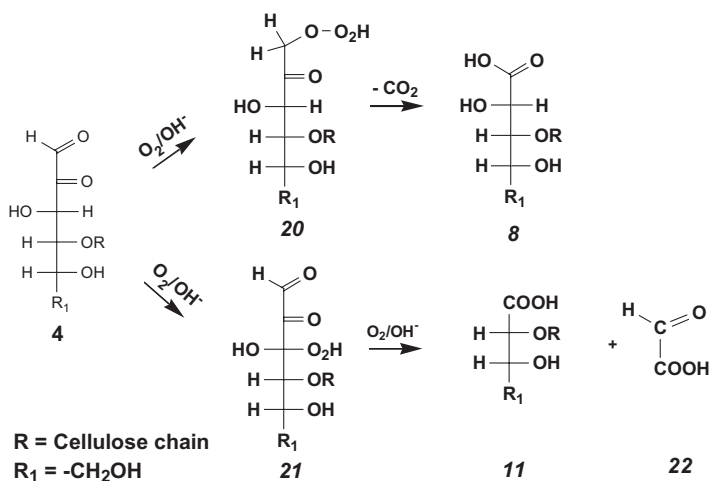
About the same proportions of aldonic acids were produced from glucosone and glucose treated with dioxygen and alkali [183], and cellobiose [190] and cello-triose [192] yielded glucosyl- and cellobiosyl-arabinonic acids as the main products. However, the presence of the substituted erythronic and mannonic acids was also significant, especially at higher alkali concentrations. Malinen and Sjöström

**R<sub>1</sub> = -CH<sub>2</sub>OH for cellulose and glucomannan**

- 10 D-erythro-2,3-hexodiulose
- 11 Erythronic acid
- 12 Glycolic acid
- 13 Arabinose
- 14 Arabinosone
- 15 4-Deoxy-D-glycero-2,3-hexodiulose
- 16 3-Deoxy-D-glycero-pentulosose
- 17 3-Deoxy-D-threo-pentonic acid
- 18 3-Deoxy-D-erythro-pentonic acid
- 19 3,4-Dihydroxybutyric acid



**Scheme 7.16** Degradation pathways of the glucosone and xylosone end-groups (adapted from Malinen [183] and Theander [185]).



**Scheme 7.17** Degradation pathways of the glucosone end-groups to the formation of arabinonic acid (8) and erythronic acid (11) (adapted from Theander [185]).

[192] reported that, when hydrocellulose was subjected to dioxygen-alkali treatment, erythronic acid was the dominating end-group, and that the reaction conditions actually have a marked effect on the composition of the aldonic acid end-groups.

Extensive studies on the formation of aldonic acid groups on cellulose [192], mannan [193], xylan [194] and the corresponding oligosaccharides under various conditions revealed that arabinonic acid was highly predominant after oxidation of 4- $\beta$ -linked mannobiose, mannotriose, and mannotetraose. The stabilization (and also peeling) reactions of glucomannan and cellulose proceed in a similar way (Schemes 7.15 and 7.16) [193]. In contrast, mannose end-groups – which react more slowly than glucose end-groups – are converted to the same reactive “fructose intermediates” as glucose, and the same aldonic acid end-groups in about the same proportions have been found from manno-oligosaccharides and mannan as from cello-oligosaccharides and hydrocellulose [193]. The monosaccharides glucose, mannose, and xylose degrade much faster under dioxygen pressure than the reducing end-groups of the corresponding oligosaccharides, the degradation rates of which are almost the same in dioxygen and nitrogen atmospheres [193].

The formation of aldonic acid end-groups after dioxygen-alkali treatment of birch xylan studied by Kolmodin and Samuelson [195] showed that xylonic (5, Scheme 7.15), lyxonic (6), threonic (8) and glyceric (11, Scheme 7.16) acids were formed as the major terminal acid residues, and xylosone 2,4-dihydroxy-butyric acid (17, 18) was also extensively formed in non-oxidative treatments [194]. Lyxonic and xylonic groups are expected from a benzilic-type rearrangement (BAR) of pentosulose end-unit (Scheme 7.15), whereas oxidative or hydrolytic cleavage leads to threonic acid (8). Glyceric acid (11) is probably formed via cleavage of *D*-glycero-2,3-pentodiulose (10) end-units formed by isomerization of pentosulose units (4), and from alkaline and oxidative degradation of the xylosone (4) through threose (13) and threosone (14) as intermediates.

#### 7.3.2.5.2 Peeling Reactions Starting from the Reducing End-Groups

The peeling removes the terminal anhydro-sugar unit, generating a new reducing end-group until a competitive stopping reaction sets in forming a stable saccharinic acid end-group (see Section 4.2.4.2, Carbohydrate reactions).

In studying the oxidative alkaline peeling reaction of cellulose by using cello-oligosaccharides and hydrocellulose, Malinen and Sjöström ([190, 192]) found in addition to the “normal” alkaline peeling products [isosaccharinic acid (27, Scheme 7.18) and lactic acid (32)], large amounts of 3,4-dihydroxybutyric acid (28), glycolic acid (33), 3-deoxy-pentonic acid (17, 18, Scheme 7.16), formic acid (34) and glyceric acid (35). The formation of the two isomeric glucoisosaccharinic acids (e.g., 27) by alkaline treatment of cellulose is much depressed in the presence of dioxygen [185], and the 4-deoxy-*D*-glycero-2,3-hexodiulose (26) is instead fragmented to 3,4-dihydroxybutyric acid (28) and glycolic acid (33). These are formed via oxidative cleavage of 4-deoxy-*D*-glycero-2,3-hexodiulose (26), which can

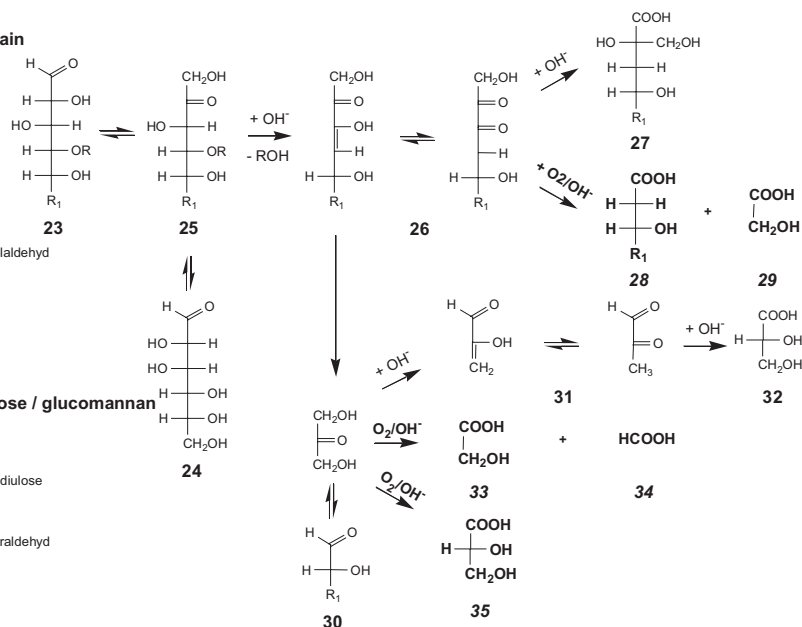
R = Polysaccharide chain

R<sub>1</sub> = -H for xylan

- 23 Xylose end-group
- 25 Xylulose end-group
- 26 4-Deoxy-2,3-pentodiulose
- 27 Xyloisaccharinic acid
- 28 2-Deoxy-glyceric acid
- 29 Glycolic acid
- 30 Dihydroxyacetone and glyceraldehyde
- 31 Methyl glyoxyl
- 32 Lactic acid
- 33 Glycolic acid
- 34 Formic acid
- 35 Glyceric acid

R<sub>1</sub> = -CH<sub>2</sub>OH for cellulose / glucomannan

- 23 Glucose end-group
- 24 Mannose end-group
- 25 Fructose end-group
- 26 4-Deoxy-D-glycero-2,3-hexodiulose
- 27 Isosaccharinic acid
- 28 3,4-Dihydroxybutyric acid
- 29 Glycolic acid
- 30 Dihydroxyacetone and glyceraldehyde
- 31 Methyl glyoxyl
- 32 Lactic acid
- 33 Glycolic acid
- 34 Formic acid
- 35 Glyceric acid



**Scheme 7.18** Peeling reactions of polysaccharides during alkaline and oxidative alkaline conditions (redrawn from Ref. [183]).

also rearrange to isosaccharinic acids (27) or cleave to yield glyceraldehyde (30) [183]. Glyceraldehyde is further converted to lactic (32), glycolic (33) and glyceric (35) acids.

Malinen and Sjöström [192] reported that the extent of the peeling reaction for cello-oligosaccharides was very low and that stabilization proceeded quickly. However, the stabilization of hydrocellulose – that is, the formation of aldonic acid end-groups – was less extensive, and peeling resulted in a loss of 10–50 sugar units, depending on the reaction.

The peeling reactions of xylan and glucomannan that take place under alkaline conditions have been described in detail (see Section 4.2.4.2, Carbohydrate reactions). In the presence of dioxygen, the peeling of xylan is more extensive than in alkali alone, and greater than that of cellulose and glucomannan. However, in the absence of dioxygen the degradation rate is lower for xylan than for cellulose and glucomannan [192,193,195]. 2,4-Dihydroxy-butyrac acid (17, 18, Scheme 7.16), 2-deoxy-glyceric acid (28, Scheme 7.18), glycolic acid (33), glyceric acid (35), xyloisaccharinic acid (27), lactic acid (32) and formic acid (34) are the main peeling products of xylan, which are analogous to the peeling products of cellulose.

The xylan chains are partly substituted with 4-O-methyl-glycuronic acid units at C2 [196], which prevent migration of the carbonyl group to the β-position relative to the glycosidic bond constraining β-elimination (see Section 4.2.4.2, Carbohydrate reactions; specific reactions of xylan). Model studies with aldobiuronic acid



[194,197] revealed that, under alkaline conditions at 80 °C, the degradation rate was rapid but much slower than that of xylobiose. Under dioxygen alkali conditions, aldobiuronic acid degraded almost as fast as xylobiose, suggesting that the substituent at C2 has a low retarding effect on the peeling reaction. The arabinose substituent at C3 position of softwood xylan is easily cleaved by  $\beta$ -elimination through the peeling process, and the chain is partly stabilized to xylometasaccharinic acid end-groups [198].

#### 7.3.2.5.3 Peeling Reactions Starting from Stabilized End-Groups

The formation of aldonic acid end-groups serves as a possible means of stabilizing the reducing end of the polysaccharide chain. In the presence of dioxygen, arabinonic acid end-groups (**8**, Scheme 7.15) are formed that are relatively stable under typical oxygen bleaching conditions, but degrade rather rapidly above 120 °C under both oxygen and nitrogen atmospheres (Scheme 7.15). The formed erythronic acid (**11**) and gluconic acid (**5**) end-groups are essentially stable up to 150 °C [192,199]. Glucitol end-groups, which are more stable against dioxygen-alkali treatment than the reducing end-groups, are relatively rapidly oxidized at higher temperatures to arabinose, and are cleaved further by  $\beta$ -elimination [183,199]. Mannitol end-groups are oxidized through the same arabinose intermediates as the glucitol end-groups. The model-compound methyl- $\alpha$ -D-mannopyranoside was oxidized more rapidly than methyl- $\alpha$ -D-glucopyranoside giving similar oxidation products, whereas the yield of furanosidic carboxylic acid was greater for methyl- $\alpha$ -D-mannopyranoside. This suggests that the oxidative attack is favored by the cis-position of the C2 and C3 hydroxyl groups [183]. Furthermore, the threonic acid end-groups that have been formed during oxidative stabilization of the reducing end-groups of xylan, show a similar degradation rate to that of arabinonic acid end-residues.

#### 7.3.2.5.4 Cleavage of the Polysaccharide Chain

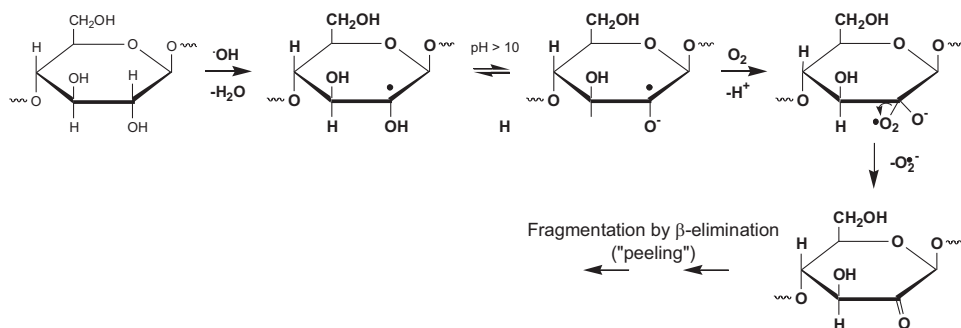
Cleavage of the cellulose chain under dioxygen-alkaline conditions has been studied with simple model compounds such as methyl-4-O-methyl- $\beta$ -D-glucopyranoside [200], methyl- $\beta$ -D-glucopyranoside [201–203] and methyl- $\beta$ -D-cellobioside [204]. These compounds represent the inner cellulose units, and result in the formation of glycolic acid, lactic acid, formic acid, acetic acid and carbon dioxide [183] and methyl- $\beta$ -D-glucoside, D-glucose, D-arabinose, D-arabinonic acid, D-erythronic acid, and D-glyceric acid [204]. Additionally, carboxy-furanosides, methyl-2-C-carboxy- $\beta$ -D-pentafuranosides, have been identified as oxidation products of both glycosides [200] and the corresponding methyl-3-C-carboxy- $\beta$ -D-pentafuranoside has also been formed from methyl- $\beta$ -D-glucopyranoside. The formation of these furanosidic acids is suggested via benzilic acid rearrangement of a diketo intermediate [201].

It has been generally suggested that the oxidative peeling of a cellulose chain proceeds via oxidation of the C2 or C3 hydroxyl group, followed by  $\beta$ -alkoxy-elim-

ination at C4 [188]. In contrast, the  $\beta$ -elimination is more pronounced when the 4-hydroxyl-group is substituted (as in cellulose), as is known from model-compound studies [185,200]. As a result of  $\beta$ -elimination at C1, preceded by oxidation at C2 or C3, the formation of methyl- $\beta$ -D-glucopyranoside from oxidation of methyl- $\beta$ -D-cellobioside can be regarded [205]. The acids which clearly result from the oxidative cleavage of the C1–C2, C2–C3, and C3–C4 linkages have been identified among the oxidation products [183]. Furthermore, an attack of the C6 hydroxyl group by a ROS seems very probable [205,206], because methyl- $\beta$ -D-glucopyranoside was more rapidly oxidized than methyl- $\beta$ -D-xylopyranoside [183,206,207] and methyl-6-deoxy- $\beta$ -D-glucopyranoside [206]. Because the products formed from methyl-4-O-methyl- $\beta$ -D-glucopyranoside under alkaline hydrogen peroxide treatment corresponded to those from alkaline dioxygen experiments with glycosides, a common reactive species was inferred [206,208,209].

Cleavage of the xylan chain studied with methyl- $\beta$ -D-xyloside as a model compound [207] showed that the oxidation reaction products were similar to those of methyl- $\beta$ -D-glucopyranoside, methyl-4-O-methyl- $\beta$ -D-glucopyranoside and methyl- $\alpha$ -D-mannopyranoside suggesting the same mechanism. Although the oxidation of methyl- $\beta$ -D-xyloside was slower, the oxidative depolymerization of xylan was more drastic compared with cellulose, but this may have been due to physical factors [183,195] such as crystallinity [80,210].

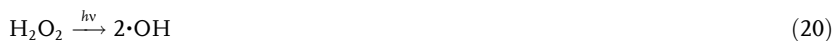
The common reactive oxygen species [206,208,209] noted previously is thought to be the hydroxyl radical [3,202–204,211]. A possible degradation mechanism for carbohydrates proposed by Gierer [3] starts with an attack of a hydroxyl radical ( $\bullet\text{OH}$ ) at the C2 position in the polysaccharide chain (Scheme 7.19), followed by oxygenation of the resultant carbon-centered radical and elimination of superoxide anion radical. This leads to the formation of a ketone in the polysaccharide chain that allows cleavage of the glycosidic linkage by  $\beta$ -elimination (see Section 4.2.4.2, Carbohydrate reactions).



**Scheme 7.19** Mechanism for oxidative cleavage of carbohydrates by hydroxyl radicals proposed by Gierer [3].

Guay et al. [204] have examined the proposed mechanism by using computational methods, which revealed that the step involving elimination of superoxide

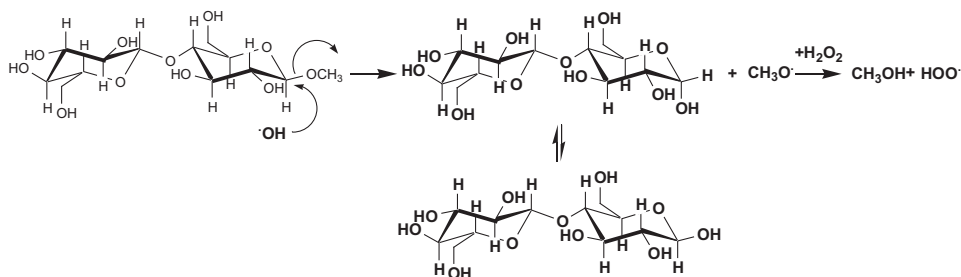
is energetically unfavorable. The highly reactive hydroxyl radical, which has been generated by using hydrogen peroxide and UV light [Eq. (20)] [204], is capable of reacting with most organic compounds, typically by hydrogen abstraction [139]. Hydroxyl radicals can react with both hydrogen peroxide and hydroperoxy anions through Eq. (21) and Eq. (22), producing hydroperoxy radicals and superoxide anions, respectively [212]. The reaction producing superoxide [Eq. (22)] is significantly faster than the hydroperoxy radical formation [Eq. (21)] [213]. As shown in Scheme 7.4, approximately half of the hydrogen peroxide is present as the conjugate base at a pH of 11.8, and formation of superoxide anions should be more important. At a lower pH, more hydroxyl radicals will be present to react with the carbohydrates.



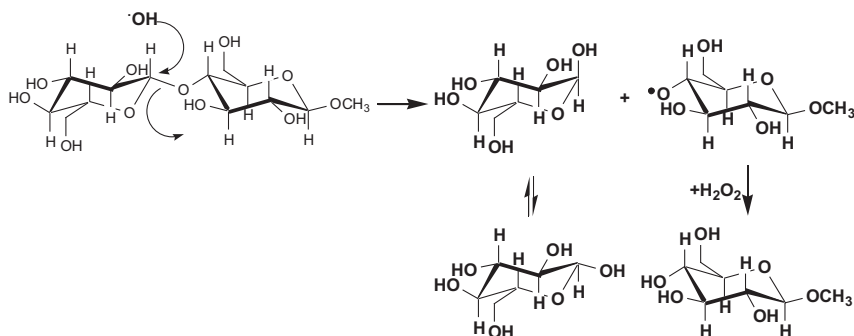
The experiments of Guay et al. with methyl- $\beta$ -cellobioside have been conducted with and without hydrogen peroxide at pH 10 and 12, and under oxygen pressure (about 4 bar) at 90 °C [204]. Beside the predominant degradation products of methyl- $\beta$ -glucoside and D-glucose, D-arabinose, D-cellobionic acid, D-arabinonic acid, D-erythronic acid, D-glyceric acid, and glycolic acid, products that have also been found by other groups [183,192,202,214–219], were identified. Moreover, no degradation products were found in the control reactions, suggesting that dioxygen, hydroxide ions, hydrogen peroxide, and hydroperoxy anions are not capable of degrading carbohydrates without a radical initiator, such as lignin or metal ions [204]. Due to the lower reactivity of methyl- $\beta$ -cellobioside at higher pH (12) [202], and the pH-dependence of the oxygen-species distribution [see Eqs. (21) and (22)], the extent of the degradation decreased but the overall chemistry was unchanged [204].

The mechanism of the formation of D-cellobioside is proposed to occur through a two-step process (Scheme 7.20), starting with a hydroxyl ion attack at the anomeric carbon displacing the methoxy radical. This radical can then abstract a hydrogen from hydrogen peroxide or another hydrogen donor, forming a hydroperoxyl radical and methanol (found experimentally).

The second degradative pathway (Scheme 7.21) is very similar to the first (Scheme 7.20), except that the cleavage is between two pyranose rings, starting with a hydroxyl attack at the anomeric carbon displacing D-glucose and methyl  $\beta$ -glucoside oxy radical at C4. The methyl  $\beta$ -glucoside radical then abstracts a hydrogen from hydrogen peroxide, forming methyl  $\beta$ -D-glucoside [204].



**Scheme 7.20** Proposed mechanism for cellobiose formation (redrawn from Guay et al. [204]).



**Scheme 7.21** Proposed mechanism for formation of methyl- $\beta$ -glucoside and D-glucose (redrawn from Guay et al. [204]).

Guay et al. [204] concluded that their experiments supported the view that hydroxyl radicals are responsible for the degradation of carbohydrates during oxygen delignification. Molecular oxygen, hydrogen peroxide, and hydroperoxy anions do not appear to degrade carbohydrates directly. Previous studies also suggested that superoxide anions do not degrade carbohydrates [3]. Guay et al. [204] reported that no experimental evidence has been found to support the reaction mechanism depicted in Scheme 7.19, though this may be due to different experimental conditions being used in these studies and in previous research, which employed pulse radiolysis to generate hydroxyl radicals. Evidence has been published suggesting that cellulose degradation during pulse radiolysis arises from direct ionization of the fibers rather than from hydroxyl radicals [216]. Moreover, the mechanism (cleavage of the glycosidic linkage) shown in Scheme 7.21 is supported by the model-compound study with 1,4-anhydrocellobiotol and cellulose [211].

Details of the mechanisms regarding the involvement of superoxide elimination [3,130] or no superoxide [204] are discussed – albeit controversially – in the literature, there appears to be no doubt that the hydroxyl ion attacks the carbohydrates, thereby starting the degradation reaction [4,220–226].

The hydroxyl radical ( $\bullet\text{OH}$ ) is one of the most reactive and short-lived of the ROS, with a lifetime of about 1 ns in biological systems [227]. Because of this, methods used to detect  $\bullet\text{OH}$  include electron spin resonance (ESR) [228] (using a spin trap such as dimethylsulfoxide, DMSO), HPLC [229,230], rapid-flow ESR [231], and fluorescence [232–237]. Two different methods can be used for the detection of  $\bullet\text{OH}$ . One is the direct reaction of a probe molecule with  $\bullet\text{OH}$ . The other method is to use a scavenger that creates a radical species with a longer lifetime. The probe molecule then reacts with this radical species [229,234]. Superoxide detection systems have also been developed using ESR spin trapping [238], cytochrome C [239,240], amperometric detection [241], or a chemiluminescence assay [242,243], which may help to clarify whether the superoxide anion radical is formed as a consequence of oxygen treatment. Moreover, a new chromatographic method to determine hydroperoxides in cellulose [244], and a new colorimetric method to determine hydroxyl radicals during the aging of cellulose [245] have been published.

A compilation of important carbohydrate degradation products in dioxigen-alkali delignification processes of kraft and sulfite pulps (glycolic acid, 2,4-dihydroxybutyric acid, 3,4-dihydroxybutyric acid, isosaccharinic acid, 2-deoxy-glyceric acid, lactic acid, glyceric acid, formic acid, and acetic acid) according to Sjöström and Välttilä [246] sums up this section.

#### 7.3.2.6 Residual Lignin–Carbohydrate Complexes (RLCC)

It is well known that lignin and carbohydrates are linked in wood, and that new linkages are formed during a kraft cook.

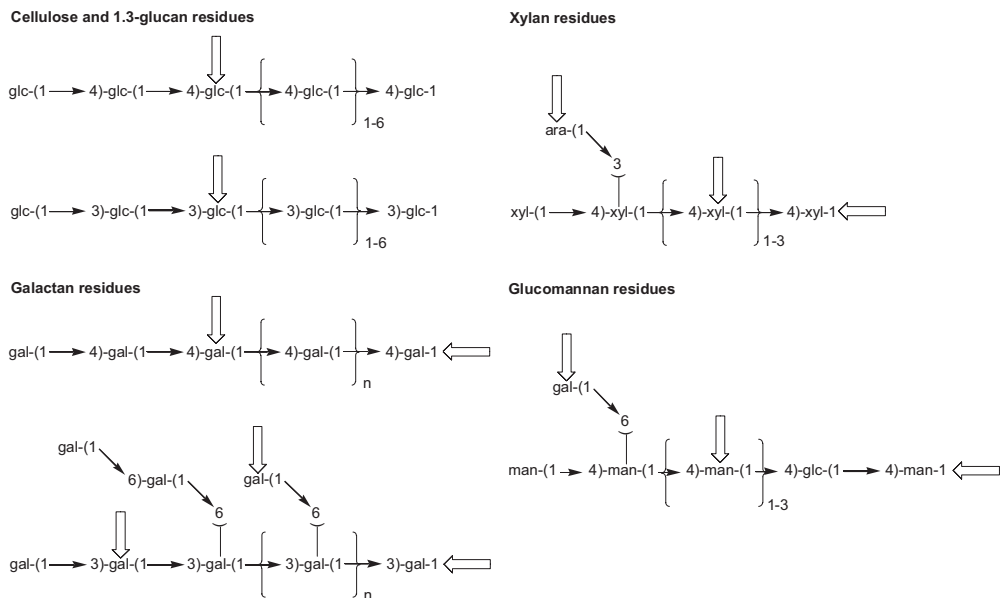
During oxygen delignification of pine pulp, the polysaccharides dissolve together with lignin in the form of lignin–carbohydrate complexes (LCC) [247]. The structures of these dissolved polysaccharides from pine and birch kraft pulps treated under oxygen delignification conditions [247], when determined by using methylation analysis [248], included 1,4-linked xylan, 1,3(,6)-linked and 1,4-linked galactan, 1,5-linked arabinan, and notable amounts of a 1,3-linked glucan, whereas the glucose-containing polysaccharide in the pine pulp effluent was 1,3-linked glucan and not cellulose [247]. From the birch pulp mainly xylan, but also traces of arabinan, 1,3-linked galactan and 1,4-linked glucan have been removed [247].

Softwood kraft pulps with a kappa number between 50 and 20 and oxygen-delignified to a similar lignin content (kappa ~6) led to the isolation of LCCs using a method based on selective enzymatic hydrolysis of the cellulose, and quantitative fractionation of the LCC [63]. The large majority (85–90%) of the residual lignin in the unbleached kraft pulp, and all of that in the oxygen-delignified pulps, when isolated as LCC, was found as one of three types of complex, namely xylan–lignin, glucomannan–lignin–xylan and glucan–lignin. Most of the lignin was linked to xylan in high-kappa number pulps, but to glucomannan when the pulping was extended to a low kappa number. Lawoko et al. [63] reported that, with increasing degree of oxygen delignification, a similar trend in the delignification

rates of LCC was observed; thus, the residual lignin was increasingly linked to glucomannan. From this it was concluded that complex LCC network structures appear to be degraded into simpler structures during delignification. Two excellent schemes for the degradation of hemicellulose networks during pulping, and possible differences in the accessibility of lignin under alkaline conditions between a xylan–lignin complex and a glucomannan–lignin complex, were described by Lawoko et al. [63]. Moreover, the chemical structure of the residual lignin bound to xylan was different from that bound to glucomannan.

Enzymatically isolated residual lignin–carbohydrate complexes (RLCC) from spruce and pine pulp ( $\kappa$  number ca. 30) contained 4.9–9.4% carbohydrates, with an enrichment of galactose and arabinose compared to the original pulp samples. The main carbohydrate units present in the RLCC were 4-substituted xylose, 4-, 3- and 3,6-substituted galactose, 4-substituted glucose, while 4- and 4,6-substituted mannose were assigned to carbohydrate residues of xylan, 1,4- and 1,3/6-linked galactan, cellulose and glucomannan [65]. The comparison of RLCC of surface material and the inner part of spruce kraft pulp fiber revealed that the 1,4-linked galactan was the major galactan in RLCC of fiber surface material of spruce kraft pulp, and towards the inner part the proportion of 1,3/6-linked galactan increased relative to 1,4-linked galactan [65]. It has been suggested that 1,3/6-linked galactan structures may have a role in restricting lignin removal from the secondary fiber wall. The RLCC of three different alkaline pine pulps studied by Lawoko et al. [65] before and after oxygen delignification revealed small differences in the carbohydrate structures of the unbleached pulps resulting from the cooking method [conventional kraft pine pulp, a polysulfide/anthraquinone (AQ) pine pulp and a soda/AQ pine pulp]. These authors found that all RLCC of oxygen-delignified pulps had more nonreducing ends and less 1,3/6-linked galactan than the corresponding RLCC of the unbleached pulps. Moreover, the oxygen-delignified soda/AQ pulp had a higher ratio of 1,4-galactan to 1,3/6-linked galactan and shorter xylan residues than the RLCCs of oxygen-delignified conventional kraft pine pulp and polysulfide/AQ pulps [65]. From the above results and the calculated degree of polymerization, conclusions were drawn on the possible positions of lignin–carbohydrate bonds (Fig. 7.27).

These authors concluded that xylan residues were partly bound to lignin via the reducing end-groups, and that the RLCC contained either long galactan chains or bonds linking galactans to lignin via the reducing ends [65]. Oxygen delignification shortened the oligosaccharide chains present in RLCC and removed preferably the 1,3/6-linked galactan compared to 1,4-linked galactan structures connected to residual lignin. The RLCC of oxygen-delignified soda/AQ pulp differed from those of the other two pulps after oxygen-delignification in that it had a higher ratio of 1,4- to 1,3/6-linked galactan, and shorter xylan residues. However, even this detailed analysis did not reveal any major differences in the soda/AQ pulp that could explain its poor bleaching response. It is possible that factors other than the chemical composition and interactions between lignin and carbohydrates affect the bleachability of the pulps. These factors may be physical rather than chemical [65].



**Fig. 7.27** Structures of carbohydrate residues in RLCC of conventional spruce kraft pulps, as suggested by Laine et al. [65]. The arrows show possible lignin binding sites.

### 7.3.2.7 Inorganics (Metals) and their Role in the Protection/Degradation of Cellulose

A study on the formation of hydrogen peroxide during oxygen bleaching of *Eucalyptus globulus* confirmed the origin of cellulose degradation, as well as the effect of metal ions on the degradation [143]. Hydrogen peroxide levels detected in the effluent of the oxygen treatment of pulps were higher when lignin was present (unbleached pulp), or in bleached pulp with the addition of phenolic lignin model compound (vanillic alcohol). Moreover, the metal ions present also influenced the content of  $H_2O_2$  in the effluents of oxygen treatments [143].

Oxygen delignification became technically feasible when Roberts showed that the addition of magnesium compounds retards the degradation of cellulose more efficiently than that of lignin [145].

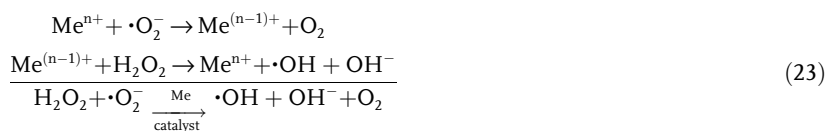
The protective effect of magnesium against hydroxyl radical formation was studied by several groups [249–254]. The influence of combined magnesium and manganese [156,255–259], transition metals [203,260–262], chelants [263–265], calcium carbonate and silicate [266–268], sulfur compounds [155] and oxygen pressure on hydroxyl radical formation has also been investigated.

Neither hydrogen peroxide [269] nor the superoxide anion radical [6] is capable of degrading carbohydrates directly. The degradation is initiated by an attack of the hydroxyl radical [6,269,270]. In the presence of metal ions, the superoxide anion radical, which is formed during oxygen bleaching, can be oxidized to oxy-

gen [see Eq. (17)] or reduced to the hydroperoxy anion [see Eq. (18)] [125]. The reduction of  $\text{Fe}^{3+}$  by the superoxide anion can also accelerate the Fenton reaction, producing a superoxide-driven Fenton reaction [Eq. (19)] [125]. In a carbohydrate model study, it was found that at pH 10.9, degradation was strongly inhibited [269], though this may have been due to the low solubility of  $\text{Fe}^{2+}$  and  $\text{Fe}^{3+}$  ions under the conditions of oxygen bleaching. In contrast, manganese proved to be a very effective catalyst for hydrogen peroxide decomposition during peroxide bleaching [271] up to pH 9, but was inactive in acidic media. Copper was seen to be the most effective transition metal to catalyze hydrogen peroxide decomposition.

The one-electron reduction of hydrogen peroxide is catalyzed primarily by mononuclear transition metal ion species. At high pH, these species may only arise when the concentration of the metal ion is very low. Copper appears to be the most efficient Fenton catalyst under the conditions of alkali bleaching [145]. At higher concentrations, most metal ions aggregate or condense to form hydroxo-bridged polynuclear species in alkaline solutions. Manganese ( $\text{Mn}^{2+}$ ) and hydroxide ions ( $\text{OH}^-$ ) form aggregates that can be oxidized by oxygen to produce  $\text{MnO}_2$  at a pH above 9. Colloidal  $\text{MnO}_2$  decomposes  $\text{H}_2\text{O}_2$  efficiently by a two-electron reduction to give oxygen and water directly, without generating any significant amount of hydroxyl radicals [145]. Colloidal particles of metal hydroxides and hydrated oxides may also catalyze the dismutation of superoxide [145].

The superoxide-driven Fenton [Eq. (19)] reaction can be written in a more common form [Eq. (23)], starting with oxidation of the superoxide anion radical by a metal ion. The second step – the reduction of hydrogen peroxide – is not an equilibrium reaction, as the radical formed will immediately react with the substrate due to the extreme reactivity of the hydroxyl radical. A maximum rate of hydroxyl formation is expected in the pH range 11–11.5 [145]; thus, conditions of oxygen delignification appear to be near-optimal.

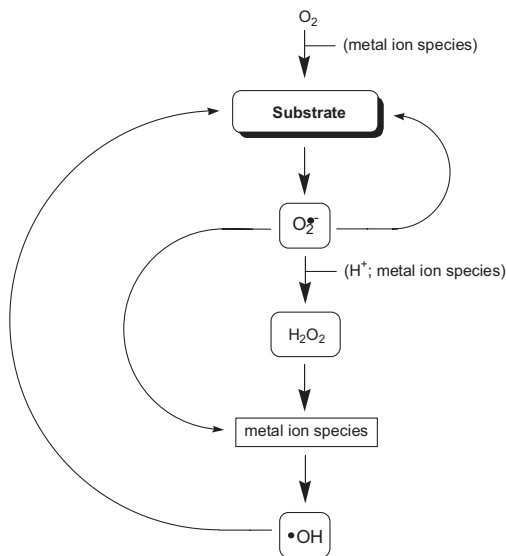


How metal ion species may affect the four oxygen reduction steps is summarized in Scheme 7.22.

Reitberger et al. [145] reported that the protective effect of magnesium compounds might have different explanations, including:

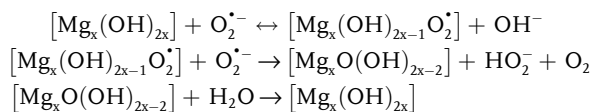
- Coprecipitation of transition metal ions with magnesium hydroxide, which should stabilize hydrogen peroxide against decomposition to give hydroxyl radicals and achieve redox stabilization of  $\text{Mn}^{2+}$ .
- Formation of Mg–cellulose complexes which protect against attack by hydroxyl radicals.





**Scheme 7.22** Catalysis by metal ion species in the oxygen reduction (from Ref. [145]).

- Association of superoxide to the  $\text{Mg}(\text{OH})_2$  colloid may catalyze the proton-dependent dismutation of superoxide – that is, the  $\text{Mg}(\text{OH})_2$  colloid mimics superoxide dismutase:



The first explanation has received wide acceptance, but magnesium salts seem to act not only by deactivation of transition metal ions [145].

Chelators, such as EDTA (ethylenediaminetetraacetic acid) or DTPA (diethylenetriaminepentaacetic acid), are often added to the pulp during bleaching to improve the viscosity. Moreover, metal ions in higher valence states are more strongly complexed than ions in a lower valence state. Therefore, the reduction of chelated metal ions by the superoxide anion radical to a lower valence state is inhibited –that is, the superoxide-driven Fenton reaction is blocked [145].

For example, residual lignin from oxygen-bleached kraft pulp subjected to oxidation with alkaline hydrogen peroxide showed a rapid but limited elimination of chromophoric groups. This resulted in the formation of carboxyl groups in the presence of magnesium ions and DTPA, which stabilizes hydrogen peroxide towards decomposition, thereby improving the chromophore elimination [272]. The effect of added stabilizer(s) was found to be particularly pronounced. The addition of transition metal ions resulted in rapid decomposition of hydrogen peroxide and the introduction of new chromophoric groups [272].

## 7.3.3

**Mass Transfer and Kinetics***Herbert Sixta*

Oxygen delignification of pulp is a three-phase reaction system consisting of an aqueous phase, suspended pulp fibers, and the oxygen gas phase (oxygen must be transferred from the gas to the liquid phase and then from the liquid to the solid phase). As a first step, oxygen dissolves in the aqueous phase and is then transported through the liquid to the liquid–pulp fiber interface. The dissolved oxygen subsequently diffuses into the fiber wall and then reacts with the wood components, preferably with the residual lignin structures.

The full description of the oxygen delignification process requires the following information:

- The solubility of oxygen in the alkaline solution.
- The oxygen mass transfer rate in the aqueous phase.
- The effective diffusion coefficient of oxygen inside the fiber wall.
- Stoichiometry and chemical kinetics of the oxygen delignification reactions.

The physical transport of oxygen gas through the immobile aqueous film layer by diffusion is the rate-determining step for oxygen delignification. Therefore, fluidization of the pulp suspension is regarded as a prerequisite for oxygen delignification.

It is generally agreed that the course of both oxygen delignification and carbohydrate degradation is mainly affected by the three primary process variables, temperature, sodium hydroxide concentration, and dissolved oxygen concentration. Furthermore, the ionic strength is also thought to influence the delignification rate. In contrast to kraft pulping, an increase in ionic strength during oxygen delignification was reported to accelerate the delignification rate [1]. Olm and Teder explained this observation by assuming that the rate-controlling reaction occurs between two negatively or two positively charged species.

The prerequisite of kinetic investigations is to avoid any mass-transfer limitations. The influence of pulp consistency on the rate of delignification has been ascribed to insufficient mixing in both the low and high consistency ranges [2,3]. Argarwal et al. reported that no significant effect of consistency is observed for oxygen delignification of mixed southern hardwood in the range 0.5 to 12%, provided that there is sufficient mixing. Nevertheless, kinetic investigations are preferably carried out at ultra-low consistencies (0.3–0.5%) in a well-mixed batch reactor to ensure constant concentrations of sodium hydroxide and dissolved oxygen (further information about mass transfer aspects are provided in Section 4.2.3).

### 7.3.3.1 Kinetics of Delignification

In the literature, three categories of mathematical models have been introduced to describe the kinetics of oxygen delignification:

- Two-stage model comprising two parallel rate equations.
- One-stage model or power-law rate equation.
- Nuclei growth concept according to Avrami-Erofeev [4]. Topochemical delignification model according to the modified equation of Prout-Thomson [5].

The first category of models considers the rapid initial rate and a considerable slow-down as the reactions proceed. Mathematically, this can be described as a two-phase model expressed by two-parallel equations, each first order on lignin. According to Macleod and Li, the rapid-reacting lignin can be assigned to a dissolved kraft lignin which is trapped in the fiber wall due to a drop in the pH during conventional brownstock washing [6]. The kraft lignin is leached to the liquid phase as soon as the conditions of high pH and high temperature are re-established during a subsequent oxygen delignification.

The apparent kinetic expression of the two-stage model is displayed in Eq. (24):

$$\begin{aligned} -\frac{d\kappa_f}{dt} &= k_f \cdot [\text{OH}^-]^{m_f} \cdot [\text{O}_2]^{n_f} \cdot \kappa_f^{q_f} \\ -\frac{d\kappa_s}{dt} &= k_s \cdot [\text{OH}^-]^{m_s} \cdot [\text{O}_2]^{n_s} \cdot \kappa_s^{q_s} \end{aligned} \quad (24)$$

where  $q_f$  and  $q_s = 1$ , and  $m$  and  $n$  are the exponents for dependencies of hydroxide and dissolved oxygen concentrations, respectively. According to the basic assumptions of this model, the kappa number,  $\kappa$ , consists of two differently reacting lignin fractions,  $\kappa_f$  the fast- and  $\kappa_s$  the slow-reacting lignin expressed as kappa numbers, respectively. Some authors have also suggested the presence of a nonreacting lignin fraction (floor kappa number level) denoted as refractory kappa number,  $\kappa_b$ , originally proposed for a kinetic delignification model for chlorination [2,7,8]. Myers and Edwards [2] proposed that 10% of the incoming kappa number (unbleached) can be attributed to the refractory kappa number, regardless of the chemical and physical nature of the residual lignin. This assumption is derived simply from the results of fitting the model using a nonlinear least-square technique, and is not really based on a measurable chemical reactivity of a certain residual lignin fraction. Similar conclusions can also be drawn for the “fast” and “slowly” eliminated lignin fraction. Their fractions vary in a rather broad range, as can be seen in Tab. 7.13.

Vincent et al. reported that the rate equations for oxygen delignification established by Myers and Edwards are inadequate for predicting results for eucalypt pulp [13]. These authors concluded that, under more extreme conditions, the residual lignin present in the eucalypt pulp is more resistant as compared to that in a softwood pulp (which was the dominating pulp source in the Myers and Edwards study [2]). Thus, Vincent et al. determined alternative rate equations,

**Tab. 7.13** Coefficients of the apparent kinetic expressions for alkaline oxygen delignification according to a two-stage model. Overview of literature data [1,2,9–12].

Reference	Wood source	Kappa number range of unbleached	Lignin fractions $\kappa_n$ $\kappa_s$	Reaction order <sup>a</sup>			Activation energy ( $E_a$ ) [kJ mol <sup>-1</sup> ]
				m	n	q	
Olm & Teder [1]							
Fast	Softwood	29.5	n.s.	0.1	0.1	1	10
Slow	Softwood	29.5	n.s.	0.3	0.2	1	45
Hsu & Hsie [9,10]							
Fast	Southern Pine	29.5	n.s.	0.78	0.35	3.07	36
Slow	Southern Pine	29.5	n.s.	0.7	0.74	3.07	71
Myers & Edwards [2]							
Fast	Softwood, Hardwood	11–128	0.225	0	0.43	1	36
Slow	Softwood, Hardwood	12–128	0.675	0.875	0.43	1	71
Iribarne & Schroeder [12]							
Fast	<i>Pinus taeda</i>	20.5–58	0.57	1.2	1.3	1	67
Slow	<i>Pinus taeda</i>	20.3–59	0.43	0,3	0,2	1	40

a. On concentrations or pressure as given in the reference  
n.s. = not separated.

based on Myers and Edward's two-stage *pseudo* first-order model, that fit the experimental results reasonably well.

A two-stage kinetic model enables a better description of the initial, rapid delignification reaction as compared to a single-stage model. Furthermore, prediction of the outlet kappa number is more reliable in case of varying initial kappa numbers, since the rate equations are mainly first order on lignin (an exception was the model proposed by Hsu and Hsie [10]). Both models, however, can be considered as pure empirical models.

More recently, it was shown that the kappa number degradation during oxygen delignification can be fitted to a power-law rate equation of apparent order q with sufficient precision using the single-stage approach [3,14]:

$$-\frac{d\kappa}{dt} = k \cdot \kappa^q \quad (25)$$

with  $\kappa$ , the kappa number and  $k$ , the rate constant of oxygen delignification according to Eq. (26):

$$k = A \cdot \text{Exp}\left(-\frac{E_A}{RT}\right) \cdot [\text{OH}^-]^m \cdot [\text{O}_2]^n \quad (26)$$

where  $A$  is the pre-exponential factor,  $E_A$  is the activation energy (in  $\text{kJ mol}^{-1}$ ),  $[\text{OH}^-]$  is the molar hydroxide ion concentration, and  $[\text{O}_2]$  is the dissolved molar oxygen concentration. Integration of Eq. (25) and implying constant conditions of dissolved oxygen and hydroxide ion concentrations leads to the following expression for the calculation of the kappa number as a function of time:

$$\kappa = \left(\kappa_0^{(1-q)} + (q-1) \cdot k \cdot t\right)^{\frac{1}{1-q}} \quad (27)$$

where  $\kappa_0$  is the initial unbleached kappa number. The parameters of the apparent kinetic expression,  $A$ ,  $E_A$ ,  $m$ , and  $n$  can be calculated by a using nonlinear least-squares technique.

It is well known that the application of a power-law representation of the rate equation yields a high reaction order  $q$  on lignin [2,3]. Using a single rate equation, the course of slow lignin degradation during the final stage of oxygen delignification can be described mathematically by a high order on lignin. The slower the final delignification rate, the higher the order on lignin. According to Axegard et al., refractory lignin structures and mass transfer limitations could account for the slow rate in the residual phase of oxygen delignification [15]. In analogy to the kinetic description of polymer degradation in petrochemical processing, Schoon suggested that a power-law applies when the oxygen delignification reactions are performed by an infinite number of parallel first-order reactions [16]. Schoon further derived a frequency function  $f(k)$  which provides a correlation between the observed order  $q$  and the distribution of the rate constants. The derived expression for the function  $f(k)$  is given in Eq. (28):

$$f(k) = \frac{\frac{1}{p^{q-1}} k^{\frac{2-q}{q-1}}}{\Gamma\left(\frac{1}{q-1}\right)} \text{Exp}(-p \cdot k) \quad (28)$$

where  $\Gamma[1/(q-1)]$  represents the gamma function evaluated at  $1/(q-1)$ .

The value of the parameter  $p$  is a function of the apparent rate order  $q$ , the reaction rate coefficient  $k$  and the initial kappa number,  $\kappa_0$ , and can be determined according to the following expression:

$$p = [(q-1) \cdot k \cdot \kappa_0^{q-1}]^{-1} \quad (29)$$

The frequency function  $f(k)$  of the rate constant distribution as determined by Eqs. (28) and (29) is defined as the fraction of the rate constants having values between  $k$  and  $k + dk$ .

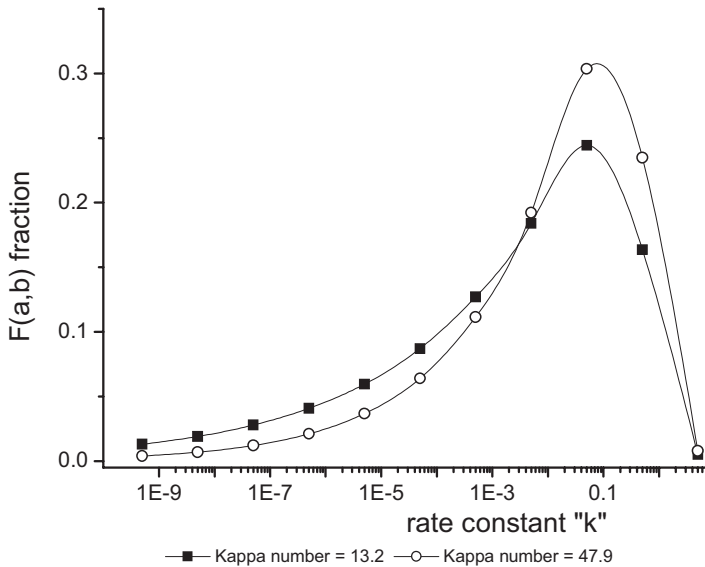
The distribution function  $F(a,b)$  is expressed as the fraction of the rate constants with the limits of integration between  $k = a$  and  $k = b$ , according to Eq. (30):

$$F(a, b) = \int_a^b f(k) dk \quad (30)$$

Oxygen delignification can be understood as a sum of an infinite number of parallel first-order reactions where the rate constants can be displayed as a distribution function. High rate constants indicate the presence of easily removable lignin.

The concept of Schoon's distribution function is exemplified by two hardwood kraft pulps of different initial kappa numbers, one with a low kappa number of 13.2 (pulp A) and the other with a high kappa number of 47.9 (pulp B).

The kinetic parameters necessary to calculate the frequency distribution functions are included in Tab. 7.14. It is assumed that oxygen delignification exhibits the same value of the rate constant,  $k_q$ , equal to  $9.62 \times 10^{-9}$  kappa  $^{(q-1)}$  min $^{-1}$  for both pulps if a hydroxide ion concentration of  $0.0852 \text{ mol L}^{-1}$  and a dissolved oxygen concentration of  $0.0055 \text{ mol g}^{-1}$  is considered (derived from an alkali charge of 2.5% on o.d. pulp at 12% consistency and an oxygen pressure of 800 kPa at a reaction temperature of  $100^\circ\text{C}$ ). The main difference between the two pulps is expressed in the different apparent reaction order  $q$  of 7.08 for pulp A and 5.15 for pulp B.



**Fig. 7.28** Distribution function for the rate constants for oxygen delignification at  $100^\circ\text{C}$ ,  $0.085 \text{ mol } [\text{OH}^-]; \text{ mol/l L}^{-1}$ ,  $0.0055 \text{ mol O}_2 \text{ L}^{-1}$  for two hardwood kraft pulps, kappa number 13.2 (pulp B) and 47.9 (pulp A), respectively. The parameter  $p$  and the frequency

functions  $f(k)$  are determined by Eqs. (29) and (28) using rate constant,  $k$ , in the range  $10^{-10}$  to  $10$  kappa  $^{(q-1)}$ .min $^{-1}$  in intervals of one order of magnitude (e.g.,  $10^{-10}$ – $10^{-9}$ ,  $10^{-9}$ – $10^{-8}$ , ...). The integral in Eq. (30) is solved numerically.

The different apparent reaction orders and initial kappa numbers are responsible for the change of the frequency functions  $f(k)$  in relation to the rate constants. The change from a reaction order of 7.08 for the low-kappa number pulp A to 5.15 for the high-kappa number pulp B results in a shift of the distribution function to higher rate constants. It can be seen from Fig. 7.28 that pulp B, with the higher starting kappa number, has a greater fraction of easily removable lignin compounds as compared to pulp A. This leads to the conclusion that the reactivity of the lignin moieties is expressed in the magnitude of the apparent reaction order  $q$ . Delignification kinetics of high-kappa number pulps predict a lower rate order as compared to low-kappa number pulps, which means that the extent of oxygen delignification increases with rising initial kappa numbers of hardwood kraft pulps. When cooking is terminated at a high kappa number, the resulting pulp contains a greater fraction of highly reactive lignin moieties as compared to a pulp derived from prolonged cooking, provided that the other cooking conditions remain constant.

Experimental data from the literature have been fitted to the power-law rate equation to demonstrate the suitability of this approach. The corresponding results are summarized in Tab. 7.14.

Apart from the results taken from Iribarne and Schroeder [12], all the laboratory oxygen delignification data were derived from a constant initial kappa number. The kappa number after oxygen delignification was calculated (Kappa\_calc after 30 min), assuming an initial kappa number of 25 and applying the parameters of the power-law rate expression given in Tab. 7.14 to evaluate the applicability of the kinetic model. The following typical reaction conditions were used for the calculations: reaction time 30 min, temperature 100 °C, 0.085 mol L<sup>-1</sup> initial hydroxide ion concentration (alkali charge of 2.5% at 12% consistency) and 0.0055 mol L<sup>-1</sup> dissolved oxygen concentration (oxygen pressure 800 kPa, 100 °C, 0.085 mol OH L<sup>-1</sup>).

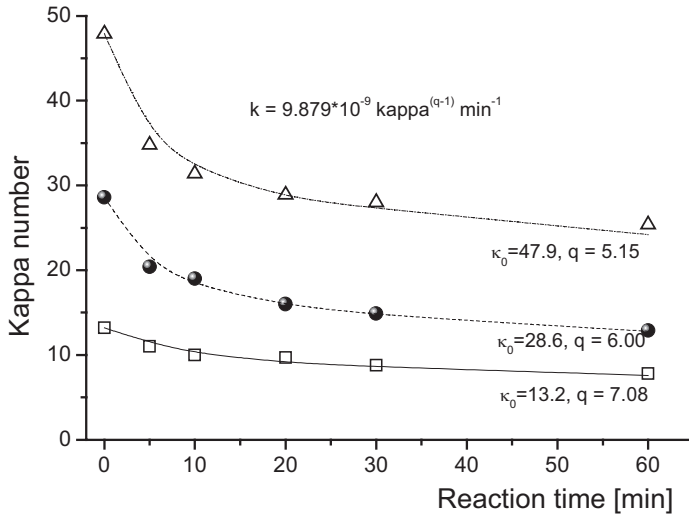
Table 7.14 illustrates that the calculated kappa numbers after oxygen delignification are reliable only for those references where the kappa number of the unbleached pulp used for the oxygen delignification trials was in the range of the assumed kappa number 25. The parameters derived from oxygen delignification of low (13.2) and high (47.9) initial kappa numbers yield either too low or too high final kappa numbers. Iribarne and Schroeder demonstrated that applying the power-law rate equation for a variety of initial kappa numbers (20.3–58), the apparent order decreases significantly [12]. The kappa number of oxygen delignified pulps can be predicted for a broad range of initial kappa numbers. However, the precision is lower as compared to the results when applying the parameters obtained from the given initial kappa number. Using the power-law rate equation, a better approach would be to adjust the apparent order  $q$ , as demonstrated by Agarwal et al. [3]. Since the rate ( $k$ ) constant is independent of the initial unbleached kappa number, it can also be applied to evaluate the apparent rate order  $q$  which best fit the experimental data with different initial kappa numbers. As seen from Tab. 7.14, the values determined for  $q$  decrease with increasing unbleached kappa number. The experimental and calculated kappa numbers throughout oxygen delignification are shown in Fig. 7.29.

Tab. 7.14 Parameters of the power-law rate equation for oxygen delignification according to Eqs. (25), (26) and (27). Recalculated from Refs. [3, 10, 12].

Reference	Wood source	Kappa unbleached	r <sup>2</sup>	Pre-exponential factor A	Reaction order#			E <sub>A</sub> [kJ mol <sup>-1</sup> ]	k [Kappa <sup>n-1</sup> · min <sup>-1</sup> ]	Kappa [calc after 30 min <sup>a</sup> ]
					m	n	q			
Hsu & Hsie [10]	Southern pine	29.5	0.94	3.20E+10	0.68	1.28	5.23	97.2	1.90E-07	12.2
Iribarne & Schroeder [12]	<i>Pinus taeda</i>	20.3–58	0.92	3.00E+06	0.70	0.70	2.00	51.0	1.02E-03	14.2
Argawal et al [3]	Southern hardwood	13.2	0.96	4.42E+07	1.20	0.23	7.08	98.9	9.91E-09	8.8
Argawal et al [3]	Southern hardwood	28.6	0.97	4.42E+07	1.20	0.23	6.00	98.9	9.91E-09	14.4
Argawal et al [3]	Southern hardwood	47.9	n.d.	4.42E+07	1.20	0.23	5.15	98.9	9.91E-09	21.8

a. assuming initial Kappa number, K<sub>0</sub> = 25.





**Fig. 7.29** Course of kappa numbers throughout oxygen delignification at 100 °C, 12% consistency, 0.085 mol L<sup>-1</sup> NaOH and 0.0048 mol L<sup>-1</sup> dissolved oxygen (equals an oxygen pressure of 690 kPa) according to Agarwal et al. [3]. Points correspond to the experimental data, the curves represent the calculated values using  $k$  equal to  $9.879 \cdot 10^{-9} \text{ kappa}^{6.7} \text{ min}^{-1}$ .

A good agreement between the experimental data and the model curves can be obtained by adjusting the apparent rate order  $q$  appropriately. The lower apparent orders  $q$  for pulps with the higher initial kappa numbers would mean a higher proportion of easily eliminated lignin. In terms of Schoon's model, the fraction of first-order rate constants with a high delignification rate increases correspondingly.

Unfortunately, this explanation does not account for unbleached pulps of equal or comparable kappa numbers, but different reactivity of the residual lignin. Zou et al. have prepared four different hardwood pulps of the same kappa number (15–16) under different cooking conditions [14]. The extent of a subsequent oxygen delignification clearly increases for pulps which are cooked with increasing amounts of effective alkali. According to Agarwal et al., the rate constant  $k$  of oxygen delignification remains constant at given reaction conditions (e.g., 90 °C, 60 min, 0.051 mol L<sup>-1</sup> [OH<sup>-</sup>], 0.005 mol L<sup>-1</sup> dissolved oxygen). This implies that the apparent order  $q$  increases parallel to the increasing fraction of easily degradable lignin to account for the accelerated delignification rate. On the other hand, the reaction rate coefficient increases while keeping the apparent reaction order  $q$  constant at the (recalculated) average value of 7.44. The results of these calculations are summarized in Tab. 7.15.

The interpretation of Agarwal et al. that a lower value of  $q$  would correlate with a lower fraction of refractory lignin structures can only be applied for pulps of different initial kappa numbers [3]. In case the initial kappa number remains unchanged, a higher extent of delignification during oxygen delignification is

**Tab. 7.15** Kinetic parameters of the power-law rate equation for oxygen delignification of hardwood kraft pulps of comparable kappa numbers obtained by different cooking conditions according to Zou et al. [14]. Rate Eq. (25) is fitted in two ways: (a) by keeping the reaction rate constant,  $k$ , constant; and (b) by keeping the apparent order,  $q$ , constant. The constant reaction rate,  $k$ , is calculated by using the kinetic parameters obtained by Agarwal et al. [3] and considering the conditions of oxygen delignification: 90 °C, 0.051 mol L<sup>-1</sup> [OH<sup>-</sup>] OH, 0.005 mol L<sup>-1</sup> dissolved oxygen, 60 min.

Cooking		Oxygen delignification								
EA-charge [% o.d.w.]	H-factor	Kappa	k = constant		Kappa_60 min		q = constant		Kappa_60 min	
			k	q	exp	calc	q	k	exp	calc
12	3051	16.3	2.20 10 <sup>-9</sup>	7.17	10.4	9.6	7.44	1.10 10 <sup>-9</sup>	10.4	9.7
15	1100	16.2	2.20 10 <sup>-9</sup>	7.32	9.4	9.1	7.44	1.63 10 <sup>-9</sup>	9.4	9.1
18	654	15.5	2.20 10 <sup>-9</sup>	7.55	8.5	8.4	7.44	2.83 10 <sup>-9</sup>	8.5	8.4
21	409	15.0	2.20 10 <sup>-9</sup>	7.73	8.3	7.9	7.44	4.40 10 <sup>-9</sup>	8.3	7.8

indicated by an increase in the rate constant,  $k$ . It may be speculated that the activation energy for oxygen delignification is shifted to higher values when the proportion of refractory lignin structures increases. It can be concluded that the power-law rate equations can be successfully applied for the description of oxygen delignification when appropriate assumptions are made [16]. This concept is characterized by an apparent high rate order with respect to the kappa number which can be explained in terms of a large number of parallel first-order reactions taking place simultaneously. Easily degradable lignin structures contribute to a high rate constant, while refractory lignin fragments account for low rate constants. The lower rate constants are possibly due to higher activation energies.

A third category of kinetic models is based on Avrami-Erofeev's concept of Nuclei Growth in phase transformation processes [5,17]. The topochemical equation of Avrami-Erofeev is predominantly used to characterize kinetics of phase-transformation processes such as crystallization, smelting, sublimation, etc. [4]. These processes are characterized by an instantaneous formation of nuclei, followed by growth of a new phase. The model assumes that the delignification rate depends on the number of reactive sites formed at the beginning of the process and the growth rate of the transformed lignin from these reactive sites. The applicability of the topochemical equation of Avrami-Erofeev on the kinetics of oxygen delignification was successfully verified, provided that the following assumptions are adopted:

- Oxygen delignification is nucleated by reactions between oxygen and reactive lignin structures, for example, ionized phenolic hydroxyl groups on the outside surface of the lignin phase.
- Delignification proceeds as a topochemical reaction in such a way that the zones of “transformed” (reacted) lignin propagate according to a power-law with respect to time. The size,  $R$ , of the reacted lignin zone at time  $t$  is assumed to be dependent on the diffusion coefficient,  $D$ , and time  $t$  according to the following expression:

$$R = \beta \cdot (D \cdot t)^n \quad (31)$$

where  $\beta$  is a constant considering the effects of temperature and lignin physical structure on the growth, and  $n$  is an exponent which depends on the nature of the chemical transportation in the transformed zones. If the growth of the reacted zone follows Fick’s law of diffusion,  $n$  would be equal to 0.5 in case of a one-dimensional system.  $D$  represents the diffusion coefficient. However, it has been shown that Fick’s law is not applicable in a system where the chemical concentration is dynamically affected by the reaction [18]. The value of  $n$  is expected to be less than 1 because the velocity of oxygen delignification slows down as time proceeds.

- The growth of a reacted zone will be interrupted by the growth of adjacent transformed zones due to spatial limitation within the lignin structure. Avrami proposed that the actual change of the reacted amount of lignin,  $dL_{RA}$ , can be calculated as the product of the residual lignin fraction,  $x_t$ , and the potential amount of degradable lignin,  $dL_R$ , according to the following expression:

$$dL_{RA} = \left(1 - \frac{L_{RA}}{L_{tot}}\right) dL_R \quad (32)$$

where  $L_{tot}$  represents the initial amount of residual lignin.

According to Eq. (32), the actual change of transformed lignin decreases with the gradual increase of transformed zones.

- Kappa number is assumed to be an appropriate indicator of the amount of unreacted lignin. Thus, the change in kappa number with time has been defined as follows:

$$-\frac{dk}{dt} = n \cdot \beta \cdot I \cdot D^n \cdot t^{(n-1)} \cdot \kappa \quad (33)$$

where  $I$  is the initial number of reactive sites per unit volume of lignin.

Equation (33) can be characterized as first-order reaction with a time-dependent rate constant. If the parameters  $n$ ,  $\beta$ ,  $I$  and  $D$  are assumed to remain constant

throughout oxygen delignification, the integral form of equation can be written as:

$$\kappa = \kappa_i \cdot \text{Exp}(-\beta \cdot I \cdot D^n \cdot t^n) \quad (34)$$

The model parameters were determined using the results obtained from experiments with a commercial eucalypt kraft pulp [17]. Oxygen delignification trials were conducted to consider the effects of temperature (100–120 °C), oxygen pressure (500–900 kPa corresponding to a dissolved oxygen concentration of 0.0046–0.0061 mol L<sup>-1</sup>) and alkali concentration (0.044–0.074 mol L<sup>-1</sup>) on the rate of delignification. The influence of temperature on the rate of oxygen delignification can be included in Eq. (34) if the diffusivity,  $D$ , is assumed to be dependent on the temperature in terms of the Arrhenius equation:

$$\kappa = \kappa_i \cdot \text{Exp}\left(-\beta \cdot I \cdot \left(D_0 \text{Exp}\left(-\frac{E}{RT}\right)\right)^n \cdot t^n\right) \quad (35)$$

The final form of the delignification rate equation according to the concept of phase transformation for the eucalypt kraft pulp has been given as follows [17]:

$$\kappa = \kappa_i \cdot \text{Exp}\left[\left(-9.99 \cdot 10^8 \cdot \text{Exp}\left(-\frac{79.7 \cdot 10^3}{RT}\right) \cdot p_{\text{oxygen}}^{0.22} \cdot [\text{OH}^-]^{0.847} \cdot t\right)^{0.32}\right] \quad (36)$$

Oxygen delignification is a heterogeneous, highly complex reaction comprising a large variety of different kinds of reactions. The reactivity of the residual lignin is predominantly determined by the wood species, the type of cooking process, and the specific cooking conditions. Consequently, the kinetics of oxygen delignification can only be described by empirical models. The model parameters of the three kinetic approaches introduced are determined using results obtained from laboratory experiments with either only one type of pulp or a very limited selection of pulps. The two- and one-stage models of Iribarne and Schroeder [12], the power-law rate equation from Agarwal et al. [19], and the topochemical reaction model derived from Avrami-Erofeev [17] are overlaid on the experimental data from Valchev et al. [5] as an example for a beech kraft pulp, and the experimental data from Zou et al. [14] and Järrehult [20,21] as examples for a softwood kraft pulp. The relevant process conditions of the two selected oxygen delignification trials are summarized in Tab. 7.16, and the kinetic parameters of the selected kinetic model in Tab. 7.17.

Figures 7.30–7.32 compare the proposed models with regressed parameters given in Tab. 7.17 and Eq. (36) to the experimental data from the researchers denoted in Tab. 7.16. The models proposed by Agarwal et al. and Nguyen and Liang successfully follow the data from oxygen delignification of the beech kraft pulp, whereas the two-stage model developed by Iribarne and Schroeder for very high-pressure oxygen delignification shows increasing deviations at reaction times longer than 50 min. Their one-stage model, however, shows a quite reasonable prediction of the final kappa numbers for both series of oxygen delignification.

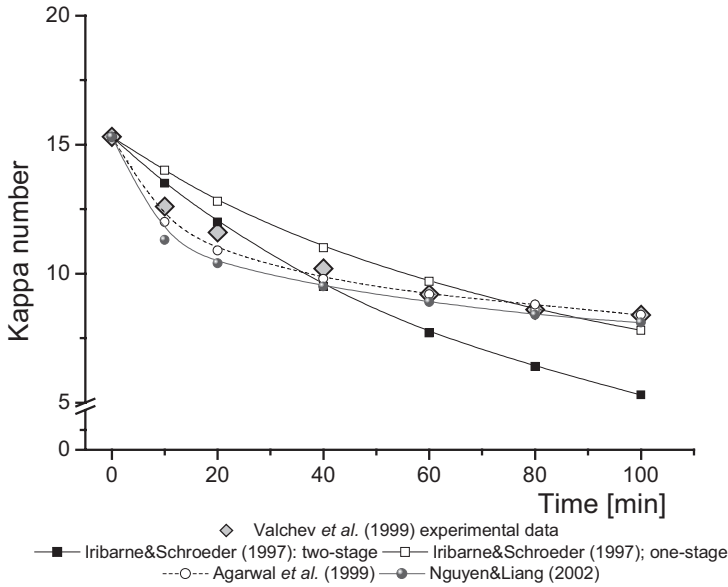
**Tab. 7.16** Conditions of two series of oxygen delignification adopted from the literature.

Parameters	Units	Valchev et al. [5]	Zou et al. [14]	Järrehult and Samuelson [21]
Wood species		beech	softwood	Scots pine
Pulp type		kraft	kraft	kraft
Kappa number (t=0)		15.3	22.8	31.5
Temperature	°C	100	100	97
Consistency	%	10	12	0.2
[OH <sup>-</sup> ] (t=0)	mol L <sup>-1</sup>	0.0556	0.0852	0.1
Pressure (t=0)	kPa	608	690	700
[O <sub>2</sub> ] (t=0)	mol L <sup>-1</sup>	0.0043	0.0047	0.00488

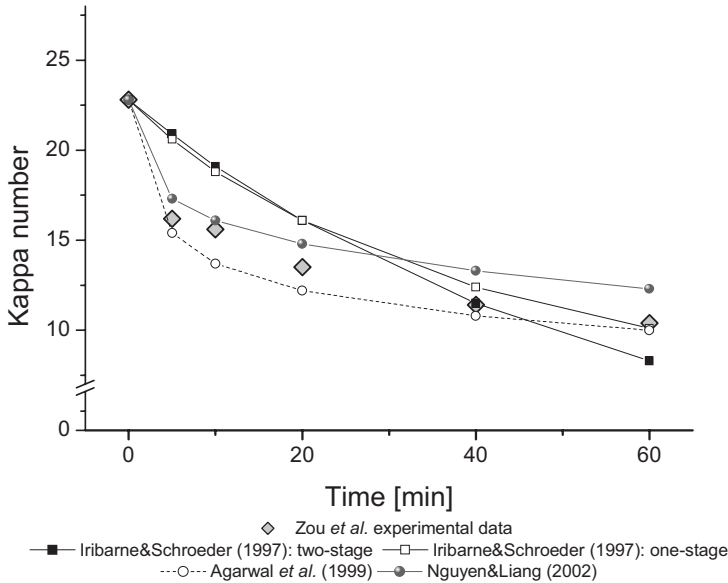
**Tab. 7.17** Kinetic parameters for models adopted from the literature used for the comparative prediction of experimental data.

Source	Model specification	kappa fraction	Model parameters			A [kappa <sup>(1-q)</sup> min <sup>-1</sup> ]	E <sub>A</sub> [kJ mol <sup>-1</sup> ]
			m	n	q		
Iribarne & Schroeder [12]	Initial	0.57	1.2	1.3	1	6.00 · 10 <sup>11</sup>	67.0
	Final	0.43	0.3	0.2	1	6.00 · 10 <sup>4</sup>	40.0
	one-stage		0.7	0.7	2	3.00 · 10 <sup>6</sup>	51.0
Agarwal et. al [19]	kappa 15.9		1.2	0.23	6.9	4.42 · 10 <sup>7</sup>	98.9
	kappa 21.2		1.2	0.23	6.5	4.42 · 10 <sup>7</sup>	98.9
	kappa 31.5		0.96	0.23	5.7	4.42 · 10 <sup>7</sup>	98.9
Nguyen & Liang [17]	Phase transformation		0.85	0.22		9.99 · 10 <sup>8</sup>	79.7

It should be noted that both the power-law model with the high order  $q$  and the phase transformation model suggested by Nguyen and Liang indicate slightly too low kappa numbers within the first 20 min reaction time. The opposite is true for the two-stage and the power-law models, with low apparent order  $q$ , as shown in Figs. 7.30 and 7.31. Their quality of prediction improves gradually with prolonged reaction time if the results from oxygen delignification of the softwood pulp are considered.

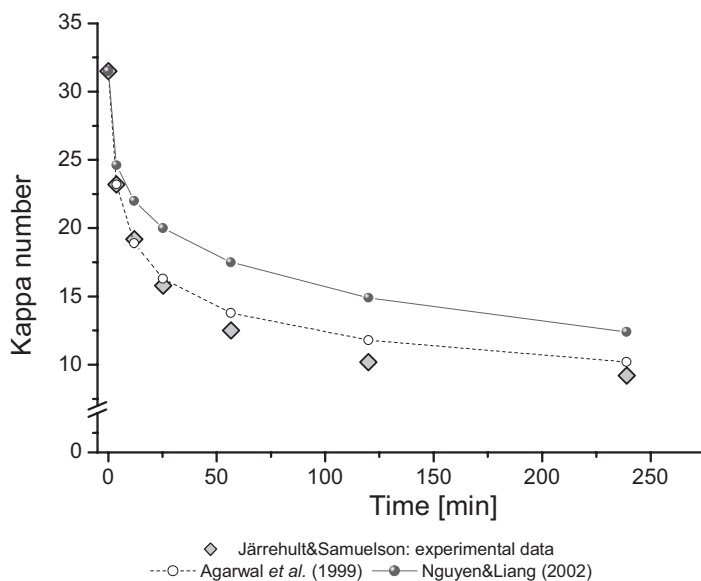


**Fig. 7.30** Comparison of model predictions against experimental data from oxygen delignification of beech wood (adapted from Valchev et al. [5]).



**Fig. 7.31** Comparison of model predictions against experimental data from oxygen delignification of softwood (adapted from Zou et al. [14]).

The development of the kappa number during oxygen delignification of a Scots pine kraft pulp, kappa number 31.5, can be predicted sufficiently well using the model of Agarwal et al., provided that the apparent order  $q$  is adjusted to the higher initial kappa number (see Tab. 7.17 and Fig. 7.32). In this particular case, the dependence on the hydroxide ion concentration has been recalculated using the experimental results from Järrehult and Samuelson determined at hydroxide ion concentrations of 0.01, 0.1 and 0.5 mol L<sup>-1</sup>, respectively, while keeping all other parameters,  $A$ ,  $E_A$ , and  $n$  constant [20,21]. The calculations revealed a slightly lower exponent  $m$  (0.96 instead of 1.2) as compared to the calculations based on the experimental data from Agarwal et al. (Tab. 7.17).



**Fig. 7.32** Comparison of model predictions against experimental data from oxygen delignification of softwood adapted from Järrehult and Samuelson [21]; reaction conditions:  $[\text{OH}^-] = 0.1 \text{ mol L}^{-1}$ ,  $[\text{O}_2] = 0.00489 \text{ mol L}^{-1}$ ; 97 °C, 0.2% consistency.

The phase transformation model using the set of model parameters determined for a eucalypt pulp, kappa number 11.6, is however not capable of predicting the course of kappa number degradation during oxygen delignification of a softwood kappa-31.5, as expected (Fig. 7.32). Softwood kraft pulps and pulps with higher initial kappa numbers are more susceptible to oxygen delignification at given conditions. Consequently, the validity of a kinetic model is more or less limited to a specific pulp type and grade. The simple model proposed by Agarwal et al. [19] seems to be well-suited to predict the course of oxygen delignification of different kinds of kraft pulps. The key contribution of this model is the utilization of a variable apparent order  $q$  which depends on the initial kappa numbers and the frac-

tion of easily eliminated lignin, while keeping parameters of the rate equation,  $A$ ,  $E_A$ ,  $m$  and  $n$  constant. The use of distribution function for the rate constants derived for different initial kappa numbers further improves the quality of prediction.

It can be concluded that so far no kinetic model exists where the susceptibility towards oxygen delignification is fully described. Thus, efforts must be undertaken to develop a model which is able to describe the reactivity of the relevant pulp components.

### 7.3.3.2 Kinetics of Cellulose Chain Scissions

A common means of following polymer degradation is to monitor the average molar mass, which is then used to calculate the rate constants for the degrading reactions. Ekenstein proposed a first-order kinetics of bond scission when studying the homogeneous degradation of the cellulose in phosphoric acid [22]:

$$\text{Ln}\left(\frac{1}{DP_t} - \frac{1}{DP_0}\right) = k \cdot t \quad (37)$$

If  $DP_t$  and  $DP_0$  are large, which is valid in the case of pulp polysaccharides, this simplifies to a zero-order kinetics:

$$\left(\frac{1}{DP_t} - \frac{1}{DP_0}\right) = k \cdot t \quad (38)$$

The degradation of cellulose chains is related to the increase in the number-average moles of cellulose per tonne of pulp,  $m_n$ . The number-average degrees of polymerization,  $DP_n$ , can be calculated in several ways. Godsays and Pearce published an equation to convert intrinsic viscosity to  $DP_n$  [23]:

$$DP_n = 961.38 \cdot \text{Log}(\eta) - 245.3 \quad (39)$$

Equation (39) implies that the polydispersity of the molecular weight distribution remains constant throughout the degradation reaction. Thus, the viscosity-average molecular weight,  $DP_v$ , calculated from intrinsic viscosity according to SCAN-CM-15:88, can be used instead, and this is certainly the most convenient way. For a polymer with a random molecular weight distribution, the viscosity average degree of polymerization,  $DP_v$  and the number average degree of polymerization,  $DP_n$ , have the following relationship [24]:

$$DP_v = DP_n[(\alpha + 1) \cdot \Gamma(\alpha + 1)]^{1/\alpha} \quad (40)$$

where  $\alpha$  = exponent of the Kuhn–Houwink equation. Since it has been found that  $\alpha$  is close to unity, Eq. (40) can be simplified to  $DP_v \approx 2 \cdot DP_n$ .



The most reliable approach would be to determine the number-average molecular weight directly, for example with gel-permeation chromatography (GPC) using MALLS detection [25]. Using Eq. (40) to calculate the number average degree of polymerization, the moles of cellulose per tonne of pulp,  $m_n$ , can be calculated as follows:

$$m_n = \frac{10^6}{162 \cdot DP_n} \quad (41)$$

The moles of cellulose per tonne of pulp,  $m_n$ , can be reconverted to the intrinsic viscosity (SCAN-CM-15:88) by the following expression:

$$[\eta] = \frac{2882.75}{m_n^{0.76}} \quad (42)$$

Assuming a zero-order reaction in  $m_n$  and a nonlinear dependency on time similar to the phase transformation concept, the following rate equation for cellulose degradation can be given:

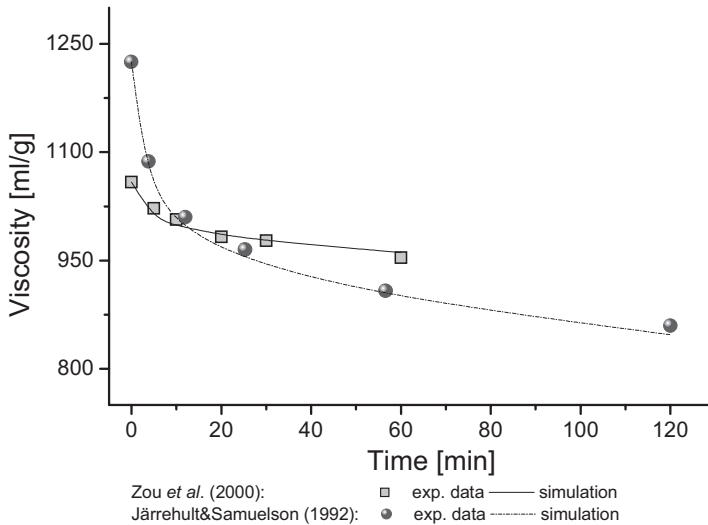
$$\begin{aligned} \frac{dm_n}{dt} &= p \cdot k \cdot t^{(p-1)} \\ m_{n(t)} &= m_{n(0)} + k \cdot t^p \\ k &= A * \text{Exp}\left(-\frac{E_A}{RT}\right) \cdot [OH^-]^m [O_2]^n \end{aligned} \quad (43)$$

The kinetic parameters  $A$ ,  $m$  and  $p$  were estimated from the regression analysis on experimental data published by Järrehult and Samuelson for a softwood kraft pulp [20], while the remaining parameters,  $E_A$ , and  $n$  were used from a study published by Iribarne and Schroeder [12]. The kinetic parameters employed are summarized in Tab. 7.18.

**Tab. 7.18** Kinetic parameters of the apparent kinetic expression for cellulose degradation during oxygen delignification adopted from Ref. [12] and recalculated using the experimental data provided by Järrehult and Samuelson [21].

Kinetic parameters	Unit	Values	Source
A	<sup>a</sup>	$2.073 \cdot 10^{11}$	Calculated
$E_A$	[kJ mol <sup>-1</sup> ]	77.0	Iribarne & Schroeder [12]
m		0.27	Calculated
n		0.30	Iribarne & Schroeder [12]
p		0.29	Calculated

a. mol cellulose t<sup>-1</sup> pulp · min<sup>-1</sup>.



**Fig. 7.33** Comparison of viscosity predictions against experimental data from oxygen delignification of northern hardwood (adapted from Zou et al. [14];  $[\text{OH}^-] = 0.042 \text{ mol L}^{-1}$ ,  $[\text{O}_2] = 0.005 \text{ mol L}^{-1}$ ,  $90^\circ\text{C}$ , medium consistency) and of Scots pine (adapted from Järrehult and Samuelson [21];  $[\text{OH}^-] = 0.1 \text{ mol L}^{-1}$ ,  $[\text{O}_2] = 0.0049 \text{ mol L}^{-1}$ ;  $97^\circ\text{C}$ , 0.2% consistency).

Figure 7.33 shows the fit to oxygen delignification data from Zou et al. for a low-kappa number hardwood kraft pulp at medium consistency, and from Järrehult and Samuelson for a high-kappa number softwood kraft pulp. The simple kinetic model is quite appropriate for the prediction of the course of viscosity during oxygen delignification. A general validity of this model cannot be expected, however, as this would require a more mechanistic approach considering the dominating delignification and carbohydrate degradation reactions.

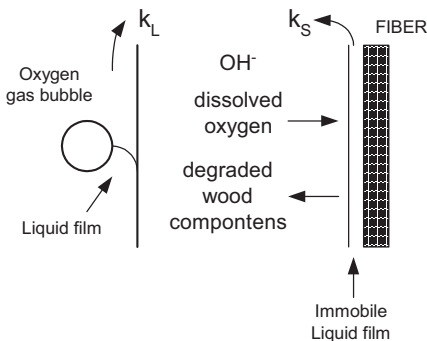
### 7.3.3.3 Application of Surfactants

Low molecular-weight ethoxy-based surfactants are able to accelerate oxygen delignification of softwood kraft pulps [26]. The extent of lignin removal was increased from 45% to 55% when 1 wt.% of surfactant (15-S-5) was added to medium consistency oxygen delignification ( $110^\circ\text{C}$ , 690 kPa, 60 min) using a commercial softwood kraft pulp, kappa number 22. The study revealed that the improved delignification efficiency can be explained rather by an accelerated chemical reaction rate than by an increased diffusion rate. It can be assumed that the presence of surfactants increases both the solubility of lignin and oxygen in the liquid phase, thus increasing the intrinsic delignification rate.

## 7.3.4

**A Model to Predict Industrial Oxygen Delignification [27]**

Industrial oxygen delignification is reported to be less efficient as compared to laboratory oxygen delignification. A study provided by Rewatkar and Bennington revealed that industrial oxygen delignification systems operate, on average, at about 20% below their potential [28]. The impaired efficiency of oxygen delignification can be attributed to mass transfer limitations which occur under industrial conditions. Oxygen delignification of pulp is a three-phase reaction system comprising pulp fibers (solid phase), an aqueous phase, and the oxygen gas phase. The mass transfer of oxygen to pulp fibers in medium consistency oxygen delignification is shown schematically in Fig. 7.34.



**Fig. 7.34** Scheme of mass transfer of oxygen to pulp fibers in medium consistency oxygen delignification process (according to Hsu and Hsieh [10]).

The process of oxygen delignification is described as follows:

- Solubilization of oxygen in the alkaline pulp suspension during high-shear mixing: first, oxygen transfer from the gas phase through a gas film into the gas–liquid interfacial boundary takes place. This is followed by oxygen transfer from the boundary through a liquid film into the bulk liquid phase.
- Diffusion of dissolved oxygen from the water surrounding the fibers through the fiber wall, where the reaction occurs: dissolved oxygen is transported from the bulk phase into the immobile liquid layer surrounding the fiber by diffusion and convection, followed by diffusion of hydroxide ions and oxygen molecules through the immobile water layer to the fiber. Finally, the process chemicals reach the reaction sites in the fiber through inter- and intrafiber mass transfer.

Quite recently, van Heiningen et al. have presented a model where the effect of mass transfer of oxygen on the efficiency of delignification in an industrial reten-

tion tower is simulated [27]. The reaction conditions that occur at the entrance of the oxygen reactor are determined by simulating the mass transfer and reaction processes in a high-shear mixer. Figure 7.35 shows a simplified oxygen delignification stage flowsheet.

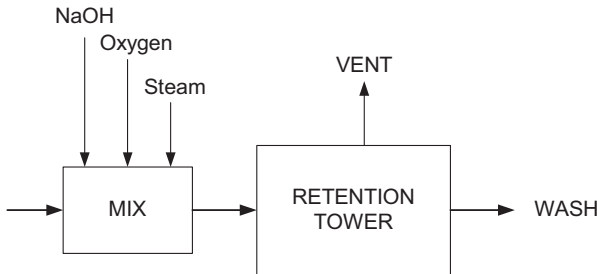


Fig. 7.35 Schematic flowsheet of oxygen delignification.

Screened and washed pulp is pumped through one or more high-shear mixers, where alkali, oxygen and steam are dispersed under pressure into a medium-consistency suspension. Pulp passes through an upflow tower and is discharged from the top of a blow tank from which gases are separated out, and the pulp finally enters subsequent washers. The model presented by van Heiningen et al. is based on this simplified process scheme. The main objective of this model is to calculate the effect of the mass transfer of oxygen on the efficiency of delignification as a function of caustic and oxygen charges, oxygen pressure, consistency and temperature.

Some minor changes and supplements have been introduced into the following model proposed by van Heiningen et al. The model considers the following elements:

- Oxygen solubilization during high shear mixing: the volumetric mass transfer rate of oxygen,  $k_L a$  (M), is obtained from an empiric equation derived by Rewatkar and Bennington [29].
- Oxygen balance through the retention tower assuming steady-state conditions at a given pulp production rate and dimensions of the retention tower.
- The gas void fraction,  $X_g$ , is calculated assuming a preset and constant gas-to-suspension linear velocity ratio.
- The oxygen consumption rate is related to the rates of pulp delignification and dissolved lignin (carryover) oxidation.
- The kinetics of kappa number degradation is described by the one-stage model proposed by Iribarne and Schroeder [12]. Due to the lack of an appropriate kinetic model, the course of dissolved organic carbon (DOC) oxidation is modeled by using the model from Iribarne and Schroeder, as well considering a DOC-to-lignin conversion factor.

- Temperature increase in the retention tower is calculated using published values of the heat of reactions of both kappa number degradation and DOC oxidation, whereas heat loss through the reactor walls is neglected.
- The saturated oxygen concentration in the aqueous phase is obtained from the empiric model provided by Broden and Simonson [30].
- Values for the mass transfer rate of oxygen,  $k_L a$  (R) in the tower are assumed in a certain range, as measured in a laboratory equipment [28].

#### 7.3.4.1 Theoretical Base of the van Heiningen Model [27]

The pulp suspension is assumed to pass through the oxygen bleaching tower by plug flow. As the steady state of the process is considered, the course of all variables through the reactor can be expressed as a function of the residence time  $t$  of the pulp suspension. The oxygen balance is governed by Eqs. (44) and (45):

$$\frac{d[O_2]}{dt} = k_L a \cdot ([O_{2,sat}] - [O_2]) \cdot \frac{\rho_l}{(\rho_s \cdot (1 - con) \cdot (1 - X_g))} - r_{O_2} \quad (44)$$

$$\frac{d[V_{O_2, g}]}{dt} = - \left( \frac{d[O_2]}{dt} + r_{O_2} \right) \cdot \dot{V}_l \quad (45)$$

where:

- $t$  = time after entering the reactor, [s]  
 $[O_2]$  = oxygen concentration in the liquor, [mol L<sup>-1</sup>]  
 $k_L a$  = mass transfer rate of oxygen to the liquid phase, [L<sub>liquid</sub><sup>-1</sup> L<sub>contactor</sub> s<sup>-1</sup>]  
 $[O_{2,sat}]$  = oxygen concentration in the liquid in equilibrium with the oxygen pressure, [mol L<sup>-1</sup>]  
 $\rho_l$  = density of the liquor, [kg L<sup>-1</sup>]  
 $\rho_s$  = density of the suspension, [kg L<sup>-1</sup>]  
 $con$  = pulp consistency, mass fraction [-]  
 $X_g$  = gas volume (void) fraction, [-]  
 $r_{O_2}$  = oxygen consumption rate caused by pulp delignification, [mol O<sub>2</sub> L<sub>liquor</sub><sup>-1</sup> s<sup>-1</sup>]  
 $V_{O_2, g}$  = oxygen flow in gas phase, [mol s<sup>-1</sup>]  
 $\dot{V}_l$  = liquor flow, calculated as  $\dot{V}_l = R \times (1 - con) / (con \times \rho_l)$ , [L s<sup>-1</sup>]  
 $R$  = rate of pulp production, [kg s<sup>-1</sup>]

It is believed that the gas void fraction,  $X_g$ , is not constant throughout the reaction, as was assumed by van Heiningen et al. due to progressive oxygen consumption [27]. Instead, it is supposed that the gas to suspension linear velocity ratio can be kept constant, which should be valid as long as the production rate remains stable. The linear gas velocity in the tower is assumed to be higher than the veloci-

ty of the suspension due to the density difference between the gas and suspension.  $X_g$  can then be calculated according to Eq. (46):

$$X_g = \frac{\dot{V}_g}{(\dot{V}_s \cdot v_g/v_s + \dot{V}_g)} \quad (46)$$

where:

$\dot{V}_g$  = gas flow, calculated as  $\dot{V}_g = V_{O_2} \cdot g \times 0.008315 \times T p^{-1}$ , [L s<sup>-1</sup>]

$T$  = temperature, [K]

$p$  = pressure, [MPa]

$\dot{V}_s$  = suspension flow, calculated as  $\dot{V}_s = R/(\text{con} \times \rho_s)$  [L s<sup>-1</sup>]

$v_g/v_s$  = ratio gas to suspension velocity [-]

The oxygen consumption rate,  $r_{O_2}$ , depends on both the degradation of residual lignin and dissolved oxidizable matter (carryover), measured as DOC according to the following expression:

$$r_{O_2} = - \frac{\left(1.5 \cdot \frac{dk}{dt} \cdot b_1 + \frac{dDOC}{dt} \cdot b_2\right) \cdot R}{32 \cdot \dot{V}_l} \quad (47)$$

where:

$b_1$  = stoichiometric coefficient for the reaction of oxygen with the residual lignin [g  $\Delta O_2$ /g  $\Delta$ lignin]. The value of  $b_1$  is taken as 1.0 [31].

DOC = dissolved organic carbon, kg t<sup>-1</sup> pulp

$b_2$  = stoichiometric coefficient for the reaction of oxygen with the dissolved black liquor [kg  $\Delta O_2$ /kg  $\Delta$ DOC]; as no experimental values are available, it is assumed that only the dissolved lignin fraction reacts with oxygen: 50% of the DOC can be assigned to lignin compounds, and 1 kg lignin relates to 0.63 kg DOC, then  $0.5/0.63 = 0.79$  kg lignin kg<sup>-1</sup> DOC; therefore,  $b_2$  can be taken as 0.79 kg  $\Delta O_2$ /kg  $\Delta$ DOC.

The kinetics of kappa number degradation is described by the model obtained by Iribarne and Schroeder [12] (Tab. 7.17), as proposed by van Heiningen et al. [27]. Any other kinetic model, as introduced in Chapter 4.2.3 (Mass transfer and kinetics) may also be used for illustration. The validity of the model from Iribarne and Schroeder is limited to softwoods (preferably *Pinus taeda*) in the kappa number range 20–58 (see Tabs. 7.14 and 7.17):

$$-\frac{dk}{dt} = \frac{3.0 \cdot 10^6}{60} \cdot \text{Exp}\left(-\frac{51000}{8.315 \cdot T}\right) \cdot [OH^-]^{0.7} \cdot [O_2]^{0.7} \cdot \kappa^{2.0} \quad (48)$$

where  $T$  is the temperature, °K after residence time  $t$ , and  $[OH^-]$  (mol L<sup>-1</sup>) is the hydroxide ion concentration in the liquor. The change in hydroxide ion concentration can be calculated as follows:

$$\frac{d[OH^-]}{dt} = - \frac{\left(1.5 \cdot \frac{dk}{dt} \cdot b_3\right) \cdot R}{17 \cdot \dot{V}_l} \quad (49)$$

where  $b_3$  = stoichiometric coefficient of hydroxide ion consumption by the residual lignin of the pulp, given as kg hydroxide ions,  $\text{OH}^-$ , consumed per kg lignin removed;  $b_3$  is taken as  $0.9 \times 17/40$ , based on recent measurements by Violette [32].

To the present authors' knowledge, a kinetic expression for DOC degradation during oxygen delignification is not yet available. In order to estimate the effect of dissolved lignin, measured as DOC, on the course of oxygen delignification, a similar kinetic expression as depicted in Eq. (48) is considered.

The heat of reaction is estimated by a value of 14 MJ per ton of pulp and removed kappa number [33]. Thus, the temperature increase caused by the oxidation reactions during oxygen delignification may be obtained from Eq. (50):

$$\frac{dT}{dt} = \frac{\left(\Delta H_L \cdot \frac{dk}{dt} \cdot 1.5 + \Delta H_{\text{DOC}} \cdot \frac{d\text{DOC}}{dt}\right)}{\left(c_{\text{pulp}} + c_{\text{H}_2\text{O}} \cdot \left(\frac{1}{\alpha \text{ON}} - 1\right) + m_{\text{O}_{2g}} \cdot c_{\text{O}_2}\right)} \quad (50)$$

where:

$\Delta H_L$  = heat of reaction of residual lignin oxidation [9.3 MJ  $\text{kg}^{-1}$  lignin], assuming that one kappa number unit,  $\kappa$  represents 1.5 kg of lignin in 1 t of pulp.

$\Delta H_{\text{DOC}}$  = heat of reaction dissolved lignin oxidation [7.4 MJ  $\text{kg}^{-1}$  DOC], assuming that 1 kg DOC contains 0.79 kg of dissolved lignin.

$m_{\text{O}_{2g}}$  = oxygen in gas phase, [kg  $\text{t}^{-1}$  pulp]

$c_{\text{pulp}}$  = specific heat capacity of pulp, 1550 kJ  $\text{t}^{-1} \text{K}^{-1}$

$c_{\text{H}_2\text{O}}$  = specific heat capacity of water, 4187 kJ  $\text{t}^{-1} \text{K}^{-1}$

$c_{\text{O}_2}$  = specific heat capacity of oxygen, 0.93 kJ  $\text{kg}^{-1} \text{K}^{-1}$ .

The pressure drop across the reactor can be calculated by Eq. (51):

$$\frac{dp}{dt} = -0.00981 \cdot \rho_s \cdot v_s = -0.00981 \cdot \rho_s \cdot \frac{\dot{V}_s \cdot H}{(1 - X_g) \cdot V} \quad (51)$$

where  $H$  and  $V$  are height (m) and volume ( $\text{m}^3$ ) of the reactor.

The model of Broden and Simonson was used to estimate the solubility of oxygen in equilibrium conditions,  $[\text{O}_2, \text{sat}]$ , as a function of oxygen pressure, temperature and hydroxide ion concentration [34]. A minimum in solubility is obtained at a temperature of about 100 °C. The presence of dissolved sodium hydroxide induces a salting-out effect which leads to a decrease in the oxygen solubility. The dissolved oxygen concentration as a function of temperature and pressure for two different sodium hydroxide concentrations is expressed by Eq. (52):

$$[\text{O}_2, \text{sat}] = (a_1 + a_2 \cdot T + a_3 \cdot p + a_4 \cdot p \cdot T^2 + a_5 \cdot p/T) \cdot 0.001 \quad (52)$$

where  $[\text{O}_2, \text{sat}]$  = oxygen concentration in the liquid in equilibrium with the oxygen pressure, [mol  $\text{L}^{-1}$ ].

The coefficients  $a_i$  are presented in Tab. 7.19.

**Tab. 7.19** Numerical values of the coefficients  $\alpha_i$  in Eq. (52) for the calculation of oxygen solubility as a function of temperature, oxygen partial pressure and hydroxide ion concentration (as determined by Broden and Simonson [34]).

Parameter	0.01 M [OH <sup>-</sup> ]	0.1 M [OH <sup>-</sup> ]
$\alpha_1$	3.236	9.582
$\alpha_2$	-0.00747	-0.02436
$\alpha_3$	-56.02	-94.77
$\alpha_4$	0.00016	0.00025
$\alpha_5$	15421	24610

Solubilization of oxygen in the alkaline pulp suspension is accomplished by high shear mixing. The volumetric mass transfer rate of oxygen to the liquid phase,  $k_L a$ , for the mixer can be calculated by an empirical equation determined by Rewatkar and Bennington [29], considering the specific power dissipation,  $\varepsilon$  [ $\text{Wm}^{-3}$ ], the gas void fraction,  $X_g$ , and the pulp consistency,  $con$ :

$$k_L a = 1.7 \cdot 10^{-4} \cdot \varepsilon^{1.0} (X_g)^{2.6} \cdot \text{Exp}(-0.386 \cdot con) \quad (53)$$

where  $\varepsilon$  = power dissipation per unit volume of the mixer, [ $\text{W m}^{-3}$ ].

The power dissipation of the mixer largely determines the achieved level of dissolved oxygen concentration at the entrance of the retention tower. So far, only limited data are available concerning the mass transfer rate,  $k_L a$ , in the tower. Based on laboratory measurements, Rewatkar and Bennington reported  $k_L a$  values in the tower as being in the range between 0.002 and 0.01  $\text{s}^{-1}$  [28]. In their chemical reactor analysis, van Heiningen et al. have not considered any relationship between the efficiency of a high-shear mixer in terms of the extent of dissolution of oxygen in the aqueous phase and the mass transfer rate,  $k_L a$ , in the tower [27]. Based on our own industrial experience, we believe that the efficiency of a high-shear mixer also determines the  $k_L a$  in the tower to a certain extent [35]. It was shown that the increase of both power dissipation and residence time in a high-shear mixer significantly improved the degree of delignification of a beech acid sulfite dissolving pulp. Therefore, we are quite convinced that there should be a relationship between the efficiency of a high-shear mixer and the mass transfer rate in an oxygen delignification tower. As bubbles of oxygen gas tend to coalesce during their transport through the tower, the  $k_L a$  would rather follow a gradient to lower values. Due to lack of information, the effect of different  $k_L a$  values in the tower on the extent of delignification is evaluated in a case study.

The second step of the mass transfer of oxygen to pulp fibers is the diffusion of dissolved oxygen from the water surrounding the fibers through the fiber wall where reaction occurs. It has been estimated by considering the ratio between the rate of oxygen consumption by reaction to oxygen diffusion into the fiber that the



liquid–fiber transfer resistance is negligible in comparison with the apparent intrinsic reaction rate [10,27]. Therefore, the intra-fiber diffusion resistance is considered insignificant for oxygen delignification. Quite recently, measurements revealed that oxygen is able to diffuse at least a distance of some 4–6 mm within the pulp suspension in a 60-min retention time of a typical pressurized retention tower at 786 kPa [36].

The effect of mass transfer of oxygen on the course of delignification through the mixer and the bleaching tower can be calculated by solving the equations numerically.

Although the model equations can be solved by any method suited for solving ordinary differential equations (ODE), we use a simple scheme which exploits the structure of the equations to yield accurate and reliable results. The tower is divided into a large number of layers, each of volume  $\Delta V$ . A total of 500 layers was used for the examples discussed below, and this resulted in an error lower than 0.0001 kappa units at the outlet of the reactor. The retention time  $\Delta t$  in the volume element  $\Delta V$  is calculated by the following expression:

$$\Delta t = \frac{(1 - X_g) \cdot \Delta V}{\dot{V}_s} \quad (54)$$

The calculation in a layer consists of two steps. In the first step, an approximation for the variables at layer outlet is obtained, while the second step applies the midpoint rule to improve the approximation.

### First Step

Use variable values at layer inlet and enter in Eq. (48) to calculate approximation for kappa at layer outlet (Euler's method), then calculate oxygen consumption rate [Eq. (47)], hydroxide consumption [Eq. (49)], temperature increase [Eq. (50)], pressure drop [Eq. (51)] and oxygen concentration at saturation [Eq. (52)]. Use the obtained values for  $r_{O_2}$  and  $[O_{2,sat}]$  and compute dissolved oxygen concentration  $[O_2]$  as exact solution [from Eq. (44)]. We use the exact solution here, because the oxygen concentration may change rapidly in the layer, as in the mixer, which is treated as single layer.

### Second Step

Calculate averages for the variables in the layer using inlet values and approximations for outlet values from first step. Carry out calculations as in first step with these averages, which is essentially an application of the midpoint rule.

The values obtained at layer outlet are the inlet values for the next layer; hence, all layers can be computed successively, starting with the bottom layer. The resulting method has convergence order 2; hence, doubling the number of layers will quarter the calculation error. The procedure can be easily extended to the more accurate classical Runge-Kutta method (convergence order 4).

#### 7.3.4.2 Case Study

Analogous to the assumptions made by van Heiningen et al., the high-shear mixer and the oxygen delignification tower are simulated for a softwood kraft pulp, a production capacity of 1000 odt d<sup>-1</sup>, a mixer with internal volume of 0.05 m<sup>3</sup>, and a tower of 3.8 m internal diameter and hydraulic height of 38 m, resulting in a residence time of about 60 min. A softwood kraft pulp of type ITC, kappa number 23, is considered for the simulation of oxygen delignification. The course of delignification of this pulp during laboratory oxygen delignification is described in the KAM report A100 [37]. A comparative evaluation of the oxygen delignification reported from laboratory bleaching and the results from modeling the operation under industrial conditions should bring out more clearly the most prominent parameters which affect the efficiency of oxygen delignification. The assumptions for the base case study are summarized in Tab. 7.20.

**Tab. 7.20** Conditions of the base case for modeling of industrial oxygen delignification. Assumptions concerning production capacity and equipment configuration and capacity according to van Heiningen et al. [27] An ITC softwood kraft pulp, kappa number 23, of which laboratory oxygen delignification is described, is selected for the process simulation [37].

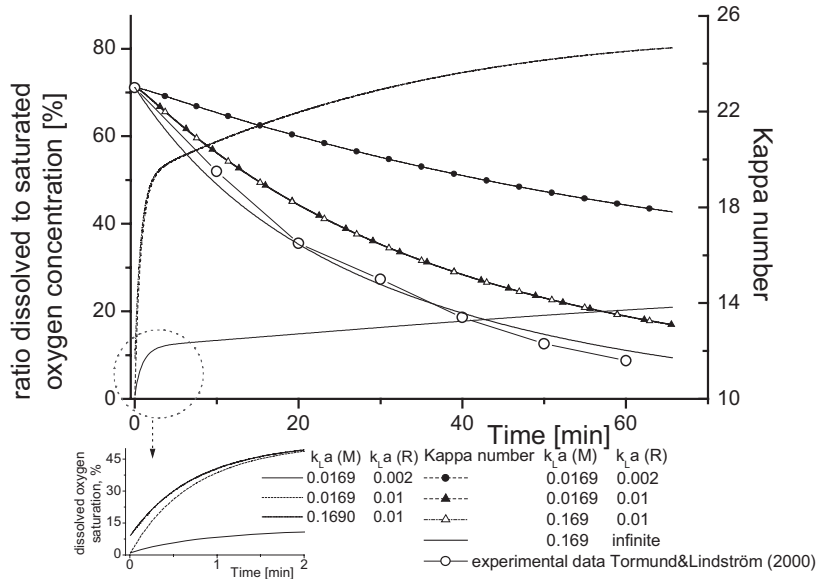
Parameter		
Production	t h <sup>-1</sup>	41.67
Consistency	[-]	0.12
Brownstock kappa		23
carry-over	kg DOC/odt	0
Mixer volume	m <sup>3</sup>	0.05
Reactor volume	m <sup>3</sup>	431
Hydraulic height	m <sup>3</sup>	38
Number of layers		500
Layer volume	m <sup>3</sup>	0.862
Layer height	m	0.076
Ratio gas to suspension velocity <sup>a)</sup>		1.8
Sodium hydroxide charge	kg odt <sup>-1</sup>	25
Oxygen charge	kg odt <sup>-1</sup>	25
Temperature	°C	100
Bottom pressure	MPa	0.8

a) assumed

### Base Case Study

#### Mixer performance

According to Bennington, the specific power dissipation,  $\varepsilon$ , for a high-shear mixer lies in the range between  $10^6$  and  $10^7 \text{ Wm}^{-3}$ . These two values are used to calculate the  $k_{L,a}$  in the mixer, using Eq. (53). Considering the conditions shown in Tab. 7.20, the corresponding  $k_{L,a}$  values calculate to  $0.0169$  and  $0.169 \text{ s}^{-1}$ , respectively, with an  $X_g$  value of  $0.171$  at the entrance of the tower. Dissolved oxygen concentration values of  $5.21 \cdot 10^{-5} \text{ mol L}^{-1}$  and  $5.013 \cdot 10^{-4} \text{ mol L}^{-1}$  are achieved in the high-shear mixer, which constitute only  $0.96\%$  and  $9.3\%$  of the saturated oxygen concentration at the base conditions, respectively. These results show that the efficiency of the mixer in terms of oxygen dissolution is rather limited. The development of the degree of dissolved oxygen relative to the saturated oxygen concentration and the resulting course of kappa number degradation are calculated by taking these two mixer performances into account and assuming  $k_{L,a}$  values in the tower to be in the range between  $0.002$  and  $0.01 \text{ s}^{-1}$ , as determined by Rewatkar and Bennington [28]. The results, which are summarized in Fig. 7.36, clearly reveal that the efficiency of the high-shear mixer, expressed as specific power dissipation,  $\varepsilon$ , has no overall influence on the development of the dissolved oxygen concentration throughout the retention tower, assuming that a constant  $k_{L,a}$  in the tower not related to the  $k_{L,a}$  in the mixer.



**Fig. 7.36** Development of the degree of dissolved oxygen relative to the saturated oxygen concentration and the resulting course of kappa number degradation as a function of  $k_{L,a}$  in the mixer (M) and the reactor (R), according to the slightly modified model from van Heiningen et al. [27]. The calculated kappa numbers are compared to those obtained from laboratory experiments published in the KAM 100 report [37].

The higher mixing intensity yields a noticeable increase in the dissolved oxygen concentration only during the first 1–2 min after mixing. The assumption of a constant  $k_{l,a}$  value in the tower independently from the  $k_{l,a}$  value in the mixer suggests that mixing intensity has no influence on the efficiency of oxygen delignification. The experimental results, already cited, are however in distinct contrast to this conclusion. The (chosen) mass transfer rate in the tower,  $k_{l,a}$  (R), has a significant influence on the extent of delignification, as depicted in Fig. 7.36 and Tab. 7.21.

Tab. 7.21 Degree of delignification as a function of  $k_{l,a}$  (R).

Parameter	$k_{l,a}$ (R) [ $s^{-1}$ ]					Lab experiments <sup>a</sup>
	0.002	0.004	0.007	0.01	1.0	
Kappa leaving the tower	17.8	15.2	13.7	13.1	11.7	11,6
Degree of delignification, %	22.6	33.9	40.3	43.0	49.1	49,6
$\Delta Kappa_{k_{l,a}}$ as given per						
$\Delta Kappa_{k_{l,a}=\infty}$	0.46	0.69	0.82	0.88	1.00	

a. Tormund & Lindström [138].

The degree of delignification for the case of no mass transfer limitation ( $k_{l,a} \geq 1 s^{-1}$ , there is no further mass transfer limitation) equals the result obtained from the laboratory. An assumption of a  $k_{l,a}$  (R) value of about  $0.004 s^{-1}$  (as proposed by van Heiningen et al.) to simulate industrial conditions of oxygen delignification appears to result in a too low a degree of delignification. A  $k_{l,a}$  (R) value of about  $0.007 s^{-1}$  would give a more reliable result. Due to a lack of experimental data, it can only be speculated that a more realistic course of  $k_{l,a}$  (R) values throughout the tower might possibly also be related to the  $k_{l,a}$  (M) value. In considering the tendency of gas bubbles to coalesce on their way through the tower, an exponential decay of  $k_{l,a}$  (R) could be envisaged.

#### *Influence of operating variables*

The mass transfer of oxygen to pulp fibers in medium-consistency oxygen delignification controls the effect of reaction variables on the efficiency of oxygen delignification. To visualize the influence of the main process variables under the constraints of mass transfer limitation in the tower, the efficiency of delignification is calculated as a function of temperature, consistency, initial pressure, and caustic and oxygen charges (Tab. 7.22; Figs. 7.37 and 7.38). For comparison, a base case scenario is defined using the initial pulp property and process conditions compiled in Tab. 7.20, and in consideration of  $k_{l,a}$  values for the mixer and tower of  $0.169$  and  $0.007 s^{-1}$ , respectively.

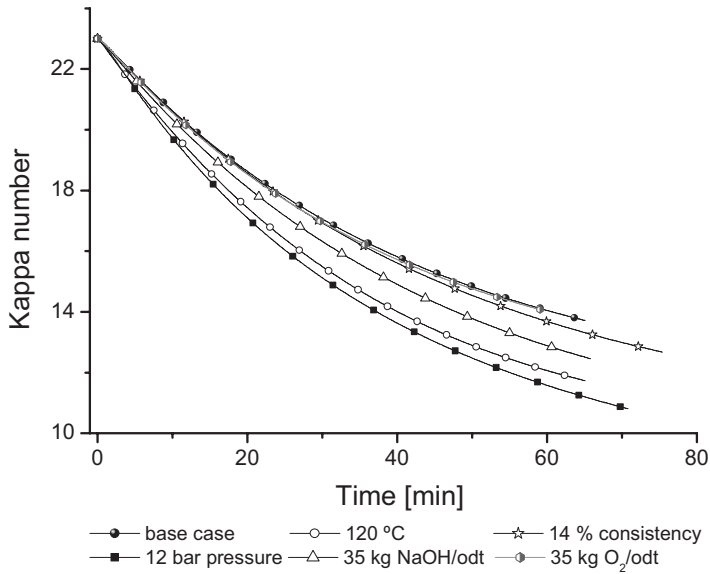
**Tab. 7.22** Effect of important process variables on the performance of oxygen delignification under the constraints of mass transfer limitation.

Parameter		Base case	High temperature	High consistency	High pressure	High NaOH-charge	High O <sub>2</sub> -charge	Carry-over
$k_{La}$ (R)	s <sup>-1</sup>	0.007	0.007	0.007	0.007	0.007	0.007	0.007
Consistency	%	12	12	14	12	12	12	12
Carry-over	kg DOC odt <sup>-1</sup>	0	0	0	0	0	0	15
Temperature	°C	100	120	100	100	100	100	100
Bottom pressure	bar	8	8	8	12	8	8	8
NaOH-charge	kg t <sup>-1</sup>	25	25	25	25	35	25	25
O <sub>2</sub> -charge	kg t <sup>-1</sup>	25	25	25	25	25	35	25
O <sub>2</sub> conc., t = 10 min	mol L <sup>-1</sup>	0.0024	0.0011	0.0020	0.0043	0.0020	0.0024	0.0020
X <sub>g</sub> at tower entrance	[-]	0.171	0.178	0.195	0.120	0.171	0.224	0.171
Temperature increase	°C	4.0	4.9	4.2	5.3	4.5	3.9	4.8
Kappa leaving the tower		13.7	11.7	12.7	10.8	12.5	14.1	14.1
Degree of delignification	%	40.3	49.1	44.9	53.0	45.8	38.8	38.7

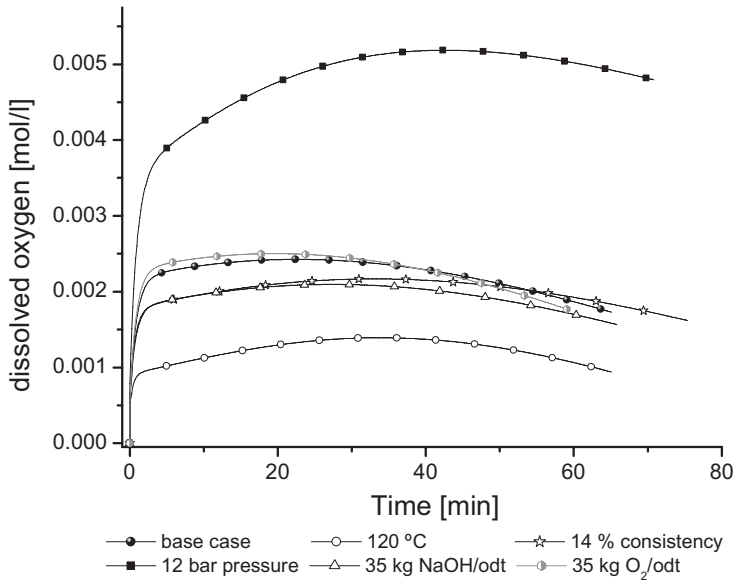
An increase in temperature by 20 °C to 120 °C clearly improves the extent of delignification, mostly determined by intrinsic chemical kinetics. Figure 7.38 confirms that the chosen mass transfer rate in the reactor of 0.007 s<sup>-1</sup> assures a sufficient supply of oxygen to allow the higher rate of lignin removal.

Oxygen delignification also benefits from an increase in consistency. Raising the consistency from 12 to 14% enables an increase in kappa number reduction by one unit (Tab. 7.22). The main reason for the improved delignification is that the residence time of the pulp in the reactor increases by 10 min (15% increase). Parallel to an increase in the consistency, the model calculates a decrease in dissolved oxygen concentration due to an increased oxygen consumption rate,  $r_{O_2}$ , which may be attributed to the lower amount of liquid available for the dissolution of oxygen. However, under real conditions an increase in consistency means a reduced thickness of the immobile water layer, which of course causes an accelerated mass transfer of oxygen to the fiber. The most pronounced effect on delignification is observed by increasing the pressure, because the oxygen concentration in the liquid phase increases almost proportionally with increasing oxygen pressure (Figs. 7.37 and 7.38). Moreover, it may also be assumed that the tendency to coalesce decreases with increasing pressure.

At a given oxygen charge, the gas void fraction reduces parallel to an increase in oxygen pressure, which again improves the mass transfer – especially in a high-



**Fig. 7.37** Calculated course of kappa number drop during oxygen delignification as a function of the main process parameters displayed in Tab. 7.22, based on the modified model of van Heiningen et al. [27].



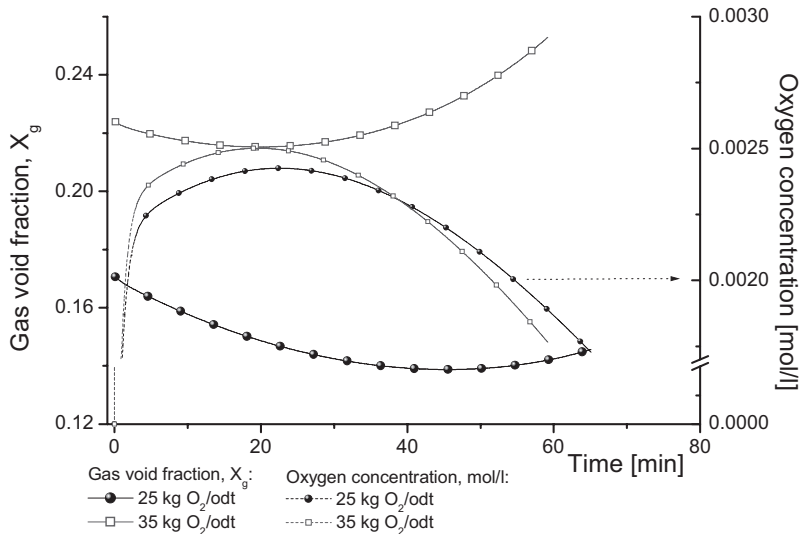
**Fig. 7.38** Calculated course of dissolved oxygen concentration during oxygen delignification as a function of the main process parameters displayed in Tab. 7.22, based on the modified model of van Heiningen et al. [27].

shear mixer. The improved delignification efficiency agrees well with practical experience. Therefore, all modern oxygen delignification concepts – including the two-reactor technology (e.g., Dualox and OxyTrac™) – favor the application of the highest possible pressure during oxygen delignification.

The effect of alkali charge in Fig. 7.37 is mainly determined by the intrinsic chemical kinetics proposed in the model. The higher extent of delignification can be explained by the more rapid consumption of the oxygen, which increases the driving force for transfer of oxygen from the gas to the bulk of the liquid.

The oxygen charge, however, has no significant effect on delignification, provided that the applied charge is sufficient to avoid limitation. On the contrary, the increase of the oxygen charge from 25 to 35 kg odt<sup>-1</sup>, causes even a slight impairment of delignification. The kappa number leaving the retention tower is approximately 0.5 unit higher than the base case (see Tab. 7.22). This result agrees well with the observation reported by Bennington and Pineault that mills with a higher oxygen charge have a lower degree of delignification [38]. The reason for the reduced kappa number drop is the shorter residence time of the pulp suspension caused by the higher gas void fraction,  $X_g$  (Fig. 7.39). However, the overall effect is diminished because the mass transfer rate,  $k_L a$ , increases with rising gas void fraction,  $X_g$ , as demonstrated in Eq. (53).

Figure 7.39 illustrates that the gas void fractions run through a minimum, while the dissolved oxygen concentrations pass through a maximum. With



**Fig. 7.39** Calculated course of dissolved oxygen concentration and gas void fraction during oxygen delignification for two different oxygen charges, 25 kg odt<sup>-1</sup> and 35 kg odt<sup>-1</sup>, respectively, based on the modified model of van Heiningen et al. [27]. Remaining parameters correspond to base case conditions (see Tab. 7.22).

increasing oxygen charge, the minimum is shifted towards a shorter retention time as expected. In this connection it must be recalled that the model assumes a ratio gas to suspension velocity greater than 1 (Tab. 7.20), which results in a lower gas void fraction according to Eq. (46).

Table 7.22 also contains the results of simulating the presence of carry-over representing an amount of 15 kg DOC  $\text{odt}^{-1}$ . However, the results are only tentative due to the lack of an appropriate kinetic expression for the description of the DOC oxidation. Therefore, a similar kinetic expression as for the degradation of residual lignin is used, taking the conversion of DOC to dissolved lignin (1 kg DOC equals 0.79 g lignin) into consideration. It is clear that the dissolved lignin competes against the residual lignin for the caustic and dissolved oxygen, which results in a slight impairment of pulp delignification. The preferred oxidation of the dissolved lignin (no mass transfer limitation) induces a higher increase in temperature ( $\Delta T = 4.8^\circ\text{C}$  instead of  $4.0^\circ\text{C}$  for the base case), which in turn accelerates pulp delignification. Consequently, the degree of pulp delignification in the presence of 15 kg DOC  $\text{odt}^{-1}$  is only slightly worse as compared to the base case scenario.

### 7.3.5

#### Process Variables

During oxygen delignification, a great variety of oxygen-containing species is involved in the reactions with pulp components. Each of these different species has a characteristic reactivity with lignin and carbohydrate structures under given conditions of pH, temperature, and concentration. The pH also controls the equilibrium concentration of other ionized species, such as phenolate and enolate anions (see Section 7.3.2).

There is a general agreement that the kappa number reduction and brightness increase during oxygen delignification are mainly governed by the alkali charge, the temperature, the reaction time, and the pressure. The most important process variables are discussed below in regard to impact on the selectivity and efficiency of oxygen delignification.

#### 7.3.5.1 Temperature

The oxygen delignification of kraft pulps requires temperatures above  $80^\circ\text{C}$  to maintain a reasonable rate of delignification. Kinetic investigations show that a low temperature during the initial phase of about 5–10 min is beneficial for the selectivity of delignification. Following the results from kinetic investigations, the temperature in the first stage of a two-reactor operation is kept at low temperature. The temperature-dependence is characterized by the activation energy,  $E_A$ , using the Arrhenius equation. The published values of  $E_A$  for both the delignification and viscosity degradation (chain scissions) during oxygen delignification of kraft pulps show large variations in the range between 50 and almost  $100\text{ kJ mol}^{-1}$  (see Tabs. 7.13, 7.14, 7.17 and 7.18). The corresponding values for lignin model compounds were determined to be in the same range, namely  $78\text{ kJ mol}^{-1}$  for the



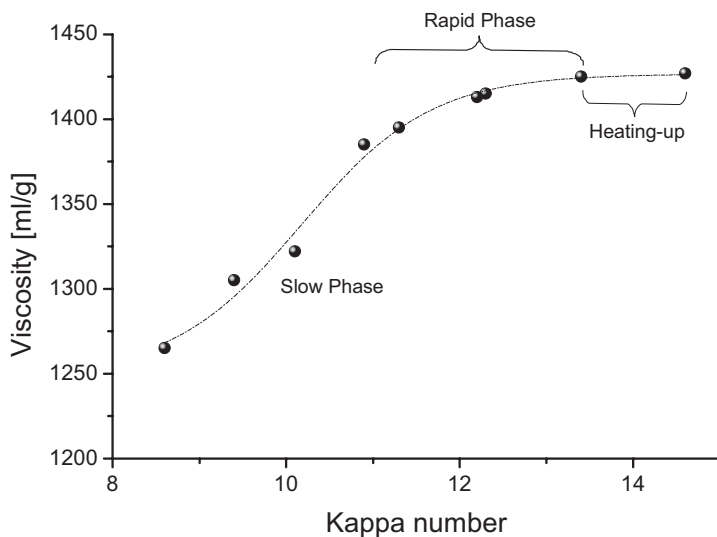
degradation of diguaiacyl stilbene and  $62 \text{ kJ mol}^{-1}$  for the degradation of a phenolic  $\beta$ -aryl ether, respectively [39].

Studies where both lignin and carbohydrate degradation kinetics have been evaluated using the same experimental set-up and substrates reveal a slightly higher activation for the chains scissions than for the lignin degradation reactions [1,12]. This implies that the selectivity of oxygen delignification tends to improve with decreasing temperature. At a given alkali charge, an increase in temperature allows the initial rapid rate to continue to a lower kappa number. Clearly, the point of alkali exhaustion is reached more rapidly at higher temperatures. The homolytic decomposition of the peroxide species apparently becomes important at temperatures well above  $110^\circ\text{C}$ . Although carbohydrate degradation becomes severe at high temperatures, increasing the temperature within the range of  $90\text{--}120^\circ\text{C}$  has little effect on pulp yield [40].

Oxygen delignification is an exothermic process. The heat of reaction is appreciable, and is reported to be range between  $12$  and  $14 \text{ MJ ton}^{-1}$  pulp and removed kappa number [33]. The removal of the heat of reaction may be a problem in high-consistency processes when little water is available to absorb the extra heat.

### 7.3.5.2 Retention Time

The selectivity of oxygen delignification varies with the degree of delignification. It is agreed that oxygen delignification proceeds as a two-stage – or, more close to reality – a multi-stage process (see Section 7.3.3, Reaction kinetics). Hartler has

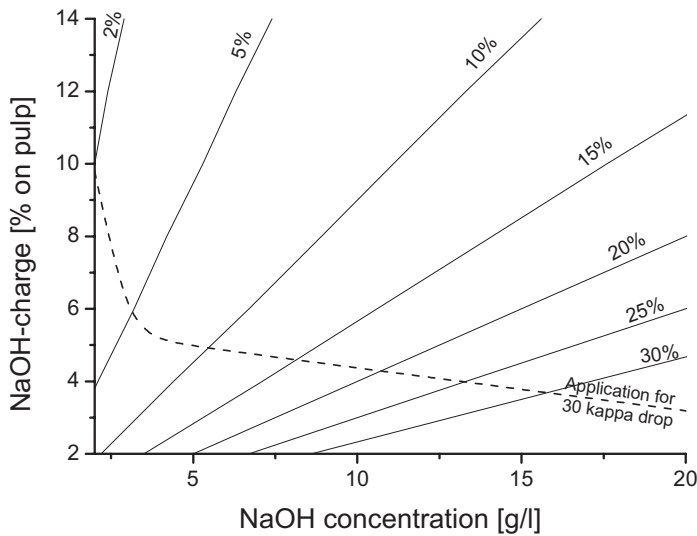


**Fig. 7.40** Selectivity plot of oxygen delignification of a *Eucalyptus globulus* kraft pulp, kappa number 14.6 (according to [42]). Process conditions:  $95^\circ\text{C}$ , 1% alkali charge on pulp, 8 bar pressure, reaction times from 1 to 120 min.

shown that a higher-viscosity pulp is obtained by using a lower temperature and thus longer retention time to reach the given kappa number [41]. The initial rapid phase is known to be more selective as compared to the latter stages [13]. Figure 7.40 illustrates the high selectivity of the initial stage of oxygen delignification of a *Eucalyptus globulus* kraft pulp, kappa 14.6, within the first 5–10 min of reaction.

### 7.3.5.3 Alkali Charge

Model compound studies revealed that the ionization of phenols to form phenolate anions is the rate-determining step in the formation of cyclohexadienone hydroperoxides [43]. The pH for most phenolic compounds is in the range of 10–11, which suggests that oxygen delignification decelerates at lower pH levels [44]. The rapid lignin degradation in the initial phase coincides with a rapid drop in pH due to the neutralization of organic acids formed by oxidation of both lignin and carbohydrate moieties. The transition from the fast initial to the slow residual delignification rate occurs at a pH of around 10 [43]. Further delignification beyond this transition point is not desirable as the rate becomes very slow, and consumption of oxygen and impairment of pulp properties continue. The transition is shifted to a lower kappa number as soon as the initial alkali charge is increased, but still occurs at the same pH value. If the pH is then raised significantly above the critical value by a second addition of sodium hydroxide, another phase of rapid delignification rate is observed [44]. An increase in alkali concentration results in both enhanced lignin and carbohydrate degradation reactions. However, the overall selectivity – expressed as the



**Fig. 7.41** Sodium hydroxide concentration versus applied caustic charge at different consistencies (values shown on individual lines) in the range from low to high consistency [45].

viscosity–kappa number relationship – is clearly impaired (see Fig. 7.51). It is clear that low-consistency pulps require a higher alkali charge (based on dry pulp) than do higher-consistency pulps to achieve a given kappa number reduction at otherwise constant conditions. The effect is most pronounced when comparing medium consistency (8–18%) to low consistency (0.5–5%), and is related to the concentration of the alkaline solution present, as shown in Fig. 7.41.

#### 7.3.5.4 pH Value

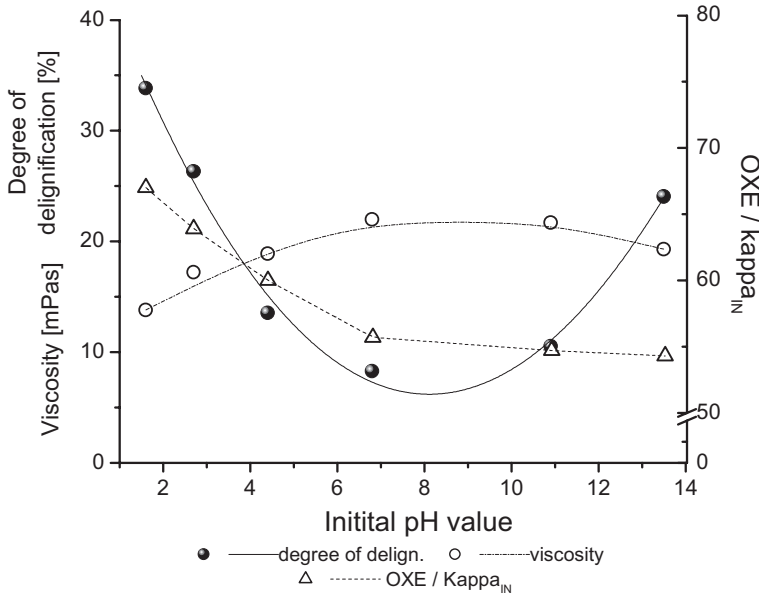
Oxygen delignification is (always) carried out at highly alkaline conditions. In a survey of North American mills, it was determined that the pH entering the oxygen delignification ranges from 10.3 to 12.1 [46]. The maximum rate of degradation for lignin model compounds such as propylguaicol is shown to be in the vicinity of pH 11, measured at room temperature in the range from pH 9 to pH 13.5 [39]. The rate increase at  $\text{pH} \geq 9$  is due to ionization of the phenolic groups, which facilitates the redox reaction with oxygen. The maximum at pH 11 may be due to the formation of further oxygen-containing species, such as superoxide anions, superoxide radicals and hydroxyl radicals which contribute to the rate of degradation. The evaluation of an industrial oxygen delignification plant revealed the optimum viscosity–kappa number relationship (selectivity) at a blowline pH of about 10.5 [47]. At lower pH, lignin begins to precipitate on the fiber, and this clearly impairs selectivity.

In the case of hardwood kraft pulps, the extent of delignification is however rather limited during oxygen delignification due to a relatively large amount of hexenuronic acid groups. A subsequent sulfuric acid treatment would efficiently remove the hexenuronic groups [48]. Taking these experiences into consideration, it may be envisaged that in a two-stage process, the first stage is conventionally run at high alkaline pH to recover the spent liquor, and the second stage at acidic pH to remove the resistant structures. With this concept in mind, the effect of pH in the range of 1.6 to 13.5 on the second stage of a two-stage oxygen delignification process of a hardwood kraft pulp was investigated while the first stage was run at alkaline pH [49].

The study revealed that the degree of delignification is highest at a pH 1.6 followed by pH 2.7, pH 13.5, and showed at minimum at pH 7. The data in Fig. 7.42 show that both the bleachability – measured as specific OXE demand, OXE/kappa, and pulp viscosity of the ECF-bleached pulp – are improved as the pH of the second oxygen delignification increases from 1.6 to 13.5.

However, at a given tensile index, the apparent density and tear index decrease with increasing the pH of the oxygen delignification, although the viscosity follows the reverse trend.

The examination of the residual dioxane lignin revealed a negative correlation between the extent of delignification during the second oxygen stage and the content of total phenolic hydroxyl groups in the residual lignins of oxygen delignified pulps. The ratio of the optical densities of the infrared bands at  $1330\text{ cm}^{-1}$  to  $1270\text{ cm}^{-1}$  indicates that the residual dioxane lignin in the oxygen-delignified pulp



**Fig. 7.42** Results of a second oxygen delignification stage of a hardwood kraft pulp as a function of pH (according to [49]). Initial substrate: oxygen-delignified hardwood kraft pulp, kappa number 13.3, viscosity 21.6 mPas delivered from a mill; constant conditions in the second oxygen delignification stage: 95 °C, 60 min, initial pressure 245 kPa, 10% consistency.

produced at pH 1.6 contains fewer guaiacyl groups relative to syringyl units than that isolated from the pulp made at pH 13.5 [49]. The lower content of phenolic hydroxyl groups of the former residual lignin (pH 1.6) suggests that it is more extensively degraded than the latter (pH 13.5).

#### 7.3.5.5 Final pH

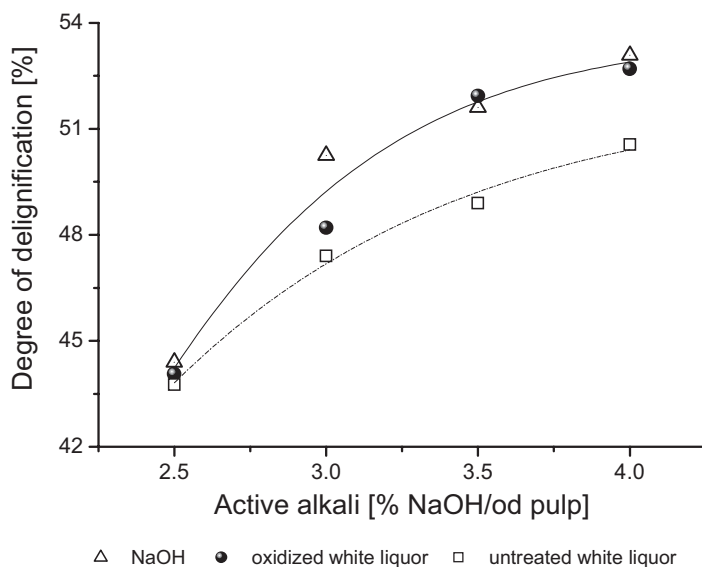
Electron spectroscopy for chemical analysis (ESCA) revealed that in conventional oxygen delignification the lignin on the fiber surface is less efficiently removed as compared to the overall decrease in lignin content, indicating possible reprecipitation of dissolved lignin [50]. It has been shown that lignin reprecipitation is primarily influenced by the final pH, but also by ionic strength, the concentration of dissolved lignin and temperature [51]. As the  $pK_a$  values of industrial kraft lignin are reported to be between 10.5 and 11.0, it can be assumed that precipitation of lignin occurs at or below these pH-values. Backa and Ragnar investigated the influence of the final pH in the range between 9.2 and 11.1, and found that the bleachability in a subsequent D(OP)D sequence is significantly improved when the final pH is raised to a value of 10.4 [52]. The improved bleachability translates into a saving of close to 10% of the total chlorine dioxide requirement to reach an ISO brightness of 89.5%. Above a pH of about 10.4, the effect on bleachability levels off, however. In order not to impair the selectivity of oxygen delignification,

the overall alkali charge should be split so that part is added to the blow tank of the oxygen delignification, stage keeping the final pH well above 10. This post-oxygen alkali addition equals an additional mild extraction stage without intermediate washing.

### 7.3.5.6 Alkali Source

The use of fresh sodium hydroxide as an alkali source for oxygen delignification of a kraft pulp would be relatively expensive, and could lead to an imbalance in the ratio of sodium to sulfur in the chemical recovery system. Alternatively, either kraft white liquor or oxidized white liquor as a source of alkali could be applied. A comparative evaluation of oxygen delignification of a radiata pine kraft pulp revealed that no change in delignification rate was observed when oxidized white liquor was used instead of fresh sodium hydroxide. Untreated white liquor, however, reduced the extent of delignification due to the presence of the sulfide (Fig. 7.43).

There are some indications that the selectivity of oxygen delignification is slightly impaired when untreated white liquor is used as a source of alkali instead of fresh sodium hydroxide or oxidized white liquor [53].



**Fig. 7.43** Influence of alkali source on the extent of delignification of a radiata pine kraft pulp during oxygen delignification (according to [53]). Constant conditions: 10% consistency, 690 kPa pressure, 100 °C.

### 7.3.5.7 Oxygen Charge, Oxygen Pressure

In contrast to the alkali charge and temperature, the charge of oxygen plays a less important role, as long as sufficient oxygen is present in the oxygen delignification system. It is agreed that an oxygen charge between 20 and 30 kg bdt<sup>-1</sup> is sufficient to avoid any oxygen-based limitation of the delignification process. In the literature, different values for specific oxygen consumption per unit kappa number reduction ( $\Delta O_2/\Delta \text{kappa number}$ ) are reported. According to laboratory studies, the oxygen consumption per unit kappa number reduction varies from 0.5 to 0.6 kg bdt<sup>-1</sup> [54,55]. The evaluation of industrial oxygen delignification plants revealed oxygen consumption values of 1.4 kg bdt<sup>-1</sup> per unit kappa number decrease for softwoods, and 1.6 kg bdt<sup>-1</sup> for hardwoods [56]. In a dissolving pulp mill using unbleached beech acid sulfite pulp, the oxygen consumption was calculated from the quantity and composition of the exhaust gas from the blow tank of the oxygen delignification stage [57]. A “helium tracer technique” was applied to control the oxygen consumption [31].

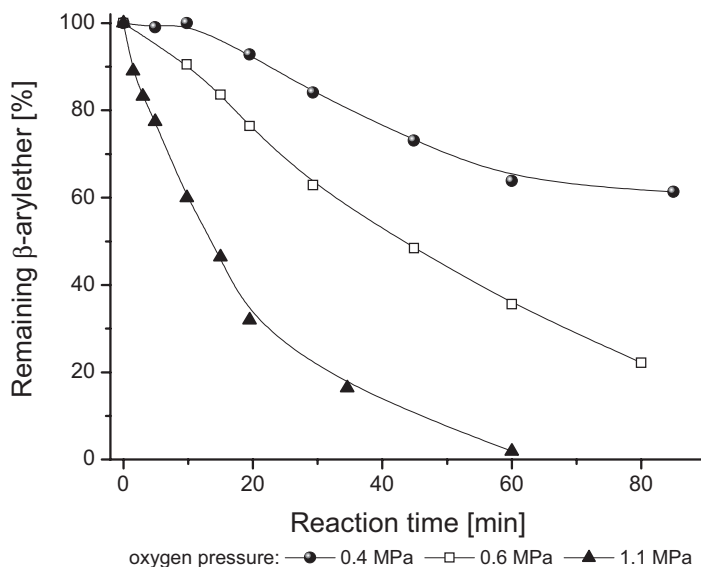
From these measurements it can be concluded that the specific oxygen consumption rate amounts to approximately 1.0 kg per unit of kappa number decrease.

With increasing temperature, the utilization of oxygen increases without significantly improving the delignification efficiency. Furthermore, it is reported that the increased oxygen consumption parallels the increased loss of pulp yield.

On the basis of detailed material balances, the amount of oxygen consumed during an industrial oxygen delignification process was estimated [58]. The study of Salmela and Alen indicates that part of the oxygen bound to the reaction products originates from alkali (about 13%), part from molecular oxygen (about 33%), and the major part from the pulp (about 54%) itself. The specific consumption of molecular oxygen needed for the oxidation reactions is, however, limited to 0.6–1.0 kg bdt<sup>-1</sup>, which is in good agreement with the results obtained from laboratory studies. An increase in the oxygen charge primarily induces increased oxidation reactions with dissolved organic and inorganic compounds.

Unlike the oxygen charge, the oxygen pressure significantly influences the degradation rate (see Section 7.3.4). Model compound studies using phenolic  $\beta$ -aryl ether confirmed the pronounced effect of oxygen pressure on degradation rate (Fig. 7.44).

Commercial oxygen delignification plants typically use pressures in the range 400 to 870 kPa with medium consistency systems applying higher pressures as compared to high consistency plants [59]. However, there is a clear trend to further increase oxygen pressure as high as technically feasible, especially in two-stage operations.



**Fig. 7.44** Influence of oxygen pressure on the degradation rate of a phenolic  $\beta$ -aryl ether compound at pH 11 and 100 °C (according to [39]).

### 7.3.5.8 Consistency

Pulp consistency affects the sodium hydroxide concentration at a given alkali charge, and also the pumping costs. Increasing pulp consistency results in a decreasing diffusion distance and in an increasing alkali concentration, both of which lead to an increased delignification rate [60]. The relationship between caustic concentration at a given alkali charge as a function of pulp consistency on the one hand, and the correlation to the extent of lignin removal on the other hand, is depicted in Fig. 7.41.

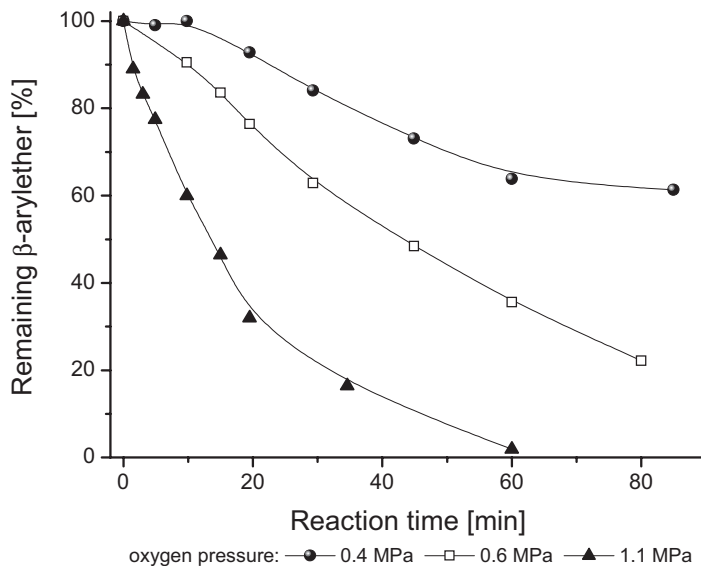
Pulp consistency plays an important role in terms of safety for a commercial system. The gaseous reaction products (predominantly carbon monoxide and volatile hydrocarbons) generated in the reaction must be removed from the oxygen delignification system comprising the reactor, blow tank, and washers. The specific carbon monoxide evolution is about 30% less at medium consistency as compared to high consistency [61].

## 7.3.6

### Pulp Components and Impurities

#### 7.3.6.1 Effect of Metal Ion Concentration

The rather poor selectivity of oxygen delignification as compared to chlorine dioxide is further impaired by the presence of transition metal ions. The wood used as



**Fig. 7.44** Influence of oxygen pressure on the degradation rate of a phenolic  $\beta$ -aryl ether compound at pH 11 and 100 °C (according to [39]).

### 7.3.5.8 Consistency

Pulp consistency affects the sodium hydroxide concentration at a given alkali charge, and also the pumping costs. Increasing pulp consistency results in a decreasing diffusion distance and in an increasing alkali concentration, both of which lead to an increased delignification rate [60]. The relationship between caustic concentration at a given alkali charge as a function of pulp consistency on the one hand, and the correlation to the extent of lignin removal on the other hand, is depicted in Fig. 7.41.

Pulp consistency plays an important role in terms of safety for a commercial system. The gaseous reaction products (predominantly carbon monoxide and volatile hydrocarbons) generated in the reaction must be removed from the oxygen delignification system comprising the reactor, blow tank, and washers. The specific carbon monoxide evolution is about 30% less at medium consistency as compared to high consistency [61].

## 7.3.6

### Pulp Components and Impurities

#### 7.3.6.1 Effect of Metal Ion Concentration

The rather poor selectivity of oxygen delignification as compared to chlorine dioxide is further impaired by the presence of transition metal ions. The wood used as



raw material in kraft pulping is the primary source of the majority of non-process elements (NPEs). The content of inorganic ions depends on the wood species and the location of the growth place. Metal ions in wood are assumed to be bound to carboxylate groups in hemicellulose, pectin, lignin, and extractives. Transition metals may also be attached to lignin and extractives by complex formation, or as metal salts of low solubility [62]. In oxygen delignification and peroxide bleaching, cellulose degradation reactions are promoted by the presence of even trace amounts of transition metal ions, such as copper, cobalt and iron [63].

The presence of cobalt (II) and iron (II) salts during oxygen bleaching of cotton linters cause the highest rate and extent of cellulose degradation, while copper has a less damaging behavior, and nickel has no visible effect. Manganese, on the other hand, demonstrates both characteristics, being a degradation catalyst below 10 ppm and a protective agent above 60 ppm [64]. The transition to a cellulose-preserving agent has also been observed for iron when present in sufficient excess. At a concentration level above 0.1% on pulp, the precipitated ferric hydroxide acts as an oxidation inhibitor, similarly to magnesium compounds [64]. Surprisingly, the effect of transition metal ions on cellulose degradation during alkali-oxygen treatment show striking similarities to the catalytic processes occurring in the aging of alkali cellulose [65,66]. The same metal ions that are found to accelerate depolymerization in alkali cellulose cause increased viscosity reduction in the course of alkali-oxygen treatment. Thus, it can be assumed that transition metal ions such as cobalt, iron and copper promote free radical generation by catalyzing the decomposition of the peroxides formed during oxygen delignification. Cobalt is shown to be an even more effective catalyst than iron [67]. Moreover, it is observed that the formation of both carbonyl and carboxyl groups is strongly favored in the presence of cobalt ions (see Tab. 7.23).

**Tab. 7.23** Influence of iron and cobalt ions on the degradation of purified cotton linters during oxygen bleaching in the presence and absence of magnesium carbonate (according to [67]).

Substrates, treatment	Additives [mmol L <sup>-1</sup> ]	Viscosity [ml g <sup>-1</sup> ]	Carbonyl groups [mmol kg <sup>-1</sup> ]	Carboxyl groups [mmol kg <sup>-1</sup> ]
Cotton linters (CL)	no	550	n.a.	3.6
CL, oxygen delignification (OD) <sup>a</sup>	no	336	3.8	16.4
CL, OD	0.05 Fe(II)	262	6.6	18.7
CL, OD	0.05 Fe(II) + 3.0 Mg (II)	373	2.8	10.4
CL, OD	0.05 Co(II)	127	19.7	64.0
CL, OD	0.05 Co(II) + 3.0 Mg(II)	194	7.1	34.5

a. 98 °C, 60 min, 6 bar, 5% NaOH.

The addition of magnesium carbonate significantly retards cellulose degradation and the formation of carbonyl and carboxyl groups in the presence of iron salts. However, the catalytic effect of cobalt ions on cellulose degradation and oxidation cannot be offset by the addition of magnesium carbonate.

The results of a detailed study on TCF-bleaching of a softwood kraft pulp indicated that even a copper content below 1 ppm on pulp promoted depolymerization of cellulose during peroxide bleaching [68].

Hydrogen peroxide undergoes Fenton-type reactions with metal ions such as iron and manganese, leading to hydroxy radicals that are then able to oxidatively cleave and/or peel polysaccharide chains [69,70]. A recent study using methyl 4-O-ethyl- $\beta$ -D-glucopyranoside as a model for cellulose indicates that Fe(II) ions are the most harmful species to carbohydrates in the presence of hydrogen peroxide [71]. The extent of glycosidic bond cleavage decreases with increasing initial pH and in the presence of oxygen, presumably due to the preferred formation of less-reactive hydroperoxyl radicals [71]. The Fenton reaction is drastically inhibited under alkaline conditions at room temperature, this most likely being due to the reduced solubility of Fe(II) and Fe(III) ions.

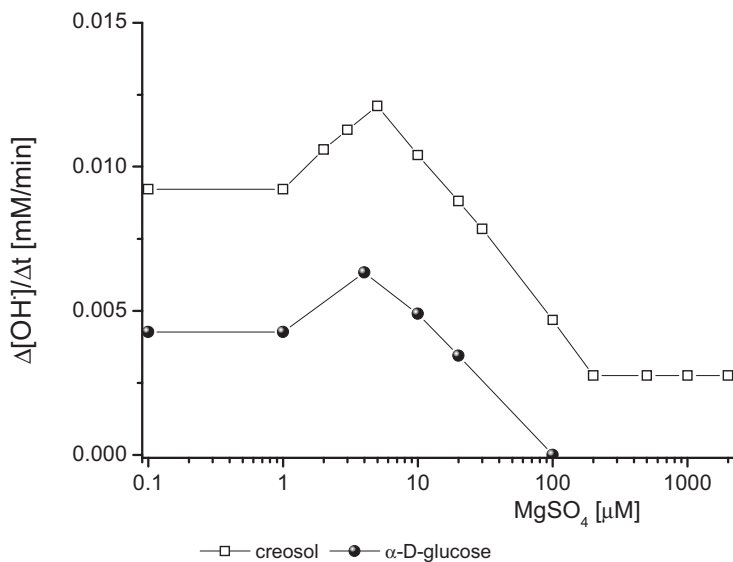
Radicals generated during the decomposition of hydrogen peroxide are also considered to be involved in delignification reactions during oxygen delignification [72]. The degradation rate of propylguaiacol (used as a lignin model) during oxygen bleaching is however generally lowered in the presence of transition metal ions [39]. Simultaneously, the maximum rate of degradation is shifted from pH 11 to pH 12. The highest rate of degradation is preserved when copper(II) ion is added. In the presence of 0.1  $\mu$ M copper (II) ion, the degradation rate of propylguaiacol is reduced by about 20% while the degradation rate is decreased by more than 40% in the presence of iron(II), cobalt(II) and manganese(II) ions at the same concentration levels. One explanation of this behavior might be the formation of a complex between the phenolate anion and the metal ion, which would make the oxygen delignification process less efficient [39].

The addition of aluminum sulfate strongly retards delignification during oxygen-alkali cooking of wood meal. It is suspected that redox active metal ions are inactivated in the presence of aluminum salts by a type of coprecipitation together with aluminum hydroxide, as is known similarly for magnesium salts [73]. The addition of lanthanum nitrate prior to oxygen delignification exerts a protective action similar to that of magnesium salts. Lanthanum salts precipitate as hydroxides under the conditions prevailing during oxygen bleaching [67].

Since the discovery by Robert and associates of the protective effect of magnesium carbonate on the cellulose fraction of the pulp, numerous investigations have clearly confirmed that the addition of magnesium salts inhibits the degradation of carbohydrates [74–76]. Consequently, several commercial oxygen delignification plants add a magnesium salt to the caustic liquor in order to prevent the metal ion-catalyzed degradation of polysaccharides. It has been proposed that magnesium cations form precipitates with iron(II) and manganese(II) ions in the presence of an anionic polymer (e.g., cellulose or polygalacturonic acid) and change their physical characteristics into a negatively charged colloidal phase.

Iron and manganese ions are redox-stabilized in their +II state by being incorporated into a solid phase; in this way they cannot further participate in a Fenton-type reaction [69,77]. Magnesium must be precipitated as the hydroxide, carbonate or silicate in order to act as stabilizer. The characterization of the precipitate revealed the presence of a so-called solid solution at a pH > 10, with a variable composition  $(\text{Mg}_{1-x}\text{Mn}_x)(\text{OH})_2(\text{ss})$ , that effectively binds a certain amount of transition metal ion [78]. In a detailed study, it has been shown that the solubility of Mn(II) decreases when the Mg(II):Mn(II) molar ratio increases. This implies that the solid-state Mn(II) will be highly diluted with Mg(II), which means that the Mn(II) will lose the opportunity to interact with dissolved hydrogen peroxide. By considering the solubility products, it can be concluded that at pH < 10, this solid solution can no longer keep the Mn(II) concentration below the catalytically active level. The reason why the Mn(II) can still be found as a co-precipitate with Mg(II) at the end of an alkaline oxygen stage with the pH below 10 has been studied in detail [79]. As a first indication, it was found that the divalent metal ions in oxygen delignification are present as carbonates, and not as hydroxides [80]. The analysis of the precipitated particles indicated that the core consists of fairly insoluble  $\text{MnCO}_3(\text{s})$  on which Mg(II), in the form of  $\text{MgCO}_3(\text{s})$ , crystallizes in layers. The latter originates from an initial precipitate,  $\text{Mg}_5(\text{OH})_2(\text{CO}_3)_4(\text{s})$ . The crystallization process is slow, which also coincides with the observation that the protection against hydrogen peroxide degradation improves either with increasing Mg(II) addition or prolonging the ageing time before hydrogen peroxide is applied. The mechanism of redox stabilization of Mn(II) by Mg(II) in oxygen delignification can be explained by assuming that manganese present in wood is transformed to  $\text{MnCO}_3(\text{s})$  already during the kraft cook. After the addition of soluble Mg(II) salts prior to oxygen delignification,  $\text{MgCO}_3(\text{s})$  crystallizes as a layer on top of the  $\text{MnCO}_3(\text{s})$  particles, and thus assures the inertness of the Mn(II) ions against hydrogen peroxide decomposition. In order to reach high redox stabilization of the catalytically active transition metal ions, high temperature, and/or prolonged ageing time is needed.

A study conducted by Lucia and Smereck indicates that the selectivity of oxygen delignification, defined as the ratio of the extent of delignification divided by the viscosity changes,  $\Delta\kappa_{(\text{initial-final})}/\Delta\text{viscosity}_{(\text{initial-final})}$  [81], is significantly improved by increasing the molar ratio Mg:Mn from 22 to 33. Interestingly, the lower lignin pulp ( $\kappa$  25) seems to be more susceptible to carbohydrate preservation due to the addition of magnesium salts as compared to the high- $\kappa$  number pulp ( $\kappa$  40). One possible reason for this observation might be the greater amount of oxidized structures in the low- $\kappa$  pulp (e.g., carboxylic groups), which clearly are necessary to bind redox active metal ions efficiently [82]. The addition of magnesium sulfate to oxygen delignification inhibits the formation of hydroxyl radicals. The effect of increasing concentrations of magnesium ions on the rate of hydroxyl radical formation in the treatment of  $\alpha$ -D-glucose and creosol under oxygen delignification conditions is shown in Fig. 7.45 [83]. The influence of magnesium ions on the formation of hydroxyl radicals is apparently independent of the substrate at concentrations <100  $\mu\text{M}$ .



**Fig. 7.45** The effect of magnesium sulfate on the rate of hydroxyl radicals formation during treatment of creosol and  $\alpha$ -D-glucose under oxygen delignification conditions (according to [83]). Substrate concentration 1.5 mM, pH 11.5, 5 bar O<sub>2</sub>, 90 °C.

The difference in behavior between  $\alpha$ -D-glucose and creosol with regard to hydroxyl radical formation at magnesium sulfate concentrations >100  $\mu$ M may be ascribed to the formation of Mg<sup>2+</sup> carbohydrate complexes, and to thermal homolytic cleavage of hydroperoxide intermediates derived from creosol to produce additional hydroxyl radicals [83].

The treatment of an unbleached softwood kraft pulp with a solution of magnesium and calcium acetate at pH 4.5 results in a decrease of the manganese content from 40 ppm to 1.9 ppm [68]. The removal efficiency is comparable to a pretreatment at pH 5.87 with 4 kg ethylen-diamine tetra-acetate EDTA t<sup>-1</sup> pulp. Effective manganese removal results in a comparable viscosity preservation as compared to magnesium addition.

Although transition metal ions are removed prior to oxygen delignification, it is confirmed that additional EDTA extraction is needed immediately prior to subsequent hydrogen peroxide bleaching in order to avoid viscosity loss [84,85]. It has been suggested that small amounts of previously embedded metals are released during bleaching, and that the metal ions released give rise to the formation of radical species during the subsequent hydrogen peroxide bleaching stage, causing severe attack on cellulose [86].

In the presence of EDTA, the catalytic effect of iron salts during oxygen-alkali treatment is enhanced. Chelation increases the oxidation potential of the redox reaction:



thereby stabilizing the +3 state relative to the +2 state while maintaining the possibility of a redox reaction in the chelated form. However, the stability of the iron chelates under the conditions prevailing during oxygen delignification is significantly less than that of copper-EDTA. Thus, it can be assumed that decomposition to simple ions takes place with accompanying catalysis. Therefore, iron activation is probably not due directly to chelated iron but is simply the result of an increased mobility of previously insoluble iron, such as oxides, by chelation, followed by redeposition in the fiber [87]. Copper is known to produce stable complexes with EDTA. However, the catalytic effect of copper is masked by EDTA only at low hydroxide concentration. At high sodium hydroxide concentration no significant protective effect of EDTA is obtained. This observation can be explained by a gradual displacement of the EDTA by hydroxide ions in the copper-EDTA complexes [67].

#### 7.3.6.2 Residual Lignin Structures

The principal pathway of oxidative degradation of phenolic units comprises the abstraction of an electron from the phenolate anion by biradical oxygen, resulting in the formation of the corresponding phenoxy and superoxide anion radicals. The unstable cyclohexadienone hydroperoxide intermediates fragment to catechols and various mono- and dicarboxylic acids, such as maleic and muconic acids, by demethoxylation, ring-opening, and side-chain elimination reactions [88]. The concentration of the catechols remain fairly constant throughout oxygen delignification, implying that they are involved in the oxidation process as intermediates [89]. Furthermore, the catechols also contribute to an improved solubility of the oxidized lignin structures due to the increase in the hydrophilicity of the lignin.

The overall outcome of these reactions is the degradation and elimination of guaiacyl (softwood and hardwood) and syringyl phenolic (hardwood) units. The degradation of the uncondensed phenolic units is more severe within the dissolved lignins (51–67%) than in the residual lignins (3–46%) [90]. Condensed phenolic units refer to those phenolic structures with C5 substituents other than methoxyl. It is reported, that 56–58% of the total phenolic units present in the residual softwood kraft lignin can be attributed to the condensed type [90,91]. The proportion of condensed phenolic units in hardwood residual lignin is considerably lower as compared to the softwood residual kraft lignin.

After applying oxygen delignification to a softwood kraft pulp, the content of condensed phenolic units in the residual lignin is decreased only by 4–29%, while the corresponding decrease within the dissolved lignin fraction is about 41–60%. It is well established that 5,5'-biphenyl [92] and diphenylmethane structures [93] are fairly resistant towards oxygen delignification. The latter structures were found to accumulate during the whole oxygen delignification process. However, some of the condensed phenolic structures seem to be susceptible to oxygen delignification, as in general most reports demonstrate an overall decrease in the total condensed phenolic units after oxygen delignification [90]. In a study by Lai

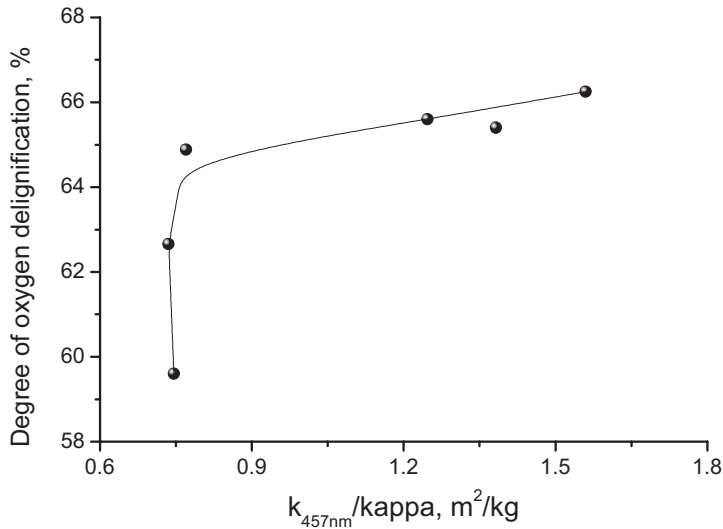
et al., it was indicated that  $\beta$ -5 linked phenylcoumaran-type structures are degraded during the initial phase of oxygen delignification [94]. At very high temperatures of about 140 °C the amount of condensed phenolic units decreases by more than 50%, which confirms that the reactivity of softwood kraft lignin substantially increases at temperatures above 110 °C.

The presence of carboxylic acid groups within the lignin structures is considered to promote lignin solubilization during alkaline oxygen delignification. The increase of the carboxylic content is particularly high in the residual softwood kraft lignin, while the corresponding carboxylic content in the hardwood residual lignin increases only moderately obviously due to the higher initial value [90]. Compared to the residual lignins, the dissolved lignins contain more carboxylic acids. It is interesting to note that the rate of carboxylic group formation increases drastically as the reaction temperature increases parallel to the degradation of the uncondensed phenolic units. A significant increase in the carboxylic acid groups is observed at temperatures greater than 120 °C [95]. After successive oxygen delignification stages, the content of carboxylic acid groups in the residual lignin decreases, which means that the lignin which is rich in carboxylic acid groups is preferably removed in the subsequent oxygen delignification stages, leaving a residual lignin containing fewer reactive groups [96]. The content of the residual lignin ( $\kappa$  number) also plays a decisive role in the overall reactivity of the lignin structures. High- $\kappa$  number pulps are known to be easier to delignify than low- $\kappa$  number pulps, clearly due to a lower proportion of condensed lignin structures, particularly 5,5'-condensed lignin units and diphenylmethane structures [93]. The extent of oxidation to carboxylic acid groups is found to be lower than that in low- $\kappa$  lignins. It can be speculated that the lower amount of condensed structures in these high- $\kappa$  number pulps requires less oxidation for the removal. Nevertheless, it has been demonstrated in a study by Chirat and Lachenal, and also later by Rööst et al., that a significant fraction of the residual lignin (>22–25% of the initial value) remains even after five oxygen treatments, which suggests that the oxygen delignification levels off [97,98]. Elucidation of the structures of residual lignin that is unsusceptible towards oxygen delignification has certainly been the focus of recent research. Based on the experience that the extent of lignin removal decreases with increasing hemicellulose content (particularly xylan), it is assumed that the residual lignin is attached to carbohydrates by lignin-carbohydrate complex (LCC) linkages [99–101]. In fact, xylan-linked lignin is more resistant to oxidative reactions, while galactan-linked lignin is readily degraded during oxygen delignification [96]. The removal of amorphous cellulose during a first oxygen delignification stage causes an increase in cellulose crystallinity, thus reducing the accessibility of residual lignin in the secondary wall.

Quite recently, the existence of *p*-hydroxyphenyl groups has been attributed to the resistant lignin structures in residual kraft lignin [93,96,102]. Model experiments indicated that these materials are less reactive than their guaiacol counterparts, although they belong to the noncondensed phenolics. The content of *p*-hydroxyphenyl groups in a residual softwood kraft lignin was shown to correlate with delignification selectivity during oxygen delignification. The stability of *p*-

hydroxybenzene during oxygen delignification is clearly confirmed by model compound studies [93]. It can thus be concluded that the accumulation of 5,5'-biphenyl structures occurring via phenoxy guaiacyl radical coupling reactions between the liquor and the fiber and the *p*-hydroxyphenyl structures are amongst the major factors impeding the efficiency of oxygen delignification.

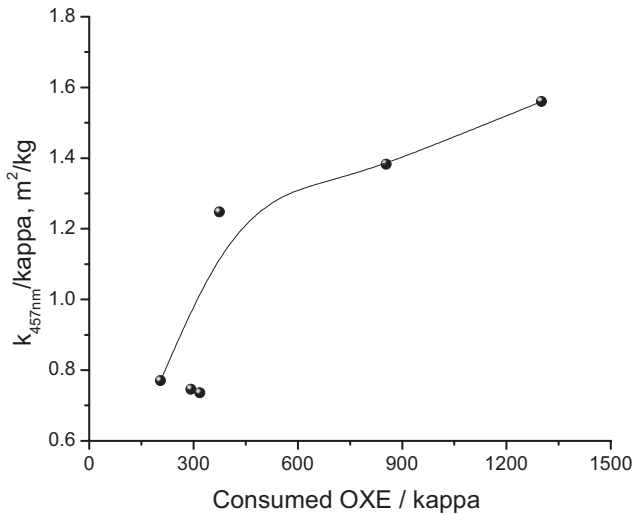
The ratio between the light absorption coefficient and kappa number corrected for the content of hexenuronic acids,  $k_{457\text{ nm}}/\kappa_{(HS)}$ , is a measure of the specific amount of chromophoric groups in the residual lignin (see Section 4.2.6, Influence on bleachability). Quite surprisingly, the degree of oxygen delignification was found to be somewhat higher for unbleached softwood kraft pulps with increasing  $k_{457\text{ nm}}/\kappa_{(HS)}$  values, as shown in Fig. 7.46 [103].



**Fig. 7.46** Extent of oxygen delignification as a function of the specific light absorption coefficient [ $k_{457\text{ nm}}/\kappa_{(HS)}$ ] (according to Gellerstedt and Al-Dajani [103]). Unbleached *Pinus sylvestris* kraft pulp, kappa numbers 15–19. Conditions for oxygen delignification are given by Gustavsson et al. [104]: 100 °C, 85 min, 12% consistency, 700 kPa pressure, 2.25% NaOH.

The slightly higher efficiency of oxygen delignification of the unbleached softwood kraft pulps with the lower brightness was mainly attributed to the higher content of reactive unsaturated aliphatic carbon atoms and phenolic hydroxyl groups, as determined by a thorough analysis of the residual lignin structures (two-dimensional NMR using the HSQC sequence) [103]. Prolonged cooking at a low hydroxide ion concentration gives rise to the formation of these degraded lignin structures due to preferred fragmentation reactions. However, the low hydroxide ion concentration during residual delignification promotes the precipitation of dissolved lignin, which then leads to a decrease in brightness and specific light absorption coefficient. Despite their higher degree of delignification in the oxygen stage, the pulps with a high unbleached  $k/\kappa_{(HS)}$ -value require more bleaching

chemicals (expressed as OXE per kappa) for subsequent bleaching to full brightness as compared to those pulps comprising a low unbleached  $k/kappa_{(87\%)}$ -value (see Fig. 7.47). The latter are produced with a high effective alkali charge and a short cooking time.



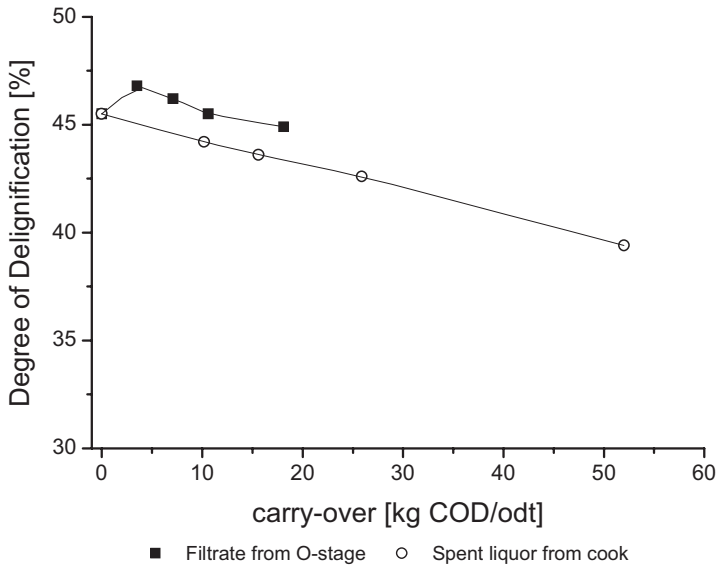
**Fig. 7.47**  $k_{457nm}/kappa_{(87\%)}$  versus quantity of oxidation equivalents consumed (OXE) in an OQPQ-sequence to a brightness of 87% ISO (according to Gellerstedt and Al-Dajani [103]). The conditions for the QPQP-sequence are given by Gustavsson et al. [104].

The better bleachability of pulps with low unbleached  $k/kappa_{(87\%)}$ -values is associated with a higher amount of  $\beta$ -O-4 structures [105]. It is generally agreed that the bleachability of softwood kraft pulps in a TCF-sequence comprising oxygen and peroxide as bleaching chemicals is positively correlated with the unbleached pulp brightness, and thus with the amount of  $\beta$ -O-4-structures in the residual lignin [106].

### 7.3.6.3 Carry-Over

The dissolved solids entering the oxygen stage originate from two different sources: the black liquor from cooking; and the filtrate from the oxygen stage. Experiments conducted by various groups have shown reproducibly that filtrates from the oxygen delignification stage have no significant effect on the performance of oxygen delignification. On the other hand, the spent liquor from the cooking stage causes a clear reduction in delignification efficiency, as reported for a hardwood kraft pulp [107]. At the same level of COD, the carry-over from the cooking stage has a more detrimental effect on delignification as compared to the filtrate of the oxygen stage (Fig. 7.48).

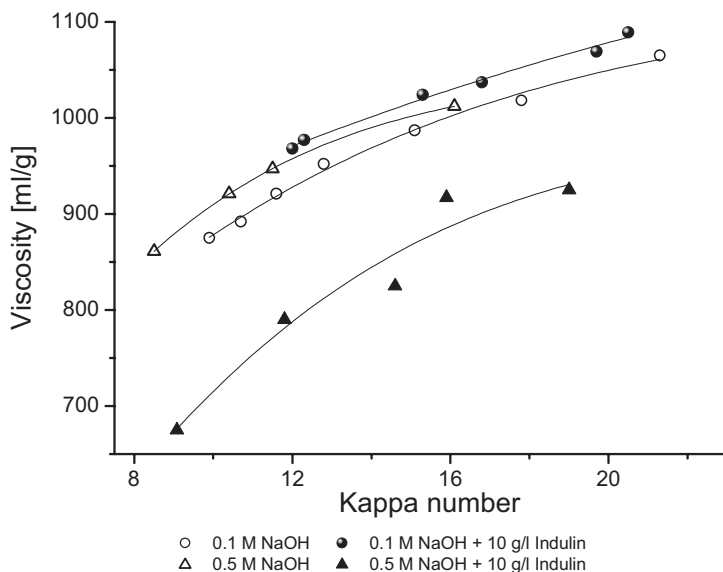




**Fig. 7.48** Influence of amount and type of carry-over on the degree of delignification in a oxygen-alkali treatment of a hardwood kraft pulp, kappa number 16.7 (according to [107]). Conditions of oxygen delignification: 10% consistency, 15 kg NaOH on pulp, 15 kg O<sub>2</sub> on pulp, 30 min, 100 °C.

Therefore, efficient upstream washing is essential to ensure a good performance of oxygen delignification. The brownstock washing losses are typically in the range of 10–30 kg COD odt<sup>-1</sup> of unbleached pulp, assuming a washing efficiency of 98–99%. Black liquor solids entering the oxygen stage may also adversely affect delignification selectivity. The effect of commercial lignin produced from kraft black liquor (Indulin A from Westvaco) added to the bleach liquor on the selectivity of oxygen delignification of a softwood kraft pulp was studied by using different caustic concentrations, while maintaining time and temperature constant [20]. The data in Fig. 7.49 show that the addition of dissolved lignin causes a significant decrease in selectivity during bleaching in 0.5 M NaOH.

The results obtained are due to a markedly decreased delignification rate and a disproportional increase in the rate of depolymerization of carbohydrates. The drop in the delignification rate may be explained in part by the decreased hydroxide ion concentration caused by the acid groups formed by the oxidation of the dissolved lignin. Additionally, an insufficient supply of oxygen may contribute to the limited delignification rate. At the same time, the depolymerization reactions of the carbohydrates are accelerated in the presence of dissolved lignin. It is assumed that the combined presence of dissolved lignin and a rather high hydroxide ion concentration (0.5 M) promotes the formation of free radicals, which in turn induces significant chain scissions. Analogous experiments with a low alkali concentration (0.1 M), however, reveal an improved selectivity in the presence of



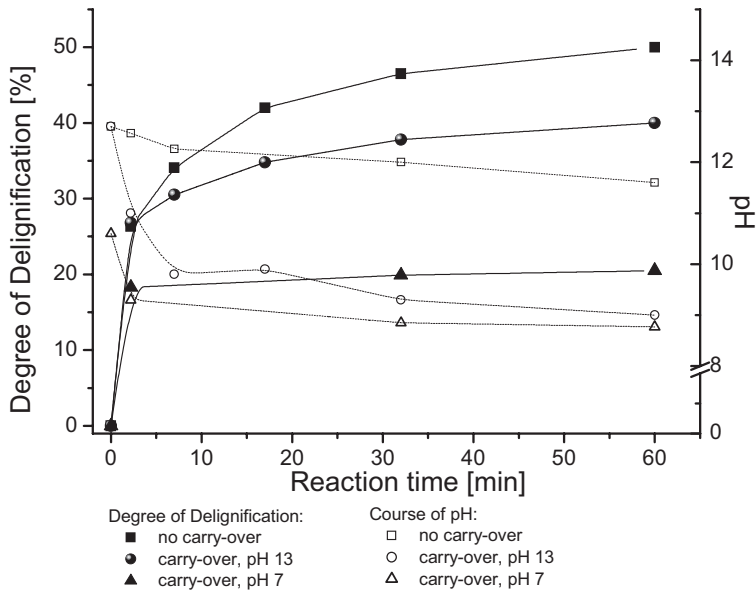
**Fig. 7.49** Effect of the addition of commercial lignin compound, Indulin A from Westvaco, on the selectivity of oxygen delignification of a Scots pine kraft pulp, kappa 32, viscosity

1220 mL g<sup>-1</sup>. Indulin A is added at a concentration of 10 g L<sup>-1</sup> in the bleach liquor; experiments were run at 97 °C, 0–14 h, 0.2% consistency, 0.7 MPa pressure [20].

dissolved Indulin A (see Fig. 7.49). At this low alkali charge, the dissolved lignin consumes a great part of the hydroxide ions present. Hence, the pH falls from 12.5 to 8.8 within 1 h, and this explains the very low rate of delignification and preservation of the carbohydrates due to a lack of free radical formation.

The effect of carry-over on the performance of oxygen delignification can be understood as a competitive consumption of alkali and oxygen between the residual lignin in the pulp and the dissolved material in the entrained liquor. Oxygen delignification appears not to be impaired as long as sufficient caustic and oxygen are available. The initial rapid phase of delignification is not affected by the presence of carry-over from the cook, clearly because the hydroxide ion concentration and oxygen supply are not limiting factors. However, in the continuation of oxygen delignification, the extent of delignification is clearly impaired by the presence of dissolved lignin. During this phase caustic and oxygen are consumed by the dissolved organic matter rather than by the residual lignin. The sole contribution of the dissolved organic matter on the performance of oxygen delignification can be studied by neutralizing the carry-over to pH 7. Corresponding experiments using a eucalyptus kraft pulp were performed by Iijima and Taneda [107]. The results depicted in Fig. 7.50 show that alkali is preferably consumed by dissolved black liquor, and this results in a rapid drop of pH.

It can be seen from Fig. 7.50 that delignification discontinues as soon as the pH falls below 9.5, and at which most phenols are no longer ionized. Thus, it can be concluded that the presence of carry-over from the cooking stage will increase the



**Fig. 7.50** Effect of carry-over from cooking stage on the performance of oxygen delignification of a hardwood kraft pulp, kappa number 16.7, and on the pH profile during the reaction (according to [107]). Conditions of oxygen delignification: 10% consistency, 20 kg NaOH on pulp, 30 kg O<sub>2</sub> on pulp, 60 min, 100 °C.

overall oxygen and alkali requirements due to their preferred consumption by the dissolved organic and inorganic compounds. Moreover, under the conditions of industrial oxygen delignification the black liquor solids adversely affect selectivity.

#### 7.3.6.4 Xylan Content

The controlled removal of hemicellulose by means of prehydrolysis prior to kraft cooking gradually improves the efficiency of delignification in a subsequent oxygen delignification stage [99]. The increasing degree of delignification, along with the removal of xylan, has been attributed to the cleavage of LCCs [108]. Similar results are obtained when the xylan content of a kraft pulp is further increased by the addition of anthraquinone. Both the rate and the extent of oxygen delignification are substantially reduced by increasing xylan content, as shown for a Northeastern hardwood kraft pulp [109]. Parallel with a higher hemicellulose content of the kraft pulp, the selectivity of oxygen delignification significantly improves. Thus, the hemicellulose polymers (specifically xylan) act as viscosity protectors for cellulose due to an enhanced accessibility of the xylan for the bleaching chemicals, for example, caustic and active oxygen species (hydroxyl free radicals) [110]. The loss in pulp yield during oxygen delignification results primarily from the xylan fraction of the pulp. This supports the assumption that the alkali present in an

oxygen stage is consumed by peeling reactions in which xylan is preferably involved. As a result, less alkali is available for both oxygen delignification and cellulose degradation.

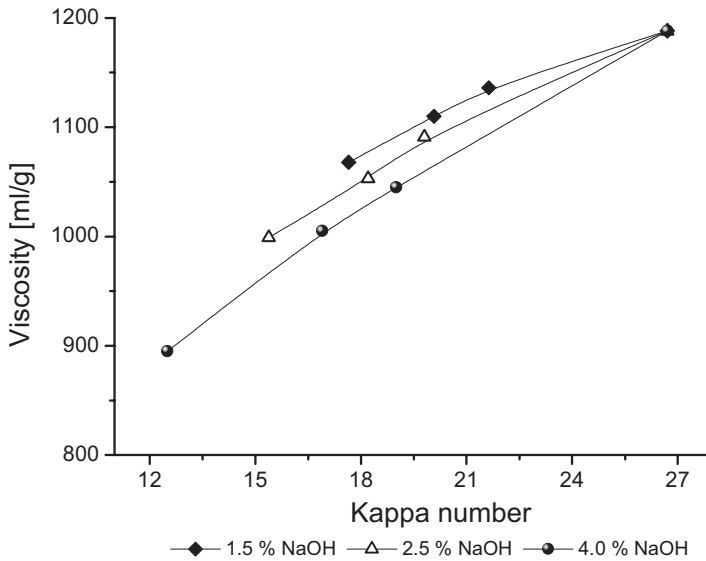
#### 7.3.6.5 Selectivity of Oxygen Delignification

Delignification selectivity is commonly defined as the change in kappa number over the change in viscosity (e.g.,  $\Delta\kappa$ ,  $\Delta\text{viscosity}$ ) or, more scientifically, as the ratio between the reaction rates of lignin removal and chain scissions of carbohydrates. Analogous to all delignification reactions, oxygen delignification is based on competitive reactions of oxygen and oxygen-active species within pulp lignin and carbohydrates. With progressive extent of delignification, the oxidation of carbohydrates becomes a more favorable process. It can be concluded that process selectivity is greatly influenced by the radical chemistry of active oxygen species as they react with both lignin and carbohydrates.

Extending delignification by reinforcing the reaction conditions often results in severe cellulose degradation. The selectivity of oxygen delignification can be estimated by comparing the delignification and polysaccharide cleavage models. As mentioned previously (see Section 7.3.3), Iribarne and Schroeder reported that low temperature combined with high alkali and oxygen concentrations during the initial delignification phase would improve the selectivity of oxygen delignification [12]. The design and recommended conditions of commercial two-reactor oxygen delignification processes are largely based on these results. Recently, it was shown that the selectivity of oxygen delignification of North-Eastern softwood kraft pulp decreases with increasing sodium hydroxide charge at given temperature and reaction time [32] (Fig. 7.51). However, the chosen temperature during the first stage was approximately 10 °C higher than that recommended by those promoting commercial, two-reactor systems.

The selectivity is significantly improved when a given alkali charge (e.g., 4.5% on pulp) in a single-stage oxygen delignification experiment with a total retention time of 90 min is split into three stages of equal retention time (30 min for each stage) in which 1.5% NaOH is added before each stage. The improved selectivity can be attributed to the rather even alkali concentration profile throughout the three stages and a lower average sodium hydroxide concentration as compared to the single-stage control experiment [32]. The same authors claimed that the selectivity of oxygen delignification is not significantly affected by raising the temperature from 90 °C to 120 °C at a level of 4.0% NaOH charge.

As mentioned above, the addition of various magnesium ion compounds (including magnesium sulfate and magnesium carbonate) provides favorable behavior in maintaining pulp viscosity during oxygen delignification [111]. The selectivity of oxygen delignification can be further improved in the presence of both phenol and magnesium sulfate in a specific amount of 0.5% on dry pulp [112]. However, this synergetic effect is limited to pulps with kappa numbers higher than 30, presumably due to the greater proportion of lignin units to be oxidized. Phenol as an additive mimics the phenolic lignin structure, and can take part in



**Fig. 7.51** Selectivity of oxygen delignification of different alkali charges (1.5%, 2.5%, and 4.0%) of a North-Eastern softwood kraft pulp with an initial kappa number 26.7 (according to [32]). Single-stage oxygen delignification at 90 °C, in the range of 60 min retention time; 10% consistency, 780 kPa pressure, 0.2% MgSO<sub>4</sub> charge.

the reaction with oxygen in an alkaline aqueous solution to produce active oxygen species, as demonstrated by J.S. Gratzl [113]. The reaction of phenolic compounds with oxygen produces active oxygen species, such as the hydroperoxy and hydroxyl radicals that contribute to the efficiency of oxygen delignification. Furthermore, the selectivity of oxygen delignification is improved in the presence of phenol due to the preferred reaction of the hydroxyl radical with the former.

### 7.3.7

#### Process and Equipment

##### 7.3.7.1 MC versus HC Technology

Following the implementation of the first commercial systems for oxygen delignification during the 1970s, and the subsequent introduction of medium consistency technology in the early 1980s, the MC and HC oxygen delignification technologies have co-existed for some time. However, medium consistency has emerged as the technology of choice due not only to simpler operation and maintenance but also to fewer safety concerns.

### 7.3.7.2 Process Technology

Conventional oxygen delignification cannot remove more than 35–50% of the residual lignin before sustaining detrimental oxidative carbohydrate degradation, which is expressed as a loss in viscosity and fiber strength. The low selectivity of oxygen delignification can be explained in part by the unfavorable conditions for lignin leaching that seem necessary to achieve access to the more resistant lignin structures (e.g., condensed phenolics). If lignin leaching does not take place, the more resistant structures might not be attacked as easily as the carbohydrates under typical conditions of a one-stage oxygen delignification process [93].

A clear overview of the physical and chemical behavior of leachable residual lignin from a Scandinavian softwood kraft pulp during oxygen delignification has been provided by Ala-Kaila and Reilama [114]. The residual lignin across an industrial two-stage oxygen delignification process was divided into four fractions by different leaching operations, representing wash loss lignin, easily leachable, slowly leachable, and resistant fraction of lignin [114]. The investigated pulp samples originate from the positions prior to the first reactor (brownstock), the transition line from the first reactor blow tank to the second reactor (O<sub>1</sub> blow), and finally from the second reactor blow tank (O<sub>2</sub> blow). The experiments revealed that most of the leachable lignin is only weakly attached on the fiber–liquid interface, and can be removed by a 5-min washing operation at 90 °C after being centrifuged to a consistency of 38% (Tab. 7.24). The amount of wash loss lignin fraction increases during the course of delignification. It can be assumed that part of the resistant lignin fraction is converted into the wash loss lignin as a result of delignification reactions in the first reactor. The unbleached softwood kraft pulp contains approximately one kappa unit of each easily (30 min at 90 °C) and slowly (24 h at 90 °C) leachable fractions, respectively. In the first reactor, the easily leachable lignin fraction diminishes almost quantitatively, whereas the slowly leachable lignin decreases significantly in the second reactor only. There, predominantly resistant and slowly leachable lignin fractions are involved in the delignification reactions. The results confirm the importance of mass-transfer processes between fiber and liquor phases in the transition from cooking over washing to oxygen delignification.

**Tab. 7.24** Residual lignin contents measured as kappa number of a softwood kraft pulp after different leaching operations in the course of a two-stage oxygen delignification process (according to [114]).

Parameter	Brownstock	O <sub>1</sub> Blow	O <sub>2</sub> Blow
Centrifuged kappa number	22.9	16.8	13.1
Kappa after 5-min washing	19.7	11.5	7.6
Kappa after 30-min leaching	18.6	11.1	7.4
Kappa after 24-h leaching	17.5	10.0	6.8

The different kappa number fractions of a birch kraft pulp were recently determined through an industrial two-reactor oxygen delignification process [115]. The leaching procedure was comparable to that described for the softwood pulp, with the exception of a shorter leaching time (2 min instead of 5 min) for the removal of the wash loss. The experimental procedure, the reaction conditions during oxygen delignification, and the applied analytical methods are described elsewhere [115]. The isolated lignin fractions were further characterized according to their chemical natures, representing residual lignin, hexenuronic acids (HexA) [116], extractives (acetone extractives) and other chemical structures contributing to the kappa number of the pulps. The residual lignin is referred to as the “actual” lignin, and is determined by means of the Oxymercuration-Demercuration (Ox-Dem) kappa number, whereas the total kappa number is denoted as “apparent lignin” [117,118]. The study results demonstrated that the amounts of wash loss were rather comparable throughout oxygen delignification for softwood and birch kraft pulps (Tabs. 7.24 and 7.25).

**Tab. 7.25** Residual lignin contents measured as kappa number of a birch kraft pulp after different leaching operations in the course of a two-stage oxygen delignification process (according to [115]).

Parameter	Brownstock	O <sub>1</sub> Blow	O <sub>2</sub> Blow
Centrifuged kappa number	22.1	18.2	16.8
Kappa after 2-min washing	16.7	12.7	11.3
Kappa after 30-min leaching	15.9	12.5	11.0
Kappa after 24-h leaching	13.9	11.6	10.4

The easily removable (apparent) lignin was also of the same magnitude for both softwood and hardwood kraft pulps, whereas the slowly removable fraction in the birch brownstock pulp was somewhat higher for the brownstock birch kraft pulp. The main difference in the performance of oxygen delignification between softwood kraft and hardwood kraft pulp is reflected in the amount of the resistant lignin. The responses for the birch kraft pulp were 2.3 units (13.9–11.6) in the first reactor and 1.2 units (11.6–10.4) in the second reactor (see Tab. 7.25). The corresponding values for the softwood kraft pulp were 7.5 units (17.5–10.0) in the first reactor, and 3.2 units (10.0–6.8) in the second (see Tab. 7.24). It is well known that a great part of the resistant lignin fraction in hardwood kraft pulp before and after oxygen delignification consists of HexA (Tab. 7.26).

The high resistance of HexA towards oxygen delignification clearly limits the removal efficiency of the resistant lignin fraction. The degree of delignification, measured as a change in kappa number, was 43% from residual lignin and 20% with regard to HexA and extractives. The leaching procedure was particularly effi-

**Tab. 7.26** Partial kappa numbers of resistant lignin fractions isolated from birch kraft pulp (received after 24 h of pulp leaching) [115].

Parameter	Brownstock	O <sub>1</sub> Blow	O <sub>2</sub> Blow
Pulp kappa no.	13.9	11.6	10.4
Residual lignin	6.5	4.7	3.7
Extractives	1.0	1.0	0.8
HexA	5.8	4.7	4.6
Others	0.6	1.2	1.3

cient with the unbleached pulp, with clear effects on the residual lignin, extractives and HexA. The course of kappa numbers prior the leaching operations are summarized in Tab. 7.27.

**Tab. 7.27** Partial kappa numbers of lignin fractions after washing isolated from birch kraft pulp (received after 2 min of pulp washing) [115].

Parameter	Brownstock	O <sub>1</sub> Blow	O <sub>2</sub> Blow
Pulp kappa no.	16.7	12.7	11.3
Residual lignin	8.2	5.3	4.1
Extractives	1.5	1.2	1.0
HexA	6.8	5.8	5.8
Others	0.2	0.4	0.4

The removal of residual lignin was more pronounced for brownstock pulp (1.7 units = 8.2 – 6.5) as compared to the oxygen-delignified pulps (0.6/0.4 units = 5.3 – 4.7 and 4.1 – 3.7). The degree of oxygen delignification was 50% based on residual lignin (from 8.2 to 4.1), but only 32% based on total lignin after washing (from 16.7 to 11.3). The removal of HexA during leaching was fairly constant for all pulps investigated. It is assumed that the removal of HexA in the first reactor is most probably caused by the dissolution of the HexA containing pulp xylan located at the surface of the fibers.

This rather simple but very useful analytical procedure for the characterization of different kappa number fractions provides valuable information on the performance of delignification reactions in general, and on the reactivity of the apparent residual lignin structures towards subsequent bleaching operations in particular.

Oxygen delignification in two stages exploits delignification reaction kinetics and allows maximum delignification efficiency and selectivity when high levels of



pressure and alkali concentration are applied in the first stage, followed by a second stage at low pressure and low alkali concentration [11]. In addition, both stages should be performed at the minimum temperature possible to achieve the desired delignification. This proposal derived from theoretical considerations was successfully put to practice [119]. The principle of two-stage operation was further developed to an “extended” OO-process by further increasing the pressure up to 1.6 MPa in the first stage according to the conditions given in Tab. 7.28.

**Tab. 7.28** Conditions proposed for the “standard” and the “extended” OO-process (according to Röst et. al. [98]).

Conditions	Unit	“Standard” O-process		“Standard” OO-process		“Extended” OO-process	
		O	O(1)	O(2)	O(1)	O(2)	
Pressure, pO <sub>2</sub>	MPa	0.6	0.9	0.6	1.6	0.6	
Temperature	°C	100	90	110	100	110	
Time	min	60	30	60	30	60	
Pulp consistency	%	10	10	10	12	12	
MgSO <sub>4</sub>	%	0.5	0.5		0.5		
NaOH	%	3	3		3		

Reinforcing the reaction conditions in the first short stage also improves the efficiency of delignification. It was shown that differences in the chromophore content of the incoming pulp originating from varying conditions in the cooking plant can be leveled out when applying “extended” oxygen delignification. It is well accepted that the bleachability of softwood kraft pulps is impaired by applying high H-factor in combination with a low alkali concentration to reach a certain kappa number [104]. The poor bleachability is characterized by a high light absorption coefficient,  $k$ , and a low amount of  $\beta$ -O-4 structures as determined by thioacidolysis [120]. If a conventional one-stage oxygen delignification process is used, the content of  $\beta$ -O-4-structures determines the demand of OXE necessary to reach full brightness (e.g., 89% ISO). If, however, the conventional O-stage is replaced by an extended OO-process, the subsequent demand of bleaching chemicals is no longer influenced by bleachability parameters, such as  $\beta$ -O-4-structures or  $k$ -values [98]. The effect of an extended OO-process prior a Q-OP-Q-PO-sequence for two different softwood kraft pulps of comparable kappa number but significantly different amounts of chromophore groups, measured as brightness,  $k$ -value and amount of  $\beta$ -O-4 structures, is indicated in Table 7.29.

**Tab. 7.29** Bleachability of pulps with different amounts of chromophore groups in an Q-OP-Q-PO sequence after oxygen delignification using either standard O- or extended OO-process technology (according to Rööst et. al. [98]). Reaction conditions of “standard” and “extended” OO-processes are listed in Tab. 7.28.

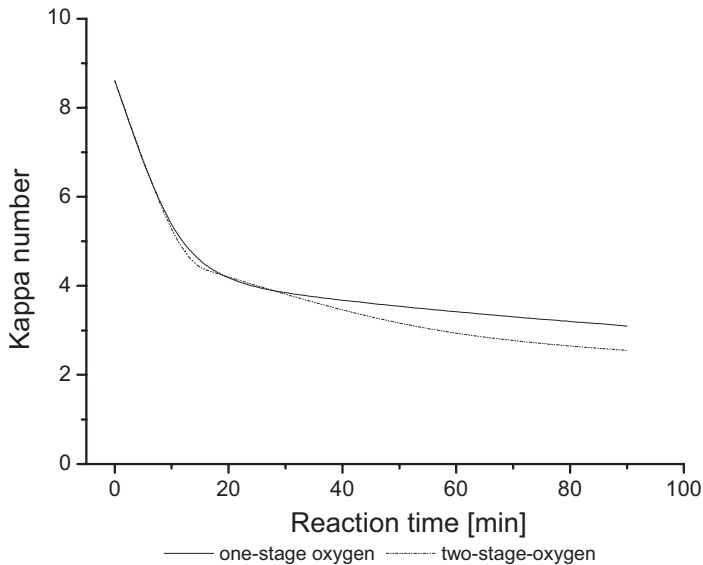
Parameters	Units	Low-alkali	High-alkali
Cooking conditions			
EA-charge	% as NaOH	17.5	22.5
Time at cooking temp.	min	300	105
Unbleached pulp characteristics			
Screened yield	%	43.8	43.8
Kappa number		18	17.2
Brightness	%ISO	30.9	36.7
Viscosity	mL g <sup>-1</sup>	973	913
Light absorption coefficient	m <sup>2</sup> kg <sup>-1</sup>	16.5	13.1
β-O-4 in residual lignin	μmol g <sup>-1</sup>	71	115
Bleachability			
After “Standard”-O			
Total peroxide consumption in Q-OP-Q-PO sequence	kg t <sup>-1</sup>	25.7	19.2
After “Extended”-OO			
Total peroxide consumption in Q-OP-Q-PO sequence	kg t <sup>-1</sup>	12.1	11.6

Thus, it can be concluded that extended oxygen delignification significantly decreases the demand of bleaching chemicals and evens out variations from the cooking stage. However, to date no information is available about the selectivity of extended oxygen delignification.

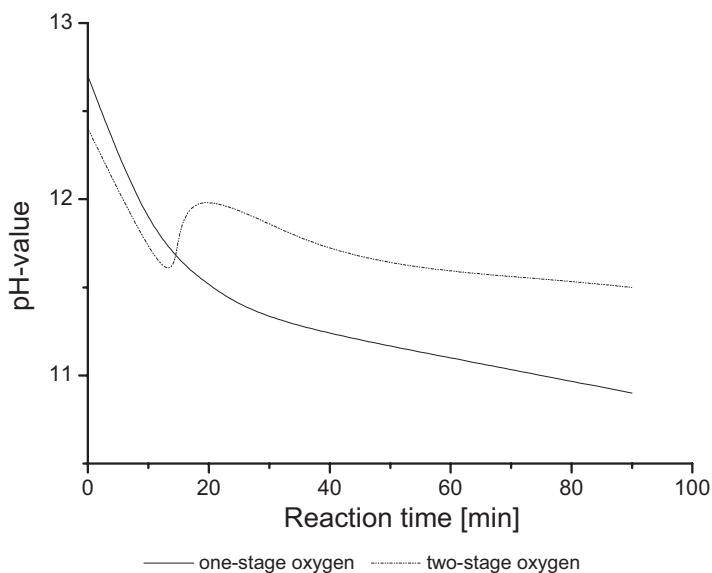
There are a number of technical set-ups where the insights from delignification reaction kinetics are realized. All of these seek to provide the best conditions in order to maximize delignification efficiency and selectivity. The first commercial two-stage oxygen delignification process was developed at Oji Seishi KK Tomakomai mill in Japan in 1985, simply by adding a second reactor to an existing one-stage oxygen delignification system. A detailed description of the practical experiences derived from this first commercial installation was provided [121]. In the same year, the first patent for a two-stage reactor oxygen delignification process was granted to Kamyr [122].

The first commercial application of a two-stage oxygen delignification stage as a pretreatment of a TCF-sequence for the manufacture of a high-purity eucalyptus prehydrolysis kraft pulp (PHK) came on stream in 1996 at the Bacell S.A. mill (since 2004, BahiaPulp) in Bahia near Salvador [123]. This concept of two-stage oxygen delignification was developed in an extensive laboratory program with a one-stage oxygen treatment as a reference [124]. In accordance with the final pulp quality requirements, the task of oxygen delignification was to reduce the kappa number from about 8–10 to below 3 in order to avoid too high ozone charges and to be able to control cellulose degradation in the subsequent ozone stage. The preliminary trials using the conventional one-stage oxygen delignification treatment resulted in a significant drop in viscosity as soon as the lignin removal rate was extended beyond 60%. Consequently, a two-stage delignification concept was investigated to achieve a higher degree of delignification without impairing viscosity. It was shown that if the given amount of caustic is split into the first and second stage in a ratio of approximately 60/40 to 75/25, then delignification can be extended in the final part of the second stage (Fig. 7.52).

The advantage of a higher delignification efficiency in a two-stage oxygen delignification process at a given charge of sodium hydroxide can be attributed for the most part to a higher pH-level (or residual effective alkali concentration) in the final part of the treatment (Fig. 7.53). Similar to kraft pulping, the selectivity of delignification improves due to the more even pH profile.



**Fig. 7.52** Course of kappa number of one- and two-stage oxygen delignification of a eucalyptus-PHK pulp, kappa 8.6, viscosity 1131 mL g<sup>-1</sup> (according to [124]). One-stage: 25 kg NaOH bdt<sup>-1</sup>, 110 °C, 10% consistency, 0.7 MPa oxygen pressure; Two-stage: first stage 15 kg NaOH bdt<sup>-1</sup>, 110 °C, 0.7 MPa oxygen pressure, 15 min; second stage 10 kg NaOH bdt<sup>-1</sup>, 115 °C, 0.4 MPa oxygen pressure; 10% consistency in both stages.

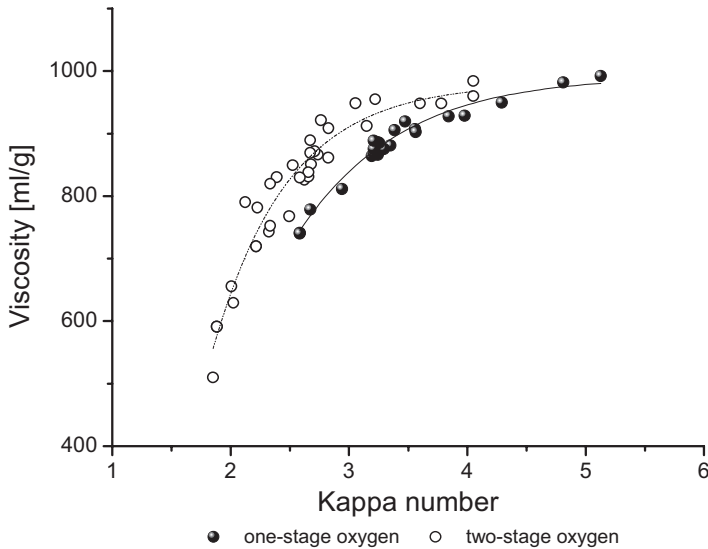


**Fig. 7.53** pH-profile during one- and two-stage oxygen delignification of a eucalyptus-PHK pulp, kappa 8.6, viscosity  $1130 \text{ mL g}^{-1}$  (according to [124]). Conditions as shown in Fig. 7.52.

The optimum overall selectivity and efficiency of two-stage oxygen delignification can be achieved by limiting the retention time in the first reactor to 10–20 min, while about 60 min appears to be the optimum retention time in the subsequent second reactor. Figure 7.54 illustrates the advantage in selectivity of a two-stage concept at an extent of delignification higher than 55%. A rather moderate and almost linear decline in viscosity can be observed as long as the kappa number is above 3.5 in case of a one-stage, and 2.9 in case of a two-stage oxygen-alkali treatment. This corresponds to an improvement in delignification efficiency from 61% to 68% (unbleached kappa number 9; see Ref. [124]).

In the meantime, the two-stage oxygen delignification process for the production of high-purity dissolving pulp has been more than nine years in operation at the Bahia pulp mill (Salvador, Brazil), and operational results have clearly exceeded expectations based on laboratory experiments. The average performance of this prebleaching stage is achieving values of about 76% delignification while maintaining a moderate level of cellulose degradation of about  $0.195 \text{ mmol AHG}^{-1}$ , expressed as the number of chain scissions (corresponds to a kappa number of 2.2 and a viscosity of  $785 \text{ mL g}^{-1}$  when compared with the pulp used for laboratory experiments in Fig. 7.54).

Extended oxygen delignification is certainly more important for paper-grade kraft pulps than for dissolving pulps, mainly because of the difficulty in removing the residual lignin present in paper-grade pulps (without prehydrolysis). Therefore, much effort was undertaken to develop appropriate two-stage delignification



**Fig. 7.54** Comparative evaluation of one- and two-stage oxygen delignification using a eucalyptus-PHK pulp, kappa 9 and viscosity  $1200 \text{ mL g}^{-1}$ . Conditions as in Fig. 7.52, and according to Refs. [124,125].

concepts. In 1995, a two-reactor oxygen delignification process was applied for patent by Sunds Defibrator (today, Metso) [126]. The delignification stage is manufactured under the trademark OxyTrac. This technology operates as a two-stage system with a high-shear mixer before each stage. It has been claimed that the selected conditions in both stages of the OxyTrac system are based on the kinetics for oxygen delignification [12,127,128]. The rather long retention time of 30–40 min in the first reactor is not exactly in line with the current knowledge on reaction kinetics (see Section 7.3.3). However, it cannot be concluded that the longer residence time in the first reactor than was predicted from kinetic considerations results in an inferior delignification performance. The first reactor is operated at a rather low temperature of 80–85 °C, but with high oxygen pressure; these conditions lead to a higher concentration of dissolved oxygen. Moreover, the gas volume at a given charge of oxygen is smaller, and this facilitates mixing of the three-phase system. All of the alkali and most of the oxygen are charged to the first reactor (Tab. 7.30).

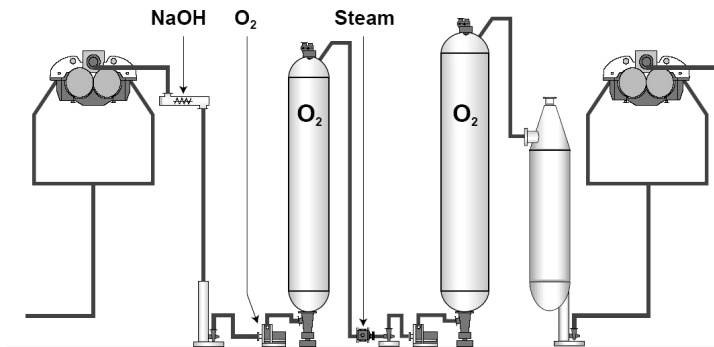
The second stage is designed as an extraction stage using a higher temperature, a longer residence time, and a lower chemical concentration to extend delignification without drastically reducing the pulp viscosity and pulp strength.

Figure 7.55 illustrates schematically a typical OxyTrac process flowsheet. Caustic is added to the dilution screw of the press before the pulp drops down into the standpipe of the medium-consistency pump. After oxygen is charged in the first high-shear mixer, the pulp-liquor-gas mixture passes through the first oxygen reactor. It then flows down to a static steam mixer, where medium-pressure steam

**Tab. 7.30** Recommended operating conditions of the OxyTrac system for two-stage delignification (according to Refs. [127,129]).

Parameters	Units	First stage	Second stage
Consistency	%	12	>10.5
NaOH-charge	kg adt <sup>-1</sup>	25	0
Oxygen charge	kg adt <sup>-1</sup>	18–25	low charge
Retention time	min	30	60
Temperature	°C	80–85	90–100
Pressure (top)	MPa	0.8–1.0	0.4

is injected to raise the temperature to the desired level for the second stage. A booster pump ensures flow through the second high-shear mixer and the second reactor to the blow tank, where gas and pulp slurry are separated. Finally, the pulp is pumped to post-oxygen washing.



**Fig. 7.55** Typical OxyTrac process flowsheet [130].

Implementation of the OxyTrac system in full scale confirms the superior delignification performance as compared to single-stage oxygen delignification systems [127,130]. It is reported that adoption of the OxyTrac system resulted in a significant increase (from 39% to >60%) in the degree of pulp delignification for the Arauco mill in Chile using radiata pine kraft pulp, while preserving strength properties. The ability to level out variations of the incoming pulp is another important feature of a two-reactor oxygen delignification system.

A second commercial solution to the two-reactor oxygen delignification system is the Dualox™ system provided by Kvaerner. The major differences from the OxyTrac system comprise the short retention time in the first reactor of only about 5 min, and the split addition of oxygen. The short retention time in the first reac-

tor is chosen by following results from kinetic investigations [14]. The first reactor was built as a long and thick tube, enabling a very space-saving design.

A typical Dualox process flowsheet is shown in Fig. 7.56. Caustic is added to the standpipe before the first medium-consistency pump. The pulp slurry is then pumped through the first high-shear mixer and the pipe-type prereactor and further on, by a booster pump, through the second high-shear mixer and the upflow reactor to the blow tank. Oxygen and steam are added both to the first and the second high-shear mixers. In the situation when a greater temperature increase is required, a dedicated static steam mixer is added to the system before the second pump [131].

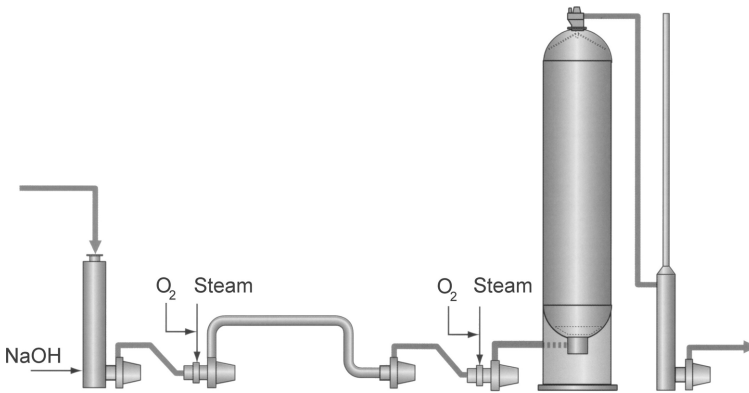


Fig. 7.56 Typical Dualox™ process flowsheet [131].

A characteristic feature of the Dualox™ system is that both reactors are run at the highest possible pressures in order to extend delignification as much as possible. In contrast to the OxyTrac system, the oxygen charge to the first reactor is kept low, while the main part of oxygen is charged to the second reactor.

According to current experiences from mill-scale operations, the Dualox™ two-reactor system provides delignification performances that are comparable to those reported for the OxyTrac system [132]. In the case of delignifying softwood kraft pulp, the kappa number reduction approaches values of about 65%, which typically ensures kappa number values of 8–12 entering the bleaching plant. The conversion of a conventional oxygen delignification system to the Dualox™ process in a hardwood kraft pulp production line was reported to improve the viscosity, despite extending delignification by almost 5 kappa number points [133].

### 7.3.7.3 Process Equipment

The process flowsheet of a typical single-stage oxygen delignification system is shown in Fig. 7.57. Medium-consistency pulp coming from brownstock washing drops into a standpipe and is mixed with caustic soda as it enters the medium-consistency pump. The pump forwards the pulp suspension to a high-shear

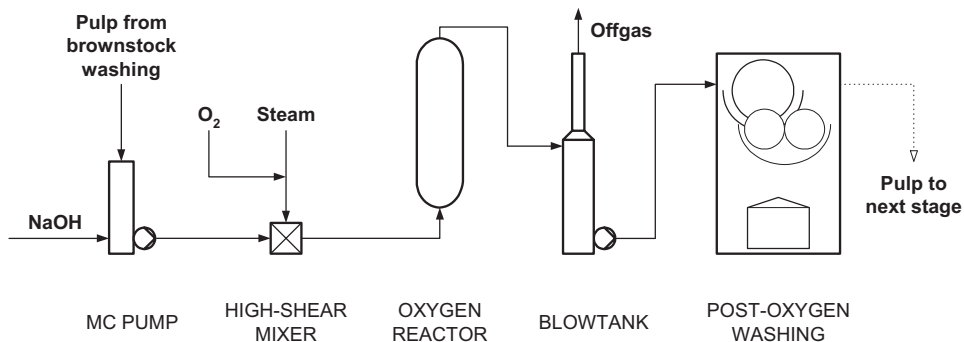


Fig. 7.57 Process flowsheet of a typical single-stage oxygen delignification system.

mixer which is charged with oxygen and also with steam to control the reaction temperature. The three-phase mixture then proceeds to a pressurized upflow reactor where the delignification reaction takes place.

It is essential that the high-shear mixer creates stable micro-bubbles with a large specific surface area. In addition, the consistency in the oxygen reactor should be above 10%, so that the fiber network forces suppress the coagulation of micro-bubbles and that sufficient mass transfer area remains available throughout the reaction time. A higher consistency also minimizes the risk of channeling in the reactor [134].

After its discharge from the reactor top, the pulp suspension is separated from the gas phase in a blowtank. The offgas from the blowtank can normally be blown to atmosphere. Depending on the feed requirements of the post-oxygen washing equipment, the pulp slurry is discharged from the blowtank either at low or medium consistency.

Two-stage oxygen delignification systems use two pressurized reactor in series. Special features of such systems are described in Section 7.3.7.2.

Post-oxygen washing requires a better washing efficiency than any other washing process in the bleach plant due to the relatively large amount of dissolved organic material and its low degree of oxidation. Post-oxygen washing systems need to have more than one washing stage. They may, for example, consist of a multi-stage Drum Displacer™, a pressure diffuser followed by a press, two presses, several vacuum drum washers, or a multi-stage belt washer.

The material from which the wetted parts in an oxygen delignification stage are constructed is usually a lower grade of austenitic stainless steel.

Further information regarding oxygen delignification equipment, including medium-consistency pumps and mixers, reactors and blowtanks is provided in Section 7.2. Details of pulp washing are provided in Chapter 5.

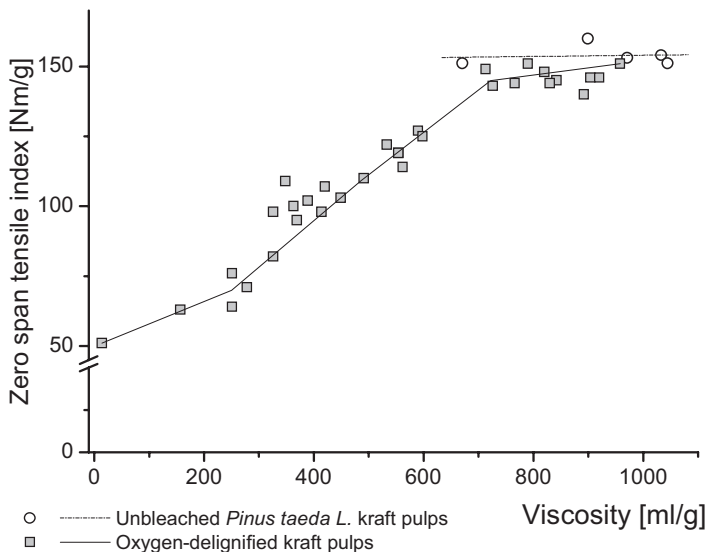


## 7.3.8

**Pulp Quality**

The kraft cooking process and subsequent oxygen delignification stage must be regarded as combined processes from the point of view of yield and pulp strength. The balance between cooking and oxygen delignification determines the quality profile of the pulp. According to today's knowledge, an unbleached kappa number between 25 and 30 (preferably around 27) ensures the lowest productions costs, taking into consideration both wood yield and chemical consumption combined with the unchanged pulp quality of a softwood kraft pulp [37,135]. In agreement with the results reported by Iribarne and Schroeder [12], strength properties are not affected as long as a certain threshold viscosity is not exceeded [135]. If the intrinsic viscosity of an oxygen-delignified softwood kraft pulp is kept above a level of about  $870 \text{ mL g}^{-1}$ , the relationship between tear index and tensile index seems not to be affected. As an example, the data in Fig. 7.58 show that the zero span tensile index of a loblolly pine kraft pulp increases proportionally to the intrinsic viscosity, and reaches a plateau value above an intrinsic viscosity of about 750–800  $\text{mL g}^{-1}$ . These values are somewhat lower than those reported before or elsewhere, most likely because of the relatively low initial viscosity of the pulps used in this study [136].

It is however important to point out that the unbleached kappa number must not fall significantly below a level of 25.



**Fig. 7.58** Relationship between intrinsic viscosity and zero-span tensile index of unbleached *Pinus taeda* L. kraft pulps and oxygen-bleached kraft pulps produced thereof according to Iribarne and Schroeder (after recalculation) [12].

Unbleached kraft pulps – and also oxygen-delignified kraft pulps – show pronounced swelling properties in an aqueous environment. The swelling properties of the pulp fibers are affected by the acid groups, predominantly carboxyl groups. These groups also determine the ion-exchange capacity of cellulose materials and they contribute to the bounding of fibers. Furthermore, cations adsorbed by the carboxyl groups play an important role in the discoloration mechanism of pulp and products made thereof (e.g., paper, cellulose fibers, films). Carboxyl groups originate from the hemicelluloses, the lignin fraction and, to a much smaller extent, also from fatty and resin acids. The carboxyl groups in the hemicelluloses are included in the 4-*O*-methyl- $\alpha$ -D-glucuronic acid side chains of the xylan fraction which are, however, degraded to hexenuronic acids during alkaline cooking. Hexenuronic acid and 4-*O*-methyl glucuronic acids are almost not degraded during oxygen delignification. The observed decrease in carboxyl groups during oxygen delignification of kraft pulp is attributed predominantly to the removal of lignin [137]. The oxygen delignification of sulfite pulps, however, also contributes to a reduction of carboxyl groups due to the dissolution of hemicelluloses.

## 7.4

### Chlorine Dioxide Bleaching

#### 7.4.1

##### Introduction

The discovery of chlorine dioxide is generally credited to Sir Humphrey Davy, who reported the results of the reaction of potassium chlorate with sulfuric acid which destroyed the color of vegetable dyes [1]. In the 1920s, Schmidt et al. reported that chlorine dioxide is a very selective bleaching agent which does not react with carbohydrates [2,3]. However, the use of chlorine dioxide on an industrial scale began only after World War II, when both suitable manufacturing processes from sodium chlorate and corrosion-resistant materials became available. In 1946, three Swedish kraft pulp mills began to apply chlorine dioxide for the production of highly bleached kraft pulps. Shortly after that, Canadian and US American kraft mills followed suit by installing chlorine dioxide bleaching stages. It can be stated that, together with the invention of the Tomlinson furnace, chlorine dioxide bleaching technology contributed to the breakthrough for the kraft process against the sulfite process. Since such modification, it became possible to produce fully bleached pulps (>88% ISO) with high strength properties (no significant decrease in strength during bleaching operations). In its early application, chlorine dioxide was solely used at, or near the end of bleaching sequences such as CEHD, CEHDED, or CEDED refer to (Tab. 7.2). The use of chlorine dioxide in the delignification stage began only when it became known that a partial replacement of chlorine by chlorine dioxide improves final pulp quality [19]. In the bleaching of hardwood sulfite pulps, it was found that the formation of sticky chlorinated res-

ins could be avoided when chlorine dioxide was used instead of chlorine. In the case of kraft pulps, 5–10% of chlorine was replaced with the equivalent amount of chlorine dioxide to further improve the strength properties of the pulps. The debate about the use of molecular chlorine for pulp bleaching evolved from reports of the research conducted during the Swedish project “Environment/Cel-lulose” [4]. As a result, the study showed that pulp mill effluents entering the Gulf of Bothnia, Sweden, severely affected the diversity, biomass, and distribution of invertebrates and plants. In the sediments outside the Swedish coast, chlorinated compounds related to bleach plant effluents were detected which indicated a high persistence of such substances. Moreover, the use of molecular chlorine for pulp bleaching produces polychlorinated dibenzo-*p*-dioxins (PCDD) and dibenzofurans (PCDF). The pattern of the tetrachlorinated congeners, as well as their concentra-tion, depends drastically on the amount of molecular chlorine applied in the first delignification stage. It has been shown that the concentration of these com-pounds decreases as the degree of substitution of chlorine with chlorine dioxide increases, and cannot usually be detected at 60% chlorine dioxide substitution or higher [5].

With this knowledge, authorities around the world began to implement new regulations that limited the amount of chlorinated organic material discharged from bleaching operations into the environment. Consequently, chlorine dioxide has become a very popular bleaching agent in place of molecular chlorine. Today, chlorine dioxide is certainly the most important bleaching chemical, since the use of elemental chlorine is increasingly abandoned. Chlorine dioxide’s high selectiv-ity towards the oxidation of chromophoric structures makes it the first choice for both delignification and pulp brightening, while retaining strength properties. Furthermore, it meets the current environmental regulations in most countries by generating approximately five times less chlorinated organic material as com-pared to chlorine.

#### 7.4.2

##### Physical and Chemical Properties and Definitions

Chlorine dioxide is a resonance-stabilized compound containing 19 valence elec-trons, nine paired electrons, and one unpaired electron (Fig. 7.59). Chlorine diox-ide shows no noticeable tendency to dimerize, probably because the electron is less localized on the central chlorine atom.

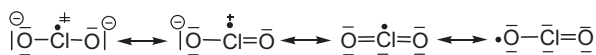


Fig. 7.59 Resonance structures of chlorine dioxide.

The chlorine–oxygen bonds, which show predominantly double-bond character, form an angle of about 117.5°, with a chlorine-oxygen bond length of 1.47 Å. The redox potential corresponding to



is 0.954 V. In aqueous solution, it depends linearly on the pH with a coefficient of  $-0.062$  V for increasing units of pH [6]. Another important half reaction involves:



with a redox potential  $E^0$  of 0.76 V. Chlorine dioxide has an oxidation state of +4, and thus can accept five electrons per molecule to be reduced to chloride ions as demonstrated by Eqs. (56) and (57). The molecular weight of chlorine dioxide is  $67.457 \text{ g mol}^{-1}$ , and that of the equivalent weight  $13.49 \text{ g mol}^{-1} e^-$  ( $67.457/5$ ). The charge of chlorine dioxide is mostly designated as “equivalent chlorine”, better known as “active chlorine”, because this allows the combined addition of chlorine and chlorine dioxide to be expressed as a single term.

To convert chlorine dioxide into active chlorine equivalents, the redox reaction of elemental chlorine must be considered:



The equivalent weight of chlorine can be calculated as  $35.46 \text{ g mol}^{-1} e^-$  ( $70.914/2$ ). The charge of chlorine dioxide can be expressed as active chlorine charge in weight units (% on o.d. pulp or  $\text{kg odt}^{-1}$  pulp) by multiplying the weight of chlorine dioxide by a factor of 2.629 ( $35.46/13.49$ ), while considering an equivalent electron transfer. The charge of chlorine dioxide, expressed as active chlorine, is often related to the kappa number of the pulp before the bleaching treatment. As an example, an unbleached softwood kraft pulp, kappa number 27, is treated in a first chlorine dioxide stage, a so-called  $D_0$ -stage. Assuming a kappa factor of 0.25 to ensure complete pre-delignification, would require the following amount of active chlorine or chlorine dioxide:

$$\begin{aligned} 27 \times 0.25 &= 6.75\% \text{ active chlorine (or equivalent chlorine) on o.d. pulp} \\ &= 67.5 \text{ kg active chlorine odt}^{-1} \text{ pulp} \\ &= 67.5/2.629 = 25.68 \text{ kg ClO}_2 \text{ odt}^{-1} \text{ pulp.} \end{aligned}$$

The freezing point of chlorine dioxide is  $-59^\circ\text{C}$ , and its boiling point  $11^\circ\text{C}$ . Chlorine dioxide is highly soluble in water. The vapor pressure, in kPa, is expressed as:

$$\log P = 6.8676 - \frac{1375.1}{T} \quad (59)$$

where T is  $^\circ\text{K}$ . Equation (59) reveals that chlorine dioxide boils at  $9.65^\circ\text{C}$ . The partition coefficient of chlorine dioxide between water and the gaseous state is 70 at  $0^\circ\text{C}$  and 21.5 at  $35^\circ\text{C}$ . The solubility of chlorine dioxide in chilled water ( $-5^\circ\text{C}$ ) is about  $10 \text{ g L}^{-1}$  while maintaining a reasonably low vapor pressure ( $\sim 6.6 \text{ kPa}$ ). This solution is rather stable, and can be stored in the dark for several months. Chlorine dioxide is known to be quite light-sensitive and decomposes through the free

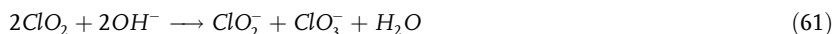
radicals O and ClO to give  $\text{ClO}_3/\text{Cl}_2\text{O}_6$  in the gas phase [6]. Chlorine dioxide is usually analyzed spectrophotometrically as it possesses a broad absorption band with a maximum near 360 nm. Lenzi reports that the extinction coefficient of  $1150 \text{ M}^{-1} \text{ cm}^{-1}$  exhibits only a slight variation with the acidity of the medium and almost no cross-sensitivity with chloride ion, chlorate ion, and chlorine [7].

#### 7.4.2.1 Behavior of Chlorine Dioxide in Aqueous Solution

Chlorine dioxide undergoes rapid electron exchange with chlorite in acid and neutral aqueous solutions [8]. Chlorine dioxide does not exchange at an appreciable rate with perchlorate, chlorate, chlorine, or chloride ions. In the presence of hypochlorous acid, however, the oxidation of chlorine dioxide to chlorate takes place fairly rapidly. Chlorine dioxide decomposes in aqueous solution according to



High acidity, the presence of chloride ions, and high temperature each promote the decomposition of chlorine dioxide [9]. There is some evidence that if there is any reaction between chloride ion and chlorine dioxide, it is very slow [10]. Bray reported that the hydrolysis of chlorine dioxide is very slow, but that the rate of decomposition is accelerated by light and heat [11]. Chlorine dioxide disproportionates in the presence of a base according to Eq. (61):

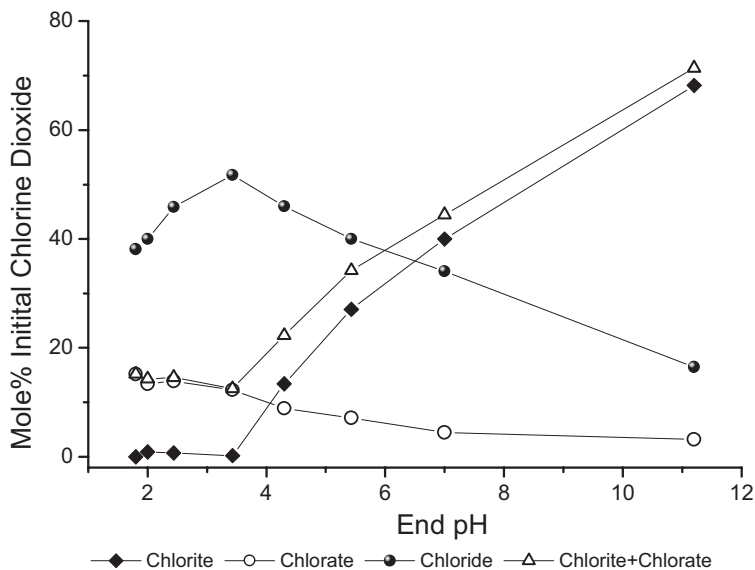


The decomposition reaction is known to be catalyzed by a variety of different bases such as carbonate and others [6]. Chlorine dioxide is converted to chlorite ions by a number of reducing agents, such as hydrogen peroxide, sulfurous acid [12], arsenite, iodide [13], and others. The reaction with hydrogen peroxide, in which the hydroperoxy anion is presumed to be the reactive species, and that with sulfurous acid, may be of some importance in pulp bleaching operations. The latter takes place at low pH values and converts chlorine dioxide to chlorite and chloride ions [12]. An aqueous  $\text{SO}_2$  solution is used after the final bleaching stage (mostly either P- or D-stages) to destroy residual oxidants prior to pulp drying. Chlorine dioxide can be oxidized by ozone to  $\text{Cl}_2\text{O}_6$  [6].

#### 7.4.2.2 Inorganic Side Reactions during Chlorine Dioxide Bleaching of Wood Pulps

The drawback of chlorine dioxide bleaching is the rather low efficiency due to the formation of chlorate and residual chlorite. The loss in oxidation power leads to a further increase in bleaching costs. Additionally, chlorate has been shown to exhibit toxic effects on brown algae, and has therefore been the focus of many studies to evaluate possibilities to minimizing the formation of chlorate and chlorite. The pH profile exhibits a significant influence on the performance of chlorine dioxide bleaching. At high pH, the efficiency of chlorine dioxide bleaching is very

low. Svenson found that when bleaching to pH 11.2 approximately 70 mol% of the initial chlorine dioxide charge is converted to chlorite, wasting 56% of the initial oxidizing power charged to the pulp [14]. Chlorite is not consumed by reactions with the residual lignin, and accounts for a large portion of lost oxidation potential. This is also reflected in a higher residual kappa number as compared to chlorine dioxide bleaching at lower pH levels. Chlorite is formed through a one-electron transfer reaction between the phenolic and nonphenolic structures present in the residual lignin and chlorine dioxide. The low chloride ion concentration also indicates that less hypochlorous acid forms at high pH (Fig. 7.60).



**Fig. 7.60** Effect of final pH in chlorine dioxide bleaching of a 27 kappa number softwood kraft pulp on chlorate, chlorite, and chloride formation (according to [14]).  $D_0$ - conditions: 5.4% active chlorine charge or 20.5 kg chlorine dioxide  $\text{odt}^{-1}$  pulp equal to a 0.2 kappa factor; 50 °C, 120 min reaction time.

The reactivity of chlorite ions increases as soon as the pH of the bleaching liquor decreases, because most reactions that consume chlorite require acidic conditions. The chlorite ions are in equilibrium with chlorous acid, its conjugated acid:



Figure 7.60 shows that the concentration of the chlorite ions linearly decreases to a very low level until a pH of 3.4 is achieved and remains constant at lower pH levels. Chlorous acid readily oxidizes lignin structures, forming hypochlorous acid according to Eq. (63):

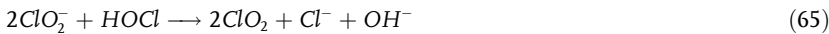


where LO represents oxidized lignin.

Under acidic conditions – preferably at a pH equal to the  $\text{pK}_a$  of chlorous acid – chlorite also undergoes a dismutation reaction that generates chlorate and hypochlorous acid as expressed in Eq. (64):



It has been confirmed that the amount of hypochlorous acid increases when the reaction pH decreases during chlorine dioxide bleaching with a kraft pulp [15]. As a result, bleaching efficiency increases significantly due to the regeneration of chlorine dioxide through chlorite oxidation. The loss of oxidation power due to chlorite formation can be recovered by oxidizing chlorite with hypochlorous acid, as illustrated in Eq. (65). This reaction represents the key step for the better performance of chlorine dioxide bleaching at acidic conditions:



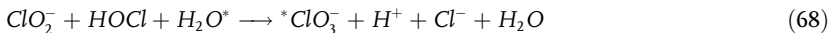
Hypochlorous acid is in equilibrium with chlorine according to Eq. (66). However, a significant amount of elemental chlorine is present only at  $\text{pH} < 2$  ( $\text{pK}_a = 1.8$ ).



In contrast to chlorite, the oxidation potential of chlorate cannot be reactivated by adjusting the reaction conditions. Figure 7.60 reveals that chlorate formation clearly increases while the final pH decreases. Chlorine dioxide decomposes in alkaline media to form chlorate and chlorite ions according to Eq. (67), with a reaction mechanism that is still the subject of debate [16]:



The initial rate of chlorine dioxide decomposition is rather slow, but largely influenced by the presence of hypochlorite ions. The reaction displayed in Eq. (68) is discussed as a further contributor to chlorate formation under neutral to alkaline conditions [17]:



Reactions containing excess hypochlorous acid favor chlorate formation according to Eq. (68), while reactions with excess chlorite generate chlorine dioxide as depicted in Eq. (65). In contrast to the results reported for reactions with wood pulps, chlorate formation increases with rising reaction pH during the reaction of chlorine dioxide with nonphenolic lignin model compounds [17]. This behavior is

attributed to the slower reaction kinetics of etherified lignin moieties as compared to phenolic ones, thereby allowing hypochlorous acid to react with chlorine dioxide to form chlorate.

Under acidic conditions chlorite oxidation was shown to proceed via a dichlorodioxide ( $\text{Cl}_2\text{O}_2$ ) intermediate [10]. This intermediate may undergo a number of possible reactions. Both nucleophiles, chlorite and water, compete for the reaction intermediate, which results in the formation of either chlorine dioxide [Eq. (65)] or chlorate [Eq. (68)].

At a pH below 3.4, where only little chlorite is present, chlorate production clearly dominates. This concludes that chlorate formation during bleaching is more pronounced when the chlorine dioxide concentration is high relative to chlorite. However, in the case of a high chlorite to chlorine dioxide ratio, and when the pH is shifted to higher values, chlorite ions react with the dichlorodioxide intermediate to form chlorine dioxide, rather than the hydrolysis product chlorate. Consequently, the level of chlorate formation can be kept at a minimum when the pH is adjusted from a high to a low level throughout chlorine dioxide bleaching. This can be achieved by splitting chlorine dioxide bleaching into two stages, where the first stage is conducted to a final pH around 7, and the second stage is run to a final pH below 3. In the first stage, a large part of chlorine dioxide is converted to chlorite, thus preventing the generation of additional chlorate in the subsequent acidic stage. The pH profiling ensures a sufficiently high chlorite to chlorine dioxide ratio to effectively suppress chlorate formation. The concentration of chloride ions increases parallel with the reduction of the chlorite ion concentration and passes a maximum at a pH level of about 3.4 (see Fig. 7.60). The decrease in chloride can be explained by a further increase in hypochlorous acid formation at low pH. This agrees well with the observation that chlorine dioxide bleaching causes an increase in AOX formation with decreasing pH below 3.4.

On closer examination of Fig. 7.60, it can be seen that the total amount of wasted oxidation potential (sum of chlorite and chlorate) does not significantly change below a final pH of 3.4. These results differ slightly from those obtained by chlorine dioxide bleaching of delignified pulps (e.g.,  $D_1$ ,  $D_2$ ) [18–20]. Chlorine dioxide bleaching (in a  $D_1$ -stage) of a CE pre-treated softwood kraft pulp requires the final pH to be between 3 and 4 in order to exhibit an optimum bleaching efficiency. The low reactivity of the oxidized lignin structures of prebleached kraft pulps favors the enhanced execution of side reactions at pH levels below 3.5, such as the disproportionation of chlorous acid to form chlorate. The higher reactivity of the unbleached kraft lignin towards chlorine dioxide bleaching promotes the oxidation of the lignin while maintaining a constant chlorate concentration.

It can be concluded, that chlorine dioxide bleaching of both unbleached and prebleached kraft pulps is most efficient when adjusting the final pH to about 3.5. In the case of unbleached kraft pulp, the oxidation power of chlorine dioxide (in a  $D_0$ -stage) remains constant even when the pH falls below 3. In contrast, chlorine dioxide bleaching of prebleached kraft pulps in  $D_1$ - or  $D_2$ -stages displays a maximum reaction efficiency only between pH 3 and 4 because the lower reactivity of



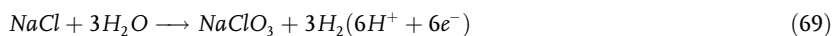
the oxidized lignin structures promotes the inorganic side reactions, predominantly associated with chlorate formation.

### 7.4.3

#### Generation of Chlorine Dioxide

Chlorine dioxide is always manufactured on site because of the risk of rapid decomposition. In most of the processes, chlorine dioxide is produced in strong acid aqueous solutions from either sodium chlorite or sodium chlorate. Sodium chlorite is used in small- and medium-scale production units mainly for water treatment and disinfection applications that require high-purity waters. Sodium chlorate is utilized in those applications not requiring high-purity waters, but very large amounts of chlorine dioxide, such as in pulp bleaching.

Generally, chlorine dioxide manufacture is based on the reduction of sodium chlorate at high acidity. In nonintegrated processes, sodium chlorate is purchased as a crystalline solid or as a concentrated (40–45%) aqueous solution, whereas in an integrated process sodium chlorate is prepared by the electrolysis of a sodium chloride solution according to the following equation:



The evolving hydrogen ( $\text{H}_2$ ) is recycled to produce hydrochloric acid, which is used in the integrated processes, known as R6, Lurgi or Chemetics processes, to reduce chlorate to chlorine dioxide. The redox reaction in the chlorine dioxide generation can be written as:



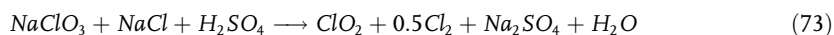
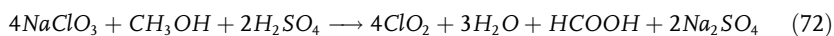
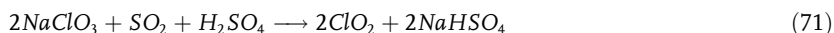
where the byproduct sodium chloride is recirculated to the electrolysis cell [Eq. (70)]. The excess chlorine gas evolved from Eq. (70) is fed to the HCl synthesis unit together with make-up chlorine, where it is burned together with the hydrogen produced from the chlorate electrolysis unit to produce hydrochloric acid (HCl). The three unit operations – chlorate electrolysis, chlorine dioxide generator and hydrochloric acid synthesis – comprise the key steps in an integrated chlorine dioxide plant [21]. The advantage of an integrated system is that it prevents the formation of any sulfur-based byproducts. However, an integrated system produces a chlorine dioxide solution with a relatively high level of residual elemental chlorine in the range 11–23% of the chlorine dioxide concentration (Tab. 7.31).

Since the first commercial use of chlorine dioxide in pulp bleaching in Canada and Sweden in 1946, both the technology of chlorine dioxide manufacture and the requirements on pulp bleaching have been changed considerably. Until the 1960s and 1970s, chlorine dioxide was preferentially used in the final bleaching stages according to CEHDED or later CEDED sequences for the production of fully bleached kraft pulp. At that time, chlorine as a byproduct from chlorine dioxide

Tab. 7.31 An overview of the different chlorine dioxide generation technologies.

Process	Type	Pressure	Reducing agent	By-products		
				Na <sub>2</sub> SO <sub>4</sub> [t/t ClO <sub>2</sub> ]	Cl <sub>2</sub> [t/t ClO <sub>2</sub> ]	[in 10 gpl ClO <sub>2</sub> ]
Mathieson	Non integrated	Atmospheric	SO <sub>2</sub>	3.5		
Solvay	Non integrated	Atmospheric	CH <sub>3</sub> OH	3.5		
R2	Non integrated	Atmospheric	NaCl	6.8	0.6	1.0
R3. SVP	Non integrated	Vacuum	NaCl	2.3	0.6	2.0
R3H	Non integrated	Vacuum	HCl	1.1	0.6	1.5–2.5
R6 Lurgi Chemetics	Integrated	Vacuum	HCl	0.0	(0.7)	1.1–2.3
R8. SVP-MeOH	Non integrated	Vacuum	CH <sub>3</sub> OH	1.1	0.01	0.1
R9	Non integrated	Vacuum	CH <sub>3</sub> OH	0–1.1	0.01	0.1
R10	Non integrated	Vacuum	CH <sub>3</sub> OH	0.9	0.01	0.1

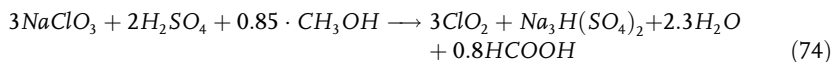
manufacture could be completely recycled to both C- and D-stages. With growing concern about the environmental impact of chlorinated organic compounds, elemental chlorine has been replaced by chlorine dioxide which produces approximately five times less AOX than the former. With the banishment of elemental chlorine from pulp bleaching sequences, the production of chlorine as a byproduct became an important criterion for the selection of chlorine dioxide generators. Hence, chlorine dioxide generation technology has advanced substantially during the past 50 years. The processes of the first generation, the Mathieson, the Solvay, and the R2, use sulfur dioxide, methanol, and sodium chloride, respectively as reducing agents. The corresponding overall reactions for the Mathieson, Solvay and R2 processes are displayed in Eqs. (71) to (73), respectively:



All three processes operate at atmospheric conditions, and thus require high charges of sulfuric acid to assure a high chlorine dioxide yield (defined as molar percentage of the sodium chlorate converted to chlorine dioxide). The drawback of these processes is the generation of large amounts of spent acid solution, expressed as tons of Na<sub>2</sub>SO<sub>4</sub> losses per ton chlorine dioxide produced (see Tab. 7.31).

The only advantage of the R2 process over the Mathieson and Solvay processes is the much faster reaction, which results in lower investment costs. However, the specific spent acid solution production is almost twice that of the Mathieson and Solvay technologies. Moreover, the R2 process generates 0.6 t of  $\text{Cl}_2$   $\text{t}^{-1}$  of  $\text{ClO}_2$ , with about 1 g  $\text{L}^{-1}$  chlorine in the chlorine dioxide solution. The residual 0.5 t  $\text{Cl}_2$   $\text{t}^{-1}$  of  $\text{ClO}_2$  is primarily used to produce sodium hypochlorite.

The R3 and SVP (single-vessel process) processes were developed in a response to reduce the amount of waste acid produced during the course of chlorine dioxide manufacture. As these processes operate under vacuum, at higher temperatures, and employ a catalyst, both high production and high yield are maintained at a far lower solution acidity as compared to the R2 process, which enables neutral anhydrous sodium sulfate to be crystallized. The neutral saltcake can be filtered-off and removed from the system. Thus, the saltcake production is approximately 34% less as compared to the Mathieson and Solvay processes, and about 66% less than that of an R2 process (see Tab. 7.31) [22]. Nonetheless, the amount of elemental chlorine formation is high due to the addition of sodium chloride as a reducing agent. The urgent need to eliminate chlorine and to further reduce the amount of sodium sulfate during chlorine dioxide production promoted the development of a new methanol-based process. This process, known as R8, SVP-MeOH and SVP-LITE processes, account for the majority of the installed  $\text{ClO}_2$  capacity [23]. The plants are similar with respect to the overall operation and the process technology employed. The generation system consists of a generator and a reboiler. In the generator, the sodium chlorate is reduced to chlorine dioxide while sodium sesquisulfate is formed as a byproduct. The chlorine dioxide is separated as a gas which, after a concentration process, is dissolved in chilled water, where a concentration of approximately 10 g  $\text{L}^{-1}$  is adjusted. The chlorine dioxide solution is pumped to storage tanks for subsequent use in the bleach plant. The sodium sesquisulfate is filtered off from the generator slurry, dissolved to a saturated, acidic aqueous solution which is stored in a tank for further use (e.g., in tall oil plant). The overall reaction comprising the R8 process may be expressed according to:

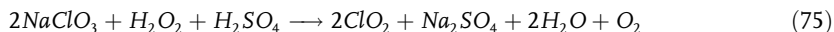


Model experiments revealed that the generation of chlorine dioxide in the methanol-chlorate process involves three distinct phases, namely initiation, start-up, and steady-state [24]. In the initial phase, no chlorine dioxide is formed, while chlorous acid and elemental chlorine are generated. Chlorous acid is generated continuously from the reduction of chlorate by methanol and then further reduced to hypochlorous acid, which then is converted to elemental chlorine. Chlorine dioxide is formed from the reaction between chlorine and chlorous acid in the presence of chloride, which acts as a catalyst. Apparently, chlorine dioxide is only generated when the chloride concentration exceeds a certain level. Chlorine is usually present in a chlorine dioxide solution because of the necessary

presence of chloride in the generator. The presence of low concentrations of chloride which actually leads to elemental chlorine formation is essential to avoid the termination of chlorine dioxide production. The situation where chlorine dioxide generation stops is known as a so-called “white-out” because a white gas consisting of chlorine and water vapor appears. In industrial practice, the chlorine dioxide solution contains elemental chlorine in a concentration ratio of 100:1, as depicted in Tab. 7.31. At the same time, methanol is oxidized stepwise by chlorate to form formaldehyde, then formic acid, and finally carbon monoxide in the case of complete oxidation [25]. Some of the methanol and its oxidation products may leave the generator along with chlorine dioxide.

Besides the very low concentration of chlorine, the R8 process has the advantage of producing less saltcake (–52%) and higher chlorine dioxide yield (97% versus 93%) as compared to the R3/SVP processes. However, the development of the methanol-based chlorine dioxide process continued by focusing on the further reduction of the amount of saltcake. The sesquisulfate is electrolyzed to form sodium hydroxide and sulfuric acid in the R9 process. There, the acid is recirculated to the generator and the alkali fed to the bleach plant. Depending on the size of the electrolytic cell, the amount of salt cake can be minimized in a range indicated in Tab. 7.31. The metathesis of the sesquisulfate into neutral sodium sulfate crystals is the key element of the R10 process. The remaining solution containing residual salt and sulfuric acid is recirculated to the generator. The metathesis is effected in such a manner as to minimize the additional evaporative load imposed on the chlorine dioxide-generating process by the metathesis medium. The extent of sulfate precipitation can be further enhanced by the addition of some methanol.

Hydrogen peroxide is another reducing agent which generates chlorine dioxide from chlorate [26]. The stoichiometry of this process is represented in Eq. (75):



The peroxide-based process exhibits faster reaction kinetics as compared to the methanol-based process. Consequently, the former can be operated at a sulfuric acid concentration of only 2 mol L<sup>-1</sup> sulfuric acid as compared to that of 4.5–5.0 mol L<sup>-1</sup> for the methanol-based process. However, the high costs of hydrogen peroxide limit the attractiveness of the peroxide-based process for chlorine dioxide generation. Alternatively, combining hydrogen peroxide and methanol causes a considerable increase in the rate of chlorine dioxide generation [27]. Furthermore, it largely eliminates molecular chlorine as a byproduct. Even when substituting only 10% of the methanol with hydrogen peroxide, the reaction rate of chlorine dioxide formation is doubled. The high reaction rate can be explained by the rapid reaction between hydrogen peroxide and chlorine, which results in chloride and oxygen formation. Additionally, the reaction of hydrogen peroxide with dichlorodioxide (Cl<sub>2</sub>O<sub>2</sub>) leads to a faster accumulation of the necessary chloride, which is a catalyst in the methanol-based chlorine dioxide generation process.

Besides costs, the most important criterion for the selection of a chlorine dioxide plant is the amount of byproducts generated. The level of elemental chlorine

must be kept to the lowest possible amount to ensure low AOX formation, while the quantities of sodium sulfate-sulfuric acid solution must be adjusted to fit the Na/S ratio of the respective kraft mill.

During the past decade, chlorine dioxide has been increasingly delivered “over-the fence” by companies specializing in chlorine dioxide generation. This concept is achieving growing acceptance as the kraft mills are no longer involved in the technology of chlorine dioxide generation.

#### 7.4.4

#### **Chemistry of Chlorine Dioxide Treatment**

*Manfred Schwanninger*

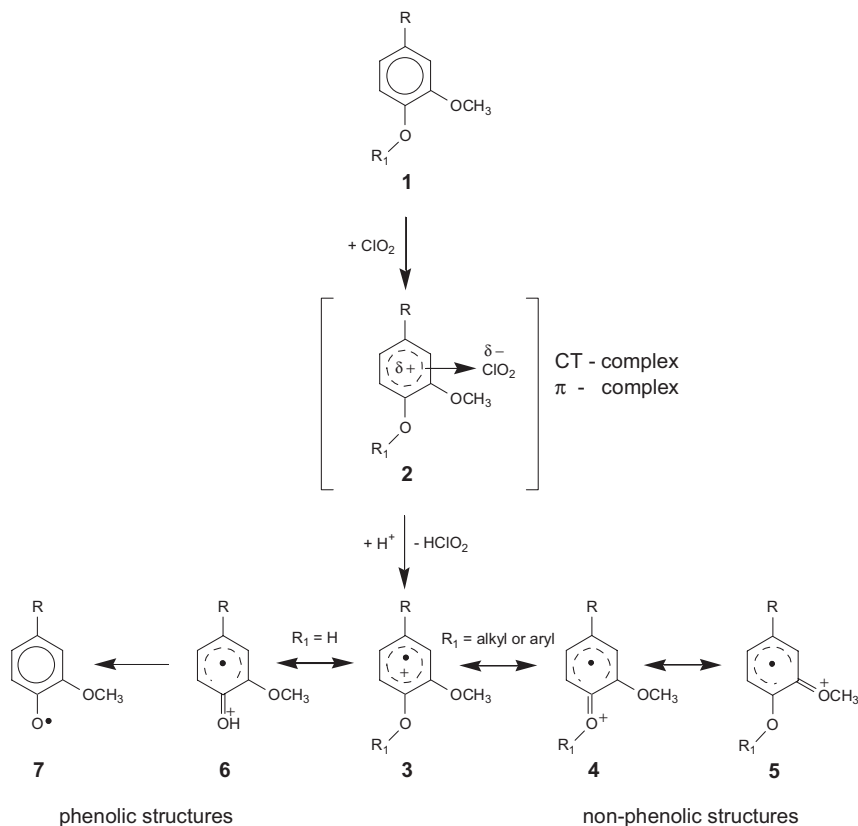
The residual lignin from unbleached or semibleached pulps, which could not be removed by pulping, must be removed from pulp through oxidative lignin degradation with bleaching reagents such as chlorine dioxide. The structure and reactivity of the residual lignin have already been described (see Section 4.2.4, Lignin structures and their reactivity; Composition of lignin, residual lignin after cooking and bleaching).

Most knowledge regarding the proposed reaction pathways of chlorine dioxide and lignin, and of compounds formed during bleaching, is derived from model compound studies [1–8], molecular orbital calculations [9,10] and from bleached residual lignin of kraft pulps [11–19]. However, whilst much information is available on the reaction pathways and degradation products formed during chlorine dioxide bleaching, for reasons of space only a minimal amount can be selected and presented in this section.

In principle, a distinction can be made between: (a) oxidations by the oxidant (chlorine dioxide), which affords a great variety of products and illustrates the complexity of chlorine dioxide bleaching; and (b) the chlorination of aromatic rings (this will be described later).

The initial steps of bleaching with chlorine dioxide are shown in Scheme 7.23. Oxidations of aromatic substrates with chlorine dioxide are initiated by electrophilic addition of the oxidant to the aromatic nuclei. This results in the generation of charge-transfer ( $= \pi$ ) complexes [1]. These complexes become protonated in acidic media, thereby enhancing the formation of corresponding resonance-stabilized cation radicals by the elimination of chlorous acid. In the case of phenolic substrates ( $R_1 = H$ ), these cation radical intermediates readily lose a proton, affording phenoxyl radicals in various mesomeric forms (Scheme 7.24; **8**, **9**, **10**, and **11**). In the case of nonphenolic substrates ( $R_1 = \text{alkyl or aryl}$ ), the intermediary cation radicals exist in various ortho- and para-oxonium ion forms (Scheme 7.25; **26** and **27**) [1].

Creosol (Scheme 7.24), a simple phenolic compound, represents structural types that were assumed to be present in residual lignin [1]. The methyl group was thought to indicate side chains lacking a free or etherified hydroxyl group in the  $\alpha$ -position [1], although finding a methyl alpha position in lignin is highly unlikely. The formation of the oxidations products (Scheme 7.242) begins from the

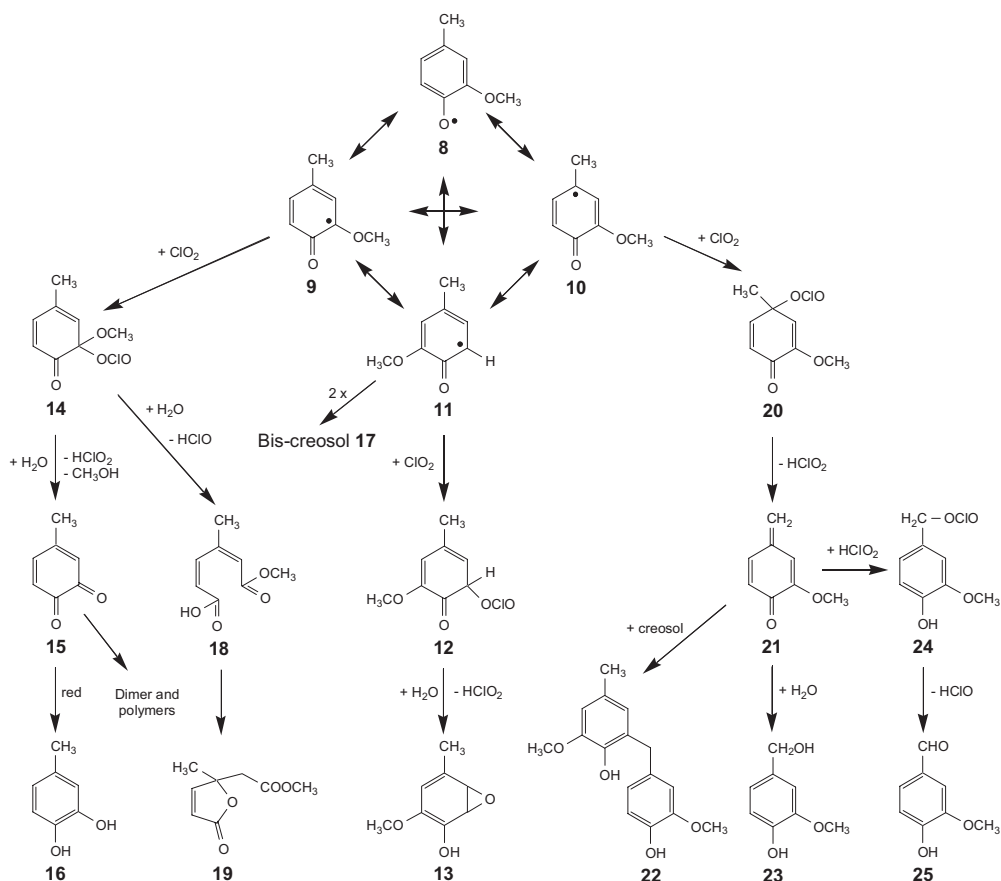


**Scheme 7.23** The initial steps of a general course of bleaching with chlorine dioxide (from Ref. [1]).

phenoxyl radical in its ortho- and para-mesomeric forms (8–11) by coupling with chlorine dioxide, yielding the chlorite esters of ortho- and para-quinols which undergo various reactions. Hydrolysis of the chlorous ester intermediate (14) accompanied by an oxidative demethoxylation gives the corresponding ortho-quinone (15), and subsequent reduction leads to 4-methylcatechol (16). Heterolytic fragmentation of the chlorous ester intermediate (14) leads to cleavage of the aromatic ring with formation of 3-methylmuconic acid monomethyl ester (18), as well as the cyclization product 4-carbomethoxymethyl-4-methylbutenolide (19). The competing reactions, the hydrolysis and the heterolytic fragmentation of the quinol chlorous ester (14), should provide quantitative correlation between the products (15, 18 and 19), which is difficult to show since the quinone (15) readily undergoes dimerization and polymerization in addition to the reduction yielding 16. Hydrolysis of the chlorous ester intermediate (12) gives a compound (13) to which an oxirane structure is tentatively ascribed. In a competitive reaction, two radicals of 11 may couple to give bis-creosol (17). Chlorine dioxide addition to the para-form of the phenoxyl radical (10) followed by elimination of chlorous acid,

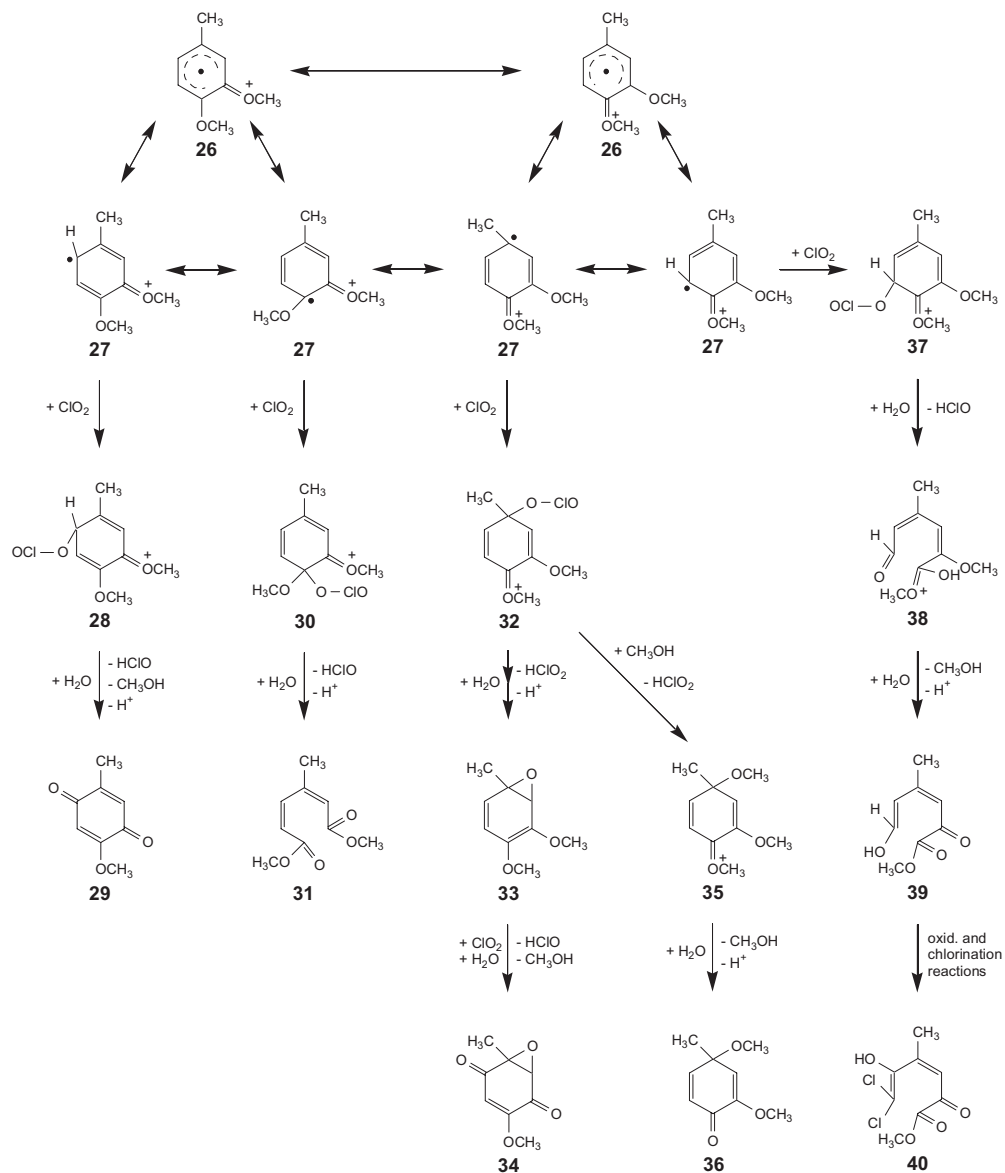
results in the formation of a quinone methide intermediate (**21**). Nucleophilic addition of water, chlorous acid or creosol to this intermediate gives rise to vanillyl alcohol (**23**), vanillin (**25**) and the diarylmethane (**22**), respectively.

The formation of quinoid structures (e.g., **15**) represents the main oxidative change of creosol-type phenols subjected to chlorine dioxide. Under the conditions usually employed, such structures are not stable and undergo reduction to catechols, and possibly also further oxidation with chlorous acid [1]. These experimental results are in good agreement with the thermodynamic results determined by computational methods [9].



**Scheme 7.24** Reactions of chlorine dioxide with creosol (from Ref. [1]).

The methylated analogue of creosol, the 4-methylveratrole, represents a simple model for nonphenolic structures in lignin, and reacts with chlorine dioxide at a much lower rate (the rate constant,  $k$ , is about seven orders lower, which illustrates the pronounced preference of chlorine dioxide for phenolic substrates [1]) than its phenolic counterpart. The reaction pathways starting from the two meth-



**Scheme 7.25** Reactions of chlorine dioxide with creosol methyl ether (4-methylveratrole) (adapted from Ref. [1]).

oxonium ions (26) are shown in Scheme 7.25. Electrophilic attack of chlorine dioxide to the unsubstituted para-position (27 left) relative to the methoxyl group, followed by elimination of hypochlorous acid and hydrolysis of the methyl aryl ether group affords the para-quinone (29). Chlorine dioxide attack on a carbon bearing



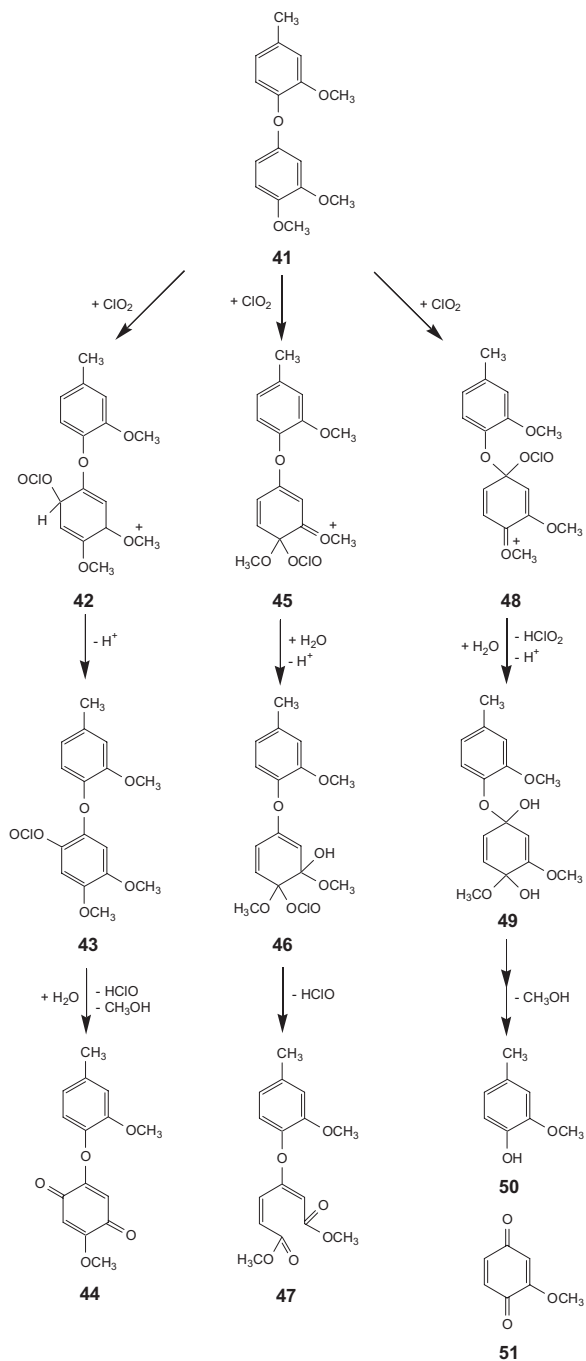
a methoxyl group yields compound **30**. In the presence of water the intermediate chlorous ester (**30**) undergoes heterolytic fragmentation and ring cleavage giving rise to 3-methylmuconic acid dimethyl ester (**31**). Hydrolysis of the chlorous ester intermediate **32**, and rearrangement forms an oxirane (**33**) that is further oxidised to oxirane (**34**). Alternatively, methanolysis of **32**, in a methanol-containing solvent, followed by hydrolysis of the methyl aryl ether bond, gives rise to the formation of the para-quinol methyl ether (**36**). A chlorine dioxide attack on an unsubstituted carbon atom ortho to a methoxyl group (**27** right), followed by heterolytic fragmentation, leads to ring opening with formation of an oxo carboxylic acid ester (**39**) which, in a series of oxidation and chlorination reactions, is converted into the dichloro-hydroxy- $\alpha$ -keto ester (**40**) [1].

4-Methyl-2,3',4'-trimethoxydiphenyl ether (Scheme 7.26; **41**) served as a model for native diaryl ether structures (unaffected during pulping) or for diaryl ether structures, arising by oxidative coupling during bleaching [2]. Electrophilic attack takes place preferentially on the aromatic moiety of the diaryl ether which is substituted by three activating ether groups, giving rise to the corresponding oxidation products (**44**, **47**, **50**, and **51**). The modes of formation of these cleavage products are analogous to those of other nonphenolic models, such as those shown in Scheme 7.25. Moreover, muconic acid esters (e.g., **31**; Scheme 7.25), monochloromuconic acid ester, a lactone (e.g., **19**; Scheme 7.24) and quinolmethylether (e.g., **36**; Scheme 7.25) are formed [2].

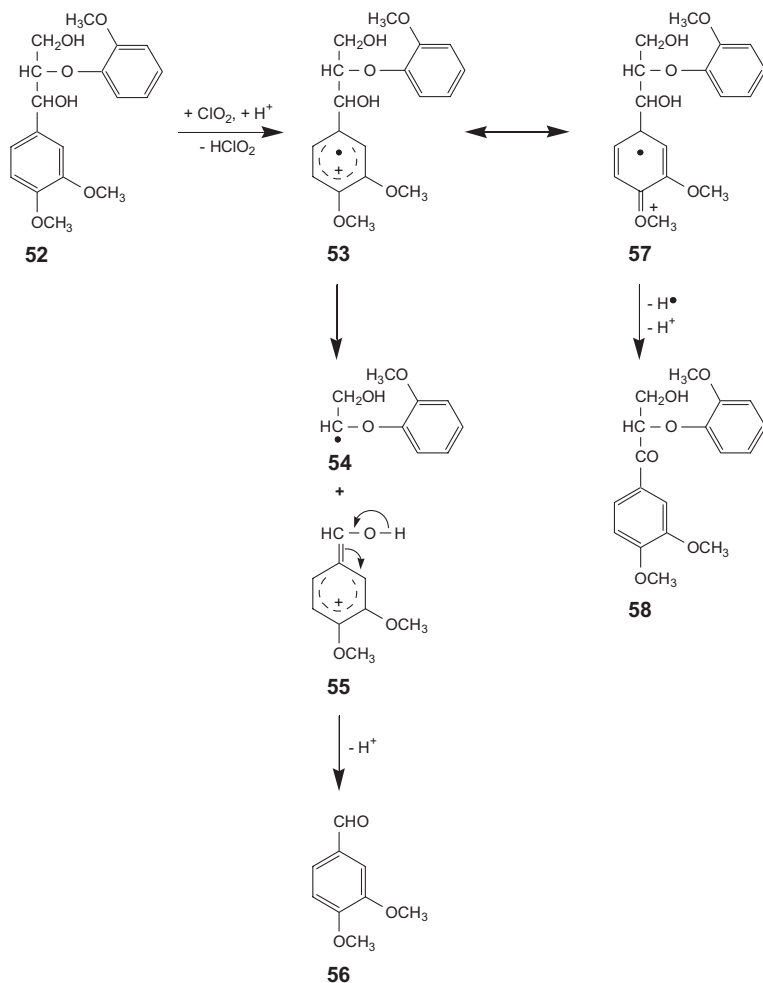
Under weakly acidic or neutral conditions, veratrylglycerol- $\beta$ -guaiacyl ether (Scheme 7.27; **52**), a nonphenolic residual lignin structure of the  $\beta$ -aryl ether type, undergo (in part) oxidation by chlorine dioxide to form the corresponding  $\alpha$ -keto structure (**58**), and in part also oxidative cleavage of the  $C_\alpha$ - $C_\beta$  bond to yield the corresponding aromatic aldehyde (e.g., veratrylaldehyde **56**) [2]. Both reactions follow the general course via the initial radical cation intermediate shown in Scheme 7.23. The  $C_\alpha$ - $C_\beta$  cleavage may be considered to involve homolytic fragmentation of the radical cation. This is analogous to the reactions of nonphenolic  $\beta$ -aryl ether structures with other reagents of the radical type, such as hydroxyl radicals during oxygen bleaching (see Scheme 7.12; Oxygen delignification, path B).

Structures of the stilbene and vinyl ether type (see Oxygen delignification, Table 7.9) were found to be more resistant to chlorine dioxide oxidation. Chlorine dioxide reacts only with the double bonds between the aromatic moieties, however extensive oxidative cleavage of the double bond did not occur and no ring-opening products were detected [3]. The initial reaction steps involved are the formation of intermediary cation radicals and their reaction with the oxidant, which are analogous to those observed when chlorine dioxide reacts with the aromatic nuclei (e.g., Scheme 7.23). The subsequent reactions of ring-conjugated structures with  $\text{ClO}_2$  differ from those of aromatic nuclei. The attack at the unsaturated side chains may be due to the high electron density at the  $\beta$ -carbon atom(s) in conjugated systems and the deactivating effect on the reactivity of aromatic nuclei exerted by the original conjugated double bonds [3].

The reaction between chlorine dioxide and different lignin model compounds (phenolic and nonphenolic, with or without an  $\alpha$ -hydroxyl group), when studied



**Scheme 7.26** Reactions of chlorine dioxide with 4-methyl-2,3',4'-trimethoxy-diphenyl ether (from Ref. [2]).



**Scheme 7.27** Homolytic fragmentation and oxidation in the  $\alpha$ -position of veratryl- $\beta$ -guaiacyl ether (**52**) on treatment with chlorine dioxide (from Ref. [2]).

under the effective elimination of hypochlorous acid by sulfamic acid during chlorine dioxide treatment [4], showed that the reaction between  $\text{ClO}_2$  and lignin model compounds is generally characterized by three independent parallel reactions: (a) demethylation (demethoxylation [20]); (b) formation of 2-methoxy-*p*-quinone; and (c) formation of muconic acid monomethyl ester and/or its derivatives [15,18,19]. Nonphenolic lignin model compounds do react with  $\text{ClO}_2$  when  $\text{ClO}_2$  is supplied in large excess [1,2,4]. These conditions are not representative of industrial  $\text{ClO}_2$  application levels; therefore, the presence of free phenolic lignin is thought to be a critical lignin component needed to increase oxidation efficiency during pulp bleaching. However, recently Svenson et al. [zz] showed that the

removal of phenolic hydroxyl groups via pulp methylation did not adversely affect the chlorine dioxide bleaching efficiency or the amount of chlorate formed during exposure to chlorine dioxide. Due to the effective elimination of hypochlorous acid, no chloroaromatic material could be detected [4], or can be substantially reduced [21]. This supports the view that the reaction intermediate hypochlorous acid (and chlorine) is solely responsible for the formation of chloro organic material during chlorine dioxide bleaching [4,5]. Without elimination of the hypochlorous acid formed during chlorine dioxide bleaching, several chlorination products of all model compounds studies have been found [1–3]. Although alkaline decomposition of chlorine dioxide has a complex behaviour and is not very well understood [31], it should be mentioned that increasing pH (although decreasing reactivity) leads to decreased formation of chlorinated organics [29].

Chlorine dioxide delignification ( $D_0$ ) preferentially oxidizes phenolic entities to both quinonoid and muconic acid structures modifying kraft residual lignin [15], indicating that quinones are significant reaction products formed in preference over muconic methyl esters during  $D_0$  stage [4]. The amount of phenolic groups of unbleached residual lignin is about 30–50% of all the phenylpropane units. Kinetic studies with model compounds have demonstrated that  $ClO_2$  preferentially oxidizes these phenolic groups orders of magnitude faster than nonphenolic entities [4,22,23]. Further, differences in the reactivity of phenolic compounds are observed and dependent on structural details [24]. Thus, it is generally accepted that  $ClO_2$  will preferably react with these phenolic groups during  $D_0$  delignification [4]. In general, these reaction products (quinonoid and muconic acid structures) are generally resistant to further oxidation by  $ClO_2$ . It is suspected that the formation of these chromophores during bleaching, and their slow elimination during later bleaching stages might explain why various bleaching sequences encounter brightness ceilings, and why different bleach sequences are more efficient at reaching higher brightness targets than others [15]. Alkali extraction (E stage), in addition to removing solubilized lignin and saponifying muconic acid methyl esters, reactivates the residual lignin towards  $ClO_2$  oxidation [13]. It appears that the E stage behaves like a reductive bleaching stage, similar to that of a Y stage (sodium hydrosulphite bleaching stages), which presumably results in the aromatization of quinones to polyhydric phenols. Chlorine dioxide oxidation of  $D_0E$  and  $D_0Y$  treated pulps generally afforded quinonoid structures onto the oxidized lignin, like that of the  $D_0$  stage, which implies that polyphenols react with  $ClO_2$  in a somewhat similar way as unbleached phenolic groups [13]. Clearly, the formation of quinones during the  $ClO_2$  oxidation of phenolic and polyphenolic moieties represents a significant reaction product.  $D_0$  stage quinones can be easily re-activated towards  $ClO_2$  again upon alkali treatment [13].

#### 7.4.4.1 Chlorination Products

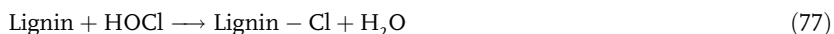
It is well established that hypochlorous acid ( $HOCl$ ) and chlorine ( $Cl_2$ ) are responsible for the chlorination products found in chlorine dioxide-bleached pulps (see Section 7.4.7) [12,25–27]. Both are in a pH-dependent equilibrium [see Section

7.4.2, Eq. (66)]. In general, the pH influences the stability [28] and the mechanism of chlorine dioxide oxidation of aromatic compounds [29]. Normally, hypochlorous acid and chlorine are found in very low concentrations, are consumed rapidly, and cannot be detected in bleaching filtrates [30].

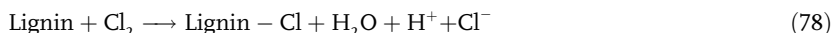
There are two possible explanations for the higher organic chlorine at pH 2 [31]. One explanation is that chlorous acid reduction by  $\text{Cl}^-$  is occurring [Eq. (76) [32,33]. The half-life of this reaction at pH 2 and 25 °C has been reported to be as low as 17 min when chloride ions are in excess of chlorite [32,33], indicating that – under the correct conditions – hypochlorous acid forms fast through:



The net result would produce more hypochlorous acid, which could further react, increasing the amount of chlorinated products at pH 2 [Eq. (77).



Another explanation for the higher amount of organic chlorine at low pH is that more elemental chlorine is present at pH 2. Hypochlorous acid is in equilibrium with elemental chlorine through a hydrolysis reaction. The rate of chlorination reactions [Eq. (78)] increases when more elemental chlorine is present because of its greater oxidation potential compared to hypochlorous acid:



The formation of chlorinated organic compounds is influenced by, for example, hexeneuronic acid (HexA) [29,34,35], and can be reduced by using dimethylsulfoxide (DMSO) [36,37], lower chlorine dioxide charges [38], or by adding sulfamic acid [4,38]. However, polychlorinated products such as dibenzo-*p*-dioxins and dibenzofurans [39, 40] and chloroform [41,42] have also been found in the process water of kraft pulp bleaching mills. The concentrations of dioxins were found to be below 1 pg TEQ  $\text{L}^{-1}$  (TEQ = toxic equivalency quantity). Approximately 30% of the chloroform produced in ECF (ECF = elemental chlorine free) bleaching of hardwood oxygen-delignified kraft pulp are discharged to bleaching effluents [42]. Chloroform in the effluents was not decomposed by activated sludge, and more than 97% was emitted to the air by volatilization. Therefore, an ecological risk of using chlorine dioxide in bleaching is immanent [43]. However, Nakamata et al. [42] suggested to introduce ECF bleaching into all mills. This would lead to a considerable fall from the chloroform discharge from ECF and chlorine bleaching mills down to about 3% (based on data from 1999). Chlorinated compound concentrations in final effluent (following secondary treatment) have been found to comprise a negligible risk to aquatic organisms in comparison with the known toxicological thresholds [43,44]. The ecological risk associated with (mono)-chlorinated compounds [45] that derived essentially from glucuronoxylan is expected to be negligible since they are easily degraded and not detected in the final mill effluent [46].

## 7.4.5

**Performance of Chlorine Dioxide Bleaching**7.4.5.1 **Standard Chlorine Dioxide Bleaching**

Since elemental chlorine is no longer used in modern kraft mills because of environmental reasons, chlorine dioxide is also used as a first bleaching stage after cooking or oxygen delignification. In fact, the first chlorine dioxide stage acts more as a delignifying stage and is commonly denoted as the  $D_0$  stage. The replacement of a conventional (C90 + D10) by a D100 stage (equal to  $D_0$ ) results in a loss of delignification efficiency. In order to obtain the same kappa number after a subsequent (EO) extraction step, the kappa factor must be increased from, for example 0.22 to 0.28, which corresponds to an increase of 27% of active chlorine charge to compensate for the loss in oxidation power [1]. In Tab. 7.32 are listed the characteristic conditions for industrial  $D_0$  stages in combination with a subsequent alkaline extraction, usually reinforced by the addition of oxygen and hydrogen peroxide. In most cases, the pulp is thoroughly washed between the  $D_0$  and the extraction stages either by a displacement press, a standard drum washer, a medium consistening drum displacer (MCDD) washer, or a diffuser washer (see Chapter 5.6).

**Tab. 7.32** Characteristic  $D_0$  and  $D_0$ (EO),  $D_0$ (EOP) conditions.

Stage	Substrate	Unit	Values	Comment
$D_0$	Consistency	%	10–14	
	Time	min	30–60	
	Temperature	°C	40–60	
	Kappa factor		0.20–0.28	
	Final pH		2–4	
(EOP)	Consistency	%	10–12	
	Time	min	60–90	
	Temperature	°C	70–90	
	NaOH-charge	kg odt <sup>-1</sup>	<sup>a</sup>	
	H <sub>2</sub> O <sub>2</sub> -charge	kg odt <sup>-1</sup>	3	
	Pressure	kPa	25–50	upward flow downward flow
	Kappa number		3–6 2–5	SW-Kraft HW-Kraft

a. typically between 15–30, more related to the incoming kappa number usually a charge equal to the kappa number entering the  $D_0$  stage.

The chlorine dioxide charge is calculated in relation to the kappa number of the pulp entering the  $D_0$  stage expressed as kappa factor,  $k_f$ :

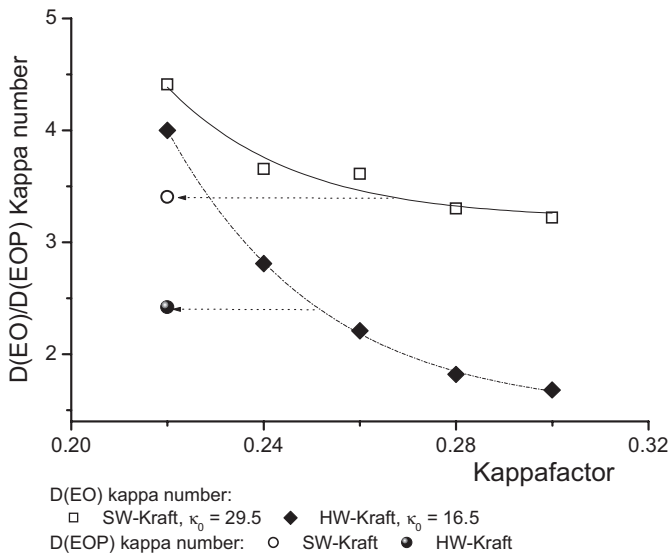
$$k_f = \frac{a \cdot Cl - \text{charge, \%odt}}{\text{kappa number}} \quad (79)$$

The stoichiometry of the chlorine dioxide delignification reaction in a  $D_0$  position (softwood kraft, initial kappa number 29–32, kappa factor 0.17–0.23, 40–50 °C) shows a linear relationship, independent of the kappa number entering the  $D_0$  stage according to the following equation [2]:

$$\frac{\Delta\kappa}{\Delta ClO_2} = 0.58 \quad (80)$$

where  $ClO_2$  is expressed in kg chlorine dioxide per o.d. ton of pulp.

Equation (80) allows the calculation of the extent of delignification during the  $D_0$  operation alone. However, this information is not very useful because a great part of the oxidized lignin compounds remains in the pulp fiber after the  $D_0$  stage, and can only be removed by a subsequent alkaline extraction stage. As expected, the charge of sodium hydroxide necessary to extract the oxidized, water-soluble material quantitatively is related to the kappa number of the pulp entering the  $D_0$  stage (Tab. 7.32). Today, it is very common to enhance the extraction stage with oxygen (EO) or hydrogen peroxide (EP), or both (EOP), to compensate for a lower chlorine dioxide charge in the preceding  $D_0$  stage. The data in Fig. 7.61 illustrate



**Fig. 7.61** Kappa number of D(EO)-treated softwood and hardwood kraft pulps as a function of kappa factor (according to [1]).  $D_0$  delignified softwood and hardwood kraft pulps, each treated with an active chlorine charge

corresponding to a kappa factor 0.22, were subjected a subsequent extraction stage, where, in addition to oxygen, 3 kg  $H_2O_2$  per ton pulp were applied.

that the addition of 3 kg H<sub>2</sub>O<sub>2</sub> odt<sup>-1</sup> in the EOP stage decreases the D(EOP) kappa numbers from 4.4 to 3.4 for the softwood kraft pulp, and from 4.0 to 2.4 for the hardwood kraft pulp.

The use of 3 kg H<sub>2</sub>O<sub>2</sub> odt<sup>-1</sup> in the EOP stage decreases the D(EOP) kappa number to a level which can be obtained after a D(EO) sequence only by increasing the kappa factor to 0.27 for the softwood and to 0.25 for the hardwood kraft pulp. Thus, the charge of 1 kg H<sub>2</sub>O<sub>2</sub> per ton pulp replaces active chlorine charges in an amount of 4.9 kg odt<sup>-1</sup> [(0.27 - 0.22) × 29.5 × 10/3 = 4.9] for the former and 1.7 kg odt<sup>-1</sup> [(0.25 - 0.22) × 16.5 × 10/3] for the latter. However, the absolute amount of active chlorine charge being replaced by the addition of H<sub>2</sub>O<sub>2</sub> in an EOP stage depends on many factors, including the amount and reactivity of residual lignin as well as the applied reactions conditions.

Chlorine dioxide is a very efficient and selective brightening agent. Therefore, chlorine dioxide stages are most commonly used in the final bleaching (ECF) sequences. A selection of different ECF-bleaching sequences comprising one or more chlorine dioxide stages which are applied to obtain full brightness (89+% ISO) are detailed in Tab. 7.33.

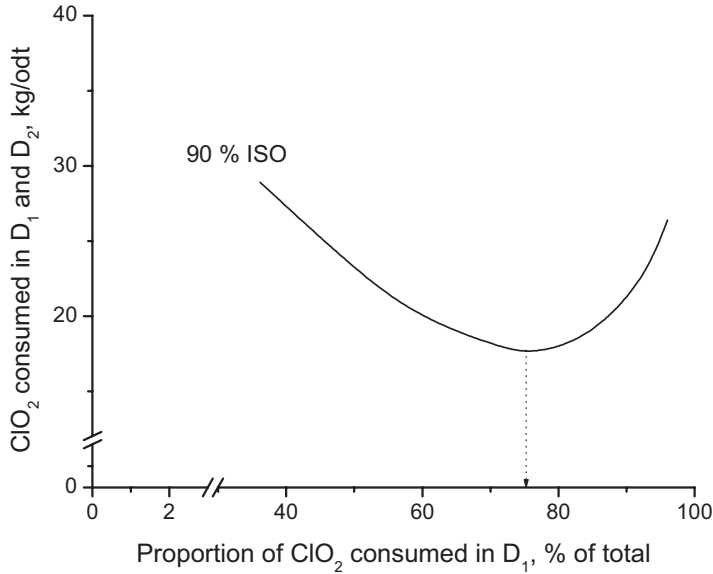
**Tab. 7.33** Examples of typical chlorine dioxide bleaching sequences.

Sequences	Preferably used for
D(EO)D	SW-, HW-Kraft
D(EOP)D	SW-, HW-Kraft
DEDED	SW-, HW-Kraft
D(EO)DED	SW-, HW-Kraft
D(EO)DD	SW-, HW-Kraft
OD(EO)D	SW-, HW-Kraft
OD(EOP)D	SW-, HW-Kraft
ODEDED	SW-, HW-Kraft
OD(EO)DED	SW-, HW-Kraft
OD(EO)DD	SW-, HW-Kraft
OQ(OP)(DQ)(PO)	SW-, HW-Kraft
OD*(EO)D	HW-Kraft
OA*D(EO)D	HW-Kraft
O(AD)*(EO)D	HW-Kraft
O(DQ)*(PO)	HW-Kraft

\* Denotes treatment with high temperature and prolonged retention time.



Bleaching of a softwood kraft pulp to full brightness (89+% ISO) is best accomplished by a sequential treatment of two chlorine dioxide steps,  $D_1$  and  $D_2$ , because it is more efficient to split the chlorine dioxide charge into two stages. The bleaching efficiency is further enhanced, when the  $D_1$  stage is followed by an alkaline extraction stage, preferably including interstage washing. To attain a particular brightness (e.g., 90% ISO), the minimum total amount of chlorine dioxide consumption is obtained when 25% of it is applied in the  $D_2$  stage (Fig. 7.62). The minimum is slightly shifted to a higher share of chlorine dioxide consumption in the  $D_2$  stage while raising the final brightness target.

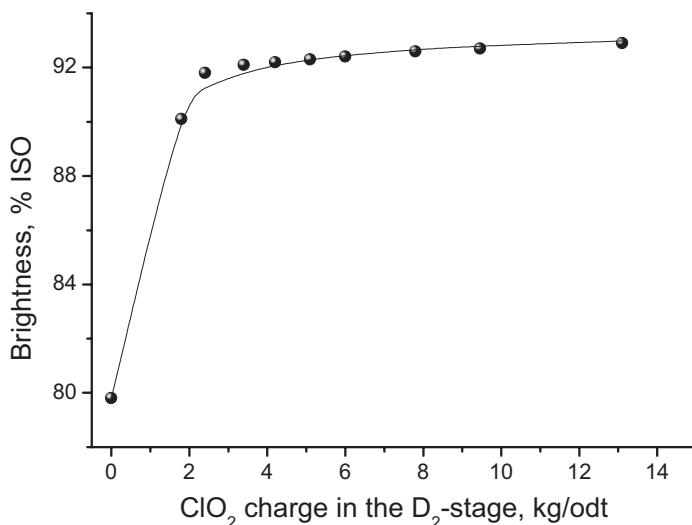


**Fig. 7.62** Effect of chlorine dioxide distribution between the  $D_1$  and  $D_2$  stages of a CEDED sequence on the total chlorine dioxide consumption in bleaching a softwood kraft pulp to attain a final brightness of 90% ISO (according to [3]).

The task of chlorine dioxide bleaching in the final bleaching sequence is to remove selectively the chromophores. The increase in brightness can be described as occurring in two distinct steps: a very rapid and short increase, followed by a much longer and slower period of reaction where the rate of decrease of the chromophores almost approaches zero. The course of brightness increase is illustrated in Fig. 7.63.

The brightening in the  $D_2$  stage responds to chlorine dioxide charge according to the following type of expression:

$$B_{D_2} = B_{D_1} + \Delta B_{\max} \cdot \left( 1 - \frac{1}{(1 + a \cdot ClO_2 ch)^b} \right)$$



**Fig. 7.63** Effect of D<sub>2</sub> stage on the brightness of a softwood kraft pulp bleached in a D<sub>0</sub>(EO)D<sub>1</sub>ED<sub>2</sub> sequence.

where  $B_{D_2}$  is the final brightness after D<sub>2</sub> treatment, and  $B_{D_1}$  is the initial brightness before ClO<sub>2</sub> addition. The term  $\Delta B_{\max}$  is the brightness increase at infinite ClO<sub>2</sub> addition. The sum of  $B_{D_1}$  and  $\Delta B_{\max}$  represents the maximum achievable brightness for the D<sub>2</sub> stage (“brightness ceiling”); a and b are constants.

The typical bleaching conditions in D<sub>1</sub> and D<sub>2</sub> stages are listed in Tab. 7.34. The amount of active chlorine required to attain full brightness is linearly related to the kappa number of the pulp entering the D<sub>1</sub> stage (after, e.g., the DE stage). The chlorine dioxide charge can thus be estimated by measuring the E<sub>1</sub> kappa number.

The brightness gain in the final D stage is different for hard- and softwood kraft pulps. In most cases, the latter requires less chlorine dioxide to target full brightness. Further information on the performance of chlorine dioxide in the final bleaching stages is available elsewhere [3].

As mentioned previously, the pH profile has a major effect in determining the efficiency of chlorine dioxide bleaching. During such bleaching, the pH is decreased considerably during the first reaction phase due to the formation of organic and hydrochloric acids. Hence, sodium hydroxide must be added to maintain the optimal end pH in the range between 3 and 3.5 (D<sub>0</sub>). According to Reeve and Rapson, approximately 0.6 kg NaOH odt<sup>-1</sup> should be added for each kg ClO<sub>2</sub> odt<sup>-1</sup> charged to the pulp to ensure an optimal end pH [3].

The final D stage is usually run with an excess amount of chlorine dioxide to ensure a chlorine dioxide residual at the end of the stage. The chlorine dioxide concentration in the filtrate of the pulp suspension leaving the final D stage is maintained at between 10 and 50 ppm, and this ensures that both the brightening

Tab. 7.34 Examples of typical chlorine dioxide bleaching sequences.

Substrate	Unit	Stage	
		D <sub>1</sub>	D <sub>2</sub>
Consistency	%	10–14	11–14
Time	min	120–240	120–240
Temperature	°C	70	70–85
Pressure		atmospheric	atmospheric
Charge			
SW-Kraft	<sup>a</sup>	3–8	1–4
HW-Kraft	<sup>a</sup>	3.5–10	1.5–5
Final pH		3.5–5	3.5–5.0

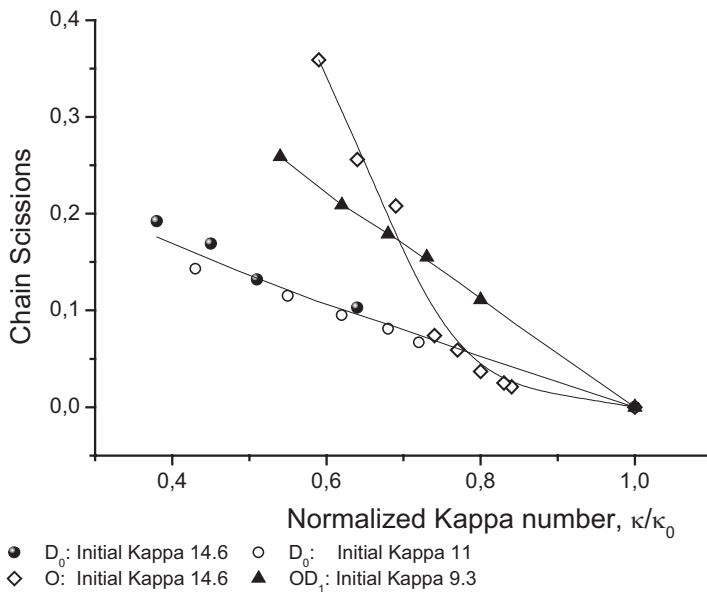
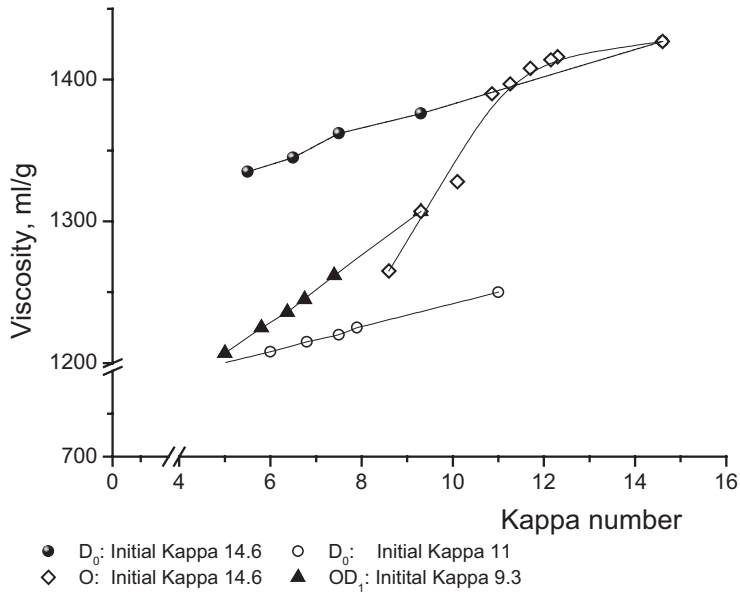
a. Multiple of the kappa number after the E-stage as active chlorine per ton of pulp.

reaction and shive removal continue. This is very important because cleanliness is characteristic for chlorine dioxide-bleached pulps. After the final bleaching stage, the residual chlorine dioxide must be converted to less harmful products. This is accomplished by the addition of either sulfur dioxide-containing water or by sodium hydroxide to increase the pH to about 7. In both cases, chlorine dioxide is reduced to chlorite and further reduced chlorine-containing compounds which are nonvolatile and much less corrosive than chlorine dioxide.

An overview of selected data on the performance of chlorine dioxide in ECF bleaching sequences of both hardwood and softwood kraft pulps is provided in Tab. 7.35 (see below).

#### 7.4.5.2 Chlorine Dioxide Bleaching of Oxygen-Delignified Kraft Pulps

The main advantage of chlorine dioxide bleaching is undoubtedly its high bleaching efficiency and selectivity. In numerous studies it has been shown that the selectivity of chlorine dioxide is largely independent of the kappa number and viscosity entering the D<sub>0</sub> stage when applied to an unbleached pulp. Due to environmental restrictions for bleach plant effluents and lower overall pulp manufacturing costs, kraft pulps – even hardwood kraft pulps – are increasingly pre-delignified in an oxygen delignification stage. The reactive species in oxygen delignification, however, compete with the same type of lignin structures as those in chlorine dioxide bleaching [4]. Consequently, the residual lignin after an oxygen stage is more resistant to chlorine dioxide as compared to the residual lignin of an unbleached kraft pulp. Barroca et al. demonstrated that the more pronounced



**Fig. 7.64** Comparison of the selectivity of oxygen delignification (O) and bleaching of both an unbleached chlorine dioxide ( $D_0$ ) and oxygen pre-delignified *E. globulus* kraft pulp ( $OD_0$ ) (according to [5]). Unbleached kraft pulps: Kappa numbers 14 and 11, viscosities  $1427 \text{ mL g}^{-1}$  and  $1250 \text{ mL g}^{-1}$ , respectively.

D stage:  $55^\circ\text{C}$ , 3% chlorine dioxide charge, maximum reaction time, 30 min. O stage:  $95^\circ\text{C}$ ,  $10 \text{ kg NaOH odt}^{-1}$ , 8 bar, maximum reaction time, 120 min.

degradation of polysaccharides during an OD-sequence (means oxygen delignification followed by chlorine dioxide treatment) cannot be attributed to the action of oxygen alone [5]. The selectivity of chlorine dioxide bleaching using an oxygen pre-delignified kraft pulp made from *E. globulus* decreases considerably with increasing extent of delignification in the oxygen stage (Fig. 7.64a,b). At a level of 40% delignification, the number of chain scission is doubled when chlorine dioxide is applied to an oxygen pre-delignified hardwood kraft pulp as compared to an untreated pulp of the same provenance. Additionally, chlorine dioxide reactions with oxidized lignin structures promote chlorate formation, as previously presented [6].

Surprisingly, oxygen delignification behaves rather selectively in the initial phase, which concludes that the best selectivity of an OD sequence can be obtained if oxygen delignification is limited to a very short reaction time of about 5–10 min. However, using an *E. eucalyptus* kraft pulp, only 25% of lignin can be removed during the first delignification phase. Therefore, the decision must be made from case to case whether the additional investment costs for this short delignification stage would be more profitable than the higher bleaching costs of a conventional pre-delignification  $D_0$  stage.

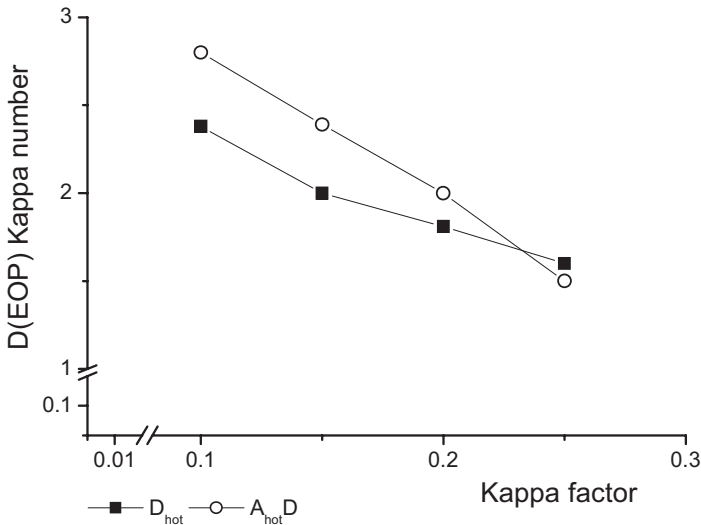
#### 7.4.5.3 Modified Chlorine Dioxide Bleaching

During the delignification process in alkaline pulping, double bonds are generated by methanol elimination from 4-*O*-methylglucuronic acid on the xylan [7]. The first indication of the source of these double bonds was the identification of 2-furancarboxylic acid as main product of its hot acid hydrolysis by Maréchal [8] (see Section 7.8, Hot acid hydrolysis). Bleaching chemicals with a reactivity towards double bonds are consumed by HexA. Consequently, the detection of HexA was directly followed by an evaluation of the different options for their removal and an analysis of the resulting savings in bleaching chemical. Hot acid hydrolysis with a retention time of about 2 h at  $>90^\circ\text{C}$  and a pH below 3 degrades HexA and lowers the kappa number. However, the resulting decrease in the demand for chlorine dioxide is moderate. Potential savings [9] of 1.5% active chlorine in hardwood pulp bleaching and 0.8% active chlorine in softwood pulp bleaching are too small to pay for the investment in a huge tower and an additional washing step. Additional costs result from the demand for up to 0.5 tons of (low-pressure) steam to heat the pulp to the required hydrolysis temperature.

In ECF bleaching a logical consideration was to combine the first chlorine dioxide stage ( $D_0$ ) with the acid hydrolysis ( $A_{\text{hot}}$ ). Both treatments require an acidic pH. The typical temperature in a chlorine dioxide stage at the beginning of an ECF sequence is 50–60 °C. The application of chlorine dioxide at even higher temperature is not a problem, because chlorine dioxide is a rather selective chemical. For the addition point for chlorine dioxide, two options exist – it could be added either at the start or at the end of a hydrolysis step. In theory, both options have advantages and disadvantages. Adding chlorine dioxide at the start of an acid hydrolysis stage will lead to a consumption of  $\text{ClO}_2$  not only by lignin but also by HexA, and therefore savings in the demand for chlorine dioxide will be difficult to

verify. However, the same is valid for adding chlorine dioxide (without intermediate washing) after an hydrolysis treatment. The products of the hydrolysis are 2-furancarboxylic acid and 2-furaldehyde-5-carboxylic acid [10]. These water-soluble compounds react very rapidly with  $\text{ClO}_2$ . If  $\text{ClO}_2$  is added to an unwashed pulp after a hydrolysis treatment, it will react therefore not only with lignin but also with the hydrolysis products. Consequently, neither combination will allow full advantage to be taken of the hydrolysis and chlorine dioxide to be saved.

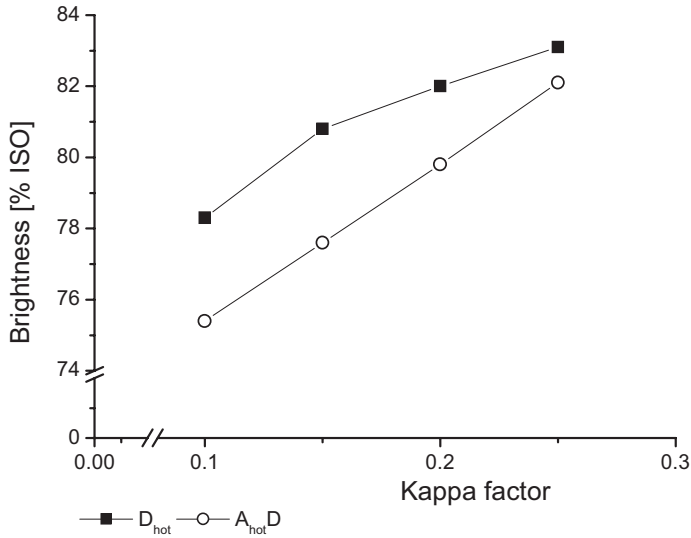
A comparison of these approaches to combine hot acid hydrolysis with chlorine dioxide treatment shows visible differences (Figs. 7.65–7.67) [11]. Figure 7.65 illustrates the resulting kappa numbers analyzed after a subsequent EOP stage. There is a visible disadvantage of adding  $\text{ClO}_2$  to the pulp containing hydrolysis products, as the reaction of  $\text{ClO}_2$  with 2-furancarboxylic acid or lignin is clearly rapid. This is certainly also affected by the water solubility of the furan compound and the need for  $\text{ClO}_2$  to diffuse into the fiber in order to oxidize the lignin. These results contradict those of Juutilainen [12], who reported a slow reaction of the hydrolysis compounds with  $\text{ClO}_2$ , but did not compare both alternatives. This disadvantage of  $A_{\text{hot}}/D$  compared to  ${}_{\text{hot}}D_0$  only disappears at very high chlorine dioxide input. With high availability of chlorine dioxide, the kappa numbers become identical. Starting with  $\text{ClO}_2$  is a clear advantage, as it reacts more rapidly with lignin than with HexA. Thus, after the rapid consumption of  $\text{ClO}_2$ , sufficient HexA sites are left to be removed by hydrolysis.



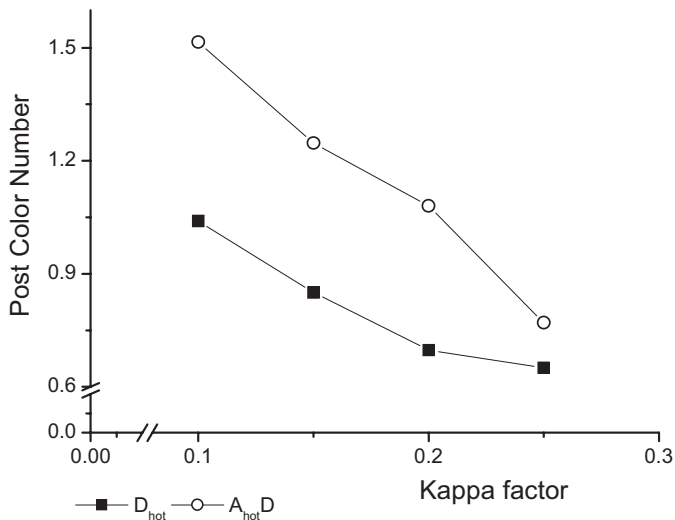
**Fig. 7.65** Effect of increasing addition of  $\text{ClO}_2$  on delignification in a hot  $D_0$  treatment. Oxygen-delignified eucalyptus kraft pulp (kappa 10). Hot  $D_0$  with  $\text{ClO}_2$  addition initially, 2 h at 95 °C, pH 3.  $A_{\text{hot}}/D$  with 110 min hydrolysis

time at pH <3 followed by  $\text{ClO}_2$  addition and additional 10 min reaction time, all at 10% consistency. EOP remained constant with 1.4% NaOH, 0.4%  $\text{H}_2\text{O}_2$ , at 85 °C, 0.3 MPa  $\text{O}_2$  pressure for 0.5 h, 1 h without pressure [11].

This effect on kappa number is mirrored by the development of brightness. The more effective reaction with lignin lowers the number of colored sites and increases brightness, which again is most obvious at low active chlorine input (Fig. 7.66).



**Fig. 7.66** Impact of addition of ClO<sub>2</sub> in the hot D<sub>0</sub> stage or in an A<sub>hot</sub>/D treatment on EOP brightness. For conditions, see Fig. 7.65 [11].

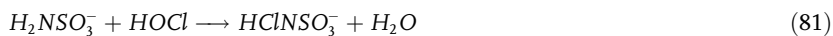


**Fig. 7.67** Impact of addition of ClO<sub>2</sub> in the hot D<sub>0</sub> stage or in an A<sub>hot</sub>/D treatment on EOP brightness stability (post color number). For conditions, see Fig. 7.65. Analysis of reversion with humid aging (2 h, 100 °C, 100% humidity) [11].

The higher brightness of the hot D<sub>0</sub>-EOP treatment in addition shows a higher stability. The data in Fig. 7.67 compare the resulting post color numbers. At low active chlorine input, the improvement is very pronounced. Even following the addition of a higher input of chlorine dioxide (high kappa factor), the advantage of keeping the chlorine dioxide treated pulp at very high temperature is still pronounced. It is a safe assumption that, at this temperature level, all chlorine dioxide added will be consumed within a few seconds. Therefore, the obvious advantage of keeping the pulp after the reaction with ClO<sub>2</sub> for an extended time at above 90 °C must have its background in additional reactions. In chlorine dioxide delignification, one may speculate that the degradation processes involve quinones as intermediates. Quinones are not stable molecules and, provided that the temperature is sufficiently high, they will react further. For example, hydrochloric acid or methanol – both compounds are present in a D stage – add to quinones in a 1,4 addition. The resulting hydroquinones can be reoxidized to another quinone. The very visible differences in AOX load are in support of this theory of additional oxidation and degradation reactions.

This hot chlorine dioxide process – which is sometimes denoted as D\*-stage and marketed as the DUALD™ process – enables an overall reduction of the AOX discharge by approximately 50%, presumably through an accelerated degradation of chlorinated structures formed in this stage to, for example, harmless chloride ions [13,14]. Moreover, when bleaching an oxygen-delignified eucalyptus kraft pulp to full brightness, the demand for chlorine dioxide could be reduced from 33 kg a.Cl odt<sup>-1</sup> to 23 kg a.Cl odt<sup>-1</sup> when replacing a conventional D<sub>0</sub> by a D\* stage in a D(EO)D sequence. The organic chlorine content of the pulp (OX), however, is not reduced in such trials, because the second D stage – which is conducted at the conventional level of 75 °C – causes a repeated production of halogenated compounds. Ragnar and Törngren have shown that the chlorination of the pulp (and thus OX formation) is related to the presence of elemental chlorine which is formed *in situ* during chlorine dioxide bleaching [13]. One way to reduce the OX level is to perform a subsequent alkaline extraction; this may be rather effective in terms of brightness increase and OX reduction if applied at the hydrogen peroxide stage [15].

Alternatively, the addition of sulfamic acid to a final D stage provides an efficient means of reducing the OX content in the pulp by almost 50%. Sulfamic acid acts as a chlorine/hypochlorous acid scavenger to form chlorosulfamic acid according to the following expression:



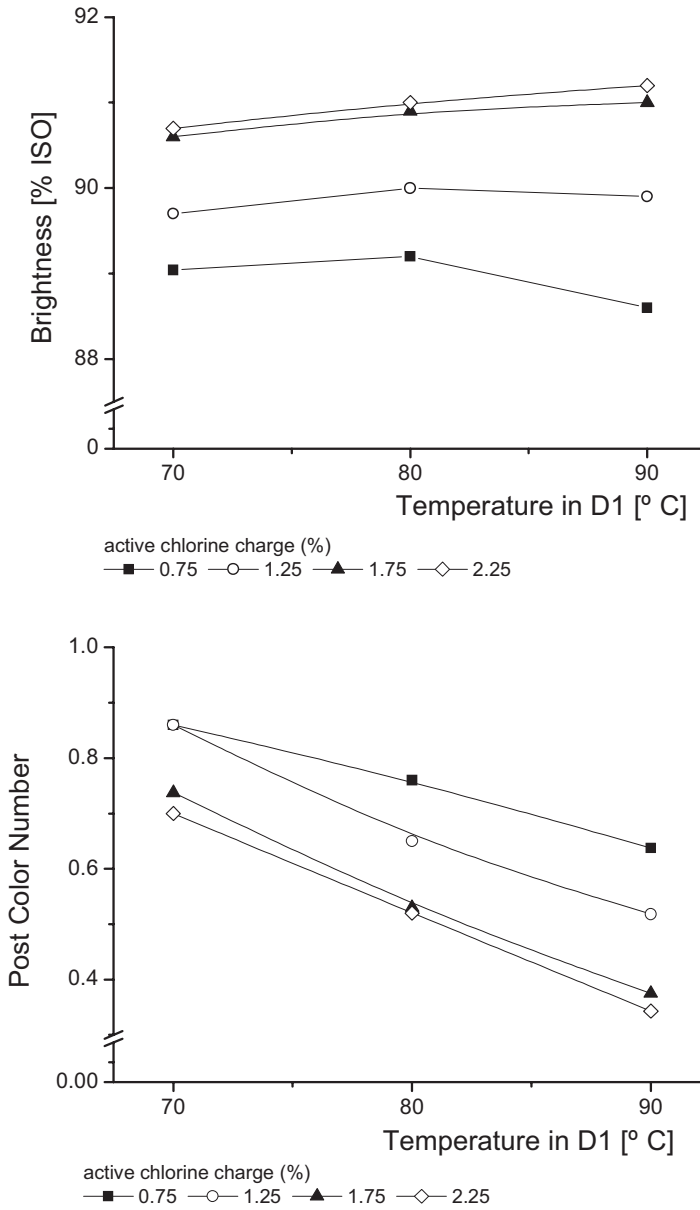
The oxidizing power of chlorine dioxide decreases (by about 20%) due to the capture of elemental chlorine by sulfamic acid. The drawback of a hot chlorine dioxide treatment (D\*) is the lower selectivity as compared to a conventional D stage. Replacing a conventional D (20 min at 70 °C) by a hot D\* stage (120 min at 90 °C) using an oxygen-delignified hardwood kraft pulp, kappa number 10.9, viscosity 1021 mL g<sup>-1</sup>, leads to an increase in the number of chain scissions from



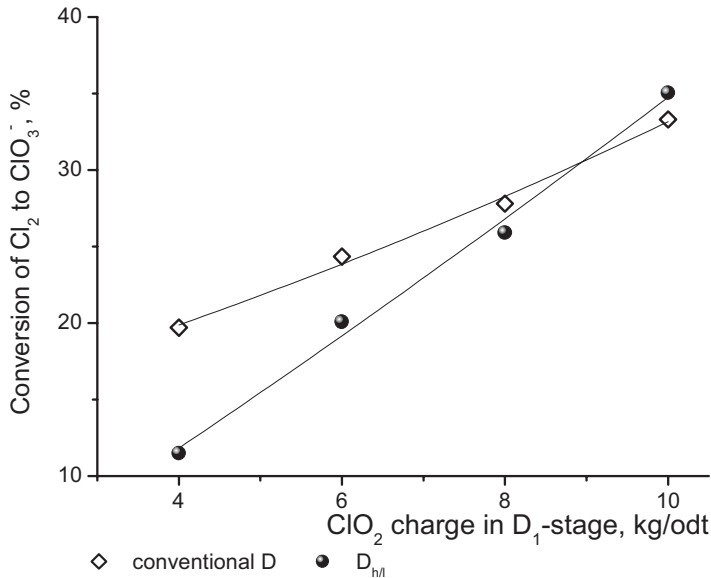
$0.224 \times 10^{-4}$  to  $0.527 \times 10^{-4}$  mol AGU<sup>-1</sup>, while the kappa number reduction over the D stage increases from 4.7 to 6.3 [14]. Considering the significantly higher efficiency of the D\* stage, the overall extent of cellulose degradation remains quite moderate in comparison to conventional chlorine dioxide bleaching. The increase of temperature from 70 °C to 90 °C, and prolongation of the reaction time from 20 min to 120 min during a first chlorine dioxide stage, is significantly more detrimental to the viscosity of a softwood kraft pulp as compared to that of a hardwood kraft pulp. Ragnar has shown in an example using an oxygen-delignified softwood kraft pulp, kappa number 12.9, viscosity 984 mL g<sup>-1</sup> that, when changing from conventional chlorine dioxide conditions to those characteristic for a D\* stage, the number of chain scissions increases from almost zero to  $0.83 \times 10^{-4}$  mol AUG<sup>-1</sup>, while the kappa number reduction over the D stage increased only by one unit, from about 7.3 to 8.3 [14]. A slight improvement in selectivity can be obtained when the hot chlorine dioxide stage is supplemented by a prestage without an interstage washing, carried out at a conventional temperature of about 60 °C with very short retention time of about 3–6 min, while preserving the beneficial effects of a D\* stage [16].

A high temperature in the final chlorine dioxide stage improves brightness stability [11]. Clearly, intermediates of chlorine dioxide bleaching are degraded and the precursors of potential chromophores are destroyed. Figure 7.68 illustrates the impact of temperature on brightness and reversion, where an oxygen-delignified pulp was pretreated with a hot D<sub>0</sub> and an EOP stage. The positive impact of a higher temperature on brightness stability already becomes visible with only a low input of active chlorine. At a higher input of chlorine dioxide, the effects are even more pronounced. Figure 7.68(a) also illustrates the potential of applying only three bleaching stages to reach full brightness. However, the need for a high input of chemical in the D<sub>1</sub> stage to guarantee >90 %ISO brightness is clear. If the brightness target is 89–90% ISO, then three bleaching stages are sufficient. Brightness stability is even more improved when the hot D<sub>1</sub> stage is followed by a final peroxide stage (see Section 7.6, Peroxide bleaching). With the D<sub>0</sub>-EOP-D<sub>1</sub>-P sequence, a brightness of >92% ISO and post color numbers as low as 0.1 are achieved.

Seger et al. found that the efficiency of chlorine dioxide bleaching can be improved by using a two-step process, denoted as D<sub>h/l</sub>, comprising a first stage for 5–15 min at an end pH of 6–7.5, and a long second stage for 150 min at an end pH of 3.5–4.0 [17]. Results obtained for OD(EOP)D and D(EO)D sequences indicate that the use of the D<sub>h/l</sub>-technology in both the D<sub>0</sub> and/or D<sub>1</sub> positions increases final brightness at a given charge of chlorine dioxide, provided that the pulp entering the D stage has a kappa number below 10. The D<sub>h/l</sub> concept is particularly efficient when applied in bleaching stages following an oxygen prebleaching stage. The results include higher final brightness and chemical savings of 4 kg ClO<sub>2</sub> odt<sup>-1</sup>, which equals a ClO<sub>2</sub> reduction of more than 20% (Tab. 7.35). The improved performance of the high/low-pH method appears to be due to a considerable reduction in chlorate formation (Fig. 7.69). Comparing the chlorate concentration at a given D<sub>1</sub> brightness, an even higher reduction (up to 45% at 78.3% ISO) can be observed using D<sub>h/l</sub> as compared to conventional chlorine dioxide



**Fig. 7.68** Impact of active chlorine amount and temperature in a D<sub>1</sub> stage on (a) brightness development and (b) brightness reversion in humid aging. Pre-bleaching with high kappa factor (0.25) in hot D<sub>0</sub> [11].



**Fig. 7.69** Chlorate formation as a function of  $\text{ClO}_2$  charge in  $D_1$  stage for a CE-prebleached softwood kraft pulp of kappa number 4.4 (according to [17]).  $D_1$  conventional: 10% consistency, 180 min, 70 °C, end pH 1.4–4.  $D_{n/1}$ : first stage: 10% consistency, 5–15 min, 70 °C, end pH 6–7.5, second stage: 10% consistency, 150–174 min, 70 °C, end pH 3.5–4.0.

bleaching. The lower chlorate formation during high/low-pH chlorine dioxide bleaching is, however, not reflected in a lower AOX formation. The generation of organochlorine compounds is seen to be comparable for D stages carried out conventionally or using the two-step technique [17].

The advantage of the two-step chlorine dioxide bleaching process over the conventional one-step technology with respect to chlorate formation diminishes with increasing kappa number prior  $D_1$  stage. It may thus be speculated that the decreasing efficiency of the two-step approach can be attributed to the changing structure of the residual lignin.

Ljunggren et al. introduced a two-step chlorine dioxide bleaching concept where the first step operates at low and the second at high pH levels, providing lower levels of AOX and OX than conventional one-stage chlorine dioxide bleaching [18]. In the first step, the pH is adjusted to about 2.8 for only 30 s after which, in the second step, the pH is raised by injection of alkali to about pH 10 for about 60 min. To avoid complete consumption of chlorine dioxide during only the first stage, two-thirds of the chlorine dioxide is charged in the first step, and one-third in the second step. The effect of chlorine dioxide bleaching with a two-step, low-to-high pH profile was investigated in the first D stage of a D(EOP)DD sequence using a pre-delignified pine kraft pulp, kappa number 12 and intrinsic viscosity 1020 mL g<sup>-1</sup> [18]. Under the most favorable conditions, comprising a pH profile from 2.8 to 10 at a kappa factor of 0.18, the AOX load in the  $D_1E$  effluents could

Tab. 7.35 Overview of literature data on the efficiency of chlorine dioxide in ECF bleaching sequences of kraft pulps.

Pulp	Sequence	kappa no.	Unbleached Pulp HexA [mmolkg <sup>-1</sup> ]	Pulp viscosity [ml g <sup>-1</sup> ]	Kappa before D [ml g <sup>-1</sup> ]	Kappa factor	D <sub>0</sub> ClO <sub>2</sub>	Chemical charges [kg odt <sup>-1</sup> ]						Total OXE
								NaOH	E <sub>1</sub> EO(P)	D <sub>1</sub> +D <sub>2</sub> ClO <sub>2</sub>	NaOH	E <sub>2</sub> H <sub>2</sub> O <sub>2</sub>	H <sub>2</sub> O <sub>2</sub>	
SW-Kraft	D(EO)DED	29.5		1130	29.5	0.22	24.7	20.0	0.0	15.0	5.0	0.0	0.0	2942
SW-Kraft	D(EOP)DED	29.5		1130	29.5	0.22	24.7	20.0	3.0	12.0	5.0	0.0	0.0	2896
SW-Kraft	D(EO)DED	29.5		1130	29.5	0.28	31.4	24.0	0.0	12.0	5.0	0.0	0.0	3218
SW-Kraft	D(EOP)DED	29.5		1130	29.5	0.28	31.4	20.0	3.0	9.5	5.0	0.0	0.0	3209
HW-Kraft	D(EO)DED	16.5		1015	16.5	0.22	13.8	16.7	0.0	11.0	5.0	0.0	0.0	1839
HW-Kraft	D(EOP)DED	16.5		1015	16.5	0.22	13.8	16.7	3.0	9.0	5.0	0.0	0.0	1867
HW-Kraft	D(EO)DED	16.5		1015	16.5	0.26	16.3	17.2	0.0	9.0	5.0	0.0	0.0	1877
HW-Kraft	D(EOP)DED	16.5		1015	16.5	0.26	16.3	17.2	3.0	8.0	5.0	0.0	0.0	1979
HW-Kraft	ODEOPDD	14.6	33	1031	7.8	0.25	7.4	12.0	3.0	9.5	0.0	0.0	0.0	1428
HW-Kraft	ODEOPDD	15.0		1090	9.5	0.22	7.9	13.6	3.0	6.1	0.0	0.0	0.0	1216
SW-Kraft	ODEOPD	16.3			7.8	0.34	10.0	13.1	2.0	7.0	0.0	0.0	0.0	1375
SW-Kraft	OD <sub>h/f</sub> EOPD	16.3			7.8	0.34	10.0	13.1	2.0	3.0	0.0	0.0	0.0	1079
SW-Kraft	DEODD	17.0			17.0	0.25	16.2	21.0	0.0	5.0	0.0	0.0	0.0	1569
SW-Kraft	D <sub>h/f</sub> EOD <sub>h/f</sub>	17.0			17.0	0.25	16.2	21.0	0.0	5.0	0.0	0.0	0.0	1569
HW-Kraft	ODEDED				9.8	0.22				2.0				756
HW-Kraft	OD*EDED				9.8	0.22				2.0				756

Tab. 7.35 Continued.

Pulp	Sequence	Pulp properties				Final bleached pulp			Chain scissions, $\times 10^4$ [mol AGU <sup>-1</sup> ] overall after O	Reference
		D(EO) pulp kappa no.	$\Delta\kappa/\Delta\text{ClO}_2$	brightn % ISO	HexA [mmol kg <sup>-1</sup> ]	viscosity [mL g <sup>-1</sup> ]	AOX [kg odt <sup>-1</sup> ]			
SW-Kraft	D(EO)DED	4.4	1.02	89.6		1050	1.9	0.288	Lachapelle et al. [1]	
SW-Kraft	D(EOP)DED	3.4	1.06	90.8		1050	1.9	0.288	Lachapelle et al. [1]	
SW-Kraft	D(EO)DED	3.3	0.83	90.9		1050	2.0	0.288	Lachapelle et al. [1]	
SW-Kraft	D(EOP)DED	2.6	0.86	91.2		1050	2.0	0.288	Lachapelle et al. [1]	
HW-Kraft	D(EO)DED	4.0	0.91	89.9		920	0.4	0.452	Lachapelle et al. [1]	
HW-Kraft	D(EOP)DED	2.4	1.02	90.8		920	0.4	0.452	Lachapelle et al. [1]	
HW-Kraft	D(EO)DED	2.4	0.86	90.3		920	0.4	0.452	Lachapelle et al. [1]	
HW-Kraft	D(EOP)DED	1.8	0.90	92.3		920	0.5	0.452	Lachapelle et al. [1]	
HW-Kraft	ODEOPDD	3.6	0.57	89.9	3.3	763	n.a.	1.559	Sixta [32]	
HW-Kraft	ODEOPDD	3.9	0.71	87.9		817	n.a.	1.375	Sixta [32]	
SW-Kraft	ODEOPD			87.5					Seger et al. [17]	
SW-Kraft	OD <sub>h/l</sub> EOPD			88.0					Seger et al. [17]	
SW-Kraft	DEODD	1.9	0.93	87.5					Seger et al. [17]	
SW-Kraft	D <sub>h/l</sub> EODh <sub>l</sub>	2.2	0.92	86.4					Seger et al. [17]	
HW-Kraft	OEDEDED	n.a.		89.4		975	0.41		Ragnar & Törngren [13]	
HW-Kraft	OD*EDED	n.a.		89.9		937	0.23		Ragnar & Törngren [13]	

n.a. = not analyzed.

be lowered from 0.33 to 0.13 kg odt<sup>-1</sup>. It is of interest to note that applying the modified pH profile in the D<sub>1</sub> stage does not result in a higher total chlorine dioxide demand to achieve a full brightness of about 90% ISO, despite a considerable increase in the kappa number after the E stage as compared to a conventional one-step chlorine dioxide bleach. Results with lignin-model studies have revealed that the chlorination of nonphenolic lignin structures is highly affected by the pH of the chlorine dioxide treatment. The extent of chlorination reactions decreases considerably when the pH is increased beyond 5.5. These results led to the conclusion that chlorine dioxide bleaching at low pH promotes delignification, while chlorination diminishes at high pH. The AOX load in the DE-effluents can also be reduced by eliminating washing between the D<sub>1</sub> and extraction stages; this is known as the Ultim-O process, and was proposed by Cook [19]. The approach shows a similar reduction of AOX but, due to the avoidance of interstage washing, the OX level in the pulp is much higher than compared to the two-step procedure.

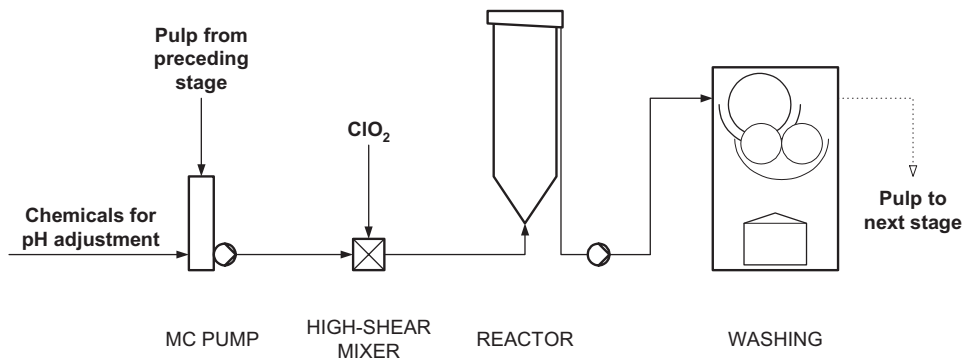
The effectiveness of chlorine dioxide in delignification can be improved by an addition of aldehydes [20]. The reaction of an aldehyde with the intermediate reaction product chlorite regenerates active chlorine dioxide and increases the delignification rate. The addition of formaldehyde or other aldehyde compounds improves the kappa number reduction by 20–35%.

#### 7.4.6

#### Technology of Chlorine Dioxide Bleaching

*Andreas W. Krotscheck*

The process flowsheet of a typical chlorine dioxide bleaching system is illustrated schematically in Fig. 7.70. Medium-consistency pulp coming from the previous bleaching stage drops into a standpipe and is mixed with chemicals for pH adjustment as it enters the medium-consistency pump. Sulfuric acid or spent liquor from the chlorine dioxide generation plant can be used to lower the pH, whilst caustic soda is applied if the pH needs to be raised.



**Fig. 7.70** Process flowsheet of a typical chlorine dioxide bleaching system.

The pump forwards the pulp suspension to a high-shear mixer which is charged with the chlorine dioxide solution. Mixing chlorine dioxide into the pulp slurry is rather unproblematic due to the dilute solution and long reaction time. Whilst in older installations the chlorine dioxide was added to the housing of the MC pump, the current state of the art is high-shear mixing with moderate power dissipation.

The pulp suspension proceeds from the mixer to an atmospheric upflow reactor, where the bleaching reaction takes place. Previously, chlorine dioxide bleaching was sometimes carried out in upflow-downflow reactor combinations, where the smaller upflow section was responsible for keeping the volatile chlorine dioxide in solution under hydrostatic pressure, while the larger downflow section was used to complete the reactions. A downflow reactor in the bleaching sequence has some operational advantages because of its capability to buffer a certain pulp volume during upsets. Depending on the feed requirements of the subsequent washing equipment, the pulp slurry is discharged from the reactor either at low or medium consistency.

Washing after a chlorine dioxide stage is usually carried out with single-stage washing equipment, for example with a wash press, a single-stage Drum Displacer™, an atmospheric diffuser, or a vacuum drum washer. The vent gases from the chlorine dioxide stage equipment and tanks must be collected and scrubbed to remove chlorine and chlorine dioxide. Scrubbing is often performed using an alkaline bleaching liquor.

The preferred material of construction for the wetted parts in a chlorine dioxide stage is titanium, but a high-molybdenum austenitic stainless steel may also be appropriate. The towers are frequently tile-lined.

Further information regarding chlorine dioxide bleaching equipment, including medium consistency pumps, mixers and atmospheric reactors is provided in Section 7.2, while details of pulp washing are collected in Chapter 5.

#### 7.4.7

#### **Formation of Organochlorine Compounds**

The negative environmental impact associated with the use of elemental chlorine is primarily related to the formation of chlorinated organic compounds. A large variety of individual chlorinated compounds are formed during the chlorination reactions, and the major part of these are released to the aqueous phase where they are summarily detected as AOX (adsorbable organic compounds). Another part of the chlorinated organic compounds remains in the bleached pulp; this is denoted organic chlorine content, known as OCl or OX. The AOX fraction can be classified into two categories of different molecular weight: (a) The high molecular fraction (molecular weight >1000 Da), which constitutes about 80% of the AOX and contains mainly hydrophilic and nonaromatic compounds; and (b) the low molecular fraction, which consists of highly chlorinated compounds (e.g., polychlorinated phenolic compounds, etc.) that are potentially problematic and toxic to aquatic organisms due to their ability to penetrate cell membranes. The substitution of elemental chlorine with 100% chlorine dioxide during the first

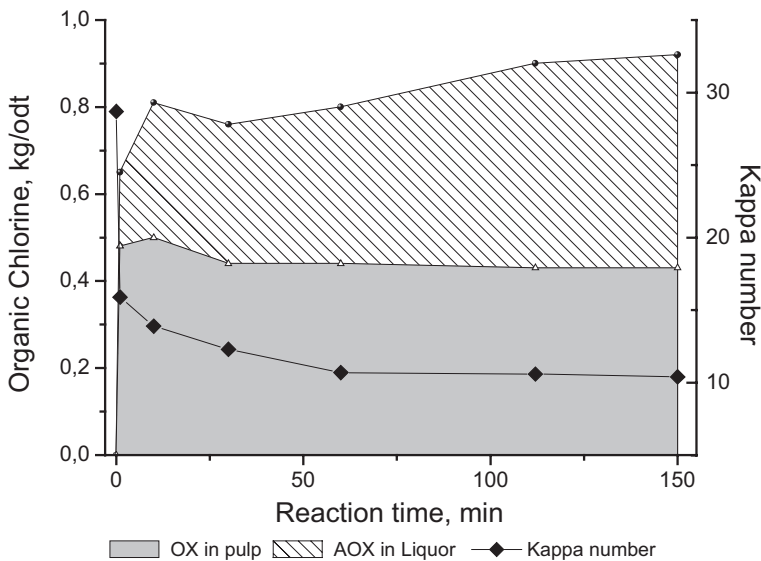
bleaching stage ( $D_0$ ) significantly reduces AOX formation, and virtually eliminates levels of polychlorinated phenols in the final effluents to below the limits of analytical detection [21]. The generation of organically bound chlorine is linearly related to the charge of active chlorine according to the following expression [22]:

$$\text{AOX} = 0.1 \cdot \left( C + \frac{D}{5} \right) \quad (82)$$

where AOX is adsorbable organic compounds (in  $\text{kg odt}^{-1}$ ),  $C$  is the amount of chlorine (in  $\text{kg odt}^{-1}$ ), and  $D$  is the amount of chlorine dioxide (in  $\text{kg}$ , calculated as active chlorine  $\text{odt}^{-1}$ ).

Equation (82), which is valid for softwood kraft pulps, indicates that chlorine dioxide introduces only about one-fifth of the AOX formed during chlorine bleaching. In the case of hardwood kraft pulps, less AOX is generated due to the different chemical structure of hardwood lignin (syringyl units) as compared to softwood lignin (guaiacyl units). The amount of AOX evolving from chlorine and chlorine dioxide bleaching of hardwood kraft pulps can be estimated from Eq. (82) by replacing the factor 0.1 through 0.05 to 0.08, depending on the hardwood species and reaction conditions.

Almost all of the chlorinated organic substances in the effluent of a multi-stage ECF sequence comprising at least two D stages are formed in the  $D_0$  and  $E_1$  stages. Kinetic studies have revealed that the generation of organic chlorine occurs very rapidly [23], with the final amount of total chlorinated organic material (AOX+OX) being produced within the first 10 min of reaction with chlorine dioxide (Fig. 7.71).



**Fig. 7.71** Kinetics of organic chlorine formation (AOX and OX) during  $D_0$  treatment of spruce kraft pulp, kappa number 28.7 (according to [23]).  $D_0$  conditions: 45 °C, 1% consistency, kappa factor 0.22.

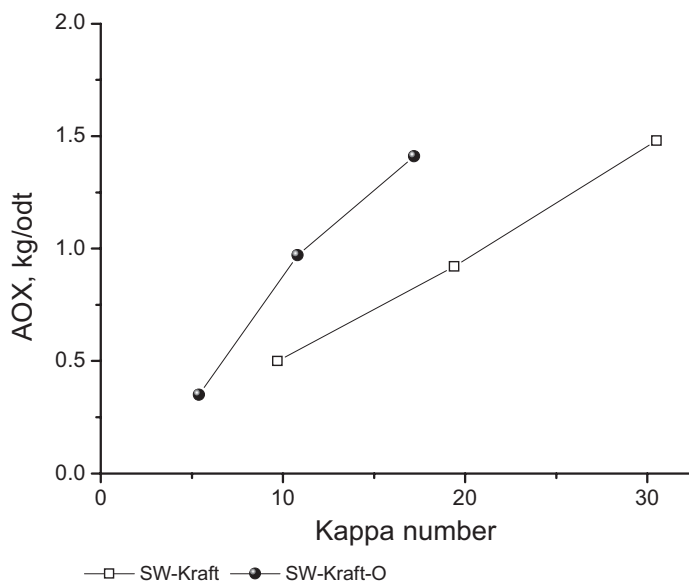


The data in Fig. 7.71 show that all the organic chlorine attached to the pulp (OX) is formed within a very short time, while the increase in AOX in the bleaching filtrate is predominantly due to increasing solubility of the chlorinated lignin in the pulp throughout chlorine dioxide treatment. The same study revealed that 86% of the sum of AOX and OX originates from the reaction with hypochlorous acid which is formed *in situ* through the step-wise reduction of chlorine dioxide [see Eqs. (61), (63) and (64)]. Hypochlorous acid reacts with the chemical structures present in lignin in a different way as compared to elemental chlorine, which is created simply by shifting the pH below 2 [Eq. (66)]. In principle, the extent of chlorination is lower for reactions with hypochlorous acid as compared to those with elemental chlorine. As an example, hypochlorous acid reacts with olefinic structures to form chlorohydrin, while chlorine converts them to dichlorinated compounds [24]. The covalently bound chlorine is more easily eliminated from chlorohydrins during subsequent alkaline extraction (by a SN reaction) than from the dichlorinated structures derived from reactions with elemental chlorine. Alkaline extraction following a D<sub>0</sub> stage generally reduces the AOX and OX level, depending on temperature and sodium hydroxide concentration. The elimination of a washing step between D<sub>0</sub> and E<sub>1</sub> provides a reduction of 65% in the total level of AOX in the effluents. This was demonstrated for an existing ECF bleaching sequence processing *E. globulus* kraft pulp, kappa 13, where a DE pre-treatment was replaced by a (DE) delignification unit, while keeping the final DED sequence unchanged [25]. Unlike the Ultim-O process described above, the temperature and pressure in the extraction stage were not altered. The sodium hydroxide in the E<sub>1</sub> stage was sufficient to neutralize the acidic carry-over in the effluent of the D<sub>0</sub> stage while maintaining the pH above 11.

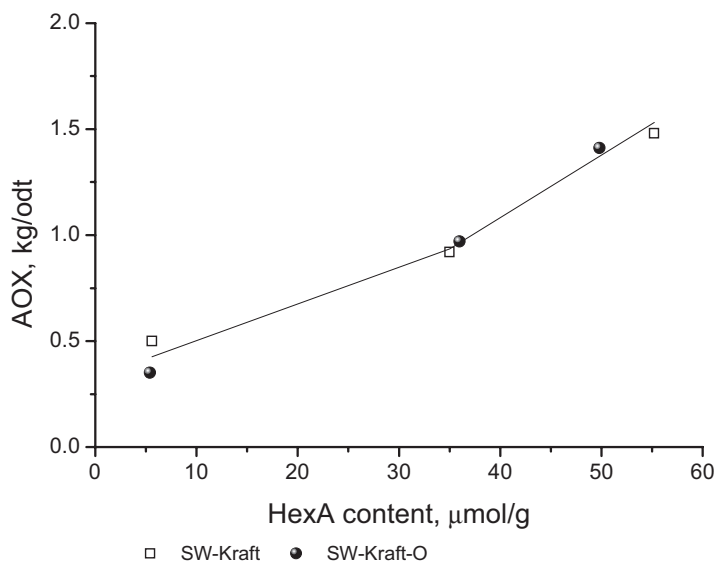
Surprisingly, it was found that the AOX levels generated in a D<sub>0</sub>(EO)D(EP)D sequence were higher for the oxygen-delignified softwood kraft pulps as compared to the non-oxygen-delignified pulps when compared at the same kappa numbers of the pulps entering the D<sub>0</sub> stage [26]. The relationship between AOX and kappa number for both types of pulp is shown graphically in Fig. 7.72.

The main difference between the unbleached and the oxygen-delignified pulps is reflected in the higher content of HexA (4-deoxy-β-D-threo-hex-4-enopyranosyluronic acid) in the latter, compared at the same kappa number, due to its resistance towards oxygen delignification [27]. This indicates that the AOX formation in the D<sub>0</sub> stage is more dependent on the HexA content than on the kappa number, as depicted in Fig. 7.73. HexA probably forms chlorinated dicarboxylic acids in the presence of chlorine dioxide, which however is easily decomposed by means of alkaline post-treatment [28].

The rule-of-thumb Eq. (82) is only valid within the conventional temperature range used in D<sub>0</sub> or D<sub>1</sub> stages. The implementation of ECF bleaching in existing bleach plants very typically was made by simply replacing chlorine with chlorine dioxide. Some mills even today still operate a low-consistency D<sub>0</sub> stage, because the equipment was not modified. Similarly, the temperature was kept at the low level required to run a C stage, or increased only moderately. Thus, typically D<sub>0</sub> stages are operated between 45 °C and 70 °C (at best), and D<sub>1</sub> or D<sub>2</sub> stages at

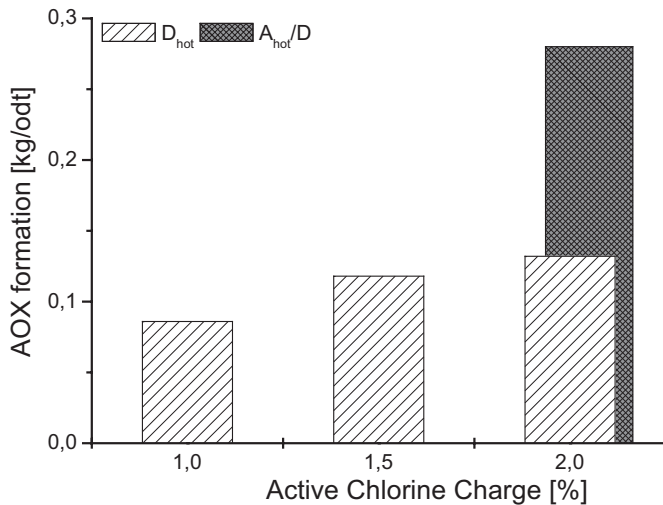


**Fig. 7.72** AOX formation in the  $D_0$  stage as a function of the kappa number of both oxygen-delignified and non-oxygen-delignified softwood kraft pulps (according to [26]).



**Fig. 7.73** AOX formation in the  $D_0$  stage as a function of the HexA content of both oxygen-delignified and non-oxygen-delignified softwood kraft pulps (according to [26]).

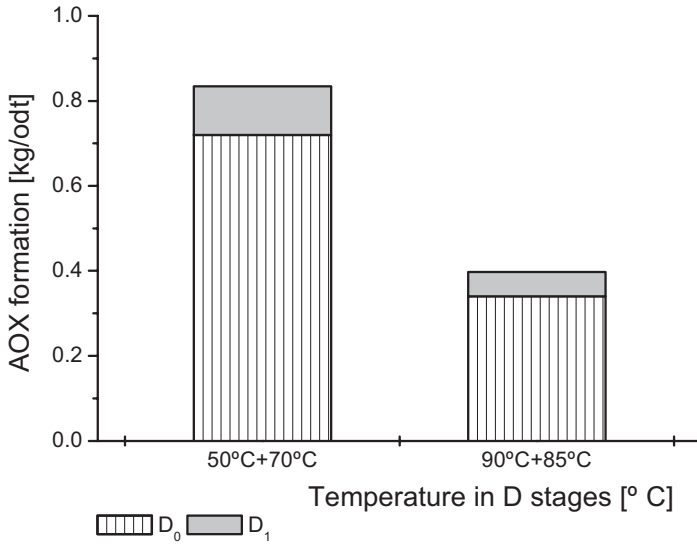
70–80 °C. The application of a hot  $D_0$  stage, as described by Lachenal [29], alters not only the bleaching results but also the effluent characteristics. Figure 7.74 compares the AOX load resulting from the treatment of a eucalyptus kraft pulp with increasing amounts of chlorine dioxide in a hot  $D_0$  stage. An increase in the chlorine dioxide, from 1% to 2% active chlorine, does not result in a doubling of the AOX load. For comparison, the other technological alternative for a combination of hot acid hydrolysis and chlorine dioxide delignification [30], hydrolysis for 110 min and addition of  $\text{ClO}_2$  (without intermediate washing), was tested. The short retention of only 10 min at 90 °C results in a significantly higher AOX residual. This is a clear indication of decomposition reactions taking place during the 2-h period at high temperature. Hydrolysis to inorganic chloride ions also occurs. If such hydrolysis is conducted well ahead of the chlorine dioxide addition, and the time following the addition is short, then degradation will not take place.



**Fig. 7.74** Impact of active chlorine amount and addition point in hot chlorine dioxide delignification on AOX load. Oxygen-delignified eucalyptus kraft pulp, kappa 10.  $D_0$  at pH 3, 90 °C, 2 h;  $A_{hot}/D$  with 110 min acid hydrolysis at pH 3, 90 °C, addition of  $\text{ClO}_2$  additional time 10 min.

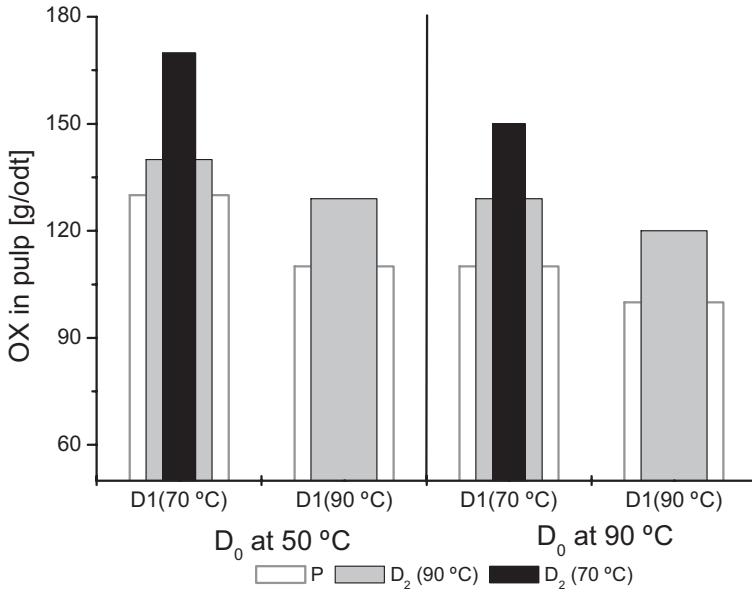
It is therefore not surprising to see similarly lower AOX and OX values also in high-temperature softwood pulp bleaching. The decrease does not require an extreme residence time, as in this example 1 h was applied to the  $D_0$  stage. The effect is clearly the result of the very high temperature.

This impact is shown graphically in Figs. 7.7.5 and 7.7.6. In comparison to conventional ECF bleaching [31], the amount of dissolved halogenated compounds (AOX) is cut by more than half by increasing the temperature in the  $D_0$  and  $D_1$  stages. Similarly, the application of high temperature in other  $D$  stages reduces the amount of halogenated compounds remaining in the pulp.



**Fig. 7.75** Impact of high temperature on the AOX load generated in bleaching oxygen-delignified (kappa 13.4) softwood kraft pulp. Constant 3.35% active chlorine (kappa factor

0.25), 1 h and pH <3 in D<sub>0</sub>, variable temperature (50 °C or 90 °C); Eop with 1.8 %NaOH, 0.5% H<sub>2</sub>O<sub>2</sub> and 0.4 MPa O<sub>2</sub>; D<sub>1</sub> with 1% active chlorine, 2 h, and 70 °C or 90 °C.



**Fig. 7.76** Impact of the temperature in D stages on the residual of halogenated compounds in pulp bleaching with the sequences D<sub>0</sub>EopD<sub>1</sub>D<sub>2</sub> or D<sub>0</sub>EopD<sub>1</sub>P. For conditions, see Fig. 7.75; D<sub>2</sub> with 0.5% active chlorine, P with 0.25% H<sub>2</sub>O<sub>2</sub>.

When not only the D<sub>0</sub> stage but also all other all D stages are operated at higher than “normal” temperature, the residual of halogenated compounds remaining in the pulp (“OX”) also decreases. When a final alkaline peroxide stage is added, which results in additional saponification and extraction, the OX level of the pulp reaches a level that would be accessible under conventional conditions only in ECF “light” bleaching – that is, with a much lower input of active chlorine [15]. The explanation for the lower AOX and OX values is the reactivity of quinones (see Section 7.4.4). A sequence with a final P stage is certainly more attractive for reaching low OX values compared to the addition of sulfamic acid. Although the addition of sulfamic acid similarly lowers the level of OX, a 25% higher charge of chlorine dioxide is required [13].

## 7.5

### Ozone Delignification

#### 7.5.1

##### Introduction

Among the oxygen-based bleaching chemicals, ozone is the most powerful oxidizing agent, reacting readily with almost any organic material. The good delignifying and brightening properties make ozone an attractive candidate to replace chlorine-based bleaching agents. The use of ozone as a bleaching agent results in an effluent which is free from organochlorine compounds and can be completely recirculated to the chemical recovery system. Thus, ozone bleaching may be a prerequisite for a closed-loop bleaching process. However, there are some difficulties concerning the application of ozone bleaching in industrial practice. First, ozone is an unstable gas which must be produced on site, most commonly by passing oxygen gas through an electrical discharge where some of the oxygen molecules are dissociated into oxygen atoms. In turn, oxygen atoms unite with oxygen molecules to form ozone. Ozone generation technology in the early stages could produce only 2–4% ozone by weight in an oxygen carrier gas. Later developments in ozone generation technology could produce 5% by weight. In the early 1990s, concentration of ozone could be raised to 8–12% by weight with power efficiency. Recent advances in ozone generation which enable ozone concentrations up to 16% by weight, as well as the lowering of oxygen cost by means of on-site production, have established ozone as a highly competitive bleaching chemical. The ozone concentration can be further increased by compressing the gas mixture; this improves the mass transfer from the gas into the liquid phase, which is a prerequisite for an efficient bleaching process. Second, the high oxidation potential of ozone makes it also prone to depolymerize and to degrade pulp polysaccharides. In fact, its delignification selectivity is significantly lower than that of chlorine dioxide. The prevalent view attributes this lack of selectivity to the generation of highly reactive and nonselective hydroxyl radicals during the bleaching process. The formation of hydroxyl radicals is usually ascribed to ozone self-decomposition

in an aqueous system, to ozone decomposition catalyzed by transition metal ions, and mostly to reactions between ozone and lignin structures, preferably containing phenolic hydroxyls. Based on a huge research effort within the past decade, the performance of ozone bleaching has been significantly improved with respect to both selectivity and production costs, making ozone a competitive bleaching agent. However, it has not yet been possible to increase the selectivity of ozone to the same level exhibited by chlorine dioxide. This is a severe drawback for the production of pulps where the high molecular weight of cellulose is a prerequisite to attain the desired properties (paper-grade pulp: high-strength properties; dissolving-grade pulp: high solution viscosity). Special emphasis will be given in future research work to further improve the efficiency and selectivity of ozone bleaching.

Although the first implementation of ozone on industrial scale was until 1990, when the first installation of an ozone bleach plant came on stream in Lenzing, ozone has long been known as an efficient bleaching agent.

The reaction of ozone with textile fibers such as cotton and linen was studied as early as 1868 [1]. In 1889, a method for bleaching “fibrous substances”, including those used in the making of paper, with a mixture of chlorine and ozone gases was patented by Brin and Brin [2]. Cunningham and Doree reported in 1912 that ozone would preferably attack the lignin part in jute, but cellulose was also affected [3]. In 1934, Campbell and Rolleston patented a process for bleaching pulp by sequential treatment with chlorine and ozone [4]. Since the studies of Brabender in 1949, in which he investigated some of the variables involved in ozonation and patented a high-consistency ozone bleaching process, many reports and patents on ozone bleaching have been published [5]. The breakthrough of ozone bleaching was the invention and development of a technology to compress ozone gas, and this is the prerequisite to apply ozone in medium-consistency technology. Since the first industrial installation of an ozone plant in 1990, more than 25 pulp mills with an annual production of about 8 million tons of pulp have implemented ozone bleaching on industrial scale (see Tab. 7.39).

### 7.5.2

#### Physical Properties of Ozone

Ozone ( $O_3$ ) is an allotropic form of oxygen. At ambient conditions, it is a pale blue gas ( $= 2.1415 \text{ g L}^{-1}$  at  $0^\circ\text{C}$  and  $101.3 \text{ kPa}$ ). It condenses into an indigo blue liquid ( $-112^\circ\text{C}$ ) and freezes to a deep blue-violet solid ( $-195.8^\circ\text{C}$ ). Ozone has a bent structure of  $C_{2v}$  symmetry with an apex angle of  $116^\circ 49'$  and equal oxygen–oxygen bond distances which are more closer to that of molecular oxygen as compared to that of hydrogen peroxide. Hence, the bonds in ozone have considerable double-bond character [6]. Data obtained from the microwave spectrum of the ozone molecule have shown it not to be significantly paramagnetic [7]. Thus, the ozone molecule can be pictured as a resonance hybrid consisting of four mesomeric structures, as shown in Fig. 7.77.

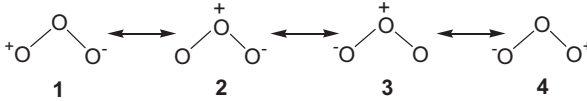
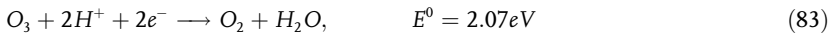


Fig. 7.77 Resonance structures of ozone.

The contributions of forms 1 and 4, which have a positively charged terminal oxygen with only six electrons, have been used to explain the electrophilic character of ozone. As such, ozone falls into a moderately large class of 1,3-dipolar compounds and will in certain reactions follow mechanisms typical of this class as a whole [8]. In a simple molecular orbital representation of the ozone molecule, each of the oxygen atoms is considered to be an  $sp^2$  hybrid and thus overlap of the p-orbitals provides a molecular orbital containing four  $\pi$  electrons. The UV spectrum of ozone shows an absorption maximum in 0.01 M  $HClO_4$  at 260 nm with an extinction coefficient of  $2930 \text{ L}\cdot\text{M}^{-1}\cdot\text{cm}^{-1}$  [9]. In acid aqueous solution, the oxidizing power is exceeded only by fluorine, atomic oxygen, OH radicals, and a few other species [6]. The oxidation potential in aqueous solution is expressed by Eq. (83):



Ozone is thermodynamically unstable, and 1 mol decomposes exothermically to 1.5 mol of molecular oxygen.

The solubility of ozone is an important criterion for ozone bleaching. The solubility of ozone in equilibrium with its partial pressure is usually defined by Henry's law according to the following expression:

$$x_{O_3} = \frac{P_{O_3}}{k_H} \quad (84)$$

where  $x_{O_3}$  is the dissolved ozone molar fraction ( $\text{mol mol}^{-1}$ ),  $P_{O_3}$  is the ozone partial pressure (kPa), and  $k_H$  is Henry's law constant ( $\text{kPa mol fraction}^{-1}$ ).

The ozone molar fraction can be transformed to a concentration of ozone,  $c_{O_3}$  (in  $\text{mol L}^{-1}$  or  $\text{mg L}^{-1}$ ) by multiplying the molar fraction by 55.51 or by  $2.664 \times 10^6$ , respectively. Ozone solubility is influenced by several factors, such as temperature, pH, ionic strength and dissolved matter. Henry's law constant,  $k_H$ , depends on the temperature,  $T$ , according to Eq. (85):

$$\frac{d \ln k_H}{d(1/T)} = -\frac{\Delta H}{R} \quad (85)$$

$$k_H = k_H^0 \cdot \text{Exp}\left(-\frac{\Delta H}{R} \left(\frac{1}{T} - \frac{1}{T^0}\right)\right)$$

where  $R$  is the gas constant and  $\Delta H$  is the heat of solution of the gas. The parameters  $k_H^0$  and  $T^0$  refer to  $k_H$  and  $T$  at standard conditions. Equations (84) and (85) show that an increase in temperature is connected with a decrease in the dissolved

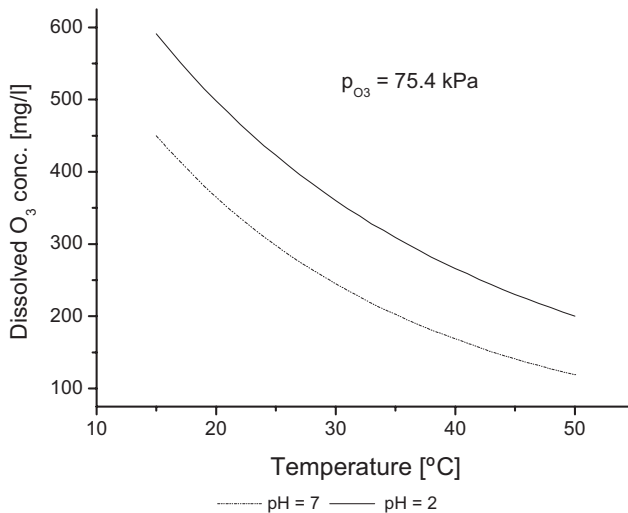
ozone concentration. The reduced ozone solubility at higher temperature can be explained by a drop in the liquid phase driving force, and by a higher decomposition rate. The pH is the predominant parameter which determines the stability of ozone in aqueous solution (see Section 7.5.4), and hence also its solubility in water. It is agreed that the dissolved ozone concentration increases with decreasing pH. This is one of the important reasons why ozone bleaching is conducted under acidic conditions, preferably in the pH range of 2–3. Quederni et al. have determined the apparent Henry's law constants for ozone solubility in water as a function of temperature at pH 2 and pH 7 [10]. The relationship between  $k_H$  and the temperature for these two different pH levels is expressed in Eq. (86):

$$k_H = 101.3 \cdot \text{Exp}\left(20.7 - \frac{3547}{T}\right) \quad (\text{pH} = 7) \quad (86)$$

$$k_H = 101.3 \cdot \text{Exp}\left(18.1 - \frac{2876}{T}\right) \quad (\text{pH} = 2)$$

The solubility of ozone in water at 1 atm,  $p_{\text{O}_3} = 101.3 \text{ kPa}$  and  $0^\circ\text{C}$  calculates to  $(101.3/1.966 \times 10^5) \times 2.664 \times 10^6 = 1.37 \text{ g L}^{-1}$  at pH 2, and to  $(101.3/2.270 \times 10^5) \times 2.664 \times 10^6 = 1.18 \text{ g L}^{-1}$  at pH 7. Figure 7.78 illustrates the course of the equilibrium dissolved ozone concentration as a function of temperature in the range of 15 to  $50^\circ\text{C}$  for the two pH levels, considering typical conditions for medium consistency ozone bleaching:

- Generated ozone concentration in oxygen gas:  $200 \text{ g m}^{-3} = 9.3 \text{ Vol}\%$
- Total pressure in the mixer:  $8 \text{ bar} = 0.81 \text{ MPa}$
- Ozone partial pressure,  $p_{\text{O}_3}$ :  $0.093 \times 810.4 = 75.4 \text{ kPa}$



**Fig. 7.78** Influence of temperature and pH on the dissolved ozone concentration in water assuming a partial pressure,  $p_{\text{O}_3}$ , of  $75.4 \text{ kPa}$  (according to results determined by Quederni et al. [10]). The ionic strength is kept constant at  $0.13 \text{ mol L}^{-1}$ .

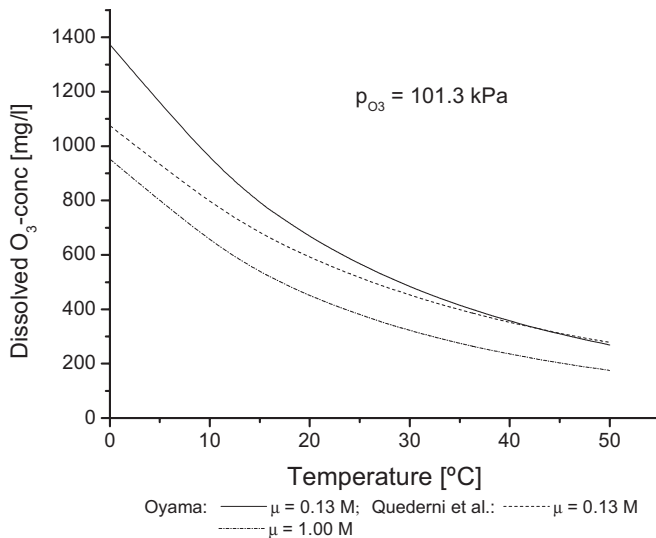


The ratio between the ozone solubility at pH 2 and pH 7 further increases with rising temperature. The dependency of the dissolved ozone concentration on pH was even more pronounced, according to results obtained by Sotelo et al. [11]. These authors found an increase by a factor of 1.6 (3.1) when comparing ozone solubilities at pH 2.5 and pH 7.0 (pH 9.0) at 10 °C and an ionic strength of 0.15 M. As already mentioned, gas absorption is also dependent on the ionic strength. Generally, the dissolved gas concentration decreases as ionic strength increases. The effect of ionic strength on the solubility of ozone is most pronounced in the presence of phosphates, chloride or carbonate ions, whereas the addition of sulfate ions exerts practically no change in solubility. According to Sotelo et al., the dissolved ozone concentration is decreased by half when increasing the ionic strength from 0.04 mol L<sup>-1</sup> to 0.49 mol L<sup>-1</sup> in the presence of sodium chloride (pH 5.94 and 1.1 kPa → 4.8 mg L<sup>-1</sup> versus 2.4 mg L<sup>-1</sup>) [11].

In more general terms, both the influence of temperature and ionic strength is described by Eq. (5) [12]:

$$k_H = \text{Exp}\left(-\frac{2297}{T} + 2.659 \cdot \mu - \frac{688 \cdot \mu}{T} + 16.808\right) \quad (87)$$

where  $k_H$ , Henry's constant is kPa.L.mol<sup>-1</sup>, T, temperature in Kelvin, and  $\mu$  is the molar ionic strength. The temperature-dependence of the dissolved ozone concentration is more pronounced using Eq. (86) than with Eq. (87), with an almost perfect correspondence at temperature higher than 35 °C (Fig. 7.79).

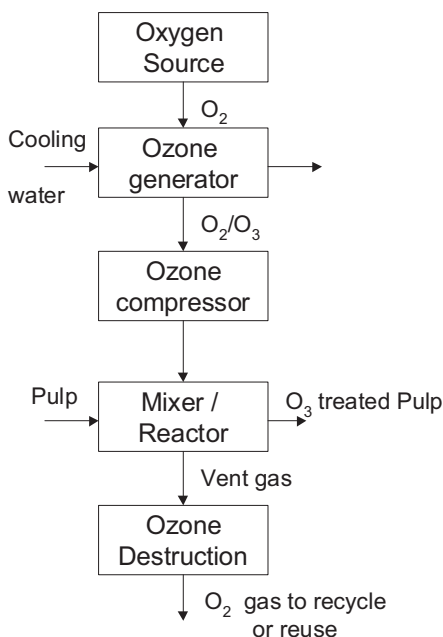


**Fig. 7.79** Comparison of calculated dissolved ozone concentration as a function of temperature using Henry's constants from different literature sources: Quederni et al. [10] versus Oyama [13]. The influence of ionic strength was assessed using Eq. (87).

## 7.5.3

**Ozone Generation**

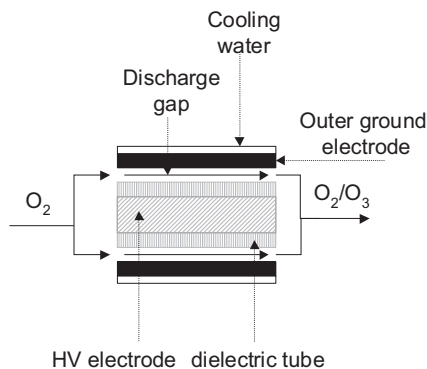
Ozone is produced at the site of use because it is unstable and cannot be stored. The ozone-generating system is selected according to the requirements on site, including the ozone bleaching technology (medium- or high-consistency), the source of oxygen (cryogenic or adsorption), the temperature of cooling water, and the possibilities to recycle the vent gas for oxygen delignification. Figure 7.80 illustrates the principal elements of an ozone bleaching system, including the oxygen source, the ozone-generating system, the ozone delivery system with an ozone compressor in the case of medium-consistency ozone bleaching technology, the mixer or reactor, the off-gas destruction system and the vent gas recovery and recycle loops.



**Fig. 7.80** Principal course of ozone in a pulp bleaching system (according to [14]).

Ozone is produced from oxygen-containing gases in ozone generators by means of silent electrical discharge in the so-called “corona discharge process”. To date, in bleaching operations only oxygen gas is used to achieve a high ozone concentration and to avoid the formation of reactive byproducts such as nitric acid. Oxygen is passed through two electrodes which are separated from each other by a dielectric and two discharge chambers (Fig. 7.81). When a high voltage is applied between two concentrically arranged electrodes, and the voltage exceeds the ionization potential of the dielectric material, then electrons flow across the gap and

provide energy for the dissociation of oxygen molecules; these then combine with oxygen molecules to form ozone. The key element of a corona discharge ozone system is the dielectric. The electrical charge is diffused over this dielectric surface, creating an electrical field where high-energy electrons bombard gas molecules so that they are ionized and a light-emitting gaseous plasma is formed, which is commonly referred to as a “corona”. Many different materials in a variety of configurations are used for the dielectric, including scientific-grade glass (e.g., borosilicate) and nonglass materials such as silicone rubber. The quantity of ozone produced is related to a number of factors, such as the voltage and frequency of the alternating current applied to the corona discharge cells, the cooling system, and the design of the ozone generator.



**Fig. 7.81** Schematic diagram of an ozone generation system.

The generally accepted technologies can be divided into three types: low-frequency (50–100 Hz); medium-frequency (100–1000 Hz); and high-frequency (1000+ Hz). Medium-frequency ozonators are now favored as they provide many benefits over the older low-frequency technology. An example of this is a greater ozone production with less electrode surface area, so that the equipment can be smaller for a given ozone output, and the power consumption per kg ozone produced is also reduced.

Since ozone generation by corona discharge is an exothermic physico-chemical reaction, and ozone decomposition increases as the gas temperature and ozone concentration increase, correct cooling is an important factor in generator design. Moreover, oxygen entering the ozone generator must be very dry (minimum  $65^\circ\text{C}$ ), because the presence of moisture affects ozone production and leads to the formation of nitric acid. Nitric acid is highly corrosive to critical internal parts of a corona discharge generator, and this can lead to premature failure and a significant increase in the frequency of maintenance. Besides the destruction of the ozone generator itself, transition metal ions are released from the stainless steel electrodes, and this can be very harmful to the pulp during the course of ozone bleaching. Depending on the strength of the electric field, cooling and the design of the ozone generator, ozone yields of up to 16% by weight ( $\sim 240\text{ g m}^{-3}$ ) can be

achieved in the production gas. The specific energy consumption for the production of 1 kg ozone is usually between 6 and 10 kWh, depending on the desired concentration. The efficiency of medium-consistency ozone bleaching is limited by a certain gas void fraction,  $X_g$  (according to Bennington, the upper operating limit is reached at  $X_g = 0.13$  [15], and according to industrial experience at  $X_g \sim 0.25$  [16]). The gas void fraction is defined by Eq. (88):

$$\begin{aligned} X_g &= \frac{V_g}{V_g + V_L} \\ X_R &= \frac{V_g}{V_L} \\ X_g &= \frac{V_R}{1 + V_R}; X_R = \frac{X_g}{1 - X_g} \end{aligned} \quad (88)$$

where:

$V_{g,T,P} = V_{g,T_0,P_0} \cdot \frac{101.3 \cdot T}{P \cdot 273.15}$  is the volume of the gas fraction, with P in kPa and T in K;

$V_L = \frac{\text{Prod}}{(\text{con} \cdot \rho_{\text{susp}})}$  is the volume of the aqueous pulp suspension;

$X_R$  is the volume ratio;

Prod is the standardized pulp production (e.g., 1 odt pulp);

$\rho_{\text{susp}} = \frac{1}{\left( \frac{\text{con}}{1.53} + \frac{(1 - \text{con})}{\rho_{\text{liquid}}} \right)}$  is the density of the pulp suspension;

con is the pulp consistency, expressed as a fraction; and

$\rho_{\text{liquid}} \sim 1$  is the density of the liquid.

Both high-concentration ozone feed and compression of the feed gas are required to ensure an efficient ozone consumption rate in medium-consistency ozone bleaching. Compression is exclusively carried out isothermally by means of liquid-ring compressors to avoid ozone destruction. The influence of ozone concentration in the feed gas to the compressor on the ozone charge being efficiently consumed in a medium-consistency mixer at a constant pressure of 8 bar at typical industrial conditions ( $T = 50^\circ\text{C}$ ,  $X_{g,\text{max}} = 0.25$ ) is shown in Tab. 7.36.

The data in Tab. 7.36 indicate that the ozone charge in a medium-consistency ozone mixer is limited to 3.2–4.2 kg odt<sup>-1</sup>. Clearly, the efficiency of medium-consistency ozone bleaching also depends on the specific energy dissipation,  $\varepsilon$ , and on the retention time (see Section 7.5.5.2, Mixing). However, in the case of a modern medium-consistency mixer the addition of higher ozone charges is connected with decreasing amounts of ozone consumption rates (see Fig. 7.107).

**Table 7.36** Effect of ozone concentration in oxygen gas prior and after compression to 0.8 MPa on the limit of ozone charge in a medium consistency ozone mixer.

Ozone concentration in oxygen				$X_g^c$	Max. $O_3$ -charge <sup>d</sup>
wt%	Vol. %	C at ST <sup>a</sup> [g Nm <sup>-3</sup> ]	c at IND <sup>b</sup> [g m <sup>-3</sup> ]	for 1 kg [O <sub>3</sub> odt <sup>-1</sup> ]	[kg O <sub>3</sub> odt <sup>-1</sup> ]
5.0	3.4	72.6	491	0.17	1.4
6.0	4.1	87.4	591	0.15	1.7
6.8	4.7	100.0	676	0.13	1.9
7.0	4.8	102.3	692	0.13	1.9
8.0	5.5	117.3	793	0.12	2.2
9.0	6.2	132.5	896	0.10	2.4
10.0	6.9	147.7	999	0.09	2.7
10.2	7.0	150.0	1014	0.09	2.7
11.0	7.6	163.0	1102	0.09	2.9
12.0	8.3	178.5	1207	0.08	3.2
13.0	9.1	194.0	1312	0.07	3.4
13.4	9.3	200.0	1352	0.07	3.5
14.0	9.8	209.7	1418	0.07	3.7
15.0	10.5	225.4	1524	0.06	3.9
16.0	11.3	241.3	1632	0.06	4.2
16.5	11.7	250.0	1691	0.06	4.3
19.6	14.0	300.0	2029	0.05	5.1

a. ST = standard conditions:  $T_0 = 273.15$  K,  $P_0 = 101.3$  kPa.

b. IND = industrial conditions:  $T = 323.15$  K,  $P = 810.6$  kPa = 8 bar.

c.  $X_g = V_g / (V_g + V_l)$  at 10% pulp consistency and IND.

d. Assuming an upper limit of  $X_g = 0.25$  to obtain a reasonably high ozone consumption rate.

#### 7.5.4

### Chemistry of Ozone Treatment

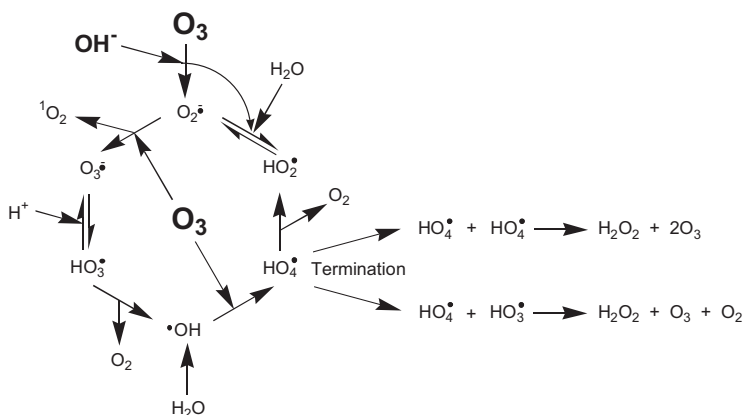
*Manfred Schwanninger*

Ozone treatment is a very effective way to remove residual lignin that remains after pulping. The structure and reactivity of the residual lignin have already been described (see Section 7.3.2.2). One of the major disadvantages of ozone as a

bleaching agent is its moderate stability in aqueous solutions [1–4]. It has the tendency to decompose in water, generating some very reactive, highly unselective radical species [1–5]. Hydroxide ions are known to catalyze ozone decomposition and to promote hydroxyl radical formation [1,3,4,6], whilst another drawback is the undesired degradation of cellulose [7–23].

#### 7.5.4.1 Ozone Decomposition

The pathways and kinetics of the decomposition of aqueous ozone are of interest for a wide range of topics, not only for pulp bleaching, and have therefore been studied intensively [1–5,24]. The chain mechanism of ozone decomposition (Scheme 7.28) is based on the studies of Bühler *et al.* [5], while Staehelin *et al.* [1] showed the decomposition of ozone and the formed intermediates (Scheme 7.28).



**Scheme 7.28** Chain mechanism of ozone decomposition according to Staehelin *et al.* [1].

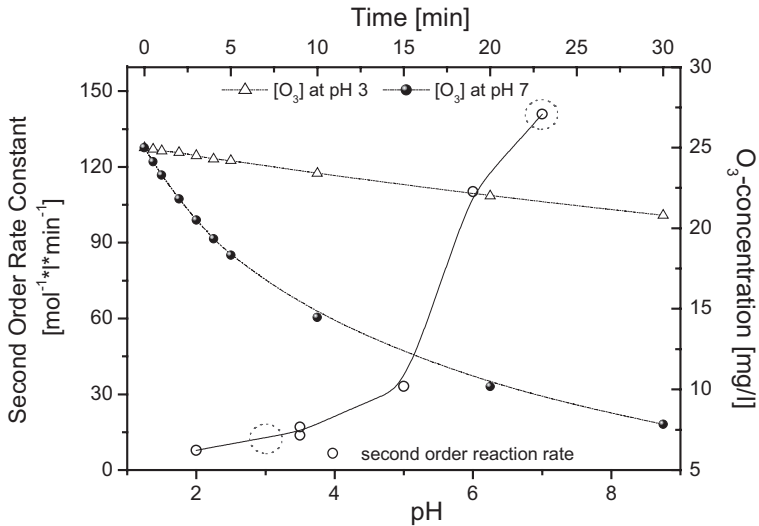
The decomposition occurs by a radical chain mechanism, which in pure water is initiated by the reaction between hydroxide ions ( $\text{OH}^-$ ) and ozone [Eq. (89)]. Superoxide  $\cdot\text{O}_2^-$  then reacts with ozone rather selectively as part of a chain cycle [1].



The hydroxide-ion-catalyzed decay of ozone is expressed in the following general rate equation (1):

$$\frac{d[\text{O}_3]}{dt} = -k \cdot [\text{O}_3]^a \cdot [\text{OH}^-]^b \quad (90)$$

The reaction order  $b$  with respect to hydroxide ion concentration varies from 0.36–1.0 and the reaction order  $a$  for ozone is reported to vary between 1.5–2.0 [aa, bb]. Pan *et al.* have studied the decomposition rate of ozone in a pure aqueous

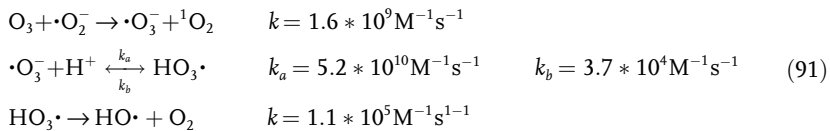


**Fig. 7.82** Effect of pH on second order rate constant of ozone decomposition and the course of ozone concentration in aqueous solution at 25 °C according to Pan et al. [25].

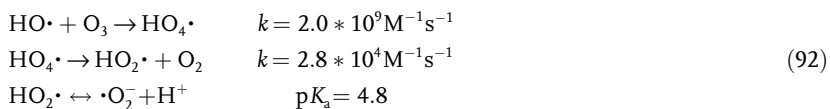
system as a function of pH at 25 °C. The results revealed a rapid increase of the second order rate constant from pH 4 to 7 as seen in Fig 7.82.

The concentration of dissolved ozone decreases rapidly at a neutral pH, while it remains quite stable under acidic conditions (pH 3) within a time frame relevant for industrial ozone bleaching applications.

The first propagation step of the chain reaction proposed by Weiss for the decomposition of aqueous ozone can be described with the intermediates  $\cdot\text{O}_3^-$  and  $\text{HO}_3\cdot$  [5]. The elementary reactions of these species and their constants are presented in Eq. (91) [5]:



In water, the decay of  $\text{HO}_3\cdot$  is very rapid, with a half-life of about 6  $\mu\text{s}$ . Since  $\cdot\text{O}_2^-$  reacts rapidly with ozone, but relatively slowly with organic compounds, the latter will interfere with ozone decomposition in aqueous solutions by scavenging OH radicals rather than  $\cdot\text{O}_2^-$  [5]. The second propagation step and the reactions of these species and their constants are presented in Eq. (92):



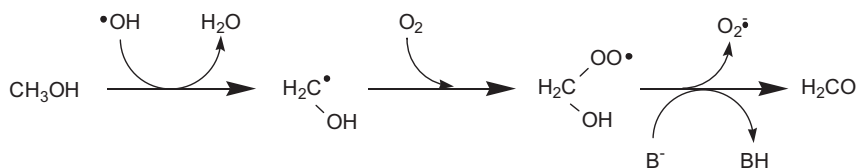
The transient  $\text{HO}_4\cdot$  might be a charge-transfer complex ( $\text{HO}\cdot\text{O}_3$ ) [1]. The lifetime of  $\text{HO}_4\cdot$  was found to be much longer than its accumulation rate, and therefore it acts as a carrier reservoir within the chain cycle. As a consequence,  $\text{HO}_4\cdot$  is the important transient for chain termination reactions (Fig. 7.82). The termination reactions shown in Eq. (93) are the dominating ones in the presence of high ozone concentrations [1].



If, at low ozone concentrations, organic solutes are present, their dominant effect will be to withdraw OH radicals; at high ozone concentrations this will similarly occur with  $\text{HO}_4\cdot$ . Some organic materials are thereby able to regenerate  $\cdot\text{O}_2^-$  in order to sustain the chain.

As the initial step of the ozone decomposition is the reaction between ozone and the hydroxide anion [Eq. (89) and Scheme 7.28], strong pH dependence is expected [6]. Gurol and Singer [4] investigated the kinetics of ozone decomposition in the pH range from 2 to 10. They found that ozone decomposes rapidly at a pH above about 6.5, but remains quite stable under acidic conditions; indeed, this finding has been confirmed by several authors [6,25,26]. Hydrogen peroxide, also used as a bleaching chemical, is incapable of initiating ozone decomposition; however, its deprotonated form, the hydroperoxy anion ( $\text{HO}_2^-$ ) has such ability [6]. At  $\text{pH} < 12$  and hydrogen peroxide concentrations  $> 10^{-7} \text{ mol L}^{-1}$ ,  $\text{HO}_2^-$  has a greater effect on the decomposition rate than the hydroxide anion ( $\text{OH}^-$ ) [3], and this might be important for bleaching sequences. In the radical-type chain reaction decomposition of ozone, inorganic and organic compounds can be divided into three categories: (a) initiators; (b) promoters; and (c) inhibitors [6,24,27,28]. Initiators are substances that are capable of initiating the decomposition of ozone to the superoxide anion radical [Eq. (89)], while promoters are radical converters forming the superoxide anion radical from the hydroxyl radical (Scheme 7.29).

Inhibitors are substances that react with the hydroxyl radical without the formation of superoxide anion radical, called radical scavengers, such as bicarbonate and carbonate, leading to the corresponding radicals [24]. Some examples are given in Tab. 7.37.



**Scheme 7.29** Reaction of methanol as a typical hydroxyl radical to superoxide anion radical converter acting as a promoter [24].



**Tab. 7.37** Typical initiators, promoters, and inhibitors for decomposition of ozone by radical-type chain reactions [6, 24–28].

Initiator	Promoter	Inhibitor
Hydroxide anion	R <sub>2</sub> CHOH, including polyalcohols and sugars	Acetate
Hydroperoxy anion	Primary alcohols	Alkyl-(R)
Superoxide anion	Aryl-(R)	<i>t</i> -butyl alcohol
Formate	Formate	HCO <sub>3</sub> <sup>-</sup> /CO <sub>3</sub> <sup>2-</sup>
Glyoxylic acid	Methanol	
Glycolic acid	Glyoxylic acid	
Fe <sup>2+</sup>	Glycolic acid	
Co <sup>2+</sup>	Phosphate ion	
Other transition/heavy metals		
UV light (254 nm)		

As shown in Tab. 7.37, transition metal ions such as Fe<sup>2+</sup> and Co<sup>2+</sup> can initiate ozone decomposition. The proposed reaction pathway for the Co<sup>2+</sup>-catalyzed ozone decomposition in sulfuric acid solution at pH 3 begins with the oxidation of Co<sup>2+</sup> to the cobaltic hydroxide ion, whereas ozone decomposes to oxygen and the hydroxyl radical [Eq. (94)] [25]:



The hydroxyl radical in turn is oxidized to the hydroperoxy radical [Eq. (91) and (95)]:



The Co<sup>3+</sup> is then reduced to Co<sup>2+</sup> by the hydroperoxy radical [Eq. (96)]. The net result is the reduction of ozone to oxygen and the regeneration of Co<sup>2+</sup>, which can initiate another decomposition cycle.



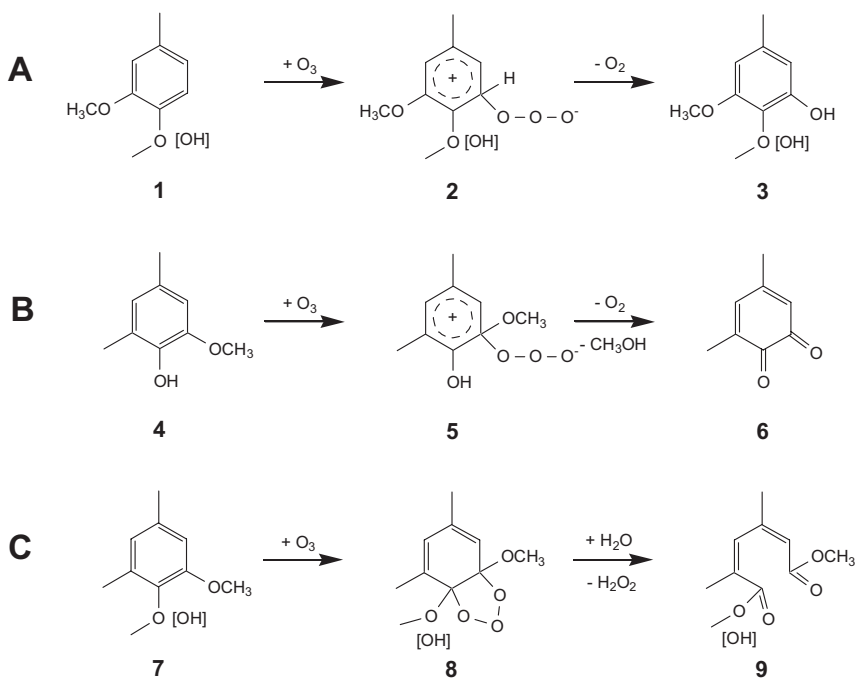
Ozone decomposition is enhanced in the presence of trace amounts of transition metals. For example, at Co<sup>2+</sup> concentration of 0.009 mmol/L (0.5 ppm) or Fe<sup>2+</sup> concentration of 0.05 mmol/L (3 ppm) ozone decomposition is dramatically increased [25]. Therefore, transition metals should be removed prior ozone treatment. However, adjusting the pH to 2 has been shown to inhibit the degradation of carbohydrates by ozone without the removal of Fe<sup>2+</sup> [10].

A collection of reaction rates of nondissociating organic compounds [27], dissociating organic compounds [28], and inorganic compounds as well as radicals [6] is available from literature sources, and so will not be described at this point.

#### 7.5.4.2 Degradation of Lignin

Ozone preferentially reacts with olefinic compounds, whereas the reactivity for the electrophilic attack is increased by substituents with +M- and +I-effect. The reactivity of lignin structures can therefore be ranked as follows: stilbenes > styroles > phenolic substances > muconic acid-like substances > nonphenolic substances > aldehydes >>  $\alpha$ -carbonyls.

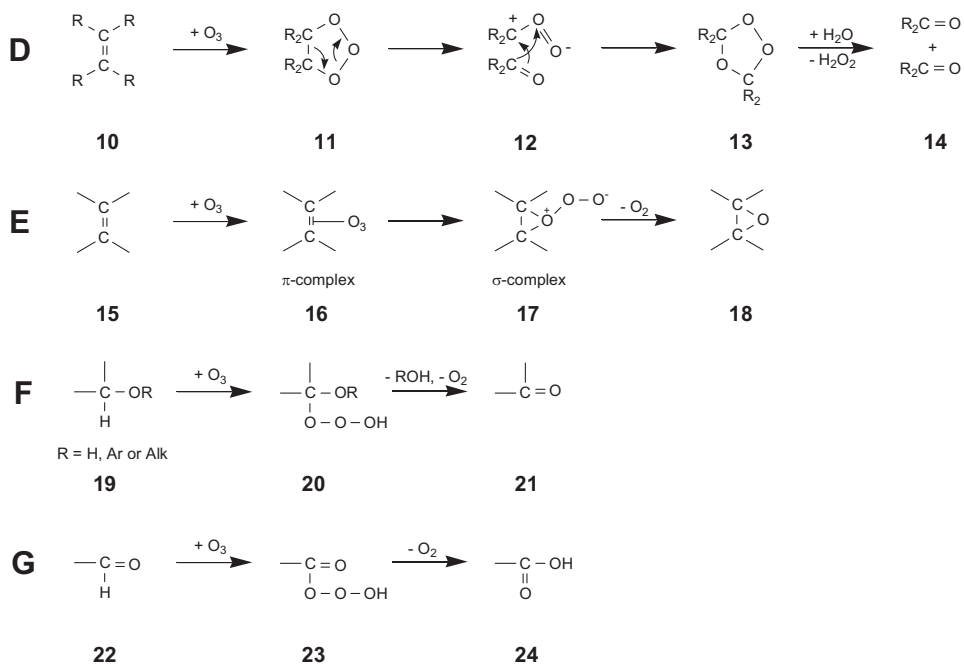
The reactions of ozone with aromatic compounds involve initial an electrophilic attack by the oxidant, followed by the loss of oxygen that results in hydroxylation of the aromatic ring (Scheme 7.30, pathway A) [29]. Formation of the hydroxyl group increases the reactivity towards electrophilic substitution reactions. Therefore, it is probable that in a subsequent step ozone reacts with the aromatic ring by a 1,3-cycloaddition. Alternatively, the electrophilic substitution can be followed by oxidative dealkylation giving an ortho quinone (Scheme 7.30, pathway B). 1,3-Dipolar cycloaddition by a concerted mechanism proceeds at C3 and C4, because these atoms have the highest negative charge density of the aromatic system. Finally, the aromatic ring is cleaved (Scheme 7.30, pathway C) [29].



**Scheme 7.30** Reactions of ozone with aromatic moieties (redrawn from Gierer [29]).

An ionic [30] 1,3-dipolar cycloaddition is also opening across olefinic double bonds (Scheme 7.31, pathway D) [29]. According to the generally accepted mechanism of Criegee, the resulting “initial ozonide” (11), a 1,2,3-trioxacyclopentane, is formed. This decomposes to a dipolar ion intermediate, a simple carbonyl compound and a carbonyl oxide (12), that recombines further to give the “final ozonide” (13) that is cleaved immediately into the ozonolysis products by hydrolysis (14). 1,1-Cycloaddition of ozone to olefins can also occur via  $\pi$ - (16) and  $\sigma$ -complexes (17) (Scheme 7.31, pathway E) forming the corresponding epoxide (18) after the loss of one molecule of oxygen (singlet state). The insertion of ozone into carbon–hydrogen bonds in alcohol-, aldehyde- and ether-type structures is a further reaction mode (Scheme 7.31, pathways F and G) [29]. In these reactions the hydrotrioxide intermediate eliminates molecular oxygen (again singlet oxygen) forming the corresponding oxidation products. In the case of aryl and alkyl ethers, the reaction thus results in the cleavage of the ether bond [29].

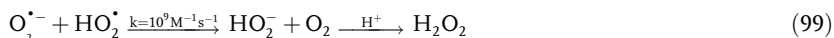
In addition to the “ionic” ozone reactions, there is an appreciable number of “radical reactions” which bear a resemblance to that of oxygen (and hydrogen peroxide bleaching) [30]. This is due to the presence and involvement of molecular oxygen (see Scheme 7.28), hydrogen peroxide (Scheme 7.31, path D) and the same radical species, superoxide and hydroxyl radicals [30]. In addition to the radical formation already described elsewhere (see Sections 7.3.2 and 7.6.4, Oxygen bleaching and hydrogen peroxide bleaching), the initial step of radical reactions of ozone may be regarded as a one-electron transfer from the substrate (SB) to the oxidant, here with the formation of a hypothetical ozonide ( $\cdot\text{O}_3^-$ )/hydrotrioxy ( $\text{HO}_3\cdot$ ) radical and a substrate radical ( $\text{SB}\cdot$ ) (Scheme 7.32, path A) [30]. This step may be followed by combination of these two radicals to give hydrotrioxides. Due to its high reduction potential, ozone reacts with the substrate much more rapidly and more comprehensively than does oxygen [30]. Thereby phenolic, nonphenolic, olefinic and aliphatic structures may be attacked. Intermediary  $\text{HO}_3\cdot$  may arise via electron transfer (Scheme 7.32, path A), which is followed by combination of the two resultant radical species.  $\text{HO}_3\cdot$  can also form through the reduction of ozone by superoxide radicals (Scheme 7.32, path B). Due to the high rate of ozone reduction by superoxide radical, path B may compete with path A. The formation of hydrotrioxides via direct insertion into C–H bonds (Scheme 7.32, path C) is a further characteristic reaction of ozone [30]. The hydroxyl radicals formed by  $\text{HO}_3\cdot$  decomposition, hydrotrioxides  $\text{SB-O}_3\text{H}$ , and possibly also by transition metal ion-catalyzed decomposition, enter the oxidation cycle and accelerate the initial step. As shown above, the efficient starting bleaching reagent ozone can be expected to compete with hydroxyl radicals for the substrate in the initial step much more successfully than oxygen. Gierer provided a tentative scheme for the course of ozone bleaching [30]. The higher efficiency and lower selectivity of ozone as compared to oxygen is due not only to the greater reactivity of ozone but also to the facile generation of hydroxyl radicals [30]. The reduction of  $\text{O}_3$  and  $\text{H}_2\text{O}_2$  can be blocked by scavenging  $\text{O}_2^{\cdot-}/\text{HO}_2\cdot$ . By the way, in water it is likely that superoxide will primarily disproportionate as it acts as a very strong lewis base. In this case, ozone bleaching should be limited to the ionic part of the process (Schemes 7.30 and



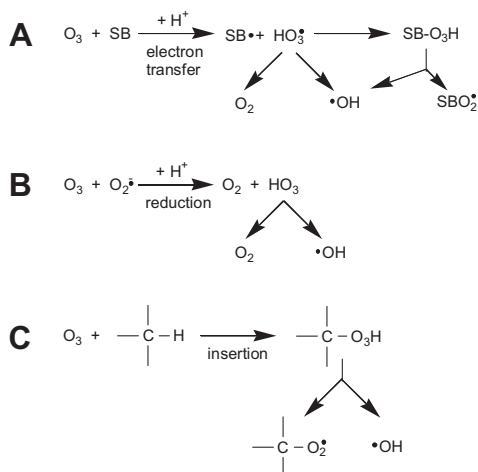
**Scheme 7.31** Reactions of ozone with olefins, alcohols, aldehydes and ethers (adapted from Gierer [29]).

7.31) and to the action of hydroxyl radicals arising directly by electron transfer from the substrate to ozone. In this way, it could be expected that the process becomes more selective without any severe loss in efficiency [30].

The formation of radicals in ozone reactions with lignin model compounds have been extensively studied by Ragnar et al. (1999) [31]. Radical formation is mainly due to a direct reaction between ozone and the substrate. By the way, in water it is likely superoxide is the primarily formed radical in acidic solution. In the presence of oxygen and ozone, superoxide is easily converted to the hydroxyl radical and vice versa, according to Eqs. (97–99).



Radical formation cannot be prevented under process conditions (e.g., by the elimination of transition metals), and they always occur, with yields being higher for syringyl compounds than for the corresponding guaiacyls. An increase in radical

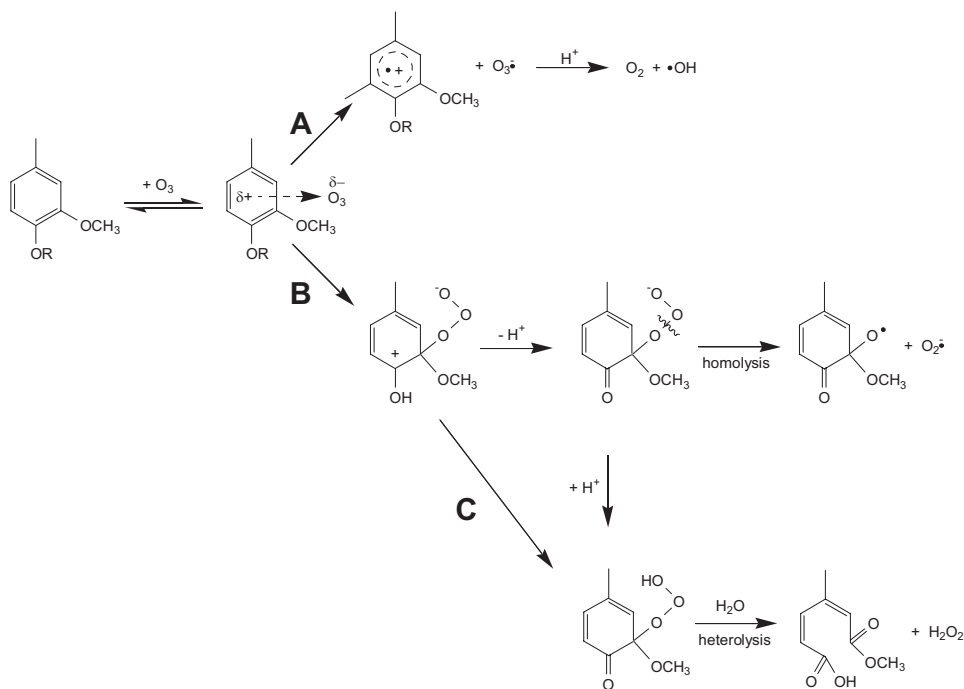


**Scheme 7.32** Radical reactions of between ozone and the substrate (SB) (redrawn from Gierer [30]).

yield was observed for all phenolic lignin model compounds, starting at pH 3. As pH is the parameter that most profoundly affects the radical formation; pH 3 may be regarded as optimal in ozone bleaching. Beside that is a self-evident impact of temperature. Moreover, the rate of ozone addition may also affect the selectivity in an ozone bleaching stage, particularly in hardwood pulp bleaching [31].

The reaction of ozone with creosol and a nonphenolic compound (3,4-dimethoxytoluene) in an aqueous medium proceeds via a charge-transfer state (Scheme 7.33) [32]. From the charge-transfer state, two reactions pathways are possible. In path A (Scheme 7.33) a complete electron-transfer takes place, and this results in the formation of an aromatic cation radical and an ozonide radical. After protonation, the ozonide radical decomposes to oxygen and a hydroxyl radical, which is a direct route to hydroxyl radical formation. In path B (Scheme 7.33), ozone adds to the aromatic ring, preferentially to the oxygen-substituted carbons, and the resulting zwitterions subsequently react via different routes. Homolytic cleavage of the trioxide yields superoxide and a quinol radical (path B) [32]. Heterolytic cleavage of the aromatic ring (path C) yields the same reaction products as does the ozonolysis, forming hydrogen peroxide. For nonphenolic structures, heterolytic ozonolysis dominates. This is supported by quantum chemical and thermochemical methods [32].

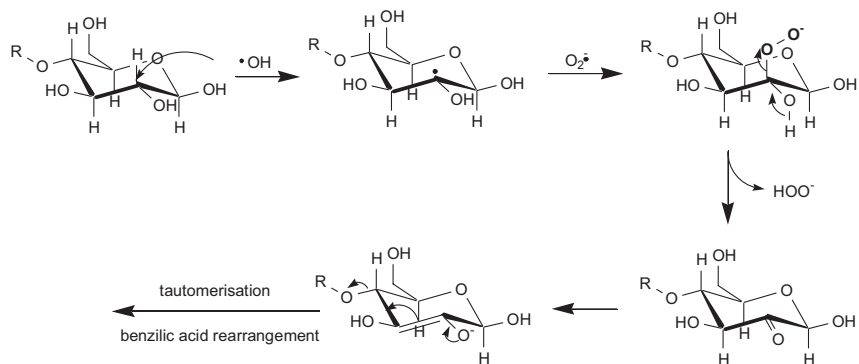
In reactions with hydroxyl radicals lignin is preferred compared to carbohydrates [33]. After ozone treatment a significant increase in hydrophilicity [34] and the number of carboxyl groups were observed in the residual lignin [34] as well as the dissolved lignin [35]. Likewise, an increase in the number of carbonyl groups was also observed [36]. In general, apart from the oxidation of double bonds of the side chain and the ring, the structure of residual lignin after ozone treatment is very close to that of the residual lignin after Kraft pulping [34]. Hoigné and Bader found that lignin-like structures react much faster with ozone than carbohydrates in the presence of radical-scavengers [27,28].



**Scheme 7.33** Proposed mechanism for the formation of superoxide and hydrogen peroxide with ozone (adapted from Ragner et al. [31]).

#### 7.5.4.3 Degradation of Carbohydrates

In carbohydrates, the attack of hydroxyl radicals begins with a hydrogen abstraction, followed by an oxygenation of the resultant carbon-centered radical, which leads to the introduction of carbonyl groups (Scheme 7.34) [30]. It is generally agreed that glycosidic bond cleavage is caused by ozone itself and radical species during ozonation in water [10], and that both are responsible for carbohydrate decomposition during ozone bleaching [xx], depending on pH, the temperature, and transition metal ions concentration [37]. Ni et al. [37] reported that from their experiments it is unlikely that in-situ-generated hydroxyl radicals mainly cause the carbohydrate degradation occurring during pulp ozonation. However, it was shown that the presence of metal ions, such as copper and iron, or a rise in temperature increases the formation of hydroxyl radicals during ozonation [yy]. They found that the increase in the number of hydroxyl radicals at pH 10.5 is not significant and concluded that a high pH molecular ozone is mainly responsible for cellulose degradation. Ozonation of unbleached pulp leads to the formation of considerable amounts of hydrogen peroxide leading to an additional degradation due to the hydroxyl radicals generated by the peroxide formed during ozonation [yy].



**Scheme 7.34** Hydrogen abstraction from carbohydrates.

Three lignin–carbohydrate model systems were studied to determine the mechanism of the effect of lignin on cellulose degradation during ozone bleaching. The three model systems were: methyl  $\alpha$ -D-glucopyranoside, dextran, and fully bleached kraft pulps in the presence of various lignin model compounds [38]. The results suggested that the lignin models can both promote and suppress degradation of the carbohydrates during ozone treatment. The presence of the lignin models can exert a protective effect by competing with the carbohydrates for the ozone available in the system. On the other hand, the ozone–lignin reactions give rise to the formation of hydroxyl radicals which promote carbohydrate degradation. It is suggested that many more hydroxyl radicals are formed via the ozone–lignin reaction route than via ozone self-decomposition. Among the lignin model compounds studied, the phenolic lignin structures have a more pronounced effect on carbohydrate degradation, though this can be explained by the easier formation of hydroxyl radicals from phenolic rather than from nonphenolic lignin models [38]. Margara et al. [14] observed a pronounced effect of free phenolic hydroxyl groups on the accelerated degradation of cellulose. Moreover, in the presence of lignin model compounds with etherified phenolic hydroxyl groups, there was a marked retardation of cellobiose degradation [14].

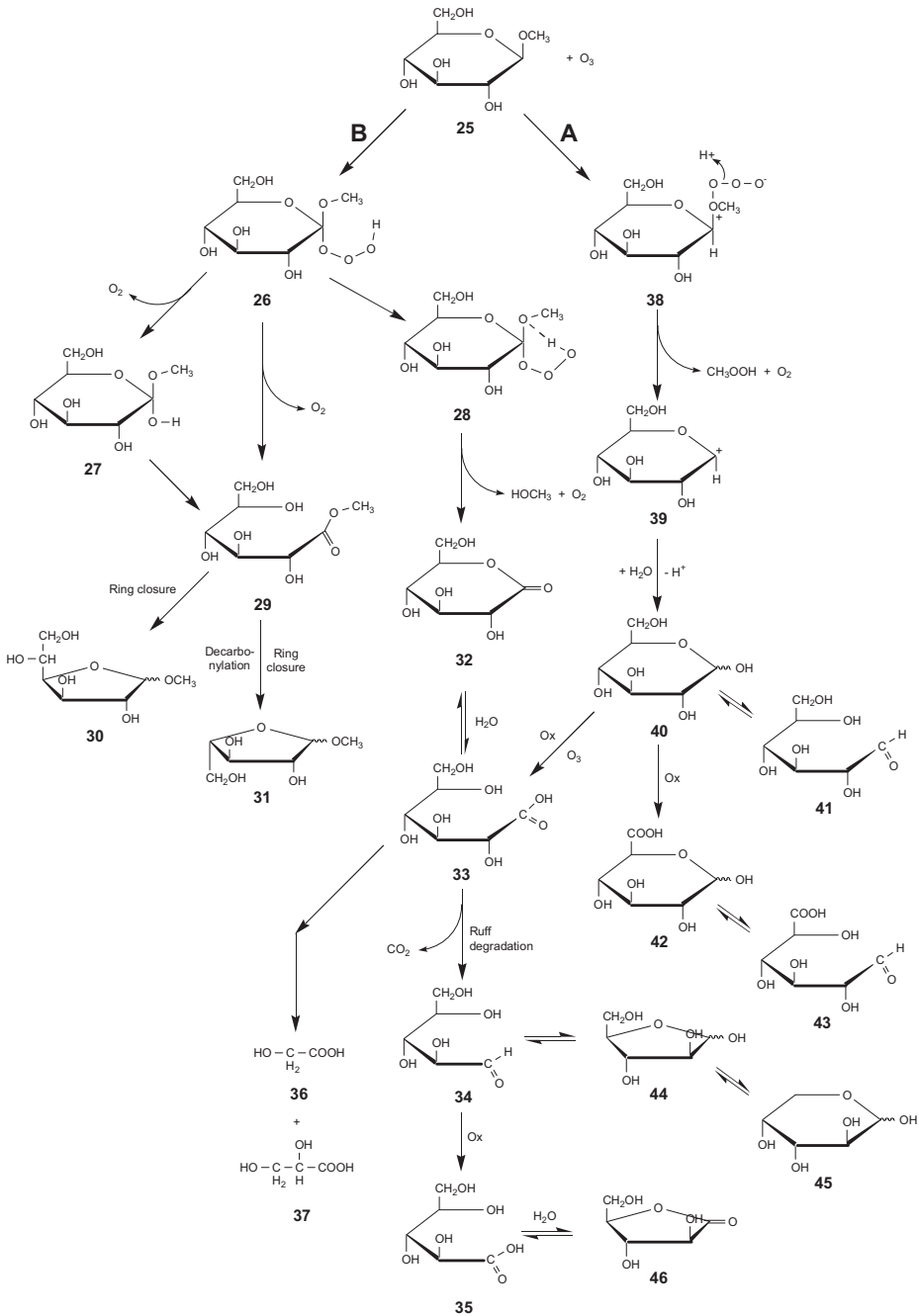
In another study, methyl beta-D-glucopyranoside was subjected to ozone treatment under different conditions. The results suggested that both direct attack by ozone and the attack of secondary radical species were responsible for degradation during the ozone treatment of aqueous solutions of carbohydrate model compounds. When ozonation occurred in water, the experimental evidence suggested that carbohydrate degradation was caused mainly by an attack of hydroxyl radicals whilst, in the presence of methanol, *tert*-butyl alcohol or acetic acid, degradation was due to direct ozone attack [39]. Moreover, radicals generated at the ozone–lignin reaction front were thought to be mainly responsible for cellulose degradation. The rate of direct cleavage of glycosidic bonds was also found to be similar to that of carbonyl group formation, providing further support that cellulose degradation is caused by radical attack. Cellulose degradation in the reacted region of the pulp contributed only a few percent of the total cellulose degradation [17].

Model compound studies using methyl 4-*O*-ethyl- $\beta$ -D-glucopyranoside were conducted to elucidate the role of radical species in the polysaccharide degradation during ozone treatment [10]. It was concluded that both ozone itself and radical species each participate in the glycosidic bond cleavage of carbohydrates during ozonation in aqueous solutions. The free radical-mediated reaction may lead to both direct cleavage and to the conversion of hydroxyl to carbonyl groups [10].

Ozonations of methylpyranosides (alpha- and beta-anomers of methyl-D-glucopyranoside, methyl-D-mannopyranoside and methyl-D-xylopyranoside), as "model compounds" for cellulose, were performed in unbuffered aqueous solution at room temperature [40]. Methyl-alpha-D-xylopyranoside was found to degrade more slowly than the other compounds, whereas the rate of degradation was highest for methyl-D-mannopyranoside. In general, the degradation of alpha-anomers was slower than that of the corresponding beta-anomers. Monosaccharides, lactones, furanosides, and acidic compounds are formed during ozonation.

A lignin-carbohydrate complex (LCC), containing a D-xylose unit connected to an aromatic part (three aromatic units and no free phenolic group) through a beta-glycosidic bond, showed, that in dilute aqueous solution (6 mg LCC/100 mL water) the initial reaction rate was extremely fast, and that the degradation of aromatic structures in the lignin-mimicking portion of the LCC was complete during the first 30 minutes of ozonation [40]. However, degradation of the carbohydrate part occurred more slowly, suggesting that lignin might provide a degree of protection against attack by ozone on cellulose in lignin-containing pulps. Ozonated LCC samples showed further that C=O structures are produced during ozonation [40]. A proposed reaction mechanism for the ozonation of methyl- $\beta$ -D-glucopyranoside (M $\beta$ G) initiated by direct ionic attack by ozone at the glycosidic linkage is described in Scheme 7.35 [40]. Electrophilic attack by ozone at the anomeric oxygen of M $\beta$ G (**25**) results in the formation of the tetroxide intermediate (**38**), which decomposes to the carbonium ion (**39**), hydroperoxide and oxygen. On reaction with water, (**39**) converts to glucose (**40**), which is further attacked by ozone and gives gluconic acid (**33**) via radical oxidation. Arabinose (**34**) is produced via a Ruff-type degradation involving hydroxyl radicals. Pan et al. [20] found that **33** was the major product in the first stages of ozonation of M $\beta$ G in buffered solution, indicating that **33** and its lactone (**32**) could be obtained from sources other than the initially formed glucose (**40**). These authors suggested that the  $\beta$ -glucoside is also attacked by ozone at the C-H bond of the anomeric carbon by a 1,3-dipolar addition mechanism (Scheme 7.35, path B). This results in the formation of a hydrotrioxide hemiorthoester (**26**), which may undergo several routes of fragmentation. Orbital-assisted fragmentation via the orthoester would produce methyl gluconate (**29**). Fragmentation assisted by the intermolecular hydrogen-bonded ring structure (**28**) would produce gluconic acid- $\delta$ -lactone (**32**). For a successful ozone attack at the anomeric C-H bond, each of the acetal groups must have an electron pair orbital antiperiplanar to the C-H bond [40]. Arabinose (**34**) may be attacked by ozone in a similar way to glucose, yielding arabinonic acid (**35**) and its  $\gamma$ -lactone (**43**), which was identified by Olkkonen et al. [40]. Methylgluconate (**29**) was not identified, but the methylfuranosides (**30**) and (**31**) were found.





**Scheme 7.35** A proposed reaction mechanism for the ozonation of methyl-β-D-glucopyranoside (redrawn from Oikkonen et al. [40]).

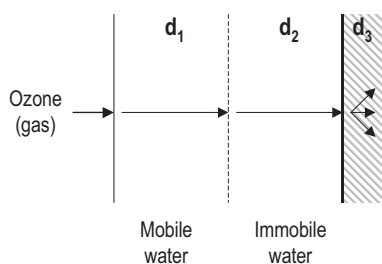
Direct attack by ozone at other positions of the hexose unit may also occur, and will result the formation of carbonyl and carboxyl groups by the insertion of ozone at the C–H bond [9]. The glucuronic acid (42) may be formed by attack at the C6-position of the glucose unit [40]. Prolonged ozonation resulted in a complex mixture of short-chain organic acids, whilst the production of hydroxyacetic acid (36) and 2,3-dihydroxypropanoic acid (37) is likely to proceed via gluconic acid (33).

### 7.5.5

#### Process Conditions

##### 7.5.5.1 Mass Transfer

In ozone bleaching, the rate-determining step is governed by the mass transfer of the oxidants to the active site in the fiber. This assumption is based on a model accounting for the reaction between ozone and the pulp fiber. This model, originally proposed by Osawa and Schuerch in 1963, involves low-consistency ozone bleaching to demonstrate the single transport processes (Fig. 7.83) [17].



**Fig. 7.83** Scheme of mass transfer in ozone bleaching according to Osawa and Schuerch [17] “Film model” infinite rapid transfer in the mobile water, and ‘ $k_a$ ’ determines transfer in immobile water.

In the first step, gaseous ozone, which is present in an oxygen/ozone gas mixture, is dissolved in the bulk or mobile water layer ( $d_1$ ) where ozone is transported by convection. The dissolved ozone (and its decomposition products) is further transported through an immobile water layer ( $d_2$ ) by diffusion. The latter becomes the rate-determining step as it is definitely slower than the convection transport in  $d_1$ . The amount of mobile water is gradually reduced by increasing the pulp consistency from low to medium. It can be assumed that at medium consistency no mobile water is present any more, and the thickness of the immobile water layer ( $d_2$ ) is controlling the reaction rate. A relationship between the thickness of the immobile layer and extent of the reaction has been recently established by Bouchard et al. [18]. The thickness of the immobile water layer surrounding the fiber as a function of pulp consistency can be easily calculated according to the concept of Bouchard et al. [18]. Fig. 7.84 shows (a quadrant of) the cross-section through a fiber considering both the dry and the swollen state.

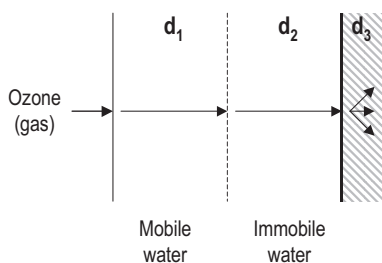
Direct attack by ozone at other positions of the hexose unit may also occur, and will result the formation of carbonyl and carboxyl groups by the insertion of ozone at the C–H bond [9]. The glucuronic acid (42) may be formed by attack at the C6-position of the glucose unit [40]. Prolonged ozonation resulted in a complex mixture of short-chain organic acids, whilst the production of hydroxyacetic acid (36) and 2,3-dihydroxypropanoic acid (37) is likely to proceed via gluconic acid (33).

### 7.5.5

#### Process Conditions

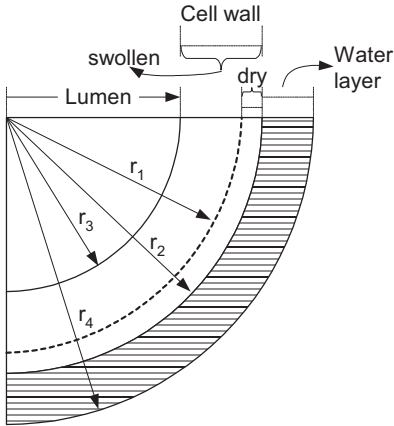
##### 7.5.5.1 Mass Transfer

In ozone bleaching, the rate-determining step is governed by the mass transfer of the oxidants to the active site in the fiber. This assumption is based on a model accounting for the reaction between ozone and the pulp fiber. This model, originally proposed by Osawa and Schuerch in 1963, involves low-consistency ozone bleaching to demonstrate the single transport processes (Fig. 7.83) [17].



**Fig. 7.83** Scheme of mass transfer in ozone bleaching according to Osawa and Schuerch [17] “Film model” infinite rapid transfer in the mobile water, and ‘ $k_1a$ ’ determines transfer in immobile water.

In the first step, gaseous ozone, which is present in an oxygen/ozone gas mixture, is dissolved in the bulk or mobile water layer ( $d_1$ ) where ozone is transported by convection. The dissolved ozone (and its decomposition products) is further transported through an immobile water layer ( $d_2$ ) by diffusion. The latter becomes the rate-determining step as it is definitely slower than the convection transport in  $d_1$ . The amount of mobile water is gradually reduced by increasing the pulp consistency from low to medium. It can be assumed that at medium consistency no mobile water is present any more, and the thickness of the immobile water layer ( $d_2$ ) is controlling the reaction rate. A relationship between the thickness of the immobile layer and extent of the reaction has been recently established by Bouchard et al. [18]. The thickness of the immobile water layer surrounding the fiber as a function of pulp consistency can be easily calculated according to the concept of Bouchard et al. [18]. Fig. 7.84 shows (a quadrant of) the cross-section through a fiber considering both the dry and the swollen state.



**Fig. 7.84** Simplified scheme of a quadrant of the cross-section through a pulp fiber in a medium-consistency pulp suspension (according to Bouchard et al. [18]).

In order to calculate the thickness of the immobile water layer ( $r_4 - r_2$ ), the following assumptions are made:

- Swelling occurs solely by shrinking the lumen.
- Fiber length ( $L$ ) remains constant during swelling.
- Cell wall thickness of an unbleached kraft pulp with 50% yield is  $1.4 \mu\text{m}$  ( $r_2 - r_1$ ) [19].
- $r_2$  is  $19.6 \mu\text{m}$  [19].
- Fiber saturation point (FSP) of an unbleached kraft pulp amounts to  $1.4 \text{ g water g}^{-1} \text{ dry pulp}$  [18].
- Specific volume of dry cell wall ( $V_{DW}$ ) amounts to  $1/1.53 = 0.654 \text{ mL g}^{-1}$ .
- Volume of the swollen cell wall ( $V_{SW}$ ) amounts to  $1/0.483 = 2.07 \text{ mL g}^{-1}$ .

Calculation of the radius of the lumen ( $r_3$ ) in the swollen state to obtain the volume of the water in the lumen ( $V_L$ ):

$$\frac{V_{SW}}{V_{DW}} = \frac{\pi(r_2^2 - r_3^2)L}{\pi(r_2^2 - r_1^2)L} \quad (100)$$

$V_L$  can be calculated according to Eq. (101) by using the value of  $r_3 = 14.7 \mu\text{m}$ :

$$\frac{V_L}{V_{DW}} = \frac{\pi \cdot r_3^2 \cdot L}{\pi \cdot (r_2^2 - r_1^2) \cdot L} \quad (101)$$

From Eq. (100), the value of  $V_L$  calculates to  $2.68 \text{ mL g}^{-1}$ . Considering this value, the amount of external water ( $V_{EW} \sim \text{immobile water}$ ) can be calculated for any

pulp consistency by subtracting the water in the cell wall ( $FSP = 1.4 \text{ mL g}^{-1}$ ) and the water in the lumen ( $V_L = 2.68 \text{ mL g}^{-1}$ ) from the total amount of water in a given pulp suspension. The thickness of the external water layer ( $V_{EW}$ ) requires the calculation of  $r_4$  (see Fig. 7.84) according to Eq. (102):

$$\frac{V_{EW}}{V_{DW}} = \frac{\pi(r_4^2 - r_2^2)L}{\pi(r_2^2 - r_1^2)L} \quad (102)$$

The thickness of the adsorbed water layer can then be estimated by  $\delta = (r_4 - r_2)$ . The calculated values for  $\delta$  are summarized in Tab. 7.39.

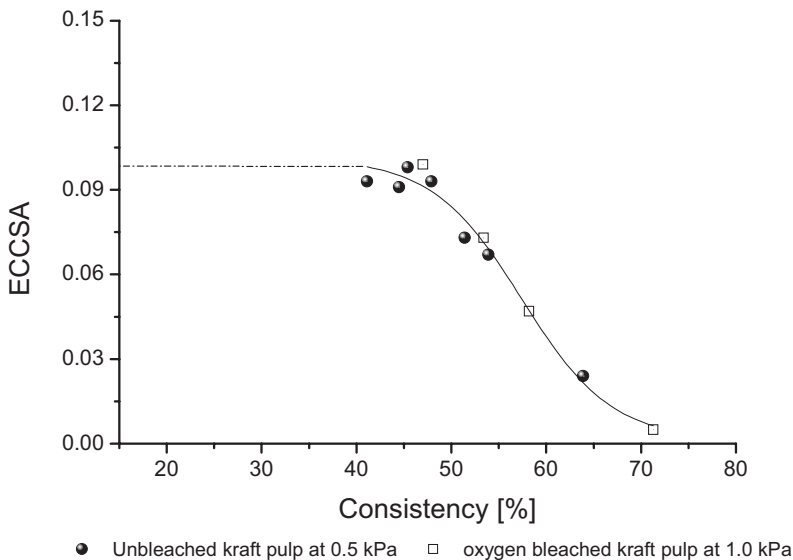
**Table 7.38** The thickness of the water layer surrounding the fiber in the consistency range from 8 to 20% estimated according to the assumptions made by Bouchard et al. [18].

Consistency [%]	Water layer thickness $(r_4 - r_2)$ [ $\mu\text{m}$ ]
8	11.8
10	8.4
12	5.8
14	3.9
16	2.3
18	1.0
20	–

Experiments on static ozone bleaching (no mixing) of black spruce kraft pulp sheets (kappa number 29.2) were carried out to investigate the influence of the thickness of the immobile water layer on the extent of delignification, while keeping the reaction conditions constant (time, temperature, pH). It transpired, clearly, that increasing the consistency of the pulp sheet leads to a reduction in kappa number at a given pulp sheet thickness [18]. This implies that there is less water to diffuse with increasing consistencies, assuming a constant rate of diffusion of ozone in water. Thus, it can be concluded that medium-consistency ozone bleaching is a diffusion-controlled process, and mixing is the key parameter to ensure fast reactions by breaking up the  $d_2$  layer. At high consistency (typically 35–40%), where both water layers,  $d_1$  and  $d_2$ , tend to zero, ozone gas is directly in contact with the wetted cellulose gel. Ozone can diffuse quickly through the thin immobile layer to the reaction site within the cell wall.

At consistencies equal to the fiber saturation point ( $\sim 1.4 \text{ g water g}^{-1}$  o.d. pulp, equal to 42% consistency) and higher, no excess liquid is present on the external

surface of the fibers or inside the lumen. In this case, the rate-determining step for the reactions with the pulp components is diffusion through the fiber wall. The reaction front gradually proceeds from the external fiber wall to the lumen during high-consistency ozonation, as has been confirmed by UV microspectrophotometry [20]. The rate of conversion of pulp components across the porous structure of the cell wall is diffusion-controlled and can be successfully modeled by using the shrinking core model [21–23]. The ozonation rate further increases with increasing consistency until a consistency of about 50% is reached [23,24]. This behavior can be explained by a reduction of the diffusion path due to shrinking of the cell wall thickness which dominates over an incipient decrease in diffusivity. The decrease in the degradation rate of pulp components (both lignin and cellulose) at consistencies above 50% during ozonation can be attributed to the reduction in the effective diffusional transport in the cell wall, expressed as the effective capillary cross-sectional area (ECCSA, defined as the ratio of effective diffusivity and molecular diffusivity), due to pore closure. The course of the ECCSA over the consistency range 40–70% is shown graphically in Fig. 7.85. According to these results, the accessibility of ozone to the cell wall components is extremely impaired at consistencies above 70%.



**Fig. 7.85** Effective capillary cross-sectional area (ECCSA) of the fiber wall as a function of pulp consistency, calculated on the basis of the shrinking core model (according to [23]). It is assumed that the ECCSA below the fiber saturation point (at consistencies <42%) remains at the same level as exactly at the fiber saturation point, since in both cases the cell wall pores are completely filled with water.

### 7.5.5.2 Mixing and Mixing Time

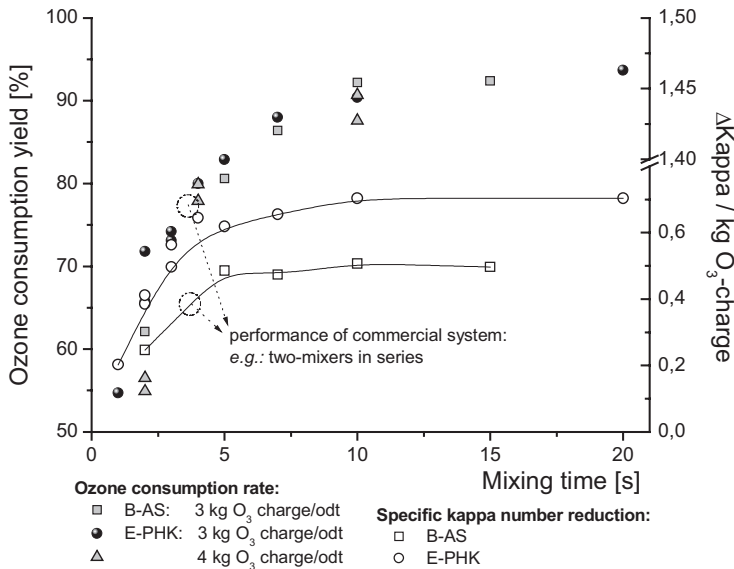
As mentioned above, the delignification rate during ozonation is determined by the rate at which ozone is transferred from the gas to the liquid phase. Thus, ozone delignification – particularly at medium consistency – depends heavily on efficient mixing of the ozone/oxygen gas with the pulp fiber suspension. The volumetric gas–liquid mass transfer coefficient,  $k_{l,a}$ , characterizes the efficiency of gas–liquid mixing. Analogous to oxygen delignification, the solubilization of ozone in the acidified pulp suspension is accomplished by high-shear mixing (see Section 7.2). The influence of process variables on  $k_{l,a}$  during the course of high-shear mixing was investigated by Rewatkar and Bennington [25]. An increase in the fiber mass concentration (pulp consistency) clearly leads to a decrease in  $k_{l,a}$ . This is explained by the increase in apparent viscosity of the suspension, which in turn reduces the extent of turbulence in the liquid phase throughout the suspension (apparent viscosity,  $\mu_a$ , relates to pulp consistency,  $C_m$ , according to the equation  $\mu_a = 1.5 \times 10^{-3} \times C_m^{3.1}$ , which gives an apparent viscosity of 1.9 Pa.s for a pulp suspension with a consistency of 10%, which is 1900-fold that of pure water [26]). In addition, pulp consistency also affects the flow regime of the suspension. As pulp consistency increases, the amount of gas dispersed in the suspension decreases because the size of the cavities that form behind the rotor blades increases [25]. Furthermore,  $k_{l,a}$  depends on power consumption per unit reactor volume,  $\varepsilon$ , and on the gas void fraction,  $X_g$ . It was shown that the energy dissipation decreases exponentially as pulp consistency increases, while the overall power consumption remains constant. Power consumption, however, decreases with increasing gas void fraction ( $X_g$ ), particularly above  $X_g = 0.3$ – $0.4$ , whereas  $k_{l,a}$  increases with increasing  $X_g$ . Rewatkar and Bennington [25] have established an empiric equation where the introduced process variables are related to  $k_{l,a}$ :

$$k_{l,a} = 1.17 \cdot 10^{-4} \cdot \varepsilon^{1.0} \cdot X_g^{2.6} \cdot \text{Exp}(-0.386 \cdot c_m) \quad (102)$$

where:  $\varepsilon$  = power dissipation per unit reactor volume ( $\text{W m}^{-3}$ );  $X_g$  = gas void fraction (–); and  $C_m$  = pulp consistency (%).

By using typical mill data [27], where  $\varepsilon = 1.47 \times 10^6 \text{ W m}^{-3}$ ,  $X_g = 0.158$  and  $C_m = 10\%$ ,  $k_{l,a}$  calculates to  $0.03 \text{ s}^{-1}$ .

As demonstrated in Chapter 7 (Section 7.2.4), high-shear mixing exerts high shear forces to the liquid–solid interface of the immersed fibers, thus reducing the thickness of the immobile water layer. Nevertheless, the reaction between ozone and the pulp constituents remains under the control of diffusion of the dissolved ozone through both the remaining immobile water layer and the cell wall (including the diffusion of reaction products through the cell wall and the water layer into the bulk solution). This leads to the conclusion that the efficiency of medium-consistency ozone bleaching also depends on mixing time, even under fully turbulent conditions. The influence of mixing time on the performance of medium-consistency ozone bleaching of two different dissolving wood pulps was investigated by using a laboratory high-shear mixing system [28]. The results (see Fig. 7.86 confirm that the retention time in commercial medium-consistency, high-shear



**Fig. 7.86** Influence of mixing time of a laboratory high-shear mixer on ozone consumption rate and specific kappa number reduction ( $\Delta\kappa$  kg<sup>-1</sup> O<sub>3</sub>-charge) of an EO-pretreated beech acid sulfite dissolving pulp (B-AS, kappa 1.8) and an OO-pretreated eucalyptus-prehydrolysis kraft (E-PHK pulp, kappa 2.6) (according to Refs. [16,28]). Ozone bleaching conditions: 50 °C, 10% consistency, pH 2,  $X_g = 0.23$  for both O<sub>3</sub>-charges (3.0 and 4.0 kg odt<sup>-1</sup>, respectively)  $P_{O_3} = 60\text{--}90$  kPa,  $\varepsilon = 2.5 \times 10^6$  W m<sup>-3</sup>, impeller speed = 50 s<sup>-1</sup>.

mixers which typically equals less than 1 s is certainly not sufficient to obtain a quantitative conversion rate [28].

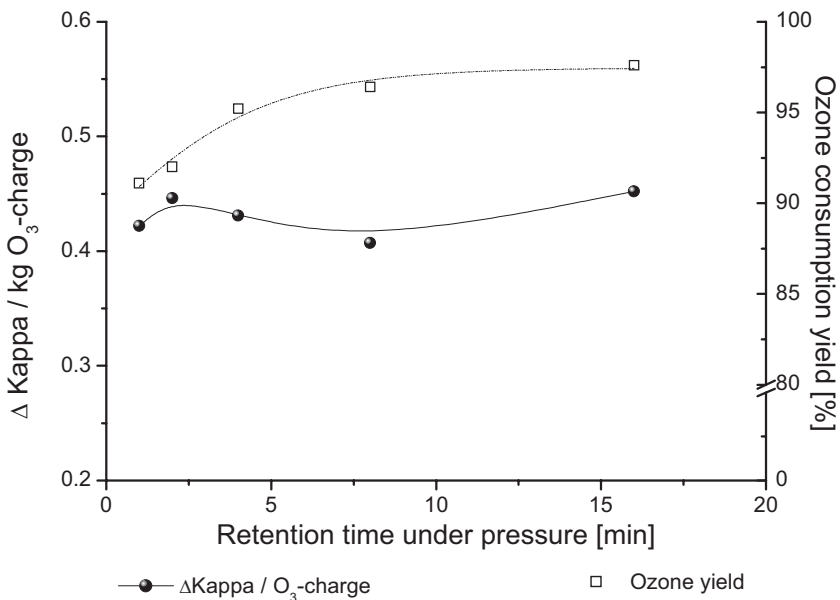
It can be seen clearly that concurrently for both pulps, a mixing time of 7–10 s under turbulent flow conditions is required to reach a complete reaction yield. Similar results have been obtained by other researchers [29–31]. [Comparisons of the performance of an industrial medium-consistency ozone bleaching system comprising the installation of two high-shear mixers in series to ensure a long mixing time are shown in Figs. 7.105 and 7.106.] Despite a mixing time of approximately 3.5 s, the large-scale medium-consistency ozone bleaching system attains only 70–75% of the efficiency of a laboratory system with a typical mixing time of 10 s, considering an ozone charge of 3–4 kg O<sub>3</sub> odt<sup>-1</sup> [16]. The prolongation of mixing time, for example, by installing several high-shear mixers in series, clearly produces both a very high specific energy consumption (a typical industrial high-shear mixer allowing a mixing time of ca. 1 s has an energy consumption of ca. 6 kWh odt<sup>-1</sup> or 11 kWh odt<sup>-1</sup> including a medium-consistency pump) and a modification of the fiber properties, mainly with respect to pulp freeness (decreases) and sheet stretch per unit tensile strength (increases) [32]. Laboratory mixer experiments revealed that fiber properties are mainly affected by the impeller geometry, especially with respect to fiber curl, and not by mixing time, whereas fiber wall dislocations are more related to residence time in the mixer [33]. Indus-



trial medium-consistency mixers produce minimal fiber curl increase, and this is attributed to a uniform shear gap between the stationary and rotating elements, as well as a very short mixing time. Mielisch et al. reported that, after prolonged high-intensity mixing, the beating resistance and tensile strength of an OP-prebleached spruce kraft pulp decreased while tear strength increased in the range of low beating degrees [29].

Thus, the question arises if – similar to oxygen delignification – retention of the ozone-containing gas and the pulp suspension in a pressurized tower leads to further oxidation of the pulp components. However, several laboratory studies revealed that no considerable delignification occurs in a pressurized tower after mixing, while the ozone consumption yield further increases, as shown graphically in Fig. 7.87.

The reason for the low reactivity of medium-consistency ozone bleaching in the absence of high-shear mixing may be explained by the low ozone concentration in the gas phase, the slow mass transfer rate of ozone through the liquid film to the reaction site in the cell wall due to long diffusion paths, and the high instability of dissolved ozone in the aqueous phase. The increasing consumption rate of ozone over time, but without any additional chemical reaction with the pulp compo-

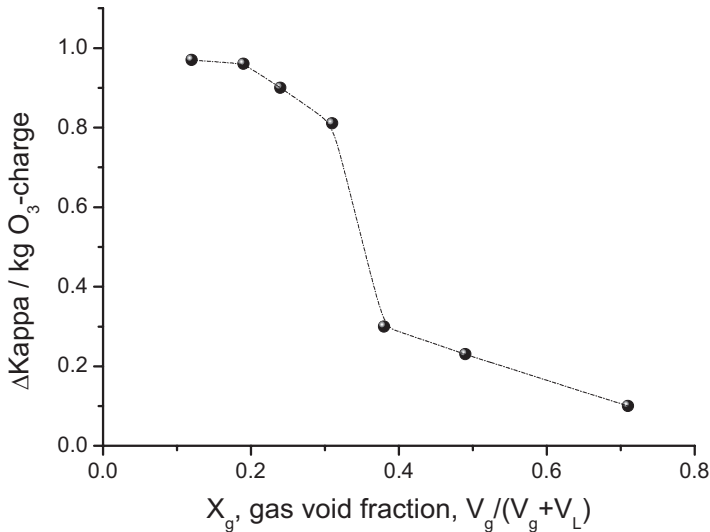


**Fig. 7.87** Influence of retention time after high-shear mixing at a given pressure (0.6 MPa) on the ozone consumption yield and specific kappa number reduction ( $\Delta \text{kappa kg}^{-1} \text{O}_3\text{-charge}$ ) of an EO-pretreated beech acid sulfite dissolving wood pulp (B-AS, kappa 1.9, viscosity  $627 \text{ mL g}^{-1}$ ). Ozone bleaching conditions:  $55^\circ\text{C}$ , 10% consistency, ozone charge: 2.2–2.3  $\text{kg odt}^{-1}$ , pH 2, carry-over 5  $\text{kg COD odt}^{-1}$ ,  $X_g = 0.23$ ,  $\varepsilon = 2.5 \times 10^6 \text{ W m}^{-3}$ , impeller speed =  $50 \text{ s}^{-1}$ .

nents, is a clear indication of ozone decomposition. The observations made in laboratory trials that a subsequent pressurized tower after mixing has almost no effect on delignification are also confirmed in industrial practice. Consequently, medium-consistency ozone bleaching operates with no subsequent bleaching tower. The system pressure is released in a subsequent blow tank with gas separation and a scrubber to clean the gas from fibers before it enters the ozone destruction unit. In some cases, a small reactor with a retention time of about 1 min is inserted between the mixer(s) and the pulp discharger.

In medium-consistency mixing, a turbulent flow regime – in the presence of gas – can only be maintained if the gas void fraction ( $X_g$ ) is limited to a certain value (see Table 7.36). By exceeding this value, gas cavities are formed which prevent efficient micro-scale mixing. The first trials of medium-consistency ozone bleaching in 1986 in Baienfurt, Germany, were unsuccessful because ozonation of the medium-consistency pulp suspension was performed at almost atmospheric pressure conditions. Finally, laboratory trials have shown that reducing the gas void fraction by compressing the ozone containing gas enables an efficient delignification performance (Fig. 7.88).

Figure 7.88 shows that efficient medium-consistency ozone bleaching is limited to a gas void fraction of about  $X_g = 0.3$ , with a mixing time of 10 s. Similar experiences were reported by others. For example, Funk et al. showed that the pilot plant



**Fig. 7.88** Influence of the gas void fraction on the specific kappa number reduction of an O-pretreated eucalyptus prehydrolysis-kraft pulp, kappa 4.7. Ozone bleaching conditions: 50 °C, 9.2% consistency, ozone charge: ~ 3.0 kg odt<sup>-1</sup>, pH 2, impeller speed = 50 s<sup>-1</sup>, 10 s mixing time.

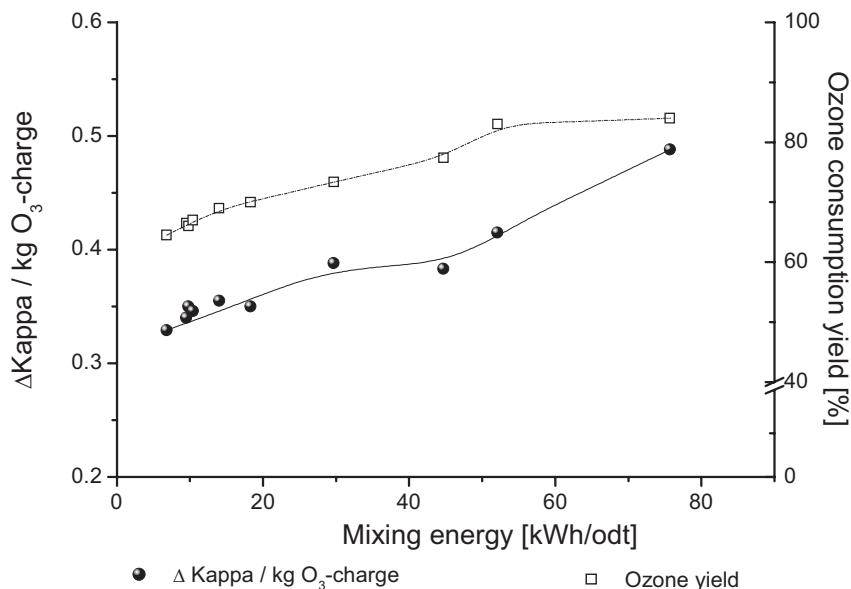
medium-consistency ozone plant operated successfully up to a gas void fraction of 0.35 [34], while pilot plant trials at Paprican revealed a significant decrease in the efficiency of delignification when exceeding a gas void fraction of about 0.36 [35].

The breakthrough for medium-consistency ozone bleaching was certainly the development of a technology to compress ozone-containing gas [36–39]. Keeping the pressure as high as possible is also advantageous, as ozone solubility and retention time both increase. In modern medium-consistency ozone plants, the pressure in the gas feeding points before the mixers is between 0.6 and 1.0 MPa. The relationship between the possible maximum ozone charge in one medium-consistency mixer at a given limit for  $X_g$  with the corresponding reaction conditions, such as ozone concentration in the feed gas, pulp consistency, pressure inside the mixer and temperature is detailed in Tab. 7.36. The technology of ozone bleaching is introduced in Section 7.5.6.

### 7.5.5.3 Effect of Pulp Consistency

The basic development of ozone bleaching of chemical pulp was exclusively carried out in the low (LC) and high (HC) consistency ranges. Medium-consistency ozone bleaching has long been considered impossible because of the lack of appropriate mixing technology and the need for mixing large volumes of gas with the pulp suspension. Even with the development of high-shear mixers, MC ozone bleaching technology has remained initially unsuccessful. The first trials on a pilot scale were carried out in 1986 at Baienfurt in Germany, but the results were poor, due mainly to the fact that ozone treatment of the medium-consistency pulp was performed at almost atmospheric pressure conditions. The breakthrough of medium-consistency ozone technology occurred only when the ozone-containing gas was compressed to below a gas void fraction,  $V_g$ , of about 0.35 to ensure homogeneous mixing of the gas with the pulp suspension [37–39]. The successful laboratory and pilot plant trials finally led to the first commercialization of ozone bleaching using medium-consistency technology at the viscose pulp mill at Lenzing AG, Lenzing Austria in 1992 [40,41]. There, an ozone stage replaced the hypochlorite stage in an EOP-H-P sequence, thus converting to EOP-Z-P.

In LC bleaching, vigorous stirring of the very dilute pulp suspension is a prerequisite to dissolving ozone in water and transferring it to the reaction site by convection through the bulk water, and by diffusion across the immobile water layer surrounding the fiber. Under these conditions, a rather homogeneous reaction between ozone and fibers can be expected. However, during the past 14 years of commercialization of ozone bleaching technology, it transpired that LC ozone bleaching was not economically applicable on an industrial scale because of the very high energy demand for mixing, high investment costs, and low bleaching/delignification efficiency due to competitive reactions with dissolved oxidizable matter. The influence of mixing energy as a function of ozone consumption rate and specific kappa number reduction of a beech acid sulfite dissolving pulp (B-AS) is shown in Fig. 7.89.



**Fig. 7.89** Low-consistency (LC) ozone bleaching of a beech acid sulfite dissolving wood pulp (B-AS, kappa after EO-pretreatment 1.8) carried out in a 500 kg day<sup>-1</sup> pilot plant at Waagner Biro, Austria. Conditions of LC ozone bleaching: pulp consistency 2%, 50 °C, average retention time 17 min, pH 2.5, ozone charge 2–2.4 kg odt<sup>-1</sup>. Influence of mixing energy on the performance of LC ozone bleaching (according to Refs. [28,42]).

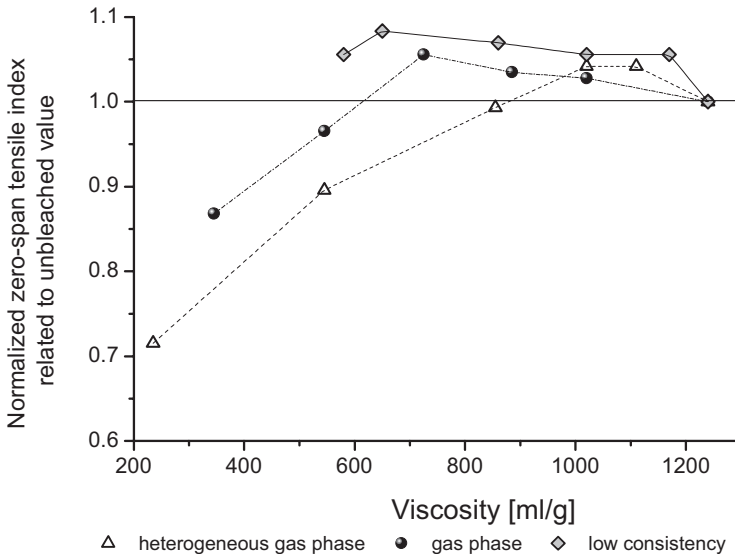
The results of these pilot plant trials clearly indicate that a high mixing energy must be employed to ensure a reasonably good performance of ozone delignification. A mixing energy of about 50–60 kWh odt<sup>-1</sup> in LC ozone technology equals the delignification efficiency of medium-consistency ozonation applying only 11 kWh odt<sup>-1</sup> (MC-pump: 5 kWh odt<sup>-1</sup>, MC-mixer: 6 kWh odt<sup>-1</sup>). The corresponding delignification performances of both ozone bleaching technologies are illustrated graphically in Figs. 7.85 and 7.88.

More detailed results of the pilot plant trials on LC ozone bleaching are reviewed elsewhere [28,42].

In high-consistency HC ozone bleaching, the fibers are surrounded by a very thin layer of water, while most of the residual water is embedded in the cell wall pores [assuming that a fiber saturation point of 1.5 mL g<sup>-1</sup> corresponds to a consistency of  $(1-1.5/2.5) = 40\%$ ]. Local variations in dry solids content may thus create fibers containing layers of immobile water of different thickness. The reactivity of ozone with the pulp fibers depends very much on the thickness of the immobile water layer. A laboratory study using a sulfite pulp revealed a maximum ozone consumption at consistencies of 30–50% comprising a consistency range from below 10% to above 90% [5]. Interestingly, the extent of ozone consumption significantly decreases at consistencies above 50%. This may be explained by a reduced accessibility of ozone to the reaction sites.

Regions of a thick immobile water layer around the fibers resist the reaction with ozone, whereas those of a thin water layer receive too high an ozone dose. Moreover, the pulp fibers must be separated from each other by fluffing as a prerequisite to enable ozone to come into contact with the water layers surrounding the single fibers.

Lindholm investigated the influence of consistency on ozone bleaching using an unbleached pine kraft pulp after acidifying to pH 2.8 [43]. Two different modes of gas phase ozone bleaching at 35% consistency were compared with LC ozone bleaching at 1% consistency (denoted *low consistency*). In one mode of HC ozone bleaching, extreme heterogeneity was simulated by separating the pulp samples into four portions which then were ozonated in series. The properties of the pulps in the four bottles were examined separately, and the average properties were calculated thereof (samples denoted *heterogeneous gas phase*). As a reference, HC ozone bleaching was performed using a standard procedure (samples denoted *gas phase*). This standard procedure included a thorough fluffing of the pulp prior to ozonation. The ozone dosage was increased step-by-step to 5.8% on o.d. pulp in the case of LC, and to 7.5% on o.d. pulp in the case of HC ozone bleaching (both modes). The heterogeneity of ozone bleaching is clearly reflected by the relationship between intrinsic pulp viscosity (average) and the zero-span tensile index. Figure 7.90 illustrates that this relationship depends heavily on the mode of operation.



**Fig. 7.90** Relationship between normalized zero-span tensile index (related to the value of the starting pine kraft pulp =  $148 \text{ Nm g}^{-1}$ ) and pulp viscosity of ozonated pine kraft pulp comprising various conditions of ozone bleaching (according to [43]): low consistency at 1% consistency versus gas phase at 40% consistency and heterogeneous gas phase.

In heterogeneous gas phase treatment, the zero-span tensile index begins to decrease at an average level of about  $950 \text{ mL g}^{-1}$ , probably due to severe carbohydrate degradation in the fibers closest to the ozone inlet. By contrast, in normal gas phase ozonation, much lower pulp viscosity levels can be tolerated without impairing strength properties. The loss of zero-span tensile strength at rather low ozone charge may be explained as a result of the greater heterogeneity in the reactions between ozone and pulp during gas phase ozonation. This may create zones with very low lignin contents, allowing intensified attack of ozone on carbohydrates.

The highest delignification selectivity was obtained in LC ozone bleaching. There, strength properties were preserved even at pulp viscosity levels as low as  $520 \text{ mL g}^{-1}$  [43]. Lindholm also found that in LC ozone bleaching of a pine kraft pulp, the zero-span tensile index remained fairly constant up to an ozone consumption of about 5% on o.d. pulp, while in HC ozonation the strength properties decreased at ozone consumption levels beyond 2% on o.d. pulp [44]. This behavior may be explained by a rather homogeneous reaction between ozone and the single pulp fibers. A similar interpretation of the results has been given when comparing the degradation processes caused by ozonation and acid hydrolysis [45]. The molar mass distribution revealed the formation of two distinct cellulose distributions during ozonation of an unbleached birch kraft pulp. However, HC ozone bleaching shows a higher efficiency of lignin removal at a given ozone charge. As a combined effect, equal selectivity was obtained for HC and LC bleaching, provided that the kappa number after ozonation was maintained above 17 (equals kappa number reduction smaller than 50% with a starting kappa number of 34). When bleaching to lower kappa numbers, the selectivity of HC ozone bleaching was inferior to that of a LC operation [44]. The higher selectivity of LC as compared to HC ozone bleaching was attributed, at least in part, to dissolved lignin fragments, which act as carbohydrate protectors [46].

The performance of medium-consistency ozone bleaching is described as resembling that of LC ozone bleaching rather than that of HC ozone bleaching, especially with respect to bleaching and delignification selectivity. Laxen et al. concluded that in the range of 1 to 10% consistency, the selectivity of ozone delignification does not depend on consistency [37]. Similar conclusions were made by others [39], though no differences with regard to delignification selectivity between laboratory HC and medium-consistency ozone bleaching have been observed for oxygen-delignified pine ASAM paper pulp and beech ASAM dissolving pulp [47]. This can be explained by both efficient fluffing prior to ozonation and to the presence of a highly accessible and easily oxidizable kappa number.

Commercial ozone bleaching installations worldwide are operated at medium (about 10%) and high (about 35%) pulp consistencies, with the majority using medium consistency (Tab. 7.39).

Table 7.39 Ozone bleaching installations in 2004 [48, 49]

Mill	Location	Bleaching sequence	Z-Stage consistency	Process supplier	Ozone generator manufacturer	Pulp process, Pulp grades	Ozone charge [kg t <sup>-1</sup> ]	Pulp capacity [adt · 10 <sup>3</sup> a <sup>-1</sup> ]
Lenzing AG	Lenzing	(EOP)ZP	MC	Kvaerner	WS-OT	HW-Sulfite, DP	2	230
Lenzing AG	Lenzing	(EOP)ZP	MC	Kvaerner	WS-OT	HW-Sulfite, DP		
Union Camp	Franklin, VA	OZ(EO)D(E)P	HC	Sunds	Ozonía	SW-Kraft, P		300
Södra Cell	Monstera	OQ(OP)(ZQ)(PO)	MC	Kvaerner	Trailigaz	SW-, HW-Kraft, P	2	700
Wisaforest	Pietarsaari	O(ZD)(EO)(ZD)(EP)D	MC	Ahlström	Trailigaz	SW-, HW-Kraft, P	2	630
M-real Husum	Husum	OQPZD	MC	Ahlström	Ozonía	HW-Kraft, P		690
Metsä-Botania	Kaskinen	OQZQ(EOP)ZP, OD(EOP)ZP	MC	Ahlström	Ozonía	SW-, HW-Kraft, P		425
Peterson Seflle	Säffle	ZEP	MC	Kvaerner	WS-OT	SW-Sulfite, P	6	50
Bahiapulp	Camacari	(OO)AZP	MC	Kvaerner	WS-OT	HW-PHK, DP	4	120
SCA Östrand	Timrå	OOQ(OP)A(ZQ)(PO)	HC	Sunds	Ozonía	SW-Kraft, P		400
Sappi	Ngodwana	OA(ZD)(EO)D	HC	Andritz, Sunds	Ozonía	SW-, HW-Kraft, P		240
Ponderosa Fibers	Memphis, TN	ZPZP	MC	Ahlström	Ozonía	Recycled Fibers		60
Metsä-Rauma	Rauma	OO(ZQ)(PO)(ZQ)(PO/PO)	MC	Ahlström	WS-OT	SW-Kraft, P		550
Stora Enso North America	Wisconsin Rapids	OAZ(EO)DD	HC	Sunds	Ozonía	HW-Kraft, P		240
Votorantim	Luiz Antonio	OO(ZD)(EOP)D	MC	Kvaerner	Ozonía	HW-Kraft, P	4	350
Votorantim	Jacarei	OQ(OP)(ZE)D	MC	Kvaerner	Ozonía	HW-Kraft, P	4-5	280
Klabin	Monte Alegre	OQ(OP)(ZQ)(PO)	MC	Kvaerner	WS-OT	SW-, HW-Kraft, P	4	140
Mattusierte (Research)	France		HC		OZONIA	recycled		
Domtar	Espanola	OA(ZD)E(Dn)D	MC	Ahlström		HW-Kraft, P	3-6	370
ZPR Rosenthal	Blankenstein	(OO)Q(OP)(DQ)Z(PO)P	HC	Sunds	WS-OT	SW-Kraft, P		280
Burgo Ardenmes	Virtou	(OO)D(Z(EO))(DD)	HC	Sunds	Ozonía	HW-Kraft, P		400
Nippon Paper	Yufutsu	O(ZD)(EOP)D	MC	Andritz	Ozonía	HW-Kraft, P		175
Nippon Paper	Yatsushiro	O(ZD)(EOP)D	MC	Andritz	Wedeco	HW-Kraft, P		210
Oji Paper	Nichinan	OaZEPD	HC	Metso	Ozonía	HW-Kraft, P		262
Votorantim	Jacarei	OA(ZE)DP	HC	Metso	Wedeco	HW-Kraft, P		735
Glatfelter	Spring Grove	O(ZD)(EOP)D	LC	Andritz	Wedeco	HW-Kraft, P		223
Neusiedler SCP	Ruzomberok	OO(A)(Z(EOP)(D <sub>n</sub> )D)	HC	Metso	Wedeco	SW-, HW-Kraft, P	3-4	370
Total	Total							8430

HW = hardwood, SW = softwood; MC = medium-consistency.

HC = high-consistency.

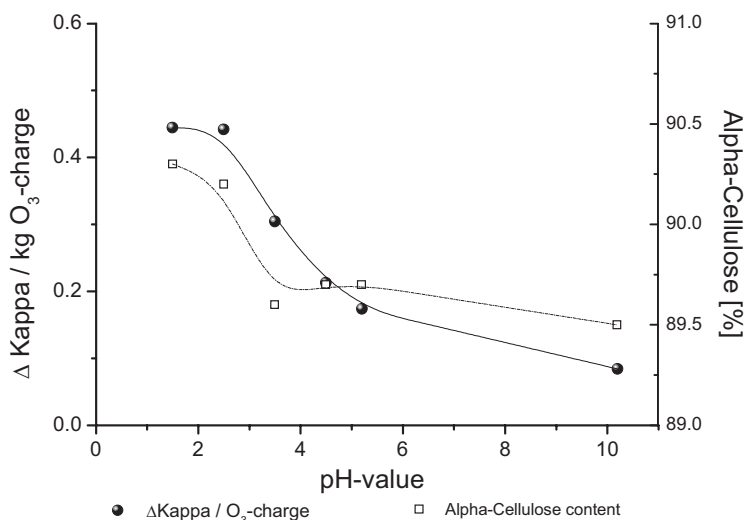
DP = dissolving pulp.

P = paper pulp

### 7.5.5.4 Effect of pH

The pH of the aqueous pulp suspension significantly affects the performance of ozone bleaching. It is generally agreed that the best efficiency of ozone delignification is achieved at a pH below 3 [50,51]. Therefore, industrial ozone bleaching is carried out in the pH range between 2 and 3 by acidifying the pulp suspension, predominantly with sulfuric acid. Lindholm found that acidification to pH 3 does not affect viscosity development, while lignin removal was enhanced [44]. The degree of delignification is increased if acidification is carried out as a pretreatment, followed by dewatering. In this particular case, this may be explained by the removal of transition metal ions during an acid prewash. The type of acid used (among sulfuric, acetic, oxalic acid and  $\text{SO}_2$  water) to adjust the pH to about 3 prior to LC ozone treatment had no influence on the performance of delignification [52]. Besides delignification efficiency, the alpha-cellulose content of a beech acid sulfite dissolving pulp is also impaired by a high pH during ozonation (Fig. 7.90). The degradation of the alpha-cellulose occurs parallel to a loss in viscosity, which strengthens the hypothesis that pH determines the yield of reactive species during ozonation [28]. This view is supported by the results obtained from reactions between ozone and carbohydrate model compounds in aqueous media, where the extent of radical reaction increases with increasing pH [53].

The beneficial effect of low pH has been ascribed to several factors. Ozone undergoes self-decomposition in water by a radical chain mechanism, initiated by hydroxide ions and propagated by the superoxide anion radical and the hydroxyl radical (see Scheme 7.28 and equation (90) [54,55]). Pan et al. have shown that, for an ozonation



**Fig. 7.91** Effect of pH on delignification efficiency,  $\Delta\kappa/\text{O}_3\text{-charge}$ , and on alpha-cellulose content during ozonation (according to [28]). Pulp: E/O-pretreated beech acid sulfite dissolving wood pulp (B-AS), kappa number 1.9,

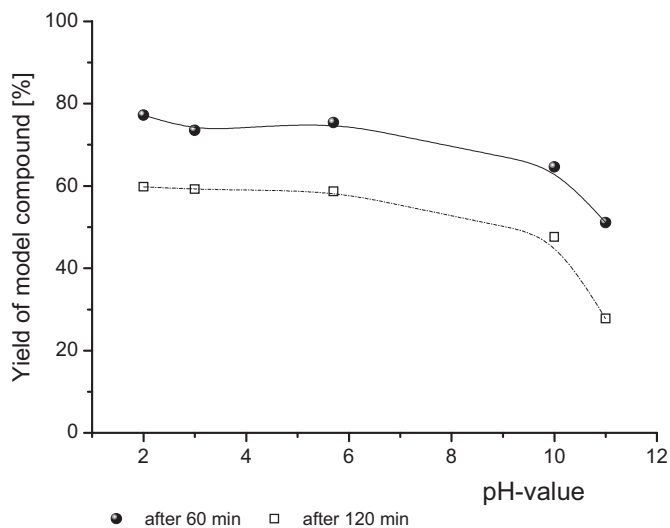
viscosity  $627 \text{ mL g}^{-1}$ ; medium-consistency Ozone bleaching: 10% consistency, temperature  $55^\circ\text{C}$ , 10 s mixing time; ozone charge:  $2.2\text{--}2.3 \text{ kg odt}^{-1}$ , carry-over:  $5 \text{ kg COD odt}^{-1}$ .



time of 10 min, 95% of the original ozone charge will remain in water at pH 3, and only 63% at pH 7 after 10 min [56]. The course of dissolved ozone concentration in pure water as a function of time at both pH levels is shown in Fig. 7.82.

In MC ozone bleaching, the reaction time is, however, less than 1 s. During this short time, the decomposition of ozone is probably not sufficiently high (<1% of  $O_3$ -charge at pH 7) to account for the difference in ozone reactivity observed between pH 3 and pH 7. The higher efficiency of ozonation at low pH has also been related to the higher ozone solubility in water, as expressed in Eq. (87). The increase in reactivity is thus explained by the higher rate of diffusion across the immobile water layer [18]. Furthermore, recent studies have suggested that the radical yield obtained in the direct reaction between ozone and phenolic lignin model compounds starts to increase rapidly at about pH 3, whereas nonphenolic compounds induce increased radical formation at pH values beyond 6 [57,58]. The pH-dependence of radical yield has been explained by the preference of reaction pathways involving homolytic cleavage of the hydrotrioxide intermediate at higher pH levels. Results from model compound studies support that the proportion of radical reactions involved in the degradation of carbohydrate structures increases with rising pH.

The results outlined in Fig. 7.92 indicate that the extent of carbohydrate degradation in acidic water (pH 2–3) is almost the same as in distilled water (pH 5.7), partly because the pH of the reaction medium decreases during ozonation due to the formation of acids (initial pH of 5.7 decreases to 3.6). However, in alkaline aqueous solution (pH 10 and 11), the contribution of radical reactions increases, as indicated by the lower relative reactivity at C1, which is shifted from 55% in distilled water to 49% at pH 11 [53].

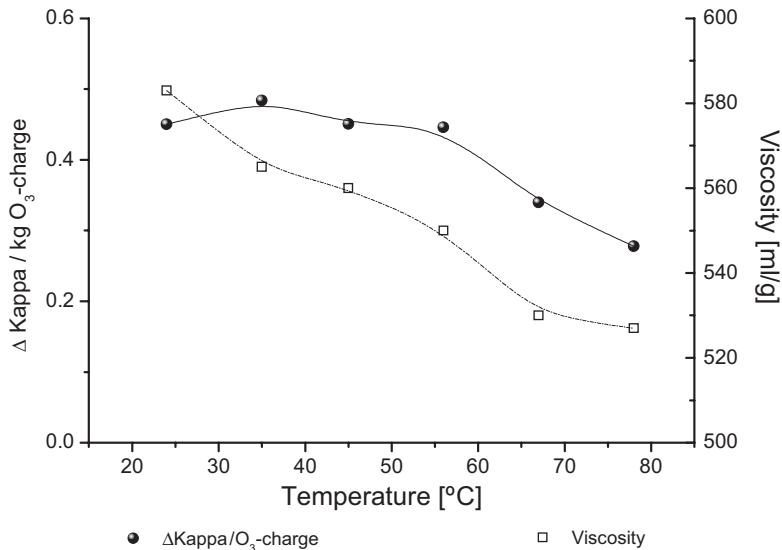


**Fig. 7.92** Effect of pH during ozonation on the yield of methyl  $\beta$ -D-glucopyranoside (according to [53]). Conditions: 0.45 mmol of the model compound are ozonated at a rate of  $0.125 \text{ mmol min}^{-1}$  at room temperature.

### 7.5.5.5 Effect of Temperature

High temperature is known to promote ozone decomposition. Most studies have concluded that an increase in temperature during ozonation of pulp impairs the selectivity and efficiency of delignification. However, different opinions have been expressed about the extent of the effect at a certain temperature level. Allison found that with radiata pine kraft pulp the extent of delignification after 1% consumed ozone decreased from only 37.1% lignin removal at 29 °C to 34.7% lignin removal at 80 °C [59]. Chandra reported that ozone is most efficient in delignifying kraft pulp at 23 °C, though selectivity gradually decreases with increasing temperature [60]. Similar observations were made by Soteland [61] and by Liebergott [24,62]. Patt et al. reported a 10% decrease in kappa number reduction when the temperature was raised from 20 to 40 °C in HC ozone bleaching of beech sulfite pulp [63]. Simoes and Castro showed that, for a given kappa number, an increase in temperature from 4 to 43 °C led to a decrease of pulp viscosity by 80 SCAN units in ultra-low consistency ozone bleaching of a pine kraft pulp [64]. The beneficial effect of a low temperature in the ozone stage was also demonstrated by Dillner and Peter [40]. In contrast to these findings, however, Lindquist reported an unchanged selectivity when increasing the temperature from 30 to 60 °C in the ozone stage [65,66].

The kappa number of an OZ(EOP)-treated softwood kraft pulp was substantially lower when medium-consistency ozone bleaching was conducted at 30 °C as compared to 50 °C and applying the same amount of ozone charge.



**Fig. 7.93** Effect of temperature on delignification efficiency,  $\Delta\text{kappa}/\text{O}_3\text{-charge}$ , and on the course of viscosity during ozonation (according to [28]). Pulp: E/O-pretreated beech acid sulfite dissolving wood pulp (B-AS), kappa

number 1.9, viscosity 627 mL g<sup>-1</sup>; medium-consistency ozone bleaching: 10% consistency, pH 2.5, 10 s mixing time; ozone charge: 2.2–2.3 kg odt<sup>-1</sup>, carry-over: 5 kg COD odt<sup>-1</sup>.

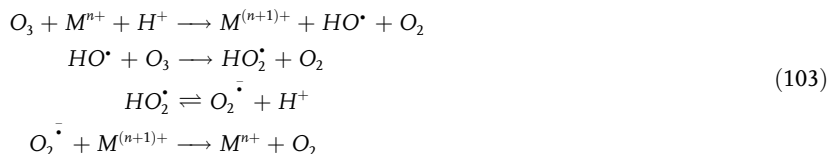
The efficiency of delignification of an (E/O)-pretreated beech acid sulfite dissolving and pulp was almost unaffected up to a temperature of 55 °C, while the viscosity gradually decreased from 580 to 550 mL g<sup>-1</sup> [28]. Temperatures above 55 °C, however, accelerated both the loss in viscosity and the reduction in delignification efficiency, as depicted in Fig. 7.93.

It can be summarized that delignification efficiency decreases at temperatures above 50 °C, mostly as a result of increased ozone decomposition [60]. Ozone bleaching in industrial practice is carried out in the temperature range between 40 and 55 °C. This temperature level is certainly significantly lower as compared to that of other bleaching stages such as oxygen or peroxide, both of which are more effective at higher temperatures. The conclusion is that the energy balance is somewhat impaired by integrating an ozone bleaching stage into a bleaching sequence.

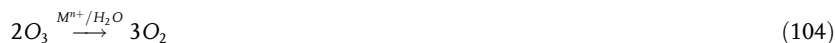
#### 7.5.5.6 Effect of Transition Metal Ions

Ozone is decomposed by the catalytic action of transition metal ions present in pulps and bleaching liquors, giving rise to hydroxyl, hydroperoxyl, and superoxide anion radical intermediates [67]. Pan et al. [56] reported that transition metal ions such as iron(II) and cobalt(II) ions enhance the decomposition of ozone, while Chirat and Lachenal [68] demonstrated that iron and copper cations exert an adverse effect on the selectivity of ozone bleaching. The detrimental effect on the viscosity is observed already at low concentration in the range between 10 and 20 ppm on pulp. Chemiluminescence and electron spin resonance (ESR) measurements confirmed the formation of hydroxyl radicals when iron cations – and, to a lesser extent, copper ions – were added to the pulp suspension subjected to ozone treatment. The presence of manganese cations, however, did not affect the selectivity of ozone bleaching, which agrees well with the result that no additional hydroxyl radicals were detected.

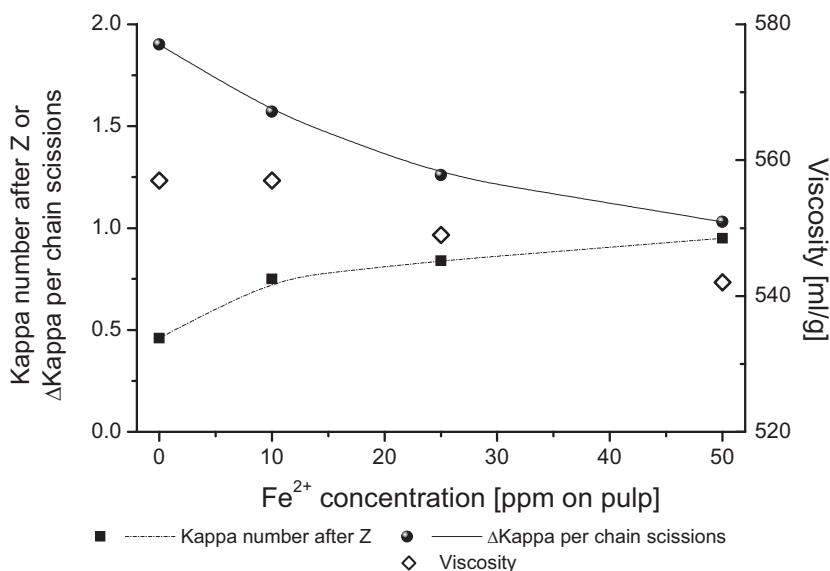
The scheme of ozone decomposition can be rationalized according to the expressions in Eqs. (103) and (104):



Net decomposition reaction:



The influence of the presence of Fe<sup>2+</sup> ions on the performance of MC ozone bleaching of a beech acid sulfite dissolving pulp (B-AS) is illustrated in Fig. 7.94. The efficiency of delignification is slightly deteriorated when Fe<sup>2+</sup> ion concentration



**Fig. 7.94** Effect of  $\text{Fe}^{2+}$  ion concentration on kappa number after Z-stage, delignification selectivity,  $\Delta$ kappa per number of chain scissions, and on the course of viscosity during ozonation (according to [28]). Pulp: E/O-pre-

treated beech acid sulfite dissolving wood pulp (B-AS), kappa number 2.1, viscosity  $614 \text{ mL g}^{-1}$  medium-consistency ozone bleaching: 10% consistency, pH 2.5, 10 s mixing time; ozone charge:  $1.9 \text{ kg odt}^{-1}$ , no carry-over.

exceeds 10 ppm on pulp. The viscosity of the ozone-treated pulp remains unaffected until an  $\text{Fe}^{2+}$  ion concentration of 20 ppm is reached. A further increase in  $\text{Fe}^{2+}$  ion concentration finally leads to a slight decrease in viscosity, while the extent of delignification further decreases; this is an indication of a shift to a higher proportion of radical reactions initiated by the decomposition of ozone.

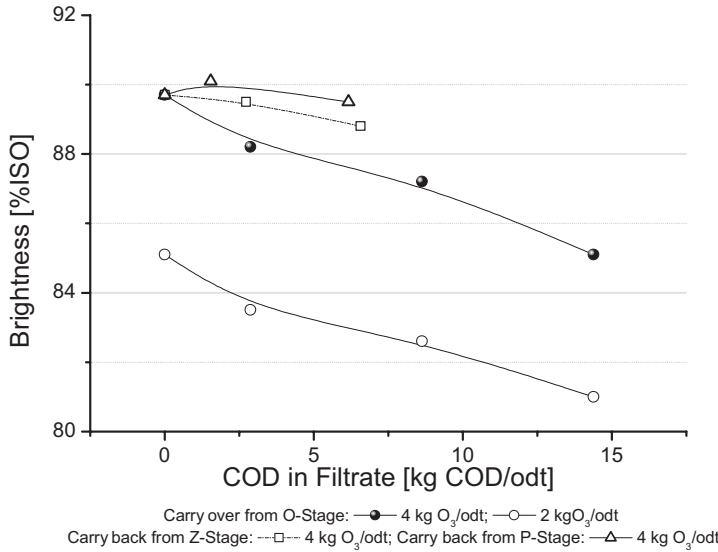
The degradation of a carbohydrate model compound, methyl 4-O-ethyl- $\beta$ -D-glucopyranoside, was enhanced when ozonation took place in an 0.5 mM  $\text{FeSO}_4$  aqueous solution compared to that in pure water (distilled water, pH 4) [53]. The additional degradation of the model compound was attributed to radical reactions initiated by the decomposition of ozone, catalyzed by the  $\text{Fe}^{2+}$  ions. Interestingly, the additional degradation of the carbohydrate model compound initiated by the presence of  $\text{Fe}^{2+}$  ions can be fully compensated for by acidifying the aqueous solution to pH 2. The observation that the removal of  $\text{Fe}^{2+}$  ions is not necessary to improve delignification selectivity if ozonation is carried out at low pH suggests that the transition metal ion-catalyzed decomposition may be completely inhibited by adjusting to low pH. Ragnar reported that the addition of various transition metal ions such as Fe(II), Co(II), Cu(II) and Mn(II) to an aqueous solution of vanillin, which served as a lignin model compound, did not affect the radical yield during ozonation [57]. It was stated that hydroxyl radicals are rather formed in a (Fenton-type) reaction with hydrogen peroxide which originates during ozonation than in a direct reaction between ozone and transition metal ions. It can be sum-

marized that the presence of transition metal ions (mainly  $\text{Fe}^{2+}$  ions) slightly impairs the performance of ozone bleaching as soon as a certain concentration is exceeded. Further investigations are required to elucidate the mechanism behind the transition metal ion-initiated decomposition of ozone.

#### 7.5.5.7 Effect of Carry-Over

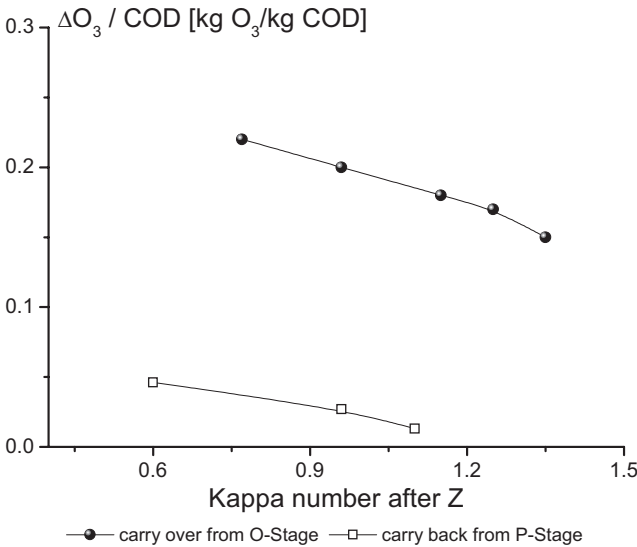
Closing the water cycle in totally chlorine (TCF) bleaching by countercurrent washing results in an accumulation of dissolved organic material in the recycled liquors. The concentration of the dissolved organic substances depends on the washing efficiency of the washing equipment and the degree of closure of the countercurrent water cycle. The waste material in the water associated with the pulp affects the performance of ozone bleaching, depending on its origin. Ozone delignification is very sensitive to dissolved material from preceding bleaching stages (carry-over), but significantly less to its own (Z-stage filtrate or carry-back) and subsequent bleaching stages (e.g., P-stage filtrate or carry-back). The high reactivity of ozone towards carry-over can be explained by the low state of oxidation of the waste material dissolved during oxygen delignification; this is roughly characterized by the chemical oxygen demand (COD):dissolved oxygen concentration (DOC) ratio being about 2.6 or slightly higher (for comparison, the COD:DOC ratio of native lignin is  $\sim 2.95$  and of neutral carbohydrates is  $\sim 2.67$ ). As the ozone stage is normally placed after an oxygen delignification stage (O), the carry-over consists predominantly of an O-stage bleaching loss. The effect of carry-over from oxygen delignification, as well as the carry-back from ozone and hydrogen peroxide stages, on medium-consistency ozone bleaching of a eucalyptus prehydrolysis-kraft (PHK) pulp was evaluated on the laboratory scale [28,41]. The load of dissolved waste substances, expressed as COD, entering the ozone stage was gradually increased to a value of  $14.4 \text{ kg odt}^{-1}$ . Medium-consistency ozone bleaching was carried out at two different levels of ozone charge, namely 2.0 and  $4.0 \text{ kg odt}^{-1}$ . The ozone-bleached pulp was thoroughly washed and finally subjected to standard hydrogen peroxide bleaching (10% consistency,  $85^\circ\text{C}$ , 180 min,  $5 \text{ kg H}_2\text{O}_2 \text{ odt}^{-1}$ ,  $7 \text{ kg NaOH odt}^{-1}$ ). As expected, the carry-over from oxygen stage had a major impact on the final brightness (Fig. 7.95).

A carry-over of  $14.4 \text{ kg COD odt}^{-1}$  from the oxygen stage caused a decrease in brightness from about 90% ISO to 85% ISO, while keeping the ozone charge constant at  $4 \text{ kg odt}^{-1}$ . The impact on brightness was the same as for an ozone charge of only  $2 \text{ kg odt}^{-1}$  (Fig. 7.95). In agreement with other studies, there was no significant effect of filtrate recirculated from the ozone stage itself on the ozone consumption and on final pulp quality [69,70]. Small amounts of carry-back from the P-stage even improved brightness, but this may be attributed to the residual hydrogen peroxide ( $\sim 1 \text{ kg H}_2\text{O}_2 \text{ odt}^{-1}$ ) present in this solution. The amount of additional ozone consumption per kg COD from the oxygen stage for a given kappa number and brightness target after ozone and peroxide bleaching increased with increasing extent of delignification in the Z-stage (Fig. 7.96).



**Fig. 7.95** Effect of dissolved organic material from O-, Z-, and P-stages on the brightness after P-stage at a constant charge of ozone in the preceding Z-stage (according to [28]). Substrate: O-delignified eucalyptus-PHK pulp,

kappa number 3.0, viscosity 942 mL g<sup>-1</sup>. Conditions in Z-stage: 9% consistency, 50 °C, pH 2.0, 10 s mixing time, ozone charges: 2.0 and 4.0 kg odt<sup>-1</sup>.



**Fig. 7.96** Additional ozone consumption per kg COD derived from dissolved organic material from O- and P-stages as a function of the kappa number after Z-stage (according to [28]). Substrate and conditions see Fig. 7.95.

The data in Fig. 7.96 illustrate that an additional amount of 0.20–0.22 kg ozone  $\text{kg}^{-1}$  COD from the oxygen filtrate is consumed to obtain a final brightness of about 90% ISO; this corresponds to a kappa number after Z-stage of 0.8 to 1.0. In other words, a COD carry-over of 10 kg  $\text{odt}^{-1}$  from the oxygen stage increases the specific ozone consumption by 85% in the case of 85% ISO brightness ( $0.17 \text{ kg O}_3 \text{ kg}^{-1} \text{ COD} \times 10 \text{ kg COD odt}^{-1} + 2.0 \text{ kg O}_3 \text{ odt}^{-1} = 3.7 \text{ kg O}_3 \text{ odt}^{-1}$ ), and by 55% in the case of 90% ISO brightness ( $0.22 \text{ kg O}_3 \text{ kg}^{-1} \text{ COD} \times 10 \text{ kg COD odt}^{-1} + 4.0 \text{ kg O}_3 \text{ odt}^{-1} = 6.2 \text{ kg O}_3 \text{ odt}^{-1}$ ).

These values are in good agreement with those reported by other investigators [70,71]. The effect of carry-back from the P-stage on additional ozone consumption amounts to only about one-eighth of that of the carry-over from oxygen stage, even when the effect of residual hydrogen peroxide is disregarded. The lack in efficiency of ozone delignification in the presence of carry-over can be compensated for by an additional ozone charge without impairing the selectivity in terms of the viscosity–brightness relationship [41,70].

The effect of the carry-over/carry-back to the ozone stage is also strongly dependent on pulp consistency. High-consistency ozone bleaching is much less affected by the presence of dissolved organic material than medium-consistency ozone treatment because of the significantly lower amount of water associated with the pulp.

#### 7.5.5.8 Effect of Pretreatments and Additives

A considerable amount of research has been devoted to finding an additive or a pretreatment that would protect cellulose and make ozone react more selective with the lignin. From among a huge list of different inorganic and organic chemicals, only a few were identified slightly to improve delignification selectivity during ozonation [24,62]. Many attempts were made to add a hydroxyl radical scavenger, but without success. The probable explanation for this is that hydroxyl radicals react very rapidly with carbohydrate structures in the pulp. The reaction rate constants of hydroxyl radicals with cellulose model compounds are about  $3 \times 10^9 \text{ M}^{-1} \text{ s}^{-1}$  (e.g., for Me- $\beta$ -D-glucopyranoside,  $3.2 \times 10^9 \text{ M}^{-1} \text{ s}^{-1}$  [72]), but are in the range of  $10^9 \text{ M}^{-1} \text{ s}^{-1}$  to  $10^{10} \text{ M}^{-1} \text{ s}^{-1}$  with the most common hydroxyl radical scavenging agents [73]. This implies that huge amounts of radical scavengers must be added to achieve a viscosity-stabilizing effect. Moreover, many of these scavenging agents react with ozone, which renders them ineffective [68].

The most promising way to improve selectivity is to exchange the associated water of the pulp suspension with media that improve the solubility of molecular ozone, act as radical scavengers, or prevent the formation of radicals, at least to some extent. Furthermore, the presence of organic solvents improves the accessibility of lignin while reducing it for cellulose; this again protects carbohydrates against degradation [74]. As an example, replacing the aqueous phase with an acetic acid medium yields an improvement in delignification performance while cellulose degradation is diminished. The selectivity advantage is particularly observed for HC ozone bleaching in 90% acetic acid in the presence of 0.95% pyrophosphate [75]. The favorable effect on selectivity is ascribed to the better stability

of ozone in acetic acid medium. Chemiluminescence measurements revealed a decrease in the amount of hydroxyl radicals with increasing acetic acid concentration [75]. The protective effect of formic acid against cellulose degradation during ozonation has been found to be even slightly better than that with acetic acid (see Tab. 7.40) [76]. The replacement of water in the pulp suspension with methanol or *tert*-butyl alcohol during an ozone stage also suppresses radical reactions with cellulose to some extent, as shown by ozone-bleaching studies in both heterogeneous and homogeneous systems [50,77]. In model compound studies, it was shown that the degradation of cellobiose in 50% methanol solution was retarded even in the presence of phenolic lignin model compounds [78]. Methanol and *tert*-butanol are more efficient in trapping hydroxyl radicals (higher rate constants) than acetic acid [73]. Therefore, the concentration of acetic acid must be significantly higher than that of methanol or *tert*-butanol in order to achieve the same scavenging ability (90 wt.% acetic acid versus 1 wt.% methanol versus 2.2 wt.% *tert*-butanol) [77]. Johansson et al. reported that the presence of ethylene glycol increased the selectivity during HC ozone delignification of an oxygen-delignified softwood kraft pulp considerably more than did methanol (Tab. 7.40) [79].

The stabilizing effect was optimal at pH 3 and 25 wt.% ethylene glycol, based on the total reaction medium. The improved selectivity in the presence of ethylene glycol was primarily attributed to a partial suppression of the free-radical reactions. Van Heiningen and Ni found that the selectivity of HC ozone bleaching could be significantly improved when the pulp was impregnated with a solution of dioxane-water at a pH of about 2 [80]. Based on this technology, a conventional softwood kraft pulp, kappa number 30 and viscosity  $1050 \text{ mL g}^{-1}$ , was delignified with 2% ozone in a ZE(O) sequence to kappa number 5 and at a viscosity at  $950 \text{ mL g}^{-1}$  [81]. The delignification selectivity, denoted as  $\Delta$ kappa number per chain scissions, calculates to about 52  $[(30 - 5)/(10^4/2800 - 10^4/3235)]$ , which is significantly better than the value of 14.2 obtained for the same sequence but applying a conventional LC ozone stage (see Tabs. 7.40 and 7.41) [82].

The addition of a small amount of methanol (ca. 3% on o.d. pulp) in the ozone gas stream (methanol in gas phase, MeOH G-P) appears to protect pulp viscosity more efficiently than impregnating the pulp with the same amount of methanol [83]. The effect on the preservation of viscosity of a reductive treatment with sodium borohydride (R) prior to the alkaline extraction stage (E) is considerably more pronounced for the MeOH G-P-ozonated pulp than for the control pulp (see Tab. 7.40). However, impregnating with a 50% methanol solution renders the pulp very selective towards an ozone treatment. Clearly, a high concentration of methanol prevents cellulose depolymerization induced by reactions with radicals. It has been speculated that the protective effect of large amounts of methanol towards the reaction with ozone is possibly due to a decrease in swelling of cellulose, thus reducing the accessibility to ozone [83]. The viscosity-preservation effect of shrinkage has however not been detected so far.

Ozonation of fully bleached kraft pulps proceeds with significantly more selectivity as compared to unbleached kraft pulps [84]. The data in Tab. 7.40 show that the protective effect of both 70% methanol and 70% *t*-butanol on cellulose



**Table 7.40** Effect of pretreatments on the selectivity of ozone treatment of unbleached, oxygen delignified and fully bleached pulps. The results are summarized from different literature sources. For more details with regard to experimental conditions it is referred to the cited literature.

Ozone consumed [kg odt <sup>-1</sup> ]	Pre-treatment	Pulp	Prior ozone Kappa [ml g <sup>-1</sup> ]	Z-Technology	Bleaching sequence	After treatment Kappa	After treatment Viscosity [ml g <sup>-1</sup> ]	CS	ΔKappa/CS	Reference
19.0	none	SW-K	34.0	LC	ZE(O)	9.5	850	1.72	14.2	Lindhölm [52]
38.0	none	SW-K	34.0	LC	ZE(O)	3.1	700	2.93	10.6	Lindhölm [52]
11.0	none	Radiata pine-KO	16.0	HC	Z	6.7	785	1.11	8.4	Ruiz et al. [76]
11.0	98% HCOOH	Radiata pine-KO	16.0	HC	Z	4.1	816	0.88	13.5	Ruiz et al. [76]
11.0	80% AcOH	Radiata pine-KO	16.0	HC	Z	4.9	820	0.85	13.1	Ruiz et al. [76]
11.0	98% HCOOH	Radiata pine-KO	16.0	HC	ZP	1.7	747	1.42	10.1	Ruiz et al. [76]
20.0	1,4-dioxane	SW-K	30.0	HC	ZE(O)	5.0	950	0.48	52.1	Ni and Ooi [81]
6.0	none	SW-KO	11.2	HC	AZE	2.5	715	1.57	5.5	Johansson et al. [79]
6.0	25 wt% MeOH	SW-KO	11.2	HC	AZE	3.4	815	0.75	10.4	Johansson et al. [79]
6.0	25 wt% EG	SW-KO	11.2	HC	AZE	3.2	870	0.39	20.6	Johansson et al. [79]
11.5	none	SW-KO	17.7	HC	ZE	3.9	665	2.06	6.7	Bouchard et al. [83]
11.5	MeOH G-P	SW-KO	17.7	HC	ZE	3.4	710	1.59	9.0	Bouchard et al. [83]
11.5	MeOH impr	SW-KO	17.7	HC	ZE	2.8	865	0.39	37.9	Bouchard et al. [83]
11.5	none	SW-KO	17.7	HC	ZRE	3.6	770	1.14	12.4	Bouchard et al. [83]
11.5	MeOH G-P	SW-KO	17.7	HC	ZRE	3.3	828	0.71	20.3	Bouchard et al. [83]
11.5	MeOH impr	SW-KO	17.7	HC	ZRE	2.3	920	0.15	100.0	Bouchard et al. [83]
20.0	none	Hemlock-KFB	n.d.	HC	Z	n.d.	800	0.70		Kang et al. [84]
20.0	70% MeOH	Hemlock-KFB	n.d.	HC	Z	n.d.	830	0.49		Kang et al. [84]
20.0	70% t-BuOH	Hemlock-KFB	n.d.	HC	Z	n.d.	820	0.56		Kang et al. [84]
20.0	none	Hemlock-K	27.7	HC	Z	9.9	695	2.14	8.3	Kang et al. [84]
20.0	70% MeOH	Hemlock-K	27.7	HC	Z	7.0	885	0.67	31.0	Kang et al. [84]
20.0	70% t-BuOH	Hemlock-K	27.7	HC	Z	7.3	785	1.34	15.2	Kang et al. [84]

SW-K softwood unbleached kraft pulp

SW-KO softwood oxygen-delignified kraft pulp

KFB kraft pulp fully bleached

EG ethylene glycol

MeOH G-P methanol addition to the ozone gas stream corresponding to an amount of approximately 3% on pulp

MeOH impr pulp suspension diluted to 2% with 50% aqueous methanol at pH 2, mixed for 5 min and pressed to a consistency of about 40%

R-stage 1% charge of sodium borohydride mixed with the pulp at 10% consistency, 15 °C for 24 h.

CS chain scissions, calculated as  $\left(\frac{10^4}{DP_t} - \frac{10^4}{DP_0}\right)$  in mmol AGU<sup>-1</sup>.

n.d. not determined

degradation is minimal for fully bleached pulp, indicating that the extent of swelling is not a decisive factor for accessibility to ozone. In the case of unbleached kraft pulp, the presence of high concentrations of methanol or *t*-butanol significantly improves the selectivity of ozone bleaching. This may be attributed to the radical-scavenging effect of the solvents. At the same ozone charge, the number of chain scissions is three-fold higher for the unbleached than for the fully bleached kraft pulp in the pure aqueous system. The ratio of chain scissions between the unbleached and bleached kraft pulps decreases to 2.4:1, and to 1.4:1 when replacing 70% of the water by *t*-butanol and by methanol, respectively. The lower advantage of selectivity for the bleached kraft pulp can be explained by a shift to direct ozone attack since the dissolved ozone concentration increases. The greater extent of cellulose degradation during ozonation of the unbleached compared to the bleached pulp suggests that even the high concentration of methanol is incapable of scavenging all of the radicals generated by the reaction between ozone and residual lignin structures. The better selectivity of an ozone treatment in the presence of methanol than in that of *t*-butanol can be explained by the more efficient radical-scavenging effect of the former. According to Hoigne and Bader, the rate constant of the reaction between hydroxyl radicals and *t*-butanol is  $0.47 \times 10^9 \text{ M}^{-1} \text{ s}^{-1}$ , while that of the reaction between hydroxyl radicals and methanol amounts to  $0.85 \times 10^9 \text{ M}^{-1} \text{ s}^{-1}$  [85]. By taking a 2.3-fold higher molar concentration of methanol compared to *t*-butanol into account, the hydroxyl radical scavenging rate of 70% methanol is more than four-fold that of *t*-butanol at the same concentration.

The application of chelants renders the ozone treatment more selective than simple acidification to pH levels below 3. Allison reported that the addition of DTPA at pH 3 before the Z stage provided a slightly better viscosity preservation than a sulfuric acid treatment alone [59]. In some cases, an additional EDTA treatment after the ozone stage makes the subsequent alkaline peroxide stage more selective. A reasonable explanation for this behavior may be the better physical and chemical accessibility of transition metal ions after the reaction of ozone with the pulp components [68].

Oxalic acid [52], acidified DMSO [52,59] and an acidic peroxide treatment at pH 2–3 [62] improved the selectivity and efficiency of an ozone treatment only slightly. A recent study showed oxalic acid to be the most efficient acid for this pretreatment [86], with a charge as low as  $0.05 \text{ kg odt}^{-1}$  providing an effective reduction in cellulose degradation during ozone treatment. The protective effect of oxalic acid against viscosity loss is attributed to a combination of different factors. Oxalic acid may act as a radical scavenger and an efficient hydrogen donor, thus inhibiting the formation of hydroxyl radicals. Moreover, oxalic acid behaves as a chelating agent. Oxalic acid, however, is formed in quite large quantities during ozone bleaching as a final oxidation product ( $\sim 0.5 \text{ kg odt}^{-1}$  at an ozone charge of  $3 \text{ kg odt}^{-1}$ ) [87], this being well above the amount needed to attain viscosity stabilization. Oxalic acid is known to form crystals of calcium oxalate that can precipitate and cause severe problems with scaling. In industrial praxis, oxalic acid formation is clearly undesirable because it prevents closure of the water cycle of the ozone stage. Therefore, partial recirculation of the effluent within the Z-stage to

adjust for oxalic acid concentration will only be carried out if it provides a significant increase in delignification selectivity and efficiency.

On occasion, an enzymatic treatment may represent an alternative choice to reduce the charge of nonselective oxidants (e.g., ozone), thereby improving the strength properties while maintaining target brightness. Xylanase treatment (Irgazyme 40 s, derived from *Trichoderma longibrachiatum*) of an oxygen-delignified softwood kraft pulp prior to medium-consistency ozone bleaching was reported to increase brightness at a given ozone charge, or to allow a reduction in ozone charge by 3 kg odt<sup>-1</sup> while maintaining the same brightness [88]. Rynänen et al. showed that xylanase treatment of an oxygen-delignified eucalypt kraft pulp prior to a HC ozone stage in an OXZQ(PO) sequence produced only slightly higher brightness levels. However, the bleaching yield was about 1–3% units lower, depending on the wood sample and the pulping process used [89].

#### 7.5.5.9 Effect of Sodium Borohydride after Treatment

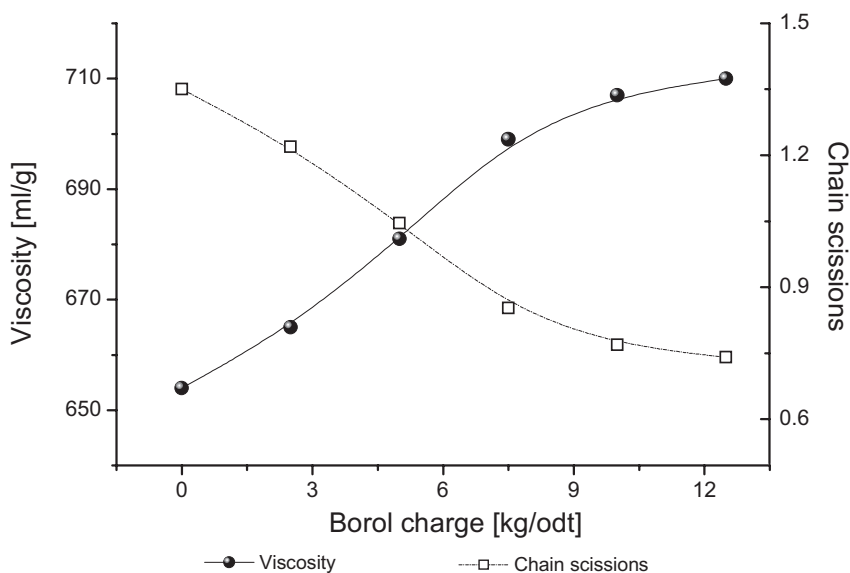
The use of organic solvents with radical-scavenging properties (e.g., methanol or multivalent alcohols) to replace part of the aqueous phase of a pulp suspension is not (yet) a realistic option for an industrial application to protect pulp viscosity during an ozone treatment. The advantage of higher strength properties does not justify the high investment and operational costs connected with the additional equipment needed to recover the solvents. The problem of finding a cheap, effective commercial inhibitor of carbohydrate depolymerization during ozone delignification remains to be solved [62]. The combined use of ozone and hydrogen peroxide for the production of a fully bleached pulp inevitably causes severe cellulose degradation. In some special cases, when ozone bleaching must be applied to the production of pulps comprising both low kappa number and high viscosity (e.g., high-purity dissolving pulps), additional measures must be undertaken to preserve viscosity. To date, the only economically feasible way to compensate in part for the viscosity loss during ozonation is a post-treatment based on sodium borohydride. It has been discussed previously that the ozonation of pulp introduces carbonyl groups within the anhydroglucose unit (AHG), giving rise to  $\beta$ -elimination reaction in a subsequent alkaline treatment that results in cleavage of the carbohydrate chain and, thus, a loss in viscosity. The carbonyl groups can be partly reduced by borohydride in a strongly alkaline environment. The chain scissions after borohydride treatment roughly correspond to the so-called direct scissions caused by the oxidation of molecular ozone on carbons C(1) and C(4) [79]. Analytically, the treatment of an ozonated pulp with sodium borohydride prior to viscosity measurement is a well-known procedure to obtain more reliable information on the respective chain length. Lindholm has established the following relationship between the viscosity before and after borohydride treatment of an oxygen-delignified softwood kraft pulp [90]:

$$[\eta_{ZR}] = 0.88 \cdot [\eta_Z] + 180 \quad (105)$$

where  $[\eta_Z]$  is the limiting viscosity after ozone treatment (Z), and  $[\eta_{ZR}]$  is the limiting viscosity after borohydride treatment (R).

It is interesting to note that, according to Eq. (105), the viscosity preservation is more pronounced for a low-viscosity pulp (e.g.,  $600 \text{ g}^{-1}$ , or 18% increase) than for a higher-viscosity pulp (e.g.,  $800 \rightarrow 884 \text{ mL g}^{-1}$ , or 11% increase). The conditions for the reductive treatment in the laboratory with a charge of sodium borohydride of far more than  $2 \text{ kg odt}^{-1}$  and long retention times are not applicable in industrial practice, due to high costs. For commercial applications, sodium borohydride is provided in the form of a strongly basic aqueous solution, containing 12% sodium borohydride and 40% sodium hydroxide, sold under the name Borol<sup>TM</sup> [91,92]. Borol can be applied immediately after ozonation, without any intermediate washing, provided that the initial pH exceeds a level of 10, preferably about 10.5. The reductive action can be optimized when the temperature is adjusted to about  $70^\circ\text{C}$  and the retention time extended to at least 30 min [93]. Pulp viscosity increases almost linearly with an increasing dosage of Borol, although improvements in viscosity gradually level off when charges  $>10 \text{ kg odt}^{-1}$  are applied (Fig. 7.97).

Figure 7.97 illustrates that the addition of 1% Borol solution (on o.d. pulp) improves pulp viscosity by more than 50 to 60 units. This may be decisive to provide either better strength or solution properties as a macromolecule, as in the case of a cellulose ether. At the same time, Borol serves as a bleaching agent, as demonstrated by an increase of brightness by 2–3 ISO points. Similar results with



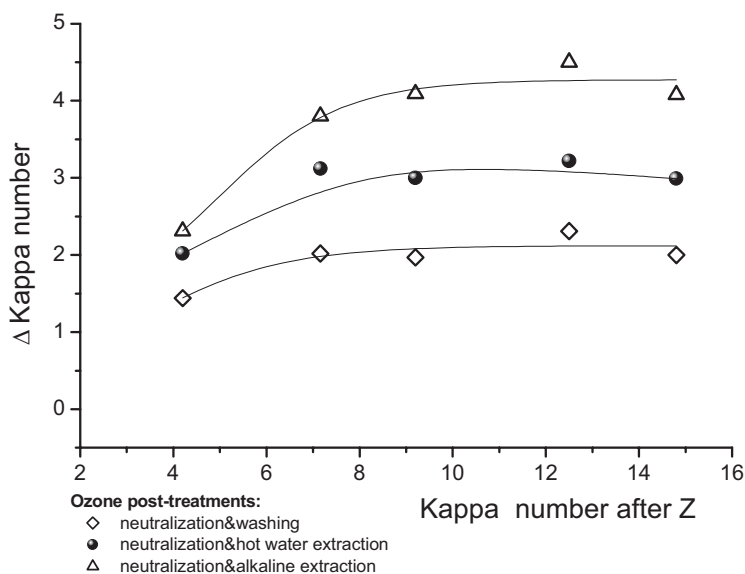
**Fig. 7.97** Effect of Borol charge on the viscosity of an OP-prebleached softwood kraft pulp after ZE- and ZER-treatments [93]. OP-delignified softwood kraft pulp: kappa number 8.2, viscosity  $890 \text{ mL g}^{-1}$ ; Z-stage: 45% consistency, pH 2,  $20^\circ\text{C}$ ,  $8.5 \text{ kg O}_3 \text{ odt}^{-1}$ ; OP-Z-treated softwood kraft pulp: kappa number 2.8, viscosity  $660 \text{ mL g}^{-1}$ ; E-stage: 10% consistency,  $70^\circ\text{C}$ , 30 min, adjusted to pH 11 by appropriate NaOH addition; R-stage: 10% consistency,  $70^\circ\text{C}$ , 30 min, pH adjustment either by NaOH or by  $\text{H}_2\text{SO}_4$ .

respect to viscosity preservation and bleaching efficiency have been observed for ozone-treated, high-purity eucalyptus PHK pulps [28]. An increase of 50–70 units in viscosity may be sufficient to meet the specifications given for high-purity, acetate-grade pulps.

Although Borol is expensive, its application has proved to be advantageous for some special applications, not least because of the very simple and inexpensive additional equipment required for its use.

#### 7.5.5.10 Effect of Alkaline Extraction

Ozone-bleached pulp may contain considerable amounts of degraded lignin that can be removed by different after-treatments. It has been shown that degraded lignin which does not contribute to the light absorption of the pulp can be removed by neutralization, followed by washing and hot water extraction [94]. The removal of colorless lignin thus shifts the brightness values to lower values at given kappa numbers. Alkaline extraction following an ozone stage removes additional lignin fragments which, contrary to neutralization, does not change the relationship between light absorption coefficient and kappa number [82,95–97]. The effect of kappa number reduction caused by various after-treatments is plotted against the kappa number measured after the ozone stage (Fig. 7.98).



**Fig. 7.98** Kappa number reduction induced by different after-treatment procedures in relation to the kappa number directly after the ozone stage (according to [94]). Substrate: oxygen-delignified pine kraft pulp, kappa number 20, intrinsic viscosity 1010 mL g<sup>-1</sup>. Ozone treat-

ment: LC; after treatment, neutralization: pH 5.5 at 1% consistency, dewatered, rediluted; alkaline extraction: 2% NaOH, 70 °C, 60 min; hot-water extraction: similar to alkaline extraction, but without addition of NaOH.

The amount of leachable kappa number is relatively constant for each post-treatment, unless the kappa number after Z-stage approaches a very low value.

Ozone is known to introduce carbonyl groups along the polysaccharide chain, and this promotes peeling reactions under alkaline conditions. The latent chain sensitivities emerge during highly alkaline viscosity measurements (cuene). Reduction of the pulps with borohydride prior to viscosity measurement provides viscosity values that are 20 to 130 mL g<sup>-1</sup> higher than without reduction, depending on the ozone dose [98,99]. Borohydride reduction after alkaline extraction does not affect the viscosity values, which correspond more or less to the unstabilized viscosity values after the ozone stage. Thus, alkaline extraction after ozone treatment decreases the molecular weight of the carbohydrates by splitting the alkali-sensitive linkages. As expected, alkaline treatment of ozone-bleached pulps in general reduces fiber strength. Again, strength reduction is more severe for HC as compared to LC ozone-bleached pulps [82]. The data in Tab. 7.41 show that alkaline extraction significantly reduces the kappa number of the ozone-treated pulp, but the viscosity level is only moderately reduced. Lignin removal can be further enhanced by using alkaline extraction reinforced with hydrogen peroxide, EP, or with oxygen, EO.

**Table 7.41** Effect of alkaline extraction (E), alkaline extraction reinforced with hydrogen peroxide (EP) or with oxygen (EO) after an ozone stage on kappa number and viscosity of a pine kraft pulp according to C.-A. Lindholm[82]. Z-stage: 1% consistency, prewash at pH 3, room temperature: E-Stage: 2% NaOH on od. pulp, 60 °C, 60 min; EP-stage: 2% NaOH on od. pulp, 0.5% H<sub>2</sub>O<sub>2</sub> on od. pulp, 60 °C, 60 min; EO-stage: 2 % NaOH on od. pulp, oxygen pressure 0.2 MPa, 90 °C, 60 min.

Ozone consumed [kg odt <sup>-1</sup> ]	Bleaching sequence	Kappa number	Viscosity [mL g <sup>-1</sup> ]	ΔKappa/CS
0		34.0	1280	
19	Z	17.6	920	12.5
19	ZE	12.6	905	15.3
19	ZEP	11.9	885	14.7
19	ZEO	9.5	850	14.2

The use of an E-stage following an ozone stage reduces the ozone charge by 25–45% when bleaching to a certain kappa number target. Intermediate washing or neutralization does not affect the extent of lignin removal during subsequent alkaline extraction. However, neutralization directly after the ozone stage appears to improve selectivity when followed by alkaline extraction.

In the case of oxygen prebleaching, being the more realistic alternative, the saving of ozone reaches almost 50% [82]. The viscosity values of the OZE-bleached pulps correspond to those determined for the OZ-bleached pulps after reduction with borohydride. Fiber strength (zero-span tensile index) is almost not impaired by the E-stage (in relation to the Z-treated pulp), at least when using LC bleaching technology. There are indications that more lignin is removed after LC and MC ozone bleaching than after HC bleaching [90], but as yet this observation is not understood.

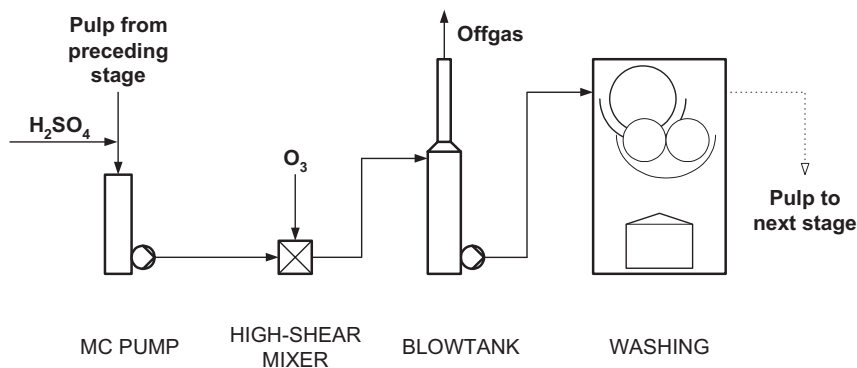
### 7.5.6

#### Technology of Ozone Treatment

*Andreas W. Krotscheck*

##### 7.5.6.1 Medium-Consistency Ozone Treatment

The process flowsheet of a typical medium-consistency ozone delignification system is shown schematically in Fig. 7.99. MC pulp coming from the previous bleaching stage falls into a standpipe after sulfuric acid has been added to adjust the pH. The pump forwards the pulp suspension to a high-shear mixer which is charged with compressed ozone/oxygen gas. The pump forwards the pulp suspension to a high-shear mixer which is charged with compressed ozone/oxygen gas.



**Fig. 7.99** Process flowsheet of a typical medium-consistency (MC) ozone delignification system.

It is of utmost importance that the ozone and pulp are mixed intensively, because the predominant portion of the delignification occurs inside the mixer. This is why the medium-consistency ozone system does not have a reactor comparable to other bleaching applications. Instead, the mixing time is prolonged at high power dissipation and, on occasion, a second high-shear mixer is installed for that purpose. Additional time for the reactions to complete after the mixer is usually provided by the pipe to the blowtank. This pipe may be increased slightly in diameter to offer about 1 min of retention time.

The pressurized three-phase flow coming from the mixer expands into the blow-tank, where the pulp suspension is separated from the gas phase. The offgas is cleaned of fibers in a scrubber and proceeds to the ozone destruction unit. The pulp slurry is discharged from the blowtank either at low or medium consistency, depending on the feed requirements of the subsequent equipment.

Washing after the ozone stage is often omitted, and the pulp is forwarded to the subsequent stage at medium consistency. Otherwise, washing can be carried out with single-stage washing equipment, for example with a single-stage Drum Displacer™, a wash press, or a vacuum drum washer.

The material for the construction of wetted parts in an ozone stage is typically a higher grade of austenitic stainless steel.

Further information regarding ozone delignification equipment including medium-consistency pumps, mixers and blowtanks is provided in Section 7.2. Details of pulp washing are provided in Chapter 5.

### 7.5.6.2 High-Consistency Ozone Treatment

High-consistency bleaching requires a press to be utilized before the stage of efficient pulp dewatering. A plain dewatering press is preferable as it achieves higher consistencies (up to 40%) than a wash press. It is necessary to adjust the desired pH in the press feed, because there is no means by which sulfuric acid can be mixed in between the press and the reactor. The fiber mat leaving the press nip must be thoroughly disintegrated in order to ensure good accessibility for the bleaching chemicals to all fiber surfaces.

The Metso ZeTrac ozone delignification system is illustrated in Fig. 7.100. Although former HC systems required a screw feeder and pulp fluffer, the Metso ZeTrac does not. Instead, the specially designed shredder screw of the press delivers well-fluffed pulp which falls into the horizontal reactor and is brought into contact with the ozone/oxygen gas mixture [100]. Paddles keep the pulp in motion as it travels concurrently with the gas through the reactor. The reactor operates at a slight vacuum, thus ensuring that no gas can escape to the ambient air [101].

The delignified pulp is discharged into a dilution screw conveyor, where it is alkalinized. The medium-consistency slurry then falls into a tank before being pumped to the subsequent stage.

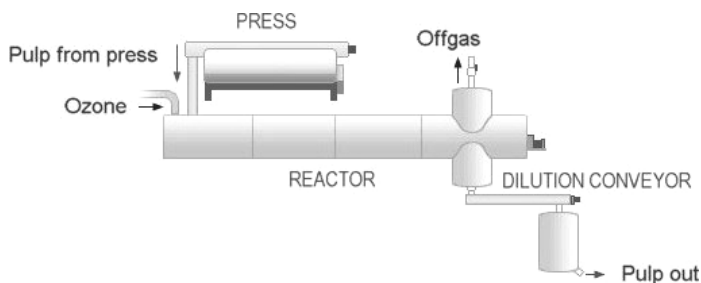


Fig. 7.100 The Metso ZeTrac high-consistency (HC) ozone bleaching system [100].



### 7.5.6.3 Ozone/Oxygen Gas Management

The oxygen gas needed for the generation of ozone can be supplied from a liquid oxygen storage tank, or it can be produced on site by oxygen plants using either a pressure swing adsorption (PSA) or vacuum swing adsorption (VSA) process.

Oxygen is by far the predominant gas in any commercially generated ozone/oxygen gas mixture. When entering the pulp delignification process, each kilogram of ozone is accompanied by 6–9 kg of oxygen. This amount of oxygen, together with oxygen which has been created by the decomposition of ozone, forms the major part of the offgas leaving the delignification process.

The flow scheme of the common once-through gas system is shown in Fig. 7.101. Oxygen is fed to the ozone generator and, if used for medium-consistency delignification, is subsequently compressed. The compression step can be omitted in the case of high-consistency delignification. After addition to the pulp, ozone is partly consumed during the delignification reaction and partly decomposed. Only small concentrations of ozone are left in the offgas, and these are destroyed in a dedicated destruction unit. Catalytic destruction is the most popular approach, followed by thermal destruction. The residual gas after destruction is available for other applications which normally require its re-compression. In the bleaching plant there are several points where residual oxygen from ozone delignification can be re-used. These include oxygen delignification, oxygen-reinforced extraction or peroxide bleaching, and white liquor oxidation. Other opportunities for re-use may exist in other areas of the mill.

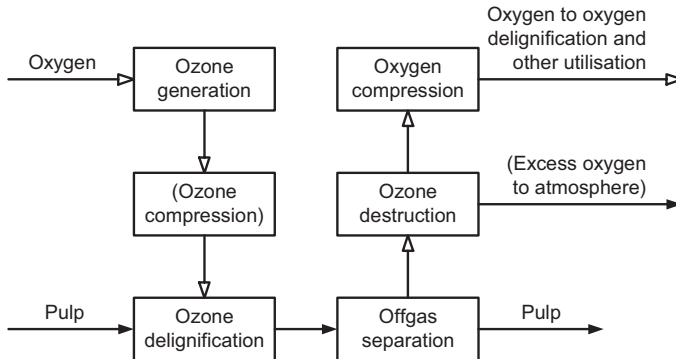


Fig. 7.101 Once-through gas management.

If the oxygen supplied with the offgas exceeds the mill's demands, the most appropriate option is to exhaust some offgas into the atmosphere. Although at first sight this may not be the most economic solution, the ambivalent operational experiences from the so-called long loop system (Fig. 7.102) seem barely worth the effort. The long loop contains an additional purification step, where gas components known to interfere with ozone generation (including moisture) are eliminated as far as possible. Since the ozone generators are very sensitive to inappropriate gas feed, the perfect function of gas purification is vital for the availability of ozone from a long loop system.

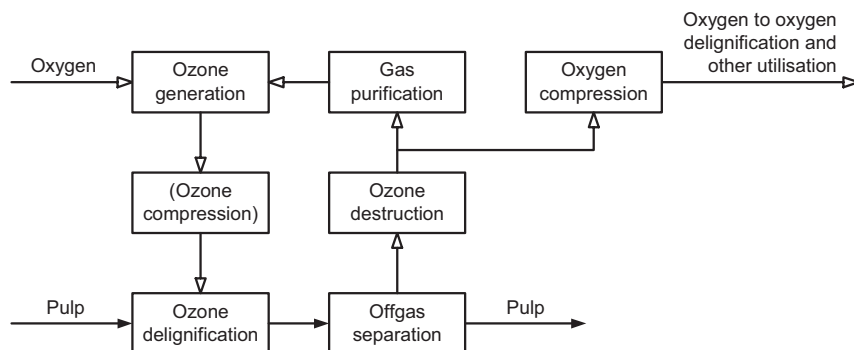


Fig. 7.102 Long loop gas management.

With modern ozone generators delivering 14% by weight of ozone, the oxygen supply and demand in the mill is balanced at ozone charges between 4 and 6 kg ton<sup>-1</sup> of pulp. Even at lower ozone concentrations in the feed gas, the majority of ozone delignification applications features specific charges below the balanced maximum. As a result, once-through gas management has become the system of choice over the past years.

## 7.5.7

### Application in Chemical Pulp Bleaching

#### 7.5.7.1 Selectivity, Efficiency of Ozone Treatment of Different Pulp Types

##### 7.5.7.1.1 Basic Considerations on the Selectivity of Ozone Bleaching

It is generally agreed that radical formation is a crucial factor that affects the selectivity and performance of an ozone bleaching stage [75,102,103]. On the basis of model compounds, the ratio of rate constants for delignification to that of carbohydrate degradation ( $k_I/k_C$ ) is more than 10<sup>5</sup> in the case of molecular ozone, whereas for hydroxyl radicals a value of only 5–6 has been determined [72,104]. However, there remains much debate about the pathways of radical formation during the ozonation of pulp. It is well-documented that radicals are formed in aqueous medium by self-decomposition of ozone [54,104]. However, the decomposition of ozone is rather slow in acidic media (see Fig. 7.82). Therefore, additional reasons have been suggested as being responsible for the unselectivity of ozone treatment. Radicals are formed in the presence of transition metal ions [56,103,105] and in a direct reaction between ozone and aromatic lignin structures [57,58,106]. Recent trials using the TNM (tetranitromethane) method, however, concluded that the addition of the transition metal ions Fe(II), Cu(II), Co(II) and Mn(II) to a lignin model compound (e.g., vanillin) do not promote additional radical formation. It has been argued that the loss in pulp viscosity in the presence of transition metal ions reported in the literature may be attributed to radical formation from the reaction with hydrogen peroxide formed during ozonation

[57,103,107]. Instead, radical formation is caused by a direct reaction between lignin model compounds and ozone [57,58]. In acidic solution, syringyl structures yield more radicals at a given ozone charge as compared to the corresponding guaiacyl compounds, mainly due to the lower oxidation potential of the former. However, no radicals are formed in direct reaction between ozone and carbohydrate model compounds. Following the finding that syringyl structures yield significantly more radicals than do corresponding guaiacyl compounds, the viscosity loss during ozone bleaching should be much more pronounced for hardwood than for softwood pulps. However, in practice the opposite is true. Ragnar has shown that the better selectivity of hardwood kraft pulps can be attributed to their higher amount of hexenuronic acids (HexA), since ozone reactions with this component do not yield radicals [108]. Magara et al. also reported that the presence of lignin model compounds with free phenolic hydroxyl groups enhanced cellobiose degradation during ozonation in water [78]. However, in the presence of nonphenolic lignin model compounds, cellobiose degradation was retarded. Based on these model compound studies, it can be concluded that the selectivity of ozone bleaching gradually improves with decreasing incoming kappa number of a pulp. In fact, this may explain the superior selectivity of oxygen-bleached pulps over unbleached kraft pulps, since oxygen reduces both the total lignin content and the phenolic structures in residual lignin [75,107]. The latter yields more radicals as compared to nonphenolic structures [57]. Cellulose is also degraded by molecular ozone according to an insertion mechanism (see Section 7.5.4.3) [53,109]. It is however doubtful if this type of reaction is responsible for the degradation reaction of pulps in the presence of residual lignin, because the reaction rate of ozone towards intact carbohydrate structures is very low ( $0.21 \text{ m}^{-1} \text{ s}^{-1}$ ), while the reaction rate of hydroxyl radicals towards similar structures is several orders of magnitudes higher [104].

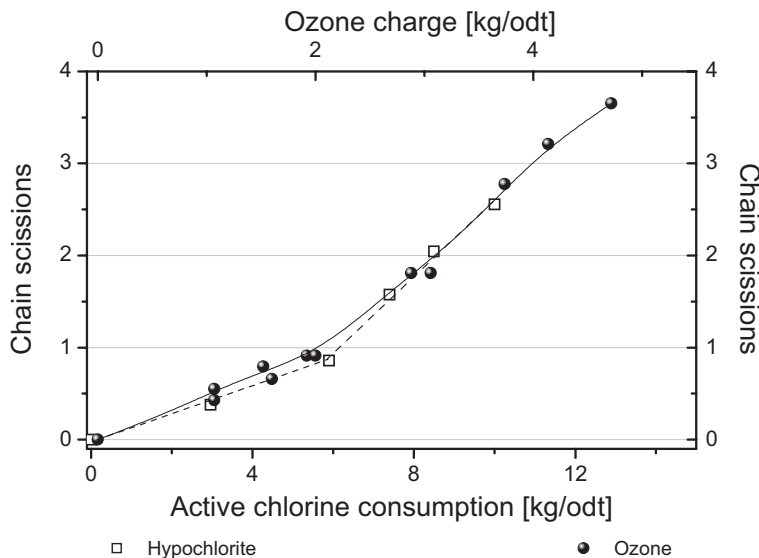
During the course of final bleaching, when the residual lignin content diminishes, it seems likely that the direct reaction between ozone and cellulose gradually becomes the predominant reaction responsible for cellulose degradation in ozone bleaching. Model compound studies using methyl 4-*O*-ethyl- $\beta$ -D-glucopyranoside were conducted to elucidate the participation of radical species in the degradation of the polysaccharide during ozone treatment [53]. From the results obtained it was concluded that both ozone itself and radical species participate in the glycosidic bond cleavage of carbohydrates during ozonation in aqueous solutions. The free radical-mediated reaction may lead to both direct cleavage and to the conversion of hydroxyl to carbonyl groups. The contribution of radical species was estimated to be about 40–70% during ozonation in distilled water acidified to pH 2 (the ratio of ionic to radical reactions was calculated by the relative reactivities at C1 towards ozone in anhydrous dichloromethane as a reference for pure ionic and toward Fenton's reagent as a reference for radical reactions). Furthermore, the model compound studies revealed that oxidation of hydroxyl groups at C2, C3, and C6 positions to carbonyl groups is caused predominantly by radical species.

#### 7.5.7.1.2 Efficiency and Selectivity of Ozone Treatment

The use of ozone for the production of paper-grade pulps is limited to low charges to prevent strength losses. Most of the industrial installations of ozone bleaching operate on hardwood kraft pulps because of a better selectivity performance compared to softwood kraft pulps; this is particularly expressed in a better preservation of strength properties. The higher selectivity of ozone towards hardwood kraft pulps may be attributed to the presence of a high proportion of HexA [106]. Ozone is known to be very effective and selective in removing HexA, without simultaneously impairing pulp properties. Therefore, it can be concluded that the use of ozone in industrial installations is primarily focused on the removal of HexA. Ozone is also used for the production of TCF-bleached dissolving pulps. The ozone treatment is preferably placed between oxygen prebleaching and the final hydrogen peroxide stage. The tasks of ozone for dissolving pulp production are both the removal of residual oxidizable impurities (measured as kappa number) and the controlled adjustment of viscosity. The ozone charge is predominantly chosen to adjust pulp viscosity, while the final brightness is regulated in the subsequent hydrogen peroxide stage. Ozone replaces the hypochlorite treatment in a conventional bleaching sequence for dissolving pulp production. Godsay and Pearce found a clear relationship between the number of chain scissions and ozone consumption (in this case even a linear relationship), and this is an important prerequisite for a controlled viscosity adjustment [99]. During the course of the development of medium-consistency ozone bleaching, a similar shape was recognized for the relationship between the number of chain scissions and the consumption of both ozone and hypochlorite (as active chlorine); this latter point was verified by Herbst and Krässig [110]. At the start of the reaction, the linear function has a shallow slope, indicating a minimal effect on carbohydrate degradation. During the second phase of the reaction, the slope increases and finally becomes straight, showing that the number of bonds broken is now proportional to the amount of chemicals consumed. The relationship between the amount of ozone and hypochlorite consumed and the number of chain scissions in a selection of experiments using beech sulfite dissolving pulp is depicted in Fig. 7.103.

With respect to chain scissions, the efficiency of 1 kg of consumed ozone is equivalent to that of about 2.8 kg of consumed active chlorine (hypochlorite). If both oxidants are expressed as oxidation equivalents (OXE), 1.0 OXE of ozone corresponds to only 0.63 OXE of active chlorine. This means that from the maximum oxidative power of ozone, representing 6 mol electrons per mol, only 3.8 are transferred, whereas in the case of hypochlorite all 2 mol electrons per mol are received.

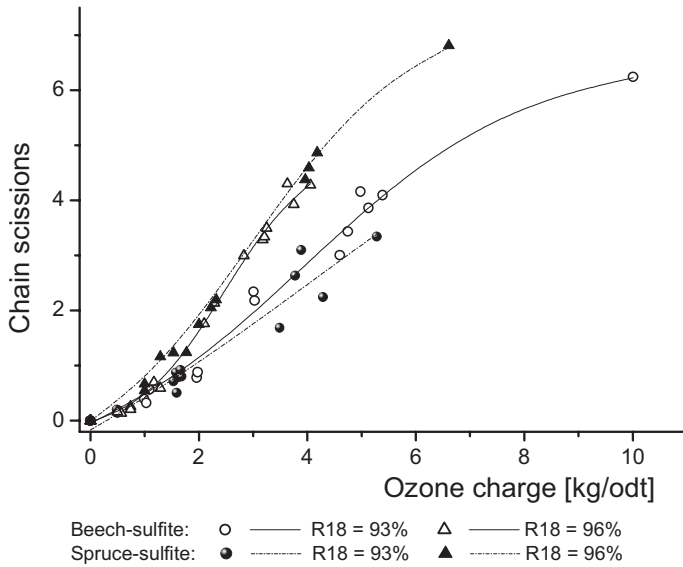
Furthermore, hypochlorite reacts slightly more selectively with the readily available residual lignin as compared to ozone, which is characterized by the lower slope during the first phase. The intercept with the abscissa and the slope of the curve are characteristic parameters for each pulp. The intercept represents the amount of ozone or hypochlorite consumed without any significant chain scissions, while the slope depends on the efficiency of bonds broken. Both parameters are related to the kappa number, the hemicellulose content, the amount of



**Fig. 7.103** Carbohydrate degradation, indicated as number of chain scissions, depending upon the amount of oxidants consumed (according to Sixta et al. [41]). Pulp: EO-pretreated beech acid sulfite dissolving wood pulp (B-AS), kappa number 2.0, viscosity  $560 \text{ mL g}^{-1}$ , alpha-cellulose content 90.2%. medium-consistency-ozone bleaching: 10% consistency, pH 2,  $50^\circ\text{C}$ , 10 s mixing time; hypochlorite treatment: 4% consistency,  $50^\circ\text{C}$ , initial pH = 9.5, reaction time 60 min.

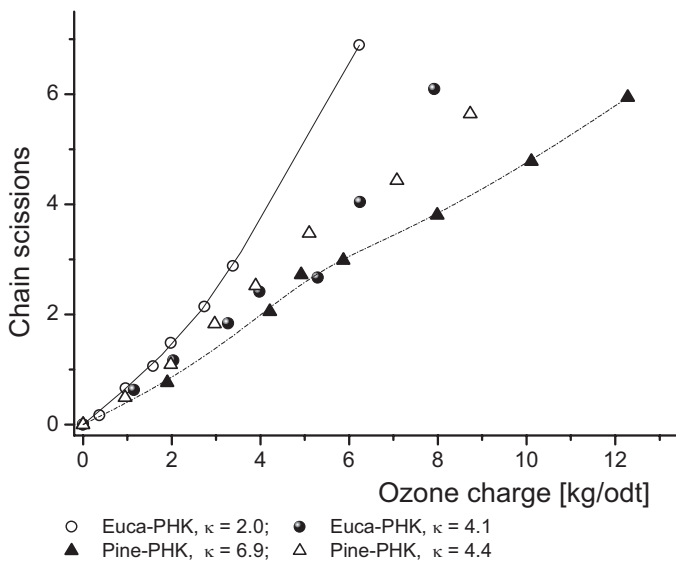
reactive groups in the cellulose chain (e.g., carbonyl groups) and the accessibility to ordered regions under given conditions of ozone bleaching. There is no indication that the selected wood species exerts any significant influence on the course of degradation during ozonation, provided that the purity (measured as R18 or hemicellulose content) and the kappa number of the corresponding pulps are at a comparable level. The development of chain scissions as a function of ozone charge for both beech and spruce sulfite dissolving pulps at two different purity levels, 93% and  $> 96\%$  R18, respectively, are shown in Fig. 7.104.

The results confirm that a correlation between cellulose degradation and ozone charge is not discernible for spruce and beech sulfite dissolving pulps at a given R18 level. The data in Fig. 7.104 also show that the presence of low molecular-weight hemicelluloses protect the pulps against cellulose degradation. Thus, high-purity dissolving pulps are exposed to more severe carbohydrate degradation at a given ozone charge.



**Fig. 7.104** Course of chain scissions as a function of ozone charge for oxygen-delignified beech and spruce Mg-based sulfite dissolving pulps of two different purity levels, 93% R18 and 96% R18, respectively (according to [131]). The remaining properties of the selected

dissolving pulps, such as hemicellulose composition and kappa number are included in Tab. 7.42 medium-consistency laboratory ozone treatment: 50 °C, 10% consistency, 150 g O<sub>3</sub> m<sup>-3</sup>, 8 bar, 10 s mixing time.



**Fig. 7.105** Course of chain scissions as a function of ozone charge for oxygen-delignified pine and eucalyptus prehydrolysis kraft pulps

at comparable purity level, 97% R18, and different kappa numbers. Reaction conditions see Fig. 7.104 and pulp properties see Tab. 7.42.

**Table 7.42** Comparative evaluation of the degradation and delignification behaviour during medium-consistency ozone bleaching of oxygen delignified pulps of different origin and composition (according to [131]).

Substrate	Initial kappa number	R18 value [%]	Xylan [%]	Mannan [%]	Ozone charge do obtain		Kappa/O <sub>3</sub> -charge	
					CS* = 2.0	CS = 3.0	at κ after Z = 1	at κ after Z = 0,5
Beech sulfite	1.2–2.0	93.3	3.4	0.9	3.1	4.2	1.0	
	1.0–1.3	96.7	1.9	0.3	2.3	2.9		0.8
Spruce sulfite	1.4–2.6	93.1	2.0	2.5	3.4	4.7	1.1	
	0.5–2.0	96.8	1.4	0.7	2.1	2.8		0.7
Beech PHK	4.4	95.5	15.6	0.5	4.6			
	2.3	95.8	5.9	0.4	2.7	3.4		
	1.5	96.4	3.1	0.3	2.1	2.7		
	1.4	97.3	2.1	0.2	1.1	1.8		
Pine PHK	6.9	96.8	2.2	2.2	4.0	5.9	0.7	
	4.4	96.7	2.2	2.2	3.2	4.5	0.8	
Eucalypt PHK	2.0	97.1	2.6	0.7	2.6	3.5	1.0	
	4.0	97.1	2.6	0.7	3.5	5.5	0.9	
Pine kraft	3.4	87.1	7.1	6.5	3.8	4.8	0.5	
	17.5	86.8	7.3	6.8	9.3			

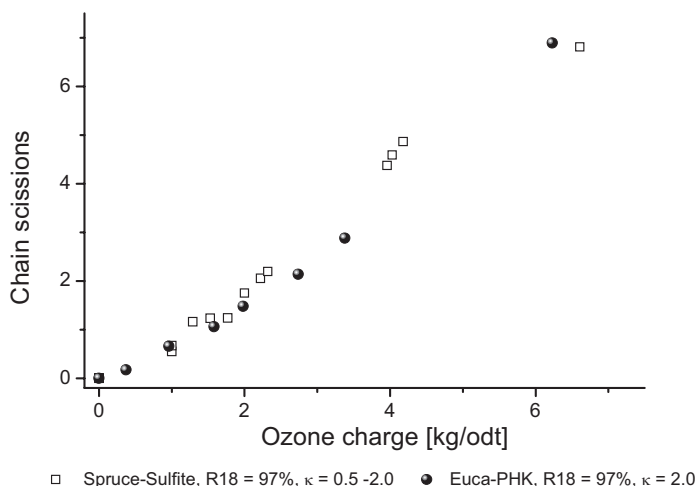
CS = chain scissions given as  $\left(\frac{10^4}{P_t} - \frac{10^4}{P_o}\right)$  in mmol AGU<sup>-1</sup>.

The course of cellulose degradation caused by ozonation is also independent on the wood species for prehydrolysis kraft pulps, as depicted in Fig. 7.105. Despite major differences in fiber morphology, oxygen-delignified pine and eucalyptus PHK pulps reveal a similar degradation pattern during ozone treatment in case of a comparable initial kappa number.

Moreover, the data in Fig. 7.105 demonstrate that the effect of ozone charge on cellulose degradation decreases with rising kappa number prior to ozone treatment.

Surprisingly, the applied cooking technology for the production of dissolving pulps appears also not to have any influence on the behavior of cellulose degradation as a function of ozone charge, provided that both pulps are of comparable R18 content. Figure 7.106 shows that the response of spruce sulfite and eucalypt PHK pulps on the number of chain scissions is quite comparable for a broad range of ozone charges.

As previously indicated, cellulose purity, determined as R18 content or residual xylan and/or mannan concentrations (see Tab. 7.42), significantly affects the degradation pattern during MC ozonation. The progressive removal of short-chain

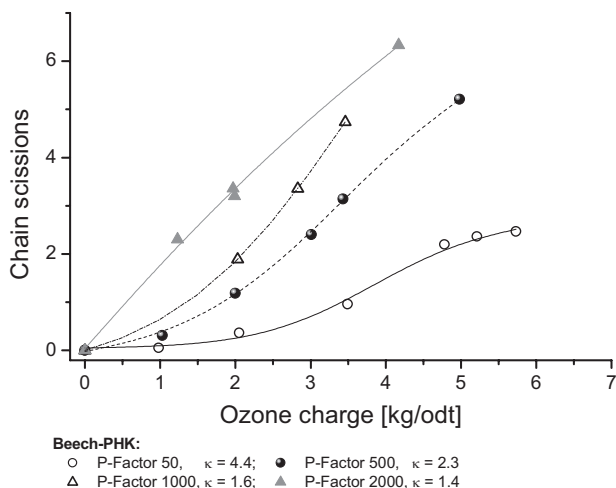


**Fig. 7.106** Comparative evaluation of the response of oxygen-delignified spruce sulfite and eucalypt prehydrolysis kraft pulps on chain scissions as a function of ozone charge at a comparable purity level, 97% R18 and kappa numbers (according to [131]). Medium-consistency laboratory ozone treatment: 50 °C, 10% consistency, 150 g O<sub>3</sub> m<sup>-3</sup>, 8 bar, 10 s mixing time.

carbohydrates leads to a growing susceptibility of the remaining high molecular-weight cellulose molecules towards ozone-induced chain scission (Fig. 7.106). Apparently, the hemicelluloses are preferentially degraded and eventually provide a sacrificial barrier for cellulose attack by ozone, and as a result, the fall in viscosity of the remaining polysaccharides is somewhat suppressed.

The high resistance of the beech pulp with the highest hemicellulose content (P-factor 50) towards chain scissions is partly due to a higher initial kappa number as compared to the other pulps of the comparison (Fig. 7.107; Tab. 7.42). The results demonstrate that the presence of both short-chain hemicelluloses and residual oxidizable impurities (kappa number) protect the high molecular-weight cellulose against degradation during ozonation. Furthermore, the laboratory results outlined in Figs. 7.104–7.107 indicate that ozone is suitable for adjusting viscosity, provided that the kappa number and viscosity of the oxygen-prebleached pulp are within certain limits. It has been shown previously that, when medium-consistency technology is applied, the reaction of ozone with pulp constituents occurs entirely in the mixer. Unlike laboratory conditions, the residence time in commercial high-shear mixers is very short, with typical retention times ranging from less than 1 s to 4 s (maximum), compared to 10 s in a typical laboratory application. The extent of reaction during medium-consistency ozone bleaching is characterized by the ozone consumption rate inside the high-shear mixer. Parallel to the increase in ozone charge, the gas void fraction,  $X_g$ , increases which in turn impairs the efficiency of ozone mass transfer. In Fig. 7.108, the relationship between ozone charge in the range from 1.0 to 5.5 kg odt<sup>-1</sup> and the extent of ozone consumption is compared for laboratory and industrial medium-consistency





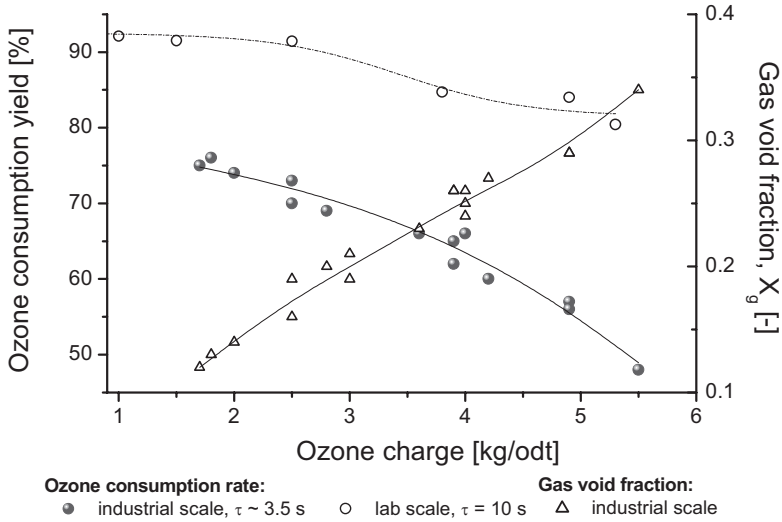
**Fig. 7.107** Influence of cellulose purity of beech prehydrolysis kraft pulps on the course of cellulose degradation during ozonation (according to [131]). The cellulose purity is adjusted by prehydrolysis intensity

characterized by the P-factor. Medium-consistency laboratory ozone treatment: 50 °C, 10% consistency, 150 g O<sub>3</sub> m<sup>-3</sup>, 8 bar, 10 s mixing time.

bleaching. The rather long residence time of approximately 3.5 s during high-shear mixing in the commercial system has been obtained by the installation of two mixers in series. The yield of reacted ozone declines in the industrial MC system, from about 75% at an ozone charge of 1.5 kg odt<sup>-1</sup> to less than 50% at an ozone charge of 5.5 kg odt<sup>-1</sup>, while the laboratory mixer keeps an ozone consumption rate beyond 80% throughout the given range of ozone charges.

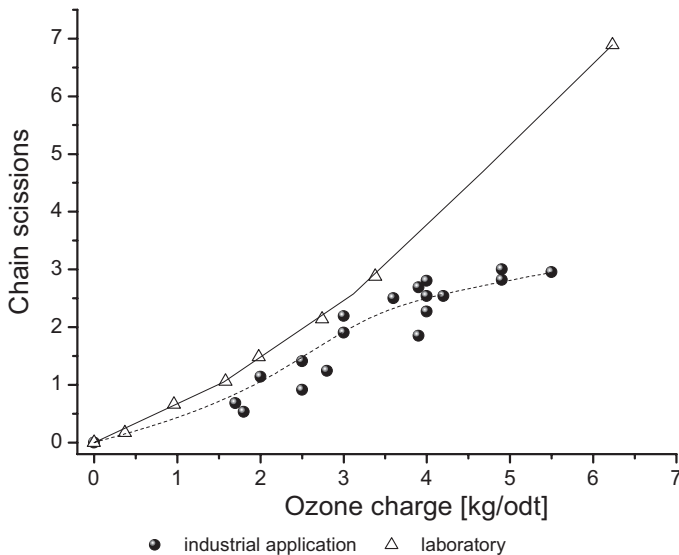
The lower ozone consumption in the commercial MC ozone installation is expressed in a reduced extent of reaction between ozone and pulp constituents as compared to the laboratory system. The data in Fig. 7.109 illustrate that, in an industrial high-shear mixing system, the number of chain scissions levels off at ozone charges exceeding 4 kg odt<sup>-1</sup>. A further improvement of the ozone consumption yield in a medium-consistency installation can only be obtained by extending the mixing time, and by reducing the gas void fraction while keeping the specific energy dissipation,  $\epsilon$ , at a fairly constant level.

The selectivity of ozone bleaching is an important criterion not only for paper-grade but also for dissolving-grade pulp production, in order to ensure an efficient delignification and bleaching performance. It has been mentioned previously that the selectivity of ozone bleaching is also affected by the type and properties of the pulps. It is well known that ozone bleaching of hardwood kraft pulp is more selective than for softwood kraft pulp in terms of the kappa number–viscosity relationship [106]. Moreover, Soteland established that sulfite pulps respond more selectively to ozone treatment than do kraft pulps [111]. The better response of sulfite pulps to ozone treatment is attributed to the lower lignin content of the unbleached pulp [112].



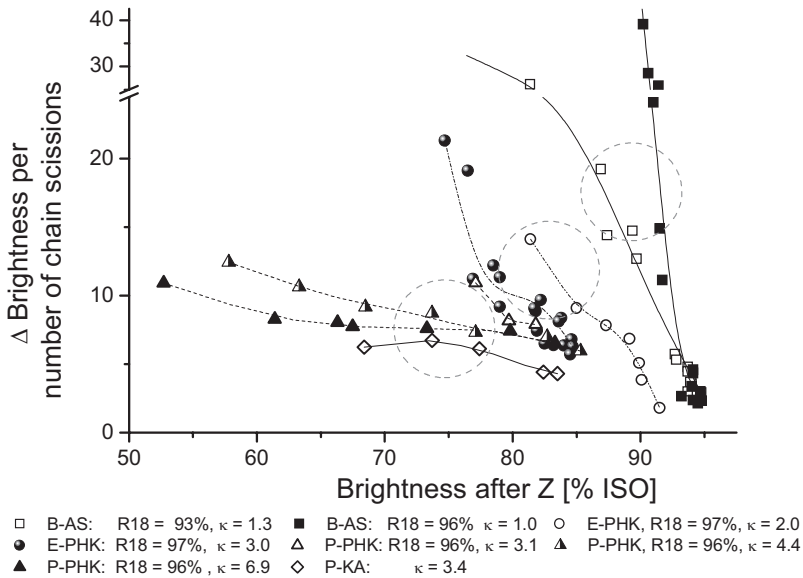
**Fig. 7.108** Comparison of industrial and laboratory medium-consistency ozone bleaching with respect to the ozone consumption rate as a function of ozone charge according to [131]). The development of the gas void fraction in the commercial system is followed over the range of ozone charges investigated.

The set-up of the commercial system comprises the installation of two high-shear mixers in series. Conditions of the commercial ozone stage: pH 2.5, ozone concentration prior to compression: 120–160 g m<sup>-3</sup>, consistency 8.5%, pressure inside the mixers 7.5 bar, 43 °C.



**Fig. 7.109** Comparison of industrial and laboratory medium-consistency ozone bleaching with respect to the ozone consumption rate as a function of ozone charge (according to [131]).

The selectivity of delignification and bleaching reactions in general – and that of ozone bleaching in particular – is defined as the ratio of the rate constant for the desired delignification or bleaching reactions (removal of chromophores) to that of the non-desired carbohydrate degradation reaction. A practical way to compare the selectivity of ozone bleaching of different pulps, and of different levels of initial viscosity, can be achieved by relating the brightness gain ( $\Delta$  brightness) per number of chain scissions (CS) to the brightness after ozonation. It can be expected that the bleaching selectivity, expressed as  $\Delta$  brightness/CS, decreases with increasing brightness after ozone treatment. The selectivity behavior of different types of dissolving pulps and of one softwood paper-grade kraft pulp was studied in a laboratory medium-consistency system under comparable conditions. The results outlined in Fig. 7.110 reveal three areas of different selectivity. The group of highest selectivity comprises the hardwood sulfite dissolving pulps, followed by the hardwood PHK pulps and the softwood kraft pulps, which cover the least-selective group of pulps. The superior selectivity of hardwood and sulfite pulps both with low initial kappa numbers is in accordance with reported values [108]. Although ozone reacts more readily with lignin structures than with carbohydrates, the bleaching selectivity decreases with increasing kappa number, due to a more efficient chromophore reduction at lower residual kappa number. These results imply that, with respect to pulp viscosity at a given kappa number, it is preferable to intensify oxygen delignification and to apply less ozone.



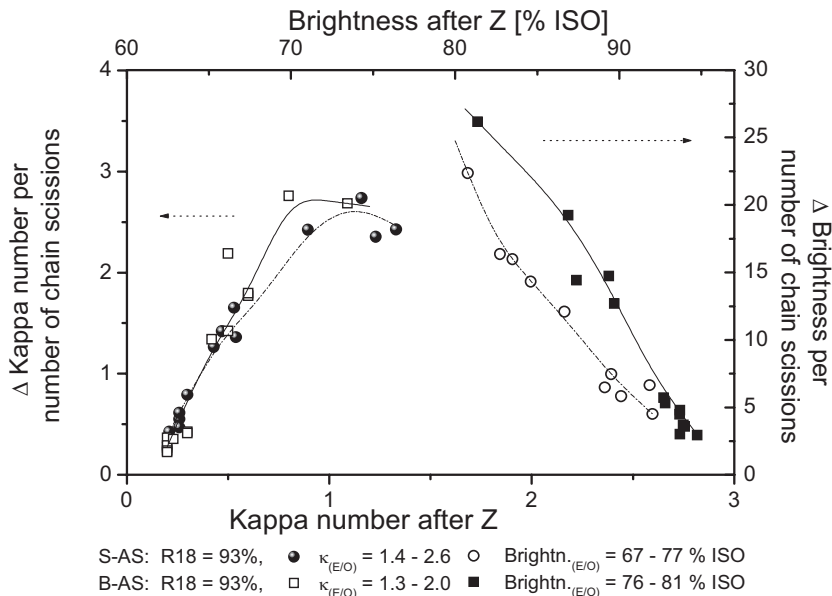
**Fig. 7.110** Bleaching selectivity of a variety of oxygen-prebleached dissolving pulps and of one softwood kraft pulp during medium-consistency ozone treatment in a laboratory high-shear mixer (according to [131]).

The pulps subjected to ozone treatment are characterized in Tab. 7.42. Constant conditions of ozone bleaching: pulp consistency 10%, 50 °C, pH 2.0, mixing time 10 s.

The reason for the higher selectivity of a hardwood over a softwood kraft pulp has been attributed to the presence of a higher amount of HexA in the former [106]. However, dissolving pulps derived from both sulfite and PHK technology contain only minor amounts of HexA, or are even free of HexA at high cellulose purity levels [113]. Therefore, the presence of HexA alone is not decisive for the superior selectivity of hardwood pulps. It may be speculated that the residual kappa number of a dissolving pulp contains no relevant amounts of phenols of the syringyl- and guaiacyl-type which promote radical formation in different yields [106]. Nevertheless, ozone bleaching is less selective for both paper-grade and dissolving-grade pulps rich in kappa number and hemicellulose content. The data in Fig. 7.110 demonstrate clearly that the pine PHK pulp behaves more selectively during ozonation as compared to a pine paper-grade pulp of comparable initial kappa number (kappa number 3.4 and 3.1, respectively).

To better elucidate the influence of wood species on the selectivity of ozonation, the performance of spruce and beech acid sulfite dissolving pulp (S-AS versus B-AS) of comparable kappa number content (1.4–2.6) and cellulose purity (R18 ~ 93%) has been investigated with regard to delignification and bleaching selectivity (Fig. 7.111).

The data in Fig. 7.111 show clearly that the selectivity of kappa number reduction is not dependent on the wood species, provided that the compositions of non-cellulosic material in the pulps are at comparable levels. The wood species, how-



**Fig. 7.111** Bleaching selectivity of a variety of oxygen-prebleached dissolving pulps and of one softwood kraft pulp during medium-consistency ozone treatment in a laboratory high-

shear mixer. The pulps subjected to ozone treatment are characterized in Tab. 7.42. Constant conditions of ozone bleaching: pulp consistency 10%, 50 °C, pH 2.0, mixing time 10 s.

ever, may exhibit an influence on the selectivity of brightness gain, as indicated in Fig. 7.111. Clearly, the beech pulp is slightly more susceptible to an increase in brightness at a given number of chain scissions as compared to the spruce pulp. The differences are small, but significant, and may be attributed to the different reflectance behavior rather than to differences in the light absorption properties of hard- and softwood fibers.

At first glance, these results appear to contradict those reported by Simoes and Castro [64], who stated that selectivity was higher for pine than for eucalyptus pulp when comparing the viscosity versus kappa number profiles. However, when converting the given changes in viscosity caused by ozonation into the number of chain scissions, in order to normalize polysaccharide degradation, the delignification selectivity was exactly the same for both pine and eucalyptus pulps [eucalyptus pulp:  $\Delta \text{Kappa}/\Delta \text{viscosity} = (15.5 - 4.0)/(1270 - 770) = 0.023$  converted to kappa number reduction per chain scissions =  $11.5/2.27 \times 10^{-4} = 51 \cdot \kappa \cdot \text{AGU} \cdot \text{mmol}^{-4}$ ; pine pulp:  $\Delta \text{Kappa}/\Delta \text{viscosity} = (18.1 - 4.0)/(970 - 615) = 0.040$  corresponds to  $50 \cdot \kappa \cdot \text{AGU} \cdot \text{mmol}^{-1}$ ] [64]. Thus, it can be summarized that the delignification selectivity of ozonation is predominantly influenced by the initial kappa number and the amount of noncellulosic components (e.g., the hemicellulose content).

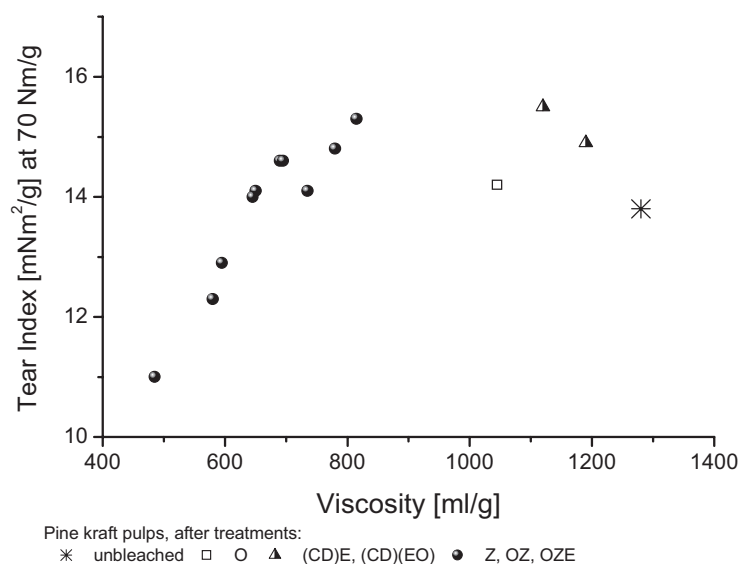
#### 7.5.7.2 Effect of Ozonation on the Formation of Carbonyl and Carboxyl Groups

The formation of carbonyl and carboxyl groups has great significance in bleaching operations. It is well known that the introduction of carbonyl groups along the polysaccharide chains leads to cleavage of glycosidic bonds when the pulp is subsequently exposed to alkali. Furthermore, carbonyl groups and uronosidic carboxyl groups exert a detrimental effect on color stability. The presence of carboxyl groups also affects the swelling characteristics and water affinity of pulp fibers, which in turn governs the sheet formation and bonding properties.

Chandra and Gratzl monitored the formation of these groups during ozonation of alpha-cellulose (produced from a softwood sulfite dissolving pulp further purified by extraction with 18% sodium hydroxide at 25 °C) [60]. The carboxyl content increased in a stepwise fashion with the degree of ozonation, while the carbonyl content underwent steep rises followed by sharp declines throughout ozonation, resulting in an overall increase at the end of the treatment. The observed pattern of carbonyl groups as a function of ozone charges was explained by the assumption that the introduction of carbonyl groups sensitizes this particular part of the polymer towards further attack by ozone [60,114]. This may lead to excessive degradation followed by dissolution of the oxidized fragments, and exposes previously protected domains to continued ozonation. The results of a comprehensive study on the generation of carbonyl and carboxyl groups along the carbohydrate chain during the course of ozonation before or after hydrogen peroxide treatment is included in Section 11.2 (paper grade pulps) and 11.3.2.2 (dissolving grade pulps).

### 7.5.7.3 Effect of Ozonation on Strength Properties

Unfortunately, ozone delignification is accompanied by a concomitant degradation of the polysaccharide fraction. As illustrated in Fig. 7.109, cellulose degradation (characterized in terms of number of chain scissions) is clearly related to ozone charge. The correlation between strength properties and carbohydrate degradation (pulp viscosity) of ozone-bleached pulps was found to differ somewhat from those of pulps subjected to conventional bleaching sequences [111,115]. Ozone-treated pulps are characterized by rapid beating, high-tensile strength but low tearing resistance. In general, the tearing strength of ozone-bleached softwood kraft pulps was found to be 10–20% lower as compared to conventionally bleached pulps of the same provenance [116]. Lindholm has investigated the impact of various ozone treatments on the tearing strength at a tensile strength of  $70 \text{ Nm g}^{-1}$  using a pine kraft pulp [116]. He reported that pulps subjected to Z, OZ, and OZE treatments had comparable strength properties to those after (CD)E and (CD)(EO) treatments, provided that the pulp viscosity of the ozone-treated pulps was greater than  $700 \text{ mL g}^{-1}$  (Fig. 7.112). The kappa numbers were about 6 (range: 5–8) for both types of pulp.



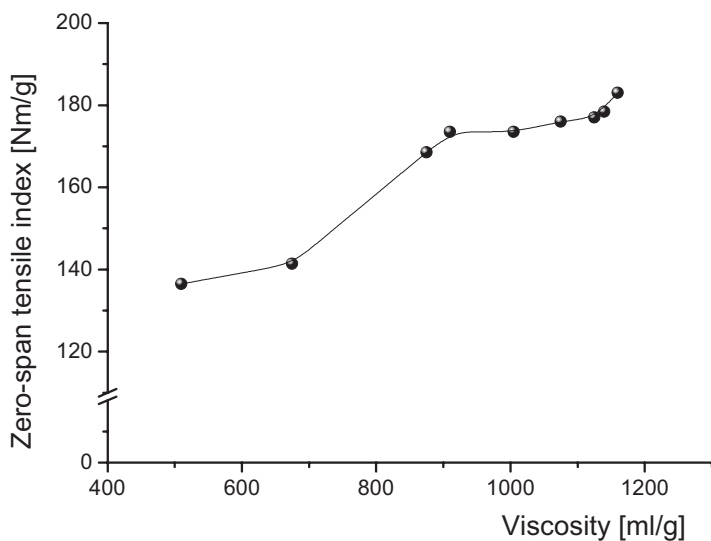
**Fig. 7.112** Tear index at  $70 \text{ Nm g}^{-1}$  versus viscosity for differently treated pine kraft pulps (according to Lindholm [116]).

Figure 7.111 demonstrates a clear relationship between viscosity and tear index at a given tensile index of the ozone-treated pulps. From this result it can be concluded that strength properties of ozone-bleached pine kraft pulps are not deteriorated, provided that pulp viscosity can be maintained above  $700 \text{ mL g}^{-1}$ . Axegard et al. reported that the tear strength at a given tensile index of an OAZQP-bleached softwood kraft pulp with a viscosity of  $710 \text{ mL g}^{-1}$  was only 5–10% lower

as compared to an OD(EO)DD softwood kraft pulp with a viscosity of  $890 \text{ mL g}^{-1}$  [117]. Similar results have been reported by Dillner and Tibbling [118], indicating that the strength–viscosity relationship presented for conventionally bleached pulps by Rydholm [119] was not valid for TCF-bleached pulps, including ozone treatment.

Strength properties of fully bleached hardwood kraft pulps with a sequence including ozone were comparable to those of a conventionally bleached pulp, although the viscosity of the ozone-bleached pulp was 20% lower [120]. The preservation of strength properties despite cellulose degradation through ozone treatment is also known for hardwood kraft pulps.

Quite recently, the relationships between the molecular weight distributions (MWDs), intrinsic viscosity and zero-span tensile index of a birch kraft pulp subjected to HC ozone bleaching were evaluated [121]. The relationship between rewetted zero-span tensile strength and viscosity is shown graphically in Fig. 7.113.



**Fig. 7.113** Zero-span tensile index versus viscosity for ozone-treated birch kraft pulp (according to [121]). Unbleached pulp: kappa number 15.5, intrinsic viscosity  $1160 \text{ mL g}^{-1}$ .

A substantial decrease in fiber strength occurred only when pulp viscosity decreased below  $800 \text{ mL g}^{-1}$ . At the highest ozone dosage, the fiber strength was still 75% of the initial value, corresponding to a viscosity of  $510 \text{ mL g}^{-1}$ . Apparently, ozone-treated pulps maintain their initial fiber strength at relatively high level, despite a substantial reduction in molecular weight. Based on gel permeation chromatography (GPC) measurements, it was shown that the degradation pattern through ozonation of kraft pulp was different from that of cotton linters. In contrast to unbleached birch kraft pulp, ozone-induced cellulose degradation

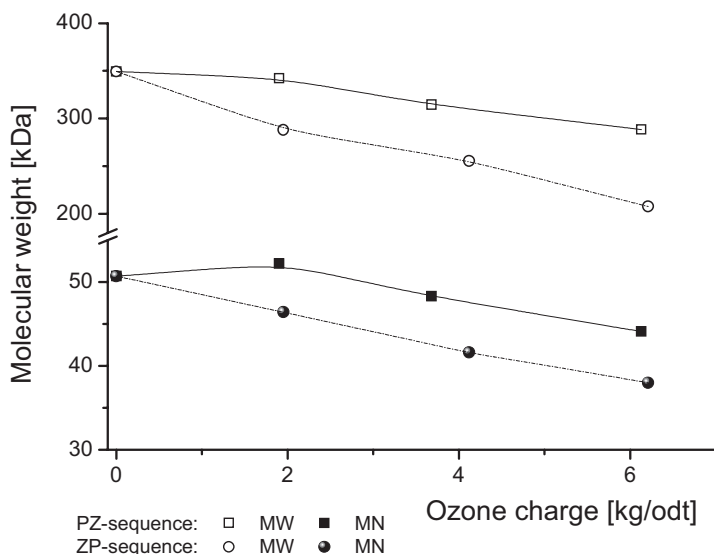
did not generate a bimodality of the cotton cellulose peak. The different action of ozone on MWD was attributed to the presence of lignin in the unbleached birch kraft pulp, as lignin is known to promote the formation of secondary radicals during ozone delignification [57]. Due to the enrichment of lignin at the surface of fibers, it is suggested that cellulose degradation of an unbleached birch kraft pulp occurs predominantly on the exterior of the fiber, thus generating two distinct cellulose distributions [21,23].

#### 7.5.7.4 Typical Conditions, Placement of Z in a Bleaching Stage

The placement of an ozone stage within a bleaching sequence must consider both technological and chemical aspects. The low pH and high sensitivity towards carry-over from the washing stage of an unbleached kraft pulp suggest that ozone should not be used in a first delignification stage. Moreover, ozone degrades part of the phenolic units and makes oxygen less reactive towards lignin in a ZO-sequence. In contrast to the observations of Lachenal et al. [122], who found that a single ozone stage (Z) behaves as selectively as an OZ-sequence, Brodin et al. [75], Ragnar [106], as well as the results shown in Fig. 7.110, show that ozone bleaching becomes more selective in terms of brightness increase per number of chain scissions by lowering the incoming kappa number; this means that oxygen delignification prior to the ozone stage is desirable for reasons of delignification selectivity. In addition, OZ is favored over Z because of better process economy due to lower chemical costs (lower ozone consumption and the possibility of recycling oxygen from the Z-stage) and better possibilities to close the water cycle. The choice between OZ and Z also depends on the applied ozone bleaching technology. In HC ozone bleaching, a sufficient quantity of ozone can be reacted in order to achieve the necessary extent of delignification in a single ozone stage, whereas ozonation at medium-consistency is limited to a kappa number reduction of maximum 5–7 units (assuming a specific kappa number reduction of about 1 unit per kg ozone charged; see also Tab. 7.36) which in most cases is not enough to complete delignification.

In a TCF-bleaching sequence consisting of O-, Z-, and P-stages, the use of hydrogen peroxide (P) is essential to remove the chromophores by oxidizing the carbonyl groups. As expected, the placement of a P-stage within such a sequence affects the final bleached pulp properties. OZP- and OPZ-sequences show the same delignification efficiency, while the latter appears to be more selective as compared to OZP [122,123]. In a recent study, the effect of placing the Z-stage prior to (ZP) and after (PZ) standard peroxide bleaching of an (E/O) pretreated beech dissolving pulp was evaluated by charging different amounts of ozone while all other reaction conditions were kept constant [123]. GPC measurements revealed that cellulose degradation was more pronounced for ZP- than for PZ-treated pulps, while the latter had slightly lower brightness values (see Tab. 7.41 and Section 11.3.2.2.2). Figure 7.114 illustrates the course of cellulose degradation in terms of weight (MW) and number (MN) average molecular weights.



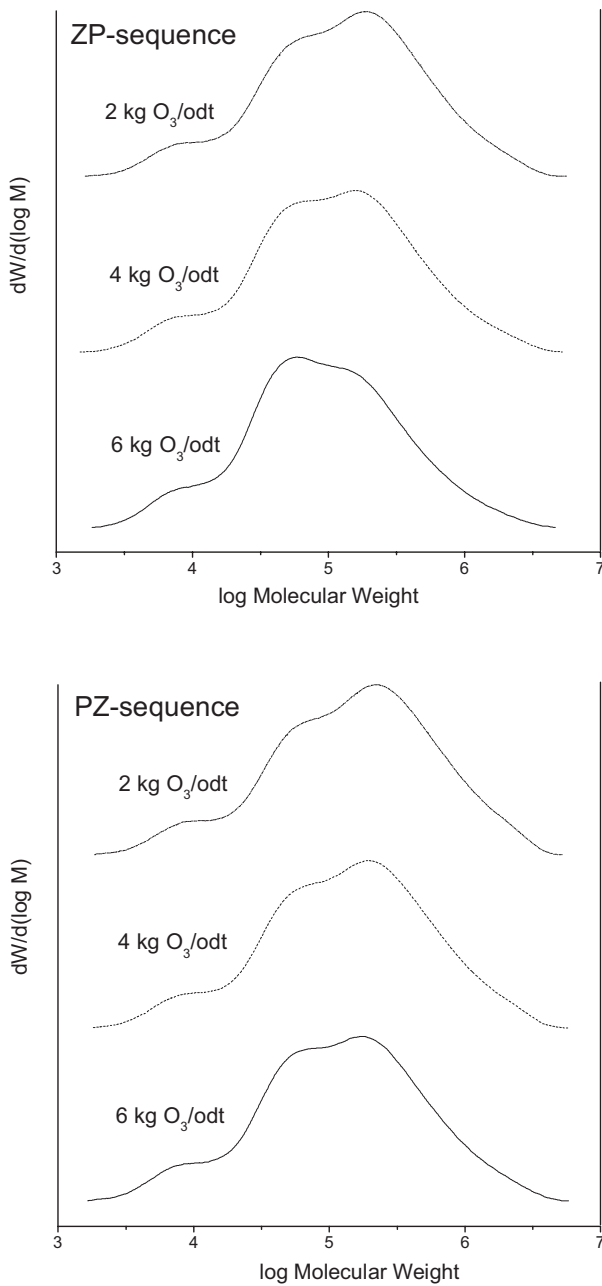


**Fig. 7.114** Course of weight (MW) and number (MN) average molecular weights of beech sulfite dissolving pulps as a function of ozone charges with Z-stage prior to (ZP) and after P-stage (PZ), applying identical conditions in each stage [123].

In contrast to the results obtained from Godsay and Pearce [99] and Berggren et al. [121], the polydispersity index (PDI) – that is, the ratio of the weight average to the number average molecular weights (MW/MN) – did not increase but rather was slightly decreased, from about 6.8 in the untreated pulp to 5.5 in the most severely degraded pulp. This may be attributed to the fact that the beech sulfite dissolving pulps were subjected to significantly less ozone dosages (2–6 kg odt<sup>-1</sup>) than those reported by either Godsay and Pearce (47.7–75.4 kg odt<sup>-1</sup>) or Berggren et al. (1–35 kg odt<sup>-1</sup>).

The placement of Z within the TCF sequence also influences the shape of the differential MWD. All samples displayed a shift of the MWD towards a lower molecular weight range as degradation proceeded. The high molecular-weight cellulose fraction of the pulp subjected to ZP treatment was considerably degraded in the presence of ozone. From the high molecular-weight peak, with a peak molecular mass ( $\log M_p$ ) = 5.3, a part of the pulp cellulose fraction was degraded and the maximum shifted to the second cellulose peak, having a  $\log M_p$  = 4.7. In the case of PZ treatment, the shape of the MWD was virtually unaffected by the ozone charge (Fig. 7.115).

It is well known that ozone treatment of pulp introduces carbonyl groups into the AHG unit along the polysaccharide chain (see Tab. 7.41 and Section 11.3.2.2.2). In a subsequent alkaline hydrogen peroxide stage (P), depolymerization of the oxidized polysaccharide components in the pulp (cellulose and hemicellulose) is favored due to  $\beta$ -elimination reaction. The high alkali instability of Z-treated



**Fig. 7.115** Differential MWDs of beech sulfite dissolving pulps prepared by TCF bleaching applying different amounts of ozone with Z-stage before (upper) (ZP) and after P-stage (lower) (PZ), applying identical conditions in each stage [123].

pulps is also the reason why pulp viscosities of PZ-treated pulps are quite comparable to those of ZP-treated pulps (despite the significantly higher MW and MN values determined by GPC measurements), provided that the pulps are not subjected to sodium borohydride reduction prior to viscosity measurements. Although OPZ bleaching results in superior strength properties, an OZP-sequence is preferred because of a significantly better brightness stability upon heat or light exposure. This better brightness stability is achieved by partly oxidizing the carbonyl groups that are introduced during ozonation. Brightness stability can also be improved by reducing the carbonyl groups with sodium borohydride after ozonation [92].

The effect of placing Z-stage on the generation of functional groups as a function of ozone dosage is discussed in detail in Section 11.3.2.2.2.

Interestingly, in an ECF-sequence comprising O-, Z-, and D-stages, OZD was found to be more selective than ODZ [124]. This can be explained by the fact that chlorine dioxide bleaching following a Z-stage shows no adverse effect on cellulose. The brightness stability after OZD is lower than after OZP bleaching, since a final chlorine dioxide treatment is less effective in oxidizing or removing carbonyl group-containing material. Contrary to a treatment in two separate bleaching stages, a sequential application of chlorine dioxide (D) and ozone (Z) without intermediate washing was shown to be very selective in delignifying softwood kraft pulp [125]. This means that the Z- and D-stages are combined into one treatment (DZ). (DZ) has been found to be more effective for unbleached pulps, whereas (ZD) seems to be superior for oxygen-delignified kraft pulps [126]. In the latter sequence, chlorine dioxide partially stabilizes the carbohydrate chain against alkaline peeling reactions due to oxidation of the carbonyl groups introduced by ozonation. In the case of an unbleached hardwood kraft pulp, however, chlorine dioxide reacts with free phenolic groups before the highly reactive ozone is introduced, the conclusion being that reaction kinetics clearly favors the (DZ) approach relative to the (ZD) treatment [127]. Furthermore, after chlorine dioxide treatment the pulp suspension is sufficiently acidic for a subsequent ozone stage. The (DZ) concept is also advantageous with respect to AOX formation, as ozone has the ability to destroy some AOX generated during D bleaching. Chlorine dioxide may act as a radical scavenger, suppressing the extent of radical reactions during the subsequent ozone treatment. However, in another study it was shown that the selectivity was not impaired when washing was carried out between D and Z, thus showing that the presence of residual chlorine dioxide seems not to be essential for maintaining a high viscosity [128]. The actual reasons for improved selectivity of a (DZ) treatment remain to be elucidated. In full ECF bleaching sequences, the replacement of a  $D_0$  stage by (DZ) stages was shown to be particularly efficient, since in the case of a hardwood kraft pulp 1 kg charged (consumed) ozone could replace 1.58 kg charged chlorine dioxide, as shown in Tab. 7.43 [128]. Ozone is added to the pulp suspension 10 min after the introduction of chlorine dioxide.

**Table 7.43** Comparison of different ECF bleaching sequences of a hardwood kraft pulp where D<sub>0</sub> is substituted either by Z or by (DZ) stages according to [128].

Sequence	Stage	Chemical	Chemical charge			Kappa no.	Bright-ness [%ISO]	Viscosity [mL g <sup>-1</sup> ]	AOX [kg odt <sup>-1</sup> ]
			[kg odt <sup>-1</sup> ]	OXE	Σ OXE				
D <sub>0</sub> EOPD <sub>1</sub> D <sub>2</sub>	Unbleached					14.8		1050	
	D <sub>0</sub>	ClO <sub>2</sub>	14.0	1038	1038				
	EOP	H <sub>2</sub> O <sub>2</sub>	5.0	294	1332				
	D <sub>1</sub>	ClO <sub>2</sub>	10.0	741	2073				
	D <sub>2</sub>	ClO <sub>2</sub>	2.5	185	2258		87.7	940	0.8
ZEOPD <sub>1</sub> D <sub>2</sub>	Unbleached					14.8		1050	
	Z	O <sub>3</sub>	6.0	750	750				
	EOP	H <sub>2</sub> O <sub>2</sub>	5.0	294	1044				
	D <sub>1</sub>	ClO <sub>2</sub>	10.0	741	1785				
	D <sub>2</sub>	ClO <sub>2</sub>	2.5	185	1970		87.5	820	0.2
(DZ)EOPD <sub>1</sub> D <sub>2</sub>	Unbleached					14.8		1050	
	(D)	ClO <sub>2</sub>	8.0	593	593				
	Z)	O <sub>3</sub>	6.0	750	1343	3.9	54.4	900	
	EOP	H <sub>2</sub> O <sub>2</sub>	5.0	294	1637		69.4	875	
	D <sub>1</sub>	ClO <sub>2</sub>	7.5	556	2193		86.2		
	D <sub>2</sub>	ClO <sub>2</sub>	1.5	111	2304		88.9	885	0.4

- D<sub>0</sub>: 3% consistency,  
 EOP: 10% consistency, 70 °C, 60 min, 3 kg MgSO<sub>4</sub>·7H<sub>2</sub>O odt<sup>-1</sup>, 0.2 MPa O<sub>2</sub>.  
 D<sub>1</sub>: 10% consistency, 75 °C, 90 min.  
 D<sub>2</sub>: 10% consistency, 80 °C, 180 min, 2 kg NaOH odt<sup>-1</sup>.  
 Z: 40% consistency, pH 2.5.  
 (DZ): 3% consistency, first 8 kg ClO<sub>2</sub> during 10 min, 50 °C, then O<sub>3</sub> is charged.

In other words, 1 kg (mol) of ozone replaces 4.2 kg (2.8 mol) of active chlorine which, in terms of OXE, represents almost the same oxidation potential (125 OXE from ozone replaces 117 OXE from chlorine dioxide). The data in Tab. 7.43 also indicate that a complete substitution of ozone for chlorine dioxide is even more efficient in replacing chlorine dioxide. There, 1 kg (mol) of ozone substitutes 6.1 kg (4.2 mol) of active chlorine, which exceeds the (nominal) oxidation power of chlorine dioxide (125 OXE from ozone replaces 173 OXE from chlorine dioxide). However, the major advantage of a (DZ) treatment over a pure Z-stage is certainly the better preservation of pulp viscosity, and this is also reflected in better strength properties. The full replacement of the D<sub>0</sub> stage by a Z stage is slightly more efficient in the case of a hardwood than for a softwood kraft pulp. In the latter case, 1 kg (mol) of ozone substitutes 3.7 kg (2.5 mol) of active chlorine. Hardwood kraft pulp is certainly more susceptible to ozone bleaching due to the presence of HexA as part of the kappa number. The AOX formation is linearly

related to the chlorine dioxide charge. The lower AOX level in the case of the (DZ) treatment is related to the lower chlorine dioxide charge, but not to a chemical breakdown during the subsequent ozone treatment.

The optimum placement of ozone within a TCF-sequence for full brightness (+88% ISO) and maximum strength properties remains an unresolved question and thus the focus of many investigations.

It has been reported that the efficiency of a TCF bleaching sequence was improved significantly when an ozone stage was arranged between two hydrogen peroxide stages [129]. This could be shown in a direct comparison of the two sequences OQP<sub>1</sub>ZP<sub>2</sub> and OZQP<sub>1</sub>P<sub>2</sub>, where identical reaction conditions were applied (the charge of OXE is equal for both sequences). It is interesting to note that the brightness level prior to the last bleaching stage P<sub>2</sub> is almost equal for both sequences. However, the brightness gain in the second peroxide stage is 5% ISO points higher when it succeeded an ozone stage rather than a hydrogen peroxide stage, as shown in Tab. 7.44.

**Table 7.44** Comparative evaluation of the two TCF sequences OZQP<sub>1</sub>P<sub>2</sub> and OQP<sub>1</sub>Z<sub>1</sub>P<sub>2</sub> with respect to pulp properties at given bleaching conditions according to [129].

Sequence	Stage	Chemical	Chemical charge			Kappa no.	Bright-ness [% ISO]	Viscosity [mL g <sup>-1</sup> ]	ΔKappa/CS*
			[kg odt <sup>-1</sup> ]	OXE	Σ OXE				
OZQP <sub>1</sub> P <sub>2</sub>	Unbleached					27.3		955	
	O					15.5		895	
	Z	O <sub>3</sub>	5.2	650	650	9.9	46.7	800	9.1
	QP <sub>1</sub>	H <sub>2</sub> O <sub>2</sub>	25	1470	2120	3.6	77.5	558	3.6
	P <sub>2</sub>	H <sub>2</sub> O <sub>2</sub>	25	1470	3590	2.8	83.9	546	3.6
OQP <sub>1</sub> ZP <sub>2</sub>	Unbleached					27.3		955	
	O					15.5		895	
	QP <sub>1</sub>	H <sub>2</sub> O <sub>2</sub>	25	1470	1470	7.1	70.3	807	14.9
	Z	O <sub>3</sub>	5.2	650	2120	2.7	77.6	730	10.8
	P <sub>2</sub>	H <sub>2</sub> O <sub>2</sub>	25	1470	3590	1.0	88.9	665	7.8

O: 10% consistency, 0.58 Mpa, 90 °C, 60 min.

Z: 10% consistency, 2 °C, pH 2.2.

P: 10 % consistency, 3% NaOH, 0.05% MgSO<sub>4</sub>, 0.2% DTPA, 85 °C, 240 min.

CS = chain scissions given as  $\left(\frac{10^4}{P_t} - \frac{10^4}{P_o}\right)$  in 10<sup>-4</sup> mol AGU<sup>-1</sup>.

These results indicate that the residual chromophore structures are activated by ozonation towards a subsequent alkaline hydrogen peroxide bleaching, presumably by introducing additional phenolic hydroxyl groups [130]. The presence of an OH in the ortho- or para-position to the α-C of the side chain containing a keto group makes this group susceptible to alkaline hydrogen peroxide, where the aro-

matic ketone structure is converted to a phenol according to a *Dakin* reaction. In subsequent oxidation reactions, the phenols are further oxidized to aliphatic carbonic acids.

Table 7.44 also shows that the overall selectivity of an OQP<sub>1</sub>ZP<sub>2</sub> sequence is better as compared to an OZQP<sub>1</sub>P<sub>2</sub> treatment, presumably because of the introduction of more alkaline-labile groups during the Z treatment directly after an oxygen stage, than after an alkaline hydrogen peroxide step with a significantly lower kappa number prior to ozonation.

## 7.6

### Hydrogen Peroxide Bleaching

*Hans-Ullrich Süß*

#### 7.6.1

##### Introduction

In 1818, J. L. Thenard discovered hydrogen peroxide (H<sub>2</sub>O<sub>2</sub>) by reacting barium peroxide with nitric acid [1]. Based on this reaction, the commercial production of H<sub>2</sub>O<sub>2</sub> began around 1880 [2]. The very diluted (~3%) H<sub>2</sub>O<sub>2</sub> produced by the barium process found only limited use due to the high production costs and a poor stability. However, the advantages of H<sub>2</sub>O<sub>2</sub> in bleaching were rapidly recognized, it was applied for example in the bleaching of precious products such as ivory. The disadvantages of the barium process were overcome by the electrochemical process, which was based on the electrolysis of a diluted sulfuric acid solution and subsequent hydrolysis of the peroxy disulfuric acid to H<sub>2</sub>O<sub>2</sub> and sulfuric acid [3]. The electrochemical process allowed the production of pure and stable, more highly concentrated (~30%) H<sub>2</sub>O<sub>2</sub> solutions. The first commercial H<sub>2</sub>O<sub>2</sub> plant using the electrochemical process started production in 1908 at Österreichische Chemische Werke, Weissenstein, Austria.

For the major part of the twentieth century, sodium peroxide played a more important role than H<sub>2</sub>O<sub>2</sub> in bleaching applications. Its relatively simple production from sodium metal by air oxidation was the cheaper route to a peroxygen compound. On dilution in water, it yields a strong alkaline solution of hydrogen peroxide, which could be applied directly in bleaching processes:



For the majority of processes, the high alkalinity is a disadvantage, and therefore acid had to be added to achieve a partial neutralization. This, and the more complicated dissolution of the solid compound Na<sub>2</sub>O<sub>2</sub> in contrast to the simple addition of the liquids caustic soda and hydrogen peroxide to a bleaching process, resulted in a slow phasing out of sodium peroxide as a bleaching chemical. The development of the anthraquinone process (the so-called AO process) in the mid-1930s at BASF [4,5] resulted in a more economical pathway to hydrogen peroxide

compared with the electrochemical reaction. In 2003, the worldwide capacity for  $\text{H}_2\text{O}_2$  production was estimated as 3.3 million tonnes, based on different variations of the AO process. The predominant proportion of  $\text{H}_2\text{O}_2$  is used in bleaching processes.

### 7.6.2

#### **$\text{H}_2\text{O}_2$ Manufacture**

The anthraquinone process for  $\text{H}_2\text{O}_2$  production starts with the catalytic hydrogenation of a 2-alkyl-9,10-anthraquinone. The resulting hydroquinone is oxidized with oxygen, usually air, to yield  $\text{H}_2\text{O}_2$  and the corresponding quinone. After separation of  $\text{H}_2\text{O}_2$  by extraction with water, the quinone is recycled within the process to the hydrogenation step [6]. The hydrogenation is dominantly made with palladium as catalyst, applied either as palladium black or supported on a carrier for slurry or fixed-bed operation. Several alternatives for the alkyl side chain are in commercial use. The patent literature cites 2-ethylanthraquinone, 2-*tert*-butylanthraquinone, mixed 2-amylanthraquinones, and 2-neopentylanthraquinone. These compounds differ in solubility in the so-called “working solution”. Because quinone and hydroquinone have different solubility, solvent mixtures are mostly used. Quinones dissolve well in nonpolar aromatic solvents, whereas hydroquinones dissolve better in polar solvents. In order to avoid losses of the active compounds, hydrogenation selectivity is important and a regeneration of the working solution is required.

Commercial  $\text{H}_2\text{O}_2$  solutions are prepared by purification and concentration steps. Hydrogen peroxide is available as a clear, colorless solution which has a specific odor and is completely miscible with water. The solutions are stabilized by acidification with phosphoric acid and the addition of stannate and small amounts of chelants. A typical stabilizer is 1-hydroxy ethylene 1,1-diphosphonic acid (HEDP). Hydrogen peroxide is stored in stainless steel or aluminum or polyethylene tanks. For storage and handling, local legislation must be considered.

For industrial applications in bleaching processes,  $\text{H}_2\text{O}_2$  is stored typically in solutions with a concentration between 50% and 70%. It may be diluted before its addition to the pulp. If effective mixing is guaranteed, an undiluted addition is possible.

### 7.6.3

#### **Physical Properties**

Hydrogen peroxide is generally supplied as an aqueous solution, typically in concentrations between 35% and 70% by weight. These acidic solutions of  $\text{H}_2\text{O}_2$  in water are very stable. Hydrogen peroxide can be stored for months in stainless steel tanks, without significant changes of the content. Some physical constants of  $\text{H}_2\text{O}_2$  are listed in Tab. 7.45. The main commercial grades are those containing between 50% and 70%  $\text{H}_2\text{O}_2$  by weight.

Tab. 7.45 The physical properties of commercial hydrogen peroxide ( $\text{H}_2\text{O}_2$ ) solutions.

Concentration (by weight)	Boiling point <sup>a</sup> [°C]	Melting point [°C]	Density <sup>b</sup> [g cm <sup>-3</sup> ]
100% $\text{H}_2\text{O}_2$	150.2	-0.42	1.443
70% $\text{H}_2\text{O}_2$	125	-40	1.288
60% $\text{H}_2\text{O}_2$	119	-56	1.241
50% $\text{H}_2\text{O}_2$	114	-52	1.196
Water	100	0	0.997

- a. Extrapolated values because decomposition will reduce boiling point continuously.  
b. 25 °C.

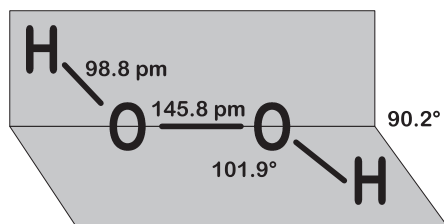
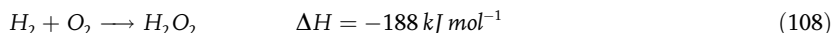
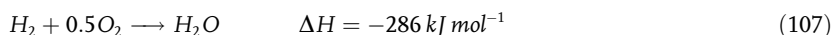


Fig. 7.116 Configuration of hydrogen peroxide in the solid phase.

The bond length between the two oxygen atoms of the  $\text{H}_2\text{O}_2$  molecule is rather long (Fig. 7.116). Compared to water, the energy content of  $\text{H}_2\text{O}_2$  is much higher. For water, the heat of formation ( $\Delta H$ ) [Eq. (107)] from the elements is as low as  $-286 \text{ kJ mol}^{-1}$ , whereas for  $\text{H}_2\text{O}_2$  [Eq. (108)] the corresponding value is only  $-188 \text{ kJ mol}^{-1}$  [7]. In consequence,  $\text{H}_2\text{O}_2$  is less stable and can disproportionate into water and oxygen:

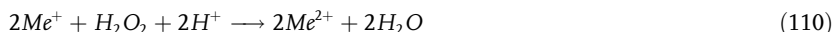


Since the activation energy for the cleavage of the oxygen–oxygen bond is rather low ( $\Delta H = -71 \text{ kJ mol}^{-1}$ ) [7], traces of contaminants can start this reaction. Basically, the decomposition is a redox process, with  $\text{H}_2\text{O}_2$  either supplying electrons and yielding oxygen, or accepting electrons and yielding water. Metal salts of different states of oxidation can start the decomposition reaction. The first step can be the reduction according to Eq. (109):





The alternative is the oxidation of a metal according to Eq. (110):



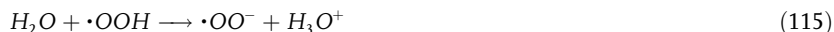
The reaction certainly can also start with the reduced form of metal. The overall reaction is identical, it being the formation of water and oxygen from  $H_2O_2$  with the redox system of the metal is acting as the catalyst [8].

The decomposition of  $H_2O_2$  is, in addition, catalyzed by alkali, with the reaction steps being as follows:



Since bleaching with  $H_2O_2$  requires alkaline conditions, this decomposition reaction is very important for its technical application.

Single electron transfer reactions of  $H_2O_2$  with catalysts yield radicals, these decomposition reactions taking place with either metals or with enzymes (e.g., catalase). Radical formation may also be the result of a thermal cleavage of the oxygen–oxygen bond:



The hydroxyl radical, the hydroperoxy radical, and the superoxide anion radical are important intermediates. Each of these cause side reactions in bleaching processes, with delignification as a positive and depolymerization of the cellulose as a negative result. In general, radicals produce more negative effects than positive results on delignification. Therefore, if present in higher amounts, transition metal ions must be removed by acid washing or “neutralized” by chelation before and during a peroxide treatment.

Tab. 7.46 Standard oxidation potential for hydrogen peroxide [7].

Reaction	pH	Oxidation potential [E°/V]
$H_2O_2 + 2H^+ + 2e^- \rightarrow 2H_2O$	0	1.776
$HO_2^- + H_2O + 2e^- \rightarrow 3OH^-$	14	0.878

The oxidation potential for  $\text{H}_2\text{O}_2$  is significantly higher under acidic conditions (Tab. 7.46). Despite this, typical bleaching reactions are conducted under alkaline conditions. Formation of the perhydroxyl anion [Eq. (111)], a nucleophile intermediate, is responsible for the oxidation of chromophores in lignin through the cleavage of side chains [9]. The effect of a  $\text{H}_2\text{O}_2$  treatment is dominantly an increase of the brightness. Delignification with  $\text{H}_2\text{O}_2$  is to a large extent the result of the action of the radicals produced in Eqs. (112–115) [10]. At moderate temperature, under buffered conditions, and in the absence of transition metals, the delignifying effect of  $\text{H}_2\text{O}_2$  is limited. The perhydroxyl anion, being a nucleophile, cannot attack the electron-rich aromatic rings of the residual lignin. Consequently a degradation of polymerized lignin, which can be the result of high-intensity pulping conditions will not occur in  $\text{H}_2\text{O}_2$  bleaching.

Under acidic conditions,  $\text{H}_2\text{O}_2$  reacts only slowly with organic compounds. At high temperature, the hydroxylation reactions that may occur do not result in any bleaching effect; on the contrary, the reaction might generate new chromophores (phenols to quinones, etc.). Because peracids have a better leaving groups, their reaction is both more rapid and more selective. For oxidation under acidic conditions therefore, peracids such as peracetic acid are the preferred reaction partners.

#### 7.6.4

#### Chemistry of hydrogen peroxide bleaching

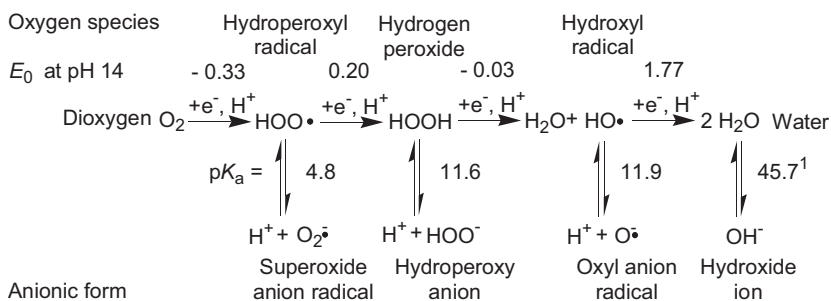
*Manfred Schwanninger*

Although the major fraction of wood lignin can be removed by pulping, the remainder of the lignin (residual lignin) is rather resistant under the pulping conditions. In order to remove the residual lignin from the pulp, oxidative lignin degradation with bleaching reagents such as dioxygen,  $\text{H}_2\text{O}_2$ , ozone, and chlorine dioxide is required. Hydrogen peroxide is mainly used to brighten pulps (removal of chromophores) during the final bleaching stages, and at the end of a conventional bleaching sequence to prevent the pulp from losing brightness over time. Carbonyl carbons or the vinylogous carbon atoms in intermediates of the enone type (quinone methide intermediate; see Section 4.2.4, Chemistry of kraft pulping, Scheme 3) are the locations where the nucleophile (the hydroperoxy anion) begins the attack [11,12]. The hydroperoxy anion is incapable of degrading polymerized lignin directly via an attack of the electron rich aromatic rings of the residual lignin, but by cleaving the sidechain i.e. Dakin and Dakin-like reactions the lignin can be depolymerised.

The parameters that influence bleachability, the composition of lignin and residual lignin after cooking and their reactivity, as well as the composition of residual lignin–carbohydrate complexes (RLCC) before and after oxygen bleaching, the influence of inorganic substances and their role in the protection/degradation of cellulose, have been described previously.

Hydrogen peroxide and the hydroperoxy anion respectively evolve *in situ* [13] during oxygen bleaching. In contrast to dioxygen, which contains multiple bonds between the O atoms,  $\text{H}_2\text{O}_2$  has only one bond, and this can be easily broken.

Under the conditions used in  $\text{H}_2\text{O}_2$  bleaching, with the pH in the range of 10–12, the standard redox potentials of the reactive species are substantially reduced (Scheme 7.36) due to the lower potential of the ionized form. Hydrogen peroxide (hydroperoxy anion) can either be oxidized by a one-electron step to the hydroperoxyl radical (superoxide anion radical), or reduced to the hydroxyl radical (oxyl anion radical) (Scheme 7.36).

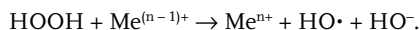


**Scheme 7.36** Dioxygen reductions proceeding in four consecutive one-electron steps ( $E^0$  standard reduction potential) (<sup>1</sup>According to [14]).

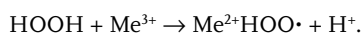
The actual concentration of the hydroperoxy anion depends on the pH of the solution (Scheme 7.36) and, of course, on the amount of  $\text{H}_2\text{O}_2$  added. The pH value is not the best measure to determine the effective hydroperoxy anion concentration, however, because of the interaction of the  $\text{OH}^-$  ion and  $\text{H}_2\text{O}_2$ , different solutions where either component is in excess might have the same pH and yet have a 10-fold difference in hydroperoxy anion concentration [15]. Conversely, two solutions may give the same approximate concentration of hydroperoxy anions and have different pH values [15]. Notably, in this very interesting study [15] it was also found that, during  $\text{H}_2\text{O}_2$  bleaching of cotton cellulose, the latter acted as a stabilizer for the peroxide.

#### 7.6.4.1 Decomposition of $\text{H}_2\text{O}_2$

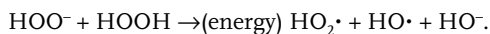
Transition metal ions such as copper, manganese, and iron can react with  $\text{H}_2\text{O}_2$  in a Fenton-type reaction:



In this reaction, a homolytic cleavage of the O–O bond occurs, generating hydroxide ion ( $\text{OH}^-$ ) and the hydroxyl radical ( $\text{OH}\cdot$ ), with the latter possibly being formed via an oxoiron(IV) intermediate [16]. The peroxide can also be effective as an oxidant, and in a transition metal-induced cleavage of the H–OO bond the hydroperoxyl radical ( $\text{HOO}\cdot$ ) is formed:



A thermal homolytic cleavage of  $\text{H}_2\text{O}_2$  also occurs:



The stabilizing effect of magnesium on  $\text{H}_2\text{O}_2$  has long been known [17], and has been confirmed in several studies [18,19]. Different possible explanations for the protective effects of magnesium compounds reported by Reitberger et al. [20] were substantiated by others (see Section 7.3.2.7, Chemistry of oxygen delignification).

The lifetime (half-life) of  $\text{H}_2\text{O}_2$  in different aqueous systems under various chemical additions (NaOH, magnesium sulfate, DTPA) in the presence and absence of fully bleached softwood kraft pulp (FBSKP) was increased significantly by the addition of magnesium sulfate and DTPA [21]. The details listed in Tab. 7.47 show a persistently longer half-life for the acid-treated pulp (FBSKP-A). In the presence of FBSKP,  $\text{MgSO}_4$  addition lengthened the peroxide half-life significantly, from 8 to 36 min, while Mg in a chelated form (Mg + Q) performed even better, increasing the half-life to 83 min. Compared to the results of Mg and DTPA alone, a synergistic effect for complexed Mg can be claimed [21]. The differences between FBSKP-A (half-life 22 min) and FBSKP (3 min) are attributable to higher concentrations of transition metals, particularly manganese, in the FBSKP (4.3 ppm compared to 0.3 ppm in the FBSKP-A) [21].

Kadla et al. [aa] subjected a technical pine kraft lignin to alkaline hydrogen peroxide oxidation at various temperatures. In the absence of DTMPA (diethylenetriaminepentamethylene-pentaphosphonic acid) the hydrogen peroxide was rapidly degraded, and accompanied by only minimal lignin oxidation. In the presence of

**Tab. 7.47** Half-lives of hydrogen peroxide ( $t_{1/2}$ , min), obtained for the different aqueous systems and various chemicals additions (OH = 2% NaOH; P = 2%  $\text{H}_2\text{O}_2$ ; Mg = 0.05% magnesium sulfate; Q = 0.2% DTPA-Na; T = 363 K) (from Ref. [21]).

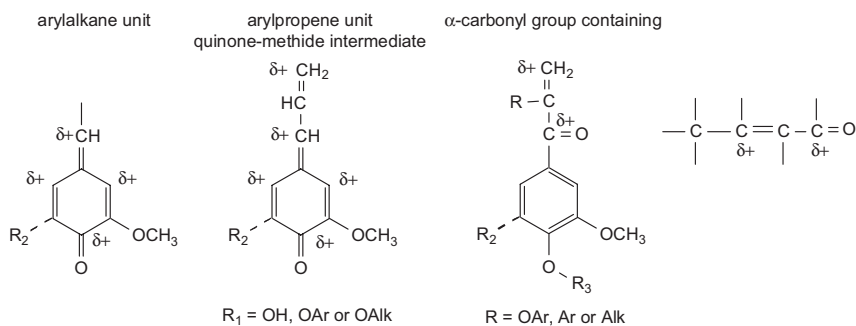
System	With pulp		Without pulp
	FBSKP-A <sup>a</sup>	FBSKP	Water
I (OH + P)	22 ± 1	8.0 ± 0.4	41 ± 24
II (OH + P + Q)	25 ± 3	12.2 ± 0.4	130 ± 40
III (OH + P + Mg)	190 ± 50	36.0 ± 13.0	300 ± 130
IV Grp 1 (Mg + Q) + Grp 2 (OH + P)	240 ± 150	83.0 ± 11.0	1330 ± 590
V Grp 1 (Mg + OH) + Grp 2 (P + Q)	370 ± 130	39.0 ± 13.0	

a. Acid-treated at pH = 1.5.

DTMPA (stabilize  $\text{H}_2\text{O}_2$  at high temperatures and alkali [bb]) the lignin undergo increasing levels of oxidation and degradation with increasing temperature. The highest degree of selectivity was observed at  $90^\circ\text{C}$ , i.e. the highest amount of phenolic hydroxyl groups degraded and the highest amount of lignin degraded as a function of hydrogen peroxide consumed. The highest amount of lignin degradation, over 80%, occurred at  $110^\circ\text{C}$ . Analyses of the degraded lignins indicated that both phenolic and nonphenolic lignin moieties were degraded [aa].

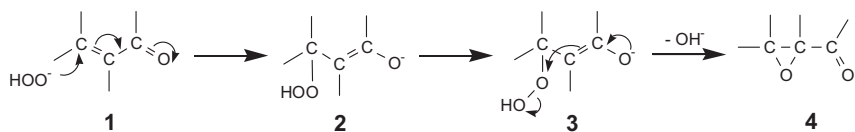
#### 7.6.4.2 Residual Lignin

The sites of nucleophilic attacks in lignins are shown in Fig. 7.116. By elimination of an  $\alpha$ - (see Section 4.2.4, Chemistry of kraft pulping) or, in conjugated structures, a  $\gamma$ -substituent, a quinone-methide intermediate is formed from the arylalkane unit (Fig. 7.116), which involves the loss of two electrons, and results in the generation of centers of low electron density ( $\delta^+$ ) that constitute the sites of attack by nucleophiles [22].



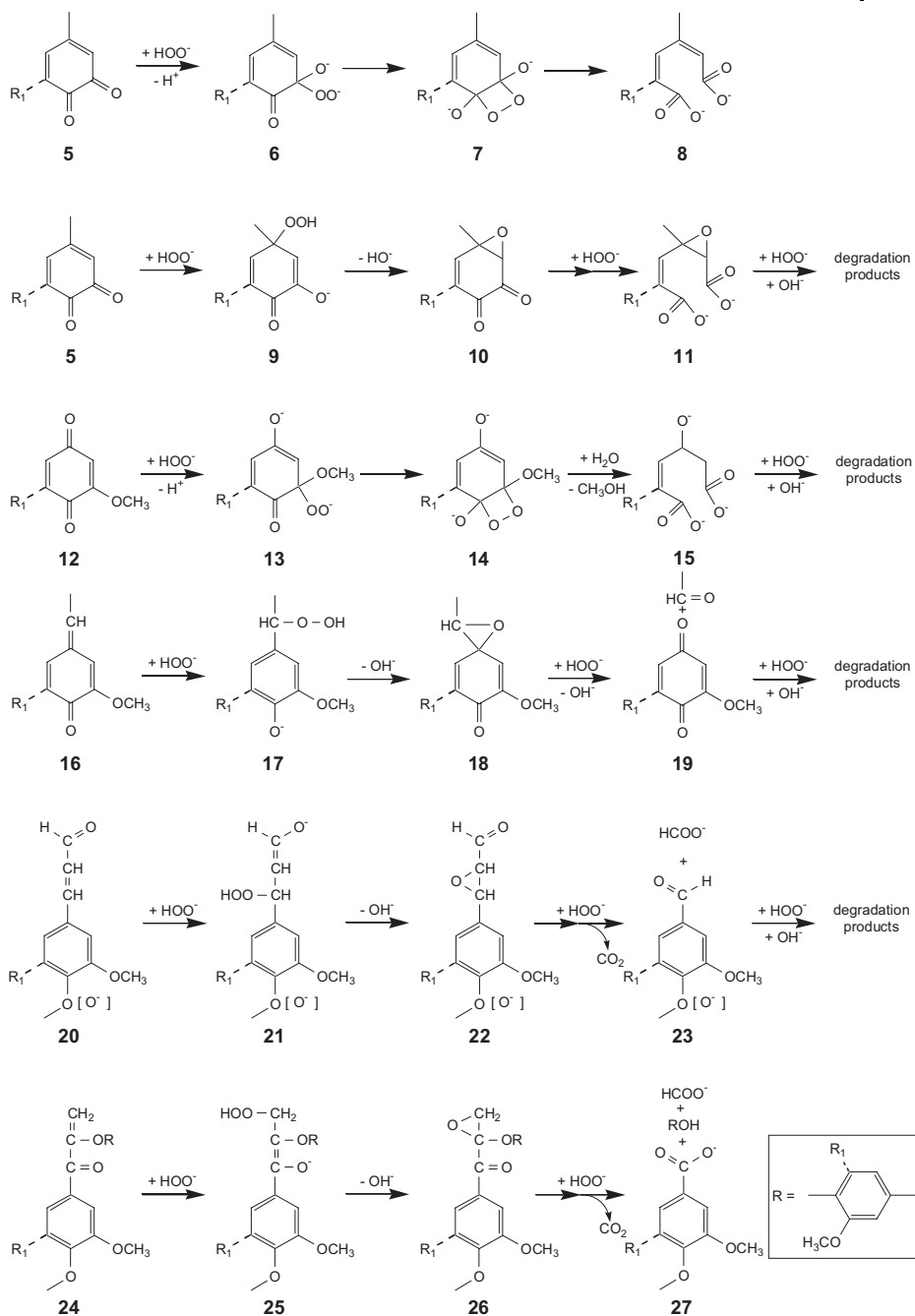
**Fig. 7.116** Sites of nucleophilic ( $\delta^+$ ) attacks in lignin (adapted from Ref. [22]).

A nucleophilic attack starts with the addition of the hydroperoxy anion to carbonyl and conjugated carbonyl structures (Scheme 7.37, **1**) giving a hydroperoxide (**2**) which forms an epoxide (**4**). After an additional nucleophilic attack the  $\text{C}_\alpha\text{-C}_\beta$  bond will be cleaved.



**Scheme 7.37** Formation of hydroperoxide via a nucleophilic reaction.

The hydroperoxide anion adds rapidly to quinoid structures (Scheme 7.38). By addition to an ortho-quinone (**5**) hydroperoxides (**6**, **9**) are formed, leading to the formation of dioxetane (**7**) or oxirane (**10**) intermediates followed by cleavage of



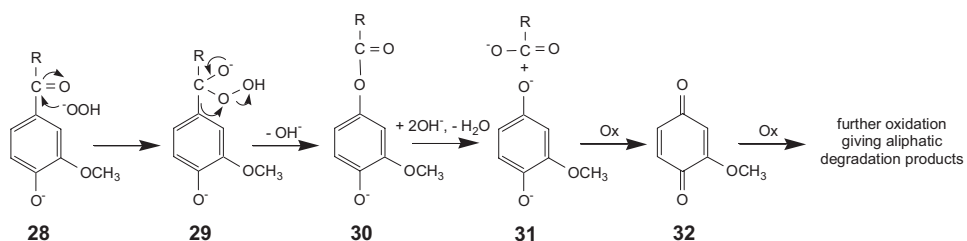
**Scheme 7.38** Addition of hydroperoxide anions to quinoid structures and to side-chain enone structures (adapted from Refs. [12,23]).

the ring giving dicarboxylic acids (**8**, **11**) that can be further degraded. Adding the hydroperoxide anion to a para-quinone with a methoxyl group (**12**) gives via a hydroperoxide (**13**), a dioxetane (**14**), and the ring is cleaved after demethoxylation, giving a dicarboxylic acid (**15**). The hydroperoxide (**17**) formed after hydroperoxide anion addition to an arylalkane (quinone methide structure) (**16**) leads to an oxirane (**18**). A further nucleophilic attack cleaves the bond between the C<sub>α</sub>-atom and the ring, thereby forming an aldehyde group and a para-quinone (**19**) which can be further degraded (**12–15**).

Side chains with enone structures (**20**, **24**) also afford hydroperoxides (**21**, **25**) and subsequently oxirane intermediates (**22**, **26**), leading to cleavage of the C<sub>α</sub>-C<sub>β</sub> bonds and producing an aldehyde (**23**) or carboxylic acid (**27**) at the aromatic ring and carboxylic acids groups on the split-off residues.

Phenylpropanols and phenylpropanones (Scheme 7.39, **28**) react with the hydroperoxide anion to form a hydroperoxide (**29**) that is rearranged to an ester (**30**) which can be cleaved to an aldehyde and a phenolate (**31**) in a Dakin-like reaction. The latter can be oxidized to a para-quinone (**32**) and further degraded (see Scheme 7.38, **12–15**).

In a lignin model study, guaiacylglycerol-β-guaiacyl-ether was oxidized with alkaline H<sub>2</sub>O<sub>2</sub> in the presence of pulp in order to simulate technical bleaching conditions [24]. The phenolic β-O-4 structure was found to react rather rapidly with H<sub>2</sub>O<sub>2</sub> and, from the mixture of products formed, it was concluded that the main reaction was a side-chain displacement that proceeded via the so-called Dakin-like mechanism. This was followed by secondary reactions that resulted in cleavage of the molecule, accompanied by an extensive formation of carboxyl groups [24].



**Scheme 7.39** Dakin reaction at the C<sub>α</sub>-keto group of a phenolic unit (adapted from Ref. [23]).

A bleaching sequence involving oxygen bleaching (O), treatment with a chelating agent EDTA (Q), and an alkaline H<sub>2</sub>O<sub>2</sub> stage (P), showed that partial removal of the residual fiber lignin was accompanied by extensive removal of chromophoric groups. It appeared that the chemical structure of lignin remaining in the fibers after the OQP sequence was mainly unaffected by the treatment. The oxidation resulted mainly in an increase in the number of hydrophilic groups, but the lignin remained phenolic to a certain extent and the aromatic structure was preserved [25].

A new mechanism for the heterogeneous alkaline peroxide brightening reactions of mechanical pulps consists of four key kinetic steps: adsorption of  $\text{H}_2\text{O}_2$  and hydroxide to the pulp fiber walls; a chromophore-removing chemical reaction on the fiber wall; desorption of “light” organic products formed from the fiber wall; and oxidation chain reduction of the cleaved organic substances. The most important step here is the surface reaction, rather than reactions occurring in the liquid phase. In general, removal of the cleaved organic substances from the fiber wall is not anticipated to occur completely during the brightening reaction operation stage [26].

As shown, the main reaction mode of  $\text{HO}_2^-$  is nucleophilic addition to enone and other carbonyl structures, removing chromophoric groups by the destruction of conjugated systems. Through addition of the hydroperoxide anion, certain peroxide (anion) structures may be formed which can subsequently react in a way similar to that of the peroxide (anion) structures arising from the addition of superoxide anion radicals to substrate radicals; this gives rise to the formation of C–C cleavage products [27–30].

Due to the fact that the number of enone and other carbonyl structures in lignin and residual lignin is usually low, the extent of degradation during bleaching with pure  $\text{H}_2\text{O}_2$  also remains low. Therefore, the main part of this bleaching step is chromophore removal and lignin retention. Due to the fact that the number of enone and other carbonyl structures in lignin and residual lignin is usually low, and the extent of degradation during bleaching with pure hydrogen peroxide remains low too. Therefore, the main part of this bleaching step is chromophore removing and lignin retaining. However, this needs to be put into context with two facts: a) most peroxide stages follow other bleaching steps where enone structures are formed, and b) at high temperature extensive delignification can occur [aa, bb].

The hydroxyl radical is considered to be responsible for the small degree of lignin degradation observed during  $\text{H}_2\text{O}_2$  bleaching. This can be interpreted as the chemical reactions of the hydroxyl radicals during oxygen bleaching (see Section 7.3.2.4, Chemistry of oxygen delignification). The occurrence of hydroxyl radicals may possibly have a distinct beneficial effect that may be ascribed to the cleavage of cross-links in the rigid lignin matrix, which will in turn facilitate the penetration of bleaching reagent(s) [31] and thereby improve the bleaching result. This interpretation is in accordance with results from studies where metal ions were removed carefully from either the pulp [32,33] or from wood shavings before kraft cooking [34], or were complexed with chelants [25,35–38], and increased the brightness gain [33].

#### 7.6.4.3 Carbohydrates

The hydroxyl radical – but not the hydroperoxy anion – is capable of degrading cellulose directly. Hydroxyl radicals, which are known to degrade carbohydrates [39], have been generated photochemically from  $\text{H}_2\text{O}_2$  in aqueous base, showing that glycosidic linkages in methyl- $\beta$ -D-glucoside and methyl- $\beta$ -cellobioside cleave



directly [40,41]. Evidence has been found for responsibility of the hydroxyl radicals in the degradation of glycosidic linkages in 1,5-anhydrocellobitol and 2-methoxytetrahydropyran by substitution reactions displacing 1-deoxyglucose, D-glucose, tetrahydropyran-2-ol, and methanol [42]. Once the glycosidic linkages are broken, the reducing carbohydrates undergo a series of reactions forming aldonic acids and lower order aldoses, in much the same manner as was described previously [40,41]. Under these same conditions, hydroxyl radicals cause a substantial degradation of cellulose, as evidenced by a loss in viscosity [42].

Peroxides can degrade cellulose in the absence of stabilizing agents, as may also decolorize it and remove stains. Both free radicals and hydroperoxy anions have been suggested as the intermediates in the reactions occurring between cellulosic products and  $H_2O_2$  [43]. The oxidation of cellulose by  $H_2O_2$  and the functional groups formed revealed that the relationships between the functional groups, degradation and stability of the celluloses enable the aging and storage behavior of the polymer to be predicted. The “active” carbonyls are responsible for the peeling reaction and formation of the yellow chromophore in alkaline solutions [44]. Experiments carried out on fully bleached pulp and viscose pulp showed clearly that colored materials were formed from carbohydrates when they were submitted to alkaline cooking conditions. However, these chromophores could be only partly removed by  $H_2O_2$  [45].

### 7.6.5

#### **Process Parameters**

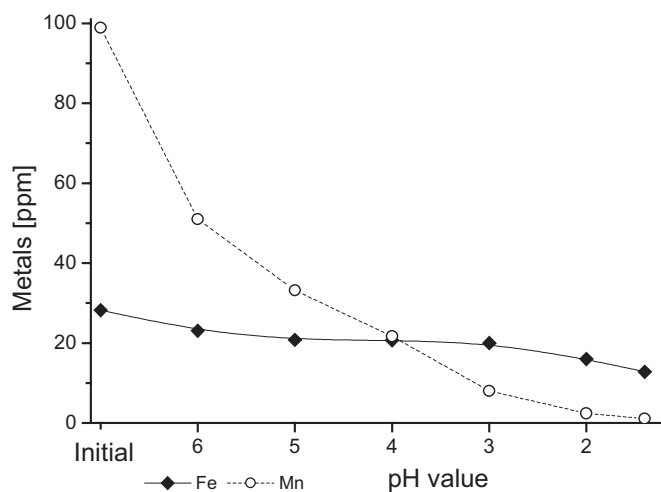
*Hans-Ullrich Süß*

##### **7.6.5.1 Metals Management**

Although transition metals cause the decomposition of  $H_2O_2$ , a controlled decomposition with the well-defined generation of radicals would be desirable from the point of improving delignification. However, to date, no such selective generation has been described. A manganese containing complex [46] has been described as catalyst for peroxide bleaching. Unfortunately, synthesis of this manganese complex is rather difficult, therefore its industrial use would be far too costly. Typically, the radicals produced by metal-catalyzed decomposition are unselective, and fiber damage dominates as a result of cellulose depolymerization. In consequence, metal impurities must be removed from the pulp before any subsequent peroxide treatment [36,46,47]. The amounts of transition metals present in pulp differ widely, as levels depend on the wood species and the soil on which the wood was grown. Normally, manganese and iron are the dominant metals, and others such as copper and cobalt are present only in trace amounts (around 1 ppm). In sulfite pulping, the removal of metal is straightforward since, under the acidic and reducing conditions of the pulping process, the metals become water-soluble and are easily removed during brownstock washing.

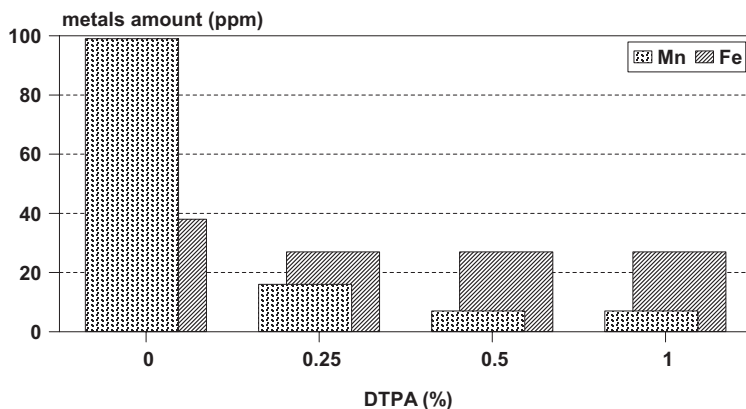
In kraft pulping, the transition metal ions become insoluble as they are reduced to a low state of oxidation and precipitate as sulfides. The sulfides are very insoluble.

ble under alkaline and neutral conditions and cannot be removed by washing. During oxygen delignification, the metals may be raised to a higher state of oxidation, although the resulting hydroxides are still insoluble under the conditions of oxygen stage washing. However, they become water-soluble under mild to strong acidic conditions. In conventional bleaching processes, the transition metals are removed during the acidic bleaching stages. Since  $\text{H}_2\text{O}_2$  typically is applied in ECF bleaching only after the first D stage, the metal profile normally is already sufficiently low, and no specific measures for metal removal are required. The effect of pH value on the elimination of iron and manganese from a softwood kraft pulp is shown graphically in Fig. 7.118. Compared with iron, the removal of manganese is clearly much easier. Strong acidic conditions are required to reduce the quantity of iron, which is very likely bound to lignin or lignin-carbohydrate structures. The iron is therefore not directly available for to decompose  $\text{H}_2\text{O}_2$ , and consequently traces remaining in the pulp after chelation do not have a negative effect on the bleaching process.



**Fig. 7.118** Removal of iron and manganese from softwood kraft pulp with increasing acidity. All trials conducted at 3% consistency, 60 °C, 0.5 h with  $\text{H}_2\text{SO}_4$  for acidification.

The removal of metals is far more important in TCF bleaching, because  $\text{H}_2\text{O}_2$  is applied early in the sequence, and at much higher charges. Since strongly acidic conditions have the disadvantage of removing not only metals such as manganese but also magnesium (which protects against loss of viscosity), metals removal at the mill scale is typically carried out at moderate pH with chelants such as diethylene triamino penta-acetate (DTPA). The impact of increasing amounts of chelant is shown in Fig. 7.119, where DTPA addition maintains a high level of magnesium. Typically, a chelation stage (Q) is operated at medium consistency, a temperature between 50 °C and 70 °C, a pH of about 6, and a retention time of about 1 h. As mentioned, it can be assumed that any remaining traces of metals are tightly



**Fig. 7.119** Removal of iron and manganese from softwood kraft pulp with diethylene triamino penta-acetate (DTPA) at pH 6. Trials were conducted at 3% consistency, 50 °C, 0.5 h, with H<sub>2</sub>SO<sub>4</sub> for acidification.

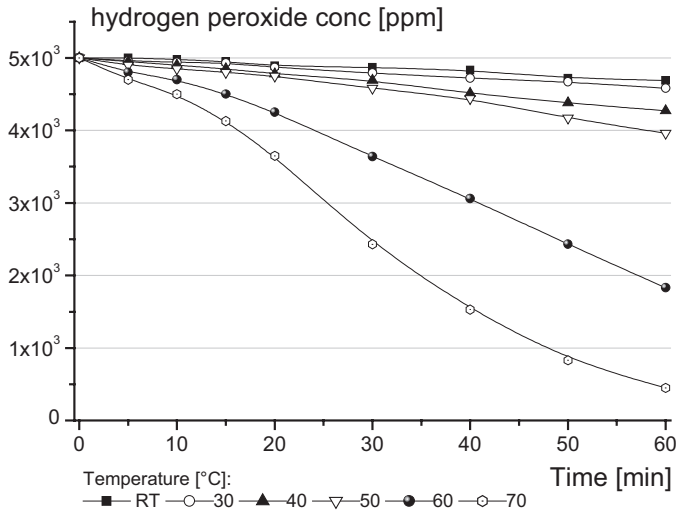
bound to the pulp; hence, it is impossible to provide a “threshold” no-effect level for a metal residual. Indeed, it is more important to have an effective washing system in place that guarantees the removal of the highly soluble metals portion.

In mechanical pulp bleaching, or in the bleaching of annual plants (e.g., bagasse), the use of phosphonates can be advantageous. The phosphonate which is homologous to DTPA – diethylene triamine penta methylene phosphonic acid (DTMPA) – forms complexes with a higher chelation constant, and is therefore more effective in removing metals that are bound tightly to cellulose or lignin complexes.

#### 7.6.5.2 Alkaline Decomposition of H<sub>2</sub>O<sub>2</sub>

The active species in H<sub>2</sub>O<sub>2</sub> bleaching is the perhydroxyl anion. This is generated under alkaline conditions, by the addition of caustic soda. Because H<sub>2</sub>O<sub>2</sub> decomposes at high pH [see Eq. (112)], a very high pH-value in bleaching is detrimental. The oxidation process generates acidic compounds, and this causes a decrease of the pH during the bleaching procedure. Typically, in peroxide bleaching the initial pH is between 10 to 11, whilst the end pH is still above 8.5. In sulfite pulp bleaching, MgO can be used during the peroxide and oxygen stages to allow recycling of effluent into the recovery of (magnesium sulfite) pulping liquor. The bleaching efficiency is lower compared with caustic soda, due mainly to limited solubility and lower pH. In addition, less hemicellulose is extracted from the pulp, which may be advantageous in mechanical pulp bleaching. There in addition, sodium silicate is added to the bleaching process, as silicate buffers the pH value and stabilizes peroxide consumption.

Other compounds producing an alkaline pH are technically not applied, mainly because of cost considerations. As an alternative to sodium silicate, the use of sodium carbonate is limited to moderate temperatures, since above about 50 °C



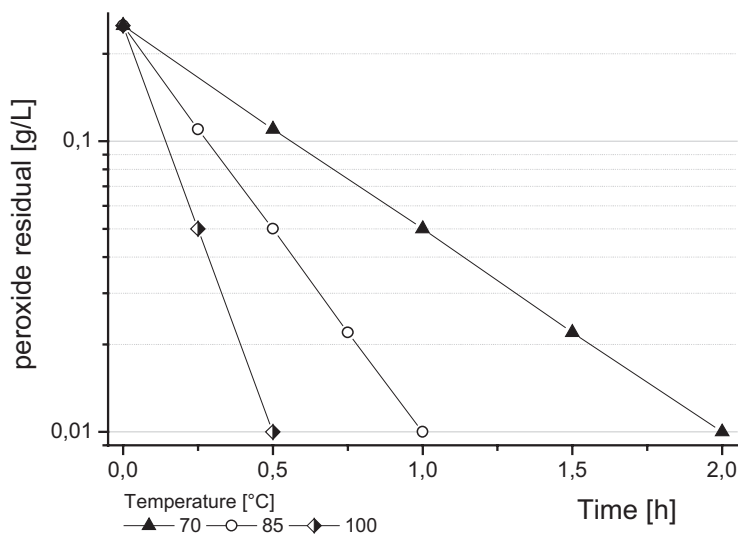
**Fig. 7.120** Stability of bicarbonate-buffered peroxide solutions in distilled water at different temperature, constant charge of analytical grade  $\text{NaHCO}_3$  ( $20 \text{ g L}^{-1}$ ).

the carbonate causes peroxide decomposition [48]. Solutions containing higher levels of carbonate ions can be used in bleaching processes only after the addition of magnesium sulfate, which precipitates the carbonate ions as very insoluble  $\text{MgCO}_3$ , or magnesium hydroxide carbonate,  $4 \text{ MgCO}_3 \cdot \text{Mg}(\text{OH})_2$ . The instability of peroxide solutions in deionized water in the presence of carbonate ions is shown in Fig. 7.120. At  $70^\circ\text{C}$ , an amount of  $5000 \text{ ppm}$  of  $\text{H}_2\text{O}_2$  decomposes almost completely within about 1 h. This decomposition of  $\text{H}_2\text{O}_2$  in the presence of carbonate ions has been described previously [49], though no satisfactory explanation was provided for any negative effects. The effects could not be explained by speculation about traces of metals and “impurities”; neither was the link recognized to the precipitation of carbonate by magnesium ions.

### 7.6.5.3 Thermal Stability of $\text{H}_2\text{O}_2$ and Bleaching Yield

The temperature in bleaching can be varied within a wide range. Logically, a lower temperature results in a slow bleaching reaction, but this can be compensated for by extending the retention time. Peroxide bleaches at ambient temperature, and this allows an application in steep bleaching with a time range of days. Mechanical pulp and sulfite pulp is bleached on an industrial scale under such conditions, but these are rare exemptions. Typically, bleaching with  $\text{H}_2\text{O}_2$  employs a temperature range between  $70^\circ\text{C}$  and  $90^\circ\text{C}$ . The huge amounts of pulp handled in continuous processes does not allow long residence times, or the bleaching towers would need to be very large. Temperature and time are interrelated. The trend to use narrow water loops with a high level of internal recycling, leads to high tem-

peratures within the loops. Pulping and refining processes are operated above 100 °C, and today even screening and cleaning of the pulp is conducted at a temperature close to the pulp's boiling point. In mechanical pulp bleaching, the temperature typically is above 70 °C, but in chemical pulp bleaching it can be as high as 90 °C. Consequently the time required for bleaching becomes short. A very high temperature (>95 °C) is critical because  $\text{H}_2\text{O}_2$  decomposes thermally. An example of this reaction at a concentration typical of a bleaching process is shown in Fig. 7.121.



**Fig. 7.121** Decomposition of diluted alkaline  $\text{H}_2\text{O}_2$  in deionized water at pH 10.5 with temperature and time. Starting concentration  $2.5 \text{ g L}^{-1}$ ; pH adjustment with NaOH.

The normal residence time for a peroxide stage is about 1.5 h. Depending on the temperature and the amount of  $\text{H}_2\text{O}_2$  to be consumed, this time may be shorter and/or extended to 2–3 h. Pressure and very high temperature were recommended for the consumption of large amounts of  $\text{H}_2\text{O}_2$  in ECF and TCF bleaching [50,51]. However, pressure is required only in so far as it allows a bleaching temperature above 100 °C. At a temperature below the boiling point of water, an increased pressure has no impact on peroxide performance. On the other hand, a very high temperature in peroxide bleaching has a negative impact on pulp quality. The energy of activation for cleavage of the oxygen–oxygen bond of  $\text{H}_2\text{O}_2$  is rather low; therefore, the side reaction “thermal decomposition” or homolytic cleavage increases strongly with temperature (see Fig. 7.120). The aftermath of this bond cleavage is the formation of other radicals, which trigger cellulose chain cleavage. Viscosity losses are also observed which, together with the improved solubility of lower molecular-weight compounds present in the pulp at high temperature and alkalinity, leads to yield losses [52,53]. Thus, extreme temperatures should be avoided in peroxide bleaching.

An example of the impact of high temperature in peroxide-supported extraction stages is provided in Tab. 7.48. The aggressive conditions allow less chlorine dioxide to be used, but the impact on viscosity and yield is pronounced. Consequently, in ECF bleaching the mill practice is to keep the temperature level below 90 °C during the peroxide stages. The exemption is TCF bleaching, where a very high temperature and even pressure must be applied to compensate for the absence of an effective delignification agent such as chlorine dioxide. In this situation, the consequences of a lower yield and decreased pulp strength must be accepted.

**Tab. 7.48** Impact of very high temperature in peroxide stages on pulp yield, effluent load, and viscosity. eucalyptus kraft pulp, bleached under standard (Eop 0.4% H<sub>2</sub>O<sub>2</sub>, P 0.2% H<sub>2</sub>O<sub>2</sub>) and hot conditions (Eop<sub>hot</sub> 0.5% H<sub>2</sub>O<sub>2</sub>, P<sub>hot</sub> 0.8% H<sub>2</sub>O<sub>2</sub>) to a brightness of >89% ISO.

Sequence	Total active chlorine [%]	Temperature in Eop or P [°C]	Viscosity [mPa.s]	COD [kg t <sup>-1</sup> ]	Yield [%]
DEopDD	5.0	85	28.4	37.5	96.0 ± 0.3
DEopDP	3.8	85	27.1	38.2	96.0 ± 0.25
DEop <sub>hot</sub> DP <sub>hot</sub>	2.5	98	18.7	44.0	95.15 ± 0.25

Magnesium sulfate (Epsom salt) is an additive applied in peroxide bleaching to prevent cellulose depolymerization. The benefit of adding magnesium ions becomes apparent in peroxide bleaching at very high temperatures and with a high peroxide input. Thus, magnesium salts are added in TCF bleaching but not normally in an Eop stage or a final P stage. The positive effect of magnesium sulfate addition becomes apparent in bleaching sequences which used acidic conditions for transition metals removal. A Q stage under mildly acidic conditions retains the magnesium and calcium traces in the pulp, thus the impact of additional magnesium is less pronounced. The same is valid in regions with a high water hardness and not very narrow water loops. The mechanism of the protective effect is not clearly understood. Magnesium will be precipitated rapidly as Mg(OH)<sub>2</sub> under the conditions of a peroxide stage. Theories discuss the absorption of other metal ions during precipitation or an action as scavenger of superoxide anion radicals [54]. Experiments with peroxide bleaching of deinked pulp in the disperger (i.e., at high temperature) did indicate any positive effect of another precipitation. Bicarbonate ions present in the water loop after CO<sub>2</sub> neutralization would decompose peroxide under the conditions of disperger bleaching. The formation of insoluble magnesium carbonate avoided peroxide losses and improved the bleaching result [55]. Since carbonate ions are present in caustic soda and are generated during bleaching, their precipitation may be part of the positive effect of magnesium salt addition.

#### 7.6.5.4 Pressurized Peroxide Bleaching

In TCF bleaching the brightness target of a final peroxide stage might require the consumption of very large amounts of peroxide, and to achieve sufficient consumption of  $H_2O_2$  high temperature will be required. The application of pressure is also recommended [50,51], with pressure applied ranging from 0.1 MPa to a maximum of 0.5 MPa. These stages are frequently labeled as P(O) stage because pressure is applied by oxygen gas addition. The positive effect was described as an acceleration of an otherwise very slow brightening of the pulp. Later, pressurized peroxide stages were also recommended for ECF sequences [56]. Several mills have installed such equipment, although many typically operate without applying pressure because bleaching is not improved by pressure or oxygen addition [57,58]. This is in line with current knowledge of the reaction mechanism of alkaline peroxide bleaching. The peroxide reactions are neither accelerated nor improved by a moderate pressure increase, however, pressurized equipment is more expensive than nonpressurized counterparts.

#### 7.6.6

#### Technology of $H_2O_2$ Bleaching

*Andreas W. Krotscheck*

##### 7.6.6.1 Atmospheric Peroxide Bleaching

The process flowsheet of a typical atmospheric peroxide bleaching system is shown schematically in Fig. 7.122. Caustic soda is added to the MC pulp coming from the previous bleaching stage, for example, to the repulper of a drum washer or to the dilution conveyor after a wash press. The alkaline pulp falls into a stand-pipe and is mixed with peroxide as it enters the MC pump.

The pump provides good mixing of the peroxide into the pulp suspension, and a dedicated mixer is often not required. The pulp proceeds to an atmospheric upflow reactor where the bleaching reaction takes place. Depending on the feed requirements of the subsequent washing equipment, the pulp slurry is discharged from the reactor either at low or medium consistency.

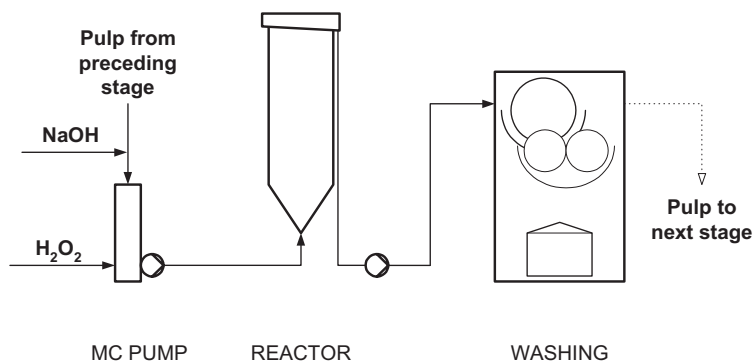


Fig. 7.122 Process flowsheet of a typical atmospheric peroxide bleaching system.

Washing after a peroxide stage is usually carried out with single-stage washing equipment, for example, with a wash press, a single-stage Drum Displacer™, an atmospheric diffuser, or a vacuum drum washer.

The material of construction for wetted parts in a peroxide stage is typically a higher grade of austenitic stainless steel.

Further information regarding atmospheric peroxide bleaching equipment, including medium-consistency pumps and atmospheric upflow reactors, is provided in Section 7.2. Pulp washing is detailed in Chapter 5.

### 7.6.6.2 Pressurized Peroxide Bleaching

The equipment used for pressurized peroxide bleaching is very similar to oxygen delignification equipment. The process flowsheet of a typical pressurized peroxide bleaching system is shown schematically in Fig. 7.123. Caustic and peroxide are added to the medium-consistency pulp coming from the previous bleaching stage, as in atmospheric peroxide bleaching. The MC pump forwards the pulp suspension to a high-shear mixer which is charged with oxygen and steam, after which the three-phase mixture proceeds to a pressurized upflow reactor where the bleaching reaction takes place.

As in oxygen delignification, it is essential that the high-shear mixer creates stable micro-bubbles which ensure a homogeneous bleaching result, without channeling in the reactor. After its discharge from the reactor top, the pulp suspension is separated from the gas phase in a blowtank. The offgas from the blowtank can normally be blown to the atmosphere. Depending on the feed requirements of the washing equipment, the pulp slurry is discharged from the blowtank either at low or medium consistency.

Washing after a peroxide stage is usually carried out with single-stage washing equipment, for example, with a wash press, a single-stage Drum Displacer™, an atmospheric diffuser, or a vacuum drum washer. Further information on pressurized peroxide bleaching equipment, including medium-consistency pumps and mixers, pressurized reactors and blowtanks is provided in Section 7.2. Details of pulp washing are provided in Chapter 5

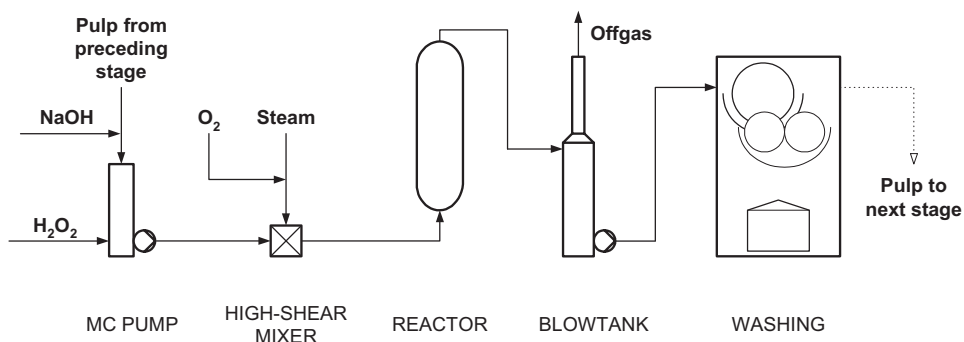


Fig. 7.123 Process flowsheet of a typical pressurized peroxide bleaching system.

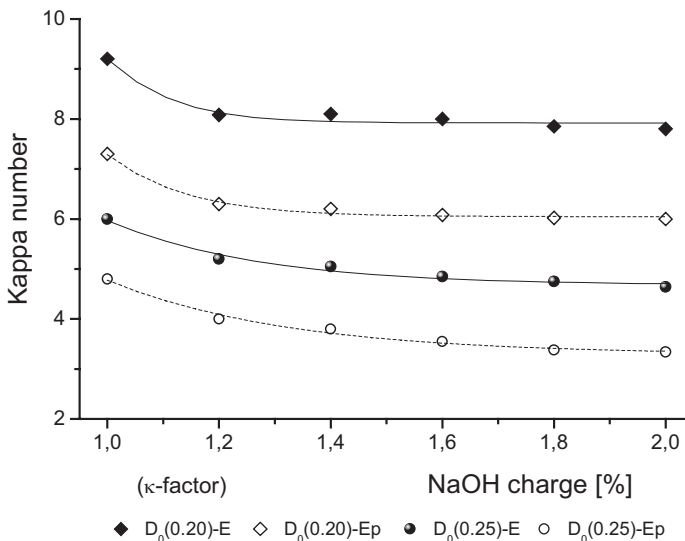


## 7.6.7

## Application in Chemical Pulp Bleaching

Hans-Ullrich Süs

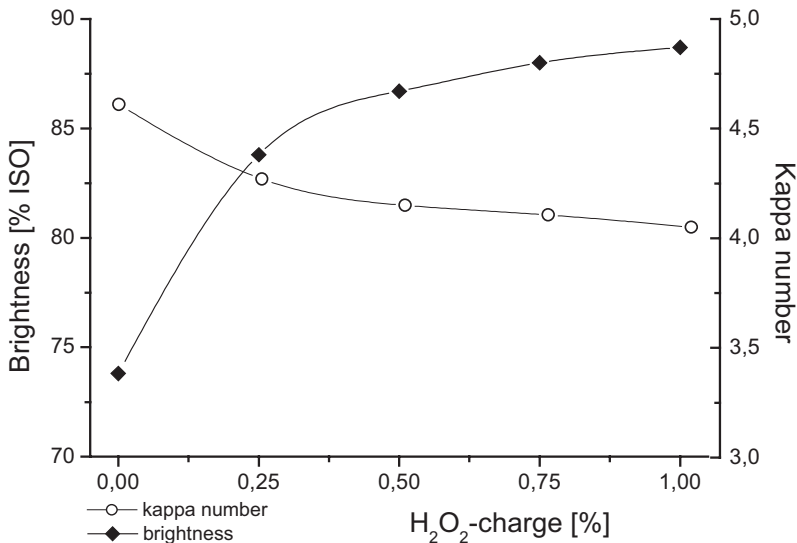
Hydrogen peroxide is applied in ECF and TCF bleaching sequences. Currently, ECF bleaching is by far the most dominant bleaching technology; indeed, in 2004 over 90% of all wood pulp was bleached with chlorine dioxide as the main bleaching agent. (In Asia, a relatively large amount of one-year-plant pulps is still bleached using chlorine and hypochlorite; thus, in relation to all pulp production, ECF bleaching might represent only 70%.) TCF bleaching has become a niche specialty, notably in Sweden and in Central European sulfite mills. Its world share in bleached pulp production is estimated at about 5%. In ECF bleaching,  $H_2O_2$  is used in the extraction stages following chlorine dioxide treatment. After the acidic D stage, a high level of oxidized lignin remains in the pulp, due to its limited solubility at acid pH. Consequently, the acidic and alkaline stages are applied alternately. The effect of an extraction is a further decrease in lignin content, because the formation of sodium salts of the carboxylic acids within the oxidized lignin residual results in a better solubility. The demand for caustic soda depends on the carry-over of acid from the D stage and the carboxylic acids content. Increasing the amount of caustic soda above a certain level has only a limited effect (Fig. 7.124). With effective washing the demand for caustic soda can decrease significantly. The temperature in an E stage is between 75 °C and 90 °C, while the pH is typically about 11 at the start of treatment and about 10 at the end.



**Fig. 7.124** Impact of increasing amounts of caustic soda in the extraction stage following a  $D_0$  stage; softwood kraft pulp, kappa 24.6. Kappa factor is the multiplier for the

kappa number value to calculate the input of active chlorine to the  $D_0$  stage. Conditions:  $D_0$  stage 50 °C, 1 h; E(p) stage 0.5%  $H_2O_2$ , 75 °C, 1.5 h, both at 10% consistency.

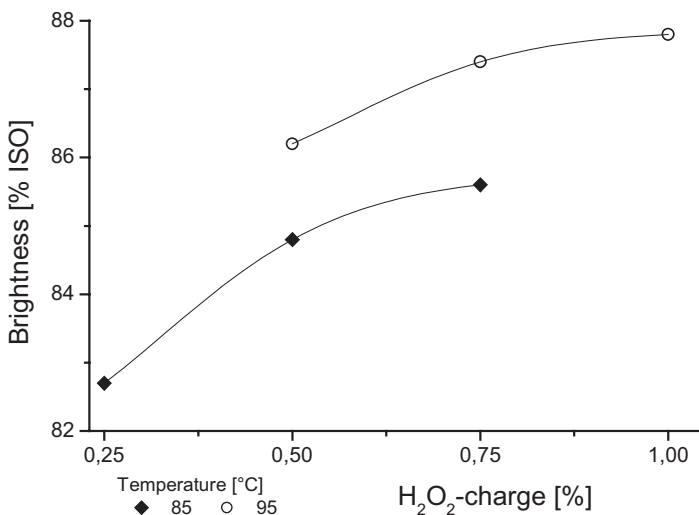
The graph in Fig. 7.124 shows the potential for reducing the amount of residual lignin by an addition of oxidants. The oxidation of quinoid structures improves the solubility of lignin. In the first E stage, typically oxygen and  $H_2O_2$  are applied. Oxygen gas is mixed with the pulp in high-shear mixers, which allow a very thorough distribution of fine gas bubbles within the fibers. The oxygen level is typically at 0.3–0.4%. While small amounts of oxygen are consumed rapidly, too-high an input can result in the re-formation of large oxygen bubbles that may channel through the tower and negatively affect pulp flow. For a moderate input of oxygen, the counter-pressure of a tower or pre-tube of 15–20 m height is sufficient. A potential solution to the problem of higher oxygen charges is to use a pressurized tower. However, such an investment is questionable because the number of oxidizable sites in the remaining lignin is normally small. Therefore, a high input of oxygen does not result in any significant benefits. The exemption are pulps with unusually high initial kappa numbers ( $>20$ ). The application of  $H_2O_2$  does not require pressure, and in most mills oxygen and  $H_2O_2$  are applied simultaneously in the first E stage. The impact of an increasing amount of  $H_2O_2$  is shown graphically in Fig. 7.125. Because of the limited availability of easily oxidizable sites, levels of  $H_2O_2$  above about 0.5% must be activated by a higher temperature. Brightness increase is accompanied by a further drop in residual lignin levels, this being the result of additional oxidation reactions improving lignin extraction. Peroxide addition can be used to balance the demand for caustic soda during the E stage (see Fig. 7.124). Increasing the addition of caustic soda has a limited impact on



**Fig. 7.125** Impact of the addition of  $H_2O_2$  to an E stage in bleaching eucalyptus kraft pulp, oxygen-delignified pulp,  $D_0$  stage at 50 °C with kappa factor 0.2. Ep stage at 85 °C for amounts of 0.25% to 0.5%  $H_2O_2$ , larger amounts applied at 95 °C, constant 1.4% NaOH, 1.5 h.

lignin removal. Rather than apply excess caustic soda, the use of moderate amounts of  $\text{H}_2\text{O}_2$  allows the brightness to be increased and the kappa number to be decreased, simultaneously.

In hardwood pulp bleaching, the impact of peroxide application on Kappa number is less pronounced. Because neither  $\text{H}_2\text{O}_2$  nor oxygen can degrade HexA, the amount of HexA remaining in the pulp after the  $\text{D}_0$  stage will remain unaffected by their addition. Both chemicals will only further oxidize the lignin residual. Therefore, the additional decrease in kappa number is small compared with softwood pulp. The impact of  $\text{H}_2\text{O}_2$  addition to an E stage following a  $\text{D}_0$  stage at  $50^\circ\text{C}$  is shown graphically in Fig. 7.125. Despite moderate changes in kappa number, the impact on brightness is significant. A temperature increase is required to trigger the consumption of larger amounts of  $\text{H}_2\text{O}_2$ . However, despite the higher temperature, above an input of about 0.4%  $\text{H}_2\text{O}_2$  a peroxide residual will remain. The impact on lignin removal decreases further if large amounts of chlorine dioxide are applied in  $\text{D}_0$ , or the temperature is raised. The use of a very high temperature ( $>90^\circ\text{C}$ ) during the first chlorine dioxide stage allows simultaneous delignification and hydrolysis, respectively destruction of HexA. In comparison to standard  $\text{D}_0$  stage conditions ( $50\text{--}70^\circ\text{C}$ ), this significantly reduces the amount of double bonds measured after the Eop stage. Values between kappa 2 and 3 are achieved with extraction only. Consequently, the impact of an oxidative support of the extraction stage with  $\text{O}_2$  and  $\text{H}_2\text{O}_2$  on the remaining double bonds becomes minimal, though the effect on brightness is still pronounced. An example of the impact of increasing  $\text{H}_2\text{O}_2$  amounts in the E stage following a hot  $\text{D}_0$  stage with kappa factor 0.2 is shown in Fig. 7.126. It is necessary to raise the temperature to enforce



**Fig. 7.126** Impact on brightness of an intensified delignification by a  $\text{hot D}_0$  stage on peroxide effectiveness in the subsequent extraction stage. E stage at 10% consistency, with 1.4% NaOH.

the consumption of a higher input of peroxide. Without peroxide addition, the E stage brightness is only at 73% ISO.

The need to add oxidants to the extraction stage might be questioned. Bleaching with the stages DEDED is possible in theory, but this would result in a rather high demand for chlorine dioxide with consequences for cost and effluent load (AOX). In order to optimize effects it is important to use the potential of other chemicals to degrade lignin and chromophores. The use of oxygen and  $H_2O_2$  in the E stages promotes the E stage from simply an extraction to a brightening and delignification stage. The improvement in pulp brightness by up to 10 points, compared to an Eo stage under identical conditions, is shown in Fig. 7.127. This advantage in brightness is still apparent after subsequent  $D_1$  and  $D_2$  stages. The right-hand portion of the graph shows, for the same input of chlorine dioxide to  $D_1$  and  $D_2$ , an advantage of about one brightness point. This represents an economical and ecological advantage which is also beneficial with regard to the operational stability of the bleaching process. The production of off-grade pulp becomes less likely if the final brightness gains are smaller, because no large variations in chemical addition are required to compensate brightness.

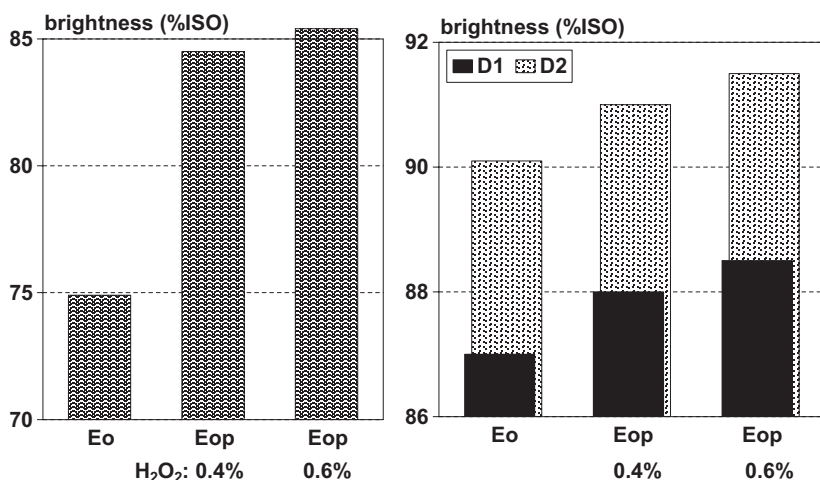
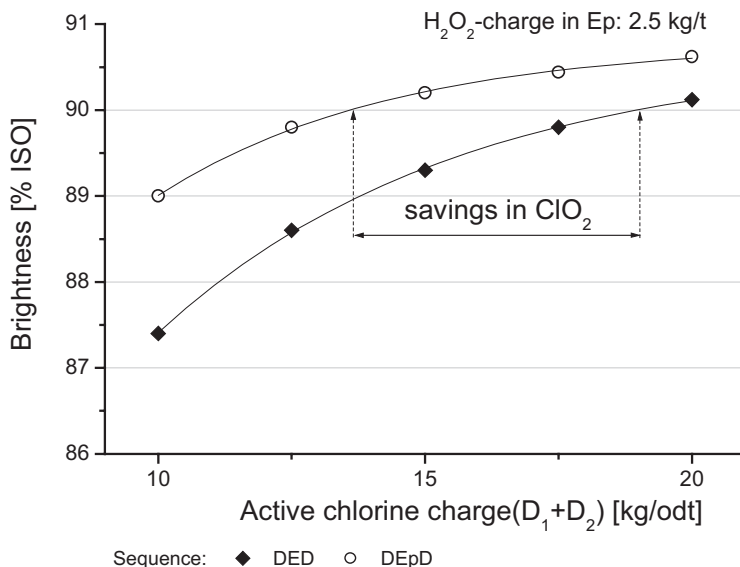


Fig. 7.127 Impact of the addition of  $H_2O_2$  to the Eop stage on brightness development in final bleaching.

One positive side effect of adding  $H_2O_2$  to the first E stage is a significant decrease in effluent color. Typically, an E-stage effluent is medium to dark brown in color, but becomes light brown on addition of  $H_2O_2$  [59]. Therefore, some mills apply  $H_2O_2$  not only for its bleaching effect but also to control effluent color. Another positive effect is the higher intensity of shives bleaching [60,61]. Even when shives are not fully bleached, they become lighter in color, which reduces their visibility.

Hydrogen peroxide is also applied advantageously in the second E stage of the longer sequences used in softwood pulp bleaching. In a  $D_0EopD_1EpD_2$  sequence,

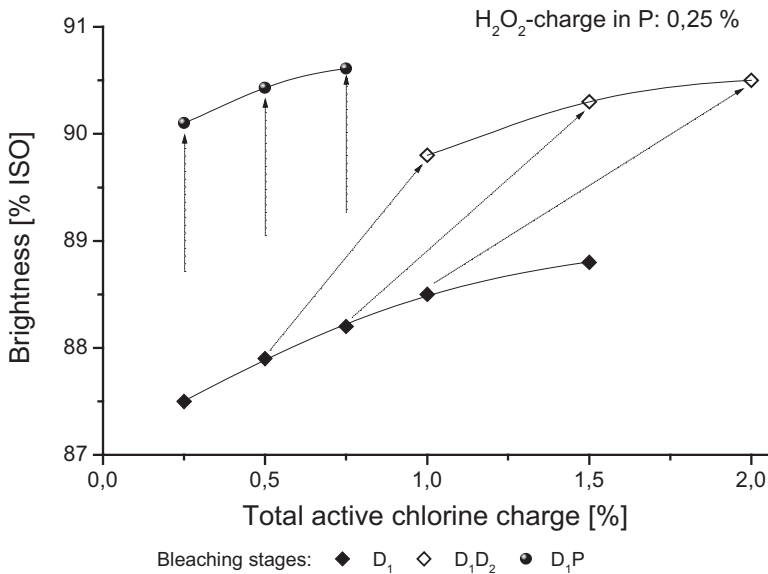
$\text{H}_2\text{O}_2$  reduces the demand for chlorine dioxide in final bleaching. The substitution of chlorine dioxide by  $\text{H}_2\text{O}_2$  in the sequence follows stoichiometric rules:  $1 \text{ kg t}^{-1}$   $\text{H}_2\text{O}_2$  replaces  $2 \text{ kg t}^{-1}$  active chlorine [62]. This is shown graphically in Fig. 7.128, where the application of  $\text{H}_2\text{O}_2$  results in a higher brightness with lower input of chlorine dioxide. The resultant flat curve crosses the 90% ISO line at lower input of  $\text{ClO}_2$ . It becomes easier to achieve a standard deviation of brightness of, for example  $\pm 0.5$  points around the 90% ISO value.



**Fig. 7.128** Substitution of chlorine dioxide by  $\text{H}_2\text{O}_2$  in final bleaching of softwood kraft pulp with the stages  $\text{D}_1\text{E}(\text{p})\text{D}_2$ . Amount of  $\text{ClO}_2$  in  $\text{D}_1$  variable, amount in  $\text{D}_2$  constant at  $5 \text{ kg t}^{-1}$  active chlorine; all stages at  $70^\circ\text{C}$ , 2 h, 10% consistency.

Most modern mills operate an oxygen stage, and therefore have a low level of lignin entering the bleach plant. This permits shorter bleaching sequences, such as a four-stage sequence with a  $\text{D}_0\text{-E}_0\text{p-D}_1\text{-D}_2$  configuration. The two D stages can be separated by a washing step, or follow each other directly. Another alternative is a short neutralization with caustic soda after  $\text{D}_1$ , which is followed by mixing the chlorine dioxide for  $\text{D}_2$ . The target of these modifications is lower investment costs. The five-stage version  $\text{D}_0\text{-E}_0\text{p-D}_1\text{ED}_2$  or  $\text{D}_0\text{-E}_0\text{p-D}_1\text{EpD}_2$  is certainly more effective, though the differences are not pronounced enough in terms of investment costs. The demand for chlorine dioxide in a shorter sequence can be rather high, especially when the target is very high brightness. Several problems of these shorter sequences are shown in Fig. 7.129. First, it becomes clear that the demand for chlorine dioxide in a three-stage sequence would become extreme if the brightness target were to be at 90% ISO. Whilst a level around 89% ISO is within reach, the flatness of the curve indicates that, to reach a much higher level, would be

very difficult. After washing the pulp, the addition of further chlorine dioxide ( $D_2$ ) becomes effective once more. Nevertheless, about 1.5% of active chlorine is required to achieve (safely) more than 90% ISO. The same brightness is achieved with much less chlorine dioxide when the second D stage is replaced by a P stage. The substitution is more than stoichiometric, as one part of peroxide replaces about four parts of active chlorine. This is the result of a more effective oxidation by two differently acting chemicals. An additional positive side effect of the P stage is an improved brightness stability (see the next section).



**Fig. 7.129** Substitution of the final D stage with a final P stage in a  $D_0EopD_1D_2$  sequence. Oxygen-delignified eucalyptus kraft pulp.  $D_0$  with factor 0.2 at 50 °C, Eop kappa 3.0, brightness 81.5% ISO. D stages at 75 °C, 2 h; P with 0.25%  $H_2O_2$ , 0.3% NaOH, 85 °C.

#### 7.6.7.1 Stabilization of Brightness with $H_2O_2$

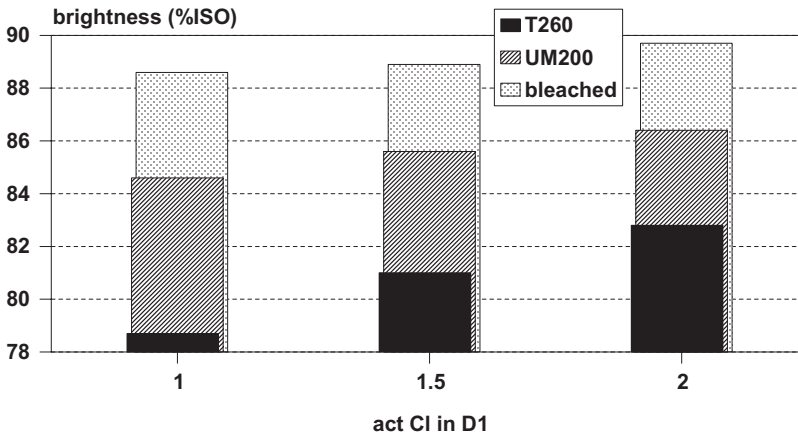
Brightness stability is affected by a number of parameters, and is typically analyzed in tests using accelerated aging. The pulp samples are exposed to elevated temperature under either dry or humid conditions. Brightness losses during dry heating are normally less pronounced compared with humid reversion tests. A standard procedure is to heat handsheets over boiling water for 1 h. This test method is described as E.4P method by Paptac [63]. The changes in light absorption and scattering are measured as post color number [64]; the smaller the number, the less reversion has taken place. Humid brightness reversion is thought to correlate more with natural aging occurring in pulp bales [65].

The intensity or aggressiveness of the bleaching process certainly has an impact. Compounds and conditions that affect brightness stability include transition metals, remaining lignin, hemicelluloses, and the pulping process used [66]. Past experience with hypochlorite pointed to rather negative effects of low pH, high temperature and high charges of this chemical on brightness stability. Losses could be attributed to oxidation of the cellulose chain, and were often very significant. 50 years ago kraft pulp was typically not bleached above about 80% ISO brightness using a typical CEHH sequence. The situation has now changed with the increasing use of chlorine dioxide, initially in a final stage (CEHD) and later with  $-D_1E_2D_2$  or  $-D_1EpD_2$  final bleaching.

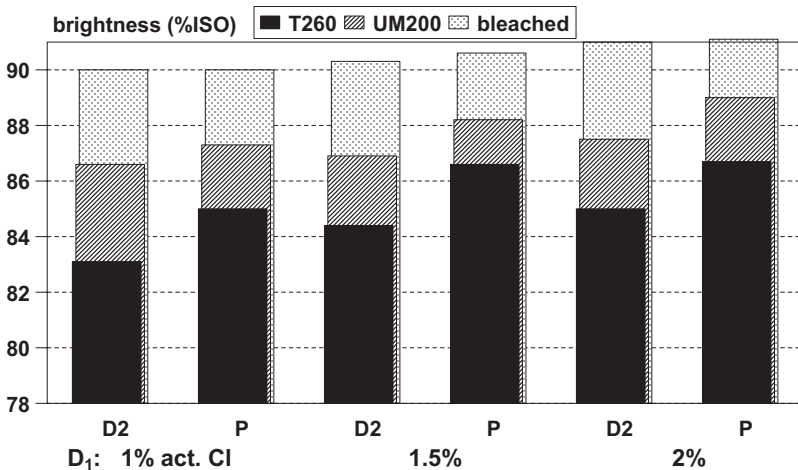
Mill experience teaches that the higher the brightness, the greater the stability, though this applies to the same sequence and moderate changes in bleaching conditions. The effectiveness of lignin removal or impurities removal is important for the stability of brightness, and therefore differences between TCF and ECF bleaching can be expected. Indeed, in TCF bleaching of birch kraft pulp HexA were identified as a source of high reversion [67]. Likewise, poor brightness stability was found for ECF “light” bleached softwood pulp [68]. However, in “normal” ECF bleaching HexA were found not to be the source for reversion [69], as it was removed completely in the process. These variances explain the importance of bleaching conditions. The TCF sequence used to bleach birch pulp with poor brightness stability [67] was conducted exclusively with alkaline bleaching steps. In order to attribute correctly the reversion to certain sources, it is important to understand how complete or ineffective potential sources for the development of colored compounds are destroyed.

A comparison of different ECF sequences, all using sufficient chemical for lignin oxidation and HexA hydrolysis or destruction [69], showed that cellulose depolymerization (apparent as a lower viscosity) has no direct influence on brightness stability. Neither hot acid hydrolysis nor ozone nor aggressive conditions and a very high temperature in the final peroxide stage had any significant impact on reversion. The positive impact of using more bleaching chemical in a  $D_0-Eop-D_1$  sequence is illustrated graphically in Fig. 7.130. A moderate input of chlorine dioxide (in this example, 1%) provided a reasonable brightness close to 89% ISO, but the brightness was not stable. With a loss of about 10 points of brightness in humid reversion, the instability was pronounced. The use of additional chemical improves bleached brightness, but not to any great degree. A doubling of the active chlorine input (from 1% to 2%) added only one brightness point, yet reversion losses decreased from 10 points to only 7 points. The more intense degradation of lignin or other “impurities” was seen to improve brightness stability.

The advantage of an additional treatment stage to improve brightness and brightness stability is illustrated in Fig. 7.131. A small amount of active chlorine (0.5%) applied in the second D stage lifts brightness to 90% ISO, and reduces losses in humid reversion to about 5 points of brightness. Even more pronounced is the improvement of a stoichiometric substitution of chlorine dioxide by  $H_2O_2$  (0.5% active Cl with 0.25%  $H_2O_2$ ). Losses in reversion decrease at best to only 3.5 points.



**Fig. 7.130** Analysis of brightness reversion of eucalyptus kraft pulp after three bleaching stages with  $D_0$ -Eop- $D_1$ . Active chlorine to  $D_0$  with kappa factor 0.23 at 50 °C, 1 h.  $D_1$  at 70 °C, 2 h. Brightness analyzed after 2 h at 100 °C, 100% humidity and 4 h at 105 °C (UM 200 test).



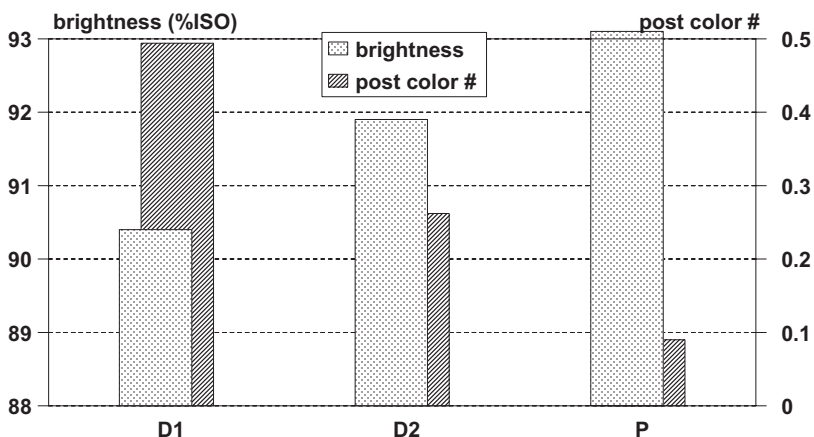
**Fig. 7.131** Analysis of brightness reversion of eucalyptus kraft pulp after four bleaching stages with  $D_0$ -Eop- $D_1$ - $D_2$ , respectively  $D_0$ -Eop- $D_1$ -P.

This advantage of an application of  $H_2O_2$  can be attributed to the destruction of carbonyl groups and quinoid structures remaining in pulp after the D stage. Using UV Raman spectroscopy, Jääskeläinen [70] detected these intermediates (or end products) of chlorine dioxide bleaching [9] in kraft pulp bleached with a final D stage. In peroxide-bleached pulp such structures were absent, the reason being the rapid reaction of alkaline peroxide with quinones.



The importance of the remaining quinoid structures, respectively their elimination by alkaline  $H_2O_2$ , explains the rather good brightness stability of TCF or ECF “light” bleached pulp. Despite their higher lignin residual, these pulps normally show very moderate reversion losses in accelerated aging. The same applies to bleached mechanical pulp, which is rather stable during heat-induced aging. Its sensitivity against light-induced yellowing has phenols as the main source, and follows a different reaction pathway [71].

The conclusion drawn regarding the source for reversion of the TCF-bleached birch pulp mentioned above [67] can now be seen from a different angle. This pulp had been subjected to a very intense peroxide treatment, but not to any acid stage capable of removing HexA. Therefore, the source for the remaining reversion of this pulp was HexA. It is not appropriate to generalize this specific finding, however. In ECF bleaching with sufficient hydrolysis or oxidation of HexA, other compounds are responsible for brightness losses in aging. The best brightness stability results from the most effective removal of all impurities. This includes sufficient bleaching chemical with different reactivities towards the impurities and definitively sufficient washing. The combination of a very high temperature in the  $D_0$  and the last D stage ( $90^\circ C$ ) with a final peroxide stage provides access to the brightness range above 93% ISO, and simultaneously to extreme brightness stability. The increase in brightness, and the development of brightness stability in humid reversion, is shown graphically in Fig. 7.132. The peroxide-bleached pulp loses less than one point of brightness during the aggressive aging treatment.



**Fig. 7.132** Development of brightness and brightness stability of eucalyptus kraft pulp bleached with the stages  $hot D_0$ -Eop- $D_1$ - $hot D_2$ -P, reversion analyzed after 2 h at  $100^\circ C$ , 100% humidity.

### 7.6.7.2 Catalyzed Peroxide Bleaching

Under acidic conditions,  $\text{H}_2\text{O}_2$  reacts very slowly with pulp, the reaction being accelerated by the presence of molybdenum and tungsten salts [72]. Such an acidic treatment can be used to activate an alkaline peroxide bleaching stage. During the period of intense searching for alternatives to chlorine bleaching – that is, before settling on ECF bleaching – molybdate-catalyzed peroxide was intensely investigated [73]. Obviously just a niche application remained [74]. In order to achieve a sufficient turnover of peroxide with a molybdate input at 0.04%, the temperature must be elevated above  $80^\circ\text{C}$ , while the required retention time is about 2 h.

A catalyst for alkaline peroxide bleaching was described by Patt [75]. The manganese complex accelerates and intensifies bleaching in both ECF and TCF applications. Unfortunately, synthesis of the manganese compound [76] (Fig. 7.133) is complicated, and this results in high – and for an industrial application – prohibitive costs. On a laboratory scale, the addition of 10–50 ppm of the complex resulted in a higher brightness at a lower demand for  $\text{H}_2\text{O}_2$ . To date, no other compounds with similar properties and lower production costs have been described in the literature.

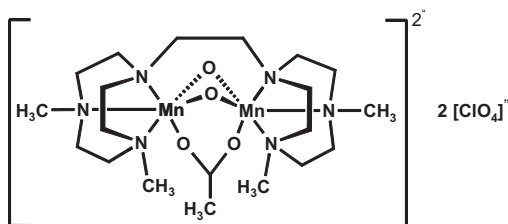
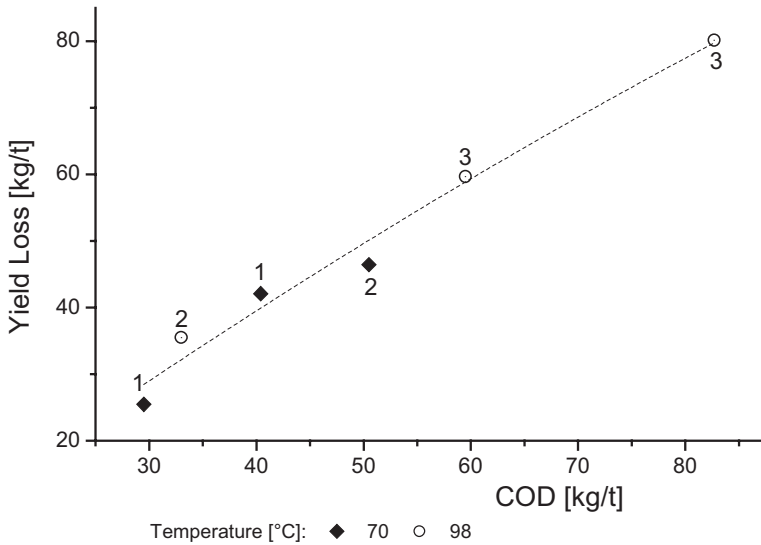


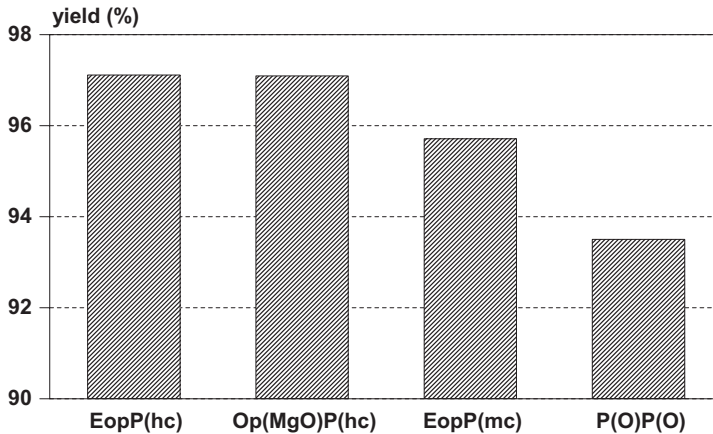
Fig. 7.133 Model of the manganese complex effective in activating peroxide bleaching of kraft and sulfite pulp.

### 7.6.7.3 Application in TCF Sulfite Pulp Bleaching

The brightening of sulfite pulp is rather easy with  $\text{H}_2\text{O}_2$ . The reason for this is a low level of residual lignin, and very little lignin condensation occurring during the pulping process. Today, therefore, most sulfite pulp is bleached under TCF conditions simply with  $\text{H}_2\text{O}_2$ . The acidic pulping process can leave a high amount of hemicelluloses in the pulp. This permits pulping with a high yield, though the hemicelluloses are soluble under alkaline conditions. Because a higher input of caustic soda is required to activate large amounts of  $\text{H}_2\text{O}_2$ , the intensity of bleaching affects both yield and effluent load. An example of the impact of temperature and caustic soda on chemical oxygen demand (COD) and yield is provided in Fig. 7.134. The graph illustrates the high likelihood of a significant yield loss when caustic soda is applied without care. The combination of a very high charge of caustic soda and very high temperature is detrimental to pulp yield and effluent load. Not surprisingly, this correlation is linear [77] within the typical range of caustic soda addition.



**Fig. 7.134** Impact of alkali amount on chemical oxygen demand (COD) and yield at two different temperature levels and NaOH charges (1%, 2%, and 3%), 10% consistency, 1 h.

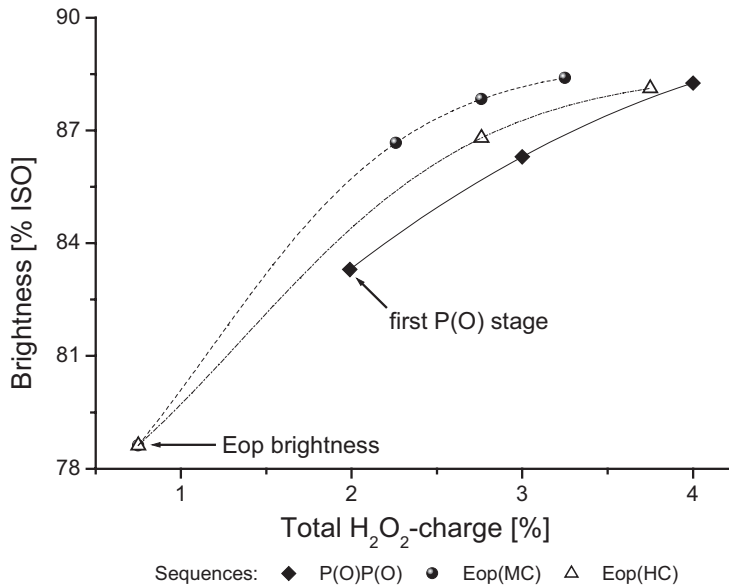


**Fig. 7.135** Yield in bleaching of spruce sulfite pulp to identical brightness (88% ISO) with four different two-stage processes. mc: medium consistency; hc: high consistency.

Bleaching to very high brightness typically begins with an MC treatment, with the application of a moderate amount of caustic soda and  $H_2O_2$ , sometimes in addition to a small amount of oxygen. Such a first step reduces the lignin level and prepares a final bleaching step. High-consistency bleaching requires less caustic soda because the higher concentration results in a higher pH with less

chemical. This becomes apparent in a comparison of different bleaching technologies. In Fig. 7.135, the yields are compared following two-stage processes. Medium-consistency delignification followed by HC peroxide bleaching (Eop-P<sub>hc</sub>) results in the highest yield. The aggressive alkalinity of a high-temperature pressurized peroxide process (PO) [78] causes a significant drop in yield. Consequently, the recommendation of such process conditions [78,79] leads in the wrong direction. The corresponding brightness increases are shown in Fig. 7.136, which also contains details of the applied process variables. The combination of MC delignification and HC bleaching clearly provides the best response. Alternatively, a combination of oxygen delignification, chelation and peroxide bleaching (O-Q-P) is applied.

The use of magnesium oxide in an oxygen/peroxide delignification allows recycling of the effluent into the recovery system in magnesium sulfite pulping [80,81]. This decreases the effluent load from final bleaching, although the effectiveness of brightening is lower – typically only the low 80s are accessible in P<sub>MgO</sub> bleaching. A sequence applied in practice uses oxygen and peroxide together with MgO and countercurrent washing from the acid stage after MgO treatment. This acid stage is necessary to remove residual MgO completely. An OP<sub>MgO</sub>-A-P sequence can reach brightness of 86–88% ISO. The effluent load is significantly



**Fig. 7.136** Brightness increase of spruce sulfite pulp ( $\kappa$  17.1) in P stage. Pre-bleaching with Eop, 1.5% NaOH, 0.75% H<sub>2</sub>O<sub>2</sub>, 1.5 h, 0.3 MPa O<sub>2</sub>, 10% consistency. Second bleaching stage: P<sub>mc</sub>: H<sub>2</sub>O<sub>2</sub> and NaOH variable, 3 h, 80 °C, 10% consistency. P<sub>hc</sub>: H<sub>2</sub>O<sub>2</sub> and NaOH variable, 0.5% sodium silicate, 4 h, 75 °C, 25% consistency. P(O) bleaching at 10% consistency. 1st stage with 2% H<sub>2</sub>O<sub>2</sub>, 1.8% NaOH, 0.3 MPa O<sub>2</sub>, 95 °C, 1.5 h; 2nd stage with 1% or 2% H<sub>2</sub>O<sub>2</sub>, 1.6% NaOH, 95 °C, 1.5 h.

decreased through the recycling procedure. Because the make-up of MgO required in pulping can be added to the bleaching stage, this process will not lead to additional costs – on the contrary, the costs for caustic soda are lowered.

#### 7.6.7.4 Activators for H<sub>2</sub>O<sub>2</sub> Bleaching

Activation steps with ozone, peracetic acid, or catalyzed acidic H<sub>2</sub>O<sub>2</sub> have been described in order to improve the performance of the final peroxide stage [82]. Cyanamide can be used to improve the performance of an MC peroxide bleaching stage [83,84], but the more effective reaction of H<sub>2</sub>O<sub>2</sub> at HC conditions [85] has outphased this application. Dissolving pulp is bleached with an ozone step to remove traces of lignin [86]. Peracetic acid has been used on a large scale to boost brightness above the 90% ISO range. This process is used to bleach magnefite pulp with the sequence O-Q-Paa/P. The activation uses on-site-mixed peracetic acid (the mixture contains equilibrium peracetic acid); thus, peracetic acid, acetic acid, H<sub>2</sub>O<sub>2</sub> and water are present. Under the slightly acidic conditions of the Paa stage, H<sub>2</sub>O<sub>2</sub> is not consumed. The excess of H<sub>2</sub>O<sub>2</sub> is activated for bleaching simply by adding caustic soda. The activation with small amounts of Paa (0.15–0.3%) allows two additional brightness points, and permits brightening to a level above 91% ISO [87].

## 7.7

### Peracetic Acid in Pulp Bleaching

Bleaching of pulp with peracids is limited on an industrial scale to the application of peracetic acid, CH<sub>3</sub>COOOH. In the past, other per-compounds were also promoted for bleaching, among these being Caro's acid, H<sub>2</sub>SO<sub>5</sub>, or mixtures of Caro's acid and peracetic acid. The interest in their application stems from the search for alternatives to chlorine bleaching. The application of peracids was tested in ECF and TCF bleaching sequences [1]. With the increasing knowledge about ECF bleaching and its good environmental performance, peracids became less interesting. Today, peracetic acid occupies a niche in TCF bleaching. The application of peracetic acid in TCF bleaching was introduced because of the need to modify residual lignin to allow its destruction in hydrogen peroxide bleaching, and to improve the economics of TCF sequences. Typically, a peracid treatment is applied under weak acidic conditions. This results in an improved delignification and a higher brightness in the following alkaline peroxide stage.

Peracetic acid has a sharp pungent odor. It has a boiling point of 103 °C and a vapor pressure of 3325 Pa at 25 °C. It is a weaker acid than acetic acid, and is produced by mixing (glacial) acetic acid with hydrogen peroxide. The addition of a strong acid (e.g., sulfuric acid) accelerates the formation of the equilibrium between acetic acid, hydrogen peroxide, water and peracetic acid:



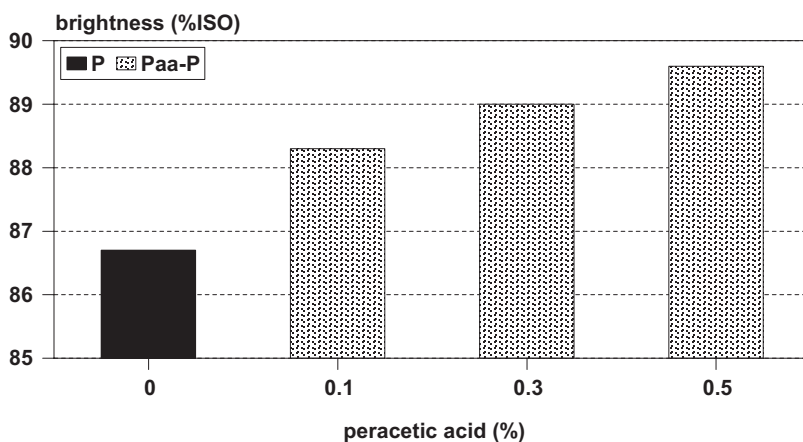
The equation shows that the equilibrium can be shifted to the right by applying high concentrations of hydrogen peroxide. However, there will always be an excess of hydrogen peroxide and unreacted acetic acid in the mixture. This increases the cost for the application of equilibrium peracetic acid in bleaching, because the reaction conditions for peracid bleaching will not allow the reaction of hydrogen peroxide. Another important factor is product safety. Storage and handling of higher concentrations of peracetic acid with a high  $\text{H}_2\text{O}_2$  content are restricted due to its potential hazards. This prevents application in mill practice.

The peracetic acid equilibrium is shifted to the right by distillation under vacuum. The resulting peroxide conversion is greater than 90%. The distillation products are the most volatile compounds, water and peracetic acid (boiling point  $103^\circ\text{C}$ ). This distillate must be cooled to prevent re-formation of the equilibrium. The ideal storage temperature for the mixture is below  $0^\circ\text{C}$ ; therefore, storage tanks require both insulation and refrigeration. Cooled distilled peracetic acid is commercially available with a content of 35–40% peracetic acid in water. Because of the absence of a strong acid, re-formation of the equilibrium is very slow. An accidentally higher storage temperature (e.g., ambient temperature) would not constitute a safety hazard, but the resulting “new” equilibrium would produce a lower concentration of peracetic acid.

Another economical alternative for peracetic acid application is on-site mixing of peracetic acid with hydrogen peroxide. At a temperature slightly above ambient, and with acid activation, the equilibrium is established within a few hours. Mixtures with a content  $>8\%$  peracetic acid and  $<40\%$   $\text{H}_2\text{O}_2$  are commercially produced on-site. In order not to waste the content of hydrogen peroxide in this equilibrium, the Paa treatment must be followed by the peroxide stage, without intermediate washing. Following an addition of caustic soda, the unused hydrogen peroxide content in the pulp reacts in the subsequent P step.

The reactions of peracid with lignin follow mainly an electrophilic pathway. With regard to reactivity, peracetic acid ( $\text{CH}_3\text{COOOH}$ ) has an advantage over Caro’s acid ( $\text{H}_2\text{SO}_5$ ). Peracetic acid has a  $\text{pK}_a$  value of 8.2, and is only partly dissociated at neutral or moderately acidic pH. Peracetic acid reacts via hydroxylation ( $\text{OH}^+$ ), splitting into a cation and an anion, acetate ( $\text{CH}_3\text{COO}^-$ ). In contrast, Caro’s acid has two  $\text{pK}_a$  values of 1 and 9.3. Thus, it is completely dissociated ( $\text{SO}_5^{2-} + 2\text{H}^+$ ). An electrophilic reaction is only possible via the mono anion ( $\text{HSO}_5^- \text{OH}^+ + \text{SO}_4^{2-}$ ), which is present only at very low concentration. This explains the slow reaction of Caro’s acid with lignin. A comparison of both compounds at identical active oxygen content favors Paa. The final kappa number is lower, and the final brightness higher after the Paa-P treatment.

The demand for peracetic acid is moderate. Figure 7.137 illustrates an example of a TCF bleaching application. An input of 0.1–0.5% peracetic acid is sufficient for the activation. Paa is applied at moderately acidic pH and at a temperature of about  $80^\circ\text{C}$ . Because the peracid reaction is slow, a retention time of 1 h is not sufficient to consume a charge of more than 0.5% at  $80^\circ\text{C}$ . On the other hand, because of the high temperature, peracetic acid is hydrolyzed into acetic acid and



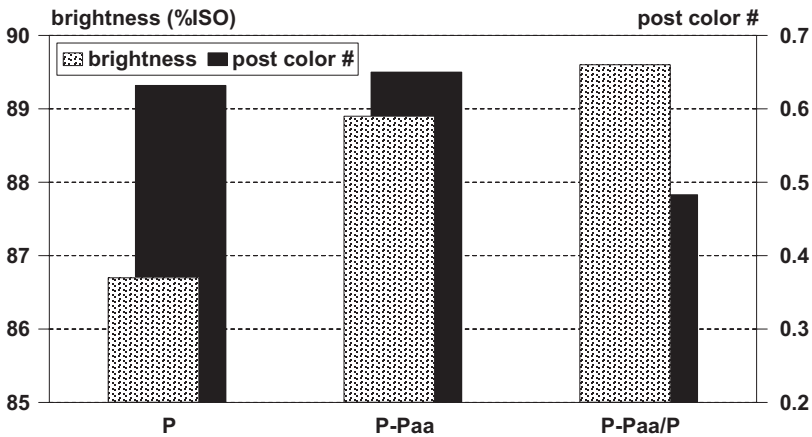
**Fig. 7.137** TCF bleaching of softwood kraft pulp with and without peracetic acid activation of a final P stage. Pulp pre-bleached with OO-Q-OP; Paa stage at 85 °C, 1 h, 10% consistency; final P stage with 2% H<sub>2</sub>O<sub>2</sub>, 1.4% NaOH, at 95 °C, 3 h, 10% consistency.

hydrogen peroxide. After about 1 h the remaining peroxy compound will be predominantly hydrogen peroxide.

Sequences with peracetic acid activation use the Paa step ahead of the final P stage. Thus, a TCF sequence could be OO-Q-OP-Paa/P or OO-Q-OP-Paa-P. Peracetic acid was also recommended as a final treatment step to boost the brightness of TCF pulp [2]. However, because of the type of reactions occurring with the remaining lignin, brightness stability is affected negatively. There is an improvement in brightness, but not in its stability. In addition, the high temperature required makes application in a high-density storage tower difficult.

Figure 7.138 illustrates the impact of a Paa post-treatment of a TCF pulp with 0.5% Paa at 80 °C. The improvement in brightness by more than 2 points is significant. Brightness stability, however, decreases. This suggests the formation of potential chromophores with Paa oxidation. These chromophore precursors are removed by treating pulp with alkaline peroxide. The change in pH changes the oxidant form from an electrophile into a nucleophile and thus removes quinones, it is likely that Paa generates phenolic intermediates. Peracid treatment is therefore more advantageous if followed with a peroxide stage.

The moderate speed of reaction of peracids with lignin is accelerated in the presence of chloride ions. Because of their high oxidation potential, peracids will oxidize chloride to chlorine. This acceleration increases the effect [3], it is, however, not environmentally sound because halogenated compounds are generated. Higher levels of AOX in the effluent and OX in pulp result from a reaction of peracid in the presence of chloride [4]. This contradicts the purpose of TCF bleaching. Peracetic acid should not be applied when there is a high level of chloride in the water loop.



**Fig. 7.138** Impact of a post-treatment with peracetic acid on brightness and brightness stability. Paa stage with 0.5% at 80 °C, 1 h 10% consistency, Paa/P at 80 °C with 0.5% Paa and alkali treatment after 0.5 h with 0.5% NaOH and continuation for 1 h. Stability analyzed after hot humid reversion (E.4P).

## 7.8 Hot Acid Hydrolysis

Kappa number – that is, permanganate demand – is generally assumed to represent the lignin content in pulp with sufficient accuracy. Because permanganate is a strong oxidizing compound, which reacts not only with the aromatic lignin but also with other double bonds, this assumption applies only with limitations. Relatively recently, a large number of “other” double bonds were identified in kraft pulp. The first indication into the source of these double bonds was the identification of furan-2-carboxylic acid as main product of its hot acid hydrolysis by Maréchal [1]. The origin was soon identified as hexenuronic acid, HexA, (Fig. 7.139), a compound generated during alkaline pulping by methanol elimination from 4-*O*-methylglucuronic acid on the xylan [2]. Therefore, permanganate consumption of a pulp describes dominantly the sum of its reaction with lignin and hexenuronic acid [3].

The ratio of substitution of the xylan backbone with 4-*O*-methylglucuronic acid in most hardwoods is about 10:1 (Xyl:Me-GluU). It is higher in most softwoods (5:1 or 4:1), however, the amount of xylan being typically significantly lower in softwood (spruce, *Picea abies* ~9%) compared with hardwood (birch, *Betula verrucosa* ~33%) [4]. Therefore, hexenuronic acids are present in softwood kraft pulp at a low level, and their share in the kappa number is only about one unit. In unbleached hardwood kraft pulp, about one-third of the permanganate consumption in kappa analysis is caused by hexenuronic acid. In oxygen-delignified hard-



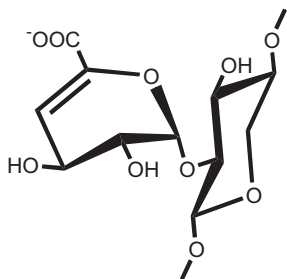


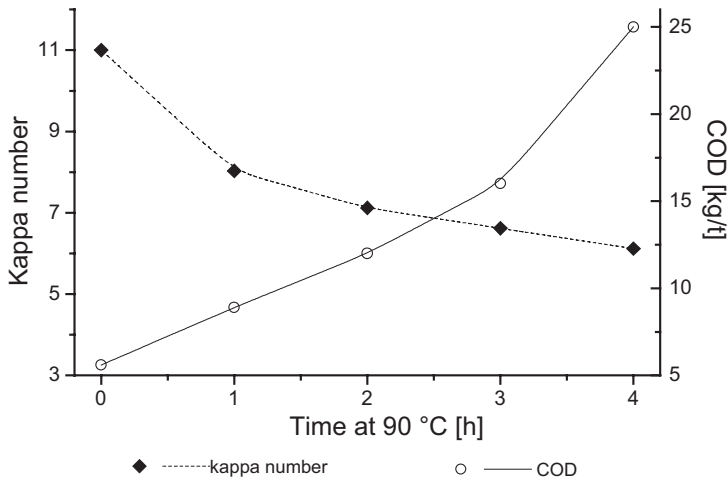
Fig. 7.139 Model of hexenuronic acid (HexA) on a xylan side chain.

wood kraft pulp, the level of “other compounds” is even higher, and can reach almost 50%. (This explains why the degree of “delignification” achieved in an oxygen stage of hardwood pulp seems more moderate compared with softwood pulp. As removed “kappa number” it might reach just 30%, but as removed real “lignin” it is typically better than 50%.)

The reason why hexenuronic acid remained undetected for decades is that the normally applied analytical method for lignin preparation uses acidic conditions, during which acid hydrolysis of the hexenuronic acid occurs.

The double bond of hexenuronic acid reacts with electrophilic bleaching agents, such as chlorine dioxide and ozone. The question of how, logically, to remove hexenuronic acid can be answered with the background of its analytical evasiveness. At elevated temperature and low pH, hexenuronic acid is rapidly hydrolyzed. The first report of the effect of hot acid treatment of hardwood pulp by Maréchal in 1993 described the conditions required, namely a temperature above 90 °C, a pH below 3.5, and extended time. The impact of time on the hot acid hydrolysis of an oxygen-delignified eucalyptus kraft pulp is shown in Fig. 7.140. The time required at 90 °C and pH 3 for complete hydrolysis of hexenuronic acid is rather long. The sharp increase of the effluent load with prolonged time indicates an increasing cellulose degradation. This becomes apparent from the parallel lowering of the pulp’s viscosity. In mill applications, therefore, a “hot acid stage” will be conducted for not more than about 2 h, in order to retain control of the pulp yield and viscosity losses. From a practical standpoint, this also keeps the size of the towers within reasonable limits. The process could be accelerated by using a higher temperature or more acid, but typically the temperature is kept below 95 °C in order to balance steam demand and to avoid pressurized conditions. A lower pH is similarly unattractive because it would only accelerate cellulose depolymerization. Hydrochloric acid may be a cost-attractive alternative to sulfuric acid, especially in mills with an on-site electrolysis for chlorate. However, the potential problem of using hydrochloric acid is corrosion of the equipment.

The high temperature and low pH used during the hydrolysis have an additional effect, in that they allow a significant reduction in the manganese content of the pulp [5,6]. It is speculated that manganese and iron might form complexes with hexenuronic acid. In bleaching, hexenuronic acid destruction and metals removal are equally important. A TCF bleaching sequence with only alkaline oxygen



**Fig. 7.140** Impact of time in hot acid hydrolysis of eucalyptus kraft pulp. Pulp delignified with oxygen to kappa 11, temperature at 90 °C, pH 3 (H<sub>2</sub>SO<sub>4</sub>).

and peroxide stages (e.g., OQPP) will maintain all hexenuronic acid sites in the bleached pulp, the consequence being a poor brightness stability [7]. The inclusion of an acid hydrolysis stage into a TCF sequence improves the bleaching process because it eliminates transition metal. At the same time it increases brightness stability, due mainly to a reduction in the level of hexenuronic acids.

Despite the very substantial drop in kappa number through the hydrolysis of hexenuronic acids, the mill application of a hot A stage is rare [8]. The reason for this is the need for an additional treatment stage that consists not only of a tower but also a washer. This additional equipment is expensive, and normally the potential savings of chlorine dioxide in an ECF sequence will not pay back the investment. Therefore, high-density storage towers are converted to a hot A stage. The lack of a washer between storage and D<sub>0</sub> stage can result in the connection of a hot A pre-treatment and chlorine dioxide addition. The result is a hotA/D<sub>0</sub> stage combination, and this has been implemented in some mills. The alternative is to use a reverse approach, with a combination of the D<sub>0</sub> stage and a subsequent hydrolysis, or hot D<sub>0</sub> with extended retention time (see Section 7.4.5.3, modified chlorine dioxide delignification).

## 7.9 Alternative Bleaching Methods

During the past few decades, there has been a constant search for environmentally benign alternatives to pulp bleaching. The search continues today, and will do so in the future. Besides the activation of peroxide stages, one such alternative is offered through biotechnological means. Although hemicellulose-degrading

enzymes (xylanases) were the first enzymes to be introduced on a large scale for pulp bleaching [1], they function more as a bleaching aid than as a direct bleaching agent. This is because they increase the efficiency of subsequent bleaching steps by loosening the structure of reprecipitated xylans on the unbleached pulp fibers, thereby saving on the amounts of bleaching chemicals required.

A direct approach might be to use lignin-degrading fungi (*Basidiomycetes* or white rot fungi) or their enzyme systems (e.g., peroxidases, laccases), all of which have long been recognized. These systems are able to selectively degrade lignin not only in wood, but also in pulp. However, the time required for this process to proceed to the desired extent is far too long for a modern pulp mill bleaching system. This problem of extended reaction times was partly tackled by the application of a so-called mediator. Discovered accidentally during the early 1990s by R. Bourbonnais of Paprican during experiments with lignin model systems, the laccase-mediator-system (LMS) was found to consist of an enzyme (laccase) and a mediator (ABTS) [2]. The mediator applied in this first LMS – a laccase substrate used for an activity assay – was impracticable for large-scale applications, however. An LMS suitable for pulp mill use was later patented by Call [3,4] which employed different mediators (e.g., 1-Hydroxy-benzotriazole, HBT) [5], and initial large-scale trials conducted with this material has shown promise.

The underlying working principle of the LMS can be summarized as follows. The enzyme laccase, as a macromolecule, is unable to penetrate the pulp fiber, despite such penetration being a prerequisite for lignin-degrading action. Moreover, due to its oxidation potential, laccase on its own is only capable of oxidizing phenolic lignin moieties, which react predominantly by dehydrogenative polymerization rather than by lignin degradation. However, both of these difficulties were overcome with the use of a low molecular-weight redox mediator. In this way, the substrate range is extended to nonphenolic lignin units, as could be shown by model compound studies, and the mediator can penetrate much more deeply into the fibers. In the LMS redox cycle, the enzyme oxidizes the mediator to a more reactive species, mainly of radical type, and these react in turn with the lignin macromolecule, either via an electron transfer process or by hydrogen atom abstraction, depending on the mediator used [6]. The reduced mediator is re-oxidized by the enzyme, which utilizes dioxygen as a co-substrate and which, in turn, is reduced to water.

Large-scale applications of the LMS remain inoperative, however, and some major restraints for eventual mill usage have been identified:

- The mediator should be a low-cost chemical which should exhibit a minimum of side reactions. These undesired processes can cause a reduction in enzyme activity or the production of harmful degradation products, which in turn raises the issue of environmental compatibility.
- A sufficient gain in kappa number reduction usually requires several LMS stages with additional extraction stages in between.
- The increase in brightness is often limited, so that additional bleaching is required.

For further information on the LMS system, the reader is referred to some excellent reviews [7,8].

Further developments include mediated electrochemical delignification systems [9], and enzyme mimicking (porphyrin derivatives, manganese-based complexes, metal–Schiff base-complexes; for a more detailed description, the reader is referred to Ref. [10]). Mimicking the action of lignolytic enzymes is also the underlying concept of bleaching system which was developed in the mid-1990s [11,12] and today is receiving increased attention. A special class of metal clusters of the Keggin-type – the polyoxometalates [13], often referred to as POMs – are utilized as the catalyst. Polyoxometalates are metal-oxo anionic clusters with chemical properties that can be largely controlled by transition metal substitution and the counteraction used. This, combined with their ability to donate and accept electrons and their stability over a wide range of conditions, makes them attractive targets for use as bleaching catalysis. To activate the cluster for delignification, one or more structural metal atoms are donated by a first-row transition metal atom (e.g., vanadium or manganese) [14]. Specific conditions (e.g., pH, type of metal cluster) allow POMs to be selective towards lignin degradation and to be thermodynamically stable in water [15]. The high-valent metal cluster anions oxidize and thus degrade and solubilize the lignin, while themselves being converted into the lower-valent reduced state. The re-oxidation with dioxygen is a process that generates radicals, but this would result in undesired cellulose damage due to highly unselective side reactions. Consequently, the POMs are reactivated in a separate stage under conditions that effect the oxidation of dissolved lignin and other dissolved organic matter to carbon dioxide and water. Actual delignification of the pulp is carried out under anaerobic conditions. POMs must be applied in stoichiometric quantities. Current types of POM are advanced products of development: they are more easily synthesized than the original representatives of this compound class, are not too costly, recyclable, and have the capability of self-buffering. Recent progress has also shown that molybdovanadophosphate heteropolyanions can be used under aerobic conditions in a single-stage process with either oxygen or ozone as the reactivating agent [16].

Further research and development is required eventually to transfer novel delignification principles to large-scale applications.

## 7.10

### **Bleach Plant Liquor Circulation**

*Andreas W. Krotscheck*

#### 7.10.1

##### **Introduction**

It is imperative for bleach plant operations to recirculate process liquors and to minimize the consumption of fresh water. On the one hand, an increasing environmental awareness calls for the responsible usage of water resources, yet on the

other hand there are strong economical arguments for liquor circulation, including the reduced consumption of bleaching chemicals, energy and water itself, and a lower hydraulic load to the effluent treatment facilities. Liquor circulation in the bleach plant has certain limits, however, that are set: (a) on the process side, by the accumulation of nonprocess elements or reaction products and by scaling; and (b) on the equipment side, by the corrosion resistance of construction materials or temperature sensitivity of machinery.

### 7.10.2

#### Intra-Stage Circulation and Circulation between Stages

It is possible to distinguish between two levels of bleaching liquor circulation, namely intra-stage circulation and circulation between stages. Intra-stage liquor circulation forms part of any modern bleach plant liquor management. As shown in Fig. 7.141, filtrate coming from the washing equipment of a bleaching stage can be used to dilute the pulp suspension in this very stage at various positions. Moreover, it can also be used on the cleaning showers of the washing equipment itself. In some cases it may be necessary to either heat or cool the dilution liquor in order to achieve a certain temperature level in the dilute suspension. It may also be required to install a fiber filter in a circulation line to protect the narrow shower nozzles from plugging.

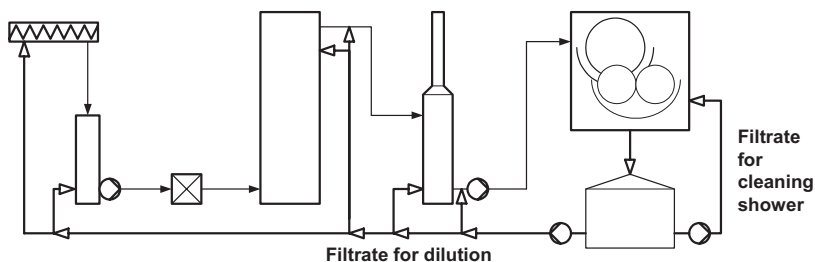


Fig. 7.141 Generic intra-stage liquor circulation.

The circulation of liquors between bleaching stages is more delicate. Starting with process matters, the advantages of liquor circulation include savings in energy and chemicals. Clearly, the circulation of hot liquor to process steps where heating is desirable and circulation of cold liquor to those steps where cooling is needed, will save steam and cooling water. Likewise, the recirculation of filtrate containing residual chemicals to the feed of a stage that uses such chemicals will reduce the chemical charge required to reach a bleaching target.

In a given bleaching stage, both energy savings and chemical savings can be usually achieved by using own filtrate as wash liquor on the preceding washer (Fig. 7.142a). Depending on the bleaching sequence, other filtrates may, however, at times be more appropriate than the own filtrate for such use (Fig. 7.142b). In special cases, other filtrates may also be utilized for the dilution of incoming pulp, reducing its consistency from the discharge consistency of the preceding washer to the desired stage feed consistency (Fig. 7.142c).

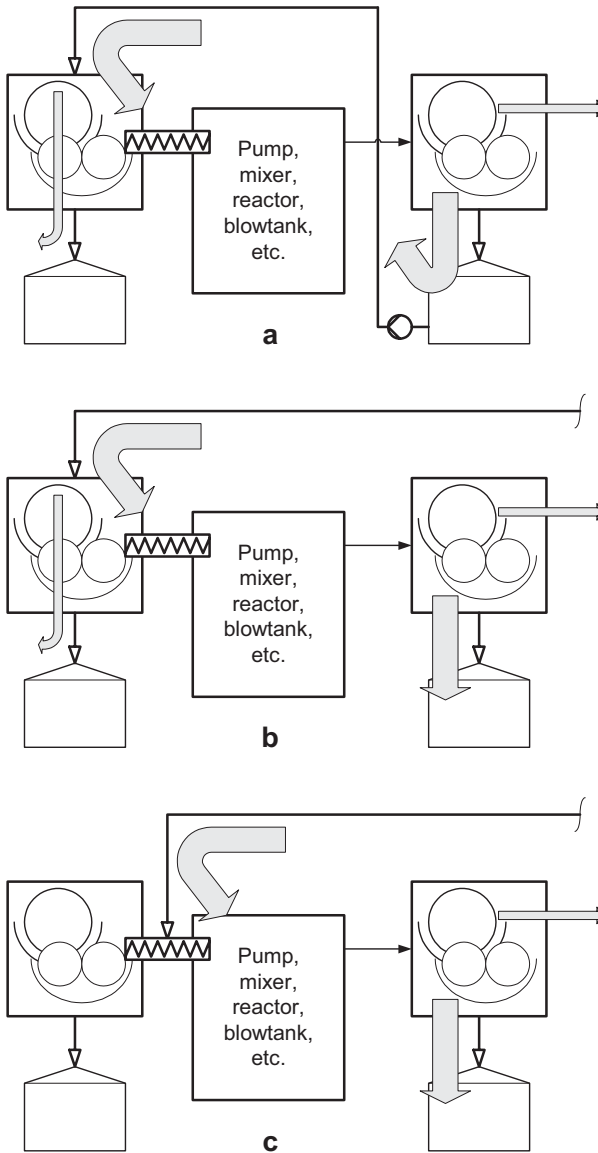


Fig. 7.142 Generic liquor circulation between stages.

The bold gray arrows in Fig. 7.142 indicate the distribution of dissolved liquor constituents moving along with circulated filtrate. If filtrate is used as washing liquor on a washer, the dissolved compounds turn to both directions – downstream to the subsequent stage, and also upstream to the preceding stage. For example, an oxygen delignification filtrate is applied to the preceding brownstock washing, thus introducing its dry matter into the cooking liquor loop for benefi-

cial recovery. On the other hand, it is problematic to recycle the filtrate from a chlorine dioxide stage to post-oxygen washing, because undesirable chlorides will also end up in the recovery loop.

### 7.10.3

#### **Open and Closed Operation of Bleaching Stages**

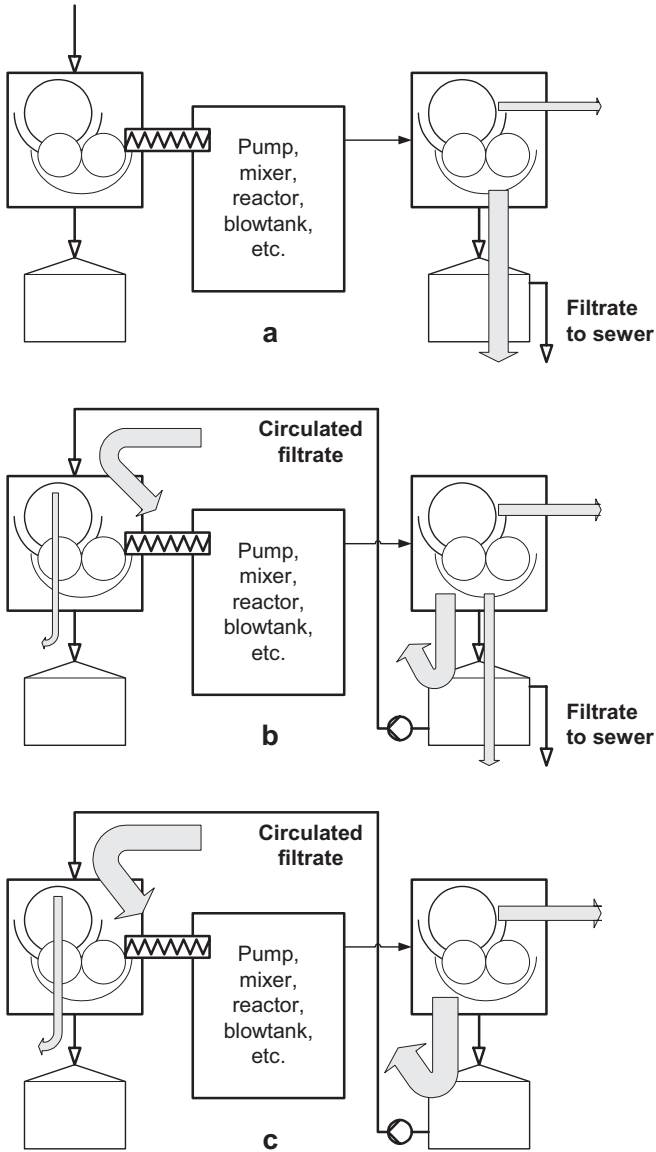
The drawback with liquor circulation is the accumulation of material in the liquor cycles. There are cases, where such accumulation is inappropriate from a process perspective, for example when transition metals build up in a totally chlorine-free bleaching sequence. In elementary chlorine-free sequences, liquor circulation can lead to an increase in the concentration levels of corrosive chloride ions. Depending on the liquor management, such stages may also be affected which are not charged with chlorine-containing chemicals and which, therefore, were not originally designed for such conditions.

The normal practice of limiting the accumulation of undesirable matter is to sewer either a part or the totality of a liquor, rather than to recirculate it. The stage is then said to be operated partly or totally open, as opposed to closed operation where all the filtrate is used elsewhere in the process (Fig. 7.143).

In an open stage, the concentrations of dissolved liquor constituents depend primarily on the pulp consistency delivered by the washer preceding this stage. If the feed pulp comes from a press at high consistency, a respectable amount of intra-stage circulation is needed to dilute the pulp before medium-consistency bleaching. This circulation brings the filtrate concentrations up to approximately double the values observed in a stage fed from a washer with medium-consistency discharge. At the same time, the effluent volume from a high-consistency fed stage is about half that from a medium-consistency fed stage (Fig. 7.144).

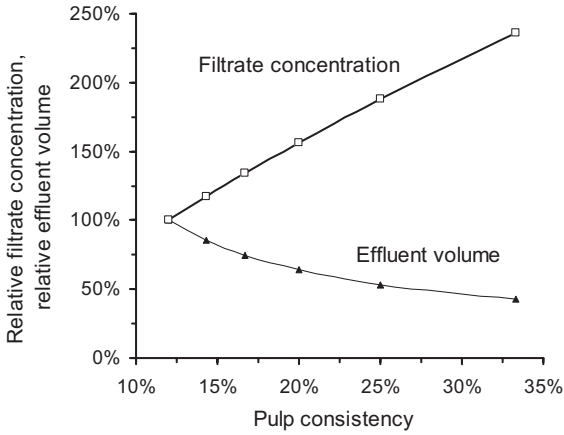
Whilst there is a near-linear dependency of the filtrate concentrations on the feed consistency to the stage, the effects of partial closure are highly nonlinear. Partial closure occurs when filtrate which is otherwise sent to the sewer is utilized elsewhere in the bleaching process. As the volume of filtrate sent to the sewer is gradually reduced, the initial change in concentrations is rather low, especially in bleaching systems using medium-consistency washing equipment. Note that a reduction in effluent load (e.g., COD load) by 50% is reached only after 65–75% of the filtrate volume is circulated back to the process (Figs. 7.145 and 7.146). In these figures, a zero degree of closure represents an open stage (as per Fig. 7.142a) and 100% closure means operation (according to Fig. 7.143c).

When a given bleaching stage is closed and concentrations rise, the carry-over of dissolved matter to the subsequent stage increases in proportion to the filtrate concentration. This fact must be carefully considered, since the amount of carry-over may affect the performance of the subsequent bleaching stage.

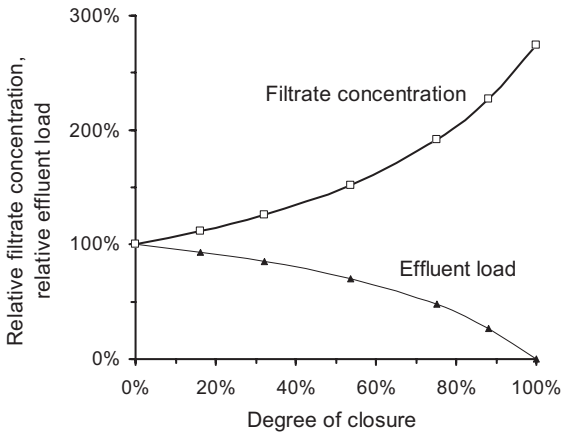


**Fig. 7.143** Stages of liquor cycle closure: (a) open; (b) partly open; (c) closed.

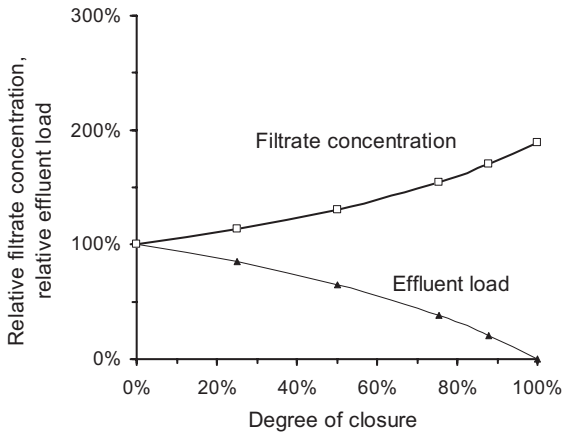




**Fig. 7.144** Relative filtrate concentration and effluent volume in an open bleaching stage with intra-stage circulation as a function of the discharge consistency from the washing equipment preceding the stage (simulation results).



**Fig. 7.145** Relative filtrate concentration and effluent load from a bleaching stage as a function of the degree of closure; bleach plant equipped with washing equipment discharging at medium consistency (simulation results).



**Fig. 7.146** Relative filtrate concentration and effluent load from a bleaching stage as a function of the degree of closure; bleach plant equipped with washing equipment discharging at high consistency (simulation results).

#### 7.10.4

##### Construction Material Compatibility

As liquor is circulated within and across the bleaching stages, chemicals accumulate in and become distributed throughout the bleach plant. The liquor management must consider that the circulation leads to concentrations acceptable to processes and construction materials. Similar issues must be addressed when a bleaching sequence retrofit requires that a particular stage be operated with a different chemical. Sequence retrofits may be driven by furnish or product grade changes, environmental pressure or capacity expansion.

Caution is always advisable when chloride-containing liquors are circulated to stages built in basic metallurgy. On the other hand, liquor circulation within a totally chlorine-free sequence is usually unproblematic.

At times, a chlorine dioxide stage may be up for a peroxide bleaching retrofit. Despite earlier doubts, the corrosion resistance of titanium against alkaline peroxide solutions under normal bleaching conditions has been confirmed, both in tests and in long-term mill operation [1,2]. In case of metallurgical reservations, expert advice together with immersion tests are highly recommended.

#### 7.10.5

##### Implications of Liquor Circulation

Process challenges by the accumulation of dissolved matter and concerns regarding the resistance of construction materials are not the only issues brought about by liquor circulation. Scaling is another important factor. For example, calcium

oxalate scaling in connection with liquor circulation has been reported to challenge bleach plant operations worldwide [3–5]. Scales often occur in an environment where the pH or temperature of a process liquor undergoes a change.

In addition, mechanical reasoning plays a role in liquor circulation. As an example, each piece of rotary washing equipment, including drum washers and presses, has its design limit with regard to the temperature difference between feed pulp and wash liquor.

Due to the large variety of bleaching sequences and installed equipment, the targets, measures and implications related to bleach plant liquor circulation differ significantly between mills. The complexity of liquor cycles is increased by the behavior of the washing equipment used. Computerized process simulation has proven very helpful for reproducing and evaluating industrial bleaching applications. Since every bleach plant is unique in processes and construction materials, a compromise must be found from case to case between the benefits and disadvantages of liquor circulation.

## References

### Section 7.1

- 1 Sixta, H., Preparation and characterization of spruce and beech dissolving pulps prepared by both acid sulfite and prehydrolysis kraft cooking. R&D, Lenzing AG: Lenzing, **2002**. p. 20.
- 2 Gierer, J., Basic principles of bleaching. Part 1: Cationic and radical processes. *Holzforschung*, **1990**; 44(5): 387–394.
- 3 Lachenal, D., M. Muguet, Degradation of residual lignin in kraft pulp with ozone. Application to bleaching. *Nordic Pulp and Paper Research Journal*, **1992**; 1: 25–29.
- 4 Lachenal, D., N.B. Nguyen-Thi. TCF bleaching – Which sequence to choose? In Tappi Proceedings, Pulping Conference, **1993**.
- 5 Grundelius, R., Oxidation equivalents, OXE – an alternative to active chlorine. *Tappi Journal*, **1993**; 76(1): 133–135.
- 6 Ragnar, M., M. Leite, Bleaching of cellulose pulp in a first chlorine dioxide bleaching step. Kvaerner pulping: PCT, **2004**, WO 2004/079087M.
- 7 Ragnar, M., Evaluation of bleachability – A recommendation against the OXE concept. *Nordic Pulp and Paper Research Journal*, **2004**; 19(3): 286–290.

### Section 7.2

- 1 Gullichsen, J., E. Härkönen, Medium consistency technology part 1, fundamental data. *Tappi J.*, **1981**; 64(6): 69–72.
- 2 Meyer, R., D. Wahren, On the elastic properties of three-dimensional fiber networks. *Svensk. Papperstidn.*, **1964**; 67(10): 432–436.
- 3 Bennington, C.P.J., R.J. Kerekes, J.R. Grace, The yield stress of fiber suspensions. *Can. J. Chem. Eng.*, **1990**; 68: 748–757.
- 4 Wikström, T., Y. Rönmark, A. Rasmuson, A new correlation for the onset of fluidisation in pulp suspensions. *Nordic Pulp Paper Res. J.*, **2002**; 17(4): 374–381.
- 5 Bennington, C.P.J., R.J. Kerekes, Power requirements for pulp suspension fluidization. *Tappi J.*, **1996**; 79(2): 253–258.
- 6 Wahren, D., Fiber structures in paper-making operations. IPC Symposium Paper Science and Technology – The Cutting Edge. Appleton: IPC, **1980**.
- 7 Pettersson, J., *An experimental investigation of the flow behaviour of fiber/liquid/gas suspensions at MC-concentrations*. Chalmers University of Technology: Göteborg, Sweden, **2002**.

- 8 Bokström, M., M. Wennerström, Ozone comes of age. *Pulp Paper Europe*, **2001**; 6(5).
- 9 Duflo Pump (product presentation). Kvaerner Pulping: Karlstad, Sweden, **2003**.
- 10 Sulzer Pumpen und Rührwerke für die Zellstoff- und Papierindustrie. Sulzer Pumps: Karhula, Finland, **2001**.
- 11 Jansson, U., Two generations of MC pumps and a third to improve the first two. *Fiberlines*, **2003**(1): 22–25.
- 12 Dual Mixers (product leaflet). Kvaerner Pulping: Karlstad, Sweden, **2000**.
- 13 S-Mixer (product leaflet). Metso Paper: Sundsvall, Sweden, **2003**.
- 14 Jetmixer (product leaflet). Kvaerner Pulping: Karlstad, Sweden, **1999**.
- 15 FlowHeater (product leaflet). Metso Paper: Sundsvall, Sweden, **2002**.
- 16 Dynamic Steam Heater (product leaflet). Andritz: Graz, Austria, **2003**.
- 17 Tower Equipment for Pulp Distribution and Discharge (product leaflet). Metso Paper: Sundsvall, Sweden, **2003**.
- 18 PREPOX Reactor (product leaflet). Kvaerner Pulping: Karlstad, Sweden, **1997**.
- 19 Sulzer, Salomix SLG Agitator (product leaflet). Sulzer Pumps: Karhula, Finland, **2001**.
- Trudy Leningrad. *Lesotekh. Akad.im. S.M. Kirova*, **1960**; 91(2): 217–225.
- 5 Nikitin, V.M., G.L. Akim, Bleaching and refining of pulp with oxygen and alkali. *Bumazh. Prom.*, **1960**; 35(12): 5–7.
- 6 Nikitin, V.M., G.L. Akim, V.P. Shchegolev, Delignification and refining of unbleached sulfite pulp by the oxygen-alkali method. III. Application of the molecular oxygen for bleaching of birch pulp. *Trudy Leningrad. Lesotekh. Akad.im. S.M. Kirova*, **1960**; 85: 3–11.
- 7 Harris, G., US Patent 2,673,148, **1954**.
- 8 Marshall, H., US Patent 2,686,120, **1954**.
- 9 Grangaard, D., G. Saunders. CAN 611,503, **1960**.
- 10 Kratzl, K., et al., Model studies on reactions occurring in oxidations of lignin with molecular oxygen in alkaline media. *Wood Sci. Technol.*, **1974**; 8(1): 35–49.
- 11 Robert, A., et al., An oxygen treatment of pulps to further subsequent bleaching. II. Bleaching pulps previously treated with oxygen. *Assoc. Techn. Ind. Papiere, Bull.*, **1964**; 18(4): 166–176.
- 12 Robert, A., et al., An oxygen treatment of pulps to further subsequent bleaching. I. Improvements obtained by using a catalyst; optimum conditions in the oxygen treatment. *Assoc. Techn. Ind. Papiere, Bull.*, **1964**; 18(4): 151–165.
- 13 Robert, A., P. Traynard, O. Martin-Borret. US Patent 3,384,533, **1968**.
- 14 Magnotta, V., et al., High-kappa pulping and extended oxygen delignification to increase yield. In *Breaking the Pulp Yield Barrier*, Symposium Proceedings. Atlanta, GA: TAPPI Press, **1998**.
- 15 Reid, D.W., J. Ayton, T. Mullen, CPPA oxygen delignification survey. *Pulp Paper Can.*, **1998**; 99(11): 43–47.
- 16 Nasman, L., G. Annergren, Medium-consistency oxygen bleaching. *Tappi*, **1980**; 63(4): 105–109.
- 17 Albert, R. In *Proceedings, International Non-Chlorine Bleaching Conference*. Orlando, Florida, **1996**.
- 18 Carter, D.N., et al., Performance parameters of oxygen delignification. *Tappi J.*, **1997**; 80(10): 111–117.

### Section 7.3.1

- 1 Hartler, N., H. Norrström, S. Rydin, Oxygen-alkali bleaching of sulphate pulp. *Svensk. Papperstidn.*, **1970**; 73(21): 696–703.
- 2 Nikitin, V.M., G.L. Akim, Delignification and chemical refining of unbleached pulp with oxygen-alkali. *Trudy Leningrad. Lesotekh. Akad.im. S.M. Kirova*, **1956**; 75: 145–155.
- 3 Nikitin, V.M., A.V. Obolenskaya, Oxidation of lignin with oxygen in alkaline medium. *Trudy Leningrad. Lesotekh. Akad.im. S.M. Kirova*, **1958**; 80: 65–75.
- 4 Nikitin, V.M., A.V. Obolenskaya, G.L. Akim, The oxidation of lignin by oxygen in alkaline medium and the practical application of this reaction.

- 19 Axegard, P., B. Backlund, Ecocyclic Pulp Mill – “KAM”. Final report, 1996–2002. STFI, Swedish Pulp and Paper Research Institute: Stockholm, Sweden, 2003.
- 20 Croon, I. In Proceedings of the 1981 TAPPI Oxidative Bleaching Seminar. Denver, CO, 1981.
- 21 Ragnar, M., The technology of oxygen delignification and bleaching of chemical pulp. Karlstadt, Sweden: Kvaerner Pulping AB, 2002.
- 22 Bergnor, E., P. Sandström, Modified cooking and oxygen bleaching for improved production economy and reduced effluent load. *Nordic Pulp Paper J.*, 1988; 3(3): 145–155.
- 23 Parsad, B., et al., Mill closure with high-kappa pulping and extended oxygen delignification. *Tappi*, 1996; 79(9): 144–152.
- 24 Kleppe, P.J., S. Storebraten, Delignifying high-yield pulps with oxygen and alkali. *Tappi*, 1985; 68(7): 68–73.
- ing. *Wood Sci. Technol.*, 1986; 20(1): 1–33.
- 8 Gierer, J., F. Imsgård, Reactions of lignins with oxygen and hydrogen peroxide in alkaline media. *Svensk. Papperstidn. – Nordisk Cellulosa*, 1977; 80(16): 510–518.
- 9 Gierer, J., The interplay between oxygen-derived radical species in the delignification during oxygen and hydrogen peroxide bleaching. In *Lignin: Historical, Biological, and Materials Perspectives*. 2000: 422–446.
- 10 Axelsson, P., M. Ek, A. Teder, The influence of alkali charge and temperature in the kraft cook on the QPQP bleachability and the kappa number composition of birch pulp. *Nordic Pulp Paper Res. J.*, 2002; 17(3): 206–212.
- 11 Backström, M., M. Häggglund, L. Olm, Effect of cooking temperature during extended delignification – Selectivity, strength properties and TCF-bleachability. *Pap. Puu*, 1996; 78(6–7): 392–397.
- 12 Ban, W.P., J. Singh, L.A. Lucia, Kraft green liquor pretreatment of softwood chips. Part III: Lignin chemical modifications. *Holzforschung*, 2003; 57(3): 275–281.
- 13 Carvalho, M.G.V., A.A. Martins, M.M.L. Figueiredo, Kraft pulping of Portuguese *Eucalyptus globulus*: Effect of process conditions on yield and pulp properties. *Appita J.*, 2003; 56(4): 267–274.
- 14 Colodette, J.L., J.L. Gomide, R. Girard, A.S. Jaaskelainen, D.S. Argyropoulos, Influence of pulping conditions on eucalyptus kraft pulp yield, quality, and bleachability. *Tappi J.*, 2002; 1(1): 14–20.
- 15 Daniel, A.I.D., C.P. Neto, D.V. Evtuguin, A.J.D. Silvestre, Hexenuronic acid contents of *Eucalyptus globulus* kraft pulps: Variation with pulping conditions and effect on ECF bleachability. *Tappi J.*, 2003; 2(5): 3–8.
- 16 Dos Santos, C.A., L.D. Shackford, W.J. Miller, Development of ECF sequence using stages in high temperatures for chlorine dioxide (DHT) and hydrogen peroxide (PHT). *O Papel (Brazül)*, 2002; 78–89.
- 17 Neto, C.P., D.V. Evtuguin, F.P. Furtado, A.P.M. Sousa, Effect of pulping conditions on the ECF bleachability of *Euca-*

### Section 7.3.2

- 1 Gierer, J., Chemistry of Delignification. 1. General Concept and Reactions During Pulping. *Wood Sci. Technol.*, 1985; 19(4): 289–312.
- 2 Gierer, J., The chemistry of delignification. A general concept. Part I. *Holz-forschung*, 1982; 36(1): 43–51.
- 3 Gierer, J., Formation and involvement of superoxide ( $O_2^{\bullet-}/HO_2^{\bullet}$ ) and hydroxyl ( $OH^{\bullet}$ ) radicals in TCF bleaching processes: A review. *Holzforschung*, 1997; 51(1): 34–46.
- 4 Gratzl, J.S., The chemical principles of pulp bleaching with oxygen, hydrogen peroxide and ozone – a short review. *Papier*, 1992; 46(10A): V1–V8.
- 5 Gierer, J., Reactions of lignin during pulping – a description and comparison of conventional pulping processes. *Svensk. Papperstidn. – Nordisk Cellulosa*, 1970; 73(18): 571–596.
- 6 Gierer, J., The Chemistry of Delignification. A General Concept Part II. *Holz-forschung*, 1982; 36(1): 55–64.
- 7 Gierer, J., Chemistry of Delignification. 2. Reactions of Lignins During Bleach-

- lyptus globulus* kraft pulps. *Ind. Eng. Chem. Res.*, **2002**; 41(24): 6200–6206.
- 18 Nilsson, D., U. Edlund, K. ElgChristofferson, M. Sjöström, R. Agnemo, The effect of designed wood storage on the brightness of bleached and unbleached thermo-mechanical pulp. *Nordic Pulp Paper Res. J.*, **2003**; 18(4): 369–376.
- 19 Olm, L., D. Tormund, Kraft pulping with sulfide pretreatment Part 2. The influence of pretreatment and cooking conditions on the pulp properties, bleachability in a TCF-sequence and strength properties. *Nordic Pulp Paper Res. J.*, **2000**; 15(1): 70–79.
- 20 Ragnar, M., Alkaline extraction and a control strategy for the chlorine dioxide charge to the final stage in DED bleaching. *Nordic Pulp Paper Res. J.*, **2003**; 18(2): 162–167.
- 21 Sjö Dahl, R.G., M. Ek, M.E. Lindström, The effect of sodium ion concentration and dissolved wood components on the kraft pulping of softwood. *Nordic Pulp Paper Res. J.*, **2004**; 19(3): 325–329.
- 22 Van Tran, A., Effect of cooking temperature on kraft pulping of hardwood. *Tappi J.*, **2002**; 1(4): 13–19.
- 23 Yang, R.M., L. Lucia, A.J. Ragauskas, H. Jameel, Oxygen delignification chemistry and its impact on pulp fibers. *J. Wood Chem. Technol.*, **2003**; 23(1): 13–29.
- 24 Van Tran, A., Effect of pH on oxygen delignification of hardwood kraft pulp. *Pap. Puu*, **2001**; 83(5): 405–410.
- 25 Axelsson, P., M. Ek, A. Teder, Influence of alkali profiling in birch kraft pulping on QPQP bleachability. *Nordic Pulp Paper Res. J.*, **2004**; 19(1): 37–43.
- 26 Bikova, T., A. Treimanis, M. Eisimonte, V. Klevinska, Relationship between the alkali solubility of hemicelluloses and lignin from unbleached hardwood kraft pulp and pulp bleachability. *J. Pulp Paper Sci.*, **2003**; 29(6): 208–212.
- 27 Björklund, M., U. Germgård, J. Basta, The influence of softwood kraft cooking conditions on the brightness development in ECF bleaching. *Appita J.*, **2004**; 57(3): 234–239.
- 28 Brannvall, E., R. Gustafsson, A. Teder, Properties of hyperalkaline polysulphide pulps. *Nordic Pulp Paper Res. J.*, **2003**; 18(4): 436–440.
- 29 Gellerstedt, G., W.W. Al-Dajani, Bleachability of alkaline pulps. Part 1. The importance of  $\beta$ -aryl ether linkages in lignin. *Holzforschung*, **2000**; 54(6): 609–617.
- 30 Gellerstedt, G., W.W. Al-Dajani, Some factors affecting the brightness and TCF-bleachability of kraft pulp. *Nordic Pulp Paper Res. J.*, **2003**; 18(1): 56–62.
- 31 Klevinska, V., T. Bykova, A. Treimanis, Multistage kraft cooking as a way of producing bleachable grade alder pulp. *Celulose Chem. Technol.*, **2000**; 34(5–6): 581–593.
- 32 Rawat, N., T.I. McDonough, Effects of pulping conditions on the bleachability of hardwood kraft pulps: 1. Effects of effective alkali charge in the pulping of birch and maple. Pulping Conference, Proceedings of the Technical Association of the Pulp and Paper Industry, **1998**: 883–891.
- 33 Sixta, H., Comparative evaluation of different concepts of sulfite pulping technology. *Papier*, **1998**; 52(5): 239–249.
- 34 Sun, Y., D.S. Argyropoulos, R.M. Berry, M. Fenster, A. Yu, The effect of metal ions on the reaction of hydrogen peroxide with Kraft lignin model compounds. *Can. J. Chem.*, **1999**: 667–675.
- 35 Lucia, L.A., A.J. Ragauskas, F.S. Chakar, Comparative evaluation of oxygen delignification processes for low- and high-lignin-content softwood kraft pulps. *Ind. Eng. Chem. Res.*, **2002**; 41(21): 5171–5180.
- 36 Friman, L., L. Logenius, R. Agnemo, H.E. Hogberg, Comparison of metal profiles in thermomechanical pulping processes in which either hydrogen peroxide or dithionite bleaching is used – Content of metals in process waters and in chips and pulp samples before and after extraction with acid or a chelating agent. *Pap. Puu*, **2003**; 85(6): 334–339.
- 37 Baptista, C., N. Belgacem, A.P. Duarte, The effect of surfactants on kraft pulping of *Pinus pinaster*. *Appita J.*, **2004**; 57(1): 35–39.
- 38 Pisuttipiched, S., E. Retulainen, R. Malinen, H. Kolehmainen, M. Ruhanen, S. Siripattanadilok, Effect

- of harvesting age on the quality of *Eucalyptus camaldulensis* bleached kraft pulp. *Appita J.*, **2003**; 56(5): 385–390.
- 39 Svedman, M., P. Tikka, M. Luhtanen, Effects of softwood morphology and chip thickness on pulping with a displacement kraft batch process. *Tappi J.*, **1998**; 81(7): 157–168.
- 40 Persson, E., J. Bergquist, T. Elowson, J. Jakara, B. Lonnberg, Brightness, bleachability and colour reversion of groundwood made of wet- and dry-stored Norway spruce (*Picea abies*) pulpwood. *Pap. Puu*, **2002**; 84(6): 411–415.
- 41 Furtado, F.P., D.V. Evtuguin, T.M. Gomes, Effect of the acid stage in ECF bleaching on *Eucalyptus globulus* kraft pulp bleachability and strength. *Pulp Paper Can.*, **2001**; 102(12): 89–92.
- 42 Ju, Y., M. Kishino, H. Ohi, Preparation of high-yielded softwood chemical pulp and its bleachability. *Sen-I Gakkaishi*, **2000**; 56(4): 199–204.
- 43 Zhan, H., B. Yue, W. Hu, W. Huang, Kraft reed pulp TCF bleaching with enzyme pretreatment. *Cellulose Chem. Technol.*, **1999**; 33(1): 53–60.
- 44 Springer, E.L., J.D. McSweeney, Treatment of softwood kraft pulps with peroxymonosulfate before oxygen delignification. *Tappi J.*, **1993**: 194–199.
- 45 Lachenal, D., L. Bourson, M. Muguet, A. Chauvet, Lignin activation improves oxygen and peroxide delignification. *Cellulose Chem. Technol.*, **1990**; 24: 593–601.
- 46 Jiang, Z.H., B. Van Lierop, A. Nolin, R. Berry, A new insight into the bleachability of kraft pulps. *J. Pulp Paper Sci.*, **2003**. 29(2): 54–58.
- 47 Gellerstedt, G., K. Gustafsson, A. Labidi, F. Pla, Alkaline delignification of hardwoods in a flow-through reactor working at a low residence time. 4. Characterization of lignins by oxidative-degradation and aminolysis. *Holzforschung*, **1992**; 46(3): 199–204.
- 48 Gellerstedt, G., D. Robert, Structural-changes in lignin during kraft cooking. 7. Quantitative C-13 NMR analysis of kraft lignins. *Acta Chim. Scand. Series B. Org. Chem. Biochem.*, **1987**; 41(7): 541–546.
- 49 Gellerstedt, G., K. Gustafsson, Structural-changes in lignin during kraft cooking. 5. Analysis of dissolved lignin by oxidative-degradation. *J. Wood Chem. Technol.*, **1987**; 7(1): 65–80.
- 50 Gellerstedt, G., E. Lindfors, Structural-changes in lignin during kraft cooking. 4. Phenolic hydroxyl-groups in wood and kraft pulps. *Svensk. Papperstidn. – Nordisk Cellulosa*, **1984**; 87(15): R115–R118.
- 51 Robert, D.R., M. Bardet, G. Gellerstedt, E.L. Lindfors, Structural-changes in lignin during kraft cooking. 3. On the structure of dissolved lignins. *J. Wood Chem. Technol.*, **1984**; 4(3): 239–263.
- 52 Gellerstedt, G., E.L. Lindfors, C. Lapiere, B. Monties, Structural-changes in lignin during kraft cooking. 2. Characterization by acidolysis. *Svensk. Papperstidn. – Nordisk Cellulosa*, **1984**; 87(9): R61–R67.
- 53 Gellerstedt, G., J. Gierer, Reactions of lignin during neutral sulphite cooking. 1. Behaviour of beta-arylether structures. *Acta Chim. Scand.*, **1968**; 22(8): 2510.
- 54 Gierer, J., Reactions of lignin during sulfite and sulfate cooking. *Papier*, **1973**; 27(12): 629–633.
- 55 Gellerstedt, G., J. Gierer, Reaction of lignin during neutral sulphite cooking. 2. Behaviour of phenylcoumaran structures. *Acta Chim. Scand.*, **1968**; 22(6): 2029.
- 56 Gierer, J., L.A. Smedman, Reactions of lignin during sulphate cooking. 10. Synthesis and alkaline treatment of model compounds representing intermediary episulphide structures. *Acta Chim. Scand.*, **1966**; 20(7): 1769.
- 57 Gierer, J., N.H. Wallin, Reactions of lignin during sulphate cooking. 9. Interaction between thiol groups and intermediary epoxide structures. *Acta Chim. Scand.*, **1965**; 19(6): 1502.
- 58 Gierer, J., L.A. Smedman, Reactions of lignin during sulphate cooking. 8. Mechanism of splitting of beta-arylether bonds in phenolic units by white liquor. *Acta Chim. Scand.*, **1965**; 19(5): 1103.
- 59 Gierer, J., N.H. Wallin, B. Lenz, Reactions of lignin during sulphate cooking. V. Model experiments on splitting of aryl-alkyl ether linkages by 2 N sodium

- hydroxide + by white liquor. *Acta Chim. Scand.*, **1964**; 18(6): 1469.
- 60** Gellerstedt, G., E.L. Lindfors, Structural-changes in lignin during kraft pulping. *Holzforschung*, **1984**; 38(3): 151–158.
- 61** Gellerstedt, G., L. Zhang, Chemistry of TCF-bleaching with oxygen and hydrogen peroxide. In *Oxidative Delignification Chemistry*, D.S. Argyropoulos, Ed. American Chemical Society, Oxford University Press: Washington, DC, **2001**: 61–72.
- 62** Tamminen, T.L., B.R. Hortling, Lignin reactions during oxygen delignification of various alkaline pulps. In *Oxidative Delignification Chemistry*, D.S. Argyropoulos, Ed. American Chemical Society, Oxford University Press: Washington, DC, **2001**: 73–91.
- 63** Lawoko, M., R. Berggren, F. Berthold, G. Henriksson, G. Gellerstedt, Changes in the lignin-carbohydrate complex in softwood kraft pulp during kraft and oxygen delignification. *Holzforschung*, **2004**; 58(6): 603–610.
- 64** Olkkonen, C., H. Tylli, I. Forsskähl, A. Fuhrmann, T. Hausalo, T. Tamminen, B. Hortling, J. Janson, Degradation of model compounds for cellulose and ligno-cellulosic pulp during ozonation in aqueous solution. *Holzforschung*, **2000**; 54(4): 397–406.
- 65** Laine, C., T. Tamminen, B. Hortling, Carbohydrate structures in residual lignin-carbohydrate complexes of spruce and pine pulp. *Holzforschung*, **2004**; 58(6): 611–621.
- 66** Antonsson, S., M.E. Lindström, M. Ragnar, A comparative study of the impact of the cooking process on oxygen delignification. *Nordic Pulp Paper Res. J.*, **2003**; 18(4): 388–394.
- 67** Rööst, C., M. Lawoko, G. Gellerstedt, Structural changes in residual kraft pulp lignins. Effects of kappa number and degree of oxygen delignification. *Nordic Pulp Paper Res. J.*, **2003**; 18(4): 395–399.
- 68** Bourbonnais, R., M. Paice, Voltammetric measurement of lignin in pulp and paper samples – An electron transfer catalytic approach with mediators. *J. Electrochem. Soc.*, **2004**; 151(7): E246–E249.
- 69** Bourbonnais, R., L. Valeanu, M.G. Paice, Voltammetric analysis of the bleachability of softwood kraft pulps. *Holz-forschung*, **2004**; 58(6): 581–587.
- 70** Lundquist, K., On the degradation of lignin during pulping conditions. In *First International Symposium on Delignification with Oxygen Ozone and Peroxides*. Raleigh, North Carolina, USA: North Carolina State University, **1975**.
- 71** Miksche, G.E., Lignin reactions in alkaline pulping processes (Rate process in soda pulping). In *First International Symposium on Delignification with Oxygen Ozone and Peroxides*. Raleigh, North Carolina, USA: North Carolina State University, **1975**.
- 72** Argyropoulos, D.S., Y. Sun, E. Palus, Isolation of residual kraft lignin in high yield and purity. *J. Pulp Paper Sci.*, **2002**; 28(2): 50–54.
- 73** Al-Dajani, W.W., G. Gellerstedt, On the isolation and structure of softwood residual lignins. *Nordic Pulp Paper Res. J.*, **2002**; 17(2): 193–198.
- 74** Jääskeläinen, A.S., Y. Sun, D.S. Argyropoulos, T. Tamminen, B. Hortling, The effect of isolation method on the chemical structure of residual lignin. *Wood Sci. Technol.*, **2003**; 37(2): 91–102.
- 75** Lachenal, D., G. Mortha, R.M. Sevillano, M. Zaroubine, Isolation of residual lignin from softwood kraft pulp. Advantages of the acetic acid acidolysis method. *C. R. Biol.*, **2004**; 327(9–10): 911–916.
- 76** Capanema, E.A., M.Y. Balakshin, C.L. Chen, An improved procedure for isolation of residual lignins from hardwood kraft pulps. *Holzforschung*, **2004**; 58(5): 464–472.
- 77** Halttunen, M., J. Vyorykka, B. Hortling, T. Tamminen, D. Batchelder, A. Zimmermann, T. Vuorinen, Study of residual lignin in pulp by UV resonance Raman spectroscopy. *Holzforschung*, **2001**; 55(6): 631–638.
- 78** Tamminen, T.L., B.R. Hortling, Isolation and characterization of residual lignin. In *Advances in Lignocellulosics Char-*



- acterization, D.S. Argyropoulos, Ed. Tappi Press: Atlanta, GA, 1999: 1–42.
- 79 Balakshin, M.Y., E.A. Capanema, C.-L. Chen, H.S. Gracz, Elucidation of the structures of residual and dissolved pine kraft lignins using an HMQC NMR technique. *J. Agric. Food Chem.*, 2003; 51(21): 6116–6127.
- 80 Fu, S.Y., L.A. Lucia, Investigation of the chemical basis for inefficient lignin removal in softwood kraft pulp during oxygen delignification. *Ind. Eng. Chem. Res.*, 2003; 42(19): 4269–4276.
- 81 Froass, P.M., A.J. Ragauskas, J. Jiang, Nuclear magnetic resonance studies. 4. Analysis of residual lignin after kraft pulping. *Ind. Eng. Chem. Res.*, 1998; 37(8): 3388–3394.
- 82 Lachenal, D., J.C. Fernandes, P. Froment, Behavior of residual lignin in kraft pulp during bleaching. *J. Pulp Paper Sci.*, 1995; 21(5): J173–J177.
- 83 Argyropoulos, D.S., Y. Liu, The role and fate of lignin's condensed structures during oxygen delignification. *J. Pulp Paper Sci.*, 2000; 26(3): 107–113.
- 84 Froass, P.M., A.J. Ragauskas, J. Jiang, Chemical structure of residual lignin from kraft pulp. *J. Wood Chem. Technol.*, 1996; 16(4): 347–365.
- 85 Froass, P.M., A.J. Ragauskas, J.E. Jiang, NMR studies Part 3: Analysis of lignins from modern kraft pulping technologies. *Holzforchung*, 1998; 52(4): 385–390.
- 86 Capanema, E.A., M.Y. Balakshin, J.F. Kadla, A comprehensive approach for quantitative lignin characterization by NMR spectroscopy. *J. Agric. Food Chem.*, 2004; 52: 1850–1860.
- 87 Zhang, L., G. Henriksson, G. Gellerstedt, The formation of  $\beta$ - $\beta$  structures in lignin biosynthesis – Are there two different pathways? *Org. Biomol. Chem.*, 2003; 3621–3624.
- 88 Kishimoto, T., A. Ueki, Y. Sano, Delignification mechanism during high-boiling solvent pulping. Part 3. Structural changes in lignin analyzed by  $^{13}\text{C}$ -NMR spectroscopy. *Holzforchung*, 2003; 57: 602–610.
- 89 Kishimoto, T., A. Ueki, H. Takamori, Y. Uraki, M. Ubukata, Delignification mechanism during high-boiling solvent pulping. Part 6. Changes in lignin structure analyzed by  $^1\text{H}$ - $^{13}\text{C}$  correlation 2-D NMR spectroscopy. *Holzforchung*, 2004; 58: 355–362.
- 90 Northey, R.A., A review of lignin model compound reactions under oxygen bleaching conditions. In *Oxidative Delignification Chemistry*, D.S. Argyropoulos, Ed. American Chemical Society, Oxford University Press: Washington, DC, 2001; 44–60.
- 91 Zou, H., J.M. Genco, A. Van Heiningen, B. Cole, R. Fort, Effect of hemicellulose content in kraft brownstock on oxygen delignification. *TAPPI Fall technical Conference and Trade Fair*, 2002: 193–209.
- 92 Saake, B., R. Lehnen, E. Schmekal, A. Neubauer, H.H. Nimz, Bleaching of formacell pulp from aspen wood with ozone and peracetic acid in organic solvents. *Holzforchung*, 1998; 52(6): 643–650.
- 93 Ruiz, J., J. Freer, J. Rodriguez, J. Baeza, Ozone organosolv bleaching of radiata pine kraft pulp. *Wood Sci. Technol.*, 1997; 31(3): 217–223.
- 94 Fu, S.Y., X.S. Chai, Q.X. Hou, L.A. Lucia, Chemical basis for a selectivity threshold to the oxygen delignification of kraft softwood fiber as supported by the use of chemical selectivity agents. *Ind. Eng. Chem. Res.*, 2004; 43(10): 2291–2295.
- 95 Francis, R.C., Y.Z. Lai, C.W. Dence, T.C. Alexander, Estimating the concentration of phenolic hydroxyl-groups in wood pulps. *Tappi J.*, 1991; 74(9): 219–224.
- 96 Gellerstedt, G., K. Gustafsson, R.A. Northey, *Nordic Pulp Paper Res. J.*, 1988; 3(2): 87–94.
- 97 Gellerstedt, G., Chemical structure of pulp components. In *Pulp Bleaching: Principles and Practice*, C.W. Dence, D.W. Reeve, Eds. Tappi Press: Atlanta, GA, 1996: 91–111.
- 98 Asgari, F., D.S. Argyropoulos, Fundamentals of oxygen delignification. Part II. Functional group formation elimination in residual kraft lignin. *Can. J. Chem.-Rev. Canadienne De Chimie*, 1998; 76(11): 1606–1615.
- 99 Yokoyama, T., Y. Matsumoto, G. Meshitsuka, Reaction selectivity of

- active oxygen species in oxygen-alkali bleaching. *J. Wood Chem. Technol.*, **1999**; 19(3): 187–202.
- 100 Johansson, E., S. Ljunggren, The kinetics of lignin reactions during oxygen bleaching. 4. The reactivities of different lignin model compounds and the influence of metal-ions on the rate of degradation. *J. Wood Chem. Technol.*, **1994**; 14(4): 507–525.
- 101 Kratzl, K., P. Claus, W. Lonsky, J.S. Gratzl, Model studies on reactions occurring in oxidations of lignin with molecular-oxygen in alkaline media. *Wood Sci. Technol.*, **1974**; 8(1): 35–49.
- 102 Sultanov, V.S., A.F.A. Wallis, Reactivities of guaiacyl and syringyl lignin model phenols towards oxidation with oxygen-alkali. *J. Wood Chem. Technol.*, **1991**; 11(3): 291–305.
- 103 Evtuguin, D.V., D. Robert, The detection of muconic acid type structures in oxidized lignins by C-13 NMR spectroscopy. *Wood Sci. Technol.*, **1997**; 31(6): 423–431.
- 104 Moe, S.T., A.J. Ragauskas, Oxygen delignification of high-yield kraft pulp part I: Structural properties of residual lignins. *Holzforschung*, **1999**; 53(4): 416–422.
- 105 Duarte, A.P., D. Robert, D. Lachenal, Eucalyptus globulus kraft pulp residual lignin Part 2. Modification of residual lignin structure in oxygen bleaching. *Holzforschung*, **2001**; 55(6): 645–651.
- 106 Lai, Y.Z., H. Xu, R. Yang. In *Lignin: Historical, Biological, and Materials Perspectives*, W.G. Glasser, R.A. Northey and T.P. Schultz, Eds. American Chemical Society, Oxford University Press: Washington D.C., **2000**.
- 107 Ede, R.M., G. Brunow, L.K. Simola, J. Lemmetyinen, 2-Dimensional H-1-H-1 chemical-shift correlation and J-resolved NMR studies on isolated and synthetic lignins. *Holzforschung*, **1990**; 44(2): 95–101.
- 108 Lundquist, K., *Nordic Pulp Paper Res. J.*, **1992**; 7(1): 4–8, 16.
- 109 Ede, R.M., R. Smit, I.D. Suckling. Oral Presentation. In 9th International Symposium of Wood and Pulping Chemistry. Montreal, **1997**.
- 110 Adler, E., Lignin chemistry – past, present and future. *Wood Sci. Technol.*, **1977**; 11(3): 169–218.
- 111 Zhang, L., G. Gellerstedt. Detection and determination of carbonyls and quinones by modern NMR techniques. In 10th International Symposium of Wood and Pulping Chemistry. Yokohama, **1999**.
- 112 Drumond, M., M. Aoyama, C.L. Chen, D. Robert, Substituent effects on C-13 chemical-shifts of aromatic carbons in biphenyl type lignin model compounds. *J. Wood Chem. Technol.*, **1989**; 9(4): 421–441.
- 113 Ahvazi, B.C., G. Pageau, D.S. Argyropoulos, On the formation of diphenylmethane structures in lignin under kraft, EMCC (R), and soda pulping conditions. *Can. J. Chem. – Rev. Canadienne De Chimie*, **1998**; 76(5): 506–512.
- 114 Chang, H.-M., H.T. Chen, J.S. Gratzl, S. Hosoya, T. Yamasaki. In SPCI International Symposium of Wood and Pulping Chemistry. Stockholm, **1981**.
- 115 Chiang, V.L., M. Funaoka, The dissolution and condensation-reactions of guaiacyl and syringyl units in residual lignin during kraft delignification of sweetgum. *Holzforschung*, **1990**; 44(2): 147–156.
- 116 Hartler, N., H. Norrström, Light-absorbing properties of pulp and pulp components. 3. Kraft pulp. *Tappi*, **1969**; 52(9): 1712–1715.
- 117 Gellerstedt, G., J. Pranda, E.L. Lindfors, Structural and molecular-properties of residual birch kraft lignins. *J. Wood Chem. Technol.*, **1994**; 14(4): 467–482.
- 118 Johansson, E., S. Ljunggren, *Nordic Pulp Paper Res. J.*, **1990**; 5(3): 148–154.
- 119 Ljunggren, S., E. Johansson, The kinetics of lignin reactions during oxygen bleaching. 3. The reactivity of 4-N-propylguaiacol and 4,4'-di-N-propyl-6,6'-biguaiacol. *Holzforschung*, **1990**; 44(4): 291–296.
- 120 Omori, S., C.W. Dence, The reactions of alkaline hydrogen-peroxide with lignin model dimers. 1. Phenacyl alpha-aryl ethers. *Wood Sci. Technol.*, **1981**; 15(1): 67–79.

- 121 Dence, C.W., A.J. Nonni. Technical Papers. In International Symposium of Wood and Pulping Chemistry. Vancouver, 1985.
- 122 Aoyagi, T., S. Hosoya, J. Nakano, A new reaction site in lignin during O<sub>2</sub>-alkali treatment. *J. Japan Wood Res. Soc. (Mokuzai Gakkaishi)*, 1979; 25(12): 783–788.
- 123 Oki, T., H. Ishikawa, K. Okubo, Oxidative Degradation of Dihydrodehydrodii-soeugenol and its methyl derivative by peroxide and oxygen alkali methods. *J. Japan Wood Res. Soc. (Mokuzai Gakkaishi)*, 1980; 26(7): 463–470.
- 124 Oki, T., H. Ishikawa, K. Okubo, On the Influence of pH on molecular oxygen and alkali degradation of guaiacylglycerol-β-guaiacyl ether derivatives. *J. Japan Wood Res. Soc. (Mokuzai Gakkaishi)*, 1976; 22(9): 518–525.
- 125 Halliwell, B., J.M.C. Gutteridge, *Free Radicals in Biology and Medicine*. Third edition. Oxford: Oxford University Press, 2000: 936.
- 126 Broden, A., R. Simonson, Solubility of oxygen. 2. Solubility of oxygen in sodium hydrogen carbonate and sodium-hydroxide solutions at temperatures less-than-or-equal-to-150-degrees-C and pressures less-than-or-equal-to-5 Mpa. *Svensk. Papperstidn. – Nordisk Cellulosa*, 1979; 82(16): 487–491.
- 127 Elstner, E.F., *Der Sauerstoff*. Mannheim: BI Wissenschaftsverlag, 1990: 529.
- 128 Barton, D.H.R., D.T. Sawyer. Introduction: The dilemmas of O<sub>2</sub> and HOOH activation. In *The Activation of Dioxygen and Homogeneous Catalytic Oxidation*. Texas A&M University, College Station: Plenum Press, 1993.
- 129 Gierer, J., The interplay between oxygen-derived radical species in the delignification during oxygen and hydrogen peroxide bleaching. *ACS Symposium Series*, 1999: 422–446.
- 130 Gierer, J., T. Reitberger, E.Q. Yang, B.H. Yoon, Formation and involvement of radicals in oxygen delignification studied by the autoxidation of lignin and carbohydrate model compounds. *J. Wood Chem. Technol.*, 2001; 21(4): 313–341.
- 131 Merenyi, G., J. Lind, M. Jonsson, Autoxidation of closed-shell organics – an outer-sphere electron-transfer. *J. Am. Chem. Soc.*, 1993; 115(11): 4945–4946.
- 132 Landucci, L.L., Electrochemical behavior of catalysts for phenoxy radical generation. *Tappi*, 1979; 62(4): 71–74.
- 133 Bielski, B.H.J., A.O. Allen, Mechanism of disproportionation of superoxide radicals. *J. Phys. Chem.*, 1977; 81(11): 1048–1050.
- 134 Luo, Q.H., S.R. Zhu, M.C. Shen, J. Wang, A pulse-radiolysis study of catalytic dismutation of superoxide anion by copper(II) complex of biscyclam dioxotetraamine. *Radiat. Physics Chem.*, 1995; 45(2): 247–250.
- 135 Belloni, J., A. Lecheheb, Heterogeneous catalysis of superoxide anion dismutation. *Radiat. Physics Chem.*, 1987; 29(2): 89–92.
- 136 Bielski, B.H.J., D.E. Cabelli, R.L. Arudi, A.B. Ross, Reactivity of HO<sub>2</sub>/O<sub>2</sub>-radicals in aqueous solution. *J. Phys. Chem. Ref. Data*, 1985; 14(4): 1041–1100.
- 137 Starnes Jr., W.H., Mechanisms of autoxidation in neutral or alkaline media. In First International Symposium on Delignification with Oxygen Ozone and Peroxides. Raleigh, North Carolina, USA: North Carolina State University, 1975.
- 138 Gierer, J., F. Imsgard, The reactions of lignin with oxygen and hydrogen peroxide in alkaline media. In First International Symposium on Delignification with Oxygen Ozone and Peroxides. Raleigh, North Carolina, USA: North Carolina State University, 1975.
- 139 Legrini, O., E. Oliveros, A.M. Braun, Photochemical processes for water-treatment. *Chem. Rev.*, 1993; 93(2): 671–698.
- 140 Machado, A.E.d.H., R. Ruggiero, M.G. Neumann, The photodegradation of lignins in the presence of hydrogen peroxide. *J. Photochem. Photobiol. A: Chemistry*, 1994; 81(2): 107–115.
- 141 Ruggiero, R., A.E.H. Machado, A. Castellan, S. Grelier, Photoreactivity of lignin model compounds in the photobleaching of chemical pulps. 1. Irradiation of 1-(3,4-dimethoxyphenyl)-2-(3'-methoxyphenoxy)-1,3-dihydroxypropane in the presence of singlet

- oxygen sensitizer or hydrogen peroxide in basic methanol solution. *J. Photochem. Photobiol. A: Chemistry*, **1997**; 110(1): 91–97.
- 142 Qiu, Y., Z. Zheng, Y. Zhou, R. Deng, Z. Dou, Study on singlet oxygen-reinforced oxygen bleaching of soda-AQ wheat straw pulp. *Zhongguo Zaozhi Xuebao/Trans. China Pulp Paper*, **1997**: 40–46.
- 143 Duarte, A.P., D. Lachenal, Hydrogen peroxide production during oxygen bleaching of *Eucalyptus globulus* kraft pulp – origin of cellulose degradation. *Pap. Puu*, **2002**; 84(4): 275–277.
- 144 Buda, F., B. Ensing, M.C.M. Gribnau, E.J. Baerends, DFT study of the active intermediate in the Fenton reaction. *Chemistry – A European Journal*, **2001**; 7(13): 2775–2783.
- 145 Reitberger, T., J. Gierer, E. Yang, B.-H. Yoon, Involvement of oxygen-derived free radicals in chemical and biochemical degradation of lignin. In *Oxidative Delignification Chemistry*, D.S. Argyropoulos, Ed. American Chemical Society, Oxford University Press: Washington, DC, **2001**: 255–271.
- 146 Chang, H.-M., J.S. Gratzl, Ring cleavage reactions of lignin models with oxygen and alkali. In *First International Symposium on Delignification with Oxygen Ozone and Peroxides*. Raleigh, North Carolina, USA: North Caroline State University, **1975**.
- 147 Aoyagi, T., S. Hosoya, J. Nakano, A new reaction site in lignin during O<sub>2</sub>-alkali treatment. In *First International Symposium on Delignification with Oxygen Ozone and Peroxides*. Raleigh, North Carolina, USA: North Caroline State University, **1975**.
- 148 Nilvebrant, N.O., J. Gierer, Oxygen and hydrogen-peroxide as bleaching reagents, their selectivity and cooperation in lignin degradation. *Abstracts, Papers Am. Chem. Soc.*, **1987**; 193: 15.
- 149 Ek, M., J. Gierer, K. Jansbo, Study on the selectivity of bleaching with oxygen-containing species. *Holzforschung*, **1989**; 43(6): 391–396.
- 150 Belgacem, M.N., D.V. Evtuguin, I. Deineko, Influence of the base nature on the lignin reactivity and oxidation selectivity during oxygen delignification of *Picea excelsa*. *Cellulose Chem. Technol.*, **2002**; 36(3–4): 327–338.
- 151 Chen, S.L., L.A. Lucia, Fundamental insight into the mechanism of oxygen delignification of kraft pulps. II. Application of surfactants. *Cellulose Chem. Technol.*, **2002**; 36(5–6): 495–505.
- 152 Chen, S.L., L.A. Lucia, Fundamental insight into the mechanism of oxygen delignification of kraft pulps: The influence of a novel carbohydrate protective system. *Cellulose Chem. Technol.*, **2002**; 36(3–4): 339–351.
- 153 Van Heiningen, A., S. Violette, Selectivity improvement during oxygen delignification by adsorption of a sugar-based-polymer. *J. Pulp Paper Sci.*, **2003**; 29(2): 48–53.
- 154 Gibson, A., M. Wajer, The use of magnesium hydroxide as an alkali and cellulose protector in chemical pulp bleaching. *Pulp Paper Can.*, **2003**; 104(11): 28–32.
- 155 Gevert, B.S., S.F. Lohmander, Influence of sulfur compounds, manganese, and magnesium on oxygen bleaching of kraft pulp. *Tappi J.*, **1997**: 263–268.
- 156 Lucia, L.A., R.S. Smereck, Effect of lignin content and magnesium-to-manganese ratio on the selectivity of oxygen delignification in softwood kraft pulp. *Pure Appl. Chem.*, **2001**; 73(12): 2059–2065.
- 157 Argyropoulos, D.S., *Oxidative delignification chemistry. Fundamentals and catalysis*. ACS Symposium Series 785. Washington, DC: American Chemical Society, **2001**: 533.
- 158 Beyer, M., C. Baurich, K. Fischer, Mechanisms of light and heat-induced discoloration of pulps. *Papier*, **1995**; 49(10A): V8–V14.
- 159 Crestini, C., M. Dauria, Photodegradation of lignin: The role of singlet oxygen. *J. Photochem. Photobiol. A Chemistry*, **1996**; 101(1): 69–73.
- 160 Machado, A.E.D., R. Ruggiero, M.G.H. Terrones, A. Nourmamode, S. Grelier, A. Castellan, Photodelignification of *Eucalyptus grandis* organosolv chemical pulp. *J. Photochem. Photobiol. A Chemistry*, **1996**; 94(2–3): 253–262.

- 161 Wang, J., G. Heitner, R.J. Manley, The photodegradation of milled-wood lignin. 2. The effect of inhibitors. *J. Pulp Paper Sci.*, **1996**; 22(2): J58–J63.
- 162 Crestini, C., M. Dauria, Singlet oxygen in the photodegradation of lignin models. *Tetrahedron*, **1997**; 53(23): 7877–7888.
- 163 Machado, A.E.H., A.J. Gomes, C.M.F. Campos, M.G.H. Terrones, D.S. Perez, R. Ruggiero, A. Castellan, Photoreactivity of lignin model compounds in the photobleaching of chemical pulps. 2. Study of the degradation of 4-hydroxy-3-methoxy-benzaldehyde and two lignin fragments induced by singlet oxygen. *J. Photochem. Photobiol. A. Chemistry*, **1997**; 110(1): 99–106.
- 164 Barclay, L.R.C., J.K. Grandy, H.D. MacKinnon, H.C. Nichol, M.R. Vinqvist, Peroxidations initiated by lignin model compounds: investigating the role of singlet oxygen in photo-yellowing. *Can. J. Chem. – Rev. Canadienne De Chimie*, **1998**; 76(12): 1805–1816.
- 165 Bonini, C., M. D'Auria, G. Mauriello, D. Viggiano, F. Zimbardi, Singlet oxygen degradation of lignin in the pulp. *J. Photochem. Photobiol. A. Chemistry*, **1998**; 118(2): 107–110.
- 166 Bonini, C., M. D'Auria, L. D'Alessio, G. Mauriello, D. Tofani, D. Viggiano, F. Zimbardi, Singlet oxygen degradation of lignin. *J. Photochem. Photobiol. A. Chemistry*, **1998**; 113(2): 119–124.
- 167 Bentivenga, G., C. Bonini, M. D'Auria, A. De Bona, Singlet oxygen degradation of lignin: a GC-MS study on the residual products of the singlet oxygen degradation of a steam exploded lignin from beech. *J. Photochem. Photobiol. A. Chemistry*, **1999**; 128(1–3): 139–143.
- 168 Bentivenga, G., C. Bonini, M. D'Auria, A. De Bona, G. Mauriello, Singlet oxygen mediated degradation of Klason lignin. *Chemosphere*, **1999**; 39(14): 2409–2417.
- 169 Castellan, A., D. Da Silva Perez, A. Nourmamode, S. Grelier, M.G.H. Terrones, A.E.H. Machado, R. Ruggiero, The improvement of the bleaching of peroxyformic sugar cane bagasse pulp by photocatalysis and photosensitization. *J. Brazil. Chem. Soc.*, **1999**: 197–202.
- 170 Bentivenga, G., C. Bonini, M. D'Auria, A. De Bona, G. Mauriello, Fine chemicals from singlet-oxygen-mediated degradation of lignin – a GC/MS study at different irradiation times on a steam-exploded lignin. *J. Photochem. Photobiol. A. Chemistry*, **2000**; 135(2–3): 203–206.
- 171 Lanzalunga, O., M. Bietti, Photo- and radiation chemical induced degradation of lignin model compounds. *J. Photochem. Photobiol. B. Biology*, **2000**; 56: 85–108.
- 172 Araujo, E., A.J. Rodriguez-Malaver, A.M. Gonzalez, O.J. Rojas, N. Penaloza, J. Bullon, M.A. Lara, N. Dmitrieva, Fenton's reagent-mediated degradation of residual Kraft black liquor. *Appl. Biochem. Biotechnol.*, **2002**; 97(2): 91–103.
- 173 Bonini, C., A. Carbone, M. D'Auria, Singlet oxygen mediated degradation of lignin – a kinetic study. *Photochem. Photobiol. Sci.*, **2002**; 1(6): 407–411.
- 174 Bonini, C., M. D'Auria, R. Ferri, Singlet oxygen mediated degradation of lignin – isolation of oxidation products from steam-exploded lignin from pine. *Photochem. Photobiol. Sci.*, **2002**; 1(8): 570–573.
- 175 Da Silva Perez, D., A. Castellan, A. Nourmamode, S. Grelier, R. Ruggiero, A.E.H. Machado, Photosensitized delignification of residual lignin and chemical pulp from *Eucalyptus grandis* wood. *Holzforschung*, **2002**; 56(6): 595–600.
- 176 D'Auria, M., C. Bonini, L. Emanuele, R. Ferri, Singlet oxygen-mediated degradation of lignin – Isolation of oxidation products from steam-exploded lignin from straw. *J. Photochem. Photobiol. A. Chemistry*, **2002**. 147(2): 153–156.
- 177 Perez, D.D., A. Castellan, A. Nourmamode, S. Grelier, R. Ruggiero, A.E.H. Machado, Photosensitized delignification of residual lignin and chemical pulp from *Eucalyptus grandis* wood. *Holzforschung*, **2002**; 56(6): 595–600.
- 178 D'Auria, M., R. Ferri, Frontier orbitals control in the reactivity of singlet oxygen with lignin model compounds – An ab initio study. *J. Photochem. Photobiol. A. Chemistry*, **2003**; 157(1): 1–4.

- 179 Hwang, K.-O., L.A. Lucia, Fundamental insights into the oxidation of lignocellulose obtained from singlet oxygen photochemistry. *J. Photochem. Photobiol. A. Chemistry*, **2004**; 168: 205–209.
- 180 Reale, S., A. Di Tullio, N. Spreti, F. De Angelis, Mass spectrometry in the biosynthetic and structural investigation of lignins. *Mass Spectrom. Rev.*, **2004**; 23(2): 87–126.
- 181 Chupka, E.I., V.V. Vershal, Role of singlet oxygen during lignin oxidation in alkali solutions. *Khimiya Prirodnykh Soedinenii*, **1986**(1): 121–122.
- 182 Lucia, L.A., M.M. Goodell, F.S. Chakar, A.J. Ragauskas, Breaking the oxygen delignification barrier: lignin reactivity and inactivity. In *Oxidative Delignification Chemistry*, D.S. Argyropoulos, Ed. American Chemical Society, Oxford University Press: Washington, DC, **2001**: 92–107.
- 183 Malinen, R., Behavior of wood polysaccharides during oxygen-alkali delignification. *Papper och Trä*, **1975**; 4a: 193–204.
- 184 Samuelson, O., L. Stolpe, Aldonic acid end groups in cellulose after oxygen bleaching. I. Model experiments with hydrocellulose. *Tappi*, **1969**; 52(9): 1709–1711.
- 185 Theander, O., Carbohydrate reactions in oxygen-alkali delignification processes. In *First International Symposium on Delignification with Oxygen Ozone and Peroxides*. Raleigh, North Carolina, USA: North Caroline State University, **1975**.
- 186 Lewin, M., Oxidation and aging of cellulose. *Macromol. Symp.*, **1997**; 118: 715–724.
- 187 Ericsson, B., B.O. Lindgren, O. Theander, Degradation of cellulose during oxygen bleaching. oxidation and alkaline treatment of D-glucosone. *Cellulose Chem. Technol.*, **1973**; 7: 581–591.
- 188 Samuelson, O., Degradation of cellulose in different bleaching processes. *Das Papier*, **1970**; 24(10A): 671.
- 189 Lindberg, B., O. Theander, Reactions between D-glucosone and alkali. *Acta Chim. Scand.*, **1968**; 22: 1782–1786.
- 190 Malinen, R., E. Sjöström, Studies on the reactions of carbohydrates during oxygen bleaching. Part I. Oxidative alkaline degradation of cellobiose. *Papper och Trä*, **1972**; 54: 451–468.
- 191 Samuelson, O., L. Thede, Identification of carboxyl groups in cellulose after aging as alkali cellulose. *Tappi*, **1969**; 52: 99–104.
- 192 Malinen, R., E. Sjöström, Studies on the reactions of carbohydrates during oxygen bleaching. Part III. Degradation of cello-oligosaccharides and hydrocellulose. *Papper och Trä*, **1973**; 55: 547–556.
- 193 Malinen, R., E. Sjöström, Studies on the reactions of carbohydrates during oxygen bleaching. Part IV. Degradation of manno-oligosaccharides and mannan. *Papper och Trä*, **1974**; 56: 895.
- 194 Malinen, R., E. Sjöström, Studies on the reactions of carbohydrates during oxygen bleaching. Part V. Degradation of xylose, xylo-oligosaccharides and birch xylan. *Papper och Trä*, **1975**; 57: 101–114.
- 195 Kolmodin, H., O. Samuelson, Oxygen-alkali treatment of hemicellulose. 2. Experiments with birch xylan. *Svensk Papperstidn.*, **1973**; 76(2): 71–77.
- 196 Jacobs, A., P.T. Larsson, O. Dahlman, Distribution of uronic acids in xylans from various species of soft- and hardwood as determined by MALDI mass spectrometry. *Biomacromolecules*, **2001**; 2: 979–990.
- 197 Aurell, R., N. Hartler, G. Persson, Alkali stability of 2-O-(4-O-methyl- $\alpha$ -D-xylopyranosyluronic acid)-D-xylopyranose. *Acta Chim. Scand.*, **1963**; 17(2): 545.
- 198 Aspinnall, G.O., R.J. Sturgeon, C.T. Greenwood, Degradation of xylans by alkali. *J. Chem. Soc.*, **1961**: 3667.
- 199 Malinen, R., E. Sjöström, J. Ylijoki, Studies on the reactions of carbohydrates during oxygen bleaching. Part II. Degradation of aldonic and glucosyl-aldonic acids. *Papper och Trä*, **1973**; 55: 5.
- 200 Ericsson, B., R. Malinen, Oxygen and hydrogen peroxide oxidation of methyl 4-O-methyl- $\beta$ -D-glucopyranoside in alkaline solution. *Cellulose Chem. Technol.*, **1974**; 8: 327–338.
- 201 Ericsson, B., B.O. Lindgren, O. Theander, Formation of methyl 2-carboxy-beta-D-pentofuranosides by oxidation of methyl beta-D-glucopyranoside

- with oxygen in alkaline, aqueous solution. *Carbohydrate Res.*, **1972**; **23**: 323–325.
- 202** Guay, D.F., B.J.W. Cole, J.R.C. Fort, J.M. Genco, M.C. Hausman, Mechanisms of oxidative degradation of carbohydrates during oxygen delignification. I. Reaction of methyl  $\beta$ -D-glucopyranoside with photochemically generated hydroxyl radicals. *J. Wood Chem. Technol.*, **2000**: 375–394.
- 203** Yokoyama, T., Y. Matsumoto, G. Meshitsuka, Enhancement of the reaction between pulp components and hydroxyl radical produced by the decomposition of hydrogen peroxide under alkaline conditions. *J. Wood Sci.*, **2002**; **48**(3): 191–196.
- 204** Guay, D.F., B.J.W. Cole, R.C. Fort, M.C. Hausman, J.M. Genco, T.J. Elder, K.R. Overly, Mechanisms of oxidative degradation of carbohydrates during oxygen delignification. II. Reaction of photochemically generated hydroxyl radicals with methyl beta-cellobioside. *J. Wood Chem. Technol.*, **2001**; **21**(1): 67–79.
- 205** Kolmodin, H., Treatment of ethyl 4-O-methyl- $\beta$ -D-glucopyranosides with oxygen-alkali. *Carbohydrate Res.*, **1974**; **34**(2): 227–232.
- 206** McCloskey, J.T., L.R. Schroeder, J.D. Sinkey, N.S. Thompson, Degradation of methyl beta-D-glucopyranoside by oxygen in alkaline-solutions. *Pap. Puu*, **1975**; **57**(3): 131.
- 207** Ericsson, B., J. Kolar, B.O. Lindgren, R. Malinen, O. Theander, Carbohydrate reactions in oxygen-alkali delignification – oxidation of methyl-beta-D-glucopyranoside, methyl-4-O-methyl-beta-D-glucopyranoside and methyl-beta-D-xylose. *Abstracts, Papers Am. Chem. Soc.*, **1974**: 41–41.
- 208** Samuelson, O., L. Stolpe, Degradation of carbohydrates during oxygen bleaching. 1. Cellobitol as a model substance. *Svensk. Papperstidn.*, **1969**; **20**: 662–666.
- 209** Sinkey, J.D., N.S. Thompson, Function of magnesium compounds in an oxygen-alkali-carbohydrate system. *Pap. Puu*, **1974**; **56**(5): 473.
- 210** De Souza, I.J., J. Bouchard, M. Methot, R. Berry, D.S. Argyropoulos, Carbohydrates in oxygen delignification. Part I: Changes in cellulose crystallinity. *J. Pulp Paper Sci.*, **2002**; **28**(5): 167–170.
- 211** Guay, D.F., B.J.W. Cole, R.C. Fort, M.C. Hausman, J.M. Genco, T.J. Elder, Mechanisms of oxidative degradation of carbohydrates during oxygen delignification. Part III: Reaction of photochemically generated hydroxyl radicals with 1,5-anhydrocellobitol and cellulose. *J. Pulp Paper Sci.*, **2002**; **28**(7): 217–221.
- 212** Sun, Y.P., A.F.A. Wallis, K.L. Nguyen, Reactivity of lignin and lignin models towards UV-assisted peroxide. *J. Wood Chem. Technol.*, **1997**; **17**(1–2): 163–178.
- 213** Buxton, G.V., C.L. Greenstock, W.P. Helman, A.B. Ross, Critical review of rate constants for reactions of hydrated electrons, hydrogen-atoms and hydroxyl radicals ( $\cdot\text{OH}/\cdot\text{O}^-$ ) in aqueous solution. *J. Phys. Chem. Ref. Data*, **1988**; **17**(2): 513–886.
- 214** Malinen, R., E. Sjöström, Oxygen-alkali oxidation of methyl glycosides. *Cellulose Chem. Technol.*, **1975**; **9**: 231–238.
- 215** Löwendahl, L., G. Petersson, O. Samuelson, Formation of dicarboxylic acids from 4-O-methyl-D-glucuronic acid in alkaline solution in the presence and absence of oxygen. *Carbohydrate Res.*, **1975**; **43**(2): 355–359.
- 216** Lind, J., G. Merenyi, N.O. Nilvebrant, Hydroxyl radical induced viscosity loss in cellulose fibres. *J. Wood Chem. Technol.*, **1997**; **17**(1–2): 111–117.
- 217** Schuchmann, M.N., C.V. Sonntag, Radiation-chemistry of carbohydrates. 14. Hydroxyl radical induced oxidation of D-glucose in oxygenated aqueous-solution. *J. Chem. Soc. -Perkin Trans. 2*, **1977** (14): 1958–1963.
- 218** Tronchet, J.M., A. Cier, C. Nofre, M.A. Ravier, Chimie organique – action du radical libre hydroxyle sur le D-ribose. *Comptes Rendus Hebdomadaires Des Seances De l'Academie Des Sciences*, **1963**; **256**(11): 2433.
- 219** Belder, A.N.D., B. Lindberg, O. Theander, Oxidation of glycosides. 13. Oxidation of methyl beta-D-glucopyranoside with Fenton's reagent. *Acta Chim. Scand.*, **1963**; **17**(4): 1012.
- 220** Gilbert, B.C., D.M. King, C.B. Thomas, Radical reactions of carbohydrates.

4. Electron-spin resonance studies of radical-induced oxidation of some aldopentoses, sucrose, and compounds containing furanose rings. *J. Chem. Soc. – Perkin Trans. 2*, **1983** (5): 675–683.
- 221 Gilbert, B.C., D.M. King, C.B. Thomas, Radical reactions of carbohydrates. 3. An electron-spin resonance investigation of base-catalyzed rearrangements of radicals derived from deuterium-glucose and related-compounds. *J. Chem. Soc. – Perkin Trans. 2*, **1982** (2): 169–179.
- 222 Gilbert, B.C., D.M. King, C.B. Thomas, Radical reactions of carbohydrates. 5. The oxidation of some polysaccharides by the hydroxyl radical – an electron-spin-resonance investigation. *Carbohydrate Res.*, **1984**; 125(2): 217–235.
- 223 Gilbert, B.C., D.M. King, C.B. Thomas, Radical reactions of carbohydrates. 2. An electron-spin resonance study of the oxidation of D-glucose and related-compounds with the hydroxyl radical. *J. Chem. Soc. – Perkin Trans. 2*, **1981** (8): 1186–1199.
- 224 McGrouther, K.G., I.D. Suckling, R.W. Allison, D. Lachenal, Carbohydrate degradation during oxygen delignification. A model study of the role of transition metals, lignin models and glucose. International Pulp Bleaching Conference: Poster Presentations, **2000**: 31–36.
- 225 Morelli, R., S. Russo-Volpe, N. Bruno, R. Lo Scalzo, Fenton-dependent damage to carbohydrates: Free radical scavenging activity of some simple sugars. *J. Agric. Food Chem.*, **2003**; 51(25): 7418–7425.
- 226 Stenman, D., M. Carlsson, T. Reitberger, Peroxynitrite mediated delignification of pulp: A comparative study on the bleaching properties of the carbonate and hydroxyl radicals. *J. Wood Chem. Technol.*, **2004**; 24(2): 83–98.
- 227 Roots, R., S. Okada, Estimation of life times and diffusion distances of radicals involved in X-ray-induced DNA strand breaks or killing of mammalian cells. *Radiat. Res.*, **1975**; 64(2): 306–320.
- 228 Yanagida, H., Y. Masubuchi, K. Minagawa, T. Ogata, J. Takimoto, K. Koyama, A reaction kinetics model of water sonolysis in the presence of a spin-trap. *Ultrason. Sonochem.*, **1999**; 5(4): 133–139.
- 229 Li, B.B., P.L. Gutierrez, N.V. Blough, Trace determination of hydroxyl radical in biological systems. *Anal. Chem.*, **1997**; 69(21): 4295–4302.
- 230 Takeda, K., H. Takedoi, S. Yamaji, K. Ohta, H. Sakugawa, Determination of hydroxyl radical photoproduction rates in natural waters. *Anal. Sci.*, **2004**; 20(1): 153–158.
- 231 Ohashi, Y., H. Yoshioka, H. Yoshioka, Detection of 2-deoxy-D-ribose radicals generated by the reaction with the hydroxyl radical using a rapid flow-ESR method. *Biosci. Biotechnol. Biochem.*, **2002**; 66(4): 847–852.
- 232 Biaglow, J.E., Y. Manevich, F. Uckun, K.D. Held, Quantitation of hydroxyl radicals produced by radiation and copper-linked oxidation of ascorbate by 2-deoxy-D-ribose method. *Free Radical Biol. Med.*, **1997**; 22(7): 1129–1138.
- 233 Manevich, Y., K.D. Held, J.E. Biaglow, Coumarin-3-carboxylic acid as a detector for hydroxyl radicals generated chemically and by gamma radiation. *Radiat. Res.*, **1997**; 148(6): 580–591.
- 234 Yang, X.F., X.Q. Guo, Study of nitroxide-linked naphthalene as a fluorescence probe for hydroxyl radicals. *Anal. Chim. Acta*, **2001**; 434(2): 169–177.
- 235 Tai, C., X.X. Gu, H. Zou, Q.H. Guo, A new simple and sensitive fluorometric method for the determination of hydroxyl radical and its application. *Talanta*, **2002**; 58(4): 661–667.
- 236 Tornberg, K., S. Olsson, Detection of hydroxyl radicals produced by wood-decomposing fungi. *FEMS Microbiol. Ecol.*, **2002**; 40(1): 13–20.
- 237 King, M., R. Kopelman, Development of a hydroxyl radical ratiometric nanoprobe. *Sensors and Actuators B – Chemical*, **2003**; 90(1–3): 76–81.
- 238 Vasquez-Vivar, J., J. Joseph, H. Karoui, H. Zhang, J. Miller, P. Martasek, EPR spin trapping of superoxide from nitric oxide synthase. *Analisis*, **2000**; 28(6): 487–492.
- 239 Ge, B., F. Lisdat, Superoxide sensor based on cytochrome c immobilized on mixed-thiol SAM with a new calibration



- method. *Anal. Chim. Acta*, **2002**; 454(1): 53–64.
- 240 Farmer, P.J., W. Liu, Cyt c modified electrodes for superoxide detection. *Free Radical Biol. Med.*, **2002**; 33: S424–S424.
- 241 Lvovich, V., A. Scheeline, Amperometric sensors for simultaneous superoxide and hydrogen peroxide detection. *Anal. Chem.*, **1997**; 69(3): 454–462.
- 242 Tarpey, M.M., I. Fridovich, Methods of detection of vascular reactive species. Nitric oxide, superoxide, hydrogen peroxide, and peroxyntirite. *Circ. Res.*, **2001**; 89(11): 224–236.
- 243 Afanas'ev, I.B., Lucigenin chemiluminescence assay for superoxide detection. *Circ. Res.*, **2001**; 89(11): E46–E46.
- 244 Kočar, D., M. Strlič, J. Kolar, B. Pihlar, A new method for determination of hydroperoxides in cellulose. *Anal. Bioanal. Chem.*, **2002**; 374(7–8): 1218–1222.
- 245 Kolar, J., M. Strlič, B. Pihlar, New colorimetric method for determination of hydroxyl radicals during ageing of cellulose. *Anal. Chim. Acta*, **2001**; 431(2): 313–319.
- 246 Sjöström, E., O. Välttilä, Inhibition of carbohydrate degradation during oxygen bleaching. 1. Comparison of various additives. *Pap. Puu*, **1972**; 54(11): 695.
- 247 Laine, C., T. Tamminen, Origin of carbohydrates dissolved during oxygen delignification of birch and pine kraft pulp. *Nordic Pulp Paper Res. J.*, **2002**; 17(2): 168–171.
- 248 Laine, C., T. Tamminen, A. Vikkula, T. Vuorinen, Methylation analysis as a tool for structural analysis of wood polysaccharides. *Holzforchung*, **2002**; 56(6): 607–614.
- 249 Gustavsson, R., B. Swan, Evaluation of the degradation of cellulose and delignification during oxygen bleaching. *Tappi*, **1975**; 58: 120–123.
- 250 Nunn, J.R., M.J.v.d. Linde. The protective action of magnesium in oxygen bleaching of pulp. Part 1: The complexing of methyl- $\alpha$ -D-glucopyranoside with magnesium ions. In First International Symposium on Delignification with Oxygen Ozone and Peroxides. Raleigh, North Carolina, USA: North Carolina State University, **1975**.
- 251 Abbot, J., D.G. Brown, G.C. Hobbs, I.J. Jewell, P.J. Wright, The influence of manganese and magnesium on alkaline peroxide bleaching of radiata pine thermomechanical pulp. *Appita J.*, **1992**; 45(2): 109.
- 252 Elashmawy, A.E., S.O. Heikal, M.H. Fadl, Effect of magnesium salts on soda-oxygen bleaching of kraft bagasse pulp. *Research and Industry*, **1983**; 28(2): 130–132.
- 253 Brown, D.G., and J. Abbot, Magnesium as a stabilizer for peroxide bleaching of mechanical pulp. *Appita J.*, **1994**; 47(3): 211–216.
- 254 Ni, Y.H., A.R.P. Van Heiningen, G.J. Kang, A. Humphrey, R.W. Thring, A. Skothos, Improved oxygen delignification for magnesium-based sulfite pulps. *Tappi J.*, **1998**; 81(10): 165–169.
- 255 Samuelson, O., U. Ojteg, Influence of manganese and magnesium on oxygen bleaching in carbonate media after a nitrogen dioxide pretreatment. *Holzforchung*, **1996**; 50(4): 379–385.
- 256 Samuelson, O., U. Ojteg, Influence of magnesium during oxygen bleaching in the presence of manganese. *Cellulose Chem. Technol.*, **1995**; 29(1): 55–63.
- 257 Liden, J., L.O. Öhman, Redox stabilization of iron and manganese in the +II oxidation state by magnesium precipitates and some anionic polymers. Implications for the use of oxygen-based bleaching chemicals. *J. Pulp Paper Sci.*, **1997**; 23(5): J193–J199.
- 258 Wiklund, L., L.O. Öhman, J. Liden, Solid solution formation between Mn(II) and Mg(II) hydroxides in alkaline aqueous solution. *Nordic Pulp Paper Res. J.*, **2001**; 16(3): 240–245.
- 259 Wiklund, L., L.-O. Öhman, J. Liden, Surface precipitation of  $MgCO_3$  on  $MnCO_3$  in aqueous solution at 90 °C. *Nordic Pulp Paper Res. J.*, **2001**; 16: 339–345.
- 260 Landucci, L.L., Effects of transition metals in oxidative delignification. In First International Symposium on Delignification with Oxygen Ozone and Peroxides. Raleigh, North Carolina, USA: North Carolina State University, **1975**.
- 261 Sun, Y., M. Fenster, A. Yu, R.M. Berry, D.S. Argyropoulos, The effect of metal ions on the reaction of hydrogen perox-

- ide with Kraft lignin model compounds. *Can. J. Chem.- Rev. Canadienne De Chimie*, **1999**; 77(5–6): 667–675.
- 262 Rodriguez, S.K., K.L. Wilson, R.C. Francis, Effect of adsorbed transition metals on hydrogen peroxide bleaching of thermomechanical pulp. Annual Meeting – Technical Section, Canadian Pulp and Paper Association, Preprints, **1996**.
- 263 Räsänen, E., L. Kärkkäinen, Modelling of complexation of metal ions in pulp suspensions. *J. Pulp Paper Sci.*, **2003**; 29(6): 196–203.
- 264 Lapierre, L., R. Berry, J. Bouchard, The effect of magnesium ions and chelants on peroxide bleaching. *Holzforschung*, **2003**; 57(6): 627–633.
- 265 Moreira, M.T., G. Feijoo, J. Canaval, J.M. Lema, Semipilot-scale bleaching of Kraft pulp with manganese peroxide. *Wood Sci. Technol.*, **2003**; 37(2): 117–123.
- 266 Wekesa, M., Y. Ni, Stabilization of peroxide systems by silicate and calcium carbonate and its application to bleaching of recycled fibres. *Pulp Paper Can.*, **2003**; 104(12): 85–87.
- 267 Qiu, Z., Y. Ni, Improving peroxide bleaching by decreasing manganese induced peroxide decomposition. International Pulp Bleaching Conference: Poster Presentations, **2000**: 139–154.
- 268 Ni, Y.H., Z.P. Qiu, Methods to decrease manganese-induced decomposition of peroxide. *Appita J.*, **2003**; 56(5): 355–358.
- 269 Kishimoto, T., F. Nakatsubo, Non-chlorine bleaching of kraft pulp – IV. Oxidation of methyl 4-O-ethyl-beta-D-glucopyranoside with Fenton's reagent: Effects of pH and oxygen. *Holz-forschung*, **1998**; 52(2): 180–184.
- 270 Yokoyama, T., Y. Matsumoto, G. Meshitsuka, The role of peroxide species in carbohydrate degradation during oxygen bleaching. Part III: Effect of metal ions on the reaction selectivity between lignin and carbohydrate model compounds. *J. Pulp Paper Sci.*, **1999**; 25(2): 42–46.
- 271 Wekesa, M., Y.H. Ni, Further understanding of the chemistry of manganese-induced peroxide decomposition. *Can. J. Chem. Eng.*, **2003**; 81(5): 968–972.
- 272 Gartner, A., G. Gellerstedt, Oxidation of residual lignin with alkaline hydrogen peroxide. Part II: Elimination of chromophoric groups. *J. Pulp Paper Sci.*, **2001**; 27(7): 244–248.

### Sections 7.3.3–7.3.8

- 1 Olm, L., A. Teder, The kinetics of oxygen bleaching. *Tappi*, **1979**; 62(12): 43–46.
- 2 Myers, M.R., L.L. Edwards, Development and verification of a predictive oxygen delignification model for hardwood and softwood kraft pulp. *Tappi J.*, **1989**; 72(9): 215–219.
- 3 Agarwal, S.B., et al., Kinetics of oxygen delignification. *J. Pulp Paper Sci.*, **1999**; 25(10): 361–366.
- 4 Avrami, M., Kinetics of phase change II – transformation-time relations for random distribution of nuclei. *J. Chem. Phys.*, **1940**; 8: 212–224.
- 5 Valchev, I., E. Valchev, E. Christova, Kinetics of oxygen delignification of hardwood kraft pulp. *Cellulose Chem. Technol.*, **1999**; 33: 303–310.
- 6 Macleod, J.M., J. Li, Alkaline leaching of kraft pulps for lignin removal. In TAPPI Pulping Conference, **1992**.
- 7 Ackert, J.E., D.D. Koch, L.L. Edwards, Displacement chlorination of kraft pulps – an experimental study and comparison of models. *Tappi*, **1975**; 58(10): 141–145.
- 8 Edwards, L., S. Norberg, *Tappi*, **1973**; 56(11): 108–111.
- 9 Hsu, C.L., J.S. Hsieh, Oxygen bleaching kinetics at ultra-low consistency. *Tappi J.*, **1987**: 107–111.
- 10 Hsu, C.L., J.S. Hsieh, Reaction kinetics in oxygen bleaching. *AIChE J.*, **1988**; 34(1): 116–122.
- 11 Iribarne, J., L.R. Schroeder, High pressure oxygen delignification of kraft pulps I – Kinetics. *Tappi Proceedings – Pulping Conference*, **1995**: 125–133.
- 12 Iribarne, J., L.R. Schroeder, High-pressure oxygen delignification of kraft

- pulps. Part I: kinetics. *Tappi J.*, **1997**; 80(10): 241–250.
- 13 Vincent, A.H.D., K.L. Nguyen, J.F. Mathews, Kinetics of oxygen delignification of eucalypt kraft pulp. *Appita*, **1994**; 47(3): 217–220.
  - 14 Zou, H., et al., Influence of kraft pulping on the kinetics of oxygen delignification. *Tappi*, **2000**; 83(2): 65–71.
  - 15 Axegard, P., S. Moldenius, L. Olm, Basic chemical kinetics equations are useful for understanding of pulping processes. *Svensk. Papperstidn.*, **1979**; 82(5): 131–136.
  - 16 Schoon, N.H., Interpretation of rate equation for kinetic studies of wood pulping and bleaching. *Svensk. Papperstidn.*, **1982**: R185–R193.
  - 17 Nguyen, K.L., H. Liang, Kinetic model of oxygen delignification. Part 1 – effect of process variables. *Appita J.*, **2002**; 55(2): 162–165.
  - 18 Quillin, D.T., et al., Crystallinity in the polypropylene/cellulose system – crystallization kinetics. *J. Appl. Polym. Sci.*, **1994**; 52: 605.
  - 19 Agarwal, S.B., et al., Kinetics of oxygen delignification. *J. Pulp Paper Sci.*, **1999**; 25(10): 361–366.
  - 20 Järrehult, B., Oxygen-alkali treatment of kraft pulp and cellobitol. In Institutionen för Teknisk Kemi. PhD-Thesis, Chalmers Tekniska Högskola: Göteborg, **1992**.
  - 21 Järrehult, B., O. Samuelson, Oxygen bleaching of kraft pulps at low consistency. *Svensk. Papperstidn.*, **1978**; 81: 533–540.
  - 22 Ekenstam, A., Über das Verhalten der Cellulose in Mineralsäure-Lösungen, II. Mitteilung: Kinetisches Studium des Abbaus der Cellulose in Säurelösungen. *Ber. Dtsch. Chem. Ges.*, **1936**; 69: 553–559.
  - 23 Godsay, M.P., E.M. Pearce, Physico-chemical properties of ozone oxidized kraft pulps. In Tappi Symposium – Oxygen Delignification, **1984**.
  - 24 Immergut, E.H., B.G. Ranby, H.F. Mark, Molecular weight of cellulose. *Journal of Industrial and Engineering Chemistry*, **1953**; 45: 2483–2490.
  - 25 Schelosky, N., T. Röder, T. Baldinger, Molmassenverteilung cellulosischer Produkte mittels Grössenausschlußchromatographie in DMAc/LiCl. *Papier*, **1999**; 53(12): 728–738.
  - 26 Chen, S.-L., L.A. Lucia, Fundamental insight into the mechanism of oxygen delignification of kraft pulps. II. Application of surfactants. *Cellulose Chem. Technol.*, **2002**; 36(5–6): 495–505.
  - 27 Heiningen, A.V., et al., A chemical reactor analysis of industrial oxygen delignification. *Pulp Paper Can.*, **2003**; 104(12): T331–T336.
  - 28 Rewatkar, V.B., V.P.J. Bennington, Gas-liquid mass transfer in pulp retention towers. In TAPPI International Pulp Bleaching Conference, **2002**.
  - 29 Rewatkar, V.B., V.P.J. Bennington, Gas-liquid mass transfer in low and medium consistency pulp suspensions. *Can. J. Chem. Eng.*, **2000**; 78: 504–512.
  - 30 Brodén, Å., R. Simonson, Solubility of oxygen. Part 2. Solubility of oxygen in sodium hydrogen carbonate and sodium hydroxide solutions at temperatures <150 °C and pressures <5 MPa. *Svensk. Papperstidn.*, **1979**; 16: 487–491.
  - 31 Hornsey, D., A. Perkins, J. Davidson. In TAPPI Annual Meeting Proceedings. Atlanta, GA, **1989**; p. 55.
  - 32 Violette, S., A.v. Heiningen. Selectivity optimization of extended alkali oxygen delignification. In Tappi Pulping Conference, **2003**.
  - 33 McDonough, T.J., Oxygen delignification. In *Pulp bleaching, principles and practice*, C.W. Dence, D.W. Reeve, Eds. Chapter 1. TAPPI Press: Atlanta, GA, USA, **1996**.
  - 34 Broden, A., R. Simonson, Solubility of oxygen. Part 2. Solubility of oxygen in sodium hydrogen carbonate and sodium hydroxide solution at temperatures below 150 °C and pressures below 5 MPa. *Svensk. Papperstidn.*, **1979** (16): 487–491.
  - 35 Ecker, A., H. Sixta, Modelling of Oxygen Delignification of Sulfite Dissolving Pulp. R&D Lenzing AG: Lenzing, **2004**: 15.
  - 36 Bouchard, J., et al., Determination of oxygen penetration rate in medium-consistency kraft pulps. In 2003 Pulping Conference. TAPPI, **2003**.

- 37 Axegard, P., B. Backlund, Ecocyclic Pulp Mill – “KAM”. Final report, 1996–2002. STFI, Swedish Pulp and Paper Research Institute: Stockholm, Sweden, **2003**.
- 38 Bennington, C.P.J., I. Pineault, Mass transfer in oxygen delignification systems: mill survey results, analysis and interpretation. *Pulp Pap. Can.*, **1999**; 100(12): T395–T402.
- 39 Johansson, E., The effect of oxygen on the degradation of lignin model compounds and residual lignin. PhD-Thesis, In Department of Pulp and Paper Chemistry and Technology. Royal Institute of Technology. Stockholm, **1997**.
- 40 Kleppe, P., H.-M. Chang, R. Eckert, Delignification of high-yield pulp with oxygen and alkali. I. preliminary studies on Southern Pines. *Pulp Paper Mag. Can.*, **1972**; 73(12): 102–106.
- 41 Hartler, N., H. Norrström, S. Rydin, Oxygen-alkali bleaching of sulphate pulp. *Svensk. Papperstidn.*, **1970**; 73(21): 696–703.
- 42 Barroca, M.J.M.C., et al., Selectivity studies of oxygen and chlorine dioxide in the pre-delignification stages of a hardwood pulp bleaching plant. *Ind. Eng. Chem. Res.*, **2001**; 40: 5680–5685.
- 43 Kratzl, K., J.S. Gratzl, P. Claus, Formation and degradation of biphenyl structures during alkaline oxidation of phenols with oxygen. *Adv. Chemistry Series*, **1966**; 59: 157–176.
- 44 Chang, H.-M., et al., Delignification of high-yield southern pine soda pulps with oxygen and alkali. Effects of temperature and alkali charge. *Tappi*, **1973**; 56(9): 116–119.
- 45 Kamy, sales literature, publicly available, **1983**.
- 46 Bennington, C.P.J., I. Pineault, Mass transfer in oxygen delignification systems: mill survey results, analysis and interpretation. *Pulp Paper Mag. Can.*, **1999**; 100(12): 123–131.
- 47 Svensson, J.E., Experiences of the SAPOXAL-Oxygen bleaching system at Skutskar mill, Sweden. In Tappi Seminar Notes, “Oxygen, Ozone and Peroxide Pulping and Bleaching”, **1978**.
- 48 Jiang, Z.-H., B.v. Lierop, R. Berry, Hexenuronic acid groups in pulping and bleaching chemistry. *Tappi*, **2000**; 83(1): 167–175.
- 49 Tran, A.V., Effect of pH on oxygen delignification of hardwood kraft pulp. *Pap. Puu*, **2001**; 83(5): 405–410.
- 50 Laine, J., P. Stenius, The effect of ECF and TCF bleaching on the surface chemical composition of kraft pulps as determined by ESCA. *Nordic Pulp Paper Res. J.*, **1996**; 11(3): 201–210.
- 51 Li, K., D.W. Reeve. Lignin adsorption on wood fibre surfaces. In International Pulp Bleaching Conference (IPBC). Portland, Oregon, **2002**.
- 52 Backa, S., M. Ragnar, The importance of high final pH in the oxygen delignification. In TAPPI Fall Conference, **2003**.
- 53 Leader, J.P., H.H.K. Lim, G.B. Byrom, Medium consistency oxygen delignification in an O (CD) (EO) D bleaching process for radiata pine kraft pulp. *Appita*, **1986**; 39(6): 451–454.
- 54 Thompson, N.S., H.M. Corbett, The effect of oxygen consumption during bleaching on the properties of a southern pine kraft pulp. *Tappi*, **1976**; 59(3): 78–80.
- 55 Berry, R., et al., Recommendations from computer modeling for improving single stage oxygen delignification systems. In 88th PAPTAC Annual meeting, Montreal, QC, Canada, **2002**.
- 56 McDonough, T.J., Oxygen delignification. In *Pulp Bleaching – Principles and Practice*, C.W. Dence, Reeve, D.W., Eds. TAPPI Press: Atlanta, GA, USA, **1996**.
- 57 Fuhrmann, F.E., W. Peter, MC-oxygenperoxide delignification, an economic alternative. Tappi Proceedings – International Oxygen Delignification Conference, **1987**: 183–189.
- 58 Salmela, M., R. Alen, Fate of oxygen in industrial oxygen-alkali delignification of softwood kraft pulp. *Nordic Pulp Paper Res. J.*, **2004**; 19(1): 97–104.
- 59 The Bleaching of Pulp (Singh, R.P., Ed.), Tappi Press, 3rd Ed., p. 186–206.
- 60 Elton, E.F., et al., New technology for medium-consistency oxygen bleaching. *Tappi*, **1980**; 63(11): 79–82.
- 61 Seifert, P., E. Elton, V. Magnotta. Engineering considerations in the design of oxygen reactors. In TAPPI Annual meeting proceedings, **1980**.

- 62 Brelid, H., T. Friberg, R. Simonson, TCF bleaching of softwood kraft pulp. Part 4. Removal of manganese from wood shavings prior to cooking. *Nordic Pulp Paper Res. J.*, **1998**; 13(1): 50–56.
- 63 Ericsson, B., B.O. Lindgren, O. Theander, *Svensk. Papperstidn.*, **1971**; 74(22): 757–765.
- 64 Gilbert, A.F., E. Pavlovova, W.H. Rapson, Mechanism of magnesium retardation of cellulose degradation during oxygen bleaching. *Tappi*, **1973**; 56(6): 95–99.
- 65 Entwistle, D., E.H. Cole, N.S. Wooding, The autoxidation of alkali cellulose. Part II. *Textile Res. J.*, **1949**; 19(9): 609–624.
- 66 Entwistle, D., E.H. Cole, N.S. Wooding, The autoxidation of alkali cellulose. Part I: An experimental study of the kinetics of the reaction. *Textile Res. J.*, **1949**; 19(9): 527–546.
- 67 Manouchehri, M., O. Samuelson, Influence of catalysts and inhibitors upon the degradation of carbohydrates during oxygen bleaching. *Svensk. Papperstidn.*, **1973**; 76(13): 486–492.
- 68 Brelid, H., T. Friberg, R. Simonson, TCF bleaching of softwood kraft pulp. Part 3. Ion exchange of softwood kraft pulp prior to oxygen delignification. *Nordic Pulp Paper Res. J.*, **1997**; 12(2): 80–85.
- 69 Liden, J., L.-O. Öhman, On the prevention of Fe- and Mn-catalyzed H<sub>2</sub>O<sub>2</sub> decomposition under bleaching conditions. *J. Pulp Paper Sci.*, **1998**; 24(9): 269–276.
- 70 Perng, Y.-S., et al., Catalytic oxygen bleaching of wood pulp with metal porphyrin and phthalocyanine complexes. *Tappi J.*, **1994**; 77(11): 119–125.
- 71 Kishimoto, T., F. Nakatsubo, Non-chlorine bleaching of kraft pulp. IV. Oxidation of methyl 4-O-ethyl-β-D-glucopyranoside with Fenton's reagent: Effects of pH and oxygen. *Holzforschung*, **1998**; 52(2): 180–184.
- 72 Ek, M., et al., Study on the selectivity of bleaching with oxygen-containing species. *Holzforschung*, **1989**; 43(6): 391–396.
- 73 Abrahamsson, K., O. Samuelson, Oxygen-alkali cooking of wood meal. Part V. Influence of metal compounds and soaking in acid. *Svensk. Papperstidn.*, **1975**; 78(4): 135–140.
- 74 Robert, A., et al., An oxygen treatment of pulps to further subsequent bleaching. II. Bleaching pulps previously treated with oxygen. *Assoc. Techn. Ind. Papietiere, Bull.*, **1964**; 18(4): 166–176.
- 75 Robert, A., et al., An oxygen treatment of pulps to further subsequent bleaching. I. Improvements obtained by using a catalyst; optimum conditions in the oxygen treatment. *Assoc. Techn. Ind. Papietiere, Bull.*, **1964**; 18(4): 151–165.
- 76 Robert, A., P. Traynard, O. Martin-Boret. US Patent 3,384,533, **1968**.
- 77 Liden, J., L.-O. Öhman, Redox stabilization of iron and manganese in the +II oxidation state by magnesium precipitates and some anionic polymers. Implications for the use of oxygen-based bleaching chemicals. *J. Pulp Paper Sci.*, **1997**; 23(5): J193–J199.
- 78 Wiklund, L., J. Liden, L.-O. Öhman, Solution formation between Mn(II) and Mg(II) hydroxides in alkaline aqueous solution. *Nordic Pulp Pap. Res. J.*, **2001**; 16(3): 240–245.
- 79 Wiklund, L., J. Liden, L.-O. Öhman, Surface precipitation of MgCO<sub>3</sub> on MnCO<sub>3</sub> in aqueous solution at 90 °C. *Nordic Pulp Pap. Res. J.*, **2001**; 16(4): 339–345.
- 80 Sjölander, C., J. Liden, L.-O. Öhman. Modelling the distribution of “free”, complexed and precipitated metal ions in a pulp suspension using Donnan equilibria. In Proceedings of 2000 International Pulp and Bleaching Conference, **2000**.
- 81 Lucia, L.A., R.S. Mereck, Effect of lignin content and magnesium-to-manganese ratio on the selectivity of oxygen delignification. *Pure Appl. Chem.*, **2001**; 73(12): 2059–2065.
- 82 Werner, J., A. Ragauskas, J.-E. Jiang, Intrinsic metal binding capacity of kraft lignins. *J. Wood Chem. Technol.*, **2000**; 20(2): 133–145.
- 83 Yang, E., Oxygen delignification. The role of hydroxyl and superoxide radicals. In Department of Pulp and Paper Chemistry and Technology. Royal Institute of Technology: Stockholm, Sweden, **1995**.

- 84 Basta, J., et al. In TAPPI Pulping Conference. Chicago, 1995.
- 85 Ek, M., et al. In TAPPI Pulping Conference. San Diego, 1994.
- 86 Chirat, C., D. Lachenal. In TAPPI Pulping Conference. Atlanta, 1993.
- 87 Landucci, L.L., N. Sanyer, Influence of transition metals in oxygen pulping. *Tappi*, 1975; 58(2): 60–63.
- 88 Gierer, J., F. Imsgard, The reactions of lignins with oxygen and hydrogen peroxide in alkaline media. *Svensk. Papperstidn.*, 1977; 80(16): 510–518.
- 89 Gellerstedt, G., E.L. Lindfors, Hydrophilic groups in lignin after oxygen bleaching. *Tappi*, 1987; 70(6): 119–122.
- 90 Sun, Y., D.S. Argyropoulos, Fundamentals of high-pressure oxygen and low-pressure oxygen-peroxide (Eop) delignification of softwood and hardwood kraft pulps: A comparison. *J. Pulp Paper Sci.*, 1995; 21(6): J185–J190.
- 91 Gellerstedt, G., E.L. Lindfors, Structural changes in lignin during kraft pulping. *Holzforschung*, 1984; 38: 151–158.
- 92 Gellerstedt, G., K. Gustafsson, E.L. Lindfors, Structural changes in lignin during oxygen bleaching. *Nordic Pulp Paper Res. J.*, 1986; 3: 14–17.
- 93 Lucia, L.A., A.J. Ragauskas, F.S. Chakar, Comparative evaluation of oxygen delignification processes for low- and high-lignin-content softwood kraft pulps. *Ind. Eng. Chem. Res.*, 2002; 41: 5171–5180.
- 94 Lai, Y.-Z., M. Funaoka, H.-T. Chen, Oxygen bleaching of kraft pulp. 1. Role of condensed units. *Holzforschung*, 1994; 48(4): 355–359.
- 95 Asgari, F., D.S. Argyropoulos, Fundamentals of oxygen delignification. Part II. Functional group formation/elimination in residual kraft lignin. *Can. J. Chem.*, 1998; 76: 1606–1615.
- 96 Fu, S., L.A. Lucia, Investigation of the chemical basis for the inefficient lignin removal in softwood kraft pulp during oxygen delignification. *Ind. Eng. Chem. Res.*, 2003; 42: 4269–4276.
- 97 Chirat, C., D. Lachenal. Limits of oxygen delignification. In TAPPI Pulping Conference. Atlanta, GA: TAPPI Press, 1998.
- 98 Rööst, C., P. Larsson, G. Gellerstedt, Reduced brightness variations by extended oxygen delignification. *Nordic Pulp Paper Res. J.*, 2000; 15(3): 211–215.
- 99 Sixta, H. Influence of prehydrolysis on pulping and bleaching. In Book of Abstracts, 211th ACS National Meeting. New Orleans, LA, 1996.
- 100 Antonsson, S., et al., A comparative study of the impact of the cooking process on oxygen delignification. *Nordic Pulp Paper Res. J.*, 2003; 18(4): 388–394.
- 101 Zou, H., et al., Effect of hemicellulose content in kraft brownstock on oxygen delignification. In TAPPI Fall Conference and Trade Fair. San Diego, CA: TAPPI Press, 2002.
- 102 Akim, L.G., J.L. Colodette, D.S. Argyropoulos, Factors limiting oxygen delignification of kraft pulp. In International Pulp Bleaching Conference. Halifax, NS, Canada: Pulp and Paper Technical Association of Canada, 2000.
- 103 Gellerstedt, G., W.W. Al-Dajani, Some factors affecting the brightness and TCF-bleachability of kraft pulps. *Nordic Pulp Paper Res. J.*, 2003; 18(1): 56–62.
- 104 Gustavsson, C., K. Sjöström, W.W. Al-Dajani, The influence of cooking conditions on the bleachability and chemical structure of kraft pulps. *Nordic Pulp Paper Res. J.*, 1999; 14(1): 71–81.
- 105 Gellerstedt, G., W.A.-D. W. Bleachability of alkaline pulps. Part 1. The importance of beta-aryl ether linkages in lignin. *Holzforschung*, 2000; 54(6): 609–617.
- 106 Rööst, C., P. Larsson, G. Gellerstedt, Brightness and kappa number – important variables to secure appropriate control of chemical charges in TCF- and ECF-bleaching sequences. *Nordic Pulp Paper Res. J.*, 2000; 15(3): 216–220.
- 107 Iijima, J.F., H. Taneda, The effect of carryover on medium-consistency oxygen delignification of hardwood kraft pulp. *J. Pulp Paper Sci.*, 1997; 23(12): J561–J564.
- 108 Pekkala, O., Some effects of extended delignification on lignin in kraft cooking. *Pap. Puu*, 1985; 67(11): 673–688.
- 109 Zou, H., et al. Effect of hemicellulose content in kraft brownstock on oxygen

- delignification. In TAPPI Fall Conference & Trade Fair, **2002**.
- 110** Violette, S., A.v. Heiningen. Selectivity improvement during oxygen delignification by adsorption of polymeric additives. In 88th Annual Meeting, PAPTAC, **2001**.
- 111** Ai, V.T., Utilization of additives in oxygen delignification of hardwood kraft pulp. *Appita*, **2000**; 53: 300–304.
- 112** Fu, S., et al., Chemical basis for a selectivity threshold to the oxygen delignification of kraft softwood fiber as supported by the use of chemical selectivity agents. *Ind. Eng. Chem. Res.*, **2004**; 43: 2291–2295.
- 113** Gratzl, J.S., Abbaureaktionen von Kohlenhydraten und Lignin durch chlorfreie Bleichmittel – Mechanismen sowie Möglichkeiten der Stabilisierung. *Das Papier*, **1987**; 41(3): 120–130.
- 114** Ala-Kaila, K., I. Reilama, Step-wise delignification response in an industrial two-stage oxygen-alkali delignification process. *Pulp Paper Canada*, **2001**; 102(6): T170–T172.
- 115** Ala-Kaila, K., et al., Apparent and actual delignification response in industrial oxygen-alkali delignification of birch kraft pulp. *Tappi*, **2003**; 2(10): 23–27.
- 116** Li, J., G. Gellerstedt, The contribution to kappa number from hexenuronic acid groups in pulp xylan. *Carbohydrate Res.*, **1997**; 302: 213–218.
- 117** Li, J., O. Sevastyanova, G. Gellerstedt, The relationship between kappa number and oxidizable structures in bleached kraft pulps. *J. Pulp Paper Sci.*, **2002**; 28(8): 262–266.
- 118** Li, J., G. Gellerstedt, Oxymercuration-demercuration kappa number: An accurate estimation of the lignin content in chemical pulps. *Nordic Pulp Paper Res. J.*, **2002**; 17(4): 410–414.
- 119** Steffes, F., M. Bokström, S. Norden. Pulp yield improvements using two-stage, extended oxygen delignification. In Breaking the pulp yield barrier symposium. Atlanta, GA, **1998**.
- 120** Rolando, C., B. Monties, C. Lapierre, Thioacidolysis. In *Methods in Lignin Chemistry*, C.W.D. S.Y. Lin, Ed. Springer-Verlag, **1992**.
- 121** Kondo, S. Two-stage oxygen delignification process and operating experiences. In Pan-Pacific Pulp & Paper Technology Conference. Tokyo, Japan, **1992**.
- 122** Backlund, A., Process for oxygen bleaching using two vertical reactors. SE-467582, **1990**.
- 123** Sixta, H., A. Borgards, New technology for the production of high-purity dissolving pulps. *Das Papier*, **1999**; 53(4): 220–234.
- 124** Sixta, H., et al., Towards effluent-free TCF-bleaching of eucalyptus prehydrolysis-kraft pulp. *Das Papier*, **1994**; 48(8): 526–537.
- 125** Sixta, H., Zellstoffherstellung unter Berücksichtigung umweltfreundlicher Aufschluß- und Bleichverfahren am Beispiel von Chemiezellstoffen. Habilitation Thesis, In Institute for Pulp, Paper and Fiber Technology. TU Graz: Graz, **1995**: 425.
- 126** Bokström, M., P. Mellander, S. Norden, Oxygen delignification of lignocellulosic pulp in two steps. SE-505141, **1997**.
- 127** Bokstrom, M., Y. Lundahl, N.K. Jain, OxyTrac process. *IPPTA*, **2002**; 14(2): 13–18.
- 128** Bokström, M., S. Norden. Extended oxygen delignification. In 52nd Appita Annual General Conference Proceedings, **1998**.
- 129** Bokström, M., T. Kobayashi, Extended oxygen delignification with the OxyTrac process. *KamiPa Gikyoshi*, **2000**; 54(9): 1214–1222.
- 130** Saldivia, M.A.G., Two-stage oxygen delignification system cuts mill's chemical use, boosts pulp quality. *PaperAge*, **2003** (Jan/Feb): 18–24.
- 131** Dualox – A two-stage oxygen delignification process (product leaflet). Kvaerner Pulping: Karlstad, Sweden, **2000**.
- 132** Ragnar, M., A compact way to extend oxygen delignification. In 7th International Conference on new available technologies. Stockholm, Sweden: SPCI, **2002**.
- 133** Aoki, I., Operating experience of two-stage oxygen delignification (DUALOX) systems. In Japan Tappi Seminar. Yonugo, Japan, **2001**.

- 134 Lindström, L.-A., Oxygen stage design and performance. In *Tappi Bleach Plant Operations Short Course*, 1991.
- 135 Bergnor, E., P. Sandström, Modified cooking and oxygen bleaching for improved production economy and reduced effluent load. *Nordic Pulp Paper Res. J.*, 1988; 3(3): 145–155.
- 136 Gustavsson, R., B. Swan, *Tappi*, 1975; 58(3): 120–123.
- 137 Chai, X.-S., Q.X. Hou, J.Y. Zhu, Carboxyl groups in wood fibers. 2. The fate of carboxyl groups during alkaline delignification and its application for fiber yield prediction in alkaline pulping. *Ind. Eng. Chem. Res.*, 2003; 42: 5445–5449.
- 138 Tormund, D., Lindström, M. Syrgas delignifiering med Karbonat som alkali-källa, STFI report BF 15, 1999, In 'Eco-cyclic Pulp Mill – "KAM"'. Final report, 1996–2002, p. 31 Stockholm, Sweden (2003), edited by Peter Axegard and Birgit Bocklund.

### Sections 7.4.1–7.4.3

- 1 Davy, H., On a combination of oxymuriatic gas and oxygene gas. *Phil. Trans.*, 1811; 101: 155.
- 2 Schmidt, E., *Ber.*, 1921; 54: 1860.
- 3 Schmidt, E., *Cellulosechem*, 1930; 11: 73.
- 4 Södergren, A., et al., Summary of results from the Swedish project "Environment/Cellulose". *Water Sci. Technol.*, 1988; 20: 49–60.
- 5 Renberg, L., N.G. Johansson, C. Blom, Destruction of PCDD and PCDF in bleached pulp by chlorine dioxide treatment. *Chemosphere*, 1995; 30(9): 1805–1811.
- 6 Gordon, G., R.G. Kieffer, D.H. Rosenblatt, The chemistry of chlorine dioxide. *Prog. Inorg. Chem.*, 1972; 15: 201–286.
- 7 Lenzi, F., W.H. Rapson, *Pulp Paper Mag. Can.*, 1962; 63: T442–448.
- 8 Dodgen, H., H. Taube, The exchange of chlorine dioxide with chlorite ion and with chlorine in other oxidation states. *J. Am. Chem. Soc.*, 1949; 71: 2501–2504.
- 9 Bray, W.C., *Z. Anorg. Allgem. Chem.*, 1906; 48: 217–250.
- 10 Taube, H., H. Dodgen, Application of radioactive chlorine to the study of the mechanisms of reactions involving changes in the oxidation state of chlorine. *J. Am. Chem. Soc.*, 1949; 71: 3330–3336.
- 11 Bray, W.C., *Z. Physik. Chem.*, 1906; 54: 569–608.
- 12 Halperin, J., H. Taube, The transfer of oxygen atoms in oxidation-reduction reactions. III. The reaction of halogenates with sulfite in aqueous solution. *J. Am. Chem. Soc.*, 1952; 74: 375–380.
- 13 Fukutomi, H., G. Gordon, Kinetic study of the reaction between chlorine dioxide and potassium iodide in aqueous solution. *J. Am. Chem. Soc.*, 1967; 89(6): 1362–1366.
- 14 Svenson, D.R., Chlorine dioxide reactions with lignin model compounds and kraft pulps. In Department of Wood and Paper Science. North Carolina State University: Raleigh, 2001.
- 15 Kolar, J., B. Lindgren, B. Pettersson, *Wood Sci. Technol.*, 1983; 17: 117–128.
- 16 Heijne, G.V., A. Teder, Kinetics of decomposition of aqueous chlorine dioxide solutions. *Acta Chim. Scand.*, 1973; 27: 4018–4019.
- 17 Svenson, D.R., et al., Effect of pH on the inorganic species involved in a chlorine dioxide reaction system. *Ind. Eng. Chem. Res.*, 2002; 41(24): 5927–5933.
- 18 Strumila, G., H. Rapson, Chlorine dioxide bleaching. In *The bleaching of pulp*, R. Singh, Ed. TAPPI: Atlanta, GA, 1979: 113.
- 19 Rapson, W.H., C.B. Anderson, *Pulp Paper Mag. Can.*, 1966; 67(1): T47–T55.
- 20 Rapson, W.H., C.B. Anderson,, *Improving the efficiency of chlorine dioxide bleaching*, 1977; 3(2): TR52–TR55.
- 21 Zabori, M., Production of chlorine dioxide – the integrated process. *Paper*, 1991; 10: 20–22.
- 22 Fredette, M.C., In *Bleach Plant Operations, Short Course*. Atlanta: TAPPI Press, 1990.
- 23 Stockburger, P., What you need to know before buying your next chlorine dioxide plant. *Tappi J.*, 1993; 76(3): 99–104.



- 24 Ni, Y., X. Wang, Mechanism of the methanol-based  $\text{ClO}_2$  generation process. *J. Pulp Paper Sci.*, **1997**; 23(7): J346–J352.
- 25 Hoq, M.F., et al., Oxidation products of methanol in chlorine dioxide production. *Ind. Eng. Chem. Res.*, **1992**; 31(7): 1807–1810.
- 26 Yin, G., Y. Ni, Using hydrogen peroxide in a methanol-based chlorine dioxide generation process. *Ind. Eng. Chem. Res.*, **1999**; 38(9): 3319–3323.
- 27 Nonni, A.J., et al., Method for producing chlorine dioxide using methanol and hydrogen peroxide as reducing agent. PCT/US, 1998.
- chlorine and chlorine dioxide. *Holz-forschung*, **1993**; 47(6): 497–500.
- 8 McKague, A.B., A. Grey, The reaction of syringol with chlorine dioxide. *J. Wood Chem. Technol.*, **1996**; 16(3): 249–259.
- 9 Elder, T., Reactions of lignin model compounds with chlorine dioxide. Molecular orbital calculations. *Holz-forschung*, **1998**; 52(4): 371–384.
- 10 Elder, T., Reactions of lignin model compounds with chlorine dioxide. Molecular orbital calculations on dimers. *J. Pulp Paper Sci.*, **1999**; 25(2): 52–59.
- 11 Pu, Y., H. Zhan, H. Wu, B. Yue, B. Li, Change of lignin structure during ECF bleaching of *Pinus elliottii* kraft pulp. *Zhongguo Zaozh Xuebao/Trans. China Pulp Paper*, **2002**; 17(1): 26–31.
- 12 Sunahara, H., H. Ohi, Structural analysis of residual lignin in eucalyptus kraft pulp by pyrolysis gas-chromatography. *Mokuzai Gakkaishi/J. Jap. Wood Res. Soc.*, **2001**; 47(1): 33–38.
- 13 Brogdon, B.N., D.G. Mancosky, L.A. Lucia, New insights into lignin modification during chlorine dioxide bleaching sequences (II): Modifications in extraction (E) and chlorine dioxide bleaching (D1). *J. Wood Chem. Technol.*, **2004**; 24(3): 221–237.
- 14 Brogdon, B.N., D.G. Mancosky, L.A. Lucia, New insights into lignin reactivation towards chlorine dioxide bleaching after caustic extraction. Tappi International Pulp Bleaching Conference, **2002**: 181–193.
- 15 Brogdon, B.N., D.G. Mancosky, L.A. Lucia, New insights into lignin modification during chlorine dioxide bleaching sequences (I): Chlorine dioxide delignification. *J. Wood Chem. Technol.*, **2004**; 24(3): 201–219.
- 16 Daniel, A.I.D., D.V. Evtuguin, A.J.D. Silvestre, C.P. Neto, Chemical features of hardwood unbleached kraft pulps and their ECF bleachability. *J. Pulp Paper Sci.*, **2004**; 30(4): 94–98.
- 17 Koda, K., H. Goto, H. Shintani, Y. Matsumoto, G. Meshitsuka, Oxidative cleavage of lignin aromatics during chlorine bleaching of kraft pulp. *J. Wood Sci.*, **2001**; 47(5): 362–367.
- 18 Vilen, E.J., A.B. McKague, D.W. Reeve, Reaction of a lignin model dimer with

#### Section 7.4.4

- 1 Brage, C., T. Eriksson, J. Gierer, Reactions of chlorine dioxide with lignins in unbleached pulps. Part I. *Holz-forschung*, **1991**; 45(1): 23–30.
- 2 Brage, C., T. Eriksson, J. Gierer, Reactions of chlorine dioxide with lignins in unbleached pulps. Part II. *Holz-forschung*, **1991**; 45(2): 147–152.
- 3 Brage, C., T. Eriksson, J. Gierer, Reactions of chlorine dioxide with lignins in unbleached pulps. Part III. Reactions with model compounds representing olefinic structures in native and residual lignins. *Holz-forschung*, **1995**; 49(2): 127–138.
- 4 Ni, Y., X. Shen, A.R.P. van Heiningen, Studies on the reactions of phenolic and nonphenolic lignin model compounds with chlorine dioxide. *J. Wood Chem. Technol.*, **1994**; 14(2): 243–262.
- 5 Vilen, E., D.W. Reeve, A.B. McKague, S.J. Rettig, J. Trotter, Reaction of lignin model compounds with pulp bleaching chemicals. Reaction of 4-methylcatechol with chlorine dioxide. *Nordic Pulp Paper Res. J.*, **1995**; 2: 119–121.
- 6 McKague, A.B., D.W. Reeve, A.A. Grey, Reaction of the hardwood lignin model compound 4-methylsyringol with chlorine dioxide. *Appita J.*, **1998**; 51(6): 448–450.
- 7 McKague, A.B., G.J. Kang, D.W. Reeve, Reaction of a lignin model dimer with

- structures in high molecular weight material from bleach plant effluents. *Holzforschung*, **2000**; 54(3): 273–278.
- 19 Vilen, E., D.W. Reeve, A.B. McKague, Identification of muconic acids in bleach plant effluent. *Holzforschung*, **1996**; 50(6): 575–578.
  - 20 Toven, K., G. Gellerstedt, R. Kleppe, S. Moe, Use of chlorine dioxide and ozone in combination in prebleaching. *J. Pulp Paper Sci.*, **2002**; 28(9): 305–310.
  - 21 Yoon, B.-H., L.-J. Wang, Chlorate reduction in ClO<sub>2</sub> prebleaching by the addition of hypochlorous acid scavengers. *J. Pulp Paper Sci.*, **2002**; 28: 274–279.
  - 22 Hoigne, J., H. Bader, Kinetics of reactions of chlorine dioxide (OClO) in water. 1. Rate constants for inorganic and organic compounds. *Water Res.*, **1994**; 28(1): 45–55.
  - 23 Barroca, M.J.M.C., J.A.A.M. Castro, Kinetics of the first chlorine dioxide bleaching stage (D1) of a hardwood kraft pulp. *Ind. Eng. Chem. Res.*, **2003**; 42(18): 4156–4161.
  - 24 Tratnyek, P.G., J. Hoigne, Kinetics of reactions of chlorine dioxide (OClO) in water. 2. Quantitative structure-activity relationships for phenolic compounds. *Water Res.*, **1994**; 28(1): 57–66.
  - 25 Rajan, P.S., C.-L. Chen, J.S. Gratzl, P.S. Rajan, Formation of chloro-organics during chlorine bleaching of softwood kraft pulp: Part 2. Chlorination of pine kraft lignin fractions. *Holz-forschung*, **1996**; 50(2): 165–174.
  - 26 Gunnarsson, P.I., S. Ljunggren, Formation of chlorinated organic material and chlorate during chlorine dioxide prebleaching of kraft pulp: Effects of sodium chloride, charge of chlorine dioxide and pH. *J. Pulp Paper Sci.*, **1996**; 22(12): J457–J463.
  - 27 Gunnarsson, N.P.I., S.C.H. Ljunggren, The kinetics of lignin reactions during chlorine dioxide bleaching. Part 1. Influence of pH and temperature on the reaction of 1-(3,4-dimethoxyphenyl)ethanol with chlorine dioxide in aqueous solution. *Acta Chim. Scand.*, **1996**; 50(5): 422–431.
  - 28 Pei, Y.S., Z.K. Luan, H. Chen, Effects of electron activity and pH on the generation and stability of chlorine dioxide. *Chinese J. Inorg. Chem.*, **2001**; 17(3): 407–413.
  - 29 Svenson, D., J.F. Kadla, H.M. Chang, H. Jameel, Effect of pH on the mechanism of OClO center dot oxidation of aromatic compounds. *Can. J. Chem. – Rev. Canadienne De Chimie*, **2002**; 80(7): 761–766.
  - 30 Gu, Y.X., L. Edwards, Virtual bleach plants, part 2: Unified ClO<sub>2</sub> and Cl<sub>2</sub> bleaching model. *Tappi J.*, **2003**; 2(7): 3–8.
  - 31 Svenson, D.R., J.F. Kadla, H.M. Chang, H. Jameel, Effect of pH on the inorganic species involved in a chlorine dioxide reaction system. *Ind. Eng. Chem. Res.*, **2002**; 41(24): 5927–5933.
  - 32 Kieffer, R.G., G. Gordon, Disproportionation of chlorous acid. 2. Kinetics. *Inorg. Chem.*, **1968**; 7(2): 239–244.
  - 33 Kieffer, R.G., G. Gordon, Disproportionation of chlorous acid. I. Stoichiometry. *Inorg. Chem.*, **1968**; 7(2): 235–238.
  - 34 Björklund, M., U. Germgård, P. Jour, A. Forsström, AOX formation in ECF bleaching at different kappa numbers – Influence of oxygen delignification and hexenuronic acid content. *Tappi J.*, **2002**; 1(9): 20–24.
  - 35 Björklund, M., U. Germgård, J. Basta, Formation of AOX and OCI in ECF bleaching of birch pulp. *Tappi J.*, **2004**; 3(8): 7–12.
  - 36 Lachenal, D., M.J. Joncourt, P. Froment, C. Chirat, Reduction of the formation of AOX during chlorine dioxide bleaching. *J. Pulp Paper Sci.*, **1998**; 24(1): 14–17.
  - 37 Joncourt, M.J., P. Froment, D. Lachenal, C. Chirat, Reduction of AOX formation during chlorine dioxide bleaching. *Tappi J.*, **2000**; 83(1): 144–148.
  - 38 Ragnar, M., A. Törngren, Ways to reduce the amount of organically bound chlorine in bleached pulp and the AOX discharges from ECF bleaching. *Nordic Pulp Paper Res. J.*, **2002**; 17(3): 234–239.
  - 39 Nakamata, K., H. Ohi, Examination of polychlorinated dibenzo-p-dioxins and polychlorinated dibenzofurans in process water of kraft pulp bleaching mill using chlorine dioxide from the aspect of environmental water quality. *J. Wood Sci.*, **2003**; 49(6): 525–530.

- 40 Ohi, H., S. Hosoya, K. Magara, Dioxins levels in chlorine dioxide bleaching of hardwood oxygen-bleached kraft pulp (I). *Kami Pa Gikyoshi/Jpn. Tappi J.*, **2002**; 56(8): 92–98.
- 41 Süß, H.U., N. Nimmerfroh, Formation of halogenated compounds bleaching chemical pulp with hypochlorite and chlorine dioxide. *Das Papier*, **1991**; 45(2): 52–61.
- 42 Nakamata, K., Y. Motoe, H. Ohi, Evaluation of chloroform formed in process of kraft pulp bleaching mill using chlorine dioxide. *J. Wood Sci.*, **2004**; 50(3): 242–247.
- 43 Bright, D.A., P.V. Hodson, K.J. Lehtinen, B. McKague, J. Rodgers, K. Solomon, Use of chlorine dioxide for the bleaching of pulp: A re-evaluation of ecological risks based on scientific progress since 1993. *Pulp Paper Can.*, **2000**; 101(1): 53–55.
- 44 Solomon, K., H. Bergman, R. Huggett, D. Mackay, B. McKague, A review and assessment of the ecological risks associated with the use of chlorine dioxide for the bleaching of pulp. *Pulp Paper Can.*, **1996**; 97(10): 35–44.
- 45 Freire, C.S.R., A.J.D. Silvestre, C.P. Neto, J.A.S. Cavaleiro, Glucuronoxylan-derived chlorinated compounds in filtrates from chlorine dioxide bleaching: a comparative study between eucalypt (*E. globulus*) and birch (*Betula* spp.) kraft pulps. *Appita J.*, **2004**; 57(1): 40–42.
- 46 Freire, C.S.R., A.J.D. Silvestre, C.P. Neto, A.M.S. Silva, D.V. Evtuguin, J.A.S. Cavaleiro, Easily degradable chlorinated compounds derived from glucuronoxylan in filtrates from chlorine dioxide bleaching of *Eucalyptus globulus* kraft pulp. *Holzforschung*, **2003**; 57(1): 81–87.
- zz Svenson, D.R., H.M. Chang, H. Jameel, J.F. Kadla, The role of non-phenolic lignin in chlorate-forming reactions during chlorine dioxide bleaching of softwood kraft pulp. *Holzforschung*, **2005**; 59(2): 110–115.

### Sections 7.4.5–7.4.7

- 1 Lachapelle, R.C., W.G. Strunk, R.J. Klein, Using hydrogen peroxide in 100% chlorine dioxide bleaching sequences. *Tappi J.*, **1992**; 181–186.
- 2 Savoie, M., P. Tessier, A mathematical model for chlorine dioxide delignification. *Tappi*, **1997**; 80(6): 145–153.
- 3 Reeve, D.W., The technology of chemical pulping. Chapter 8: Chlorine dioxide in bleaching stages. In *Pulp Bleaching – Principles and Practice*, D.W. Reeve, C.W. Dence, Ed. TAPPI Press: Atlanta, GA, **1996**: 381–394.
- 4 Gierer, J., Chemistry of delignification. Part 2: Reactions of lignins during bleaching. *Wood Sci. Technol.*, **1986**; 20: 1–33.
- 5 Barroca, M.J.M.C., et al., Selectivity studies of oxygen and chlorine dioxide in the pre-delignification stages of a hardwood pulp bleaching plant. *Ind. Eng. Chem. Res.*, **2001**; 40: 5680–5685.
- 6 Svenson, D.R., et al., Effect of pH on the inorganic species involved in a chlorine dioxide reaction system. *Ind. Eng. Chem. Res.*, **2002**; 41(24): 5927–5933.
- 7 Teleman, A., et al., Characterization of 4-deoxy- $\beta$ -L-threo-hex-4-enopyranosyluronic acid attached to xylan in pine kraft pulp and pulping liquor by  $^1\text{H}$  and  $^{13}\text{C}$  NMR spectroscopy. *Carbohydrate Res.*, **1995**; 272: 55–71.
- 8 Marechal, A., Acid extraction of the alkaline wood pulps (Kraft or Soda/AQ) before or during bleaching, reason and opportunity. *J. Wood Chem. Technol.*, **1993**; 13(2): 261–281.
- 9 Vuorinen, T., et al. Selective hydrolysis of hexenuronic acid groups and its applications in ECF and TCF bleaching of kraft pulps. In 1996 International Pulp Bleaching Conference. Washington, **1996**.
- 10 Teleman, A., et al., Identification of the acidic degradation products of hexenuronic acid and characterization of hexenuronic acid-substituted xylooligosaccharides by NMR spectroscopy. *Carbohydrate Res.*, **1996**; 280: 197–208.
- 11 Suess, H.U. and C.L. Filho. Progress in bleaching to top brightness with low

- reversion. in 37th ABTCP Annual Conf. 2004. Sao Paolo, Brazil.
- 12 Juutilainen, D., et al. Combining chlorine dioxide bleaching of birch kraft pulp with an A stage at high temperature. In Tappi Pulping Conference, 1999.
  - 13 Ragnar, M., A. Torngren, Ways to reduce the amount of organically bound chlorine in bleached pulp and the AOX discharges from ECF bleaching. *Nordic Pulp Paper Res. J.*, 2002; 17(3): 234–239.
  - 14 Ragnar, M. Compact bleaching – a concept for fully bleached HW kraft pulp in only 2 stages. In 35th Congresso e Exposicao Anual de Celulose e Papel. Sao Paolo, Brazil: Associacao Brasileira Tecnica de Celulose e Papel, 2002.
  - 15 Suess, H.U., C.L. Filho, K. Schmidt. Bleaching of eucalyptus kraft pulp with low residual halogenated compounds (OX) “ECF”-light”. In 32nd ABTCP Annual Meeting. Sao Paolo, Brazil, 1999.
  - 16 Ragnar, M., M. Leite, Bleaching of cellulose pulp in a first chlorine dioxide bleaching step. *Kvaerner Pulping: PCT*, 2004.
  - 17 Seger, G.E., H. Jameel, H.-M. Chang, A two-step high-pH/low-pH method for improved efficiency of D-stage bleaching. *Tappi J.*, 1992; 174–180.
  - 18 Ljunggren, S., E.B. Gidnert, J. Kolar, Chlorine dioxide bleaching with a two-step low-high pH profile. *Tappi*, 1996; 79(12): 152–160.
  - 19 Cook, R.A., A bleaching process for minimizing AOX discharges. *Appita J.*, 1991; 44(3): 179–183.
  - 20 Jiang, Z.-H., B.v. Lierop, R. Berry. Improving chlorine dioxide bleaching with aldehydes. In International Pulp Bleaching Conference. Portland, OR, 2002.
  - 21 Solomon, K., et al., A review and assessment of the ecological risks associated with the use of chlorine dioxide for the bleaching of pulp. *Pulp Paper Can.*, 1996; 97(10): 35–44.
  - 22 Germgaard, U., S. Larsson, Oxygen bleaching in the modern softwood kraft pulp mill. *Pap. Puu*, 1983; 65(4): 287–290.
  - 23 Ni, Y., A.R.P.v. Heiningen, G.J. Kubes, Mechanism of formation of chloroorganics during chlorine dioxide prebleaching of kraft pulp. *Nordic Pulp Paper Res. J.*, 1993; 4: 350–351.
  - 24 Solomon, K.R., Chlorine in the bleaching of pulp and paper. *Pure Appl. Chem.*, 1996; 68(9): 1721–1730.
  - 25 Barroca, M.J.M.C., Seco, I.M., Fernandez, P.M.M., Ferreira, L.M.G.A., Castro, J.A.A.M., Reduction of AOX in the bleach plant of a pulp mill. *Environ. Sci. Technol.*, 2001; 35(21): 4390–4393.
  - 26 Björklund, M., et al., AOX formation in ECF bleaching at different kappa numbers – influence of oxygen delignification and hexenuronic acid content. *Tappi*, 2002; 1(7): 20–24.
  - 27 Buchert, J., et al., Effect of cooking and bleaching on the structure of xylan in conventional pine kraft pulp. *Tappi*, 1995; 78(11): 125–130.
  - 28 Vuorinen, T., et al. Selective hydrolysis of hexenuronic acid groups opens new possibilities for development of bleaching processes. In 9th International Symposium on Wood and Pulping Chemistry. Montreal, Canada, 1997.
  - 29 Lachenal, D., C. Chirat. High temperature ClO<sub>2</sub> bleaching of Kraft pulp. In International Pulp Bleaching Conference. Helsinki, Finland, 1998.
  - 30 Ohlavi, P., V. Janne. Ozone bleaching and AHL-stage acid treatment in a modern multichemical bleach plant. In 35th ABTCP Annual Conference. Sao Paolo, Brazil, 2002.
  - 31 Suess, H.U., et al., Approaches to minimize the formation of AOX in kraft pulp bleaching. *Das Papier*, 1990; 44(7): 339–348.
  - 32 Sixta, H., ECF bleaching of HW-Kraft pulps. *Internal Report*, R&D Lenzing AG, 2002.

### Sections 7.5.1–7.5.3, and 7.5.5

- 1 Kolb, M.J., *Bull. Soc. Ind. Mulhouse*, 1868; 38: 259.
- 2 Brin, A., L.Q. Brin. US Patent Application, 1889.

- 3 Cunningham, M., C. Doree, *Chem. Soc.*, **1912**; 101: 497.
- 4 Campbell, J., L.O. Rolleston. US Patent Application, **1930**.
- 5 Brabender, G.J., J.W. Bard, J.M. Daily. US Patent Application. **1949**.
- 6 Cotton, F.A., G. Wilkinson, *Advanced Inorganic Chemistry*. 5th edn. New York: John Wiley & Sons, **1988**: 452–454.
- 7 Trambarulo, R., et al., The molecular structure, dipole moment, and g factor of ozone from its microwave spectrum. *J. Chem. Phys.*, **1953**; 21: 851–855.
- 8 Huisgen, R., 1,3-Dipolar cycloadditions. *Angew. Chem.*, **1963**; 75(13): 604–637.
- 9 Kilpatrick, M.L., C.C. Herrick, M. Kilpatrick, The decomposition of ozone in aqueous solution. *J. Am. Chem. Soc.*, **1956**; 78: 1784–1789.
- 10 Quederni, A., J.C. Mora, R.S. Bes, Ozone absorption in water: Mass transfer and solubility. *Ozone Sci. Eng.*, **1987**; 9: 1–12.
- 11 Sotelo, J.L., et al., Henry's law constant for the ozone-water system. *Water Res.*, **1989**; 23(10): 1239–1246.
- 12 Kosak-Channing, L.F., G.R. Helz, *Environ. Sci. Technol.*, **1983**; 17(3): 145–149.
- 13 Oyama, S.T., Chemical and catalytic properties of ozone. *Catal. Rev. – Sci. Eng.*, **2000**; 42(3): 279–322.
- 14 Owen, D., J.R. Anderson, G. Homer, Bleaching Chemicals. In *Pulp Bleaching: Principles and Practice*, C.W. Dence, D.W. Reeve, Eds. Tappi Press: Atlanta, Georgia, **1996**: 71–90.
- 15 Bennington, C.P.J., Mixing gases into medium-consistency pulp suspensions using rotary devices. *Tappi J.*, **1993**; 76(7): 77–86.
- 16 Sixta, H., Evaluation of new mixing system. R&D Lenzing AG: Lenzing, **1997**.
- 17 Osawa, Z., C. Schuerch, The action of gaseous reagents on cellulosic materials. I. Ozonization and reduction of unbleached kraft pulp. *Tappi*, **1963**; 46(2): 79–87.
- 18 Bouchard, J., H.M. Nugent, R.M. Berry, The role of water and hydrogen ion concentration in ozone bleaching of kraft pulp at medium consistency. *Tappi J.*, **1995**; 78(1): 74–82.
- 19 Scallan, A.M., H.V. Green, *Wood Fiber*, **1975**; 7(3): 226–233.
- 20 Zhang, X.-Z., et al., Initial delignification and cellulose degradation of conventional and ethanol-assisted ozonation. *J. Wood Chem. Technol.*, **1998**; 18(2): 129–157.
- 21 Zhang, X.Z., Ozone bleaching of chemical pulp. PhD Thesis, University of New Brunswick: Fredericton, NB, **1998**.
- 22 Levenspiel, O., *The Chemical Reaction Omnibook*. Corvallis, Oregon: Oregon State University Book Stores, Inc., **1989**.
- 23 Griffin, R., Y. Ni, A.R.P.v. Heiningen, The development of delignification and lignin-cellulose selectivity during ozone bleaching. *J. Pulp Paper Sci.*, **1998**; 24(4): 111–115.
- 24 Liebergott, N., B.v. Lierop, A. Skothos, A survey of the use of ozone in bleaching pulps, Part 1. *Tappi J.*, **1992**; 75(1): 145–152.
- 25 Rewatkar, V.B., C.P.J. Bennington, Gas-liquid mass transfer in low- and medium-consistency pulp suspensions. *Can. J. Chem. Eng.*, **2000**; 78(3): 504–512.
- 26 Bennington, C.P.J., R.J. Kerekes, Power requirements for pulp suspension fluidization. *Tappi J.*, **1996**; 79(2): 253–258.
- 27 Gerzer, T., Medium consistency ozone bleaching in mill application. Lenzing AG: Lenzing, **2004**.
- 28 Sixta, H., Zellstoffherstellung unter Berücksichtigung umweltfreundlicher Aufschluß- und Bleichverfahren am Beispiel von Chemiezellstoffen. Habilitation Thesis, In Institute for Pulp, Paper and Fiber Technology. TU Graz: Graz, **1995**: 425.
- 29 Mielisch, H.-J., et al., TCF bleaching of kraft pulp: Investigation of the mixing conditions in an MC ozone stage. *Holz-forschung*, **1995**; 49(5): 445–452.
- 30 Sreeram, C., et al., Laboratory-scale medium-consistency ozone bleaching system. *Tappi J.*, **1994**; 77(10): 161–168.
- 31 Hurst, M.M., Effects of pulp consistency and mixing intensity on ozone bleaching. *Tappi J.*, **1993**; 76(4): 156–161.
- 32 Seth, R.S., C.P.J. Bennington, Fiber morphology and the response of pulps to medium-consistency fluidization. *Tappi J.*, **1995**; 78(12): 152–154.

- 33 Ellis, M.J., et al., Fibre deformation during medium consistency mixing: role of residence time and impeller geometry. *Appita J.*, 1998; 51(1): 29–34.
- 34 Funk, E., et al. Espanola ozone bleaching pilot plant: status report. In Tappi Pulping Conference, Boston, 1992.
- 35 Berry, R.M., et al. Medium consistency bleaching with high concentration ozone gas in the Paprican pilot plant and a comparison with laboratory bleaching. In International Pulp Bleaching Conference, Vancouver, Canada, 1994.
- 36 Henricson, K., J. Peltonen, T. Laxen, Bleaching of foamed pulp with ozone. European Patent Application, Ahlstrom, A., Corp., Finland, 1990.
- 37 Laxén, T., H. Ryyänänen, K. Henricson, Medium-consistency ozone bleaching. *Pap. Puu*, 1990; 72(5): 504–507.
- 38 Sixta, H., et al., Process for the chlorine-free bleaching of pulp. European Patent Application. Lenzing AG, Austria, 1991.
- 39 Sixta, H., et al., Medium consistency ozone bleaching: laboratory and mill experience. *Das Papier*, 1991; 45(10): 610–624.
- 40 Dillner, B., W. Peter, Application of MC ozone delignification to bleaching chemical pulp. *Pap. Puu*, 1992; 74(9): 720–726.
- 41 Sixta, H., et al., Towards effluent-free TCF-bleaching of eucalyptus prehydrolysis-kraft pulp. *Das Papier*, 1994; 48(8): 526–537.
- 42 Prutsch, W., et al. Chlorine-free bleaching of wood and annual plant pulp. In Wood and Pulping Chemistry Symposium, Raleigh, NC, 1989.
- 43 Lindholm, C.-A., Effect of heterogeneity in pulp bleaching with ozone. *Pap. Puu*, 1986; 4: 283–290.
- 44 Lindholm, C.-A., Effect of pulp consistency and pH in ozone bleaching; Part 2. Lignin removal and carbohydrate degradation. In Tappi Proceedings – International Oxygen Delignification Conference, 1987.
- 45 Berggren, R., Cellulose degradation in pulp fibers studied as changes in molar mass distributions. PhD-Thesis, In Department of Fibre and Polymer Technology. Royal Institute of Technology: Stockholm, 2003.
- 46 Lindholm, C.-A., Effect of dissolved reaction products on pulp viscosity in low consistency ozone bleaching. *Pap. Puu*, 1990; 72(3): 254–256.
- 47 Oltmann, E., et al., Ozone bleaching technology: a comparison between high and medium consistency. Part I. *Das Papier*, 1992; 7: 341–350.
- 48 Ragner, M., Ozone bleaching installations. Personal communication, 2004.
- 49 Krotscheck, A., A. Wimmer, Ozone bleaching installations. Personal communication, 2004.
- 50 Jakobson, B., P.O. Lindblad, N.-O. Nilvebrandt. Lignin reactions affect the attack of ozone on carbohydrates. In 1991 International Pulp Bleaching Conference, SPCI. Stockholm, Sweden, 1991.
- 51 Rutkowski, J., R. Szopinski, Investigations on bleaching of sulfate pine pulp with ozone. *Cellulose Chem. Technol.*, 1984; 18: 323–333.
- 52 Lindholm, C.-A., *Cellulose Chem. Technol.*, 1989; 23(3): 307–319.
- 53 Kishimoto, T., F. Nakatsubo, Non-chlorine bleaching of kraft pulp. V. Participation of radical species in ozonation of methyl 4-O-ethyl-β-D-glucopyranoside. *Holzforschung*, 1998; 52(2): 185–190.
- 54 Staehelin, J., J. Hoigné, Decomposition of ozone in water: rate of initiation by hydroxide ions and hydrogen peroxide. *Environ. Sci. Technol.*, 1982; 16(10): 676–681.
- 55 Staehelin, J., R.E. Bühler, J. Hoigné, Ozone decomposition in water studied by pulse radiolysis. 2. OH and HO<sub>4</sub> as chain intermediates. *J. Phys. Chem.*, 1984; 88: 5999–6004.
- 56 Pan, G.Y., et al., Studies on ozone bleaching. I. The effect of pH, temperature, buffer systems and heavy metal ions on stability of ozone in aqueous solution. *J. Wood Chem. Technol.*, 1984; 4(3): 367–387.
- 57 Ragnar, M., T. Eriksson, T. Reitberger, Radical formation in ozone reactions with lignin and carbohydrate model compounds. *Holzforschung*, 1999; 53(3): 292–298.

- 58 Ragnar, M., et al., A new mechanism in the ozone reaction with lignin-like structures. *Holzforschung*, 1999; 53(4): 423–428.
- 59 Allison, R.W., Effects of temperature and chemical pretreatment on pulp bleaching with ozone. In International Pulp Bleaching Conference, CPPA. Quebec, Canada, 1985.
- 60 Chandra, S., Studies on ozonization of softwood pulps and evaluation of oxygen prebleaching options. In Department of Wood and Paper Science. NC State University: Raleigh, NC, 1985.
- 61 Soteland, N., Comparison between oxygen and ozone delignification of sulphite pulps. In Tappi Symposium – Oxygen Delignification, 1984.
- 62 Liebergott, N., B.v. Lierop, A. Skothos, A survey of the use of ozone in bleaching pulps, Part 2. *Tappi J.*, 1992; 2: 117–124.
- 63 Patt, R., O. Kordsachia, D.L.-K. Wang, Einsatz von Ozon zur Zellstoffbleiche. *Das Papier*, 1988; 42(10A): V14–V23.
- 64 Simoes, R.M.S., J.A.A.M.e. Castro, Ozone delignification of pine and eucalyptus kraft pulps. 2. Selectivity. *Ind. Eng. Chem. Res.*, 1999; 38: 4608–4614.
- 65 Lindqvist, B., et al., Ozone bleaching of sulfite pulps. In Tappi Proceedings – International Sulfite Pulping Conference, 1982.
- 66 Lindqvist, B., A. Marklund, Ozone bleaching of sulfite pulps. *Svensk. Papperstidn.*, 1984; 6: 54–64.
- 67 Staehelin, J., J. Hoigné, Decomposition of ozone in water in the presence of organic solutes acting as promoters and inhibitors of radical chain reactions. *Environ. Sci. Technol.*, 1985; 19(12): 1206–1213.
- 68 Chirat, C., D. Lachenal, Minimizing pulp degradation during totally chlorine free bleaching sequences including an ozone stage. In International Pulp Bleaching Conference Papers, 1994.
- 69 Szopinski, R., B. Stromberg, High brightness using totally chlorine free (TCF) bleaching sequences. In Non-Chlorine Bleaching Conference. Hilton Head, 1993.
- 70 Gause, E., et al., Ozone bleaching technology: a comparison between high and medium consistency. Part II. *Das Papier*, 1993; 47(7): 331–337.
- 71 Funk, E., et al., Espanola ozone bleaching pilot plant: progress update. In 47th Annual General Conference, APPITA. Parkville, Victoria, Australia, 1993.
- 72 Ek, M., et al., Study on the selectivity of bleaching with oxygen-containing species. *Holzforschung*, 1989; 43(6): 391–396.
- 73 Buxton, G.V., Greenstock, C.L., Helman, W.P., Ross, A.B., Critical review of rate constants for reactions of hydrated electrons, hydrogen atoms and hydroxyl radicals in aqueous solution. *J. Phys. Chem. Ref. Data*, 1988; 17(2): 513–886.
- 74 Kamishima, K., T. Fujii, I. Akkatsu, Factors affecting the carbohydrate protection of methanol during ozone bleaching. *Mokuzai Gakkaishi*, 1983; 29(7): 474–480.
- 75 Brolin, A., J. Gierer, Z. Zhang, On the selectivity of ozone delignification of softwood kraft pulps. *Wood Sci. Technol.*, 1993; 27: 115–129.
- 76 Ruiz, J., et al., Ozone organosolv bleaching of radiata pine kraft pulp. *Wood Sci. Technol.*, 1997; 31: 217–223.
- 77 Zhang, Y., et al., Degradation of wood polysaccharide model compounds during ozone treatment. *J. Pulp Paper Sci.*, 1997; 23(1): J23–J27.
- 78 Magara, K., et al., Accelerated degradation of cellulose in the presence of lignin during ozone bleaching. *J. Pulp Paper Sci.*, 1998; 24(8): 264–268.
- 79 Johansson, E.E., J. Lind, S. Ljunggren, Aspects of the chemistry of cellulose degradation and the effect of ethylene glycol during ozone delignification of kraft pulps. *J. Pulp Paper Sci.*, 2000; 26(7): 239–244.
- 80 Heiningen, A.R.P.v., Y. Ni, Ozone dioxane bleaching of chemical pulp. US Patent Application. University of New Brunswick, CA, 1994.
- 81 Ni, Y., T. Ooi, Laboratory study on bleaching softwood kraft pulp by a totally chlorine-free process including the novel ozone bleaching. *Tappi J.*, 1996; 79(10): 167–172.
- 82 Lindholm, C.-A., Effect of pulp consistency and pH in ozone bleaching. Part

4. Alkaline extraction of ozone-bleached pulp. *Pap. Puu*, **1989**; 2: 145–154.
- 83 Bouchard, J., E. Morelli, R.M. Berry, Gas-phase addition of solvent to ozone bleaching of kraft pulp. *J. Pulp Paper Sci.*, **2000**; 26(1): 30–34.
- 84 Kang, G.J., Y. Ni, A.R.P.V. Heiningen, Further understanding on the cause of cellulose degradation during ozone bleaching. *Ippita*, **2001**; 13(4): 1–5.
- 85 Hoigné, J., H. Bader, The role of hydroxyl radical reactions in ozonation processes in aqueous solutions. *Water Res.*, **1976**; 10: 377–386.
- 86 Roncero, M.B., J.F. Colom, T. Vidal, Why oxalic acid protects cellulose during ozone treatments? *Carbohydrate Polymers*, **2002**; 52: 411–422.
- 87 Lindeberg, O., Concurrent bleaching and metal management by addition of EDTA to chlorine dioxide and ozone stages, degradation of EDTA and formation of oxalic acid. In International Pulp Bleaching Conference. Tappi, **1996**.
- 88 Brown, J., et al., Medium-consistency ozone bleaching with enzyme pretreatment. *Tappi J.*, **1994**; 77(11): 105–109.
- 89 Rynnänen, H., P.J. Nelson, C.W.J. Chin, Ozone bleaching of eucalypt kraft pulps. *Appita*, **1995**; 48(6): 440–444.
- 90 Lindholm, C.-A., Alkaline extraction of ozone-bleached pulp. Part 1. General aspects and outlines for further research. *Pap. Puu*, **1992**; 74(3): 224–231.
- 91 Odermatt, J., et al., The application of sodium tetrahydroborate to improve the properties of ozonized softwood kraft pulp. *Cellulose Chem. Technol.*, **1998**; 32(3–4): 309–325.
- 92 Chirat, C., D. Lachenal, Effect of ozone on pulp components application to bleaching of kraft pulps. *Holzforschung*, **1994**; 48 (Suppl.): 133–139.
- 93 Patt, R., TCF bleaching of softwood kraft pulp with particular emphasis on Borol solution stabilization of ozone treated pulp. Report, University of Hamburg: Hamburg, **1995**.
- 94 Lindholm, C.-A., Alkaline extraction of ozone-bleached pulp. Part 2. Effect of leachable lignin. *Nordic Pulp Paper Res. J.*, **1992**; 2: 95–102.
- 95 Liebergott, N., B.v. Liero, The use of ozone in bleaching and brightening wood pulps. Part I. Chemical pulps. In Tappi – Oxygen, Ozone and Peroxide Bleaching. New Orleans, **1978**.
- 96 Liebergott, N., et al., Bleaching a softwood kraft pulp without chlorine compounds. In Tappi Proceedings – Pulping Conference, **1983**.
- 97 Lorás, V., N. Soteland, Bleaching of sulphite pulps with oxygen and ozone. In Tappi Proceedings – International Pulp Bleaching Conference, **1982**.
- 98 Gupta, M.K., R.C. Eckert, OZ prebleaching: Influence on viscosity and sheet strength. In Tappi Symposium – Oxygen Delignification, **1984**.
- 99 Godsay, M.P., E.M. Pearce. Physicochemical properties of ozone oxidized kraft pulps. In Tappi Symposium – Oxygen Delignification, **1984**.
- 100 Bokström, M., M. Wennerström, Ozone comes of age. *Pulp Paper Europe*, **2001**; 6(5).
- 101 Metso, PulpWay (brochure). Metso Paper: Sundsvall, Sweden, **2001**.
- 102 Eriksson, T., T. Reitberger, Formation of hydroxyl radicals from direct ozone reactions with pulp constituents. In 8th International Symposium on Wood and Pulping Chemistry (ISWPC). Helsinki, Finland, **1995**.
- 103 Chirat, C., D. Lachenal, Effect of hydroxyl radicals on cellulose and pulp and their occurrence during ozone bleaching. *Holzforschung*, **1997**; 51(2): 147–154.
- 104 Zhang, Y., On the selectivity of ozone delignification during bleaching. PhD Thesis, In Department of Fibre and Polymer Technology. Kungliga Tekniska Högskolan (KTH): Stockholm, Sweden, **1994**.
- 105 Gratzl, J.S., Die chemischen Grundlagen der Zellstoffbleiche mit Sauerstoff, Wasserstoffperoxid und Ozon – ein kurzer Überblick. *Das Papier*, **1992**; 10A: V1–V8.
- 106 Ragnar, M., On the importance of radical formation in ozone bleaching. PhD Thesis, In Pulp and Paper Research Institute. KTH: Stockholm, Sweden, **2000**.



- 107 Gierer, J., Y. Zhang. The role of hydroxyl radicals in ozone bleaching process. In Seventh International Symposium on Wood and Pulping Chemistry (ISWPC). Beijing, China, 1993.
- 108 Ragnar, M., On the importance of the structural composition of pulp for the selectivity of ozone and chlorine dioxide bleaching. *Nordic Pulp Paper Res. J.*, 2001; 16(1): 72–79.
- 109 Pan, G., et al., Model experiments on the splitting of glycosidic bonds by ozone. In International Symposium of Wood and Pulping Chemistry (ISWPC), Stockholm, Sweden 1981.
- 110 Herbst, H.E., H. Krässig, The distribution of oxidant consumption in bleaching. *Tappi*, 1959; 42(8): 660–664.
- 111 Soteland, N., Bleaching of chemical pulps with oxygen and ozone. *Pulp Paper Mag. Can.* 1974; 75(4): 91–96.
- 112 Patt, R., et al. In TAPPI Oxygen Delignification Symposium, 1984.
- 113 Antonsson, S., et al., A comparative study of the impact of the cooking process on oxygen delignification. *Nordic Pulp Paper Res. J.*, 2003; 18(4): 388–394.
- 114 Chandra, S., Studies on ozonation of softwood pulps and evaluation of oxygen prebleaching options. PhD Thesis, Department of Wood and Paper Science, NC State University, Raleigh NC.
- 115 Secrist, R.B., R.P. Singh, Kraft pulp bleaching. II. Studies on the ozonation of chemical pulps. *Tappi*, 1971; 54(4): 581–584.
- 116 Lindholm, C.-A., Effect of pulp consistency and pH in ozone bleaching. Part 6. Strength properties. *Nordic Pulp Paper Res. J.*, 1990; 1: 22–27.
- 117 Axegard, P., et al., Bleaching of softwood kraft pulps with H<sub>2</sub>O<sub>2</sub>, O<sub>3</sub>, and ClO<sub>2</sub>. *Tappi J.*, 1996; 79(1): 113–119.
- 118 Dillner, B., P. Tibbling, Optimum use of peroxide and ozone in TCF bleaching. In International Pulp Bleaching Conference. Vancouver, BC: TAPPI Press, 1994.
- 119 Rydholm, S.A., Pulping Processes. Malabar, Florida. Robert E. Krieger Publishing Co., Inc., 1965: 971.
- 120 Liebergott, N., B.v. Lierop, Ozone delignification of black spruce and hardwood kraft, kraft-anthraquinone, and soda-anthraquinone pulps. *Tappi*, 1981; 64(6): 95–99.
- 121 Berggren, R., et al., Fiber strength in relation to molecular mass distribution of hardwood kraft pulp. Degradation by ozone and acid hydrolysis. *Nordic Pulp Paper Res. J.*, 2001; 16(4): 333–338.
- 122 Lachenal, D., N.B. Nguyen-Thi. TCF bleaching – Which sequence to choose? In Tappi Proceedings – Pulping Conference, 1993.
- 123 Baldinger, T., A. Potthast, Evaluation of keto groups generated along the cellulose chain from combined GPC-CCOA measurement. CD Laboratory, Internal Report: Vienna, 2004.
- 124 Lachenal, D., M.T. Taverdet, M. Muguet. Improvement in the ozone bleaching of kraft pulps. In International Pulp Bleaching Conference. Stockholm, Sweden, 1991.
- 125 Lachenal, D., M. Muguet, Degradation of residual lignin in kraft pulp with ozone. Application to bleaching. *Nordic Pulp Paper Res. J.*, 1992; 1: 25–29.
- 126 Chirat, C., et al., (DZ) and (ZD) bleaching: Fundamentals and application. *J. Pulp Paper Sci.*, 1997; 23: 289–292.
- 127 Homer, G., et al., State of the art ECF bleaching. Part 3: Effects of ozone and chlorine dioxide on bleaching and effluent chemistry. In Emerging Technologies Conference. Orlando, Florida, 1997.
- 128 Chirat, C., D. Lachenal, Other ways to use ozone in a bleaching sequence. *Tappi J.*, 1997; 80(9): 209–214.
- 129 Lierop, B.v., R.M. Berry, B.P. Roy, High-brightness bleaching of softwood kraft pulps with oxygen, ozone and peroxide. *J. Pulp Paper Sci.*, 1997; 23(9): 428–432.
- 130 Lachenal, D., J. Papadopoulos, Improvement of hydrogen peroxide delignification. *Cellulose Chem. Technol.*, 1988; 22: 537–546.
- 131 Sixta, H., Influence of pulp properties on the ozone bleaching performance. R&D Lenzing AG, Lenzing, 2002.

## Section 7.5.4

- 1 Staehelin, J., R.E. Bühler and J. Hoigné, Ozone decomposition in water studied by pulse-radiolysis. 2. OH and HO<sub>4</sub> as chain intermediates. *J. Phys. Chem.*, **1984**; *88*(24): 5999–6004.
- 2 Staehelin, J., J. Hoigné, Mechanism and kinetics of decomposition of ozone in water in the presence of organic solutes. *Vom Wasser*, **1983**; *61*: 337–348.
- 3 Staehelin, J., J. Hoigné, Decomposition of ozone in water – rate of initiation by hydroxide ions and hydrogen-peroxide. *Environ. Sci. Technol.*, **1982**; *16*(10): 676–681.
- 4 Gurol, M.D., P.C. Singer, Kinetics of ozone decomposition – a dynamic approach. *Environ. Sci. Technol.*, **1982**; *16*(7): 377–383.
- 5 Bühler, R.E., J. Staehelin, J. Hoigné, Ozone decomposition in water studied by pulse-radiolysis. 1. HO<sub>2</sub>/O<sub>2</sub>- and HO<sub>3</sub>/O<sub>3</sub>- as intermediates. *J. Phys. Chem.*, **1984**; *88*(12): 2560–2564.
- 6 Hoigné, J., H. Bader, W.R. Haag, J. Staehelin, Rate constants of reactions of ozone with organic and inorganic-compounds in water. 3. Inorganic-compounds and radicals. *Water Res.*, **1985**; *19*(8): 993–1004.
- 7 Chirat, C., D. Lachenal, Effect of hydroxyl radicals on cellulose and pulp and their occurrence during ozone bleaching. *Holzforschung*, **1997**; *51*(2): 147–154.
- 8 Kang, G.J., Y. Ni, A.R.P. van Heiningen, Mechanism of cellulose protection in a novel and selective ozone pulp bleaching process. Annual Meeting – Technical Section, Canadian Pulp and Paper Association, Preprints, **1996**.
- 9 Kishimoto, T., F. Nakatsubo, Non-chlorine bleaching of kraft pulp. II. Ozonation of methyl 4-O-ethyl-beta-D-glucopyranoside. Quantitative analysis of reaction products. *Holzforschung*, **1996**; *50*(4): 372–378.
- 10 Kishimoto, T., F. Nakatsubo, Non-chlorine bleaching of kraft pulp. V. Participation of radical species in ozonation of methyl 4-O-ethyl-beta-D-glucopyranoside. *Holzforschung*, **1998**; *52*(2): 185–190.
- 11 Lemeune, S., J.M. Barbe, A. Trichet, R. Guillard, Degradation of cellulose models during an ozone treatment. Ozonation of glucose and cellobiose with oxygen or nitrogen as carrier gas at different pH. *Ozone: Science and Engineering*, **2000**: 447–460.
- 12 Lewin, M., Oxidation and aging of cellulose. *Macromolecular Symposia*, **1997**; *118*: 715–724.
- 13 King, J.E., A.R.P. van Heiningen, Effect of pulp species and pretreatment on the rates of delignification and cellulose degradation during ozone bleaching. *Pulp Paper Can.*, **2003**; *104*(10): 38–42.
- 14 Magara, K., T. Ikeda, Y. Tomimura, S. Hosoya, Accelerated degradation of cellulose in the presence of lignin during ozone bleaching. *J. Pulp Paper Sci.*, **1998**; *24*(8): 264–268.
- 15 Kang, G.J., Y. Ni, A.R.P.V. Heiningen, Further understanding on the cause of cellulose degradation during ozone bleaching. *Appita*, **2001**; *13*(4): 1–5.
- 16 Johansson, E.E., J. Lind, S. Ljunggren, Aspects of the chemistry of cellulose degradation and the effect of ethylene glycol during ozone delignification of kraft pulps. *J. Pulp Paper Sci.*, **2000**; *26*(7): 239–244.
- 17 Zhang, X.Z., Y. Ni, A. van Heiningen, Kinetics of cellulose degradation during ozone bleaching *J. Pulp Paper Sci.*, **2000**; *26*(9): 335–340.
- 18 Magara, K., T. Ikeda, Y. Tomimura, S. Hosoya, Accelerated degradation of cellulose by lignin during ozonolysis. *Mokuzai Gakkaishi*, **1994**; *40*(10): 1152–1154.
- 19 Sakai, K., J.M. Uprichard, Ozone degradation of cellulose model compounds. *J. Faculty Agric. Kyushu University*, **1991**; *36*(1–2): 45–53.
- 20 Pan, G.Y., C.L. Chen, J.S. Gratzl, and H.M. Chang, Model-compound studies on the cleavage of glycosidic bonds by ozone in aqueous-solution. *Res. Chem. Intermediates*, **1995**; *21*(3–5): 205–222.
- 21 Zhang, X.Z., G.J. Kang, Y. Ni, A.R.P. van Heiningen, A. Mislankar, A. Darabie, D. Reeve, Initial delignification and cellulose degradation of con-

- ventional and ethanol-assisted ozonation. *J. Wood Chem. Technol.*, **1998**; 18(2): 129–157.
- 22 Zhang, X.Z., G.J. Kang, Y. Ni, A.R.P. van Heiningen, Delignification and cellulose degradation rates during novel and conventional ozone bleaching. *Abstracts, Papers Am. Chem. Soc.*, **1996**; 211: 199-CELL.
- 23 Roncero, M.B., M.A. Queral, J.F. Colom, T. Vidal, Why acid pH increases the selectivity of the ozone bleaching processes. *Ozone Sci. Eng.*, **2003**; 25(6): 523–534.
- 24 Staehelin, J., J. Hoigné, Decomposition of ozone in water in the presence of organic solutes acting as promoters and inhibitors of radical chain reactions. *Environ. Sci. Technol.*, **1985**; 19(12): 1206–1213.
- 25 Pan, G.Y., C.-L. Chen, H.-M. Chang, J.S. Gratzl, Studies on ozone bleaching. I. The effect of pH, temperature, buffer systems and heavy metal-ions on stability of ozone in aqueous solution. *J. Wood Chem. Technol.*, **1984**; 4(3): 367–387.
- 26 Parthasarathy, V.R., R.C. Peterson. Ozone Bleaching. Part I. The decomposition of ozone in aqueous solution – Influence of pH, temperature and transition metals on the rate kinetics of ozone decomposition. In *Tappi Symposium Notes – Oxygen Delignification*, **1990**.
- 27 Hoigné, J., H. Bader, Rate constants of reactions of ozone with organic and inorganic-compounds in water. 1. Non-dissociating organic compounds. *Water Res.*, **1983**; 17(2): 173–183.
- 28 Hoigné, J., H. Bader, Rate constants of reactions of ozone with organic and inorganic-compounds in water. 2. Dissociating organic compounds. *Water Res.*, **1983**; 17(2): 185–194.
- 29 Gierer, J., The chemistry of delignification. A general concept. Part II. *Holzfor-schung*, **1982**; 36(1): 55–64.
- 30 Gierer, J., Formation and involvement of superoxide ( $O_2^{\bullet-}/HO_2^{\bullet}$ ) and hydroxyl ( $OH^{\bullet}$ ) radicals in TCF bleaching processes: A review. *Holzfor-schung*, **1997**; 51(1): 34–46.
- 31 Ragnar, M., T. Eriksson, T. Reitberger, Radical formation in ozone reactions with lignin and carbohydrate model compounds. *Holzfor-schung*, **1999**; 53(3): 292–298.
- 32 Ragnar, M., T. Eriksson, T. Reitberger, P. Brandt, M. Ragnar, A new mechanism in the ozone reaction with lignin like structures. *Holzfor-schung*, **1999**; 53(4): 423–428.
- 33 Ek, M., J. Gierer, K. Jansbo, Study on the selectivity of bleaching with oxygen-containing species. *Holzfor-schung*, **1989**; 43(6): 391–396.
- 34 Chirat, C., D. Lachenal, Effect of ozone on pulp components application to bleaching of kraft pulps. *Holzfor-schung*, **1994**; 48: 133–139.
- 35 Soteland, N., Some attempts to characterize the oxidized lignin after ozone treatment of western hemlock groundwood. Part II. *Norsk Skogindustri.*, **1971**; 5: 135–139.
- 36 Plonka, A.M., J. Rutkowski, R. Szopinski, Changes of the chromophore system in sulfate pine pulp treated with ozone. *Cellulose Chem. Technol.*, **1987**; 21(5): 535–541.
- 37 Ni, Y., G.J. Kang, A.R.P. van Heiningen, Are hydroxyl radicals responsible for degradation of carbohydrates during ozone bleaching of chemical pulp? *J. Pulp Paper Sci.*, **1996**; 22(2): J53–J57.
- 38 Kang, G.J., Y.J. Zhang, Y.G. Ni, A.R.P. van Heiningen, Influence of lignins on the degradation of cellulose during ozone treatment. *J. Wood Chem. Technol.*, **1995**; 15(4): 413–430.
- 39 Zhang, Y., G. Kang, Y. Ni, A.R.P. van Heiningen, Degradation of wood polysaccharide model compounds during ozone treatment. *J. Pulp Paper Sci.*, **1997**; 23(1): J23–J27.
- 40 Olkkonen, C., H. Tylli, I. Forsskahl, A. Fuhrmann, T. Hausalo, T. Tamminen, B. Hortling, J. Janson, Degradation of model compounds for cellulose and ligno-cellulosic pulp during ozonation in aqueous solution. *Holzfor-schung*, **2000**; 54(4): 397–406.
- aa Hewes, C. G., R. R. Davison, Kinetics of Ozone Decomposition and Reaction with Organics in Water. *Aiche Journal*, **1971**; 17(1): 141–&.
- bb Alder, M. G., G. R. Hill. The Kinetics and Mechanism of Hydroxide Ion Cata-

- lyzed Ozone Decomposition in Aqueous Solution. *Journal of the American Chemical Society*, **1950**; 72(5): 1884–1886.
- xx Zhang, X.-Z., Y. Ni, A. van Heiningen, Kinetics of Cellulose Degradation During Ozone Bleaching. *J. Pulp Paper Sci.*, **2000**; 26(9): 335–339.
- yy Chirat, C., D. Lachenal, Effect of hydroxyl radicals on cellulose and pulp and their occurrence during ozone bleaching. *Holzforschung* **1997**; 51(2): 147–154.
- ### Section 7.6
- 1 Thenard, L.J., *Ann. Chim. Phys.*, **1818**; 8: 306.
  - 2 Schumb, W.C., C.N. Satterfield, R.L. Wenworth, *Hydrogen Peroxide*. Reinhold Publ. Co.: New York, **1955**: 18.
  - 3 Berthelot, H., *Compt. Rend.*, **1878**; 86: 71.
  - 4 BASF, in DRP 649234, **1934**.
  - 5 BASF, in DRP 6583767, **1935**.
  - 6 Goor, G., Hydrogen peroxide: Manufacture and industrial use for production of organic chemicals. In *Catalytic Oxidations with Hydrogen Peroxide as Oxidant*, G. Strukal, Ed. Kluwer Academic Publishers, **1992**: 13–43.
  - 7 Greenwood, N.N., A. Earnshaw, *Chemie der Elemente*. VCH, **1988**.
  - 8 Takagi, J., K. Ishigure, Thermal decomposition of hydrogen peroxide and its effect on reactor water monitoring of boiling water reactors. *Nuclear Sci. Eng.*, **1985**; 89: 177–186.
  - 9 Gierer, J., The chemistry of delignification. A general concept. Part II. *Holz-forschung*, **1982**; 36(2): 55–64.
  - 10 Gellerstedt, G., I. Pettersson, Chemical aspects of hydrogen peroxide bleaching. Part II. The bleaching of kraft pulps. *J. Wood Chem. Technol.*, **1982**; 2(3): 231–250.
  - 11 Gierer, J., Chemistry of delignification. 2. Reactions of lignins during bleaching. *Wood Sci. Technol.*, **1986**; 20(1): 1–33.
  - 12 Gierer, J., The chemistry of delignification. A general concept. Part II. *Holz-forschung*, **1982**; 36(1): 55–64.
  - 13 Duarte, A.P., D. Lachenal, Hydrogen peroxide production during oxygen bleaching of *Eucalyptus globulus* kraft pulp – origin of cellulose degradation. *Pap. Puu*, **2002**; 84(4): 275–277.
  - 14 Barton, D.H.R., D.T. Sawyer. O<sub>2</sub> and HOOH activation. In *The Activation of Dioxygen and Homogeneous Catalytic Oxidation*. Texas A&M University, College Station: Plenum Press, **1993**.
  - 15 Brooks, R.E., S.B. Moore, Alkaline hydrogen peroxide bleaching of cellulose. *Cellulose*, **2000**; 7: 263–286.
  - 16 Buda, F., et al., DFT Study of the Active Intermediate in the Fenton Reaction. *Chemistry – A European Journal*, **2001**. 7(13): 2775–2783.
  - 17 Nunn, J.R., M.J.v.d. Linde. The protective action of magnesium in oxygen bleaching of pulp. Part 1: The complexing of methyl-alpha-D-glucopyranoside with magnesium ions. In First International Symposium on Delignification with Oxygen Ozone and Peroxides. Raleigh, North Carolina, USA: North Carolina State University, **1975**.
  - 18 Qiu, Z., Improvement in hydrogen peroxide bleaching by decreasing manganese-induced peroxide decomposition. In The University of New Brunswick. The University of New Brunswick: Fredericton, **2000**: 88.
  - 19 Wiklund, L., L.-O. Ohman, J. Liden, Solid solution formation between Mn(II) and Mg(II) hydroxides in alkaline aqueous solution. *Nordic Pulp Paper Res. J.*, **2001**; 16: 240–245.
  - 20 Reitberger, T., et al., Involvement of oxygen-derived free radicals in chemical and biochemical degradation of lignin. In *Oxidative Delignification Chemistry*, D.S. Argyropoulos, Ed. American Chemical Society, Oxford University Press: Washington, DC, **2001**: 255–271.
  - 21 Lapierre, L., R. Berry, J. Bouchard, The effect of magnesium ions and chelants on peroxide bleaching. *Holzforschung*, **2003**; 57(6): 627–633.
  - 22 Gierer, J., The chemistry of delignification. A general concept. Part I. *Holz-forschung*, **1982**; 36(1): 43–51.
  - 23 Gierer, J., F. Imsgard. The reactions of lignin with oxygen and hydrogen peroxide in alkaline media. In First International Symposium on Delignification with Oxygen Ozone and Peroxides.

- Raleigh, North Carolina, USA: North Carolina State University, 1975.
- 24 Heuts, L., G. Gellerstedt, Oxidation of guaiacylglycerol-beta-guaiacyl-ether with alkaline hydrogen peroxide in the presence of kraft pulp. *Nordic Pulp Paper Res. J.*, 1998; 13(2): 107–111.
  - 25 Gellerstedt, G., L. Heuts, Changes in the lignin structure during a totally chlorine free bleaching sequence. *J. Pulp Paper Sci.*, 1997; 23(7): J335–J340.
  - 26 Liu, S.J., Chemical kinetics of alkaline peroxide brightening of mechanical pulps. *Chem. Eng. Sci.*, 2003; 58(11): 2229–2244.
  - 27 Gierer, J., ( $O_2\bullet$ -/ $HO_2\bullet$ ) and hydroxyl ( $OH\bullet$ ) radicals in TCF bleaching processes: A review. *Holzforschung*, 1997; 51(1): 34–46.
  - 28 Gierer, J., Formation and involvement of superoxide ( $O_2$ -/ $HO_2$ -) and hydroxyl ( $OH\bullet$ ) radicals in TCF bleaching processes: A review. *Holzforschung*, 1997; 51(1): 34–46.
  - 29 Gierer, J., The interplay between oxygen-derived radical species in the delignification during oxygen and hydrogen peroxide bleaching. In *Lignin: Historical, Biological, and Materials Perspectives*. ACS, 2000: 422–446.
  - 30 Gierer, J., The interplay between oxygen-derived radical species in the delignification during oxygen and hydrogen peroxide bleaching. *ACS Symposium Series*, 1999: 422–446.
  - 31 Gierer, J., K. Jansbo, T. Reitberger, Formation of hydroxyl radicals from hydrogen-peroxide and their effect on bleaching of mechanical pulps. *J. Wood Chem. Technol.*, 1993; 13(4): 561–581.
  - 32 Abbot, J., et al., The influence of manganese and magnesium on alkaline peroxide bleaching of radiata pine thermomechanical pulp. *Appita J.*, 1992; 45(2): 109.
  - 33 Brelid, H., T. Friberg, R. Simonson, TCF bleaching of softwood kraft pulp. Part 3. Ion exchange of softwood kraft pulp prior to oxygen delignification. *Doktorsavhandlingar vid Chalmers Tekniska Högskola*, 1998.
  - 34 Brelid, H., T. Friberg, R. Simonson, TCF bleaching of softwood kraft pulp. Part 4. Removal of manganese from wood shavings prior to cooking. *Doktorsavhandlingar vid Chalmers Tekniska Högskola*, 1998.
  - 35 Lapiere, L., Bouchard, J., Berry, R.M., van Lierop, V., Chelation prior to hydrogen peroxide bleaching of kraft pulps: an overview. *J. Pulp Paper Sci.*, 1995; 21(8): 268–273.
  - 36 Bouchard, J., H.M. Nugent, R.M. Berry, A comparison between acid treatment and chelation prior to hydrogen peroxide bleaching of kraft pulps. *J. Pulp Paper Sci.*, 1995; 21(6): 203–208.
  - 37 Phinney, S., Less bleach – Brighter paper. *Chemical Innovation*, 2001: 3–5.
  - 38 Sjogren, B., J. Hook, Extended oxygen delignification – The effect of pretreatments and process conditions. 2000 International Pulp Bleaching Conference: Oral Presentations, 2000: 89–96.
  - 39 Gratzl, J.S., The chemical principles of pulp bleaching with oxygen, hydrogen peroxide and ozone – a short review. Die chemischen Grundlagen der Zellstoffbleiche mit Sauerstoff, Wasserstoffperoxid und Ozon – ein kurzer Überblick. *Papier*, 1992; 46(10A): V1–V8.
  - 40 Guay, D.F., Cole, B.J.W., Fort, R.C., Hausman, M.C., Genco, J.M., Elder, T.J., Overly, K.R., Mechanisms of oxidative degradation of carbohydrates during oxygen delignification. II. Reaction of photochemically generated hydroxyl radicals with methyl beta-cellobioside. *J. Wood Chem. Technol.*, 2001; 21(1): 67–79.
  - 41 Guay, D.F., Cole, B.J.W., Fort, Jr. R.C., Genco, J.M., Hausman, M.C.,  $\beta$ -D-glucopyranoside with photochemically generated hydroxyl radicals. *J. Wood Chem. Technol.*, 2000: 20: 375–394.
  - 42 Guay, D.F., Cole, B.J.W., Fort, Jr. R.C., Hausman, M.C., Genco, J.M., Elder, T.J., Mechanisms of oxidative degradation of carbohydrates during oxygen delignification. Part III: Reaction of photochemically generated hydroxyl radicals with 1,5-anhydrocellobitol and cellulose. *J. Pulp Paper Sci.*, 2002; 28(7): 217–221.
  - 43 Zeronian, S.H., M.K. Inglesby, Bleaching of cellulose by hydrogen peroxide. *Cellulose*, 1995; 2(4): 265–272.

- 44 Lewin, M., Oxidation and aging of cellulose. *Macromolecular Symposia*, **1997**; 118: 715–724.
- 45 Chirat, C., Mateo, C., Furstoss, H., Jeunet, A., Lachenal, D., Formation of chromophores from carbohydrates during pulping and their impact on bleaching. *Pulp Paper Canada*, **2002**; 103(2): 28–30.
- 46 Mielisch, H.-J., O. Kordsachia, and R. Patt, Katalysierte Wasserstoffperoxidbleiche. *Das Papier*, **1996**; 50: V16–V23.
- 47 Suess, H.U., W. Eul, O. Hemling, Semi-bleaching of Kraft pulp using oxygen and hydrogen peroxide. *Das Papier*, **1989**; 43(7): 318–323.
- 48 Suess, H.U., J.D. Kronis. Impact of carbonate ions on hydrogen peroxide in sodium carbonate solutions. In International Pulp Bleaching Conference, Portland, OR, **2002**.
- 49 Lee, H.H.B., A.-H. Park, C. Oloman, Stability of hydrogen peroxide in sodium carbonate solutions. *Tappi J.*, **2000**; 83(8): 94.
- 50 Stromberg, C.B., R. Szopinski. Pressurized hydrogen peroxide bleaching for improved TCF bleaching. In International Pulp Bleaching Conference, Vancouver, BC, TAPPI Press, **1994**.
- 51 Dillner, B., Tibbling. Optimum use of peroxide and ozone in TCF bleaching. In International Pulp Bleaching Conference. Vancouver, BC: TAPPI Press, **1994**.
- 52 Suess, H.U., C.L. Filho. ECF Bleaching: Balancing hydrogen peroxide bleaching effects and pulp yield. In ABTC Annual Meeting, **1997**.
- 53 Suess, H.U., N. Nimmerfroh, H.D. Kronis, The naked truth on hot peroxide bleaching. *Pulp Paper Canada*, **1998**; 99(4): T122–T125.
- 54 Colodette, J.L., S. Rothenburger, C.W. Dence, Factors affecting hydrogen peroxide stability in the brightening of mechanical and chemimechanical pulps. Part III: Hydrogen peroxide stability in the presence of magnesium and combinations of stabilizers. *J. Pulp Paper Sci.*, **1989**; 15(2): J45.
- 55 Suess, H.U., B. Hopf, K. Schmidt, Optimising peroxide bleaching of deinked pulps in the disperser. *Wochenblatt für Papierfabrikation*, **2002**; 130(11/12): 738–745.
- 56 Sjödin, L., S. Noren. Extended delignification with oxygen and hydrogen peroxide in ECF and TCF sequences. In Tappi Pulping Conference, **1994**.
- 57 Ragnar, M., Alkaline extraction and a control strategy for the chlorine dioxide charge to the final stage in DED bleaching. *Nordic Pulp Paper Res. J.*, **2003**; 18(2): 162–167.
- 58 Milanez, A., J.L. Colodette. Optimum conditions for bleaching eucalyptus kraft pulp with a three stage sequence. In International Pulp Bleaching Conference, Stockholm, **2005**.
- 59 Strunk, W.G., Kraft bleach plants increase use of hydrogen peroxide as benefits mount. *Pulp Paper*, **1990**; 10: 112–116.
- 60 Höök, J., L. Mueller, S. Wallin, Väteperoxid i alkalistegen höjer kvaiteten. *Nordisk Cellulosa*, **1985**; 2: 47–50.
- 61 Andersson, L., et al. The use of hydrogen peroxide bleaching for bleaching of chemical pulp. In Tappi Pulping Conference, **1985**.
- 62 Loufti, H., The use of hydrogen peroxide in bleaching of North-Eastern softwood pulp. In CPPA Annual Meeting, **1981**.
- 63 PAPTAC, Standard Testing Methods, Montreal, Sep. 2003.
- 64 Gullichsen, J., The influence of temperature and humidity in the color reversion of pulp. *Pap. Puu*, **1965**; 47: 215.
- 65 Hausalo, T., L. Söderhjelm, Chemical analysis of pulps. In *Pulp and Paper Testing*, J.E. Levlin, L. Söderhjelm, Eds. Fapet Oy: Helsinki, **1999**: 128–129.
- 66 Rydholm, S.A., *Pulping Processes*. Malabar, Florida: Robert E. Krieger Publishing Co., Inc., **1965**: 851–854.
- 67 Gellerstedt, G., O. Dahlman. Recent hypothesis for brightness reversion of hardwood pulps. In International Colloquium on Eucalyptus Kraft pulp. Universidade Federal de Vicosá, MG, Brazil, **2003**.
- 68 Tenkanen, M., et al., Heat-induced brightness reversion of ECF-light bleached pine kraft pulp. In 7th European Workshop on Lignocellulosics and Pulp. Turku, **2002**.

- 69 Suess, H.U., K. Schmidt, B. Hopf, ECF bleaching: Improving brightness stability of kraft pulp. *IPW/Papier*, 2004; 6: T105–T111.
- 70 Jääskeläinen, A.-S., et al., Characterization of residual lignin structures by UV Raman spectroscopy and the possibilities of Raman spectroscopy in the visible region with Kerr-gated fluorescence rejection. In International Symposium on Wood and Pulping Chemistry, Madison, WI, 2003.
- 71 Fischer, K., Vergilbung von Hochausbeutezellstoff. *Das Papier*, 1990; 44(10A): V11.
- 72 Eckert, R.C. US Patent 894561, 1978.
- 73 Jäkärä, J., A. Paren, J. Patola, Peroxide activation – a key to high brightness in TCF bleaching of softwood Kraft pulp. In International Symposium on Wood and Pulping Chemistry. Helsinki, Finland, 1995.
- 74 Hämäläinen, H., et al., Mill scale application of a molybdate activated peroxide delignification process in ECF and TCF production of softwood and hardwood Kraft pulp. In International Symposium on Wood and Pulping Chemistry. Madison, WI, 2003.
- 75 Patt, R., T. Jaschinski, H.-J. Mielisch, Stabilisierte und katalysierte Peroxidbleiche. *Wochenblatt für Papierfabrikation*, 1996; 17: 750–755.
- 76 Wieghardt, K., Die aktiven Zentren in manganhaltigen Metallproteinen und anorganische Modellkomplexe. *Angew. Chem.*, 1989; 101: 1179–1198.
- 77 Suess, H.U., J.D. Kronis, B. Taylor. Selection of the best available technology for TCF bleaching of sulfite pulp. In Tappi Pulping Conference, 1998.
- 78 Wackerberg, E., et al., High temperature peroxide stage optimization on hardwood and softwood sulfite pulp. In Tappi Pulping Conference, 1997.
- 79 Heimbürger, S.A., K.F. French, N. Weber. Optimizing pressurized peroxide bleaching of a hardwood sulfite pulp. In Tappi Pulping Conference, 1997.
- 80 Böttcher, H., R. Kamprath, Umweltfreundliche Zellstoffherzeugung auf Basis des konventionellen Magnesium-Bisulfit-Verfahrens. *Das Papier*, 1990; 44(10A): V26–V32.
- 81 Nimmerfroth, N., et al., The German approach to the closed-cycle sulfite mill – development and implementation. *Pulp Paper Canada*, 1995; 96(12): T414–T420.
- 82 Suess, H.U., K. Schmidt, M.d. Grosso. Options to improve TCF-bleaching of sulfite pulp. In 57th Appita Annual Conference, Melbourne, Australia, 2003.
- 83 Sturm, W., Hochweisse Sulfitzellstoffe durch absolut chlorfreie Bleiche – Aktivierung von Peroxid durch Nitrilamin. *Wochenblatt für Papierfabrikation*, 1990; 118(10): 423–424.
- 84 Kuchler, J.G., W.G.J. Sturm, H.E. Teichmann, Hohe Weißgrade und deutlich bessere Delignifizierungsleistung in der OPMgO-Stufe – Aktivierung von Peroxid durch Nitrilamin (Teil 2). *Das Papier*, 1993; 2: 53–55.
- 85 Kappel, J., M. Grengg, Bräuer, High-consistency bleaching technology for TCF pulps. *Pulp Paper Canada*, 1994; 95(1): T1–T6.
- 86 Sixta, H., et al., Medium consistency ozone bleaching: laboratory and mill experience. *Das Papier*, 1991; 45(10): 610–624.
- 87 Wickström, P., Improved brightness by adding a peracetic acid stage. In International Pulp Bleaching Conference, Stockholm, Sweden, 2005: p. 216–221.
- [aa] Kadla, J. F., H.-M. Chang, H. Jameel, The Reactions of Lignins with High Temperature Hydrogen Peroxide Part 2. The Oxidation of Kraft Lignin. *Holz-forschung*, 1999; 53(3): 277–284.
- [bb] Kadla, J. F., H. M. Chang, Jameel, H., The reactions of lignins with hydrogen peroxide at high temperature .1. The oxidation of lignin model compounds. *Holz-forschung*, 1997; 51(5): 428–434.

## Section 7.7

- 1 Ruohoniemi, K., et al. Experience in the use of peracetic acid in ECF and TCF bleaching. In International Pulp Bleaching Conference, Helsinki, 1998.

- 2 Jäkärä, J., A. Parén, P. Autio. The use of peracetic acid as a brightening agent. In *Appita Conference Proceedings*, 1999.
- 3 Francis, R.C., et al., Caraoate delignification enhanced by halides. *Tappi*, 1994; 77(7): 135–141.
- 4 Stüss, H.U., K. Schmidt, Generation of halogenated compounds in bleaching without chlorine. Can TCF be chlorine-free? *IPW/Papier*, 2000; 1(5): T69–T73.

## Section 7.8

- 1 Marechal, A., Acid extraction of the alkaline wood pulps (Kraft or Soda/AQ) before or during bleaching, reason and opportunity. *J. Wood Chem. Technol.*, 1993; 13(2): 261.
- 2 Teleman, A., et al., Characterization of 4-deoxy- $\beta$ -L-threo-hex-4-enopyranosyluronic acid attached to xylan in pine kraft pulp and pulping liquor by  $^1\text{H}$  and  $^{13}\text{C}$  NMR spectroscopy. *Carbohydrate Res.*, 1995; 272: 55–71.
- 3 Li, J., G. Gellerstedt, The contribution to kappa number from hexenuronic acid groups in pulp xylan. *Carbohydrate Res.*, 1997; 302: 213–218.
- 4 Fengel, D., G. Wegener, *Wood: chemistry, ultrastructure, reactions*. New York: de Gruyter, 1983: 49, 109–112.
- 5 Vuorinen, T., et al., Selective hydrolysis of hexenuronic acid groups and its applications in ECF and TCF bleaching of kraft pulps. In *International Pulp Bleaching Conference*. Washington, 1996.
- 6 Jiang, Z.-H., B.v. Lierop, R. Berry, Hexenuronic acid groups in pulping and bleaching chemistry. *Tappi*, 2000; 83(1): 167–175.
- 7 Gellerstedt, G., O. Dahlman. Recent hypothesis for brightness reversion of hardwood pulps. In *International Colloquium on Eucalyptus Kraft pulp*. Universidade Federal de Vicosa, MG, Brazil, 2003.
- 8 Ohlavi, P., V. Janne. Ozone bleaching and AHL-stage acid treatment in a modern multichemical bleach plant. In *35th ABTCP Annual Conference*. Sao Paolo, Brazil, 2002.

## Section 7.9

- 1 Viikari, L., Ranua, M., Kantelinen, A., Sundquist, J., Linko, M. 3rd International Conference on Biotechnology in the Pulp and Paper Industry, STFI, Stockholm, 1986.
- 2 2,2'-azinobis(3-ethylbenzothiazoline-6-sulfonic acid).
- 3 Call, H.P., PCT World Patent Application No. WO 94/29510, 1994.
- 4 Call, H.P., PCT World Patent Application No. WO 97/36041, 1997.
- 5 1-Hydroxybenzotriazole.
- 6 Galli, C., Gentili, P., *J. Phys. Org. Chem.*, 2004; 17: 973.
- 7 Call, H.P., Mücke, I., *J. Biotechnol.*, 1997; 53: 163.
- 8 Rochefort, D., Leech, D., Bourbonnais, R., *Green Chem.*, 2004; 6: 14
- 9 Rochefort, D., Bourbonnais, R., Leech, D., Renaud, S., Paice, M., *J. Electrochem. Soc.*, 2002; 149: D15.
- 10 ACS Symposium Series 785, Oxidative Delignification Chemistry, Argyropoulos, D.S. Ed., ACS, Washington, 2001.
- 11 Weinstock, I.A., Hill, C.L., US Patent 5,302,248, 1994.
- 12 Evtuguin, D.V., Pascoal Neto, C., Portuguese Patent 101 857, 1996.
- 13 For more information on polyoxometalates see: Polyoxometalates, *Chem. Rev.*, 1998; 98: 1.
- 14 Atalla, R.H., Weinstock, I.A., Bond, J.S., Reiner, R.S., Sonnen, D.M., Houtman, C.J., Heintz, R.A., Hill, C.G., Hill, C.L., Wemple, M.W., Geletii, Yu.V., Barbuzzi, E.M.G., Polyoxometalate-based closed systems for oxidative delignification of wood pulp fibers. In ACS Symposium Series 785, Oxidative Delignification Chemistry, Argyropoulos, D.S. Ed., ACS, Washington, 2001: 313.
- 15 Weinstock, I.A., Barbuzzi, E.M.G., Wemple, M.W., Cowan, J.J., Reiner, R.S., Sonnen, D.M., Heintz, R.A., Bond, J.S., Hill, C.L., *Nature*, 2001; 414: 191.
- 16 Evtuguin, D.S., Pascoal Neto, C., Catalytic oxidative delignification with Keggin-type molybdovanadophosphate het-



eropolyanions. In ACS Symposium Series 785, Oxidative Delignification Chemistry, Argyropoulos, D.S. Ed., ACS, Washington, 2001: 313.

### Section 7.10

- 1 Süß, H.U., N. Nimmerfroh, Hydrogen peroxide in chemical pulp bleaching. ABTCP Meeting. Vitoria, Brazil, 1996.
- 2 Süß, H.U., Personal communication, 2004.
- 3 Annergren, G.E., M.G. Boman, P.E. Sandström, Towards the closed cycle bleach plant. 5th International Conference on Newly Available Techniques. Stockholm, Sweden, 1996.
- 4 Zolio, A., M.R. Silva, M.A.L. Peixoto, Calcium oxalate scaling in bleach plants: VCP experience. 33rd Pulp and Paper Annual Congress. Sao Paulo, Brazil, 2000.
- 5 Reid, D.W., M.L. Hinck, Factors contributing to calcium oxalate scale at the Simpson Tacoma kraft mill. *Tappi J.*, 2003; 2(2): 8–13.

## 8

# Pulp Purification

Herbert Sixta

### 8.1

#### Introduction

The production of dissolving pulp involves the removal of short-chain carbohydrates, denoted as hemicelluloses, which negatively influence either the processing behavior of the pulp or the quality of the final product. (The technical definition of hemicelluloses comprises both alkali-soluble heteropolysaccharides and degraded cellulose soluble in the steeping lye.) Purification processes for dissolving pulps include both the removal of noncellulosic material (e.g., extractives, lignin, hemicelluloses), and the change of the molecular distribution to a narrow, monomodal type of distribution with a minimum amount of low molecular-weight carbohydrates. The extent of purification should thus be adjusted to the need of the dissolving process, and pulp grades of varying purity level are available. It is a well-known fact that the mechanical properties of the viscose fibers correlate quite well with the amount of short-chain molecules. As early as 1941, Hermans stated that the chain-length distribution in the dissolving pulp is a crucial property in the production of rayon fibers [1]. In addition, by using sulfite and prehydrolysis-kraft (PHK) pulps of different purity levels, Avela et al. were able to demonstrate that all strength characteristics are significantly reduced with an increase in the low molecular-weight fraction [2]. The short-chain molecules represent the weakest part in the fiber; this means that, the shorter the molecules, the lower will be the number of molecules linking the crystalline regions. In a recent study, a correlation between the strength properties of rayon fibers and the amount of low molecular-weight fraction (expressed as the DP50-fraction) was established, using a set of dissolving pulps prepared by different organosolv processes [3].

In general, caustic extraction steps are conducted to remove short-chain carbohydrates from wood pulp that resisted the pulping process, in order to obtain favorable product characteristics such as improved material properties (e.g., increased fiber strength), higher brightness and brightness stability. These alkaline purification procedures can be carried out in two different ways – as either cold or hot caustic extractions. While the cold process, which is conducted at 20–

40 °C and high sodium hydroxide concentration (1.2–3.0 mol L<sup>-1</sup>), involves mainly physical changes, the hot purification process, operated in the range between 70 °C and 130 °C and low sodium hydroxide concentration (0.1–0.4 mol L<sup>-1</sup>), induces multiple carbohydrate degradation reactions. In addition to cleavage of the terminal glycosyl groups, one by one via  $\beta$ -alkoxy elimination (*peeling* reaction) until the reducing end group is converted into a corresponding aldonic acid (alkali-resistant metasaccharinic acid end group), a series of fragmentations to mainly short-chain organic acids (mainly C<sub>2</sub> and C<sub>3</sub> hydroxy acids) occurs at elevated temperatures. This explains why the alkali consumption does not correspond to 1 mol per degraded monosaccharide, but rather to 1.6 mol, indicating that fragmentation to smaller acids takes place [4].

Unlike PHK pulps, acid sulfite pulps require the application of both technologies to achieve purification levels appropriate to produce high-tenacity regenerated fibers (e.g., continuous-filament industrial rayons), cellulose acetate or cellulose ethers of pure quality. Cold alkali purification is certainly the most selective way of increasing the alpha-cellulose content of the pulp. The yield losses are in the range of 1.2–1.5% per increase of 1% in alpha-cellulose content [4]. In the case of hot caustic extraction, a yield loss of about 3% per 1% increase in alpha-cellulose content is experienced. However, cold caustic extraction is rarely used on a technical scale because of the huge amounts of alkali needed. When working at 10% consistency and 10% NaOH concentration, 1 t NaOH odt<sup>-1</sup> pulp is necessary to charge. In combination with a PHK process, part of the press-lye can be re-used in the cooking process or, alternatively, white liquor can be used for the cold extraction process. Another means of employing the excess lye is to use it for hot alkaline purification, with the prerequisite that the production of hot alkali-purified pulp considerably exceeds that of cold alkali-purified pulp. Recirculation of the lye (after pressing) significantly deteriorates the result of the purification, due to an accumulation of impurities derived from short-chain carbohydrate degradation products, being characterized as beta- and gamma-celluloses. Beta-cellulose is defined as the precipitate formed upon acidification of an aqueous alkaline solution containing the dissolved pulp constituents, while gamma-cellulose comprises the carbohydrate residue in solution. The former consists of higher molecular-weight, the latter of lower molecular-weight material.

These compounds can be (partly) removed by means of dialysis of (part of) the press-lye [4,5]. In addition, inter- and even intramolecular swelling of pulps under the conditions of cold caustic extraction (low temperature combined with high alkali concentration in the vicinity of the swelling maximum) impedes the removal of excess lye during the course of subsequent washing. An optimum between purification performance and limitation of fiber swelling can be found by adjusting the temperature and caustic charge.

The treatment of pulp with aqueous sodium hydroxide solution still represents the principal means of producing highly purified dissolving pulp. When applying these caustic treatments, the extent of purification can be controlled by adjusting the appropriate conditions. The relationship between the process conditions, involving both sodium hydroxide concentration and temperature, and the course of

reaction comprising the carbohydrate constituents of a selected hardwood sulfite dissolving pulp is described in the next section.

## 8.2

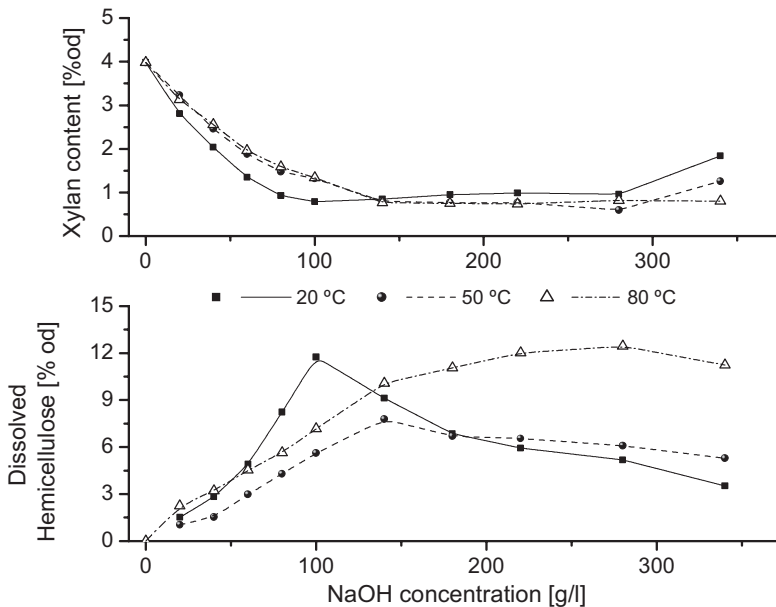
### Reactions between Pulp Constituents and Aqueous Sodium Hydroxide Solution

Wood pulp obtained by the acid sulfite process still contains considerable amounts of low molecular-weight carbohydrates (hemicelluloses). These make the pulp less suitable for many purposes as known for the production of cellulose acetate, high-purity cellulose ethers or high-tenacity regenerated fibers. As mentioned previously, the pulp is refined with alkali either at temperatures below 50 °C whereby strong solutions of sodium hydroxide are used (characterized as cold caustic extraction, CCE), or at higher temperatures using weaker alkaline solutions (characterized as hot caustic extraction, HCE). In some cases, both processes are applied subsequently (in any order: CCE before or after HCE) to obtain the highest purity dissolving pulp derived from the sulfite cooking process. It is well known that the extraction of wood pulp with strong sodium hydroxide solutions at low temperatures produces higher levels of alpha-cellulose than with dilute solutions at high temperatures, while the yields obtained are considerably higher. The basis of both purification processes was developed during the 1940s and 1950s. Hempel studied the solubility of viscose pulps at 20 °C in the range of NaOH concentration between 1 and 20%, with the emphasis on maximum solubility [6]. Shogenji and associates treated chlorinated sulfite pulp at 25 °C with 3 to 12% NaOH and investigated the alkaline solutions after treatment for total and combined alkali [7]. Wilson and coworkers tested the alkali solubility of pulp in relation to the alpha-cellulose determination, and stated that wood originally contains appreciable amounts of gamma-cellulose of low degree of polymerization (10–30), but no beta-cellulose [8]. The latter is formed during the pulping processes from alpha-cellulose. Many studies have been conducted to determine phase-transition during the treatment of pulp or cotton linters with alkaline solutions of varying concentrations, using X-ray diffraction. Ranby studied the appearance of cellulose hydrate when treating different cellulose substrates at 0 °C with increasing concentrations of sodium hydroxide [9]. With cotton, the first indication of hydrate cellulose occurs at 8% NaOH, whereas with wood pulp it occurs already at 6% NaOH. The NaOH concentration necessary for transition is related to the water sorption of the original cellulose, which means that cellulose undergoing transition at low NaOH concentration has a high water sorption. An electron-microscopic study of spruce holocellulose indicated that alpha-cellulose is built up of micelle strings about 8 nm wide, whereas gamma-cellulose contains no strings [10]. The beta-cellulose fraction appears to be a mixture of short string fragments and small particles. An X-ray investigation showed that both alpha- and beta-celluloses show the same type of lattice (cellulose II). The gamma-cellulose seems to consist of several phases different from cellulose II. The beta-cellulose is assumed

to originate from alpha-cellulose by degradation during the pulping and bleaching processes.

The composition of the beta- and gamma-celluloses fractions removed from the wood pulp during cold and hot extraction processes with respect to the amount of unchanged carbohydrates has been the focus of few studies. Corbett and Kidd studied the degradation of a mixture of beta- and gamma-celluloses extracted by hot alkali from spruce pulp [11]. These authors found that the insoluble residue essentially consists of glucan, and whereas the beta-cellulose fraction is made predominantly of xylan, the gamma-cellulose originates from a mixture of glucan and mannan. In a recent study, the change in composition of the alpha- (residue), beta- and gamma-celluloses fractions created during treatment of a beech sulfite dissolving pulp with aqueous NaOH of various concentrations ranging from 20 to 340 g L<sup>-1</sup> at 20 °C, 50 °C and 80 °C, was investigated [12]. The pulp consistency was kept constant at 5%, which is a typical value for the industrial steeping process. The profile of the xylan content of the residue (alpha-cellulose) and the weight fraction of the dissolved hemicelluloses (sum of beta- and gamma-cellulose) related to the initial amount of pulp is illustrated graphically in Fig. 8.1.

As expected, xylan removal is more efficient at 20 °C than at higher temperatures. To obtain the lowest possible xylan content in the pulp residue (about 0.7% appears to be alkali-resistant), the NaOH concentration must be increased from

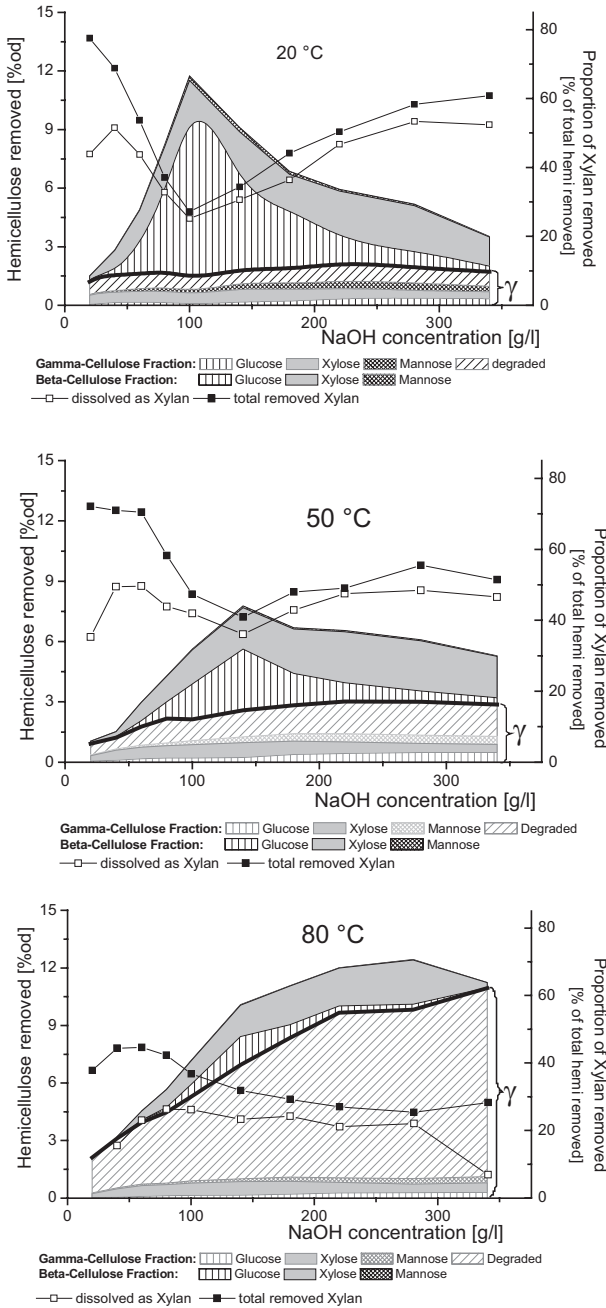


**Fig. 8.1** Profiles of xylan content in the pulp residue (upper) and the amount of dissolved hemicelluloses (sum of beta- and gamma-cellulose) (lower) during alkaline treatment of a beech sulfite dissolving pulp (93.4% R18, 4.0% xylan) at different temperatures [12]. Caustic treatment: 5% consistency, 30 min reaction time, NaOH concentrations: 20, 40, 60, 80, 100, 140, 180, 280, and 340 g L<sup>-1</sup>.

100 g L<sup>-1</sup> to about 140 g L<sup>-1</sup> when raising the temperature from 20 to 50 °C. The alkaline treatments at 50 °C and 80 °C reveal a comparable pattern of xylan removal up to a lye concentration of about 280 g L<sup>-1</sup>. The xylan removal efficiency remains unchanged at 80 °C and also at NaOH concentration up to 340 g L<sup>-1</sup>, but is slightly reduced at lower temperatures.

The profile of the amount of hemicelluloses dissolved during alkaline treatment resembles the swelling behavior of cellulose in dependence on lye concentration, as experienced by Saito [13,14]. At low temperature (20 °C), the amount of dissolved hemicelluloses increases rapidly with increasing NaOH concentration, and passes through a maximum at 100 g NaOH L<sup>-1</sup>. While the residual xylan content remains fairly constant with increasing lye concentration, the amount of dissolved hemicellulose decreases significantly to values less than half of the amount determined at maximum solubility. In the low lye concentration range up to 170 g NaOH L<sup>-1</sup>, the solubility of pulp constituents is significantly lower at 50 °C as compared to 20 °C, whereas the maximum solubility is shifted to 140 g NaOH L<sup>-1</sup>. At higher NaOH concentrations, the pattern of the solubility of hemicelluloses develops quite comparably for both temperatures, 20 °C and 50 °C, respectively. In contrast, alkaline treatment at 80 °C causes a steady increase in hemicellulose solubility up to a NaOH concentration of 280 g L<sup>-1</sup>. Beyond this lye concentration, the amount of dissolved hemicelluloses experiences a slight reduction (see Fig. 8.1, lower). In hot alkali treatments (80 °C), the removal of short-chain carbohydrates is essentially governed by chemical degradation reactions involving endwise depolymerization reactions (the *peeling* reaction). With increasing temperature, the peeling reaction becomes the dominant pathway for the degradation of pulp carbohydrates. This explains the different pattern of hemicelluloses removal as compared to the alkaline treatment at lower temperatures (20 °C and 50 °C). In contrast, cold alkali treatment at 20 °C induces intermicellar and intramicellar swelling, permitting short-chain material to dissolve. The physical interaction between cellulose and aqueous sodium hydroxide proceeds in several steps. According to Bartunek [15] and Dobbins [16], the addition of low amounts of electrolytes (e.g., NaOH) seems to create unbound or “monomeric” water by shifting the equilibrium between clustered and free water. Swelling can thus be explained by the penetration of the unbound water molecules into the cellulose structure, while destroying intermolecular hydrogen bonds. Moreover, swelling facilitates the accessibility of the hydrated ions into the crystalline structure. The degree of swelling is governed by both the number of water molecules present as hydrates of the alkali ions entering the cellulose structure, which decreases with increasing lye concentration, and the penetration depth of these alkali ions into the structure, which increases with lye concentration until the conversion to alkali cellulose is completed. Thus, swelling passes through a maximum at a lye concentration that is sufficient to ensure complete penetration of the whole structure. The decrease in swelling beyond this value can be explained by a disproportionately large reduction of the hydration number when further increasing the NaOH concentration.

It can be assumed that the extent of hemicellulose dissolution proceeds parallel to the swelling behavior of the pulp. The monomeric sugar composition of the

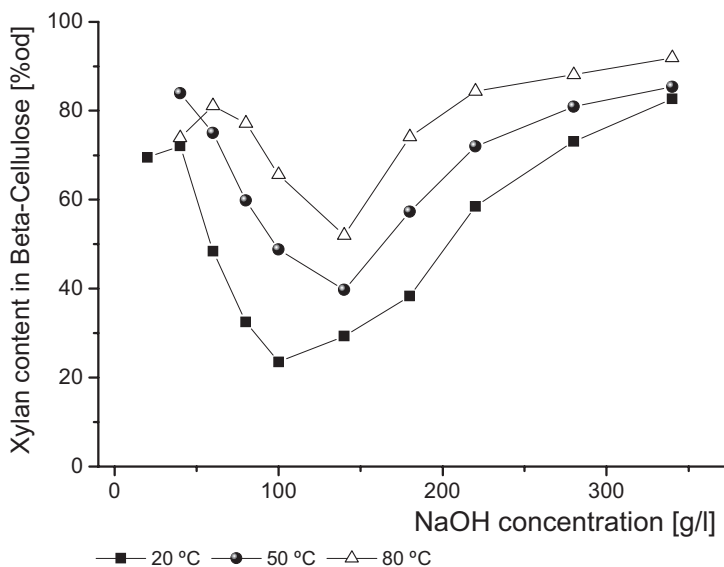


**Fig. 8.2** Profiles of carbohydrate composition of the gamma- and beta-celluloses fractions dissolved during alkalinization of a beech sulfite dissolving pulp (93.4% R18, 4.0% xylan) at three different temperatures: (a) 20 °C; (b) 50 °C; (c) 80 °C [12]. Caustic treatment: 5% consistency, 30 min reaction time, NaOH concentrations: 20, 40, 60, 80, 100, 140, 180, 280, and 340 g L<sup>-1</sup>.

dissolved hemicelluloses was analyzed by anion-exchange chromatography (AEC) with pulsed amperometric detection (PAD) after separation into beta- and gamma-cellulose fractions [17]. It is noted that the proportion of beta-cellulose decreases with increasing temperature, particularly above 50 °C. While the absolute amount of gamma-cellulose remains fairly constant at 20–50 °C throughout the whole range of NaOH concentrations investigated, the increase in the total amount of dissolved hemicelluloses at 80 °C is mainly attributed to an increase in the gamma-cellulose fraction (see Fig. 8.2). The fact that up to 90% of the gamma-cellulose fraction consists of degraded carbohydrates (equal to non-neutral sugars) clearly indicates that the removal of hemicelluloses through alkaline treatment at 80 °C is mainly governed by chemical degradation reactions (e.g. peeling reaction). As stated previously, the extent of chemical degradation reactions decreases with decreasing temperatures. Accordingly, the amount of degraded carbohydrates decreases at lower temperatures. The beta-cellulose fraction originating from any alkaline treatment consists almost exclusively of neutral sugars (except for uronic acid side chains and oxidized end groups). As anticipated, the maximum yield of beta-cellulose corresponds with the maximum solubility of the hemicelluloses (sum of beta- and gamma-celluloses) at an alkaline treatment at 20 °C and 50 °C, and with the lowest xylan content in the pulp residue at any temperature investigated. Parallel to its highest yield, the beta-cellulose consists of the highest glucan content (74 wt.%, 59 wt.% and 47 wt.% based on beta-cellulose for 20 °C, 50 °C, and 80 °C, respectively). It can be assumed that the glucan fraction derives from degraded cellulose and comprises the highest molecular weight within the beta-cellulose. Surprisingly, the treatment at 80 °C also produces a beta-cellulose fraction enriched with degraded cellulose at the same conditions where a complete removal of alkali soluble xylan occurs. This indicates that at a lower lye concentration the cellulose structure is opened by inter- and intramolecular swelling, even at high temperatures. Apart from degraded cellulose, the predominant hemicellulose fraction in beech sulfite dissolving pulps is made up of xylan, while the glucmannan content is almost negligible. Therefore, the main objective of the alkali purification processes comprises removal of the residual xylan content.

By comparing the amount of xylan removed from the pulp with the amount recovered in both the beta- and gamma-cellulose fractions, it can be concluded that most xylan is recovered in oligomeric and polymeric structures. The proportion of degraded xylan is greater only in the lower NaOH concentration range (up to 80 g L<sup>-1</sup>) where the easily degradable fraction is removed. Apart from the minimum at a NaOH concentration of 100 g L<sup>-1</sup> at 20 °C and 140 g L<sup>-1</sup> at 50 °C and 80 °C due to the increased dissolution of degraded cellulose, the beta-cellulose becomes increasingly enriched with xylan as both the NaOH concentration and temperature are raised (Fig. 8.3). This means that the xylan part in the hemicelluloses is clearly more resistant to alkaline degradation than the other carbohydrate components. The major part of the xylan remains stable even after hot caustic extraction (100 °C, 0.25 N NaOH, 1–4 h) as exemplified in a study conducted by Corbett and Kidd [11].



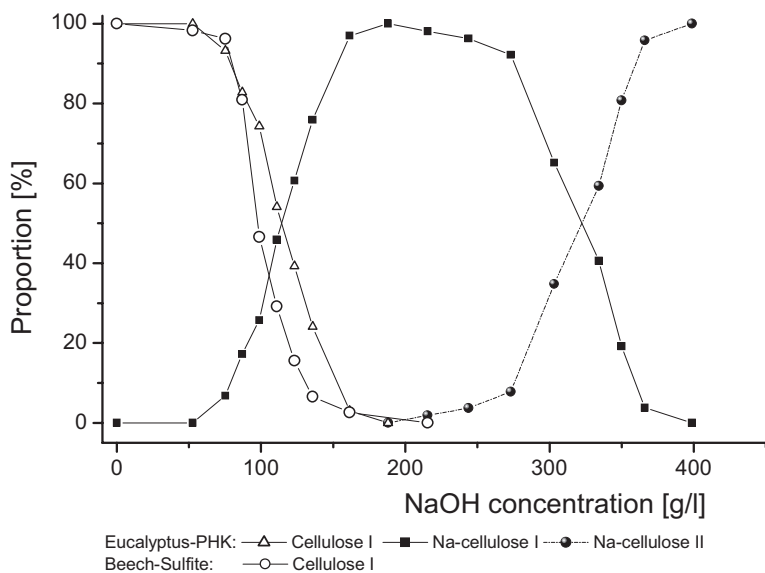


**Fig. 8.3** Xylan content in beta-cellulose as a function of NaOH concentration and temperature [12]. Caustic treatment: 5% consistency, 30 min reaction time, NaOH concentrations: 20, 40, 60, 80, 100, 140, 180, 280, and 340 g L<sup>-1</sup>.

Model compound studies using aldobiouronic (4-*O*-methyl- $\beta$ -D-glucuronic acid-(1 $\rightarrow$ 2)-xylose) (4OMeGlcA) and aldotriouronic acid (4-*O*-methyl- $\beta$ -D-glucuronic acid-(1 $\rightarrow$ 2')-xylobiose), confirmed that substitution at position 2 of the terminal, reducing xylose unit strongly inhibits alkaline degradation [18]. In the absence of a C-2 substituent, the xylose chain is rapidly shortened according to classical peeling pathways, until the next C-2 substituted xylose unit is reached. The results explain the observed higher stability of the xylan fraction as compared to the glucan fraction isolated from the steeping lye. Thus, the decreased alkaline degradation of the xylan isolated from the beta-cellulose fraction can be attributed to the presence of side branches consisting of 4-*O*-methyl-glucuronic acid as detected by FT-IR-spectra and by MALDI-MS with a 4OMeGlcA:Xylose-ratio of 5:100 at the maximum [19].

The interaction between aqueous NaOH and cellulose also affects the supramolecular structure of cellulose. Increasing the NaOH concentration beyond 70–80 g L<sup>-1</sup> at room temperature leads gradually to a change from the native cellulose I structure into the Na-cellulose I structure. Thereby, the plane distance of the 101-lattice planes is widened from the original 0.61 nm to more than 1.2 nm due to incorporation of the sodium hydrate ion [20]. At a NaOH concentration between 160 and 190 g L<sup>-1</sup> the lattice transformation to Na-cellulose I is completed. This structure gives rise to a better reactivity with chemical reactants due to the better accessibility of the hydroxyl groups on C<sub>6</sub> and C<sub>2</sub> (e.g., CS<sub>2</sub> in the case of the viscose process). It is well known that the transition curve from cellulose I to Na-

cellulose I depends also on the supramolecular structure of the dissolving pulp. Sulfite pulps generally require a lower lye concentration to achieve full lattice conversion than do PHK pulps [21]. The somewhat higher mercerization resistance may be due to the less degraded primary cell wall of the latter, restricting swelling by NaOH [20]. The changes in supramolecular structure upon alkali treatment of two dissolving pulps, beech acid sulfite and eucalyptus PHK pulps, have been investigated using solid-state CP-MAS  $^{13}\text{C}$ -NMR spectroscopy (Fig. 8.4).



**Fig. 8.4** Lattice transition from cellulose I to Na-cellulose I and Na-cellulose II of beech sulfite and eucalyptus-PHK pulps depending on NaOH concentration. Data were recorded using solid-state CP-MAS  $^{13}\text{C}$ -NMR spectroscopy (according to [22]).

Over the range of NaOH concentration from about  $160 \text{ g L}^{-1}$  to  $270 \text{ g L}^{-1}$ , the structure of Na-cellulose I prevails, while beyond this concentration level a further lattice conversion to Na-cellulose II arises. The NMR-spectrum of this lattice type indicates cleavage of the intramolecular hydrogen bond between O-3-H and O-5', and thus the coordination of an additional  $\text{Na}^+$  ion to O-3 [23]. A series of comprehensive reports provides further information on the changes in supramolecular structure that occur during the treatment of cellulose with aqueous solutions [20,22,24–26].

### 8.3

#### Cold Caustic Extraction

The extent of purification, measured in terms of R18 and R10 values and residual hemicellulose content (xylan in case of hardwood pulp), depends primarily on the NaOH concentration and the temperature (see Section 8.2). Additionally, the reaction time, the position of the cold caustic extraction (CCE) within the sequence, and the presence of dissolved hemicelluloses may have an influence on the efficiency of purification. In industrial CCE treatment, emphasis is placed on efficient washing. The pulp entering the CCE stage must be thoroughly washed and dewatered to a high consistency (>35%) in order to avoid dilution of the added caustic solution through the pulp slurry. The conditions of CCE include the homogeneous distribution of pulp in 5–10% NaOH for at least 10 min at temperatures between 25 and 45 °C in a downflow, unpressurized tower. Due to the rapid interaction between alkali and cellulose, a separate retention tower is not really needed (in industrial praxis, a tower would perfectly act as a surge tank). Removal of the lye from the highly swollen pulp is rather difficult, and requires efficient post-CCE washing in a series of more than three washers [27]. Special attention must be paid to the washing concept in order to avoid reprecipitation of dissolved polymeric hemicelluloses (beta-cellulose) during the course of washing.

The most important parameters influencing the degree of purification are presented in the following section.

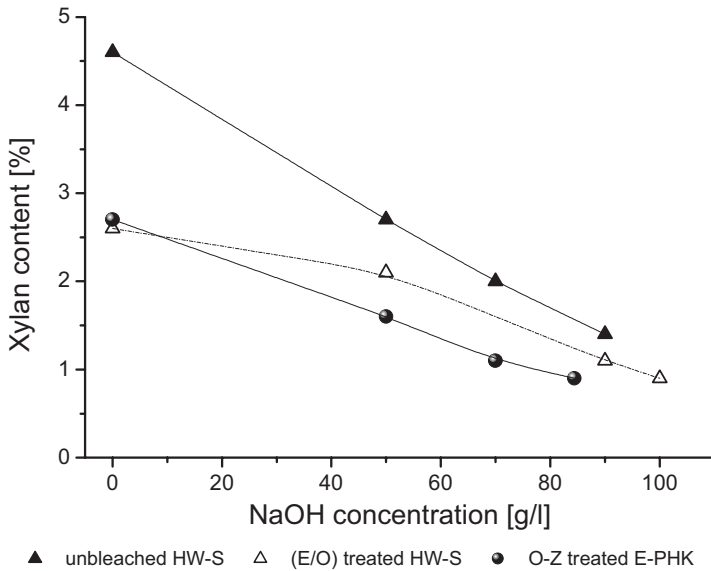
#### 8.3.1

##### NaOH Concentration

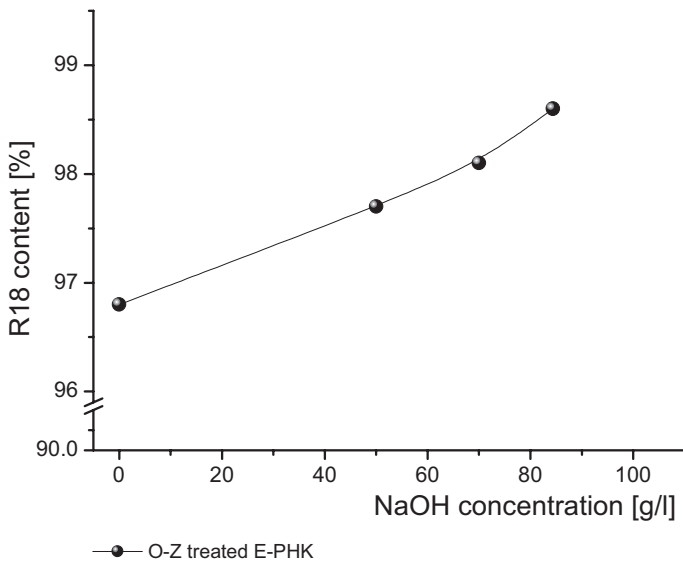
As anticipated, the hemicellulose content in the pulp, determined as xylan, decreases linearly with increasing NaOH concentration in the aqueous phase of the pulp suspension, up to a value of about 100 g L<sup>-1</sup> (Fig. 8.5).

Parallel to the decrease in residual xylan content, an increase in R18 content can be observed. The course of R18 content during CCE treatment as a function of NaOH concentration is illustrated graphically in Fig. 8.6.

The purification efficiency of both sulfite and PHK pulps is quite comparable, provided that the initial xylan contents are at the same level. The xylan content of the unbleached sulfite pulp was reduced by a mild hot caustic extraction followed by oxygen delignification without interstage washing ((E/O)-stage). Purification during CCE proceeds for both pulps to levels close to 1% xylan (or slightly below), even at NaOH concentrations significantly lower than 100 g L<sup>-1</sup>, which prevents the conversion of significant parts to Na-cellulose I (see Fig. 8.4). A subsequent change of the crystalline lattice to the cellulose II-type alters the fiber structure and thus deteriorates pulp reactivity towards acetylation [29]. A xylan content of about 3% in the untreated pulp must be ensured in order to avoid a change in the supramolecular structure while attaining a sufficiently low xylan content to meet the required specifications for high-purity pulps (see Section 11.3, Tab. 11.7, Pulp properties). The relationship between initial pulp purity (R18) and final xylan content

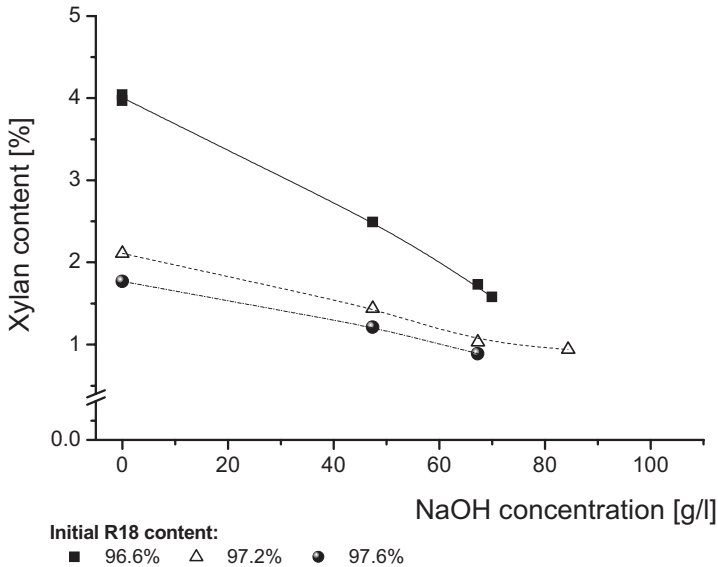


**Fig. 8.5** Purification of hardwood sulfite pulps (HW-S) and eucalyptus prehydrolysis-kraft pulp (E-PHK) with cold aqueous NaOH solution of varying strength [28]. HW-S: unbleached, kappa number 6; (E/O) pretreated: kappa 1.6. E-PHK: OZ pretreated, kappa 0.6. CCE-treatment: 10% consistency, 30 °C, 30 min.



**Fig. 8.6** Purification of eucalyptus prehydrolysis-kraft pulp (E-PHK) with cold aqueous NaOH solution of varying strength [28]. E-PHK: OZ pretreated, kappa number 0.6. CCE-treatment: 10% consistency, 30 °C, 30 min.

through alkaline treatment, depending on NaOH concentration, is further illustrated in Fig. 8.7. The different levels of R18 content after cooking and subsequent oxygen delignification (O) of the eucalyptus PHK pulps have been adjusted by prehydrolysis intensity (P-factor). Even though xylan removal efficiency increases with increasing initial hemicellulose content, the initial purity must exceed a certain level in order to achieve a sufficiently high purity without approaching a change in the supramolecular structure.



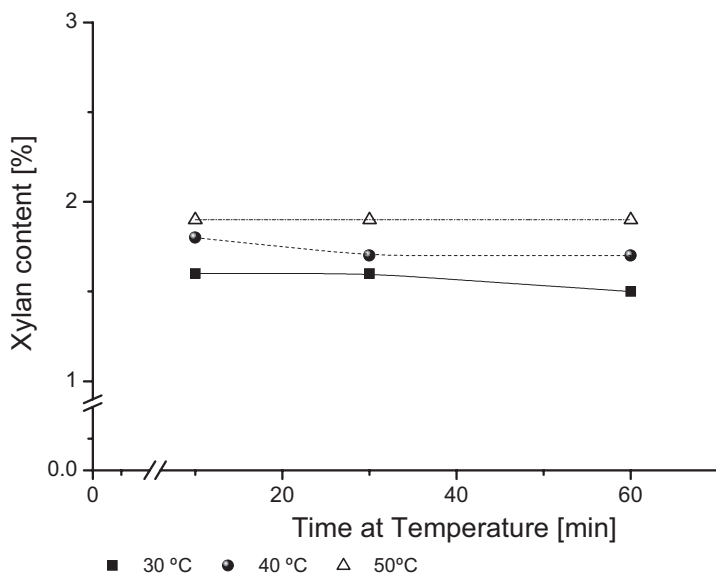
**Fig. 8.7** Purification of eucalyptus prehydrolysis-kraft pulps (E-PHK) of three different initial purity levels with cold aqueous NaOH solution of varying strength [28]. O-pretreated E-PHK pulps: (a) R18 = 96.6%, kappa number 3.4; (b) R18 = 97.4%, kappa number 2.5; (c) R18 = 97.6%, kappa number = 2.2. CCE-treatment: 10% consistency, 30 °C, 30 min.

### 8.3.2

#### Time and Temperature

The influence of temperature on the performance of caustic extraction has been discussed in detail in Section 8.2. It is well established that lower temperatures cause a high degree of swelling, and this enhances the solubility of hemicelluloses. The effect of temperature and retention time in the range 30–50 °C and 10–60 min, respectively, while keeping the NaOH concentration constant at 70 g L<sup>-1</sup>, is illustrated in Fig. 8.8.

It can be seen that extraction time has no influence on the purification efficiency in the range investigated. The retention time during alkalization is not a critical parameter because swelling takes place almost instantaneously [4]. However, the increase in temperature from 30 °C to 50 °C induces a decreased removal of xylan content of 0.4% (from 1.5% to 1.9% in the residue). This temperature



**Fig. 8.8** Influence of time and temperature during CCE treatment of eucalyptus prehydrolysis-kraft pulp (E-PHK) at a constant NaOH concentration of  $70 \text{ g L}^{-1}$  [28]. E-PHK: OZ pre-treated, kappa 0.6. CCE-treatment: 10% consistency, 30 min,  $70 \text{ g NaOH L}^{-1}$ .

increase equally affects purification, as would a decrease in NaOH concentration by  $17 \text{ g L}^{-1}$ , from  $70$  to  $53 \text{ g L}^{-1}$ , at  $30^\circ\text{C}$ , respectively. The processability of the CCE treatment is worsened at low temperature because washing is deteriorated due to an increased lye viscosity. At a given washer capacity, this may result in additional alkali losses. In industrial praxis, a compromise must be found between economic considerations and pulp quality demand. In most cases, the temperature level is adjusted to about  $35^\circ\text{C}$ , which might fulfill both targets.

### 8.3.3

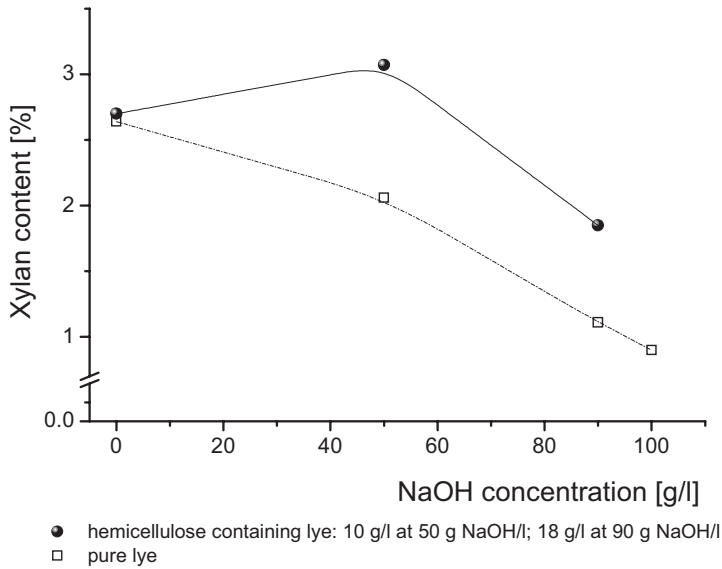
#### Presence of Hemicelluloses in the Lye

CCE treatment requires a comparatively high dosage of NaOH. Maintaining a NaOH concentration of  $80 \text{ g L}^{-1}$  ( $74 \text{ kg NaOH t}^{-1}$ ) at 10% pulp consistency requires a total NaOH charge of  $666 \text{ kg odt}^{-1}$ . The total alkali loss to the sewer is economically by no means acceptable, however, and consequently methods to reuse the entire quantity of the lye must be evaluated. In the case of cold caustic purification of a PHK pulp, the excess lye may be completely recycled to the kraft cook, provided that the demand of alkali for cooking is not lower than the amount of alkali originating from the CCE treatment. In this particular case, white liquor must be used as the alkali source. The efficacy of the white liquor with respect to purification efficiency is equal to a pure NaOH if the strength of the white liquor

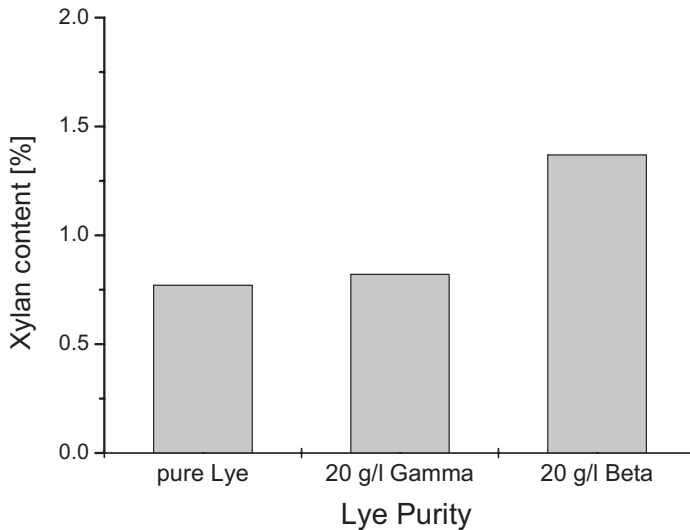
is calculated as effective alkali (EA). Assuming total EA losses (including EA consumption through CCE treatment and washing losses of about  $50 \text{ kg odt}^{-1}$ ), an amount of 616 (equals  $666-50$ )  $\text{kg odt}^{-1}$  of EA is recycled to the cooking plant (note that the CCE filtrate must be evaporated in order to reach the white liquor EA-concentration). Supposing a bleached yield of 35% (o.d.), this amount of alkali corresponds to an EA charge of  $216 \text{ kg odt}^{-1}$  wood which, for cooking, seems to be a rather too-low than a too-high amount (depending on the wood species, cooking technology and intensity of prehydrolysis, the required EA amount for cooking ranges from 22% to 26% on o.d. wood). This brief example shows that the excess lye of cold alkali purification balances quite well with the demand in PHK cooking. However, the situation is different when combining acid sulfite cooking with a CCE treatment. There, the opportunities to re-use the excess lye quantitatively are limited to special cases. For example, one possibility of disposing of the excess lye from the CCE treatment would be to use it for hot caustic extraction, provided that the production of hot alkali-purified pulp considerably exceeds that of cold alkali-purified pulp. If this is not the case, the only chance of preventing too-high losses of alkali would be to recirculate the pressed lye to the sodium hydroxide circuit for re-use in CCE treatment. A closed loop operation, however, inevitably leads to an accumulation of dissolved hemicelluloses in the lye circulation system. Depending on the amount of hemicelluloses removed from the pulp and the leaks from the circuit (e.g., the discharge with the press cake), a certain level of dissolved hemicelluloses is allowed to be reached under equilibrium conditions. It has been reported that the extent of purification is much deteriorated by the presence of dissolved hemicelluloses and other impurities [4]. Surprisingly, if an (E/O) treated hardwood acid sulfite dissolving pulp is subjected to mild cold caustic extraction at 5% NaOH concentration in the presence of  $10 \text{ g L}^{-1}$  hemicelluloses, the xylan content even slightly increases, clearly due to xylan reprecipitation (Fig. 8.9).

As expected, the purification efficiency increases when raising the NaOH concentration to  $90 \text{ g L}^{-1}$  while keeping the ratio to the hemicellulose concentration constant at 5:1. Nonetheless, the presence of hemicelluloses significantly impairs pulp purification (see Fig. 8.9). In the light of the previous discussion about the nature of hemicelluloses, it was interesting to examine which of the two hemicellulose fractions would have the greater impact on purification efficiency. The gamma-cellulose fraction was separated by nanofiltration, while the beta-cellulose was prepared by precipitation upon acidification. The data in Fig. 8.10 show that the presence of the low molecular-weight gamma-cellulose fraction during CCE treatment does not affect purification, whereas the presence of the high molecular-weight beta-cellulose clearly impedes xylan removal.

This observation strengthens the presumption that xylan, when exceeding a certain molecular weight, precipitates onto the surface of the pulp fiber even at rather high NaOH concentration ( $2.5 \text{ mol L}^{-1}$ ). Xylan redeposition is clearly the main reason for a reduced purification efficiency, if CCE is carried out with a lye containing dissolved beta-cellulose.



**Fig. 8.9** Effect of hemicelluloses in the lye on the xylan removal efficiency during CCE treatment of hardwood acid sulfite dissolving pulp (HW-S) in the range of 0 to 100 g L<sup>-1</sup> NaOH [28]. HW-S: (E/O) pretreated, kappa 1.6, 2.7% xylan.



**Fig. 8.10** Effect of the presence of low (gamma) and high (beta) molecular-weight hemicelluloses on xylan removal efficiency during CCE treatment of hardwood acid sulfite dissolving pulp (HW-S) at 100 g L<sup>-1</sup> NaOH and 25 °C [28]. Unbleached HW-S: kappa number 5.7; total bleaching sequence: CCE (E/O)ZP.

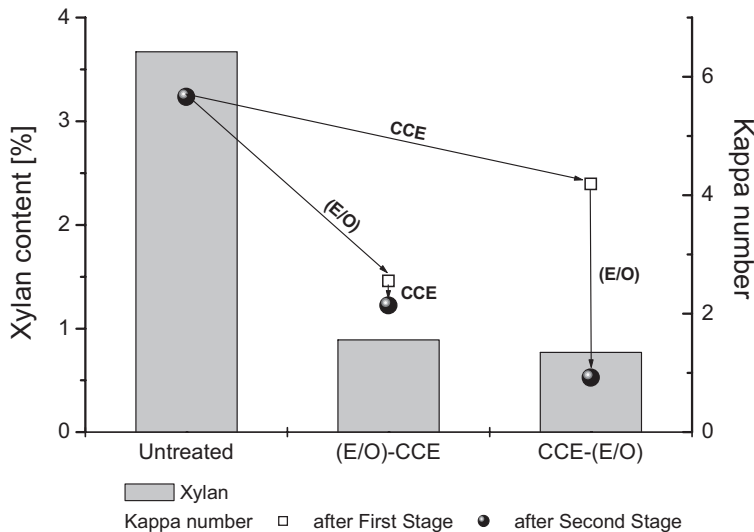


## 8.3.4

## Placement of CCE in the Bleaching Sequence

The efficiency of cold alkali purification is reported to be improved by a preceding hot caustic extraction stage in the case of a sulfite dissolving pulp [4]. More recently, it has been shown that the position of the CCE stage within a bleaching sequence has no significant impact on the degree of purification, provided that washing takes place between both purification stages (Fig. 8.11). In contrast, when oxygen delignification (O) follows hot caustic extraction (E) without inter-stage washing, denoted as (E/O) sequence, a CCE treatment preceding (E/O) seems to be advantageous over the reversed sequence with respect to delignification, as illustrated in Fig. 8.11. The simple reason for the higher overall delignification efficiency of the latter is that unbleached pulp exhibits a higher level of alkaline-extractable lignin than an (E/O) pretreated pulp, while the efficiency of oxygen delignification appears to be unaffected by the prehistory of pulp treatment.

Likewise, the position of CCE within a final bleaching sequence of a hardwood TCF-bleached PHK pulp proved to have no influence on the purification efficiency, as shown in Fig. 8.12. Nevertheless, placing CCE before the ozone stage (Z) is preferred compared to both other alternatives because of a loss in viscosity (in the case of CCE after Z) or higher capital costs (in the case of CCE after P). Moreover, CCE treatment on the bleached pulp might be disadvantageous with

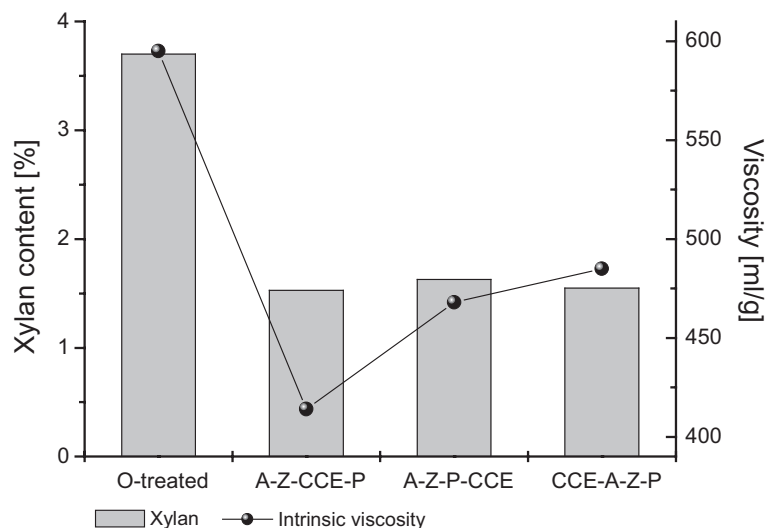


**Fig. 8.11** Influence of the positions of CCE and (E/O) versus (E/O)CCE; CCE-treatment: 100 g L<sup>-1</sup> NaOH, 30 min, 30 °C; (E/O)-treatment: E: 30 kg NaOH odt<sup>-1</sup>, 85 °C, 120 min; O: 85 °C, 90 min,  $p_{O_{2H=0}} = 8$  bar (abs). Unbleached HW-S: kappa number 5.7; CCE

regard to possible impurities of the final product. It is also reported that pretreating pulp with cold alkali prior to hot caustic extraction reduces the amount of alpha-cellulose being degraded during the latter process [11]. The reduction in viscosity loss is most pronounced when the pulp is partly converted from cellulose I into cellulose II.

However, in cases where oxidative degradation is desired to reduce pulp viscosity, the CCE treatment should be placed immediately after ozonation.

The placement of CCE in the bleach sequence is open to debate, but depends ultimately on the prevailing circumstances in industrial practice.



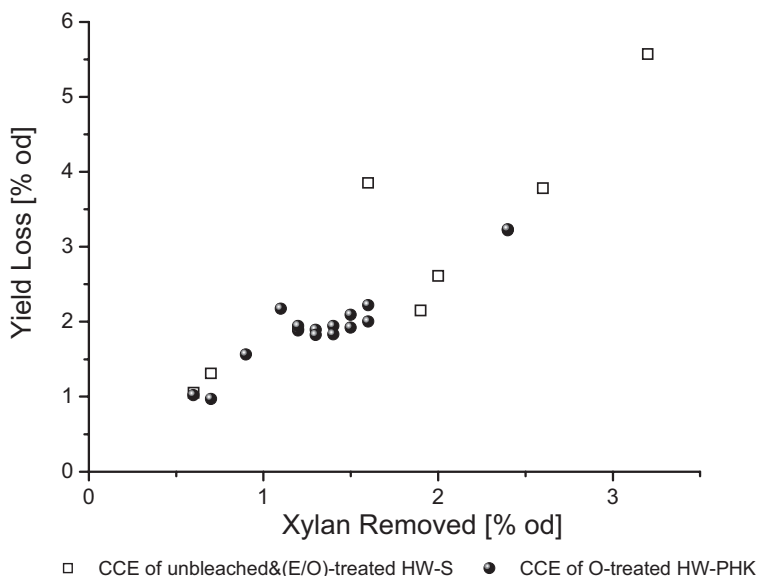
**Fig. 8.12** Influence of CCE placement within an AZP sequence on xylan removal efficiency and final viscosity of a hardwood PHK pulp [28]. O-treated E-PHK: kappa number 2.4; CCE-treatment: 70 g L<sup>-1</sup> NaOH, 30 min, 30 °C.

### 8.3.5

#### Specific Yield Loss, Influence on Kappa Number

Cold caustic extraction is a rather selective purification process because it mainly involves physical changes in the corresponding pulp substrate. The yield losses reported in the literature are 1.2–1.5% per 1% increase in alpha-cellulose content [4] or 1.2–1.8% for a 1% gain in R10 [27]. These values are in close agreement with recent results obtained from hardwood sulfite and PHK dissolving pulps [28], as illustrated in Fig. 8.13.

On average, the yield loss calculates to 1.6% for a 1% reduction in xylan content. Closer examination of the results shows that CCE treatment on HW-PHK pulps is slightly more selective as compared to that of HW-S pulps, as indicated by a specific yield loss per 1% decrease in xylan of 1.4% for the former, and 1.8% for the latter.



**Fig. 8.13** Yield loss as a function of the amount of xylan removed from hardwood sulfite (HW-S) and hardwood prehydrolysis-kraft (HW-PHK) dissolving pulps during CCE treatment [28]. CCE-treatment for HW-S: 50–100 g L<sup>-1</sup> NaOH, 25–30 °C, 30–60 min; CCE-treatment for HW-PHK: 40–70 g L<sup>-1</sup> NaOH, 30–50 °C, 10–60 min.

It has already been pointed out that a certain lignin fraction is removed through CCE treatment. It may be speculated that the delignifying performance of CCE exceeds that of normal alkaline extraction (E) at elevated temperature, known as operation to remove leachable residual lignin (see Section 7.3.7.2, tables 7.24 and 7.25, Process technology: oxygen delignification), because part of the xylan being removed during CCE may be covalently linked to the residual lignin. The rather high delignification removal efficiency of CCE (14–25%) despite the very low initial lignin content ( $2.1 \times 0.15 - 6.0 \times 0.15 = 0.3\% - 0.9\%$ ) is demonstrated in Tab. 8.1.

**Tab. 8.1** Average kappa number values before and after CCE treatment of differently pretreated hardwood sulfite and hardwood PHK dissolving pulps [28]. For details of CCE treatments, see Fig. 8.13.

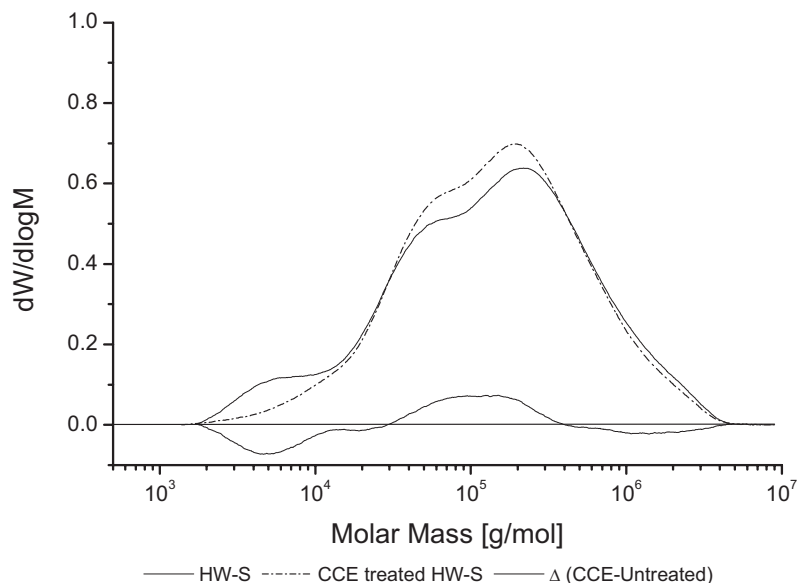
Treatment	HW-Sulfite		HW-PHK
	Unbleached	(E/O)	O
Untreated	6.0	2.1	2.8
CCE	4.5	1.8	2.3

Clearly, delignification is most pronounced for the unbleached pulp. However, significant parts of the residual lignin structures are even removed after oxygen delignification through CCE, but this may be attributed to the dissolution of xylan linked to residues of oxidizable structures (degraded lignin and/or HexA?).

### 8.3.6

#### Molecular Weight Distribution

The aim of CCE is selectively to remove short-chain carbohydrates and other alkaline-soluble impurities, and this leads to a narrowing of the molar mass distribution. The effect of CCE on molecular weight distribution (MWD) has been investigated using a standard hardwood sulfite dissolving pulp (HW-S). The data in Fig. 8.14 show that the main part of the short-chain carbohydrates with molecular weights ranging from 2.5 to 12 kDa (maximum at 5 kDa) is removed through CCE. At the same time, the mid-molecular weight region between 30 and 380 kDa becomes enriched. CCE treatment at low temperature (23 °C) proves to be rather selective. Only a very small proportion of the very high molecular-weight fractions (>1000 kDa) is degraded through CCE. Numerical evaluation of the MWD confirms the removal of short-chain material (Tab. 8.2). It should be noted that the polydispersity and amount of low molecular-weight fractions (below DP50 and DP 200) are significantly decreased, while the high molecular-weight fraction remains largely unchanged (beyond DP2000).



**Fig. 8.14** Molar mass distribution of a hardwood-sulfite dissolving pulp (HW-S) before and after CCE treatment [12]. CCE-treatment: 80 g L<sup>-1</sup> NaOH, 23 °C, 45 min.

**Tab. 8.2** Numerical evaluation of molecular weight distribution of HW-S pulp before and after CCE treatment [12]. DP: degree of polymerization, I: weight fraction.

Pulp	DPw	DPn	PDI	I < P50 [wt.%]	I < P200 [wt.%]	I > P2000 [wt.%]
HW-S	1950	245	8.0	5.1	17.4	27.9
HWS-CCE	1880	355	5.3	2.0	13.4	26.6

## 8.4

### Hot Caustic Extraction

The purpose of hot caustic extraction (HCE) is to remove the short-chain hemicelluloses (determined as S18, S10 fractions) for the production of reactive dissolving pulps based on acid sulfite cooking. In contrast to cold caustic purification, which relies on physical effects such as swelling and solubilization to remove short-chain noncellulosic carbohydrates, hot alkali extraction utilizes primarily chemical reactions on the entire pulp substrate for purification.

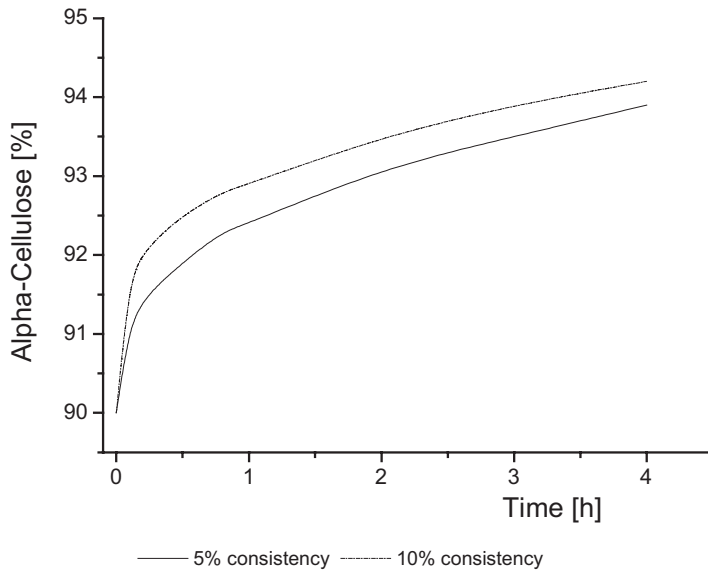
The treatment is carried out at low caustic concentration, typically 3–18 g L<sup>-1</sup> NaOH, with pulp consistencies of 10–15% at temperatures ranging from 70 °C to 120 °C (occasionally 140 °C). As mentioned previously, HCE is carried out solely for sulfite pulps, because the same carbohydrate degradation reactions are involved in alkaline cooks (kraft, soda), at less severe conditions and thus avoiding alkaline hydrolysis reactions. Therefore, HCE does not contribute much to the purity of pulps derived from alkaline cooking processes. From the chemistry point of view, HCE should be placed before any oxidative bleaching stage, as the efficiency of purification is impaired as soon as aldehyde groups are oxidized to carboxyl groups. It has been found that the gain in alpha-cellulose is related to the copper number (or carbonyl content) of the unpurified pulp [30]. Consequently, if measures are undertaken to stabilize the carbohydrates against alkaline degradation either by oxidation (HClO<sub>2</sub>) or reduction (sodium borohydride), virtually no purification is achieved [31,32]. However, for the production of low-grade dissolving pulps with a focus on viscose applications, hot caustic extraction (E) and oxygen delignification (O) are often combined into one single stage (EO) to reduce costs. The reduction in purification efficiency is negligible, provided that the degree of purification is limited to R18 values well below 94–95%.

## 8.4.1

## Influence of Reaction Conditions on Pulp Quality and Pulp Yield

## 8.4.1.1 NaOH Charge and Temperature in E, (EO), and (E/O) Treatments

The NaOH charge is the most important parameter controlling the degree of purification during HCE. At a given alkali dosage, the consistency determines the alkali concentration in the purifying lye. According to Leugering [30], the gain in alpha-cellulose is accelerated with increasing consistency at a given alkali charge, as shown in Fig. 8.15.



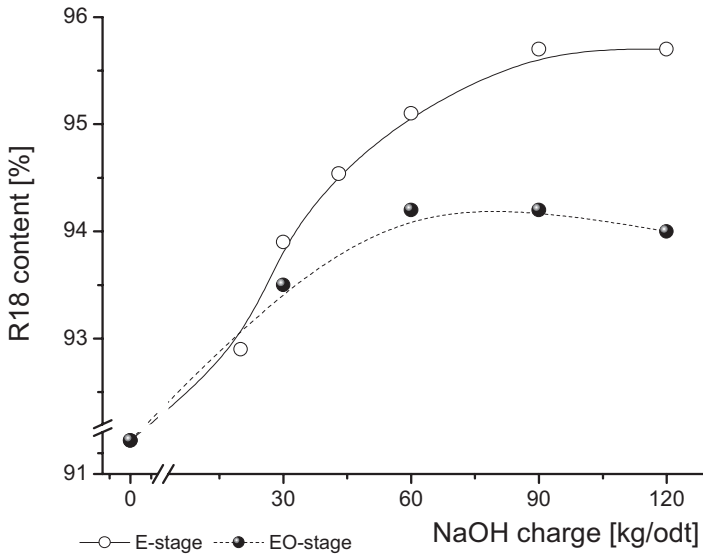
**Fig. 8.15** Alpha-cellulose versus time, calculated according to the empiric formula developed by Leugering [30], with the following assumptions: Initial alpha-cellulose content 90%, 4% NaOH charge, 90 °C.

The relationship between the gain in alpha-cellulose content ( $\Delta\alpha$ ) and NaOH concentration multiplied by retention time has been derived on the basis of spruce acid sulfite pulps:

$$\Delta\alpha = [(3.3 - 0.1 \cdot \text{con}) + 0.13 \cdot (T - 80)] \cdot \left( \frac{\text{NaOHch} \cdot \text{con}}{100 - \text{con}} \cdot t \right)^{\left( \frac{1}{2 + 0.2 \cdot \text{con}} \right)} \quad (1)$$

where: con = consistency (%; validity range 5–15%); T = temperature (°C; validity range 80–97 °C); NaOHch = NaOH charge (kg odt<sup>-1</sup>; validity range 34–228 kg odt<sup>-1</sup>); and t = time (h; validity range 0–4 h).

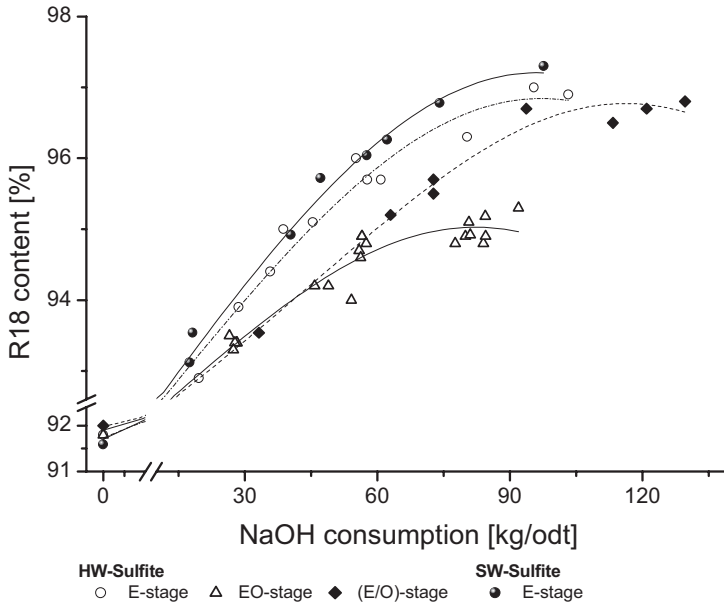
HCE is usually carried out at medium consistency of 10–18%, though in some cases a consistency of 25–30% is practiced. The presence of oxygen at elevated pressure during HCE, aiming to reduce the kappa number parallel to pulp purification, clearly impairs the degree of purification (Fig. 8.16).



**Fig. 8.16** R18 content as a function of NaOH charge comparing E- and (EO)-treatments of hardwood sulfite dissolving pulp (HW-S) [33]. HW-S: kappa number 5.1, 91.8% R18 content. Process conditions: E: 90 °C, 0–120 kg NaOH odt<sup>-1</sup>, 90 min; (EO): equal to E plus oxygen: 8.4 bar (abs) at t = 0.

The data in Fig. 8.16 indicate clearly that purification levels off at about 94% R18 if (EO) is applied. At a given alkali charge, temperature and time are adjusted to achieve a minimal caustic residual. The amount of NaOH consumed relates to both the gain in R18 and pulp yield. The curve characterizing the increase in R18 as a function of the caustic consumed is comparable for spruce and beech sulfite pulps; these data are in agreement with the report of Leugering [30].

When oxygen delignification follows HCE treatment without interstage washing [characterized as (E/O)], the relationship between R18 and the amount of caustic consumption proceeds parallel to pure HCE treatment (E), with a shift to higher NaOH consumption due to an additional consumption during oxygen delignification (Fig. 8.17). When oxygen delignification and HCE occur simultaneously, the degree of purification is leveled off at ca. 95% R18. By further intensifying the reaction conditions during (EO) treatment through increased temperature and caustic charge, no additional gain in R18 content can be attained while caustic consumption continues to increase. This unselective behavior of (EO) is also reflected in the relationship between purification yield and R18 content (see Fig. 8.18). As anticipated, E and (E/O) treatments with hardwood sulfite pulps



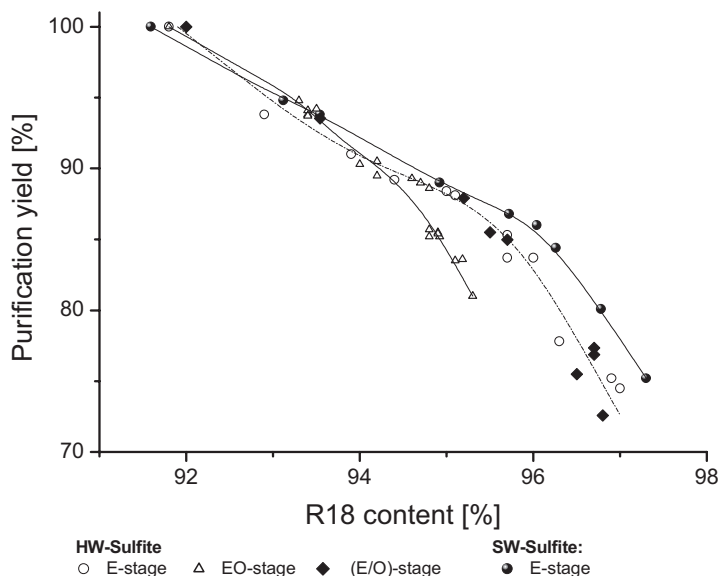
**Fig. 8.17** R18 content as a function of the amount of NaOH consumed comparing E-, (EO)- and (E/O)-treatments of hardwood sulfite dissolving pulp (HW-S) and E-treatment of spruce sulfite dissolving pulp (SW-S) [33]. HW-S: kappa number 4.6–7.1, 91.4–92.0% R18 content; SW-S: kappa number 4.6–12, R18 content: 90–91.6%. Process conditions: E: 82–110°C, 40–120 kg NaOH odt<sup>-1</sup>, 90–240 min; (EO): 85–110°C, 150–300 min, 35–145 kg NaOH odt<sup>-1</sup>, 8.4 bar (abs) at t = 0; (E/O): 90–110°C, 30–120 kg NaOH odt<sup>-1</sup>, 90–240 min, 8.4 bar (abs) at t = 0.

follow the same pattern in terms of yield versus R18 content. The gain in R18 content during HCE of spruce sulfite pulps appears to develop slightly more selectively as compared to beech sulfite pulps (see Fig. 8.18). The reaction of purification can be divided into two phases: first, a more-selective course; and second, a less-selective course. Transition between the two phases appears for E and (E/O) stages at R18 values of 95.5–96.0%, and in the case of (EO) treatment at R18 values of 94.0–94.5%.

A yield loss of about 3% per 1% increase in alpha-cellulose content has been reported elsewhere [4,27,30]. Recent studies on beech and spruce dissolving pulps have confirmed this “rule-of-thumb” in general. However, small deviations are experienced as the yield loss is related to R18 content which, in contrast to alpha-cellulose or R10 values, is rather independent of viscosity in the range investigated. A summary of the specific yield losses and NaOH consumption values is provided in Tab. 8.3.

The data in Tab. 8.3 show that HCE is very unselective at R18 values greater than 96%. The one-stage hot purification and oxygen delignification behaves slightly less selectively when exceeding R18 values of 94%. NaOH consumption is a good indication for the degree of purification. Similar to kraft cooking,





**Fig. 8.18** Purification yield as a function of R18 content comparing E-, (EO)-, and (E/O)-treatments of hardwood sulfite dissolving pulp (HW-S) and E-treatment of spruce sulfite dissolving pulp (SW-S) [33]. Pulps and conditions are as in Fig. 8.17.

**Tab. 8.3** Specific yield losses and NaOH consumption values in the course of E-, (EO), and (E/O) treatments of beech and spruce sulfite pulps.

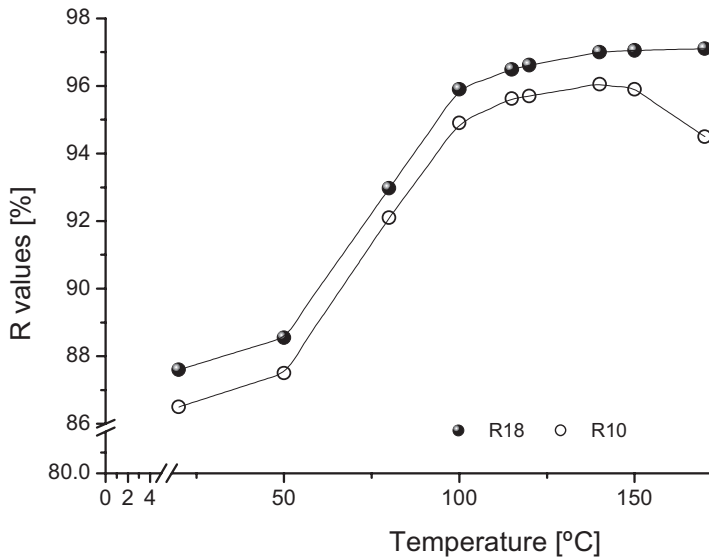
Pulp	Purification	Yield loss per 1% R18 increase		NaOH cons per C6 sugar dissolved	
		<96% [% o.d. pulp]	>96%	<96%	>96% [mol mol <sup>-1</sup> ]
HW-S	E	3.7	5.0	1.4	1.6
HW-S	EO <sup>a</sup>	4.0		2.0	
HW-S	(E/O)	3.2	5.0	2.0	2.0
SW-S	E	3.3	4.1	1.4	1.6

a. Max. 95% R18.

the alkali consumption in pure E stages amounts to between 1.4 and 1.6 mol mol<sup>-1</sup> monosaccharide unit (calculated as C6) dissolved, indicating that the end products of degradation must be fragmented to smaller units than isosaccharinic acid, such

as glycolic, lactic, pyruvic and 3,4-dihydroxybutyric acids, as described by MacLeod and Schroeder [34]. As anticipated, specific alkali consumption increases to a value of about  $2 \text{ mol mol}^{-1}$  monosaccharide unit when oxygen delignification is integrated into the purification reaction, either in the same (EO) or in a separate stage (E/O).

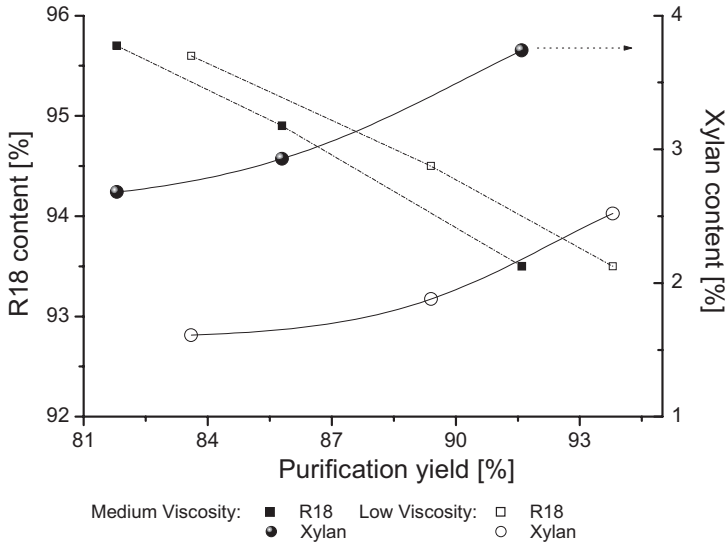
An elevated temperature between 80 and  $120 \text{ }^\circ\text{C}$  is necessary to activate peeling reactions in the presence of sufficient alkali to achieve an increase in R18 and R10, and a decrease in hemicelluloses. As shown in Fig. 8.19, cellulose degradation begins at temperatures exceeding  $140 \text{ }^\circ\text{C}$ , as suggested by a decrease in R10 content, indicating the fragmentation of microfibrils. Clearly, temperatures beyond  $140 \text{ }^\circ\text{C}$  do not contribute to further purification due to alkaline hydrolysis.



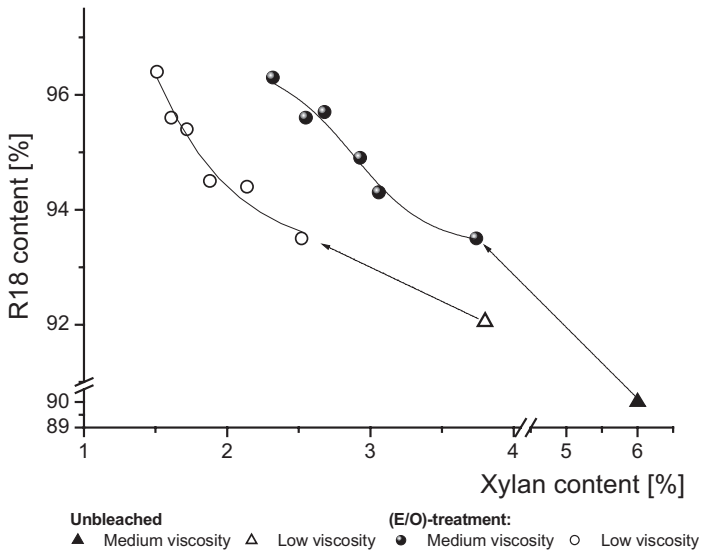
**Fig. 8.19** Development of R18 and R10 contents as a function of temperature of a high-viscosity spruce sulfite pulp during HCE [4]: HCE-conditions:  $120 \text{ kg NaOH odt}^{-1}$ , 4 h.

#### 8.4.1.2 Xylan versus R18 Contents

Prolonged acid sulfite cooking causes both the removal of hemicelluloses (e.g., xylan) and the degradation of cellulose, resulting in a low-viscosity pulp. HCE treatment of low-viscosity sulfite pulps allows reduction to a very low xylan content, while the R18 content remains rather close to that of pulps with a higher initial viscosity at a comparable yield level (Fig. 8.20). These data conclude that the R18 content of medium- to high-viscosity pulps partly contains alkaline-stable hemicelluloses. On the other hand, part of the degraded cellulose is not included in the R18 fraction of the low-viscosity pulp.



**Fig. 8.20** R18 and xylan contents related to purification yield during (E/O)-treatment of hardwood sulfite dissolving pulp (HW-S) [33]. Low-viscosity pulp: viscosity 490 mL g<sup>-1</sup>, kappa number 6.2, xylan content 4.5%; Medium-viscosity pulp: viscosity 730 mL g<sup>-1</sup>, kappa number 6.2, xylan content 6.5%.



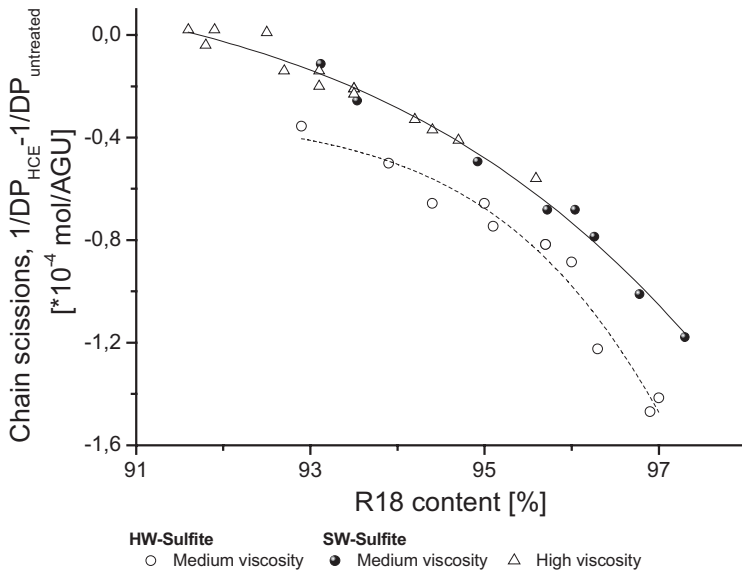
**Fig. 8.21** R18 versus xylan content during (E/O)-treatment of hardwood sulfite dissolving pulp (HW-S) [33]. Low-viscosity pulp: viscosity 490 mL g<sup>-1</sup>, kappa number 6.2, xylan content 4.5%; Medium-viscosity pulp: viscosity 730 mL g<sup>-1</sup>, kappa number 6.2, xylan content 6.5%.

The distinct difference in the residual xylan contents of low- and medium-viscosity hardwood sulfite dissolving pulps at a given R18 content is clearly shown in Fig. 8.21. The xylan content of the medium-viscosity pulp is approximately 1% higher than that of the low-viscosity pulp when compared at a level of 95% R18 (2.8% versus 1.8% xylan).

### 8.4.1.3 Purification versus Viscosity

The removal of short-chain carbohydrates through HCE treatment results in a slight increase in viscosity because stepwise degradation (peeling) has only a small effect on the molecular weight of long-chain cellulose. The effect of HCE on viscosity has been expressed as a negative change of chain scissions for both spruce and beech dissolving pulps to consider different levels of initial viscosity.

The data in Fig. 8.22 reveal a clear relationship between the degree of purification and viscosity increase, reflecting the removal of short-chain material. The change in viscosity is more pronounced for beech dissolving pulp, indicating that the molecular weight of the removed hemicelluloses is lower than that from spruce dissolving pulp. Alternatively, a greater amount of low molecular-weight material is removed from the beech dissolving pulp during HCE treatment; this suggestion would be in line with the higher specific yield loss when compared to spruce dissolving pulp.

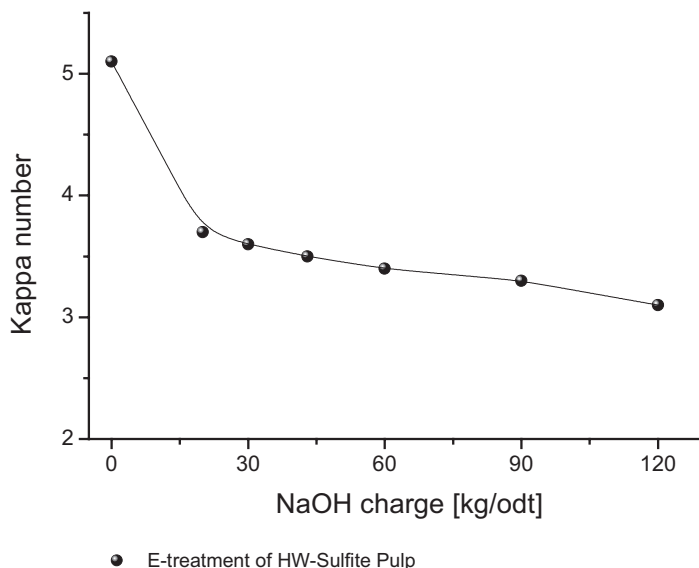


**Fig. 8.22** Change in pulp viscosity, expressed as negative number of chain scissions, as a function of the degree of purification, characterized as R18 content, during E-treatment of hardwood and softwood sulfite dissolving

pulps (HW-S, SW-S) [33]. Medium-viscosity HW-S: viscosity 590 mL g<sup>-1</sup>, kappa number 4.6; Medium-viscosity SW-S: viscosity 625 mL g<sup>-1</sup>, kappa number 4.6; High-viscosity SW-S: viscosity 890 mL g<sup>-1</sup>, kappa number 12.2.

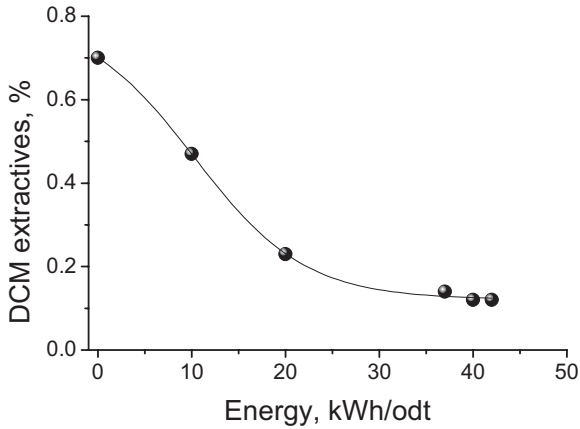
#### 8.4.1.4 Purification versus Kappa Number and Extractives

Hot caustic purification also removes other pulp impurities such as lignin and extractives. Most of the kappa number reduction occurs already at low NaOH charge, and this can be attributed to a readily available lignin (Fig. 8.23). The more alkali-resistant lignin is gradually decreased with increasing NaOH charge. It may be speculated that part of the removed lignin is associated with the extracted (and degraded) xylan.



**Fig. 8.23** Course of kappa number as a function of NaOH charge during E-treatment of hardwood sulfite dissolving pulps (HW-S) [33]. HW-S: viscosity  $580 \text{ mL g}^{-1}$ , kappa number 5.1; E conditions:  $90^\circ\text{C}$ , 240 min.

Hot caustic extraction is a very efficient stage in the removal of resin constituents of sulfite pulps [27]. The saponification of fats, waxes and other esters is the key reaction responsible for the removal of extractives. The removal efficiency can be further enhanced by the addition of surfactants (nonyl phenol with attached polyoxyethylene chain), and this may also solubilize the nonsaponifiables. The de-resination of softwood pulps with large amounts of resin can be further improved by subjecting the pulp to increased mechanical forces that allow removal of the encapsulated resin from the ray cells. A process developed by Domsjö involves the use of a Frotapulper, along with the addition of caustic for the de-resination of sulfite pulps (Fig. 8.24) [35,36].



**Fig. 8.24** Course of dichloromethane (DCM) extractives in fully bleached softwood dissolving pulps as a function of energy input in a Frotapulper [35,36].

#### 8.4.1.5 Composition of Hot Caustic Extract

Hot caustic extract contains a large amount of low molecular-weight hydroxycarbonic acids, with glucoisosaccharinate as the main component, derived from purification of softwood sulfite pulp [37]. A typical extract composition is shown in Tab. 8.4.

**Tab. 8.4** Typical composition of hot caustic extract [37].

Compounds	% of solids as sodium Salts
Chloride <sup>a</sup>	3.3
Formate	17.0
Acetate	3.4
Glucoisosaccharinate	27.0
Other Hydroxy acids	38.0
“Complex” acids	11.3

a. C stage preceding HCE treatment.

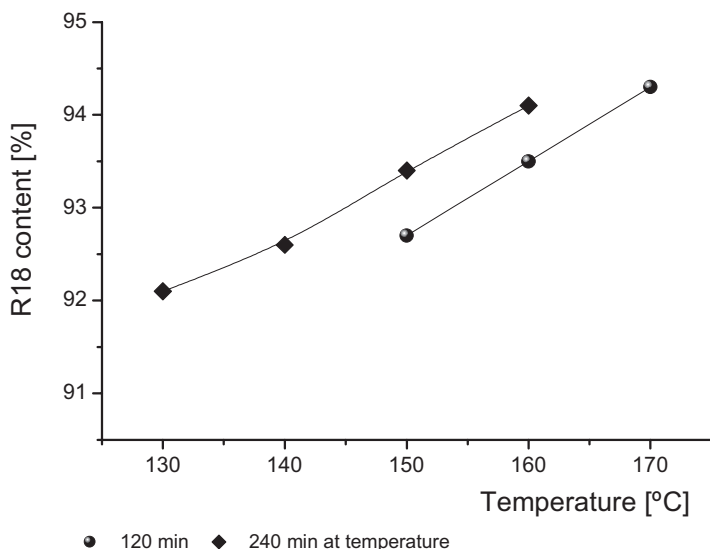
The combined saccharinic acids and other hydroxy acids constitute about 65% of the hot caustic extract. These compounds are readily biodegradable in a wastewater treatment plant. However, the COD load is significant and calculates to about  $180 \text{ kg odt}^{-1}$ , assuming an average yield loss of about 15% on bleached pulp across the stage ( $150 \text{ kg carbohydrates/odt} \times 1.185 \text{ kg COD/kg carbohydrates}$ ). As

a consequence, several sulfite dissolving pulp mills have recently installed evaporation plants and recovery furnaces (soda boiler) to concentrate and burn the filtrates from hot caustic extraction. To date, no products are prepared from the thick liquor, mainly because of the high costs to isolate, purify, and modify the saccharinic acids. Reintjes and Cooper have proposed a scheme to utilize these compounds where the acids are lactonized and converted to amides; they may then be further processed to anionic and nonionic surfactants by reaction with chlorosulfonic acid or ethylene oxide [37].

#### 8.4.2

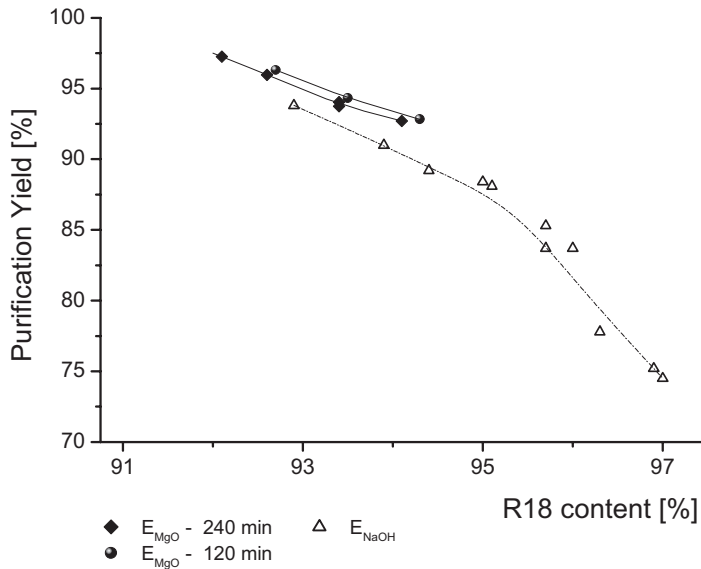
##### MgO as an Alternative Alkali Source

The main disadvantage of using NaOH as an alkali source for HCE is that the evaporated caustic extract cannot be recycled to the spent sulfite liquor (SSL) of a Mg-based cooking process due to the formation of low-melting Na-Mg eutectic mixtures. Thus, efforts were undertaken to investigate the possibility of using  $\text{Mg}(\text{OH})_2$  as an alkali source for hot caustic extraction, as this enables the combined recovery of hot caustic extract and Mg-based SSL [38]. As known from weak bases such as sodium carbonate, sodium sulfite and others, a higher temperature than is used for NaOH is required for the purification. The time and temperature of MgO-based HCE ( $E_{\text{MgO}}$ ) are the two main parameters that determine the degree of purification, rather than the  $\text{Mg}(\text{OH})_2$  charge. Charges higher than  $15 \text{ kg odt}^{-1}$  have no effect on purification, due mainly to the low solubility of  $\text{Mg}(\text{OH})_2$  in aqueous solution.



**Fig. 8.25** R18 content of a hardwood sulfite pulp (HW-S) as a function of temperature during hot caustic extraction using MgO as a base, at two different reaction times [39]. HW-S for 120 min reaction time: kappa number 6.2, viscosity  $640 \text{ mL g}^{-1}$ , 91.0% R18; HW-S for 240 min reaction time: kappa number 9.9, viscosity  $600 \text{ mL g}^{-1}$ , 90.9% R18.

Figure 8.25 illustrates the successful use of MgO to obtain degrees of purification sufficiently high for the production of viscose staple fiber pulps. The main drawback when using MgO is the high temperature needed to achieve the necessary purification. Another problem may be to achieve homogeneous distribution of  $\text{Mg}(\text{OH})_2$  within the pulp suspension in order to obtain a uniform pulp quality. The prolongation of retention time from 120 to 240 min may reduce the temperature by almost  $10^\circ\text{C}$ , while maintaining the same R18 content. Moreover, the MgO-based hot caustic extraction appears to be more selective than the conventional system, with a specific yield loss of only 2.4% per 1% increase in R18 (Fig. 8.26).



**Fig. 8.26** Purification yield as a function of R18 content for MgO- and NaOH-based hot extraction processes of a hardwood sulfite pulp (HW-S) [39]. Pulp substrate and conditions:  $E_{\text{MgO}}$  according to Fig. 8.25;  $E_{\text{NaOH}}$  according to Fig. 8.18.

## References

- 1 Hermans, P.H., The analogy between the mechanism of deformation of cellulose and that of rubber. *J. Phys. Chem.*, **1941**; 45: 827–836.
- 2 Avela, E., et al., Sulfite pulps for HWM-fibres. *Pure Appl. Chem.*, **1967**: 289–301.
- 3 Sixta, H., et al., Evaluation of new organosolv dissolving pulps. Part I: Preparation, analytical characterization and viscose processability. *Cellulose*, **2004**; 11: 73–83.
- 4 Rydholm, S.A., *Pulping Processes*. Malabar, Florida: Robert E. Krieger Publishing Co., Inc., **1965**: 992–1023.
- 5 Richter, G.A., Production of high alpha-cellulose wood pulps and their properties. *Tappi*, **1955**; 38(3): 129–150.



- 6 Hempel, K., Solubility of cellulose in alkalies and its technical significance. *Przegląd Papierniczy*, **1949**; 5: 62–69, 73–81.
- 7 Shogenji, T., H. Takahasi, K. Akashi, The cold alkaline purification of sulfite pulp. Use of ion-exchange resin for the analysis of waste liquor and some information on alkali consumption. *J. Jap. Tech. Assoc. Pulp Paper Ind.*, **1952**; 6: 201–211.
- 8 Wilson, K., E. Ringstrom, I. Hedlund, The alkali solubility of pulp. *Svensk. Papperstidn.*, **1952**; 55: 31–37.
- 9 Ranby, B.G., The mercerization of cellulose. II. A phase-transition study with X-ray diffraction. *Acta Chim. Scand.*, **1952**; 6: 116–127.
- 10 Ranby, B.G., The physical characteristics of alpha-, beta- and gamma-cellulose. *Svensk. Papperstidn.*, **1952**; 55: 115–124.
- 11 Corbett, W.M., J. Kidd, Some aspects of alkali refining of pulps. *Tappi*, **1958**; 41(3).
- 12 Sixta, H., A. Schrittwieser, Alkalization of hardwood dissolving pulps. R&D Lenzing AG: Lenzing, **2004**: 1–10.
- 13 Saito, G.-I., The behaviour of cellulose in solutions of alkalies. *Kolloid-Beihefte*, **1939**; 49: 365–366.
- 14 Saito, G.-I., The behaviour of cellulose in solutions of alkalies. I. Cross-sectional swelling of fibers of different celluloses in sodium hydroxide solutions at different temperatures. *Kolloid-Beihefte*, **1939**; 49: 367–387.
- 15 Bartunek, R., The reactions, swelling and solution of cellulose in solutions of electrolytes. *Das Papier*, **1953**; 7: 153–158.
- 16 Dobbins, R.J., Role of water in cellulose-solute interactions. *Tappi*, **1970**; 53(12): 2284–2290.
- 17 Sixta, H., et al., Characterization of alkali-soluble pulp fractions by chromatography. In 11th ISWPC. Nice, France, **2001**.
- 18 Sartori, J., Investigations of alkaline degradation reactions of cellulosic model compounds. In Institute of Chemistry. University of Natural Resources and Applied Life Science: Vienna, **2003**: 134.
- 19 Mais, U., H. Sixta, Characterization of alkali-soluble hemicelluloses of hardwood dissolving pulps. In ACS Symposium Series, **2004**: 94–107.
- 20 Krässig, H.A., *Cellulose: Structure, Accessibility and Reactivity*. Polymer Monographs. M.B. Huglin, Ed. Vol. 11. Gordon and Breach Science Publishers, **1993**: 258–323.
- 21 Sixta, H., Comparative evaluation of TCF bleached hardwood dissolving pulps. *Lenzinger Berichte*, **1999**; 79: 119–128.
- 22 Fink, H.-P., J. Kunze, Solid state <sup>13</sup>C NMR studies of alkalization of hardwood dissolving pulps. Fraunhofer, Institut für Angewandte Polymerforschung: Golm, **2003**: 1–5.
- 23 Fink, H.-P., B. Philipp, Models of cellulose physical structure from the viewpoint of the cellulose I → cellulose II transition. *J. Appl. Polym. Sci.*, **1985**; 30(9): 3779–3790.
- 24 Fink, H.-P., et al., The composition of alkali cellulose: a new concept. *Polymer*, **1986**; 27(6): 944–948.
- 25 Fink, H.-P., et al., The structure of amorphous cellulose as revealed by wide-angle X-ray scattering. *Polymer*, **1987**; 28(8): 1265–1270.
- 26 Fink, H.-P., et al., <sup>13</sup>C-NMR studies of cellulose alkalization. *Cellulose and Cellulose Derivatives, Physico-chemical Aspects and Industrial Applications*. J.F. Kennedy, G.O. Williams, L. Piculell, Eds. Woodhead Publishing Ltd: Cambridge, **1995**: 523–528.
- 27 Hinck, J.F., R.L. Casebier, J.K. Hamilton, Dissolving pulp manufacturing. In *Sulfite Science & Technology*. J.K.O. Ingruber, P.E. Al Wong, Eds. TAPPI, CPPA: Atlanta, **1985**: 213–243.
- 28 Borgards, A., A. Lima, H. Sixta, Cold caustic extraction of various hardwood dissolving pulps. Internal Report, R&D Lenzing AG, **1998**.
- 29 Sears, K.D., J.F. Hinck, C.G. Sewell, Highly reactive wood pulps for cellulose acetate production. *J. Appl. Polym. Sci.*, **1982**; 27(12): 4599–4610.
- 30 Leugering, H.-J., Zur Kenntnis der Zellstoffveredelung durch Heissalkalisierung. *Das Papier*, **1953**; 7(3/4): 47–51.

- 31 Meller, A., Studies on modified cellulose. I. The alkali stability of oxidized, hydrolyzed, and methanolized cellulose. *Tappi*, **1951**; 34: 171–179.
- 32 Samuelson, O., C. Ramsel, Effect of chlorine and chlorine dioxide bleaching on the copper number, hot-alkali solubility, and carboxyl content of sulfite cellulose. *Svensk. Papperstidn.*, **1950**; 53: 155–163.
- 33 Yaldez, R., H. Sixta, Hot caustic extraction of sulfite dissolving pulps. Internal Report, R&D Lenzing AG, **1998**.
- 34 MacLeod, J.M., L.R. Schroeder,  $\beta$ -D-(glucopyranosyl)-D-glucose-3.6-anhydro-4-O-methyl-D-glucose, and D-glucose. *J. Wood Chem. Technol.*, **1982**; 2(2): 187–205.
- 35 Lindahl, J.A.I., Process and apparatus for the deresination and brightness improvement of cellulose pulp. Mo och Domsjö Aktebolag: US Patent, **1981**.
- 36 Assarsson, A., et al., Control of rosin-induced complications in pulp. *Przegląd Paperniczy*, **1982**; 38(2): 53–55.
- 37 Reintjes, M., G.K. Cooper, Polysaccharide alkaline degradation products as a source of organic chemicals. *Ind. Eng. Chem. Prod. Res. Dev.*, **1984**; 23: 70–73.
- 38 Sixta, H., T. Gerzer, W. Müller, Verfahren zur Veredelung von Zellstoffen. Österreichische Patentanmeldung, **2002**.
- 39 Sixta, H., Hot caustic extraction of hardwood sulfite pulp with MgO as a base. Internal Report, R&D Lenzing AG, **2002**.

## 9

### Recovery

Andreas W. Krotscheck, Herbert Sixta

#### 9.1

##### Characterization of Black Liquors

###### 9.1.1

###### Chemical Composition

Kraft black liquor contains most of the organic compounds removed from the wood during the cook and the inorganic chemicals charged, mainly in the form of salts with organic acids. A major portion part of the extractives removed from the wood during kraft pulping is, however, not included in the black liquor solids. The volatile wood extractives such as low molecular-weight terpenes are recovered from the digester relief condensates (turpentine). The resin and fatty acids, as well as some neutral resins (e.g.,  $\beta$ -sitosterol), are suspended in the diluted black liquor (in the form of stable micelles). During the course of black liquor evaporation, when a concentration of 25–28% of total solids is reached, these extractives are separated from the aqueous phase as “soap skimmings”. Crude tall oil is obtained from the soap skimmings after acidification with sulfuric acid. The composition of the tall oil is described elsewhere [1].

The remaining kraft black liquor contains organic constituents in the form of lignin and carbohydrate degradation products. The composition of the spent liquor depends greatly on the wood species, the composition and amount of white liquor charged, the unbleached pulp yield, and the amount of recycled bleach filtrates (predominantly from the oxygen delignification stage). During kraft pulping, lignin and a large part of carbohydrates mainly derived from hemicelluloses, are degraded by alkali-catalyzed reactions. Thus, the organic material of the black liquor consists primarily of lignin fragments (mainly high molecular-mass fragments) and low molecular-weight aliphatic carboxylic acids originating from wood carbohydrates. The approximate composition of a black liquor from birch and pine kraft cooks is shown in Tab. 9.1.

Organic material also contains minor amounts of polysaccharides mainly derived from xylan (part of “Other organics” in Tab. 9.1). Quite recently, it was shown that black liquor from *Eucalyptus globulus* kraft cooking contains substantial amounts of dissolved polysaccharides (BLPS = black liquor dissolved polysaccharides) [4]. BLPS represent about 20% of the total dissolved and/or degraded wood polysaccharides. The major component of BLPS is xylan, with a molecular

**Tab. 9.1** Composition of the dry matter of pine (*Pinus sylvestris*) and birch (*Betula pendula*) kraft black liquors. Values are % of total dry matter [2,3].

Component	Pine	Birch
Lignin	33	27
Aliphatic carboxylic acids	31	32
Formic acid	6	4
Acetic acid	4	9
Glycolic acid	2	2
Lactic acid	3	2
2-Hydroxybutanoic acid	1	5
3,4-Dideoxypentonic acid	2	1
3-Deoxypentonic acid	1	1
Xyloisosaccharinic acid	1	2
Glucosisosaccharinic acid	7	3
Others	4	3
Other Oganics	8	12
Inorganics <sup>a</sup>	28	29
Sodium bound to organics	12	12
Inorganic compounds	16	17
Total	100	100

a. Including sodium bound to organic material.

weight in the range 17–19 kDa. During pulping, the black liquor xylans are progressively enriched in hexenuronic acid.

Black liquor is concentrated by evaporation and then combusted in the recovery furnace for the recovery of cooking chemicals and the generation of energy. The heating value of black liquor has a major impact on the steam generation rate, knowledge of which is essential in the design and operation of a recovery boiler. The higher heating (gross calorific) value (HHV) is determined by oxidizing the black liquor quantitatively, condensing the water vapor produced, and cooling the products to 25 °C (TAPPI method T 684 om-90). The net heating (net calorific) value (NHV), which better reflects the actual energy release, accounts for the fact that the generated water is not condensed during combustion and steam generation. NHV is obtained by subtracting the heat of vaporization of the water from the HHV value. In addition, any sulfur is completely oxidized in the oxygen bomb calorimeter, whereas with kraft black liquor it always appears as sodium sulfide ( $\text{Na}_2\text{S}$ ). The reduction process of  $\text{Na}_2\text{S}$  to  $\text{Na}_2\text{SO}_4$  is endothermic by 13 090 kJ  $\text{kg}^{-1}$  of  $\text{Na}_2\text{S}$ . The NHV can be calculated according to the following expression:

$$\text{NHV} = \text{HHV} - 2440 \cdot \left[ \frac{18}{2} \cdot H \right] - 13090 \cdot \left[ \frac{78}{32} \cdot S \cdot \eta_{RED} \right] \quad (1)$$

where NHV is the net heating value of black liquor solids (BLS; in  $\text{kJ kg}^{-1}$  BLS); HHV is the higher heating value of BLS (in  $\text{kJ kg}^{-1}$  BLS);  $H$  and  $S$  are the weight fractions of hydrogen (H) and sulfur (S) in BLS; and  $\eta_{\text{RED}}$  is the degree of reduction given as a weight fraction.

Typical values for the HHV of kraft black liquor range between  $13 \text{ MJ kg}^{-1}$  BLS (predominantly derived from hardwoods) and  $15.5 \text{ MJ kg}^{-1}$  BLS (predominantly derived from softwoods), as indicated in Tab. 9.2.

It should be noted that the recycling of bleach (e.g., oxygen delignification) and purification (e.g., cold caustic extraction) filtrates has an impact on the composition and heating value of the BLS due to a generally lower content of organic compounds.

Tab. 9.2 Chemical analysis and heating values of black liquor solids [5–8].

Components		A	B	C	D	E	F	G
Wood species	Unit	hardwood	hardwood	hardwood	softwood	softwood	softwood	softwood
Elemental analysis								
C	wt% on DS	32.3	33.3	33.4	35.8	37.8	35.8	38.0
H	wt% on DS	3.8	3.6	3.9	3.5	4.2	3.6	3.8
N	wt% on DS		0.2	0.1	0.1	0.2	0.1	
O	wt% on DS	35.8						33.6
S	wt% on DS	3.0	5.4	4.4	4.1	4.8	4.6	3.7
Na	wt% on DS	18.2	19.9	20.7	19.9	17.9	19.6	19.2
K	wt% on DS	3.0	1.5	1.7	1.1	1.2	1.8	0.6
Cl	wt% on DS	0.7	0.6	0.3	0.2	2.9	0.5	1.0
HHV	$\text{MJ kg}^{-1}$	13.2	13.2	13.2	14.1	15.4		15.1
NHV (calculated <sup>a</sup> )	$\text{MJ kg}^{-1}$	11.5	10.9	11.1	12.2	13.1		13.2
Reference	[5]		[6]	[6]	[6]	[6]	[7]	[8]

a. Assuming a degree of reduction of 90%.

## 9.1.2

**Physical Properties**

The most important physical properties which affect evaporator and recovery boiler design and operation include liquor viscosity, boiling point rise, surface tension, density, thermal conductivity and heat capacity.

9.1.2.1 **Viscosity**

The viscosity of the black liquor is determined by its composition, the dry solids content, and temperature. At low shear rates, black liquor behaves as a Newtonian fluid, and the macromolecular components such as lignin and polysaccharide molecules control the rheological properties. At a dry solids content of about 15%, the viscosity of the black liquor is only three-fold that of water at a given temperature. At about 50% solids content, however, black liquor behaves as a polymer blend with water as plasticizer, and the viscosity increases exponentially with solids content. The relationship between dry solids content and viscosity at a low shear rate is expressed in Eq. (2) [8]:

$$\text{Log} \left( \frac{\mu_{bl}}{\mu_w} \right) = \frac{\frac{DS \cdot 373}{T}}{0.679 - 0.656 \cdot \frac{DS \cdot 373}{T}} \quad (2)$$

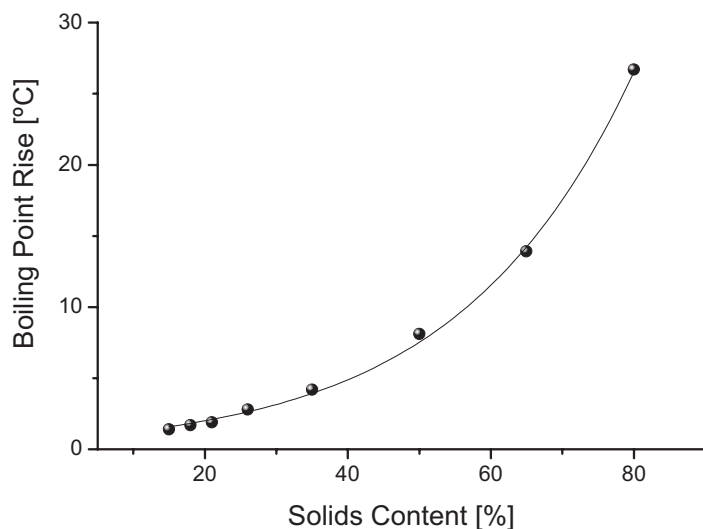
where  $\mu_{bl}$  is the viscosity of black liquor (in Pa.s);  $\mu_w$  is the viscosity of water (in Pa.s); DS is the weight fraction of dry solids in black liquor; and T is temperature (in K).

According to Eq. (2), viscosity can change by five orders of magnitude over the range of dry solids contents typical for kraft black liquor recovery.

The shape of the dissolved lignin molecules is influenced by the content of residual effective alkali of the black liquor. With decreasing pH, the volume occupied by the lignin molecules increases. The larger spheres can entangle more easily, and this contributes to a higher viscosity. Dissolved polysaccharides such as xylan tend to form expanded random coils which greatly influence the viscosity of black liquor. The viscosity of black liquor can be reduced by a heat treatment. The black liquor is heated up to 180–190 °C to further degrade the polymeric material in the presence of residual alkali. The resulting reduced viscosity allows the black liquor to be concentrated up to 80% dry solids in order to maximize the benefits of high dry solids in black liquor combustion [9].

9.1.2.2 **Boiling Point Rise (BPR)**

According to Raoult's law, the vapor pressure of the solvent decreases proportionally to the molal concentration of the solute. Thus, the boiling point of the black liquor increases with increasing dry solids content. The BRP can increase up to values of close to 30 °C for black liquors leaving the concentrator (BLS about 80%) [8]. The dependency of BRP on dry solids content is illustrated graphically in Fig. 9.1[8].



**Fig. 9.1** Boiling point rise (BPR) as a function of dry solids content (according to Frederick [8]).

The inorganic compounds (sodium, potassium, etc.) constitute more than 90% of the solute on a molar basis. Therefore, the BPR is mainly influenced by the salt concentration in the black liquor. The BPR is an important parameter for evaluating the efficiency of black liquor evaporators. Heat transfer is dependent upon the temperature difference between the condensing steam and the evaporating black liquor. More detailed information regarding the calculation of BPR as a function of pressure and molal concentration are provided in Ref. [8].

#### 9.1.2.3 Surface Tension

The surface tension of black liquor is influenced by the temperature, as well as by the nature and concentration of the dissolved components. Inorganic compounds such as sodium salts increase the surface tension, whereas some organic substances (e.g., extractives, lignin, etc.), which are known as surface-active agents, reduce the surface tension of water. It has been shown that the latter effect outweighs that of the inorganic compounds. The surface tension comprises a value of 40–60% of the value for pure water ( $72.8 \text{ mN m}^{-1}$  at  $20^\circ\text{C}$ ) in the range between 15% and 40% dry solids content. The effect of temperature on the surface tension is about the same as for pure water.

#### 9.1.2.4 Density

The density of black liquor is predominantly influenced by the concentration of inorganic components; this is a near-linear function of the dry solids content. The

density of black liquors at 25 °C can be predicted up to a dry solids content of 50% by the following expression [10]:

$$\rho_{25} = 997 + 649 \cdot DS \quad (3)$$

where DS is the weight fraction of dry solids in black liquor.

The influence of temperature on black liquor density can be estimated by Eq. (4):

$$\frac{\rho_T}{\rho_{25}} = 1 - 3.69 \cdot 10^{-4} \cdot (T - 25) - 1.94 \cdot (T - 25)^2 \quad (4)$$

where T is the temperature (in °C).

#### 9.1.2.5 Thermal Conductivity

The capability of a material to transfer heat is described by its thermal conductivity. As water shows the highest contribution to thermal conductivity, the latter decreases with increasing dry solids content and increases with increasing temperature. This relationship is expressed by the following empirical equation:

$$k = 1.44 \cdot 10^{-3} \cdot T - 0.335 \cdot DS + 0.58 \quad (5)$$

where K is thermal conductivity (in  $W m^{-1} \text{°C}^{-1}$ ); and T is temperature (in °C).

#### 9.1.2.5 Heat Capacity [8,11]

The specific heat capacity represents the heat necessary to raise the temperature of 1 kg of a material by 1 °C. Enthalpy data for black liquor are essential for estimating energy balances of kraft recovery boilers. The heat capacity of the black liquor decreases along with the increase in dry solids content. It can be approximated by a linear addition of the specific enthalpy contributions of water and black liquor solids. Moreover, an excess heat capacity function is incorporated to account for changes in black liquor heat capacity.

$$Cp_{bl} = (1 - DS) \cdot Cp_w + DS \cdot Cp_{DS} + Cp_E \quad (6)$$

where  $Cp_{bl}$  is the heat capacity of black liquor (in  $J kg^{-1} \text{°C}^{-1}$ );  $Cp_w$  is the heat capacity of water ( $4216 J kg^{-1} \text{°C}^{-1}$ );  $Cp_{DS}$  is the heat capacity of black liquor solids (in  $J kg^{-1} \text{°C}^{-1}$ ); and  $Cp_E$  is the excess heat capacity (in  $J kg^{-1} \text{°C}^{-1}$ ).

The temperature-dependence of the heat capacity of dry black liquor solids is expressed by Eq. (7):

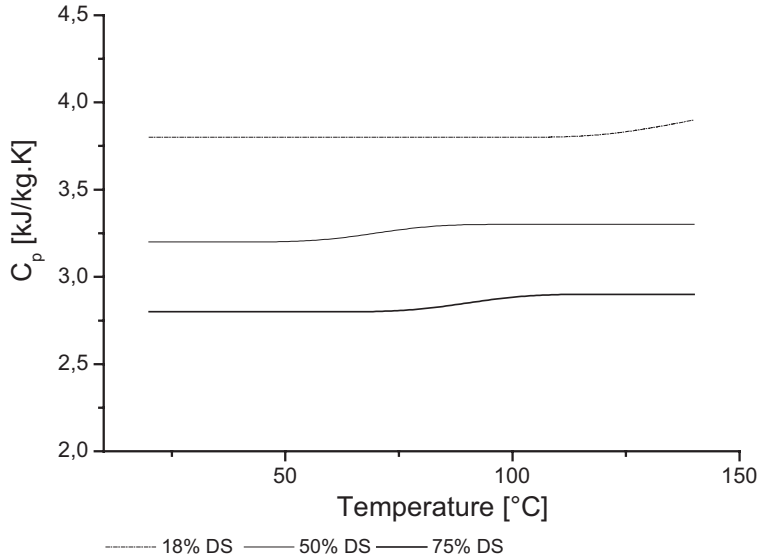
$$Cp_{DS} = 1684 + 4.47 \cdot T \quad (7)$$



The dependence of excess heat capacity on temperature and dry solids content is described by the empirical equation:

$$C_{pE} = (4930 - 29 \cdot T) \cdot (1 - DS) \cdot (DS)^{3.2} \quad (8)$$

The dependency of the heat capacity of black liquor,  $C_{p,bl}$ , for different dry solids contents is illustrated graphically in Fig. 9.2 ( $c_{p,w}$ ), as shown in Fig. 9.2.



**Fig. 9.2** Heat capacity of black liquor for different dry solids contents as a function of temperature.

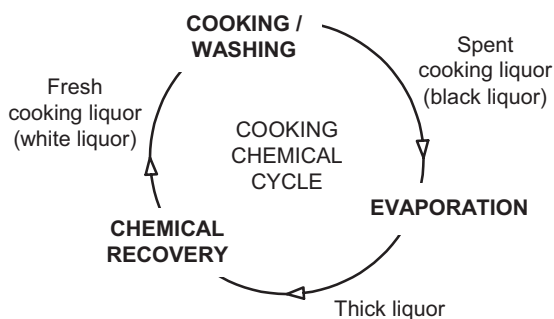
## 9.2 Chemical Recovery Processes

### 9.2.1 Overview

The chemical recovery processes contribute substantially to the economy of pulp manufacture. On the one hand, chemicals are separated from dissolved wood substances and recycled for repeated use in the fiberline. This limits the chemical consumption to a make-up in the amount of losses from the cycle. On the other hand, the organic material contained in the spent cooking liquor releases energy for the generation of steam and electrical power when incinerated. A modern pulp mill can, in fact, be self-sufficient in steam and electrical power.

The main stations in the cooking chemical cycle are illustrated in Fig. 9.3. The digester plant is provided with fresh cooking chemicals, which are consumed during the course of the pulping process. Spent cooking liquor contains, besides

chemicals, the organic material dissolved from wood. The spent liquor proceeds to the evaporation plant, where it is concentrated to a level suitable for combustion. The thick liquor goes on to the chemical recovery system, which comprises a recovery boiler and a number of installations for the preparation of fresh cooking liquor. The recovery boiler separates the inorganic cooking chemicals from the totality of spent liquor solids, and in parallel generates steam by combustion of the organic matter in the spent liquor. The inorganics proceed to the cooking liquor preparation system, which in the kraft industry consists of the causticizing and lime reburning areas. Fresh kraft cooking liquor is referred to as white liquor, and spent kraft liquor is called black liquor.



**Fig. 9.3** The cooking chemical cycle.

Besides serving the purposes of chemical recovery and energy generation, the combustion units in the chemical recovery areas are used for the disposal of odorous vent gases from all areas of the pulp mill. From an environmental perspective, these combustion units represent the major sources of a pulp mill's emissions to air.

The following sections provide a brief overview over the main processes employed in evaporation and chemical recovery, with particular focus on the kraft process. Those readers requiring further detail are referred to the relevant (information on recovery in the alkaline pulping processes e.g. Refs. [12–14]), and to Ref. [15] for sulfite recovery.

## 9.2.2

### Black Liquor Evaporation

#### 9.2.2.1 Introduction

Spent cooking liquor coming from the digester or wash plant typically contains 13–18% dry solids, the remainder being water. In order to recover the energy bound in the black liquor organics, it is necessary to remove most of the water from the weak liquor. This is done by evaporation, and this in turn raises the dry solids concentration in the black liquor for the purpose of firing the thick liquor

in a recovery boiler. Depending on the process used, a final solids concentration in thick liquor from kraft pulping up to 85% is achievable. Most commonly, kraft thick liquor concentrations are in the range of 65% to 80% dry solids. Thick liquors from sulfite pulping reach 50–65% dry solids.

Either steam or electrical power can be used to provide the energy to evaporate water from the black liquor. As there are usually sufficient quantities of low-pressure steam available in a pulp mill, the most economic solution in almost all cases is multi-effect evaporation with steam as the energy source. The use of mechanical vapor recompression (an electrical power-consuming process) is economically restricted to the evaporation of liquors with a low boiling point rise. Vapor recompression is therefore viable mainly for the *pre-thickening* of kraft black liquors at low dry solids concentrations, or for the evaporation of liquors from sulfite pulping.

### 9.2.2.2 Evaporators

Today's evaporators are mainly of the falling film type, with plates or tubes as heating elements. For applications involving high-viscosity liquor, or liquor with a strong tendency to scaling, forced circulation evaporators are also employed. Evaporators are usually constructed from stainless steel.

A schematic diagram of a falling film evaporator equipped with plate (lamella) heating elements is shown in Fig. 9.4. Thin liquor is fed to the suction side of the circulation liquor pump, which lifts the black liquor up to the liquor distribution. The liquor distribution ensures uniform wetting of the heating element surfaces. As the liquor flows downwards on the hot surface by gravity, the water is evaporated and the concentration of the liquor increases. The concentrated liquor is collected in the sump at the bottom of the evaporator. The generated vapor escapes from between the lamellas to the outer sections of the evaporator body, and then proceeds to the droplet separator, where the entrained liquor droplets are retained.

The steam, which drives the evaporation on the liquor side, is condensed inside the lamellas. Steam may actually be fresh steam or vapor coming from elsewhere, for example, another evaporator. In the latter case, the vapor often contains gases which are not condensable under the given conditions, such as methanol and reduced sulfur compounds from kraft black liquor or sulfur dioxide from spent sulfite liquor. If not removed, noncondensable gases (NCG) accumulate on the steam side of the heating element and adversely affect heat transfer by reducing both the heat transfer coefficient and the effective heating surface. When NCG are present, the evaporators require continuous venting from the steam side. The NCG are odorous and may be inflammable. Kraft NCG are typically forwarded to incineration, whereas sulphite NCG can be re-used for cooking acid preparation.

Evaporators are usually arranged in groups in order to improve the steam economy, and to accommodate the large heat exchange surfaces. When black liquor is transferred from one evaporator body to the other, the thickened liquor may be separately extracted from the evaporator sump (see Fig. 9.4), or branched off after the circulation liquor pump. The separate extraction of thick liquor before

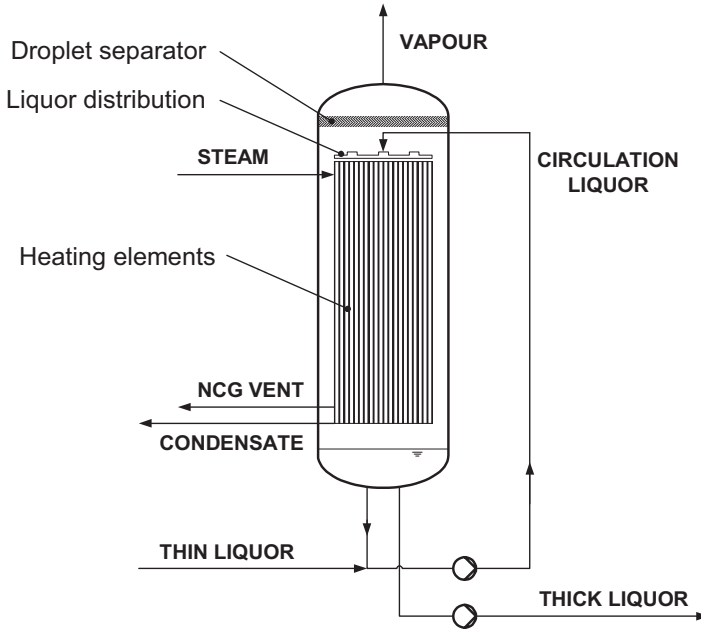


Fig. 9.4 Example of a plate-type falling film evaporator.

dilution with thin liquor keeps the concentration level in the evaporator comparatively low. This is especially helpful at high dry solids concentrations, where the boiling point rise can considerably reduce the evaporator performance.

The performance of an evaporator is determined by the heat transfer rate,  $Q$  (W). The very basic equation of heat transfer relates the transfer rate to the overall heat transfer coefficient,  $U$  ( $\text{W m}^{-2} \text{K}^{-1}$ ), the surface of the heating elements,  $A$  ( $\text{m}^2$ ), and the effective temperature difference,  $\Delta T_{\text{eff}}$  ( $^{\circ}\text{C}$ ):

$$Q = UA\Delta T_{\text{eff}} \quad (9)$$

The effective temperature difference which drives the evaporation is given by the difference between the steam side condensing temperature and the vapor side gas temperature,  $\Delta T$ , minus the boiling point rise, BPR:

$$\Delta T_{\text{eff}} = \Delta T - \text{BPR} \quad (10)$$

The overall heat transfer coefficient  $U$  depends on evaporator design, on the physical properties of the liquor (especially its dry solids concentration and viscosity), and on potential fouling of heat exchange surfaces. Typical heat transfer coefficients for falling film evaporators are between  $700$  and  $2000 \text{ W m}^{-2} \text{K}^{-1}$ , with low-end values related to high dry solids concentrations. The heat transfer rate is pro-

portional to the evaporation capacity. Thus, more surface area and a higher temperature difference result in increased capacity.

As concentrations rise during evaporation, fouling of the heat exchanger surfaces on the liquor side can be caused by the precipitation of inorganic and organic liquor compounds. Inorganics with a tendency to scaling include calcium carbonate, sodium salts, gypsum, silicates, or oxalates. Scaling worsens with higher concentrations and higher temperatures. A high fiber content in the feed liquor, as well as insufficiently removed soap, also accelerate fouling. Scales reduce the heat transfer, and by that the capacity of the evaporation plant. Hence, scales must be removed periodically by, in order of increasing operational disturbance: switching the evaporator body to liquor of a lower concentration; rinsing with clean condensate; cleaning with chemicals (mostly acids); or hydroblasting. High-temperature, high-concentration stages may require daily cleaning, whereas low-temperature low-concentration stages may continue for several months without cleaning.

### 9.2.2.3 Multiple-Effect Evaporation

The basic idea of multiple-effect evaporation is the repeated use of vapor to achieve a given evaporation task. Compared to single-stage evaporation, only a fraction of the fresh steam is required for the same amount of water evaporated.

The principle is illustrated in Fig. 9.5. Multiple-effect evaporation plants consist of a number of evaporators connected in series, with countercurrent flow of vapor and liquor. Live steam is passed to the heating elements of effect I and is condensed there, evaporating water from the liquor and producing thick liquor. The vapor released in this effect is condensed in the heating elements of the second effect at a somewhat lower temperature. The vapor released in turn on the liquor side of the second effect proceeds to the third effect and so forth, until the vapor from the last effect is condensed in a surface condenser at 55–65 °C. The vacuum needed at the last effect is most favorably provided by a liquid-ring vacuum pump.

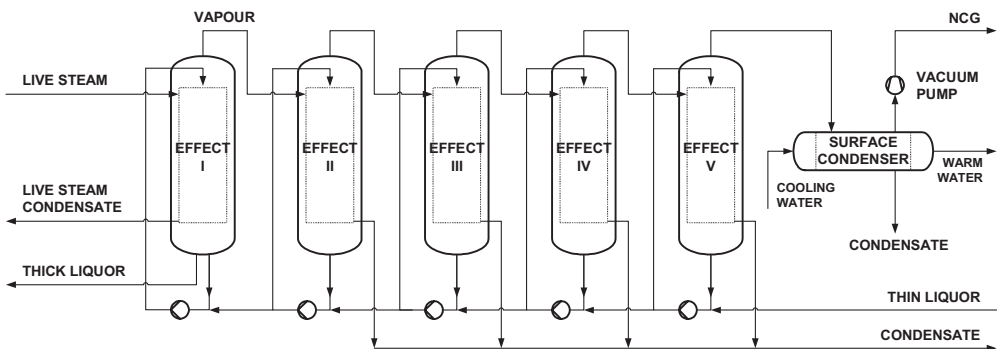


Fig. 9.5 The principle of multiple-effect evaporation demonstrated on a five-effects system.

Vapor condensates of different degrees of contamination come from the surface condenser, and from all the effects but the first. The live steam condensate from the first effect is collected separately from the vapor condensate for re-use as boiler feedwater.

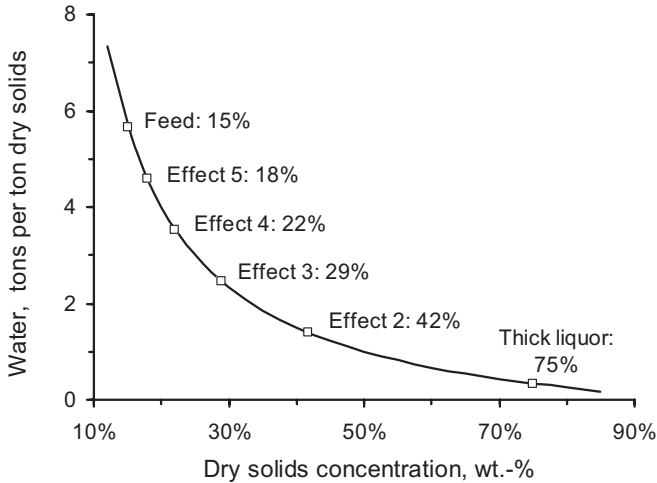
In Fig. 9.5, the thin liquor is fed to the last effect. The actual feed position of thin liquor in a multiple-effect system depends on the temperature of the weak liquor, on the course of temperatures over the effects, and on other unit operations which may be combined with evaporation such as stripping of foul condensate, soap skimming or black liquor heat treatment. The vapor from the stage, into which the thin liquor is fed, contains most of the volatile compounds from the black liquor. The place where this vapor is condensed delivers the foul condensate. In Fig. 9.5, this would be the surface condenser. The condensate from the other effects is less contaminated. Foul condensate is usually subjected to stripping for the removal of volatile substances such as methanol and organic sulfur compounds. Cleaner condensates can be used elsewhere in the mill instead of fresh water, for example for pulp washing or in the causticizing plant.

If the thick liquor concentration needs to be raised to above approximately 75%, the associated boiling point rise may require the use of medium-pressure steam in the first effect. The first effect – often called the “concentrator” – usually incorporates two or three bodies due to the more frequent cleaning required at the high-end temperature and concentration levels. Other effects may also need to be cleaned during operation from time to time. Depending on the cleaning procedure, arrangements may need to be provided for switching feed liquor between the bodies of an effect, or for by-passing a body when it is in cleaning mode.

In the last stages of a multiple-effect evaporation plant, the dry solids concentration of the black liquor changes only slightly. This is due to the large quantities of water to be evaporated at low concentrations. The amount of water in black liquor as a function of the dry solids concentration, together with calculated concentration levels in a five-effect plant starting with a 15% feed and thickening to 75%, is shown graphically in Fig. 9.6. Note that the rise in dry solids concentration is just 7% over effects 4 and 5, but more than 30% over effect 1 alone.

The steam economy of a multiple-effect evaporation plant depends mainly on the number of effects and on the temperature of the thin liquor. Other factors influencing the economy are, for example, the use of residual energy contained in condensates by flashing, venting practices, and cleaning procedures for scale removal. Typical multiple-effect evaporation plants in the pulp industry comprise five to seven effects, and have a gross specific steam consumption of between 0.17 and 0.25 tons of steam per ton of water evaporated. The specific consumption is roughly calculated by dividing 1.2 through the number of effects.

Evaporation plants which deliver high-end thick liquor concentrations usually have mixing of recovery boiler ash and chemical make-up to an intermediate liquor before the concentrator. The suspended solids then act as crystallization seeds for salts precipitating in the concentrator, thus making heating surfaces less susceptible to fouling. Thick liquors of high dry solids concentrations require a pressurized tank for storage at temperatures of 125–150 °C.



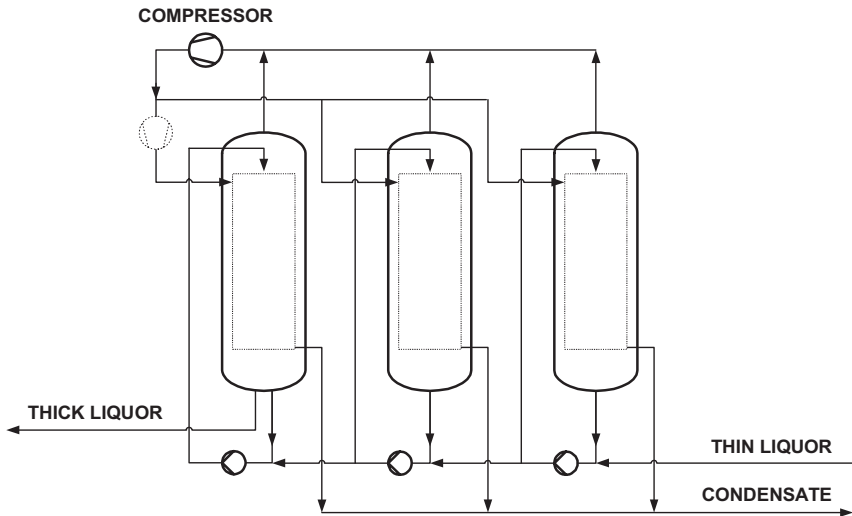
**Fig. 9.6** Water in black liquor as a function of the dry solids concentration. □, calculated dry solids concentrations in a five-effect evaporation plant with 15% dry solids in weak liquor feed and 75% dry solids in thick liquor.

Increasing the dry solids concentration brings a number of considerable advantages for subsequent firing in the recovery boiler, including more stable furnace conditions, higher boiler capacity, and better steam economy.

#### 9.2.2.4 Vapor Recompression

The concept of mechanical vapor recompression is based on a process where evaporation is driven by electrical power. In general, vapor coming from the liquor side of an evaporator body is compressed and recycled back to the steam side of the same body for condensation. The principle is shown schematically in Fig. 9.7. The vapors from all bodies are collected and fed to a fan-type, centrifugal compressor. The compressed vapors then return, at an elevated temperature, to the different bodies and condense at the steam sides, by that evaporating new water on the liquor sides.

The liquor is pumped from body to body. In contrast to multiple-effect plants, where the flow rates of condensate from all effects are similar (at the same surface area), vapor recompression plants have the highest condensate flow rate from the thin liquor stage and the lowest flow rate from the thick liquor stage. This is caused by the reduced driving temperature difference due to the increasing boiling point rise at higher dry solids concentrations. In some applications, it is useful to install a second fan in series to the first one. The second fan (shown in dotted style in Fig. 9.7) is dedicated to supplying the higher-concentration bodies with vapor of more elevated temperature, thus considerably improving their performance.



**Fig. 9.7** Principle of vapor recompression evaporation demonstrated on a system with three evaporator bodies.

Compression increases the vapor pressure, but at the same time the vapor is also superheated. The vapor must be de-superheated by injection of condensate before feeding it to the steam side of the heating element in order to make the heat transfer effective. The temperature rise across the fan compressor and de-superheater is typically around 6 °C. The resulting driving temperature difference is low, and hence vapor recompression plants require comparatively large heating surfaces.

Vapor recompression systems need steam from another source for start-up. Depending on the electrical power input and thin liquor temperature, they may also need a small amount of steam make-up during continuous operation. The specific power consumption for evaporation in a vapor recompression plant depends mainly on the boiling point rise, the heat exchange surface, and the thin liquor temperature. Typical specific power consumption figures range from 15 to 25 kWh t<sup>-1</sup> of water evaporated.

### 9.2.3

#### **Kraft Chemical Recovery**

##### **9.2.3.1 Kraft Recovery Boiler**

###### **9.2.3.1.1 Processes and Equipment**

A kraft recovery boiler converts the chemical energy of the black liquor solids into high-pressure steam, recovers the inorganics from the black liquor, and reduces the inorganic sulfur compounds to sulfides.



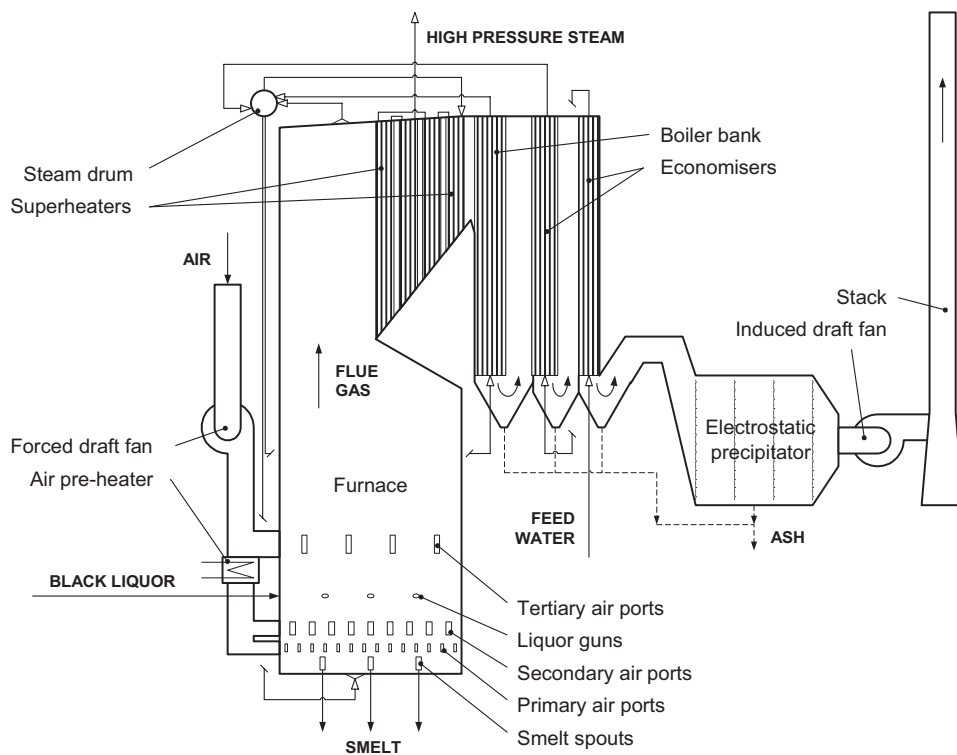


Fig. 9.8 Schematic of a kraft recovery boiler with single-drum design.

The recovery boiler consists mainly of the furnace and several heat exchange units, as illustrated in Fig. 9.8. Pre-heated black liquor is sprayed into the furnace via a number of nozzles, the liquor guns. The droplets formed by the nozzles are typically 2–3 mm in diameter. On their way to the bottom of the furnace, the droplets first dry quickly, and then ignite and burn to form char. After the char particles reach the char bed situated on top of the smelt, carbon reduces the sulfate to sulfide, forming carbon monoxide and carbon dioxide gases. Most of the inorganic black liquor constituents remain in the char and finally form a smelt at the bottom of the furnace, consisting mainly of sodium carbonate and sodium sulfide. Some of the inorganic material is also carried away as a fume by the flue gas. The liquid smelt leaves the furnace through several smelt spouts.

Air is sucked from the boiler house through the forced draft fan and enters the recovery boiler at three or four levels. The portion of the air going to the primary and secondary air ports is pre-heated with steam. The oxygen provided to the furnace with primary and secondary air creates a reducing environment in the lowest section of the furnace, which is necessary to provoke the formation of sodium sulfide. The oxygen supplied with tertiary air completes the oxidation of gaseous reaction products. The hot flue gas then enters the superheater section after passing the bull nose, which protects the superheaters from the radiation heat of the

hearth. As the flue gas flows through superheaters, boiler bank and economizers, its temperature is continuously falling to about 180 °C. After the superheaters, heat exchanger surfaces are located only in drafts with downward flow in order to minimize disadvantageous ash caking. After leaving the boiler, the flue gas still carries a considerable dust load. An electrostatic precipitator ensures dust separation before the induced draft fan blows the flue gas into the stack.

Ash continuously settles on the heat exchanger surfaces and so reduces the heat transfer. The most common means of keeping the surfaces clean is by periodical sootblowing – that is, cleaning with steam of 20–30 bar pressure.

Feed water enters the boiler at the economizer, where it is heated countercurrently by flue gas up to a temperature close to the boiling point. It enters the boiler drum and flows by gravity into downcomers supplying the furnace membrane walls and the boiler bank. Note that most of the evaporation of water takes place in the furnace walls, and only 10–20% in the boiler bank. As water turns into steam, the density of the mixture is reduced and the water/steam mixture is pushed back into the steam drum, where the two phases are separated. The saturated steam from the drum enters the superheaters, where it is finally heated to a temperature of 480–500 °C at a pressure of 70–100 bar. The temperature of the superheated steam leaving the boiler is controlled by attemperation with water before final superheating. The high-pressure steam proceeds to a steam turbine for the generation of electrical power and process steam at medium- and low-pressure levels. Excess steam not needed in the process continues to the condensing part of the turbine.

#### 9.2.3.1.2 Material Balance

A summary of a simplified calculation of smelt and flue gas constituents from black liquor solids is provided in Tab. 9.3. An analysis of the black liquor sampled is required before the boiler ash is mixed. In addition, any chemical make-up must be considered and the resulting composition is taken as the starting point for the calculation.

The computation is performed line by line. First, it is assumed that potassium and chlorine react completely to potassium sulfide and sodium chloride, respectively. In this simplified model, all the potassium from the black liquor (18 kg t<sup>-1</sup> of black liquor solids) turns into K<sub>2</sub>S in the smelt. Using the molecular weights of potassium (39 kg kmol<sup>-1</sup>) and sulfur (32 kg kmol<sup>-1</sup>), the sulfur bound in K<sub>2</sub>S is then  $18 \times 32 / (2 \times 39) = 7 \text{ kg t}^{-1}$  of black liquor solids. The remaining sulfur,  $46 - 7 = 39 \text{ kg}$ , is distributed between sodium sulfide and sodium sulfate according to the degree of reduction, *DR*, also termed the “reduction efficiency”:

$$DR = \frac{Na_2S}{Na_2S + Na_2SO_4} \quad (11)$$

Values for the chemicals in Eq. (11) can be inserted on a molar basis, equivalent basis or sulfur weight basis, all of which give the same result. Assuming 95%

Tab. 9.3 Simplified calculation of smelt and flue gas constituents from black liquor solids.

System input/output	Composition [wt.%]	Smelt constituents [kg ton <sup>-1</sup> dry solids]					Flue gas constituents [kg ton <sup>-1</sup> d.s.]			
		Na <sub>2</sub> CO <sub>3</sub>	Na <sub>2</sub> S	K <sub>2</sub> S	Na <sub>2</sub> SO <sub>4</sub>	NaCl	N <sub>2</sub>	H <sub>2</sub> O	CO <sub>2</sub>	O <sub>2</sub>
<i>Black liquor solids</i>	100%									
Potassium, K	1.8%		18							
Chlorine, Cl	0.5%					5				
Sulphur, S	4.6%		37	7	2					
Sodium, Na	19.6%	137	53		3	3				
Carbon, C	35.8%	36						322		
Hydrogen, H	3.6%						36			
Oxygen, O	34.1%	143			4		288	859	-953	
<b>Smelt total</b>		<b>316</b>	<b>89</b>	<b>25</b>	<b>9</b>	<b>8</b>				
<i>Air</i>	100.0%									
Nitrogen, N	75.6%					3.765				
Oxygen, O	23.0%								1.144	
Humidity	1.4%						70			
<i>Water and steam</i>										
Water in black liquor								333		
Soot blowing steam								100		
<b>Flue gas total</b>							<b>3.765</b>	<b>827</b>	<b>1.181</b>	<b>191</b>

reduction efficiency,  $0.95 \times 39 = 37$  kg sulfur are with Na<sub>2</sub>S, and the remaining 2 kg are with Na<sub>2</sub>SO<sub>4</sub>. Next comes sodium, with  $37 \times (2 \times 23)/32 = 53$  kg bound to Na<sub>2</sub>S,  $2 \times (2 \times 23)/32 = 3$  kg in Na<sub>2</sub>SO<sub>4</sub> and  $5 \times 23/35.5 = 3$  kg in NaCl. The remaining sodium is converted to sodium carbonate:  $196 - 53 - 3 - 3 = 137$  kg. Na<sub>2</sub>CO<sub>3</sub> binds  $137 \times 12/(2 \times 23) = 36$  kg carbon. The rest of the carbon is oxidized to CO<sub>2</sub>. Hydrogen from the black liquor is converted to water vapor. Finally, the oxygen demand can be calculated by summing up oxygen bound in carbonate, sulfate, water vapor and carbon dioxide:

$$137 \times (3 \times 16)/(2 \times 23) + 2 \times (4 \times 16)/32 + 36 \times 16/(2 \times 1) + 322 \times (2 \times 16)/12 = 1294 \text{ kg.}$$

As the black liquor solids contain just 341 kg of oxygen per ton, 953 kg must be provided with combustion air. Assuming 20% excess air, the oxygen in air is  $1.2 \times 953 = 1144$  kg. Nitrogen and humidity follow from the air composition. For calculating the total flue gas flow, we need to consider the water content of the black liquor and the steam used for sootblowing. Supposing 75% black liquor solids, the water coming with 1 ton of solids is  $1000/0.75 - 1000 = 333$  kg. The final total is about 450 kg of smelt and 6000 kg of wet flue gas per ton of dry liquor solids. The flue gas mass is equivalent to a volume of around 4800 standard cubic meters. Note that the above is a quite rough approach to the boiler mass balance, as minor streams are neglected, such as dust, sulfur dioxide, reduced sulfur compounds (TRS), carbon monoxide and nitrogen oxides ( $\text{NO}_x$ ) in the flue gas, as well as other inorganic matter and unburned carbon in the smelt.

#### 9.2.3.1.3 Energy Balance

Once the material balance of the recovery boiler has been calculated, a rough energy balance is easily obtained (see Tab. 9.4). At first, the enthalpies of input and output streams to the boiler are listed. Output streams have negative enthalpies. The reaction enthalpy is then calculated from the higher heating value (HHV) of the black liquor solids. Since the major part of the sulfur leaves the boiler in a reduced state, the corresponding energies of reduction must be subtracted from the HHV. The energy available for steam generation results from summing up all the stream and reaction enthalpies. In our example, the heat to steam amounts to  $9.9 \text{ GJ t}^{-1}$  black liquor solids. We assume a feedwater of  $120^\circ\text{C}$  and 95 bar, as well as high-pressure steam of  $480^\circ\text{C}$  and 80 bar. Then, the gross amount of steam generated is 3.5 tons per ton of black liquor solids. Note that some of the generated steam is consumed by the boiler itself. Sootblowing steam, steam for air/liquor pre-heating and feedwater preparation need to be deducted from the gross steam generation to obtain the net steam quantity available for the mill.

The data in Tab. 9.4 show that the humidity of the flue gas accounts for a considerable energy loss from the boiler. The humidity comes mainly from the water in the black liquor, from water formed out of hydrogen in organic material, and from sootblowing steam. Increasing the dry solids concentration of the black liquor, and thereby reducing the water input to the boiler, leads to a higher steam generation per mass unit of black liquor solids (Fig. 9.9).

Tab. 9.4 Simplified recovery boiler heat balance.

System input/output	Mass [kg ton <sup>-1</sup> dry solids]	Specific enthalpy [kJ kg <sup>-1</sup> ]	Enthalpy [MJ ton <sup>-1</sup> dry solids]
<i>Enthalpy of input/output streams</i>			
Black liquor	1.333	$2.8 \times 130$	485
Pre-heated air (dry)	4.909	$1.0 \times 120$	589
Humidity of pre-heated air	70	2.725	190
Sootblowing steam	100	2.820	282
Flue gas (dry)	5.137	$0.96 \times 180$	-888
Humidity of flue gas	827	2.840	-2.349
Smelt	448	1.500	-672
<i>Reaction enthalpy</i>			
HHV of black liquor solids	1.000	14.000	14.000
Reduction to Na <sub>2</sub> S	89	13.090	-1.170
Reduction to K <sub>2</sub> S	25	9.625	-244
<i>Losses</i>			-300
<b>Heat to steam</b>			9.923
<i>Feedwater/steam</i>			
Feedwater	3.494	510	1.782
<b>Total steam generation</b>	3.494	3.350	11.705

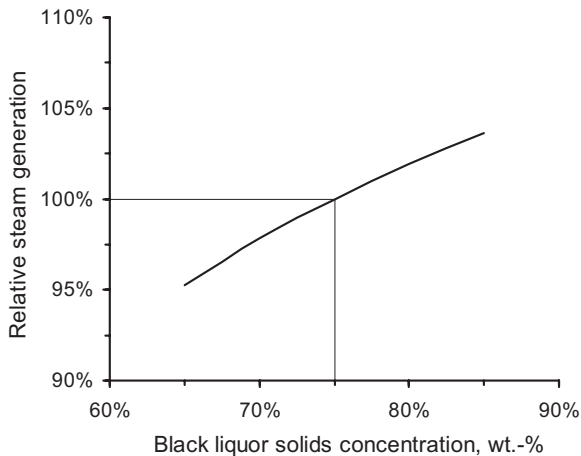
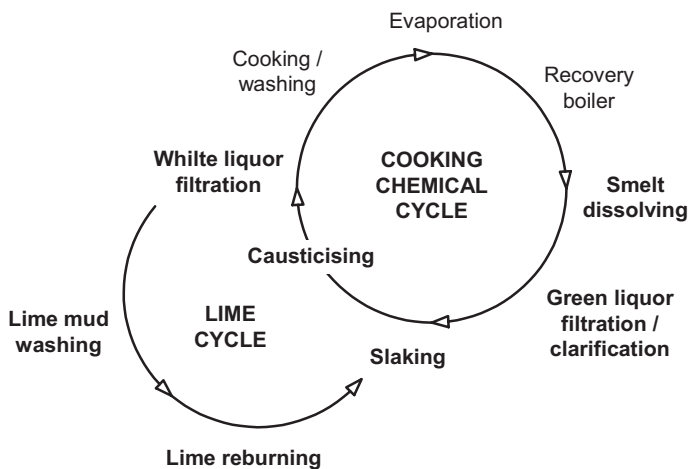


Fig. 9.9 Steam generation in a recovery boiler as a function of the black liquor solids concentration; typical curve normalized to 100% at 75% solids concentration.

### 9.2.3.2 Causticizing and Lime Reburning

#### 9.2.3.2.1 Overview

The causticizing and lime reburning operations target at the efficient conversion of sodium carbonate from the smelt to sodium hydroxide needed for cooking. As a part of the cooking chemical cycle, the preparation of white liquor consists of several process steps, and is accompanied by a separate chemical loop, the lime cycle (Fig. 9.10). The generated white liquor ought to contain a minimum of residual sodium carbonate in order to maintain the dead solids load in the cooking chemical cycle as low as possible.

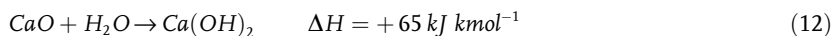


**Fig. 9.10** Major unit operations of causticizing and lime reburning in the context of the kraft chemical recovery cycle.

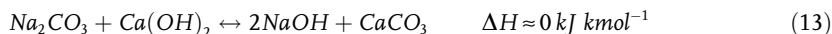
Process wise, the smelt coming from the smelt spouts of the recovery boiler drops into the smelt dissolving tank and becomes dissolved in weak wash, thereby forming green liquor. Since the smelt carries impurities which disturb the subsequent process steps, those must be removed by clarification or filtration of the green liquor. Then follow slaking, causticizing and white liquor filtration. After separation from the white liquor, the lime is washed and reburned for re-use in causticizing.

#### 9.2.3.2.2 Chemistry

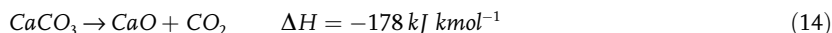
The basic chemical reactions in the causticizing plant and lime kiln start with the exothermic slaking reaction, where burned lime,  $\text{CaO}$ , is converted into calcium hydroxide,  $\text{Ca}(\text{OH})_2$  (slaked lime):



Then the causticizing reaction transforms sodium carbonate from the smelt,  $\text{Na}_2\text{CO}_3$ , to sodium hydroxide needed for cooking, thereby giving rise to calcium carbonate,  $\text{CaCO}_3$ :



Calcium carbonate is separated from the white liquor and reburned at a temperature above  $820^\circ\text{C}$  following the endothermic calcination reaction:



From a chemical perspective, white liquor is fundamentally characterized by active or effective alkali concentration, by sulfidity, as well as by causticizing and reduction efficiencies (see Section 4.2.2). In the causticizing plant, the total titratable alkali (TTA) is also of interest. Causticizing efficiency, CE, and TTA are defined as follows:

$$\text{CE} = \frac{\text{NaOH}}{\text{NaOH} + \text{Na}_2\text{CO}_3} \cdot 100\% \quad (15)$$

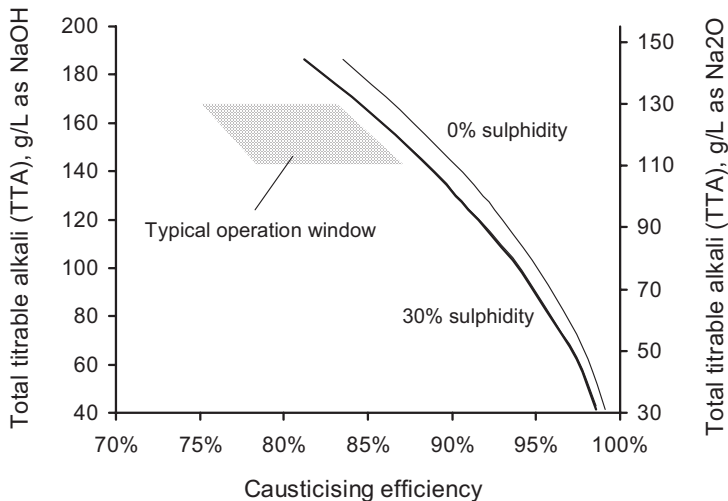
$$\text{TTA} = \text{NaOH} + \text{Na}_2\text{S} + \text{Na}_2\text{CO}_3 \quad (16)$$

The concentrations of the sodium salts in Eqs. (15) and (16) are, by convention, expressed in  $\text{g L}^{-1}$  and in terms of NaOH or  $\text{Na}_2\text{O}$  equivalents.

Lime ( $\text{CaO}$ ), calcium hydroxide ( $\text{Ca}(\text{OH})_2$ ) and calcium carbonate ( $\text{CaCO}_3$ ), also referred to as “lime mud”, all have a very low solubility in water. Reactions related to these components are basically happening in the solid phase.

The equilibrium of the slaking reaction is far on the product side of Eq. (12), and slaking is completed within 10–30 min. In contrast, the equilibrium of the causticizing reaction in a typical kraft pulp mill would be reached at a causticizing efficiency of about 85–90% (Fig. 9.11). The equilibrium conversion rate depends mainly on total alkali, sulfidity, lime quality, and temperature. A higher TTA and sulfidity reduce the equilibrium causticizing efficiency through product inhibition. As the retention time proceeds, the causticizing reaction is increasingly limited by the diffusion of reactants and reaction products through the increasingly thicker layer of  $\text{CaCO}_3$  around the hydroxide core of the particle. The equilibrium efficiency can be reached only with an excess of lime and at very long retention times.

Actual mill operations deal with time restrictions, and must avoid over-liming in order to maintain good filterability of the white liquor. As a consequence, the average achievable causticizing efficiency on mill scale is 3–10% lower than the equilibrium efficiency. Typical total retention times provided in the causticizers are around 2.5 h.



**Fig. 9.11** Equilibrium causticizing efficiencies at 0% and 30% sulfidity [14] and typical operating window for kraft mill causticizing systems. Sulfidity in this diagram is defined as  $\text{NaOH}/(\text{Na}_2\text{S} + \text{NaOH} + \text{Na}_2\text{CO}_3)$ .

#### 9.2.3.2.3 White Liquor Preparation Processes and Equipment

The preparation of white liquor begins with smelt dissolving. Weak wash and smelt form the green liquor, a solution of mainly sodium carbonate and sodium sulfide. The green liquor carries some unburned carbon and insoluble inert material from the smelt, which are detrimental to the downstream recovery and pulping processes if not removed, together with lime mud particles. While the removal of these so-called “dregs” was traditionally carried out by sedimentation, the requirements of today’s increasingly closed mills are best met with green liquor filtration. Since filters retain much smaller particles than clarifiers, the levels of insoluble metal salts are kept low. Several types of filters with and without lime mud filter aid are in use, such as candle filters, cassette filters, crossflow filters or disk filters.

The dregs separated from the green liquor are subjected to washing for recovery of valuable cooking chemicals. Dregs washers are typically rotary drum filters with a lime mud precoat. As the filter drum rotates, the dregs are dewatered, washed, and finally discharged from the drum at 35–50% dry solids by a slowly advancing scraper together with a thin layer of precoat. The consumption of lime mud for the precoat amounts to at least the same quantity as the dregs. This consumption is, however, not considered a loss because some lime mud must be sluiced from the lime cycle anyway for process reasons. Otherwise, nonprocess elements would accumulate in the lime cycle to problematical levels.

Clear green liquor coming from clarification or filtration proceeds to slaking. An example of a slaker is shown in Fig. 9.12. Lime mud and green liquor enter the equipment from the top of the cylindrical slaker bowl and are intensely mixed



by an impeller. Not only the slaking reaction, but also a major part of causticizing occurs in the slaker. The slurry flows from the slaker to the classifier section, from where it overflows to the causticizers. Grits – that is, heavy insoluble particles such as sand and overburned lime – settle in the classifier. These are transported by an inclined screw conveyor through a washing zone, and leave the cooking chemical cycle for landfill, together with dregs.

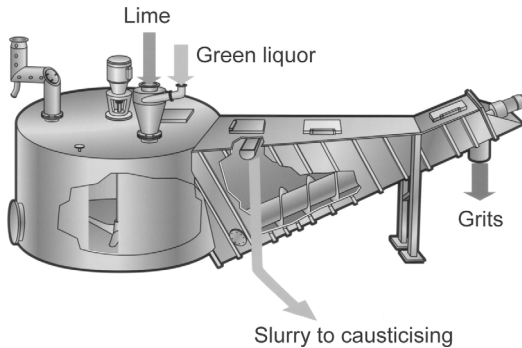


Fig. 9.12 A slaker [16].

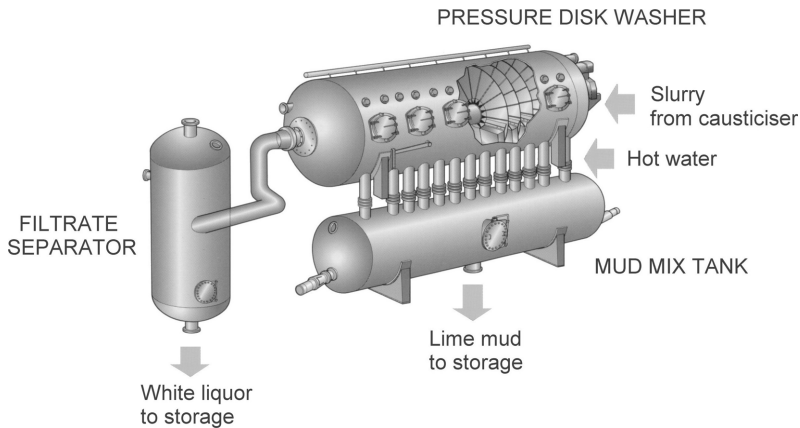
The slurry from the slaker enters the first of typically three causticizers, each of which is divided into two or three compartments (Fig. 9.13). The slurry flows from one unit to the next by gravity. Minimum backmixing between compartments ensures that the causticizing efficiency advances to a maximum. Agitation in slakers and causticizers needs special attention in order to avoid particle disintegration, since small lime mud particles reduce the white liquor filterability.



Fig. 9.13 A causticizer train [17].

After causticizing, the lime mud is removed from the slurry by pressure disk filters or candle (pressure tube) filters. The use of clarifiers for that purpose is fading out. A pressure disk filter, where the slurry from the last causticizer enters the filter vessel at the bottom of the horizontal shell, is shown in Fig. 9.14. White liquor is pushed by gas pressure through the precoat filter medium on the rotat-

ing disks into the center shaft, and flows to the filtrate separator. There, the white liquor and gas are separated. While the white liquor proceeds to storage, a fan blows back the gas from the top of the filtrate separator to the shell of the disk filter to provide the driving force for filtration. Lime mud accumulates on the filter medium as it rotates submerged in slurry, is then washed and continuously scraped from the surface of the disc at 60–70% dry solids. The lime mud is then discharged through a number of chutes into the mud mix tank. The washing step leads to a minor dilution of the white liquor, but reduces the requirements of downstream lime mud washing.



**Fig. 9.14** A pressure disk filter [18].

The examples of equipment solutions described above are what will most likely be found in a new mill. Existing causticizing plants are likely to appear quite different, as they may have seen certain pieces of equipment taken into different service over time as causticizing capacity increased. Equipment with potential application in changed positions includes rotary drum filter for the washing of dregs or lime mud; candle filters for white liquor filtration or lime mud washing; and sedimentation clarifiers for clarification of green liquor or white liquor, or for lime mud washing.

#### 9.2.3.2.4 Lime Cycle Processes and Equipment

Lime mud from the white liquor filter is pumped to storage and then washed on a rotary drum filter for the removal of soluble liquor constituents. The wash filtrate resulting from lime mud washing, termed “weak wash”, is used for smelt dissolving.

The lime mud coming from the lime mud washer contains 75–85% dry solids. It is either dried with flue gas in a separate, pneumatic lime mud dryer or is fed directly to the rotary kiln for drying and subsequent calcination. The diagram in Fig. 9.15 shows how solids and gas flow countercurrently through a lime kiln with a drying zone. Lime mud enters the refractory lined kiln at the cold end. The kiln slopes towards the firing end, and the solids move downwards as the kiln

slowly rotates. At first, water is evaporated from the lime mud in the drying section, and then the carbonate is brought to calcination temperature in the heating zone; finally, the calcination reaction takes place in the calcination zone. The high lime temperature at the firing end causes agglomeration and slight sintering. The overall retention time in the lime kiln is typically 2–4 h. Before leaving the kiln, the lime is cooled in tubular satellite coolers and in turn heats up fresh combustion air. After that, the larger lime particles are crushed and the lime is stored in a silo for re-use in slaking.

The quality of the burned lime is characterized mainly by the amount of residual calcium carbonate, typically 2–4%, and by the lime availability – that is, the percentage of lime which reacts with acid, typically 85–95%. Lime make-up requirements are usually in the range of 3–5%.

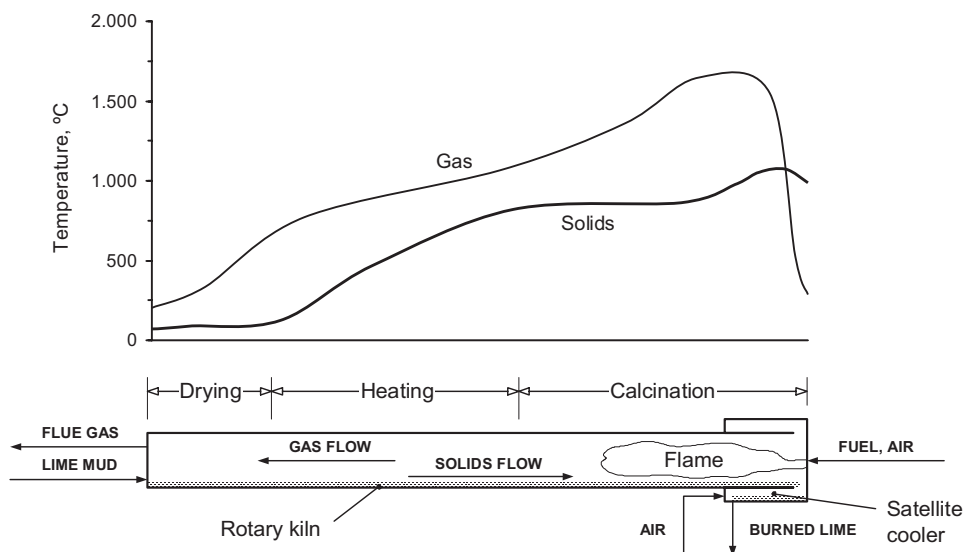


Fig. 9.15 Schematic of a lime kiln with temperature profiles of solids and gas.

The energy supply for the very endothermic calcination reaction usually comes from firing of fuel oil or natural gas. Approximately 150 kg of fuel oil or 200 Nm<sup>3</sup> natural gas are needed per ton of lime product. The oxygen for fuel combustion is supplied by air. The flame extends into the calcination zone, where the major part of the energy is transferred by radiation. As the flue gas passes through the kiln, its temperature falls gradually. Only about one-half of the chemical energy in the fuel is consumed by the calcination reaction, while about one-quarter is needed for evaporation of water from the lime mud. The remainder of the energy is lost with the flue gas and via the kiln shell. The flue gas which exits the kiln carries dust and, depending on the type of fuel, also sulfur dioxide. It is cleaned in an electrostatic precipitator for the elimination of particulates and, if needed, in a wet scrubber for SO<sub>2</sub> removal.

### 9.2.3.3 The Future of Kraft Chemical Recovery

#### 9.2.3.3.1 Meeting the Industry's Needs

The core technology of the Tomlinson-type chemical recovery boiler was developed in the 1930s. Various improvements have been made since then, and especially the energy efficiency has improved dramatically. However, certain inherent disadvantages of today's recovery systems are inflexibility regarding the independent control of sodium and sulfur levels in white liquor, as well as the safety risk connected to explosions caused by smelt/water contact.

Future recovery technologies are challenged by the technical requirements of modern kraft cooking processes with regard to liquor compositions, by increasingly stringent environmental demands, and last – but not least – by the industry's everlasting strive for improving the economic efficiency of pulping. In fact, the ongoing developments address all of these issues, and novel recovery techniques provide for the appealing long-term perspective that product diversification will once make pulp mill economics less dependent on pulp prices alone.

With regard to the near future, the two technologies which have conceivable potential to change the face of kraft chemical recovery are black liquor gasification (BLG) and in-situ causticization. Major achievements have been made in these fields since the 1990s, and commercialization is currently in progress [19–22].

#### 9.2.3.3.2 Black Liquor Gasification

Black liquor gasification is founded chemically on the pyrolysis of organic material under reducing conditions, or on steam reforming with the objective to form a combustible product gas of low to medium heating value. The main gasification products are hydrogen, hydrogen sulfide, carbon monoxide, and carbon dioxide. Gasification processes are divided into low-temperature techniques, where the inorganics leave the reactor as solids, and into high-temperature techniques, which produce a slag. Both gasification types allow the separation of sodium and sulfur, and both bear insignificant risk of smelt/water incidents.

*High-temperature gasification* occurs at about 1000 °C in an entrained flow reactor. Air is used as oxidant in low-pressure gasifiers, whereas high-pressure systems operate with oxygen. The black liquor decomposes in the reactor to form product gas and smelt droplets, both of which are quenched after exiting the reaction chamber. The smelt droplets dissolve in weak wash to form green liquor. The product gas serves as fuel after particulate removal and cooling [23].

*Low-temperature gasification* is carried out in an indirectly heated fluidized bed reactor, with sodium carbonate bed material and at a temperature around 600 °C. Superheated steam provides for bed fluidization, and the required energy is supplied by burning a portion of the product gas in pulsed tubular heaters immersed in the bed. Green liquor is produced from surplus bed solids. The product gas proceeds to cleaning and further on to utilization as a fuel [24].

Due to the separation of sulfur to the product gas, the salts recovered from gasification have a high carbonate content. Despite the flexibility in producing cooking

liquors of different compositions, the overall mill balance for sodium and sulfur must be observed. Selective scrubbing of hydrogen sulfide from the product gas and absorption in alkaline liquor is a must for kraft mills which operate at typical sulfidity levels. Depending on the set-up of hydrogen sulfide absorption, mills may run into increased loads on causticizing and lime kiln processes [25].

BLG is particularly energy efficient when applied together with combined-cycle technology – that is, when the product gas is burned in a gas turbine with subsequent heat recovery by steam generation (BLGCC; see Fig. 9.16). In such a case, the yield of electrical power from pulp mill operations can be increased by a factor of two compared with the conventional power generation by steam turbines alone. The related benefits range from the income generated from selling excess electrical power to the environmental edge of replacing fossil fuel elsewhere.

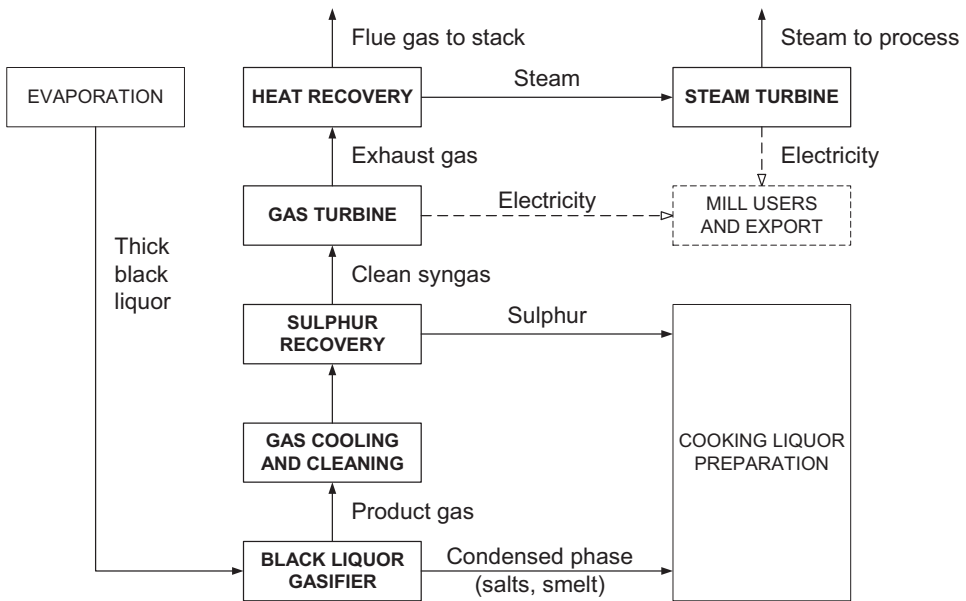


Fig. 9.16 The principle of black liquor gasification with combined cycle (BLGCC).

At present, some BLG installations are operating on a mill scale, mostly providing incremental capacity for handling black liquor solids. The encountered difficulties are mainly the adequate carbon conversion for the low-temperature process and the choice of materials for the high-temperature process. With regard to black liquor solids, the capacities of the currently installed systems are less than 10% of today's largest recovery boilers. When the process and material issues are settled, appropriate scale-up will be the next challenge. Nevertheless, it is expected that gasifier-based recovery systems will operate a number of reactors in parallel because physical limitations restrict the maximum size of a unit.

With regard to the combined-cycle systems, the BLG processes must be followed by efficient gas-cleaning steps. Cleaning of the synthesis gas is especially needed

because some volatile tar is formed during gasification, and this must be kept from entering the gas turbine.

#### 9.2.3.3.3 *In-Situ Causticization*

The second group of technologies on the brink of commercialization includes *autocausticization*. This is based on the formation of sodium hydroxide in the recovery furnace by means of soluble borates circulating in the cooking chemical cycle. Under certain conditions of causticizing or lime kiln limitations, partial autocausticizing can remove a bottleneck. Mill trials have demonstrated the technical feasibility, improved causticizing efficiency, and energy savings in lime reburning, and the process has been applied in one mill [26].

Another technique of in-situ causticization is that of *direct causticizing*. The process is still in the conceptual phase, and builds on the formation of sodium titanates or manganates in combination with BLG. The reactions in the gasifier release carbon dioxide to the product gas. Titanates are more efficient at converting carbonates to carbon dioxide than are manganates. The metal oxides proceed from the gasifier to a leaching step, where sodium hydroxide is formed in the presence of water. The insoluble metal oxides are then separated from the liquor and returned to the gasifier [27].

#### 9.2.3.3.4 *Vision Bio-Refinery*

Although a general breakthrough in novel recovery techniques is not expected before 2010–2015, it is likely that over the next decades a number of technologies will emerge to match certain applications. Fully commercialized BLGCC applications will add substantial flexibility to pulp mill operations, and will represent a most important step towards the pulp mill as a bio-refinery. Developments in the future may then involve the production of liquid biofuels from product gas, export of pure hydrogen or fabrication of hydrogen-based products [28].

### 9.2.4

#### **Sulfite Chemical Recovery**

The recovery of cooking chemicals from the sulfite pulping process can be split into primary and secondary recovery steps. This definition relates to the recovery of sulfur dioxide (see Fig. 9.17). In sulfite cooking, gas is continuously relieved from the digester for pressure control during the time at temperature, and the cook is also terminated by a pressure relief. The resulting relief gas contains considerable amounts of sulfur dioxide together with a bulk of water vapor and some NCG such as carbon oxides. In the primary recovery system, this gas is subjected to countercurrent absorption by fresh cooking acid in a number of vessels operated under staged pressure levels.

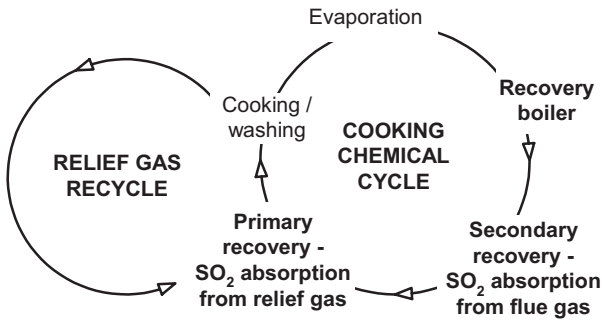


Fig. 9.17 The sulphite cooking chemical cycle.

Following evaporation, thick spent sulfite liquor is usually fired in a recovery boiler under an oxidative environment. Sulfur leaves the boiler in the form of  $\text{SO}_2$  with the flue gas, and is subsequently absorbed from the flue gas in the secondary recovery system. The design of both recovery boilers and secondary recovery systems is largely different between sulfite cooking bases. While magnesium and sodium bases can be recovered from the spent cooking liquor and re-used for cooking acid preparation, the recovery of calcium and ammonium bases is not practicable.

The sulfite pulping process is of declining relevance. New developments in the area of sulfite recovery are minor and very site-specific. They target mainly at reduced emissions to atmosphere and at more flexibility regarding combined and free  $\text{SO}_2$  in the cooking acid.

## References

- 1 Sjöström, E., *Wood Chemistry: Fundamentals and Applications*. Academic Press, Inc.: San Diego, California, 1981: 200–202.
- 2 Alen, R., Conversion of cellulose-containing materials into useful products. In *Cellulose Sources and Exploitation – Industrial Utilization, Biotechnology and Physico-Chemical Properties*. Ellis Horwood Ltd: Chichester, England, 1990: 453–464.
- 3 Alen, R., Analysis of degradation products: a new approach to characterizing the combustion properties of kraft black liquors. *J. Pulp Paper Sci.*, 1997; 23(2): J62–J66.
- 4 Lisboa, S.A., et al., Isolation and structural characterization of xylans from eucalyptus globulus kraft black liquors. In Eighth European Workshop on Lignocellulosics and Pulp. Riga, Latvia, 2004.
- 5 Zeng, L., A.R.P.v. Heiningen, Pilot fluidized-bed testing of kraft black liquor gasification and its direct causticization with  $\text{TiO}_2$ . *J. Pulp Paper Sci.*, 1997; 23(11): J511–J516.
- 6 Söderhjelm, L., M. Hupa, T. Noopila, Combustibility of black liquors with different rheological and chemical properties. *J. Pulp Paper Sci.*, 1989; 15(7): J117–J122.
- 7 Forsen, H., M. Hupa, P. Hellström, Liquor-to-liquor differences in combustion and gasification processes: nitrogen oxide formation tendency. *Tappi J.*, 1999; 82(3): 221–227.

- 8 Frederick, J., Black liquor properties. In *Kraft Recovery Boilers*, T.N. Adams, Ed. TAPPI Press: Atlanta, GA, 1997: 61–99.
- 9 Ryham, R., High solids evaporation of kraft black liquor using heat treatment. In Proceedings, Engineering Conference. Seattle, WA, 1990.
- 10 Fricke, A.L., Physical properties of kraft black liquors: Final Report – Phase I and II. DOE Report no. DOE/CE 40606-T5 (DE88002991), 1987.
- 11 Zamann, A.A., S.A. Tavares, A.L. Fricke, Studies on the heat capacity of slash pine kraft black liquors: effect of temperature and solids concentrations. *J. Chem. Eng. Data*, 1996; 41: 266–271.
- 12 *Chemical Pulping. Papermaking Science and Technology*, Book 6B, J. Gullichsen, H. Paulapuro, Eds. Helsinki: Fapet Oy, 2000.
- 13 Kocurek, M.J., Ed. *Alkaline pulping. Pulp and paper manufacture*, 3rd edn. Vol. 5. Atlanta, Montreal: The joint textbook committee of the paper industry (TAPPI/CPPIA), 1989.
- 14 Hough, G., Ed. *Chemical Recovery in the Alkaline Pulping Processes*. TAPPI: Atlanta, GA, USA, 1985: 196.
- 15 Kocurek, M.J., Ed. *Sulfite Pulping Science and Technology. Pulp and Paper Manufacture*, 3rd edn., Vol. 4. Atlanta, Montreal: The joint textbook committee of the paper industry (TAPPI/CPPIA), 1989.
- 16 Caustec Lime slaker (product leaflet). Kvaerner Pulping: Karlstad, Sweden, 2003.
- 17 Caustec Causticizers (product leaflet). Kvaerner Pulping: Karlstad, Sweden, 2003.
- 18 Caustec PDW filter (product leaflet). Kvaerner Pulping: Karlstad, Sweden, 2000.
- 19 Kordsachia, O., Stand und Perspektiven der Schwarzlaugenvergasung. *Das Papier*, 2002; 10: 50–53.
- 20 Patrick, K., Gasification edges closer to commercial reality with three new N.A. mill startups. *PaperAge*, 2003; October: 30–33.
- 21 Jopson, N., What tomorrow may bring. *Pulp & Paper International*, 2004 (5).
- 22 Stigsson, L., et al., Recovery of strongly alkaline chemicals for the NovaCell Process. International Chemical Recovery Conference. Charleston, SC, USA: TAPPI/PAPTEC, 2004.
- 23 Lindblom, M., An overview over Chemrec process concepts. Colloquium on Black Liquor Combustion and Gasification. Park City, UT, USA, 2003.
- 24 Mansour, M.N., R.R. Chandran, L. Rockvam. The evolution of and advances in steam reforming of black liquor. TAPPI Fall Technical Conference. San Diego, CA, USA, 2002.
- 25 Larson, E.D., et al., A cost-benefit assessment of BLGCC technology. *Tappi J.*, 2000; 83(6): 57.
- 26 Thorp, B., Agenda 2020. Reachable Goals Can Double Industry Cash Flow. PIMA's Leadership Conference. New Orleans, LA, USA, 2004.
- 27 Nohlgren, I., S. Siquefield, X. Zeng. In situ caustification for low temperature black liquor gasification. Colloquium on Black Liquor Combustion and Gasification. Park City, UT, USA, 2003.
- 28 Thorp, B., Industry/Government Partnership Targets New Energy Strategies. *Solutions! for People, Processes and Paper*, 2003(9): 35–36.



## 10 Environmental Aspects of Pulp Production

*Hans-Ulrich Süß*

### 10.1 Introduction

Since the production of pulp uses the renewable resource wood, the environmental impact starts with the selection of the tree species and their planting. All forestry operations have an environmental impact. Forestry certification, for example by the Forest Stewardship Council (FSC), is used to describe “best” conditions. Logging processes and the transport of wood similarly have an impact, as can wood storage and debarking. Bark can be described as the natural protection of trees against biological activity. Fungi and bacteria use wood as nutrition source, and therefore trees naturally produce compounds (e.g., resin acids) that have a certain toxicity and a very high concentration of poorly biodegradable organic matter to hinder rapid decay. The leaching of bark with water can result in a rather high level of toxicity in such an effluent, and dry debarking is therefore preferred. Bark is burned and used as energy source. Because bark is generally richer in minerals than the corresponding wood [1], the ash content is usually more than 10% – which is ten times higher than that in wood. The resulting ashes contain high levels of elements such as calcium, magnesium, potassium, sodium, iron, manganese, zinc, and phosphorus. These trace elements are important to the nutrition of trees, and should be returned into the forest, though this is not always permitted.

This chapter will focus briefly on the impact of the pulping process. The dominant process for chemical pulp production is the kraft or sulfate process. Apart from some specific differences, other processes such as sulfite pulping or soda pulping have a rather comparable environmental impact. Although the operation of a pulping process requires energy, modern mills do not require fossil fuel as the source for all energy is combustion of the compounds dissolved during the pulping process. The resultant emissions are the release of volatile compounds during the high-temperature pulping process and during brown stock washing. Evaporation and combustion of the recovered liquor causes additional emissions. In alkaline pulping the operation of the lime kiln represents an emission source.

The standard measures to reduce the impact of volatile and odorous compounds is by the sophisticated management of these sources. This comprises their collection, combustion and scrubbing of the remaining noncondensable gases. These methods are applied similarly for the on-site generation of bleaching chemicals such as chlorine dioxide and ozone. The build-up of nonprocess elements (chloride ions, potassium, or transition metals) in the process requires the introduction of cleaning steps that cause additional liquid or solid emissions. Washing of the fibers in the bleach plant removes organic matter, these dissolved compounds require a biological treatment of the effluent.

The impact of pulping, and the measures to control and limit the emissions, have been described in a variety of publications, with the European Commission publishing standards in 2000 [2]. Integrated Pollution and Prevention Control (IPPC) is used to describe the “best available techniques in the pulp and paper industry”. Similarly guidelines for a potential kraft pulp mill in Tasmania [3] describe the requirements for an environmentally sound operation.

## 10.2

### A Glimpse of the Historical Development

Over the years, pulp mills have become significantly larger with the development of technology. During the late nineteenth century, a mill with an annual production above 10 000 tons of fiber was considered to be a huge operation. Recovery of the pulping chemicals and treatment of the effluent was not usual [4], and for the sulfite process in some regions this approach was maintained for almost 100 years. The cheap pulping chemicals – limestone and sulfur – did not require expensive recovery, and consequently all wood compounds dissolved during pulping were discharged into the rivers. Assuming a pulping yield (on wood) of less than 50%, more dissolved material such as carbohydrates and sulfonated lignin was discharged than fiber produced.

This situation was different in kraft pulping, however, as the rather expensive caustic soda made recovery economical. The process acquired its other name – sulfate pulping – from the addition of sodium sulfate as sulfur make-up ahead of the reduction and combustion steps. As the processes changed slowly to provide better recoveries, huge amounts of organic material were removed from the effluent. Today, in sulfite pulping magnesium is the cation of choice. Following evaporation and combustion of the dissolved wood material, it is recovered as MgO from the dust filters. The combustion gases contain SO<sub>2</sub>, which is recovered by absorption by a magnesium oxide slurry. The small number of calcium sulfite mills remaining in operation also include an evaporation stage, and produce different types of lignosulfonates as valued byproducts. The sulfur dioxide remaining in the combustion gases is recycled and used to prepare fresh pulping acid solution. Therefore, sulfite mills do not contribute as excessively as in the past to the problem of “acid rain”, and sulfur dioxide emission using the best available techniques (BAT) is now running at 0.5–1.0 kg t<sup>-1</sup> pulp (as sulfur) [2].

In alkaline pulping, the intensity of pulping chemical recovery has been increased significantly. This had a pronounced impact on the color of the effluent. In general the effectiveness of brownstock washing and measures to avoid spills were intensified. Special basins are required to handle spills. The use of an oxygen stage as an “extension” of the pulping process has become common practice, as this permits to combust additional amounts of lignin dissolved by the oxygen treatment. This requires a higher evaporation and boiler capacity, but has the advantage of reducing the amount of dissolved organic material from the bleach plant.

Initially, the bleaching of chemical pulp was limited to treatment with hypochlorite in a hollander, and effluent from the bleach plant was discharged without further treatment. Sulfite pulp responds much better to bleaching than do kraft pulps, and by the end of the nineteenth century the demand for bright paper was satisfied by the wide use of sulfite pulp. The intensity of the exposure to hypochlorite cannot be enforced without damaging the fiber properties, however. A multi-stage treatment with intermediate washing reduced the demand for hypochlorite in a HEH treatment and permitted higher brightness at about 80% ISO (using current scales for better comparison).

Bleaching in towers with elemental chlorine was first introduced during the mid-1920s, whereupon the standard bleaching sequence became a CEH configuration. Because chlorination causes less fiber damage at low temperature, and the solubility of chlorine gas in water is higher at low temperature, chlorine was applied using and discharging large amounts of water. Indeed, for the very bleachable sulfite pulp this sequence remained standard until the early 1970s.

During the 1950s, chlorine dioxide became the standard chemical for the production of brighter kraft pulp. Initially, chlorine dioxide was applied simply as an additional final stage (CEHD). This procedure rapidly gained acceptance, due mainly to its high effectiveness in brightening without causing fiber damage. Consequently, bleaching sequences such as CEHDED became commonplace.

Increasing pulp production resulted in increasing effluent volumes and loads. The discharge without any treatment became a significant problem, especially for mills located on streams with poor water flow. The need to reduce the amount of organic material was most pronounced in highly populated countries, where filtered river water was used as source for drinking water. In other countries, a low availability of water did not allow high pollution levels. Already in the late 1960s, Sappi in South Africa began to develop oxygen delignification with the target of cutting the demand for bleaching chemical and decreasing the remaining discharge of organic compounds [5]. In Germany, the effluent of the extraction stage was evaporated together with the calcium sulfite pulping liquor at Schwäbische Zellstoff [6]. The aim of another project was to adsorb all higher molecular-weight compounds in the effluent on aluminum oxide [7], and then to reactivate the adsorbent by thermal treatment in a rotating kiln. However, serious corrosion problems as a result of high levels of chloride ions and hydrochloric acid stopped this project. In a Canadian project, the target was an effluent-free pulp mill, and water consumption and the bleach plant configuration and operation were modi-

fied stepwise over a number of years [8]. During these investigations, many lessons were learned about corrosion and bleaching efficiency in narrow loops, and it became obvious that the bleaching process was extremely difficult to operate in a “highly closed” mode.

The biological treatment of an effluent from chlorine bleaching, for example with CEH or CEDED, is of limited effectiveness. Some of the halogenated compounds produced are toxic, and most are poorly biodegradable [9]. Their amounts could be measured using absorption on to activated carbon. After washing to remove inorganic chloride, combustion of the loaded carbon provides an indication of the amount of absorbable organically bound halogen (AOX). The use of chlorine in the bleaching process led to the generation of very large amounts of organically bound chlorine. As a rule of thumb, about 10% of the chlorine applied in a C stage was detected as AOX in the effluent (50 kg Cl<sub>2</sub> t<sup>-1</sup> pulp generated about 5 kg AOX) [10]. The different reaction of hypochlorite with lignin led to the generation of only about half of the AOX for the same amount of active chlorine. Chlorine dioxide reacts with lignin dominantly as an oxidant. Typically, only 0.5–1% of the active chlorine is converted into halogenated compounds (50 kg active chlorine would generate about 250–500 g of AOX). There appeared to be no correlation between the AOX value and effluent toxicity [11], and whilst some toxic compounds contain halogen atoms, they are not all necessarily toxic.

During the 1980s, however, the detection of polychlorinated dioxins and furans in chlorination effluent [12] led to the relatively rapid development of alternative bleaching processes. Chlorine was eliminated from most bleaching sequences, the initial intention being the complete replacement of all chlorinated compounds (termed “totally chlorine-free”, or TCF bleaching). This could be easily achieved with sulfite pulps, which typically have good bleachability. The conversion of sulfite bleaching sequences from CEH (or CEHD) to shorter two-stage processes with PP stages took only a few years, and put an end to discussions about the relevance of AOX quantities in the description of potential or real hazards. The absence of chlorinated products in the effluent allowed for effective biodegradation. A sulfite mill having a lower brightness target applied the option to use magnesium oxide as an alkalization source for the peroxide stage. This permitted countercurrent water flow from the bleach plant to the pulping chemical recovery, which in turn led to very low amounts of organic material remaining and the mill being described as a (nearly) closed-cycle process [13].

Kraft pulp mills have been converted predominantly to elemental chlorine-free (ECF) bleaching, with such processes using modified pulping and oxygen delignification to achieve low residual lignin levels. In bleaching, chlorine dioxide and oxidative supported extraction stages (Eop and Ep) are applied alternately, which results in sequences such as DEopDEpD or DEopDP. Some mills use ozone to further reduce the demand for active chlorine as chlorine dioxide, and this has resulted in very low AOX discharge levels, whilst maintaining the pulp quality. Depending on the intensity of the use of other chemicals and the temperature applied in the chlorine dioxide treatment, ECF bleaching can become ECF-“light” bleaching. This is reflected in the detectable residuals of halogenated compounds

remaining in the fully bleached pulp. Such residuals are analyzed in similar manner to AOX, and labeled as OX (“halogenated residual”). An ECF-“light” pulp can have a residual of “OX” comparable to the “OX” background value of halogenated organic material present in TCF pulp.

TCF bleaching of kraft pulp is much more complicated because the condensed lignin is difficult to bleach without effective electrophilic oxidation. The compounds available – ozone or peracid (peracetic acid or Caro’s acid) – are much less selective than chlorine dioxide, and cannot be applied in large amounts without risking fiber damage and pulp yield loss. Thus, high brightness or top strength targets are typically difficult to meet simultaneously.

In 1990, only about 5% of the world’s bleached pulp was produced using ECF bleaching sequences, but by 2002 this level had increased to more than 75%, representing 64 million tons of pulp [14]. The level of pulp still bleached with chlorine has been affected by a slower than anticipated conversion of pulp mills in Japan, and its relative high use in the multitude of small non-wood pulp mills in Asia (mainly China and India). The huge kraft pulp mills in Western Europe, in the Americas, in Australia and New Zealand, as well as those in South Africa, are operating in the ECF mode at a level above 90%. These mills reach annual pulp production rates of between 400 000 and 1 000 000 tons. The mills that still use chlorine are much smaller, and produce pulp in amounts between 1000 and several 10 000 tons. These are typically old-fashioned, non-wood mills pending an upgrade or closure. Some of these mills do not even operate a chemical recovery unit, and therefore pollution caused by the bleaching process can unfortunately be labeled as minor compared to the total discharge of waste.

Currently, the extent of TCF bleaching remains static, though the process is maintaining its niche market position at around 5% of pulp production. TCF bleaching remains the method of choice for sulfite mills, though the slow decrease in sulfite operations and the continuing construction of new pulp mills using ECF bleaching will in time lead to a fall in the share of TCF bleaching.

In developed countries, kraft pulp mills began to use biodegradation plants for effluent treatment at an early stage. These included the use of large lagoons with aerators and anaerobic decomposition zones, while activated sludge systems were less common. The chemical oxygen demand (COD) or total organic carbon (TOC) are decreased by bacteria which consume the organic material. Today, rather narrow limits are set for COD and BOD (biochemical oxygen demand). The AOX are removed in these plants predominantly by adsorption [11], and not by actual biodegradation.

Compared with the pollution levels of the early pulping operations – and also compared to the situation just 10 to 20 years ago – pulp mills have more recently developed into very clean operations. Their typical water demand has fallen from more than  $50 \text{ m}^3 \text{ t}^{-1}$  pulp to below  $30 \text{ m}^3 \text{ t}^{-1}$ , while some mills operate with volumes below  $10 \text{ m}^3 \text{ t}^{-1}$ . However, at such low levels of water usage other problems such as scaling may become a serious threat to the operation. Although water saving may lead to additional environmental emissions – perhaps via a higher demand for bleaching chemicals or a higher energy input – sophisticated water

management and “kidneys” for the separation of nonprocess elements and pollutants become essential for such an operation.

New mills are typically erected based on the continuing development of technology, and current terms used to describe the state of the art are “accepted modern technology” (AMT) or “best available technology” (BAT). As new or “emerging” technology will develop into “accepted technology” once its applicability is proven, pulping and bleaching technology cannot be described as established processes. Indeed, all processes are undergoing continual development and further improvement.

### 10.3 Emissions to the Atmosphere

Typically, the combustion processes in the recovery or the bark boiler or lime kiln result in the emission of particulate matter. Such emission may be controlled using effective scrubbers or electrostatic precipitators.

During the pulping process, volatile organic compounds (VOC = volatile organic carbon) are generated. The typical odor of the kraft process is caused by mercaptans. These can be released either during the blow (discharge) of the digester or during brownstock washing or evaporation of the black liquor. All gaseous emissions must be collected and sent to a combustion unit. These malodorous emissions are described as “total reduced sulfur” (TRS) and expressed as hydrogen sulfide ( $H_2S$ ). These sulfur compounds are removed by oxidation to sulfur dioxide. During the combustion process, nitrogen is oxidized to a mixture of nitrogen oxides; they are described as  $NO_x$ . The amount of sulfur dioxide or nitrogen oxides within the gaseous effluent must not exceed certain threshold values that vary slightly different depending upon the type of combustion unit and the fuel material. The emission sources, the emissions and the interrelation between the different process steps are shown schematically in Fig. 10.1.

The emissions of all these compounds are controlled using either BAT or AMT. This could be achieved either by combustion or by washing in scrubbers with suitable liquids. The combustion itself must be controlled to avoid the emission of carbon monoxide or incomplete incineration. Likewise, nitrogen oxide and sulfur dioxide emission must be controlled. Examples of the emissions permitted from the recovery boiler and the lime kiln, the most important parts of the process, are listed in Tab. 10.1.

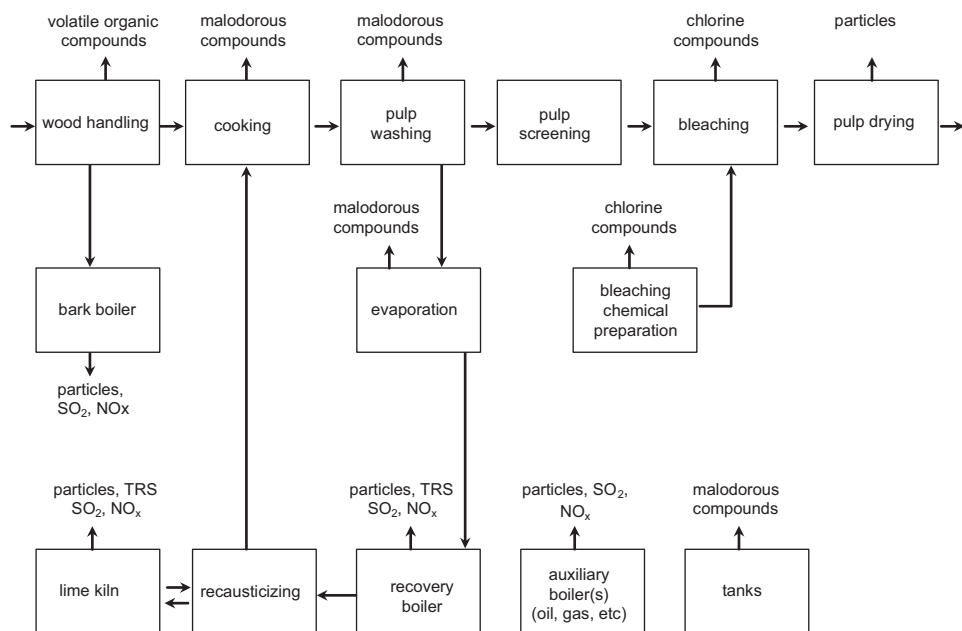


Fig. 10.1 Sources and emissions to the atmosphere from kraft pulp mills [2].

Tab. 10.1 Selected emission limits to the atmosphere described in 2004 for a potential pulp mill in Tasmania using “accepted modern technology” (AMT) [3].

Emission point	Pollutant	Units	Annual/monthly average
Recovery boiler	PM	mg NDm <sup>-3</sup>	50 @ 3% O <sub>2</sub>
	TRS	mg H <sub>2</sub> S NDm <sup>-3</sup>	7 @ 3% O <sub>2</sub>
	PCDD/PCDF	pg I-TEQ NDm <sup>-3</sup>	100 @ 3% O <sub>2</sub>
Lime kiln	PM	mg NDm <sup>-3</sup>	40 @ 3% O <sub>2</sub>
	TRS	mg H <sub>2</sub> S NDm <sup>-3</sup>	16 @ 3% O <sub>2</sub>
	PCDD/PCDF	pg I-TEQ NDm <sup>-3</sup>	100 @ 3% O <sub>2</sub>
All sources	NO <sub>x</sub>	kg NO <sub>2</sub> adt <sup>-1</sup>	1.3
All sources	SO <sub>2</sub>	kg S adt <sup>-1</sup>	0.4

PM = Particulate matter (or dust).

TRS = Total reduced sulfur.

NO<sub>x</sub> = Nitrogen oxides.

SO<sub>2</sub> = Sulfur dioxide.

PCDD/PCDF = Polychlorinated dioxins and furans.

NDm<sup>3</sup> = normal cubic meter of dry gas.

pg I-TEQ = pg International Toxicity Equivalents.

Detailed data on the typical emissions and the impact of different measures using BAT, for example, wet scrubbing only or with an electrostatic precipitator, are available in the European Commission report [2].

#### 10.4

##### Emissions to the Aquatic Environment

Washing following the pulping and bleaching process requires water, the demand for which has decreased significantly during the past few decades. This is the result of more effective washing procedures with improved equipment, and a higher degree of countercurrent water flow. The process, which is typically described as “loop closure”, became possible with the elimination of chlorine and hypochlorite from the bleaching sequences, both of which required a low treatment temperature and therefore cold dilution water. ECF bleaching allows a rather constant high temperature range to be maintained from brownstock washing to the dryer machine. The positive side effect is a lower demand for energy to heat the process water, while the downside is a higher tendency for scaling, for example with barium sulfate and calcium oxalate.

Cleaning of the effluent begins with the sedimentation of suspended solids, which describes mostly the recovery of fiber losses; this step is labeled as “primary effluent treatment”.

As mentioned previously, wood handling and debarking should be made without generating a higher volume of effluent. If de-icing or log washing is required, the effluent must be made nontoxic by a biological treatment. An example of this is woodyard effluent (rain water), which must be collected and treated biologically (unlike other rain water).

The pulping liquor should be recovered very effectively. Screening and brownstock washing should be conducted in a closed loop mode. Spills and leakages should be avoided by an optimized process control, but if they do occur enough temporary storage volume and evaporation capacity must be made available to deal with these problems. Brownstock washing following an oxygen delignification step must remove dissolved organic compounds and inorganic pulping chemicals effectively. Typically, the level of washing efficiency asked for is recovery of 99% of the dissolved organic material. Similarly, the lime mud generated in the green liquor clarification requires efficient washing.

Evaporation condensates must be stripped and appropriately reused. The condensates of acidic pulping processes (e.g., sulfite pulping) contains compounds such as methanol, acetic acid and furfural. These compounds may be separated, and represent a valuable byproduct; alternatively, they can be used as an energy source in a boiler. Water can be saved by recycling all clean cooling and sealing water.

The typical secondary effluent treatment unit for kraft pulp mills uses aerated lagoons in which the biomass is degraded by bacteria. Zones with a low oxygen content allow anaerobic fermentation and sludge decomposition, which decreases the generation of excess biomass (sludge).



The energy demand for oxygen addition is rather high [11], with about 1 kWh kg<sup>-1</sup> BOD<sub>5</sub> being required for the aeration. About half of the organic material is converted into carbon dioxide, while the other half is converted into biomass and must be separated as sludge. Sludge dewatering and disposal, followed by combustion of the sludge, leads to additional costs. Anaerobic fermentation may be an attractive alternative, as conversion of the organic matter leaves only 5% of the input carbon as residual for disposal or combustion. The process requires energy, predominantly for pumping, but also generates biogas consisting of methane containing a large amount of carbon dioxide. The typical process has four steps: (a) the fermentation and dissolution of insoluble residuals (fibers); (b) acidic degradation into alcohols and aldehydes; (c) conversion of these intermediates into acetic acid and acetates by micro-organisms; and (d) conversion into methane. For an effective process, acetogenic and methanogenic bacteria must exist in a close symbiosis. However, the surplus of energy generated by the conversion of waste sludge from the sustainable source wood into biogas does make anaerobic treatment very attractive.

A tertiary treatment is the final precipitation of remaining suspended or dissolved compounds by chemical coagulation. Usually, compounds used for such treatments include aluminum salts, ferric salts (Fe<sup>3+</sup>), and lime slurries, while charged polymers can be used for a further intensification. This process reduces the residual of recalcitrant compounds such as high molecular-weight degradation products of lignin. The resultant sludges may be rather difficult to dewater and are rich in inorganic material; thus, their combustion without additional fuel is difficult. The tertiary treatment is mainly used to remove excess nutrients such as phosphorus [2], but it can also reduce higher levels of COD and AOX. In the Tasmanian guidelines, the tertiary treatment is not considered to be AMT [3].

For the production of kraft pulp, the European Commission describes the BAT for the discharge of water, with the emission data summarized in Tab. 10.2.

The biological degradation of the organic material – carbon – requires in addition trace elements and ammonia, as well as phosphate. These nutrients are typically not available in a suitable ratio in pulp mill effluents, and must be added. Likewise, their levels must be controlled in order to avoid eutropic conditions in the receiving waters.

**Tab. 10.2** Best available technology (BAT) emission levels to the aquatic environment for bleached kraft pulp [2].

Water flow [m <sup>3</sup> adt <sup>-1</sup> ]	COD [kg adt <sup>-1</sup> ]	BOD [kg adt <sup>-1</sup> ]	TSS [kg adt <sup>-1</sup> ]	AOX [kg adt <sup>-1</sup> ]	Total N [kg adt <sup>-1</sup> ]	Total P [kg adt <sup>-1</sup> ]
30–50	8–23	0.3–1.5	0.6–1.5	<0.25	0.1–0.25	0.01–0.03

TSS = total suspended solids.

BOD<sub>5</sub> = biological oxygen demand (5 days).

COD = chemical oxygen demand.

AOX = absorbable halogenated compounds.

The Tasmanian mill guidelines exclude any discharge of effluent to a river. It is obviously assumed that rapid dilution of the effluent with sea water reduces the environmental impact. This limits the potential sites for a pulp mill to the coastline. The data listed in Tab. 10.3 show the comparability of the emission limits with the values described by the European Commission.

**Tab. 10.3** Selected emission limits to the marine environment described in 2004 for a potential pulp mill in Tasmania using “accepted modern technology” (AMT) [3].

Parameter	Unit	Monthly average maximum	Daily maximum
TSS	kg adt <sup>-1</sup>	2.6	4.5
BOD <sub>5</sub>	kg adt <sup>-1</sup>	2.1	3.6
COD	kg adt <sup>-1</sup>	20	34
AOX	kg adt <sup>-1</sup>	0.2	0.4

In North America, effluent color is a parameter which must be monitored. Color is more of aesthetic value than a parameter of toxicity. The presence of small amounts of humic acids represent a natural source for the brown color of water. However, in the past black liquor spills and the extraction stage effluent following a chlorination stage may have been responsible for the dark brown color of a pulp mill’s effluent. Therefore, color still can be an effluent control parameter, and is analyzed in color units (CU) using different dilutions of a mixture of a platinum complex and a cobalt salt.

## 10.5 Solid Waste

Solid waste results from a variety of sources, including inorganic sludge from the chemical recovery consisting of dregs and lime mud, bark and wood residues, as well as sand from wood handling. Sludge results from the effluent treatment, and consists of inorganic and organic material. In addition, there are dust and ashes from boilers and furnaces. Most of the organic waste products are burned for energy generation. The ash resulting from bark burning typically contains nutrients taken with the wood from the forest, and may be suitable as a fertilizer as long as it is not contaminated with other trace elements such as mercury, lead, or cadmium. The metal traces that occur naturally in wood are in part collected in the lime sludge and in the wastewater treatment sludge. These are then partly discharged with the effluent.

Sludge from the wastewater treatment constitutes the main group of waste, and large amounts may be generated in the primary and secondary treatment stages.

The amounts of sludge become smaller with anaerobic treatment conditions. Because aerobic sludge can be difficult to dewater, primary sludge (with fibers) or bark is frequently added to improve results. The amount of inorganic material in sludge may be rather high; a few ppm of transition metals in the wood and bark will translate, together with the lime mud and other waste, into over 40 kg adt<sup>-1</sup> of solid waste [2]. It should be noted that this value is the sum of all waste, consisting of dewatered wastewater treatment sludge, wood and other ash and wood waste.

Lime mud and green liquor clarification dregs can be disposed of in landfills. However, they must be washed very well to avoid the emission of H<sub>2</sub>S during mud drying, and to avoid the leaching of caustic soda residual. Sludge with a high content of combustible material may be dried and incinerated.

## 10.6 Outlook

Hopefully, this short summary on the environmental impact of pulp production has highlighted the point that there is no simple solution to all negative impacts. The close interrelation of the different process steps makes it almost impossible to avoid one problem without raising or increasing the size of another one. To name a few examples: An effluent-free mill will need to dispose of more solid waste and consequently may require more fossil fuel or more energy in general. Very tight water loops might require more chemical for more frequent cleaning steps, or the application of poorly biodegradable chelants. They might at the same time increase pollution by causing a higher demand for a chemical to achieve identical results. Pulping to very low kappa number for less bleaching chemical demand and effluent load might result in a lower yield, and so require more wood. It can in addition negatively affect fiber strength, which in turn triggers a higher demand for strong reinforcement fiber. Taken together, all of these “pros” and “cons” can result in a negative ecobalance for the positive intention.

Slogans such as effluent-free, chlorine-free or closed loop must be placed into perspective and analyzed very carefully for their total impact. Unfortunately, the tendency to simplify a complicated matter, and the desire to impress with achievements, have caused misleading impressions about the feasibility and impact of loop closure. On occasion, frequent loop opening is described as the use of kidneys, and the yield on wood as a parameter to be neglected. One study which aims to bring together all parameters into a realistic perspective is the Ecocyclic pulp mill project [15]. It demonstrates the potential for improvements and aims to set priorities. An increasing knowledge of the processes will doubtless generate the potential to balance the different interests of the conservation and the intelligent use of resources, with a minimum impact on the environment at best fiber quality, to name only three parameters.

## References

- 1 D. Fengel, G. Wegener, *Wood: Chemistry, ultrastructure, reactions*. De Gruyter, New York, 1983.
- 2 Integrated pollution prevention and control, Reference document on best available techniques in the pulp and paper industry, European Commission, Sevilla, Spain, December, 2001.
- 3 Draft main report: Development of new environmental emission guide lines for any new bleached eucalyptus kraft pulp mill in Tasmania, Vols. 1–3. Resource Planning and Development Commission, Hobart, Tasmania, 2004 <http://www.rpdc.tas.gov.au>.
- 4 W. Sandermann, *Die Kulturgeschichte des Papiers*. Springer-Verlag, 1988.
- 5 P. Perolle, H.H. Myburgh, A. Roberts, *Pulp Pap.* 1969; 43(10): 148–150; G. Rowlandson, Continuous oxygen bleaching in commercial production. *Tappi J.*, 1971; 54(6): 962–967.
- 6 H. Klein, J.P. Franzreb, *Delignifizierende Bleiche von Sulfitzellstoffen mit Wasserstoffperoxid*. Eucepa Tagung, Helsinki, 1980: 9:1–9:25.
- 7 H. Solbach, Erfahrungen mit der Abwasserbehandlung in einer integrierten Zellstoff- und Papierfabrik. *Papier*, 1977; 31(10A): V87–V91.
- 8 D.W. Reeve, G. Rowlandson, W.H. Rapson, The effluent-free bleached kraft pulp mill. *Pulp Paper Canada*, 1977; 78(3): T50–T56; D.W. Reeve, The effluent-free bleached kraft pulp mill – Part XIII: The second fifteen years of development. *Pulp Paper Canada*, 1984; 85(2): T24–T27.
- 9 K. Kringstad, K. Lindström, Spent liquors from pulp bleaching. *Environ. Sci. Technol.*, 1984; 18(8): 236–238.
- 10 H.U. Süss, Die peroxidgestützte Sauerstoffdelignifizierung von Sulfitzellstoff – ein Schritt zur Verringerung der AOX-Belastung. *Papier*, 1986; 40(4): 150–153; H.U. Süss, N. Nimmerfroh, W. Eul, J. Meier, Approaches to minimize the formation of AOX in Kraft pulp bleaching. *Papier*, 1990; 44(7): 339–348.
- 11 C.H. Möbius, Abwasser der Papier- und Zellstoffindustrie, 3. Auflage, 2002, revised December, 2004. Available as pdf file at: [www.cm-consult.de](http://www.cm-consult.de).
- 12 F. de Souza, M.-C Kolar, K.P. Kringstad, S.E. Swanson, C. Rappe, B. Glas, Influence of chlorine ratio and oxygen bleaching on the formation of PCDFs and PCDDs in pulp bleaching. *Tappi J.*, 1989; 72(4): 147–153.
- 13 N. Nimmerfroh, H.U. Süss, H.P. Boettcher, W. Luetngen, A. Geisenheiner, The German approach to the closed-cycle sulfite mill – development and implementation. *Pulp Paper Canada*, 1995; 96(12): T414–T420.
- 14 [www.aet.org/reports/markets/trends90-01](http://www.aet.org/reports/markets/trends90-01).
- 15 Kretsloppsanpassad massafabrik, *Ecocyclic pulp mill*, Final report KAM 1, 1996–1999. English version.

## 11

# Pulp Properties and Applications

Herbert Sixta

### 11.1

#### Introduction

Pulp represents the major raw material basis for two main applications: (a) for paper and board production, where the pulp fibers are mechanically modified to give a coherent sheet; and (b) for chemical conversion to products such as regenerated fibers and cellulose derivatives. The former is denoted as *paper grade*, the latter as *dissolving grade* pulp. Paper-grade pulp is by far the most dominant field of pulp production. With an annual production of about 190 million tonnes in 2002, paper-grade pulp accounts for almost 98% of the total wood pulp production (see Chapter 1, Tab. 2, Tab. 3 in Part I). A large variety of different unbleached and bleached mechanical and chemical pulps comprise the raw material basis for paper and board products. The kraft process represents the dominating pulping technology (130 million tonnes in 2004), while the sulfite process (being the most important pulping method until the 1930s) continuously loses ground and finds application only in certain niche markets.

Sulfite pulp is characterized by rather weak strength properties, and is typically used in products that require good sheet formation and moderate strength. Historically, sulfite has been most widely used in newsprint furnish. However, its importance in newsprint has been declining in recent years with the increasing use of stronger mechanical pulps such as thermomechanical pulp (TMP) and chemo-thermomechanical pulp (CTMP). However, their use is mostly restricted to applications such as newsprint, toilet tissues, and paperboard as they tend to yellow on age due to the high content of residual lignin (20–25%).

Semi-chemical pulps with a typical residual lignin content of 10–15% represent the transition from mechanical to chemical pulps. There are several types of semi-chemical pulps in production, but the most important of these is Neutral Sulfite Semi-Chemical (NSSC). NSSC is made primarily from hardwood species, and is noted for its exceptional stiffness and high rigidity. Its primary use is for the production of corrugating medium as well as printing papers, greaseproof papers, and bond papers.

Kraft pulp is noted for its superior strength characteristics, and can be used in virtually all paper and paperboard grades in order to improve strength properties. In fact, the word kraft is the Swedish and German word for strength. Unbleached kraft is usually made with softwood and is used primarily in furnishes of kraft linerboard, wrapping paper and bag papers such as grocery bags. Semi-bleached kraft is used in furnishes of such grades which do not require high brightness, like newsprint and other groundwood-based papers. Bleached kraft is used in a much wider range of products than either unbleached or semi-bleached. Its greatest importance is in the printing and writing grades. In these grades, softwood kraft is used for its strength characteristics, while hardwood kraft, having shorter fibers, is used for its superior printing properties.

For dissolving pulp production, only acid sulfite cooking and the prehydrolysis kraft process are of major practical importance. Unlike paper-grade pulping, the acid sulfite process is the dominant system for the production of dissolving pulps, and accounts for approximately 60% of the total production. Compared to paper-grade production, the manufacture of dissolving wood pulp represents a niche production. However, the high demands for cellulose purity and reactivity – as well as its manifold routes of utilization – are the reason for its advanced state of technology within the pulp industry.

In this chapter, the main emphasis is placed on a comprehensive discussion of the physical and chemical properties of dissolving pulps because they serve as appropriate substrates of which many aspects of pulp characterization may also be transferred to paper-grade pulps. The papermaking properties of pulp are extensively described and reviewed in the relevant literature [1–3]. The following section on paper-grade pulp is limited to a short description of certain chemical and macromolecular properties which are rarely presented in the literature. (The chemical and macromolecular properties of chemical paper pulps, however, were rarely the subjects of published literature. This section is therefore concerned with a very short description of important differences in chemical and macromolecular properties of a selection of chemical paper pulps.)

## 11.2

### Paper-Grade Pulp

Chemical paper-grade pulps can be categorized into hardwood and softwood sulfite and kraft pulps. The definite differences in pulp properties between sulfite and kraft pulps have been the subject of numerous studies [4]. Jayme and Kortzen advanced a hypothesis that, for a given degree of delignification, sulfite pulps were more degraded on the outside of the fiber than were kraft pulps [5]. This hypothesis was supported by Luce, who developed the method of “chemical pulping” to study the radial distribution of different properties across the cell wall [6]. According to his results, the molecular weight of the polysaccharides of the kraft pulp was uniform throughout the fiber wall, while in the sulfite pulp it was low at the outermost layers and increased towards the inner layers. The significantly

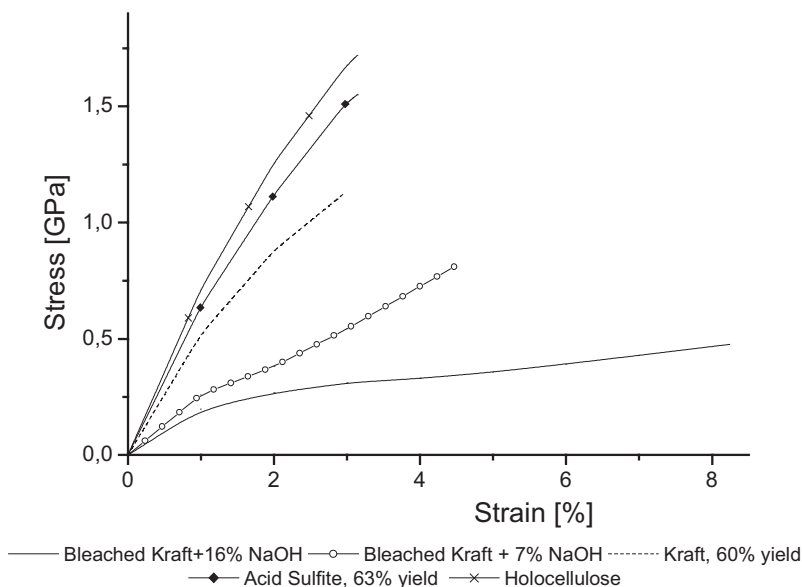
lower molecular weight of the residual hemicellulose fraction in sulfite as compared to kraft pulps has been also pointed out by Jayme and Köppen [7]. It can be concluded that (acid) sulfite cooking liquor penetrates through the pits into the porous middle lamella where delignification proceeds from the primary wall. The degradation reaction involving both lignin and carbohydrates thus proceeds from the outer to the inner cell wall layers, and this results in a broad molecular weight distribution of the polysaccharide fraction. In contrast, alkaline cooking conditions promote rather uniform pulping reactions due to the high swelling properties. Hamilton and Thompson have studied the main differences in the carbohydrate constituents of wood celluloses prepared by the sulfite and kraft pulping processes [8]. According to their findings, xylan from hardwoods is converted to low molecular-weight 4-*O*-methylglucuronoxylan by the acid sulfite pulping procedure, and to a rather high molecular-weight xylan with a low number of uronic acid side chains. The glycosidic bond between uronic acid and the xylan backbone is particularly sensitive to alkaline cleavage. The decrease in uronic acid content results in a drastic decrease in the solubility of the xylan in aqueous alkaline solutions. This leads to the well-known phenomenon of xylan reprecipitation onto the surface of pulp fibers during the final kraft cooking phase, as demonstrated by Yllner-Enström when treating a mixture of cotton linters and xylan extracted from birch at kraft cooking conditions [9,10]. The significantly higher enrichment of xylan in the surface layers of kraft pulps as compared to sulfite pulps has been confirmed by Dahlmann and Sjöberg, who applied an enzymatic peeling technique to characterize carbohydrate composition across the cell wall layers of both softwood and hardwood pulp fibers [11].

When examining the properties of paper pulps, sulfite and kraft pulps differ in two major characteristics. First, kraft pulps show a much higher resistance towards beating than do sulfite pulps. For sulfite pulps it requires less time to reach a given drainage resistance as compared to kraft pulps. Second, sheets from sulfite pulps are considerably lower in tear (22%) and burst (17%) strengths, and somewhat lower in tensile (10%) as compared to kraft pulp sheets [12]. At the same tensile index, kraft pulps typically exceed sulfite pulps in tearing strength by 40–80% [13]. It was reported that over the cellulose content range of 44–80%, the fiber strength is directly proportional to the cellulose content, but above a value of 80% cellulose content the fiber strength greatly diminishes [14]. This may be due to the replacement of flexible cellulose–hemicellulose–cellulose bonds by the more rigid cellulose–cellulose bonds.

Page proposed a concept based on supramolecular properties to explain differences between sulfite and kraft pulps. Sulfite pulp is seen as containing largely crystalline and paracrystalline cellulose, whereas in kraft pulp substantial transformation of the paracrystalline regions to the amorphous state has occurred. The relationship to the degree of order has been established by measuring the level-off DP (LODP), which is a simple means of determining the mean crystalline length [13]. Furthermore, Page suggested that paracrystalline regions in native cellulose fibrils are transformed into amorphous regions during pulp processing that are viscoelastic and capable of absorbing more energy under mechanical stress. The

high LODP, the high modulus in the stress-strain curve, the excellent swelling properties [15,16], the low tear strength, and the high beating rate of sulfite pulps were attributed to the greater amounts of crystalline and paracrystalline regions compared to kraft pulps.

Sulfite pulps contain large amounts of crystalline and paracrystalline cellulose, while kraft pulps consist predominantly of amorphous cellulose domains. Page recognized an increase in tear strength of a pulp with increasing proportion of amorphous cellulose. This is also reflected in the low modulus of the stress-strain curve of a single fiber, as illustrated in Fig. 11.1.



**Fig. 11.1** Stress-strain curves of single fibers prepared by various pulping treatments using black spruce with low fibril angles ( $0^{\circ}$ – $10^{\circ}$ ) [13].

Fibers, particularly of low fibril angle between  $0^{\circ}$  and  $10^{\circ}$ , have shown that the shape of the stress-strain curve depends on the pulping process. Figure 11.1 illustrates the decreasing modulus with increasing proportion of amorphous cellulose. The modulus decreases in the order holocellulose > acid sulfite > 60% kraft > bleached kraft + 7% NaOH > bleached kraft + 16% NaOH, which corresponds well with the order of decreasing beating rate and increasing tear strength. The rate at which a pulp beats is virtually a measure of the rate at which the wet cell wall splits and breaks up while applying mechanical stress. Fibers of amorphous structure thus containing viscoelastic properties are more likely to withstand stress without fracture, since the stresses will be relaxed and the energy dissipated in the viscoelastic regions. Fibers of high modulus and elasticity tend to peel their bonds at low strains, while those of low modulus will peel at larger strains because



they relax stresses in viscoelastic elements. From that it has been concluded that higher tearing strength is likely to be associated with a higher proportion of amorphous regions.

The differences between sulfite and kraft pulps are also reflected in their chemical and macromolecular properties. Representative fully bleached commercial soft- and hardwood kraft and sulfite paper pulps have been selected for comprehensive chemical and macromolecular characterization. Additionally, elemental chlorine-free (ECF) and totally chlorine-free (TCF) -bleached pulps have been chosen from each softwood kraft and sulfite pulps. A comparison of the four categories of chemical paper pulps, including TCF and ECF variants for both softwood kraft and sulfite pulps and two representatives of hardwood kraft pulps, on the basis of extended chemical characterization, is provided in Tab. 11.1.

**Tab. 11.1** Comprehensive chemical characterization of a representative selection of commercial paper-grade pulps [17].

Parameter		Pine	Spruce	Eucalyptus	Beech	Spruce	Spruce	Beech
		Kraft		Kraft		Sulfite		Sulfite
		ECF	TCF	ECF	ECF	TCF	ECF	TCF
Basic characteristics								
Kappa number	–	0.5	0.5	0.5	0.8	2.7	0.3	6.2
Brightness	% ISO	89.0	90.7	89.7	87.6	85.9	92.7	90.3
Viscosity	mL g <sup>-1</sup>	793	635	833	802	1020	868	1123
Extractives								
DCM	% od pulp	0.03	0.03	0.12	0.17	0.15	0.10	0.15
Acetone	% od pulp	0.05	0.02	0.16	0.18	0.12	0.12	0.18
Alkali resistancies								
R <sub>10</sub> content	% od pulp	87.0	87.2	91.9	90.0	87.7	87.4	84.6
R <sub>18</sub> content	% od pulp	87.1	88.0	94.6	93.6	89.8	90.5	87.6
Carbohydrates								
Glucose	% od pulp	84.7	86.1	80.4	73.3	89.7	91.6	84.9
Mannose	% od pulp	6.6	5.8	0.3	0.2	5.2	5.0	1.2
Galactose	% od pulp	0.2	0.2	0.1	0.1	0.0	0.0	0.0
Xylose	% od pulp	7.3	6.9	18.4	25.5	4.1	2.7	12.2
Arabinose	% od pulp	0.5	0.5	0.0	0.0	0.0	0.0	0.0

Tab. 11.1 Continued.

Parameter		Pine	Spruce	Eucalyptus	Beech	Spruce	Spruce	Beech
		Kraft		Kraft		Sulfite		Sulfite
		ECF	TCF	ECF	ECF	TCF	ECF	TCF
Hexenuronic acid (HexA)	$\mu\text{mol g}^{-1}$	1.1	1.5	1.4	1.1	0.7	0.7	0.6
Organochloric compounds	ppm	130	33	203	n.d.	<6	61	<6
Functional groups								
Copper number	%	0.3	0.2	0.8	0.5	1.0	1.3	1.4
Carbonyl groups (CCOA)	$\mu\text{mol g}^{-1}$	15		9	12	57		37
Carboxyl groups	$\mu\text{mol g}^{-1}$	37	46	84	131	54	40	70
Inorganic Compounds								
Total ash	%	0.33	0.19	0.19	0.34	0.30	0.20	0.23
Ca	ppm	199	130	175	1208	655	453	916
Mg	ppm	404	195	70	319	550	130	237
Si	ppm	293	50	59	73	115	63	10
Fe	ppm	49	11	6	16	25	4	2
Mn	ppm	1.7	2.0	2.3	2.7	4.1	< 0.2	0.4
Water retention value (WRV)	%	83.7	80.6	78.3	92.8	76.2	81.2	84.3
Zero-Span tensile index								
dry	$\text{Nm g}^{-1}$	130.8	133.7	147.1	n.d.	113.1	103.6	98.8
rewetted	$\text{Nm g}^{-1}$	116.2	109.4	n.d.	n.d.	96.5	82.9	84.4

The residual lignin content of all ECF- and the TCF-bleached softwood kraft pulps is far below 1, indicating a low tendency of light-induced yellowing. The two TCF-bleached sulfite pulps reveal slightly elevated kappa numbers, which may be attributed to the applied bleaching concept, namely sequential alkaline oxidative bleaching step comprising oxygen delignification and hydrogen peroxide bleaching.

There are also some noticeable differences in pulp viscosity ranging from low level in the case of TCF-bleached softwood kraft pulp to generally high levels in the case of the TCF-bleached sulfite pulps. The high bleaching selectivity of the latter is reflected in the high viscosity at a given brightness level.

The extractives content of a fully bleached commercial pulp depends on many different parameters, with the wood species, pulping, and bleaching processes being the most important influencing factors. The data in Tab. 11.1 confirm the predominant influence of the cooking process on the extractives content when comparing sulfite and kraft pulps based on spruce wood. The bleaching sequence, however, seems not to exhibit a major influence on the extractives content. TCF- and ECF-bleached spruce sulfite pulps reveal similar resin contents. A further significant decrease in the extractives content due to bleaching operations may only be expected when high dosages of, for example, ozone, or other bleaching chemicals of high oxidation potential are applied.

The alkali resistance determined at 18% ( $R_{18}$ ) and 10% ( $R_{10}$ ) NaOH concentration at room temperature is a measure of estimating the cellulose content (total for  $R_{18}$  and long-chain cellulose for  $R_{10}$ ), and is usually used to characterize the degree of purity of dissolving pulps (see Tab. 11.7, Dissolving pulp characterization). Although not very common in paper pulp analysis, the R-values provide insight into many aspects of pulp origin and properties, including the type of pulp, wood species (at least allowing a distinction to be made between hardwood and softwood), molecular weight of carbohydrates, supramolecular structure, chemical composition of hemicelluloses, and functional groups (which for example indicate oxidative damage of carbohydrates).

In general, the R-values of paper pulps are typically at higher levels as predicted from the cellulose content, indicating that part of the hemicelluloses are alkali-insoluble. The low difference between  $R_{18}$  and  $R_{10}$ , as observed particularly for softwood kraft pulps, refers to both high molecular-weight cellulose and alkali-insoluble hemicellulose fractions that mainly derive from xylan with a low content of uronic acid side chains. It is interesting to note that the pulps containing the highest amount of hemicelluloses, the hardwood kraft pulps, exhibit extremely high R-values at the same time, completely comparable to those of dissolving pulps. In a first approximation, this can be attributed to high molecular-weight xylan comprising a low degree of substitution of uronic acid side chains. However, the contrary is true for sulfite pulps. Even though the R-values of sulfite pulps are generally lower as compared to kraft pulps, their cellulose content is considerably higher, as indicated from carbohydrate analysis. Moreover, the higher values of ( $R_{18} - R_{10}$ ) as compared to kraft pulps suggest a higher fraction of low molecular-weight cellulose and differences in the supramolecular structure.

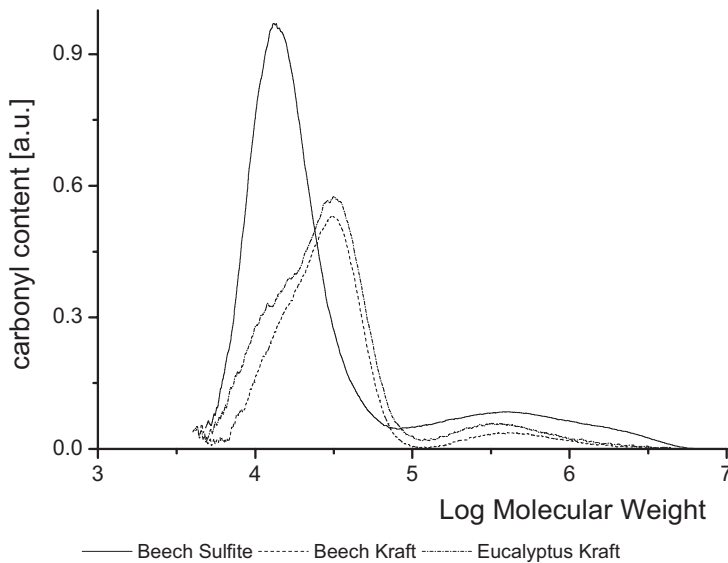
The carbohydrate analysis of pulp provides a variety of valuable information about the wood species, the pulping process, and even pulping and bleaching conditions. Sulfite pulps have a significantly lower content of hemicelluloses than kraft pulps, which may be attributed in general to both a better preservation of cellulose and higher losses of hemicelluloses. It is well established that virtually no cellulose is lost, while the hemicellulose fraction (particularly from hardwood) is rather unstable in acid sulfite pulping, and this results in a low (hemicellulose) yield and low molecular weight of the residual hemicelluloses. Generally, kraft pulps obtain higher yields in the case of hardwoods, whereas sulfite pulps preserve better yields in the case of softwoods. When examining one particular cook-

ing process, for example the kraft process, the cellulose:hemicellulose ratio is rather indicative of pulp strength [18]. Molin and Teder have shown convincingly that the specific bond strength (relationship between Z-strength/Scott Bond energy and density) as well as the fiber strength (dry and rewetted zero-span tensile strength) are unaffected by the hemicellulose content of spruce kraft pulps comprising a cellulose:hemicellulose ratio between 3 and 9 (equal to a hemicellulose content of 10–25%). On the other hand, the tensile index decreases by 30% when the cellulose:hemicellulose ratio is increased from 3 to 9 when compared at the same density. In parallel with the decrease in tensile strength, the tear strength increases by up to 100%. In contrast to fiber strength, the sheet strength is highly dependent upon the hemicellulose content. The stiffness of the fibers has been identified as the major influencing parameter of sheet strength properties. It has been shown that fibers become stiffer and more brittle with increasing proportions of hemicelluloses in the kraft pulp. One of several explanations for this is that the shrinkage of the fibers during drying may increase with a decreasing cellulose:hemicellulose ratio. Fibers with higher shrinkage are subjected to higher stress during drying of sheets, which in turn increases the E-modulus of the fibers [19]. Fibers with a high E-modulus show high tensile strength, but low tear strength (see also Ref. [14]).

During kraft cooking, 4-O-methylglucuronic acid groups attached to xylan are partially converted to hexenuronic acid (HexA) groups (see Section 4.2.6.2, Modified Kraft cooking, “Effect on carbohydrate composition”). These groups react with electrophilic bleaching chemicals such as chlorine dioxide and ozone. Additionally, acid treatment at elevated temperature may also be used selectively to remove the HexA groups. Fully bleached kraft pulps with kappa numbers below 1 contain only traces of residual HexA, as shown in Tab. 11.1.

In contrast to dissolving pulp specification, the standard characterization of paper-grade pulp does not include the determination of functional groups. However, many important pulp properties originate from carboxyl and carbonyl groups, depending on the amount and their distribution along the polysaccharide chains (see Tab. 11.7, Dissolving pulp characterization). The carboxyl groups, mainly derived from uronic acid side chains of hemicelluloses, and aldonic acid groups created by the oxidation of reducing end groups, determine the surface charge (distribution) and hydrophilicity, which in turn exhibits an influence on wettability of the pulp (the ability of the sample to absorb liquids). The carboxyl groups relate also to the swelling behavior of a pulp sample, which may be estimated by the water retention value (WRV). The data in Tab. 11.1 indicate that the WRV values of the selected pulps differ only slightly. The only significant difference is observed for beech kraft pulp, which seems to correlate with the enhanced carboxyl group content. The carbonyl group content of a pulp is made up of the reducing end-groups and oxidized groups such as keto and aldehyde groups, which are introduced by pulping and bleaching operations. The reliable and accurate determination of those oxidized structures in cellulose remains a major challenge. A novel method based on fluorescence labeling with carbazole-9-carboxylic acid [2-(2-aminooxyethoxy)ethoxy]amide (CCOA) allows the precise evaluation of

the carbonyl groups relative to the molecular weight, as it is combined with gel-permeation chromatography (GPC) measurement [20,21]. Even though the average molecular weight is higher for sulfite pulps, their carbonyl group content is considerably higher as compared to kraft pulps (see Tab. 11.1). It may be assumed that the high carbonyl content of sulfite pulps originates from low molecular-weight hemicelluloses and oxidized groups along the cellulose chain. In a first approximation, the carbonyl group profile may be estimated by subtracting the contribution of the reducing end groups from the total amount of carbonyls, assuming that the amount of reducing end groups relates to the number average molecular weight determined from GPC measurement [22]. The pattern of carbonyl groups along the polysaccharide chains has been determined for the hardwood paper pulps to obtain a first indication about the influence of pulping processes on the generation of carbonyl groups. Figure 11.2 indicates that the major part of the carbonyl groups in the beech sulfite pulp is centered around a molecular weight of about 13 kDa (DP ~80), whereas in both hardwood kraft pulps the maximum of carbonyl groups introduced along the polysaccharide chains is shifted to a higher molecular weight (32 kDa or DP ~200).

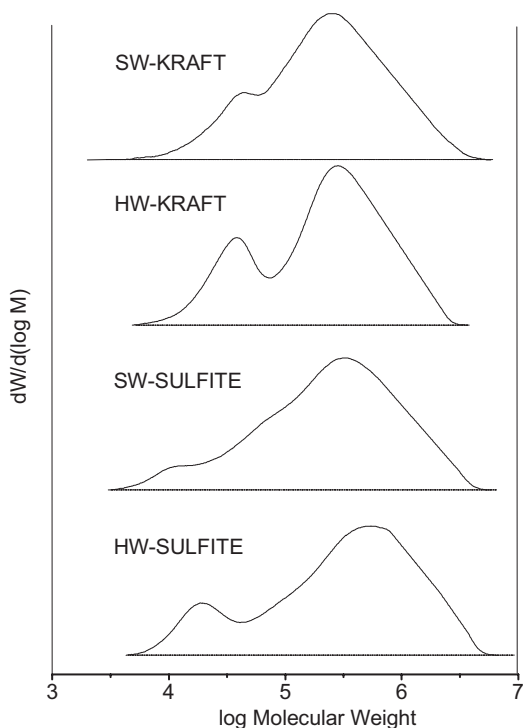


**Fig. 11.2** Profile of carbonyl groups relative to the molecular weight of hardwood kraft and sulfite pulps [17]. For more detailed characterization, see Tab. 11.1.

The large amount of oxidized structures in sulfite pulps correlates well with their low R-values, and indicates the presence of an increased level of alkali-labile groups.

The majority of pulp constituents are composed of polymers of varying type and size. A polymer is typically characterized by its molar mass and molar mass distri-

bution. The decrease in molar mass of the wood polymers during pulping and bleaching procedures is normally estimated by measuring the intrinsic viscosity of the pulp fibers. Since celluloses from natural sources and after chemical treatment are always polydisperse, the determination of intrinsic viscosity is insufficient to predict specific fiber properties. Additional information is provided by measuring the molecular weight distribution of paper pulps. The results of GPC measurements of cellulose solutions in LiCl/DMAc with MALLS/RI detection according to Schelosky et al. [23] are provided in Tab. 11.2 and Fig. 11.3.



**Fig. 11.3** Molar mass distribution of a representative selection of fully bleached commercial paper pulps [17].

The typical pattern of molecular weight distribution of the four different categories of chemical paper grade pulps is clearly demonstrated in Fig 3. The kraft pulps can easily be distinguished from the sulfite pulps by a hemicellulose distribution centered at a rather high molecular weight. The bimodal character of the molecular weight distribution is particularly pronounced for the hardwood pulps, comprising a clear minimum between the cellulose and hemicellulose distributions.

The polydispersity index (PDI) calculated from the ratio of mass-weighted ( $M_w$ ) and number-weighted ( $M_n$ ) molar masses ( $PDI = M_w/M_n$ ), as shown in Tab. 11.2. is significantly higher for the sulfite as compared to the kraft pulps, and indicates

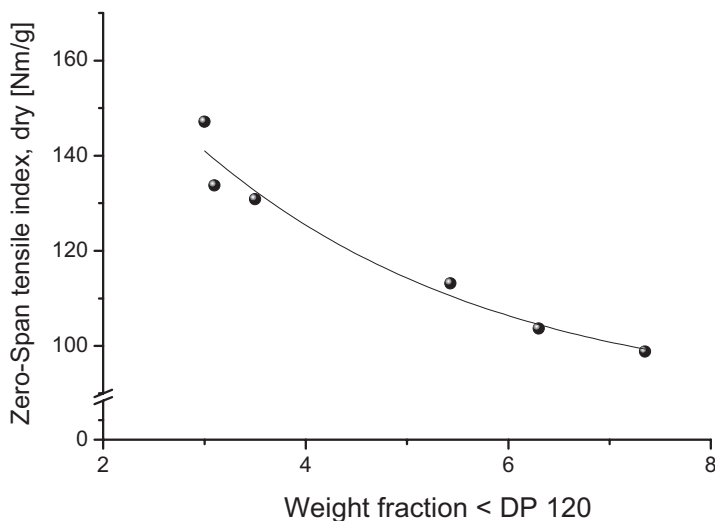
**Tab. 11.2** Numerical evaluation of molecular weight distribution of fully bleached commercial paper pulps [17].

Parameter		Pine	Spruce	Eucalyptus	Beech	Spruce	Spruce	Beech
		Kraft		Sulfite		Sulfite		
		ECF	TCF	ECF	ECF	TCF	ECF	TCF
DP <sub>v</sub> (Cuen)		2207	1648	2355	2240	3074	2486	3489
DP <sub>w</sub>		2827	2251	2847	2636	3648	3144	4050
DP <sub>n</sub>		659	650	612	590	572	504	517
PDI		4.3	3.5	4.6	4.5	6.4	6.2	7.8
DP < 120	wt%	3.5	3.1	3.0	3.5	5.4	6.3	7.4
DP < 200	wt%	8.2	7.9	8.2	10.7	8.8	8.7	12.8
DP > 2000	wt%	38.7	29.7	40.5	39.5	49.8	44.0	53.4
Zero-span tensile strength								
dry	Nm · g <sup>-1</sup>	130.8	133.7	147.1	n.d.	113.1	103.6	98.8
wet	Nm · g <sup>-1</sup>	116.2	109.4	n.d.	n.d.	96.5	82.9	84.4

a broader distribution of the former. The high PDI of the sulfite pulps originates from rather high molecular-weight cellulose and very low molecular-weight hemicellulose fractions owing to the heterogeneous degradation of the wood pulp constituents across the cell wall layers. Intrinsic strength properties from a polymeric material are always related to the weakest part in the polymer, which is represented by the short-chain molecules. A detailed evaluation of the numerical data from GPC measurement revealed that zero-span tensile strength correlates well with the weight percent of the DP <120 fraction, as illustrated in Fig. 11.4.

The intrinsic viscosity as well as standard information from GPC measurements such as PDI or DP<sub>w</sub> and DP<sub>n</sub> are not suited to predict the fiber strength properties accurately. However, the amount of low molecular-weight fraction comprising the DP range between 100 and 150 is a suitable measure to estimate fiber strength properties, regardless of the origin of pulp (wood species, pulping, bleaching processes). This example clearly demonstrates that the macromolecular properties are a decisive element of strength characteristics of a pulp fiber. These results are in good agreement with the findings of Kettunen et al. that tearing strength of a pulp increased with increasing amounts of high molecular-weight xylan [24].

However, sheet properties are determined by many other parameters such as the cellulose:hemicellulose ratio, as previously discussed. Another important factor for pulp sheet properties is fiber morphology, characterized by fiber length, fiber length distribution, and coarseness. It is widely accepted that especially



**Fig. 11.4** Relationship between zero-span tensile index and the weight fraction <DP 120 of a representative selection of commercial hardwood and softwood kraft and sulfite pulps [17]. For more detailed information on these pulps, see Tabs. 11.1 and 11.2.

tearing strength is influenced by fiber length. Based on the comparison between hardwood and softwood kraft pulps, the poorer tearing strength of the former is generally attributed to the shorter fiber length. The results of the measurement of the fiber dimensions of the selected paper pulps are provided in Fig. 11.5 and Tab. 11.3.

By comparing the fiber length distribution of both spruce pulps, it is apparent that the sulfite pulp shows a higher proportion of short fibers as compared to the kraft pulp. This may be attributed to the degraded cellulose fraction formed during the late stage of cooking. The beech pulp shows the characteristic peak at a fiber length below 0.2 mm, indicating the presence of large amounts of fines derived by both parenchymal cells (primary fines) and degraded pulp fibers (secondary fines). In contrast, eucalyptus pulps are characteristic for a narrow fiber length distribution and an extremely low coarseness which contributes to a high accessible surface area of the pulp fibers.



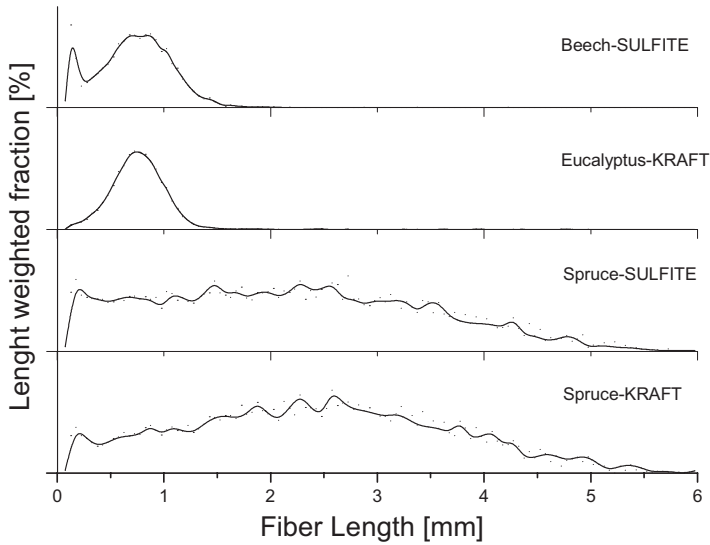


Fig. 11.5 Fiber dimensions of a representative selection of commercial hardwood and softwood kraft and sulfite pulps [17]. Fiber dimensions determined using Kajaani FS200.

Tab. 11.3 Fiber dimensions of fully bleached commercial paper pulps, as determined with Kajaani FS200 [17].

Parameter		Pine	Spruce	Eucalyptus	Beech	Spruce	Spruce	Beech
		Kraft		Kraft		Sulfite		Sulfite
		ECF	TCF	ECF	ECF	TCF	ECF	TCF
Average fiber length								
arithmetic	mm	0.90	1.04	0.55	n.d.	0.79	0.52	0.28
length-weighted	mm	2.16	2.36	0.72	n.d.	2.15	1.89	0.66
weight-weighted	mm	2.82	3.01	0.91	n.d.	2.93	2.91	0.86
Fines ( $P < 0.2$ mm)	wt%	3.5	2.7	2.0	n.d.	4.2	7.9	12.8
Coarseness	$\text{mg m}^{-1}$	0.213	0.215	0.074	n.d.	0.227	0.219	0.122

n.d. = not determined

### 11.3

#### Dissolving Grade Pulp

##### 11.3.1

###### Introduction

Dissolving pulp refers to pulp of high cellulose content which is used to manufacture various cellulose-derived products such as regenerated fibers or films (e.g., Viscose, Lyocell), cellulose esters (acetates, propionates, butyrates, nitrates) and cellulose ethers (carboxymethyl-, ethyl-, methyl-celluloses). The wood-derived celluloses which account for about 85–88% of the total dissolving pulp market are made by the prehydrolysis kraft and acid sulfite processes comprising additional purification stages such as hot and cold caustic extraction. The residual amount of dissolving pulps is based on cotton linters. The linters fibers, being attached to the cotton seeds, are removed by the delinting process, producing fibers of different lengths. The shortest fibers or second-cut linters are used as chemical feedstock. Purification is accomplished by a combination of mechanical and chemical steps comprising mild alkali treatment at elevated temperature to remove proteins, waxes, pectins and other polysaccharides and bleaching to achieve the required brightness level. Purified cotton linters represent the dissolving pulp of highest cellulose purity particularly used for manufacturing acetate plastics and high-viscosity cellulose ethers.

When using softwoods and hardwoods as a raw material, more drastic conditions in pulping and bleaching operations are required in order to obtain a high-quality dissolving pulp. However, even least amounts of residual impurities such as resins or inorganic compounds can adversely affect the filterability of viscose, and some residual noncellulosic carbohydrates can promote yellowing of cellulose acetate spinning dope. Since the (almost) complete removal of noncellulosic impurities would be very expensive and, moreover environmentally harmful (high yield loss, high chemical charges, additional equipment, etc.), the main emphasis is placed on adjusting the refining processes on the demands of each cellulose product.

The suitability of dissolving pulps can be adequately determined only by simulating the conversion processes to the final products (e.g., to regenerated fibers or cellulose derivatives) on a small scale. Sometimes, even pilot plant or mill-scale tests are needed to approve the dissolving pulp for further processing. This is particularly true in the case of new applications such as the Lyocell process. Since the early days of cellulose research, much effort has been undertaken to develop analytical methods that provide rapid and reliable assessment of the quality of dissolving pulp. There are many established methods for evaluating pulp quality [1–3], but they are insufficient to provide a full picture of the dissolving pulps' properties. The relationships between structure, chemical composition and behavior with regard to topochemical reactions are too complex. The difficulty of reliable cellulose characterization has been expressed appropriately by L.E. Wise, an important pioneer of cellulose chemistry and technology, by the statement that "Cellulose is a system, not a pure individual" [1].

The processability of a dissolving pulp is often characterized as its reactivity towards derivatizing chemicals or solvents. Reactivity is related to the accessibility of chemicals to the cellulose, which virtually means the relative ease by which the hydroxyl groups can be reached by the reactants. The structure and morphology of cellulose is responsible for the homogeneity of the conversion process and the final product quality. A reliable analysis of the property profile of dissolving pulps involves the extensive characterization of the cellulose structure at three different levels: (a) the molecular level of the single macromolecule; (b) the supramolecular level of aggregation of macromolecules to highly ordered structural entities; and (c) the morphological level comprising the architecture of well-organized fibrillar elements [4]. Moreover, the pore system providing access to the molecular structure is an important characteristic of dissolving pulps. Finally, the qualitative and quantitative determination of organic and inorganic impurities completes the analytical characterization of a dissolving pulp.

The quality profile of dissolving pulps is comparatively evaluated in the following sections of this chapter, according to the following scheme (see Tab. 11.4).

**Tab. 11.4** Characterization scheme of dissolving pulps.

---

Pulp Origin, Pulp Consumers
Chemical properties (molecular level)
Chemical composition
Organic compounds
Carbohydrates
Extractives
Residual Lignin
Inorganic compounds
Macromolecular properties
Molar mass, Molar mass distribution
Functional groups
Supramolecular structure
Crystallinity, Crystallite dimensions
Lattice transition to sodium cellulose I
Cell wall structure
Distribution of hemicelluloses across the fiber wall
Fiber morphology
Pore structure, Accessibility
Degradation of dissolving pulps
Alkaline oxidative degradation (ageing)
Radiation degradation (electron beam treatment)
Overall pulp specification

---

## 11.3.2

**Dissolving Pulp Characterization**11.3.2.1 **Pulp Origin, Pulp Consumers**

Despite much effort to develop alternative pulping routes, dissolving pulp is still solely produced by acid sulfite and prehydrolysis kraft processes. The most promising alternative processes under development are organosolv processes such as that originally proposed by Kleinert in 1931 [5] and further developed by Peter and Höglinger using only a mixture of ethanol and water [6]. Other approaches include the recently evaluated Formacell procedure [7], as well as the prehydrolysis-ASAM (alkaline sulfite with anthraquinone and methanol) and prehydrolysis-ASA (alkaline sulfite process) processes which enable the manufacture of high-purity, high-viscosity dissolving pulps due to their high purification and delignification selectivity [8]. The progress in kraft cooking during the past two decades owing to the principles of modified cooking has formed the basis for the development of the new Visbatch<sup>®</sup> and VisCBC processes, both of which combine the advantages of displacement technology and steam prehydrolysis (see Section 4.2.7.2). These new environmentally friendly pulping processes are characterized by their short cover-to-cover times, low energy requirements and very homogeneous and high product quality, and promote a gradual shift from traditional softwood sulfite pulps to hardwood prehydrolysis kraft pulps [9].

Despite the world production of dissolving pulp having been reduced constantly in the past, the latest forecasts reveal a slight change in this trend (see Chapter 1.3). A stabilization of the production amounts, followed by a pronounced growth until the year 2006 is predicted, mainly due to new installations of Viscose (and presumably also Lyocell) plants manufacturing regenerated cellulose fibers in Asia.

Alkaline and acid processing routes constitute the main applications of dissolving pulps. The former comprises the viscose and etherification processes, which involve steeping of the pulp in aqueous solutions of high NaOH concentration (18–25 wt.%), followed by the addition of appropriate chemicals for subsequent derivatization (e.g., CS<sub>2</sub> for xanthation or alkylhalides for cellulose ethers). The acidic esterification processes yield cellulose nitrate and cellulose acetate. The latter, more important, conversion process involves a pretreatment with acetic acid prior to esterification to triacetate on the addition of acetic anhydride and a catalyst, usually sulfuric acid. In a second step, the triacetate is hydrolyzed to the so-called secondary acetate (DS between 1.8 and 2.5) on dilution with water and precipitation of the flakes. These are then dissolved in acetone to a spinning dope (polymer concentration above 30%) from which fibers (e.g., filter tow, textile filaments), lacquers or plastic are processed.

Since the commercialization of the Lyocell process in 1992, the direct solution of pulp in an organic solvent without the formation of an intermediate cellulose derivative represents a new processing route for dissolving pulp comprising challenging demands on pulp quality [10–12].

For over 80 years, regenerated fibers of high quality and special uses have also been spun from a cuprammonium solution (*cupram*), a metal complex solvent for cellulose. Less than 2% is estimated for cuprammonium rayon within the world rayon production. The high demand on processability and pulp quality requires the use of high-purity cotton linters which, compared to the viscose process, is not a decisive cost factor.

Table 11.5 provides a rough overview of the raw material sources, dissolving pulp technologies and main applications.

**Tab. 11.5** Overview of different applications of dissolving pulps.

Product	Simplified reaction scheme	Raw material	Pulping processes	Bleaching processes
Viscose				
Staple	$CellOH (I) \xrightarrow{NaOH} CellONa$	B, E, S, H, P*)	AS, PHK	ECF, TCF
Textile filaments	$CellONa + CS_2 \rightarrow Cell(OCSSNa)_{0.4-0.5}$	E, S, H, P*)	AS, PHK	ECF, TCF
Technical Filament	$\xrightarrow{H^+, Zn^{2+}, Na^+} CellOH (II)$	P*), MHW	PHK (CCE)	ECF
Cuprammonium Rayon	$CellOH (I) \xrightarrow{Cu[(NH_3)_4(OH)_2]} CellOH (II)$	CL, S	SO, AS	ECF
Lyocell				
Textile	$CellOH (I) \xrightarrow{NMMO \bullet H_2O} CellOH (II)$	E, P*), H	AS, PHK	TCF, ECF
Non-Wovens		B, E, S, H, P*)	AS, (PHK), K	TCF, ECF
Ethers				
MC	$CellONa + CH_3Cl \rightarrow Cell(OCH_3)_x$	S, E, P, H, MHW, CL	AS, (PHK), SO	ECF
MHPC	$CellONa + CH_3Cl \xrightarrow{PO} Cell[(OCH_2CHOCH_3)_x(OCH_3)_y]$	S, E, P, H, MHW, CL	AS, (PHK), SO	ECF
HEC	$CellOH + EO \xrightarrow{OH^-} Cell[(OCH_2CH_2O)_x(CH_2CH_2O)_y]$	S, E, P, H, MHW, CL	AS, (PHK), SO	ECF
CMC	$CellONa + ClCH_2COO^- \rightarrow Cell[(OCH_2COONa)_x]$	S, E, P, H, MHW, CL	AS, (PHK), SO	ECF

Tab. 11.5 Continued.

Product	Simplified reaction scheme	Raw material	Pulping processes	Bleaching processes
Acetate				
Tow	$CellOH + (CH_3CO)_2O \xrightarrow{H^+} Cell(OCOCH_3)_{2-3}$	MHW, H, S, E, P	AS (CCE), PHK (CCE)	ECF, CONV
Plastics		P, CL	PHK-CCE, SO	ECF, CONV
Nitrocellulose (NC)				
High-N-NC ( $x = 3$ )	$CellOH + HNO_3 \xrightarrow{H^+} Cell(ONO_2)_x$	CL	SO	CONV
Low-N-NC ( $x = 2$ )		CL, S	SO, AS	CONV, ECF
Microcrystalline Cellulose (MCC)	$CellOH \xrightarrow{H^+} CellOH_{crist}$	MHW, H, S, E, P	(AS), PHK	ECF

**Raw Material:**

B (beech), E (eucalypt), S (spruce), H (hemlock), P (pine), MHW (mixed hardwood), CK (cotton linters)

\*) sulfite cooking with pine and other resinous wood requires different pH profile → two-stage processes, or measures to remove the resins

**Pulping Purification Processes:**

AC (acid sulfite), PHK (prehydrolysis kraft), CCE (cold caustic extraction), SO (soda).

**Products:**

EO = ethylene oxide, PO = propylene oxide

MC (methylcellulose), MHPC (methylhydroxypropylcellulose), HEC (hydroxyethylcellulose).

**11.3.2.2 Chemical Properties****11.3.2.2.1 Chemical Composition****Organic Compounds***Hemicelluloses (short-chain alkali-soluble carbohydrates)*

One of the main objectives of dissolving pulp production is the removal of noncellulosic carbohydrates which constitute the major part of the short-chain material in the polymer. The available purification processes – particularly the hot and cold caustic extraction processes – contribute to a considerable increase in production costs, mainly due to high yield loss and high chemical charges (see Sections 8.3 and 8.4). Therefore, the extent of purification is adjusted to the demands on the particular further processing. However, even small amounts of alien polysaccharides may influence the processability and properties of the final product.

During steeping, the first step of alkaline processing of dissolving pulps for the viscose and etherification procedures, alkali-soluble hemicelluloses are removed to an extent depending on pulp quality, the process conditions and the

equilibrium concentration level in the recycled steeping liquor. In this definition, the hemicelluloses consist of both alkali-soluble degraded cellulose and heteropolysaccharides such as degraded xylan or mannan. The accumulation of hemicelluloses in the steeping lye inhibits cellulose degradation during ageing due to the additional oxygen consumption through these degraded carbohydrates [13]. In addition, they react preferentially with carbon disulfide in the subsequent xanthation process, thus leading to inhomogeneously substituted cellulose which consequently adversely affects viscose filterability [14]. A good quality of viscose solution, characterized by low particle content ( $< 3 \mu\text{m}$ ) and good viscose filterability, is governed by a low content of noncellulosic impurities, particularly pentosans, certain inorganic substances, and resins [15].

Lenz et al. have shown that fiber tenacity is altered due to incorporation of low molecular-weight hemicellulose if they exceed a certain concentration level in the steeping liquor (Tab. 11.6) [13].

**Tab. 11.6** Influence of hemicellulose concentration in steeping lye on fiber tenacity [13]. Pulp substrate: ECF-bleached beech acid sulfite dissolving pulp.

alpha-Cellulose [%]	Hemicellulose content in steeping lye [ $\text{g L}^{-1}$ ]	Fibre- $\text{DP}_n$	Tenacity (cond) [ $\text{cN tex}^{-1}$ ]	Elongation (cond) [%]
90.5	17.3	254	27.5	15.3
90.5	20.5	253	26.6	15.5
90.5	37.0	261	26.0	15.0
91.3	17.6	254	28.6	16.8
91.3	35.4	255	28.0	16.2

Siclari reports that the use of dissolving pulps with increasing amounts of low molecular-weight carbohydrates is closely related to a decrease in the wet tenacity of a Polynosic-type fiber [16]. An increase of the low molecular-weight fraction determined by gel permeation chromatography (GPC) measurement and an increase in the xylan content in the respective viscose fibers clearly support the assumption that the decrease in fiber tenacity is caused by the incorporation of the acid-insoluble hemicellulose fraction (beta-cellulose) which occurs during the regeneration process in the highly acidic spin bath.

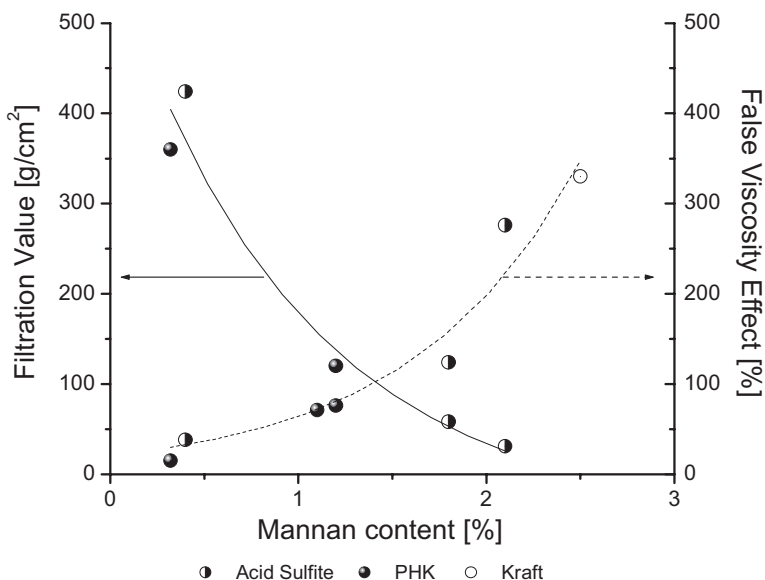
Hemicelluloses also contribute to discoloration of the resulting cellulose products during both alkaline (e.g., Viscose) and acidic conversion (e.g., acetate) steps [13,17]. The chromophore formation of the hemicelluloses under alkaline conditions is closely associated with the presence of carbonyl and carboxyl groups.

Quite recently, it could be shown that hemicelluloses, particularly xylans, are involved in the discoloration of Lyocell dopes [18]. Pentoses generally revealed a significantly higher rate of chromophore formation as compared to hexoses. In

addition, the glucuronic acid side chains have been shown to be a source of enhanced chromophore formation, while the corresponding gluconic acid revealed no measurable yellowing [18]. The detailed mechanism of the preferred chromophore formation of pentoses over hexoses in both acidic and alkaline processing is still under investigation.

Acid processing generally requires pulps of higher purity as compared to alkaline processes. Acetate pulps are high-purity pulps containing hemicelluloses in an amount less than 1.5% and no detectable residual lignin. Experimental findings strongly suggest that even very small amounts of certain hemicellulose fractions play an important role in the formation of haze and color of cellulose tri- and diacetate solutions. Glucomannan from both acid sulfite and prehydrolysis kraft (PHK) pulps is a major source for diacetate haze, false viscosity, and poor filtration [17]. False or anomalous viscosity determines production capacity, and is defined as the percent increase in dope viscosity compared to that of a dope prepared from cotton linters diacetate of the same composition and intrinsic viscosity. The effect of the pulp mannan content on false viscosity and filterability of a diacetate solution in acetone is illustrated in Fig. 11.6.

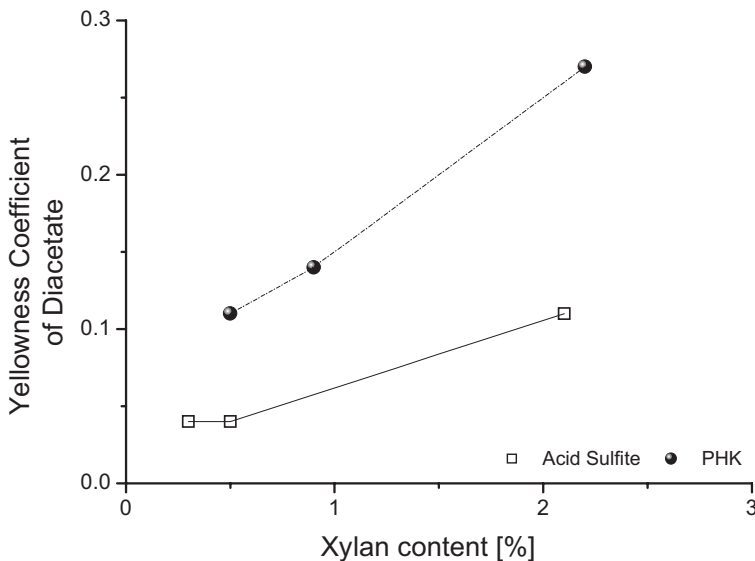
Glucomannan is very detrimental to diacetate filterability (obtained from the filtration of 18% diacetate acetone dope through a cotton fabric media at 275 kPa), whether it comes from acid sulfite, PHK or conventional kraft pulp. Even small



**Fig. 11.6** Effect of mannan content in various pulps on diacetate filterability and false viscosity [17,19]. Pulp acetylation according to the high-catalyst process using 14% sulfuric acid catalyst based on initial amount of cellulose. Diacetate dope consists of 18% acetate, 1.35% water, and 80.65% acetone.



amounts of glucomannan seem to deteriorate filtration of the dope. It is assumed that glucomannan is competing against cellulose for acetylation, leaving swollen fiber fragments in the solution. Xylan causes only a moderate drop in filtration in the range below 2%, but this is the major contributor to acetate color and thermal instability. Diacetate color is measured by determining the yellowness coefficient [ $Cy = (T_{640} - T_{440})/T_{640}$ ] of a 12% diacetate dispersion in a mixed solvent of dichloromethane and methanol. The xylan originating from PHK pulps causes more intense yellowing than that present in acid sulfite pulps (Fig. 11.7). This behavior has been explained by the lower content of uronic acid side chains of the kraft xylan compared to sulfite xylan which, on acetylation, produces hazy solutions [20]. Kraft cooking conditions favor the removal of 4-*O*-methylglucuronic acid substituents from xylan, whereas xylan retains its branched structure during acid sulfite pulping.

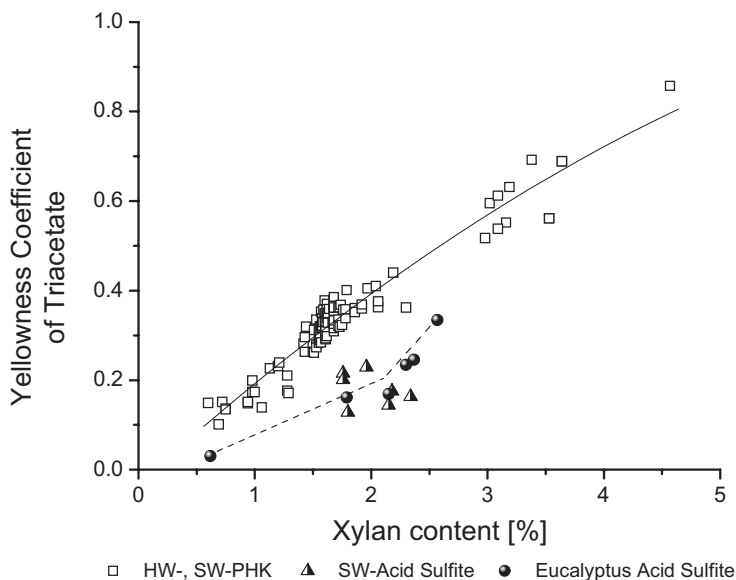


**Fig. 11.7** Effect of the xylan content originating from acid sulfite and PHK pulps on yellowness coefficient of diacetate solution [17,19]. For pulp acetylation, see Fig. 11.6.

Moreover, the higher molecular weight of the kraft xylan as compared to the sulfite xylan gives rise to a higher yellowness coefficient. It has been assumed that the diacetate color is caused by undissolved particles in the size range of 1  $\mu\text{m}$ , since centrifugation eliminated both color and fiber fragments [21].

The yellowness of the cellulose triacetate solution is also closely related to the xylan content of the initial pulps, and again, at equal xylan content, the PHK pulps reveal a higher yellowness coefficient than the corresponding sulfite pulps (Fig. 11.8).

These findings agree with the results reported by Conca and associates, who showed that xylans of low uronic acid content gave poor acetate solution properties [23]. Later, Wells and coworkers [24], as well as Gardner and Chang [25], con-



**Fig. 11.8** Effect of xylan content originating from acid sulfite and PHK pulps on yellowness coefficient of triacetate solution [22]. Pulp acetylation according to the low-catalyst process using 0.3% sulfuric acid catalyst based on initial amount of cellulose.

firmed the poor acetylation performance of xylans derived in particular from alkaline processes and which are known to possess a lower degree of branching and have a higher molecular weight as compared to acid sulfite xylan.

Quite recently, residual chromophores in cellulose triacetate were isolated by treating the cellulosic material with a boron trifluoride:acetate acid complex,  $\text{BF}_3 \cdot 2\text{HOAc}$ , in the presence of small amounts of sodium sulfite. The identified structures of the compounds causing the yellowish appearance indicate that the formation pathways of chromophores involves thermal condensation of degraded cellulose or hemicellulose compounds to form aromatic condensation products (primary chromophores such as 2,5-dihydroxybenzoquinone, *o*-dihydroxybenzene, and others), self-condensation of acetic acid derivatives and the reaction of primary chromophores with acetic acid [11].

The detailed mechanism of the preferred chromophore formation of pentoses over hexoses in both acidic and alkaline processing is, however, still under investigation.

#### *Extractives, resins*

Pulp resins, determined as acetone or dichloromethane (DCM) extractives, play an ambivalent role in dissolving pulp processing. When exceeding a certain threshold concentration, resins may cause severe problems along the process chain such as precipitation (preferably taking place through sudden changes from alkaline to acid pH), haze in the viscose, clogging of the spinnerets, and yellowing

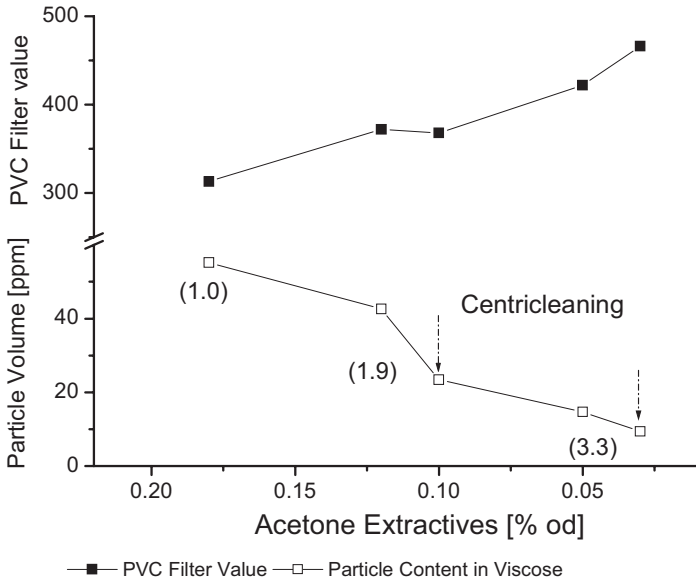
of the yarn. On the other hand, the presence of resins considerably improves the accessibility of reagents to the cellulose substrate (e.g., alkali cellulose) due to lowered surface tension. The amount of extractives in the dissolving pulp is determined by both the wood species used and the pulping and bleaching operations.

Acid sulfite cooking is rather sensitive to wood that is rich in resins. The major problems arise with phenolic extractives originating from pine, larch, Douglas fir and other extractive-rich wood species, which tend to undergo condensation reactions with reactive lignin structures. The formation of high molecular-weight resinous products may cause uncontrollable pitch problems in subsequent operation steps. These may be largely overcome by applying a two-stage process with an initial bisulfite or neutral sulfite stage. Thereby, the most reactive groups of lignin are protected by sulfonation. Hardwoods are generally better suited for acid sulfite pulping than softwoods. In the case of some resinous hardwoods, such as birch or some aspen species, the delignification of parenchyma cells with a high content of resins remains incomplete. Subsequent chlorine-free bleaching sequences – particularly those containing ozone stages – contribute significantly to reducing the resin content. Additionally, the short parenchymal cells may be removed by fractionation, though this is connected with high yield loss.

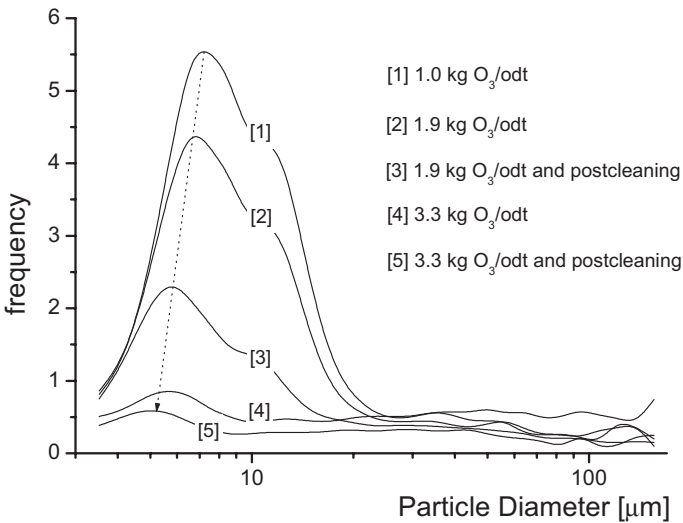
Kraft cooking is less sensitive to wood raw materials that are rich in resins because most acidic extractives, together with part of the neutral lipophilic compounds, are dissolved in the cooking liquor, leaving little resin in the unbleached pulp. However, if the fraction of unsaponifiable compounds is high (as with many hardwoods), the fatty acid soaps formed do not possess sufficient micellar-forming properties to carry less polar compounds into solution. During PHK pulping of *Eucalyptus globulus* L., nearly all polyphenols, phenols, fatty acids are dissolved. Two-thirds of the neutral compounds are left in the unbleached pulp, while two-thirds consists of  $\beta$ -sitosterol [26]. During bleaching, the unsaponifiables are modified to more polar compounds containing carboxyl groups; these compounds, together with other polar extractives such as fatty acids, are favorable as surface active agents in the viscose process and account in part for good filtration of the viscose prepared from this pulp [27,28].

Resins derived from pulps of high resin content – and particularly those containing higher amounts of nonpolar neutral substances such as hydrocarbons and waxes – show a tendency to accumulate in the spinnerets. The deposits of resin inside the holes in the spinnerets increase the adhesion of precipitated zinc sulfide, and this ultimately leads to clogging of the spinnerets [29]. In times of conventional bleaching, chlorination of extractives caused viscose turbidity, which was closely associated with spinning jet clogging [30]. The introduction of hydrophilic groups by means of oxidation during bleaching operations (O, D, Z, P) improves the dispersibility of pulp resin in sodium hydroxide [30].

Viscose quality was greatly affected by the ozone charge during the course of TCF bleaching (O-A-Z-P) of an aspen PHK pulp [31]. A step-wise increase in ozone charge from 1.0 to 3.3 kg odt<sup>-1</sup> significantly decreased the content of acetone extractives while improving viscose quality, characterized as the relationship between the average particle volume and viscose filterability (Fig. 11.9).



**Fig. 11.9** Relationship between the content of acetone extractives of a TCF-bleached aspen-PHK pulp and viscose quality [31]. The reduction of acetone extractives was achieved by increasing charges of ozone and additional post cleaning with a centricleaner. Pulping according to the VisCBC process: P-factor 750, H-factor 600, EA concentration in cooking liquor 0.875 g L<sup>-1</sup>; TCF-bleaching according to O-A-Z-P to achieve brightness >91% ISO.



**Fig. 11.10** Particle size distribution of viscose samples made from aspen PHK pulps of varying ozone charges and additional post cleaning operations [31]. Pulping conditions according to Fig. 11.9.

Additional post cleaning by means of a centricleaner further reduced the amount of resins, thus improving viscose filterability. The particle spectrum in the viscose demonstrates both a clear reduction in the particle volume and a shift of the average particle size to lower values (Fig. 11.10).

The results confirm that reinforced oxidation, for example by ozone, contributes to an improved dispersibility of pulp resins, and this is an important prerequisite for the effective separation of these impurities. The efficiency of resin removal can be further enhanced by additional post-cleaning operations.

Although a certain amount of pulp resin may be beneficial for subsequent processing steps, by improving accessibility to the cellulose substrate, practical experience has taught that the best way to control extractives is to take measures to keep them at a low level [32]. When the resin content falls below a certain level, the homogeneity of subsequent reactions may be impaired because of a lowered surface activity. In this case, the addition of small amounts of synthetic surface active agents overcomes that deficiency.

#### *Residual lignin, brightness*

The residual lignin content in dissolving pulps is generally very low. The kappa number, which specifies the amount of oxidizable (by  $\text{KMnO}_4$ ) structures containing double bonds in the pulp, is typically between 0.2 and 0.5 units which translates to a residual lignin content of about 0.05% [33]. The main reason for aiming at a low kappa number is the high demand on optical properties. Residual lignin structures strongly contribute to yellowing of the cellulosic products. The highest demands on brightness and brightness stability are given for viscose, lyocell, and acetate pulps. Similar brightness levels are required for dissolving pulps converted to cellulose ethers for application in foodstuff and pharmaceuticals. Residual lignin is, however, not the only factor determining the optical properties of cellulosic substances. Therefore, the relationship between pulp brightness and brightness of the final product is also dependent upon the processing conditions, especially in the case of alkaline derivatization procedures (e.g., viscose, ethers). In industrial operations using constant conditions, pulp brightness is clearly reflected in the brightness of the final product.

Brightness – and thus residual lignin – is not a concern for pulps used for technical-grade cellulose ethers (major applications: textile, paper, drilling muds, ceramics, etc.). Nevertheless, bleaching to brightness levels of about 70–75% ISO is necessary to improve pulp reactivity and prevent precipitation of lignin compounds in subsequent processing steps.

The residual lignin is not only a concern for optical properties, but also governs the processability of dissolving pulps. It is reported that viscose filterability (determined by the clogging constant) gradually deteriorates when increasing the residual lignin content from about 0.17 to 0.36% [34].

#### **Inorganic Compounds**

The presence of certain inorganic compounds such as silicates, Ca salts, and catalytically active transition metal ions (Fe, Mn, Co, etc.) clearly impairs the filterabil-

ity and spinnability of a cellulose spinning dope (e.g., viscose or lyocell type of fibers). Moreover, pulp contamination with inorganic compounds leads to a gradual clogging of the spinnerets, and this alters the uniformity of the fiber titer [13]. In particular, the cations  $\text{Ca}^{2+}$  and  $\text{Fe}^{2+}$ , as well as silicates, are considered to be detrimental in this respect. Although  $\text{Fe(II)}$ , and to a lesser extent  $\text{Cu(II)}$ , promote light-induced yellowing, both cations are involved in detrimental degradation reactions in the presence of hydrogen peroxide bleaching (Fenton-type reaction). Thus, all necessary measures must be undertaken (acid wash, chelation stage, etc.) to remove catalytically active cations.

Surprisingly, most of the harmful ash components are not distributed homogeneously in the pulp, but are present as particulates in certain cell fractions, particularly in the parenchyma cells [35]. Therefore, the only promising way to reduce the amount of harmful ash components is an efficient mechanical pulp treatment which applies combined pressure screening of unbleached pulp and centrifugal cleaning after bleaching. This treatment ensures the removal of extremely small debris such as sand, bark specks, and shives. Again, the best way to control inorganic compounds is to reduce them to the lowest level economically feasible.

#### 11.3.2.2.2 Macromolecular Properties

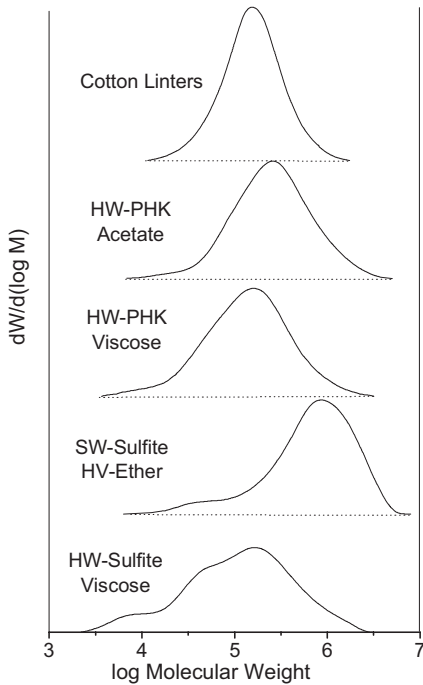
##### **Molar mass, molar mass distribution**

Since celluloses from natural sources and after chemical treatment are always polydisperse, the determination of the average molecular weight (e.g., by viscosimetry) is insufficient to predict specific product properties. Additional information is provided by the measuring molecular weight distribution (MWD) of dissolving pulps.

Measurements of MWD reveal a multimodal distribution for pulps produced according to acid sulfite cooking, while the PHK pulps show a rather uniform MWD. Dissolving pulps, being representative of various applications including viscose, acetate and high-viscosity ether, are compared in Fig. 11.11.

The numerical evaluation of the MWD, as well as additional pulp quality parameters, are included in Tab. 11.7. As expected, the sulfite dissolving pulps (viscose, high-viscosity ether) reveal a rather broad MWD, as indicated by the high PDI. This is also reflected in the higher amount of short-chain molecules ( $\text{DP} < 100$ ), lower values for the alkali resistances, and the large difference between  $R_{18}$  and  $R_{10}$  when comparing at a similar viscosity level. In the case of a high-viscosity ether pulp, the comparison is not valid because the entire molecular weight is shifted to higher values (Tab. 11.7).

There are many reports which confirm that the chain-length distribution in the dissolving pulp is a crucial property in the production of rayon fibers [37]. The short-chain molecules represent the weakest part in the fiber: the shorter the molecules, the lower will be the number of molecules linking the crystalline regions. Avela et al. were able to show that all strength characteristics are significantly reduced with an increase in the low molecular-weight fraction [38]. Treiber



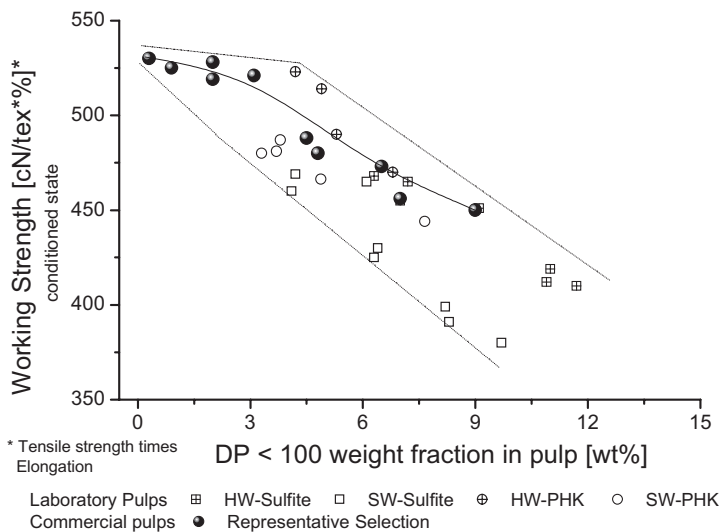
**Fig. 11.11** Molecular weight distribution (MWD) of different grades of sulfite and PHK wood dissolving pulps and cotton linters. GPC measurement of cellulose solutions in LiCl/DMAc with MALLS/RI detection according

to Schelosky et al. [36]. Detailed characterization of these pulps including numerical evaluation of GPC measurements is included in Tab. 11.7.

reported an increase in wet strength of regular and high wet modulus viscose fibers with decreasing amount of the DP <200 fraction in the dissolving pulp [39,40]. Clearly, the physico-mechanical properties of fibrous substrates are influenced not only by the macromolecular properties but also by the crystallite dimensions, the degree of lateral order, and the orientation with respect to the fiber axis. In order to bring out the effect of MWD on the strength properties of viscose fibers more clearly, the conditions of viscose preparation and viscose fiber production must be kept constant. Recently, detailed bench-scale trials were conducted imitating the regular production of rayon fibers. To obtain a representative view on the suitability of dissolving pulps for viscose fiber production, laboratory pulps covering all four categories of dissolving pulps, namely HW-sulfite, SW-sulfite, HW-PHK and SW-PHK, as well as a selection of commercial dissolving pulps were converted to regular viscose rayon staple fibers with a titer of 1.3 dtex. The results depicted in Fig. 11.7 clearly confirm the relationship between the maximum strength properties in the conditioned state, calculated as the product of tenacity and elongation, corresponding to a so-called working strength, and the amount of short-chain molecules characterized as DP <100 fraction.

Tab. 11.7 Characterization of a selection of representative dissolving pulps.

Raw Material	Cooking Process	Preferred Application				
		Viscose	Ether (HV)	Viscose	Acetate	Acetate
		Hardwood Sulfite	Softwood Sulfite	Hardwood PHK	Hardwood PHK	Cotton Linters
Brightness	% ISO	92.2	90.2	90.7	92.2	87.9
R <sub>18</sub> content	%	93.4	95.2	97.9	98.2	99.0
R <sub>10</sub> content	%	87.6	93.8	93.3	97.7	97.4
Xylan	%	3.6	3.1	1.5	0.9	0.2
Carbonyl	μmol g <sup>-1</sup>	18.8	6.0	4.3	4.4	3.7
Carboxyl	μmol g <sup>-1</sup>	35.6	59.8	32.0	15.0	12.4
DP <sub>w</sub>		1790	4750	1400	2100	1250
DP <sub>n</sub>		277	450	460	650	700
PDI		6.5	10.6	3.0	3.2	1.8
DP<100	wt%	9.0	0.5	2.5	2.0	0.3
DP>2000	wt%	26.8	61.0	19.9	35.0	15.5

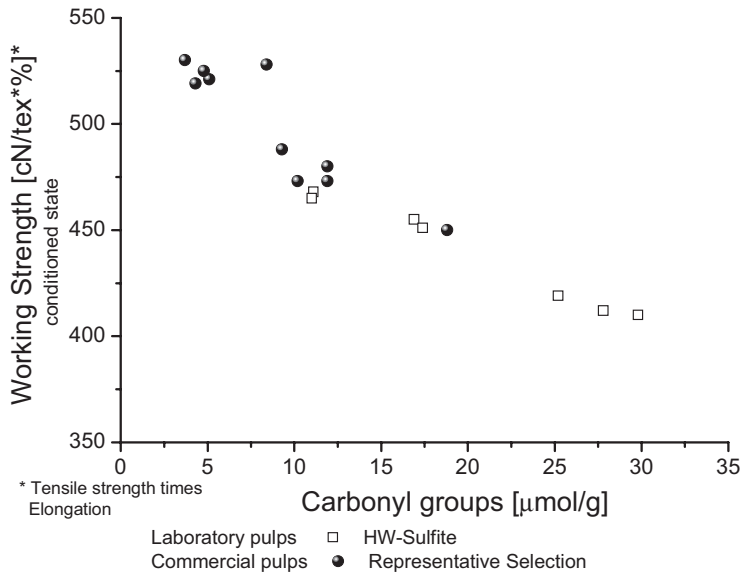


**Fig. 11.12** Maximum strength properties of 1.3 dtex regular viscose fibers in the conditioned state related to the DP <100 fraction of dissolving pulps covering the whole spectrum of pulp purity (R<sub>18</sub> 93–99%). DP <100

determined from GPC measurements carried out according to [36]. Conditions for viscose and viscose fiber production are described elsewhere [7].



The data in Fig. 11.12 also indicate that the viscose fibers derived from sulfite pulps generally exhibit slightly lower mechanical properties at a given DP <100 weight fraction as compared to those made from PHK pulps. This may be caused by the higher carbonyl content of the sulfite pulps at a comparable purity level. GPC measurements of the corresponding fibers indicate that the increase in the amount of low molecular-weight carbohydrates during alkaline degradation (ageing) is more pronounced for sulfite than for PHK pulps. Surprisingly, a clear correlation between the carbonyl content of the pulps and the working strength of the regular viscose fibers made thereof could be established, as illustrated in Fig. 11.13.



**Fig. 11.13** Maximum strength properties of 1.3 dtex regular viscose fibers in the conditioned state related to the carbonyl content of dissolving pulps (selection of Fig. 11.12). The content of carbonyl groups was determined according to the CCOA method [41].

The content of carbonyl groups reflects both the amount of reducing endgroups (short-chain molecules) and the oxidized groups thus undergoing degradation reactions under strongly alkaline conditions.

#### Functional Groups (Carbonyl, Carboxyl)

Cellulose, particularly from wood pulp, contains small amounts of oxidized groups. The carbonyl groups originate from the reducing endgroups and oxidized groups along the cellulose chain. Carboxyl groups are present in the residual hemicelluloses (predominantly as uronic acids), but are also introduced by pulping, bleaching, and other oxidation processes. Oxidized positions in cellulose,

such as keto or aldehyde groups, are sources of polymer instability, where subsequent cleavage will primarily occur, especially under alkaline conditions [42]. The carbonyl groups are a main reason for strength loss and decreased performance parameters in textiles, paper and other cellulosic materials, and they govern ageing kinetics and promote thermal and light-induced yellowing processes [43]. Discoloration, or color reversion, is a serious deterioration of dissolving pulp quality. The heat-induced brightness loss is particularly attributed to low molecular-weight carbohydrates (hemicelluloses), uronic acids, and carbonyl groups [44]. During pulping and bleaching operations, and particularly when strong oxidizing agents (e.g., ozone) are used, carbonyl groups are introduced into the pulp, thus enhancing color reversion.

In a comprehensive study, the effect of placing ozonation before (Z-P) and after (P-Z) standard peroxide bleaching for three different ozone charges (2, 4, and 6 kg O<sub>3</sub> odt<sup>-1</sup>, respectively) on the effect of yellowing and the introduction of carbonyl groups was investigated by using an (E/O) pretreated beech sulfite dissolving pulp [46]. With increasing ozone dosage from 2 to 6 kg odt<sup>-1</sup>, the overall carbonyl content increased from 22.9 to 38.4 μmol g<sup>-1</sup> in the case of a PZ-sequence, whereas reversing the sequence to ZP the carbonyl content changed only marginally, from 22.3 to 24.2 μmol g<sup>-1</sup>. The courses of viscosity and carboxyl group contents were quite comparable for both sequences, as shown in Tab. 11.8.

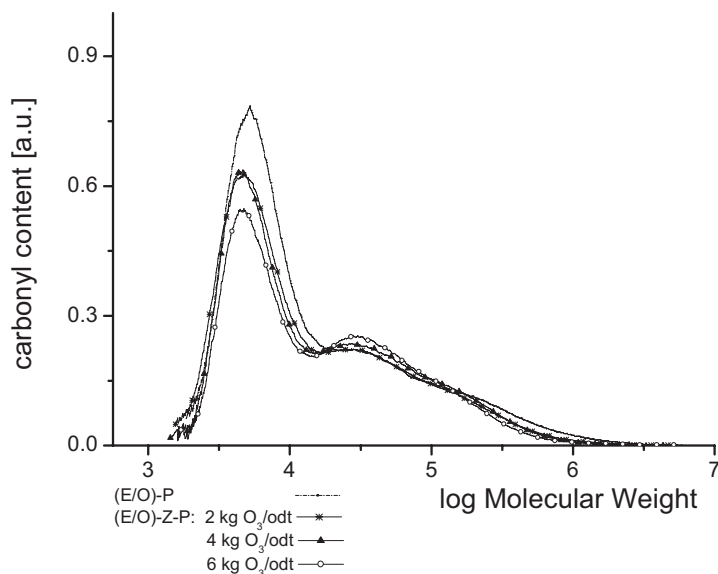
However, the optical properties are considerably better with peroxide (P) as a final bleaching stage, which clearly relates to both the low overall carbonyl group content and the specific profile of the additionally introduced carbonyl groups along the cellulose chain. The data in Fig. 11.14 reveal that the pattern of keto groups generated along the cellulose chain is not influenced by the ozone charge, provided that the ozone treatment is followed by an alkaline treatment.

**Tab. 11.8** Comparison of ZP and PZ treatments on (E/O) pretreated hardwood sulfite dissolving pulps [46].

Sequence	Ozone charge [kg odt <sup>-1</sup> ]	Viscosity <sup>a)</sup> [mL g <sup>-1</sup> ]	Brightness		Carbonyl <sup>a</sup> [μmol g <sup>-1</sup> ]	Carboxyl [μmol g <sup>-1</sup> ]
			Initial [% ISO]	72 h, 105 °C [% ISO]		
P		640	87.2	81.8	16.8	34.4
PZ	2	575	93.2	87.9	22.9	33.7
	4	460	94.3	88.8	29.9	36.6
	6	390	94.4	88.4	38.4	42.7
ZP	2	529	94.3	91.0	22.3	31.3
	4	463	95.4	92.8	21.0	35.0
	6	390	95.4	92.5	24.2	40.9

a. CCOA method.

\*) no borohydride treatment prior to viscosity measurement



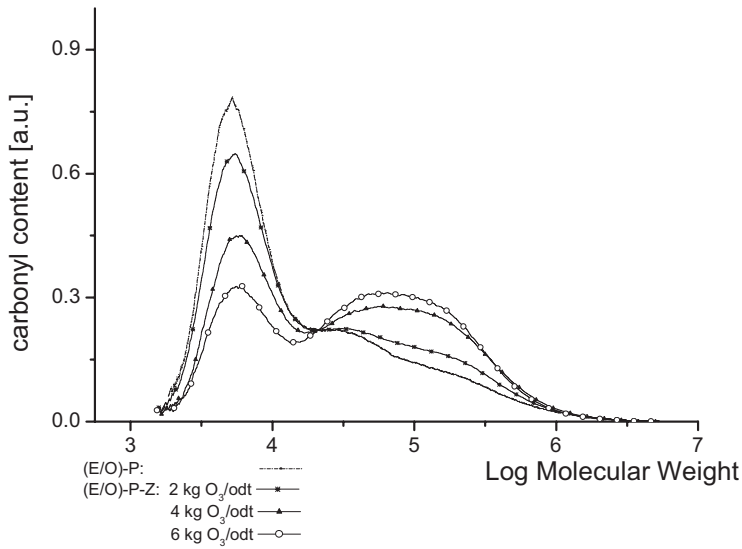
**Fig. 11.14** Profile of carbonyl groups generated through ZP-treatment of an (E/O) pretreated beech sulfite dissolving pulp as a function of increasing ozone charges. For a more detailed characterization, see Tab. 11.8 and [46]. Estimation of the carbonyl group profile by

subtracting the contribution of the reducing endgroups from the total amount of carbonyls, assuming that the amount of reducing endgroups relates to the  $MW_n$  determined from GPC measurement [45]

The profile of carbonyl groups changes completely when the bleaching sequence is reversed and ozonation represents the final treatment. Parallel to a continuous increase of the overall carbonyl group content, the amount of carbonyl groups introduced into the high molecular-weight region increases relative to the amount generated into the low molecular-weight region, as depicted in Fig. 11.15.

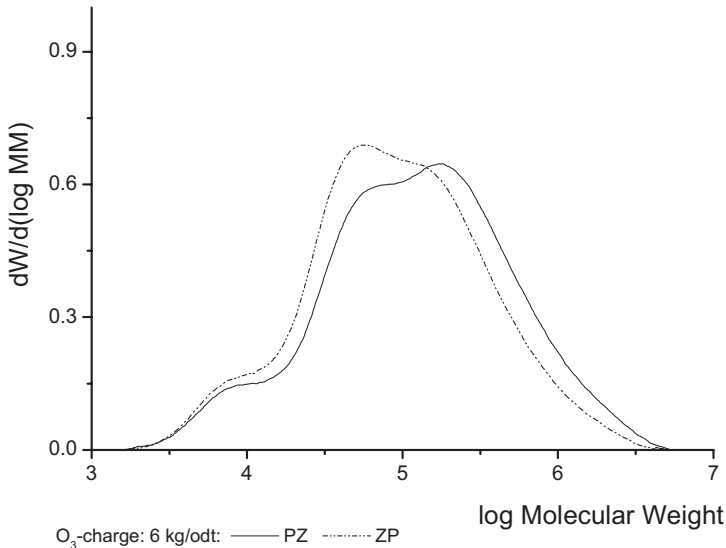
The generation of carbonyls during ozonation gives rise to enhanced depolymerization of the oxidized cellulose in a subsequent alkaline hydrogen peroxide stage (P) due to  $\beta$ -elimination reaction, thus stabilizing the cellulose chain against further alkaline processing (e.g., steeping). The higher selectivity of a PZ over a ZP treatment can be recognized by GPC measurement in LiCl/DMAc, while simple viscosity measurement additionally induces depolymerization due to strong alkaline conditions (Fig. 11.16; see Tab. 11.8).

Stabilization of the cellulose chain against alkaline degradation also improves the brightness stability of pulps. The thermal-induced color reversion, measured as standardized brightness change,  $\Delta R/R$  (after 72 h treatment at 105 °C), relates to the overall carbonyl group content, as depicted in Fig. 11.17



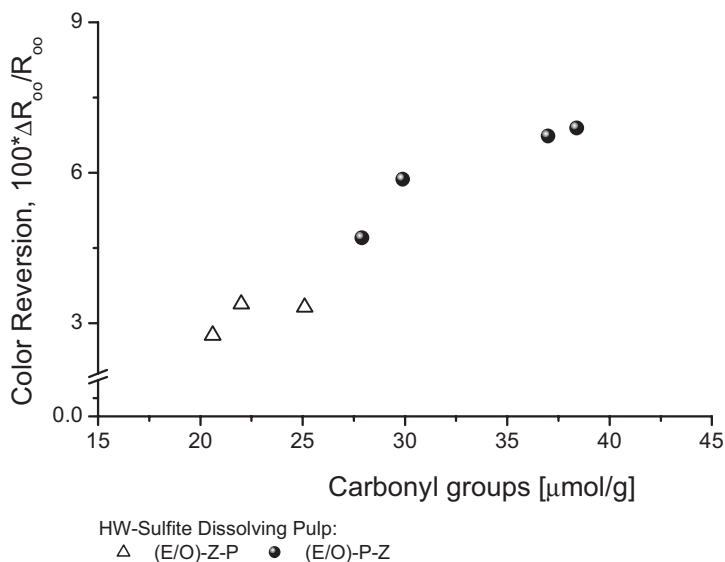
**Fig. 11.15** Profile of carbonyl groups generated through PZ-treatment of an (E/O) pretreated beech sulfite dissolving pulp as a function of increasing ozone charges. For more detailed characterization, see Tab. 11.8 and [46]. Estimation of the carbonyl group profile by

subtracting the contribution of the reducing endgroups from the total amount of carbonyls assuming that the amount of reducing endgroups relates to the  $MW_n$  determined from GPC measurement [45].



**Fig. 11.16** Differential MWDs of beech sulfite dissolving pulps prepared by TCF bleaching with Z-stage prior and after P-stage according to (E/O)ZP and (E/O)PZ, applying identical

conditions in each stage [46]. Molecular weight ( $MW_n$  in brackets) after (E/O)ZP: 205 (38) kDa, after (E/O)PZ: 290 (45) kDa; for more detailed characterization, see Tab. 11.8.



**Fig. 11.17** Color reversion,  $\Delta R/R$  after 72 h treatment at 105 °C, as a function of the overall carbonyl group content of beech sulfite dissolving pulps prepared by TCF bleaching with Z-stage prior and after P-stage according to (E/O)ZP and (E/O)PZ, applying a series of different ozone charges: (E/O)ZP: 2, 4, 6 kg odt<sup>-1</sup>; (E/O)PZ: 2, 4, 6, 6.2 kg odt<sup>-1</sup> [46].

The results indicate clearly that carbonyl groups promote both cellulose degradation reactions and color reversion [47]. Even though delignification and bleaching is more selective when ozonation represents the final stage according to an (E/O)-P-Z-sequence, yellowing can only be reduced when the final bleaching sequence is reversed and the peroxide step follows an ozone stage. The important role of carbonyl groups with respect to stability of polysaccharides is comprehensively reviewed by Gratzl [47].

Upon oxidative bleaching treatments, carbonyl groups are partly oxidized to carboxylic acids (see Tab. 11.8). Higher concentrations of carboxyl groups have shown not to adversely affect viscose fiber processing. However, the thermal stability of the pulp is negatively influenced with an increasing amount of carboxyl groups [48]. Moreover, carboxyl groups – particularly from the uronic acids present in the pulp – are considered to promote heat-induced yellowing of kraft hardwood and softwood pulps [49]. Acetate-grade pulps, which are used for plastic molding, should therefore have a carboxyl group content which is as low as possible [42].

### 11.3.2.3 Supramolecular Structure

The supramolecular structure of cellulose is adequately characterized by the widely accepted two-phase model (fringe fibrillar model) representing low-ordered (amorphous) and highly ordered (crystalline) regions. The ratio of crystalline-to-amorphous domains – the so-called “degree of crystallinity” (order) – is predomi-

nantly determined from the wide-angle X-ray scattering (WAXS) pattern [50], and more recently also from solid state  $^{13}\text{C}$ -CP/MAS-NMR [51] and vibrational spectroscopy (e.g., FTIR applying the ratio of the absorption intensities at  $1370\text{ cm}^{-1}$  and  $2900\text{ cm}^{-1}$ ) [52]. The degree of crystallinity of different cellulose I samples (pulp) covers a rather narrow range, and depends on origin and processing conditions of the particular sample. The reduction of pulp molecular weight during the final phase of acid sulfite cooking proceeds parallel to the degradation of the polysaccharide fraction (cellulose and hemicellulose), and occurs particularly in the amorphous region. The preferred removal of amorphous hemicelluloses is finally expressed in a slight (but clear) increase in the degree of crystallinity when reducing unbleached pulp viscosity from about  $730\text{ mL g}^{-1}$  to  $490\text{ mL g}^{-1}$ . Crystallinity is further altered by subsequent bleaching and purification processes. This has also been reported by Fink et al., who identified an increase in the degree of crystallinity and a change of the crystallite dimensions due to recrystallization in the course of full bleaching operations [53]. During bleaching with high dosages of ozone, crystallinity increases obviously due to removing amorphous pulp components, while the amorphous regions are slightly extended by a subsequent hot caustic extraction. When cellulose undergoes a transition from the glassy to the softened state, the concentration of intermolecular bonds decreases and the segmental mobility increases. In the glassy state, virtually all hydroxyl groups are involved in intra- and intermolecular hydrogen bonds. The softened state favors chemical reactions, and diffusion is accelerated [54].

The influence of pulping, bleaching and purification treatments on the degree of crystallinity of a beech acid sulfite pulp is detailed in Tab. 11.9.

As mentioned previously, the structural parameters also depend on the origin of the pulp sample. The degrees of order differ only slightly among the dissolving wood pulps comprising different types of pulps (sulfite versus PHK) and purity levels, whereas the perfection of crystallite order is considerably higher in the case of cotton linters. The same ranking clearly holds true for the anisometry of the crystallites – that is, the ratio of length ( $D_{021}$ ) to width ( $D_{002}$ ), as depicted in Tab. 11.10.

**Tab. 11.9** Degrees of crystallinity,  $x_c$ , of a beech sulfite pulp subjected to prolonged cooking (unbleached viscosity), mild and intensive ozone bleaching as well as reinforced hot caustic extraction (HCE).

Unbleached viscosity [ $\text{mL g}^{-1}$ ]	Low ozone charge <sup>a</sup>	High ozone charge <sup>b</sup>	Reinforced HCE <sup>c</sup>
490	55	56	54
599	53	55	51
729	52	54	52

a. 1–2 kg  $\text{odt}^{-1}$  (medium-consistency).

b. 4–5 kg/ $\text{odt}^{-1}$  (medium-consistency).

c. 75–115 kg NaOH  $\text{odt}^{-1}$ , 85 °C.

**Tab. 11.10** Structural parameters of different dissolving pulps grades including cotton linters by wide-angle X-ray scattering (WAXS) and wet chemistry methods (LODP, WRV).

Pulp	$x_c$ [%]	Cellulose II [%]	Crystallite dimensions		LODP	WRV [%]
			$D_{021}$ [nm]	$D_{002}$ [nm]		
HW-S	54	0	5.5	4.5	265	73
HW-PHK	56	0	6.7	5.0	190	71
HW-PHK-CCE <sup>a</sup>	58	64			175	80
Cotton linters	63	0	9.3	7.4	160	54

a. NaOH concentration of lye during CCE treatment about 10%.

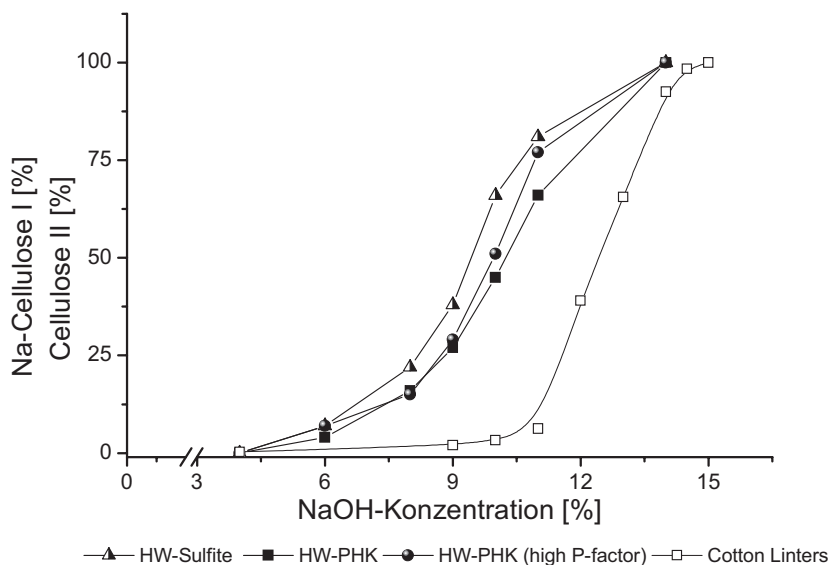
The level-off DPs (LODP) show a clear dependency on the purity of the pulps (expressed as  $R_{18}$  content), which is in agreement with results reported by Steege and Philipp [55] and later by Sixta [56]. The mean length of fibrillar aggregations (which is characterized by the LODP or limiting degree of polymerization) decreases in parallel with the removal of noncellulosic impurities in different levels for sulfite and PHK pulps [56]. The lower LODP values of the PHK pulps and cotton linters might be explained by their lower polydispersity.

To summarize the structural characteristics of dissolving pulps shown in Tab. 11.10, it can be concluded – in accordance with literature data [4] – that crystallite dimensions decrease in the order cotton linters > PHK pulp > sulfite pulp. Interestingly, the resistance to mercerization, which refers to the concentration of NaOH required to rearrange native cellulose crystal structure, follows the same order (cotton linters highest, sulfite pulp lowest).

The alkali concentration necessary to promote lattice transition from cellulose I to Na-cellulose I (and after neutralization to cellulose II) is an important criterion for characterizing pulp reactivity towards alkali cellulose formation as an intermediate for the production of viscose fibers and cellulose ethers. These intermediates exhibit a markedly enhanced reactivity compared with the initial cellulose substrate. The reagents can penetrate more easily into the swollen cellulose structure and thus react with the hydroxyl groups. The lattice transformation is accompanied with a disruption of microfibrils into smaller fibrillar units. This may well be the cause for the lowering of the LODP observed in acid hydrolysis of cellulose substrates regenerated from alkali cellulose, as reported by Schleicher and Philipp [57].

The transformation to Na-cellulose I begins at a NaOH concentration of about 6–7% for wood pulps and beyond 10% for cotton linters, respectively, and is completed at about 14–15% NaOH for both cellulose substrates (Fig. 11.18).

The resistance of cotton linters to mercerization is connected with its different supramolecular and fibrillar structure compared to dissolving pulps derived from

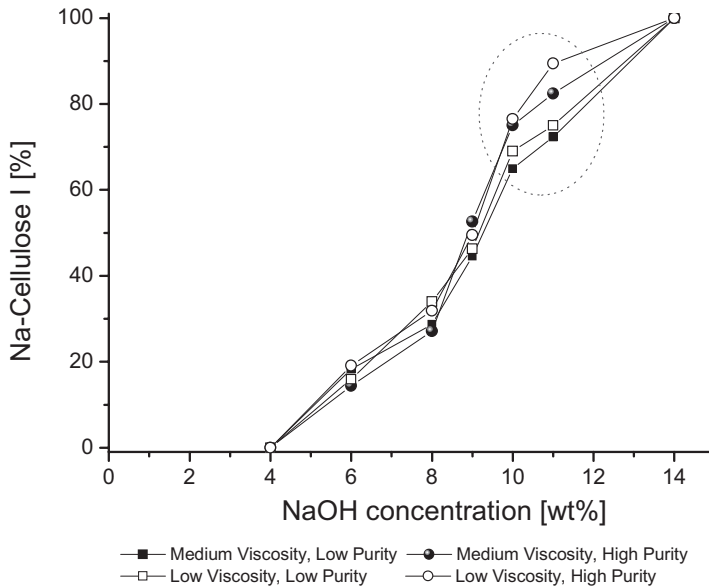


**Fig. 11.18** Lattice transition from cellulose I to Na-cellulose I of HW-sulfite and HW-PHK pulps of different purity, depending upon steeping lye concentration at room temperature [56]. An overlay of the lattice transition curve from cellulose I to cellulose II of cotton linters is marked for comparison [58].

wood or other lignocellulosic substrates. The rather uniform cellulose molecules (low polydispersity) in cotton linters are arranged as highly organized architecture of fibrillar elements. The high packing density of the microfibrils paired with a dense and specific build-up of the primary wall in which the fibrillar elements are arranged in a network-like helical fashion around the secondary wall lead to a decreased accessibility of reagents which is (also) expressed in a reduced accessible pore volume as determined by the water retention value (see Tab. 11.10). Within the wood dissolving pulps, acid sulfite pulps generally require a lower lye concentration for the lattice conversion than PHK pulps [9]. The data in Fig. 11.19 illustrate that the difference in lye concentration between the two types of dissolving wood pulps necessary to transform 50% to Na-cellulose I is about 0.9% (9.4% for sulfite versus 10.4% for PHK pulps). Compared to cotton linters, the difference from sulfite pulps is small and can be further reduced by reinforcing the prehydrolysis conditions. The more complete removal of xylan by increasing prehydrolysis intensity (see Fig. 11.18: HW-PHK high P-factor) clearly changes the supramolecular structure and results in a shift of the transition curve to a lower NaOH concentration. Above 11% NaOH, the curve of the highly purified PHK pulp proceeds similar to that of the sulfite pulp.

Closer examination of the mercerization behavior reveals that even between different sulfite dissolving pulps, differences in the course of the curve have been reported [58]. Recently, it was shown that pulping and subsequent purification





**Fig. 11.19** Lattice transition from cellulose I to Na-cellulose I of HW-sulfite dissolving pulps subjected to different pulping and purification pretreatments in dependence on steeping lye concentration at room temperature [56].

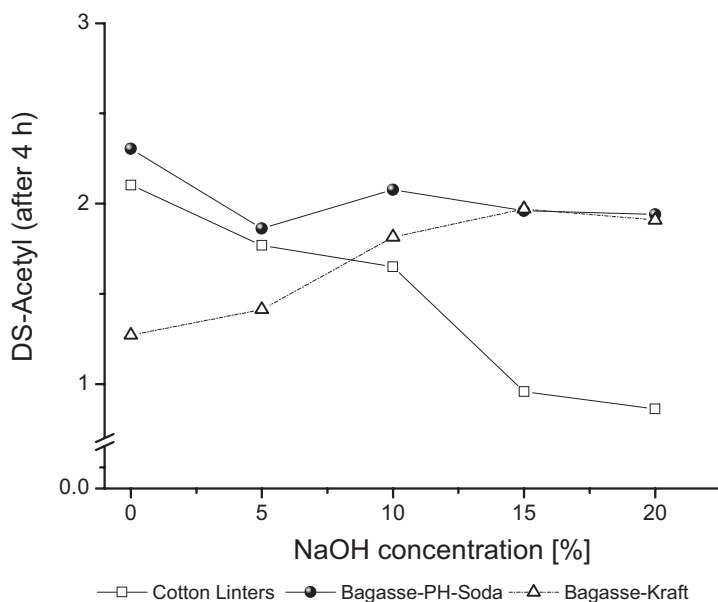
procedures of hardwood sulfite dissolving pulps clearly exert an influence on the shape of the transition curve, especially beyond an NaOH concentration of 10% at room temperature.

The enhanced viscosity degradation during final phase of sulfite cooking, combined with reinforced purification during hot caustic treatment, accelerates the transition to Na-cellulose I in the range of NaOH concentration of 10–12%. This type of activation towards alkali cellulose formation is also expressed in a better viscose filterability, thus indicating an improved reactivity.

During the course of a cold alkali extraction treatment for the manufacture of high-purity wood dissolving pulps, a partial lattice transformation from cellulose I to cellulose II usually occurs, depending on NaOH concentration in the aqueous pulp suspension (see Fig. 8.4). For the manufacture of very high-purity pulps ( $R_{18} > 98\%$ ), NaOH concentrations up to 10–11% are required, thus leading to a significant shift in the crystalline structure to cellulose II, as shown in Tab. 11.10 (HW-PHK-CCE). After drying, the reactivity of the mercerized dissolving pulps may alter [59]. It is reported that dried, partly mercerized dissolving pulps cannot be converted to cellulose acetate under the normal processing conditions, but the reactivity during nitration is not affected [60,61].

However, different pulps respond differently to cold alkali extraction, and hence behave differently towards acetylation. Thus, bond cleavage and solution of hemicelluloses may lead to increased reactivity, while drying may lead to decreased

reactivity. It was shown that the reactivity of a cotton linters pulp towards acetylation decreases steadily with increasing the concentration during cold caustic extraction (Fig. 11.20). The loss in reactivity is due to drying of the pulp after the cold caustic refining, which induces the formation of hydrogen bonding. With rising alkali concentration the hydrogen bonds become more dense, and this finally impairs the accessibility of the acetylation agent. When subjecting a low-grade dissolving pulp with a residual pentosan content of 7.8% to cold alkali extraction, the reactivity towards acetylation changes only marginally. This may be explained by two counteracting effects. On the one hand, the removal of higher amounts of low molecular-weight hemicelluloses, especially when using 10% NaOH, results in the formation of a more homogeneous pulp with increased accessibility to the reagent. On the other hand, a denser network of hydrogen bonds ensures that pores are closed and accessibility becomes more difficult. In contrast, reactivity of the kraft pulp increases continuously with increasing the NaOH concentration which may be accounted for by removal of the hemicelluloses. In the case of unpurified kraft pulp, the effect of improving reactivity due to pulp homogenization prevails up to a NaOH concentration of about 15%. However, by exceeding this NaOH concentration a slight decrease in reactivity is observed due to a decreasing accessibility.



**Fig. 11.20** Effect of NaOH concentration during cold caustic extraction on the reactivity towards acetylation of cotton linters, bagasse-PH-Soda and bagasse-kraft pulps [62]. Initial pulp purities, measured in terms of alpha-cellulose content: 99.1%, 91.9%, and 75.8% for cotton linters, bagasse-PH-Soda and bagasse-kraft pulps, respectively.

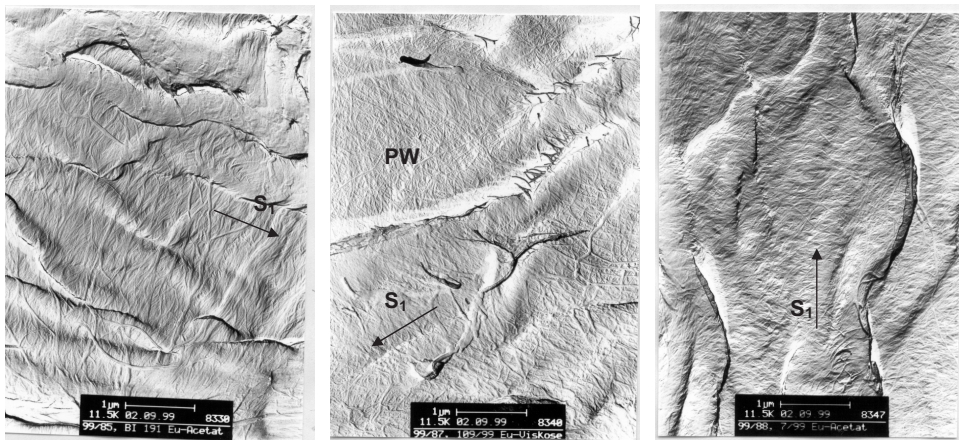
### 11.3.2.4 Cell Wall Structure

The architecture of both native (cellulose I) and regenerated fibers (cellulose II) is constituted by micro- and macrofibrils. The latter are the structural elements of a single cellulose fiber. The cross-section of cotton linters fibers amounts to 17–27  $\mu\text{m}$ , while that of spruce sulfite pulp fibers is 21–40  $\mu\text{m}$  [63]. The cellulose I fibers are a buildup of single cell-wall layers that differ in their fibril texture, and this contributes to the fiber properties.

The fibrillar morphology of pulps is highly dependent upon the pulping process and pulping conditions. It is assumed that the active sulfite cooking chemicals, comprising hydrogen sulfite and hydrated sulfur dioxide, penetrate through the pits into the middle lamella where the pulping reaction starts from the primary wall across the cell wall. As a consequence, the primary wall is sometimes completely removed after acid sulfite pulping. Pulping under alkaline conditions (the kraft process), however, enables rather uniform pulping reactions across the cell wall layers due to the high swelling properties of white liquor. The morphology of cellulose samples is evaluated mainly using electron microscopy (scanning and transmission electron). A very good resolution of the fibrillar structure is obtained by the transmission electron microscopy (TEM) surface replica technique described by Purz et al. [64] and by Fink et al. [53]. A characteristic micrograph of eucalyptus sulfite dissolving pulp is shown in Fig. 11.21a, with the primary wall having been largely removed. The morphological architecture of the sulfite pulp is clearly dominated by the S1 layer (Fig. 11.21a).

Identification of the cell wall layers is possible by the preferred orientation of the exposed cellulose microfibrils with respect to the cell axis. The latter is indicated by arrows in the micrographs.

On the other hand, residues of the primary wall can be detected for the PHK viscose pulp (low P-factor) (Fig. 11.21b, top). Apparently, the type of pulp – as well as process conditions during pulp manufacture – exert an influence on the exposure



**Fig. 11.21** Transmission electron microscopic surface replica of (a) eucalypt sulfite dissolving pulp (b) eucalypt PHK pulp (c) eucalypt PHK pulp with high P-factor [56].

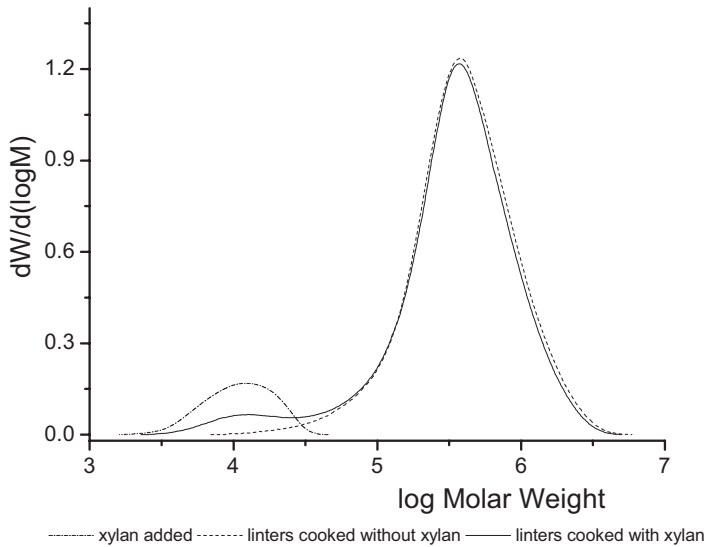
of cell wall layers. Clearly, mild prehydrolysis combined with alkaline cooking is less detrimental to cellulose microfibrils than acid sulfite cooking, thus leaving the primary cell wall morphology largely unaffected. However, PHK cooking, using intensified prehydrolysis conditions to produce pulps of very low residual hemicellulose content (e.g., xylan), further removes the primary cell wall layers, as shown in Fig. 11.21c. Therefore, the microfibrillar structure of this PHK pulp (high P-factor) is almost comparable to that of the sulfite pulps.

The different behavior of the three dissolving pulps with regard to lattice transition as a function of NaOH concentration can be explained by their different morphological structure. It is interesting to note that the supramolecular structure may be influenced by the cell wall structure of the dissolving pulps. Also, the markedly higher reactivity of sulfite and highly purified PHK pulps in ageing of alkali cellulose and xanthation may well be caused by a weakening of the outer layers of the wood fiber cell wall due to the higher hydrolytic action during final phase sulfite cooking and intensified prehydrolysis.

#### 11.3.2.4.1 Distribution of Hemicelluloses across the Fiber Wall

In the manufacture of dissolving pulps, the objective is to remove as much hemicelluloses as possible without causing too-severe cellulose deterioration. An important topic with regard to further process development is how the remaining hemicelluloses are located within the fiber wall. The different chemistry of acid sulfite and alkaline cooking procedures, as well as the heterogeneous distribution of hemicellulose across the different cell wall layers, suggest that there is a difference in the arrangement of hemicelluloses in the fiber walls of PHK and acid sulfite fibers which presumably influences their chemical properties. Moreover, during the final phase of alkaline pulping dissolved hemicelluloses (e.g., xylan) are taken back by the fibers from solution. The redeposition of xylan plays an important role in the papermaking properties of the resulting pulp fibers, but could also adversely affect the manufacture of cellulose acetate. Yllner and Enström showed that on heating pentosan-free cotton linters with birch wood chips in kraft cooking liquor, considerable quantities of xylan were taken up from the solution [65,66]. Quite recently it was shown that during kraft cooking of cotton linters at 150 °C for 2 h, more than 70% of a xylan, which was added to the cooking liquor (isolated from a eucalyptus pulp), was retained on the cellulose surface at a residual effective alkali concentrations of approximately 10 g L<sup>-1</sup>, and still more than 20% in the case of alkali concentrations up to 50 g L<sup>-1</sup> [67]. Xylan redeposition has been demonstrated unequivocally by carbohydrate and GPC analysis (Fig. 11.24).

The xylan distributions across the fiber wall of TCF-bleached acid sulfite and PHK dissolving pulps, obtained from both spruce and beech wood, were investigated employing a new enzymatic peeling technique [69,70]. A general characterization of the pulp substrates subjected to enzymatic peeling is provided in Tab. 11.11.



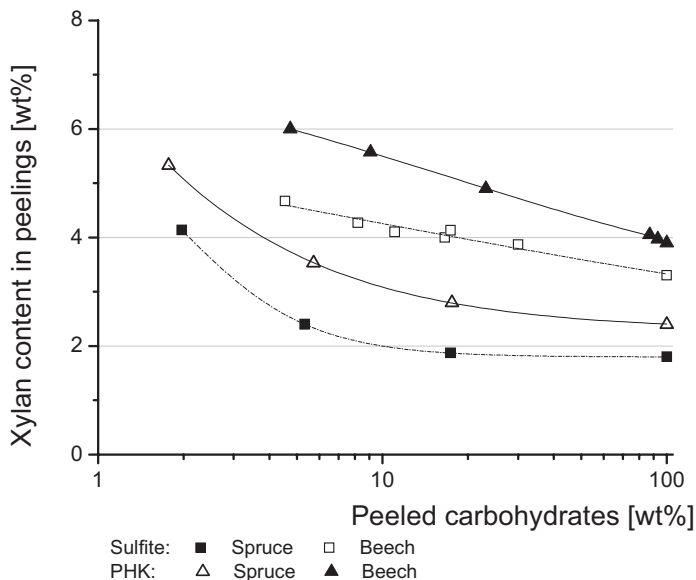
**Fig. 11.24** Molar mass distribution of cotton linters after cooking for 2 h at 150 °C with a residual EA-concentration of 10 g L<sup>-1</sup> in the absence and presence of xylan [67]. The xylan was isolated from a eucalyptus kraft pulp. GPC measurements were made according to [68].

**Tab. 11.11** Characterization of TCF-bleached dissolving pulps made from spruce and beech wood produced by acid sulfite and prehydrolysis kraft (PHK) cooking procedures [70].

Pulp type	Bleaching sequence	Bleached yield [%]	Viscosity [mL g <sup>-1</sup> ]	Brightness [% ISO]	Xylan [%]	Glucomannan [%]
Beech-S	(E/O)-Z-P	39.7	573	91.4	3.3	0.6
Beech-PHK	O-A-Z-P	38.1	465	91.1	6.4	0.4
Spruce-S	(E/O)-Z-P	42.3	526	90.0	1.8	2.4
Spruce-PHK	O-A-Z-P	38.5	439	83.4	2.3	1.3

The enzyme treatment causes a peeling effect which removes fiber material, starting from the fiber surface. An analysis of the removed material by capillary zone electrophoresis (CZE) revealed fundamental differences in the radial distributions of hemicelluloses, as shown in Fig. 11.25. These differences may account for some of the differences in dissolving properties of acid sulfite and PHK pulps.

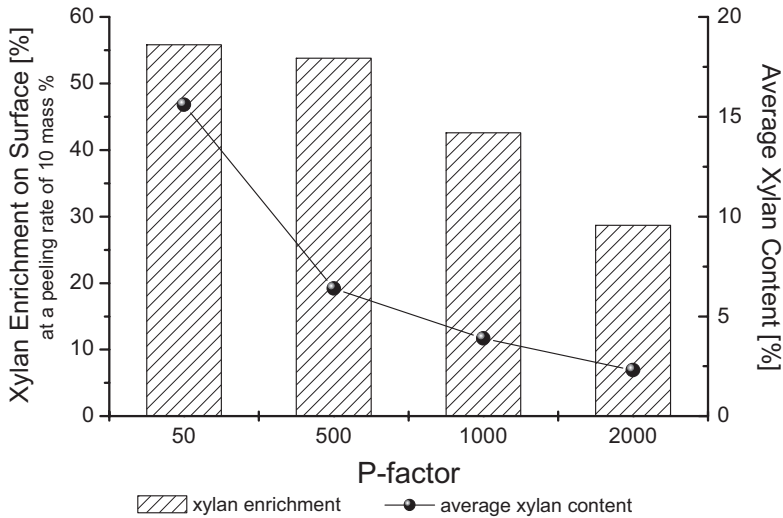
The results show that all dissolving pulps investigated have a higher xylan content in the surface layer than in the inner fiber wall. This is in agreement with results obtained from paper-grade pulps [70,71]. The enrichment, however, is



**Fig. 11.25** Radial distribution of xylan in TCF-bleached spruce and beech sulfite and PHK dissolving pulps, according to Tab. 11.11. Xylan content determined in aliquots of the hydrolyzate (mass % of carbohydrates), collected after 1, 3, 10 min and 48 h of enzymatic peeling, and after total hydrolysis [70].

highly dependent upon both the process and the wood species used. The high xylan content located in the outermost layers of the beech PHK fibers suggests that xylan precipitation occurs in the final kraft cooking phase, as shown for cotton linters in Fig. 11.24. Beech sulfite dissolving pulp, however, shows a comparable even cross-sectional concentration profile, as was determined for paper-grade pulps [71]. For spruce PHK and acid sulfite dissolving pulps, only a very thin outermost surface enrichment of xylan is found. But again, xylan is more enriched at the surface of the PHK fibers as compared to the acid sulfite fibers. It is known from practice that sulfite pulp behaves satisfactorily during the manufacture of cellulose acetate, whereas kraft pulp with a similar (average) chemical analysis does not. The enrichment of hemicellulose in PHK pulps may be one reason for the impaired properties. Therefore, it is important to know if the pronounced xylan profile through the cell wall can be leveled out by reinforced purification conditions. Indeed, the enrichment of xylan was shown to decrease considerably when prehydrolysis conditions were gradually intensified (increasing P-factor) while the kraft cooking conditions were kept constant (Fig. 11.26).

A general characterization of the beech PHK pulps subjected to enzymatic peeling is provided in Tab. 11.12.



**Fig. 11.26** Xylan enrichment on surface at a peeling rate of 10 mass % of beech PHK pulps prepared by increasing P factors while Visbatch® cooking conditions were kept constant. For enzymatic peeling conditions, see Fig. 11.25.

**Tab. 11.12** Characterization of TCF-bleached beech PHK pulps prepared according to the Visbatch® process comprising four different levels of P-factor [72].

Pulp type	Bleaching sequence	Bleached yield [%]	Viscosity [mL g <sup>-1</sup> ]	Brightness [% ISO]	Xylan [%]	Glucomannan [%]
50	O-A-Z-P	44.4	466	90.7	15.6	0.6
500	O-A-Z-P	38.1	465	91.1	6.4	0.4
1000	O-A-Z-P	34.7	488	91.2	3.9	0.3
2000	O-A-Z-P	30.4	470	89.0	2.3	0.2

The decrease in surface xylan concentration may be explained by both the enhanced removal of xylan from the outermost surface layers through reinforced prehydrolysis conditions, and the diminished reprecipitation of xylan from solution during the final phase of cooking due to a significant reduction in xylan concentration.

### 11.3.2.5 Fiber Morphology

Hardwoods contain a wide variety of cell types of extremely heterogeneous morphology, and this is reflected in the distribution of fiber dimensions in the fully bleached pulp (e.g., fiber length, coarseness, etc.). This complex cell morphology

of predominantly hardwood dissolving pulps (e.g., beech, birch, aspen) might cause problems in subsequent conversion processes due to an inhomogeneous course of reaction. Moreover, some of the cell types such as the parenchyma cells are highly enriched in noncellulosic compounds, the removal of which during pulping and bleaching operations remains insufficient. This material does not react completely with reagents to form homogeneous solutions and products (e.g., viscose, acetate). Gruber et al. reported that even the short fiber fraction of spruce yields lower degrees of substitution during the course of heterogeneous nitration and carbanilation than do the long fiber fractions [73]. Moreover, their derivatives are less soluble and contain a large proportion of gels. The lower reactivity of the short fiber fraction in sulfite spruce dissolving pulp is due to its more rapid swelling, which impedes diffusion of the reagents.

Therefore, much effort has been undertaken since the early days of dissolving pulp production to fractionate the pulp fiber into more homogeneous fractions in order to overcome the problems in subsequent processing steps. Several attempts were pursued to construct suitable devices for selective separation of the short fiber fraction (wood ray, "0-fibers", etc.). By using special drum filters with a 0.3-mm mesh screen [74] or so-called "side hills", the total pulp losses were usually kept at 4–6%, while the extent of resin removal was reported to be between 50 and 90%. Moreover, bleachability of the screened pulps from which the wood rays were removed was greatly improved, owing to a lowering of the lignin content. The cost:benefit ratio of pulp fractionation was poor, mainly due to the high costs caused by the extensive pulp losses and the need for additional equipment. Consequently, pulp fractionation was discontinued in the early 1980s. Quite recently, pilot plant trials were conducted using a specially designed pressure screen with drilled screening plates [75]. Even though the fractionator was operated with a split ratio of 15% short fibers and 85% long fibers, the reactivity of the latter fraction towards xanthation was only marginally improved. However, the more homogeneous long-fiber fraction revealed a narrower MWD and improved optical properties, which also could be translated to a higher brightness of viscose fibers. Again, these pilot plant trials confirm that pulp fractionation simply does not pay unless the removed short-fiber fraction could be recovered as a product with a price comparable to that of the long-fiber fraction.

#### 11.3.2.6 Pore Structure, Accessibility

The cell wall of a pulp fiber is a hydrogel, and consists of carbohydrates that can take up water and thereby increase in volume. The interaction between polysaccharides and water within the whole cell wall structure is an important prerequisite for the subsequent conversion of cellulose to its derivatives. Otherwise, the reaction would be limited to the available surface. The swelling behavior of a pulp depends strongly on its supramolecular structure which finally determines the pore volume and pore structure. It has been shown that there are three distinct fractions of water within the cell wall: (a) bulk water located in large macropores; (b) freezing bound water held in micropores within the amorphous region of the



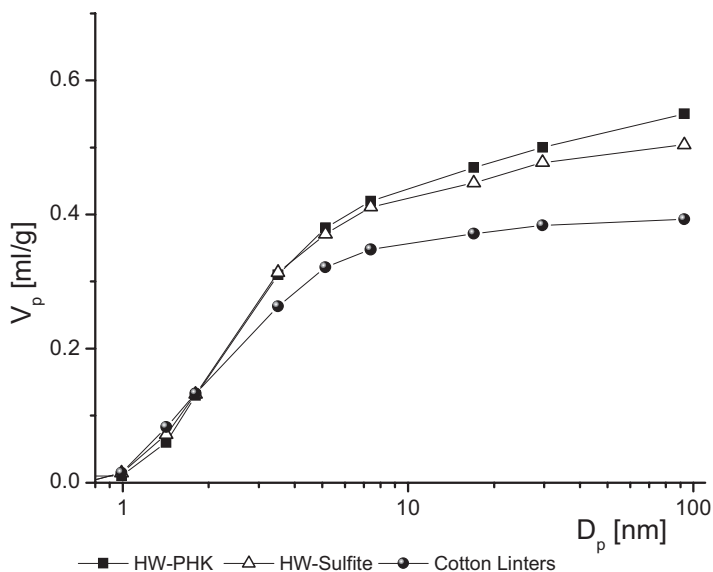
cell wall; and (c) nonfreezing bound water which is adsorbed on to hydrophilic sites of the carbohydrates and can be designated as water of hydration [76,77]. The latter amounts to approximately  $0.34\text{--}0.39\text{ g g}^{-1}$  o.d. pulp, and is only slightly decreased after drying and rewetting. It is proposed that the nonfreezing and freezing bound water fractions are in small pores (micropores), and that the bulk water in the cell wall is in large pores that are formed when lignin and hemicelluloses dissolve out of the cell wall during pulping (macropores). The amount of water within the cell wall – the so-called fiber saturation point (FSP) – can be adequately measured with a solute exclusion technique [78,79]. Based on this technique, Brederick et al. [80,81] developed an inverse size-exclusion chromatography (ISEC) technique in which the macromolecules used are a series of dextran fractions and mono-, di-, tri-, and tetrasaccharides. (The diameters of the macromolecules are calculated from their diffusion coefficients using the Einstein–Stokes formula.) The uptake of water by a pulp sample can be simply determined by measuring the so-called water retention value (WRV), which comprises the weight gain (in %) of a dry sample after swelling in a large excess of water and subsequent centrifugation under defined conditions [82]. Scallan showed the WRV to be a good measure of the FSP up to values of  $1.8\text{ H}_2\text{O g}^{-1}$  o.d. pulp [83]. The values determined from WRV and ISEC measurements listed in Tab. 11.13 demonstrate the important influence of the supramolecular structure of dissolving pulps on water swelling.

**Tab. 11.13** Results of ISEC and WRV measurements obtained from a selection of typical dissolving pulps.  $V_p$  = pore volume;  $D_p$  = average pore diameter;  $O_p$  = specific pore surface of water-swollen pulps. The values were calculated according to the model published by Brederick et al. [81].

Pulp type	$V_p$ [mL g <sup>-1</sup> ]	FSP [mL g <sup>-1</sup> ]	WRV [%]	$D_p$ [nm]	$O_p$ [m <sup>2</sup> g <sup>-1</sup> ]
HW-S	0.60	0.50	73	5.1	235
HW-PHK	0.65	0.55	71	5.5	240
Cotton linters	0.45	0.39	54	4.8	190

As expected, the water-accessible pore volume of cotton linters is clearly lower than that of the dissolving wood pulps. Only minor differences in integral pore volume ( $V_p$ ), WRV and specific pore surface ( $O_p$ ) were seen between acid sulfite and PHK dissolving pulps. A slight advantage of the PHK over the acid sulfite pulp with regard to total pore volume was apparent (Fig. 11.27), though closer examination revealed that the PHK pulp provided a larger number of small pores with an average diameter of 1.5–2.0 nm.

Never-dried cellulose substrates showed a considerably higher accessibility for water than did either the dried or rewetted samples. When pulps are dried, an



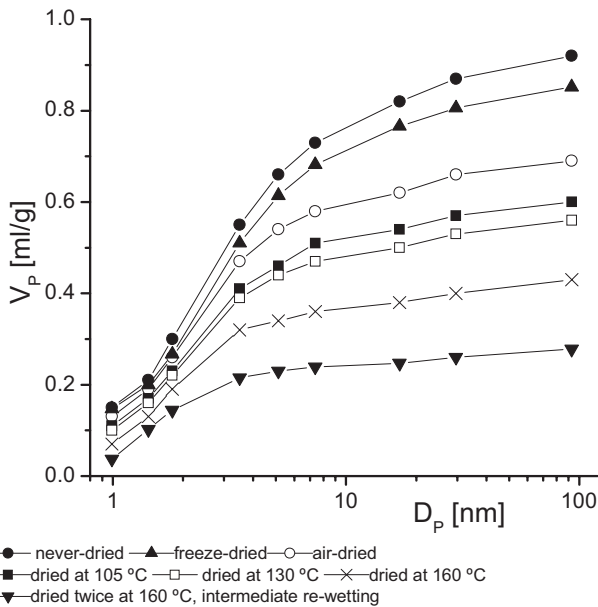
**Fig. 11.27** Pore volume versus pore diameter of a selection of dissolving pulps, as determined by the ISEC method.

irreversible loss of fiber swelling occurs; indeed, Maloney and Paulapuro reported that most macropores may be rendered inaccessible, while none of the micropores was irreversibly collapsed after drying and rewetting [77]. The mechanism leading to these irreversible changes is termed “hornification”. Moreover, drying and even thermal treatment has a negligible effect on the amount of nonfreezing bound water. On drying, the water molecules are partially removed and new hydrogen bonds are formed directly between cellulose molecules [84]. It is likely that, in addition to hydrogen bonds, van der Waals bonds are also involved in hornification, though the exact nature of irreversible bonding in pulp fibers has not yet been established. Newman and Hemmingson have postulated a co-crystallization in microcrystalline areas as the main reason for hornification [85]. The effect of thermal treatment on the physical and chemical properties was examined by using a never-dried beech acid sulfite pulp [86]. When the temperature exceeds 105 °C, thermal degradation proceeds in parallel with hornification, as shown in Tab. 11.14.

The content of carboxyl groups decreased while the content of carbonyl groups increased, particularly at temperatures above 105 °C. The increase in carbonyl groups is caused by the cellulose degradation, thus creating new reducing end-groups (see Tab. 11.14). The course of brightness reveals the effect of heat-induced yellowing caused by the formation of chromophores, with a probable participation of carbonyl groups and residual noncellulosic compounds such as hemicellulose, resins, and certain metal ions. The effect of pore collapse along with the decrease in pore volume is clearly illustrated in Fig. 11.28.

**Tab. 11.14** Chemical and physical characterization of a never-dried beech acid sulfite pulp during the course of different drying conditions [86]. Thermal treatment was carried out for 12 h.

Sample treatment	Brightness [% ISO]	Viscosity [mL g <sup>-1</sup> ]	WRV [%]	V <sub>p</sub> [mL g <sup>-1</sup> ]	COOH [μmol g <sup>-1</sup> ]	CO [μmol g <sup>-1</sup> ]
Never-dried	91.2	581	91.2	0.92		24.5
Freezed-dried				0.86		
Air-dried	91.2	581	91.2	0.69	30.9	25.6
105 °C	90.1	546	90.1	0.60	30.5	27.5
130 °C	88.9	489	88.9	0.56	28.2	29.7
160 °C	79.1	350	79.1	0.43	27.6	37.3



**Fig. 11.28** Pore volume versus pore diameter (ISEC method) of a beech acid sulfite pulp subjected to different drying procedures [86].

As expected, freeze-drying is the only drying procedure which largely preserves the pore and void system of a never-dried pulp fiber. The loss in pore volume is negligible compared to all other drying procedures (see Fig. 11.28 and Tab. 11.14). When discussing hornification, the question always arises to what extent pulp reactivity is affected by this irreversible loss of pore volume. The reaction with

acetic anhydride in acid solution is more sensitive to accessibility as compared to alkaline processing due to limited swelling conditions. The results indicate that drying at 105 °C is unfavorable over drying at room temperature with respect to the homogeneity of the cellulose triacetate solution, as expressed by the increased turbidity value (Tab. 11.15).

**Tab. 11.15** Chemical and physical characterization of a never-dried beech acid sulfite pulp in the course of different drying conditions [86].

Sample treatment	Triacetate solution quality	
	Yellowness coefficient	Turbidity
Air-dried		
105 °C	0.59	296
130 °C	0.59	367
160 °C	0.89	1030

The loss in pore volume by drying at 160 °C is clearly reflected in a significant increase in the yellowness coefficient, haze, and the amount of undissolved particles. The severe decrease in reactivity has also been described by Gruber et al., using comparable conditions [87].

To summarize, water uptake is largely controlled by morphological features of the cellulose fiber, consisting of a hierarchy of domains of gradually different accessibility. By drying swollen fibers, some of these domains become inaccessible (hornification). In agreement with many previous reports, chemical reactivity in particular has been found to be sensitive to drying conditions.

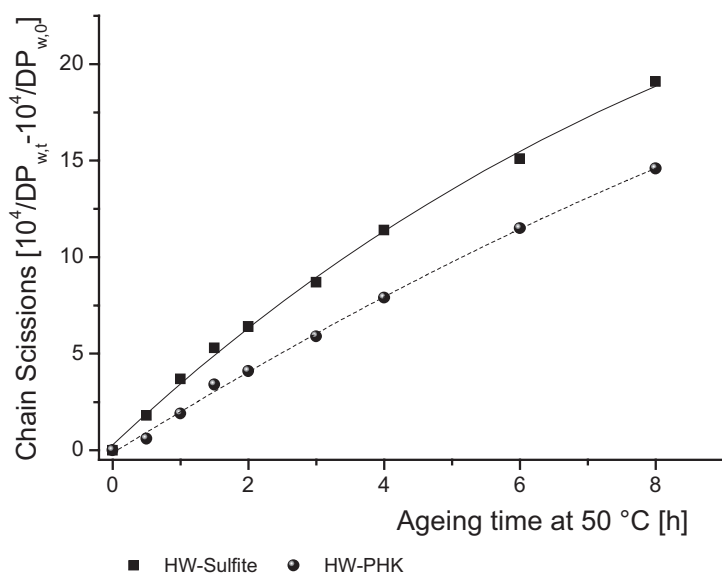
### 11.3.2.7 Degradation of Dissolving Pulps

The behaviour of dissolving pulps within heterogeneous degradation reactions provides insight into their supramolecular structures, functionalities, and changes in MWD. A comprehensive description of all relevant cellulose degradation processes is reviewed in Ref. [4]. The different modes of cellulose degradation comprise chemical, mechanical, thermal, and radiation degradation. In many conversion processes of cellulose, the molecular weight must be adjusted by controlled degradation procedures.

The degradation of cellulose plays an important role in the chemical processing of dissolving pulps. The aim of controlled cellulose degradation is to adjust polymer properties related to the molecular weight such as solution viscosity (ethers) or strength properties of the final product (regenerated fibers). The most important conversion processes of dissolving pulps, viscose and cellulose ethers, operate

under alkaline conditions. There, molar mass is adjusted by oxidative alkaline degradation, also known as ageing of alkali cellulose. In recent years, a new route of controlled degradation of the dissolving pulp prior alkalization by high-energy radiation has been extensively investigated and technologically developed by Fischer et al. [88].

Alkali cellulose with a typical composition of 34% cellulose and 16% NaOH ( $\sim 1.9 \text{ mol NaOH mol}^{-1}$  cellulose) is rather rapidly degraded at only a slightly elevated temperature ( $30\text{--}50^\circ\text{C}$ ), initiated by the uptake of oxygen. The reaction rate can be accelerated by the addition of transition metal ions, particularly Co or Mn salts. The course of the chain scissions, calculated from the weighted molecular weight (determined by GPC measurement [68]) of alkali celluloses prepared from both hardwood sulfite and PHK dissolving pulps as a function of reaction time at  $50^\circ\text{C}$ , is illustrated graphically in Fig. 11.29.



**Fig. 11.29** Course of chains scissions (based on weighted molecular weight) of alkali celluloses prepared from hardwood sulfite and PHK dissolving pulps as a function of time at  $50^\circ\text{C}$ .

The ageing of alkali cellulose follows a pseudo zero-order reaction kinetics based on the number-average degree of polymerization  $DP_n$ , according to the following expression [56]:

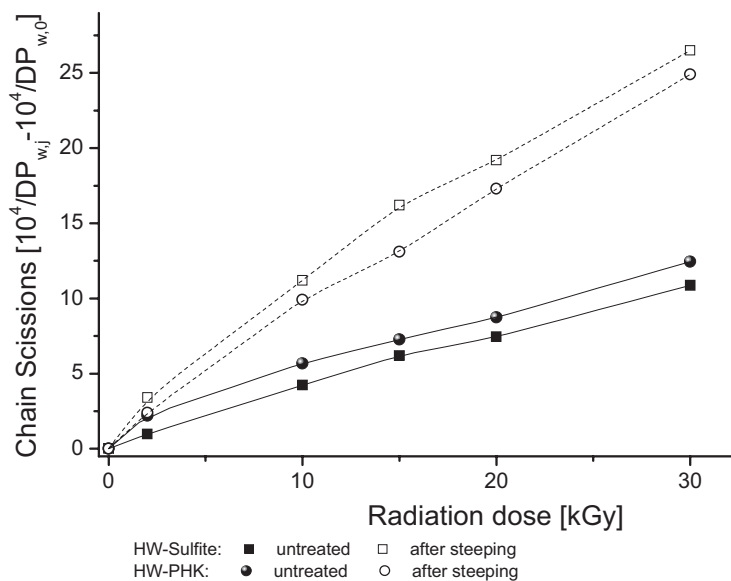
$$\left[ \frac{10^4}{DP_{n,t}} - \frac{10^4}{DP_{n,0}} \right] = k_A \cdot t \quad (1)$$

where  $k_A$  is the reaction rate of the ageing process.

The deviation from linearity, which is particularly discernible for alkali cellulose made from a hardwood sulfite pulp, can be attributed to the change (decrease) in polydispersity during degradation. Based on today's knowledge of the reaction mechanism, chain scission is initiated by the reducing endgroups. In agreement with these considerations, oxidative alkaline degradation of sulfite pulp proceeds faster as compared to the more narrowly distributed PHK dissolving pulp (see Fig. 11.29).

The arguments in favor of electron beam treatment of dissolving pulp are a better control of viscosity degradation following a strict random scission mechanism, which results in better reactivity towards derivatization due to a better accessibility in the crystalline regions.

Hardwood sulfite and PHK dissolving pulps were irradiated by means of a 10 MeV accelerator, applying dosages of between 0 and 30 kGy (Fig. 11.30).



**Fig. 11.30** Course of chain scissions (based on weighted molecular weight) of hardwood sulfite and PHK dissolving pulps, before and after steeping as a function of radiation dose.

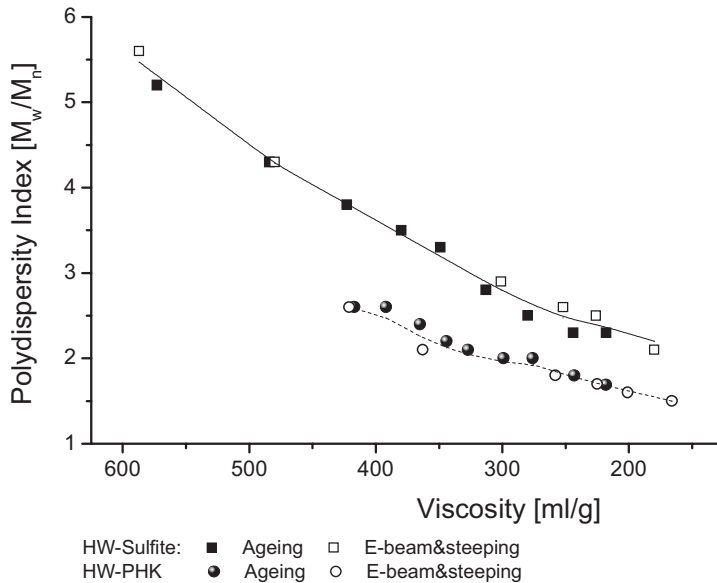
After irradiation, the molecular weight was determined without any further treatment and after alkalization with a caustic solution of 17.5% NaOH (steeping). Degradation kinetics can be described by means of zero order, whereby using the model equation from Sakurada:

$$\left[ \frac{10^4}{DP_{n,t}} - \frac{10^4}{DP_{n,0}} \right] = k_D \cdot D^n \quad (2)$$

where  $k_D$  is the reaction rate of the radiation degradation.

The exponent  $n$  takes into account the fact that the polydispersity changes during radiation degradation. According to Fig. 11.30, the course of chain scissions is comparable for both pulps investigated. Because of a larger amount of carbonyl groups (including reducing end groups), the degradation rate of a sulfite pulp is more enhanced after a subsequent steeping step as compared to a PHK pulp. As mentioned previously, the statistical character of molecular weight degradation has been proposed as one important advantage of the electron beam treatment compared to chemical degradation processes. If random chain scission is assumed, then nonuniformity ( $U = \text{PDI} - 1$ ) would approach unity, as indicated by Kuhn [89].

The data in Fig. 11.31 show that the MWD curves through progressive degradation are practically equal for both degradation processes, namely electron beam treatment followed by steeping and oxidative alkaline ageing. Furthermore, the results suggest that the statistical degradation performance applies to both degradation processes. The conclusion is that radiation degradation and alkaline ageing successively reduce the molecular weight, making the MWD progressively narrower. In both processes, the reaction kinetics is governed by the content of carbonyl groups, indicating that the degradation rate of sulfite pulps is higher than that of PHK pulps.



**Fig. 11.31** Polydispersity index (PDI) as a function of cellulose viscosity indicating the course of degradation: comparison of electron beam treatment for both hardwood sulfite and PHK dissolving pulps. The PDI was determined from GPC-MALLS measurement (according to [68]).

### 11.3.2.8 Overview of Pulp Specification

As stated previously, the suitability of dissolving pulps can be adequately determined simply by simulating the conversion processes to the final products, at least on a laboratory scale. The most important property of virtually all dissolving pulps can be expressed by the term “chemical reactivity”. Pulp reactivity, however, cannot be described by a single structural feature, but rather by both the physical structure of the cellulosic material and the type of chemical interaction with the reagent. Additionally, all three structural levels – the molecular, supramolecular, and fibrillar – must be considered when using the term reactivity [90].

Reactivity is related to the accessibility of chemicals to the cellulose, which means the relative ease by which the hydroxyl groups can be reached by the reactants. Structure and morphology of the fiber determines the homogeneity of the conversion process and final product quality [91].

One of the most informative parameters in commercial specification sheets (quality card) is that of alkali solubility tests at room temperature. Here, the pulps are subjected to extractions with 10% (highest alkaline solubility) and 18% NaOH (concentration of steeping lye), respectively. Thereby, differentiation must be made between methods based on the gravimetric determination of the extraction residue (R-values) and determination of the soluble fraction (S-values) using potassium dichromate oxidation of the filtrate, followed by titration. The results are specified as a percentage based on the dry starting material. The concentration of NaOH is given as a subscript index ( $R_{10}$ ,  $R_{18}$  or  $S_{10}$ ,  $S_{18}$ ). The alkali resistances are directly related to alkaline processing of dissolving pulps, as for viscose and etherification processes. There, the  $R_{18}$  or (in some cases preferred)  $R_{21.5}$  values have been cited as being representative of the yield of alkaline-processed products (viscose fiber and cellulose ether) [92]. It has been shown that the cellulose content corresponds well with the  $R_{18}$  value. For sulfite pulps with low molecular weight, the  $R_{18}$  value lies below the cellulose content, because low molecular-weight material becomes dissolved. For PHK pulps and high-viscosity sulfite pulps (ether application), the  $R_{18}$  value exceeds the cellulose content because high molecular-weight, alkali-stable hemicelluloses remain in the pulp [93]. The difference between the two extraction results is sometimes used as a measure for low molar mass cellulose ( $R_{18} - R_{10}$  or  $S_{10} - S_{18}$ ).

Moreover, the  $S_{18}$  or  $(100 - R_{18})$  values are good indicators for estimating the organic wastewater load associated with the production of viscose fibers or cellulose ethers.

The data in Tab. 11.16 represents a simplified specification profile of the most important dissolving pulps, derived from hardwood, softwood and cotton linters and produced according to acid sulfite and PHK procedures.



Tab. 11.16 Chemical and physical characterization profile of selected dissolving pulps.

Parameters	Viscose products				Cellulose acetate				High-viscosity ether				
	Hardwood	Hardwood	Softwood	Cotton	Hardwood	Hardwood	Softwood	Cotton	Hardwood	Hardwood	Softwood	Cotton	
Pulp origin	Reference	Acid sulfite ECF	PHK TCF	Acid sulfite ECF	PHK ECF	Acid sulfite ECF	PHK ECF	Acid sulfite ECF	Soda ECF	Reference	Acid sulfite ECF	PHK ECF	Acid sulfite ECF
Wood	Method												
Process													
Cooking													
Bleaching													
<b>Chemical properties</b>													
<b>Chemical Composition</b>													
Carbohydrates													
Glucan		rel%	96.3	97.0	98.8	97.5	98.8	94.8	99.6	[25]			
Mannan	AX/EC-PAD	rel%	0.2	0.5	0.2	1.2	0.2	2.0	0.0				
Xylan	AX/EC-PAD	rel%	3.5	2.5	3.5	1.3	1.0	3.2	0.4				
Extractives, Resins													
Acetone extractives	ISO 624 (mod.)	%	0.1	0.2	0.05	0.05	0.05	0.07	0.06				
DCM extractives	ISO 624	%	0.06	0.07	0.04	0.04	0.02	0.06	0.03				
Kappa number	T 236 cm-85 mod.		0.3	0.3	0.2	0.2	0.2	0.5	0.1				
Organohalogen (OX)	DIN 52355	ppm	25	100	25	55	100	130	120				
Total ash	LAG Z614	%	0.08	0.1	0.07	0.1	0.07	0.2	0.02				
Metal ions													
Mn	ICP-AES	ppm	0.2	0.2	0.3	0.3	0.6	0.5	0.5				
Fe	ICP-AES	ppm	5	3	3	3	3	5	10				
Mg	ICP-AES	ppm	50	10	10	10	15	100	15				
Ca	ICP-AES	ppm	15	15	15	15	20	100	60				
Si	ICP-AES	ppm	20	20	15	15	10	15	10				
<b>Macromolecular properties</b>													
Viscosity	SCAN-CM 15:99	mL g <sup>-1</sup>	450	500	820	820	730	1500	2000				
Mn	GPC-MALLS	kg mol <sup>-1</sup>	58	56	100	100	121	119	722	[36]			
Mw	GPC-MALLS	kg mol <sup>-1</sup>	175	250	400	400	340	950	1300	[36]			
PDI	GPC-MALLS		3.0	4.5	4.0	4.0	2.8	8.0	1.8	[36]			
DP < 100	GPC-MALLS	wt%	2.8	5.0	2.0	2.0	1.5	0.0	0.0	[36]			
DP > 2000	GPC-MALLS	wt%	15.0	25.0	45.0	45.0	38.0	65.0	95.0	[36]			



## References

## Sections 11.1–11.2

- 1 Niskanen, K., *Paper Physics. Papermaking Science and Technology*; J. Gullichsen, H. Paulapuro, Eds. Vol. 16. Fapet Oy, 1998.
- 2 Levlin, J.-E., L. Söderhjelm, *Pulp and Paper Testing. Papermaking Science and Technology*, J. Gullichsen, H. Paulapuro, Eds. Vol. 17. Fapet Oy, 1999.
- 3 Rydholm, S.A., *Pulping Processes*. Malabar, Florida 1965: Robert E. Krieger Publishing Co., Inc., 1965: 1135–1166.
- 4 Young, R.A., Comparison of the properties of chemical cellulose pulps. *Cellulose*, 1994; 1: 107–130.
- 5 Jayme, G., A.v. Köppen, Strukturelle und chemische Unterschiede zwischen Sulfit- und Sulfatzellstoffen. *Das Papier*, 1950; 4(23/24): 455–462.
- 6 Luce, J.E., Radial distribution of properties through the cell wall. *Pulp Paper Mag. Can.*, 1964: 419–423.
- 7 Jayme, G., A.v. Köppen, Strukturelle und chemische Unterschiede zwischen Sulfit- und Sulfatzellstoffen. *Das Papier*, 1950; 4(21/22): 415–420.
- 8 Hamilton, J.K., N.S. Thompson, A chemical comparison of kraft and sulphite pulps. *Pulp Paper Mag. Can.*, 1960: 263–272.
- 9 Yllner, S., B. Enström, Studies of the adsorption of xylan on cellulose fibres during the sulphate cook. Part 1. *Svensk. Papperstidn.*, 1956; 59: 229–234.
- 10 Yllner, S., B. Enström, Studies of the adsorption of xylan on cellulosic fibres during the sulphate cook. Part 2. *Svensk. Papperstidn.*, 1957; 60(15): 549–554.
- 11 Dahlmann, O., J. Sjöberg, Comparative study of different approaches for analyzing carbohydrates at the surface of chemical pulp fibers. In Seventh European Workshop on Lignocellulosics and Pulp. Turku/Abo, Finland: Abo Akademi, 2002; 111–114.
- 12 Pettersson, S.E., S.A. Rydholm, Hemicelluloses and paper properties of birch pulps. III. *Svensk. Papperstidn.*, 1961; 64(1): 4–17.
- 13 Page, D.H., The origin of the differences between sulphite and kraft pulps. *J. Pulp Paper Sci.*, 1983; 9(1): TR15–TR20.
- 14 Page, D.H., The mechanism of strength development of dried pulps by beating. *Svensk. Papperstidn.*, 1985; 88(3): R30–R35.
- 15 Scallan, A.M. In *Fibre Water Interactions in Papermaking*. Clowes: London, 1978.
- 16 Koeppen, A.V., Structural and chemical differences between sulfite and kraft pulps. *Tappi*, 1964; 47(10): 589–595.
- 17 Sixta, H., R. Möslinger, Characterization of commercial paper grade pulps. R&D Lenzing AG, Internal Report: Lenzing, 2004.
- 18 Molin, U., A. Teder, Importance of cellulose/hemicellulose-ratio for pulp strength. *Nordic Pulp Paper Res. J.*, 2002; 17(1): 14–19.
- 19 Jenzen, C.A., The effect of stress applied during drying on some of the properties of individual pulp fibers. *Tappi*, 1964; 47(7): 412–418.
- 20 Röhrling, J., et al., A novel method for the determination of carbonyl groups in cellulose by fluorescence labeling. 2. Validation and applications. *Biomacromolecules*, 2002; 3: 969–975.
- 21 Röhrling, J., et al., A novel method for the determination of carbonyl groups in cellulose by fluorescence labeling. 1. Method development. *Biomacromolecules*, 2002; 3: 959–968.
- 22 Baldinger, T., A. Potthast, Evaluation of keto groups generated along the cellulose chain from combined GPC-CCOA measurement. CD Laboratory, Internal Report: Vienna, 2004.
- 23 Schelosky, N., T. Roder, T. Baldinger, Molecular mass distribution of cellulosic products by size exclusion chromatography in DMAc/LiCl. *Das Papier*, 1999; 53(12): 728–738.
- 24 Kettunen, J., et al., Aspects of strength development in fibre produced by different pulping methods. *Pap. Puu*, 1982; Specialnummer 4: 205–211.

## Section 11.3

- 1 Treiber, E., Charakterisierung von Chemiefaserzellstoffen. *Das Papier*, **1971**; 25(12): 830–833.
- 2 Treiber, E., Probleme bei der Charakterisierung von Chemiefaserzellstoffen. *Faserforschung und Textiltechnik*, **1974**; 25(9): 387–391.
- 3 Treiber, E., The viscose process surveyed from an industrial and laboratory point of view. *Tappi J.*, **46**(10), 594–600.
- 4 Klemm, D., et al., *Comprehensive Cellulose Chemistry*. Vol. 1. Weinheim, Germany: Wiley-VCH Verlag GmbH, **1998**: 9–42.
- 5 Kleinert, T.N., *Z. Angew. Chem.*, **1931**; 44(39): 788.
- 6 Peter, W., Herstellung von Kunstfaserzellstoff nach dem Organosolv-Aufschlußverfahren. *Lenzinger Ber.*, **1986**; 61: 12–16.
- 7 Sixta, H., et al., Evaluation of new organosolv dissolving pulps. part I: Preparation, analytical characterization and viscose processability. *Cellulose*, **2004**; 11: 73–83.
- 8 Kordsachia, O., S. Roßkopf, R. Patt, Production of spruce dissolving pulp with the prehydrolysis-alkaline sulfite process (PH-ASA). *Lenzinger Ber.*, **2004**; 83: 24–34.
- 9 Sixta, H., A. Borgards, New technology for the production of high-purity dissolving pulps. *Das Papier*, **1999**; 53(4): 220–234.
- 10 Rosenau, T., et al., The chemistry of side reactions and byproduct formation in the system NMMO/cellulose (Lyocell process). *Prog. Polym. Sci.*, **2001**; 26: 1763–1837.
- 11 Rosenau, T., et al., Isolation and identification of residual chromophores in cellulosic materials. *Polymer*, **2004**; 45: 6437–6443.
- 12 White, P., Lyocell: the production process and market development. In *Regenerated Cellulose Fibres*, C. Woodings, Ed. Woodhead Publishing Limited: Cambridge, England, **2001**: 62–87.
- 13 Lenz, J., et al., Der Einfluß der Begleit-substanzen des Zellstoffs auf Verarbeitbarkeit und Fasereigenschaften im Viskoseprozeß. *Lenzinger Ber.*, **1981**; 51: 10–13.
- 14 Jayme, G., N. Nikoliew, The reactivity of the hemicelluloses of pulp in the xanthation reaction. *Angew. Chemie*, **1948**; A60: 15–18.
- 15 Micic, M., Correlation between the filtration constant and alpha-cellulose, pentosans, brightness, impurities, mineral substances, resins, and viscose of pulp. *Hemijaska Vlakna*, **1988**; 28(3): 9–13.
- 16 Siclari, F., Polynosic fibres from different types of dissolving pulps. *Pure Appl. Chem.*, **1967**; 14(3–4): 423–433.
- 17 Wilson, J.D., R.S. Tabke, Influence of hemicelluloses on acetate processing in high catalyst systems. In *Dissolving Pulps Conference*. Atlanta, GA: TAPPI, **1973**: 55–68.
- 18 Adorjan, I., et al., Discoloration of cellulose solutions in *N*-methylmorpholine-*N*-oxide (Lyocell). Part 1: Studies on model compounds and pulps. *Cellulose*, **2005**; 12: 51–57.
- 19 Wilson, J.D., R.S. Tabke, Influence of hemicelluloses on acetate processing in high catalyst systems. *Tappi*, **1974**; 57(8): 77–80.
- 20 Gardner, P.E., M.Y. Chang, The acetylation of native and modified hemicelluloses. In *Dissolving Pulps Conference*. Atlanta: Tappi, **1973**: 93–95.
- 21 Neal, J.L., Factors affecting the solution properties of cellulose acetates. *J. Appl. Polymer Sci.*, **1965**; 9(3): 947–961.
- 22 Borgards, A., H. Sixta, Evaluation of Cellulose Triacetate. Lenzing AG, Internal Report, **2000**.
- 23 Conca, R.L., J.K. Hamilton, H.W. Kircher, Haze in cellulose acetate. *Tappi*, **1963**; 46(11): 644–648.
- 24 Wells, F.L., W.C. Schattner, A. Walker, Hemicellulose and false viscosity in cellulose acetate. *Tappi*, **1963**; 46(10): 581–586.
- 25 Sixta, H. et al., Characterisation of alkali-soluble pulp fractions by chromatography, 11<sup>th</sup> Intern. Symp. on Wood and Pulping Chem. (ISWPC), Nice, France, **2001**: 655–658.
- 26 Swan, B., Extractives of unbleached and bleached prehydrolysis-kraft pulp from

- Eucalyptus globulus*. *Svensk. Papperstidn.*, **1967**; 70(19): 616–619.
- 27 Rydholm, S.A., Production and properties of eucalyptus pulp. *Papier*, **1966**; 20(10): 711–720.
  - 28 Croon, I., Resins, waxes, and fats present in wood pulp. *Papier*, **1965**; 19(10A): 711–719.
  - 29 Assarsson, A., H. Jonsén, O. Samuelson, Influence of resin in viscose upon the clogging of spinnerets. *Svensk Papperstidn.*, **1968**; 5: 137–141.
  - 30 Göransson, S., Effect of pulp extractives in the viscose process. *Svensk. Papperstidn.*, **1968**; 16: 533–543.
  - 31 Sixta, H., The use of aspen wood for the production of viscose pulp. R&D Lenzing AG: Lenzing, **2004**.
  - 32 Räsänen, R.H., J. Erva, M. Saaristo. Evaluation of viscose pulp at a pulp mill. In *Dissolving Pulp Conference*. Atlanta, GA: Tappi, **1973**: 25–41.
  - 33 Berzings, V., J.E. Tasman, The relationship of the kappa number to the lignin content of pulp materials. *Pulp Paper Canada*, **1957**; 9: 154–158.
  - 34 Chinchloe, P.R. Residual lignin in dissolving grade pulp. In *Dissolving Pulps Conference*. Atlanta, GA: Tappi, **1973**.
  - 35 Bergner, C., B. Philipp, S. Schulze, Untersuchungen zur Menge und Verteilung mineralischer Verunreinigungen in Buchensulfit-Textilzellstoffen. *Zellstoff und Papier*, **1990**; 39(1): 11–16.
  - 36 Schelosky, N., T. Röder, T. Baldinger, Molecular mass distribution of cellulose products by size exclusion chromatography in DMAC/LiCl. *Das Papier*, **1999**; 53(12): 728–738.
  - 37 Hermans, P.H., The analogy between the mechanism of deformation of cellulose and that of rubber. *J. Phys. Chem.*, **1941**; 45: 827–836.
  - 38 Avela, E., et al., Sulphite pulps for HWM-fibres. *Pure Appl. Chem.*, **1967**; 14(3–4): 289–301.
  - 39 Treiber, E.E., Zellstoffe für Modalfasern. *Lenzinger Ber.*, **1988**; 64: 19–22.
  - 40 Treiber, E. Gegenwärtiger Stand und Zukunftstrend des Viskoseverfahrens und seines Rohstoffes. In 4th International Symposium on Man-Made Fibres. Kalinin, USSR, **1986**.
  - 41 Röhring, J., et al., A novel method for the determination of carbonyl groups in cellulose by fluorescence labeling. 2. Validation and applications. *Biomacromolecules*, **2002**; 3: 969–975.
  - 42 Schleicher, H. and H. Lang, Carbonyl- und Carboxylgruppen in Zellstoffen und Celluloseprodukten. *Das Papier*, **1994**; 12: 765–768.
  - 43 Beyer, M., C. Baurich, K. Fischer, Mechanism of light- and thermal-induced yellowing of pulps. *Das Papier*, **1995**; 49(10A): V8–V14.
  - 44 Beving, H.F.G., O. Theander, Degradation of methyl alpha-D-glucohexo-1,5-dialdopyranoside in aqueous solution. *Acta Chim. Scand., Ser. B*, **1975**; 29(5): 577–581.
  - 45 Baldinger, T., A. Potthast, Evaluation of keto groups generated along the cellulose chain from combined GPC-CCOA measurement. CD Laboratory, Internal Report: Vienna, **2004**.
  - 46 Sixta, H., R. Möslinger, Influence of ozone bleaching with Z-stage in various positions within a TCF sequence on thermal-induced discoloration of a beech sulfite dissolving pulp. R&D Lenzing AG: Lenzing, **2004**.
  - 47 Gratzl, J.S., Lichtinduzierte Vergilbung von Zellstoffen – Ursachen und Verhütung. *Das Papier*, **1985**; 39(10A): V14–V23.
  - 48 Philipp, B., J. Baudisch, W. Stöhr, Zum Einfluß einiger chemischer Faktoren auf den thermischen Abbau der Cellulose. *Cellulose Chem. Technol.*, **1972**; 6: 379–392.
  - 49 Buchert, J., et al., Significance of xylan and glucomannan in the brightness reversion of kraft pulps. *Tappi*, **1997**; 80(6): 165–171.
  - 50 Fink, H., E. Walenta, Röntgenbeugungsuntersuchungen zur übermolekularen Struktur von Cellulose im Verarbeitungsprozeß. *Das Papier*, **1994**; 48: 739–748.
  - 51 Kunze, J., A. Ebert, H.-Fink, Characterization of cellulose and cellulose ethers by means of <sup>13</sup>C-NMR spectroscopy. *Cellulose Chem. Technol.*, **2000**; 34: 21–34.
  - 52 Baldinger, T., J. Moosbauer, H. Sixta, Supermolecular structure of cellulosic materials by FTIR spectroscopy calibrat-

- ed by WAXS and  $^{13}\text{C}$  NMR. *Lenzinger Ber.*, **2000**; 79: 15–17.
- 53 Fink, H.-P., et al., Evaluation of new organosolv dissolving pulps. Part II: Structure and NMMO processability of the pulps. *Cellulose*, **2004**; 11: 85–98.
- 54 Akim, E.L., Manufacture and chemical treatment of dissolving pulps. *Tappi*, **1978**; 61(9): 111–114.
- 55 Steege, H.H., B. Philipp, Production, characterization, and use of microcrystalline cellulose. *Zellst. Pap.*, **1974**; 23(3): 68–73.
- 56 Sixta, H., Comparative evaluation of TCF bleached hardwood dissolving pulps. *Lenzinger Ber.*, **2000**; 79: 119–128.
- 57 Schleicher, H., B. Philipp, Effect of activation on the reactivity of cellulose. *Das Papier*, **1980**; 34(12): 550–555.
- 58 Philipp, B., R. Lehmann, C. Rauscher, Influence of cellulose material on the course of alkali cellulose formation. *Faserforschung und Textiltechnik*, **1959**; 10: 22–35.
- 59 Hinck, J.F., R.L. Casebier, J.K. Hamilton, Dissolving Pulp Manufacturing. In *Sulfite Science & Technology*, J.K.O. Ingruber, P.E. Al Wong, Eds. TAPPI, CPPA: Atlanta, **1985**: 213–243.
- 60 Wallis, A.F.A., R.H. Wearne, Preparation of chemical cellulose from radiata pine bisulfite pulps without using chlorine-containing reagents. *Appita*, **1992**; 45(4): 239–242.
- 61 Sioumis, A.A., A.F.A. Wallis, Chemical celluloses derived from *Pinus radiata* wood pulps for nitrocellulose preparation. *Polymer Int.*, **1991**; 25: 203–209.
- 62 El-Din, N.M.S., F.F.A. El-Megeid, The effect of cold alkali pretreatment on the reactivity of some cellulosic pulps towards acetylation. *Holzforschung*, **1994**; 48: 496–500.
- 63 Temming, H., H. Grunert, Temming linters: technical informations about cotton cellulose, ed. Peter Temming AG. Glückstadt: J.J. Augustin, **1972**.
- 64 Purz, H.J., H. Graf, H.-Fink, Electron microscopic investigations of fibrillar and coagulation structure of cellulose. *Das Papier*, **1995**; 49(12): 714–730.
- 65 Yllner, S., B. Enström, Studies of the adsorption of xylan on cellulose fibres during the sulphate cook. Part 1. *Svensk. Papperstidn.*, **1956**; 59: 229–234.
- 66 Yllner, S., B. Enström, Studies of the adsorption of xylan on cellulosic fibres during the sulphate cook. Part 2. *Svensk. Papperstidn.*, **1957**; 60(15): 549–554.
- 67 Sixta, H., Investigation of xylan precipitation during kraft cooking. R&D, Lenzing AG: Lenzing, **2002**: 8.
- 68 Hüpfel, J., J. Zauner, Testing dissolving pulps by use of a laboratory-scale viscose plant. *Das Papier*, 20(3): 125–132.
- 69 Dahlmann, O., J. Sjöberg. Comparative study of different approaches for analyzing carbohydrates at the surface of chemical pulp fibers. In Seventh European Workshop on Lignocellulosics and Pulp. Turku/Abo, Finland: Abo Akademi, **2002**: 111–114.
- 70 Sjöberg, J., et al., Fiber surface and inner layer analysis of the polysaccharide composition in sulfate and sulfite dissolving pulps using enzymatic peeling and CZE. In 227th ACS National Meeting, Anaheim, CA., **2004**.
- 71 Luce, J.E., Radial distribution of properties through the cell wall. *Pulp Paper Mag. Can.*, **1964**: 419–423.
- 72 Sixta, H., Preparation and characterization of spruce and beech dissolving pulps prepared by both acid sulfite and prehydrolysis kraft cooking. R&D, Lenzing AG: Lenzing, **2002**.
- 73 Gruber, E., S. Ezzat, J. Schurz, Zellstoff-Eigenschaften und Faserlänge. II. Chemische Reaktivität bei homogenen und heterogenen Reaktionen. *Das Papier*, **1976**; 30(4): 133–138.
- 74 Dubach, M., M. Rutishauser, Deresinification of sulfite pulps by fiber fractionation. *Das Papier*, **1957**; 11: 37–43.
- 75 Yaldez, R., Fractionation of beech dissolving pulp. *Lenzinger Ber.*, **2000**; 79: 143–148.
- 76 Maloney, T.C., T. Johansson, H. Paulapuro, Removal of water from the cell wall during drying. *Paper Technol.*, **1998**; 39(6): 39–42, 44–57.
- 77 Maloney, T.C., H. Paulapuro, The formation of pores in the cell wall. *J. Pulp Paper Sci.*, **1999**; 25(12): 430–436.
- 78 Stone, J.E., A.M. Scallan, Studies of component removal upon the porous structure of the cell wall of wood. II.

- Swelling in water and the fiber saturation point. *Tappi*, **1967**; 50(10): 496–501.
- 79 Stone, J.E., A.M. Scallan, Structural model for the cell wall of water-swollen wood pulp fibers based on their accessibility to macromolecules. *Cellulose Chem. Technol.*, **1968**; 2(3): 343–358.
- 80 Bredereck, K., W.A. Schick, E. Bader, Characterization of the pore structure of water-swollen cellulose fibers. *Makromolekulare Chemie*, **1985**; 186(8): 1643–1655.
- 81 Bredereck, K., A. Blueher, A. Hoffmann-Frey, The determination of pore structure of cellulose fibers by exclusion measurement. *Papier*, **1990**; 44(12): 648–656.
- 82 Jayme, G., L. Rothamel, Development of a standard centrifugal method for determining the swelling values of pulps. *Papier*, **1948**; 2: 7–18.
- 83 Scallan, A.M., J.E. Carles, Correlation of the water retention value with the fiber saturation point. *Svensk. Papperstidn.*, **1972**; 75(17): 699–703.
- 84 Urquhart, A.R., The mechanism of adsorption of water by cotton. *J. Textile Inst.*, **1929**; 20: T125–T132.
- 85 Newman, R.H., J.A. Hemmingson. Cellulose cocrystallization in hornification of kraft pulp. In 9th International Symposium of Wood and Pulp Chemistry. Montreal, Canada, **1997**.
- 86 Röder, T., H. Sixta. Thermal treatment of cellulose pulps and its influence to cellulose reactivity. In ISWPC. Madison, WI, **2003**.
- 87 Gruber, E., C. Schneider, W. Schempp, Measuring the extent of hornification of pulp fibers. *Int. Papierwirtsch.*, **2001**; 4: T72–T75.
- 88 Fischer, K., W. Goldberg, M. Wilke, Radiation pre-treatment of pulp for the production of regenerated fibre production. *Lenzinger Ber.*, **1985**; 59(8): 32–37.
- 89 Kuhn, W., Kinetics of the destruction of high-molecular chains. *Ber. Chem. Dtsch. Ges.*, **1930**; 63: 1503–1509.
- 90 Philipp, B., Struktur und Reaktivität der Cellulose als Schwerpunkte der Celluloseforschung im Institut für Polymerenchemie in Teltow-Seehof. *Das Papier*, **1991**; 12: 764–772.
- 91 Krässig, H.A., *Cellulose: Structure, Accessibility and Reactivity. Polymer Monographs*. M.B. Huglin, Ed.. Vol. 11. Gordon and Breach Science Publishers, **1993**: 258–323.
- 92 Schenker, C., M.A. Heath, Development of high purity dissolving wood pulp for tire cord production. *Tappi*, **1959**; 42(8): 709–712.
- 93 Patt, R., D.L.-K. Wang, Qualitätsbeurteilung von Chemiezellstoffen. Teil 2: Alkalilöslichkeit und Gesamtzuckeranalyse. *Das Papier*, **1987**; 41(1): 7–12.
- 94 Methylenblue method, In *Methods in Carbohydrate Chemistry*, Academic Press, New York, ed.: R.L. Whistler, Vol. III, 35–36.
- 95 Steinmeier, H., Acetate manufacturing, process and technology. Chemistry of Cellulose Acetylation. In *Macromol. Symp.* 208; [Cellulose Acetates: Properties and Applications, ed.: R. Rustemeyer, Wiley-VCH], **2004**, 49–60.

## II

### **Mechanical Pulping**

*Jürgen Blechschmidt, Sabine Heinemann, and Hans-Ulrich Süss*



## 1

## Introduction

*Jürgen Blechschmidt and Sabine Heinemann*

There are two technological principles to produce paper pulp from wood, namely mechanical processes or chemical processes. Whereas in chemical pulping the yields are only about 45–55%, mechanical pulping uses about 80–95% of the fiber wood. Whilst this represents a source for the economic potential of mechanical pulps, the higher yield results in certain unfavorable properties compared to chemical pulp. Thus, from the same portion of wood, a double quantity of mechanical pulp is produced compared to chemical pulp. The increasing demand for paper and board has led to a permanent increase in mechanical pulp production (Fig. 1.1).

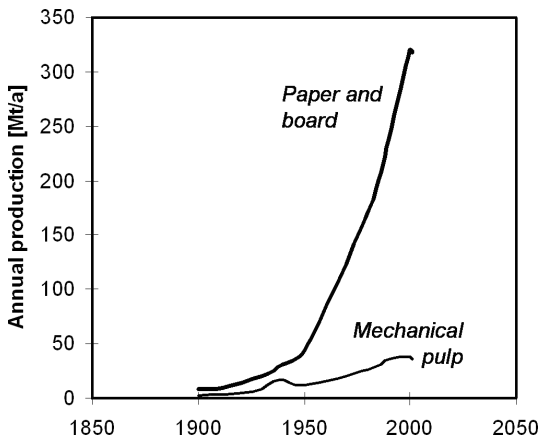


Fig. 1.1 Worldwide development of mechanical pulp production [1].

Among the total amount of paper pulp produced, mechanical pulp accounts for about 20%.

Although mechanical pulping is a thermomechanical process, chemical processes may also play a certain role. The mechanical defibration of wood is carried out in two different ways (Fig. 1.2), namely as a grinding process or as a refining process. The following definitions have been formulated for the products of those processes:

- Mechanical pulp: this is manufactured by mechanical defibration using a variety of mechanical procedures.
- Stone groundwood: this is manufactured from round logs in a grinder.
- Refiner mechanical pulp: this is manufactured by the mechanical defibration of wood chips in a disc refiner.

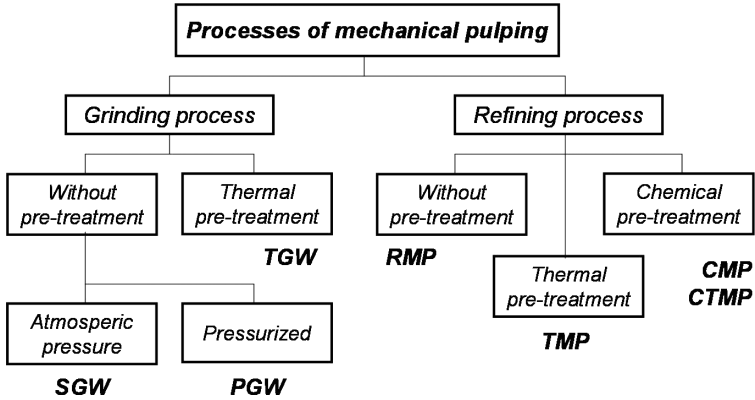


Fig. 1.2 An overview of the basic mechanical pulping procedures.

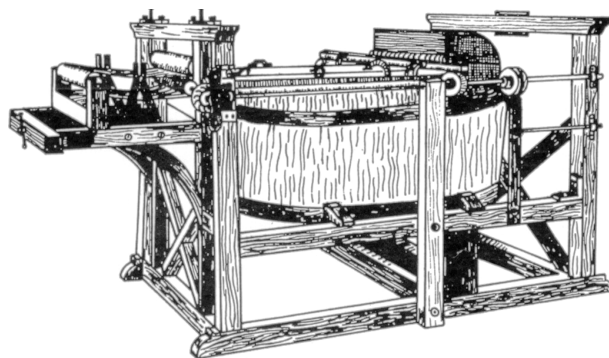
## 2

### A Short History of Mechanical Pulping

*Jürgen Blechschmidt and Sabine Heinemann*

Along with the development of mankind there has been an ever-increasing demand for writing materials. It is said that papermaking was invented in China in the year 105 AD and, after a long journey, the procedure arrived in Europe in 1144 (Spain) and finally in Germany in 1390 (Nuremberg). When Gutenberg invented letterpress printing in 1445, to replace hand-written books with printed books, the demand for paper increased immensely. During this evolution, the raw materials used for paper have ranged from rags to hemp, and from flax and cotton as well as worn-out hemp ropes.

Up until the end of the eighteenth century, paper was only made by hand, but in 1799 Nicolas-Louis Robert developed the first papermaking machine in France (Fig. 2.1).

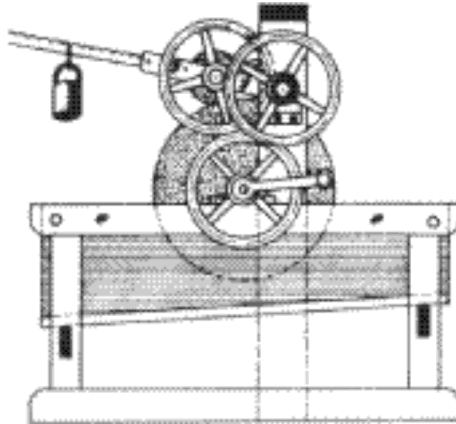


**Fig. 2.1** Papermaking machine, developed in 1799 by N.-L. Robert (1761–1826).

At about in the same time, in 1805, Bramah invented the cylinder machine in England, and as a result of these inventions paper production was subsequently increased during the following years. The problem was that this increased production resulted in an increasing lack of raw materials.

In 1843, the Saxon weaver Friedrich Gottlob Keller (Fig. 2.2) successfully developed the mechanical defibration of wood to produce groundwood. "Because this

epochal invention turned the paper production into a totally new direction, it represents – together with the invention of the paper machine – one of the largest technical progress since the invention of paper itself” [2].



**Fig. 2.2** Left: Friedrich Gottlob Keller (1816–1895), the inventor of stone groundwood. Right: the second version of Keller's grinding machine.

### 3

## Raw Materials for Mechanical Pulp

*Jürgen Blechschmidt and Sabine Heinemann*

### 3.1

#### Wood Quality

The quality of wood obtained from the forest is of special importance for mechanical pulping. This raw material that is useful for mechanical pulp and chemical pulping is often also termed “pulpwood”. In mechanical pulping, the requirements of fiber wood are higher for grinding than for refining. The most important requirements of fiber wood include:

- Wood quality: The wood should be healthy, possibly grown straight, less knotty and free from rot.
- Wood moisture: The moisture of the wood should be as high as possible. It should be over 35% in order to exceed the fiber saturation point.
- Wood diameter: Useful wood diameters in grinding are 10–20 cm. In refining, the thinnings (diameter 7–10 cm) can also be processed.
- Debarking state: Three different debarking states can be distinguished for the wood:
  - Bark is completely removed from wood (tanned, white peeled).
  - Bark is removed from wood with some retention of phloem (spotted, barked).
  - Wood is completely or partly surrounded by bark (not debarked).
- Resin content: A high resin content in wood is disadvantageous in mechanical pulping as it causes foam; the situation is especially poor with pine.
- Wood species: Spruce uniquely serves the purpose for mechanical pulping, especially in grinding. In refining procedures, both softwood and hardwood species can be processed. Poplar and aspen are also suitable for grinding.

In mechanical pulping, those fibers that are responsible for strength properties are of major importance. In softwood, these are tracheids, and in hardwood they are the libriform fibers. Tracheids cover about 90% of cell material in softwood

species, whilst in hardwoods the amount of libriform fibers differs, depending upon the wood species. As a mean value, they cover only 50% of the cell material, and this is the reason why different wood species show different suitabilities in mechanical pulping.

## 3.2

### Processing of Wood

#### 3.2.1

##### Wood Log Storage

In mechanical pulping, the wood should have a high moisture content, and the processing of forest-fresh wood is the best way to achieve this. The storage period of wood should be of short duration, and the wood should be processed in as fresh a state as possible. Nevertheless, most mills have high-capacity wood storage units with capacities of between 10 000 and 500 000 m<sup>3</sup>.

The storage of wood can be performed using four basic approaches:

- as irregular round log stacks (piles)
- as round log water storage
- as chip storage for refiner pulps
- as regular round log stacks

Today, irregular piles are the preferred storage form, with the cone-shaped piles reaching heights of up to 30 m and being fed by so-called stackers. In summer, and in order to keep the moisture content high enough, water sprayers are used. Water storage – or even better, under-water storage – is the best way to maintain a high moisture content of the wood. For this, the wood is stored in bundles in lakes, sea bays or watering ponds, with the log bundles being moved and turned using special boats.

#### 3.2.2

##### Wood Log Debarking

For further processing, the wood must be debarked. Bark cells are formed outside the living part of the tree (the cambium), and consist of the phloem (inner bark) and bark (outer bark). Phloem cells are responsible for the transportation of assimilates and storage, while the bark protects the living parts of the wood from drying, temperature influences or damage. Depending on the wood type, the thickness of the bark layer is between 2 and 40 mm. This corresponds to a bark portion of 5 to 28%, in relation to the total wood stem.

The different chemical and morphological composition of the bark compared to that of the wood makes it necessary to remove the bark from the wood before mechanical pulping is carried out. Bark particles are responsible for dirty points in the paper and reduced paper quality. The higher the quality of the paper, the

fewer bark particles should be retained on the wood stems after debarking. In line with the morphological construction of the bark layer, bark removal should take place at the contact area between the phloem and cambium. One measure of characterization of the ability to wood be debarked is the debarking resistance or the power and force, respectively, per  $\text{cm}^2$  of bark that is needed to remove the bark from the wood stem. Debarking resistance is influenced by:

- Wood type
- Felling time (season)
- Moisture content of the wood
- Storage duration of the wood
- Temperature in the cambium area
- Type of pretreatment

For example, debarking resistance is highest for birch, followed by spruce and pine, but it also depends very heavily on the felling season of the wood (Fig. 3.1). Seasonal differences in debarking resistance are also related to the morphological differences, depending on growth. During spring and summer, when cell division activity is very high, the radial walls of the cambial cells and the neighboring phloem cells are very thin and weak, and at this time the debarking resistance is low. However, if cell division activity is low or is stopped, and liquid transportation through the cells is very restricted, debarking resistance is increased significantly.

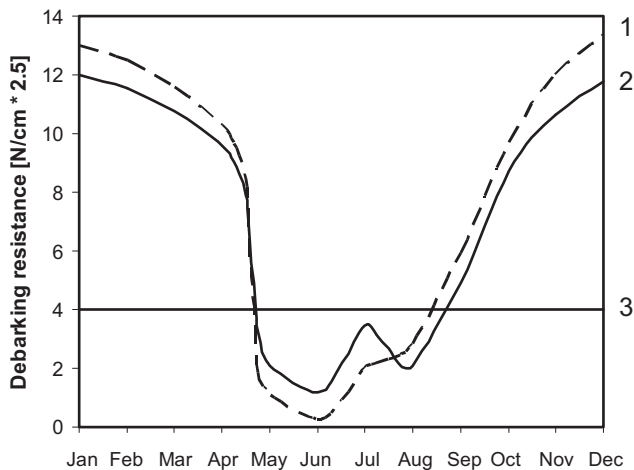


Fig. 3.1 Seasonal development of debarking resistance.

1, Transversal resistance; 2, Longitudinal resistance; 3, Tanning limit.

Debarking resistance also increases with decreasing moisture content of the wood. Wood that has been stored under dry conditions for a longer time has a higher debarking resistance. When the type of storage keeps the moisture content high and rather constant, a longer storage time does not increase the debarking resistance to any great degree. In order to maintain the state of low debarking

resistance from wood that has been felled in the spring, water storage would be the best approach.

Although wet debarking may be carried out with a lower debarking resistance and better debarking results, dry debarking in continuous drum debarkers is preferred in the industrial situation in order to avoid problems of pollution and also to achieve lower investment costs (shorter drum constructions, no effluent treatment). For technical applications of dry debarkers, see Chapter I-3, Wood yard operations.

### 3.2.3

#### Wood Log Chipping

The uniformity of chip size distribution, bulk density and wood source are the most important factors that determine chip quality for mechanical pulping. The average chip length of 22 mm is less than that of chips used for kraft pulping. The shorter the chip is along the grain, the more fibers have been cut; consequently, short chips result especially in a lower tear strength. The impact of extreme chip fractions on thermomechanical pulp (TMP) are detailed in Tab. 3.1.

**Tab. 3.1** Impact of extreme chip size fractions on thermomechanical pulp processing and quality.

Chip fraction	Impact
Over-large fraction	<ul style="list-style-type: none"> <li>– Causes uneven feed to the refiner.</li> <li>– Reduces pulp quality.</li> </ul>
Over-thick fraction	<ul style="list-style-type: none"> <li>– Contains most knot wood present in groundwood logs.</li> <li>– Causes unstable refining and increase of energy consumption.</li> <li>– Decreases fiber length and long fiber portion.</li> <li>– Impairs strength properties and brightness.</li> </ul>
Fines fraction	<ul style="list-style-type: none"> <li>– Lowers energy consumption.</li> <li>– Decreases pulp strength, sheet density, brightness and light-Scattering coefficient.</li> <li>– Increases shives content and causes linting problems.</li> </ul>

The technical applications of wood chipping are explained in detail in Chapter I-3, Wood yard operations.



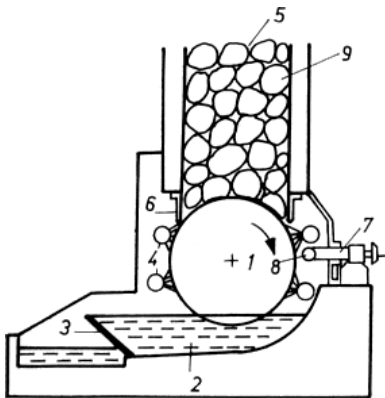
## 4 Mechanical Pulping Processes

Jürgen Blechschmidt and Sabine Heinemann

### 4.1 Grinding Processes

#### 4.1.1 Principle and Terminology

Round logs are pressed against a rotating pulp stone under specified conditions of pressure and temperature (Fig. 4.1).



**Fig. 4.1** Grinding principle. 1, Pulp stone; 2, grinder pit; 3, weir; 4, shower water pipe; 5, wood magazine; 6, finger plate; 7, pulp stone sharpener; 8, sharpening roll; 9, wood logs.

Depending on the position of the log in the grinder magazine, it can be distinguished between:

- Transversal groundwood: Wood logs (and evidently also the fibers) are loaded in the magazine or pocket of the grinder transversally (perpendicularly) to the rotational direction of the stone (in practice the only used orientation).
- Longitudinal groundwood: Wood logs are loaded parallel to the rotational direction of the stone (only applied in research studies).

Grinding procedures may be categorized as atmospheric grinding, pressure grinding, and thermo grinding. The principles of each process are illustrated schematically in Fig. 4.2.

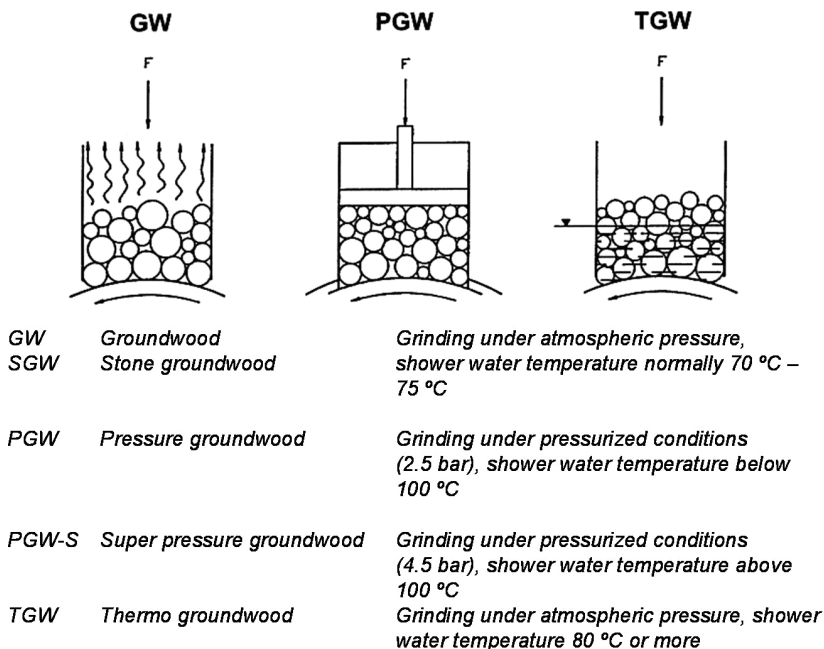


Fig. 4.2 Principles of the grinding procedures.

#### 4.1.2

#### Mechanical and Thermal Processes in Grinding

Grinding is a thermomechanical process that is divided into two parts, each of which overlaps one another: (a) Softening and breakdown of the fiber structure; and (b) peeling of the softened fibers from the wood matrix in the grinding zone

##### 4.1.2.1 Softening of the Fibers

The wood logs are pressed against a rotating pulp stone, applying suitable pressure and temperature conditions (see Fig. 4.2). Just before entering the grinding zone, the wood logs are still cold and thermally untreated. The stone grits pass over the wood matrix at very high frequencies. In a so-called compression/decompression process, the fibers are cyclically stressed or relaxed. Depending on the rotational speed of the pulp stone, and also on the surface profile of the stone, pressure pulsations up to 40 kHz occur on the logs.

The fiber matrix is loosened due to the fatigue work done by the grits. Finally, when they enter the boundary area between the revolving stone surfaces, the

fibers are peeled from the outermost layer of the softened wood, much in the same way that tape is torn from a paper surface. Both processes warm up the wood and break down the fiber structure. Due to the viscoelastic nature of the wood, the temperature at 1–2 mm above the actual grinding zone increases very quickly, and this rise in temperature causes the lignin to soften. The resulting so-called “softening temperature” depends on the water content of lignin and the frequency. In 1963, Goring [3] demonstrated how the softening temperature of lignin is dependent upon the water content (Fig. 4.3).

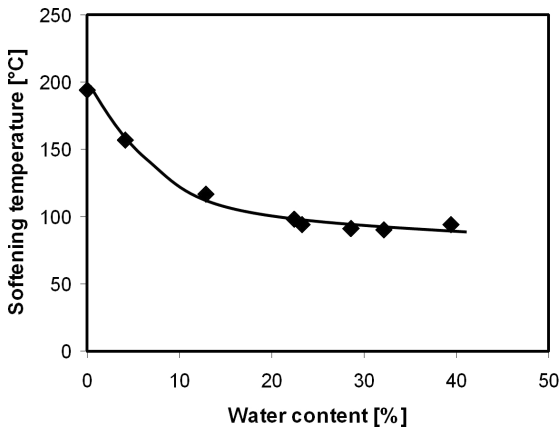
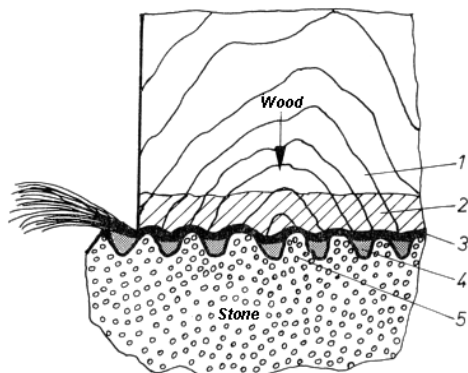


Fig. 4.3 Softening temperature of lignin depending on water content (according to Goring [3]).

The softening temperature is understood to represent the transition of an amorphous polymer such as lignin from a glass-like and brittle state into a weak and plastic one. Goring [3] identified the softening temperatures for lignin as 135 °C to 235 °C, whereas according to Styan and Bramshall [4] the softening temperatures for softwoods are about 135 °C and for hardwoods about 100 °C. In lignin, the plasticizing effect of water has a limit at water contents as low as 5%. For water-saturated isolated lignin, the softening takes place at 80–90 °C, and additional water does not result in any considerable further softening of lignin. Under typical mechanical pulping conditions, the softening temperature for lignin as part of the wood fiber matrix is higher (in the range of 100–130 °C). The lignin polymer, being the stiffest wood component under the conditions used in mechanical pulping, represents the most important component for the thermal softening of wood. Preferably, wood for mechanical pulping should have a moisture:wood ratio of over 0.5.

Knowledge of the thermal processes in grinding is important step when completing the grinding process. In evaluating investigations made by Luhde [5], the relationship between thermal relationships during grinding process is illustrated schematically in Fig. 4.4, while the five temperature-dependent regions of Fig. 4.4 are described in more detail in Tab. 4.1.



**Fig. 4.4** Thermal relationships in the grinding process.  
1, Cool wood; 2, strongly heated wood layer; 3, actual grinding zone; 4, fiber suspension zone; 5, pulp stone surface.

**Tab. 4.1** Temperatures at different zones during the grinding process.

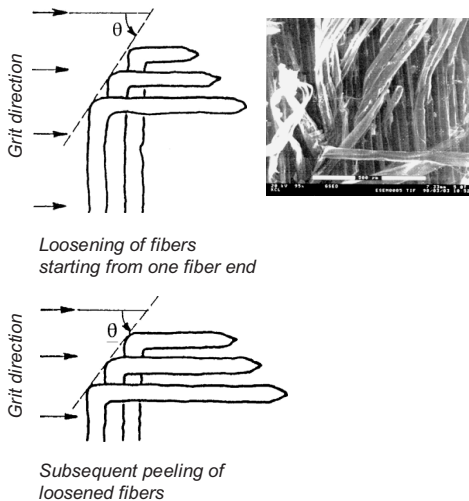
Zone	Temperature	Process
1 <i>Cold wood</i>	Depending on surrounding temperature (related to season)	The wood is cold and thermally untreated when entering zone 2.
2 <i>Strongly heated wood layer</i>	100–170 °C	The temperature in the wood about 0.1 mm above the grinding zone is high, due to by heat impound, but below the carbonizing temperature of wood (206 °C) [6]. These high temperatures are the reason for the softening of lignin. The resulting equilibrium temperature depends on the water content in the wood.
3 <i>Actual grinding zone</i>	80 °C (SGW) 125 °C (PGW)	The actual grinding zone is only ca. 0.1 mm thick (according to Steenberg and Nordstrand [7]), and has a temperature usually close to 100 °C (higher in pressurized grinding). This temperature increases with increasing pit consistency and pit temperature. At this point, the fibers are deliberated from the fiber compound. Here, the resulting equilibrium temperature also depends on the water content in the wood.
4 <i>Fiber suspension zone</i>	80–100 °C (SGW) 100–140 °C (PGW)	It is assumed that the temperatures in the pulp suspension zone and the actual grinding zone are similar. The pulp suspension is a mixture of water, fibers and broken fiber parts moving along the grinding zone towards its end. This pulp suspension also acts as a lubricating and cooling agent.
5 <i>Pulp stone surface</i>	100 °C or more	The surface temperature of the pulp stone is under 100 °C, and depends on the shower water temperature and pit consistency.

It can be summarized that the temperatures in the grinding zone vary over a wide range, depending on the moisture content of the wood and of the system used (atmospheric or pressurized grinding). According to Steenberg and Nordstrand [7], the actual grinding zone is only 0.1 mm thick. Above this zone, the temperatures in the wood are higher. In practical trials, Attack and May [8] have measured the upper limit of the wood temperature as 206 °C, which corresponds to the carbonizing temperature.

#### 4.1.2.2 Defibration (Deliberation) of Single Fibers from the Fiber Compound

The pressure pulsations cause deformation of the fibers in the wood. Because of the macro structure of the pulp stone surface, the fibers will be compressed and expanded with frequencies from 40 kHz. This leads to a breakdown of intermolecular bondings between the fibers and of intramolecular bondings within the fiber, as described by Attack and Pye [9]. The breakdown of bonds is the basic prerequisite for delibration of the fibers from the wood. In addition, these deformations support the water absorption of lignin.

The pulp stone grit, when meeting the fiber, causes “treatment” of the fiber surface. Depending on the macrostructure and microstructure of the pulp stone surface, the fiber will be crushed, scratched, compressed, sheared off and cut. The strict subsequent loosening and peeling of fibers from wood surface, starting generally from one end of the fiber, is shown schematically in Fig. 4.5. The fiber surface will be fibrillated, the primary wall is opened, and finally the fiber delibrated from the fiber compound, with the “treatment”-phase lasting only 20–40 ms. The higher the feeding speed of wood, the less a single fiber is treated until the next grit appears.



**Fig. 4.5** Schematic diagram of fiber loosening and peeling in a grinding process (according to Attack [10]).

## 4.1.3

**Influence of Parameters on the Properties of Groundwood**

In the mechanical defibration of wood by grinding, several process parameters have significant influences on the final properties of the stone groundwood. Among these, the most important include:

- Moisture of the wood logs
- Logs feeding speed or grinding pressure respectively
- Pulp stone rotational speed
- Temperatures
- Process consistency
- Surface profile of the pulp stone
- Specific grinding energy consumption

Basically, it can be said that an increase in grinding pressure produces a groundwood with better dewatering behavior (high freeness) and less strength properties, assuming that all other parameters are kept constant. Such pulps are coarse groundwoods, whereas pulps with low freeness are fine groundwoods. Increasing the pulp stone speed, and keeping all other conditions constant, produces a pulp with shorter fibers and lower freeness.

From a practical standpoint, the efficiency of the grinding process will be improved by increasing both parameters – grinding pressure *and* pulp stone speed. However, the relationship between both of these parameters can be held constant and high-quality groundwood produced.

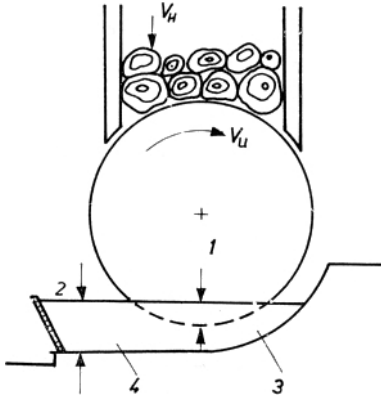
The temperature relationship during grinding also affects the properties of the final groundwood. Functions which describe the temperature relationship in grinding include:

- Temperature of the pit pulp
- Temperature of the shower water
- Temperature at the end of the grinding zone

In practice, the temperature of the pit pulp is used to control the grinding process, with typical shower water temperatures of 60–75 °C being used in atmospheric grinders.

The pit consistency, in practical terms, is set from 1.0% to 2.5%, and interacts with the pit temperature. Increasing the pit consistency also enables the pit temperature to be increased, at constant shower water temperature. Depending on either the pit consistency or possible stone immersion in the pit (Fig. 4.6), a certain amount of pit pulp is transported with the stone and passes back into the grinding zone. Here, regrinding takes place, so that the pulp suspension from the grinder pit is passed to the grinding zone instead of the shower water.

A deeper immersion of the stone into the pit, or a higher weir height in the pit, leads to a larger quantity of circulating pulp. The stone surface will be lubricated by pulp particles and appears duller than it really is, and this in turn reduces the freeness of the pulp.



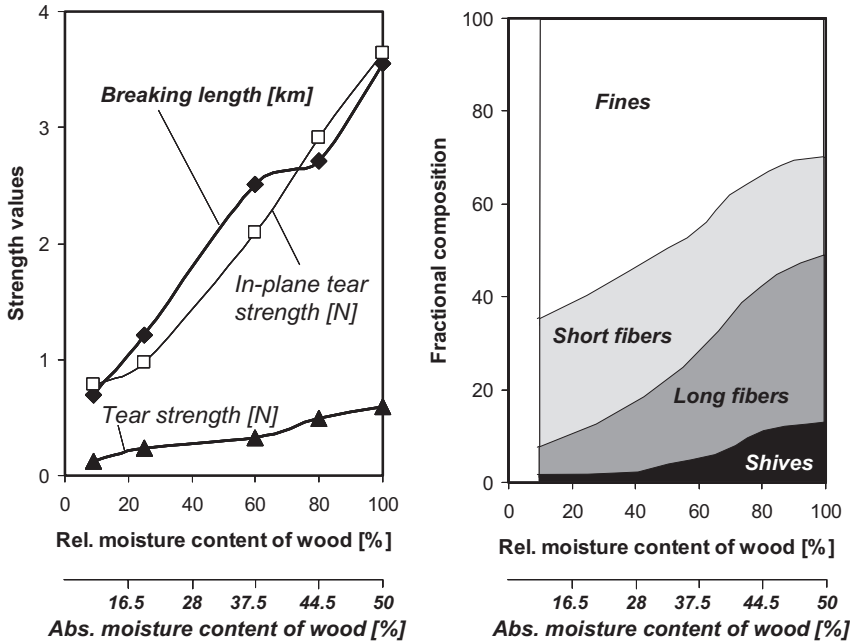
**Fig. 4.6** Pulp stone immersion and weir height in grinding. 1, Pulp stone immersion; 2, weir height; 3, grinder pit; 4, measuring point of pit temperature and pit consistency;  $V_H$ , feeding speed = grinding pressure;  $V_U$ , pulp stone rotational speed.

A high shower water pressure [at least 350 kPa (3.5 bar)] and the position of the shower water pipes at front of the grinding zone cleans the pulp stone surface, and complete stone sharpening can occur. If pit-less grinding is carried out, these influences and interactions disappear, while high shower water pressures are applied.

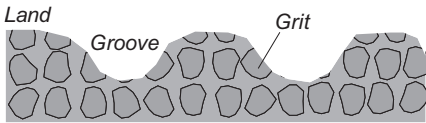
The moisture of the wood is the most important parameter in grinding, as high-quality pulp can be produced from moist wood, at a lower specific grinding energy consumption. Neither technical nor technological developments can replace the effect of moisture in wood. The highest possible quality values are not found in the range of fiber saturation (moisture of wood  $\geq 23\%$ ), but rather at a wood saturation of 50–60% moisture content. The request by grinding mills to receive pulpwood with at least 30% moisture content represents an objective need for the optimal use of a wood source.

Groundwood made from logs with a higher moisture content has a higher brightness, higher strength properties (see Fig. 4.7), and a higher long fiber content with high-quality fines.

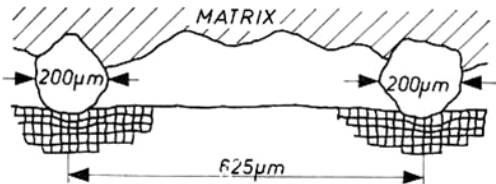
The pulp stone requires a certain surface structure (stone surface profile) to produce a certain pulp quality, and distinction must be made between the macrostructure and microstructure of that profile. The macrostructure is gained by sharpening of the stone (see also Section II-4.1.4). A typical sharpness profile is shown in Fig. 4.8, while the grit material of the pulp stone estimates the microstructure (Fig. 4.9).



**Fig. 4.7** Influence of wood moisture content on groundwood properties. Left: Effect on tensile strength and tear strength. Right: Effect on fractional composition.



**Fig. 4.8** Cross-section of a pulpstone pattern.

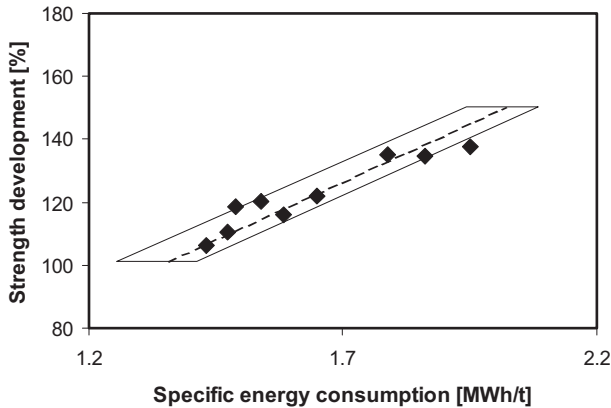


**Fig. 4.9** Ideal grit positioning (according to Attack).

The mechanical defibration of wood to groundwood is a highly energy-intensive process. The specific grinding energy consumption can be used to characterize the energy used, and with this the groundwood quality. In grinding, values between  $0.6 \text{ MWh t}^{-1}$  and  $2.0 \text{ MWh t}^{-1}$  o.d. pulp are typical for the production of



pulp grades from board to high value printing pulps. Thus, high specific energy consumption will lead to the production of a finer groundwood pulp with higher strength properties (see Fig. 4.10). The parameter of specific grinding energy consumption is of major importance for process control in grinding.



**Fig. 4.10** Strength properties of stone groundwoods, depending upon specific grinding energy consumption (according to Süttinger [22]).

#### 4.1.4

#### **Grinders and Auxiliary Equipment for Mechanical Pulping by Grinding**

A typical flow sheet for a groundwood process is shown in Fig. 4.11.

Today, grinding can strictly be divided into two different processes – atmospheric and pressurized grinding. In contrast, the ring grinder, which operates in a totally different manner (Fig. 4.12), was developed in 1939 and used in the USA and Canada. The manually fed logs are ground inside a drum, but this system has now almost disappeared completely because of the very high manual effort involved.

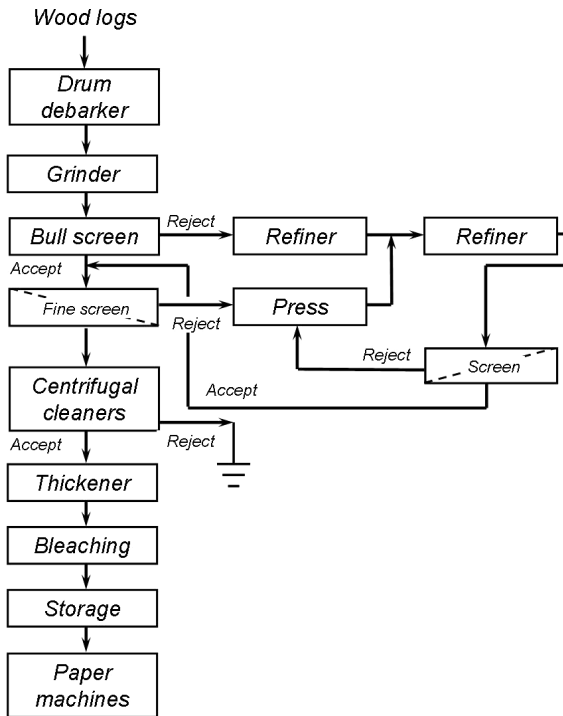


Fig. 4.11 A typical flow sheet for a groundwood process.

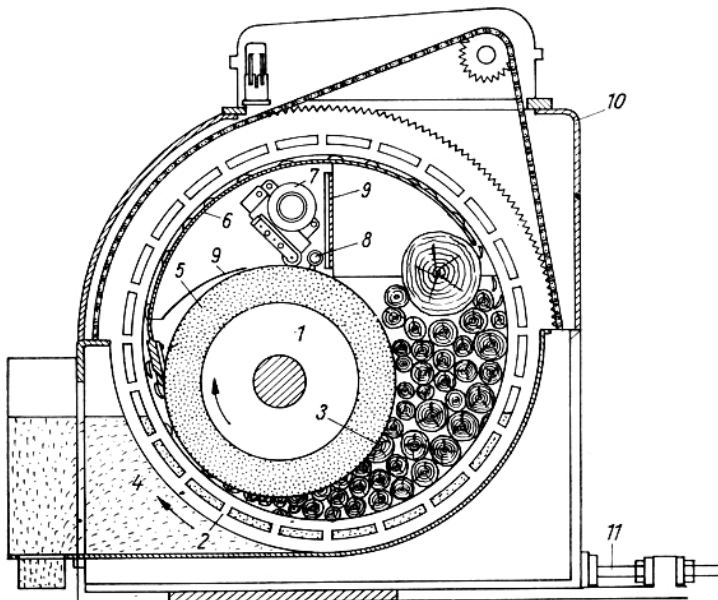
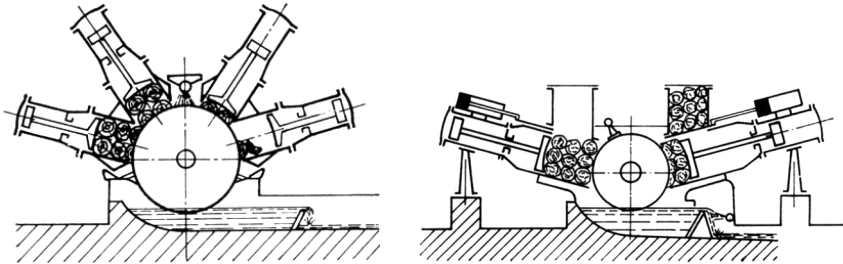


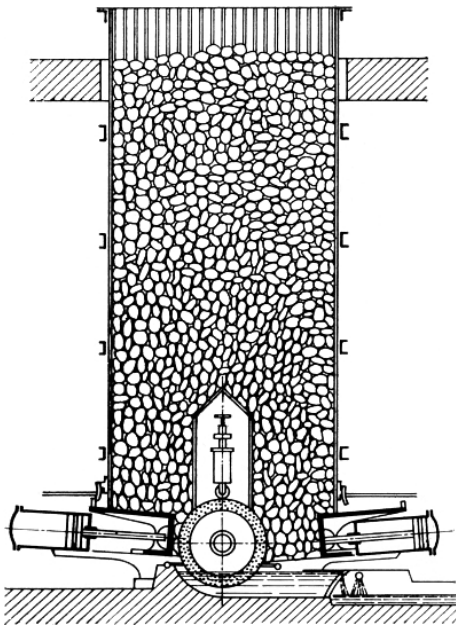
Fig. 4.12 A ring grinder.

#### 4.1.4.1 Pocket Grinders

Pocket grinders were the first designs of industrial grinders, and were further developed from the spindle-type grinder (first built in 1867). Figure 4.13 (left) shows a pocket grinder with four magazines that has to be fed manually. A further development of the pocket grinder is the magazine-type grinder (Fig. 4.14), which was first built in 1910 to improve the manual feeding of logs to the pockets.



**Fig. 4.13** Pocket grinders. Left: A pocket grinder with four magazines. Right: An atmospheric, two-pocket grinder.



**Fig. 4.14** A magazine-type grinder.

Today, pocket grinders are widely used in Scandinavia and America as two-pocket grinders (Fig. 4.13, right). The two-pocket pocket grinder has, in accordance with its name, two separate grinding pockets that operate batch-wise. The

magazine above a pocket can hold just one pocket filling of logs. Irrespectively as the one pocket filling is pressed hydraulically towards the pulp stone and grinded, the other pocket can be filled for the next batch. Today, the Metso grinders have pulp stone diameters of 1.8 m, and both grinding zones are from 1.0 to 1.5 m in length. The width of the feeding gate opening is 600 mm, and the pocket reloading time is approximately 30 s. A hydraulic pressure of between 1.2 and 5 MPa (12 and 50 bar) – it is about 120 kPa and 500 kPa on the wood – moves the logs towards the pulp stone.

The advantages of modern pocket grinders compared to chain grinders include:

- Small design height
- Simple operating
- Short pocket changing times
- Quick pulp stone change

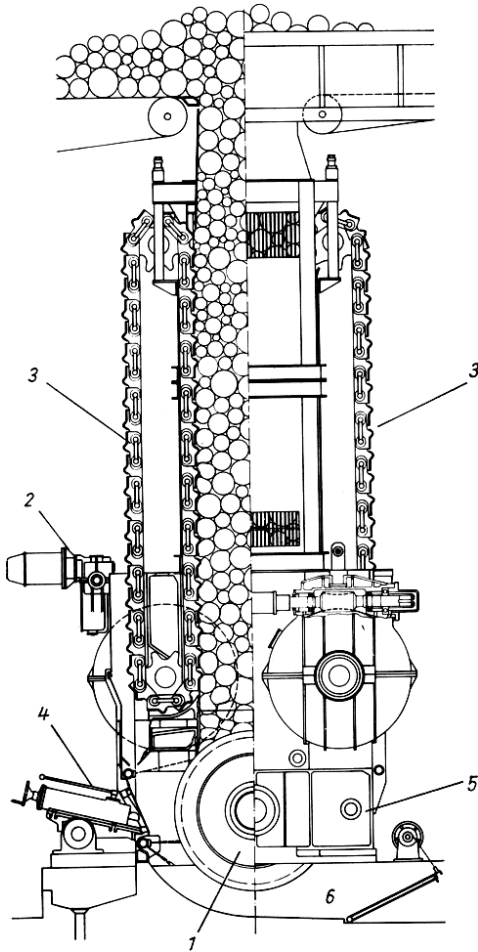
The increased importance of the pocket grinders is related to the development of pressurized grinding (see Section II-4.1.5).

#### 4.1.4.2 Chain Grinders

The chain grinder, which is widely distributed throughout Europe, except for Scandinavia, was first designed 1921 by Voith, in Heidenheim. The operating principle is shown schematically in Fig. 4.15. The logs are stored in the log magazine, located above the pulp stone. From the magazine, the logs are caught by the cams of the permanent moving chain elements and pressed down continuously towards the pulp stone with a pressure which is related to the feeding speed. The chains are driven hydraulically by gears or screw gears (Fig. 4.16), and the magazine is fed continuously, as shown in Fig. 4.17.

The chain grinder operation can be controlled either by constant feed (grinding pressure) or by constant load, though from a technological aspect the constant-pressure operation is preferred. The pulp produced has an even quality, although problems with automatic feeding (e.g., uneven log distribution) cause load fluctuations, and a better approach with regard to economy of energy may be to operate under constant load.

Today, chain grinders are designed with up to 5 MW driving power, and pulp stone speeds of  $30 \text{ m s}^{-1}$  (circumferential speed). A daily production may be up to 70 t, with log lengths of 1–1.5 m and pulp stone diameters of 1.5, 1.6, 1.8, 1.9 or 2.0 m. Water is important as a lubricant and a cooling agent. A shower water flow of  $2000\text{--}3000 \text{ L min}^{-1}$  have pressures of 350 to 600 kPa (3.5–6 bar). Coming from closed loops, the shower water must be filtered to remove, for example, pulp particles. The weir level can be regulated either manually or by mechanical adjustment of the overflow.



**Fig. 4.15** The chain grinder. 1, Pulp stone; 2, feeding drive; 3, feeding chains; 4, stone sharpening equipment; 5, shower water pipe; 6, grinding pit.

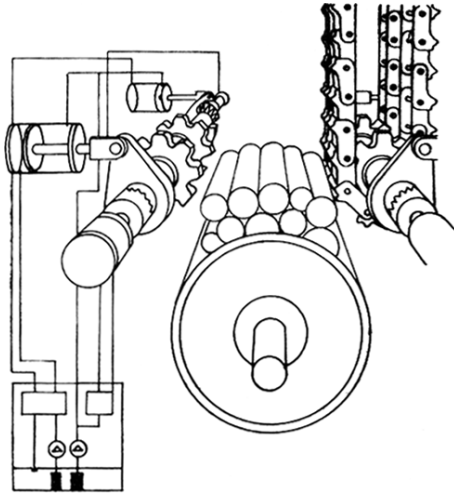


Fig. 4.16 The feeding hydraulics system in a chain grinder.

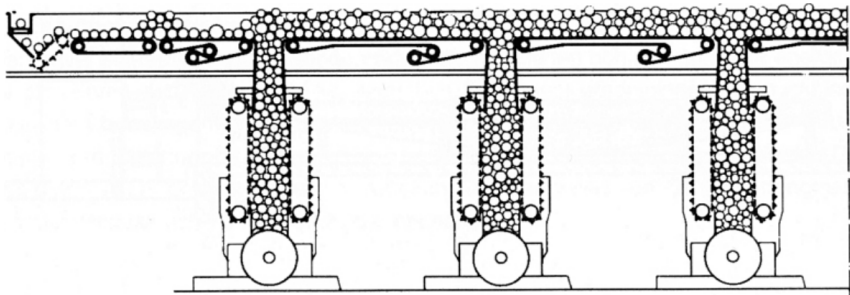


Fig. 4.17 The continuous feeding system for a chain grinder.

Several scientific-technological investigations and further developments, especially in the field of grinding control, have allowed the optimization of chain grinding to obtain modified groundwood pulps. One example is the thermo groundwood (TGW), as introduced by Voith in 1984. The most important difference to the conventional chain grinder is the temperature impound in the grinder shaft (the lower part of the log magazine) and control of the grinding zone temperature.

#### 4.1.4.3 Pulp Stones

The pulp stone is the most important part of the groundwood process. During the early days of industrial grinding natural stones were used, but for more than 100 years these have been replaced by artificial pulp stones. In Europe, the pulp stones were made from cement-based concrete, whilst in North America the modern-day

ceramic-based stones were developed. The use of artificial stones has enabled tailor-made surface structures of the pulp stones to be developed. After an exact adjustment of the pulp stone, it is fixed on the grinder shaft with flanges (see Fig. 4.18), and the free distance between the stone and flange is sealed with either concrete or sulfur.

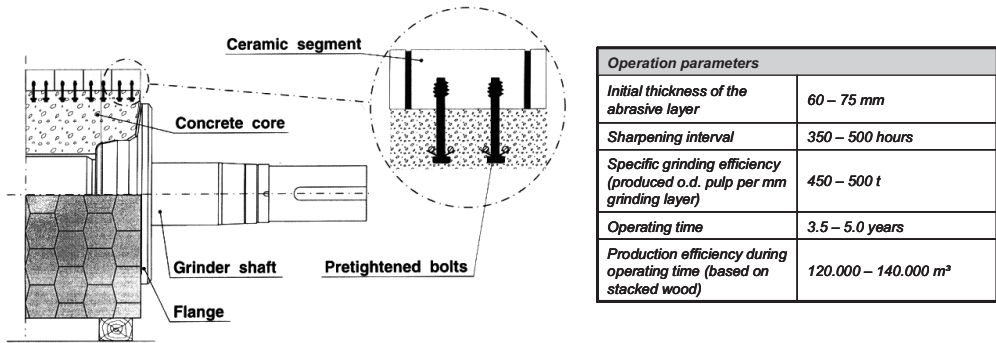


Fig. 4.18 Structure of an artificial pulp stone.

The structure of a ceramic stone that is most commonly used today is shown in Fig. 4.18 (left). The stone consists of a steel-reinforced core to which the honey-combed ceramic segments are fixed with anchor screws. The spaces between the segments have elastic joint material filling. Although the abrasive layer, at 60–75 mm thickness, is much thinner than that of a concrete pulp stone, much longer operating times are attained. The abrasive layer material estimates the quality of the ceramic pulp stone, and differs in basic mineral, grit size, and grit size distribution. The basic abrasive minerals used are aluminum oxide (Alundum) or silicon carbide (Crystolon), and these are manufactured in several grades of hardness and density. The ceramic bonding is achieved with the use of a sintered silicon-based bonding agent.

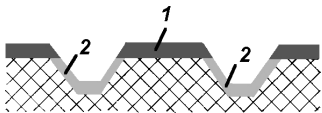


Fig. 4.19 Scheme of a macrostructure before and after sharpening (according to Süttinger). 1, Material removed by abrasion during a sharpening interval; 2, material removed by the subsequent sharpening.

#### Pulp Stone Sharpening

The pulp stone requires a certain surface structure to produce a certain ground-wood quality, the so-called “macrostructure” (Fig. 4.19). This is achieved by sharpening the pulp stone with a special device, although the abrasive layer becomes worn-out during grinding. The top area of the structure profile becomes wider,

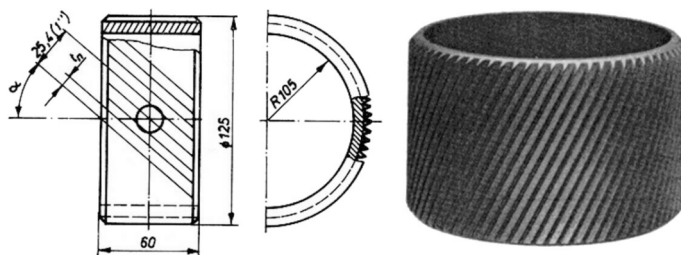
and the pulp stone becomes dull so that the quality and quantity of the groundwood produced is changed. To regain the original surface structure, the stone must be sharpened. The surface profile (macrostructure) before and after the sharpening process is shown in Fig. 4.19. The sharpening interval is the time between two sharpening actions, during which the groundwood quality changes significantly.

Traditionally, sharpening of the pulp stone has been carried out with metallic burrs. For this purpose, a sharpening lathe is installed on the top of a pocket grinder, or on the side of a chain grinder. The burr itself is installed into a burr holder that is fastened to the sharpening lathe. The burr sharpening produces a spiral pattern having grooves and areas, in turn, in the pulpstone surface. Sharpening deepens the grooves and reduces the land area, and also exposes fresh abrasive grits and removes impurities from the stone pores and surface. A smaller land area provides a higher unit grinding pressure, which results in a coarser pulp having a higher degree of freeness. The deeper grooves with a higher void area at the stone surface bring more water to the grinding zone, and consequently are able to carry more pulp out of the grinding zone.

The most important parameters that can be varied in the sharpening pattern include:

- Tooth frequency of the burr, pitch of the burr, pitch of the burr
- Tooth angle (mainly  $28^\circ$  in spiral burrs)
- Sharpening depth

The pitch of the burr and sharpening depth are used for burr specification. For each pulpstone type, there is a minimum width for the base of the land to be strong enough to support the grinding load. If finer burrs are used, it is highly probable that the lands break and the pulp quality is impaired. Some characteristics of spiral burrs are shown in Fig. 4.20.



$t_n$  – Pitch (distance of teeth, i.e. number of teeth per inch)  
 $\alpha$  – Tooth angle ( $28^\circ$ )

**Fig. 4.20** Characteristics of spiral burrs.

The sharpening of grinding stones with spiral burrs is being increasingly replaced by the use of ultrahigh-pressure water. This waterjet conditioning with water pressures set at 50 to 240 MPa (500 to 2400 bar) allows accurate control of the pulpstone sharpness, and results in a stable pulp quality and higher produc-



tion. This in turn leads to an improved stability of the total grinding and screening process. Compared to conventional spiral burr sharpening, waterjet conditioning is carried out during the grinding process, and variations in pulpstone sharpness may be reduced by 50–60%. The resultant groundwood had a more even distribution of well-bonding fibrillar particles. The tensile index of long fibers was increased by 15% and the tear index by 15–20%, while the apparent density was reduced by 30%.

#### 4.1.5

#### **Pressure Grinding**

Groundwood production has been carried out under atmospheric pressure, as indicated by Keller with its invention. Further investigations into temperature relationships in grinding have led to the introduction of higher pressures in grinding processes [11]. Although early small-scale trials have been successful, the technical realization required much development. By 1970, only the former Tampella factory [today part of Metso Paper (Metso Corp.)] had been able to develop the first industrial pressure grinder [12], though by 1982 almost 2.5% of the world's production of groundwood was manufactured by pressure grinding.

Goring [3] highlighted the importance of water content in wood during mechanical defibration. A high water content lowers the softening temperature of lignin and hemicelluloses (see Fig. 4.3). Still in atmospheric grinding, the Defibration takes place at temperatures below the softening temperature of wood. With high pressures of 100–300 kPa (1–3 bar), the boiling temperature of water increases; from the vapor–pressure relationship, the boiling temperature is seen to be 120 °C at a pressure of 100 kPa (1 bar). Pressurized grinding prevents the water from boiling in the grinding zone. The temperatures in the grinding zone are higher when compared to atmospheric grinding (see Fig. 4.21). According to Goring, water in the grinding zone can be used completely for softening purposes; consequently, the pressurized grinding of dry wood produces groundwood of a better quality than does atmospheric grinding.

The design of the Metso pressure groundwood (PGW) grinder (also called the Tampella-grinder or Valmet PGW grinder, depending on the year of publication) (Fig. 4.22) is similar to the atmospheric two-pocket grinder, though the total internal space of the grinder (including the two magazines) is now pressurized. Two magazines above the check damper to the pressurized area have been added for the feeding of wood logs, because of pressure equalization. Pressure grinding causes much higher forces to the housing materials and the pulp stone, and hence the atmospheric grinder concept has been redesigned. Currently, the grinder body is constructed from welded heavy steel plates, whilst all surfaces in contact with the pulp are clad with stainless steel. The end blocks are constructed from stronger stainless steel castings.

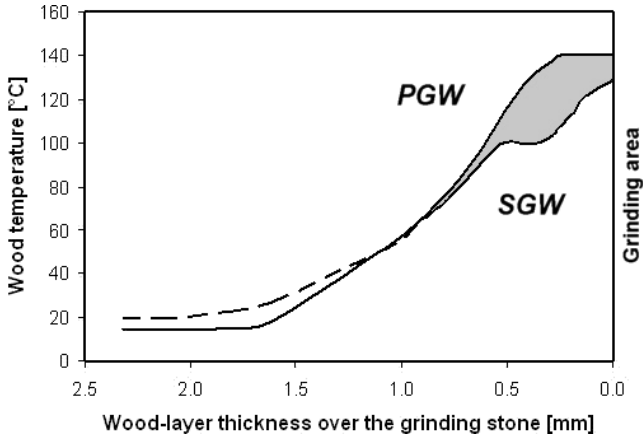


Fig. 4.21 Temperature rises in wood during grinding.

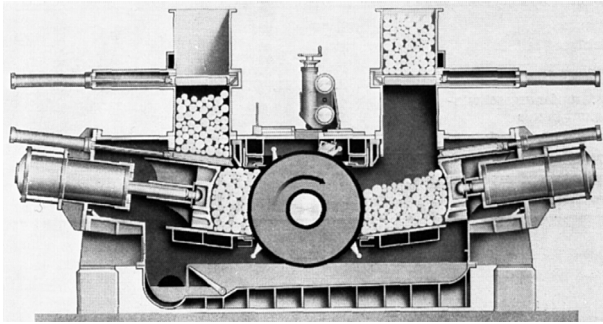


Fig. 4.22 The Metso PGW grinder.

The pressure inside the grinder casing is adjusted by compressed air, though this is mainly required only when pressurizing the grinder for start-ups. Pulp stone showering and the water hydraulic system are similar to those of the atmospheric grinder. Due to the higher temperatures utilized, cooling of the hydraulic water is necessary and a separate water-filtering loop is also included. Two-sided mechanical seals are used for the grinder shaft to minimize the use of fresh water in the PGW proves, and to prevent the colder seal waters from bleeding onto the ceramic pulp stones.

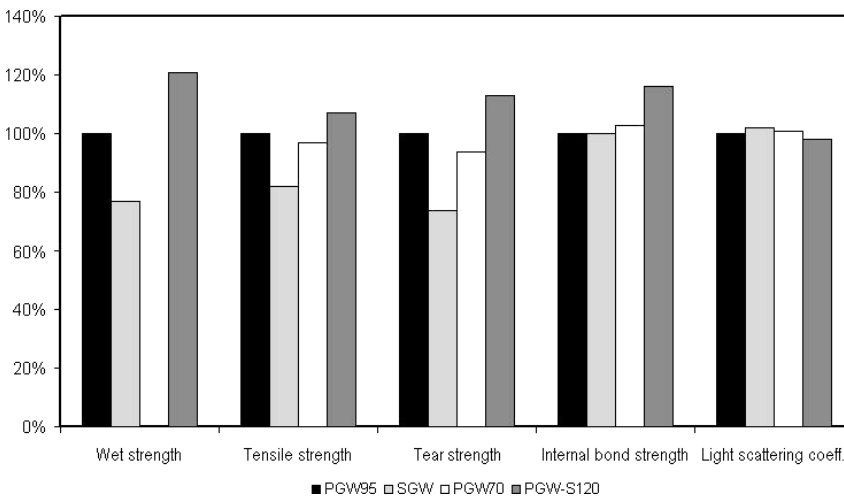
When it became clear that stronger pulps may be produced at a grinding pressure of 500 kPa (5 bar) and temperatures up to 140 °C [13], the design of a new series of pressure grinders with a stronger body rated for this higher grinder pressure was introduced. These grinders, which are known as “super pressure grinders” (PGW-S grinders), were first utilized in Finland in 1988 [14].

The entire grinding process from log feeding to the groundwood outlet occurs under pressure. The groundwood is passed through to a shredder to cut down in

size the very coarse wood pieces, after which the shives are so small that the groundwood can be passed directly to the pressure screening.

In pressure grinding, the grinder shower water temperature and flow are adjusted so that the pulp temperature is maintained well below the water boiling temperature at the set grinder pressure. A variety of combinations of pressure groundwood process, depending on shower water temperature and grinding pressure, are utilized in the following examples:

- PGW95: The maximum grinder casing pressure is 300 kPa (3 bar) and the shower water temperature is 95 °C. Hot filtrate water from the thickener is led back to the grinder as shower water with temperatures of about 95 °C (“Hot Loop”, PGW95 process). The steam is removed in the cyclone and can be used, by heat recovery, for several other process steps.
- PGW-S120: The maximum grinder casing pressure is 500 kPa (5 bar) and the shower water temperature is 120 °C.
- PGW70: The use of groundwood in SC and LWC paper grades raised the requirements for excellent pulp brightness and light scattering. Higher fines content is preferred, and low coarse long fiber amounts are favored. This can be reached by lower shower water temperatures; the strength decreased only slightly compared to PGW95 pulp. To achieve a shower water temperature of 70 °C, a hot loop is no longer used, and the grinding process is simplified. In mill applications, white water is cooled in a separate heat exchanger installed in the grinder shower water line.



**Fig. 4.23** Relative pit pulp properties at CSF 80 mL for different groundwood types (data are based on Refs. [14–18]). The reference pulp is PGW95.

The properties of PGW differ from the conventional stone groundwood (SGW). Especially important is the higher long-fiber content that causes increased initial wet web strength and tear resistance [about 40% higher strength values for PGW-S120 compared to atmospheric SGW; see Fig. 4.23]. Average values for the fiber length are 1.3–1.5 mm for PGW from spruce, compared to 0.7–0.8 mm for SGW from the same wood species.

An overview of the different groundwood pulp properties, depending on the grinding method, is provided in Fig. 4.23. All pulps are compared at the same freeness level of CSF 80 mL, while the reference pulp is PGW95, set as 100% in all properties.

Pressure grinding produces a pulp with higher long-fiber content and higher strength level than does atmospheric grinding, and their properties are comparable to those from refiner mechanical pulp (see Section II-4.2). One main advantage of pressure grinding is a better exploitation of the raw material without additional specific energy input and loss in optical properties, and a pulp quality that enables the saving of amounts of chemical pulp in pulp blends.

## 4.2

### Refiner Processes

#### 4.2.1

##### Principle and Terminology

A typical flow sheet of a refining process is shown in Fig. 4.24.

Fiber logs are cut down into wood chips that are then defibrated to mechanical pulp by means of disc refiners. Depending on the type of chip pre-treatment or chip post-treatment, several processes can be carried out, each of which is specifically defined.

- RMP (Refiner mechanical pulp): The refining of chips at atmospheric pressure in a refiner (in some cases, the refiner outlet may be pressurized).
- TMP (Thermo-mechanical pulp): Thermal pre-treatment and refining of the chips under pressure, with the second refiner also under pressure in most cases (the pressure allows heat recovery)
- RTS<sup>TM</sup> (Retention time, temperature, speed): Chips are pre-heated very briefly at a high temperature and then refined at high speed.
- Thermopulp<sup>TM</sup> (Thermo pulp): This differs from TMP in that the pulp is heated to a very high temperature (ca. 170 °C) briefly before the second refining stage.
- CMP (Chemimechanical pulp): Chips are pre-treated, usually with sodium sulfite and caustic, and then refined without pressure.

- CTMP (Chemithermo mechanical pulp): Chips are pre-treated in the same way as for CMP, but with a lower chemical charge, and then refined under pressure.

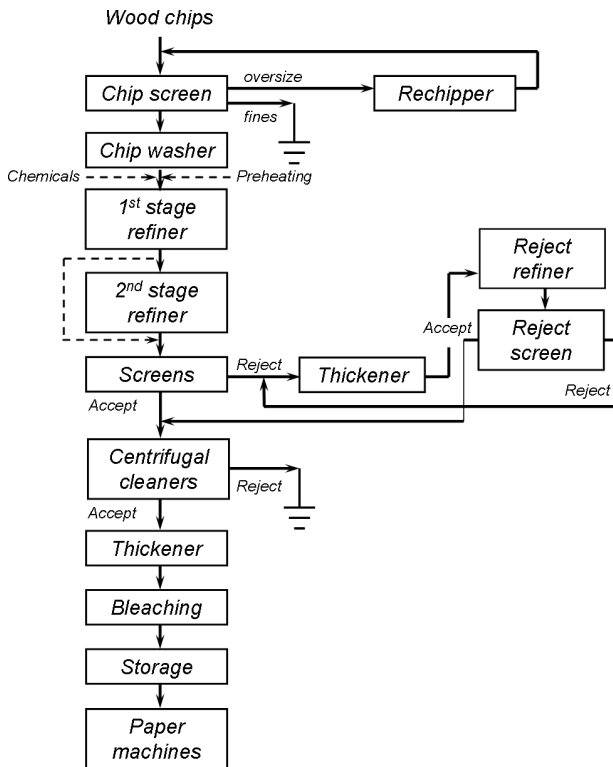


Fig. 4.24 Typical flow sheet of a modern refining process.

The industrial production of RMP began in 1960, since which time the refiner process has been extensively developed as result of the increasing demand for pulp fibers and the commissioning of large and highly efficient paper machines.

The advantages of refiner processes can be summarized as follows:

- Chips as a raw material allows the processing of wood that cannot be used for grinding (size of the logs, wood species), for example, saw mill chips or sawdust. With chemical pretreatment, some hardwoods can also be used successfully.
- There are good possibilities of process automation and minimal operating effort. Wood transportation and log handling are no longer necessary.
- Pulps with a high content of long fibers and good strength properties can be produced.

- The quality of the mechanical pulp produced is constant over a longer time interval than for groundwood, because there are no sharpening fluctuations.

The development of the refiner process has been enforced by much better designs of the refiners, highly efficient refiners, and the development of wear-resistant plate materials.

#### 4.2.2

#### **Mechanical, Thermal, and Chemical Processes in the Refiner Process**

Fiber delimitation from the fiber compound can occur in the refiner process as follows:

- Softening of the lignin in the middle lamella and in the primary wall of the wood fiber by pressure load frequencies in the refiner; this is mechanical softening.
- Softening of the lignin in the middle lamella and in the primary wall of the wood fiber by thermal influences; this is thermal softening.
- Softening of the lignin in the middle lamella and in the primary wall of the wood fiber by chemical pretreatment; this is chemical softening.

Many process parameters are considered responsible for the character and properties of the mechanical pulp produced, including: (a) the pressure and temperature during thermal pretreatment; (b) the duration of thermal pretreatment; (c) the addition of chemicals; (d) the specific energy consumption; (e) the energy distribution within the refining stages; (f) the consistency in the refining zone of the first refining stage; (g) the wood chip quality; (h) the refiner design; and (i) refining intensity caused by plate design and rotational speed.

The duration of thermal pre-treatment has only minimal influence on pulp quality, since in practical terms this stage lasts for only 1–3 min, and a minimum time is striven for.

The defibration temperature is as important as for the grinding process, and should be 100–130 °C. By raising the temperature to 140 °C, the lignin becomes well-softened and the fiber requires minimal mechanical energy for its liberation from the fiber compound. This mechanical pulp has an unsuitable quality for papermaking, however, as it is harsh and coarse. The softened lignin solidifies at the fiber surface to a hard substance; the pulp has a high refining resistance. If the defibration temperature is lower than the softening temperature of the lignin, then the mechanical pulp produced is coarse and has only a low level of strength properties. When the refining temperature is very close to the softening temperature, a high percentage of the fibers can be defibrated without being destroyed. The primary wall of these fibers can be damaged, and this allows fibrillation of the secondary wall. According to Giertz [19], the shearing frequency in a refiner is be-

tween 10 kHz and 1 MHz. Based on the fact that the softening temperature for high polymers increases by 7° when the frequency increases by 1 tenth, it can be assumed that the lignin of moist chips will be softened in the refiner at 120–135 °C.

The shearing frequency is estimated by rotational speed, disc diameter, and plate pattern. Moreover, the type of refining – whether single disc, double disc or conical disc – is also important. If the refining temperature is slightly above the softening temperature of the wood chips, then defibration occurs mainly in the zones with a high lignin concentration (i.e., in the middle lamella). In this way, a high proportion of fibers is deliberated without being damaged. At the same time, the middle lamella and primary wall are removed and milled down to fines, while the outer secondary wall (S1) is fibrillated [19]. The mechanical and thermal processes during refining can be divided into three phases:

1. Reduction of the chips sizes to units of matches.
2. Reduction of those “matches” to fibers.
  - Stress by pressure pulsation and shearing of the fiber – fatigue of the middle lamella
  - Thermal softening of lignin and hemicellulose
  - Rolling effect (= agglomeration of deliberated fibers)
  - Fiber cutting
3. Fibrillation of the deliberated fibers and fiber bundles.

Chemimechanical pulping involves a gentle chemical treatment stage combined with mechanical defibration such as disc refining. The yields of these pulps are generally in the range of 80–95%, and their properties are intermediate between those of high-yield chemical pulps and mechanical pulps. Chemithermomechanical pulp (CTMP) is produced with pressurized refining. Relatively low chemical doses are applied, and the yield is typically above 90%. Chemimechanical pulp (CMP) can be produced with refining at atmospheric pressure; the chemical treatment stage is more severe than in the CTMP process, and the yield is typically below 90%. CMP is also the general name for all chemimechanically produced pulps. CTMP and CMP have been developed for the better use of hardwood and the improvement of the bonding ability of the stiff long TMP-fibers, with the first pulping lines beginning operation during the 1950s and 1960s for hardwood applications. The breakthrough in chemimechanical pulping occurred during the 1970s as result of the improved TMP technology. Because the key subprocess in chemimechanical pulping is refining, all developments of the TMP process could also be utilized for CMP production. This caused a rapid growth in the production of softwood CTMPs during the late 1970s and 1980s.

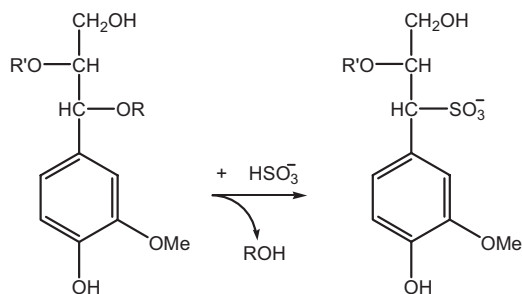
The difference between chemithermomechanical and chemimechanical pulping relates mainly to the process conditions utilized (see Tab. 4.2), and is apparent mainly in terms of the intensity of chemical treatment and pulp yield.

**Tab. 4.2** Possible defibration conditions for the production of chemithermomechanical pulp (CTMP) and chemimechanical pulp (CMP).

	Wood type	Pre-damping [min]	Impregnation	Preheating	Cooking	Yield [%]
CTMP	Softwood	10	1–5% Na <sub>2</sub> SO <sub>3</sub>	2–5 min 120–135 °C		91–96
	Hardwood	10	1–3% Na <sub>2</sub> SO <sub>3</sub> 1–7% NaOH	0–5 min 60–120 °C		88–95
CMP	Softwood	10	12–20% Na <sub>2</sub> SO <sub>3</sub>		10–60 min 140–175 °C	87–91
	Hardwood	10	10–15% Na <sub>2</sub> SO <sub>3</sub>		10–60 min 130–160 °C	80–88

Chemimechanical pulps can be produced, in principle, by a variety of combinations of chemical treatments and mechanical defibration. In practical operation, sodium sulfite is the dominating chemical in softwood pulping, while sodium hydroxide and/or sodium sulfite are the common chemicals in hardwood pulping.

Sulfonation opens the wood structure and enables the access of water to the fiber. Attack and Heitner [20] described this procedure (see Fig. 4.25), and assumed that the softening of lignin could be led back to an exchange of the aliphatic hydroxyl groups or ether groups participating in hydrogen bonding between the lignin molecule chains, by solvated groups that cannot take over any bond between the molecule chains.

**Fig. 4.25** Exchange of hydroxyl groups by sulfonate groups (according to Attack et al. [21]).

Attack and Heitner [20] also assumed that the hydrophilicity of wood is caused by an exchange of the aliphatic hydroxyl or ether groups – acting between the chains in hydrogen bonding – by solvated groups that cannot build bonding between the chains, and this results in a softening of lignin. This permanent lignin softening affects the following defibration in two important ways:



- The addition of sulfonate groups up to about 1.2% on o.d. wood leads to an almost complete fiber separation and to diminution of the disturbing influence of stiff long fibers caused by softening of the middle lamella [20].
- The addition of a larger quantity of sulfonate groups (>1.2% up to 2.0% on o.d. wood) makes the stiff long fibers more flexible and deformable, and this increases the bonding ability, caused by softening of the fiber walls [20].

In practical CTMP and CMP operations, the chemical treatment of wood is carried out as pretreatment by the impregnation of wood chips. Besides refining, this impregnation is one of the most important process steps in chemimechanical pulping. Generally, impregnation is defined as penetration of the chemicals into the microstructure of the wood. The physical processes of penetration and diffusion ensure the distribution of a maximum amount of chemical in a minimum of time evenly within the wood structure.

A practical solution to this procedure is to dampen and compress the chips on their way to the impregnator in the feeding screw, and then to expand them in the cold impregnation liquid. This expansion and condensation effect causes the chemical to soak into the wood structure. Depending on the chemical concentration and impregnation time, a chemical consumption of 2% up to 20% on o.d. wood can be achieved. This means also an increase in wood moisture of 5% to 30%. Because of their anatomic structure, hardwoods are able to absorb more liquid than softwoods.

The efficacy of impregnation can be estimated by the sulfonate content in the pulp. This value expresses the chemical amount of sulfonate groups in lignin, related to o.d. matter, and can be calculated as:

$$\text{Sulfonate content} = \frac{\text{Amount of SO}_3\text{H (in mg)}}{\text{o.d. matter (in mg)}} \times 100\%$$

A maximum sulfonate content of about 2% on o.d. matter corresponds to a degree of sulfonation of ca. 0.15. The degree of sulfonation is defined as the ratio between sulfur and methoxy groups; a value of ca. 0.15 represents complete sulfonation of the X-groups as part of the A-groups in spruce lignin.

The degree of sulfonation may be calculated as:

$$\text{Degree of sulfonation} = \frac{\text{Sulfur (S)}}{\text{Methoxy groups (-OCH}_3\text{)}}$$

The specific energy consumption affects the property of mechanical pulps, and is at least 2 MWh t<sup>-1</sup> o.d. pulp for strongly fibrillated TMP and CTMP pulps from spruce. The processing of pine chips increases specific energy consumption by 15–20%. The data in Fig. 4.26 illustrates how strength properties are dependent upon on specific energy consumption. The so-called F-value in Fig. 4.26 is a

strength value that combines tensile strength and tear strength, according to the following equation:

$$F\text{-value} = 10 \times \text{breaking length (km)} + 0.1 \times \text{tear strength (mJ m}^{-1}\text{)}$$

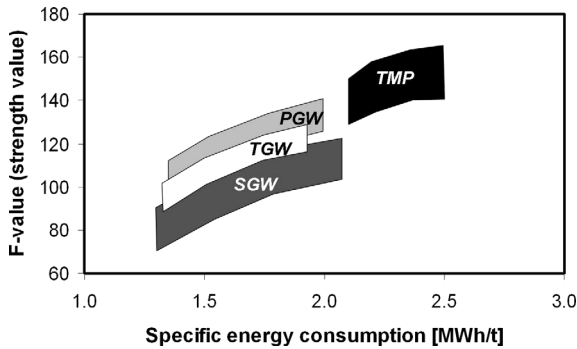


Fig. 4.26 F-value (strength value) depending on specific energy consumption (according to Süttinger [22]).

The refiner process is carried out mostly as a one- or two-stage process. In two-stage processes, the main part of energy is used in the first stage. The defibration concentration in the refining zone of the first refining stage is of major importance for the quality of the mechanical pulp, and should range from 20 to 45%, with 25% as an optimal value.

As for grinding, spruce wood is also the most suitable raw material for refining, though pine or hardwood with a low density may also be used. Again as with grinding, a high wood moisture is needed for refining. The size distribution of the wood chips should constitute only a small part of fines fraction, and they must be of a certain degree of purity. Sand and other minerals are abrasive for the refiner plates; hence, the wood chips are often washed before defibration.

#### 4.2.3

##### Machines and Aggregates for Mechanical Pulping by Refining

Disc refiners of different construction are widely used in the refining procedure, mostly as single-disc or double-disc variants. Other commercially available designs include several types of large-capacity refiners, such as the Twin concept or conical disc concept.

Single-disc refiners have one fixed and one rotating disc (Fig. 4.27), while double-disc refiners have two counter-rotating discs (Fig. 4.28). Two types of large-capacity TMP refiners are available: the Twin concept was introduced by Sprout (today Andritz), and is characterized by two parallel single-disc refiner gaps (i.e., three discs, with the center disc rotating and the outer discs fixed; see Fig. 4.29).

Somewhat later, Sunds Defibrator (today Metso) developed the RGP CD (= conical disc) system. Conical-disc refiners have a single-disc refining gap followed by a conical refining gap inside one refiner housing (Fig. 4.30).

The latest developments on the market are cylindrical refiners; the Papillon™ (Andritz) (Fig. 4.31) incorporates the advantages of hollaender beating with the continuous refiner principle. Also available are multiconical refiners; an example is the TriConic® (Pilão) (Fig. 4.32), which is a medium-angle, double-flow conical refiner with a low refining intensity and low no-load.

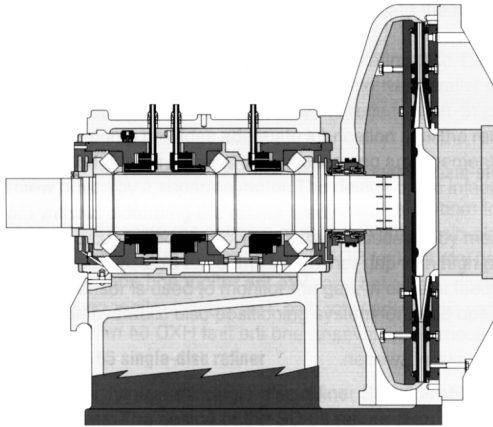


Fig. 4.27 The single-disc refiner (Metso RGP 268).

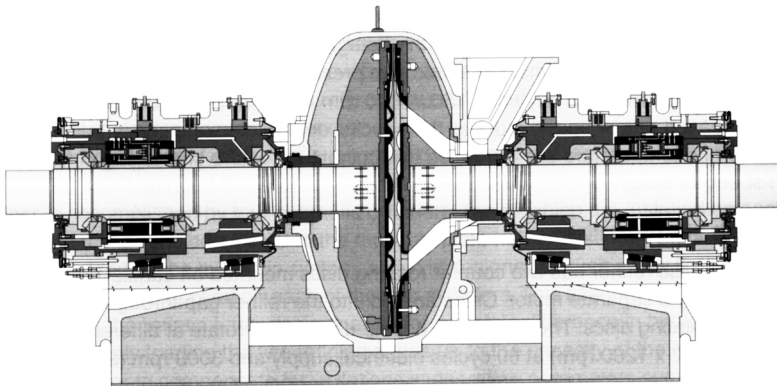
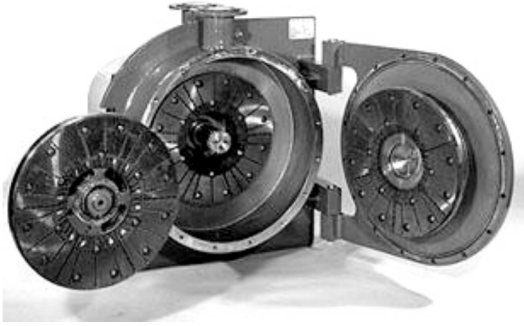
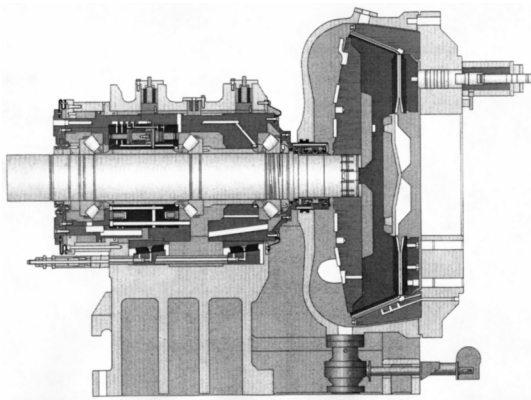


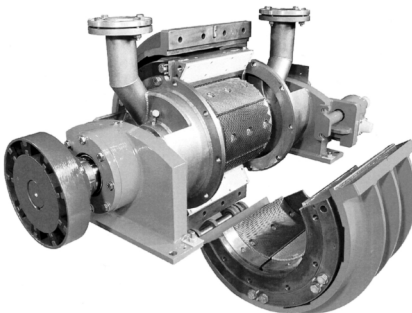
Fig. 4.28 The double-disc refiner (Metso RGP 68 DD).



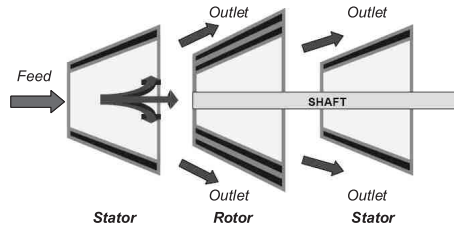
**Fig. 4.29** The twin-refiner TwinFlo™ (Andritz).



**Fig. 4.30** The conical-disc refiner (Metso RPG 82 CD).

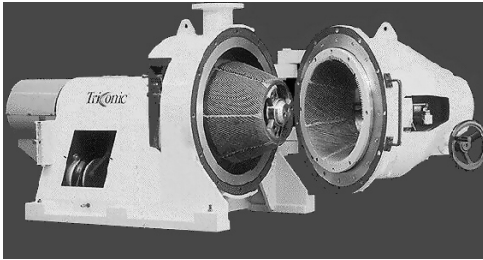


**Fig. 4.31** The cylindrical refiner Papillon™ (Andritz), with an open housing for plate change.

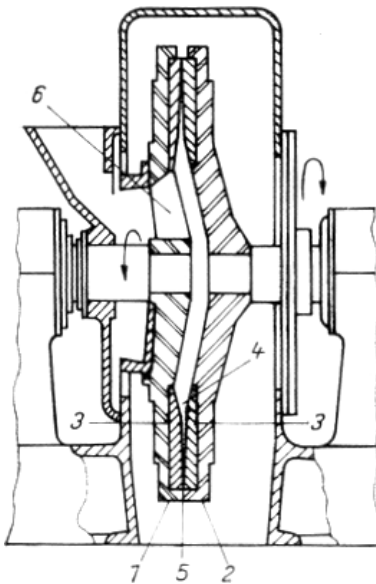


Positios of special plate design from stainless steel

Inner side of the conus      Outer side AND inner side of the conus      Outer side of the conus



**Fig. 4.32** The multiconical refiner TriConic® (Pilão). Left: Refiner with an open housing. Right: TriConic®; upper diagram, principle of operation; lower diagram, plate design.



**Fig. 4.33** Double disc refiner concept. 1 and 2, Rotating discs; 3, active parts of the discs (refiner plates); 4, entrance area into the refining zone; 5, outlet from the refining zone; 6, chip feed.

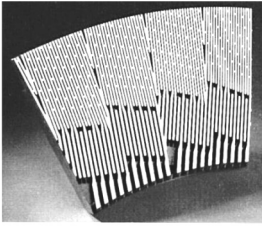
The working principle of mechanical pulp refiners is explained by means of the double disc concept in Fig. 4.33. The pulp is treated between two refiner discs, enters in the center at the shaft, and passes the discs from center to side. Refining plates constructed from high-strength steel and with different profiles are mounted on the refiner discs, which are pressed together hydraulically. The refining gap has an important influence on mechanical pulp quality.

An overview of the design of selected refiner types is provided in Tab. 4.3.

**Tab. 4.3** Characteristics of selected large-size refiner types.

Refiner type	Characteristics
RGP 268 SD	<u>Single-disc refiner (Metso)</u> Motor size 15 MW, disc diameter 1728 mm (68 in), rotational speed 1500 r.p.m.
RGP 68 DD	<u>Double-disc refiner (Metso)</u> Motor size 30 MW, disc diameter 1730 mm (68 in), rotational speed 1500 r.p.m. (50 Hz) or 1800 r.p.m. (60 Hz); designed pressure 1.4 MPa
RGP 82 CD	<u>Conical-disc refiner (Metso)</u> Motor size 30 MW, disc diameter 2080 mm (82 in), rotational speed 1500 r.p.m. (50 Hz) or 1800 r.p.m. (60 Hz); designed pressure 1.4 MPa; refining surface 3.2 m <sup>2</sup>
Twin 66	<u>Twin refiner (Andritz)</u> Motor size 24 MW, nominal disc diameter at 1800 r.p.m.: 1680 mm (66 in)
Papillon CC-600	<u>Cylindrical refiner with center feed (Andritz)</u> Motor size 2000 kW, diameter of refining area 600 mm, idle load 160 kW
TriConic Type RTC 6000	<u>Multiconical refiner (Pilão)</u> Motor size 880–1470 kW, throughput 200–1800 t day <sup>-1</sup>

Refiner plates are the “heart” of the refining process. The type of refiner plate design chosen is specified for a certain pulp quality and depends on the requirements of the paper machine. These depend on the type of paper produced and on the control strategy of the paper machine. Varying refiner positions (1<sup>st</sup> stage, 2<sup>nd</sup> stage, reject) also require different refiner plate designs. Refiner plate designs are always under further development, and some selected examples of actual plate design are illustrated in Fig. 4.34. Bi-directional refiner plates are standard in TMP production, and perform independently of the direction of rotation of the refiner. Turbine™ segments are the latest development by Metso Paper for the conical disc refiner RGP 82 CD (see Fig. 4.30); this system operates at low pressure during chip defibration stage, and this results in improved optical properties of the refined pulp.



**Bi-directional refiner plate**    **Turbine™ segments**  
*(DURAMETAL, member of the Andritz-Group)*    **for RGP 82 CD**  
*(Metso Paper)*    *(Metso Paper)*

Fig. 4.34 Selected examples of refiner plate designs.

Refiner plates are hard-wearing tools with a working lifetime of between 300 and 1000 h. Selected examples of mechanical pulp lines using the refiner process are shown in Figs. 4.35–4.37.

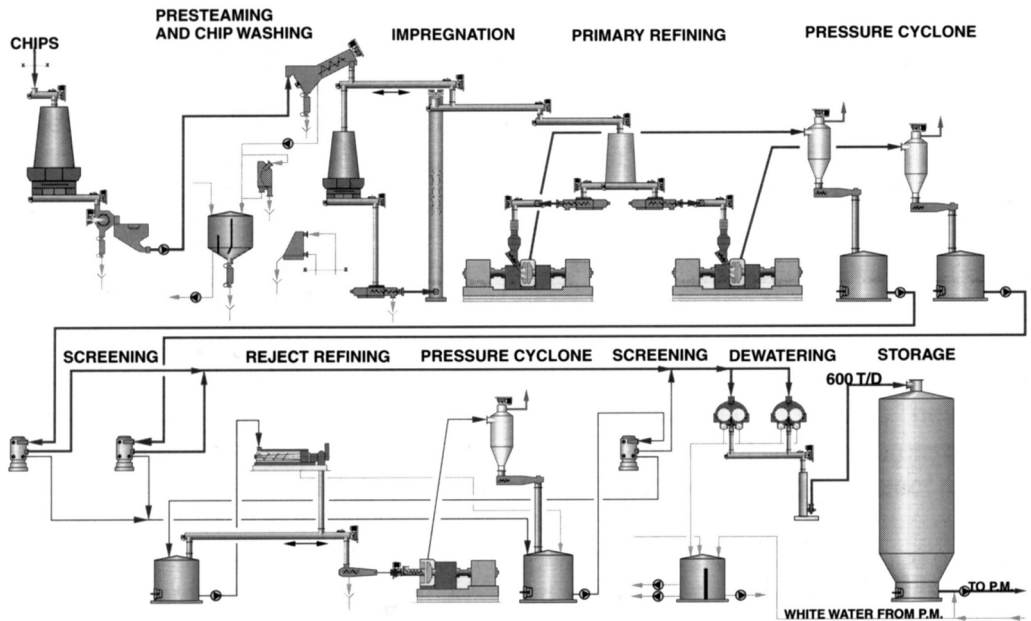


Fig. 4.35 Single-stage TMP line with Metso-Double disc refiners RGP 68 DD (Union Bruk Norway, 1999).

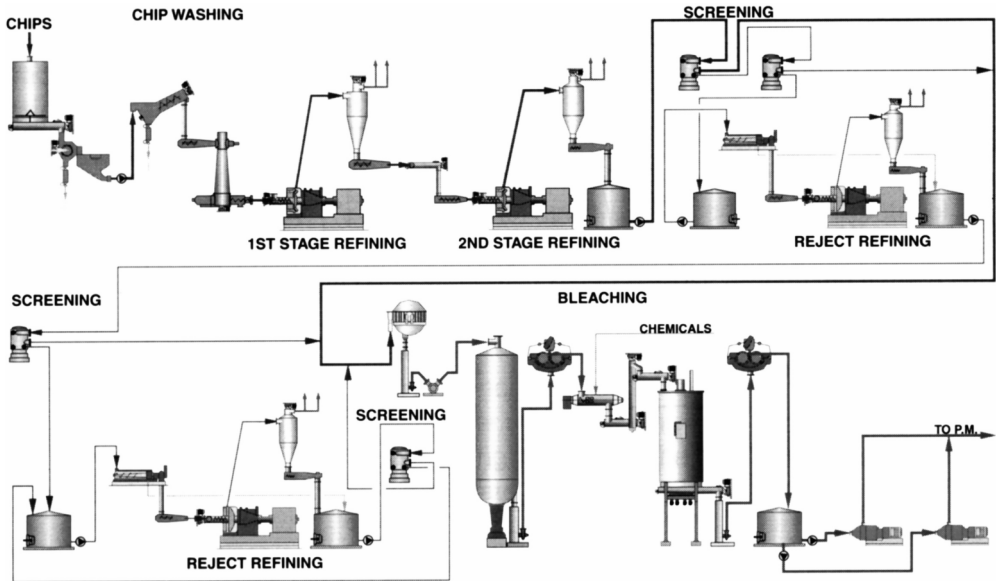


Fig. 4.36 Two-stage TMP line with two-stage reject refining and fractionation for LWC paper (Metso Paper).

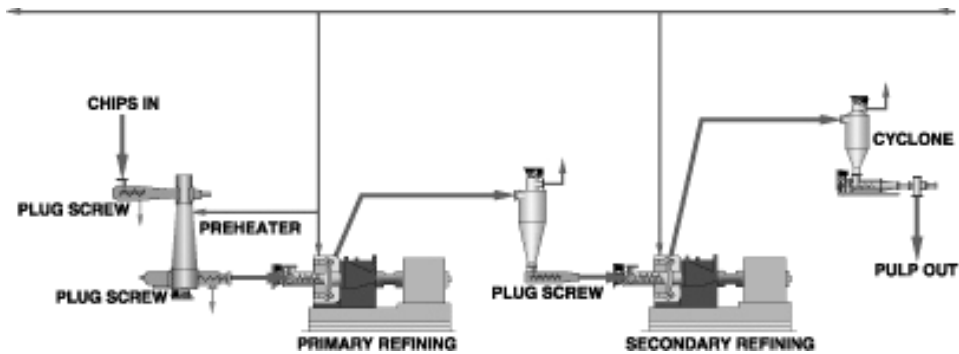


Fig. 4.37 Modern CTMP refining in one or two stages (Metso Paper).

To date, the production of pulp for fluting has been the most common use of semi-chemical hardwood pulps. The dominant process for this product is the neutral sulfite semi-chemical process (NSSC), with sodium or ammonium sulfite as cooking chemicals. The pulp yield is in the range of 70–80% depending on the wood species. Birch, beech, maple, oak and eucalyptus are the most frequently used hardwoods for fluting production, often as the sole component in furnish.

Primarily, the demand on a fluting pulp is high stiffness and good crush resistance. A combination of short, stiff fibers and a high proportion of hemicellulose in hardwoods makes them more favorable than softwoods for this purpose. A semi-mechanical pulping process is illustrated schematically in Fig. 4.38.



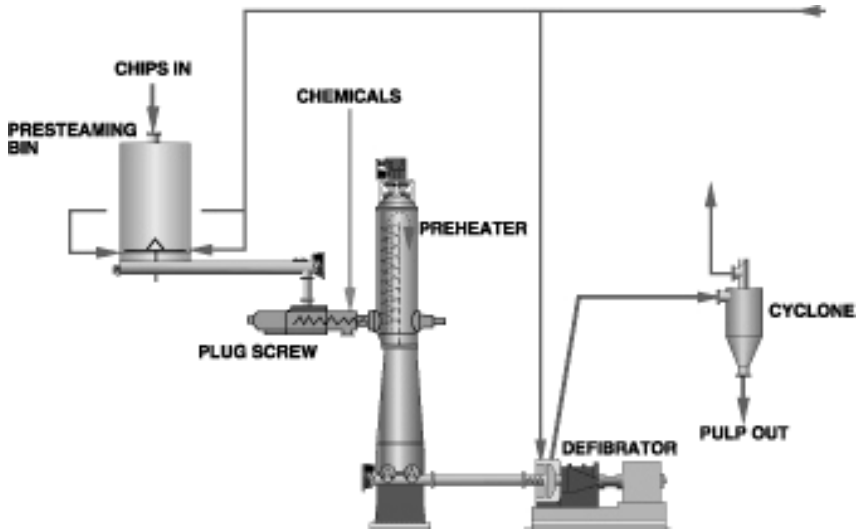


Fig. 4.38 Semi-mechanical pulping process.

## 5

# Processing of Mechanical Pulp and Reject Handling: Screening and Cleaning

*Jürgen Blechschmidt and Sabine Heinemann*

### 5.1

#### Basic Principles and Parameters

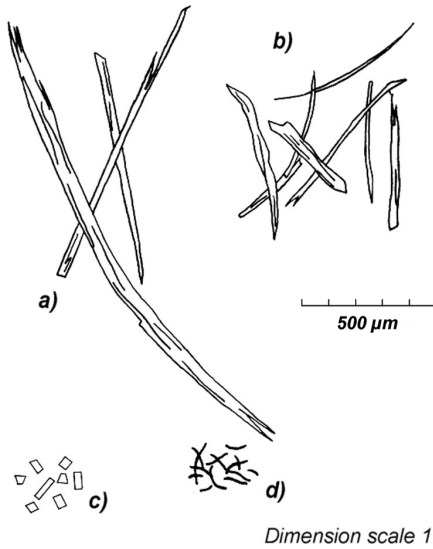
The aim of mechanical defibration of wood is the delimitation of fibers from the wood, without their destruction. This happens only ideally, and in reality a mixture of different fiber components and debris is created immediately after defibration, and is characterized as follows:

- Shives (unsuitable particles that must be separated from the pulp).
- Fibers, divided into:
  - Long fibers; length 800–4500  $\mu\text{m}$ ; width 25–80  $\mu\text{m}$
  - Short fibers; length 200–800  $\mu\text{m}$ ; width 2.5–25  $\mu\text{m}$
- Fines, divided into:
  - Fibrillar fines (slime stuff); length up to 200  $\mu\text{m}$ , width about 1  $\mu\text{m}$
  - Flake-like fines (flour stuff); length 20–30  $\mu\text{m}$ ; width 1–30  $\mu\text{m}$

Additionally, wood pieces of different dimensions and shapes, sand and other nonwood particles are found (Fig. 5.1).

Separating by suitable screening brings the mechanical pulp to the following composition, depending on its process parameters during defibration:

- Shives content: 2–6% (extreme values up to 20%)
- Fiber content: 50–80%
  - Long fiber content: 25–55%
  - Short fiber content: 25–40%
- Fines content: 20–50%

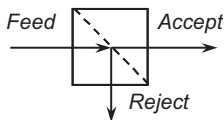


**Fig. 5.1** Ground wood components. (a) Long fibers; (b) short fibers; (c) flake-like fines; (d) fibrillar fines.

There are two basic process principles for screening in mechanical pulping:

- Pulp classification – that is, separation of the pulp into fractions of different particles size (applied for shives removal from the pulp).
- Separation according to particle density – that is, separation of pulp and minerals such as sand and other heavy material (applied for pulp cleaning).

The separation process can be characterized by a simple scheme, as shown in Fig. 5.2.



**Fig. 5.2** Parameters of the screening principle.

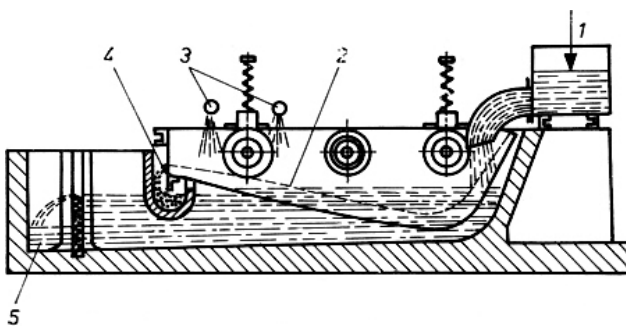
## 5.2 Machines and Aggregates for Screening and Cleaning

No screening process can result in a complete or exact separation of accepts and rejects. There are always particles retained in the reject that are smaller than the separation size (slot width or mesh size), and there are also larger but slender and flexible particles in the accept.

The screening efficiency depends on the following influences [23]:

- Parameters of the material to be screened (inlet pulp).
  - Type of material (mechanical pulp, chemical pulp, recycled pulp)
  - Shape of the particles to be separated (cube-like, flake-like, stretched length directionally)
  - Particle size distribution
  - Flexibility of the particles
  - Drainage resistance and consistency of the inlet slurry
- Parameters of the screening elements
  - Shape of the element (mesh, hole, slit)
  - Size of the element (mesh opening, hole diameter, slit width)
  - Position and distance of the elements
  - Portion of open screening surface
- Process or design parameters
  - Evenness of flow
  - Evenness of composition and consistency
  - Type of inlet feeding to the screening elements
  - Geometry of feeding stream contact with the screening surface
  - Speed and length of feeding stream over the screening element
  - Transportation force of accept through the screening elements
  - Slurry height over the screening surface and specific feed to the screening surface
  - Mechanical measures to prevent plugging of the screening elements surfing mater

The coarse rejects in the grinding process are separated in the coarse screening using vibration screens (Fig. 5.3) with holes of 6-mm diameter. The flow rate is between 40 and 50 t day<sup>-1</sup> at a feeding consistency of 1% and a screen area of 1.5 m<sup>2</sup>.

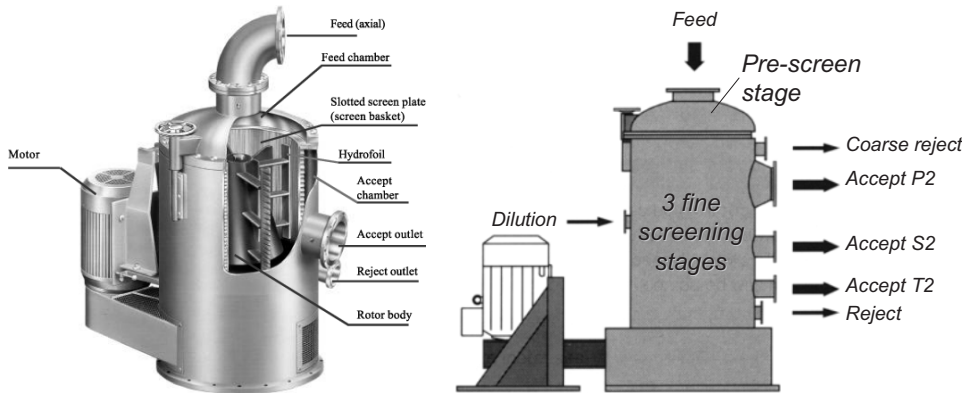


**Fig. 5.3** Bull screen (vibration screen). 1, Groundwood feed from grinder pit; 2, screen plate; 3, shower water; 4, coarse reject; 5, accept.

The coarse reject is further treated in shredders. In pressure grinding, this shredder treatment is applied to the whole pulp before pressure relaxation.

In refiner mechanical pulping, there is virtually no such coarse material in the pulps (TMP, CTMP, and CMP) any longer. These pulps contain more mini-shives, chops and long fibers than can be separated in fine screening steps, and are further treated by reject refining.

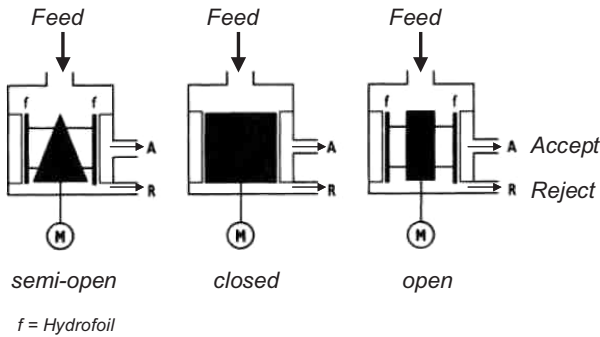
Pressure screens are the most common equipment in screening and fractionation of mechanical pulp (Fig. 5.4, left). The pressure screen consists of a cylindrical screen basket as a screening element, and a concentric positioned rotor to keep the screen openings unplugged (see also Fig. 5.5). The pulp suspension is fed from above, either axially or tangentially, with the flow operating either centrifugally, centripetally, or as a combination of the two. Either the rotor or the screen basket can rotate, but today the major application is centrifugal flow with a rotor. Single-stage screens operate with low-consistency or medium-consistency pulps, whereas in multistage screens several stages are run in one screening apparatus (Fig. 5.4, right). In future, these screens will increasingly replace existing single-stage screens. The shives and stiff long fibers are removed as rejects from below, while the filtrate moves easily through the screen openings, causing a thickening of the reject flow. Any pad build-up will be repeatedly destroyed by the rotor wings.



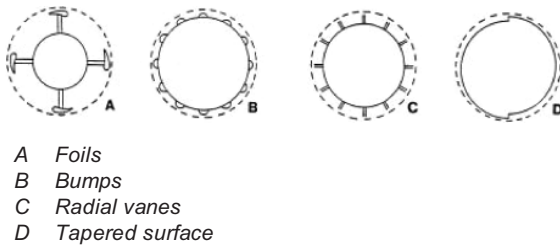
**Fig. 5.4** Left: Single-stage pressure screen (Metso TAP) [24].

Right: Multistage pressure screen (Metso MuST) [25].

The capacity and runnability of a screen, and also the screening efficiency to some extent, can be controlled by means of pulsation. Today, several designs of foil-type pulsation element are available. The aim is to obtain adequate pulsation by adjusting the number of foils and their shape, width, clearance, incident angle, and tip speed. A small difference between the peaks of positive and negative pulses is advantageous for screening efficiency, but the negative pulses should be sufficiently strong to enable the suction flow to remix flocks, fibers and contaminants resting on the edge of the screen opening [26]. The general construction of rotors is shown in Fig. 5.5, with a cross-sectional view on different pulsation elements of rotors in Fig. 5.6.

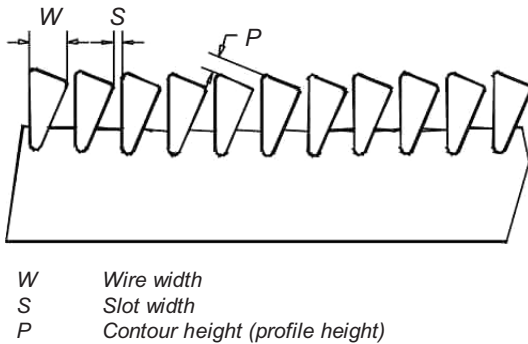


**Fig. 5.5** General construction forms of pressure screen rotors (according to Niinimäki et al. [27]).

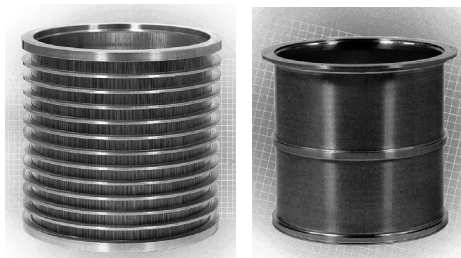


**Fig. 5.6** Rotor types with different pulsation elements (according to Bliss [28]).

Slotted screen plates have been found to have superior shives removal efficiency compared to holed screen plates, but the capacity of the latter is better because of a larger open area. Contoured screen plates have further increased the capacity of slotted screens, and slotted screens manufactured from wedge wires (Fig. 5.7) provide about 100% greater open surface area than screen plates with machine slots.

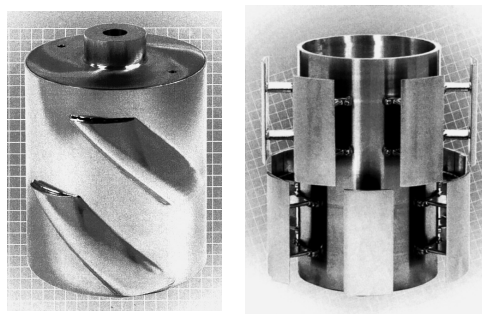


**Fig. 5.7** Example of a wedge wire screen basket [29].



*Continuous slotted screen*    *Perforated cylinder*  
AFT MacroFlow™

**Fig. 5.8** Pressure screen basket designs (AFT).



*AFT Gladiator™*  
*HC Rotor*

*AFT EP Rotor™*  
*Engineered Pulse™*

**Fig. 5.9** Pressure screen rotor designs (AFT).

Some examples of industrial designs of screen baskets and rotors are shown in Figs. 5.8 and 5.9.

Separation according to material density is carried out using hydrocyclones (Tab. 5.1 and Fig. 5.10). In almost all of these apparatus, the pulp suspension is fed tangentially by pump pressure into a cylindrical or conical pipe and moves as a spiral downwards at the outer wall of the pipe. Heavy particles are found outside of the downward stream moving slowly through an opening at the lower end of the pipe into a dirt collector. The main stream is turned up above this opening and rises in the middle of the pipe to the outlet. Depending on the design, the pressure drop in this hydrocyclones is from 60 to 300 kPa (0.6 to 3 bar).

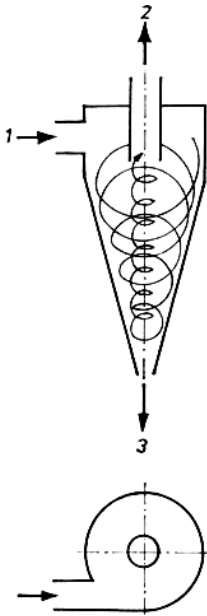


Fig. 5.10 Operation principle of a hydrocyclone.  
1, Pulp suspension inlet; 2, accepts; 3, rejects.

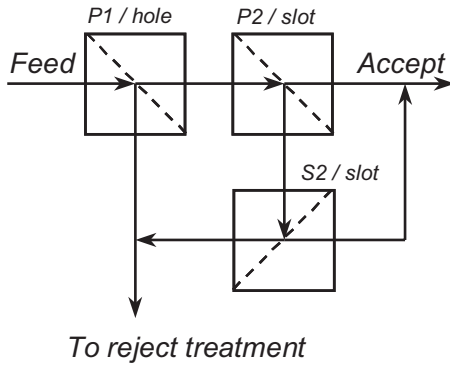
Tab. 5.1 Parameters of centrifugal separation principle for different cleaner types.

Parameter	Centricleaner	Low-consistency cleaner
Pulp consistency [%]	< 1	< 1
Pressure drop, [kPa (bar)]	300 (3)	160 (1.6)
Acceleration	550 g	150 g
Inlet flow rate [ $\text{m s}^{-1}$ ]	20	12
Fiber loss [%]	2	Practically none
Specific energy consumption [ $\text{kWh t}^{-1}$ ]	0.4–0.5	0.08

It is impossible to design a screen for mechanical pulps that is able to separate particles depending on the screen size absolutely. In practice, there is always only a certain amount of shives separated, and this depends mainly on the overflow rate. In addition to the efficiency grades of the single separation aggregates, a combination of all single screens estimates the efficiency and economy of the screening stage.

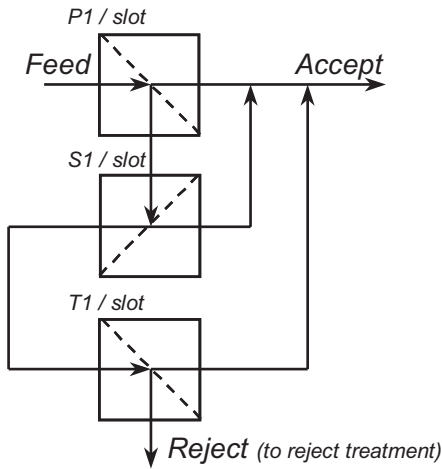
Some schematic examples of modern screening concepts are illustrated in Figs. 5.11–5.13.





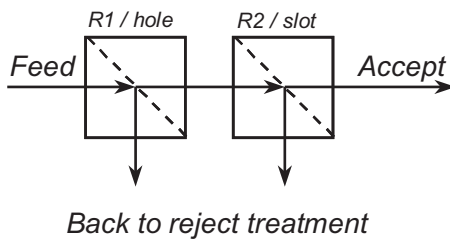
- P1 Primary screen 1, hole basket
- P2 Primary screen 2, slot basket
- S2 Secondary screen 2, slot basket

Fig. 5.11 Modern main line screening.



- P1 Primary screen 1, slot basket
- S1 Secondary screen 1, slot basket
- T1 Tertiary screen 1, slot basket

Fig. 5.12 Thermomechanical pulp (TMP) screening.



- R1 Reject screen 1, hole basket
- R2 Reject screen 2, slot basket

Fig. 5.13 Screening concept for refined groundwood rejects.

### 5.3 Reject Treatment and Heat Recovery

The separated coarse reject is treated in special reject disc refiners. In grinding, a high-consistency refining of the reject is also useful. The technological scheme of a high-consistency reject refining stage is shown in Fig. 5.14. The pulp arrives from the reject bin with 2.5% consistency and is thickened up to 25–30%.

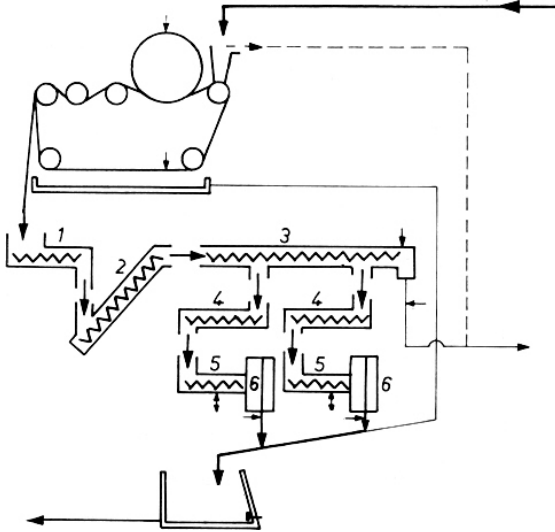


Fig. 5.14 Technological scheme of a high-consistency reject refining stage.

In a TMP mill, heat recovery plays an essential role in economic operating. Normally, around two-thirds of the refining energy can be recovered in the form of clean steam. The TMP steam generated in the refiners is separated from the fibers in the cyclones (see Figs. 4.35–4.37), and then condensed in the reboiler against vaporizing clean steam. The main components of a typical heat recovery unit are illustrated in Fig. 5.15.

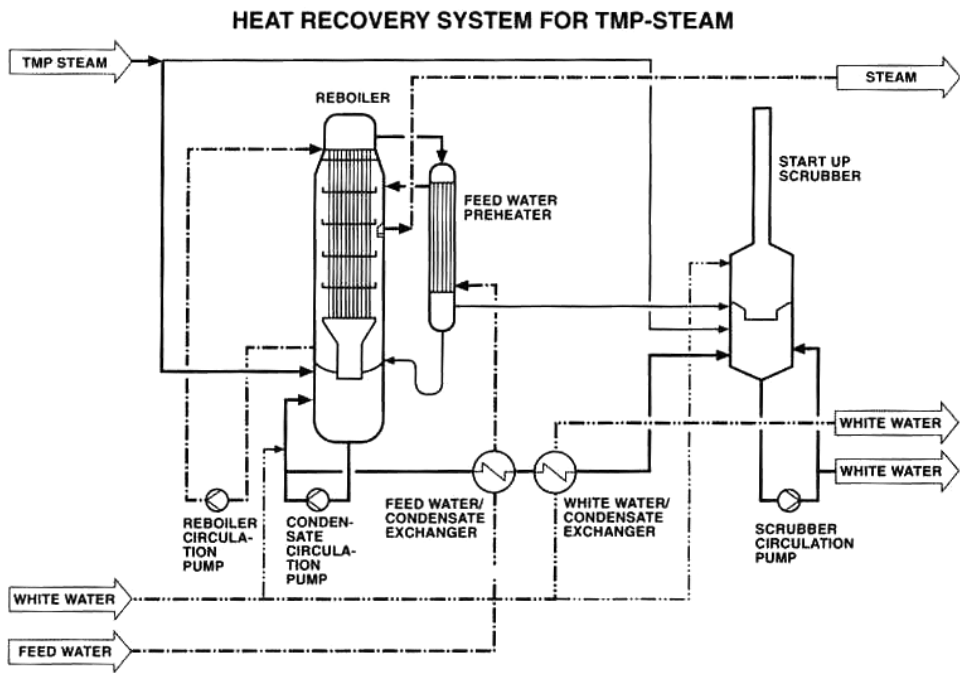


Fig. 5.15 Typical thermomechanical pulp (TMP) heat recovery flow sheet (Rinheat).

## 6 Bleaching of Mechanical Pulp

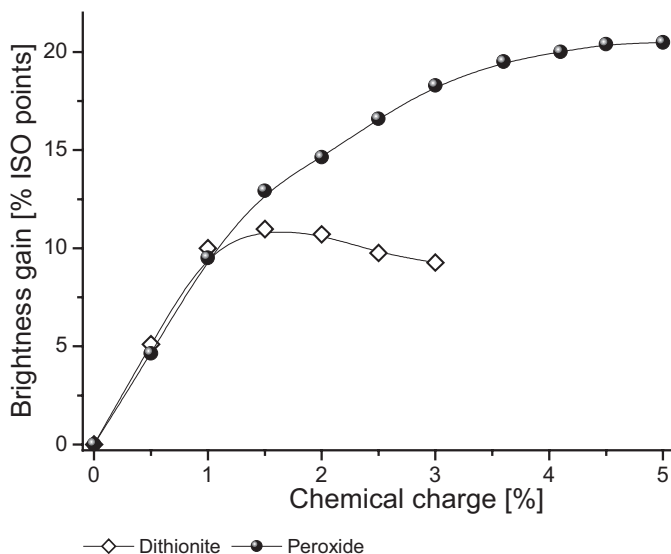
*Hans-Ulrich Süß*

Mechanical defiberization leaves most of the lignin compounds in the fiber. A bleaching process using the aggressive chemicals applied in chemical pulp bleaching would result in the oxidation and removal of this lignin. This cannot be the target of the process, as it would decrease the yield dramatically, require an enormous amount of chemical, and also destroy the optical properties of the fiber. Bleaching of mechanical pulp has to apply chemicals with limited aggressivity, as well as conditions which keep the extraction of lower molecular-weight carbohydrates and lignin compounds as moderate as possible. The high temperature of the defiberization process causes the solubilization of polyoses and starts the hydrolysis of acetyl groups. Resins and lignans are partially dispersed and dissolved [30–32]. A higher pH and a high temperature in bleaching will intensify these effects; consequently, neutral or moderately acidic bleaching conditions are required in order to maintain the pulp yield.

Softwood from forest thinning or wood chips from sawmills has an unbleached brightness level which is sufficiently high as to allow its application in newsprint production, without any bleaching process. The initial brightness typically is between 55% ISO and 65% ISO. The intensity of the bark removal, the wood species, and the storage time between wood harvest and refining has a huge impact on the unbleached brightness level. The use of sawmill waste normally provides a lower unbleached brightness. Generally the use of a mechanical pulp in higher quality paper grades such as SC or LWC paper requires a bleaching step.

Lignin is the dominant source of chromophores in mechanical pulp, with aromatic ring structures with conjugated side chains, quinones, quinone methids and metal–catechol complexes being the origin of the color. Chemically, decolorization or destruction of these compounds is accomplished by either reductive or oxidative processes.

An example of the brightness gains achieved in bleaching with dithionite or hydrogen peroxide is shown in Fig. 6.1. Based on the initial brightness levels, the range between 70% ISO to about 80% ISO is accessible for softwood. Hardwood pulps can be bleached to >85% ISO. The top brightness requires more than one bleaching stage. The higher the brightness target, the more complicated the bleaching technology becomes. The simplest way to improve brightness is to treat



**Fig. 6.1** Typical response of mechanical pulp to oxidative or reductive bleaching with hydrogen peroxide or dithionite (hydrosulfite).

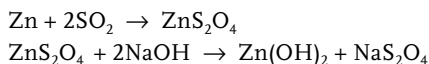
the pulp with sulfur dioxide. The reduction of transition metals decolorizes the above-mentioned catechol–metal complexes. Metal ions reduction not only decolorizes the chromophores but also solubilizes the metals and allows their removal by washing and subsequent dewatering. Because the reduction is easily reverted by air oxidation, all reductive bleaching treatments require “closed” systems. Because air can be excluded from pulp slurries more easily at a lower consistency, reductive bleaching in the past was conducted in up-flow towers at only 3–5% consistency. The de-aeration which takes place in modern medium-consistency pumps permits reductive bleaching at consistencies from 8% to 14% (see Section II-6.3). This allows a smaller size of reactors to be used (tubes instead of towers) and a lower volume of process water.

### 6.1 Bleaching with Dithionite

The impact of the reduction process is intensified with the application of dithionite, which in addition reduces quinones and quinone methids. (In English-speaking countries, dithionite is frequently still labeled as “hydrosulfite”, an incorrect description of the product, but this was rectified in 1881.) The dominant compound used in bleaching processes is sodium dithionite, and in the description of bleaching processes the normal abbreviation for dithionite bleaching is “Y”.

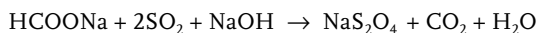
Sodium dithionite is produced using several processes, but historically the zinc dust process is the most important. The reaction of zinc dust in an aqueous slurry

with sulfur dioxide generates zinc dithionite which is reacted further with caustic soda:



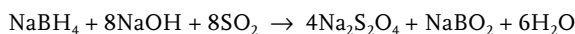
Initially, the zinc hydroxide is filtered off and reprocessed to zinc dust. Then, after concentration of the liquor by evaporation, sodium dithionite is precipitated by the addition of sodium chloride. The salt, which is dried before shipment, contains up to 300 p.p.m. zinc.

The dominant process is the reaction of sodium formate with sulfur dioxide and caustic soda under pressure. The reaction is described by:



Commercial grades of sodium dithionite powder typically have a content of about 88% sodium dithionite, with the sodium salts of bisulfite, sulfite, sulfate and carbonate as the byproducts. Solutions of dithionite in water must be prepared on-site. In pulp bleaching, the use of returnable steel containers with up to 2000 kg of technical-grade product is common. Typically, a small amount of a chelant (e.g., ethylene diamine tetra-acetic acid; EDTA) is added. This avoids scaling (precipitation of calcium carbonate) caused by the hardness of the dilution water. An analysis of the stability of dithionite solutions in the presence of iron and manganese [33] contradicted the speculation about the metal ion (Fe, Mn) -induced decomposition of dithionite [34]. The fine powder reacts exothermically with atmospheric oxygen; the heat of oxidation can lead to ignition. Sodium dithionite is therefore classified as “spontaneously combustible goods”, and the corresponding transport and storage regulations must be applied.

Alternatively, some mills operate an on-site process using a solution of sodium borohydride (~12% by weight) with caustic soda (~40%). This mixture is reacted with sulfur dioxide to yield dithionite solutions:



Some pulp mills are supplied with an alkaline solution (pH > 12) of sodium dithionite. Transportation requires cooling to a temperature below 10 °C to maintain the content at ca. 11–12% dithionite. Cooling of the storage tank is not required when there is a rapid turnover of the product. Exclusion of air is required to avoid product losses, as dithionite reacts rapidly with oxygen in the air to yield sulfite. In the absence of air, decomposition reactions take place, with one of the products being thiosulfate; this, in turn, may accelerate corrosion reactions.

Bleaching with dithionite typically is conducted at moderately acidic pH, between pH 4.5 and 6.5. The temperature in tower or tube bleaching is maintained at 60–80 °C, although a higher temperature produces a faster response to the chemical addition. The reduction of chromophores occurs very quickly, so the

reaction time required is short – 15–60 min is sufficient. The amounts of dithionite vary, but are normally ca.  $10 \text{ kg t}^{-1}$  or 1% on fiber. As the number of available chromophores for the reduction process is limited, a brightness plateau is typically reached at an input of between 1.2% and 1.5%. An addition above these levels triggers decomposition and the formation of thiosulfate. A technological alternative to tower bleaching is the application of dithionite in the refiner. Although the brightness gains are slightly inferior, the application is simple and can eliminate the need for a bleach plant.

As can be imagined, the reduction reactions may be reversible. For example, the reduction of an *o*-quinone to the catechol generates the leuco form, which can be re-oxidized by oxygen in the air. Despite this, the brightness of dithionite-bleached pulp is relatively stable in heat-induced aging. Stability is affected by light, UV radiation or transition metal-induced reactions of the phenolic groups within the lignin, easily generating chromophores [35].

## 6.2 Bleaching with Hydrogen Peroxide

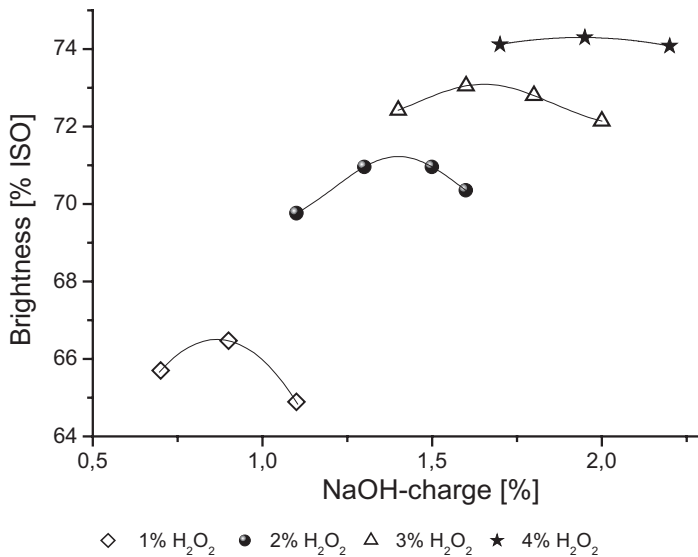
The application of hydrogen peroxide in bleaching mechanical pulp is by far older than its use in chemical pulp bleaching. A prerequisite of peroxide bleaching is the “neutralization” of peroxide-decomposing transition metals (e.g., Mn). Chelation of the metal ions is achieved with compounds such as diethylene diamine penta-acetic acid (DTPA) or ethylene diamine tetra-acetic acid (EDTA) (see Section II-5.4.2.4.5.1, Prerequisites of hydrogen peroxide application). The chelants are added most beneficially during screening after the refining process. This allows sufficient residence time and typically has the correct pH level (slightly acidic) for effective chelation. The demand for chelant is between 0.1% and 0.3% on fiber (of the commercial product with an active content of ~40%). The addition of chelant, together with the other chemicals ( $\text{H}_2\text{O}_2$ , NaOH, silicate) is another option, though it is slightly less effective because of the higher pH.

The limited aggressivity of hydrogen peroxide might be a disadvantage where delignification is required, but it may be advantageous if an improvement of brightness is the only target. In the past therefore, hydrogen peroxide bleaching was often labeled as being “lignin-conserving”. As described in previous chapters, this is not the case, and lignin is in fact removed during peroxide bleaching. Lignin side chains are cleaved and quinones oxidized to more water-soluble carboxylic acids. However, because hydrogen peroxide will not react easily with the aromatic systems of lignin, its level of removal is moderate. In mechanical pulp bleaching, this is an advantage, and the yield and optical properties (opacity) are only moderately affected by the bleaching process. An example of the response of mechanical pulp to hydrogen peroxide is shown in Fig. 6.1.

Peroxide addition yields increasing brightness with charges up to about 5%. The plateau is reached at about 82% ISO for softwood pulp, spruce (*Picea* spp.) and pine (*Pinus* spp.), and 86% ISO for hardwood mechanical pulp, poplar and aspen (*Populus*

spp.). The wood species, the age of the wood, storage of the logs and the bark content each have a huge impact on bleachability and the brightness ceiling.

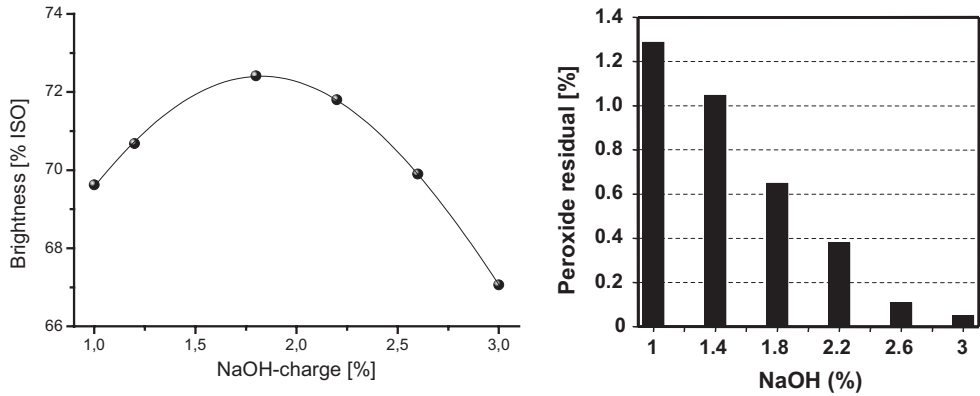
During the bleaching process, a variety of compounds are dissolved, the main ones being acetic acid (from acetyl groups on carbohydrates) and low molecular-weight polyoses. Lignin dissolves only to a small extent. However, because the pulping process solubilizes only a small part of the wood, rather high effluent loads can result from bleaching. Top brightness requires a high peroxide input and, for its activation, a similarly large amount of caustic soda. The resultant brightness in bleaching softwood TMP with increasing input of hydrogen peroxide is shown graphically in Fig. 6.2, where different amounts of caustic soda were applied to achieve the best response in brightness. For a given residence time and temperature, there is an optimum level of activation. The shape of the curves shows, for the ratio of  $\text{H}_2\text{O}_2$  to  $\text{NaOH}$ , an increasingly wider range of tolerance. Clearly, the more peroxide applied, the less critical is the correct amount of caustic soda added.



**Fig. 6.2** Increase in brightness with optimized charges of  $\text{NaOH}$  for different peroxide amounts. Bleaching at  $65^\circ\text{C}$ , 3 h, 20% consistency, with a constant addition of 2% sodium silicate.

An inadequate activation results in an insufficient consumption of  $\text{H}_2\text{O}_2$ , but too-high charges are similarly detrimental, and the alkalinity consumes peroxide and brightness decreases again. The process cannot be operated with the aim of consuming all of the hydrogen peroxide applied. An example of the brightness resulting from a constant input of hydrogen peroxide but a variation of the amount of caustic soda is shown in Fig. 6.3. The comparison of best brightness and remaining residual allows the conclusion to be made that the residual must be higher than about 10–15% of the peroxide input in order to achieve the best result. As a lower residual results in a poorer gain in brightness, it is therefore



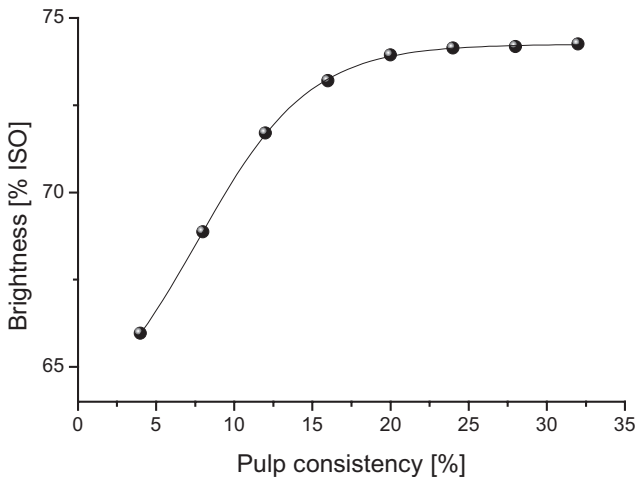


**Fig. 6.3** Impact of the variation of the caustic soda charge on brightness. Bleaching of softwood TMP with 4%  $\text{H}_2\text{O}_2$  and 2% sodium silicate, constant: 25% consistency, 3 h, 70 °C.

important to control the peroxide residual and to evaluate the ratio between residual and input.

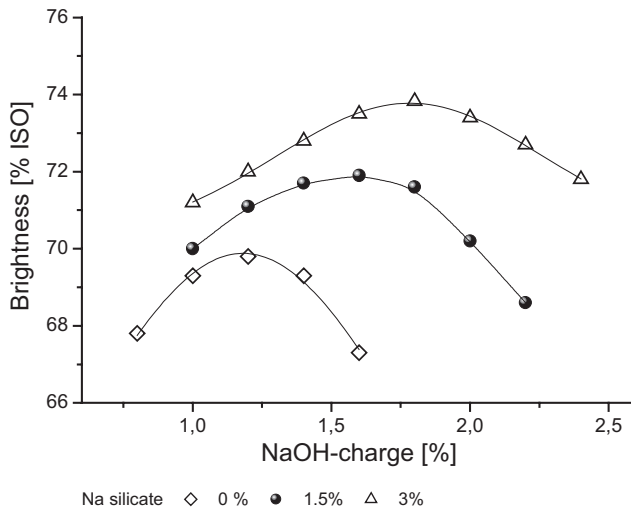
Bleaching response is improved with consistency. The reason for this is the higher relative concentration of the chemicals and the lower level of dissolved compounds. The steep increase in bleaching efficiency with the consistency is visualized in Fig. 6.4. Because of the importance of high-consistency, modern bleach plants operate well above a level of 25%.

The addition of sodium silicate in bleaching has several effects. First, it acts as a buffer, and therefore reduces the peak value of the pH. The instability of diluted



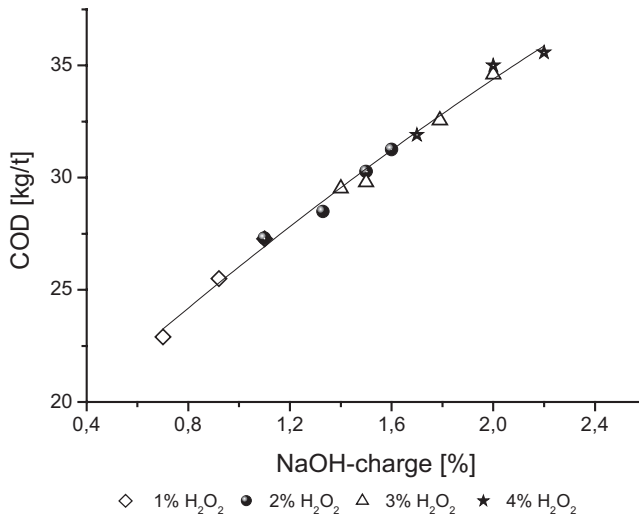
**Fig. 6.4** Impact of consistency on mechanical pulp bleaching. Constant application of 1.5%  $\text{H}_2\text{O}_2$ , 3% sodium silicate at 70 °C, 2 h, amount of NaOH adjusted.

silicate solutions favors the precipitation of silicates (silicic acid sols), and this can lead to the removal of potential decomposing compounds. Because such precipitation can cause problems with scaling, the amounts of silicate added are typically adjusted to lower levels. Despite these difficulties, the advantage of silicate addition normally keeps this product in the mill's receipt. A clear example of the benefit is shown in Fig. 6.5, where silicate addition leads to a higher brightness and a wider maximum. In the presence of silicate, the receipt for composition of the chemicals tolerates deviations more easily. The standard addition of silicate is around 2%, calculated as commercial solution with 38–40 Bé density. Silicate solutions with a higher alkalinity have a lower average molecular weight for the silicic acid polymer, and this permits a lower level of addition, with identical effects.



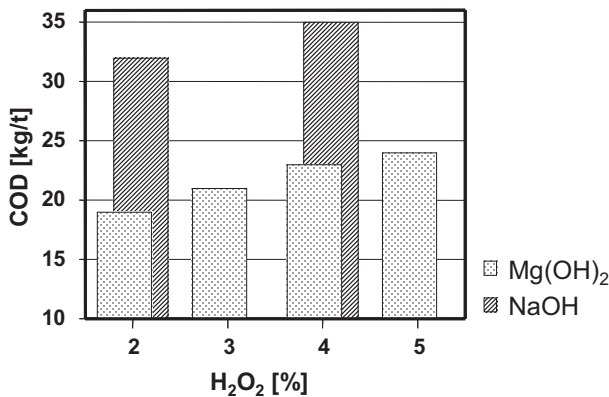
**Fig. 6.5** Impact of sodium silicate stabilization on brightness development in thermomechanical pulp (TMP) bleaching.

The amount of caustic soda applied correlates directly with the effluent load [35]. Taking the data from Fig. 6.2 and plotting the input of caustic soda against the resulting COD load, the points in the graph show the linear dependency (Fig. 6.6). This applies not only to the COD but in parallel to total organic carbon (TOC). Because the amount of dissolved compounds must correlate with the pulp yield, bleaching to a very high brightness decreases the yield. Fines are extracted and freeness is increased. The extraction effect not only affects pulp yield and opacity, but also has an impact on fiber properties. With intense extraction, hardwood fibers collapse, making it difficult to produce highly bleached fiber with a high volume (bulk). For most paper-grade applications, fiber volume should be low in order to allow a smooth surface. In the production of white board, the opposite is valid and stiff fibers with a high volume are an advantage; however, this requires to carry out bleaching with other alkali sources.



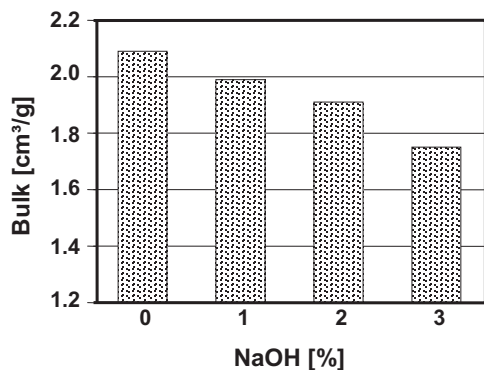
**Fig. 6.6** Increase of the COD load with increasing caustic soda addition in bleaching with hydrogen peroxide.

The substitution of caustic soda with magnesium hydroxide is a useful alternative [36], although because of the limited solubility of  $\text{Mg}(\text{OH})_2$ , effective mixing becomes even more important. The particle size is similarly important, as a fine product is distributed better. The amount of  $\text{Mg}(\text{OH})_2$  can be kept low; the limited solubility would only result in a high neutralization demand. It is sufficient to add about 1–1.2% to activate the bleaching process with 2–4%  $\text{H}_2\text{O}_2$ . The demand for sodium silicate is even lower, and an input of only 0.5–1% will result in the best response. The moderate impact on hemicellulose extract becomes apparent with a lower COD load (see Fig. 6.7).



**Fig. 6.7** Impact of an exchange of NaOH by  $\text{Mg}(\text{OH})_2$  in bleaching pressurized groundwood with increasing amounts of  $\text{H}_2\text{O}_2$  and NaOH or  $\text{Mg}(\text{OH})_2$  as alkalization source [NaOH amount variable,  $\text{Mg}(\text{OH})_2$  input 0.75% at 2%  $\text{H}_2\text{O}_2$ , all other bleaches 1%, 2% sodium silicate, 70 °C, 3 h, 20% consistency].

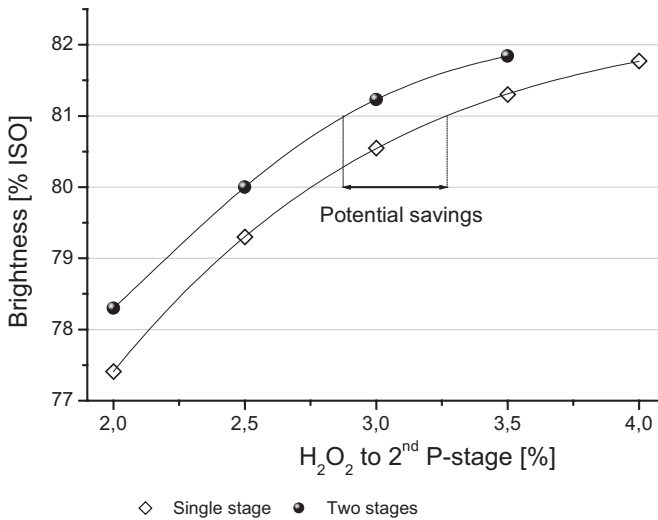
When bleaching aspen pulp, the impact on fiber volume of using  $\text{Mg}(\text{OH})_2$  is pronounced. Conventional bleaching to very high brightness (>85% ISO) is accompanied by a decrease in the specific volume from  $>2 \text{ cm}^3 \text{ g}^{-1}$  to  $1.4 \text{ cm}^3 \text{ g}^{-1}$ , or even less. The substitution allows the specific volume (also labeled as “bulk”) to be maintained. In a set-up using the  $\text{Mg}(\text{OH})_2$  stage as the main (high consistency) stage and an additional (medium-consistency) stage with caustic soda as a brightness adjustment step, it is possible to balance the parameters of bulk and tensile strength to all levels in between (Fig. 6.8). The more moderate response in bleaching to the activation with  $\text{Mg}(\text{OH})_2$  is compensated by a final hydrosulfite treatment. Consequently, brightness is very high (>85% ISO) and will not effect any physical properties.



**Fig. 6.8** Decrease in specific volume of aspen TMP with input of caustic soda in a  $\text{P}_{\text{Mg}(\text{OH})_2}$ - $\text{P}_{\text{NaOH}}$ -Y sequence (high consistency–medium consistency–low consistency).

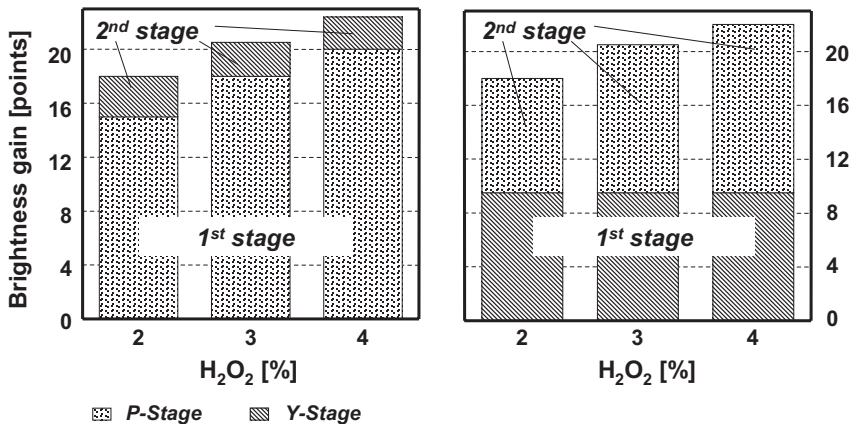
Very high brightness can be achieved with two-stage peroxide bleaching, although the equipment required is rather complicated (see Section 6.3). A two-stage process can use the high excess of peroxide from the main bleaching stage in a first step. This excess must be activated with an addition of caustic soda. The volume of liquid to be recycled depends on the dilution and dewatering conditions following the main bleaching step. Typically, volumes are so high that the first stage must be conducted at medium consistency. The potential savings of this approach (Fig. 6.9) are reasonable only for a very high brightness target, and this becomes apparent from the shape of the curves.

Some mills apply in-refiner-bleaching with sodium dithionite. Because of the high temperature, this reaction is very rapid; sulfonation of the lignin occurs and typically the residual of sulfite detected in the pulp is extremely small. Therefore, a peroxide bleaching stage can be added without any fear of activity losses. Y-P bleaching typically is applied in integrated mills producing paper with different brightness grades. A part of the reductive bleaching effect is lost by the oxidation with peroxide, the reason for this being the re-formation of some conjugated structures with the oxidation. However, the total brightness gain in a Y-P treat-



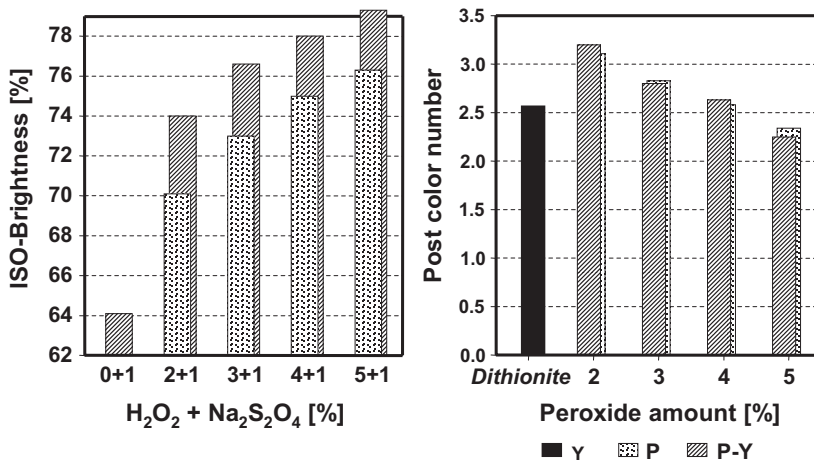
**Fig. 6.9** Impact of single-stage (high consistency) or two-stage (medium/high consistency) peroxide bleaching of a spruce TMP pulp. The second stage saves significant amounts of peroxide for very high brightness targets.

ment using dithionite in the refiner and peroxide under high-consistency conditions delivers comparable results with the more conventional P-Y treatment. Post bleaching with dithionite requires destruction of the excess hydrogen peroxide with sodium bisulfite or sulfur dioxide gas. These effects are explained graphically in Fig. 6.10.



**Fig. 6.10** Comparison of P-Y and Y-P bleaching. Bleaching of softwood TMP with constant 1% Na<sub>2</sub>S<sub>2</sub>O<sub>4</sub> and variable amounts of peroxide. P-Y with destruction of peroxide excess by bisulfite, Y-P sequence with refiner application of dithionite.

The brightness stability of mechanical pulp is much lower compared with fully bleached chemical pulp. The reason for this is the high level of lignin remaining in the fiber. Following bleaching, the structural elements which will re-generate chromophores easily are mostly eliminated, although the presence of phenols allows sufficient oxidation processes to yield a low brightness stability [35]. Post color numbers after heat- or light- induced reversion are significantly higher in comparison to chemical pulp. This is understandable in light of the large quantities of phenols and phenol ethers in the remaining lignin. The light-induced brightness reversion of mechanical pulp can be significant. However, whilst the reversion of a newspaper in the summer sun might become apparent after only an hour, this is of limited practical impact. Paper typically is not excessively exposed to light, and its reversion in the dark is more important. Accelerated aging in dry or humid tests can describe the stability of a brightness gain. The response of a TMP to peroxide and P-Y bleaching and to accelerated aging using hot and humid conditions is compared in Fig. 6.11. Brightness losses described as points of brightness are relatively constant for the whole range tested. Losses with humid reversion (100 °C, 100% humidity, 2 h) are around three points, with a clear tendency for lower losses the higher the brightness. This results in a decreasing post color number. The results confirm the experience with chemical pulp, that the greater the removal of chromophores, the better the resulting stability. The reductive post-treatment has post color numbers that are approximately equivalent to the results after the P stage; thus, the brightness gained is not easily lost.



**Fig. 6.11** Bleaching and aging of spruce TMP with Y, P, or P-Y bleaching. Initial brightness 55.5% ISO, peroxide bleaching with silicate stabilization, destruction of the peroxide excess with bisulfite, constant input of 1% dithionite in Y.

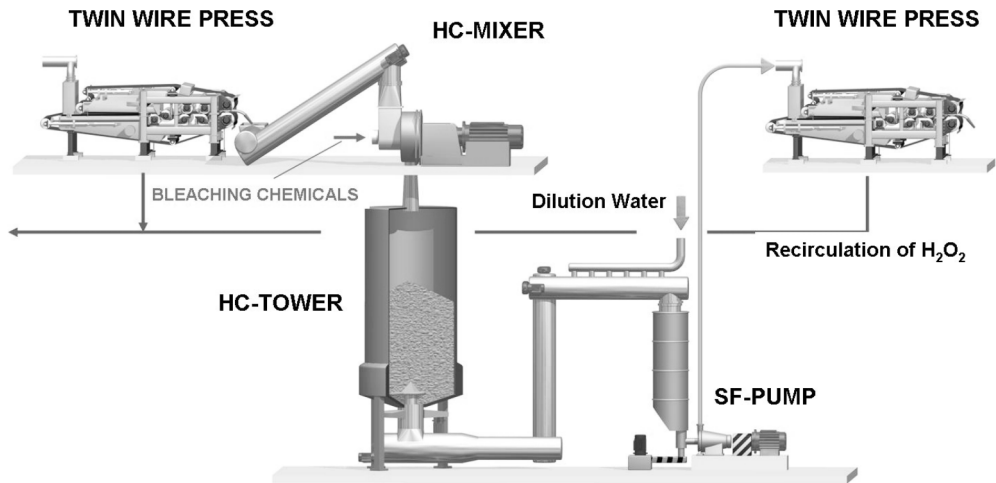
### 6.3 Technology of Mechanical Pulp Bleaching

Reductive bleaching is the most simple option for bleaching, not only because just one chemical has to be added to the pulp, but also because the available low or medium consistency after screening and latency chest can be applied. Other than using an effective mixer and a tower or tube, no additional equipment is required.

Peroxide bleaching is more complicated, however. High-consistency dewatering is an essential requirement for bleaching effectiveness. Modern twin-wire presses easily reach a consistency above 40%, and today – even when large amounts of chemical must be added – consistency in the bleaching tower is well above 30%. Four different chemicals must be mixed with the pulp. The chelant can be added as a pre-treatment prior to the latency chest. Caustic soda, sodium silicate, and hydrogen peroxide are either premixed with additional dilution water in a descending cascade to a concentration of less than 10%  $H_2O_2$  in the mixture. Alternatively, these chemicals can be added directly, using a very effective mechanical mixer, and mixed immediately with the pulp. Special attention must be paid to the design of the chemical addition. A backflow of liquor into the storage tanks is a serious safety threat, and may occur during a production halt. However, such a hazard can be avoided by installing back-pressure valves, or even more effectively by a system using the free flow of liquor into a small intermediate tank.

An example of a high-consistency peroxide bleach plant is shown in Fig. 6.12. The retention time in the tower can be adjusted by controlling the filling height. Mechanical discharge is essential for correct control, and older bleach plants operating at a lower consistency (<25%) can be discharged by injecting water at the base of the tower. An agitator (propeller) provides sufficient shear force to mix water and fiber bundles to a uniform discharge consistency below 5%. At very high consistency, simple stirring does not provide sufficient mixing, and the fiber bundles and water remain separate. Discharge at a higher consistency requires less volume of dilution water and allows post-bleaching with dithionite at medium consistency after destruction of the peroxide excess with bisulfite. The second twin-wire press is not required in the case of post-bleaching with dithionite. It is, however, a technological advantage because it separates the water loop of the bleach plant from the paper machine, and this may be important for retention control. After an intense peroxide treatment the amount of anionic compounds (“trash”) in the water circuit is high, and may cause problems.

Somewhat more complicated is a bleach plant with two peroxide stages (Fig. 6.13). Three presses are required to allow recycling of the peroxide excess. The pulp is dewatered to a high consistency, and excess liquor from the main bleaching step is then added. This dilutes the consistency to a level between 10% and 12%. In order to initiate a reaction, an addition of caustic soda to the peroxide content might be required. Following this MC-stage, the next press generates the high consistency required in the main bleaching stage. The effluent of this press is discharged to the effluent treatment plant. After the main bleaching stage, the



**Fig. 6.12** Schematic of a high-consistency peroxide bleach plant with twin-wire press, mixer and tower with mechanical discharge (courtesy Andritz AG, Graz, Austria).

pulp is diluted to generate sufficient liquid for recycling of the excess. With the pulp, the major part of the excess leaves the system, and this amount can only be decreased further if additional dilution and “washing” within the press is possible. However, this depends on the freeness. Typically, the washing of a mechanical pulp is difficult because of the high fines content and a low freeness. As mentioned above, a two-stage bleach plant only makes commercial sense for very high brightness targets.



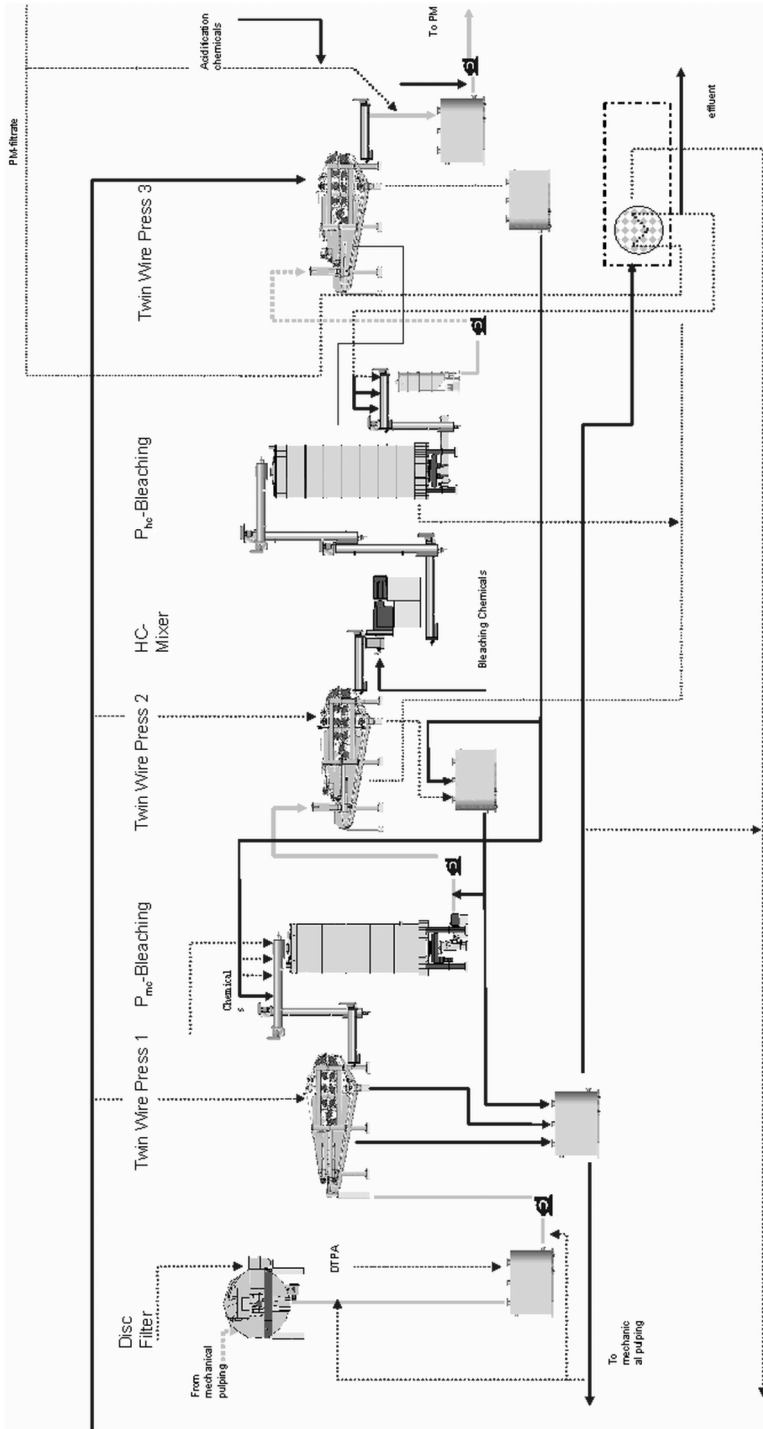


Fig. 6.13 Two-stage medium/high-consistency bleaching plant for bleaching to very high brightness (courtesy Andritz AG, Graz, Austria).

## 7

### Latency and Properties of Mechanical Pulp

Jürgen Blechschmidt and Sabine Heinemann

#### 7.1

##### Latency of Mechanical Pulp

When fibers are defiberized at high temperatures and high consistencies, they are deformed due to stresses that they encounter. The fibers are compressed, twisted and curled (Fig. 7.1a). However, when cooling down at high consistency, the fibers remain twisted and curly (Fig. 7.1b). This behavior is mainly found in refiner mechanical pulps [37], but it also occurs in pressure groundwood [38], and is termed “latency”. Latency can be removed by agitating the pulp at low consistency and high temperature. The fibers are re-straightened (Fig. 7.1c), and this pulp has a lower freeness and a higher tensile index. Thus, latency can be defined as the difference of mechanical pulp properties between the initial hot state (Fig. 7.1b) and the cooled state (Fig. 7.1c) that can be removed to a large extent [39].

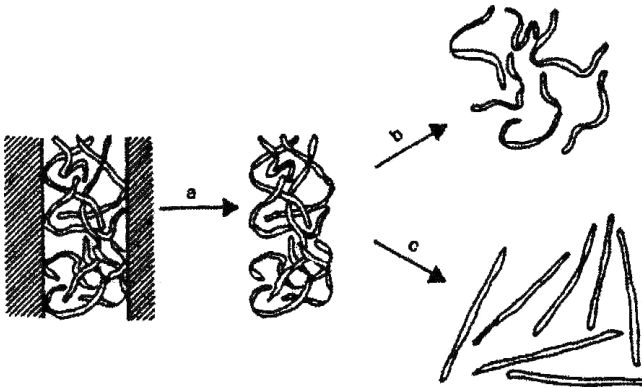


Fig. 7.1 Fiber deformation in mechanical pulping (latency).

## 7.2

## Properties of Mechanical Pulp

Figure 7.2 provides the comparative characteristics of mechanical pulps and chemical pulps, in relation to various yields.

Pulp type		Mechanical pulp			CMP	Semi-chemical pulp		Chemical pulp	
		SGW TMP	CTMP						
Yield	%	97	95	90		80	70	60	40
Biological oxygen demand (BOD)	kg/t	10	20		50	100			200
Grinding or refining energy	kWh/t	1200	2200	2500		1000	500	200	100
Freeness CSF	ml	100	120	200	400		600		800
Tensile index	Nm/g	30	40	50	60		70	80	100
Light-scattering coefficient	m <sup>2</sup> /kg	65	60	50		40			30

increase with refining
decrease with refining

Fig. 7.2 Characteristics of mechanical, semi-chemical, and chemical pulps.

With decreasing yield, an increased effluent load (biological oxygen demand; BOD) and an increased strength potential is found, but this is to the disadvantage of light-scattering properties. In conventional chemical pulping, specific energy consumption is lower and the chemical consumption higher compared with the other processes. Freeness is measured with about 100 mL for (fines-containing) stone groundwood (SGW) and 800 mL (ca. 12 SR) for chemical pulp with a high long-fiber content. Light-scattering values are provided for the pulp before it undergoes additional mechanical treatment. The post-refining of a mechanical pulp increases the light-scattering coefficient, whereas the refining of a chemical pulp decreases this measure.

The grinding and refining processes separate the fibers in different ways. Figure 7.3 shows the fractional composition according to the McNett principle versus the yield of various pulps. The amount of long fibers in mechanical pulps (fraction McNett R28) increases in the range SGW, RMP, TMP, CTMP more to the debit of the middle fraction than of the fines fraction.

The bonding ability of mechanical pulp fractions can vary widely, as shown in Fig. 7.4 [41]. The high bonding ability of middle fractions is clear.

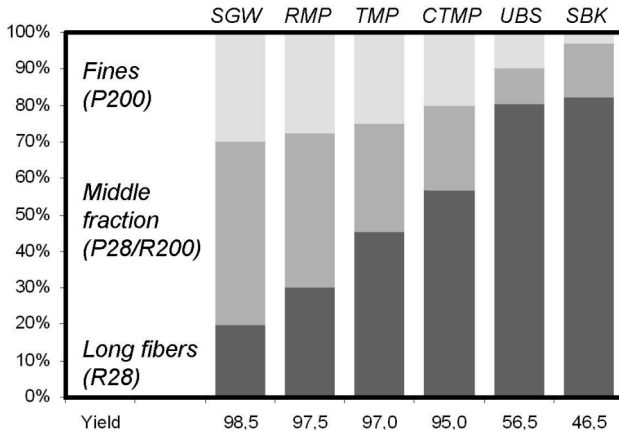


Fig. 7.3 Comparative fractional composition of various pulps according to the McNett principle [40].

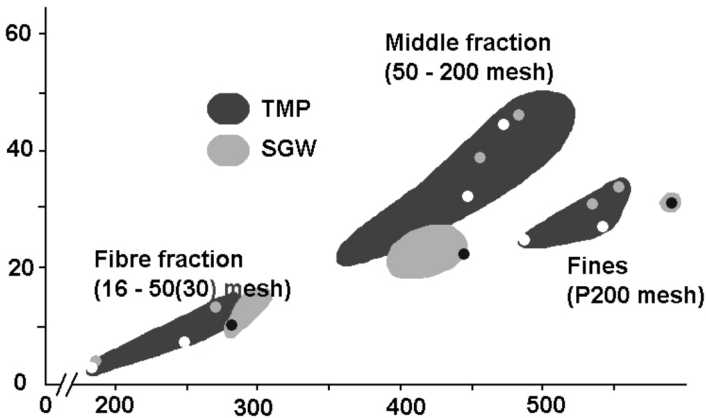
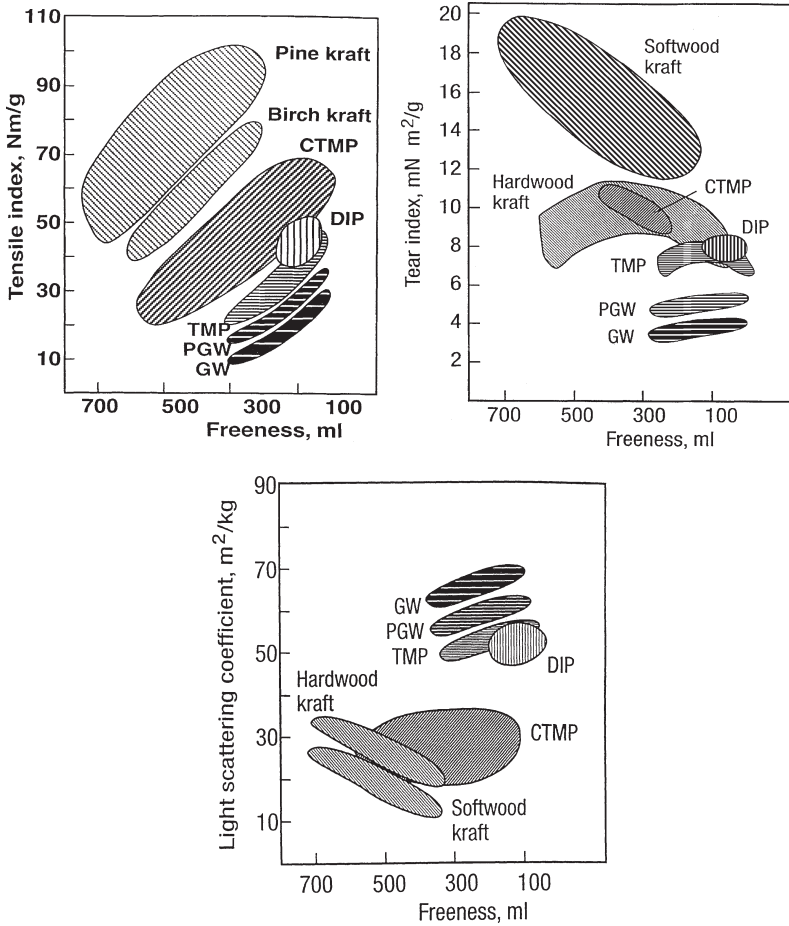


Fig. 7.4 Tensile index versus apparent density for the coarse fiber fraction, middle fraction and fines fraction of different mechanical pulps (according to Mohlin [41]).

Mechanical pulps typically form bulky sheets with high light scattering (Fig. 7.5). Thus, it is possible to produce paper with acceptable stiffness and opacity at a considerably lower basis weight by using a mechanical pulp than a chemical pulp. When compared at the same freeness levels, TMP normally has the highest bulk and CTMP the lowest bulk of mechanical pulps. With regard to the mechanical pulps in Fig. 7.5, groundwood pulps usually exhibit the best optical properties (Fig. 7.5, below), whereas TMP and CTMP exhibit the best strength properties (Fig. 7.5, left and right). Because of their good strength properties, these mechanical pulps require less reinforcement pulps when manufacturing,



**Fig. 7.5** Tensile index, tear index, and light-scattering coefficient of different pulps depending on freeness [42].

for example, LWC paper. This compensates their lower light-scattering power and makes their use economically viable.

Höglund et al. [43] have compared the same types of mechanical pulps with chemical pulps according to their strength properties. The mechanical pulps were from spruce wood (SGW, RMP, TMP, and CTMP), and the chemical pulps from pine were either unbleached (USB) or semi-bleached (SBK). The possible property fields for these pulps are illustrated in Figs. 7.6–7.8.

Strength properties increased in the range SGW, RMP, TMP, CTMP, USB, and SBK. The tear resistance of CTMP pulps was close to that of unbleached chemical pulp USB (Fig. 7.6). The tensile index of CTMP covered large parts of the semi-bleached chemical pulp SBK and unbleached chemical pulp USB, but at lower apparent densities (Fig. 7.7). When considering the light-scattering coefficient,

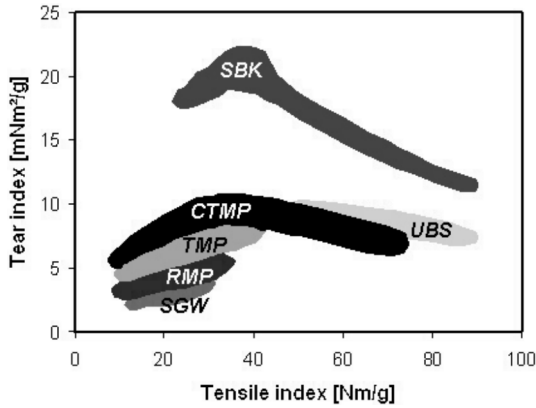


Fig. 7.6 Tear resistance versus tensile index for various mechanical pulps compared with chemical pulps.

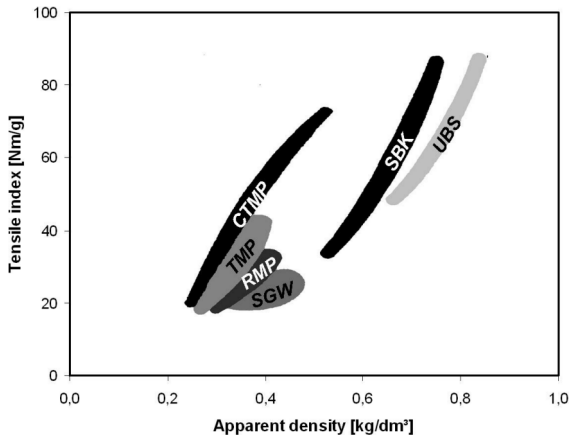
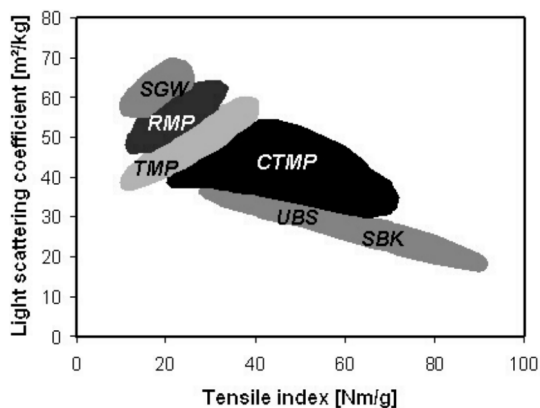


Fig. 7.7 Tensile index versus apparent density for various mechanical pulps compared with chemical pulps.

SGW had the highest values, followed by RMP and TMP. The light-scattering coefficient of CTMP was in the same range as TMP, but at higher levels of tensile index. The chemical pulps had the lowest light-scattering coefficient, and could be distinguished by type (USB or SBK) (Fig. 7.8).



**Fig. 7.8** Light-scattering coefficient versus tensile index for various mechanical pulps compared with chemical pulps.

Selected properties from different mechanical pulps, made from Norway spruce and compared at freeness level 40 mL, are listed in Tab. 7.1. General quality requirements of mechanical pulp for use in LWC and SCA grades are detailed in Tab. 7.2.

**Tab. 7.1** Properties of mechanical pulps for printing paper grades (Norway spruce, CSF 40 mL).

Parameter	Unit	Groundwood	Pressure groundwood	TMP
Minishives	%	0.1	0.1	<0.1
Coarse fibers (R14)	%	1	3	10
Long fibers (P14/R28)	%	11	22	30
Fines (P200)	%	38	33	30
Fiber length	mm	0.65	0.85	1.5
Apparent density	kg m <sup>-3</sup>	520	510	500
Gurley	s	150	200	250
Tensile index	Nm g <sup>-1</sup>	35	43	52
Tear index	mNm <sup>2</sup> g <sup>-1</sup>	3.2	4.2	7.2
Scott Bond	J m <sup>-2</sup>	280	320	250
Light scattering coefficient	m <sup>2</sup> kg <sup>-1</sup>	75	72	60
Brightness	%	65	64	62

Tab. 7.2 General quality requirements of mechanical pulp for use in LWC and SCA grades.

Pulp grade		SGW	PGW	TMP	TMP
Paper grade	Unit	SC/LWC	SC/LWC	SC	LWC
Freeness	mL	30–40	30–40	30–40	40–50
Shives content	%	<0.05	<0.05	<0.05	<0.05
Coarse fibers (R14)	%	<1.0	<1.0	<7.0	<3.0
Long fibers (P14/R28)	%	10–15	14–20	28–33	22–27
Fines (P200)	%	>36	>32	>28	>28
Apparent density	kg m <sup>-3</sup>	450–500	440–500	450–520	450–500
Tensile index	Nm g <sup>-1</sup>	>40	>45	>50	>50
Tear index	mNm <sup>2</sup> g <sup>-1</sup>	>3.5	>4.5	>7.0	>6.5
Light-scattering coefficient	m <sup>2</sup> kg <sup>-1</sup>	>70	>68	>58	>58

## References

- 1 vdp Verband Deutscher Papierfabriken e.V.
- 2 Sittauer, H.L., Friedrich Gottlob Keller, Leipzig, 1982.
- 3 Goring, D.A.J., Thermal softening of lignin, hemicellulose and cellulose. *Pulp Paper Mag. Can.*, 1963; 64(12): T517–T527.
- 4 Styan, G.E., Bramshall, A.E., Lignin-solvation improves mechanical pulp processing. *Pulp Paper Can.*, 1979; 80(1): 74–77.
- 5 Luhde, F., Temperature within the grinding zone. Part 1. *Pulp Paper Mag. Can.*, 1959; 60(9): T269–T271.
- 6 Süttinger, R., *The Technology of the Wood Grinding Process*. Heidenheim: Voith Forschung und Konstruktion, Nr. 26, 1979.
- 7 Steenberg, M.B., Nordstrand, A., Production and dissipation of frictional heat in the mechanical wood grinding process. *Tappi J.*, 1962; 45(4): 333–336.
- 8 May, W.D., Atack, D., A laboratory study of a new mechanical pulping process. *Pulp Paper Mag. Can.*, 1965; 66(8): T422–T435.
- 9 Atack, D., Pye, I.T., The measurement of grinding zone temperature. *Pulp Paper Mag. Can.*, 1964; 65(9): T363–T376.
- 10 Atack, D., *Mechanics of Wood Grinding Trend*. The Activities of the Pulp and Paper Research Institute of Canada, Report No. 19, 1971: 6–11.
- 11 Powell, F.G., Luhde, F., Logan, K.C., Super groundwood by grinding. *Pulp Paper Mag. Can.*, 1965; 66(8): T399–T406.
- 12 Aario, M., Haikkala, P., Lindahl, A., Pressure grinding – a new process for mechanical pulping. *Wochenbl. f. Papierfabr.*, 1978; 106(19): 723–730.
- 13 Pietarila, V., Mitchell, G., Haikkala, P., Tuominen, R., PGW at high temperatures and pressures. International Mechanical Pulping Conference, Vancouver, Canada, Preprints, CPPA, Montreal, 1987: 19.
- 14 Pasanen, K., Peltonen, E., Haikkala, P., Liimatainen, H., Experiences using super-pressurized groundwood at a Finnish supercalender paper mill. *Tappi J.*, 1991; 74(12): 63.



- 15 Murtola, C., Peltonen, E., Industrial pressure grinding at low shower water temperatures in a paper mill. PTS-TUD-Symposium Technology of Chemical and Mechanical Pulp 1995, PTS Verlag München, 1995.
- 16 Valmet, Groundwood Systems, Pressure Groundwood, Tampere, 1996.
- 17 Tuovinen, O., Liimatainen, H., Fibers, fibrils and fractions – an analysis of various mechanical pulps. *Pap. Puu*, 1994; 76(8): 508–515.
- 18 Asunmaa, P., The selection, process flowcharts, optimization and results obtained from the new PGW-S mill at the Kaukas Oy Voikkaa paper mill in Finland. Annual Meeting CPA Montreal, Proceedings, 1993: B71.
- 19 Giertz, H.W., Different qualities of groundwood, refiner mechanical pulp and thermomechanical pulp, *Wochenbl. f. Papierfabr.*, 1976; 104(19): 736–737.
- 20 Atack, D., Heitner, C., State of the art of chemimechanical wood pulping processes for printing paper. *Das Papier*, 1982; 36(10A): V114–V127.
- 21 Beatson, R., Heitner, C., Atack, D., Factors affecting the sulphonation of spruce. *J. Pulp Paper Sci.*, 1984; 10(1): J12.
- 22 Süttinger, K., Analysis of energy consumption in mechanical pulping. *Wochenbl. f. Papierfabr.*, 1979; 107(2): 40–43.
- 23 Strauss, J., Screening by classifying – a more and more important process in stock preparation. *Zellstoff und Papier*, 1981; 30(4): 170–176.
- 24 Ämmälä, A., Fractionation of thermo-mechanical pulp in pressure screening – an experimental study on the classification of fibres with slotted screen plates. Acta Universitatis Oululensis, Technica, C156, 2001 (Thesis).
- 25 *Papermaking Science and Technology. Book 5, Mechanical Pulping.* Fapet Oy Helsinki 1999: 270.
- 26 Yu, C.J., DeFoe, R.J., Fundamental study of screening hydraulics. Part 1: Flow patterns at the fed-side surface of screen baskets. Mechanism of fiber mat formation and re-mixing. *Tappi J.*, 1994; 77(9): 767–782.
- 27 Niinimäki, J., On the fundamentals of pressure screening – an experimental study of conditions and phenomena in the screen basket. Acta Universitatis Oululensis, Technica, C124, 1998 (Thesis).
- 28 Bliss, T., Screening in the Stock Preparation System. Stock Preparation Short Course, Atlanta, GA, USA, Proceedings, 1990: 59–75.
- 29 Kleinhappel, S., Lipponen, J., Jussila, T., Groundwood pulp quality improvements with economical benefit by improved screening efficiency. International Mechanical Pulping Conference, Ottawa, Canada, Proceedings, 1995: 267–270.
- 30 Schmidt, G., Schempp, W., Krause, T., Wasserlösliche Holzschliffbestandteile, Analyse und Auswirkung bei der Papierherstellung. *Das Papier*, 1990; 44(10A): V49–V55.
- 31 Roick, T., Schmidt, G., Schempp, W., Störstoffe in Holzstofffiltraten: Identifizierung, Veränderungen im Verlauf der Bleiche, analytische Beurteilung der Wirkung von Bekämpfungsmitteln. *Wochenbl. f. Papierfabr.*, 1994; 122(12): 506–509.
- 32 Roick, T., Schempp, W., Krause, T., Holzstoff-Feinstoffe: einige Ursachen ihrer schlechten Bleichbarkeit. *Das Papier*, 1991; 45(10A): V23–V26.
- 33 Melzer, J., Stabilität von Natriumdithionit in wässrigen Lösungen. *Wochenbl. f. Papierfabr.*, 1990; 118(22): 925–931.
- 34 Ellis, M.E., Hydrosulfit (dithionite) bleaching. In: *Pulp Bleaching, Principles and Practice.* Tappi Press, Atlanta, 1996: 500–501.
- 35 Fischer, K., Vergilbung von Hochofensbeutezellstoff. *Das Papier*, 1990; 44(10A): V11.
- 36 Süß, H.U., Del Grosso, M., Schmidt, K., Hopf, B., Options for bleaching mechanical pulp with a lower COD load. Appita Annual Conference, Proceedings, 2001.
- 37 Htun, M., Engstrand, P., Salmén, L., The implication of lignin softening on latency removal of mechanical and chemimechanical pulps. *J. Pulp Paper Sci.*, 1988; 14(3): 109–112.

- 38 Karojärvi, R., Nerg, H., Latency in pressure groundwood. International Mechanical Pulping Conference, Vancouver, Canada, Proceedings, 1987: 25–28.
- 39 Blechschmidt, J., About latency behavior of mechanical pulps. *Zellstoff und Papier*, 1976; 25(10): 293–298.
- 40 Sundholm, J., What is mechanical pulping? In: *Papermaking Science and Technology. Book 5, Mechanical Pulping*. Fapet Oy Helsinki, 1999: 17–21.
- 41 Mohlin, U.-B., Properties of TMP fractions and their importance for the quality of printing papers. Part 1: Large variations in properties within fractions are observed. *Svensk. Papperstidn.*, 1980; 16: 461–466.
- 42 Heikkurinen, A., Leskelä, L., The character and properties of mechanical pulps. In: *Papermaking Science and Technology. Book 5, Mechanical Pulping*. Fapet Oy Helsinki 1999: 395–413.
- 43 Höglund, H., Modified thermomechanical pulp in newsprint furnishes. International Mechanical Pulping Conference, Helsinki, Proceedings Vol. III, 1977: 17B.

### III

## Recovered Paper and Recycled Fibers

*Hans-Joachim Putz*

## 1

## Introduction

During the era before the introduction of industrialized paper production 200 years ago, the most common fiber furnish was secondary fibers recovered from used textiles. These were rags based on hemp, linen, and cotton. Only after the invention of mechanical woodpulp in 1843 and chemical woodpulp during the second half of the nineteenth century was paper production no longer as reliant on recycled material as in the previous 2000 years.

Before industrialized paper production and the invention of the paper machine in 1799, stationery or writing paper made from rags was recycled to produce low-grade board. As early as 1774, Claproth in Göttingen, Germany, improved the processing of used, hand-made writing papers. His process removed optically disturbing inks or printing ink. Today, we call this method “deinking”.

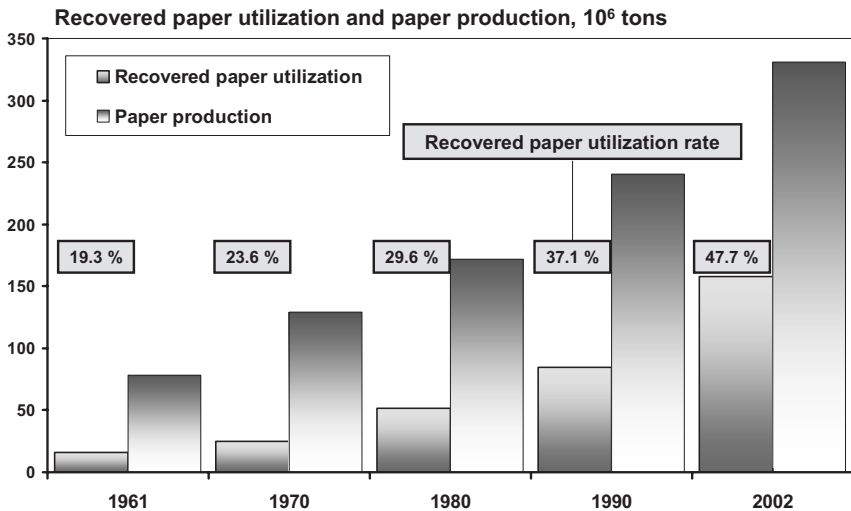
With growing industrialization and gross national product, the global paper production increased significantly from almost 44 million tons in 1950 to 339 million tons in 2003. The data in Tab. 1.1 indicate that between 1960 and 2000, for a doubling of the paper production worldwide, in the CEPI countries (all EU countries plus Czech Republic, Hungary, Norway, Slovak Republic, and Switzerland) or in Germany, an approximate period of 20 years was necessary, whereas between 1950 and 1960 only a 10-year period was required for the first doubling of paper production. In all of these time periods no doubling appeared in the USA where,

Tab. 1.1 Development of paper production between 1950 and 2003, in million tons [1–6].

Country	Year						
	1950	1960	1970	1980	1990	2000	2003
Germany	1.6	3.4	6.6	8.8	12.8	18.2	19.3
CEPI	10.5	20.5	36.7	40.7	63.1	90.8	95.2
USA	22.1	31.3	47.6	56.8	72.2	85.8	80.2
World	43.8	74.4	129.3	171.7	240.8	324.0	338.8

in 1950, about 50% of the global paper production was produced. This proportion decreased until 2002 to 25% and becomes also expressed in the lowest average annual growth rate between 1950 and 2002 in this comparison of: 2.5% for USA; 4.0% worldwide; 4.2% for the CEPI countries; and 4.8% for Germany.

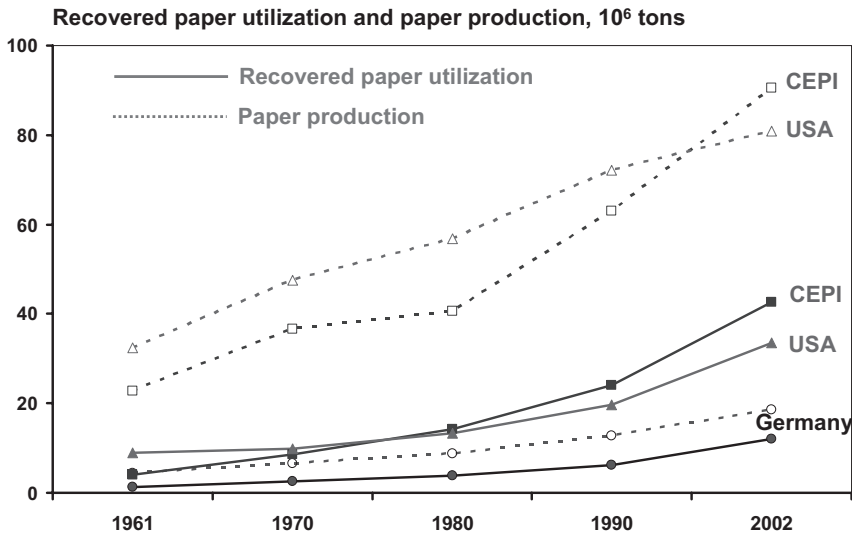
Compared with the situation today, the recycling of used paper products manufactured from woodpulp fibers was of little importance during the first half of the twentieth century. During the 1950s and 1960s, increasing use was made of recycled fiber furnish, especially for the production of packaging paper and board. International statistics related to the use of recovered paper published in the official yearbooks of the German association of the paper industry (VDP) stated first in 1979 international data for the utilization of recovered paper. In 1963, the annual review of PPI (Pulp & Paper International) published earlier international data on recovered paper for the year 1961 [7]. Figure 1.1 illustrates the global increase of recovered paper utilization and paper production between 1961 and 2002.



**Fig. 1.1** Global development of recovered paper utilization and paper production between 1961 and 2002 [1–4,7].

In Fig. 1.2, the development of recovered paper utilization and paper production is split into the USA, the CEPI countries, and Germany. It is clear that since 1990, the use of recovered paper has increased over-proportionally, with average annual growth rates between 1961 and 2002 for recovered paper use as 3.3% for the USA, 5.8% for Germany and worldwide, and 5.9% for the CEPI countries.

These higher values compared to paper production imply an increasing relevance of recovered paper in the selected regions.



**Fig. 1.2** Development of recovered paper utilization and paper production in the USA, the CEPI countries, and Germany between 1961 and 2002 [1–4,7].

Recovered paper use is most attractive in densely populated regions with a high paper consumption per capita, where the so-called “urban forest” growth occurs. The region must also have a paper industry with sufficient technology and a long tradition in recycled fiber processing. The most prominent regions are Japan and Europe outside Scandinavia. Recovered paper is not the only material increasingly collected and reused in developed countries. National recycling management, enforced by legal measures, encourages the population to collect metal, glass, and plastics also. Consumers in many countries participate in recycling; in this way they are involved as consumers of commodities while producing secondary raw materials for reuse.

Cost competition and the legal requirements in many countries primarily promote the use of recovered paper. The impact of environmentalists through “green” movements and the level of acceptance in the market of paper made from recycled fibers are additional driving forces that vary by country. Recovered paper use is an environmentally friendly issue according to the recycled fiber processing paper industry, environmentalists, governmental authorities, and often even the marketplace. It is accepted that recycling preserves forest resources and energy used for production of mechanical pulps for paper manufacturing. Additionally, recovery and recycling of used paper products avoids unnecessary landfilling.

The processing of recycled products requires relatively little fresh water per ton of paper produced. However, the solid waste rejects and sludge (e.g., deinking sludge) from recovered paper processing mills typically present a problem. The rate of formation of such residues is between 5% and 40%, depending on the recovered paper grade processed and the paper grade produced. The average rate

of rejects and sludges totals about 15%, calculated on the recovered paper input on an air-dried basis. Because landfilling of organic matter has no future in many countries, most organic waste requires burning in order to reduce its volume. Effective, clean incineration technologies are available that control flue gas emissions, and the heat content of the residues and sludges contributes to self-supporting incineration. The final waste (ashes) can either be discarded or used as raw materials in other industries. An increasing volume of rejects and sludges can be used in brick works, the cement industry, and for other purposes.

## 2

### Relevance of Recycled Fibers as Paper Raw Material

Recovered paper has become the most important fiber raw material for paper production. At 153 million tons in 2001, the volume of recovered paper used globally in the paper industry has exceeded for the first time the total volume of virgin fibers, such as chemical pulp (113 million tons) and mechanical pulp (36 million tons) [1]. These figures make it evident that recycled fibers play a very important role today in the global paper industry as a substitute for virgin pulps. Together with nonwood fibers, the virgin fiber share reached 54% in 2002, whereas the proportion of recovered paper was 46%.

Global and European usage values are illustrated in Fig. 2.1. By comparing the annual average growth in recovered paper utilization and paper production since 1971, it becomes clear that in Germany, in the CEPI countries, in the USA and globally, the increase in recovered paper use was between 1.7% p.a. and 3.0% p.a.

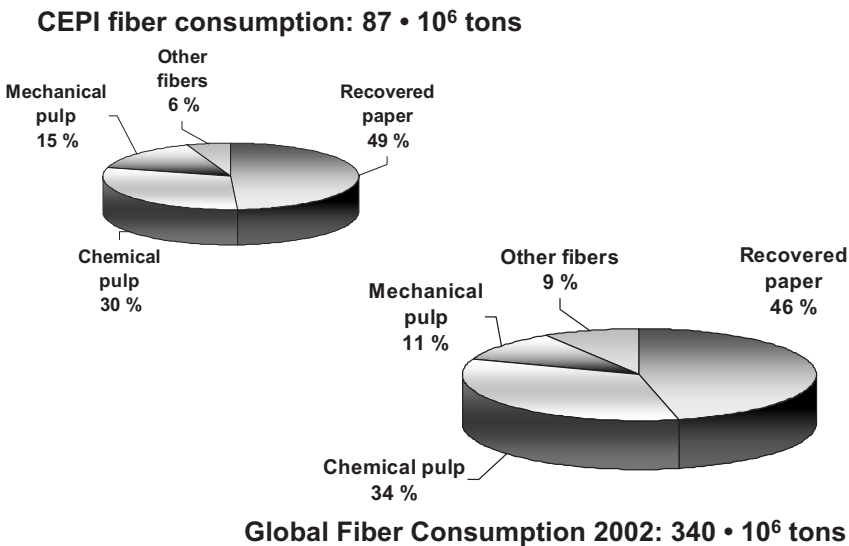


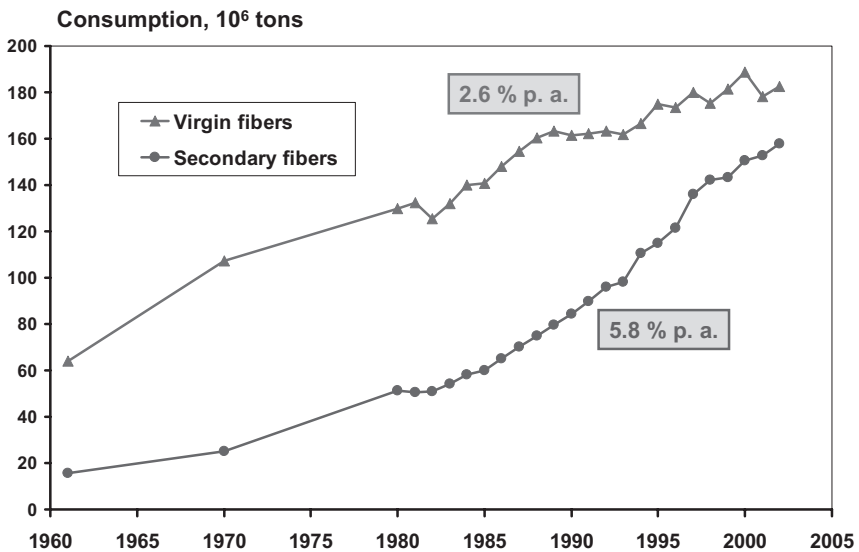
Fig. 2.1 Fiber material consumption for paper and board production in the CEPI countries and in the world for 2002 [1].



higher than the annual growth in paper production. This underlines once again the increasing importance of recovered paper as fiber raw material for the paper industry in general. Indeed, in many countries of the world, the paper industry could not exist as it does today without recycled fibers. In Central, Southern, or Western Europe, this is due to economic reasons, whereas in places such as Japan, Korea, Taiwan, or Mexico, the additional reason is a scarcity of native pulpwood resources.

The paper industry is the exclusive relevant user of recovered paper as secondary raw material – at least in terms of material recycling. Various mechanical and chemical processes generate recycled fibers for the production of new paper and board grades. These processes use different recovered paper grades that contain either chemical or mechanical fibers, or mainly an undefined mixture of both. Some paper and board grades can use recycled fibers exclusively. This includes corrugating medium and test liner, for example, in Central, Western and Southern Europe or newsprint in Germany. Other grades use blends of recycled and virgin fibers. Examples are newsprint produced in North America or Northern Europe. The proportion of recycled fibers in the furnish can vary from about 5% for fine papers to 100%, depending on the paper grade or geographic region.

The data in Fig. 2.2 indicate the global increase in fiber raw material consumption during the past four decades. Over this time period, the consumption of virgin fibers increased annually by 2.6%, whereas the increase in secondary fiber consumption was more than twice as high. The use of recovered paper accelerated especially in the 1980s. Between 1980 and 2002, the global paper production



**Fig. 2.2** Global development of the use of virgin fibers and recovered paper for paper and board production [1–4,7].

grew by 3.0% annually. For this production the use of recovered paper increased by 5.2% p.a. on average, whereas the annual growth of all kinds of virgin fibers (chemical and mechanical pulp as well as nonwood pulp) was only 1.6% p.a.. Increasing application of improved deinking processes also influenced the growth in use of recovered paper during the 1980s and 1990s. This allows the use of recycled fibers in higher-grade hygiene papers, newsprint and recycled graphic papers such as copying and writing papers.

The proportion of recovered paper as fiber raw material for paper and board production has been increased in the following regions between 1980 and 2002, from 28% to 46% worldwide; from 31% to 48% in the CEPI countries; and from 46% to 68% in Germany.

During the period of time under examination, an increase of about 20%-points can be observed in each region.

## 3

### Recovered Paper Grades

#### 3.1

##### Europe

In Europe, recovered paper was traded until 1998 by various national recovered paper grade lists [8–10]. In 1999, the CEPI (Confederation of European Paper Industries) and B.I.R. (Bureau International de la Récupération) agreed on a European list of standard grades for recovered paper and board. This list had become a European Standard in 2001 by CEN (European Committee for Standardization) as EN 643 [11]. Subsequently, the national recovered paper grade lists have been withdrawn, so that only one list is valid throughout Europe.

In total, 67 recovered paper grades and sub-grades are listed in the EN 643 and are classified in the following five groups:

1. Ordinary grades
2. Medium grades
3. High grades
4. Kraft grades
5. Special grades.

The first number of the recovered paper grade specification indicates the category to which the grade belongs; for example, grade 1.11 is “Sorted graphic paper for deinking”, which belongs to the group of “ordinary grades” (No. 1). The grade 4.02 is “Used corrugated kraft I” and belongs to the fourth group of “kraft grades”.

Recovered paper grades are generally not specified with quantified quality characteristics. Unusable materials are defined according to EN 643 as materials that are unusable in production. They consist of nonpaper components and paper and board detrimental to production. Nonpaper components are any foreign matter in the recovered paper that can cause damage to machines, interruption to production, or reduce the value of the finished product. Such items include the following components:

- Metal
- Plastic
- String

- Glass
- Textiles
- Wood
- Sand and building materials
- Synthetic materials
- “Synthetic papers.”

According to EN 643, recovered paper must be supplied free of nonpaper components and unusable paper and board. Certain amounts of unusable materials may be included, but only if this has been agreed individually between the paper mill and the supplier.

According to EN 643, paper and board detrimental to production are those grades treated such that, for a basic or standard level of equipment, they are unsuitable as raw material for the manufacture of paper and board, or actually damaging, or whose presence makes the whole consignment of recovered paper unusable. No special paper grades or paper products are listed, but the following paper products are intended, for example:

- Bitumenized board
- Carbon paper
- Parchment and greaseproof paper
- Wet-strength paper
- Waxed paper.

Especially in the (white) recovered paper grades intended for deinking, (brown) packaging materials and colored papers are also considered as unusable components.

Moreover, EN 643 specifies that recovered paper should be supplied with a moisture content of not more than 10%.

It is very important to clarify that, according to EN 643, recovered paper from refuse sorting stations is not suitable for use in the paper industry. Additionally, recovered paper and board originating from multi-material collection systems, containing only material of a valuable, recyclable nature must be specifically marked. It is not allowed to mix recovered paper from this origin unmarked with other recovered paper and board.

The naming of recovered paper in all lists uses one of the following criteria:

- Places of occurrence, such as supermarket corrugated paper and board (1.04) or sorted office paper (2.05).
- Former paper grades contained in the recovered paper, such as mixed magazines and newspapers (1.10) or white wood-free computer print-out (3.07).
- Mixed category, such as mixed paper and board, unsorted, but unusable materials removed (1.01) or mixed papers and boards (sorted) (1.02).

The descriptions of the individual recovered paper grades are as follows:

- Primarily solely descriptive, without further specifications:
  - New shavings of corrugated board (4.01); shavings of corrugated board, with liners of kraft or testliner
  - Old corrugated containers (1.05); used boxes and sheets of corrugated board of various qualities
- One specification stating which grades should not be part of the recovered paper grade or limited to a certain percentage:
  - Colored letters (2.06); correspondence, in mixed papers colored in the mass, with and without print, of printing or writing paper. Free from carbon paper and hard covers.
  - White newsprint (3.14); shavings and sheets of white unprinted newsprint, free from magazine paper.
- Minimum or maximum demand for a certain paper grade as components of the recovered paper grade:
  - Mixed papers and board (sorted) (1.02); a mixture of various qualities of paper and board, containing a maximum of 40% newspapers and magazines.
  - Supermarket corrugated paper and board (1.04); used paper and board packaging, containing a minimum of 70% of corrugated board, the remainder being solid board and wrapping papers.

A satisfactory description of a wood-containing recovered paper mix, commonly used for deinking called “Sorted graphic paper for deinking” (1.11), originating primarily from household collections has the following characterization:

- Sorted graphic papers from households, newspapers and magazines, each at a minimum of 40%. The percentage of non-deinkable paper and board should be reduced over time to a maximum level of 1.5%. The actual percentage is to be negotiated between buyer and seller.

In this special case, the limit to a maximum 1.5% of paper and board unsuitable for deinking includes packaging papers, corrugated board boxes, and board as well as dyed papers.

The group of special recovered paper grades comprises (according to EN 643) seven grades such as unsorted mixed recovered paper and board (5.01), mixed packaging (5.02), liquid board packaging (5.03), wrapper kraft (5.04), wet labels (5.05), and unprinted as well as printed white wet-strength wood-free papers (5.06 and 5.07).

The structure of the EN 643 and most of the grade descriptions has its origin in the former German recovered paper grade list. The German association of the paper industry (VDP) and the associations of secondary raw material collectors and dealers (BDE and bvse) had agreed on this former list. Used paper and board from industrial and commercial facilities is relatively easy to recover, but increasing demands of the paper industry requires more intensified collection from

private households. During the past two decades, it has become clear that in Germany the additional recovered paper volumes have been collected predominantly from private households, which belong to the group of ordinary paper grades. Therefore, in Germany the proportion of ordinary paper grades increased significantly between 1980 and 2002 from 60% to 78% (Fig. 3.1). During the same period, the total volume of recovered paper collection increased from 3.3 million tons to 13.7 million tons.

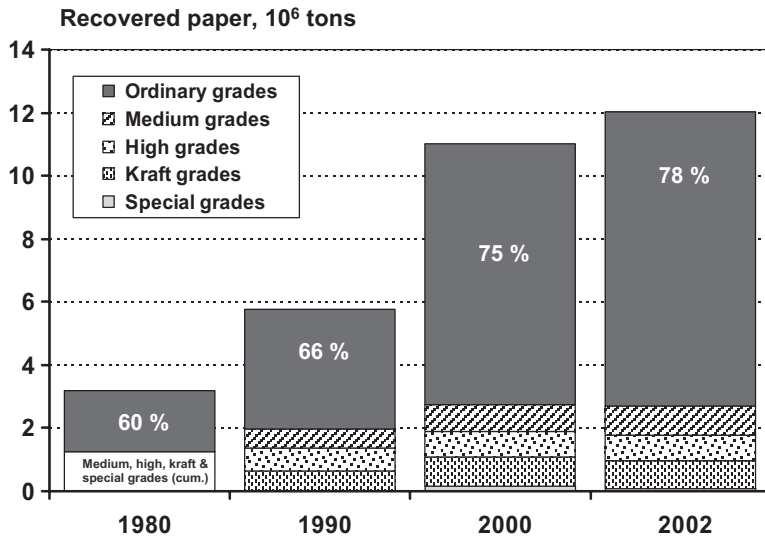


Fig. 3.1 Recovered paper demand (1980–2002) by groups in Germany [1–3].

The complete list of recovered paper grades is published in the Appendix of this chapter, and is also available on the German website of GesPaRec ([www.altpapierrohstoff.de](http://www.altpapierrohstoff.de)).

The examples of these grade names and definitions shows that the specifications of recovered paper in the official grade list do not define physically verifiable quality criteria. In contrast, such definitions are available for chemical pulp as virgin fibers using optical characteristics or minimum strength parameters depending on freeness levels.

The use of recovered paper in paper production in the CEPI countries varies greatly by grade of recovered paper. In 2002, the consumption of recovered paper of all CEPI countries was as follows:

- 41% corrugated and kraft grades
- 26% deinking grades
- 20% mixed grades
- 13% other grades including high grades.

Figure 3.2 illustrates in which paper grades the various groups of recovered paper are used. Whereas corrugated and kraft as well as mixed grades (91% by weight) primarily find use in the production of packaging papers and board, almost all deinking grades (80% by weight) go to graphic paper production. The latter recovered paper grades are also used for hygiene papers with an addition of nearly two-thirds high grades. The production of other papers requires almost equal proportions of all four recovered paper grade groups.

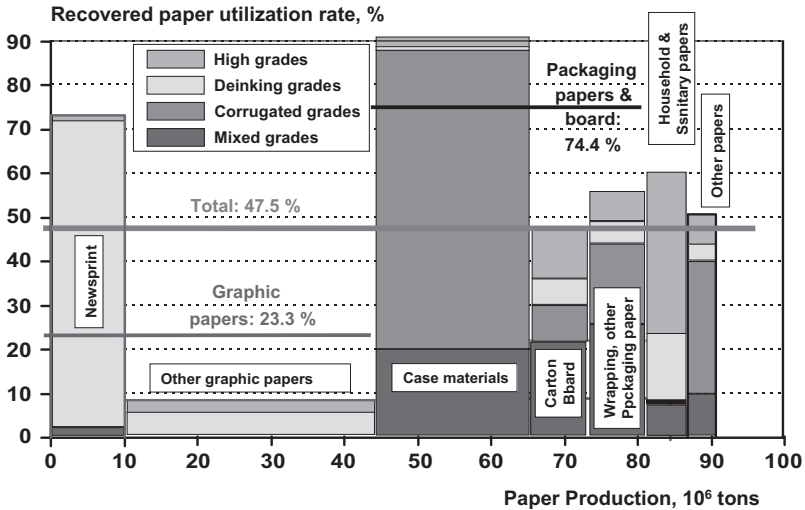


Fig. 3.2 Recovered paper utilization by grades in the CEPI countries in 2002 [12].

The total amount of 43 million tons of recovered paper was used in the following production areas: 45% case materials; 17% newsprint; 10% wrappings and other packaging papers; 9% carton boards; 8% household and sanitary papers; 7% other graphic papers; and 4% other paper grades.

The individual paper grades need specific recovered paper grades as raw materials. Thus, collection and sorting of these resources must be carried out accordingly to satisfy the needs of the industry.

### 3.2 North America and Japan

Neither the United States nor the Japanese grade lists for recovered paper use the European classification of four or five different groups. Instead, they define 26 grades in Japan and 51 grades in the USA. According to the guidelines for recovered paper stock export transactions (PS-2003) of the United States, seven grades are currently not in use. The names of the used grades are based on the original paper or packaging materials. Some grade descriptions generally refer to the

paper and board products as printed or unprinted and wood-containing or wood-free papers according to what is assumed to be contained in the recovered paper grade concerned.

### 3.2.1

#### **United States**

The United States grade list does not permit the presence of individual paper or board grades in several grades, including coated, printed, or waxed papers [13]. In some grades, the contents of mechanical fibers, or of colored papers, are limited. Unusable materials in the recovered paper are divided into outthrows and prohibitive materials. Outthrows are defined as all papers that are so manufactured or treated or in such a form which renders them unsuitable for consumption in the grade specified. Prohibitive materials have the following definition:

- Any materials that by their presence in the packaging of paper stock in excess of the amount allowed will make the packaging unusable as the grade specified.
- Any materials that may be damaging to equipment.

For both definitions, a material can be an outthrow in one grade and a prohibitive material in another grade. For example, carbon paper is unsuitable in mixed paper (#2) and is therefore classified as an outthrow, whereas it is unusable in sorted white ledger (#40). The classification in this case is prohibitive material.

Prohibitive materials are allowable in 13 of the 44 recovered paper grades, but not in the remaining 31. The total including both outthrows and prohibitive material ranges from 0% to 12%.

The American grade list also currently includes 35 specialty grades called 1-S to 35-S which are not part of the regular grades. Generally, these require a special processing system. The recovered specialty paper grades do not have more definite specifications. The grade name reflects their origin. The majority of these grades relate to the following:

- Waxed cup cuttings, waxed boxboard cuttings, and waxed corrugated cuttings.
- Wet strength corrugated cuttings, white or brown, printed and/or colored wet-strength waste.
- Polycoated milk carton, diaper stock, bleached kraft, or boxboard cuttings.

Other special grades include asphalt laminated corrugated cuttings, carbonless treated ledger, or textile boxes. The term “soft” describes the American grade list for short fiber stock consisting of predominantly soda pulp, hardwood fibers, or both. “Hard” refers to long fiber stock predominantly sulfite or sulfate made of softwood fibers.

In the USA, almost 48 million tons of used paper products were recovered in 2002. The most important grades considering recovery in the USA are the OCC



grades (49%), followed by deinking grades (32%) which include old news, high-quality recovered graphic paper grades as well as pulp substitutes (wood-free recovered papers). The remaining 19% are mixed grades [14].

### 3.2.2

#### **Japan**

Two-thirds of the 27 grades on the Japanese list are pre-consumer recovered paper. They refer to grades that occur at printing plants, bookbinders, corrugated board plant operations, or in board or paper-converting plants [15]. Remarkably, the Japanese grade list does not recognize any mixed recovered paper grades. In almost half of all grades, no objectionable materials at all are permitted. In the remaining ones, limits of objectionable materials range from 1% to 3%.

In 2002, old corrugated containers (#23) and kraft browns (#19 to #22) had a share of 46% of the total recovered paper tonnage, followed by old news (#17) with 25% and the remaining grades (#1 to #16, #18, #24 to #27) with 29%. (The symbol “#” is used to indicate the number of recovered paper grades.)

## 4

### Basic Statistics

Consideration of recovered paper use and recovery of used paper products requires the definition of three statistical parameters:

- Recovered paper utilization rate (in %) is the amount of recovered paper used as raw material in the paper industry (in tons), divided by paper production (in tons), on an annual basis, multiplied by 100.
- Recovery or collection rate (in %) is the amount of recovered paper for all material recycling (in tons), divided by paper consumption (in tons), on an annual basis, multiplied by 100.
- Recycling rate (in %) is the amount of recovered paper used as raw material in the paper industry (in tons), divided by paper consumption (in tons), on an annual basis, multiplied by 100.

The above mentioned parameters can be calculated either globally or for a country or a certain region such as Europe. Calculating these factors for certain paper grades or categories of paper grades such as newsprint or graphic papers globally or for a country or region is often even more relevant. Naturally, this calculation presupposes that the data for recovered paper used, collected, or recovered are recorded and documented using the same criteria in each country.

From these definitions it becomes clear that the utilization rate is related to recovered paper usage in paper production, whereas the recovery rate is related to the amount of collected paper related to paper consumption. Both rates can be affected directly either by the paper industry by the usage of more or less recovered paper in paper production, or by the waste management industry collecting more or less recovered paper of the paper consumption. The recycling rate is a more theoretical value which places recovered paper usage in relation to paper consumption. A high level of recovered paper usage in paper production, combined with strong net paper export rate, will result in a high recycling rate, which must be satisfied by recovered paper imports from abroad.

However, calculating the recovered paper utilization rate does not provide any indication of the proportion of recycled fibers (with or without minerals) that ultimately is found in specific paper grades. This is because the yield in recovered paper processing differs by paper grade produced and is usually not statistically

documented but only estimated. This factor is often of more interest for technical, quality, ecological, and economic reasons than for monitoring the recovered paper utilization rate. Many years of industrial experience have provided the following ranges of yields for recovered paper processing for different production segments:

- Packaging papers and board: 90–95%
- Graphic papers: 65–90%
- Hygiene papers: 60–75%
- Specialty papers: 70–95%
- Market deinked pulp (DIP) (wood-free): 60–70%
- Market DIP (wood-containing): 80–85%.

The yields of recycled fiber pulps for packaging papers and board are high because these are mostly “brown” recovered papers processed without deinking. The yield loss results primarily from the removal of nonpaper components such as metal, glass, plastics, wood, and textiles as rejects from slushing, cleaning, and screening.

Besides a careful coarse and fine cleaning and screening in several stages, a flotation deinking process is necessary to improve the optical characteristics of recycled fibers for graphic papers. The low yield of about 65% applies to the preparation of wood-containing DIP for higher-grade printing papers such as lightweight coated (LWC) paper with ink removal and partial de-ashing. The higher yields relate to DIP for the production of newsprint. Depending on the system concept, this includes a one- or two-stage flotation process with yields between 80% and 90%.

The processing of deinked pulp for hygiene paper is a special case. The multi-stage deinking process, including flotation and washing, must ensure removal not only of printing ink and other impurities but also of almost all fillers and coating pigments. The required residual ash content of less than 5% results in the low yield of 60%.

Specialty papers cover a wide spectrum with greatly varying quality requirements. The high yield of about 95% relates to processing of ordinary recovered paper grades for the production of automobile board or core board. Wallpaper is an example of a low-yield material due to the necessity of an additional deinking process.

Especially exacting demands for cleanliness, brightness, and freedom from ash, stickies, and other impurities are necessary for market DIP produced from wood-free mixed office waste (MOW) to permit its use as a pulp substitute in wood-free printing paper and stationery. For this reason, low yields of 60–70% result when processing MOW, depending on the ash content of the recovered paper grades processed. Wood-containing market DIP for newsprint is less demanding, and this results in a higher yield ranging between 80% and 85%.

When estimating the required proportion of recycled pulp in furnishes containing recycled fibers and virgin fibers, the recovered paper utilization rate itself is not as important as the proportion of recycled fibers considering the process-specific yield in recovered paper processing. However, the following discussion refers

to the recovered paper utilization rate defined above, according to common convention and availability of statistical data.

#### 4.1 Utilization Rate

Recovered paper utilization rates globally and nationally can provide comparisons. Such statistics can give, however, a false impression of the recycling activities in different countries as the following discussion explains.

The range of national utilization rates extends globally from 5% to more than 100%. Figure 4.1 shows the 12 largest papermaking countries accounting for almost 80% of the global paper production in 2002, with 255 million tons. Simultaneously, these countries consumed about three-quarters of the world's recovered paper volume. Heading the list are South Korea, Germany, Indonesia and Japan. The lowest utilization rates are for Finland and Sweden. This is due to a paper production of which more than 84% are exported, the low population figures, and the related low level of national paper consumption.

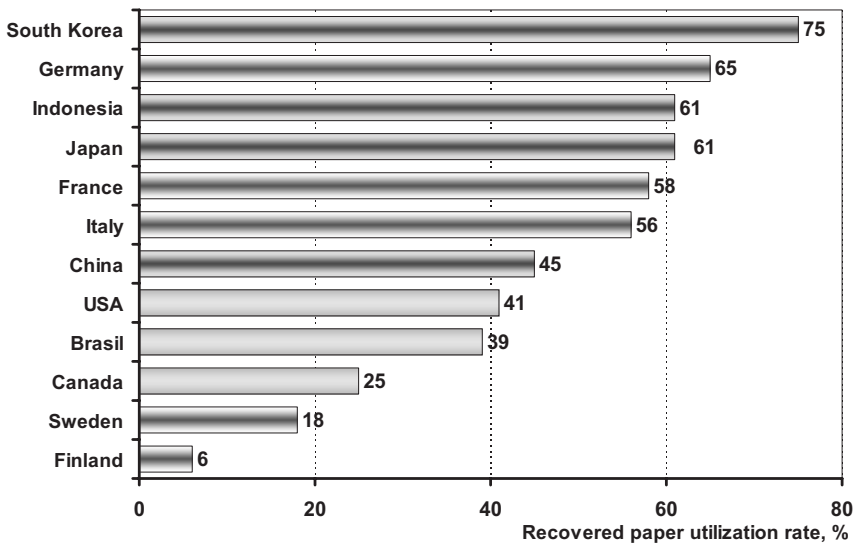
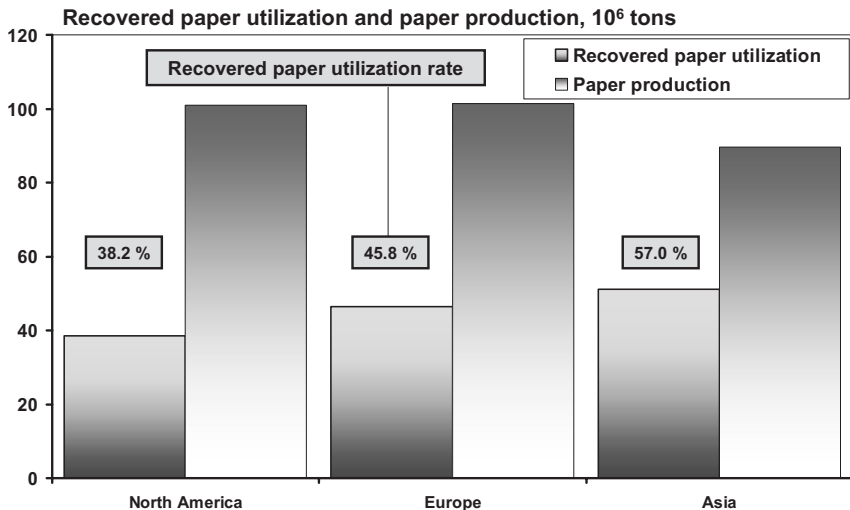


Fig. 4.1 Utilization rate of recovered paper for the 12 largest papermaking countries in the world (2002) [1].

Among the leading industrialized nations, United Kingdom, Denmark and Spain have raised their recovered paper utilization rates to a high level of at least 74%, followed by Germany and the Netherlands with 65%. Ireland records a level of more than 100% due to the structure and size of its paper industry. Utilization rates in excess of 100% occur because the figure includes the loss of yield in recov-

ered paper processing as rejects and sludge. In addition, the share of packaging paper and board in the production of those countries is exceptionally high.

Figure 4.2 shows the utilization rate for the three largest paper production regions in the world where the paper industry uses 86% of the global recovered paper volume: Asia, Europe, and North America. Paper production in these three regions is between 90 and 100 million tons each, resulting in recovered paper utilization rates of roughly 57% in Asia, 46% in Europe, and 38% in North America.



**Fig. 4.2** Utilization rate of recovered paper for Asia, Europe, and North America (2002) [1].

Utilization rates for different countries should not be compared without further comment. Knowing the structure of the production program of the different national paper industries in the main product categories of packaging papers and board, graphic papers, hygiene papers, and specialty papers is important, because the utilization rates for these product segments can differ significantly, as Fig. 4.3 shows for Germany.

Traditionally, packaging papers and board have the highest recovered paper utilization rate. In Germany this ratio has reached 97%, and has been higher than 90% for more than 20 years. Demanding quality specifications must be fulfilled by these recycled fiber-based papers and board to ensure trouble-free converting, for example, to corrugated board boxes or folding boxes and adequate functional characteristics of the finished products.

Occupying second place in many countries is the utilization rate of hygiene papers. Due to high yield losses in flotation and washing steps, the actual proportion of recycled fibers in hygiene paper produced in Germany is not higher than 45% on average. The figure of 45% deinked pulp derives from a 60% yield of a 74% utilization rate.

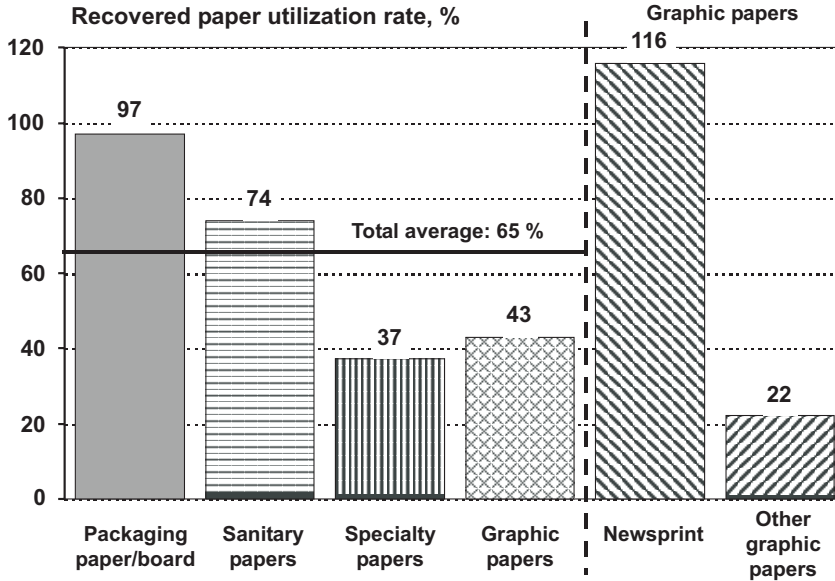


Fig. 4.3 Recovered paper utilization rates for different paper grades produced in Germany in 2002 [1].

Specialty papers now achieve a 37% utilization rate in Germany due to the inclusion of core board made from 100% secondary fibers. Many grades of specialty paper such as cigarette paper, filter paper, or banknote paper can never use recycled fibers. This causes stagnation of the average utilization rate in this product group.

Finally, the level of utilization for graphic papers has increased to 43% in Germany. Due to the wide spectrum of the produced paper grades, a distinction is necessary for this product segment because newsprint has reached a level of 116%. The utilization rate of the other graphic papers averages 22%. Included among these other graphic papers are wood-containing and wood-free papers that are coated or uncoated. Some use 100% recycled fiber furnish such as recycling copy paper. The latest development in the use of recycled fibers is occurring with supercalendered (SC) and LWC papers. Some of these papers contain no or only a small amount of recycled fibers. Nevertheless, some German companies manufacture offset LWC paper even from 100% DIP.

The proportions of the paper production segments vary from country to country, and this results in different national recovered paper utilization rate levels. A higher utilization rate means that the fibers undergo the following steps of the complete recycling loop more frequently:

- Paper production
- Paper converting and printing
- Consumption of paper products
- Collection of used paper products

- Sorting of recovered paper
- Processing of recovered paper.

## 4.2

### Recovery Rate

As far as national recycling activities are concerned, an assessment of the paper recovery rates of different countries is more relevant than a comparison between national recovered paper utilization rates. Figure 4.4 shows the development of recovery rates (recovered paper for material recycling) since 1991 for the CEPI countries and Germany, as well as those European countries collecting more than 2 million tons of used paper products each year. Due to intensified collecting in several countries, the CEPI average rose from 41% to 56% in 2002, corresponding to a total volume of recovered paper of 46 million tons in that year. During the same period, the recovery rate in Japan increased from 51% to 65%. The rate for the USA was 37% in 1991, and reached 48% in 2002. It becomes clear that in all regions the recovery of used paper products was significantly intensified; in Europe as well as in Japan by about 15%-points, and in the USA by 11%-points. However, it must be pointed out that an additional increase in recovery of a certain level becomes more difficult the higher the basic value.



**Fig. 4.4** Development of the recovered paper collection rate of selected CEPI countries (1991–2002) [12,16].

Europe requires a distinction to be made between two categories of countries. Some have a high recovery rate, while others have a lower rate. Due to comprehensive, country-wide collection measures, Finland, Germany, the Netherlands,

Norway, Sweden and Switzerland have succeeded in achieving and stabilizing recovery rates above 65% during the past years. In Belgium, France, Italy, Portugal, and the United Kingdom, a corresponding development did not occur, resulting in recovery rates below 50%. As a result of this stagnation, growth in paper production during this period depended on increasing imports of recovered paper from countries with higher recovery rates. This satisfied the industry demand for recovered paper and maintained the utilization rate at a high level.

Figure 4.5 shows the collection rates depending on the utilization rates of recovered paper in the CEPI countries. The bubble size is equivalent to the tonnage of recovered paper used in each country. It becomes clear that the highest collection rates in Europe are established in Germany and Finland (72%), followed by Switzerland (70%), Sweden (69%), Norway (68%), the Netherlands (65%), and Austria (61%). The listed seven countries collect 46% of the total European volume of recovered paper of 46 million tons in 2002. The highest utilization rates are reached in Ireland, Denmark, Spain, Greece, United Kingdom and the Netherlands, and are in a range from 71% to 109%. In these countries the production share of packaging papers, board and newsprint is in a range of 56% to 100%, and with an average of 61% – significantly above the CEPI average of 52%. Due to the fact that a high use of recovered paper is relatively easy to manage in packaging grades and newsprint, it becomes clear that those countries reach high utilization rates. The largest tonnages of recovered paper are used in Germany, France, Italy, United Kingdom and Spain. Those five countries consume 74% of the total recovered paper demand of all CEPI countries of 43 million tons. Due to the fact that

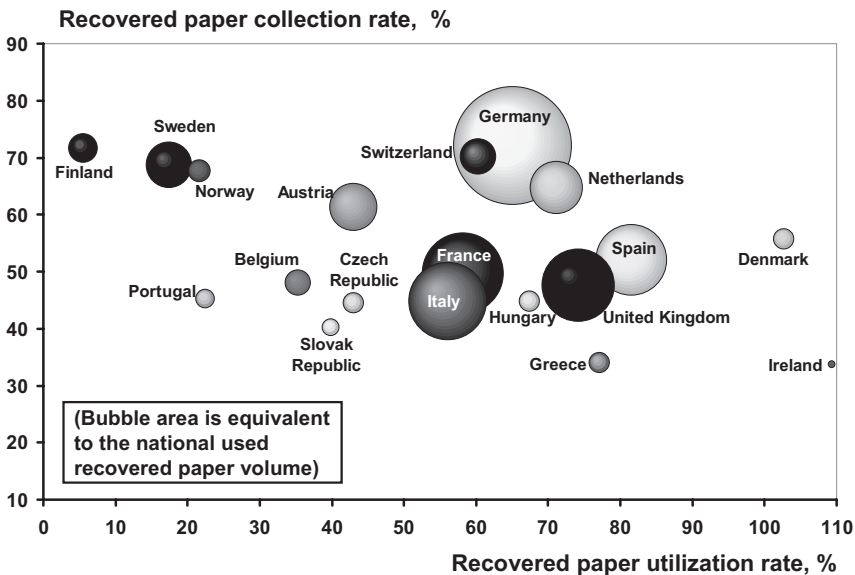


Fig. 4.5 Collection rate versus utilization rate for the CEPI countries (2002) [12].



paper consumption in Spain, United Kingdom, Italy, France and Belgium has a sufficiently high level (minimum 3.4 million tons, maximum 12.4 million tons), and the recovery rates have capacities still to be further developed, it becomes clear that significant additional recovered paper potentials in Europe can be generated in these countries.

The maximum paper recovery rate in an industrialized country with a well-developed infrastructure is about 80% [17]. The theoretical limit of the recovery rate is obtained since approximately 20% of the used paper products are not collectible, because they are contaminated, long-living products or are destroyed by disposal or burning. This includes hygiene paper, specialty paper products, long-life paper products, papers used in industrial applications, and papers used for other purposes in private homes such as fuel or compost material. Considering the theoretical recovery rate of 80%, the recovery rate of 75% achieved already in 2002 in Germany is equivalent to a paper collection efficiency of about 94%. Collecting additional used paper is probably not economically feasible.

Germany is the largest exporter of recovered paper in Europe, with 3.4 million tons in 2002, of which about 75% goes to destinations within Europe. Some 20% of the export volume of recovered paper goes to Indonesia, Taiwan and China. Because of the large demand for fiber material in Asia, Europe could easily activate its still dormant recovered paper potentials. The USA did this by exporting about 11 million tons in 2002, primarily to Asia, Canada, Mexico, and the Pacific Rim. For 2005, the global flow of recovered paper is expected as shown in Fig. 4.6, with dominant exports from North America to Asia, whereas Europe becomes more self-supplying, with only a small excess of recovered paper being exported to Asia [18].

#### Expected global recovered paper trade 2005: $13 \cdot 10^6$ tons

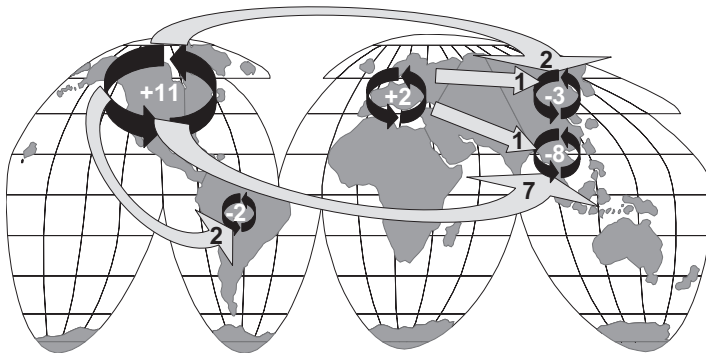


Fig. 4.6 Expected global recovered paper trade, 2005 [18].

Production residues from paper converting such as the corrugated board industry or printing houses, and the used paper products from packaging in product distribution such as supermarkets, are totally collected and recycled in industrialized countries. A high collection rate also applies to private homes, provided that corresponding collection systems are available in sufficient numbers with conve-

nient pick-up and drop-off systems. Some potential exists to increase the level of paper collection in offices for the production of higher-grade recovered paper. These would be largely wood-free paper grades that are scarce due to increasing needs of the paper industry.

### 4.3 Recycling Rate

The recycling rate was introduced by CEPI for the first time and describes the relation of recovered paper utilization to paper and board consumption. Related to the consumption of paper and board, the figure indicates the internal material recycling of recovered paper in a country or a region. Nevertheless, recycling rates close to 100% indicates that either a large amount of recovered paper is imported, or a high volume of produced paper and board is exported. According to studies initiated by CEPI, about 19% of the total paper and board products are not available for recovery because they are contaminated or long-living products or are destroyed for collection by disposal or burning. That means that the maximum recycling rate will reach 81% in a closed system. Figure 4.7 shows a comparison of the recovered paper utilization, collection and recycling rates within the CEPI countries in 2003.

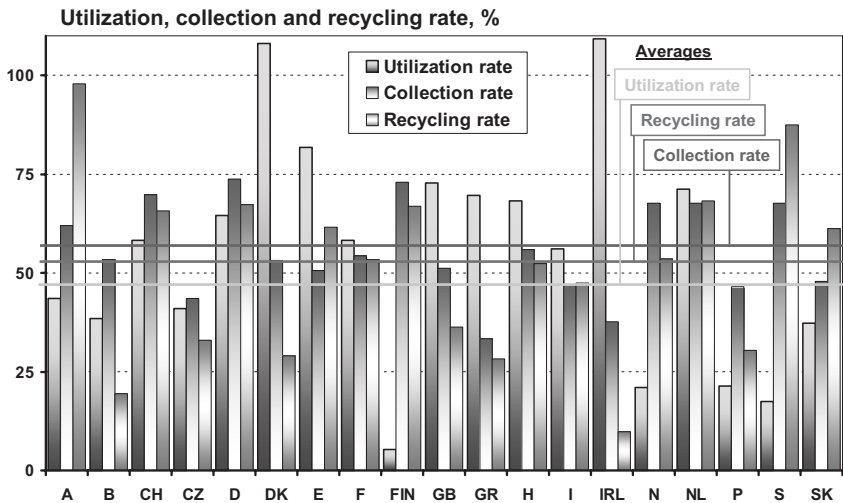


Fig. 4.7 Recovered paper utilization, collection and recycling rates of the CEPI countries (2003) [19].

The average collection rate in the CEPI countries is the highest when compared to other continents using significant recovered paper shares (see Tab. 4.1). This finding is based on the already-existing sophisticated recovered paper collection systems in most European countries. In a few countries, additional developments

are necessary to fulfill the demands of the paper industry for their raw material. In Asia, the utilization and recycling rates are higher than in the CEPI countries; this is based on the fact that in Asia the production of packaging papers at almost 45% is much higher than in Europe (40%), and the use of recovered paper (especially in this paper grade) is dominant. In North America, all recovered paper rates are on a lower level compared to Europe and Asia.

**Tab. 4.1** Utilization, collection and recycling rates for Asia, the CEPI countries, North America and the World (2002) [1].

Rate	Asia [%]	CEPI [%]	North America [%]	World [%]
Utilization	55	47	38	48
Collection	45	56	49	47
Recycling	56	53	40	48

#### 4.4

#### Deinked Pulp Capacities

The first deinking system which operated according to the flotation principle was installed during the late 1950s in the USA. The first European operation started production at a Dutch paper mill in 1959, and had a capacity of 10 tons per day for the production of hygiene papers. Figure 4.8 shows the flotation capacities for different continents. In 1975, the global capacity was 1.2 million tons, only, and has reached 39.2 million tons in 2004. Between 1975 and 2002, the annual growth of the flotation deinking capacity worldwide was 13.3% – four-fold higher than the annual increase in paper production (3.3% p.a.). In Europe, a similar development took place, resulting in a three-fold higher annual increase in the flotation deinking capacity compared to paper production (13.4% p.a. versus 4.1% p.a.). In 2002, the global flotation deinking capacity totaled 35.2 million tons, corresponding to 22% of global recovered paper use.

The largest share (45%) of the global deinking capacities is in Europe, while Asia has achieved second place at 30% and North America has a share of 21%. The deinking capacities in Latin America, Africa, and Oceania are below 4%. Globally and in Europe, the use of DIP in newsprint dominates (64%), followed by magazine, printing and writing grades (11–13%) and hygiene papers (10–12%). Included under the heading of other grades is a wide spectrum of paper grades which reaches a share of 13% such as magazine papers, white-lined chipboard (top layer), wallpapers, and molded products such as egg cartons. In the past, especially the share of DIP in wood-containing printing papers such as newsprint, SC and LWC papers has been increased, and it can be expected that this development will continue in the future.

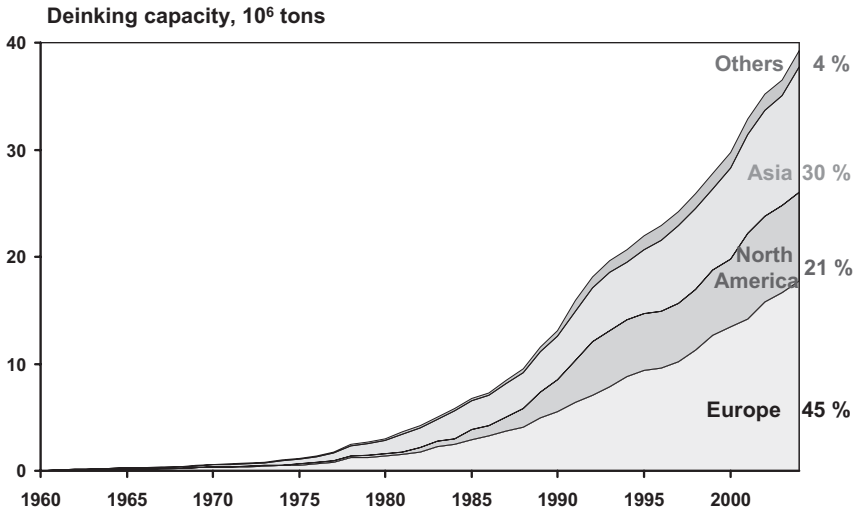
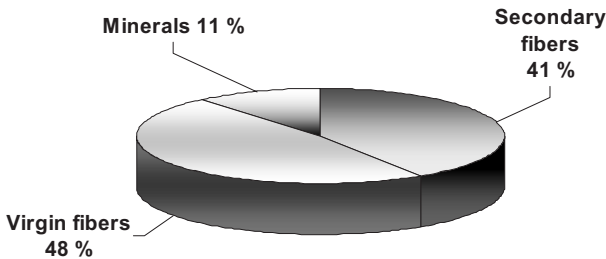


Fig. 4.8 Development of the global flotation deinking capacities.

**4.5  
Future Development of the Use of Recovered Paper**

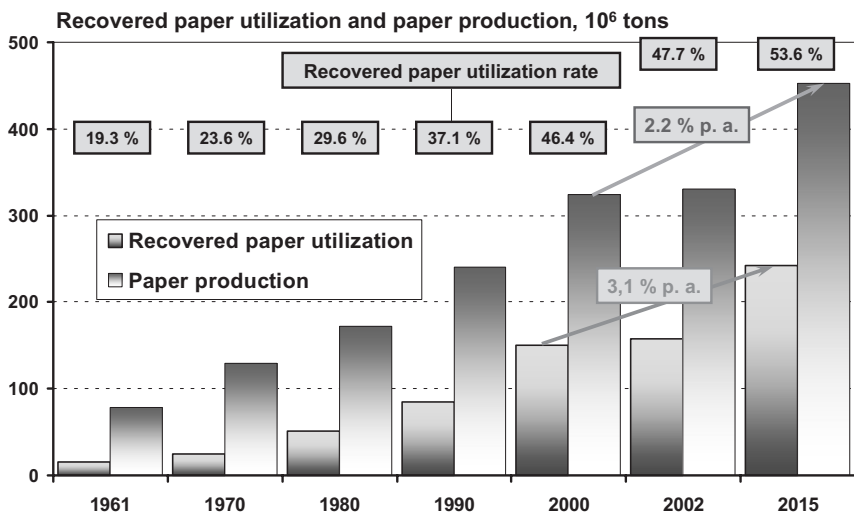
The global recovered paper utilization rate approached 48% in 2002. Based on the fact that rejects and sludges are generated by recovered paper processing, this corresponds to a lower share of recycled fibers used for paper and board manufacturing. Therefore, the average recycled fiber content (including minerals) amounts to 40.8% using an average yield in recovered paper processing of 85%. According to Fig. 4.9, the use of minerals in terms of fillers and pigments totals globally at 11%, and this results in a virgin fibers consumption of 48.2%.



**Global paper production: 331 • 10<sup>6</sup> tons**

Fig. 4.9 Global raw material consumption, 2002.

When looking ahead to the next decade, all forecasts expect a further global increase of the recovered paper utilization rate. According to Jakko Pöyry, by 2015 the recovered paper utilization rate will reach almost 54% on a global level. The increase of recovered paper utilization will be 3.1% p.a. larger than for paper production (2.2% p.a.), as shown in Fig. 4.10. In 2015, global paper production will reach about 450 million tons, while the use of recovered paper will be roughly 240 million tons [20]. Using the same basis as an average of 15% rejects and sludges for all processing technologies for all papers and board grades, the utilized amount of recycled fibers in paper may reach about 206 million tons. In estimating a higher amount of 15% fillers and pigments, the average raw material utilization in 2015 might be 45% for recycled fibers, 40% for virgin fibers, and 15% for minerals.



**Fig. 4.10** Global development of recovered paper utilization and paper production (1961–2015) [20].

Utela forecasts an even more rapid increase in recovered paper utilization, with – by 2010 – a global utilization rate of 54% and a recovered paper utilization of 225 million tons for a paper production of 417 million tons [21]. Nevertheless, it becomes clear that in the future, recovered paper will become even more important than it is today as the most important raw material for the paper industry.

## 5 Collection of Recovered Paper

In general, the collection of recovered paper is accomplished by:

- collection in private households and small commercial enterprises;
- collection from industrial and business operations, sites where unwrapping is carried out (e.g., supermarkets), offices, authorities and administration; and
- returns of recovered paper from converting facilities such as printing houses and corrugated board industry as well as over-issues.

Depending on the origin of the collected recovered paper, a clear distinction exists between pre- and post-consumer recovered paper. The U.S. EPA defines these two types of recovered paper as follows [22]:

- Post-consumer recovered paper comprises paper, paperboard, and fibrous material recovered from retail stores, offices, and homes after these products have served their end-uses as consumer items and papers separated from municipal solid waste.
- Pre-consumer recovered paper is material from manufacturing, other waste from the papermaking process, and finished paper from obsolete inventories.

For paper recovery, differentiation is made by collection systems, the equipment, and their mode of operation. In the “drop-off” system, generators of the used paper product, perhaps end-users, carry the material to a centralized collection point. Alternatively, when the material is collected at each individual point of generation (e.g., households or offices) it is named a “pick-up” system.

The two systems operate somewhat differently depending on whether pre- or post-consumer recovered paper is handled.

## 5.1

### **Pre-Consumer Recovered Paper**

The collection of pre-consumer recovered paper in the form of over-issues and converting residues such as shavings and cuttings uses pick-up systems that, traditionally, are organized via the recovered paper dealers using containers at individual points of generation. Pick-up systems collect recovered paper from industrial and business operations. Containers are exchanged or emptied at regular intervals, either with or without the benefit of stationary compressing compactors. Collection vehicles which compress refuse are seldom used.

The traditional recovered paper trading industry is facing increasing competition from waste management companies, who tend to offer their services to industrial and business operations and to the retail trade, not only for paper but also for the collection of other materials such as glass, plastics, or wood. Thus, they provide a greater convenience and flexibility.

Consequently, most pre-consumer collections are handled in the pick-up mode.

## 5.2

### **Post-Consumer Recovered Paper**

Recovered paper from operations, where unwrapping occurs (e.g., supermarkets) belongs to post-consumer recovered paper. In these facilities, the same collection systems are installed as for collection of pre-consumer recovered paper – that is, in the pick-up mode. In contrast, many different collection systems are available for recovered paper collection from private households. The choices made are based on population structure (population density and rural or urban regions), housing structure (inner city, high-rise developments, single-family housing), and the customary use for the collected recovered paper. A distinction exists here between pick-up and drop-off systems, both of which have been in long-term practice in Germany.

### 5.2.1

#### **Pick-Up Systems**

For paper pick-up, collection systems placed in households, containers (volume 120–240 L) are used primarily either as mono-bins or as multi-compartment containers to collect different secondary materials such as paper, metal, or glass. Special vehicles are necessary for the collection of multi-compartment containers in order to ensure that the different materials remain separated.

With the most common collection of used paper products from private households using mono-bins, printed graphic paper products are mixed with paper and board packaging material. Avoiding this requires two paper containers or a multi-compartment container for the separate disposal and collection of used graphic paper products and used paper and board packaging. Use of the recovered paper

is then possible in different recycling areas, without any need for labor-intensive manual sorting that is necessary with mixed paper collection.

Besides container collections, curbside collection systems exist at a few places. This approach is also used at certain intervals by charitable or private organizations, and usually involves the collection of bundles of printed graphic paper products. The population collects and bundles used paper products, and bundles of newspapers and/or magazines are placed at the curbside at specific times. The collecting organizations pick them up and usually deliver them to nearby paper mills, where they are paid for the service.

Unfortunately, strongly fluctuating prices for recovered paper have almost completely discouraged curbside collections in Germany. In Switzerland, however, such collections of recovered paper continue to have major importance for the national paper industry. The difference may be due to the fact that the Swiss paper industry has continually supported and financed the curbside collection, even when it was more economic for the paper manufacturing companies to buy the recovered paper from the market.

### 5.2.2

#### **Drop-Off Systems**

For drop-off systems, larger containers ( $>5 \text{ m}^3$ ) are used. These are placed at central, publicly accessible locations and are emptied at regular intervals. They can be either single-compartment containers intended only for collecting paper, or multi-compartment containers for collecting different materials such as paper, glass, and metal that remain separate within the container. Besides the greater space that is necessary for multi-compartment containers, the decision on whether to install single-compartment or multi-compartment containers depends on the availability of suitable vehicles and the occurrence of the materials concerned at the installation sites.

Containers can simply be emptied into a suitable refuse collection vehicle for single-compartment containers or exchanged, as in the case of drop-off containers. For multi-compartment containers, the refuse collection vehicle must suit the multi-compartment system of the container to avoid mixing the individual materials. With multi-compartment containers, exchanging or emptying the entire container when collecting the materials is necessary, despite the fact that individual compartments may not be totally full. This means the collection frequency must consider the material whose compartment fills first.

Standard vehicles are useful for emptying single-compartment containers by the exchange method. Avoiding overflowing containers is essential; otherwise, the tendency to throw materials in still-empty containers for other materials increases, or the sites can turn into rubbish dumps. Single-compartment containers offer the basic advantage that the collection intervals of single containers can be linked to the occurrence of material. Containers that fill more quickly can be emptied more frequently than those that fill more slowly. Larger containers can also be selected. In principle, separate collection of used graphic paper products



and packaging material is possible with at least two different containers or a multi-compartment container.

In some regions recyclable materials are collected at so-called drop-off recycling centers where municipal employees accept a range of different materials. Here, the collection has supervision which is not available with container collection in public places. However, a disadvantage of the drop-off recycling centers is that disposal is available only at certain times. The ability to dispose of difficult materials such as paints, varnishes, used batteries, or motor oils can compensate for this disadvantage [23].

### 5.3 Efficiency of Different Collection Systems

For the different systems, the specific amount of paper collected per inhabitant depends on many different marginal conditions, such as collection frequency, population density, and sizes of the containers used. A detailed analysis in 1994 in Germany resulted in the following average specific recovered paper collection figures (values are per capita and year) [24]:

- Drop-off container system: 32 kg
- Curbside collection: 43 kg
- Recycling center: 45 kg
- Pick-up container system: 53 kg

Densely populated regions should therefore use a pick-up container system, although the space required for an additional paper container at home requires consideration. In less populated areas, drop-off container systems are useful. Finding the most suitable locations for the containers (clean and attractive, accessible by automobile, and close to home) is especially important to ensure that the collectable volume and the standard of purity of the recovered paper satisfy the requirements. Bundled paper collections in densely populated areas are always suitable if containers cannot be installed in sufficient numbers.

A few regions of Germany collect used papers from private households as one component of the so-called multi-component recyclable container collection. Here, one container is used in private households for collecting several recyclable materials such as printed products, packaging materials including liquid packaging, plastic, metal, and textiles. Glass is usually collected separately due to the danger of breaking and subsequent occurrence of glass splinters in the paper and board fraction, even after manual sorting.

Although paper recovery by this multi-component container collection is possible, it requires especially intensive and consequently expensive manual sorting. Generally, contamination of the moisture-absorbing recovered paper with liquid and foodstuff residues from liquid packages, plastic bottles, and tin cans can also occur. The paper industry therefore has major reservations about the use of recovered paper from this collection system. In accordance with European standard EN

643, recovered paper from this collection system requires express identification as such.

Recovered paper from multi-component collection systems has not been used for materials and articles of paper and board for contact with foodstuffs that must comply with international or national hygiene regulations. It is not permissible to mix recovered paper from multi-component collection systems with other recovered paper grades, without special identification [25].

## 5.4

### Municipal Solid Waste

Despite all efforts to recover paper as a raw material for the paper industry, domestic waste also includes paper and board, though in increasingly smaller quantities. In the USA, according to the EPA definition, municipal solid waste (MSW) consists of durable goods, containers and packaging, food scraps, yard trimmings, and miscellaneous wastes from residential, commercial, and industrial resources. In 1996 in the USA, MSW contained about 38% paper and paperboard, of which about half was recycled. Finally, about 19% paper content remained in MSW and went to landfill or to incineration plants [26].

In Germany, according to the most recent National Household Recovery Analysis (NHWA) from 1985, the share of paper, paperboard, and composite paper contained in household waste was only about 18%. This result was achieved much sooner than in the USA due to the totally higher level of separate paper recovery in Germany, and also due to different categories of waste counted as domestic waste.

Despite the fact that no NHWA was performed since 1985 all recent results from individual German cities reveal even lower figures [23]. According to Intecus an actual average proportion of paper products in household waste have to be estimated for Germany between 9 and 10% [27]. In principle, the paper industry takes a negative stance regarding the use of recovered paper which is sorted from general domestic waste collections. This is also reflected in EN 643 by the specification that "... paper recovered from general refuse is not suitable for use in the paper industry".

## 6 Sources of Recovered Paper

At the global level, no data are currently available for the different sources of collection systems of recovered paper by tonnage. In Europe, the CEPI has conducted recovered paper surveys for several years, and in 2003 the following five sources of recovered paper were indicated for the recovery of 48 million tons:

- Recovered paper from households: 38%
- Recovered paper from trade and industry: 33%
- Recovered paper from converting and printing: 15%
- Recovered paper from offices: 10%
- Recovered paper from unsold news and magazines: 4%.

Figure 6.1 provides a total view for paper recovery in Europe in 2003. The figure includes the tonnages of paper at all production and consumption stages. It considers all product groups of graphic paper, packaging paper and board, hygiene paper and specialty paper.

In 2003, almost 95 million tons of paper and board were produced in Europe. For this, 45 million tons (47% utilization rate) of recovered paper and 62 million tons of other raw materials (including nonfibrous components) were used. The European market demanded 87 million tons of paper and board, and the net export was 8.3 million tons.

Considering the recovered paper from converting and printing such as cuttings and shavings, a market supply of 80 million tons of converted paper and board products was realized. After recovery of 2.0 million tons of over-issues, a product use of 78 million tons was established at the end-users. By subtracting the volumes of long-life paper, nonrecoverable paper and board products, and the unusable recovered paper, the theoretical recovered paper potential from among final consumers was 63 million tons. This is the maximum tonnage of paper products which could be recovered from final consumers.

Some 39 million tons of used paper products were recovered through household and industrial collections. If one considers paper material from converting, printing and over-issues, 48 million tons of recovered paper was collected in Europe, resulting in a 56% recovery rate. After subtracting the net export of 3.5 million tons, 45 million tons of recovered paper remain for use in paper production. The 39 million tons of paper not recovered from the end-users are disposed of by

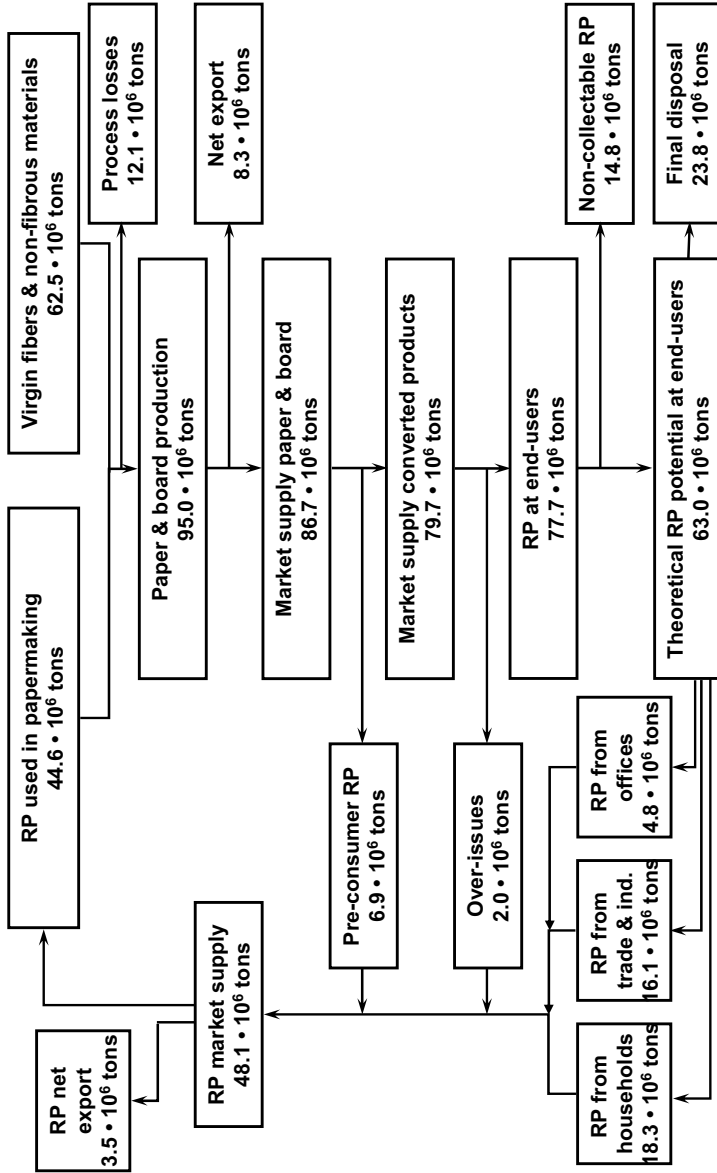


Fig. 6.1 Paper and recovered paper (RP) cycle in Europe in 2003 [19].

landfilling, incineration and composting, or they are used for other recovery options. This proportion corresponds to 45% of the market supply of paper and board products which were not recycled in the CEPI countries in 2003.

Similar (but simplified) calculations are performed in Fig. 6.2 for Germany, which is one of the leading countries in paper recycling. Starting from paper consumption, paper products were made with the help of 3% paper additives (e.g., glues, staples, tapes, printing inks). For Germany, the paper products were 19.1 million tons in 2003. The amount of nonrecoverable paper was estimated at 18%, resulting in a theoretical recovered paper potential of 15.7 million tons. The non-recoverable paper was either destroyed (e.g., toilet or cigarette paper), contaminated (e.g., filter papers for oil or air) or long-living products in libraries. From the recovered paper, a potential of 71% (corresponding to 13.7 million tons) was collected effectively. From this recovered paper 12.5 million tons were used for the domestic paper production, and the remainder corresponds to the final net export. Only 11% (2 million tons) were disposed of to landfilling, incineration or composting, mainly together with household garbage. Together with the nonrecoverable paper products, the proportion of not-collected paper products reached 29% (5.4 million tons) of the paper product consumption.

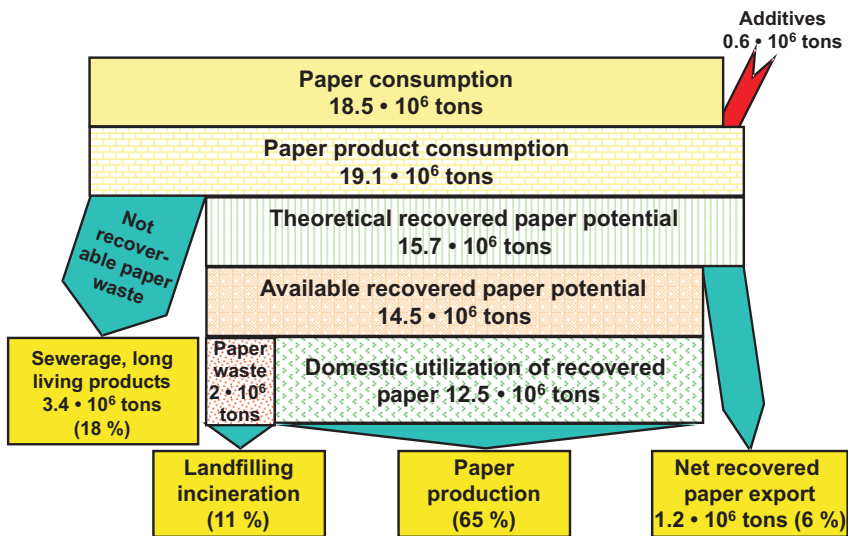


Fig. 6.2 Balance of paper, recovered paper collection and paper waste in Germany (2003).

When the estimation of the proportion of nonrecoverable paper is correct, 18% of the consumed paper products can never be collected. Figure 6.3 shows, for Germany, that the amount of not-recovered paper products decreased significantly, from 67% in 1980 to 29% in 2003. The main reasons for this are the demand of the paper industry, the economy of the recycled fibers, and the political circumstances supporting recycling in general.

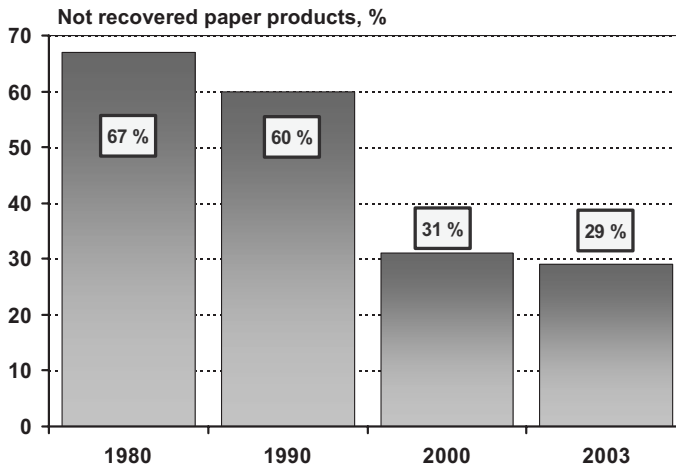


Fig. 6.3 Development of not-recovered paper products in Germany.

Due to the fact that a final 12% proportion of paper products are very difficult to collect, it must be expected that in the CEPI about 30% of the paper product consumption will not be collected, even in the future. By using the same recovery rate for all CEPI countries as in Germany (in 2003), an additional 12 million tons (approximately) of recovered paper would be collectable in 2003 in the CEPI countries [28]. This corresponds to 28% of the actual tonnage of collected recovered paper within the CEPI. Such an estimation shows that, even in Europe where a high recycling level is already achieved, there is still a significant potential for paper recovery.

## 7

# Sorting, Handling, and Storage of Recovered Paper

### 7.1

#### Sorting

Despite many technical developments, the sorting of recovered paper continues to be predominantly a manual, labor-intensive activity, which is increasing as the recovered paper becomes more and more heterogeneous and contaminated with nonpaper components. If recovered paper is a component of a multi-component collection of different materials for example, its sorting will be especially troublesome and will require machines such as grid drums to remove small components, magnetic separators to eliminate metals automatically, and blowers to remove especially lightweight components from the material stream. Nevertheless, the received paper fraction has required a labor- and time-intensive manual sorting. However, in the future more automatic recovered paper sorting plants will be developed and introduced in the recovered paper-dealing business.

Recovered paper intended for use as a raw material for the paper industry is usually collected separately from other materials so that an exclusively manual sorting is sufficient. Besides an inclined conveyor and a speed-adjustable sorting belt that is usually installed at a higher level, no further mechanical auxiliary equipment is necessary. Several persons work at this sorting belt to remove unusable materials manually. This includes nonpaper components such as wood, metal, glass and plastic, as well as paper and board that are detrimental to production, such as liquid packaging. The workers throw these items into containers provided for this purpose below the sorting belt.

The amount of work involved in the manual sorting depends primarily on the origin of the recovered paper. Pre-consumer recovered paper such as cuttings or shavings from paper converting requires only a very low level of sorting. It can often go to recovered paper processing after inspection on the spot. In contrast, post-consumer recovered paper such as from household collections always requires sorting to satisfy the quality standards specified for the different recovered paper grades. This is especially true for recovered graphic paper for deinking.

A distinction is made between positive and negative sorting:

- With positive sorting, the material to be recovered is removed from the incoming stream. This sorting technology produces a relatively clean material, but an unfortunate disadvantage is the low specific sorting output per person and unit of time.
- Because separately collected recovered paper consists primarily of paper and board with relatively small amounts of unusable materials, the negative sorting method is utilized almost without exception to obtain a greater sorting productivity. In this case, only the unusable materials are removed from the incoming material stream. The sorted recovered paper can be marketed in accordance with its composition such as mixed recovered paper or origin such as recovered paper from department stores.

Negative sorting usually results in a lower level, since unusable materials can be overlooked and may remain in the sorted product. Excessively high speeds of the sorting belt or insufficient personnel can cause a high proportion of unusable materials even in the sorted, recovered paper.

The growing demand for recovered paper for deinking has caused a situation in which recovered paper from post-consumer collections that consists basically primarily of a higher proportion of graphic papers and a lower proportion of packaging materials, undergoes a modified negative sorting. Besides the unusable materials, packaging materials are also separated into different containers. The remaining recovered paper should then be free of unusable and packaging materials. This allows offering it as recovered paper for deinking. The removed packaging paper and board fraction is marketed as mixed paper or supermarket corrugated paper and board, depending on its composition. With this type of sorting, small-component packaging or torn board such as corrugated board boxes cannot be completely sorted by a justifiable effort. This results in a certain amount of packaging material remaining in the recovered paper for deinking.

Accordingly, paper mills with deinking operations demand a separate collection of graphic paper and packaging materials for post-consumer recovered paper. From the start, this ensures that the proportion of packaging materials contained in the collected graphic paper is considerably smaller. This improves the quality of the sorted recovered paper for deinking.

The sorting productivity depends highly on the recovered paper collection system.

- For the sorting of mixed papers and boards collected in containers, a sorting productivity of 0.7–1.2 tons per person and hour ( $\text{t p}^{-1} \text{h}^{-1}$ ) is possible.
- Sorting productivity decreases to 0.7–1.0  $\text{t p}^{-1} \text{h}^{-1}$  when generating recovered paper for deinking from mixed collected papers.
- The sorting productivity for recovered graphic papers collected in bundles is 1.0–1.5  $\text{t p}^{-1} \text{h}^{-1}$ .



- If recovered paper is collected as a component in a multi-component material collection system, the sorting productivity drops independent of the additional mechanization of the sorting system to  $0.4\text{--}0.7 \text{ t p}^{-1} \text{ h}^{-1}$  [25].

A dramatic reduction in sorting productivity occurs if the recovered paper undergoes compression before sorting (e.g., in compactor-type refuse vehicles) to increase the load. Recovered paper treated in this way can usually only be marketed as mixed recovered paper [23].

## 7.2 Handling

The additional handling of sorted recovered paper depends on the transport conditions of the recovered paper operation, the storage conditions at this operation and at the mills, and the additional agreements between the dealer of secondary raw material and the mill. It may, for example, include shredding which usually is performed on office papers and confidential listings.

The simplest approach is to load the sorted recovered paper as loose material onto large trucks and transport it directly to the paper mill. Due to the large space requirements resulting from the low settled bulk of such paper, it is stored in large quantities only in the paper mill, where appropriate unloading equipment and storage bunkers are installed in accordance with safety regulations. These storage facilities must always be covered by roofs.

The trade and supply of loose recovered paper involves almost exclusively recovered paper for deinking. Settled apparent density is approximately  $330 \text{ kg m}^{-3}$ . In Germany, the majority of the recovered paper for deinking is supplied as loose material; the other recovered paper grades are delivered primarily in bales.

To produce bales, the sorted recovered paper enters the hopper of a stationary baling press where it is compressed hydraulically at pressures of 8 MPa. This produces compact bales having a typical size of  $1.2 \times 1.0 \times 0.8 \text{ m}$  weighing 500 to 600 kg. These are then tied with wire within the baling press. With larger baling presses and higher pressures, bales of larger size and weight can also be produced.

The individual bales can be simply transported and stacked by fork-lift trucks equipped with bale clamps. Bale density ranges from 250 to  $900 \text{ kg m}^{-3}$  depending on the recovered paper grade and pressing conditions. Additional transport can use almost all modes such as truck, railcar, and ship. For this reason, the trade, transport, and storage of recovered paper in bales is a global business [25].

**7.3****Storage**

Recovered paper, especially in bales, is stored on plain areas, under a roof or in the open air, whereas loose recovered paper is stored in special bunkers or enclosed facilities with roofs. Mixed recovered paper that is traded at a low price is often stored outdoors. Inside storage is more used with higher quality and therefore more expensive grades. Recovered paper stored outdoors is exposed to weather influences such as rain, snow, frost, or sunshine.

## 8

### Legislation for the Use of Recycled Fibers

The limited capacities of landfill sites and (municipal) incineration plants, increasing waste disposal costs, and environmental awareness of the general public are the most important reasons for the efforts being made by all governments in industrialized countries to limit or even to reduce the quantities of waste from private homes, businesses, and industrial operations. In many industrialized countries the annual population growth increased less compared to the generation of municipal solid waste. Avoiding waste and promotion of material recycling are the most important means of limiting the generation and growth of municipal and industrial waste.

A wide range of legislation in various countries has attempted to promote material recycling and to reduce further the generation of waste that requires disposal in appropriate facilities. Legislation can be categorized into general regulations (sometimes also for other material categories), special regulations for certain paper or board grades by products, and regulations relating to private households for reduction of municipal waste. This area is subject to rapid change involving testing of many different political approaches. Some approaches oriented towards paper products include the following:

- Directives and ordinances
- Procurement policy guidelines
- Voluntary agreements
- Formulation of national recovery or utilization rates of recovered paper
- Eco-labeling of paper.

Other regulations that cover packaging materials or graphic paper products include:

- Packaging ordinance for packaging material (e.g., in Austria or Germany).
- Voluntary agreement of the graphic paper chain (e.g., in Germany).
- Stipulation of minimum contents of recycled fibers for example in newsprint (e.g., in the USA).

- Executive orders for purchasing graphic papers with a minimum content of recycled fibers by public funds (e.g., in the USA) [25].

These regulations set responsibilities for taking back used paper products, independently of the public disposal system, and recycling them. Alternatively, they may specify the content of secondary fibers used to manufacture a certain paper grade. Other efforts describe recycling objectives in general or stipulate the installation of collection systems aimed at household and municipal waste [17].

The legal conditions relating to recycling objectives and waste disposal measures globally are changing rapidly, and this means that the laws, guidelines and voluntary agreements described in the following sections may be out of date by the time that this book is published. Simultaneously, no uniform objectives exist regarding the recycling of recovered paper. The survey in this book therefore covers examples from a limited number of countries, and for this reason, the following information concentrates less on statistical objectives and more on the basic intentions of waste avoidance strategies and recycling philosophies [25].

## 8.1

### Europe

In Europe, Germany was the pioneer for the following three-pronged waste strategy with priority in the order listed:

- Avoidance of waste
- Reuse or recycling of used paper products
- Disposal of waste.

The European Union (EU) has subsequently adopted this concept with its waste management directives in which the European Waste Guideline 91/156/EEC of 1991 and the EU Packaging Directive 94/62/EC of 1994 have special importance. The latter also places top priority on avoiding packaging waste and covers packaging made from paper and board, glass, metal, plastic, and composite material. The other main principles are the reuse of packaging material, recycling of packaging material and other uses of packaging waste, and a consequent reduction in the amount of waste for final disposal.

The EU member states must establish systems for take-back, collection, and utilization of waste as a secondary raw material. All parties involved in the production, conversion, import, and distribution of packaging and packaged products must become more aware of the degree to which packaging becomes waste. They must also take responsibility for this waste in accordance with the “polluter pays” principle. Final consumers play a decisive part in the avoidance and use of packaging and packaging waste, and they must therefore be educated in this respect. The efficient sorting of waste at its source – for example in private households – has a major importance for a high recycling level.

Independent of the packaging material, a distinction exists among the following three categories of packaging:

- Sales packaging or first packaging: this is offered to the final user or consumer at the sales outlet as a sales unit such as a bottle or can of beer, a box of washing powder, or a cigarette box.
- Re-packaging or second packaging: this contains a certain number of sales units given to the final user or consumer at the sales outlet, or that serves only to stock the shelves. Removing this packaging does not influence the characteristics of the goods. Examples are a case, tray, or pack of bottles or cans. (This category of packaging is of minor importance.)
- Transport packaging or third packaging: this facilitates the handling and transport of several sales units in such a way that direct contact with them and transport damage are avoided. Examples are corrugated boxes for carrying one or many purchased items (e.g., a new TV set or a dozen jars of jam). Containers for road, rail, ship, or air transportation are not part of the category of transport packaging.

According to the EU Packaging Directive, the term “utilization” means the following for various packaging materials:

- Material recycling: the reprocessing of packaging materials in a production process for the original purpose or for other purposes including organic use, but not combustion for generation of energy.
- Energy recovery: the use of combustible packaging materials for energy production purposes by direct combustion with or without other types of waste, but with heat recovery.
- Organic utilization: the aerobic treatment (biological use) or anaerobic treatment (biogas production) with microorganisms in a controlled process of the biologically degradable components of the packaging materials to produce stabilized organic residue or methane. Landfill disposal, however, is not a form of organic utilization.

The EU Packaging Directive has the following objectives:

- Since 2001, national legislation must guarantee that at least 50% and at most 65% by weight of packaging waste must be used.
- Within this utilization objective, at least 25% and at most 45% by weight of the total packaging material contained in the packaging waste and at least 15% by weight of each individual packaging material must be processed by material recycling [25].

All EU member states had to translate the EU packaging directive into national law. The scope of measures implemented in the individual EU states ranged from

issuing directives to reaching voluntary agreements with their national industries. All countries have set very high objectives for the collection of used packaging, averaging 70–80% of the total material [29]. By the year 2000, the material recycling objectives in the individual EU member states exceeded the levels of the EU directive.

All such regulations are based on the principle of producer responsibility. Producers, material suppliers, businesses, and authorities bear the specific responsibility for disposal covering the entire life of a product, from its production until its final use. The producer is the most important player, as he or she sets to a high degree the conditions for waste disposal. In the opinion of the EU Commission, the producer makes the decisions that determine how the product will be handled as waste. This covers the concept, use of specific materials, composition, and marketing. With careful use of natural resources, renewable raw materials, or harmless substances, the producer can help to avoid waste and to design products so that they will be suitable for utilization. The EU Commission has adopted a spirit of cooperation, emphasizing the active participation of all parties involved to meet the objectives of the waste policy. The objectives will be reached only with the active cooperation of authorities, private and public organizations, environmental organizations, and especially the general public as final consumer [30]. The latest EU concept for waste avoidance set prior options to the avoidance and the reduction of waste. This should be realized by extended duration times of products, an improved ability to reuse products, and increased recycling.

In 2000, and in accordance with this EU strategy, the CEPI and ERPA (European Recovered Paper Association) published a voluntary European Declaration on paper recovery. The main target of this European Declaration is to reach a 56% ( $\pm 1.5\%$ ) European recycling rate of the paper and board products consumed in Europe in 2005. The increase in the recycling rate from 49% corresponds at that time (1998) to an additional recycling of recovered paper of 10 million tons or a 26.6% higher recovered paper utilization compared to 1998. In order to guarantee the credibility and transparency, a European Recovered Paper Council (ERPC) was established. In the meantime the European Federation of Corrugated Board Manufacturers (FEFCO) signed the declaration additionally. The European Federation of Waste Management and Environmental Services (FEAD), the European Paper Merchants Association (EUGROPA) as well as the International Confederation of Printing and Allied Industries (INTERGRAF) are also supporting the European Declaration. Beside the recycling rate to be obtained in 2005, the signatories of the declaration are also committed to achieve the following:

- Further reduction of the generation of residues during all processes in the paper and board life-cycle.
- Further improvement of the efficient use of raw and auxiliary materials.
- Optimization of recovered paper collection systems by sharing expertise with those responsible for collecting recovered paper for recycling purposes.

- Improvement of technical, operational and environmentally benign solutions by stimulating and supporting research and development.
- Improvement of the awareness of paper recycling by informing the consumers about their role in closing the paper loop [31].

The European paper industry is a good way to meeting the target, because the recycling rate achieved in 2003 was already 54% and the recovered paper use has increased since 1998 by 6.1 million tons [32].

There are, however, significant challenges still to be met – not only in terms of collecting the volume of recovered paper needed, but also in remaining focused on the quality of paper collected. Stakeholders in the paper recycling chain are looking at initiatives that will promote separate collection streams for paper. Therefore, the industry has begun to prepare guidelines for the responsible sourcing of recovered paper, covering everything from collection, sorting and transportation through to the storage and end-uses of recovered paper. As a result, the CEPI and ERPA have adopted a set of quality control guidelines to be used by suppliers and buyers of recovered paper [33]. Food contact papers are another challenge to be faced in this respect. The paper industry and its partners in the supply chain are also looking at new ways of improving the recyclability of paper and board products.

## 8.2

### United States of America

As the USA has a population of more than 270 million in 50 states, it is not possible to describe the total recycling situation under a single heading. Several federal government Executive Orders are now in existence, but a general assumption is that the federal government will not introduce any radical changes during the next few years. Many individual states have issued laws and promulgated rules that promote recycling, reduce the amount of waste material, or prohibit individual objects from being disposed of in landfills.

To date, about 40 states have passed recycling laws or have implemented voluntary goals and directives. Most states have determined a recycling goal between 20% (Maryland) and 70% (Rhode Island) for used paper products. With its Act 335, Wisconsin issued the most comprehensive and far-reaching recycling and waste material avoidance law as early as 1989. Besides numerous promotional and educational programs, the law established Responsible Units (RUs) which oversee local recycling activities and are eligible for grants to maintain their administrative function [14,34].

In contrast to European directives, which define specific recovery rates for paper and board packaging and partly also for printed material, a recycled fiber content for specific new paper grades or paper products is effective in the USA. This began in 1976 with the Resource Conservation and Recovery Act that led to the

introduction by the U.S. Environmental Protection Agency (EPA) of a set of Procurement Guidelines for government agencies in 1991.

Dissatisfaction with these guidelines motivated the U.S. Recycling Advisory Council (RAC) to promulgate a minimum recycled fiber content (including post-consumer recovered paper) for the paper procurements of the federal authorities. In 1998, President Clinton renewed the EPA acquisition guidelines by the Executive Order called Greening the Government by Waste Prevention, Recycling, and Federal Acquisition. According to this order, all writing, printing and office papers purchased after 1998 with public funds must contain at least 30% post-consumer recovered paper, or not less than 50% recovered material including pre-consumer recovered paper. All price increases must be offset by a reduction in the amount of waste material produced and by lower consumption. This constitutes a rare example of an officially decreed consumption limitation.

In 1995, the EPA issued a Guidance Document on the Acquisition of Environmental Preferable Products and Services. This was the first comprehensive articulation of its "Green Products" policy. The document contains seven principles to ensure that environmentally friendly products receive greater consideration for orders placed by state procurement agents. This considered both quantity and quality. The first principle of this environmental preference did not consider whether one "green product" can substitute for another. Instead, it questioned whether a function must be improved, and realized this while minimizing negative effects to the environment. The intention was that federal agencies should acquire more environmentally friendly products and services and initiate voluntary pilot projects.

For paper and paper products, the EPA Office for Solid Waste has published a Paper Products Recovered Materials Advisory Notice [35]. This guidance note promotes paper recycling by centralized acquisition, and expands the markets for papers containing recycled fibers. Two important agencies for paper acquisition in the United States are the General Services Administration (GSA) and the Government Printing Office. The EPA guidance notice has special importance in that it extends beyond governmental agencies and is also applicable on a wide scale for purchases in the private sector. Such purchases represent 95% or more of total paper requirements.

U.S. Postal Service (USPS) faced in 1995 the problem of stickies in paper mills by the more widely used pressure sensitive postage stamps. Together with members of the pulp and paper industry, the adhesive industry, the converting industry and the USDA Forest Products Laboratory a large research investigation was started to develop environmentally benign pressure sensitive adhesives (PSA). The team specified environmentally benign adhesives (EBA) for stamps and label products, developed laboratory and pilot scale tests and set specifications for the allowable level of stickies from an EBA. Additionally, mill scale trials with EBA were conducted to validate laboratory and pilot tests. Finally a list of identified qualified environmentally benign PSA's was published in 2001. Nevertheless, the use and acceptance of EBA paper labels is still infancy in the United States. That is the reason that IPEBA (Initiative to Promote Environmentally Benign Adhe-



sives) was founded in 2003 as a consortium of adhesive manufacturers to promote the successful implementation of the United States Executive Order 13148 Section 702, which rules the public order of PSA label products [36].

EPA has defined conditions for the minimum recycled fiber content in different paper grades. A two-tier level exists consisting of post-consumer fiber content and total recycled fiber content. According to the American Forest & Paper Association (AF&PA), almost all pre-consumer recovered paper is collected and recycled. Therefore, the EPA believes that the two-tier approach leads to greater use of post-consumer recovered paper. To date, the EPA has not defined environmentally preferable paper in an even stricter sense. For example, it has not taken into account major environmental influences on paper production such as the type of forests from which the virgin fiber furnish is derived.

Table 8.1 shows the minimum content of recycled fibers for different paper grades. It includes a comparison of the recycled fiber content proposed by RAC for government acquisitions since 1992 with the EPA guidelines. At first glance, the EPA conditions appear to more strict. However, the statistical values must be interpreted very carefully as the definitions differ somewhat [17].

**Tab. 8.1** Recycling Advisory Council (RAC) and Environmental Protection Agency (EPA) guidelines for government paper products [17].

Product line	RAC 1992		EPA 1995	
	Total recycled fiber content [%]	Post-consumer fiber content [%]	Total recycled fiber content [%]	Post-consumer fiber content [%]
Newsprint	40	40	40–100	40–85
Printing and writing	40–50	10–15	10–50	10–20
Tissue	60–80	50–70	20–100	20–60
Construction paper	80	65	n/a	n/a
Packaging paper	40	20	5–40	5–20
Uncoated paper: corrugated	40	35	30–50	30–50
Uncoated paper: other	100	60	n/a	n/a
Coated paperboard	90	45	100	45–100

n/a = not announced.

Besides general laws, ordinances, and guidelines, many federal laws exist in the USA to avoid waste material. Typically, these laws cover the fields of separation of discarded paper at the source, procurement preference, and recycled fiber content

in newsprint. They achieve the aim of the EPA to reduce the amount of waste material for disposal in landfills or in incineration plants. These laws include the following:

- Mandated separation of newspapers by households.
- Federal, state, and municipal procurement policies favoring recycled materials.
- Laws requiring consumers of newsprint to use recycled fiber containing newsprint for a certain portion of their total requirements.

The goals to be achieved as recycled fiber content in newsprint in the state regulations are mainly between 30% and 50% and mandatory or voluntary. The various states have no general definition, either for the penalties or for the basis of the recycling goals. Such regulations therefore force mills in the USA or Canada to invest in paper recycling plants to produce papers with the stipulated proportion of recycled fibers. Customers of paper are limited in their choice of supplier. A lack of methods also exists to monitor the secondary fiber content in paper and board grades produced with certain proportions of recovered paper. From the European viewpoint, legislation stipulating contents of recycled fibers in certain paper grades is not acceptable by the paper industry and the consumers of paper products.

Against this background, guidelines for a national recovered paper collection rate, recycling rate – or both – make more sense because they give the paper industry considerably greater freedom in its efforts to achieve the targets, particularly concerning technical and economical matters. Depending on the availability of recovered paper grades and technical possibilities of recovered paper processing, corporate decisions could insure the recycled fiber content of future paper production on a national level. This also allows newsprint mills that operate near major cities to make predominant use of recovered paper as fiber material, whereas mills located in rural, thinly populated areas can continue to produce newsprint from virgin fibers. Both paper grades can be marketed everywhere and compete directly with one another. For this reason, the AF&PA specified a recovered paper collection rate of 50% of paper consumption by 2000 as a goal for the American paper industry, but this failed by 4%-points. In 2002, a recovery rate of 48% was realized and the new target set by AF&PA is now 55%, to be achieved in 2012 [37].

### 8.3

#### **Japan**

Japan is still the world's second-largest consumer of recovered paper, at 18.3 million tons in 2002. Only the USA has a greater volume. Considering the structure of the paper grades produced, balanced and small paper exports and imports (about 5% of the paper production), and the fact that Japan in the mid-1980s had already achieved high utilization rates, a consideration of the political goals for recovered paper recycling is useful. The Waste Disposal Law enacted in 1970 was

amended in 1991 when the Resource Recycling Facilitation Law (called the Recycling Law) was added. Article 1 describes the purpose of this law: “Considering that Japan relies on importing many important resources, but a large part of these resources are now being discarded without being used, the purpose of this law is to provide the basic mechanism for promoting the use of recyclable resources, and thereby promote the healthy development of the nation’s economy”.

According to Ministerial Ordinance No. 53 of the Ministry of International Trade and Industry (MITI), a further increase in the utilization rate of recovered paper of 55% was to be realized in domestic paper production by the end of the Fiscal Year 1994 (April 1994 to March 1995). Paper producers must also do the following:

- Install processing systems for the utilization of recovered paper and provide the necessary storage space for recovered paper.
- Improve recovered paper processing technology in cooperation with machine manufacturers and chemical suppliers.
- Develop a recovered paper utilization plan for each fiscal year.
- Publicize statistical data on the percentage use of recovered paper.

The MITI contribution to increase the utilization rate of recovered paper consists of regulations that create financial and tax incentives on the recovered paper market. These include reduced corporate taxes, special rate of depreciation allowance, low credit rates for purchasing machines for pre-treating recovered paper such as bale presses and wiring machines, and a model for collection systems. Paper producers were offered reduced tax rates and special depreciation rates for machines for processing recovered paper and favorable loans for the installation of deinking systems.

The MITI itself launched several advertising campaigns for the use of recycled fiber products. Two private associations also promoted use of recycled paper among consumers. The Paper Recycling Promotion Center introduced “Green Mark Labels” for magazines, toilet paper, and books produced from recycled fibers. The Japan Environment Association developed the Eco-Mark project for products manufactured with recycled fibers. Unfortunately, due to the unclear definition of the recycled fiber contents in paper and board products, both programs had only limited influence on the consumers’ decisions.

The objective of a 55% utilization rate for recovered paper in 1994 was determined in 1989, when the rate was 50%. This rate was accepted without reservation by the industry as it represented a realistic goal. Nevertheless, a utilization rate for recovered paper of only 53% occurred in 1994, despite the market having an oversupply of recovered paper. Some factors that contributed to this failure to reach the projected utilization rate included:

- Reduced production share of those grades of packaging papers and board that contain large proportions of recycled fibers.
- Increased demand for high-quality paper products.
- Rising costs for processing recovered paper due to environmental legislation.

- Efforts by industry to increase profits.
- Inadequate legislation.

This failure by the paper industry to achieve the goal of recovered paper use of 55% motivated the Ministry of Health and Welfare (MHW) to accuse MITI of taking an excessively lenient approach towards paper producers. Economic studies concerning the use of recycled papers at private businesses showed that the consumers of recycled papers either demanded identical quality as with papers manufactured from virgin fibers, or much lower prices for them. The studies also revealed that a precondition for raising the level of use of recovered paper is improvement of public knowledge and understanding of recycled paper products.

To overcome these problems, MITI established a Study Committee on Basic Issues of the Japanese Paper and Pulp Industry. This committee comprised representatives of newspaper, banking, and trading companies and the pulp and paper manufacturing, paper distribution, paper converting, printing, and recovered paper industries. The industry calls for government support to:

- Establish a policy of improving the separation of recovered paper at the source;
- Expand the collection of office papers by establishing a support system;
- Expand consumer demand for recycled paper;
- Negotiate an agreement between industry and consumers on standard qualities for printing and writing paper with a clear statement on the content of recycled fibers;
- Promote increasing transparency on the domestic and export market for recycled paper products;
- Subsidize improved recovered paper processing methods;
- Re-evaluate the tax system to promote increased use of recycled products;
- Establish a policy to reduce transport costs of recovered paper;
- Develop alternative recovered paper uses other than recycling into paper and board products;
- Increase recycling for energy recovery; this means that low-grade recovered paper can also have use for energy recovery; and
- Increase international recycling with increased export of recovered paper [25,38].

MITI supported the research and consulting activities of this committee, used it to establish a new political orientation and to help companies develop new strategies. In 1994, the Study Committee presented a new program called “Recycle 56”; this was aimed at achieving a recovered paper utilization rate of 56% by 2000, and this was exceeded by 1%-point. In fact, the program was so effective that in 2002 a utilization rate of 61% was achieved.

## References

- 1 Anonymous, *Papier 2005 – Ein Leistungsbericht* (VDP, Ed.), Bonn, 2005, 85 pp.
- 2 Anonymous, *Papier 1993 – Ein Leistungsbericht* (VDP, Ed.), Bonn, 1993, 64 pp.
- 3 Anonymous, *Papier 1983 – Ein Leistungsbericht* (VDP, Ed.), Bonn, 1983, 50 pp.
- 4 Anonymous, 1972 Annual Review. *Pulp Paper Int.*, 1972; 14(9): 67–185.
- 5 Anonymous, 1962 Annual Review. *Pulp Paper Int.*, 1962; 4(9): 77–200.
- 6 Anonymous, 1959 Annual Review. *Pulp Paper Int.*, 1959; 1(9): 7–140.
- 7 Anonymous, 1963 Annual Review. *Pulp Paper Int.*, 1963; 5(9): 83–212.
- 8 Anonymous, *Altpapierliste der Deutschen Standardsorten und ihre Qualitäten*. BDE/Köln, bvse/Bonn, VDP/Bonn, Germany, 1997.
- 9 Anonymous, *CEPI List of European Standard Qualities of Recovered Paper*. CEPI, Brussels, 1995.
- 10 Anonymous, *General List of Standard Qualities of Recovered Paper, B.I.R.* Bureau International de la Récupération, Barcelona, Spain, 1996.
- 11 Anonymous, *DIN EN 643, Europäische Altpapier-Standardsorten-Liste*. Beuth Verlag, Berlin, 2001.
- 12 Anonymous, *Special Recycling 2002 Statistics – October 2003*. CEPI/Brussels, 2003.
- 13 Anonymous, *Scrap Specifications Circular 2003, Guidelines for Nonferrous Scrap, Ferrous Scrap, Glass Cullet, Paper Stock, Plastic Scrap Electronics Scrap*. Institute of Recovered Recycling Industries (ISRI), Washington D.C., 2003: 19–31.
- 14 Anonymous, Information from Internet Web-Site of American Forest & Paper Association. Available online: <http://www.afandpa.org/state/newsprint>, 1998.
- 15 Anonymous, *2002 Statistics of Recovered Paper in Japan*. Paper Recycling Promotion Center, Tokyo, 2002.
- 16 Anonymous, *CEPI 10-Year Statistical Summary*. CEPI/Brussels, 2002.
- 17 Anonymous, *Towards a Sustainable Paper Cycle*. International Institute for Environment and Development (IIED), London, 1996.
- 18 Putz, H.-J., Göttsching, L., Altpapier – ist sein Einsatz noch zu steigern? *ipw* 2001; (11): T189–T193.
- 19 Anonymous, *Special Recycling 2003 Statistics – October 2004*. CEPI/Brussels, 2004.
- 20 Pihlajamäki, P., Hytonen, H., Gemischtes tropisches Hartholz – eine unbedeutende und schrumpfende Faser-Rohstoffquelle für Papier. *Together – Magazin der Papiertechnik*, 2004; 17: 2–6.
- 21 Anonymous, Weltweiter Altpapierverbrauch wird bis 2010 auf 225 Mio. Tonnen steigen. *EUWID Papier und Zellstoff*, 2004; 49: 16.
- 22 Mulligan, D.B., Sourcing and grading of secondary paper. In: *Secondary Fiber Recycling*, Spangenberg, R.J. (Ed.), Tappi Press, Atlanta, GA, 1993: Chapter 8.
- 23 Bilitewski, B., Härdtle, G., Marek, K., *Waste Management*. Springer-Verlag, Berlin, 1994.
- 24 Bilitewski, B., Heilmann, A., Apitz, B., et al., Wissenschaftliche Untersuchung und Begleitung von Modellversuchen zur getrennten Erfassung graphischer Papiere. Phase I: Erfassung und Bewertung vorhandener Sammelsysteme. INTECUS, Dresden, Germany, 1994.
- 25 Göttsching, L., Pakarinen, H., *Recycled fiber and deinking*. Fapet Oy, Helsinki, 2000.
- 26 Andersen, S.L. In: *Recycling*, Abubakr, S. (Ed.). Tappi Press, Atlanta, GA, 1997: 3–6.
- 27 Kügler, T., Private communication on household recovery analysis. Intecus, Dresden, April 8., 2005.
- 28 Putz, H.-J., Schabel, S., Rohstoff Altpapier – ein ausblick. *Wochenbl. f. Papierfabr.*, 2005; 133(3/4): 103–111.
- 29 Kibat, K.-D., Altpapier und Produktverantwortung in Europa. *Wochenbl. f. Papierfabr.*, 1996; 124(14/15): 656.
- 30 Kibat, K.-D., Altpapiereinsatz im Spektrum der europäischen Abfallpolitik.

*Wochenbl. f. Papierfabr.*, **1998**; 126(16): 742.

- 31 Anonymous, *European Declaration on Paper Recovery*. CEPI/Brussels, **2000**.
- 32 Anonymous, *The European Declaration on Paper Recovery*. CEPI/Brussels, **2003**.
- 33 Anonymous, *Responsible Management of Recovered Paper: Guidelines on responsible sourcing and quality control*. CEPI/Brussels, **2004**.
- 34 Anonymous, *Waste Reduction and Recycling Initiative*. PUBL-IE-041, REV 2/93, Wisconsin Department of Natural Resources, Madison, **1993**.
- 35 Anonymous, Information from Internet Web-Site of EPA. Available online: [www.epa.gov/epaoswer/non-hw/procure/paper/response.txt](http://www.epa.gov/epaoswer/non-hw/procure/paper/response.txt), 1996.
- 36 Oldack, R.C., Gustafson, F.J., Initiative to promote environmentally benign adhesives (IPEBA): Solving a "Sticky" issue. *Progress in Paper Recycling*, **2005**; 14(2): 6–8.
- 37 Anonymous, Information from Internet Web-Site of American Forest & Paper Association. Available online: <http://www.afandpa.org>, **2004**.
- 38 Carbonnier, S., Paper Recycling and the Waste Paper Business in Japan. Sub-Study No. 16 for IIED Study: *Towards a Sustainable Paper Cycle*. Tokyo, **1996**.

## **Appendix: European List of Standard Grades of Recovered Paper and Board (February, 1999)**

This document has been developed jointly by the Confederation of European Paper Industries (CEPI) and the Bureau of International Recycling (B.I.R.) as a revision of the CEPI list dated January 1995.

### **Preface**

This list of European standard grades of recovered paper and board provides a general description of the standard grades by defining what they do, and do not, contain.

The list is for use by industry professionals, organizations and individuals with an interest in the recovered paper sector to assist in the buying and selling of this raw material intended for recycling by the paper and board industry.

The list also provides help and support for Customs and Excise Officers who are required to classify these raw materials from waste in the context of supranational legislation on the control of waste movement.

It is not the purpose of the list to specify all the qualities of recovered paper and board that exist in the different markets, but rather to define those qualities most commonly traded in Europe. The description of the grades is brief, and for this reason it is recognized that specific deals between buyer and supplier for grades with special specifications will still be necessary to meet individual requirements and will not be excluded by any implied regulations associated with the publication of this list.

Paper and board mills may ask for a declaration from the supplier about the origin of the material, in relation to national regulations or standard requirements.

Recovered paper from refuse sorting stations is not suitable for use in the paper industry.

Recovered paper and board originating from multi-material collection systems, containing only material of a valuable, recyclable nature, must be specifically marked. It is not permissible to mix it unmarked with other recovered paper and board.

The list contains a group of recovered paper grades (Group 5 “Special Grades”) that, in most cases, can only be recycled using specific processes, or can cause some particular constraints to recycling. Their inclusion in the list is justified by the existence of a significant European market. Actual recycling of the specific qualities can only be done by a limited number of mills located in a few countries only.

## **Definitions**

### **Unusable Materials**

Materials which are unusable in the production of paper and board consist of “nonpaper components”, and “paper and board detrimental to production”. Recovered paper and board should, in principle, be supplied free of unusable materials, but where for specific grades a certain proportion of unusable materials is agreed between purchaser and supplier, it shall refer solely to the element described as “paper and board detrimental to production”.

### **Nonpaper Components**

These consist of any foreign matter in the recovered paper and board which, during processing, may cause damage to machines or interruptions to production or may reduce the value of the finished product, such as:

- metal
- plastic
- glass
- textiles
- wood
- sand and building materials
- synthetic materials
- “synthetic papers”

### **Paper and Board Detrimental to Production**

These are grades of paper and board which have been recovered or treated in such a way that they are, for a basic or standard level of equipment, unsuitable as raw material for the manufacture of paper and board, or are actually damaging, or whose presence makes the whole consignment of paper unusable.

A growing number of mills have, however, adapted treatment plants to handle such grades and the range of papers and boards capable of being recycled is increasing all the time as technology develops. The criteria for defining the per-



centage of “unusable materials” for these grades will be subject to individual mills’ specifications.

### Moisture Content

Recovered paper and board will, in principle, be supplied with moisture of not more than the naturally occurring level. Where the moisture content is higher than 10% (of air-dried weight), the additional weight in excess of 10% may be claimed back – with the method of testing and sampling to be agreed between buyer and seller.

### To the Numbering System

Recovered paper grades have been numbered in this list according to a numerical code system of “x.yy.ww”, where: x = group; y = grade; and w = subgrade.

- Group 1 – Ordinary grades
- Group 2 – Medium grades
- Group 3 – High grades
- Group 4 – Kraft grades
- Group 5 – Special grades

#### Group 1: Ordinary grades

- |      |   |
|------|---|
| 1.01 | Mixed paper and board, unsorted, but unusable materials removed<br>A mixture of various grades of paper and board, without restriction on short fibre content.              |
| 1.02 | Mixed papers and board (sorted)<br>A mixture of various qualities of paper and board, containing a maximum of 40% of newspapers and magazines.                              |
| 1.03 | Gray board<br>Printed and unprinted white lined and unlined grey board or mixed board, free from corrugated material.   |
| 1.04 | Supermarket corrugated paper and board.<br>Used paper and board packaging, containing a minimum of 70% of corrugated board, the rest being solid board and wrapping papers. |
| 1.05 | Old corrugated containers<br>Used boxes and sheets of corrugated board of various qualities.  |
| 1.06 | Unsold magazines<br>Unsold magazines, with or without glue.<br>1.06.01 – Unsold magazines without glue<br>Unsold magazines without glue.                                    |

- 1.07 Telephone books  
New and used telephone books, with unlimited content of pages colored in the mass, with and without glue. Shavings allowed.
- 1.08 Mixed newspapers and magazines I  
A mixture of newspapers and magazines, containing a minimum of 50% of newspapers, with or without glue.
- 1.09 Mixed newspapers and magazines II  
A mixture of newspapers and magazines, containing a minimum of 60% of newspapers, with or without glue.
- 1.10 Mixed magazines and newspapers  
A mixture of newspapers and magazines, containing a minimum of 60% of magazines, with or without glue.
- 1.11 Sorted graphic paper for deinking  
Sorted graphic paper from households, newspapers and magazines, each at a minimum of 40%. The percentage of non-deinkable paper and board should be reduced over time to a maximum level of 1.5%. The actual percentage is to be negotiated between buyer and seller.

#### Group 2: Medium grades

- 2.01 Newspapers  
Newspapers, containing a maximum of 5% of newspapers or advertisements colored in the mass.
- 2.02 Unsold newspapers  
Unsold daily newspapers, free from additional inserts or illustrated material colored in the mass.  
2.02.01 – Unsold newspapers, no flexographic printing allowed  
Unsold daily newspapers, free from additional inserts or illustrated material colored in the mass, strings allowed. No flexographic printed material allowed.
- 2.03 Lightly printed white shavings  
Lightly printed white shavings, mainly mechanical pulp-based paper.  
2.03.01 – Lightly printed white shavings without glue  
Lightly printed white shavings, mainly mechanical pulp-based paper, without glue.
- 2.04 Heavily printed white shavings  
Heavily printed white shavings, mainly mechanical pulp-based paper.  
2.04.01 – Heavily printed white shavings without glue  
Heavily printed white shavings, mainly mechanical pulp-based paper, without glue
- 2.05 Sorted office paper  
Sorted office paper.

- 2.06 Colored letters  
Correspondence, in mixed papers colored in the mass, with or without print, of printing or writing paper. Free from carbon paper and hard covers.
- 2.07 White wood-free books  
Books, including misprints of books, without hard covers, mainly of wood-free white paper, black printed only. Containing a maximum of 10% of coated paper.
- 2.08 Colored wood-free magazines  
Coated or uncoated magazines, white or colored in the mass, free from nonflexible covers, bindings, non-dispersible inks and adhesives, poster papers, labels or label trim. May include heavily printed circulars and colored in the mass shavings. Containing a maximum of 10% mechanical pulp-based papers.
- 2.09 Carbonless copy paper  
Carbonless copy paper.
- 2.10 Bleached wood-free PE-coated board  
Bleached wood-free PE-coated board from board manufacturers and converters.
- 2.11 Other PE-coated board  
Other PE-coated board. May contain unbleached board and paper from board manufacturers and converters.
- 2.12 Mechanical pulp-based computer print-out  
Continuous computer print-out, mechanical pulp based, sorted by colors, may include recycled fibers.

### Group 3: High grades

- 3.01 Mixed lightly colored printers shavings  
Mixed shavings of printing and writing papers, lightly colored in the mass, containing a minimum of 50% of wood-free paper.
- 3.02 Mixed lightly colored wood-free printer shavings  
Mixed shavings of printing and writing papers lightly colored in the mass, containing a minimum of 90% of wood-free paper.
- 3.03 Wood-free binders  
White wood-free lightly printed shavings with glue, free from paper colored in the mass. May contain a maximum of 10% of mechanical pulp-based paper.
- 3.04 Tear white shavings  
White wood-free lightly printed shavings without glue, free from wet-strength paper and paper colored in the mass.
- 3.05 White wood-free letters  
Sorted white wood-free writing papers, originating from office records, free from cash books, carbon paper and non-water-soluble adhesives.

- 3.06 White business forms  
White wood-free printed business forms.
- 3.07 White wood-free computer print-out  
White wood-free computer print-out, free from carbonless paper and glue.
- 3.08 Printed bleached sulfate board  
Heavily printed sheets of bleached sulfate board, without glue, poly-coated or waxed materials.
- 3.09 Lightly printed bleached sulfate board  
Lightly printed sheets of bleached sulfate board, without glue, poly-coated or waxed materials.
- 3.10 Multi printing  
Wood-free, coated, lightly printed, free from wet-strength paper or paper colored in the mass.
- 3.11 White heavily printed multiply board  
New cuttings of heavily printed white multiply board, containing wood-free, mechanical or thermomechanical pulp plies, but without gray plies.
- 3.12 White lightly printed multiply board  
New cuttings of lightly printed white multiply board, containing wood-free, mechanical or thermomechanical pulp plies, but without gray plies.
- 3.13 White unprinted multiply board  
New cuttings of unprinted white multiply board, containing wood-free, mechanical or thermomechanical pulp plies, but without gray plies.
- 3.14 White newsprint  
Shavings and sheets of white unprinted newsprint, free from magazine paper.
- 3.15 White mechanical pulp based coated and uncoated paper  
Shavings and sheets of white unprinted coated and uncoated mechanical pulp-based paper.  
3.15.01 – White mechanical pulp-based paper containing coated paper  
Shavings and sheets of white unprinted mechanical pulp-based coated paper.
- 3.16 White wood-free coated paper, without glue  
Shavings and sheets of white unprinted wood-free coated paper, without glue.
- 3.17 White shavings  
Shavings and sheets of white unprinted paper, free from newsprint and magazine paper containing a minimum of 60% of wood-free paper; may contain a maximum of 10% of coated paper. Without glue.

- 3.18 White wood-free shavings  
Shavings and sheets of white unprinted wood-free paper; may contain a maximum of 5% of coated paper. Without glue.  
3.18.01 – White wood-free uncoated shavings  
Shavings and sheets of white unprinted wood-free paper, free from coated paper. Without glue.
- 3.19 Unprinted bleached sulfate board  
Unprinted sheets of bleached sulfate board, without glue, polycoated or waxed materials.

Group 4: Kraft grades

- 4.01 New shavings of corrugated board  
Shavings of corrugated board, with liners of kraft- or testliner  
4.01.01 – Unused corrugated kraft  
Unused boxes, sheets and shavings of corrugated board, with kraftliners only, the fluting made from chemical or thermochemical pulp.  
4.01.02 – Unused corrugating material  
Unused boxes, sheets and shavings of corrugated board, with liners of kraft- or testliner.
- 4.02 Used corrugated kraft I  
Used boxes of corrugated board, with kraftliners only, the fluting made from chemical or thermochemical pulp.
- 4.03 Used corrugated kraft II  
Used boxes of corrugated board, with liners of kraft- or testliners but having at least one liner made of kraft
- 4.04 Used kraft sacks  
Clean used kraft sacks. Wet-strength and non-wet-strength.  
4.04.01 – Used kraft sacks with polycoated papers  
Clean used kraft sacks. Wet-strength and non-wet-strength. May include polycoated papers.
- 4.05 Unused kraft sacks  
Unused kraft sacks. Wet-strength and non-wet-strength.  
4.05.01 – Unused kraft sacks with polycoated papers  
Unused kraft sacks. Wet-strength and non-wet-strength, may include polycoated papers.
- 4.06 Used kraft  
Used kraft paper and board of a natural or white shade.
- 4.07 New kraft  
Shavings and other new kraft paper and board of a natural shade.
- 4.08 New carrier kraft  
New carrier kraft, may include wet-strength paper.

Group 5: Special grades

- 5.01 Mixed recovered paper and board  
Unsorted paper and board, separated at source.
- 5.02 Mixed packaging  
A mixture of various qualities of used paper and board packaging, free from newspapers and magazines.
- 5.03 Liquid board packaging  
Used liquid packaging board including used PE-coated liquid packaging board (with or without aluminum content), containing a minimum of 50% by weight of fibers, and the balance being aluminum or coatings.
- 5.04 Wrapper kraft  
Poly-lined, sprayed, or laminated used kraft. Must not contain bitumen or wax coatings.
- 5.05 Wet labels  
Used wet labels from wet-strength papers, containing a maximum of 1% glass content, and a maximum of 50% moisture, without other unusable materials.
- 5.06 Unprinted white wet-strength wood-free papers  
Unprinted white wet-strength wood-free papers.
- 5.07 Printed white wet-strength wood-free papers  
Printed white wet-strength wood-free papers.

## **IV** **Analytical Characterization of Pulps**

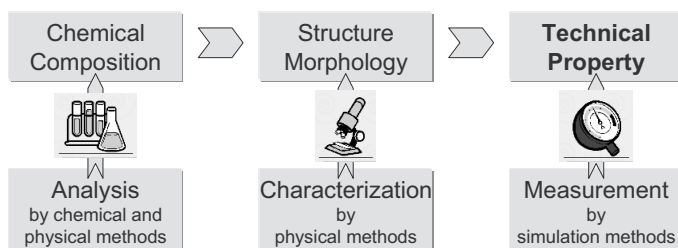
*Erich Gruber*

# 1

## Fundamentals of Quality Control Procedures

Quality is the sum of all properties relevant for a specified use. So, primarily quality control (QC) means the monitoring of certain key application properties of a product. Which technical features have to be controlled, depends on the kind of application. Dissolving pulps must meet other criteria than do pulps for paper. The important features of a paper are determined by the envisaged application. Technical properties normally are measured using a laboratory method that simply simulates the use (e.g., filtering a solution, tearing a strip of paper) under strictly controlled conditions.

Chemical composition is indirectly important, as most technical properties of a product depend heavily on its chemical components. Of equal importance is the macromolecular structure and morphology of the specimen (fiber morphology, paper structure). Quality control uses all of these approaches to acquire information about this group of important technical properties, and this is shown schematically in Fig. 1.1.



**Fig. 1.1** Direct and indirect quality control approaches of relevant technical properties.

For chemical composition, we should differentiate between major and minor components (Tab. 1.1).



Tab. 1.1 Concentration ranges of chemical components in a product.

Component	Concentration in sample [g kg <sup>-1</sup> ]
Main component	>10
Accompanying (minor) component	1 to 10
Trace component	0.1 to 1
Micro component	<0.1

## 1.1 The Role of QC

Quality control deals not only with product and material properties, which are important for application, but also with properties that control the production process. Those purposes for which QC-measurements are used and evaluated to monitor any indication for deviation from the specified profile are listed in Tab. 1.2.

Tab. 1.2 The role of quality control in production.

Raw material check	Process control	Product check
Checking specified properties	In-line measurements	Checking specified properties
Checking unspecified, properties for production control	On-line-measurements	Checking unspecified, properties for production feedback
Data-monitoring	Data-monitoring	Data-monitoring

## 1.2 Basics of QC-statistics

In order to obtain reliable information about any property, a statistical approach of testing and evaluation of measurement results is necessary for several reasons. First, no practical measurement is able to yield a totally reliable result. An experimental value for a property of a product generally differs from the true value of this property. The product itself may not be completely uniform and may show some variation of the property in question. Thus, different samples have to yield a different number, as shown schematically in Fig. 1.2 (variance of sampling). In addition, there is always a certain inaccuracy in the measurement (variance of measurement). Indeed, the variance of measurement is a measure of the reliability of the method applied.

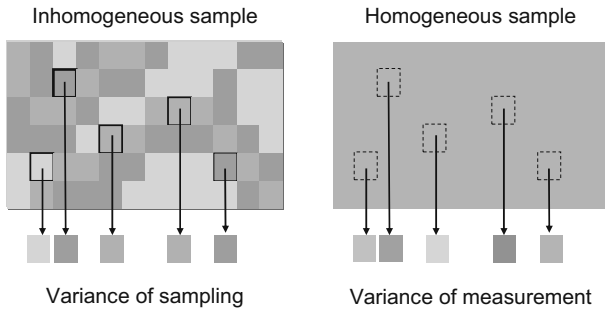


Fig. 1.2 Major reasons for variance of data.

So, each value of property data must be complemented by a measure of reliability, and this can be deduced from repeated measurements by statistical evaluation. In order to evaluate a method of measurement, the “repeatability” must be checked, which means checking the variation of a measuring result using a homogeneous sample, the same method and the apparatus, as well as the same experimenter for various measurements. “Reproducibility” signifies the variance of measurement results, derived by different laboratories when using the same method.

In any case, multiple measurements yield different values, and consequently which is the most probable “true” value must be derived from a statistical analysis of all measurements available. Variance of data can be made visible by grouping them appropriately, as shown in Fig. 1.3.

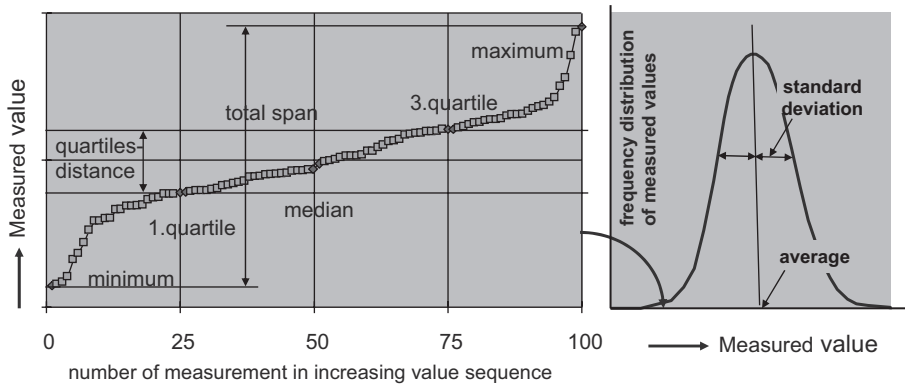


Fig. 1.3 Distribution of measured values and statistical evaluation thereof.

The reliability of a measuring result should be indicated by the confidence interval, which is the range within which an average value of a certain number of equal tests may be expected at a given probability. Unless specified otherwise, a probability of 95% is used. In a graph, the result is presented by a bar or a data point, and the confidence range is indicated by a bar of variance. Alternatively, data may

be represented by a box plot, which indicates the data distribution by quantile values. The different measures for reliability, and their graphical representations in data plots, is shown in Fig. 1.4.

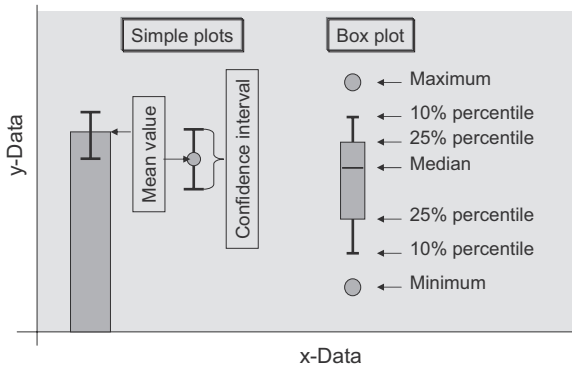


Fig. 1.4 Graphical presentation of data, indicating reliability.

Erroneously, such an interval bar is sometimes used to point out the span of the standard deviation, which however does not directly indicate the reliability of measurements.

Statistics also are applied to compare sets of data (ANOVA = analysis of variation). For example, a so-called *t-test* is used to determine whether different samples differ significantly in a specific quantitative property.

### 1.3

#### Sampling

Guidelines for sampling chemical or mechanical pulp are described in ISO 7213 [1] for paper and for board by ISO 186 [2].

### 1.4

#### Conditions for Testing and/or Conditioning

Unless a specific testing method advises otherwise, the pulp to be tested must be in an exactly defined condition. As pulp has a certain tendency to adsorb water, measures must be taken that an equilibrium state of water up-take at defined conditions has been obtained. Before analysis, the pulp is conditioned by keeping it in a standard atmosphere, normally at a temperature of  $(23 \pm 1)^\circ\text{C}$  and a relative humidity of  $(50 \pm 2)\%$ . In tropical countries, conditions of  $(27 \pm 1)^\circ\text{C}$  and  $(65 \pm 2)\%$  may be applied.

## 1.5 Disintegration

Except for the delivery information of bales and sheets, the fiber material to be tested must be disintegrated into separated fiber fluff. This may be done either in dry or in wet status. In any case, mechanical shear stress should be kept at a minimum in order to keep the fibers as intact as possible.

Standardized laboratory methods shall be applied, according to the following references:

- For fiber disintegration, a special disintegrator or a high-speed mixer is used. Using the disintegrator, the pulp portion is immersed in 1 L of test water and the slurry is stirred at 13 000 r.p.m. for 5 min. Using a high-speed mixer, normally only 500 mL of water is added and stirred at 13 000 r.p.m. for 2 min, after which the fiber suspension is diluted to 1 L [3].

Details for special pulps may be taken from the relevant literature:

- Disintegration of chemical pulps [4]
- Mechanical pulps [5]
- Latency removal [6]

## 2

### Determination of Low Molecular-Weight Components

#### 2.1

##### Moisture

The easiest way to determine the relevant content of water of a pulp is to measure the weight loss on drying. The mechanically fluffed pulp is placed into a weighing dish, which then is exposed to a temperature of  $(105 \pm 2)^\circ\text{C}$  for as long as necessary to reach constant weight [7]. The pulp then is “oven-dry (o.d.)”, but still contains some bound and trapped water, which cannot be removed at this temperature. This water usually is neglected. The moisture content is defined as the percentage of weight loss of the sample by drying; the residue is called “dry matter”.

Some older standards use a temperature of  $(103 \pm 2)^\circ\text{C}$  [8], or refer to determining the moisture content of pulp in bales [9].

More modern, less time-consuming methods are drying by infra-red radiation, measurement of dielectric or neutron absorbance, thermo-gravimetry, or differential scanning calorimetry. A chemical approach is titration by the Karl-Fischer method. These methods are not standardized for pulp and should be calibrated by the drying method.

#### 2.2

##### Inorganic Components

Inorganic compounds may be present in pulp as ions (e.g., sodium or chloride) or as crystalline matter (e.g., silica). Their concentration in pulp is rather low, being normally in the range of a trace component or infrequently of a minor one (see Tab. 1.1). Basically, the classic methods of inorganic analysis may be applied either directly or, more frequently, by using the residue of incineration (ashes). In order to apply a wet chemical analysis, the insoluble material must be transferred into soluble compounds by alkaline or acid digestion.

## 2.2.1

**Ashes**2.2.1.1 **Total Ash**

Ash is the residue of a sample, which has been incinerated completely, and consists of mineral salts and oxides. Sulfite pulps may contain Ca, Mg, SiO<sub>2</sub>, and kraft pulp contains sodium, whilst trace elements of Fe, Mn, Cu, etc., are found in all pulps, with the cations being bound as oxides, halides, sulfates, sulfites, phosphates, silicates, and carbonates. Heavy-metal ions are less abundant in acid-processed pulp than in alkaline-processes versions.

As the salts may be decomposed at higher temperatures (most frequently by loss of bound water or carbon dioxide), they may also form more volatile salts or react further with oxygen to a higher state of oxidation. So, the incineration temperature must be controlled rather accurately. According to ISO [10] and corresponding standard methods, the sample is incinerated at  $(575 \pm 25)^\circ\text{C}$  in a crucible, which is placed in an electric muffle furnace. The treatment must be repeated until constant weight after cooling down in an exsiccator is achieved. The ash content is specified as a percentage of the original sample (normally o.d.).

In practice, there are various apparatus and variations of the incineration method available to accelerate and/or automatize the determination procedure. For instance, the sample may be burned in a flow of oxygen in a tube oven. These methods are not standardized, however, and must be calibrated against a standard procedure.

2.2.1.2 **Sulfated Ash**

In order to avoid ambiguities, it is sometimes recommended to treat the ash with sulfuric acid and to repeat the incineration at  $(700 \pm 25)^\circ\text{C}$  for 3 h [11]. However, statistical studies have shown that this method of sulfated ash does not yield more constant and reliable results than does simple incineration.

2.2.1.3 **Acid-Insoluble Ash**

By incineration, the metals have been transformed to either water-soluble salts or to oxides, which commonly are soluble in acid. Among the elements normally present in pulp, only silica is found as SiO<sub>2</sub>, which is insoluble in moderately concentrated HCl. Some partly soluble silicates, phosphates and sulfates will also remain in the residue of acid treatment.

To determine acid-insoluble ash, the total ash is treated several times with 6 N HCl, evaporated, and digested with dilute HCl. The insoluble residue is filtered over an ash-free paper filter, which is incinerated after being washed free of chlorides [12].

## 2.2.2

**Determination of Single Elements**2.2.2.1 **Survey of Chemical Procedures**

Chemical methods normally are not sufficiently sensitive to be applied directly to the fiber material. For each element, a specific test procedure is applied, normally starting from ash. The stages of the chemical analysis include:

- incineration or chemical digestion;
- dissolution;
- separation from disturbing elements by specific reactions and an appropriate separation procedure;
- transfer into the compound of identification and
- measuring the amount of identification product.

Some elements which form volatile compounds may be partly lost by incineration (e.g., mercury, chlorine, sulfur, arsenic). In such a case, an acid or alkaline wet digestion is preferable, and this is normally carried out in an autoclave.

The final step during the course of a chemical analysis may be different; indeed, the methods are classified according to this step of quantitative determination (Tab. 2.1).

Tab. 2.1 Operating principle of different chemical analytical methods.

Analytical method	Key property of identification product	Method of determination of the identification product	Use for simple identification (qualitative analysis)
Gravimetry	Insoluble	Filtering, drying and weighing	Observing precipitation
Acidimetry	Acidic or alkaline	Titration by a standard solution of base or acid, resp.	Checking pH
Photometry	Absorbance of visible or UV light	Measuring the absorbance (extinction) of a solution	Observing coloration
Oxidimetry	Reducing or oxidizing	Titration by a standard solution of oxidizing or reducing agent, resp.	Discoloration or coloration resp. of a I <sub>2</sub> /KI/starch-solution
Complexometry	Soluble strong, non-ionic complex	Titration by a standard solution of complexing agent	

Complexometry is a suitable method for measuring calcium and magnesium [13,14]. Among the methods mentioned in Tab. 2.1, photometric determination is most widely applied, as it generally exhibits the best sensitivity. The details of some photometric methods are provided in Tab. 2.3.

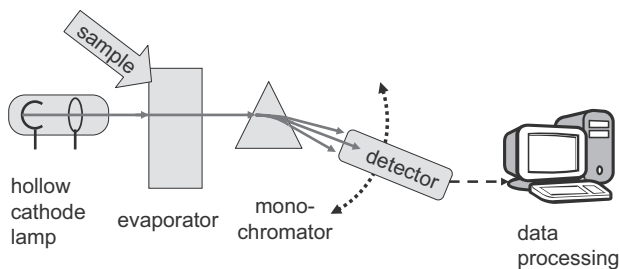
**Tab. 2.2** Major photometric methods for the determination of metal ions in pulp and paper.

Element	Colored identification product	Standard methods
Manganese [Mn]	Oxidation by $\text{HNO}_3$ and $\text{NaIO}_4$ to colored $\text{MnO}_4^{-1}$ -ion	ISO [15,16]; DIN [17]; Zellcheming [18]; SCAN [19]; Tappi [20]
Iron [Fe]	Complex with <i>o</i> -phenanthroline	ISO [21], DIN [22], Scan [23], Tappi
	Complex with bathophenanthroline	Zellcheming [24]
Copper [Cu]	Complex with sodium diethyldithiocarbamate	ISO [25], DIN [26], Zellcheming [27], Scan [28], Tappi [29]
	Complex with bathocuproin	Zellcheming [30]
Cobalt [Co]	Nitroso-R-salt	

#### 2.2.2.2 Atomic Absorption Spectroscopy (AAS)

The principle of AAS is rather simple. It is based on the fact that an element will emit photons of a specific energy (corresponding to light of a certain wavelength), when excited electrons fall back to the base energy level. When exposed to the same kind of light electrons may be excited again, thus absorbing photons of the same wavelength. Suitable light for detecting a certain element can be easily generated by emission from a cathode, coated by material containing the element in question.

The essential components of an apparatus for measuring atomic absorption spectra are shown schematically in Fig. 2.1.



**Fig. 2.1** The measurement principles of atomic absorption spectroscopy (AAS).



A hollow cathode lamp emits light containing mainly the excitation wavelengths of the element(s) to be detected. This light is passed through the evaporated sample. There are various methods for evaporating the sample, the most frequent being evaporation in a flame. If the element sought is present in the sample, it will absorb light in proportion to its concentration. The light, which passed the sample vapors is analyzed by a spectrophotometer consisting of a monochromator (prism, grid, or filter) and a detector.

### 2.2.2.3 X-ray Fluorescence Spectroscopy (XFS)

X-ray fluorescence spectroscopy may be used in various formats to determine the elemental composition of a sample. The major methods use X-ray absorption and X-ray fluorescence, respectively. The X-ray radiation interacts with non-binding electrons of lower energy levels, initiating a quantum leap of such electrons by absorption of a  $\gamma$ -photon. The energies needed for such transitions are unambiguously significant for a specific element. The essentials of the analytical equipment are shown schematically in Fig. 2.2.

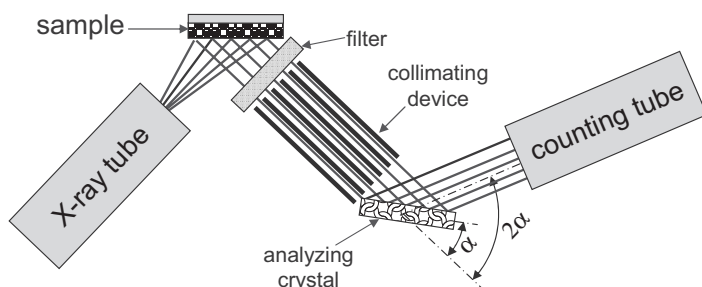


Fig. 2.2 X-ray fluorescence analyzer.

The irradiated sample emits fluorescent photons, which may be analyzed by using an analyzing crystal. This reflects the X-ray radiation most effectively under the angle of reflection,  $\alpha$ , which is linked to the energy (or to the wavelength respectively) of the fluorescence radiation by Bragg's law:

$$n \cdot \lambda = d \sin \alpha$$

where  $n$  is an integer number;  $\lambda$  is the wave length; and  $d$  is the crystal lattice distance.

### 2.2.2.4 Electron Spectroscopy for Chemical Application (ESCA)

ESCA uses the phenomenon, that an electron of an atom may be expelled by soft X-ray radiation. The energy of such an electron depends on the energy of the X-ray radiation applied, and on the binding energy within the atom. The latter prop-

erty is characteristic for each element, and so this type of spectroscopy may be used to determine the concentration of a certain element in a sample. The primary energy of the X-ray source must be known, and the energy of the emitted electrons measured. The number of emitted electrons is proportional to the concentration of the element in the sample. As electrons are very strongly absorbed by matter, they are unable to penetrate thicker layers of a sample. Hence, this type of method is normally only applicable for the analysis of surfaces (e.g., fiber surfaces).

## 2.3

### Extractives

“Extractives” is a general term for those components in pulps, which may be extracted by solvents without disintegrating the structures of the pulp fibers. Extractives are predominately low molecular-weight inorganic or organic compounds. Inorganics are frequently soluble in water, while organic extractives are soluble in organic solvents. A good solvent for a compound must have a strong affinity to the solute, which is the case when there are similar interactions among the molecules of the solvent and the solute respectively. A solvent of high polarity dissolves polar compounds, while nonpolar compounds are only soluble in nonpolar solvents.

Inorganic extractives are mainly ions, which are not integrated in an insoluble crystalline compound, and thus may be completely solvated by water molecules.

#### 2.3.1

##### Water Extractives

Only a small amount of a pulp material is water-soluble, and its presence is in fact an indication of an incomplete washing process during pulp production. This material may consist of soluble salts such as chlorides and acetates and of low molecular-weight carbohydrates.

Normally, the total amount of water extractives is not of major interest, but water extracts may serve as vehicle to determine the presence of specific detrimental compounds.

##### 2.3.1.1 Test Water

For analytical purposes, water of high purity must be used. This is obtained by distillation, de-ionization, or a combination of both. For tests where oxygen, carbon dioxide or pH matters, the purified water should be deaerated immediately before use under a nitrogen atmosphere.

The conductivity of water of high purity grade should not exceed  $0.2 \text{ mS m}^{-1}$ , though some tests are less demanding. In any case, the conductivity of water used for a test should be measured and specified.

### 2.3.1.2 Cold Water Extraction

As there are no general standards for the cold water extraction of pulps, it may be convenient to use a method which was originally designed for plastic materials [31]. Here, the pulp material is kept in test water at 20 °C for 24 h with occasional shaking and following filtration. For specific tests on water extracts, such as the determination of conductivity [32], the conditions of extraction are specified by the standard method.

### 2.3.1.3 Hot Water Extraction

Hot water extracts may be derived in different ways. The sample may simply be flooded by boiling water and kept for 2 h at a temperature just below boiling point [33]; alternatively, it may be treated with boiling water under reflux for 1 h [34].

### 2.3.1.4 Analysis of Water Extracts

Hot and cold water extracts can be used to determine soluble components, and may be characterized by their intrinsic properties, which are characteristic for important chemical features of the sample. Hence, they may be directly useful in evaluating the behavior of the material by technical processing. Some of the most important properties of extracts are listed in Tab. 2.3.

Tab. 2.3 General properties of aqueous extracts.

Property of extract	Principle of determination	Standard methods
pH	Potentiometric by using a pH-sensitive glass electrode	ISO [35]; TAPPI [36]; SCAN [37]
Electrical conductivity	Conductometric measurement	ISO [35]
Acid content	Titration by NaOH to pH = 7	Zellcheming [38]
Alkali content	Titration by H <sub>2</sub> SO <sub>4</sub> to pH = 7	

## 2.4

### Chlorine Compounds

Chlorine may be present in pulps as soluble or insoluble chloride, or as organically bound chlorine.

Soluble chlorides [39] can be determined in aqueous extracts by a gravimetric method using AgNO<sub>3</sub> [40,41]; alternatively, for sheets of pulp or paper the chloride content of the surface may be determined potentiometrically by using a chloride-sensitive electrode.

In order to determine the content of total chlorine, the sample should be preferably burned in a pure oxygen atmosphere in a tightly closed vessel. The ashes are dissolved in NaOH and chloride is determined gravimetrically in the solution. If there are no interfering elements, conductometric titration may also be used for the determination. The sample is dissolved in acetone and titrated by using a solution of  $\text{AgNO}_3$  as titration agent and an Ag/AgCl-electrode [42].

## 3 Macromolecular Composition

The main polymeric compounds in pulp are of course cellulose, lignin and polyoses, and partial degradation products thereof. While the main component cellulose is chemically the same irregardless of its origin, lignin and polyoses may vary widely from plant to plant. Lignin is generally not welcome in a pulp. Polyoses, however, generally should only be absent from a dissolving pulp, as in paper pulp they may be quite useful.

### 3.1 Lignin Content

By pulping, most of the lignin is removed, although the small amount of residual lignin is responsible for many (mostly undesirable) properties. The methods used to determine lignin in pulp must differentiate selectively between polysaccharides and lignin.

In the majority of cases, the lignin content is estimated directly from the demand for an oxidation or chlorination reagent in the bleaching reaction, using the Kappa number, Roe number, or chlorine number. However, these methods are not very selective, as carbohydrates may also react with the oxidizing reagents. The oxidation demand also depends on the degree of pre-oxidation of the residual lignin by the bleaching process. In addition, lignins of different plant origin do not exhibit the same specific reduction potential. Hence, these numbers should rather be considered as a relative measure of residual lignin for a given raw material and in a given pulping process. Accordingly, this situation will be discussed in Section 3.2.

A more selective oxidizing agent is hypochlorite, which is also used for the determination of chlorite holocellulose. Shadenbock suggested extracting residual lignin by reaction with sodium hypochlorite and then determining the lignin content by the UV-absorption of the extract [43]. Simionescu used the same reagent for lignin determination by measuring the heat of reaction in a micro-calorimetric apparatus [44].

A different approach to lignin determination is to remove all the carbohydrates by selective hydrolysis, usually by treating with concentrated mineral acid. The

residue from hydrolysis with 72% sulfuric acid is called *Klasen*-lignin [45,46]. The organic extractives should be removed from the pulp sample by extraction by benzene:methanol (1:1) prior to hydrolysis. The thoroughly washed residue after hydrolysis may still contain insoluble inorganic material, which should be determined separately by incineration.

Up to 10–15% of ligninous components in parts may be also acid-soluble.

## 3.2

### Extent of Delignification

In order to evaluate the extent of delignification while following the course of cooking, it is not necessary to know the exact amount of residual lignin. A simple practical method will suffice, which correlates with the lignin content. Usually, this is carried out by monitoring the consumption of an oxidizing bleaching agent, predominantly of potassium permanganate or chlorine.

#### 3.2.1

##### Roe Number [47]

The Roe number is obtained by reacting the moist sample with chlorine gas. It is defined by the amount (in g) of chlorine consumed by 100 g of moist pulp. The consumption of chlorine gas within a 20-min exposure period is measured volumetrically and the Roe number is calculated.

#### 3.2.2

##### Chlorine Number [48]

The chlorine number is defined as the amount of chlorine (in g) consumed by 100 g of pulp (on a dry basis). The determination is similar to that of the Roe number, but differs in details. The moist sample is exposed for 15 min to chlorine gas, which is generated by acidifying hypochlorite solution. The unreacted amount of chlorine gas is determined iodometrically. The chlorine number may also be used for semi-chemical and high-yield pulps, which are beyond the range which is covered by kappa-number.

#### 3.2.3

##### Kappa Number (Permanganate Number) [49–52]

Since the handling of gas reactions is not simple, over a period of time the Roe number has lost ground as a measure of delignification and is being increasingly substituted by the Kappa number. The latter is defined by the volume (in mL) of 0.02 M potassium permanganate solution consumed by 1 g of pulp (on a dry weight basis).

$\text{KMnO}_4$  reacts preferentially (but not completely) and exclusively with lignin. When longer reaction times are permitted, carbohydrates are also oxidized; consequently, the method requires that the reaction conditions are maintained very accurately.

The reaction is carried out under standard conditions in sulfuric acid, and is limited to 10-min reaction time. The amount of reagent used should contain an excess of approximately the same amount of permanganate as consumed by the reaction; this quantity should be determined by a pretest.

The standardized method applies only to pulps within the kappa-number range of 5 to 100, although it may also be adapted to the lower lignin contents found in bleached chemical pulps.

### 3.3

#### Alkali Resistance and Solubility

The molecular components of pulp may be partially soluble in aqueous alkali, their solubility depending heavily on the alkali concentration. Of course, normally a major part of the alkali-soluble components is removed during the alkaline stages of pulping and bleaching. Only that part of material which is only soluble at higher alkali concentration (i.e., 10–18% NaOH) may be still found in pulp. This residue consists mainly of more- or less-oxidized polyoses and strongly degraded and/or oxidized cellulose. These components have a strong influence on the application properties of the pulp, so alkali solubility is an important measure of quality assurance. However, this number is simply a sum parameter and is useful only for comparing similar pulps. Originally, this method served to evaluate the yield of cellulose after alkalization in the xanthate process.

#### 3.3.1

##### Alkali-Soluble Components

The solubility of plant polysaccharides depends on their degree of polymerization (DP), monomer composition, and degree of branching. Cellulose and hemicelluloses differ strongly in their alkali solubility: cellulose in plant fibers is less soluble, and its resistance against alkali treatment increases with a rising DP.

#### 3.3.2

##### $\alpha$ -, $\beta$ -, and $\gamma$ -cellulose [53]

Previously, Ross and Bevan [54] used the term  $\alpha$ -cellulose to indicate the content of cellulose material which was insoluble in the lye used for alkalization. The soluble portions which could be precipitated by acidification were termed  $\beta$ -cellulose, and the remaining residues  $\gamma$ -cellulose. Classically, “pure” cellulose is called “alpha-cellulose”, which is defined as the carbohydrate residue after treatment of the pulp material by 17.5% NaOH at room temperature. By using this treatment,

low molecular-weight degraded cellulose is also dissolved to some extent. Quite surprisingly, cellulose is more soluble in less concentrated NaOH, with alkali of 10% NaOH being most effective. The reason for this unexpected behavior is that cellulose swells best at a lye concentration of approximately 10% [55], whereas at concentrations above 10–15% Na-cellulose is formed, which is a rather stable compound. A practical problem arises, however, when Na-cellulose is washed with water, as the solubility is increased temporarily and part of the less-soluble alkali cellulose will dissolve. Thus, washing conditions are critical for the determination of alpha-cellulose, and the conditions of treatment must be controlled precisely.

The alkali-soluble carbohydrates, which comprise rather short molecular chains, are even soluble in water. This fraction is called gamma-cellulose, and it can be determined by neutralizing the alkali extract using acetic acid. The residue, which is insoluble under neutral conditions, is termed beta-cellulose. An overview on the fractionation of pulp components according to alkali solubility is provided in Fig. 3.1.

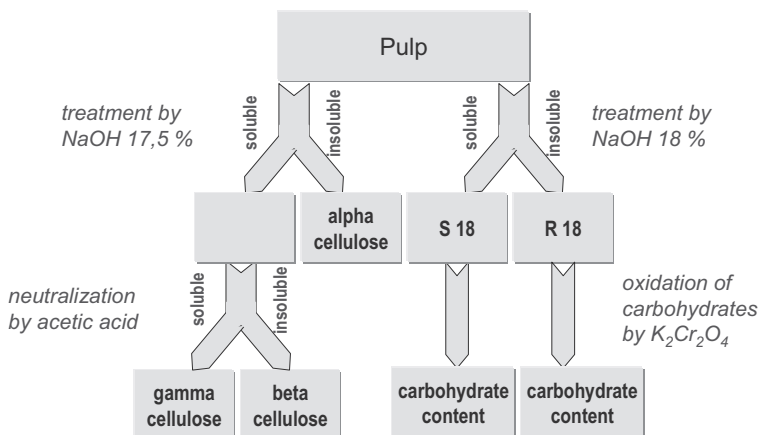


Fig. 3.1 Fractionation of poly- and oligosaccharides by alkali solubility.

### 3.3.3

#### $R_{18}$ and $S_{18}$ values

Nowadays, instead of alpha-cellulose content the insoluble residue after treatment by 18% NaOH is used. This number is termed  $R_{18}$ , and it is determined by the ISO method [56]. The corresponding method to determine alkali solubility ( $S_{18}$ ) is also standardized [57]. For softwood pulps, there is no major difference between alpha-cellulose and  $R_{18}$ , whilst for hardwood pulps 18% NaOH dissolves substantially less material than 17.5% NaOH.



### 3.4 Composition of Polysaccharides

Polysaccharides of plant origin consist mainly of glucose units. However, besides glucose, all functional biopolymers also contain other carbohydrates that are specific for a certain polymer. Thus, the carbohydrate composition of a fiber material is also an indication of the presence of polysaccharides other than cellulose.

For analysis, the polysaccharides are hydrolyzed using either acid or an enzyme catalyst to monosaccharides, which are determined either qualitatively or quantitatively, using chromatographic methods. The acidic conditions must not be too strong, since under severe reaction conditions pentoses may be converted to furfural, and hexoses to methyl furfural (see Fig. 3.4).

#### 3.4.1 Determination of Monosaccharides after Hydrolysis

##### 3.4.1.1 Gas Chromatography

In order to analyze sugar molecules with gas chromatography, the compounds must be volatilized by derivatization with hydrophobic groups, which inhibit hydrogen bonding. The most common method is to treat the sugars with trimethylsilyl chloride in pyridine solution to produce trimethylsilyl (TMS) ethers. In the reaction medium, the acetal group of monosaccharides can be opened such that there will be a final equilibrium of  $\alpha$ - and  $\beta$ -forms, as well pyranosic as furanose conformers for each sugar; this leads to the formation of four peaks in the gas chromatogram. An example of the four possible ring trimethylsilyl derivatives of glucose is shown in Fig. 3.2.

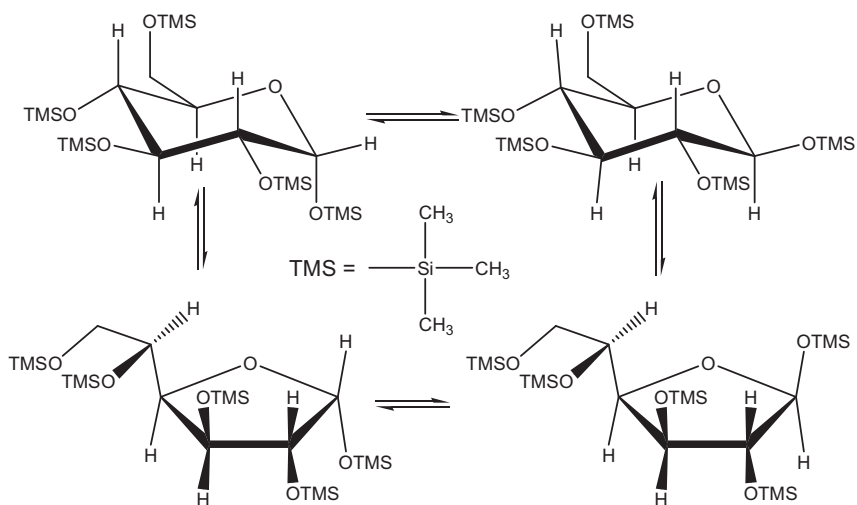
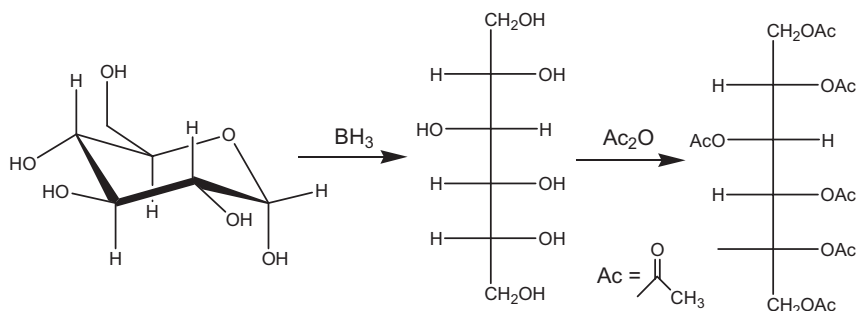


Fig. 3.2 The different conformers of trimethylglucose.

A better-suited approach to quantitative determination consists of reducing the acetal to an alcohol by borohydride, before esterifying all alcoholic functions of the resulting alditol with acetic anhydride (Fig. 3.3). Using this method, each sugar yields only a single product.



**Fig. 3.3** Synthesis of alditol acetate for gas chromatographic identification.

Such acetates are readily soluble in methylene chloride, thereby producing gas chromatograms of high reproducibility, with nicely separated peaks for glucose, xylose, mannose, arabinose, and galactose [58]. A suitable gas chromatograph should be equipped with a flame ionization detector and a device to integrate peak areas of the chromatogram.

#### 3.4.1.2 Thin-Layer Chromatography

The sugars xylose, arabinose, mannose, glucose, and galactose may be separated effectively using thin-layer chromatography [59]. Phosphated silica gel is used as a stationary phase, with ethanol as the mobile developer. The carbohydrate patches are made visible by staining with aniline phthalate and quantified using spectrophotometry.

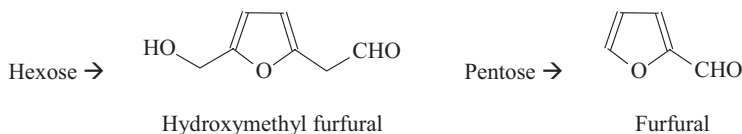
#### 3.4.1.3 Liquid Chromatography

While gas chromatography requires volatile compounds to function, liquid chromatography requires solutions. As a solution can be handled more easily, the latter method is increasingly replacing gas chromatography for sugar analysis. The monomeric sugars produced after hydrolysis are water-soluble in water; hence, the liquid chromatography column must be packed with a suitable adsorbing material. Measurements of compounds in the column eluent are carried out using a suitable detector such as a refractometer or a UV-photometer.

## 3.4.2

**Determination of Pentosans after Hydrolysis**

Pentosans may be determined by hydrolyzing polysaccharides to the pentoses. Under strong acidic conditions, pentoses form furfural, while hexoses will be transformed to hydroxymethyl-furfural (Fig. 3.4).



**Fig. 3.4** Conversion products from pentoses and hexoses from polyoses.

Furfural is isolated from the reaction mixture by distillation. It reacts with orcinol-ferric chloride, forming a deeply colored complex that is monitored photometrically at a wavelength of 630 nm [60]. In addition to this standardized method, many colorimetric reactions have been reported in literature that are better suited to the photometric determination of pentose-based furfural [61].

## 3.4.3

**Determination of Uronic Acids after Hydrolysis**

Ionic derivatives of sugars can be determined using ion chromatography. This method uses separation columns packed with ion-exchange material to which ions are bound by electrostatic forces, depending on their net charge and their hydrated radius. The predominantly aqueous sample solution contains the salts of uronic acid or onic acid. After loading the exchange resin material, an eluent solution containing ions of higher affinity is passed through the column, and these replace the carbohydrate. Different carbohydrates appear at the column outlet after various residence times within the column, and normally are detected using a conductivity sensor. The equipment used for ion chromatography resembles that used for size-exclusion chromatography (see Fig. 3.20), and differs only in the separating medium (column filler) and the sensors used.

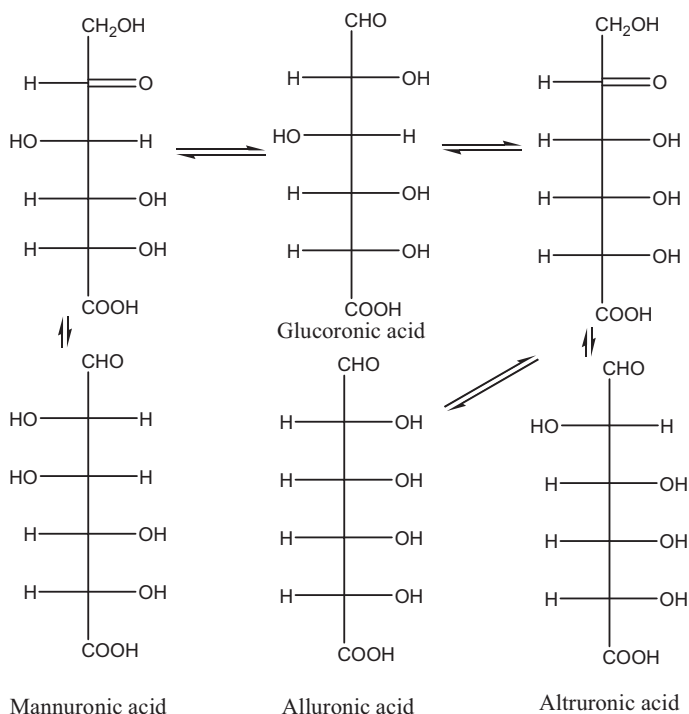
Uronic acids may be detected using ion chromatography, paper chromatography, or electrophoresis (paper or gel electrophoresis). Alternatively, the sugars may be transferred to their TMS derivatives and analyzed using gas chromatography.

For paper chromatography, *p*-anisidine-HCl is used as a staining reagent when developing the chromatograms.

In any case, pure uronic acids must be applied as a “standard”. These reference standards may be synthesized by bromine oxidation of the corresponding sugar.

For the interpretation of the results, consideration must be made that uronic acids readily tend to isomerize. Thus, glucuronic acid may isomerize to uronic acids of the corresponding ketoses by the Lobry de Bruyn–Alberda van Ekenstein

mechanism (Fig. 3.5). These products may easily form aldo-hexuronic acids such as mannuronic, altruronic, and alluronic acids. Thus, any chromatographic method will yield a mixture of uronic products, which may or may not stem from a common origin.



**Fig. 3.5** Isomerization products of glucuronic acid.

### 3.5

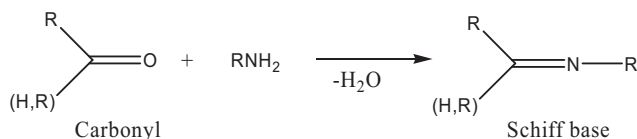
#### Functional Groups

##### 3.5.1

#### Carbonyl Functions

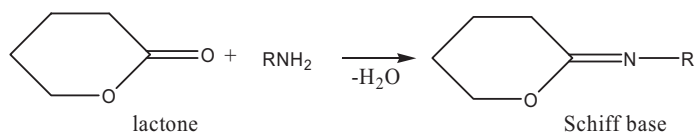
Carbonyl groups, such as keto or aldehyde functions, in sugar units of polysaccharides increase the reactivity of the carbohydrate ring. Consequently, these groups are considered to be responsible for degradation and yellowing of the polysaccharides by chemical action, or simply by aging. Such groups are generated predominantly by bleaching processes. Normally, the concentration of carbonyl in pulp is very low, so that conventionally spectroscopic methods such as IR, UV, and nuclear magnetic resonance (NMR) are not sufficiently sensitive to yield reliable quantitative results.

Chemical methods of determination use specific reactions to monitor the amount of carbonyl groups. As carbonyl groups may be hidden as lactones, it is advisable to open such bonds by alkali treatment. Aldehydes may be oxidized to the corresponding acid, and both, aldehydes and ketones may be reduced to alcohols. A convenient, rather selective type of reaction is the formation of Schiff bases (Scheme 3.1).



**Scheme 3.1** Formation of Schiff bases.

Whilst under appropriate conditions, the C=O of carboxyl does not react, lactones may also react with the amine reagent (Scheme 3.2), with or without opening of the lactone ring.



**Scheme 3.2** Reaction of lactones with amine (to be complemented by a ring-opening reaction).

These reactions proceed less readily than with the open carbonyl, and the reaction may not be quantitative. In this case, the pulp should be treated with zinc acetate solution to open the lactone rings before reacting it with amine [62].

Conventional methods of determination are the copper-number, oxime, and cyanohydrine methods.

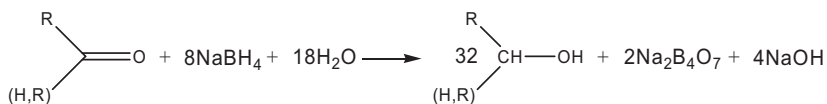
#### 3.5.1.1 Copper Number [63–65]

The copper number is a general measure for characterizing the reducing properties of a specimen. In pulp, it mainly monitors aldehyde functions, albeit not exclusively. When polysaccharides are degraded hydrolytically or by oxidation, the number of aldehyde functions increases. So, aging may be monitored by the increase in copper number as well as the decrease in DP [66].

The copper number is defined as the number of grams of metallic copper (as  $\text{Cu}_2\text{O}$ ) resulting from the reduction of  $\text{CuSO}_4$  by 100 g of pulp or paper fibers. Pulp is exposed to hot  $\text{Cu(II)}$  solution in an alkaline-buffered medium. The  $\text{Cu}_2\text{O}$  generated is adsorbed onto the fiber material; after washing the fibers, the  $\text{Cu}_2\text{O}$  is dissolved by a complexing agent and titrated using potassium permanganate.

## 3.5.1.2 Sodium Borohydride Method

$\text{NaBH}_4$  reduces carbonyl to hydroxyl groups, according to Scheme 3.3. For the reaction, an excess of the reducing agent is used.



**Scheme 3.3** Reduction of carbonyl groups by sodium borohydride [67,68].

Sodium borohydride, which is not consumed by reaction with carbonyl groups, is subsequently decomposed to hydrogen gas by sulfuric acid (Scheme 3.4).

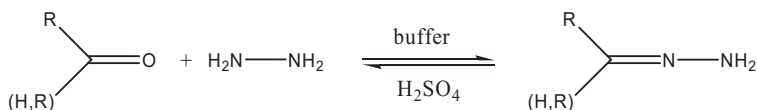


**Scheme 3.4** Decomposition of excess sodium borohydride to hydrogen gas.

The amount of hydrogen produced is then measured volumetrically.

## 3.5.1.3 Hydrazine Method [69]

When pulp is suspended in a solution containing hydrazine, the carbonyl groups form hydrazones according to Scheme 3.5.

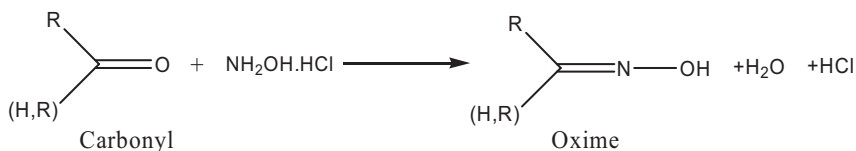


**Scheme 3.5** Formation and decomposition of hydrazones.

After reaction with hydrazine and washing, the cellulose hydrazone is dissolved in sulfuric acid and the liberated hydrazine is determined colorimetrically.

## 3.5.1.4 Oxime Method [62]

As reagent, hydroxyl amine hydrochloride is used which reacts according to Scheme 3.6.



**Scheme 3.6** Oxime formation of carbonyl groups.

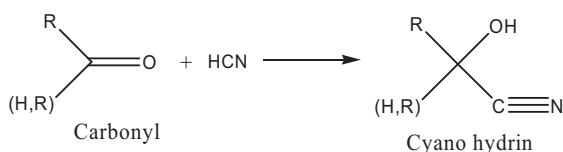
The concentration of carbonyl groups can be concluded from the amount of hydrochloric acid generated, or by determining the content of nitrogen in the modified pulp.

### 3.5.1.5 Girard-P Method [70]

Girard P reagent is a pyridinium hydrazide, which reacts with carbonyl groups to introduce cationic groups. The degree of substitution corresponds to the number of carbonyls. It is either determined by the nitrogen content of the compound or by the absorption of picric acid, the extent of which is measured colorimetrically.

### 3.5.1.6 Cyanohydrin Method

Hydrogen cyanide is easily added to carbonyl groups to form cyanohydrins (Scheme 3.7).



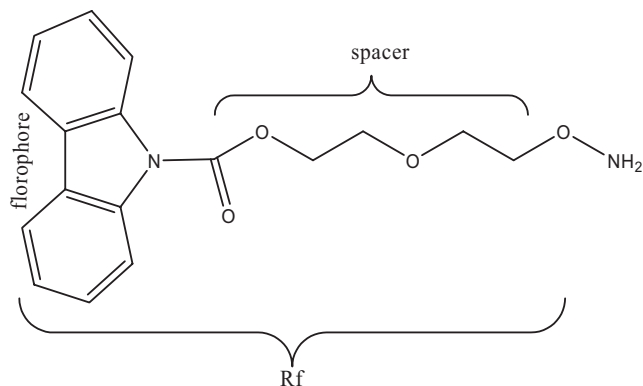
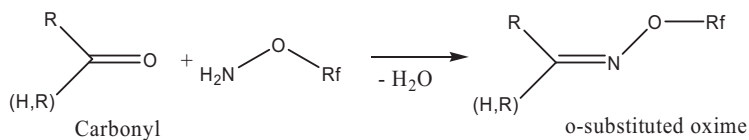
**Scheme 3.7** Formation of cyanohydrin [71].

The degree of substitution of the compound is determined via the nitrogen content.

### 3.5.1.7 Fluorescent Dying

Röhring et al. [72] described a highly efficient method of analyzing carbonyls, using a reactive fluorescent compound, carbazole-9-carboxylic acid [2-(2-aminoxy-ethoxy)-ethoxy]-amide (CCOA), the structure and reaction of which is shown in Scheme 3.8.

As this reactive labeling is also stable in dimethylacetamide-lithium chloride (DMAc/LiCl) solvent, the labeled cellulose may be dissolved and investigated in solution. Using gel-permeation chromatography (GPC) equipment with both SALS- (small angle light scattering) and fluorescence detection, information regarding molecular weight distribution can be correlated with the carbonyl content of the different molecular weight fractions.



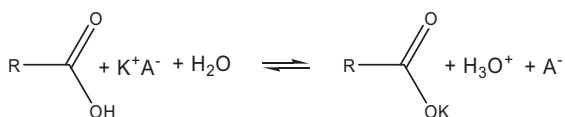
**Scheme 3.8** Staining of carbonyls using the fluorescent reactive dye, CCOA.

### 3.5.2

#### Carboxyl Functions

Carboxyl groups are originally present to some extent in polyoses, and may be still be found in the pulp fibers. A larger amount is generated by oxidation reactions during bleaching operations. The presence of carboxylic groups is the main reason for the anionic surface charge of pulp. These groups also have a bearing on the swelling and ion uptake of pulp.

Carboxylic functions bound in any way onto a macromolecular component of pulp may be determined chemically using ion-exchange reactions (see Scheme 3.9).



**Scheme 3.9** Ion exchange reaction of carboxylic functions.

The electrophile  $\text{K}^+$  must show a stronger affinity to carboxylic groups than to the counter-ion  $\text{A}^-$ . The concentration of carboxylic groups may then be determined by the increase in acidity, or by consumption of the electrophile reagent  $\text{K}^+$ .

Among the variety of methods available for determining carboxyl groups (see Tab. 3.1), the only one which is standardized works with  $\text{NaHCO}_3$ . All ion-exchange methods will also detect sulfonic acid. Thus, liginosulfonic acid, which is present in sulphite pulp, increases the apparent carboxyl content.



Tab. 3.1 Methods for the determination of carboxylic groups.

Reagent	Principle of measurement	Reference(s)
Ca(CH <sub>3</sub> COO) <sub>2</sub>	Acidity	73
	Ca(CH <sub>3</sub> COO) <sub>2</sub>	74
Zn(CH <sub>3</sub> COO) <sub>2</sub>	Zn(CH <sub>3</sub> COO) <sub>2</sub>	75
NaCl + NaHCO <sub>3</sub>	NaHCO <sub>3</sub> -consumption	76,77
NaCl + NaOH	NaOH-consumption	78 (potentiometrically)
		79 (conductometrically)
Crystal violet	Dye-consumption	80
Methylene blue	Dye-consumption	81

### 3.6

#### Degree of Polymerization (Molecular Mass)

Many macroscopic properties of macromolecular compounds depend heavily on the chain length of its molecules, including the DP or molecular mass of the molecules. In cellulose products, the DP also indicates how severely the native material has been degraded during cooking and bleaching. Any polymeric material contains molecules of different mass, which is represented by a distribution function, as shown in Fig. 3.6.

The DP is decreased as a result of aging, by both hydrolytic and oxidative degradation (see Section IV-4.6.4). Both the average size of the molecules as well as the relative amount of very large and small molecules, have a bearing on virtually

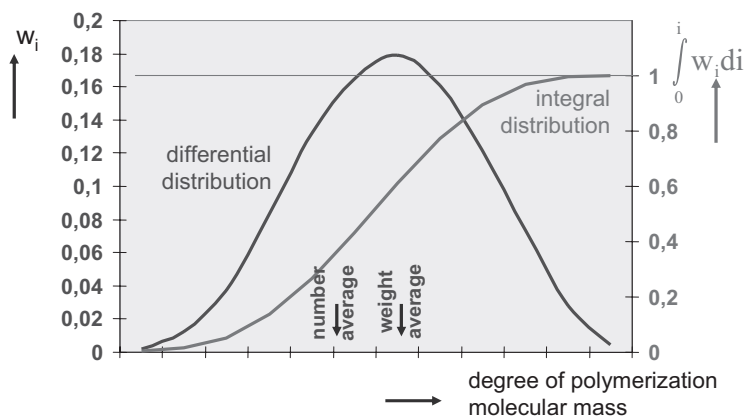


Fig. 3.6 Distribution function of molecular mass (resp. degree of polymerization).

all technical properties. This information is derived from measuring special physical properties in solution. Most methods yield an average value for the molecular mass, but methods are also available that provide information about the details of the distribution function.

### 3.6.1

#### Solvents for Cellulose

In order to determine the sizes of single macromolecules, these must first be dissolved. Cellulose may be dissolved in special aqueous solvents, or may be solubilized in normal organic solvents by derivatization, for example transformation to cellulose nitrates or acetates (esters of nitric or acetic acid, respectively) or carbaniates (phenylurethanes).

A survey of the most common aqueous solvents for cellulose is presented in Tab. 3.2. Those solvents which contain metal ions form metal complexes between cellulose and a chelating compound. Controversy persists, however, as to whether in such solutions all cellulose molecules are fully separated or whether they are rather “dissolved” as aggregated molecular bundles (micro gel particles). All of these solvents are alkaline and lead to more or less harsh hydrolytic degradation of the dissolved carbohydrate. Such degradation is most severe when there are carbonyl functions present in the carbohydrate. In some cases it is also fostered by the presence of oxygen, forming intermediate carbonyls. To prevent excess degradation, the carbonyls should be reduced, for example using borohydride treatment before dissolving the cellulosic material in a complexing solvent.

**Tab. 3.2** Aqueous solvents for the molecular weight determination of cellulose.

Acronym	Composition	Remarks
CUOXAM (Schweizer's reagent)	Copper oxide-ammonia	Deep blue color; dissolved polysaccharides hydrolyze easily, even in absence of oxygen; technically applied for regenerated cellulose production
CUENE (CED)	Copper ethylenediamine	Blue color; causes less carbohydrate depolymerization
CADOXEN (CADOX),	Cadmium oxide in ethylene diamine	Even better carbohydrate stability
EWNN	Iron and sodium tartrate	Green color; only modest hydrolysis, possibly gel-solution
DMA/LiCl	Dimethylacetamide-lithium chloride	Modestly hydrolytic, probably molecular disperse cellulose solutions
NMNO	<i>N</i> -morpholine <i>N</i> -oxide hydrate	

### 3.6.1.1 CUOXAM

Tetra-ammin-copper(II)-hydroxide,  $[\text{Cu}(\text{NH}_3)_4](\text{OH})_2 \cdot 3\text{H}_2\text{O}$  (Schweizer's reagent), is prepared by dissolving copper powder in 20% ammonia and oxidizing the copper simultaneously to dissolve the oxide by aerating. Alternatively, freshly precipitated  $\text{CuO}$  is dissolved in 20% ammonia [82]. Carbohydrates are dissolved under the formation of a  $\text{Cu}(\text{II})$ tetramino-complex. This solvent is sometimes used to determine the DP of cellulose. A standard method has been documented by Zellcheming [83].

### 3.6.1.2 CUEN [84]

The name "cuen" is used as a shortened version of cupri-ethylene-diamine-solution (CDE). To prepare such a solution,  $\text{Cu}(\text{OH})_2$  is precipitated from a copper sulfate solution by ammonia and  $\text{NaOH}$ . The dry copper hydroxide is dissolved in ethylene diamine.

### 3.6.1.3 Iron Sodium Tartrate (EWNN) [85]

An alkaline solution of iron sodium tartrate complex is prepared by adding  $\text{FeCl}_3 \cdot 6\text{H}_2\text{O}$  to a solution of sodium tartrate and adding  $\text{NaOH}$  and a small quantity of sorbitol for stabilization of the solution [86].

## 3.6.2

### Diverse Average Values of Molecular Mass and Index of Nonuniformity

All methods that do not fractionate the sample provide only an average number of the molecular mass for all molecules. It would be expected that a common arithmetic mean would be obtained, which is calculated by dividing the sum of the weights of all molecules by their number. However, some methods are not directly sensitive to the number of molecules in the sample (these methods are not able to "count"). For example, light scattering by a single macromolecule is dependent upon that molecule's molecular mass. Consequently, this method does not count but rather "weighs" the molecules, and provides a mean value based on the individual masses of the uniform particle fractions [weight average, as defined by Eq. (1)].

$$m_w = \frac{\sum_0^i m_i^2}{\sum_0^i m_i} = \frac{\sum_0^i w_i m_i}{\sum_0^i w_i} \quad (1)$$

$$w_i = \frac{m_i}{\sum_0^i m_i}$$

where  $m_w$  = average particle mass ("weight average") and  $w_i$  = weight of the  $i$ -fraction.

Other analytical methods are sensitive for other derived properties of molecules, which are in some way related to the molecular weight (see Tab. 3.3).

**Tab. 3.3** Different mean values of molecular mass and degree of polymerization (DP), obtained by different methods.

Type of mean	Weighing factor	Average molecular weight	Average DP	Analytical method
General formula	$r$	$M_r = \frac{\sum n_i M_i^{r+1}}{\sum n_i M_i^r} = \frac{\sum w_i M_i^r}{\sum w_i M_i^{r-1}}$	$P_r = \frac{\sum n_i P_i^{r+1}}{\sum n_i P_i^r}$	
Number average weight	$0$	$M_r = \frac{\sum n_i M_i}{\sum n_i}$	$P_r = \frac{\sum n_i P_i}{\sum n_i}$	End-group determination Osmosis
Weight average	$1$	$M_r = \frac{\sum n_i M_i^2}{\sum n_i M_i} = \frac{\sum w_i M_i}{\sum w_i}$	$P_r = \frac{\sum n_i P_i^2}{\sum n_i P_i}$	Light scattering Sedimentation equilibrium (ultracentrifuge)
z-average	$2$	$M_r = \frac{\sum n_i M_i^3}{\sum n_i M_i^2} = \frac{\sum w_i M_i^2}{\sum w_i M_i}$	$P_r = \frac{\sum n_i P_i^3}{\sum n_i P_i^2}$	Sedimentation velocity (ultracentrifuge)
a-average	$A$	$M_r = \frac{\sum n_i M_i^{a+1}}{\sum n_i M_i^a} = \frac{\sum w_i M_i^a}{\sum w_i M_i^{a-1}}$	$P_a = \frac{\sum n_i P_i^{a+1}}{\sum n_i P_i^a}$	Diffusion
Viscosity average	Inconsistent	$M_\eta = \left( \frac{\sum n_i M_i^{a+1}}{\sum n_i M_i} \right)^{\frac{1}{a}}$	$P_\eta = \left( \frac{\sum n_i P_i^{a+1}}{\sum n_i P_i} \right)^{\frac{1}{a}}$	Viscosity

In polydisperse samples the different types of averages differ considerably. Higher-order averages have larger values than lower-order averages ( $M_{r+1} > M_r$ ).

A simple value signifying polydispersity is the nonuniformity-index,  $U$ , which is zero for monodisperse samples and increases with increasing polydispersity [Eq. (2)]:

$$U = \frac{M_w}{M_n} - 1 \quad (2)$$

## 3.6.3

**Methods to Determine Molar Mass (“Molecular Weight”)**

Many properties of a solution containing macromolecules depend not only on the mass concentration of solute but also on the size of the dissolved particles, or on their molecular weight. The specific property  $E_{\text{specific}}$ , as defined in Eq. (3), is a function of molecular mass,  $M$ , and mass-concentration,  $c$ :

$$E_{\text{specific}} = \frac{E - E_{\text{solvent}}}{c \cdot E_{\text{solvent}}} = f(c; M) \quad (3)$$

$$\lim_{c \rightarrow 0} E_{\text{specific}} = f(M)$$

By measuring several solutions of different concentrations and extrapolating the specific properties derived to zero concentration, a value is obtained which is an explicit measure of molecular mass of the solute. The main methods used for molecular mass determination are listed in Tab. 3.4.

**Tab. 3.4** Survey of methods to determine molecular mass.

Method	absolute/ relative	Specific property measured
Osmosis	a	Osmotic pressure
Light scattering	a	Light, scattered in the direction of an incident beam of light
Small-angle X-ray scattering		
Small-angle neutron scattering		
Ultracentrifuge	a	Sedimentation constant and diffusion constant. Concentration gradient of particle atmosphere
Diffusion	r	Diffusion constant
Size-exclusion chromatography (gel-permeation chromatography)	r	Retention time in a permeated gel
Viscosity	r	Viscosity (ideally at zero shear)

3.6.3.1 **Osmosis**

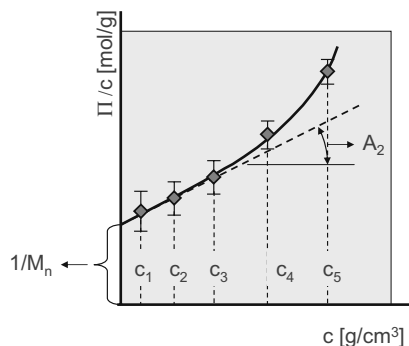
The osmotic pressure  $\Pi$  of a solution depends on molecular mass  $M$  and concentration  $c$  [Eq. (4)]:

$$\frac{\Pi}{c} = \frac{1}{M_n} + A_2c + A_3c^2 + \dots \quad (4)$$

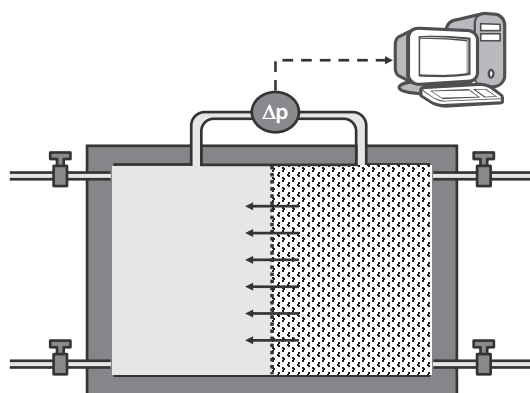
where  $A_2$ ;  $A_3$  = second and third virial coefficient of osmotic pressure and  $M_n$  = molecular mass of solute (number average).

The osmotic pressure is inversely proportional to molecular mass, so high molecular-weight compounds contribute very little. Thus, measurement must be very accurate. Moreover, it must be guaranteed that there are no low molecular-weight compounds (e.g., salts) present when using this method. This is rarely true for aqueous cellulose solutions, and consequently osmometry is normally only applied to cellulose derivatives in organic solvents.

The molecular mass is derived from the reduced osmotic pressure, which is free from intermolecular effects (formally at concentration 0, obtained by the extrapolation of values received at higher concentrations, numerically according to Scheme 3.13, or graphically, as shown in Fig. 3.7.



**Fig. 3.7** Evaluation of measurements of osmotic pressure.  $A$  = second virial coefficient  $c_1, c_2, c_3$ , etc. = concentrations.



**Fig. 3.8** The principle of determining osmotic pressure by membrane osmometry.  $\Delta p$  = pressure difference (= osmotic pressure).

Osmotic pressure may be measured directly by using a semi-permeable membrane, which separates two adjacent chambers containing the solution and solvent, respectively. As small solvent molecules diffuse through the membrane, the pressure in the solvent chamber increases. The difference in pressure between the two chambers corresponds to the osmotic pressure. The measuring cell of an apparatus for measuring osmotic pressure is shown schematically in Fig. 3.8. Polyelectrolytes may cause deviations in the values determined as a consequence of electro-osmotic effects.

Alternatively, the osmotic pressure may be determined indirectly by the change of vapor pressure, the depression of vapor pressure,  $p$ , in a solution being proportional to the osmotic pressure,  $\Pi$  [Eq. (5)]:

$$\Pi = K_{\Pi p}(p_{\text{solvent}} - p_{\text{solution}}) \quad (5)$$

Normally, the difference in vapor pressure is determined by an indirect method, such as pressure compensation via temperature adjustment. Very small differences are difficult to measure, so this method is preferred for relatively low molecular weights and is not suitable for native or only slightly degraded cellulose.

### 3.6.3.2 Scattering Methods

Scattering methods determine the radiation, which is diffusely scattered by the dissolved macromolecules. The source of radiation may be visible light from a laser, X-rays, or temperate neutrons from a nuclear reactor. The most convenient among these methods uses visible light. Here, it is not easily possible to use colored solvents as Cu- and Fe-containing complexes; consequently, cellulose is normally derivatized and dissolved in an organic solvent for measurement. The preferred derivatives are trinitrate and tricarbanilate.

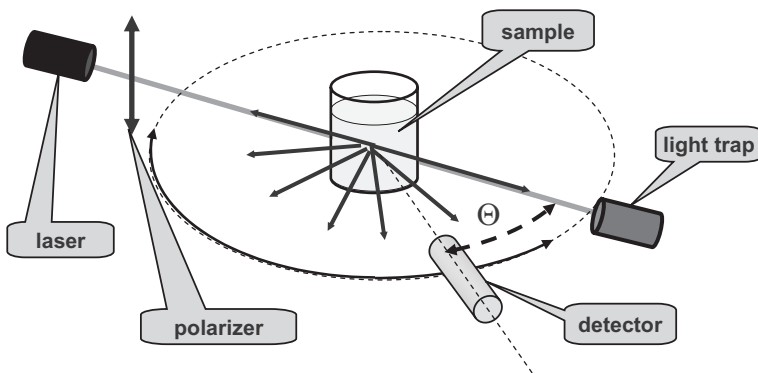


Fig. 3.9 Principle of measuring the diffusely scattered light (variable detecting angle).

Visible light scattering is measured by an apparatus according to Fig. 3.9. The sample-solution must be free of dust particles which, due to their oversize, have a

strong light-scattering capacity and will therefore influence the result considerably. For this reason, dust is removed using ultra-fine filters or centrifugation prior to measurements being made.

The vertically polarized incident light is scattered by the macromolecules in solution. The scattered light is detected by a photometer, which encircles the sample in a horizontal plane. The emitted light intensity is recorded as a function of the scattering angle,  $\Theta$ . Alternatively, a number of fixed detectors may simultaneously detect the light at various scattering angles.

The relative intensity of light scattered in a certain scattering direction ( $R_{\Theta} = I_{\text{scattered}}/I_{\text{incident}}$ ) depends on:

- the concentration of the solution ( $c$ );
- the difference in index of refraction between solute and solvent, resp. the index of refraction increment ( $\Delta n/c = (n_{\text{solution}} - n_{\text{solvent}})/c$ );
- the molecular mass of dissolved particles ( $M$ ); and
- the scattering angle ( $\Theta$ ).

The angular dependence of scattering intensity reflects the diminution of light intensity by intra-particle interference. For particles comparable in size to the wavelength of light, scattering intensity depends on the scattering angle according to a formula derived by Guinier [Eq. (6)]:

$$R_{\Theta} = R_{\Theta=0} e^{-K \cdot S^2 \sin^2 \frac{\Theta}{2}}$$

$$\frac{1}{R_{\Theta}} \approx \frac{1}{R_{\Theta=0}} \left( 1 + K \cdot S^2 \cdot \sin^2 \frac{\Theta}{2} + \dots \right) \quad (6)$$

$$K = \frac{1}{3} \left( \frac{4\pi}{\lambda} \right)^2$$

where  $S$  = radius of gyration and  $\lambda$  = wavelength of light in the solution (app. approximation by Zimm).

The formulae in Eq. (6) allow an extrapolation of intensities, measured at various scattering angles to scattering angle zero ( $R_{\Theta=0}$ ) which is not directly accessible to measurement, as that is the location of the primary incident beam, which overlaps the scattered light.

Now,  $R_{\Theta=0}$  is proportional to the molecular weight of solute for infinite dilution. At a higher concentration of solution, the intensity of scattering light is further diminished by inter-particle interference. The dependence on concentration of the reduced scattering intensity is given by Eq. (7), and is similar to the dependence of osmotic pressure [see Eq. (4)].

$$\frac{K_v c}{R_{\Theta=0}} = \frac{1}{M_w} + A_2 c + A_3 c^2 + \dots \quad (7)$$



$$K_v = \frac{4\pi^2 n_{\text{solvent}}^2}{N_A \lambda_0^4} \left( \frac{\partial n}{\partial c} \right)^2$$

where  $A_2$ ;  $A_3$  = second and third virial coefficient of osmotic pressure;  $M_w$  = molecular mass of solute (weight average);  $\lambda_0$  = wavelength of light *in vacuo*;  $N_A$  = Avogadro's number; and  $n$  = index of refraction.

By applying Eqs. (6) and (7), the measured data may be extrapolated to zero concentration, as well as to zero degree scattering angle. This is normally done by using a so-called Zimm-plot (see Fig. 3.10). This is a two-dimensional projection of the three-dimensional function  $R = f(c)g(\Theta)$ . The Zimm-constant  $Z$  may be chosen arbitrarily, so that a well-resolved grid will result consisting of grid-lines that are neither too flat, nor too steep.

The refractive increment must be measured separately by using a differential refractometer.

From the Zimm grid, three valuable quantities can be derived:

- Molecular mass (number average)  $M_w$
- Radius of gyration (z-average)  $S_z$
- Second virial coefficient of osmotic pressure  $A_2$

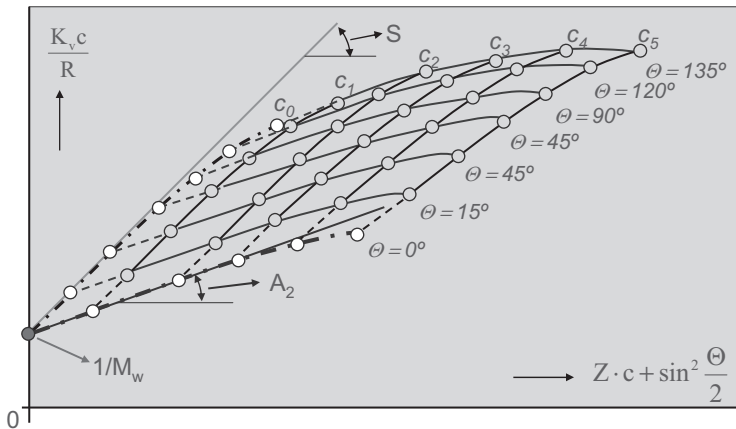


Fig. 3.10 ZIMM-plot for the evaluation of light-scattering data.

If there are super-molecular gel particles in the solution, the scattering at low angles is very high, so that linear extrapolation is not possible. In this case, a special scattering curve analysis may help.

The light-scattering method is rather tedious, but it yields an absolute value for molecular mass and further valuable information about the state of solution (e.g., coil expansion, thermodynamic solution stability). A light-scattering apparatus may also be used as a detecting device for size-exclusion chromatography (see Section 3.6.5.2)

## 3.6.4

## Viscosity Measurements

## 3.6.4.1 Solution Viscosity as a Measure of Macromolecular Chain Length

Polymers are generally less soluble in solvents than their chemically similar low molecular-weight compounds. When polymers are dissolved, the solutions obtained excel by their high viscosity, and the viscosity rise increases with the average chain length of the polymer molecules. Considering that the viscosity of a solution can be easily measured by simple means, viscosity measurements clearly offer a widely applicable means of determining the DP of cellulose.

The reason for the viscosity increase is that large molecules, when dissolved, considerably impede the flow of a liquid. When a liquid is under shear stress it will flow such that it will undergo shear deformation. During this shear process, the molecules constantly change their position towards their neighbors, as do people in a moving crowd. The binding forces must be surmounted, and for this the mechanical deformation energy applied externally onto the liquid body is consumed. When new bonds are formed temporarily to new neighbors, some energy is released in the form of thermal energy. Thus, viscosity is a measure of internal friction. As sand under wheels of an automobile increases the friction of the tires, macromolecules increase the internal friction of a liquid.

When a pure liquid is exposed to shear stress it flows. In the liquid body, layers of liquid move parallel to each other, as shown in Fig. 3.11 for the case of simple Newtonian liquid.

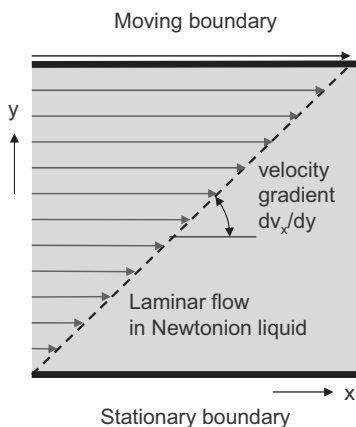


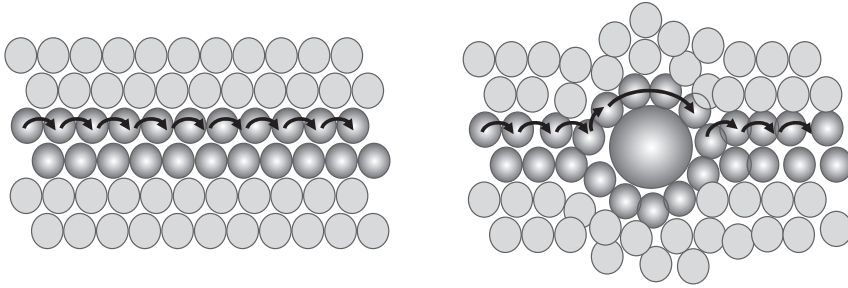
Fig. 3.11 Laminar flow in a Newtonian liquid under shear stress.

The force necessary for this deformation is proportional to the velocity gradient in the liquid. The factor of proportionality, which is called “viscosity”, depends on the forces of attraction between the moving layers [Eq. (8)]:

$$\tau = \eta \cdot \frac{\partial v_x}{\partial y} = \eta \cdot D \quad (8)$$

where  $\tau$  (Pa) = shear stress;  $\eta$  (Pa·s) = viscosity; and  $D$  ( $s^{-1}$ ) = velocity gradient (= shear rate).

In reality, these layers consist of molecules that change their mutual positions. For each jump from one position to another, energy is required to break the attractions to the former neighbors. In a solution, alien particles which are large compared to the molecules of the solvent must be circum-flowed, as shown in Fig. 3.12.



**Fig. 3.12** Change of positions of molecules in a liquid under shear. Left, pure liquid; right, solution.

The disturbing effect of dispersed particles depends on the number of solvent molecules which have to be displaced, so that the relative increase in viscosity is proportional to the volume of the alien large particle.

Einstein showed that in a dispersion or solution containing large particles, the relative increase in viscosity is proportional to the total volume of the dispersed phase [Eqs. (9) and (10)].

$$\eta_{sp} = \frac{\eta_{solution} - \eta_{solvent}}{\eta_{solvent}} = f\varphi_{solute} = f \frac{V_{solute}}{V_{solution}} \quad (9)$$

where  $\eta_{sp}$  = specific viscosity;  $V$  = volume; and  $f$  = viscosity factor (for solid spherical particles,  $f = 2.5$ ).

$$\lim_{c \rightarrow 0} \frac{\eta_{sp}}{c} = \frac{f}{d} = \frac{2.5}{d_{he}} \quad (10)$$

where  $c$  ( $g \text{ mL}^{-1}$ ) = mass concentration of the solute per volume solution;  $d$  ( $g \text{ cm}^{-3}$ ) = density of disperse particles; and  $d_{he}$  = density of a hydrodynamically equivalent sphere.

$\lim_{c \rightarrow 0} \frac{\eta_{sp}}{c} = [\eta]$  is the reduced viscosity of a solution at infinitely diluted conditions. It is named the “limiting viscosity number”, or “intrinsic viscosity” or the “Staudinger-index”. As we only can use sufficiently concentrated solutions for real measurements, the intrinsic viscosity value is derived by extrapolation of a series of measurements at concentrations which are high enough to obtain reliable data, but low enough to find a linear dependence on concentration, in order to be able to extrapolate the data to zero concentration (see Fig. 3.13).

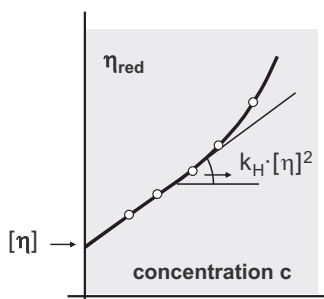


Fig. 3.13 Extrapolation of reduced viscosities to obtain the intrinsic viscosity ( $\eta$ ).

According to Scheme 3.19, viscosity measurements are a convenient way to determine the hydrodynamically equivalent density of dissolved particles. Dissolved macromolecules form statistically irregular coils, the sizes of which increase with chain length by an exponential law. A snapshot cartoon of a molecular coil and its hydrodynamically active volume is shown in Fig. 3.14.

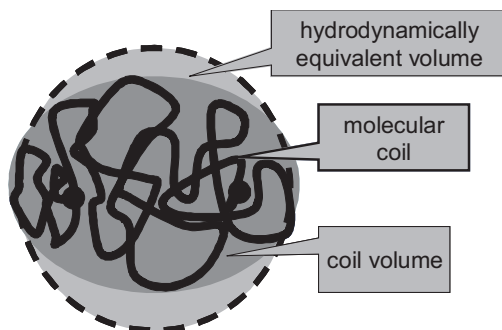


Fig. 3.14 The hydrodynamically equivalent volume of a macromolecule in solution.

As the particle mass is proportional to chain length, the hydrodynamically equivalent density of the molecular coils likewise decreases with molecular mass by an exponential law (the Staudinger–Mark–Houwink equation) [Eq. (11)]:

$$\begin{aligned}
 d_h &= g \cdot M^{-a} \\
 [\eta] &= \frac{2,25}{d_h} = K_M M^a = K_P P^a \\
 K_M &= K_P m_0
 \end{aligned}
 \tag{11}$$

where  $M$  = molecular mass;  $P$  = degree of polymerization; and  $m_0$  = mass of polymer repeating unit.

The constants  $K_M$  and  $a$  must be determined experimentally for each polymer-solvent system, by using standard samples of known molecular weight. For most practical systems, these values can be found in data handbooks [87]. For most cellulose solutions, factors for extrapolating to concentration zero are also listed. In such a case, measuring the solution viscosity of a specific concentration is sufficient for calculating the intrinsic viscosity.

#### 3.6.4.2 Viscosity Measurements on Cellulose Pulps

The relative viscosity,  $\eta_{rel} = \eta_{solution}/\eta_{solvent}$ , is determined by measuring the viscosities of solution and solvent by a capillary type of viscometer. In the viscometer, a defined volume of liquid flows downward through a fine capillary, driven by its own weight. The time needed for passage of that volume is proportional to the viscosity of the liquid, provided that the densities are equal (or in the case of differently concentrated dilute solutions, nearly equal). In solutions of pulps, the vastly dominating factor for viscosity is the cellulose. A small amount of polyoses does not contribute much to the viscosity, and may be neglected. The same is valid for soluble degradation products of lignin. The fiber material of higher lignin content which must be extracted normally is not completely soluble in cellulose solvents. In this case, the insoluble component must be filtered off before measuring. The concentration is calculated on a dry weight basis of the soluble part of pulp.

Viscosity measurements mostly use complexing solvents to determine the limiting viscosity number.

#### 3.6.5

##### Molecular Weight Distribution

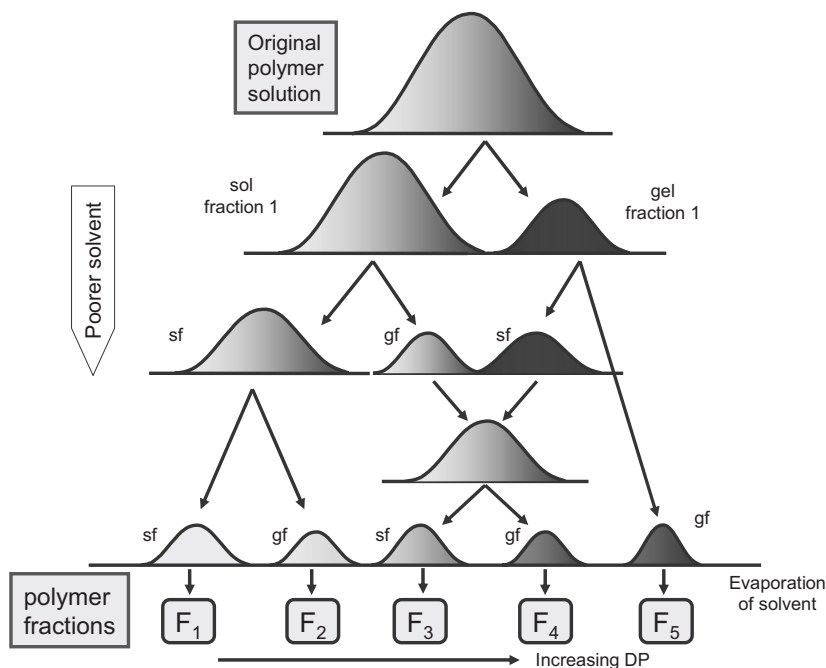
The index of nonuniformity,  $U = M_w/M_n - 1$  (see Section IV-3.6.2) only signifies whether the distribution of molecular mass is wide or narrow. For a better understanding of macromolecular properties, further knowledge of the details of polydispersity is necessary. Therefore, the polydispersity function (see Fig. 3.6) should be determined.

##### 3.6.5.1 Fractional Precipitation or Solution

In general, the solubility of macromolecules decreases with increasing chain length. This fact can be used to precipitate only the highest molecular species

from a solution, by cautiously weakening the dissolving capacity of a solvent. This can be done by lowering the temperature or by adding a small amount of nonsolvent.

Polymers do not precipitate clearly, but rather form a gel phase which still contains solvent. This gel phase is separated from the remaining solution (sol phase). Thus, step by step small fractions of narrowly distributed polymer are removed from the sample. The principle of this procedure is demonstrated in Fig. 3.15.



**Fig. 3.15** Principle of polymer fractionation by stepwise precipitation.

This method is rather time- and labor-consuming, although an advantage is that it may also be used to produce larger quantities of fractionated material.

### 3.6.5.2 Size-Exclusion (Gel-Permeation) Chromatography

Chromatography is a very powerful instrument for polymer analysis. The technique uses the fact that different molecules, when in solution and passing along a stationary phase, are more or less retained by that phase.

The basic set-up of the equipment used for liquid chromatography is shown in Fig. 3.16. Within a hollow tube (column), sphere-like resin beads are packed which act as a stationary phase (Fig. 3.17). In size-exclusion chromatography, the stationary phase consists of a loosely cross-linked polymer gel containing immobilized solvent into which molecules of the solute may penetrate.

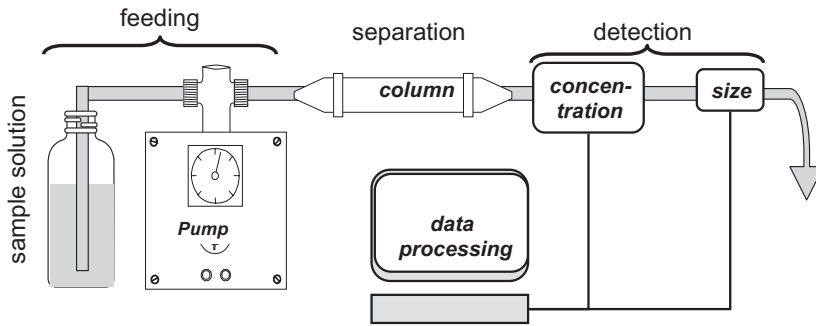


Fig. 3.16 Schematic set-up of equipment for liquid chromatography.

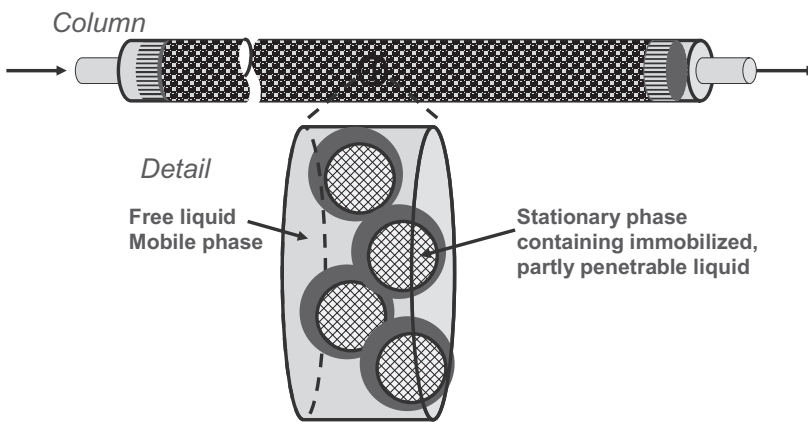


Fig. 3.17 Construction of a chromatographic separation column.

The rate of penetration depends on the difference of concentration between the mobile phase and the stationary phase, and additionally on the size of the dissolved molecules. Small molecules may penetrate more quickly and more deeply into the gel material. When a polymer solution passes a separation gel, small molecules “dissolve” quickly in the gel and block this part of gel against the penetration of larger molecules. The latter then progress to an area of the solid phase which is still free. Thus, molecules of different sizes are spatially separated in the gel. When successively pure solvent is passed through the column along the loaded gel, the larger molecules, which were absorbed last, will be eluted first. So, for a given molecular fraction,  $i$ , its retention time  $t_i$  is a direct function of the resulting separation coefficient  $k_i$  between the mobile and stationary phases [Eq. (12)]:

$$t_i = a \cdot k_i^b$$

$$k_i = \frac{C_{i,\text{stationary}}}{C_{i,\text{mobile}}} \quad (12)$$

where  $i$  = index of fraction of molecules of certain size;  $t$  = retention time;  $c$  = concentration;  $k_i$  = separation coefficient (gel/solution); and  $a$  and  $b$  are constants ( $b \approx 1$ ).

The separation coefficient  $k$  is determined by interaction forces between solute/solvent and solute/gel (enthalpic effects; adsorption) as well as entropic effects (space demand of interacting molecules). Both enthalpic and entropic effects depend on the molecular mass of the solute. Adsorption and size-exclusion chromatography may be differentiated by the prevailing effects of interaction (Tab. 3.5).

Tab. 3.5 Modes of chromatographic separation.

Mode of chromatography	Adsorption chromatography	Size-exclusion (gel-permeation) chromatography
<b>Characteristic feature</b>		
Prevailing effects	Enthalpic	Entropic
Mechanism	Adsorption	Penetration
Effect of sizes of macromolecules on retention	Retention increases with molar mass	Retention decreases with molar volume
Type of solvent for polymer	Poor solvent	Good solvent
Degree of swelling of gel	Moderately swollen	Highly swollen

By balancing these enthalpic and entropic effects, a special chromatographic set-up is obtained, which is termed “chromatography at the critical state”. By varying the solvent, a state may be achieved where retention time is virtually independent of molecular mass. This type of chromatography is used to determine slight differences in chemical composition of polymers (e.g., end groups, functional groups).

The size-exclusion chromatography (SEC) mode uses very good solvents, so that interactions between the solute and the gel material are comparatively negligible. In this case, the coefficient of separation increases as a function of molecular volume (approximately the hydrodynamic volume).

$k_i$  may be interpreted as a measure of the relative volume of the total liquid in the column (free plus imbibed volume), which is accessible to the species  $i$  of macromolecules. Each column is characterized by an exclusion characteristic shown schematically in Fig. 3.18. Ideally, very small molecules are not retained by the gel material formally corresponding to complete penetration of the liquid volume (“pores”) of the gel-particles. On the other hand, very large molecules may not penetrate the gels at all. Medium-sized molecules penetrate the gel to a certain degree, depending on their size.



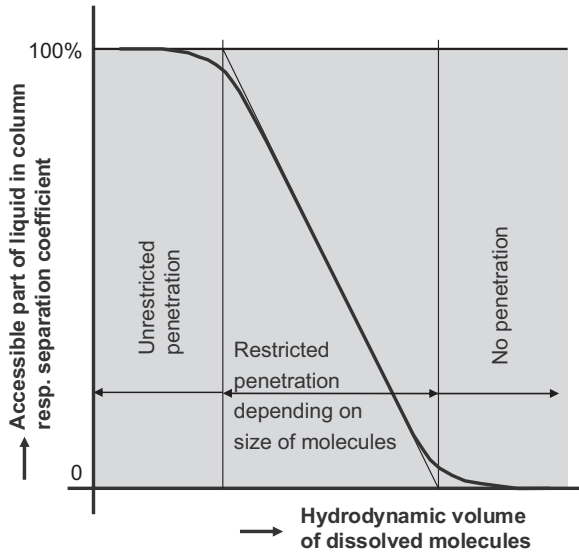


Fig. 3.18 Size exclusion characteristics of a gel column.

The penetration properties of a specific column are represented by plotting the accessible volume for molecules of different sizes against molecular size (Fig. 3.18). Such a column characteristic may be determined by using standard samples of known molecular size. It corresponds to a plot  $[\eta]$  (as a measure of the specific hydrodynamic molecular volume) versus retention time or volume (corresponding to the coefficient of separation) (Fig. 3.19).

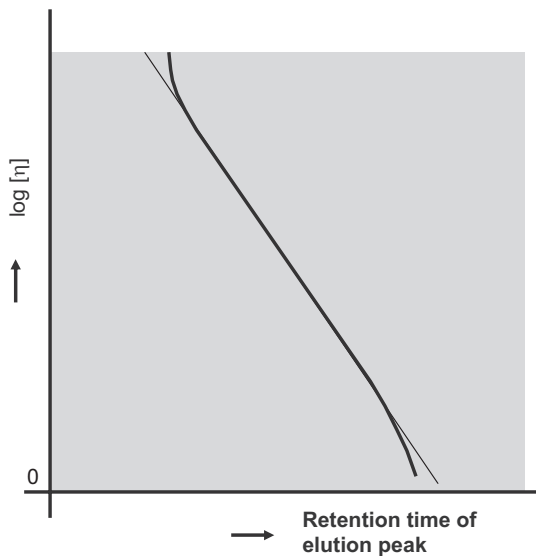


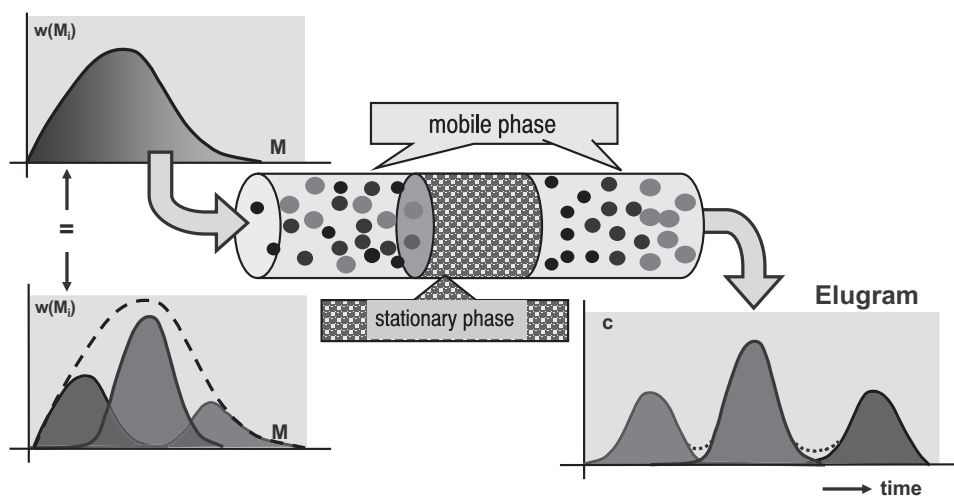
Fig. 3.19 Size-exclusion calibration curve for a given gel/solvent system.

For the SEC mode, the separation coefficient for a certain fraction of molecules is linked to their specific hydrodynamic volumes by the relationship shown in Eq. (13):

$$\begin{aligned} k_i &= f(v_{\text{hydr}}) \\ v_{\text{hydr}} &\approx [\eta] = K_{\eta} M^a \end{aligned} \quad (13)$$

where  $v_{\text{hydr}}$  = specific hydrodynamic volume of polymer fraction;  $[\eta]$  = Staudinger index (limiting viscosity number; intrinsic viscosity); and  $K_{\eta}$ ;  $a$  = Staudinger–Mark–Howink constants.

Based on these relationships, the retention time of a certain molecular species is seen to depend on its molecular size. Figure 3.20 illustrates, schematically, how the elugram mirrors the original molecular size distribution, which is linked to molecular weight distribution.



**Fig. 3.20** The principle of gel-permeation chromatography.

Depending on the column characteristics, the retention time of an elution peak decreases within a broad range logarithmically with increasing hydrodynamic volume of the molecular fraction (see Fig. 3.18). The performance of a column may be calibrated by using known standard polymer samples.

## 4 Characterization of Supermolecular Structures

### 4.1 Crystallinity

#### 4.1.1 Degree of Crystallinity

Among the polymer components in plant fibers, cellulose has a strong tendency to crystallize. This inclination is due to the straight, linear and rather stiff nature of the cellulose chains, their molecular regularity, and the presence of hydroxyl groups which may easily form hydrogen bonds between chains. However, even pure cellulose does not crystallize completely; rather, it only builds crystalline domains embedded in less well-ordered (“amorphous”) material. In native cellulose the supermolecular structure is determined by biosynthesis and the morphology of the plant fiber wall. In regenerated cellulose, the supermolecular structure stems from the specific conditions of precipitation and the transition from sol to gel state.

There are no clear-cut boundaries between crystalline and amorphous domains – there are only soft transitions. The characteristic structural unit of solid cellulose is a fringed micelle crystallite, as shown schematically in Fig. 4.1.

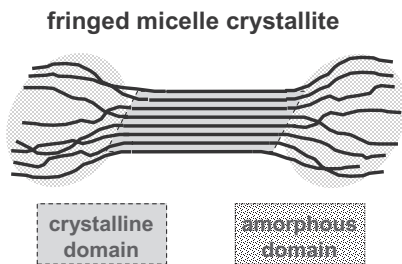


Fig. 4.1 Subunit of partially crystalline structure of cellulose.

The cellulose may be thought of as being constituted of a continuous network predominantly oriented with fringed micelle crystallites. In this way, the mainly crystalline and rather amorphous domains alternate (a two-phase model).

This situation also can be described by a single-phase model, with a spatially fluctuating degree of order. Local physical properties such as density or refractive index fluctuate throughout the material. The two models are demonstrated in Fig. 4.2.

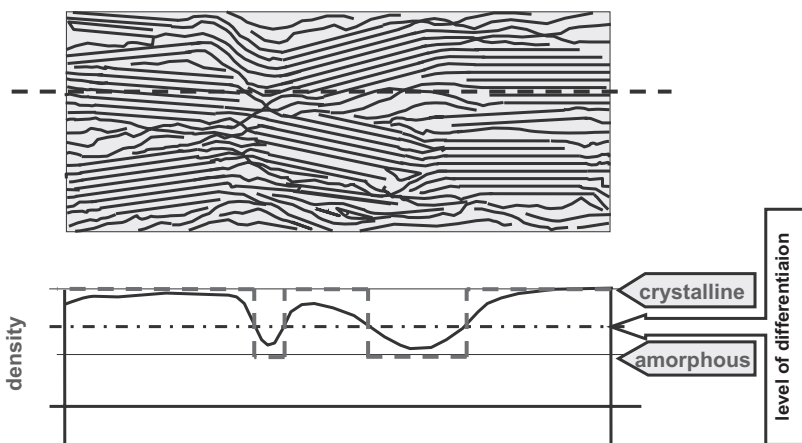


Fig. 4.2 The partial crystalline structure of cellulose.

In a one-phase model, there is visible in the cellulose material an average degree of ordering, consistent with a “fuzzy” crystal, a so-called “para-crystal”. Such a model is probably nearer to reality, but it is less comprehensive. A model which sees the material as being composed of distinct domains of crystals embedded in an amorphous matrix is easier to imagine. The level above which the measured property is attributed to a crystal depends on the method applied.

In order to describe the relative amount of crystalline domains in such a two-phase model, the degree of crystallinity “DI” is defined as the weight fraction of crystalline component [Eq. (1)]:

$$DI = w_c = \frac{m_c}{m_c + m_a} \quad (1)$$

where  $m_c$  = mass of the crystalline component; and  $m_a$  = mass of the amorphous component.

As the boundary between crystalline and amorphous is not sharp, any physical method, which is able to differentiate between these two states, will draw this fictive boundary differently. The parameter measured is a relative index, the crystallinity index (CI), which is related to the method applied. Any suitable method  $m$  measures a property  $E_m$ , which is supposed to be an additive function of the con-

tribution of the amorphous and the crystalline component. The crystallinity index is calculated using Eq. (2)]:

$$CI_m = w_{c:m} = \frac{E_m - E_{m;a}}{E_{m;c} - E_{m;a}} \quad (2)$$

where  $E_m$  = specific property of the two phase material;  $E_{m;a}$  = specific property of the amorphous component; and  $E_{m;c}$  = specific property of the crystalline component.

A survey of the most common methods to determine the index of crystallinity is presented in Tab. 4.1.

**Tab. 4.1** Methods for determining the index of crystallinity.

Method	Contrasting property	Mechanism
X-ray diffraction	Long-distance periodicity (molecular order) Bragg versus diffuse reflectance	Angular dependence of diffracted X-ray
NMR	Mobility $m$ of H-atoms $m_{\text{cryst}} < m_{\text{amorph}}$	Selective absorption of radio-waves by resonance of spin orientation
IR	Different absorption wavelength of OH-valence vibration	Influence of the relative number of H-bonded OH-groups
Densitometry	Densities $d_{\text{cryst}} > d_{\text{amorph}}$	Average density
Reaction kinetics	Reaction velocities $v_{\text{cryst}} < v_{\text{amorph}}$	Preferred accessibility of amorphous domains

#### 4.1.1.1 X-Ray Diffraction

To measure the CI, the fibrous material is normally pressed into a thin disc, where the fibers are orientated only in planar fashion. This specimen is irradiated by a filtered and collimated X-ray beam of known wavelength  $\lambda$  (normally Cu- $K_{\alpha}$ -line). By using a device called a goniometer, the intensity of scattered radiation is measured as a function of the diffraction angle  $2\alpha$ . The arrangement of such a device is shown in Fig. 4.3, while the X-ray diffractogram obtained is illustrated in schematic form in Fig. 4.4.

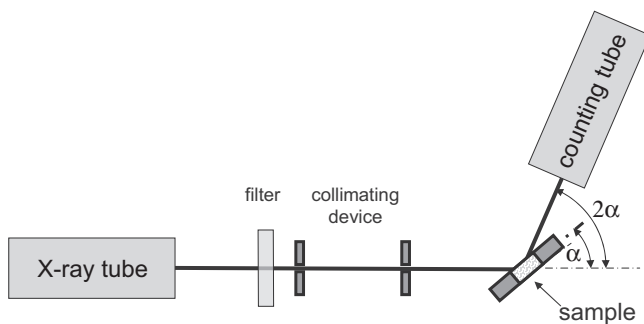


Fig. 4.3 X-ray diffractometer (goniometer).

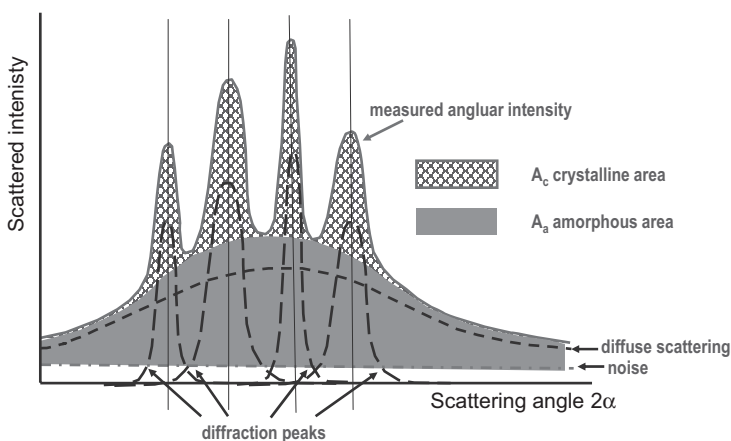


Fig. 4.4 X-ray diffractogram of a partially crystalline material.

The scattering intensity varies with the angle of observation, and comprises three components:

- radiation and measuring noise (space radiation; noise of counter, etc.);
- scattering of the amorphous phase due to density fluctuations; and
- distinct reflection on crystal planes.

By graphically analyzing the scattering functions, the amorphous part may be separated from the crystalline part. The X-ray index of crystallinity ( $CI_X$ ) is then calculated using Eq. (3), from the respective areas  $A_c$  and  $A_a$ , as shown in Fig. 4.4.

$$CI_X = \frac{A_c}{A_c + A_a} \quad (3)$$

The dimensions of the crystal unit cell (distances between crystal planes,  $d_i$ ) may be calculated from the angular position of the scattering peak maxima, according to Bragg's law [Eq. (4)]:

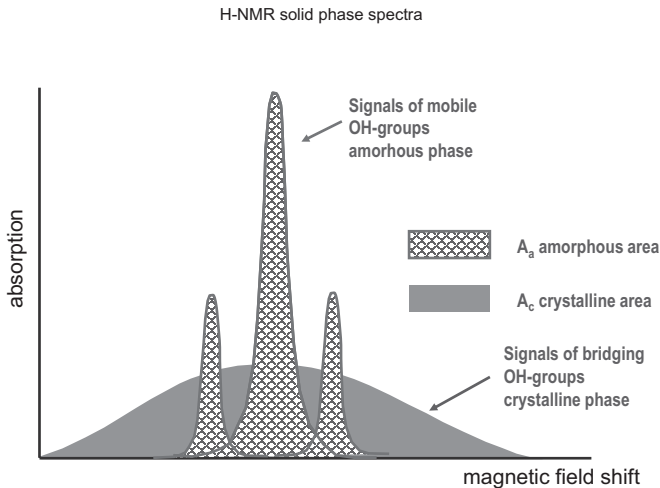
$$d_i = \frac{n \cdot \lambda_x}{2 \sin \alpha} \quad (4)$$

where  $n$  = integer number.

When using the normal graphical method of evaluation according to Fig. 4.4, the amorphous contribution is somewhat overestimated, as overlapping crystalline peaks appear lead to a higher base line. In order to obtain a more faithful value of crystallinity, the diffractogram should be analyzed numerically with software as is used for analyzing spectra.

#### 4.1.1.2 Solid-phase NMR-Spectroscopy

The proton NMR method uses the fact, that protons in chemical compounds may be orientated either parallel or anti-parallel to a magnetic field. The transition of one state to another may be triggered by electromagnetic radiation, the wavelength of which depends on the chemical environment (state of bonding) of the proton. OH-protons which are engaged in hydrogen bridges abundantly present in the crystalline state require different wavelengths of excitation (resonance) from protons in detached OH-groups. These bridging protons are furthermore rather fixed and orientated compared to the magnetic field. They cannot spin freely, which would be prerequisite for producing sharp NMR signals. Thus, in the NMR spectrum – in contrast to the X-ray diffractogram – there are sharp H-signals from the amorphous phase, and only a diffuse broad absorption area for the crystalline phase. The shape of a solid-phase H-NMR spectrum and the split into amorphous and crystalline absorption areas is shown schematically in Fig. 4.5.



**Fig. 4.5** H-NMR solid-phase spectrum of partially crystalline material containing OH-groups.

The index of crystallinity is derived according to Eq. (5):

$$CI_{NMR} = \frac{A_c}{A_c + A_a} \quad (5)$$

#### 4.1.1.3 Reaction Kinetics

As the amorphous domains of cellulose are more easily accessible to chemical reagents, these domains react first, when the material is exposed to the reagent. Only later are the crystalline domains attacked, when the reaction is proceeding more slowly.

How the degree of crystallinity is derived from reaction kinetics is illustrated in Fig. 4.6. After having reached a critical yield,  $Y_{cr}$ , all amorphous material is consumed. This point is derived by the intersection of the tangents at low and high yields to the reaction curve.

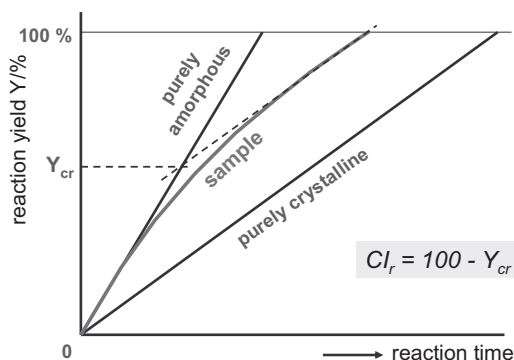


Fig. 4.6 Determination of crystallinity index ( $CI_r$ ) by reaction kinetics.

#### 4.1.1.4 Density Measurements

A straightforward method for determining the degree of crystallinity would be a simple measurement of the density [88]. The method is based on the assumption, that the specific volume  $\bar{v}$  is an additive function of the amorphous and the crystalline component ( $\bar{v} = w_a \bar{v}_a + w_c \bar{v}_c$ ).

The index of crystallinity can be easily calculated according to Eq. (6):

$$CI_d = \frac{\frac{1}{\bar{d}} - \frac{1}{\bar{d}_a}}{\frac{1}{\bar{d}_c} - \frac{1}{\bar{d}_a}} \quad (6)$$



where  $d$  = density of sample;  $d_a$  = density of the amorphous component; and  $d_c$  = density of the crystalline component.

For this method, the densities of completely crystalline and completely amorphous cellulose must be known. The density of a hypothetical macro crystal of cellulose can be calculated from the known dimensions of the crystal unit cell and the mass of the cellulose repeating unit. The density of amorphous cellulose may be roughly determined by measuring a cellulose sample, which has been made amorphous by extensive grinding. Extensive ball milling leads to near-complete loss of X-ray crystallinity, but this intense mechanical treatment also results in a low DP of such an “amorphous” cellulose [89].

However, it is not as easy to measure the true density of normal cellulose sample, as most celluloses contain pores and voids. If the total pore volume is measured separately, it can be considered in the evaluation (see Section 4.2. “Accessibility, voids and pores”).

#### 4.1.2

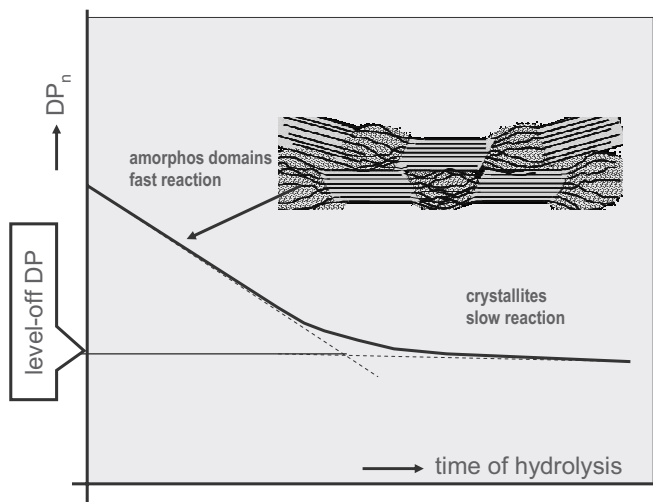
##### Dimension of Crystallites

A variety of methods are available for determining the average crystallite length:

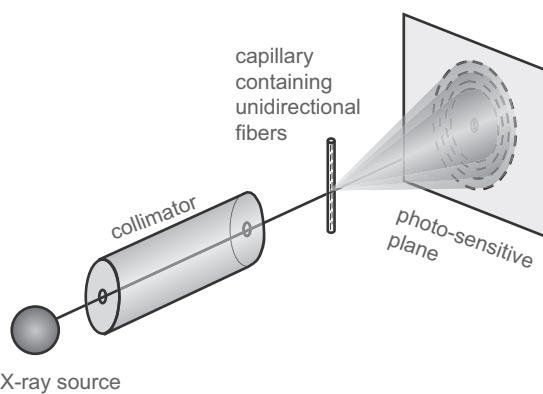
- Calculation from the band width of the 040-plane of the crystallite measured by wide angle X-ray scattering of native fibers. The band width is inversely dependent on crystallite length. As, normally, bands overlap in the diffractogram and are additionally blurred by the amorphous scattering halo, a careful numerical band separation must be applied. To do this, a Cauchy distribution curve is used for the shape of scattering bands.
- Small angle scattering on fragments of hydrolyzed fiber samples.
- Determining the length distribution of the fragments of elementary fibrils in highly degraded fiber samples by electron microscopy.
- Extended acid hydrolysis and determining the leveling-off-DP (see Fig. 4.7). The crystallite length is calculated from the DP, under the assumption that it consists of parallel, intact cellulose chains

The width of crystallites can be also derived from wide-angle X-ray diffractograms analyzing the band width of lateral reflections, or from a fiber diagram (see Fig. 4.9).

For a comprehensive X-ray analysis of fibers, a set-up as shown in Fig. 4.8 is used. This equipment is ideal for long fibers (as in cotton or rayon), but short fibers (as in pulp) must be orientated alongside parallel by placing them in a capillary tube. The reflections obtained are always less clear and differentiated as with long fibers, however.



**Fig. 4.7** Determination of level-off- $DP$ , for calculation of the average crystallite length.



**Fig. 4.8** The instrumental set-up used for determining X-ray fiber diagrams.

The angle of reflection is calculated from the distance of reflections from the center of the diagram. This yields the characteristic interplanar repetition length by applying Bragg's law.

Information regarding the dimensions of the crystallites can be deduced from the size of the reflections. The dimensions of reflections correspond to the width of the corresponding peaks in the diffractogram. Figure 4.9 indicates how the reflections in a fiber diagram are evaluated. The long period reflections near the center are normally only found with long fibers, which frequently show a regular density fluctuation in the direction of the fiber axis.

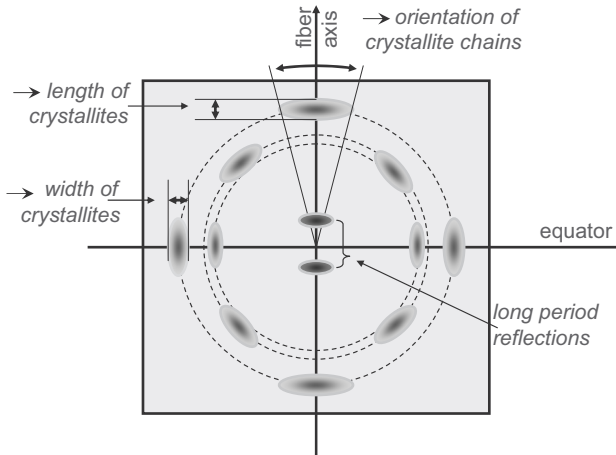


Fig. 4.9 Evaluation of reflections of a fiber X-ray diagram.

#### 4.1.3

##### Orientation of Crystallites

A measure of orientation of the anisotropic crystallites relative to the fiber axis can be derived from the fiber X-ray diagram (see Section 4.1.2).

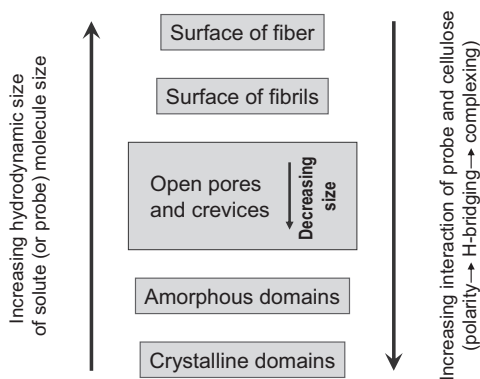
The orientation of crystallites is also mirrored by the optical axis, which can be determined by birefringence measurements (polarization microscopy). If in a microscope using polarized light, both the polarizer and analyzer are set parallel to a crystallite, then light penetrates through the crystallites and their shape is seen. The preferred angle of orientation is found, when the maximum of light intensity passes through the sample. The prerequisite is that the sample contains only fibers which are orientated parallel.

Polarization microscopy may also be used favorably to differentiate between fibers of different plant origin (see Section 5.4.1).

#### 4.2

##### Accessibility, Voids, and Pores

Cellulose fibers are a multi-phase body. When immersed in a liquid, the molecules of the liquid will try to penetrate into the polymer, because the osmotic pressure of the liquid considerably exceeds that of the polymer. At equilibrium, the location of solute molecules will depend on the accessibility of the specific domain; this situation is explained in Fig. 4.10.



**Fig. 4.10** Accessibility of different elements of fiber morphology towards molecules of a solvent.

Accessibility is a key factor for monitoring the swelling properties and chemical reactivity of pulps. As it is determined by the internal fiber structure, it may also be used successfully to obtain information about this structure. For such analyses, the solvent molecules and specific foreign molecules dissolved in it may be used as probes.

#### 4.2.1

##### **Porosity**

The cell wall of a native plant fiber consists of an integer polymer compound, and does not contain a substantial number of voids called pores. The large void in the center of the fiber, the lumen, is not considered to be a pore.

However, the isolated pulp fiber normally includes pores and voids generated by the removal of lignin and polyoses, as well as by mechanical impairment during the pulping process [90]. In the original wet state after pulping (never-dried), these voids are filled by water and the fibers show a maximal degree of swelling (as, for example, indicated by the water retention value). On drying, the pore water diffuses either through bottle-necks or through the cell wall material, evaporates, and the pores collapse, in part irreversibly. After drying, the original degree of swelling can no longer be obtained. Repeated drying and wetting cycles lead to increasingly less solvent accessibility and flexibility of the fiber material. This phenomenon is termed “hornification”.

The pores are characterized by accessibility of the pulp towards various compounds, which act as molecular probes. In this way, only those pores which are open can be detected, as completely closed pores are inaccessible to non-swelling agents. Water, lye or various other solvents may also penetrate the cellulose matrix and more or less and fill the closed pores.

Based on the findings of previous studies [91], Stone and Scallan developed a method for determining the pore size distribution of fibers in aqueous medium

by using dextran molecules of different sizes as probes [92]. When pulp is immersed in a solution of defined dextran, the dissolved polysaccharides will penetrate into the fiber matrix according to accessibility. Based on the depletion of dextran in the solution, the volume of pores with an open diameter equal to or bigger than the hydrodynamic diameter of the dextran molecules can be deduced. This method was further developed by using dextrans marked with reactive dyes, so that photometric determination of concentration could be applied [93]. Low molecular-weight sugars may be used as probing molecules for small pores, and by using this method it is possible to detect pore diameters of between 1 and 60 nm. In order to reduce experimental time demands, a mixture of probing molecules of different sizes may be applied simultaneously in one solution. The change of concentration of the probing species is then measured using size-exclusion chromatography [94].

As an alternative to accessibility measurements, scattering experiments such as small-angle X-ray scattering may be utilized that provide indirect information related to the pore content of fibers.

#### 4.2.2

##### **Accessible Surface**

The accessible surface area of fibers depends on their history. In dry fibers, the cell wall structure of cellulose is collapsed to a great extent, so that only the outer fiber surface may be reached. In swollen fibers, molecules may penetrate into voids, and consequently the specific accessible surface may differ considerably, from 0.5 to 2 m<sup>2</sup> g<sup>-1</sup> for dry fibers, and from 100 to 500 m<sup>2</sup> g<sup>-1</sup> for wet fibers.

The specific surface of dry fibers is most frequently determined using the nitrogen adsorption method (the BET method) [95]. This was adapted for pulp fiber measurement by several groups [96,97]. The swollen state of the fibers can be approximately conserved by using a stepwise solvent exchange. The water of wet fibers can be substituted successively by ethanol, acetone, and other increasingly less-polar solvents. Thus, the formation of new hydrogen bonds between approaching cellulose chains is diminished and collapse of the pore structure by final drying is minimized. In this way the swollen pore structure is almost preserved in the dry state and the total accessible surface can be determined by nitrogen adsorption [98].

Other methods to determine the surface use either water vapor adsorption [99], or the take-up of iodine [100] or bromine [101] from aqueous solution. The rate of deuterium (D) exchange may also be used as an indication of surface size, as accessible -OH on the surface is rapidly converted to -OD that are subsequently detected using infra-red spectroscopy [102]. A survey of various methods for free surface determination has been provided by Stamm [103].

### 4.3

#### Water and Solvent Retention

##### 4.3.1

##### Total Water Uptake

When cellulose is exposed to moisture, it will take up water due to its hydrophilic nature. Initially, up to five layers of water molecules will be adsorbed to the accessible cellulose surfaces in the pulp, after which water penetrates into capillaries, crevices and open pores of the pulp fibers.

The swelling of pulp fibers is also influenced by their chemical composition – polyoses endorse fiber swelling, while lignins reduce it. The swelling of chemical pulp fibers is increased with beating. With mechanical pulps, refining also increases the water retention value (WRV), but this is mainly because of an increased fines content rather than because of increased fiber swelling.

The overall uptake of water may be determined by immersing the pulp material into water and removing excess water by centrifugation. Under standardized conditions, this allows the WRV to be calculated [104,105], which is a good indication of the amount of water retained within the fibers. A modified version of WRV measurement has recently been reported [106] which uses preformed sheets rather than disintegrated fibers as samples.

Cotton linters have a WRV of approximately 50% (35% free, 15% bound water), while pulps and regenerated cellulose fibers reach values of 60–90% [107].

The WRV decreases with freeness and with thermal exposure by drying. Never-dried pulp may store as much as 135% [108].

##### 4.3.2

##### Free and Bound Water

Water molecules may be bound directly to a polysaccharide of pulp fibers by hydrogen bonds. Strictly, this applies only to a mono molecular layer of water on the outer or on inner surfaces (walls of pores, etc.). However, water tends to form molecular clusters which are also bound by hydrogen bridging. The first layer is strongly immobilized, while the second layer shows enhanced mobility of molecules. Some water in swollen cellulose fibers even shows a very high order and may be taken as crystalline. At a greater distance from the surface, the water molecules are no longer restricted in any way (bulk or free water). Thus, it is not easy to define the amount of bound water as the boundary towards bulk water is not sharp. Bound water in equilibrium swollen cotton and ordinary pulp amounts to approximately 30% of the total water content.

One way to differentiate between bound and free water is to detect the restricted mobility of bound water by phase-transition phenomena. Bound water boils at a higher temperature and freezes at a lower temperature than free water. Freezing and boiling point can be measured very accurately using differential scanning calorimetry (DSC), as this measures the enthalpy of phase transition as a function of temperature [109]. The different forms of water in swollen cellulose may also be differentiated using the NMR-method [110].

## 5 Fiber Properties

### 5.1 Identification of Fibers

Cellulose fibers may originate from various plant species, each of which shows specific characteristic features that may also be identified microscopically. These specific morphological features of fibers include fiber length, fiber width, thickness of cell wall, shape of fiber tips, pits, and fenestrations.

#### 5.1.1 Morphological Characterization

The most important morphological features of pulp fibers can be seen using normal light microscopy. Each species of plant consists of very specific cells, so that the plant origin of a pulp can be directly revealed from identifying the fibers stemming from the cells of wooden tissue.

To make morphological details more visible, a variety of additional techniques may be applied for preparing samples and visualizing them, including:

- differential staining, using visual or fluorescent dyes (Tab. 5.1);
- applying swelling reagents; and/or
- optical contrasting (birefringence, phase-contrasting, interference-contrasting, fluorescence).

The morphology of the fiber walls may be made better visible by using mild swelling reagents (see Tab. 5.2). When the cell wall swells, its fibrils are increasingly separated and become discernable. Pits and damaged fiber areas are also seen under better contrast. Most of the dye formulations also contain swelling components, which enhances the penetration and interaction of the dyestuff.

Tab. 5.1 A selection of staining methods used for fiber identification.

Staining reagent	Reference(s)	Staining reactions
Chlorine-stannous-iodine	111,112	cellulose: blue violet wood fibers: yellow to brownish
Iodine-potassium iodide	113	cellulose: colorless to grey wood fibers: brown
Iodine-cadmium iodide	114,115	cotton: red unbleached wood pulp: gray bleached pulp: blue wood fibers: yellow
Iodide-calcium chloride	116	
Iodine-potassium chloride- calcium chloride	117	
Malachite green – I <sub>2</sub> – SnCl <sub>4</sub> (Herzberg solution)	118	cellulose: blue wood fibers: brown
Basic violet and basic green	114	Lignin-containing pulps: blue Bleached chemical pulps: colorless
Phloroglucinol		Wood fibers: red

Details of these and additional staining methods are compiled by Werthmann [119].

Tab. 5.2 Characteristic morphological features of wood pulp fibers.

Component of wood	Soft wood	Hard wood
Conducting tissue systems	Bordered pits of early wood tracheids	Open and perforated vessels (fenestriform pits)
Bearing tissue system	Striation of late wood tracheids	Libriform fibers
Parenchyme	Bulky cells with simple pits	Elongated cells containing many simple pits



## 5.1.2

**Visible and UV Microscopy**

The various characteristic aspects of pulp fibers are too numerous and diverse to be described here. In order to identify the type of pulp according to plant source, much empirical expertise is necessary, though for purposes of comparison, a fiber atlas may be used (e.g. [120]). Some examples of pulp fibers are shown in Fig. 5.1.

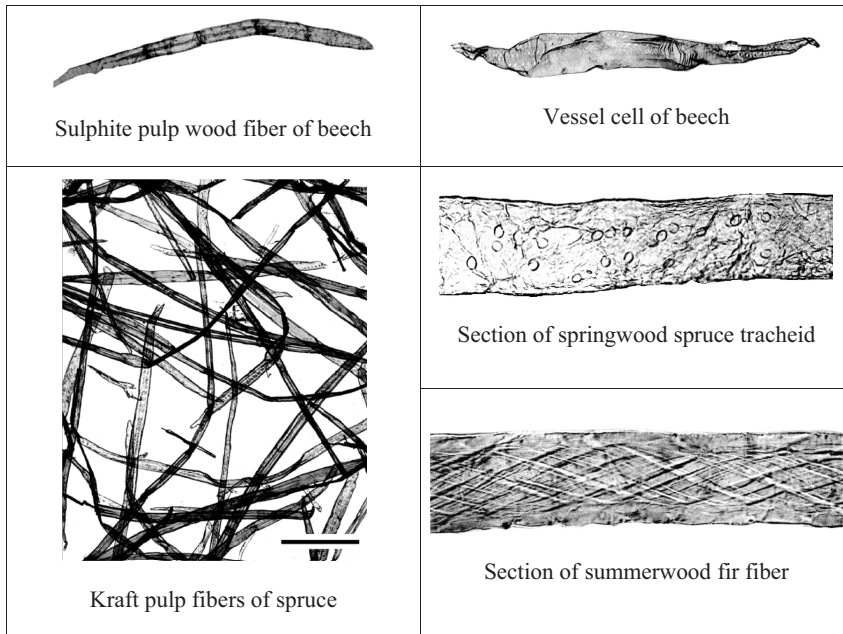


Fig. 5.1 Examples of pulp fiber characteristics.

## 5.1.3

**Electron Microscopy**

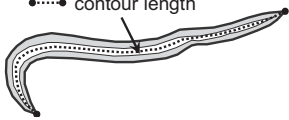
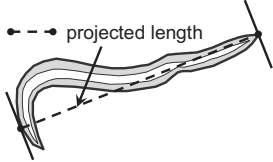

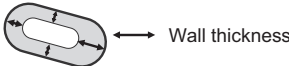
Scanning electron microscopy (SEM) is a very valuable tool in the study of detailed fiber morphology, for example examining the structures of tracheids and vessels, and the dimensions of cell wall and cell wall layers, pits and fenestrations.

## 5.2 Fiber Dimensions

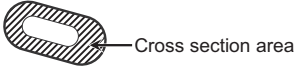
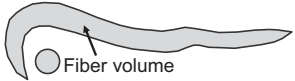
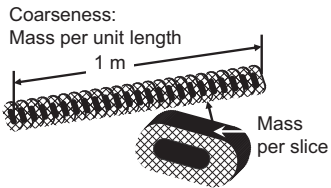
A sample of pulp or paper fiber material consists of a variety of fibers and pieces thereof. Typically, the length of a softwood fiber is 100 times its width, while the width of the open (not collapsed) fiber is approximately ten times the wall thickness. Fiber dimensions depend primarily on the fiber source species, and within any one species these dimensions will vary according to the growing conditions and age.

Each property derives from contributions of each fiber, and is described by statistical numbers: mean, shape, and width of distribution (see Tab. 5.3). In order to determine a property of single fibers, many fibers must be measured and the results calculated using a statistical approach.

**Tab. 5.3** Characteristic parameters of average dimensions of suspended single fibers.

Fiber parameter	Preferred dimension	Average of	Explanation
Contour length	mm	Length of straightened fiber	
Projected length	mm	Length of curled fiber	
Curl	%	Extent of curling of fiber	$CU/\% = \left( \frac{\text{contour length}}{\text{projected length}} - 1 \right) \cdot 100$
Width	$\mu\text{m}$	Dimension of cross section	
Wall	$\mu\text{m}$	Thickness of fiber wall	

Tab. 5.3 Continued.

Fiber parameter	Preferred dimension	Average of	Explanation
Cross-sectional area	$\mu\text{m}^2$	Cross section area of fiber wall	
Fiber volume	$\mu\text{m}^3$	Total volume of swollen fiber	
Coarseness	$\text{g m}^{-1}$	Mass per unit length	Coarseness: Mass per unit length 

### 5.2.1

#### Fiber Length [121] and Width

##### 5.2.1.1 Microscopic Methods and Image Analysis

A straightforward way of determining fiber lengths is to measure the individual length of each fiber in a microscopic sample. This can be done manually, conveniently by projecting the microscopic image to a screen and measuring the lengths of fibers by using a screen grid [122]. Alternatively, image analysis may be used.

Various methods detect, optically, the dimensions of fibers that are suspended in water flowing through a measuring cell. The fibers are orientated in the flow direction, and images of individual fibers taken by a camera are evaluated by mathematical image analysis. To differentiate between fibers and nonfiber particles, polarized light may be applied, which detects only the birefringent fiber material. This technique is described by a TAPPI standard method [123]. Another principle consists of sensing the beginning and the end of a flowing fiber passing a light bar. Fiber length is then calculated by using the shadowing time and flow velocity.

Today, commercial equipment such as the “Kajaani fiber analyzer”, “Fiber master” (developed by STFI), or the “Pulp Expert” are available. These instruments provide information about fiber length distribution, the average fiber length, and the fiber coarseness of a sample. For different properties, different averages are most appropriate; for example, in the case of fiber length the length-weighted average is best suited.

More modern instruments (e.g., “Fiberlab”; Metso Automation; “Kajaani FS-200”) also provide additional information about fiber width and fiber wall thickness. In addition, shape parameters such as kinks and fiber curl may be quantified by proper image analysis. Different curl indices are used in characterizing the curliness of a fiber, with the most widely used index being that defined as in Tab. 5.3.

### 5.2.1.2 Fiber Fractionation by Screening

Quantitatively, the fiber length distribution of a pulp and its fines content can be determined by stepwise consecutive screening through screens of decreasing slot size. Fibers are retained predominantly according to their lengths, although other fiber dimensions and fiber flexibility also affect the fractionation result. The fines content is received as the material that passes through the screen with smallest slot. A typical example of such equipment is the Bauer-McNett apparatus, which consists of a series of tanks with screens of different aperture (Fig. 5.2).

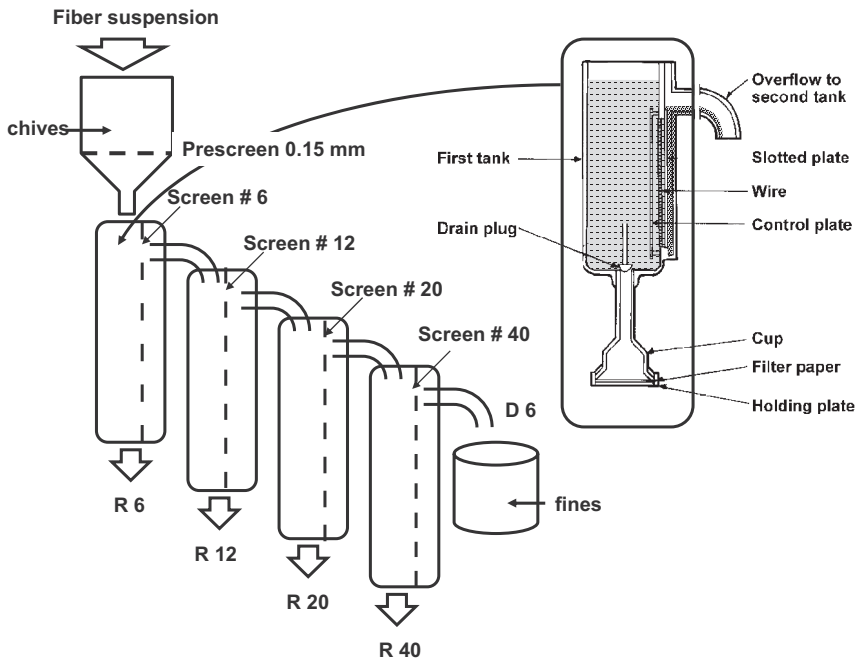


Fig. 5.2 Fiber fractionation according to Bauer-McNett.

Typical screen slots used for mechanical pulp are 30, 50, 100, and 200 mesh. Material passing the 200 mesh is often considered as fines, while long fibers are the fraction retained on the 30-mesh screen. A dynamic drainage jar (DDJ) with a 200-mesh wire screen can also be used to measure the fines content [124].

## 5.2.2

**Coarseness [125]**

Coarseness is a measure of the mass of a slice of fiber cross-section of a certain thickness, and is taken as the weight of 1 m of fiber. Hence, the units of coarseness are mass per unit length. Coarseness can be calculated from the number of fibers, their average length, and the total dry weight of the fibers in a sample. Advanced fiber analyzers provide direct information on coarseness, the prerequisite being that the total dry weight of the fibers in the sample is known exactly.

## 5.3

**Mechanical Properties**

## 5.3.1

**Single Fiber Properties**

Fibers are usually processed in the wet stage, and for pumping, mixing, screening, sheet formation and pressing the wet fiber properties are decisive. In a fibrous product, dry fiber properties form the basis of the product's properties.

5.3.1.1 **Wet Fiber Properties**

The prevailing features of fibers in a liquid (predominantly aqueous) medium are swelling and specific properties of the swollen fibers; these include collapsibility, flexibility, and conformability. These terms are illustrated schematically in Fig. 5.3. Conformability is a combined property which is not measured separately. Indirect information about conformability can be deduced from a combination of swelling (water retention), flexibility and collapsibility measurements.

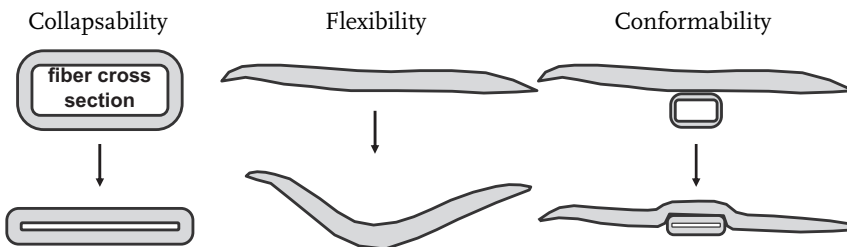


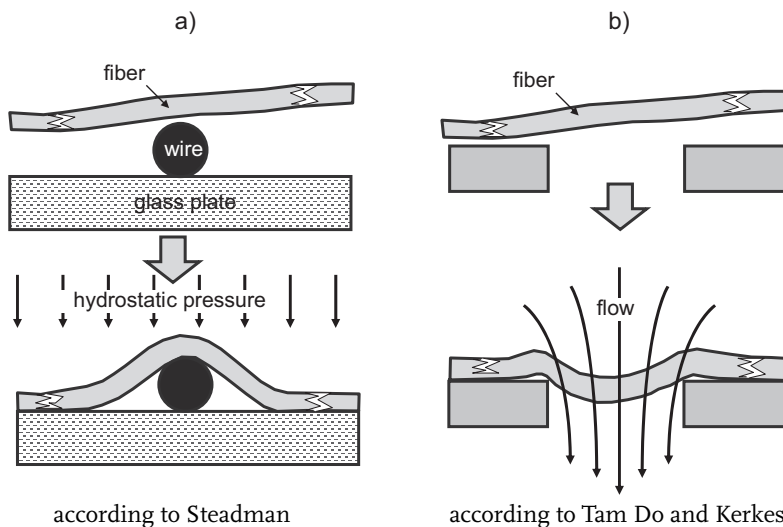
Fig. 5.3 Parameters of deformability of single wet fibers.

By applying lateral pressure, the fiber may collapse and change the tube structure into a double-layered strip. The compression force required can be measured directly using a tensiometer. Typical compression forces needed to collapse the fiber laterally are in the range of 80 to 500 N m<sup>-1</sup> for normal pulps, and decrease with the degree of pulping. Compression values for Norway spruce are listed in Tab. 5.4.

**Tab. 5.4** Compression forces ( $\text{n M}^{-1}$ ) for wet Norway spruce pulp [126].

	Spring wood	Summer wood
Sulfite pulp	100–120	150–200
Kraft pulp	250–300	300–400

Flexibility or its inverse stiffness is less easily measured, and attempts to calculate fiber stiffness from fiber mat compressibility have been unsuccessful. Various methods use the cantilever concept, wherein a single fiber is clamped from one end, with the other end protruding freely into the measuring chamber. A bending force is applied by a mechanical micro device, or hydrodynamically by a tangent stream, and the deflection of the fiber is measured. According to Steadman, fibers are positioned over a metal string on a glass plate. By applying hydrodynamic pressure, a fiber is partially pressed against the glass plate, though a section of the fiber does not touch it as it is hindered by the wire. The more flexible the fiber, the more it will wrap around the wire contour, leading to a smaller area of non-contact (Fig. 5.4).



**Fig. 5.4** Principles of measuring single fiber flexibility.

The most reliable method appears to be that suggested by Tam Do and Kerekes [127]. According to this method, a fiber is positioned transversely over a hole, without clamping. When a stream of water is passed through the hole, the fiber bends. From the hydrodynamic force and curvature of the fiber, its stiffness may

be deduced. Stiffness is higher for kraft pulps than for sulfite pulps, and decreases with increasing degree of delignification [128]. Generally, spring wood fibers are approximately twice as flexible as summer wood fibers, and the flexibility increases linearly with degree of beating (Schopper-Riegler) [129].

### 5.3.1.2 Mechanical Properties of Dry Fibers

The quality of a pulp is mirrored by the deformability of single fibers and sheets from which it is made. Highly informative data may be acquired from the stress–strain characteristics, as shown in Fig. 5.5. When mechanical stress is applied to a body, it will yield to this stress to a certain degree by becoming deformed (strain). By deforming the body, its internal structure is also deformed, rearranged, and finally broken. In cellulose fibers, the strongest domains are the micro crystals, the strength of which can only be augmented by chemical cross-linking. Any other deviation from the crystal structure diminishes strength. Such weak points include: lattice shifts in cellulose crystals, chain scission of the cellulose macromolecule, ring scission of glucose units, alien chemical groups on the cellulose backbone, low-density packing (“amorphous” domains), voids (pores) and crevices, and imbibed low molecular-weight compounds (impurities, solvents). All weak points lower the modulus of elasticity and breaking force, and in general also increase breaking deformation.

For the characterization of pulps and paper, the most commonly applied type of deformation is elongation. A tear experiment provides the modulus of elongation, the breaking load and stretch at break. The tensile index is derived from the breaking load, which in turn depends on the dimensions of the sample.

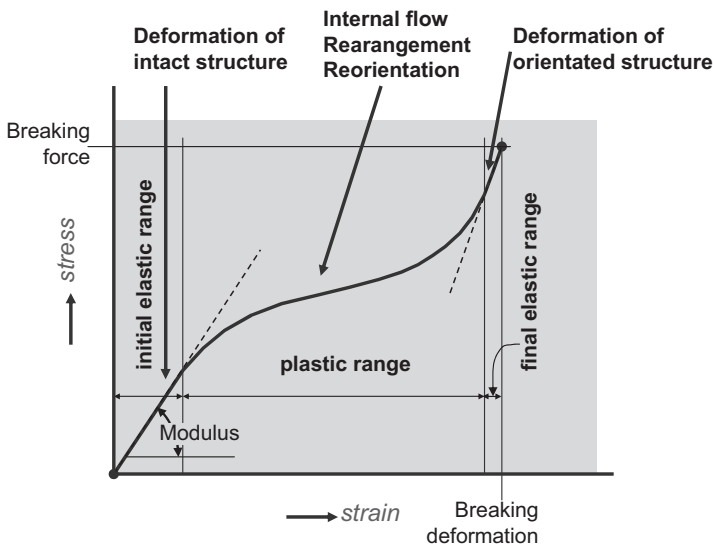


Fig. 5.5 Stress–strain characteristics of single pulp fibers or sheets made of such.

The tensile strength of single fibers may be measured directly using a micro-tensiometer. However, clamping a single fiber is not easy and may damage the fiber wall such that a predetermined breaking zone is introduced. To determine a meaningful average value, a large number of fibers must be measured, notably because of the wide distribution of fiber properties of a pulp.

A quick and convenient way to obtain information about single fiber strength is to determine the zero-span strength of sheets. A sheet is clamped in the tear apparatus so that the clamps at rest are in contact, and most of the fibers bridging the gap are clamped from both sides. When the clamps separate, these fibers will be torn. The load-elongation behavior of various cellulose fibers is similar. Differences are due to the origin and type of fiber, as well as defects relating to the fiber's history, especially pulping and refining. Such weak points may include pores, cracks, and dislocations. The elastic modulus of elongation is determined by the initial linear section of the load-elongation curve; beyond the linear section, the fiber offers less resistance towards further stress of elongation.

Some nonlinearity in the load-elongation behavior of single fibers can be attributed to curl, and certain defects – for example, crimps, kinks, and micro-compressions – may be rectified by the elongation.

The typical tensile strengths of wood fibers are in the range of 100 to 200 mN. As the noncellulosic components do not contribute much to the elongational strength of fibers, pulp may show comparable fiber strength as wood. More severe pulping (especially under acid conditions) causes degradation of the cellulose, leading to poor fiber tensile strength and fiber stiffness. Bleaching chemicals may also have a similar degrading effect.

Mild beating may toughen the fiber by closing pores and crevices, and even causing some recrystallization. However, stronger beating damages the structure of the fibers, leading to poorer mechanical strength properties.

Drying generally makes fibers more brittle, this being due to the closing of pores and the formation of glassy amorphous cellulose domains in the fiber structure.

### 5.3.2

#### **Sheet Properties**

The mechanical properties of fiber sheets derive from the fiber properties, fleece structure and bonding. Inter-fiber bonds may form within a contact zone where two fibers are so close that hydrogen bridging, van der Waals interaction, or molecular entanglement may occur. In addition, the entanglement of intertwining fibers would render some degree of mechanical strength to a fiber mat, even in absence of bonding.

#### **5.3.2.1 Preparation of Laboratory Sheets for Physical Testing [130–133]**

In a laboratory sheet former, a much-diluted pulp suspension drains slowly through a wire screen. The sheets are couched from the wire with blotters, wet-



pressed, and dried under standard conditions. The wet-pressing of laboratory sheets involves pressing the sheets between press plates and blotters. The required pressure of 400–500 kPa is applied to the sheets for a few minutes.

Sheet-forming standards differ slightly, though in central Europe the Rapid-Köthen former is widely used.

#### 5.3.2.2 Determination of Mechanical Pulp Sheet Properties

In the tensile strength test, the breaking load and strain at rupture are determined as values characteristic of sheet strength [134,135]. The breaking load, together with the sample width, provides the tensile strength per unit width (measured in  $\text{N m}^{-1}$ ) which, when combined with the sample thickness, gives the tensile strength (measured in kPa).

In paper technology, the breaking length is also of some importance as a relative measure of strength. This is the length of a freely suspended paper strip of any constant width and thickness that breaks at the point of suspension due to its own weight.

The resistance to flexural stress is measured as the bending stiffness under approximately pure elastic deformation, and is monitored using a beam deflection method. In a Lorentzen and Wettre-type tester, the sample strip is clamped and the open end is gradually moved towards a blunt knife mounted on a pressure transducer [136]. Alternatively, the sample rests on two points of suspension [137]. When using the resonance length method, resonance is generated by a clamp vibrating at 25 Hz [138].

## 5.4

### Optical Properties of Laboratory Sheets

The optical properties of a fibrous sheet depend on the intrinsic optical features of the fiber (e.g., index of refraction, spectrum of light absorption, specific surface, porous structure) and on web properties (e.g., fraction of bonded fiber surface). UV/visible absorptivity is minimally influenced by the web structure of the sheet, and consequently a sheet yields comparable absorption spectra as unbounded fibers. More generally, summation parameters such as brightness and opacity are taken as measures, using specially defined white light illumination. According to the well-known Kubelka–Munk theory, all directly measurable properties are linked to two individual material factors, namely the absorption factor  $k$  and scattering factor  $s$ .

An object is termed “white” when reflectance intensity and absorption capacity do not vary with wavelength of incident light. Deviations confer a more or less pronounced color shade on the surface.

The whiteness or brightness of a sheet is determined by collecting and measuring the total reflected light of a diffusely illuminated sample [139]. For the ISO test, a filter is used which has an intensity maximum at a wavelength of 457 nm.

The reflectance (blue component) measured in a reflectometer under specified conditions is known as brightness, and is expressed as a percentage of the brightness of a white standard (compressed MgO-powder).

Another important optical property of a sheet is its transparency – that is, a measure of its light transmittance. This is calculated from the reflectance factors  $R_0$ ,  $R_w$ , which are determined in accordance with DIN 53 145 [140,141], Part 1 or Part 2. The reflectance factor of the individual sheet over a completely black background is  $R_0$ ,  $R_w$  is the reflectance factor of the individual sheet on a white background, and  $R_{(w)}$  is the reflectance factor of the white base.

The opacity (O) is a measure of light-tightness, and is defined in ISO 2471 (1977) as the ratio of the reflectance factor  $R_0$  to the reflectance factor  $R_\infty$ :

$$O/\% = \frac{R_0}{R_\infty} \cdot 100$$

Both reflectance factors are determined in accordance with DIN 53 145.  $R_0$  is measured as the reflectance factor of an individual sheet on a completely black background, and  $R_\infty$  as the reflectance factor of an “infinitely” thick stack of the same paper.

## 6 Papermaking Properties of Pulps

### 6.1 Beating

Originally, real beating was used to enhance the binding power of plant fibers in paper sheets, but today, instead of beating by hammers, the aqueous fiber slurry is milled by a device called a “valley beater” or by a “refiner”. By performing such mechanical treatment, the fiber wall is squeezed, kneaded and plasticized, and the fiber surface is partly disintegrated. Mechanical shear separates parts of cellulose fibrils so that the fiber surface becomes hairy and fluffy. Fibrils may involuntarily be completely liberated from the fiber material, and some fibers may even be completely torn to fiber fragments.

A major effect of “beating” is a drastic increase of water uptake by the fiber material. The kneaded cell wall will swell, and the fibril fur on the surface will store water by capillary forces, while the isolated cellulose fibrils aggregate to hydrogels containing huge amounts of immobilized water. The hydrodynamic volume of the fibers is increased substantially, so that filtration – as in the sheet-forming process – is severely hampered. This effect is used to characterize the effectiveness of beating, by measuring drainability.

For the beating of small quantities of pulp, a JOKRO mill [142,143], a PFI mill [144], or a small refiner may be used.

### 6.2 Drainage Resistance

The filtration behavior of fiber slurry depends largely on the overall hydration state of the fibers. Compact unswollen fibers form an open fiber mat, including protruding free channels (“freeness”), and will filter readily. On the other hand, swollen and defibrillated fibers form a fiber-containing, gel-like filter cake which dewateres only hesitatingly.

Thus, freeness is an indirect measure of compactness, stiffness and partial density of fibers suspended in water. By cooking and mechanical treatment (beating, refining) the fiber wall is plasticized and made more swellable. At the same time,

the fiber surface is fibrillated to form a high-volume hydrogel that covers the fiber. Freeness is measured by determining the rate of dewatering when the fiber slurry is filtered under defined conditions.

The two common methods are the Canadian Standard Freeness (CSF) [145] and Schopper–Riegler (SR) [146]. Both methods are a relative measure of the drainability of a pulp suspension, and both use a similar device for determining the rate of dewatering.

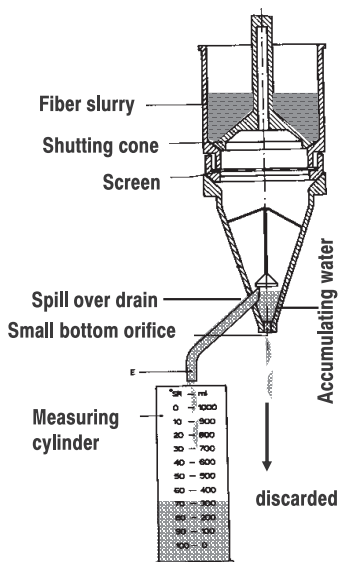


Fig. 6.1 Determination of freeness (Schopper–Riegler method).

The principle of determining freeness is shown in Fig. 6.1. The SR number corresponds to the amount of water passing through the side opening (spill) of the testing apparatus. A volume of pulp suspension (1 L) with a consistency of  $2 \text{ g L}^{-1}$  is filtered through the screen of the testing device. Slower drainage leads to less spill-over and a higher SR number. The measurement principle of the CSF number is the same as for SR (except that a consistency of  $3 \text{ g L}^{-1}$  of fiber slurry is applied). The measuring vessel is calibrated inversely to the SR system, so the CSF number is inversely proportional to drainage resistance. SR numbers can be easily be converted to CSF numbers (Fig. 6.2).

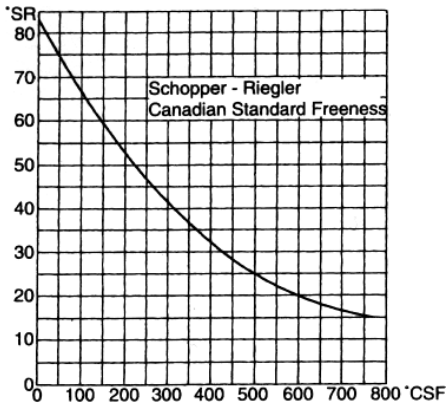


Fig. 6.2 Correlation of Schopper-Riegler (SR) numbers with Canadian Standard Freeness (CSF) numbers.

Freeness is an overall empirical measure for the degree of beating; it does not specify explicit properties such as swelling or defibrillation. The values also depend on the quality of water used. The SR number decreases with increasing salt concentration, due to the fact that the anionic charge of the fibers contributes to the degree of swelling. The effect of the charged pulp groups is shielded by ion concentration in the slurry. Today, automatic equipment is available which determines the degree of freeness by using a similar set-up, but measures the degree and speed of drainage by a registering balance.

### 6.3

#### Drainage (Dewatering) Time

Drainage time is a relative indication of drainability determined by a simple sheet formation process using a special laboratory sheet former (dynamic drainage analyzer, DDA) [147]. Drainage time is defined as the time for a specified volume of water to drain through the forming wire during sheet formation. The drainage time depends heavily on conditions during the measurement, such as pressure difference created by drainage, density of the fiber mat on the wire, and fiber properties including length, flexibility, and degree of swelling. Today, automated laboratory equipment is available which is able to measure drainage time and retention simultaneously (e.g., Drainage Freeness Retention-Analyzer; BTG-Mutek).

## 6.4

### Aging

The properties of pulp and paper are changed in time by the influence of oxygen, moisture, acid atmosphere, and radiation (light, UV, or occasionally high-energy radiation). Polysaccharides may be oxidized, and carbonyl and carboxylic functions are generated. Oxidation also fosters hydrolytic degradation. The most important molecular changes during aging were investigated extensively by Klei-nert and coworkers [148–150].

As a consequence, fiber strength suffers. Harsh thermal treatment of fibrous material may cause hornification, a phenomenon based on the formation of a glassy brittle phase of amorphous cellulose or other polysaccharide. Following the formation of free radicals, of carbonyl, and carboxyl functions, cross-linking between adjacent cellulose chains may take place [151]. At the same time, discoloration may occur by the formation of chromophores. Saccharides can form chromophores by dehydration and the formation of double carbon–carbon bonds. Major discoloration is based on the oxidation of heavy metal ions (predominantly Fe) to colored oxides. Also, residual lignin is sensitive to yellowing, by oxidative reactions, intensified by UV-light. Aggressive gases (ozone, sulfur dioxide, oxides of nitrogen, etc.), a higher temperature and moisture will also intensify the aging processes. Virtually any molecular, fiber, or hand sheet property may be used to monitor the process of aging.

#### 6.4.1

##### Accelerated Aging

As aging under normal environmental conditions is a slow process, special physical or chemical laboratory methods are applied to accelerate aging processes in order to study relative stability and changes of related properties.

Methods used include exposure to heat, visible and UV-light and sulfur dioxide gas. ISO standards refer to the aging of paper and board at elevated temperatures (e.g., 105 °C) [152], under low relative humidity conditions (e.g., 90 °C and 25% relative humidity) [153], and under high relative humidity conditions (e.g., 80 °C and 65% relative humidity) [154], respectively. The most effective acceleration of aging is achieved by applying temperature and humidity cycles to the cellulose samples [155].

## References

- 1 DIN ISO 7213 (1981); Pulps – Sampling for testing.
- 2 DIN EN ISO 186 (2002); Paper and board – Sampling to determine average quality.
- 3 ISO 5263 (1995); Pulps – Laboratory wet disintegration.
- 4 ISO 5263 – 1 (2003); Wet disintegration. Part 1: Disintegration of chemical pulps.
- 5 ISO 5263 – 2 (2003); Wet disintegration. Part 2: Disintegration of mechanical pulps at 20 °C.
- 6 ISO 5263 – 3 (2003); Wet disintegration. Part 3: Disintegration of mechanical pulps at >85 °C (latency removal).
- 7 ISO 287 (1994); Paper and board – Determination of moisture content: Oven-drying method.
- 8 ISO 638 (1978); Pulps – Determination of dry matter content.
- 9 SCAN C 3:61 (1961); Dry matter in pulp.
- 10 ISO 1762 (1974); Pulps – Determination of ash.
- 11 Zellcheming-Merkblatt IV/41/67 (1967); Bestimmung der Sulfatasche.
- 12 ISO 776 (1982); Pulps – Determination of acid-insoluble ash.
- 13 ISO 777 (1982); Pulps – Determination of calcium content – EDTA Titrimetric and flame atomic absorption spectrometric methods.
- 14 Zellcheming-Merkblatt IV/45/67 (1967); Prüfung von Zellstoff; Bestimmung von Ca und Mg.
- 15 ISO 777 (1982); Pulps – Determination of calcium content – EDTA; Titrimetric and flame atomic absorption spectrometric methods.
- 16 ISO 9668 (1990); Pulps – Determination of magnesium content; Flame atomic absorption spectrometric method.
- 17 DIN 54363 (1980); Testing of pulp and paper; determination of iron, manganese, copper, calcium and magnesium contents; determination by atomic absorption spectroscopy.
- 18 Zellcheming-Merkblatt IV/48/68 (1967); Prüfung von Zellstoff, Mangan in Zellstoff.
- 19 SCAN C 14:62 (1962); Manganese in pulp.
- 20 TAPPI T 241 hm-83 (1983); Manganese in pulp.
- 21 ISO 779 (1982); Pulps; Determination of iron content; 1,10-Phenanthroline photometric and flame atomic absorption spectrometric methods.
- 22 DIN (1982); Prüfung von Zellstoff, Papier und Pappe; Bestimmung des Mangengehaltes; Photometrisches Verfahren.
- 23 SCAN C 12:62 (1962); Copper.
- 24 Zellcheming-Merkblatt IV/59/68 (1968); Prüfung von Zellstoff und Papier; Bestimmung des Eisengehaltes, Photometrische Bestimmung mit Bathophenanthrolin-Reagenz.
- 25 ISO 778 (1982); Pulps; Determination of copper content; Extraction-photometric and flame atomic absorption spectrometric methods.
- 26 DIN (1970); Prüfung von Zellstoff, Papier und Pappe; Bestimmung des Kupfergehaltes.
- 27 Zellcheming-Merkblatt IV/60/86 (1986); Prüfung von Zellstoff und Papier; Bestimmung des Kupfergehaltes; Photometrische Bestimmung mit Bathocuproin-Reagenz.
- 28 SCAN C 12:62 (1962); Copper.
- 29 TAPPI T 243 hm-83 (1983); Copper in pulp.
- 30 Zellcheming-Merkblatt IV/47/68 (1968); Prüfung von Zellstoff, Kupfer in Zellstoff.
- 31 BGA BIII – XXXVI – A1; 9. Mitteilung zur Untersuchung von Kunststoffen: Kaltwasserextrakt Deutsches Bundes Gesundheitsamt, 1997.
- 32 DIN 53114 (1990) Prüfung von Papier, Pappe und Zellstoff; Bestimmung der spezifischen elektrischen Leitfähigkeit von wässrigen Auszügen.
- 33 BGA BIII – XXXVI – A2; 9. Mitteilung zur Untersuchung von Kunststoffen: Heißwasserextrakt. Deutsches Bundes Gesundheitsamt, 1997.
- 34 ISO 6587 (1992); Paper, board and pulps; Determination of conductivity of aqueous extracts.

- 35 ISO 6588 (1981); Paper, board and pulps; Determination of pH of aqueous extracts.
- 36 TAPPI om T 252 (1985); pH and electrical conductivity of hot water extract of pulp, paper and paperboard.
- 37 SCAN P 16:65 (1965); pH of aqueous extracts of paper.
- 38 Zellcheming-Merkblatt IV/58/80 (1980); Prüfung von Papier, Karton und Papp; Säure- und Alkaligehalt in wässrigen Extrakten.
- 39 ISO 9197-1 (1989); Paper, board and pulps; Determination of water soluble chlorides; General method.
- 40 DIN 38405 T1 (1985); Deutsche Einheitsverfahren zu Wasser-, Abwasser- und Schlammuntersuchung; Anionen (Gruppe D) Bestimmung der Chloridionen.
- 41 ISO 9197-2 (1990); Paper, board and pulps; Determination of water-soluble chlorides. Method for high purity products.
- 42 ISO 9197-1 (1989); Paper, board and pulps – Determination of water-soluble chlorides. General method.
- 43 W. Shadenböck, V. Prey: Eine neue quantitative Ligninbestimmung mit Hilfe der UV-Spektrophotometrie. *Papier*, 1972; 261(3): 116–118.
- 44 Cr. I. Simionescu, A. Stoleriu, Gh. Rozmarin: Microcalorimetric method for residual lignin determination in sulfite pulps. *Cellulose Chem. Technol.*, 1989; 23: 585–590.
- 45 TAPPI om T 222 (1998); Acid-insoluble lignin in wood and pulp.
- 46 Th. Krause, Ed., *Chemische und mikrobiologische Verfahren*. Springer, Berlin, 1991: 10–11.
- 47 E. Merck, Ed., *Chemisch-technische Untersuchungsmethoden für die Zellstoff und Papierfabrikation*. Verlag Chemie, Darmstadt, 1957: 112.
- 48 ISO 3260 (1982); Pulps; Determination of chlorine consumption (Degree of delignification).
- 49 ISO 302 (2004); Pulps; Determination of kappa-number.
- 50 Zellcheming-Merkblatt (1980); Prüfung von Zellstoff; Bestimmung der Kappa-Zahl.
- 51 SCAN C1 (1962); Kappa number of pulp.
- 52 TAPPI om T236 (1985); Kappa number of pulp.
- 53 TAPPI om 203 (1993); Alpha-, beta- and gamma-cellulose in pulp.
- 54 C.F. Cross, E.J. Bevan, Eds., *Researches on Cellulose*. Longman, London, 1912.
- 55 E. Bartunek, R. Heuser: *Cellulose Chem.*, 1925: 9.
- 56 ISO 699 (1982); Pulps – Determination of alkali resistance.
- 57 ISO 692 (1982); Pulps – Determination of alkali solubility.
- 58 TAPPI (1985); Carbohydrate composition of extractive-free wood and wood pulp by gas-liquid chromatography.
- 59 Th. Krause, H. Teubner: Dünnschichtchromatographische Trennung und quantitative Bestimmung von Zuckern aus Zellstoffhydrolysaten. *Holz-forschung*, 1963; 27(4): 123–126.
- 60 TAPPI cm T 223 (1984); Pentosans in wood and pulp.
- 61 J. Cerny, M. Stanek, J. Kocourek, J. Pacak: *The Monosaccharides*. Academic Press, New York, London, 1963.
- 62 W. Rehder, B. Phillip, H. Lang: Ein Beitrag zur Analytik der Carbonylgruppen in Oxycellulose und technischen Zellstoffen. *Das Papier*, 1965; 19(9): 502–509.
- 63 SCAN 22 (1966); Copper number of pulp.
- 64 TAPPI om T430 (1994); Copper number of pulp, paper, and paperboard.
- 65 Zellcheming-Merkblatt IV/30 (1970); Prüfung von Zellstoff; Bestimmung der Kupferzahl.
- 66 D.C. Chamberlain, D.J. Priest: Comparison of physical and chemical methods for analysing cellulose degradation following artificial ageing treatment. *Cellulose Chem. Technol.*, 1998; 32: 35–41.
- 67 B. Misiorny, B. Lindberg: Quantitative analysis of reducible carbohydrates by means of sodium borohydride. *Svensk. Papperstidn.*, 1952; 55: 13–14.
- 68 B. Theander, A. Lindberg: Quantitative analysis of carbonyl groups in oxycellulose by means of sodium borohydride. *Svensk. Papperstidn.*, 1954; 57: 83–85.



- 69 I. Samuelson, O. Norstedt: Quantitative determination of carbonyl groups in bleached wood pulps. *Svensk. Papperstidn.*, 1966; 69: 441–446.
- 70 J.W. Green. In: *Methods in Carbohydrate Chemistry. III Cellulose*. R.L. Whistler, Ed. Academic Press, New York, London, 1963: 49–54.
- 71 M. Eppstein, J.A. Lewin. *J. Polymer Sci.*, 1962; 58: 1023.
- 72 J. Potthast, A. Röhring, Th. Rosenau, H. Sixta, P. Kosma: *Cellulose Chemiker Rundgespräch*. Wiesbaden, 2002: 73–90.
- 73 M. Lüdtke: *Papierfabrikant*, 1934: 509–528.
- 74 M. Okubo, H. Sobue: Determination of carboxyl groups in cellulosic materials with the “Dynamic ion exchange method”. *Tappi J.*, 1956; 39: 415–417.
- 75 H. Doering: Carboxylgruppenbestimmung in Zellstoffen mit Komplexon. *Das Papier*, 1956; 10: 140–141.
- 76 K. Wilson: Determination of carboxyl groups in cellulose. *Svensk. Papperstidn.*, 1966; 69: 386–390.
- 77 TAPPI om T 237 (1993); Carboxyl content of pulp.
- 78 O. Ant-Wuorinen: The reactivity of the carboxyl groups of cellulose. *Pap. Puu*, 1952; 34: 195–201.
- 79 S. Beatson, R.P. Katz, A.M. Scallan: The determination of strong and weak acidic groups in sulphite pulps. *Svensk. Papperstidn.*, 1984; 87: R48–R53.
- 80 M. Beck, H. Rebek: Zur Charakterisierung des Verhaltens von Cellulose mit Hilfe von Kristallviolettbase. *Das Papier*, 1955; 13: 1–5.
- 81 G.F. Davidson: The acidic properties of cotton cellulose and derived oxycelluloses. Part II: The adsorption of methylene blue. *J. Text. Inst.*, 1948; 39: T65–T71.
- 82 E. Merck, Ed., *Chemisch-technische Untersuchungsmethoden für die Zellstoff und Papierfabrikation*. Verlag Chemie Darmstadt, 1957: 134.
- 83 Zellcheming-Merkblatt IV/30/68 (1967); Schnellbestimmung der Kupferviskosität von Zellstoffen (Betriebsmethode).
- 84 ISO 5351–1 (1981); Cellulose in dilute solution; Determination of limiting viscosity number; Method in cupriethylene-diamine (CDE) solution.
- 85 ISO 5351–2 (1981); Cellulose in dilute solution; Determination of limiting viscosity number; Method in iron (III) sodium tartrate complex (EWNN<sub>mod</sub> NaCl) solution).
- 86 Zellcheming-Merkblatt (1969); Determination of the Intrinsic Viscosity Number in EWNN(mod, NaCl).
- 87 J. Immergut, E.H. Brandrup, E.A. Grulk, Eds., *Polymer Handbook*. John Wiley, New York, 1999.
- 88 P.H. Weidinger, A. Hermans: *J. Polymer Sci.*, 1949: 135.
- 89 T. Serimaa, R. Paakari, H.P. Fink: *Acta Polym.*, 1989; 40: 731–734.
- 90 T.C. Maloney, H. Paulapuro: The formation of pores in the cell wall. *J. Pulp Paper Sci.*, 1999; 25(12): 430–436.
- 91 L.G. Aggrebrandt, O. Samuelson: *J. Appl. Polymer Sci.*, 1964; 8: 2801.
- 92 J.E. Stone, C.T. Maloney: A structural model of the cell wall of water swollen wood pulp fibres based on their accessibility to macromolecules. *Cellulose Chem. Technol.*, 1968; 2(3): 343–358.
- 93 J. Böttger, P.C. Le Thi, Th. Krause: Untersuchungen zur Porenstruktur von Zellstofffasern. *Das Papier*, 1983; 37(10A): V14–V21.
- 94 Th. Krause, P.C. Le Thi: Faserstruktur, Wasserbindung, Trocknung. *Das Papier*, 1985; 39(10A): V24–V31.
- 95 S. Brunauer, P.H. Emmet, E.J. Teller: The adsorption of gases in multimolecular layers. *J. Am. Chem. Soc.*, 1938; 60: 309.
- 96 W.R. Hasselton: Gas adsorption by wood, pulp, and paper. I. The low-temperature adsorption of nitrogen, butane, carbon dioxide by sprucewood and its components. *Tappi J.*, 1954; 37(9): 404–412.
- 97 J.E. Stone, L.F. Nickerson: A dynamic nitrogen adsorption method for surface area measurement of paper. *Pulp Paper Can.*, 1963; 64(3): T155–T161.
- 98 M.V. Merchant: A study of water-swollen cellulose fibers which have been liquid-exchanged and dried from hydrocarbons. *Tappi J.*, 1957; 40(9): 771–781.
- 99 M. Lewin, H. Guttman, N. Saa: New aspects of the accessibility of cellulose. *J. Appl. Polymer Sci.*, 1976; 29: 791–808.

- 100 K. Schwertassek: Beschreibung der Methode zur Bestimmung der Iodadsorption, der reduzierten Iodadsorption und der Normalmercerisation. *Faserforsch. Textiltechn.*, 1952; 3(3): 87–95.
- 101 M. Lewin, J.A. Eppstein: *J. Polymer Sci.*, 1962; 58: 1023.
- 102 J. Dechant: Eine Methode zur Bestimmung der Zugänglichkeit von Cellulose durch Deuteriumaustausch. *Faserforsch. Textiltechn.*, 1967; 18(6): 263–265.
- 103 A.J. Stamm: *Internal surface and accessibility in wood and cellulose science*. Ronald Press, New York, 1964: 186–200.
- 104 Zellcheming-Merkblatt IV/33/57 (1957); Bestimmung des Wasserrückhaltevermögens.
- 105 ISO 23713 (2003); Water Retention Value.
- 106 U. Weise, T. Maloney, H. Paulapuro: Quantification of water in different states of interaction with wood pulp fibres. *Cellulose*, 1996; 3(3): 189.
- 107 W. Kiessig, H. Koblitz: Der Anteil von Adsorptionswasser bei der Quellung von Cellulosefasern. *Das Papier*, 1960; 14(5): 179–185.
- 108 D. Klemm, et. al. *Comprehensive Cellulose Chemistry*, Vol. 1. Wiley-VCH, Weinheim, 1998: 48.
- 109 R.A. Nelson: The determination of moisture transitions in cellulose materials using differential scanning calorimetry. *J. Appl. Polymer Sci.*, 1977; 21: 645–654.
- 110 M.F. Froix, R. Nelson: The interaction of water with cellulose from NMR relaxation time. *Macromolecules*, 1975; 8(6): 726–730.
- 111 SCAN G-4 (1972); Fibre analysis of pulp and paper; Herzberg stain.
- 112 ISO/DIN 9184 (1990); Paper, board and pulps; Fibre furnish analysis Herzberg staining tests.
- 113 P. Klemm: *Handbuch der Papierkunde*, Grieben, Leipzig, 1923.
- 114 Zellcheming-Merkblatt IV/55/74 (1974); Prüfung von Zellstoff und Papier. Anfärbemethoden für mikroskopische Untersuchungen.
- 115 TAPPI om T 401 (1988); Fiber analysis of paper and board.
- 116 E. Sutermeister: *Chemistry of pulp and paper making*. New York, 1920.
- 117 E.L. Selleger: *Papierfabrikant*, 1903: 537.
- 118 H. Bucher: *Textil-Rundschau*, 1964: 119–132.
- 119 B. Werthmann. In: *Prüfung von Papier, Pappe, Zellstoff und Holzstoff*, W. Franke, Ed. Springer, Berlin, 1993: 66–99.
- 120 A. Herzog: *Mikroskopischer Atlas der technisch wichtigen Pflanzenfasern*, E. Correns, W. Frenzel, Eds. Akademie Verlag, Berlin, 1955.
- 121 ISO 16065–1 (2001); Pulps; Determination of fibre length by automated optical analysis. Part 1: Polarized light method.
- 122 TAPPI cm T 232 (1985); Fiber length of pulp by projection.
- 123 TAPPI om T 271(1998); Fiber length of pulp and paper by automated optical analyzer using polarized light.
- 124 TAPPI pm T 261 (1990); Fines fraction of paper stock by wet screening.
- 125 ISO 9184–6 (1990); Paper, board and pulps – Fiber furnish analysis. Determination of fibre coarseness.
- 126 N. Hartler, J. Nyrén: *Tappi J.*, 1970; 53(5): 820.
- 127 P.A. Tam Doo, R.J. Kerekes: A method to measure wet fiber flexibility. *Tappi J.*, 1981; 64: 113–116.
- 128 R.J. Kerekes, P.A. Tam Doo: Wet Fibre Flexibility of Some Major Softwood Species Pulped by Various Processes. *J. Pulp Paper Sci.*, 1985; 11(2): 160.
- 129 T. Hattula, H. Niemi: Sulphate pulp fibre flexibility and its effect on sheet strength. *Pap. Puu*, 1988; 2: 356–361.
- 130 ISO 5269–1 (1989); Testing of pulps; preparation of laboratory sheets for physical testing Conventional sheet former method.
- 131 ISO 5269–2 (1989); Testing of pulps; preparation of laboratory sheets for physical testing; Rapid-Köthen method.
- 132 TAPPI om T 205 (1988); Forming hand-sheets for physical test of pulp.
- 133 SCAN C 26 (1976); Pulp; Preparation of laboratory sheets for physical testing.
- 134 ISO 1924–1 (1992); Paper and board; determination of tensile properties; part 1: Constant rate of loading method.
- 135 ISO 1924–2 (1992) Paper and board; determination of tensile properties; part 2: Constant rate of elongation method.

- 136 TAPPI pm T 556 (1995); Bending resistance of paper and paperboard (Lorentzen & Wettre type tester).
- 137 DIN 53121 (1996); Testing of paper and board; Determination of the bending stiffness by the beam method.
- 138 DIN 53123 (1978 ); Bestimmung der Biegesteifigkeit: Resonanzlängenverfahren.
- 139 ISO 3688 (1977); Pulps; Measurement of diffuse blue reflectance factor (ISO-brightness).
- 140 DIN 53145-1 (2000); Testing of paper and board; Basic parameters for determination of reflectance factor – Part 1: Measurements made on non-fluorescent specimens.
- 141 DIN 53145-2 (2000); Testing of paper and board; Basic parameters for determination of reflectance factor – Part 2: Measurements made on fluorescent specimens.
- 142 ISO 5264-3 (2000); Pulps; Laboratory beating. Part 3: Jokro mill method.
- 143 DIN 54360 (2004 ); Faserstoff – Labor-mahlung; Jokro-Mühle-Verfahren.
- 144 ISO 5264-2 (1979); Pulps; Laboratory beating. PFI mill method.
- 145 TAPPI om T 227 (1994); Freeness of pulp (Canadian standard method).
- 146 DIN EN ISO 5267-1 (2000); Pulps; Determination of drainability. Part 1: Schopper-Riegler method (ISO 5267-1:1999).
- 147 S. Forsberg, M. Bengtsson: *The Dynamic Drainage Analyzer (DDA)*. Papermakers Conference Atlanta, GA. Tappi Press, 1990: 239.
- 148 N.T. Kleinert, L-M. Marracini: Aging and colour reversion of bleached pulps. Part 1: Peroxide formation during aging. *Svensk. Papperstidn.*, 1962; 65(4): 126–131.
- 149 N.T. Kleinert, L.-M. Marracini: Aging and color reversion of bleached pulps. Part 2: Influence of air and moisture. *Svensk. Papperstidn.*, 1963; 66(6): 189–195.
- 150 N.T. Kleinert, L.-M. Marracini: Aging and color reversion of bleached pulps. Part 4: The role of aldehyde groups. *Svensk. Papperstidn.*, 1963; 69(3): 69–71.
- 151 E.L. Back: Thermal auto-crosslinking in cellulose material. *Pulp Paper Can.*, 1967; 68: T165–T171.
- 152 ISO 5630-1 (1982); Paper and board; Accelerated ageing; Part 1: Dry heat treatment.
- 153 ISO 5630-2 (1982); Paper and board; Accelerated ageing; Part 2: Moist heat treatment at 90 degrees C and 25% relative humidity.
- 154 ISO 5630-3 (1996); Paper and board; Accelerated ageing; Part 3: Moist heat treatment at 80 °C and 65% relative humidity.
- 155 M. Käßberger, G. Dessauer, H. Stark: Der Grazer Alterungstest: der dynamische Alterungstest von Papier und Karton. *Das Papier*, 1998; 52 (9): 529–531.

## Index

### a

- AA *see* active alkali
- AAS *see* atomic absorption spectroscopy
- abaca, cell dimensions and chemical composition 4
- Abies alba*
  - average cell dimensions 52
  - inorganic composition 40
  - resin acid composition 36
- Abies balsamea*
  - chemical composition of wood 23
  - hemicelluloses, nonglucosic units 29
- Abies grandis*, resin acid composition 36
- abietic acid, structure 183
- abrasive minerals, pulp stone 1093
- absorbed sulfide ions, saturation level 242
- absorbency, beechwood sulfite dissolving pulp 433–434
- absorption coefficient spectra, unbleached and bleached hardwood sulfite pulp 611
- Acacia mollissima*, chemical composition of wood 23
- Acanthamoeba castellanii* 24
- accelerated aging 1284
- accept flow rate, screening operating parameters 575
- accessibility
  - cell wall 1052–1056
  - towards molecules of a solvent 1265–1267
- accessory compounds
  - hardwoods 37–39
  - softwoods 35–37
  - woods 33
- Acer pseudoplatanus*, density and void volume 128
- Acer rubrum*
  - chemical composition of wood 23
  - hemicelluloses, nonglucosic units 29
  - inorganic composition 40
  - kinetic parameters for xylan water prehydrolysis 333
- Acer saccharum*
  - chemical composition of wood 23
  - chip storage 99
- acetate
  - hot caustic extract 961
  - ozone decomposition, inhibitor 789
- acetic acid
  - black liquor composition 968
  - cellulose protecting additive 819
  - content as function of H-factor 447
  - polysaccharide chain cleavage 662
  - spent liquor content as function of viscosity 457
- acetone extractives, dissolving pulp characterization 1061
- acetone extractives content 1032
- acetovanillone, structure 308
- acetyl, content as function of pH 474
- acetylation, cold alkali extraction 1046
- acid–base equilibria, white liquor 117
- acid bisulfite pulping process, pH range 393
- acid-catalyzed hydrolysis, dissolved hemicellulose fragments 341
- acid degradation reactions, wood hemicelluloses 327–329
- acid dissociation constants, white liquor 117
- acid hydrolysis
  - carbohydrates reactions 416–425
  - cellulose 416–418
  - influence of substituents 417
- acid-insoluble ash, inorganic components 1220
- acid sulfite cook
  - aspen 468
  - beech magnesium 435–437, 439
- acid sulfite cooking
  - chemistry 405–427

- one-stage cooking parameters 452
- acid sulfite cooking chemistry, lignin reactions 407–416
- acid sulfite cooking cycle, temperature-, pressure- and H-factor profiles 427
- acid sulfite cooking liquor
  - parameters 396
  - SO<sub>2</sub> partial pressure 402
- acid sulfite dissolving pulp 806
- acid sulfite processes, dissolving pulp 1024
- acid sulfite pulping process chemistry 427–465
  - cooking conditions 459–465
  - influence of reaction conditions 449–464
- acid-treated pulp, hydrogen peroxide lifetime 855
- acidic conditions, hydrogen peroxide application 877
- acidic peroxide, ozone treatment 821
- acidic sulfite cooking, side reactions 423
- acidification 811
- acidified DMSO, ozone treatment 821
- acidifying 815
- acidimetry, operating principle 1221
- activation, dioxygen 642–644
- activation energy
  - delignification 201–202
  - xylan hydrolysis from *Eucalyptus saligna* 343
- activators, hydrogen peroxide bleaching 880
- active alkali, kraft cooking active chemicals 114
- active chlorine
  - oxidation capacity 613
  - oxidation equivalents (OXE) 264
- active chlorine amount, effect on brightness development 766
- active kraft cooking chemicals, specific consumption in selected model of kraft cooking kinetics 221
- active species, polysulfide CBC cooking 291
- additives, ozone bleaching 818–822
- ADS *see* air density separator
- adsorbable organic compounds 771
- adsorbable organic halogen *see* AOX
- adsorbable organically bound halogen 1000
- adsorbed water layer, thickness 800
- advanced liquor management 366
- AEC *see* anion-exchange chromatography
- AFM *see* atomic force microscopy
- ageing
  - accelerated 1284
  - alkali cellulose 1057
  - pulp 1284
- agitators
  - bleaching equipment 627–628
  - pulp bleaching 1134
- agricultural fibers, cell dimensions and chemical composition 4
- AGU *see* anhydroglucose units
- Ahlmix, Sulzer 621
- AHQ
  - AQ/AHQ redox system 318
  - pulping aid 170, 315, 318–321
- air core, hydrocyclone 580
- air density separator 94
- air entrainment
  - in relation to relative pressure washer capacity 534
  - pulp washing parameter 534–535
- air impact, wind screening 93
- air removal, effect of steaming 131
- air replacement, kraft cooking pretreatment 129
- Al-Dajani *see* Gustavson and Al-Dajani kinetic model
- alcohols, ozone reactions 792
- aldehydes, ozone reactions 792
- alditol acetate, synthesis 1232
- aldonic acid
  - formation 423
  - residues, relative composition 658
  - stabilization of reducing end-groups 657
- alien particles, solution 1249
- aliphatic carboxylic acids, black liquor composition 968
- aliphatic hydroxyl, content in lignin samples 636
- aliphatic hydroxyl groups, elimination during kraft cooking 261
- alkali
  - concentration profile 237–241, 276–277
  - consumption 220–221
  - kraft cooking active chemicals 114
- alkali amount, effect on chemical oxygen demand 878
- alkali cellulose, ageing 1057
- alkali charge
  - effect on delignification 700
  - oxygen delignification 703–704
  - selectivity improvement 720
- alkali resistances 347, 353, 365, 439–441, 448, 832–835, 838–839, 943–944, 953–959, 963, 1015–1016, 1043–1044, 1060, 1062, 1229
- alkali solubility tests 1060

- as function of H-factor 442
- as function of P-factor in unbleached Visbatch<sup>®</sup> pulp 354
- commercial paper-grade pulp 1013
- comparison with xylan contents 957–959
- dissolving pulp characterization 1062
- NaOH dependence 954–955
- paper pulp 1015
- purification yield 958
- temperature dependence 957, 962
- viscosity as function of R18 363
- *see also* R10, R18
- alkali solubility, pulp specification 1060
- alkali-soluble components, pulp 1229
- alkali source 706–708
  - alternative 962–963
- alkali-stable chromophores 258
- alkaline ageing, molecular weight reduction 1059
- alkaline decomposition, hydrogen peroxide decomposition 862–863
- alkaline extraction 824–826
- alkaline hydrolysis 178
  - glycosidic linkages 178
- alkaline peroxide bleaching, catalyst 877
- alkaline pulp suspension, solubility of oxygen 693
- alkaline-soluble impurities, removal 951
- alkaline sulfite 475–482
- alkaline sulfite-anthraquinone-methanol *see* ASAM
- alkaline sulfite pulping process, pH range 393
- alkalinity, black liquor 120
- alkalization 938
- $\beta$ -alkoxy elimination 177, 934
- alkyl-(R), ozone decomposition, inhibitor 789
- Alnus incana*, chemical composition of wood 23
- alternative bleaching methods 885–887
- alternative sulfite pulping concepts 465–482
  - alkaline sulfite 475–482
  - AS/AQ 476–482
  - magnefite process 466–467
  - Sivola processes 468–471
  - Stora processes 472–475
  - two-stage neutral magnefite process 467–468
- aluminum sulfate, addition 710
- American beech, average moisture content 125
- American Elm, average moisture content 125
- [2-(2-aminooxyethoxy)ethoxy]amide 1016
- ammonium hydrogen sulfite 404
- Andritz Dynamic steam heater 622
- Andritz HHQ<sup>™</sup> chipper 83–84
- Andritz HQ<sup>™</sup>-sizer 86–87
- Andritz Lo-Level heat recovery system 391
- Andritz TurboFeed system 381–382
- Andritz two-stage DD washer 550
- angiosperms, lignin 30
- anhydro-sugar units
  - hemicelluloses 28
  - peeling 175–176
- anhydroglucose units 822
  - cellulose structure 24
- anion-exchange chromatography 939
- anion radical, superoxide 646
- anisotropy, orientation 1265
- annual ring, softwoods 51
- annular differential volume element, screening theory 566
- anthraquinone *see* AQ
- anthraquinone pulping 314–325
  - *see also* AQ
- AOX 17, 609, 740–742, 764, 767–777, 846–848, 1000–1001, 1005–1006
  - efficiency of chlorine dioxide 769
  - formation 774, 843
  - levels 773
  - load 775
  - *see also* adsorbable organically bound halogen
- aperture velocity 565
  - in relation to fiber passage ratio 576
- apex flow, hydrocyclone 579–580
- apparent rate constants, hardwood prehydrolysis 334
- AQ 195, 200–201, 476–481, 667
  - *a*-aryl ether structures degradation paths 320
  - combined effects of PS and AQ pulping 314–316
  - effect on kappa number–H-factor relationship 322
  - PS/AQ mill experience 316
  - *see also* soda-AQ
- AQ/AHQ redox system 318
- aquatic environment 1004–1007
- aqueous acidic compounds, polysaccharides treatment 327
- aqueous extracts, general properties 1225
- aqueous sodium hydroxide solution
  - pulp treatment 934
  - reactions 935–941

- aqueous solvents, cellulose molecular weight determination 1240
- arabinoglucuronoxylan *see* AX
- arabinonic acid
  - content in aldonic acid residues 658
  - formation 659
- D-arabinonic acid, polysaccharide chain cleavage 662
- arabinose
  - commercial paper-grade pulp 1013
  - concentration development in beechwood prehydrolysis 337–338
  - content as function of H-factor 447
  - ozonation 796
  - pulp fraction 440
- arabinoxylan
  - yield as function of lignin yield 481
  - *see also* AX
- aromatic compounds, from sugar dehydration under acidic conditions 420
- aromatic molecules, ozone reactions 790
- aromatic rings
  - chlorination 745
  - hydroxylation 790
- aromatic structures
  - carbohydrate dehydration to 419–421
  - hydroxyl radical adducts 653–654
- aryl-(R), ozone decomposition, promotor 789
- $\alpha$ -aryl ether structures, AQ degradation paths 320
- $\beta$ -aryl ether structures
  - correlation with bleachability 265
  - correlation with H-factor 266
  - oxygen pressure influence 708
  - residual lignin 174
  - sulfonation and condensation 410
- AS *see* alkaline sulfite pulping
- AS pulp, bleachability 478
- AS/AQ 17–18, 476–482
  - course of pH and temperature in pine pulping 479
  - liquor composition and yields in comparison to kraft pulping 476
  - spruce selectivity plot 479
  - wood component yield–lignin yield relation 481
- ASAM 273–274, 478, 809, 1024
  - alternative to kraft pulping 17
  - spruce wood nanostructure during pulping 57
- ASAM pulp
  - bleachability 273
  - brightness gain in relation to consumed OXE 273
- ash
  - acid-insoluble 1220
  - components, distribution in pulp 1034
  - density and void volume 128
  - inorganic components 39
  - pulp 1220
  - pulping yields 110
  - sulfated 1220
  - white (average moisture content) 125
- aspen
  - average moisture content 125
  - chemical composition 451
  - density and void volume 128
  - Sivola process cooks 468
  - viscosity–H-factor relationship 452
- aspiration, pits closing 47
- atmospheric diffuser
  - Kvaerner double 553
  - pulp washing equipment 552–554
- atmospheric downflow reactors, bleaching equipment 624–625
- atmospheric emissions 1002–1004
  - kraft pulp mills 1003
- atmospheric peroxide bleaching 866–867
- atmospheric screens, screening and cleaning equipment 604–605
- atmospheric steam mixers, bleaching equipment 622–623
- atmospheric upflow reactors, bleaching equipment 623–624
- atomic absorption spectroscopy 1222–1223
- atomic force microscopy 60
- Aucoumea klaineana*, diffuse-porous hardwoods 53
- autocatalysis 644
- autocausticization 994
- autohydrolysis 326
- automation, wood yard operations 95
- autoxidation, oxygen 644–645
- average crystallite length 1263
- average moisture content, green wood 125
- avoidance of waste, waste strategy 1192
- Avrami-Erofeev's concept, nuclei growth 679
- AX 285–286
  - arabinoglucuronoxylan 251–252, 276
  - arabinoxylan 198, 211, 215
  - dissolution in CBC process 284
  - 4-O-methylglucuronoarabinoxylan 110, 186–188, 226
  - removal in CBC process 286

- axial concentration profile
  - Kazi and Chornet diffusion model of impregnation 153
  - numerical solution of diffusion equation 162–163
- axial impregnation, NaOH concentration profile 154
- axial parenchyma
  - hardwoods 54
  - softwoods 51
- axial velocity profile, hydrocyclone 581
- AZP sequence 949
  
- b**
- B.I.R. *see* Bureau International de la Recuperation
- baldcypress, average moisture content 125
- balsam fir, chemical composition of wood 23
- bamboo fibers, cell dimensions and chemical composition 4
- BAR *see* benilic acid rearrangement
- bark
  - lignins 33
  - selective removal 593
- bark and chips, waste generation 105
- bark cells 1076
- barrier separation 563
- base flow, hydrocyclone 579–580
- basic statistics, recovered paper 1165–1176
- Basidiomycetes*, alternative bleaching methods 886
- bast fibers, cell dimensions and chemical composition 4
- batch cooking
  - comparison of results 274–295
  - equipment in comparison to continuous cooking 366
  - standard 229–234
  - technology and equipment 367–376
- batch digesters 367–368
- Bauer-McNett apparatus, fiber fractionation 1274
- beating, pulp 1281
- beating resistance, pulp 1011
- beech, chemical composition 360, 451
  - density and void volume 128
  - Visbatch<sup>®</sup> process conditions 365
  - viscosity–H-factor relationship 452
- beech acid sulfite dissolving pulp 806
  - drying conditions 1056
- beech magnesium acid sulfite cook
  - carbohydrate derived components as function of H-factor 447
  - cellulose, R10/R18 and H-factor 442
  - $\beta$ - and  $\gamma$ -cellulose as function of H-factor 443
  - COOH and xylan content 441
  - dissolved wood components and degradation products 446
  - H-factor–SO<sub>2</sub> amount relation 435
  - pulp composition 439
  - residual xylan–H-factor relation 444
  - wood component yield 438
- beech sulfite cooks, pulp and spent liquor compositions 448
- beech sulfite dissolving pulp
  - alkalization 938
  - degree of crystallinity 1042
  - differential MWD 845, 1040
  - PZ-treatment 1040
  - ZP-treatment 1039
- beechwood
  - carbohydrates and xylose concentration in prehydrolysis 336
  - composition 330
  - kinetic parameters for prehydrolysis weight-loss 332
  - water prehydrolysis wood yield temporal development 331
  - *see also Fagus sylvatica*
- beechwood acid magnesium bisulfite pulping, HSO<sub>3</sub><sup>–</sup>–H-factor relation 460
- beechwood acid sulfite cooking, wood components degradation 437–449
- beechwood sulfite dissolving pulp, viscosity–extinction 433
- belt conveyor, log handling 98
- belt washers, pulp washing equipment 551–552
- benilic acid rearrangement 176
- benzylum cation
  - electron density distribution 409
  - formation 409
  - LUMO-distribution 409
- benzylum ion, condensation reaction with weakly nucleophilic resonance form 415
- BET method 1267
- Betula* 37
- Betula papyrifera*
  - chemical composition of wood 23
  - inorganic composition 40
  - kinetic parameters for xylan water prehydrolysis 333
- Betula pendula*
  - black liquor composition 968
  - chemical composition 360, 451



- Betula verrucosa*
  - chemical composition of wood 23
  - diffusion coefficient 148–149
  - hemicelluloses, nonglucosic units 29
- Bevan, Edward J. 7
- bicarbonate-buffered peroxide solutions, stability in water 863
- bio-refinery 994
- biochemical oxygen demand (BOD) 72, 629, 1001, 1005, 1138
  - increased 72
- biodegradation plants, effluent treatment 1001
- biological oxygen demand 1138
- biomass, yearly production 15
- birch
  - black liquor composition 968
  - chemical composition 360, 451
  - diffusion coefficient 148–149
  - Lo-Solids™ laboratory cooks 301–302
  - Visbatch® process conditions 365
  - viscosity–H-factor relationship 452
- birch lignin 33
- birch wood 37
- bisulfite, pH range 393
- bisulfite-acid sulfite process 468–469
- bisulfite-MgO process 467–468
- bisulfite-neutral sulfite process 468–469
- bisulfite processes 466–471
- bisulfite(-soda) cook, aspen 468
- bitternut hickory, average moisture content 125
- Bjerrum diagram, conventional kraft cook 118
- black cooks 406
- black liquor
  - acetic acid 968
  - aliphatic carboxylic acids 968
  - alkalinity 120
  - boiling point 970
  - characterization 967–970
  - chemical composition 967–970
  - composition 120, 967–970
  - density 971
  - 3-deoxypentonic acid 968
  - dry solids content 971
  - dynamic viscosity 136
  - evaporation 974–980
  - excess heat capacity 973
  - fatty acids 967
  - fiber removal 371, 380
  - formic acid 968
  - gasification 18, 992–994
  - glucoisosacharinic acid 968
  - glycolic acid 968
  - heat capacity 973
  - heating values 969
  - hot *see* hot black liquor
  - 2-hydroxybutanoic acid 968
  - kraft pulping 111–112
  - kraft recovery boiler 985
  - lactic acid 968
  - neutralization curve 121
  - organic constituents 967
  - physical properties 970–973
  - pre-thickening 975
  - recovery furnace 968
  - regeneration 112
  - resin 967
  - surface properties 136
  - surface tension 971
  - thermal conductivity 972
  - viscosity 970–973
  - warm black liquor 372–376
  - water content 979
  - xyloisosaccharinic acid 968
  - *see also* liquor(s), white liquor
- black liquor dissolved polysaccharides 967
- black liquor solids 983
  - heating values 969
- black spruce
  - effect of steam pressure during pre-steaming 130
  - kraft pulp sheets 800
- black wattle, chemical composition of wood 23
- bleach plant liquor circulation 887–894
- bleachability 634
  - $\beta$ -aryl ether structures 265
  - AS pulp 478
  - ASAM pulp 273
  - chromophore groups 726
  - correlation with  $\beta$ -aryl ether structures content 265
  - influence of modified kraft cooking 264–274
  - MCC-cooked pulp 296
  - TCF pulp bleaching 267
- bleached chemical pulp, global production 10
- bleached commercial paper pulp
  - fiber dimensions 1021
  - molecular weight distribution 1019
- bleached hardwood sulfite pulp, reflectance and absorption coefficient spectra 611
- bleached kraft pulp, emission levels 1005

- bleaching 25
  - activators 880
  - additives 818–822
  - alkaline peroxide bleaching 877
  - alternative bleaching methods 885–887
  - atmospheric downflow reactors 624–625
  - atmospheric peroxide bleaching 866–867
  - atmospheric steam mixers 622–623
  - atmospheric upflow reactors 623–624
  - *Basidiomycetes* 886
  - bis-creosol 746
  - brightening stages 613
  - brightness *see* brightness
  - 4-carbomethoxymethyl-4-methylbutenolide 746
  - carbonyl groups 1234
  - catalyzed peroxide bleaching 877
  - caustic soda charge 1128
  - CEHDED 313
  - chelation 1126
  - chemical 868–880
  - chlorine dioxide *see* chlorine dioxide bleaching
  - chlorite formation 738
  - cobalt (II) salts 709
  - consistency 1128
  - delignification selectivity 809
  - diarylmethane 747
  - diffusion control 800
  - dithionite 1124–1126
  - ECF *see* ECF bleaching
  - effluent volume 892
  - electrochemical delignification 887
  - elemental chlorine-free 1000
  - final stage 756, 1038
  - generic stage set-up 616–617
  - hardwoods 1126
  - high consistency ozone 617, 806, 827
  - high-shear mixers 620
  - hydrogen peroxide *see* hydrogen peroxide bleaching
  - hydroxyl radical 777
  - iron (III) salts 709
  - Keggin-type metal clusters 887
  - laccase mediator-system 886
  - lignin-conserving 1126
  - lignin-degrading fungi 886
  - low-consistency ozone 806–807, 809
  - magnesium hydroxide 1130
  - mechanical pulp 1123–1136
  - medium consistency (MC) 616
  - metal clusters 887
  - modified 761–771
  - offgas 867
  - operations 613–628
  - operations and equipment 613–628
  - OXE 271, 612–613, 847
  - oxidative bleaching 1041
  - oxygen delignification 628–734
  - oxygen-alkali 633
  - ozone *see* ozone bleaching
  - peroxide 1132, 1134
  - phenolic hydroxyl groups 848
  - *Picea* 1126
  - *Pinus* 1126
  - polyoses 1123
  - polyoxometalates 887
  - *Populus* 1126
  - pressurized peroxide 866–867
  - pressurized reactors 625–627
  - pulp 609–894
  - P-Y 1132
  - QPQP bleaching 267–271
  - reactors 866–867
  - reductive 1134
  - retention time 802
  - sodium borohydride 1125
  - sodium peroxide 849
  - sodium silicate stabilization 1129
  - softwoods 882, 1126
  - specific volume 1131
  - static ozone bleaching 800
  - TCF *see* TCF bleaching
  - two-stage processes 878
  - vanillin 747
  - washing 628, 866–867
  - white rot fungi 886
  - yield 863–865, 878
  - Y-P bleaching 1131
  - *see also* pulp bleaching
- bleaching chemicals
  - classification 610–613
  - most important 264
  - oxygen-based 777
  - reactivity 611
- bleaching equipment, agitators 627–628, 1134
  - blowtank 627
  - medium consistency mixers 619–623
  - medium consistency pumps 617–619
  - medium consistency reactors 623–627
- bleaching methods, alternative 885–887
- bleaching plant, two-stage 1136
- bleaching reactions 1227
  - selectivity 838
- bleaching sequence, CCE 948–949

- bleaching stages
    - operation 890–893
    - ozone placement 843–849
  - BLG *see* black liquor gasification
  - blowtank
    - bleaching equipment 627
    - medium-consistency ozone delignification system 826
    - pressurized peroxide bleaching system 867
  - BLPS *see* black liquor dissolved polysaccharides
  - Blue gum, chemical composition of wood 23
  - board, recovered, european list of standard grades 1203–1210
  - board production, fiber material consumption 1153
  - BOD *see* biochemical oxygen demand, *see also* biological oxygen demand
  - boiler bank, kraft recovery boiler 981
  - boiling point
    - hydrogen peroxide 851
    - rise 970–971
  - bongossi, stem section 58
  - boom-type stacker reclaimer, chip storage 103
  - bordered pits 47
    - cell components 46
    - softwood fibers 123
  - borol charge 823
  - Bouchard, concept 798
  - bound water 1268
  - BPR *see* boiling point rise
  - Bragg's law 1223
  - brightening, chlorine dioxide bleaching 757
  - brightening stages, pulp bleaching 613
  - brightness 1033
    - as function of residual effective alkali 272
    - commercial paper-grade pulp 1013
    - dependence on delignification 870
    - dissolving pulp characterization 1062
    - effect of adding chlorine dioxide 763
    - effect of dissolved organic material 817
    - efficiency of chlorine dioxide 769
    - in ITC-type and ASAM pulp 273
    - ISO Standard method 610
    - ITC-type pulp 273
    - post-treatment with peracetic acid 883
    - pulp bleaching 1127–1130
    - QPQP bleaching 271
    - second chlorine dioxide stage 758
    - spruce sulfite pulp 879
    - stability 876
      - stabilization with hydrogen peroxide 873–876
      - TCF-bleached dissolving pulp 1049
  - brightness decrease, carry-over effect 816
  - brightness development 876
    - chlorine amount 766
    - hydrogen peroxide application 871
    - in QPQP bleaching as function of consumed OXE 271
  - brightness gain 758
    - in relation to consumed OXE 273
    - selectivity comparison 838
  - brightness increase 879
    - hydrogen peroxide application 867
    - peroxide amounts 1127
    - spruce sulfite pulp 879
  - brightness level, pulp 1123
  - brightness losses, aging 876
  - brightness measurement, ISO Standard method 610
  - brightness reversion 875
  - bromination, lignin 316
  - brownish cooks 406
  - brownstock washing 1004
  - BS *see* bisulfite processes
  - BS-AS *see* bisulfite-acid sulfite process
  - BS-NS *see* bisulfite-neutral sulfite process
  - bucket elevator, log handling 98
  - bulk phase, kraft pulping reactions overview 184
  - bulk water 1052
  - bull screen 1115
  - bump rotor, cross section 564
  - buoyancy force, on settling particle 581
  - Bureau International de la Recuperation 1157
  - Burgess, Hugh 5
  - t*-butyl alcohol, ozone decomposition, inhibitor 789
- c**
- <sup>13</sup>C-CP/MAS-NMR, degree of crystallinity 1042
  - Cadoxen, cellulose molecular weight determination 1240
  - calcium hydrogen sulfite, diffusion coefficient at 20 °C 404
  - camphor 37
  - Canadian Standard Freeness
    - freeness determination 1282
    - values 1283
  - caoutchouc 38

- capacity
  - pressure screen 575
  - pressure washer 533–536
  - rotary drum pressure washer 529
- capillary electrophoresis *see* CE
- carbazole-9-carboxylic acid [2-(2-aminooxy-ethoxy)-ethoxy]-amide *see* CCOA
- carbohydrate composition 938
  - effect of modified kraft cooking 251–256
  - jack pine sulfite and kraft pulp 470
  - spruce 251
- carbohydrate degradation 832
  - kinetics 215–216
- carbohydrate-derived chromophores 181
- carbohydrate-derived components, as function of H-factor 447
- carbohydrate oxidation, charge transfer complexes 321
- carbohydrate reactions
  - acid hydrolysis 416–425
  - dioxygen-alkali delignification processes 657–666
- carbohydrate residues, structures 668
- carbohydrate yield
  - effect of polysulfide added to impregnation liquor 292
  - in relation to lignin content in alkaline pulping 186
  - increase by polysulfide pretreatment 311
- carbohydrates
  - alkali-soluble 1230
  - commercial paper-grade pulp 1013
  - composition of pulp in conventional batch and CLF (continuous liquor flow) cook 255
  - concentration development in beechwood prehydrolysis 336, 338
  - degradation 794
  - degradation in kraft cooking kinetics models 193–198
  - dehydration to aromatic structures 419–421
  - dissolution in CBC process 284
  - glycosidic bond cleavage 830
  - hydrogen abstraction 795
  - hydrogen peroxide reactions 859–860
  - kraft pulping reactions 174–181
  - low molecular weight 933
  - molecular weight decrease 825
  - oxidative cleavage 663
  - pulping yields 110
  - removal 951
  - sulfur-containing 421–425
- 4-carbomethoxymethyl-4-methylbutenolide, chlorine bleaching 746
- carbon dioxide, polysaccharide chain cleavage 662
- carbon-hydrogen bonds, ozone insertion 791
- carbonate ion, molar concentration in white liquor 115
- carbonium-oxonium ion
  - electron density distribution 417
  - LUMO-distribution 417
- carbonyl
  - dissolving pulp characterization 1062
  - functional groups 1037–1041
- $\alpha$ -carbonyl, structure and relative oxygen susceptibility 640
- carbonyl formation, ozonation effect 840
- carbonyl functions 1234–1238
- carbonyl groups 1039–1040
  - commercial paper-grade pulp 1014
  - profile 1017
  - reduction by sodium borohydride 1236
- $\alpha$ -carbonyl groups, photodegradation 655
- carboxy-furanosides, polysaccharide chain cleavage 662
- carboxyl
  - dissolving pulp characterization 1062
  - functional groups 1037–1041
- carboxyl functions 1238–1239
- carboxyl groups
  - commercial paper-grade pulp 1014
  - formation, ozonation effect 840
- carboxylic acid 714
- carboxylic acid groups
  - content as function of xylan 441
  - content in lignin samples 636
- carboxylic groups
  - determination 1239
  - enrichment during kraft cooking 261
- C-carboxy- $\beta$ -D-pentafuranoside, polysaccharide chain cleavage 662
- Carman–Kozeny relationship 513
- Caro's acid 880
- carry-over 716–719
  - dissolved matter 890
  - effect 816–818
- cascade feed-forward arrangement, two-stage screening 598
- cascade feedback arrangement
  - four-stage cleaning 597
  - three-stage screening 596
  - two-stage fractionation system 600
- catalyzed peroxide bleaching 877

- cathode lamp, atomic absorption spectroscopy 1223
- cation affinity, to cellulose 519
- caustic concentration, low 952
- caustic extraction 944
  - dissolving pulp 1026
- caustic soda 862
  - pulp bleaching 1128
- causticization, *in-situ* 994
- causticizer train 989
- causticizing 986–991
- CBC 9, 110, 282–294, 308, 346–347, 481–482
  - cooking cycle 376
  - course of temperature, pressure and effective alkali 283
  - effect of [OH<sup>-</sup>] 287–289
  - results 282–287
  - simplified flowsheet 375
  - technology and equipment 375–376
  - wood component removal in comparison to conventional cooking 286
  - wood component yield–lignin yield relation 481
  - *see also* VisCBC
- CBC process, effect of polysulfide added to impregnation liquor 290–293
- CBC pulp, strength properties 293–295
- CCE
  - placement 948–949
  - *see also* cold caustic extraction
- CCOA 1237
- CD *see* cold displacement
- CE 135, 181, 434, 629, 740, 767
  - acid sulfite cooking liquor analysis 433
- CED, cellulose molecular weight determination 1240
- CED-intrinsic viscosity 451
- CEHDED, bleaching sequence 313
- cell dimensions
  - agricultural fibers 4
  - average 52
- cell structure, wood characterization level 21
- cell types 48–50
- cell wall
  - structure 21, 1047–1051
  - ultrastructure 41–44
- cell wall layers
  - average thickness 43
  - S2 473
  - schematic illustration 41
  - Transmission electron micrographs 43
- cellobiose formation 665
- D-cellobioside, formation 664
- cellophane, global production 11
- cellular UV spectroscopy 44
- cellulose 11, 22, 26–27, 41, 47, 1034, 1240–1241, 1268
  - acid hydrolysis 416–418
  - alkali 1057
  - as function of H-factor 442
  - cation affinity 519
  - cell wall components 41
  - cellulose I 941, 1045
  - cellulose II 27
  - cellulose triacetate 1030
  - crystalline 1012
  - depolymerization 819
  - dissolving pulp applications 1026
  - DP *see* DP
  - $\beta$ -elimination of glycosidic bond 177
  - fibrillar structure 41–42
  - first indication 935
  - in relation to  $\beta$ - and  $\gamma$ -cellulose 443
  - lattice 935, 941, 1044–1045
  - molecular structure 25
  - molecular weight determination 1240
  - partially crystalline structure 1257–1258
  - phases 26
  - polymorphs 27
  - production of regenerated cellulose fibers 7
  - pulp fraction 440
  - pulping yields 110
  - purity 834, 836
  - relative acid hydrolysis rates 417
  - removal in CBC process 286
  - solubility in alkali 1229–1230
  - solvents 1025, 1240–1241
  - specific consumption in selected model of kraft cooking kinetics 221
  - structure 24, 939
  - supramolecular structure 25, 940
- $\alpha$ -cellulose 10–11, 279, 322, 470–471, 811, 840, 935, 1027, 1046, 1229–1230
  - as function of third stage pH and temperature 471
  - gain during HCE 952
  - time dependence 953
- $\alpha$ -cellulose content
  - ozonation 811
  - specific yield loss 949
- $\beta$ -cellulose 442–445, 934–936, 939–940, 946, 1027, 1229–1230
  - molecular weight distribution 443
  - weight-average molecular weight 445
- $\beta$ -cellulose fraction 939

- $\gamma$ -cellulose 442–443, 934–936, 938–940, 946, 1229–1230
- cellulose acetate, dissolving pulp
  - characterization 1061
- cellulose bleaching 1042
- cellulose chain scissions 685–687
  - effect of hydroxide concentration 195
  - kinetics 217
  - rate 194
- cellulose chains 41
  - oxidative peeling 663
  - stabilization 1039
- cellulose-containing materials, chemical composition 24
- cellulose content
  - high 1022
  - in relation to tear index 294
  - in softwoods and hardwoods 22
  - tear index 294
- cellulose degradation 720, 859
  - apparent kinetic expression 686
  - carbonyl groups reactions 1041
  - dependence on wood species 834
  - lignin effect 795
  - metals 668–671
  - under alkaline conditions 175
- cellulose fibers 1047
  - regenerated 7
- cellulose fraction, DP in relation to pulp yield for conventional and MCC<sup>®</sup> cook 256
- cellulose microfibrils, bordered pits 47
- cellulose products, discoloration 1027
- cellulose protection 710–711, 819
  - metals 668–671
- cellulose pulp, viscosity measurements 1251
- cellulose substrates, never-dried 1053
- cellulose viscosity 1059
- cellulose yield
  - as function of H-factor 438
  - as function of lignin yield 481
  - CBC process 283
- cellulose/hemicellulose ratio, pulp strength 1016
- celluloseether, global production 11
- centrifugal cleaning theory 579–586
  - flow regime 580–581
  - sedimentation 581–584
  - selective separation 585–586
  - underflow thickening 584–585
- CEPI *see* Confederation of European Paper Industries
- cereal straw fibers, cell dimensions and chemical composition 4
- CH *see* carbohydrates
- Chaetamorpha melagonicum* 24
- chain conveyors, log handling 98
- chain grinder, mechanical pulping 1090–1092
- chain length
  - dissolving pulp 1034
  - macromolecular 1248–1251
- chain scissions 831
  - alkali cellulose 1057
  - development 832
  - DP 216–217
  - effect of hydroxide concentration 195
  - efficiency of chlorine dioxide 769
  - kinetics 217, 685–687
  - ozone charge dependence 833, 835
  - pulp 1058
  - reducing end groups content 1058
- chain scissions number 260
- chain terminations, ozone 788
- Chamaecyparis*, sesquiterpenic tropolone derivatives 35
- charge-transfer state, ozone reactions 792
- chelants 821, 859, 860, 1007, 1125–1126, 1134
  - influence on manganese sorption 523
  - metal removal 861
- chelation 712
  - pulp bleaching 1126
- chelators 670
- Chem-Washer 551–552
- chemical additives, effect on kraft cooking models 211
- chemical analytical methods, operating principle 1221
- chemical charges, efficiency of chlorine dioxide 768
- chemical composition
  - agricultural fibers 4
  - black liquors 967–970
- chemical oxygen demand *see* COD
- chemical procedures, survey 1221
- chemical pulp
  - tear resistance 1141
  - tensile index 1141
- chemical pulp bleaching 829–849, 868–880, 999
- chemical pulp fiber, global production 9
- chemical pulping 109–508
  - overview 3–20
  - sulfite 392–482
- chemical reactivity, pulp specification 1060
- chemical recovery, kraft 980

- chemical recovery processes 973
- chemicals, bleaching 264
- chemimechanical pulp 1098
  - defibrillation conditions 1102
- chemimechanical pulping 1101
- chemithermomechanical pulp 1099, 1101
  - defibrillation conditions 1102
- chip conditioner 87–88
  - textured stainless steel segments 87
- chip dimensions, recommended 80
- chip feeding 380–382
  - continuous cooking process step 378
  - conventional 380
- chip filling
  - acid sulfite pulping process chemistry 428
  - displacement cooking process step 369
- chip moisture, redistribution during storage 99
- chip pile, changes 99
- chip preparation, impregnation 405
- chip quality, wood moisture content 82
- chip screening 89–90
- chip size, thermomechanical pulp processing 1078
- chip steaming 380–382
  - continuous cooking process step 378
- chip storage 98–100
- chip storage systems 100–104
- chipper canter
  - softwood sawmills 88
  - tool arrangement 88
- chipping, wood 80
- chips
  - mechanical screening 89–93
  - thickness 82
- chlorate 737, 739
  - chlorine dioxide charge 767
- chloride, hot caustic extract 961
- chlorination
  - amount of reagent 1227
  - aromatic rings 745
- chlorination products 752–754
- chlorination reactions, decrease with pH 770
- chlorine compounds 1225–1226
- chlorine dioxide
  - distribution 757
  - efficiency of chlorine dioxide 768
  - generation 741–745
  - generation technologies 742
  - in aqueous solution 737
  - oxidation 745
  - oxidation capacity 613
  - oxidation equivalents (OXE) 264
  - oxidizing power 764
  - physical and chemical properties 735
  - resonance structures 735
  - substitution 872
  - treatment 745–754
- chlorine dioxide bleaching 734–777
  - ecological risk 753
  - oxygen-delignified kraft pulp 759–761
  - performance 754–770
  - process flowsheet 770
  - sequences 759
  - side reactions 737–741
  - technology 770–771
- chlorine dioxide decomposition, initial rate 739
- chlorine dioxide delignification 752, 755
- chlorine gas, Roe number 1228
- chlorine number 1228
- chlorite formation, during bleaching 738
- chlorite ions, reactivity 739
- chlorite oxidation, acidic conditions 740
- chlorohydrin 772
- chlorous ester intermediate, chlorine bleaching 746
- Chornet *see* Kazi and Chornet diffusion model of impregnation
- chromatographic methods, saccharides composition 1231–1233
- chromatographic separation column 1253
- chromatography
  - at the critical state 1254
  - HP-AEC 340–341
  - separation modes 1254
  - size-exclusion 340
- chromophores
  - alkali-stable 258
  - carbohydrate-derived 181
  - cellulose triacetate 1030
  - kraft pulping reactions 172
  - removal 838
  - removal through hydrogen peroxide 853
- CI see* crystallinity index
- Cinnamomum camphora*, camphor 37
- circulation between stages, liquor 888–890
- cleaning
  - applications 592–594
  - centrifugal *see* centrifugal cleaning
  - equipment 600–606
  - four-stage (cascade feedback arrangement) 597
  - machines and aggregates 1114–1120
  - pulp 561–606, 1113–1122
  - separation efficiency 588–592

- theory 579–586
- cleavage, polysaccharide chain 662–666
- CLF *see* continuous liquor flow
- ClO<sub>2</sub> *see* chlorine dioxide
- closed rotor 564
- closure, degree of 893
- CMP *see* chemimechanical pulp
- CO<sub>3</sub><sup>2-</sup> *see* carbonate ion
- coarse material, refiner process 1115
- coarseness 1275
- cobalt (II) salts, cotton bleaching 709
- COD 17, 537–539, 544, 961, 1001, 1005–1006, 1129–1130
- cold alkali extraction 1046
- cold alkali purification 934
  - efficiency after hot caustic extraction 948
- cold aqueous NaOH solution, eucalyptus prehydrolysis-kraft pulp 943
- cold blow technology 274–275
- cold caustic extraction 942–952
  - NaOH concentration 1046
  - pulp purification 935
  - temperature dependence 945
- cold displacement
  - displacement cooking process step 370
  - prehydrolysis-kraft process 348–350
- cold water extraction 1225
- collection rate versus utilization rate, CEPI countries 1171
- collection systems
  - efficiency 1180–1181
  - recovered paper 1177
- color, acid sulfite cooking liquor analysis 433
- color reversion 1041
- combined-cycle technology, black liquor gasification 993
- commercial lignin 717–718
- commercial paper pulp
  - chemical characterization 1013–1014
  - fiber dimensions 1021
  - molecular weight distribution 1019
- compact feed system 381–382
- compact press, Kvaerner 557
- comparative evaluation, sodium ion diffusion coefficient 149–150
- complex acids, hot caustic extract 961
- complexometry, operating principle 1221
- compression forces
  - Norway spruce pulp 1276
  - single wet fibers 1275
- compression wood 55
- compressive dewatering 525–526
  - pulp washing theory 517
- concentration profile, Kazi and Chornet diffusion model of impregnation 153
- concept of Bouchard 798
- condensation
  - β-O-4 arylether structures 410
  - degradation products with lignin units 420
  - lignin 167–168
  - sulfite cooking chemistry 414–415
  - with phenols 424–425
- conditioning 1216
- conditions, ozonization 843–849
- conducting system, functional elements 46–48
- conductivity, acid sulfite cooking liquor analysis 433
- Confederation of European Paper Industries 1157
- conical-disc refiners 1105–1106
- coniferous woods
  - structure 50
  - terpenes 35
- coniferyl-type structures, formation 170
- coniferylaldehyde 342
- coniferylaldehyde-type structures, sulfonation of α-position 412
- consistency
  - as function of screening zone length 570
  - pulp 708
  - pulp bleaching 1128
  - two-stage delignification operating conditions 730
- construction material compatibility 893
- consumer demand, recycled papers 1199
- contaminant removal 594–600
  - arrangements 596–598
  - design principles 594–596
  - efficiency 598–599
  - selective 592–594
- contaminants
  - centrifugal cleaning operating parameters 588
  - screening operating parameters 579
- continuous batch cooking *see* CBC
- continuous cooking
  - equipment in comparison to batch cooking 366
  - outline of single-vessel system 377
  - principles 377–378
  - process steps 378–380
  - results 295–306
  - technology and equipment 377–391



- continuous digester, in conventional chip feeding system 380
- continuous liquor flow
  - carbohydrate composition of pulp 255
  - comparison with standard batch cooking 245
- contoured-drum rotor (S-rotor), pressure pulse profile 573
- convective air movement, pile interior 99
- conventional cooking, effective alkali profile 276–277
- conventional drum washers, pulp washing equipment 547–549
- conventional heat recovery system 391
- conventional kraft pulp
  - effect of polysulfide 312
  - residual lignin structures 262
  - RLCC composition 640–641
- conveyor systems, stationary 97–98
- cooking
  - acid sulfite pulping process chemistry 430
  - chemical cycle 973–974, 986
  - continuous cooking process step 379
  - prehydrolysis-kraft process 348–350
  - standard batch 229–234
- cooking chemicals
  - recovery 968, 994
  - selected model of kraft cooking kinetics 217–220
  - sulfite chemical pulping 395–403
- cooking conditions, influence on acid sulfite pulping process chemistry 459–465
- cooking liquor
  - acid sulfite 396
  - analysis methods 433
  - displacement 430–434
- cooking temperature
  - decrease in modified kraft cooking 249–250
  - effect on modified kraft cooking 248–251
  - in relation to kappa number and dissolved xylose 463
  - in relation to pentosan and screened yield 463
  - influence on CBC process 289–290
  - influence on pulp yield in standard batch cooking process 231–233
- copper number
  - commercial paper-grade pulp 1014
  - dissolving pulp characterization 1062
  - functional groups determination 1235
  - unpurified pulp 952
- copper number method 441
- corn straw fibers, cell dimensions and chemical composition 4
- corona discharge, ozone generation 783
- cotton linters
  - acetylation 1046
  - cell dimensions and chemical composition 4
  - dissolving grade pulp 1022
  - low polydispersity 1044
  - molar mass distribution 1049
  - molecular weight distribution 1035
  - representative dissolving pulp 1036
  - water-accessible pore volume 1053
- cottonwood, average moisture content 125
- countercurrent cascade, pulp washing mixing stages 539
- creosol
  - chlorine bleaching 746
  - ozone reactions 792
  - reactions with chlorine dioxide 747
- creosol methyl ether, reactions with chlorine dioxide 748
- critical state, chromatography 1254
- Cross, Charles F. 7
- crude tall oil, kraft pulping 112
- crude turpentine, kraft pulping 112
- crystalline cellulose 26
- crystalline lattice, packing 27
- crystalline material
  - H-NMR solid-phase spectrum 1261
  - X-ray diffractogram 1260
- crystallinity 1042, 1257–1265
  - degree of 1041, 1258
- crystallinity index 1262
  - determination 1258–1259
- crystallites, dimension 1263–1265
- Crystolon, pulp stone 1093
- CS chip screen 90
- CSF *see* Canadian Standard Freeness
- CTMP *see* chemithermo mechanical pulp
- CTMP refining 1110
- CTO *see* crude tall oil
- CUENE 1241
  - cellulose molecular weight determination 1240
- CUOXAM 1241
  - cellulose molecular weight determination 1240
- cupram 1025
- cuprammonium, dissolving pulp applications 1025
- Cupressus*, sesquiterpenic tropolone derivatives 35

- cupri-ethylene-diamine(-solution) *see* CUENE
- cutting geometry, disc chipper 81
- cyanohydrin method, functional groups  
determination 1237
- 1,3-cycloaddition, lignin degradation 790
- cyclone parameters, centrifugal cleaning  
586–587
- cylindrical coordinates, Fick's second law of  
diffusion in 152
- cylindrical refiners 1105–1106
- cymene, conversion of *a*-pinene during sulfite  
pulping 426
- d**
- D\*-stage 764
- DAE *see* differential algebraic equations
- Dahl, Carl 5
- Dakin-like reaction 858
- Darcy's law 132, 147, 513
- DCM, extractive 234, 330, 342, 360, 365,  
450–451, 961, 1013, 1030, 1061
- deacetylation, glucomannan in superbath  
process 280
- debarker, Nicholson A2 78
- debarking 71–80  
– methods 72–80
- debarking resistance, seasonal development  
1077
- debarking state, wood quality 1075
- debris passage ratio, in relation to screening  
efficiency 590
- Debye–Hückel–Onsager equation 142
- decayed wood, waste generation 105
- deciduous woods, structure 50
- decomposition  
– chlorine dioxide 737  
– homolytic 651  
– hydrogen peroxide 854–856  
– metal ion-catalyzed 791
- decreasing-permeability model 517
- defiberization, lignin compounds 1123
- defibration  
– conditions 1102  
– single fibers 1083
- deflocculation, fibers 562
- degradation  
– carbohydrates 794–798, 859  
– cellulose 1056–1059  
– cellulose/hemicellulose under alkaline  
conditions 175  
– end products 956  
– lignin 790–794  
– pathways for glucosone and xylosone end-  
groups 659  
– pentoses and hexoses 420  
– products 446  
– wood components 437–449
- degradation acids, relative frequencies  
(oxidative degradation) 637
- dehydration, carbohydrates 419–421
- deinking 1165, 1174–1175
- deliberation 1113  
– single fibers 1083
- delignification 16–17, 61, 79, 110–112,  
158–162, 705–706, 828–829  
– activation energy literature data 201–202  
– alkali charge 700  
– alternative bleaching methods 887  
– as function of pH 473  
– beechwood acid sulfite cooking 437  
– behaviour 834  
– bleaching 809, 887  
– blowtank 826  
– brightness dependence 870  
– carbohydrate reactions 657  
– chain scissions number 260  
– chlorine dioxide 752, 755  
– degree of 697, 717  
– dioxygen-alkali delignification processes  
657–666  
– Dualox™ system 730  
– effect of carry-over 717  
– effect of impregnation on delignification  
uniformity 158–162  
– effect of increasing chlorine dioxide 762  
– electrochemical 887  
– *Eucalyptus saligna* prehydrolysis kraft pulp  
with oxygen delignification 260  
– extent 1228–1229  
– final pH 705  
– hemicellulose degradation in initial phase  
251  
– H-factor 259  
– high-shear mixers 826  
– industrial 688, 695  
– kappa number 258, 678, 684  
– kinetics 211–215, 671–685  
– kraft cooking 184, 189, 211  
– lignin solubilization 714  
– low-consistency ozone bleaching 809  
– mass transfer rate 697  
– medium-consistency ozone delignification  
system 826  
– NaOH-charge 730  
– offgas 826

- oxygen *see* oxygen delignification
- OxyTrac system 730
- ozone 777–849
- pH 473
- phases in kraft cooking 184
- pine 473
- predicted by selected model of kraft cooking kinetics 223
- pressure 730
- process equipment 731
- profiles within handmade chip 160
- relation to oxygen delignification efficiency 259
- retention time 730
- selectivity 363, 809, 815
- temperature 730
- two-stage 473, 730
- washing 826
- *see also* kappa number
- delignification chemistry 632
- (di)oxygen and derivatives 641–649
- delignification efficiency
  - *Eucalyptus saligna* prehydrolysis kraft pulp with oxygen delignification 260
  - temperature effect 813
- delignification rate 802
- equation 681
- prehydrolysis effect in prehydrolysis-kraft process for *Eucalyptus saligna* 351
- delignification reactions, selectivity 838
- DeltaCombi, Metso 603
- DeltaScreen, Metso 602
- demethylation reaction, lignin 169
- density
  - black liquor 971
  - crystallinity 1262
  - dissolving pulp characterization 1062
  - hydrogen peroxide 851
  - white liquor 116
  - wood species 127–128
- dentated discs 92
- chip screens 91
- deoxy-hexoses, hemicelluloses 28
- 3-deoxypentonic acid, black liquor composition 968
- depolymerization reactions 937
- design principles, contaminant removal and fractionation systems 594–596
- detrimental effect, viscosity 814
- dewatering
  - compressive 517, 525–526
  - press 827
  - time 1283
- DF *see* dilution factor
- DI *see* crystallinity, degree of
- diacetate filterability 1028
- diamond rolls
  - chip screens 92
  - thickness screen 93
- diarylmethane, chlorine bleaching 747
- diarylmethane-type structures, lignin chemistry 169
- dichloromethane *see* DCM
- 3,4-dideoxypentonic acid, black liquor composition 968
- diequatorial intramolecular interactions, glycone 327
- diethylene diamine penta-acetic acid *see* DTPA
- diethylene triamino penta-acetate 670
  - metals removal 861
- different pulp types, ozone treatment 829–840
- differential algebraic equations 228–229
- differential form, Fick's second law of diffusion 152
- differential MWD
  - ozone treatment 845
  - shape 844
- differential volume element, annular (screening theory) 566
- diffuse-porous woods 133
  - *Aucoumea klaineana* 53
  - *Fagus sylvatica* 50
  - vessels 53
- diffusely scattered light, scattering methods 1245
- diffusion
  - control 800
  - dissolved ozone 798
  - Fick's first law 142–143, 220, 517
  - Fick's second law 138, 219, 518
  - kraft cooking mass transfer 123, 137–150
  - mass transfer 518
  - model *see* Kazi and Chornet diffusion model of impregnation
  - oxygen gas 671
  - parameters 156
  - pulp washing theory 517–518
  - rate 149
  - Stokes–Einstein model 147
- diffusion coefficient 138–142
  - activation energy dependency 140
  - comparative evaluation for sodium ions 149–150
  - dependency on wood species 148–149

- determination apparatus 142
- numerically evaluated for different conditions 155
- sulfur(IV) species 404
- temperature dependency 140–141
- yield dependence 141
- diffusion washers, pulp washing equipment 552–555
- digester
  - batch 367–368
  - discharge 370
  - dissolved lignin concentration at different locations 298
  - downflow hydraulic single-vessel 390
  - effective alkali 300
  - evacuation 129
  - hydraulic single-vessel 386, 388
  - pressure 403
  - single-vessel hydraulic 383
- 9,10-dihydroxyanthracene, AQ reduction product 317
- diluted alkaline hydrogen peroxide, decomposition in deionized water 864
- dilution conveyor 827
- dilution factor, pulp washing parameter 529–532, 545–546
- dilution/extraction washing 523
- dioxane lignin, residual 704
- dioxins, concentrations 753
- dioxygen 641–649
  - electronic structure 642
  - electrophilic-nucleophilic reactions 647–649
  - principles of activation 642–644
  - reactions and reduction products 644
  - redox potentials 643
  - reductions 854
  - simplified bonding scheme 642
  - *see also* oxygen
- dioxygen-alkali delignification processes, carbohydrate reactions 657–666
- dipertenes, softwoods 35
- diphenylmethane *see* DPM
- 1,3-dipolar cycloaddition, lignin degradation 791
- Dipterocarpus*, apitonene 37
- direct causticizing 994
- dirty points, paper 1076
- disc chipper 80–84
- disc refiners 1104
- disc thickness screen
  - diamond roll 93
  - raised roll 91
- discharge
  - acid sulfite pulping process chemistry 430–434
  - consistency 530, 532–533
  - gate operating mode 75
- discolored wood 57
- discs
  - chipper canter 88
  - dentated 91
- dismutation reaction 739
- displacement
  - applied on prehydrolysis kraft process 327
  - cooking liquor 430–434
- displacement cooking
  - principles 367
  - process steps 368
- displacement ratio, pulp washing 538–539, 543
- displacement washing 524–525
- disproportionation, hydroxyl radical adducts 653
- dissociation constant, temperature dependence for SO<sub>2</sub> 397
- dissolution
  - of AX, carbohydrate, GGM and lignin in CBC process 284
  - single elements determination 1221
- dissolved lignin
  - different digester locations 298
  - effect on kraft cooking kinetics models 207
  - influence on alkalinity 246
- dissolved oxygen, diffusion 693
- dissolved ozone 780–781, 798
- dissolved solids
  - effect on modified kraft cooking 244–248
  - sources 716
- dissolved wood components, beech magnesium acid sulfite cook 446
- dissolved xylan, concentration in cooking liquor 303–304
- dissolved xylose
  - as function of cooking temperature 463
  - as function of HSO<sub>3</sub><sup>-</sup> 461
- dissolving grade pulp 1009, 1022–1062
- dissolving pulp
  - applications 1025
  - characterization 1024, 1061
  - chemical composition 1026
  - degradation 1056–1059
  - functional groups specification 1016
  - global production 11
  - organic compounds 1026

- processability 1023
  - quality profile 1023
  - representative 1036
  - structural parameters 1043
  - dithionite, pulp bleaching 1124–1126
  - DMA/LiCl, cellulose molecular weight determination 1240
  - DOC degradation during oxygen delignification 692
  - domains, crystalline 1257
  - Donnan theory 393
    - pulp washing 521
  - double disc refiner 1105
    - concept 1107
  - Douglas fir
    - average moisture content 125
    - chemical composition of wood 23
    - lignin weight fractions 213
    - spiral thickenings 44
  - downflow reactors
    - atmospheric 624–625
    - low consistency discharge 625
  - downflow single-vessel hydraulic digester, Lo-Solids™ process 390
  - DP 25, 1020, 1036, 1058
    - alkali cellulose 1057
    - carbohydrate degradation in kraft cooking kinetics models 193–197
    - carbohydrates 174–175
    - cellulose 42, 256, 935
    - cellulose acid hydrolysis 416
    - cellulose chain scissions 216–217
    - degree of packing 428
    - dissolving pulp characterization 1061
    - hemicelluloses 28
    - polymer fractionation 1252
    - reduction in cellulose acid hydrolysis 416
    - water prehydrolyzate neutral sugar fraction 340
    - *see also* polymerization, degree of
  - DPM 165, 167–168, 173, 638, 656
    - structure and relative oxygen susceptibility 640
    - structures 713
  - DR 115–116
    - *see also* displacement ratio, reduction efficiency
  - drag force, on settling particle 581
  - drainage, pulp washing theory 513–516
  - drainage resistance
    - pulp 1281–1283
    - specific 515
  - drainage time, pulp 1283
  - drainage velocity equation 516
  - dregs, white liquor preparation processes 988
  - driving unit, drum debarker 74
  - drop-off systems, paper collection 1179–1180
  - drum, support 74
  - drum chipper 84–86
    - layout 86
  - drum debarker 72–76
  - drum displacer (DD), pulp washing equipment 549–550
  - drum rotation speed, in relation to relative pressure washer capacity 536
  - drum washers
    - conventional 547–549
    - rotary 547–550
  - DrumMatic™ 95–96
  - dry debarking 74
  - dry fibers
    - mechanical properties 1277
    - specific surface 1267
  - dry solid content 124, 129
    - black liquor density 971
    - black liquor heat capacity 972
  - drying, pulp weight loss 1219
  - DS *see* dry solid content
  - DTPA 523, 671, 821, 855, 861–862, 1126
  - Dual mixer, Kvaerner 620
  - DUALD™ process 764
  - Dualox™ system, two-stage delignification 730–730
  - Duflo impeller, Kvaerner 618
  - Duflo pump, Kvaerner 617
  - dynamic steam heater, Andritz 622
  - dynamic viscosity, black liquor and water 136
- E
- $E_{10}$  *see* modified efficiency factor
  - E factor *see* efficiency factor
  - (E/O) sequence 948
  - (E/O) treatments, NaOH charge 953–957
  - E-pH plot, AQ redox equilibria 317
  - E/O *see* hot caustic extraction
  - EA *see* effective alkali
  - earlywood, bordered pits 47
  - eastern hemlock
    - average moisture content 125
    - chemical composition of wood 23
  - ECCSA 144–146, 148, 801
    - pH-dependency in Aspen 145
    - pulp yield dependency 146
    - relation to pH and pulp yield in kraft cooking kinetics model 218

- ECF bleaching 10, 1000
  - hydrogen peroxide application 868
  - superbatch process 281
- ECF bleaching sequences
  - comparison 847
  - efficiency of chlorine dioxide 768–769
- Ecocyclic pulp mill project 1007
- ecological risk, chlorine dioxide bleaching 753
- economizers, kraft recovery boiler 981
- EDTA 670, 712–713, 821, 858, 1125–1126
- EDXA *see* energy dispersive X-ray analysis
- effective alkali 946
  - as function of cooking temperature and H-factor in conventional kraft cooking 232
  - at different digester locations 300
  - calculated consumption in Visbatch<sup>®</sup> cook of *Eucalyptus urograndis* 351
  - CBC process 283
  - in relation to brightness 272
  - in relation to H-factor after 120 min cooking 238
  - in relation to intrinsic viscosity 270
  - in relation to light absorption coefficient 269
  - in relation to pine total pulp yield 239
  - in relation to xylan content in unbleached Visbatch<sup>®</sup> pulp 358
  - influence on pulp yield in standard batch cooking process 229
  - kraft cooking active chemicals 114–115, 118–119, 159–161
  - Lo-Solids<sup>™</sup> laboratory cooks 301–303, 305
  - predicted concentration in selected kraft cooking kinetics model 223, 227
  - white liquors 244
- effective capillary cross-sectional area *see* ECCSA
- effective filtration pressure, in relation to relative pressure washer capacity 536
- efficiency 765
  - chlorine dioxide 768–769
  - fractionation 590–592
  - ozone treatment 829–840
  - pulp washing 531, 537–546
- efficiency factor (*E* factor)
  - determination 544
  - modified 545–546
  - Norden 539–544
- effluent
  - biological treatment 999
  - pulping processes 998
  - treatment 1004–1005
- effluent-free mill 1007
- effluent load
  - avoiding 999
  - mechanical pulp 1138
  - temperature effect 865
- effluent volume, open bleaching stage 892
- Einstein *see* Stokes–Einstein model
- electrochemical delignification, alternative bleaching methods 887
- electron density distribution
  - benzylium cation 409
  - carbonium-oxonium ion 417
  - phenylpropene unit 2 633
- electron microscopy, fiber morphology 1271
- electron spectroscopy for chemical application 1223
- electron-transfer reactions, lignin 170
- electronic structure, dioxygen 642
- electrophilic attack, ozone 790
- electrophilic attack sites, lignin 648
- electrophilic-nucleophilic reactions, (di)oxygen and derivatives 647–649
- electrostatic precipitator, kraft recovery boiler 981
- elemental chlorine, redox reaction 736
- elemental chlorine-free bleaching *see* ECF bleaching
- elementary fibrils, cellulose 41
- $\beta$ -elimination, glycosidic bond 177
- elimination reactions, lignin 169–170
- ellagic acid, structure 425
- EMCC<sup>®</sup>
  - dissolved lignin concentration at different digester locations 298
  - effect of polysulfide 312
  - process steps and flow regime 387
  - residual lignin structures 262
  - results 297–298
  - single-vessel hydraulic digester 386
  - technology and equipment 386–388
  - yield–kappa number plot 248–249
- emission levels
  - aquatic environment 1005
  - Tasmanian 1005
- emission limits, selected 1003
- EN 643, paper grades 1157
- end-groups, reducing 657–660
- energy balance, kraft recovery boiler 984–985
- energy consumption, TMP 13
- energy dispersive X-ray spectroscopy 40, 404
- enol ethers, formation 169
- enolic structures, hydroperoxide formation 651

- enone, nucleophilic addition 859
- entrained air 534–535
  - screening operating parameters 579
- environmental aspects
  - elemental chlorine 771
  - pulp production 997–1008
- enzyme treatment 1049
- epoxides, intramolecular formation 171
- equilibria, sulfite chemical pulping 395–403
- equipment
  - batch cooking 367–376
  - bleaching 613–628
  - continuous cooking 377–391
  - EMCC® 386–388
  - ITC 386–388
  - kraft pulping 366–391
  - lime cycle 990–991
  - Lo-Solids™ cooking 388–390
  - MCC 383–386
  - parameters 572–575
  - pulp washing 547–558
  - RDH 372–373
  - screening and cleaning 600–606
  - specific pulp washing parameters 535–536
  - superbatch process 373–374
- equivalent volume, hydrodynamically 1250
- erythronic acid
  - content in aldonic acid residues 658
  - formation 659
- D-erythronic acid, polysaccharide chain cleavage 662
- ESCA *see* electron spectroscopy for chemical application
- ethanol-benzene, organic solvents 342
- ether
  - dissolving pulp applications 1025
  - ozone reactions 793
- $\alpha$ -O-4 ether, structure 164–165
- $\beta$ -O-4 ether 172–174
  - structure 413
- ethoxy-based surfactants 687
- 4-O-ethyl- $\beta$ -D-glucopyranoside 830
  - polysaccharide degradation 796
- ethylene diamine tetra-acetic acid *see* EDTA
- EU packaging directive 1193
- Euca*-PHK-pulp, P-factor 259
- eucalypt
  - sulfite dissolving pulp 1047
  - Visbatch® process conditions 365
- eucalyptus
  - chemical composition 451
  - PHK pulp 1048
  - prehydrolysis-kraft pulp 943–945
    - viscosity–H-factor relationship 452
- Eucalyptus globulus* 967
  - chemical composition 451
  - chemical composition of wood 23
  - lignin mass balance during impregnation and kraft cooking 162
- Eucalyptus grandis*, AQ effects on kraft and soda pulping 325
- Eucalyptus saligna*
  - kinetic parameters for prehydrolysis weight-loss 332
  - kinetic parameters for xylan water prehydrolysis 333
  - lignin species degradation during kraft pulping 213
  - prehydrolysis effect on delignification rates in prehydrolysis-kraft process 351
  - prehydrolysis kraft pulp 260
  - xylan hydrolysis activation energy 343
- Eucalyptus urograndis*
  - chemical composition 360
  - RDH kraft pulping 279
  - wood component mass balance in Visbatch® cook 349–350
- Eucalyptus urophylla*, Lo-Solids™ laboratory cooks 304–305
- European Declaration on paper recovery 1194
- European list of standard grades of recovered paper and board 1203–1210
- evacuation, digester 129
- evaporation
  - black liquor 974–980
  - multiple-effect 977–979
  - vapor recompression 980
- evaporators 975
  - concentration level 976
  - falling film 976
  - performance 976
- EWNN
  - cellulose molecular weight determination 1240
  - *see also* iron sodium tartrate
- excess heat capacity, black liquor 973
- excess lye 946
- exchange reaction, carboxyl functions 1238
- Executive Order, US legislation 1196
- extended modified cooking concept *see* EMCC®
- external water layer, thickness 800
- extinction, in relation to viscosity 433
- extraction residue, alkali solubility tests 1060

- extraction washing *see* dilution/extraction washing
- extractives 1030–1033
  - commercial paper-grade pulp 1013
  - commercial pulp 1015
  - DCM *see* DCM
  - dissolving pulp characterization 1061
  - fractions obtained after kraft cooking 182
  - hardwoods 38
  - hot caustic 961–962
  - kraft pulping reactions 181–183
  - percentage 35
  - pulp 1224–1225
  - pulping yields 110
  - purification dependence 960–961
  - sulfite cooking chemistry 425–427
  - topochemical distribution 61–63
  - woods 33–39

## f

*F-value*, refiner process 1104

$f_{\text{void}}$  *see* void volume fraction

*Fagus sylvatica* 33, 39

- chemical composition 360, 451
- chemical composition of wood 23
- composition 330
- density and void volume 128
- diffuse-porous hardwoods 50
- earlywood transition 49
- facultative heartwood formation 57
- fibers 45
- inorganic composition 40
- kinetic parameters for prehydrolysis 332–333
- nonglucosic hemicelluloses units 29
- tissue 63
- tyloses 48
- woodyard storage 70
- falling film evaporator 975
- “false” lignin 257
- false viscosity 1028
- fats
  - fats and waxes 34
  - softwoods 36
- fatty acid esters, hydrolyzation in acid sulfite cook 427
- fatty acids
  - black liquor 967
  - kraft cooking extractives 182–183
  - softwoods 36
- Fe<sup>2+</sup> ion concentration 815

- feed consistency 529
  - centrifugal cleaning operating parameters 587
  - in relation to relative pressure washer capacity 533
  - pulp washing parameter 532–533
  - screening operating parameters 577
- feeding hydraulics, chain grinder 1092
- feedwater, kraft recovery boiler 985
- Fenton-type reactions 854
  - hydrogen peroxide 710
  - superoxide-driven 669
- fiber analyzers, pulp 1274
- fiber bundle, kraft cooked 60
- fiber concentration
  - in relation to permeability, porosity and specific surface 514
  - in relation to specific drainage resistance 515
- fiber content, minimum recycled 1196
- fiber–fiber bonding 473
- fiber fractionation 591–592
  - screening 1274
  - tensile index 1139
- fiber length 1273
  - concept of Bouchard 799
  - fractionation 1051
  - in relation to fiber passage ratio 571, 578
  - spruce pulp 1020
- fiber loss
  - grinding 1083
  - relation to contaminant removal efficiency 598–599
- fiber passage
  - screening theory 566–570
  - selective 570–572
- fiber passage ratio 566
  - as function of aperture velocity 576
  - as function of fiber length 571, 578
  - as function of hole size 578
  - as function of screening zone length 569
- fiber removal
  - efficiency 590–591
  - from black liquor 371, 380
- fiber saturation point 126, 1053
- fiber slurry, pulp 1281
- fiber strength 1019
  - pulp viscosity 842
- fiber swelling, limitation 934
- fiber tenacity, hemicellulose concentration 1027
- fiber wall
  - hemicelluloses distribution 1048–1051



- model of contact with external solution 520
- thickness distributions after centrifugal cleaning 585
- fibers
  - agricultural fibers 4
  - cell components 46
  - cell dimensions and chemical composition 4
  - cellulose 1047
  - commercial paper pulp 1021
  - compression forces 1275
  - defibrillation 1083
  - deflocculation 562
  - deformation 1137
  - deliberation 1113
  - dimensions 1021, 1272–1275
  - dry 1267, 1277
  - *Fagus sylvatica* 45
  - FSP *see* fiber saturation point
  - hardwoods 4, 123–124
  - heterogeneity 123
  - hornification 1284
  - identification 1269–1271
  - material consumption, paper production 1153
  - morphology 180–181, 1051–1052, 1269–1271
  - nano-structure 59–61
  - native fibers 1047
  - nonwood 9, 13
  - oxygen 688
  - ozone 807
  - pits 123
  - polymer components 1257
  - polynosic-type 1027
  - properties 1269–1280
  - rattan 50
  - recycled 1147–1210
  - regenerated 7, 1047
  - selective passage (screening theory) 570–572
  - single *see* single fibers
  - softening 1080–1083
  - softwoods 4, 123
  - specific surface 514, 1267
  - strength properties 1036–1037
  - stress-strain characteristics 1277
  - suspended 1272
  - viscose 1036–1037, 1061
  - wet 1275–1277
  - width 1273–1274
  - wood cells 49
  - X-ray diagrams 1264
  - xylan 180–181
  - *see also* pulp fibers
- fibrillar morphology, pulp 1047
- fibrillar structure, cellulose 41–42
- fibrous bark, ring debarkers 77
- Fick's laws of diffusion
  - first 142–143, 220, 517
  - second 138, 152, 219, 518
- field emission-SEM 60
- filtrate concentration
  - degree of closure 892–893
  - open bleaching stage 892
- filtrate separator 990
- filtration behavior, pulp 1281
- filtration pressure, in relation to relative pressure washer capacity 536
- final bleaching
  - chlorine dioxide 756
  - peroxide 1038
- final chlorine dioxide stage, high temperature 765
- final pH
  - chlorine dioxide bleaching 738
  - oxygen delignification 705–706
- fines
  - beech pulp 1020
  - deliberation 1113
- finite difference method 228
- finite geometric progression 541
- flavonoids
  - hardwoods 38
  - softwoods 37
- flax fibers, cell dimensions and chemical composition 4
- flexibility, single fiber 1276
- flexural stress, resistance 1279
- flow discharger, Sulzer 627
- flow pattern, hydrocyclone 580
- flow rate, centrifugal cleaning operating parameters 587
- flow regime
  - centrifugal cleaning theory 580–581
  - EMCC<sup>®</sup>/ITC 387
  - Lo-Solids<sup>™</sup> process 389
  - MCC 385
  - screening theory 564–565
- flow vectors, screen basket 565
- FlowHeater, Metso 622
- FlowScraper
  - Metso 625–626
- flue gas
  - constituents 982–983

- humidity 984
  - kraft recovery boiler 985
  - lime cycle processes 991
  - fluidization, pulp 614–615
  - fluorescent dyeing, functional groups
    - determination 1237
  - foil rotor, cross section 564
  - forces, acting on a particle in a hydrocyclone 583
  - formaldehyde, elimination kraft pulping
    - reactions 169
  - formate
    - hot caustic extract 961
    - ozone decomposition, initiator 789
  - formic acid
    - black liquor composition 968
    - cellulose protecting additive 819
    - polysaccharide chain cleavage 662
  - 5-formylfuran carboxylic acid, formation 421
  - foul condensate 978
  - four-stage cleaning, cascade feedback arrangement 597
  - Fourier transmission infra-red 159
  - fractional washing 528
  - fractionation
    - capacity, chip screens 91
    - efficiency 590–592
    - pulp 561–606
    - screening and cleaning applications 594
  - fractionation index 591–592
    - as function of the mass reject ratio 600
  - fractionation systems 594, 599–600
    - design principles 594–596
  - Fraxinus excelsior*
    - density and void volume 128
    - hemicelluloses, nonglucosic units 29
    - ring-porous hardwoods 53
  - free radical, hydroxyl 647
  - free water 1268
  - freeness 1268
    - mechanical pulp 1138
    - Schopper-Riegler method 1282
    - water suspended fibers 1172
  - freeze-drying, pore preservation 1055
  - freezing bound water 1053
  - frequency functions, change 676
  - fringe fibrillar model, supramolecular structure 1041
  - FS-SEM *see* field emission-SEM
  - FSP *see* fiber saturation point
  - FTIR *see* Fourier transmission infra-red
  - functional groups 1037–1041, 1234–1239
    - commercial paper-grade pulp 1014
    - determination 1016
    - dissolving pulp characterization 1062
    - residual lignin 635
  - furans, effluent content 1000
  - furfural 328–338, 419, 444–449, 1004, 1231, 1233
    - content as function of H-factor 447
    - formation 455
    - spent liquor content as function of viscosity 456
  - furnace 968
    - kraft recovery boiler 981
  - furnish parameters
    - centrifugal cleaning 587–588
    - screening 578–579
- g**
- G-factor model for viscosity loss 195–197, 356–357
  - G-layer *see* gelatinous layer
  - galactan, relative acid hydrolysis rates 417
  - galactoglucomannan *see* GGM
  - galactose
    - commercial paper-grade pulp 1013
    - concentration development in beechwood prehydrolysis 337–338
    - content as function of H-factor 447
    - pulp fraction 440
  - gallic acid, structure 425
  - gas chromatography, monosaccharides
    - determination 1231
  - gas management 828
    - continuous cooking process step 380
    - displacement cooking process step 372
  - gas phase ozone bleaching 808
  - gas void fraction 690, 701, 805
    - ozone generation 784
  - gasification 992
    - low-temperature 482
  - gel column, size exclusion characteristics 1255
  - gel permeation 1252
  - gel permeation chromatography (GPC)
    - measurements 181, 255–256, 263, 415, 1237, 1256
    - functional groups 1017
    - lignosulfonates 415
    - measurements 842
  - gel phase, polymers 1252
  - gelatinous layer 55
  - GentleFeed system, debarking 74
  - geometric progression, finite 541

- GGM 186–187, 211, 215–216, 234, 251–252, 283–286, 291–293, 476
  - dissolution in CBC process 284
  - pulping yields 110–111
  - removal in CBC process 286
- Girard-P method, functional groups determination 1237
- GL&V Impco HI-Q Knotter 602
- glassy state, cellulose bleaching 1042
- global production capacity, oxygen-delignified pulp 631
- glucan
  - dissolving pulp characterization 1061
  - residue 936
- glucoisosaccharinate, hot caustic extract 961
- glucoisosaccharinic acid, black liquor composition 968
- glucomannan 1028
  - deacetylation in superbatch process 280
  - degradation rate in Gustavson–Al-Dajani kinetic model 253
  - molecular structure 28
  - pulping yields 110
  - specific consumption in selected model of kraft cooking kinetics 221
  - specific kraft pulping reactions 180
  - TCF-bleached dissolving pulp 1049, 1051
  - yield as function of lignin yield 481
- Gluconacetobacter xylinum* 24
- gluconic acid
  - content in aldonic acid residues 658
  - ozonation 796
- glucose
  - commercial paper-grade pulp 1013
  - concentration development in beechwood prehydrolysis 337–338
  - content as function of H-factor 447
  - polysaccharide chain cleavage 662
  - reactions with sulfonic acid 422
  - spent liquor content as function of viscosity 459
- glucosone end-groups, degradation pathways 659
- glucuronic acid, isomerization products 1234
- glucuronoxylan, pulping yields 110
- D-glyceric acid, polysaccharide chain cleavage 662
- glycolic acid
  - black liquor composition 968
  - ozone decomposition, initiator 789
  - polysaccharide chain cleavage 662
- glycone, steric diequatorial intramolecular interactions 327
- glycosidic bond
  - $\beta$ -elimination 177
  - ozonation 830
- glycosidic linkages
  - alkaline hydrolysis 178
  - degradation 859
- glyoxylic acid, ozone decomposition, initiator 789
- GM *see* glucomannan
- goniometer, X-ray diffractometer 1260
- GPC *see* gel permeation chromatography
- graphic papers, utilization rate 1169
- grass fibers, cell dimensions and chemical composition 4
- gravimetry, operating principle 1221
- gravitational field, earth 582
- gravity separators, hydrocyclone 579
- gray alder, chemical composition of wood 23
- green liquor 112, 117, 243, 394, 986–992, 1004, 1007
  - clarified 988
  - kraft pulping 112
  - Na<sub>2</sub>S 241
- green wood, average moisture content 125
- Greening the Government by Waste Prevention, Recycling, and Federal Acquisition, US legislation 1196
- grinders, mechanical pulping 1089–1090
- grinding
  - machines and aggregates 1087–1095
  - mechanical and thermal processes 1080–1083
  - parameters 1084
  - pulping 1079–1098
  - zonal temperatures 1082
- grits, white liquor preparation processes 989
- groundwood
  - components 1114
  - flow sheet 1088
  - properties 1084–1087
- Guaiacum officinale*, caoutchouc 38
- guaiaacyl 713
- guaiaacylglycerol- $\beta$ -guaiaacyl-ether 858
- guaiaacylpropane
  - lignin 165
  - molecular structure 32
- Gustavson and Al-Dajani kinetic model
  - degradation rates for xylan, glucomannan and HexA 253
  - hemicellulose degradation 252
- gutta 38
- gymnosperms, lignin 30

**h**

## H-factor

- acid sulfite cooking 427
- acid sulfite pulping 431–432
- as function of  $\text{HSO}_3^-$  460
- as function of kappa number effected by AQ 322
- as function of residual EA concentration 238
- beech magnesium acid sulfite cook 440
- correlation with  $\beta$ -aryl ether structures content 266
- in relation to  $\beta$ - and  $\gamma$ -cellulose 443
- in relation to kappa number 258, 287, 356
- in relation to oxygen delignification efficiency 259
- in relation to pentosan and viscosity 464
- in relation to residual xylan 444
- in relation to  $\text{SO}_2$  amount 435–436
- in relation to viscosity for different wood species 452
- in relation to wood component yield 438
- in unbleached Visbatch<sup>®</sup> pulp 357
- influence on kappa number–P-factor relation 359
- influence on pulp yield in standard batch cooking process 231–233

## H-factor concept

- kraft cooking kinetics model predictions 224
- kraft cooking kinetics models 189–191

## Hagen–Poiseuille's law, laminar flow 132–133

## half-bordered pits 47

halogen, adsorbable organic *see* AOX

## halogenated residual 1001

## handling

- recovered paper 1187–1190
- sorted recovered paper 1189

## handling systems, wood yard operations 95–106

## hardwood chips, silo-stored 99

## hardwood fibers

- cell dimensions and chemical composition 4
- heterogeneity 123–124

## hardwood kraft pulp, oxygen delignification 723

## hardwood PHK, representative dissolving pulp 1036

## hardwood prehydrolysis

- apparent rate constants 334
- kinetic model 329–343

## hardwood structure 50–54

- hardwood sulfite dissolving pulp 1036
  - degree of polymerization 952
  - molar mass distribution 951
  - pretreated 1038
  - R18 content 955
  - selectivity 838

## hardwood sulfite pulp

- purification 943
- reflectance and absorption coefficient spectra 611

## hardwoods

- accessory compounds 37–39
- apparent prehydrolysis rate constants 334
- axial parenchymal cells 54
- bleaching 1126
- cellulose 22
- chemical composition of wood 23
- defibration conditions 1102
- diffuse-porous hardwoods 50, 53
- extractives 38
- flavonoids 38
- hemicellulose 22
- homocellular rays 54
- isoflavones 38
- kinetic prehydrolysis model 329–343
- lignans 38
- lignin 22
- lignins 33
- macromolecular substances 22
- parenchymal cells 54
- penetrability 135
- phenolic compounds 38
- pits 46
- pulp 1010
- pulp bleaching 1126
- rays 54
- resin-rich 465
- ring porous hardwoods 53
- sapwood conversion to 59
- semi-ring-porous hardwoods 53
- steroids 37
- tannins 38
- triglycerides 38
- vessels 53
- xylan chains 29

HBL *see* hot black liquor

## HC cleaner, Metso 606

## HC technology 721

HCE *see* hot caustic extractionHD *see* hot displacementheartwood, *Pinus monophylla* 36

## heartwood formation 57

- heat capacity, black liquor 972–973
- heat exchange, kraft recovery boiler 981
- heat management
  - continuous cooking process step 380
  - displacement cooking process step 371
- heat recovery 1121–1122
  - Andritz Lo-Level 391
  - conventional 391
  - flow sheet 1122
- heat transfer rate, evaporator 976
- heating and cooking, displacement cooking process step 370
- heating-up, acid sulfite pulping process chemistry 430
- heating values, black liquor solids 969
- heavy metals, ozone decomposition, initiator 789
- hemicellulose 28, 835, 1026–1030
  - *Abies balsamea* 29
  - *Acer rubrum* 29
  - acid degradation reactions 327–329
  - acid hydrolysis 418
  - acid-catalyzed hydrolysis 341
  - amount 936
  - anhydro-sugars 28
  - *Betula verrucosa* 29
  - Carboxyl groups 1037
  - CBC process 286
  - cell wall components 41
  - cellulose/hemicellulose ratio 1016
  - concentration 1026
  - content as function of P-factor in unbleached Visbatch<sup>®</sup> pulp 361
  - content in lye 947
  - content in pulp from modified kraft cooking 240
  - content in softwoods and hardwoods 22
  - controlled removal 719
  - degradation 175, 251
  - delignification 251
  - deoxy-hexoses 28
  - discoloration 1027
  - distribution 1048–1051
  - DP 28
  - enrichment 1050
  - *Fagus sylvatica* 29
  - fiber tenacity 1027
  - fiber wall 1048–1051
  - *Fraxinus excelsior* 29
  - Gustavson and Al-Dajani kinetic degradation model 252
  - hardwoods 22
  - hexoses 28
    - hydrolysis 325–326
    - in relation to screened yield 362
    - in relation to viscosity-to-kappa number ratio 364
    - *Larix decidua* 29
    - pentoses 28
    - P-factor 361
    - *Picea abies* 29
    - *Picea mariana* 29
    - *Pinus strobus* 29
    - *Pinus sylvestris* 29
    - *Populus tremuloides* 29
    - prehydrolysis 325–326
    - presence 945–947, 947
    - pulp 240, 361
    - removal 952, 957
    - short-chain hemicelluloses removal 952
    - softwoods 22
    - *Tsuga canadensis* 29
    - *Ulmus americana* 29
- hemp fibers, cell dimensions and chemical composition 4
- heterogeneity
  - hardwood fibers 123–124
  - softwood fibers 123
  - wood structure 123–129
- heterogeneous gas phase, ozone bleaching 808
- heterolytic fragmentation 749
  - chlorine bleaching 746
- heterolytic ozonolysis 792
- heteropolysaccharides 28
- HexA 187, 240, 251–254, 257–259, 267–270, 278–279, 302, 774, 830, 1016
  - commercial paper-grade pulp 1014
  - degradation rate in Gustavson–Al-Dajani kinetic model 253
  - efficiency of chlorine dioxide 768
  - formation 180
  - hydrolysis 874, 884
  - in conventional and RDH pulp 278–279
  - influence on kappa number 180
  - model 884
  - presence 839
  - reactions under acidic conditions 421
- hexenuronic acid *see* HexA
- hexoses
  - degradation 420
  - hemicelluloses 28
  - spent liquor content as function of viscosity 459
- HHV 968
  - kraft recovery boiler 984

- hi-heat washing 384, 558
- HI-Q Fine Screen, Impco 601
- HI-Q Knotter, GL&V Impco 602
- high consistency ozone stage, bleaching 617, 806, 827
- high molecular fraction, adsorbable organic compounds 771
- high-performance anion-exchange chromatography, water prehydrolyzate neutral sugar fraction 340–341
- high-purity *Eucalyptus* prehydrolysis kraft pulp 727
- high resin content, pulp 1031
- high-shear mixers 731
  - bleaching equipment 620
  - medium-consistency ozone delignification system 826
  - oxygen gas addition 867
  - ozone solubilization 802
- high-temperature gasification 992
- high-viscosity ethers, dissolving pulp characterization 1061
- high-volume low-concentration 372
- higher heating value *see* HHV
- Himalaya spruce, spiral thickenings 44
- HMF *see* hydroxymethylfurfural
- hole size, in relation to fiber passage ratio 578
- HOMO-distribution, phenylpropene unit 2 633
- homocellular rays, hardwoods 54
- homolytic decomposition 651
- homolytic fragmentation, veratryl- $\beta$ -guaiacyl ether 751
- hornification 1054
  - fibers 1284
- hot acid hydrolysis 883–885
  - comparison with chlorine dioxide 762
  - time dependence 885
- hot black liquor 136–137, 346, 348, 372–374
- hot caustic extract, composition 961–962
- hot caustic extraction (HCE) 948, 952–963
  - pulp purification 935
  - treatment without interstage washing 954
- hot chlorine dioxide process 764
- hot displacement
  - displacement cooking process step 369
  - prehydrolysis-kraft process 348–350
- hot purification process 934
- hot water extraction 1225
- hot white liquor 346, 348, 372–374
- HP-AEC *see* high-performance anion-exchange chromatography
- [HS<sup>-</sup>]/[OH<sup>-</sup>] ratio, at different digester locations 300
- HS<sup>-</sup> *see* hydrogen sulfide ion
- HSO<sub>3</sub><sup>-</sup> *see* hydrogen sulfite ion
- Hückel *see* Debye–Hückel–Onsager equation
- humidity, kraft recovery boiler 985
- HVLC *see* high-volume low-concentration
- HW-S *see* hardwood-sulfite dissolving pulp
- HWL *see* hot white liquor
- hybrid poplar, lignin weight fractions 213
- hydrate cellulose, first indication 935
- hydraulic cook 275
- hydraulic digester
  - downflow single-vessel 390
  - single-vessel 383, 386, 388
- hydrazine method, carbonyl groups determination 1236
- hydrazones, formation 1236
- hydrocyclone 562, 1118
  - axial and tangential velocity profile 581
  - flow pattern 580
  - forces acting on a particle 583
  - gravity separator 579
  - operation principle 1119
  - screening and cleaning equipment 605–606
  - streams 579
- hydrodynamically equivalent volume, macromolecule 1250
- hydrogel 1052
- hydrogen abstraction, carbohydrates 795
- hydrogen bonds, cellulose 26
- hydrogen peroxide 646–647
  - chlorine dioxide generation 744
  - decomposition 852, 854
  - efficiency of chlorine dioxide 768
  - formation 794
  - manufacture 850–853
  - one-electron reduction 669
  - oxidation 613, 854
  - oxygen 264
  - physical properties 850–853
  - thermal stability 863–865
  - *see also* hydroperoxides
- hydrogen peroxide bleaching 849–879, 1123, 1126–1133
  - activators 880
  - chemistry 853–860
  - technology 866
- hydrogen sulfide, addition to quinone methide 167
- hydrogen sulfide consumption, selected model of kraft cooking kinetics 220–221

- hydrogen sulfide ion
    - concentration in selected model of kraft cooking kinetics 217–220
    - effect on kraft cooking kinetics models 203–206
    - effect on modified kraft cooking 241–244
    - molar concentration in white liquor 115
  - hydrogen sulfite
    - concentration in cooking liquor 400–401
    - Stora process 472–475
  - hydrogen sulfite ion
    - in relation to H-factor 460
    - in relation to kappa number and dissolved xylose 461
    - in relation to screened yield and xylan 462
  - hydrolysis
    - acid-catalyzed 341
    - alkaline 178
    - hemicelluloses 325–326
    - hot acid 883–885
    - lignin 407–414
  - hydrolyzation, fatty acid esters 427
  - hydroperoxide anions 857
  - hydroperoxides 645–652, 655–658, 855–859
    - formation by enolic structures
      - autoxidation 651
    - formation by phenolic structures
      - autoxidation 652
    - formation in alkaline media 650
    - formation, lignin 856
  - hydroperoxy anions
    - concentration 854
    - formation 651–652
    - ozone decomposition, initiator 789
  - hydroperoxy radical
    - hydrogen peroxide intermediates 852
    - ozone decomposition 789
  - hydrostatic pressurization, impregnation 405
  - hydrosulfite *see* dithionite
  - hydrotrioxide hemioorthoester, ozonation 796
  - hydroxide ion
    - concentration in selected model of kraft cooking kinetics 217–220
    - during VisCBC hardwood cooking process 347
    - effect on CBC process 287–289
    - effect on cellulose chain scissions 195
    - effect on kraft cooking kinetics models 203–206
    - effect on modified kraft cooking 237–241
    - in relation to pine total pulp yield 240
    - molar concentration in white liquor 115
    - ozone decomposition, initiator 789
  - (4-hydroxy-3-methoxyphenyl)-glyoxylic acid, structure 308
  - hydroxy acids, hot caustic extract 961
  - hydroxy carboxylic acids monitoring, role in H-factor control 191–193
  - 2-hydroxybutanoic acid, black liquor
    - composition 968
  - hydroxycarbonic acids, low molecular-weight 961
  - hydroxycyclohexadienyl radicals, formation 652
  - $\alpha$ -hydroxyl, structure and relative oxygen susceptibility 640
  - hydroxyl groups
    - aliphatic 261
    - exchange 1102
    - phenolic 173
  - hydroxyl radical 647, 794
    - cellulose degradation 859
    - during bleaching 777
    - formation 712
    - hydrogen peroxide intermediates 852
    - methanol 788
    - phenoxyl radical formation 650
  - hydroxyl radical adducts
    - disproportionation 653
    - phenolic coupling 654
    - reactions 653–654
  - hydroxymethylfurfural, formation 419
  - p*-hydroxyphenyl, monolignol structural units 31
  - p*-hydroxyphenyl groups, resistant lignin 714
  - p*-hydroxyphenylpropane units
    - lignin 165
    - molecular structure 32
    - wheat straw 209
  - $\alpha$ -hydroxysulfonates, formation 423
  - hygiene papers, utilization rate 1168
  - hypochlorite
    - consumption 831
    - oxidation capacity (OXE) 613
  - hypochlorous acid 737
    - excess 739
- i**
- +I-effect, lignin degradation 790
  - image analysis, pulp 1274
  - Impco HI-Q Fine Screen 601
  - Impco HI-Q Knotter, GL&V 602
  - impregnation 208–209
    - acid sulfite pulping process chemistry 428
    - axial 154
    - continuous cooking process step 378

- displacement cooking process step 369
- effect on delignification uniformity 158–162
- Kazi and Chornet diffusion model 151–158
- kraft cooking mass transfer 122–123
- lignin mass balance of *Eucalyptus globulus* 162
- radial 155
- refiner process 1103
- sulfite chemical pulping 403–405
- two-vessel MCC<sup>®</sup> system 385
- impurities, pulp 708
- in-digester washing 557–558
- in-situ causticization 992
- incineration
  - pulp sample 1220
  - single elements determination 1221
- index of nonuniformity 1241–1242, 1251
- industrial oxygen delignification
  - base case parameters 695
  - prediction model 688–701
- infeed rings, debarkers 79
- inhibitors
  - ozone 788
  - ozone generation 788
- initial NaOH charge, in relation to kappa number and selectivity 480
- initial phase
  - chlorine dioxide selectivity 761
  - kraft pulping reactions overview 183–184
- initiators, ozone generation 788
- inorganic compounds 1033–1037
  - black liquor composition 968
  - cellulose protection/degradation 668–671
  - commercial paper-grade pulp 1014
  - pulp 1219–1224
  - woods 39–41
- inorganic reactions, kraft pulping 184–185
- integral level, wood characterization 21
- intercellular layer, cell components 44
- interstage washing 948
- intra-stage circulation, liquor 888–890
- intramolecular formation, epoxides 171
- intramolecular hydrogen bond, cleavage 941
- intrinsic viscosity 1250
  - as function of H-factor 357
  - as function of P-factor 353
  - as function of residual EA 270, 272, 302
  - CED 451
  - in relation to pulp strength for kraft softwood pulp 236
- inverse size-exclusion chromatography 1053

- ion diffusion, effect of pressure steaming 149
- ionic strength
  - effect on kraft cooking kinetics models 207
  - effect on modified kraft cooking 244–248
- iron, removal 862
- iron (III) salts, cotton bleaching 709
- iron sodium tartrate 1241
- irregular piles, wood log storage 1076
- ISEC *see* inverse size-exclusion chromatography
- ISO Standard method
  - brightness measurement 610
  - *see also* brightness
- isoflavones, hardwoods 38
- isoprene units, terpenes 35
- isotherm, Langmuir 519
- isothermal cooking *see* ITC
- ITC 9, 269–274, 297, 695
  - brightness gain in relation to consumed OXE 273
  - process steps and flow regime 387
  - single-vessel hydraulic digester 386
  - technology and equipment 386–388

## j

- jack pine, carbohydrate composition of sulfite and kraft pulp 470
- Japan
  - legislation 1198
  - recovered paper grades 1161, 1163
- Jetmixer, Kvaerner 621
- Juniperus*, sesquiterpenic tropolone derivatives 35
- Juniperus communis*, chemical composition of wood 23
- jute fibers, cell dimensions and chemical composition 4
- juvenile wood 56–59

## k

- $K_{a,1}$ , temperature dependence for SO<sub>2</sub> 397
- Kadant Black Clawson Chemi-Washer 551–552
- kappa, efficiency of chlorine dioxide 768
- kappa factor 755
  - efficiency of chlorine dioxide 768
- kappa number 17, 111, 137, 190–193, 208–211, 229–245, 249–275, 278–298, 301–305, 312–316, 322–325, 351, 354–357, 363–365, 475–482, 529, 715, 727, 755, 868, 1033, 1228
  - as function of alkali ratio in spruce AS/AQ pulping 479



- as function of AQ charge 323–324
- as function of CBC cooking temperature 290
- as function of cooking temperature 463
- as function of H-factor 191, 259, 287, 356
- as function of  $\text{HSO}_3^-$  461
- as function of initial NaOH charge 480
- as function of  $[\text{OH}^-]$  value 288–289
- as function of P-factor in unbleached Visbatch® pulp 355
- as function of polysulfide addition effect 292–293
- as function of white liquor sulfidity 355
- as function of yield in pine/spruce conventional kraft cooking 233
- average values with CCE 950
- bisulfite-MgO process 467
- calculated 699
- change during oxygen delignification 678
- commercial paper-grade pulp 1013
- degradation 673
- dependency on oxygen delignification 258
- development during oxygen delignification 684
- effect of impregnation on uniformity 159
- hot acid hydrolysis 883
- hydrogen peroxide application 868–870
- influence of HexA 180
- lignin content 188
- oxymercuration-demercuration 723
- ozone consumption 803
- pine kraft pulp 825
- prediction by G-factor model 197
- pulp yield–kappa number relationship 320
- purification dependence 960–961
- refractory 672
- relation to H-factor effected by AQ 322
- relation to P-factor at different H-factor levels 359
- relation to pine/spruce kraft pulp yield in EMCC 249
- relation to pulp yield 230, 321
- relation to tear index of kraft softwood pulp 235
- residual lignin content 432
- selectivity plot for CLF and standard batch cooking 245
- selectivity plot for conventional, MCC® and EMCC® cooking 297
- selectivity plot for different wood species 453
- selectivity plot for oxygen bleaching 629
- selectivity plot for pine/spruce kraft cooking 226, 232, 243
- selectivity plot for radiata pine kraft pulp 247
- specific yield loss 949
- viscosity–kappa number relationship 452–453, 479–480
- *see also* delignification
- kappa number reduction 804–805
  - effect of different after-treatment procedures 824
  - temperature effect 813
- Kaufmann diagram 406
- Kazi and Chornet diffusion model of impregnation 151–158
  - calculated parameters 156–157
  - comparison with experimental data of *Populus tremuloides* heartwood 153–154
  - concentration profile 153
  - influence of wood chip dimensions 158
  - pressure influence equation 151
- Keggin-type metal clusters, alternative bleaching methods 887
- Keller, Friedrich Gottlob 5, 1073
- kenaf fibers, cell dimensions and chemical composition 4
- kinetic model
  - degradation rates for xylan, glucomannan and HexA 253
  - Gustavson and Al-Dajani 252
  - hardwood prehydrolysis 329–343
- kinetics
  - carbohydrate degradation 215–216
  - cellulose chain scissions 217
  - chain scissions 685–687
  - kraft pulping 185–229
  - oxygen delignification 671–687
- knot screens, secondary (screening and cleaning equipment) 604–605
- knots, selective removal 593
- Kozeny *see* Carman–Kozeny relationship
- “kraft”, word origin 5
- kraft chemical recovery 980
  - future 992–994
- kraft cooking 733
  - active chemicals 114–116, 221, 988
  - aliphatic hydroxyl groups elimination 261
  - Bjerrum diagram 118
  - carboxylic groups enrichment 261
  - chemicals 221
  - delignification phases 184
  - diffusion mass transfer 123, 137–150
  - experiments 225

- extractives fractions 182–183
  - fiber bundle 60
  - lignin mass balance of *Eucalyptus globulus* 162
  - liquors 113–121
  - modified *see* modified kraft cooking
  - PHK *see* PHK process
  - pine *see* pine
  - prehydrolysis *see* PHK process
  - pretreatment 129–130
  - process chemistry 229–325
  - Purdue model 198–199
  - kraft cooking kinetics
    - alkali and hydrogen sulfide consumption 220–221
    - concentration of cooking chemicals 217–220
    - delignification kinetics 211–215
    - numerical solution of cooking chemical concentration equations 228–229
    - parameters 221–227
    - structure 211–229
    - validation and application 223–227
  - kraft cooking kinetics models
    - carbohydrate degradation 193–198
    - delignification 189–198
    - H-factor concept 189–191
    - kraft cooking kinetics 199–211
    - pseudo first-principle 198–199
    - pulping selectivity 197–198
    - review 188–211
  - kraft cooking mass transfer, diffusion 123, 137–150
    - impregnation 122–123
    - penetration 122, 129, 132–137
  - kraft cooking pretreatment
    - digester evacuation 129
    - steaming 129–132
  - kraft process 12, 17
    - development 6
    - dissolving pulp 1024
    - prehydrolysis- 345–365
    - uniform pulping reactions 1047
    - *see also* kraft pulping
  - kraft pulp 1010
    - beating resistance 1011
    - carbohydrate composition 470
    - conventional *see* conventional kraft pulp
    - emission levels 1005
    - global fiber production 9
    - hardwoods 723
    - R-values 1015
    - sheets 800
    - softwoods *see* softwood kraft pulp
  - kraft pulping
    - black liquor 111–112
    - carbohydrates reactions 174–181
    - chemistry 163–185
    - chromophore reactions 172
    - extractives 181–183
    - formaldehyde 169
    - glucomannan 180
    - green liquor 112
    - kinetics 185–229
    - levopimaric acid 183
    - liquor composition 476
    - low-lignin pulp production 323
    - multistage 325–365
    - nucleophiles addition 167
    - processes 111–391
    - reactions overview 183–184
    - selectivity plot *see* selectivity plot
    - tall oil soap 112
    - technology and equipment 366–391
    - toxic compounds 112
    - transition metals 859
    - white liquor 111
    - xylan 179
    - *see also* kraft process, *see also* lignin
  - kraft recovery boiler 980–985
    - emission limits 1003
    - schematic 981
    - *see also* kraft chemical recovery
  - kraft residual lignin, linkage frequencies 638
  - Kramfors process 465
  - Kubelka-Munk theory 610, 1279
  - Kvaerner compact press 557
  - Kvaerner double atmospheric diffuser 553
  - Kvaerner Dual mixer 620
  - Kvaerner Duflo impeller 618
  - Kvaerner Duflo pump 617
  - Kvaerner Jetmixer 621
  - Kvaerner pressure diffuser 555
  - Kvaerner's Compact Feed system 381–382
- I**
- laboratory methods, material testing 1217
  - laboratory sheets, optical properties 1279–1280
  - laccase mediator-system, alternative bleaching methods 886
  - lactic acid
    - black liquor composition 968
    - polysaccharide chain cleavage 662
  - laminar flow, Hagen–Poiseuille's law 132–133

- Langmuir isotherm 519
- Laplace *see* Young–Laplace equation
- Larix decidua*, hemicelluloses, nonglucosic units 29
- Larix sibirica*, chemical composition of wood 23
- latency, mechanical pulp 1137–1143
- latewood, bordered pits 47
- latewood tracheids, *Picea abies* 62
- lattice conversion, wood dissolving pulp 1044
- lattice transition
  - alkali concentration 1043
  - cellulose I 941, 1045
- layers
  - cell wall 42
  - model calculation 694
- LCC *see* lignin–carbohydrate-complexes, *see also* lower cook circulation
- leaf fibers, cell dimensions and chemical composition 4
- legislation, recycled fibers 1191–1210
- level-off DP 1011
  - crystallite length 1264
- levopimaric acid, conversion to abietic acid during kraft process 183
- levulinic acid 419
- lifetime, hydrogen peroxide 855
- light absorption coefficient
  - as function of residual effective alkali 269
  - kappa number 715
  - residual softwood lignin 266
  - unbleached pine 269
- light-scattering coefficient 1142
  - pulp 1140–1141
- lignans
  - hardwoods 38
  - softwoods 37
- lignification of the cell walls 44–46
- lignin 30–31, 33, 713–716, 749, 856–858, 1033
  - addition of nucleophiles 167
  - alternative bleaching methods 886
  - angiosperms 30
  - arabinoxylan 481
  - bark 33
  - birch 33
  - bleaching 886, 1126
  - bromination 316
  - carbohydrate degradation 795
  - $\alpha$ -carbonyl group-containing 655
  - cell wall components 41
  - charge transfer complexes 321
    - chemical structure 858
    - chromophore formation 172
    - cold caustic extraction 950
    - commercial 717–718
    - composition after cooking and bleaching 634–640
    - concentration *see* delignification, kappa number
    - condensation 167–168, 420
    - content 1230
    - conventional kraft pulp 262
    - 1,3-cycloaddition 790
    - defiberization 1123
    - degradation 213, 790–794
    - demethylation reaction 169
    - diarylmethane-type structures 169
    - diffusion rate 149
    - digester 298
      - 1,3-dipolar cycloaddition 791
    - dissolution in CBC process 284
    - dissolved 207, 246, 284, 298
    - Douglas fir 213
    - electro-/nucleophilic attack sites 648
    - electron-transfer reactions 170
    - elimination kraft pulping reactions 169–170
      - “false” 257
    - fraction 173, 724, 950
    - frequencies in kraft residual lignin 638
    - functional group content 635
    - fungi 886
    - guaiacylpropane unit 165
    - gymnosperms 30
    - hardwoods 22, 33
    - hydrogen peroxide 853
    - hydrolysis 407–414
    - hydroperoxide formation 856
    - *p*-hydroxyphenyl groups 714
    - *p*-hydroxyphenyl-propane unit 165
    - kappa number reduction 960
    - kraft pulping reactions 163–174, 323
    - light absorption coefficient 266
    - linkage frequencies 638
    - mass balance during impregnation and kraft cooking of *Eucalyptus globulus* 162
    - milled wood 262
    - modification with peracetic acid 880
    - modified kraft cooking 31, 244–248, 257–264
    - molecular structure 32
    - nucleophilic attack 856
    - nucleophilic attack sites 648
    - oxidation 874

- oxygen susceptibility (relative) 640
- partial kappa numbers 724
- phenolic hydroxyl 263, 636
- phenolic hydroxyl groups 173
- phenolic polymer 31
- phenolic subunits 164
- phenylpropane building blocks 32
- PHK process 348
- photodegradation 655
- polymerized 853
- production in AQ-kraft process 323
- pteridophytes 30
- pulp bleaching 1126
- pulp fraction 440
- pulping yields 110
- *para*-quinone methide 164–165
- reactions with acid sulfite 407–416
- reactions with ozone 795
- reactions with peracid 881
- reactivity 634–641
- redox mechanisms 319
- relative oxygen susceptibility 640
- removal in CBC process 286
- removal rate in prehydrolysis-kraft process 348
- residual 174, 635, 704
- residual structure 173–174, 257–264
- resistant fractions 724
- selective bromination 316
- selective hydrolysis 1227
- side chain 635
- side-chain enone structures 857
- softening temperature 1081
- softwoods 22, 33
- solubilization 714
- specific consumption in selected model of kraft cooking kinetics 221
- spermatophytes 30
- spruce 213
- structure *see* lignin structures
- sulfitolysis 407
- sulfonation 407–408
- syringylpropane unit 165
- topochemical distribution 61–63
- units 164, 170–172, 420
- weight fractions 213
- yield as function of H-factor 438
- *see also* RLCC
- lignin-carbohydrate complexes 181, 258, 796
  - formation and structure 171
  - residual *see* RLCC
- lignin content 1227–1228
  - in relation to carbohydrate yield in alkaline pulping 186
  - in relation to wood component yields 481
  - in softwoods and hardwoods 22
  - residual 1014, 1033
- lignin model compounds
  - *a*-carbonyl group-containing 655
  - relative oxygen susceptibility 640
- lignin species, degradation during kraft pulping 213
- lignin structures 164–165, 173–174, 261–263
  - $\beta$ -O-4 263
  - phenolic 795
  - reactivity 634–641
  - residual 262, 713–716
  - responsible for bleaching reactivity 261
- lignosulfonates, structure 415–416
- lime cycle processes 990–991
- lime kiln
  - emission limits 1003
  - schematic 991
- lime mud 987
- lime reburning 986–991
- limiting-consistency model 517
- limiting degree of polymerization 1043
- linkages, frequencies in kraft residual lignin 638
- liquid chromatography 1232
- liquid-ring vacuum pump 977
- Liquidamber styraciflua*, kinetic parameters for xylan water prehydrolysis 333
- liquor charging, acid sulfite pulping process chemistry 428
- liquor circulation 887
  - implications 893–894
  - schematic 889
- liquor composition, AS/AQ and kraft pulping 476
- liquor cycle closure, stages 891
- liquor management, advanced 366
- liquor-to-wood ratio, prehydrolysis 326
- liquors
  - kraft cooking 113–121
  - spent liquor composition 448
  - *see also* black liquor, green liquor, orange liquor, white liquor
- LMS *see* laccase mediator- system
- Lo-Level heat recovery system, Andritz 391
- Lo-Solids™ process
  - birch laboratory cooks 301–302
  - dissolved lignin concentration at different digester locations 298

- downflow single-vessel hydraulic digester 390
  - *Eucalyptus urophylla* laboratory cooks 304–305
  - introduction 299
  - process steps and flow regime 389
  - results 298–306
  - single-vessel hydraulic digester 388
  - technology and equipment 388–390
  - lobolly pine
    - average moisture content 125
    - lignin weight fractions 213
    - photosensitized degradation 656
  - Lobry de Bruyn-Alberda van Ekenstein mechanism 1233–1234
  - LODP *see* level-off DP
  - log handling, wood yard operations 97
  - log storage, wood 1076
  - long fiber removal, as function of short fiber loss 592
  - long loop gas management 829
  - longitudinal diffusion
    - dependency on temperature and activation energy 140
    - residual sodium fractions 139
  - longitudinal groundwood 1079
  - Lophira alata*, stem section 58
  - low consistency discharge
    - downflow reactor 625
    - Metso Tower scrapers 624
  - low-consistency ozone bleaching 806–807
    - delignification selectivity 809
  - low-lignin pulp, production in AQ-kraft process 323
  - low molecular fraction, adsorbable organic compounds 771
  - low molecular-weight components, determination 1219–1226
  - low-temperature gasification 482, 992
  - low unbleached kappa-values 716
  - low-viscosity pulp 464
    - sulfite cooking 957
  - low-volume high-concentration 372
  - lower cooking circulation 298
  - Lowest Unoccupied Molecule Orbital
    - benzylum cation 409
    - carbonium-oxonium ion 417
    - quinone-methide 166
  - LUMO *see* Lowest Unoccupied Molecule Orbital
  - LVHC *see* low-volume high-concentration
  - Lyocell dopes, discoloration 1027
  - Lyocell process 1022
- m**
- +M-effect 790
  - macrofibrils, cellulose 41
  - macromolecular chains, solution viscosity 1248–1251
  - macromolecular composition 1227–1256
  - macromolecular substances, wood 22
  - macropores, accessibility 1054
  - macroscopic level, wood characterization 21
  - macrostructure, pulp stone 1093
  - magazine-type grinder, mechanical pulping 1089
  - magnetite process 466–467
    - pH range 393
    - two-stage neutral 467–468
  - magnesium
    - protective effect 668
    - stabilizing effect on hydrogen peroxide 855
  - magnesium acid sulfite cook, beech 435–437, 439
  - magnesium carbonate, cellulose protection 710–711
  - magnesium hydrogen sulfite
    - diffusion coefficient 404
    - solution 392
  - magnesium hydroxide, pulp bleaching 1130
  - magnesium oxide 879
  - magnolia, average moisture content 125
  - manganese
    - distribution between fiber wall and external solution 419
    - pulp sorption as function of pH 523
    - removal 862
  - manganese complex, model 877
  - mannan 834
    - content 1028
    - content as function of P-factor in unbleached Visbatch® pulp 361
    - dissolving pulp characterization 1061
    - in relation to screened yield 362
    - in relation to viscosity-to-kappa number ratio 364
    - relative acid hydrolysis rates 417
    - structure 30
  - mannonic acid
    - content in aldonic acid residues 658
    - stabilization of reducing end-groups 657
  - mannose
    - commercial paper-grade pulp 1013
    - concentration development in beechwood prehydrolysis 337–338
    - content as function of H-factor 447

- pulp fraction 440
- spent liquor content as function of viscosity 459
- maple, density and void volume 128
- maple chips, storage 99
- market situation, pulping processes 8–15
- mass balance
  - contaminant removal efficiency 598–599
  - screening theory 567
  - Visbatch<sup>®</sup> cook of *Eucalyptus urograndis* 349–350
- mass reject ratio
  - in relation to fractionation index 600
  - in relation to screening efficiency 589
- mass transfer
  - by diffusion 518
  - degree of delignification 697
  - kraft cooking 122–163
  - oxygen delignification 671–687
  - ozone bleaching 798–801
- material balance
  - kraft recovery boiler 982–984
  - one-stage acid sulfite cooking 458
  - prehydrolysis-kraft process 347–351
- Mathieson process, chlorine dioxide generation 742
- M $\beta$ G *see* methyl- $\beta$ -D-glucopyranoside
- MC ozone bleaching, ozone charge dependence 837
- mc pump, pressurized peroxide bleaching system 866
- MC technology 721
- MCC 298
  - cellulose DP in relation to pulp yield 256
  - global production 11
  - process steps and flow regime 385
  - pulp bleachability 296
  - reaction scheme 1026
  - results 295–297
  - strength properties of softwood pulp 297
  - technology and equipment 383–386
- mechanical pulp
  - bleaching 1123–1136
  - definition 1072
  - printing paper grades 1142
  - processing 1113
  - properties 1137–1143
  - raw materials 1075–1078
  - tear resistance 1141
  - tensile index 1141
- mechanical pulp fiber
  - deformation 1137
  - global production 9
- mechanical pulping 1069–1146
  - by refining 1104–1112
  - history 1073–1074
  - machines and aggregates 1087–1095
- mechanical screening, chips 89–93
- medium consistency discharge, Metso Tower scrapers 624
- medium consistency mixers, bleaching equipment 619–623
- medium consistency ozone bleaching 834
- medium-consistency ozone delignification system, flowsheet 826
- medium-consistency ozone treatment 826–827
- medium consistency pumps
  - arrangement with an external vacuum pump 618
  - bleaching equipment 617–619
- medium consistency reactors, bleaching equipment 623–627
- medium consistency stage, bleaching 616
- melting point, hydrogen peroxide 851
- membrane osmometry 1244
- mercaptane, formation 169
- mercerization 1044
  - cellulose 27
- mercerization resistance 941
- metal clusters, alternative bleaching methods 887
- metal-containing logs, waste generation 105
- metal ion concentration 708–713
- metal ion species, catalysis 670
- metal oxides, separation 994
- metals
  - cellulose protection/degradation 668–671
  - inorganic components 1220
  - management 860–862
  - removal 860
  - selective removal 594
- methanol 788
  - cellulose protecting additive 819
  - content as function of H-factor 447
  - formation 425
  - ozone decomposition, promotor 789
- methanol-based process, chlorine dioxide generation 743
- methanol elimination 761
- methoxyl, relative reactivity 635
- methyl-2-, polysaccharide chain cleavage 662
- 2-methyl butadiene, terpenes 35
- 4-methyl catechol, chlorine bleaching 746
- methyl- $\beta$ -D-cellobioside, polysaccharide chain cleavage 662

- methyl- $\beta$ -D-glucopyranoside
  - ozonation 796
  - ozone treatment 795
  - polysaccharide chain cleavage 662
  - pH dependence 812
  - reaction mechanism 797
- methyl- $\beta$ -glucoside, formation 665
- methyl- $\beta$ -D-glucoside, polysaccharide chain cleavage 662
- 4-O-methyl-glucuronic acid 940
  - kraft cooking 1016
  - methanol elimination 761
  - substitution 883
- 4-O-methyl- $\alpha$ -D-glucuronic acid 328
- 4-O-methyl glucuronic acid side chains, peeling reaction stopping 179
- 4-O-methyl glucuronic acid substituents, removal from xylan 1029
- 4-O-methyl- $\beta$ -D-glucuronic add-(1 $\rightarrow$ 2)-xylose 940
- 4-O-methyl glucuronarabinoxylan *see* AX
- 4-O-methyl glucuronoxylan 1011
- methyl-D-mannopyranoside, ozonation 796
- methyl-4-O-methyl- $\beta$ -D-glucopyranoside 662
- 3-methyl muconic acid monomethyl ester, chlorine bleaching 746
- methyl pyranosides, ozonation 796
- methyl- $\beta$ -pyranosides, relative hydrolysis rates 328
- 4-methyl-2,3',4'-trimethoxydiphenyl, native diaryl ether structures 749–750
- 4-methyl veratrole, chlorine bleaching 747
- methyl-D-xylopyranoside, ozonation 796
- Metso DeltaCombi 603
- Metso DeltaScreen 602
- Metso FlowHeater 622
- Metso FlowScraper 626
  - medium consistency discharge 625
- Metso HC cleaner 606
- Metso PGW grinder 1096
- Metso S-Mixer 620
- Metso Tower scrapers 624
- Mg(HSO<sub>3</sub>)<sub>2</sub> 392
- Mg(OH)<sub>2</sub>, titrator base 399
- MgO, alkali source 962–963
- microcrystalline cellulose 11
- microfibrils, cellulose 41
- micropores, accessibility 1054
- microscopy techniques 60
  - fiber morphology 1271
  - pulp 1274
- middle lamella, cell components 42, 44
- mill experience
  - polysulfide pulping 314
  - PS/AQ 316
- milled wood lignin, residual lignin structures 262
- mineral components, *Fagus sylvatica* 39
- minimum recycled fiber content 1196
- minor streams, kraft recovery boiler 984
- Mitscherlich, Alexander 6
- Mitscherlich process, sulfite chemical pulping 392
- mixed-flow model 566, 568
- mixed office waste, woodfree 1166
- mixers
  - atmospheric steam 622–623
  - high-shear 620
  - medium consistency 619–623
  - performance 695
  - static 621–622
- mixing, medium-consistency 805
- mixing energy, ozone technology 807
- mixing stages, pulp washing 539
- mixing time
  - ozone bleaching 802–806
- ML *see* middle lamella
- model parameters, selected model of kraft cooking kinetics 221–227
- modified chlorine dioxide bleaching 761–771
- modified continuous cooking *see* MCC
- modified cooking circulation *see* MCC
- modified efficiency factor ( $E_{10}$ ), pulp washing 545–546
- modified kraft cooking
  - cold blow technology 274–275
  - comparison of results 274–306
  - continuous batch cooking 282–287
  - continuous cooking 295–306
  - effect on carbohydrate composition 251–256
  - EMCC<sup>®</sup> 297–298
  - influence on bleachability 264–274
  - interdependence of temperature, cooking time and effective alkali 251
  - Lo-Solids™ process 298–306
  - MCC 295–297
  - principles 237–274
  - process chemistry 235–306
  - pulp strength delivery 256–257
  - rapid displacement heating 275–280
  - residual lignin structures 257–264
  - structural changes of softwood xylan 252–256
  - superbatch process 280–282

- moisture 1205, 1219  
 – green wood 125  
 – grinding process parameters 1084  
 – wood 124, 1085  
 molar fraction, ozone 779  
 molar mass 1034–1037  
 – average values 1241–1243  
 – determination 1243–1246  
 – distribution 951, 1018, 1049  
 – polymerization 1239  
 molecular weight 1058  
 – dependence on bleaching stage 844  
 molecular weight distribution 951–952, 1251  
 – bleached commercial paper pulp 1019  
 –  $\beta$ -cellulose 443  
 – dissolving pulp 1034  
 – wood dissolving pulp 1035  
 molybdovanadophosphate heteropolyanions,  
 alternative bleaching methods 887  
 monoglignol  
 – lignin 31  
 – structural units 31  
 monomeric sugars, concentration  
 development in beechwood prehydrolysis  
 339  
 monomodal distribution, molecular 933  
 monosaccharides  
 – after hydrolysis 1231–1232  
 – in water prehydrolyzate from beechwood  
 340  
 monosulfite-acid sulfite Stora process  
 472–475  
 monoterpenes, softwoods 35  
 Monterey pine, chemical composition of  
 wood 23  
 morphological characterization, pulp fibers  
 1269  
 morphology, wood 41–48  
 MOW *see* mixed office waste  
 MOXY process 307, 313  
 – white liquor oxidation 311  
 MSW *see* municipal solid waste  
 multiconical refiner 1107  
 multiple-effect evaporation 977–979  
 – principles 977  
 multistage kraft pulping 325–365  
 multistage washing 526–527  
 municipal solid waste 1181–1182  
 Munk *see* Kubelka-Munk theory
- n**
- Na-cellulose 1045  
 – lattice transition 941, 1043, 1045  
 ( $\text{Na}_2\text{S}_4$ ), polysulfide liquor 306  
 Na(trium) *see* sodium  
 nano-structure, fibers 59–61  
 NaOH  
 – charge 730, 953–957  
 – concentration profile 154–155, 942–944  
 – dosage in cold caustic extraction 945  
 – efficiency of chlorine dioxide 768  
 – initial charge 480  
 – titrator base 399  
 native diaryl ether structures 749  
 native fibers 1047  
 NCG *see* noncondensable gases  
 negative sorting, recovered paper 1188  
 Nernst equation 309  
 net heating value 968  
 neutral magnefite process, two-stage  
 467–468  
 neutral sugars,  $\beta$ -cellulose fraction 939  
 neutral sulfite-acid sulfite process 468–469  
 neutral sulfite pulping 412–414  
 – pH range 393  
 neutral sulfite semi-chemical process *see*  
 NSSC  
 neutralization 872  
 – black liquor 121  
 – prehydrolysis-kraft process 348–350  
 – white liquor 119  
 Newtonian liquid, laminar flow 1248  
 Newton's law, terminal settling velocity 582  
 Nicholson A2/A8 Debarker 78–79  
 nitric acid, ozone generation 783  
 nitrocellulose, dissolving pulp applications  
 1026  
 nitrogen adsorption method, specific surface  
 of dry fibers 1267  
 NMNO, cellulose molecular weight  
 determination 1240  
 NMR spectroscopy 31, 168, 173–174  
 – solid-phase 1261–1262  
 – xylan 254  
 nonaromatic compounds, adsorbable organic  
 compounds 771  
 noncellulosic material 933  
 – carbohydrates 1026  
 noncondensable gases, falling film  
 evaporator 975  
 nonfreezing bound water 1053  
 nonpaper components, contained in recovered  
 paper 1204  
 nonphenolic compound, ozone reactions 790  
 nonphenolic lignin units 170–172  
 – structure 171



- nonrecoverable paper 1186
  - germany 1185
  - world 1183
- nonuniformity-index *see* index of nonuniformity
- nonwood plant fibers, economic potential 13
- nonwood pulp fiber, global production 9
- Norden efficiency (*E*) factor
  - definition 542
  - pulp washing 539–546
  - standardized 558
- North America, recovered paper grades 1161
- northern red oak, average moisture content 125
- Norway spruce, chemical composition of wood 23
- Noss Radiclone AM 606
- Noss Radiscreen 603–604
- Noss Raditrim 604
- NS-AS *see* neutral sulfite-acid sulfite process
- NSSC 1009, 1110
  - role in global pulp production 12
- nuclei growth, Avrami-Erofeev's concept 679
- nucleophiles
  - addition in kraft pulping reactions 167
  - addition of water, chlorine bleaching 747
  - lignin attack 648, 856
- nucleophilic opening, oxiran 171
- nucleophilic reactions, (di)oxygen and derivatives 647–649
- numbering system, European list of standard grades of recovered paper and board 1205
- numerical solution
  - cooking chemical concentration equations in selected kinetics model 228–229
  - diffusion model with cylindrical symmetries 162–163
- O
- oak species 37
- ODE *see* ordinary differential equation
- offgas
  - medium-consistency ozone delignification system 826
  - pressurized peroxide bleaching system 867
- OH<sup>-</sup> *see* hydroxide ion
- old growth redwood, average moisture content 125
- olefins, ozone reactions 793
- oleoresin, softwood species 35
- oligosaccharides
  - fractionation 1230
  - in water prehydrolyzate from beechwood 340
- 4OMeGlcA 940
- once-through gas management 828
- one-stage acid sulfite cooking
  - material balance for different wood species 458
  - parameters 452
- one-stage oxygen-delignified pulp 631
- Onsager *see* Debye–Hückel–Onsager equation
- opacity 1280
- open-air chip storage 101
- open rotor 564
- operating parameters, screening 575–578
- operating variables, base case study 697
- OQP sequence, effect on lignin structure 858
- orange liquor 311
- ordinary differential equation 159, 229
- organic chlorine
  - formation kinetics 772
  - low pH 753
- organic compounds
  - dissolving pulp 1026–1033
  - volatile 1002
- organic constituents, black liquor 967
- organic halogen, adsorbable *see* AOX
- organic solutes, effect on ozone concentration 788
- organic solvents 342
- organochlorine compounds
  - commercial paper-grade pulp 1014
  - *see also* OX
- organohalogen, dissolving pulp characterization 1061
- organosolv pulping 16
- osmosis, molar mass determination 1243
- osmotic pressure, evaluation 1244
- outlet consistency ( $N_{Std}$ ), standardized 545
- outthrow materials, recovered paper 1162
- overall selectivity, optimum 728
- overflow, hydrocyclone 579–580
- oversized logs, waste generation 105
- OX 17, 628, 764, 767–777, 882, 1001, 1061
- Ox-Dem *see* oxymercuration-demercuration
- oxalic acid, ozone treatment 821
- OXE 70, 264–265, 314, 705, 716
  - bleaching chemicals 612–613
  - formation during bleaching 847
  - ITC-type and ASAM pulp 273
  - QPQP bleaching 271
- oxidants, extraction stage 869
- oxidation
  - amount of reagent 1227

- veratryl- $\beta$ -guaiacyl ether 751
- oxidation capacity 612
- oxidation equivalents *see* OXE
- oxidation potential
  - hydrogen peroxide 852
  - wasted 740
- oxidative bleaching, carbonyl groups 1041
- oxidative degradation, relative degradation
  - acid frequencies 637
- oxidative peeling 177
  - cellulose chain 663
- oxidimetry, operating principle 1221
- oxidizable impurities, removal 831
- oxidizing power, ozone 779
- oxime method, functional groups
  - determination 1236–1237
- oxiran, nucleophilic opening 171
- oxirane intermediates 858
- oxygen 641–649
  - autooxidation 644–645
  - consumption 707, 869
  - mass transfer to pulp fibers 688
  - oxidation capacity (OXE) 613
  - phenoxyl radical formation 650
  - reduction energetics 643
  - single O<sub>2</sub>–excited state 645–646
  - solubility under equilibrium conditions 692
  - *see also* dioxygen
- oxygen-alkali bleaching, initial step 633
- oxygen charge
  - delignification process 707
  - effect on delignification 700
  - two-stage delignification operating conditions 730
- oxygen delignification 675, 681, 948, 950, 952
  - alkali charge 703
  - bleaching 628–734
  - chemistry 632–670
  - comparison between model and experiment 683
  - effect of carry-over 718–719
  - efficiency in relation to P-factor 259
  - first commercial application 727
  - flowsheet 689
  - industrial 688, 722
  - ITC-type and ASAM pulp 274
  - kappa number 258, 678, 684, 721
  - kinetics 671
  - kraft pulp 701, 759–761
  - mass transfer 671
  - paper-grade pulp 728
  - P-factor 259
  - pH Value 704
  - pine pulp 667
  - power law kinetic parameters 677, 679
  - principal reaction schema 649–656
  - process variables 701
  - pulp bleaching 628
  - residual xylan content, delignification efficiency and chain scissions number 260
  - selectivity 629, 702, 720–721
  - softwood kraft pulp 713, 723
  - temperature effect 813
  - under mass transfer limitation 698
  - xylan 260
- oxygen-delignified pulp 631
- oxygen gas management 828
- oxygen-oxygen bond, cleavage activation energy 851
- oxygen pressure, delignification process 707
- oxygen susceptibility (relative), lignin model compounds 640
- oxymercuration-demercuration kappa number 723
- OxyTrac system 730
- OZE-bleached pulp 825
- ozonation 840, 1038
  - degree of 840
  - low pH 812
  - rate 801
- ozone
  - charge 834, 1039–1040
  - concentration 785
  - consumption 803, 817, 831
  - consumption rate 803
  - consumption yield 804
  - containing gas 806
  - decomposition 786–790
  - delignification 777–849
  - dissolved 798
  - generation 782–785
  - oxidation capacity 613
  - oxidation equivalents (OXE) 264
  - physical properties 778–782
  - radical reactions 792
  - reactivity with pulp fibers 807
  - resonance structures 779
  - self-decomposition 811
- ozone bleaching 793, 798
  - basic considerations 829–830
  - comparison of different stages 843–846
  - efficiency 784
  - installations 810
  - medium-consistency 805

- selectivity 836
  - ozone gas management 828
  - ozone-lignin reactions 795
  - ozone placement, bleaching stage 843–849
  - ozone stage 948
  - ozone technology 806
  - ozone treatment 831–840
    - chemistry 785–798
    - high-consistency 827
    - medium-consistency 826–827
    - selectivity 820
    - technology 826–829
  - ozonide hydrotrioxy radical 791
  - ozonolysis 793
- p**
- P-factor
    - alkali resistances 354
    - beechwood water prehydrolysis 344–345
    - concept 343–345
    - different H-factor levels 359
    - modified 345
    - oxygen delignification efficiency 259
    - TCF-bleached dissolving pulp 1051
    - unbleached Visbatch® pulp 352–353, 355, 361
  - P-Y bleaching 1132
  - P(O) stage 866
  - packaging, categories 1192–1193
  - packaging papers, utilization rate 1168
  - packing, degree of 428
  - PAD *see* pulsed amperometric detection paper
    - average moisture content, birch 125
    - chemical composition of wood 23
    - collection 1178–1180
    - dirty points 1076
    - making 4–7, 1073, 1281–1290
    - production 1147, 1153
    - properties, unbleached spruce pulp 109
    - recovered 1147–1210
    - recovered, european list of standard grades 1203–1210
    - recycled 1199
    - structure 59
    - “tree-free” 14
  - paper chromatography, uronic acids determination 1233
  - paper grade 1009, 1142, 1162, 1169
    - EN643 1157
    - Europe 1157, 1205
    - graphic 1169
    - Japan 1161, 1163
    - North America 1161
    - United States 1162
    - utilization rate 1167–1169
  - paper-grade pulp 1010–1021
    - chemical characterization 1013
    - extended oxygen delignification 728
  - paper machine, invention 5
  - Paper Products Recovered Materials Advisory Notice, US legislation 1196
  - paper pulp
    - alkali resistances 1015
    - fiber dimensions 1021
    - molecular weight distribution 1019
  - paper raw material, recycled fibers 1153–1156
  - para-crystallinity, single-phase model 1258
  - para*-quinone methide, lignin chemistry intermediate molecule 164–165
  - parenchymal cells
    - connection 46
    - hardwoods 54
    - rattan 50
    - wood cells 49
  - partial kappa numbers
    - lignin fractions after washing 724
    - resistant lignin fractions 724
  - partial pressure, ozone 779
  - particle size distribution, viscose samples 1032
  - passage ratio
    - debris *see* debris passage ratio
    - fibers *see* fiber passage ratio
  - passing velocity 565
  - PDI *see* polydispersity index
  - pectin 30
  - peeling
    - anhydro-sugar unit removal 175–176
    - oxidative 177
    - secondary 188
  - peeling effect, fiber walls 1049
  - peeling reactions 937
    - polysaccharides 661
    - pulp purification 934
    - starting from reducing end-groups 660–662
    - starting from stabilizing end-groups 662
    - stopping at 4-*O*-methylglucuronic acid side chains 179
  - penetrability, wood species 135
  - penetration, kraft cooking mass transfer 122, 129, 132–137
  - penetration factor 134

- penetration rate, effect of steam pressure
  - during pre-steaming 130
- pentosan
  - as function of cooking temperature 463
  - as function of H-factor 464
  - determination 1233
- pentoses
  - degradation 420
  - hemicelluloses 28
  - spent liquor content as function of viscosity 456
- peracetic acid
  - demand 881
  - equilibrium 881
  - oxidation capacity 613
  - oxidation equivalents (OXE) 264
  - post-treatment 883
  - pulp bleaching 880
- perforation plates, patterns 53
- permanganate demand, hot acid hydrolysis 883
- permanganate number 1228–1229
- permeability 513
  - as function of fiber concentration 514
- peroxide bleaching 1132, 1134–1135
  - catalyzed 877
  - ozonation 1038
  - pressurized 866–867
- peroxide solutions, stability in water 863
- peroxide stage, residence time 865
- peroxide-supported extraction stages, temperature effect 865
- PGW *see* pressure groundwood
- pH
  - acid sulfite cooking liquor analysis 433
  - oxygen delignification 704–705
  - pine delignification 473
  - profile 728
  - pulp washing parameter 533–534
  - Rauma three-stage sulfite cook 471
  - sorbed sodium 520
  - spruce pulp yield and acetyl content 474
  - sulfite pulping processes 393
  - temporal development in AS/AQ pine pulping 479
- pH effect, ozone bleaching 811–812
- pH fall during bleaching, oxidation processes 863
- phase transformation model, kappa numbers 684
- phases, cellulose I 26
- phenolate anions 703
- phenolic compounds
  - absorbance spectra 58
  - hardwoods 38
  - softwoods 37
- phenolic coupling, hydroxyl radical adducts of aromatic structures 654
- phenolic extractives, topochemical distribution 61–63
- phenolic hydroxyl
  - content in lignin samples 636
  - content in residual lignin 263
  - relative reactivity 635
- phenolic hydroxyl groups
  - bleaching 848
  - in lignin fractions 173
- phenolic lignin subunits
  - carbohydrate degradation 795
  - chemistry 164
  - chromophore formation 172
  - structure 164
- phenolic phenylcoumaran structures 411
- phenolic phenylcoumarans, neutral sulfite pulping reactions 413
- phenolic pinoresinol structures 410
  - neutral sulfite pulping reactions 414
- phenolic polymer, lignin 31
- phenolic structures, hydroperoxide formation 652
- phenols
  - in condensation reactions 424–425
  - ionization 703
- phenoxy radical
  - chlorine bleaching 746
  - formation by oxygen or by hydroxyl radical 650
- phenylcoumaran structures, phenolic 411
- phenylpropane  $\alpha$ -carbonyl- $\beta$ -arylether structures, sulfonation 412
- phenylpropane building blocks, lignin 32
- phenylpropanols 858
- phenylpropanones 858
- phenylpropene unit 2, HOMO- and electron density distribution 633
- PHK process 11, 345–365, 816
  - development 7
  - dissolving pulp 1024
  - influence of process conditions 351–358
  - influence of wood species 358–365
  - lignin and xylan removal rate 348
  - *see also* prehydrolysis
- PHK pulp
  - purification efficiency 942
  - selectivity 838

- phosphate ion, ozone decomposition, promotor 789
- photochemical oxidation, lignin models 655
- photodegradation,  $\alpha$ -carbonyl group-containing lignin model compounds 655
- photometric methods, metal ions determination 1222
- photometry, operating principle 1221
- photosensitized degradation, loblolly pine (*Pinus taeda*) 656
- physical properties, hydrogen peroxide 850–853
- Picea*, pulp bleaching 1126
- Picea abies* 33
  - average cell dimensions 52
  - bordered pits 47
  - carbohydrate composition 251
  - cell wall layers 43
  - chemical composition 23, 360, 451
  - density and void volume 128
  - diffusion coefficient 148–149
  - earlywood transition 49
  - hemicelluloses, nonglucosic units 29
  - inorganic composition 40
  - latewood tracheids 62
  - resin acid composition 36
  - resin canals 52
  - stem section 55
- Picea glauca*, chemical composition of wood 23
- Picea marina*
  - effect of steam pressure during pre-steaming 130
  - hemicelluloses, nonglucosic units 29
- Picea smithii*, spiral thickenings 44
- pick-up systems, paper collection 1178–1179
- pile dimensions, softwood chips 99
- pine
  - AS/AQ pulping 479–480
  - black liquor composition 968
  - comparison of kraft cooking experiments with predictions of selected kinetics model 225
  - delignification as function of pH 473
  - density and void volume 128
  - diffusion coefficient 148–149
  - effect of steaming on air removal 131
  - kraft cooking selectivity plot 226, 232, 243
  - specific light absorption coefficient of unbleached kraft pulp 269
  - structural xylan changes during conventional kraft cook 254
- pine/spruce conventional kraft cooking 233
- $\alpha$ -pinene, conversion to cymene during sulfite pulping 426
- pinoresinol structures, phenolic 410
- pinosylvin, structure 425
- Pinus*
  - inorganic composition 40
  - pulp bleaching 1126
- Pinus eliottii*, resin acid composition 36
- Pinus monophylla*, resin acid composition 36
- Pinus radiata*
  - AQ effects on kraft pulping 325
  - chemical composition of wood 23
- Pinus strobus*
  - hemicelluloses, nonglucosic units 29
  - inorganic composition 40
  - resin acid composition 36
- Pinus sylvestris* 36
  - average cell dimensions 52
  - black liquor composition 968
  - chemical composition of wood 23
  - density and void volume 128
  - diffusion coefficient 148–149
  - effect of steaming on air removal 131
  - extractives 35
  - hemicelluloses, nonglucosic units 29
  - specific light absorption coefficient of unbleached kraft pulp 269
  - total kraft cooking yield as function of residual EA concentration 239
  - woodyard storage 71
- Pinus taeda* 33
  - EMCC<sup>®</sup> pulp 297
  - photosensitized degradation 656
  - resin acid composition 36
- pit consistency, grinding process parameters 1084
- pit pulp properties 1097
- “pitch”, acid pulping 426
- pits
  - closing 47
  - in hardwoods and softwoods 46
  - secondary wall 46
  - softwood fibers 123
- plant biomass, yearly production 15
- plasmodesmata, cell components 46
- plastics, selective removal 594
- plate heating elements, falling film evaporator 975
- plate-type falling film evaporator 976
- plug-flow model 566, 568, 591
- pocket grinders, mechanical pulping 1089–1090

- polluter-pays principle *see* producer responsibility
- pollution prevention options 105–106
- polyalcohols, ozone decomposition, promotor 789
- polychlorinated dioxins, effluent content 1000
- polychlorinated phenols, adsorbable organic compounds 771
- polydispersity
- changes 1059
  - degradation reaction 685
  - index 844, 1018
- polyelectrolytes, osmotic pressure 1245
- polylignol, lignin 31
- polymer components, plant fibers 1257
- polymeric compounds, pulp 1227
- polymerization, degree of *see also* DP, 952, 1229, 1239
- polymerized lignin, hydrogen peroxide 853
- polymers
- cell wall 30
  - fractionation 1252
  - instability 1038
  - phenolic 31
  - precipitation 1252
  - wood 1018
- polynosic-type fiber, wet tenacity 1027
- polyoses
- conversion products 1233
  - pulp bleaching 1123
- polyoxometalates, alternative bleaching methods 887
- polysaccharide chain, cleavage 662–666
- polysaccharide degradation 796, 841
- polysaccharides
- composition 1231–1234
  - fractionation 1230
  - peeling reactions 661
  - treatment with aqueous acidic compounds 327
  - wood 30
- polysulfide 195, 201–202, 211
- disproportionation kinetics 307–308
- polysulfide addition, effect on CBC impregnation liquor 290–293
- polysulfide ions, formation under kraft cooking conditions 185
- polysulfide liquor 306
- polysulfide pretreatment, yield increase as function of redox potential 310
- polysulfide pulping 306–316
- combined effects of PS and AQ pulping 314–316
  - mill experience 314
- POM *see* polyoxometalates
- ponderosa pine, average moisture content 125
- poplar
- lignin weight fractions 213
  - radial diffusion coefficient 144
- Populus*
- average cell dimensions 52
  - inorganic composition 40
  - pulp bleaching 1126
  - steroids 37
- Populus deltoides carolinensis*, radial diffusion coefficient 144
- Populus rubrum*, kinetic parameters for xylan water prehydrolysis 333
- Populus tremula*
- chemical composition 451
  - density and void volume 128
- Populus tremuloides*
- comparison of experimental data with diffusion model 153–154
  - hemicelluloses, nonglucosic units 29
  - kinetic parameters for xylan water prehydrolysis 333
- pores 1265–1267
- collapse 1054
  - structure, cell wall 1052–1056
- porosity 1266
- as function of fiber concentration 514
- porous woods, vessels 53
- portal cranes, log handling 97
- positive sorting, recovered paper 1188
- post-consumer recovered paper 1177–1180
- post-oxygen washing 731
- post-treatment with peracetic acid, effect on brightness 883
- Pourbaix diagram, AQ redox equilibria 317
- power dissipation, as function of pulp consistency 615
- pre-consumer recovered paper 1177–1180
- pre-heated air, kraft recovery boiler 985
- pre-steaming, kraft cooking pretreatment 130
- pre-thickening, kraft black liquors 975
- precipitation
- pulp resins 1031
  - xylan 1050
- prehydrolysis
- general discussion 325–345

- intensity *see* P-factor
- kinetic weight-loss parameters 332
- kraft process *see* PHK process
- liquor-to-wood ratio 326
- P-factor concept 343–345
- prehydrolysis-kraft process 347–350
- wood yield temporal development for beechwood 331
- pressure
  - acid sulfite cooking cycle 427
  - calculated influence on impregnation in Kazi and Chornet model 157
  - CBC process 283
  - during VisCBC hardwood cooking process 347
  - grinding process parameters 1084
  - influence equation in Kazi and Chornet diffusion model 151
  - predicted time-dependency in selected model of kraft cooking kinetics 224
  - Rauma three-stage sulfite cook 471
  - two-stage delignification operating conditions 730
- pressure diffuser
  - Kvaerner 555
  - pulp washing equipment 554–555
- pressure disk filter 990
- pressure drop, centrifugal cleaning operating parameters 587
- pressure grinding 1095–1098
- pressure groundwood grinder 1095
- pressure pulse profile, contoured-drum rotor (S-rotor) 573
- pressure relief, acid sulfite pulping process chemistry 430–434
- pressure screen 568
  - basket design 1118
  - capacity 575
  - equipment 601–604
  - protecting 597
  - rotors 1117–1118
  - single-stage 1116
- pressure steaming, effect on ion diffusion 149
- pressure swing adsorption 828
- pressure washer
  - drum rotation speed and effective filtration pressure 536
  - pulp feed air content 534
  - pulp feed consistency 533
  - pulp temperature 535
  - rotary drum 529
- pressurization, hydrostatic 405
- pressurized peroxide bleaching 866–867
- pressurized reactors, bleaching equipment 625–627
- prestige, hot chlorine dioxide stage 765
- pretreatments, ozone bleaching 818–822
- primary alcohols, ozone decomposition, promotor 789
- primary effluent treatment 1004
- primary fines, beech pulp 1020
- primary wall, cell components 42, 44
- printing paper grades, mechanical pulp properties 1142
- probability separation 563
- process chemistry
  - acid sulfite pulping 427–465
  - kraft cooking 229–325
- process control
  - flow chart 96
  - wood yard operations 95
- process steps
  - continuous cooking 378–380
  - displacement cooking 368
  - EMCC®/ITC 387
  - Lo-Solids™ process 389
  - MCC 385
- process variables 698
  - kraft cooking kinetics models 199–211
  - oxygen delignification 701–708
- processing rings, debarkers 78
- producer responsibility 1192, 1194
- profiling line 88
- profiling router, tool arrangement 88
- prohibitive materials, recovered paper 1162
- promoters, ozone generation 789
- protecting pressure screen 597
- protective layer, cell components 48
- protons, NMR-spectroscopy 1261
- Prunus*, semi-ring-porous hardwoods 53
- PS *see* polysulfide
- PS/AQ
  - mill experience 316
  - pulp RLCC composition 640–641
- PSA *see* pressure swing adsorption
- pseudo first-principle models, kraft cooking kinetics 198–199
- Pseudotsuga menziesii*
  - chemical composition of wood 23
  - inorganic composition 40
  - resin acid composition 36
  - spiral thickenings 44
- pteridophytes, lignin 30
- pulp 1113–1122
  - alkali resistances 1013, 1015, 1229

- analytical characterization 1211–1280
- AS 478
- ASAM 273
- beech *see* beech
- beech sulfite dissolving *see* beech sulfite dissolving
- birch *see* birch
- bleachability 273, 296–297
- brightening 853
- brightness *see* brightness
- carbohydrate composition 255
- carbohydrates 937
- cellulose *see* cellulose
- chain scissions 260, 1058
- characteristics 1138
- chemical *see* chemical pulp(ing)
- chemimechanical 1098–1102
- chemithermomechanical 1099–1102
- cleaning 561–606
- comparative fractional composition 1139
- consumers 1024
- cooking 231–233, 395–403, 459–465
- copper number 952, 1014, 1062
- cotton linters 1022, 1036
- delignification *see* delignification
- discharge, continuous cooking process step 379
- dissolving *see* dissolving pulp
- effective alkali content 229, 239, 358
- extractives *see* extractives
- fibrillar morphology 1047
- fractionation 561–606
- hardwood *see* hardwood(s)
- hemicellulose 240, 361
- impregnation 403–405, 428
- intrinsic viscosity *see* intrinsic viscosity
- ITC-type pulp 273, 695
- kappa number *see* kappa number
- kraft *see* kraft pulp(ing)
- latency 1137–1143
- lignin *see* lignin
- low-viscosity 464, 957
- mannan 361, 1061
- mannose 440, 1013
- manufacture 973
- mechanical *see* mechanical pulp
- mechanical properties 1275–1280
- molecular weight distribution 1019, 1034–1035
- organic chlorine content 764
- origin 1024
- oxygen delignification *see* oxygen delignification
- paper-grade 728, 1010–1021
- papermaking properties 1281–1290
- PHK *see* PHK process
- pine *see* pine
- prehydrolysis *see* PHK process
- properties 769, 1009–1068
- purification 933–966
- purity 1043–1044
- quality 223, 733–734, 843, 953–963
- raw material 21–63, 1075–1078
- RDH 255
- reflectance and absorption coefficient spectra 611
- screening 561–606, 1113–1122
- softwoods *see* softwood(s)
- spruce *see* spruce
- sulfite *see* sulfite pulp
- tensile index 808, 1140
- thermomechanical *see* thermomechanical pulp
- unbleached *see* unbleached pulp
- viscosity *see* viscosity
- water retention value 1014, 1062
- wood dissolving 1035, 1044
- xylan *see* xylan
- yield *see* pulp yield
- zero-span tensile index 808, 1014, 1020
- pulp acidification 811
- pulp bleaching 609–894, 1123–1136
  - chemical 868–880
  - dithionite 1124
  - ECF *see* ECF bleaching
  - general principles 609–610
  - hydrogen peroxide 1123, 1126–1133
  - magnesium hydroxide 1130
  - oxygen delignification 628–734
  - ozone generation 782
  - peracetic acid 880
  - TCF *see* TCF bleaching
  - technology 1134–1136
  - *see also* bleaching, chlorine dioxide bleaching, ozone bleaching
- pulp components 708
  - reactions 935–941
  - yields 110
- pulp composition
  - beech and spruce sulfite cooks 448
  - beech magnesium acid sulfite cook 439
- pulp consistency 708
  - ECCSA 801
  - effect 806–810
  - in relation to power dissipation 615



- pulp fibers
  - cell wall 1052
  - centrifugal cleaning operating parameters 587
  - fractionation 1051
  - morphological features 1270
  - schematic crosssection 799
  - screening operating parameters 578
  - stress-strain characteristics 1277
  - *see also* fibers
- pulp-liquor systems, basic rheology 614–615
- “pulp mat” 512
- pulp mill effluents, environmental effect 735
- pulp mill wood yard, schematic material flow 70
- pulp production
  - environmental aspects 997–1008
  - raw material 21–63
  - worldwide development 1071
- pulp resins 1030
- pulp sheet properties, mechanical 1279
- pulp specification 1060–1062
- pulp stone 1079, 1092–1095
  - grinding process parameters 1084
  - immersion 1085
  - softening 1080
  - structure 1093
- pulp strength 1016
  - as function of intrinsic viscosity for kraft softwood pulp 236
  - modified kraft cooking 256–257
  - strength 293–295, 297
- pulp washer
  - diffusion 552–555
  - flows and concentrations 538–539
  - mass balance 530–531
  - streams 529
- pulp washing 511–558
  - compressive dewatering 525–526
  - countercurrent washing 527
  - dilution factor 529–532, 545–546
  - dilution/extraction 524
  - discharge consistency 532–533
  - displacement ratio 538–539, 543
  - displacement washing 524–525
  - Donnan theory 521
  - efficiency 531, 537–546
  - fractional 528
  - in-digester 557–558
  - mixing stages 539
  - most important equation 543
  - multi-stage 526–527
  - parameters 528–536
  - pH 533–534
  - principles 523–528
  - simplified illustration 512
  - theory 512–523
- pulp washing equipment 547–558
  - atmospheric diffuser 552–554
  - belt washers 551–552
  - conventional drum washers 549–550
  - drum displacer (DD) 549–550
  - pressure diffuser 554–555
  - roll presses 556–557
- pulp yield 953–962
  - as function of H-factor 440
  - as function of kappa number 230, 233, 249, 321
  - as function of pH 474
  - as function of residual  $[\text{OH}^-]$  concentration 240
  - as function of standard batch cooking process parameters 229–234
  - temperature effect 865
  - unbleached 469
- pulping 25
  - alternative sulfite pulping concepts 465–482
  - anthraquinone 314–325
  - chemical 109–508
  - definition 109
  - effluents 998, 1138
  - future developments 16–17
  - historical development 998–1002
  - kraft *see* kraft pulping
  - market situation 8–15
  - MCC<sup>®</sup> 256, 296–297
  - mechanical *see* mechanical pulping
  - Mitscherlich process 392
  - multistage kraft pulping 325–365
  - neutral sulfite pulping 393, 412–414
  - polysulfide *see also* PS/AQ, 306–316
  - reject handling 1113–1122
  - Ritter–Kellner process 392
  - selectivity 197–198
  - semi-mechanical 1111
  - sulfite *see* sulfite pulping
  - sulfite chemical *see* sulfite chemical pulping
  - sulfonation 412
  - technology, end-uses, and the market situation 8–15
- pulping liquor, recovery 1004
- pulsed amperometric detection 939

- pumps
- atmospheric peroxide bleaching system 867
  - medium consistency 617–619
- Purdue model, kraft cooking kinetics 198–199
- pure liquid, shear stress 1248
- purification 959–962
- cold alkali 934, 948
  - cold caustic extraction 935
  - degree 953, 959
  - efficiency after hot caustic extraction 948
  - *Eucalyptus* prehydrolysis-kraft pulp 943–944
  - extractives 960–961
  - hardwood sulfite pulp 943
  - hot 934
  - hot caustic extraction 935
  - kappa number 960–961
  - levels 954
  - phases 955
  - pulp 933–966
  - pulp viscosity 959
  - selectivity 363
  - Visbatch<sup>®</sup> process 363
- purification efficiency
- NaOH concentration 946
  - PHK pulp 942
  - sulfite pulp 942
- purification yield 958
- alkali resistances 958
  - R18 content 963
  - R18 dependence 956
  - xylan content 958
- purified cotton linters, influence of salts on degeneration 709
- purity levels, eucalyptus prehydrolysis-kraft pulp 944
- pyranosyl cation 416
- pyrolysis, organic material 992
- PZ treatments 1038
- q**
- QC *see* quality control
- QPQP bleaching 267–271
- brightness development as function of consumed OXE 271
- quality control, fundamentals 1213–1218
- quality profile, dissolving pulp 1023
- quality requirements, mechanical pulp 1143
- quercetin, formation from taxifolin under acid sulfite conditions 426
- Quercus* 37
- Quercus alba*, inorganic composition 40
- Quercus nigra*, pulp yield–kappa number relationship in soda-AQ cook 321
- Quercus robur*
- average cell dimensions 52
  - extractives 35
  - obligate heartwood formation 57
- Quercus rubra*, kinetic parameters for xylan water prehydrolysis 333
- quinoid structures
- elimination by alkaline hydrogen peroxide 875
  - lignin 857
  - residual lignin 174
- quinone-methide
- addition of hydrogen sulfide 167
  - formation 166
  - LUMO-distribution 166
  - reduction 170
- quinone-methide intermediate
- chlorine bleaching 747
  - lignin 856
- r**
- R-values *see* alkali resistances
- R10 *see* alkali resistances
- R18
- lignin content 1230
  - *see also* alkali resistances
- R2 process, chlorine dioxide generation 742
- radial concentration profile
- Kazi and Chornet diffusion model of impregnation 153
  - numerical solution of diffusion equation 162–163
- radial diffusion coefficient
- as function of NaOH concentration 145
  - Poplar 144
- radial impregnation, NaOH concentration profile 155
- radiation degradation, molecular weight reduction 1059
- radical formation 792, 829
- radical part, ozone reactions 791
- radical reactions 792
- radical-scavenging
- methanol 821
  - organic solvents 822
- radical-type chain reactions 789
- radical yield 812
- Radiclon AM, Noss 606
- Radiscreen, Noss 603–604
- Raditrim, Noss 604

- raised roll thickness screen 91–92
- Raman spectroscopy 117, 178
- Raoult's law 970
- rapid displacement heating *see* RDH
- rare sugar, yield as function of H-factor 438
- rattan, cell types 50
- Rauma three-stage sulfite cook
  - *a*-cellulose as function of third stage pH and temperature 471
  - pH, temperature and pressure course 471
- raw material
  - mechanical pulp 1075–1078
  - paper 1153–1156
  - pulp production 21–63
  - storage 69–71
  - unsuitable 1157
- rays
  - hardwoods 54
  - softwoods 51
- RDH 9
  - cooking cycle 373
  - effective alkali profile 276–277
  - hydraulic cook 275
  - results 275–280
  - sulfide ions concentration 278
  - technology and equipment 372–373
- RDH pulp
  - HexA content 278–279
  - xylan content 255
- reaction conditions
  - acid sulfite pulping process chemistry 449–464
  - pulp quality 953–962
- reaction enthalpy, kraft recovery boiler 984
- reaction kinetics, crystallinity 1262–1263
- reaction wood 54–56
- reactive oxygen species *see* ROS
- reactivity
  - bleaching chemicals 611
  - chlorite ions 739
  - lignin model compounds 635
  - lignin structures 634–641
  - pulp specification 1060
- reactors 827
  - atmospheric downflow 624–625
  - atmospheric peroxide bleaching system 867
  - atmospheric upflow 623–624
  - medium consistency 623–627
  - pressurized 625–627
  - pressurized peroxide bleaching system 866
- rechipper 86–87
- reclaimer, chip storage 102–103
- recovered paper 1147–1210
  - annual flow in comparison to virgin paper 15
  - basic statistics 1165–1176
  - collection 1165, 1170, 1177–1182
  - cycle, Europe 1184
  - demand, Germany 1160
  - different rates 1173
  - future development 1175–1176
  - global trade, expected 1172
  - grades 1157–1164, 1203–1210
  - handling 1187–1190
  - industrial volume 1153
  - Japan 1161, 1163
  - naming criteria 1158
  - nonpaper components 1204
  - outthrow materials 1162
  - prohibitive materials 1162
  - recycling rate 1165, 1173–1175
  - sorted 1189
  - sorting, handling, and storage 1187–1190
  - sources 1183–1186
  - unusable materials 1204
  - usage 1151
- recovered paper utilization
  - CEPI countries 1161
  - global development 1148
  - rate 1165, 1167–1168
  - rate for different paper grades 1169
- recovery 967–997
- recovery boiler *see* kraft recovery boiler
- recovery furnace, black liquor 968
- recovery rate 1170–1173
- recovery systems, sulfite compounds 994–995
- recycled fibers 1147–1210
  - relevance as paper raw material 1153–1156
- recycled fibers use, legislation 1191–1210
- recycling, waste strategy 1192
- recycling rate, recovered paper 1173–1175
- red hickory, average moisture content 125
- red maple, chemical composition of wood 23
- redox cycle, laccase mediator-system 887
- redox mechanisms, lignin 319
- redox potential
  - dioxygen 643
  - in kraft pulp with polysulfide pretreatment 310
- reducing end-groups
  - chains scissions 1058
  - peeling reactions 660–662

- stabilization 657–660
- reduction, degree of *see* DR
- reduction efficiency 982
- reduction energetics, oxygen 643
- reduction products, dioxygen 644
- reductive bleaching 1134
- refiner mechanical pulp 1098
  - definition 1072
- refiner plates 1108
  - designs 1109
- refiner process 1098–1112
- refiner types, characteristics 1108
- reflectance, sheets 1280
- reflectance spectra, hardwood sulfite pulp 611
- refractive index, acid sulfite cooking liquor analysis 433
- refractory kappa number 672
- regenerated cellulose fibers, production by viscose process 7
- regenerated fibers 1047
  - global production 11
- regeneration
  - black liquor 112
  - cellulose II 27
- reject handling, pulp processing 1113–1122
- reject rate, screening operating parameters 575
- reject ratio, volumetric 568–569, 576
- reject refining stage 1121
- reject thickening, in relation to volumetric reject ratio 568–569, 576
  - screening theory 566–570
- reject treatment 1121–1122
- relative hydrolysis rates, methyl-b-pyranosides and 328
- relative oxygen susceptibility, lignin model compounds 640
- reliability, quality control 1215
- removal efficiency, fibers 590–591
- repeatability, quality control 1215
- reprecipitation, xylan 1011
- reproducibility, quality control 1215
- residual chromophores 1030
- residual lignin 174, 704, 856–859, 1033
  - composition after cooking and bleaching 634–640
  - contents 722
  - functional group content 635
  - linkage frequencies 638
  - modification with peracetic acid 880
  - phenolic hydroxyl content 263
  - $\beta$ -O-4-structures content 263
- residual lignin-carbohydrate complex *see* RLCC
- residual lignin structures 173–174, 713–716, 749
  - milled wood lignin, conventional and EMCC® kraft pulp 262
  - modified kraft cooking 257–264
- residual phase, kraft pulping reactions overview 184
- residual sodium, unidirectional longitudinal diffusion 139
- resin 1030–1033
  - black liquor 967
  - dissolving pulp characterization 1061
- resin acids
  - kraft cooking extractives 183
  - softwoods 35–36
- resin canals, softwoods 52
- resin content, wood quality 1075
- resin ducts, softwoods 51
- resin reduction 960
- resin-rich, softwoods and hardwoods 465
- resistance to chlorine dioxide oxidation 749
- resistant lignin fractions, partial kappa numbers 724
- resonance structures, chlorine dioxide 735
- Resource Conservation and Recovery Act, US legislation 1195
- Resource Recycling Facilitation Law, Japanese legislation 1198
- retention time 702–703, 804
  - ozone bleaching 802
  - temperature, speed 1098
  - two-stage delignification operating conditions 730
- rheology, pulp-liquor systems 614–615
- ribonic acid, content in aldonic acid residues 658
- rice straw fibers, cell dimensions and chemical composition 4
- ring-conjugated structures, hydroxyl radical adducts 653
- ring debarkers 77–80
- ring grinder, mechanical pulping 1088
- ring-porous hardwoods, *Fraxinus excelsior* 53
- ring-porous woods
  - liquid flow 133
  - vessels 53
- Ritter–Kellner process 6
  - sulfite chemical pulping 392
- RLCC 634, 666–668
  - composition before and after after bleaching 640–641

- enzymatically isolated 667
- *see also* lignin-carbohydrate complexes
- RMP *see* refiner mechanical pulp
- Robert, Louis-Nicholas 5, 1073
- Robinia pseudoacacia*, tyloses 48
- Roe number 1228
- roll presses, pulp washing equipment 556–557
- roller conveyor, log handling 98
- ROS 647–649, 655, 663, 666
- rotary debarker 72, 76–77
- rotary drum pressure washer, empirical capacity model 529
- rotary drum washers, pulp washing equipment 547–550
- rotor
  - categories 564
  - screening equipment parameters 573–575
- rotor tip velocity, screening operating parameters 577
- rotor types, pulsation elements 1117
- RTS™ *see* retention time, temperature, speed
- Ruff-type degradation 796
  
- s**
- S-factor 430–431
- S-Mixer, Metso 620
- S-rotor, pressure pulse profile 573
- S-values, alkali solubility tests 1060
- S2, cell wall layer 473
- saccharinic acids, hot caustic extract 961
- Salomix agitator, Sulzer 628
- saltcake loss 537
- sampling, data 1216
- sand, selective removal 593
- santalol 37
- Santalum album*, santalol 37
- sapwood
  - conversion to hardwood 59
  - *Pinus monophylla*, resin acid composition 36
- saturation approach, pulp washing sorption theory 519
- saturation level, absorbed sulfide ions 242
- scalping screen section, chip screens 92
- scanning electron microscopy 60, 404
- scanning UV microspectrophotometry 60–61
- scattering intensity, angular dependence 1246
- scattering methods 1245
- schedule management, batch cooking 376
- Schiff bases, formation 1235
- Schoon's distribution function 675
- Schopper-Riegler method
  - freeness determination 1282
  - values 1283
- Schweizer's reagent 1241
  - cellulose molecular weight determination 1240
- Scots pine
  - chemical composition of wood 23
  - total kraft cooking yield as function of residual EA concentration 239
- scraper conveyor, log handling 98
- screen, streams 563
- screen basket 572–573
  - flow vectors 565
  - wedge wire 1117
- screen operating curves 592
- screen plates, slotted 1117
- screened yield
  - as function of cooking temperature 463
  - as function of  $\text{HSO}_3^-$  462
  - as function of viscosity 454
  - conventional, MCC® and EMCC® cooking 297
  - different  $[\text{OH}^-]$  values 289
  - different AQ charges 324
  - polysulfide addition effect 292
  - unbleached Visbatch® pulp 353, 357, 362
- screening 563–572
  - applications 592–594
  - chips 89
  - elements 1114
  - equipment parameters 572–575, 600–606
  - fiber fractionation 1274
  - fiber passage and reject thickening 566–570
  - flow regime 564–565
  - furnish parameters 578–579
  - machines and aggregates 1114–1120
  - mechanical 89–93
  - operating parameters 575–578
  - pulp 561–606
  - pulp processing 1113–1122
  - selective fiber passage 570–572
  - three-stage (cascade feedback arrangement) 596
  - two-stage (cascade feed-forward arrangement) 598
  - wood 80–88
- screening efficiency 588–592
  - as function of debris passage ratio and volumetric reject ratio 590
  - as function of screening quotient and mass reject ratio 589

- definition 588
- screening quotient (Q) 588
- in relation to screening efficiency 589
- screening zone length 567
- in relation to consistency 570
- in relation to fiber passage ratio 569
- screw conveyor
  - log handling 98
  - shredding 550
- screw reclaimer, chip storage 103
- SEC *see* size-exclusion chromatography
- second chlorine dioxide stage, effect on brightness 758
- secondary effluent treatment 1004
- secondary fines, beech pulp 1020
- secondary knot screens, screening and cleaning equipment 604–605
- secondary peeling 188
- secondary wall, cell components 42
- sedimentation, centrifugal cleaning theory 581–584
- seed and fruit fibers, cell dimensions and chemical composition 4
- selective contaminant removal 592–594
- selective fiber passage, screening theory 570–572
- selective hydrolysis, lignin content 1227
- selective lignin bromination 316
- selective separation, centrifugal cleaning theory 585–586
- selectivity
  - as function of initial NaOH charge 480
  - chlorine dioxide bleaching 760
  - delignification/purification in Visbatch® process 363
  - oxygen delignification 702, 720–721
  - ozone treatment 829–840
- selectivity plot
  - comparison of CLF and standard batch cooking 245
  - conventional, MCC® and EMCC® cooking 297
  - different alkali ratios in spruce AS/AQ pulping 479
  - different AQ charges 323–324
  - different wood species 453
  - effect of polysulfide addition in CBC process 292–293
  - influence of [OH<sup>-</sup>] in CBC cooking liquor 288–289
  - influence of CBC cooking temperature 290
  - oxygen bleaching 629
  - pine/spruce kraft cooking 226, 232
  - pretreated pine/spruce kraft cooking 243
  - radiata pine kraft pulp 247
- self-decomposition, ozone 811
- SEM *see* scanning electron microscopy
- semi-chemical pulp 1009
  - global production 9
- semi-open rotor 564
- semi-ring-porous woods, vessels 53
- sensitivity to wood raw material, pulping processes 1031
- separate extraction, thick liquor 975
- separation
  - selective (centrifugal cleaning theory) 585–586
  - single elements determination 1221
- separation efficiency
  - definition 588
  - fractionation 590–592
  - pulp screening and cleaning 588–592
- sequential treatment, CCE and (E/O) stages 948
- series feedback arrangement, two-stage fractionation system 600
- sesquiterpenic tropolone derivatives, softwoods 35
- SET *see* single electron transfer
- settling particle, forces 581
- settling velocity, Newton's law 582
- SF *see* S-factor
- SGW *see* stone groundwood
- sheet properties 1278–1280
  - mechanical 1279
- shives
  - deliberation 1113
  - selective removal 593
- short-chain alkali-soluble carbohydrates 1026–1030
- short-chain carbohydrates, removal 951
- short-chain hemicelluloses, removal 952
- short fiber loss, in relation to long fiber removal 592
- shredding screw conveyor 550
- siberian larch, chemical composition of wood 23
- side chain structures
  - hydroxyl radical adducts 654
  - lignin 857
- side reactions
  - acidic sulfite cooking 423
  - inorganic 737–741
  - sulfur-containing carbohydrates 422–424

- side relief, acid sulfite pulping process
  - chemistry 429
- silo reclaimer, chip storage 102
- silo storage, chips 101
- silo-stored hardwood chips, *Acer saccharum* 99
- silver birch, chemical composition of wood 23
- silver maple, average moisture content 125
- simple pit, softwood fibers 123
- single-disc refiner 1105
- single electron transfer
  - degradation mechanism 320
  - hydrogen peroxide reactions 852
- single elements, determination 1221–1224
- single fibers
  - cell dimensions and chemical composition 4
  - defibrillation 1083
  - flexibility 1276
  - properties 1275–1278
  - stress-strain curves 1012
  - suspended 1272
- single log layer chipping 82
- single O<sub>2</sub>–excited state 645–646
- single-phase model, crystallinity 1258
- single pulp fibers, stress-strain characteristics 1277
- single-stage oxygen delignification system, process flowsheet 732
- single-vessel continuous cooking system, outline 377
- single-vessel hydraulic digester
  - downflow 390
  - EMCC<sup>®</sup>/ITC 386
  - Lo-Solids™ process 388
  - MCC 383
- single wet fibers, parameters 1275
- sisal, cell dimensions and chemical composition 4
- Sitka spruce, average moisture content 125
- β*-sitosterol 37
- Sivola processes 468–471
  - aspen cooks 468
- size-exclusion chromatography 1252, 1254
  - water prehydrolyzate from beechwood 340
- slaked lime 986
- slaker 989
- slaking 987–988
- slash pine, sorbed sodium–pH relation 520
- slewing screw reclaimer, chip storage 103
- sludge 1004
  - wastewater treatment 1007
- smelt 982, 986
  - calculation 983
  - kraft recovery boiler 985
  - sodium carbonate 987
- smelt dissolving 988
  - weak wash 990
- SO<sub>2</sub> *see* sulfur dioxide
- soap skimming 967
  - displacement cooking process step 371
- soda-AQ 178, 194–195, 201–202, 211, 321, 345
  - effects on *Eucalyptus grandis* pulping 325
  - *see also* AQ
- soda boiler 962
- soda pulping process, discovery 6
- sodium
  - comparative evaluation of diffusion coefficients 149–150
  - distribution between fiber wall and external solution 419
  - effect on kraft cooking kinetics models 207
  - sorption as function of pH 520
- sodium-based two-stage sulfite pulping, pH-dependency of delignification, pulp yield and acetyl content 473–474
- sodium borohydride
  - cellulose protecting additive 819
  - decomposition by hydrogen gas 1236
  - post-treatment 822–824
  - pulp bleaching 1125
- sodium carbonate 987
  - conversion 986
- sodium chlorate, reduction 741
- sodium dithionite, commercial grades 1125
- sodium hydroxide 987
  - concentration 703
- sodium peroxide, industrial bleaching 849
- sodium silicate stabilization, pulp bleaching 1129
- softening, fibers 1080–1083
- softwood fibers
  - cell dimensions and chemical composition 4
  - heterogeneity 123
- softwood kraft pulp
  - comparison of different cooking conditions 234
  - oxygen delignification 713, 723
  - selectivity 838
  - TCF bleaching with peracetic acid 882

- softwood kraft pulping, interdependence of
  - temperature, cooking time and effective alkali 251
- softwood PHK, representative dissolving pulp 1036
- softwood sawmills, profiling line 88
- softwood structure 50–54
- softwood-sulfite dissolving pulp 1036
  - R18 content 955
- softwood xylan, structural changes 252–256
- softwoods
  - accessory compounds 35–37
  - annual ring 51
  - axial parenchyma 51
  - bleaching 882, 1126
  - bordered pits 123
  - cellulose 22
  - chemical composition of wood 23
  - chip pile dimensions 99
  - chipper canter 88
  - defibration conditions 1102
  - diterpenes 35
  - fats and fatty acids 36
  - flavonoids 37
  - hemicellulose 22
  - lignans 37
  - lignin 22
  - lignins 33
  - macromolecular substances 22
  - monoterpene 35
  - oleoresin 35
  - penetrability 135
  - phenolic compounds 37
  - pits 46, 123
  - pulp 1010
  - pulp bleaching 1126
  - rays 51
  - resin acids 35–36
  - resin canals 52
  - resin ducts 51
  - resin-rich 465
  - sesquiterpenic tropolone derivatives 35
  - stilbene 37
  - tall oil 36
  - tracheids 51
  - tropolone derivatives 35
  - waxes 36
  - xylan 29, 252–256
- soil-contaminated, waste generation 105
- solid-phase NMR spectroscopy 1261–1262
- solid-solid separation, liquid environment 562
- solid-state NMR spectroscopy 168
- solid waste 1006
  - municipal 1181–1182
- solids concentration, thick liquor 974
- solubility
  - alkali 1229
  - ozone 780–781
  - pulp constituents 937
- solubility of oxygen, equilibrium conditions 692
- solubilization, ozone 802
- soluble fraction, alkali solubility tests 1060
- solution viscosity 1248–1251
- Solvay process, chlorine dioxide generation 742
- solvent retention 1268
- solvents, cellulose 1240–1241
- sootblowing steam, kraft recovery boiler 985
- sorbed manganese, as function of pH 523
- sorbed sodium, as function of pH 520
- sorption, pulp washing theory 519–523
- sorted recovered paper, handling 1189
- sorting, recovered paper 1187–1190
- southern pine, effect of polysulfide 312
- southern mixed hardwood, pulp yield as function of kappa number 230
- southern pine, pulp yield as function of kappa number 230
- southern red oak, average moisture content 125
- specialty papers, utilization rate 1169
- specific consumption, active kraft cooking chemicals 221
- specific drainage resistance 515
- specific light absorption coefficient
  - residual softwood lignin 266
  - unbleached pine 269
- specific surface
  - as function of fiber concentration 514
  - dry fibers 1267
- specific volume, pulp bleaching 1131
- specific yield loss 949
- spectroscopy
  - cellular UV 44
  - energy dispersive X-ray spectroscopy 40
  - Fourier transmission infra-red 159
  - NMR 31, 168, 173–174, 254
  - Raman 117, 178
  - solid-phase NMR spectroscopy 1261–1262
  - time-of-flight secondary ion mass spectroscopy 60
  - X-ray photoelectron spectroscopy 60
- spent sulfite liquor 448, 962
- spermatophytes, lignin 30



- spinnability, cellulose 1034
- spiral burrs, pulp stone 1094
- spiral thickenings 44
- spruce
  - average moisture content 125
  - characterization of unbleached kraft pulp in CBC and conventional cooking 285
  - chemical composition 360, 451
  - comparison of kraft cooking experiments with predictions of selected kinetics model 225
  - density and void volume 128
  - diffusion coefficient 148–149
  - kraft cooking selectivity plot 226, 232, 243
  - lignin weight fractions 213
  - pH, pulp yield and acetyl content 474
  - pulp 109
  - selectivity plot for different alkali ratios in AS/AQ pulping 479
  - Sivola process pulp properties 469
  - stem section 55
  - Visbatch<sup>®</sup> process conditions 365
  - viscosity–H-factor relationship 452
- spruce CBC pulp 285, 292
- spruce sulfite cooks, pulp and spent liquor compositions 448
- spruce sulfite pulp, brightness increase 879
- spruce wood, ASAM pulping process 59
- SR *see* Schopper-Riegler method
- stabilization, reducing end-groups 657–660
- stabilized end-groups, peeling reactions 662
- stacker reclaimer, boom-type 103
- stages, liquor circulation 888–890
- staining methods, fiber identification. 1270
- stalk fibers, cell dimensions and chemical composition 4
- standard batch cooking process 229–234
  - carbohydrate composition of pulp 255
  - parameters 234
- standard chlorine dioxide bleaching 754–759
- standard grades of recovered paper and board, European list 1203–1210
- standardized Norden efficiency factor 545–546, 558
- standardized outlet consistency 545
- starch, wood content 30
- static mixers, bleaching equipment 621–622
- static ozone bleaching 800
- stationary conveyor systems, log handling 97–98
- Staudinger-Mark-Houwink equation 1250–1251
- steam
  - generation, kraft recovery boiler 985
  - pressurized peroxide bleaching system 867
- steam consumption, reduced with cold blow technology 274
- steam drum, kraft recovery boiler 981
- steam economy, multiple-effect evaporation 978
- steam mixers, atmospheric 622–623
- steam pressure, effect on penetration rate during pre-steaming 130
- steaming
  - acid sulfite pulping process chemistry 428
  - effect on air removal 131
  - impregnation 405
  - kraft cooking pretreatment 129–132
- steel plate conveyor, log handling 98
- steeping, dissolving pulp 1026
- stem section, *Lophira alata* 58
- stem structure, wood characterization level 21
- step rotor, cross section 564
- stepwise degradation, effect on molecular weight 959
- steric intramolecular interactions, glycone 327
- steroids, hardwoods 37
- stilbene
  - formation and reactions 411
  - relative oxygen susceptibility 640
  - softwoods 37
  - structure 640
- stilbene structures, resistance to chlorine dioxide oxidation 749
- stoker discharger, chip storage 104
- Stokes–Einstein model, diffusion 147
- Stokes' law 582
- stone groundwood 1087, 1098
  - definition 1072
- stones, selective removal 593
- Stora processes 465, 472–475
- storage
  - recovered paper 1187–1190
  - wood yard 69–71
- streams
  - around a hydrocyclone 579
  - around a screen 563
- strength delivery, pulp 256–257
- strength F-value 1104
- strength properties
  - CBC pulp 293–295
  - MCC<sup>®</sup> softwood pulp 297

- ozonation effect 841–843
- viscose fibers 1036–1037
- stress-strain characteristics, single pulp fibers 1012, 1277
- structural changes, xylan 254
- structural levels, wood characterization 21
- $\beta$ -1 structures, reaction to stilbenes 411
- $\beta$ -O-4-structures 31–32, 183–184, 261–270, 273, 407–413, 475, 638–640, 655, 716, 725
- content in relation to consumed OXE 268
- content in residual lignin 263
- phenolic 309, 858
- substrate radical reactions 793
- ozone 790
- sugar cane bagasse fibers, cell dimensions and chemical composition 4
- sugar maple, chemical composition of wood 23
- sugars
  - concentration development in beechwood prehydrolysis 339
  - dehydration products 420
  - ozone decomposition, promotor 789
- sulfamic acid, addition 764
- sulfated ash, inorganic components 1220
- sulfide
  - concentration profile 241–244
  - sorption in wood 242
- sulfide ions, concentration as function of cooking time in RDH process 278
- sulfide-lean/rich white liquors, composition 244
- sulfidity
  - in relation to kappa number 355
  - influence on pulp yield in standard batch cooking process 230–233
  - kraft cooking active chemicals 114, 116
  - white liquors 244
- sulfidolytic cleavage,  $\beta$ -O-4 ether 172
- sulfite, concentration in sulfite cooking liquor 400–401
- sulfite chemical pulping 392–482
  - cooking chemicals and equilibria 395–403
  - historical development 392–395
  - impregnation 403–405
- sulfite chemical recovery 994
- sulfite cooking 957
  - carbohydrates acid hydrolysis 416–425
  - chemistry 405–427
  - condensation 414–415
  - extractives reactions 425–427
  - lignin reactions 407–416
  - one-stage acid cooking parameters 452
  - Rauma three-stage 471
- sulfite cooking liquor
  - acid 396
  - ionic species concentrations 400–401
- sulfite dissolving pulp, beechwood 433
- sulfite pulp 1009
  - beating resistance 1011
  - carbohydrate composition 470
  - fibers, global production 9
  - purification efficiency 942
  - reflectance and absorption coefficient spectra 611
  - resin reduction 960
  - R-values 1015
- sulfite pulping
  - alkaline 475–482
  - alternative concepts 465–482
  - pH ranges 393
- sulfitolysis, lignin 407
- sulfonation
  - $\beta$ -O-4 aryether structures 410
  - lignin 407–408
  - phenylpropane  $\alpha$ -carbonyl- $\beta$ -arylether structures 412
  - $\alpha$ -position of coniferylaldehyde-type structures 412
  - reactions in neutral sulfite pulping 412
- sulfonic acid
  - formation from xylose under neutral sulfite conditions 422
  - reactions with glucose 422
- sulfur-containing carbohydrates, formation 421–425
- sulfur dioxide 998
  - amount as function of H-factor 435
  - balance 434–449
  - bound–free equilibrium 405
  - concentration in sulfite cooking liquor 400–401
  - diffusion coefficient at 20 °C 404
  - partial pressure–temperature relation in sulfite cooking liquor 402
  - temperature dependence of dissociation constant  $K_{a,1}$  397
- sulfur species, balance 436–437
- sulfuric acid, pulp acidification 811
- Sulzer Ahlmix 621
- Sulzer flow discharger 627
- Sulzer Salomix agitator 628
- super pressure grinders 1096
- Superbatch® process
  - cooking cycle 136–137, 374
  - results 280–282

- simplified flowsheet 374
  - technology and equipment 373–374
  - superheaters, kraft recovery boiler 981
  - supermolecular structures, characterization 1257–1268
  - superoxide anion, ozone decomposition, initiator 788
  - superoxide anion radical 646
    - converter 788
    - hydrogen peroxide intermediates 852
  - superoxide formation, ozone reactions 794
  - supramolecular structure 1041–1047
  - surface, accessible 1267
  - surface area, specific *see* specific surface
  - surface condenser 978
  - surface tension
    - black liquor 971
    - black liquor and water 136
  - surfactants, application 687
  - surge bin, chip storage 102
  - suspended single fibers, characteristic parameters 1272
  - sweetgum, average moisture content 125
  - swelling 937
    - concept of Bouchard 799
    - pulp 1052
    - pulp fibers 1268
    - unbleached kraft pulp 733
  - synthesis gas, cleaning 994
  - syringyl
    - monolignol structural units 31
    - structures 830
  - syringylpropane
    - lignin 165
    - molecular structure 32
- t**
- TA *see* total alkali
  - tall oil
    - crude 967
    - kraft pulping 112
    - softwoods 36
  - Tampella-grinder 1095
  - tandem infeed rings, debarkers 79
  - tangential velocity profile, hydrocyclone 581
  - tangential walls, cell components 44
  - tannins, hardwoods 38
  - Tasmanian emission levels, marine environment 1005
  - taxifolin 449
    - formation of quercetin under acid sulfite conditions 426
  - TCF-bleached acid sulfite 1048
  - TCF-bleached dissolving pulp, characterization 1049, 1051
  - TCF bleaching 10, 816, 1040
    - bleachability 267
    - hydrogen peroxide application 868
    - sulfite 877–880
  - TCF bleaching sequence 843
    - groups 727
    - ozone placement 848
  - tear index 235–236
    - as function of cellulose content 294
    - as function of tensile index 294, 482
    - of kraft softwood pulp as function of kappa number 235
    - viscosity dependence 841
  - tear resistance, pulp 1141
  - tear strength, CBC pulp 293
  - tear-tensile plot
    - for AS/AQ and kraft CBC cooking 482
    - for CBC, CBC-PS and conventional kraft pulp 294
  - Tectona grandis*, gutta 38
  - temperature 701–702
    - acid sulfite cooking cycle 427
    - AS/AQ pine pulping 479
    - caustic extraction 944–945
    - CBC process 283
    - centrifugal cleaning operating parameters 587
    - during VisCBC hardwood cooking process 347
    - grinding process parameters 1084
    - in relation to kappa number and dissolved xylose 463
    - in relation to pentosan and screened yield 463
    - in relation to relative pressure washer capacity 535
    - influence on CBC process 289–290
    - influence on pulp yield in standard batch cooking process 231–233
    - Lo-Solids™ cook 303
    - predicted time-dependency in selected model of kraft cooking kinetics 224
    - pulp washing parameter 535
    - Rauma three-stage sulfite cook 471
    - screening operating parameters 577
    - two-stage delignification operating conditions 730
  - temperature distribution, softwood chip pile 99
  - temperature effect
    - on kraft cooking kinetics models 200–203

- on modified kraft cooking 248–251
- oxygen delignification 813–814
- tensile index 235–236
- commercial paper-grade pulp 1014
- in relation to tear index 294, 482
- pulp 808, 1140
- tensile strength
  - single fibers 1278
  - zero-span 1019
- tension wood 55–56
- terpenes
  - hartwoods 37
  - isoprene 35
- tert-butanol, cellulose protecting additive 819
- tertiary treatment 1005
- test water, analytical purposes 1224
- tetra-ammin-copper(II)-hydroxide *see* CUOX-AM
- tetranitromethane method 829
- textile filaments, dissolving pulp
  - applications 1025
- TGW *see* thermo groundwood
- thermal conductivity, black liquor 972
- thermal pre-treatment, refiner process 1100
- thermal processes, refiner process 1101
- thermal stability, hydrogen peroxide 863–865
- thermo groundwood 1092
- thermomechanical pulp 1098
  - energy consumption 13
  - role in global pulp production 12
  - screening system 1120
- thick liquor, separate extraction 975
- thickening factor (T) 584–585
- thickness distribution, fiber wall (after centrifugal cleaning) 585
- thin-layer chromatography 1232
- thiosulfate
  - formation 423
  - model reaction with vanillyl alcohol 424
  - role in sulfur-containing carbohydrates formation 422–424
- three-stage screening, cascade feedback arrangement 596
- three-stage sequence, hydrogen peroxide application 872
- Tilghman, Benjamin 6, 392
- Tilia americana*, inorganic composition 40
- time-of-flight secondary ion mass spectroscopy 60
- tissue structure, wood characterization level 21
- titration curve
  - titrator base Mg(OH)<sub>2</sub> 399
  - titrator base NaOH 399
- TMP *see* thermomechanical pulp
- TMP line
  - single-stage 1109
  - two-stage 1110
- TMS *see* trimethylsilyl ethers
- TNM *see* tetranitromethane method
- ToF-SIMS 60
- Tomlinson-type chemical recovery boiler 992
- torus, cellulose microfibrils 47
- total alkali, kraft cooking active chemicals 114
- total ash
  - commercial paper-grade pulp 1014
  - pulp 1220
- total reduced sulfur 1002
- total titratable alkali, kraft cooking active chemicals 114–115, 988
- total weight of wet wood 124
- totally chlorine free bleaching *see* TCF bleaching
- Tower scrapers, Metso 624
- toxic compounds, kraft pulping 112
- tracheids
  - cell components 46
  - softwoods 51
  - wood cells 49
- transition metal ions 814–816
  - reactions with hydrogen peroxide 854
- transition metals
  - hydrogen peroxide decomposition 860
  - ozone decomposition 789
- transparency, sheets 1280
- transport systems, wood yard operations 95–106
- transversal diffusion coefficient, dependency on temperature and activation energy 140
- transversal groundwood 1079
- traveling screw reclaimer, chip storage 103
- “tree-free” paper 14
- Trichoderma longibrachiatum* 822
- triglycerides, hardwoods 38
- trimethylglucose, conformers 1231
- trimethylsilyl ethers, monosaccharides determination 1231
- tropolone derivatives 37
  - softwoods 35
- TSR *see* total reduced sulfur
- Tsuga*, inorganic composition 40
- Tsuga canadensis*
  - chemical composition of wood 23
  - hemicelluloses, nonglucosic units 29
- TTA *see* total titratable alkali

- TurboFeed system 381–382
  - turpentine 967
  - twin-refiner 1106
  - two-stage bleaching processes 879
  - two-stage delignification, operating conditions 730
  - two-stage fractionation system 600
  - two-stage neutral magnefite process 467–468
  - two-stage oxygen delignification 631
    - first commercial application 727
    - industrial fractions 722
  - two-stage screening, cascade feed-forward arrangement 598
  - two-stage sulfite pulping, pH-dependency of delignification, pulp yield and acetyl content 473–474
  - two-step chlorine dioxide bleaching, advantages 767
  - two-vessel MCC<sup>®</sup> system, impregnation vessel 385
  - tyloses, cell components 48
- u**
- UCC *see* upper cooking circulation
  - Ulmus*, steroids 37
  - Ulmus americana*
    - hemicelluloses, nonglucosic units 29
    - kinetic parameters for xylan water prehydrolysis 333
  - ultrastructure
    - cell wall components 41–44
    - wood characterization 21
  - UMSP *see* scanning UV microspectrophotometry
  - unbleached hardwood sulfite pulp, reflectance and absorption coefficient spectra 611
  - unbleached pulp 348–350
    - quality, predicted by selected model of kraft cooking kinetics 223
    - yield, Sivola process spruce pulp 469
  - unbleached softwood kraft pulp, comparison of different cooking conditions 234
  - unbleached spruce kraft pulp, parameters in CBC and conventional cooking 285
  - unbleached spruce pulp, paper properties 109
  - underflow, hydrocyclone 579–580
  - underflow thickening, centrifugal cleaning theory 584–585
  - unidirectional longitudinal diffusion, residual sodium fractions 139
  - United States
    - legislation 1195–1198
    - recovered paper grades 1162
  - UP *see* unbleached pulp
  - upflow reactors, atmospheric 623–624
  - upper cooking circulation 388
  - urban forest 1151
  - uronic acids, determination 1233–1234
  - utilization, packaging materials 1193
  - utilization rate 1167
  - UV microscopy, fiber morphology 1271
- v**
- Va-Purge process 130
  - vacuum swing adsorption 828
  - validation, selected model of kraft cooking kinetics 223–227
  - valley beater, pulp beating 1281
  - Valmet PGW grinder 1095
  - Valonia ventricosa* 24
  - van Heiningen model 689
    - theoretical base 690–701
  - vanillin
    - chlorine bleaching 747
    - structure 308
  - vanillyl alcohol
    - chlorine bleaching 747
    - model reaction with thiosulfate 424
  - vapor recompression 979–980
  - vascular cells, cell components 46
  - velocity
    - aperture/passing 565
    - rotor tip (screening operating parameters) 577
  - velocity profile, hydrocyclone 581
  - veratryl- $\beta$ -guaiaicyl ether, homolytic fragmentation and oxidation 751
  - veratrylglycerol- $\beta$ -guaiaicyl ether 749
  - vessels
    - cell components 46
    - hardwoods 53
    - rattan 50
    - wood cells 50
  - vibrating conveyor, log handling 98
  - vibratory screens 605
  - Vilamo method 403
  - vinyl ether
    - resistance to chlorine dioxide oxidation 749
    - structure and relative oxygen susceptibility 640
  - virgin paper, annual flow in comparison to recovered paper 15
  - virgin pulp fiber
    - consumption for paper production 1154

- global production 8–9
  - Visbatch<sup>®</sup> process 7, 327, 346–350, 352–365, 1024, 1051
    - development 327
    - process conditions for beech, birch, eucalypt and spruce 365
  - VisCBC 7, 346–348, 1024, 1032
    - hardwood cooking process 347
  - viscose
    - dissolving pulp applications 1025
    - production of regenerated cellulose fibers 7
    - quality 1031–1032
  - viscose fibers
    - dissolving pulp characterization 1061
    - strength properties 1036–1037
  - viscosity 959–960
    - adjustment, ozone task 831
    - as function of extinction 433
    - as function of H-factor 440, 464
    - as function of residual effective alkali 270, 272
    - beech sulfite pulp 1042
    - black liquor 970–973
    - borol charge dependence 823
    - CBC cooking liquor 288
    - CED-intrinsic 451
    - commercial paper-grade pulp 1013
    - conventional, MCC<sup>®</sup> and EMCC<sup>®</sup> cooking 297
    - degradation, sulfite cooking 1045
    - detrimental effect 814
    - different wood species 452–453
    - dissolving pulp characterization 1061
    - during ozonation, temperature effect 813
    - efficiency of chlorine dioxide 768–769
    - in relation to R18 363
    - in relation to screened yield 454
    - in relation to xylan 455
    - in spent liquor 456–457, 459
    - increase, polymers in solution 1248
    - kraft softwood pulp 236
    - Lo-Solids<sup>™</sup> laboratory cooks 302
    - loss in G-factor model 195–197, 356–357
    - measurements 1248–1251
    - oxygene bleaching 629
    - pine kraft pulp 825
    - pine/spruce kraft cooking 226, 232, 243
    - polysulfide addition effect 293
    - predictions, comparison against experiment 687
    - preservation 819, 823
    - radiata pine kraft pulp 247
    - reduced 1250
    - selectivity plot for different AQ charges 323
    - selectivity plot for different CBC cooking temperatures 290
    - spruce AS/AQ pulping 479
    - standard batch cooking 245
    - TCF-bleached dissolving pulp 1049, 1051
    - temperature effect 865
    - unbleached Visbatch<sup>®</sup> pulp 353, 357
  - viscosity–kappa number relationship 364, 452–453, 479–480
  - visible microscopy, fiber morphology 1271
  - VOC *see* volatile organic compounds
  - void volume fraction 127–128
  - voids 1265–1267
  - volatile compounds, single elements determination 1221
  - volatile oils 34
  - volatile organic compounds 1002
  - volume element, annular differential (screening theory) 566
  - volumetric reject ratio, as function of reject thickening factor 568–569, 576
    - volumetric reject ratio 590
  - VSA *see* vacuum swing adsorption
- W**
- warm black liquor 372–373, 375–376
  - wash filtrate 990
  - wash yield 537–538
  - washing
    - atmospheric peroxide bleaching system 867
    - bleaching 628, 866–867
    - bleaching equipment 628
    - cold caustic extraction 942
    - continuous cooking process step 379
    - delignification 826
    - fractional 528
    - HCE treatment 954
    - hi-heat 384, 558
    - in-digester 557–558
    - interstage 948
    - lignin fractions 724
    - medium-consistency ozone delignification system 826
    - multi-stage 526–527
    - parameters 528–536
    - pH 533–534
    - post-oxygen 731
    - pressurized peroxide bleaching system 867

- pulp 511–558
- washing zone, hi-heat 384
- waste disposal, waste strategy 1192
- Waste Disposal Law, Japanese legislation 1198
- waste generation, causes 105
- waste reduction 104–106
- wasted oxidation potential 740
- water, surface properties 136
- water-accessible pore volume, cotton linters 1053
- water extractives 1224–1225
- water fractions, cell wall 1052
- water layer
  - adsorbed 800
  - immobile 808
- water oak, pulp yield–kappa number relationship in soda-AQ cook 321
- water retention 1053, 1268
  - commercial paper-grade pulp 1014
  - dissolving pulp characterization 1062
  - value (WRV) 1016
- water uptake, cellulose 1268
- waterjet conditioning, pulp stone 1094
- Watt, Charles 5
- waxes, softwoods 36
- WAXS *see* wide-angle X-ray scattering methods
- WBL *see* warm black liquor
- weak wash 990
- weakly nucleophilic resonance form, condensation reaction with benzylium ion 415
- wedge-shaped knife, disc chipper 81
- wedge-wire screen basket 573, 1117
- weight force, on settling particle 581
- weight fraction, commercial pulp 1020
- western hemlock
  - average moisture content 125
  - lignin weight fractions 213
- western red cedar, average moisture content 125
- wet debarking 74
- wet fibers, properties 1275–1277
- wheat straw fibers, cell dimensions and chemical composition 4
- wheel loaders, log handling 97
- white fir, average moisture content 125
- white liquor
  - acid–base equilibria 117
  - carbonate ion 115
  - composition 113, 244
  - density 116
  - dregs 988
  - effective alkali 244
  - filterability 987
  - grits 989
  - hot white liquor 346, 348, 372–374
  - hydrogen sulfide ion 115
  - hydroxide ion 115
  - influence on superbatch process 281
  - kraft pulping 111
  - neutralization curve 119
  - oxidation in MOXY process 311
  - preparation processes 988–990
  - sulfide-lean/rich 244
  - sulfidity 244
  - *see also* black liquor, liquor(s)
- white oak, average moisture content 125
- white rot fungi, alternative bleaching methods 886
- white spruce, chemical composition of wood 23
- whiteness, sheets 1279
- wide-angle and small-angle X-ray scattering methods 60
- wind screening 93–94
- wood
  - characterization 21
  - chemical composition 22–23
  - elementary composition 22
  - inorganic composition 40
  - macromolecular substances 22
  - mechanical defibration 1073, 1086
  - microscopic structure 48–59
  - polysaccharides content 30
  - processing 1076–1078
  - pulp raw material 21–59
  - quality 1075
  - storage 1076
  - structure 123–129
  - structure and morphology 41–48
  - water content 1095
- wood age, effect on kraft cooking kinetics models 210
- wood chip dimensions 127
  - effect on kraft cooking kinetics models 208–211
  - influence on Kazi and Chornet diffusion model of impregnation 158
- wood component yield
  - as function of lignin yield 481
  - AS/AQ and kraft pulping 476
  - beech magnesium acid sulfite cook 438
- wood components
  - degradation 437–449

- dissolved 446
  - wood dissolving pulp
    - lattice conversion 1044
    - molecular weight distribution 1035
  - wood extractives
    - major classes 34
    - volatile 967
  - wood fibers, cell dimensions and chemical composition 4
  - wood hemicelluloses *see* hemicellulose
  - wood log
    - chipping 1078
    - debarking 1076–1078
    - storage 1076
  - wood moisture content
    - chip quality 82
    - groundwood properties 1086
  - wood polymers, molar mass decrease 1018
  - wood pulp
    - chlorine dioxide bleaching 737–741
    - morphological features 1270
  - wood resins 34
  - wood species
    - effect on kraft cooking kinetics models 208–211
    - influence on acid sulfite pulping process chemistry 449–459
    - influence on prehydrolysis-kraft process 358–365
    - influence on viscosity–H-factor relationship 452
    - material balances in one-stage acid sulfite cooking 458
  - wood yard losses 104–106
  - wood yard operations 69–108
    - process control 95
  - wood yield, temporal development in water prehydrolysis of beechwood 331
  - wooden debris, waste generation 105
  - woodfree mixed office waste 1166
  - WRV *see* water retention value
- x**
- X-ray diffraction, crystallinity index 1259
  - X-ray diffractometer, goniometer 1260
  - X-ray fiber diagrams 1264
  - X-ray fluorescence spectroscopy (XFS) 1223
  - X-ray photoelectron spectroscopy (XPS) 60
  - XFS *see* X-ray fluorescence spectroscopy
  - XPS *see* X-ray photoelectron spectroscopy
  - xylan 834
    - alkali resistant 445
    - beechwood water prehydrolysis 344–345
    - CBC pulp 285
    - cooking liquor 303–304
    - degradation rate in Gustavson–Al-Dajani kinetic model 253
    - dissolving pulp characterization 1061
    - enrichment 1051
    - hydrolysis 343
    - in relation to COOH 441
    - in relation to screened yield 362
    - in relation to viscosity-to-kappa number ratio 364
    - influence on fiber morphology 180–181
    - kinetic modeling of hardwood prehydrolysis 329
    - molecular structure 28
    - pulp fraction 440
    - pulp residue 936
    - radial distribution 1050
    - redeposition 1048
    - relative acid hydrolysis rates 417
    - removal 936, 947, 949
    - removal rate in prehydrolysis-kraft process 348
    - reprecipitation 302, 1011
    - residual content 260, 332, 444
    - softwoods 29
    - specific consumption in selected model of kraft cooking kinetics 221
    - specific kraft pulping reactions 179
    - structural changes 252–256
    - TCF-bleached dissolving pulp 1049, 1051
    - unbleached Visbatch<sup>®</sup> pulp 352, 358, 361
    - viscosity 455
    - yield as function of H-factor 438
  - xylan backbone, substitution 883
  - xylan chains
    - cleavage 663
    - hardwoods 29
  - xylan content 719–721, 940, 1029
    - comparison with R18 contents 957–959
    - purification yield 958
    - specific yield loss 949
    - yellowness coefficient 1030
  - xylanase treatment 822
  - xylem, age dependent changes 56
  - xyloisosaccharinic acid, black liquor composition 968
  - xyloic acid, content as function of H-factor 447
  - xylose
    - commercial paper-grade pulp 1013
    - concentration development in beechwood prehydrolysis 336, 338



- content as function of H-factor 447
- decomposition 335
- degradation pathways 659
- formation of sulfonic acid under neutralsulfite conditions 422

**y**

- Y-P bleaching 1131
- yellow birch, average moisture content 125
- yellow-poplar, average moisture content 125
- yellowing 1038
- yellowness coefficient
  - diacetate solution 1029
  - triacetate solution 1030
- yield
  - carbohydrate amount in relation to lignin content in alkaline pulping 186
  - increase achieved by polysulfide pretreatment 310–311
  - pulp washing 537–538

- wood components 438, 476
- *see also* pulp yield, screened yield
- yield loss 950, 956
  - specific 949–951
- Young–Laplace equation 132

**z**

- zero-span strength, sheets 1278
- zero-span tensile index
  - commercial paper-grade pulp 1014
  - commercial pulp 1020
  - heterogeneous gas phase treatment 809
  - pulp viscosity dependence 808
  - viscosity dependence 842
- zero-span tensile strength 1019
- Zimm-constant 1247
- Zimm-plot 1247
- ZP treatment 1038
  - beech sulfite dissolving pulp 1039